FITNESS-FOR-SERVICE

API 579-1/ASME FFS-1, December 2021

AN INTERNATIONAL CODE

[Intentionally Left Blank]

All rights reserved. No part of this work may be reproduced, stored in a retrieval system, or transmitted by any means, electronic, mechanical, photocopying, recording, or otherwise, without prior written permission from the publisher.
Contact the Publisher, API Publishing Services, 1220 L Street, N.W., Washington, D.C. 20005.

Copyright © 2021 by the American Petroleum Institute and The American Society of Mechanical Engineers

ISBN 978-0-7918-7449-3

[Intentionally Left Blank]

CONTENTS

FOREWORD ..... **XXIX**

SPECIAL NOTES ..... **XXXI**

SUMMARY OF CHANGES ..... **XXXIII**

PART 1 – INTRODUCTION **1-1**

1.1 INTRODUCTION 1-1
1.1.1 Construction Codes and Fitness-For-Service *1-1*
1.1.2 Fitness-For-Service Definition *1-1*
1.2 SCOPE 1-2
1.2.1 Supplement to In-Service Inspection Codes *1-2*
1.2.2 Application Construction Codes *1-2*
1.2.3 Other Recognized Codes and Standards *1-2*
1.2.4 Remaining Life *1-3*
1.2.5 Assessment Methods for Flaw Types and Damage Conditions *1-3*
1.2.6 Special Cases *1-3*
1.3 ORGANIZATION AND USE 1-4
1.4 RESPONSIBILITIES 1-4
1.4.1 Owner-User *1-4*
1.4.2 Inspector *1-4*
1.4.3 Engineer *1-4*
1.4.4 Plant Engineer *1-5*
1.5 QUALIFICATIONS 1-5
1.5.1 Education and Experience *1-5*
1.5.2 Owner-User *1-5*
1.5.3 Inspector *1-5*
1.5.4 Engineer *1-6*
1.6 DEFINITION OF TERMS 1-6
1.7 REFERENCES 1-6
1.7.1 Types *1-6*
1.7.2 Code, Standards and Recommended Practices *1-6*
1.7.3 Technical reports and Other Publications *1-6*
1.8 TABLES 1-7

ANNEX 1A – GLOSSARY OF TERMS AND DEFINITIONS **1A-1**

PART 2 – FITNESS-FOR-SERVICE ENGINEERING ASSESSMENT PROCEDURE **2-1**

2.1 GENERAL 2-1
2.1.1 Fitness-For-Service and Continued Operation *2-1*
2.1.2 Organization by Flaw Type and Damage Mechanism *2-2*
2.1.3 FFS Assessment Procedure *2-2*
2.2 APPLICABILITY AND LIMITATIONS OF THE FFS ASSESSMENT PROCEDURES 2-3
2.2.1 FFS Procedures for Pressurized or Unpressurized Components *2-3*
2.2.2 Component Definition *2-3*
2.2.3 Construction Codes *2-3*

2.2.4 Specific Applicability and Limitations *2-3*
2.3 DATA REQUIREMENTS 2-4
2.3.1 Original Equipment Design Data *2-4*
2.3.2 Maintenance and Operational History *2-5*
2.3.3 Required Data/Measurements for an FFS Assessment *2-6*
2.3.4 Recommendations for Inspection Technique and Sizing Requirements *2-6*
2.4 ASSESSMENT TECHNIQUES AND ACCEPTANCE CRITERIA 2-6
2.4.1 Assessment Levels *2-6*
2.4.2 FFS Acceptance Criteria *2-7*
2.4.3 Data Uncertainties *2-8*
2.5 REMAINING LIFE ASSESSMENT 2-9
2.5.1 Remaining Life *2-9*
2.5.2 Guidance on Remaining Life Determination *2-10*
2.6 REMEDIATION 2-10
2.6.1 Requirements for Remediation *2-10*
2.6.2 Guidelines for Remediation *2-10*
2.7 IN-SERVICE MONITORING 2-10
2.8 DOCUMENTATION 2-11
2.8.1 General *2-11*
2.8.2 Applicability and Limitations *2-11*
2.8.3 Data Requirements *2-11*
2.8.4 Assessment Techniques and Acceptance Criteria *2-11*
2.8.5 Remaining Life Assessment *2-12*
2.8.6 Remediation Methods *2-12*
2.8.7 In-Service Monitoring *2-12*
2.8.8 Retention *2-12*
2.9 NOMENCLATURE 2-12
2.10 REFERENCES 2-13
2.11 TABLES 2-14
2.12 FIGURES 2-16

ANNEX 2A – TECHNICAL BASIS AND VALIDATION – FITNESS-FOR-SERVICE ENGINEERING ASSESSMENT PROCEDURE 2A-1

2A.1 TECHNICAL BASIS AND VALIDATION 2A-1
2A.2 REFERENCES 2A-1

ANNEX 2B – DAMAGE MECHANISMS 2B-1

2B.1 DETERIORATION AND FAILURE MODES 2B-1
2B.2 FFS ASSESSMENT AND THE IDENTIFICATION OF DAMAGE MECHANISMS 2B-1
2B.3 PRE-SERVICE DEFICIENCIES 2B-2
2B.3.1 Types of Pre-Service Deficiencies *2B-2*
2B.3.2 In-Service Inspection *2B-2*
2B.4 IN-SERVICE DETERIORATION AND DAMAGE 2B-2
2B.4.1 Overview *2B-2*
2B.4.2 General Metal Loss Due to Corrosion and/or Erosion *2B-3*
2B.4.3 Localized Metal Loss Due to Corrosion and/or Erosion *2B-3*
2B.4.4 Surface Connected Cracking *2B-4*
2B.4.5 Subsurface Cracking and Microfissuring/Microvoid Formation *2B-5*
2B.4.6 Metallurgical Changes *2B-6*

2B.5 REFERENCES 2B-7
2B.6 TABLES 2B-8

ANNEX 2C – THICKNESS, MAWP AND STRESS EQUATIONS FOR AN FFS ASSESSMENT 2C-1

2C.1 GENERAL 2C-2
2C.1.1 Scope 2C-2
2C.1.2 MAWP and MFH 2C-2
2C.1.3 Construction Codes and Common Rules 2C-2
2C.1.4 Use of VIII-2 Design Equations 2C-3
2C.2 CALCULATION OF T_{MIN}, MAWP (MFH), AND MEMBRANE STRESS 2C-3
2C.2.1 Overview 2C-3
2C.2.2 Minimum Required Wall Thickness and MAWP (MFH) 2C-3
2C.2.3 Code Revisions 2C-4
2C.2.4 Determination of Allowable Stresses 2C-4
2C.2.5 Treatment of Weld and Riveted Joint Efficiency, and Ligament Efficiency 2C-5
2C.2.6 Treatment of Damage in Formed Heads 2C-6
2C.2.7 Thickness for Supplemental Loads 2C-7
2C.2.7.1 Definition 2C-7
2C.2.7.2 Required Thickness 2C-7
2C.2.7.3 Vertical Vessels 2C-7
2C.2.7.4 Design-by-Rule Using VIII-2 ..... 2C-8
2C.2.7.5 Piping Systems 2C-8
2C.2.8 Determination of Metal Loss and Future Corrosion Allowance 2C-8
2C.2.9 Treatment of Metal Loss and Future Corrosion Allowance 2C-8
2C.2.10 Treatment of Shell Distortions 2C-8
2C.3 PRESSURE VESSELS AND BOILER COMPONENTS – INTERNAL PRESSURE 2C-9
2C.3.1 Overview 2C-9
2C.3.2 Shell Tolerances 2C-9
2C.3.3 Shell Thickness and MAWP 2C-9
2C.3.3.1 Cylindrical Shells 2C-9
2C.3.3.2 Spherical Shell or Hemispherical Head 2C-10
2C.3.3.3 Elliptical Head 2C-11
2C.3.3.4 Torispherical Head 2C-11
2C.3.3.5 Conical Shell 2C-12
2C.3.3.6 Toriconical Head 2C-13
2C.3.3.7 Conical Transition 2C-13
2C.3.4 Nozzles Connections in Shells 2C-16
2C.3.4.1 General 2C-16
2C.3.4.2 Required Reinforcement 2C-16
2C.3.4.3 Weld Strength Analysis 2C-17
2C.3.5 Junction Reinforcement Requirements at Conical Transitions 2C-19
2C.3.6 Other Components 2C-19
2C.4 PRESSURE VESSELS AND BOILER COMPONENTS – EXTERNAL PRESSURE 2C-20
2C.5 PIPING COMPONENTS AND BOILER TUBES 2C-20
2C.5.1 Overview 2C-20
2C.5.2 Metal Loss 2C-20
2C.5.3 Required Thickness and MAWP – Straight Pipes Subject to Internal Pressure 2C-20
2C.5.4 Required Thickness and MAWP – Boiler Tubes 2C-21
2C.5.5 Required Thickness and MAWP – Pipe Bends Subject to Internal Pressure 2C-21
2C.5.6 Required Thickness and MAWP for External Pressure 2C-23
2C.5.7 Branch Connections 2C-23

2C.6 API 650 STORAGE TANKS 2C-23
2C.6.1 Overview *2C-23*
2C.6.2 Metal Loss *2C-24*
2C.6.3 Required Thickness and MFH for Liquid Hydrostatic Loading *2C-24*
2C.7 ESTIMATION OF BURST PRESSURE 2C-24
2C.7.1 Svensson's Method *2C-24*
2C.7.2 Cylindrical Shell Burst Pressure *2C-25*
2C.7.3 Spherical Shell Burst Pressure *2C-25*
2C.8 NOMENCLATURE 2C-26
2C.9 REFERENCES 2C-32
2C.10 TABLES 2C-34
2C.11 FIGURES 2C-36

ANNEX 2D – STRESS ANALYSIS OVERVIEW FOR AN FFS ASSESSMENT 2D-1

2D.1 GENERAL REQUIREMENTS 2D-1
2D.1.1 Scope *2D-1*
2D.1.2 ASME B&PV Code, Section VIII, Division 2 (VIII-2) *2D-1*
2D.1.3 Applicability *2D-2*
2D.1.4 Protection Against Failure Modes *2D-2*
2D.1.5 Numerical Analysis *2D-2*
2D.1.6 Material Properties *2D-2*
2D.1.7 Applicable Loads and Load Case Combinations *2D-3*
2D.1.8 Loading Histogram *2D-3*
2D.2 PROTECTION AGAINST PLASTIC COLLAPSE 2D-4
2D.2.1 Overview *2D-4*
2D.2.2 Elastic Stress Analysis Method *2D-4*
2D.2.3 Limit Load Analysis Method *2D-4*
2D.2.4 Elastic-Plastic Stress Analysis Method *2D-4*
2D.2.5 Treatment of the Weld Joint Efficiency *2D-4*
2D.3 PROTECTION AGAINST LOCAL FAILURE 2D-5
2D.3.1 Overview *2D-5*
2D.3.2 Elastic Analysis Method *2D-5*
2D.3.3 Elastic-Plastic Analysis Method *2D-6*
2D.4 PROTECTION AGAINST COLLAPSE FROM BUCKLING 2D-6
2D.4.1 Assessment Procedure *2D-6*
2D.4.2 Supplemental Requirements for Components with Flaws *2D-6*
2D.5 SUPPLEMENTAL REQUIREMENTS FOR STRESS CLASSIFICATION IN NOZZLE NECKS 2D-6
2D.6 NOMENCLATURE 2D-6
2D.7 REFERENCES 2D-7
2D.8 TABLES 2D-8

ANNEX 2E – MATERIAL PROPERTIES FOR STRESS ANALYSIS 2E-1

2E.1 GENERAL 2E-1
2E.1.1 Material Properties Required *2E-1*
2E.1.2 Material Properties and In-Service Degradation *2E-2*
2E.2 STRENGTH PARAMETERS 2E-2
2E.2.1 Yield and Tensile Strength *2E-2*
2E.2.1.1 Mean Estimates of Tensile Strength from Hardness Tests 2E-2
2E.2.1.2 Minimum Specified Yield and Tensile Strength from MPC Correlations 2E-2

2E.2.1.3 Minimum Specified Yield and Tensile Strength from API Std 530 and WRC Bulletin 541 ..... 2E-3
2E.2.1.4 Minimum Specified Yield and Tensile Strength Data from ASME Code, Section II, Part D 2E-3
2E.2.1.5 Mean Values of Yield and tensile Strength from Minimum Specified Values 2E-3
2E.2.2 Flow Stress 2E-3
2E.2.2.1 Definition 2E-3
2E.2.2.2 Estimation of Flow Stress 2E-3
2E.3 MONOTONIC STRESS-STRAIN RELATIONSHIPS 2E-4
2E.3.1 MPC True Stress-Strain Curve Model 2E-4
2E.3.2 MPC Tangent Modulus Model 2E-5
2E.3.3 Ramberg-Osgood Stress-Strain Model 2E-6
2E.3.3.1 True Stress-Strain Curve 2E-6
2E.3.3.2 Engineering Stress-Strain Curve 2E-7
2E.3.4 Ramberg-Osgood Tangent Modulus Model 2E-8
2E.3.5 Engineering Stress-Strain Models for API 5L Pipeline Materials 2E-8
2E.3.5.1 Stress-Strain Model from CSA Z662 ..... 2E-8
2E.3.5.2 API 5L Grades X52 to X80 ..... 2E-8
2E.3.5.3 API 5L Grades X80 to X100 ..... 2E-8
2E.3.6 Tangent Modulus Model for API 5L Pipeline Materials 2E-10
2E.4 CYCLIC STRESS-STRAIN RELATIONSHIPS 2E-10
2E.4.1 Ramberg-Osgood Equation 2E-10
2E.4.2 Estimation of Cyclic Stress-Strain Curve Parameters 2E-10
2E.4.2.1 Estimation from Monotonic Properties 2E-10
2E.4.2.2 Uniform Material Law 2E-11
2E.5 PHYSICAL PROPERTIES 2E-11
2E.5.1 Elastic Modulus 2E-11
2E.5.2 Poisson's Ratio 2E-11
2E.5.3 Coefficient of Thermal Expansion 2E-11
2E.5.4 Thermal Conductivity 2E-11
2E.5.5 Thermal Diffusivity 2E-11
2E.5.6 Density 2E-12
2E.6 NOMENCLATURE 2E-12
2E.7 REFERENCES 2E-14
2E.8 TABLES 2E-16

ANNEX 2F – ALTERNATIVE METHOD FOR ESTABLISHING THE REMAINING STRENGTH FACTOR 2F-1

2F.1 OVERVIEW 2F-1
2F.2 ESTABLISHING AN ALLOWABLE REMAINING STRENGTH FACTOR – RSF_A 2F-1
2F.3 NOMENCLATURE 2F-2
2F.4 REFERENCES 2F-2

PART 3 – ASSESSMENT OF EXISTING EQUIPMENT FOR BRITTLE FRACTURE 3-1

3.1 GENERAL 3-2
3.1.1 Evaluation of Resistance to Brittle Fracture 3-2
3.1.2 Avoidance of Catastrophic Brittle Fracture 3-2
3.1.3 Use of Construction Codes and Standards for Brittle Fracture Assessment 3-2
3.1.4 Boilers and Boiler External Piping 3-2
3.1.5 Supplemental Brittle Fracture Assessment to Other FFS Assessment Procedures 3-2
3.1.6 Critical Exposure Temperature (CET) 3-3
3.1.7 Minimum Allowable Temperature (MAT) 3-3
3.2 APPLICABILITY AND LIMITATIONS OF THE PROCEDURE 3-3

3.2.1 Equipment Covered ... 3-3
3.2.2 Components Subject to Metal Loss ... 3-4
3.2.3 Requirements for In-Service Inspection and Maintenance Programs ... 3-4
3.2.4 Supplemental Guidance for SA-212 Grade B Material ... 3-4
3.3 DATA REQUIREMENTS ... 3-4
3.3.1 Original Equipment Design Data ... 3-5
3.3.2 Maintenance and Operational History ... 3-5
3.3.3 Required Data/Measurements for an FFS Assessment ... 3-5
3.3.4 Recommendations for Inspection Technique and Sizing Requirements ... 3-6
3.4 ASSESSMENT TECHNIQUES AND ACCEPTANCE CRITERIA ... 3-6
3.4.1 Overview ... 3-6
3.4.2 Level 1 Assessment ... 3-7
3.4.3 Level 2 Assessment ... 3-10
3.4.4 Level 3 Assessment ... 3-15
3.5 REMAINING LIFE ASSESSMENT ... 3-16
3.5.1 Acceptability for Continued Service ... 3-16
3.5.2 Pressure Vessels ... 3-17
3.5.3 Piping Systems ... 3-17
3.5.4 Atmospheric and Low Pressure Storage Tanks ... 3-17
3.6 REMEDIATION ... 3-17
3.6.1 Potential Use of Remediation Methods ... 3-17
3.6.2 Remediation Methods ... 3-17
3.7 IN-SERVICE MONITORING ... 3-19
3.7.1 In-Service Monitoring and Control of Process Conditions ... 3-19
3.7.2 Monitoring for Degradation of Low Alloy Steel Notch Toughness ... 3-19
3.7.3 Monitoring for Criticality of Growing Flaws ... 3-19
3.7.4 Assessment of Non-Growing Flaws Detected In-Service ... 3-19
3.8 DOCUMENTATION ... 3-19
3.8.1 Documentation Requirements for Each Assessment Level ... 3-19
3.8.2 Documentation Retention ... 3-20
3.9 NOMENCLATURE ... 3-20
3.10 REFERENCES ... 3-21
3.11 TABLES ... 3-22
3.12 FIGURES ... 3-28

ANNEX 3A – TECHNICAL BASIS AND VALIDATION – ASSESSMENT OF EXISTING EQUIPMENT FOR BRITTLE FRACTURE ... 3A-1

3A.1 TECHNICAL BASIS AND VALIDATION ... 3A-1
3A.2 REFERENCES ... 3A-1

PART 4 – ASSESSMENT OF GENERAL METAL LOSS ... 4-1

4.1 GENERAL ... 4-1
4.1.1 Assessment Procedures for General Metal Loss ... 4-1
4.1.2 Thickness Averaging Approach Used for the Assessment ... 4-1
4.2 APPLICABILITY AND LIMITATIONS OF THE PROCEDURE ... 4-2
4.2.1 General Metal Loss Assessment ... 4-2
4.2.2 Limitations Based on Flaw Type ... 4-2
4.2.3 Calculation of the $MAWP_r$ and MFH_r and Coincident Temperature ... 4-2

4.2.4 Limitations Based on Temperature *4-2*
4.2.5 Definition of Component Types *4-2*
4.2.6 Applicability of the Level 1 and Level 2 Assessment Procedures *4-2*
4.2.7 Applicability of the Level 3 Assessment Procedures *4-3*
4.3 DATA REQUIREMENTS 4-3
4.3.1 Original Equipment Design Data *4-3*
4.3.2 Maintenance and Operational History *4-3*
4.3.3 Required Data/Measurements for an FFS Assessment *4-4*
4.3.4 Recommendations for Inspection Technique and Sizing Requirements *4-6*
4.4 ASSESSMENT TECHNIQUES AND ACCEPTANCE CRITERIA 4-7
4.4.1 Overview *4-7*
4.4.2 Level 1 Assessment *4-8*
4.4.3 Level 2 Assessment *4-9*
4.4.4 Level 3 Assessment *4-11*
4.5 REMAINING LIFE ASSESSMENT 4-12
4.5.1 Thickness Approach *4-12*
4.5.2 MAWP Approach *4-12*
4.6 REMEDIATION 4-13
4.6.1 Objectives *4-13*
4.6.2 Methods *4-13*
4.7 IN–SERVICE MONITORING 4-15
4.7.1 Objectives *4-15*
4.7.2 Monitoring Methods *4-15*
4.7.3 Calibration *4-15*
4.8 DOCUMENTATION 4-15
4.8.1 General *4-15*
4.8.2 Inspection Data *4-15*
4.9 NOMENCLATURE 4-15
4.10 REFERENCES 4-18
4.11 TABLES 4-19
4.12 FIGURES 4-28

ANNEX 4A – TECHNICAL BASIS AND VALIDATION – ASSESSMENT OF GENERAL METAL LOSS 4A-1

4A.1 TECHNICAL BASIS AND VALIDATION 4A-1
4A.2 REFERENCES 4A-1

PART 5 – ASSESSMENT OF LOCAL METAL LOSS 5-1

5.1 GENERAL 5-1
5.1.1 Assessment Procedures for Local Metal Loss *5-1*
5.1.2 Choice of Part 4 or Part 5 Assessment Procedures *5-2*
5.1.3 Pitting Damage *5-2*
5.2 APPLICABILITY AND LIMITATIONS OF THE PROCEDURE 5-2
5.2.1 Local Metal Loss Assessment *5-2*
5.2.2 Limitations Based on Flaw Type *5-2*
5.2.3 Calculation of the $MAWP_r$ and MFH_r, and Coincident Temperature *5-2*
5.2.4 Limitations Based on Temperature *5-3*
5.2.5 Applicability of the Level 1 and Level 2 Assessment Procedures *5-3*
5.2.6 Applicability of the Level 3 Assessment Procedures *5-3*

5.2.7 Assessment of Blend Ground Areas for Crack-Like Flaw Removal *5-4*
5.3 DATA REQUIREMENTS 5-4
5.3.1 Original Equipment Design Data *5-4*
5.3.2 Maintenance and Operational History *5-4*
5.3.3 Required Data/Measurements for an FFS Assessment *5-4*
5.3.4 Recommendations for Inspection Technique and Sizing Requirements *5-5*
5.4 ASSESSMENT TECHNIQUES AND ACCEPTANCE CRITERIA 5-6
5.4.1 Overview *5-6*
5.4.2 Level 1 Assessment *5-6*
5.4.3 Level 2 Assessment *5-8*
5.4.4 Level 3 Assessment *5-14*
5.5 REMAINING LIFE ASSESSMENT 5-14
5.5.1 Thickness Approach *5-14*
5.5.2 MAWP Approach *5-15*
5.6 REMEDIATION 5-15
5.7 IN-SERVICE MONITORING 5-15
5.8 DOCUMENTATION 5-15
5.8.1 General *5-15*
5.8.2 Inspection Data *5-15*
5.9 NOMENCLATURE 5-16
5.10 REFERENCES 5-20
5.11 TABLES 5-21
5.12 FIGURES 5-27

ANNEX 5A – TECHNICAL BASIS AND VALIDATION – ASSESSMENT OF LOCAL METAL LOSS 5A-1

5A.1 TECHNICAL BASIS AND VALIDATION 5A-1
5A.2 REFERENCES 5A-1

PART 6 – ASSESSMENT OF PITTING CORROSION 6-1

6.1 GENERAL 6-1
6.1.1 Assessment of Pitting Corrosion *6-1*
6.1.2 Assessment of Blister Arrays *6-1*
6.2 APPLICABILITY AND LIMITATIONS OF THE PROCEDURE 6-1
6.2.1 Assessment of Four Types of Pitting Corrosion *6-2*
6.2.2 Calculation of the $MAWP_r$ and MFH_r and Coincident Temperature *6-2*
6.2.3 Limitations Based on Flaw Type *6-2*
6.2.4 Limitations Based on Temperature *6-2*
6.2.5 Applicability of the Level 1 and Level 2 Assessment Procedures *6-2*
6.2.6 Applicability of the Level 3 Assessment Procedures *6-3*
6.2.7 Assessment for Active Pitting Corrosion *6-3*
6.2.8 Future Corrosion Allowance *6-3*
6.3 DATA REQUIREMENTS 6-4
6.3.1 Original Equipment Design Data *6-4*
6.3.2 Maintenance and Operational History *6-4*
6.3.3 Required Data/Measurements for an FFS Assessment *6-4*
6.3.4 Recommendation for Inspection Technique and Sizing Requirements *6-5*
6.4 ASSESSMENT TECHNIQUES AND ACCEPTANCE CRITERIA 6-6
6.4.1 Overview *6-6*

6.4.2 Level 1 Assessment *6-6*
6.4.3 Level 2 Assessment *6-8*
6.4.4 Level 3 Assessment *6-13*
6.5 Remaining Life Assessment 6-14
6.5.1 MAWP Approach *6-14*
6.5.2 MAWP Procedure for Remaining Life Determination *6-14*
6.6 Remediation 6-15
6.7 In-Service Monitoring 6-15
6.8 Documentation 6-15
6.8.1 General *6-15*
6.8.2 Inspection Data *6-15*
6.9 Nomenclature 6-15
6.10 References 6-18
6.11 Tables 6-19
6.12 Figures 6-21

ANNEX 6A – TECHNICAL BASIS AND VALIDATION – ASSESSMENT OF PITTING CORROSION 6A-1

6A.1 Technical Basis and Validation 6A-1
6A.2 References 6A-1

PART 7 – ASSESSMENT OF HYDROGEN BLISTERS AND HYDROGEN DAMAGE ASSOCIATED WITH HIC AND SOHIC 7-1

7.1 General 7-2
7.1.1 Assessment Procedures for Hydrogen Blisters, HIC and SOHIC *7-2*
7.1.2 HIC Definition *7-2*
7.1.3 SOHIC Definition *7-2*
7.1.4 Hydrogen Blistering Definition *7-2*
7.1.5 HIC, SOHIC and Blistering Distinct Damage Types *7-3*
7.2 Applicability and Limitations of the Procedure 7-3
7.2.1 HIC, SOHIC and Blistering Distinct Damage Types *7-3*
7.2.2 Calculation of the $MAWP_r$ and MFH_r and Coincident Temperature *7-3*
7.2.3 Limitations Based on Temperature *7-3*
7.2.4 Applicability of the Level 1 and Level 2 Assessment Procedures *7-3*
7.2.5 Applicability of the Level 3 Assessment Procedure *7-4*
7.3 Data Requirements 7-4
7.3.1 Original Equipment Design Data *7-4*
7.3.2 Maintenance and Operational History *7-4*
7.3.3 Required Data/Measurements for an FFS Assessment *7-4*
7.3.4 Recommendations for Detection, Characterization, and Sizing *7-7*
7.4 Assessment Techniques and Acceptance Criteria 7-7
7.4.1 Overview *7-7*
7.4.2 Level 1 Assessment *7-8*
7.4.3 Level 2 Assessment *7-10*
7.4.4 Level 3 Assessment *7-14*
7.5 Remaining Life Assessment 7-15
7.5.1 HIC and SOHIC Growth Rates *7-15*
7.5.2 Blister Growth *7-16*
7.6 Remediation 7-16

7.6.1 Elimination of Hydrogen Charging *7-16*
7.6.2 Controlling Hydrogen Charging *7-16*
7.6.3 Venting of Blisters *7-16*
7.6.4 Blend Grinding *7-16*
7.6.5 Repair and Replacement of Damaged Material *7-17*
7.6.6 NACE Standard SP0296-10 ..... *7-17*
7.7 IN-SERVICE MONITORING 7-17
7.7.1 Monitoring for Hydrogen Charging *7-17*
7.7.2 Inspection Methods for Monitoring *7-17*
7.7.3 Detection of HIC, SOHIC, or Blister Damage Growth *7-17*
7.8 DOCUMENTATION 7-17
7.8.1 General *7-17*
7.8.2 Inspection Data *7-17*
7.8.3 In-Service Monitoring *7-18*
7.9 NOMENCLATURE 7-18
7.10 REFERENCES 7-19
7.11 TABLES 7-20
7.12 FIGURES 7-22

ANNEX 7A – TECHNICAL BASIS AND VALIDATION – ASSESSMENT OF HYDROGEN BLISTERS AND HYDROGEN DAMAGE ASSOCIATED WITH HIC AND SOHIC 7A-1

7A.1 TECHNICAL BASIS AND VALIDATION 7A-1
7A.2 REFERENCES 7A-1

PART 8 – ASSESSMENT OF WELD MISALIGNMENT AND SHELL DISTORTIONS 8-1

8.1 GENERAL 8-1
8.1.1 Evaluation of Weld Misalignment and Shell Distortions *8-1*
8.1.2 ASME B&PV Code, Section VIII, Division 2 ..... *8-1*
8.2 APPLICABILITY AND LIMITATIONS OF THE PROCEDURE 8-2
8.2.1 Types of Weld Misalignment and Shell Distortions *8-2*
8.2.2 Limitations Based on Flaw Type *8-2*
8.2.3 Calculation of the $MAWP_r$ and MFH_r and Coincident Temperature *8-2*
8.2.4 Limitations Based on Temperature *8-2*
8.2.5 Applicability of the Level 1 and Level 2 Assessment Procedures *8-3*
8.2.6 Applicability of the Level 3 Assessment *8-3*
8.3 DATA REQUIREMENTS 8-4
8.3.1 Original Equipment Design Data *8-4*
8.3.2 Maintenance and Operational History *8-4*
8.3.3 Required Data/Measurements for an FFS Assessment *8-4*
8.3.4 Recommendations for Inspection Technique and Sizing Requirements *8-4*
8.4 EVALUATION TECHNIQUES AND ACCEPTANCE CRITERIA 8-6
8.4.1 Overview *8-6*
8.4.2 Level 1 Assessment *8-6*
8.4.3 Level 2 Assessment *8-7*
8.4.4 Level 3 Assessment *8-12*
8.5 REMAINING LIFE ASSESSMENT 8-13
8.5.1 Categories – Metal Loss, Cyclic Loading, High Temperature Operation *8-13*
8.5.2 Requirements for a Level 3 Assessment *8-14*

8.6 REMEDIATION 8-14
8.6.1 Addition of Reinforcement *8-14*
8.6.2 Correction of Tolerances by Mechanical Means *8-14*
8.7 IN-SERVICE MONITORING 8-14
8.7.1 Overview *8-14*
8.7.2 Groove-Like and Crack-Like Flaws *8-14*
8.8 DOCUMENTATION 8-14
8.9 NOMENCLATURE 8-14
8.10 REFERENCES 8-19
8.11 TABLES 8-20
8.12 FIGURES 8-34

ANNEX 8A – TECHNICAL BASIS AND VALIDATION – ASSESSMENT OF WELD MISALIGNMENT AND SHELL DISTORTIONS 8A-1

8A.1 TECHNICAL BASIS AND VALIDATION 8A-1
8A.2 REFERENCES 8A-1

PART 9 – ASSESSMENT OF CRACK-LIKE FLAWS 9-1

9.1 GENERAL 9-1
9.1.1 Assessment Procedures for Crack-Like Flaws *9-1*
9.1.2 ASME B&PV Code, Section VIII, Division 2 (VIII-2) *9-2*
9.1.3 Crack-Like Flaw Definition *9-2*
9.1.4 Treatment of Volumetric Flaws as Crack-Like Flaws *9-2*
9.1.5 Use of Assessment Procedures to Evaluate Brittle Fracture *9-2*
9.1.6 Service Environment and Material Interactions with Crack-Like flaws *9-2*
9.2 APPLICABILITY AND LIMITATIONS OF THE PROCEDURE 9-3
9.2.1 Overview *9-3*
9.2.2 Applicability of the Level 1 and Level 2 Assessment Procedures *9-3*
9.2.3 Applicability of the Level 3 Assessment Procedure *9-4*
9.2.4 Assessment Procedures for Notches in Groove-Like Flaws *9-4*
9.3 DATA REQUIREMENTS 9-4
9.3.1 General *9-4*
9.3.2 Original Equipment Design Data *9-5*
9.3.3 Maintenance and Operating History *9-5*
9.3.4 Required Data/Measurements for an FFS Assessment – Loads and Stresses *9-6*
9.3.5 Required Data/Measurements for an FFS Assessment – Material Properties *9-7*
9.3.6 Required Data/Measurements for an FFS Assessment – Flaw Characterization *9-8*
9.3.7 Recommendation for Inspection Technique and Sizing Requirements *9-12*
9.4 ASSESSMENT TECHNIQUES AND ACCEPTANCE CRITERIA 9-13
9.4.1 Overview *9-13*
9.4.2 Level 1 Assessment *9-14*
9.4.3 Level 2 Assessment *9-15*
9.4.4 Level 3 Assessment *9-19*
9.5 REMAINING LIFE ASSESSMENT 9-21
9.5.1 Subcritical Crack Growth *9-21*
9.5.2 Leak-Before-Break Analysis *9-23*
9.6 REMEDIATION 9-25
9.6.1 Objectives of Remediation *9-25*

9.6.2 Remediation Methods *9-25*
9.7 In-Service Monitoring 9-26
9.7.1 Monitoring of Subcritical Crack Growth *9-26*
9.7.2 Validation of Monitoring Method *9-26*
9.8 Documentation 9-26
9.8.1 General *9-26*
9.8.2 Assessment Procedure *9-27*
9.8.3 Remediation Methods *9-27*
9.8.4 In-Service Monitoring *9-28*
9.9 Nomenclature 9-28
9.10 References 9-29
9.11 Tables 9-30
9.12 Figures 9-34

ANNEX 9A – TECHNICAL BASIS AND VALIDATION – ASSESSMENT OF CRACK-LIKE FLAWS 9A-1

9A.1 Technical Basis and Validation 9A-1
9A.2 References 9A-2

ANNEX 9B – COMPENDIUM OF STRESS INTENSITY FACTOR SOLUTIONS 9B-1

9B.1 General 9B-1
9B.2 Stress Analysis 9B-2
9B.3 Stress Intensity Factor Solutions for Plates 9B-4
9B.4 Stress Intensity Factor Solutions for Plates with Holes 9B-15
9B.5 Stress Intensity Factor Solutions for Cylinders 9B-21
9B.6 Stress Intensity Factor Solutions for Spheres 9B-30
9B.7 Stress Intensity Factor Solutions for Elbows and Pipe Bends 9B-33
9B.8 Stress Intensity Factor Solutions for Nozzles and Piping Tees 9B-33
9B.9 Stress Intensity Factor Solutions for Ring-Stiffened Cylinders 9B-35
9B.10 Stress Intensity Factor Solutions for Sleeve Reinforced Cylinders 9B-36
9B.11 Stress Intensity Factor Solutions for Round Bars and Bolts 9B-36
9B.12 Stress Intensity Factor Solutions for Cracks at Fillet Welds 9B-39
9B.13 Stress Intensity Factor Solutions Cracks in Clad Plates and Shells 9B-41
9B.14 The Weight Function Method for Surface Cracks 9B-41
9B.15 Nomenclature 9B-45
9B.16 References 9B-50
9B.17 Tables 9B-54
9B.18 Figures 9B-225

ANNEX 9C – COMPENDIUM OF REFERENCE STRESS SOLUTIONS FOR CRACK-LIKE FLAWS 9C-1

9C.1 General 9C-1
9C.2 Stress Analysis 9C-2
9C.3 Reference Stress Solutions for Plates 9C-9
9C.4 Reference Stress Solutions for Plates with Holes 9C-12
9C.5 Reference Stress Solutions for Cylinders 9C-13
9C.6 Reference Stress Solutions for Spheres 9C-22
9C.7 Reference Stress Solutions for Elbows and Pipe Bends 9C-23
9C.8 Reference Stress Solutions for Nozzles and Piping Tees 9C-24

9C.9 REFERENCE STRESS SOLUTIONS FOR RING-STIFFENED CYLINDERS 9C-25
9C.10 REFERENCE STRESS SOLUTIONS FOR SLEEVE REINFORCED CYLINDERS 9C-25
9C.11 REFERENCE STRESS SOLUTIONS FOR ROUND BARS AND BOLTS 9C-25
9C.12 REFERENCE STRESS SOLUTIONS FOR CRACKS AT FILLET WELDS 9C-27
9C.13 REFERENCE STRESS SOLUTIONS FOR CRACKS IN CLAD PLATES AND SHELLS 9C-27
9C.14 REFERENCE STRESS SOLUTIONS FOR CRACKS IN HEAVY WALL CYLINDERS $\mathbf{1} \leq \boldsymbol{t/Ri} \leq \mathbf{3}$ 9C-27
9C.15 NOMENCLATURE 9C-28
9C.16 REFERENCES 9C-31
9C.17 TABLES 9C-33
9C.18 FIGURES 9C-45

ANNEX 9D – RESIDUAL STRESSES IN A FITNESS-FOR-SERVICE EVALUATION 9D-1

9D.1 GENERAL 9D-2
9D.1.1 Scope 9D-2
9D.1.2 Crack Driving Force Associated with Residual Stress 9D-2
9D.2 APPLICABILITY AND LIMITATIONS 9D-2
9D.2.1 Residual Stress Solutions for In-Service and New Welded Joints 9D-2
9D.2.2 Technical Basis 9D-3
9D.2.3 Applicable Materials 9D-3
9D.2.4 Weld Joint Geometry 9D-3
9D.2.5 Residual Stress Distributions 9D-3
9D.2.6 Residual Stress Distribution Reference Point 9D-3
9D.2.7 Use of Alternative Residual Stress Solutions 9D-3
9D.2.8 Residual Stress Distributions from Welding Simulation 9D-3
9D.3 DATA REQUIREMENTS AND DEFINITION OF VARIABLES 9D-4
9D.3.1 Required Data 9D-4
9D.3.2 Optional Data 9D-4
9D.3.3 Yield Strength in Residual Stress Calculations 9D-4
9D.4 RESIDUAL STRESS DISTRIBUTION MODIFYING FACTORS 9D-4
9D.4.1 Post Weld Heat Treatment 9D-4
9D.4.2 Pressure Tests 9D-5
9D.5 FULL PENETRATION CIRCUMFERENTIAL WELDS IN PIPING & PRESSURE VESSEL CYLINDRICAL SHELLS 9D-5
9D.5.1 Residual Stress Perpendicular to the Weld Seam (Circumferential Flaw) 9D-5
9D.5.2 Residual Stress Parallel to the Weld Seam (Longitudinal Flaw) 9D-6
9D.5.3 Technical Basis 9D-7
9D.6 FULL PENETRATION LONGITUDINAL WELDS IN PIPING & PRESSURE VESSEL CYLINDRICAL SHELLS 9D-7
9D.6.1 Residual Stress Perpendicular to the Weld Seam (Longitudinal Flaw) 9D-7
9D.6.2 Residual Stress Parallel to the Weld Seam (Circumferential Flaw) 9D-7
9D.6.3 Technical basis 9D-8
9D.7 FULL PENETRATION CIRCUMFERENTIAL WELDS IN SPHERES AND PRESSURE VESSEL HEADS 9D-8
9D.7.1 Residual Stress Perpendicular to the Weld Seam (Circumferential Flaw) 9D-8
9D.7.2 Residual Stress Parallel to the Weld Seam (Meridional Flaw) 9D-8
9D.7.3 Technical Basis 9D-8
9D.8 FULL PENETRATION MERIDIONAL (SEAM) WELDS IN SPHERES AND PRESSURE VESSEL HEADS 9D-9
9D.8.1 Residual Stress Perpendicular to the Weld Seam (Meridional Flaw) 9D-9
9D.8.2 Residual Stress Parallel to the Weld Seam (Circumferential Flaw) 9D-9
9D.8.3 Technical Basis 9D-9
9D.9 FULL PENETRATION WELDS IN STORAGE TANKS 9D-9
9D.10 FULL PENETRATION WELDS AT CORNER JOINTS (NOZZLES OR PIPING BRANCH CONNECTIONS) 9D-9
9D.10.1 Corner Joint, Set-In Nozzle Weld (See Figure 9D.7 and Figure 9D.8, Weld Joint A) 9D-9

9D.10.1.1 Residual Stress Perpendicular to the Weld Seam (See Figure 9D.9) 9D-9
9D.10.1.2 Residual Stress Parallel to the Weld Seam (See Figure 9D.9) 9D-10
9D.10.2 Corner Joint, Set-On Nozzle Weld (See Figure 9D.7 and Figure 9D.8, Weld Joint B) 9D-10
9D.10.2.1 Residual Stress Perpendicular to the Weld Seam 9D-10
9D.10.2.2 Residual Stress Parallel to the Weld Seam 9D-11
9D.10.3 Reinforcing Pad Shell Fillet Weld (See Figure 9D.7 and Figure 9D.8, Weld Joint C) 9D-11
9D.10.3.1 Residual Stress Perpendicular to the Weld Seam 9D-11
9D.10.3.2 Residual Stress Parallel to the Weld Seam 9D-11
9D.10.4 Piping Branch Connection (See Figure 9D.11) 9D-11
9D.10.4.1 Residual Stress Perpendicular to the Weld Seam (See Figure 9D.11) 9D-11
9D.10.4.2 Residual Stress Parallel to the Weld Seam (see Figure 9D.11) 9D-12
9D.10.5 Technical Basis 9D-12
9D.11 Full Penetration and Fillet Welds at a Tee Joint 9D-13
9D.11.1 Main Plate (See Figure 9D.12, Figure 9D.13 and Figure 9D.15) 9D-13
9D.11.1.1 Residual Stress Perpendicular to the Weld Seam 9D-13
9D.11.1.2 Residual Stress Parallel to the Weld Seam 9D-13
9D.11.2 Stay Plate (See Figure 9D.12, Figure 9D.14 and Figure 9D.15) 9D-14
9D.11.2.1 Residual Stress Perpendicular to the Weld 9D-14
9D.11.2.2 Residual Stress Parallel to the Weld Seam 9D-14
9D.11.3 Technical Basis 9D-14
9D.12 Repair Welds 9D-15
9D.12.1 Residual Stress Perpendicular to the Weld 9D-15
9D.12.2 Residual Stress Parallel to the Weld Seam 9D-15
9D.12.3 Technical Basis 9D-15
9D.13 Welding Simulation-Based Stress Distributions 9D-16
9D.13.1 General 9D-16
9D.13.2 Description of Simplified Method 9D-16
9D.13.3 Simulation References 9D-17
9D.14 Nomenclature 9D-18
9D.15 References 9D-19
9D.16 Tables 9D-23
9D.17 Figures 9D-25

ANNEX 9E – CRACK OPENING AREAS 9E-1

9E.1 Introduction 9E-1
9E.1.1 Scope 9E-1
9E.1.2 Overview of Crack Opening Area Calculations 9E-1
9E.2 Crack Opening Areas (COA) for Cylinders and Spheres 9E-2
9E.2.1 Longitudinal Cracks in Cylinders 9E-2
9E.2.2 Circumferential Cracks in Cylinders 9E-2
9E.2.3 Meridional Cracks in Spheres 9E-4
9E.2.4 Plasticity Correction for the COA 9E-4
9E.2.5 Nomenclature 9E-5
9E.2.6 References 9E-6
9E.2.7 Tables 9E-7

ANNEX 9F – MATERIAL PROPERTIES FOR CRACK-LIKE FLAWS 9F-1

9F.1 General 9F-2

9F.2 CHARPY V-NOTCH IMPACT ENERGY 9F-3
9F.2.1 Definition 9F-3
9F.2.2 Charpy V-Notch (CVN) Test 9F-3
9F.2.3 Charpy V-Notch Transition Curve 9F-5
9F.2.4 Charpy Transition Curves and ASME Division 1 and 2 Toughness Exemption Curves 9F-6
9F.2.4.1 Section VIII, Divisions 1 and 2 Toughness Requirements 9F-6
9F.2.4.2 Charpy Transition Curve for Toughness Exemption 9F-6
9F.2.4.3 Reference Temperature Determination 9F-7
9F.2.4.4 Reference Temperature for Part 9, Level 1 Assessments 9F-7
9F.2.4.5 Reference Temperature for Part 12 Assessments of Gouges and Dent-Gouge Combinations 9F-7
9F.3 FRACTURE TOUGHNESS 9F-8
9F.3.1 Definition 9F-8
9F.3.2 Fracture Toughness Parameters 9F-8
9F.3.3 Fracture Toughness Testing 9F-9
9F.3.3.1 Obtaining Samples for Toughness Testing 9F-9
9F.3.3.2 Fracture Toughness Tests 9F-9
9F.3.3.3 JR-Curve 9F-10
9F.3.4 Fracture Toughness Estimation from Charpy V-Notch Data 9F-10
9F.3.5 ASME B&PV Code, Section VIII Division 1 and 2 Fracture Toughness 9F-10
9F.4 FRACTURE TOUGHNESS ESTIMATION FOR AN FFS ASSESSMENT 9F-11
9F.4.1 Introduction 9F-11
9F.4.2 ASME Section XI Fracture Toughness 9F-11
9F.4.2.1 Indexing Procedure for Fracture Toughness Determination 9F-11
9F.4.2.2 Lower Bound Toughness Based on ASME Section XI Reference Curves 9F-12
9F.4.3 Fracture Toughness Master Curve 9F-12
9F.4.3.1 Overview 9F-12
9F.4.3.2 Determining the Master Curve Reference Transition Temperature $T0$ 9F-13
9F.4.3.3 Fracture Toughness Prediction Using the Master Curve 9F-17
9F.4.3.4 Determining the Master Curve Reference Transition Temperature T_0 for Modern Cr-Mo Steels 9F-18
9F.4.4 Upper Shelf Fracture Toughness 9F-18
9F.4.4.1 Overview 9F-18
9F.4.4.2 Fracture Toughness Prediction 9F-18
9F.4.5 Dynamic and Crack Arrest Fracture Toughness 9F-19
9F.4.5.1 Overview 9F-19
9F.4.5.2 Dynamic Fracture Toughness Prediction 9F-19
9F.4.5.3 Arrest Fracture Toughness Prediction 9F-20
9F.4.6 Fracture Toughness for Materials Subject to In-Service Degradation 9F-21
9F.4.6.1 Service Environment Effects on Fracture Toughness 9F-21
9F.4.6.2 Hydrogen Effects on Fracture Toughness and Flaw Assessment 9F-21
9F.4.6.3 Overview of Metallurgical Embrittlement that Reduces Ductility and Fracture Toughness 9F-22
9F.4.7 Aging Effects on the Fracture Toughness of Cr-Mo Steels 9F-23
9F.4.7.1 Overview 9F-23
9F.4.7.2 Effect of Tramp Elements on the Fracture Toughness of 1.25Cr-0.5Mo 9F-23
9F.4.7.3 Effect of Tramp Elements on the Fracture Toughness of 2.25Cr-1Mo 9F-24
9F.4.8 Fracture Toughness of Electroslag Welds in 2.25Cr-1Mo Vessels 9F-25
9F.4.9 Fracture Toughness as a Function of Temperature for Ferritic Materials 9F-26
9F.4.10 The Effect of Warm Pre-stress on Fracture Toughness 9F-26
9F.4.10.1 Introduction 9F-26
9F.4.10.2 Benefits 9F-26
9F.4.10.3 Procedure 9F-26
9F.4.10.4 Conditions to be Satisfied 9F-27
9F.4.11 Fracture Toughness Estimation for Brittle Fracture Assessments 9F-27
9F.4.12 Fracture Toughness of Austenitic Stainless Steel 9F-28
9F.4.13 Ductile Tearing Assessment Using a JR-curve 9F-28

9F.5 MATERIAL DATA FOR CRACK GROWTH CALCULATIONS 9F-28
9F.5.1 Categories of Crack Growth *9F-28*
9F.5.1.1 Crack Growth by Fatigue 9F-28
9F.5.1.2 Crack Growth by Stress Corrosion Cracking (SCC) 9F-29
9F.5.1.3 Crack Growth by Hydrogen Assisted Cracking (HAC) 9F-29
9F.5.1.4 Crack Growth by Corrosion Fatigue 9F-29
9F.5.2 Fatigue Crack Growth Equations *9F-30*
9F.5.2.1 Overview 9F-30
9F.5.2.2 Paris Equation 9F-30
9F.5.2.3 Modified Paris Equation for Welded Joints 9F-31
9F.5.2.4 Walker Equation 9F-31
9F.5.2.5 Trilinear and Bilinear Equations 9F-32
9F.5.2.6 Modified Forman Equation 9F-32
9F.5.2.7 NASGRO Equation 9F-33
9F.5.2.8 Collipriest Equation 9F-33
9F.5.2.9 ASME B&PV Code, Section VIII, Division 3 ..... 9F-33
9F.5.3 Fatigue Crack Growth Data *9F-34*
9F.5.3.1 Sources for Crack Growth Data 9F-34
9F.5.3.2 ASME B&PV Code, Section VIII, Division 3 ..... 9F-34
9F.5.3.3 ASME B&PV Code, Section XI 9F-34
9F.5.3.4 AFCEN Code, RSE-M 9F-34
9F.5.3.5 Barsom Original Crack Growth Data 9F-34
9F.5.3.6 Crack Growth Data for Welds 9F-34
9F.5.3.7 BS 7910 Crack Growth Data for Screening 9F-35
9F.5.3.8 BS 7910 Bilinear Crack Growth Data 9F-35
9F.5.3.9 Crack Growth Data for Pipeline Steels 9F-35
9F.5.3.10 NASGRO Crack Growth Data 9F-36
9F.5.4 Hydrogen Assisted Crack Growth *9F-36*
9F.5.4.1 ASME B31.12 ..... 9F-36
9F.5.4.2 ASME B&PV Code, Section VIII, Division 3 ..... 9F-36
9F.5.5 Stress Corrosion Crack (SCC) Growth Equations *9F-36*
9F.5.6 Stress Corrosion Crack Growth Data *9F-37*
9F.5.7 Conversion of Units for Crack Growth Data *9F-37*
9F.5.7.1 Cyclic Crack Growth Conversion Method 9F-37
9F.5.7.2 Time-Dependent Crack Growth Conversion Method 9F-37
9F.6 NOMENCLATURE 9F-38
9F.7 REFERENCES 9F-43
9F.8 TABLES 9F-46
9F.9 FIGURES 9F-59

ANNEX 9G – STRESS ANALYSIS FOR CRACK-LIKE FLAWS 9G-1

9G.1 GENERAL REQUIREMENTS 9G-1
9G.1.1 Scope *9G-1*
9G.1.2 ASME B&PV Code, Section VIII, Division 2 (VIII-2) *9G-2*
9G.1.3 FAD-Based Assessment Procedure *9G-2*
9G.1.4 Assessment Using Stress Analysis Results – Uncracked Configuration *9G-2*
9G.1.5 Assessment Using Stress Analysis Results – Crack Incorporated into the Model *9G-2*
9G.1.6 Assessment of Growing Cracks *9G-2*
9G.1.7 Numerical Analysis *9G-2*
9G.1.8 Applicable Loads and Load Case Combinations *9G-2*
9G.2 STRESS ANALYSIS OF THE UN-CRACKED CONFIGURATION 9G-3
9G.2.1 Overview *9G-3*

9G.2.2 Categorization and Linearization of Stress Results *9G-3*
9G.2.3 Fitting Stress Results to a Polynomial *9G-3*
9G.2.4 The Weight Function Method *9G-3*
9G.3 FINITE ELEMENT ANALYSIS OF COMPONENTS WITH CRACKS 9G-4
9G.3.1 Overview *9G-4*
9G.3.2 Output Quantity *9G-4*
9G.3.3 Mesh Design *9G-4*
9G.3.4 Crack Tip Modeling Approaches *9G-4*
9G.3.5 Focused Mesh Approach *9G-4*
9G.3.6 Finite Radius Approach *9G-5*
9G.3.7 Small Strain vs. Large Strain Analysis *9G-6*
9G.3.8 Convergence *9G-6*
9G.3.9 Initial and Thermal Strains *9G-7*
9G.3.10 Modeling Procedure *9G-7*
9G.4 FAD-BASED METHOD FOR NON-GROWING CRACKS 9G-8
9G.4.1 Overview *9G-8*
9G.4.2 Assessment Procedure *9G-8*
9G.5 DRIVING FORCE METHOD FOR NON-GROWING CRACKS 9G-10
9G.5.1 Overview *9G-10*
9G.5.2 Assessment Procedure *9G-10*
9G.6 ASSESSMENT OF GROWING CRACKS 9G-11
9G.6.1 Crack Growth Models *9G-11*
9G.6.2 Crack Parameter Solutions *9G-11*
9G.6.3 Determination of a Remaining Life *9G-11*
9G.6.4 Crack Growth Using Numerical Methods *9G-11*
9G.7 NOMENCLATURE 9G-11
9G.8 REFERENCES 9G-12
9G.9 FIGURES 9G-14

ANNEX 9H – CONSTRAINT EFFECTS FOR SURFACE FLAWS IN CARBON AND LOW-ALLOY STEEL COMPONENTS IN THE DUCTILE-BRITTLE TRANSITION REGION 9H-1

9H.1 GENERAL 9H-1
9H.1.1 Overview *9H-1*
9H.1.2 Applicability and Limitations of the Procedure *9H-1*
9H.1.3 Fracture Toughness Estimation Procedure *9H-2*
9H.2 NOMENCLATURE 9H-4
9H.3 REFERENCES 9H-5
9H.4 TABLES 9H-6
9H.5 FIGURES 9H-11

ANNEX 9I – ALTERNATIVE ESTIMATE OF MODE I STRESS INTENSITY FACTORS FOR FFS ASSESSMENTS IN THE DUCTILE-BRITTLE TRANSITION REGION 9I-1

9I.1 GENERAL 9I-1
9I.1.1 Overview *9I-1*
9I.1.2 Applicability and Limitations of the Procedure *9I-1*
9I.1.3 Alternative Estimate of Mode I Stress Intensity Factors for K_r Determination *9I-2*
9I.2 NOMENCLATURE 9I-3
9I.3 REFERENCES 9I-4

9I.4 FIGURES 9I-5

ANNEX 9J – DETERMINATION OF THE MINIMUM ALLOWABLE TEMPERATURE (MAT) USING A LEVEL 2 FRACTURE MECHANICS APPROACH CONSISTENT WITH PARTS 3 AND 9 ..... 9J-1

9J.1 INTRODUCTION 9J-1
9J.2 PROCEDURE TO DETERMINE THE MAT 9J-1
9J.2.1 General Procedure 9J-1
9J.2.2 Simplified Procedure 9J-3
9J.3 REQUIRED MODIFICATIONS FOR HYDROGEN SERVICE 9J-4
9J.3.1 Overview 9J-4
9J.3.2 2.25 Cr – 1 Mo 9J-4
9J.3.3 2.25 Cr – 1 Mo - V 9J-5
9J.3.4 Carbon Steel and Other Low-Chrome Alloys 9J-5
9J.4 MAT ENVELOPE 9J-6
9J.5 NOMENCLATURE 9J-6
9J.6 REFERENCES 9J-7
9J.7 TABLES 9J-8
9J.8 FIGURES 9J-11

PART 10 – ASSESSMENT OF COMPONENTS OPERATING IN THE CREEP RANGE 10-1

10.1 GENERAL 10-2
10.1.1 FFS Procedures and Temperature Limits 10-2
10.1.2 Remaining Life of Components with and without Crack-Like Flaws 10-2
10.2 APPLICABILITY AND LIMITATIONS OF THE PROCEDURE 10-2
10.2.1 Suitability for Service and Remaining Life 10-2
10.2.2 Applicability and Limitations 10-2
10.2.3 Recommendations for Life Predictions Exceeding 35 Years 10-4
10.3 DATA REQUIREMENTS 10-4
10.3.1 General 10-4
10.3.2 Original Equipment Design Data 10-4
10.3.3 Maintenance and Operational History 10-4
10.3.4 Required Data for an FFS Assessment – Loads and Stresses 10-5
10.3.5 Required Data for an FFS Assessment – Material Properties 10-6
10.3.6 Required Data for an FFS Assessment – Damage Characterization 10-7
10.3.7 Recommendation for Inspection Technique and Sizing Requirements 10-8
10.4 ASSESSMENT TECHNIQUES AND ACCEPTANCE CRITERIA 10-10
10.4.1 Overview 10-10
10.4.2 Level 1 Assessment 10-11
10.4.3 Level 2 Assessment 10-12
10.4.4 Level 3 Assessment 10-13
10.5 REMAINING LIFE ASSESSMENT 10-13
10.5.1 Overview 10-13
10.5.2 Creep Rupture Life 10-15
10.5.3 Creep-Fatigue Interaction 10-22
10.5.4 Creep Crack Growth 10-22
10.5.5 Creep Buckling 10-27
10.5.6 Creep-Fatigue Assessment of Ferritic-Austenitic Dissimilar Weld Joints 10-29
10.5.7 Microstructural Approach 10-32

10.6 REMEDIATION 10-34
10.6.1 Components with and without a Crack-Like Flaw *10-34*
10.6.2 Components with a Crack-Like Flaw *10-34*
10.7 IN-SERVICE MONITORING 10-34
10.8 DOCUMENTATION 10-34
10.8.1 General *10-34*
10.8.2 Assumptions Used in the Assumption *10-34*
10.8.3 Documentation for Life Assessment *10-34*
10.8.4 Supplemental Documentation for Creep Crack Growth *10-35*
10.8.5 Supplemental Documentation for Microstructural Approaches *10-35*
10.9 NOMENCLATURE 10-36
10.10 REFERENCES 10-43
10.11 TABLES 10-44
10.12 FIGURES 10-51

ANNEX 10A – TECHNICAL BASIS AND VALIDATION – ASSESSMENT OF COMPONENTS OPERATING IN THE CREEP RANGE 10A-1

10A.1 TECHNICAL BASIS AND VALIDATION 10A-1
10A.2 TECHNICAL BASIS AND VALIDATION REFERENCES 10A-1
10A.3 ADDITIONAL REFERENCES 10A-3

ANNEX 10B – MATERIAL DATA FOR CREEP ANALYSIS 10B-1

10B.1 GENERAL 10B-1
10B.2 CREEP RUPTURE DATA 10B-1
10B.2.1 MPC Project Omega *10B-1*
10B.2.2 API Std 530, 6th Edition, September 2008 ..... *10B-3*
10B.2.3 WRC Bulletin 541 ..... *10B-3*
10B.3 TANGENT AND SECANT MODULUS 10B-4
10B.4 CREEP STRAIN-RATE DATA 10B-5
10B.5 ISOCHRONOUS STRESS-STRAIN CURVES 10B-5
10B.6 CREEP REGIME FATIGUE CURVES (CRACK INITIATION) 10B-6
10B.7 CREEP CRACK GROWTH DATA 10B-6
10B.8 NOMENCLATURE 10B-7
10B.9 REFERENCES 10B-9
10B.9.1 Technical References – High Temperature Assessment *10B-9*
10B.9.2 Creep Rupture Strength and Creep Strain Rate Data *10B-10*
10B.9.3 Creep Crack Growth Data *10B-12*
10B.10 TABLES 10B-14
10B.11 FIGURES 10B-59

PART 11 – ASSESSMENT OF FIRE DAMAGE 11-1

11.1 GENERAL 11-1
11.1.1 Assessment of Fire Damage *11-1*
11.1.2 Assessment of Process Upsets *11-1*
11.1.3 Guidelines and Assessment Flowchart *11-2*
11.1.4 Forms of Fire Damage *11-2*
11.1.5 Alternative Methods for Equipment Not Suitable for Operation *11-2*

11.2 Applicability and Limitations of the Procedure 11-2
11.2.1 Equipment and Components Covered by the Assessment Procedure 11-2
11.2.2 Equipment and Components Not Covered by the Assessment Procedure 11-2
11.3 Data Requirements 11-3
11.3.1 Original Equipment Design Data 11-3
11.3.2 Maintenance and Operational History 11-3
11.3.3 Required Data/Measurements for an FFS Assessment 11-3
11.3.4 Recommendations for Inspection Techniques and Sizing Requirements 11-7
11.4 Assessment Techniques and Acceptance Criteria 11-8
11.4.1 Overview 11-8
11.4.2 Level 1 Assessment 11-9
11.4.3 Level 2 Assessment 11-9
11.4.4 Level 3 Assessment 11-11
11.5 Remaining Life Assessment 11-12
11.5.1 Thinning and Crack-Like Flaw Damage 11-12
11.5.2 Creep Damage 11-12
11.6 Remediation 11-12
11.6.1 Techniques 11-12
11.6.2 Need for Repair or Replacement 11-12
11.7 In-Service Monitoring 11-12
11.8 Documentation 11-12
11.8.1 General 11-12
11.8.2 Heat Exposure Zones 11-13
11.8.3 Record Retention 11-13
11.9 Nomenclature 11-13
11.10 References 11-13
11.11 Tables 11-14
11.12 Figures 11-38

ANNEX 11A – TECHNICAL BASIS AND VALIDATION – ASSESSMENT OF FIRE DAMAGE 11A-1

11A.1 Technical Basis and Validation 11A-1
11A.2 References 11A-1

ANNEX 11B – METALLURGICAL INVESTIGATION AND EVALUATION OF MECHANICAL PROPERTIES IN FIRE DAMAGE ASSESSMENT 11B-1

11B.1 General 11B-2
11B.1.1 Metallurgical Investigations 11B-2
11B.1.2 Materials Covered 11B-2
11B.1.3 Change in material properties from Fire Damage 11B-2
11B.2 Applicability and Limitations of the Procedure 11B-2
11B.3 Specific Responsibilities and Qualifications 11B-2
11B.3.1 Overview 11B-2
11B.3.2 Field Assessment Team 11B-2
11B.3.3 Laboratory Assessment Team 11B-3
11B.4 Evaluation Techniques 11B-3
11B.5 Field Assessment Techniques 11B-3
11B.5.1 Field Hardness Testing 11B-3
11B.5.2 In-situ Metallography or Replication 11B-4

11B.5.3 Positive Material Identification *11B-4*
11B.6 Laboratory Assessment Techniques 11B-5
11B.6.1 Coupon or Sample Removal *11B-5*
11B.6.2 Metallurgical Mounts and Mechanical Testing Specimens *11B-5*
11B.7 Work Procedure 11B-5
11B.7.1 STEP 1 – Select Equipment and Component Subject to Analysis *11B-5*
11B.7.2 STEP 2 – Select Sampling Technique(s) *11B-6*
11B.7.3 STEP 3 – Perform In-situ Metallography or Replica Evaluation *11B-6*
11B.7.4 STEP 4 – Take Field Hardness Readings *11B-6*
11B.7.5 STEP 5 – Remove Samples for Laboratory Analysis and Mechanical Testing (Optional) *11B-7*
11B.8 Guidance for Metallographic Analysis and Mechanical Testing Interpretation 11B-7
11B.8.1 Overview *11B-7*
11B.8.2 Reduction in Tensile Strength *11B-7*
11B.8.3 Reduction in Toughness *11B-7*
11B.8.4 Decrease of Corrosion Resistance *11B-8*
11B.8.5 Consideration for Reuse *11B-8*
11B.8.6 Heat Treatment *11B-8*
11B.9 Example of Metallography Analysis and Hardness Testing Results 11B-8
11B.9.1 Overview *11B-8*
11B.9.2 Samples *11B-9*
11B.9.3 Test Sequence *11B-9*
11B.9.4 Test Results – Metallography *11B-9*
11B.9.5 Test Results – Hardness *11B-10*
11B.10 Figures 11B-11

PART 12 – ASSESSMENT OF DENTS, GOUGES, AND DENT-GOUGE COMBINATIONS 12-1

12.1 General 12-1
12.1.1 Assessment Procedures for Dents, Gouges and Dent-Gouge Combinations *12-1*
12.1.2 Assessment Procedures for LTAs, Grooves, and Other Shell Distortions *12-2*
12.2 Applicability and Limitations of the Procedure 12-2
12.2.1 Overview *12-2*
12.2.2 Calculation of the MAWP and Coincident Temperature *12-2*
12.2.3 Limitations Based on Flaw Type *12-2*
12.2.4 Limitations Based on Temperature *12-2*
12.2.5 Applicability of the Level 1 and Level 2 Assessment Procedures *12-3*
12.2.6 Applicability of the Level 3 Assessment Procedure *12-4*
12.3 Data Requirements 12-4
12.3.1 Original Equipment Design Data *12-4*
12.3.2 Maintenance and Operational History *12-4*
12.3.3 Required Data/Measurements for an FFS Assessment *12-4*
12.3.4 Recommendations for Inspection Technique and Sizing Requirements *12-7*
12.4 Assessment Techniques and Acceptance Criteria 12-7
12.4.1 Overview *12-7*
12.4.2 Level 1 Assessment *12-8*
12.4.3 Level 2 Assessment *12-10*
12.4.4 Level 3 Assessment *12-13*
12.5 Remaining Life Assessment 12-14
12.5.1 Categories of Remaining Life Assessment *12-14*
12.5.2 Requirements for a Level 3 Assessment *12-14*
12.6 Remediation 12-14

12.6.1 Flaw Severity and Evaluation of Material Condition *12-14*
12.6.2 Reinforcement of Dents, Gouges and Dent-Gouge Combinations *12-14*
12.6.3 Use of General Corrosion Remediation Methods *12-14*
12.7 IN-SERVICE MONITORING 12-15
12.7.1 Requirements for In-Service Monitoring *12-15*
12.7.2 Visual Inspection and Field Measurements of Distortion *12-15*
12.8 DOCUMENTATION 12-15
12.8.1 Requirements *12-15*
12.8.2 Inspection and Field Measurements *12-15*
12.9 NOMENCLATURE 12-15
12.10 REFERENCES 12-17
12.11 TABLES 12-18
12.12 FIGURES 12-21

ANNEX 12A – TECHNICAL BASIS AND VALIDATION – ASSESSMENT OF DENTS, GOUGES, AND DENT-GOUGE COMBINATIONS 12A-1

12A.1 TECHNICAL BASIS AND VALIDATION 12A-1
12A.2 REFERENCES 12A-1

PART 13 – ASSESSMENT OF LAMINATIONS 13-1

13.1 GENERAL 13-1
13.1.1 Assessment Procedures for Laminations *13-1*
13.1.2 Definition of Laminations *13-2*
13.1.3 Laminations in Hydrogen Charging Service *13-2*
13.1.4 Detection of Laminations *13-2*
13.1.5 Acceptance of Laminations *13-2*
13.2 APPLICABILITY AND LIMITATIONS OF THE PROCEDURE 13-2
13.2.1 Applicability and Limitations of the Assessments Procedures for Laminations *13-2*
13.2.2 Calculation of MAWP and Coincident Temperature *13-2*
13.2.3 Limitations Based on Temperature *13-2*
13.2.4 Limitations Based on Flaw Type *13-3*
13.2.5 Applicability of the Level 1 and Level 2 Assessment Procedures *13-3*
13.2.6 Applicability of the Level 3 Assessment *13-3*
13.3 DATA REQUIREMENTS 13-4
13.3.1 Original Equipment Design Data *13-4*
13.3.2 Maintenance and Operational History *13-4*
13.3.3 Required Data/Measurements for an FFS Assessment *13-4*
13.3.4 Recommendations for Inspection Technique and Sizing Requirements *13-5*
13.4 ASSESSMENT TECHNIQUES AND ACCEPTANCE CRITERIA 13-5
13.4.1 Overview *13-5*
13.4.2 Level 1 Assessment *13-5*
13.4.3 Level 2 Assessment *13-6*
13.4.4 Level 3 Assessment *13-7*
13.5 REMAINING LIFE ASSESSMENT 13-7
13.6 REMEDIATION 13-7
13.7 IN-SERVICE MONITORING 13-7
13.8 DOCUMENTATION 13-7
13.8.1 General *13-7*

13.8.2 Documentation of Flaw Size and Conditions *13-8*
13.8.3 Documentation of Flaw Growth *13-8*
13.9 NOMENCLATURE 13-8
13.10 REFERENCES 13-8
13.11 TABLES 13-9
13.12 FIGURES 13-10

ANNEX 13A – TECHNICAL BASIS AND VALIDATION – ASSESSMENT OF LAMINATIONS 13A-1

13A.1 TECHNICAL BASIS AND VALIDATION 13A-1
13A.2 REFERENCES 13A-1

PART 14 – ASSESSMENT OF FATIGUE DAMAGE 14-1

14.1 GENERAL 14-2
14.1.1 Assessment Procedures for Fatigue Damage *14-2*
14.1.2 Damage Tolerance *14-2*
14.1.3 Fatigue Evaluation in the Creep Range *14-2*
14.1.4 Fatigue Evaluation and Crack-Like Flaws *14-2*
14.1.5 ASME B&PV Code, Section VIII, Division 2 (VIII-2) *14-3*
14.1.6 Use of Fatigue Curves in Performing Assessments *14-3*
14.1.7 Adjustment for Mean Stress *14-3*
14.1.8 Ratcheting *14-3*
14.2 APPLICABILITY AND LIMITATIONS OF THE PROCEDURE 14-3
14.2.1 Applicability and Limitations of the Assessment Procedures *14-3*
14.2.2 Calculation of MAWP and Coincident Temperature *14-3*
14.2.3 Limitations Based on Temperature *14-4*
14.2.4 Limitations Based on Flaw Type *14-4*
14.2.5 Applicability of the Level 1 and Level 2 Assessment Procedures *14-4*
14.2.6 Applicability of the Level 3 Assessment *14-4*
14.3 DATA REQUIREMENTS 14-5
14.3.1 Original Equipment Design Data *14-5*
14.3.2 Maintenance and Operational History *14-5*
14.3.3 Required Data/Measurements for an FFS Assessment *14-5*
14.3.4 Recommendations for Inspection Technique and Sizing Requirements *14-5*
14.4 ASSESSMENT TECHNIQUES AND ACCEPTANCE CRITERIA 14-6
14.4.1 Overview *14-6*
14.4.2 Level 1 Assessment *14-6*
14.4.2.1 Overview 14-6
14.4.2.2 Method A – Fatigue Screening Based on Experience with Comparable Equipment 14-7
14.4.2.3 Method B – Fatigue Screening 14-7
14.4.2.4 Method C – Fatigue Screening 14-8
14.4.2.5 Method D – Fatigue Screening, Welded Joints 14-10
14.4.2.6 Level 1 Assessment Results 14-12
14.4.3 Level 2 Assessment *14-12*
14.4.3.1 Overview 14-12
14.4.3.2 Method A – Fatigue Assessment Using Elastic Stress Analysis and Equivalent Stresses 14-13
14.4.3.3 Method B – Fatigue Assessment Using Elastic-Plastic Stress Analysis and Equivalent Strain 14-17
14.4.3.4 Method C – Fatigue Assessment of Welds Using the Equivalent Structural Stress 14-19
14.4.3.5 Ratcheting Assessment – Elastic Stress Analysis 14-23
14.4.3.6 Ratcheting Assessment – Elastic-Plastic Stress Analysis 14-25
14.4.3.7 Ratcheting Assessment – Non-Integral Connections 14-26

14.4.3.8 Level 2 Assessment Results 14-26
14.4.4 Level 3 Assessment 14-26
14.4.4.1 Overview 14-26
14.4.4.2 Method A – Elastic Stress Analysis and Critical Plane Approach 14-27
14.4.4.3 Method B – Elastic-Plastic Stress Analysis and Critical Plane Approach 14-28
14.4.4.4 Method C – Recognized Codes and Standards 14-29
14.5 REMAINING LIFE ASSESSMENT 14-29
14.5.1 Included in Level 2 and Level 3 Assessments 14-29
14.5.2 Loading Time History 14-29
14.6 REMEDIATION 14-29
14.6.1 Overview 14-29
14.6.2 Removal or Reduction of the Driving Energy Source or Forces. 14-30
14.6.3 Alteration of Component Constraint, Mechanical Design, or Weld Quality 14-30
14.6.4 Reduction of Temperature Differentials or Gradients 14-31
14.7 IN-SERVICE MONITORING 14-31
14.8 DOCUMENTATION 14-31
14.8.1 General 14-31
14.8.2 Assessment Level 14-31
14.8.3 Loading Time History 14-31
14.8.4 Material Properties 14-32
14.8.5 Stress Analysis Results 14-32
14.8.6 Assessment Results 14-32
14.8.7 Remaining Life Assessment 14-32
14.8.8 Remediation Methods 14-32
14.8.9 In-Service Monitoring 14-32
14.9 NOMENCLATURE 14-32
14.10 REFERENCES 14-41
14.11 TABLES 14-42
14.12 FIGURES 14-65

ANNEX 14A – TECHNICAL BASIS AND VALIDATION – ASSESSMENT OF FATIGUE DAMAGE 14A-1

14A.1 TECHNICAL BASIS AND VALIDATION 14A-1
14A.2 REFERENCES 14A-1

ANNEX 14B – MATERIAL PROPERTIES FOR FATIGUE ANALYSIS 14B-1

14B.1 SMOOTH BAR DESIGN FATIGUE CURVES – ASME CODE, SECTION VIII, DIVISION 2 ..... 14B-1
14B.1.1 Temperature Correction 14B-1
14B.1.2 Interpolation 14B-1
14B.1.3 Design Fatigue Curves Based on Testing in Air 14B-1
14B.1.4 Design Fatigue Curve Models 14B-2
14B.1.5 Computation of Allowable Cycles 14B-4
14B.2 SMOOTH BAR DESIGN FATIGUE CURVES – MEAN CURVE WITH EXPLICIT MARGINS 14B-4
14B.3 UNIFORM MATERIAL LAW 14B-5
14B.4 WELDED JOINT FATIGUE CURVES – ASME CODE, SECTION VIII, DIVISION 2 ..... 14B-5
14B.4.1 Fatigue Curve Models 14B-5
14B.4.2 Computation of Allowable Cycles 14B-5
14B.5 NOMENCLATURE 14B-6
14B.6 REFERENCES 14B-8
14B.7 TABLES 14B-10

14B.8 FIGURES 14B-17

ANNEX 14C – PLASTICITY CORRECTION AND CYCLE COUNTING FOR FATIGUE ANALYSIS 14C-1

14C.1 INTRODUCTION 14C-1
14C.1.1 Cycle Counting 14C-1
14C.1.2 Plasticity Correction 14C-1
14C.1.3 Definitions 14C-2
14C.1.4 Histogram Development 14C-3
14C.2 PLASTICITY CORRECTION 14C-3
14C.2.1 Uniaxial Plasticity Correction 14C-3
14C.2.2 Multiaxial Plasticity Correction 14C-3
14C.3 UNIAXIAL CYCLE COUNTING 14C-8
14C.3.1 Rainflow Cycle Counting – With Reordering 14C-8
14C.3.2 Additional Rainflow Cycle Counting – Without Reordering 14C-10
14C.4 MULTIAXIAL CYCLE COUNTING 14C-10
14C.4.1 Wang-Brown Cycle Counting 14C-10
14C.4.2 Critical Plane Cycle Counting 14C-14
14C.5 NOMENCLATURE 14C-18
14C.6 REFERENCES 14C-24
14C.7 FIGURES 14C-25

[Intentionally Left Blank]

FOREWORD

In contrast to the straightforward and conservative calculations that are typically found in design codes, more sophisticated assessment of metallurgical conditions and analyses of stresses and strains can more precisely indicate whether operating equipment is fit for its intended service or whether fabrication defects or in-service deterioration threaten its integrity. Such analyses offer a sound basis for decisions to continue to run as is or to alter, repair, monitor, retire or replace the equipment.

The publication of the American Petroleum Institute's Recommended Practice 579, Fitness-For-Service, in January 2000 provided the refining and petrochemical industry with a compendium of consensus methods for reliable assessment of the structural integrity of equipment containing identified flaws or damage. API RP 579 was written to be used in conjunction with the refining and petrochemical industry's existing codes for pressure vessels, piping and aboveground storage tanks (i.e., API 510, API 570 and API 653). The standardized Fitness-For-Service Assessment procedures presented in API RP 579 provide technically sound consensus approaches that ensure the safety of plant personnel and the public while aging equipment continues to operate and can be used to optimize maintenance and operation practices, maintain availability and enhance the long-term economic performance of plant equipment.

API RP 579 was prepared by a committee of the American Petroleum Institute with representatives of the Chemical Manufacturers Association, as well as some individuals associated with related industries. It grew out of a resource document developed by a Joint Industry Program on Fitness-For-Service administered by The Materials Properties Council. Although it incorporated the best practices known to the committee members, it was written as a Recommended Practice rather than as a mandatory standard or code.

While API was developing Fitness-For-Service methodology for the refining and petrochemical industry, the American Society of Mechanical Engineers (ASME) also began to address post-construction integrity issues. Realizing the possibility of overlap, duplication, and conflict in parallel standards, ASME and API formed the Joint Fitness-For-Service Committee in 2001 to develop and maintain a Fitness-For-Service standard for equipment operated in a wide range of process, manufacturing, and power generation industries. It was intended that this collaboration would promote the widespread adoption of these practices by regulatory bodies. The Joint Committee included the original members of the API Committee that were involved in the development of API Recommended Practice 579, complemented by a similar number of ASME members representing similar areas of expertise in other industries such as chemicals, power generation, and pulp and paper. In addition to owner representatives, it included substantial international participation and subject matter experts from universities and consulting firms.

In June 2007, the API and ASME Fitness-For-Service Joint Committee published the first edition of API 579-1/ASME FFS-1 Fitness-For-Service. The main enhancement in this publication relative to 2000 Edition API 579 was the addition of Part 10 covering the assessment of components operating in the creep range.

The 2016 Edition of API 579-1/ASME FFS-1 included many modifications and technical improvements. Some of the more significant changes are the following: reorganized the standard to facilitate use and updates by renumbering annexes that are directly associated with the relevant part of the document, Expanded equipment design code coverage, added a new annex for establishing an allowable Remaining Strength Factor (RSF), re-wrote weld residual stress solution annex for use in the assessment of crack-like flaws, updated guidance on material toughness predictions for use in the assessment of crack-like flaws, updated evaluation procedures for the assessment of creep damage, added an annex covering metallurgical investigation and evaluation of mechanical properties in a fire damage assessment, and developed new Part 14 covering the assessment of fatigue damage.

Numerous changes have been made for the 2021 Edition of API 579-1/ASME FFS-1 to address user feedback and to introduce new technology. A summary of these changes is provided on pages xxxv to xl.

This publication is written as a standard. Its words *shall* and *must* indicate explicit requirements that are essential for an assessment procedure to be correct. The word *should* indicate recommendations that are good practice but not essential. The word *may* indicate recommendations that are optional.

Most of the original technology that underlies this standard was developed by the Joint Industry Program on Fitness-For-Service, administered by The Materials Properties Council of the Welding Research Council, Inc., (WRC). The sponsorship of the member companies of this research consortium and the voluntary efforts of their company representatives are acknowledged with gratitude. Most of the next generation technology has been developed by WRC with some funding from API and ASME.

The committee encourages the broad use of the state-of-the-art methods presented here for evaluating all types of pressure vessels, boiler components, piping and tanks. The committee intends to continuously improve this standard as improved methodology is developed and as user feedback is received. All users are encouraged to inform the committee if they discover areas in which these procedures should be corrected, revised or expanded. Suggestions should be submitted to the Secretary, API/ASME Fitness-For-Service Joint Committee, The American Society of Mechanical Engineers, Two Park Avenue, New York, NY 10016, or SecretaryFFS@asme.org.

There is an option available to receive an e-mail notification when errata are posted to a particular code or standard. This option can be found on the Committee Web at http://go.asme.org/ffscommittee after selecting “errata” in the “Publication Information” section.

This standard is under the jurisdiction of the ASME Board on Pressure Technology Codes and Standards and the API CRE Committee and is the direct responsibility of the API/ASME Fitness-For-Service Joint Committee. The American National Standards Institute approved API 579-1/ASME FFS-1 2021 in December 2021.

Although every effort has been made to assure the accuracy and reliability of the information that is presented in this standard, API and ASME make no representation, warranty, or guarantee in connection with this publication and expressly disclaim any liability or responsibility for loss or damage resulting from its use or for the violation of any regulation with which this publication may conflict.

SPECIAL NOTES

This international Code was developed under the ASME/API Joint Committee on Fitness-For-Service Policies and Procedures, which were approved by ANSI and accredited as meeting the criteria for American National Standards and it is an American National Standard. The Standards Committee that approved this Code was balanced to assure that individuals from competent and concerned interests have had an opportunity to participate. The proposed Code was made available for public review and comment that provides an opportunity for additional public input from industry, academia, regulatory agencies, and the public-at-large.

This document addresses problems of a general nature. With respect to particular circumstances, local, state, and federal laws and regulations should be reviewed.

Nothing contained in this document is to be construed as granting any right, by implication or otherwise, for the manufacture, sale, or use of any method, apparatus, or product covered by letters patent. Neither should anything contained in this document be construed as insuring anyone against liability for infringement of letters patent.

Neither API nor ASME nor any employees, subcontractors, consultants, committees, or other assignees of API or ASME make any warranty or representation, either express or implied, with respect to the accuracy, completeness, or usefulness of the information contained herein, or assume any liability or responsibility for any use, or the results of such use, of any information or process disclosed in this document. Neither API nor ASME nor any employees, subcontractors, consultants, or other assignees of API or ASME represent that use of this document would not infringe upon privately owned rights.

This document may be used by anyone desiring to do so. Every effort has been made to assure the accuracy and reliability of the data contained herein; however, API and ASME make no representation, warranty, or guarantee in connection with this document and hereby expressly disclaim any liability or responsibility for loss or damage resulting from its use or for the violation of any requirements of authorities having jurisdiction with which this document may conflict.

This document is published to facilitate the broad availability of proven, sound engineering and operating practices. This document is not intended to obviate the need for applying sound engineering judgment regarding when and where this document should be utilized. The formulation and publication of this document is not intended in any way to inhibit anyone from using any other practices.

Classified areas may vary depending on the location, conditions, equipment, and substances involved in any given situation. Users of this Code should consult with the appropriate authorities having jurisdiction.

Work sites and equipment operations may differ. Users are solely responsible for assessing their specific equipment and premises in determining the appropriateness of applying the Instructions. At all times users should employ sound business, scientific, engineering, and judgment safety when using this Code.

Users of this Code should not rely exclusively on the information contained in this document. Sound business, scientific, engineering, and safety judgment should be used in employing the information contained herein.

API and ASME are not undertaking to meet the duties of employers, manufacturers, or suppliers to warn and properly train and equip their employees, and others exposed, concerning health and safety risks and precautions, nor undertaking their obligations to comply with authorities having jurisdiction.

Information concerning safety and health risks and proper precautions with respect to particular materials and conditions should be obtained from the employer, the manufacturer or supplier of that material, or the material safety data sheet.

[Intentionally Left Blank]

SUMMARY OF CHANGES

A summary of editorial corrections, updates, and clarifications that are included throughout the standard along with several technical changes and enhancements are described below.

Part 2: *Fitness-For-Service Engineering Assessment Procedure*

- Added provision that permits $MAWP$ to be determined using the stress analysis procedures in Annex 2D.

Annex 2C: *Thickness, $MAWP$, and Stress Equations for an FFS Assessment*

- Added Svensson method for burst pressure calculation.
- Removed option to use ASME VIII-2 allowable stress for ASME VIII-1 equipment. This was originally a carryover from API 510 before the allowable stress criteria in ASME VIII-2 changed from a factor of safety of 3.0 to a factor or safety of 2.4.
- Removed requirement for nozzle reinforcement check for small nozzles to be consistent with ASME VIII-1.
- Removed legacy limit load nozzle reinforcement procedure which was previously eliminated in ASME VIII-1.

Annex 2D: *Stress Analysis Overview for an FFS Assessment*

- Elastic load cases reference ASME VIII-2 for simplicity.
- Removed option to use ASME VIII-2 allowable stress for ASME VIII-1 equipment.
- Modified coefficients for use in elastic-plastic calculation to cover the appropriate design margins with various current and legacy construction codes (including the appropriate design margins for pipelines).
- Added explicit guidance on capping the yield stress used in a limit load analysis to the yield stress at temperature to prevent misapplication of the method when evaluating components fabricated from materials that have a design Code elastic allowable stress equal to 90% of the Minimum Specific Yield Stress (MSYS).
- Limited the allowable remaining strength factor, RSF_a, for buckling assessments to no lower than 0.9.

Annex 2E*: Material Properties for Stress Analysis*

- Updated the Ramberg-Osgood stress-strain model for use in a Level 3 evaluation.
- Added guidance for material properties for Level 3 evaluations involving pipeline materials.
- Updated correlations for estimating material Ultimate Tensile Strength (UTS) using hardness testing.

Part 3: *Assessment of Existing Equipment for Brittle Fracture*

- Clarified that the use of design codes/standards as an alternative to Part 3 is considered a Level 3 Assessment.
- Corrected errors related to the Minimum Allowable Temperature (MAT) for bolting and nut material specifications.
- Expanded the definition of shock chilling and added the requirement that a Level 3 evaluation is necessary to evaluate conditions where the shock chilling screening is not satisfied.
- Added thickness limits for Level 1 impact test exemption curves to be consistent with ASME VIII-1.
- Clarified that no $PWHT$ credit is permitted in a brittle fracture evaluation of a component if previous repairs were completed using alternative weld methods (such as high preheat or temper bead).
- Added supplemental inspection requirements for brittle fracture evaluations performed on component identified to have metal loss that exceeds the original design tolerances.
- Explicitly excluded mill tolerance effects in a brittle fracture assessment.

- Modified impact test exemptions for flanges to address recent changes to ASME VIII-1.
  - Flanges Fabricated Pre-1989:
    - As-Forged SA-105 is Curve B. Heat-treated condition is Curve C.
    - MAT for ferritic flanges meeting ASME B16.5, ASME B16.47, or the Long Weld Neck (LWN) requirements of ASME VIII-1, UCS-66(c)(4) in the as-forged condition is -29°C (-20°F).
  - Flanges Fabricated in 1989 or Later:
    - As-Forged SA-105 is Curve A
    - Heat-treated condition SA-105 is Curve B
    - MAT for ferritic flanges meeting ASME B16.5, ASME B16.47, or LWN requirements in the as-forged is 0°F. Note: The basis for the 1989 cutoff comes from a 1996 report indicating "a number of flange failures have been reported during the past 5 years within the various Amoco operating units" and a Chemical Risks Directive requiring impact testing of all flanges in Europe being issued in response to a failure that occurred in 1998 on a flange that was installed in 1990.
  - MAT for ferritic flanges meeting ASME B16.5, ASME B16.47, or the LWN requirements in the normalized condition after forging shall be set at -29°C (-20°F) regardless of the year of manufacturing. (Note: Wording regarding "produced to fine grain practice" as currently included in ASME VIII-1 is not included).
  - For all ASME B16.5, ASME B16.47, and LWN flanges, MAT is set equal to the impact test exemption temperature "unless the MAT determined by the governing thickness at the flange nozzle neck weld joint together with the curve associated with the flange material gives a higher value."
- Added requirement that components not exposed to general primary membrane tensile stress shall be evaluated using the pressure rating basis in a Level 2 Assessment.

$$R_{ts} = \frac{P_a}{P_{rating}}$$

  - Added guidance that pressure rating in the stress ratio calculation can be calculated using paragraph 2C.3.4 for nozzle assemblies and paragraph 2C.3.6 for flanges.
  - Limited MAT to no lower than -48°C (-55°F) in as-welded condition even if Level 1 MAT was established using impact testing. (Note: MAT can still be reduced to -104°F (-155°F) if $PWHT$.)
    - Impact tested at or below -46°C (-50°F):

$$MAT = \max\left[\left(MAT_{Level\,1} - T_R\right),\ -104^\circ F\,(-155^\circ F)\right]$$

    - Impact tested above -46°C (-50°F):

$$MAT = \max\left[\left(MAT_{Level\,1} - T_R\right),\ -48^\circ F\,(-55^\circ F)\right] \quad \left(As-Welded\ Condition\right)$$

$$MAT = \max\left[\left(MAT_{Level\,1} - T_R\right),\ -104^\circ F\,(-155^\circ F)\right] \quad \left(PWHT\ Condition\right)$$

Part 4: *Assessment of General Metal Loss*

- Moved component type definitions and examples to a table to simplify designations.
- Exempted the cylinder side of 2:1 elliptical head-to-shell junctions as Type C components and structural discontinuities for metal loss assessments (applicable to Part 4, Part 5, and Part 6 Assessments).
- Revised qualifications to utilize Point Thickness Reading (PTR) approach to prevent misapplication of the method and "washing out" of local damage.

- Eliminated the check on Coefficient of Variation (COV).
- Added limitation on minimum measured thickness, i.e., $t_{mm} \geq 0.9 \cdot t_{avg}$.

- Revised length for thickness averaging at nozzles (Figure 4.13) to ensure method does not permit greater damage at nozzle junctions vs. away from nozzle junctions.

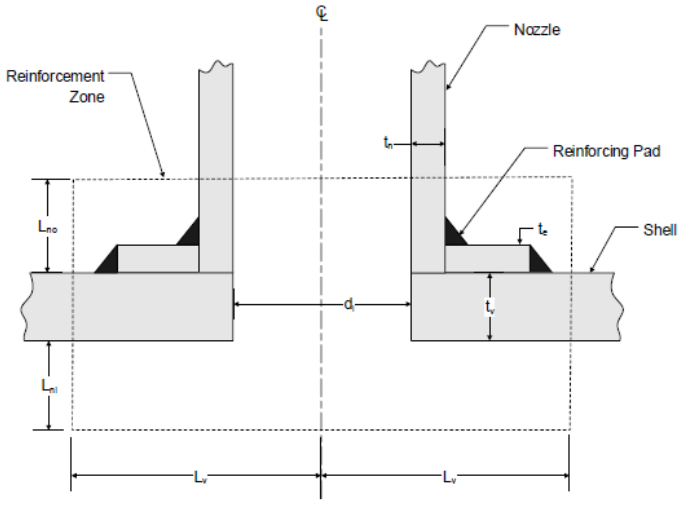

Nozzle with a Reinforcement Element

Notes:

1. Thickness averaging zone in the horizontal direction (see paragraph 4.3.3.4.a): $L_H = \min[L,\ L_v]$. L is calculated using Equation 4.7. $L_v = \max[d_i,\ (d_i/2 + t_n + t_v)]$.
2. Thickness averaging zone in the vertical direction on the outside of the shell (see paragraph 4.3.3.4.a). $L_{vno} = \min[L, L_{no}]$ L is calculated using Equation 4.7. $L_{no} = \min[2.5t_v,\ (2.5t_n + t_e)]$.
3. Thickness averaging zone in the vertical direction on the inside of the shell (see paragraph 4.3.3.4.a): $L_{vni} = \min[L, L_{ni}]$. L is calculated using Equation 4.7. $L_{ni} = \min[2.5t_v,\ 2.5t_n]$.

Figure 4.13 – Zone for Thickness Averaging – Nozzles and Fabricated Branch Connections

- Revised recommended UT grid spacing for scenarios when "corroded surface is not accessible for visual inspection, $L_s = \min[2t_{rd}, 25\ mm\ (1\ inch)]$.
- Documented the purpose of the minimum measured thickness limit in Level 1 and Level 2 Assessments.
- Included recommendations for validation of inspection results when thickness readings are less than or equal to 2.5 mm (0.100 inches) (also referenced in Part 5 *Assessment of Local Wall Loss* and Part 6 *Assessment of Pitting*).

Part 9: *Assessment of Crack-Like Flaws*

- Redefined crack-like flaw interaction and recategorization rules to reduce conservatism and for better alignment with ASME Section XI.
- Table 9.2 updated to reflect new Wallin Master Curve fracture toughness correlation for carbon and low alloy steels in Annex 9F.

Annex 9B: *Compendium of Stress Intensity Factor Solutions for Crack-like Flaws*

- Expanded K-solutions to cover thick-wall cylinders.

Annex 9C: *Compendium of Reference Stress Solutions for Crack-like Flaws*

- Updated solutions for circumferential flaws in cylinders.
- Expanded reference solutions to cover thick-wall cylinders.

Annex 9F: *Material Properties for Crack-like Flaws*

- Updated Wallin Master Curve fracture toughness correlation for carbon and low alloy steels,

$$K_{Jc} = 20 + \left(11 + 77\exp\left[0.0190\left(T - T_0\right)\right]\right)\left(\ln\left[\frac{1}{1-P_f}\right]\cdot\left(\frac{25}{L}\right)\right)^{0.25} \qquad \left(MPa\sqrt{m}, {}^{\circ}C, mm\right)$$

$$K_{Jc} = 18.2 + \left(9.9 + 70.1\exp\left[0.0106\left(T - T_0\right)\right]\right)\left(\ln\left[\frac{1}{1-P_f}\right]\cdot\left(\frac{1}{L}\right)\right)^{0.25} \qquad \left(ksi\sqrt{in}, {}^{\circ}F, in\right)$$

- Added ductile tearing material property data. The data was included in the 2007 edition of API 579, but mistakenly removed in the 2016 edition.
- Updated guidance on fracture toughness estimates for stainless-steel base metal and welds.
- Incorporated guidance from WRC Bulletin 562 *Recommendations for Establishing the Minimum Pressurization Temperature (MPT) for Equipment* and the API white paper *The Effects of Hydrogen for Establishing a Minimum Pressurization Temperature (MPT) for Heavy Wall Steel Reactor Vessels* to address material toughness modifications due to hydrogen and temper embrittlement effects.
- Added guidance for ASME VIII-3 equipment (high pressure).

New Annex 9H: *Constraint Effects for Surface Flaws in Carbon and Low-Alloy Steel Components in the Ductile-Brittle Transition Region*

- Established a procedure to adjust material fracture toughness to take advantage of constraint effects for surface flaws in a Level 2 Assessment.
- Technical basis is documented in WRC Bulletin 577 *Constraint Effects on Fracture Toughness in Ductile-Brittle Transition*.

New Annex 9I: *Alternative Estimate of Mode I Stress Intensity Factors*

- Established a procedure to reduce conservatism with the Mode I stress intensity factors using an integrated crack driving force over the crack front (rather than peak values) in a Level 2 assessment.
- Technical basis is documented in WRC Bulletin 577 *Constraint Effects on Fracture Toughness in Ductile-Brittle Transition*.

New Annex 9J: *Determination of the Minimum Allowable Temperature (MAT) using a Fracture Mechanics Approach*

- Established procedure for using fracture mechanics to determine the MAT.
- Included a simplified brittle fracture screening procedure developed using fracture mechanics.
- Provided guidance on the necessary adjustments for 2.25Cr-1Mo steel in hydrogen service.

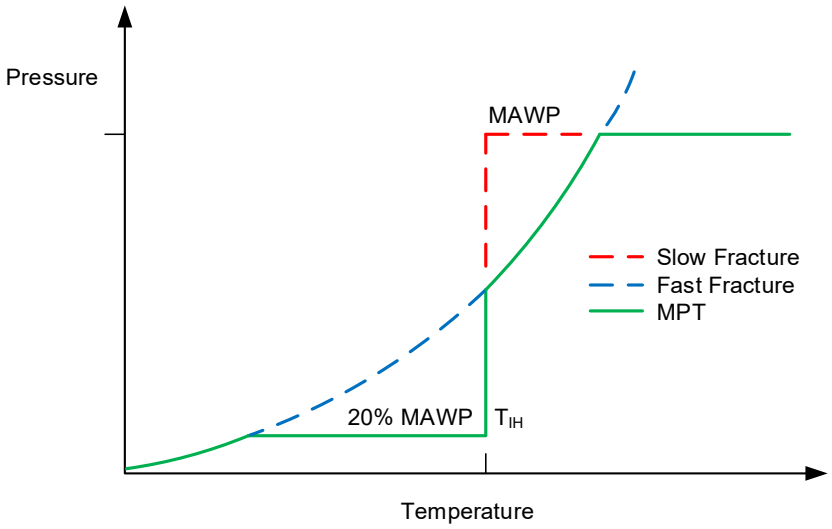

Part 10: *Assessment of Components Operating in the Creep Range*

- Updated Level 1 screening curves to ensure consistency with results from a Level 2 Assessment and incorporate technology updates (updated material coefficients, etc.).

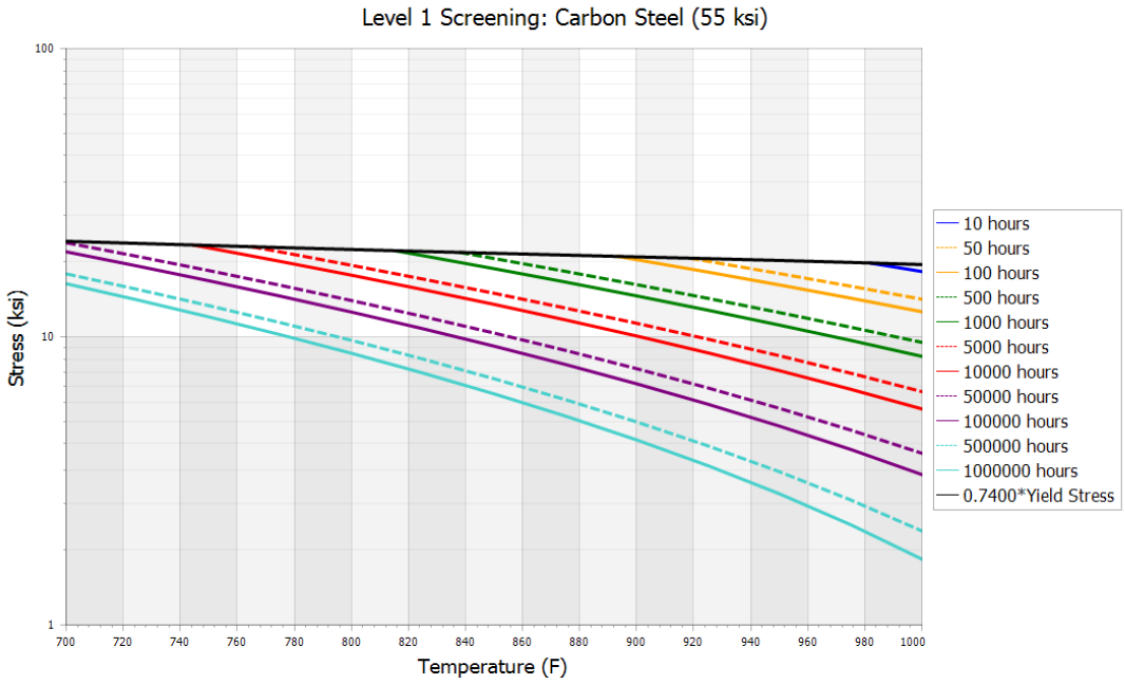

- Revised Level 1 maximum permissible damage limit to 0.8 in the evaluation of multiple operating conditions.
- Add structural thickness limit to Level 1 and Level 2 Assessments to protect against loss of containment due to the challenges and limitations associated with inspection of furnace tubes.

$$t_{\lim} = \min\left[0.9t_{nom},\ 2.5\,mm\ (0.100\ inches)\right]$$

Annex 10B: *Material Data for Creep Analysis*

- Updated existing and added new MPC Omega material coefficients.

- Added WRC Bulletin 541 revision 3 Larson-Miller material coefficients.
- Fixed elevated temperature fatigue curve coefficients.

Part 11: *Assessment of Fire Damage*

- Extended the use of hardness testing to cover carbon steel, low chrome, and stainless-steel materials.

Part 12: *Assessment of Dents, Gouges, and Dent-Gouge Combinations*

- Updated Level 1 and Level 2 procedures, applicability and limitations, and acceptance criteria to align with The Pipeline Defect Assessment Manual (PDAM).
- Table 12.2 updated to reflect new Wallin Master Curve fracture toughness correlation for carbon and low alloy steels in Annex 9F.

Part 14: *Assessment of Fatigue Damage*

- Added closed-form equation for smooth bar fatigue curves and data for new materials.
- Added smooth bar fatigue curves based on fatigue testing in air.
- Added bounds for use of smooth bar fatigue curve equations.
- Updated fatigue screening Method C and Method D.
- Corrected plasticity correction factor, $K_{e,k}$.
- Elastic ratcheting procedure re-written using Bree Diagram.
- Updated Level 2 procedure for Method C Fatigue Assessment.

Annex 14B: *Material Properties for Fatigue Analysis*

- Added closed-form equation for smooth bar fatigue curves and added data for new materials.
- Added smooth bar fatigue curves based on fatigue testing in air.
- Added bounds for use of smooth bar fatigue curve equations.

PART 1 – INTRODUCTION

CONTENTS

PART 1 – INTRODUCTION 1-1

1.1 INTRODUCTION 1-1
1.1.1 Construction Codes and Fitness-For-Service 1-1
1.1.2 Fitness-For-Service Definition 1-1
1.2 SCOPE 1-2
1.2.1 Supplement to In-Service Inspection Codes 1-2
1.2.2 Application Construction Codes 1-2
1.2.3 Other Recognized Codes and Standards 1-2
1.2.4 Remaining Life 1-3
1.2.5 Assessment Methods for Flaw Types and Damage Conditions 1-3
1.2.6 Special Cases 1-3
1.3 ORGANIZATION AND USE 1-4
1.4 RESPONSIBILITIES 1-4
1.4.1 Owner-User 1-4
1.4.2 Inspector 1-4
1.4.3 Engineer 1-4
1.4.4 Plant Engineer 1-5
1.5 QUALIFICATIONS 1-5
1.5.1 Education and Experience 1-5
1.5.2 Owner-User 1-5
1.5.3 Inspector 1-5
1.5.4 Engineer 1-6
1.6 DEFINITION OF TERMS 1-6
1.7 REFERENCES 1-6
1.7.1 Types 1-6
1.7.2 Code, Standards and Recommended Practices 1-6
1.7.3 Technical reports and Other Publications 1-6
1.8 TABLES 1-7

1.1 Introduction

1.1.1 Construction Codes and Fitness-For-Service

The ASME and API new construction codes and standards for pressurized equipment provide rules for the design, fabrication, inspection and testing of new pressure vessels, piping systems, and storage tanks. These codes typically do not provide rules to evaluate equipment that degrades while in-service and deficiencies caused by degradation or from original fabrication that may be found during subsequent inspections. API 510, API 570, API 653, and NB-23 Codes/Standards for the inspection, repair, alteration, and rerating of in-service pressure vessels, piping systems, and storage tanks do address the fact that equipment degrades while in service.

1.1.2 Fitness-For-Service Definition

Fitness-For-Service (FFS) Assessments are quantitative engineering evaluations that are performed to demonstrate the structural integrity of an in-service component that may contain a flaw or damage, or that may be operating under a specific condition that might cause a failure. This Standard provides guidance for conducting FFS Assessments using methodologies specifically prepared for pressurized equipment. The guidelines provided in this Standard can be used to make run-repair-replace decisions to help determine if components in pressurized

equipment containing flaws that have been identified by inspection can continue to operate safely for some period of time. These FFS Assessments are currently recognized and referenced by the API Codes and Standards (510, 570, and 653), and by NB-23 as suitable means for evaluating the structural integrity of pressure vessels, piping systems and storage tanks where inspection has revealed degradation and flaws in the equipment.

1.2 Scope

1.2.1 Supplement to In-Service Inspection Codes

The methods and procedures in this Standard are intended to supplement and augment the requirements in API 510, API 570, API 653, and other post construction codes that reference FFS evaluations such as NB-23.

1.2.2 Application Construction Codes

The assessment procedures in this Standard can be used for FFS Assessments and/or rerating of equipment designed and constructed to the following codes:

a) ASME B&PV Code, Section VIII, Division 1

b) ASME B&PV Code, Section VIII, Division 2

c) ASME B&PV Code, Section I

d) ASME B31.1 Piping Code

e) ASME B31.3 Piping Code

f) ASME B31.4 Piping Code

g) ASME B31.8 Piping Code

h) ASME B31.12 Piping Code

i) API Std 650

j) API Std 620

k) API Std 530

1.2.3 Other Recognized Codes and Standards

The assessment procedures in this Standard may also be applied to pressure containing equipment constructed to other recognized codes and standards, including international and internal corporate standards. This Standard has broad applications since the assessment procedures are based on allowable stress methods and plastic collapse loads for non-crack-like flaws, and the Failure Assessment Diagram (FAD) Approach for crack-like flaws (see Part 2, paragraph 2.4.2).

a) If the procedures of this Standard are applied to pressure containing equipment not constructed to the codes listed in paragraph 1.2.2, then the user is advised to first review the validation discussion in Annexes 3A through 14A. The information in these Annexes, along with knowledge of the differences in design codes, should enable the user to factor, scale, or adjust the acceptance limits of this Standard such that equivalent FFS in-service margins can be attained for equipment not constructed to these codes. When evaluating other codes and standards, the following attributes of the ASME and API design codes should be considered:

1) Material specifications
2) Upper and lower temperature limits for specific materials
3) Material strength properties and the design allowable stress basis
4) Material fracture toughness requirements
5) Design rules for shell sections
6) Design rules for shell discontinuities such as nozzles and conical transitions
7) Design requirements for cyclic loads
8) Design requirements for operation in the creep range
9) Weld joint efficiency or quality factors
10) Fabrication details and quality of workmanship
11) Inspection requirements, particularly for welded joints

b) As an alternative, users may elect to correlate the pressure-containing component's material specification to an equivalent ASME, or API listed material specification to determine a comparable allowable stress. This approach provides an entry point into the ASME or API codes wherein the pressure-containing component is reconciled or generally made equivalent to the design bases assumed for this Standard (see Annex 2C, paragraph 2C.1.3). Hence, general equivalence is established, and the user may then directly apply the acceptance limits of the FFS procedures contained in this Standard. Equivalent ASME and ASTM material specifications provide a satisfactory means for initiating reconciliation between the ASME and API design codes and other codes and standards. However, the user is cautioned to also consider the effects of fabrication and inspection requirements on the design basis (e.g., joint efficiency with respect to minimum thickness calculation).

1.2.4 Remaining Life

The FFS Assessment procedures in this Standard cover both the present integrity of the component given a current state of damage and the projected remaining life. Qualitative and quantitative guidance for establishing remaining life and in-service margins for continued operation of equipment are provided in regards to future operating conditions and environmental compatibility.

1.2.5 Assessment Methods for Flaw Types and Damage Conditions

Assessment methods as well as material properties, Nondestructive Examination (NDE) guidelines, and documentation requirements are included to evaluate flaws including: general and localized corrosion, widespread and localized pitting, blisters and hydrogen damage, weld misalignment and shell distortions, crack-like flaws including environmental cracking, laminations, dents, and gouges. In addition, evaluation techniques are provided for condition assessment of equipment including resistance to brittle fracture, creep damage, and fire damage.

1.2.6 Special Cases

The FFS Assessment procedures in this Standard can be used to evaluate flaws commonly encountered in pressure vessels, piping, and tankage. The procedures are not intended to provide a definitive guideline for every possible situation that may be encountered. However, flexibility is provided to the user in the form of an advanced

assessment level to handle uncommon situations that may require a more detailed analysis.

1.3 Organization and Use

The organization, applicability and limitations, required information, analysis techniques and documentation requirements are described in Part 2 of this Standard. In addition, an overview of the acceptance criteria utilized to qualify a component with a flaw is provided. First time users of the FFS Assessment technology in this Standard should carefully review Part 2 prior to starting an analysis.

1.4 Responsibilities

1.4.1 Owner-User

The Owner-User of pressurized equipment shall have overall responsibility for FFS Assessments completed using the procedures in this Standard, including compliance with appropriate jurisdictional and insurance requirements. The Owner-User shall ensure that the results of the assessment are documented and filed with the appropriate permanent equipment records. Many of the Owner-User responsibilities are given to the Plant Engineer (see paragraph 1.4.4).

1.4.2 Inspector

The Inspector, working in conjunction with the Nondestructive Examination (NDE) engineer, shall be responsible to the Owner-User for determining that the requirements for inspection and testing are met. In addition, the Inspector shall provide all necessary inspection data required for an FFS Assessment in accordance with the appropriate Part of this Standard and be responsible for controlling the overall accuracy of the flaw detection and sizing activities. In some instances, as determined by the Owner-User, the Inspector may also be responsible for the FFS Assessment, i.e., a Level 1 Assessment (see Part 2, paragraph 2.4.1.1).

1.4.3 Engineer

1.4.3.1 The Engineer is responsible to the Owner-User for most types of FFS Assessments, documentation, and resulting recommendations. The exception is that a Level 1 Assessment may be performed by an Inspector or other non-degreed specialist (see Part 2, paragraph 2.4.1.1). However, in these cases the Engineer should review the analysis.

1.4.3.2 In the context of this Standard, the term Engineer applies to the combination of the following disciplines unless a specific discipline is cited directly. A FFS Assessment may require input from multiple engineering disciplines as described below.

a) Materials or Metallurgical Engineering – Identification of the material damage mechanisms, establishment of corrosion/erosion rates, determination of material properties including strength parameters and crack-like flaw growth parameters, development of suitable remediation methods and monitoring programs, and documentation.

b) Mechanical or Structural Engineering – Computations of the minimum required thickness and/or $MAWP$ (MFH) for a component, performance of any required thermal and stress analysis, and knowledge in the design of and the practices relating to pressure containing equipment including pressure vessel, piping, and tankage codes and standards.

c) Inspection Engineering – Establishment of an inspection plan that is capable of detecting, characterizing, sizing flaws or damage, and selection and execution of examination procedures in conjunction with available Nondestructive Examination expertise.

d) Fracture Mechanics Engineering – Assessment of crack-like flaws using the principles of fracture mechanics.

e) Nondestructive Examination (NDE) Engineering – Selection and development of methods to detect, characterize, and size flaws or quantify the amount of damage, and the analysis and interpretation of inspection data.

f) Process Engineering – Documentation of past and future operating conditions, including normal and upset conditions, and identification of the contained fluid and its contaminant levels that may affect degradation of the component being evaluated.

1.4.4 Plant Engineer

In the context of this Standard, the term Plant Engineer applies to an engineer with knowledge of the equipment containing the component requiring the FFS Assessment. The Plant Engineer may perform both a Level 1 Assessment and Level 2 Assessment and typically has certain knowledge of the engineering disciplines, or access to personnel with the necessary engineering disciplines knowledge required for the FFS Assessment to be performed, described in paragraph 1.4.3.2.

1.5 Qualifications

1.5.1 Education and Experience

The level or amount of education and experience of all participants shall be commensurate with the complexity, rigor, requirements and significance of the overall assessment. All individuals involved shall be able to demonstrate their proficiency to the satisfaction of the Owner-User.

1.5.2 Owner-User

The Owner-User shall understand the overall process, the importance of each piece of equipment to that process, and the failure consequences of each piece of equipment such that the Owner-User can assume overall responsibility for the results of the FFS Assessment performed (see paragraph 1.4.1). The Owner-User shall have the ability and experience to recognize potentially damaging operations or equipment conditions and to take remedial steps.

1.5.3 Inspector

The Inspector shall be qualified and certified in accordance with the applicable post-construction Code, API 510, API 570, API 653, NB-23, or other post-construction code or standard required by the jurisdiction (see paragraph 1.4.2). Nondestructive examination personnel responsible for data used in an FFS Assessment shall be certified to at least Level II in accordance with industry standards such as the American Society for Nondestructive Testing (ASNT) SNT-TC-1A, CP-189, ACCP, or equivalent. The Inspector shall have experience in the inspection, examination, or both, of the type of equipment and associated process that is the subject of the FFS Assessment.

1.5.4 Engineer

The Engineer shall be competent to perform the level of assessment required (see paragraph 1.4.3). The Engineer shall meet all required qualifications to perform engineering work within the applicable jurisdiction and any supplemental requirements stipulated by the Owner-User.

1.6 Definition of Terms

Definitions of common technical terms used throughout this Standard may be found in Annex 1A.

1.7 References

1.7.1 Types

Throughout this Standard, references are made to various international codes, standards, recommended practices, and technical reports that cover:

a) Design, fabrication, inspection, and testing of pressure vessels, piping, and tankage.

b) In-service inspection of pressure vessels, piping, and tankage.

c) FFS standards applicable to welded components.

d) Materials selection and behavior in process plants or other industrial environments.

1.7.2 Code, Standards and Recommended Practices

Rules for the use of these codes, standards, recommended practices and technical reports are stated in each Part and Annex of this Standard. The referenced codes, standards, and recommended practices in this Standard are listed in Table 1.1. The edition of the codes, standards, and recommended practices used in the FFS Assessment shall be either the latest edition, the edition used for the design and fabrication of the component, or a combination thereof. The Engineer responsible for the assessment shall determine the edition(s) to be used. The principles cited in paragraph 1.2.3 and Annex 2C, paragraph 2C.3 should be considered when making this determination.

1.7.3 Technical reports and Other Publications

References to other publications that provide background and other pertinent information to the assessment procedures used in this Standard are included in each Part and Annex, as applicable.

1.8 Tables

Table 1.1 – Codes, Standards and Recommended Practices

Title	Identification
Pressure Vessel Inspection Code: In-Service Inspection, Rating, Repair and Alteration	API 510
Calculation of Heater-Tube Thickness in Petroleum Refineries	API Std 530
Piping Inspection Code: In-Service Inspection, Repair, and Alteration of Piping Systems	API 570
Damage Mechanisms Affecting Fixed Equipment in the Refining Industry	API RP 571
Inspection of Pressure Vessels	API RP 572
Inspection of Fired Boilers and Heaters	API RP 573
Inspection Practices for Piping System Components	API RP 574
Inspection Practices for Atmospheric and Low-pressure Storage Tanks	API RP 575
Inspection of Pressure-Relieving Devices	API RP 576
Welding Processes, Inspection, and Metallurgy	API RP 577
Material Verification Program for New and Existing Alloy Piping Systems	API RP 578
Risk-Based Inspection	API RP 580
Risk-Based Inspection Methodology	API RP 581
Design and Construction of Large, Welded, Low-Pressure Storage Tanks	API Std 620
Welded Tanks for Oil Storage	API Std 650
Tank Inspection, Repair, Alteration, and Reconstruction	API Std 653
Materials and Fabrication of 2-1/4Cr-1Mo, 2 1/4Cr-1Mo-1/4V, 3Cr-1Mo, and 3Cr-1Mo-1/4V Steel Heavy Wall Pressure Vessels for High-temperature, High Pressure Hydrogen Service	API RP 934–A
Materials and Fabrication of 1 1/4Cr-1/2 Mo Steel Heavy Wall Pressure Vessels for High-pressure Hydrogen Service Operating at or Below 825 Degrees F (440 Degrees C)	API RP 934–C
Closed Recommended Practice for Materials and Fabrication of 1 1/4 CR-1/2 Mo Steel Pressure Vessels for Service Above 825 degrees F (440 C)	API RP 934–E
Steels for Hydrogen Service at Elevated Temperatures and Pressures in Petroleum Refineries and Petrochemical Plants	API RP 941
Avoiding Environmental Cracking in Amine Units	API RP 945
Assessment and Management of Cracking in Pipelines	API RP 1176
Assessment and Management of Dents in Pipelines	API RP 1183

Table 1.1 – Codes, Standards and Recommended Practices

Title	Identification
API-ASME Code for the Design, Construction, Inspection and Repair of Unfired Pressure Vessels for Petroleum Liquids and Gases	API-ASME Code 1934-1954
National Board Inspection Code	NBBI NB-23
Minimum Design Loads and Associated Criteria for Buildings and Other Structures	ASCE 7
Section I: Rules for Construction of Power Boilers	ASME B&PV Code Section I
Section II: Materials – Part A: Ferrous Material Specifications	ASME B&PV Code Section II, Part A
Section II: Materials – Part B: Nonferrous Material Specifications	ASME B&PV Code Section II, Part B
Section II: Materials – Part D: Properties (Customary)	ASME B&PV Code Section II, Part D
High Temperature Reactors	ASME B&PV Code Section III, Division 5
Unfired Pressure Vessels	ASME Section VIII, 1950 to 1965 Edition
Unfired Pressure Vessels	ASME Section VIII, prior to the 1950
Boiler and Pressure Vessel Code, Section VIII, Pressure Vessels Division 1	ASME B&PV Code Section VIII, Division 1
Boiler and Pressure Vessel Code, Section VIII, Pressure Vessels Division 2, Alternative Rules	ASME B&PV Code Section VIII, Division 2
Rules for In-Service Inspection of Nuclear Power Plant Components	ASME B&PV Code Section XI
Alternative Method to Area Replacement Rules for Openings Under Internal Pressure, Section VIII, Division 1	ASME B&PV Code Case 2168
Alternative Rules for Determining Allowable External Pressure and Compressive Stresses for Cylinders, Cones, Spheres, and Formed Heads, Section VIII, Divisions 1, and 2	ASME B&PV Code Case 2286
Factory-Made Wrought Buttwelding Fittings	ASME B16.9
Manual for Determining the Remaining Strength of Corroded Pipelines: Supplement to ASME B31 Code for Pressure Piping	ASME B31G
Power Piping	ASME B31.1
Process Piping	ASME B31.3
Pipeline Transportation Systems for Liquids and Slurries	ASME B31.4
Gas Transmission and Distribution Piping System	ASME B31.8
Hydrogen Piping and Pipelines	ASME B31.12
Standard Specification for General Requirements for Steel Plates for Pressure Vessels	ASTM A20
Standard Specification for Electric-Fusion-Welded Austenitic Chromium-Nickel Stainless Steel Pipe for High-Temperature Service and General Applications	ASTM A358

Table 1.1 – Codes, Standards and Recommended Practices

Title	Identification
Standard Test Methods and Definitions for Mechanical Testing of Steel Products	ASTM A370
Standard Specification for General Requirements for Specialized Carbon and Alloy Steel Pipe	ASTM A530
Standard Specification for Electric-Fusion-Welded Steel Pipe for Atmospheric and Lower Temperatures	ASTM A671
Standard Specification for Electric-Fusion-Welded Steel Pipe for High-Pressure Service at Moderate Temperatures	ASTM A672
Standard Specification for Carbon and Alloy Steel Pipe, Electric-Fusion-Welded for High-Pressure Service at High Temperatures	ASTM A691
Standard Test Methods of Tension Testing of Metallic Materials	ASTM E8
Standard Test Method for Measurement of Fatigue Crack Growth Rates	ASTM E647
Standard Practices for Cycle Counting in Fatigue Analysis	ASTM E1049
Standard Test Method for Measurement of Fracture Toughness	ASTM E1820
Standard Test Method for Determination of Reference Temperature, T_0, for Ferritic Steels in the Transition Range	ASTM E1921
Standard Guide for Examination and Evaluation of Pitting Corrosion	ASTM G46
Specification for Unfired Pressure Vessels	BS PD 5500
Guide to Methods for the Assessment of the Influence of Crack Growth on the Significance of Defects in Components Operating at High Temperatures	BS PD 6539
Method for Determination of K_{IC}, Critical CTOD and Critical J Values of Welds in Metallic Materials	BS 7448: Part 2
Guide to Fatigue Design and Assessment of Steel Products	BS 7608
Guide to Methods for Assessing the Acceptability of Flaws in Metallic Structures	BS 7910
Design of Steel Pressure Pipes	DIN 2413 Part 1
Design of Steel Bends Used in Pressure Pipelines	DIN 2413 Part 2
Unfired pressure vessels	EN 13445
Summary of Average Stress Rupture Properties of Wrought Steels for Boilers and Pressure Vessels	ISO/TR 7468-1981(E)
Guidelines for Detection, Repair, and Mitigation of Cracking of Existing Petroleum Refinery Pressure Vessels in Wet H_2S Environments	NACE Std RP0296
Assessment Procedure for High Temperature Response of Structures	EDF Energy R-5

Table 1.1 – Codes, Standards and Recommended Practices

Title	Identification
Assessment of the Integrity of Structures Containing Defects	EDF Energy R-6
A combined deterministic and probabilistic procedure for safety assessment of components with cracks – Handbook	SSM Report 2008:01
Method of Assessment for Flaws in Fusion Welded Joints with Respect to Brittle Fracture and Fatigue Crack Growth	JWES 2805

ANNEX 1A – GLOSSARY OF TERMS AND DEFINITIONS

(NORMATIVE)

This Annex contains definitions of terms that are used in this Standard, or terms that may be found elsewhere in documents related to Fitness-For-Service evaluation.

1A.1 **Abs[a] or |a| –** The definition of a mathematical function that indicates that the absolute value of the arguments, a, is to be computed.

1A.2 **AET –** Acoustic Emission Testing.

1A.3 **Alteration –** The definition depends on the equipment type and in-service code as shown below.

1) Pressure vessels (API 510) – A physical change in any component having design implications that affect the pressure-containing capability of a pressure vessel beyond the scope of the items described in existing data reports. It is not intended that any comparable or duplicate replacement, such as the addition of any reinforced nozzle equal to or less than the size of existing reinforced nozzles, the addition of nozzles not requiring reinforcement, or rerating be considered an alteration.
2) Piping Systems (API 570) – A physical change in any component or pipe routing (including support system modifications), which have design implications affecting the pressure-containing capability of the piping system, including the pressure vessels, tanks, and/or equipment it services. For example, an alteration that involves the installation of a heavy valve near a vessel nozzle may have design implications for the pressure vessel as well as the piping system itself.
3) Storage tanks (API 653) – Any work on a tank involving cutting, burning, welding, or heating operations that change the overall physical dimensions and/or configuration of a tank.
4) Pressure Vessels (NB-23) – Any change in the item described in the original Manufacturer's Data Report that affects the pressure containing capability of the pressure retaining item. Non-physical changes such as an increase in the maximum allowable working pressure (internal or external) or design temperature of a pressure retaining item is considered an alteration. A reduction in minimum temperature such that additional mechanical tests are required is also considered an alteration.

1A.4 **ASCC (Alkaline Stress Corrosion Cracking)** – The cracking of a metal produced by the combined action of corrosion in an aqueous alkaline environment containing H_2S, CO_2, and tensile stresses (residual or applied). The cracking is branched and intergranular in nature, and typically occurs in carbon steel components that have not been subjected to $PWHT$. This form of cracking has often been referred to as carbonate cracking when associated with alkaline sour waters, and as amine cracking when associated with alkanolamine treating solutions.

1A.5 **Bending Stress –** The variable component of normal stress, the variation may or may not be linear across the section thickness (see Annex 2C).

1A.6 **Bifurcation Buckling –** The point of instability where there is a branch in the primary load versus displacement path for a structure (see Annex 2C).

1A.7 **CET (Critical Exposure Temperature) –** The CET is defined as the lowest (coldest) metal temperature derived from either the operating or atmospheric conditions at the maximum credible coincident combination of pressure and supplemental loads that result in primary stresses. Note that operating conditions include startup, shutdown and upset conditions. The CET may be a single temperature at the

maximum credible coincident combination of pressure and primary supplemental loads if that is also the lowest (coldest) metal temperature for all other combinations of pressure and primary supplemental loads. If lower (colder) temperatures at lower pressures and supplemental loads are credible, the CET can be defined by an envelope of temperatures and pressures (see Part 3).

1A.8 Corrosion – The deterioration of metal caused by chemical or electrochemical attack as a result of its reaction to the environment (see Part 4).

1A.9 Crack-Like Flaw – A flaw that may or may not be the result of linear rupture, but which has the physical characteristics of a crack when detected by an NDE technique (see Part 9).

1A.10 Creep – The special case of inelasticity that characterizes the stress induced time-dependent deformation under load, usually occurring at elevated temperatures (see Part 10).

1A.11 Creep Damage – In polycrystalline materials (e.g., metals) creep damage results from the motion of dislocations within grains, grain boundary sliding and microstructural diffusion processes within the crystalline lattice. The resultant grain boundary voids, or grain and grain boundary distortions (damage), generally impairs the materials strain hardening capability (see Part 10).

1A.12 Creep Rupture – An extension of the creep process to the limiting condition of gross section failure (frequently termed creep fracture). The stress that will cause creep fracture at a given time in a specified environment is the creep rupture strength (see Part 10 and Annex 10B).

1A.13 Cycle – A cycle is a relationship between stress and strain that is established by the specified loading at a location in a vessel or component. More than one stress-strain cycle may be produced at a location, either within an event or in transition between two events, and the accumulated fatigue damage of the stress-strain cycles determines the adequacy for the specified operation at that location. This determination is made with respect to the stabilized stress-strain cycle.

1A.14 Cyclic Loading – The application of repeated or fluctuating stresses, strains, or stress intensities to locations on structural components (see Part 14).

1A.15 Cyclic Service – A service in which fatigue becomes significant as a result of the cyclic nature of mechanical and/or thermal loads. A screening criterion is provided in Part 14 that can be used to determine if a fatigue analysis is required as part of a Fitness-For-Service Assessment.

1A.16 Damage Mechanism – A phenomenon that induces deleterious micro and/or macro changes in the material conditions that are harmful to the material condition or mechanical properties. Damage mechanisms are usually incremental, cumulative, and unrecoverable. Common damage mechanisms are associated with chemical attack, creep, erosion, fatigue, fracture, embrittlement, and thermal aging (see Part 2 and Annex 2B).

1A.17 Design Pressure – The pressure used in the design of a pressure component together with the coincident design metal temperature, for the purpose of determining the minimum permissible thickness or physical characteristics of the different zones of the pressure equipment. Static head and other static or dynamic loads are included in addition to the equipment design pressure where applicable.

1A.18 Ductility – The ability of a material to plastically deform without fracturing. Ductility is measured as either the reduction in area or elongation in a tensile test specimen.

1A.19 Elastic Follow-up – A structural behavior where the elastic material surrounding a region with material non-linearity (i.e., plasticity, creep or combined plasticity and creep) results in the region experiencing loading conditions between the extremes of load-controlled (primary stress) and strain-controlled (secondary stress). The material non-linearity in the region results in a reduction in structural stiffness and subsequent strain concentration.

1A.20 Equipment Design Pressure – The overall design pressure of the pressure equipment or assemblage. For pressure vessels, it is the design pressure required at the top of the vessel in its operating position.

1A.21 Equipment $MAWP$ – The maximum permissible pressure of the pressure equipment or assemblage at the designated coincident design metal temperature. It is the smallest of the values found for maximum allowable working pressure of all the essential parts/components of the equipment minus the static head (if any) for that component. For pressure vessels, it is the maximum permissible pressure at the top of the vessel in its normal operating position for a designated temperature. For pressure vessels built to the ASME B&PV Code, this is the nameplate $MAWP$ and is the basis for the set point pressure of the relieving devices protecting the vessel.

1A.22 Erosion – The destruction of metal by the abrasive action of a liquid or vapor (see Part 4).

1A.23 Event – The Owner-Users' Specification may include one or more events that produce fatigue or creep damage. Each event consists of loading components specified at a number of time points over a time period and is repeated a specified number of times. For example, an event may be the startup, shutdown, upset condition, or any other cyclic action. The sequence of multiple events may be specified or random.

1A.24 exp[x] – The mathematical function e^x.

1A.25 FAD (Failure Assessment Diagram) – The FAD is used for the evaluation of crack-like flaws in components (see Part 2 and Part 9).

1A.26 Fatigue – The damage mechanism resulting in fracture under repeated or fluctuating stresses having a maximum value less than the tensile strength of the material (see Part 14).

1A.27 Fatigue Limit – The fatigue limit or fatigue endurance limit is the highest stress or range of stress that can be repeated indefinitely without failure of the material.

1A.28 Fatigue Strength – The maximum cyclic stress a material can withstand for a given number of cycles before failure occurs.

1A.29 Fatigue Strength Reduction Factor – A stress intensification factor which accounts for the effect of a local structural discontinuity (stress concentration) on the fatigue strength. It is the ratio of the fatigue strength of a component without a discontinuity or weld joint to the fatigue strength of that same component with a discontinuity or weld joint. Values for some specific cases are empirically determined (e.g., socket welds). In the absence of experimental data, the stress intensification factor can be developed from a theoretical stress concentration factor derived from the theory of elasticity or based on the guidance provided in Annex 14B.

1A.30 FCA (Future Corrosion Allowance) – The corrosion allowance required for the future operational period of a component.

1A.31 Fillet Weld – A weld of approximately triangular cross section joining two surfaces approximately at right angles to each other in a lap joint, tee joint, or corner joint.

1A.32 *FFS* (Fitness-For-Service) Assessment – A methodology whereby flaws or a damage state in a component is evaluated in order to determine the adequacy of the component for continued operation (see Part 2).

1A.33 Flaw – A discontinuity, irregularity, or defect that is detected by inspection.

1A.34 Fracture Mechanics – An engineering discipline concerned with the behavior of cracks in materials. Fracture mechanics models provide mathematical relationships for critical combinations of stress, crack size and fracture toughness that lead to crack propagation. Linear Elastic Fracture Mechanics (LEFM) approaches apply to cases where crack propagation occurs during predominately elastic loading with negligible plasticity. Elastic-Plastic Fracture Mechanics (EPFM) methods are suitable for materials that undergo significant plastic deformation during crack propagation (see Part 9).

1A.35 Girth Weld – A butt weld joining plate sections along the circumferential direction of a cylinder or cone.

1A.36 Gouge – An elongated local mechanical removal and/or relocation of material from the surface of a component, causing a reduction in wall thickness at the defect; the length of a gouge is much greater than the width and the material may have been cold worked in the formation of the flaw. Gouges are typically caused by mechanical damage; for example, denting and gouging of a section of pipe by mechanical equipment during the excavation of a pipeline (see Part 12).

1A.37 Groove – A local elongated thin spot caused by directional erosion or corrosion; the length of the metal loss is significantly greater than the width (see Part 5).

1A.38 Gross Structural Discontinuity – Another name for a Major Structural Discontinuity (see 1A.55).

1A.39 Groove-Like Flaw – A surface flaw with a small, but finite, tip (or frontal) radius wherein the flaw length is very much greater than its depth. Groove-like flaws are categorized as either a groove or gouge (see Part 5 and Part 12).

1A.40 HAZ (Heat-Affected Zone) – A portion of the base metal adjacent to a weld that has not been melted, but whose metallurgical microstructure and mechanical properties have been changed by the heat of welding, usually with undesirable effects.

1A.41 HIC (Hydrogen-Induced Cracking) – Stepwise internal cracks that connect adjacent hydrogen blisters on different planes in the metal, or to the metal surface. An externally applied stress is not needed for the formation of HIC. In steels, the development of internal cracks (sometimes referred to as blister cracks) tends to link with other cracks by a transgranular plastic shear mechanism because of internal pressure resulting from the accumulation of hydrogen. The link-up of these cracks on different planes in steels has been referred to as stepwise cracking to characterize the nature of the crack appearance. HIC is commonly found in steels with: (a) high impurity levels that have a high density of large planar inclusions, and/or (b) regions of anomalous microstructure produced by segregation of impurity and alloying elements in the steel (see Part 7).

1A.42 Hydrogen Blistering – The formation of subsurface planar cavities, called hydrogen blisters, in a metal resulting from excessive internal hydrogen pressure. Growth of near-surface blisters in low-strength

metals usually results in surface bulges. Hydrogen blistering in steel involves the absorption and diffusion of atomic hydrogen produced on the metal surface by the sulfide corrosion process. The development of hydrogen blisters in steels is caused by the accumulation of hydrogen that recombines to form molecular hydrogen at internal sites in the metal. Typical sites for the formation of hydrogen blisters are large non-metallic inclusions, laminations, or other discontinuities in the steel. This differs from the voids, blisters, and cracking associated with high-temperature hydrogen attack (see Part 7).

1A.43 Inclusion – A discontinuity in a material, usually consisting of a non-metallic compound (oxides, silicate, etc.) encapsulated in a metallic matrix as unintentional impurity.

1A.44 Incomplete Fusion – Lack of complete melting and coalescence (fusion) of some portion of the metal in a weld joint.

1A.45 Incomplete Penetration – Partial penetration of the weld through the thickness of the joint.

1A.46 In-Service Margin – Stated in terms of applied loads, the ratio of the load that will produce a limiting condition to the applied load in the assessed condition. Similar definitions may be developed for parameters other than load. For example, the safety margin on fracture toughness is defined as the ratio of the fracture toughness of the material being assessed to the fracture toughness to produce a limiting condition (see Part 9).

1A.47 Jurisdiction – A legally constituted government administration that may adopt rules relating to pressurized components.

1A.48 Limit Analysis – Limit Analysis is a special case of plastic analysis in which the material is assumed to be ideally plastic (non-strain-hardening). In limit analysis the equilibrium and flow characteristics at the limit state are used to calculate the collapse load (see Annex 2C).

1A.49 Limit Analysis Collapse Load – The methods of limit analysis are used to compute the maximum load a structure made of an ideally plastic material can carry. The deformations of an ideally plastic structure increase without bound at this load, which is termed the collapse load (see Annex 2C).

1A.50 Local Primary Membrane Stress – A membrane stress produced by pressure, or other mechanical loading associated with a primary and/or a discontinuity effect would, if not limited, produce excessive distortion in the transfer of load to other portions of the structure. To be conservative, this stress is classified as a local primary membrane stress even though it has some characteristics of a secondary stress (see Annex 2C).

1A.51 Local Structural Discontinuity – A source of stress or strain intensification that affects a relatively small volume of material and does not have a significant effect on the overall stress or strain pattern, or on the structure as a whole. Examples are small fillet radii, small attachments, and partial penetration welds (see Annex 2C).

1A.52 Longitudinal Weld – A full penetration butt weld joining plate sections along the longitudinal axis of a cylinder or cone.

1A.53 LTA – Locally Thin Area (see Part 5).

1A.54 Major Structural Discontinuity – A source of stress or strain intensification that affects a relatively large portion of a structure and has a significant effect on the overall stress or strain pattern of the structure as a whole. Examples are head-to-shell and flange-to-shell junctions, nozzles, and junctions between shells of different diameters or thicknesses (see Annex 2C).

1A.55 MAT (Minimum Allowable Temperature) – The lowest permissible metal temperature for a given material at a specified thickness based on its resistance to brittle fracture. It may be a single temperature, or an envelope of allowable operating temperatures as a function of pressure. The MAT is derived from mechanical design information, materials specifications, and/or materials data (see Part 3).

1A.56 MAWP (Maximum Allowable Working Pressure) – The maximum gauge pressure adjusted for liquid head for a component in its operating position at the design temperature, based on calculations using the current minimum thickness, exclusive of thickness required for future corrosion allowance and supplemental loads. Note that this term is also applied to piping components. For components containing a flaw, the $MAWP$ is also a function of the Remaining Strength Factor (see Part 2).

1A.57 $MAWP_r$ (Reduced Maximum Allowable Working Pressure) – Reduced maximum allowable working pressure of the damaged component.

1A.58 Max[a_1, a_2, a_3,.., a_i] – The definition of a mathematical function that indicates that the maximum value of all of the arguments, a_i, is to be computed.

1A.59 Membrane Stress – The component of normal stress that is uniformly distributed and equal to the average value of stress across the thickness of the section under consideration (see Annex 2C).

1A.60 MFH (Maximum Fill Height) – The maximum height permitted for a liquid with a given specific gravity in an atmospheric storage tank at the design temperature based on calculations using the current minimum thickness for all critical shell elements, exclusive of thickness required for future corrosion allowance and supplemental loads. For components containing a flaw, the MFH is also a function of the Remaining Strength Factor (see Part 2).

1A.61 Min[a_1, a_2, a_3,.., a_i] – The definition of a mathematical function that indicates that the minimum value of all of the arguments, a_i, is to be computed.

1A.62 Minimum Allowable Thickness – The thickness required for each element of a vessel based on calculations considering temperature, pressure, and all loadings (see Annex 2B).

1A.63 MDMT (Minimum Design Metal Temperature) – The lowest temperature at which a significant load can be applied to a pressure vessel as defined by the ASME Code, Section VIII, Division 1 (see Part 3).

1A.64 MT – Magnetic particle examination.

1A.65 NDE – Nondestructive examination.

1A.66 Nil-Ductility Temperature – A temperature at which an otherwise ductile material subject to a load, cracks in a manner characteristic of a brittle fracture.

1A.67 Normal Stress – The component of stress normal to the plane of reference (this is also referred to as a direct stress). Usually, the distribution of normal stress is not uniform through the thickness of a part, so this stress may be considered to be made up of two components. One stress component is uniformly

distributed and equal to the average value of stress across the thickness of the section under consideration, and the other stress component varies with the location across the section thickness.

1A.68 Notch Sensitivity – A measure of the reduction in the strength of a metal caused by the presence of a stress concentration.

1A.69 Notch Toughness – The ability of a material to resist brittle fracture under conditions of high stress concentration, such as impact loading in the presence of a notch.

1A.70 On-Stream Inspection – The use of any of a number of nondestructive examination procedures to establish the suitability of a pressurized component for continued operation. The pressurized component may, or may not, be in operation while the inspection is performed.

1A.71 Operational Cycle – An operational cycle is defined as the initiation and establishment of new conditions followed by a return to the conditions that prevailed at the beginning of the cycle. Three types of operational cycles are considered: the startup-shutdown cycle, defined as any cycle that has atmospheric temperature and/or pressure as one of its extremes and normal operating conditions as its other extreme; the initiation of, and recovery from, any emergency or upset condition that must be considered in the design; and the normal operating cycle, defined as any cycle between startup and shutdown that is required for the vessel to perform its intended purpose.

1A.72 Peak Stress – The basic characteristic of a peak stress is that it does not cause any noticeable distortion and is objectionable only as a possible source of a fatigue crack or a brittle fracture. A stress that is not highly localized falls into this category if it is of a type, which cannot cause noticeable distortion (see Annex 2C). Examples of peak stress are the thermal stress in the austenitic steel cladding of a carbon steel vessel, the thermal stress in the wall of a vessel or pipe caused by a rapid change in temperature of the contained fluid, and the stress at a local structural discontinuity.

1A.73 Pitting – Localized corrosion in the form of a cavity or hole such that the surface diameter of the cavity is on the order of the plate thickness (see Part 6).

1A.74 Plastic Analysis – A stress analysis method where the structural behavior of a component under load is computed considering the plasticity characteristics of the material including strain hardening and stress redistribution (see Annex 2C).

1A.75 Plastic Instability Load – The plastic instability load for a structure under predominantly tensile or compressive loading is defined as the load at which unbounded plastic deformation can occur without further load increase. At the plastic tensile instability load, the true stress in the material increases faster than the strain hardening can accommodate (see Annex 2C).

1A.76 Plasticity – A general characterization of material behavior in which the material undergoes time independent non-recoverable deformation (see Annex 2C).

1A.77 POD (Probability Of Detection) – A measure of the ability to detect a flaw or indication in a component using a standard NDE technique on a consistent basis.

1A.78 Primary Stress – A normal or shear stress developed by the imposed loading that is necessary to satisfy the laws of equilibrium of external and internal forces and moments. The basic characteristic of a primary stress is that it is not self-limiting. Primary stresses that considerably exceed the yield strength will result

in failure or at least in gross distortion. A thermal stress is not classified as a primary stress. Primary membrane stress is divided into general and local categories. A general primary membrane stress is one that is distributed in the structure such that no redistribution of load occurs as a result of yielding. Examples of primary stress are general membrane stress in a circular cylindrical or a spherical shell due to internal pressure or to distributed live loads and the bending stress in the central portion of a flat head due to pressure. Cases arise in which a membrane stress produced by pressure or other mechanical loading and associated with a primary and/or a discontinuity effect would, if not limited, produce excessive distortion in the transfer of load to other portions of the structure. To be conservative, this stress is classified as a local primary membrane stress even though it has some characteristics of a secondary stress. A primary bending stress can be defined as a bending stress developed by the imposed loading that is necessary to satisfy the laws of equilibrium of external and internal forces and moments (see Annex 2C).

1A.79 PSF (Partial Safety Factor) – A deterministic parameter (derived from statistical considerations) that represents a level of uncertainty or importance for a specific field variable. For example, in a fracture mechanics analysis, distinct PSF's may be applied to each of the loading, material toughness and crack sizing variables. In combination these factors yield a desired level of confidence (i.e., degree of safety) in the calculated fracture assessment result. Where the method is prescribed, tabulations are provided that map the required (or critical) analysis variables to a user selected risk level and the associated PSF multiplier. As an application example, the PSF methodology is well established in the Load and Resistance Factor Design Manual of the American Institute of Steel Construction (see Part 2 and Part 9).

1A.80 PT – Liquid penetrant examination.

1A.81 PWHT (Postweld Heat Treatment) – Uniform heating of a weldment to a temperature below the critical range to relieve a major part of the welding residual stresses, followed by uniform cooling in still air.

1A.82 Ratcheting – A progressive incremental inelastic deformation or strain that can occur in a component subjected to variations of mechanical stress, thermal stress, or both (thermal stress ratcheting is partly or wholly caused by thermal stress). Ratcheting is produced by a sustained load acting over the full cross section of a component, in combination with a strain controlled cyclic load or temperature distribution that is alternately applied and removed. Ratcheting causes cyclic straining of the material, which can result in failure by fatigue and at the same time produces cyclic incremental growth of a structure, which could ultimately lead to collapse (see Part 14).

1A.83 Recognized Code or Standard – A term used to define a code or standard that is recognized by a local jurisdiction (see Part 1, paragraphs 1.2.2 and 1.2.3).

1A.84 Reference Stress – A quantity that is used to account for plasticity effects in the FAD method. The reference stress is computed by multiplying the primary stress by a dimensionless factor that is a function of the component geometry and crack dimensions as shown in Part 9 and Annex 9C. Traditionally, the reference stress has been defined from yield load solutions, such that the net cross section is fully plastic when the reference stress is equal to the yield strength. An alternative definition of the reference stress is based on an elastic-plastic J-integral analysis (see Annex 2C). This newer definition is more technically sound because it greatly reduces geometry effects in the FAD curve.

1A.85 Repair – Restoration of a pressure containing component, the definition is dependent on the equipment type as shown below:

1) Pressure vessels (API 510) – The work necessary to restore a vessel to a condition suitable for safe operation at the design conditions. Repairs also include the addition or replacement of pressure or non-pressure parts that do not change the rating of a vessel.
2) Piping systems (API 570) – The work necessary to restore a piping system to a condition suitable for safe operation at the design conditions. Such repairs are typically completed in compliance with the schedule and pressure class requirements of the piping system. Repairs resulting in schedule/class deviations (e.g., use of lower pressure class fittings) may impact the system design conditions.
3) Storage tanks (API 653) – Any work on a tank necessary to restore a tank to a condition suitable for safe operation.
4) Pressure Vessels (NB-23) – The work necessary to restore pressure retaining items to a safe and satisfactory operating condition.

1A.86 Rerating – A change in either or both the temperature rating and the maximum allowable working pressure rating of a vessel (see Part 2).

1A.87 RSF (Remaining Strength Factor) – The ratio of the collapse pressure of a damaged component (e.g., cylinder containing an LTA) to the collapse pressure of the undamaged component (see Part 2).

1A.88 RT – Radiographic examination.

1A.89 Secondary Stress – A normal stress or a shear stress developed by the constraint of adjacent parts or by self-constraint of a structure. The basic characteristic of a secondary stress is that it is self-limiting. Local yielding and minor distortions can satisfy the conditions that cause the stress to occur and failure from one application of the stress is not to be expected (see Annex 2C). Examples of secondary stress are a general thermal stress and the bending stress at a gross structural discontinuity.

1A.90 Sensitivity Analysis – A statistical or parametric process of varying the independent variables (or inputs) in order to determine the response (or sensitivity) of the dependent variables (or outputs). For example, in a Fitness-For-Service analysis, determination of the maximum permissible crack length may have a strong sensitivity to temperature variation if the material fracture toughness (a material property) is also strongly influenced by temperature (see Part 2).

1A.91 Shakedown – A process caused by cyclic loads or cyclic temperature distributions which produce plastic deformations in some regions of the component when the loading or temperature distribution is applied, but upon removal of the loading or temperature distribution, only elastic primary and secondary stresses are developed in the component, except in small areas associated with local stress (strain) concentrations. These small areas exhibit a stable hysteresis loop, with no indication of progressive deformation. Further loading and unloading, or applications and removals of the temperature distribution produce only elastic primary and secondary stresses (see Part 14).

1A.92 Shear Stress – The component of stress tangent to the plane on which forces act (see Annex 2C).

1A.93 Shock Chilling – Shock chilling is a rapid decrease in metal temperature caused by the sudden contact of liquid or a two-phase (gas/liquid) fluid with a metal surface when the liquid or two phase fluid is colder than the metal temperature at the instant of contact (see Part 3).

1A.94 SOHIC (Stress-Oriented Hydrogen-Induced Cracking) – Arrays of cracks that are aligned nearly perpendicular to the applied stress, which is formed by the link-up of small HIC cracks in steel. Tensile stress (residual or applied) is required to produce SOHIC. SOHIC is commonly observed in the base metal adjacent to the Heat-Affected Zone (HAZ) of a weld, oriented in the through-thickness direction. SOHIC may also be produced in susceptible steels at other high stress points such as from the tip of mechanical cracks and defects, or from the interaction between HIC on different planes in the steel (see Part 7).

1A.95 Strain Limiting Load – The load associated with a given strain limit (see Annex 2C).

1A.96 Stress Concentration Factor – A multiplying factor applied stress equal to the ratio of the maximum stress to the average section stress (see Annex 2C).

1A.97 Stress Cycle – A stress cycle is a condition in which the alternating stress difference goes from an initial value through an algebraic maximum value and an algebraic minimum value and then returns to the initial value. A single operational cycle may result in one or more stress cycles (see Part 14).

1A.98 Stress Intensity Factor – The stress intensity factor is used in fracture mechanics to predict the stress state or stress intensity near the tip of a crack in a linear elastic body caused by a remote loading or residual stresses (see Part 9 and Annex 9B). There are three basic modes for a stress intensity factor: opening (Mode I), in-plane shear (Mode II) and out-of-plane tearing (Mode III). Mode I corresponds to normal separation of the crack faces under the action of tensile stresses. The difference between Mode II and Mode III is that the shearing action in the former case is normal to the crack front in the plane of the crack whereas the shearing action in Mode III is parallel to the crack front. A cracked body in reality can be loaded in any one of these three, or a combination of these three modes.

1A.99 SSC (Sulfide Stress Cracking) – Cracking of a metal under the combined action of tensile stress and corrosion in the presence of water and H_2S (a form of hydrogen stress cracking). SSC involves hydrogen embrittlement of the metal by atomic hydrogen that is produced by the sulfide corrosion process on the metal surface. The atomic hydrogen can diffuse into the metal and produce embrittlement. SSC usually occurs more readily in high-strength steels or in hard weld zones of steels than in other types of steels or weld zones.

1A.100 Tensile Strength – The maximum load per unit of original cross sectional area that a tensile test specimen of a material sustains prior to fracture. The tensile strength may also be identified as the ultimate tensile strength (see Annex 2D).

1A.101 Thermal Stress – A self-balancing stress produced by a nonuniform distribution of temperature or by differing thermal coefficients of expansion. Thermal stress is developed in a solid body whenever a volume of material is prevented from assuming the size and shape that it normally would under a change in temperature. For the purpose of establishing allowable stresses, two types of thermal stress are recognized, depending on the volume or area in which distortion takes place. A general thermal stress that is associated with distortion of the structure in which it occurs. If a stress of this type, neglecting stress concentrations, exceeds twice the yield strength of the material, the elastic analysis may be invalid and successive thermal cycles may produce incremental distortion. Therefore, this type is classified as a secondary stress. Examples of general thermal stress are the stress produced by an axial temperature distribution in a cylindrical shell, the stress produced by the temperature difference between a nozzle and

the shell to which it is attached, and the equivalent linear stress produced by the radial temperature distribution in a cylindrical shell. A local thermal stress is associated with almost complete suppression of the differential expansion and thus produces no significant distortion. Such stresses are considered only from the fatigue standpoint and are therefore classified as local stresses. Examples of local thermal stresses are the stress in a small hot spot in a vessel wall, the difference between the actual stress and the equivalent linear stress resulting from a radial temperature distribution in a cylindrical shell, and the thermal stress in a cladding material that has a coefficient of expansion different from that of the base metal (see Annex 2C).

1A.102 Toughness – The ability of a material to absorb energy and deform plastically before fracturing (see Annex 9F).

1A.103 Transition Temperature – The temperature at which a material fracture mode changes from ductile to brittle (see Annex 9F).

1A.104 Undercut – An intermittent or continuous groove, crater or channel that has melted below, and thus undercut, the surface of the base metal adjacent to the toe of a weld and is left unfilled by weld metal.

1A.105 UT – Ultrasonic examination.

1A.106 Volumetric Flaw – A flaw characterized by a loss of material volume or by a shape imperfection. Examples include general and local corrosion, pitting, blisters, out-of-roundness, bulges, dents, gouges, and dent-gouge combinations, and weld misalignment.

1A.107 Weld – A localized coalescence of metal wherein coalescence (i.e., fusion) is produced by heating to suitable temperatures, with or without the application of pressure, and with or without the use of filler metal. If a filler metal is used, it typically has a melting point approximately the same as that of the base metal.

1A.108 Yield Strength – The stress at which a material exhibits a specified deviation from the linear proportionality of stress versus strain (see Annex 2E).

[Intentionally Left Blank]

PART 2 – FITNESS-FOR-SERVICE ENGINEERING ASSESSMENT PROCEDURE

CONTENTS

PART 2 – FITNESS-FOR-SERVICE ENGINEERING ASSESSMENT PROCEDURE 2-1

2.1 GENERAL 2-1
2.1.1 Fitness-For-Service and Continued Operation 2-1
2.1.2 Organization by Flaw Type and Damage Mechanism 2-2
2.1.3 FFS Assessment Procedure 2-2
2.2 APPLICABILITY AND LIMITATIONS OF THE FFS ASSESSMENT PROCEDURES 2-3
2.2.1 FFS Procedures for Pressurized or Unpressurized Components 2-3
2.2.2 Component Definition 2-3
2.2.3 Construction Codes 2-3
2.2.4 Specific Applicability and Limitations 2-3
2.3 DATA REQUIREMENTS 2-4
2.3.1 Original Equipment Design Data 2-4
2.3.2 Maintenance and Operational History 2-5
2.3.3 Required Data/Measurements for an FFS Assessment 2-6
2.3.4 Recommendations for Inspection Technique and Sizing Requirements 2-6
2.4 ASSESSMENT TECHNIQUES AND ACCEPTANCE CRITERIA 2-6
2.4.1 Assessment Levels 2-6
2.4.2 FFS Acceptance Criteria 2-7
2.4.3 Data Uncertainties 2-8
2.5 REMAINING LIFE ASSESSMENT 2-9
2.5.1 Remaining Life 2-9
2.5.2 Guidance on Remaining Life Determination 2-10
2.6 REMEDIATION 2-10
2.6.1 Requirements for Remediation 2-10
2.6.2 Guidelines for Remediation 2-10
2.7 IN-SERVICE MONITORING 2-10
2.8 DOCUMENTATION 2-11
2.8.1 General 2-11
2.8.2 Applicability and Limitations 2-11
2.8.3 Data Requirements 2-11
2.8.4 Assessment Techniques and Acceptance Criteria 2-11
2.8.5 Remaining Life Assessment 2-12
2.8.6 Remediation Methods 2-12
2.8.7 In-Service Monitoring 2-12
2.8.8 Retention 2-12
2.9 NOMENCLATURE 2-12
2.10 REFERENCES 2-13
2.11 TABLES 2-14
2.12 FIGURES 2-16

2.1 General

2.1.1 Fitness-For-Service and Continued Operation

This Standard contains Fitness-For-Service (FFS) Assessment procedures that can be used to evaluate pressurized components containing flaws or damage. If the results of an FFS Assessment indicate that the equipment is suitable for the current operating conditions, then the equipment can continue to be operated at these conditions provided suitable monitoring/inspection programs are established. If the results of the FFS Assessment indicate that the equipment is not suitable for the current operating conditions, then the equipment

can be rerated using the calculation methods in this Standard. These calculation methods can be used to find a Reduced Maximum Allowable Working Pressure ($MAWP_r$) and/or coincident temperature for pressurized components (e.g., pressure vessels drums, headers, tubing, and piping). The calculation methods can also be used to determine a reduced Maximum Fill Height (MFH_r) for tank components (e.g., shell courses).

2.1.2 Organization by Flaw Type and Damage Mechanism

The FFS Assessment procedures in this Standard are organized by flaw type and/or damage mechanism. A list of flaw types and damage mechanisms and the corresponding Part that provides the FFS Assessment methodology is shown in Table 2.1. In some cases, it may be necessary to use the assessment procedures from multiple Parts if the primary type of damage is not evident. For example, the metal loss in a component may be associated with general corrosion, local corrosion, and pitting. If multiple damage mechanisms are present, a damage class, e.g., corrosion/erosion, can be identified to assist in the evaluation. An overview of damage classes in this Standard is shown in Figure 2.1. As indicated in this figure, several flaw types and damage mechanisms may need to be evaluated to determine the FFS of a component. Each Part referenced within a damage class includes guidance on how to perform an assessment when multiple damage mechanisms are present.

2.1.3 FFS Assessment Procedure

The general FFS Assessment procedure used in this Standard for all flaw types and damage mechanisms is provided in this Part. An overview of the procedure is provided in the following eight STEPs. The remaining Parts in this Standard utilize this assessment methodology for a specific flaw type or damage mechanism and provide specific details covering STEPs 2 through 8 of this procedure.

a) STEP 1 – *Flaw and Damage Mechanism Identification:* The first STEP in an FFS Assessment is to identify the flaw type and cause of damage, see paragraph 2.1.2. The original design and fabrication practices, the material of construction, and the service history and environmental conditions can be used to ascertain the likely cause of the damage. An overview of damage mechanisms that can assist in identifying likely causes of damage, is provided in Annex 2B. Once the flaw type is identified, the appropriate Part of this Standard can be selected for the assessment, see Table 2.1 and Figure 2.1.

b) STEP 2 – *Applicability and Limitations of the FFS Assessment Procedures:* The applicability and limitations of the assessment procedure are described in each Part, and a decision on whether to proceed with an assessment can be made.

c) STEP 3 – *Data Requirements:* The data required for an FFS Assessment depend on the flaw type or damage mechanism being evaluated. Data requirements may include original equipment design data, information pertaining to maintenance and operational history, expected future service, and data specific to the FFS Assessment such as flaw size, state of stress in the component at the location of the flaw, and material properties. Data requirements common to all FFS Assessment procedures are covered in this Part. Data requirements specific to a damage mechanism or flaw type are covered in the Part containing the corresponding assessment procedures.

d) STEP 4 – *Assessment Techniques and Acceptance Criteria:* Assessment techniques and acceptance criteria are provided in each Part. If multiple damage mechanisms are present, more than one Part may have to be used for the evaluation.

e) STEP 5 – *Remaining Life Evaluation:* An estimate of the remaining life or limiting flaw size should be made for establishing an inspection interval. The remaining life is established using the FFS Assessment

procedures with an estimate of future damage. The remaining life can be used in conjunction with an inspection code to establish an inspection interval.

f) STEP 6 – *Remediation:* Remediation methods are provided in each Part based on the damage mechanism or flaw type. In some cases, remediation techniques may be used to control future damage associated with flaw growth and/or material deterioration.

g) STEP 7 – *In-Service Monitoring:* Methods for in-service monitoring are provided in each Part based on the damage mechanism or flaw type. In-service monitoring may be used for those cases where a remaining life and inspection interval cannot adequately be established because of the complexities associated with the service environment.

h) STEP 8 – *Documentation:* Documentation should include a record of all information and decisions made in each of the previous STEPs to qualify the component for continued operation. Documentation requirements common to all FFS Assessment procedures are covered in this Part. Documentation requirements specific to a damage mechanism or flaw type are covered in the Part containing the corresponding assessment procedures.

2.2 Applicability and Limitations of the FFS Assessment Procedures

2.2.1 FFS Procedures for Pressurized or Unpressurized Components

The FFS Assessment procedures in this Standard were developed to evaluate the pressure boundaries of pressure vessels, boiler components, piping, and shell courses of storage tanks with a flaw resulting from single or multiple damage mechanisms. The concepts presented in this Standard may also be used for the assessment of non-pressure-boundary components such as supports. FFS procedures for fixed and floating roof structures, and bottom plates of tanks are covered in API 653, Part 4.

2.2.2 Component Definition

In the context of this Standard, a component is defined as any part that is designed and fabricated to a recognized code or standard, and equipment is defined to be an assemblage of components, see Part 1, paragraphs 1.2.2 and 1.2.3. Therefore, the equipment $MAWP$ is the lowest $MAWP$ of all the components in the assemblage.

2.2.3 Construction Codes

The assessment procedures in this Standard have been formulated based on the assumption that the component was constructed to a recognized code or standard. For components that have not been constructed to a recognized construction or code or standard, the principles in this Standard may be used to evaluate the in-service damage and as-built condition relative to the intended design. FFS Assessments of this type shall be performed by an Engineer (except for Level 1 Assessment) knowledgeable and experienced in the design requirements of the applicable code, see Part 1, paragraph 1.4.3.

2.2.4 Specific Applicability and Limitations

Each Part in this Standard where an FFS Assessment procedure is described includes a statement of the applicability and limitations of the procedure. The applicability and limitations of an analysis procedure are stated relative to the level of assessment, see paragraph 2.4.

2.3 Data Requirements

2.3.1 Original Equipment Design Data

2.3.1.1 The following original equipment design data should be assembled to perform an FFS Assessment. The extent of the data required depends on the damage mechanism and assessment level. A data sheet is included in Table 2.2 to record the required information that is common to all FFS Assessments. In addition, a separate data sheet is included with each Part of this Standard to record information specific to the flaw type, damage mechanism, and assessment procedure.

a) Data for pressure vessels and boiler components may include some or all the following:

1) An ASME Manufacturer's Data Report or, if the vessel or system is not Code stamped, other equivalent documentation or specifications.

2) Fabrication drawings showing enough details to permit calculation of the $MAWP$ of the component containing the flaw. If a rerate to a different condition of pressure and/or temperature is desired (i.e., increase or decrease in conditions), this information should be available for all affected components. Detailed sketches with data necessary to perform $MAWP$ calculations may be used if the original fabrication drawings are not available.

3) The original or updated design calculations for the load cases in Annex 2C, Table 2C.2, as applicable, and anchor bolt calculations.

4) The inspection records for the component at the time of fabrication.

5) User Design Specification if the vessel is designed to the ASME Code, Section VIII, Division 2.

6) Material test reports.

7) Pressure-relieving device information including pressure relief valve and/or rupture disk setting and capacity information.

8) A record of the original hydrotest including the test pressure and metal temperature at the time of the test or, if the metal temperature is unavailable, the water or ambient temperature.

b) Data for piping components may include some or all the following:

1) Piping Line Lists or other documentation showing process design conditions, and a description of the piping class including material specification, pipe wall thickness and pressure-temperature rating.

2) Piping isometric drawings to the extent necessary to perform an FFS Assessment. The piping isometric drawings should include enough details to permit a piping flexibility calculation if such an analysis is deemed necessary by the Engineer to determine the $MAWP$ of all piping components. Detailed sketches with data necessary to perform $MAWP$ calculations may be used if the original piping isometric drawings are not available.

3) The original or updated design calculations for the load cases in Annex 2C, Table 2C.2, as applicable.

4) The inspection records for the component at the time of fabrication.

5) Material test reports.

6) A record of the original hydrotest including the test pressure and metal temperature at the time of the test, or if the metal temperature is unavailable, the water or ambient temperature.

c) Data for tanks may include some or all the following:

1) The original API data sheet.

2) Fabrication drawings showing enough details to permit calculation of the maximum fill height (MFH) for atmospheric storage tanks and the $MAWP$ for low-pressure storage tanks. Detailed data with sketches where necessary may be used if the original fabrication drawings are not available.

3) The original or updated design calculations for the load cases in Annex 2C, Table 2C.2, as applicable, and anchor bolt calculations.

4) The inspection records for the component at the time of fabrication.

5) Material test reports.

6) A record of the last hydrotest performed including the test pressure and metal temperature at the time of the test or, if the metal temperature is unavailable, the water or ambient temperature.

2.3.1.2 If some of these data are not available, physical measurements or field inspection of the component should be made to provide the information necessary to perform the assessment.

2.3.2 Maintenance and Operational History

2.3.2.1 A progressive record including, but not limited to, the following should be available for the equipment being evaluated. The extent of the data required depends on the damage mechanism and assessment level.

a) The actual operating envelope consisting of pressure and temperature, including upset conditions should be obtained. If the actual operating conditions envelope is not available, an approximation of one should be developed based upon available operational data and consultation with operating personnel. An operating histogram consisting of pressure and temperature data recorded simultaneously may be required for some types of FFS Assessments (e.g., Part 10 for components operating in the creep regime).

b) Documentation of any significant changes in service conditions including pressure, temperature, fluid content and corrosion rate. Both past and future service conditions should be reviewed and documented.

c) The date of installation and a summary of all alterations and repairs including required calculations, material changes, drawings, and repair procedures, including $PWHT$ procedures if applicable. The calculations should include the required wall thickness and $MAWP$ (MFH) for atmospheric storage tanks) with definition and allowances for supplemental loads such as static liquid head, wind, and earthquake loads.

d) Records of all hydrotests performed as part of any repairs including the test pressure and metal temperature at the time of the tests or, if the metal temperature is unavailable, the water or ambient temperature at the time of the test if known.

e) Results of prior in-service examinations including wall thickness measurements and other NDE results that may assist in determining the structural integrity of the component and in establishing a corrosion rate.

f) Records of all internal repairs, weld build-up and overlay, and modifications of internals.

g) Records of "out-of-plumb" readings for vertical vessels or tank shells.

h) Foundation settlement records if corrosion is being evaluated in the bottom plate or shell courses of the tank.

2.3.2.2 If some of these data are not available, physical measurements should be made to provide the information necessary to perform the assessment.

2.3.3 Required Data/Measurements for an FFS Assessment

2.3.3.1 Each Part in this Standard that contains FFS Assessment procedures include specific requirements for data measurements and flaw characterization based on the damage mechanism being evaluated. Examples of flaw characterization include thickness profiles for local corrosion/erosion, pitting depth, and dimensions of crack-like flaws. The extent of information and data required for an FFS Assessment depends on the assessment level and damage mechanism being evaluated.

2.3.3.2 The Future Corrosion Allowance (FCA) should be established for the intended future operating period. The FCA should be based on past inspection information or corrosion rate data relative to the component material in a similar environment. Corrosion rate data may be obtained from API Publication 581 or other sources, see Annex 2C, paragraph 2C.2.8. The FCA is calculated by multiplying the anticipated corrosion rate by the future service period considering inspection interval requirements of the applicable inspection code. The FFS Assessment procedures in this Standard include provisions to ensure that the FCA is available for the future intended operating period.

2.3.4 Recommendations for Inspection Technique and Sizing Requirements

Recommendations for Nondestructive Examination (NDE) procedures regarding detection and sizing of a particular damage mechanism and/or flaw type are provided in each Part.

2.4 Assessment Techniques and Acceptance Criteria

2.4.1 Assessment Levels

Three Levels of assessment are provided in each Part of this Standard that cover FFS Assessment procedures. A logic diagram is included in each Part to illustrate how these assessment levels are interrelated. In general, each assessment level provides a balance between conservatism, the amount of information required for the evaluation, the skill of the personnel performing the assessment, and the complexity of analysis being performed. Level 1 is the most conservative but is easiest to use. Practitioners usually proceed sequentially from a Level 1 to a Level 3 analysis (unless otherwise directed by the assessment techniques) if the current assessment level does not provide an acceptable result, or a clear course of action cannot be determined. A general overview of each assessment level and its intended use are described below.

2.4.1.1 Level 1 Assessment

The assessment procedures included in this level are intended to provide conservative screening criteria that can be utilized with a minimum amount of inspection or component information. A Level 1 Assessment may be performed either by plant inspection or engineering personnel, see Part 1, paragraphs 1.4.2 and 1.4.3.

2.4.1.2 Level 2 Assessment

The assessment procedures included in this level are intended to provide a more detailed evaluation that produces results that are more precise than those from a Level 1 Assessment. In a Level 2 Assessment, inspection information like that required for a Level 1 Assessment is needed; however, more detailed calculations are used in the evaluation. Level 2 Assessments would typically be conducted by plant engineers, or engineering specialists experienced and knowledgeable in performing FFS Assessments.

2.4.1.3 Level 3 Assessment

The assessment procedures included in this level are intended to provide the most detailed evaluation that produces results that are more precise than those from a Level 2 Assessment. In a Level 3 Assessment the most

detailed inspection and component information is typically required, and the recommended analysis is based on numerical techniques such as the finite element method or experimental techniques when appropriate. A Level 3 Assessment is primarily intended for use by engineering specialists experienced and knowledgeable in performing FFS Assessments.

2.4.2 FFS Acceptance Criteria

Each of the FFS Assessment methodologies presented in this Standard utilize one or more of the following acceptance criteria.

2.4.2.1 Allowable Stress

This acceptance criterion is based upon calculation of stresses resulting from different loading conditions, classification and superposition of stress results, and comparison of the calculated stresses in an assigned category or class to an allowable stress value. An overview and aspects of these acceptance criteria are included in Annex 2C. The allowable stress value is typically established as a fraction of yield, tensile or rupture stress at room and the service temperature, and this fraction can be associated with a design margin. This acceptance criteria method is currently utilized in most new construction design codes. In FFS applications, this method has limited applicability because of the difficulty in establishing suitable stress classifications for components containing flaws. As an alternative, assessment methods based on elastic-plastic analysis may be used, see Annex 2C. Elastic-plastic analysis methods were used to develop the Remaining Strength Factor, see paragraph 2.4.2.2.

2.4.2.2 Remaining Strength Factor

Structural evaluation procedures using linear elastic stress analysis with stress classification and allowable stress acceptance criteria provide only a rough approximation of the loads that a component can withstand without failure. A better estimate of the safe load carrying capacity of a component can be provided by using non-linear stress analysis to develop limit and plastic collapse loads, evaluate the deformation characteristics of the component (e.g., deformation or strain limits associated with component operability), and assess fatigue and/or creep damage including ratcheting.

a) In this Standard, the concept of a remaining strength factor is utilized to define the acceptability of a component for continued service. The Remaining Strength Factor (RSF) is defined as:

$$RSF = \frac{L_{DC}}{L_{UC}} \tag{2.1}$$

b) With this definition of the RSF, acceptance criteria can be established using traditional code formulas, elastic stress analysis, limit load theory, or elastic-plastic analysis. For example, to evaluate local thin areas, the FFS Assessment procedures provide a means to compute a RSF, see Part 5. The reduced maximum allowable working pressure, $MAWP_r$, for the component can then be calculated from the RSF using Equations (2.2) and (2.3). The resulting value of the $MAWP_r$, minus the static head as appropriate, should be compared with the existing equipment design pressure or equipment $MAWP$, see paragraph 2.4.2.2(e).

$$MAWP_r = MAWP\left(\frac{RSF}{RSF_a}\right) \qquad \left(for \quad RSF < RSF_a\right) \tag{2.2}$$

$$MAWP_r = MAWP \qquad \left(for \quad RSF \geq RSF_a\right) \tag{2.3}$$

c) For tankage, the RSF acceptance criteria are:

$$MFH_r = H_f + (MFH - H_f)\left(\frac{RSF}{RSF_a}\right) \qquad \left(for \quad RSF < RSF_a\right) \tag{2.4}$$

$$MFH_r = MFH \qquad \left(for \quad RSF \geq RSF_a\right) \tag{2.5}$$

d) The recommended value for the allowable Remaining Strength Factor, RSF_a, is 0.90. Alternative values for the RSF_a may be used based on the information provided in Annex 2F.

e) The $MAWP_r$ for the component with the static head subtracted as appropriate shall be compared to either the equipment design pressure or equipment $MAWP$. If the $MAWP_r$ is greater than or equal to the equipment design pressure or equipment $MAWP$, the component is acceptable for operating at the equipment design pressure or equipment $MAWP$. If the $MAWP_r$ is less than the equipment design pressure or equipment $MAWP$, the component is unacceptable for operating at the equipment design pressure or equipment $MAWP$.

f) If unacceptable, the equipment shall be rerated, repaired or the equipment retired. Options specific to damage type are listed in the corresponding Part.

g) The $MAWP$ and the $MAWP_r$ may be established using the stress analysis procedures defined in Annex 2D.

2.4.2.3 Failure Assessment Diagram

The Failure Assessment Diagram (FAD) is used for the evaluation of crack-like flaws in components.

a) The FAD approach was adopted because it provides a convenient, technically based method to provide a measure for the acceptability of a component with a crack-like flaw when the failure mechanism is measured by two distinct criteria: unstable fracture and limit load. Unstable fracture usually controls failure for small flaws in components fabricated from a brittle material and plastic collapse typically controls failure for large flaws if the component is fabricated from a material with high toughness. In an FFS analysis of crack-like flaws, the results from a stress analysis, stress intensity factor and limit load solutions, the material strength, and fracture toughness are combined to calculate a toughness ratio, K_r, and load ratio, L_r. These two quantities represent the coordinates of a point that is plotted on a two-dimensional FAD to determine acceptability. If the assessment point is on or below the FAD curve, the component is suitable for continued operation. A schematic that illustrates the procedure for evaluating a crack-like flaw using the Failure Assessment Diagram is shown in Figure 2.2.

b) The in-service margin for a component with a crack-like flaw provides a measure of how close the component is to the limiting condition in the FAD. The in-service margin is defined by how far the assessment point, which represents a single operating condition, is within the failure envelope of the FAD. This point is determined based on the results from stress and fracture mechanics analyses. The in-service margin is defined to be greater than or equal to one when the point resides underneath or on the FAD failure curve. The recommended minimum allowable value for the in-service margin is set at 1.0.

2.4.3 Data Uncertainties

The FFS Assessment procedures provided in this Standard are deterministic in that all information required for an analysis (independent variables) is assumed to be known. However, in many instances not all the important independent variables are known with a high degree of accuracy. In such cases, conservative estimates of the independent variables are made to ensure an acceptable safety margin; this approach can lead to overly

conservative results. The following types of analyses can be used to provide insight into the dependency of the analysis results with variations in the input parameters. The deterministic FFS Assessment procedures in this standard can be used with any of these analyses.

2.4.3.1 Sensitivity Analysis

The purpose of such an analysis is to determine if a change in any of the independent (input) variables has a strong influence on the computed safety factors. The sensitivity analysis should consider the effects of different assumptions about loading conditions, material properties and flaw sizes. For example, there may be uncertainties in the service loading conditions; the extrapolation of materials data to service conditions; and the type, size, and shape of the flaw. Confidence is gained in an assessment when it is possible to demonstrate that small changes in input parameters do not dramatically change the assessment results; and when realistic variations in the input parameters, on an individual or combined basis, still lead to the demonstration of an acceptable safety margin. If a strong dependence on an input variable is found, it may be possible to improve the degree of accuracy used to establish the value of that variable.

2.4.3.2 Probabilistic Analysis

The dependence of the safety margin on the uncertainty of the independent variables can be evaluated using this type of analysis. All or a limited number of the independent variables are characterized as random variables with a distribution of values. Using Monte Carlo simulation, first order reliability methods or other analytical techniques, the failure probability is estimated. These methods can be used to combine a deterministic FFS Assessment model with the distributions prescribed for the independent variable to calculate failure probabilities. Once a probability of failure has been determined, an acceptable level can be established based on multiple factors such as jurisdictional regulations and the consequence of failure.

2.4.3.3 Partial Safety Factors

Partial Safety Factors are individual safety factors that are applied to the independent variables in the assessment procedure. The partial safety factors are probabilistically calibrated to reflect the effect that each of the independent variables has on the probability of failure. Partial safety factors are developed using probabilistic analysis techniques considering a limit state model, distributions of the main independent variables of the model, and a target reliability or probability of failure. The advantage of this approach is that uncertainty can be introduced in an assessment by separately combining the partial safety factors with the independent variables in a deterministic analysis model; the format of the analysis is similar to that used by many design codes. In this Standard, partial safety factors are only considered in a Level 3 Assessment of a crack-like flaw.

2.5 Remaining Life Assessment

2.5.1 Remaining Life

Once it has been established that the component containing the flaw is acceptable at the current time, the user should determine a remaining life for the component. The remaining life in this Standard is used to establish an appropriate inspection interval, an in-service monitoring plan, or the need for remediation. The remaining life is not intended to provide a precise estimate of the actual time to failure. Therefore, the remaining life can be estimated based on the quality of available information, assessment level, and appropriate assumptions to provide an adequate safety factor for operation until the next scheduled inspection.

2.5.2 Guidance on Remaining Life Determination

Each FFS Assessment Part in this Standard provides guidance on calculating a remaining life. In general, the remaining life can be calculated using the assessment procedures in each Part with the introduction of a parameter that represents a measure of the time dependency of the damage taking place. The remaining life is then established by solving for the time to reach a specified operating condition such as the $MAWP$ (MFH) or a reduced operating condition $MAWP_r$ (MFH_r), see paragraph 2.4.2.2(b) and paragraph 2.4.2.2(c). Remaining life estimates typically fall into one of the following categories:

a) *The Remaining Life Can be Calculated with Reasonable Certainty* – An example is general uniform corrosion, where a future corrosion allowance can be calculated and the remaining life is the future corrosion allowance divided by the assumed corrosion rate from previous thickness data, corrosion design curves, or experience in similar services. Another example may be long term creep damage, where a future damage rate can be estimated. An appropriate inspection interval can be established at a certain fraction of the remaining life. The estimate of remaining life should be conservative to account for uncertainties in material properties, stress assumptions, and variability in future damage rate.

b) *The Remaining Life Cannot be Established with Reasonable Certainty* – Examples may be a stress corrosion cracking mechanism where there are no reliable crack growth rate data available or hydrogen blistering where a future damage rate cannot be estimated. In these examples, remediation methods should be employed, such as application of a lining or coating to isolate the environment, drilling of blisters, or monitoring. Inspection would then be limited to assuring remediation method acceptability, such as lining or coating integrity.

c) *There is Little or No Remaining Life* – In this case remediation, such as repair of the damaged component, application of a lining or coating to isolate the environment, and/or frequent monitoring is necessary for future operation.

2.6 Remediation

2.6.1 Requirements for Remediation

In some circumstance's remediation should be used, see paragraph 2.5.2. Examples include where a flaw is not acceptable in its current condition; the estimated remaining life is minimal or difficult to estimate; or the state-of-the-art analysis/knowledge is insufficient to provide an adequate assessment. Appropriate remediation methods are covered within each Part of this standard that contains an FFS Assessment procedure.

2.6.2 Guidelines for Remediation

Only general guidelines are provided in this Standard; each situation will require a customized approach to remediation. Periodic checks should be made to ensure that the remediation actions have prevented additional damage and can be expected to prevent future damage. The user may need to refer to other standards for detailed remediation procedures; for example, weld repair guidelines can be found in applicable repair codes, such as API 510, API 570, API 653, and ANSI/NB-23.

2.7 In-Service Monitoring

Under some circumstances, the future damage rate/progression cannot be estimated easily, or the estimated remaining life is short. In-service monitoring is one method whereby future damage or conditions leading to future damage can be assessed, or confidence in the remaining life estimate can be increased. Monitoring methods typically utilized include corrosion probes to determine a corrosion rate; hydrogen probes to assess hydrogen

activity; various ultrasonic examination methods and acoustic emission testing to measure metal loss or cracking activity; and measurement of key process variables and contaminants. Appropriate in-service monitoring methods are covered within each Part of this standard that contains an FFS Assessment procedure.

2.8 Documentation

2.8.1 General

FFS analysis should be sufficiently documented such that the analysis can be repeated later. Documentation requirements specific to a particular assessment are described in the corresponding Part covering the FFS Assessment procedure.

2.8.2 Applicability and Limitations

Applicability and limitation requirements should be documented along with any assumptions.

2.8.3 Data Requirements

The following items should be included in the documentation.

a) Original equipment design data as described in paragraph 2.3.1.

b) Maintenance and operational history as described in paragraph 2.3.2.

c) Type of flaw and characterization of the flaw including all sizing data. Inspection data including all readings utilized in the FFS Assessment as described in paragraph 2.3.3.

2.8.4 Assessment Techniques and Acceptance Criteria

The assessment level used, i.e., Levels 1, 2 and/or 3, and acceptance criteria.

a) Part, edition, and assessment level of this Standard and any other supporting documents used to evaluate the flaw or damage.

b) Documentation of the criteria used in the FFS Assessment.

c) The material specification of the component containing the flaw and all applicable material properties required for the assessment.

d) Loading conditions considered in the assessment including normal operation and upset conditions and the stress analysis methods (handbook or numerical techniques such as finite-element analysis).

e) Method used to evaluate data uncertainties.

f) Any assumptions, deviations or modifications used for the assessment level including:

- Future operating and design conditions including pressure, temperature, and abnormal operating conditions.
- Description of how time dependent damage is modeled. For example, a description of the basis for the future corrosion allowance for a Part 4 or Part 5 Assessment should be documented.

g) Assessment results.

2.8.5 Remaining Life Assessment

A description of the method used to determine a remaining life.

a) Volumetric flaw – the assumptions used to determine the Future Corrosion Allowance (FCA) should be documented.

b) Crack-Like Flaw – the assumptions used to include the crack growth model and associated constants should be documented.

c) Fatigue – the fatigue curve for fatigue crack initiation, and the crack growth model and associated constants for fatigue crack growth should be documented.

d) Creep Damage – the material model and associated constants should be documented.

2.8.6 Remediation Methods

If applicable, all remediation methods shall be documented including the type of method and reason for application of the method.

2.8.7 In-Service Monitoring

If applicable, a complete description of the reason for in-service monitoring and the in-service monitoring method utilized shall be documented.

2.8.8 Retention

The documentation of the FFS Assessment should be permanently stored with the equipment record files.

2.9 Nomenclature

FCA	future corrosion allowance.
H_f	distance between the bottom of the flaw and the tank bottom.
L_{DC}	limit or plastic collapse load of the damaged component (component with flaws).
L_{UC}	limit or plastic collapse load of the undamaged component.
$LOSS$	uniform metal loss away from the damage area at the time of the inspection.
$MAWP$	maximum allowable working pressure of the undamaged component (see Annex 2C, paragraph 2C.1.2).
$MAWP_r$	reduced maximum allowable working pressure of the damaged component.
MFH	maximum fill height of the undamaged component (see Annex 2C, paragraph 2C.1.2).
MFH_r	reduced maximum fill height of the damaged tank course.
RSF	remaining strength factor computed based on the flaw and damage mechanism in the component.
RSF_a	allowable remaining strength factor.

2.10 References

References for this Part are provided in Annex 2A – Technical Basis and Validation – Fitness-For-Service Engineering Assessment Procedure.

2.11 Tables

Table 2.1 – Overview of Flaw and Damage Assessment Procedures

Flaw or Damage Mechanism	Part	Overview
Brittle Fracture	Part 3	Assessment procedures are provided for evaluating the resistance to brittle fracture of existing carbon and low alloy steel pressure vessels, piping, and storage tanks. Criteria are provided to evaluate normal operating, start-up, upset, and shut-down conditions.
General Metal Loss	Part 4	Assessment procedures are provided to evaluate general corrosion. Thickness data used for the assessment can be either point thickness readings or detailed thickness profiles. A methodology is provided to utilize the assessment procedures of Part 5 when the thickness data indicates that the metal loss can be treated as localized.
Local Metal Loss	Part 5	Assessment techniques are provided to evaluate single and networks of Local Thin Areas and groove-like flaws in pressurized components. Detailed thickness profiles are required for the assessment. The assessment procedures can also be utilized to evaluate individual pits or blisters as provided for in Part 6 and Part 7, respectively.
Pitting Corrosion	Part 6	Assessment procedures are provided to evaluate widely scattered pitting, localized pitting, pitting which occurs within a region of local metal loss, and a region of localized metal loss located within a region of widely scattered pitting. The assessment procedures can also be utilized to evaluate a network of closely spaced blisters as provided for in Part 7.
Blisters and HIC/SOHIC Damage	Part 7	Assessment procedures are provided to evaluate isolated and networks of blisters and HIC/SOHIC Damage. The assessment guidelines include provisions for blisters and HIC/SOHIC damage located at weld joints and structural discontinuities such as shell transitions, stiffening rings, and nozzles.
Weld Misalignment and Shell Distortions	Part 8	Assessment procedures are provided to evaluate stresses resulting from geometric discontinuities in shell type structures including weld misalignment and shell distortions (e.g., out-of-roundness and bulges).
Crack-Like Flaws	Part 9	Assessment procedures are provided to evaluate crack-like flaws. Solutions for stress intensity factors and reference stress (limit load) are included in Annex 9B and Annex 9C, respectively. Methods to evaluate residual stress as required by the assessment procedure are described in Annex 9D. Material properties required for the assessment are provided in Annex 9E. Recommendations for evaluating crack growth including environmental concerns are also covered.
High Temperature Operation and Creep	Part 10	Assessment procedures are provided to determine the remaining life of a component operating in the creep regime. Material properties required for the assessment are provided in Annex 10B. Analysis methods for evaluating crack growth including environmental concerns are also covered.
Fire Damage	Part 11	Assessment procedures are provided to evaluate equipment subject to fire damage. A methodology is provided to rank and screen components for evaluation based on the heat exposure experienced during the fire. The assessment procedures of the other Parts of this publication are utilized to evaluate component damage.
Dent, Gouge, and Dent Gouge Combinations	Part 12	Assessment techniques are provided to evaluate dent, gouge, and dent gouge combinations in components.
Laminations	Part 13	Assessment procedures are provided to evaluate laminations. The assessment guidelines include provisions for laminations located at weld joints and structural discontinuities such as shell transitions, stiffening rings, and nozzles.
Fatigue	Part 14	Assessment procedures are provided to evaluate pressurized components subject to cyclic loading. The assessment procedures include specific requirements for welded joints.

Table 2.2 – Overview of Data Required for Flaw and Damage Assessment

The following data are required for most types of Fitness-For-Service Assessments and it is recommended that this completed table accompany the data table completed for the specific damage type that are located in the respective Part of this standard.

Equipment Identification: _____
Equipment Type: ___ Pressure Vessel ___ Piping Component ___ Boiler Component ___ Storage Tank
Component Type & Location: _____
Design Code: _____ ASME Section VIII Div. 1 _____ ASME Section VIII Div. 2 _____ ASME Section I
_____ ASME B31.1 _____ ASME B31.3 _____ API 650 _____ API 620
_____ other: _____
Material of Construction (e.g., ASTM Specification): _____
$MAWP$ or MFH: _____
Minimum Required Wall Thickness: _____
Temperature: _____
Cyclic Operation: _____

Type of Damage
Metal Loss – General: _____
Metal Loss – Local: _____
Metal Loss – Pitting: _____
HIC, SOHIC & Blisters: _____
Misalignment or Out-Of-Roundness: _____
Bulge: _____
Crack-Like Flaw: _____
Creep Damage: _____
Fire Damage: _____
Dent, Gouge & Dent/Gouge Combinations: _____
Laminations: _____
Fatigue: _____

Location of Damage (provide a sketch)
Internal/External: _____
Near weld: _____
Orientation: _____

Environment
Internal: _____
_____
External: _____
_____

Repair and Inspection History (Including any Previous FFS Assessments)
_____
_____

Operations History
_____
_____
_____

Future Anticipated Operations
_____
_____

2.12 Figures

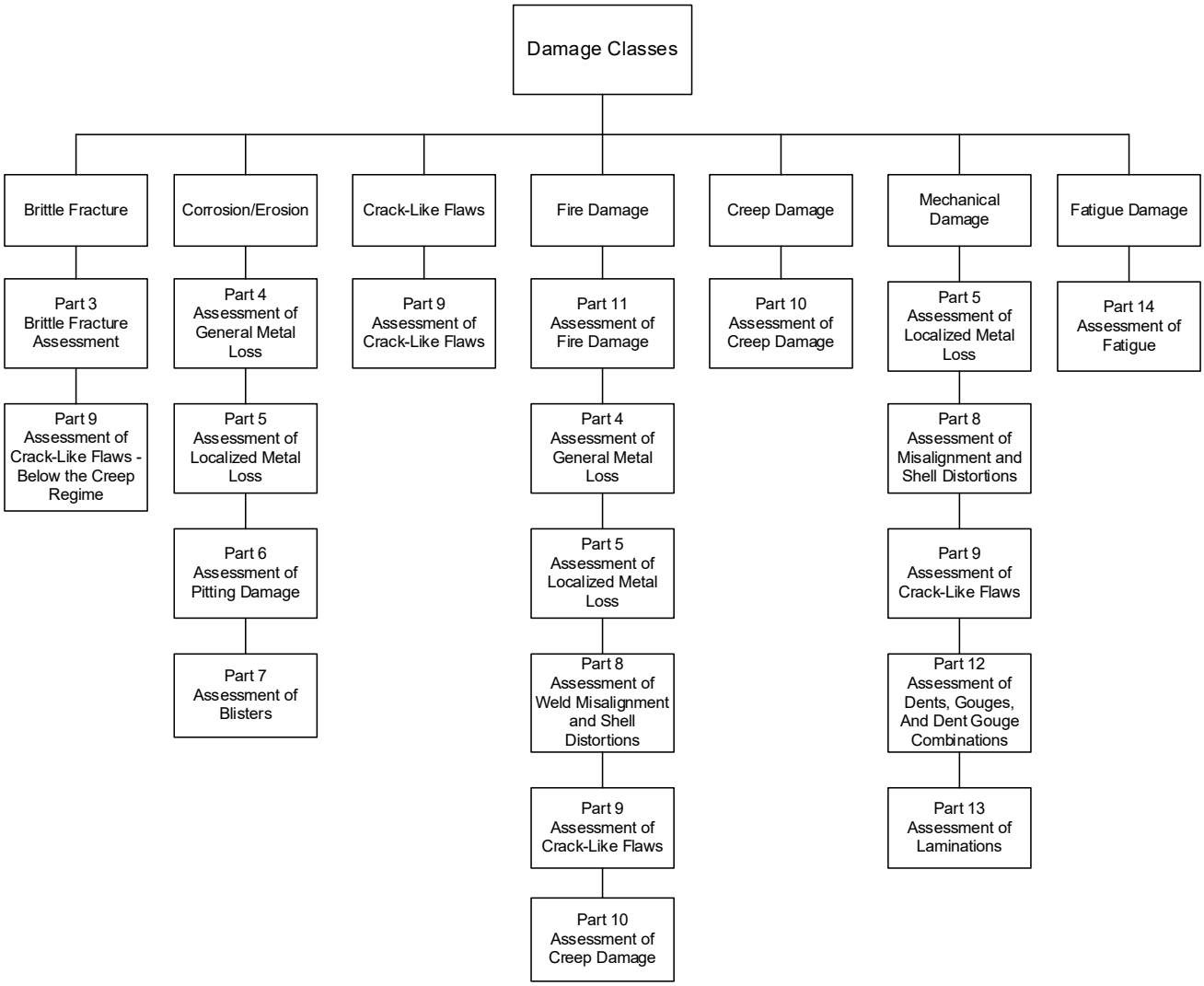

Figure 2.1 – *FFS* Assessment Procedures for Various Damage Classes

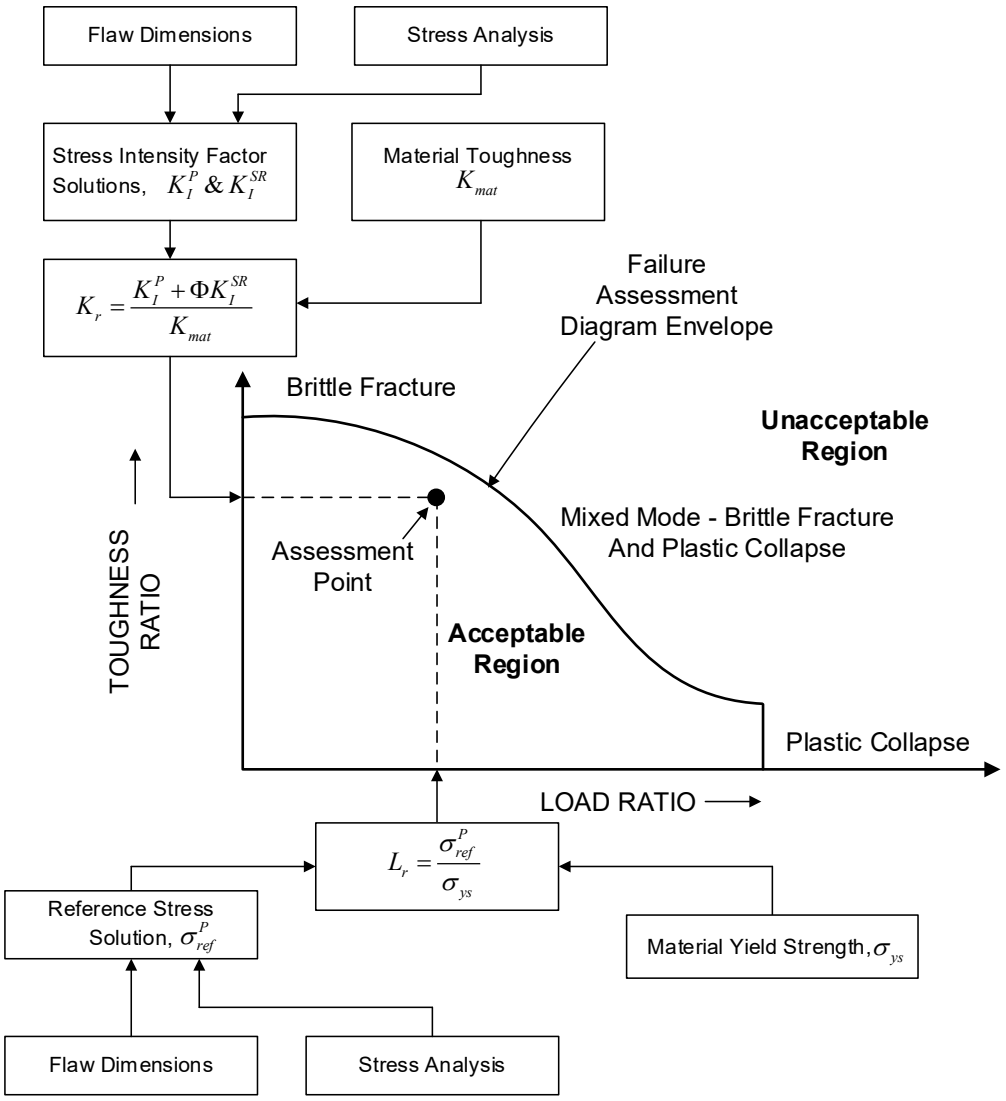

Figure 2.2 – Overview of an *FFS* Analysis for Crack-Like Flaws Using the Failure Assessment Diagram

Intentionally Left Blank

ANNEX 2A – TECHNICAL BASIS AND VALIDATION – FITNESS-FOR-SERVICE ENGINEERING ASSESSMENT PROCEDURE

(INFORMATIVE)

CONTENTS

ANNEX 2A – TECHNICAL BASIS AND VALIDATION – FITNESS-FOR-SERVICE ENGINEERING ASSESSMENT PROCEDURE 2A-1

2A.1 TECHNICAL BASIS AND VALIDATION 2A-1
2A.2 REFERENCES 2A-1

2A.1 Technical Basis and Validation

The primary references for the basis of the assessment procedures in this standard are summarized in references [9] and [11]. The remaining references provide additional information on specific damage mechanisms or industry experience with Fitness-For-Service technologies.

2A.2 References

[1] Anderson, T.L., and Osage, D.A., “API 579: A Comprehensive Fitness-For-Service Guide”, International Journal of Pressure Vessels and Piping 77, pages 953-963, 2000.

[2] Ainsworth, R.A., Ruggles, M.B., and Takahashi, Y., "Flaw Assessment Procedure for High-Temperature Reactor Components," Journal of Pressure Vessel Technology, Vol. 114, American Society of Mechanical Engineers, New York, NY, May 1992, pp. 166-170.

[3] API, Base Resource Document on Risk-Based Inspection, API Publication 581, American Petroleum Institute, Washington DC, 1996.

[4] Buchheim, G.M., Osage, D.A., Prager, M., and Warke, W.R., "Fitness-For-Service and Inspection for the Petrochemical Industry," ASME PVP-Vol. 261, American Society of Mechanical Engineers, New York, NY, 1993, pp. 245-256.

[5] Buchheim, G.M., Osage, D.A., Warke, W.R., and Prager, M., "Update for Fitness-For-Service and Inspection for the Petrochemical Industry," ASME PVP-Vol. 288, American Society of Mechanical Engineers, New York, NY, 1994, pp. 253-260.

[6] Janelle, J.L., Osage, D.A., and Burkhart, S.J., *An Overview and Validation of the Fitness-For-Service Assessment Procedures for Local Thin Areas*, WRC Bulletin 505, Welding Research Council, Inc., New York, NY, 2005.

[7] Kim, D.S., and Reynolds, J.T., "Fitness-For-Service Analysis in Turnaround Decision Making," ASME PVP-Vol. 261, American Society of Mechanical Engineers, New York, NY, 1993, pp. 283-294.

[8] Osage, D.A. and Prager, M., "Status and Unresolved Technical Issues of Fitness-For-Service Assessment Procedures for the Petroleum Industry," ASME PVP-Vol. 359, American Society of Mechanical Engineers, New York, NY, 1997, pp. 117-128.

[9] Osage, D.A., Krishnaswamy, P., Stephens, D.R., Scott, P., Janelle, J., Rohan, R., and Wilkowski, G.M., Technologies for the Evaluation of Non-Crack-Like Flaws in Pressurized Components – Erosion/Corrosion, Pitting, Blisters, Shell Out-Of-Roundness, Weld Misalignment, Bulges and Dents, WRC Bulletin 465, Welding Research Council, Inc., New York, NY, 2001.

[10] Osage, D.A., “API 579 – A Comprehensive Fitness-For-Service Standard,” ASME PVP-Vol. 463, Flaw Evaluation, Service Experience, and Reliability, Vol. 463, pages, 71-84, 2003.

[11] Scott, P.M., Anderson, T.L., Osage, D.A., and Wilkowski, G.M., *Review of Existing Fitness-For-Service Criteria for Crack-Like Flaws*, WRC Bulletin 430, Welding Research Council, Inc., New York, NY, 1998.

[12] Yin, H., and Bagnoli, D.L., "Case Histories Using Fitness-For-Service Methods," ASME PVP-Vol. 288, American Society of Mechanical Engineers, New York, 1994, pp. 315-328.

ANNEX 2B – DAMAGE MECHANISMS

(NORMATIVE)

CONTENTS

ANNEX 2B – DAMAGE MECHANISMS 2B-1

2B.1 DETERIORATION AND FAILURE MODES 2B-1
2B.2 FFS ASSESSMENT AND THE IDENTIFICATION OF DAMAGE MECHANISMS 2B-1
2B.3 PRE-SERVICE DEFICIENCIES 2B-2
2B.3.1 Types of Pre-Service Deficiencies 2B-2
2B.3.2 In-Service Inspection 2B-2
2B.4 IN-SERVICE DETERIORATION AND DAMAGE 2B-2
2B.4.1 Overview 2B-2
2B.4.2 General Metal Loss Due to Corrosion and/or Erosion 2B-3
2B.4.3 Localized Metal Loss Due to Corrosion and/or Erosion 2B-3
2B.4.4 Surface Connected Cracking 2B-4
2B.4.5 Subsurface Cracking and Microfissuring/Microvoid Formation 2B-5
2B.4.6 Metallurgical Changes 2B-6
2B.5 REFERENCES 2B-7
2B.6 TABLES 2B-8

2B.1 Deterioration and Failure Modes

This Annex provides a general overview of the types of flaws and damage observed, concentrating on service-induced damage mechanisms. It also provides general information about mitigation and monitoring methods. A more complete overview of the damage mechanisms that occur in the following industries are shown below.

a) API RP 571 *Damage Mechanisms Affecting Fixed Equipment in the Refining Industry*

b) Welding Research Council, Inc. (WRC), WRC Bulletin 489 *Damage Mechanisms Affecting Fixed Equipment in the Refining Industry*

c) Welding Research Council, Inc. (WRC), WRC Bulletin 488 *Damage Mechanisms Affecting Fixed Equipment in the Pulp and Paper Industry*

d) Welding Research Council, Inc. (WRC), WRC Bulletin 490 *Damage Mechanisms Affecting Fixed Equipment in the Fossil Electric Power Industry*

e) Materials Technology Institute (MTI) *Guidance for Failure Mechanisms*

2B.2 FFS Assessment and the Identification of Damage Mechanisms

When conducting an FFS Assessment, it is very important to determine the cause(s) of the damage or deterioration observed to date and the likelihood and degree of further damage that might occur in the future. Flaws and damage that are discovered during an in-service inspection can be the result of a preexisting condition before the component entered service and/or could be service-induced. The root causes of deterioration could be due to inadequate design considerations including material selection and design details, or the interaction with aggressive environments/conditions that the equipment is subjected to during normal service or during transient periods.

2B.3 Pre-Service Deficiencies

2B.3.1 Types of Pre-Service Deficiencies

a) *Material Production Flaws* – Flaws which occur during production including laminations and laps in wrought products, voids, segregation, shrinks, cracks, and bursts in cast products.

b) *Welding Related Flaws* – Flaws which occur as a result of the welding process including lack of penetration, lack of fusion, delayed hydrogen cracking, porosity, slag, undercut, weld cracking, and hot shortness.

c) *Fabrication Related Flaws* – Imperfections associated with fabrication including out-of-roundness, forming cracks, grinding cracks and marks, dents, gouges, dent-gouge combinations, and lamellar tearing.

d) *Heat Treatment Related Flaws or Embrittlement* – Flaws associated with heat treatment including reheat cracking, quench cracking, sensitization, 475°C (885°F) embrittlement, and sigma phase embrittlement. Similar flaws are also associated with in-service elevated temperature exposure.

e) *Wrong Material of Construction* – Due to either faulty material selections, poor choice of a specification break (i.e., a location in a component where a change in material specification is designated), or due to the inadvertent substitution of a different alloy or heat treatment condition due to a lack of Positive Material Identification (PMI), the installed component does not have the expected resistance or needed properties for the service or loading.

2B.3.2 In-Service Inspection

2B.3.2.1 In most instances, one or more of these pre-service deficiencies do not lead to an immediate failure. Usually, only gross errors cause a failure during a pre-service hydrostatic or pneumatic test.

2B.3.2.2 Flaws or damage associated with pre-service deficiencies or damage are often only discovered during an In-Service Inspection (ISI), because in many cases the ISI techniques used are more sensitive or the inspection scope is wider than the inspection techniques or extent of inspection used during the original construction. Some damage can be classified relatively easily as pre-service, based on its characteristics and location (e.g., void in the interior of a weld is porosity). However, some pre-service damage is indistinguishable from service-induced damage (e.g., delayed hydrogen cracking and sulfide stress cracking). Therefore, the key decision that needs to be made is whether the flaw and associated deterioration (regardless of its origin) is likely to progress in the future based on the material, stress, service conditions, and flaw size.

2B.4 In-Service Deterioration and Damage

2B.4.1 Overview

2B.4.1.1 Once equipment enters service, it is subjected to operating and/or downtime conditions that can deteriorate or damage the equipment. One factor that complicates an FFS analysis is that material/environmental condition interactions are extremely varied; many plants contain numerous processing units, each having its own combination of aggressive process streams and temperature/pressure conditions. In general, the following types of damage are encountered in process equipment:

a) General and local metal loss due to corrosion and/or erosion.

b) Surface connected cracking.

c) Subsurface cracking.

d) Microfissuring or microvoid formation.

e) Metallurgical changes.

f) Plastic deformation.

2B.4.1.2 Each general type of damage is caused by a multitude of damage mechanisms, which are specific types of corrosion (e.g., naphthenic acid corrosion of carbon steel), Stress Corrosion Cracking (SCC – e.g., Polythionic Acid Stress Corrosion Cracking of sensitized austenitic stainless steels (PASCC)), or types of embrittlement (e.g., temper embrittlement of 2-1/4 Cr -1 Mo alloy steel). Each of the damage mechanisms occurs under very specific combinations of materials, process environments, and operating conditions.

2B.4.1.3 The following sections of this Annex describe each of the damage types and provide some typical examples of damage mechanisms and potential mitigation methods. These sections are intended to introduce the concepts of service-induced deterioration and failure modes to an engineer (see Part 1). The user is urged to consult with engineers familiar with damage modes and to refer to publications such as API RP 571 and WRC Bulletins 488, 489, and 490 that provide a more detailed description of damage mechanisms in various industries (see paragraph 2B.1).

2B.4.1.4 When performing an FFS Assessment it is important that the potential for further damage is considered or that steps are taken to preclude further damage from occurring by means of mitigation methods. A list of the types of information needed for an engineer (see Part 1) to judge whether, and at what rate, further damage is likely to occur is provided in Table 2B.1 for damage mechanisms in the refining industry.

2B.4.2 General Metal Loss Due to Corrosion and/or Erosion

2B.4.2.1 General metal loss is defined as relatively uniform thinning over a significant area of the equipment (see Part 4). Examples of general corrosion for carbon steel and low alloy steels are sulfidation in crude units, H_2/H_2S corrosion in hydrotreaters, and sour water corrosion in moderate velocity situations in sour water strippers.

2B.4.2.2 A corrosion rate can usually be calculated from past and current thickness readings, for example see API 510, API 570, and API 653. The corrosion rate can also be predicted from standard corrosion curves/references, such as the modified McConomy Curves for sulfidation of carbon and low alloy steels (these curves are a function of temperature and sulfur content versus alloy). The measured or calculated rate, or a modified rate if conditions have changed, can be factored into an FFS Assessment to evaluate future operation.

2B.4.2.3 Remediation and monitoring methods for general metal loss are described in Part 4.

2B.4.3 Localized Metal Loss Due to Corrosion and/or Erosion

2B.4.3.1 Unlike general metal loss, localized metal loss rates can vary significantly within a given area of the equipment. Examples of localized metal loss are under deposit corrosion in crude unit overhead systems, naphthenic acid corrosion, injection point corrosion, and corrosion under insulation. Localized corrosion can take many forms, such as pitting resulting in numerous surface cavities, selective galvanic corrosion in the region between two electrochemically different metals, selective corrosion attack along a weld Heat-Affected Zone (HAZ), corrosion attack in crevices resulting from the concentration of aggressive chemical specie(s), or local grooving due to impingement. In general, the more resistant an alloy is to general corrosion, the more likely it is that corrosion, if it occurs, will be localized.

2B.4.3.2 When localized metal loss is detected, it is important to locate and characterize all of the locally thinned areas and obtain accurate measurements to calculate a metal loss rate. Predicting a localized corrosion rate is difficult, since the damage may only occur under very specific operating conditions (temperatures, chemical species, flow velocity) and is more of an on/off situation and usually does not occur at a steady constant pace.

Since localized corrosion rates are extremely sensitive to minor variations in process conditions/materials it is difficult to find applicable reference sources of corrosion data.

2B.4.3.3 Remediation and monitoring methods for local metal loss are described in Part 5.

2B.4.4 Surface Connected Cracking

2B.4.4.1 Most service-induced cracking mechanisms initiate at the surface of the component. Examples of service-induced surface cracking are mechanical and thermal fatigue and various forms of Stress Corrosion Cracking (SCC), such as Polythionic Acid Stress Corrosion Cracking (PASCC) or chloride SCC of austenitic stainless steels, amine type cracking of carbon steels, and sulfide stress cracking of carbon and low alloy steels. Fatigue cracking data are available from a number of reference sources and future crack growth rate can be calculated if the stresses can be characterized (see Annex 9F).

2B.4.4.2 The occurrence of SCC requires a combination of three conditions to be present: a susceptible material or material condition, a chemically aggressive environment, and a sufficiently high tensile stress. Since three factors are involved, generalizations about environments that can cause SCC are difficult even when restricted to a specific class of material. However, experiments and service experience have identified environments that can or have caused SCC in carbon and low alloy steels, and these have been tabulated and described in API RP 571.

2B.4.4.3 The metallurgical condition of the material is an important determinant of the severity of the SCC problem. For example, high hardness and strength make steel, particularly the HAZ of welds, more susceptible to sulfide stress cracking. Another material condition is sensitization of austenitic steels (chromium-rich carbide precipitation at grain boundaries) that is necessary for PASCC. The environmental and operating conditions of the component are also important. For example, there is a threshold level of caustic concentration and temperature that must be exceeded before carbon steel is susceptible to caustic cracking. In general, the greater the concentration of the causative agent, Cl, ammonia, H_2S, CN, etc., the greater the likelihood of SCC. For some mechanisms, increasing temperature increases susceptibility, while for others it decreases susceptibility. Concentration of the causative agents due to boiling, crevices, etc. can lead to problems where bulk stream composition would not predict susceptibility. Tensile stress is the third required ingredient for SCC. High tensile stresses, both applied and residual, increase the severity of the problem. Residual stress estimation is very important, because many cracks in practice arrest when they enter a lower residual stress field.

2B.4.4.4 Surface cracks often are found by surface inspection techniques, such as visual, PT and MT, although UT methods and AET are also used to detect cracks. Sizing surface connected cracking, in particular SCC, is very difficult, because in many cases the cracks are branched. PT or MT examination methods can be used to determine the length of surface cracks and UT examination methods can be used to determine the depth of cracking. Crack depth can also be determined by destructive grinding.

2B.4.4.5 Predicting crack growth rates for SCC is also very difficult, because of a lack of relevant data and lack of precise knowledge of the environmental conditions near the crack tip, which can be different from the bulk stream composition. SCC is also more of an on/off damage type, i.e., cracks can grow very rapidly if all the conditions are conducive, but it can also be dormant for a very long time.

2B.4.4.6 Mitigation methods to slow/prevent further SCC without removing cracks are somewhat limited. Strip lining the area and possibly coating the area if the cracks are tight is possible. Other methods are to alter the environment by means of chemical treatments, changing the temperature, or removing contaminants. Monitoring

methods consist of periodic UT measurements or continuous passive AET monitoring. Stream sampling/analysis and process variable monitoring to predict when conditions conducive to SCC are present can also be used.

2B.4.4.7 If cracks are removed, additional mitigation options are available, such as $PWHT$ or heat treatment to remove residual stresses and/or improve the metallurgical condition such as grain refining, weld overlays and coatings to isolate the susceptible material from the environment.

2B.4.5 Subsurface Cracking and Microfissuring/Microvoid Formation

2B.4.5.1 Service-induced damage that is not surface connected or initiates subsurface cracking falls into the general class of low-temperature hydrogen related phenomena or high temperature mechanisms such as creep and hydrogen attack. Hydrogen damage consisting of blistering, HIC, and SOHIC is primarily encountered in carbon steels operating in wet H_2S or HF environments. Much of refinery equipment is subject to wet H_2S charging conditions during service or shutdown. For example, deethanizers in fluid catalytic cracking light ends units typically have an environment with a high pH and cyanides that causes severe hydrogen charging leading to damage. Low-temperature hydrogen related damage occurs because of a local surface corrosion reaction that allows hydrogen atoms to diffuse into the steel. Once the hydrogen charging reaches a threshold concentration, damage can occur. Subsurface service-induced hydrogen damage can also eventually connect with the surface, or this type of damage can initiate because of surface cracks, such as sulfide stress cracking.

2B.4.5.2 This mechanism is similar to SCC in that susceptible material and an aggressive environment must be present. Hydrogen blistering and HIC are however, not stress related, but SOHIC is. Hydrogen damage often is an on/off mechanism, occurring under very specific environmental conditions that may be present only during upsets and startup/shutdowns. Damage often occurs very quickly at first and once surface films buildup they inhibit further damage, although if films are disturbed in-service or intentionally during inspections accelerated damage can recur. Since hydrogen charging normally only occurs from the process side of the equipment, the hydrogen concentration decreases through the wall and in practice many cracks arrest mid-wall and blisters are less prevalent on the external surfaces.

2B.4.5.3 Metallurgical and microstructural details (e.g., the sulfur impurity level of the steel) affect the susceptibility to damage or threshold level for damage by a certain level of hydrogen charging. Environmental variables, such as pH, temperature, CN, H_2S content, and stream velocity influence the level of hydrogen charging. Applied and residual stresses also influence SOHIC susceptibility. Much of the equipment that will be evaluated for FFS will contain hydrogen damage. It is recommended that an expert in this field be consulted because it is very important to assess the future potential and rate of hydrogen damage. Reference publications that can be used in this assessment are API RP571; and MTI *Guidance for Failure Mechanisms*, NACE Publications 8X194, 8X294, and RP0296, and API 939-A.

2B.4.5.4 Finding subsurface hydrogen damage is normally accomplished using various UT methods. Assessing the damage is very difficult because this is more a damage mechanics than fracture mechanics problem, since there often is no discreet single crack, cracks may be interconnected, and stacked in arrays. Various UT methods are used to characterize the damage.

2B.4.5.5 Mitigation for low temperature hydrogen damage can consist of chemical treatment and/or water washing to minimize hydrogen charging, strip lining or coatings to isolate the steel from the environment, and venting for blisters to relieve the internal stress. If properly performed, $PWHT$ may also reduce the propensity for SOHIC cracking by lowering the residual stress. Monitoring methods consist of hydrogen probes that measure hydrogen flux and periodic UT inspections to monitor damage extent.

2B.4.5.6 Creep and/or High Temperature Hydrogen Attack (HTHA) are mechanisms that form voids and fissuring only during latter stages of damage. These mechanisms can be either surface-connected or initiate subsurface. The variables that affect creep damage are the creep strength and strain capability of the material and the exposure conditions (stress and temperature). The variables that affect hydrogen attack are similar, but in addition the hydrogen partial pressure in the process stream and the alloy chemistry are very important. Subsurface creep and hydrogen attack damage that is detectable with UT methods, indicates that the component is at late stages of life for most common alloys. Creep and hydrogen attack damage rates can only be reduced by lowering the severity of the operating conditions. Field metallography may be effective for monitoring creep; however, the best monitoring method involves removing samples and conducting destructive tests while recording the temperature and pressure of the process.

2B.4.6 Metallurgical Changes

2B.4.6.1 Metallurgical properties, such as strength, ductility, toughness, and corrosion resistance can change while a component is in-service due to microstructural changes because of thermal aging at elevated temperatures. In addition, properties can also change because of hydrogen charging. Examples of embrittlement are shown below:

a) Carbon steels can strain age embrittle, spheroidize, or graphitize.

b) Ferritic, austenitic, and duplex stainless steels may form sigma phase or can sensitize.

c) Ferritic and duplex stainless steels may experience 475°C (885°F) embrittlement.

d) 2.25 Cr-1Mo Steel may experience temper embrittlement.

2B.4.6.2 These changes in properties are often difficult to detect, since damage may not have occurred yet. Sometimes inferences can be made from examining samples or surface replicas. Steel composition and microstructure, operating temperature, and accumulated strain are the most important factors that determine susceptibility to metallurgical changes. Often, an equilibrium state of change is reached and further changes will not occur. Hydrogen charging, even without material damage, will typically lower the ductility and possibly even the toughness of the material. Hydrogen charging is a reversible reaction and if it does not cause damage, has no permanent effect.

2B.4.6.3 Once the metallurgical properties are changed in-service, they usually are not recoverable. Heat treatment can be effective, although this often is only a temporary solution. To prevent further damage or degradation to metallurgical properties, the operating conditions can be adjusted to a lower severity. If the degradation in properties is known, then operating precautions such as start-up and shutdown procedures can be altered to prevent damage from occurring despite the degraded physical properties.

2B.4.6.4 As previously discussed, loss of toughness can occur in-service because of the process environment and service conditions. This form of metallurgical damage will have significant impact on the structural integrity of a component containing a crack-like flaw. In addition, experimental evidence indicates that loss of toughness may also have an effect on the structural integrity of components with blunt flaws that are typically associated with localized corrosion, groove-like flaws or pitting. Some of the service and materials combinations that may be susceptible to loss of toughness are listed below. An evaluation of the material toughness may be required depending on the flaw type, the severity of the environment, and the operating conditions.

a) Carbon steel in wet H_2S service and hydrofluoric acid service (hydrogen embrittlement).

b) Carbon steel and C-0.5 Mo between 149°C – 316°C (300°F – 600°F) (strain age embrittlement).

c) Carbon steel above 427°C (800°F) (graphitization).

d) Carbon steel, low alloy steels (i.e., 0.5 Cr to 9 Cr), and 12 Cr in fire situation when temperatures exceed 704°C (1300°F) (various damage mechanisms, see Part 11).

e) Alloy steels (0.5 Cr – 9 Cr) above 593°C (1100°F) (carburization).

f) 1.25 Cr-0.5 Mo above 482°C (900°F) (reheat cracking/creep embrittlement).

g) 2.25 Cr-1 Mo above 399°C (750°F) (temper embrittlement).

h) 12 Cr above 371°C (700°F) (475°C – 885°F embrittlement).

i) Austenitic stainless steel above 593°C (1100°F) (sigma phase embrittlement).

2B.5 References

[1] API, Damage Mechanisms Affecting Fixed Equipment in The Refining Industry, Third Edition, API Recommended Practice 571, American Petroleum Institute, Washington DC, 2020.

[2] API, *Research Report on Characterization and Monitoring of Cracking in Wet H_2S Service*, API Publication 939-A, American Petroleum Institute, Washington DC, 1994.

[3] Dobis, J.D. and Prager, M., *Damage Mechanisms Affecting Fixed Equipment in the Pulp and Paper Industry*, WRC Bulletin 488, Welding Research Council, Inc., New York, NY, 2004.

[4] Dobis, J.D. and Prager, M., *Damage Mechanisms Affecting Fixed Equipment in the Refining Industry*, WRC Bulletin 489, 2nd Edition, Welding Research Council, Inc., New York, NY, 2019.

[5] Dobis, J.D. and Prager, M., *Damage Mechanisms Affecting Fixed Equipment in Fossil Electric Power Industry*, WRC Bulletin 490, Welding Research Council, Inc., New York, NY, 2004.

[6] Rose, L., McLaughlin, J., Dean Jr., S.W., Hurst Jr., L, and Grubb, J.F., *Guidance for Failure Mechanisms*, Materials Technology Institute of the Chemical Process Industries, Inc. (MTI), 2020.

[7] Logan, H.L., The Stress Corrosion of Metals, Wiley, 1966.

[8] McConomy, H.F., "High Temperature Sulfuric Corrosion in Hydrogen Free Environments," Proc. API, Vol. 43 (III), pp. 78-96, 1963.

[9] NACE, “Guidelines for Detection, Repair, and Mitigation of Cracking of Existing Petroleum Refinery Pressure Vessels in Wet H_2S Environments,” NACE Publication RP0296, National Association of Corrosion Engineers, Houston, TX, 1996.

[10] NACE, “Materials and Fabrication Practices for New Pressure Vessels Used in Wet H_2S Refinery Service,” NACE Publication 8X194, National Association of Corrosion Engineers, Houston, TX, 1994.

[11] NACE, “Review of Published Literature on Wet H_2S Cracking of Steels Through 1989,” NACE Publication 8X194, National Association of Corrosion Engineers, Houston, TX, 1994.

2B.6 Tables

Table 2B.1 – Damage Mechanisms Affecting Fixed Equipment

General Information	Data		
Processing Unit/Item			
Year of Construction			
Material Specification			
Material Chemical Composition			
PWHT (Yes/No)			
Lining/Coating Material			
Item (1)	**Operating Information (2)**		
	Normal	**Start-Up /Shutdown**	**Upset**
Crude Fraction Sulfur Content (%)			
Crude Fraction Neut Number			
Water Content (%/pH)			
H_2S (ppm in water)			
NH_3 (ppm in water)			
NH_3 (%)			
H_2S (%)			
HCl (%)			
Chlorides (%)			
Sulfuric Acid (%)			
HF Acid (%)			
Amine Type (MEA/DEA/etc.)			
Amine Concentration (%)			
Amine Loading (mole H_2S & CO_2/mole amine)			
Caustic Concentration (%)			
H_2S Partial Pressure (bar:psia)			
H_2 Partial Pressure (bar:psia)			
Cyanides (Yes/No)			
Water Wash/Injection (Yes/No)			
Polysulfide Injection (Yes/No)			
Neutralizing Amine Injection (Yes/No)			
Filming Amine Injection (Yes/No)			
Caustic Injection (Yes/No)			
Hydrogen Absorption Injection Inhibitor			
Temperature (°C:°F)			
Pressure (barg:psig)			
Flow Velocity (m/sec:ft/sec)			

Notes:
1. Other process stream constituents or operating parameters that may affect the Fitness-For-Service Assessment can be entered at the end of this list.
2. Values for the process stream constituents and operating parameters for the start-up, shutdown, and upset conditions, as well as the normal operating condition, need to be defined because significant damage may occur during these phases of operation.

ANNEX 2C – THICKNESS, MAWP AND STRESS EQUATIONS FOR AN FFS ASSESSMENT

(NORMATIVE)

CONTENTS

ANNEX 2C – THICKNESS, MAWP AND STRESS EQUATIONS FOR AN FFS ASSESSMENT 2C-1

2C.1 GENERAL 2C-2
2C.1.1 Scope 2C-2
2C.1.2 MAWP and MFH 2C-2
2C.1.3 Construction Codes and Common Rules 2C-2
2C.1.4 Use of VIII-2 Design Equations 2C-3
2C.2 CALCULATION OF T_{MIN}, MAWP (MFH), AND MEMBRANE STRESS 2C-3
2C.2.1 Overview 2C-3
2C.2.2 Minimum Required Wall Thickness and MAWP (MFH) 2C-3
2C.2.3 Code Revisions 2C-4
2C.2.4 Determination of Allowable Stresses 2C-4
2C.2.5 Treatment of Weld and Riveted Joint Efficiency, and Ligament Efficiency 2C-5
2C.2.6 Treatment of Damage in Formed Heads 2C-6
2C.2.7 Thickness for Supplemental Loads 2C-7
2C.2.7.1 Definition 2C-7
2C.2.7.2 Required Thickness 2C-7
2C.2.7.3 Vertical Vessels 2C-7
2C.2.7.4 Design-by-Rule Using VIII-2 ..... 2C-8
2C.2.7.5 Piping Systems 2C-8
2C.2.8 Determination of Metal Loss and Future Corrosion Allowance 2C-8
2C.2.9 Treatment of Metal Loss and Future Corrosion Allowance 2C-8
2C.2.10 Treatment of Shell Distortions 2C-8
2C.3 PRESSURE VESSELS AND BOILER COMPONENTS – INTERNAL PRESSURE 2C-9
2C.3.1 Overview 2C-9
2C.3.2 Shell Tolerances 2C-9
2C.3.3 Shell Thickness and MAWP 2C-9
2C.3.3.1 Cylindrical Shells 2C-9
2C.3.3.2 Spherical Shell or Hemispherical Head 2C-10
2C.3.3.3 Elliptical Head 2C-11
2C.3.3.4 Torispherical Head 2C-11
2C.3.3.5 Conical Shell 2C-12
2C.3.3.6 Toriconical Head 2C-13
2C.3.3.7 Conical Transition 2C-13
2C.3.4 Nozzles Connections in Shells 2C-16
2C.3.4.1 General 2C-16
2C.3.4.2 Required Reinforcement 2C-16
2C.3.4.3 Weld Strength Analysis 2C-17
2C.3.5 Junction Reinforcement Requirements at Conical Transitions 2C-19
2C.3.6 Other Components 2C-19
2C.4 PRESSURE VESSELS AND BOILER COMPONENTS – EXTERNAL PRESSURE 2C-20
2C.5 PIPING COMPONENTS AND BOILER TUBES 2C-20
2C.5.1 Overview 2C-20
2C.5.2 Metal Loss 2C-20
2C.5.3 Required Thickness and MAWP – Straight Pipes Subject to Internal Pressure 2C-20
2C.5.4 Required Thickness and MAWP – Boiler Tubes 2C-21
2C.5.5 Required Thickness and MAWP – Pipe Bends Subject to Internal Pressure 2C-21
2C.5.6 Required Thickness and MAWP for External Pressure 2C-23

2C.5.7 Branch Connections *2C-23*
2C.6 API 650 STORAGE TANKS 2C-23
2C.6.1 Overview *2C-23*
2C.6.2 Metal Loss *2C-24*
2C.6.3 Required Thickness and MFH for Liquid Hydrostatic Loading *2C-24*
2C.7 ESTIMATION OF BURST PRESSURE 2C-24
2C.7.1 Svensson's Method *2C-24*
2C.7.2 Cylindrical Shell Burst Pressure *2C-25*
2C.7.3 Spherical Shell Burst Pressure *2C-25*
2C.8 NOMENCLATURE 2C-26
2C.9 REFERENCES 2C-32
2C.10 TABLES 2C-34
2C.11 FIGURES 2C-36

2C.1 General

2C.1.1 Scope

The minimum required wall thickness, $MAWP$, and membrane stress for common pressure components are required for many of the Level 1 and Level 2 Fitness-For-Service Assessments in this Standard. These parameters may be computed using the appropriate equations and other requirements from the construction code. Equations for thickness, $MAWP$, and membrane stress for internal pressure and external pressure are provided in this Annex for easy reference, but they are not intended to replace those of the original construction code. It is the Users' responsibility to ensure that equations and other requirements for the calculation of thickness, $MAWP$, and membrane stress used in a Fitness-For-Service Assessment are correct for the code of construction of the equipment. The equations are presented in an organized fashion to facilitate use and are adjusted for metal loss and future corrosion allowance.

2C.1.2 MAWP and MFH

In this Annex, the safe operating pressure capability of a pressure vessel is described in terms of $MAWP$. This terminology is also used for piping instead of the usual term, maximum allowable operating pressure. For atmospheric storage tanks, the pressure capability is defined in terms of a Maximum Fill Height (MFH).

2C.1.3 Construction Codes and Common Rules

The design-by-rule equations in this Annex are based on the following construction codes.

a) ASME B&PV Code, Section 1

b) ASME B&PV Code, Section VIII, Division 1 (VIII-1)

c) ASME B&PV Code, Section VIII, Division 2 (VIII-2)

d) ASME B31.3 Process Piping Design (B31.3)

e) API 650 Welded Steel Tanks for Oil Storage (API-650)

In the development of VIII-2, an effort was made to harmonize the design-by-rule requirements in this new code with VIII-1. Based on this effort, the design rules in VIII-2 are either identical to the rules in VIII-1 or represent a more restrictive subset of the design rules in VIII-1. A comparison of the design-by-rule procedures in VIII-2 and VIII-1 is shown in Table 2C.1. Based on the development of the new VIII-2, ASME has initiated a Common Rules effort to standardize the design-by-rule procedures in the VIII-1, VIII-2, and VIII-3 Construction Codes. Common Rules are defined as those rules in VIII-1, VIII-2, and VIII-3 that are identical and difficult to maintain because of

complexity (i.e., either computationally or editorially complex), or frequent updating due to the introduction of new technologies. Common rules typically occur in the design-by-rule or design-by-analysis parts of the code; but also exist in material, fabrication, and examination requirements.

Some of the most used design rules from VIII-1, B31.3, and API-650 have been re-produced for the convenience of the user. These rules typically encompass procedures for design for internal pressure. Rules for external pressure are addressed by reference.

2C.1.4 Use of VIII-2 Design Equations

The overall objective of the ASME Common Rules initiative is to have the design-by-rule and design-by-analysis procedures in VIII-2 and reference these procedures from other ASME Codes. Therefore, design-by-rule procedures from VIII-2 are only referenced for use in the Annex. Additionally, the design-by-rule procedures from VIII-2 may be used in place of the procedures in VIII-1 in accordance with VIII-1, Mandatory Appendix 46. The design equations of VIII-2 may be used in lieu of those of VIII-1. The design rules of VIII-2 typically provide benefits for the following:

a) Torispherical and elliptical heads,

b) Conical transitions,

c) Knuckles and flares,

d) Nozzle junctions (i.e., reinforcement requirements), and

e) Shells under combined loading

2C.2 Calculation of t_{min}, MAWP (MFH), and Membrane Stress

2C.2.1 Overview

Computation of the minimum wall thickness, $MAWP$ or MFH, and membrane stress for existing equipment typically requires judgment on the part of the user to determine factors and parameters that may significantly affect the final results (e.g., code revisions, determination of allowable stresses for in-service components, weld joint efficiency in corroded regions). Methods to determine these factors and parameters for in-service equipment are provided in paragraph 2C.2.2.

2C.2.2 Minimum Required Wall Thickness and MAWP (MFH)

a) The minimum wall thickness and the $MAWP$ or MFH of a component can be determined using one of the following options:

   1) Option 1 – If the original design conditions have not been changed and $t_{nom} - LOSS - FCA \geq t_{\min}$, then the $MAWP$ or MFH as shown in the original documentation for the equipment may be used. The $MAWP$ for a component may be taken as the design pressure and the MFH for a tank may be taken as the maximum design liquid level. In this case, the minimum required wall thickness may be determined using one of the following alternatives:

      i) The minimum required wall thickness as shown in the original documentation for the equipment.

      ii) The nominal or furnished thickness t_{nom} minus the original specified corrosion allowance.

   2) Option 2 – The $MAWP$ or MFH and minimum required wall thickness may be calculated as follows.

      i) The $MAWP$ and minimum required wall thickness for pressure vessel and piping components may

be calculated if the design pressure (including liquid head), supplemental loads (see paragraph 2C.2.7) design temperature, component geometry, current measured thickness, future corrosion allowance, material specification and allowable stress are known.

ii) The MFH and minimum required wall thickness for atmospheric storage tank shell courses may be calculated if the design fill height, fluid specific gravity, supplemental loads (see paragraph 2C.2.7) design temperature, component geometry, current measured thickness, future corrosion allowance, design temperature, material specification and allowable stress are known.

b) If the component contains a flaw, the $MAWP$ or MFH may be reduced as a function of the Remaining Strength Factor (see Part 2, paragraph 2.4.2.2(b) or 2.4.2.2(c)).

2C.2.3 Code Revisions

The minimum wall thickness, $MAWP$ or MFH, and membrane stress of a component can be determined using the latest edition of the applicable construction code if the following essential details are known to comply with that code. If any of the essential details do not comply with the latest edition of the code, the minimum thickness, $MAWP$ or MFH, and membrane stress may be established using the edition of the code to which the component was originally constructed. However, an assessment of the component using the latest edition of the code should be made to ensure that the original construction code rules provide an adequate margin of safety.

a) Material specifications

b) Upper and/or lower temperature limits for specific materials

c) Design details (e.g., nozzles, nozzle reinforcement, and conical transitions)

d) Special design requirements for cyclical and/or high temperature design conditions

e) Fabrication details and quality of workmanship

f) Inspection requirements

g) Weld joint efficiency

h) Material toughness (Charpy Impact Energy) requirements

2C.2.4 Determination of Allowable Stresses

The allowable stress to be used in the calculation of the minimum required wall thickness and $MAWP$ or MFH can be determined based on one of the following items.

a) The allowable stress for all components can be based on the original construction code. Recommendations pertaining to the revision of the construction code to use for an assessment are contained in paragraph 2C.2.3.

b) If a pressure vessel was constructed to VIII-1, the allowable stress may be determined from VIII-1, 1999 Addenda and subsequent editions and addenda subject to all the following:

1) The pressure vessel was constructed to the 1968 or later edition of the Code,

2) The essential details listed in paragraph 2C.2.3 comply with the latest edition of the Code, and

3) The pressure vessel satisfies one of the assessment levels of Part 3 of this Standard (note that pressure vessels constructed to the 1987 edition of the code, or later edition automatically satisfy this requirement unless the exemption of VIII-1, paragraph UG-20(f) was used in the original design).

c) If the specification for the material of construction cannot be identified, an allowable stress can be estimated based on the material chemistry determined by chemical analysis, methods used for positive materials identification (see API RP 578) or other physical attributes, e.g., magnetic properties, atmospheric corrosion behavior, hardness, color, etc. This chemistry can then be compared to material specifications and grade in the original construction code. The allowable stress should be based on a specification and grade with a comparable chemistry that results in the lowest value of the code allowable stress at the design temperature.

d) If a component was constructed to more stringent requirements than required by the original construction code, the allowable stress may be established considering the higher quality aspects of the component while considering the basis for establishing the design allowable stress in the code. Examples include guaranteed strength properties, increased inspection, design details that minimize stress concentration, and/or material selection to mitigate the effects of environmental damage and/or to provide higher fracture toughness. If the allowable stresses are established based on the enhanced quality of the component, the basis should be documented and included in the assessment records.

2C.2.5 Treatment of Weld and Riveted Joint Efficiency, and Ligament Efficiency

The minimum thickness, $MAWP$ or MFH, and membrane stress of a component shall include the appropriate weld or riveted joint, or ligament efficiency utilized in the original design unless alternative values for these parameters can be established by stress analysis and/or inspection.

a) For damaged regions (e.g., corrosion/erosion, pitting, etc.) at a weld or riveted joint, the weld or riveted joint efficiency or weld joint quality factor, as applicable, shall be included in the minimum thickness and $MAWP$ or MFH calculations. A damaged region is considered to be at a weld or riveted joint if any part of it is located within the weld or riveted joint band. The weld band is defined to be centered on the weld and has a width of 50.8 mm (2 inches) or twice of the furnished plate thickness, whichever is greater. The riveted joint band is defined to begin at the centerline of the riveted joint and extend 152.4 mm (6 inches) beyond the outermost row of rivets either side of the riveted joint.

b) For damaged regions (e.g., corrosion/erosion, pitting, etc.) outside of the weld or riveted joint band (see subparagraph a above) in components without closely spaced openings, a joint efficiency of 1.0 can be utilized in the minimum thickness and $MAWP$ or MFH calculations. For components with multiple closely spaced openings, the ligament efficiency associated with the hole pattern shall be utilized in the calculations.

c) The joint efficiency of a riveted lap joint, E, may be determined by the following procedures, or determined by a more detailed stress analysis. Alternatively, for atmospheric storage tanks designed and fabricated to API 12A, paragraph 4.3.4 of API 653 may be used and for atmospheric storage tanks designed to API 650, paragraph 4.3.4 or Table 4.3 of API 653 may be used.

1) STEP 1 – Determine allowable stresses: σ_{bp}, σ_{br}, σ_{sr}, and σ_{tp}.

2) STEP 2 – Determine the unit width, w_r, over which the riveted joint efficiency will be determined and the thickness of the plate to be used in the calculation, t_c.

3) STEP 3 – Determine the rivet shear load.

$$P_{rs} = \frac{N_r \cdot \pi \cdot d_r^2 \cdot \sigma_{sr}}{4} \qquad \textit{for a single lap joint} \tag{2C.1}$$

$$P_{rs} = \frac{N_r \cdot \pi \cdot d_r^2 \cdot \sigma_{sr}}{2} \qquad \textit{for a double lap joint} \tag{2C.2}$$

4) STEP 4 – Determine the plate or rivet compressive load.

$$P_{rc} = \min\left[\left(N_r \cdot d_p \cdot t_c \cdot \sigma_{bp}\right), \left(N_r \cdot d_r \cdot t_c \cdot \sigma_{br}\right)\right] \quad (2C.3)$$

5) STEP 5 – Determine the plate tension load. The plate tension load shall be computed using Equation (2C.4) for the j^{th} row of rivets. The plate tension loads should be calculated for each row of rivets to determine the governing load, this load is designated as $P_{rj,\max}$.

$$P_{rj} = \left(w_r - j \cdot d_p\right) \cdot t_c \cdot \sigma_{tp} \cdot \left(\frac{N_r}{N_r - \sum_{(j-1)}^{N} n_{rm}}\right) \quad (2C.4)$$

6) STEP 6 – Determine the limiting load.

$$P_{rl} = \min\left[P_{rs}, P_{rc}, P_{rj,\max}\right] \quad (2C.5)$$

7) STEP 7 – Determine the strength of the plate without a riveted joint.

$$P_{rp} = w_r t_c \sigma_{tp} \quad (2C.6)$$

8) STEP 8 – Determine the riveted joint efficiency.

$$E = \frac{P_{rl}}{P_{rp}} \quad (2C.7)$$

2C.2.6 Treatment of Damage in Formed Heads

If damage (e.g., corrosion/erosion, pitting, etc.) occurs in the center section of an elliptical or torispherical head, the minimum thickness, $MAWP$, and membrane stress can be determined as follows:

a) Elliptical Heads:

1) The minimum thickness and $MAWP$ of the knuckle region for an elliptical head may be calculated by the equations in paragraph 2C.3.5.

2) The minimum thickness and $MAWP$ of the spherical region of an elliptical head may be calculated by the equation for spherical shells in paragraph 2C.3.3.2 using an equivalent radius. The spherical region of an ellipsoidal head is the area located entirely within a circle whose center coincides with the center of the head and whose diameter is equal to 80 percent of the shell diameter. The equivalent radius of the spherical segment is the equivalent spherical radius $K_c D$ where K_c is given in paragraph 2C.3.3.5(b) and D is the inside shell diameter.

b) Torispherical Heads:

1) The minimum thickness and $MAWP$ of the knuckle region for a torispherical head may be calculated by the equations in paragraph 2C.3.3.4.

2) The minimum thickness and $MAWP$ of the spherical region of a torispherical head may be calculated by the equation in paragraph 2C.3.3.4 with $M = 1.0$.

2C.2.7 Thickness for Supplemental Loads

2C.2.7.1 Definition

Supplemental loads may result in an axial force and/or bending moment being applied to the end of a cylindrical shell, conical shell, or pipe section. This type of loading results in longitudinal membrane and bending stresses (stresses acting on a circumferential plane) in addition to the longitudinal and circumferential (hoop) membrane stress caused by pressure loading. The effects of supplemental loads for other loading conditions and/or shell geometries can be evaluated using the stress analysis methods in Annex 2D.

2C.2.7.2 Required Thickness

The required thickness for supplemental loads shall be considered in the determination of the minimum thickness, $t_{\min}$, $MAWP$ or MFH, and/or membrane stress.

a) Supplemental loads include but are not limited to the weight of the component, contained fluid, insulation, or refractory; loads resulting from the constraint of free thermal expansion, thermal gradients, or differences in thermal expansion characteristics; occasional loads due to wind, earthquake, snow, and ice; loads due both to environmental and operating conditions; reaction forces from fluid discharges; loads resulting from support displacements; and loads due to process upset conditions.

b) An overview of supplemental loads, loading conditions, and allowances for pressure and/or temperature variations that should be considered in an assessment are shown in Table 2C.2. Load definitions and load case combinations that shall be considered in an assessment are shown in Annex 2D, Tables 2D.1 and 2D.2, respectively.

c) Supplemental loads may be considered to be negligible if these loads do not affect the minimum required thickness, $MAWP$ or MFH, fatigue life or creep remaining life of a component with a flaw, or the remaining life of a component operating in the creep regime. Otherwise, these loads are considered to be significant and must be included in an assessment.

d) Typical pressure vessel and piping configurations and flaw locations where the required thickness for supplemental loads may be significant are listed below.

   1) Vertical vessels subject to wind or earthquake loading, with the flaw located in the lower section of the vessel.

   2) Horizontal pressure vessels, with the flaw located in the mid-span between saddle support points or close to the saddle (see paragraph 2C.2.7.4).

   3) Piping systems, with the flaw located at support point locations or in the mid-span of piping sections.

2C.2.7.3 Vertical Vessels

Two Options are provided for evaluating supplemental loads on vertical vessels.

a) Option A – A thickness is computed based on the applied supplemental loading using Equation (2C.8) with F and M equal to the weight of the tower, attachments, and contents, and the bending moment from the wind or earthquake loading, respectively. Note that the thickness will vary with the elevation of the vertical vessel based on the values of F and M that change with the elevation. Equation (2C.8) is applicable to both thick and thin shells. For compressive stresses, the allowable stress shall be established using VIII-2, Part 4, paragraphs 4.3 and 4.4. The loads resulting from wind and earthquake load may be calculated using the procedure in ASCE 7.

$$t_{sl} = \frac{2F}{SE\pi\left(D_o + D\right)\cos\left[\alpha\right]} + \frac{16D_oM}{SE\pi\left(D_o + D_c\right)\left(D_o^2 + D^2\right)\cos\left[\alpha\right]} \quad \text{(2C.8)}$$

b) Option B – Detailed evaluation procedures are described in VIII-2, Part 4, paragraphs 4.3 and 4.4. Note that the evaluation procedures in VIII-2 are based on computation of stress components and an equivalent stress. Hence, the parameter t_{sl} is not explicitly calculated. This stress basis is also used in Parts 5 and 6 of this Standard.

2C.2.7.4 Design-by-Rule Using VIII-2

The thickness for supplemental loads may be computed using VIII-2, Part 4, paragraph 4.15.

2C.2.7.5 Piping Systems

Typically, t_{sl} is not explicitly calculated for piping systems because of the relationship between the component thickness, piping flexibility or stiffness, and applied loading, both sustained and thermal. When evaluating requirements for supplemental loads, a piping stress analysis is typically performed where the piping system is modeled, and all loads are applied. Separate cases are analyzed for pressure and sustained loads as well as secondary loads.

2C.2.8 Determination of Metal Loss and Future Corrosion Allowance

a) The metal loss ($LOSS$) is defined as the amount of uniform metal loss at the time of inspection, or the uniform metal loss away from the damage area at the time of the inspection.

b) The Future Corrosion Allowance (FCA) is defined as the anticipated metal loss for the next period of operation. The FCA is established based on the operating conditions and service. This corrosion allowance may be estimated based upon previous thickness measurements, from corrosion rates on equipment in a similar service, or from information obtained from corrosion design curves.

2C.2.9 Treatment of Metal Loss and Future Corrosion Allowance

The equations presented in this Annex shall be adjusted for mill tolerance, $LOSS$ and FCA. When calculating the required thickness for future operation, the $LOSS$ and FCA shall be applied to component dimensions. When calculating the $MAWP$ or MFH, the wall thickness as well as component dimensions shall be adjusted for $LOSS$ and FCA. The location of metal loss should be considered when determining the adjusted dimensions. For example, for internal corrosion the inside diameter and wall thickness are adjusted for $LOSS$ and FCA while for external corrosion the outside diameter and wall thickness are adjusted for $LOSS$ and FCA. If corrosion occurs on both sides, the inside diameter, outside diameter and wall thickness are adjusted for $LOSS$ and FCA. Note that in this case, $LOSS$ and FCA may have more than one value for internal and external corrosion.

2C.2.10 Treatment of Shell Distortions

While in-service, components may evolve into a configuration that no longer satisfies the fabrication tolerances of the original design code. This distortion in shape may result in areas with high localized stresses, and for components subject to a compressive stress field, a reduction in structural stability. Assessment procedures for shell out-of-roundness and/or shell misalignment are covered in Part 8.

2C.3 Pressure Vessels and Boiler Components – Internal Pressure

2C.3.1 Overview

The minimum required thickness and $MAWP$ of a pressure vessel component subject to internal pressure may be calculated based on the original construction code. Alternatively, the equations in this section may be utilized in the calculation of these parameters. The effects of supplemental loads (see paragraph 2C.2.7) are included in these equations only for cylindrical and conical shells (i.e., longitudinal stress direction) subject to a net section axial force and/or bending moment. The effects of supplemental loads for other component geometries and loading conditions can be evaluated using the stress analysis methods in Annex 2D.

2C.3.2 Shell Tolerances

The equations presented in this section are valid if the out-of-roundness tolerances for the shell satisfy the tolerances in Part 8, Table 8.3.

2C.3.3 Shell Thickness and MAWP

The equations for shell thickness and $MAWP$ in this paragraph are based on VIII-1. Alternatively, the equations for thickness and $MAWP$ in the design-by-rule procedures in VIII-2, Part 4, paragraph 4.3 may be used.

2C.3.3.1 Cylindrical Shells

The minimum thickness, $MAWP$, and membrane stress equations are as follows:

a) Circumferential Stress when $P \le 0.385SE$ and $t^C_{\min} \le 0.5R$ (Longitudinal Joints):

$$t^C_{\min} = \frac{PR}{SE - 0.6P} \tag{2C.9}$$

$$MAWP^C = \frac{SEt}{R + 0.6t} \tag{2C.10}$$

$$\sigma^C_m = \frac{P}{E}\left(\frac{R}{t} + 0.6\right) \tag{2C.11}$$

b) Circumferential Stress when $P > 0.385SE$ or $t^C_{\min} > 0.5R$ (Longitudinal Joints):

$$t^C_{\min} = R\left(\exp\left[\frac{P}{SE}\right] - 1\right) \tag{2C.12}$$

$$MAWP^C = SE \cdot \ln\left[\frac{R+t}{R}\right] \tag{2C.13}$$

$$\sigma^C_m = \frac{P}{E}\left(\ln\left[\frac{R+t}{R}\right]\right)^{-1} \tag{2C.14}$$

c) Longitudinal Stress when $P \le 1.25SE$ and $t^L_{\min} \le 0.5R$ (Circumferential Joints):

$$t^L_{\min} = \frac{PR}{2SE + 0.4P} + t_{sl} \tag{2C.15}$$

$$MAWP^L = \frac{2SE(t - t_{sl})}{R - 0.4(t - t_{sl})} \tag{2C.16}$$

$$\sigma_m^L = \frac{P}{2E}\left(\frac{R}{t - t_{sl}} - 0.4\right) \tag{2C.17}$$

d) Longitudinal Stress when $P > 1.25SE$ or $t_{\min}^L > 0.5R$ (Circumferential Joints):

$$t_{\min}^L = R\left(\left(\frac{P}{SE} + 1\right)^{1/2} - 1\right) + t_{sl} \tag{2C.18}$$

$$MAWP^L = SE\left(\left(\frac{R + \left(t - t_{sl}\right)}{R}\right)^2 - 1\right) \tag{2C.19}$$

$$\sigma_m^L = \frac{P}{E}\left(\left(\frac{R + \left(t - t_{sl}\right)}{R}\right)^2 - 1\right)^{-1} \tag{2C.20}$$

e) Final Values:

$$t_{\min} = \max\left[t_{\min}^C,\ t_{\min}^L\right] \tag{2C.21}$$

$$MAWP = \min\left[MAWP^C, MAWP^L\right] \tag{2C.22}$$

$$\sigma_{\max} = \max\left[\sigma_m^C,\ \sigma_m^L\right] \tag{2C.23}$$

2C.3.3.2 Spherical Shell or Hemispherical Head

a) If $P \le 0.665SE$ and $t_{\min} \le 0.356R$, then the minimum thickness, $MAWP$, and membrane stress equations are as follows:

$$t_{\min} = \frac{PR}{2SE - 0.2P} \tag{2C.24}$$

$$MAWP = \frac{2SEt}{R + 0.2t} \tag{2C.25}$$

$$\sigma_m = \frac{P}{2E}\left(\frac{R}{t} + 0.2\right) \tag{2C.26}$$

b) If $P > 0.665SE$ or $t_{\min} > 0.356R$, then the minimum thickness, $MAWP$, and membrane stress equations are as follows:

$$t_{\min} = R\left(\left(\frac{2\left(SE + P\right)}{2SE - P}\right)^{\frac{1}{3}} - 1\right) \tag{2C.27}$$

$$MAWP = 2SE\left(\left(\frac{R + t}{R}\right)^3 - 1\right)\left(\left(\frac{R + t}{R}\right)^3 + 2\right)^{-1} \tag{2C.28}$$

$$\sigma_m = \frac{P}{2E} \cdot \left(\left(\frac{R + t}{R}\right)^3 + 2\right)\left(\left(\frac{R + t}{R}\right)^3 - 1\right)^{-1} \tag{2C.29}$$

2C.3.3.3 Elliptical Head

The minimum thickness, $MAWP$, and membrane stress equations may be computed using the equations shown below with the following limitations (see Figure 2C.1):

a) Nominal values:

$$t_{\min} = \frac{PDK}{2SE - 0.2P} \tag{2C.30}$$

$$MAWP = \frac{2SEt}{KD + 0.2t} \tag{2C.31}$$

$$\sigma_m = \frac{P}{2E}\left(\frac{DK}{t} + 0.2\right) \tag{2C.32}$$

where,

$$K = \frac{1}{6}\left(2.0 + R_{ell}^2\right) \tag{2C.33}$$

b) Values in the center portion of the head – To compute the minimum thickness, $MAWP$, and membrane stress for the center section of an elliptical head (a section within $0.8D$ centered on the head centerline), use K_c instead of K in the above equations.

$$K_c = 0.25346 + 0.13995R_{ell} + 0.12238R_{ell}^2 - 0.015297R_{ell}^3 \tag{2C.34}$$

c) Limitations – If these limitations are not satisfied, the rules of VIII-2 may be used.

$$1.7 \le R_{ell} \le 2.2 \tag{2C.35}$$

$$\frac{D\left(0.44R_{ell} + 0.02\right)}{t_{\min}} \le 500 \qquad or \qquad \frac{D\left(0.44R_{ell} + 0.02\right)}{t} \le 500 \tag{2C.36}$$

2C.3.3.4 Torispherical Head

The minimum thickness, $MAWP$, and membrane stress equations may be computed using the equations shown below with the following limitations (see Figure 2C.1):

a) Nominal values:

$$t_{\min} = \frac{PC_rM}{2SE - 0.2P} \tag{2C.37}$$

$$MAWP = \frac{2SEt}{C_rM + 0.2t} \tag{2C.38}$$

$$\sigma_m = \frac{P}{2E}\left(\frac{C_rM}{t} + 0.2\right) \tag{2C.39}$$

where,

$$M = \frac{1}{4}\left(3.0 + \sqrt{\frac{C_r}{r_k}}\right) \tag{2C.40}$$

b) Values in the center or spherical portion of the head – To compute the minimum thickness, $MAWP$, and membrane stress for the center section of a torispherical head, use $M = 1.0$ in the above equations.

c) Limitations – If these limitations are not satisfied, the rules of VIII-2 may be used.

$$0.7 \le \frac{C_r}{D} \le 1.2 \tag{2C.41}$$

$$\frac{r_k}{D} \ge 0.06 \tag{2C.42}$$

$$\frac{C_r}{t_{\min}} \le 500 \qquad or \qquad \frac{C_r}{t} \le 500 \tag{2C.43}$$

2C.3.3.5 Conical Shell

The minimum thickness, $MAWP$, and membrane stress equations may be computed using the following procedures (see Figure 2C.2):

a) Circumferential Stress (Longitudinal Joints):

$$t_{\min}^{C} = \frac{PD}{2\cos[\alpha](SE - 0.6P)} \tag{2C.44}$$

$$MAWP^{C} = \frac{2SEt\cos[\alpha]}{D + 1.2t\cos[\alpha]} \tag{2C.45}$$

$$\sigma_m^{C} = \frac{P}{2E}\left(\frac{D}{t\cos[\alpha]} + 1.2\right) \tag{2C.46}$$

b) Longitudinal Stress (Circumferential Joints):

$$t_{\min}^{L} = \frac{PD}{2\cos[\alpha](2SE + 0.4P)} + t_{sl} \tag{2C.47}$$

$$MAWP^{L} = \frac{4SE(t - t_{sl})\cos[\alpha]}{D - 0.8(t - t_{sl})\cos[\alpha]} \tag{2C.48}$$

$$\sigma_m^{L} = \frac{P}{2E}\left(\frac{D}{2(t - t_{sl})\cos[\alpha]} - 0.4\right) \tag{2C.49}$$

c) Final Values:

$$t_{\min} = \max\left[t_{\min}^{C},\ t_{\min}^{L}\right] \tag{2C.50}$$

$$MAWP = \min\left[MAWP^{C}, MAWP^{L}\right] \tag{2C.51}$$

$$\sigma_{\max} = \max\left[\sigma_m^{C},\ \sigma_m^{L}\right] \tag{2C.52}$$

d) When determining the minimum thickness or $MAWP$ of a corroded area on a conical shell section, the inside diameter at the location of the minimum thickness reading adjusted for metal loss and corrosion allowance may be used in the above equations instead of maximum cone diameter.

e) Eccentric Cone – The minimum thickness of an eccentric cone shall be taken as the greater of the two thicknesses obtained using both the smallest and largest α in the calculations (see Figure 2C.3).

2C.3.3.6 Toriconical Head

The minimum thickness, $MAWP$, and membrane stress equations are computed on a component basis (see Figure 2C.2):

a) Conical Section – The equations in paragraph 2C.3.3.5 can be used to compute the minimum required thickness, $MAWP$ and membrane stress of the cone section, designate these values as $t_{\min}^{C}$, $MAWP^{C}$, and σ_m^c, respectively.

b) Knuckle Section – The following equations can be used to compute the minimum required thickness, $MAWP$ and membrane stress:

$$t_{\min}^{k} = \frac{PL_kM}{2SE - 0.2P} \tag{2C.53}$$

$$MAWP^{k} = \frac{2SEt_k}{L_kM + 0.2t_k} \tag{2C.54}$$

$$\sigma_m^k = \frac{P}{2E}\left(\frac{L_kM}{t_k} + 0.2\right) \tag{2C.55}$$

where,

$$L_k = \frac{R - r_k\left(1 - \cos[\alpha]\right)}{\cos[\alpha]} \tag{2C.56}$$

$$M = \frac{1}{4}\left(3.0 + \sqrt{\frac{L_k}{r_k}}\right) \tag{2C.57}$$

c) Final Values – Expressions for the minimum required wall thickness, $MAWP$, and membrane stress are provided on a component basis in paragraph 2C.3.3.6(a) and paragraph 2C.3.3.6(b). The values of these quantities to be used in an assessment depend on the location of the flaw. The following equations can be used if a single expression is required for the cone-knuckle configuration.

$$t_{\min} = \max\left[t_{\min}^{c}, t_{\min}^{k}\right] \tag{2C.58}$$

$$MAWP = \min\left[MAWP^{c}, MAWP^{k}\right] \tag{2C.59}$$

$$\sigma_{\max} = \max\left[\sigma_m^c, \sigma_m^k\right] \tag{2C.60}$$

2C.3.3.7 Conical Transition

a) The minimum thickness, $MAWP$, and membrane stress equations are computed on a component basis (see Figure 2C.3).

b) Conical Section – The equations in paragraph 2C.3.3.5 can be used to compute the minimum required thickness, $MAWP$, and membrane stress of the cone section, designate these values as $t_{\min}^{C}$, $MAWP^{C}$, and σ_m^c, respectively.

c) Knuckle Section (If Used) – Use the following equations to compute the minimum required thickness, $MAWP$, and membrane stress.

$$t_{\min}^{k} = \frac{PL_kM}{2SE - 0.2P} \tag{2C.61}$$

$$MAWP^{k} = \frac{2SEt_k}{L_kM + 0.2t_k} \tag{2C.62}$$

$$\sigma_m^k = \frac{P}{2E}\left(\frac{L_kM}{t_k} + 0.2\right) \tag{2C.63}$$

where,

$$L_k = \frac{R_L - r_k\left(1 - \cos[\alpha]\right)}{\cos[\alpha]} \tag{2C.64}$$

$$M = \frac{1}{4}\left(3 + \sqrt{\frac{L_k}{r_k}}\right) \tag{2C.65}$$

d) Flare Section (If Used) – Use the following equations to compute the minimum required thickness, $MAWP$, and membrane stress.

$$t_{\min}^{f} = \frac{PL_fM}{2SE - 0.2P} \tag{2C.66}$$

$$MAWP^{f} = \frac{2SEt_f}{L_fM + 0.2t_f} \tag{2C.67}$$

$$\sigma_m^f = \frac{P}{2E}\left(\frac{L_fM}{t_f} + 0.2\right) \tag{2C.68}$$

where,

$$L_f = \frac{R_S + r_f\left(1 - \cos\alpha\right)}{\cos\alpha} \tag{2C.69}$$

$$M = \frac{1}{4}\left(3 + \sqrt{\frac{L_f}{r_f}}\right) \tag{2C.70}$$

e) Final Values – Expressions for the minimum required wall thickness, $MAWP$, and membrane stress are provided on a component basis in paragraph 2C.3.3.7(b), 2C.3.3.7(c), and 2C.3.3.7(d). The values of these quantities to be used in an assessment depend on the location of the flaw. The following equations can be used if a single expression is required for the conical transition.

1) Case 1 – The conical transition only contains a cone (see Figure 2C.3(a)).

$$t_{\min} = t^{c}_{\min} \tag{2C.71}$$

$$MAWP = MAWP^{c} \tag{2C.72}$$

$$\sigma_{\max} = \sigma^{c}_{m} \tag{2C.73}$$

2) Case 2 – The conical transition contains a cone and knuckle (see Figure 2C.3(b)).

$$t_{\min} = \max\left[t^{c}_{\min}, t^{k}_{\min}\right] \tag{2C.74}$$

$$MAWP = \min\left[MAWP^{c}, MAWP^{k}\right] \tag{2C.75}$$

$$\sigma_{\max} = \max\left[\sigma^{c}_{m}, \sigma^{k}_{m}\right] \tag{2C.76}$$

3) Case 3 – The conical transition contains a cone, knuckle, and flare (see Figure 2C.3(c)).

$$t_{\min} = \max\left[t^{c}_{\min}, t^{k}_{\min}, t^{f}_{\min}\right] \tag{2C.77}$$

$$MAWP = \min\left[MAWP^{c}, MAWP^{k}, MAWP^{f}\right] \tag{2C.78}$$

$$\sigma_{\max} = \max\left[\sigma^{c}_{m}, \sigma^{k}_{m}, \sigma^{f}_{m}\right] \tag{2C.79}$$

4) Case 4 – The conical transition contains a knuckle and flare (see Figure 2C.3(d)).

$$t_{\min} = \max\left[t^{k}_{\min}, t^{f}_{\min}\right] \tag{2C.80}$$

$$MAWP = \min\left[MAWP^{k}, MAWP^{f}\right] \tag{2C.81}$$

$$\sigma_{\max} = \max\left[\sigma^{k}_{m}, \sigma^{f}_{m}\right] \tag{2C.82}$$

5) Case 5 – The conical transition contains a cone and flare (see Figure 2C.4(d)).

$$t_{\min} = \max\left[t^{c}_{\min}, t^{f}_{\min}\right] \tag{2C.83}$$

$$MAWP = \min\left[MAWP^{c}, MAWP^{f}\right] \tag{2C.84}$$

$$\sigma_{\max} = \max\left[\sigma^{c}_{m}, \sigma^{f}_{m}\right] \tag{2C.85}$$

f) The half-apex angle of a conical transition can be computed knowing the shell geometry with the following equations. These equations were developed with the assumption that the conical transition contains a cone section, knuckle, and flare. If the transition does not contain a knuckle or flare, the radii of these components should be set to zero when computing the half-apex angle.

1) If $(R_L - r_k) \geq (R_S + r_f)$,

$$\alpha = \phi + \beta \tag{2C.86}$$

$$\beta = \arctan\left[\frac{(R_L - r_k) - (R_S + r_f)}{L_c}\right] \tag{2C.87}$$

2) If $(R_L - r_k) < (R_S + r_f)$,

$$\alpha = \phi - \beta \tag{2C.88}$$

$$\beta = \arctan\left[\frac{(R_S + r_f) - (R_L - r_k)}{L_c}\right] \tag{2C.89}$$

3) In both cases shown above, the angle ϕ is given by the following equation.

$$\phi = \arcsin\left[\frac{(r_f + r_k)\cos[\beta]}{L_c}\right] \tag{2C.90}$$

2C.3.4 Nozzles Connections in Shells

2C.3.4.1 General

The nozzle reinforcement procedures in this paragraph are based on VIII-1. Alternatively, the design-by-rule procedures in VIII-2, Part 4, paragraph 4.5 may be used.

2C.3.4.2 Required Reinforcement

The following assessment procedure is the one used for design of nozzles in VIII-1. This procedure can be used to evaluate the required reinforcement for nozzle connections to most shell types with or without a reinforcing pad. The procedure is known to produce conservative results for small nozzles. If the applicability and limitations shown below are not satisfied, it is recommended the nozzle be evaluated using VIII-2, Part 4, paragraph 4.5, or the Design-By-Analysis (DBA) procedures in VIII-2, Part 5.

a) Applicability and Limitations:

1) Openings in shells and heads satisfying the exemption criteria in VIII-1, UG-36(c)(3) do not require reinforcement other than that inherent in the construction.

2) For openings in cylindrical shells, the opening shall not exceed the following.

i) For vessels 1524 mm (60 inches) in diameter and less, $\min[D/2,\ 508\ mm\ (20\ in.)]$.

ii) For vessels over 1524 mm (60 inches), $\min[D/3,\ 1016\ mm\ (40\ in.)]$.

3) For openings in spherical shells or formed heads there is no restriction on the opening size.

4) The effects of nozzle loading are not included in this procedure. If nozzle loads are significant, a stress analysis should be performed to evaluate the acceptability of the nozzle configuration. The significance of nozzle loads may be evaluated using VIII-2, Part 4.5. paragraph 4.5.15.

b) The condition required for satisfactory reinforcement of a branch nozzle connection is given by the following:

1) The basic equations for all configurations are shown below:

$$A_r = d_c t_r F + 2t_n t_r F\left(1 - f_{r1}\right) \tag{2C.91}$$

$$A_1 = \max\left[\left(d_c\left(E_1 t - F t_r\right) - B\right),\ \left(2\left(t + t_n\right)\cdot\left(E_1 t - F t_r\right) - B\right)\right] \tag{2C.92}$$

$$B = 2t_n\left(E_1 t - F t_r\right)\left(1 - f_{r1}\right) \tag{2C.93}$$

$$A_3 = \min\left[\left(5t\cdot t_i\cdot f_{r2}\right),\ \left(5t_n^2\cdot f_{r2}\right),\ \left(2h\cdot t_i\cdot f_{r2}\right)\right] \tag{2C.94}$$

$$A_{43} = w_h^2 f_{r2} \tag{2C.95}$$

2) For nozzles without a reinforcing pad (see Figure 2C.5) for the definition of areas:

$$A_1 + A_2 + A_3 + A_{41} + A_{43} \geq J_r A_r \tag{2C.96}$$

$$A_2 = \min\left[\left(5\left(t_n - t_{rn}\right) f_{r2} t\right),\ \left(5\left(t_n - t_{rn}\right) f_{r2} t_n\right)\right] \tag{2C.97}$$

$$A_{41} = w_n^2 f_{r2} \tag{2C.98}$$

3) For nozzles with a reinforcing pad (see Figure 2C.5) for the definition of areas:

$$A_1 + A_2 + A_3 + A_{41} + A_{42} + A_{43} + A_5 \geq J_r A_r \tag{2C.99}$$

$$A_2 = \min\left[\left(5\left(t_n - t_{rn}\right) f_{r2} t\right),\ \left(2\left(t_n - t_{rn}\right) \cdot \left(2.5 t_n + t_e\right) f_{r2}\right)\right] \tag{2C.100}$$

$$A_{41} = w_n^2 f_{r3} \tag{2C.101}$$

$$A_{42} = w_p^2 f_{r4} \tag{2C.102}$$

$$A_5 = \left(D_p - d_c - 2t_n\right) t_e f_{r4} \tag{2C.103}$$

4) In the above equations:

$$A_1 < 0.0 \qquad then \qquad c_b = LOSS_b + FCA \tag{2C.104}$$

$$A_2 < 0.0 \qquad then \qquad A_2 = 0.0 \tag{2C.105}$$

$$f_{r1} = \frac{S_n}{S_v} \qquad for\ a\ set-in\ nozzle \tag{2C.106}$$

$$f_{r1} = 1.0 \qquad for\ a\ set-on\ nozzle \tag{2C.107}$$

$$f_{r2} = \frac{S_n}{S_v} \tag{2C.108}$$

$$f_{r3} = \frac{\min\left[S_n, S_p\right]}{S_v} \tag{2C.109}$$

$$f_{r4} = \frac{S_p}{S_v} \tag{2C.110}$$

2C.3.4.3 Weld Strength Analysis

A weld strength analysis is required for nozzles with a reinforcing pad. Integrally reinforced nozzles, i.e., nozzles without a reinforcing pad, are exempt from a weld strength analysis per VIII-1, UW-15(b)(1). However, if the attachment welds are subject to corrosion or erosion in excess of the corrosion allowance, a weld strength analysis shall be performed.

a) If the nozzle connection is subject to corrosion, the corroded dimensions of the groove and fillet welds should be used in the strength calculations.

b) The following analysis should be used when the nozzle neck is inserted through the vessel wall (set-in nozzle), (see Figure 2C.6); the reinforcement areas to be used in the calculations are defined in paragraph 2C.3.4.2.

1) The required strength is:

$$W = \left[A - A_1 + 2t_n f_{r1} \left(E_1 t - F t_r \right) \right] S_v \tag{2C.111}$$

$$W_{11} = \left(A_2 + A_{41} + A_{42} + A_5 \right) S_v \tag{2C.112}$$

$$W_{22} = \left(A_2 + A_3 + A_{41} + A_{43} + 2t_n \cdot t \cdot f_{r1} \right) S_v \tag{2C.113}$$

$$W_{33} = \left(A_2 + A_3 + A_5 + A_{41} + A_{42} + A_{43} + 2t_n \cdot t \cdot f_{r1} \right) S_v \tag{2C.114}$$

2) The computed strength with a reinforcing pad is:

$$W^c = \min\left[W_{11}^c, W_{22}^c, W_{33}^c \right] \tag{2C.115}$$

$$W_{11}^c = \frac{\pi}{2} D_p w_p \left(0.49 S_{wp} \right) + \frac{\pi}{2} d_m t_n \left(0.7 S_n \right) \tag{2C.116}$$

$$W_{22}^c = \begin{pmatrix} \frac{\pi}{2} d_o w_n \left(0.49 S_{wn} \right) + \frac{\pi}{2} d_o w_{pg} \left(0.74 S_{wpg} \right) + \\ \frac{\pi}{2} d_o w_{ng} \left(0.74 S_{wng} \right) + \frac{\pi}{2} d_o w_h \left(0.49 S_{wh} \right) \end{pmatrix} \tag{2C.117}$$

$$W_{33}^c = \frac{\pi}{2} D_p w_p \left(0.49 S_{wp} \right) + \frac{\pi}{2} d_o w_{ng} \left(0.74 S_{wng} \right) + \frac{\pi}{2} d_o w_h \left(0.49 S_{wh} \right) \tag{2C.118}$$

3) The computed strength without a reinforcing pad is:

$$W^c = \min\left[W_{11}^c, W_{22}^c \right] \tag{2C.119}$$

$$W_{11}^c = \frac{\pi}{2} d_o w_n \left(0.49 S_{wn} \right) + \frac{\pi}{2} d_m t_n \left(0.7 S_n \right) \tag{2C.120}$$

$$W_{22}^c = \frac{\pi}{2} d_o w_n \left(0.49 S_{wn} \right) + \frac{\pi}{2} d_o w_{ng} \left(0.74 S_{wng} \right) + \frac{\pi}{2} d_o w_h \left(0.49 S_{wh} \right) \tag{2C.121}$$

$$W_{33}^c = 0.0 \tag{2C.122}$$

4) The acceptance criteria are given by the following equations:

$$W^c \geq W \tag{2C.123}$$

$$W_{11}^c \geq \min\left[W_{11}, W \right] \tag{2C.124}$$

$$W_{22}^c \geq \min\left[W_{22}, W \right] \tag{2C.125}$$

$$W_{33}^c \geq \min\left[W_{33}, W \right] \tag{2C.126}$$

c) The following analysis should be used when the nozzle neck abuts the vessel wall (set-on nozzle), (see Figure 2C.7); the reinforcement areas to be used in the calculations are defined in paragraph 2C.3.4.2.

1) The required strength is:

$$W = \left[A - A_1 \right] S_v \tag{2C.127}$$

$$W_{11} = \left(A_2 + A_5 + A_{41} + A_{42} \right) S_v \tag{2C.128}$$

$$W_{22} = \left(A_2 + A_{41} \right) S_v \tag{2C.129}$$

2) The computed strength with a reinforcing pad is:

$$W^c = \min\left[W_{11}^c, W_{22}^c \right] \tag{2C.130}$$

$$W_{11}^c = \frac{\pi}{2} D_p w_p \left(0.49 S_{wp} \right) + \frac{\pi}{2} d_m w_{ng} \left(0.60 S_{wng} \right) \tag{2C.131}$$

$$W_{22}^c = \frac{\pi}{2} d_o w_n \left(0.49 S_{wn} \right) + \frac{\pi}{2} d_m w_{ng} \left(0.60 S_{wng} \right) \tag{2C.132}$$

3) The computed strength without a reinforcing pad is:

$$W^c = W_{11}^c \tag{2C.133}$$

$$W_{11}^c = \frac{\pi}{2} d_o w_n \left(0.49 S_{wn} \right) + \frac{\pi}{2} d_m w_{ng} \left(0.60 S_{wng} \right) \tag{2C.134}$$

$$W_{22}^c = 0.0 \tag{2C.135}$$

4) The acceptance criteria are given by the following equations:

$$W^c \geq W \tag{2C.136}$$

$$W_{11}^c \geq \min\left[W_{11}, W \right] \tag{2C.137}$$

$$W_{22}^c \geq \min\left[W_{22}, W \right] \tag{2C.138}$$

d) The reinforcement and weld strength calculations above are given in terms of thicknesses and areas. Therefore, to compute an $MAWP$, an iterative procedure is required. In this procedure, a pressure is assumed and the corresponding wall thicknesses, reinforcement areas, and weld strengths are computed are checked against required values. This process is repeated until a pressure is found that results in satisfaction of all required values. This resulting pressure is the $MAWP$ of the nozzle component.

2C.3.5 Junction Reinforcement Requirements at Conical Transitions

Junction reinforcement at the small end and large end of a conical transition may be evaluated based on the original construction code. Alternatively, VIII-1, Appendix 1-5 or the design-by-rule procedures in VIII-2, Part 4, paragraph 4.3 may be used.

2C.3.6 Other Components

Calculation procedures for other components should be evaluated based on the original construction code. References for these components constructed to VIII-1, VIII-2, or the TEMA standard are cited below.

a) Tubesheets: VIII-1 Part UHX, VIII-2, Part 4, paragraph 4.18 or TEMA.

b) Flat head to cylinder connections: VIII-1 paragraph UG-34 or VIII-2, Part 4, paragraph 4.3.

c) Bolted Flanges: VIII-1, Appendix 2 or VIII-2, Part 4, paragraph 4.16.

2C.4 Pressure Vessels and Boiler Components – External Pressure

The minimum thickness and $MAWP$ of a pressure vessel or boiler component subject to external pressure may be computed based on the original construction code. Alternatively, the design-by-rule procedures in VIII-2, Part 4, paragraph 4.4 may be used because these rules are superior to those in VIII-1.

2C.5 Piping Components and Boiler Tubes

2C.5.1 Overview

The minimum thickness and $MAWP$ of a straight section or curved section of pipe subject to internal or external pressure with supplemental loads may be computed based on the original construction code. Alternatively, the equations in this section may be utilized in the calculation of these parameters. In addition, a procedure to evaluate branch connections subject to internal pressure is provided. These equations are based upon the ASME B31.3 and ASME Section I. The effects of supplemental loads (see paragraph 2C.2.7) are included in these equations only for straight pipe (i.e., longitudinal stress direction) subject to a net-section axial force and/or bending moment. The effects of supplemental loads for other component geometries or loading conditions can be evaluated using the stress analysis methods in Annex 2D.

2C.5.2 Metal Loss

The equations in paragraph 2C.5 are written in terms of outside diameter of the pipe, D_o; therefore, the equations do not need to be adjusted for metal loss and future corrosion allowance which occur on the inside surface. If metal loss has occurred on the outside diameter (e.g., corrosion under insulation), then D_o would need to be modified to account for this metal loss.

2C.5.3 Required Thickness and MAWP – Straight Pipes Subject to Internal Pressure

The minimum thickness, $MAWP$, and membrane stress equations for straight sections of pipe subject to internal pressure are as follows:

a) Circumferential stress (Longitudinal Joints):

$$t_{\min}^{C} = \frac{PD_o}{2\left(SE + PY_{B31}\right)} + MA \tag{2C.139}$$

$$MAWP^{C} = \frac{2SE\left(t - MA\right)}{D_o - 2Y_{B31}\left(t - MA\right)} \tag{2C.140}$$

$$\sigma_m^{C} = \frac{P}{E}\left[\frac{D_o}{2\left(t - MA\right)} - Y_{B31}\right] \tag{2C.141}$$

b) Longitudinal stress (Circumferential Joints):

$$t_{\min}^{L} = \frac{PD_o}{4(SE + PY_{B31})} + t_{sl} + MA \tag{2C.142}$$

$$MAWP^L = \frac{4SE(t - t_{sl} - MA)}{D_o - 4Y_{B31}(t - t_{sl} - MA)} \quad (2C.143)$$

$$\sigma_m^L = \frac{P}{E}\left(\frac{D_o}{4\left(t - t_{sl} - MA\right)} - Y_{B31}\right) \quad (2C.144)$$

c) Final Values:

$$t_{\min} = \max\left[t_{\min}^C, t_{\min}^L\right] \quad (2C.145)$$

$$MAWP = \min\left[MAWP^C, MAWP^L\right] \quad (2C.146)$$

$$\sigma_{\max} = \max\left[\sigma_m^C, \sigma_m^L\right] \quad (2C.147)$$

2C.5.4 Required Thickness and MAWP – Boiler Tubes

The minimum thickness, $MAWP$, and membrane stress equations for straight sections of pipe and pipe bends subject to internal pressure are shown below. These equations only cover circumferential stress. If longitudinal stresses are significant, the equation in paragraph 2C.3.3 may be used.

a) Circumferential Stress when $t_c \leq 0.5R$ and $D \leq 125\ mm\ (5.0\ in.)$ (Longitudinal Joints):

$$t_{\min}^C = \frac{PD}{2S + P} + 0.005D + e_t \quad (2C.148)$$

$$MAWP^C = \frac{2S\left(t - 0.005D - e_t\right)}{D - \left(t - 0.005D - e_t\right)} \quad (2C.149)$$

$$\sigma^C = \frac{P\left[D - \left(t - 0.005D - e_t\right)\right]}{2\left(t - 0.005D - e_t\right)} \quad (2C.150)$$

b) Circumferential Stress when $t_c > 0.5R$ and $D \leq 125\ mm\ (5.0\ in.)$ (Longitudinal Joints) – the equations in paragraph 2C.3.3.3(b) may be used.

2C.5.5 Required Thickness and MAWP – Pipe Bends Subject to Internal Pressure

The results for circumferential stress, and the minimum required thickness and $MAWP$ are shown below for thin wall bends $(R_m/t_c \geq 10)$. Results for thick wall pipe bends which do not satisfy this criterion can be found in DIN 2413, Parts 1 and 2.

a) Circumferential stress

1) The results for any location defined by the angle θ (see Figure 2C.8) are given by the following equations:

$$t_{\min}^C = \frac{PD_o}{2\left(\frac{SE}{L_f} + PY_{B31}\right)} + MA \quad (2C.151)$$

$$MAWP^C = \frac{2\left(\frac{SE}{L_f}\right)(t - MA)}{D_o - 2Y_{B31}(t - MA)} \quad (2C.152)$$

$$\sigma_m^C = \frac{PL_f}{E}\left[\frac{D_o}{2(t - MA)} - Y_{B31}\right] \quad (2C.153)$$

2) In equations shown above, L_f is the Lorentz factor which is a measure of the stress magnitude in an elbow relative to that in a straight pipe. If $L_f = 1.0$, then equations for stress, minimum required wall thickness and $MAWP$ are the same as those for straight pipe. If the pipe bend contains a flaw, the position defined by the angle θ should coincide with the centerline of the location of the flaw if the flaw is in the center section or middle one-third of the bend. If the flaw is not located in the center section of the bend, then use the calculated value of L_f.

i) The Lorentz factor is computed using Equation (2C.154).

$$L_f = \left(\frac{\frac{R_b}{R_m} + \frac{\sin\theta}{2}}{\frac{R_b}{R_m} + \sin\theta}\right) \quad (2C.154)$$

ii) At the intrados ($\theta = -90°$) or ($\theta = 270°$) the Lorentz factor is:

$$L_f = \left(\frac{\frac{R_b}{R_m} - 0.5}{\frac{R_b}{R_m} - 1.0}\right) \quad (2C.155)$$

iii) At the extrados ($\theta = 90°$) the Lorentz factor is:

$$L_f = \left(\frac{\frac{R_b}{R_m} + 0.5}{\frac{R_b}{R_m} + 1.0}\right) \quad (2C.156)$$

iv) If the bend angle, β, is greater than $2\beta_a$ where β_a is computed in degrees using Equation (2C.157), the equations in paragraph 2C.5.5(a)(1) will give the correct value for the maximum circumferential stress. Otherwise, the actual maximum circumferential stress will be less than that given by these equations because of the strengthening effect of the attached straight pipe sections.

$$\beta_a = \left(\frac{121.5R_m}{R_b - R_m}\right)\sqrt{\frac{t}{R_m}} \quad (2C.157)$$

b) Longitudinal Stress – The equations in paragraph 2C.5.3(b) can be used.

c) Final Values – The equations in paragraph 2C.5.3(c) can be used.

2C.5.6 Required Thickness and MAWP for External Pressure

The minimum thickness and $MAWP$ for straight and curved sections of pipe subject to external pressure can be determined using the methods in paragraph 2C.4.

2C.5.7 Branch Connections

Branch connections in piping systems have a thickness dependency and are evaluated in a Level 2 Assessment procedure. The following analysis method based on the area replacement rules in ASME B31.3 may be used for a Level 2 Assessment. The condition for satisfactory reinforcement of a branch nozzle connection may be determined using the equations shown below (see Figure 2C.9).

$$A_2 + A_3 + A_4 \geq A_r \tag{2C.158}$$

where,

$$A_r = t_h d_1 \left(2 - \sin\left[\beta\right]\right) \tag{2C.159}$$

$$A_2 = \left(2d_2 - d_1\right)\left(T_h - t_h\right) \tag{2C.160}$$

$$A_3 = \frac{2L_4\left(T_b - t_b\right)}{\sin\left[\beta\right]} \tag{2C.161}$$

$$A_4 = A_{41} + A_{42} + A_{43} \tag{2C.162}$$

$$A_{41} = w_n^2 f_w \tag{2C.163}$$

$$A_{42} = w_p^2 f_w \tag{2C.164}$$

$$A_{43} = \left(D_p - \frac{D_b}{\sin\left[\beta\right]}\right) T_r f_r \tag{2C.165}$$

with,

$$d_2 = \max\left[d_1, \left(T_b + T_h + d_1/2\right)\right] \tag{2C.166}$$

$$L_4 = \min\left[2.5T_h, \left(2.5T_b + T_r\right)\right] \tag{2C.167}$$

$$f_w = \min\left[\left(\frac{S_w}{S}\right), 1.0\right] \tag{2C.168}$$

$$f_r = \min\left[\left(\frac{S_r}{S}\right), 1.0\right] \tag{2C.169}$$

In the above equations, if $A_1 < 0.0$ use $A_1 = 0.0$, and if $A_2 < 0.0$ use $A_2 = 0.0$.

2C.6 API 650 Storage Tanks

2C.6.1 Overview

The equations to evaluate the minimum thickness and maximum fill height of an atmospheric storage tank are covered in Part 4 of API 653. The minimum thickness and Maximum Fill Height (MFH) can be computed by the

1-Foot Method (see paragraph 2C.6.3) or the Variable Point Method described in API 650.

2C.6.2 Metal Loss

The equations in this paragraph are written in terms of the nominal diameter of the tank, D_n; therefore, the diameter does not need to be adjusted for metal loss and future corrosion allowance. The wall thickness is adjusted for metal loss and future corrosion allowance.

2C.6.3 Required Thickness and MFH for Liquid Hydrostatic Loading

a) The minimum thickness and MFH in Metric Units are shown below. In these equations, the tank nominal diameter D is in meters, the design fill height H is in meters, the allowable stress S is in MPa, the wall thicknesses $t_{\min}$ and t are in millimeters.

$$t_{\min} = \frac{4.9DG(H-0.3)}{S} \tag{2C.170}$$

$$MFH = \frac{tS}{4.9DG} + 0.3 \tag{2C.171}$$

b) The minimum thickness and MFH in US Customary Units are shown below. In these equations, the tank nominal diameter D is in feet, the design fill height H is in feet, the allowable stress S is in psi, the wall thicknesses $t_{\min}$ and t are in inches.

$$t_{\min} = \frac{2.6DG(H-1)}{S} \tag{2C.172}$$

$$MFH = \frac{tS}{2.6DG} + 1 \tag{2C.173}$$

2C.7 Estimation of Burst Pressure

2C.7.1 Svensson's Method

Solution for the burst pressure of a cylindrical or spherical shell under internal pressure are provided in the following paragraphs. These solutions were developed and validated by Svensson [16] for a material that has the following stress-strain relationship:

$$\sigma = \sigma_0 \varepsilon^n \tag{2C.174}$$

The parameters n and σ_0 define the plastic part of the true stress-strain curve. The constant σ_0 in Equation (2C.174) may be related to the engineering ultimate tensile strength, σ_{uts}, using Equation (2C.175).

$$\sigma_0 = \sigma_{uts} \cdot \left(\frac{e}{n}\right)^n \tag{2C.175}$$

The parameter n may be taken as m_2 from the MPC stress-strain curve model (see Annex 2E, Table 2E.8) or as n_{RO} from the Ramberg-Osgood stress-strain curve model (see Annex 2E, paragraph 2E.3.3).

Validation of the Svensson approximation for burst pressure and the predicted strain at failure are provided in reference [17].

2C.7.2 Cylindrical Shell Burst Pressure

The burst pressure for a thick wall cylindrical shell is given by the following equation.

$$P_{burst} = \sigma_0 \int_{\varepsilon_1}^{\varepsilon_2} \frac{\varepsilon^n}{1 - e^{\sqrt{3}\varepsilon}} d\varepsilon \tag{2C.176}$$

At the burst pressure, Svensson shows that the following equations must be satisfied. Equations (2C.177) and (2C.178) represent two equations with two unknowns, ε_1 and ε_2. For a given true stress-strain curve, the parameter n is determined and these equations may be solved for ε_1 and ε_2.

$$\left(\frac{\varepsilon_1}{\varepsilon_2}\right)^n = \frac{e^{\sqrt{3}\varepsilon_1}}{\left[1 - \left(1 - e^{\sqrt{3}\varepsilon_1}\right)\left(\frac{R_o}{R}\right)^{-2}\right]} \tag{2C.177}$$

$$\varepsilon_2 = \frac{1}{\sqrt{3}} \ln\left[1 - \left(1 - e^{\sqrt{3}\varepsilon_1}\right)\left(\frac{R_o}{R}\right)^{-2}\right] \tag{2C.178}$$

The resulting values of ε_1 and ε_2 are substituted into Equation (2C.176) to determine the burst pressure. The parameter σ_0 is determined using Equation (2C.175).

An approximate solution for both thick and thin wall cylinders can be made using Equation (2C.179).

$$P_{burst} = \sigma_{uts}\left(\frac{2}{\left(\sqrt{3}\right)^{n+1}}\right)\left(\frac{t}{R_m}\right) \tag{2C.179}$$

2C.7.3 Spherical Shell Burst Pressure

The burst pressure for a thick wall spherical shell is given by the Equation (2C.180).

$$P_{burst} = \sigma_0 \int_{\varepsilon_1}^{\varepsilon_2} \frac{\varepsilon^n}{1 - e^{3\varepsilon/2}} d\varepsilon \tag{2C.180}$$

At the burst pressure, Svensson shows that the following equations must be satisfied. Equations (2C.181) and (2C.182) represent two equations with two unknowns, ε_1 and ε_2. For a given true stress-strain curve, the parameter n is determined and these equations may be solved for ε_1 and ε_2.

$$\left(\frac{\varepsilon_1}{\varepsilon_2}\right)^n = \frac{e^{3\varepsilon_1/2}}{\left[1 - \left(1 - e^{3\varepsilon_1/2}\right)\left(\frac{R_o}{R}\right)^{-3}\right]} \tag{2C.181}$$

$$\varepsilon_2 = \frac{2}{3} \cdot \ln\left[1 - \left(1 - e^{3\varepsilon_1/2}\right)\left(\frac{R_o}{R}\right)^{-3}\right] \tag{2C.182}$$

The resulting values of ε_1 and ε_2 are substituted into Equation (2C.180) to determine the burst pressure. The parameter σ_0 is determined using Equation (2C.175).

An approximate solution for both thick and thin wall sphere can be made using Equation (2C.183).

$$P_{burst} = \sigma_{uts}\left(\frac{2^{n+1}}{3^n}\right)\left(\frac{t}{R_m}\right) \tag{2C.183}$$

2C.8 Nomenclature

A cross-sectional area of cylinder.

A_r required reinforcement area.

A_1 available reinforcement area resulting from excess thickness in the shell.

A_2 available reinforcement area resulting from excess thickness in the nozzle or run pipe, as applicable.

A_3 available reinforcement area resulting from excess thickness in the nozzle internal projection or branch pipe, as applicable.

A_4 available reinforcement area provided by the welds and, for piping, the reinforcement pad.

A_5 available reinforcement area provided by a reinforcing pad.

A_{41} available reinforcement area provided by the nozzle to pad or nozzle to pipe attachment welds.

A_{42} available reinforcement area provided by the reinforcement pad attachment welds.

A_{43} available reinforcement area provided by the reinforcement pad.

α one-half apex angle of the cone in a conical shell or toriconical head (radians).

α_1 offset cone angle.

α_2 offset cone angle.

β angle between the axis of the header and branch pipe, or an angle used to compute the geometry of a conical transition with a knuckle and/or flare, as applicable.

β_a angle used to determine the applicability of the Lorentz factor.

C_r inside crown radius of a torispherical head.

D inside shell diameter.

D_c diameter.

D_n tank nominal diameter.

D_L cone outside diameter, large end.

D_{LS} cylinder outside diameter, large end.

D_S cone outside diameter, small end.

D_{SS} cylinder outside diameter, small end.

D_b outside diameter of the branch pipe.

D_o outside diameter.

D_p outside diameter of the reinforcing pad.

D_1 diameter used in the flare stress calculation.

d_c diameter of the circular opening, or chord length at the vessel wall mid-surface of a non-radial opening, in the plane under consideration.

d_o outside diameter of the nozzle.

d_r diameter of the rivet.

d_p diameter of the rivet hole in the plate.

d_1 effective length removed from the pipe at the branch location.

d_2 half-width of reinforcement zone.

e Euler's number, $e = 2.7182818284$.

e_t parameter used for computing the boiler tube thickness determined as follows: $e_t = 0.0$ for tubes strength-welded to headers and drums, and $e_t = 0.004$ over a length equal to the length of the seat plus 25 mm (1 inch) for tubes expanded into tube seats except $e_t = 0.0$ for tubes expanded into tube seats provided the thickness of the tube ends over a length of the seat plus 25 mm (1 inch) is not less than the following:

- 2.41 mm (0.095 inch) for tubes 32 mm (1.25 inches) OD and smaller,
- 2.67 mm (0.105 inch) for tubes above 32 mm (1.25 inches) and up to 51 mm (2 inches) inclusive,
- 3.05 mm (0.120 inch) for tubes above 51 mm (2 inches) and up to 76 mm (3 inches) inclusive,
- 3.43 mm (0.135 inch) for tubes above 76 mm (3 inches) and up to 102 mm (4 inches) inclusive,
- 3.81 mm (0.150 inch) for tubes above 102 mm (4 inches) and up to 127 mm (5 inches) inclusive.

E weld joint efficiency or quality factor from the original construction code if unknown use 0.7.

E_1 equal to 1.0 when the opening is in solid plate or in a Category B butt joint, otherwise, the joint efficiency of the weld joints the nozzle intersects.

ε_1 strain at the inside surface.

ε_2 strain at the outside surface.

f_v shear stress from applied loads.

f_r weld strength factor.

f_w weld strength factor.

F applied net-section axial force, use a negative value if the axial force produces a compressive stress at the location of the assessment point.

f_{r1} strength reduction factor.

f_{r2} strength reduction factor.

f_{r3} strength reduction factor.

f_{r4} strength reduction factor.

G fluid density.

H height of the horizontal vessel head, or the design liquid level in an atmospheric storage tank, as applicable.

h height of the elliptical head measured to the inside surface or the inside nozzle projection, as applicable.

j rivet row number.

J_r reinforcement factor equal to 1.0 for internal pressure and 0.5 for external pressure.

K elliptical head coefficient.

K_c equivalent radius coefficient.

L_f Lorentz factor.

$LOSS$ uniform metal loss away from the damage area at the time of the inspection.

M applied net-section bending moment, use a negative value if the bending moment produces a compressive stress at the location of the assessment point. For a formed head M is the knuckle factor.

MA mechanical allowances (thread or groove depth); for threaded components, the nominal thread depth (dimension h of ASME B.1.20.1) shall apply.

$MAWP$ maximum allowable working pressure.

$MAWP^C$ maximum allowable working pressure based on circumferential stress.

$MAWP^L$ maximum allowable working pressure based on longitudinal stress.

$MAWP^c$ maximum allowable working pressure for the cone.

$MAWP^f$ maximum allowable working pressure for the flare.

$MAWP^k$ maximum allowable working pressure for the knuckle.

MFH maximum fill height of the liquid to be stored in an atmospheric storage tank.

n Strain hardening parameter.

n_{rm} number of rivets.

N_r total number of rivets over the width w_r, for a butt joint, this will encompass one half of the joint pattern.

P internal design pressure.

P_{rs} rivet shear load.

P_{rc} minimum compressive load in a riveted joint.

P_{rj} plate tension load for the j^{th} row of rivets in a riveted joint.

$P_{rj,\max}$ governing plate tension load for a riveted joint.

P_{rl} limiting load of a riveted plate.

P_{rp} limiting load of a plate without a rivet.

ϕ angle used to compute the cone geometry.

R inside radius of the component.

R_m mean radius of the component.

R_o outside radius of the component.

R_L large end radius at a conical transition.

R_S small end radius at a conical transition.

R_b centerline bend radius (see Figure 2C.8).

R_{ell} ratio of the major-to-minor axis of an elliptical head (see Figure 2C.1).

R_m mean radius of the component; use the large end radius for a conical shell.

r_f inside radius of the flare at a conical transition.

r_k inside knuckle radius of a torispherical head, toriconical head, or conical transition.

S allowable stress.

S_n allowable stress for the nozzle.

S_r allowable stress for the reinforcing pad.

S_v allowable stress for the vessel.

S_w allowable stress for the weld metal.

S_{wh} allowable stress for the nozzle-to-vessel (inside surface) attachment weld.

S_{wn} allowable stress for the nozzle-to-reinforcing pad or nozzle-to-vessel fillet weld.

S_{wp} allowable stress for the shell to reinforcing pad fillet weld.

S_{wpg} allowable stress for the nozzle-to-pad groove weld.

S_{wng} allowable stress for nozzle-to-vessel groove weld.

σ_{bp} allowable bearing stress of plate.

σ_{br} allowable bearing stress of rivets.

σ_{sr} allowable shear stress of rivets.

σ_{tp} allowable tensile stress of plate.

σ_m nominal membrane stress.

σ_m^C nominal circumferential membrane stress for a cylinder or cone, as applicable.

σ_m^L nominal longitudinal membrane stress for a cylinder or cone, as applicable.

σ_m^c maximum stress in the cone.

σ_m^f maximum stress in the flare.

σ_m^k maximum stress in the knuckle.

$\sigma_{\max}$ maximum stress.

σ_0 Stress-strain curve coefficient.

σ_{uts} ultimate tensile stress of material at the assessment temperature.

T_b nominal or furnished branch pipe thickness.

T_h nominal or furnished header or run pipe thickness.

T_r nominal or furnished thickness of the reinforcing pad.

t thickness of the shell or pipe adjusted for mill tolerance, $LOSS$ and FCA, or cylinder thickness at a conical transition for a junction reinforcement calculation adjusted for mill tolerance, $LOSS$ and FCA, as applicable.

t_b required thickness of the branch pipe (see paragraph 2C.5.3).

t_e nominal thickness of the reinforcing pad.

t_f flare thickness.

t_h required thickness of the header or run pipe (see paragraph 2C.5.3); for welded pipe, when the branch pipe does not intersect the longitudinal weld on the run pipe, the basic allowable stress for

the pipe may be used in determining the required wall thickness. If the branch pipe does intersect the longitudinal weld of the run pipe, then the product of the basic allowable stress and the weld joint efficiency should be used in calculating the required wall thickness.

t_i nominal thickness of the internal projection of the nozzle wall.

t_k knuckle thickness.

$t_{\min}$ minimum required thickness.

$t_{\min}^{C}$ minimum required thickness based on the circumferential membrane stress for a cylinder or cone, as applicable.

$t_{\min}^{L}$ minimum required thickness based on the longitudinal membrane stress for a cylinder or cone, as applicable.

$t_{\min}^{c}$ minimum required thickness for the cone.

$t_{\min}^{f}$ minimum required thickness for the flare.

$t_{\min}^{k}$ minimum required thickness for the knuckle.

t_{nom} nominal thickness.

t_r required vessel shell thickness for the nozzle reinforcement calculation computed with $E = 1.0$.

(1) Cylindrical shell (see paragraphs 2C.3.3.1 and 2C.4).

(2) Spherical shell (see paragraphs 2C.3.3.2 and 2C.4).

(3) Elliptical head (see paragraphs 2C.3.3.3 and 2C.4); for the internal pressure calculation, when the nozzle opening and its reinforcement are completely within a circle the center of that coincides with the center of the head and the diameter of which is 80% of the shell diameter, the required wall thickness shall be determined using K_c instead of K.

(4) Torispherical head (see paragraphs 2C.3.3.4 and 2C.4); for the internal pressure calculation, when the nozzle opening is entirely within the spherical of a torispherical head the required wall thickness is computed using $M = 1.0$.

(5) Conical shell (see paragraphs 2C.3.3.5 and 2C.4); when the nozzle opening is in a cone, the required wall thickness is determined based on the shell diameter where the nozzle axis intersects the conical shell.

t_{req} required thickness for future operation.

t_{rn} required thickness of a seamless nozzle wall.

t_{sl} supplemental thickness for mechanical loads other than pressure that result in longitudinal stress; this thickness is usually obtained from the results of a weight case in a stress analysis of the piping system (see paragraph 2C.2.7).

t_{std} nominal thickness of ANSI B36.10 standard weight pipe.

θ angle around the elbow circumference where results are to be computed (degrees).

w_h weld leg size of the nozzle-to-vessel attachment weld on the inside surface of the vessel.

w_n weld leg size of the nozzle-to-vessel or nozzle-to-reinforcing pad (if a pad is used) attachment weld.

w_{ng} depth of nozzle-to-shell groove weld; for a set-on nozzle with a full penetration weld $w_{ng} = t_n$; for a set-in nozzle with a full penetration weld $w_{ng} = t$.

w_p weld leg size of the reinforcing pad-to-vessel attachment weld.

w_r unit width over which the riveted joint efficiency will be determined.

w_{pg} depth of nozzle-to-pad groove weld; for a full penetration weld $w_{pg} = t_p$.

W required weld stress.

W_{11} required weld stress calculation parameter.

W_{22} required weld stress calculation parameter.

W_{33} required weld stress calculation parameter.

W^c computed weld stress.

W_{11}^c computed weld stress calculation parameter.

W_{22}^c computed weld stress calculation parameter.

W_{33}^c computed weld stress calculation parameter.

Y_{B31} coefficient from ASME B31 Piping codes used for determining the pipe wall thickness, the coefficient can be determined from the following table that is valid for $t_{\min} < D_o/6$.

Value of Y_{B31} (interpolate for intermediate temperatures)						
Materials	Temperature °C (°F)					
	≤ 482 (≤ 900)	510 (950)	538 (1000)	566 (1050)	593 (1100)	≥ 621 (≥ 1150)
Ferritic Steels	0.4	0.5	0.7	0.7	0.7	0.7
Austenitic Steels	0.4	0.4	0.4	0.4	0.5	0.7
Other Ductile Metals	0.4	0.4	0.4	0.4	0.4	0.4
Cast iron	0.0	---	---	---	---	---

2C.9 References

[1] ASME B&PV Code, Section VIII, Division 1, *Rules for Construction of Pressure Vessels*, ASME, New York, NY.

[2] ASME B&PV Code, Section VIII, Division 2, *Rules for Construction of Pressure Vessels – Alternative Rules*, ASME, New York, NY.

[3] ASME B31.3, *Process Design Piping Code*, 2013, ASME, New York, NY.

[4] ASCE-7, *Minimum Design Loads for Buildings and Other Structures*, American Society of Civil Engineers, Reston, VA.

[5] Osage, D., and Sowinski, J., *ASME Section VIII – Division 2 Criteria and Commentary*, PTB-1-2013, ASME, New York, NY, 2014.

[6] Cao, Z. Ph.D., Bildy, L., Osage, D.A., and Sowinski, J.*, Development of Nozzle Rules for ASME B&PV Code, Section VIII, Division 2*, WRC Bulletin 529, Welding Research Council, Inc., New York, NY, 2011.

[7] Farr, J.R. and Jawad, M.H., Guidebook for The Design of ASME Section VIII Pressure Vessels, ASME, New York, NY, 1998.

[8] Miller, C.D. and Moktarian, K, "A Comparisons of Proposed Alternative Rules with ASME Code Rules for Determining Allowable Compressive Stresses," The Eighth International Conference on Pressure Vessel Technology, Montreal, Canada, July 1996.

[9] Osage, D.A., Buchheim, G.M., Brown, R.G., and Poremba, J., "An Alternate Approach for Inspection Scheduling Using the Maximum Allowable Working Pressure for Pressurized Equipment," PVP-Vol. 288, American Society of Mechanical Engineers, 1994, pp. 261-273.

[10] Sowinski, J.C., Osage, D.A., and Brown, R.G., *ASME Section VIII - Division 2 Example Problem Manual*, PTB-3-2013, ASME, New York, NY, 2013.

[11] Sowinski, J.C. and Osage, D.A., *ASME Section VIII - Division 1 Example Problem Manual*, PTB-4-2013, ASME, New York, NY, 2013.

[12] Sowinski, J.C., Cao, Z., Osage, D.A., Brubaker, J.E., and Carr, N.A., *Development of Design Rules for Conical Transitions in Pressure Vessels for the ASME B&PV Code, Section VIII, Division 2*, WRC Bulletin 521, Welding Research Council, Inc., New York, NY, 2009.

[13] Rodabaugh, E.C., Duffy, A.R., and Atterbury, T.J., "The Internal Pressure Capacity of Butt Welding Elbows," American Gas Association, NG-18, Report No. 22, September 1969.

[14] Rodabaugh, E.C., "Review of Area Replacement Rules for Pipe Connections in Pressure Vessels and Piping, WRC-335, Welding Research Council, Inc., New York, NY, October 1988.

[15] Miller, C.D. and Moktarian, K., *Proposed Rules for Determining Allowable Compressive Stresses for Cylinders, Cones, Spheres and Formed Heads*, WRC Bulletin 406, Welding Research Council, Inc., New York, NY, 1995.

[16] Svensson, N., "The Bursting Pressure of Cylindrical and Spherical Vessels," Journal of Applied Mechanics, pgs. 326-334, 1958.

[17] Janelle, J., Osage, D.A., and Burkhart, S.J., *An Overview and Validation of the Fitness-For-Service Assessment Procedures for Local Thin Areas*, WRC Bulletin 505, Welding Research Council, Inc., New York, NY, 2005.

2C.10 Tables

Table 2C.1 – Comparison of Design Rules Between VIII-2 and VIII-1

Paragraph in Section VIII, Division 2	Comments Pertaining to Section VIII, Division 1
4.1	General Requirements, harmonized with VIII-1, i.e., $MAWP$ introduced, etc.
4.2	Design Rules for Welded Joints, a restrictive subset of rules in VIII-1, UG & UW
4.3	Design Rules for Shells Under Internal Pressure, mostly new technology
4.4	Design Rules for Shells Under External Pressure and Allowable Compressive Stresses, almost identical to CC2286 with exception of stiffening ring requirements at cone-to-cylinder junctions
4.5	Design Rules for Shells Openings in Shells and Heads, new technology
4.6	Design Rules for Flat Heads, identical to UG-34
4.7	Design Rules for Spherically Dished Bolted Covers, identical to Appendix 1-6 and Appendix 14 except Soehern's stress analysis method for Type 6D Heads is included
4.8	Design Rules for Quick Actuating (Quick Opening) Closures, identical to UG-35.2
4.9	Design Rules for Braced and Stayed Surfaces, a restrictive subset of rules in paragraph UG-47(a)
4.10	Design Rules for Ligaments, identical to paragraph UG-53
4.11	Design Rules for Jacketed Vessels, a more restrictive subset of rules in Appendix 9
4.12	Design Rules for Non-circular vessels, identical to Appendix 13 but re-written for clarity
4.13	Design Rules for Layered Vessels, identical to Part ULW
4.14	Evaluation of Vessels Outside of Tolerance, new technology per API 579-1/ASME FFS-1
4.15	Design Rules for Supports and Attachments, new for VIII-2 using existing technology
4.16	Design Rules for Flanged Joints, almost identical to Appendix 2
4.17	Design Rules for Clamped Connections, identical to Appendix 24
4.18	Design Rules for Shell and Tube Heat Exchangers, identical to Part UHX
4.19	Design Rules for Bellows Expansion Joints, identical to Appendix 26
4.20	Design Rules for Flexible Shell Element Expansion Joints, identical to Appendix 6

Notes:

1. During the VIII-2 re-write project, an effort was made to harmonize the design-by-rule requirements in VIII-2 with VIII-1. As shown in this table, based on this effort, the design rules in VIII-2 are either identical to the rules in VIII-1 or represent a more restrictive subset of the design rules in VIII-1.
2. In the comparison of code rules presented in this table, the term identical is used but is difficult to achieve and maintain because of coordination of ballot items on VIII-1 and VIII-2. There may be slight differences, but the objective is to make the design rules identical. The restrictive subset of the rules in VIII-1 was introduced in VIII-2 mainly in weld details. In general, it was thought by the committee that full penetration welds should be used in most of the construction details of a VIII-2 vessel.

Table 2C.2 – Loads, Load Cases, and Allowable Stresses to Be Considered in an FFS Assessment

Loading Condition	Load Description	Typical Allowable Membrane Stress
Erection	1. Dead load of component less: insulation, fireproofing, piping, all loose internals, catalyst, packing, etc. 2. Temporary loads and forces caused by erection 3. Full wind or earthquake, whichever is greater.	Code of construction design allowable stress as determine in paragraph 2C.2.4.
Pressure Testing	1. Dead load of component plus insulation, fireproofing, installed internals, platforms and other equipment supported from the component in the installed position. 2. Piping loads including pressure thrust 3. Applicable live loads excluding vibration and maintenance live loads. 4. Pressure and fluid loads (water) for testing and flushing equipment and piping unless a pneumatic test is specified. 5. Wind load for a wind speed of 56.3 Km/hr (35 mph).	Code of construction design allowable stress as determined in paragraph 2C.2.4. In addition, the following limits may be considered: 1. Tensile membrane stresses shall not exceed 90% of the minimum specified yield strength at 38°C (100°F) multiplied by the applicable weld joint efficiency. 2. Longitudinal compressive membrane stresses shall not exceed the allowable compressive stress calculated at 38°C (100°F).
Normal Operation	1. Dead load of component plus insulation, refractory, fireproofing, installed internals, catalyst, packing, platforms, and other equipment supported from the component in the installed position. 2. Piping loads including pressure thrust 3. Applicable live loads. 4. Pressure and fluid loading during normal operation. 5. Thermal loads.	Code of construction design allowable stress as determined in paragraph 2C.2.4.
Normal Operation plus Occasional (Note: occasional loads are usually governed by wind and earthquake; however, other load types such as snow and ice loads may govern, see ASCE-7)	1. Dead load of component plus insulation, refractory, fireproofing, installed internals, catalyst, packing, platforms, and other equipment supported from the component in the installed position. 2. Piping loads including pressure thrust 3. Applicable live loads. 4. Pressure and fluid loading during normal operation. 5. Thermal loads 6. Full wind, earthquake, or other occasional loads, whichever is greater.	Code of construction design allowable stress as determined in paragraph 2C.2.4. Load definitions and load case combinations that shall be considered are shown in Annex 2D, Tables 2D.1 and 2D.2, respectively.
Abnormal or Start-up Operation plus Occasional (See Note Above).	1. Dead load of component plus insulation, refractory, fireproofing, installed internals, catalyst, packing, platforms, and other equipment supported from the component in the installed position. 2. Piping loads including pressure thrust 3. Applicable live loads. 4. Pressure and fluid loading associated with the abnormal or start-up conditions 5. Thermal loads 6. Wind load for a wind speed of 35 mph.	Code of construction design allowable stress as determined in paragraph 2C.2.4 modified as follows: Vessels – Abnormal or start-up operation is considered part of normal operation in the ASME B&PV Code; modification of design allowable stress not permitted. Piping – per Paragraph 302.3.5, limits for occasional loads per Paragraph 302.3.6, allowances for pressure and temperature variations per Paragraph 302.2.4. of the ASME B31.3 Piping Code.

2C.11 Figures

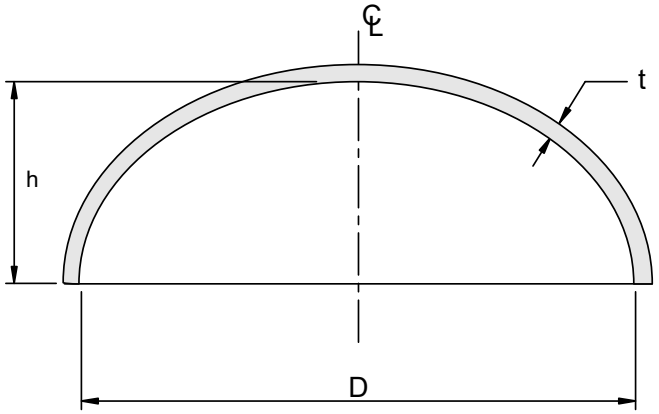

R_{ell}= D/2h

(a) Elliptical Head Geometry

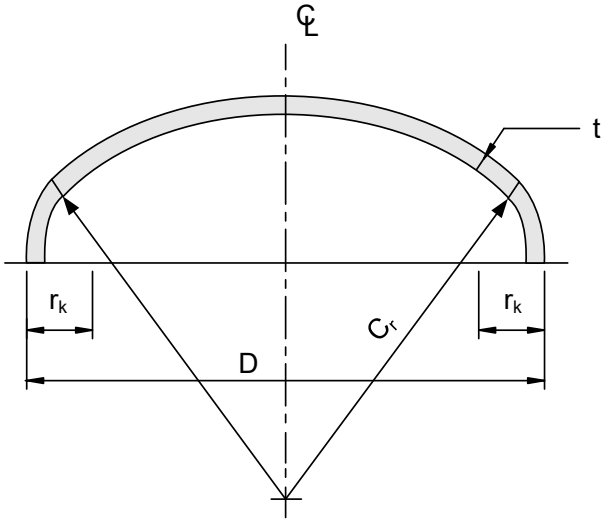

r_k/C_r x 100 ≥ 6%

(b) Torispherical Head Geometry

Figure 2C.1 – Elliptical and Torispherical Head Geometries

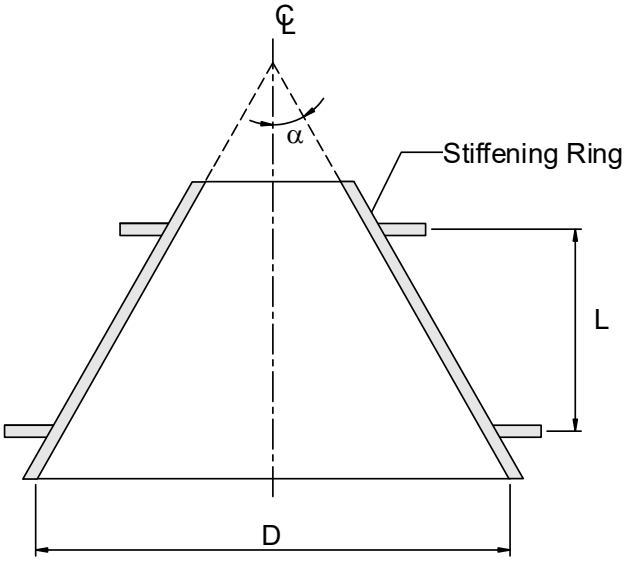

(a) Conical Shell Geometry

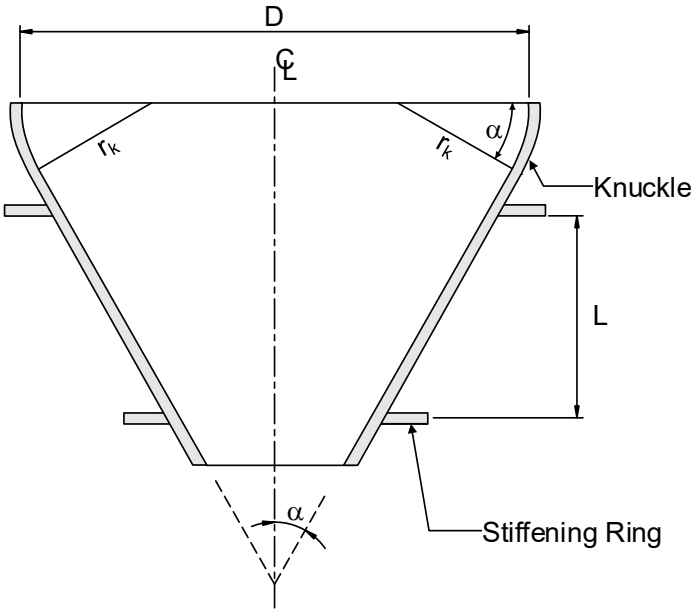

(b) Toriconical Head Geometry

Figure 2C.2 – Conical Shell and Toriconical Head Geometries

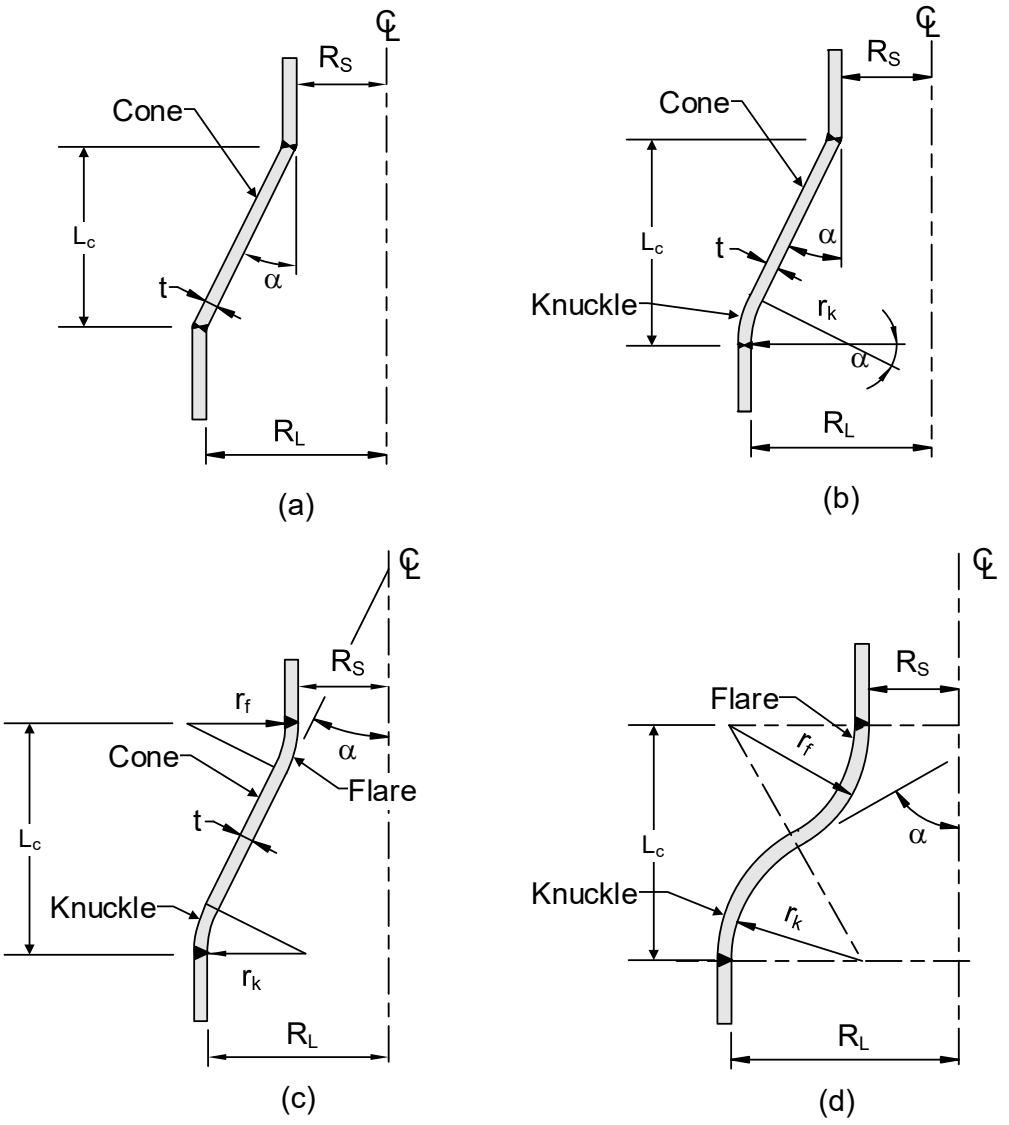

Note: r_k => max[0.12(R_L + t), 3t_c]; R_s has no dimensional requirements.

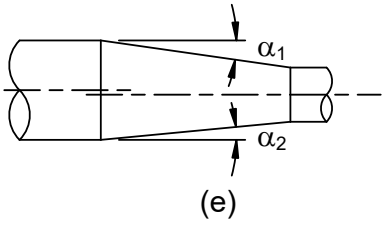

$\alpha_1 > \alpha_2$; Therefore use $\alpha 1$ in design equations.

Figure 2C.3 – Conical Transition Geometries

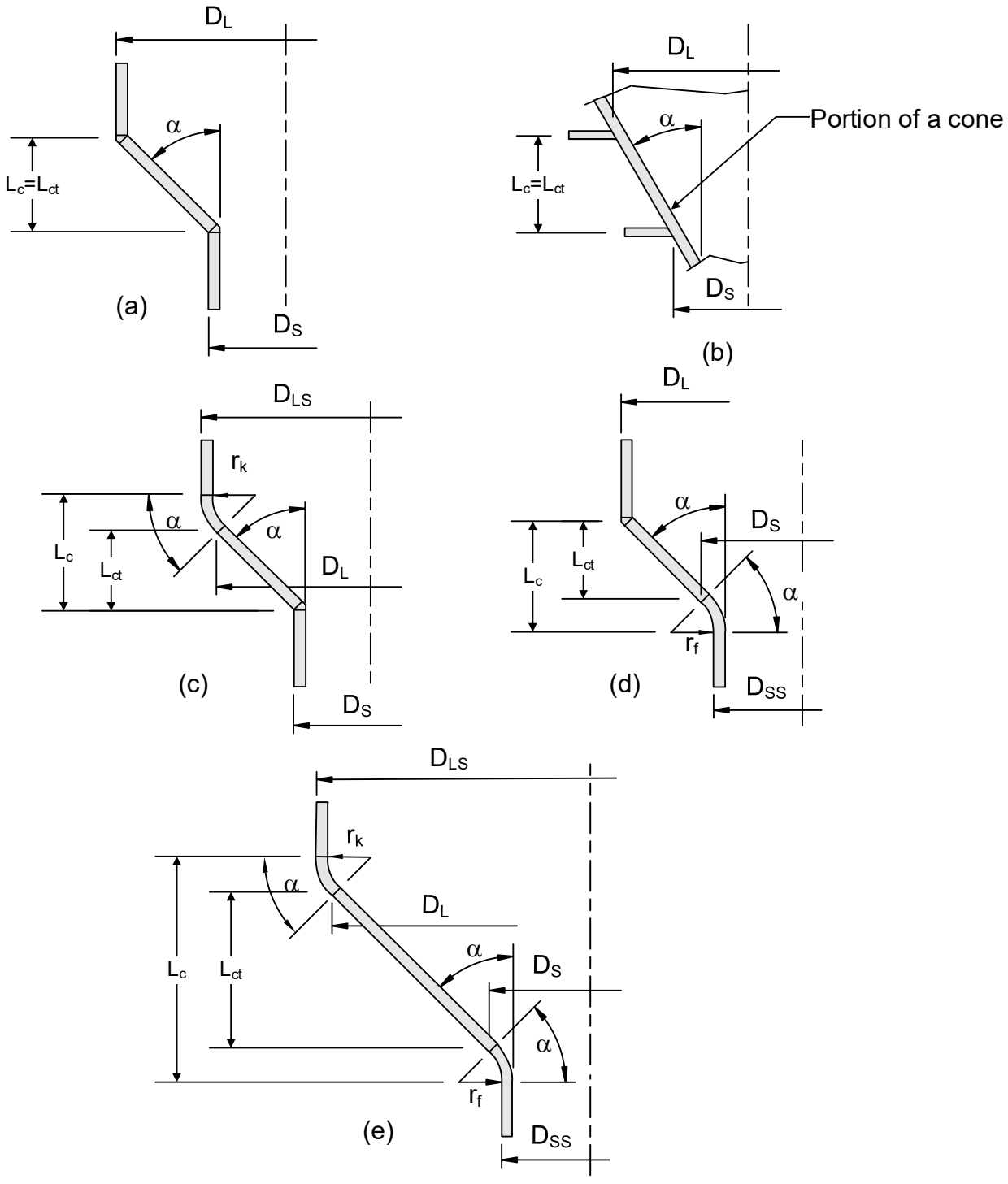

Figure 2C.4 – Unsupported Length for Conical Transitions

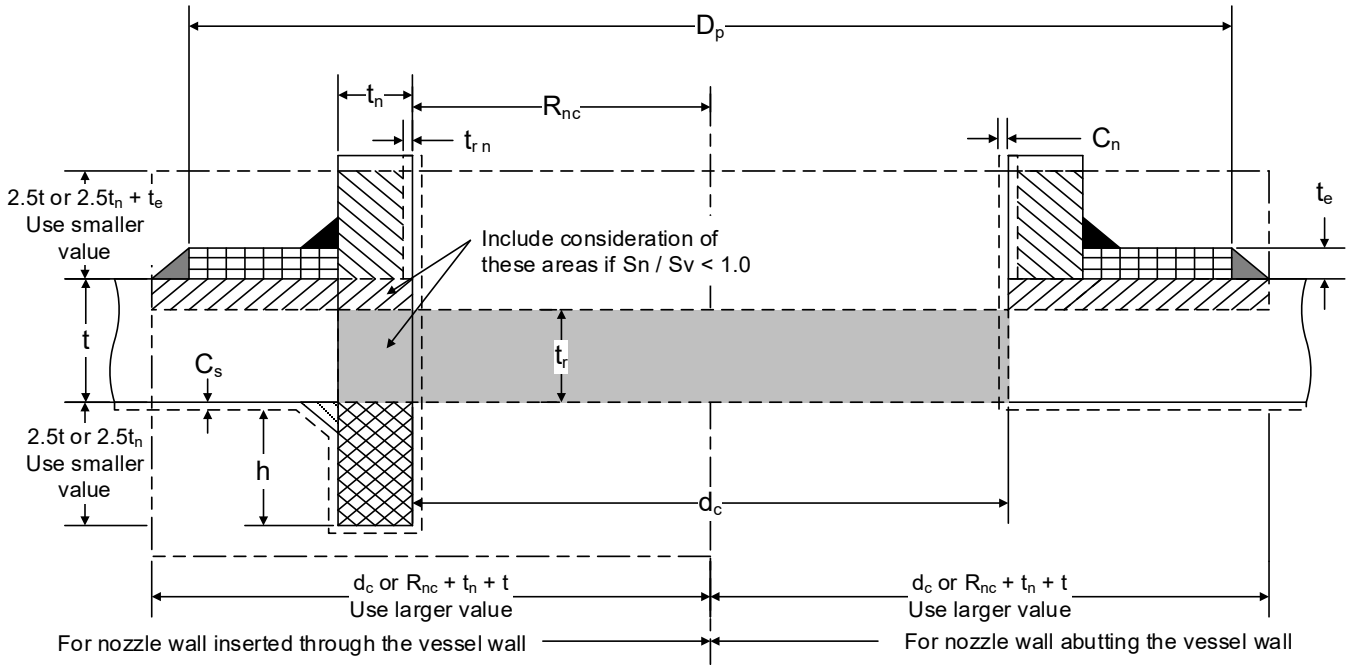

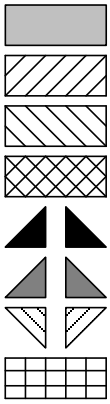

- A_r Required reinforcement area
- A_1 Available reinforcement area in the shell
- A_2 Available reinforcement area in the nozzle
- A_3 Available reinforcement area, inside nozzle projection
- A_{41} Available reinforcement area in the nozzle to pad or vessel weld
- A_{42} Available reinforcement area in the nozzle to weld, inside surface
- A_{43} Available reinforcement area in the reinforcing pad attachment weld
- A_5 Available reinforcement area in the reinforcing pad

Figure 2C.5 – Nozzle Parameters – Area Replacement Method

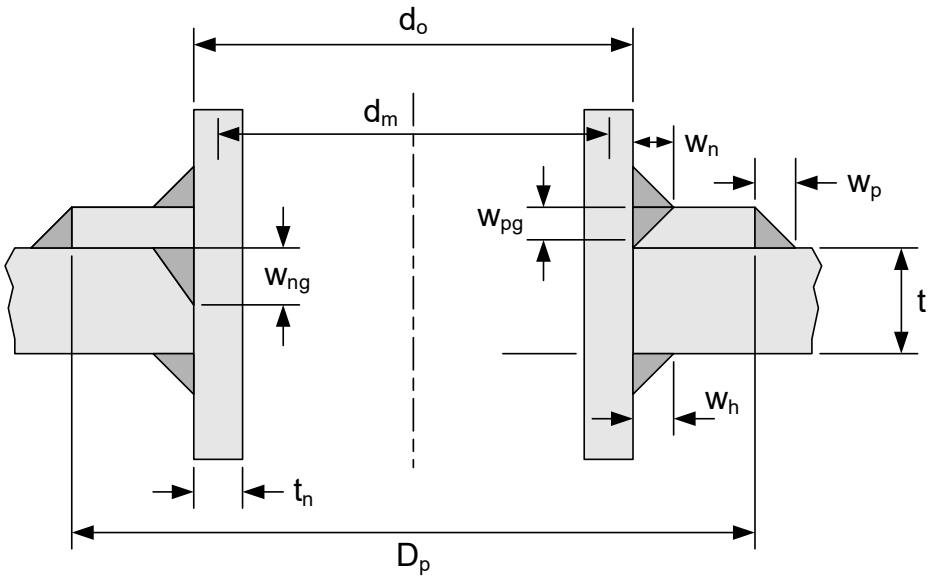

(a) Nozzle and Weld Dimensions

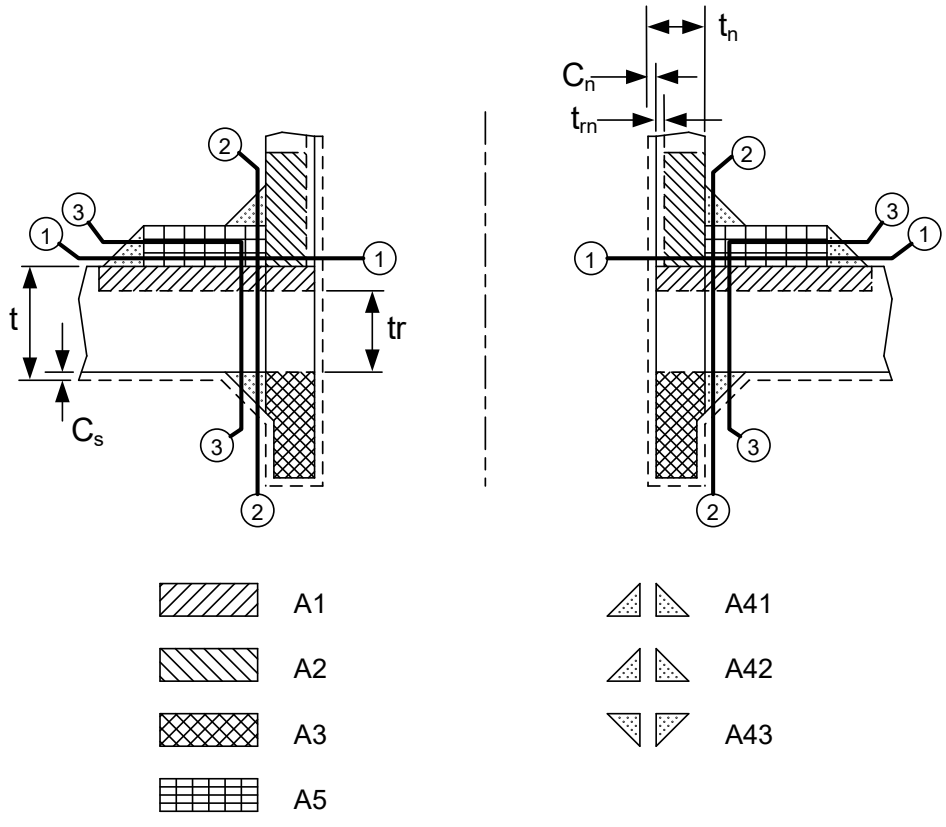

(b) Weld Strength Paths

Figure 2C.6 – Definition of Paths for a Nozzle Weld Strength Analysis – Set-in Nozzle

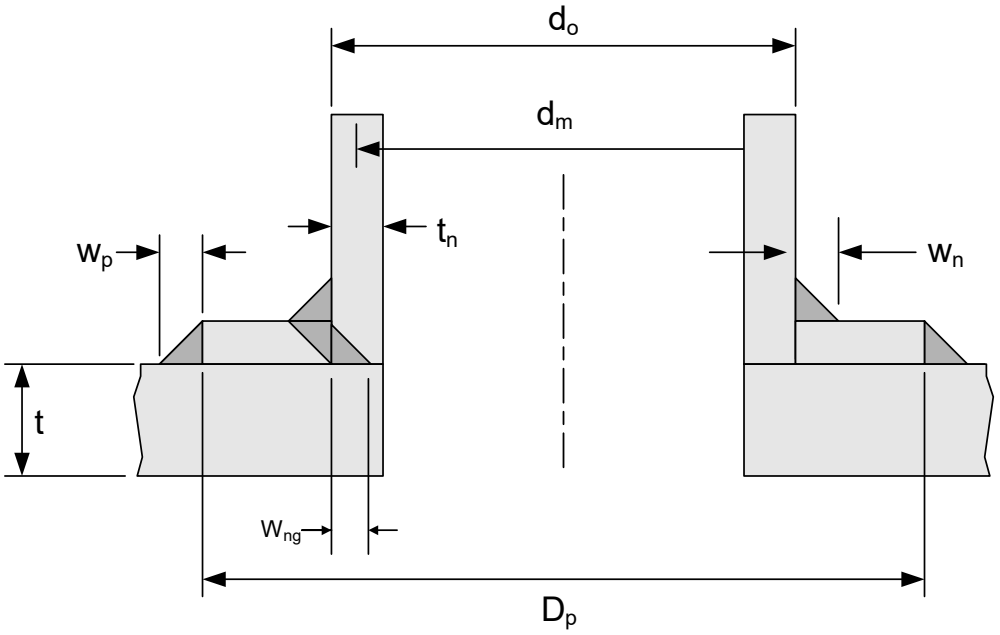

(a) Nozzle and Weld Dimensions

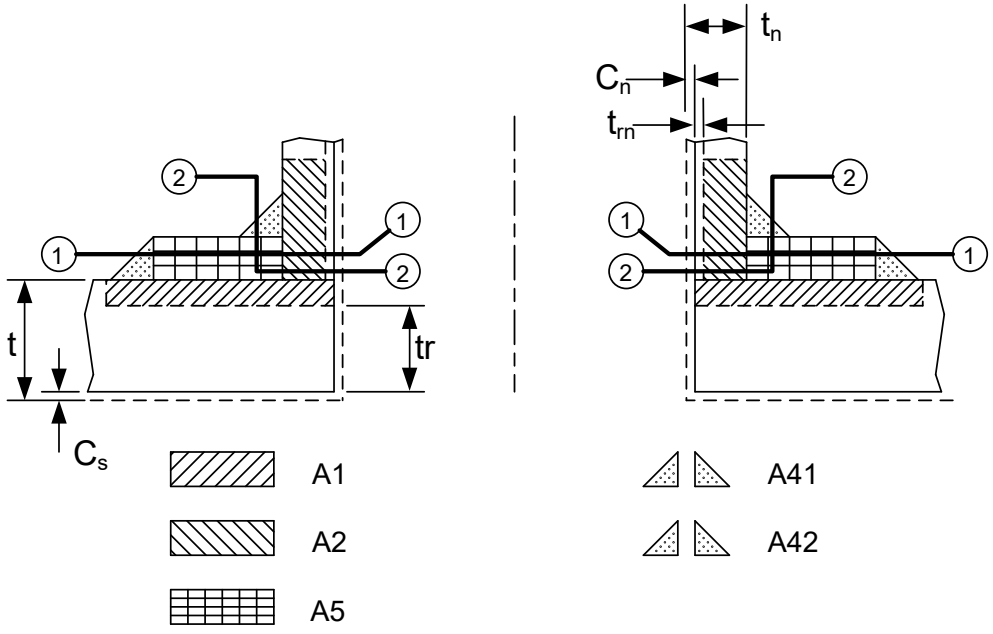

(b) Weld Strength Paths

Figure 2C.7 – Definition of Paths for a Nozzle Weld Strength Analysis – Set-on Nozzle

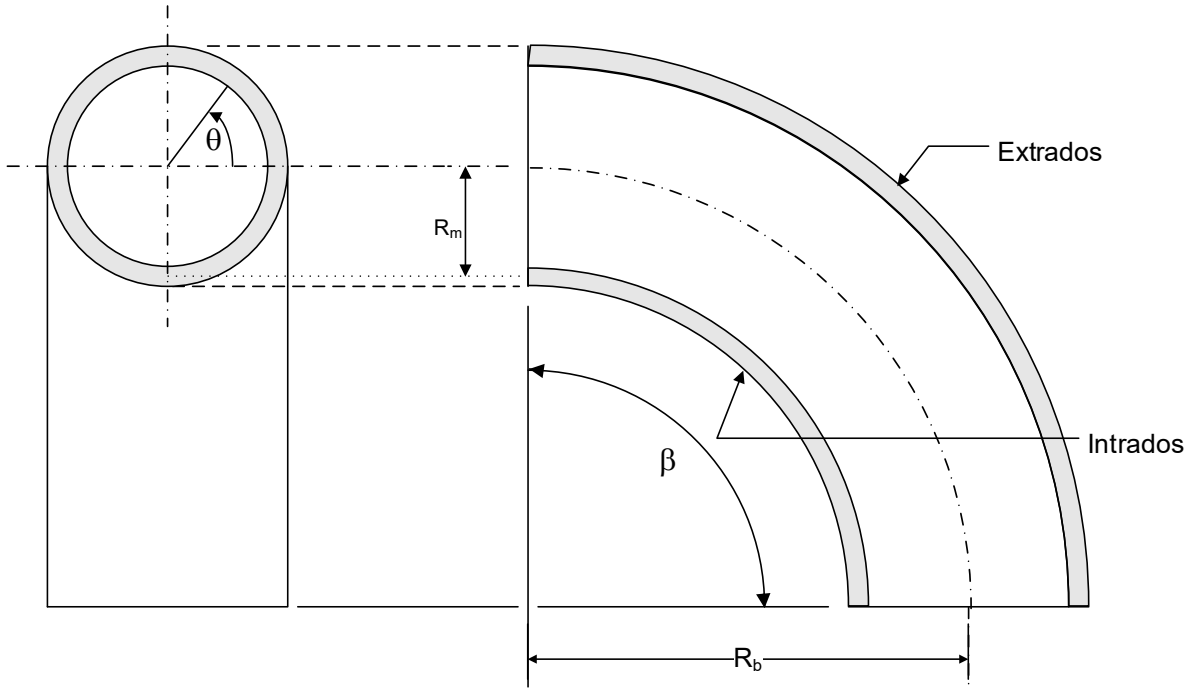

(a) Bend Geometry

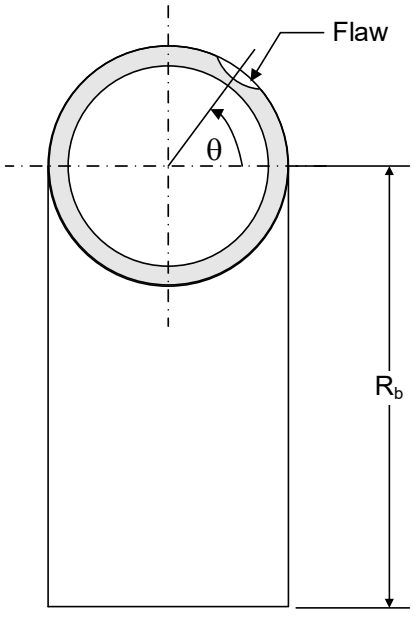

(b) Flaw Location

Figure 2C.8 – Definition of Variables for Piping Bends

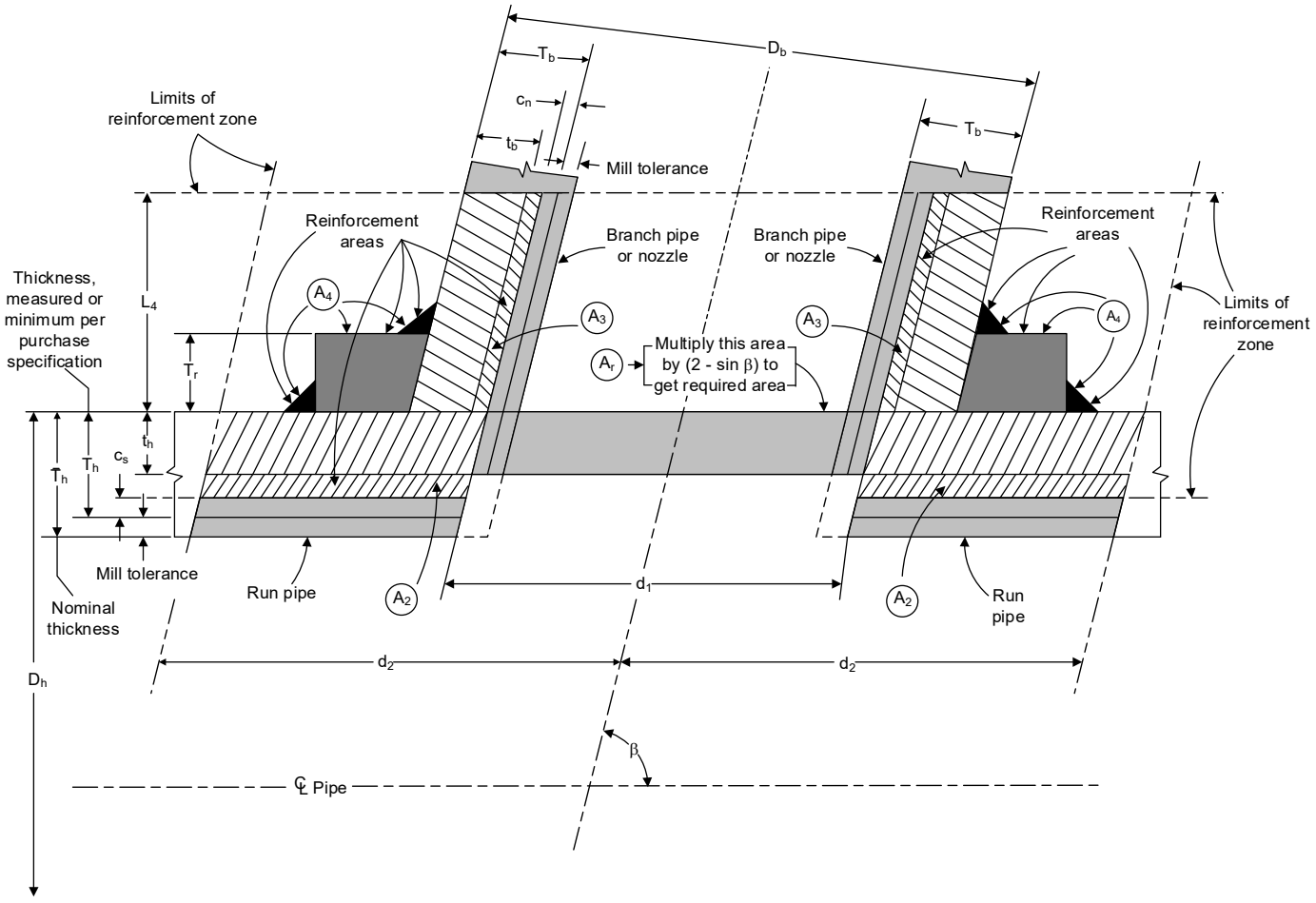

Figure 2C.9 – Definition of Variables for Branch Reinforcement Calculation in Piping Systems

ANNEX 2D – STRESS ANALYSIS OVERVIEW FOR AN FFS ASSESSMENT

(NORMATIVE)

CONTENTS

ANNEX 2D – STRESS ANALYSIS OVERVIEW FOR AN FFS ASSESSMENT 2D-1

2D.1 GENERAL REQUIREMENTS 2D-1
2D.1.1 Scope 2D-1
2D.1.2 ASME B&PV Code, Section VIII, Division 2 (VIII-2) 2D-2
2D.1.3 Applicability 2D-2
2D.1.4 Protection Against Failure Modes 2D-2
2D.1.5 Numerical Analysis 2D-2
2D.1.6 Material Properties 2D-3
2D.1.7 Applicable Loads and Load Case Combinations 2D-3
2D.1.8 Loading Histogram 2D-3
2D.2 PROTECTION AGAINST PLASTIC COLLAPSE 2D-4
2D.2.1 Overview 2D-4
2D.2.2 Elastic Stress Analysis Method 2D-4
2D.2.3 Limit Load Analysis Method 2D-4
2D.2.4 Elastic-Plastic Stress Analysis Method 2D-4
2D.2.5 Treatment of the Weld Joint Efficiency 2D-5
2D.3 PROTECTION AGAINST LOCAL FAILURE 2D-5
2D.3.1 Overview 2D-5
2D.3.2 Elastic Analysis Method 2D-6
2D.3.3 Elastic-Plastic Analysis Method 2D-6
2D.4 PROTECTION AGAINST COLLAPSE FROM BUCKLING 2D-6
2D.4.1 Assessment Procedure 2D-6
2D.4.2 Supplemental Requirements for Components with Flaws 2D-6
2D.5 SUPPLEMENTAL REQUIREMENTS FOR STRESS CLASSIFICATION IN NOZZLE NECKS 2D-6
2D.6 NOMENCLATURE 2D-7
2D.7 REFERENCES 2D-7
2D.8 TABLES 2D-8

2D.1 General Requirements

2D.1.1 Scope

The analytical methods contained within this Annex can be used for stress analysis when performing a Fitness-For-Service (FFS) Assessment of a component with a volumetric flaw. These methods are typically employed in either a Level 2 or Level 3 Assessment. Detailed assessment procedures utilizing the results from a stress analysis are provided to evaluate components for plastic collapse, local failure, and buckling.

Recommendations are provided on how to perform and utilize results from a stress analysis in an FFS Assessment. Procedures for performing linear and non-linear analysis, determination of stress categories and classification of stress results obtained from a linear analysis, and a methodology to perform an elastic-plastic analysis to determine a collapse load or to perform a fatigue evaluation are among the items covered in this Annex.

2D.1.2 ASME B&PV Code, Section VIII, Division 2 (VIII-2)

The stress analysis methods in this Annex are based on ASME B&PV Code, Section VIII, Division 2 (VIII-2), Part 5. The methods in this Annex reference VIII-2 directly and provide exceptions that are to be used in an FFS Assessment.

2D.1.3 Applicability

The assessment procedures in this Annex may only be used if the allowable stress from the applicable construction code evaluated at the design temperature is governed by time-independent properties unless otherwise noted in a specific design procedure. If the allowable stress from the applicable construction code evaluated at the design temperature is governed by time-dependent properties and the fatigue screening criteria of Part 14 are satisfied, then the elastic stress analysis procedures in this Annex may be used.

2D.1.4 Protection Against Failure Modes

The analysis requirements for volumetric flaws are organized based on protection against the failure modes listed below. If multiple assessment procedures are provided for a failure mode, only one of these procedures must be satisfied to qualify the component for continued operation. In addition, the component shall be evaluated for each applicable failure mode.

a) Protection Against Plastic Collapse – The requirements of paragraph 2D.2 shall be satisfied.

b) Protection Against Local Failure – The requirements of paragraph 2D.3 shall be satisfied.

c) Protection Against Collapse from Buckling – The requirements of paragraph 2D.4 shall be satisfied.

d) Protection Against Creep or Creep-Fatigue Damage – Assessment procedures for components subject to cyclic operation in the creep regime are covered in Part 10.

e) Protection Against Fatigue Damage – Assessment procedures for components subject to cyclic operation below the creep regime are covered in Part 14.

2D.1.5 Numerical Analysis

a) The assessment methods in this Annex are based on the use of results obtained from a detailed stress analysis of a component. Depending on the loading condition, a thermal analysis to determine the temperature distribution and resulting thermal stresses may also be required.

b) Procedures are provided for performing stress analyses to determine protection against plastic collapse, local failure, buckling, and cyclic loading. These procedures provide the necessary details to obtain a consistent result with regards to development of loading conditions, selection of material properties, post-processing of results, and comparison to acceptance criteria to determine the suitability of a component.

c) Recommendations on a stress analysis method, modeling of a component, and validation of analysis results are not provided. While these aspects of the assessment process are important and shall be considered in the analysis, a detailed treatment of the subject is not provided because of the variability in approaches and design processes. However, an accurate stress analysis including validation of results shall be provided as part of the assessment.

2D.1.6 Material Properties

The following material properties for use in the stress analysis may be determined using the data and material models in Annex 2E. Material properties may also be obtained from test data from the actual material being evaluated.

a) Physical properties – Young's Modulus, thermal expansion coefficient, thermal conductivity, thermal diffusivity, density, Poisson's ratio.

b) Strength Parameters – Allowable stress, minimum specified yield strength, minimum specified tensile strength.

c) Monotonic Stress-Strain Curve – Elastic perfectly plastic and elastic-plastic true stress-strain curve with strain hardening.

d) Cyclic Stress-Strain Curve – Stabilized true stress-strain amplitude curve.

2D.1.7 Applicable Loads and Load Case Combinations

a) All applicable applied loads on the component shall be considered when performing an FFS Assessment. Supplemental loads shall be considered in addition to the applied pressure in the form of applicable load cases. An overview of the supplemental loads and loading conditions that shall be considered in a design are shown in Annex 2C, Table 2C.2.

b) Load case combinations shall be considered in the FFS Assessment.

   1) Load definitions and load case combination for elastic analysis are defined in VIII-2, Part 5, Table 5.2 and 5.3.

   2) Load definitions and load case combinations for limit analysis and elastic-plastic analysis are defined in Table 2D.1, Table 2D.2 and Table 2D.3, respectively.

   3) In evaluating load cases involving the pressure term, P, the effects of the pressure being equal to zero shall be considered.

   4) The applicable load case combinations shall be considered in addition to any other combinations defined by the Owner-User.

2D.1.8 Loading Histogram

If any of the loads vary with time, a loading histogram shall be developed to show the time variation of each specific load. The loads in the histogram shall satisfy the requirements of this Annex. In addition, these loads shall be evaluated for creep, fatigue, or creep-fatigue in accordance with Part 10 and Part 14, as applicable.

a) The loading histogram shall include all significant operating temperatures, pressures, supplemental loads, and the corresponding cycles or time periods for all significant events that are applied to the component. The following shall be considered in developing the loading histogram.

   1) The number of cycles associated with each event during the operation life, these events shall include start-ups, normal operation, upset conditions, and shutdowns.

   2) When creating the histogram, the history to be used in the assessment shall be based on the anticipated sequence of operation.

3) Applicable loadings such as pressure, temperature, supplemental loads such as weight, support displacements, and nozzle reaction loadings.

4) The relationship between the applied loadings during the time history.

b) If an accurate histogram cannot be generated, then an approximate histogram shall be developed based on information obtained from plant personnel. This information shall include a description of all assumptions made and include a discussion of the accuracy in establishing points on the histogram. A sensitivity analysis (see Part 2, paragraph 2.4.3.1) shall be included in the FFS Assessment to determine and evaluate the effects of the assumptions made to develop the operating history.

2D.2 Protection Against Plastic Collapse

2D.2.1 Overview

Three alternative analysis methods are provided in VIII-2, Part 5 for evaluating protection against plastic collapse. A brief description of the analysis methods is provided below.

a) Elastic Stress Analysis Method – Stresses are computed using an elastic analysis, classified into categories, and limited to allowable values that have been conservatively established such that a plastic collapse will not occur.

b) Limit Load Method – A calculation is performed to determine a lower bound to the limit load of a component. The allowable load on the component is established by applying design factors to the limit load such that the onset of gross plastic deformations (plastic collapse) will not occur.

c) Elastic-Plastic Stress Analysis Method – A collapse load is derived from an elastic-plastic analysis considering both the applied loading and deformation characteristics of the component. The allowable load on the component is established by applying design factors to the plastic collapse load.

2D.2.2 Elastic Stress Analysis Method

a) Assessment procedure – The assessment procedures for the Elastic Stress Analysis Method including the basis for determining stresses based on elastic analysis, stress categorization, and linearization shall be in accordance with VIII-2, Part 5, paragraph 5.2.2 except that the allowable stresses that incorporate the Allowable Remaining Strength Factor (RSF_a) may be used in the assessment, i.e., S/RSF_a and S_{PL}/RSF_a.

b) Allowable Equivalent Stress – The allowable equivalent stress, S, to be used in conjunction with the Elastic Stress Analysis Method in an FFS Assessment is the allowable stress from the original construction code.

2D.2.3 Limit Load Analysis Method

The assessment procedures for the Limit Load Analysis Method shall be in accordance with VIII-2, Part 5, paragraph 5.2.3 except that the load case combinations that incorporate the Allowable Remaining Strength Factor (RSF_a) as shown in Table 2D.2 may be used in the assessment, and the yield strength used in the limit load analysis shall be based on the following:

$$\sigma_{ysll} = \min\left[1.5S,\ S_y\right] \tag{2D.1}$$

2D.2.4 Elastic-Plastic Stress Analysis Method

The assessment procedures for the Elastic-Plastic Analysis Method shall be in accordance with VIII-2, Part 5, paragraph 5.2.4 except that the load case combinations that incorporate the construction code design margin and

the RSF_a as shown in Table 2D.3 shall be used in the assessment. The value of β in Table 2D.3 is shown in Table 2D.4 as a function of the construction code.

2D.2.5 Treatment of the Weld Joint Efficiency

The weld joint efficiency is included in the analysis through either Method A or B as detailed below. Method A takes a global approach and Method B takes a local approach. The material response guidelines in Method B can be applied to an entire component or specifically to a weld band region as defined in paragraph 2C.2.5.

a) Method A

- Elastic Stress Analysis – The material allowable stress is reduced by multiplying by the governing weld joint efficiency.
- Limit Load Analysis – The limit load is computed and subsequently reduced by the governing weld joint efficiency or the load multipliers on sustained loads as defined in paragraph 2D.2.3 are increased by multiplying by the inverse of the governing weld joint efficiency prior to determination of the limit load.
- Elastic-Plastic Analysis – The load multipliers on sustained loads as defined in paragraph 2D.2.4 are increased by multiplying by the inverse of the governing weld joint efficiency prior to determination of the plastic collapse load. The material true stress-strain curve is unaffected.

b) Method B

- Elastic Stress Analysis – The allowable stress for a component or weld band region shall be multiplied by the weld joint efficiency for the weld.
- Limit Load Analysis – The elastic perfectly-plastic yield strength limit for a component or weld band region shall be multiplied by the weld joint efficiency for the weld. The load multipliers used in the analysis are as defined in paragraph 2D.2.3.
- Elastic-Plastic Analysis – When defining the material true stress-strain curve for a component or weld band region, both the engineering yield strength and the engineering ultimate tensile strength shall be multiplied by the weld joint efficiency for the weld. The load multipliers used in the analysis are as defined in paragraph 2D.2.4.

2D.3 Protection Against Local Failure

2D.3.1 Overview

In addition to demonstrating protection against plastic collapse as defined in paragraph 2D.2, the applicable local failure criteria below shall be satisfied for a component. The strain limit criterion typically does not need to be evaluated if the component design is in accordance with the applicable construction code and the presence of a flaw does not result in a significant strain concentration. If the significance of a strain concentration cannot be established, then the strain limit criterion should be evaluated as part of the assessment.

Two analysis methodologies are provided for evaluating protection against local failure to limit the potential for fracture under applied design loads.

a) Elastic Analysis Method – An approximation of the protection against local failure based on the results of an elastic analysis.

b) Elastic-Plastic Analysis Method – A more accurate estimate of the protection against local failure of a component is obtained based on the results of an elastic-plastic stress analysis.

If a limit load analysis is used to evaluate protection against plastic collapse, the elastic-plastic analysis method for local failure shall be used to evaluate protection against local failure (see Table 2D.2).

2D.3.2 Elastic Analysis Method

The assessment procedures for the Elastic Analysis Method shall be in accordance with VIII-2, Part 5, paragraph 5.3.2 except the acceptance criterion may be $4S/RSF_a$ rather than $4S$.

2D.3.3 Elastic-Plastic Analysis Method

The assessment procedures for the Elastic-Plastic Analysis Method shall be in accordance with VIII-2, Part 5, paragraph 5.3.3 except that the RSF_a may be applied for load case combinations as shown in Table 2D.3.

2D.4 Protection Against Collapse from Buckling

2D.4.1 Assessment Procedure

The assessment procedures for Protection Against Collapse from Buckling shall be in accordance with VIII-2, Part 5, paragraph 5.4 except that the buckling load computed using these procedures may be divided by $\max[RSF_a, 0.9]$ to determine the permissible buckling load.

2D.4.2 Supplemental Requirements for Components with Flaws

a) Assessment of the structural stability of a component with flaws should consider growth aspects and remaining life. The location, size and reduced thickness associated with a flaw will affect the structural stability of a component. Therefore, the assessment should be performed for the flaw size at the end of its useful life. For volumetric-type flaws, account should be taken of the possibility of increased metal loss and expansion of the corroded area with time. For crack-like flaws, account should be taken of the possibility of crack growth by fatigue, corrosion-fatigue, stress corrosion cracking and creep.

b) The significance of planar flaws parallel to a plate or shell surface in the direction of compressive stress (laminations, laminar tears, etc.) should be assessed by checking the buckling strength of each part of the material between the flaw and the component surface. This may be done by calculation as if the individual parts of the material are separate plates of the same area as the flaw using the distance between the flaw and the surface as an effective thickness.

c) If a flaw occurs parallel to the surface under the weld attaching a stiffener to a shell or plate loaded in compression, it will reduce the effective length over which the stiffener is attached to the plate. If a flaw of this type is located, it should be assessed assuming that the stiffener is intermittently welded to the plate and that the flaw forms a "space" between two welds. Rules for determining the allowable weld spacing for stiffener attachment from the original design code may be used in this evaluation.

d) The allowable compressive stress for a shell component with a flaw can be established using the compressive stress equations in VIII-2, Part 4, paragraph 4.4. The thickness to be used in the compressive stress calculation should be the minimum thickness less any future corrosion allowance unless another thickness can be justified.

2D.5 Supplemental Requirements for Stress Classification in Nozzle Necks

Classification of stresses for nozzle necks shall be in accordance with VIII-2, Part 5, paragraph 5.6.

2D.6 Nomenclature

β load multiplier used in an elastic-plastic analysis that is based on a design margin in a construction code.

F design factor used in the ASME B31.4, B31.8 and B31.12 Piping Codes.

H_f materials performance factor for pipelines used in the ASME B31.12 Piping Code.

M a design margin of the construction code.

M_f materials performance factor for industrial piping used in the ASME B31.12 Piping Code.

RSF_a allowable remaining strength factor (see Part 2).

S allowable stress based on the material of construction, design temperature, and construction code.

S_y yield strength based on the material of construction, design temperature, and construction code.

S_T allowable stress based on the material of construction, pressure-test temperature, and construction code.

S_{PL} allowable limit on the local primary membrane and local primary membrane plus bending stress categories (see VIII-2, Part 5).

σ_{ysll} yield strength to be used in a limit-load analysis.

T design load parameter to represent the self-restraining load case or the temperature derating factor used in the ASME B31.8 and B31.12 Piping Codes.

2D.7 References

[1] Bushnell D., Computerized Buckling Analysis and Shells, Kluwer Academic Publishers, Norwell, MA, 1985.

[2] Gerdeen, J.C., Rodabaugh, E.C., and O'Donnell, W.J., A Critical Evaluation of Plastic Behavior Data and a Unified Definition of Plastic Loads for Pressure Components, WRC Bulletin 254, Welding Research Council, Inc., New York, NY, 1979.

[3] Miline, I., Ainsworth, R.A., Dowling, A.R., and Stewart, A.T., "Assessment of the Integrity of Structures Containing Defects," International Journal of Pressure Vessels and Piping 32, 1988, pp. 66-72.

[4] Osage, D., ASME Section VIII – Division 2 Criteria and Commentary, PTB-1-2013, ASME, New York, NY, 2014.

[5] Osage, D.A., Krishnaswamy, P., Stephens, D.R., Scott, P., Janelle, J., Mohan, R., and Wilkowski, G.M., *Technologies for the Evaluation of Non-Crack-Like Flaws in Pressurized Components – Erosion/Corrosion, Pitting, Blisters, Shell Out-Of-Roundness, Weld Misalignment, Bulges and Dents*, WRC Bulletin 465, Welding Research Council, Inc., New York, NY, September 2001.

[6] Sowinski, J.C., Osage, D.A., and Brown, R.G., *ASME Section VIII - Division 2 Example Problem Manual*, PTB-3-2013, ASME, New York, NY, 2013.

[7] 3DS Simulia, Abaqus/CAE User's Guide, Dassault Systèmes.

2D.8 Tables

Table 2D.1 – Load Descriptions

Design Load Parameter	Description
P	Internal and external maximum allowable working pressure
P_s	Static head from liquid or bulk materials (e.g., catalyst)
D	Dead weight of the vessel, contents, and appurtenances at the location of interest, including the following: • Weight of vessel including internals, supports (e.g., skirts, lugs, saddles, and legs), and appurtenances (e.g., platforms, ladders, etc.) • Weight of vessel contents under operating and test conditions • Refractory linings, insulation • Static reactions from the weight of attached equipment, such as motors, machinery, other vessels, and piping • Transportation loads
L	• Appurtenance live loading • Effects of fluid momentum, steady state and transient • Wave loading
E	Earthquake loads (for example, see ASCE/SEI 7 for the specific definition of the earthquake load, as applicable)
W	Wind Loads
W_{pt}	The pressure-test wind load case. The design wind speed for this case shall be specified by the Owner-User.
S_s	Snow Loads
T	Is the self-restraining load case (i.e., thermal loads, applied displacements). This load case does not typically affect the collapse load but should be considered in cases where elastic follow-up causes stresses that do not relax sufficiently to redistribute the load without excessive deformation.

Table 2D.2 – Load Case Combinations and Load Factors for a Limit-Load Analysis

Design Conditions		
Criteria	**Required Factored Load Combinations**	
Global Criteria	Load Case	Load Combination
	1	$\left[1.5\left(P+P_s+D\right)\right]\cdot RSF_a$
	2	$\left[1.3\left(P+P_s+D+T\right)+1.7L+0.54S_s\right]\cdot RSF_a$
	3	$\left[1.3\left(P+P_s+D\right)+1.7S_s+\left(1.1L\ or\ \ 0.54W\right)\right]\cdot RSF_a$
	4	$\left[1.3\left(P+P_s+D\right)+1.1W+1.1L+0.54S_s\right]\cdot RSF_a$
	5	$\left[1.3\left(P+P_s+D\right)+1.1E+1.1L+0.21S_s\right]\cdot RSF_a$
Local Criteria	Per Table 2D.3 using an Elastic-Plastic Analysis.	
Serviceability Criteria	Per User's Design Specification, if applicable (see VIII-2, Part 5, paragraph 5.2.4.3.b).	
Hydrostatic Test Conditions		
Global Criteria	$\max\left[1.43, 1.25\left(\frac{S_T}{S}\right)\right]\cdot\left(P+P_s+D\right)+W_{pt}$	
Serviceability Criteria	Per User's Design Specification, if applicable.	
Pneumatic Test Conditions		
Global Criteria	$1.15\left(\frac{S_T}{S}\right)\cdot\left(P+P_s+D\right)+W_{pt}$	
Serviceability Criteria	Per User's Design Specification, if applicable.	

Notes:
1. The parameters used in the Design Load Combination column are defined in Table 2D.1. See VIII-2, Part 5, paragraph 5.2.3.4 for descriptions of global and serviceability criteria.
2. Loads listed herein shall be considered to act in the combinations described above; whichever produces the most unfavorable effect in the component being considered. Effects of one or more loads not acting shall be considered.

Table 2D.3– Load Case Combinations and Load Factors for an Elastic-Plastic Analysis

Design Conditions		
Criteria	**Required Factored Load Combinations**	
Global Criteria	Load Case	Load Combination
	1	$\beta\left(P+P_s+D\right)$
	2	$0.88\beta\left(P+P_s+D+T\right)+1.13\beta L+0.36\beta S_s$
	3	$0.88\beta\left(P+P_s+D\right)+1.13\beta S_s+\left(0.71\beta L \text{ or } 0.36\beta W\right)$
	4	$0.88\beta\left(P+P_s+D\right)+0.71\beta W+0.71\beta L+0.36\beta S_s$
	5	$0.88\beta\left(P+P_s+D\right)+0.71\beta E+0.71\beta L+0.14\beta S_s$
Local Criteria	$1.7\left(P+P_s+D\right)\cdot RSF_a$	
Serviceability Criteria	Per User's Design Specification, if applicable (see VIII-2, Part 5, paragraph 5.2.4.3.b).	
Hydrostatic Test Conditions		
Global and Local Criteria	$\max\left[0.95\beta,\ 0.83\beta\left(\frac{S_T}{S}\right)\right]\cdot\left(P+P_s+D\right)+0.42\beta W_{pt}$	
Serviceability Criteria	Per User's Design Specification, if applicable.	
Pneumatic Test Conditions		
Global and Local Criteria	$0.75\beta\left(\frac{S_T}{S}\right)\cdot\left(P+P_s+D\right)+0.42\beta W_{pt}$	
Serviceability Criteria	Per User's Design Specification, if applicable.	

Notes:

1. The parameters used in the Design Load Combination column are defined in Table 2D.1. See VIII-2, Part 5, paragraph 5.2.4.3 for descriptions of global and serviceability criteria.
2. Loads listed herein shall be considered to act in the combinations described above; whichever produces the most unfavorable effect in the component being considered. Effects of one or more loads not acting shall be considered.

Table 2D.4 – Values of M and β for an FFS Assessment Based on Elastic-Plastic Analysis

Construction Code	Design Margin, M (1)	β (2)
PD 5500	2.35	$M \cdot RSF_a$
EN 13345	2.4	$M \cdot RSF_a$
ASME Section VIII, Division 2, 2017 Edition and later, Class 1 Vessel	3.0	$M \cdot RSF_a$
ASME Section VIII, Division 2, 2017 Edition and later, Class 2 Vessel	2.4	$M \cdot RSF_a$
ASME Section VIII, Division 2, 2007 up to the 2017 Edition	2.4	$M \cdot RSF_a$
ASME Section VIII, Division 2, prior to the 2007 Edition	3.0	$M \cdot RSF_a$
ASME Section VIII, Division 1, 1999 Addenda of the 1998 Edition and later	3.5	$M \cdot RSF_a$
ASME Section VIII, Division 1, 1968 Edition up to the 1999 Addenda of the 1998 Edition	4.0	$M \cdot RSF_a$
ASME Section VIII, 1950 Edition up to the 1968 Edition	4.0	$M \cdot RSF_a$
ASME Section VIII, prior to the 1950 Edition (3)	5.0	$M \cdot RSF_a$
API-ASME Code 1934-1954 (3)	4.0	$M \cdot RSF_a$
API 650	2.5	$M \cdot RSF_a$
API 620	3.3	$M \cdot RSF_a$
ASME B31.1 2007 Edition and later	3.5	$M \cdot RSF_a$
ASME B31.1 prior to the 2007 Edition	4.0	$M \cdot RSF_a$
ASME B31.3	3.0	$M \cdot RSF_a$
ASME B31.4	$\frac{1}{F}$	$\max\left[1.25,\ M \cdot RSF_a\right]$

Table 2D.4 – Values of M and β for an FFS Assessment Based on Elastic-Plastic Analysis

Construction Code	Design Margin, M (1)	β (2)
ASME B31.8	$\frac{1}{F \cdot T}$	$\max\left[1.25,\ M \cdot RSF_a\right]$
ASME B31.12 – Industrial Piping	$\frac{3.0}{M_f}$	$M \cdot RSF_a$
ASME B31.12 – Pipelines	$\frac{1}{F \cdot T \cdot H_f}$	$\max\left[1.25,\ M \cdot RSF_a\right]$

Notes:
1. For the ASME B31.4, ASME B31.8, and B31.12 Piping Codes, the value of Beta $(\beta)$is determined differently because the design margin in these codes is applied to the specified minimum yield strength while design margins in the other codes is applied to both the yield strength and the specified ultimate tensile strength.
2. Beta $(\beta)$is used in Table 2D.3.
3. A quality factor for some materials was applied to the margin on the Minimum Ultimate Tensile Strength, this factor is noted in the applicable code and shall be applied to the design margin shown in this table.

ANNEX 2E – MATERIAL PROPERTIES FOR STRESS ANALYSIS

(NORMATIVE)

CONTENTS

ANNEX 2E – MATERIAL PROPERTIES FOR STRESS ANALYSIS 2E-1

2E.1 GENERAL 2E-1
2E.1.1 Material Properties Required 2E-1
2E.1.2 Material Properties and In-Service Degradation 2E-2
2E.2 STRENGTH PARAMETERS 2E-2
2E.2.1 Yield and Tensile Strength 2E-2
2E.2.1.1 Mean Estimates of Tensile Strength from Hardness Tests 2E-2
2E.2.1.2 Minimum Specified Yield and Tensile Strength from MPC Correlations 2E-2
2E.2.1.3 Minimum Specified Yield and Tensile Strength from API Std 530 and WRC Bulletin 541 ..... 2E-3
2E.2.1.4 Minimum Specified Yield and Tensile Strength Data from ASME Code, Section II, Part D 2E-3
2E.2.1.5 Mean Values of Yield and tensile Strength from Minimum Specified Values 2E-3
2E.2.2 Flow Stress 2E-3
2E.2.2.1 Definition 2E-3
2E.2.2.2 Estimation of Flow Stress 2E-3
2E.3 MONOTONIC STRESS-STRAIN RELATIONSHIPS 2E-4
2E.3.1 MPC True Stress-Strain Curve Model 2E-4
2E.3.2 MPC Tangent Modulus Model 2E-5
2E.3.3 Ramberg-Osgood Stress-Strain Model 2E-6
2E.3.3.1 True Stress-Strain Curve 2E-6
2E.3.3.2 Engineering Stress-Strain Curve 2E-7
2E.3.4 Ramberg-Osgood Tangent Modulus Model 2E-8
2E.3.5 Engineering Stress-Strain Models for API 5L Pipeline Materials 2E-8
2E.3.5.1 Stress-Strain Model from CSA Z662 ..... 2E-8
2E.3.5.2 API 5L Grades X52 to X80 ..... 2E-8
2E.3.5.3 API 5L Grades X80 to X100 ..... 2E-8
2E.3.6 Tangent Modulus Model for API 5L Pipeline Materials 2E-10
2E.4 CYCLIC STRESS-STRAIN RELATIONSHIPS 2E-10
2E.4.1 Ramberg-Osgood Equation 2E-10
2E.4.2 Estimation of Cyclic Stress-Strain Curve Parameters 2E-10
2E.4.2.1 Estimation from Monotonic Properties 2E-10
2E.4.2.2 Uniform Material Law 2E-11
2E.5 PHYSICAL PROPERTIES 2E-11
2E.5.1 Elastic Modulus 2E-11
2E.5.2 Poisson's Ratio 2E-11
2E.5.3 Coefficient of Thermal Expansion 2E-11
2E.5.4 Thermal Conductivity 2E-11
2E.5.5 Thermal Diffusivity 2E-11
2E.5.6 Density 2E-12
2E.6 NOMENCLATURE 2E-12
2E.7 REFERENCES 2E-14
2E.8 TABLES 2E-16

2E.1 General

2E.1.1 Material Properties Required

The information in this Annex is intended to provide guidance on the materials information required for the Fitness-For-Service (FFS) Assessments covered in this Standard. Specific materials data are provided for strength

parameters, monotonic stress-strain curve relationships, cyclic stress-strain curve relationships, and physical properties; however, some of the materials data are provided in terms of references to published sources. To include, and keep up to date, the property information required by the assessment methods in this Standard would be prohibitive. This is especially true for properties that are affected by the service environment.

2E.1.2 Material Properties and In-Service Degradation

The FFS Assessment procedures in this Standard cover situations involving flaws commonly encountered in pressure vessels, piping and tankage that have been exposed to service for long periods of time. Therefore, when selecting materials properties for an analysis, care must be taken to evaluate these properties in terms of equipment that has been in-service; the properties used in the assessment should reflect any change or degradation, including aging, resulting from the service environment or past operation.

2E.2 Strength Parameters

2E.2.1 Yield and Tensile Strength

2E.2.1.1 Mean Estimates of Tensile Strength from Hardness Tests

It may be necessary to obtain samples from a component and use a standard test procedure to directly determine the yield and tensile strength when accurate estimates of these properties can affect the results of an FFS Assessment. The yield strength and ultimate tensile strength for plate and pipe material can be determined in accordance with ASTM A370, ASTM E8, or an equivalent standard method, and reported on a mill test report for the heat of steel.

Hardness tests based on Brinell (HB) and Vickers (HV) hardness measurements can be used to estimate the mean tensile strength using the equations shown below (see reference [1]) with values corresponding to those shown in Table 2E.1. The standard deviation for the HB correlation is 50 MPa (7.25 ksi) and for the HV correlation is 53.7 MPa (7.79 ksi). These conversions may be used for carbon and alloy steels in the annealed, normalized, and quenched and tempered conditions, and austenitic stainless steels. The conversions are not applicable for cold worked materials, and other high alloy, nickel based, or nonferrous materials.

$$\sigma_{uts} = 0.002 \cdot (HB)^2 + 2.222 \cdot (HB) + 164.71 \qquad (HB, MPa) \qquad \text{(2E.1)}$$

$$\sigma_{uts} = 0.0003 \cdot (HB)^2 + 0.3223 \cdot (HB) + 23.889 \qquad (HB, ksi) \qquad \text{(2E.2)}$$

$$\sigma_{uts} = 0.001 \cdot (HV)^2 + 2.6396 \cdot (HV) + 77.14 \qquad (HV, MPa) \qquad \text{(2E.3)}$$

$$\sigma_{uts} = 0.0001 \cdot (HV)^2 + 0.3828 \cdot (HV) + 11.188 \qquad (HV, ksi) \qquad \text{(2E.4)}$$

2E.2.1.2 Minimum Specified Yield and Tensile Strength from MPC Correlations

Analytical expressions for the minimum specified yield strength as a function of temperature and the applicable temperature range are provided in Table 2E.2. The minimum specified yield strength at a temperature is determined by multiplying the value at room temperature by a temperature reduction factor in these tables. The room temperature value of the minimum specified yield strength can be found in the applicable construction code. The analytical expressions for the minimum specified yield strength for a limited number of materials are listed in terms of a material pointer, PYS, which can be determined for a specific material of construction using Table 2E.3.

Analytical expressions for the minimum specified ultimate tensile strength as a function of temperature and the applicable temperature range are provided in Table 2E.4. The minimum specified ultimate tensile strength at a temperature is determined by multiplying the value at room temperature by a temperature reduction factor in these tables. The room temperature value of the minimum specified ultimate tensile strength can be found in the applicable construction code. The analytical expressions for the minimum specified ultimate tensile strength for a limited number of materials are listed in terms of a material pointer, PUS, which can be determined for a specific material of construction using Table 2E.5.

2E.2.1.3 Minimum Specified Yield and Tensile Strength from API Std 530 and WRC Bulletin 541

A method to compute the minimum yield and tensile strength as a function of temperature for pipe and tube materials is provided in Table 2E.6. The data used to develop these equations are from API Std 530, 6th Edition, September 2008 (see reference [2]). The yield and tensile properties of API Std 530 have been updated in the 7th Edition, April 2015 to reflect modern steel making practices for alloys currently produced and used for petroleum refinery heater applications (see Annex 10.B, paragraph 10B.2.3). The yield and tensile values from WRC Bulletin 541 (see reference [3]) are provided in Table 2E.7.

2E.2.1.4 Minimum Specified Yield and Tensile Strength Data from ASME Code, Section II, Part D

Values for the yield and tensile strength below the creep regime for pressure vessel, piping, and tankage steels can be found in the ASME Code, Section II, Part D (see reference [4]).

2E.2.1.5 Mean Values of Yield and tensile Strength from Minimum Specified Values

In the absence of heat specific data, mean values for the tensile and yield strength can be approximated using the following equations:

$$\sigma_{uts}^{mean} = \sigma_{uts}^{min} + 69\,MPa \tag{2E.5}$$

$$\sigma_{uts}^{mean} = \sigma_{uts}^{min} + 10\ ksi \tag{2E.6}$$

and,

$$\sigma_{ys}^{mean} = \sigma_{ys}^{min} + 69\,MPa \tag{2E.7}$$

$$\sigma_{ys}^{mean} = \sigma_{ys}^{min} + 10\ ksi \tag{2E.8}$$

2E.2.2 Flow Stress

2E.2.2.1 Definition

The flow stress, σ_f, can be thought of as the effective yield strength of a work hardened material. The use of a flow stress concept permits the real material to be treated as if it were an elastic-plastic material that can be characterized by a single strength parameter. The flow stress can be used, for example, as the stress level in the material that controls the resistance of a cracked structure to failure by plastic collapse.

2E.2.2.2 Estimation of Flow Stress

Several relationships for estimating the flow stress have been proposed which are summarized below. The flow stress to be used in an assessment will be covered in the appropriate Part of this Standard. In the absence of a material test report for plate and pipe, and for weld metal, the specified minimum yield strength and the specified minimum tensile strength for the material can be used to calculate the flow stress.

a) Average of the yield and tensile strengths (recommended for most assessments):

$$\sigma_f = \frac{\left(\sigma_{ys} + \sigma_{uts}\right)}{2} \tag{2E.9}$$

b) The yield strength plus 69 MPa (10 ksi):

$$\sigma_f = \sigma_{ys} + 69 \text{ MPa} \tag{2E.10}$$

$$\sigma_f = \sigma_{ys} + 10 \text{ ksi} \tag{2E.11}$$

c) For austenitic stainless steels, a factor times the average of the yield and tensile strengths:

$$\sigma_f = \frac{1.15 \cdot \left(\sigma_{ys} + \sigma_{uts}\right)}{2} \tag{2E.12}$$

d) For ferritic steels and austenitic stainless steels, the maximum allowable stress (S) in accordance with the ASME Code, Section VIII, Division 2, multiplied by an appropriate factor:

$$\sigma_f = 2.4 \cdot S \qquad \textit{for ferritic steels} \tag{2E.13}$$

$$\sigma_f = 3 \cdot S \qquad \textit{for austenitic stainless steels} \tag{2E.14}$$

e) If Ramberg-Osgood parameters are available (see paragraph 2E.3.3), the flow stress can be computed using the following equation for materials where a 0.2 percent offset is used to establish the yield strength of a material.

$$\sigma_f = \frac{\sigma_{ys}}{2}\left(1 + \frac{\left(\frac{n_{RO}}{0.002}\right)^{n_{RO}}}{\exp\left[n_{RO}\right]}\right) \tag{2E.15}$$

2E.3 Monotonic Stress-Strain Relationships

2E.3.1 MPC True Stress-Strain Curve Model

The following model for the true stress-strain curve may be used in FFS calculations where required by this Standard when the strain hardening characteristics of the true stress-strain curve are to be considered. The development of the stress-strain curve should be limited to a value of true ultimate tensile stress at the ultimate tensile strain. The stress strain curve beyond this point should be perfectly plastic.

$$\varepsilon_t = \frac{\sigma_t}{E_y} \qquad \textit{if } \left(\gamma_1 + \gamma_2\right) \le \varepsilon_p \tag{2E.16}$$

$$\varepsilon_t = \frac{\sigma_t}{E_y} + \gamma_1 + \gamma_2 \qquad \textit{if } \left(\gamma_1 + \gamma_2\right) > \varepsilon_p \tag{2E.17}$$

where,

$$\gamma_1 = \frac{\varepsilon_1}{2}\left(1.0 - \tanh\left[H\right]\right) \tag{2E.18}$$

$$\gamma_2 = \frac{\varepsilon_2}{2}\left(1.0 + \tanh\left[H\right]\right) \tag{2E.19}$$

$$\varepsilon_1 = \left(\frac{\sigma_t}{A_1}\right)^{\frac{1}{m_1}} \tag{2E.20}$$

$$A_1 = \frac{\sigma_{ys}\left(1+\varepsilon_{ys}\right)}{\left(\ln\left[1+\varepsilon_{ys}\right]\right)^{m_1}} \tag{2E.21}$$

$$m_1 = \frac{\ln\left[R\right] + \left(\varepsilon_p - \varepsilon_{ys}\right)}{\ln\left[\frac{\ln\left[1+\varepsilon_p\right]}{\ln\left[1+\varepsilon_{ys}\right]}\right]} \tag{2E.22}$$

$$\varepsilon_2 = \left(\frac{\sigma_t}{A_2}\right)^{\frac{1}{m_2}} \tag{2E.23}$$

$$A_2 = \frac{\sigma_{uts}\exp\left[m_2\right]}{m_2^{\,m_2}} \tag{2E.24}$$

$$H = \frac{2\left[\sigma_t - \left(\sigma_{ys} + K\cdot\left(\sigma_{uts} - \sigma_{ys}\right)\right)\right]}{K\left(\sigma_{uts} - \sigma_{ys}\right)} \tag{2E.25}$$

$$R = \frac{\sigma_{ys}}{\sigma_{uts}} \tag{2E.26}$$

$$\varepsilon_{ys} = 0.002 \tag{2E.27}$$

$$K = 1.5R^{1.5} - 0.5R^{2.5} - R^{3.5} \tag{2E.28}$$

The parameters m_2 and ε_p are provided in Table 2E.8, and σ_t is determined using Equation (2E.37).

The true ultimate tensile stress and the true strain at ultimate tensile stress are:

$$\sigma_{uts,t} = \sigma_{uts}\cdot\exp\left[m_2\right] \tag{2E.29}$$

$$\varepsilon_{uts,t} = m_2 \tag{2E.30}$$

2E.3.2 MPC Tangent Modulus Model

The tangent modulus based on the MPC true stress-strain curve model in paragraph 2E.3.1 is given by Equation (2E.31).

$$E_t = \frac{\partial\sigma_t}{\partial\varepsilon_t} = \left(\frac{\partial\varepsilon_t}{\partial\sigma_t}\right)^{-1} = \left(\frac{1}{E_y} + D_1 + D_2 + D_3 + D_4\right)^{-1} \tag{2E.31}$$

where,

$$D_1 = \frac{\sigma_t^{\left(\frac{1}{m_1}-1\right)}}{2m_1 \cdot A_1^{\left(\frac{1}{m_1}\right)}} \tag{2E.32}$$

$$D_2 = -\frac{1}{2}\left(\frac{1}{A_1^{\left(\frac{1}{m_1}\right)}}\right)\cdot\left(\sigma_t^{\left(\frac{1}{m_1}\right)}\cdot\left(\frac{2}{K\left(\sigma_{uts}-\sigma_{ys}\right)}\right)\cdot\left(1-\tanh^2\left[H\right]\right)+\frac{1}{m_1}\cdot\sigma_t^{\left(\frac{1}{m_1}-1\right)}\cdot\tanh\left[H\right]\right) \tag{2E.33}$$

$$D_3 = \frac{\sigma_t^{\left(\frac{1}{m_2}-1\right)}}{2m_2 \cdot A_2^{\left(\frac{1}{m_2}\right)}} \tag{2E.34}$$

$$D_4 = \frac{1}{2}\left(\frac{1}{A_2^{\left(\frac{1}{m_2}\right)}}\right)\cdot\left(\sigma_t^{\left(\frac{1}{m_2}\right)}\cdot\left(\frac{2}{K\left(\sigma_{uts}-\sigma_{ys}\right)}\right)\cdot\left(1-\tanh^2\left[H\right]\right)+\frac{1}{m_2}\cdot\sigma_t^{\left(\frac{1}{m_2}-1\right)}\cdot\tanh\left[H\right]\right) \tag{2E.35}$$

2E.3.3 Ramberg-Osgood Stress-Strain Model

2E.3.3.1 True Stress-Strain Curve

The true stress-strain curve of a material can be represented by Equations (2E.36). This equation is one form of the Ramberg-Osgood Equation (see reference [5]). The development of the stress-strain curve should be limited to a value of true ultimate tensile stress at the ultimate tensile strain. The stress strain curve beyond this point should be perfectly plastic. The denominator of the exponent of the true stress-strain curve, n_{RO}, may be used for a J-integral calculation.

$$\varepsilon_t = \varepsilon_e + \varepsilon_p = \frac{\sigma_t}{E_y} + \left(\frac{\sigma_t}{H_{RO}}\right)^{\frac{1}{n_{RO}}} \tag{2E.36}$$

The relationship between true stress-strain and engineering stress-strain is provided in the following equations.

$$\sigma_t = \left(1+\varepsilon_{es}\right)\sigma_{es} \tag{2E.37}$$

$$\varepsilon_t = \ln\left(1+\varepsilon_{es}\right) \tag{2E.38}$$

Equation (2E.37) and Equation (2E.38) are valid for $\sigma_t \leq \sigma_{uts,t}$ where the true ultimate stress, $\sigma_{uts,t}$, is given by Equation (2E.39), and the true strain, $\varepsilon_{uts,t}$, at the true ultimate tensile stress is given by Equation (2E.40).

$$\sigma_{uts,t} = \sigma_{uts}\cdot\exp\left[n_{RO}\right] \tag{2E.39}$$

$$\varepsilon_{uts,t} = n_{RO} \tag{2E.40}$$

If multiple data points for a stress-strain curve are provided, the data fitting constants n_{RO} and H_{RO} can be derived using regression techniques. If only the yield and ultimate tensile strengths are known, the exponent for the true stress-strain curve, n_{RO}, can be estimated by solving Equation (2E.41).

$$\frac{\sigma_{uts}}{\sigma_{ys}} = \frac{\left(\frac{n_{RO}}{\varepsilon_{ys}}\right)^{n_{RO}}}{\exp\left[n_{RO}\right]} \tag{2E.41}$$

Alternatively, n_{RO}, can be determined using Equation (2E.42). The parameters A_{RO} and B_{RO} are provided in the table shown below based on the percent offset used to determine the yield strength of the material (see reference [6]).

$$n_{RO} = \frac{1}{A_{RO}} \ln\left[\frac{\sigma_{uts}}{\sigma_{ys}}\right]^{B_{RO}} \qquad \left(Valid\ \ for\ 1.2 \le \frac{\sigma_{uts}}{\sigma_{ys}} \le 2.0\right) \tag{2E.42}$$

Parameters to Determine the Ramberg-Osgood Exponent n_{RO} for the True Stress-Strain Curve		
Yield Offset Strain, ε_{ys}	**A_{RO}**	**B_{RO}**
0.002	3.93	0.754
0.005	3.27	0.690
0.010	2.86	0.610

The constant H_{RO} is subsequently determined using Equation (2E.43).

$$H_{RO} = \frac{\sigma_{uts} \exp\left[n_{RO}\right]}{n_{RO}^{\ n_{RO}}} \tag{2E.43}$$

2E.3.3.2 Engineering Stress-Strain Curve

The Ramberg-Osgood equation may also be used to represent an engineering stress-strain curve.

$$\varepsilon_{es} = \varepsilon_e + \varepsilon_p = \frac{\sigma_{es}}{E_y} + \left(\frac{\sigma_{es}}{H_{RO}}\right)^{\frac{1}{n_{RO}}} \tag{2E.44}$$

If the uniform elongation e_{LU} is known, then n_{RO} for an engineering stress-strain curve may be determined by Equation (2E.45) (see reference [7]).

$$\frac{1}{n_{RO}} = \frac{\log_{10}\left[\frac{E \cdot e_{LU}}{\sigma_u} - 1\right] - \log_{10}\left[\frac{E \cdot \varepsilon_y}{\sigma_{ys}} - 1\right]}{\log_{10}\left[\frac{\sigma_{uts}}{\sigma_{ys}}\right]} + 1 \tag{2E.45}$$

The constant H_{RO} is computed using Equation (2E.46).

$$H_{RO} = \frac{\sigma_{ys}}{\left(\varepsilon_{ys}\right)^{n_{ro}}} \tag{2E.46}$$

2E.3.4 Ramberg-Osgood Tangent Modulus Model

The tangent modulus based on the Ramberg-Osgood stress-strain curve model in paragraph 2E.3.3.1 is given by Equation (2E.47).

$$E_t = \frac{\partial \sigma_t}{\partial \varepsilon_t} = \left(\frac{\partial \varepsilon_t}{\partial \sigma_t} \right)^{-1} = \left(\frac{1}{E_y} + \frac{1}{n_{RO}} \left(\frac{\sigma_t}{H_{RO}} \right)^{\frac{1}{n_{RO}}-1} \cdot \left(\frac{1}{H_{RO}} \right) \right)^{-1} \tag{2E.47}$$

2E.3.5 Engineering Stress-Strain Models for API 5L Pipeline Materials

2E.3.5.1 Stress-Strain Model from CSA Z662

The engineering stress-strain model used for pipeline materials is based on CSA Z662 (see reference [8]) and is given by Equation (2E.48) (see reference [9]).

$$\varepsilon_t = \varepsilon_e + \varepsilon_p = \frac{\sigma_t}{E_y} + \left(0.005 - \frac{\sigma_{ys}}{E_y} \right) \left(\frac{\sigma_t}{\sigma_{ys}} \right)^{N_{RO}} \tag{2E.48}$$

2E.3.5.2 API 5L Grades X52 to X80

The strain hardening exponent may be estimated based on the yield to tensile ratio of the material using the following Equation (2E.49).

$$N_{RO} = \frac{\ln \left[\frac{\varepsilon_t}{0.005} \right]}{\ln \left[\frac{1}{\sigma_{ys} / \sigma_{uts}} \right]} \tag{2E.49}$$

Where the yield to ultimate tensile stress ratio is estimated as:

$$\frac{\sigma_{ys}}{\sigma_{uts}} = \frac{1}{1 + 2 \left(\frac{149.96}{\sigma_{ys}} \right)^{2.3}} \qquad (MPa) \tag{2E.50}$$

$$\frac{\sigma_{ys}}{\sigma_{uts}} = \frac{1}{1 + 2 \left(\frac{21.75}{\sigma_{ys}} \right)^{2.3}} \qquad (ksi) \tag{2E.51}$$

and the total strain at the ultimate tensile stress is given by:

$$\varepsilon_t = -0.000254 \cdot \sigma_{ys} + 0.22 \qquad (MPa) \tag{2E.52}$$

$$\varepsilon_t = -0.00175 \cdot \sigma_{ys} + 0.22 \qquad (ksi) \tag{2E.53}$$

2E.3.5.3 API 5L Grades X80 to X100

a) The full engineering stress-strain curve for the pipe material is determined using the following procedure (see reference [10]).

1) STEP 1 – Determine the yield strength and ultimate tensile strength.

2) STEP 2 – Calculate σ_{ys}/σ_{uts}.

3) STEP 3 – Compute N_{RO}.

$$N_{RO} = \frac{3.14}{\left(1 - \frac{1}{\sigma_{ys}/\sigma_{uts}}\right)} \qquad \left(Valid\ \ for\ 0.80 \le \sigma_{ys}/\sigma_{uts} \le 0.95\right) \tag{2E.54}$$

4) STEP 4 – Compute ε_0.

$$\varepsilon_0 = \frac{\sigma_{uts}}{E} + \left(0.005 - \frac{\sigma_{ys}}{E}\right)\left(\frac{1}{\sigma_{ys}/\sigma_{uts}}\right)^{N_{RO}} \tag{2E.55}$$

5) STEP 5 – Compute uEL.

$$uEL = 1.25 \cdot \varepsilon_0 \tag{2E.56}$$

6) STEP 6 – Construct the 1st part of the stress-strain curve using Equation (2E.48) for strains up to ε_0.

7) STEP 7 – Construct the 2nd part of the stress-strain curve by extending a horizontal line of constant stress from ε_0 to uEL.

b) The full engineering stress-strain curve for the weld material is determined as follows (see reference [10]).

1) STEP 1 – Determine ultimate tensile strength.

2) STEP 2 – Determine yield strength.

$$\sigma_{ys} = \sigma_{uts} - 91.0 \qquad (MPa) \tag{2E.57}$$

$$\sigma_{ys} = \sigma_{uts} - 13.2 \qquad (ksi) \tag{2E.58}$$

3) STEP 3 – Calculate σ_{ys}/σ_{uts}.

4) STEP 4 – Compute N_{RO}.

$$N_{RO} = \frac{2.58}{\left(1 - \frac{1}{\sigma_{ys}/\sigma_{uts}}\right)^{1.17}} \qquad \left(valid\ \ for\ 0.80 \le \sigma_{ys}/\sigma_{uts} \le 0.95\right) \tag{2E.59}$$

5) STEP 5 – Construct the stress-strain curve using the following equations.

$$\varepsilon = \frac{\sigma}{E} \qquad if \quad \varepsilon \le \frac{\sigma_{ys}}{E} \tag{2E.60}$$

$$\sigma = \sigma_{ys} \qquad if \quad \frac{\sigma_{ys}}{E} < \varepsilon \le 1\% \tag{2E.61}$$

$$\varepsilon = \frac{\sigma}{E} + \left(0.005 - \frac{\sigma_{ys}}{E}\right)\left(\frac{\sigma}{\sigma_{ys}}\right)^{N_{RO}} + 0.005 \qquad if \quad 1\% < \varepsilon \le uEL \tag{2E.62}$$

2E.3.6 Tangent Modulus Model for API 5L Pipeline Materials

A numerical approach may be used to determine the tangent modules for the stress-strain curve described in paragraphs 2E.3.5.2 and 2E.3.5.3.

2E.4 Cyclic Stress-Strain Relationships

2E.4.1 Ramberg-Osgood Equation

The cyclic stress-strain curve of a material (i.e., strain amplitude versus stress amplitude (see reference [11]) may be represented by the Equation (2E.63). The material constants for this model are provided in Table 2E.9.

$$\varepsilon_{ta} = \frac{\sigma_a}{E_y} + \left[\frac{\sigma_a}{K_{css}}\right]^{\frac{1}{n_{css}}} \tag{2E.63}$$

The hysteresis loop stress-strain curve of a material (i.e., strain range versus stress range) obtained by scaling the cyclic stress-strain curve by a factor of two is represented by Equation (2E.64). The material constants provided in Table 2E.9 are also used in this equation.

$$\varepsilon_{tr} = \frac{\sigma_r}{E_y} + 2\left[\frac{\sigma_r}{2K_{css}}\right]^{\frac{1}{n_{css}}} \tag{2E.64}$$

2E.4.2 Estimation of Cyclic Stress-Strain Curve Parameters

2E.4.2.1 Estimation from Monotonic Properties

A review of estimation methods for determining the cyclic Ramberg-Osgood stress-strain parameters of steels from their monotonic properties including a discussion of the material database used in the study and statistical analysis is provided in reference [12]. A recommendation from this publication for estimating the Ramberg-Osgood stress-strain parameters of steels from their monotonic properties is shown below.

a) For $\sigma_{uts}/\sigma_{ys} > 1.2$:

$$K_{css} = 1.16 \cdot \sigma_{uts} + 593 \qquad (MPa) \tag{2E.65}$$

$$n_{css} = -0.37 \cdot \log\left[\frac{0.75 \cdot \sigma_{ys} + 82}{1.16 \cdot \sigma_{uts} + 593}\right] \qquad (MPa) \tag{2E.66}$$

$$K_{css} = 1.16 \cdot \sigma_{uts} + 86.0074 \qquad (ksi) \tag{2E.67}$$

$$n_{css} = -0.37 \cdot \log\left[\frac{0.75 \cdot \sigma_{ys} + 11.8931}{1.16 \cdot \sigma_{uts} + 86.0074}\right] \qquad (ksi) \tag{2E.68}$$

b) For $\sigma_{uts}/\sigma_{ys} \leq 1.2$:

$$K_{css} = 3(10)^{-4} \cdot \left(\sigma_{uts}\right)^2 + 0.23 \cdot \sigma_{uts} + 619 \qquad (MPa) \tag{2E.69}$$

$$n_{css} = -0.37 \cdot \log\left[\frac{3(10)^{-4} \cdot \left(\sigma_{ys}\right)^2 - 0.15 \cdot \sigma_{ys} + 526}{3(10)^{-4} \cdot \left(\sigma_{uts}\right)^2 + 0.23 \cdot \sigma_{uts} + 619}\right] \qquad (MPa) \tag{2E.70}$$

$$K_{css} = 2.0684(10)^{-3} \cdot (\sigma_{uts})^2 + 0.23 \cdot \sigma_{uts} + 89.7783 \qquad (ksi) \qquad \text{(2E.71)}$$

$$n_{css} = -0.37 \cdot \log\left[\frac{2.0684(10)^{-3} \cdot (\sigma_{ys})^2 - 0.15 \cdot \sigma_{ys} + 76.2898}{2.0684(10)^{-3} \cdot (\sigma_{uts})^2 + 0.23 \cdot \sigma_{uts} + 89.7783}\right] \qquad (ksi) \qquad \text{(2E.72)}$$

2E.4.2.2 Uniform Material Law

Baumel and Seeger developed a Uniform Material Law (see reference [13]) for estimating the mean cyclic stress-strain curve and strain life properties for plain carbon and low to medium alloy steels, and for aluminum and titanium alloys. The method is shown in Table 2E.10. The Uniform Material Law provides generally satisfactory agreement with measured material properties and may on occasion provide an exceptional correlation. It is the general method recommended for estimating cyclic stress-strain curves and strain life properties when actual data for a specific material are not provided in the form of a correlation or actual data points.

2E.5 Physical Properties

2E.5.1 Elastic Modulus

The elastic or Young's modulus is required to perform stress analysis of a statically indeterminate component. Values for the elastic modulus for a full range in temperatures can be found in WRC Bulletin 503 (see reference [14]) or the ASME B&PV Code, Section II, Part D (see reference [4]).

2E.5.2 Poisson's Ratio

The value of Poisson's ratio in the elastic range, ν, can normally be taken as 0.3 for steels. Data for specific steels can be found in WRC Bulletin 503 (see reference [14]) or the ASME B&PV Code, Section II, Part D (see reference [4]).

2E.5.3 Coefficient of Thermal Expansion

The coefficient of thermal expansion is required to perform a thermal stress analysis of a component. Values for the thermal expansion coefficient for a full range in temperatures can be found in the WRC Bulletin 503 (see reference [14]) or the ASME B&PV Code, Section II, Part D (see reference [4]).

2E.5.4 Thermal Conductivity

The thermal conductivity is required to perform a heat transfer analysis of a component. The results from this analysis are utilized in a thermal stress calculation. Values for the thermal conductivity for a full range in temperatures can be found in WRC Bulletin 503 (see reference [14]) or the ASME B&PV Code, Section II, Part D.

2E.5.5 Thermal Diffusivity

The thermal diffusivity is required to perform a transient thermal heat transfer analysis of a component. The results from this analysis are utilized in a transient thermal stress calculation. Values for the thermal diffusivity for a full range in temperatures can be found in WRC Bulletin 503 (see reference [14]) or the ASME B&PV Code, Section II, Part D (see reference [4]).

2E.5.6 Density

The material density is required to perform a transient thermal heat transfer analysis, and in cases where body force components are to be considered in a stress analysis of a component. The results from this analysis are utilized in a transient thermal stress calculation. Values for the density for a full range in temperatures can be found in WRC Bulletin 503 (see reference [14]) or the ASME B&PV Code, Section II, Part D (see reference [4]).

2E.6 Nomenclature

a	parameter used in the Uniform Material Law.
$A_0 \rightarrow A_5$	curve-fit coefficients for the yield strength data from API Std 530.
A_{RO}	Ramberg Osgood curve-fit coefficient.
b	fatigue strength exponent (Basquin's exponent).
$B_0 \rightarrow B_5$	curve-fit coefficients for the tensile strength data from API Std 530.
B_{RO}	Ramberg Osgood curve-fit exponent.
c	fatigue strength exponent (Coffin-Manson exponent) in the Uniform Material Law.
$C_0 \rightarrow C_5$	material coefficients for the yield strength or ultimate tensile strength data, as applicable.
$D_1 \rightarrow D_4$	material coefficients used in the tangent modulus calculation.
E_t	tangent Modulus.
E_y	Young's Modulus at the temperature of interest.
ε_{es}	engineering strain.
ε_e	true elastic strain.
ε_p	true plastic strain or fitting parameter for MPC true stress-strain curve model.
ε_t	true strain or total true strain.
ε_{ta}	total true strain amplitude.
ε_{tr}	total true strain range.
ε_y	total strain at yield stress.
e_{LU}	uniform elongation which is equal to total strain at the ultimate tensile stress.
ε_{ys}	Engineering offset strain as defined by material specification.
$\varepsilon_{uts,t}$	true strain at true ultimate tensile stress.
ε_1	true plastic strain in the micro-strain region of the stress-strain curve.
ε_2	true plastic strain in the macro-strain region of the stress-strain curve.
ε_f^*	fatigue ductility coefficient.

ε_0 stress-strain curve parameter.

γ_1 true strain in the micro-strain region of the stress-strain curve.

γ_2 true strain in the macro-strain region of the stress-strain curve.

H Prager doctor factor.

H_{RO} constant in Ramberg-Osgood Stress Strain Model.

K elastic crack driving force parameter, stress intensity factor, or a parameter in the MPC stress-strain curve model, as applicable.

K_{css} material parameter for the cyclic stress-strain curve model.

m_1 curve fitting exponent for the stress-strain curve equal to the true strain at the proportional limit and the strain hardening coefficient in the large strain region.

m_2 curve fitting exponent for the stress-strain curve equal to the true strain at the true ultimate stress.

n_{css} exponent for the cyclic stress-strain curve model.

n_{RO} exponent for Ramberg-Osgood stress-strain curve model.

N_{RO} exponent for Ramberg-Osgood stress-strain curve model for pipeline materials.

N_f number of cycles to failure in accordance with the Uniform Material Law.

R the ratio of the engineering yield stress to engineering tensile stress evaluated at the assessment temperature, as applicable.

S allowable stress.

σ_a total stress amplitude.

σ_r total stress range.

σ_t true stress.

σ_f flow stress.

σ_r applied stress range.

σ_{ys} yield stress at the temperature of interest.

σ_{uts} engineering ultimate tensile stress evaluated at the temperature of interest.

$\sigma_{uts,t}$ true ultimate tensile stress evaluated at the temperature of interest.

σ_{uts}^{rt} minimum specified ultimate tensile strength at room temperature.

σ_{ys}^{rt} minimum specified yield strength at room temperature.

$\sigma_{ys}^{T_{\min}}$ ultimate tensile strength at $T_{\min}$.

$\sigma_{uts}^{T_{\min}}$ yield strength at $T_{\min}$.

σ_{uts}^{mean} mean value of the ultimate tensile strength.

$\sigma_{uts}^{\min}$ minimum specified ultimate tensile strength from the original construction code.

σ_{ys}^{mean} mean value of the yield strength.

$\sigma_{ys}^{\min}$ minimum specified yield strength.

σ_{f}^{*} fatigue strength coefficient.

T temperature.

$T_{\min}$ minimum temperature for applicability of material data from API Std 530.

$T_{\max}$ maximum temperature for applicability of material data from API Std 530.

uEL uniform elongation at the ultimate tensile strength.

2E.7 References

[1] Grumbach, M., Regnier, L., Roesch, L., and Roche, R., "Conversion of hardness values into tensile strength estimates," Bulletin du Cercle d'Etudes des Metaux, Page (EN)23.1-23.3, 23.5-23.7, (FR)23.3-23.7, 1983.

[2] API Std 530, Calculation of Heater-tube Thickness in Petroleum Refineries, American Petroleum Institute.

[3] Prager, M., Osage, D.A., and Panzarella, C.H., *Evaluation of Material Strength Data for Use in API Std 530, WRC Bulletin 541*, Welding Research Council, Inc., New York, NY, 2015.

[4] ASME, Boiler and Pressure Vessel Code, Section II, Part D *Properties*, ASME Code Section II, Part D, ASME, New York, NY

[5] Ramberg, W. and Osgood, W.R., "Description of Stress-Strain Curves by Three Parameters," Technical Note No. 902., National Advisory Committee for Aeronautics, July 1943.

[6] Kamaya, Masayuki, "Ramberg-Osgood type stress-strain curve estimation using yield and ultimate strengths for failure assessments," International Journal of Pressure Vessels and Piping 137 (2016) 1-12.

[7] BS 7910:2105, Guide to methods for assessing the acceptability of flaws in metallic structures, British Standards Institute.

[8] CSA Z662, *Oil and Gas Pipeline Systems*, Canadian Standards Association, 2015.

[9] API 1104:2013, *Welding of Pipelines and Related Facilities*, 21st Edition, American Petroleum Institute.

[10] PRCI, *Second Generation Models for Strain-based Design*, Pipeline Research Council International, Contract PR-ABD-1 – Project 2, Catalog No. L5XXXX, 2011.

[11] Draper, J., Modern *Metal fatigue Analysis*, EMAS Publishing, FESI-UK Forum for Engineering Structural Integrity, Whittle House, The Quadrant, Birchwood Park, Warrington, WA3 6FW, UK, 2008.

[12] Marohnic, T., Basan, R., and Franulovic, M., "Evaluation of Methods for Estimation of Cyclic Stress-Strain Parameters from Monotonic Properties of Steel," Metals 2017,7,17; doi:10.3390/met7010017, www.mdpi.com/journal/metals.

[13] Baumel A. Jr. and Seeger, T., *Materials Data for Cyclic Loading – Supplement 1*, Elsevier Science Publishing BV, 1987.

[14] Osage, D.A., Janelle, J.A., Sutton, N.G., Kowalski, P., Orosz, K.T., and Bednarz, J., *Compendium of Temperature-Dependent Physical Properties for Pressure Vessel Materials*, WRC Bulletin 503, Welding Research Council, Inc., New York, NY, 2019.

2E.8 Tables

Table 2E.1 –Hardness Number to Mean Tensile Strength for Carbon and Alloy Steels in the Annealed, Normalized, and Quench-and Tempered Conditions, and Austenitic Stainless Steels

Brinell Hardness HB2.5, HB5, HB10	Mean Tensile Strength		Vickers Hardness HV5, HV10, HV30, HV50, HV100	Mean Tensile Strength	
	(MPa)	(ksi)		(MPa)	(ksi)
441	1534	224	470	1539	213
433	1502	220	460	1503	208
425	1470	215	450	1467	204
415	1431	209	440	1432	199
405	1393	204	430	1397	194
397	1362	199	420	1362	190
388	1328	194	410	1327	185
379	1294	189	400	1293	180
369	1257	184	390	1259	176
360	1224	179	380	1225	171
350	1187	173	370	1191	167
341	1155	169	360	1157	162
331	1119	163	350	1124	157
322	1088	159	340	1090	153
313	1056	154	330	1057	148
303	1022	149	320	1024	144
294	991	145	310	992	139
284	957	140	300	959	135
280	944	138	295	943	133
275	927	135	290	927	131
270	910	133	285	911	128
265	894	130	280	895	126
261	881	128	275	879	124
256	865	126	270	863	122
252	852	124	265	847	120
247	836	122	260	831	117
243	823	120	255	815	115
238	807	118	250	800	113
233	791	115	245	784	111
228	775	113	240	768	109
219	747	109	230	737	105
209	716	104	220	706	100
200	689	100	210	676	96
190	659	96	200	645	92
181	632	92	190	615	88
171	603	88	180	585	83
162	577	84	170	555	79
152	549	80	160	525	75
143	523	76	150	496	71
133	496	72	140	466	67
124	471	68	130	437	63
114	444	65	120	408	59

Table 2E.2 – MPC Minimum Specified Yield Strength as a Function of Temperature

Material Pointer (PYS)	Temperature (°F)		$\sigma_{ys} = \sigma_{ys}^{rt} \cdot \exp\left[C_0 + C_1 T + C_2 T^2 + C_3 T^3 + C_4 T^4 + C_5 T^5 \right] \quad \left({}^{o}F, ksi \right)$					
	Min	Max	C_0	C_1	C_2	C_3	C_4	C_5
1	70	1100	7.32895590E-02	-1.17762521E-03	2.38047105E-06	-3.41856446E-09	2.30957367E-12	-6.50662295E-16
2	70	1100	6.74115307E-02	-1.14022133E-03	2.93774604E-06	-4.04287814E-09	3.37044043E-12	-1.42534965E-15
3	70	1100	8.64892939E-02	-1.46822432E-03	4.43698029E-06	-7.48574857E-09	6.52970740E-12	-2.49641702E-15
4	70	1500	1.15119384E-01	-1.64008687E-03	1.40737810E-06	-6.87419020E-10	4.10067600E-13	-2.28537801E-16
5	70	1500	6.54193489E-02	-9.16571466E-04	1.97469205E-07	9.82045387E-11	3.83196021E-13	-3.00033395E-16
6	70	1500	1.29553432E-01	-1.83405205E-03	1.90867347E-06	-7.72504653E-10	-2.35102806E-13	1.49090484E-16
7	70	1500	7.22867367E-02	-1.18789668E-03	2.93345768E-06	-4.65145193E-09	3.62287974E-12	-1.09404474E-15
8	70	1500	5.02134175E-02	-7.23768917E-04	4.55342493E-07	-9.74792542E-10	1.21882955E-12	-5.03459802E-16
9	70	1500	1.71228796E-01	-2.75036658E-03	5.44467782E-06	-6.11640012E-09	3.62507062E-12	-8.78106064E-16

Table 2E.2M – MPC Minimum Specified Yield Strength as a Function of Temperature

Material Pointer (PYS)	Temperature (°C)		$\sigma_{ys} = \sigma_{ys}^{rt} \cdot \exp\left[C_0 + C_1 T + C_2 T^2 + C_3 T^3 + C_4 T^4 + C_5 T^5 \right] \quad \left({}^{o}C, MPa \right)$					
	Min	Max	C_0	C_1	C_2	C_3	C_4	C_5
1	21	593	3.79335351E-02	-1.86385965E-03	6.69470079E-06	-1.82518378E-08	2.31521177E-11	-1.22947065E-14
2	21	593	3.38037095E-02	-1.73554380E-03	8.32638097E-06	-2.11471664E-08	3.29874954E-11	-2.69329508E-14
3	21	593	4.38110535E-02	-2.17153985E-03	1.21747825E-05	-3.89315704E-08	6.43532344E-11	-4.71714972E-14
4	21	816	6.40556561E-02	-2.79373298E-03	4.35401064E-06	-3.71656211E-09	3.92086989E-12	-4.31837715E-15
5	21	816	3.62948800E-02	-1.62644958E-03	6.77655338E-07	8.40865268E-10	3.51869766E-12	-5.66933503E-15
6	21	816	7.27926926E-02	-3.08574021E-03	5.93930041E-06	-4.67184681E-09	-2.21760045E-12	2.81716608E-15
7	21	816	3.71292469E-02	-1.82515595E-03	8.12857283E-06	-2.44881384E-08	3.61939674E-11	-2.06727194E-14
8	21	816	2.74884019E-02	-1.25543600E-03	1.19583839E-06	-4.80520518E-09	1.19491660E-11	-9.51321531E-15
9	21	816	8.85957654E-02	-4.35640722E-03	1.58095415E-05	-3.30171850E-08	3.65796603E-11	-1.65924112E-14

Table 2E.3 – Material Description for the MPC Minimum Specified Yield Strength

PYS	Applicable Materials
1	Carbon Steel (YS<275.9 MPa) (YS< 40 ksi)
2	C-1/2Mo, 1-1/4Cr-1/2Mo Annealed, 2-1/4Cr-1Mo Annealed, 3Cr-1Mo, 5Cr-1/2Mo, 9Cr-1Mo
3	1-1/4Cr-1/2Mo N&T, 2-1/4Cr-1Mo N&T, 2-1/4Cr-1Mo Q&T, 2-1/4Cr-1Mo -V, 9Cr-1Mo-V
4	Type 304, Type 316
5	Type 310, Type 321, Type 347
6	Type 316L
7	Alloy 800
8	Alloy 800H, Alloy 800HT
9	HK-40

Table 2E.4 – MPC Minimum Specified Ultimate Tensile Strength as a Function of Temperature

Material Pointer (PUS)	Temperature (°F)		$\sigma_{uts} = \sigma_{uts}^{rt} \cdot \exp\left[C_0 + C_1 T + C_2 T^2 + C_3 T^3 + C_4 T^4 + C_5 T^5 \right] \quad \left({}^{o}F, ksi \right)$					
	Min	Max	C_0	C_1	C_2	C_3	C_4	C_5
1	70	1100	4.96592236E-02	-3.77753186E-04	-2.22995759E-06	9.37412910E-09	-1.08177336E-11	3.38063139E-15
2	70	1100	1.03059502E-01	-1.50239969E-03	1.23729610E-06	2.88144828E-09	-3.79884518E-12	7.81749069E-16
3	70	1100	6.32622065E-02	-9.67153551E-04	1.22766678E-06	8.18123287E-10	-2.12906253E-12	5.21468764E-16
4	70	1500	1.32974273E-01	-2.10253189E-03	4.12208906E-06	-4.23720525E-09	2.51092690E-12	-7.88154028E-16
5	70	1500	1.34525275E-01	-2.14511512E-03	4.94560236E-06	-5.06503095E-09	2.39919595E-12	-5.62207065E-16
6	70	1500	1.05691876E-01	-1.63492458E-03	2.65859303E-06	-1.24506534E-09	-3.85312660E-13	1.68156273E-16
7	70	1500	1.31877934E-01	-2.43123502E-03	9.41969068E-06	-1.70606702E-08	1.47018626E-11	-4.92753399E-15
8	70	1500	1.41247151E-01	-2.64436746E-03	1.08241364E-05	-2.09316450E-08	1.90667084E-11	-6.59569764E-15
9	70	1500	1.63465185E-01	-2.70857567E-03	5.77561099E-06	-5.13107773E-09	1.83255377E-12	-2.70855733E-16

Table 2E.4M – MPC Minimum Specified Ultimate Tensile Strength as a Function of Temperature

Material Pointer (PUS)	Temperature (°C)		$\sigma_{uts} = \sigma_{uts}^{rt} \cdot \exp\left[C_0 + C_1 T + C_2 T^2 + C_3 T^3 + C_4 T^4 + C_5 T^5 \right] \quad \left({}^{o}C, MPa \right)$					
	Min	Max	C_0	C_1	C_2	C_3	C_4	C_5
1	21	593	3.55835868E-02	-8.87531986E-04	-4.52108819E-06	4.67964163E-08	-1.07882077E-10	6.38793289E-14
2	21	593	5.63401650E-02	-2.54673855E-03	4.83029306E-06	1.40154694E-08	-3.85657189E-11	1.47716803E-14
3	21	593	3.35950169E-02	-1.59542267E-03	4.19028077E-06	3.21310030E-09	-2.14741795E-11	9.85350689E-15
4	21	816	6.97780335E-02	-3.33253782E-03	1.20867754E-05	-2.28840524E-08	2.50349101E-11	-1.48927063E-14
5	21	816	7.07824139E-02	-3.31892068E-03	1.44954873E-05	-2.77818452E-08	2.42415074E-11	-1.06232848E-14
6	21	816	5.60554916E-02	-2.64356837E-03	8.21908457E-06	-7.53881321E-09	-3.76242022E-12	3.17742712E-15
7	21	816	6.31803836E-02	-3.38199124E-03	2.55006790E-05	-8.88172175E-08	1.46057908E-10	-9.31091055E-14
8	21	816	6.70451917E-02	-3.62422838E-03	2.89321732E-05	-1.08234025E-07	1.89076439E-10	-1.24630192E-13
9	21	816	8.25387660E-02	-4.23802883E-03	1.71532015E-05	-2.85726267E-08	1.87824828E-11	-5.11800326E-15

Table 2E.5 – Material Descriptions for the MPC Minimum Ultimate Tensile Strength

PUS	Applicable Materials
1	Carbon Steel (YS<275.9 MPa) (YS< 40 ksi)
2	C-1/2Mo, 1-1/4Cr-1/2Mo Annealed, 2-1/4Cr-1Mo Annealed, 3Cr-1Mo, 5Cr-1/2Mo, 9Cr-1Mo
3	1-1/4Cr-1/2Mo N&T, 2-1/4Cr-1Mo N&T, 2-1/4Cr-1Mo Q&T, 2-1/4Cr-1Mo -V, 9Cr-1Mo-V
4	Type 304, Type 347
5	Type 310, Type 316, Type 321
6	Type 316L
7	Alloy 800
8	Alloy 800H, Alloy 800HT
9	HK-40

Table 2E.6 – Minimum Yield and Tensile Strength Values from API Std 530, 6th Edition, September 2008, (1), (2)

Material	Temperature Limits and Strength Parameters at Minimum Temperature (3), (4)	Yield Strength: σ_{ys} (3)		Tensile Strength: σ_{uts} (4)	
Low Carbon Steel (Figure 4A) A161 A192	$T_{min} = 149^o C\ (300^o F)$ $T_{max} = 621^o C\ (1150^o F)$ $\sigma_{ys}^{T_{min}} = 157\ MPa\ (22.8\ ksi)$ $\sigma_{uts}^{T_{min}} = 298\ MPa\ (43.2\ ksi)$	A_0	1.6251089E+00	B_0	1.1720989E+00
		A_1	-3.3124966E-03	B_1	-2.0580032E-03
		A_2	5.0904910E-06	B_2	7.6239020E-06
		A_3	-3.3374441E-09	B_3	-9.9459690E-09
		A_4	4.9690402E-13	B_4	3.7189699E-12
		A_5	0.0	B_5	0.0
Medium Carbon Steel (Figure 4B) A53 Grade B A106 Grade B A210 Grade A-1	$T_{min} = 149^o C\ (300^o F)$ $T_{max} = 621^o C\ (1150^o F)$ $\sigma_{ys}^{T_{min}} = 210\ MPa\ (30.5\ ksi)$ $\sigma_{uts}^{T_{min}} = 379\ MPa\ (55.0\ ksi)$	A_0	1.6434698E+00	B_0	1.1872106E+00
		A_1	-3.5201715E-03	B_1	-2.2083065E-03
		A_2	5.8080277E-06	B_2	8.0934859E-06
		A_3	-4.2398160E-09	B_3	-1.0510434E-08
		A_4	8.7536764E-13	B_4	3.9529036E-12
		A_5	0.0000000E+00	B_5	0.0000000E+00
C-0.5Mo (Figure 4C) A 161 T1 A 209 T1 A 335 P1	$T_{min} = 149^o C\ (300^o F)$ $T_{max} = 621^o C\ (1150^o F)$ $\sigma_{ys}^{T_{min}} = 186\ MPa\ (27.0\ ksi)$ $\sigma_{uts}^{T_{min}} = 395\ MPa\ (57.3\ ksi)$	A_0	1.0875314E+00	B_0	-8.3107781E-02
		A_1	-2.1270293E-04	B_1	6.7591546E-03
		A_2	-4.4780776E-07	B_2	-1.3556423E-05
		A_3	8.4688943E-10	B_3	1.1122871E-08
		A_4	-5.6614129E-13	B_4	-3.5429684E-12
		A_5	0.0000000E+00	B_5	0.0000000E+00
1.25Cr-0.5Mo (Figure 4D) A 213 T11 A 335 P11 A 200 T11	$T_{min} = 149^o C\ (300^o F)$ $T_{max} = 621^o C\ (1150^o F)$ $\sigma_{ys}^{T_{min}} = 183\ MPa\ (26.5\ ksi)$ $\sigma_{uts}^{T_{min}} = 379\ MPa\ (55.0\ ksi)$	A_0	1.1345901E+00	B_0	1.7526113E+00
		A_1	-4.8648764E-04	B_1	-7.0066393E-03
		A_2	3.9401132E-08	B_2	2.3037863E-05
		A_3	4.2209296E-10	B_3	-3.2685799E-08
		A_4	-3.8709072E-13	B_4	2.0963053E-11
		A_5	0.0	B_5	-5.2442438E-15
2.25Cr-1Mo (Figure 4E) A 213 T22 A 335 P22 A 200 T22	$T_{min} = 149^o C\ (300^o F)$ $T_{max} = 732^o C\ (1350^o F)$ $\sigma_{ys}^{T_{min}} = 186\ MPa\ (27.0\ ksi)$ $\sigma_{uts}^{T_{min}} = 364\ MPa\ (52.8\ ksi)$	A_0	1.2398072E+00	B_0	2.0398036E+00
		A_1	-1.5494280E-03	B_1	-7.5239262E-03
		A_2	3.2430371E-06	B_2	1.7967199E-05
		A_3	-2.3756026E-09	B_3	-1.6168512E-08
		A_4	3.1331338E-13	B_4	4.6189330E-12
		A_5	0.0000000E+00	B_5	0.0000000E+00

Table 2E.6 – Minimum Yield and Tensile Strength Values from API Std 530, 6th Edition, September 2008, (1), (2)

Material	Temperature Limits and Strength Parameters at Minimum Temperature (3), (4)	Yield Strength: σ_{ys} (3)		Tensile Strength: σ_{uts} (4)	
3Cr-1Mo (Figure 4F) A 213 T5 A 335 P5 A 200 T5	$T_{min} = 149^o C\ (300^o F)$ $T_{max} = 732^o C\ (1350^o F)$ $\sigma_{ys}^{T_{min}} = 179\ MPa\ (26.0\ ksi)$ $\sigma_{uts}^{T_{min}} = 393\ MPa\ (57.0\ ksi)$	A_0	1.3109507E+00	B_0	1.2922744E+00
		A_1	-1.8522910E-03	B_1	-1.7583742E-03
		A_2	3.3285320E-06	B_2	3.5081428E-06
		A_3	-2.1885193E-09	B_3	-2.9914715E-09
		A_4	2.7268140E-13	B_4	6.7845610E-13
		A_5	0.0000000E+00	B_5	0.0000000E+00
5Cr-0.5Mo (Figure 4G) A 213 T5 A 335 P5 A 200 T5	$T_{min} = 149^o C\ (300^o F)$ $T_{max} = 732^o C\ (1350^o F)$ $\sigma_{ys}^{T_{min}} = 175\ MPa\ (25.4\ ksi)$ $\sigma_{uts}^{T_{min}} = 362\ MPa\ (52.5\ ksi)$	A_0	1.1392352E+00	B_0	1.2563698E+00
		A_1	-1.3518395E-03	B_1	-1.9619215E-03
		A_2	4.3886534E-06	B_2	5.1583250E-06
		A_3	-5.1308445E-09	B_3	-5.4836935E-09
		A_4	1.6914766E-12	B_4	1.7207470E-12
		A_5	0.0000000E+00	B_5	0.0000000E+00
5Cr-0.5Mo-Si (Figure 4H) A 213 T5b A 335 P5b	$T_{min} = 149^o C\ (300^o F)$ $T_{max} = 732^o C\ (1350^o F)$ $\sigma_{ys}^{T_{min}} = 186\,MPa\ (27.0\ ksi)$ $\sigma_{uts}^{T_{min}} = 356\,MPa\ (51.7\ ksi)$	A_0	1.2324252E+00	B_0	1.2773067E+00
		A_1	-1.6940271E-03	B_1	-2.3196405E-03
		A_2	4.3681713E-06	B_2	6.5893951E-06
		A_3	-4.8983328E-09	B_3	-7.2379937E-09
		A_4	1.6079702E-12	B_4	2.3466718E-12
		A_5	0.0000000E+00	B_5	0.0000000E+00
7Cr-0.5Mo (Figure 4I) A 213 T7 A 335 P7 A 200 T7	$T_{min} = 149^o C\ (300^o F)$ $T_{max} = 732^o C\ (1350^o F)$ $\sigma_{ys}^{T_{min}} = 172\,MPa\ (25.0\ ksi)$ $\sigma_{uts}^{T_{min}} = 400\,MPa\ (58.0\ ksi)$	A_0	6.9288533E-01	B_0	9.9596073E-01
		A_1	3.4867283E-03	B_1	2.4796284E-05
		A_2	-1.3498948E-05	B_2	3.3129703E-07
		A_3	2.2065464E-08	B_3	-1.4772664E-09
		A_4	-1.6085361E-11	B_4	6.5165864E-13
		A_5	4.1090437E-15	B_5	0.0
9Cr-1Mo (Figure 4J) A 213 T9 A 335 P9 A 200 T9	$T_{min} = 149^o C\ (300^o F)$ $T_{max} = 732^o C\ (1350^o F)$ $\sigma_{ys}^{T_{min}} = 179\,MPa\ (26.0\ ksi)$ $\sigma_{uts}^{T_{min}} = 370\,MPa\ (53.6\ ksi)$	A_0	1.3645782E+00	B_0	1.6002250E+00
		A_1	-2.4184891E-03	B_1	-3.8196855E-03
		A_2	5.3798831E-06	B_2	8.1545162E-06
		A_3	-5.0826095E-09	B_3	-7.4536524E-09
		A_4	1.4540216E-12	B_4	2.1749553E-12
		A_5	0.0000000E+00	B_5	0.0000000E+00

Table 2E.6 – Minimum Yield and Tensile Strength Values from API Std 530, 6th Edition, September 2008, (1), (2)

Material	Temperature Limits and Strength Parameters at Minimum Temperature (3), (4)	Yield Strength: σ_{ys} (3)		Tensile Strength: σ_{uts} (4)	
9Cr-1Mo-V (Figure 4K) A 213 T91 A 335 P91 A 200 T91	$T_{min} = 149^o C\ (300^o F)$ $T_{max} = 660^o C\ (1220^o F)$ $\sigma_{ys}^{T_{min}} = 379\,MPa\ (55.0\ ksi)$ $\sigma_{uts}^{T_{min}} = 538\,MPa\ (78.0\ ksi)$	A_0	1.1559737E+00	B_0	1.3561147E+00
		A_1	-1.3027523E-03	B_1	-2.5814516E-03
		A_2	3.6718335E-06	B_2	6.4611130E-06
		A_3	-3.9082343E-09	B_3	-6.6563640E-09
		A_4	1.1136278E-12	B_4	2.0875274E-12
		A_5	0.0000000E+00	B_5	0.0000000E+00
Type 304 & 304H (Figure 4L) A 213 Type 304&304H A 271 Type 304&304H A 312 Type 304&304H A 376 Type 304&304H	$T_{min} = 204^o C\ (400^o F)$ $T_{max} = 843^o C\ (1550^o F)$ $\sigma_{ys}^{T_{min}} = 143\,MPa\ (20.8\ ksi)$ $\sigma_{uts}^{T_{min}} = 414\,MPa\ (60.0\ ksi)$	A_0	1.6894159E+00	B_0	1.2907427E+00
		A_1	-3.3500871E-03	B_1	-1.8958334E-03
		A_2	6.0887433E-06	B_2	4.2634694E-06
		A_3	-6.3277196E-09	B_3	-3.7649126E-09
		A_4	3.4413453E-12	B_4	9.8390933E-13
		A_5	-7.8762940E-16	B_5	0.0
Type 316 & 316H (Figure 4M) A 213 Type 316&316H A 271 Type 316&316H A 312 Type 316&316H A 376 Type316&316H	$T_{min} = 204^o C\ (400^o F)$ $T_{max} = 843^o C\ (1550^o F)$ $\sigma_{ys}^{T_{min}} = 148\,MPa\ (21.4\ ksi)$ $\sigma_{uts}^{T_{min}} = 452\,MPa\ (65.5\ ksi)$	A_0	1.3224680E+00	B_0	1.2454373E+00
		A_1	-8.7683155E-04	B_1	-1.6314830E-03
		A_2	-1.3646107E-07	B_2	3.7350778E-06
		A_3	8.9906963E-10	B_3	-3.3393727E-09
		A_4	-4.2098578E-13	B_4	8.7044694E-13
		A_5	0.0000000E+00	B_5	0.0000000E+00
Type 316L (Figure 4N) A 213 Type 316L A 312 Type 316L	$T_{min} = 204^o C\ (400^o F)$ $T_{max} = 688^o C\ (1270^o F)$ $\sigma_{ys}^{T_{min}} = 119\,MPa\ (17.3\ ksi)$ $\sigma_{uts}^{T_{min}} = 391\,MPa\ (56.7\ ksi)$	A_0	1.6764367E+00	B_0	1.4209808E+00
		A_1	-2.7911113E-03	B_1	-2.3830395E-03
		A_2	3.5200992E-06	B_2	4.6717029E-06
		A_3	-2.0849191E-09	B_3	-3.7247428E-09
		A_4	3.9274747E-13	B_4	9.0385624E-13
		A_5	0.0000000E+00	B_5	0.0000000E+00
Type 321 (Figure 4O) A 213 Type 321 A 271 Type 321 A 312 Type 321 A 376 Type 321	$T_{min} = 204^o C\ (400^o F)$ $T_{max} = 843^o C\ (1550^o F)$ $\sigma_{ys}^{T_{min}} = 142\,MPa\ (20.6\ ksi)$ $\sigma_{uts}^{T_{min}} = 430\,MPa\ (62.4\ ksi)$	A_0	1.6512149E+00	B_0	1.1069812E+00
		A_1	-2.5517760E-03	B_1	2.4195844E-04
		A_2	2.7303828E-06	B_2	-3.4616380E-06
		A_3	-1.0524840E-09	B_3	7.9148731E-09
		A_4	3.6127158E-14	B_4	-6.6204087E-12
		A_5	0.0000000E+00	B_5	1.7648940E-15

Table 2E.6 – Minimum Yield and Tensile Strength Values from API Std 530, 6th Edition, September 2008, (1), (2)

Material	Temperature Limits and Strength Parameters at Minimum Temperature (3), (4)	Yield Strength: σ_{ys} (3)		Tensile Strength: σ_{uts} (4)	
Type 321H (Figure 4P) A 213 Type 321H A 271 Type 321H A 312 Type 321H A 376 Type 321H	$T_{min} = 204^o C\ (400^o F)$ $T_{max} = 843^o C\ (1550^o F)$ $\sigma_{ys}^{T_{\min}} = 142\,MPa\ (20.6\ ksi)$ $\sigma_{uts}^{T_{\min}} = 427\,MPa\ (62.0\ ksi)$	A_0	1.5939147E+00	B_0	1.1972163E+00
		A_1	-2.2764479E-03	B_1	-3.3091580E-04
		A_2	2.3000206E-06	B_2	-2.1198718E-06
		A_3	-7.7700412E-10	B_3	6.4820833E-09
		A_4	-2.6637614E-14	B_4	-5.9046170E-12
		A_5	0.0000000E+00	B_5	1.6286232E-15
Type 347 & 347H (Figure 4Q) A 213 Type 347&347H A 271 Type 347&347H A 312 Type 347&347H A 376 Type 347&347H	$T_{min} = 204^o C\ (400^o F)$ $T_{max} = 843^o C\ (1550^o F)$ $\sigma_{ys}^{T_{\min}} = 165\,MPa\ (24.0\ ksi)$ $\sigma_{uts}^{T_{\min}} = 387\,MPa\ (56.2\ ksi)$	A_0	1.3337499E+00	B_0	1.5437300E+00
		A_1	-7.4852863E-04	B_1	-2.4368121E-03
		A_2	-8.1021768E-07	B_2	3.3229020E-06
		A_3	1.8974804E-09	B_3	-1.5387323E-09
		A_4	-8.3958005E-13	B_4	3.9373670E-14
		A_5	0.0000000E+00	B_5	0.0000000E+00
Alloy 800H (Figure 4R) B407 Alloy 800H	(See Note 5)	---	(See Note 5)	---	(See Note 5)
HK-40 (Figure 4S) A608 Grade HK-40	(See Note 5)	---	(See Note 5)	---	(See Note 5)

Note:

1. Data for tensile and yield strength in this table are from Figures 4A through 4S of API Std 530 *Calculation of Heater Tube Thickness in Petroleum Refineries*, 6th Edition, September 2008.
2. Units for the equations in this table are as follows: σ_{ys} and σ_{uts} are in ksi and the temperature, T, is in degrees Fahrenheit (See Notes 3 and 4).
3. σ_{ys} is the value of the yield stress at temperature where $\sigma_{ys}^{T_{\min}}$ is the value of the yield stress (minimum, average, or maximum as applicable) at the minimum temperature limit defined in this table.

$$\sigma_{ys} = \sigma_{ys}^{T_{\min}} \cdot \left(A_0 + A_1 T + A_2 T^2 + A_3 T^3 + A_4 T^4 + A_5 T^5 \right) \qquad \left(ksi, {}^o F \right)$$

4. σ_{uts} is the value of the ultimate tensile stress at temperature where $\sigma_{uts}^{T_{\min}}$ is the value of the ultimate tensile stress (minimum, average, or maximum as applicable) at the minimum temperature limit defined in this table.

$$\sigma_{uts} = \sigma_{uts}^{T_{\min}} \cdot \left(B_0 + B_1 T + B_2 T^2 + B_3 T^3 + B_4 T^4 + B_5 T^5 \right) \qquad \left(ksi, {}^o F \right)$$

5. Data for Figures 4R and 4S are not provided in API Std 530.

Table 2E.7 – Minimum Yield and Tensile Strength in ksi as a Function of Temperature (°F) from WRC Bulletin 541, 3rd Edition

Material	Parameter	Yield Strength (ksi)	Tensile Strength (ksi)
Low Carbon Steel	σ^{rt}	26	47
	C_0	1.4088389E-02	1.0807518E-01
	C_1	-1.9932341E-04	-2.3290664E-03
	C_2	-2.0694516E-08	1.2941407E-05
	C_3	-1.0013720E-10	-2.6166794E-08
	C_4	0	2.2225699E-11
	C_5	0	-7.0569264E-15
Medium Carbon Steel	σ^{rt}	35	60
	C_0	1.4088389E-02	1.0807518E-01
	C_1	-1.9932341E-04	-2.3290664E-03
	C_2	-2.0694516E-08	1.2941407E-05
	C_3	-1.0013720E-10	-2.6166794E-08
	C_4	0	2.2225699E-11
	C_5	0	-7.0569264E-15
C-0.5Mo	σ^{rt}	30	52
	C_0	1.3089229E-02	1.1433749E-01
	C_1	-1.9903245E-04	-2.4719083E-03
	C_2	1.8433603E-07	1.3823832E-05
	C_3	-1.7552202E-10	-2.7995759E-08
	C_4	0	2.3927060E-11
	C_5	0	-7.5170846E-15
1.25Cr-0.5Mo	σ^{rt}	30	60
	C_0	2.1540371E-02	1.4704266E-02
	C_1	-3.2503600E-04	-1.9874800E-04
	C_2	2.2155200E-07	-2.9115300E-07
	C_3	4.1358400E-10	2.0040500E-09
	C_4	-6.4839900E-13	-2.2341400E-12
	C_5	1.5027000E-16	5.9263200E-16

Table 2E.7 – Minimum Yield and Tensile Strength in ksi as a Function of Temperature (°F) from WRC Bulletin 541, 3rd Edition

Material	Parameter	Yield Strength (ksi)	Tensile Strength (ksi)
2.25Cr-1Mo	σ^{rt}	30	60
	C_0	2.1540371E-02	1.4704266E-02
	C_1	-3.2503600E-04	-1.9874800E-04
	C_2	2.2155200E-07	-2.9115300E-07
	C_3	4.1358400E-10	2.0040500E-09
	C_4	-6.4839900E-13	-2.2341400E-12
	C_5	1.5027000E-16	5.9263200E-16
3Cr-1Mo	σ^{rt}	30	60
	C_0	4.4186141E-02	4.3741544E-02
	C_1	-7.1542041E-04	-7.3028160E-04
	C_2	1.2664132E-06	1.6372698E-06
	C_3	-9.3458131E-10	-1.9656642E-09
	C_4	3.6214293E-13	1.2727055E-12
	C_5	-1.6088326E-16	-4.6917217E-16
5Cr-0.5Mo	σ^{rt}	30	60
	C_0	1.2855425E-02	-1.5076613E-03
	C_1	-1.9373113E-04	1.6602155E-04
	C_2	1.2449247E-07	-2.4425324E-06
	C_3	3.0404621E-10	5.7486446E-09
	C_4	-3.5555955E-13	-4.9777060E-12
	C_5	-5.7953915E-18	1.3635365E-15
5Cr-0.5Mo-Si	σ^{rt}	30	60
	C_0	1.2855425E-02	-1.5076613E-03
	C_1	-1.9373113E-04	1.6602155E-04
	C_2	1.2449247E-07	-2.4425324E-06
	C_3	3.0404621E-10	5.7486446E-09
	C_4	-3.5555955E-13	-4.9777060E-12
	C_5	-5.7953915E-18	1.3635365E-15

Table 2E.7 – Minimum Yield and Tensile Strength in ksi as a Function of Temperature (°F) from WRC Bulletin 541, 3rd Edition

Material	Parameter	Yield Strength (ksi)	Tensile Strength (ksi)
7Cr-0.5Mo	σ^{rt}	30	60
	C_0	1.3532100E-01	9.9054977E-03
	C_1	-2.5870657E-03	-1.7559652E-04
	C_2	1.0664886E-05	5.5881927E-07
	C_3	-2.0092622E-08	-1.0648485E-09
	C_4	1.7366385E-11	5.6685649E-13
	C_5	-5.6740415E-15	-1.9197713E-16
9Cr-1Mo	σ^{rt}	30	60
	C_0	1.3571242E-02	2.1597188E-02
	C_1	-1.7082315E-04	-3.1031668E-04
	C_2	-4.3400952E-07	-6.1394577E-08
	C_3	1.6036654E-09	1.3545273E-09
	C_4	-1.5678560E-12	-1.6448546E-12
	C_5	3.6386453E-16	4.1818392E-16
9Cr-1Mo-V	σ^{rt}	60	85
	C_0	3.3650472E-02	1.8096292E-02
	C_1	-5.5446746E-04	-2.5065398E-04
	C_2	1.0944031E-06	-1.9394875E-07
	C_3	-5.7019722E-10	1.2610086E-09
	C_4	-1.9770030E-13	-1.3855450E-12
	C_5	0	3.4264520E-16
Alloy 115 (10.5Cr-V)	σ^{rt}	65	90
	C_0	1.231708E-02	2.908092E-03
	C_1	-1.790514E-04	1.406736E-04
	C_2	-7.122579E-07	-2.267740E-06
	C_3	2.724685E-09	5.749854E-09
	C_4	-2.811096E-12	-5.548227E-12
	C_5	7.679149E-16	1.692498E-15

Table 2E.7 – Minimum Yield and Tensile Strength in ksi as a Function of Temperature (°F) from WRC Bulletin 541, 3rd Edition

Material	Parameter	Yield Strength (ksi)	Tensile Strength (ksi)
Type 304L SS	σ^{rt}	25	70
	C_0	4.5888791E-02	7.7361661E-02
	C_1	-6.9508400E-04	-1.2718700E-03
	C_2	5.7950900E-07	2.4999900E-06
	C_3	-2.1178000E-10	-1.7023100E-09
	C_4	6.5466400E-15	1.2739600E-13
	C_5	-1.2730800E-17	7.2563700E-17
Type 304/304H SS	σ^{rt}	30	75
	C_0	9.8188514E-03	6.7196226E-02
	C_1	-5.0551619E-05	-1.1080527E-03
	C_2	-1.4866719E-06	2.2413756E-06
	C_3	3.0912775E-09	-1.8350694E-09
	C_4	-2.3688742E-12	5.9804933E-13
	C_5	6.0840262E-16	-1.2196459E-16
Type 316L SS	σ^{rt}	25	70
	C_0	4.947300E-02	2.825000E-02
	C_1	-7.820685E-04	-3.814120E-04
	C_2	9.205307E-07	-1.664940E-07
	C_3	-9.753774E-10	1.406040E-09
	C_4	7.836576E-13	-1.341640E-12
	C_5	-2.709835E-16	3.241850E-16
Type 316/316H SS	σ^{rt}	30	75
	C_0	1.4975350E-02	6.3571170E-02
	C_1	-1.4884480E-04	-9.8280180E-04
	C_2	-1.2120110E-06	2.1574480E-06
	C_3	2.2017160E-09	-1.7514100E-09
	C_4	-1.3187870E-12	4.1529270E-13
	C_5	2.3810670E-16	-1.6233610E-17

Table 2E.7 – Minimum Yield and Tensile Strength in ksi as a Function of Temperature (°F) from WRC Bulletin 541, 3rd Edition

Material	Parameter	Yield Strength (ksi)	Tensile Strength (ksi)
Type 317L SS	σ^{rt}	25	70
	C_0	4.947300E-02	2.825000E-02
	C_1	-7.820685E-04	-3.814120E-04
	C_2	9.205307E-07	-1.664940E-07
	C_3	-9.753774E-10	1.406040E-09
	C_4	7.836576E-13	-1.341640E-12
	C_5	-2.709835E-16	3.241850E-16
Type 321 SS	σ^{rt}	30	75
	C_0	6.863218E-02	6.278852E-02
	C_1	-1.184702E-03	-1.080116E-03
	C_2	3.244156E-06	2.863153E-06
	C_3	-4.905795E-09	-3.697114E-09
	C_4	3.536365E-12	2.478506E-12
	C_5	-9.654898E-16	-7.256524E-16
Type 321H SS	σ^{rt}	25	70
	C_0	1.0112716E-02	5.1423451E-02
	C_1	-1.4446737E-04	-8.3118863E-04
	C_2	0	1.4451218E-06
	C_3	0	-9.5441766E-10
	C_4	0	2.5659891E-13
	C_5	0	-8.2941763E-17
Type 347 SS	σ^{rt}	30	75
	C_0	4.9734437E-02	6.9844688E-02
	C_1	-8.6863733E-04	-1.2173646E-03
	C_2	2.5602354E-06	3.4825694E-06
	C_3	-4.5554196E-09	-5.2044883E-09
	C_4	3.7224192E-12	3.8869832E-12
	C_5	-1.0967259E-15	-1.1567466E-15

Table 2E.7 – Minimum Yield and Tensile Strength in ksi as a Function of Temperature (°F) from WRC Bulletin 541, 3rd Edition

Material	Parameter	Yield Strength (ksi)	Tensile Strength (ksi)
Type 347H SS	σ^{rt}	30	75
	C_0	4.9734437E-02	6.9844688E-02
	C_1	-8.6863733E-04	-1.2173646E-03
	C_2	2.5602354E-06	3.4825694E-06
	C_3	-4.5554196E-09	-5.2044883E-09
	C_4	3.7224192E-12	3.8869832E-12
	C_5	-1.0967259E-15	-1.1567466E-15
Type 347LN SS (UNS S34751)	σ^{rt}	30	75
	C_0	3.104110E-02	4.701130E-02
	C_1	-4.327040E-04	-7.548550E-04
	C_2	-2.174960E-07	1.141080E-06
	C_3	7.572260E-10	-9.874450E-10
	C_4	-3.583780E-13	5.854640E-13
	C_5	0.0	-2.099690E-16
Advanced 347 AP (UNS S34752)	σ^{rt}	30	75
	C_0	9.4858959E-02	3.5792780E-02
	C_1	-1.4774538E-03	-4.9495358E-04
	C_2	4.9109700E-06	5.9380604E-07
	C_3	-8.0109761E-09	-4.9866467E-10
	C_4	5.7965728E-12	4.4038093E-13
	C_5	-1.5178862E-15	-2.0950161E-16
Alloy 800	σ^{rt}	30	75
	C_0	3.4030711E-02	3.4512216E-02
	C_1	-5.9044935E-04	-6.1931709E-04
	C_2	1.6819983E-06	2.0239806E-06
	C_3	-2.9084079E-09	-3.3262726E-09
	C_4	2.4078033E-12	2.7021246E-12
	C_5	-7.5887806E-16	-8.8727065E-16

Table 2E.7 – Minimum Yield and Tensile Strength in ksi as a Function of Temperature (°F) from WRC Bulletin 541, 3rd Edition

Material	Parameter	Yield Strength (ksi)	Tensile Strength (ksi)
Alloy 800H	σ^{rt}	25	65
	C_0	9.1352894E-03	8.4274949E-04
	C_1	-6.7153045E-05	8.2765885E-05
	C_2	-1.0330418E-06	-1.5893549E-06
	C_3	1.9114308E-09	3.5471048E-09
	C_4	-1.1936454E-12	-2.7606359E-12
	C_5	2.1862178E-16	6.5642052E-16
Alloy 800HT	σ^{rt}	25	65
	C_0	8.8300983E-03	2.8694938E-02
	C_1	-1.0077128E-04	-3.7098086E-04
	C_2	-1.0539062E-06	1.3818833E-07
	C_3	2.0373420E-09	1.0103445E-09
	C_4	-1.3054492E-12	-1.1807267E-12
	C_5	2.5069564E-16	3.0723317E-16
HK-40	σ^{rt}	35	62
	C_0	4.3689351E-03	4.7208139E-03
	C_1	4.5144996E-05	-1.3979452E-07
	C_2	-1.7279747E-06	-1.1239086E-06
	C_3	2.8459599E-09	2.4482148E-09
	C_4	-1.6093404E-12	-1.8461449E-12
	C_5	2.7808712E-16	4.2367166E-16

Notes:

1. In the parameter column, the term σ^{rt} is used to represent both the room temperature value of the yield strength, σ_{ys}^{rt}, and the room temperature value of the ultimate tensile strength, σ_{uts}^{rt}.
2. The yield strength as a function of temperature is computed using the following equation.

$$\sigma_{ys} = \sigma_{ys}^{rt} \cdot \left(10^{\left[C_0+C_1T+C_2T^2+C_3T^3+C_4T^4+C_5T^5\right]}\right) \qquad \left(ksi, {}^{o}F\right)$$

3. The tensile strength as a function of temperature is computed using the following equation.

$$\sigma_{uts} = \sigma_{uts}^{rt} \cdot \left(10^{\left[C_0+C_1T+C_2T^2+C_3T^3+C_4T^4+C_5T^5\right]}\right) \qquad \left(ksi, {}^{o}F\right)$$

Table 2E.7M – Minimum Yield and Tensile Strength in MPa as a Function of Temperature (°C) from WRC Bulletin 541 3rd Edition

Material	Parameter	Yield Strength (MPa)	Tensile Strength (MPa)
Low Carbon Steel	σ^{rt}	179	324
	C_0	7.6855674E-03	4.5962691E-02
	C_1	-3.6171986E-04	-2.8409842E-03
	C_2	-9.8196907E-08	3.4226184E-05
	C_3	-5.8400015E-10	-1.3643478E-07
	C_4	0	2.2146357E-10
	C_5	0	-1.3334542E-13
Medium Carbon Steel	σ^{rt}	241	414
	C_0	7.6855674E-03	4.5962691E-02
	C_1	-3.6171986E-04	-2.8409842E-03
	C_2	-9.8196907E-08	3.4226184E-05
	C_3	-5.8400015E-10	-1.3643478E-07
	C_4	0	2.2146357E-10
	C_5	0	-1.3334542E-13
C-0.5Mo	σ^{rt}	207	358
	C_0	6.9031992E-03	4.8499500E-02
	C_1	-3.3799347E-04	-3.0061607E-03
	C_2	5.4265437E-07	3.6549739E-05
	C_3	-1.0236444E-09	-1.4585873E-07
	C_4	0	2.3855089E-10
	C_5	0	-1.4204043E-13
1.25Cr-0.5Mo	σ^{rt}	207	414
	C_0	1.1378966E-02	8.1095353E-03
	C_1	-5.5740661E-04	-3.8072714E-04
	C_2	8.3372179E-07	-3.6384086E-07
	C_3	1.9369687E-09	1.0055235E-08
	C_4	-6.5542374E-12	-2.2457714E-11
	C_5	2.8394538E-15	1.1198185E-14

Table 2E.7M – Minimum Yield and Tensile Strength in MPa as a Function of Temperature (°C) from WRC Bulletin 541 3rd Edition

Material	Parameter	Yield Strength (MPa)	Tensile Strength (MPa)
2.25Cr-1Mo	σ^{rt}	207	414
	C_0	1.1378966E-02	8.1095353E-03
	C_1	-5.5740661E-04	-3.8072714E-04
	C_2	8.3372179E-07	-3.6384086E-07
	C_3	1.9369687E-09	1.0055235E-08
	C_4	-6.5542374E-12	-2.2457714E-11
	C_5	2.8394538E-15	1.1198185E-14
3Cr-1Mo	σ^{rt}	207	414
	C_0	2.2559245E-02	2.1986005E-02
	C_1	-1.1469499E-03	-1.1364669E-03
	C_2	3.8195248E-06	4.7181910E-06
	C_3	-5.1897478E-09	-1.0541703E-08
	C_4	3.5314095E-12	1.2572324E-11
	C_5	-3.0399986E-15	-8.8653272E-15
5Cr-0.5Mo	σ^{rt}	207	414
	C_0	6.7930991E-03	1.4870730E-03
	C_1	-3.3277719E-04	4.8085242E-05
	C_2	4.9084202E-07	-6.2233879E-06
	C_3	1.5074276E-09	2.9891688E-08
	C_4	-3.7422560E-12	-4.9963749E-11
	C_5	-1.0950786E-16	2.5764949E-14
5Cr-0.5Mo-Si	σ^{rt}	207	414
	C_0	6.7930991E-03	1.4870730E-03
	C_1	-3.3277719E-04	4.8085242E-05
	C_2	4.9084202E-07	-6.2233879E-06
	C_3	1.5074276E-09	2.9891688E-08
	C_4	-3.7422560E-12	-4.9963749E-11
	C_5	-1.0950786E-16	2.5764949E-14

Table 2E.7M – Minimum Yield and Tensile Strength in MPa as a Function of Temperature (°C) from WRC Bulletin 541 3rd Edition

Material	Parameter	Yield Strength (MPa)	Tensile Strength (MPa)
7Cr-0.5Mo	σ^{rt}	207	414
	C_0	6.2815365E-02	4.8243350E-03
	C_1	-3.5351839E-03	-2.5745402E-04
	C_2	2.8644302E-05	1.4904443E-06
	C_3	-1.0455509E-07	-5.7985052E-09
	C_4	1.7277515E-10	5.6281848E-12
	C_5	-1.0721487E-13	-3.6275384E-15
9Cr-1Mo	σ^{rt}	207	414
	C_0	7.7113926E-03	1.1646861E-02
	C_1	-3.4897841E-04	-5.5853681E-04
	C_2	-9.3821107E-07	1.9009432E-07
	C_3	8.2039083E-09	6.6966996E-09
	C_4	-1.5847572E-11	-1.6564637E-11
	C_5	6.8754677E-15	7.9018695E-15
9Cr-1Mo-V	σ^{rt}	414	586
	C_0	1.7009291E-02	9.9166405E-03
	C_1	-8.7516580E-04	-4.6687084E-04
	C_2	3.3645764E-06	-2.6338749E-07
	C_3	-3.4729727E-09	6.3403610E-09
	C_4	-2.0753787E-12	-1.3969385E-11
	C_5	0	6.4745141E-15
Alloy 115 (10.5Cr-V)	σ^{rt}	450	620
	C_0	5.996168E-03	-4.496855E-04
	C_1	-3.907281E-04	1.885860E-05
	C_2	-1.500992E-06	-5.630629E-06
	C_3	1.378814E-08	2.935645E-08
	C_4	-2.817128E-11	-5.519726E-11
	C_5	1.450945E-14	3.187894E-14

Table 2E.7M – Minimum Yield and Tensile Strength in MPa as a Function of Temperature (°C) from WRC Bulletin 541 3rd Edition

Material	Parameter	Yield Strength (MPa)	Tensile Strength (MPa)
Type 304L SS	σ^{rt}	172	483
	C_0	2.4232587E-02	3.9166165E-02
	C_1	-1.1855614E-03	-2.0107495E-03
	C_2	1.8118539E-06	7.5730942E-06
	C_3	-1.2309742E-09	-9.8284378E-09
	C_4	4.7341153E-14	1.4592314E-12
	C_5	-2.4055712E-16	1.3711405E-15
Type 304/304H SS	σ^{rt}	207	517
	C_0	6.7776790E-03	3.3974200E-02
	C_1	-2.4571713E-04	-1.7462956E-03
	C_2	-3.9018162E-06	6.7030526E-06
	C_3	1.6296309E-08	-1.0262967E-08
	C_4	-2.3845611E-11	6.0732290E-12
	C_5	1.1496181E-14	-2.3046039E-15
Type 316L SS	σ^{rt}	172	483
	C_0	2.5358283E-02	1.5919003E-02
	C_1	-1.3068893E-03	-6.9826034E-04
	C_2	2.6944503E-06	-1.2846913E-07
	C_3	-5.1195868E-09	7.2178566E-09
	C_4	7.7713758E-12	-1.3539494E-11
	C_5	-5.1204175E-15	6.1256960E-15
Type 316/316H SS	σ^{rt}	207	517
	C_0	9.0419880E-03	3.4273780E-02
	C_1	-3.9567860E-04	-1.5300920E-03
	C_2	-3.2680950E-06	6.4536220E-06
	C_3	1.1870160E-08	-9.9051770E-09
	C_4	-1.3444170E-11	4.3323110E-12
	C_5	4.4991880E-15	-3.0674510E-16

Table 2E.7M – Minimum Yield and Tensile Strength in MPa as a Function of Temperature (°C) from WRC Bulletin 541 3rd Edition

Material	Parameter	Yield Strength (MPa)	Tensile Strength (MPa)
Type 317L SS	σ^{rt}	172	483
	C_0	2.5358283E-02	1.5919003E-02
	C_1	-1.3068893E-03	-6.9826034E-04
	C_2	2.6944503E-06	-1.2846913E-07
	C_3	-5.1195868E-09	7.2178566E-09
	C_4	7.7713758E-12	-1.3539494E-11
	C_5	-5.1204175E-15	6.1256960E-15
Type 321 SS	σ^{rt}	207	517
	C_0	3.3886654E-02	3.1038104E-02
	C_1	-1.7850387E-03	-1.6342392E-03
	C_2	9.0545388E-06	8.1752335E-06
	C_3	-2.6028373E-08	-1.9754710E-08
	C_4	3.5501693E-11	2.4799547E-11
	C_5	-1.8243586E-14	-1.3711696E-14
Type 321H SS	σ^{rt}	172	483
	C_0	5.4897602E-03	2.6274211E-02
	C_1	-2.6004127E-04	-1.3348793E-03
	C_2	0	4.3903525E-06
	C_3	0	-5.3795670E-09
	C_4	0	2.5543624E-12
	C_5	0	-1.5672410E-15
Type 347 SS	σ^{rt}	207	517
	C_0	2.4414318E-02	3.4288668E-02
	C_1	-1.2929298E-03	-1.8179369E-03
	C_2	6.9511812E-06	9.7408692E-06
	C_3	-2.3853932E-08	-2.7520039E-08
	C_4	3.7234389E-11	3.8861105E-11
	C_5	-2.0723382E-14	-2.1857514E-14

Table 2E.7M – Minimum Yield and Tensile Strength in MPa as a Function of Temperature (°C) from WRC Bulletin 541 3rd Edition

Material	Parameter	Yield Strength (MPa)	Tensile Strength (MPa)
Type 347H SS	σ^{rt}	207	517
	C_0	2.4414318E-02	3.4288668E-02
	C_1	-1.2929298E-03	-1.8179369E-03
	C_2	6.9511812E-06	9.7408692E-06
	C_3	-2.3853932E-08	-2.7520039E-08
	C_4	3.7234389E-11	3.8861105E-11
	C_5	-2.0723382E-14	-2.1857514E-14
Type 347LN SS (UNS S34751)	σ^{rt}	205	515
	C_0	1.699630E-02	2.399260E-02
	C_1	-7.998200E-04	-1.232610E-03
	C_2	-4.762950E-07	3.401400E-06
	C_3	4.148610E-09	-5.334270E-09
	C_4	-3.762110E-12	5.793300E-12
	C_5	0	-3.967510E-15
Advanced 347AP (UNS S34752)	σ^{rt}	205	515
	C_0	5.2352794E-02	2.0546437E-02
	C_1	-2.1366173E-03	-8.2516548E-04
	C_2	1.3533587E-05	1.7773710E-06
	C_3	-4.2483542E-08	-2.5919811E-09
	C_4	5.8300636E-11	4.2710605E-12
	C_5	-2.8681492E-14	-3.9586755E-15
Alloy 800	σ^{rt}	207	517
	C_0	1.6765895E-02	1.6660434E-02
	C_1	-8.8456405E-04	-8.9937202E-04
	C_2	4.5921687E-06	5.5759413E-06
	C_3	-1.5209739E-08	-1.7434684E-08
	C_4	2.4001532E-11	2.6875549E-11
	C_5	-1.4339517E-14	-1.6765582E-14

Table 2E.7M – Minimum Yield and Tensile Strength in MPa as a Function of Temperature (°C) from WRC Bulletin 541 3rd Edition

Material	Parameter	Yield Strength (MPa)	Tensile Strength (MPa)
Alloy 800H	σ^{rt}	172	448
	C_0	5.9899466E-03	1.9771172E-03
	C_1	-2.2959200E-04	-1.5146142E-05
	C_2	-2.7760533E-06	-4.1004763E-06
	C_3	1.0269469E-08	1.8665113E-08
	C_4	-1.2163211E-11	-2.7877517E-11
	C_5	4.1310072E-15	1.2403512E-14
Alloy 800HT	σ^{rt}	172	448
	C_0	4.5916166E-03	1.6996934E-02
	C_1	-2.9183824E-04	-6.4653512E-04
	C_2	-2.8066821E-06	7.3880969E-07
	C_3	1.0922238E-08	5.0292690E-09
	C_4	-1.3283011E-11	-1.1878762E-11
	C_5	4.7370647E-15	5.8053797E-15
HK-40	σ^{rt}	241	427
	C_0	4.1357071E-03	3.6437596E-03
	C_1	-1.0244174E-04	-1.1661981E-04
	C_2	-4.7451719E-06	-2.9162717E-06
	C_3	1.5412879E-08	1.2925150E-08
	C_4	-1.6427132E-11	-1.8668485E-11
	C_5	5.2546452E-15	8.0055641E-15

Notes:

1. In the parameter column, the term σ^{rt} is used to represent both the room temperature value of the yield strength, σ_{ys}^{rt}, and the room temperature value of the ultimate tensile strength, σ_{uts}^{rt}.
2. The yield strength as a function of temperature is computed using the following equation.

$$\sigma_{ys} = \sigma_{ys}^{rt} \cdot \left(10^{\left[C_0+C_1T+C_2T^2+C_3T^3+C_4T^4+C_5T^5\right]}\right) \qquad \left(MPa, {}^{o}C\right)$$

3. The tensile strength as a function of temperature is computed using the following equation.

$$\sigma_{uts} = \sigma_{uts}^{rt} \cdot \left(10^{\left[C_0+C_1T+C_2T^2+C_3T^3+C_4T^4+C_5T^5\right]}\right) \qquad \left(MPa, {}^{o}C\right)$$

Table 2E.8 – Stress-Strain Curve Parameters

Material	Temperature Limit	m_2 (2)	ε_p
Ferritic Steel (1)	480°C (900°F)	$0.60(1.00-R)$	2.0E-5
Stainless Steel and Nickel Base Alloys	480°C (900°F)	$0.75(1.00-R)$	2.0E-5
Duplex Stainless Steel	480°C (900°F)	$0.70(0.95-R)$	2.0E-5
Precipitation hardening, nickel based austenitic alloys	540°C (1000°F)	$1.09(0.93-R)$	2.0E-5
Aluminum	120°C (250°F)	$0.52(0.98-R)$	5.0E-6
Copper	65°C (150°F)	$0.50(1.00-R)$	5.0E-6
Titanium and Zirconium	260°C (500°F)	$0.50(0.98-R)$	2.0E-5

Notes:

1. Ferritic steels include carbon, low alloy, alloy steels, and ferritic, martensitic, and iron-based age-hardening stainless steels.
2. The parameter R is the ratio of the engineering yield stress to engineering tensile stress evaluated at the assessment temperature (see Equation (2E.26)).

Table 2E.9 – Cyclic Stress-Strain Curve Data, ksi and (°F)

Material Description	Temperature (°F)	n_{css}	K_{css} (ksi)
Carbon Steel (0.75 in. – base metal)	70	0.128	109.8
	390	0.134	105.6
	570	0.093	107.5
	750	0.109	96.60
Carbon Steel (0.75 in. – weld metal)	70	0.110	100.8
	390	0.118	99.60
	570	0.066	100.8
	750	0.067	79.60
Carbon Steel (2 in. – base metal)	70	0.126	100.5
	390	0.113	92.20
	570	0.082	107.5
	750	0.101	93.30
Carbon Steel (4 in. – base metal)	70	0.137	111.0
	390	0.156	115.7
	570	0.100	108.5
	750	0.112	96.90
1Cr–1/2Mo (0.75 in. – base metal)	70	0.116	95.70
	390	0.126	95.10
	570	0.094	90.40
	750	0.087	90.80
1Cr–1/2Mo (0.75 in. – weld metal)	70	0.088	96.90
	390	0.114	102.7
	570	0.085	99.10
	750	0.076	86.90
1Cr–1/2Mo (2 in. – base metal)	70	0.105	92.50
	390	0.133	99.20
	570	0.086	88.00
	750	0.079	83.70
1Cr–1Mo–1/4V	70	0.128	156.9
	750	0.128	132.3
	930	0.143	118.2
	1020	0.133	100.5
	1110	0.153	80.6
2-1/4Cr–1/2Mo	70	0.100	115.5
	570	0.109	107.5
	750	0.096	105.9
	930	0.105	94.60
	1110	0.082	62.10

Table 2E.9 – Cyclic Stress-Strain Curve Data, ksi and (°F)

Material Description	Temperature (°F)	n_{css}	K_{css} (ksi)
9Cr–1Mo	70	0.177	141.4
	930	0.132	100.5
	1020	0.142	88.30
	1110	0.121	64.30
	1200	0.125	49.70
Type 304	70	0.171	178.0
	750	0.095	85.60
	930	0.085	79.80
	1110	0.090	65.30
	1290	0.094	44.40
Type 304 (Annealed)	70	0.334	330.0
800H	70	0.070	91.50
	930	0.085	110.5
	1110	0.088	105.7
	1290	0.092	80.20
	1470	0.080	45.70
Aluminum (Al–4.5Zn–0.6Mn)	70	0.058	65.70
Aluminum (Al–4.5Zn–1.5Mg)	70	0.047	74.10
Aluminum (1100-T6)	70	0.144	22.30
Aluminum (2014-T6)	70	0.132	139.7
Aluminum (5086)	70	0.139	96.00
Aluminum (6009-T4)	70	0.124	83.70
Aluminum (6009-T6)	70	0.128	91.80
Copper	70	0.263	99.10

Table 2E.9M – Cyclic Stress-Strain Curve Data, MPa and (°C)

Material Description	Temperature (°C)	n_{css}	K_{css} (MPa)
Carbon Steel (20 mm – base metal)	20	0.128	757
	200	0.134	728
	300	0.093	741
	400	0.109	666
Carbon Steel (20 mm – weld metal)	20	0.110	695
	200	0.118	687
	300	0.066	695
	400	0.067	549
Carbon Steel (50 mm – base metal)	20	0.126	693
	200	0.113	636
	300	0.082	741
	400	0.101	643
Carbon Steel (100 mm – base metal)	20	0.137	765
	200	0.156	798
	300	0.100	748
	400	0.112	668
1Cr–1/2Mo (20 mm – base metal)	20	0.116	660
	200	0.126	656
	300	0.094	623
	400	0.087	626
1Cr–1/2Mo (20 mm – weld metal)	20	0.088	668
	200	0.114	708
	300	0.085	683
	400	0.076	599
1Cr–1/2Mo (50 mm – base metal)	20	0.105	638
	200	0.133	684
	300	0.086	607
	400	0.079	577
1Cr–1Mo–1/4V	20	0.128	1082
	400	0.128	912
	500	0.143	815
	550	0.133	693
	600	0.153	556
2-1/4Cr–1/2Mo	20	0.100	796
	300	0.109	741
	400	0.096	730
	500	0.105	652
	600	0.082	428

Table 2E.9M – Cyclic Stress-Strain Curve Data, MPa and (°C)

Material Description	Temperature (°C)	n_{css}	K_{css} (MPa)
9Cr–1Mo	20	0.177	975
	500	0.132	693
	550	0.142	609
	600	0.121	443
	650	0.125	343
Type 304	20	0.171	1227
	400	0.095	590
	500	0.085	550
	600	0.090	450
	700	0.094	306
Type 304 (Annealed)	20	0.334	2275
800H	20	0.070	631
	500	0.085	762
	600	0.088	729
	700	0.092	553
	800	0.080	315
Aluminum (Al–4.5Zn–0.6Mn)	20	0.058	453
Aluminum (Al–4.5Zn–1.5Mg)	20	0.047	511
Aluminum (1100-T6)	20	0.144	154
Aluminum (2014-T6)	20	0.132	963
Aluminum (5086)	20	0.139	662
Aluminum (6009-T4)	20	0.124	577
Aluminum (6009-T6)	20	0.128	633
Copper	20	0.263	683

Table 2E.10 – Uniform Material Law for Estimating the Mean Cyclic Stress-Strain Curve and Strain Life Properties

Parameter	Plain Carbon and Low to Medium Alloy Steels	Aluminum and Titanium Alloys
n_{css}	0.15	0.11
K_{css}	$1.65 \cdot \sigma_{uts}$	$1.61 \cdot \sigma_{uts}$
σ_f^*	$1.5 \cdot \sigma_{uts}$	$1.67 \cdot \sigma_{uts}$
ε_f^*	$0.59 \cdot a$	0.35
b	-0.087	-0.095
c	-0.58	-0.69

Cyclic Stress-Strain Curve:

$$\varepsilon_{tr} = \frac{\sigma_r}{E_y} + 2\left[\frac{C_{usm} \cdot \sigma_r}{2K_{css}}\right]^{\frac{1}{n_{css}}}$$

Strain-Life Equation:

$$\frac{\varepsilon_{tr}}{2} = \frac{\sigma_f^*}{E_y}\left(2N_f\right)^b + \varepsilon_f^*\left(2N_f\right)^c$$

where,

$$a = 1.0 \qquad for \qquad \frac{\sigma_{uts}}{E_y} < 0.003$$

$$a = 1.375 - 125.0\left(\frac{\sigma_{uts}}{E_y}\right) \qquad for \qquad \frac{\sigma_{uts}}{E_y} \geq 0.003$$

ANNEX 2F – ALTERNATIVE METHOD FOR ESTABLISHING THE REMAINING STRENGTH FACTOR

(NORMATIVE)

CONTENTS

ANNEX 2F – ALTERNATIVE METHOD FOR ESTABLISHING THE REMAINING STRENGTH FACTOR 2F-1
2F.1 OVERVIEW 2F-1
2F.2 ESTABLISHING AN ALLOWABLE REMAINING STRENGTH FACTOR – RSF_A 2F-1
2F.3 NOMENCLATURE 2F-2
2F.4 REFERENCES 2F-2

2F.1 Overview

As described in Part 2, paragraph 2.4, structural evaluation procedures using linear elastic stress analysis with stress classification and allowable stress acceptance criteria provide only an approximation of the loads that a component can withstand without failure. A better estimate of the safe load carrying capacity of a component can be provided by using non-linear stress analysis to develop limit and plastic collapse loads, evaluate the deformation characteristics of the component (e.g., deformation or strain limits associated with component operability), and assess fatigue and/or creep damage including ratcheting.

In this Standard, the concept of a remaining strength factor is utilized to define the acceptability of a component for continued service. The Remaining Strength Factor (RSF) is defined as:

$$RSF = \frac{L_{DC}}{L_{UC}} \tag{2F.1}$$

With this definition of the RSF, acceptance criteria can be established using traditional code formulas, elastic stress analysis, limit load theory, or elastic-plastic analysis. For example, to evaluate local thin areas (see Part 5), the Fitness-For-Service (FFS) assessment procedures provide a means to compute a RSF. The reduced maximum allowing working pressure, $MAWP_r$, for the component can then be calculated from the RSF using Equations (2F.2) and (2F.3). The resulting value of the $MAWP_r$, minus the static head as appropriate, should be compared to the existing equipment design pressure or equipment $MAWP$.

$$MAWP_r = MAWP\left(\frac{RSF}{RSF_a}\right) \qquad for \quad RSF < RSF_a \tag{2F.2}$$

$$MAWP_r = MAWP \qquad for \quad RSF \geq RSF_a \tag{2F.3}$$

2F.2 Establishing an Allowable Remaining Strength Factor – RSF_a

The recommended value for the allowable Remaining Strength Factor, RSF_a, is 0.90 (see Part 2, paragraph 2.4.2.2). This value was established based on evaluation of burst test results as discussed in references [1], [2] and [3], and has been shown to be conservative. However, the value of RSF_a, may be modified based on the original construction code. The dependence of RSF_a on the original construction code is a result of the allowable stress criteria used in the code. The allowable stress criterion for service below the creep range is typically set to address protection against collapse. A lower design margin in a construction code will result in a lower burst

pressure ratio defined as the burst pressure divided by the $MAWP$ computed using the applicable code rules and allowable stresses. If an in-service margin on the burst pressure ratio is set, then a RSF_a may be selected to produce this margin based on the allowable stress criterion in the construction code. The information to select an RSF_a based on a burst pressure ratio and the design margins in various international construction codes is provided in WRC Bulletin 505 reference [1].

If a value of RSF_a less than 0.90 is used in an assessment, the assumptions and technical basis used for determining this RSF_a shall be included in the documentation of the Fitness-For-Service Assessment.

In addition, the value of the RSF_a, may be modified based on the type of loading (e.g., normal operating loads, occasional loads, short-time upset conditions) and/or the consequence of failure. For example, a lower RSF_a could be utilized for low-pressure piping containing a flaw that conveys cooling water.

2F.3 Nomenclature

L_{DC} limit or plastic collapse load of the damaged component (component with flaws).

L_{UC} limit or plastic collapse load of the undamaged component.

$MAWP$ maximum allowable working pressure of the undamaged component.

$MAWP_r$ reduced maximum allowable working pressure of the damaged component.

RSF remaining strength factor computed based on the flaw and damage mechanism in the component.

RSF_a allowable remaining strength factor.

2F.4 References

[1] Janelle, J.A. and Osage, D.A., An Overview and Validation of the Fitness-For-Service Assessment Procedures for Local Thin Areas in API 579, WRC Bulletin 505, Welding Research Council, Inc., New York, NY, 2005.

[2] Osage, D.A., Janelle, J. and Henry, P.A., “Fitness-For-Service Local Metal Loss Assessment Rules in API 579,” PVP Vol. 411, Service Experience and Fitness-For-Service in Power and Petroleum Processing, ASME, 2000, pp. 143-176.

[3] Osage, D.A., Krishnaswamy, P., Stephens, D.R., Scott, P., Janelle, J., Mohan, R., and Wilkowski, G.M., Technologies for the Evaluation of Non-Crack-Like Flaws in Pressurized Components – Erosion/Corrosion, Pitting, Blisters, Shell Out-Of-Roundness, Weld Misalignment, Bulges and Dents, WRC Bulletin 465, Welding Research Council, Inc., New York, NY, September 2001.

PART 3 – ASSESSMENT OF EXISTING EQUIPMENT FOR BRITTLE FRACTURE

CONTENTS

PART 3 – ASSESSMENT OF EXISTING EQUIPMENT FOR BRITTLE FRACTURE 3-1

3.1 GENERAL 3-2
3.1.1 Evaluation of Resistance to Brittle Fracture 3-2
3.1.2 Avoidance of Catastrophic Brittle Fracture 3-2
3.1.3 Use of Construction Codes and Standards for Brittle Fracture Assessment 3-2
3.1.4 Boilers and Boiler External Piping 3-2
3.1.5 Supplemental Brittle Fracture Assessment to Other FFS Assessment Procedures 3-2
3.1.6 Critical Exposure Temperature (CET) 3-3
3.1.7 Minimum Allowable Temperature (MAT) 3-3
3.2 APPLICABILITY AND LIMITATIONS OF THE PROCEDURE 3-3
3.2.1 Equipment Covered 3-3
3.2.2 Components Subject to Metal Loss 3-4
3.2.3 Requirements for In-Service Inspection and Maintenance Programs 3-4
3.2.4 Supplemental Guidance for SA-212 Grade B Material 3-4
3.3 DATA REQUIREMENTS 3-4
3.3.1 Original Equipment Design Data 3-5
3.3.2 Maintenance and Operational History 3-5
3.3.3 Required Data/Measurements for an FFS Assessment 3-5
3.3.4 Recommendations for Inspection Technique and Sizing Requirements 3-6
3.4 ASSESSMENT TECHNIQUES AND ACCEPTANCE CRITERIA 3-6
3.4.1 Overview 3-6
3.4.2 Level 1 Assessment 3-7
3.4.3 Level 2 Assessment 3-10
3.4.4 Level 3 Assessment 3-15
3.5 REMAINING LIFE ASSESSMENT 3-16
3.5.1 Acceptability for Continued Service 3-16
3.5.2 Pressure Vessels 3-17
3.5.3 Piping Systems 3-17
3.5.4 Atmospheric and Low Pressure Storage Tanks 3-17
3.6 REMEDIATION 3-17
3.6.1 Potential Use of Remediation Methods 3-17
3.6.2 Remediation Methods 3-17
3.7 IN-SERVICE MONITORING 3-19
3.7.1 In-Service Monitoring and Control of Process Conditions 3-19
3.7.2 Monitoring for Degradation of Low Alloy Steel Notch Toughness 3-19
3.7.3 Monitoring for Criticality of Growing Flaws 3-19
3.7.4 Assessment of Non-Growing Flaws Detected In-Service 3-19
3.8 DOCUMENTATION 3-19
3.8.1 Documentation Requirements for Each Assessment Level 3-19
3.8.2 Documentation Retention 3-20
3.9 NOMENCLATURE 3-20
3.10 REFERENCES 3-21
3.11 TABLES 3-22
3.12 FIGURES 3-28

3.1 General

3.1.1 Evaluation of Resistance to Brittle Fracture

This Part provides guidelines for evaluating the resistance to brittle fracture of existing carbon and low alloy steel pressure vessels, piping, and storage tanks. Other materials that could be susceptible to brittle fracture, such as ferritic, martensitic, and duplex stainless steels, are not addressed in this Standard. The principles of some of the methods in Part 3 (e.g., Level 2, Methods B and C and Level 3) can be used to evaluate these materials. However, the user is cautioned that the methodology in Part 3 may not apply to materials that have a transition curve slope that is different from that for carbon and low alloy steels.

3.1.2 Avoidance of Catastrophic Brittle Fracture

The purpose of this assessment is to avoid a catastrophic brittle fracture failure. It is intended to prevent the initiation of brittle fracture; however, it does not ensure against service-induced cracks resulting in leakage nor does it ensure arrest of a running brittle fracture. Unlike other Parts in this Standard, this Part is used to screen for the propensity for brittle fracture. If a crack-like flaw is found, Part 9 should be used for the assessment. A flow chart for the brittle fracture assessment procedure is shown in Figure 3.1 for pressure vessels and piping and Figure 3.2 for storage tanks.

3.1.3 Use of Construction Codes and Standards for Brittle Fracture Assessment

As an alternative to the procedures in Part 3, the user may perform a Level 3 brittle fracture assessment using a construction code or standard (e.g., ASME Section VIII, Division 1, or Division 2). However, the user is cautioned that the methods in construction codes or standards may not provide the same level of protection from potential brittle fracture failures when applied to in-service equipment, especially if brittle fracture was not identified as a failure mode in the original design.

3.1.4 Boilers and Boiler External Piping

Brittle fracture is not considered in boilers constructed in accordance with the ASME Code, Section I and associated piping constructed to ASME B31.1. However, boiler components and boiler external piping may be evaluated using the rules for pressure vessels and piping respectively in this Part if brittle fracture has been identified as a failure mode and if all other applicability limits in this Part are met.

3.1.5 Supplemental Brittle Fracture Assessment to Other FFS Assessment Procedures

A brittle fracture assessment may be required as part of the assessment procedure of another Part in this Standard. In addition, the following circumstances may indicate the need for a brittle fracture assessment.

a) A change in process operating conditions, including startup, shutdown and upset conditions, that increase the possibility of low metal temperatures.

b) A process hazards review indicates that process temperatures, including those during start up, shutdown and upset conditions, could be lower than anticipated in the original design.

c) The equipment was constructed to a pressure vessel or piping code or standard that did not have requirements for the prevention of brittle fracture similar to those in the ASME Code, Section VIII, Division 1, 1987 or later Editions. For example, equipment constructed to earlier Editions of the ASME Code, Section VIII, Division 1 may not meet the requirements for exemption from impact testing and may not have been impact tested as would be required by later Editions.

d) The equipment item is rerated using a lower design margin, to change the MAT, or to modify $MAWP$.

e) A minimum temperature is needed for a hydrotest (see paragraph 3.6.2.3).

f) The status of $PWHT$ has changed (e.g., use of controlled deposition as an alternative to $PWHT$).

g) Continued operation of equipment where an active cracking mechanism remains in service (i.e., Level 1 and Level 2 Assessment no longer valid; Level 3 Assessment required).

h) The equipment is expected to be exposed to a general primary membrane tensile stress (including any stresses due to net section bending) greater than 55 MPa (8 ksi) at or near ambient temperature and either of the following is true:

   1) The equipment has a wall thickness equal to or greater than 50 mm (2 inches).

   2) The equipment has been subjected to conditions that may cause embrittlement.

The owner/user may identify other circumstances where a brittle fracture assessment of equipment items may be warranted based on operating conditions and/or the condition of the component.

3.1.6 Critical Exposure Temperature (CET)

The Critical Exposure Temperature (CET) as used in this Part is defined as the lowest (coldest) metal temperature derived from either the operating or atmospheric conditions at the maximum credible coincident combination of pressure and supplemental loads that result in general primary membrane tensile stress (including any stresses due to net section bending) greater than 55 MPa (8 ksi). Note that operating conditions include startup, shutdown, upset and standby conditions. The CET is specified and may be a single temperature at the maximum credible coincident combination of pressure and supplemental loads if that is also the lowest (coldest) metal temperature for all other combinations of pressure and supplemental loads. If lower (colder) temperatures at lower pressures and supplemental loads are credible, the CET should be defined by an envelope of temperatures and pressures (see paragraph 3.3.3). The CET for atmospheric storage tanks constructed to API 650 is defined as the lower of either the lowest one-day mean atmospheric temperature plus 8°C (15°F), or the hydrostatic test temperature. The CET for low-pressure storage tanks constructed to API 620 should be established using the methodology for pressure vessels (see paragraph 3.3.3).

3.1.7 Minimum Allowable Temperature (MAT)

The Minimum Allowable Temperature (MAT) is the lowest (coldest) permissible metal temperature for a given material and thickness based on its resistance to brittle fracture. It may be a single temperature, or an envelope of allowable operating temperatures as a function of pressure. The MAT is derived from mechanical design information, materials specifications, and/or materials data using the guidelines in this Part.

3.2 Applicability and Limitations of the Procedure

3.2.1 Equipment Covered

This Part should be applied only to the following equipment:

a) Pressure vessels constructed in accordance with any edition of the ASME Code, Section VIII, Divisions 1 and 2. However, the same guidelines may be used for pressure vessels constructed to other recognized codes and standards (see Part 2, paragraphs 2.2.2 and 2.2.3).

b) Boilers constructed in accordance with the ASME Code, Section I if brittle fracture has been identified as a failure mode and if all other applicability limits in this Part are met.

c) Welded, non-welded, and riveted pressure vessels constructed in accordance with any edition of the former API or API/ASME Code for Unfired Pressure Vessels for Petroleum Liquids and Gases.

d) Piping systems constructed in accordance with the ASME B31.3 or ASME B31.1 Codes. However, the same guidelines may be used for piping systems constructed to other recognized codes and standards (see Part 2, paragraphs 2.2.2 and 2.2.3).

e) Atmospheric or low-pressure above ground storage tanks that are welded or riveted, non-refrigerated, or operating at atmospheric or low pressure, and constructed in accordance with any edition of API 650 or API 620.

3.2.2 Components Subject to Metal Loss

The Level 1 and 2 Assessment procedures in this Part may be applied to components subject to general corrosion, local metal loss and pitting damage provided the assessment criteria in Part 4, Part 5, and Part 6, respectively, are satisfied and supplemental inspection is performed in accordance with paragraph 5.3.4.3 of Part 5 to confirm no crack-like flaws exist. In the Level 1 and Level 2 Assessment procedures in this Part, the component shall be evaluated in the undamaged condition (i.e., without any adjustments or modifications for the wall loss that is qualified through Part 4, Part 5, and Part 6). Components with known crack-like flaws shall be evaluated using the procedures in Part 9.

3.2.3 Requirements for In-Service Inspection and Maintenance Programs

The assessment methods in this Part apply only to equipment that has been and will continue to be included in a plant inspection and maintenance program that is consistent with API 510, API 570, API 653, NB 23, or other applicable in-service inspection code. If environmental cracking (e.g., wet H_2S) or a service condition that may result in a loss in the material toughness is credible, the Level 3 procedures of this Part shall be utilized in the assessment. For example, low alloy steels such as 2¼Cr–1Mo may lose toughness at ambient temperature if exposed to high temperatures, above 400°C (750°F), for long periods because of thermal aging degradation mechanisms (see API RP 571 and API 934 series). Components made from these types of materials require special precautions if a hydrotest or other low temperature pressurization is required.

3.2.4 Supplemental Guidance for SA-212 Grade B Material

There have been a number of brittle fracture failures in industry involving pressure components constructed from SA-212 Grade B material. SA-212 Grade B is known to be a relatively low toughness material, and in some instances the material has been found to exhibit toughness lower than the typical lower bound predictions for similar materials. Additionally, the material is also known to be prone to the issue of “dynamic strain age embrittlement.” Thorough and detailed NDE focused on crack detection is recommended as a supplement to the brittle fracture screening procedures in this Part. Any weld repair of such materials should also include thorough and detailed NDE. Supplemental $PWHT$ can decrease the risk of brittle fracture failures.

3.3 Data Requirements

Data that may be needed for a brittle fracture analysis are described in this paragraph. The specific data requirements depend on the type of equipment and the level of the assessment.

3.3.1 Original Equipment Design Data

Mechanical design information, materials of construction, and specific material properties test data, such as Charpy V-notch and tensile data, if available, should be obtained for all components. These data should be obtained for the base metal, weld metal and heat affected zones, if available. An overview of the original equipment data that may be required for an assessment is provided in Part 2, paragraph 2.3.1. A summary of the original equipment design data typically used for an assessment is shown in Table 3.1.

3.3.2 Maintenance and Operational History

In addition to original equipment design data, information pertaining to repair history, and past and future operating conditions should be gathered. These data should include a summary of repairs and alterations and include the current design pressure and temperature as well as the current wall thickness. Previous or proposed operating pressures and temperatures should be included, as well as startup, shutdown, transient and/or upset operating conditions, and extreme environmental conditions. These data are used to establish the most severe operating and exposure conditions encountered during the life of the equipment. Of special concern with existing equipment is any change in the original design that has occurred after the equipment was placed into service that could result in a higher (warmer) MAT than established in the original design (such as repairs or alterations involving different materials or any changes in the applied or residual stresses). Information related to environmental exposure will also be needed to determine whether there is a probability of environmental cracking that would necessitate a Level 3 evaluation. If the equipment was originally $PWHT$, but subsequent repairs were completed without $PWHT$, no credit for stress relief should be applied in the evaluation. An overview of the maintenance and operational history information that should be obtained for an assessment if it is available is provided in Part 2, paragraph 2.3.2. A summary of the maintenance and operational history data typically used for an analysis is shown in Table 3.1.

3.3.3 Required Data/Measurements for an FFS Assessment

The CET loading-temperature envelope should be determined after consideration of all potential operating conditions (including startup, shutdown, upset and standby conditions) using procedures encompassing hazard analysis or other comparable assessment methodologies. Of special concern with existing equipment is any change in the operation that has occurred after the equipment was placed into service that could result in a lower (colder) CET than accounted for in the original design. In determining the CET, the current process design and safety philosophies should be employed. The CET loading-temperature envelope should consider the following process conditions and ambient factors:

a) The lowest (coldest) one-day mean atmospheric temperature, unless a higher (warmer) temperature is specified (e.g., specifying a minimum required startup temperature and coincident pressure). If a higher (warmer) temperature is specified, it shall be confirmed that the system has control capabilities and/or that operating procedures are in place to maintain the higher temperature.

b) The lowest metal temperature under normal operating conditions.

c) The lowest metal temperature associated with startup, shutdown, upset conditions, and standby. The following items should be considered:

   1) Failure of warning and/or shutdown systems (e.g., a pump stops, control valve shuts, etc.).

   2) A colder than expected warming stream.

   3) Reboiler failure or stall (e.g., flow loss of reboiling medium, failure of a control valve, etc.).

d) Potential for autorefrigeration due to depressurization, either during operations or due to equipment failure (e.g., a safety relief valve sticks open). In some services where autorefrigeration can occur, equipment can be chilled to a temperature below the CET at an applied pressure less than that defined in paragraph 3.1.6. When this occurs, the possibility of any repressurization of equipment before the material has had sufficient time to warm up to the CET should be considered.

e) Potential for shock chilling. Shock chilling is defined as a rapid decrease in metal temperature caused by the sudden contact of liquid or a two-phase (gas/liquid) fluid with a metal surface under the following two conditions:

1) The liquid or two-phase fluid shall be colder than the metal temperature at the instant of contact by more than 56°C (100°F) or the temperature difference determined from Figure 3.3, whichever is greater. If the heat transfer properties used in Figure 3.3 are not known, shock chilling should be considered to occur when the liquid or two phase fluid is 56°C (100°F) colder than the metal at the instant of contact. Interpolation may be used for intermediate values of thickness when using Figure 3.3.

2) The liquid or two-phase fluid temperature shall be colder than the Level 1 MAT (see paragraph 3.4.2) for the affected component(s).

Shock chilling does not typically result from rapid changes in temperature in a flowing liquid or two-phase fluid, but rather from the sudden contact of a liquid or two phase fluid with a hot surface. One example of this is a flare header that receives sub-cooled or flashing liquid from a safety valve discharge. The CET shall not be higher (warmer) than the temperature of the liquid causing the shock chilling. With the exception of piping meeting the requirements in Figure 3.4, when the shock chilling criteria above are satisfied, the Level 1 and Level 2 Assessment procedures in this Part are not acceptable and a Level 3 Assessment is required to evaluate components subject to shock chilling.

3.3.4 Recommendations for Inspection Technique and Sizing Requirements

The current component wall thickness is required for Level 2 and Level 3 Assessments. Methods for establishing this thickness are provided in Part 4, paragraph 4.3.4.

3.4 Assessment Techniques and Acceptance Criteria

3.4.1 Overview

An overview of the assessment levels for pressure vessels and piping is shown in Figure 3.1. A separate assessment procedure is provided for tankage as shown in Figure 3.2. A summary of the 3 Assessment levels is described below.

a) The Level 1 Assessment procedures are based on the requirements in the ASME Code, Section VIII, Divisions 1 and 2. Level 1 can be satisfied based on impact test results or impact test exemption curves. At this Level, a single value for the MAT is determined. Development of a load (e.g., pressure) vs. temperature envelope in accordance with the Code requires a Level 2 analysis.

b) The Level 2 Assessment procedures for pressure vessels and piping are divided into three methods (see Figure 3.1). In the first method (Method A), equipment may be exempt from further assessment if it can be shown that the operating pressure and temperature are within an acceptable envelope. In the second method (Method B), equipment may be qualified for continued service based on a hydrotest. In the third method (Method C), equipment may be qualified for continued service based on materials of construction, operating

conditions, service environment and past operating experience. Results from Level 2 Method A, Method B, and Method C evaluations may be combined to develop a single MAT curve. A separate assessment procedure is provided for tankage (see Figure 3.2) that is based on a combination of these three methods.

c) A Level 3 Assessment may be used for equipment that does not meet the acceptance criteria for Levels 1 and 2 and is required for equipment subject to shock chilling and where credible active cracking mechanisms exist. This equipment shall be evaluated on an individual basis with the help of process, materials, mechanical, inspection, safety, and other specialists as appropriate. A Level 3 Assessment normally involves a more detailed evaluation using a fracture mechanics methodology (see Part 9). A Level 3 Assessment should include a systematic evaluation of all of the factors that control the susceptibility of the component to brittle fracture: stress, flaw size, and material toughness.

3.4.2 Level 1 Assessment

3.4.2.1 Pressure Vessels

a) The Level 1 Assessment procedure is based on the toughness rules in the ASME Code, Section VIII, Division 1. The Level 1 Assessment procedure shall be used for vessels constructed to any Edition of Division 1 and vessels constructed to any Edition of Division 2 prior to 2007. The toughness requirements in the current edition of ASME Code, Section VIII, Division 2 should be used for vessels constructed to the 2007 or subsequent Editions of Division 2.

b) Acceptability can be determined from impact test results or from the use of impact test exemption curves.

c) Pressure vessels that have a CET equal to or greater than the MAT, as demonstrated by the following procedure, are exempt from further brittle fracture assessment provided conditions do not change in the future. If a change in the operating conditions is made that affects the CET, a reassessment should be completed. These vessels require no special treatment other than to continue their inclusion in a normal plant inspection and maintenance program encompassing generally accepted engineering practices such as those contained in API 510, NB-23, or other recognized inspection codes.

d) A general procedure for determining the MAT for a component is described below. The MAT for a pressure vessel or for a boiler evaluated as a pressure vessel is the highest (warmest) value of the MAT for any of its components.

1) STEP 1 – Determine the starting point for the MAT using one of the following two options:

i) Option A – Determine the starting point for the MAT using a governing thickness and the impact test exemption curves shown in Figure 3.5 as described below. Consistent with ASME Section VIII, Division 1, UCS-66(f), the use of impact test exemption curves is only permitted for materials, other than bolting, having a specified minimum yield strength of 450 MPa (65 ksi) or less. Materials, other than bolting, having a specified minimum yield strength greater than 450 MPa (65 ksi) that were not impact tested will require a Level 3 Assessment.

I) STEP 1.1 – For the component under consideration, determine the following parameters:

A. Nominal uncorroded thickness at each weld joint, t_n.

B. Material of construction.

II) STEP 1.2 – Determine the uncorroded governing thickness, t_g, (see paragraph 3.4.2.1(e)) based on the nominal uncorroded thickness of the component.

III) STEP 1.3 – Determine the applicable material impact test exemption curve from Figure 3.5. The applicable material impact test exemption curve can be determined from the material specification (see Table 3.2), heat treatment, and steel-making practice. If this information is not available, Curve A should be used.

IV) STEP 1.4 – Determine the MAT from Figure 3.5 based on the applicable material impact test exemption curve and the governing thickness, t_g (see paragraph 3.4.2.1(e)). The MAT for ASME Code, Section VIII, Division 1, Table UCS-23 materials with a governing thickness of 2.5 mm (0.098 inch) or less shall be -48°C (-55°F). The MAT for bolting and nut materials is shown in Table 3.3. The MAT for ferritic flanges meeting ASME B16.5, ASME B16.47, or the Long Weld Neck requirements of ASME Code, Section VIII, Division 1, UCS-66(c)(3) shall be determined as the warmest temperature from the criteria listed below.

A. The MAT shall be set at -18°C (0°F) for ferritic flanges in the as-forged condition and manufactured in 1989 or later, or if the year of manufacturing is unknown.

B. The MAT shall be set at -29°C (-20°F) for ferritic flanges in the as-forged condition and manufactured prior to 1989.

C. The MAT shall be set at -29°C (-20°F) for ferritic flanges in the normalized condition after forging regardless of the year of manufacturing

V) STEP 1.5 – The MAT determined in STEP 1.4 can be reduced further using Equation (3.1) if all of the following are true:

A. The MAT in STEP 1.4 was determined using Figure 3.5,

B. The component was fabricated from ASME P1 Group 1 or P1 Group 2 material,

C. The component has a weld thickness that is less than or equal to 38 mm (1.5 inches), and

D. The component was subjected to $PWHT$ and the status of the $PWHT$ has not been changed because of repairs and/or alterations. For scenarios where a repair or alteration is performed using alternative methods in lieu of $PWHT$ (such as high preheat or temperbead welding, etc.), no credit for $PWHT$ shall be permitted in the evaluation.

$$MAT = \max\left[MAT_{STEP1.4} - 17^{o}C\ (30^{o}F), -48°C(-55°F)\right] \quad (3.1)$$

ii) Option B – If impact test results are available for the component, then the MAT may be set at the temperature at which the impact test values required by the ASME Code, Section VIII, Division 1 or 2, as applicable, or other international codes and standards are satisfied. However, the reduction in the MAT for $PWHT$ that is described in STEP 1.5 above shall not be applied to impact tested components.

2) STEP 2 – Repeat STEP 1 for all components that make-up the equipment being evaluated. The MAT for the equipment is the highest (warmest) value obtained for any component.

e) When determining the MAT, parts such as shells, heads, nozzles, manways, reinforcing pads, flanges, tubesheets, flat cover plates, skirts, and attachments that are essential to the structural integrity of the vessel shall be treated as separate components. Each component shall be evaluated based on its individual material classification (see Tables 3.2 and 3.3, and Figure 3.5) and governing thickness shown in Figure 3.6.

Additionally, the MAT shall be assessed on a weld joint-by-weld joint basis. For welds joining materials of different material impact test exemption curves (per Table 3.2), the more limiting material classification shall be assigned to the weld joint under evaluation. The following governing thickness definitions apply:

1) The uncorroded governing thickness, t_g, of a welded component, excluding castings, is as follows:

   i) For butt joints except those in flat heads and tubesheets, t_g is the nominal thickness of the component at the weld joint (see Figure 3.6(a)),

   ii) For corner, fillet or lap welded joints, including attachments as defined above, t_g is the nominal thickness of the thinner of the two parts joined (see Figure 3.6(b), 3.6(f) and 3.6(g)),

   iii) For blind flanges, flat heads, or tubesheets, t_g is the thinner of the two parts joined at a weld, or the flat component thickness divided by 4, whichever is larger (see Figure 3.6(c), (d) and (e)), and

   iv) For welded assemblies consisting of more than two components (e.g., nozzle-to-shell joint with a reinforcing pad), the t_g and permissible MAT of each of the individual components of the assembly shall be determined and the warmest MAT shall be assigned to the welded assembly (see Figure 3.6(b)).

   v) If the governing thickness at any welded joint exceeds 100 mm (4 inches) and the CET is colder than 50°C (120°F), use of the impact test exemption curves in Figure 3.5 is not permitted.

2) For formed heads, the minimum specified thickness after forming may be used as the governing thickness, t_g, in lieu of the nominal thickness.

3) For components made from pipe, the nominal thickness neglecting the mill tolerance may be used as the governing thickness, t_g. Note that ASME Code, Section VIII, Division 1, Figure UCS-66.2, Note 1 requires that mill tolerance be deducted from the nominal thickness. However, use of nominal thickness results in a more conservative value for the Level 1 MAT and is consistent with the requirements of ASME B31.3.

4) The governing thickness of a casting is its largest nominal thickness.

5) The governing thickness of flat non-welded parts, such as bolted blind flanges (see STEP 1.4 in paragraph 3.4.2.1(d)), tubesheets, and flat heads, is the component thickness divided by four (see Figure 3.6(c)).

6) The governing thickness of a non-welded dished head (see ASME Section VIII, Division 1, Appendix 1, Figure 1-6, Sketch (c)) is the greater of the flat flange thickness divided by four (4) or the minimum thickness of the dished portion.

7) If the governing thickness of a non-welded component exceeds 150 mm (6 inches) and the CET is colder than 50°C (120°F), use of the impact test exemption curves in Figure 3.5 is not permitted.

3.4.2.2 Piping Systems

Piping systems should be evaluated on a component and weld joint-by-weld joint basis using the procedures in paragraph 3.4.2.1. The MAT for a piping system is the highest (warmest) MAT obtained for any of the components in the system.

3.4.2.3 Atmospheric and Low Pressure Storage Tanks

a) Atmospheric storage tanks constructed to API 650 shall meet the Level 1 Assessment criteria contained in Figure 3.2, as applicable, and the accompanying notes. The Level 1 Assessment criteria require that these tanks meet the toughness requirements contained in API 650 or an equivalent construction code.

b) Low-pressure storage tanks constructed to API 620 shall be evaluated as pressure vessels using the assessment procedures of paragraph 3.4.2.1.

c) The Level 1 procedure is not applicable for atmospheric or low-pressure storage tanks that contain a refrigerated product or for tanks with lap-welded components.

3.4.2.4 If the component does not meet the Level 1 Assessment requirements, then a Level 2 or Level 3 Assessment may be performed.

3.4.3 Level 2 Assessment

3.4.3.1 Pressure Vessels – Method A

a) Pressure vessels may be exempt from further assessment at this level if it can be demonstrated that the operating pressure and temperature is within an acceptable envelope with respect to component design stress and the MAT.

b) The MAT may be adjusted from the value determined in the Level 1 Assessment by considering temperature reduction allowances as described below. If the Level 1 MAT was determined from impact test values and these values exceed the code minimum requirement, then the MAT from Level 1 may be used as the starting point for a Level 2 Assessment. A reduction in the MAT from the Level 1 value may be applied to pressure vessels with excess thickness due to lower actual operating stresses at the low temperature pressurization condition. These temperature reductions can also be applied to vessels designed for elevated temperatures that have excess thickness at low-temperature conditions because of the difference in design allowable stresses. A procedure for determining the MAT considering the temperature reductions is shown below. This procedure can only be used for components with an allowable stress value less than or equal to 172.5 MPa (25 ksi); otherwise, a Level 3 Assessment is required.

   1) STEP 1 – Determine the starting point for the MAT using one of the following two options:

      i) Option A – The MAT is determined using Option A, STEP 1.4 of paragraph 3.4.2.1(d).

      ii) Option B – The MAT is determined using Option B, STEP 1.4 of paragraph 3.4.2.1(d).

   2) STEP 2 – For the component under consideration, determine the following parameters:

      i) All applicable loads and coincident CET. A summary of the loads that should be considered is included in Annex 2C, Table 2C.2.

      ii) Previous metal loss associated with the nominal thickness, $LOSS$.

      iii) Future corrosion allowance associated with the nominal thickness, FCA.

      iv) Weld joint efficiencies, E and E^*.

      v) Required thickness in the corroded condition for all applicable loads, t_{min}, using the applicable weld joint efficiency, E, and evaluated at the low-temperature (i.e., < 50°C (120°F)) operating condition under consideration.

3) STEP 3 – Determine the stress ratio, R_{ts}, using one of the equations shown below. Note that this ratio can be computed in terms of the quantities shown below. When determining these quantities, the minimum required thickness, applied general primary membrane stress (including any stress due to net section bending), and applied pressure are based on the tensile stress state associated with the low-temperature operating condition being evaluated. For components not exposed to general primary membrane tensile stress, the Pressure-Temperature Rating Basis shown in Equation (3.4) shall be used. For welded assemblies consisting of more than two components (e.g., nozzle-to-shell joint with a reinforcing pad), the starting point for the Level 2 MAT is the Level 1 MAT for the welded assembly established in accordance with paragraph 3.4.2.1(e)(iv). Compressive stress states (e.g., external pressure, axial compressive stress due to weight of a vertical vessel, net section bending compressive stress due to wind acting on a vertical vessel, net section bending compressive stress at mid-span of saddle-supported horizontal vessels, etc.), are not considered in a Part 3 analysis.

$$R_{ts} = \frac{t_{\min} E^*}{t_n - LOSS - FCA} \qquad (Thickness\ Basis) \tag{3.2}$$

$$R_{ts} = \frac{S^* E^*}{SE} \qquad (Stress\ Basis) \tag{3.3}$$

$$R_{ts} = \frac{P_a}{P_{rating}} \qquad (Pressure - Temperature\ Rating\ Basis) \tag{3.4}$$

The pressure rating in Equation (3.4), P_{rating}, may be calculated as shown below for nozzle assemblies and flange assemblies:

i) For a nozzle assembly, P_{rating} may be calculated using Annex 2C, paragraph 2C.3.4.

ii) For a flange assembly, P_{rating} may be calculated using Annex 2C, paragraph 2C.3.6 or from ASME/ANSI pressure-temperature ratings (e.g., ASME B16.5, ASME B16.47).

4) STEP 4 – Determine the reduction in the MAT based on the R_{ts} ratio.

i) If the starting point for the MAT is established using Option A in STEP 1, then:

I) If the computed value of the R_{ts} ratio from STEP 3 is less than or equal to the R_{ts} ratio threshold from Figure 3.7, then set the MAT to -104°C (-155°F).

II) If the computed value of the R_{ts} ratio from STEP 3 is greater than the R_{ts} ratio threshold from Figure 3.7, then determine the temperature reduction, T_R, based on the R_{ts} ratio using Figure 3.7. The reduced MAT can be calculated using the following equation:

$$MAT = \max\left[\left(MAT_{STEP1} - T_R\right),\ -48^o C\,(-55^o F)\right] \tag{3.5}$$

ii) If the starting point for the MAT is established using Option B in STEP 1, then:

I) If the computed value of the R_{ts} ratio from STEP 3 is less than or equal to the R_{ts} ratio threshold from Figure 3.7, then set the MAT to -104°C (-155°F).

II) If the computed value of the R_{ts} ratio from STEP 3 is greater than the R_{ts} ratio threshold from Figure 3.7, then the reduced MAT is determined as follows.

A. For components with base metal and weld procedures that are impact tested at or below -48°C (-50°F), the reduced MAT is determined using Equation (3.6).

$$MAT = \max\left[\left(MAT_{STEP1} - T_R\right),\ -104^oC\,(-155^oF)\right] \quad (3.6)$$

B. For components that are impact tested above -48°C (-50°F), the reduced MAT is determined using Equation (3.7) for the as-welded condition or Equation (3.8) if the component was subjected to $PWHT$ and the status of the $PWHT$ has not been changed because of repairs and/or alterations. For scenarios where a repair or alteration is performed using alternative methods in lieu of $PWHT$ (such as high preheat or temper bead welding, etc.), no credit for $PWHT$ shall be permitted in the evaluation.

$$MAT = \max\left[\left(MAT_{STEP1} - T_R\right), -48^oC\,(-55^oF)\right] \quad \left(As\text{-}Welded\ Condition\right) \quad (3.7)$$

$$MAT = \max\left[\left(MAT_{STEP1} - T_R\right),\ -104^oC\,(-155^oF)\right] \quad \left(PWHT\ Condition\right) \quad (3.8)$$

5) STEP 5 – The MAT determined in STEP 4 can be reduced further if all of the following conditions are met:

i) the starting point for the MAT in STEP 1 was determined using Figure 3.5,

ii) the component was fabricated from P1 Group 1 or P1 Group 2 material,

iii) the component has a weld thickness that is less than or equal to 38 mm (1.5 inches), and

iv) the component was subject to $PWHT$ and the status of the $PWHT$ has not been changed because of repairs and/or alterations. For scenarios where a repair or alteration is performed using alternative methods in lieu of $PWHT$ (such as high preheat or temperbead welding, etc.), no credit for $PWHT$ shall be permitted in the evaluation.

$$MAT = \max\left[\left(MAT_{STEP4} - 17^oC\ (30^oF)\right), -104^oC\ (-155^oF)\right] \quad (3.9)$$

6) STEP 6 – Repeat STEPs 1 through 5 for all components that make up the equipment being evaluated. The MAT for the equipment is the highest (warmest) value obtained for any component. When specified as an envelope of pressure-temperature points, the MAT for the equipment is the highest (warmest) temperature value obtained from all components in the vessel at the associated pressure. A vessel MAT curve may consist of a composite of component MAT curves if the same component does not govern for all pressures.

3.4.3.2 Pressure Vessels – Method B

a) A vessel may be qualified for continued service based on a hydrotest. A minimum acceptable temperature for operating pressures below the hydrotest pressure can be determined using Figure 3.8. This method is limited to a maximum hydrotest pressure of 125%, 130% or 150% (i.e., the hydrotest factor based on the code of construction) of the design pressure corrected for the ratio of the allowable stress at test temperature to the allowable stress at design temperature; this method is also limited to materials with an allowable design stress equal to or less than 172.5 MPa (25 ksi).

1) The risk associated with a potential brittle fracture during the hydrotest shall be considered prior to commencement of the test.

2) Qualification through Method B does not confirm adequacy for any particular crack-like flaw size, nor does it ensure protection from potential brittle fracture in the event future crack-like flaws or defects are introduced into the vessel. Additionally, if a repair is required, re-evaluation is necessary.

3) The test pressure should be corrected for the difference in allowable stresses between the design and hydrotest temperatures, but the test pressure should be limited as required above and to a value that will not produce a general primary membrane stress (including any stresses due to net section bending) higher than 90% of the ambient specified minimum yield strength for the steel used in the construction of the vessel. This can provide an additional advantage for vessels designed for elevated temperatures that have a design stress value lower than the allowable stress at ambient temperature.

4) The metal temperature during hydrotest, rather than water temperature, is the relevant parameter in a brittle fracture assessment. Therefore, it is preferable to measure and use this value directly. Records of the measured metal temperature used in the assessment should be kept.

5) If the hydrotest is performed at a temperature colder than the MAT plus 17°C (30°F), a brittle fracture may occur during the hydrotest. In this evaluation, the MAT shall be determined using a Level 1 assessment.

6) The MAT shall not be less than -104°C (-155°F) after adjustments using this procedure.

b) If the vessel is subject to multiple operating conditions, a MAT curve may be established using Figure 3.8 by plotting the pressure versus the permissible temperature.

3.4.3.3 Pressure Vessels – Method C

a) Pressure vessels that meet all of the criteria in items 1 through 9 below, may be considered to be acceptable for continued service without further assessment when the additional requirements in b), c), and d) are satisfied. Vessels that satisfy these criteria shall be assigned a MAT consistent with the service experience. Note that the MAT may be a single temperature or a pressure-temperature operating envelope for the vessel.

1) Pressure vessels fabricated from P-1 and P-3 steels (as defined in the ASME Code, Section IX) where the maximum design temperature is less than or equal to 343°C (650°F). P-4 and P-5 steels may also be evaluated at this level, provided the proper precautions (e.g., preheating prior to pressurization) are taken to avoid brittle fracture due to in-service embrittlement.

2) The equipment satisfied all requirements of a recognized code or standard (see Part 2, paragraph 2.2.2) at the time of fabrication.

3) The nominal operating conditions have been essentially the same and consistent with the specified design conditions for a period of at least 5 years, and more severe conditions (i.e., lower temperature and/or higher stress) are not expected in the future. Records shall be kept of the measured metal temperature(s) or justification for assumed metal temperature(s) along with the corresponding pressure(s) used in the assessment.

4) The CET at the equipment design pressure or equipment $MAWP$ is greater than or equal to -29°C (-20°F).

5) The nominal uncorroded governing thickness is not greater than 50.8 mm (2 inches).

6) Cyclic service as defined in Part 14 is not a design requirement.

7) The equipment is not subject to environmental cracking (see Annex 2B).

8) The equipment is not subject to shock chilling (see paragraph 3.3.3(e) for a definition of shock chilling).

9) The component material allowable design stress value is less than or equal to 172.5 MPa (25 ksi).

b) Pressure vessels that are assessed using Method C of the Level 2 Assessment procedure are qualified for continued operation based on their successful performance demonstrated during past operation.

1) If a repair is required, re-evaluation is necessary. The guidelines in paragraph 3.6 should be followed to ensure that the probability of brittle fracture does not increase.

2) Records shall be kept of the measured metal temperature(s) or justification for assumed metal temperature(s), and corresponding pressure(s) used in the assessment.

3) Qualification through Method C neither confirms adequacy for any particular crack-like flaw size nor does it ensure protection from potential brittle fracture in the event future crack-like flaws or defects are introduced into the vessel.

c) A documented pressure and metal temperature combination from the operating history of a component may be extrapolated to a pressure no more than 10% above the documented pressure using Figure 3.9. In no case shall the resulting pressure be higher than the equipment $MAWP$.

d) A documented pressure and metal temperature combination from the operating history of a component shall be used as the basis for developing a MAT pressure-temperature operating envelope as follows:

1) STEP 1 – Determine the stress ratio, R_{ts}, for a series of metal temperatures below the documented temperature from the operating history. The stress ratio, R_{ts}, is defined in paragraph 3.4.3.1(b)(3).

2) STEP 2 – Determine the temperature reduction, T_R, based on the R_{ts} ratio from STEP 1 and the R_{ts} ratio threshold from Figure 3.7.

3) STEP 3 – Determine the reduction in the MAT based on the R_{ts} ratio from STEP 1.

i) If the computed value of the R_{ts} ratio from STEP 1 is less than or equal to the R_{ts} ratio threshold from Figure 3.7, then set the MAT to -104°C (-155°F).

ii) If the computed value of the R_{ts} ratio from STEP 1 is greater than the R_{ts} ratio threshold from Figure 3.7, then determine the temperature reduction, T_R, from Figure 3.7 based on the R_{ts} ratio. The reduced MAT can be calculated using the following equation:

$$MAT = \max\left[\left(MAT_{STEP1} - T_R\right),\ -48^o C\,(-55^o F)\right] \tag{3.10}$$

3.4.3.4 Piping Systems – Method A

a) Piping systems are acceptable if it can be demonstrated that the operating pressure/temperature is within an acceptable envelope with respect to component design stress and the MAT. The provisions in paragraph 3.4.3.1 can be applied to piping to lower the MAT when the operating stress level is below the design allowable stress.

b) Assessments of piping systems shall consider component stress due to combined sustained and thermal loads and the following guidelines:

1) The circumferential stress shall be calculated based on the nominal wall thickness minus the metal loss, future corrosion allowance, mechanical allowances, and the manufacturing mill tolerance.

2) The longitudinal stress shall be calculated based on the combined stress resulting from pressure, dead weight, and displacement strain. In calculating the longitudinal stress, the forces and moments in the piping system should be determined using section properties based on the nominal dimensions adjusted for metal loss and future corrosion allowance, and the stress should be calculated using section properties based on the nominal dimensions minus the metal loss, future corrosion allowance, and mechanical allowances. Stress intensification factors associated with pipe bends, elbows, tees, etc., should not be included in the longitudinal stress calculation. It is not necessary that the thermal stress calculation consider a full design range, such as would result from a system with a high design temperature. It should best reflect the actual stress imposed at low temperature.

3.4.3.5 Piping Systems – Method B

a) Piping systems are acceptable if it can be demonstrated that the operating pressure and coincident temperature are within an acceptable envelope with respect to a hydrotest condition. The approach discussed in paragraph 3.4.3.2 that provides for a reduction in the MAT shall be applied to piping.

b) Assessments of piping systems shall consider component stress due to combined sustained and thermal loads and following the guidelines of paragraph 3.4.3.4(b).

3.4.3.6 Piping Systems – Method C

Piping systems are acceptable if the assessment criteria in Figure 3.4 and the accompanying notes are satisfied. This method is limited to piping components with a thickness of 38 mm (1.5 inches) or less and for materials with an allowable design stress value less than or equal to 172.5 MPa (25 ksi). Piping systems that are assessed using Method C of the Level 2 Assessment procedure are qualified for continued operation based on their successful performance demonstrated during past operation.

3.4.3.7 Atmospheric and Low Pressure Storage Tanks

a) Atmospheric and low-pressure storage tanks that operate at ambient temperature (including those that contain a heated product) shall meet the Level 2 Assessment criteria contained in Figure 3.2 and the accompanying notes.

b) Low pressure storage tanks constructed to API 620 shall be evaluated as pressure vessels using the assessment procedures in paragraphs 3.4.3.1, 3.4.3.2 and 3.4.3.3.

c) The Level 2 procedure is not applicable for atmospheric or low-pressure storage tanks that comprise lap-welded components or tanks that contain a refrigerated product unless a detailed stress analysis is performed.

3.4.3.8 If the component does not meet the Level 2 Assessment requirements, then a Level 3 Assessment may be performed.

3.4.4 Level 3 Assessment

3.4.4.1 Pressure vessels, piping, and tankage that do not meet the criteria for Level 1 or 2 Assessments may be evaluated using a Level 3 Assessment. Level 3 Assessments are required for components subjected to shock chilling. Level 3 Assessments are also required for any components in which an active cracking mechanism

exists. Level 3 Assessments normally involve more detailed determinations of one or more of the three factors that control the susceptibility to brittle fracture: stress, flaw size and material toughness.

3.4.4.2 Part 9 may be used as a basis for a Level 3 Assessment. A risk analysis considering both the probability and potential consequences of a brittle fracture in the specific service should also be considered in a Level 3 Assessment. A procedure that may be used to determine the MAT is provided in Annex 9J.

3.4.4.3 At this assessment level, the judgment of the engineer involved (see Part 1, paragraph 1.4.3) may be used to apply some of the principles of Levels 1 and 2 without the specific restrictions used at those levels. Examples of some other approaches that may be considered are described below.

a) A heat transfer analysis may be performed to provide a less conservative estimate of the lowest metal temperature to which the vessel will be exposed in service.

b) If loadings are always quasi-static, the additional credits due to the temperature shift between dynamic (e.g., Charpy V-notch) and quasi-static toughness may be considered.

c) Inspection of seam welds and attachment welds to the pressure shell can be made to determine the presence and size of crack-like flaws. Guidance on acceptable flaw sizes based on a flaw assessment (see Part 9) can be used. The extent of subsequent inspections should be based upon the severity of the service considering the conditions given in paragraph 3.3.3. Ultrasonic examination from the outside is permissible if the inside surface cannot be inspected directly.

3.4.4.4 It may be necessary to evaluate stresses using advanced techniques such as finite element analysis. Consideration should be given to all relevant loads including those that produce localized stresses (e.g., forces and moments at nozzles), thermal transient effects, and residual stress. These additional considerations may result in different criteria for different locations within a piece of equipment. Probable locations and orientations of crack-like flaws should be determined to guide the stress analyst.

3.4.4.5 A Level 3 Assessment normally relies on a determination of maximum expected flaw sizes at locations of high stress. In general, these postulated flaws should be assumed to be surface breaking and oriented transverse to the maximum stress. For welded structures, this often implies that the flaw is located within the residual stress field parallel to a longitudinal weld or transverse to a circumferential weld. The maximum expected flaw size should be detectable with standard NDE techniques. The detectable flaw size will depend on factors such as surface condition, location, accessibility, operator competence, and NDE technique, Part 9 can be used to derive limiting sizes for crack-like flaws. In this assessment, the aspect ratio of the assumed flaw should be large enough to ensure that the calculations are not highly sensitive to small variations in flaw depth in the through thickness direction. To reduce this sensitivity, a minimum crack-like flaw aspect ratio of 6:1 is recommended.

3.4.4.6 The use of material toughness data from appropriate testing is the preferred basis for a Level 3 Assessment. Where this is not practical, appropriate, and sufficiently conservative estimates should be made. Methods for obtaining or estimating fracture toughness are described in Annex 9F. The effects from any potential toughness degradation mechanisms should be appropriately addressed. The effect of warm prestress (or hydrotest) on fracture toughness can be quantified using the procedure in WRC Bulletin 562.

3.5 Remaining Life Assessment

3.5.1 Acceptability for Continued Service

Remaining life is not normally an issue associated with equipment's resistance to brittle fracture. Therefore, equipment evaluated using the Level 1 or 2 Assessment procedures is acceptable for future operation if operating

conditions do not become more severe and there is no active damage mechanism that can result in loss of material toughness or the propagation of a crack-like flaw. If this is not the case, a Level 3 Assessment shall be performed, and the remaining life associated with the time for a flaw to grow to critical size should be calculated.

3.5.2 Pressure Vessels

Pressure vessels constructed of materials that satisfy the requirements of a Level 1, 2, or 3 Assessment are considered acceptable for continued service. Pressure vessels can be fully pressurized within the limits of their design parameters at any metal temperature above the MAT.

3.5.3 Piping Systems

Piping systems constructed of materials that satisfy the requirements of a Level 1, 2, or 3 Assessment are considered acceptable for continued service. Piping systems can be fully pressurized within the limits of their design parameters at metal temperatures above the MAT. The acceptability of piping systems for continued service can be determined by using similar methods as those to evaluate pressure vessels. There are two facts that distinguish piping from pressure vessels and make piping less likely to experience brittle fracture:

a) A lower MAT is more easily attainable because the component is usually thinner (see Figure 3.5, Note 4); and,

b) There is a lower probability that crack-like flaws will be oriented perpendicular to the highest stress direction in piping systems because there are fewer longitudinal weld seams (i.e., seamless pipe). However, some piping systems may have high bending stresses in circumferential seams at low temperature due to thermal contraction.

3.5.4 Atmospheric and Low Pressure Storage Tanks

Atmospheric and low-pressure storage tanks constructed of materials that satisfy the requirements of a Level 1, 2, or 3 Assessment are considered acceptable for continued service. A Level 3 Assessment for storage tanks should follow the same general guidelines as used for pressure vessels. However, the analysis shall reflect the special design considerations used for storage tanks such as the bottom plate-to-shell junction.

3.6 Remediation

3.6.1 Potential Use of Remediation Methods

An FFS analysis typically provides an evaluation of the condition of a component for continued operation for a period based upon a degradation rate. In the case of brittle fracture, a component is suitable for continued service as long as the operating conditions do not become more severe and/or there is no active material degradation mechanism that can result in loss of material toughness or the propagation of crack-like flaws. However, in many cases, future degradation rates are very difficult to predict, or little or no further degradation can be tolerated. Therefore, the Owner-User may choose to apply mitigation methods to prevent or minimize the rate of further damage.

3.6.2 Remediation Methods

Remediation methods are provided below. These methods are not inclusive for all situations, nor are they intended to be a substitute for an engineering evaluation of a particular situation. The Owner-User should consult

a qualified metallurgist/corrosion engineer and a pressure vessel engineer as to the most appropriate method to apply for the relevant damage mechanism(s).

3.6.2.1 Limiting Operation – The limitation of operating conditions to within the acceptable operating pressure-temperature envelope is the simplest type of remediation effort. This method, however, may be impractical in many cases because of the requirements for stable process operation. The most successful, and effective, technique for limiting operation has been to implement a controlled start-up procedure. This is because many petroleum and chemical processes that undergo this type of assessment for brittle fracture were originally designed for substantially warmer temperatures, above the temperature range where the probability of brittle fracture is of concern.

3.6.2.2 Post Weld Heat Treatment ($PWHT$) – If the component has not been subject to $PWHT$, $PWHT$ may be performed to enhance the damage tolerance to crack-like flaws and resistance to brittle fracture. The effects of $PWHT$ are described below.

a) The beneficial effects of $PWHT$ are:

   1) A reduction in the residual stresses that contribute to the driving force for brittle fracture.

   2) Improvement in the resistance of hard heat affected zones to environmental cracking and a potential improvement in the toughness. Conducting $PWHT$ in certain active cracking mechanism services such as Wet H_2S service can mitigate the potential for future cracking.

b) The detrimental effects of $PWHT$ are:

   1) A potential reduction in the toughness of the heat affected zone.

   2) The potential for reheat cracking in certain materials (see API RP 571).

   3) A potential for increased cracking due to the thermal gradients/constraint imposed during $PWHT$ when the equipment is in an active cracking mechanism service or the $PWHT$ is not engineered or executed properly.

3.6.2.3 Hydrostatic Test – If the component has not been subjected to a hydrotest, then a hydrotest may be performed to enhance the damage tolerance to crack-like flaws and resistance to brittle fracture. The beneficial effect of a hydrotest is that crack-like flaws located in the component are blunted resulting in an increase in brittle fracture resistance. The beneficial effects of a hydrotest can be quantified using a Level 2 Assessment (see paragraph 3.4.3.2) or a Level 3 Assessment. If a hydrotest is performed, it should be conducted at a metal temperature that will permit plastic flow without the possibility of brittle fracture (i.e., conduct the test at a metal temperature that is in the upper shelf region of the transition curve). A typical hydrotest temperature that has been used is 17°C (30°F) above the MAT.

3.6.2.4 Rerate Using Higher Allowable Stresses – If the equipment or component meets the requirements in Annex 2C, paragraph 2C.2.4 and a rerate is performed using a lower design margin, the lower stress ratio in a Level 2 evaluation will result in a lower MAT.

3.6.2.5 Reduce the Future Corrosion Allowance – If the FCA for the component is reduced, the lower stress ratio in a Level 2 evaluation will result in a lower MAT. Consideration can be given to reducing the FCA to obtain a few years of future operation until a permanent mitigation can be implemented.

3.6.2.6 Replace the component/equipment – Components or entire pieces of equipment that fail to meet brittle fracture requirements may be replaced with an acceptable metallurgy and/or impact tested to meet CET requirements.

3.6.2.7 External Heating Source – The use of external heating sources (e.g., steam tracing, electrical tracing, etc.) may provide adequate protection from potential brittle fracture scenarios, even if temporarily until a permanent mitigation can be implemented.

3.7 In-Service Monitoring

3.7.1 In-Service Monitoring and Control of Process Conditions

In-service monitoring and control of process conditions, with operating procedures in place to remain within a defined pressure-temperature envelope, can reduce the probability of brittle fracture.

3.7.2 Monitoring for Degradation of Low Alloy Steel Notch Toughness

Certain materials, such as the chromium-molybdenum low alloy steels, experience a loss of notch toughness due to long-term exposure at high temperatures (e.g., temper embrittlement). This degradation may be monitored over the service life by means of sentinel material included within a pressure vessel. Periodically, a portion of this material is removed and tested to monitor for the degradation of material toughness. The degradation of material properties is evaluated against a minimum acceptable brittle fracture criterion that has previously been established. A Level 3 Assessment is usually required to justify continued use when the material no longer meets this criterion.

3.7.3 Monitoring for Criticality of Growing Flaws

Flaws that develop or propagate during the service life of equipment can increase the probability of brittle fracture. The assessment of each type of flaw is prescribed in other Parts of this Standard; see Part 2 for an overview.

3.7.4 Assessment of Non-Growing Flaws Detected In-Service

In-service inspections may result in the detection of flaws that are original material or fabrication flaws. These flaws may or may not be in excess of the requirements of the original design and construction code. While these flaws may have been innocuous relative to the original design code, their presence may affect current or altered design and operating parameters. Alternatively, flaws may have developed or resulted from service exposure, excessive operating conditions, or maintenance-related activities. The influence of such flaws on the increased susceptibility for brittle fracture should be assessed. This assessment generally requires a Level 3 analysis.

3.8 Documentation

3.8.1 Documentation Requirements for Each Assessment Level

The documentation for each level of brittle fracture assessment should include the information cited in Part 2, paragraph 2.8, and the following specific requirements:

3.8.1.1 Level 1 Assessment – Documentation covering the assessment, the specific data used, and the criteria that have been met by the results obtained from the evaluation.

3.8.1.2 Level 2 Assessment – The documentation should address the reason(s) for the assessment, the assessment level used, the engineering principles employed, the source of all material data used, identification of

any potential material property degradation mechanisms and their associated influence on the propagation of flaws, and the criteria applied in the assessment procedure.

3.8.1.3 Level 3 Assessment – The documentation should cover the reason(s) for performing a Level 3 Assessment and all issues pertaining to the Fitness-For-Service Assessment. The documentation should also address the engineering principles employed including stress analysis methods and flaw sizing, the source of all material data used, identification of any potential material property degradation mechanisms and their associated influence on the propagation of flaws, and the criteria applied in the assessment procedure.

3.8.2 Documentation Retention

All documents pertaining to the assessment for brittle fracture should be retained for the life of the equipment in the equipment history file. This includes all supporting documentation, data, test reports, and references to methods and criteria used for such assessments and evaluations. For geometrically identical vessels exposed to identical conditions, a single document with appropriate references is adequate.

3.9 Nomenclature

CET	Critical Exposure Temperature.
α	coefficient of thermal expansion.
C_1	55 MPa for SI Units, 8000 psi for US Customary Units.
$\Delta T_{\max}$	temperature difference between the liquid and metal temperatures.
E_y	elastic modulus.
E	joint efficiency (e.g., see Table UW-12 of the ASME Code, Section VIII, Division 1) used in the calculation of t_{min}. For castings, the quality factor or joint efficiency E, whichever governs design, should be used.
E^*	is equal to E except that E^* shall not be less than 0.80, or $E* = \max[E, 0.80]$.
FCA	future corrosion allowance associated with the governing thickness.
h	convective heat transfer coefficient.
k	thermal conductivity of the metal.
$LOSS$	previous metal loss associated with the governing thickness.
MAT	Minimum Allowable Temperature.
$MAWP$	Maximum Allowable Working Pressure of the undamaged component.
ν	Poisson's ratio.
P_a	applied pressure for the condition under consideration. When developing a pressure vessel MAT curve, P_a should not exceed the vessel $MAWP$ plus static head acting on the component of interest.
P_I	per cent increase in pressure above the initial point.
P_{rating}	component pressure rating at the MAT. For Equation (3.4), this is calculated using a weld joint efficiency of E/E^* in the corroded condition.

R_{ts} stress ratio defined as the applied general primary tensile stress for the operating condition under consideration divided by the allowable stress at the MAT. The stress ratio may also be defined in terms of required and actual thicknesses, and for components with pressure-temperature ratings, the stress ratio is computed as the applied pressure for the condition under consideration divided by the pressure rating at the MAT.

S allowable stress value in tension from the applicable code at the condition under consideration.

S^* applied general primary membrane tensile stress, including stress due to net section bending, calculated using a weld joint efficiency (E) of one (1) in the corroded condition; for piping systems, the applied general primary membrane tensile stress is computed using the guidelines of paragraph 3.4.3.4(b).

t component thickness (see Figure 3.3).

t_g governing uncorroded thickness of the component (see paragraph 3.4.2.1(d).

t_{gi} governing thickness of the component at weld joint i.

t_n nominal uncorroded thickness of the component.

t_{min} minimum required thickness of the component in the corroded condition for all applicable loads that result in general primary membrane tensile stress at the operating condition based on E.

T_I increase in temperature above the initial point.

T_{pwht} MAT adjustment for components subject to $PWHT$.

T_R reduction in MAT based on available excess thickness.

T_{RH} reduction in MAT based on the operating-to-hydrotest ratio.

T_S shell metal temperature.

3.10 References

References for this Part are provided in Annex 3A – Technical Basis and Validation – Assessment of Existing Equipment for Brittle Fracture.

3.11 Tables

Table 3.1 – Overview of Data for the Assessment of Brittle Fracture

Use this form to summarize the data obtained from a field inspection.

Equipment Identification: _____

Equipment Type: __ Pressure Vessel __ Storage Tank __ Piping Component __ Boiler (1)

Component Type & Location: _____

Year of Fabrication: _____

Data Required for A Level 1 Assessment (V – indicates data needed for pressure vessels, P – indicates data needed for piping, and T – indicates data needed for tankage):

Design Temperature (V, P, T): _____

Original Hydrotest Pressure (V, P): _____

Product Specific Gravity & Design Liquid Height (T): _____

Temperature During Original Hydrotest Pressure (V, P, T): _____

Nominal Wall Thickness of all components (V, P, T): _____

Critical Exposure Temperature (CET) (V, P, T): _____

Minimum Allowable Temperature (MAT) (V, P): _____

PWHT done at initial construction? (V, P, T): _____

PWHT after all repairs? (V, P, T): _____

Additional Data Required for Level 2 Assessment (In Addition to the Level 1 Data):

Weld Joint Efficiency (Level 2) (V, P, T): _____

Metal Loss (V, P): _____

Future Corrosion Allowance (V, P): _____

Weld Joint Efficiency (V, P): _____

Maximum Operating Pressure (V, P): _____

Charpy Impact Data, if available (V, P, T): _____

Note (1): Boiler components and boiler external piping may be evaluated using the rules for pressure vessels and piping respectively in this Part if brittle fracture has been identified as a failure mode and if all other applicability limits in this Part are met.

Table 3.2 – Assignment of Materials to the Material Temperature Exemption Curves in Figure 3.5

Curve	Material, (1), (2), (6)
A	All carbon and all low alloy steel plates, structural shapes and bars not listed in Curves B, C, and D below. SA-216 Grades WCB and WCC if normalized and tempered or water-quenched and tempered; SA -217 Grade WC6 if normalized and tempered or water-quenched and tempered. The following specifications for obsolete materials: A7, A10, A30, A70, A113, A149, A150 (3). The following specifications for obsolete materials from the 1934 Edition of the ASME Code, Section VIII: S1, S2, S25, S26, and S27 (4). A201 and A212 unless it can be established that the steel was produced by a fine-grain practice (5). SA-105 forged flanges that are supplied in the as-forged condition if manufactured in 1989 or later.
B	SA-216 Grades WCA if normalized and tempered or water-quenched and tempered. SA-216 Grades WCB and WCC for thicknesses not exceeding 2 inches if produced to a fine grain practice and water-quenched and tempered. SA -217 Grade WC9 if normalized and tempered. SA-285 Grades A and B SA-414 Grade A SA-442 Grade 55 > 1 inch if not to fine grain practice and normalized. SA-442 Grade 60 if not to fine grain practice and normalized. SA-515 Grades 60 SA-516 Grades 65 and 70 if not normalized. SA-612 if not normalized. SA-662 Grade B if not normalized. Except for cast steels, all materials of Curve A if produced to fine grain practice and normalized which are not listed for Curve C and D below. All pipe, fittings, forgings, and tubing not listed for Curves A, C or D. Parts permitted from paragraph UG-11 of the ASME Code, Section VIII, Division 1, shall be included in Curve B even when fabricated from plate that otherwise would be assigned to a different curve. A201 and A212 if it can be established that the steel was produced by a fine-grain practice. SA-105 forged flanges that are normalized, normalized and tempered, or quenched and tempered if manufactured in 1989 or later and SA-105 forged flanges that are supplied in the as-forged condition if manufactured prior to 1989.
C	SA-182 Grades 21 and 22 if normalized and tempered. SA-302 Grades C and D. SA-336 Grades F21 and F22 if normalized and tempered. SA-387 Grades 21 and 22 if normalized and tempered. SA-442 Grades 55 < 1 inch if not to fine grain practice and normalized. SA-516 Grades 55 and 60 if not normalized. SA-533 Grades B and C.

Table 3.2 – Assignment of Materials to the Material Temperature Exemption Curves in Figure 3.5

Curve	Material, (1), (2), (6)
	SA-662 Grade A. All material of Curve B if produced to fine grain practice and normalized and not listed for Curve D below. SA-105 forged flanges that are normalized, normalized and tempered, or quenched and tempered if manufactured prior to 1989.
D	SA-203. SA-442 if to fine grain practice and normalized. SA-508 Class 1. SA-516 if normalized. SA-524 Classes 1 and 2. SA-537 Classes 1 and 2. SA-612 if normalized. SA-662 if normalized. SA-738 Grade A.

Notes:

1. When a material class or grade is not shown, all classes or grades are included.
2. The following apply to all material assignment notes.
   a. Cooling rates faster than those obtained in air, followed by tempering, as permitted by the material specification, are considered equivalent to normalizing and tempering heat treatments.
   b. Fine grain practice is defined as the procedures necessary to obtain a fine austenitic grain size as described in SA-20.
3. The first edition of the API Code for Unfired Pressure Vessels (discontinued in 1956) included these ASTM carbon steel plate specifications. These specifications were variously designated for structural steel for bridges, locomotives, and rail cars or for boilers and firebox steel for locomotives and stationary service. ASTM A 149 and A150 were applicable to high-tensile-strength carbon steel plates for pressure vessels.
4. The 1934 Edition of Section VIII of the ASME Code listed a series of ASME steel specifications, including S1 and S2 for forge welding; S26 and S27 for carbon steel plates; and S25 for open-hearth iron. The titles of some of these specifications are similar to the ASTM specifications listed in the 1934 Edition of the API Code for Unfired Pressure Vessels.
5. These two steels were replaced in strength grades by the four grades specified in ASTM A 515 and the four grades specified in ASTM A 516. Steel in accordance with ASTM A 212 was made only in strength grades the same as Grades 65 and 70 and has accounted for several known brittle failures. Steels in conformance with ASTM A 201 and A 212 should be assigned to Curve A unless it can be established that the steel was produced by fine-grain practice, which may have enhanced the toughness properties.
6. No attempt has been made to make a list of obsolete specifications for tubes, pipes, forgings, bars, and castings. Unless specific information to the contrary is available, all of these product forms should be assigned to Curve A.

Table 3.3 – Impact Test Exemption Temperature for Bolting Materials

Specification	Grade	Impact Test Exemption Temperature	
		(°C)	(°F)
SA-193	B5	-29	-20
SA-193	B7 $\{Dia \le 63.5\ mm\ (2.5\ in.)\}$	-48	-55
SA-193	B7 $\{Dia > 63.5\ mm\ (2.5\ in.)\}$	-40	-40
SA-193	B7M	-48	-55
SA-193	B16	-30	-20
SA-307	B	-30	-20
SA-325	1, 2	-30	-20
SA-354	BC	-18	0
SA-354	BD	-7	+20
SA-449	---	-30	-20
SA-540	B23/24	-12	+10
SA-194	2, 2H, 2HM, 3, 4, 7, 7M, and 16	-48	-55
SA-540	B31/B22/B23/B24/B24V	-48	-55

Note:

1. Use of Figure 3.7 is not permitted for bolts and nuts due to loading conditions.
2. SA-320, SA-333, SA-334, SA-350, SA-352, SA-420, SA-437, SA-540 (except for those material specifications noted in the Table above), and SA-765 are impacted tested per the material specification.

Table 3.4 – Equations for the Curves Included in Figures 3.3, 3.5, 3.7, 3.8, 3.9 and 3.10

Figure	Equation
3.3 (1)	$\Delta T_{\max} = \max\left[\frac{C_1(1-\nu)}{E\alpha}\left(1.5+\frac{3.25k}{ht}-0.5\exp\left[\frac{-16k}{ht}\right]\right),\ C_2\right]$
3.5 (2)	**Curve A** $MAT = 18 \quad (for\ 0 < t \le 0.394)$ $MAT = \frac{-76.911+284.85t-27.560t^2}{1.0+1.7971t-0.17887t^2} \quad (for\ 0.394 < t \le 6.0)$ **Curve B** $MAT = -20 \quad (for\ 0 < t \le 0.394)$ $MAT = \left(\begin{array}{l}-135.79+171.56t^{0.5}+103.63t- \\ 172.0t^{1.5}+73.737t^2-10.535t^{2.5}\end{array}\right) \quad (for\ 0.394 < t \le 6.0)$ **Curve C** $MAT = -55 \quad (for\ 0 < t \le 0.394)$ $MAT = 101.29-\frac{255.50}{t}+\frac{287.86}{t^2}-\frac{196.42}{t^3}+\frac{69.457}{t^4}-\frac{9.8082}{t^5} \quad (for\ 0.394 < t \le 6.0)$ **Curve D** $MAT = -55 \quad (for\ 0 < t \le 0.50)$ $MAT = \left(\begin{array}{l}-92.965+94.065t-39.812t^2+ \\ 9.6838t^3-1.1698t^4+0.054687t^5\end{array}\right) \quad (for\ 0.50 < t \le 6.0)$
3.7 (2)	$T_R = 100.0(1.0-R_{ts}) \quad (for\ R_{ts} \ge 0.6,\ see\ Note\ 2)$ $T_R = \left(\begin{array}{l}-9979.57-14125.0R_{ts}^{1.5}+ \\ 9088.11\exp[R_{ts}]-17.3893\frac{\ln[R_{ts}]}{R_{ts}^2}\end{array}\right) \quad (for\ 0.6 > R_{ts} > 0.3,\ see\ Note\ 2)$ $T_R = 105.0\ to\ 275 \quad (for\ R_{ts} \le 0.40,\ see\ Note\ 2\ in\ Figure\ 3.7)$ $T_R = 140.0\ to\ 275 \quad (for\ R_{ts} \le 0.35,\ see\ Note\ 3\ in\ Figure\ 3.7)$ $T_R = 200.0\ to\ 275 \quad (for\ R_{ts} \le 0.30,\ see\ Note\ 4\ in\ Figure\ 3.7)$
3.8 (2)	$T_{RH} = 52.1971-53.3079H_R-15.7024H_R^2+\frac{16.7548}{H_R} \quad (for\ H_r > 0.25)$ $T_{RH} = 105\ to\ 275.0 \quad (for\ H_R \le 0.25)$

Table 3.4 – Equations for the Curves Included in Figures 3.3, 3.5, 3.7, 3.8, 3.9 and 3.10

Figure	Equation
3.9 (2)	$P_I = 0.5T_I$
3.10 (2)	$T_S = 30 \quad (for\ 0 < t \le 0.50)$ $T_S = 191.03 - 0.48321t^2 - \frac{133.75}{t^{0.5}} + \frac{10.775}{t^{1.5}} \quad (for\ 0.50 < t < 0.875)$ $T_S = 60 \quad (for\ 0.875 \le t \le 2.0)$

Notes:

1. The SI and U.S. Customary Units for this equation are shown below. Note that the screening curve was developed based on: $K = 2.3\ BTU/hr-in-F$, $E_y = 29.3E6\ psi$, and $\alpha = 6.13E-6\ in/in-F$.

   $\Delta T_{\max}$ Temperature difference between the liquid and metal temperatures, °C, °F.

   C_1 55.2 MPa for SI Units, 8000 psi for U.S. Customary Units.

   C_2 55.6°C for SI Units, 100°F for U.S. Customary Units.

   E_y Elastic modulus, MPa, psi.

   α Coefficient of thermal expansion, mm/mm-°C, in/in-°F.

   k Thermal conductivity of the metal, J/s-m-°C, BTU/hr-in-°F.

   h Convective heat transfer coefficient, J/s-m2-°C, BTU/hr-in2-°F.

   t Component Thickness, mm, in.

   ν Poisson's ratio.

2. The equations are based on the U.S. Customary units shown below. When working in the SI system of units, the SI units used for input to the equations should be converted to U.S. Customary units to at least four significant figures. Similarly, the U.S. Customary output should be converted back to the SI system.

   MAT Minimum Allowable Temperature in degrees Fahrenheit.

   P_I per cent increase in pressure above the initial point.

   T_I increase in temperature above the initial point in degrees Fahrenheit.

   T_R reduction in MAT based on available excess thickness in degrees Fahrenheit.

   T_{RH} reduction in MAT based on the operating-to-hydrotest ratio in degrees Fahrenheit.

   T_S component metal temperature is in degrees Fahrenheit.

   t component thickness in inches.

3.12 Figures

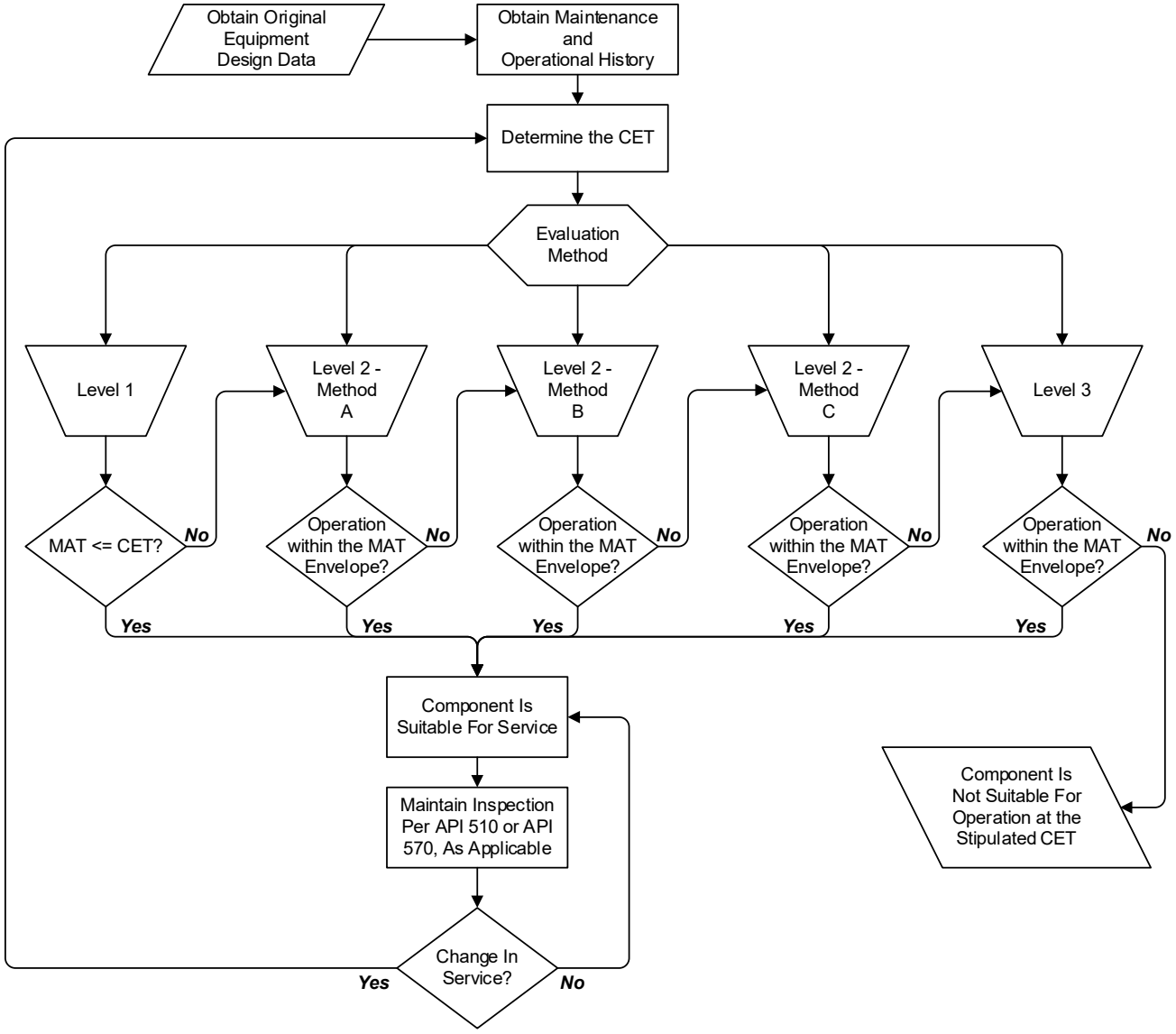

Figure 3.1 – Overall Brittle Fracture Assessment Procedure for Pressure Vessels and Piping

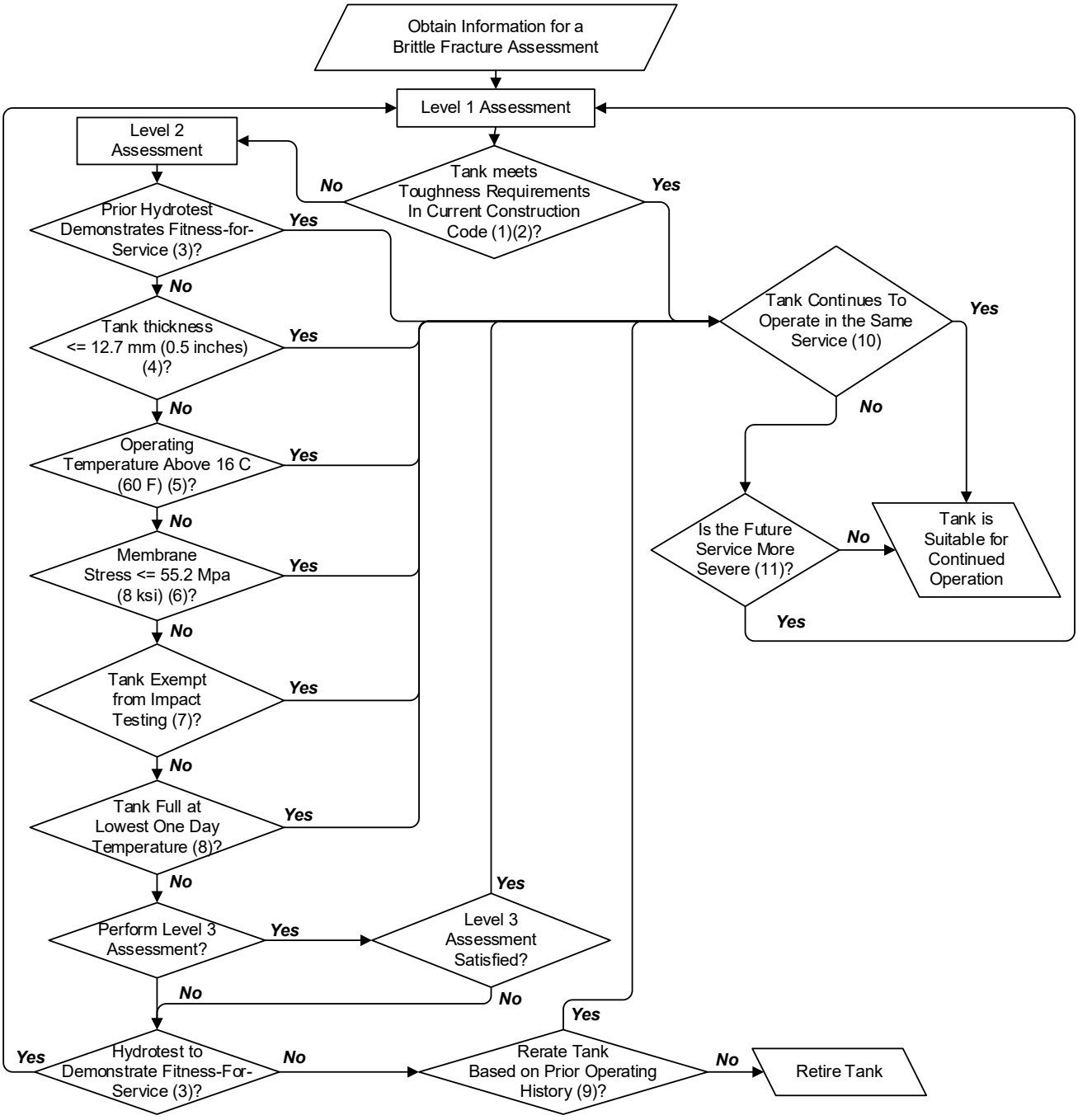

Figure 3.2 – Brittle Fracture Assessment Procedure for Storage Tanks

Notes for Figure 3.2

The assessment procedure as illustrated in Figure 3.2 shall be used for Level 1 and Level 2 Assessment of aboveground atmospheric storage tanks in petroleum and chemical services. Each of the key steps on the decision tree is numbered corresponding to the explanation provided as follows:

1. Atmospheric storage tanks constructed in accordance with API Standard 650 (seventh edition or later) include requirements to minimize the probability of failure due to brittle fracture. Tanks constructed to earlier versions of this Standard may also be shown to meet the API 650 (seventh edition or later) toughness requirements by impact testing coupon samples from a representative number of shell plates.
2. Many tanks continue to operate successfully in the same service that were not constructed to the requirements of API Standard 650 (seventh edition or later). These tanks are potentially susceptible to failure due to brittle fracture and require a Level 2 Assessment.
3. For purposes of this assessment, hydrostatic testing demonstrates that an aboveground atmospheric storage tank in a petroleum or chemical service is fit for continued service and at minimal probability of failure due to brittle fracture, provided that all governing requirements for repair, alterations, reconstruction, or change in service are in accordance with API Standard 653 (including a need for hydrostatic testing after major repairs, modifications, or reconstruction). The effectiveness of the hydrostatic test in demonstrating fitness for continued service is shown by industry experience.
4. If a tank shell thickness is no greater than 12.7 mm (0.5 inch), the probability of failure due to brittle fracture is minimal, provided that an evaluation for suitability of service per API 653, Section 4 has been performed. The original nominal thickness for the thickest tank shell plate shall be used for this assessment.
5. No known tank failures due to brittle fracture have occurred at shell metal temperatures of 16°C (60°F) or warmer. Similar assurance against brittle fracture can be gained by increasing the metal temperature by heating the tank contents.
6. Industry experience and laboratory tests have shown that a membrane stress in tank shell plates of at least 55.2 MPa (8 ksi) is required to cause failure due to brittle fracture.
7. Tanks constructed from steel listed in API Standard 650 can be used in accordance with their exemption curves, provided that an evaluation for suitability of service per Section 4 of API Standard 653 has been performed. Tanks fabricated from steels of unknown toughness thicker than 12.7 mm (0.5 inch) and operating at a shell metal temperature below 16°C (60°F) can be used if the tank meets the requirements of Figure 3.10. The original nominal thickness for the thickest tank shell plate shall be used for the assessment. For unheated tanks, the shell metal temperature shall be the design metal temperature as defined in API Standard 650.
8. The probability of failure due to brittle fracture is minimal once a tank has demonstrated that it can operate at a specified maximum liquid level at the lowest expected temperature without failing unless repairs or alterations have been made. For the purpose of this assessment, the lowest expected temperature is defined as the lowest one day mean temperature as shown in API Standard 650 for the continental United States. It is necessary to check tank log records and meteorological records to ensure that the tank has operated at the specified maximum liquid level when the one-day mean temperature was as low as shown in API Standard 650.
9. An evaluation can be performed to establish a safe operating envelope for a tank based on the past operating history. This evaluation shall be based on the most severe combination of temperature and liquid level experienced by the tank during its life. The evaluation may show that the tank needs to be rerated or operated differently. Several options exist such as: restrict the liquid level, restrict the minimum metal temperature, change the service to a stored product with a lower specific gravity, or combinations of these options.
10. An assessment shall be made to determine if the change in service increases the probability of failure due to brittle fracture. The service can be considered more severe, therefore creating a greater probability of brittle fracture if the service temperature is reduced (for example, changing from heated oil service to ambient temperature product), or the product is changed to one with a greater specific gravity and thus increasing stresses.
11. A change in service shall be evaluated to determine if it increases the probability of failure due to brittle fracture. In the event of a change to a more severe service (such as operating at a lower temperature or handling product at a higher specific gravity), it is necessary to consider the future service conditions in the Fitness-For-Service Assessment.

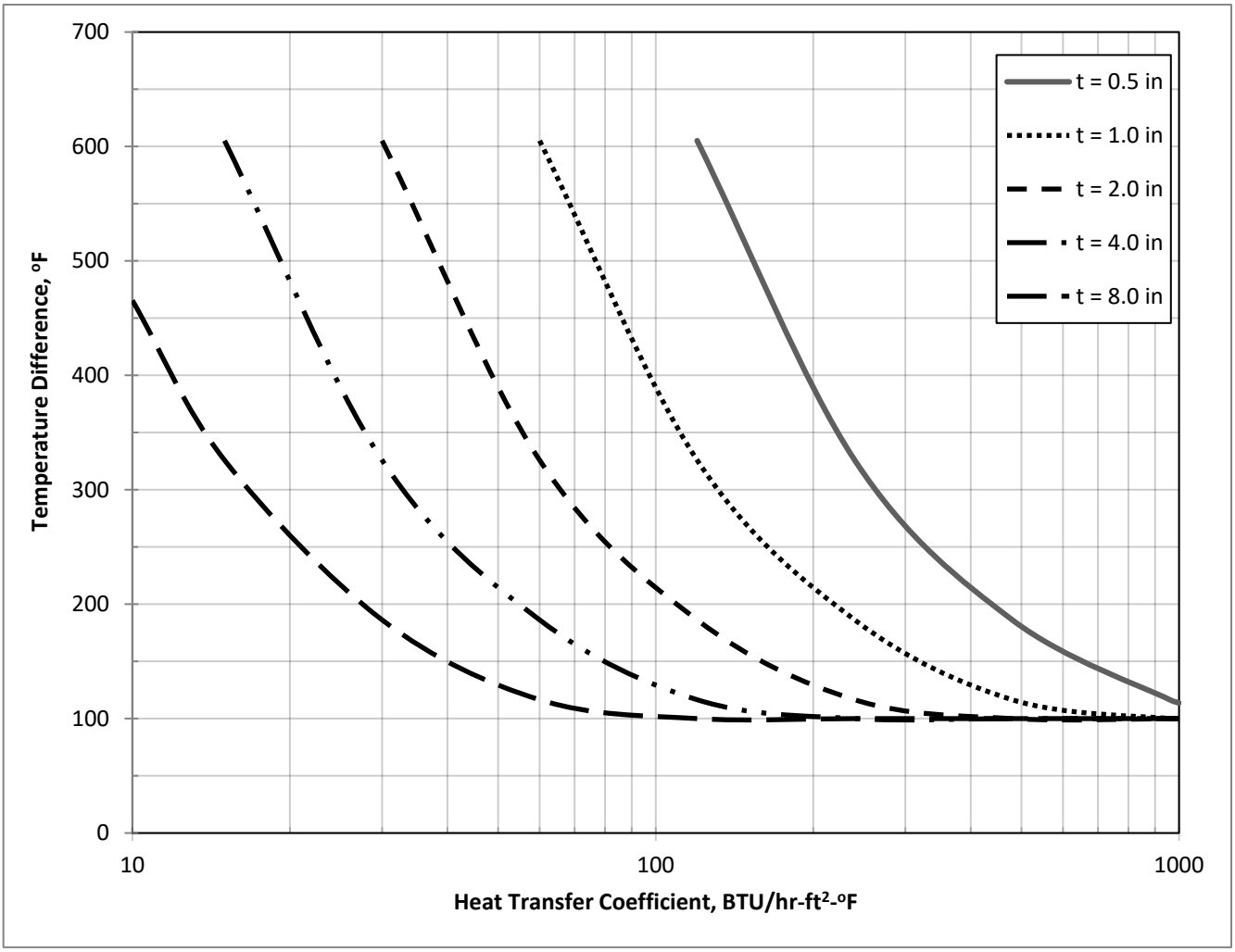

Note: The equations for these curves in this figure are provided in Table 3.4.

Figure 3.3 – Definition of Shock Chilling for Carbon and Low Alloy Steels Conditions Above and to the Right of the Line are Considered to be Shock Chilling when the Liquid or Two-Phase Fluid Temperature is Also Colder than the Affected Component(s) Level 1 MAT

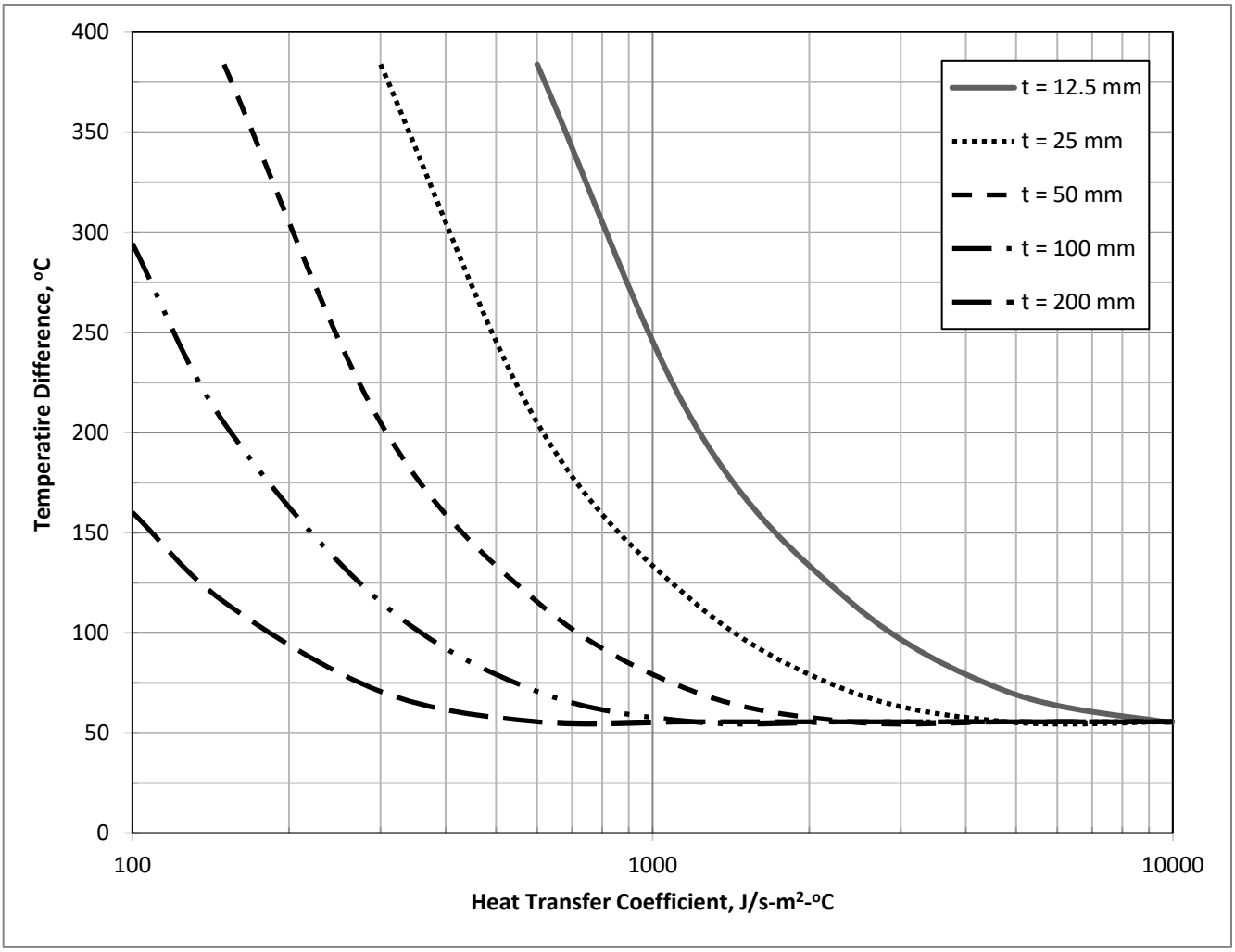

Note: The equations for these curves in this figure are provided in Table 3.4.

Figure 3.3M – Definition of Shock Chilling for Carbon and Low Alloy Steels Conditions Above and to the Right of the Line are Considered to be Shock Chilling when the Liquid or Two-Phase Fluid Temperature is Also Colder than the Affected Component(s) Level 1 MAT

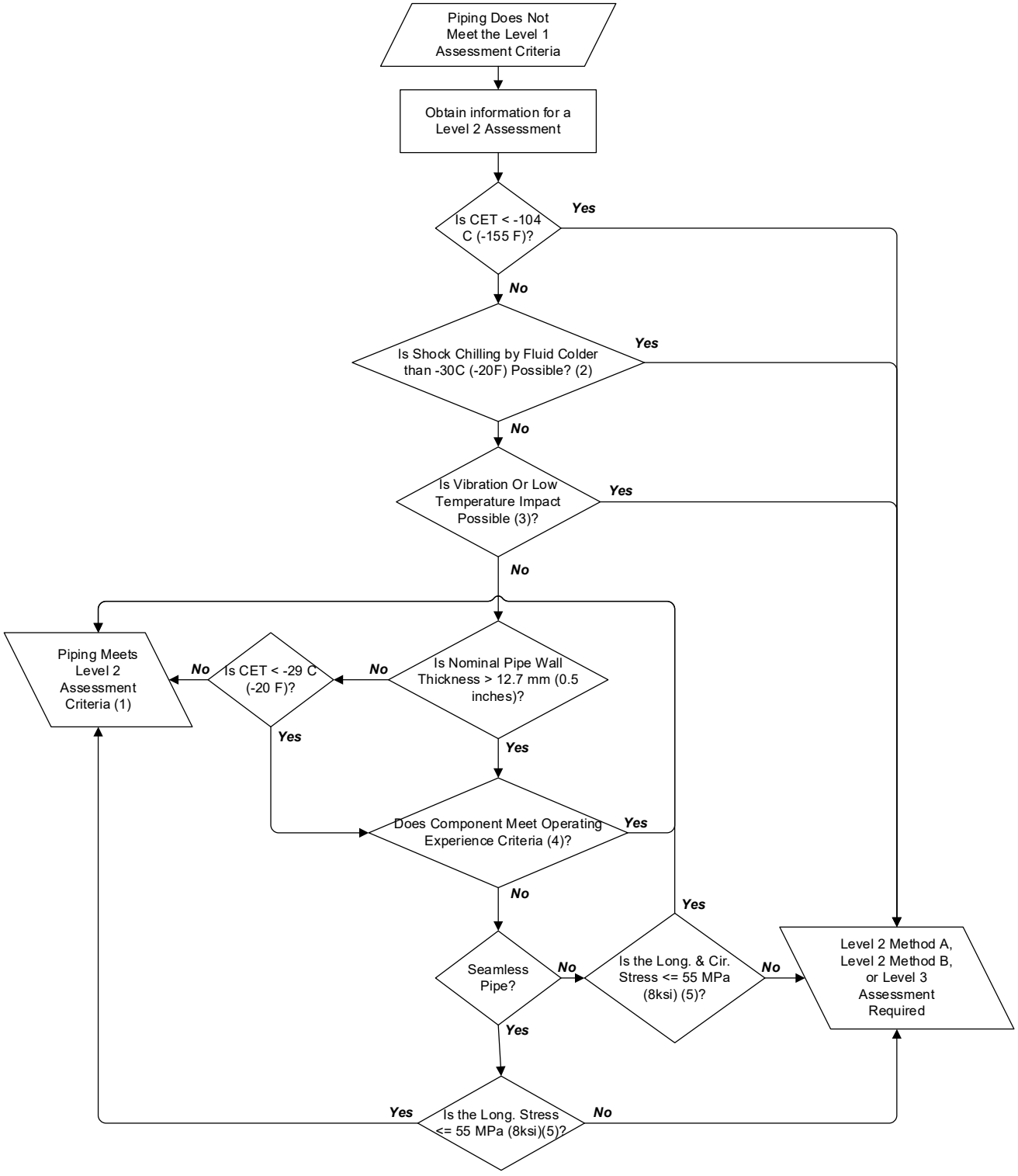

Figure 3.4 – Level 2 Method C Assessment for Carbon Steel Piping

Notes for Figure 3.4

1. If the piping system satisfies the Method C criteria, the MAT should be set equal to the CET and the CET shall be based on successful performance demonstrated during past operation. Records shall be kept of the measured metal temperature(s) or justification for the assumed metal temperature(s) along with the corresponding pressure(s) used in the assessment. Qualification through Method C neither confirms adequacy for any particular crack-like flaw size nor does it ensure protection from potential brittle fracture in the event future crack-like flaws or defects are introduced into the piping system.
2. See definition of shock chilling in paragraph 3.3.3(e).
3. Vibrations in a portion of the piping system could initiate cracks that are cause for a high level of concern of brittle fracture. If the system could be subject to cyclic operating or impact load while it is operating below the CET, then an assessment shall be made to determine whether the resulting cyclic stresses could result in the initiation and propagation of a crack. If crack initiation and/or propagation are determined to be possible, then a Level 3 Assessment is required. Impact loads include hammering from flow or aggressive repeated strikes from tools or mobile equipment, etc. Minor impact loads from hand tools other than deliberate hammering are not generally a cause for concern.
4. Acceptance based on successful operating experience is based on the following:
   i) The nominal operating conditions have been essentially the same and consistent for a significant period of time and more severe conditions (i.e., lower temperature and/or higher pressure or stress) are not expected in the future. In addition, the maximum design temperature and pressure have not been exceeded for a significant period of time. Note that safety valve discharge lines usually do not meet this criterion (see Note 2).
   ii) The piping is not in a stress corrosion cracking environment such as non-$PWHT$ piping in DEA, MEA, NaOH, or KOH. This restriction does not apply to seamless pipe in wet H_2S service or seamless and welded pipe in anhydrous ammonia service unless there are clear indications of cracking in the piping.
   iii) The piping system is in good condition as determined by an inspection using API 570 or other applicable inspection code or standard.
   iv) The piping system has adequate flexibility by virtue of layout, freedom for thermal growth or contraction, and the supports as determined by visual inspection are in good condition.
   v) The CET for the piping system is no lower than -59°C (-55°F).
5. Guidelines for stress calculations are provided in paragraph 3.4.3.4(b).

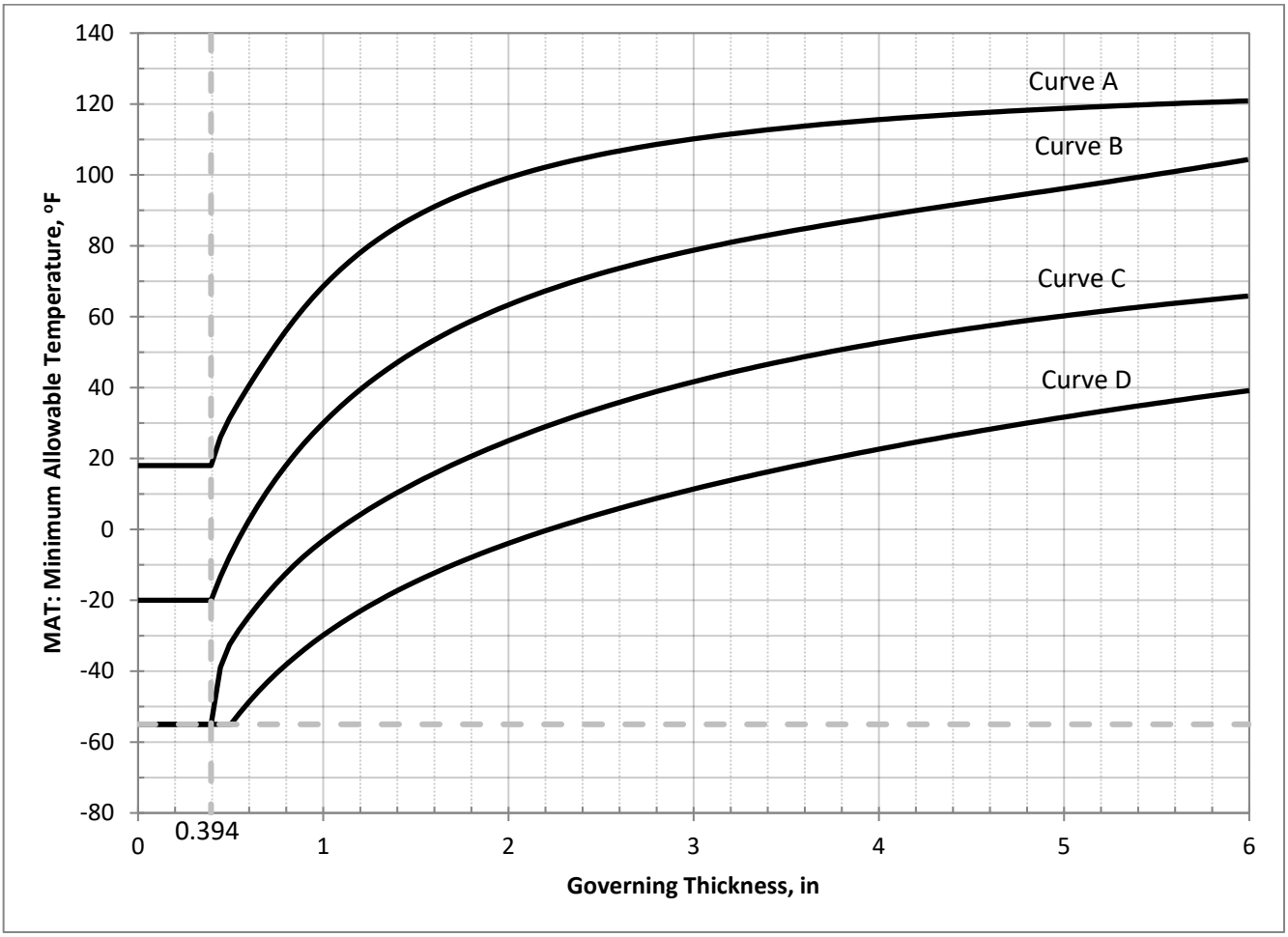

Notes:

1. Curves A through D define material specification classes in accordance with Table 3.2.
2. This figure is from the ASME Code Section VIII, Division 1, paragraph UCS-66.
3. Curve A intersects the MAT -axis at 18°F, Curve B intersects the MAT -axis at -20°F, and Curves C and D intersect the MAT -axis at -55°F.
4. These curves can also be used to evaluate piping components. In this case, Curve B should be shifted to the right so that 0.5 inch corresponds to a temperature of -20°F. To account for this shift in an assessment, an effective governing thickness equal to the actual governing thickness minus 0.106 inch can be used to determine the MAT.
5. The equations for the curves in this figure are provided in Table 3.4.
6. Use of the impact test exemption curves is only applicable up to a maximum governing thickness of 4 inches for welded parts and 6 inches for nonwelded parts.

Figure 3.5 – Minimum Allowable Metal Temperature

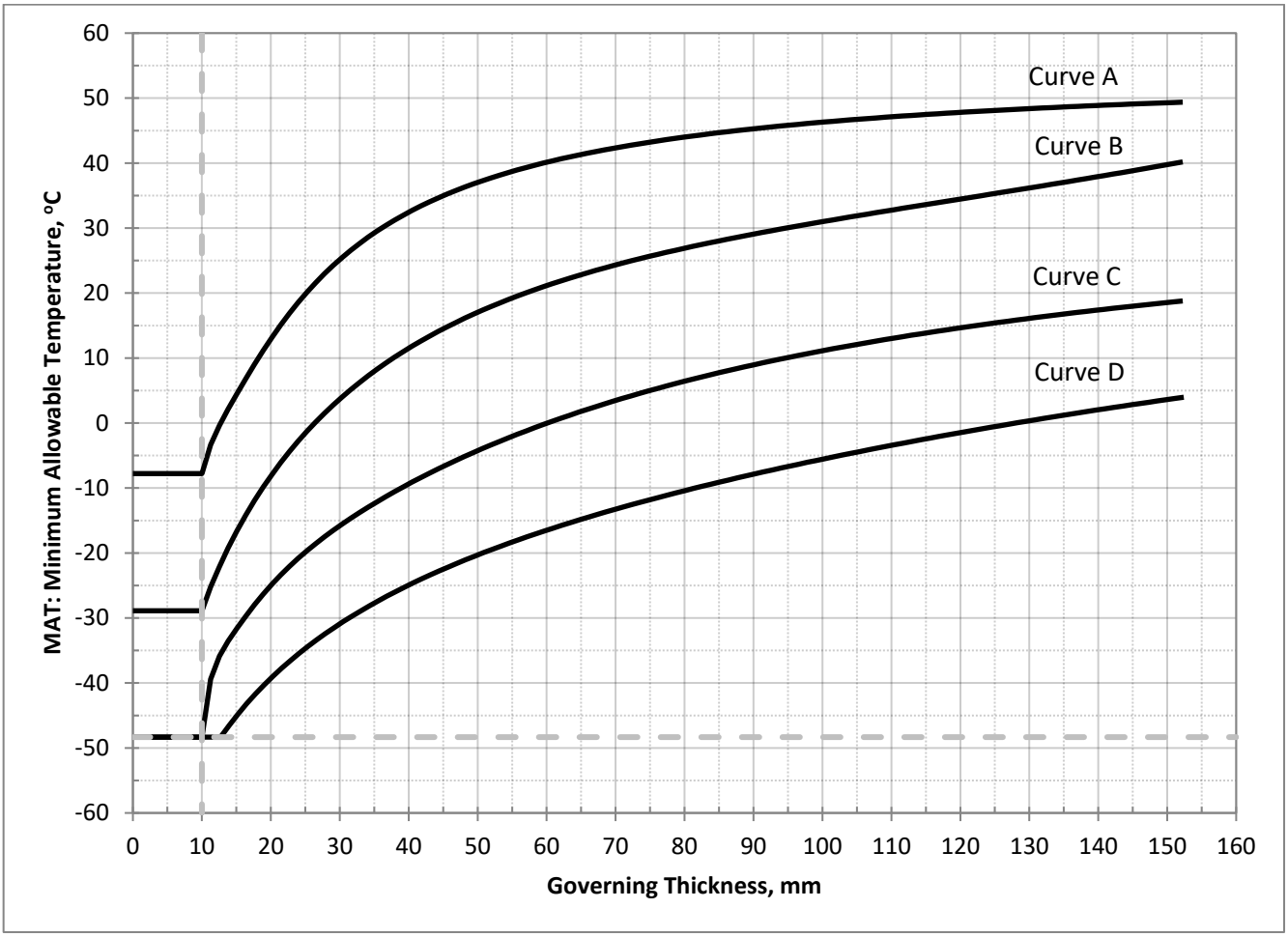

Notes:

1. Curves A through D define material specification classes in accordance with Table 3.2.
2. This figure is from the ASME Code Section VIII, Division 1, paragraph UCS-66.
3. Curve A intersects the MAT -axis at -8°C, Curve B intersects the MAT -axis at -29°C, and Curves C and D intersect the MAT -axis at -48°C.
4. These curves can also be used to evaluate piping components. In this case, Curve B should be shifted to the right so that 12.7 mm corresponds to a temperature of -29°C. To account for this shift in an assessment, an effective governing thickness equal to the actual governing thickness minus 2.69 mm can be used to determine the MAT.
5. The equations for the curves in this figure are provided in Table 3.4.
6. Use of the impact test exemption curves is only applicable up to a maximum governing thickness of 100 mm for welded parts and 150 mm for nonwelded parts.

Figure 3.5M – Minimum Allowable Metal Temperature

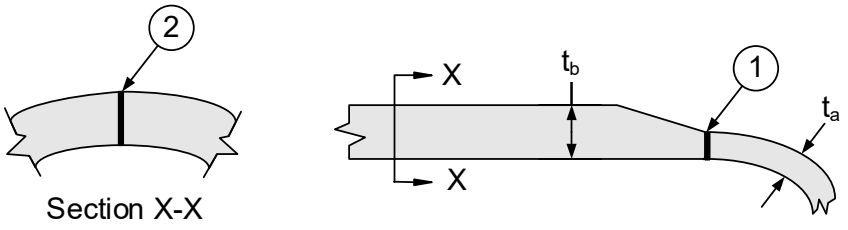

$t_{g1}=t_a$

$t_{g2}=t_a$ (seamless) or t_b (welded)

(a) Butt Welded Components

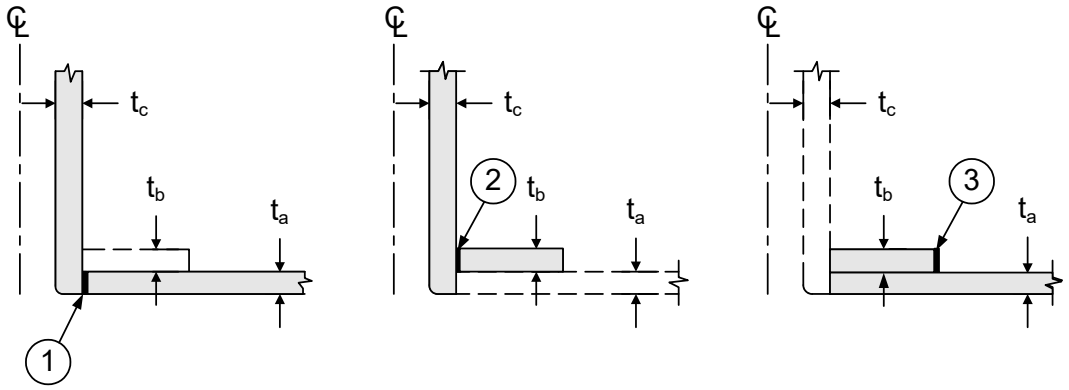

t_{g1}= min (t_a, t_c) t_{g2}= min (t_b, t_c) t_{g3}=min (t_a, t_b)

(b) Welded Connection with or without a Reinforcing Plate

Figure 3.6 – Some Typical Vessel Details Showing the Governing Thickness

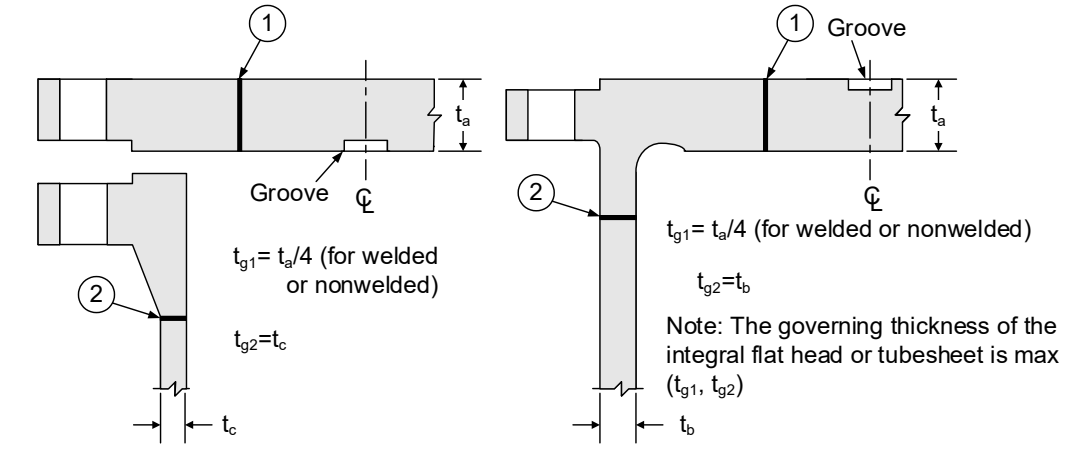

(c) Bolted Flat Head or Tubesheet and Flange (d) Integral Flat Head or Tubesheet

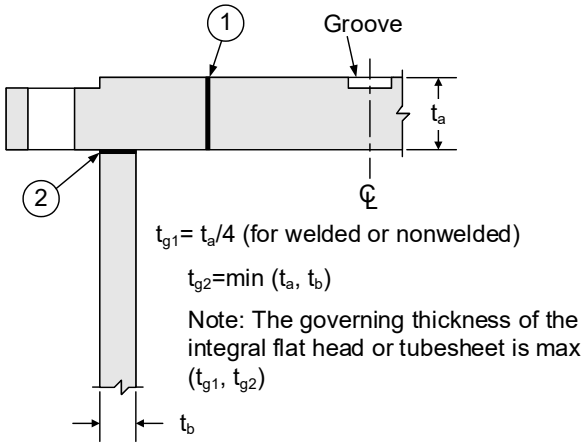

(e) Flat Head or Tubesheet with a Corner Joint

Figure 3.6 – Some Typical Vessel Details Showing the Governing Thickness – Continued

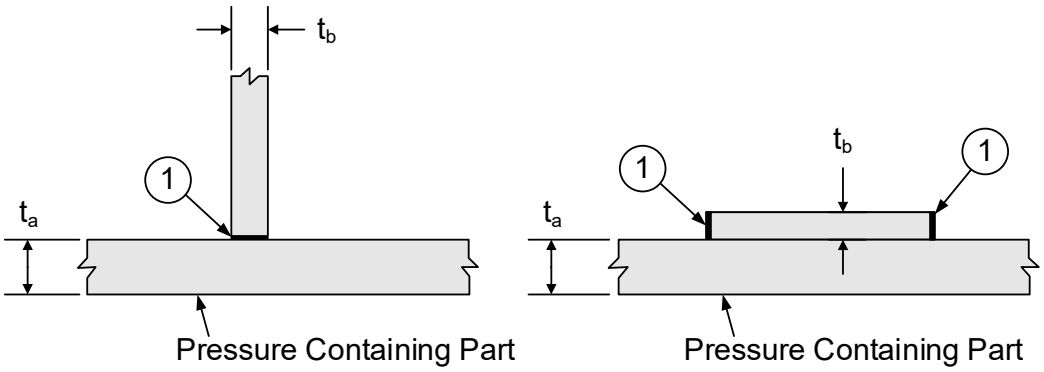

$t_{g1}=\min(t_a, t_b)$

(f) Welded Attachments

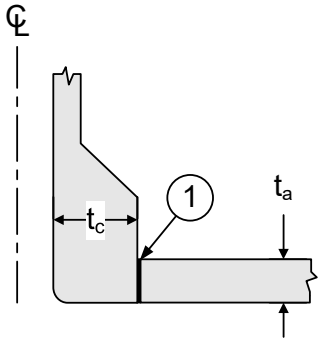

$t_{g1}=\min(t_a, t_c)$

(g) Integrally Reinforced Welded Connection

Notes:

1. In general, the governing thickness is the thinner of the two parts at the welded joint.
2. In details Figure 3.6(a) to Figure 3.6(g), t_{gi}, governing thickness at weld joint i.
3. The MAT of a component is evaluated at each governing thickness, t_{gi}, as applicable.

Figure 3.6 – Some Typical Vessel Details Showing the Governing Thickness – Continued

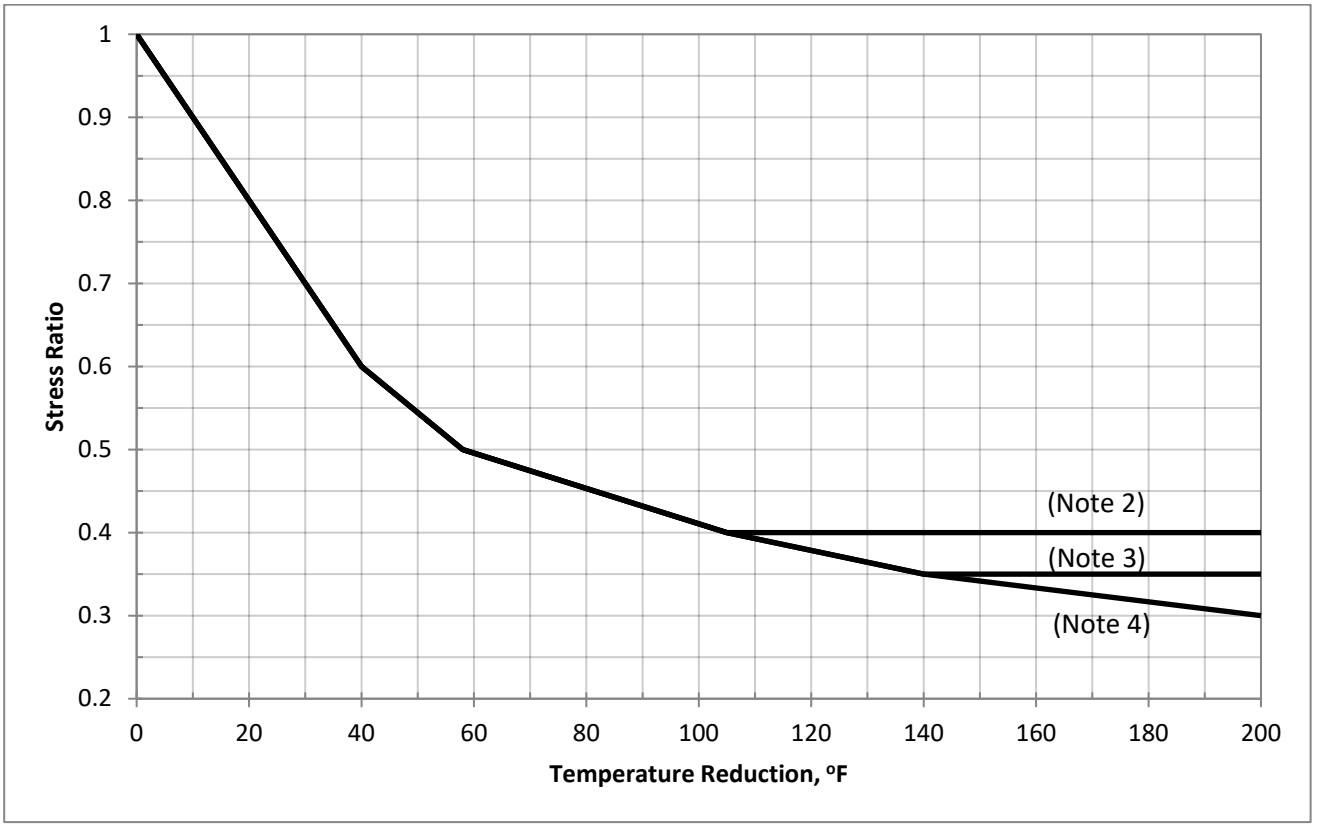

Notes:

1. A definition of the parameters used in this curve is provided in paragraph 3.9.
2. Use this curve for components with a design allowable stress at room temperature less than or equal to 17.5 ksi. This curve can be used for vessels constructed to all Editions and Addenda prior to 1999 of the ASME Code, Section VIII, Division 1; and piping constructed to all Editions and Addenda prior to 2002 of ASME B31.1. The threshold value for this curve is 0.40.
3. Use this curve for components with a design allowable stress at room temperature less than or equal to 20 ksi but greater than 17.5 ksi. This curve can be used for vessels constructed to the 1999 Addenda and later Editions and Addenda of the ASME Code, Section VIII, Division 1; and piping constructed to the 2002 Addenda and later Editions and Addenda of ASME B31.1. The threshold value for this curve is 0.35.
4. Use this curve for components with a design allowable stress at room temperature less than or equal to 25 ksi but greater than 20 ksi. This curve can be used for vessels designed and constructed to the ASME Code, Section VIII, Division 2 prior to the 2007 Edition, and piping designed to ASME B31.3. The threshold value for this curve is 0.30.
5. The equations for the curves in this figure are provided in Table 3.4.

Figure 3.7 – Reduction in the MAT Based on Available Excess Thickness for Carbon and Low Alloy Steel Components

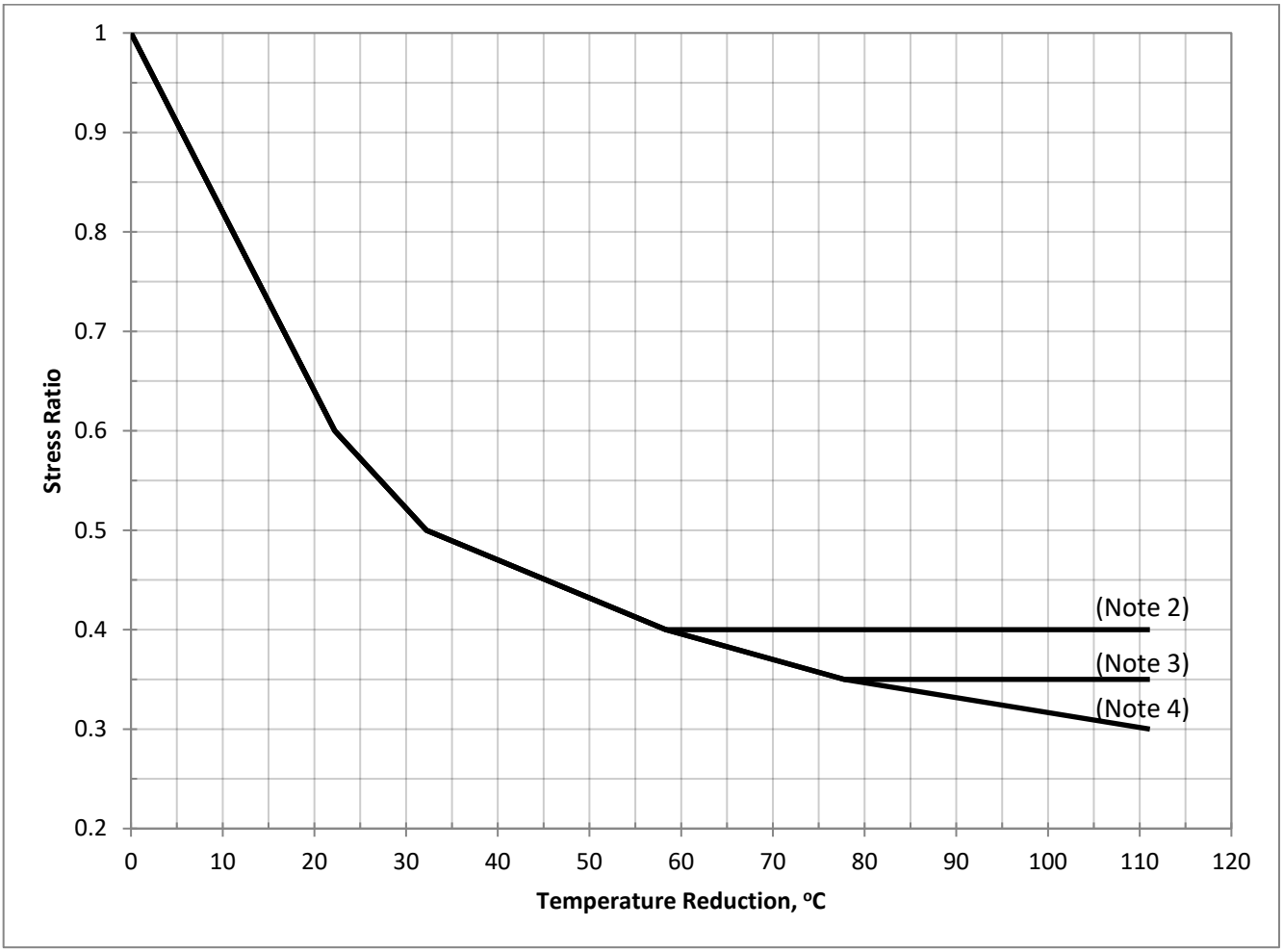

Notes:

1. A definition of the parameters used in this curve is provided in paragraph 3.9.
2. Use this curve for components with a design allowable stress at room temperature less than or equal to 120.8 MPa. This curve can be used for vessels constructed to all Editions and Addenda prior to 1999 of the ASME Code, Section VIII, Division 1; and piping constructed to all Editions and Addenda prior to 2002 of ASME B31.1. The threshold value for this curve is 0.40.
3. Use this curve for components with a design allowable stress at room temperature less than or equal to 138 MPa but greater than 120.8 MPa. This curve can be used for vessels constructed to the 1999 Addenda and later Editions and Addenda of the ASME Code, Section VIII, Division 1; and piping constructed to the 2002 Addenda and later Editions and Addenda of ASME B31.1. The threshold value for this curve is 0.35.
4. Use this curve for components with a design allowable stress at room temperature less than or equal to 172.5 MPa but greater than 138 MPa. This curve can be used for vessels designed and constructed to the ASME Code, Section VIII, Division 2 prior to the 2007 Edition, and piping designed to ASME B31.3. The threshold value for this curve is 0.30.
5. The equations for the curves in this figure are provided in Table 3.4.

Figure 3.7M – Reduction in the MAT Based on Available Excess Thickness for Carbon and Low Alloy Steel Components

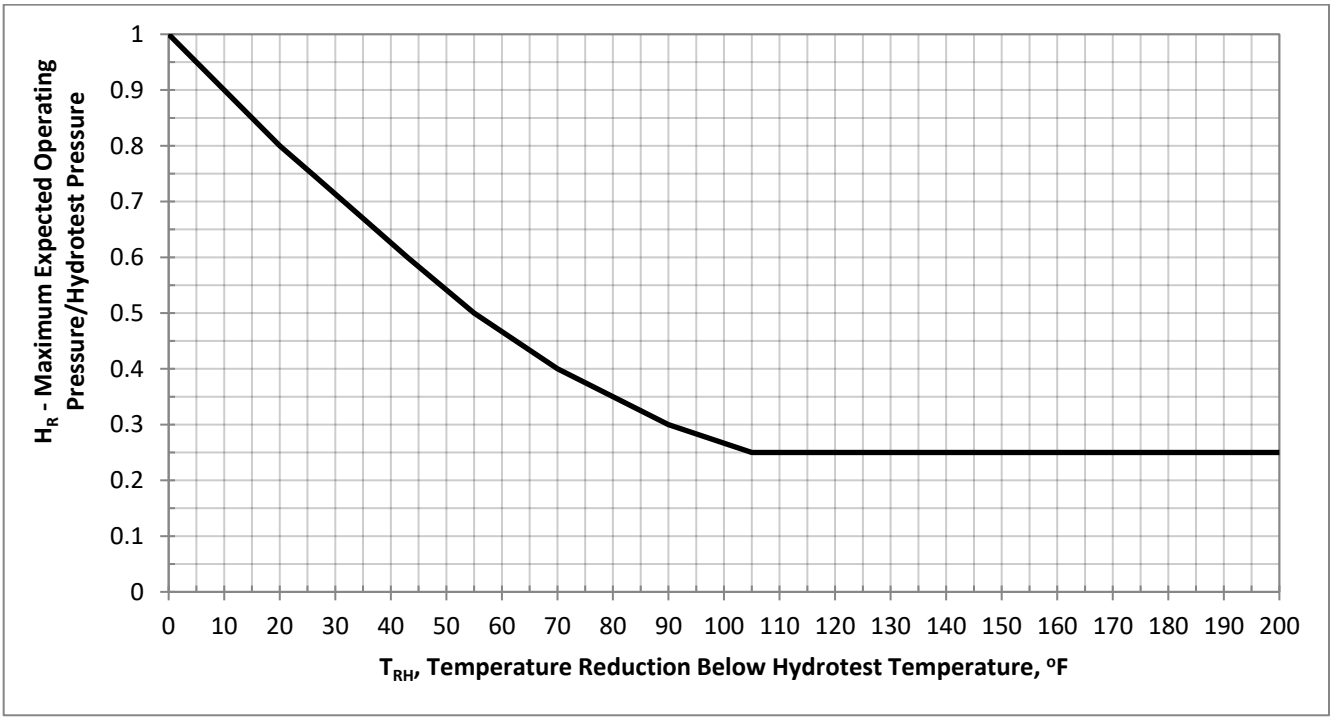

Note: The equations for the curve in this figure are provided in Table 3.4.

Figure 3.8 – Allowable Reduction in the MAT Based on Hydrostatic Proof Testing

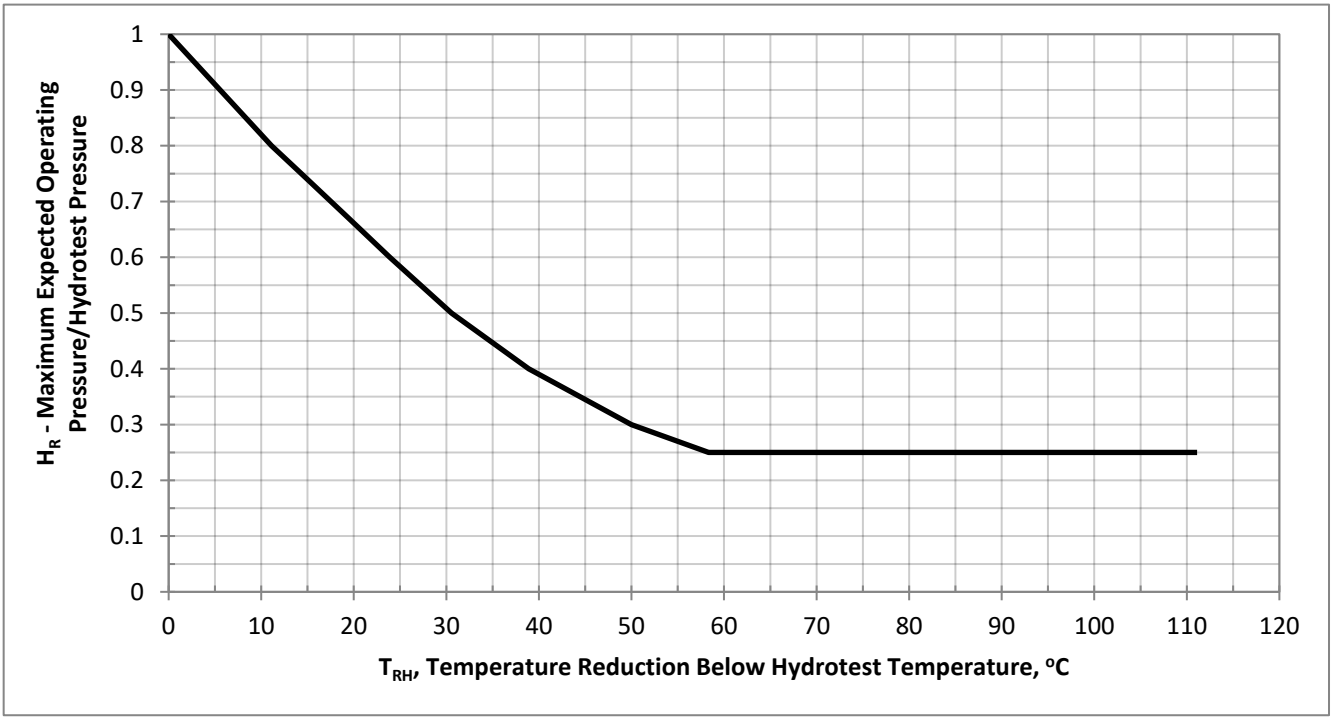

Note: The equation for the curves in this figure are provided in Table 3.4.

Figure 3.8M – Allowable Reduction in the MAT Based on Hydrostatic Proof Testing

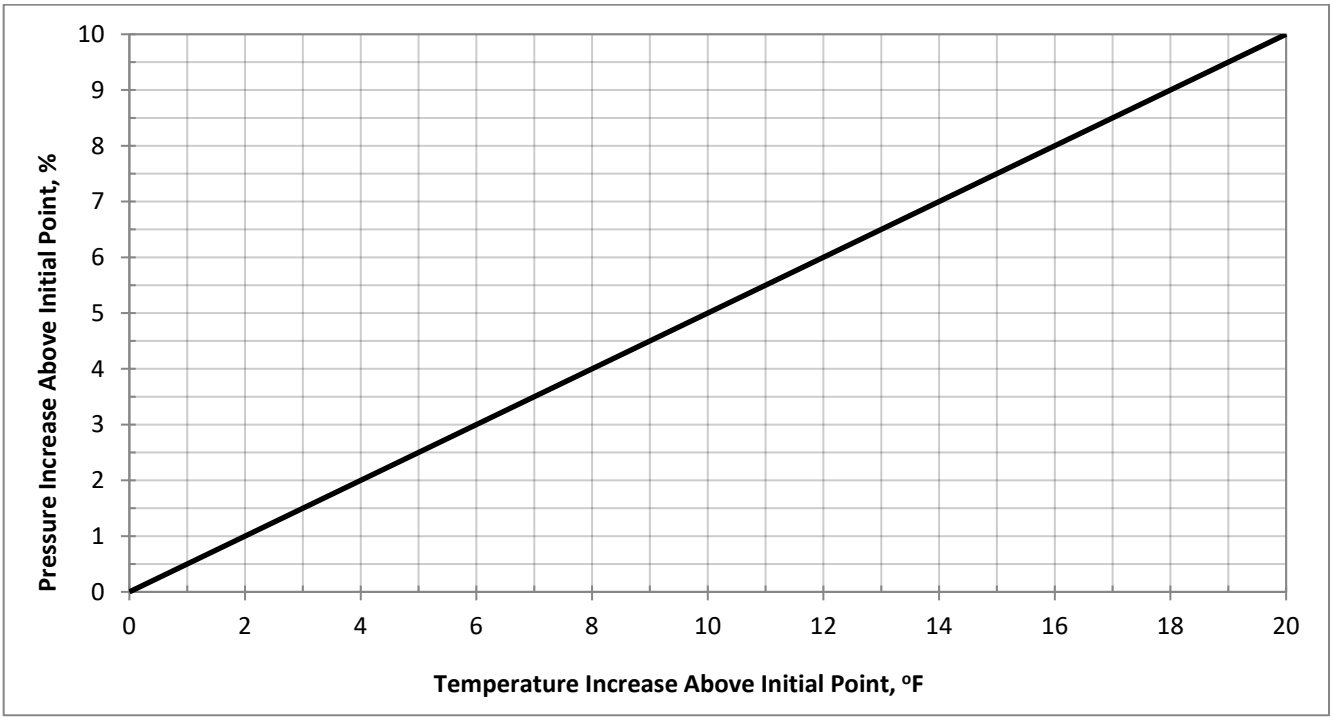

Note: The equation for the curve in this figure is provided in Table 3.4.

Figure 3.9 – Pressure-Temperature Curve

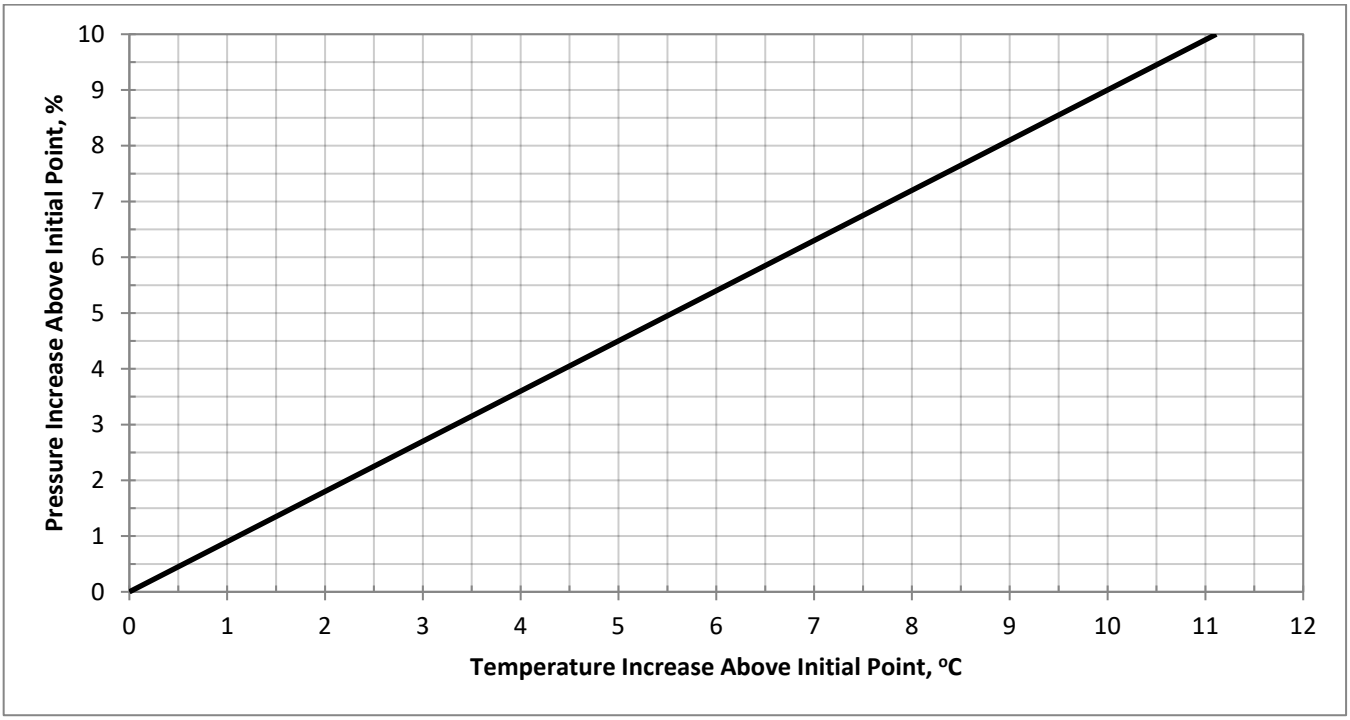

Note: The equation for the curve in this figure is provided in Table 3.4.

Figure 3.9M – Pressure-Temperature Curve

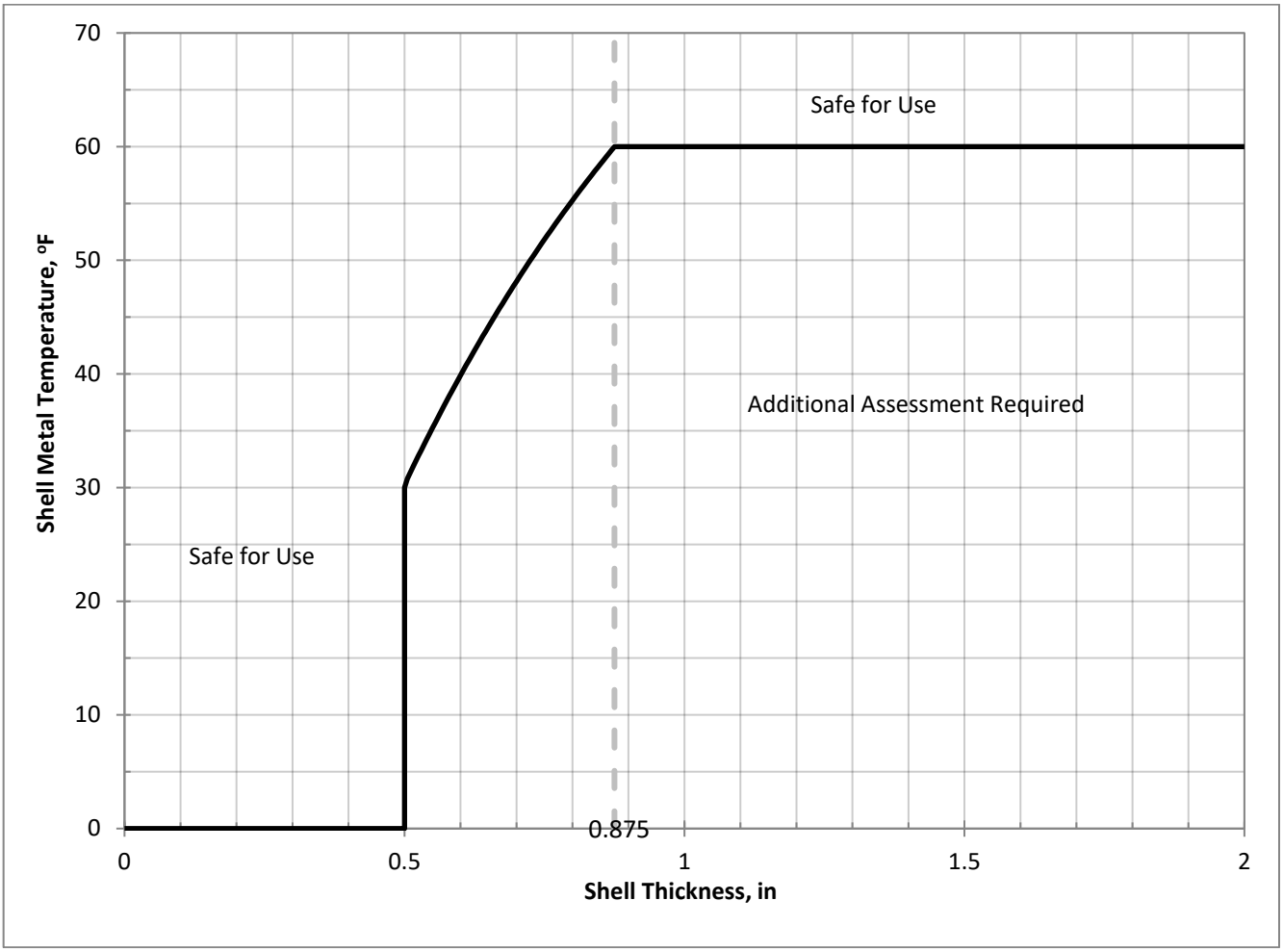

Note: The above exemption curve between 30°F and 60°F is based on Curve A in Figure 3.5. The other parts of the curve were established based on successful operating experience. The equations for the curve in this figure are provided in Table 3.4.

Figure 3.10 – Exemption Curve for Tanks Constructed from Carbon Steel of Unknown Toughness Thicker Than 1/2 inch and Operating at a Shell Metal Temperature Below 60°F

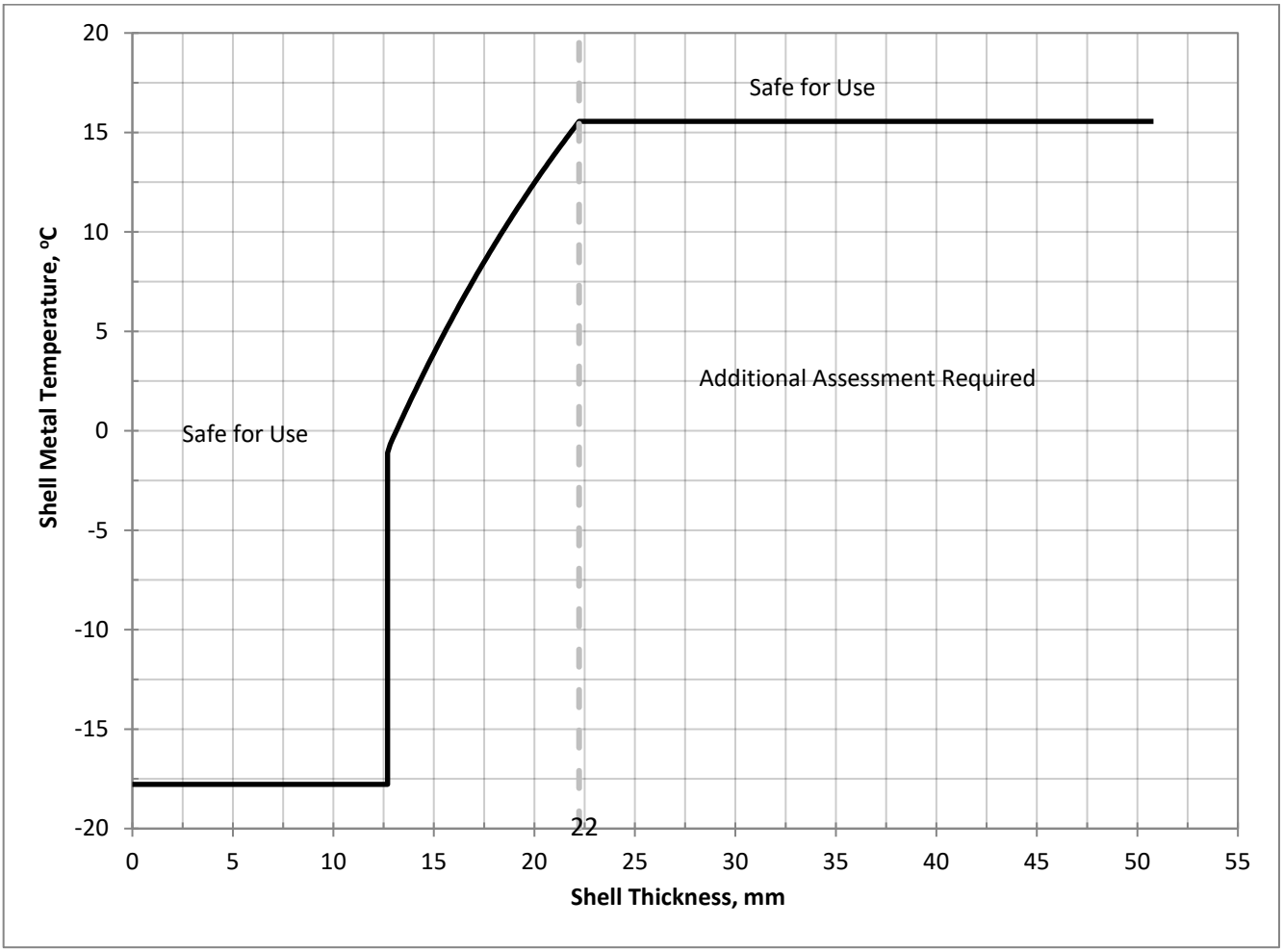

Note: The above exemption curve between -1°C and 16°C is based on Curve A in Figure 3.5. The other parts of the curve were established based on successful operating experience. The equations for the curve in this figure are provided in Table 3.4.

Figure 3.10M – Exemption Curve for Tanks Constructed from Carbon Steel of Unknown Toughness Thicker Than 12.7 mm and Operating at a Shell Metal Temperature Below 16°C

[Intentionally Left Blank]

ANNEX 3A – TECHNICAL BASIS AND VALIDATION – ASSESSMENT OF EXISTING EQUIPMENT FOR BRITTLE FRACTURE

(INFORMATIVE)

CONTENTS

ANNEX 3A – TECHNICAL BASIS AND VALIDATION – ASSESSMENT OF EXISTING EQUIPMENT FOR BRITTLE FRACTURE 3A-1

3A.1 TECHNICAL BASIS AND VALIDATION 3A-1
3A.2 REFERENCES 3A-1

3A.1 Technical Basis and Validation

The assessment procedures for prevention of brittle fracture for pressure vessel and piping components in Part 3 are based on the design requirements contained in the ASME B&PV Code, Section VIII, Division 1. The technical basis to these rules is presented in references [1], [2], [3], and [4]. A comparison of other international pressure vessel codes to the ASME rules is provided in reference [5]. The use of the ASME toughness rules for evaluation of in-service equipment is described in references [6] and [7]. The assessment procedure for prevention of brittle fracture for tank components in Part 3 is based on the rules in API 653. The technical basis to these rules is provided in reference [8].

3A.2 References

[1] M. Prager, D.A. Osage, Macejko and J. Staats, Development of Material Fracture Toughness Rules for ASME B&PV Code Section VIII Division 2, Welding Research Council, Inc., WRC Bulletin 528, New York, NY, 2008.

[2] Jacobs, W.S., “ASME Code Material Toughness Requirements for Low Temperature Operation, Section VIII, Division 1 & Division 2, 1998 Edition, 1999 Addenda,” PVP-Vol. 407, Pressure Vessel and Piping Codes and Standards - 2000, ASME 2000, pages 23 through 38.

[3] Mooney, J.L., “Application of the New ASME Section VIII, Division 1 Toughness Requirements to a Typical Vessel,” Mechanical Engineering, ASME, New York, NY, March 1999, pp. 99-101.

[4] Selz, A, “New Toughness Rules in Section VIII, Division 1 of the ASME Boiler and Pressure Vessel Code,” 88-PVP-8, ASME, 1988.

[5] Kent, L., “Comparison of Pressure Vessel Codes Requirements for Brittle Fracture Prevention,” Proc. ICPVT-9, 1992, pp 970-990.

[6] Findlay, M., McLaughlin, J.E., and Sims, J.R., “Assessment of Older Cold Service Pressure Vessels for Brittle Fracture During Temperature Excursions Below the Minimum Design Temperature,” ASME PVP-Vol. 288, American Society of Mechanical Engineers, New York, NY, pp. 297-305 1994.

[7] McLaughlin, J.E. and Sims, J.R., "Assessment of Older Equipment for Risk of Brittle Fracture," ASME PVP-Vol. 261, American Society of Mechanical Engineers, New York, NY, 1993, pp. 257-264.

[8] McLaughlin, J.E., "Preventing Brittle Fracture of Aboveground Storage Tanks – Basis for the Approach Incorporated in API 653," Proceedings Case Studies: Sessions III and IV of the IIW Conference, Fitness-For-Purpose of Welded Structures, Key Biscayne, Florida, USA, October 23-24, 1991.

[9] TWI, Fracture -Safe Designs for Large Storage Tanks, ed. A.A. Willoughby, The Welding Institute, 1986.

PART 4 – ASSESSMENT OF GENERAL METAL LOSS

CONTENTS

PART 4 – ASSESSMENT OF GENERAL METAL LOSS 4-1

4.1 GENERAL 4-1
4.1.1 Assessment Procedures for General Metal Loss 4-1
4.1.2 Thickness Averaging Approach Used for the Assessment 4-2
4.2 APPLICABILITY AND LIMITATIONS OF THE PROCEDURE 4-2
4.2.1 General Metal Loss Assessment 4-2
4.2.2 Limitations Based on Flaw Type 4-2
4.2.3 Calculation of the $MAWP_r$ and MFH_r and Coincident Temperature 4-2
4.2.4 Limitations Based on Temperature 4-2
4.2.5 Definition of Component Types 4-2
4.2.6 Applicability of the Level 1 and Level 2 Assessment Procedures 4-2
4.2.7 Applicability of the Level 3 Assessment Procedures 4-3
4.3 DATA REQUIREMENTS 4-3
4.3.1 Original Equipment Design Data 4-3
4.3.2 Maintenance and Operational History 4-3
4.3.3 Required Data/Measurements for an FFS Assessment 4-4
4.3.4 Recommendations for Inspection Technique and Sizing Requirements 4-6
4.4 ASSESSMENT TECHNIQUES AND ACCEPTANCE CRITERIA 4-7
4.4.1 Overview 4-7
4.4.2 Level 1 Assessment 4-8
4.4.3 Level 2 Assessment 4-9
4.4.4 Level 3 Assessment 4-11
4.5 REMAINING LIFE ASSESSMENT 4-12
4.5.1 Thickness Approach 4-12
4.5.2 MAWP Approach 4-12
4.6 REMEDIATION 4-13
4.6.1 Objectives 4-13
4.6.2 Methods 4-13
4.7 IN–SERVICE MONITORING 4-15
4.7.1 Objectives 4-15
4.7.2 Monitoring Methods 4-15
4.7.3 Calibration 4-15
4.8 DOCUMENTATION 4-15
4.8.1 General 4-15
4.8.2 Inspection Data 4-15
4.9 NOMENCLATURE 4-15
4.10 REFERENCES 4-18
4.11 TABLES 4-19
4.12 FIGURES 4-28

4.1 General

4.1.1 Assessment Procedures for General Metal Loss

Fitness-For-Service (FFS) Assessment procedures for pressurized components subject to general metal loss resulting from corrosion, erosion, or both corrosion and erosion are provided in this Part. The procedures can be used to qualify a component for continued operation or for rerating. A flow chart for the assessment procedure for general metal loss is shown in Figure 4.1.

4.1.2 Thickness Averaging Approach Used for the Assessment

The assessment procedures in this Part are based on a thickness averaging approach. If local areas of metal loss are found in the component, the thickness averaging approach may produce conservative results. For these cases, the assessment procedures of Part 5 can be utilized to reduce the conservatism in the analysis. The exact distinction between uniform and local metal loss cannot be made without knowing the characteristics of the metal loss profile. For most evaluations, it is recommended to first perform an assessment using Part 4.

4.2 Applicability and Limitations of the Procedure

4.2.1 General Metal Loss Assessment

The assessment procedures in this Part can be used to evaluate general metal loss (uniform or local) that exceeds or is predicted to exceed the corrosion allowance before the next scheduled inspection. The general metal loss may occur on the inside or outside surface of the component. Assessment procedures based on point thickness readings and thickness profiles are provided. The assessment procedure to be used in an evaluation depends on the type of thickness data available, i.e., point thickness readings or thickness profiles (see paragraph 4.3.3), the characteristics of the metal loss (i.e., uniform or local), and the degree of conservatism acceptable for the assessment. The methodology shown in Figure 4.2 can be used to determine the assessment procedure to be used in the evaluation.

4.2.2 Limitations Based on Flaw Type

Unless otherwise specified, this Part is limited to the evaluation of metal loss. Other flaw types shall be evaluated in accordance with Part 2, Table 2.1.

4.2.3 Calculation of the $MAWP_r$ and MFH_r and Coincident Temperature

Calculation methods are provided to rerate the component if the acceptance criteria in this Part are not satisfied. For pressurized components, the calculation methods can be used to find a reduced maximum allowable working pressure ($MAWP_r$) and coincident temperature. For tank components (i.e., shell courses), the calculation methods can be used to determine a reduced maximum fill height (MFH_r) and coincident temperature.

4.2.4 Limitations Based on Temperature

The assessment procedures only apply to components that are not operating in the creep range; the design temperature is less than or equal to the value in Table 4.1. The Materials Engineer should be consulted regarding the creep range temperature limit for materials not listed in this table. Assessment procedures for components operating in the creep range are provided in Part 10.

4.2.5 Definition of Component Types

In this Part, the component definitions provided in Table 4.2 are used in determining the permissible assessment level for a component.

4.2.6 Applicability of the Level 1 and Level 2 Assessment Procedures

The Level 1 or 2 Assessment procedures in this Part apply only if all of the following conditions are satisfied.

a) The original design criteria were in accordance with a recognized code or standard (see Part 1, paragraphs 1.2.2 or 1.2.3).

b) The region of metal loss has relatively smooth contours without notches, i.e., negligible local stress concentrations.

c) The component is not in cyclic service. If the component is subject to less than 150 cycles, i.e., pressure and/or temperature variations including operational changes and start-ups and shut-downs, throughout its previous operating history and future planned operation, or satisfies the cyclic service screening procedure in Part 14, then the component is not in cyclic service.

d) The following limitations on component types and applied loads are satisfied:

1) Level 1 Assessment – Type A Components (see paragraph 4.2.5) subject to internal pressure or external pressure.

2) Level 2 Assessment – Type A and Type B Components (see paragraph 4.2.5) subject to internal pressure, external pressure, supplemental loads (see Annex 2C, paragraph 2C.2.7) or any combination thereof.

e) The Level 1 or Level 2 Assessment procedures may be applied if the region of metal loss is located a distance L_{msd} from the Type C component (see Figure 4.6).

f) The Level 1 and Level 2 Assessment procedures include a limitation on the minimum measured thickness, t_{mm}. The limitation on t_{mm} is to guard against potential inadequacy in inspection method capabilities to accurately characterize excessively thinned areas. If the limitation on t_{mm} is not satisfied, a Level 3 Assessment may be performed. Future inspection frequency shall be established based on a detailed investigation of all applicable damage mechanisms and inspection results shall be appropriately validated (see paragraph 4.3.4.6).

4.2.7 Applicability of the Level 3 Assessment Procedures

A Level 3 Assessment can be performed when the Level 1 and 2 Assessment procedures do not apply, or when these assessment levels produce overly conservative results, i.e., would not permit operation at the current design conditions. Examples include but are not limited to the following.

a) Type A, B, or C Components subject to internal pressure, external pressure, supplemental loads, and any combination thereof.

b) Components with a design based on proof testing, e.g., piping tee or reducer produced in accordance with ASME B16.9 where the design may be based on proof testing.

c) Components in cyclic service or components where a fatigue analysis was performed as part of the original design calculations; the assessment should consider the effects of fatigue on the FFS calculations used to qualify the component for continued operation.

4.3 Data Requirements

4.3.1 Original Equipment Design Data

An overview of the original equipment data required for an assessment is provided in Part 2, paragraph 2.3.1.

4.3.2 Maintenance and Operational History

An overview of the maintenance and operational history required for an assessment is provided in Part 2, paragraph 2.3.2.

4.3.3 Required Data/Measurements for an FFS Assessment

4.3.3.1 Thickness readings are required on the component where the metal loss has occurred to evaluate general metal loss. An overview of the Level 1 and Level 2 Assessment options are shown in Figure 4.2, and described in paragraph 4.4.

a) Two options for obtaining thickness data are presented:

   1) Point thickness readings – point thickness readings can be used to characterize the metal loss in a component if there are no significant differences in the thickness readings obtained at inspection monitoring locations.

   2) Thickness profiles – thickness profiles should be used to characterize metal loss in a component if there is a significant variation in the thickness readings. In this case, the metal loss may be localized, and thickness profiles (thickness readings on a prescribed grid) should be used to characterize the remaining thickness and size of the metal loss area.

b) The thickness quantities used in this Part for the assessment of general metal loss are the average measured thickness and the minimum measured thickness. If thickness readings indicate that the metal loss is general, the procedures in this Part will provide an adequate assessment. However, if the metal loss is localized and thickness profiles are obtained, the assessment procedures of this Part may produce conservative results, and the option for performing the evaluation using the assessment procedures of Part 5 is provided.

4.3.3.2 Point thickness readings may be used in the assessment if all of the following requirements are satisfied. Otherwise, thickness profiles shall be used per paragraph 4.3.3.3.

a) The damage shall be confirmed to be uniform wall loss. The point thickness reading approach shall not be used when there is an indication of localized metal loss.

b) Additional inspection may be required such as visual examination, radiography or other NDE methods.

c) A minimum of 15 thickness readings should be used unless the level of NDE utilized can be used to confirm that the metal loss is general. In some cases, additional readings may be required based on the size of the component, the construction details utilized, and the nature of the environment resulting in the metal loss. A sample data sheet to record thickness readings is shown in Table 4.3.

d) To prevent smoothing out significant local variations in thickness readings during the averaging process, the minimum measured thickness, t_{mm}, shall satisfy the following requirement:

$$t_{mm} \geq 0.9 t_{am} \tag{4.1}$$

4.3.3.3 If thickness profiles are used in the assessment, the following procedure shall be used to determine the required inspection locations and the Critical Thickness Profiles (CTPs).

a) STEP 1 – Locate the region of metal loss in the component and determine the location, orientation, and length of the inspection plane(s).

b) STEP 2 – To determine the inspection plane(s) for thickness readings the following shall be considered:

   1) Pressure Vessel Heads and Spheres – Both the circumferential and meridional directions shall be set as inspection plane(s) (see Figure 4.7).

2) Cylindrical Shells, Conical Shells and Elbows – The critical inspection plane(s) are meridional (longitudinal) if the circumferential stress due to pressure governs, and circumferential if the longitudinal stress due to pressure and supplemental loads governs (see Figure 4.8).

3) Atmospheric Storage Tanks – The critical inspection plane(s) are in the meridional (longitudinal) direction (see Figure 4.9).

4) Low Pressure Storage Tanks – The critical inspection plane(s) are assigned based on the component geometry. For general shells with a single vertical axis of revolution and curvature along the meridian, e.g., storage sphere, the critical inspection planes may be determined using subparagraphs 1 and 2 above, as applicable. For flat bottom storage tanks with hydrostatic liquid loading, e.g., double wall LPG or LNG tanks constructed to API 620, the critical inspection planes are determined using subparagraph 3 above.

5) If the critical inspection plane(s) for a component are not known at the time of the inspection, a minimum of two planes at right angles to each other should be utilized to record thickness readings.

c) STEP 3 – Mark each inspection plane on the component; the length of the inspection plane for the corroded/eroded region should be sufficient to characterize the metal loss.

d) STEP 4 – Determine the uniform thickness away from the local metal loss at the time of the assessment, t_{rd}.

e) STEP 5 – Measure and record the wall thickness readings at intervals along each inspection plane and determine the minimum measured wall thickness, t_{mm}. The spacing distance for thickness readings should allow for an accurate characterization of the thickness profile.

1) If the corroded surface is not accessible for visual inspection, then the recommended spacing for thickness readings along each inspection plane, L_s, is given by Equation (4.2); however, a minimum of five thickness readings is recommended for each inspection plane(s). The length for thickness averaging L is computed using Equation (4.7).

$$L_s = \min\left[2t_{rd},\ 25\ mm\ (1.0\ inch)\right] \tag{4.2}$$

2) The above recommended spacing for thickness readings can be modified based on the actual size of the region of metal loss. If visual inspection or other NDE methods are utilized to quantify the metal loss, an alternative spacing can be used as long as the metal loss can be adequately characterized. For example, if the region of metal loss is determined to be uniform based on a visual inspection, the spacing utilized to take thickness readings can be increased without impacting the FFS Assessment result.

3) A sample data sheet to record thickness readings is shown in Table 4.3. If more than four inspection planes are utilized, additional copies of this sheet can be used to record the thickness profile data.

f) STEP 6 – Determine the CTP in the meridional and circumferential directions. The CTP in each direction is determined by projecting the minimum remaining thickness for each position along all parallel inspection planes onto a common plane as shown in Figure 4.10. The length of the profile is established by determining the end point locations where the remaining wall thickness is greater than or equal to t_{rd} in the meridional and circumferential directions.

1) The CTP in the meridional or longitudinal direction is obtained by projecting the minimum thickness at each interval along M1 – M5 inspection planes onto a common plane. The length of the metal loss in the longitudinal direction, denoted as s, is determined using the CTP and t_{rd} as shown in Figure 4.10.

2) The CTP in the circumferential direction is obtained by projecting the minimum thickness at each interval along C1 – C7 inspection planes onto a common plane. The length of the metal loss in the circumferential direction, denoted as c, is determined using the CTP and t_{rd} as shown in Figure 4.10.

3) If there are multiple flaws in close proximity to one another, then the size of the flaw to be used in the assessment is established considering the effects of neighboring flaws using the methodology shown in Figure 4.11. The final CTP for the flaw, or network of flaws, can be established as shown in Figure 4.12. The thickness profile for both the longitudinal and circumferential planes should be evaluated in this manner.

4) For large regions of metal loss, it may be overly conservative to project the minimum thicknesses on to a single plane to determine a CTP. For these cases, more than one CTP in the longitudinal or circumferential directions may be utilized in the assessment. The number of CTP's to be used in an assessment depends on the uniformity of the metal loss. A sensitivity analysis (see Part 2, paragraph 2.4.3.1) can be performed to evaluate the benefits of using multiple CTP's in the assessment of the longitudinal and circumferential directions. Alternatively, a Level 3 Assessment can be completed to reduce conservatism.

4.3.3.4 If the region of metal loss is close to or at a major structural discontinuity, the remaining thickness can be established using the procedure in paragraphs 4.3.3.2 or 4.3.3.3. However, additional thickness readings should be taken to include sufficient data points in the region close to the major structural discontinuity. This involves taking adequate thickness readings within the zones defined as follows for the components listed below:

a) Nozzle or branch connection (see Figure 4.13) for the thickness zone, L_v, L_{no} and L_{ni}.

b) Conical shell transition (see Figure 4.14) for the thickness zone, L_v.

c) Flange connections (see Figure 4.15) for the thickness zone, L_{vh} and L_{vt}.

d) Cylinder to flat head junctions (see Figure 4.16) for the thickness zone, L_v.

e) Integral tubesheet connections (see Figure 4.17) for the thickness zone, L_v.

f) Stiffening or insulation support rings (see Figure 4.18) for the thickness zone, L_v.

4.3.3.5 Additional thickness readings are required if discrepancies are noted in the reported thickness measurements. For example, if the latest thickness reading is greater than the reading at the time of the last inspection, additional readings may be required to resolve the discrepancies in the data.

4.3.4 Recommendations for Inspection Technique and Sizing Requirements

4.3.4.1 Thickness readings can be made using straight beam Ultrasonic Thickness examination (UT). This method can provide high accuracy and can be used for point thickness readings and in obtaining thickness profiles. Continuous line scans or area scans can also be used to obtain thickness profiles. The limitations of UT are associated with uneven surfaces and access. Examples include measuring the thickness at a weld or the thickness of the shell located underneath a reinforcing pad from the outside of a vessel.

4.3.4.2 Obtaining accurate thickness readings using UT depends on the surface condition of the component. Surface preparation techniques vary depending on the surface condition, but in many cases, wire brushing is sufficient. However, if the surface has a scale build-up or is pitted, grinding may be necessary.

4.3.4.3 All UT thickness readings should be made after proper calibration for the wall thickness, ultrasonic velocity, and temperature ranges of the component. Special UT couplants are required if the thickness readings

are obtained on high temperature components. It may be preferable to obtain readings with probes less than 12.7 mm (0.5 inches) in diameter to provide greater assurance that pitting/localized corrosion is not present.

4.3.4.4 Radiographic Testing (RT) may also be used to determine metal loss; however, accurate thickness data may only be obtained by moving the component containing the metal loss or moving the source around the component to obtain multiple views. This type of manipulation may not be possible for all pressure-containing components. However, RT examination can be effectively used to qualify the existence, extent, and depth of a region of metal loss, and may be used in conjunction with UT to determine whether the metal loss on a component is general or local.

4.3.4.5 For components susceptible to brittle fracture (see Part 3, paragraph 3.2.2), supplemental inspection in accordance with paragraph 5.3.4.3 of Part 5 is required to confirm no crack-like flaws exist.

4.3.4.6 Special precautions shall be made to validate inspection results when measured thickness readings are 2.5 mm (0.100 inches) or less. Recommendations for consideration are listed below:

a) Confirm appropriate instrument calibration for the full range of measured thickness values.

b) Perform multiple forms of NDE or utilize multiple inspectors to validate inspection findings.

c) Validate inspection method accuracy with a mock-up sample representing the actual field conditions (considering operating temperature, measured thickness ranges, damage profile, etc.), insofar as possible.

d) Increase inspection frequency to confirm damage progression rate.

4.4 Assessment Techniques and Acceptance Criteria

4.4.1 Overview

4.4.1.1 If the metal loss is less than the specified corrosion/erosion allowance and adequate thickness is available for the future corrosion allowance, no further action is required other than to record the data; otherwise, an assessment is required.

4.4.1.2 An overview of the assessment levels is provided in Figure 4.1.

a) Level 1 Assessments are limited to Type A components subject to internal pressure or external pressure.

b) Level 2 Assessments may be used to evaluate Type A components that do not satisfy the Level 1 Assessment criteria and may be used to evaluate Type B Class 1 components and the following Type B Class 2 components subject to internal pressure or external pressure.

- Pressure vessel nozzles, tank nozzles and piping branch connections.
- The reinforcement zone of conical transitions.
- Flanges.

c) Level 3 Assessments may be used to evaluate Type A and B components that do not satisfy the Level 1 or Level 2 Assessment criteria and may be used to evaluate Type C components using stress analysis methods (see Annex 2D).

4.4.1.3 If thickness readings indicate that the metal loss is localized and thickness profiles are obtained, the assessment procedures in this Part can still be used for the assessment. However, the results may be conservative, and the option for performing the analysis using the assessment procedures of Part 5 is provided.

4.4.1.4 FFS Assessments for the components listed below require special consideration because of the complexities associated with the design requirements of the original construction code. In each case, an Engineer knowledgeable and experienced in the design requirements of the applicable code should perform the assessment (see Part 1, paragraph 1.4.3). If the metal loss is in a component that was not subject to special design requirements per the original construction code (i.e., design requirements based on stress analysis), then the Level 1 or Level 2 Assessment procedures may be applied. If the corrosion/erosion damage is in a component subject to special design requirements, then the calculations required in the original design to qualify the component should be repeated considering a reduced wall thickness.

a) Pressure Vessels Designed to The ASME Code, Section VIII, Division 2 – A user design specification is required where the operational parameters for the original design were established. In addition, detailed heat transfer and stress calculations, and a fatigue analysis may have been performed to satisfy the design-by-analysis rules required in this code.

b) Low Pressure Storage Tanks Designed to API 620 – The design rules for low–pressure storage tanks contained in API 620 require a thorough knowledge of engineering mechanics in that the required thickness of a shell component is based upon the evaluation of free body diagrams, the development of equilibrium equations, and the consideration of a biaxial stress field to determine an allowable design stress.

c) Piping Designed to ASME B31.3 – Metal loss in piping systems can be evaluated using a Level 1 Assessment if the supplemental loads on the piping system are negligible (see Annex 2C, paragraph 2C.2.7). Supplemental loads on piping systems are negligible if the piping satisfies the requirements for a Type A component (see Table 4.2). If supplemental loads are not negligible, a piping stress analysis is required. The piping analysis should consider the relationship between the component thickness, piping flexibility, and the resulting stress (see paragraph 4.4.3.3).

4.4.2 Level 1 Assessment

4.4.2.1 The following assessment procedure shall be used to evaluate Type A Components (see paragraph 4.2.5) subject to internal or external pressure when Point Thickness Reading (PTR) data are used to characterize the metal loss (see paragraph 4.3.3.2).

a) STEP 1 – Take the point thickness reading data in accordance with paragraph 4.3.3.2. From these data determine the minimum measured thickness, t_{mm}, and the average measured thickness, t_{am}.

b) STEP 2 – If Equation (4.1) is satisfied, then proceed to STEP 3 to complete the assessment using the average thickness, t_{am}. If Equation (4.1) is not satisfied, then thickness profiles shall be used for the assessment (see paragraph 4.4.2.2).

c) STEP 3 – The acceptability of the component for continued operation can be established using the Level 1 criteria in Table 4.4, Table 4.5, Table 4.6 and Table 4.7. The averaged measured thickness or $MAWP$ acceptance criterion may be used. In either case, the minimum thickness criterion shall be satisfied. For $MAWP$ acceptance criterion, see Part 2, paragraph 2.4.2.2(e) to determine the acceptability of the equipment for continued operation.

4.4.2.2 The following assessment procedure shall be used to evaluate Type A Components (see paragraph 4.2.5) subject to internal or external pressure when Critical Thickness Profile (CTP) data are used to characterize the metal loss (see paragraph 4.3.3.3).

a) STEP 1 – Determine the thickness profile data in accordance with paragraph 4.3.3.3 and determine the minimum measured thickness, t_{mm}.

b) STEP 2 – Determine the wall thickness and diameter to be used in the assessment using Equation (4.3) and Equation (4.4) or Equation (4.5).

$$t_{ml} = t_{nom} - FCA_{ml} \tag{4.3}$$

$$D_{ml} = D + 2 \cdot FCA_{ml} \qquad \left(for\ Internal\ FCA\right) \tag{4.4}$$

$$D_{ml} = D \qquad \left(for\ External\ FCA\right) \tag{4.5}$$

c) STEP 3 – Compute the remaining thickness ratio, R_t.

$$R_t = \left(\frac{t_{mm} - FCA_{ml}}{t_{ml}} \right) \tag{4.6}$$

d) STEP 4 – Compute the length for thickness averaging, L where the parameter Q is evaluated using Table 4.8.

$$L = Q\sqrt{D_{ml} \cdot t_{ml}} \tag{4.7}$$

e) STEP 5 – Establish the Critical Thickness Profiles (CTP's) from the thickness profile data (see paragraph 4.3.3.3). Determine the average measured thickness t_{am}^{s} based on the longitudinal CTP and the average measured thickness t_{am}^{c} based on the circumferential CTP. The average measured thicknesses t_{am}^{s} and t_{am}^{c} shall be based on the length L determined in STEP 4 (see Figure 4.19). The length L shall be located on the respective CTP such that the resulting average thickness is a minimum.

f) STEP 6 – Based on the values of t_{am}^{s} and t_{am}^{c} from STEP 5, determine the acceptability of the component for continued operation using the Level 1 criteria in Table 4.4, Table 4.5, Table 4.6 and Table 4.7, as applicable. The averaged measured thickness or $MAWP$ acceptance criterion may be used. In either case, the minimum measured thickness, t_{mm}, shall satisfy the criterion in Table 4.4, Table 4.5, Table 4.6 and Table 4.7. For $MAWP$ acceptance criterion, see Part 2, paragraph 2.4.2.2(e) to determine the acceptability of the equipment for continued operation.

4.4.2.3 If the component does not meet the Level 1 Assessment requirements (see Part 2, paragraph 2.4.2.2(e)), then the following, or combinations thereof, shall be considered:

a) Rerate, repair, or replace the component.

b) Adjust the FCA_{ml} by applying remediation techniques (see paragraph 4.6).

c) Adjust the weld joint efficiency or quality factor, E, by conducting additional examination and repeat the assessment. Note: To raise the value of E from 0.7 to 0.85, or from 0.85 to 1.0, would require that the weld seams be spot or 100% radiographed, respectively, and these examinations may reveal additional flaws that will have to be evaluated.

d) Conduct a Level 2 or a Level 3 Assessment.

4.4.3 Level 2 Assessment

4.4.3.1 The assessment procedure in paragraph 4.4.2.1 may be used to evaluate Type A and Type B Class 1 Components (see paragraph 4.2.5) subject to internal pressure, external pressure, supplemental load or combined

loads when Point Thickness Reading (PTR) data are used to characterize the metal loss (see paragraph 4.3.3.2). Note that the Level 2 Acceptance Criteria in Table 4.4, Table 4.5, Table 4.6 and Table 4.7 shall be used in conjunction with STEP 3.

4.4.3.2 The assessment procedure in paragraph 4.4.2.2 may be used to evaluate Type A and Type B Class 1 Components (see paragraph 4.2.5) subject to internal pressure, external pressure, supplemental load or combined loads when CTP data are used to characterize the metal loss (see paragraph 4.3.3.3). Note that the Level 2 Acceptance Criteria in Table 4.4, Table 4.5, Table 4.6 and Table 4.7 shall be used in conjunction with STEP 6.

4.4.3.3 The following assessment procedure can be used to evaluate Type B Class 2 Components (see paragraph 4.4.1.2(b)) subject to internal pressure or external pressure load.

a) STEP 1 – Compute the $MAWP_r$ based upon the average measured thickness minus the future corrosion allowance applied to the region of metal loss and the thickness required for supplemental loads (see Annex 2C, paragraph 2C.2.7), for each component using the equations in the original construction. The calculated $MAWP_r$ should be equal to or exceed the equipment design pressure or equipment $MAWP$. The average thickness of the region, t_{am}, shall be obtained as follows for components with a thickness interdependency:

   1) Nozzles and Branch Connections – Determine the average thickness within the nozzle reinforcement zone shown in Figure 4.13 (see paragraph 4.3.3.4). The assessment procedures in Annex 2C, paragraph 2C.3.4 or 2C.5.7, as applicable, can be utilized to evaluate metal loss at a nozzle or piping branch connection, respectively. The weld load path analysis in this paragraph should also be checked, particularly if the metal loss has occurred in the weldments of the connection.

   2) Axisymmetric Structural Discontinuities – Determine L using Equation (4.7) and L_v based on the type of structural discontinuity listed below. The average thickness is computed based on the smaller of these two distances. If $L < L_v$, then the midpoint of L should be located at t_{mm} to establish a length for thickness averaging unless the location of t_{mm} is within $L/2$ of the zone for thickness averaging. In this case, t_{mm} should be positioned so that it is entirely within L before the average thickness is computed.

      i) Conical shell transition (see Figure 4.14) for the zone for thickness averaging and L_v.

      ii) Flange connections (see Figure 4.15) for the zone for thickness averaging and L_v. If the flange has a hub, and the metal loss is uniform along the hub, then the average thickness may be proportioned in accordance with the original hub dimensions for the flange calculation. If the metal loss is non-uniform or the flange does not have a hub, then the flange calculation should be performed using a uniform hub section with a thickness equal to the average thickness.

      iii) Cylinder to flat head junctions (see Figure 4.16) for the zone for thickness averaging and L_v.

      iv) Integral tubesheet connections (see Figure 4.17) for the zone for thickness averaging and L_v.

      v) Stiffening or insulation support rings (see Figure 4.18) for the thickness zone, L_v.

   3) Piping Systems – Piping systems that are not classified as Type A components in Table 4.2 are classified as Type B Class 1 Components in Table 4.2 because of the relationship between the component thickness, piping flexibility, and the resulting stress. For straight sections of piping, determine L using Equation (4.7) and compute the average thickness based on L to represent the section of pipe with metal loss in the piping analysis. For elbows or bends, the thickness readings should be averaged within the bend and a single thickness used in the piping analysis (i.e., to compute the flexibility factor, system stiffness and stress intensification factor). For branch connections, the thickness should be averaged

within the reinforcement zones for the branch and header, and these thicknesses should be used in the piping model (to compute the stress intensification factor). An alternative assumption is to use the minimum measured thickness to represent the component thickness in the piping model. This approach may be warranted if the metal loss is localized; however, this may result in an overly conservative evaluation. In these cases, a Level 3 Assessment may be required to reduce the conservatism in the assessment (see paragraph 4.4.4.4).

b) STEP 2 – The minimum measured wall thickness, t_{mm}, shall satisfy the criterion in Table 4.4, Table 4.5, Table 4.6 and Table 4.7.

4.4.3.4 If the component does not meet the Level 2 Assessment requirements, then the following, or combinations thereof, can be considered:

a) Rerate, repair, or replace the component.

b) Adjust the FCA_{ml} by applying remediation techniques (see paragraph 4.6).

c) Adjust the weld joint efficiency factor, E, by conducting additional examination and repeat the assessment (see paragraph 4.4.2.3).

d) Conduct a Level 3 Assessment.

e) Evaluate the region of metal using the Part 5 Assessment procedures.

4.4.4 Level 3 Assessment

4.4.4.1 The stress analysis techniques discussed in Annex 2D can be utilized to evaluate regions of general or local metal loss in pressure vessels, piping, and tanks. The finite element method is typically used to compute the stresses in a component; however, other numerical methods such as the boundary element or finite difference method may also be used. Handbook solutions may also be used if the solution matches the component geometry and loading condition. The evaluation may be based on a linear stress analysis with acceptability determined using stress categorization, or a non-linear stress analysis with acceptability determined using a plastic collapse load. Non-linear stress analysis techniques are recommended to provide the best estimate of the acceptable load carrying capacity of the component. Guidelines for performing and processing results from a finite element analysis for an FFS analysis are provided in Annex 2D.

4.4.4.2 If a component is subject to external pressure and/or other loads that result in compressive stresses, a structural stability analysis should be performed using the methods in Annex 2D to determine suitability for continued service. In addition, methods to evaluate fatigue are also included in Part 14 if a component is subject to cyclic loading.

4.4.4.3 Thickness data per paragraph 4.3.3 as well as the component geometry, material properties and loading conditions are required for a Level 3 Assessment. The thickness data can be used directly in finite element model of the component. If thickness profile data are available, the thickness grid can be directly mapped into a three-dimensional finite element model using two or three dimensional continuum elements, as applicable. This information can also be used if the component is modeled using shell elements.

4.4.4.4 If the region of local metal loss is close to or at a major structural discontinuity, details of the component geometry, material properties, and imposed supplemental loads (see Annex 2C, paragraph 2C.2.7) at this location are required for the assessment. Special consideration is required if there are significant supplemental loads at a nozzle, piping branch connection, or pipe bend. The location and distribution of the metal loss in these components may significantly affect both the flexibility and stress distribution in a manner that cannot be evaluated

using the approaches employed in the design. In addition, the localized metal loss may significantly reduce the plastic collapse load capability depending on the nozzle geometry, piping system configuration, and/or applied supplemental loads.

4.5 Remaining Life Assessment

4.5.1 Thickness Approach

4.5.1.1 The remaining life of a component can be determined based upon computation of a minimum required thickness for the intended service conditions according to Table 4.4, Table 4.5, Table 4.6 and Table 4.7, thickness measurements from an inspection, and an estimate of the anticipated corrosion rate. This method is suitable for determination of the remaining life for Type A and Type B Class 1 Components (see paragraph 4.2.5).

$$R_{life} = \frac{t_{am} - t_{min}}{C_{rate}} \tag{4.8}$$

4.5.1.2 The remaining life determined using the Thickness Approach may produce non-conservative results when applied to Type B Class 2 or Type C Components (see paragraph 4.2.5). For these cases, the remaining life should be established using the $MAWP$ approach.

4.5.2 MAWP Approach

4.5.2.1 The $MAWP$ approach provides a systematic method for determining the remaining life of Type A, B, and C components (see Annex 4A, reference [2]). This method is also the only method suitable for determining the remaining life of Type B and C components. In addition, the $MAWP$ approach ensures that the design pressure is not exceeded during normal operation if the future corrosion rate is accurately established.

4.5.2.2 The following procedure can be used to determine the remaining life of a component using the $MAWP$ approach.

a) STEP 1 – Determine the metal loss of the component, t_{loss}.

$$t_{loss} = t_{nom} - t_{am} \tag{4.9}$$

b) STEP 2 – Determine the $MAWP_r$ for a series of increasing time increments using an effective corrosion allowance and the nominal thickness in the computation. The effective corrosion allowance is determined as follows:

$$CA_e = t_{loss} + C_{rate} \cdot time \tag{4.10}$$

c) STEP 3 – Using the results from STEP 2, determine the remaining life from a plot of the $MAWP$ versus time. The time at which the $MAWP_r$ curve intersects the equipment design pressure or equipment $MAWP$ is the remaining life of the component.

d) STEP 4 – Repeat the STEPS 1 through 3 for each component. The equipment remaining life is taken as the smallest value of the remaining life computed for each of the individual components.

4.5.2.3 This approach may also be applied to tanks using the maximum fill height, MFH, instead of the $MAWP$.

4.6 Remediation

4.6.1 Objectives

A FFS Assessment provides an evaluation of the condition of a component for continued operation for a period based upon a future corrosion or degradation rate. However, in many cases, future degradation rates are very difficult to predict, or little or no further degradation can be tolerated. Therefore, remediation methods may be applied to prevent or minimize the rate of further damage.

4.6.2 Methods

Remediation methods for general corrosion/erosion as well as local corrosion/erosion and pitting are provided below. These methods may also be suitable for mitigation of crack-like flaws in some process environments. The methods described below are not inclusive for all situations, nor are they intended to be a substitute for an engineering evaluation of a particular situation. The Owner–User should consult a qualified Metallurgist/Corrosion Engineer and Mechanical Engineer as to the most appropriate method to apply for the relevant damage mechanism(s).

4.6.2.1 Remediation Method 1 – Performing Physical Changes to the Process Stream; the following can be considered.

a) Increasing or decreasing the process temperature, pressure, or both – If the degradation mode is temperature or pressure sensitive, a process change may minimize the progression of the damage. However, the component must be evaluated so that the design still meets the changed conditions. Note that a reduction in the pressure or temperature may result in a reduction of the minimum required wall thickness, thereby increasing the life of the component.

b) Increasing or decreasing the velocity of the stream – Some damage mechanisms, such as erosion, sour water corrosion, under-deposit corrosion, and naphthenic acid corrosion are very velocity sensitive. A slight decrease or increase in stream velocity can change the rate of damage.

c) Installing scrubbers, treaters, coalescers and filters to remove certain fractions and/or contaminants in a stream.

4.6.2.2 Remediation Method 2 – Application of solid barrier linings or coatings to keep the environment isolated from the base metal that has experienced previous damage.

a) Organic coatings – The coating must be compatible with the service (temperature and stream composition) and must be resistant to all service conditions, including steaming–out. Surface preparation, particularly filling of pits, cracks, etc., is critical to achieve a solid bond. Curing conditions are also very important to assure a reliable lining. These fall into the following general classes:

    1) Thin film coatings – Typically, these include epoxy, epoxy phenolic, and baked phenolic coatings applied in dry film thickness less than 0.25 mm (0.010 inch).

    2) Thick film coatings – Typically, these include vinyl ester and glass fiber reinforced coatings that are applied in dry film thickness greater than 0.25 mm (0.010 inch).

b) Metallic linings – These fall into three general classes:

    1) Metal spray linings – Various metal spray processes are available. In general, higher velocity processes such as HVOF (High Velocity Oxy–Fuel) produce denser coatings, which are less susceptible to spalling or undermining. Coatings are often applied in multiple layers, with different compositions in each layer.

The coating material in contact with the process environment should be corrosion resistant. Surface preparation is critical in achieving a solid bond. One advantage of metal spray linings is that the base material is not heated to high temperatures as in welding.

2) Strip linings – Thin strips of a corrosion resistant metal are applied to the area of concern. They are fastened to the backing metal by small welds, which help to minimize the size of the weld heat affected zone. Note that strip linings may crack at the lining attachment-to-component wall weld and may need periodic maintenance. In addition, corrosion of the underlying wall by leaking fluid at these cracks may be difficult to detect.

3) Weld overlay (see paragraph 4.6.2.4).

c) Refractory linings – Many materials fall into this category. Depending on the damage mechanism, insulating refractories can be used to decrease the metal temperature, erosion resistant refractories can be used for erosion protection, and corrosion resistant refractories can be used to protect the base material. Selection of the refractory type and anchoring system and curing of the refractory are critical elements for this remediation method. A refractory specialist should be consulted for details.

4.6.2.3 Remediation Method 3 – Injection of water and/or chemicals on a continuous basis to modify the environment or the surface of the metal. Important variables to consider when injecting chemicals are the particular stream contaminants, injection point location and design, rate of injection, eventual disposition and any adverse reactions, the effect of process upsets, and monitoring for effectiveness. Examples of this type are as follows:

a) Water washing to dilute contaminants – This strategy is often applied in fluid catalytic cracking light end units and hydrodesulfurization reactor outlet systems. Important variables to consider when stipulating a retrofit water wash installation are location of injection, distribution of water, water rate, water quality, injection point design and disengagement, and monitoring for effectiveness.

b) Injection of chemicals to change the aggressiveness of the solution – Neutralizing chemicals as used in atmospheric distillation unit overheads, polysulfide, and oxygen scavengers all fall into this category. Important variables to consider include the injection location and design, possible adverse side effects, and monitoring for effectiveness.

c) Injection of filming type chemicals to coat the metal surface – Filming chemicals attach to the metal surface to form a thin barrier that protects the metal. Important variables to consider are the injection location and design, response to upsets, and monitoring effectiveness.

4.6.2.4 Remediation Method 4 – Application of weld overlay for repair of the base material or for the addition of a corrosion resistant lining. If weld overlay is applied, the weldability of the base metal considering the effects of the environment should be evaluated (see Annex 2B). Note that the application of a weld overlay may necessitate a $PWHT$.

a) Repair of Base Material – Weld overlay with the same chemistry (P-Number) as the base metal of the component is added to the component to provide the necessary increase in wall thickness to compensate for corrosion/erosion. Note that this method does not eliminate/reduce the rate of degradation. The weld overlay may be added either to the inside or outside surface regardless of the surface on which the metal loss is occurring. For some applications, a repair procedure can be developed which permits deposition of the weld overlay while the component is in operation. Since this process changes the geometry of the component, an analysis considering bending stresses should be made to determine the acceptability of the proposed design.

b) Application of corrosion resistant lining – A corrosion/erosion resistant material is applied to the surface of the base material.

4.7 In–Service Monitoring

4.7.1 Objectives

As discussed above, mitigation methods can be applied, but in some cases, these are not feasible or, if they are applied, it still is important to confirm that they are effective. Therefore, in-service monitoring methods can be applied to directly monitor any further damage or to monitor indirectly conditions that might lead to further damage.

4.7.2 Monitoring Methods

Typical monitoring methods include the use of the following tools or procedures:

a) Corrosion probes

b) Hydrogen probes

c) Retractable corrosion coupons and physical probes

d) Spot UT measurements and scanning

e) Radiographic examination

f) Stream samples for H_2S, Cl, NH_3, CO_2, Fe, Ni, pH, water content, Hg, etc.

g) Infrared thermography

h) Thermocouples

4.7.3 Calibration

Care must be exercised in defining the in–service monitoring method, determining the required measurement sensitivity of the method based on the environment, and locating monitoring stations on the component to insure that the damage mechanism resulting in the metal loss can adequately be measured and evaluated during operation.

4.8 Documentation

4.8.1 General

The documentation of the FFS Assessment should include the information cited in Part 2, paragraph 2.8.

4.8.2 Inspection Data

Inspection data including all thickness readings and corresponding locations used to determine the average measured thickness, t_{am}, and the minimum measured thickness, t_{mm}, should be recorded and included in the documentation. A sample data sheet is provided in Table 4.3 for this purpose. A sketch showing the location and orientation of the inspection planes on the component is also recommended.

4.9 Nomenclature

A_R vessel stiffening ring cross-sectional area or the remaining wall thickness area.

CTP Critical Thickness Profile.

C_{rate} future corrosion rate.

CA_e effective corrosion allowance used to determine a remaining life.

c extent of the metal loss established using the CTP in the circumferential direction.

D inside diameter of the vessel.

D_{ml} inside diameter of the shell corrected for FCA_{ml}, as applicable.

d_i current inside diameter of the nozzle including the specified FCA_{ml}.

E weld joint efficiency or quality factor.

FCA Future Corrosion Allowance applied to the region away from the metal loss (see Annex 2C, paragraph 2C.2.8 and Figure 4.19).

FCA_{ml} Future Corrosion Allowance applied to the region of metal loss (see Figure 4.19).

L length for thickness averaging along the shell.

L_H length for thickness averaging in the horizontal direction along the shell at nozzle junction.

L_{ni} length for thickness averaging at a nozzle in the vertical direction on the inside of the shell based on area reinforcement requirements.

L_{no} length for thickness averaging at a nozzle in the vertical direction on the outside of the shell based on area reinforcement requirements.

L_s recommended spacing of thickness readings.

L_{ss} length between saddle supports for horizontal pressure vessels and heat exchangers.

L_v length for thickness averaging along the shell at shell discontinuities such as stiffening rings, conical transitions, and skirt attachment locations.

L_{vh} length for thickness averaging for the flange hub.

L_{vf} length for thickness averaging for a flange.

L_{vni} length for thickness averaging at a nozzle in the vertical direction on the inside of the shell.

L_{vno} length for thickness averaging at a nozzle in the vertical direction on the outside of the shell.

$LOSS$ uniform metal loss away from the damage area at the time of the inspection.

$MAWP$ Maximum Allowable Working Pressure of the undamaged component.

$MAWP_r$ reduced maximum allowable working pressure of the damaged component.

$MAWP_r^C$ reduced $MAWP$ of a conical or cylindrical shell based on the stresses in the circumferential or hoop direction (see Annex 2C, paragraph 2C.2).

$MAWP_r^L$ reduced $MAWP$ of a conical or cylindrical shell based on the stresses in the longitudinal direction (see Annex 2C, paragraph 2C.2).

MFH Maximum Fill Height of the undamaged tank.

MFH_r reduced maximum fill height of the damaged tank.

P internal or external design pressure.

Q factor used to determine the length for thickness averaging based on an allowable Remaining Strength Factor (see Part 2) and the remaining thickness ratio, R_t (see Table 4.8).

R inside radius of the component.

R_S small end inside radius at a conical transition corrected for $LOSS$ and FCA as applicable.

R_L large end inside radius at a conical transition corrected for $LOSS$ and FCA as applicable.

R_t remaining thickness ratio.

R_{life} remaining life.

RSF_a allowable remaining strength factor (see Part 2).

s extent of the metal loss established using the CTP in the longitudinal direction with t_{min}.

t_{am} average measured wall thickness of the component based on the Point Thickness Readings (PTR) measured at the time of the inspection.

t_{am}^c average measured wall thickness of the component based on the circumferential CTP determined at the time of the inspection.

t_{am}^s average measured wall thickness of the component based on the longitudinal CTP determined at the time of the inspection.

t_c wall thickness away from the damaged area adjusted for $LOSS$ and FCA, as applicable (see Figure 4.19).

t_{co} furnished cone thickness at a conical transition.

t_e reinforcing pad thickness.

t_{lim} limiting thickness.

t_L furnished large end cylinder thickness at a conical transition.

t_{loss} the nominal thickness minus the average measured thickness.

t_{min} minimum required wall thickness of the component (see Annex 2C, paragraph 2C.2).

t_{min}^C minimum required thickness of a conical or cylindrical shell based on the stresses in the circumferential or hoop direction (see Annex 2C, paragraph 2C.2).

t_{min}^L minimum required thickness of a conical or cylindrical shell based on the stresses in the longitudinal direction (see Annex 2C, paragraph 2C.2).

t_{ml} nominal thickness in the region of corrosion corrected for FCA_{ml}, as applicable.

t_{mm} minimum measured thickness determined at the time of the inspection (see Figure 4.19).

t_{nom} nominal or furnished thickness of the component adjusted for mill undertolerance as applicable (see Figure 4.19).

t_n nozzle thickness.

t_{rd} uniform thickness away from the local metal loss location established by thickness measurements at the time of the assessment (see Figure 4.19).

t_s furnished small end cylinder thickness at a conical transition.

t_{sl} required shell thickness for supplemental loads.

t_v furnished vessel thickness.

$time$ time allocated for future operation.

4.10 References

References for this Part are provided in Annex 4A – Technical Basis and Validation – Assessment of General Metal Loss.

4.11 Tables

Table 4.1 – Temperature Limit Used to Define the Creep Range

Material	Temperature Limit
Carbon Steel $\left(UTS \le 414MPa\ (60\ ksi)\right)$	343°C (650°F)
Carbon Steel $\left(UTS > 414MPa\ (60\ ksi)\right)$	371°C (700°F)
Carbon Steel – Graphitized	371°C (700°F)
C-1/2Mo	399°C (750°F)
1-1/4Cr-1/2Mo – Normalized & Tempered	427°C (800°F)
1-1/4Cr-1/2Mo – Annealed	427°C (800°F)
2-1/4Cr-1Mo – Normalized & Tempered	427°C (800°F)
2-1/4Cr-1Mo – Annealed	427°C (800°F)
2-1/4Cr-1Mo – Quenched & Tempered	427°C (800°F)
2-1/4Cr-1Mo – V	441°C (825°F)
3Cr-1Mo-V	441°C (825°F)
5Cr-1/2Mo	427°C (800°F)
7Cr-1/2Mo	427°C (800°F)
9Cr-1Mo	427°C (800°F)
9Cr-1Mo – V	454°C (850°F)
12 Cr	482°C (900°F)
AISI Type 304 & 304H	510°C (950°F)
AISI Type 316 & 316H	538°C (1000°F)
AISI Type 321	538°C (1000°F)
AISI Type 321H	538°C (1000°F)
AISI Type 347	538°C (1000°F)
AISI Type 347H	538°C (1000°F)
Alloy 800	565°C (1050°F)
Alloy 800H	565°C (1050°F)
Alloy 800HT	565°C (1050°F)
HK-40	649°C (1200°F)

Table 4.2 – Definitions of Component Types

Component Type	Definition	Examples
Type A	A component that has a design equation that specifically relates pressure (or liquid fill height for tanks) and supplemental loads, as applicable, to a required wall thickness, and the supplemental loads in combination with pressure do not govern the required wall thickness, i.e., the required thickness is based on pressure only.	• Pressure vessel cylindrical and conical shell sections with dimensions that satisfy the criteria in Figure 4.3 and Figure 4.4. • Spherical pressure vessels and storage spheres. • Spherical, elliptical and torispherical formed heads. • Straight sections of piping systems and elbows or pipe bends that do not have structural attachments that satisfy the temperature criteria in Figure 4.5. • Cylindrical atmospheric storage tank shell courses.
Type B, Class 1	Components have the same geometry and loading conditions as described above for Type A but are not classified as Type A components because supplemental loads in combination with pressure may govern the required wall thickness.	• Pressure vessel cylindrical and conical shell sections that are not classified as Type A components in accordance with the criteria above. • Piping systems (see paragraph 4.4.3.3(a)(3)) that are not classified as Type A components in accordance with the criteria above.
Type B, Class 2	Components do not have a design equation that specifically relates pressure (or liquid fill height for tanks) and/or other loads, as applicable, to a required wall thickness. These components have a code design procedure to determine an acceptable configuration. Type B, Class 2 components typically exist at a major structural discontinuity and involve the satisfaction of a local reinforcement requirement (e.g., nozzle reinforcement area), or necessitate the computation of a stress level based upon a given load condition, geometry, and thickness configuration (e.g., flange design). These rules typically result in one component with a thickness that is dependent upon that of another component. Design rules of this type have thickness interdependency, and the definition of a minimum thickness for a component is ambiguous.	• Pressure vessel nozzles, tank nozzles and piping branch connections. • The reinforcement zone of conical transitions. • Flanges. • Cylinder to flat head junctions. • Integral tubesheet connections.

Table 4.2 – Definitions of Component Types

Component Type	Definition	Examples
Type C	A component that does not have a design equation which specifically relates pressure (or liquid fill height for tanks) and/or other loads, as applicable, to a required wall thickness. In addition, these components do not have a code design procedure to determine local stresses.	• Pressure vessel head to shell junctions. However, the cylinder side of junctions between cylinders and 2:1 elliptical head may be treated as Type A components in metal loss evaluations (Part 4, Part 5, and Part 6) when the required thickness of the components is governed exclusively by internal pressure. When this condition is satisfied, the head to shell junction is exempt from being considered as a major structural discontinuity for metal loss evaluations on the cylinder side of the junction. • Stiffening rings attached to a shell (see paragraph 4.3.3.4(f)). • Skirt and lug-type supports on pressure vessels. • Tank shell bottom course to tank bottom junction.

Table 4.3 – Inspection Summary Required for The Assessment of General Metal Loss

Use this form to summarize the data obtained from a field inspection.

Equipment Identification: _____
Equipment Type: _____ Pressure Vessel _____ Storage Tank _____ Piping Component
Component Type & Location: _____

Data Required for Level 1 And Level 2 Assessment
Future Corrosion Allowance: _____
Inside Diameter: _____
Minimum Required Thickness: _____
Flaw Dimensions (s & c): _____

Enter the thickness data for each of the inspection planes in the table shown below.

Inspection Plane:__		**Inspection Plane:__**		**Inspection Plane:__**		**Inspection Plane:__**	
Location	**Thickness**	**Location**	**Thickness**	**Location**	**Thickness**	**Location**	**Thickness**
t_{mm}		t_{mm}		t_{mm}		t_{mm}	
t_{am}		t_{am}		t_{am}		t_{am}	

Table 4.4 – Acceptance Criteria for Level 1 And 2 Assessment for Cylindrical and Conical Shells, and Elbows – Pressure Vessels and Piping

Assessment Parameter	Level 1 Assessment Acceptance Criteria	Level 2 Assessment Acceptance Criteria
Average Measured Thickness from Point Thickness Readings (PTR)	Determine $t^C_{\min}$ using P $t_{am} - FCA_{ml} \ge t^C_{min}$	Determine t^C_{min}, t^L_{min} using $P \cdot RSF_a$ $t_{am} - FCA_{ml} \ge \max\left[t^C_{min}, t^L_{min}\right]$
Average Measured Thickness from Critical Thickness Profiles (CTP)	Determine $t^C_{\min}, t^L_{\min}$ using P $t^s_{am} - FCA_{ml} \ge t^C_{min}$ $t^c_{am} - FCA_{ml} \ge t^L_{min}$	Determine t^C_{min}, t^L_{min} using $P \cdot RSF_a$ $t^s_{am} - FCA_{ml} \ge t^C_{min}$ $t^c_{am} - FCA_{ml} \ge t^L_{min}$
MAWP from Point Thickness Readings (PTR)	Determine $MAWP^C_r$ using $\left(t_{am} - FCA_{ml}\right)$ $MAWP^C_r \ge MAWP$	Determine $MAWP^C_r$ using $\left(t_{am} - FCA_{ml}\right)$ Determine $MAWP^L_r$ using $\left(t_{am} - t_{sl} - FCA_{ml}\right)$ $\dfrac{\min\left[MAWP^C_r, MAWP^L_r\right]}{RSF_a} \ge MAWP$
MAWP from Critical Thickness Profiles (CTP)	Determine $MAWP^C_r$ using $\left(t^s_{am} - FCA_{ml}\right)$ Determine $MAWP^L_r$ using $\left(t^c_{am} - FCA_{ml}\right)$ $\min\left[MAWP^C_r, MAWP^L_r\right] \ge MAWP$	Determine $MAWP^C_r$ using $\left(t^s_{am} - FCA_{ml}\right)$ Determine $MAWP^L_r$ using $\left(t^c_{am} - t_{sl} - FCA_{ml}\right)$ $\dfrac{\min\left[MAWP^C_r, MAWP^L_r\right]}{RSF_a} \ge MAWP$
Minimum Measured Thickness	$\left(t_{mm} - FCA_{ml}\right) \ge \max\left[0.5t_{min}, t_{lim}\right]$ $t_{min} = \max[t^C_{min}, t^L_{min}]$ $t_{lim} = \max\left[0.2t_{nom}, 2.5\ mm\ (0.10\ inches)\right]$ *for Pressure Vessels* $t_{lim} = \max\left[0.2t_{nom}, 1.3\ mm\ (0.05\ inches)\right]$ *for Piping*	

Notes:

1. Procedures to compute t^C_{min}, t^C_{min}, t_{min}, $MAWP^C_r$, $MAWP^L_r$, and $MAWP$ are provided in Annex 2C.
2. Procedures to compute the effects of supplement loads, i.e., t_{sl}, are provided in Annex 2C. Supplemental loads or the required thickness for supplemental loads may be reduced by RSF_a, e.g., $t_{sl} \cdot RSF_a$, in a Level 2 Assessment.
3. In the above equations, t_{mm} may be substituted for t_{am}, t^s_{am}, or t^c_{am} to produce a conservative result.

Table 4.5 – Acceptance Criteria for Level 1 and 2 Assessment for Spherical Shells and Formed Heads – Pressure Vessels

Assessment Parameter	Level 1 Assessment Acceptance Criteria	Level 2 Assessment Acceptance Criteria
Average Measured Thickness from Point Thickness Readings (PTR)	Determine $t_{\min}$ using P $t_{am} - FCA_{ml} \geq t_{min}$	Determine t_{min} using $P \cdot RSF_a$ $t_{am} - FCA_{ml} \geq t_{min}$
Average Measured Thickness from Critical Thickness Profiles (CTP)	Determine t_{min} using P $t^s_{am} - FCA_{ml} \geq t_{min}$ $t^c_{am} - FCA_{ml} \geq t_{min}$	Determine t_{min} using $P \cdot RSF_a$ $t^s_{am} - FCA_{ml} \geq t_{min}$ $t^c_{am} - FCA_{ml} \geq t_{min}$
MAWP from Point Thickness Readings (PTR)	Determine $MAWP_r$ using $\left(t_{am} - FCA_{ml}\right)$ $MAWP_r \geq MAWP$	Determine $MAWP_r$ using $\left(t_{am} - FCA_{ml}\right)$ $\frac{MAWP_r}{RSF_a} \geq MAWP$
MAWP from Critical Thickness Profiles (CTP)	Determine $MAWP^C_r$ using $\left(t^s_{am} - FCA_{ml}\right)$ Determine $MAWP^L_r$ using $\left(t^c_{am} - FCA_{ml}\right)$ $\min\left[MAWP^C_r, MAWP^L_r\right] \geq MAWP$	Determine $MAWP^C_r$ using $\left(t^s_{am} - FCA_{ml}\right)$ Determine $MAWP^L_r$ using $\left(t^c_{am} - FCA_{ml}\right)$ $\frac{\min\left[MAWP^C_r, MAWP^L_r\right]}{RSF_a} \geq MAWP$
Minimum Measured Thickness	$\left(t_{mm} - FCA_{ml}\right) \geq \max\left[0.5t_{min}, t_{lim}\right]$ $t_{lim} = \max\left[0.2t_{nom}, 2.5\ mm\ (0.10\ inches)\right]$	

Notes:

1. Procedures to compute t^C_{min}, t^C_{min}, t_{min}, $MAWP^C_r$, $MAWP^L_r$, and $MAWP$ are provided in Annex 2C.
2. In the above equations, t_{mm} may be substituted for t_{am}, t^s_{am}, or t^c_{am} to produce a conservative result.

Table 4.6 – Acceptance Criteria for Level 1 and 2 Assessment for Atmospheric Storage Tanks

Assessment Parameter	Level 1 Assessment Acceptance Criteria	Level 2 Assessment Acceptance Criteria
Average Measured Thickness from Point Thickness Readings (PTR)	Determine t_{min} using MFH, S_a $t_{am} - FCA_{ml} \geq t_{\min}$	Determine t_{min} using $MFH, S_a \cdot H_f$ $t_{am} - FCA_{ml} \geq t_{min}$
Average Measured Thickness from Critical Thickness Profiles (CTP)	Determine $t_{\min}$ using MFH, S_a $t^s_{am} - FCA_{ml} \geq t_{\min}$	Determine $t_{\min}$ using $MFH, S_a \cdot H_f$ $t^s_{am} - FCA_{ml} \geq t_{\min}$
MFH from Point Thickness Readings (PTR)	Determine MFH_r using $\left(t_{am} - FCA_{ml}\right), S_a$ $MFH_r \geq MFH$	Determine MFH_r using $\left(t_{am} - FCA_{ml}\right), S_a \cdot H_f$ $MFH_r \geq MFH$
MFH from Critical Thickness Profiles (CTP)	Determine MFH_r using $\left(t^s_{am} - FCA_{ml}\right), S_a$ $MFH_r \geq MFH$	Determine MFH_r using $\left(t^s_{am} - FCA_{ml}\right), S_a \cdot H_f$ $MFH_r \geq MFH$
Minimum Measured Thickness	$\left(t_{mm} - FCA_{ml}\right) \geq \max\left[0.6t_{min}, t_{lim}\right]$ $t_{lim} = \max\left[0.2t_{nom}, 2.5\ mm\ (0.10\ inches)\right]$	

Notes:

1. The value of H_f is:

$$H_f = 1.0 \qquad \left(for\ API-653\ allowable\ stress\ values\right)$$

$$H_f = \frac{1.0}{RSF_a} \qquad \left(for\ API-650\ or\ API-620\ allowable\ stress\ values\right)$$

2. Procedures to compute the minimum required thickness (i.e., t^C_{min} and t_{min}, as applicable) for atmospheric storage tank shells are provided in Annex 2C.
3. Procedures to compute the maximum fill height, MFH, for atmospheric storage tank shells are provided in Annex 2C.
4. In the above equations, t_{mm} may be substituted for t_{am} or t^s_{am} to produce a conservative result.

Table 4.7 – Acceptance Criteria for Level 1 and 2 Assessment for Low Pressure Storage Tanks

Assessment Parameter	Level 1 Assessment Acceptance Criteria		Level 2 Assessment Acceptance Criteria	
	Flat Bottom Storage Tanks with Hydrostatic Liquid Loading	General Shells with Curvature Along the Meridian	Flat Bottom Storage Tanks with Hydrostatic Liquid Loading	General Shells with Curvature Along the Meridian
Average Measured Thickness from Point Thickness Readings (PTR)	See Table 4.6	See Table 4.4 or Table 4.5, as applicable	See Table 4.6	See Table 4.4 or Table 4.5, as applicable
Average Measured Thickness from Critical Thickness Profiles (CTP)	See Table 4.6	See Table 4.4 or Table 4.5, as applicable	See Table 4.6	See Table 4.4 or Table 4.5, as applicable
MAWP from Point Thickness Readings (PTR)	Not Applicable	See Table 4.4 or Table 4.5, as applicable	Not Applicable	See Table 4.4 or Table 4.5, as applicable
MAWP from Critical Thickness Profiles (CTP)	Not Applicable	See Table 4.4 or Table 4.5, as applicable	Not Applicable	See Table 4.4 or Table 4.5, as applicable
MFH from Point Thickness Readings (PTR)	See Table 4.6	Not Applicable	See Table 4.6	Not Applicable
MFH from Critical Thickness Profiles (CTP)	See Table 4.6	Not Applicable	See Table 4.6	Not Applicable
Minimum Measured Thickness	See Table 4.6	See Table 4.4 or Table 4.5, as applicable	See Table 4.6	See Table 4.4 or Table 4.5, as applicable

Table 4.8 – Parameters to Compute the Length for Thickness Averaging

R_t	Q				
	$RSF_a = 0.90$	$RSF_a = 0.85$	$RSF_a = 0.80$	$RSF_a = 0.75$	$RSF_a = 0.70$
0.900	50.00	50.00	50.00	50.00	50.00
0.895	21.19	50.00	50.00	50.00	50.00
0.875	4.93	50.00	50.00	50.00	50.00
0.850	2.82	50.00	50.00	50.00	50.00
0.845	2.62	29.57	50.00	50.00	50.00
0.825	2.07	6.59	50.00	50.00	50.00
0.800	1.68	3.65	50.00	50.00	50.00
0.795	1.62	3.38	36.82	50.00	50.00
0.775	1.43	2.63	8.01	50.00	50.00
0.750	1.26	2.11	4.35	50.00	50.00
0.745	1.23	2.03	4.01	42.94	50.00
0.725	1.12	1.77	3.10	9.20	50.00
0.700	1.02	1.54	2.45	4.93	50.00
0.695	1.00	1.51	2.36	4.53	47.94
0.675	0.93	1.37	2.05	3.47	10.16
0.650	0.86	1.24	1.77	2.73	5.39
0.625	0.80	1.13	1.56	2.26	3.77
0.600	0.74	1.04	1.40	1.95	2.94
0.575	0.70	0.96	1.27	1.71	2.43
0.550	0.65	0.89	1.16	1.53	2.07
0.525	0.61	0.83	1.07	1.38	1.81
0.500	0.58	0.77	0.99	1.26	1.61
0.475	0.55	0.72	0.92	1.15	1.45
0.450	0.51	0.68	0.86	1.06	1.32
0.425	0.49	0.64	0.80	0.98	1.20
0.400	0.46	0.60	0.74	0.91	1.10
0.375	0.43	0.56	0.70	0.84	1.01
0.350	0.41	0.53	0.65	0.78	0.93
0.325	0.38	0.50	0.61	0.73	0.86
0.300	0.36	0.46	0.57	0.67	0.79
0.275	0.34	0.43	0.53	0.63	0.73
0.250	0.31	0.40	0.49	0.58	0.67
0.200	0.27	0.35	0.42	0.49	0.57

Notes:

1. The equation for Q is:

$$Q = 1.123\left[\left(\frac{1-R_t}{1-R_t/RSF_a}\right)^2 - 1\right]^{0.5} \qquad \left(for\ R_t < RSF_a\right)$$

$$Q = 50.0 \qquad \left(for\ R_t \geq RSF_a\right)$$

2. The length for thickness averaging is given by Equation (4.7).

4.12 Figures

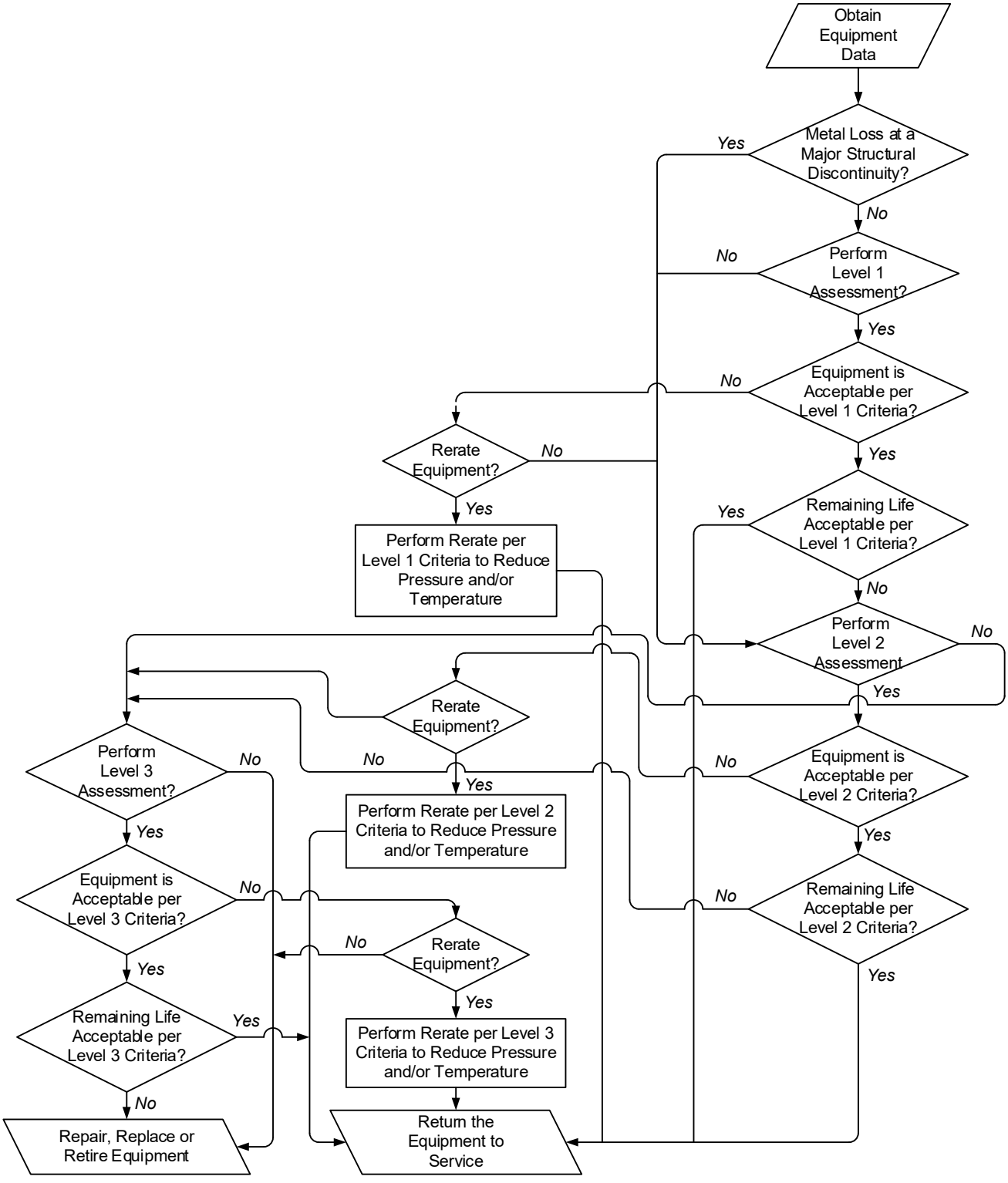

Figure 4.1 – Overview of the Assessment Procedures to Evaluate a Component with General Metal Loss

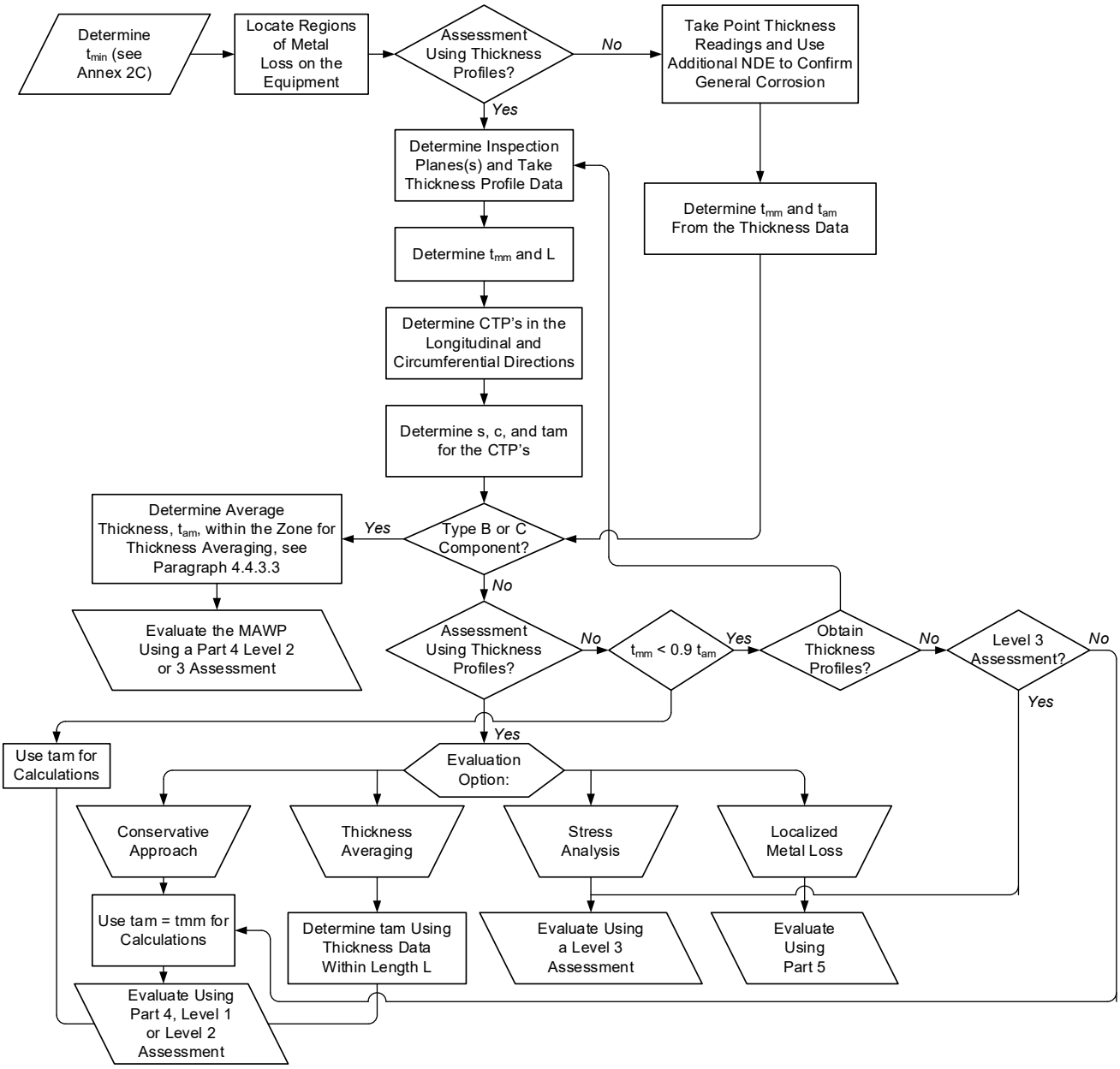

Figure 4.2 – Assessment Procedure to Evaluate a Component with Metal Loss Using Part 4 and Part 5

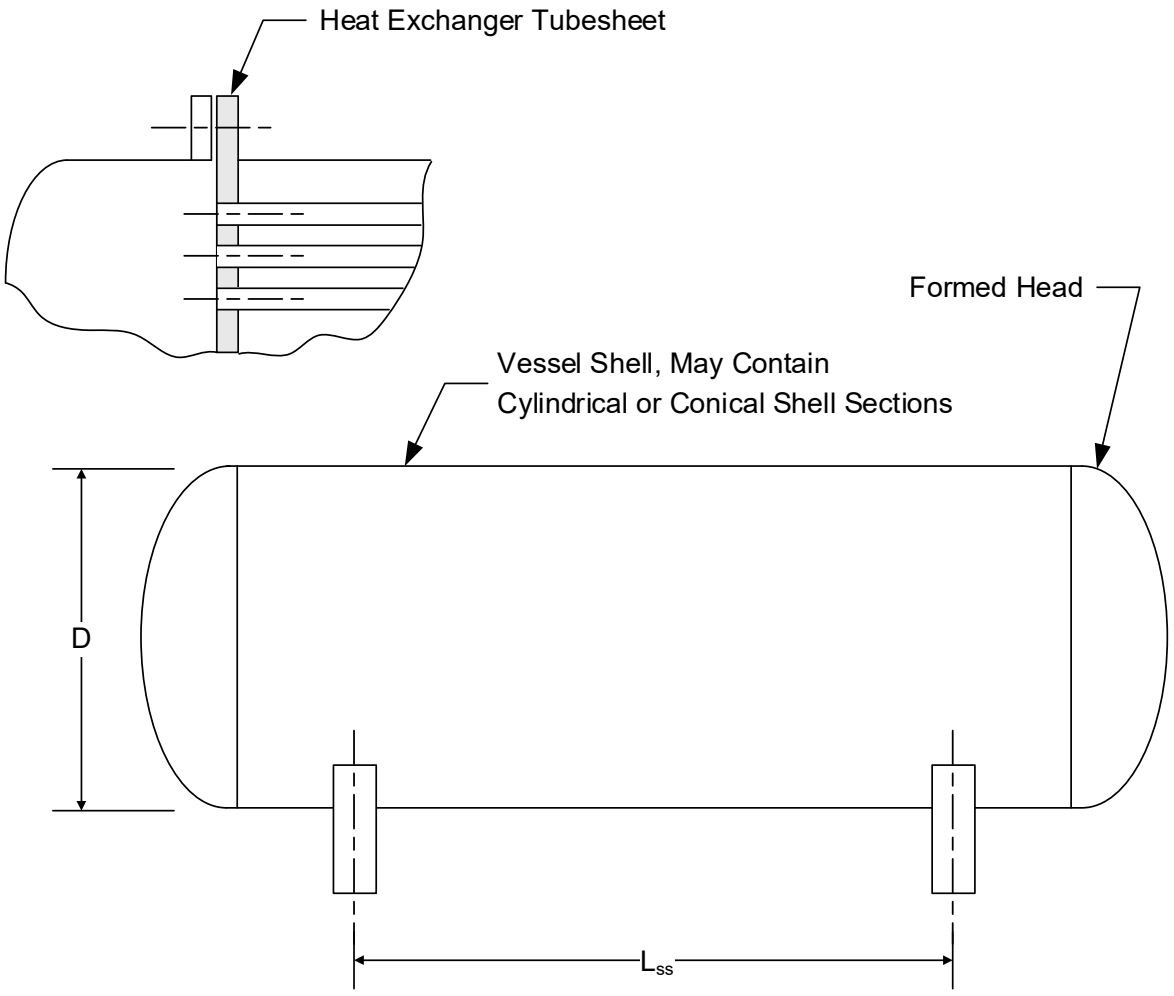

Type A Component Criteria – If $L_{ss}/D \leq 2.5$ and $D \leq 3.05\ m\ (10\ ft)$, the horizontal vessel or heat exchanger shell between the supports may be considered to be a Type A Component. If the horizontal vessel or heat exchanger contains conical transitions, the diameter D shall be based on the minimum inside diameter.

Figure 4.3 – Criteria for a Horizontal Pressure Vessel or Heat Exchanger to be Categorized as Type A Components

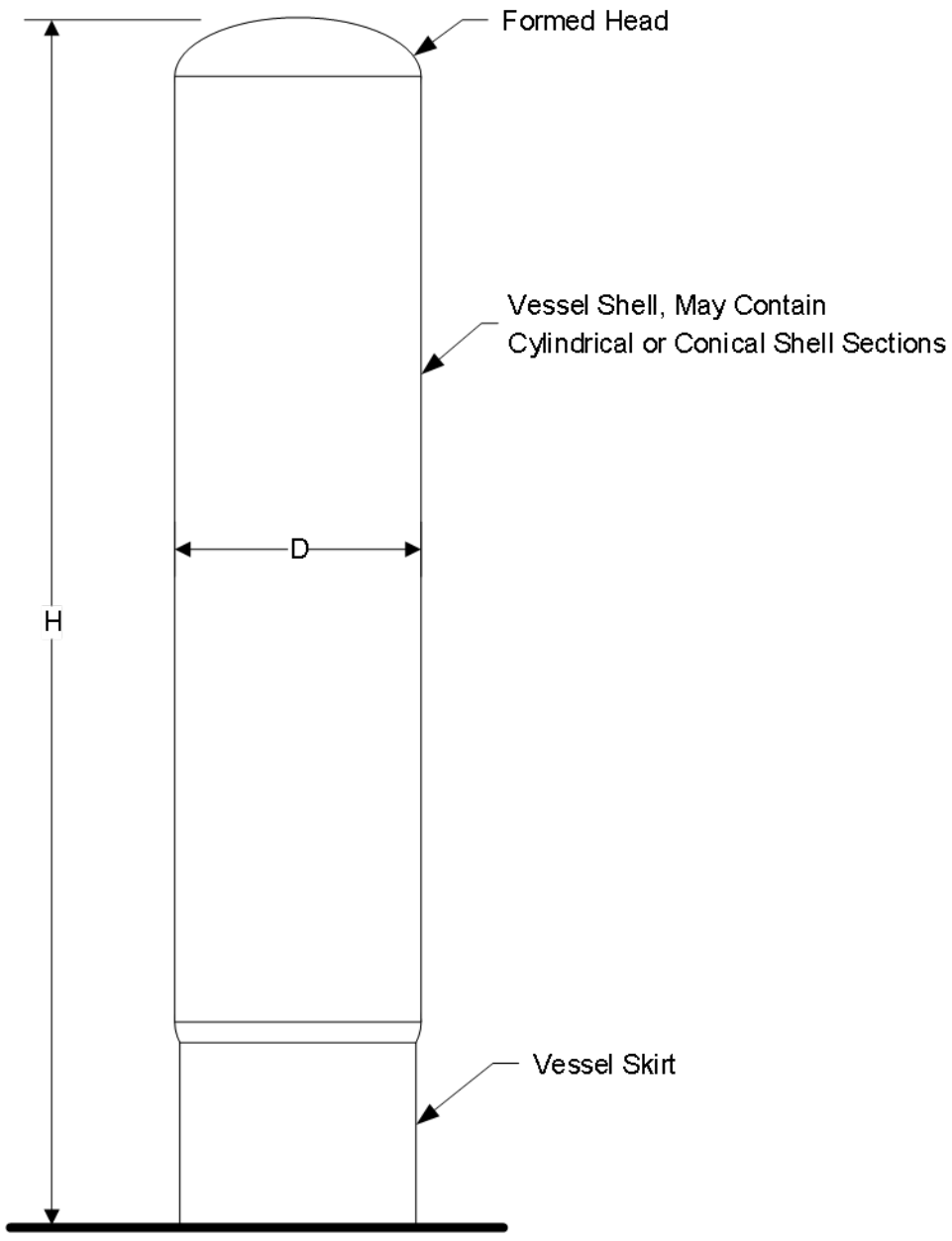

Type A Component Criteria – If $H/D \leq 3$ and $H \leq 30.5\ m\ (100\ ft)$, the vertical vessel may be considered to be a Type A Component. If the vertical vessel contains conical transitions, the diameter D shall be based on the minimum inside diameter of all vessel courses.

Figure 4.4 – Criteria for a Vertical Pressure Vessel to be Categorized as Type A Components

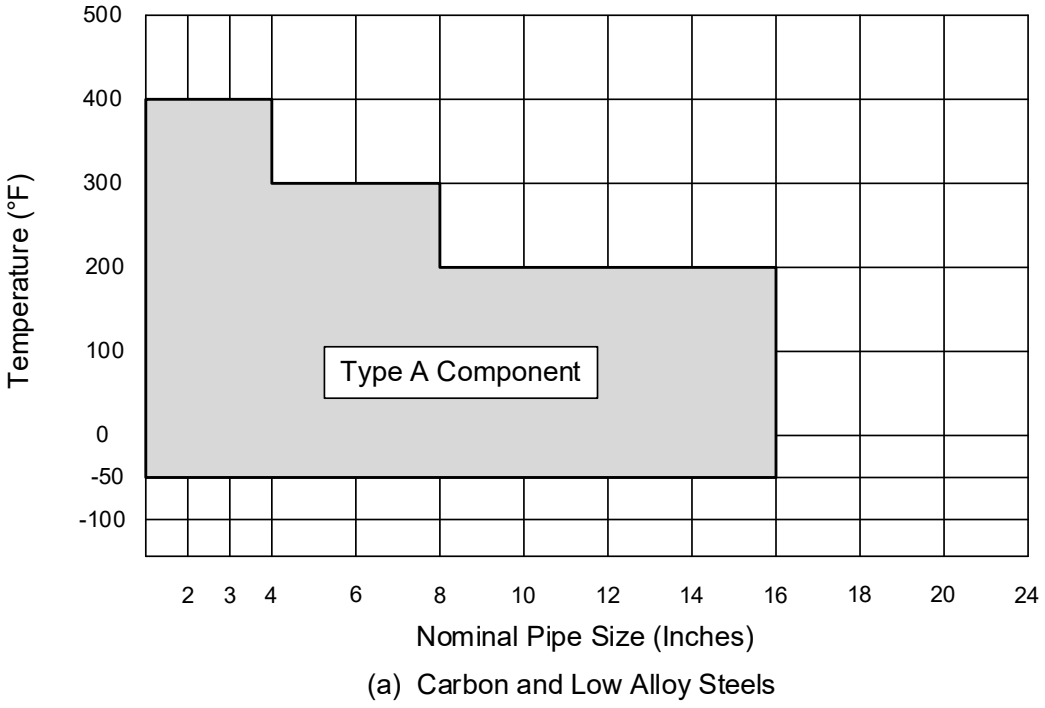

(a) Carbon and Low Alloy Steels

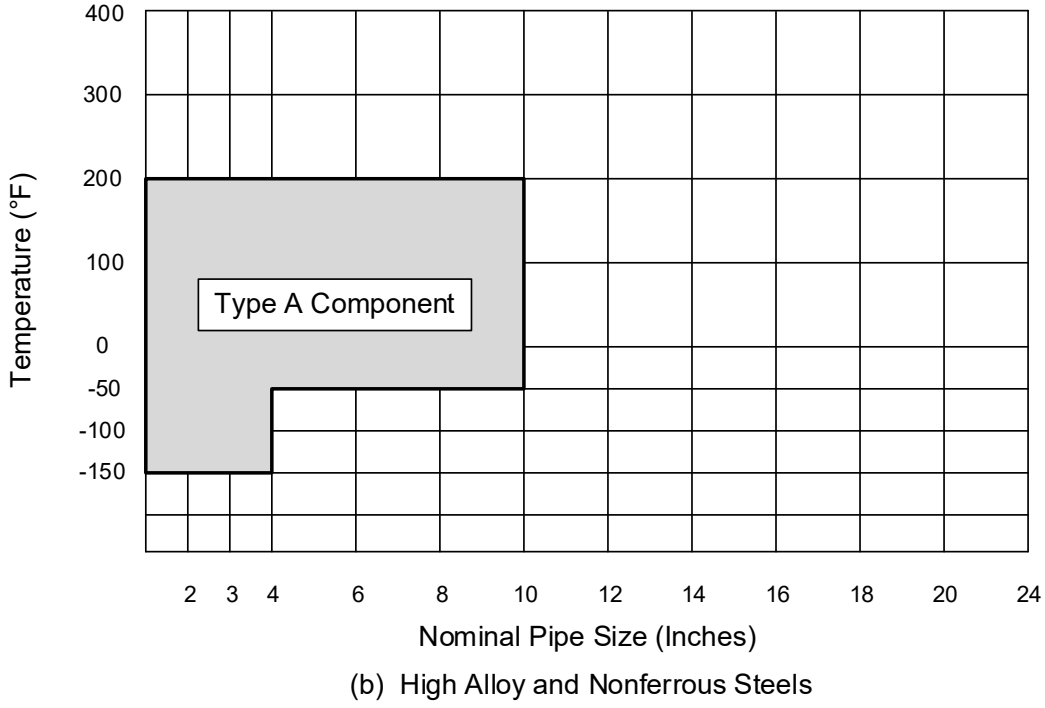

(b) High Alloy and Nonferrous Steels

Type A Component Criteria – If the design temperature and nominal pipe size of a straight section of pipe, or elbow or pipe bend that does not have a structural attachment, are within the shaded region, the pipe may be considered to be a Type A component.

Figure 4.5 – Temperature Criteria for Piping Categorized as a Type A Component

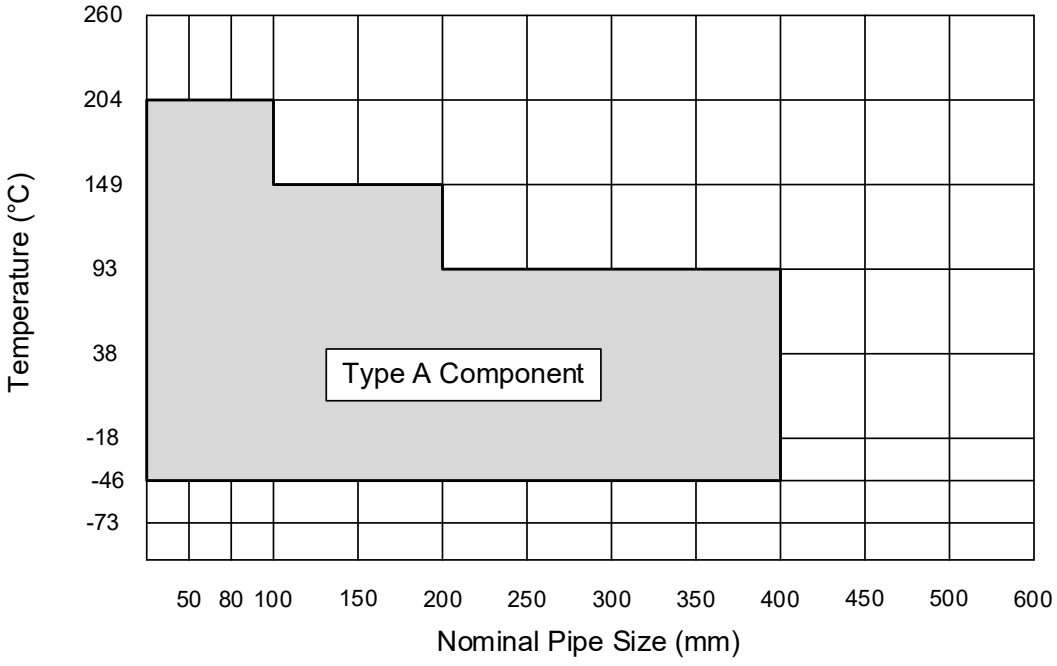

(a) Carbon and Low Alloy Steels

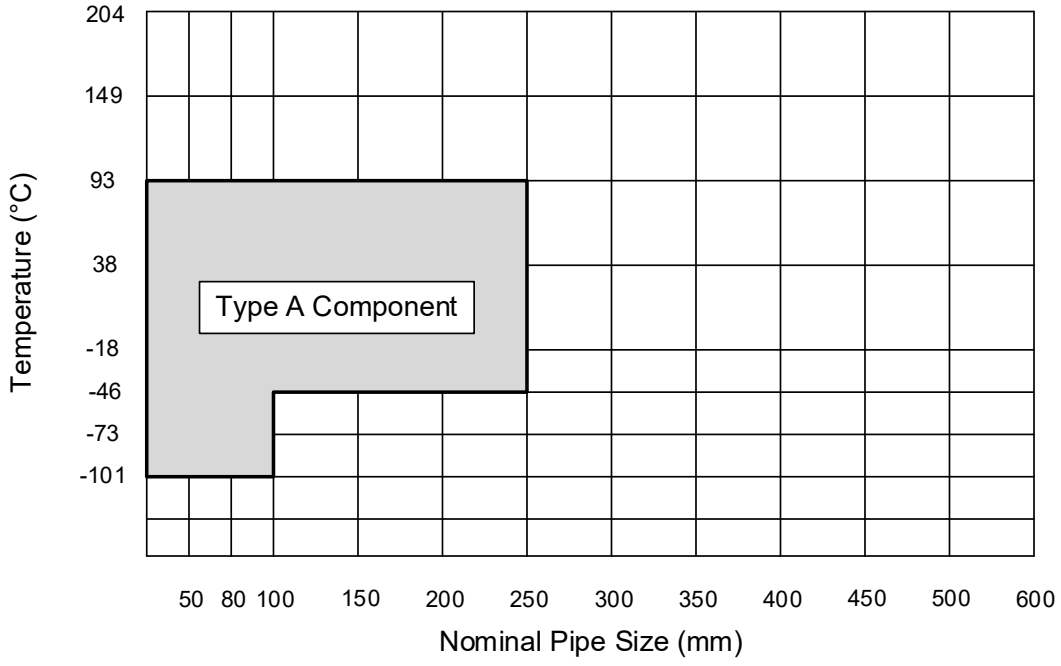

(b) High Alloy and Nonferrous Steels

Type A Component Criteria – If the design temperature and nominal pipe size of a straight section of pipe, or elbow or pipe bend that does not have a structural attachment, are within the shaded region, the pipe may be considered to be a Type A component.

Figure 4.5M – Temperature Criteria for Piping Categorized as a Type A Component

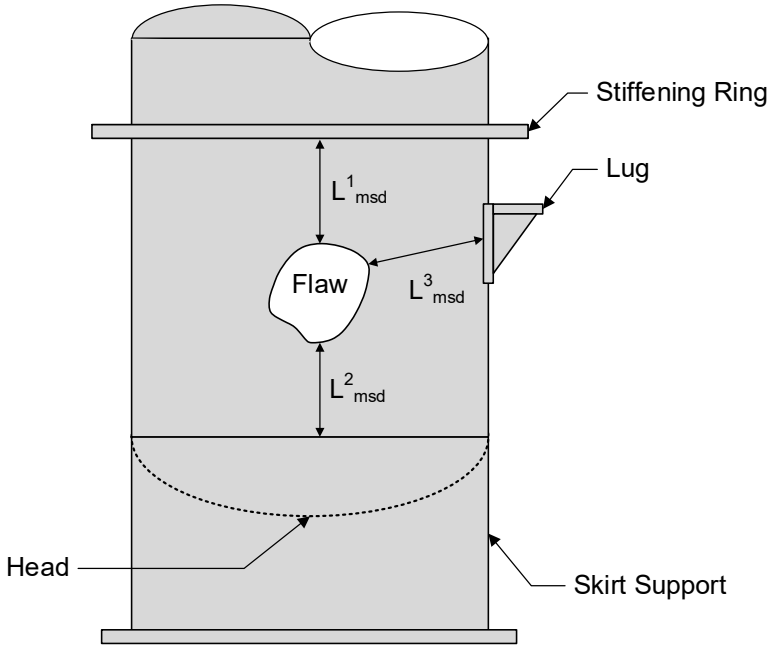

(a) Type C Component Spacing Limitation - Pressure Vessels

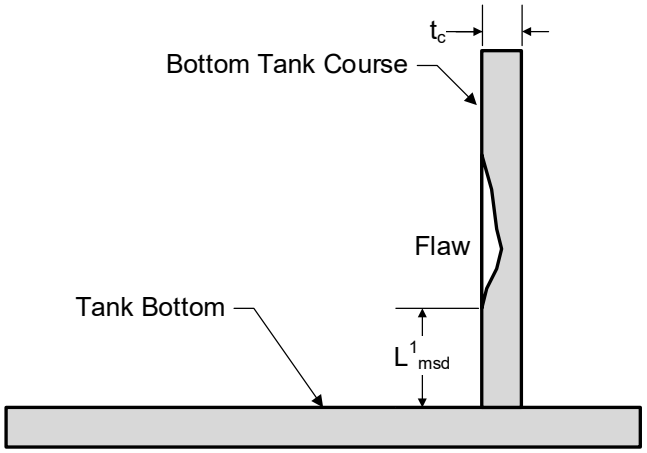

(b) Type C Component Spacing Limitation – Tank Bottom

Notes:

1. Spacing Criteria is: $L_{msd} \geq 1.8\sqrt{Dt_c}$.
2. For the example shown above, the minimum distance to a major structural discontinuity is: $L_{msd} = \min\left[L^1_{msd}, L^2_{msd}, L^3_{msd}\right]$.
3. Typical major structural discontinuities associated with vertical vessels are shown in this figure. For horizontal vessels, the saddle supports would constitute a major structural discontinuity and for a spherical storage vessel, the support locations (shell-to-leg junction) would constitute a major structural discontinuity.
4. The measure of the minimum distances defined in this figure is from the nearest edge of the region of local metal loss to the nearest weld of the structural discontinuity.

Figure 4.6 – Flaw Spacing Criteria to Type C Components

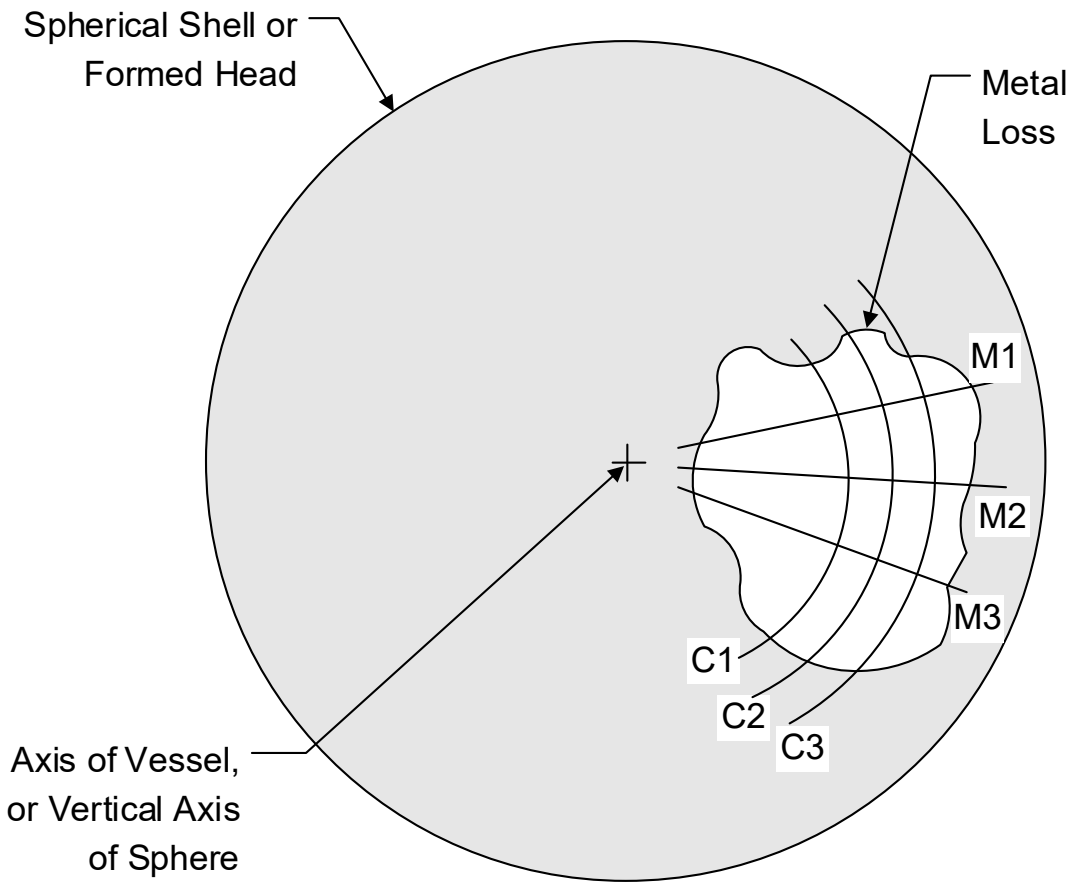

Note: M1 – M3 are meridional inspection planes and C1 – C3 are circumferential inspection planes.

Figure 4.7 – Inspection Planes for Pressure Vessel Heads and Spheres

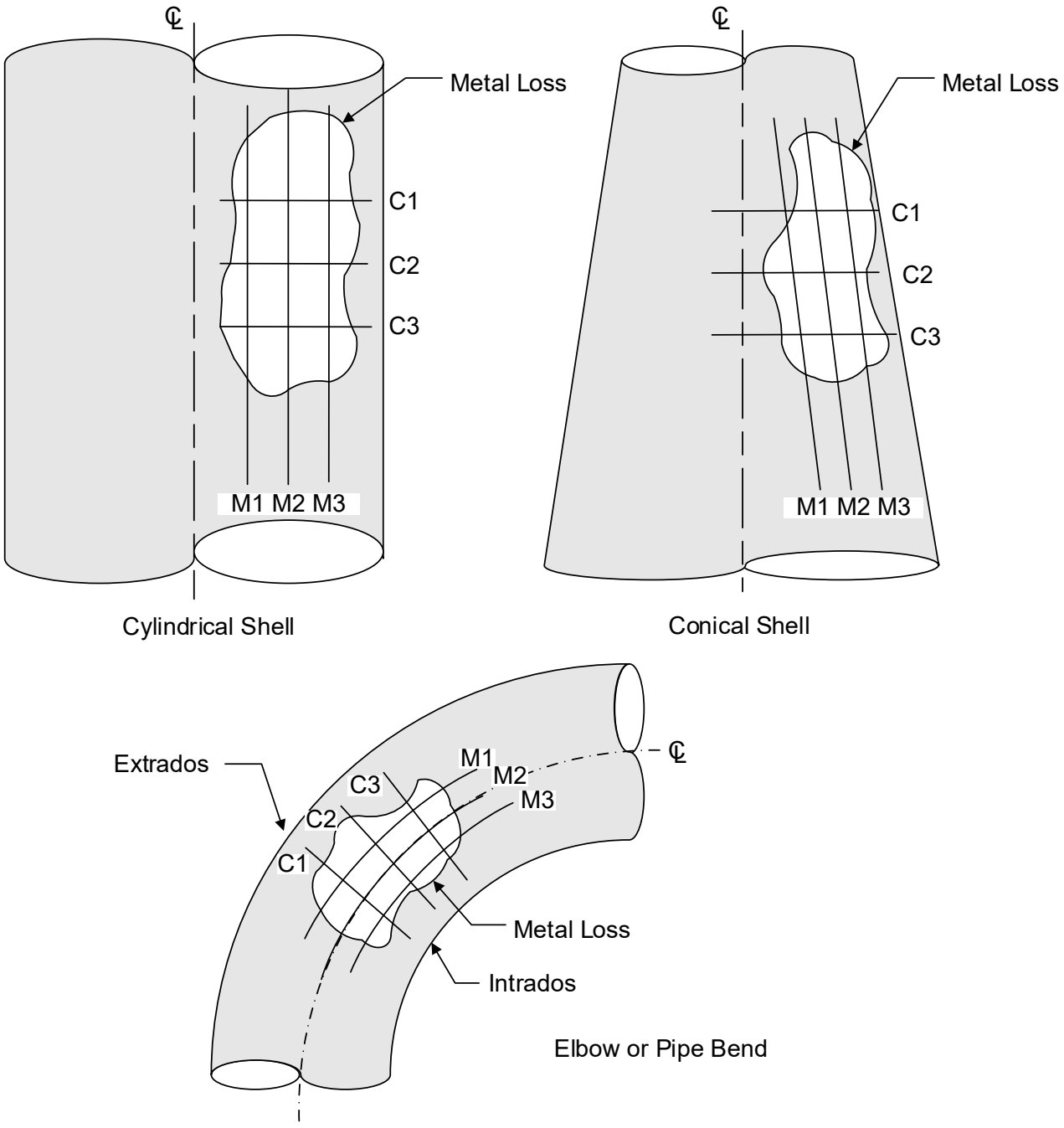

Notes:

1. For cylindrical and conical shells, M1 – M3 are meridional (longitudinal direction) inspection planes and C1 – C3 are circumferential inspection planes.
2. For elbows and pipe bends, M1 – M3 are longitudinal inspection planes and C1 – C3 are circumferential inspection planes.

Figure 4.8 – Inspection Planes for Cylindrical Shells, Conical Shells, and Pipe Bends

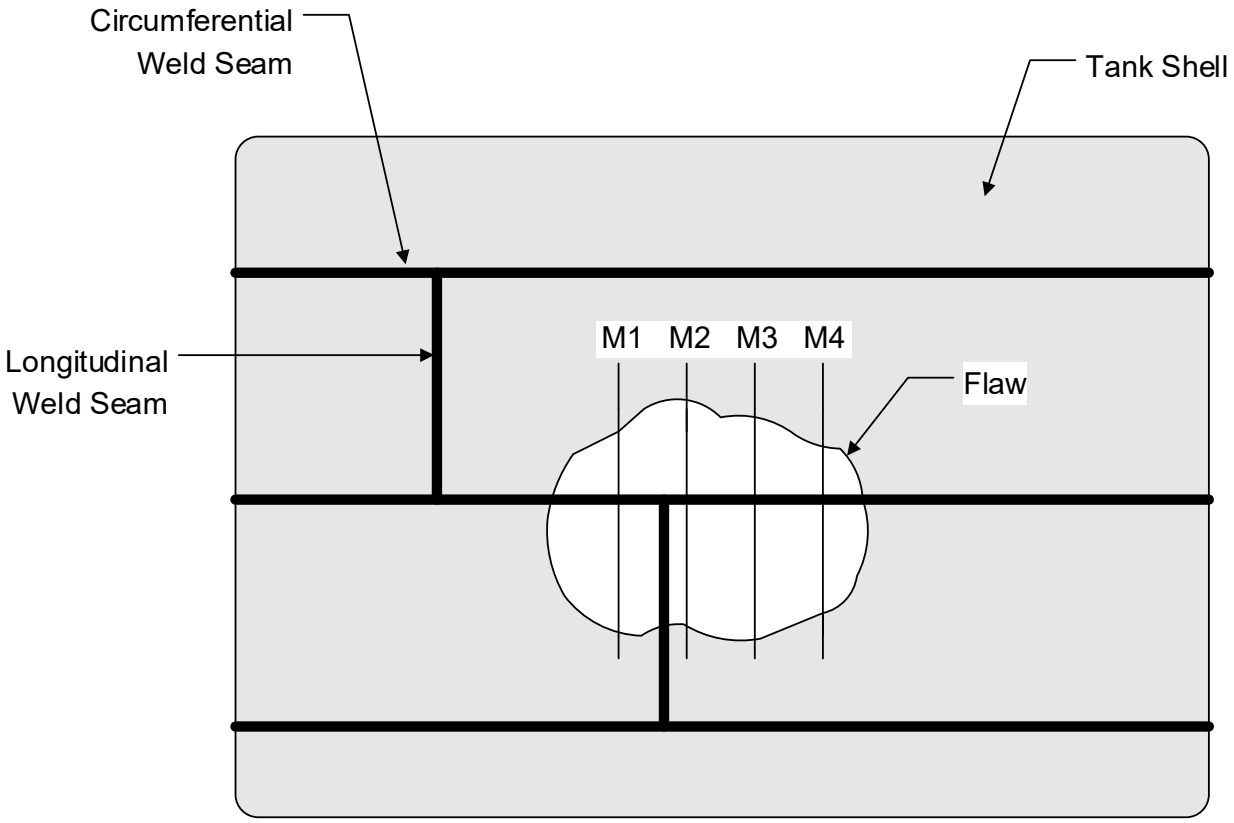

Notes:

1. M1 – M4 are meridional (longitudinal direction).
2. Circumferential inspection planes are not required because the stress normal to this direction is negligibly small and does not govern the design thickness calculation.

Figure 4.9 – Inspection Planes for Atmospheric Storage Tanks

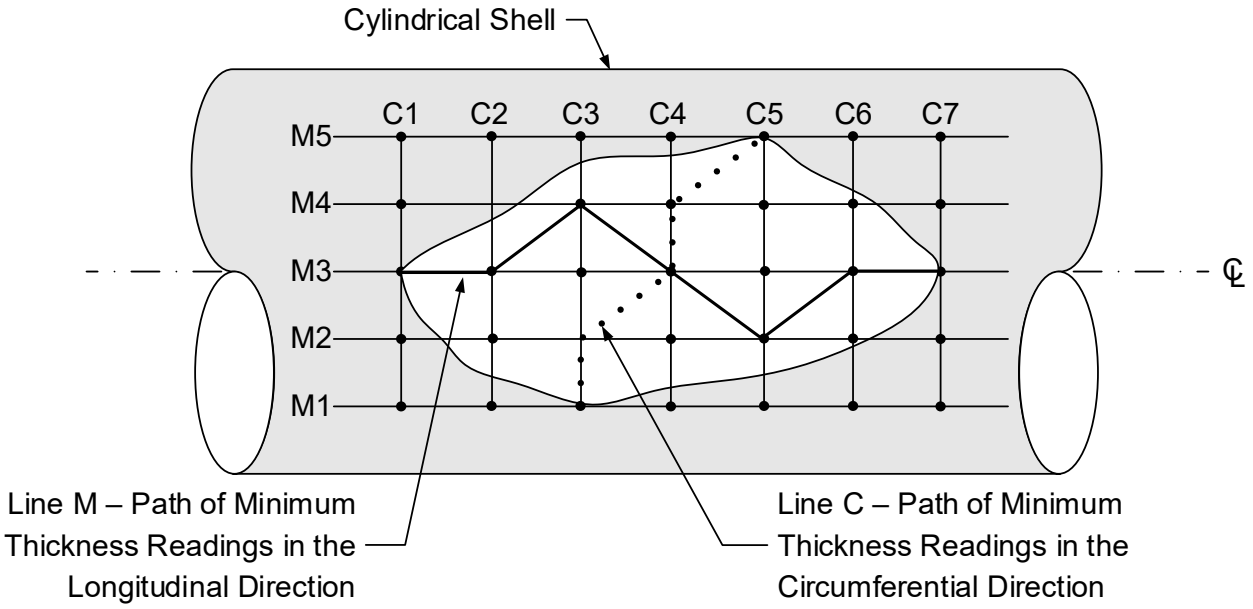

(a) Inspection Planes and the Critical Thickness Profile

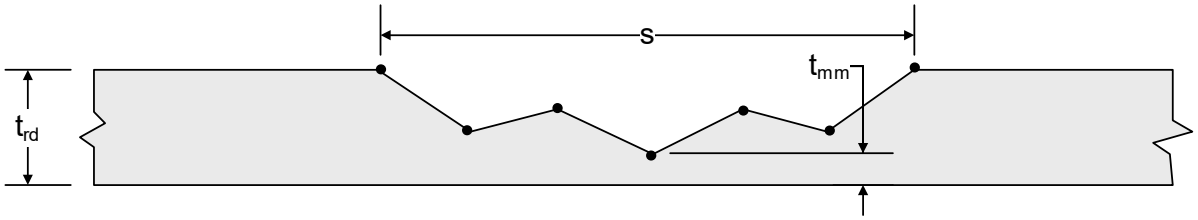

(b) Critical Thickness Profile (CTP) - Longitudinal Plane (Projection of Line M)

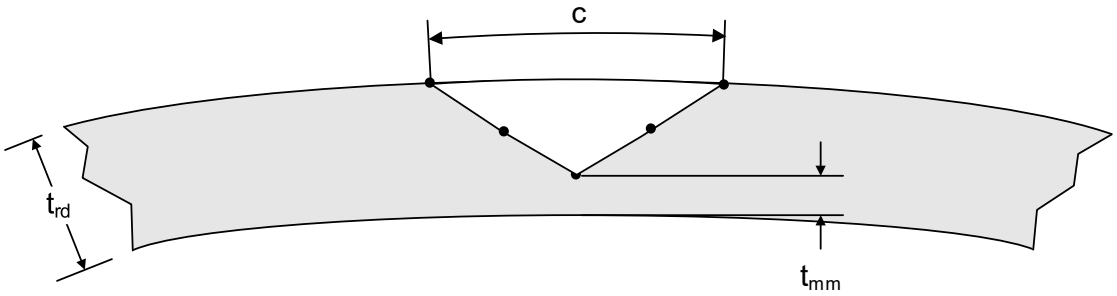

(c) Critical Thickness Profile (CTP) - Circumferential Plane (Projection of Line C)

Notes:

1. M1 – M5 are meridional (longitudinal) inspection planes.
2. C1 – C7 are circumferential inspection planes.

Figure 4.10 – Method for Determining the Plane of Maximum Metal Loss (Critical Thickness Profile)

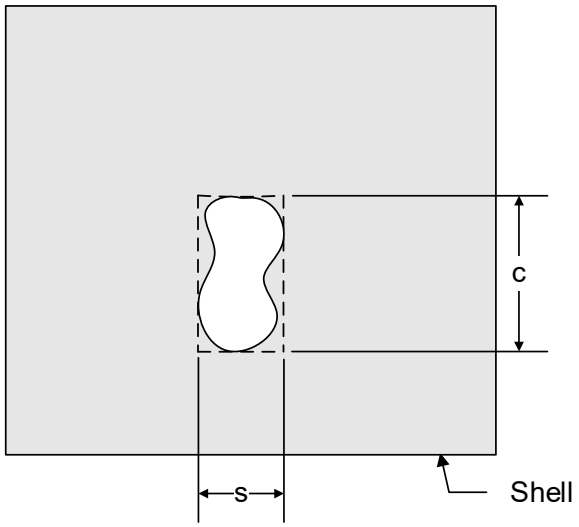

Step 1 - Draw a box that completely encloses each LTA. Measure the maximum longitudinal (axial) extent, s (in. or mm.) and the maximum circumferential extent, c (in. or mm.) of this box. This will be the dimensions of the thinned area used in the assessment.

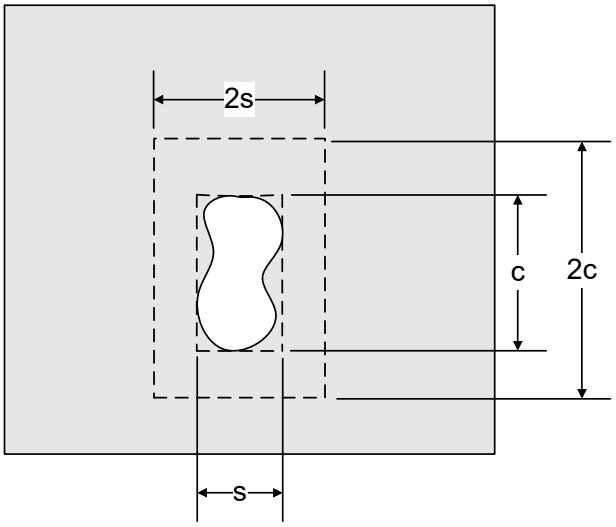

Step 2 - Draw a second box twice the size of the first box (2s x 2c) around each LTA.

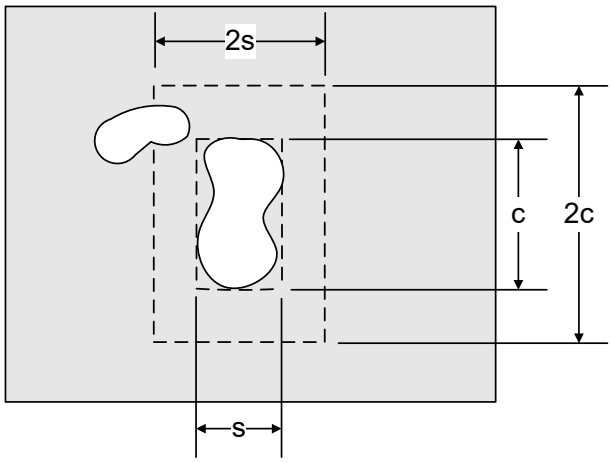

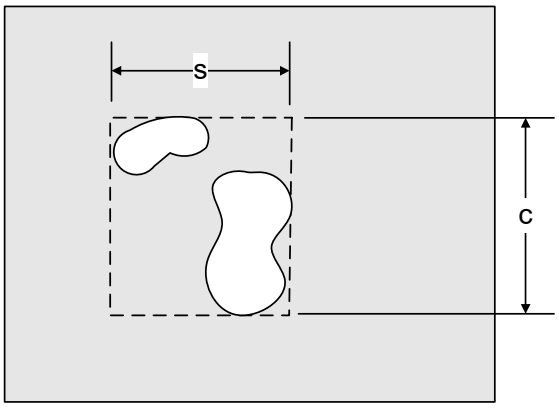

Step 3 - If another LTA is within the larger box, the dimensions s and c should be adjusted to include the additional thinned area. Go back to step 2.

Figure 4.11 – Sizing of a Region with Multiple Areas of Metal Loss for an Assessment

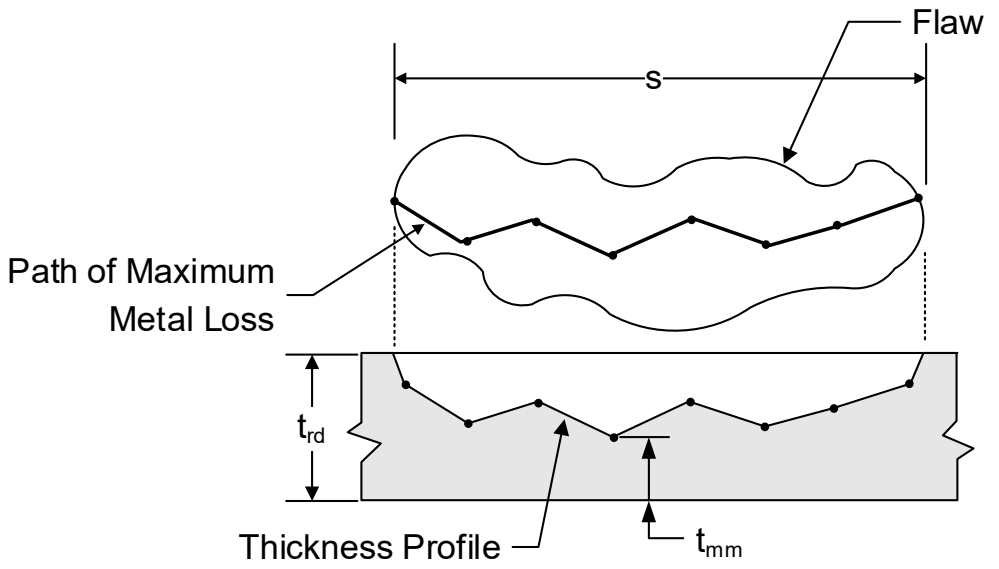

(a) Isolated Flaw

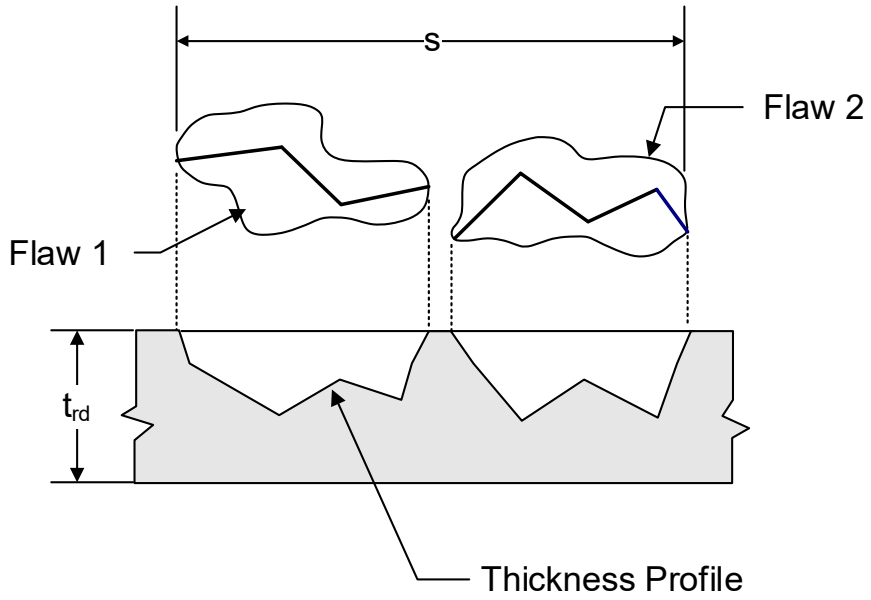

Note: Flaw 1 and Flaw 2 Are Combined Based on the Criterion Shown In Figure 4.11 To Form A Single Flaw For The Assessment

(b) Network Of Flaws

Figure 4.12 – Sizing of an Isolated Metal Loss Region and a Network of Metal Loss Regions

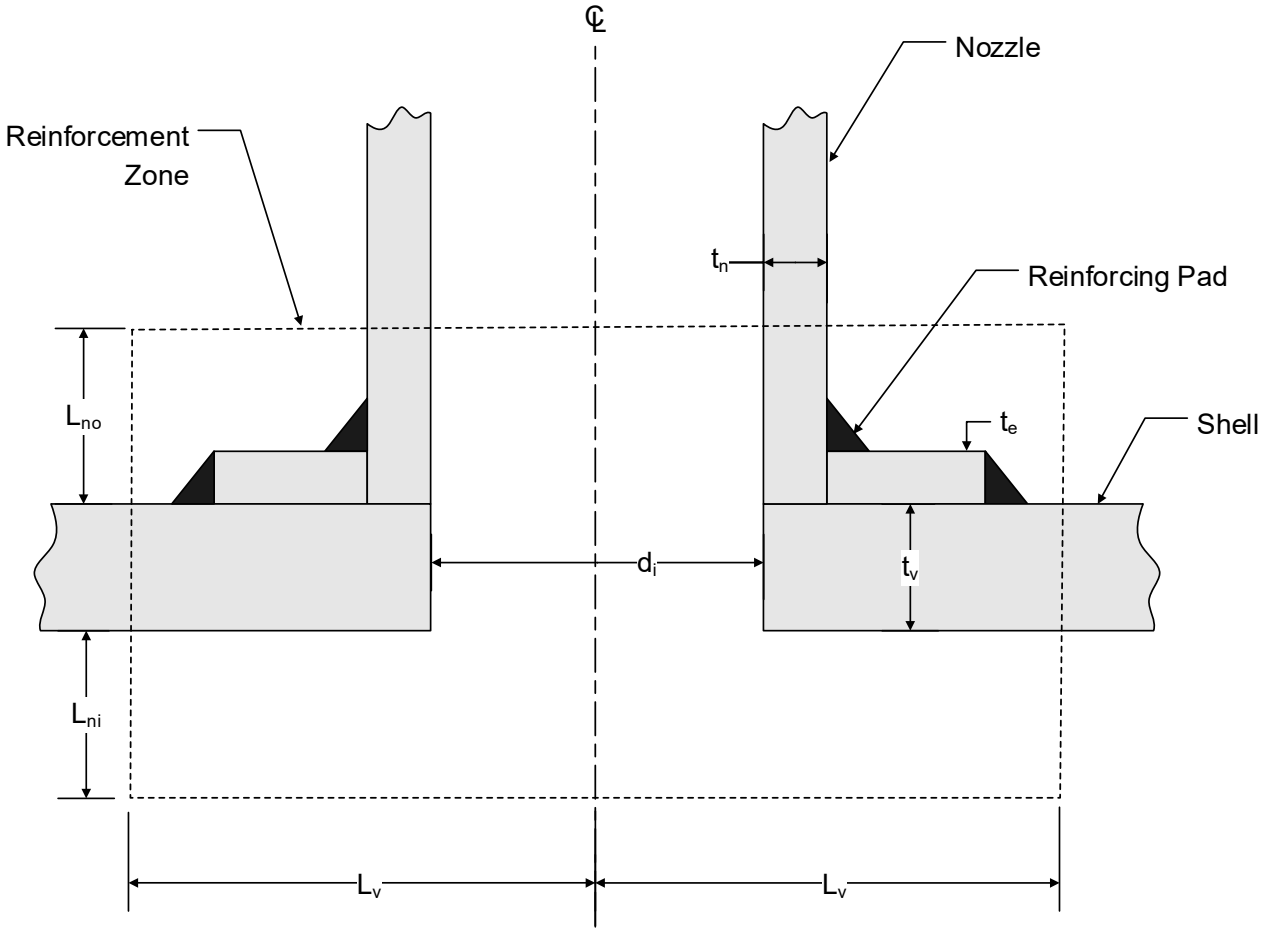

Nozzle with a Reinforcement Element

Notes:

1. Thickness averaging zone in the horizontal direction (see paragraph 4.3.3.4(a)): $L_H = \min[L, L_v]$. L is calculated using Equation (4.7), $L_v = \max[d_i, (d_i/2 + t_n + t_v)]$.
2. Thickness averaging zone in the vertical direction on the outside of the shell (see paragraph 4.3.3.4(a)): $L_{vno} = \min[L, L_{no}]$. L is calculated using Equation (4.7), $L_{no} = \min[2.5t_v, (2.5t_n + t_e)]$.
3. Thickness averaging zone in the vertical direction on the inside of the shell (see paragraph 4.3.3.4(a)): $L_{vni} = \min[L, L_{ni}]$. L is calculated using Equation (4.7), $L_{ni} = \min[2.5t_v,\ 2.5t_n]$.

Figure 4.13 – Zone for Thickness Averaging – Nozzles and Fabricated Branch Connections

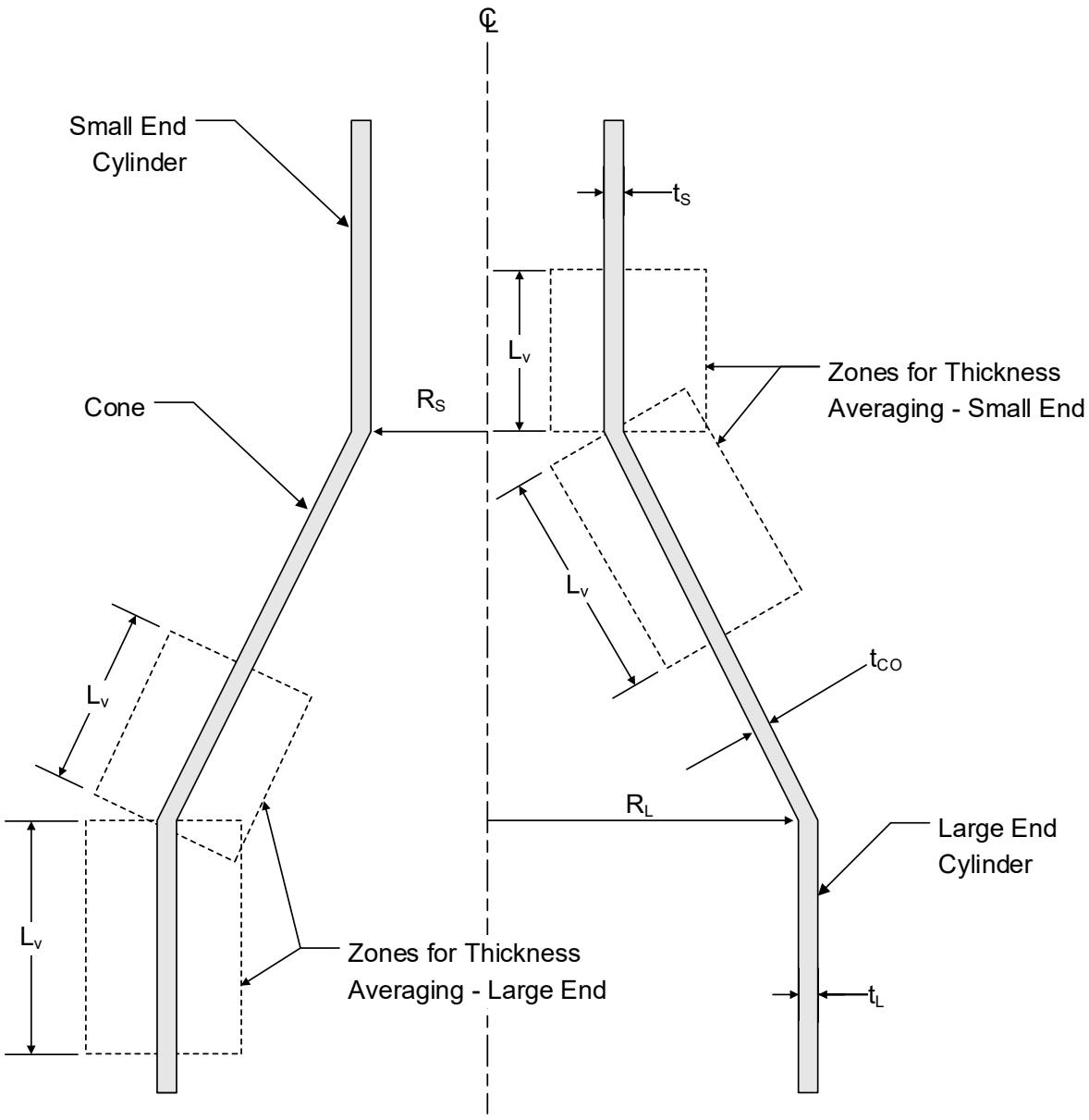

Notes:

1. $L_v = 0.78\sqrt{R_S t_S}$ – thickness averaging zone for the small end cylinder (see paragraph 4.3.3.4(b)).
2. $L_v = 0.78\sqrt{R_S t_{CO}}$ – thickness averaging zone for the small end cone (see paragraph 4.3.3.4(b)).
3. $L_v = 1.0\sqrt{R_L t_{CO}}$ – thickness averaging zone for the large end cone (see paragraph 4.3.3.4(b)).
4. $L_v = 1.0\sqrt{R_L t_L}$ – thickness averaging zone for the large end cylinder (see paragraph 4.3.3.4(b)).
5. See paragraph 4.4.3.3(a)(2) to determine the length for thickness averaging.

Figure 4.14 – Zone for Thickness Averaging – Conical Transitions

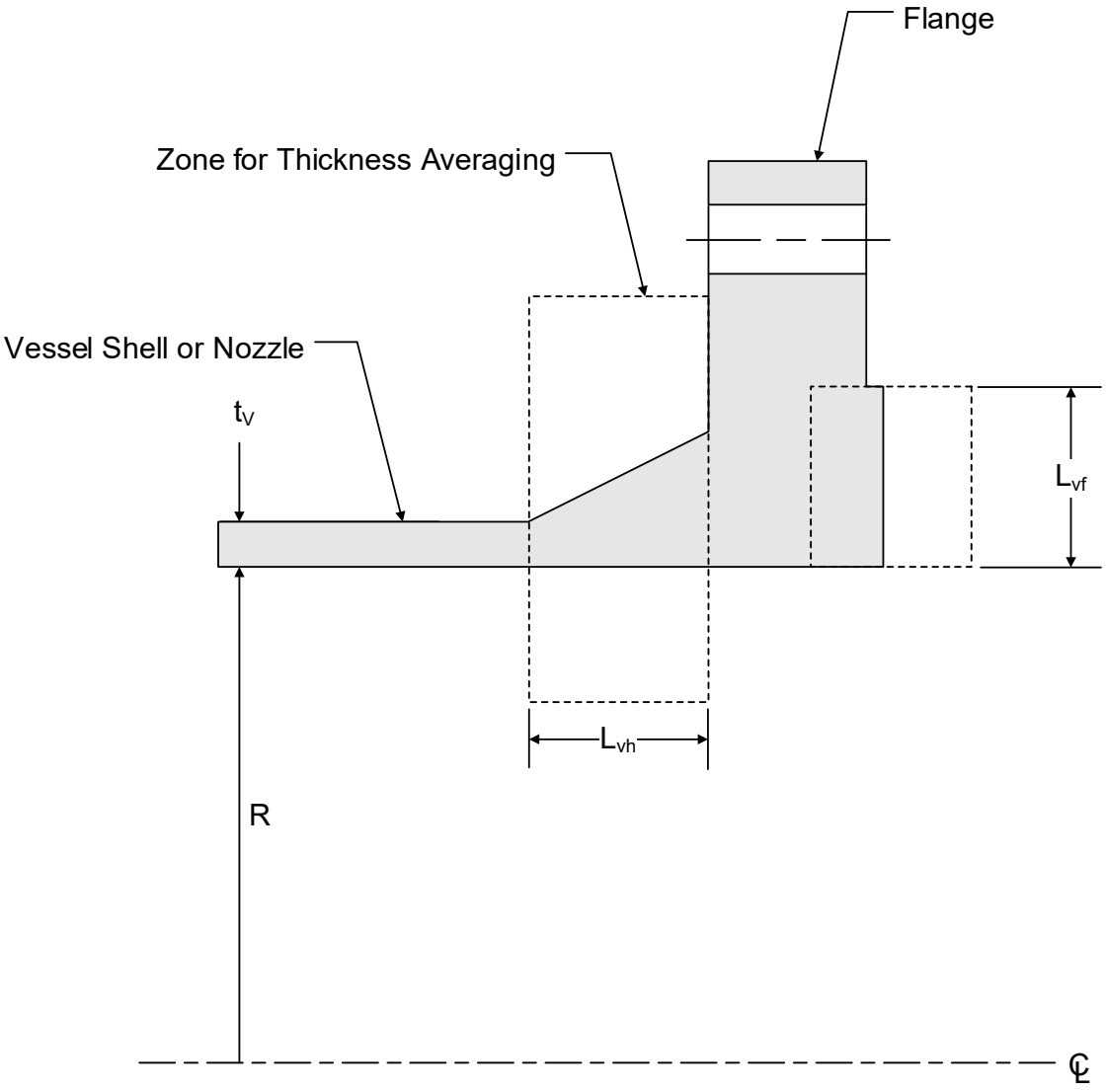

Notes:

1. L_{vh} is thickness averaging zone for the hub.
2. L_{vf} is thickness averaging zone for the flange.

Figure 4.15 – Zone for Thickness Averaging – Flange Connections

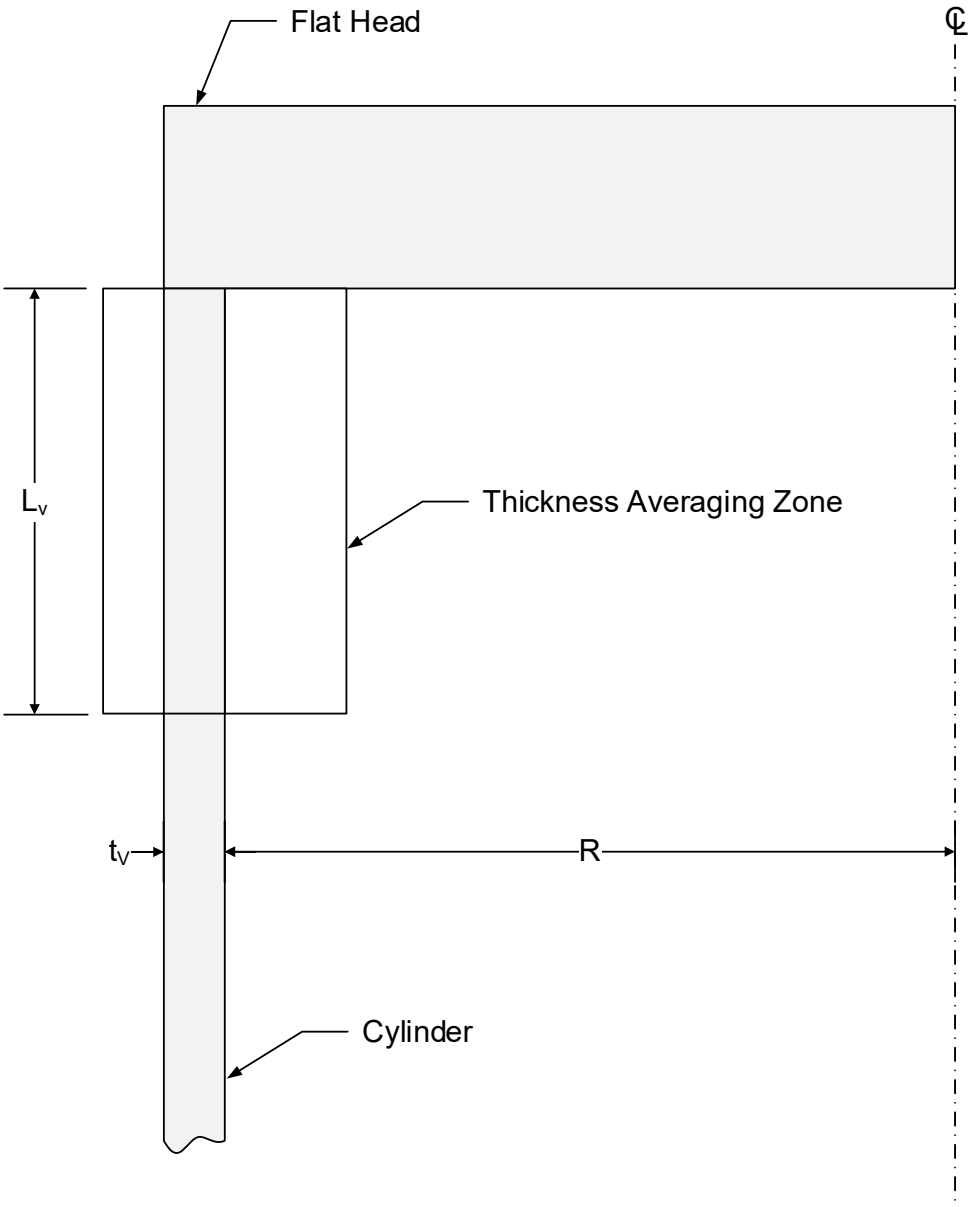

Notes: $L_v = 1.0\sqrt{Rt_v}$ is thickness averaging zone for the cylinder.

Figure 4.16 – Zone for Thickness Averaging – Cylinder to Flat Head Junctions

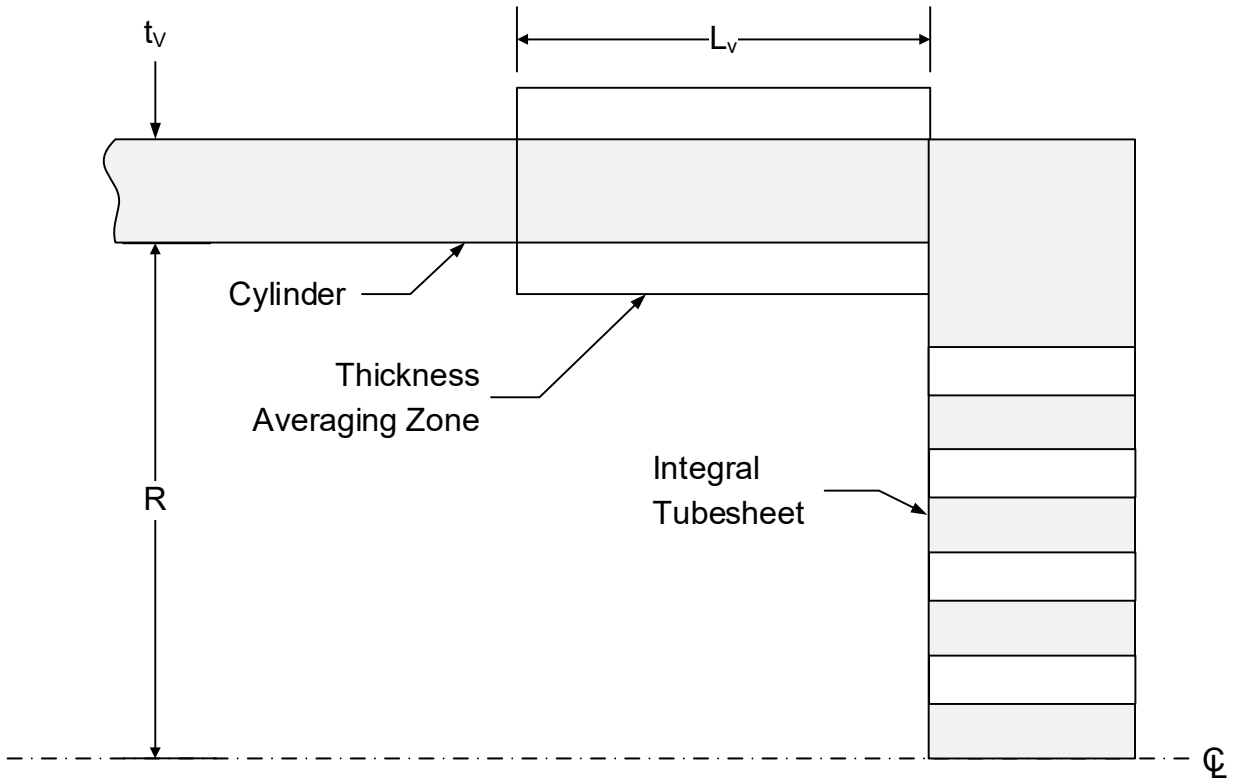

Notes: $L_v = 2.5\sqrt{Rt_v}$ is thickness averaging zone for the cylinder.

Figure 4.17 – Zone for Thickness Averaging – Integral Tubesheet Connections

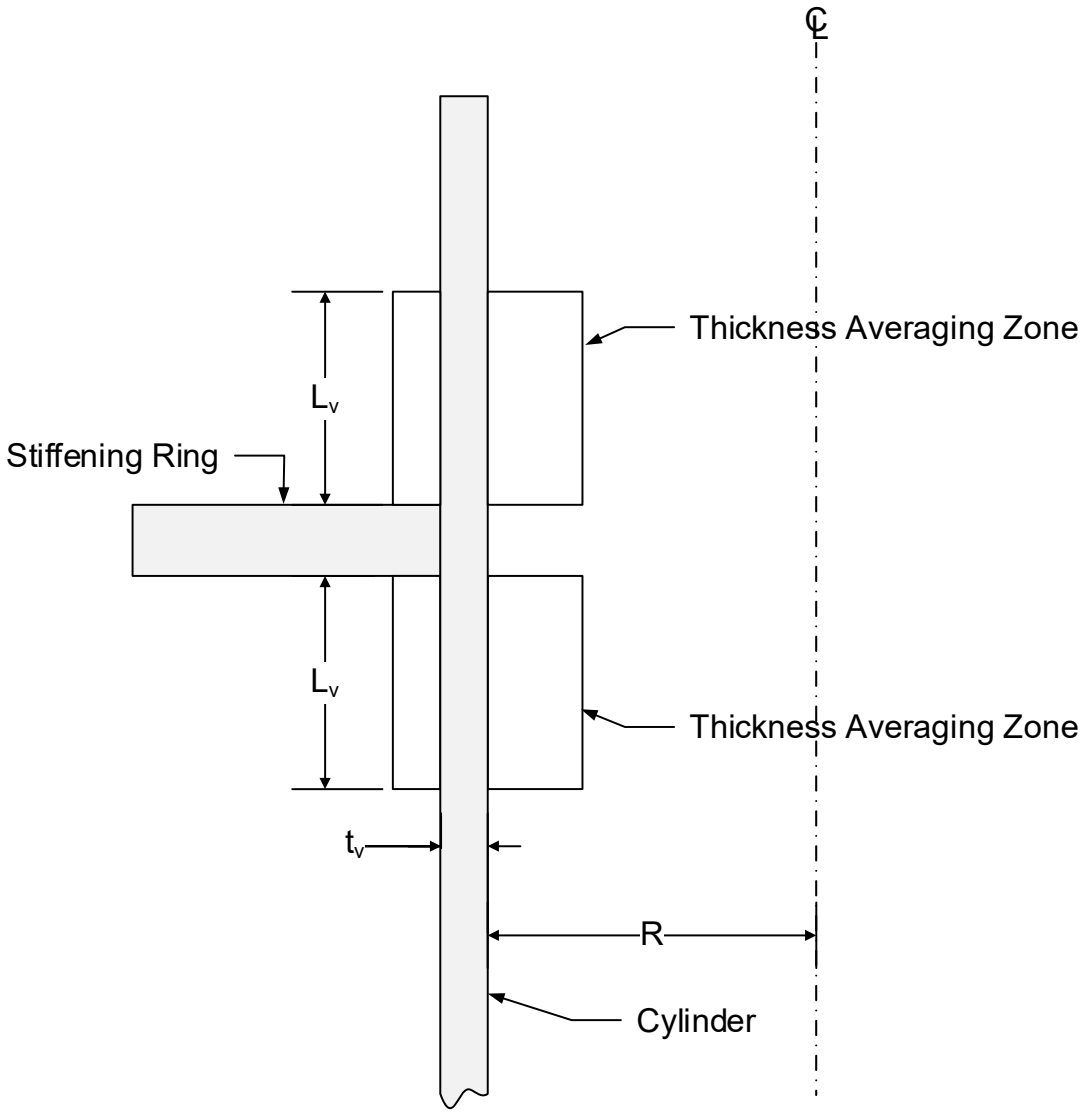

Notes:

1. Criteria for determining if the stiffening ring is a structural discontinuity

$$\frac{A_R}{A_R + 1.56 t_v \sqrt{R t_v}} > 0.38 \quad \left(Stiffening\ Ring\ is\ a\ Structural\ Discontinuity \right)$$

$$\frac{A_R}{A_R + 1.56 t_v \sqrt{R t_v}} \le 0.38 \quad \left(Stiffening\ Ring\ is\ NOT\ a\ Structural\ Discontinuity \right)$$

2. $L_v = 2.5\sqrt{R t_v}$ is thickness averaging zone for the cylinder on each side of the stiffening ring.

Figure 4.18 – Zone for Thickness Averaging – Stiffening Ring

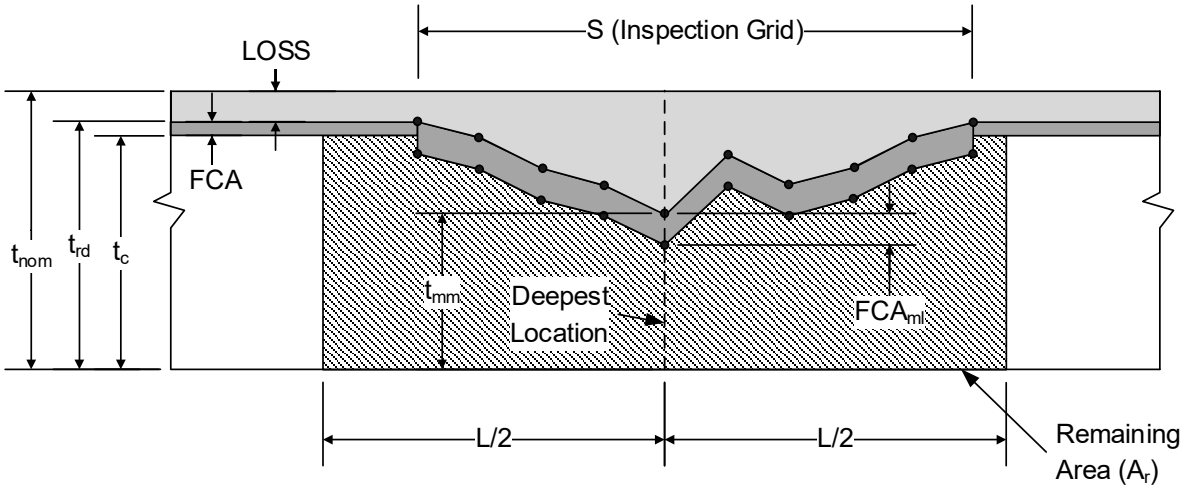

(a) The Length for Thickness Averaging is Greater Than the Inspection Grid Dimension

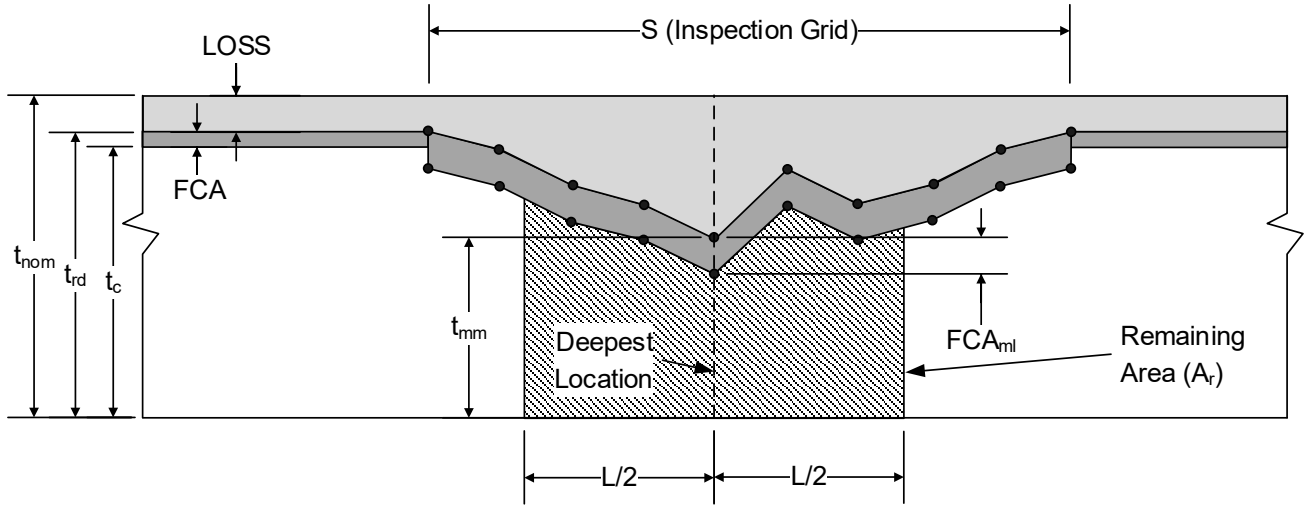

(b) The Length for Thickness Averaging is Less Than the Inspection Grid Dimension

Notes: The average thickness is: $t_{am} = \frac{A_r}{L}$

Figure 4.19 – Calculation of Average Thickness Based on the CTP

[Intentionally Left Blank]

ANNEX 4A – TECHNICAL BASIS AND VALIDATION – ASSESSMENT OF GENERAL METAL LOSS

(INFORMATIVE)

CONTENTS

ANNEX 4A – TECHNICAL BASIS AND VALIDATION – ASSESSMENT OF GENERAL METAL LOSS 4A-1

4A.1 TECHNICAL BASIS AND VALIDATION 4A-1
4A.2 REFERENCES 4A-1

4A.1 Technical Basis and Validation

The technical basis and validation of the assessment procedures for general metal loss and local metal loss contained in Part 4 and Part 5 are provided in references [1], [2], [3], and [4]. In each of these references, a comparison is made between the assessment methods in this Standard and the assessment methods contained in other standards. A comparison of assessment methodologies for the pipeline industry (i.e., B31G, RSTRENG, BS 7910) is provided in reference [5]. However, in the comparison of methods for the assessment of local thin areas, the methods in API 579-1/ASME FFS-1 were not considered in reference [5]. In order to provide a complete comparison of the methodologies currently being used for the assessment of local thin areas, the Materials Properties Council Joint Industry Project on Fitness-For-Service commissioned an additional study. The results of this comparison are provided in reference [1].

4A.2 References

[1] Janelle, J.A. and Osage, D.A., An Overview and Validation of the Fitness-For-Service Assessment Procedures for Local Thin Areas in API 579, WRC Bulletin 505, Welding Research Council, Inc., New York, NY, 2005.

[2] Osage, D.A., Buchheim, G.M., Brown, and R.G., Poremba, J., "An Alternate Approach for Inspection Scheduling Using the Maximum Allowable Working Pressure for Pressurized Equipment," ASME PVP–Vol. 288, American Society of Mechanical Engineers, New York, NY, 1994, pp. 261–273.

[3] Osage, D.A., Janelle, J. and Henry, P.A., “Fitness-For-Service Local Metal Loss Assessment Rules in API 579,” PVP Vol. 411, Service Experience and Fitness-For-Service in Power and Petroleum Processing, ASME, 2000, pp. 143-176.

[4] Osage, D.A., Krishnaswamy, P., Stephens, D.R., Scott, P., Janelle, J., Mohan, R., and Wilkowski, G.M., Technologies for the Evaluation of Non-Crack-Like Flaws in Pressurized Components – Erosion/Corrosion, Pitting, Blisters, Shell Out-Of-Roundness, Weld Misalignment, Bulges and Dents, WRC Bulletin 465, Welding Research Council, Inc., New York, NY, September 2001.

[5] Fu B., Stephens, D., Ritchie, D., and Jones, C.L., *Methods for Assessing Corroded Pipeline – Review, Validation and Recommendations*, Catalog No. L5878, Pipeline Research Council International, Inc. (PRCI), 2002.

[6] Prueter, P.E., Dewees, D.J., and Brown, R.G., “Evaluating Fitness-For-Service Assessment Procedures for Pressurized Components Subject to Local Thin Areas Near Structural Discontinuities,” ASME PVP 2013-97575, American Society of Mechanical Engineers, New York, NY, 2013.

[Intentionally Left Blank]

PART 5 – ASSESSMENT OF LOCAL METAL LOSS

CONTENTS

PART 5 – ASSESSMENT OF LOCAL METAL LOSS 5-1

5.1 GENERAL 5-1
5.1.1 Assessment Procedures for Local Metal Loss 5-1
5.1.2 Choice of Part 4 or Part 5 Assessment Procedures 5-2
5.1.3 Pitting Damage 5-2
5.2 APPLICABILITY AND LIMITATIONS OF THE PROCEDURE 5-2
5.2.1 Local Metal Loss Assessment 5-2
5.2.2 Limitations Based on Flaw Type 5-2
5.2.3 Calculation of the $MAWP_r$ and MFH_r, and Coincident Temperature 5-2
5.2.4 Limitations Based on Temperature 5-3
5.2.5 Applicability of the Level 1 and Level 2 Assessment Procedures 5-3
5.2.6 Applicability of the Level 3 Assessment Procedures 5-3
5.2.7 Assessment of Blend Ground Areas for Crack-Like Flaw Removal 5-4
5.3 DATA REQUIREMENTS 5-4
5.3.1 Original Equipment Design Data 5-4
5.3.2 Maintenance and Operational History 5-4
5.3.3 Required Data/Measurements for an FFS Assessment 5-4
5.3.4 Recommendations for Inspection Technique and Sizing Requirements 5-5
5.4 ASSESSMENT TECHNIQUES AND ACCEPTANCE CRITERIA 5-6
5.4.1 Overview 5-6
5.4.2 Level 1 Assessment 5-6
5.4.3 Level 2 Assessment 5-8
5.4.4 Level 3 Assessment 5-14
5.5 REMAINING LIFE ASSESSMENT 5-14
5.5.1 Thickness Approach 5-14
5.5.2 MAWP Approach 5-15
5.6 REMEDIATION 5-15
5.7 IN-SERVICE MONITORING 5-15
5.8 DOCUMENTATION 5-15
5.8.1 General 5-15
5.8.2 Inspection Data 5-15
5.9 NOMENCLATURE 5-16
5.10 REFERENCES 5-20
5.11 TABLES 5-21
5.12 FIGURES 5-27

5.1 General

5.1.1 Assessment Procedures for Local Metal Loss

Fitness-For-Service (FFS) Assessment procedures for pressurized components subject to local metal loss resulting from corrosion/erosion and/or mechanical damage are provided in this Part. These procedures can be used to qualify a component for continued operation or rerating and can also be used to evaluate regions of local metal loss resulting from blend grinding of crack-like flaws. A flow chart for the assessment procedures for local metal loss is shown in Figure 5.1.

5.1.2 Choice of Part 4 or Part 5 Assessment Procedures

The assessment procedures of this Part are for the analysis of local metal loss whereas the procedures of Part 4 are for general metal loss. The methodology shown in Part 4, Figure 4.2 can be used to determine whether the assessment procedures of Part 4 or Part 5 should be used in the evaluation. For most evaluations, it is recommended to first perform an assessment using Part 4. The local metal loss assessed with the procedures in this Part can only be established using thickness profiles because the size of the region of metal loss as well as thickness data are required for the assessment.

5.1.3 Pitting Damage

Damage associated with pitting and blisters can also be evaluated using the assessment procedures in this Part in conjunction with the assessment procedures of Part 6 and Part 7, respectively.

5.2 Applicability and Limitations of the Procedure

5.2.1 Local Metal Loss Assessment

The procedures in this Part can be used to evaluate components subject to local metal loss from corrosion/erosion, mechanical damage, or blend grinding that exceeds, or is predicted to exceed, the corrosion allowance before the next scheduled inspection. The local metal loss may occur on the inside or outside surface of the component. The types of flaws that are characterized as local metal loss are defined as follows:

a) Local Thin Area (LTA) – local metal loss on the surface of the component; the length of a region of metal loss is the same order of magnitude as the width.

b) Groove-Like Flaw – the following flaws are included in this category; a sharp radius may be present at the base of a groove-like flaw.

   1) Groove – local elongated thin spot caused by directional erosion or corrosion; the length of the metal loss is much greater than the width.

   2) Gouge – elongated local mechanical removal and/or relocation of material from the surface of a component, causing a reduction in wall thickness at the defect; the length of a gouge is much greater than the width and the material may have been cold worked in the formation of the flaw. Gouges are typically caused by mechanical damage, for example, denting and gouging of a section of pipe by mechanical equipment during the excavation of a pipeline. Gouges are frequently associated with dents due to the nature of mechanical damage. If a gouge is present, the assessment procedures of Part 12 shall be used.

5.2.2 Limitations Based on Flaw Type

Unless otherwise specified, this Part is limited to the evaluation of local metal loss. Other flaw types shall be evaluated in accordance with Part 2, Table 2.1.

5.2.3 Calculation of the $MAWP_r$ and MFH_r, and Coincident Temperature

Calculation methods are provided to rerate the component if the acceptance criteria in this Part are not satisfied. For pressurized components, the calculation methods can be used to find a reduced maximum allowable working pressure, $MAWP_r$, and coincident temperature. For tank shell courses, the calculation methods can be used to determine a reduced maximum fill height (MFH_r) and coincident temperature.

5.2.4 Limitations Based on Temperature

The assessment procedures only apply to components that are not operating in the creep range; the design temperature is less than or equal to the value in Part 4, Table 4.1. A Materials Engineer should be consulted regarding the creep range temperature limit for materials not listed in this table. Assessment procedures for components operating in the creep range are provided in Part 10.

5.2.5 Applicability of the Level 1 and Level 2 Assessment Procedures

The Level 1 and 2 Assessment procedures in this Part apply only if all the following conditions are satisfied.

a) The original design criteria were in accordance with a recognized code or standard (see Part 1, paragraphs 1.2.2 or 1.2.3).

b) The material is considered to have sufficient material toughness. If there is an uncertainty regarding the material toughness, then a Part 3 assessment should be performed. If the component is subject to embrittlement during operation due to temperature and/or the process environment, a Part 3, Level 3 Assessment should be performed. Temperature and/or process conditions that result in material embrittlement are discussed in Annex 2B.

c) The component is not in cyclic service. If the component is subject to less than 150 cycles (i.e., pressure and/or temperature variations including operational changes and start-ups and shut-downs) throughout its previous operating history and future planned operation or satisfies the cyclic service screening procedure in Part 14, then the component is not in cyclic service.

d) The following limitations on component types and applied loads are satisfied:

   1) Level 1 Assessment – Type A Components (see Part 4, paragraph 4.2.5) subject to internal pressure.

   2) Level 2 Assessment – Type A and Type B, Class 1 components (see Part 4, paragraph 4.2.5) subject to internal pressure, external pressure, and supplemental loads (see Annex 2C, paragraph 2C.2.7).

e) The Level 1 and Level 2 Assessment procedures include a limitation on the minimum measured thickness, t_{mm}. The limitation on t_{mm} is to guard against potential inadequacy in inspection method capabilities to accurately characterize excessively thinned areas. If the limitation on t_{mm} is not satisfied, a Level 3 Assessment may be performed. Future inspection frequency shall be established based on a detailed investigation of all applicable damage mechanisms and inspection results shall be appropriately validated (see Part 4, paragraph 4.3.4.6).

5.2.6 Applicability of the Level 3 Assessment Procedures

A Level 3 Assessment can be performed when the Level 1 and Level 2 Assessment procedures do not apply, or when these assessment procedures produce conservative results (i.e., would not permit operation at the current design conditions). Examples include, but are not limited to the following:

a) Type A, B, or C Components (see Part 4, paragraph 4.2.5) subject to internal pressure, external pressure, supplemental loads, and any combination thereof.

b) Components with a design based on proof testing (e.g., piping tee or reducer produced in accordance with ASME B16.9 where the design may be based on proof testing).

c) Components in cyclic service or components where a fatigue analysis was performed as a part of the original design calculations; the assessment should consider the effects of fatigue on the Fitness-For-Service calculations used to qualify the component for continued operation.

d) The metal loss is in the knuckle region of elliptical heads (outside of the $0.8D$ region), torispherical and toriconical heads, or conical transitions.

5.2.7 Assessment of Blend Ground Areas for Crack-Like Flaw Removal

The assessment procedures in this Part can be used to evaluate a region of local metal loss that is created when a crack-like flaw is removed by blend grinding. However, the potential for future cracking should be considered based on the relevant damage mechanisms.

5.3 Data Requirements

5.3.1 Original Equipment Design Data

An overview of the original equipment data required for an assessment is provided in Part 2, paragraph 2.3.1. These data can be entered in the form provided in Part 2, Table 2.2, and Table 5.1 for each component under evaluation.

5.3.2 Maintenance and Operational History

An overview of the maintenance and operational history required for an assessment is provided in Part 2, paragraph 2.3.2.

5.3.3 Required Data/Measurements for an FFS Assessment

5.3.3.1 To assess local corrosion/erosion, thickness readings are required on the component in the area where the metal loss has occurred. If the metal loss is less than the specified corrosion/erosion allowance and adequate thickness is available for the future corrosion allowance, no further action is required other than to record the data.

5.3.3.2 The following information is required for a Level 1 and Level 2 Assessment.

a) Thickness Profiles – The region of local metal loss on the component should be identified and inspection planes should be established to record thickness data. Based on these inspection planes, Critical Thickness Profiles (CTP) and the minimum measured thickness, t_{mm}, can be established for the flaw types shown below using the procedures in Part 4, paragraph 4.3.3.3.

   1) Local Thin Area (LTA) – A grid should be established to obtain thickness readings and to establish the CTP in the meridional (longitudinal direction for a cylinder) and circumferential directions. For an atmospheric storage tank, only the longitudinal CTP is required.

   2) Groove-Like Flaw – For groove-like flaws oriented in the circumferential and longitudinal directions, a grid similar to that used for an LTA can be utilized. For all other groove-like flaw orientations, the inspection planes of the grid should be located parallel and perpendicular to the groove.

b) Flaw Dimensions – The following procedures can be used to establish the flaw dimensions.

   1) Local Thin Area (LTA) – The relevant dimensions are s and c (see Figure 5.2), that are defined as the longitudinal and circumferential dimensions, respectively, of the extent of the local metal loss based on the corresponding CTP. The CTP is determined using the procedure in Part 4, paragraph 4.3.3.3. Both s and c should include the projected future corrosion growth.

   2) Groove-Like Flaw – The relevant parameters are g_l, g_w, g_r, and β, the dimensions that define the length, width, radius and orientation of the Groove-Like Flaw, respectively (see Figures 5.3 and 5.4). The flaw dimensions g_l and g_w are based on the corresponding CTP measured parallel and perpendicular to the

groove and should include the projected future corrosion growth. In the Level 1 and Level 2 Assessment procedures, the Groove-Like Flaw is treated as an equivalent LTA with dimensions s and c established as shown in Figure 5.4. For cylinders and cones, if the groove is orientated at an angle to the longitudinal axis, then the groove-like flaw profile can be projected on to the longitudinal and circumferential planes using the following equations to establish the equivalent LTA dimensions (see Figure 5.4). Alternatively, the flaw may be treated as an LTA with dimensions s and c established using subparagraph 1) above.

$$s = g_l \cos\beta + g_w \sin\beta \qquad \left(for \quad \beta < 90 \ Degrees\right) \tag{5.1}$$

$$c = g_l \sin\beta + g_w \cos\beta \qquad \left(for \quad \beta < 90 \ Degrees\right) \tag{5.2}$$

c) Flaw-To-Major Structural Discontinuity Spacing – The distance to the nearest major structural discontinuity should be determined (see Figure 5.5).

d) Vessel Geometry Data – The information required depends on the shell type as summarized in paragraphs 5.4.2 and 5.4.3 for a Level 1 and Level 2 Assessment, respectively.

e) Materials Property Data – The information required is summarized in paragraphs 5.4.2 and 5.4.3 for a Level 1 and Level 2 Assessment, respectively.

5.3.3.3 The information required to perform a Level 3 Assessment depends on the analysis method utilized. In general, a limit load procedure using a numerical technique can be used to establish the acceptable operating or design conditions as appropriate. For this type of analysis, a description of the local metal loss including size and thickness profiles (similar to that required for a Level 2 Assessment) shall be obtained along with the material strength (see paragraph 5.4.4).

5.3.4 Recommendations for Inspection Technique and Sizing Requirements

5.3.4.1 Recommendations for obtaining thickness measurements to characterize the local metal loss are covered in Part 4, paragraph 4.3.4.

5.3.4.2 The radius at the base of the groove-like flaw can be established by using a profile gauge. Alternatively, a mold can be made of the flaw using clay or a similar material and the radius can be directly determined from the mold.

5.3.4.3 In addition to thickness readings to establish the thickness profile, the following inspections are recommended. For components susceptible to brittle fracture (see Part 3, paragraph 3.2.2), these inspections are required.

a) All weld seams within a “2s x 2c box” (see Figure 5.2), and the entire surface of the flaw should be examined using Magnetic Particle (MT), Dye Penetrant (PT), or Ultrasonic (UT) techniques,

b) Any portion of a weld seam with a thickness less than the required thickness, t_{min}, within a “2s x 2c box” (see Figure 5.2) should be volumetrically examined with Radiographic (RT) or Ultrasonic (UT) techniques, and

c) If crack-like flaws or porosity not meeting the acceptance criteria of the original construction code are found, they shall either be repaired or an assessment in accordance with Part 9 be performed.

5.4 Assessment Techniques and Acceptance Criteria

5.4.1 Overview

5.4.1.1 If the metal loss is less than the specified corrosion/erosion allowance and adequate thickness is available for the future corrosion allowance, no further action is required other than to record the data; otherwise, an assessment is required.

5.4.1.2 An overview of the assessment levels is provided in Figure 5.1.

a) Level 1 Assessments are limited to Type A Components (see Part 4, paragraph 4.2.5). The only load considered is internal pressure, and a single thickness with one or two surface area dimensions are used to characterize the local metal loss.

b) Level 2 Assessment rules provide a better estimate of the structural integrity of a Type A or Type B, Class 1 component subject to internal pressure when significant variations in the thickness profile occur within the region of metal loss. Level 2 Assessment rules also provide procedures for assessing a Type A or Type B Class 1 component of cylindrical shape subject to external pressure as well as supplemental loads.

c) Level 3 Assessment rules are intended to evaluate components that do not pass Level 1 and 2 Assessments as well as components with complex geometries and/or regions of localized metal loss. Numerical stress analysis techniques are normally utilized in a Level 3 Assessment.

5.4.2 Level 1 Assessment

5.4.2.1 The Level 1 Assessment procedures can be used to evaluate a Type A Component with local metal loss subject to internal pressure. The procedures can be used to determine acceptability and/or to rerate a component with a flaw. If there are significant thickness variations over the length of the flaw or if a network of flaws is closely spaced, this procedure may produce conservative results, and a Level 2 Assessment is recommended.

5.4.2.2 The procedure shown below is developed for pressurized components where an $MAWP$ can be determined. For an atmospheric storage tank, the same procedure can be followed to determine a MFH by replacing them $MAWP$ with the MFH, and determining the MFH using the applicable code equations for a tank shell.

a) STEP 1 – Determine the CTP (see paragraph 5.3.3.2).

b) STEP 2 – Determine the wall thickness to be used in the assessment using Equation (5.3) or (5.4), as applicable.

$$t_c = t_{nom} - LOSS - FCA \tag{5.3}$$

$$t_c = t_{rd} - FCA \tag{5.4}$$

c) STEP 3 – Determine the minimum measured thickness in the LTA, t_{mm}, and the dimensions, s and c (see paragraph 5.3.3.2(b)) for the CTP.

d) STEP 4 – Determine the remaining thickness ratio using Equation (5.5) and the longitudinal flaw length parameter using Equation (5.6).

$$R_t = \frac{t_{mm} - FCA_{ml}}{t_c} \tag{5.5}$$

$$\lambda = \frac{1.285s}{\sqrt{Dt_c}} \tag{5.6}$$

e) STEP 5 – Check the limiting flaw size criteria; if the following requirements are satisfied, proceed to STEP 6; otherwise, the flaw is not acceptable per the Level 1 Assessment procedure.

$$R_t \geq 0.20 \tag{5.7}$$

$$t_{mm} - FCA_{ml} \geq 2.5\ mm\ (0.10\ inches) \qquad (for\ vessels\ \&\ tanks) \tag{5.8}$$

$$t_{mm} - FCA_{ml} \geq 1.3\ mm\ (0.05\ inches) \qquad (for\ piping) \tag{5.9}$$

$$L_{msd} \geq 1.8\sqrt{Dt_c} \tag{5.10}$$

f) STEP 6 – If the region of metal loss is categorized as an LTA (i.e., the LTA is not a groove), then proceed to STEP 7. If the region of metal loss is categorized as a groove and Equation (5.11) is satisfied, then proceed to STEP 7. Otherwise, the Level 1 Assessment is not satisfied and proceed to paragraph 5.4.2.3.

$$\frac{g_r}{(1-R_t)t_c} \geq 0.5 \tag{5.11}$$

g) STEP 7 – Determine the $MAWP$ for the component (see Annex 2C, paragraph 2C.2) using the thickness from STEP 2.

h) STEP 8 – Enter Figure 5.6 for a cylindrical shell or Figure 5.7 for a spherical shell with the calculated values of λ and R_t. If the point defined by the intersection of these values is on or above the curve, then the longitudinal extent (circumferential or meridional extent for spherical shells and formed heads) of the flaw is acceptable for operation at the $MAWP$ determined in STEP 7. If the flaw is unacceptable, then determine the RSF using Equation (5.12). If $RSF \geq RSF_a$, then the region of local metal loss is acceptable for operation at the $MAWP$ determined in STEP 7. If $RSF < RSF_a$, then the region of local metal loss is acceptable for operation at $MAWP_r$, where $MAWP_r$ is computed using the equations in Part 2, paragraph 2.4.2.2. The $MAWP$ from STEP 7 shall be used in this calculation. See Part 2, paragraph 2.4.2.2(e) to determine the acceptability of the equipment for continued operation.

$$RSF = \frac{R_t}{1 - \frac{1}{M_t}(1-R_t)} \tag{5.12}$$

The parameter M_t in Equation (5.12) is determined from Table 5.2.

i) STEP 9 – The assessment is complete for all component types except cylindrical shells, conical shells, and elbows. If the component is a cylindrical shell, conical shell, or elbow, then evaluate the circumferential extent of the flaw using the following procedure.

1) STEP 9.1 – If Equation (5.13) is satisfied, the circumferential extent is acceptable, and no further evaluation is required. Otherwise, proceed to STEP 9.2.

$$c \leq 2s\left(\frac{E_C}{E_L}\right) \tag{5.13}$$

2) STEP 9.2 – Calculate the minimum thickness required for longitudinal stresses, t_{min}^{L}, using $MAWP_r$ determined in STEP 8.

3) STEP 9.3 – If Equation (5.14) is satisfied, the circumferential extent is acceptable, and no further evaluation is required. Otherwise, proceed to STEP 9.4.

$$t_{\min}^{L} \le t_{mm} - FCA_{ml} \tag{5.14}$$

4) STEP 9.4 – The $MAWP_r$ for the component can be adjusted using Equation (5.15). Otherwise, a Level 2 or Level 3 Assessment may be performed. Note that the $MAWP_r$ on the right hand side of Equation (5.15) is determined in STEP 8.

$$MAWP_r = MAWP_r \left(\frac{t_{mm} - FCA_{ml}}{t_{\min}^{L}} \right) \tag{5.15}$$

5.4.2.3 If the equipment is not acceptable for continued operation per Level 1 Assessment requirements, then the following, or combinations thereof, shall be considered:

a) Rerate, repair, or replace, the component or equipment.

b) Adjust the FCA_{ml} by applying remediation techniques (see Part 4, paragraph 4.6).

c) Adjust the weld joint efficiency factor by conducting additional examination and repeat the assessment (see Part 4, paragraph 4.4.2.3(c)).

d) Conduct a Level 2 or Level 3 Assessment.

5.4.3 Level 2 Assessment

5.4.3.1 The Level 2 Assessment procedures provide a better estimate of the Remaining Strength Factor than the Level 1 procedure for local metal loss in a component subject to internal pressure if there are significant variations in the thickness profile. These procedures account for the local reinforcement effects of the varying wall thickness in the region of the local metal loss and ensure that the weakest ligament is identified and properly evaluated. The procedures can be used to evaluate closely spaced regions of local metal loss in lieu of the interaction rules specified in Part 4, Paragraph 4.3.3.3(f)(3)). The procedures can also be used to evaluate local metal loss in a Type A or Type B Class 1 component of cylindrical shape subject to external pressure and supplemental loads.

5.4.3.2 The following assessment procedure can be used to evaluate Type A Components subject to internal pressure (see paragraph 5.2.5(d)). The procedure shown below is developed for pressurized components where a $MAWP$ can be determined. For an atmospheric storage tank, the same procedure can be followed to determine a MFH by replacing the $MAWP$ with the MFH, and determining the MFH using the applicable code equations for a tank shell.

a) STEP 1 – Determine the CTP (see paragraph 5.3.3.2).

b) STEP 2 – Determine the wall thickness to be used in the assessment using Equation (5.3) or (5.4), as applicable.

c) STEP 3 – Determine the minimum measured thickness, t_{mm}, and the flaw dimensions s and c (see paragraph 5.3.3.2(b)).

d) STEP 4 – Determine the remaining thickness ratio, R_t, using Equation (5.5) and the longitudinal flaw length parameter, λ, using Equation (5.6).

e) STEP 5 – Check the limiting flaw size criteria in paragraph 5.4.2.2(e). If all these requirements are satisfied, then proceed to STEP 6; otherwise, the flaw is not acceptable per the Level 2 Assessment procedure.

f) STEP 6 – If the region of metal loss is categorized as an LTA (i.e., the LTA is not a groove), then proceed to STEP 7. If the region of metal loss is categorized as a groove, then proceed as follows:

1) If Equation (5.11) is satisfied, then proceed to STEP 7.

2) If Equation (5.16) is satisfied, then the groove shall be evaluated as an equivalent crack-like flaw using the assessment procedures in Part 9. In this assessment, the crack depth shall equal the groove depth, i.e., $a = (1 - R_t)t_c$, the crack length shall equal the groove length, and the fracture toughness shall be evaluated using Table 5.3 or Part 9.

$$0.1 < \frac{g_r}{(1-R_t)t_c} < 0.5 \tag{5.16}$$

3) If Equation (5.17) is satisfied, then the groove shall be evaluated as an equivalent crack-like flaw using the assessment procedures in Part 9. In this assessment, the crack depth shall equal the groove depth, i.e., $a = (1 - R_t)t_c$, the crack length shall equal the groove length, and the fracture toughness shall be evaluated using Part 9.

$$\frac{g_r}{(1-R_t)t_c} \le 0.1 \tag{5.17}$$

g) STEP 7 – Determine the $MAWP$ for the component (see Annex 2C, paragraph 2C.2) using the thickness from STEP 2.

h) STEP 8 – Determine the Remaining Strength Factor for the longitudinal CTP using the following procedure.

1) STEP 8.1 – Rank the thickness readings in ascending order based on metal loss profile.

2) STEP 8.2 – Set the initial evaluation starting point as the location of maximum metal loss. This is the location in the thickness profile where t_{mm} is recorded. Subsequent starting points should be in accordance with the ranking in STEP 8.1.

3) STEP 8.3 – At the current evaluation starting point, subdivide the thickness profile into a series of subsections (see Figure 5.8). The number and extent of the subsections should be chosen based on the desired accuracy and should encompass the variations in metal loss.

4) STEP 8.4 – For each subsection, compute the Remaining Strength Factor using Equation (5.18).

$$RSF^i = \frac{1-\left(\frac{A^i}{A_o^i}\right)}{1-\frac{1}{M_t^i}\left(\frac{A^i}{A_o^i}\right)} \tag{5.18}$$

with,

$$A_o^i = s^i t_c \tag{5.19}$$

The parameter M_t^i in Equation (5.18) is determined from Table 5.2 using $\lambda = \lambda^i$ and with $s = s^i$ in Equation (5.6).

5) STEP 8.5 – Determine the minimum value of the Remaining Strength Factors, RSF^i, found in STEP 8.4 for all subsections (see Figure 5.8). This is the minimum value of the Remaining Strength Factor for the current evaluation point.

6) STEP 8.6 – Repeat STEPs 8.3 through 8.5 of this calculation for the next evaluation starting point that corresponds to the next thickness reading location in the ranked thickness profile list.

7) STEP 8.7 – The Remaining Strength Factor to be used in the assessment, RSF, is the minimum value determined for all evaluation points.

i) STEP 9 – Evaluate the longitudinal extent of the flaw for cylindrical and conical shells. For spherical shells and formed heads evaluate the larger of the circumferential extent and meridional extent of the flaw. If $RSF \geq RSF_a$, then the region of local metal loss is acceptable for operation at the $MAWP$ determined in STEP 7. If $RSF < RSF_a$, then the region of local metal loss is acceptable for operation at $MAWP_r$, where $MAWP_r$ is computed using the equations in Part 2, paragraph 2.4.2.2. The $MAWP$ from STEP 7 shall be used in this calculation. See Part 2, paragraph 2.4.2.2(e) to determine the acceptability of the equipment for continued operation.

j) STEP 10 – The assessment is complete for all components except for cylindrical shells, conical shells, and elbows. For cylindrical shells, conical shells, or elbows, evaluate the circumferential dimension, c, of the flaw determined from the circumferential CTP using the criterion in paragraph 5.4.2.2(i). If this failed, the supplemental load procedure in paragraph 5.4.3.4 can be used for a more detailed analysis.

5.4.3.3 The following assessment procedure can be used to evaluate a Type A or Type B Class 1 component of cylindrical shape subject to external pressure. If the flaw is found to be unacceptable, the procedure can be used to establish a new $MAWP$.

a) STEP 1 – Determine the CTP (see paragraph 5.3.3.2).

b) STEP 2 – Subdivide the CTP in the longitudinal direction using a series of cylindrical shells that approximate the actual metal loss (see Figure 5.9). Determine the thickness and length of each of these cylindrical shells and designate them t_i and L_i.

c) STEP 3 – Determine the allowable external pressure, P_i^e, of each of the cylindrical shells defined in STEP 2 using $(t_i - FCA_{ml})$ within the region of corrosion or $(t_i - FCA)$ outside the region of corrosion and the total length, L_T, given by Equation (5.20), and designate this pressure as P_i^e. Methods for determining the allowable external pressure are provided in Annex 2C.

$$L_T = \sum_{i=1}^{n} L_i \tag{5.20}$$

d) STEP 4 – Determine the allowable external pressure of the actual cylinder using the following equation:

$$MAWP_r = \frac{L_T}{\sum_{i=1}^{n} \frac{L_i}{P_i^e}} \tag{5.21}$$

e) STEP 5 – If $MAWP_r \geq MAWP$, then the component is acceptable for continued operation. If $MAWP_r < MAWP$, then the component is acceptable for continued operation at $MAWP_r$. See Part 2, paragraph 2.4.2.2.e to determine the acceptability of the equipment for continued operation.

5.4.3.4 The assessment procedure in this paragraph can be used to determine the acceptability of the circumferential extent of a flaw in a cylindrical or conical shell subject to internal pressure and supplemental loads. Note that the acceptability of the longitudinal extent of the flaw is evaluated using paragraph 5.4.3.2 or paragraph 5.4.3.3, as applicable.

a) Supplemental Loads – These types of loads may result in a net-section axial force, bending moment, torsion, and shear being applied to the cross section of the cylinder containing the flaw (see Annex 2C, paragraph 2C.2.7). Supplemental loads will result in longitudinal membrane, bending, and shear stresses acting on the flaw, in addition to the longitudinal and circumferential (hoop) membrane stress caused by pressure.

1) The supplemental loads included in the assessment should include loads that produce both load-controlled and strain-controlled effects. Therefore, the net-section axial force, bending moment, torsion, and shear should be computed for two load cases, weight, and weight plus thermal. The weight load case includes pressure effects, weight of the component, occasional loads from wind or earthquake, and other loads that are considered as load controlled. The weight plus thermal load case includes the results from the weight case plus the results from a thermal case that includes the effects of temperature, support displacements and other loads that are considered as strain-controlled.

2) For situations where the results of a detailed stress analysis are unavailable, the following modification may be made to the procedure in subparagraph c).

i) Calculate the longitudinal stress due to pressure and designate this value as S_{lp}.

ii) Subtract S_{lp} from the allowable stress for load-controlled effects, S_{al} and the allowable stress for strain-controlled effects, S_{as}.

iii) Multiply each of the resulting stress values obtained in subparagraph ii) above by the section modulus of the cylinder in the uncorroded condition using the original nominal thickness to obtain the maximum allowable load-controlled bending moment, M_{al}, and the strain-controlled bending moment, M_{as}.

iv) Calculate the longitudinal stress at Point A, σ_{lm}^{A}, for the two load cases using Equation (5.27) by setting the axial force term, F, to zero and substituting M_{al} for M_x and setting M_y to zero to obtain the maximum load-controlled longitudinal stress, and M_{as} for M_x and setting M_y to zero to obtain the maximum strain-controlled longitudinal stress.

v) Calculate the longitudinal stress at Point B, σ_{lm}^{B}, for the two load cases using Equation (5.28) by setting the axial force term, F, to zero and substituting M_{al} for M_x and setting M_y to zero to obtain the maximum load-controlled longitudinal stress, and substituting M_{as} for M_x and setting M_y to zero to obtain the maximum strain-controlled longitudinal stress.

vi) Proceed to STEP 7 to evaluate the load-controlled and strain-controlled load cases values of σ_{lm}^{A} and σ_{lm}^{B}. When evaluating the results in STEP 7, set the shear stress, τ, to zero.

b) Special Requirements for Piping Systems – The relationship between the component thickness, piping flexibility or stiffness, and the resulting stress should be considered for piping systems.

1) The forces and moments acting on the circumferential plane of the defect resulting from supplemental loads can be computed from a piping stress analysis. The model used in this analysis should consider the effects of metal loss. Recommendations for modeling piping components are provided in Part 4, paragraph 4.4.3.3.a.2. Alternatively, a maximum value of the moments can be computed using the procedure in paragraph 5.4.3.4(a)(2).

2) Special consideration may be required if the local metal loss is located at an elbow or pipe bend (see Part 4, paragraph 4.4.4.4). A Level 3 Assessment with a detailed stress analysis performed using shell or continuum elements may be required in some cases.

c) Assessment Procedure – If the metal loss in the circumferential plane can be approximated by a single area (see Figure 5.10), then the following procedure can be used to evaluate the permissible membrane, bending and shear stresses resulting from pressure and supplemental loads. If the metal loss in the circumferential plane is composed of several distinct regions, then a conservative approach is to define a continuous region of local metal loss that encompasses all these regions (as an alternative see STEP 6 below).

1) STEP 1 – Determine the Critical Thickness Profiles(s) in the circumferential direction (see paragraph 5.3.3.2).

2) STEP 2 – For the circumferential inspection plane being evaluated, approximate the circumferential extent of metal loss on the plane under evaluation as a rectangular shape (see Figure 5.10).

i) For a region of local metal loss located on the inside surface,

$$D_f = D_o - 2\left(t_{mm} - FCA_{ml}\right) \tag{5.22}$$

ii) For a region of local metal loss located on the outside surface:

$$D_f = D + 2\left(t_{mm} - FCA_{ml}\right) \tag{5.23}$$

iii) The circumferential angular extent of the region of local metal loss is:

$$\theta = \frac{c}{D_f} \qquad (\theta \text{ in radians}) \tag{5.24}$$

3) STEP 3 – Determine the remaining strength factor, RSF, the reduced maximum allowable working pressure, $MAWP_r$, and supplemental loads on the circumferential plane. The remaining strength factor and reduced maximum allowable working pressure for the region of local metal loss can be established using the procedures in paragraph 5.4.2.2 or paragraph 5.4.3.2. The supplemental loads are determined in accordance with paragraphs 5.4.3.4(a) and 5.4.3.4(b).

4) STEP 4 – For the supplemental loads determined in STEP 3, compute the components of the resultant longitudinal bending moment (i.e., excluding torsion) in the plane of the defect relative to the region of metal loss as shown in Figure 5.10. This will need to be done for the weight and weight plus thermal load cases.

5) STEP 5 – Determine the pressure to be used in the supplemental load calculation, P_{sl}. This pressure is determined as follows:

$$P_{sl} = \min\left[MAWP_r,\ P_d\right] \tag{5.25}$$

6) STEP 6 – Compute the circumferential stress resulting from pressure for both the weight and weight plus thermal load cases at Points A and B in the cross section (see Figure 5.11).

$$\sigma_{cm} = \frac{P_{sl}}{RSF \cdot \cos\alpha}\left(\frac{D}{D_o - D} + 0.6\right) \tag{5.26}$$

7) STEP 7 – Compute the longitudinal membrane stress and shear stress for the weight and weight plus thermal load cases at Points A and B in the cross section (see Figure 5.11). All credible load combinations should be considered in the calculation. If the circumferential plane of the metal loss can be approximated by a rectangular area, then the section properties required for this calculation are provided in Table 5.4 (see Figure 5.10). If the metal loss in the circumferential plane cannot be approximated by a rectangular area because of irregularities in the thickness profile, then a numerical procedure may be used to compute the section properties and the membrane and bending stresses resulting from pressure and supplemental loads.

$$\sigma_{lm}^{A} = \frac{M_s^C}{E_C \cdot \cos\alpha}\left(\begin{array}{l}\dfrac{A_w}{A_m - A_f}\cdot P_{sl} + \dfrac{F}{A_m - A_f} + \\ \dfrac{y_A}{I_{\bar{X}}}\left(F\cdot\bar{y} + \left(\bar{y}+b\right)\cdot P_{sl}\cdot A_w + M_x\right) + \dfrac{x_A}{I_{\bar{Y}}}\cdot M_y\end{array}\right) \tag{5.27}$$

$$\sigma_{lm}^{B} = \frac{M_s^C}{E_C \cdot \cos\alpha}\left(\begin{array}{l}\dfrac{A_w}{A_m - A_f}\cdot P_{sl} + \dfrac{F}{A_m - A_f} + \\ \dfrac{y_B}{I_{\bar{X}}}\left(F\cdot\bar{y} + \left(\bar{y}+b\right)\cdot P_{sl}\cdot A_w + M_x\right) + \dfrac{x_B}{I_{\bar{Y}}}\cdot M_y\end{array}\right) \tag{5.28}$$

$$\tau = \frac{M_T}{2\left(A_t + A_{tf}\right)\left(t_{mm} - FCA_{ml}\right)} + \frac{V}{A_m - A_f} \tag{5.29}$$

where,

$$M_s^C = \frac{1 - \left(\dfrac{1}{M_t^C}\right)\left(\dfrac{d}{t_c}\right)}{1 - \left(\dfrac{d}{t_c}\right)} \tag{5.30}$$

$$M_t^C = \frac{1.0 + 0.1401\left(\lambda_c\right)^2 + 0.002046\left(\lambda_c\right)^4}{1.0 + 0.09556\left(\lambda_c\right)^2 + 0.0005024\left(\lambda_c\right)^4} \tag{5.31}$$

$$\lambda_c = \frac{1.285c}{\sqrt{Dt_c}} \tag{5.32}$$

Equation (5.30) is valid for $\lambda_c \leq 9$. If the value of $\lambda > 9$, then a Level 3 Assessment is required except that if the circumferential extent of the LTA is 360˚, then $M_t^c = 1.0$.

8) STEP 8 – Compute the equivalent membrane stress for both the weight and weight plus thermal load cases at Points A and B in the cross section (see Figure 5.11):

$$\sigma_e^A = \left[\left(\sigma_{cm}\right)^2 - \left(\sigma_{cm}\right)\left(\sigma_{lm}^A\right) + \left(\sigma_{lm}^A\right)^2 + 3\tau^2 \right]^{0.5} \tag{5.33}$$

$$\sigma_e^B = \left[\left(\sigma_{cm}\right)^2 - \left(\sigma_{cm}\right)\left(\sigma_{lm}^B\right) + \left(\sigma_{lm}^B\right)^2 + 3\tau^2 \right]^{0.5} \tag{5.34}$$

9) STEP 9 – Evaluate the results as follows:

i) Equation (5.35) shall be satisfied for either a tensile or compressive longitudinal stress for the weight and weight plus thermal load cases.

$$\max\left[\sigma_e^A, \sigma_e^B\right] \le H_f\left(\frac{S_a}{RSF_a}\right) \tag{5.35}$$

ii) If the maximum longitudinal stress computed in STEP 7 is compressive, then this stress should be less than or equal to the allowable compressive stress computed using the methodology in Annex 2C, paragraph 2C.4 or the allowable tensile stress, whichever is smaller. When using this methodology to establish an allowable compressive stress, an average thickness representative of the region of local metal loss in the compressive stress zone should be used in the calculations.

10) STEP 10 – If the equivalent stress criterion in STEP 9 is not satisfied, the $MAWP$ and/or supplemental loads determined in STEP 3 should be reduced, and the evaluation outlined in STEPs 1 through 9 should be repeated. Alternatively, a Level 3 Assessment can be performed.

5.4.3.5 If the equipment is not acceptable for continued operation per the Level 2 Assessment requirements, then the following, or combinations thereof, can be considered:

a) Rerate (i.e., reduce the $MAWP$ and/or supplemental loads), repair, or replace the equipment/component.

b) Adjust the FCA_{ml} by applying remediation techniques (see Part 4, paragraph 4.6).

c) Adjust the weld joint efficiency factor by conducting additional examination and repeat the assessment (see Part 4, paragraph 4.4.2.3.c).

d) Conduct a Level 3 Assessment.

5.4.4 Level 3 Assessment

The recommendations for a Level 3 Assessment of local metal loss are the same as those for general metal loss (see Part 4, paragraph 4.4.4). An assessment technique for a groove-like flaw with a geometry satisfying the requirements of Equation (5.16) is described in WRC Bulletin 562 (see Annex 5A, reference [30]).

5.5 Remaining Life Assessment

5.5.1 Thickness Approach

5.5.1.1 The remaining life of a component with a region of local metal loss can be estimated based upon computation of a minimum required thickness for the intended service conditions, actual thickness and region size measurements from an inspection, and an estimate of the anticipated corrosion/erosion rate and rate of change of the size of the flaw. If this information is known, or can be estimated, the equations in paragraph 5.4.2.2 or paragraph 5.4.3.2 can be solved iteratively with the following substitutions to determine the remaining life:

$$RSF \rightarrow RSF_a \tag{5.36}$$

$$R_t \rightarrow \frac{t_{mm} - \left(C_{rate} \cdot time\right)}{t_{rd} - \left(C_{rate}^{rd} \cdot time\right)} \tag{5.37}$$

For an LTA or groove-like flaw evaluated as an equivalent LTA.

$$s \rightarrow s + C_{rate}^{s} \cdot time \tag{5.38}$$

$$c \rightarrow c + C_{rate}^{c} \cdot time \tag{5.39}$$

5.5.1.2 The rate-of-change in the size or characteristic length of a region of local metal loss can be estimated based upon inspection records. If this information is not available, engineering judgment should be applied to determine the sensitivity of the remaining life of the component to this parameter.

5.5.1.3 The remaining life determined using the thickness-based approach can only be utilized if the region of local metal loss is characterized by a single thickness. If a thickness profile is utilized (Level 2 Assessment procedure), the remaining life should be established using the $MAWP$ Approach.

5.5.2 MAWP Approach

The $MAWP$ approach can be used to determine the remaining life of a pressurized component with a region of local metal loss characterized by a thickness profile. To use this approach, the methodology in Part 4, paragraph 4.5.2.2 is applied in conjunction with the assessment methods of this Part. When determining a remaining life with the $MAWP$ approach, the change in the flaw size should be considered as discussed in paragraph 5.5.1.

5.6 Remediation

The remediation methods for general corrosion provided in Part 4, paragraph 4.6 is applicable to local metal loss. Because of the localized damage pattern, it may be necessary in some cases to fill deep areas of metal loss with substances such as caulking, before applying linings.

5.7 In-Service Monitoring

The remaining life may be difficult to establish for some regions of local metal loss in services where an estimate of the future metal loss and enlargement of the LTA cannot be adequately characterized. In these circumstances, remediation and/or in-service monitoring may be required to validate the assumptions made to establish the remaining life. Typical monitoring methods and procedures are provided in Part 4, paragraph 4.7.

5.8 Documentation

5.8.1 General

The documentation of the FFS Assessment should include the information cited in Part 2, paragraph 2.8.

5.8.2 Inspection Data

Inspection data including all thickness readings and corresponding locations used to establish the thickness profile and the minimum measured thickness, t_{mm}, should be recorded and included in the documentation. A sample data sheet is provided in Table 5.1 for this purpose. A sketch showing the location and orientation of the inspection planes on the component is also recommended.

5.9 Nomenclature

a equivalent crack depth for a groove that is being evaluated as a crack-like flaw.

A^i area of metal loss based on s^i including the effect of FCA_{ml} (see Figure 5.8).

A_o^i original metal area based on s^i.

A_a cylinder aperture cross-section.

A_f cross-sectional area of the region of local metal loss, (the unshaded area labeled “Metal Loss” in Figure 5.11).

A_m metal area of the cylinder’s cross-section.

A_t mean area to compute torsion stress for the region of the cross section without metal loss.

A_{tf} mean area to compute torsion stress for the region of the cross section with metal loss.

A_w effective area on which pressure acts.

α cone half-apex angle.

b location of the centroid of area A_w, measured from the $x - x$ axis.

β orientation of the groove-like flaw with respect to the longitudinal axis or a parameter to compute an effective fracture toughness for a groove being evaluated as a crack-like flaw, as applicable.

C_{rate} anticipated future corrosion rate in the local metal loss area.

C_{rate}^c estimated rate of change of the circumferential length of the region of local metal loss.

C_{rate}^{rd} anticipated future corrosion rate away from the local metal loss.

C_{rate}^s estimated rate of change of the meridional length of the region of local metal loss.

c circumferential extent or length of the region of local metal loss (see Figures 5.2 and 5.10), based on future corroded thickness, t_c.

C_K Fracture toughness conversion factor.

D inside diameter of the cylinder, cone (at the location of the flaw), sphere, or formed head corrected for $LOSS$ and FCA as applicable; for the center section of an elliptical head an equivalent inside diameter of $K_c D_c$ is used where D_c is the inside diameter of the head straight flange and K_c is a factor defined in Annex 2C, paragraph 2C.3.5; for the center section of a torispherical head two times the crown radius of the spherical section is used. The cylinder inside diameter D shall be corrected for $LOSS$ and FCA as applicable.

D_f diameter at the base of the region of local metal loss (see Figure 5.11).

D_o outside diameter of the cylinder, corrected for $LOSS$ and FCA as applicable.

d maximum depth of the region of local metal loss.

E_C circumferential weld joint efficiency.

E_L longitudinal weld joint efficiency.

E_y modulus of elasticity.

F applied net-section axial force for the weight or weight plus thermal load case.

FCA_{ml} future corrosion allowance applied to the region of local metal loss.

FCA future corrosion allowance applied to the region away from the local metal loss.

g_l length of the Groove-Like Flaw based on future corroded condition.

g_w width of the Groove-Like Flaw based on future corroded condition.

g_r radius at the base of a Groove-Like Flaw based on future corroded condition.

H_f allowable stress factor depending on the load case being evaluated. $H_f = 1.0$ for the weight (i.e., sustained) load case, and $H_f = 1.5$ for the weight (i.e., sustained) plus thermal (i.e., displacement controlled) load case.

θ angle describing the circumferential extent of the region of local metal loss on the cross section, (see Figure 5.10 and Figure 5.11).

I_{LX} moment of inertia of area A_f about a local x-axis (see Figure 5.11).

I_{LY} moment of inertia of area A_f about a local y-axis (see Figure 5.11).

I_X cylinder moment of inertia about the $x - x$ axis.

I_Y cylinder moment of inertia about the $y - y$ axis.

$I_{\bar{X}}$ moment of inertia of the cross section with the region of local metal loss about the $\bar{x}$-axis (see Figure 5.11).

$I_{\bar{Y}}$ moment of inertia of the cross section with the region of local metal loss about the $\bar{y}$-axis (see Figure 5.11).

$K_{mat,g}$ effective fracture toughness of a groove being evaluated as a crack-like flaw.

$LOSS$ the amount of uniform metal loss away from the local metal loss location at the time of the assessment.

L_i length of the cylinder i that is used to determine the maximum allowable external pressure of a cylindrical shell with an LTA (see Figure 5.9).

L_{msd} distance to the nearest major structural discontinuity.

L_T total length of the cylinder.

λ longitudinal flaw length parameter.

λ^i incremental longitudinal flaw length parameter.

λ_c circumferential flaw length parameter.

M_{al} maximum allowable load controlled bending moment.

M_{as} maximum allowable strain controlled bending moment.

M_T applied net-section torsion for the weight or weight plus thermal load, as applicable (see Figure 5.10).

M_x applied section bending moment for the weight or weight plus thermal load case about the x-axis, as applicable, that is defined as the component of the net-section bending moment that is perpendicular to M_y as shown in Figure 5.10.

M_y applied section bending moment for the weight or weight plus thermal load case about the y-axis, as applicable, that is defined as the component of the net-section bending moment that is perpendicular to M_x as shown in Figure 5.10.

M_t Folias factor based on the longitudinal extent of the LTA for a through-wall flaw (see Annex 9C, paragraph 9C.2.3).

M_t^i Folias factor based on the longitudinal extent of the LTA for a through-wall flaw for the current subsection being evaluated.

M_t^C Folias factor based on the circumferential extent of the LTA for a through-wall flaw.

M_s^C Folias factor based on the circumferential extent of the LTA for a surface flaw.

$MAWP$ maximum allowable working pressure of the undamaged component (see Annex 2C, paragraph 2C.2).

$MAWP_r$ reduced maximum allowable working pressure of the damaged component.

MFH maximum fill height of the undamaged tank (see Annex 2C, paragraph 2C.2).

MFH_r reduced maximum fill height of the damaged tank.

P_d equipment design pressure or $MAWP$.

P_{sl} pressure used in the Level 2 supplemental load calculation.

P_i^e allowable external pressure of cylinder i that is used to determine the maximum allowable external pressure of a cylindrical shell with an LTA.

R outside radius of area A_f corrected for $LOSS$ and FCA as applicable.

R_t remaining thickness ratio.

RSF computed remaining strength factor based on the meridional extent of the LTA.

RSF^i RSF for the current subsection being evaluated.

RSF_a allowable remaining strength factor (see Part 2, paragraph 2.4.2.2).

s longitudinal extent or length of the region of local metal loss based on future corroded thickness, t_c.

s^i longitudinal extent or length increment of metal loss (see Figure 5.8).

S_a allowable stress determined based on the component's original construction code at the design temperature.

S_{al} allowable stress for load-controlled effects

S_{as} allowable stress for strain-controlled effects.

S_{lp} longitudinal stress due to pressure.

σ_{cm} maximum circumferential stress, typically the hoop stress from pressure loading for both the weight and weight plus thermal load cases.

σ_{lm}^A maximum longitudinal membrane stress computed for both the weight and weight plus thermal load cases at Point A (see Figure 5.11).

σ_{lm}^B maximum longitudinal membrane stress computed for both the weight and weight plus thermal load cases at Point B (see Figure 5.11).

σ_e^A equivalent stress computed for both the weight and weight plus thermal load cases at Point A (see Figure 5.11).

σ_e^B equivalent stress computed for both the weight and weight plus thermal load cases at Point B (see Figure 5.11).

t_c future corroded wall thickness away from the damage area.

t_i wall thickness of the cylinder i that is used to determine the maximum allowable external pressure of a cylindrical shell with an LTA.

$t_{\min}$ minimum required thickness for the component based on equipment design pressure or equipment $MAWP$ (see Annex 2C).

t_{mm} minimum measured thickness determined at the time of the assessment.

t_{nom} nominal or furnished thickness of the component adjusted for mill undertolerance as applicable.

t_{rd} uniform thickness away from the local metal loss location established by thickness measurements at the time of the assessment.

t_{sl} thickness required for supplemental loads (see Annex 2C, paragraph 2C.2).

$time$ time for future operation.

τ maximum shear stress in the region of local metal loss for both the weight and weight plus thermal load cases.

V applied net-section shear force for both the weight and weight plus thermal load cases.

$\overline{x}$ location of the neutral axis (see Figure 5.11).

x_A distance along the x-axis to Point A on the cross section shown in Figure 5.11.

x_B distance along the x-axis to Point B on the cross section shown in Figure 5.11.

$\overline{y}$ location of the neutral axis (see Figure 5.11).

y_A distance from the $\bar{x} - \bar{x}$ axis measured along the y-axis to Point A on the cross section shown in Figure 5.11.

y_B distance from the $\bar{x} - \bar{x}$ axis measured along the y-axis to Point B on the cross section shown in Figure 5.11.

$\overline{y}_{LX}$ distance from the centroid of area A_f to the x-axis (see Figure 5.11).

5.10 References

References for this Part are provided in Annex 5A – Technical Basis and Validation – Assessment of Local Metal Loss.

5.11 Tables

Table 5.1 – Data Required for the Assessment of Local Metal Loss

Use this form to summarize the data obtained from a field inspection.

Equipment Identification: _____
Equipment Type: _____ Pressure Vessel _____ Storage Tank _____ Piping Component
Component Type & Location: _____

Data Required for A Level 1 And Level 2 Assessment
Future Corrosion Allowance: _____
Inside Diameter: _____
Uniform Thickness (t_{rd}): _____
Minimum Measured Wall Thickness (t_{mm}): _____
Distance to the Nearest Structural Discontinuity (L_{msd}): _____
LTA Dimensions $(s \ \& \ c)$: _____
Groove-Like Flaw Dimensions $(g_l, g_r, g_w \ \& \ \beta)$: _____

Additional Data Required for A Level 2 Assessment
Distance to the Nearest LTA: _____

The thickness data for each of the inspection planes may be entered in a table as shown below.

Inspection Plane:__		**Inspection Plane:__**		**Inspection Plane:__**		**Inspection Plane:__**	
Location	**Thickness**	**Location**	**Thickness**	**Location**	**Thickness**	**Location**	**Thickness**
t_{mm}		t_{mm}		t_{mm}		t_{mm}	

Table 5.2 – Folias Factor, M_t, Based on the Longitudinal or Meridional Flaw Parameter, λ, for Cylindrical, Conical and Spherical Shells

λ	M_t	
	Cylindrical or Conical Shell	Spherical Shell
0.0	1.001	1.000
0.5	1.056	1.063
1.0	1.199	1.218
1.5	1.394	1.427
2.0	1.618	1.673
2.5	1.857	1.946
3.0	2.103	2.240
3.5	2.351	2.552
4.0	2.600	2.880
4.5	2.847	3.221
5.0	3.091	3.576
5.5	3.331	3.944
6.0	3.568	4.323
6.5	3.801	4.715
7.0	4.032	5.119
7.5	4.262	5.535
8.0	4.492	5.964
8.5	4.727	6.405
9.0	4.970	6.858
9.5	5.225	7.325
10.0	5.497	7.806
10.5	5.791	8.301
11.0	6.112	8.810
11.5	6.468	9.334
12.0	6.864	9.873
12.5	7.307	10.429
13.0	7.804	11.002
13.5	8.362	11.592
14.0	8.989	12.200
14.5	9.693	12.827
15.0	10.481	13.474
15.5	11.361	14.142

Table 5.2 – Folias Factor, M_t, Based on the Longitudinal or Meridional Flaw Parameter, λ, for Cylindrical, Conical and Spherical Shells

λ	M_t	
	Cylindrical or Conical Shell	Spherical Shell
16.0	12.340	14.832
16.5	13.423	15.544
17.0	14.616	16.281
17.5	15.921	17.042
18.0	17.338	17.830
18.5	18.864	18.645
19.0	20.494	19.489
19.5	22.219	20.364
20.0	24.027	21.272

Notes:

1. λ is the longitudinal or meridional flaw length parameter computed using Equation (5.6).

   Interpolation is permitted for intermediate values of λ, Figure 5.12 may also be used.

2. The equation for the cylindrical shell is shown below. If $\lambda > 20$, then use $\lambda = 20$ in the calculation.

$$M_t = \left(\begin{array}{l} 1.0010 - 0.014195\lambda + 0.29090\lambda^2 - 0.096420\lambda^3 + 0.020890\lambda^4 - \\ 0.0030540\lambda^5 + 2.9570\left(10^{-4}\right)\lambda^6 - 1.8462\left(10^{-5}\right)\lambda^7 + 7.1553\left(10^{-7}\right)\lambda^8 - \\ 1.5631\left(10^{-8}\right)\lambda^9 + 1.4656\left(10^{-10}\right)\lambda^{10} \end{array} \right)$$

3. The equation for the spherical shell is shown below. Note that the value of λ is limited by the inside circumference of the shell.

$$M_t = \left(\frac{1.0005 + 0.49001(\lambda) + 0.32409(\lambda)^2}{1.0 + 0.50144(\lambda) - 0.011067(\lambda)^2} \right)$$

4. Both s and c are based on the future corroded thickness, t_c.

Table 5.3 – Effective Toughness for A Groove Being Evaluated as a Crack-like Flaw with a Geometry that Satisfies Equation (5.16)

Material	Toughness Coefficients					
	A_0	A_1	A_2	A_3	A_4	A_5
High-Sulfur Steels (Greater than 0.01 percent)	90.93	0.107416	502.3968	7.206574	1191.002	0.0
Low-Sulfur Steels (0.01 percent or less)	146.27	-11.03721	-1626.36	62.67731	10229.16	-28.1154

$$K_{mat,g} = \left(\frac{A_0 + A_2\beta + A_4\beta^2}{1 + A_1\beta + A_3\beta^2 + A_5\beta^3} \right) \cdot C_K$$

Where:

$$\beta = \frac{g_r}{a}\left(\frac{a}{t_c}\right)^{0.9}$$

$$a = \left(1 - R_t\right)t_c$$

$$C_K = 1.0 \qquad for\ ksi\sqrt{in}$$

$$C_K = 1.09884 \quad for\ MPa\sqrt{m}$$

Table 5.4 – Section Properties for Computation of Longitudinal Stress in a Cylinder with an *LTA*

For Local Metal Loss on the Inside and Outside Surface

$$I_{\bar{X}} = I_X + A_m \bar{y}^2 - I_{LX} - A_f \left(\bar{y}_{LX} + \bar{y} \right)^2$$

$$I_{\bar{Y}} = I_Y - I_{LY}$$

$$I_X = I_y = \frac{\pi}{64}\left(D_o^4 - D^4 \right)$$

$$I_{LX} = R^3 d \left[\begin{array}{l} \left(1 - \frac{3d}{2R} + \frac{d^2}{R^2} - \frac{d^3}{4R^3} \right)\left(\theta + \sin\theta\cos\theta - \frac{2\sin^2\theta}{\theta} \right) + \\ \frac{d^2 \sin^2\theta}{3R^2\theta\left(2 - d/R\right)}\left(1 - \frac{d}{R} + \frac{d^2}{6R^2} \right) \end{array} \right]$$

$$I_{LY} = R^3 d \left[\left(1 - \frac{3d}{2R} + \frac{d^2}{R^2} - \frac{d^3}{4R^3} \right)\left(\theta - \sin\theta\cos\theta \right) \right]$$

$$\bar{y}_{LX} = \frac{2R\sin\theta}{3\theta}\left(1 - \frac{d}{R} + \frac{1}{2 - d/R} \right)$$

$$A_t = \frac{\left[0.5\pi\left(D + D_o \right) - c \right]\left(D + D_o \right)}{8}$$

$$A_a = \frac{\pi}{4} D^2$$

$$A_m = \frac{\pi}{4}\left(D_o^2 - D^2 \right)$$

Table 5.4 – Section Properties for Computation of Longitudinal Stress in a Cylinder with an *LTA*

For a Region of Local Metal Loss Located on the Inside Surface	For a Region of Local Metal Loss Located on the Outside Surface
$A_f = \frac{\theta}{4}\left(D_f^2 - D^2\right)$ $A_w = A_a + A_f$ $\overline{y} = \frac{1}{12}\frac{\sin\theta\left(D_f^3 - D^3\right)}{A_m - A_f}$ $x_A = 0.0$ $y_A = \overline{y} + \frac{D_o}{2}$ $x_B = \frac{D_o}{2}\sin\theta$ $y_B = \overline{y} + \frac{D_o}{2}\cos\theta$ $b = \frac{1}{12}\frac{\sin\theta\left(D_f^3 - D^3\right)}{A_a + A_f}$ $R = \frac{D_f}{2}$ $d = \frac{\left(D_f - D\right)}{2}$ $t_{mm} = \frac{\left(D_o - D_f\right)}{2}$ $A_{tf} = \frac{c\left(D_o + D_f\right)}{8}$	$A_w = A_a$ $A_f = \frac{\theta}{4}\left(D_o^2 - D_f^2\right)$ $\overline{y} = \frac{1}{12}\frac{\sin\theta\left(D_o^3 - D_f^3\right)}{A_m - A_f}$ $x_A = 0.0$ $y_A = \overline{y} + \frac{D_f}{2}$ $x_B = \frac{D_f}{2}\sin\theta$ $y_B = \overline{y} + \frac{D_f}{2}\cos\theta$ $b = 0$ $R = \frac{D_o}{2}$ $d = \frac{\left(D_o - D_f\right)}{2}$ $t_{mm} = \frac{\left(D_f - D\right)}{2}$ $A_{tf} = \frac{c\left(D + D_f\right)}{8}$

5.12 Figures

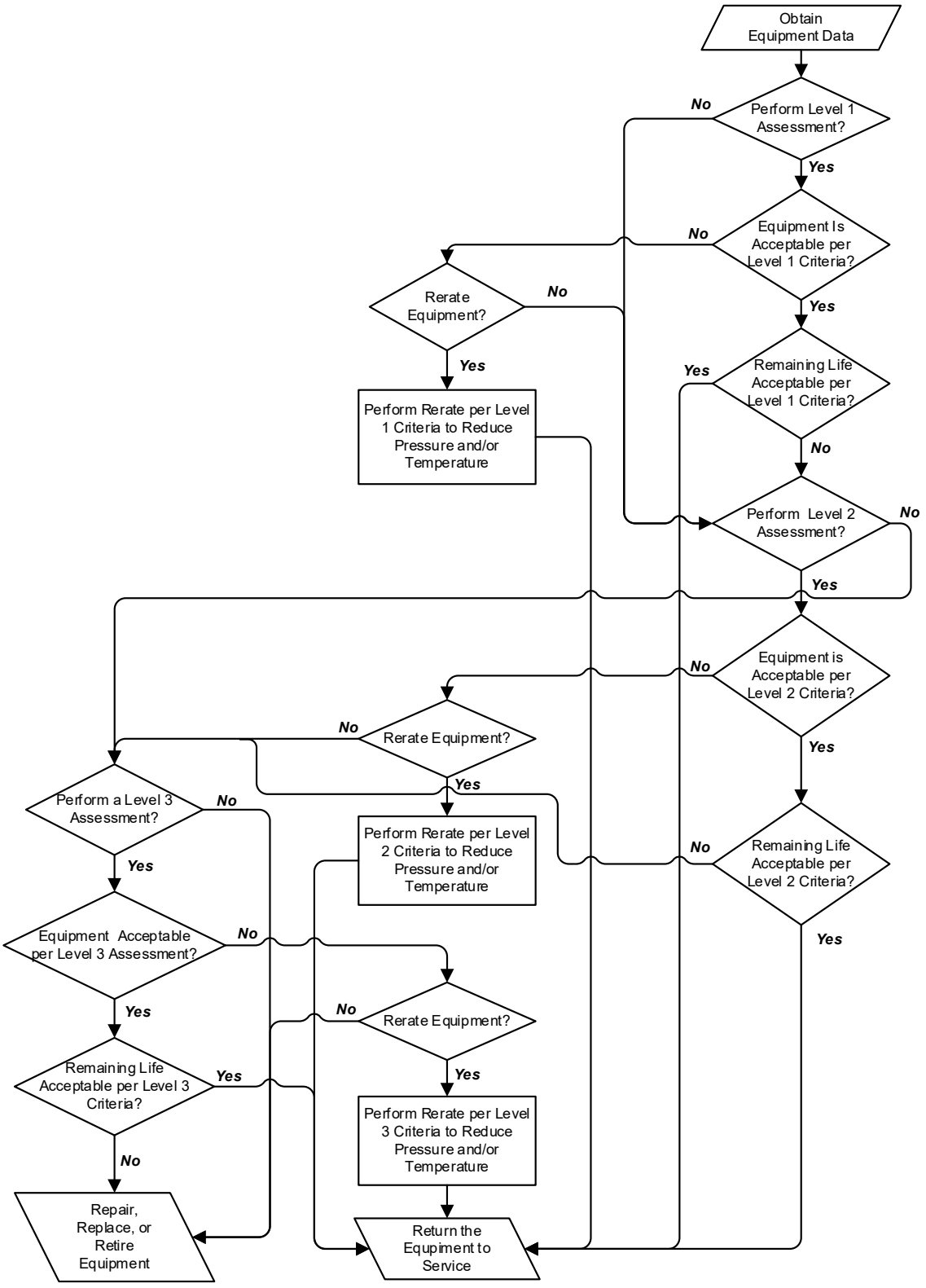

Figure 5.1 – Overview of the Assessment Procedures to Evaluate a Component with Local Metal Loss

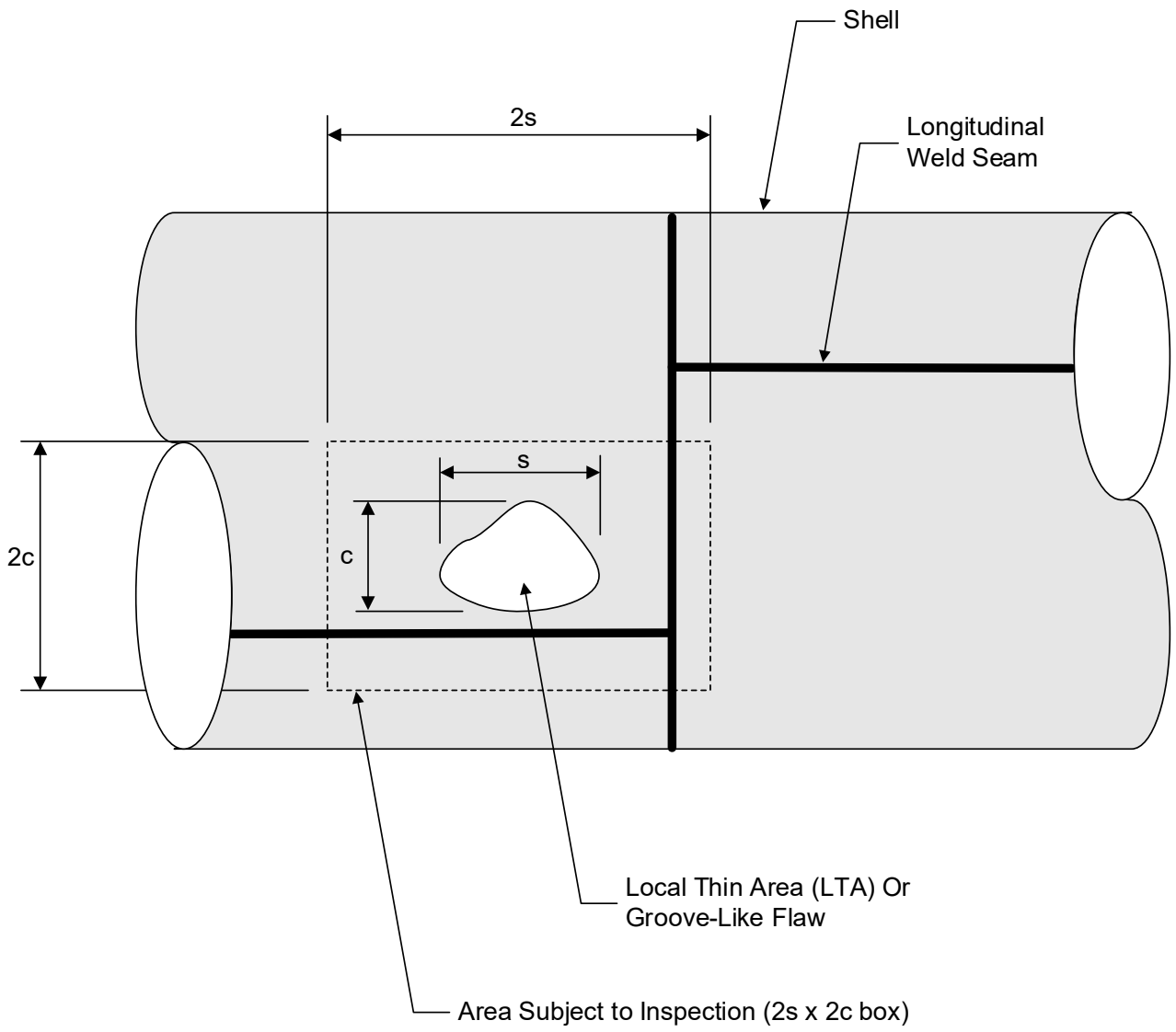

Notes: 1. See Part 4, paragraph 4.3.3.3 for the procedure to determine s and c.

2. Both s and c are based on the future corroded thickness, t_c.

Figure 5.2 – LTA Flaw Dimensions

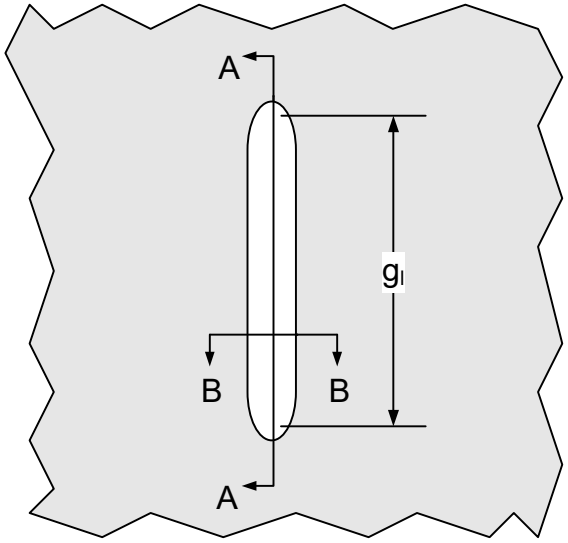

(a) Groove-Like Flaw - Plan View

(b) Groove-Like Flaw -Section A-A

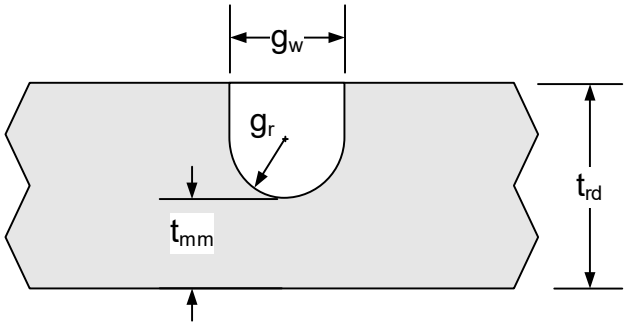

(c) Groove-Like Flaw - Section B-B

Note: g_l, g_w, and g_r are based on the future corroded condition, t_c.

Figure 5.3 – Groove-Like Flaw Dimensions – Flaw Profile

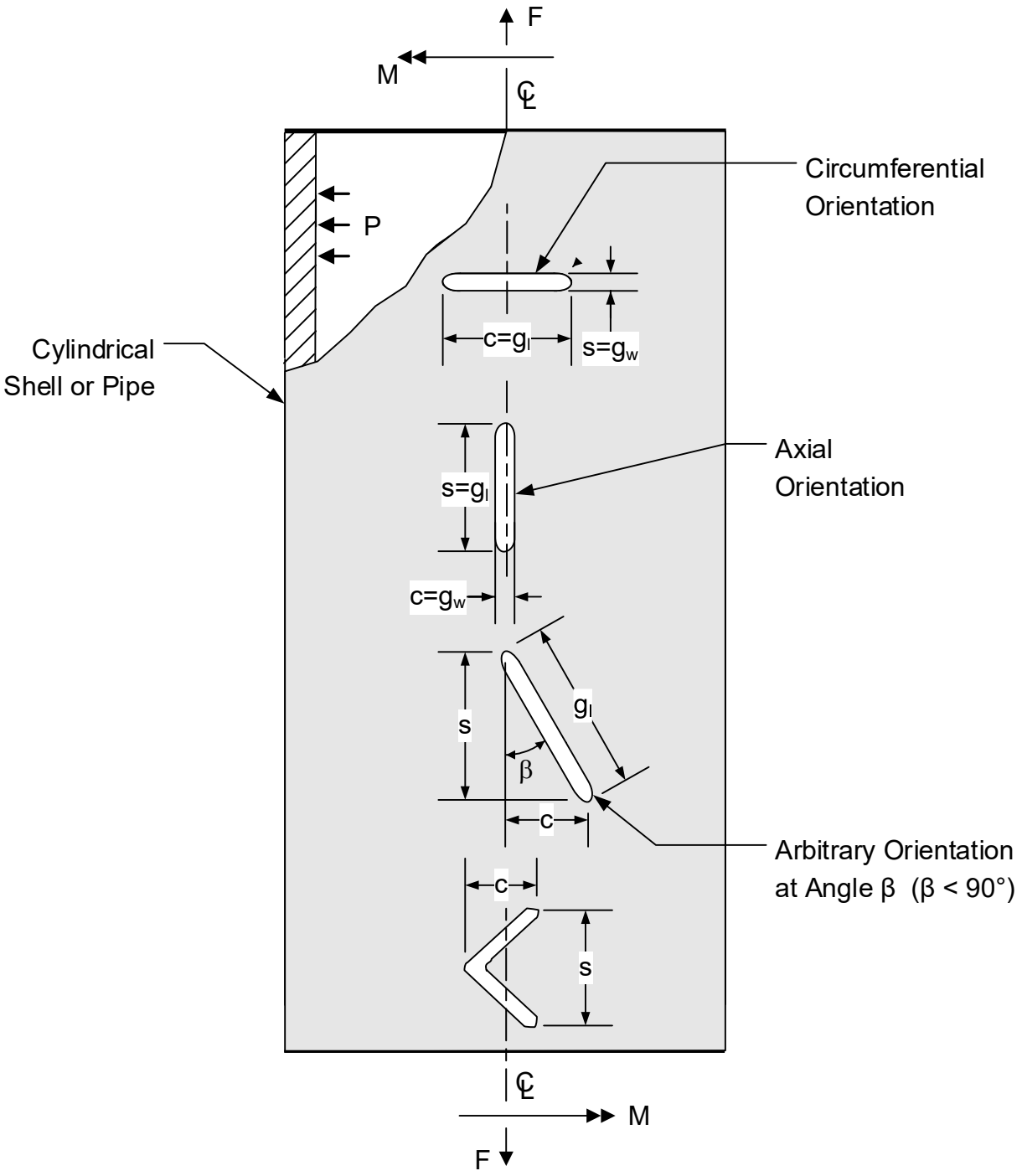

Figure 5.4 – Groove-Like Flaw Dimensions – Flaw Orientation on a Cylindrical Shell

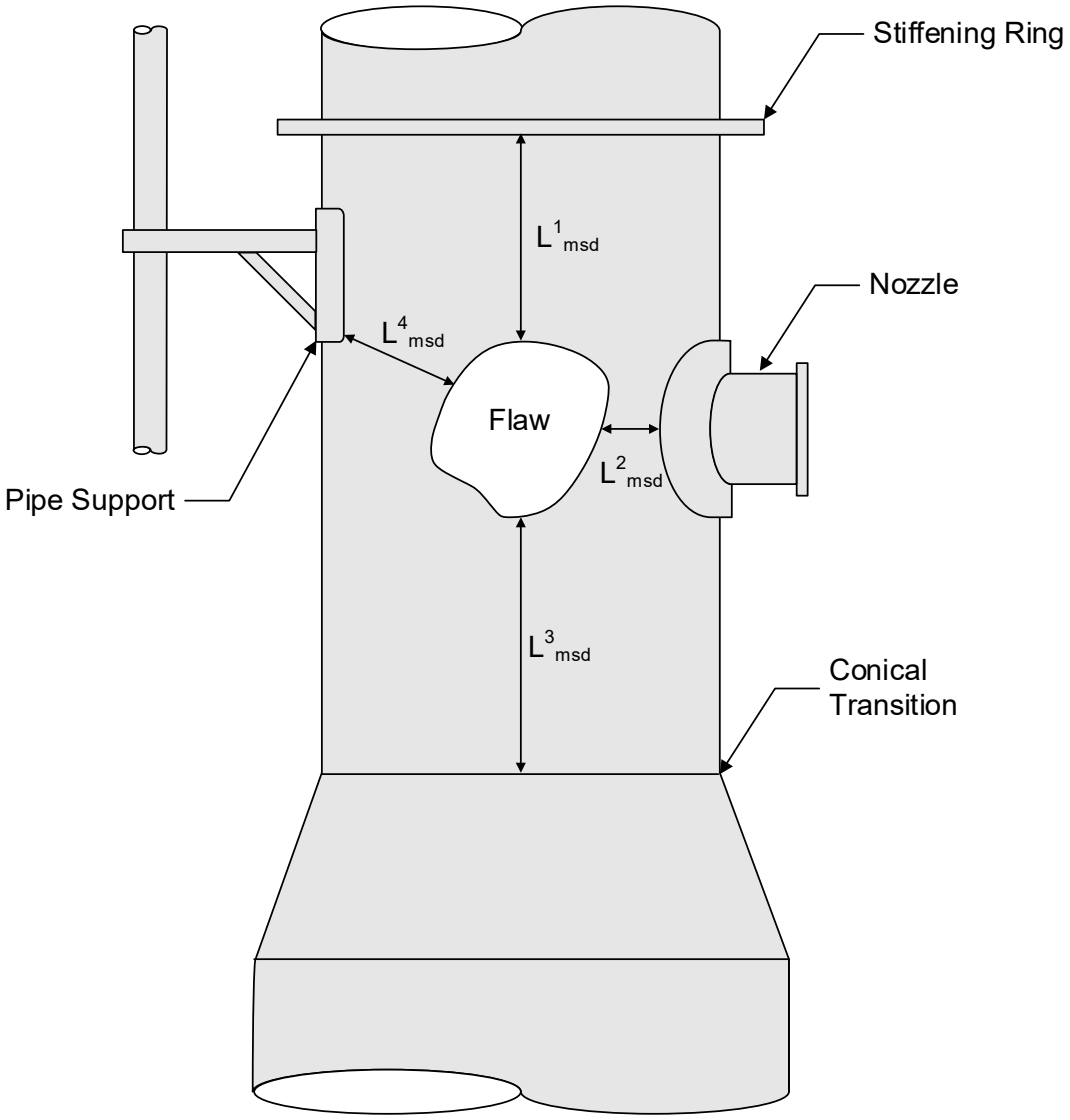

Notes:

1. For the example shown above, the minimum distance to a major structural discontinuity is: $L_{msd} = \min\left[L^1_{msd}, L^2_{msd}, L^3_{msd}, L^4_{msd}\right]$.
2. Typical major structural discontinuities associated with vertical vessels are shown in this figure. For horizontal drums, the saddles support would constitute a major structural discontinuity and for a spherical storage vessel, the support locations (shell-to-leg junction) would constitute a major structural discontinuity. The location of the flaw from these support locations would need to be considered in determining L_{msd} as well as the distances from the nearest nozzle, piping/platform support, conical transition, and stiffening ring.
3. The measure of the minimum distances defined in this figure is from the nearest edge of the region of local metal loss to the nearest weld of the structural discontinuity.

Figure 5.5 – Procedure to Determine L_{msd}

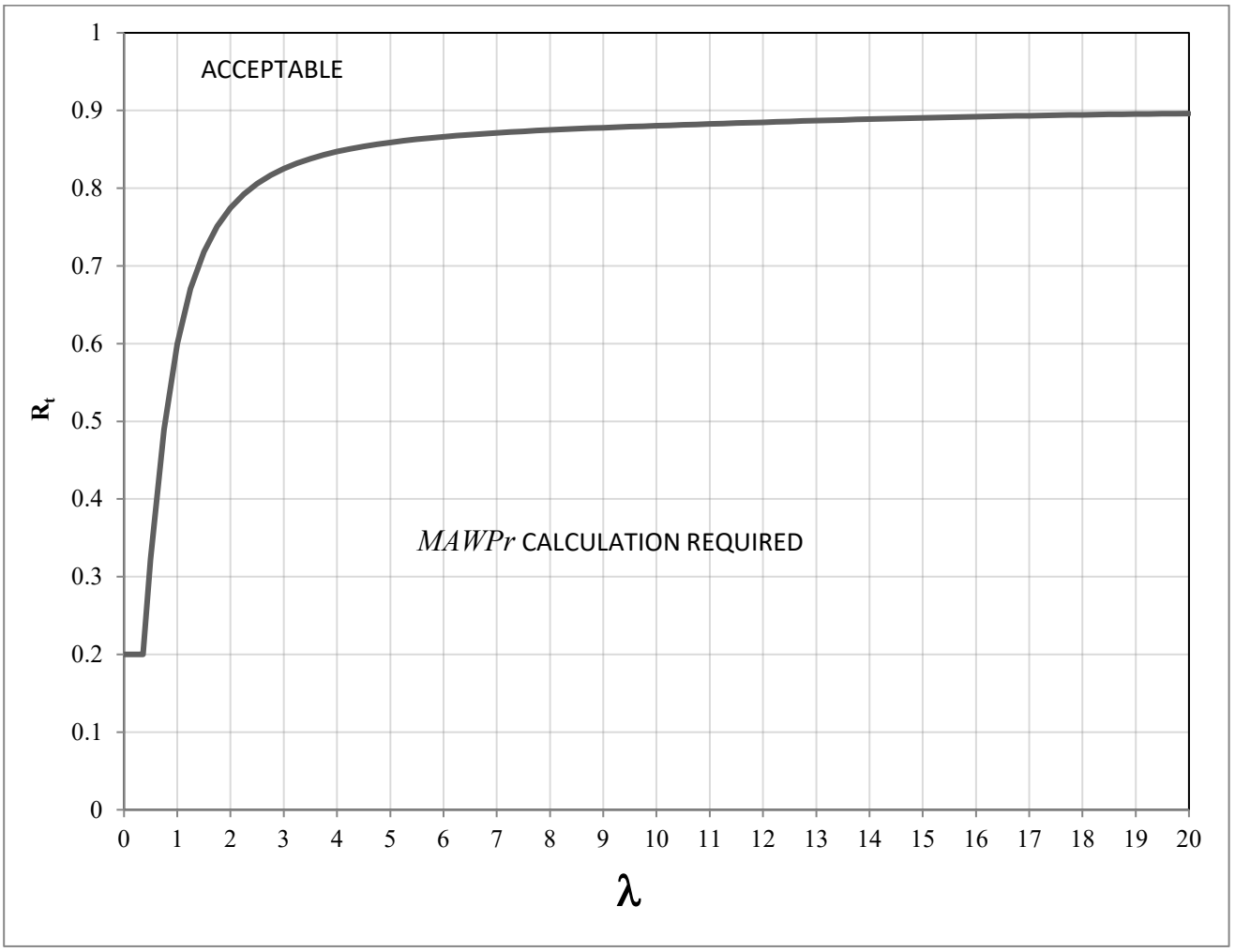

Note: The allowable remaining strength factor for this curve is $RSF_a = 0.90$. Equations for the curves in this figure are provided below where M_t for a cylindrical shell is determined using Table 5.2.

$$R_t = 0.2 \qquad \left(for\ \lambda \le 0.354\right) \tag{5.40}$$

$$R_t = \left(RSF_a - \frac{RSF_a}{M_t}\right)\left(1.0 - \frac{RSF_a}{M_t}\right)^{-1} \qquad \left(for\ 0.354 < \lambda < 20\right) \tag{5.41}$$

$$R_t = 0.90 \qquad \left(for\ \lambda \ge 20\right) \tag{5.42}$$

Figure 5.6 – Level 1 Screening Criteria for Local Metal Loss in a Cylindrical Shell

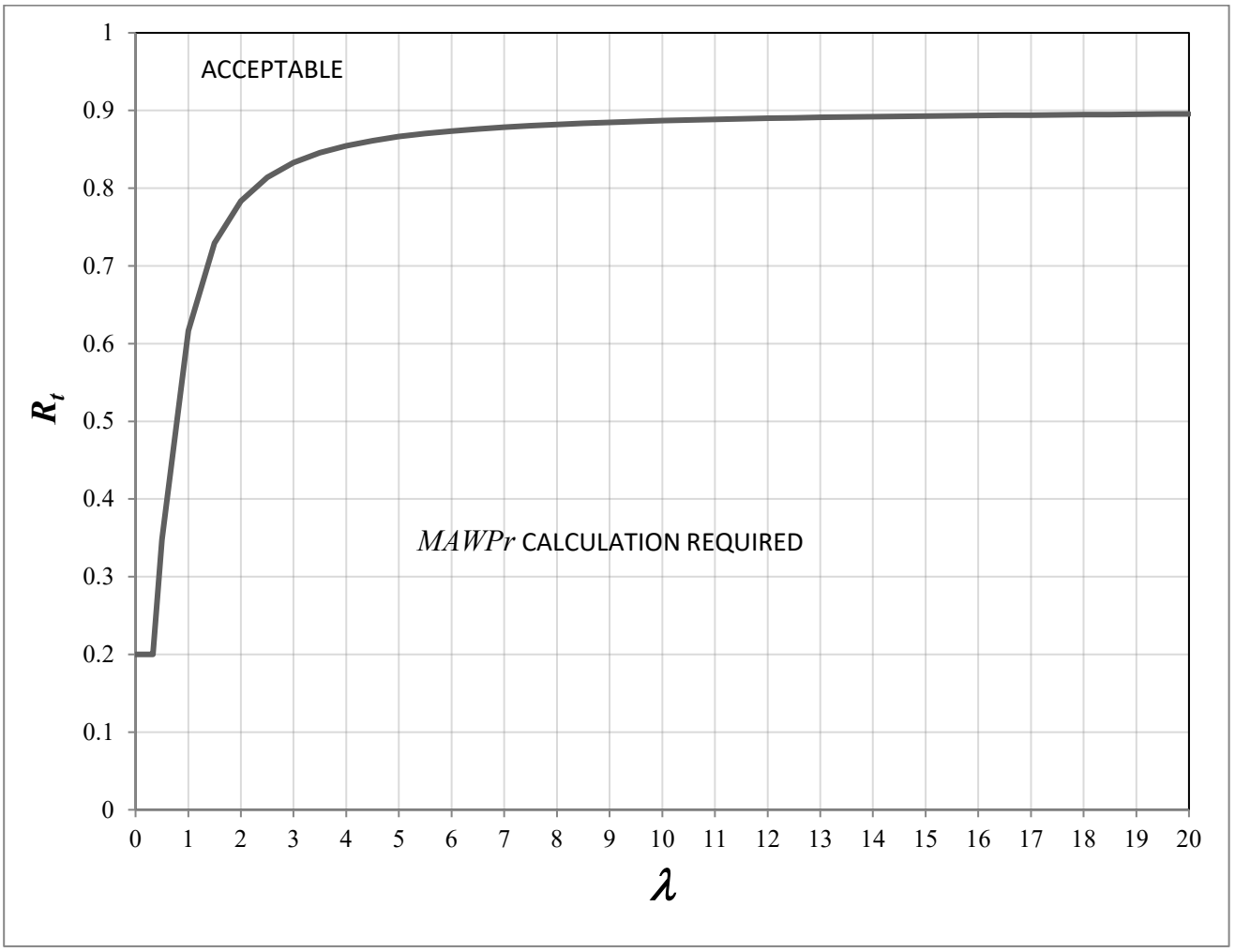

Note: The allowable remaining strength factor for this curve is $RSF_a = 0.90$. Equations for the curves in this figure are provided below where M_t for a spherical shell is determined using Table 5.2.

$$R_t = 0.2 \qquad \left(for\ \lambda \le 0.330\right) \tag{5.43}$$

$$R_t = \left(RSF_a - \frac{RSF_a}{M_t}\right)\left(1.0 - \frac{RSF_a}{M_t}\right)^{-1} \qquad \left(for\ 0.330 < \lambda < 20\right) \tag{5.44}$$

$$R_t = 0.90 \qquad \left(for\ \lambda \ge 20\right) \tag{5.45}$$

Figure 5.7 – Level 1 Screening Criteria for Local Metal Loss in a Spherical Shell

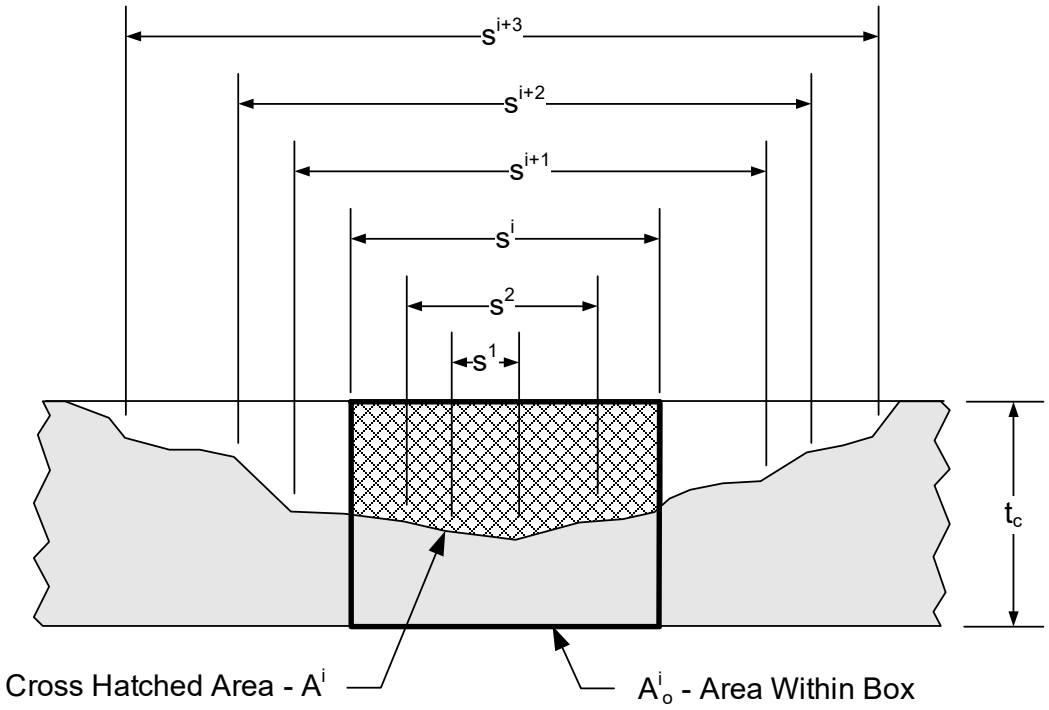

(a) Subdivision Process for Determining the RSF

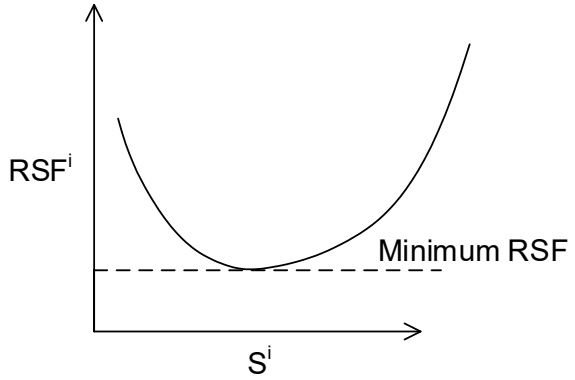

(b) Determining the Minimum RSF Value

Notes:

A^i = Area of metal loss associated with length s^i (cross-hatched area). This area can be evaluated using a numerical integration technique (e.g., Simpson's or Trapezoidal Rule).

A_o^i = Total original area associated with length s^i and thickness t_c, or $A_o^i = s^i t_c$.

Figure 5.8 – Definition of Areas Used to Compute the RSF for a Region of Local Metal Loss in a Level 2 Assessment

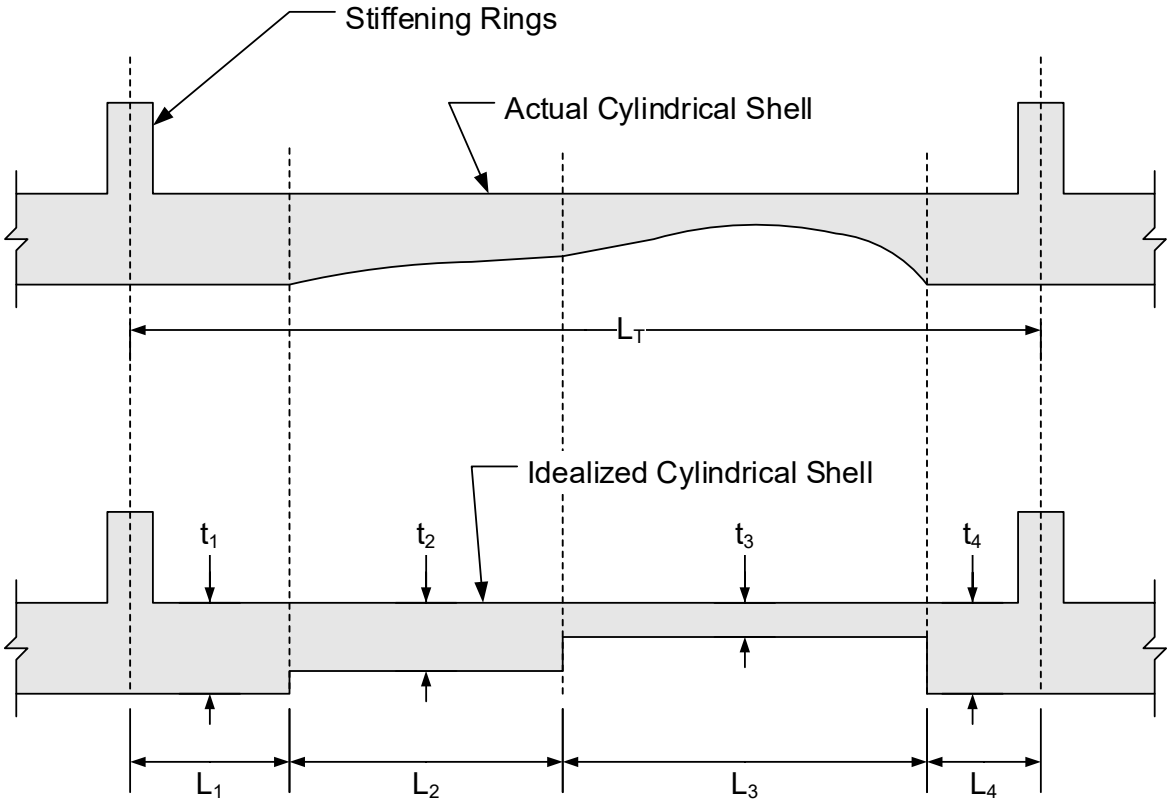

Figure 5.9 – Parameters for Determining the Maximum Allowable External Pressure of a Cylinder with an LTA

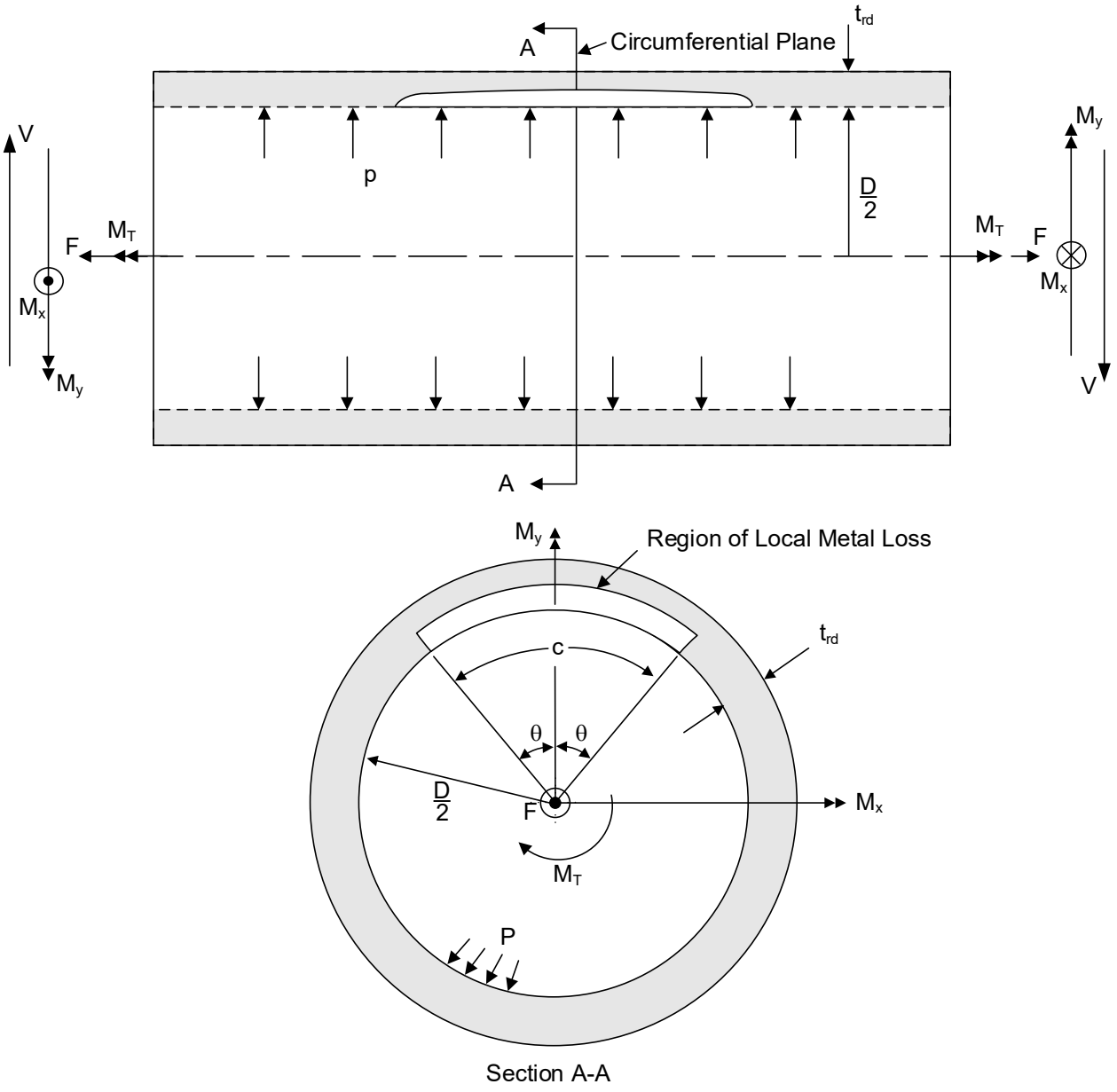

Figure 5.10 – Parameters for Permissible Bending Moment, Axial Force, and Pressure for a Cylinder with an LTA

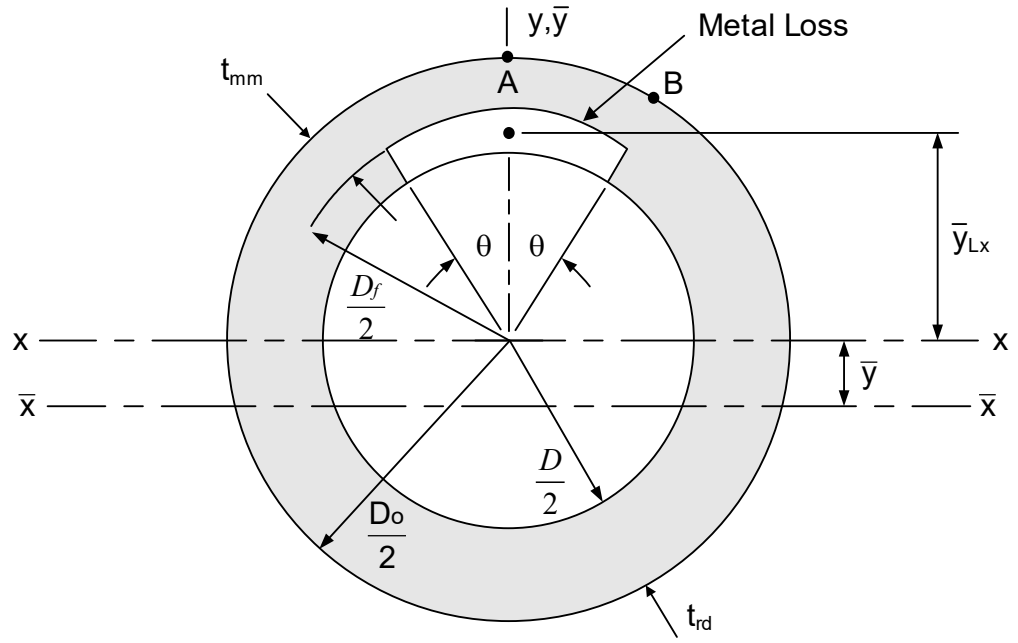

(a) Region Of Local Metal Loss Located on the Inside Surface

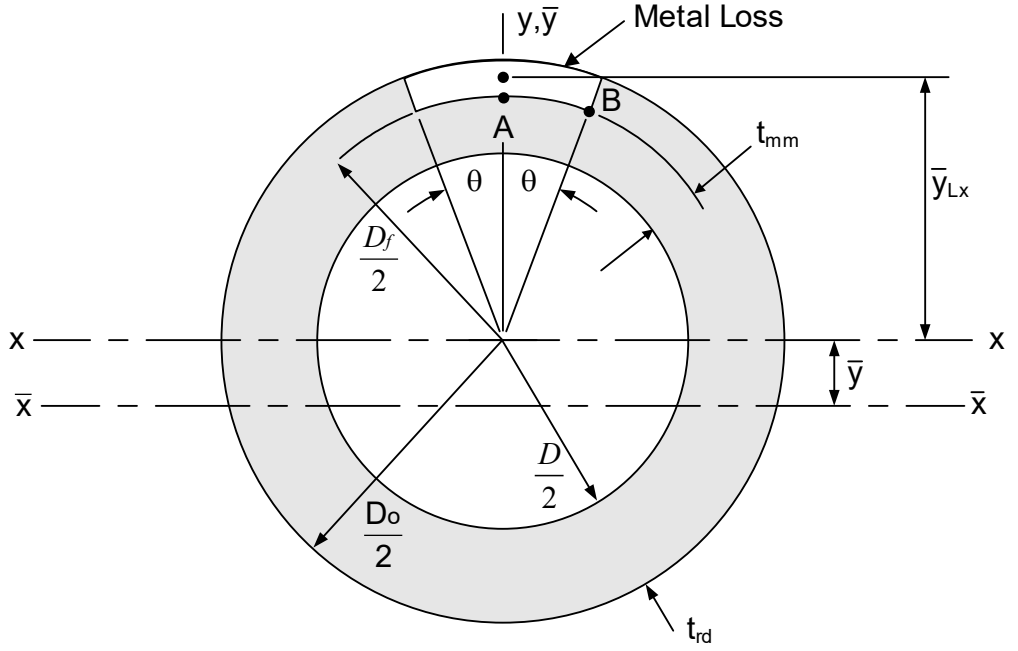

(b) Region Of Local Metal Loss Located on the Outside Surface

Figure 5.11 – Parameters for Determining Section Properties of a Cylinder with an LTA

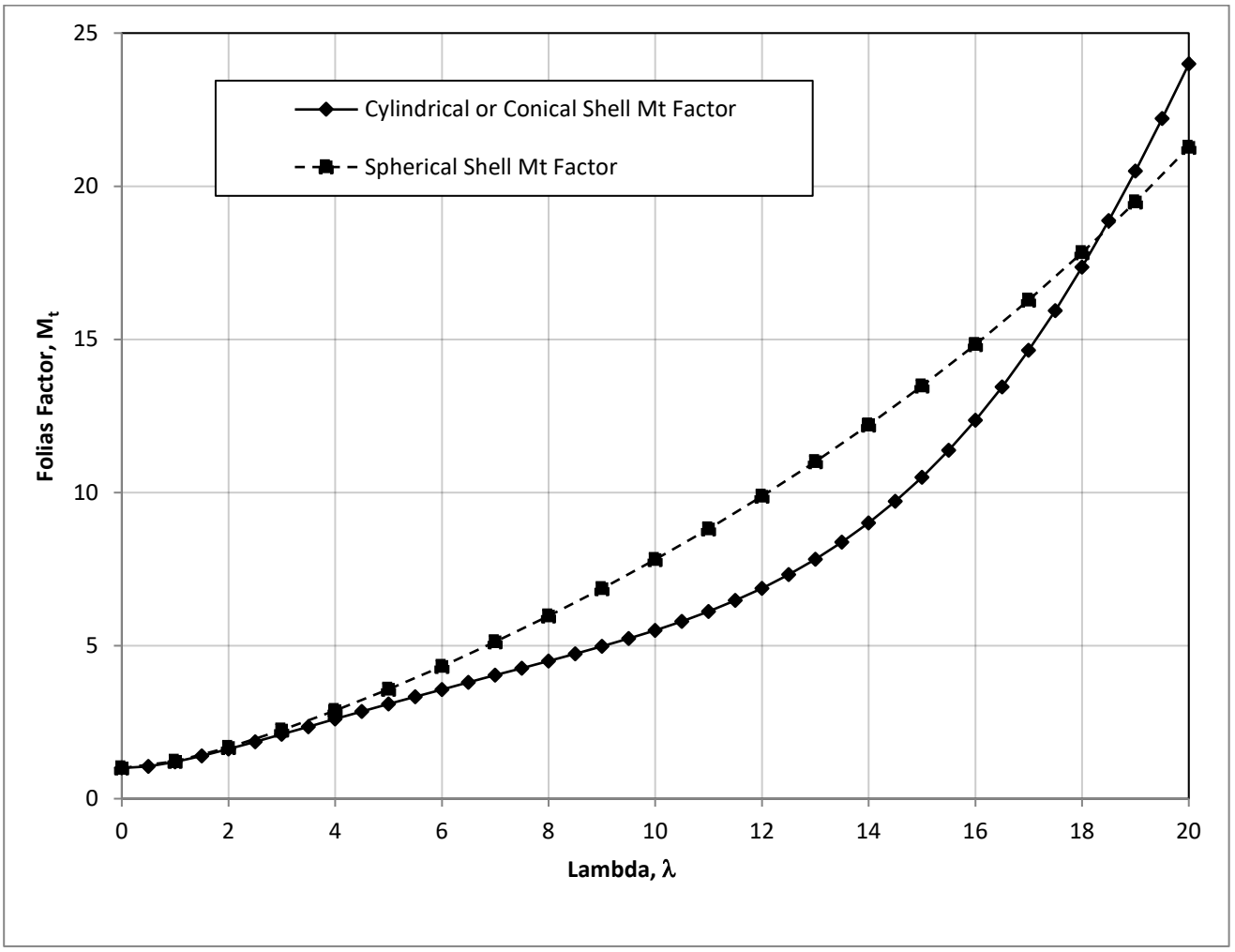

Figure 5.12 – M_t Parameter from Table 5.2

ANNEX 5A – TECHNICAL BASIS AND VALIDATION – ASSESSMENT OF LOCAL METAL LOSS

(INFORMATIVE)

CONTENTS

ANNEX 5A – TECHNICAL BASIS AND VALIDATION – ASSESSMENT OF LOCAL METAL LOSS 5A-1

5A.1 TECHNICAL BASIS AND VALIDATION 5A-1
5A.2 REFERENCES 5A-1

5A.1 Technical Basis and Validation

The technical basis and validation of the assessment procedures for general metal loss and local metal loss contained in Part 4 and Part 5 are provided in references [1] through [30]. A comparison is made between the assessment methods in this Standard and the assessment methods contained in other standards in references [9], [15], and [16]. A comparison of assessment methodologies for the pipeline industry (i.e., B31G, RSTRENG, DNV F-101) is provided in reference [6]. However, in the comparison of methods for the assessment of local thin areas, the methods in API 579-1/ASME FFS-1 were not considered in reference [6]. In order to provide a complete comparison of the methodologies currently being used for the assessment of local thin areas, the Materials Properties Council Joint Industry Project on Fitness-For-Service commissioned an additional study. The results of this comparison are provided in reference [9].

5A.2 References

[1] Bubenik, T.A., Olsen, R.J., Stephens, D.R. and Francini, R.B., “Analyzing the Pressure Strength of Corroded Line Pipe,” Offshore Mechanics and Arctic Engineering Symposium, OMAE Volume V-A, Pipeline Technology, American Society of Mechanical Engineers, pp. 225-231, 1992.

[2] Bubenik, T.A. and Rosenfeld, M.J., “Assessing the Strength of Corroded Elbows,” NG-18 Report No. 206, Pipeline Research Committee of the American Gas Association, 1993.

[3] Chouchaoui, B.A. and Pick, R.J., “A Three Level Assessment of the Residual Strength of Corroded Line Pipe,” Offshore Mechanics and Arctic Engineering Symposium, OMAE Volume V, Pipeline Technology, American Society of Mechanical Engineers, pp 9-18, 1994.

[4] Eiber, R.J., Maxey, W.A., Duffy, A.R. and Atterbury, T.J., “Investigation of the Initiation and Extent of Ductile Pipe Rupture,” BMI-1908, Battelle Columbus Laboratories, Ohio, 1971.

[5] Folias, E.S., “On the Effect of Initial Curvature on Cracked Flat Sheets,” International Journal of Fracture Mechanics, Vol. 5, No. 4, December 1969, pp. 327-346.

[6] Fu B., Stephens, D., Ritchie, D., and Jones, C.L., Methods for Assessing Corroded Pipeline – Review, Validation and Recommendations, Catalog No. L5878, Pipeline Research Council International, Inc. (PRCI), 2002.

[7] Hantz, B.F., Sims, J.R., Kenyon, C.T. and Turbak, T.A., “Fitness For Service: Groove Like Local Thin Areas on Pressure Vessels and Storage Tanks,” ASME PVP-Vol. 252, American Society of Mechanical Engineers, New York, 1992.

[8] Herter, K.H., Julisch, P., Stoppler, W. and Sturm, D., “Behavior of Pipes Under Internal Pressure and External Bending Moment – Comparison between Experiment and Calculation,” Fracture Mechanics Verification by Large-Scale Testing, EGF/E5158, Edited by K. Kussmaul, Mechanical Engineering Publications, London, 1991, pp. 223-241.

[9] Janelle, J.A. and Osage, D.A., An Overview and Validation of the Fitness-For-Service Assessment Procedures for Local Thin Areas in API 579, WRC Bulletin 505, Welding Research Council, Inc., New York, NY, September 2005.

[10] Kastner, W., Rehrich, E., Schmitt, W., and Steinbuch, R., “Critical Crack Sizes in Ductile Piping,” International Journal of Pressure Vessels & Piping, 9, 1981, pp. 197-219.

[11] Kiefner, J.F., Maxey, W.A., Eiber, R.J., and Duffy, A.R., “Failure Stress Levels of Flaws in Pressurized Cylinders,” ASTM STP 536, American Society for Testing and Materials, 1973, pp. 461-481.

[12] Kiefner, J.F. and Vieth, P.H., A Modified Criterion for Evaluating the Remaining Strength of Corroded Pipe, RPC International Catalog No. L51609, 1989.

[13] Leggatt, R.H., Hodgson, A.P., Hayes, B., and Chan, S.W.K., “Safety Factors in Flaw Assessment of Girth Welds,” For the American Gas Association, Contract No: PR 164 509, The Welding Institute, 1988.

[14] Maxey, W.A., Kiefner, J.F., Eiber, R.J., and Duffy, A.R., “Ductile Fracture Initiation, Propagation, and Arrest in Cylindrical Shells,” ASTM STP 514, American Society for Testing and Materials, 1972, pp. 70-81.

[15] Osage, D.A., Krishnaswamy, P., Stephens, D.R., Scott, P., Janelle, J., Mohan, R., and Wilkowski, G.M., Technologies for the Evaluation of Non-Crack-Like Flaws in Pressurized Components – Erosion/Corrosion, Pitting, Blisters, Shell Out-Of-Roundness, Weld Misalignment, Bulges and Dents, WRC Bulletin 465, Welding Research Council, Inc., New York, NY, September 2001.

[16] Osage, D.A., Janelle, J. and Henry, P.A., “Fitness-For-Service Local Metal Loss Assessment Rules in API 579,” PVP Vol. 411, Service Experience and Fitness-For-Service in Power and Petroleum Processing, ASME, 2000, pp. 143-176.

[17] Sims, J.R., Hantz, B.F., Kuehn, K.E., “A Basis for the Fitness For Service Evaluation of Thin Areas in Pressure Vessels and Storage Tanks,” ASME PVP-Vol 233, American Society of Mechanical Engineers, New York, 1992.

[18] Stephens, D.R., Bubenik, T.A., Francini, R.B., Residual Strength of Pipeline Corrosion Defects Under Combined Pressure and Axial Loads, NG-18 Report No. 216, Pipeline Research Committee of the American Gas Association, 1995.

[19] Stephens, D.R., Krishnaswamy, P., Mohan, R., Osage, D.A. and Wilkowski, G., “A Review of Analysis Methods and Acceptance Criteria for Local Thinned Areas in Piping and Piping Components,” 1997 Pressure Vessels and Piping Conference, Orlando, FL, July 1997.

[20] Strum, D., Stoppler, W. and Schiedermaier, “The Behavior of Dynamically Loaded Pipes with Circumferential Flaws Under Internal Pressure and External Bending Loads,” Nuclear Engineering and Design, 96, 1986, pp. 99-113.

[21] Rosenfeld, M.J., Vieth, P.H. and Haupt, R.W., “A Proposed Corrosion Assessment Method and In-Service Safety Factors for Process and Power Piping Facilities,” PVP-Vol. 353, ASME, pp. 395-405, 1997.

[22] Rosenfeld, M.J., Serviceability of Corroded Girth Welds, RPC International, Catalog No. L 51742, 1996.

[23] Turbak, T.A. and Sims, J.R., “Comparison of Local Thin Area Assessment Methodologies,” ASME PVP-Vol. 288, American Society of Mechanical Engineers, New York, 1994, pp. 307-314.

[24] Turbak, T.A. and Sims, J.R., “Fitness-For-Service Local Thin Areas Comparison of Finite Element Results to Physical Test Results,” ASME PVP-Vol. 315, American Society of Mechanical Engineers, New York, 1995, pp. 285-292.

[25] Vieth, V.H. and Kiefner, J.F., “RSTRENG2 User’s Manual, RPC International Catalog No. L51688, 1993.

[26] Vieth, V.H. and Kiefner, J.F., Database of Corroded Pipe Tests, RPC International Catalog No. L51689, 1993.

[27] Wang, K.C. and Smith, E.D., “The Effect of Mechanical Damage on Fracture Initiation in Linepipe Part II – Gouges,” Metals Technology Laboratories, Report MTL 88-16(TR), March 1988.

[28] Wilkowski, G.M. and Scott, P.M., “A Statistical Based Circumferentially Cracked Pipe Fracture Mechanics Analysis for Design or Code Implementation,” Nuclear Engineering and Design, 111, 1989, pp. 173-187.

[29] Willoughby, A.A., “A Survey of Plastic Collapse Solutions Used in the Failure Assessment of Part Wall Defects,” The Welding Institute, 1982.

[30] Brown, G.W., Parietti, L., Rose, B.D. and Anderson, T.L., “Evaluation of Groove Radius Assessment Criteria Based on Brittle and Ductile Local Failure Models.” Proceedings of the ASME 2016 Pressure Vessels and Piping Conference, Volume 1A: Codes and Standards. Vancouver, British Columbia, Canada. July 17-21, 2016. V01AT01A004. ASME. https://doi.org/10.1115/PVP2016-63756.

[Intentionally Left Blank]

PART 6 – ASSESSMENT OF PITTING CORROSION

CONTENTS

PART 6 – ASSESSMENT OF PITTING CORROSION 6-1

6.1 GENERAL 6-1
6.1.1 Assessment of Pitting Corrosion 6-1
6.1.2 Assessment of Blister Arrays 6-1
6.2 APPLICABILITY AND LIMITATIONS OF THE PROCEDURE 6-2
6.2.1 Assessment of Four Types of Pitting Corrosion 6-2
6.2.2 Calculation of the $MAWP_r$ and MFH_r and Coincident Temperature 6-2
6.2.3 Limitations Based on Flaw Type 6-2
6.2.4 Limitations Based on Temperature 6-2
6.2.5 Applicability of the Level 1 and Level 2 Assessment Procedures 6-2
6.2.6 Applicability of the Level 3 Assessment Procedures 6-3
6.2.7 Assessment for Active Pitting Corrosion 6-3
6.2.8 Future Corrosion Allowance 6-3
6.3 DATA REQUIREMENTS 6-4
6.3.1 Original Equipment Design Data 6-4
6.3.2 Maintenance and Operational History 6-4
6.3.3 Required Data/Measurements for an FFS Assessment 6-4
6.3.4 Recommendation for Inspection Technique and Sizing Requirements 6-5
6.4 ASSESSMENT TECHNIQUES AND ACCEPTANCE CRITERIA 6-6
6.4.1 Overview 6-6
6.4.2 Level 1 Assessment 6-6
6.4.3 Level 2 Assessment 6-8
6.4.4 Level 3 Assessment 6-13
6.5 REMAINING LIFE ASSESSMENT 6-14
6.5.1 MAWP Approach 6-14
6.5.2 MAWP Procedure for Remaining Life Determination 6-14
6.6 REMEDIATION 6-15
6.7 IN-SERVICE MONITORING 6-15
6.8 DOCUMENTATION 6-15
6.8.1 General 6-15
6.8.2 Inspection Data 6-15
6.9 NOMENCLATURE 6-15
6.10 REFERENCES 6-18
6.11 TABLES 6-19
6.12 FIGURES 6-21

6.1 General

6.1.1 Assessment of Pitting Corrosion

The assessment procedures in this Part can be utilized to evaluate metal loss from pitting corrosion. Pitting is defined as localized regions of metal loss that can be characterized by a pit diameter on the order of the plate thickness or less, and a pit depth that is less than the plate thickness. Assessment procedures are provided to evaluate both widespread and localized pitting in a component with or without a region of local metal loss. A flowchart for the evaluation procedure of equipment with pitting is shown in Figure 6.1.

6.1.2 Assessment of Blister Arrays

The procedures in this Part can be used to assess an array of blisters as described in Part 7.

6.2 Applicability and Limitations of the Procedure

6.2.1 Assessment of Four Types of Pitting Corrosion

The assessment procedures in this Part can be used to evaluate four types of pitting: widely scattered pitting that occurs over a significant region of the component, a Local Thin Area (LTA) located in a region of widely scattered pitting, localized regions of pitting, and pitting confined within a region of an LTA. A flowchart that provides details of the assessment procedures required is shown in Figure 6.2. Depending on the type of pitting corrosion, either assessment methods in Part 6 or a combination of assessment methods in Parts 5 and 6 are used in the evaluation.

6.2.2 Calculation of the $MAWP_r$ and MFH_r and Coincident Temperature

Calculation methods are provided to rerate the component if the acceptance criteria in this Part are not satisfied. The calculation methods can be used to define a reduced Maximum Allowable Working Pressure, $MAWP_r$, and/or temperature for pressurized components, i.e., pressure vessels and piping. For tank shell courses, the calculation methods can be used to determine a reduced Maximum Fill Height, MFH_r.

6.2.3 Limitations Based on Flaw Type

Unless otherwise specified, this Part is limited to the evaluation of pitting corrosion. Other flaw types shall be evaluated in accordance with Part 2, Table 2.1.

6.2.4 Limitations Based on Temperature

The assessment procedures in this Part shall only apply to components that are not operating in the creep range, i.e., when the design temperature is less or equal to the value in Part 4, Table 4.1. The Materials Engineer should be consulted regarding the creep range temperature limit for materials not listed in Part 4, Table 4.1.

6.2.5 Applicability of the Level 1 and Level 2 Assessment Procedures

6.2.5.1 The Level 1 and 2 Assessment procedures in this Part shall apply only if all the following conditions are satisfied.

a) The original design criteria were in accordance with a recognized code or standard (see Part 1, paragraphs 1.2.2 or 1.2.3).

b) The material is considered to have sufficient material toughness. If there is uncertainty regarding the material toughness, then a Part 3 assessment should be performed. If the component is subject to embrittlement during operation due to temperature and/or the process environment, a Level 3 Assessment should be performed. Temperature and/or process conditions that result in material embrittlement are discussed in Annex 2B.

c) The component is not in cyclic service. If the component is subject to less than 150 cycles, i.e., pressure and/or temperature variations including operational changes and start-ups and shut-downs, throughout its previous operating history and future planned operation, or satisfies the cyclic service screening procedure in Part 14, then the component is not in cyclic service.

d) The following limitations on component types and applied loads are satisfied:

   1) Level 1 Assessment – Type A Components (see Part 4, paragraph 4.2.5) subject to internal pressure.

   2) Level 2 Assessment – Type A Components and Type B Class 1 components (see Part 4, paragraph 4.2.5, subject to internal pressure and supplemental loads (see Annex 2B).

e) The pitting corrosion is located on only one surface of the component, i.e., inside or outside diameter.

f) The pitting corrosion is composed of many pits; individual pits or isolated pairs of pits should be evaluated as LTA s using the assessment procedures in Part 5.

g) For a Level 1 Assessment, the pitting corrosion is arrested.

h) The Level 1 and Level 2 Assessment procedures include a limitation on the minimum measured thickness, t_{mm}. The limitation on t_{mm} is to guard against potential inadequacy in inspection method capabilities to accurately characterize excessively thinned areas. If the limitation on t_{mm} is not satisfied, a Level 3 Assessment may be performed. Future inspection frequency shall be established based on a detailed investigation of all applicable damage mechanisms and inspection results shall be appropriately validated (see Part 4, paragraph 4.3.4.6).

6.2.5.2 A Level 2 Assessment shall be performed if:

a) An appropriate pit comparison chart cannot be found (see paragraph 6.3.3.1).

b) A more detailed assessment of widespread pitting, e.g., inclusion of the pit-couple orientation is required.

c) The pitting corrosion is not arrested.

d) The pitting corrosion is characterized as an LTA located in a region of widely scattered pitting or pitting that is confined within an LTA.

6.2.6 Applicability of the Level 3 Assessment Procedures

A Level 3 Assessment may be performed where Level 1 and Level 2 Assessment procedures do not apply, or when these assessment procedures produce conservative results, i.e., would not permit operation at the $MAWP$. Examples include, but are not limited to the following:

a) When the component geometry and loading conditions are as described in Part 5, paragraph 5.2.6.

b) When the pitting corrosion is in a component with a non-uniform through-wall stress distribution, e.g., bending stress.

c) When the pitting corrosion is located on both surfaces of the component (see Figure 6.3).

6.2.7 Assessment for Active Pitting Corrosion

In Level 2 and 3 Assessments, pitting corrosion shall be assessed at a specific future inspection date, with the available pitting data at the current inspection date. The user shall determine the acceptability of the pitting corrosion at the future inspection date by performing a series of assessments for various pitting progression rates to simulate the change in the pit depths, diameters, spacing or density at the specific time interval (see paragraphs 6.3.3.4 and 6.5).

6.2.8 Future Corrosion Allowance

The Future Corrosion Allowance (FCA) shall be based on the projected future metal loss in the pitting region. The FCA is not applied to the depth or diameter of the pits (see Figure 6.4). The FCA is used to determine the value of t_c.

6.3 Data Requirements

6.3.1 Original Equipment Design Data

An overview of the original equipment data required for an assessment is provided in Part 2, paragraph 2.3.1.

6.3.2 Maintenance and Operational History

An overview of the maintenance and operational history required for an assessment is provided in Part 2, paragraph 2.3.2.

6.3.3 Required Data/Measurements for an FFS Assessment

6.3.3.1 In a Level 1 Assessment, a measure of the surface damage in terms of pitted area and the maximum pit depth are used to quantify the extent of pitting corrosion. The depth of a pit should be carefully measured because of the variety of pit types that can occur in service (see Figure 6.5). The measure of surface area damage is determined using standard pit charts by comparing the actual damage on the component to the damage represented on the pit chart (see Figures 6.6 through 6.13). A pit chart is found by comparing the surface damage (black areas) to the surface damage on the actual component. This chart along with an estimate of the corresponding maximum pit depth is used to directly determine acceptability. Therefore, the data required for an assessment should include a photograph (with a reference scale) and/or rubbing of the surface of the damaged component with an estimate of the maximum pit depth. A cross-sectional UT thickness scan can also be performed to determine the pitting profile. Guidelines for determining the maximum pit depth are included in paragraph 6.3.4.1.

6.3.3.2 In a Level 2 Assessment, the measure of damage used to evaluate pitting is the pit-couple. A pit-couple is composed of two pits separated by a solid ligament (see Figure 6.14). The metal loss of each pit in a pit-couple is modeled as an equivalent cylinder. To define a pit-couple, the diameter and depth of each pit, and the distance between the pit centers are required. The orientation of the pit-couple in the biaxial stress field may also be included in the assessment (see Figure 6.14). The depth and diameter of a pit should be carefully measured because of the variety of pit types that can occur in service (see Figure 6.5). If the pit has an irregular shape, a diameter and depth that encompasses the entire shape should be used in the assessment.

a) The occurrence of pits and their relative size in a region of a component are typically random. User judgment is required to select a population of pits that adequately represents the damage in the component.

b) To evaluate a region with pitting, a representative number of pit-couples in the damaged area should be used. If the pitting is uniform, a minimum sample size of ten pit-couples is recommended. If the pitting is non-uniform, additional pit-couple data should be taken.

c) The following procedure should be followed to select the pit-couples for an assessment.

   1) STEP 1 – Select a minimum of ten pits covering a broad area that are representative of the pitting corrosion. The pits selected should be unique, if possible, based on the number of pits present.

   2) STEP 2 – Select the nearest pits to each of the selected pits in STEP 1. For example, as shown in Figure 6.14, Pit 1 is nearest and assessed against Pits 2, 4, 5, 6, 7 and 8.

   3) STEP 3 – Compute the average RSF for all pit couples per paragraph 6.4.

d) The orientation of the pit-couple in a biaxial stress field is used only in a Level 2 Assessment. These data typically do not improve the assessment results unless the pitting corrosion is preferential (e.g., the pitting corrosion is concentrated along a longitudinal, circumferential, or spiral weld seam). Therefore, the extra

effort associated with obtaining this information should be balanced with the potential increase in remaining strength it could demonstrate.

e) To determine the effects that additional pit-couples would have on the assessment results, additional independent pit-couples can be included in the sample size, and the assessment can be repeated. This procedure will provide a measure of the sensitivity of the data about assessment results (see Part 2, paragraph 2.4.3.1). Alternatively, distributions can be developed for the parameters that define a pit-couple, i.e., diameter and depth of each pit, and the distance between the pit centers, and a probabilistic analysis (see Part 2, paragraph 2.4.3.2) may be performed using the assessment procedure in paragraph 6.4.3.

f) An overview of the required information for a Level 2 Assessment is defined below.

1) The specific information required for a Level 2 Assessment is given in paragraph 6.4.3.2. The form shown in Table 6.1 can be used to record this information.

2) The parameters s and c using the CTP procedure described in Part 5 and shown in Figure 6.15 shall be determined if the pitting corrosion is localized or confined to a localized region of metal loss (see Figure 6.16).

6.3.3.3 The information required to perform a Level 3 Assessment depends on the analysis method utilized. In general, a limit load procedure using a numerical technique can be used to establish the acceptable operating or design conditions as appropriate. A description of the pitting, like that required for a Level 2 Assessment, should be obtained along with the material yield strength and stress-strain curve.

6.3.3.4 The future Pitting Progression Rate (PPR) should be estimated. This is not a straightforward procedure because pits can increase in size (depth and diameter), increase in density, and a region of local pitting may increase in size. All pit dimensions used in the assessments in this Part should be based on the best estimate of future size. The determination of a remaining life for a component with pitting corrosion is discussed in paragraph 6.5.

6.3.4 Recommendation for Inspection Technique and Sizing Requirements

6.3.4.1 Precise measurement of pitting is difficult. Care should be taken to ensure that the correct dimensions are measured because pits often have irregular shapes as shown in Figure 6.5 or are filled with scale. Pit gauges are used to measure pit depth and rulers or calipers to measure pit diameter and the distance between pits. Ultrasonic methods can also be used to measure the wall thickness of pits with large diameters and the average plate thickness in non-pitted areas adjacent to the pitting.

6.3.4.2 It is difficult to detect small diameter pits or to measure the depth of pits using ultrasonic methods. Radiography may also be used to characterize the damage in pitted regions.

6.3.4.3 If the surface is scaled, dirty or has a damaged coating, cleaning (e.g., sandblasting) may be required to obtain accurate pit measurements.

6.3.4.4 Inspection techniques that characterize pitting corrosion from the opposite surface should only be used when they have sufficient resolution and coverage to ensure that significant damage cannot be overlooked.

6.3.4.5 For components susceptible to brittle fracture (see Part 3, paragraph 3.2.2), supplemental inspection in accordance with paragraph 5.3.4.3 of Part 5 is required to confirm no crack-like flaws exist.

6.4 Assessment Techniques and Acceptance Criteria

6.4.1 Overview

6.4.1.1 If the depth of all the pits is less than the specified corrosion/erosion allowance and adequate thickness is available for future pitting corrosion (see paragraph 6.5.1), no further action is required other than to record the data; otherwise, an assessment is required. The procedures in this Part can be used to determine the acceptability of a component for continued operation to a future date when an estimate on the pitting progression rate can be determined (see paragraph 6.3.3.4).

6.4.1.2 An overview of the assessment levels is provided in Figure 6.1.

a) Level 1 Assessments are limited to Type A components with one-sided, widespread pitting corrosion that are designed to a recognized code or standard. The only load considered is internal pressure.

b) The Level 2 Assessment procedures are used to evaluate all four categories of pitting: widespread pitting, localized pitting, pitting within a locally thin area, and a locally thin area in a region of widespread pitting. The Level 2 Assessment rules provide a better estimate of the structural integrity of a component than the Level 1 Assessment rules because a measure of the actual damage parameter, the pit-couple, is directly used in the assessment.

c) The Level 3 Assessment procedures are intended to evaluate more complex regions of pitting, loading conditions, and/or components with details where only limited design rules are provided in the original construction code or standard. Detailed stress analysis techniques should be utilized in a Level 3 Assessment. A Level 3 Assessment should be used when the pitting corrosion occurs on both sides of the component.

6.4.2 Level 1 Assessment

6.4.2.1 The Level 1 Assessment technique utilizes standard pit charts and the maximum pit depth in the area being evaluated to estimate a Remaining Strength Factor, RSF. The surface damage of the pitted region is characterized by making a visual comparison between the actual damage and a standard pit chart. Based on the pit chart that best approximates the present damage, the remaining strength factor can be determined using the measured maximum pit depth.

6.4.2.2 The following assessment procedure can be used to evaluate Type A components subject to internal pressure that meet the conditions stipulated in paragraph 6.2.5.1 that are applicable to a Level 1 Assessment. For an atmospheric storage tank, the same procedure can be followed to determine a MFH by replacing the $MAWP$ with the MFH, and determining the MFH using the applicable code equations for a tank shell.

a) STEP 1 – Determine the following parameters: D, FCA, either t_{rd} or t_{nom} and $LOSS$.

b) STEP 2 – Determine the wall thickness to be used in the assessment using Equation (6.1) or Equation (6.2), as applicable.

$$t_c = t_{nom} - LOSS - FCA \tag{6.1}$$

$$t_c = t_{rd} - FCA \tag{6.2}$$

c) STEP 3 – Locate the area on the component that has the highest density of pitting corrosion based on the number of pits. Obtain photographs (include a reference scale) or rubbings of this area to record the amount of surface damage.

d) STEP 4 – Determine the maximum pit depth, w_{max}, and the minimum measured thickness for the pit with the maximum depth, t_{mm}, in the region of pitting corrosion being evaluated (see Figure 6.5).

$$t_{mm} = t_{rd} - w_{\max} \tag{6.3}$$

e) STEP 5 – Determine the ratio of the remaining wall thickness to the future wall thickness in the pitted region using the following equations. If the t_{mm} criterion is satisfied and $R_{wt} \geq 0.2$, proceed to STEP 6. Otherwise, the Level 1 Assessment criterion is not satisfied. The limit on t_{mm} and R_{wt} is intended to prevent a local failure characterized by pinhole type leakage.

1) Pitting and corrosion damage are acting on the same side and the pit depth is greater than the FCA:

$$t_{mm} \geq 2.5\ mm\ (0.10\ inches) \qquad (for\ vessels\ \&\ tanks) \tag{6.4}$$

$$t_{mm} \geq 1.3\ mm\ (0.05\ inches) \qquad (for\ piping) \tag{6.5}$$

$$R_{wt} = \frac{t_{mm}}{t_c} \tag{6.6}$$

2) Pitting and corrosion damage are acting on opposite sides:

$$t_{mm} - FCA \geq 2.5\ mm\ (0.10\ inches) \qquad (for\ vessels\ \&\ tanks) \tag{6.7}$$

$$t_{mm} - FCA \geq 1.3\ mm\ (0.05\ inches) \qquad (for\ piping) \tag{6.8}$$

$$R_{wt} = \frac{t_{mm} - FCA}{t_c} \tag{6.9}$$

f) STEP 6 – If Equation (6.10) is not satisfied for an individual pit, then the pit should be evaluated as a local thin area using the Level 2 Assessment procedure in paragraph 6.4.3.4. The value of Q in Equation (6.10) shall be determined using Part 4, Table 4.8 and is a function of the remaining thickness ratio, R_{wt}, defined in STEP 5 substituting $w_{i,k}$ for w_{max} into Equation (6.3).

$$d \leq Q\sqrt{D \cdot t_c} \tag{6.10}$$

g) STEP 7 – Determine the $MAWP$ for the component (see Annex 2C) using the thickness from STEP 2.

h) STEP 8 – Compare the surface damage from the photographs or rubbings to the standard pit charts shown in Figures 6.6 through 6.13. Select a pit chart that has a measure of surface damage that approximates the actual damage on the component. If the pitting corrosion is more extensive than that shown in Figure 6.13, then compute the RSF using the following equation and proceed to STEP 10.

$$RSF = R_{wt} \tag{6.11}$$

i) STEP 9 – Determine the RSF from the table shown at the bottom of the pit chart that was chosen in STEP 8 using the value of R_{wt} calculated in STEP 5. Interpolation of the RSF is acceptable for intermediate values of R_{wt}.

j) STEP 10 – If $RSF \geq RSF_a$, then the pitting corrosion is acceptable for operation at the $MAWP$ determined in STEP 7. If $RSF < RSF_a$, then the region of pitting corrosion is acceptable for operation at $MAWP_r$, where $MAWP_r$, is computed using the equations in Part 2, paragraph 2.4.2.2. The $MAWP$ from STEP 7 shall be used in this calculation.

6.4.2.3 If the component does not meet the Level 1 Assessment requirements, then the following, or combinations thereof, can be considered:

a) Rerate, repair, or replace the component.

b) Adjust the FCA by applying remediation techniques (see Part 4, paragraph 4.6).

c) Conduct a Level 2 or Level 3 Assessment.

6.4.3 Level 2 Assessment

6.4.3.1 The assessment procedure in paragraphs 6.4.3.2, 6.4.3.3 and 6.4.3.4 are used to determine the acceptability for the circumferential stress direction. The assessment procedure in paragraph 6.4.3.5 is used to determine the acceptability for the longitudinal stress direction. A Level 2 Assessment provides a better estimate of the RSF than a Level 1 Assessment for pitting corrosion in a component subject to internal pressure loading and supplemental loading for cylindrical and conical shells. This procedure accounts for the orientation of the pit-couple with respect to the maximum stress direction. Guidance for conducting an assessment for the four categories of pitting described in paragraph 6.2.1 is shown in Figure 6.2. The procedure in this Part or the pitting charts in Level 1 can be used to determine the acceptability of a component at a future date when an estimate on the pitting progression rate can be determined (see paragraph 6.3.3.4).

6.4.3.2 The following assessment procedure can be used to evaluate components with widespread or localized pitting when conditions described in paragraph 6.2.5.1 are met. If the flaw is found to be unacceptable in the circumferential stress direction, the procedure can be used to establish a reduced $MAWP$. For an atmospheric storage tank, the same procedure can be followed to determine a MFH by replacing the $MAWP$ with the MFH, and determining the MFH using the applicable code equations for a tank shell.

d) STEP 1 – Determine the following parameters: D, FCA, either t_{rd} or t_{nom} and $LOSS$.

e) STEP 2 – Determine the wall thickness to be used in the assessment using Equation (6.1) or Equation (6.2), as applicable.

f) STEP 3 – Determine the pit-couple sample for the assessment (see paragraph 6.3.3.2) and the following parameters for each pit-couple, k, $d_{i,k}$, $d_{j,k}$, P_k, $w_{i,k}$ and $w_{j,k}$. In addition, determine the orientation of the pit-couple measured from the direction of the σ_2 stress component, θ_k (see Figure 6.14); for a conservative analysis set $\theta_k = 0.0$ degrees.

g) STEP 4 – Determine the minimum measured thickness for each pit (see paragraph 6.4.2.2, STEP 4).

h) STEP 5 – Determine the ratio of the remaining wall thickness to the future wall thickness for each pit (see paragraph 6.4.2.2, STEP 5). If the t_{mm} criterion is satisfied and $R_{wt} \geq 0.2$, proceed to STEP 6. Otherwise, the Level 2 assessment criterion is not satisfied.

i) STEP 6 – Check the pit diameter limitation using paragraph 6.4.2.2, STEP 6.

j) STEP 7 – Compute the average R_{wt} ratio for each pit-couple. In Equation (6.12), the subscript k represents a calculation for pit-couple k.

$$R_{wt,avg,k} = \frac{\left(R_{wt,i,k} + R_{wt,j,k}\right)}{2} \tag{6.12}$$

k) STEP 8 – Calculate the components of the membrane stress field, σ_1 and σ_2 (see Figure 6.14). Membrane stress equations for shell components are included in Annex 2C.

l) STEP 9 – Determine the $MAWP$ for the component (see Annex 2C) using the thickness from STEP 2.

m) STEP 10 – For pit-couple k, compute the Remaining Strength Factor using Equation (6.13) where $R_{wt,avg,k}$ is from STEP 7.

$$RSF_k = 1-\left(1-R_{wt,avg,k}\right)\cdot\left(1-E_{avg,k}\right) \tag{6.13}$$

$$E_{avg,k} = \min\left[\frac{\Phi_k}{\sqrt{\Psi_k}},\ 1.0\right] \tag{6.14}$$

$$\Phi_k = \mu_{avg,k}\cdot\max\left[\left|\rho_{1,k}\right|,\ \left|\rho_{2,k}\right|,\ \left|\rho_{1,k}-\rho_{2,k}\right|\right] \tag{6.15}$$

$$\Psi_k = \left(\begin{array}{l}\left(\cos^4\left[\theta_k\right]+\sin^2\left[2\theta_k\right]\right)\left(\rho_{1,k}\right)^2 - \dfrac{3\left(\sin^2\left[2\theta_k\right]\right)\rho_{1,k}\cdot\rho_{2,k}}{2} + \\ \left(\sin^4\left[\theta_k\right]+\sin^2\left[2\theta_k\right]\right)\left(\rho_{2,k}\right)^2\end{array}\right) \tag{6.16}$$

$$\rho_{1,k} = \frac{\sigma_1}{\mu_{avg,k}} \tag{6.17}$$

$$\rho_{2,k} = \frac{\sigma_2}{\mu_{avg,k}} \tag{6.18}$$

$$\mu_{avg,k} = \frac{P_k - d_{avg,k}}{P_k} \tag{6.19}$$

$$d_{avg,k} = \frac{d_{i,k}+d_{j,k}}{2} \tag{6.20}$$

n) STEP 11 – Repeat STEP 10 for all pit-couples, n, recorded at the time of the inspection. Determine the average value of the Remaining Strength Factors, RSF_k, found in STEP 10 and designate this value as RSF_{pit} for the region of pitting.

$$RSF_{pit} = \frac{1}{n}\cdot\sum_{k=1}^{n} RSF_k \tag{6.21}$$

o) STEP 12 – Evaluate results based on the type of pitting corrosion (see Figure 6.2):

1) Widespread Pitting – For widespread pitting that occurs over a significant region of the component, if $RSF_{pit} \geq RSF_a$, then the pitting corrosion is acceptable for operation at the $MAWP$ determined in STEP 9. If $RSF_{pit} < RSF_a$, then the region of pitting corrosion is acceptable for operation at $MAWP_r$, where $MAWP_r$ is computed using the equations in Part 2, paragraph 2.4.2.2. The $MAWP$ from STEP 9 shall be used in this calculation.

2) Localized Pitting – If the pitting corrosion is localized, then the damaged area is evaluated as an equivalent region of localized metal loss (see Part 5 and Figure 6.15). The meridional and circumferential dimensions of the equivalent LTA for this evaluation should be based on the physical bounds of the observed pitting. The equivalent thickness, t_{eq}, for the LTA can be established using the following equation. To complete the analysis, the LTA is then evaluated using the Level 1 or Level 2 Assessment

procedures in Part 5 with $t_{mm} = t_{eq}$, where t_{eq} is given as follows. Note that in this calculation, t_{mm} is not adjusted for FCA when using the Part 5 procedure.

$$t_{eq} = RSF_{pit} \cdot t_c \tag{6.22}$$

6.4.3.3 *Pitting Confined Within a Region of Localized Metal Loss* – If the pitting corrosion is confined within a region of localized metal loss (see Figure 6.16), then the results can be evaluated using the following methodology. This procedure assumes that the pitting depths and LTA will corrode an equivalent amount given by FCA.

a) STEP 1 – Determine parameters per paragraph 6.4.3.2, STEP 1.

b) STEP 2 – Determine t_c per paragraph 6.4.3.2, STEP 2.

c) STEP 3 – Determine the $MAWP$ for the component (see Annex 2C) using the thickness from STEP 2.

d) STEP 4 – Determine the CTP for the LTA per Part 4, paragraph 4.3.3.3.

e) STEP 5 – Using the CTP and the extent of the LTA, determine the RSF_{LTA} using procedures in Part 5.

f) STEP 6 – Determine the equivalent thickness for the pitting assessment using Equation (6.23).

$$t_{eq} = RSF_{LTA} \cdot t_{rd} \tag{6.23}$$

g) STEP 7 – For the pits within the LTA, determine the pit couple data per paragraph 6.4.3.2, STEP 3. Pit depths shall be measured from the equivalent thickness, t_{eq}, calculated in STEP 6.

h) STEP 8 – Determine the depth of each pit below the equivalent thickness, t_{eq}, for all pit couples $w_{i,k}$ and $w_{j,k}$. Determine the average R_{wt} ratio per Equation (6.12).

i) STEP 9 – Determine the maximum pit depth, w_{max}, and the minimum measured thickness for the pit with the maximum depth, t_{mm}, in the region of pitting corrosion being evaluated (see paragraph 6.4.2.2, STEP 4).

j) STEP 10 – Determine the ratio of the remaining wall thickness to the future wall thickness (see paragraph 6.4.2.2, STEP 5). If the t_{mm} criterion is satisfied and $R_{wt} \geq 0.2$, proceed to STEP 11. Otherwise, the Level 2 Assessment criterion is not satisfied.

k) STEP 11 – Check the pit diameter limitation using paragraph 6.4.2.2, STEP 6.

l) STEP 12 – Determine RSF_{pit} using the pit couple data and the procedures in paragraph 6.4.3.2, STEPs 7 through 11.

m) STEP 13 – Determine RSF_{comb} from Equation (6.24).

$$RSF_{comb} = RSF_{pit} \cdot RSF_{LTA} \tag{6.24}$$

n) STEP 14 – If $RSF_{comb} \geq RSF_a$, then the pitting corrosion is acceptable for operation at the $MAWP$ determined in STEP 3. If $RSF_{comb} < RSF_a$, then the region of pitting corrosion is acceptable for operation at $MAWP_r$ where $MAWP_r$ is computed using the equations in Part 2, paragraph 2.4.2.2. The $MAWP$ from STEP 3 shall be used in this calculation.

6.4.3.4 *Region of Local Metal Loss Located in An Area of Widespread Pitting* – If a region of local metal loss (LTA) is in an area of widespread pitting, then a combined Remaining Strength Factor can be determined using Equation (6.24) and the following procedure. This procedure assumes that the pitting depths and LTA will corrode an equivalent amount given by FCA.

a) STEP 1 – Determine parameters per paragraph 6.4.3.2, STEP 1.

b) STEP 2 – Determine t_c per paragraph 6.4.3.2, STEP 2.

c) STEP 3 – Determine the $MAWP$ for the component (see Annex 2C) using the thickness from STEP 2.

d) STEP 4 – For the pitting, determine the pit couple data per paragraph 6.4.3.2, STEP 3. Determine the depth of each pit below t_{rd} for all pit couples $w_{i,k}$ and $w_{j,k}$. Determine the average R_{wt} ratio using Equation (6.12).

e) STEP 5 – Determine the maximum pit depth, w_{max}, and the minimum measured thickness for the pit with the maximum depth, t_{mm}, in the region of pitting corrosion being evaluated (see paragraph 6.4.2.2, STEP 4).

f) STEP 6 – Determine the ratio of the remaining wall thickness to the future wall thickness (see paragraph 6.4.2.2, STEP 5). If the t_{mm} criterion is satisfied and $R_{wt} \geq 0.2$, proceed to STEP 7. Otherwise, the Level 2 assessment criterion is not satisfied.

g) STEP 7 – Check the pit diameter limitation using paragraph 6.4.2.2, STEP 6.

h) STEP 8 – Determine RSF_{pit} using the pit couple data and the procedures in paragraph 6.4.3.2, STEPs 7 through 11.

i) STEP 9 – Determine the CTP for the LTA per Part 4, paragraph 4.3.3.3.

j) STEP 10 – Using the CTP and the extent of the LTA, determine the RSF_{LTA} using procedures in Part 5.

k) STEP 11 – Determine RSF_{comb} from Equation (6.24).

l) STEP 12 – If $RSF_{comb} \geq RSF_a$, then the pitting corrosion is acceptable for operation at the $MAWP$ determined in STEP 3. If $RSF_{comb} < RSF_a$, then the region of pitting corrosion is acceptable for operation at $MAWP_r$, where $MAWP_r$ is computed using the equations in Part 2, paragraph 2.4.2.2. The $MAWP$ from STEP 3 shall be used in this calculation.

6.4.3.5 The assessment procedures in this paragraph should be used to determine the acceptability of the longitudinal stress direction in a cylindrical or conical shell or pipe with pitting corrosion subject to internal pressure and supplemental loads. The acceptability of the circumferential stress direction is evaluated using paragraph 6.4.3.2.

a) Supplemental Loads – These types of loads may result in a net section axial force, bending moment, torsion, and shear being applied to the cross-section containing the flaw (see Annex 2C, paragraph 2C.2.7). The supplemental loads included in the assessment should include loads that produce both load-controlled and strain-controlled effects. Therefore, the net-section axial force, bending moment, torsion, and shear should be computed for two load cases, weight, and weight plus thermal (see Part 5, paragraph 5.4.3.4(a)).

b) Special Requirements for Piping Systems – Requirements in Part 5, paragraph 5.4.3.4(b) are required because of the relationship between the component thickness, piping flexibility or stiffness, and resulting stress.

c) Assessment for Widespread Pitting – The following procedure should be used to evaluate the permissible membrane, bending and shear stresses resulting from pressure and supplemental loads.

1) STEP 1 – Determine the following parameters: D, D_o, FCA, either t_{rd} or t_{nom} and $LOSS$.

2) STEP 2 – Determine the wall thickness to be used in the assessment using Equation (6.1) or Equation (6.2), as applicable.

3) STEP 3 – Determine the remaining strength factor, RSF_{pit} from Equation (6.21), the allowable remaining strength factor, RSF_a, the reduced maximum allowable working pressure, $MAWP_r$, and supplemental loads on the circumferential plane. The remaining strength factor, allowable remaining strength factor, and the reduced maximum allowable working pressure for the region with pitting corrosion can be established using the procedures in paragraph 6.4.3.2. The supplemental loads are determined in accordance with paragraphs 6.4.3.5(a) and 6.4.3.5(b).

4) STEP 4 – Compute the equivalent thickness of the cylinder with pitting corrosion using Equation (6.22).

5) STEP 5 – For the supplemental loads determined in STEP 3, compute the components of the resultant bending moment and torsion. This should be done for the weight and the weight plus thermal load cases.

6) STEP 6 – Determine the pressure to be used in the supplemental load calculation, P_{sl}. This pressure is determined as the minimum value of $MAWP_r$ and the equipment design pressure, P_d.

$$P_{sl} = \min\left[MAWP_r,\ P_d\right] \tag{6.25}$$

7) STEP 7 – Compute the circumferential stress resulting from pressure for both the weight and weight plus thermal load cases.

$$\sigma_{cm} = \frac{P_{sl}}{RSF_{pit} \cdot \cos\left[\alpha\right]}\left(\frac{D}{D_o - D} + 0.6\right) \tag{6.26}$$

8) STEP 8 – Compute the maximum section longitudinal membrane stress and the shear stress for the weight and the weight plus thermal load cases. All credible load combinations should be considered in the calculation. The section properties required for the calculations are provided in Table 6.2.

$$\sigma_{lm} = \frac{1}{E_C \cdot \cos\left[\alpha\right]}\left[P_{sl} \cdot \left(\frac{A_a}{A_m}\right) + \frac{F}{A_m} \pm \frac{Ma}{I_{\bar{x}}}\right] \tag{6.27}$$

$$\tau = \frac{M_T}{2A_t t_{eq}} + \frac{V}{A_m} \tag{6.28}$$

9) STEP 9 – Compute the equivalent membrane stress for the weight and the weight plus thermal load cases.

$$\sigma_e = \left[\sigma_{cm}^2 - \sigma_{cm}\sigma_{lm} + \sigma_{lm}^2 + 3\tau^2\right]^{0.5} \tag{6.29}$$

10) STEP 10 – Evaluate the results as follows:

i) Equation (6.30) shall be satisfied for either a tensile or compressive longitudinal stress for the weight and weight plus thermal load cases.

$$\sigma_e \le H_f\left(\frac{S_a}{RSF_a}\right) \tag{6.30}$$

ii) If the maximum longitudinal stress computed in STEP 8 is compressive, then this stress should be less than or equal to the allowable compressive stress computed using the methodology in Annex 2C, paragraphs 2C.4 and 2C.5 or the allowable tensile stress, whichever is smaller. When using this methodology to establish an allowable compressive stress, an equivalent thickness

representative of the region of pitting corrosion in the compressive stress zone should be used in the calculations.

11) STEP 11 – If the equivalent stress criterion of STEP 10 is not satisfied, the $MAWP$ and/or supplemental loads determined in STEP 3 should be reduced, and the evaluation outlined in STEPs 1 through 10 should be repeated. Alternatively, a Level 3 Assessment can be performed.

d) Assessment For Localized Pitting – If the flaw is categorized as localized pitting, a LTA located in a region of widely scattered pitting, or pitting confined within a region of an LTA, the assessment procedure in Part 5, paragraph 5.4.3.2 can be used once an equivalent LTA has been derived using the procedures in paragraph 6.4.3.2, 6.4.3.3 or 6.4.3.4.

6.4.3.6 Type B Class 2 Components with pitting may be evaluated using the assessment procedure in Part 4, paragraph 4.4.3.3. For this analysis, the average measure thickness, t_{am}, calculated using the following equation shall be used.

$$t_{am} = RSF_{pit} \cdot t_{rd} \tag{6.31}$$

6.4.3.7 If the component does not meet the Level 2 Assessment requirements, then the following, or combinations thereof, can be considered:

a) Rerate, repair, or replace the component.

b) Adjust the FCA by applying remediation techniques, (see Part 4, paragraph 4.6).

c) Conduct a Level 3 Assessment.

6.4.4 Level 3 Assessment

6.4.4.1 The stress analysis techniques discussed in Annex 2D can be utilized to assess pitting corrosion in pressure vessels, piping, and tankage. The limit load techniques described in Annex 2D are typically recommended for this evaluation.

6.4.4.2 If a numerical computation (e.g., finite element method) is used to evaluate pitting, two alternatives for modeling the pits may be considered. In the first method, the pits can be modeled directly using three- dimensional continuum finite elements. This method may be impractical based upon the pit density. In the second method, the reduced stiffness of the plate with pits can be approximated by using effective elastic constants or by developing an equivalent thickness. Effective elastic constants for plates with holes with triangular and rectangular pitch patterns are provided in the ASME B&PV Code Section VIII, Division 1, Part UHX. Either of these methods will facilitate modeling of pitting corrosion using either shell or continuum finite elements; however, representative values of the effective elastic constants or equivalent thickness should be validated for use in the assessment. In addition, if a limit analysis is being performed, the validity of the effective elastic constants or equivalent thickness in the plastic regime should also be determined.

6.4.4.3 *Multiple Layer Analysis* – This analysis is used to account for pitting on both sides of the component (see Figure 6.3) when the pitting corrosion is not overlapping. In this analysis, $E_{avg,k}$ is calculated for each pit-couple using Equations (6.14) through (6.20). The value of $E_{avg,k}$ is then used along with the thickness of all layers that the pit-couple penetrates to calculate a value of RSF_k for the pit couple. The selection of the number of layers, N, is based on the depth of pits on both sides of the component. Each layer thickness, t_L, is determined by the depth of the deeper of the two pits in the pit-couple that establishes the layer. For layers where a pit-couple does not penetrate the layer, and the solid layer for all pit couples, $E_{avg,k}$ in Equation (6.22) equals 1.0. The

$MAWP$ used with this expression should be based on t_c. A procedure for overlapping pitting analysis has not been provided (see Figure 6.3(b)).

$$RSF_k = 1 - \sum_{L=1}^{N} \left(\frac{t_L}{t_c} \right) \cdot \left(1 - E_{avg,k} \right)_L \tag{6.32}$$

6.5 Remaining Life Assessment

6.5.1 MAWP Approach

6.5.1.1 The $MAWP$ approach (see Part 4, paragraph 4.5.2) provides a systematic way of determining the remaining life of a pressurized component with pitting. When estimating the remaining life of pitting corrosion, a Pit Propagation Rate should be determined based on the environmental and operating conditions.

6.5.1.2 Pits can grow in three different modes and suitable estimates for a propagation rate should be established for each mode. In addition to these individual modes, pitting corrosion can also grow from a combination of these modes.

a) Increase in Pit Size – an estimate as to how the pit characteristic diameter and depth will increase with time should be made. For a given pit-couple, as the pit diameter and/or depth increases, the RSF decreases.

b) Increase in Pit Density – in addition to existing pits continuing to grow, new pits can form, thus increases the pit density. This decreases the pit spacing distance and the RSF.

c) Increase in Pit Region Size – if the pitting is localized, future operation may result in an enlargement of the localized region. The enlargement of a local region with pits has similar effects as the enlargement of an LTA.

6.5.1.3 If an estimate of the propagation rates cannot be made, remediation methods may be used to minimize future pitting corrosion.

6.5.2 MAWP Procedure for Remaining Life Determination

The following procedure should be used to determine the remaining life of a component with pitting using the $MAWP$ approach.

a) STEP 1 – Determine the uniform metal loss, $LOSS$ in the region with pitting.

b) STEP 2 – Using the procedures described in Level 2, determine the $MAWP$ for a series of increasing time increments using a Pit Propagation Rate applied to the pit depth and diameter. Use a statistical analysis to predict the likely depth of the deepest pit that was not measured. The statistical value is then used as the pit depth in the formulas.

c) STEP 3 – The effective pit size and rate of change in the characteristic dimensions are determined as follows:

$$w_f = w_c + PPR_{pit-depth} \cdot time \tag{6.33}$$

$$d_f = d_c + PPR_{pit-diameter} \cdot time \tag{6.34}$$

d) STEP 4 – If remediation is not performed, an estimate of the future pit density should be made and included in the estimation of the $MAWP$ in STEP 2.

e) STEP 5 – If the pitted region is localized, an estimate of the future enlargement of this region should be made and included in the estimation of the $MAWP$ in STEP 2. If there is an interaction between pitting and an LTA, then this interaction shall also be considered in a $MAWP$ versus time calculation.

f) STEP 6 – Determine the remaining life from a plot of the $MAWP$ versus time. The time at which the curve intersects the design $MAWP$ for the component is defined as the remaining life of the component. The equipment $MAWP$ is taken as the smallest value of the $MAWP$ for the individual components.

6.5.2.1 This approach may also be applied to tankage; however, in this case, the liquid maximum fill height, MFH, is evaluated instead of the $MAWP$.

6.6 Remediation

The remediation methods for general corrosion provided in Part 4 are typically applicable to pit damage. It is very difficult to properly remediate active pitting because the environment in a pit can be different from the bulk fluid environment; therefore, chemical treatments may not be effective. Coatings may be ineffective because they depend on proper surface preparation which can be difficult when removing scale in pits. Therefore, replacement of component sections or welded strip linings may be the remediation method of choice.

6.7 In-Service Monitoring

The remaining life may be difficult to establish for some services where an estimate of the future metal loss and enlargement of the pitted region cannot be adequately characterized. In these circumstances, remediation alone or with in-service monitoring may be required to qualify the assumptions made to establish the remaining life. It is often difficult to monitor pitting progression non-intrusively with ultrasonic methods. Radiography may be an alternative.

6.8 Documentation

6.8.1 General

The documentation of the FFS assessment should include the information cited in Part 2, paragraph 2.8.

6.8.2 Inspection Data

Inspection data including readings and locations used to determine the pitting corrosion RSF should be recorded and included in the documentation. A sample data sheet is provided in Table 6.1 for this purpose.

6.9 Nomenclature

A_m cylinder metal cross-section.

A_a cylinder aperture cross-section.

A_t area used in the torsional shear stress calculation.

a distance from the centroidal axis to the point where the net-section bending stress is to be computed.

α cone half apex angle.

D inside diameter of the cylinder, cone (at the location of the flaw), sphere, or formed head corrected for $LOSS$ and FCA; for the center section of an elliptical head, an equivalent inside diameter of $K_c D_c$ is used where D_c inside diameter of the head straight flange and K_c is a factor defined in Annex 2C, paragraph 2C.3.5; for the center section of a torispherical head, two times the crown radius of the spherical section is used. The inside diameter D shall be corrected for $LOSS$ and FCA, as applicable.

D_f modified cylinder diameter to account for pitting corrosion.

D_o outside diameter of the cylinder, corrected for $LOSS$ and FCA, as applicable.

d_c current characteristic pit diameter.

d_f estimated future characteristic pit diameter.

$d_{i,k}$ diameter of pit i in pit-couple k.

$d_{j,k}$ diameter of pit j in pit-couple k.

$d_{avg,k}$ average diameter of pit-couple k.

E_C circumferential weld joint efficiency.

E_L longitudinal weld joint efficiency.

E_y modulus of elasticity at the assessment temperature.

F applied section axial force for the weight or weight plus thermal load case, as applicable.

FCA future corrosion allowance to account for uniform metal loss, or future corrosion allowance to account for uniform metal loss away from damage area. FCA is not applied to the depth of the individual pits.

H_f allowable stress factor depending on the load case being evaluated. $H_f = 1.0$ for the weight (i.e., sustained) load case, and $H_f = 1.5$ for the weight (i.e., sustained) plus thermal (i.e., displacement controlled) load case.

$LOSS$ amount of uniform metal loss at the time of inspection, or uniform metal loss away from the damage area at the time of the inspection.

LTA local thin area.

I_x cylindrical shell moment of inertia.

M applied section bending moment for the weight or weight plus thermal load case, as applicable.

$MAWP$ maximum allowable working pressure of the undamaged component.

$MAWP_r$ reduced maximum allowable working pressure of the damaged component.

MFH maximum fill height of the tank.

MFH_r reduced maximum fill height of the damaged tank.

M_T applied net-section torsion for the weight or weight plus thermal load case, as applicable.

n number of pits used in the assessment.

N number of layers in a multiple layer analysis.

P_k distance between pit centers in pit-couple k.

$PPR_{pit-depth}$ estimated rate of change of pit characteristic depth.

$PPR_{pit-diameter}$ estimated rate of change of the pit characteristic diameter.

Q factor used to determine the length for thickness averaging based on an allowable Remaining Strength Factor (see Part 2) and the remaining thickness ratio (R_t) (see Part 4, Table 4.8).

$R_{wt,avg,k}$ average remaining wall thickness ratio for the k^{th} pit couple.

RSF Remaining Strength Factor.

RSF_a allowable Remaining Strength Factor.

RSF_{comb} combined Remaining Strength Factor that includes the effects of pitting corrosion and a local thin area.

RSF_k Remaining Strength Factor for pit-couple k.

RSF_{lta} Remaining Strength Factor for a local thin area computed using the methods provided in Part 5 (note that individual pits should be ignored in this calculation).

RSF_{pit} Remaining Strength Factor for pitting corrosion.

S_a allowable stress determined based on the component's original construction code at the design temperature.

σ_{cm} maximum circumferential stress, typically the hoop stress from pressure loading for the weight and weight plus thermal load case, as applicable.

σ_e equivalent membrane stress.

σ_{lm} maximum section longitudinal membrane stress computed for the weight or weight plus thermal load case, as applicable.

σ_1 principle membrane stress in direction 1.

σ_2 principle membrane stress in direction 2.

t_c future corroded wall thickness away from the damage area.

t_{eq} equivalent thickness.

t_L thickness of a layer.

t_{mm} minimum measured thickness determined at the time of the assessment.

t_{nom} nominal or furnished thickness of the component adjusted for mill undertolerance as applicable.

t_{rd} uniform thickness away from the damage area established by thickness measurements at the time of the inspection.

θ_k angle between σ_2 direction and the line joining pit 1 and 2 of pit-couple k (see Figure 6.14).

$time$ time allocated for future operation.

maximum shear stress for the weight or weight plus thermal load case, as applicable.

V applied net-section shear force for the weight or weight plus thermal load case, as applicable.

$w_{\max}$ maximum measured pit depth in the region of pitting corrosion.

w_c current characteristic pit depth.

w_f estimated future characteristic pit depth.

$w_{i,k}$ measured depth of the pit i in pit-couple k.

$w_{j,k}$ measured depth of the pit j in pit-couple k.

6.10 References

References for this Part are provided in Annex 6A – Technical Basis and Validation – Assessment of Pitting Corrosion.

6.11 Tables

Table 6.1 – Required Data for Assessment of Pitting Corrosion

Use this form to summarize the data obtained from a field inspection.

Equipment Identification: _____
Equipment Type: _____ Pressure Vessel _____ Storage Tank _____ Piping Component
Component Type & Location: _____

Data Required for Level 1:
Pitting Chart Grade: _____
Remaining Wall Thickness Ratio, R_{wt}: _____
(Note: A photograph or etching with comparison to the respective pitting chart grade should be documented.)

Data Required for Level 2:

Pit-Couple	P_k	θ_k	$d_{i,k}$	$w_{i,k}$	$d_{j,k}$	$w_{j,k}$

Table 6.2 – Section Properties for Computation of Longitudinal Stress in a Cylinder with Pitting

Pitting Corrosion on the Inside Surface	Pitting Corrosion on the Outside Surface
$D_f = D_o - 2t_{eq}$	$D_f = D + 2t_{eq}$
$I_{\bar{X}} = \frac{\pi}{64}\left(D_o^4 - D_f^4\right)$	$I_{\bar{X}} = \frac{\pi}{64}\left(D_f^4 - D^4\right)$
$A_m = \frac{\pi}{4}\left(D_o^2 - D_f^2\right)$	$A_m = \frac{\pi}{4}\left(D_f^2 - D^2\right)$
$A_t = \frac{\pi}{16}\left(D_o + D_f\right)^2$	$A_t = \frac{\pi}{16}\left(D_f + D\right)^2$
$a = \frac{D_o}{2}$	$a = \frac{D_f}{2}$
$A_a = \frac{\pi}{4}D_f^2$	$A_a = \frac{\pi}{4}D^2$

6.12 Figures

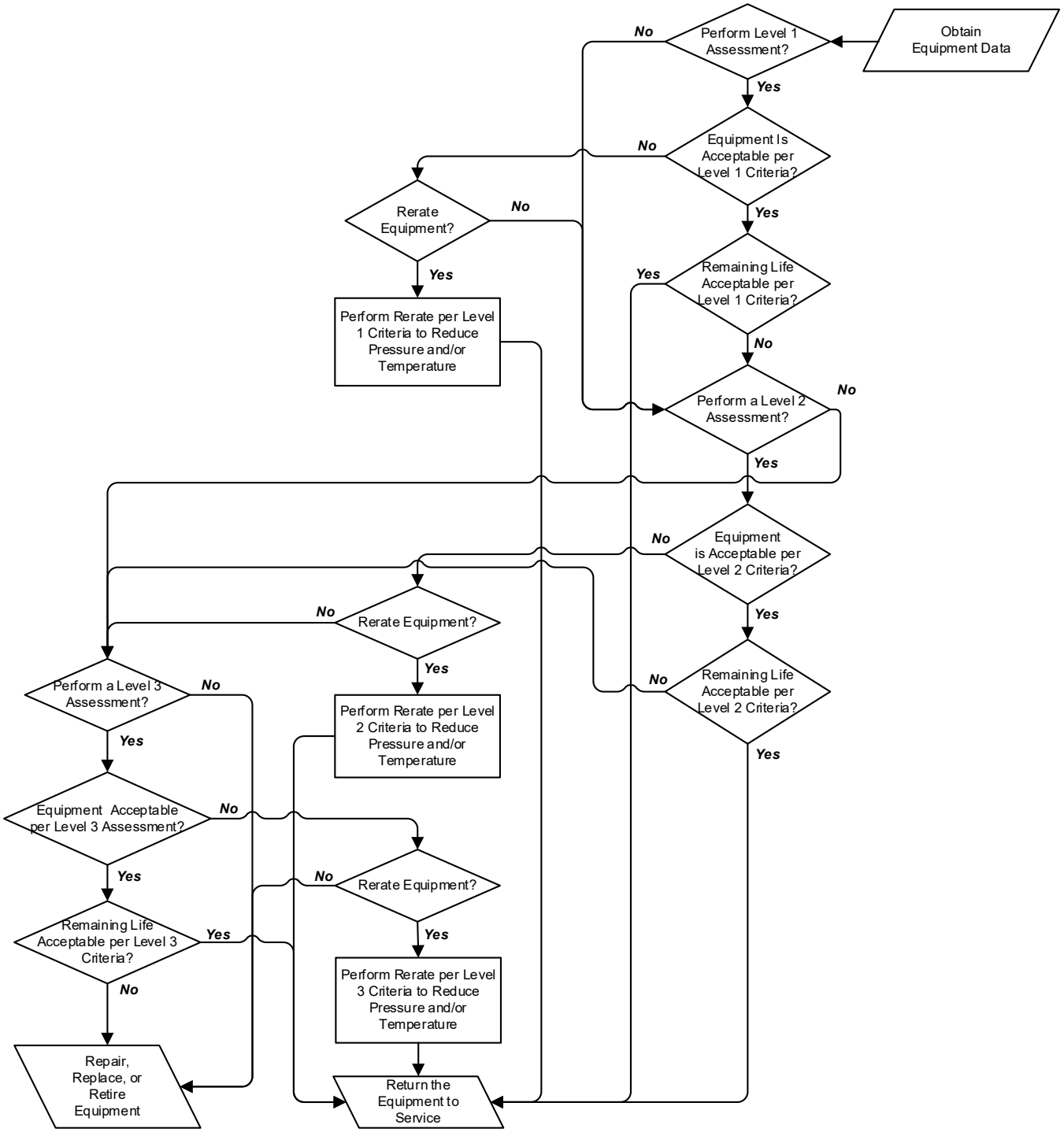

Figure 6.1 – Overview of the Assessment Procedures to Evaluate a Component with Pitting Corrosion

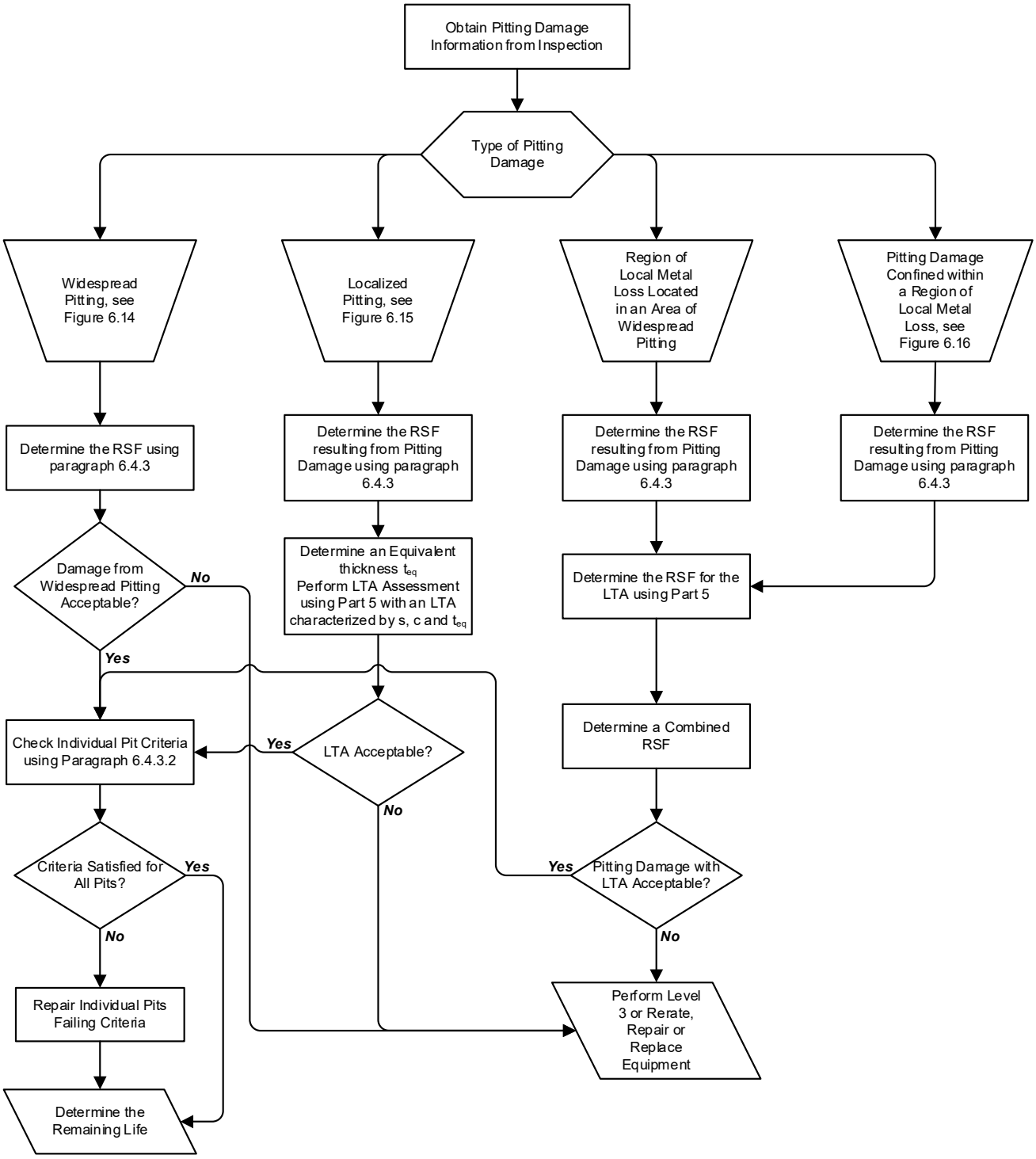

Figure 6.2 – Categories and Analysis Methodology of the Level 2 Pitting Corrosion Assessment

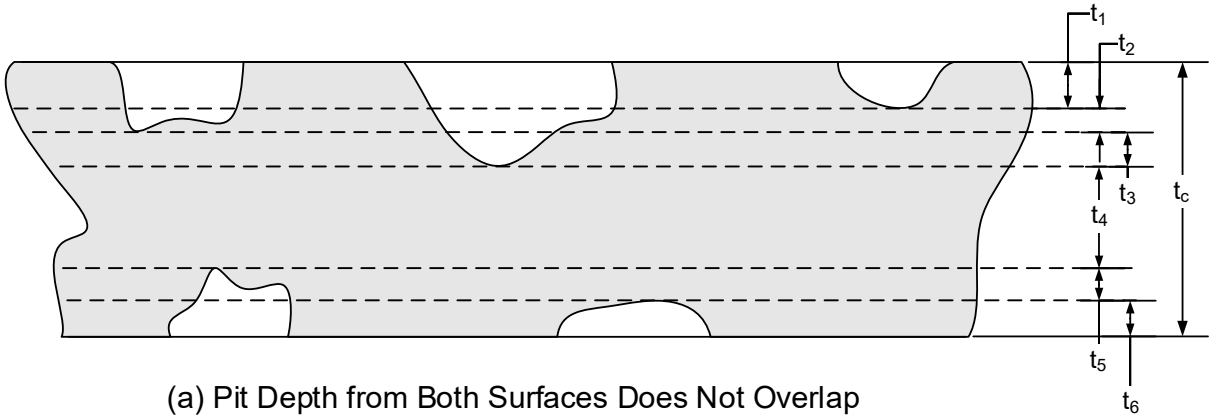

(a) Pit Depth from Both Surfaces Does Not Overlap

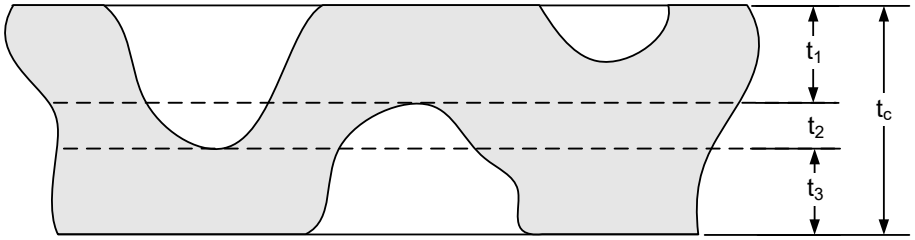

(b) Pit Depth from Opposing Surfaces Overlaps

Notes:

1. The number of layers used in the assessment is established based on the deepest penetration of the individual pits included in the pit-couple data. A layer is assigned based on the depth of each pit until all pits are accounted for. Using this procedure, a single layer of material will exist (see Detail (a) above) if the depth of pitting corrosion from the inside and outside surface of the component does not overlap (see Detail (b) above).
2. Overlapping pit depth from opposing surfaces can be assessed in a Level 3 Assessment.

Figure 6.3 – Layered Shell Model to Evaluate Pitting Corrosion on Both Surfaces

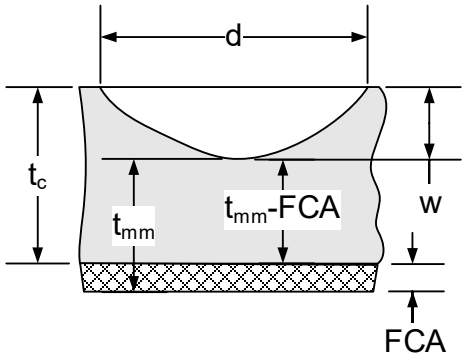

(a) Pitting and Corrosion Damage on Opposite Sides

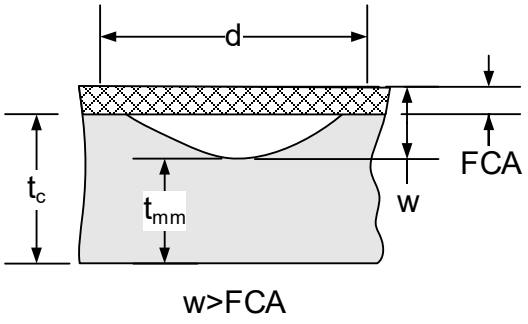

(b) Pitting and Corrosion Damage on the Same Side

Figure 6.4 – Pitting on Opposite Side and Same Side as Corrosion

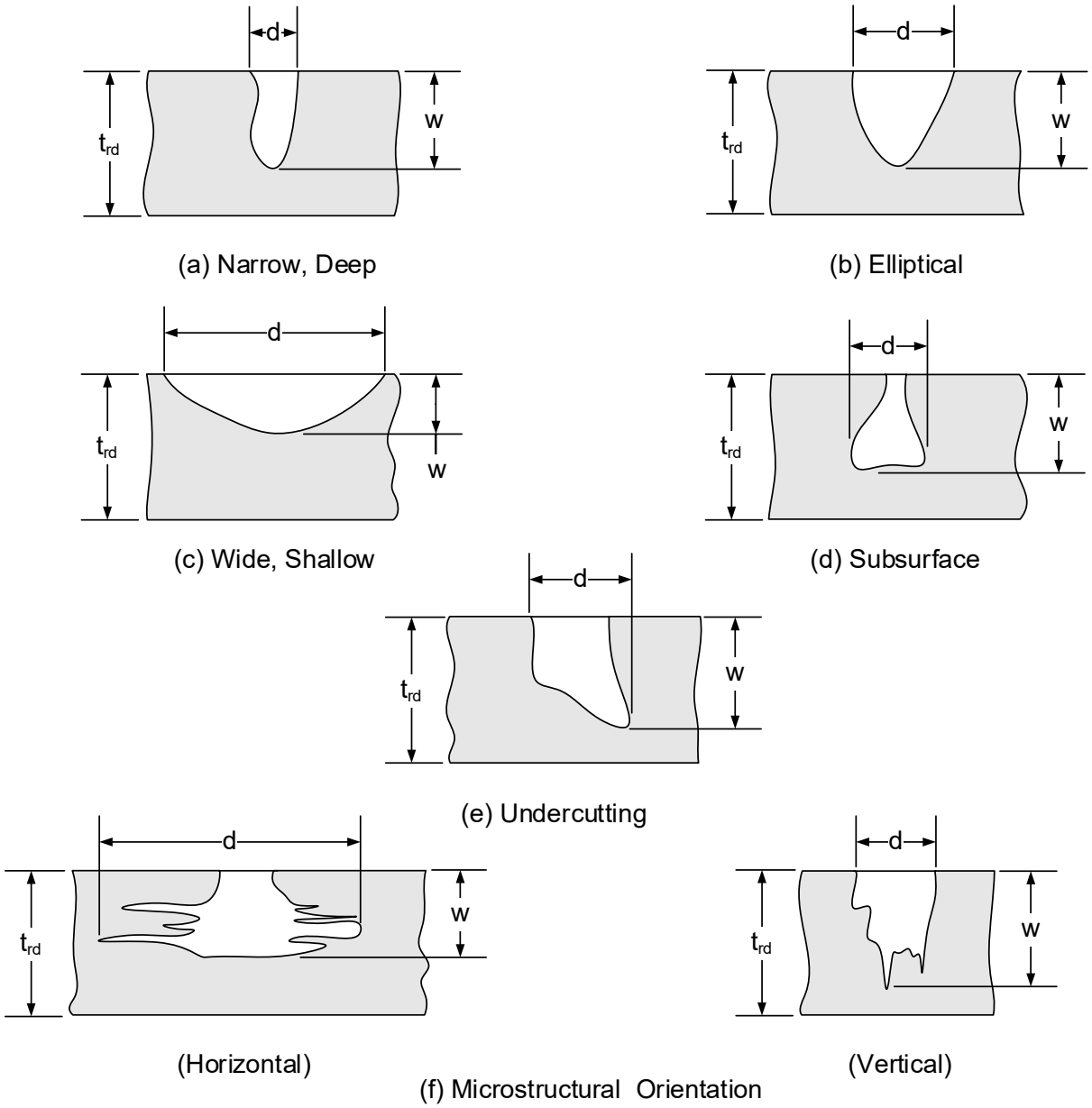

Figure 6.5 – Variation in the Cross-Sectional Shapes of Pits

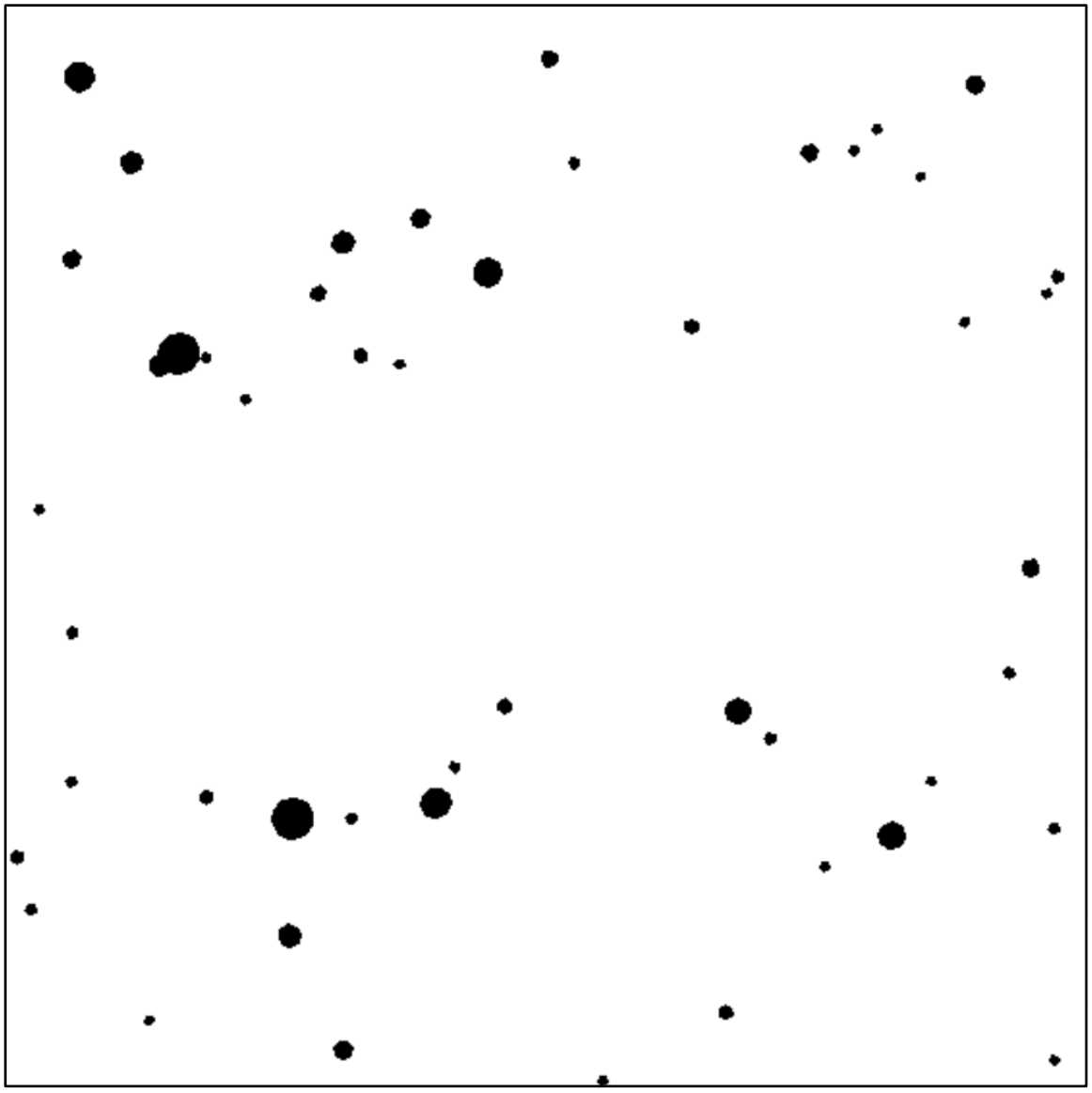

Note: The scale of this figure is 150 mm by 150 mm (6 in. by 6 in.).

R_{wt}	Level 1 RSF	
	Cylinder	Sphere
0.8	0.98	0.97
0.6	0.97	0.95
0.4	0.96	0.92
0.2	0.94	0.90

Figure 6.6 – Pitting Chart for Grade 1 Pitting Corrosion

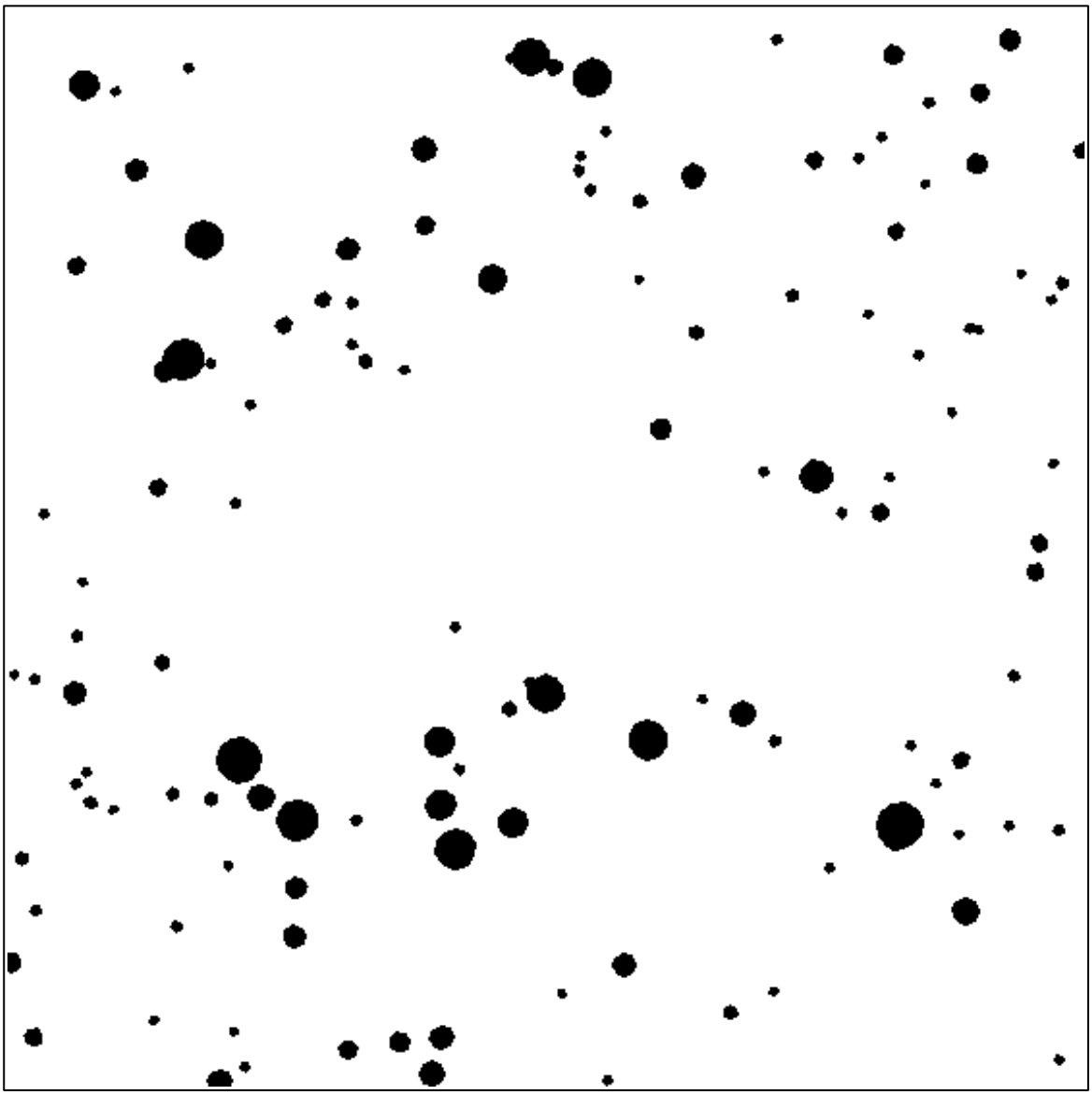

Note: The scale of this figure is 150 mm by 150 mm (6 in. by 6 in.).

R_{wt}	Level 1 RSF	
	Cylinder	Sphere
0.8	0.97	0.96
0.6	0.95	0.91
0.4	0.92	0.87
0.2	0.89	0.83

Figure 6.7 – Pitting Chart for Grade 2 Pitting Corrosion

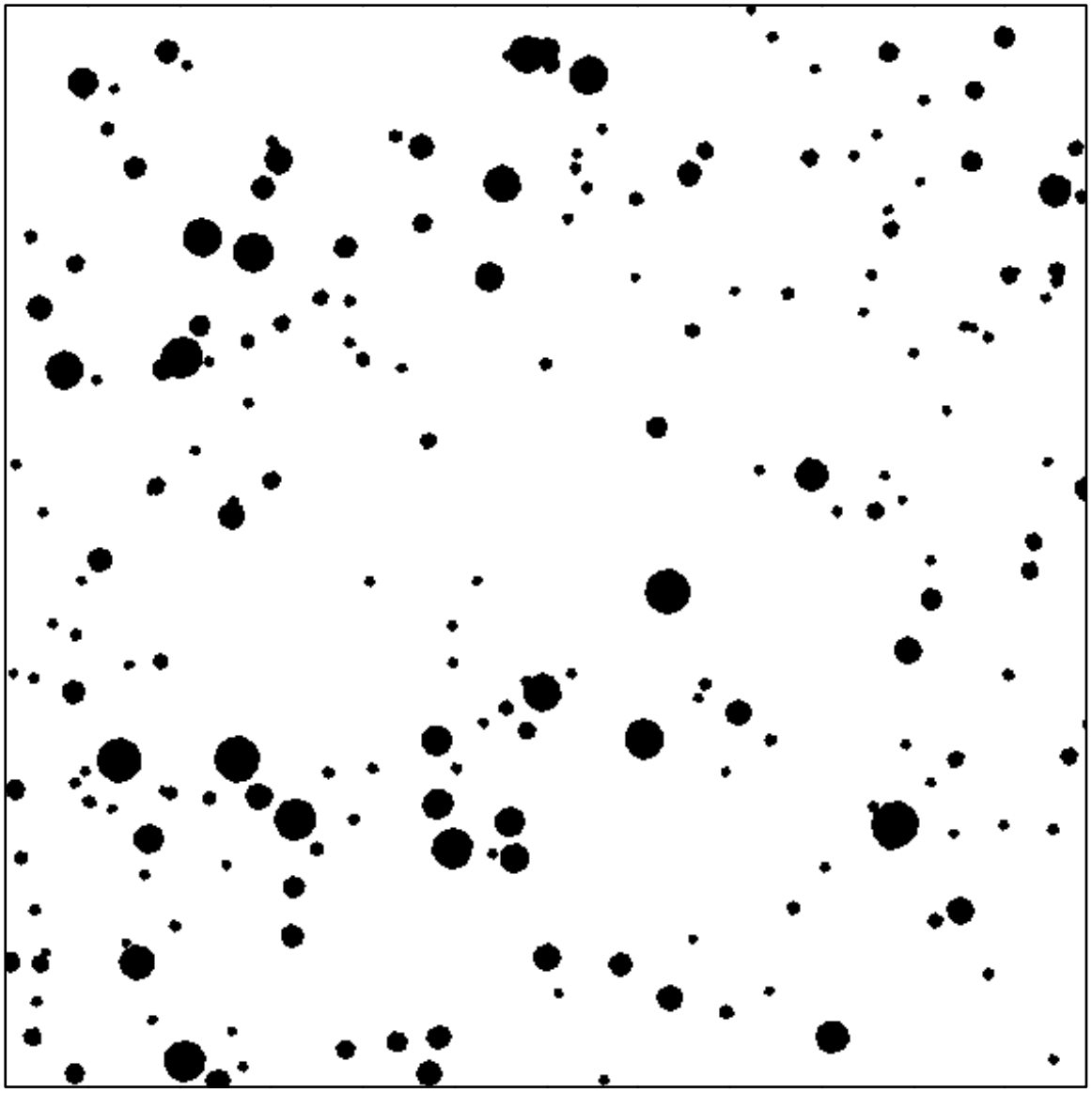

Note: The scale of this figure is 150 mm by 150 mm (6 in. by 6 in.).

R_{wt}	Level 1 RSF	
	Cylinder	Sphere
0.8	0.96	0.95
0.6	0.93	0.89
0.4	0.89	0.84
0.2	0.86	0.79

Figure 6.8 – Pitting Chart for Grade 3 Pitting Corrosion

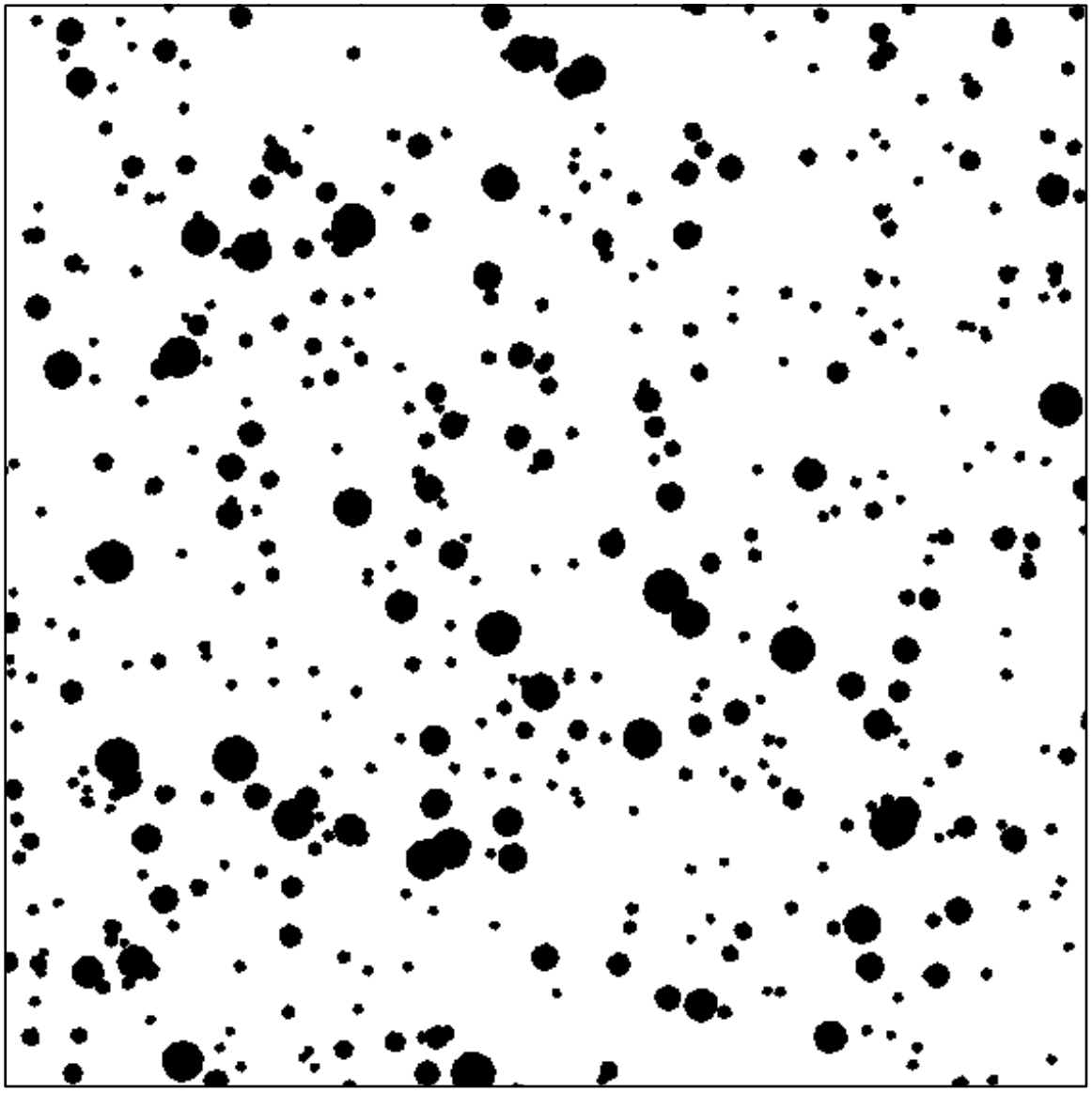

Note: The scale of this figure is 150 mm by 150 mm (6 in. by 6 in.).

R_{wt}	Level 1 RSF	
	Cylinder	Sphere
0.8	0.95	0.93
0.6	0.90	0.86
0.4	0.85	0.79
0.2	0.79	0.72

Figure 6.9 – Pitting Chart for Grade 4 Pitting Corrosion

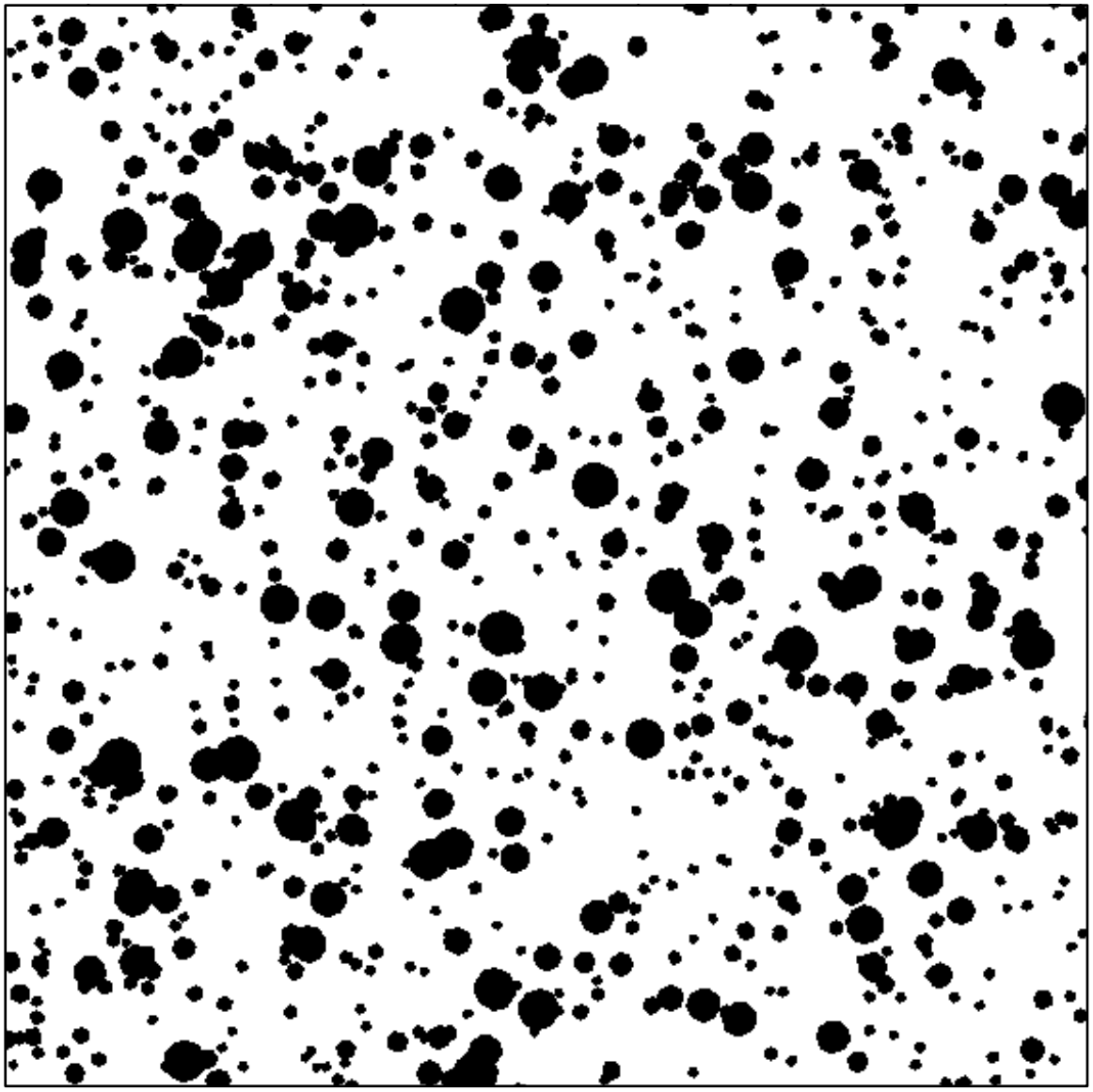

Note: The scale of this figure is 150 mm by 150 mm (6 in. by 6 in.).

R_{wt}	Level 1 RSF	
	Cylinder	Sphere
0.8	0.93	0.91
0.6	0.85	0.81
0.4	0.78	0.72
0.2	0.70	0.62

Figure 6.10 – Pitting Chart for Grade 5 Pitting Corrosion

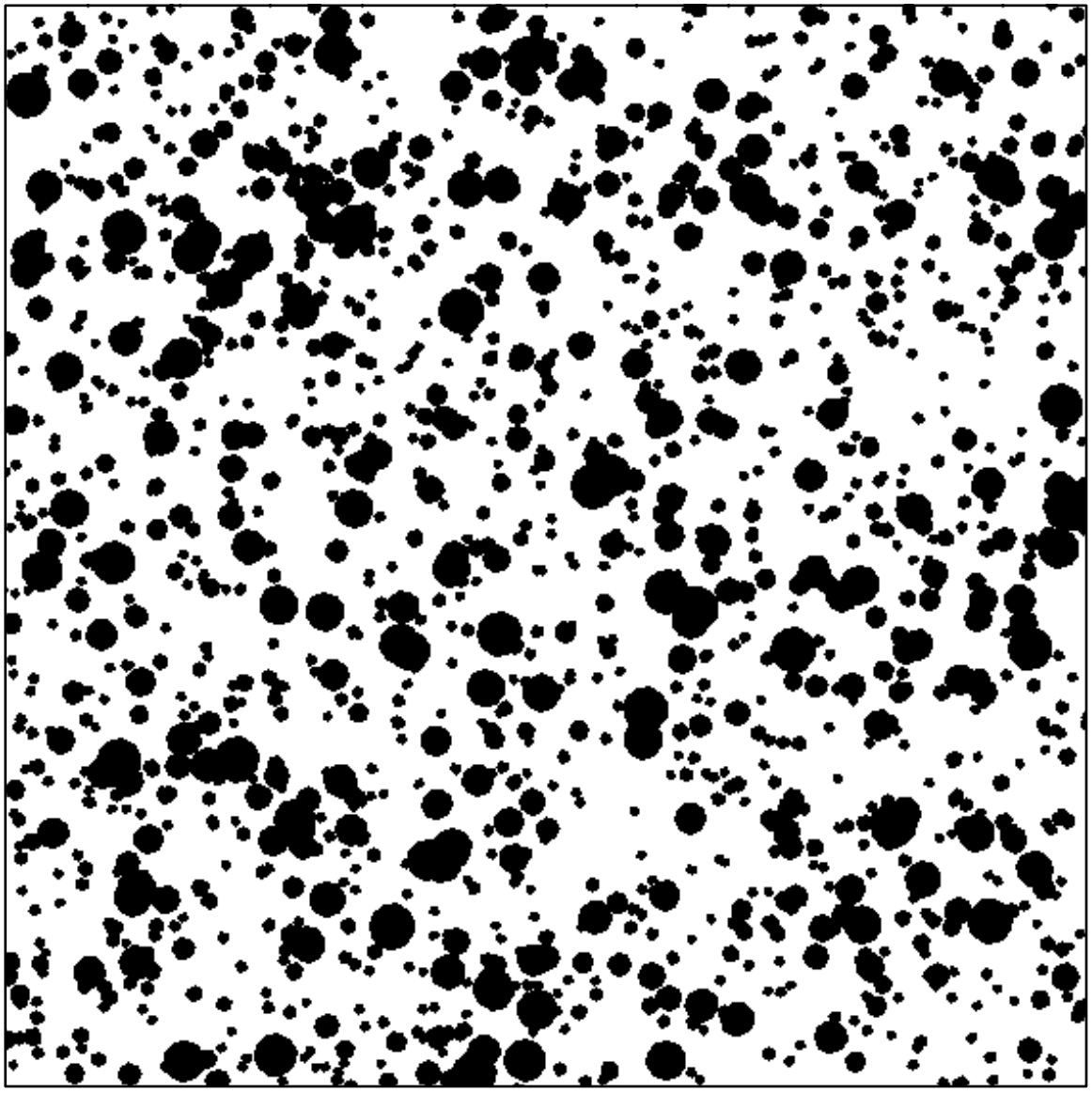

Note: The scale of this figure is 150 mm by 150 mm (6 in. by 6 in.).

R_{wt}	Level 1 RSF	
	Cylinder	Sphere
0.8	0.91	0.89
0.6	0.82	0.78
0.4	0.73	0.67
0.2	0.64	0.56

Figure 6.11 – Pitting Chart for Grade 6 Pitting Corrosion

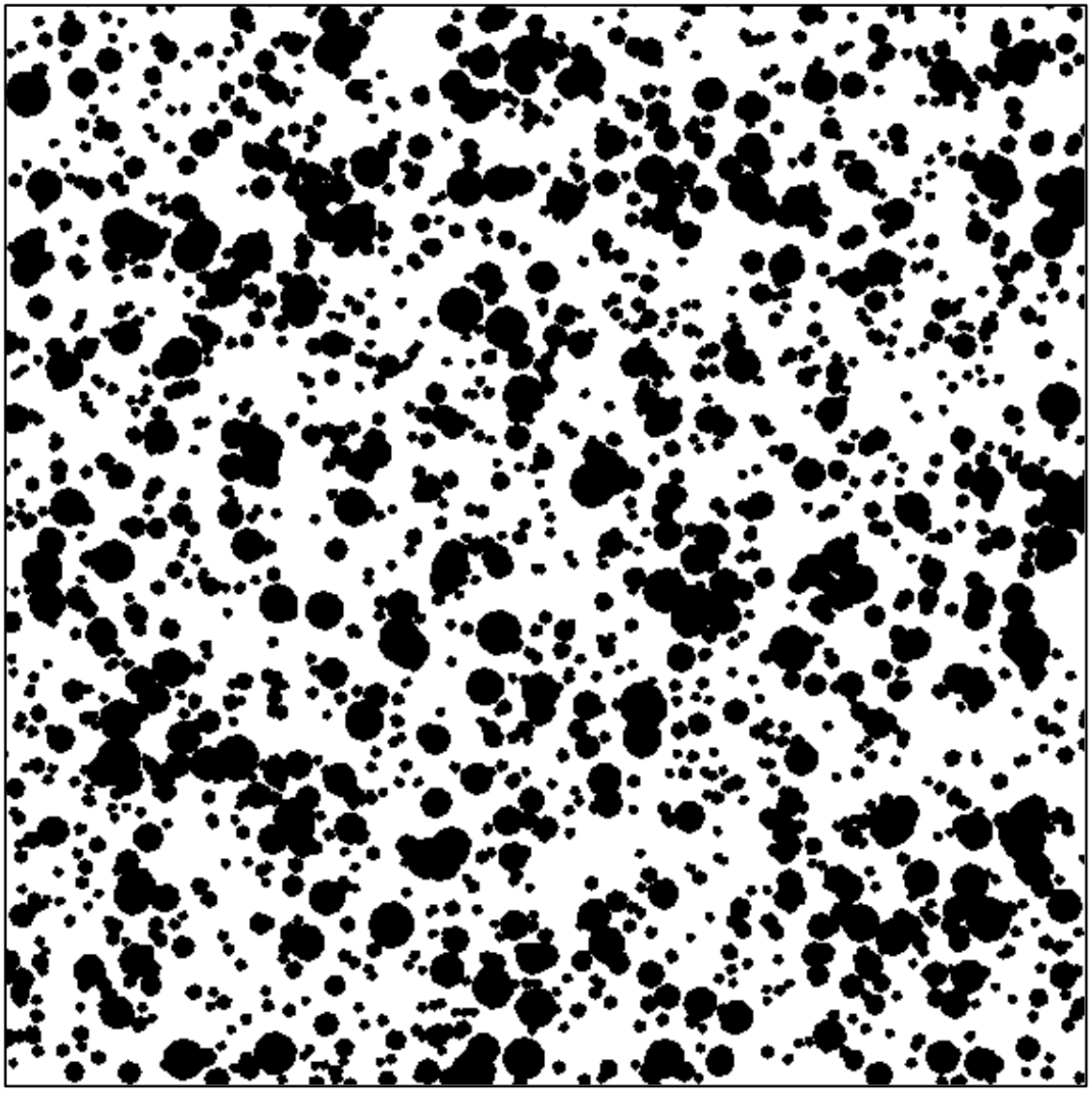

Note: The scale of this figure is 150 mm by 150 mm (6 in. by 6 in.).

R_{wt}	Level 1 RSF	
	Cylinder	Sphere
0.8	0.89	0.88
0.6	0.79	0.76
0.4	0.68	0.63
0.2	0.58	0.51

Figure 6.12 – Pitting Chart for Grade 7 Pitting Corrosion

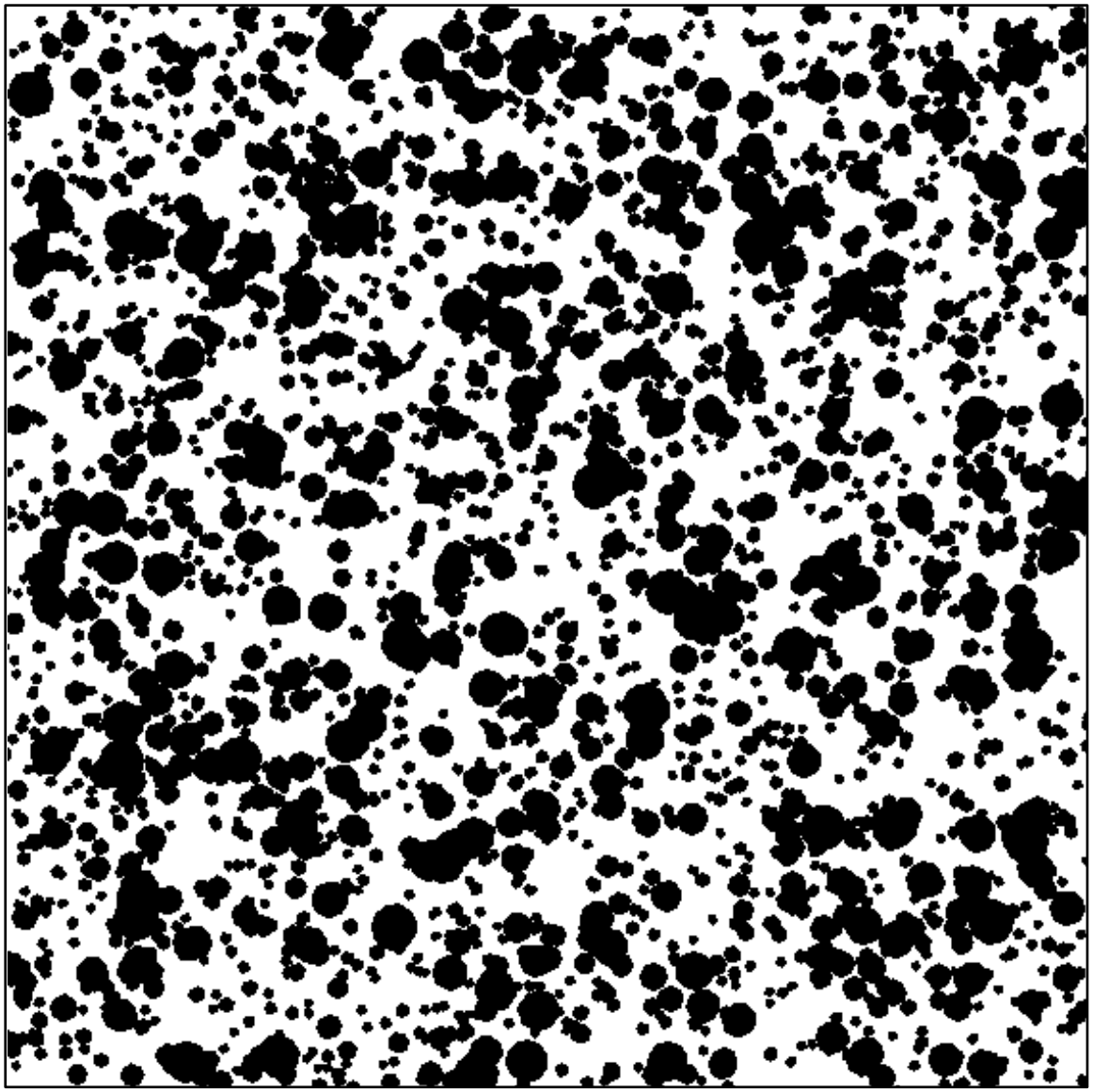

Note: The scale of this figure is 150 mm by 150 mm (6 in. by 6 in.).

R_{wt}	Level 1 RSF	
	Cylinder	Sphere
0.8	0.88	0.87
0.6	0.77	0.74
0.4	0.65	0.60
0.2	0.53	0.47

Figure 6.13 – Pitting Chart for Grade 8 Pitting Corrosion

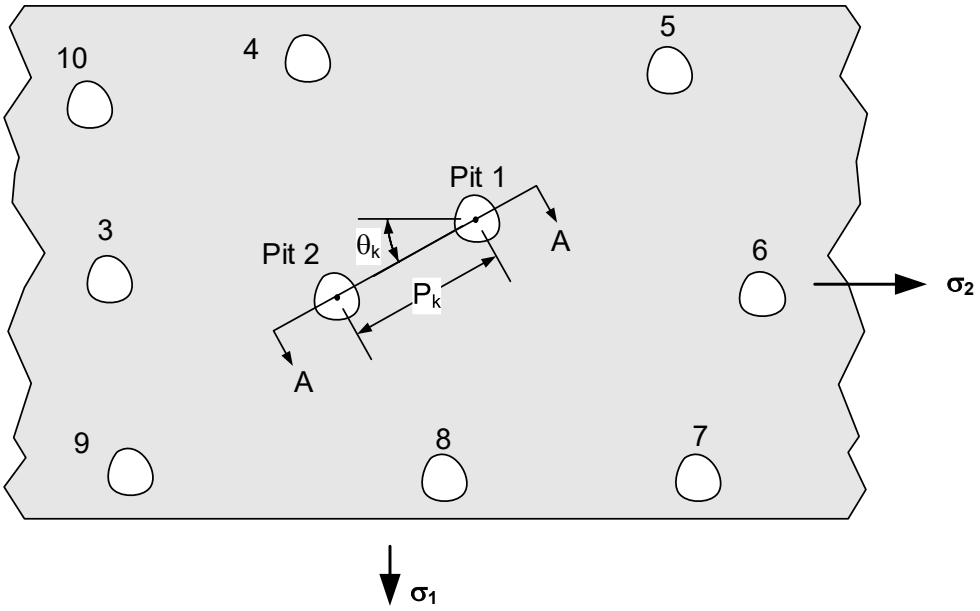

Note: In the example above: $P_k = P_{12}$ and $\theta_k = \theta_{12}$ because the closest pit to pit 1 is pit 2 (i.e. pit 2 is the nearest neighbor to pit 1).

(a) Pit-couple in a Plate Subject to a Biaxial Membrane Stress Field with $\sigma_1 \geq \sigma_2$

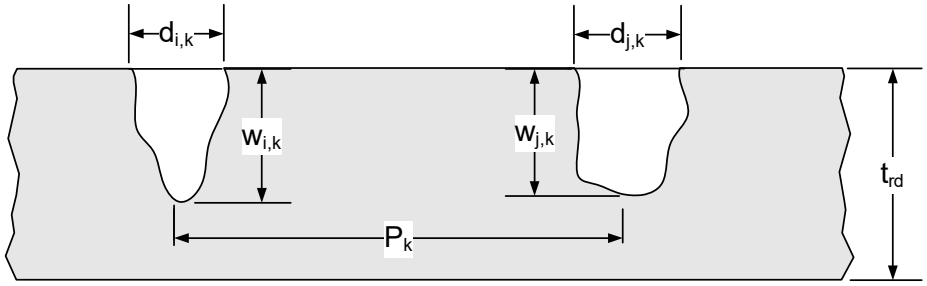

$d_{avg,k} = 0.5(d_{i,k} + d_{j,k})$

(b) Section A-A

Figure 6.14 – Parameters for the Analysis of Pitting Corrosion

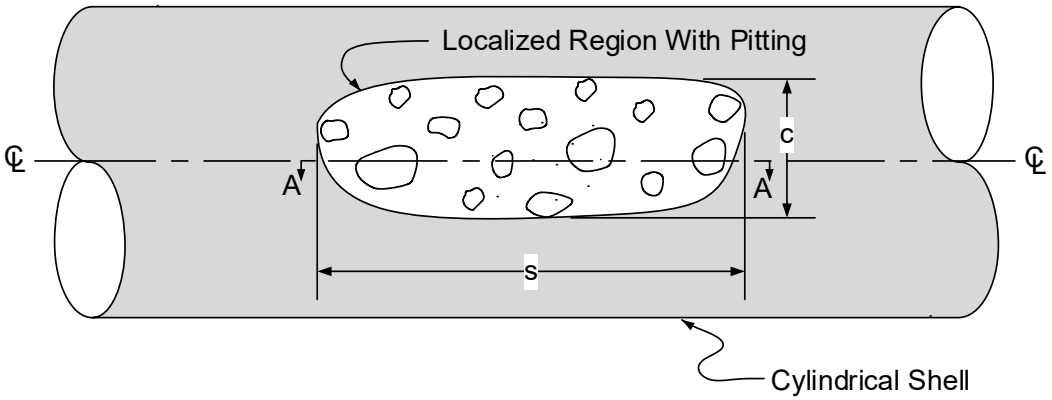

(a) Cylinder With Localized Pitting

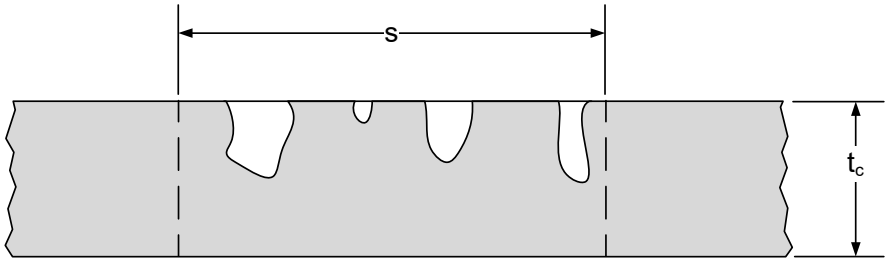

(b) Section A-A

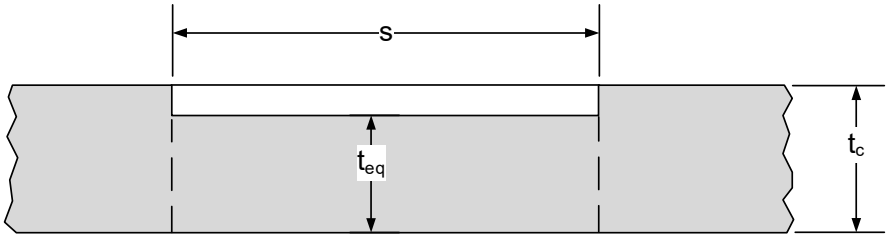

(c) Equivalent Plate Section for LTA Analysis

Figure 6.15 – Additional Parameters for the Analysis of a Localized Region of Pitting Corrosion

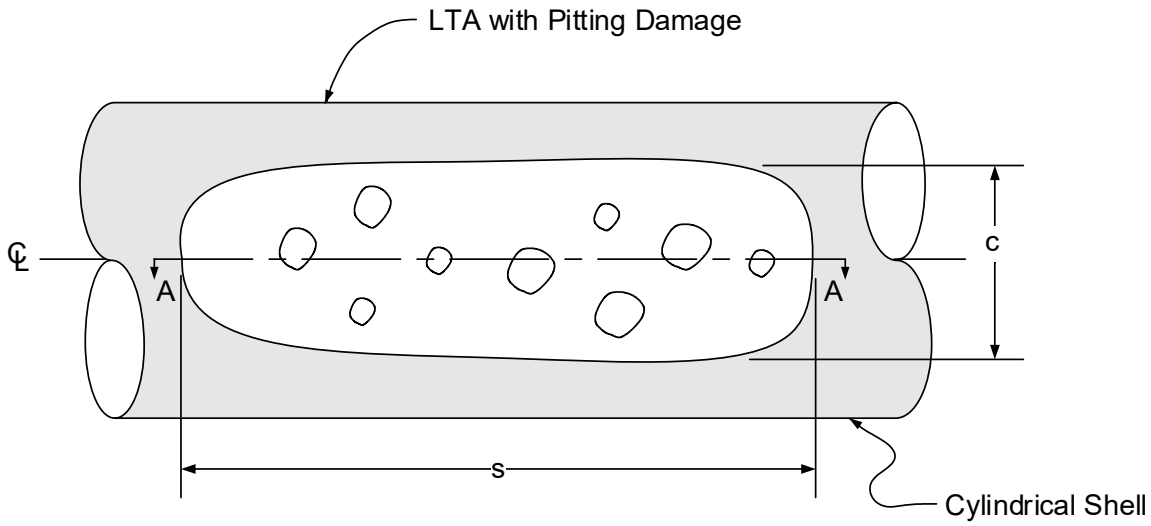

(a) Cylinder With Pitting Damage Confined to an LTA

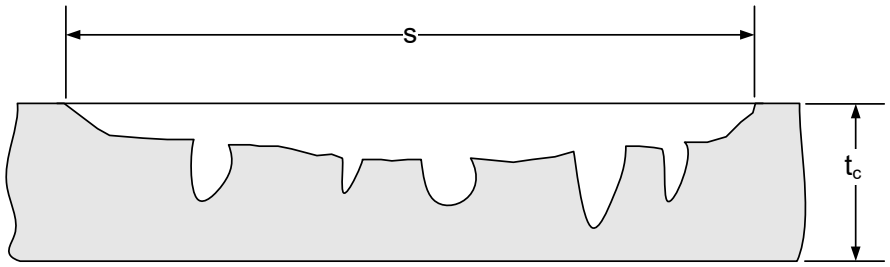

(b) Section A-A

Notes:

1. The dimensions s and c define the region of localized pitting corrosion or local metal loss.
2. A combined RSF is used in the assessment (see paragraph 6.4.3.2).
3. Section A-A is defined based on the $CTPS$.

Figure 6.16 – Pitting Corrosion Confined to an LTA

ANNEX 6A – TECHNICAL BASIS AND VALIDATION – ASSESSMENT OF PITTING CORROSION

(INFORMATIVE)

CONTENTS

ANNEX 6A – TECHNICAL BASIS AND VALIDATION – ASSESSMENT OF PITTING CORROSION.....6A-1

6A.1 TECHNICAL BASIS AND VALIDATION.....6A-1
6A.2 REFERENCES.....6A-1

6A.1 Technical Basis and Validation

The technical basis of the assessment procedures for pitting damage in Part 6 is provided in references [1] and [2]. The limit analysis used to develop the assessment procedures described in reference [2] was also used to develop the rules for the design of perforated plates included in the ASME Code, Section VIII, Division 2, Appendix 4 and Section III, Division 1, Article-8000, and Non-mandatory Appendix A. The pitting damage assessment procedures could not be compared to experimental results because of lack of data. However, these rules have been used extensively in the industry without incident and have been proven to provide acceptable results.

6A.2 References

[1] Osage, D.A., Krishnaswamy, P., Stephens, D.R., Scott, P., Janelle, J., Mohan, R., and Wilkowski, G.M., Technologies for the Evaluation of Non-Crack-Like Flaws in Pressurized Components – Erosion/Corrosion, Pitting, Blisters, Shell Out-Of-Roundness, Weld Misalignment, Bulges and Dents, WRC Bulletin 465, Welding Research Council, New York, NY, September 2001.

[2] Porowski, J.S., Osage, D.A. and Janelle, J.A., “Limit Analysis of Shells with Random Pattern of Spread Pits,” ASME PVP, 2002.

[3] ASM, *Metals Handbook, Ninth Edition, Volume 13, Corrosion*, ASM International, Metals Park, Ohio, pp. 231-233, 1987.

[4] ASM, *Metals Handbook, Ninth Edition, Volume 13, Corrosion*, ASM International, Metals Park, Ohio, pp. 113-122, 1987.

[5] Daidola, J.C., Parente, J. and Orisamolu, I.R., “Strength Assessment of Pitted Panels”, SSC-394, Ship Structures Committee, D.C., 1997.

[6] Gumbel, E.J., “Statistical Theory of Extreme Values”, National Bureau of Standards, AMS 33, 1954.

[7] Kowaka, Masamichi, Introduction to Life Prediction of Industrial Plant Materials – Application of the Extreme Value Statistical Method for Corrosion Analysis, Allerton Press, Inc., 1994.

[8] O’Donnell, W.J. and Porowski, J.S., “Yield Surfaces for Perforated Materials”, Transactions of the ASME, Journal of Applied Mechanics, American Society of Mechanical Engineers, NY, pp. 263-270, 1973.

[9] Porowski, W.J., O’Donnell, J.S., and Farr, J.R., “Limit Design of Perforated Cylindrical Shells per ASME Code”, Journal of Pressure Vessel Technology, American Society of Mechanical Engineers, NY, pp. 646-651, 1977.

[10] Porowski, W.J. and O'Donnell, J.S., "Effective Elastic Constants for Perforated Materials", Transactions of the ASME, Journal of Pressure Vessel Technology, American Society of Mechanical Engineers, NY, pp. 234-241, 1974.

PART 7 – ASSESSMENT OF HYDROGEN BLISTERS AND HYDROGEN DAMAGE ASSOCIATED WITH HIC AND SOHIC

CONTENTS

PART 7 – ASSESSMENT OF HYDROGEN BLISTERS AND HYDROGEN DAMAGE ASSOCIATED WITH HIC AND SOHIC 7-1

7.1 GENERAL 7-2
7.1.1 Assessment Procedures for Hydrogen Blisters, HIC and SOHIC 7-2
7.1.2 HIC Definition 7-2
7.1.3 SOHIC Definition 7-2
7.1.4 Hydrogen Blistering Definition 7-2
7.1.5 HIC, SOHIC and Blistering Distinct Damage Types 7-3
7.2 APPLICABILITY AND LIMITATIONS OF THE PROCEDURE 7-3
7.2.1 HIC, SOHIC and Blistering Distinct Damage Types 7-3
7.2.2 Calculation of the $MAWP_r$ and MFH_r and Coincident Temperature 7-3
7.2.3 Limitations Based on Temperature 7-3
7.2.4 Applicability of the Level 1 and Level 2 Assessment Procedures 7-3
7.2.5 Applicability of the Level 3 Assessment Procedure 7-4
7.3 DATA REQUIREMENTS 7-4
7.3.1 Original Equipment Design Data 7-4
7.3.2 Maintenance and Operational History 7-4
7.3.3 Required Data/Measurements for an FFS Assessment 7-4
7.3.4 Recommendations for Detection, Characterization, and Sizing 7-7
7.4 ASSESSMENT TECHNIQUES AND ACCEPTANCE CRITERIA 7-7
7.4.1 Overview 7-7
7.4.2 Level 1 Assessment 7-8
7.4.3 Level 2 Assessment 7-10
7.4.4 Level 3 Assessment 7-14
7.5 REMAINING LIFE ASSESSMENT 7-15
7.5.1 HIC and SOHIC Growth Rates 7-15
7.5.2 Blister Growth 7-16
7.6 REMEDIATION 7-16
7.6.1 Elimination of Hydrogen Charging 7-16
7.6.2 Controlling Hydrogen Charging 7-16
7.6.3 Venting of Blisters 7-16
7.6.4 Blend Grinding 7-16
7.6.5 Repair and Replacement of Damaged Material 7-17
7.6.6 NACE Standard SP0296-10 7-17
7.7 IN-SERVICE MONITORING 7-17
7.7.1 Monitoring for Hydrogen Charging 7-17
7.7.2 Inspection Methods for Monitoring 7-17
7.7.3 Detection of HIC, SOHIC, or Blister Damage Growth 7-17
7.8 DOCUMENTATION 7-17
7.8.1 General 7-17
7.8.2 Inspection Data 7-17
7.8.3 In-Service Monitoring 7-18
7.9 NOMENCLATURE 7-18
7.10 REFERENCES 7-19
7.11 TABLES 7-20
7.12 FIGURES 7-22

7.1 General

7.1.1 Assessment Procedures for Hydrogen Blisters, HIC and SOHIC

Fitness-For-Service (FFS) Assessment procedures are provided in this Part for low strength ferritic steel pressurized components with Hydrogen Induced Cracking (HIC) and blisters, stress oriented HIC (SOHIC) damage, and components with laminations that Part 13 directs that Part 7 shall be used (e.g., the component operates in a hydrogen charging environment or closely spaced laminations at different depths in through-thickness direction). These forms of damage are further described below and in NACE Standard SP0296-10 Detection, Repair, and Mitigation of Cracking in Refinery Equipment in Wet H_2S Environments. The assessment procedures for HIC and blister damage are shown in the flow chart contained in Figure 7.1. This Part excludes Sulfide Stress Cracking (SSC) and hydrogen embrittlement of high strength steels which generally occur in steels with a hardness above Rockwell C 22 (Brinell 237) or with tensile strengths above 793 MPa (115 ksi). The technical basis for Part 7 is summarized in Annex 7A.

7.1.2 HIC Definition

Hydrogen Induced Cracking (HIC) is characterized by laminar (in-plane) cracking with some associated through-thickness crack linkage. This is sometimes referred to as step-wise cracking, due to its morphology. This type of damage typically occurs in carbon steel plates exposed to an aqueous phase containing hydrogen sulfide, cyanides, hydrofluoric acid, or other species which charge atomic hydrogen into the steel. It is less common in forgings and seamless pipes than in plates. The atomic hydrogen combines at non-metallic inclusions or other imperfections to form hydrogen molecules that are too large to diffuse through the steel. This build-up of internal hydrogen can result in HIC. Typical HIC damage is shown in Figures 7.2 and 7.3.

7.1.3 SOHIC Definition

Stress Oriented HIC (SOHIC) is defined in NACE Standard SP0296-10 as follows: “Array of cracks, aligned nearly perpendicular to the stress, that are formed by the link-up of small HIC cracks in steel.” Tensile stress (residual or applied) is required to produce SOHIC. SOHIC is commonly observed in the base metal adjacent to the Heat-Affected Zone (HAZ) of a weld, oriented in the through-thickness direction. SOHIC may also be produced in susceptible steels at other high stress points such as from the tip of mechanical cracks and defects, or from the interaction among HIC on different planes in the steel. The hydrogen charging phenomenon is the same as that which causes HIC. Typical SOHIC damage is shown in Figure 7.4.

7.1.4 Hydrogen Blistering Definition

Hydrogen blistering is characterized by physical bulging of the surface(s) of equipment. It is caused by hydrogen accumulation at imperfections in the steel, such as laminations or inclusions. Atomic hydrogen generated by wet H_2S or hydrofluoric acid environments combines at imperfections to form hydrogen molecules that are too large to diffuse through the steel. The hydrogen accumulates and results in the build-up of high pressure that causes local stresses that exceed the yield strength of the material near these imperfections. The yielding of the material and subsequent plastic deformation in the form of bulging due to pressure loading results in a blister. Sometimes cracks can extend from the periphery of a blister and can propagate in a through-wall direction, particularly if the blister is located near a weld. Typical hydrogen blistering is shown in Figures 7.5 through 7.9.

7.1.5 HIC, SOHIC and Blistering Distinct Damage Types

HIC, SOHIC, and blistering are distinct from other forms of damage that may be related to hydrogen in steels which are addressed elsewhere in this document, including:

a) Discrete or singular cracks shall be assessed as crack-like flaws per Part 9. This includes hydrogen embrittlement or sulfide stress cracking of high strength or high hardness base metals and weldments.

b) Laminations are planar defects that exist on one or more planes in the equipment, but cause no bulging of the metal surface, have no cracking in the through thickness direction, and are not linked. Laminations may be present in equipment whether it is operating in a hydrogen charging environment. Assessment procedures for laminations are covered in Part 13 of this Standard; however, they may also be covered in Part 7 if Part 13 directs the user to use Part 7. Depending on the detailed nature of the lamination(s) the most similar type of damage (blistering, HIC, or SOHIC) would be applicable.

7.2 Applicability and Limitations of the Procedure

7.2.1 HIC, SOHIC and Blistering Distinct Damage Types

The FFS Assessment procedures described below may be used to evaluate the acceptability of HIC, SOHIC, blisters, and laminations if Part 13 directed the user to Part 7 subject to the limitations in this Part. Unless otherwise specified, this Part is limited to the evaluation of HIC, SOHIC, or blister damage, associated with hydrogen charging from the process environment and laminations if Part 13 directed the user to Part 7. Other flaw types shall be evaluated in accordance with Part 2, Table 2.1.

7.2.2 Calculation of the $MAWP_r$ and MFH_r and Coincident Temperature

Calculation methods are provided to rerate the component if the acceptance criteria in this Part are not satisfied. For pressurized components, the calculation methods can be used to find a reduced $MAWP$ or $MAWP_r$. The calculation methods may be used to determine a reduced MFH for tank components or MFH_r.

7.2.3 Limitations Based on Temperature

The procedures apply to components whose operating temperature is less than 204°C (400°F) for carbon or low alloy steels or are below the applicable design curve in API RP 941 Steels for Hydrogen Service at Elevated Temperatures and Pressures in Petroleum Refineries and Petrochemical Plants, whichever is greater. Damage associated with high temperature hydrogen attack is specifically excluded from this assessment.

7.2.4 Applicability of the Level 1 and Level 2 Assessment Procedures

The Level 1 and Level 2 Assessment procedures for HIC, blisters, and laminations if Part 13 directed the user to Part 7 apply only if all the following conditions are satisfied:

a) The original design criteria were in accordance with a recognized code or standard (see Part 1, paragraphs 1.2.2 or 1.2.3).

b) The material is considered to have sufficient toughness. If there is uncertainty regarding the material toughness, then a brittle fracture analysis per Part 3 should be performed. Temperature and/or process conditions that result in material embrittlement are discussed in API RP 571 Damage Mechanisms Affecting Fixed Equipment in the Refining Industry.

c) The component is not in cyclic service. If the component is subject to less than 150 cycles (i.e., pressure and/or temperature variations including operational changes and start-ups and shut-downs) throughout its

history and future planned operation or satisfies the cyclic service screening procedure in Part 14, paragraph 14.4.2, then the component is not in cyclic service.

d) The following limitations on component types and applied loads are satisfied:

1) Level 1 Assessment – Type A components (see Part 4, paragraph 4.2.5) subject to internal pressure.

2) Level 2 Assessment – Type A components subject to internal pressure and supplemental loads and Type B Class 1 components (see Part 4).

Level 1 and Level 2 Assessments are not provided for SOHIC Damage.

7.2.5 Applicability of the Level 3 Assessment Procedure

A Level 3 Assessment for HIC, SOHIC, blister damage, and laminations if Part 13 directed the user to Part 7 should be performed when:

a) The requirements of Level 1 and Level 2 are not satisfied.

b) The HIC, SOHIC, blister damage or laminations are located close to a weld seam or a major structural discontinuity (see Equation (7.11)).

c) A component contains a multitude of closely spaced blisters (see Figure 7.9).

7.3 Data Requirements

7.3.1 Original Equipment Design Data

An overview of the original equipment data required for an assessment is provided in Part 2, paragraph 2.3.1.

7.3.2 Maintenance and Operational History

An overview of the maintenance and operational history required for an assessment is provided in Part 2, paragraph 2.3.2.

7.3.3 Required Data/Measurements for an FFS Assessment

7.3.3.1 The required data and measurements for assessment of HIC damage is listed below:

a) HIC Spacing to Nearest HIC or Blister, L_H and L_{Hs} – Measurements should be made to determine the edge-to-edge spacing between HIC damage and the nearest HIC or blister damage, L_H, (see Figure 7.3). In addition, the longitudinal spacing, L_{Hs}, should also be determined (see Figure 7.3). This information should be detailed and provided on an inspection sketch.

b) HIC Spacing to Weld Joints, L_w – Measurements should be made to determine the spacing between the edge of the HIC damage and the nearest weld joint (see Figure 7.3). This information should be detailed and provided on an inspection sketch.

c) HIC Spacing to Major Structural Discontinuities, L_{msd} – Measurements should be made to determine the spacing between the edge of the HIC and the nearest major structural discontinuity. This information should be detailed and provided on an inspection sketch.

d) HIC Through-Thickness Extent of Damage, w_H – This is the maximum extent of the HIC damage measured in the through-thickness direction of the damaged component (see Figure 7.2).

e) Minimum Remaining Wall Thickness of Undamaged Metal, Internal Side, t_{mm-ID} – For subsurface HIC, this is the distance from the HIC damaged zone to the internal surface of the component (see Figure 7.2) modified by the Future Corrosion Allowance (FCA) as required.

f) Minimum Remaining Wall Thickness of Undamaged Metal, External Side, t_{mm-OD} – For subsurface HIC, this is the distance from the HIC damaged zone to the external surface of the component (see Figure 7.2) modified by the Future Corrosion Allowance (FCA) as required.

g) Minimum Remaining Wall Thickness of Undamaged Metal, t_{mm} – For subsurface HIC, this is the sum of the distances from the HIC damage zone to the internal surface and from the HIC damage zone to the external surface, or $t_{mm} = t_{mm-ID} + t_{mm-OD}$ (see Figure 7.2). For surface breaking HIC, this is the distance from the HIC damaged zone to the non-damaged surface of the component (see Figure 7.2) modified by the Future Corrosion Allowance (FCA) as required.

h) HIC damage shall be classified as either surface breaking HIC or subsurface HIC. If Equations (7.1) and (7.2) are satisfied (see Figure 7.2), then the HIC damage is classified as subsurface. Otherwise, the HIC damage shall be classified as surface breaking.

$$t_{mm-ID} \geq 0.2t_c \tag{7.1}$$

$$t_{mm-OD} \geq 0.2t_c \tag{7.2}$$

i) HIC Damage Dimensions s and c – The dimensions in the longitudinal and circumferential directions shall be determined as follows:

1) If $L_H \geq 8t_c$, then the HIC damage dimensions, s and c, are taken as the longitudinal and circumferential extent of the damaged zone, respectively. For example, for HIC Damage Zone 1 in Figure 7.3, the HIC damage dimensions, s and c, are given by Equations (7.3) and (7.4).

$$s = s_1 \tag{7.3}$$

$$c = c_1 \tag{7.4}$$

2) If $L_H < 8t_c$, then the HIC damage dimensions, s and c, for HIC Damage Zones 1 and 2 in Figure 7.3 are established using the procedure described in Part 4, Figure 4.11.

7.3.3.2 The required data and measurements for assessment of SOHIC damage are as follows:

a) SOHIC Spacing to Nearest HIC or Blister, L_{SH} – Measurements should be made to determine the spacing between SOHIC damage and the nearest HIC or blister damage. This information should be detailed and provided on an inspection sketch.

b) SOHIC Spacing to Nearest Major Structural Discontinuity, L_{msd} – Measurements should be made to determine the spacing between the SOHIC and the nearest major structural discontinuity. This information should be detailed and provided on an inspection sketch.

c) SOHIC Damage Dimensions, a and $2c$ – The dimensions of the crack-like flaw that will be used to evaluate the SOHIC damage (see Figure 7.4).

7.3.3.3 The required data and measurements for assessment of blister damage are as follows:

a) Blister Diameter – The blister dimensions to be recorded depend on the assessment level and are defined below.

1) Level 1 Assessment – The largest dimension in either the longitudinal or circumferential direction, s or c, should be taken as the blister diameter (see Figure 7.5).

2) Level 2 Assessment – The blister dimensions in the longitudinal and circumferential directions, s and c, should be recorded consistent with the method used to characterize a region of localized metal loss in Part 5.

b) Blister Spacing to Nearest HIC or Blister, L_B – Measurements should be made to determine the edge-to-edge spacing between a blister and the nearest HIC or blister damage. This information should be detailed and provided on an inspection sketch. If there are multiple blisters near one another, the size of the blister to be used in the assessment is established considering the effects of neighboring blisters using the criterion for local metal loss described in Part 5 (see Figure 5.2). In addition, if the distance between two adjacent blisters zones (measured edge-to-edge) is less than or equal to two times the corroded thickness, t_c, the blisters should be combined and evaluated as a single blister.

c) Bulge Direction and Projection, B_p – The blister bulge direction, inside or outside of the pressure containing component, and the blister projection above the shell surface (see Figure 7.5) should be recorded.

d) Minimum Remaining Wall Thickness, t_{mm} – For an internal blister this is the distance from the outside surface to the blister, and for an external blister, this is the distance from the inside surface to the blister (see Figure 7.5).

e) Blister Periphery Cracking – The blister should be examined to determine if there are any cracks extending in the plane of the blister and/or in a through-thickness direction. This type of cracking typically occurs at the periphery of the blister and can lead to cracking in the through thickness direction.

f) Blister Crown Cracking and Vent Hole Size, s_c – Cracks or vent holes on the crown of blisters affect the strength calculation; therefore, the dimension s_c should be recorded if cracks or vent holes are present (see Figures 7.6 and 7.7).

g) Blister Spacing to Weld Joints, L_W – Measurements should be made to determine the spacing between the blister and the nearest weld joint (see Figure 7.8). This information should be detailed and provided on an inspection sketch.

h) Blister Spacing to Nearest Major Structural Discontinuity, L_{msd} – Measurements should be made to determine the spacing between the blister and the nearest major structural discontinuity. This information should be detailed and provided on an inspection sketch.

7.3.3.4 The required data and measurements for laminations if Part 13 directed the user to Part 7 should be per paragraph 7.3.3.1 for laminations treated as HIC damage or paragraph 7.3.3.3 for laminations treated as blisters.

7.3.3.5 The information in paragraph 7.3.3.1 and paragraph 7.3.3.3 should be recorded in a format similar to the ones shown in Table 7.1 for HIC damage and Table 7.2 for blister damage. In addition, a detailed sketch should be created showing this information. The data format of Part 9 of this Standard may be used to record the information in paragraph 7.3.3.2.

7.3.4 Recommendations for Detection, Characterization, and Sizing

7.3.4.1 Recommendations for Detection, Characterization, and Sizing of HIC Damage are given below:

a) HIC damage that is open to the surface may be detected by magnetic particle, liquid penetrant, or other methods used to detect surface breaking crack-like flaws, depending on the extent and severity of the damage.

b) HIC damage is, by definition, a three-dimensional array of linear indications. Ultrasonic examination or other suitable techniques shall be used to detect HIC damage that is subsurface and to determine the subsurface dimensions of the HIC damage, including the remaining undamaged thickness at the HIC location. Neither radiography nor surface examination methods are sufficient. Figure 7.10 illustrates how ultrasonic examination may be used to assess the dimensions of HIC damage.

c) When HIC damage and/or blisters are present in the proximity of welds, structural discontinuities, or other stress concentrating features, the possibility of stress oriented hydrogen induced cracking (SOHIC) should be considered, and appropriate inspection conducted using UT or other methods. Details regarding this type of cracking and examination techniques are provided in NACE Standard SP0296-10.

7.3.4.2 Recommendations for Detection, Characterization, and Sizing of SOHIC Damage are given below:

a) SOHIC damage that is open to the surface may be detected by magnetic particle, liquid penetrant, or other methods used to detect surface breaking crack-like flaws, depending on the extent and severity of the damage. However, SOHIC damage may be entirely subsurface.

b) Sizing of SOHIC damage is a challenge, particularly if there is also HIC damage present. Typically, the crack depth can be determined by grinding or by use of angle beam or time of flight diffraction UT methods. Further guidance is given in NACE Standard SP0296-10.

7.3.4.3 Recommendations for Detection, Characterization, and Sizing of Blister Damage are shown below:

a) Blisters are usually discovered by visual observation of surface bulging on either the inside or outside of the equipment. During an in-service inspection/monitoring blisters may also be discovered with UT examination.

b) Ultrasonic examination can be used to determine the depth of the blister and remaining thickness at the blister location.

c) The periphery of the blister(s) should be inspected for subsurface and surface breaking cracks. The crown of the blister should also be examined to detect and size any crown cracks. Inspection techniques to identify and size crack-like flaws are covered in Part 9 of this Standard.

7.4 Assessment Techniques and Acceptance Criteria

7.4.1 Overview

7.4.1.1 If the HIC or blister is located within the region of the specified corrosion/erosion allowance, the assessment procedures of this Part should still be followed. For laminations in a component in hydrogen charging service use:

a) the blister assessment procedure for a single lamination or widely spaced laminations, or

b) The HIC assessment procedure for closely spaced laminations at different depths in a through-thickness direction.

7.4.1.2 An overview of the assessment levels for HIC damage is provided below:

a) The Level 1 Assessments are limited to Type A components. The assessment procedures provide screening criteria to evaluate HIC damage, considering the damage from the perspective of local metal loss. Steps shall be taken to ensure the damage will not propagate.

b) The Level 2 Assessments are limited to Type A components and Type B Class 1 components subject to internal pressure and supplemental loads. The assessment procedures utilize the methodologies of Part 5 and Part 9 to evaluate the damage zone as a region of local metal loss and as a crack. Steps shall be taken to control or periodically monitor the progression of damage. An overview of the Level 2 Assessment procedure for HIC is shown in Figure 7.11.

c) The Level 3 Assessment procedures are intended to evaluate components that do not pass Level 1 and 2 Assessment as well as components of larger or more complex regions of HIC damage or components that require detailed stress analysis because of complex geometry, complex loading conditions or both.

7.4.1.3 An overview of the assessment levels for SOHIC damage is provided below:

a) The Level 1 and Level 2 Assessment procedures are not provided for SOHIC Damage.

b) The Level 3 Assessment procedures utilize the methodologies of Part 9 to evaluate the SOHIC damage as a crack. Steps shall be taken to control or periodically monitor the progression of damage.

c) The Level 3 Assessment procedures may also be used to evaluate more complex regions of SOHIC damage or components that require detailed stress analysis because of complex geometry, complex loading conditions or both.

7.4.1.4 An overview of the assessment levels for blisters is provided below:

a) The Level 1 Assessment procedures provide screening criteria to evaluate blisters on Type A components subject to internal pressure.

b) The assessment procedures in Level 2 utilize the methodology of Part 5 to evaluate the blister as an equivalent region of local metal loss of Type A components subject to internal pressure and supplemental loads and Type B Class 1 components subject to internal pressure and supplemental loads. An overview of the Level 2 Assessment procedure for blisters is shown in Figure 7.12.

c) The Level 3 Assessment procedures are intended to evaluate larger or more complex regions of blister damage or components that require detailed stress analysis because of complex geometry, complex loading conditions or both.

7.4.2 Level 1 Assessment

7.4.2.1 HIC Assessment Procedure

The Level 1 Assessment procedure for determining the acceptability of HIC damage in Type A components subject to internal pressure is as shown below:

a) STEP 1 – Determine the wall thickness to be used in the assessment using Equation (7.5) or (7.6), as applicable.

$$t_c = t_{nom} - LOSS - FCA \tag{7.5}$$

$$t_c = t_{rd} - FCA \tag{7.6}$$

b) STEP 2 – Determine the information in paragraph 7.3.3.1.

c) STEP 3 – If all the following requirements are satisfied, then proceed to STEP 4. Otherwise, the Level 1 Assessment is not satisfied.

1) The planar dimensions of the HIC damage satisfy Equations (7.7) and (7.8).

$$s \le 0.60\sqrt{Dt_c} \tag{7.7}$$

$$c \le 0.6\sqrt{Dt_c} \tag{7.8}$$

2) The through-thickness extent of the damage satisfies Equation (7.9).

$$w_H \le \min\left[\frac{t_c}{3}, 13\ mm\ (0.5\ in)\right] \tag{7.9}$$

3) The HIC damage is not surface breaking in accordance with paragraph 7.3.3.1(h) (see Equations (7.1) and (7.2)).

4) The distance between the edge of the HIC damage and the nearest weld seam satisfies Equation (7.10).

$$L_w > \max\left[2t_c,\ 25\,mm\ (1.0\,in)\right] \tag{7.10}$$

5) The distance from the edge of the HIC damage to the nearest major structural discontinuity satisfies Equation (7.11).

$$L_{msd} \ge 1.8\sqrt{Dt_c} \tag{7.11}$$

6) Further HIC damage has been prevented by one of the following means:

i) A barrier coating or overlay (e.g., an organic coating, metal spray, weld overlay, etc.) has been applied to prevent contact between the process environment and the metal.

ii) The equipment has been moved or the process environment altered such that no further hydrogen charging of the metal will occur.

d) STEP 4 – The Level 1 Assessment is complete; the component may be returned to service.

7.4.2.2 SOHIC Assessment Procedure

A Level 1 Assessment procedure for determining the acceptability of SOHIC damage is not provided; refer to paragraph 7.4.4.2 for assessment options.

7.4.2.3 Blister Assessment Procedure

The Level 1 Assessment procedure for determining the acceptability of blister damage in Type A components subject to internal pressure is shown below:

a) STEP 1 – Determine the information in paragraph 7.3.3.3.

b) STEP 2 – Determine the wall thickness to be used in the assessment using Equation (7.5) or (7.6), as applicable.

c) STEP 3 – If all the following requirements are satisfied, then proceed to STEP 4. Otherwise, the Level 1 Assessment is not satisfied.

1) The blister diameter and venting requirements meet one of the following criteria.

   i) The blister diameter is less than or equal to 50 mm (2 inches), or

   ii) The blister is vented either intentionally or by crown cracking and the dimensions satisfy Equations (7.7) and (7.8).

2) The minimum measured undamaged thickness measured from the side that is not bulged (see Figure 7.5) satisfies Equation (7.12).

$$t_{mm} \geq 0.5 t_c \tag{7.12}$$

3) The blister projection satisfies Equation (7.13).

$$B_p \leq 0.10 \cdot \min\left[s, c\right] \tag{7.13}$$

4) There are no periphery cracks directed towards the inside or outside surface of the component as shown in Figure 7.5.

5) The distance between the edge of the blister and the nearest weld seam satisfies Equation (7.10).

6) The distance from the blister edge to the nearest major structural discontinuity satisfies Equation (7.11).

d) STEP 4 – The Level 1 Assessment is complete; the component may be returned to service.

7.4.2.4 If the component does not meet the Level 1 Assessment requirements, then the following, or combinations thereof, can be considered:

a) The damaged material may be removed, repaired, or replaced.

b) The damage can be removed by blend grinding as shown in Figure 7.13, and the area evaluated as a local thin area per the assessment procedures of Part 5.

c) A Level 2 or Level 3 Assessment can be conducted.

7.4.3 Level 2 Assessment

7.4.3.1 HIC Assessment Procedure

The Level 2 Assessment procedure for determining the acceptability of HIC damage in Type A components subject to internal pressure and supplemental loads and Type B Class 1 components subject to internal pressure and supplemental loads is shown below. A logic diagram for a Level 2 Assessment is shown in Figure 7.11. The procedure shown below is developed for pressurized components where an $MAWP$ can be determined. For an atmospheric storage tank, the same procedure can be followed to determine a MFH by replacing the $MAWP$ with the MFH, and determining the MFH using the applicable code equations for a tank shell.

a) STEP 1 – Determine the information in paragraph 7.3.3.1.

b) STEP 2 – Determine the wall thickness to be used in the assessment using Equation (7.5) or (7.6).

c) STEP 3 – If the distance between the edge of the HIC damage and the nearest weld seam satisfies Equation (7.10), then proceed to STEP 4. Otherwise, the Level 2 Assessment is not satisfied.

d) STEP 4 – If the distance from the edge of the HIC damage to the nearest major structural discontinuity satisfies Equation (7.11), then proceed to STEP 5. Otherwise, the Level 2 Assessment is not satisfied.

e) STEP 5 – Classify the damage as either subsurface HIC or surface breaking HIC in accordance with paragraph 7.3.3.1(h) (see Equations (7.1) and (7.2)) and proceed to STEP 6.

f) STEP 6 – Determine the $MAWP$ for the component (see Part 4) using the thickness from STEP 2.

g) STEP 7 – Calculate the Remaining Strength Factor based on the type of HIC damage. In both cases, the damage parameter for HIC damage shall be set equal to 80%, or $D_H = 0.80$.

1) The Remaining Strength Factor for surface-breaking HIC damage is computed using Equation (7.14). The parameter M_t in Equation (7.14) is determined from Part 5, Table 5.2 using the value of λ given by Equation (7.15).

$$RSF = \frac{1 - \left[\frac{w_H \cdot D_H}{t_c}\right]}{1 - \frac{1}{M_t}\left[\frac{w_H \cdot D_H}{t_c}\right]} \tag{7.14}$$

$$\lambda = \frac{1.285s}{\sqrt{Dt_c}} \tag{7.15}$$

2) The Remaining Strength Factor for subsurface HIC damage is computed using Equation (7.16). The parameter L_R in Equation (7.16) is given by Equation (7.17) where L_{Hs} is determined in accordance with Figure 7.3.

$$RSF = \frac{2L_R + s\left[1 - \left(\frac{w_H \cdot D_H}{t_c}\right)\right]}{2L_R + s} \tag{7.16}$$

$$L_R = \min\left[\frac{L_{Hs}}{2}, 8t_c\right] \tag{7.17}$$

h) STEP 8 – If $RSF \geq RSF_a$, then the longitudinal extent of the HIC damage satisfies the LTA portion of the assessment at the $MAWP$ determined in STEP 6. If $RSF < RSF_a$, then the HIC damage is acceptable for operation at $MAWP_r$, where $MAWP_r$ is computed using the equations in Part 2, paragraph 2.4.2.2. The $MAWP$ from STEP 6 shall be used in this calculation. See Part 2, paragraph 2.4.2.2(e) to determine the acceptability of the equipment for continued operation.

i) STEP 9 – For cylindrical shells, conical shells, and elbows, evaluate the circumferential extent of the HIC damage using an equivalent LTA and the procedures in Part 5 paragraph 5.4.2.2(i); Proceed to STEP 10 if passes, otherwise the supplemental load procedure in paragraph 5.4.3.4 can be used for a more detailed analysis. The equivalent LTA shall have a depth computed using Equation (7.18) and a length equal to the circumferential extent of the HIC damage zone. If the HIC damage is located on the outside surface or is sub-surface, then the equivalent LTA shall be assumed to be on the outside surface. If the HIC is on the inside surface, then the equivalent LTA shall be assumed to be on the inside surface.

$$d_{HIC} = w_H D_H \tag{7.18}$$

j) STEP 10 – Determine whether a fracture assessment is required. If any of the following criteria apply, then proceed to STEP 11; otherwise, proceed to STEP 12.

1) The equipment remains in hydrogen charging service, and hydrogen charging has not been halted by means of a barrier coating, overlay, or process change.

2) The HIC damage is classified as surface-breaking (see paragraph 7.3.3.1(h)).

3) The through-wall extent of the HIC damage satisfies Equation (7.19).

$$w_H > \min\left[\frac{t_c}{3}, 13\,mm\ (0.5\ in.)\right] \tag{7.19}$$

k) STEP 11 – Evaluate the HIC damage as a crack-like flaw in accordance with the procedures of Part 9 in conjunction with the requirements shown below. If the Part 9 assessment is acceptable, then proceed to STEP 12. Otherwise, the Level 2 Assessment is not satisfied.

1) Flaw Size – two crack-like flaw assessments shall be performed, one for the longitudinal direction and one for the circumferential direction.

i) The longitudinal crack-like flaw length shall be set equal to the longitudinal extent of HIC damage, s. The crack-like flaw depth shall be set equal to the maximum extent of HIC damage in the through thickness direction, w_H.

ii) The circumferential crack-like flaw length shall be set equal to the circumferential extent of HIC damage, c. The crack-like flaw depth shall be set equal to the maximum extent of HIC damage in the through thickness direction, w_H.

2) Fracture Toughness – If hydrogen charging of the steel has not been halted by means of a barrier coating, overlay, or process change, then the toughness used in the Part 9 assessment shall include the effects of hydrogen charging and shall be indexed to the lower bound fracture arrest curve K_{IR} in accordance with the methods specified in Annex 9F of this Standard.

l) STEP 12 – Confirm that further HIC damage has been either prevented or is limited to a known or verifiable rate by one or more of the following means, then proceed to STEP 13. Otherwise, the Level 2 Assessment is not satisfied.

1) Establishment of a barrier coating (e.g., organic, inorganic, metal spray, etc.).

2) Use of corrosion inhibitors or other process chemicals that reduce the severity of hydrogen charging.

3) Modification of process or operating conditions to reduce the severity of hydrogen charging.

4) Use of devices that monitor hydrogen permeation through the equipment.

5) Review of historical records indicating that HIC damage size and extent is stable or progressing at a well-defined rate.

6) Monitoring of defects at an established interval to ensure growth rates are within expected limits.

m) STEP 13 – The Level 2 Assessment is complete; the component may be returned to service.

7.4.3.2 SOHIC Assessment Procedure

A Level 2 Assessment procedure for determining the acceptability of SOHIC damage is not provided; refer to paragraph 7.4.4.2 for assessment options.

7.4.3.3 Blister Assessment Procedure

The Level 2 Assessment procedure for determining the acceptability of blister damage in Type A components subject to internal pressure and supplemental loads and Type B class 1 components subject to internal pressure and supplemental loads is given below. A logic diagram for a Level 2 Assessment is provided in Figure 7.12. The procedure shown below is developed for pressurized components where an $MAWP$ can be determined. For an atmospheric storage tank, the same procedure can be followed to determine a MFH by replacing the $MAWP$ with the MFH, and determining the MFH using the applicable code equations for a tank shell.

a) STEP 1 – Determine the information in paragraph 7.3.3.3.

b) STEP 2 – Determine the wall thickness to be used in the assessment using Equation (7.5) or Equation (7.6).

c) STEP 3 – If the distance from the blister edge to the nearest major structural discontinuity satisfies Equation (7.11), then proceed to STEP 4. Otherwise, the Level 2 Assessment is not satisfied.

d) STEP 4 – If the blister has periphery cracks toward either the internal or external surface, then proceed to STEP 5; otherwise, proceed to STEP 6.

e) STEP 5 – If the blister is bulged toward the internal surface and has periphery cracks toward the external surface, or if the blister is bulged toward the external surface and has periphery cracks toward the internal surface (i.e., periphery cracks are on the opposite side from the bulging), then the blister does not pass the Level 2 Assessment. If the periphery cracks are on the same side as the bulging, then proceed to STEP 9.

f) STEP 6 – If the blister does not have a crown crack, then proceed to STEP 7. If the blister has a crown crack, then proceed to STEP 9.

g) STEP 7 – If the blister projection above the surface satisfies Equation (7.13), then proceed to STEP 8. Otherwise, proceed to STEP 9.

h) STEP 8 – If the blister is vented, then go to STEP 10. If the blister is unvented, then proceed to STEP 11. Note that venting is recommended for an unvented blister, except that venting of a blister to the inside surface is not recommended for components in hydrofluoric acid service because of the safety concerns regarding contamination, decontamination, and the potential for corrosion and scale build-up within the blister.

i) STEP 9 – The blister shall be evaluated as an equivalent local thin area using the methods of Part 5. The remaining sound metal thickness to use in the LTA analysis is t_{mm}, as shown in Figures 7.5 through 7.8. The diameter of the local thin area shall be determined using the following criteria.

   1) If the blister projection does not satisfy Equation (7.13) and the blister does not have periphery cracks, then the blister diameter shall be used as the size of the region of local metal loss.

   2) If the blister projection satisfies Equation (7.13) and the blister has only crown cracks, then the blister diameter or the length of the crown crack (see paragraph 7.3.3.3) can be used as the size of the region of local metal loss with a remaining thickness equal to t_{mm} (see Figure 7.6).

   3) If the blister has periphery cracks, then the size of local metal loss to use in the assessment is the blister diameter plus any crack growth extension at the periphery.

j) STEP 10 – If the distance between the edge of the blister and the nearest weld seam satisfies Equation (7.10) then go to STEP 12; otherwise go to STEP 11.

k) STEP 11 – An in-service monitoring system should be developed to monitor blister growth while the component is in service, go to STEP 12.

l) STEP 12 – The Level 2 Assessment is complete; the component may be returned to service.

7.4.3.4 If the component does not meet the Level 2 Assessment requirements (see Part 2, paragraph 2.4.2.2(e)) then the following, or combinations thereof, can be considered:

a) The component may be rerated, and the Level 2 Assessment procedures repeated.

b) The damaged material may be removed, repaired, or replaced.

c) A Level 3 Assessment can be conducted.

7.4.4 Level 3 Assessment

7.4.4.1 HIC Assessment Procedure

The Level 3 Assessment procedure for determining the acceptability of HIC damage is given below.

a) All Level 3 Assessments of HIC damage shall explicitly address the following:

   1) Potential for failure due to loss of load bearing capability, and the remaining strength of the component.

   2) Potential for failure due to fracture.

   3) The expected future progression (if any) of the damage.

   4) Future inspection requirements, including whether in-service monitoring is required.

b) If the HIC damage does not satisfy the Level 2 Assessment criteria because of complex component geometry, applied loading, or the damage is close to structural discontinuities, then the Level 3 analysis should include a detailed stress analysis per the techniques discussed in Annex 2D of this Standard.

c) A Level 3 Assessment of HIC damage may be performed using the Level 2 Assessment procedure with a HIC damage parameter value of less than 80%, or $D_H = 0.80$. If a value less than 80% is utilized, this value shall correspond to inspection information and appropriate correlations between the inspection information and the remaining strength of the HIC Damaged Zone. The final value of the HIC damage parameter utilized in the assessment shall be fully documented and included in the assessment results.

d) A Level 3 Assessment of HIC damage may be performed using a numerical method such as Finite Element Analysis (FEA) considering explicit modeling of HIC damaged and undamaged areas in accordance with Annex 2D of this Standard. In this analysis, the HIC damaged area may be modeled as elastic-perfectly plastic material and the undamaged area may be modeled using an elastic-perfectly plastic material or elastic-plastic material with strain hardening unless information is available to justify alternative material models for each of these areas.

e) A fracture mechanics analysis in accordance with Part 9 of this Standard shall be considered for all Level 3 Assessments. If a fracture mechanics assessment is performed, then effects of hydrogen on the fracture toughness of the steel shall be considered unless hydrogen is precluded from entering the steel during operation.

7.4.4.2 SOHIC Assessment Procedure

A Level 3 Assessment of SOHIC shall be based on the assessment procedures of Part 9, with particular attention given to potential hydrogen effects on future crack growth and fracture toughness.

a) There is currently no accepted method for predicting SOHIC crack growth rate, and therefore no basis for returning actively growing cracks to service. The arrest of SOHIC cracks shall be provided by one of the following or comparable means, and shall be documented in the analysis:

   1) Reduction and control of the hydrogen flux rate to a level below that which caused the existing damage.

   2) Reduction of the crack tip stress intensity that caused the damage.

   3) Alteration of the microstructure ahead of the damage zone to preclude further crack propagation.

b) A fracture assessment is required in accordance with the procedures of Part 9, and the following additional requirements:

   1) Inspection techniques shall be applied that can interrogate the affected volume of material and assess the subsurface extent of the damage. The efficacy of the method(s) used should be demonstrated specifically for SOHIC damage, including suitable provisions for sizing accuracy.

   2) An analysis shall be performed to assess the stress state of the SOHIC damage zone, including primary, secondary, and residual stresses that may affect the crack tip stress intensity. This shall include all stresses which may contribute to the subcritical growth of SOHIC damage, even those that are not normally considered to contribute to brittle fracture.

   3) If the hydrogen charging of the steel has not been halted by means of a barrier coating, overlay, or process change, then the material toughness used in the fracture assessment shall account for the effect of hydrogen charging by indexing to the lower bound fracture arrest curve K_{IR}, in accordance with the methods specified in Annex 9F of this Standard, or an alternative method that is fully documented.

c) Periodic monitoring can be used to confirm the absence of crack growth. However, when conditions for SOHIC are favorable, crack growth may be so rapid as to render periodic monitoring impractical.

7.4.4.3 Blister Assessment Procedure

A Level 3 Assessment for blisters consists of performing a detailed stress analysis in accordance with the techniques in Annex 2D of this Standard. In addition, if cracks are detected at the blister location by inspection, a fracture mechanics assessment in accordance with Part 9 of this Standard shall be performed. If a component has a multitude of closely spaced blisters (see Figure 7.9), then it is recommended to first use the concepts of this Part to evaluate individual blisters. If the criterion for individual blisters is not satisfied, the array of blisters can then be modeled as equivalent pitting damage, and the assessment procedures of Part 6 can be used to evaluate the overall weakening effect due to the blister array.

7.5 Remaining Life Assessment

7.5.1 HIC and SOHIC Growth Rates

At the present time, there is no widely accepted method to predict the growth rate of active HIC or SOHIC damage; therefore, a standard method to assess the remaining life of a damaged structure cannot be established.

Therefore, unless the determination can be made that the HIC or SOHIC damage is dormant, periodic monitoring is required.

7.5.2 Blister Growth

The growth rate and the remaining life of a blister cannot be adequately evaluated using analytical techniques. However, a remaining life evaluation is not required because the presence of blisters in equipment does not have a direct effect on the internal inspection interval except for the special inspection requirements required for in-service monitoring.

7.6 Remediation

7.6.1 Elimination of Hydrogen Charging

Elimination or reduction of hydrogen charging by means of a barrier coating (e.g., organic, metal spray, weld overlay, etc.) or lining, or by changing the process environment is required for Level 1 Assessments of HIC damage (see paragraph 7.4.2.1) and for Level 3 Assessment of SOHIC damage (see paragraph 7.4.4.2).

7.6.2 Controlling Hydrogen Charging

Even when not required, the progression of HIC, SOHIC, and blister damage can be reduced or eliminated by controlling the hydrogen charging. Consideration should be given to applying a barrier coating (e.g., organic, metal spray, weld overlay, etc.) or lining to the inside surface of equipment with HIC, SOHIC, or blister damage to prevent further hydrogen charging and damage, particularly in the weld regions. In addition, process changes and/or inhibitor additions that would decrease the hydrogen charging should also be evaluated and considered.

7.6.3 Venting of Blisters

Blisters meeting the acceptance criteria of any assessment level should be considered for venting if the blister is deeper than 3 mm (0.125 inches) from the bulged surface and the blister diameter exceeds 50 mm (2 inches).

a) Venting of blisters may involve risk and all applicable plant safety guidelines should be reviewed and followed. If the component is in-service, additional inspection is required prior to drilling.

b) Venting of blisters can typically be accomplished by drilling a small diameter hole (e.g., 3 mm (0.125 inches)) in the center of the blister from the surface where the bulging is observed. Blisters located on the inside surface of equipment may be vented to the inside, or may be vented from the outside during downtime periods provided:

   1) The blister is parallel to the surface as confirmed by inspection.

   2) The blister is not already vented to the inside by crown or periphery cracking.

   3) The component is not in hydrofluoric acid service.

c) Electric drills should not be used to vent blisters because of the presence of hydrogen in the blister cavity. Air-driven drills should be used, and suitable safety provisions should be made to ensure that ignition of the hydrogen released during the drilling operation does not occur (see NACE Standard SP0296-10). An inert gas and other safety provisions can be utilized to purge the area to help ensure that ignition does not occur.

7.6.4 Blend Grinding

Blend grinding and weld repair techniques can be used to repair HIC, SOHIC, or blister damage. Caution should be exercised when conducting weld repairs on hydrogen charged steel to prevent crack growth and/or subsequent

re-cracking. A hydrogen bake-out should be considered prior to welding or grinding. The application of a suitable coating after blend grinding or weld repairs should be considered. All blend ground areas should be rechecked using either MT or PT examination techniques.

7.6.5 Repair and Replacement of Damaged Material

If the material is severely damaged and cannot be accepted per the assessment procedures or repaired, it should be replaced. The metallurgy and design of the replacement material, weld details and weld procedures should be reviewed by a materials engineer and a mechanical engineer (see Part 1, paragraph 1.4.3).

7.6.6 NACE Standard SP0296-10

Additional information regarding remediation and repair of HIC and SOHIC damage can be found in NACE Standard SP0296-10.

7.7 In-Service Monitoring

7.7.1 Monitoring for Hydrogen Charging

Periodic monitoring of the process stream for hydrogen charging conditions and/or of the equipment for additional damage should be considered, once HIC, SOHIC, or blister damage has been observed. Monitoring of such damage, particularly damage adjacent to welds that are not vented, is important when the driving force for blister formation and growth (i.e., hydrogen pressure in the blister cavity) has not been relieved.

7.7.2 Inspection Methods for Monitoring

Various inspection methods can be used to monitor HIC, SOHIC, and blister damage growth. Common methods are straight beam UT for HIC and blisters and angle beam UT for HIC and SOHIC damage. Hydrogen charging levels can be monitored by either intrusive or non-intrusive hydrogen probes attached to the external surface of the equipment to measure hydrogen activity either directly, by pressure build up, or by electrochemical means. The inspection monitoring interval can be adjusted based on the measured hydrogen charging levels.

7.7.3 Detection of HIC, SOHIC, or Blister Damage Growth

If the HIC, SOHIC, or blister damage is found to grow during the monitoring process, the evaluation procedures in paragraph 7.4 and the remediation guidelines in paragraph 7.6 should be reviewed and implemented based on the severity of the damage that is anticipated.

7.8 Documentation

7.8.1 General

The documentation of the FFS Assessment should include the information cited in Part 2, paragraph 2.8.

7.8.2 Inspection Data

The location, size, spacing and condition of existing HIC, SOHIC, and blister damage should be recorded along with the results of the assessments performed. Sample data sheets for HIC and blister damage are shown in Tables 7.1 and 7.2, respectively. The data sheet for crack-like flaws included in Part 9 can be used for SOHIC damage.

7.8.3 In-Service Monitoring

If HIC, SOHIC, or blister damage growth is detected during the monitoring process, the physical dimensions and location of the damage should be recorded along with the time period between measurements. In addition, the associated operating conditions and process stream constituents should be recorded to permit an evaluation of the hydrogen-charging environment relative to the operation of the equipment. This information may be valuable in determining suitable process changes in the operation of the equipment, if possible, to mitigate further damage.

7.9 Nomenclature

a depth of a SOHIC crack (see Figure 7.4 and Part 9).

B_p blister bulge projection.

c HIC damage or blister dimension in the circumferential direction.

$2c$ length of a SOHIC crack (see Figure 7.4 and Part 9).

c_1 HIC or blister dimension for HIC damage area 1 in the circumferential direction.

c_2 HIC or blister dimension for HIC damage area 2 in the circumferential direction.

d_{HIC} effective through thickness extent of HIC damage after accounting for the remaining strength of the damaged material.

D inside diameter corrected for $LOSS$ and FCA allowance as applicable.

D_H HIC Damage parameter that relates the strength of HIC damaged steel to that of undamaged steel. For example, zero percent of HIC damage corresponds to $D_H = 0.0$, 80% HIC damage corresponds to $D_H = 0.80$, and 100% HIC damage corresponds to $D_H = 1.0$. A $D_H = 1.0$ indicates that the HIC damaged area does not have any structural strength.

FCA future corrosion allowance in the damage area.

$LOSS$ amount of uniform metal loss at the time of inspection, or uniform metal loss away from the damage area at the time of the inspection.

L_B blister-to-blister or blister-to-HIC spacing.

L_H edge-to-edge spacing between HIC damage and the nearest HIC or blister damage.

L_{Hs} HIC-to-HIC or HIC-to-blister spacing in the longitudinal direction.

L_{SH} SOHIC to HIC or blister damage spacing.

L_R extent of non-damaged material available for reinforcement of the HIC damaged area.

L_{msd} spacing to nearest major structural discontinuity.

L_W spacing to nearest weld joint.

λ longitudinal flaw length parameter.

$MAWP$ maximum allowable working pressure of the undamaged component (see Annex 2C, paragraph 2C.2).

$MAWP_r$ reduced maximum allowable working pressure of the damaged component.

MFH maximum fill height of the undamaged component.

MFH_r reduced maximum fill height of the damaged component.

M_t Folias Factor based on the longitudinal or meridional flaw parameter.

RSF computed remaining strength factor based on the meridional extent of the HIC or blister.

RSF_a allowable remaining strength factor (see Part 2, paragraph 2.4.2.2).

s HIC or blister dimension in the longitudinal direction.

s_c length of a blister crown crack or diameter of a vent hole.

s_1 HIC or blister dimension for HIC damage area 1 in the longitudinal direction.

s_2 HIC or blister dimension for HIC damage area 2 in the longitudinal direction.

t_c corroded wall thickness, allowing for future corrosion loss.

t_{mm} minimum measured thickness of undamaged metal at the blister or HIC being evaluated, modified by the future corrosion allowance (FCA) as required.

t_{mm-ID} minimum measured thickness of undamaged metal on the internal side of HIC damage, modified by the future corrosion allowance (FCA) as required.

t_{mm-OD} minimum measured thickness of undamaged metal on the external side of HIC damage, modified by the future corrosion allowance (FCA) as required.

t_{nom} nominal or furnished thickness of the component adjusted for mill under tolerance as applicable.

t_{rd} uniform thickness away from the damage area established by thickness measurements at the time of the inspection.

w_H thickness of HIC damage as measured in the through-thickness direction, modified by the future corrosion allowance (FCA) as required.

W width of the weld.

7.10 References

References for this Part are provided in Annex 7A – Technical Basis and Validation – Assessment of Hydrogen Blisters and Hydrogen Damage Associated with HIC and SOHIC.

7.11 Tables

Table 7.1 – Size, Location, Condition, and Spacing for HIC Damage

Enter the data obtained from a field inspection on this form.

Inspection Date: _____

Equipment Identification: _____

Equipment Type: _____ Pressure Vessel _____ Storage Tank _____ Piping Component

Component Type & Location: _____

_____

_____

t_{nom}: _____

$LOSS$: _____

FCA: _____

t_{rd}: _____

Data Required for Level 1 and Level 2 Assessment					
HIC Identification					
Diameter s (1)					
Dimension c (1)					
Edge-To-Edge Spacing to Nearest HIC or Blister L_H (2)					
Minimum Measured Thickness to Internal Surface t_{mm-ID} (3)					
Minimum Measured Thickness to External Surface t_{mm-OD} (3)					
Minimum Measured Thickness; Total of Both Sides t_{mm} (3)					
Spacing to Nearest Weld Joint L_W (2)					
Spacing to Nearest Major Structural Discontinuity L_{msd}					

Notes:
1. The HIC-to-HIC spacing may affect the size of the HIC damage to be used in the evaluation (see paragraph 7.3.3.1(i)).
2. See Figure 7.3.
3. See Figure 7.2.

Table 7.2 – Size, Location, Condition, and Spacing for Blisters

Enter the data obtained from a field inspection on this form.

Inspection Date: _____

Equipment Identification: _____

Equipment Type: _____ Pressure Vessel _____ Storage Tank _____ Piping Component

Component Type & Location: _____

_____

_____

Data Required for Level 1 and Level 2 Assessment					
Blister Identification					
Diameter s (1)					
Dimension c (1)					
Edge-To-Edge Spacing to Nearest Blister L_B (1)					
Bulge Direction (inside/ outside)					
Blister Projection B_p					
Minimum Measured Thickness t_{mm}					
Cracking at Periphery (Yes/No)					
Crown Cracking or Venting (Yes/No) (2)					
Length of Crown Crack or Diameter of Vent Hole s_c (2)					
Spacing to Nearest Weld Joint L_W (3)					
Spacing to Nearest Major Structural Discontinuity L_{msd}					

Notes:

1. The blister-to-blister spacing may affect the size of the blister to be used in the evaluation (see paragraph 7.3.3.3(a) and 7.3.3.3(b)).
2. If the blister has crown cracks, enter the length of the crack (see dimension s_c in Figure 7.6). If the blister has a vent hole, indicate as such with the diameter of the hole (see Figure 7.7).
3. See Figure 7.8.

7.12 Figures

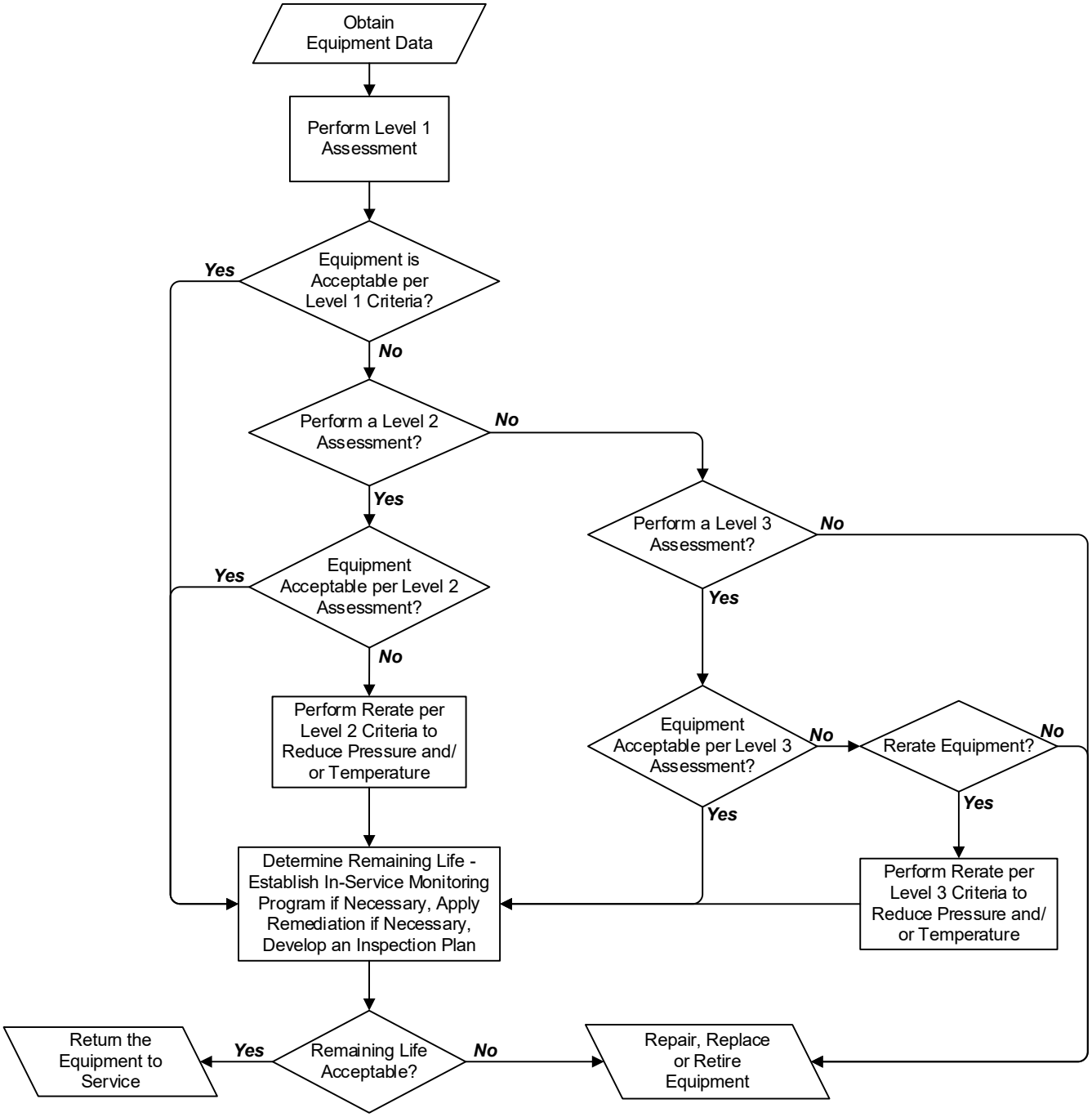

Figure 7.1 – Overview of the Assessment Procedure to Evaluate a Component with HIC or Hydrogen Blisters

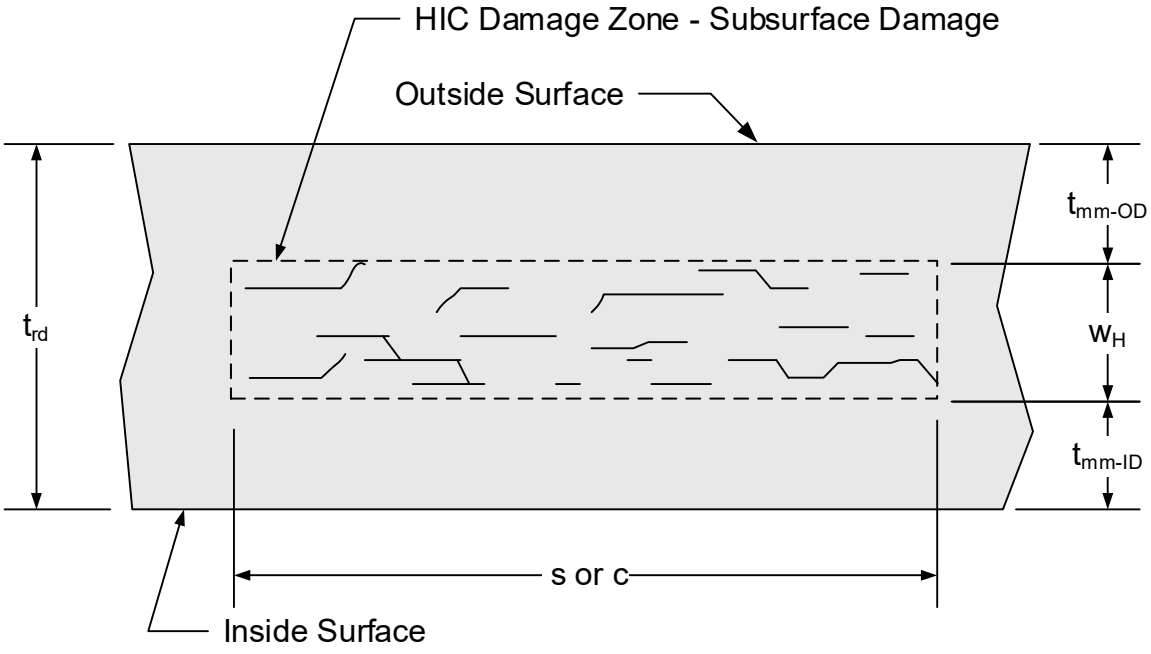

a) Typical Subsurface HIC Damage

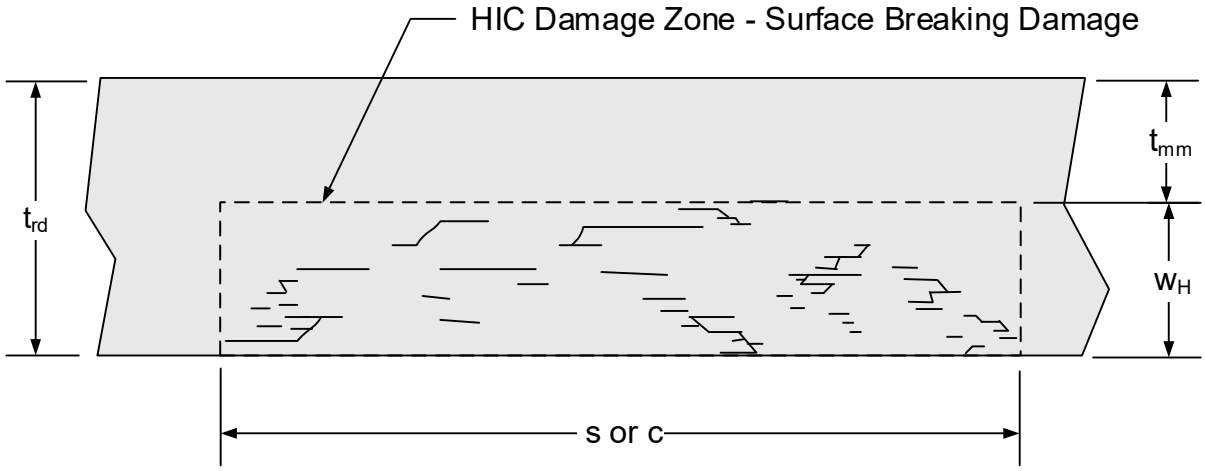

b) Typical Surface Breaking HIC Damage

Note: w_H, t_{mm}, t_{mm-ID}, *and* t_{mm-OD}, shall be modified by the FCA as appropriate.

Figure 7.2 – Surface and Subsurface HIC Damage

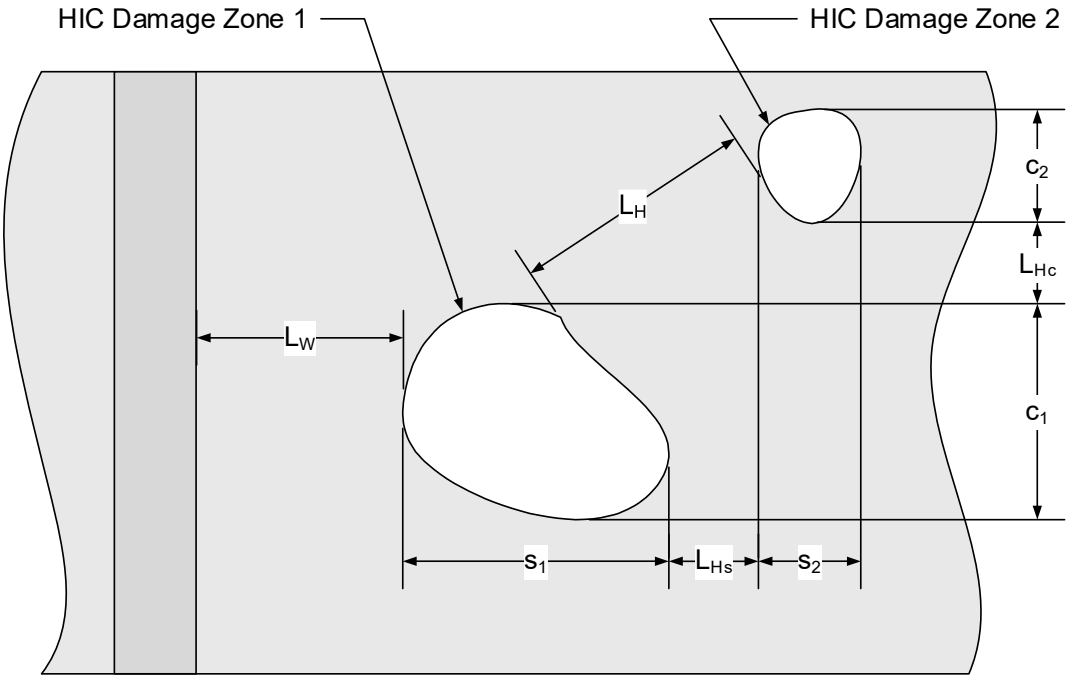

a) Planar View of HIC Damage Close to a Weld Seam and to Other HIC Damaged Zones

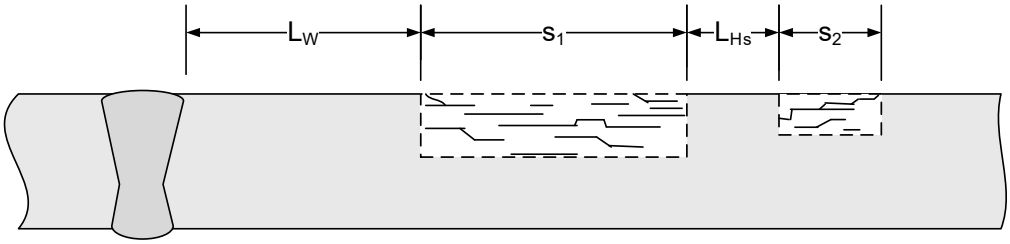

b) Cross Sectional View of HIC Damage Close to a Weld Seam and to Other HIC Damage

Figure 7.3 – HIC Damage in Proximity to a Weld or Other HIC damage

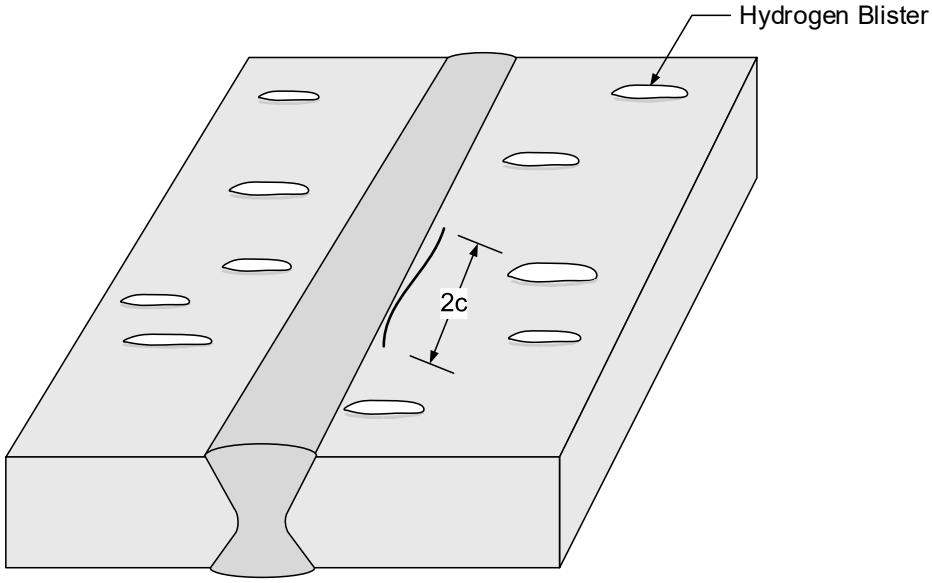

Note: The Length of the Crack-Like Flaw Should be Established Using Applicable NDE Methods. If a Series of Crack-Like Flaws are Present, the Individual Flaws Shall be Combined in Accordance with the Flaw Interaction Procedures of Part 9.

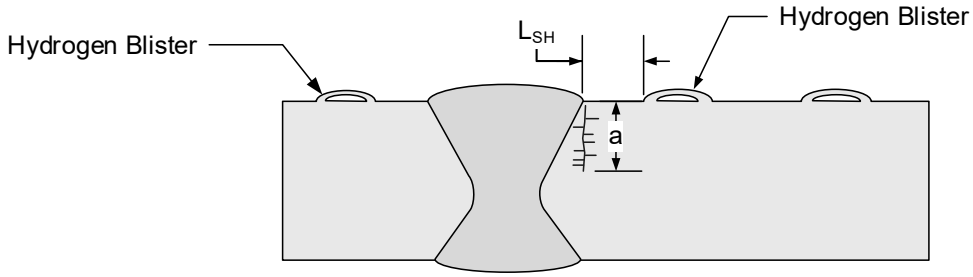

Figure 7.4 – SOHIC Damage

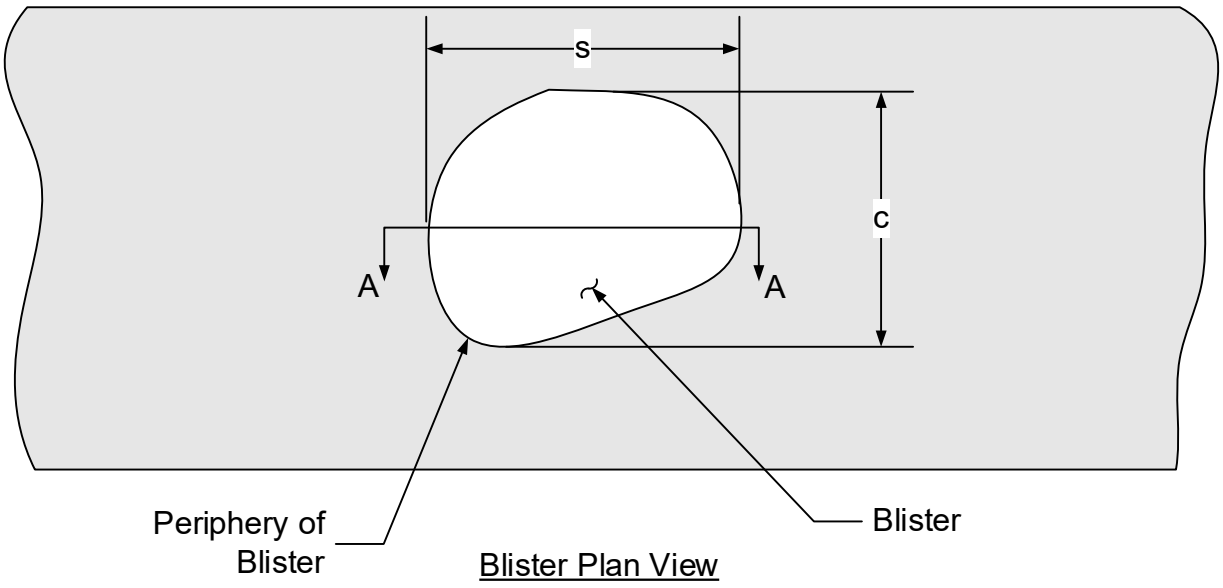

Blister Plan View

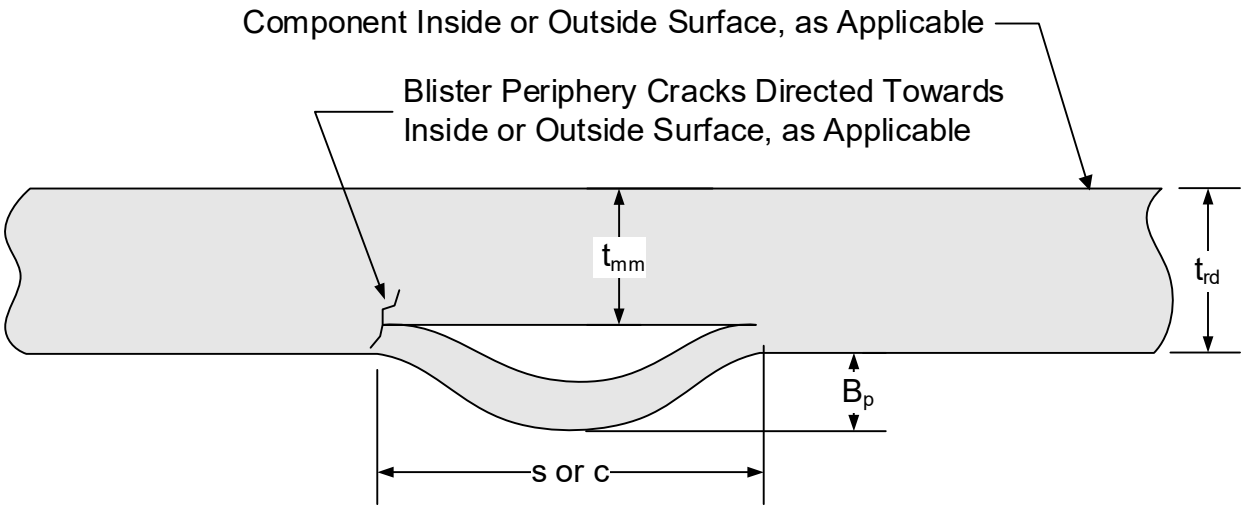

Section A-A
Cross Section Of Blister

Notes:

1. The blister diameter to be used in the assessment is defined in paragraph 7.3.3.3(a).
2. t_{mm} shall be modified by the FCA as appropriate.

Figure 7.5 – Typical Hydrogen Blister

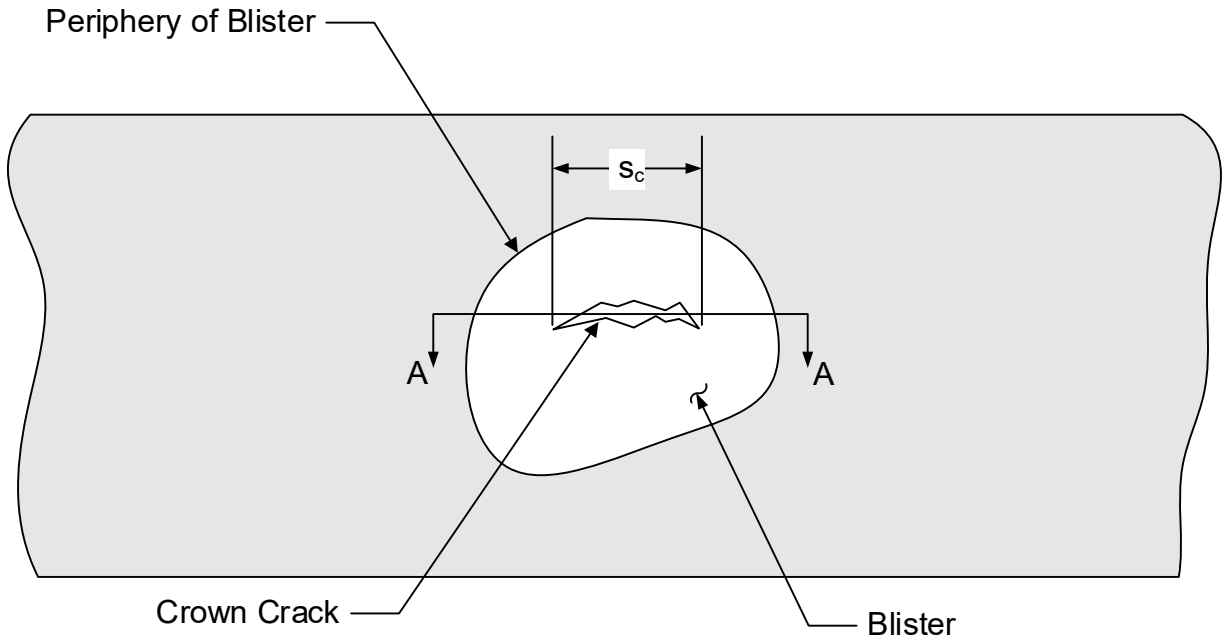

Blister Plan View

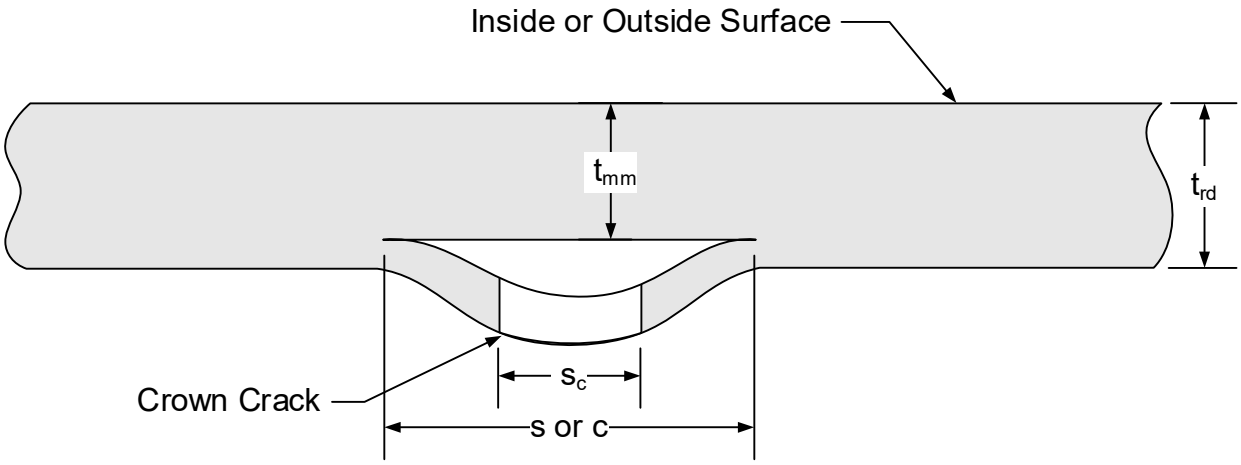

Section A-A
Cross Section of Blister

Notes:

1. The blister diameter to be used in the assessment is defined in paragraph 7.3.3.3(a).
2. t_{mm} shall be modified by the FCA as appropriate.
3. The dimension s_c can be used to characterize the length of an equivalent LTA for a blister with a crown crack that satisfies the HIC projection criterion; alternatively, the dimension $\max[s, c]$ can be used.

Figure 7.6 – Blister with a Crown Crack

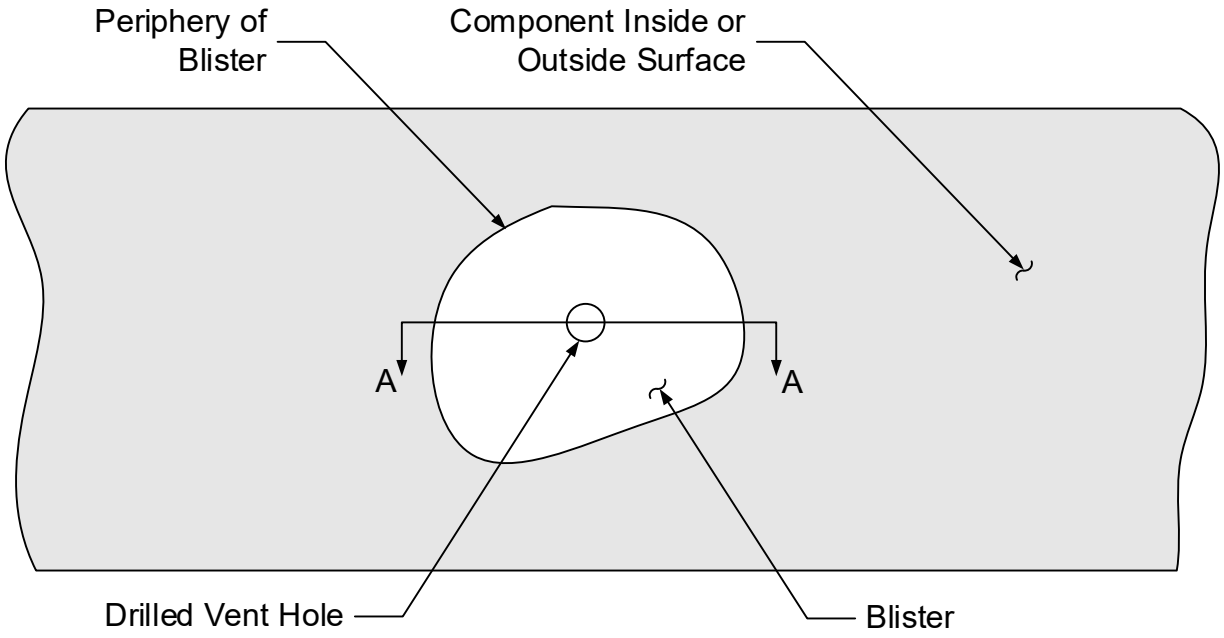

Blister Plan View

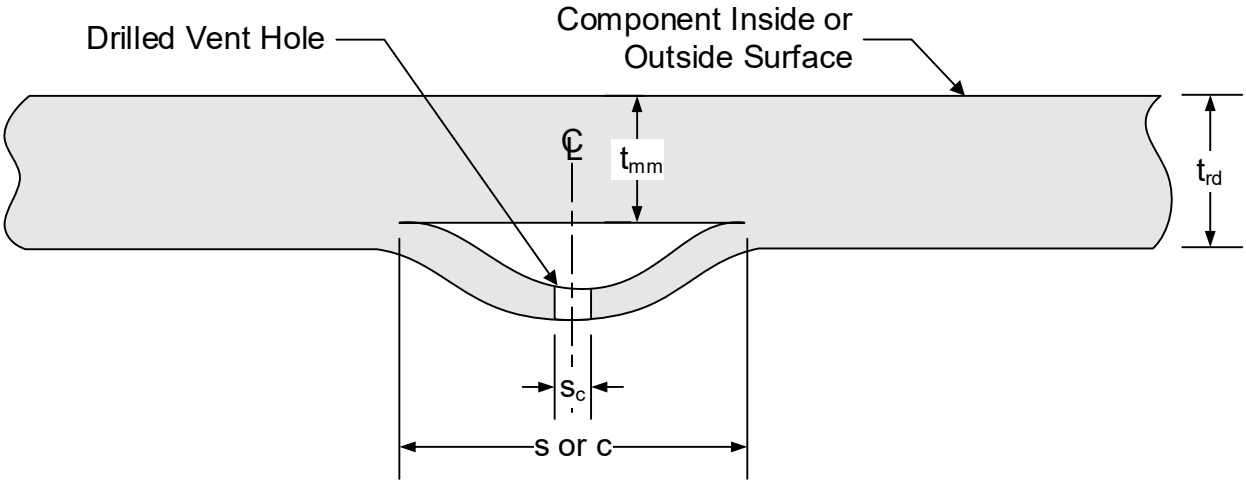

Section A-A
Cross Section of Blister

Notes:

1. The blister diameter to be used in the assessment is defined in paragraph 7.3.3.3(a).
2. t_{mm} shall be modified by the FCA as appropriate.

Figure 7.7 – Blister with a Vent Hole

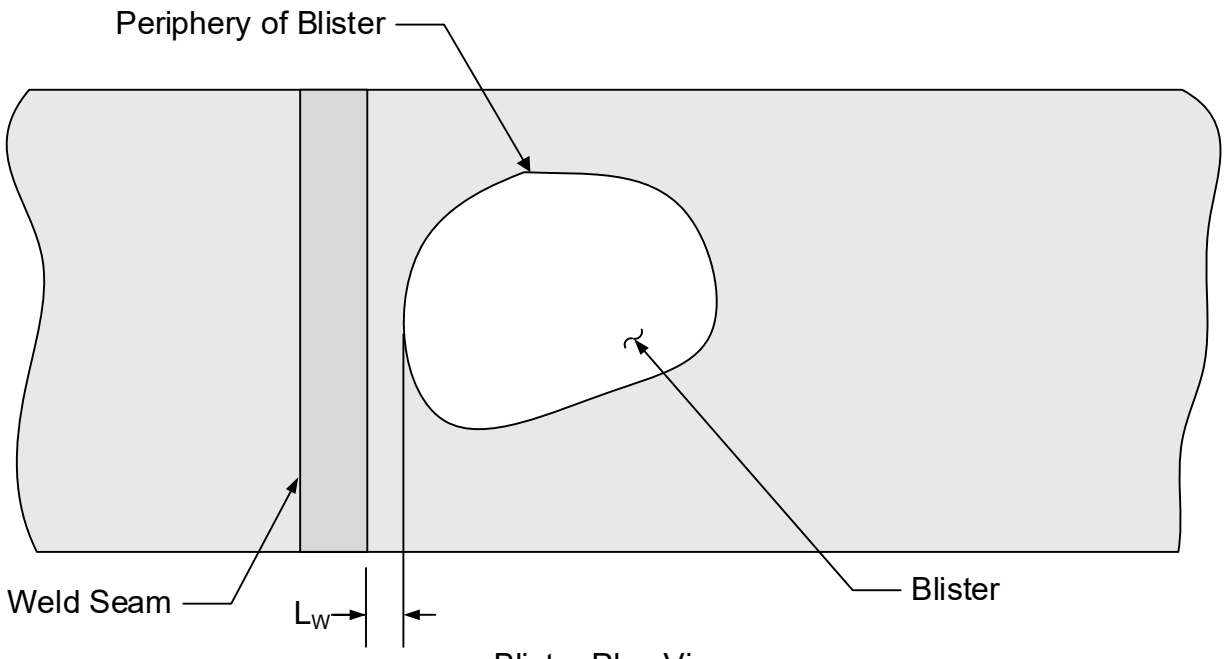

a) Blister Spacing to a Weld Seam

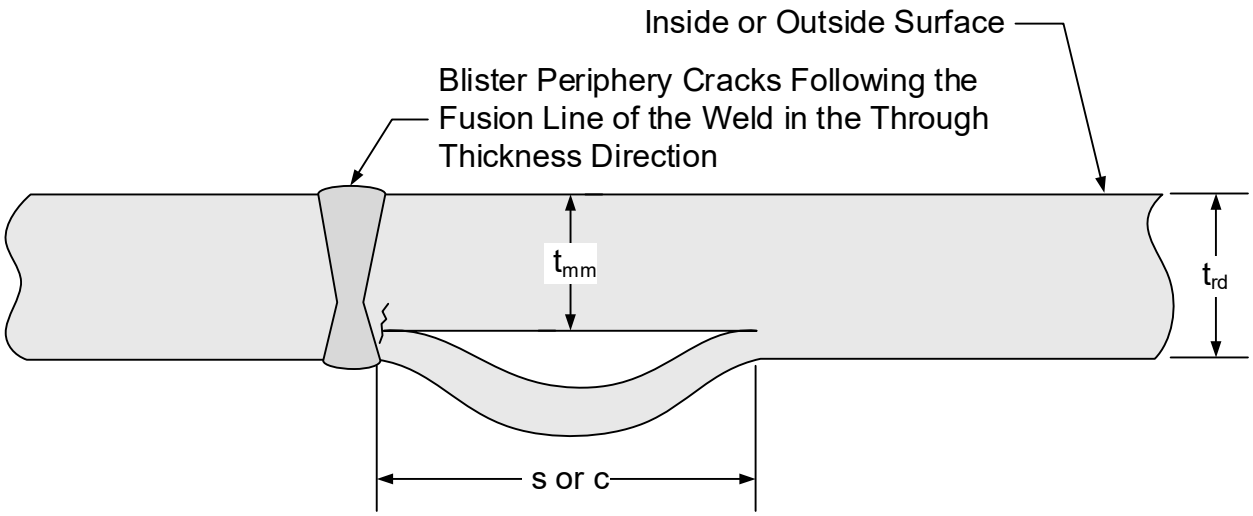

b) Blister Periphery Cracks at the Weld Joint

Notes:

1. The blister is considered to be close to a weld seam if $L_w < \max[2t_c, 25\ mm\ (1.0\ in.)]$.
2. The blister diameter to be used in the assessment is defined in paragraph 7.3.3.3(a).
3. t_{mm} shall be modified by the FCA as appropriate.

Figure 7.8 – Blister Periphery Cracks at a Weld

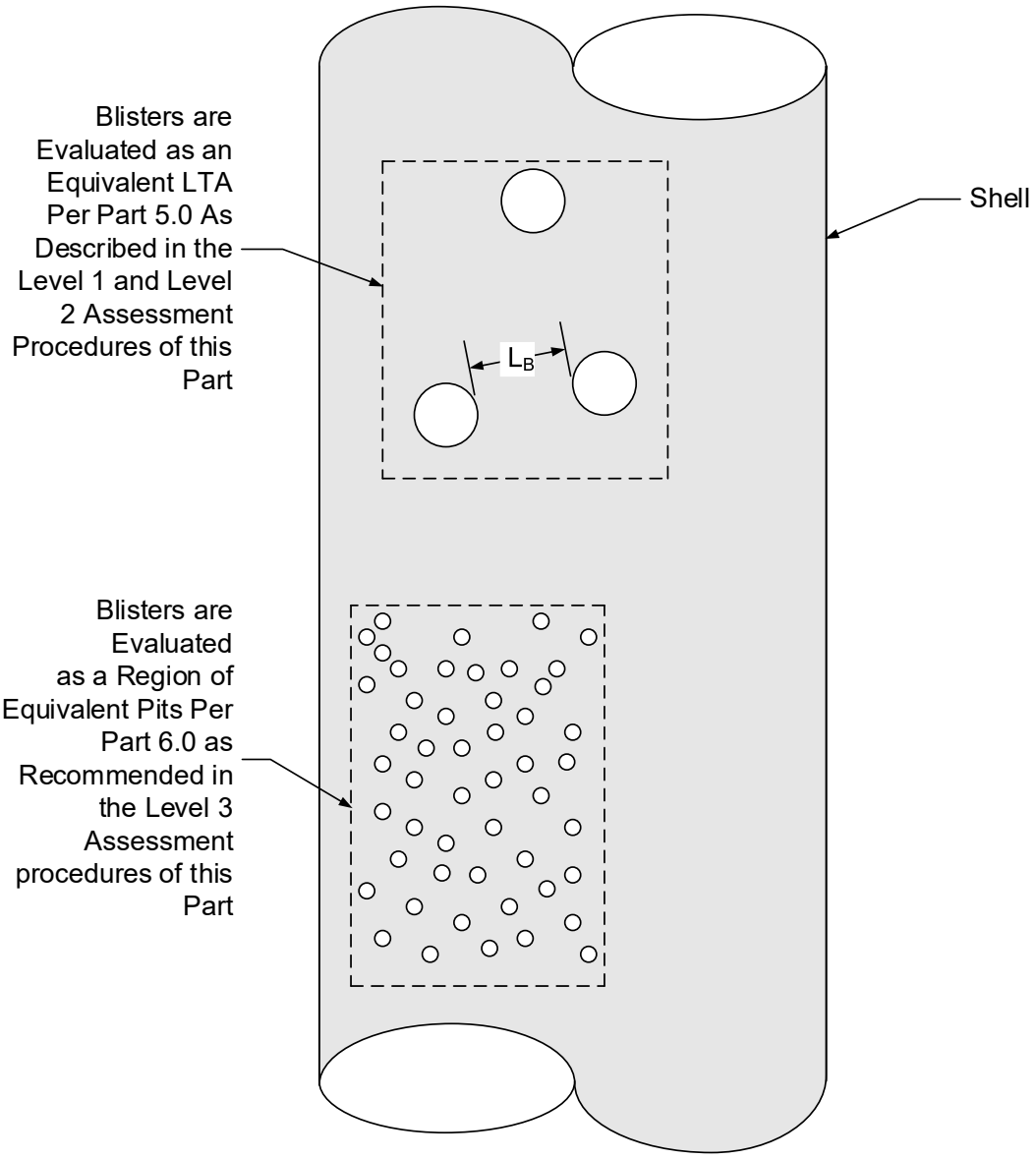

Figure 7.9 – Additional Assessment Requirements for Closely Spaced Blisters

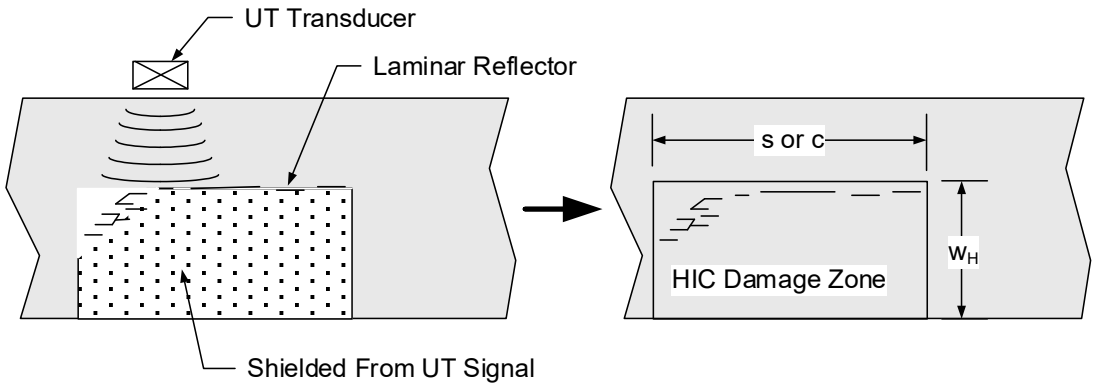

Single Sided UT Exam; if HIC Damage is Found, Treat the Associated Area Shielded From UT Signal as Also Being HIC Damaged.

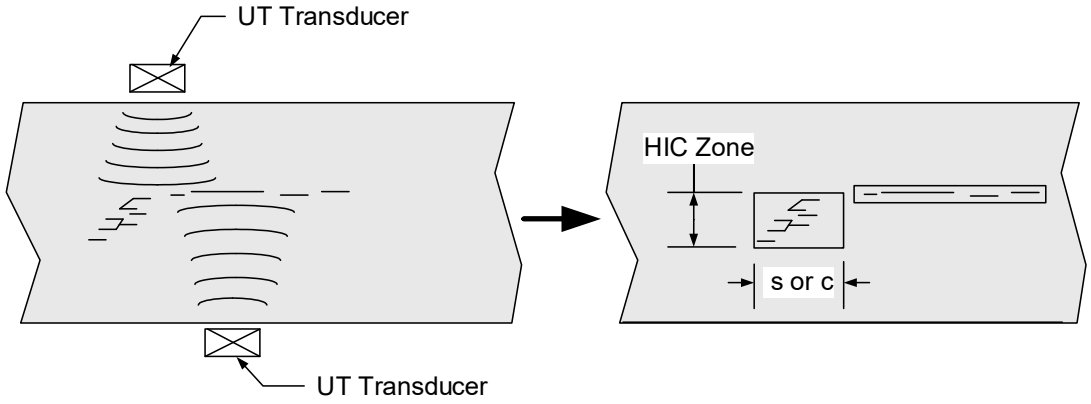

Two Sided UT Exam; Material Under Laminar Defect can be Interrogated. HIC Damage Size is Confirmed to be Limited.

Figure 7.10 – Characterization and Sizing of HIC Damage Zones Using Ultrasonic Examination

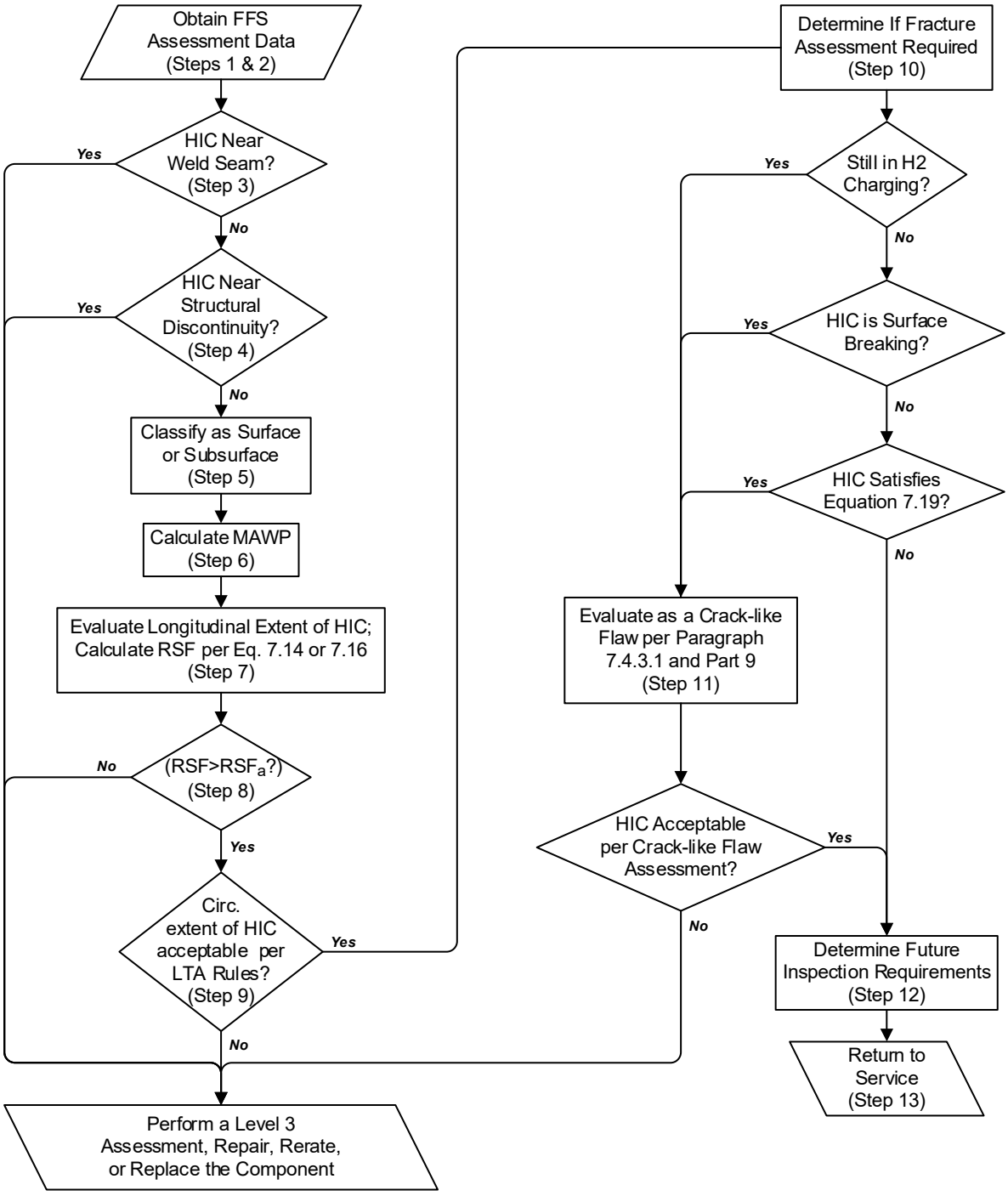

Figure 7.11 – Level 2 Assessment Procedure for HIC Damage

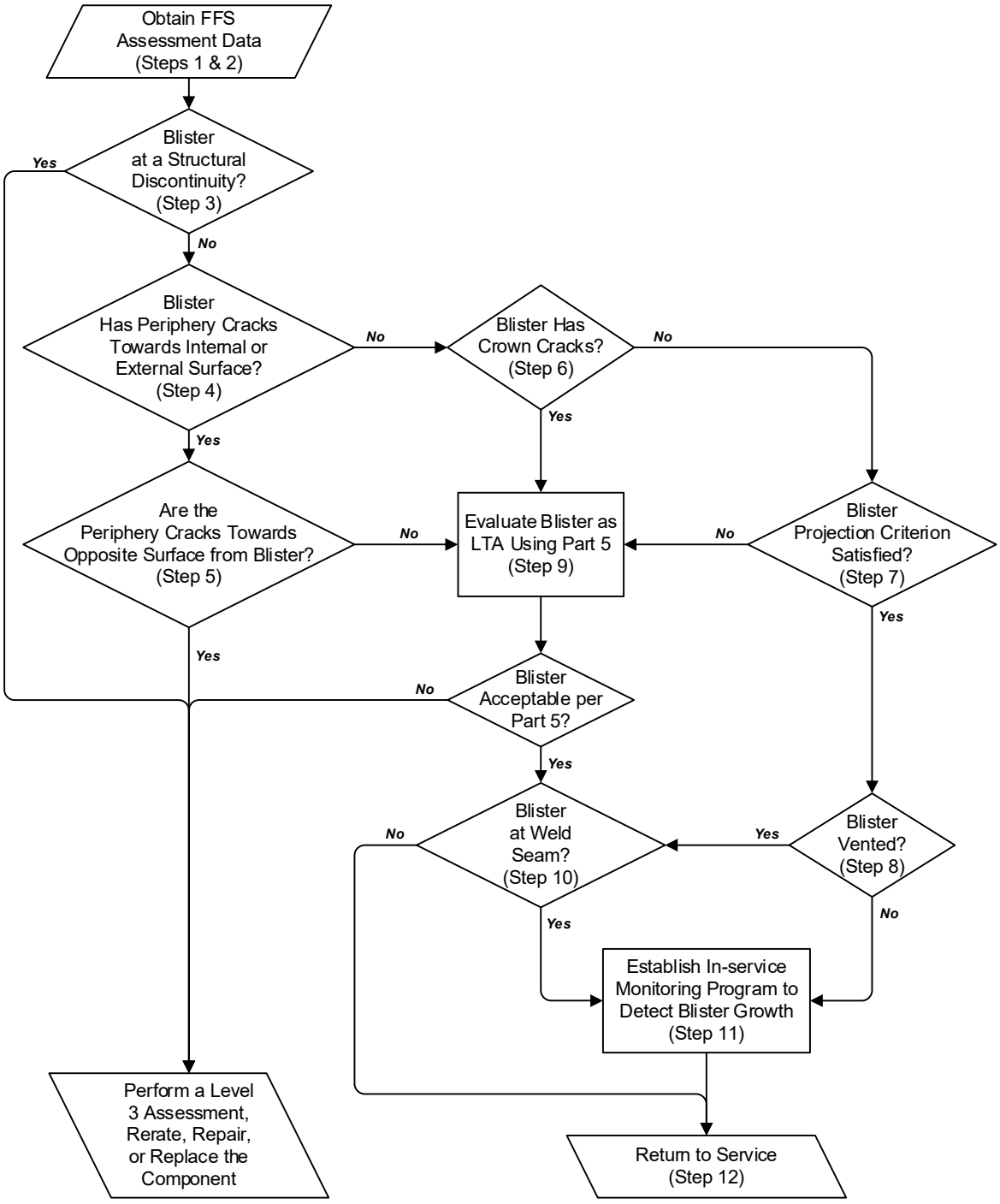

Figure 7.12 – Level 2 Assessment Procedure for Blisters

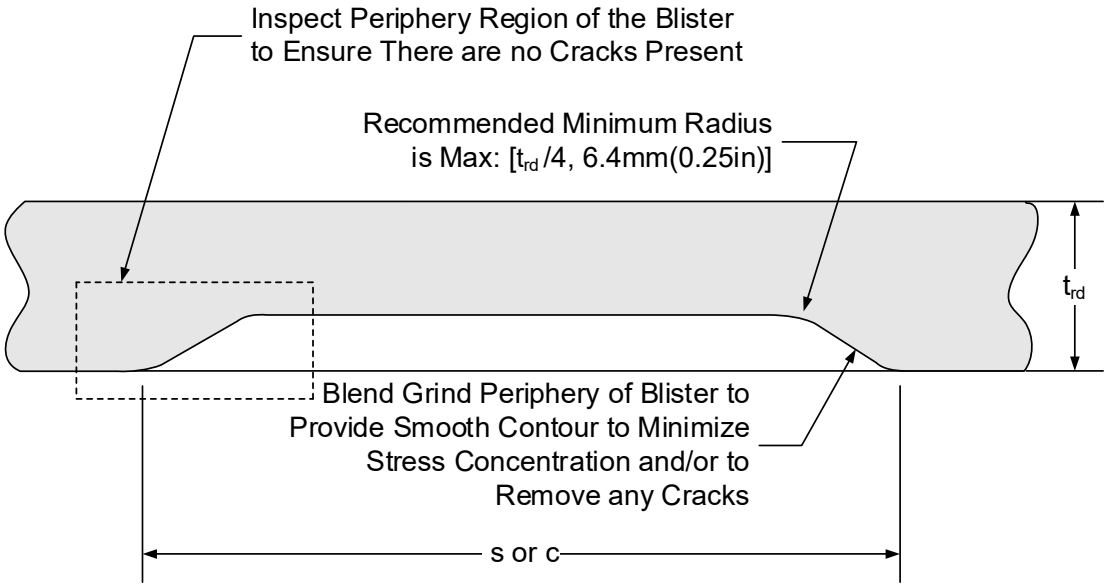

Note: Blisters Removed by Blend Grinding Should be Evaluated as an LTA Using the Assessment Procedures in Part 5.

Figure 7.13 – Blend Ground Area Remaining After Removal of a HIC Damage Zone or a Blister

ANNEX 7A – TECHNICAL BASIS AND VALIDATION – ASSESSMENT OF HYDROGEN BLISTERS AND HYDROGEN DAMAGE ASSOCIATED WITH HIC AND SOHIC

(INFORMATIVE)

CONTENTS

ANNEX 7A – TECHNICAL BASIS AND VALIDATION – ASSESSMENT OF HYDROGEN BLISTERS AND HYDROGEN DAMAGE ASSOCIATED WITH HIC AND SOHIC 7A-1

7A.1 TECHNICAL BASIS AND VALIDATION 7A-1
7A.2 REFERENCES 7A-1

7A.1 Technical Basis and Validation

The technical basis of the assessment procedures for blisters damage in Part 7 is provided in references [1], [2], and [3]. The blister damage assessment procedures could not be compared to experimental results because of lack of data. However, these rules have been used extensively in the industry without incident, have been proven to provide acceptable results, and are consistent with NACE guidelines, see reference [4]. The technical basis of the assessment procedures for HIC/SOHIC damage in Part 7 is provided in reference [5]. The development of a remaining strength factor approach, similar to that used for local thin areas, and experiments to validate the approach are described in this publication. The rules in Part 7 requiring a crack-like flaw check are based on Part 9 and the validation work for Part 9. Process conditions that can result in blisters/HIC/SOHIC damage are discussed in API RP 571, see reference [6]. Damage associated with high temperature hydrogen attack is specifically excluded from the assessment procedures, see reference [7].

7A.2 References

[1] Prager, M., Fitness-For-Service Evaluation Procedures for Operating Pressure Vessels, Tanks, and Piping in Refinery and Chemical Service, FS-26, Consultants Report, MPC Program on Fitness-For-Service, WRC Bulletin 547, Welding Research Council, Inc., New York, NY, 2014.

[2] Buchheim, G.M., “Fitness-For-Service Hydrogen Blistering and Lamination Assessment Rules in API 579,” PVP Vol. 411, Service Experience and Fitness-For-Service in Power and Petroleum Processing, ASME, 2000, pp. 177-190.

[3] Osage, D.A., Krishnaswamy, P., Stephens, D.R., Scott, P., Janelle, J., Mohan, R., and Wilkowski, G.M., Technologies for the Evaluation of Non-Crack-Like Flaws in Pressurized Components – Erosion/Corrosion, Pitting, Blisters, Shell Out-Of-Roundness, Weld Misalignment, Bulges and Dents, WRC Bulletin 465, Welding Research Council, Inc., New York, NY, September 2001.

[4] NACE Standard SP0296-10, “Detection, Repair, and Mitigation of Cracking in Refinery Equipment in Wet H2S Environments”, NACE International, Houston, TX, 2010.

[5] Staats, J.C., Buchheim, G.M., and Osage, D.A., Development of Fitness-For-Service Rules for the Assessment of Hydrogen Blisters, HIC and SOHIC, WRC Bulletin 531, Welding Research Council, Inc., New York, NY, 2010.

[6] API, Damage Mechanisms Affecting Fixed Equipment in the Refining Industry, API RP 571, 2nd Edition, April 2011, American Petroleum Institute, Washington, DC.

[7] API, Steels for Hydrogen Service at Elevated Temperatures and Pressures in Petroleum Refineries and Petrochemical Plants, API RP 941, 7th Edition, August 2008, American Petroleum Institute, Washington, DC.

PART 8 – ASSESSMENT OF WELD MISALIGNMENT AND SHELL DISTORTIONS

CONTENTS

PART 8 – ASSESSMENT OF WELD MISALIGNMENT AND SHELL DISTORTIONS 8-1

8.1 GENERAL 8-1
8.1.1 Evaluation of Weld Misalignment and Shell Distortions 8-1
8.1.2 ASME B&PV Code, Section VIII, Division 2 8-2
8.2 APPLICABILITY AND LIMITATIONS OF THE PROCEDURE 8-2
8.2.1 Types of Weld Misalignment and Shell Distortions 8-2
8.2.2 Limitations Based on Flaw Type 8-2
8.2.3 Calculation of the $MAWP_r$ and MFH_r and Coincident Temperature 8-2
8.2.4 Limitations Based on Temperature 8-3
8.2.5 Applicability of the Level 1 and Level 2 Assessment Procedures 8-3
8.2.6 Applicability of the Level 3 Assessment 8-4
8.3 DATA REQUIREMENTS 8-4
8.3.1 Original Equipment Design Data 8-4
8.3.2 Maintenance and Operational History 8-4
8.3.3 Required Data/Measurements for an FFS Assessment 8-4
8.3.4 Recommendations for Inspection Technique and Sizing Requirements 8-4
8.4 EVALUATION TECHNIQUES AND ACCEPTANCE CRITERIA 8-6
8.4.1 Overview 8-6
8.4.2 Level 1 Assessment 8-7
8.4.3 Level 2 Assessment 8-7
8.4.4 Level 3 Assessment 8-12
8.5 REMAINING LIFE ASSESSMENT 8-14
8.5.1 Categories – Metal Loss, Cyclic Loading, High Temperature Operation 8-14
8.5.2 Requirements for a Level 3 Assessment 8-14
8.6 REMEDIATION 8-14
8.6.1 Addition of Reinforcement 8-14
8.6.2 Correction of Tolerances by Mechanical Means 8-14
8.7 IN-SERVICE MONITORING 8-15
8.7.1 Overview 8-15
8.7.2 Groove-Like and Crack-Like Flaws 8-15
8.8 DOCUMENTATION 8-15
8.9 NOMENCLATURE 8-15
8.10 REFERENCES 8-19
8.11 TABLES 8-20
8.12 FIGURES 8-34

8.1 General

8.1.1 Evaluation of Weld Misalignment and Shell Distortions

Fitness-For-Service (FFS) Assessment procedures for pressurized components with weld misalignment and shell distortion, including out-of-roundness and bulges, are provided in this part. A flow chart for the evaluation procedure of equipment with a weld misalignment or shell distortion is shown in Figure 8.1.

8.1.2 ASME B&PV Code, Section VIII, Division 2

Some of the analysis methods in this Part are based on ASME B&PV Code, Section VIII, Division 2 (VIII-2), Part 4. The methods in this Part reference VIII-2 directly and provide exceptions that are to be used in an FFS Assessment.

8.2 Applicability and Limitations of the Procedure

8.2.1 Types of Weld Misalignment and Shell Distortions

8.2.1.1 Overview

The procedures in this part can be used to assess weld misalignments and shell distortions in components made up of flat plates; cylindrical, conical, and spherical shells; and formed heads. The types of flaws referred to as weld misalignment and shell distortion in this part are defined in the following paragraphs. If the current geometry of a component with a weld misalignment or shell distortion satisfies the original fabrication tolerances only a Level 1 Assessment is typically required. Exceptions include components subject to cyclic service and components that have a localized shell distortion such as a bulge.

8.2.1.2 Weld Misalignment – Categories covered include centerline offset, angular misalignment (peaking), and a combination of centerline offset and angular misalignment of butt weld joints in flat plates, cylindrical shells, and spherical shells (see Figures 8.2 through 8.6).

8.2.1.3 Shell Distortion – Categories of shell distortion are defined as follows:

a) General Shell Distortion – A deviation of a shell from an ideal geometry that occurs in the longitudinal and/or circumferential direction and exceeds the deviation permitted by the applicable code or standard. This type of distortion exhibits significant shape variation of the shell (i.e., multiple local curvatures), and typically requires a Level 3 Assessment based on a numerical analysis method. Flat spots on a shell are classified as general shell distortion.

b) Out-of-roundness – A deviation of the cross-section of a cylindrical shell or pipe bend from an ideally circular geometry. The out-of-roundness of a cylinder is assumed to be constant in the longitudinal direction (see Figure 8.7 and paragraph 8.2.5.2(d)), and either global (oval shape) or arbitrarily shaped in the circumferential direction. The out-of-roundness of a pipe elbow is assumed to be global (oval shape) in the mid-elbow region when the ovality at the end equals or exceeds 50% of the mid-elbow value.

c) Bulge – An outward deviation of a cross-section of a shell member from an ideal geometry that can be characterized by local radii and angular extent. The local bulge geometry may be either spherical or cylindrical. Flat spots (infinite radius of curvature) are not considered to be bulges; they are classified as general shell distortions. If the bulge occurs at a blister, the analysis procedures in Part 7 should be utilized for the assessment.

8.2.2 Limitations Based on Flaw Type

Unless otherwise specified, this Part is limited to the evaluation of weld misalignment and shell distortions. Other flaw types shall be evaluated in accordance with Part 2, Table 2.1.

8.2.3 Calculation of the $MAWP_r$ and MFH_r and Coincident Temperature

Calculation methods are provided to rerate the component if the acceptance criteria in this part are not satisfied. For pressurized components, the calculation methods determine a reduced maximum allowable working pressure

($MAWP_r$) and/or coincident temperature. For tank components (shell courses), the calculation methods determine a reduced maximum fill height (MFH_r).

8.2.4 Limitations Based on Temperature

The assessment procedures only apply to components that are not operating in the creep range; the design temperature is less than or equal to the value in Part 4, Table 4.1. The Materials Engineer should be consulted regarding the creep range temperature limit for materials not listed in this table. Assessment procedures for components operating in the creep range are provided in Part 10.

8.2.5 Applicability of the Level 1 and Level 2 Assessment Procedures

8.2.5.1 Level 1 Assessment procedures are based on the criteria in the original construction code. If these criteria are not completely defined by the original construction code and are not in the original owner-user design specification, a Level 2 or Level 3 Assessment may be performed. Level 1 Assessment procedures shall not be used if the component is in cyclic service. A screening procedure to determine if a component is in cyclic service is provided in Part 14.

8.2.5.2 The Level 2 Assessment procedures in this part apply only if all the following conditions are satisfied:

a) The original design criteria were in accordance with a recognized code or standard (see Part 1, paragraphs 1.2.2 or 1.2.3).

b) The component geometry is one of the following:

   1) Flat plate

   2) Pressure vessel cylindrical or conical shell section

   3) Spherical pressure vessel

   4) Straight section of a piping system

   5) Elbow or pipe bend that does not have structural attachments

   6) Shell course of an atmospheric storage tank

c) The applied loads are limited to pressure and/or supplemental loads (see Annex 2C) that result in a membrane state of stress in the component, excluding the effects of the weld misalignment and shell distortion (i.e., through-wall bending stresses in the component are a result of the weld misalignment or shell distortion). The assessment procedures can be used to evaluate stresses resulting from both internal and external pressure. Level 2 stability assessment procedures are provided only for cylindrical and conical shells subject to external pressure. The Level 2 stability assessment rules do not apply to cylinders subject to external pressure in combination with supplemental loads that result in significant longitudinal compressive stresses.

d) If the component under evaluation is a cylinder with out-of-roundness, the out-of-roundness is constant along the axis of the cylinder. If local deviations of the cylindrical shell occur in the longitudinal direction, the Level 2 Assessment procedure can produce non-conservative results, and the shell distortion should be classified as general shell distortion.

8.2.6 Applicability of the Level 3 Assessment

A Level 3 Assessment may be performed where Level 1 and 2 methods do not apply, such as for the following conditions:

a) Type A, B, or C Components (see Part 4, paragraph 4.2.5) subject to internal pressure, external pressure, supplemental loads, and any combination thereof.

b) Components with a design based on proof testing (e.g., piping tee or reducer produced in accordance with ASME B16.9 where the design may be based on proof testing).

c) The shell distortion is classified as general shell distortion (see paragraph 8.2.1.3).

d) The loading conditions result in significant stress gradients at the location of the weld misalignment or shell distortion.

e) The component is subject to a loading condition that results in compressive stresses where structural stability is a concern. Guidelines for performing a structural stability assessment are provided in Annex 2D, paragraph 2D.4.

8.3 Data Requirements

8.3.1 Original Equipment Design Data

An overview of the original equipment data required for an assessment is provided in Part 2, paragraph 2.3.1.

8.3.2 Maintenance and Operational History

An overview of the maintenance and operational history required for an assessment is provided in Part 2, paragraph 2.3.2.

8.3.3 Required Data/Measurements for an FFS Assessment

8.3.3.1 The information typically used for a Level 1 and Level 2 Assessment is covered in paragraphs 8.4.2 and 8.4.3, respectively. A summary of these data is provided in Table 8.1.

8.3.3.2 The information required to perform a Level 3 Assessment depends on the analysis method utilized. A detailed stress analysis or limit load procedure using a numerical technique can be used to establish acceptable operating conditions. For such analyses, an accurate description of the weld misalignment or shell distortion should be obtained along with the material properties, including the elastic modulus and the yield stress (see Annex 2E). The description of the weld misalignment or shell distortion should include field measurements that adequately characterize the deformed shape.

8.3.4 Recommendations for Inspection Technique and Sizing Requirements

8.3.4.1 Measurement of the radial (offset) and angular (peaking) misalignment at the weld joint is required to use the assessment procedures for weld misalignment.

a) For flat plates, these two quantities can be established by knowing the plate thicknesses, disposition of the surfaces of the plates in the weld joint (e.g., internal surfaces are flush), the maximum offset between the plate centerlines at the weld joint, and for angular misalignment, the effective height and length used to characterize the deviation.

b) For cylindrical or spherical shells, the radial misalignment can be established by knowing the plate thicknesses and the disposition of the surfaces of the plates in the weld joint (e.g., internal surfaces are flush).

The angular misalignment at the joint can be established by using a template as shown in Figure 8.8. The arc length of the template should extend beyond the locally deformed region resulting from the angular misalignment (or the contact point as shown in Figure 8.8) and should be established using the inside or outside radius of the cylinder, as applicable. The template should be notched as shown in Figure 8.8 so that no part of it is in contact with the area of weld reinforcement (weld cap). Using this technique, the maximum deviation can be calculated using either of the following equations. For a center template,

$$\delta = \frac{(a_1 + a_2)}{2} \tag{8.1}$$

and for a rocked template,

$$\delta = \frac{(b_1 + b_2)}{4} \tag{8.2}$$

where a_1, a_2, b_1, and b_2 are defined in Figure 8.8.

8.3.4.2 Measurement of the radius and associated deviation from the mean radius at positions around the circumference are required to use the assessment procedures for circumferential out-of-roundness of cylindrical shells.

a) For the case of global out-of-roundness, the maximum, minimum and mean diameters are required. If these quantities are difficult to measure in the field, the measurement procedure for arbitrary out-of-roundness presented in item (b) below is recommended.

b) An accurate measurement of the cylinder radius at various stations should be made to apply the assessment procedures for an arbitrary circumferential out-of-roundness.

1) Radii at an even number of equally spaced intervals around the circumference of the cylinder sufficient to define the profile of the cross section under evaluation should be measured (see Figure 8.9). The recommended minimum number of measurement locations is 24. If access to the inside of the vessel is not possible, an alternative means for measuring the cross section profile will be required. For a vessel that has stiffening rings, the shape deviation of the shell located between the stiffening rings can be measured by placing a level on the outside diameter of the rings and measuring the radial offset to the deformed surface. This method can produce accurate results if the stiffening rings are not significantly out-of-round. For a vessel without stiffening rings, a vertical level or plumb line placed alongside the vessel shell can be used to measure the radial offset (see Part 11, Figure 11.4).

2) To determine the deviation from the mean circle, the radius measurements should be corrected for the mean and for the error in positioning the center of measurement. If the radius at i discrete points around the circumference can be represented by the Fourier Series shown in Equation (8.3), then the radius at an angular location, θ, is given by Equation (8.4).

$$R_i = R_m + \sum_{n=1}^{N}\left(A_n \cos\left[\frac{2\pi(i-1)}{M} n\right] + B_n \sin\left[\frac{2\pi(i-1)}{M} n\right]\right) \tag{8.3}$$

$$R(\theta) = R_m + A_1 \cos[\theta] + B_1 \sin[\theta] + \varepsilon \tag{8.4}$$

3) The corrected radius and deviation from the mean circle can be calculated using Equations (8.5) and (8.6), respectively.

$$R_i^c = R_i - A_1 \cos\left[\frac{2\pi(i-1)}{M}\right] - B_1 \sin\left[\frac{2\pi(i-1)}{M}\right] \tag{8.5}$$

$$\varepsilon_i = R_i^c - R_m \tag{8.6}$$

4) The mean radius in Equation (8.6) can be calculated using Equation (8.7). The coefficients of the Fourier Series may be determined using Equations (8.8) and (8.9) or the procedure shown in Table 8.2. The parameters A_1 and B_1 in Equation (8.5) are equal to the second value of the sine and cosine terms, respectively, of the computed Fourier coefficients.

$$R_m = \frac{1}{M}\sum_{i=1}^{M} R_i \tag{8.7}$$

$$A_n = \frac{2}{M}\sum_{i=1}^{M} R_i \cos\left[\frac{2\pi(i-1)}{M}n\right] \tag{8.8}$$

$$B_n = \frac{2}{M}\sum_{i=1}^{M} R_i \sin\left[\frac{2\pi(i-1)}{M}n\right] \tag{8.9}$$

8.3.4.3 An estimate of the local radius, R_L, is required to use the assessment procedures for local imperfections in cylindrical shells subject to external pressure. The local radius, R_L, can be estimated using the guidelines shown in Figure 8.10.

8.3.4.4 Estimates of the local bulge radii and the bulge angular extent are required to use the assessment procedures for bulges. In addition, if the bulge is caused by local heating, hardness values and other in-situ testing should be considered to evaluate the condition of the material.

8.4 Evaluation Techniques and Acceptance Criteria

8.4.1 Overview

An overview of the assessment levels is provided in Figure 8.1.

a) The Level 1 Assessment is based on the fabrication tolerances of the original construction code. If the current geometry of the component conforms to the original fabrication tolerances, the Level 1 Assessment criteria are satisfied. Additional analysis is not required unless the component is in cyclic service as defined in Part 14, or if a fatigue analysis was conducted as part of the original design; in these cases, a Level 2 or Level 3 Assessment is required.

b) Level 2 Assessments provide a means to estimate the structural integrity of a component with weld misalignment or shell distortion characterized as out-of-roundness. Level 2 Assessments can consider pressure and supplemental loads as well as complicated geometries (e.g., pipes with different wall thickness and locations of welds).

c) Level 3 Assessments are intended for the evaluation of components with general shell distortions, complex component geometries and/or loadings. Level 3 Assessments involve detailed stress analysis techniques including fracture, fatigue, and numerical stress analysis. Level 3 Assessments typically require significant field measurements to characterize the weld misalignment or shell distortion.

8.4.2 Level 1 Assessment

8.4.2.1 The Level 1 Assessment procedures are based on the fabrication tolerances provided in the original construction code. Tables 8.3 through 8.7 provide an overview of these tolerances for the following construction codes. For equipment or components designed to other recognized construction codes, standards, or specifications, fabrication tolerances in those documents may also be followed (see paragraph 8.2.5.1).

a) ASME Boiler and Pressure Vessel Code, Section VIII, Division 1 and Division 2 – see Table 8.3

b) ASME B31.3 Piping Code – see Table 8.4

c) API 620 Standard – see Table 8.5

d) API 650 Standard – see Table 8.6

e) API 653 Standard (reconstructed tanks) – see Table 8.7

8.4.2.2 If the component does not meet the Level 1 Assessment requirements, then a Level 2 or Level 3 Assessment can be conducted.

8.4.3 Level 2 Assessment

8.4.3.1 The Level 2 Assessment procedures are computational procedures for assessment of a weld misalignment or shell distortion in a component subject to pressure and supplemental loads. Calculation methods are provided to rerate the component if the acceptance criteria in this part are not satisfied.

8.4.3.2 Weld Misalignment

a) STEP 1 – Identify the component and misalignment type (see Tables 8.8, 8.9, 8.10, and 8.11) and determine the following variables as applicable (see Figures 8.2 through 8.6): A, e, E_y, F, FCA, H_f, L, $LOSS$, M, P, R, S_a, t_1, t_2, t_{nom}, t_{rd}, RSF_a, R_1, R_2, Z, δ, θ_p, and v.

b) STEP 2 – Determine the wall thickness to be used in the assessment using Equation (8.10) or (8.11), as applicable.

$$t_c = t_{nom} - LOSS - FCA \tag{8.10}$$

$$t_c = t_{rd} - FCA \tag{8.11}$$

c) STEP 3 – Determine the membrane stress from pressure, σ_m, (see Annex 2C). Note that for cylindrical shells, σ_m^C should be used for misalignment of longitudinal joints, and σ_m^L should be used for misalignment of circumferential joints. For centerline offset in flat plates and circumferential joints in cylindrical shells, determine the resulting longitudinal membrane stress using the following equation if supplemental loads exist.

$$\sigma_{ms} = \frac{F}{A} + \frac{M_{ns}}{Z} \tag{8.12}$$

d) STEP 4 – Calculate the ratio of the induced bending stress to the applied membrane stress using the equations Tables 8.8 through 8.11 based on the type of component and weld misalignment, and the thickness determined in STEP 2. The ratio of the induced bending stress to the applied membrane stress equals zero if no centerline offset or angular misalignment exists. The quantity R_b is the ratio of the induced bending stress to the applied membrane stress resulting from pressure. The parameter R_{bs} is the ratio of the induced bending stress to the membrane stress resulting from supplemental loads.

1) Flat Plates (note that a pressure induced bending stress shall be categorized as σ_{ms} and R_{bs} is applicable; therefore, $\sigma_m = 0$):

$$\sigma_m = 0.0 \tag{8.13}$$

$$R_{bs} = R_{bs}^{pc} + R_{bs}^{pa} \tag{8.14}$$

2) Cylinders – Circumferential Joints (Longitudinal Stress):

$$R_b = R_b^{ccjc} + R_b^{ccja} \tag{8.15}$$

$$R_{bs} = R_{bs}^{ccjc} + R_{bs}^{ccja} \tag{8.16}$$

3) Cylinders – Longitudinal Joints (Circumferential Pressure Stress; therefore, $\sigma_{ms} = 0.0$):

$$R_b = R_b^{cljc} + R_b^{clja} \tag{8.17}$$

$$\sigma_{ms} = 0.0 \tag{8.18}$$

4) Spheres – Circumferential Joints (Circumferential Stress):

$$R_b = R_b^{scjc} + R_b^{scja} \tag{8.19}$$

$$\sigma_{ms} = 0.0 \tag{8.20}$$

e) STEP 5 – Determine the Remaining Strength Factor:

$$RSF = \min\left[\left\{\frac{H_f S_a}{\sigma_m\left(1+R_b\right)+\sigma_{ms}\left(1+R_{bs}\right)}\right\},\ 1.0\right] \tag{8.21}$$

f) STEP 6 – Evaluate the results. If $RSF \geq RSF_a$, then the weld misalignment is acceptable per Level 2; otherwise, refer to paragraph 8.4.3.7.

8.4.3.3 Out-Of-Roundness – Cylindrical Shells and Pipe Elbows

a) STEP 1 – Determine the following variables based on the type of out-of-roundness.

1) For Global Out-Of-Roundness (see Figure 8.7), the following parameters are required: θ, C_s, D_m, D_o, $D_{\max}$, $D_{\min}$, E_y, FCA, $LOSS$, t_{nom}, t_{rd}, v and L_f.

2) For General (Arbitrary Shape) Out-Of-Roundness (see Figure 8.9), the parameter θ and the cross sectional profile of the cylinder at various angles around the vessel circumference when the cylinder is not pressurized are required. The cross sectional profile data can be represented by the Fourier Series in Equation (8.3). The coefficients to this Fourier Series may be determined using the procedure shown in Table 8.2.

b) STEP 2 – Determine the wall thickness to be used in the assessment, t_c, using Equation (8.10) or (8.11), as applicable.

c) STEP 3 – Determine the circumferential membrane stress using the thickness from STEP 2 (see Annex 2C).

d) STEP 4 – Determine the ratio of the induced circumferential bending stress to the circumferential membrane stress at the circumferential position (denoted by the angle θ) of interest.

1) Global Out-Of-Roundness of a cylinder, θ is measured from the major axis of the oval:

$$R_b^{or}(\theta) = \frac{1.5\left(D_{\max} - D_{\min}\right)\cos\left[2\theta\right]}{t_c\left(1+\left[\frac{C_s P\left(1-\nu^2\right)}{E_y}\right]\left[\frac{D_m}{t_c}\right]^3\right)} \tag{8.22}$$

2) General (Arbitrary Shape) Out-Of-Roundness of a cylinder:

$$R_b^{or}(\theta) = \left(\frac{6}{t_c}\right)\cdot\sum_{n=2}^{N}\left\{\frac{\left(A_n\cos\left[n\theta\right] + B_n\sin\left[n\theta\right]\right)}{1+k_n}\right\} \tag{8.23}$$

where,

$$k_n = \frac{PR^3}{\left(n^2-1\right)D_c} \tag{8.24}$$

$$D_c = \frac{E_y t_c^3}{12\left(1-\nu^2\right)} \tag{8.25}$$

3) Global Out-Of-Roundness of Long Radius Elbow (note: limitations for the terms of Equation (8.26) are shown in Equations (8.28) and (8.29)), (see subparagraph 4 below if these limitations are not satisfied).

$$R_b^{or}(\theta) = \frac{C_b\cdot\cos\left[2\theta\right]}{L_f} \tag{8.26}$$

where,

$$C_b = \begin{pmatrix} -0.007281 + 0.05671Y + 0.0008353X + 0.01210XY + \\ 0.00001313X^2 - 0.00008362X^2Y + 0.04889W + 0.1827WY - \\ 0.003201WX - 0.01697WXY - 0.00003506WX^2 - \\ 0.0001021WX^2Y - 0.1386W^2 - 0.09795W^2Y + 0.007906W^2X + \\ 0.004694W^2XY - 0.00003833W^2X^2 + 0.0002649W^2X^2Y \end{pmatrix} \tag{8.27}$$

$$W = \frac{1000\cdot PR}{E_y t_c} \qquad \left(valid\ \ for\ 0.045 \le W \le 0.50\right) \tag{8.28}$$

$$X = \frac{R}{t_c} \qquad \left(valid\ \ for\ 20 \le X \le 40\right) \tag{8.29}$$

$$Y = \frac{100\left(D_{\max} - D_{\min}\right)}{D_o} \tag{8.30}$$

4) Global Out-Of-Roundness of an Elbow or Pipe Bend (no limitation on bend radius).

$$R_b^{or}(\theta) = \frac{\dfrac{3R\cos[2\theta]}{t_c L_f}\left(\dfrac{D_{\max} - D_{\min}}{D_o}\right)}{\left[1 + 3.64\left(\dfrac{PR}{E_y t_c}\right)\left(\dfrac{R}{t_c}\right)^2\right]} \tag{8.31}$$

e) STEP 5 – Determine the remaining strength factor using Equation (8.21) with $R_b = \text{abs}[R_b^{or}]$ and $R_{bs} = -1.0$.

f) STEP 6 – Evaluate the results. If $RSF \geq RSF_a$, then the out-of-roundness is acceptable per Level 2; otherwise, refer to paragraph 8.4.3.7.

8.4.3.4 Combined Weld Misalignment and Out-Of-Roundness in Cylindrical Shells Subject to Internal Pressure

a) The ratio of the induced circumferential bending stress to the circumferential membrane stress, R_b, due to weld misalignment can be calculated at the location of the weld using the equations in paragraph 8.4.3.2. The R_b ratio due to out-of-roundness should be calculated at the location of the longitudinal weld joint (i.e., the position of the weld as defined by θ) using the equations in paragraph 8.4.3.3.

b) The assessment procedure for weld misalignment and out-of-roundness in cylindrical shells subject to internal pressure is as follows:

1) STEP 1 – Determine the wall thickness to be used in the assessment, t_c, using Equation (8.10) or Equation (8.11), as applicable.

2) STEP 2 – Determine the circumferential membrane stress using the thickness from STEP 1 (see Annex 2C).

3) STEP 3 – Calculate the ratio of the induced bending stress to the applied membrane stress for weld misalignment using paragraph 8.4.3.2, and for circumferential out of roundness using paragraph 8.4.3.3 (note: when computing R_b^{or} per paragraph 8.4.3.3, do not take the absolute value of the result as indicated in STEP 5 of paragraph 8.4.3.3).

$$R_b = R_b^{cljc} + R_b^{clja} + R_b^{or} \tag{8.32}$$

4) STEP 4 – Determine the remaining strength factor using Equation (8.21) with the value of R_b determined in STEP 3 and $R_{bs} = -1.0$.

5) STEP 5 – Evaluate the results. If $RSF \geq RSF_a$, then the weld misalignment and out-of-roundness is acceptable per Level 2; otherwise, refer to paragraph 8.4.3.7.

8.4.3.5 Out-Of-Roundness – Cylindrical Shells Subject to External Pressure (Buckling Assessment)

a) Cylindrical shells subject to external pressure should satisfy the stress criteria in paragraph 8.4.3.3 or 8.4.3.4, as applicable, and the buckling criteria set out in this paragraph.

b) The assessment procedure for out-of-roundness for cylindrical and conical shells subject to external pressure is as follows:

1) STEP 1 – Determine the following variables (see Figure 8.10): e_d, E_y, FCA, FS, L, $LOSS$, P, R_o, R_L, t_{nom}, t_{rd}, ν and σ_{ys}.

2) STEP 2 – Determine the wall thickness to be used in the assessment, t_c, using Equation (8.10) or Equation (8.11), as applicable.

3) STEP 3 – If a conical shell is being evaluated, determine the equivalent length and outside diameter as defined in VIII-2, Part 4, paragraph 4.4.6. The equivalent length and equivalent outside radius $(R_o = D/2)$ are to be used in all subsequent steps.

4) STEP 4 – Find the value of n (the number of waves into which the cylinder will buckle in the circumferential direction to give a minimum value of P_{eL}) for the perfect cylinder $(e_d = 0.0)$.

   i) Approximate method – determine the value of n using the equations in VIII-2, Part 4, paragraph 4.4.4.1 with $R_m = R_o$.

   ii) Exact method – determine the value of n in the following equation that results in a minimum value of P_{eL}. This calculation assumes the value of n to be a floating point number. Starting with $n = 2$, increase n in increments of 0.10 until a minimum value of P_{eL} is found.

$$P_{eL} = \frac{1}{n^2 + 0.5\lambda^2 - 1}\left(\frac{E_y t_c}{R_o}\right)\left[\frac{\left(n^2 + \lambda^2 - 1\right)^2}{12\left(1-\nu^2\right)}\left(\frac{t_c}{R_o}\right)^2 + \frac{\lambda^4}{\left(n^2 + \lambda^2\right)^2}\right] \tag{8.33}$$

with,

$$\lambda = \frac{\pi R_o}{L_u} \tag{8.34}$$

5) STEP 5 – Determine the value of the local radius, R_L, of the imperfection using the procedure shown in Figure 8.10 with the measured value of the deviation from the true cylinder, e_d, and the value of n determined in STEP 4.

6) STEP 6 – Substitute R_L for R_o into Equation (8.33) and find a new value of n along with the associated value of the minimum elastic buckling pressure and designate this pressure as P_{ec}. In calculating P_{ec}, start with $n = 2$ and increase n in increments of 0.10 until a minimum value of P_{ec} is found.

7) STEP 7 – Determine the inelastic buckling pressure using Equation (8.35). The parameter F_{ic} in Equation (8.35) is determined using VIII-2, Part 4, paragraph 4.4.5.1 with the value of F_{ic} calculated using Equation (8.36).

$$P_c = \frac{F_{ic} t_c}{R_o} \tag{8.35}$$

$$F_{he} = \frac{P_{ec} R_o}{t_c} \tag{8.36}$$

8) STEP 8 – Determine the permissible external pressure using Equation (8.37):

$$P_{ext} = \frac{\min\left[P_{ec}, P_c\right]}{FS} \tag{8.37}$$

9) STEP 9 – Evaluate the results. If $P_{ext} \geq P$, then the component is suitable for continued operation; otherwise, refer to paragraph 8.4.3.7.

8.4.3.6 Bulges

A Level 2 Assessment procedure for determining the acceptability of a bulge is currently not provided; refer to paragraph 8.4.4 for Level 3 Assessment options.

8.4.3.7 Rerating Components

If $RSF \geq RSF_a$, the component is acceptable per Level 2. If this criterion is not satisfied, then the component may be rerated using the equations in Part 2, paragraph 2.4.2.2. In the cases where the R_b factor is a function of pressure; an iterative analysis is required to determine the final $MAWP_r$. See paragraph 2.4.2.2(e) to determine the acceptability of the equipment for continued operation.

8.4.3.8 Fatigue Analysis

a) If the component is in cyclic service, or if a fatigue analysis was performed as part of the original design calculations, the fatigue strength including the effects of the weld misalignment or shell distortion should be checked. A screening procedure to determine if a component is in cyclic service is provided in Part 14.

b) The procedure for fatigue assessment that follows may be used to evaluate fatigue in components with weld misalignment, shell out-of-roundness, or a combination of weld misalignment and shell out-of-roundness subject to the restrictions in paragraphs 8.4.3.2, 8.4.3.3, or 8.4.3.4, respectively. A Level 3 Assessment is required for a component with bulges.

   1) STEP 1 – Determine the nature of loading the associated membrane stress (see Annex 2C), and the number of operating cycles. For loading that results in a variable membrane stress range the equivalent number of operating cycles may be determined from the methods provided in Part 14.

   2) STEP 2 – Determine the ratio of the induced bending stress to membrane stress, R_b, resulting from weld misalignment, shell out-of-roundness or combination of weld misalignment and shell out-of-roundness, as applicable, using the procedures in paragraphs 8.4.3.2, 8.4.3.3, or 8.4.3.4, respectively.

   3) STEP 3 – Using the loading history and membrane stress from STEP 1 and the R_b parameters from STEP 2, calculate the stress range for the fatigue analysis using Table 8.12.

   4) STEP 4 – Compute the number of allowed cycles using the stress range determined in STEP 3 using Part 14, as applicable.

   5) STEP 5 – Evaluate the results. If the computed number of cycles determined in STEP 4 equals or exceeds the number of operating cycles in STEP 1, then the component is acceptable per Level 2.

8.4.3.9 If the component does not meet the Level 2 Assessment requirements, then the following, or combinations thereof, should be considered:

a) Rerate, repair, or replace the component.

b) Adjust the FCA by applying remediation techniques (see Part 4, paragraph 4.6).

c) Conduct a Level 3 Assessment.

d) Retire the equipment.

8.4.4 Level 3 Assessment

8.4.4.1 The stress analysis techniques in Annex 2D can be used to assess the weld misalignment or shell distortion discussed in this part in pressure vessels, piping, and tankage.

8.4.4.2 Linear stress analysis and the stress categorization techniques discussed in Annex 2D, paragraph 2D.2.2 can be used to analyze misalignment at weld joints. In the Level 2 Assessment, the induced bending stress resulting from misalignment is considered a secondary bending stress for most applications. In some cases, this stress should be taken as a primary bending stress if elastic follow-up occurs. The limit load techniques described in Annex 2D, paragraph 2D.2.3 may be utilized in the analysis to resolve issues pertaining to stress categorization.

8.4.4.3 The non-linear stress analysis techniques described in Annex 2D, paragraph 2D.2.4 may be utilized to analyze general shell distortions.

a) Typically, the localized bending stresses resulting from general shell distortion will tend to decrease due to the rounding effect of the shell when subject to internal pressure. This effect is more pronounced in thinner shells and can be directly evaluated using a non-linear analysis that includes the effects of geometric non-linearity. The rounding effect is introduced in a Level 2 analysis of out-of-roundness through the correction factor, C_f. If material non-linearity is included in the analysis, the plastic collapse strength of the component can also be determined and used to qualify the component for continued operation.

b) An accurate representation of the deformed shell profile is critical in obtaining accurate analysis results. This is especially important for a shell with significant deviations (or kinks) in the longitudinal and circumferential direction. To obtain an accurate profile of the shell geometry, a grid should be established over the deformed region and measurements taken to determine the actual profile of the shell. The data should then be curve-fit with piece-wise cubic splines to obtain an accurate representation of the deformed shape and ensure that the slope and curvature of the deformed shell profile is continuous. Alternatively, cubic splines may be used to model the deformed shape in the meridional direction and a Fourier series expansion used to model the deformation in the circumferential direction.

c) If a kink or sharp local radius exists in the shell surface, traditional shell theory will not provide an accurate estimate of the stress state. A sharp local radius is defined $R_{Lm} < 5t_c$ and is measured in the meridional or circumferential direction of the shell. In this case, a continuum model including the effects of plasticity is recommended for the evaluation.

d) For shell structures with significant localized distortion resulting from contact with another component or mechanical device, a non-linear stress analysis to simulate the deformation process should be used to determine the magnitude of permanent plastic strain developed. To simulate the distortion process, perform an analysis that includes geometric and material non-linearity as well as the contact interaction between the original undeformed shell structure and the contacting body. The contacting component may be explicitly modeled as a deformable body or as a simple rigid surface. The analysis should include applicable loadings to develop the final distorted configuration of the shell structure. The calculated inelastic strains should be compared to the allowable strain limits given in Annex 2D, paragraph 2D.3.

8.4.4.4 If the component is subject to a compressive stress field, the non-linear stress analysis techniques described in Annex 2D, paragraph 2D.2.4 may be used for the assessment. If geometric non-linearity is included along with material non-linearity in the assessment, the stability of the component can be evaluated in the same analysis utilized to determine the plastic collapse strength. Alternatively, the stress categorization and structural stability techniques discussed in Annex 2D, paragraph 2D.2.2 and Annex 2C, paragraph 2C.4, respectively, may be utilized in the assessment.

8.4.4.5 If the component is operating in the creep range, a non-linear analysis that includes both material (plasticity and creep) and geometric non-linearity should be performed. Stresses due to a localized weld

misalignment or shell distortion may not sufficiently relax with time because of the surrounding compliance of the component. In this case, creep strains can accumulate and could result in significant creep damage or cracking. The assessment procedures in Part 10 are recommended for such situations.

8.4.4.6 If the component contains a weld misalignment or shell distortion with highly localized stresses, a detailed non-linear stress analysis and assessment should be performed. This assessment should also include an evaluation of the material toughness requirements. Otherwise, repair or replacement of the component is recommended.

8.5 Remaining Life Assessment

8.5.1 Categories – Metal Loss, Cyclic Loading, High Temperature Operation

A remaining life assessment of a component with a weld misalignment or shell distortion generally consists of one of the following three categories:

a) *Metal Loss Resulting from a Corrosive/Erosive Environment* – In this case, adequate protection from a corrosive/erosive environment can be established by setting an appropriate value for the future corrosion allowance. The remaining life as a function of time can be established using the $MAWP$ Approach described in Part 4, paragraph 4.5.2.

b) *Cyclic Loading* – The Level 2 assessment procedures include a fatigue evaluation for weld misalignment and out-of-roundness (see paragraph 8.4.3.8 and Part 14). The remaining life can be established by combining the results from this analysis with the operational history of the component.

c) *High Temperature Operation* – If the component is operating in the creep regime, the assessment procedures in Part 10 should be utilized to determine a remaining life.

8.5.2 Requirements for a Level 3 Assessment

If the component's operation is not within one of the above categories, a detailed Level 3 analysis should be performed to determine the remaining life of the component.

8.6 Remediation

8.6.1 Addition of Reinforcement

Weld misalignment, out-of-roundness and bulges may be reinforced using stiffening plates and lap patches depending on the geometry, temperature and loading conditions. The reinforcement, if utilized, should be designed using the principles and allowable stresses of the original construction code.

8.6.2 Correction of Tolerances by Mechanical Means

Cylindrical shell sections that are out-of-round can be brought to within original fabrication tolerances or to a shape that reduces the local stress to within acceptable limits by mechanical means. Hydraulic jacks have been used successfully to alter the out-of-round shape of stiffened cylindrical shells. The design of the jacking arrangement and loads should be carefully established and monitored during the shaping process to minimize the potential for damage to the shell and attachments.

8.7 In-Service Monitoring

8.7.1 Overview

The weld misalignment and shell distortion covered in this part do not normally require in-service monitoring unless an unusually corrosive environment exists and future corrosion allowance cannot adequately be estimated, or if the component is subject to a cyclic operation and the load history cannot be adequately established. In these cases, the in-service monitoring usually entails visual inspection and field measurements of the components weld misalignment or shell distortion at regular intervals. The type of measurements made depends on the procedure utilized in the assessment.

8.7.2 Groove-Like and Crack-Like Flaws

In-service monitoring is typically required when a Level 3 Assessment is performed to qualify a component that contains weld misalignment or shell distortion with a groove-like or crack-like flaw for continued operation.

8.8 Documentation

The documentation of the FFS Assessment should include the information cited in Part 2, paragraph 2.8.

8.9 Nomenclature

A area of the metal cross section, $2\pi Rt_1$; used for centerline offset of circumferential joints in cylinders when supplemental loads are present.

A_n coefficient of cosine term in the Fourier series used to model arbitrary out-of-roundness of a cylindrical shell.

A_1 correction factor or offset from the center of measurement to the true center of the mean circle (see Figure 8.9).

B_n coefficient of sine term in the Fourier series used to model arbitrary out-of-roundness of a cylindrical shell.

B_1 correction factor or offset from the center of measurement to the true center of the mean circle (see Figure 8.9).

$C_1 \rightarrow C_{11}$ curve fit coefficients.

C_f correction factor for angular weld misalignment in the longitudinal joint of a cylindrical shell.

C_s factor to account for the severity of the out of roundness, use $C_s = 0.5$ for a purely oval shape and $C_s = 0.1$ for shapes which significantly deviate from an oval shape.

D inside diameter corrected for $LOSS$ and FCA as applicable.

D_L cone outside diameter, large end, corrected for $LOSS$ and FCA allowance as applicable.

D_m mean diameter.

$D_{\max}$ maximum outside diameter corrected for $LOSS$ and FCA as applicable.

$D_{\min}$ minimum outside diameter corrected for $LOSS$ and FCA as applicable.

D_o outside diameter of a pipe bend corrected for $LOSS$ and FCA as applicable.

D_S cone outside diameter, small end corrected for $LOSS$ and FCA as applicable.

D_x cone outside diameter at a location within the cone corrected for $LOSS$ and FCA as applicable.

D_1 outside diameter of component 1 with a wall thickness of t_1 in the joint (used for centerline offset in circumferential joints of cylinders (see Figure 8.3) corrected for $LOSS$ and FCA, as applicable.

D_2 outside diameter of component 2 with a wall thickness of t_2 in the joint (used for centerline offset in circumferential joints of cylinders (see Figure 8.3) corrected for $LOSS$ and FCA, as applicable.

d inward or outward peaking in a cylinder resulting from an angular weld misalignment.

δ height of the angular peaking (see Figures 8.4, 8.5 and 8.6).

ΔS_P range of primary plus secondary plus peak equivalent stress.

$\Delta\sigma_b$ structural bending stress range.

$\Delta\sigma_m$ structural membrane stress range.

E weld joint efficiency.

E_y Young's modulus.

e centerline offset of the plate sections at the welded joint or the maximum inward deviation that occurs within an 2θ arc length when evaluating shells subject to external pressure.

e_d maximum deviation from a true cylinder.

ε deviation from the mean circle at a location defined by θ (see Equation (8.4)).

ε_i deviation from the true mean radius at point i (see Equation (8.6)).

F net-section axial force; used only for flat plates and for centerline offset of circumferential joints in cylinders.

FCA future corrosion allowance.

FS in-service margin (see VIII-2, Part 4, paragraph 4.4.2).

h_1 distance from a datum line to the outside surface of component 1 with a wall thickness of t_1 in the joint (used for centerline offset in circumferential joints of cylinders (see Figure 8.3) corrected for $LOSS$ and FCA as applicable.

h_2 distance from a datum line to the outside surface of component 2 with a wall thickness of t_2 in the joint (used for centerline offset in circumferential joints of cylinders (see Figure 8.3) corrected for $LOSS$ and FCA as applicable.

H_f factor dependent on whether the induced stress from the shape deviation is categorized as a primary or secondary stress (see Annex 2D); $H_f = 3.0$ if the stress is secondary and $H_f = 1.5$ if the stress is primary.

i index of the current radius measurement point on the cylinder's circumference.

K_c equivalent radius coefficient for an elliptical head.

K_f fatigue strength reduction factor.

L characteristic length used to establish the amount of angular misalignment (see Figures 8.4 and 8.6); the definition of this length is shown in Figure 8.6.

L_f Lorenz factor (see Annex 2C, paragraph 2C.5.5).

L_u unsupported length of a cylindrical or conical shell used in an external pressure calculation (see Annex 2C, paragraph 2C.4).

L_{msd} distance from the edge of the bulge under investigation to the nearest major structural discontinuity or adjacent flaw.

$LOSS$ amount of uniform metal loss away from the local metal loss location at the time of the assessment.

λ buckling parameter.

M number of equally spaced measurement locations around the cylinder's circumference, a minimum of 24 points is recommended, M must be an even number.

M_{ns} net section bending moment; used only for flat plates and for centerline offset of circumferential joints in cylinders.

n harmonic number associated with the Fourier series, or the number of waves for a buckled cylindrical shell.

N number of Fourier coefficients used in the calculation equal to $M/2$.

P internal or external design pressure, as applicable.

P_c inelastic buckling pressure of a cylindrical shell subject to external pressure.

P_{ec} minimum elastic buckling pressure of a cylindrical shell subject to external pressure.

P_{eL} elastic buckling pressure of a cylinder.

P_{ext} permissible external pressure.

R mean radius of the cylinder or sphere measured to mid thickness.

R_b ratio of the induced bending stress to the applied membrane stress in a component that results from pressure.

R_{bs} ratio of the induced bending stress to the applied membrane stress in a component that results from supplemental loads.

R_m average radius.

$R(\theta)$ radius at a location defined by θ corrected for $LOSS$ and FCA as applicable.

R_i measured radius at point i on a cylinder.

R_i^c corrected radius at point i on a cylinder.

R_L local outside radius of imperfect shell (see Figure 8.10) corrected for $LOSS$ and FCA as applicable.

R_{Lm} local mean radius of the shell surface measured in the meridional or circumferential direction, as applicable.

R_o outside radius of the perfect shell (see Figure 8.10) corrected for $LOSS$ and FCA as applicable.

R_1 mean radius of component 1 with a wall thickness of t_1 in the joint (used for centerline offset in circumferential joints of cylinders (see Figure 8.3) corrected for $LOSS$ and FCA as applicable).

R_2 mean radius of component 2 with a wall thickness of t_2 in the joint (used for centerline offset in circumferential joints of cylinders (see Figure 8.3) corrected for $LOSS$ and FCA as applicable).

RSF calculated remaining strength factor for a component.

RSF_a allowable remaining strength factor (see Part 2).

R_{bs}^{pc} R_{bs} factor for a plate, centerline offset.

R_{bs}^{pa} R_{bs} factor for a plate, angular misalignment.

R_b^{ccjc} R_b factor for a cylinder, circumferential joint, centerline offset.

R_b^{ccja} R_b factor for a cylinder, circumferential joint, angular misalignment.

R_{bp}^{ccja} R_b factor for a cylinder, circumferential joint, angular misalignment, peak location.

R_{bt}^{ccja} R_b factor for a cylinder, circumferential joint, angular misalignment, trough location.

R_{bs}^{ccjc} R_{bs} factor for a cylinder, circumferential joint, centerline offset.

R_{bs}^{ccja} R_{bs} factor for a cylinder, circumferential joint, angular misalignment.

R_b^{cljc} R_b factor for a cylinder, longitudinal joint, centerline offset.

R_b^{clja} R_b factor for a cylinder, longitudinal joint, angular misalignment.

R_b^{scjc} R_b factor for a sphere, circumferential joint, centerline offset.

R_b^{scja} R_b factor for a sphere, circumferential joint, angular misalignment.

R_b^{or} R_b factor for out-of-roundness.

S_a allowable stress for the component at the assessment temperature based on the original construction code.

S_p parameter for misalignment calculation.

σ_m membrane stress from pressure.

σ_{ms} membrane stress from supplemental loads.

σ_m^C circumferential membrane stress in a cylindrical shell.

σ_m^L longitudinal membrane stress in a cylindrical shell.

σ_r stress range in a component used in determining the permitted number of cycles in a fatigue analysis.

σ_{ys} yield stress at the assessment temperature (see Annex 2E).

T temperature (°C or °F).

t furnished thickness of the component.

t_B minimum local wall thickness in the bulge.

t_c corroded wall thickness.

t_{nom} nominal or furnished thickness of the component adjusted for mill under tolerance as applicable.

t_{rd} uniform thickness away from the local metal loss location established by thickness measurements at the time of the assessment.

t_1 wall thickness of component 1 in the joint where $t_2 \geq t_1$; used for centerline offset weld misalignment in cylindrical shell circumferential weld joints (see Figure 8.3).

t_2 wall thickness of component 2 in the joint where $t_2 \geq t_1$; used for centerline offset weld misalignment in cylindrical shell circumferential weld joints (see Figure 8.3).

t_{1c} wall thickness of component 1, adjusted for $LOSS$ and FCA using Equation (8.10) or Equation (8.11), as applicable.

t_{2c} wall thickness of component 2, adjusted for $LOSS$ and FCA using Equation (8.10) or Equation (8.11), as applicable.

θ angle to define the location where the stress will be computed (see Figure 8.5, Figure 8.7, and Figure 8.9).

θ_p angle associated with angular misalignment.

ν Poisson's Ratio.

Z section modulus of the cylindrical shell cross section.

8.10 References

References for this Part are provided in Annex 8A – Technical Basis and Validation – Assessment of Weld Misalignment and Shell Distortions.

8.11 Tables

Table 8.1 – Data Required for the Assessment of a Weld Misalignment or Shell Distortion

Use this form to summarize the data obtained from a field inspection.

Equipment Identification: _____
Equipment Type: _____ Pressure Vessel _____ Storage Tank _____ Piping Component
Component Type & Location: _____

Data required For Level 1 Assessment

Future Corrosion Allowance: _____

Out-Of-Roundness (Cylindrical Shell Subject to Internal Pressure)
Maximum Measured Internal Diameter ($D_{\max}$): _____
Minimum Measured Internal Diameter ($D_{\min}$): _____
Nominal Diameter: _____

Weld Misalignment
Wall Thickness: _____
Radial Misalignment (e): _____

Data required For Level 2 Assessment

Temperature: _____
Internal and/or External Pressure: _____
Allowable Stress and Weld Joint Efficiency: _____
Component Inside Diameter (D): _____

Weld Misalignment
Component Wall Thickness (t *or* t_1 *and* t_2): _____
Component Geometry (R *or* R_1 *and* R_2): _____
Measure of Misalignment (e *or* δ): _____
Characteristic Length (L): _____
Net Section Force, (F), and Bending Moment (M): _____

Out-Of-Roundness
Component Wall Thickness (t): _____
Mean Radius (R_o): _____
Local Radius (R_L): _____
Young's Modulus (E_y): _____

Bulges
Component Furnished Thickness (t): _____
Minimum Thickness in Bulge (t_b): _____
Bulge Measurements: _____
Distance to Nearest Structural Discontinuity (L_{msd}): _____

Table 8.2 – Pseudocode for Computation of Fourier Series Coefficients on a Discrete Range for the Analysis of Out-Of-Roundness Radius Data

```
Fourier (Npoints, RAD, Ncoeff, An, Bn)

Ncoeff = Npoints/2

An(1) = 0.0
Bn(1) = 0.0

sp = 0.0
cp = 1.0
rn = 2.0 / Npoints
arg = 3.14159265*rn
c = cos[arg]
s = sin[arg]

FOR i = 1 TO Npoints
   An(1) = An(1) + RAD(i)
ENDFOR

An(1) = rn * An(1) / 2.0

FOR k = 1 TO Ncoeff
   x = (c * cp) - (s * sp)
   sp = (c * sp) + (s * cp)
   cp = x
   u = 0.0
   v = 0.0

    FOR ii = 2 TO Npoints
        j = np - ii + 2
        w = RAD(j) + (2 * cp * v) - u
        u = v
        v = w
    ENDFOR

    An(k + 1) = rn * (RAD(1) + (cp * v) - u)
    Bn(k + 1) = rn * sp * v
ENDFOR
```

Notes:

1. Definitions of variables
   - Npoints – number of radius reading points.
   - RAD – array of radius readings values at a total number of points equal to Npoints.
   - Ncoeff – number of Fourier coefficients to be computed.
   - An – array of computed coefficients of the cosine portion of the Fourier series.
   - Bn – array of computed coefficients of the sine portion of the Fourier series.
2. This algorithm may only be used for an even number of equal spacing of readings for a full period or 360°. For example, in Figure 8.9, Npoints=24 readings are indicated with an equal spacing of 15°. The radius readings at 0°, 15°, 30°, …, 345° correspond to RAD(1), RAD(2), RAD(3),…, RAD(Npoints). The radius reading at 360° is assumed to be equal to the reading at 0°.
3. The results from the routine produce Ncoeff Fourier coefficients where An(1), Bn(1) correspond to the A_0 and B_0, An(2), Bn(2) correspond to the A_1 and B_1, and in general, An(k), Bn(k) correspond to the A_{k-1} and B_{k-1}.

Table 8.3 – Overview of Fabrication Tolerances – ASME B&PV Code, Section VIII, Division 1 and Division 2

Fabrication Tolerance	Requirement	Code Reference
Out-Of-Roundness in Cylindrical Shells Under Internal Pressure	$(D_{max} - D_{min})$ shall not exceed 1% of D where: D_{max} Maximum measured internal diameter D_{min} Minimum measured internal diameter D Nominal internal diameter At nozzle openings, this tolerance is increased by 2% of the inside diameter of the opening.	UG-80(a) (6.1.2.7)
Out-Of-Roundness in Cylindrical Shells Under External Pressure	The diameter tolerance for internal pressure shall be satisfied. Using a chord length equal to twice the arc length determined from Figure 8.11, the maximum deviation from true circle shall not exceed the value e determined from Figure 8.12. Take measurements on the unwelded plate surface. For shells with a lap joint, increase tolerance by t. Do not include future corrosion allowance in t.	UG-80(b) (6.1.2.7)
Shape of Formed Heads	The inside surface shall not deviate outside the shape by more than 1.25% of the inside diameter nor inside the shape by more than 0.625% of the inside diameter.	UG-81 (6.1.2.7)
Cylindrical Shell-To-Head Attachment Weld	The centerline (radial) misalignment between the shell and the head shall be less than one-half the difference between the actual shell and head thicknesses.	UW-13(b)(3) (Table 4.2.5 Details 2-5)
Centerline Offset Weld Misalignment – Longitudinal Joints (Category A)	For $t \leq$ 13 mm (1/2 in) e = t/4 For 13 mm (1/2 in) < $t \leq$ 19 mm (3/4 in) e = 3 mm (1/8 in) For 19 mm (3/4 in) < $t \leq$ 38 mm (1-1/2 in) e = 3 mm (1/8 in) For 38 mm (1-1/2 in) < $t \leq$ 51 mm (2 in) e = 3 mm (1/8 in) For $t >$ 51 mm (2 in) e = min(t/16, 10 mm) or e = min(t/16, 3/8 in) Where t is the plate thickness and e the allowable centerline offset.	UW-33 (6.1.6)
Centerline Offset Weld Misalignment - Circumferential Joints (Category B, C and D)	For $t \leq$ 19 mm (3/4 in) e = t/4 For 19 mm (3/4 in) < $t \leq$ 38 mm (1-1/2 in) e = 5 mm (3/16 in) For 38 mm (1-1/2 in) < $t \leq$ 51 mm (2 in) e = t/8 For $t >$ 51 mm (2 in) e = min(t/8, 19 mm) or e = min(t/8, 3/4 in) Where t is the plate thickness and e the allowable centerline offset.	UW-33 (6.1.6)
Angular Weld Misalignment	None stated in Division 1 or Division 2	
Peaking of Welds (Category A)	The inward or outward peaking dimension, d , shall be measured using a template and included in the fatigue analysis of Division 2 vessels as required. The Manufacturer's Design Report shall stipulate the permitted value.	(6.1.6.3)

Table 8.4 – Overview of Fabrication Tolerances – ASME B31.3

Fabrication Tolerance	Requirement	Code Reference
Out-Of-Roundness in Piping Under Internal Pressure	Default ASTM Standard the pipe was purchased to, for example: • ASTM 530 – For thin wall pipe, the difference in extreme outside diameter readings (ovality) in any one cross-section shall not exceed 1.5% of the specified outside diameter. Thin wall pipe is defined as having a wall thickness of 3% or less of the outside diameter. • ASTM 358 – Difference between major and minor outside diameters, 1% of specified diameter. • ASTM 671 – Difference between major and minor outside diameters, 1% of specified diameter. • ASTM 672 – Difference between major and minor outside diameters, 1% of specified diameter. • ASTM 691 – Difference between major and minor outside diameters, 1% of specified diameter. For wrought steel butt-welding fittings (e.g., elbows, tees, reducers, weld caps), requirements are provided in ASME B16.9.	---
Out-Of-Roundness in Piping Under External Pressure	Same as for internal pressure	---
Centerline Offset Weld Misalignment – Longitudinal Joints	The tolerance defaults to the tolerance of ASTM standard pipe as purchased, or requirement stipulated for centerline offset misalignment of circumferential joints.	328.4.3(b)
Centerline Offset Weld Misalignment - Circumferential Joints	Inside surfaces of components at ends to be joined in girth or miter groove welds shall be aligned within dimensional limits in the WPS and the engineering design.	328.4.3(a)
Angular Weld Misalignment	An angular offset of three degrees (3°) or less is considered acceptable without additional design considerations.	304.2.3

Table 8.5 – Overview of Fabrication Tolerances – API Standard 620

Fabrication Tolerance	Requirement	Code Reference
Out-Of-Plumbness for Tank Shells	Out of plumbness from top of shell to bottom of shell shall not exceed 1/200 of the total tank height.	6.5.2
Out-Of-Roundness for Tank Shells	Maximum allowable out-of-roundness for tank shells, measured as the difference between the maximum and minimum diameters, shall not exceed 1% of average diameter or 300 mm (12 in), whichever is less, except as modified for flat bottom tanks for which the radii measured at 300 mm (12 in) above the bottom corner weld shall not exceed the tolerances shown below. D < 12 m (40 ft) Tol = 13 mm (1/2 in) 12 m (40 ft) ≤ D < 46 m (150 ft) Tol = 19 mm (3/4 in) 46 m (150 ft) ≤ D < 76 m (250 ft) Tol = 25 mm (1 in) D ≥ 76 m (250 ft) Tol = 32 mm (1-1/4 in) Where D is the diameter of the tank in meters or feet and Tol the tolerance on the radius. Skirts or cylindrical ends of formed tops shall have a maximum difference between maximum and minimum diameters of 1% of the nominal diameter.	6.5.3
Centerline Offset Weld Radial Misalignment – All Butt Joints	For t ≤ 6 mm (1/4 in) e = 2 mm (1/16 in) For t > 6 mm (1/4 in) e = min [t/4, 3 mm] or e = min [t/4, 1/8 in] Where t is the plate thickness and e the allowable radial misalignment or offset.	6.14
Local Deviations Such as Angular Weld Misalignment (Peaking) and or Flat Spots	Using a 910 mm (36 in) horizontal sweep board with a radius equal to the nominal radius of the tank, peaking at vertical joints shall not exceed 13 mm (1/2 in) for steel shells and 25 mm (1 in) for aluminum shells (see API 620, Appendix Q). Using a 910 mm (36 in) vertical straight sweep board, banding at horizontal joints shall not exceed 13 mm (1/2 in) for steel shells and 25 mm (1 in) for aluminum shells (see API 620, Appendix Q). Flat spots shall not exceed appropriate flatness and waviness requirements specified in ASTM A6 or ASTM A20 for carbon and alloy steels, ASTM A480 for stainless steels, and Table 5.13 of ANSI H35.2 for aluminum.	6.5.4

Table 8.6 – Overview of Fabrication Tolerances – API Standard 650

Fabrication Tolerance	Requirement	Code Reference
Out-of-Plumbness	The maximum out of plumbness of the top of the shell of revolution to the bottom of the shell shall not exceed 1/200 of the total tank height.	7.5.2
Out-Of-Roundness for Tank Shells	Radii measured at 300 mm (12 in) above the bottom corner weld shall not exceed the tolerances shown below. D < 12 m (40 ft) Tol = 13 mm (1/2 in) 12 m (40 ft) ≤ D < 46 m (150 ft) Tol = 19 mm (3/4 in) 46 m (150 ft) ≤ D < 76 m (250 ft) Tol = 25 mm (1 in) D ≥ 76 m (250 ft) Tol = 32 mm (1-1/4 in) Where D is the diameter of the tank in meters or feet and Tol the tolerance on the radius.	7.5.3
Centerline Offset Weld Misalignment – Longitudinal Joints	For t ≤ 16 mm (5/8 in) e = 2 mm (1/16 in) For t > 16 mm (5/8 in) e = min [t/10, 3 mm] or e = min [t/10, 1/8 in] Where t is the plate thickness and e the allowable radial misalignment or offset.	7.2.3.1
Centerline Offset Weld Misalignment - Circumferential Joints	The upper plate shall not project by more than 20 percent of the thickness of the upper plate, with a maximum projection of 3mm (1/8 in); however, for upper plates less than 8 mm (5/16 in) thick, the maximum projection shall be limited to 2 mm (1/16 in).	7.2.3.2
Local Deviations Such as Angular Weld Misalignment (Peaking) and or Flat Spots	Using a 910 mm (36 in) horizontal sweep board with a radius equal to the nominal radius of the tank, peaking at vertical joints shall not exceed 13 mm (1/2 in). Using a 910 mm (36 in) vertical straight sweep board, banding at horizontal joints shall not exceed 13 mm (1/2 in). Flat spots shall not exceed appropriate flatness and waviness requirements specified in ASTM A6 or ASTM A20.	7.5.4

Table 8.7 – Overview of Fabrication Tolerances for Reconstructed Tanks – API Standard 653

Fabrication Tolerance	Requirement	Code Reference
Out-of-Plumbness	The maximum out of plumbness of the top of the shell of revolution to the bottom of the shell shall not exceed 1/100 of the total tank height, with a maximum deviation of 130 mm (5 in).	10.5.2.1
Out-Of-Roundness for Tank Shells	Radii measured at 304 mm (12 in) above the shell-to-bottom weld shall not exceed the tolerances shown below. D < 12 m (40 ft) — Tol = 13 mm (1/2 in) 12 m (40 ft) ≤ D < 46 m (150 ft) — Tol = 19 mm (3/4 in) 46 m (150 ft) ≤ D < 76 m (250 ft) — Tol = 25 mm (1 in) D ≥ 76 m (250 ft) — Tol = 32 mm (1-1/4 in) Where D is the diameter of the tank in meters or feet and Tol the tolerance on the radius. Radius tolerances measured higher than one foot above the shell-to-bottom weld shall not exceed three times the tolerances given above.	10.5.3
Centerline Offset Weld Misalignment – Longitudinal Joints	For t ≤ 16 mm (5/8 in) — e = 2 mm (1/16 in) For t > 16 mm (5/8 in) — e = min[t/10, 3 mm] or e = min[t/10, 1/8 in] Where t is the plate thickness and e is the allowable radial misalignment or offset.	10.4.4.1
Centerline Offset Weld Misalignment - Circumferential Joints	The upper plate shall not project by more than 20 percent of the thickness of the upper plate, with a maximum projection of 3 mm (1/8 in); however, for upper plates less than 8 mm (5/16 in) thick, the maximum projection shall be limited to 2 mm (1/16 in).	10.4.4.2
Local Deviations Such as Angular Weld Misalignment (Peaking) and / or Flat Spots	Using a 910 mm (36 in) horizontal sweep board with a radius equal to the nominal radius of the tank, peaking at vertical joints shall not exceed 13 mm (1/2 in). Using a 910 mm (36 in) vertical straight sweep board, banding at horizontal joints shall not exceed 25 mm (1 in).	10.5.4 & 10.5.5

Table 8.8 – Equations for the Ratio of Induced Bending Stress to Applied Membrane Stress for a Flat Plate with Centerline Offset and Angular Misalignment

Type of Misalignment	Equations For R_{bs}
Flat Plate – Centerline Offset (see Figure 8.2) (1)	$R_{bs}^{pc} = 6\left(\frac{e}{t_{1c}}\right)\left(1+\left(\frac{t_{2c}}{t_{1c}}\right)^{1.5}\right)^{-1}$ Limitations: $0.0 \le e \le t_{1c}$, $t_{2c} \ge t_{1c}$
Flat Plate – Angular Misalignment (see Figure 8.4) (1)	$R_{bs}^{pa} = 3\left(\frac{\delta}{t_c}\right)C_f$ where: $\delta = \frac{L\theta_p}{4}$ $(\theta_p \text{ in radians})$ $C_f = \left(\frac{2}{\beta}\right)\cdot\tanh\left[\frac{\beta}{2}\right]$ (for fixed ends) $C_f = \left(\frac{2}{\beta}\right)\cdot\tanh\left[\beta\right]$ (for pinned ends) $\beta = \frac{L}{t_c}\sqrt{\frac{3\sigma_m}{E_y}}$ (in radians) Limitations: $\theta_p \ge 0.0$
Note: The equation for R_b and R_{bs} are dimensionless.	

Table 8.9 – Equations for the Ratio of Induced Bending Stress to Applied Membrane Stress for the Circumferential Joints of a Cylinder with Centerline Offset and Angular Misalignment

Type of Misalignment	Equations for R_b
Cylinder – Circumferential Joint, Centerline Offset (see Figure 8.3) (1)	$R_b^{ccjc} = \text{abs}\left[\frac{12}{R_1 t_{1c}}\left(0.25672 R_2 t_{2c}\left(\frac{C_1}{C_3}\right)+\frac{e\cdot R_a}{2}\left(\frac{C_2}{C_3}\right)\right)\right]$ $R_{bs}^{ccjc} = \left(\frac{6\cdot e}{t_{1c}}\right)\left(1+\rho^{1.5}\right)^{-1}$ where: $C_1 = (\rho-1)\left(\rho^2-1\right)$ $C_2 = \rho^2 + 2\rho^{1.5} + 1$ $C_3 = \left(\rho^2+1\right)^2 + 2\rho^{1.5}(\rho+1)$ $\rho = \frac{t_{2c}}{t_{1c}}$ *where* $t_{2c} \ge t_{1c}$ $R_a = 0.5(R_1 + R_2)$ $R_1 = 0.5(D_1 - t_{1c})$ $R_2 = 0.5(D_2 - t_{2c})$ $e = D_1 - D_2 + h_1 - h_2 + 0.5(t_2 - t_1)$ *e is positive if* $h_2 + D_2 - 0.5t_2 < h_1 + D_1 - 0.5t_1$ *in Figure* 8.3 *e is negative if* $h_2 + D_2 - 0.5t_2 > h_1 + D_1 - 0.5t_1$ *in Figure* 8.3 Limitations: $\frac{R_1}{t_{1c}} \ge 10.0$, $\frac{R_2}{t_{2c}} \ge 10.0$, and $0.0 < \frac{abs[e]}{t} \le 1.0$

Table 8.9 – Equations for the Ratio of Induced Bending Stress to Applied Membrane Stress for the Circumferential Joints of a Cylinder with Centerline Offset and Angular Misalignment

Type of Misalignment	Equations for R_b
Cylinder – Circumferential Joint, Angular Misalignment (see Figure 8.6) (1)	$R_b^{ccja} = \max\left[R_{bp}^{ccja},\ R_{bt}^{ccja}\right] \qquad (\delta \geq 0)$ $R_b^{ccja} = 0.0 \qquad (\delta = 0)$ where $\theta_p = \arctan\left[\dfrac{2\cdot\delta}{L}\right] \qquad (in\ radians)$ $R_b^{ccja} = \dfrac{\left(\begin{array}{l} C_1 + C_2\cdot\ln\left(S_p\right) + C_3\cdot\theta_p + C_4\cdot\ln\left(S_p\right)^2 + \\ C_5\cdot{\theta_p}^2 + C_6\cdot\theta_p\cdot\ln\left(S_p\right)\end{array}\right)}{\left(\begin{array}{l} 1.0 + C_7\cdot\ln\left(S_p\right) + C_8\cdot\theta_p + C_9\cdot\ln\left(S_p\right)^2 + \\ C_{10}\cdot{\theta_p}^2 + C_{11}\cdot\theta_p\cdot\ln\left(S_p\right)\end{array}\right)}$ $\left(\begin{array}{ll} C_1 = 5.0993384(10)^{-4} & , C_2 = 5.16375(10)^{-5} \\ C_3 = 12.710179 & , C_4 = -6.8895492(10)^{-4} \\ C_5 = -16.054574 & , C_6 = 1.20587 \\ C_7 = -0.24477649 & , C_8 = -1.0837891 \\ C_9 = 0.02263272 & , C_{10} = 0.49373892 \\ C_{11} = 0.51540822 & \end{array}\right) \quad \left(for\ R_{bp}^{ccja}\right)$ $\left(\begin{array}{ll} C_1 = 5.7545948(10)^{-3} & , C_2 = 4.2129576(10)^{-3} \\ C_3 = 12.609416 & , C_4 = -4.0643269(10)^{-3} \\ C_5 = -30.793641 & , C_6 = 0.77497182 \\ C_7 = -0.25724978 & , C_8 = -1.9582039 \\ C_9 = 0.019325187 & , C_{10} = 0.6770323 \\ C_{11} = 0.70900192 & \end{array}\right) \quad \left(for\ R_{bt}^{ccja}\right)$ $S_p = \sqrt{\dfrac{12\left(1-\nu^2\right)PR^3}{E_y t_c^3}}$ Note: In the above equations, θ_p is in radians. Equations for R_{bs}^{ccja} are currently under development. Limitations: $10.0 \leq \dfrac{R}{t_c} \leq 500.0$, $0.0^o \leq \theta_p \leq 10.0^o$, and $0.0 \leq S_p \leq 67.5$
Note: The equation for R_b and R_{bs} are dimensionless.	

Table 8.10 – Equations for the Ratio of Induced Bending Stress to Applied Membrane Stress for the Longitudinal Joints of a Cylinder with Centerline Offset and Angular Misalignment

Type of Misalignment	Equations for R_b
Cylinder – Longitudinal Joints, Centerline Offset (see Figure 8.2) (1)	$R_b^{cljc} = C_1 \cdot \ln\left(S_p + 1\right)^3 + C_2 \cdot \ln\left(S_p + 1\right)^2 + C_3$ where: $C_1 = \left(0.00038430935\left(\frac{e}{t_c}\right)^3 + 0.0073689734\left(\frac{e}{t_c}\right)^2 - 0.0075497567\left(\frac{e}{t_c}\right) \right)$ $C_2 = \left(-0.021263219\left(\frac{e}{t_c}\right)^3 - 0.023904130\left(\frac{e}{t_c}\right)^2 + 0.019662850\left(\frac{e}{t_c}\right) \right)$ $C_3 = \left(0.079070679\left(\frac{e}{t_c}\right)^3 + 0.24470862\left(\frac{e}{t_c}\right)^2 + 2.9331524\left(\frac{e}{t_c}\right) \right)$ The parameter S_p from Table 8.9. Limitations: $10.0 \le \frac{R}{t_c} \le 400.0$, $0.0 \le \frac{e}{t_c} \le 1.0$, and $1.0 \le S_p \le 50.0$

Table 8.10 – Equations for the Ratio of Induced Bending Stress to Applied Membrane Stress for the Longitudinal Joints of a Cylinder with Centerline Offset and Angular Misalignment

Type of Misalignment	Equations for R_b
Cylinder – Longitudinal Joint, Angular Misalignment, Local Peaking (see Figures 8.4 and 8.5) (1), (2)	$R_b^{clja} = 6\left(\frac{\delta}{t_c}\right)C_f \qquad (\delta \geq 0.0)$ where: $\theta_p = \arccos\left[\frac{R}{R+\delta}\right] \qquad (in\ radians)$ $C_f = 1 - \frac{\theta_p}{3\pi} - \frac{4}{\pi\theta_p^2}\left(\theta_p - \sin\left[\theta_p\right]\right) - \frac{4S_p^2}{\pi\theta_p^2}\sum_{n=2}^{\infty}\left(\frac{\left(n\theta_p - \sin\left[n\theta_p\right]\right)}{n^3\left(n^2 - 1 + S_p^2\right)}\right)$ The parameter S_p from Table 8.9. Alternatively, the values of C_f can be determined from Figure 8.13. Limitations: $\frac{R}{t_c} \geq 10.0$ and $0.0 \leq S_p \leq 30.0$
Cylinder – Longitudinal Joint, Angular Misalignment, Global Peaking (see Figures 8.4 and 8.5) (1), (2)	$R_b^{clja} = 6\left(\frac{\delta}{t_c}\right)C_f \qquad (\delta \geq 0.0)$ where: $C_f = 0.5 - \frac{\pi}{2k}\coth\left[k\pi\right] - \frac{k^2-1}{2k^2} + \frac{1}{2k^2-1} \qquad (for\ S_p^2 < 1.0)$ $C_f = 0.5 + \frac{\pi}{2k}\coth\left[k\pi\right] - \frac{k^2+1}{2k^2} - \frac{1}{k^2+1} \qquad (for\ S_p^2 \geq 1.0)$ $k^2 = 1 - S_p^2 \qquad (for\ S_p^2 < 1.0)$ $k^2 = S_p^2 - 1 \qquad (for\ S_p^2 \geq 1.0)$ The parameter S_p from Table 8.9.

Notes:
1. The equation for R_b is dimensionless.
2. Establish an appropriate cutoff for the series solution for C_f, e.g., the change in C_f is less than 0.01%.

Table 8.11 – Equations for the Ratio of Induced Bending Stress to Applied Membrane Stress for the Circumferential Joints of a Sphere with Centerline Offset and Angular Misalignment

Type of Misalignment	Equations for R_b
Sphere – Circumferential Joint, Centerline Offset (see Figure 8.2) (1)	$R_b^{scjc} = 3.032556\left(\frac{e}{t_c}\right)$ Limitations: $10.0 \le \frac{R}{t_c} \le 400.0$ and $0.0 \le \frac{e}{t_c} \le 1.0$.
Sphere – Circumferential Joint, Angular Misalignment (see Figures 8.4 and 8.5)	$R_b^{scja} = \frac{C_1 + C_2 \cdot \ln(S_p) + C_3 \cdot \theta_p + C_4 \cdot \theta_p^{\,2} + C_5 \cdot \theta_p^{\,3}}{1.0 + C_6 \cdot \ln(S_p) + C_7 \cdot \ln(S_p)^2 + C_8 \cdot \ln(S_p)^3 + C_9 \cdot \theta_p}$ $(\delta > 0)$ $R_b^{scja} = 0.0$ $(\delta = 0)$ where: $\theta_p = \arccos\left[\frac{R}{R+\delta}\right]$ $(in\ radians)$ $\begin{pmatrix} C_1 = -1.4304468 & , C_2 = 0.35940205 \\ C_3 = 21.179401 & , C_4 = -24.388672 \\ C_5 = 25.735686 & , C_6 = -0.25763931 \\ C_7 = 0.039519591 & , C_8 = -3.0092784(10)^{-3} \\ C_9 = -0.31903642 & \end{pmatrix}$ $(for\ \theta_p \ge 0.1309)$ $\begin{pmatrix} C_1 = -1.4997207(10)^{-4} & , C_2 = 6.6708435(10)^{-5} \\ C_3 = -0.28544055 & , C_4 = 96.112344 \\ C_5 = -162.72803 & , C_6 = -0.60993664 \\ C_7 = 0.14674857 & , C_8 = -0.013907169 \\ C_9 = 1.2550312 & \end{pmatrix}$ $(for\ \theta_p < 0.1309)$ The parameter S_p is from Table 8.9. Limitations: $10.0 \le \frac{R}{t_c} \le 300.0$, $0.0^o \le \theta_p \le 25.0^o$ and $0.0 \le S_p \le 30.0$
Note: The equation for R_b is dimensionless.	

Table 8.12 – Stress Data Required for a Fatigue Assessment

Type of Fatigue Analysis	Stress Data
Elastic Stress Analysis using welded joint fatigue curves (see Part 14)	Flat Plate – Weld misalignment $\Delta\sigma_m = \sigma_{ms}$ $\Delta\sigma_b = \sigma_{ms}\left(R_b^{pc} + R_b^{pa}\right)$ Cylinder, Circumferential Weld Joint – Weld misalignment $\Delta\sigma_m = \sigma_m + \sigma_{ms}$ $\Delta\sigma_b = \sigma_m\left(R_b^{ccjc} + R_b^{ccja}\right) + \sigma_{ms}\left(R_{bs}^{ccjc} + R_{bs}^{ccja}\right)$ Cylinder, Longitudinal Weld Joint – Weld misalignment and out-of-roundness $\Delta\sigma_m = \sigma_m$ $\Delta\sigma_b = \sigma_m\left(R_b^{cljc} + R_b^{clja} + R_b^{or}\right)$ Spheres, Circumferential Weld Joint – Weld misalignment $\Delta\sigma_m = \sigma_m$ $\Delta\sigma_b = \sigma_m\left(R_b^{scjc} + R_b^{scja}\right)$
Elastic Stress Analysis using smooth bar fatigue curves (see Part 14)	Flat Plate – Weld misalignment (See Note Below) $\Delta S_P = \sigma_{ms}\left(1 + R_b^{pc} + R_b^{pa}\right)K_f$ Cylinder, Circumferential Weld Joint – Weld misalignment (See Note Below) $\Delta S_P = \left[\sigma_m\left(1 + R_b^{ccjc} + R_b^{ccja}\right) + \sigma_{ms}\left(1 + R_{bs}^{ccjc} + R_{bs}^{ccja}\right)\right]K_f$ Cylinder, Longitudinal Weld Joint – Weld misalignment and out-of-roundness (See Note Below) $\Delta S_P = \sigma_m\left(1 + R_b^{cljc} + R_b^{clja} + R_b^{or}\right)K_f$ Spheres, Circumferential Weld Joint – Weld misalignment (See Note Below) $\Delta S_P = \sigma_m\left(1 + R_b^{scjc} + R_b^{scja}\right)K_f$
Note: Recommendations for determining the fatigue strength reduction factor, K_f are provided in Part 14.	

8.12 Figures

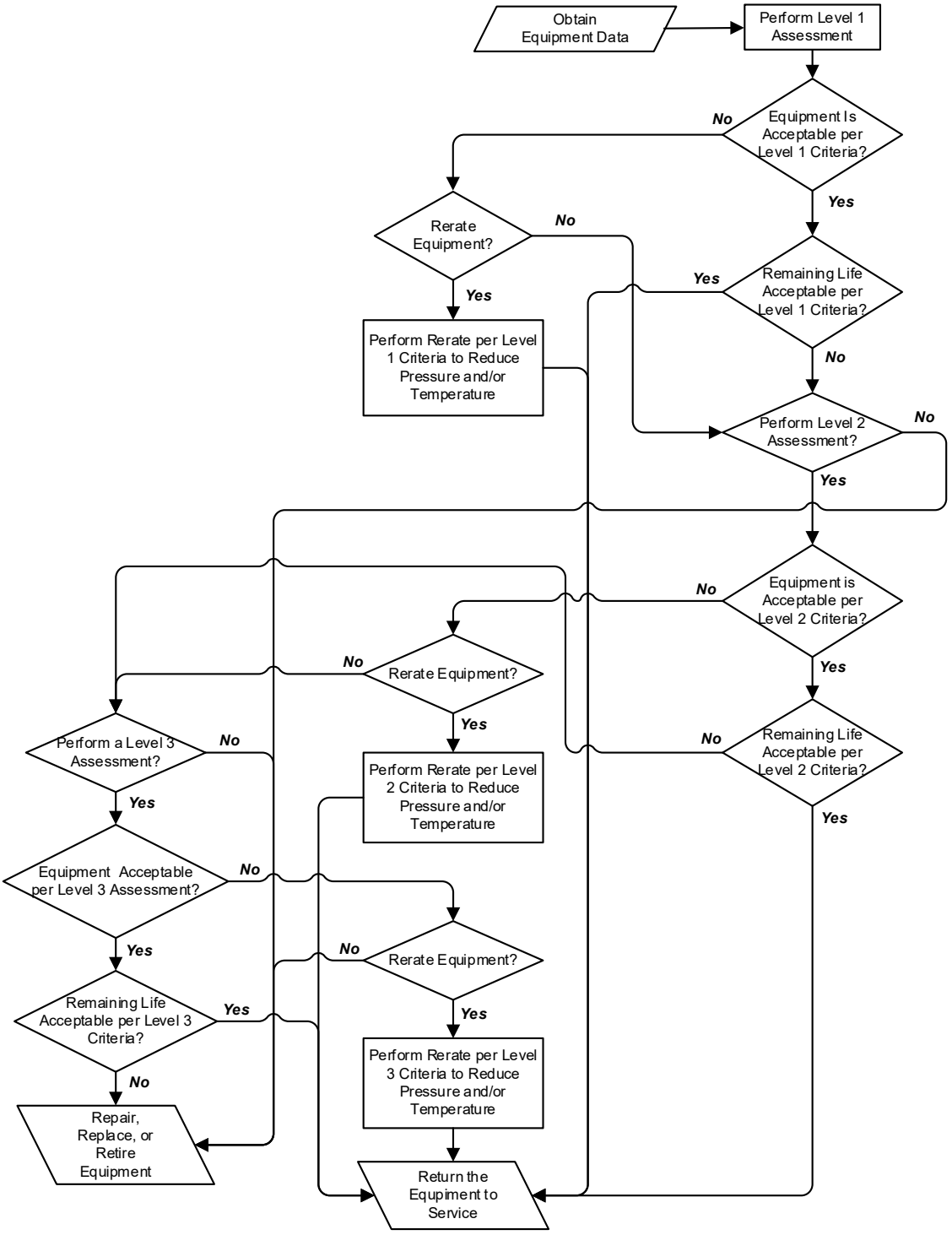

Figure 8.1 – Overview of the Assessment Procedures to Evaluate a Component with a Weld Misalignment or Shell Distortion

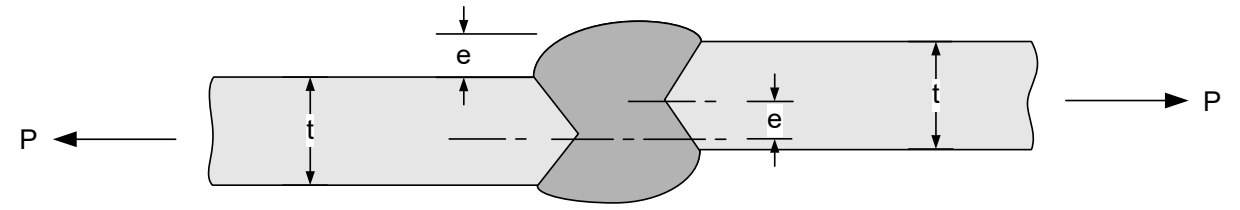

(a) Same Thickness -- Inside and Outside Surfaces Not Aligned

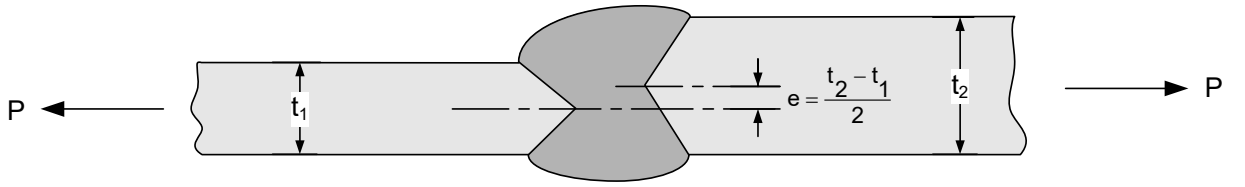

(b) Different Thickness -- Alignment With One Surface

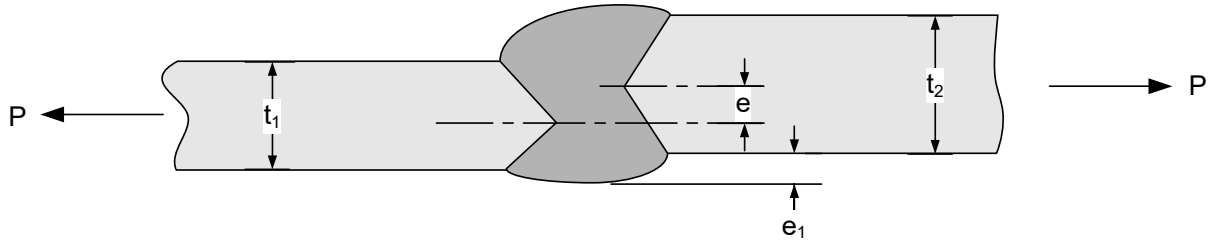

(c) Different Thickness -- Inside and Outside Surfaces Not Aligned

Figure 8.2 – Centerline Offset Weld Misalignment in Butt Weld Joints in Flat Plates

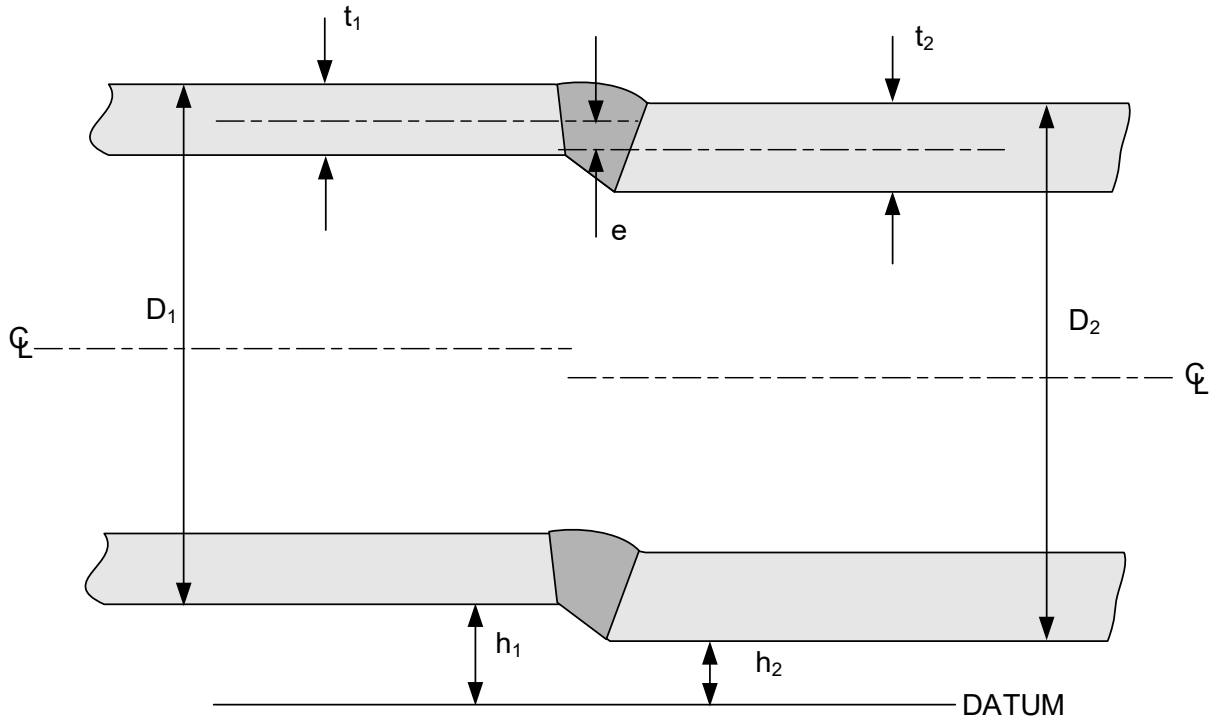

(a) Weld Misalignment - Equal Diameters ($D_1 = D_2$)

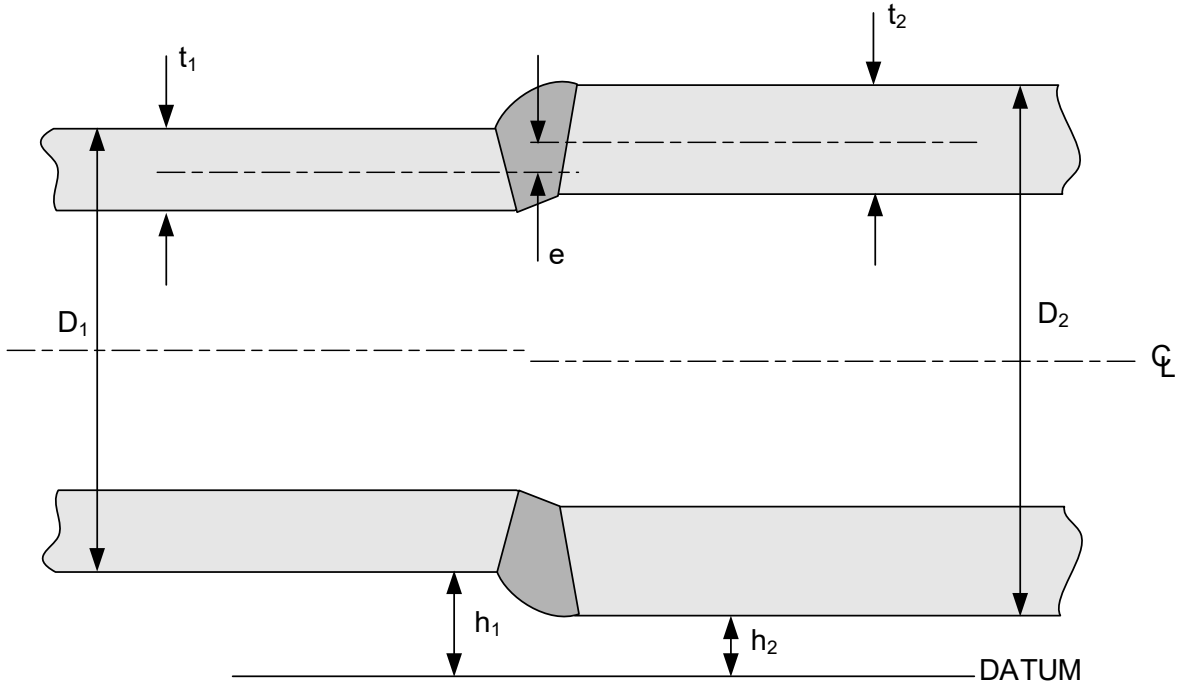

(b) Weld Misalignment - Unequal Diameters ($D_1 \neq D_2$)

Note: For Both Case (a) and (b) $e = (h_1 – h_2) + (D_1 – D_2) + 0.5\ (t_2 – t_1)$

Figure 8.3 – Centerline Offset Weld Misalignment in Cylindrical Shell Circumferential Weld Joints

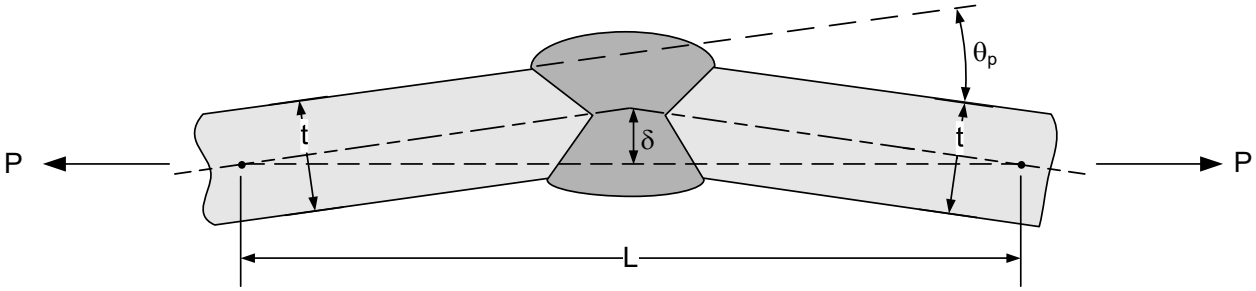

(a) Angular Weld Misalignment

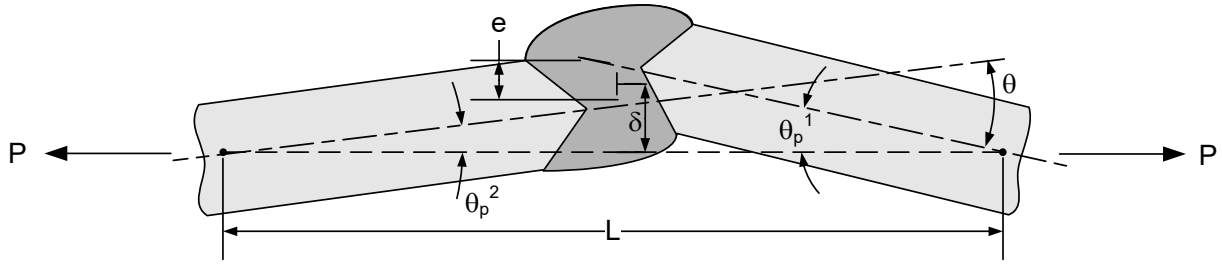

(b) Angular and Centerline Offset Weld Misalignment

Notes: The dimension L is established as shown in Figure 8.6.

Figure 8.4 – Angular Misalignment in Butt Weld Joints in Flat Plates

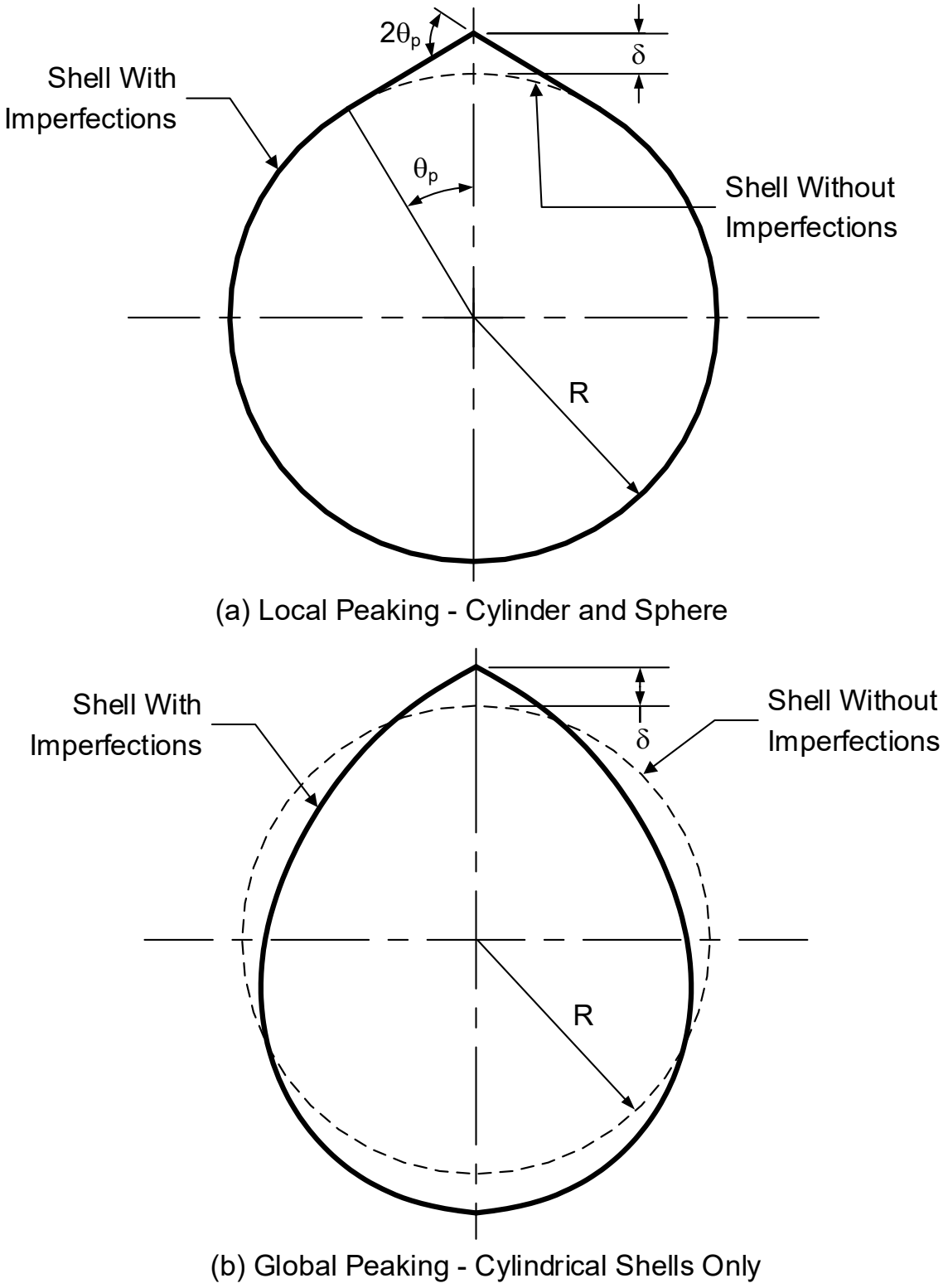

Figure 8.5 – Angular Misalignment in a Cylindrical Shell Longitudinal Weld and Spherical Shell Circumferential Weld

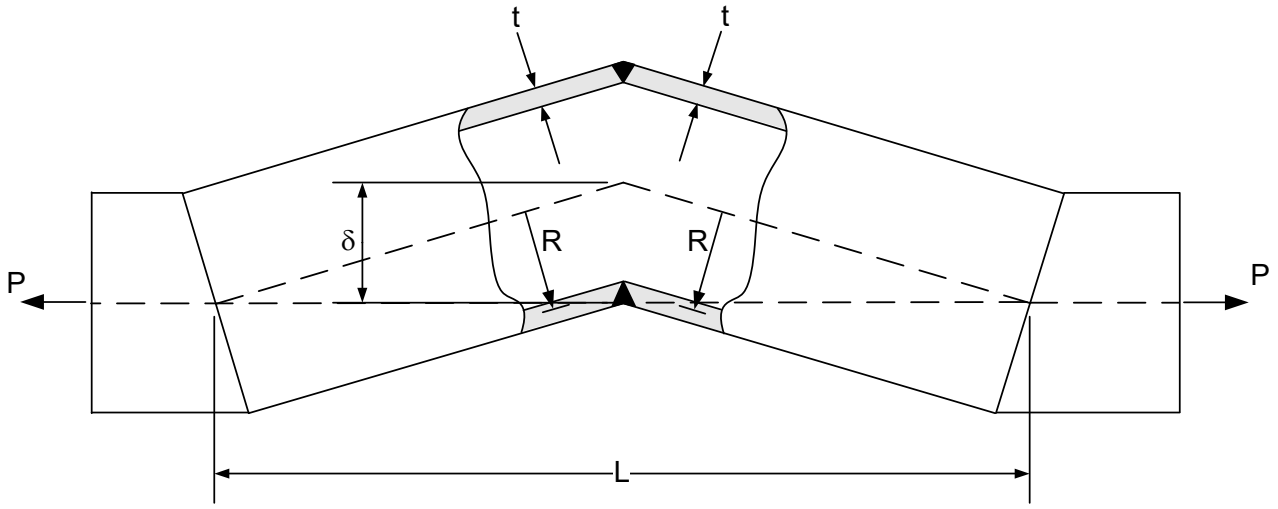

Notes:

1. The dimension L is defined as the length of the base of a triangle whose height is measured from the line of force, P, and whose height equals the angular peaking, δ.
2. Note that as the height of the angular peaking, $\delta \to 0$, $L \to \infty$.

Figure 8.6 – Angular Misalignment in a Cylindrical Shell Circumferential Seam

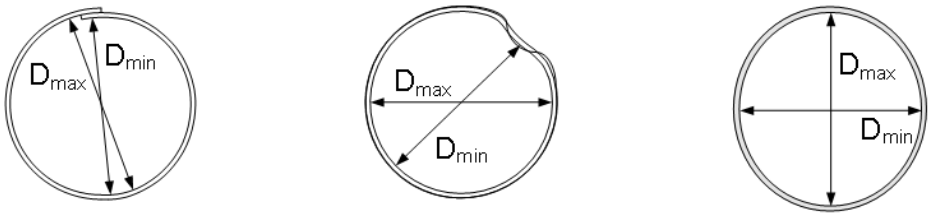

(a) Examples of Differences Between Maximum and Minimum Diameters In Cylindrical, Conical, and Spherical Shells

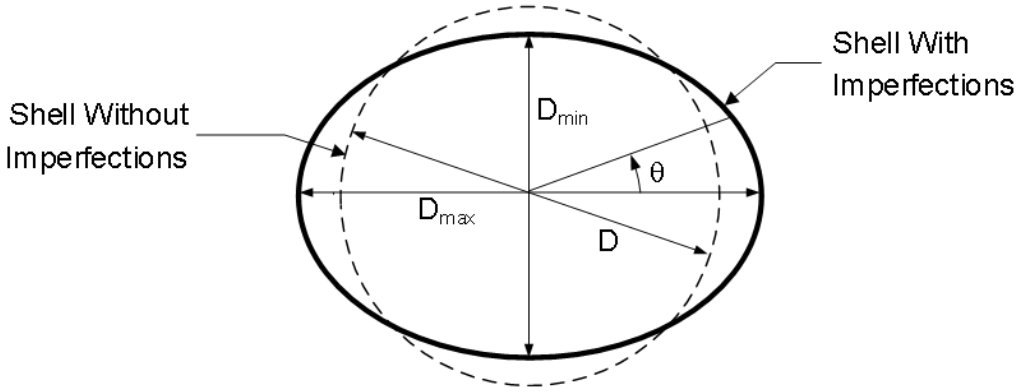

(b) Global Out-Of-Roundness

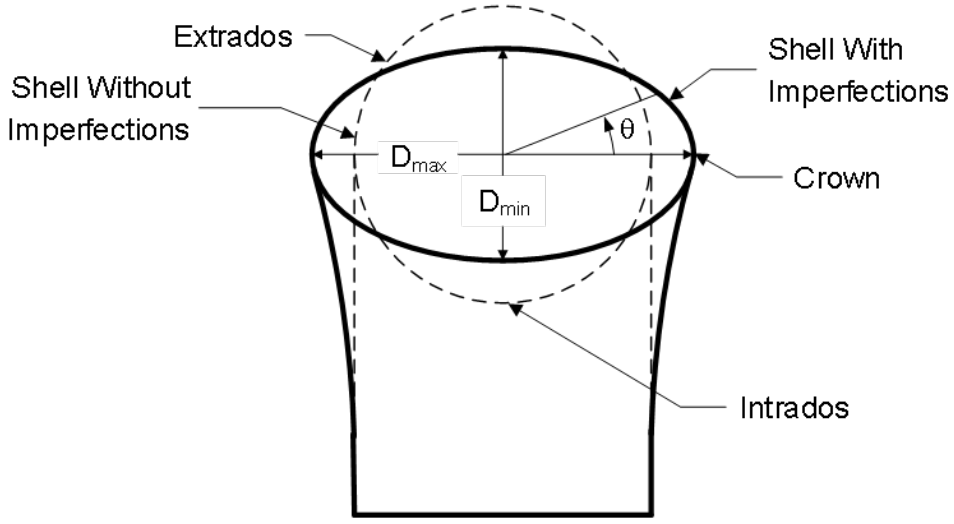

(c) Ovalization of a Pipe Bend

Figure 8.7 – Global Circumferential Out-Of-Roundness

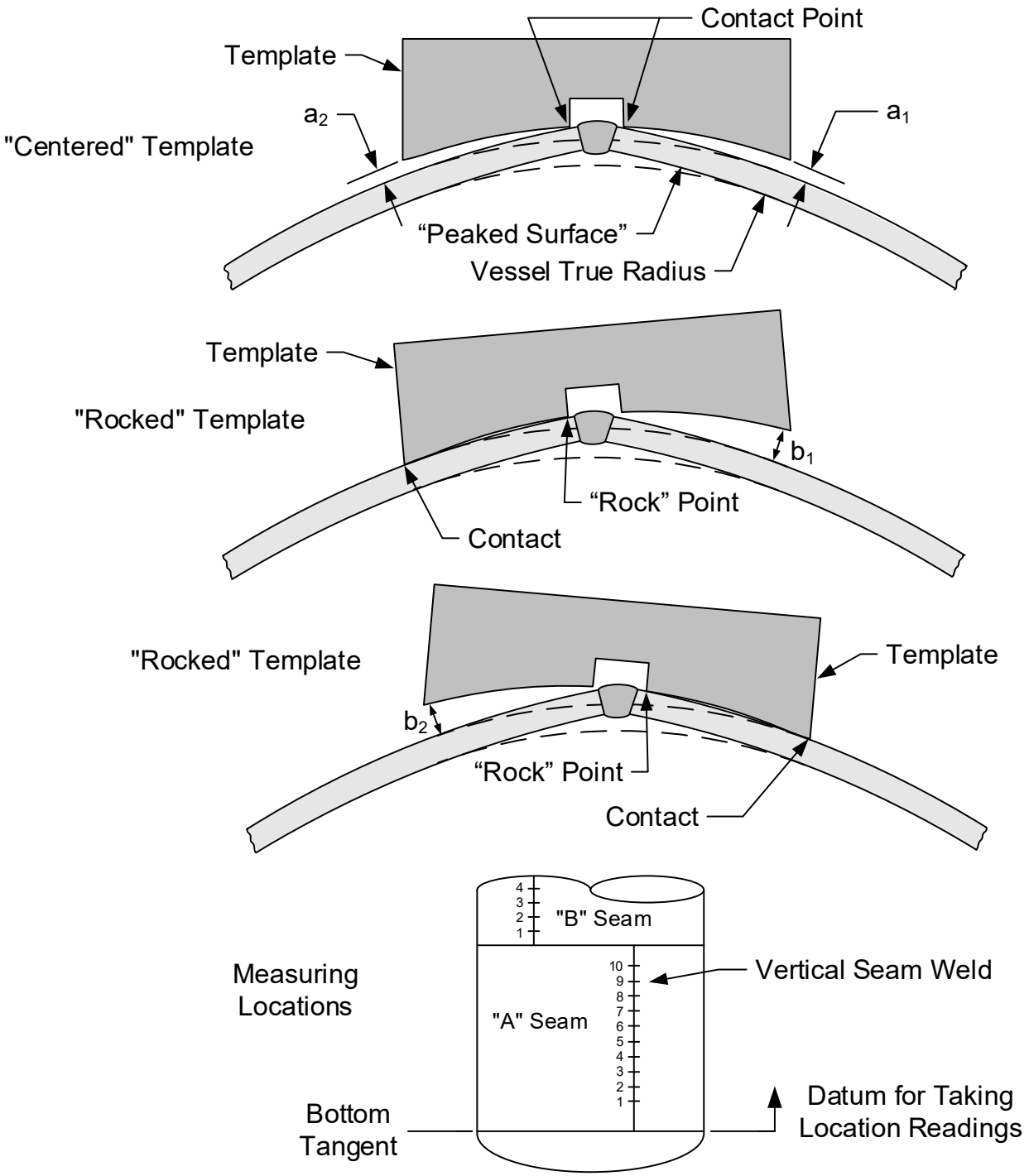

Figure 8.8 – Method of Measurement to Determine the Extent of Peaking in a Shell

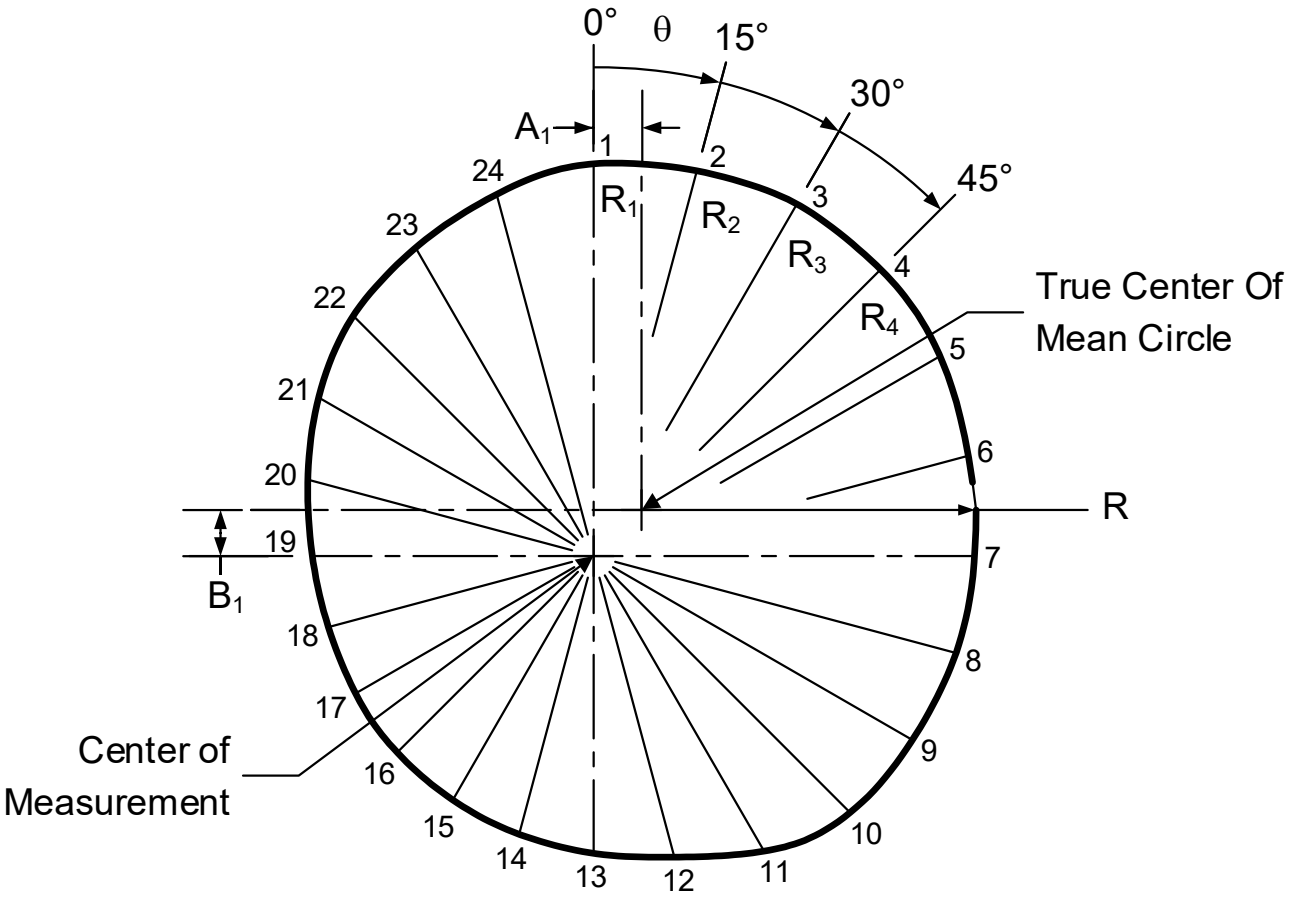

Figure 8.9 – Method of Measurement to Determine the Extent of Out-Of-Roundness in a Cylinder

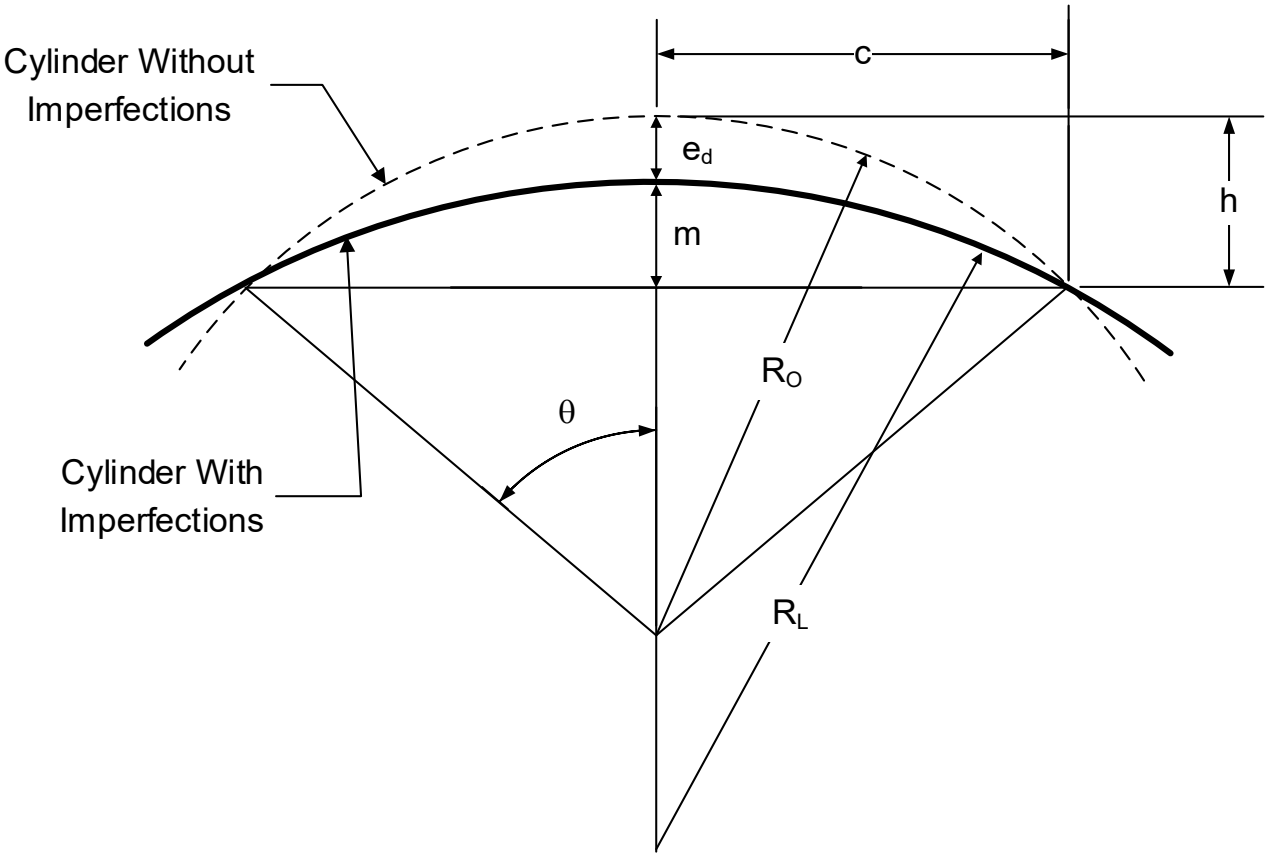

Notes: The following equations can be used to compute the local radius, R_L. The value n is computed using the equations in paragraph 8.4.3.5(b). The maximum deviation from a true cylinder, e_d, is obtained by measurement.

$$\theta = \frac{90}{n} \tag{8.38}$$

$$h = R_o\left(1 - \cos\left[\theta\right]\right) \tag{8.39}$$

$$c = R_o \sin\left[\theta\right] \tag{8.40}$$

$$m = h - e_d \tag{8.41}$$

$$R_L = \frac{m^2 + c^2}{2m} \tag{8.42}$$

Figure 8.10 – Definition of Local Radius Used to Compute the Permissible External Pressure in a Cylindrical Shell with a Geometrical Deviation

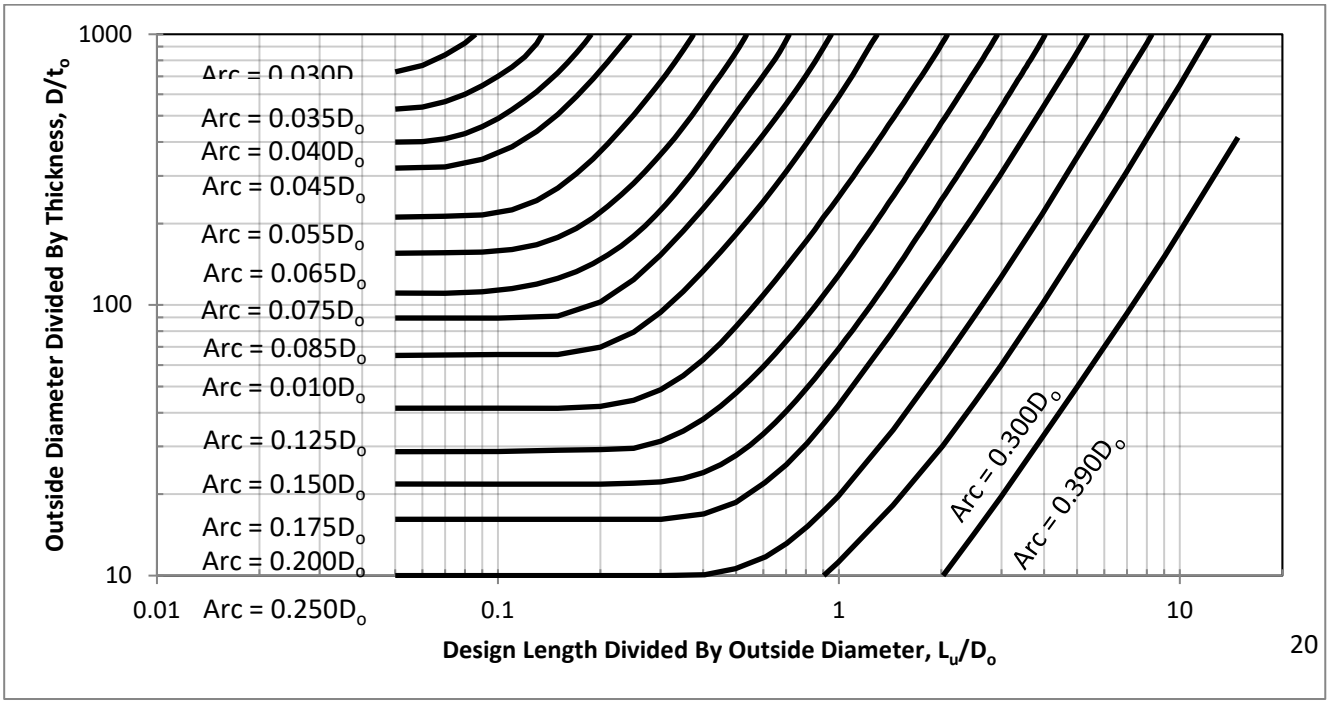

Notes:

1. Cylindrical Shells – L_u unsupported length of the cylinder and D_o outside diameter.
2. Conical Shells – L_u and D_o are established using the following equations for any cross section having a diameter D_x. In these equations D_L and D_S are the cone large end and small end outside diameters, respectively and L unsupported length of the conical section under evaluation (See Annex 2C, Figure 2C.2).

$$L_u = \left(\frac{L}{2}\right)\left(1+\frac{D_S}{D_L}\right)\left(\frac{D_L}{D_x}\right) \tag{8.43}$$

$$D_o = D_x \tag{8.44}$$

3. Spherical Shell – L_u is one-half of the outside diameter D_o of the sphere.
4. Elliptical Head – L_u is $K_c D_o$ (see Annex 2C, paragraph 2C.3.5.b) and D_o is the outside diameter of the cylinder at the head attachment point.
5. Torispherical Head – L_u crown radius and D_o outside diameter of the cylinder at the head attachment point.
6. For vessels with butt joints, $t = t_c$. For vessels with lap joints, $t = t_c$ and the permissible deviation is $e + t_c$. Where the shell at any cross section is made from plates of different thicknesses t corroded wall thickness (i.e., including metal loss and future corrosion allowance) of the thinnest plate. For cones and conical sections, t shall be determined using the previous rules except that t shall be replaced by $t/cos\alpha$.

Figure 8.11 – Maximum Arc of a Shell Used as a Basis to Determine the Deviation from Circular Form

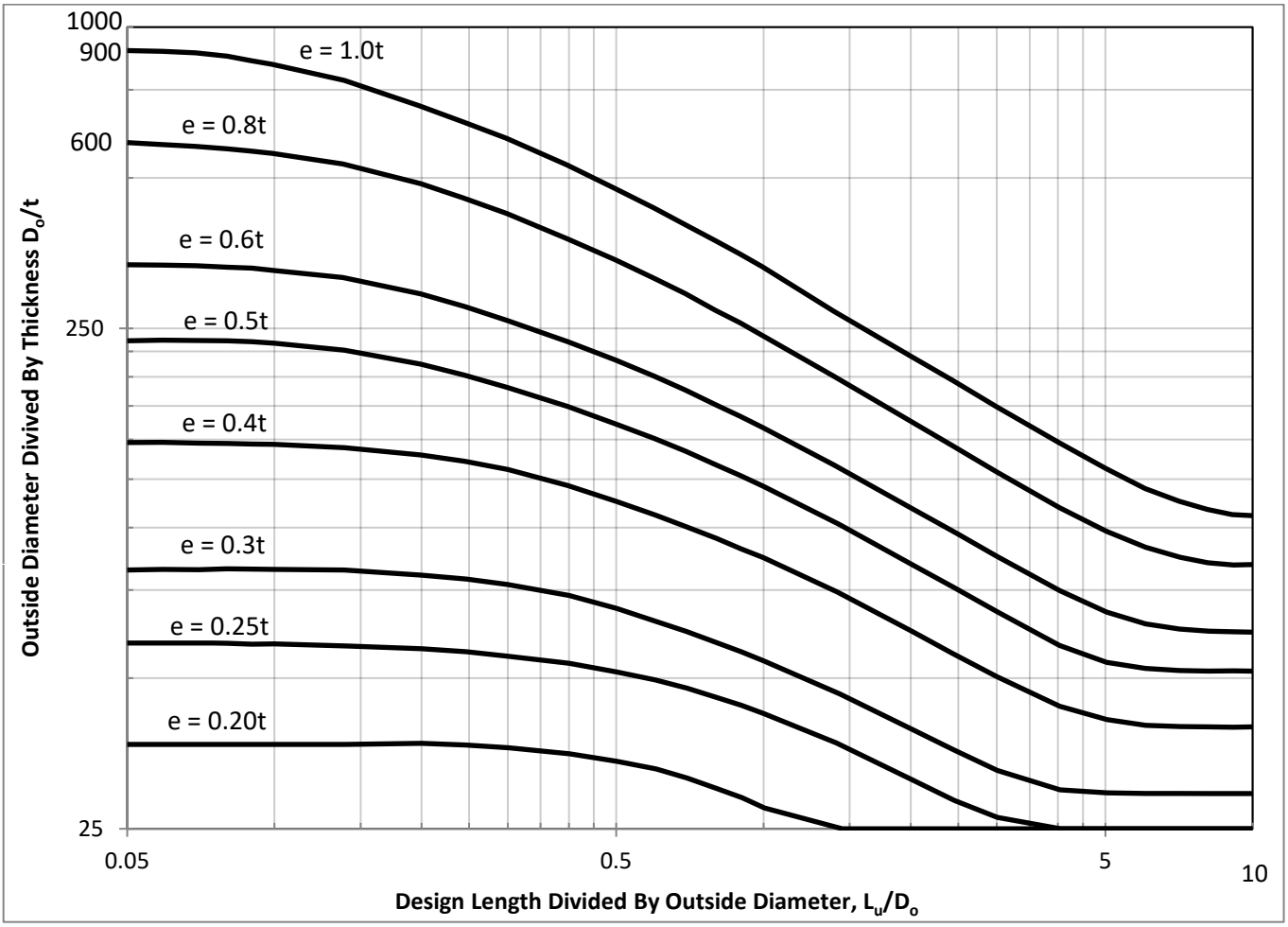

Notes:

1. Cylindrical Shells – L_u unsupported length of the cylinder and D_o outside diameter.
2. Conical Shells – L_u and D_o are established using Equations (8.43) and (8.44) respectively for any cross section having a diameter D_x. In these equations D_L and D_S are the cone large end and small end outside diameters, respectively and L unsupported length of the conical section under evaluation (see Annex 2C, Figure 2C.2).
3. Spherical Shell – L_u is one-half of the outside diameter D_o of the sphere.
4. Elliptical Head – L_u is of $K_c D_o$ (see Annex 2C, paragraph 2C.3.5.b) and D_o is the outside diameter of the cylinder at the head attachment point.
5. Torispherical Head – L_u crown radius and D_o outside diameter of the cylinder at the head attachment point.
6. For vessels with butt joints, $t = t_c$. For vessels with lap joints, $t = t_c$ and the permissible deviation is $e + t_c$. Where the shell at any cross section is made from plates of different thicknesses t corroded wall thickness (i.e., including metal loss and future corrosion allowance) of the thinnest plate. For cones and conical sections, t shall be determined using the previous rules except that t shall be replaced by $t/cos\alpha$.

Figure 8.12 – Maximum Permissible Deviation from a Circular Form for Vessels Subject to External Pressure

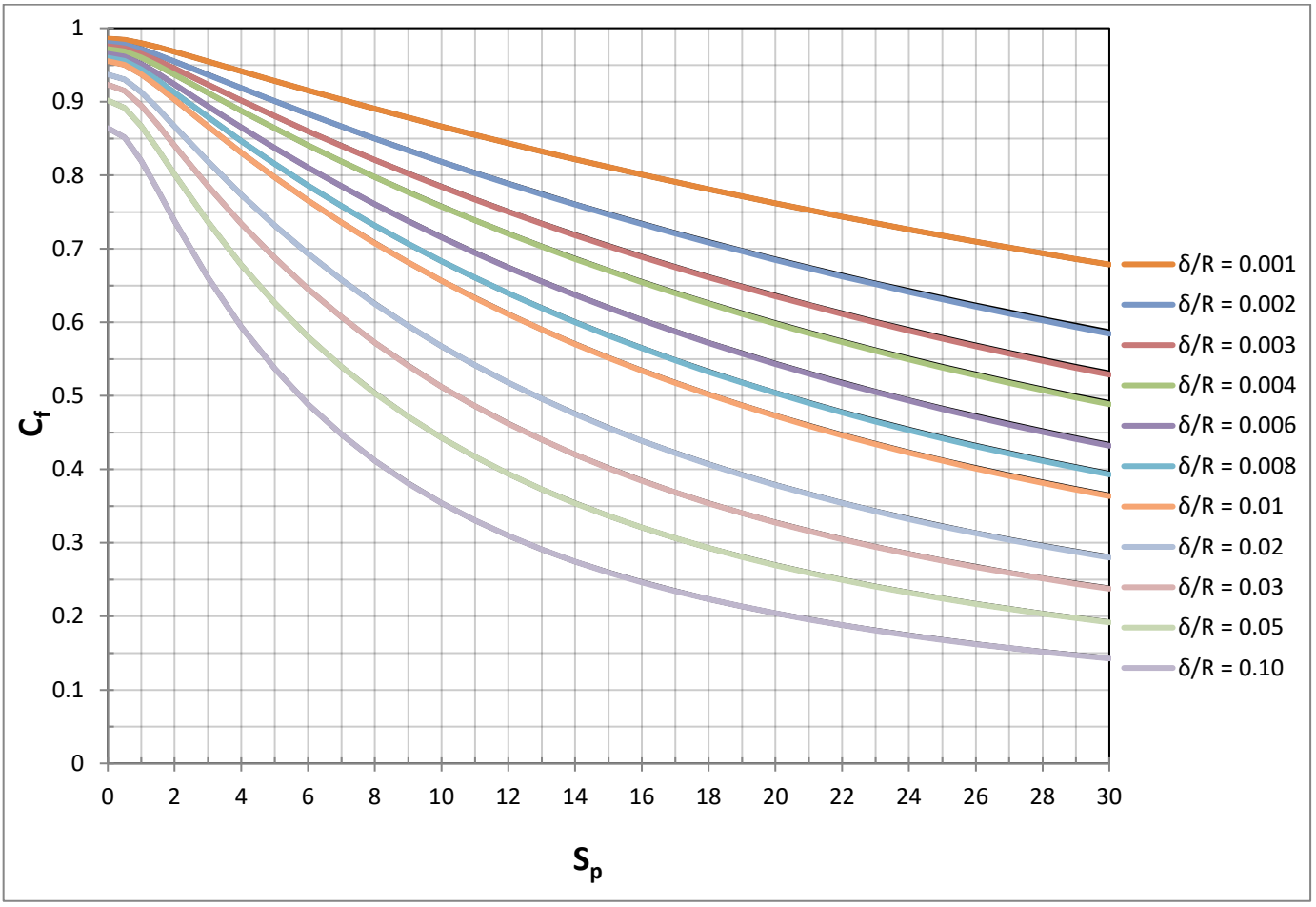

Figure 8.13 – Correction Factor for Angular Weld Misalignment in the Longitudinal Joint of a Cylindrical Shell

ANNEX 8A – TECHNICAL BASIS AND VALIDATION – ASSESSMENT OF WELD MISALIGNMENT AND SHELL DISTORTIONS

(INFORMATIVE)

CONTENTS

ANNEX 8A – TECHNICAL BASIS AND VALIDATION – ASSESSMENT OF WELD MISALIGNMENT AND SHELL DISTORTIONS 8A-1

8A.1 TECHNICAL BASIS AND VALIDATION 8A-1
8A.2 REFERENCES 8A-1

8A.1 Technical Basis and Validation

The technical basis of the assessment procedures in Part 8 for weld misalignment and shell distortions (i.e., out-of-roundness) is provided in references [1], [2], and [3]. Reference [3] provides an overview of the method and reference [1] provides the basis for the development of the equations for the R_b-factor defined as the ratio of the induced bending stress to the applied membrane stress.

The predominant mode of failure associated with weld misalignment and shell distortions for components in cyclic operation is fatigue. Three methods for fatigue assessment are provided in Part 14. Two of these methods utilize a fatigue curve derived from smooth bar test specimens while the third method utilizes a fatigue curve based on test specimens that include weld details. The fatigue assessment method and smooth bar fatigue curves are based on the ASME B&PV Code, Section VIII, Division 2. The fatigue assessment method that utilizes the fatigue curves based on welded joint test specimens is described in references [4] and [5]. The fatigue assessment methods provided in Part 14 correspond to those provided in The ASME Boiler & Pressure Vessel Code, Section VIII, Division 2, Part 5.

8A.2 References

[1] Osage, D.A., Janelle, J.L., and Gassama, E., An Overview of the Fitness-For-Service Assessment Procedures for Weld Misalignment and Shell Distortions in API 579-1/ASME FFS-1, WRC Bulletin 549, Welding Research Council, Inc., New York, NY, 2015.

[2] Osage, D.A., Brown, R.G., and Janelle, J.L., “Fitness-For-Service Rules for Shell Distortions and Weld Misalignment in API 579,” PVP-Vol. 411, Service Experience and Fitness-For-Service in Power and Petroleum Processing, ASME, 2000, pp. 191-220.

[3] Osage, D.A., Krishnaswamy, P., Stephens, D.R., Scott, P., Janelle, J., Mohan, R., and Wilkowski, G.M., Technologies for the Evaluation of Non-Crack-Like Flaws in Pressurized Components – Erosion/Corrosion, Pitting, Blisters, Shell Out-Of-Roundness, Weld Misalignment, Bulges and Dents, WRC Bulletin 465, Welding Research Council, Inc., New York, NY, September 2001.

[4] Dong, P., Hong, J.K., Osage, D.A., and Prager, M., *Master S-N Curve Method for Fatigue Evaluation of Welded Components*, WRC Bulletin 474, Welding Research Council, Inc., New York, NY, August 2002.

[5] Dong, P., Hong, J.K, and DeJesus, A.M.P., “Analysis of Recent Fatigue Data Using the Structural Stress Procedure in ASME Div2 Rewrite,” ASME PVP2005-71511, Proceedings of PVP2005, Denver, Colorado, ASME, New York, NY, 2005.

[6] Becht IV, C., Cehn, Y., and Lyow, B., “Jacking to Correct Out-Of-Roundness Of A Ring-Stiffened Vessel,” PVP-Vol. 315, Fitness-For-Service and Decisions for Petroleum and Chemical Equipment, ASME, 1995, pp. 447-451.

[7] Berge, S., and Myrhe, H., “Fatigue Strength of Misaligned Cruciform and Butt Joints,” Norwegian Maritime Research, No. 1, 1977, pp. 29-39.

[8] Bizon, P.T, “Elastic Stresses At A Mismatched Circumferential Joint In A Pressurized Cylinder Including Thickness Changes And Meridional Load Coupling,” NASA TN D-3609, NTIS, Springfield, Va., D.C., September, 1966.

[9] Bock, N. and Zeman, J.L., “On Bending Stress at Longitudinal Weld Joints of Cylindrical Shells Due to Peaking,” International Journal of Pressure Vessels & Piping, 60, 1994, pp 103-106.

[10] Buchheim, M.B., Osage, D.A., Brown, R.G., and Dobis, J.D., “Failure Investigation of A Low Chrome Long-Seam Weld in a High -Temperature Refinery Piping System,” PVP-Vol. 288, ASME, 1994, pp 363-386.

[11] Chuse, R. and Carson, B.E., *The ASME Code Simplified*, 7th Ed., McGraw-Hill, Inc., New York, NY, 1993.

[12] Connelly, L.M., and Zettlemoyer, N., “Stress Concentrations at Girth Welds of Tubulars with Axial Wall Misalignment,” Tubular Structures, E & FN Spon., 1993.

[13] Eiber, R.J., Maxey, W.A., Bert, C.W., and McClure, G.M., “The Effects of Dents on the Failure Characteristics of Line Pipe,” Battelle NG-18 Report No. 125, May 8 , 1981.

[14] Hopkins, P., Jones, D.G., and Clyne, A.J., “The Significance Of Dents And Defects In Transmission Pipelines,” C376/049, ImechE, 1989.

[15] Haigh, B.P., “An Estimate of Bending Stresses Induced by Pressure in a Tube That is Not Quite Circular,” Appendix IX in the Welding Research Committee Second Report.

[16] Hechmer, J.L., *Report 2: Fatigue Strength-Reduction-Factors for Welds Based on NDE*, WRC Bulletin 432, Welding Research Council, Inc., New York, NY, 2003.

[17] Johns, R.H. and Orange, T.W., “Theoretical Elastic Stress Distributions Arising from Discontinuities and Edge Loads in Several Shell-Type Structures,” NASA TR R-103, NTIS, Springfield, Va., September 1966.

[18] Kendrick, S., “The Measurement of Shape in Pressure Vessels,” Institute of Mechanical Engineers, C96/80, 1980, pp. 261-267.

[19] Maddox, S.J., *Fatigue Strength of Welded Structures*, 2nd Ed., Abington Publishing, Cambridge, England, 1991.

[20] Miller, C.D., *The Effect of Initial Imperfections on the Buckling of Cylinders Subjected to External Pressure*, WRC Bulletin 443, Report 1, Welding Research Council, Inc., New York, NY, January 1995.

[21] Morgan, W.C. and Bizon, P.T, “Technical Note D-1200 – Experimental Investigation of Stress Distributions Near Abrupt Change in Wall Thickness in Thin-Walled Pressurized Cylinders,” NASA TN D-1200, NTIS, Springfield, VA, September 1966.

[22] Morgan, W.C. and Bizon, P.T, “Comparison of Experimental and Theoretical Stresses at a Mismatch in a Circumferential Joint in a Cylindrical Pressure Vessel,” NASA TN D-3608, NTIS, Springfield, VA, September 1966.

[23] Partanen, T., “Factors Affecting the Fatigue Behavior of Misaligned Transverse Butt Joints in Stiffened Plate Structures,” Engineering Design in Welded Constructions. Proceedings, International Conference, Madrid, Spain, Pergamon Press for the International Institute of Welding (IIW), Oxford, UK, Sept, 1992, pp. 65-72.

[24] Ong, L.S. and Hoon, K.H., “Bending Stresses at Longitudinal Weld Joints of Pressurized Cylindrical Shells Due to Angular Distortion,” Journal of Pressure Vessel Technology, Vol. 118, ASME, August, 1996, pp. 369-373.

[25] Ong, L.S., “Allowable Shape Deviation in a Pressurized Cylinder,” Transactions of the ASME, Vol. 116, August 1994, pp. 274-277.

[26] Rodabaugh, E.C. and Pickett, A.G., “Survey Report on Structural Design of Piping Systems and Components,” Report TID-25553, NTIS, December, 1970, pp. 10.3-10.7.

[27] Schwarz, M., and Zeman, J.L., “Bending Stresses at Longitudinal Weld Joints of Pressurized Cylindrical Shells Due to Angular Misalignment,” Journal of Pressure Vessel Technology, Vol. 119, ASME, May, 1997, pp. 245-246.

[28] Thomas, K., “The Effects of Geometric Irregularities on the Design Analysis of Thin-Walled Piping Elbows,” Journal of Pressure Vessel Technology, Vol. 102, ASME, November, 1980, pp. 410-418.

[29] Tooth, A.S., and Ong, L.S., “The Derivation of the Stresses in a Pressurized Pipe or Cylindrical Vessel with Initial Geometric Imperfections,” Strain, February, 1988, pp. 7-13.

[30] Zeman, J.L., “Aufdachung an Langsnahten Zylindrischer Schusse,” TU Bd. 34, Nr. 7/8, 1993, pp 292-295.

[31] Zeman, J.L., “On the Problem of Angular Misalignment at Longitudinal Weld Joints of Cylinder Shells,” International Journal of Pressure Vessels & Piping, 58, 1994, pp. 179-184.

[32] Sofronas, A., Fitzgerald, B.J., and Harding, E.M., “The Effect of Manufacturing Tolerances on Pressure Vessels in High Cyclic Service,” PVP Vol. 347, ASME, New York, NY 1997, pp. 15-32.

[Intentionally Left Blank]

PART 9 – ASSESSMENT OF CRACK-LIKE FLAWS

CONTENTS

PART 9 – ASSESSMENT OF CRACK-LIKE FLAWS 9-1

9.1 GENERAL 9-2
9.1.1 Assessment Procedures for Crack-Like Flaws 9-2
9.1.2 ASME B&PV Code, Section VIII, Division 2 (VIII-2) 9-2
9.1.3 Crack-Like Flaw Definition 9-2
9.1.4 Treatment of Volumetric Flaws as Crack-Like Flaws 9-2
9.1.5 Use of Assessment Procedures to Evaluate Brittle Fracture 9-2
9.1.6 Service Environment and Material Interactions with Crack-Like flaws 9-2
9.2 APPLICABILITY AND LIMITATIONS OF THE PROCEDURE 9-3
9.2.1 Overview 9-3
9.2.2 Applicability of the Level 1 and Level 2 Assessment Procedures 9-3
9.2.3 Applicability of the Level 3 Assessment Procedure 9-4
9.2.4 Assessment Procedures for Notches in Groove-Like Flaws 9-4
9.3 DATA REQUIREMENTS 9-5
9.3.1 General 9-5
9.3.2 Original Equipment Design Data 9-5
9.3.3 Maintenance and Operating History 9-5
9.3.4 Required Data/Measurements for an FFS Assessment – Loads and Stresses 9-6
9.3.5 Required Data/Measurements for an FFS Assessment – Material Properties 9-7
9.3.6 Required Data/Measurements for an FFS Assessment – Flaw Characterization 9-8
9.3.7 Recommendation for Inspection Technique and Sizing Requirements 9-12
9.4 ASSESSMENT TECHNIQUES AND ACCEPTANCE CRITERIA 9-13
9.4.1 Overview 9-13
9.4.2 Level 1 Assessment 9-14
9.4.3 Level 2 Assessment 9-15
9.4.4 Level 3 Assessment 9-19
9.5 REMAINING LIFE ASSESSMENT 9-21
9.5.1 Subcritical Crack Growth 9-21
9.5.2 Leak-Before-Break Analysis 9-23
9.6 REMEDIATION 9-25
9.6.1 Objectives of Remediation 9-25
9.6.2 Remediation Methods 9-25
9.7 IN-SERVICE MONITORING 9-26
9.7.1 Monitoring of Subcritical Crack Growth 9-26
9.7.2 Validation of Monitoring Method 9-26
9.8 DOCUMENTATION 9-26
9.8.1 General 9-26
9.8.2 Assessment Procedure 9-27
9.8.3 Remediation Methods 9-27
9.8.4 In-Service Monitoring 9-28
9.9 NOMENCLATURE 9-28
9.10 REFERENCES 9-29
9.11 TABLES 9-30
9.12 FIGURES 9-34

9.1 General

9.1.1 Assessment Procedures for Crack-Like Flaws

Fitness-For-Service (FFS) Assessment procedures for evaluating crack-like flaws in components are covered in this Part. These assessment procedures are based on the Failure Assessment Diagram (FAD) method. Details regarding the background and development of the methodology and assessment procedures can be found in Annex 9A.

9.1.2 ASME B&PV Code, Section VIII, Division 2 (VIII-2)

The stress analysis concepts and methods in this Part are based on ASME B&PV Code, Section VIII, Division 2 (VIII-2), Part 5, and reference to VIII-2 is made directly.

9.1.3 Crack-Like Flaw Definition

Crack-like flaws are planar flaws that are predominantly characterized by a length and depth, with a sharp root radius. Crack-like flaws may either be surface breaking, embedded, or through-wall. Examples of crack-like flaws include planar cracks, lack of fusion and lack of penetration in welds, sharp groove-like localized corrosion, and branch type cracks associated with environmental cracking.

9.1.4 Treatment of Volumetric Flaws as Crack-Like Flaws

In some cases, it is conservative and advisable to treat volumetric flaws such as aligned porosity or inclusions, deep undercuts, root undercuts, and overlaps as planar flaws, particularly when such volumetric flaws may contain micro-cracks at the root. This is because an NDE examination may not be sensitive enough to determine whether micro-cracks have initiated from the flaw.

9.1.5 Use of Assessment Procedures to Evaluate Brittle Fracture

The likelihood of brittle fracture of an existing component may be assessed by postulating a standard reference flaw and using the Level 2 or Level 3 Assessment procedure to solve for the Minimum Allowable Temperature (MAT) as defined in Part 3. A Level 2 procedure for determining the MAT is provided in Annex 9J.

9.1.6 Service Environment and Material Interactions with Crack-Like flaws

a) Crack-like flaws may be associated with a wide variety of process environment/material interactions and material damage mechanisms. These environmental/material interactions and the associated damage mechanisms tend to be industry specific; however, the mechanisms associated with similar services (e.g., steam) are common for all industries.

b) An overview of the failure modes and damage mechanisms that are covered by this Standard is given in Annex 2B. Knowledge of the damage mechanism may affect decisions regarding the following:

   1) The choice of material properties to be used in an FFS Assessment.

   2) The choice of an appropriate crack growth rate.

   3) The permissible amount of crack extension prior to the final fracture or the time between inspections.

   4) The mode of final failure, e.g., unstable fracture, yielding due to overload of remaining ligament, or leak.

   5) The interaction between damage mechanisms, e.g., corrosion and fatigue, creep and fatigue, hydrogen embrittlement and temper-embrittlement, or environmental assisted cracking.

c) Environmental cracks typically occur in multiples and may be branched. The assessment procedures in this Part can be applied to such cracks provided a predominant crack whose behavior largely controls the structural response of the equipment can be identified. The predominant crack in the presence of multiple cracks or branched cracks can be defined through the flaw characterization techniques described in paragraph 9.3.6. When a predominant crack cannot be defined even after re-characterization, more advanced FFS techniques such as damage mechanics, which are outside the scope of this document, are available.

9.2 Applicability and Limitations of the Procedure

9.2.1 Overview

The assessment procedures of this Part can be used to evaluate pressurized components containing crack-like flaws. The pressurized components covered include pressure vessels, piping, and tanks that are designed to a recognized code or industry standard. Specific details pertaining to the applicability and limitations of each of the assessment procedures are discussed below.

9.2.2 Applicability of the Level 1 and Level 2 Assessment Procedures

The Level 1 and 2 Assessment procedures in this Part apply only if all the following conditions are satisfied:

a) The original design criteria were in accordance with Part 2, paragraph 2.2.3.

b) The component is not operating in the creep range (see Part 4, paragraph 4.2.3).

c) Dynamic loading effects are not significant (e.g., earthquake, impact, water hammer, etc.).

d) The crack-like flaw is subject to loading conditions and/or an environment that will not result in crack growth. If a flaw is expected to grow in service, it should be evaluated using a Level 3 Assessment, and the remaining life should be evaluated using the procedures of paragraph 9.5.

e) The following limiting conditions are satisfied for a Level 1 Assessment.

1) Limitations on component and crack-like flaw geometries:

i) The component is a flat plate, cylinder, or sphere.

ii) Cylinders and spheres are limited to geometries with $R/t \geq 5$ where R is the inside radius and t is the current thickness of the component.

iii) The wall thickness of the component at the location of the flaw is less than 38 mm (1.5 inches).

iv) The crack-like flaw geometry can be of the surface or through-thickness type, specific limitations for the crack-like flaw depth are included in the Level 1 Assessment procedure (see paragraph 9.4.2). The maximum permitted crack length is 200 mm (8 inches).

v) For cylindrical and spherical shell components, the crack-like flaw is oriented in the axial or circumferential direction (i.e., perpendicular to a principal stress direction) and is located at a distance greater than or equal to $1.8\sqrt{Dt}$ from any major structural discontinuity where D is the inside diameter and t is the current thickness of the component. For a flat plate, the crack-like flaw is oriented such that the maximum principal stress direction is perpendicular to the plane of the flaw. If the crack-like flaw is oriented such that it is not perpendicular to a principal stress plane, then the flaw may be characterized by the procedure in paragraph 9.3.6.2(b).

2) Limitations on component loads:

   i) The loading on the component is from pressure that produces only a membrane stress field. Pressurized components subject to pressure that result in bending stresses (e.g., head-to-cylinder junction, nozzle intersections, rectangular header boxes on air-cooled heat exchangers) and/or components subject to supplemental loading (see Annex 2C) shall be evaluated using a Level 2 or Level 3 Assessment.

   ii) The membrane stresses during operation are within the design limits of the original construction code.

   iii) If a component being evaluated is to be subject to a pressure test, the component's metal temperature shall be above the MAT during the test (see Part 3, paragraph 3.1.6 and paragraph 3.6.2.3). After the pressure test, the crack-like flaw shall be re-examined to ensure that the flaw has not grown.

   iv) The weld joint geometry is either a Single-V or Double-V configuration; the residual stresses are based on the solutions provided in Annex 9D.

3) The material meets the following limitations:

   i) The material is carbon steel (P1, Group 1 or 2) with an allowable stress in accordance with the original construction code that does not exceed 172 MPa (25 ksi).

   ii) The specified minimum yield strength for the base material is less than or equal to 276 MPa (40 ksi), the specified minimum tensile strength for the base material is less than or equal to 483 MPa (70 ksi), and the weldments are made with an electrode compatible with the base material.

   iii) The fracture toughness is greater than or equal to the lower bound K_{IC} value obtained from Annex 9F. This will be true for carbon steels where the toughness has not been degraded because of environmental damage (e.g., fire damage, over-heating, graphitization, hydrogen damage, etc.).

9.2.3 Applicability of the Level 3 Assessment Procedure

A Level 3 Assessment should be performed when the Level 1 and 2 methods cannot be applied or produce overly conservative results. Conditions that typically require a Level 3 Assessment include the following.

a) Advanced stress analysis techniques are required to define the state of stress at the location of the flaw because of complicated geometry and/or loading conditions.

b) The flaw is determined or expected to be in an active subcritical growth phase or has the potential to be active because of loading conditions, e.g., cyclic stresses, and/or environmental conditions, and a remaining life assessment or on-stream monitoring of the component is required.

c) High gradients in stress, (either primary or secondary as defined in VIII-2) material fracture toughness, or material yield and/or tensile strength exist in the component at the location of the flaw (e.g., mismatch between the weld and base metal).

9.2.4 Assessment Procedures for Notches in Groove-Like Flaws

Assessment procedures to evaluate a notch at the base of a groove-like flaw are covered in Part 12.

9.3 Data Requirements

9.3.1 General

9.3.1.1 The information required for a Level 1 Assessment is shown below:

a) Original Equipment Design Data (see paragraph 9.3.2).

b) Maintenance and Operating History (see paragraph 9.3.3).

c) Material reference temperature, i.e., toughness curve.

d) Flaw Characterization (see paragraph 9.3.6).

9.3.1.2 The information required to perform a Level 2 or Level 3 Assessment is covered in paragraphs 9.3.2 through 9.3.7. The choice of input data should be conservative to compensate for uncertainties. In a Level 2 or Level 3 Assessment, a sensitivity analysis, partial safety factors or a probabilistic analysis shall be used to evaluate uncertainties.

9.3.1.3 The datasheet shown in Table 9.2 should be completed before the FFS Assessment is started. This ensures that all the pertinent factors are considered, communicated, and incorporated into the assessment. The information on this datasheet is used for a Level 1 or Level 2 Assessment. In addition, this information is generally applicable for a Level 3 Assessment. Guidelines for establishing the information to be entered on this datasheet are provided in paragraphs 9.3.2 through 9.3.7.

9.3.2 Original Equipment Design Data

9.3.2.1 An overview of the original equipment data required for an assessment is provided in Part 2, paragraph 2.3.1.

9.3.2.2 Equipment data is required to compute the stress intensity factor and reference stress solution based on the geometry of the component at the crack location.

a) For pressure equipment with uniform thickness such as vessels, pipes, and tanks, the important dimensions are the inside diameter and wall thickness.

b) For pressurized equipment with a non-uniform thickness, or where structural discontinuities are involved, e.g., vessel head-to-shell junctions, conical transitions, nozzles, piping tees, and valve bodies, the dimensions required include the diameter, wall thickness, and the local geometric variables required to determine the stress distribution at a structural discontinuity.

9.3.3 Maintenance and Operating History

9.3.3.1 An overview of the maintenance and operating history required for an assessment is provided in Part 2, paragraph 2.3.2.

9.3.3.2 Maintenance and operational input should be provided by personnel familiar with the operational and maintenance requirements of the component containing the crack-like flaw. These data provide a basis for determining the following:

a) The most probable mechanism of the cracking.

b) Whether or not the crack is growing.

c) Reasonable estimates for the flaw size based on prior records of cracking or experience with other components in a similar service.

d) The most probable mechanism of the failure expected.

e) Potential remediation measures.

9.3.4 Required Data/Measurements for an FFS Assessment – Loads and Stresses

9.3.4.1 Load Cases

The stress distribution at the cracked region of the component should be determined for all relevant loads based on the planned future operating conditions. An overview of the load cases to consider in a stress analysis is provided in Annex 2C and Annex 2D. It is important that the combination of pressure and temperature be determined for all load cases because of the dependence of the material fracture toughness with temperature.

9.3.4.2 Stress Computation

The stress distributions from each load case are calculated based on the uncracked component geometry using loads derived from the anticipated future operating conditions.

a) A non-uniform stress distribution may occur through the wall thickness or along the surface of the component. Examples include the through-wall stresses in a pressurized thick wall cylinder, the stress attenuation that occurs at a major structural discontinuity (e.g., nozzle-to-shell and head-to-shell junctions), and the stress distribution caused by a thermal gradient that typically occurs at a skirt-to-vessel attachment. The method used to determine the state of stress in a component should include capabilities to compute stress distributions based on loading conditions and structural configuration.

b) Stress analysis methods based on handbook solutions may be used if these solutions accurately represent the component geometry and loading condition. Otherwise, numerical analysis techniques such as the finite element method shall be used to determine the stress field at the crack location.

c) If it is necessary to linearize computed through-wall stress profiles into membrane and bending stress components to compute a stress intensity factor and reference stress for certain crack geometries and load conditions, then the linearization of the through-wall stress field in the presence of a crack shall be performed in accordance with VIII-2, Part 5.

d) If it can be verified that the crack-like flaw in the component occurred after application of load, then the stress distribution may be computed using an elastic-plastic analysis.

e) Stress computation shall be performed with a weld joint efficiency equal to 1.0.

9.3.4.3 Stress Classification

The stress analysis methods in this Part are based on VIII-2, Part 5. For each loading condition under consideration, the stress distributions at the cracked region of the component shall be classified into the following stress categories to complete a Level 2 Assessment.

a) Primary Stress – The stress distribution developed by the imposed load-controlled loading that is necessary to satisfy the laws of equilibrium (see VIII-2, Part 5). In addition, the primary stress shall also include any recategorized secondary stresses. In accordance with VIII-2, Part 5, primary stresses are categorized as follows:

- General Primary Membrane Stress
- Local Primary Membrane Stress
- Primary Membrane (General or Local) Plus Primary Bending Stress

b) Secondary Stress – A secondary stress distribution is developed by the constraint of adjacent parts or by self-constraint of a component (sees VIII-2, Part 5). If it is uncertain whether a given stress is a primary or secondary stress, it is more conservative to treat it as primary stress. It should be noted that in certain cases secondary stresses that are self-equilibrating over the entire structure or component might still result in plastic collapse in the net-section local to the crack-like flaw. This can occur when the flaw is small compared to the spatial extent of the secondary stress distribution, or there is significant elastic follow-up from the surrounding structure. In these cases, the secondary stress should be treated as a primary stress in the assessment. In accordance with VIII-2, Part 5, Secondary Stresses may be comprised of both membrane and bending stresses.

c) Residual Stress – Crack extension can occur locally if the crack tip is in a tensile residual stress field. Therefore, residual stresses resulting from welding shall be included in the assessment. The magnitude and distribution of residual stress shall be determined using Annex 9D.

9.3.5 Required Data/Measurements for an FFS Assessment – Material Properties

9.3.5.1 Material Yield and Tensile Strength

The yield and tensile strength of the material are required in the FFS Assessment to determine the effects of plasticity on the crack driving force, estimate the residual stress, and evaluate the fracture toughness using correlations with other material toughness parameters.

a) If heat-specific yield and tensile strengths for the material and/or weldments are not available, then estimates may be made using the information in Annex 2E. Otherwise, the specified minimum values of yield stress and tensile stress for the base and weld material shall be used.

b) In general, use of minimum values of yield and tensile strengths will result in a conservative assessment. However, if there are residual stresses in the region of the crack-like flaw, the use of the specified minimum yield strength will tend to underestimate the magnitude of the residual stresses. Therefore, when estimating the magnitude of residual stresses, the actual yield strength should be used. If the actual yield strength is not known, the value of the minimum yield strength shall be adjusted using the procedure in Annex 9D before the residual stresses are computed.

c) The material yield and tensile strength for the region(s) ahead of the crack tip should be adjusted, as appropriate, to take account of temperature, strain aging, thermal aging, or other prevalent forms of degradation.

d) The material stress-strain curve or Ramberg-Osgood constants are required if a $J - integral$ evaluation or elastic-plastic stress analysis is performed as part of the assessment.

9.3.5.2 Material Fracture Toughness

The fracture toughness of the material is a measure of its ability to resist failure by the onset of crack extension to fracture.

a) Guidance for determining fracture toughness for various materials and environments is provided in Annex 9F.

b) The process environment, service temperature envelope, and any related material/service degradation mechanisms such as embrittlement shall be accounted for when determining the fracture toughness.

c) Local variations in the fracture toughness near the crack tip shall be considered in the assessment.

d) When material specific toughness is not available, then lower bound values may be used.

9.3.5.3 Crack Growth Model

A crack growth model and associated constants are required if an estimate of the remaining life of the component with a crack-like flaw is to be made based on a fracture mechanics approach. An overview of crack growth models and data are provided in Annex 9F. The model chosen for the assessment shall account for environmental effects and may be related to cyclic behavior (da/dN), time to failure (da/dt), or both.

9.3.5.4 Material Physical Constants

Material properties such as the elastic modulus, Poisson's ratio, and the thermal expansion coefficient may be required to perform an evaluation. Guidelines for determining these quantities are provided in Annex 2E.

9.3.6 Required Data/Measurements for an FFS Assessment – Flaw Characterization

9.3.6.1 Overview

The flaw characterization rules allow existing or postulated crack geometry to be modeled by a geometrically simpler one to make the actual crack geometry more amenable to fracture mechanics analysis. The nomenclature and idealized shapes used to evaluate crack-like flaws are shown in Figure 9.1. Multiple flaws may need to be combined per paragraph 9.3.6.5. Embedded or surface flaws may need to be recategorized in accordance with paragraph 9.3.6.6. The rules used to characterize crack-like flaws are necessarily conservative and intended to lead to idealized crack geometries that are more severe than the actual crack geometry they represent. These characterization rules account for flaw shape, orientation, and interaction.

For Level 3 Assessment, individual flaws may be explicitly modeled by finite element analysis without idealizing flaw shape, applying flaw proximity rules in paragraph 9.3.6.5, or applying flaw recategorization rules in paragraph 9.3.6.6.

9.3.6.2 Characterization of Flaw Length

If the flaw is oriented perpendicular to the plane of the maximum principal tensile stress in the component, then the flaw length to be used in calculations (c or $2c$) is the measured length c_m or $2c_m$. If the flaw is not oriented in a principal plane, then an equivalent flaw dimension with a Mode I orientation shall be determined by one of the following options.

a) Option 1 – The flaw dimension, c, to be used in the calculations shall be set equal to the measured length, c_m, irrespective of orientation. For fracture assessments, the plane of the flaw shall be assumed to be normal to the maximum principal tensile stress.

b) Option 2 – The procedure for defining an equivalent Mode I flaw dimension is shown in Figure 9.2.

   1) STEP 1 – Project the flaw onto a principal plane. In the case of uniaxial loading, there is only one possible principal plane. When the loading is biaxial (e.g., a pressurized component which is subject to a hoop stress and an axial stress), there is a choice of principal planes on which to project the flaw. In most cases, the flaw should be projected to the plane normal to the maximum principal tensile stress (the σ_1 plane), but there are instances where the σ_2 plane would be more appropriate (e.g., when the angle between the flaw and the principal plane (α) is greater than 45-degrees).

   2) STEP 2 – Compute the equivalent flaw length.

      i) For the plane of the flaw projected onto the plane normal to σ_1:

$$\frac{c}{c_m} = \cos^2\alpha + \frac{(1-B)\sin\alpha\cos\alpha}{2} + B^2\sin^2\alpha \tag{9.1}$$

ii) For the plane of the flaw projected onto the plane normal to σ_2:

$$\frac{c}{c_m} = \frac{\cos^2\alpha}{B^2} + \frac{(1-B)\sin\alpha\cos\alpha}{2B^2} + \sin^2\alpha \tag{9.2}$$

iii) In the Equations (9.1) and (9.2), the dimension c corresponds to the half flaw length (or total length for corner or edge cracks) to be used in calculations, c_m is the measured half-length for the flaw oriented at an angle α from the σ_1 plane, and B is the biaxiality ratio defined using Equation (9.3). If stress gradients occur in one or more directions, the sum of membrane and bending components shall be used for computing σ_1 and σ_2.

$$B = \frac{\sigma_2}{\sigma_1} \qquad where\ \sigma_1 \geq \sigma_2\ and\ 0.0 \leq B \leq 1.0 \tag{9.3}$$

iv) Equations (9.1) and (9.2) are only valid when both σ_1 and σ_2 are positive. If σ_2 is compressive or equal to zero, then Equation (9.1) shall be used to compute the equivalent flaw length with $B = 0$, or

$$\frac{c}{c_m} = \cos^2\alpha + \frac{\sin\alpha\cos\alpha}{2} \tag{9.4}$$

v) The relationship between c/c_m, α, and B is shown in Figure 9.3.

9.3.6.3 Characterization of Flaw Depth

The part through-wall depth of a flaw can be considerably more difficult to estimate than the length. Either a default value or a value based on detailed measurements may be used for the flaw depth in the assessment. In services where the owner determines that a leak is not acceptable, the flaw size shall be characterized by actual measurement in accordance with sub-paragraph (b) below.

a) Flaw Depth by Default Values

1) Through-Wall Flaw – If no information is available about the depth of a flaw, a conservative assumption is that the flaw penetrates the wall, i.e., $a = t$ for a surface flaw. In pressurized components, an actual through-wall flaw would most likely lead to leakage, and thus would not be acceptable in the long term. However, if it can be shown that a through-wall flaw of a given length would not lead to brittle fracture or plastic collapse, then the component should be acceptable for continued service with a part-through-wall flaw of that same length. Additional special considerations may be necessary for pressurized components containing a fluid where a leak can result in autorefrigeration of the material near the crack tip, or other dynamic effects.

2) Surface Flaw – Flaw depths less than the full wall may be assumed if justified by service experience with the type of cracking observed. If service experience is not available, then the assumed flaw depth should not be less than the following where length of the flaw is $2c$ (see Figure 9.1(b)).

$$a = \min[t, c] \tag{9.5}$$

b) Flaw Depth from Actual Measurements

The definition of the appropriate depth dimensions, a for a surface flaw, $2a$ and d for an embedded flaw, when relatively accurate measurements are available is illustrated in Figure 9.1 and Figure 9.4. If the flaw is normal to the surface, the depth dimension, a, is taken as the measured dimension, a_m. However, if the flaw is not normal to the surface, e.g., a lack of fusion flaw that is parallel to the bevel angle or a lamination (see Figure 9.4) the following procedure may be used to compute the depth dimension, a.

1) STEP 1 – Project the flaw onto a plane that is normal to the plate surface, designate this flaw depth as a_m.

2) STEP 2 – Measure the angle to the flaw, θ, as defined in Figure 9.4, and determine W using Equations (9.6) and (9.7) or Figure 9.5 where θ is measured in degrees.

$$W = \max[W_{Theta},\ 1.0] \tag{9.6}$$

$$W_{Theta} = \begin{pmatrix} 0.99999 + 1.0481\left(10^{-5}\right)\theta + 1.5471\left(10^{-4}\right)\theta^2 + \\ 3.4141\left(10^{-5}\right)\theta^3 - 2.0688\left(10^{-6}\right)\theta^4 + 4.4977\left(10^{-8}\right)\theta^5 - \\ 4.5751\left(10^{-10}\right)\theta^6 + 1.8220\left(10^{-12}\right)\theta^7 \end{pmatrix} \tag{9.7}$$

3) STEP 3 – Multiply a_m by W to obtain the dimension a, which is used in calculations. Note that the dimension d for buried flaws may decrease when the flaw depth is determined using this approach.

9.3.6.4 Characterization of Branched Cracks

Determination of an idealized flaw is complicated when a branched network of cracks forms in a component because the idealized flaw must be equivalent to the network of cracks from a fracture mechanics approach. The methodology for assessing a network of branched cracks is shown in Figure 9.6. As shown in this figure, the network is idealized as a single planar predominant flaw by means of the following procedure:

a) STEP 1 – Draw a rectangle around the affected region. Define the measured flaw length, $2c_o$, as the length of the rectangle (see Figure 9.6(a) and Figure 9.6(b)).

b) STEP 2 – Rotate the idealized flaw so that it is perpendicular to the maximum principal stress, σ_1. Define an effective length according to the procedure in paragraph 9.3.6.2 (see Figure 9.6(c)). Alternatively, for a conservative estimate of the flaw size, set $c = c_o$.

c) STEP 3 – Measure the maximum through-wall depth of the branched network, a_0 (see Figure 9.6(d)). If an actual depth measurement is made, then the flaw depth to be used in the assessment is shown in Figure 9.6(d). Alternatively, the default value defined in paragraph 9.3.6.3(a) can be used if accurate measurements are not possible.

9.3.6.5 Characterization of Multiple Flaws

The following procedure applies to multiple discrete flaws that are close to one another. A branched network of cracks is treated as a single flaw, as discussed in paragraph 9.3.6.4.

a) If two or more flaws are close to one another, they shall be evaluated for the need to combine them into a single equivalent flaw for the purpose of analysis. If separation distances are sufficient such that flaw alignment or combination is not required, the flaws can be analyzed independently, and only the worst-case flaw needs to be considered. This assumes that the stress fields at each flaw are similar.

b) The procedure for assessing multiple flaws in a local region is illustrated in Figure 9.7 and Figure 9.8, and outlined below:

1) STEP 1 – Rotate each flaw so that it coincides with a principal plane and determine the effective flaw length according to the procedure in paragraph 9.3.6.2. Determine the flaw depth according to the procedure outlined in paragraph 9.3.6.3. All flaws in the local region should now be parallel, as illustrated in Figure 9.7(b).

2) STEP 2 – Apply flaw alignment criteria to check for interaction between parallel flaws. Surface-connected or embedded flaws located in parallel planes spaced 0.5 inch (13 mm) or less shall be considered to be coplanar flaws. Flaw alignment criteria are illustrated in Figure 9.8(a). Project all interacting flaws onto a single plane, as illustrated in Figure 9.7(c). Some flaws may overlap after projection and shall be combined. If two or more flaws are combined due to overlap, define flaw dimensions using the rectangle inscribed around the combined flaw, as illustrated in Figure 9.7(d).

3) STEP 3 – Apply flaw combination criteria to check for interaction between flaws on a given plane. Flaw combination criteria are in Figure 9.8(b) and (c). If the separation distance between any two flaws satisfies the flaw combination criteria, the two flaws are combined, as illustrated in Figure 9.7(c). The dimensions of the combined flaw are inferred from a rectangle inscribed around the two interacting flaws. If two or more flaws are combined after applying the flaw combination criteria, it is not required to further evaluate interactions based on the dimensions of the combined flaw with other flaws. Also, it is not required to recategorize flaws as per paragraph 9.3.6.6 based on the dimensions of the combined flaw.

c) It is not required to combine multiple flaws into an equivalent flaw for crack growth analysis due to fatigue or stress corrosion cracking.

d) As an alternative to applying the procedure of flaw alignment and combination as described above, multiple flaws do not have to be combined into an equivalent flaw for evaluation if a stress intensity factor and limit load solution can be obtained for the interacting flaw geometries.

9.3.6.6 Recategorization of Flaws

a) Flaw recategorization may be necessary for the following reasons:

- For an embedded flaw close to the surface or for a deep surface flaw where the remaining ligament is small, the results obtained in the assessment may be overly conservative because the reference stress (see Annex 9C) in the remaining ligament may over-estimate the plasticity effects on the crack driving force. Recategorization of an embedded flaw to a surface flaw, or a surface flaw to a through-wall flaw, may result in the associated assessment being more accurate than without recategorization.
- Most of the stress intensity factor solutions in Annex 9B are not accurate for very deep cracks due to high strain/plasticity effects. For example, the commonly published stress intensity factor (K) solutions for a semi-elliptical surface flaw are only accurate for $a/t < 0.8$. Therefore, recategorization to a through-thickness flaw may be necessary to achieve a more accurate solution.
- Reliable sizing of the remaining ligament may be difficult by Non-Destructive Examination (NDE). Therefore, categorization of an embedded flaw to a surface flaw, or a surface flaw to a through-wall flaw, may be advisable due to measurement uncertainty.
- Ligament failure may occur for an embedded flaw near the surface. This potential “snap-through” can increase the length of the resulting surface flaw.

b) Guidelines for recategorization of flaws are provided below. An embedded or buried flaw can be recategorized as a surface flaw, while a surface flaw can be recategorized as a through-wall flaw. The dimensions of the initial and recategorized crack-like flaws are shown in Figure 9.9. As an alternative to applying the procedures for flaw recategorization, flaws do not need to be recategorized if stress intensity factor and limit load solutions can be obtained by explicitly modeling flaw to surface interaction (i.e., finite element analysis).

1) Embedded Flaw

i) An embedded flaw shall be recategorized to a surface flaw when $d < 0.4a_b$ (see Figure 9.9(a)). The length and depth of the surface flaw are given by the equations shown below. Note that the crack length is increased twice the ligament dimension. When the plastic strain on the remaining ligament is large, the flaw may grow to the free surface by ductile tearing, in which case the flaw is assumed to also extend in the length direction by the same amount on each side.

$$2c_s = 2c_b + 2d \tag{9.8}$$

$$a_s = 2a_b + d \tag{9.9}$$

ii) An embedded flaw with ligament length $d \geq 0.4a_b$ may be recategorized. The length and depth of the recategorized flaw are given by Equations (9.8) and (9.9), respectively.

2) Surface Flaw

i) A surface flaw may be recategorized as a through-thickness flaw when $a_s/t > 0.8$ (see Figure 9.9(b)). The length of the through-wall flaw is given by the following equation. Note that the crack length is increased twice the ligament dimension. When the plastic strain on the remaining ligament is large, the flaw may grow to the free surface by ductile tearing, in which case the flaw is assumed to also extend in the length direction by the same amount on each side.

$$2c_t = 2c_s + 2\left(t - a_s\right) \tag{9.10}$$

ii) Alternatively, for flaws deeper than $a_s/t > 0.8$, the solutions for crack driving force (K) and reference stress may be obtained by interpolation between the $a_s/t = 0.8$ surface flaw and through-wall solutions based on size of the remaining ligament, provided applicable solutions exist for the applied loading. This may be beneficial provided the assessment point for the surface flaw falls within the Failure Assessment Diagram (FAD). The length provided in Equation (9.10) should be used for the through-thickness flaw when interpolating. However, the length shall not be less than $2c_s + 0.4a_s$. The greater of the through-thickness stress intensity values between the inner and outer surface should be used for interpolation. Values for the interpolated stress intensity factor and reference stress should be no less than the values obtained for the surface flaw. If the interpolation results in the assessment point falling outside the FAD, the flaw may be recategorized as a through-thickness flaw with the flaw length given by Equation (9.10).

9.3.7 Recommendation for Inspection Technique and Sizing Requirements

9.3.7.1 Reliable sizing of the flaws by Non-Destructive Examination (NDE) is important. Therefore, the choice of the NDE method should be based on its ability to detect and size the depth and length of the flaw.

9.3.7.2 As previously discussed in paragraph 9.3.6, the crack dimensions required as input for an FFS analysis are the crack depth, crack length, crack angle with the plate surface, crack location from the surface, and the spacing between the cracks if the component has multiple cracks.

a) Surface Cracks – The crack length, angle relative to the principal stress direction (see Figure 9.2) and distance to other surface cracks may be determined using Magnetic Particle (MT) or Dye Penetrant (PT) examination technique. The depth and angle of the flaw relative to the surface (see Figure 9.4) are typically determined using Ultrasonic (UT) examination techniques.

b) Embedded Cracks – The crack depth, length, angle, and distance to other surface breaking or embedded cracks are typically determined using angle beam Ultrasonic (UT) examination techniques, e.g., Time-Of-Flight-Diffraction (TOFD) or pulse echo techniques. The calibration settings may need to be more sensitive than are used for new construction weld quality inspections.

9.3.7.3 Accurate sizing of crack-like flaws depends on both the available technology and the skill of the inspector. Parameters to be considered in the uncertainties of flaw sizing include the crack length, depth, flaw orientation, whether the flaw is surface breaking, and the number of flaws, i.e., single flaw or multiple flaws. PT or MT should be used to enhance surface breaking flaws prior to determining the crack length. A visual examination should not be used to determine the length of the flaw because the ends of the crack may be closed.

9.3.7.4 Determination of the depth, orientation, and position, i.e., the location below the surface for an embedded crack, of a crack-like flaw is usually done by using ultrasonic examination techniques. Radiographic examination techniques may also be used; however, accurate flaw depth and orientation information can be obtained only by moving the component containing the flaw or moving the source around the component to obtain multiple views. This type of manipulation is typically not possible for many pressure-containing components. A level of qualitative depth and orientation information can sometimes be obtained with electrical resistance (potential drop), magnetic leakage field, and eddy current techniques. The accuracy of the electrical resistance techniques is seriously affected by conditions in the crack (i.e., touching surface and impurities such as oxides). Therefore, ultrasonic examination is the recommended sizing technique for depth and inclination of crack-like flaws.

9.3.7.5 If part of a component is inaccessible for inspection due to the component configuration, materials used, or obstruction by other flaws, and a flaw is suspected in this region because of the surrounding conditions, the possibility of the existence of a flaw the size of the region that cannot be inspected should be considered in the assessment.

9.4 Assessment Techniques and Acceptance Criteria

9.4.1 Overview

9.4.1.1 The Fitness-For-Service Assessment procedure used to evaluate crack-like flaws is shown in Figure 9.10. The three assessment levels used to evaluate crack-like flaws are summarized below.

a) Level 1 Assessments are limited to crack-like flaws in pressurized cylinders, spheres, or flat plates away from all structural discontinuities.

b) Level 2 Assessments can be used for general shell structures including crack-like flaws located at structural discontinuities. A flow diagram for the Level 2 Assessment is provided in Figure 9.11. In Level 2 Assessments, detailed information on material properties and loading conditions is required, and a stress

analysis is required to determine the state of stress at the location of the flaw. The stress analysis at this level may be based on code equations, closed form solutions, or a numerical analysis.

c) Level 3 Assessments can be used to evaluate those cases that do not meet the requirements of Level 1 or Level 2 Assessments. Level 3 Assessments are also required for flaws that may grow in service because of loading or environmental conditions.

9.4.1.2 The assessment levels designated in this document are based on the definitions in Part 2 and are different from the assessment levels described in BS PD6493, BS 7910, and EDF Energy Nuclear Generation Limited R-6 (see Part 1, Table 1.1).

9.4.2 Level 1 Assessment

9.4.2.1 The Level 1 Assessment is applicable to components that satisfy the limitations in paragraph 9.2.2(e)(1).

9.4.2.2 The following procedure can be used to determine the acceptability of a crack-like flaw using a Level 1 Assessment.

a) STEP 1 – Determine the load cases and temperatures to be used in the assessment based on operating and design conditions (see paragraph 9.3.4). The CET (see Part 3) should be considered in establishing the temperature for the assessment.

b) STEP 2 – Determine the length, $2c$, and depth, a, of the crack-like flaw from inspection data. The flaw should be characterized using the procedure in paragraph 9.3.6.

c) STEP 3 – Determine the Figure from the list below to be used in the assessment based on the component geometry and crack-like flaw orientation with respect to the weld joint.

1) Flat Plate, Crack-Like Flaw Parallel to the Joint (see Figure 9.12).

2) Cylinder, Longitudinal Joint, Crack-Like Flaw Parallel to the Joint (see Figure 9.13).

3) Cylinder, Longitudinal Joint, Crack-Like Perpendicular to the Joint (see Figure 9.14).

4) Cylinder, Circumferential Joint, Crack-Like Flaw Parallel to the Joint (see Figure 9.15).

5) Cylinder, Circumferential Joint, Crack-Like Flaw Perpendicular to the Joint (see Figure 9.16).

6) Sphere, Circumferential Joint, Crack-Like Flaw Parallel to the Joint (see Figure 9.17).

7) Sphere, Circumferential Joint, Crack-Like Flaw Perpendicular to the Joint (see Figure 9.18).

d) STEP 4 – Determine the screening curve from the Figure selected in STEP 3. The following should be noted when selecting a screening curve.

1) For each Figure in STEP 3, two sets of screening curves, 1/4-t and 1-t crack depths, are provided for three conditions; base metal, weld metal that has been subject to $PWHT$, and weld metal that has not been subject to $PWHT$.

2) If the depth of the flaw can be accurately determined using qualified NDE procedures, then the 1/4-t flaw curve can be used in the assessment based on the criteria in 3) below; otherwise, the 1-t flaw curve should be used.

3) The screening curve to be used in the assessment shall be based on the following criteria.

i) For $t \leq 25\ mm\ (1\ in)$:

I) If $a \leq t/4$, then the 1/4-t screening curves shall be used.

II) If $a > t/4$, then the 1-t screening curves shall be used.

ii) For $25\ mm\ (1\ in) < t \leq 38\ mm\ (1.5\ in)$:

I) If $a \leq 6\ mm\ (0.25\ in)$, then the 1/4-t screening curves shall be used.

II) If $a > 6\ mm\ (0.25\ in)$, then the 1-t screening curves shall be used.

4) If the location of the flaw is at the weld, or within two times the nominal plate thickness measured from the centerline of the weld, then the curves for weld metal should be used; otherwise, the curve for base metal may be used. For flaws located at a weld, the applicable assessment curve is based on heat treatment of the component. If there is question regarding the type and/or quality of $PWHT$, Curve C (i.e., no $PWHT$) should be used.

e) STEP 5 – Determine the reference temperature. Based on the material specification determine the Material Temperature Exemption Curve using Part 3, Table 3.2 and the Specified Minimum Yield Strength (SMYS) at ambient temperature based on the original construction code. With the Material Temperature Exemption Curve and the SMYS of the material, enter Table 9.2 to determine the reference temperature. If the material is a carbon steel, then the reference temperature is based on the 20 Joule or 15 ft-lb transition temperature. For example, for an A516 grade 70 material, the exemption curve from Part 3, Table 3.2 is B. The SMYS for this material is 262 MPa (38 ksi). The material is carbon steel; therefore, is based on the 20 Joule or 15 ft-lb transition temperature. Based on these data, the reference temperature from Table 9.2 is $T_{ref} = 10.3℃\ (51.1°F)$.

f) STEP 6 – Determine the maximum permissible crack-like flaw length. Enter the assessment Figure established in STEP 3 with the assessment temperature and reference temperature determined in STEPs 1 and 5, respectively, to determine the maximum length of the flaw $(2c)$ using the applicable screening curve.

g) STEP 7 – Evaluate Results – if the permissible flaw size determined in STEP 6 is greater than or equal to the length of the crack-like flaw determined in STEP 2, then the component is acceptable for future operation.

9.4.2.3 The Level 1 Assessment may be based on the Level 2 Assessment calculation procedure subject to the restrictions and requirements stipulated in paragraph 9.2.2(e)(1).

9.4.2.4 If the component does not meet the Level 1 Assessment requirements, then the following actions, or combination thereof, shall be taken:

a) The data used in the analysis can be refined and the Level 1 Assessment can be repeated (i.e., refinement of data) entails performing additional NDE to better characterize the flaw dimensions and determining the future operating conditions accurately to establish the operating temperature envelope.

b) Rerate (e.g., temperature), repair, replace, or retire the component.

c) Conduct a Level 2 or Level 3 Assessment.

9.4.3 Level 2 Assessment

9.4.3.1 The Level 2 Assessment is applicable to components and loading conditions that satisfy the conditions given in paragraph 9.2.2(e)(1). The assessment procedure in Level 2 provides a better estimate of the structural integrity of a component than a Level 1 Assessment with a crack-like flaw. A flow diagram for a Level 2 Assessment is shown in Figure 9.11.

9.4.3.2 The following procedure can be used to determine the acceptability of a crack-like flaw using a Level 2 Assessment.

a) STEP 1 – Evaluate the operating conditions and determine the pressure, temperature, and supplemental loading combinations to be evaluated (see paragraph 9.3.4.1).

b) STEP 2 – Determine the stress distributions (see paragraph 9.3.4.2) at the location of the flaw based on the applied loads in STEP 1 and classify the resulting stresses into the following stress categories (see paragraph 9.3.4.3):

   1) Primary stress

   2) Secondary stress

   3) Residual stress

c) STEP 3 – Determine the yield strength and tensile strength for the conditions being evaluated in STEP 1 (see paragraph 9.3.5.1). The yield and tensile strength shall be established using actual values or nominal values defined as the specified minimum values per the applicable material specification.

d) STEP 4 – Determine the fracture toughness, K_{mat}, for the conditions being evaluated in STEP 1 (see paragraph 9.3.5.2). If actual fracture toughness data is available for the component being evaluated, these data may be used in the assessment. Otherwise, the fracture toughness may be estimated using one of the following methods.

   1) Methods for estimating fracture toughness for carbon and low alloy steels are provided below. In all cases, in-service degradation of the fracture toughness shall be considered in accordance with Annex 9F, paragraph 9F.4.6 or 9F.4.7, as applicable.

      i) Lower bound fracture toughness estimation in accordance with Annex 9F, paragraph 9F.4.2.

      ii) Transition region fracture toughness estimate in accordance with Annex 9F, paragraph 9F.4.3.

      iii) Upper Shelf fracture toughness estimate in accordance with Annex 9F, paragraph 9F.4.4.

      iv) Dynamic and crack arrest fracture toughness estimate in accordance with Annex 9F, paragraph 9F.4.5.

   2) Annex 9F, paragraph 9F.4.12 shall be used to estimate fracture toughness for austenitic stainless steels.

e) STEP 5 – Determine the crack-like flaw dimensions from inspection data. The flaw should be categorized using the procedure in paragraph 9.3.6.

f) STEP 6 – Compute the reference stress for primary stresses, σ_{ref}^{P}, based on the primary stress distribution and flaw size from STEPs 2 and 5, respectively, and the reference stress solutions in Annex 9C.

g) STEP 7 – Compute the Load Ratio or the abscissa of the FAD using the reference stress for primary loads from STEP 6 and the yield strength from STEP 3.

$$L_r^P = \frac{\sigma_{ref}^P}{\sigma_{ys}} \tag{9.11}$$

h) STEP 8 – Compute the stress intensity attributed to the primary loads, K_I^P, using the primary stress distribution and flaw size from STEPs 2 and 5, respectively, and the stress intensity factor solutions in Annex 9B. If $K_I^P < 0.0$, then set $K_I^P = 0.0$.

i) STEP 9 – Compute the stress intensity attributed to the secondary and residual stresses, K_I^{SR}, using the secondary and residual stress distributions from STEP 2, the flaw size from STEP 5, and the stress intensity factor solutions in Annex 9B. If $K_I^{SR} < 0.0$, then set $K_I^{SR} = 0.0$. The value of K_I^{SR} should be determined at the same location along the crack front as that used to determine K_I^P.

j) STEP 10 – Compute the plasticity interaction factor, Φ, using the following procedure. The procedure shown is for computing the plasticity interaction associated with the flaw depth, a. For a surface or embedded flaw, the procedure should be repeated using the half-flaw length, c. Note for a through- thickness flaw, the procedure need only be used to compute the plasticity interaction factor for the half-flaw length, c.

1) STEP 10.1 – Compute the parameter Φ_0.

$$\Phi_0 = \left(\frac{a_{eff}}{a}\right)^{0.5} \tag{9.12}$$

$$a_{eff} = a + \left(\frac{1}{6\pi}\right) \cdot \left(\frac{K_I^{SR}}{\sigma_{ys}}\right)^2 \qquad (Plane\ Strain\ Conditions) \tag{9.13}$$

$$a_{eff} = a + \left(\frac{1}{2\pi}\right) \cdot \left(\frac{K_I^{SR}}{\sigma_{ys}}\right)^2 \qquad (Plane\ Stress\ Conditions) \tag{9.14}$$

2) STEP 10.2 – Compute the stress intensity factor for secondary and residual stresses corrected for plasticity effects, K_J^{SR},

$$K_J^{SR} = \Phi_0 \cdot K_I^{SR} \tag{9.15}$$

3) STEP 10.3 – If $K_I^P = 0$, set $\Phi = \Phi_0$ and proceed to STEP 11; otherwise, compute the parameter, X, and proceed to STEP 10.4.

$$\mathrm{X} = K_J^{SR} \cdot \left(\frac{L_r^P}{K_I^P}\right) \tag{9.16}$$

4) STEP 10.4 – Determine the parameter ξ from Table 9.3.

5) STEP 10.5 – Compute the plasticity interaction factor Φ.

$$\Phi = \Phi_0 \cdot \xi \tag{9.17}$$

k) STEP 11 – Determine toughness ratio or ordinate of the FAD assessment point where K_I^P is the applied stress intensity due to the primary stress distribution from STEP 8, K_I^{SR} is the applied stress intensity due to the secondary and residual stress distributions from STEP 9, K_{mat} is the material toughness from STEP 4, and Φ is the plasticity correction factor from STEP 10.

$$K_r = \frac{K_I^P + \Phi K_I^{SR}}{K_{mat}} \tag{9.18}$$

l) STEP 12 – Evaluate results; the FAD assessment point for the current flaw size and operating conditions (stress levels) is defined as (K_r, L_r^P).

1) STEP 12.1 – Determine the cut-off for the L_r^P-axis of the FAD (see Figure 9.19).

2) STEP 12.2 – Plot the point on the FAD shown in Figure 9.19. If the point is on or inside the FAD (on or below and/or to the left), then the component is acceptable per the Level 2 Assessment procedure. If the point is outside of the FAD (above and/or to the right), then the component is unacceptable per the Level 2 Assessment procedure. Note that the value of K_I^P and K_I^{SR} will vary along the crack front; therefore, the assessment may have to be repeated at several points along the crack front to ensure that the critical location is found.

9.4.3.3 Constraint effects for surface flaws may be included in the assessment using Annex 9H by modifying the fracture toughness, K_{mat}, in STEP 11 of paragraph 9.4.3.2. The procedure in Annex 9H applies only to carbon and low-alloy steels that operate in the ductile-brittle transition region.

9.4.3.4 Calculation of the Mode I stress intensity factors in STEPs 8 and 9 of paragraph 9.4.3.2 may be modified using Annex 9I. The procedure in Annex 9I applies only to carbon and low-alloy steels that operate in the ductile-brittle transition region.

9.4.3.5 A limiting flaw size can be established using the following procedure. Determination of the limiting flaw size may be useful in selecting an appropriate NDE technique for inspection.

a) Increase the crack-like flaw dimensions by a small increment; for a surface flaw compute $a = a_0 + \Delta a$ and $c = c_0 + \Delta c$, where a_0 and c_0 are the initial flaw sizes found at the time of the inspection. The flaw increments should be proportioned based on the flaw aspect ratio or ratio of the stress intensity factor values at the surface and deepest part of the crack.

b) For the new flaw size, complete the steps in paragraph 9.4.3.2 and determine if the new flaw size is inside of the FAD curve.

c) Continue to increment the flaw size until the calculated assessment point is on the FAD curve. The resulting flaw size is defined as the limiting flaw size.

9.4.3.6 If the component does not meet the Level 2 Assessment requirements, then the following actions, or combination thereof, shall be taken:

a) The data used in the analysis can be refined and the Level 2 Assessment can be repeated. Refinement of data entails performing additional NDE to better characterize the flaw dimensions, reviewing equipment documentation to justify the use of other than lower bound material properties, and/or determining the future operating conditions and associated stress levels more accurately. If the assessment point lies within the Level 2 FAD after data refinement, the component is acceptable for continued operation.

b) Rerate, repair, replace, or retire the component, and/or

c) A Level 3 Assessment can be performed.

9.4.4 Level 3 Assessment

9.4.4.1 The Level 3 Assessment procedure provides the best estimate of the structural integrity of a component with a crack-like flaw. In addition, this assessment level is required if subcritical crack growth is possible during future operation. Five Methods are permitted in a Level 3 Assessment.

a) Method A Assessment – The basis of this method is the Level 2 Assessment procedure using the FAD in Figure 9.19.

b) Method B Assessment – The basis of this method is the Level 2 Assessment procedure except that the FAD is constructed based on the actual material properties. This method is only suitable for base and weld materials because it requires a specific material dependent stress-strain curve; the method should not be used for assessment of crack-like flaws in the HAZ. The procedure for the assessment is as follows:

1) STEP 1 – Obtain engineering stress-strain data for the material containing the crack-like flaw at the assessment temperature. If a stress-strain curve for the actual material containing the flaw cannot be obtained, a stress-strain curve for a material with the same specification and similar stress-strain response can be used. The 0.2% offset yield strength, tensile strength, and modulus of elasticity should be determined together with enough data points to accurately define the stress-strain curve. It is recommended that the engineering stress-strain curve be accurately defined at the following ratios of applied stress to yield stress: $\sigma_{uts}/\sigma_{ys} = 0.7, 0.8, 0.98, 1.0, 1.02, 1.1, 1.2$ and intervals of 0.1 up to σ_{uts}.

2) STEP 2 – Convert the engineering stress-strain curve obtained in STEP 1 to a true stress-strain curve. The true stress and strain can be computed from the engineering strain as shown in Annex 2E, paragraph 2E.3.3.1.

3) STEP 3 – Determine the material-specific FAD using the following equations:

$$K_r(L_r^P) = \left(\frac{E\varepsilon_{ref}}{L_r^P \sigma_{ys}} + \frac{\left(L_r^P\right)^3 \sigma_{ys}}{2E\varepsilon_{ref}} \right)^{-1/2} \qquad \left(for \quad 0.0 < L_r^P \le L_{r(\max)}^P \right) \tag{9.19}$$

$$K_r(L_r^P) = 1.0 \qquad \left(for \quad L_r^P = 0.0 \right) \tag{9.20}$$

4) STEP 4 – The plasticity interaction factor, Φ, may be determined using the approach in Level 2 or using the method provided in Annex 9A, reference [39].

5) STEP 5 – Complete the assessment using the Level 2 Assessment procedure except the material-specific FAD is utilized in STEP 12 (see paragraph 9.4.3.2(l)).

c) Method C Assessment – The basis of this method is the Level 2 Assessment procedure except that the FAD is constructed based on the actual loading conditions, component geometry, and material properties. A procedure to construct the geometry and material dependent FAD, and to complete the assessment for a known crack-like flaw is covered in Annex 9G.

d) Method D Assessment – This method is a ductile tearing analysis where the fracture tearing resistance is defined as a function of the amount of stable ductile tearing. This method should only be used for materials that exhibit stable ductile tearing, e.g., ferritic steels on the upper shelf and austenitic stainless steels. The procedure for the assessment is as follows:

1) STEP 1 – Obtain a JR curve for the material containing the crack-like flaw at the assessment temperature (see Annex 9F). If a JR curve for the actual material containing the flaw cannot be obtained, a JR curve for a material with the same specification and similar ductile tearing response can be used.

2) STEP 2 – Determine a FAD to be used in the assessment from Methods A, B, or C as defined above.

3) STEP 3 – Follow the Level 2 Assessment procedure (see paragraph 9.4.3.2) to generate a series of assessment points (see Figure 9.20(a)). For each assessment point, the crack depth, a, is determined by adding a crack depth increment, Δa_j, to the measured or initial crack depth, a_i (i.e., the first point is $a = a_i + \Delta a_1$, the second point is $a = a_i + \Delta a_1 + \Delta a_2$, the third point is $a = a_i + \Delta a_1 + \Delta a_2 + \Delta a_3$, etc.). The magnitude of the crack depth increment, Δa_j, used to generate the series of assessment points can be inferred from the JR curve. For surface and embedded flaws, the magnitude of crack depth increment should also be applied to the flaw length. The material fracture toughness used for each assessment point is determined from the JR curve (J can be converted to K using the procedures in Annex 9F) at the crack depth associated with ductile tearing, a_{JR} (i.e., the first point is $a_{JR} = \Delta a_1$, the second point is $a_{JR} = \Delta a_1 + \Delta a_2$, the third point is $a_{JR} = \Delta a_1 + \Delta a_2 + \Delta a_3$, etc.). Note that for a rising JR Curve, the fracture toughness will increase with the crack depth.

4) STEP 4 – Plot the series of assessment points on the FAD. The three possible outcomes of a tearing analysis are shown in Figure 9.20(b). If all the assessment points fall inside of the FAD, then unstable crack growth will not occur. If the first few assessment points fall outside of the FAD and subsequent points fall within the FAD, then a finite amount of crack growth or stable ductile tearing will occur. Ductile instability is predicted when all the assessment points fall outside of the FAD. If the load is fixed, the locus of the assessment typically exhibits a "fishhook" shape where the value of K_r reaches a minimum and then increases. The point of instability occurs when the locus of the assessment points is tangent to the FAD.

e) Method E Assessment – The basis of this method is the use of the following recognized assessment procedures.

1) BS 7910 (see Part 1, Table 1.1).

2) EDF Energy R-6 (see Part 1, Table 1.1).

3) SSM Research Report 2008:01 (see Part 1, Table 1.1).

4) WES 2805 (see Part 1, Table 1.1).

5) DPFAD Methodology (see Annex 9A, references [7] and [8]).

6) EPFM using the J-integral (see Annex 9A, references [3], [22], and [25]).

7) The J-integral-Tearing Modulus method (see Annex 9A, references [3], [31], and [34]).

9.4.4.2 For each Method, a sensitivity analysis, partial safety factors or a probabilistic analysis shall be used in the assessment to evaluate uncertainties in the input parameters.

9.4.4.3 It is the responsibility of the Engineer to meet all limitations and requirements imposed by the selected method. In addition, the Engineer must ensure that the method used including all assumptions, analysis parameters, results and conclusions is clearly documented.

9.5 Remaining Life Assessment

9.5.1 Subcritical Crack Growth

9.5.1.1 Overview

There is special emphasis in the assessment procedures in this Part for evaluating subcritical crack growth in pressure containing components. There are a wide variety of process environments and material degradation mechanisms that increase the occurrence of environmentally and service induced cracking (see Annex 2B).

a) For purposes of this document, in-service crack growth may be categorized into four main types; crack growth by fatigue, crack growth by stress corrosion cracking, crack growth by hydrogen assisted cracking, and crack growth by corrosion fatigue. Details regarding these crack growth mechanisms are covered in Annex 9F.

b) The methodology for crack growth evaluation used in this document is based on fracture mechanics. In this methodology, the growth of a pre-existing crack is controlled by a crack tip stress intensity factor. In addition, it is assumed that the growth of a crack is controlled by a crack growth model for each combination of material, environment, and crack tip stress intensity factor that can be measured or determined independently and applied to a component with a crack-like flaw. An important requirement for this methodology is that the material properties such as yield and flow stress, material toughness, and crack growth model including appropriate coefficients should be determined as closely as possible from conditions that represent the combination of material, equipment age, environment, loading conditions, and applied stress intensity level for the component being evaluated.

c) A major difficulty that must be addressed with environmental cracking data is that crack growth rates can be highly sensitive to changes in the process environment. While the environment is carefully controlled in an experiment, the composition and temperature of an actual process is subject to fluctuations, and the applicability of laboratory data is inappropriate in many cases. Another problem with predicting crack growth rates in structures is that the cracking often occurs as the result of an upset in operating conditions. For example, cracking that is detected after several years of service may have occurred over the space of several hours or days when atypical operating conditions were present; no cracking occurred before or after this upset. An average crack growth rate, obtained by dividing the crack size by the total time in service, would be meaningless in such instances.

d) For cases involving fatigue, or environmentally assisted cracking, new cracks can initiate at other locations in the structure remote from the known cracks being analyzed. This occurs because corrosion, erosion, local cyclic or static stresses or local concentration of the environment is such that threshold values for crack extension are exceeded. Hence, when assessing the significance of known or postulated cracks for in-service crack extension and structural failure, the implications of exceeding such threshold values elsewhere in the structure must be considered.

e) Closed form estimates for the time to reach a limiting flaw size are complicated by random loading, fatigue threshold and retardation effects, and the complexity of the stress intensity solution. Therefore, crack growth is typically done using a numerical algorithm that explicitly increments the crack growth for some repeated block of representative service loading. For complicated loading histories, load blocks may be developed for a representative time period using the rainflow or other cycle-counting method.

f) In addition to the complexities described above, sources of error in computing the time to reach a limiting flaw size include uncertainty in sizing the initial defect, variability in material behavior, and oversimplification

of the load spectrum. Despite the difficulties of performing crack growth calculations, estimates of crack growth time to failure are useful for establishing inspection intervals and prioritizing repairs.

g) All cases in which subcritical crack growth is included in the assessment should be referred to and analyzed by an engineer sufficiently knowledgeable about the interactions between cracks, environment, component (structural) design, and loading history, including cyclic loads, using Level 3 procedures of this document.

h) In cases where subcritical crack growth data is minimal or nonexistent, periodic monitoring of crack growth using appropriate NDE methods is recommended. The incremental growth data resulting from the periodic monitoring can be used as input data to an assessment.

9.5.1.2 Evaluation and Analysis Procedures for Components with Growing Cracks

Analysis of equipment containing growing cracks requires specialized skills, expertise, and experience because of the inherent uncertainties with the methodology. The analysis involves the use of a Level 3 Assessment per paragraph 9.4.4 and the numerical integration of a crack growth model. The overall evaluation methodology for growing cracks is shown in Figure 9.21. Guidance for conducting a crack growth analysis is shown in Figure 9.22. Highlights of the evaluation include the following.

a) STEP 1 – Perform a Level 3 Assessment for the initial crack size. If the component is demonstrated to be acceptable per a Level 3 Assessment, then an attempt to apply remedial measures to prevent further crack growth should be made (see paragraph 9.6).

b) STEP 2 – If effective remedial measures are not possible and slow subcritical crack growth is expected, then determine if a crack growth model and associated data exist for the material and service environment. If a crack growth model and data exist, then a crack growth analysis can be performed. If crack growth data does not exist, it may be determined in accordance with a recognized standard for crack growth testing. The selection of an appropriate crack growth model, the specification of the test conditions that represent the full range of operating conditions the component is subjected to, and selection of the test material are the responsibility of the engineer performing the assessment (see paragraph 9.5.1.1). As an alternative to a subcritical crack growth analysis, a leak-before break analysis may be performed to determine if an acceptable upper bound crack size can be established (see paragraph 9.5.2).

c) STEP 3 – Compute the stress at the flaw based on the future operating conditions. In these calculations, all relevant operating conditions including normal operation, start-up, upset, and shutdown should be considered.

d) STEP 4 – Determine an increment in crack growth based on the previous flaw size, stress, estimated stress intensity, and the crack growth model. To initialize the process, the previous flaw size is the initial flaw size determined in STEP 1. For surface and embedded flaws, the increment of crack growth will have a component in the depth and length dimension. For embedded flaws, the increment of crack growth may also include a component to model the flaw location in the wall thickness direction. The increment of crack growth is established based on the applied stress intensity associated with the component of the crack and the crack growth equation. For example, if a surface flaw is being evaluated, the crack depth is incremented based on the stress intensity factor at the deepest portion of the crack and the length is incremented based on the stress intensity factor at the surface. The flaw size to be used in STEP 5 is the previous flaw size plus the increment of crack growth. A description of methodologies for performing crack growth calculations subject to constant amplitude and variable amplitude loading is contained in Annex 9A, references [3], [9], [17], and [26].

e) STEP 5 – Perform a Level 3 Assessment for the current crack size. Demonstrate that for the current crack size, the applied stress intensity factor is less than the critical stress intensity factor for the applicable crack growth mechanism. If the assessment point for the current flaw size is outside of the FAD or the crack is recategorized as a through-wall crack (see paragraph 9.3.6.6) then go to STEP 6; otherwise, go to STEP 4 and continue to grow the crack.

f) STEP 6 – Determine the time or number of stress cycles for the current crack size (a_o, c_o) to reach the limiting flaw size. The component is acceptable for continued operation provided:

1) The time or number of cycles to reach the limiting flaw size, including an appropriate in-service margin, is more than the required operating period.

2) The crack growth is monitored on-stream or during shutdowns, as applicable, by a validated technique.

3) The observed crack growth rate is below the value used in the remaining life prediction as determined by an on-stream monitoring or inspections during shutdowns.

4) Upset conditions in loading or environmental severity are avoidable.

5) If the depth of the limiting flaw size is recategorized as a through-wall thickness crack, the conditions for an acceptable Leak-Before-Break (LBB) criterion should be satisfied (see paragraph 9.5.2).

g) STEP 7 – At the next inspection, establish the actual crack growth rate, and re-evaluate the new flaw conditions per procedures of this Part. Alternatively, repair or replace the component or apply effective mitigation measures.

9.5.1.3 Alternative Analysis Procedure for Components with Growing Fatigue Cracks

As an alternative to the provisions of paragraph 9.5.1.2, components with growing fatigue cracks may be evaluated using the methodology in ASME B&PV Code, Section VIII, Division 3, Article KD-4 and Nonmandatory Appendix D. When this method is used, the design margin provided in Article KD-4, paragraph KD-412 should be used in the assessment. The crack growth factors may be taken from Article KD-4 and Nonmandatory Appendix D if the materials under consideration are listed therein. Alternatively, crack growth factors C and m, as well as the threshold for crack growth, ΔK_{th} may be taken from Appendix F. However, in all cases, the mean stress correction, $f(R_k)$, shall be applied. If the material under consideration is not listed, the material closest in composition should be used to calculate $f(R_k)$. For example, the equations and values for high strength low alloy steel should be used for all ferritic alloys and the values for austenitic stainless steel should be used for nickel-based alloys.

9.5.2 Leak-Before-Break Analysis

9.5.2.1 Overview

In certain cases, it may be possible to show that a flaw can grow through the wall of a component without causing a catastrophic failure. In such cases, a leak can be detected, taking into consideration the contained fluid and type of insulation, and remedial action could be initiated to avoid a component failure. This type of examination is called a Leak-Before-Break (LBB) analysis. The leak-before-break methodology may be useful to determine an upper bound for a part-through flaw that is growing at an unknown rate; although the remaining life cannot be determined, detection of a leak can serve as an early warning. A leak-before-break analysis begins by re-categorizing the flaw as through-wall, and then evaluating the new geometry according to the procedures in paragraph 9.4.3 or 9.4.4. If the postulated through-wall flaw is acceptable, the existing flaw can be left in service if it does not grow through the wall.

9.5.2.2 Limitations of LBB

There are limitations of the leak-before-break methodology. This approach should not be applied to certain situations that are outlined below.

a) The leak should be readily detectable. The LBB approach may not be appropriate if the affected area is covered by insulation, or if the cracking mechanism produces very tight cracks that do not produce leaks when they grow through the wall. The ability to detect a leak may also be influenced by the contained fluid (e.g., liquid or gas).

b) The LBB methodology may not be suitable for flaws near stress concentrations or regions of high residual stress. The pitfalls of LBB in these situations are illustrated in Figure 9.23. When the stresses are higher on the surface than in the interior of the wall, the flaw may grow faster in the surface direction than in the depth direction. In some cases, the flaw can grow virtually around the entire circumference of the vessel before advancing in the depth direction. Therefore, LBB should not be applied to non-post weld heat treated cylindrical shell components with cracks in a circumferential weld joint, e.g., girth seams and head-to-shell junctions, or shell-to-nozzle junctions with circumferential cracks unless it can be shown that the stress distribution will not promote accelerated crack growth at the surface.

c) The LBB approach should not be applied when the crack growth rate could potentially be high. When a leak occurs, adequate time must be available to discover the leak and take the necessary action. This consideration is particularly important when the component is subject to pneumatic pressure.

d) The possible adverse consequences of developing a leak must be considered, especially when the component contains hazardous materials, fluids operating below their boiling point, and fluids operating above their auto-ignition temperature. Pressurized components that contain gas at high pressure can experience pneumatic loading or other dynamic effects at the crack tip making LBB impractical. Pressurized components that contain light hydrocarbon liquids, or other liquids with a low boiling point, can experience autorefrigeration that also make LBB impractical.

9.5.2.3 LBB Procedure

The procedure for assuring that a leak-before-break criterion is satisfied is shown below.

a) STEP 1 – Using methods of paragraph 9.4.3 or paragraph 9.4.4, demonstrate that the largest initial flaw size left in the structure will not lead to fracture for all applicable load cases.

b) STEP 2 – Using methods of paragraph 9.4.3 or paragraph 9.4.4, determine the largest or critical crack length of a full through-wall crack below which catastrophic rupture will not occur for all applicable load cases.

c) STEP 3 – Compute the corresponding leak areas associated with the critical crack lengths determined in STEP 2.

d) STEP 4 – Determine the leakage rate associated with the crack area computed in STEP 3, and demonstrate that the associated leaks are detectable with the selected leak detection system (see paragraph 9.5.2.5).

9.5.2.4 Flaw Dimensions for LBB

The crack-like flaw dimensions to be used in an LBB analysis are determined as follows:

a) If the component meets all the conditions outlined in paragraph 9.5.2.2, the assumed LBB flaw can be defined as follows:

$$2c_{LBB} = 2c + 2t \tag{9.21}$$

b) The above equation, which applies to both surface and buried flaws, is more restrictive than the recategorization procedure in paragraph 9.3.6.6. If the current flaw was initially recategorized as a through-wall flaw, the length of the flaw should be redefined using subparagraph a) above if an LBB analysis is to be performed.

9.5.2.5 Leak Area Calculations for LBB Analysis

The Crack Opening Area (COA) of a potential through-wall crack-like flaw is required to estimate leakage flow rates. The COA depends on the crack geometry (effective length, shape, orientation, etc.), component geometry, material properties, and the loading conditions. Methods to compute the crack opening area are provided in Annex 9E of this Standard.

9.5.2.6 Leak Rate Calculations for Through-Wall Cracks

The calculation of the fluid flow or leak rate through a crack-like flaw involves the crack geometry, the flow path length, fluid friction effects, and the thermodynamics of the flow through the crack. A method to compute the leak rate using approximate solutions for isothermal or polytropic flows of gases is provided in Annex 9A, reference [18]. Methods to compute the leak rate for two phase flow of steam/water mixtures are provided in Annex 9A, reference [32].

9.5.2.7 Analysis of Critical Leak Length (CLL) of Through-Wall Cracks

If a leak is expected and acceptable, and if conditions for LBB methodology are met, then the critical length of a through-wall crack for the component under the conditions of the prevalent stresses and material properties shall be performed using paragraph 9.4.3 or paragraph 9.4.4. The acceptance criteria of the CLL will depend on the capability and reliability of the in-service monitoring and the leak detection system.

9.6 Remediation

9.6.1 Objectives of Remediation

A FFS analysis provides the determination of the remaining life of a component containing a flaw so that operation can be assured until the next scheduled inspection. The remaining life of a component containing crack-like flaws can only be determined if information about the crack growth rate in the service environment is known. Typically, this information is not readily available or established for many of the process environments. Therefore, a combination of analytical techniques, i.e., LBB (see paragraph 9.5.2) in-service monitoring (see paragraph 9.7) and remediation methods may be used to provide assurance that a component can be operated until the next scheduled inspection.

9.6.2 Remediation Methods

Remediation methods for crack-like flaws generally fall into one of the categories shown below. One or a combination of these methods may be employed.

9.6.2.1 *Remediation Method 1* – Removal or repair of the crack. The crack may be removed by blend grinding. The resulting groove is then repaired using a technique to restore the full thickness of material and the weld repair is subject to $PWHT$ in accordance with the in-service inspection code. Alternatively, repair of the groove is not required if the requirements of FFS Assessment procedures in Part 5 are satisfied.

9.6.2.2 *Remediation Method 2* – Use of a crack arresting detail or device. For components that are not a pressure boundary, the simplest form of this method is to drill holes at the end of an existing crack to effectively reduce the crack driving force. For pressurized components, a device can be added to the component to control unstable crack growth (for example, crack arresting devices for pipelines), (see Annex 9A, reference [44]).

9.6.2.3 *Remediation Method 3* – Performing physical changes to the process stream (see Part 4, paragraph 4.6.2.1). This method can be used to reduce the crack driving force (reduction in pressure) or to provide an increase in the material toughness at the condition associated with highest stress state. This may involve the introduction of a warm start-up and/or shut-down cycle into equipment operating procedures such that the temperature of the component is high enough to ensure adequate material toughness at load levels associated with the highest state of stress.

9.6.2.4 *Remediation Method 4* – Application of solid barrier linings or coatings to keep the environment isolated from the metal (see Part 4, paragraph 4.6.2.2). In this method, the flaw is isolated from the process environment to minimize the potential for environmentally assisted subcritical crack growth.

9.6.2.5 *Remediation Method 5* – Injection of water and/or chemicals on a continuous basis to modify the environment or the surface of the metal (see Part 4, paragraph 4.6.2.3). In this method, the process environment is controlled to minimize the potential for environmentally assisted subcritical crack growth.

9.6.2.6 *Remediation Method 6* – Application of weld overlay (see Part 4, paragraph 4.6.2.4). In this method, weld overlay is applied to the component surface opposite to the surface containing the cracks to introduce a compressive residual stress field at the location of the crack (for an example see Annex 9A, reference [9]). The compressive residual stress field should eliminate any future crack growth. This type of repair also increases the structural integrity of the component containing the flaw by the addition of extra wall thickness provided by the weld overlay.

9.6.2.7 *Remediation Method 7* – Use of leak monitoring and leak-sealing devices.

9.7 In-Service Monitoring

9.7.1 Monitoring of Subcritical Crack Growth

In all cases where subcritical in-service crack growth is permitted by the methods of this document, in-service monitoring or monitoring at a shutdown inspection, as applicable, of the crack growth by NDE may be required. The applicable NDE method will depend on the specific case.

9.7.2 Validation of Monitoring Method

Before returning the component to service, the monitoring method should be validated to ensure that it could adequately detect the size of the flaw under service conditions. The NDE sensitivity and flaw sizing uncertainty associated with the in-service monitoring procedure should be considered when specifying a limiting maximum flaw size for continued operation.

9.8 Documentation

9.8.1 General

The documentation of the FFS Assessment should include the information cited in Part 2, paragraph 2.8.

9.8.2 Assessment Procedure

The following information should be documented for an FFS Assessment carried out according to the procedures of this Part.

a) Loading Conditions – normal operation and upset conditions (see Annex 2C and Annex 2D for a summary of loading conditions) additional loads and stresses considered in the assessment, e.g., stresses from supplement loads, thermal gradients, and residual stresses; the stress analysis methods from handbooks or numerical solution technique such as finite-element analysis; and categorization of stress results (Levels 1, 2, and 3).

b) Material Properties – The material specification of the component containing the flaw; yield stress, ultimate tensile stress, and fracture toughness at the temperature of interest including whether the data was obtained by direct testing or indirect means and the source and validity of data; and a description of the process environment including its effect on material properties (Levels 1, 2, and 3).

c) Characterization of Flaw – The flaw location, shape, and size; NDE method used for flaw sizing and allowance for sizing errors; and whether re-characterization of the flaw was required (Levels 1, 2, and 3).

d) Assessment Level – Calculation results and any assumptions, deviations or modifications used for the assessment level (Levels 1, 2, and 3).

e) Partial Safety Factors – A list of the Partial Safety Factors used in the assessment (Level 3).

f) Reference Stress Solution – The source of the reference stress solutions, e.g., handbook solution or finite-element analysis, used in the assessment including whether the local and/or global collapse was considered (Levels 2 and 3).

g) Stress Intensity Factor Solution – The source of stress intensity factor solutions, e.g., handbook solution or finite-element analysis, used in the assessment (Levels 2 and 3).

h) Failure Assessment Diagram – whether the Level 2 recommended curve, a material specific curve including the source and validity of stress-strain data, or a curve derived from J-analysis is used in the assessment (Level 3).

i) Flaw Growth – whether any allowance is made for crack extension by sub-critical crack growth mechanism, e.g., fatigue or stress corrosion cracking; the crack growth models, and associated constants utilized from technical publications or laboratory measurements should be summarized (Level 3).

j) In-Service Margins – The results calculated for each loading condition of interest and for each category of analysis undertaken; assessment points should be displayed on the appropriate failure assessment diagram (Level 3).

k) Sensitivity Analysis – A listing of the input parameters used to perform sensitivity studies including loads, material properties, flaw size, etc.; the results of each individual study should be summarized (Levels 2 and 3).

9.8.3 Remediation Methods

All remediation methods shall be documented including the type of method and reason for application of the method.

9.8.4 In-Service Monitoring

If an in-service monitoring system is instituted because of the potential for sub-critical crack growth (see paragraph 9.7) or a leak detection system is installed as the result of a LBB assessment (see paragraph 9.5.2.7), then the following documentation should be kept with the equipment files:

a) Specification for the system,

b) Procedures for installation of the system,

c) System validation and calibration,

d) Procedures for recording data, and

e) All data readings while the component is in-service readings.

9.9 Nomenclature

a	depth of the crack-like flaw.
a_{eff}	effective depth of the crack-like flaw.
a_m	measured depth of the crack-like flaw.
α	angle of the crack measured from the principal plane (see Figure 9.2).
B	biaxial stress ratio.
c_m	measured half length of the crack-like flaw.
c_o	initial half length of the crack-like flaw.
CET	Critical Exposure Temperature (see Part 3).
COA_p	crack opening area of a plate.
COA_s	crack opening area of a shell.
c	half-length of the existing flaw.
$2c$	full length of the existing flaw.
c_{LBB}	half-length of the postulated through-wall flaw.
d	size of the ligament for an embedded flaw (see Figure 9.1(c)).
d_m	measured size of the ligament for an embedded flaw (see Figure 9.1(c)).
D	inside diameter of the component containing the crack-like flaw including metal loss and future corrosion allowance, as applicable.
E	Young's Modulus.
ε_{ref}	reference strain obtained from the true stress-strain curve at a true stress equal to $L_r^P \sigma_{ys}$.
J^{SR}	$J-integral$ based on residual stress.
K_I^P	stress intensity factor based on primary stresses.

K_I^{SR} stress intensity factor based on secondary and residual stresses.

K_J^{SR} stress intensity factor based on secondary and residual stresses corrected for plasticity.

K_{mat} value of the material fracture toughness used in the assessment.

K_r toughness ratio.

L_r^P load ratio based on primary stress.

$L_{r(\max)}^P$ maximum permitted value of L_r^P (see Figure 9.19).

ν Poisson's ratio.

P_m primary membrane stress.

P_b primary bending stress.

R inside radius of the component containing the crack-like flaw including metal loss and future corrosion allowance, as applicable.

S_{srf} secondary and residual stress reduction factor.

σ applied tensile stress.

σ_f flow stress (see Annex 2E).

σ_{ys} yield strength at the assessment temperature (see Annex 2E).

σ_{ref}^P reference stress based on the primary stress.

σ_{ref}^{SR} reference stress based on the secondary and residual stress.

ξ parameter used in the calculation of plasticity correction factor Φ.

Φ plasticity correction factor.

t thickness of the component containing the crack-like flaw including metal loss and future corrosion allowance, as applicable.

T_{ref} reference Temperature.

W correction factor for flaw depth.

W_{Theta} parameter used to determine the correction factor for flaw depth.

X parameter used in the calculation of plasticity correction factor Φ.

9.10 References

References for this Part are provided in Annex 9A – Technical Basis and Validation – Assessment of Crack-Like Flaws.

9.11 Tables

Table 9.1 – Data Required for the Assessment of a Crack-Like Flaw

A summary of the data that should be obtained from a field inspection is provided on this form.

Equipment Identification: _____
Equipment Type: _____ Pressure Vessel _____ Storage Tank _____ Piping Component
Component Type & Location: _____

Data Required for Level 1:
Assessment Temperature (typically the minimum temperature at full pressure): _____
Assessment Pressure: _____
Location of Flaw (*Base Metal, Weld Metal or HAZ*): _____
Surface Location (*ID, OD or Through-Wall*): _____
Flaw Type (*Surface or Embedded*): _____
Flaw Orientation to Weld Seam (*Parallel or Perpendicular*): _____
Flaw Depth and Length (a and $2c$): _____
Flaw Depth Below Surface (d – Embedded Flaw): _____
Axial or Circumferential Crack: _____
Post Weld Heat Treated ($PWHT$): _____
Design Code: _____
Base Material Specification: _____
Weld Material Specification: _____
Wall Thickness: _____
$MAWP$: _____
Process Environment: _____
Design Pressure & Temperature: _____
Cyclic Loading Conditions: _____
Inspection Method – Flaw Length: _____
Inspection Method – Flaw Depth: _____
Inspection Method – Flaw Depth Below Surface: _____

Additional Data Required for Level 2 (In Addition to the Level 1 Data):
Yield Stress (Base Metal): _____
Tensile Stress (Base Metal): _____
Fracture Toughness (Base Metal): _____
Source of Material Data (Base Metal): _____
Yield Stress (Weld Metal): _____
Tensile Stress (Weld Metal): _____
Fracture Toughness (Weld Metal): _____
Source of Material Data (Weld Metal): _____
Yield Stress (HAZ): _____
Tensile Stress (HAZ): _____
Fracture Toughness (HAZ): _____
Source of Material Data (HAZ): _____
Probability of Failure Category: _____

Table 9.2 – Reference Temperature for Use in a Level 1 Assessment

Carbon Steels – 20 Joule or 15 ft-lb Transition Temperature for Each ASME Exemption Curve				
Specified Minimum Yield Strength (SMYS) (ksi)	ASME Exemption Curve			
	A (ºF)	B (ºF)	C (ºF)	D (ºF)
30	90.3	52.3	14.3	-11.7
32	90.0	52.0	14.0	-12.0
34	89.7	51.7	13.7	-12.3
36	89.4	51.4	13.4	-12.6
38	89.1	51.1	13.1	-12.9
40	88.7	50.7	12.7	-13.3
42	88.4	50.4	12.4	-13.6
44	88.1	50.1	12.1	-13.9
46	87.8	49.8	11.8	-14.2
48	87.5	49.5	11.5	-14.5
50	87.1	49.1	11.1	-14.9
Low Alloy Steels – 27 Joule or 20 ft-lb Transition Temperature for Each ASME Exemption Curve				
Specified Minimum Yield Strength (SMYS) (ksi)	ASME Exemption Curve			
	A (ºF)	B (ºF)	C (ºF)	D (ºF)
30	96.8	58.8	20.8	-5.2
32	96.6	58.6	20.6	-5.4
34	96.4	58.4	20.4	-5.6
36	96.1	58.1	20.1	-5.9
38	95.9	57.9	19.9	-6.1
40	95.7	57.7	19.7	-6.3
42	95.5	57.5	19.5	-6.5
44	95.2	57.2	19.2	-6.8
46	95.0	57.0	19.0	-7.0
48	94.8	56.8	18.8	-7.2
50	94.5	56.5	18.5	-7.5
52	94.3	56.3	18.3	-7.7
54	94.0	56.0	18.0	-8.0
56	93.8	55.8	17.8	-8.2
58	93.6	55.6	17.6	-8.4
60	93.3	55.3	17.3	-8.7
62	93.1	55.1	17.1	-8.9
64	92.8	54.8	16.8	-9.2
66	92.5	54.5	16.5	-9.5
68	92.3	54.3	16.3	-9.7
70	92.0	54.0	16.0	-10.0
72	91.8	53.8	15.8	-10.2
74	91.5	53.5	15.5	-10.5
76	91.2	53.2	15.2	-10.8
78	91.0	53.0	15.0	-11.0
80	90.7	52.7	14.7	-11.3
Note: The transition temperatures in this table are determined using Annex 9F, paragraph 9F.2.4.4.				

Table 9.2M – Reference Temperature for Use in a Level 1 Assessment

Carbon Steels – 20 Joule or 15 ft-lb Transition Temperature for Each ASME Exemption Curve				
Specified Minimum Yield Strength (SMYS) (MPa)	ASME Exemption Curve			
	A (ºC)	B (ºC)	C (ºC)	D (ºC)
200	32.3	11.1	-10.0	-24.4
210	32.1	10.9	-10.1	-24.6
220	32.0	10.8	-10.3	-24.7
230	31.9	10.7	-10.4	-24.8
240	31.8	10.6	-10.5	-24.9
260	31.5	10.3	-10.8	-25.2
280	31.3	10.1	-11.0	-25.4
300	31.0	9.8	-11.3	-25.7
320	30.7	9.5	-11.5	-26.0
340	30.5	9.3	-11.8	-26.2
360	30.2	9.0	-12.1	-26.5
Low Alloy Steels – 27 Joule or 20 ft-lb Transition Temperature for Each ASME Exemption Curve				
Specified Minimum Yield Strength (SMYS) (MPa)	ASME Exemption Curve			
	A (ºC)	B (ºC)	C (ºC)	D (ºC)
200	36.0	14.8	-6.3	-20.7
210	35.9	14.7	-6.3	-20.8
220	35.8	14.6	-6.4	-20.9
230	35.7	14.5	-6.5	-21.0
240	35.7	14.5	-6.6	-21.0
250	35.6	14.4	-6.7	-21.1
260	35.5	14.3	-6.8	-21.2
270	35.4	14.2	-6.9	-21.3
280	35.3	14.1	-7.0	-21.4
290	35.2	14.0	-7.1	-21.5
300	35.1	13.9	-7.2	-21.6
310	35.0	13.8	-7.3	-21.7
320	34.9	13.7	-7.3	-21.8
330	34.8	13.6	-7.4	-21.9
340	34.7	13.5	-7.5	-22.0
360	34.5	13.3	-7.7	-22.2
380	34.3	13.1	-7.9	-22.4
400	34.1	12.9	-8.1	-22.6
420	33.9	12.7	-8.3	-22.8
440	33.7	12.5	-8.5	-23.0
460	33.5	12.3	-8.7	-23.2
480	33.3	12.1	-8.9	-23.4
500	33.1	11.9	-9.2	-23.6
520	32.9	11.7	-9.4	-23.8
540	32.7	11.5	-9.6	-24.0
560	32.4	11.2	-9.8	-24.3

Note: The transition temperatures in this table are determined using Annex 9F, paragraph 9F.2.4.4.

Table 9.3 – Plasticity Interaction Factor – Parameter ξ as a Function of L_r^P and X

L_r^P	X																		
	0	0.02	0.04	0.06	0.08	0.1	0.2	0.3	0.4	0.5	1	1.5	2	2.5	3	3.5	4	4.5	≥5
0		1	1	1	1	1	1	1	1	1	1	1	1	1	1	1	1	1	1
0.01	1	1.000	1.000	1.000	1.000	1.000	1.001	1.001	1.002	1.003	1.011	1.019	1.023	1.026	1.028	1.029	1.030	1.031	1.032
0.02	1	1.000	1.000	1.001	1.001	1.001	1.002	1.003	1.004	1.006	1.019	1.031	1.038	1.042	1.044	1.046	1.048	1.051	1.047
0.03	1	1.001	1.001	1.001	1.001	1.002	1.003	1.004	1.006	1.008	1.026	1.040	1.048	1.053	1.056	1.059	1.060	1.061	1.062
0.04	1	1.001	1.001	1.001	1.002	1.002	1.004	1.006	1.008	1.011	1.031	1.047	1.056	1.061	1.065	1.068	1.071	1.076	1.081
0.06	1	1.002	1.002	1.003	1.003	1.004	1.006	1.009	1.012	1.016	1.039	1.058	1.068	1.074	1.078	1.083	1.087	1.092	1.099
0.08	1	1.002	1.003	1.004	1.004	1.005	1.008	1.012	1.016	1.020	1.045	1.066	1.077	1.084	1.088	1.093	1.098	1.103	1.112
0.1	1	1.004	1.004	1.005	1.006	1.007	1.011	1.015	1.020	1.024	1.050	1.072	1.084	1.092	1.097	1.102	1.108	1.114	1.122
0.12	1	1.005	1.006	1.007	1.008	1.009	1.013	1.018	1.023	1.028	1.054	1.077	1.090	1.099	1.104	1.110	1.116	1.122	1.132
0.14	1	1.007	1.008	1.009	1.010	1.011	1.016	1.022	1.027	1.032	1.057	1.082	1.096	1.105	1.111	1.117	1.123	1.131	1.142
0.16	1	1.008	1.010	1.011	1.012	1.013	1.019	1.025	1.031	1.035	1.060	1.086	1.101	1.111	1.117	1.123	1.130	1.138	1.149
0.18	1	1.010	1.012	1.013	1.014	1.016	1.022	1.029	1.034	1.038	1.063	1.090	1.106	1.116	1.124	1.129	1.137	1.145	1.158
0.2	1	1.012	1.014	1.015	1.017	1.018	1.026	1.033	1.038	1.041	1.066	1.094	1.110	1.121	1.128	1.136	1.144	1.153	1.166
0.3	1	1.027	1.029	1.031	1.033	1.035	1.045	1.051	1.054	1.055	1.080	1.113	1.133	1.146	1.155	1.165	1.175	1.187	1.205
0.4	1	1.049	1.052	1.054	1.057	1.059	1.068	1.071	1.071	1.071	1.099	1.135	1.157	1.173	1.184	1.196	1.209	1.225	1.248
0.5	1	1.082	1.085	1.087	1.089	1.091	1.096	1.096	1.095	1.095	1.126	1.164	1.187	1.203	1.215	1.229	1.246	1.266	1.292
0.6	1	1.126	1.128	1.129	1.130	1.131	1.131	1.129	1.128	1.129	1.161	1.196	1.218	1.234	1.248	1.262	1.284	1.311	1.337
0.7	1	1.176	1.175	1.175	1.175	1.174	1.171	1.169	1.168	1.169	1.195	1.224	1.242	1.256	1.269	1.288	1.314	1.343	1.365
0.8	1	1.215	1.214	1.212	1.211	1.210	1.204	1.200	1.198	1.196	1.210	1.228	1.241	1.252	1.267	1.291	1.316	1.341	1.355
0.9	1	1.215	1.212	1.210	1.208	1.206	1.198	1.191	1.185	1.180	1.178	1.184	1.190	1.199	1.218	1.240	1.259	1.271	1.272
1	1	1.133	1.130	1.128	1.125	1.123	1.112	1.102	1.094	1.087	1.070	1.067	1.069	1.080	1.098	1.105	1.104	1.094	1.073
1.1	1	0.951	0.948	0.946	0.943	0.941	0.930	0.921	0.912	0.905	0.884	0.877	0.882	0.887	0.879	0.861	0.842	0.820	0.801
1.2	1	0.710	0.708	0.707	0.705	0.703	0.695	0.688	0.682	0.677	0.661	0.658	0.649	0.633	0.613	0.597	0.583	0.571	0.561
1.3	1	0.498	0.497	0.496	0.495	0.494	0.490	0.486	0.483	0.480	0.471	0.461	0.449	0.439	0.426	0.427	0.420	0.415	0.413
1.4	1	0.376	0.375	0.375	0.375	0.374	0.373	0.371	0.370	0.368	0.363	0.361	0.359	0.358	0.357	0.355	0.354	0.351	0.351
1.5	1	0.334	0.334	0.333	0.333	0.333	0.332	0.331	0.331	0.330	0.330	0.331	0.332	0.333	0.332	0.333	0.331	0.333	0.331
1.6	1	0.320	0.319	0.319	0.319	0.319	0.318	0.318	0.317	0.317	0.317	0.319	0.320	0.321	0.320	0.320	0.322	0.319	0.319
1.7	1	0.308	0.308	0.308	0.308	0.308	0.307	0.307	0.306	0.306	0.306	0.307	0.308	0.309	0.309	0.308	0.309	0.308	0.308
1.8	1	0.296	0.296	0.296	0.296	0.296	0.295	0.295	0.294	0.294	0.294	0.295	0.296	0.296	0.295	0.297	0.295	0.297	0.292
1.9	1	0.283	0.283	0.283	0.283	0.282	0.282	0.282	0.281	0.281	0.281	0.281	0.282	0.282	0.284	0.283	0.281	0.280	0.280
≥2	1	0.268	0.268	0.268	0.268	0.268	0.267	0.267	0.267	0.266	0.266	0.266	0.266	0.266	0.262	0.261	0.256	0.263	0.266

9.12 Figures

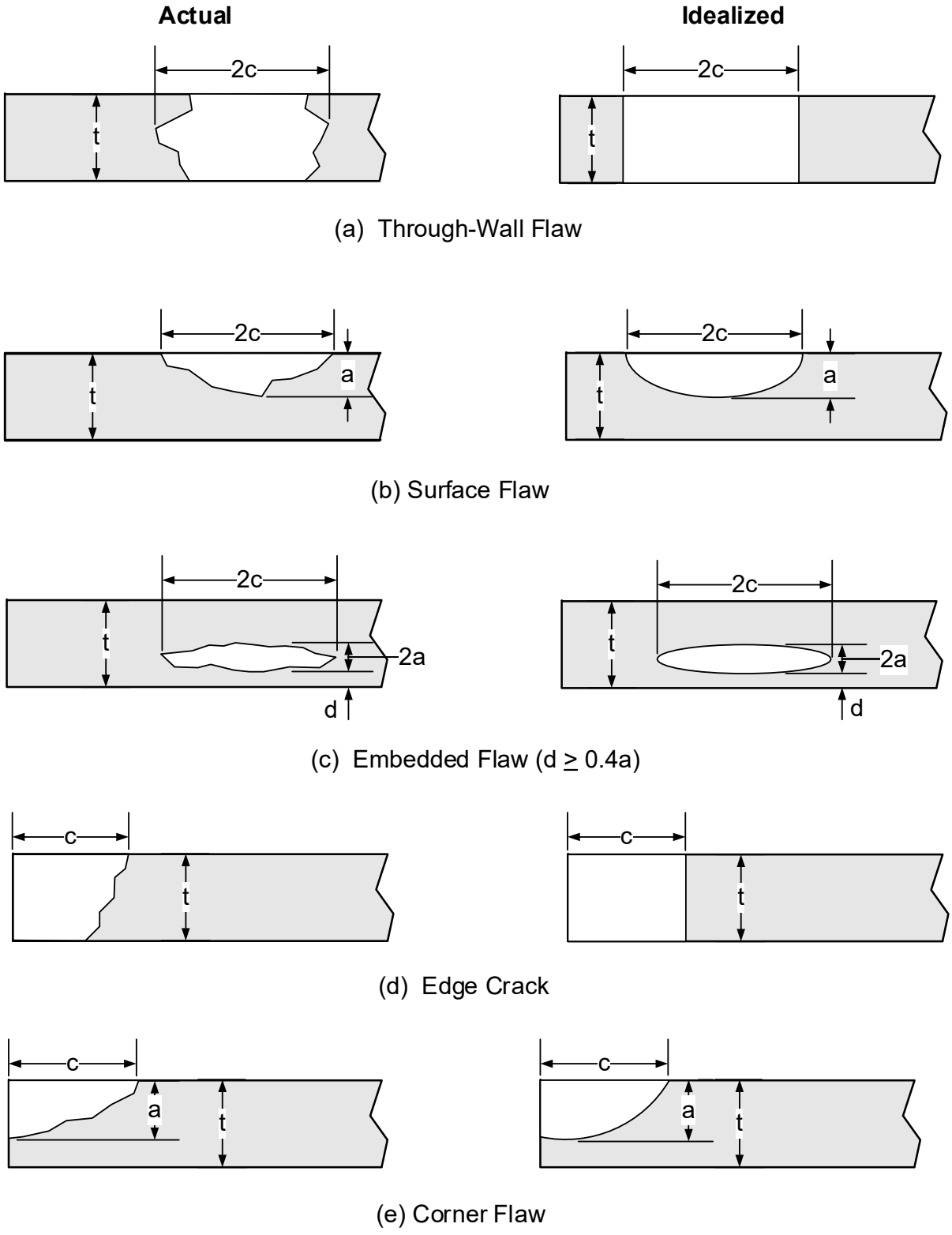

(a) Through-Wall Flaw

(b) Surface Flaw

(c) Embedded Flaw (d ≥ 0.4a)

(d) Edge Crack

(e) Corner Flaw

Figure 9.1 – Nomenclature and Idealized Shapes of Crack-Like Flaws

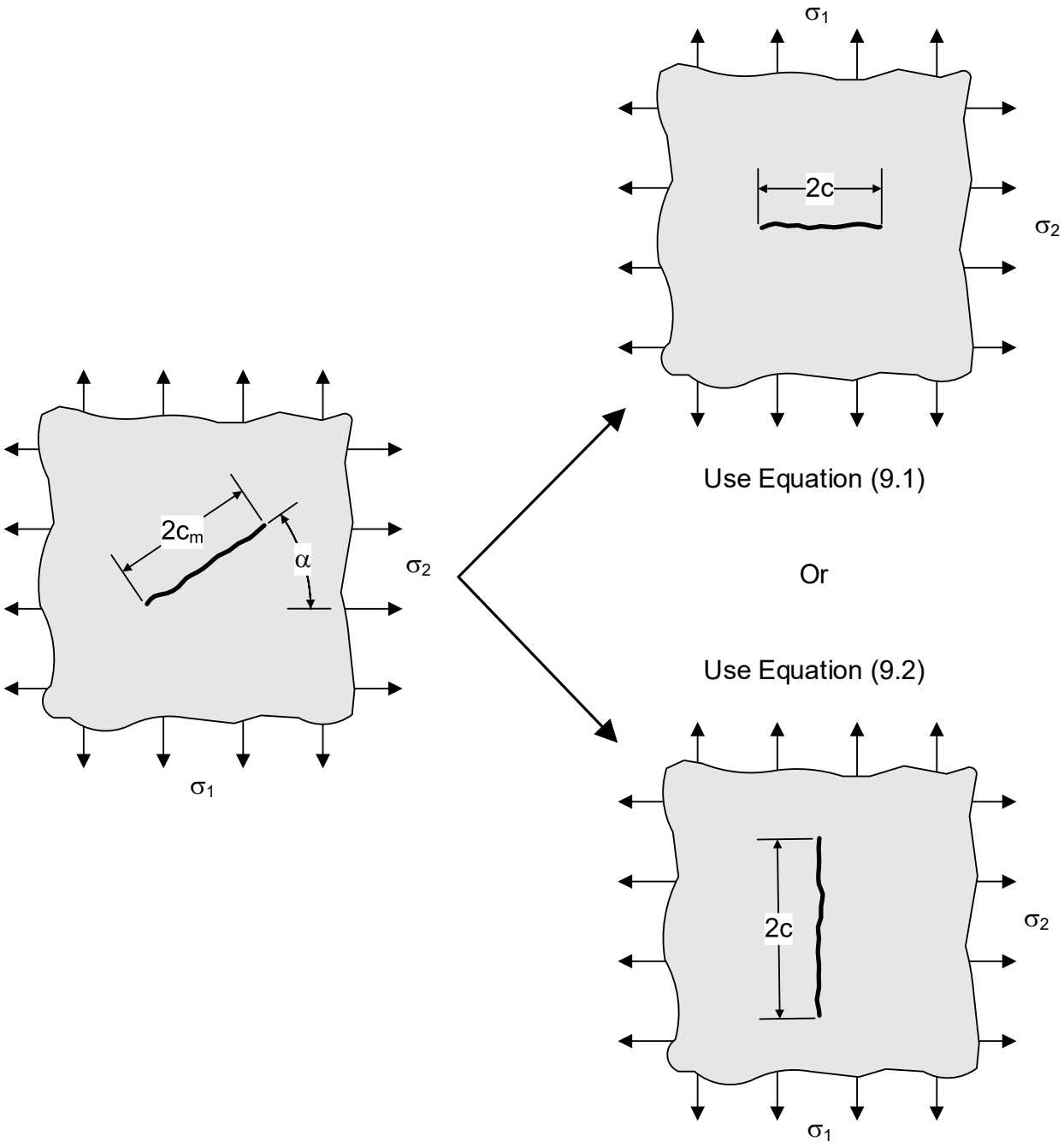

Figure 9.2 – Procedure for Defining an Effective Flaw Length on a Principal Stress Plane

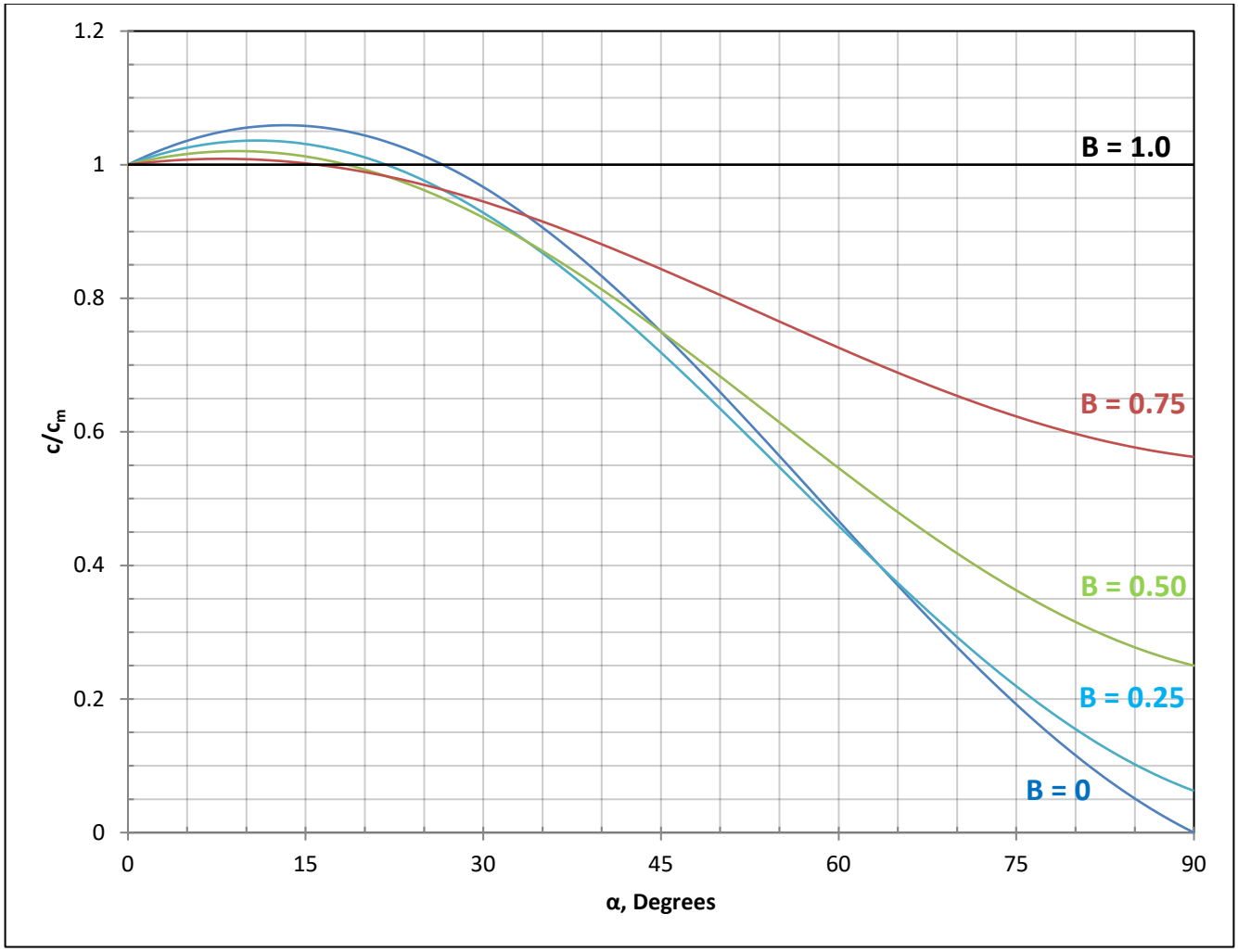

Notes:

1. The figure is a plot of Equation (9.1).
2. B in this figure is the biaxial stress ratio (see Equation (9.3)).

Figure 9.3 – Equivalent Mode I Crack Length as a Function of α and the Stress Biaxiality Ratio

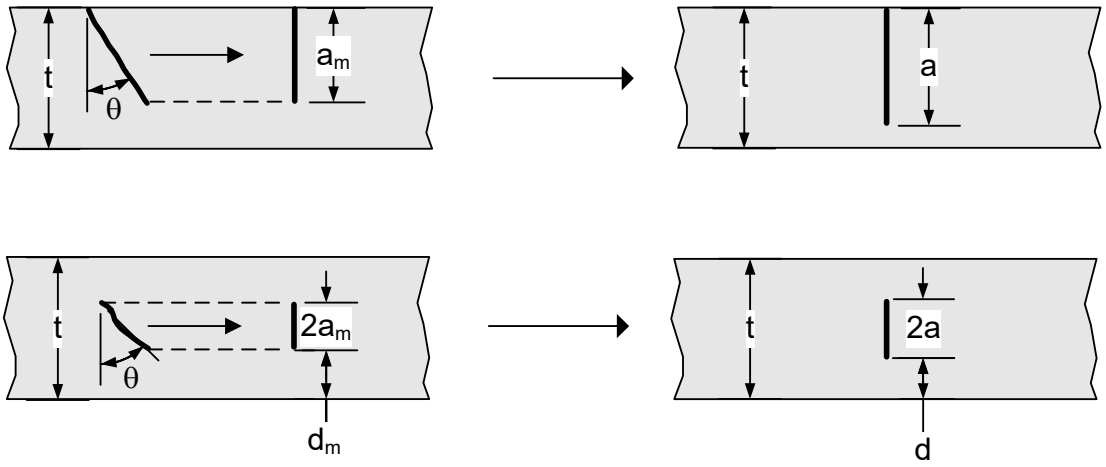

Project the Flaw Onto the Principal Plane a = Wa_m, W is Determined Using Figure 9.5

(a) Planar Crack-Like Flaw

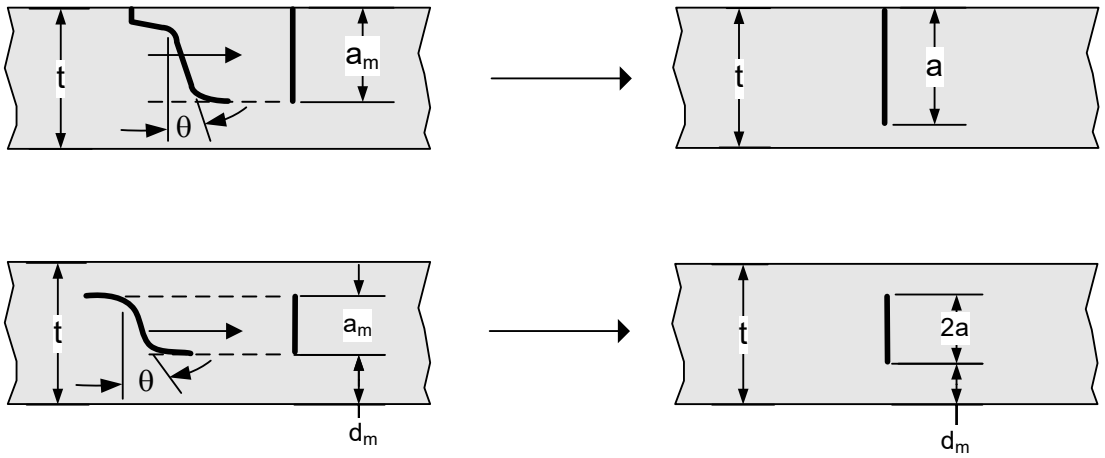

Project the Flaw Onto the Principal Plane a = Wa_m, W is Determined Using Figure 9.5

(b) Stepwise Crack-Like Flaw

Note:

1. Project the flaw onto the principle plane. For a surface flaw, $a = W \cdot a_m$, and for an embedded flaw $2a = W \cdot 2a_m$, were W is determined using Figure 9.5.
2. For an embedded flaw, d_m and d are the minimum distance from the flaw to the surface.

Figure 9.4 – Procedure for Defining the Effective Depth of a Flaw that is Oriented at an Oblique Angle

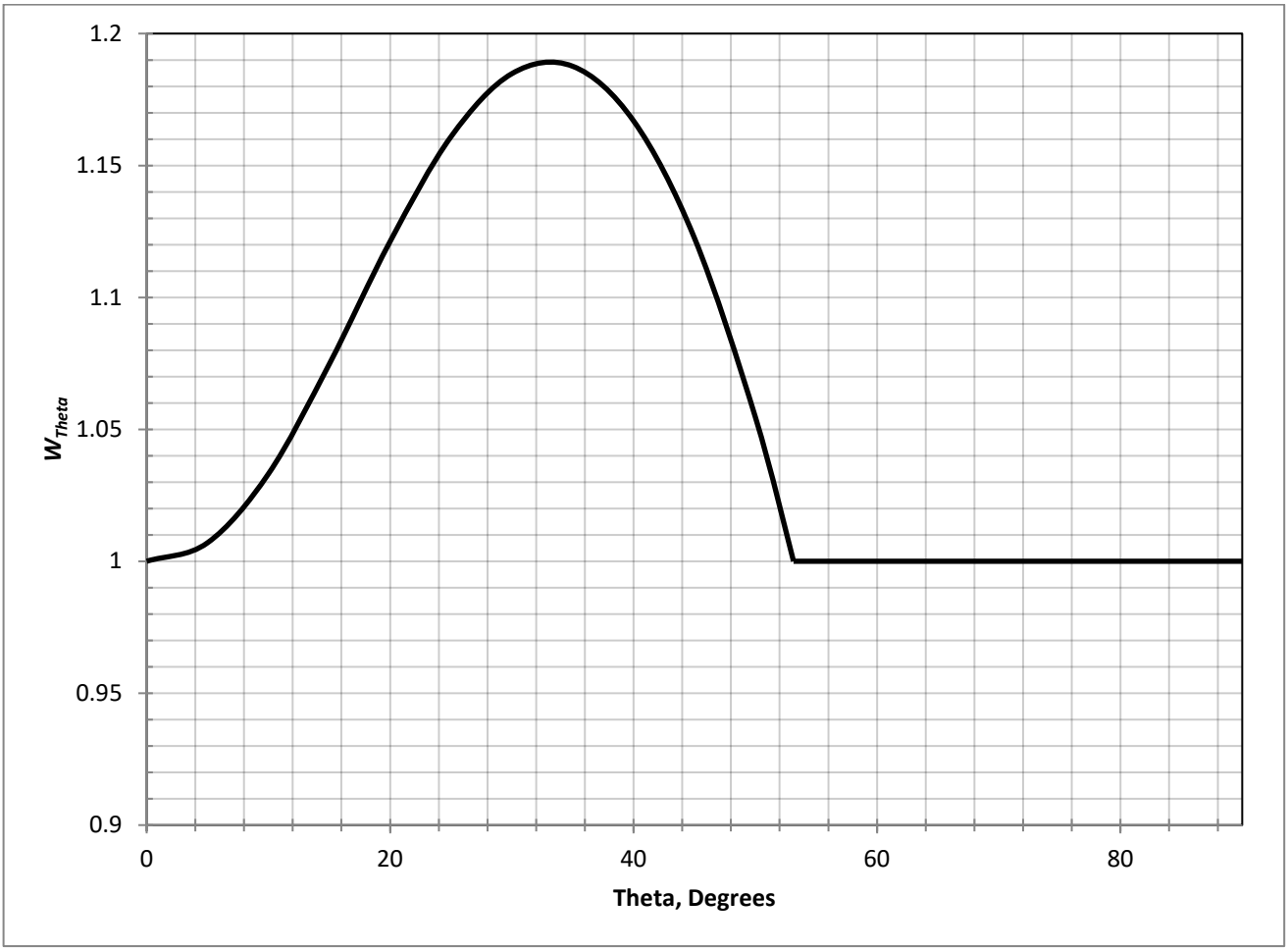

Notes:

1. The figure is a plot of Equation (9.7).
2. Theta in this figure angle of the flaw measured from the normal in the through-thickness direction (see Figure 9.4).

Figure 9.5 – Equivalent Mode I Crack Depth as a Function of the θ Angle.

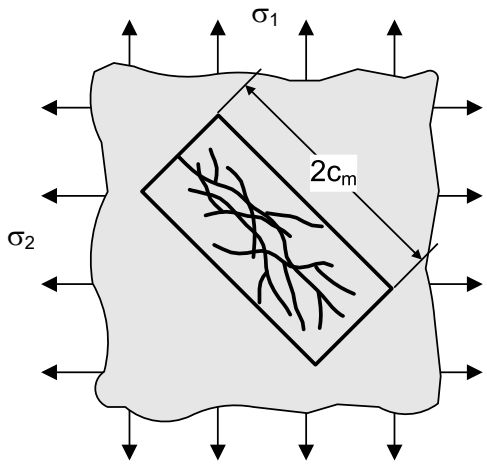

(a) Draw a Rectangle Around the Affected Area

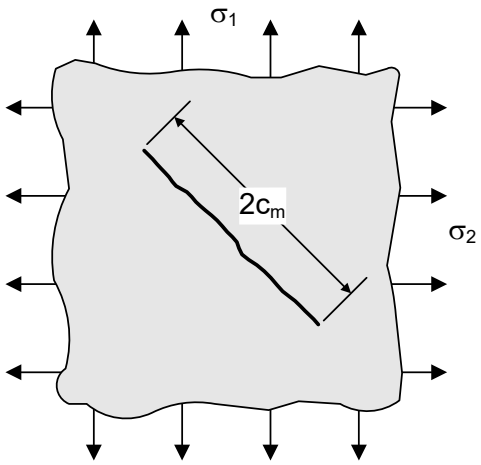

(b) Idealize the Area as a Planar Flaw with Length Equal to the Length of the Rectangle

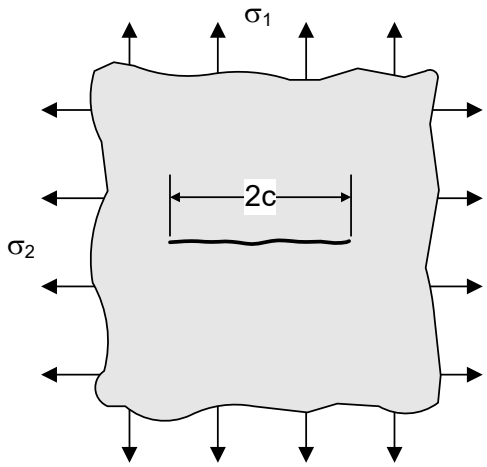

(c) Define an Effective Flaw Length on a Principal Stress Plane ($\sigma_1 \geq \sigma_2$)

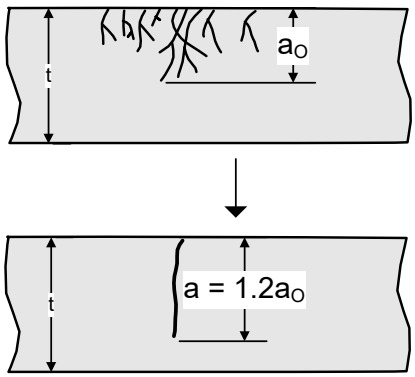

(d) Define the Effective Flaw Depth as 1.2 Times the Maximum Depth of the Branched Network

Figure 9.6 – Procedure for Treating Branched Cracking

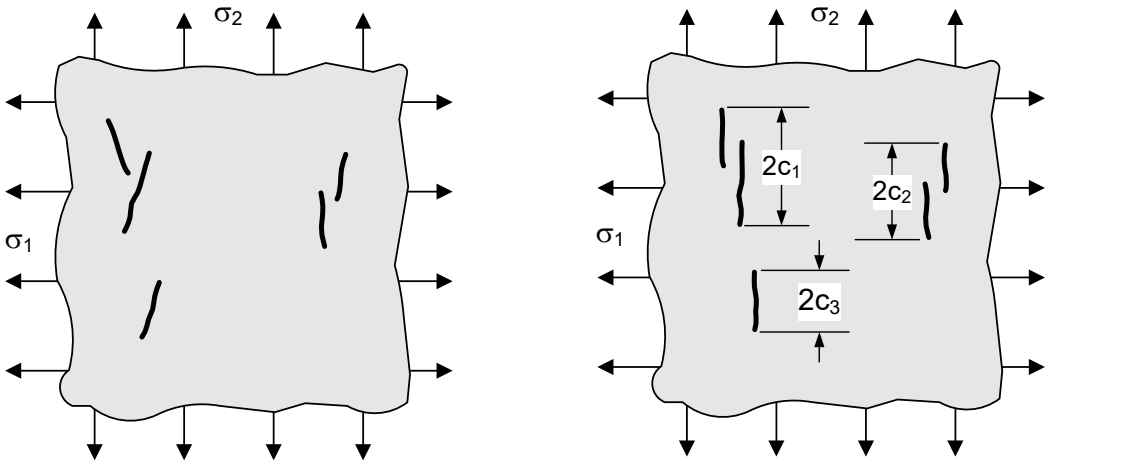

(a) Initial Configuration

(b) After Application of STEP-1 in Paragraph 9.3.6.5

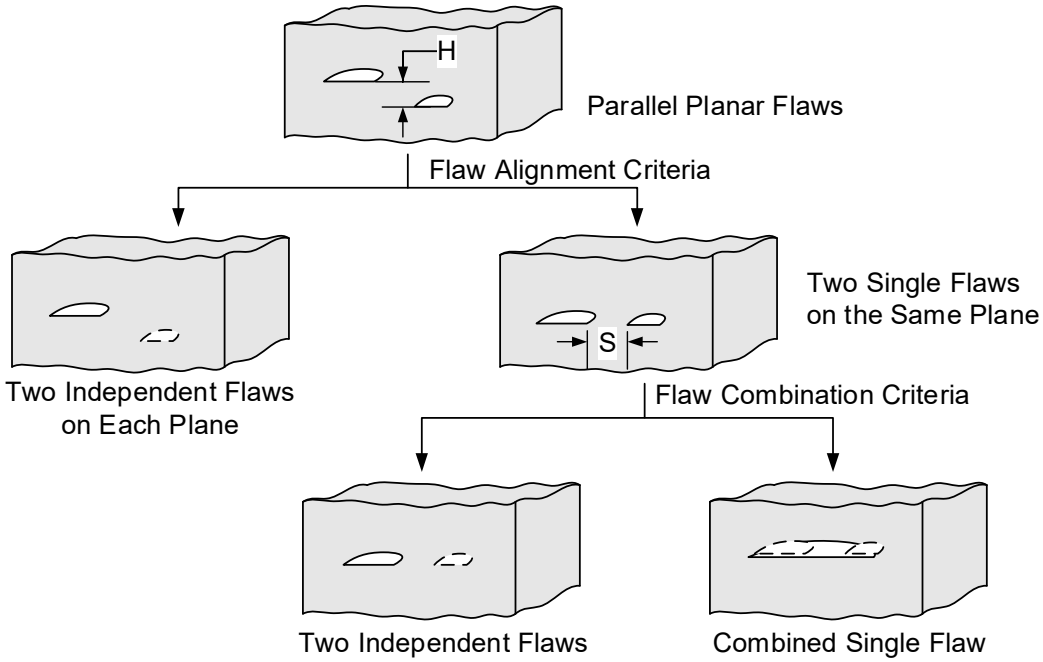

(c) After Projecting Interacting Flaws Onto a Single Plane

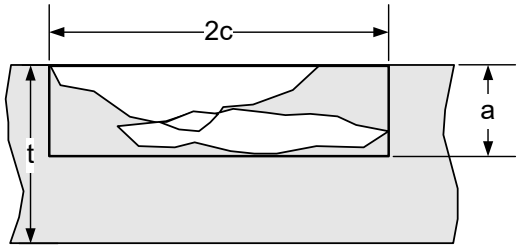

(d) Definition of Effective Dimensions of Flaws that Overlap After Projection Onto a Single Plane

Figure 9.7 – Treatment of Multiple Crack-Like Flaws

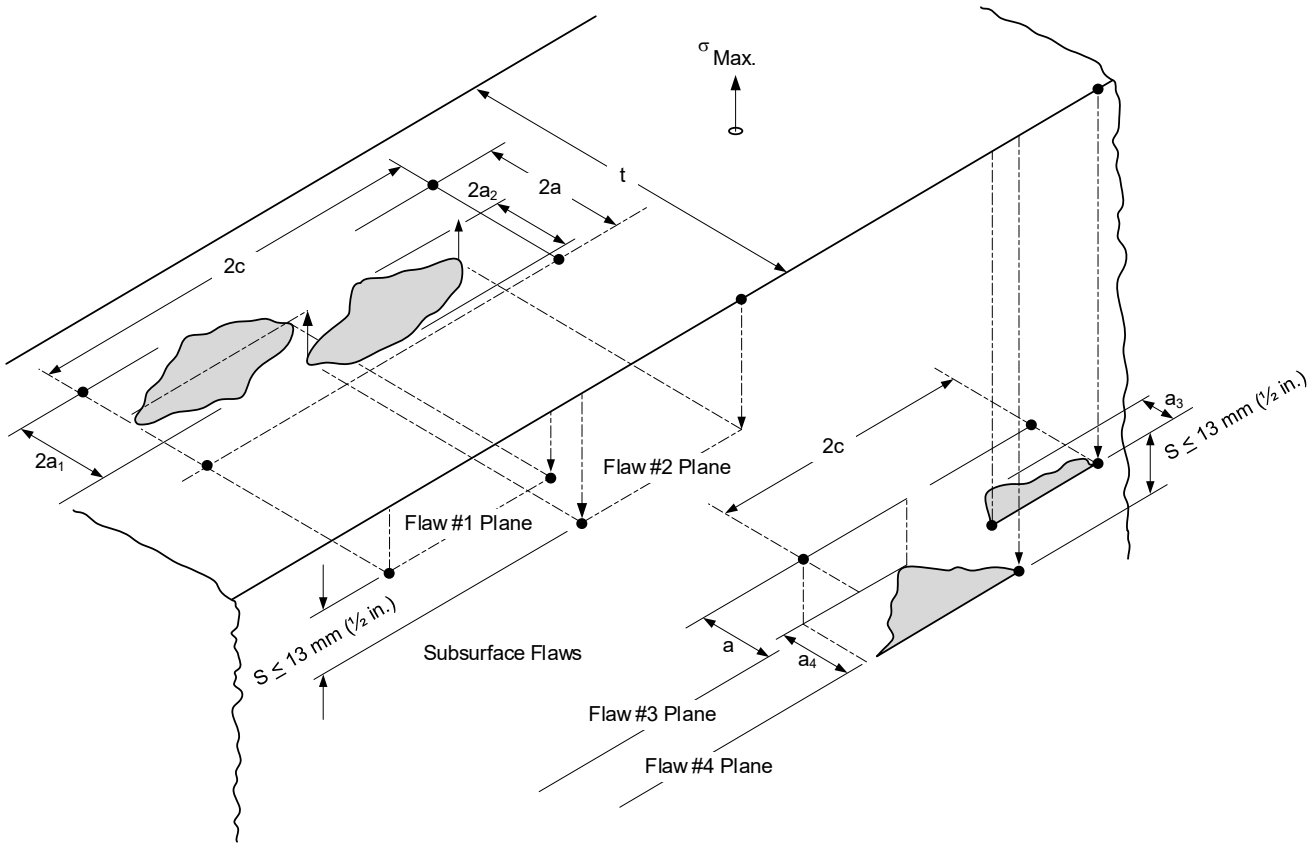

Figure 9.8(a) – Flaw Alignment and Combination Criteria – Alignment Criteria for Parallel Planar Flaws

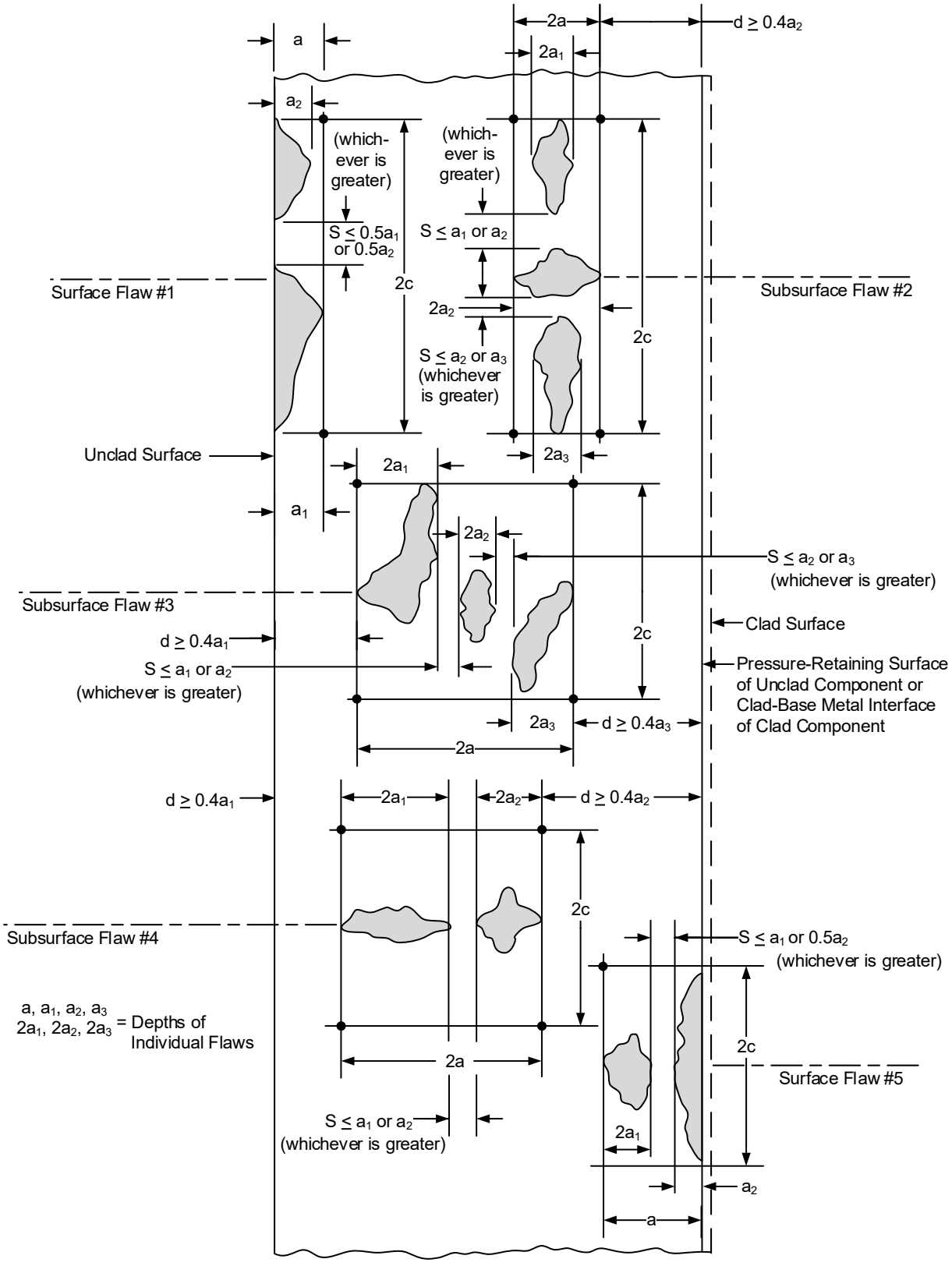

Figure 9.8(b) – Flaw Alignment and Combination Criteria – Combination Criteria for Multiple Planar Flaws

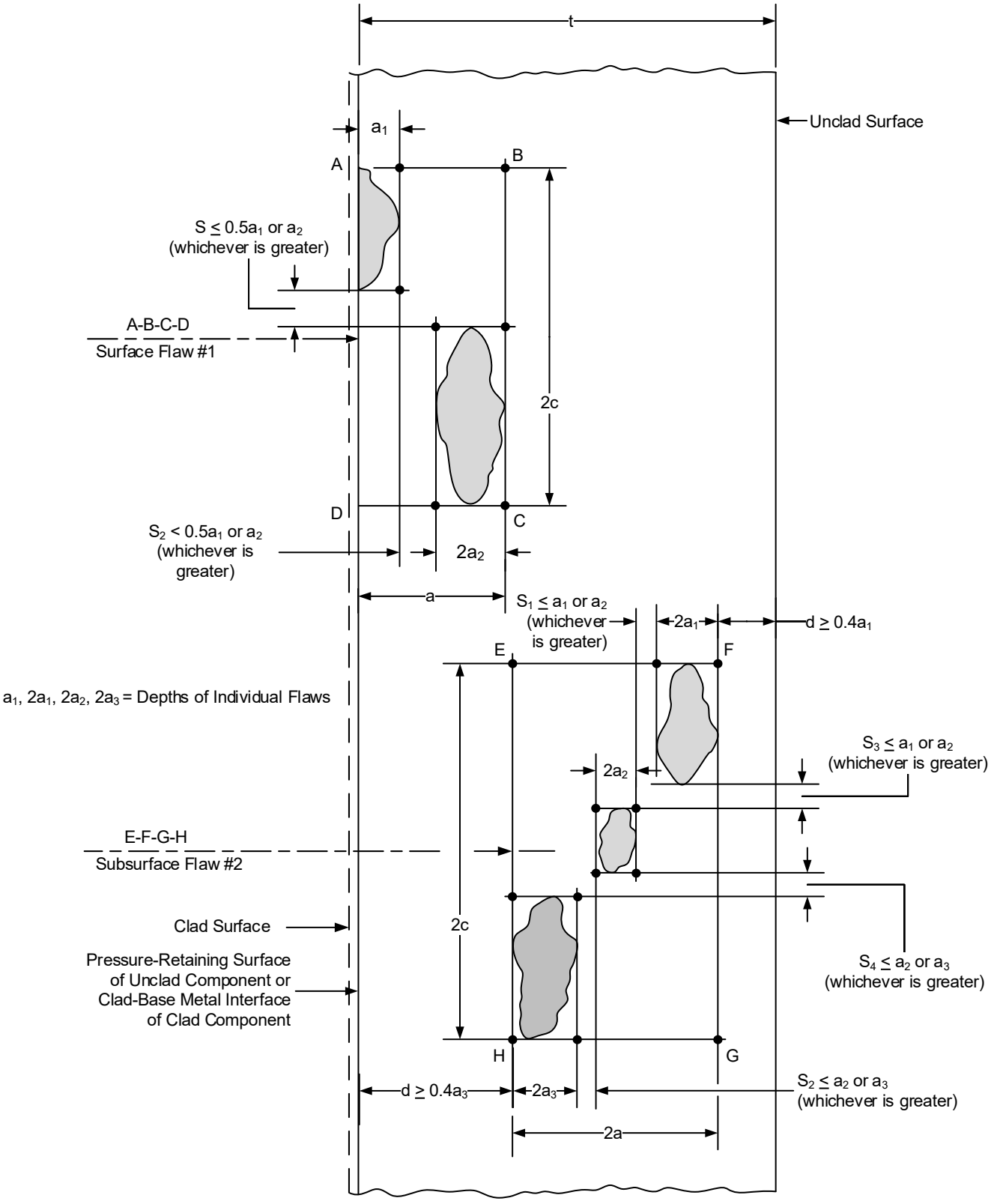

Figure 9.8(c) – Flaw Alignment and Combination Criteria – Combination Criteria for Nonaligned Coplanar Flaws

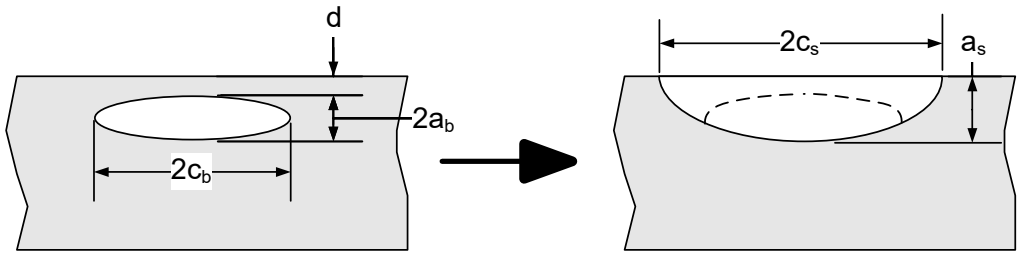

$2c_s = 2c_b + 2d$
$a_s = 2a_b + d$

(a) Embedded Flaw Re-categorized as a Surface Flaw

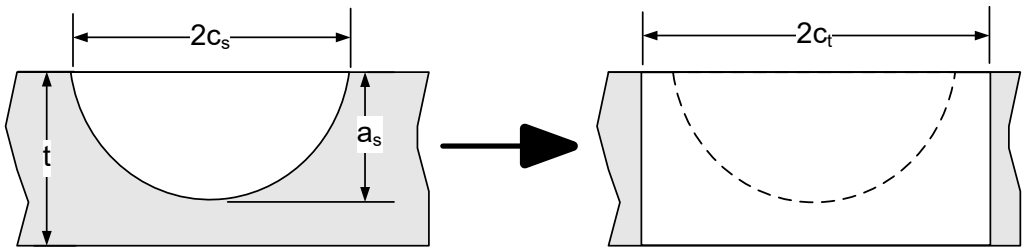

$2c_t = 2c_s + 2(t - a_s)$

(b) Surface Flaw Re-categorized as a Through-Wall Flaw

Figure 9.9 – Flaw Dimensions after Recategorization

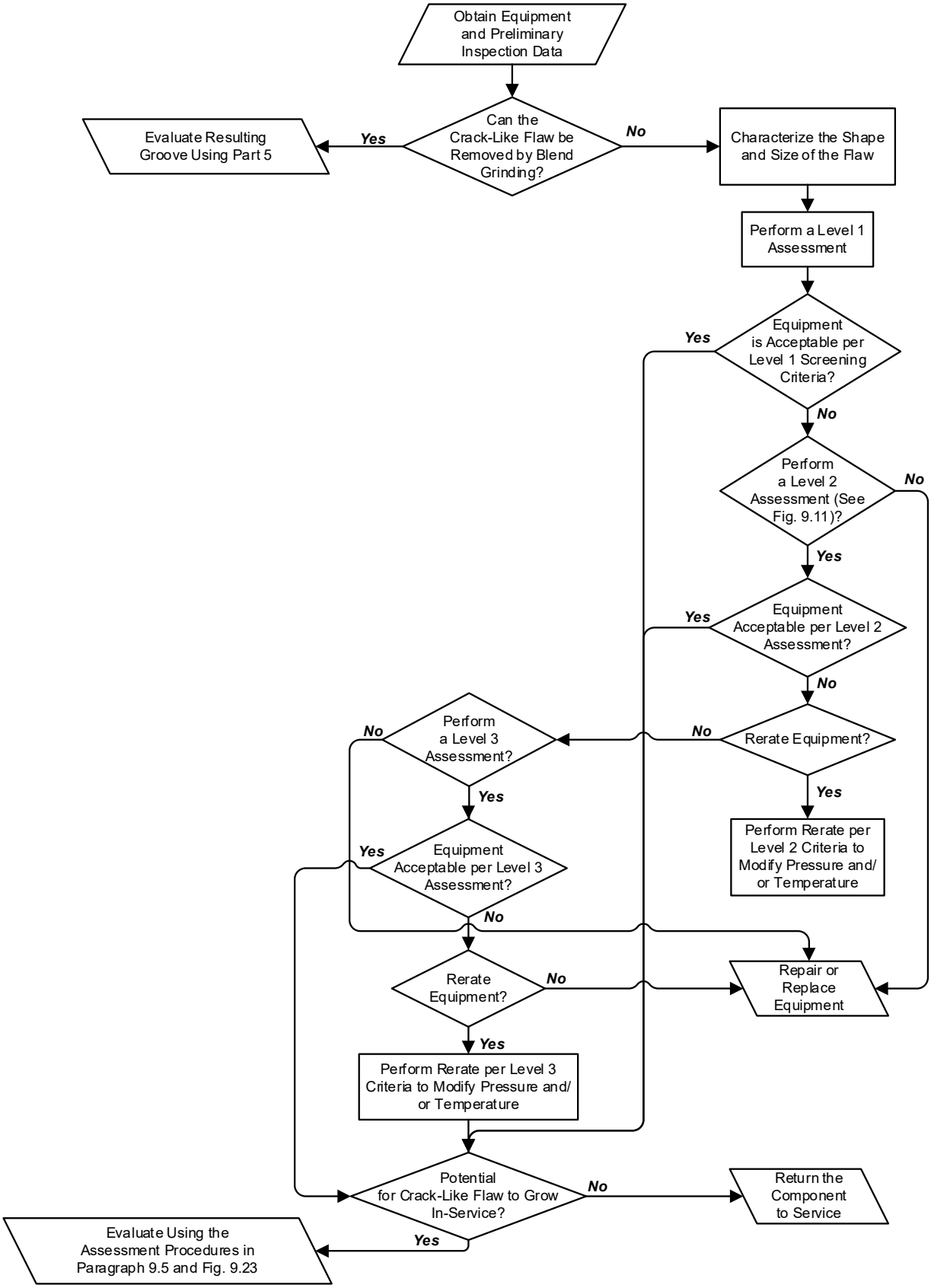

Figure 9.10 – Overview of the Assessment Procedures to Evaluate a Component with Crack-Like Flaws

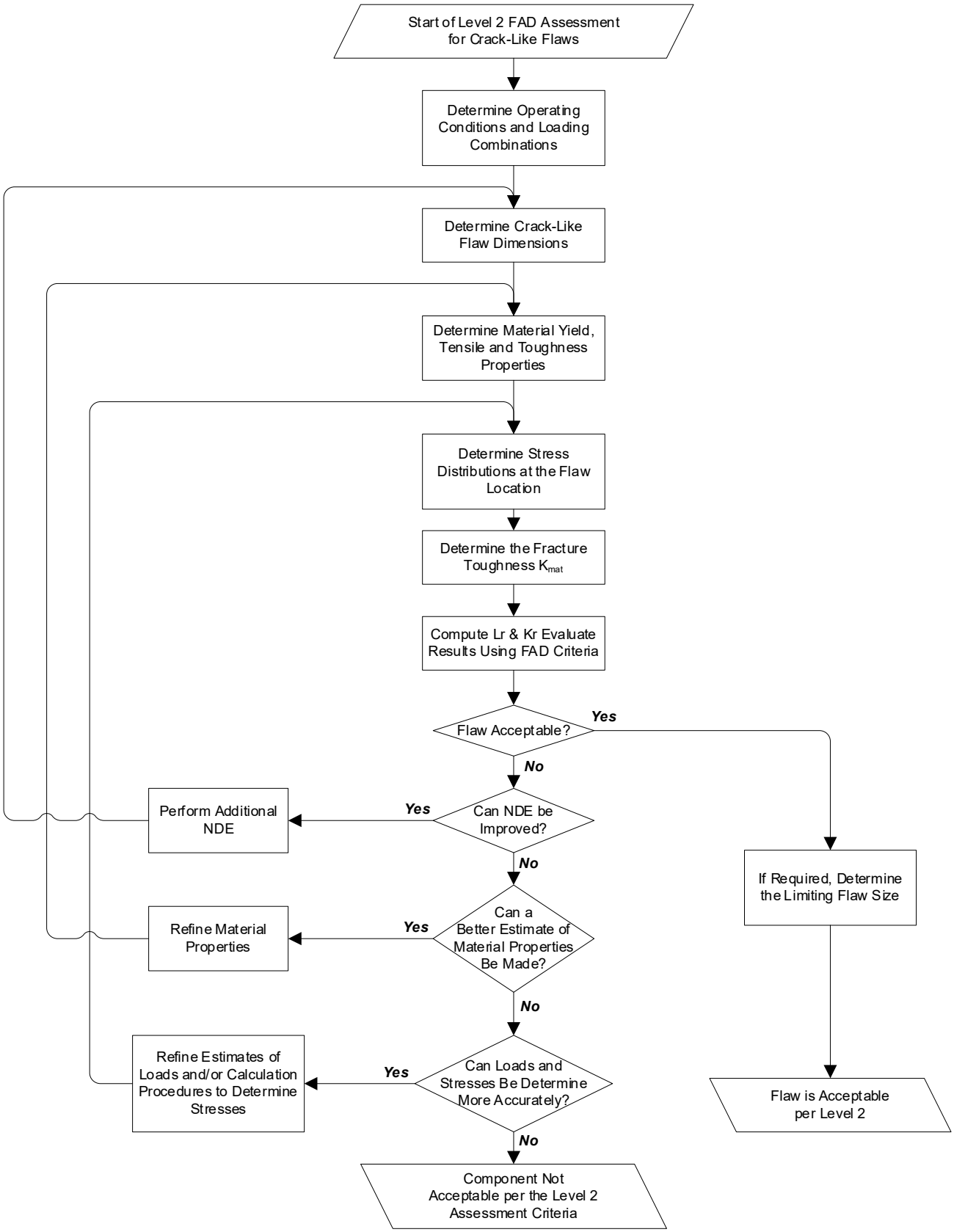

Figure 9.11 – Overview of the Level 2 Assessment Procedure for a Non-Growing Crack-Like Flaw

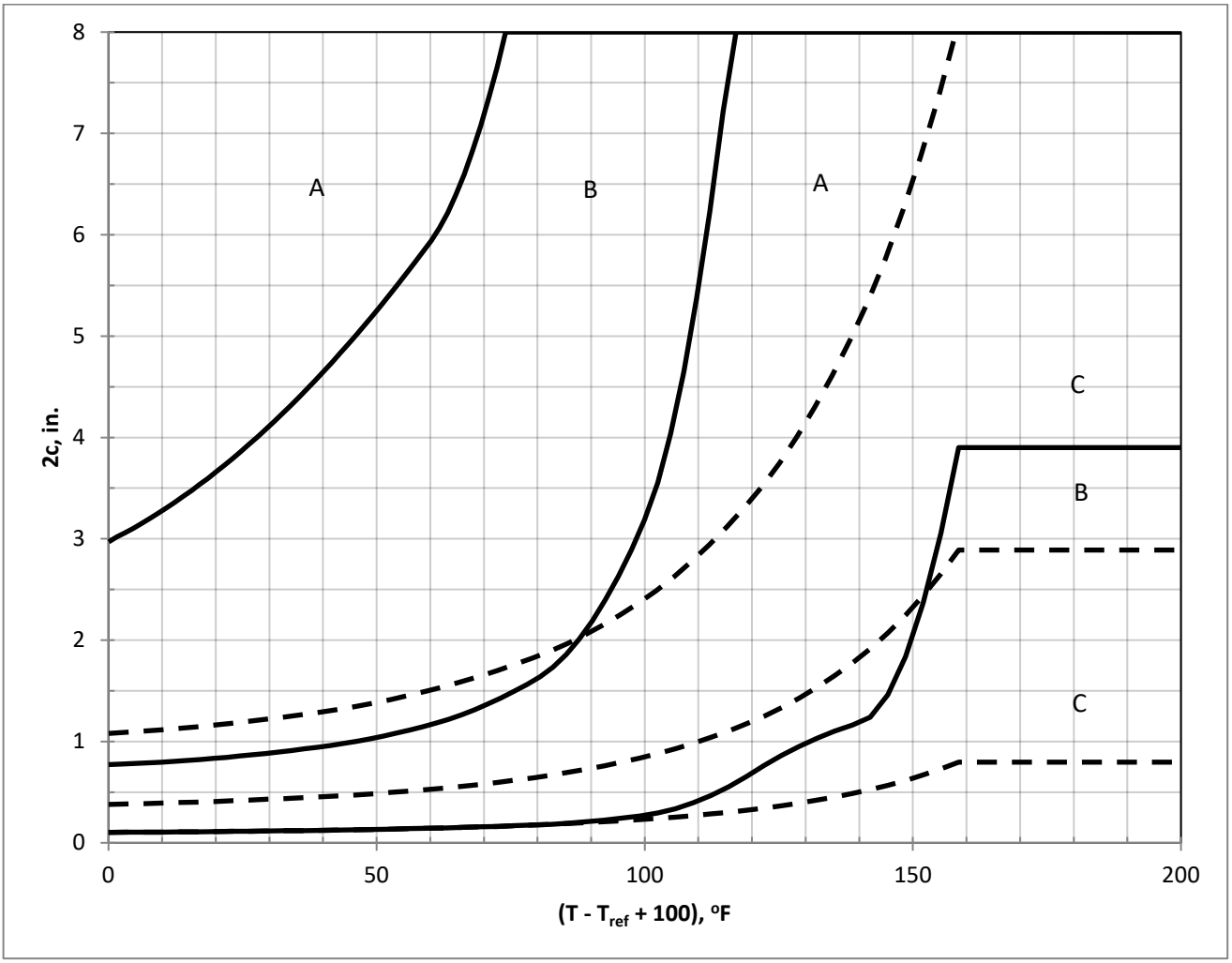

Notes:

1. Definition of Screening Curves (solid line ¼-t flaw, dashed line 1-t flaw):
   A – Allowable flaw size in base metal.
   B – Allowable flaw size in weld metal that has been subject to $PWHT$.
   C – Allowable flaw size in weld metal that has not been subject to $PWHT$.
2. Crack dimension for a 1-t and ¼-t flaw are shown in Annex 9B, Figures 9B.1 and 9B.2.
3. See paragraph 9.2.2(e)(1) for restrictions and limitations.
4. Guidelines for establishing the Reference Temperature, T_{ref}, are covered in paragraph 9.4.2.2(e).
5. The maximum permitted flaw length from this curve is $2c = 8\ in.$

Figure 9.12 – Level 1 Assessment – Flat Plate

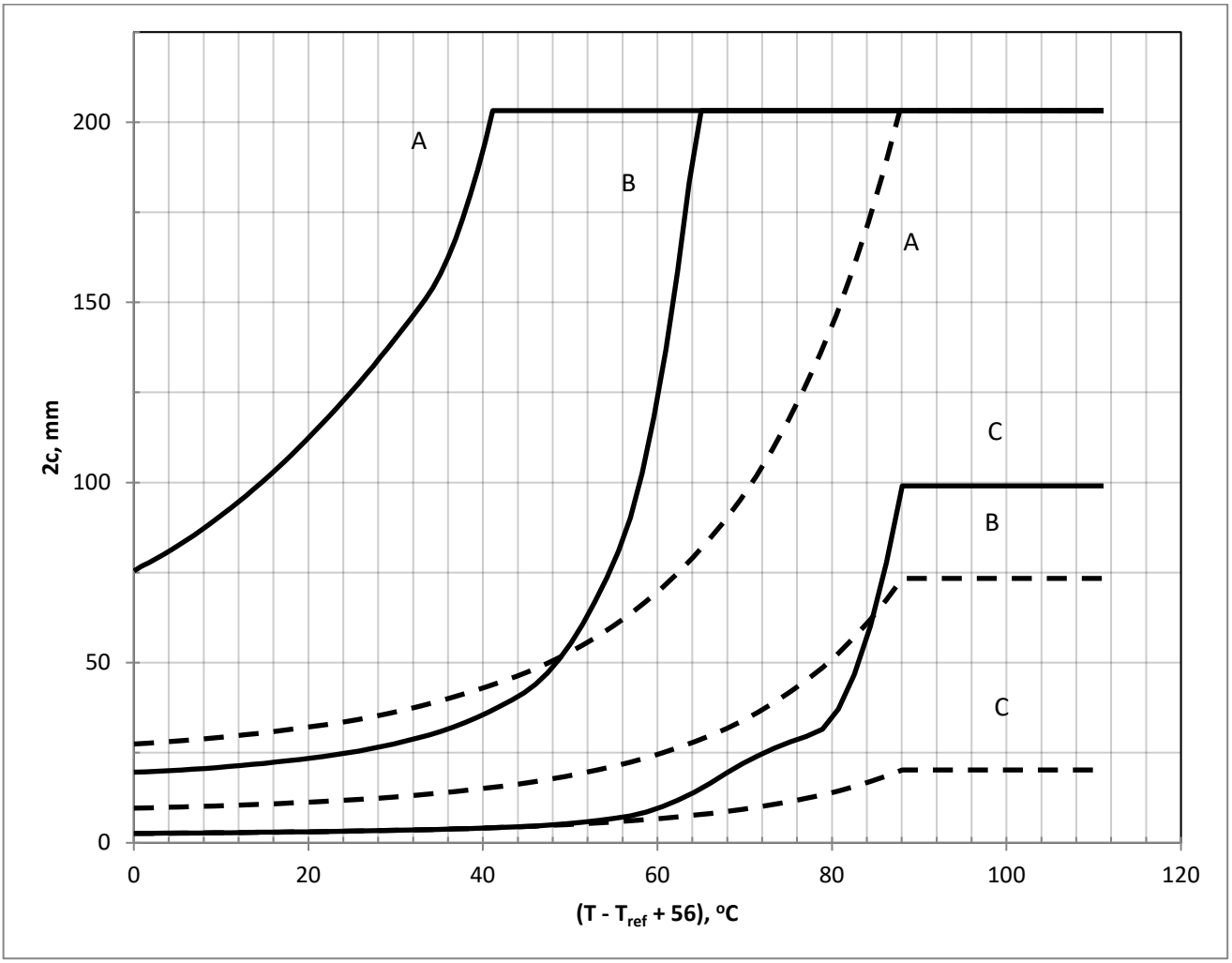

Notes:

1. Definition of Screening Curves (solid line ¼-t flaw, dashed line 1-t flaw):
   A – Allowable flaw size in base metal.
   B – Allowable flaw size in weld metal that has been subject to $PWHT$.
   C – Allowable flaw size in weld metal that has not been subject to $PWHT$.
2. Crack dimension for a 1-t and ¼-t flaw are shown in Annex 9B, Figures 9B.1 and 9B.2.
3. See paragraph 9.2.2(e)(1) for restrictions and limitations.
4. Guidelines for establishing the Reference Temperature, T_{ref}, are covered in paragraph 9.4.2.2(e).
5. The maximum permitted flaw length from this curve is $2c = 200\ mm$.

Figure 9.12M – Level 1 Assessment – Flat Plate

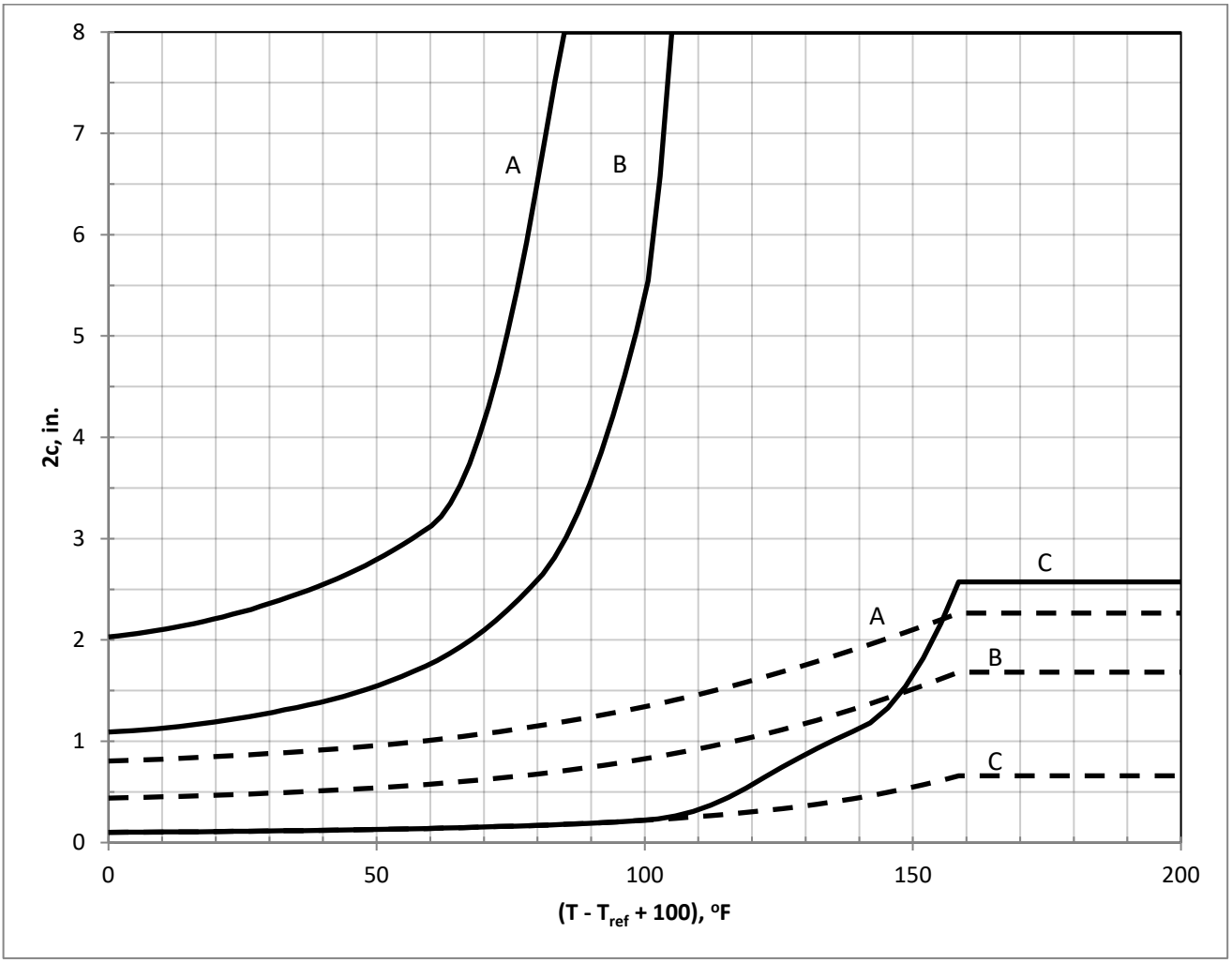

Notes:

1. Definition of Screening Curves (solid line ¼-t flaw, dashed line 1-t flaw):
   A – Allowable flaw size in base metal.
   B – Allowable flaw size in weld metal that has been subject to $PWHT$.
   C – Allowable flaw size in weld metal that has not been subject to $PWHT$.
2. Crack dimension for a 1-t and ¼-t flaw are shown in Annex 9B, Figures 9B.11 and 9B.15.
3. See paragraph 9.2.2(e)(1) for restrictions and limitations.
4. Guidelines for establishing the Reference Temperature, T_{ref}, are covered in paragraph 9.4.2.2(e).
5. The maximum permitted flaw length from this curve is $2c = 8\ in.$

Figure 9.13 – Level 1 Assessment – Cylinder, Longitudinal Joint, Crack-Like Flaw Parallel to the Joint

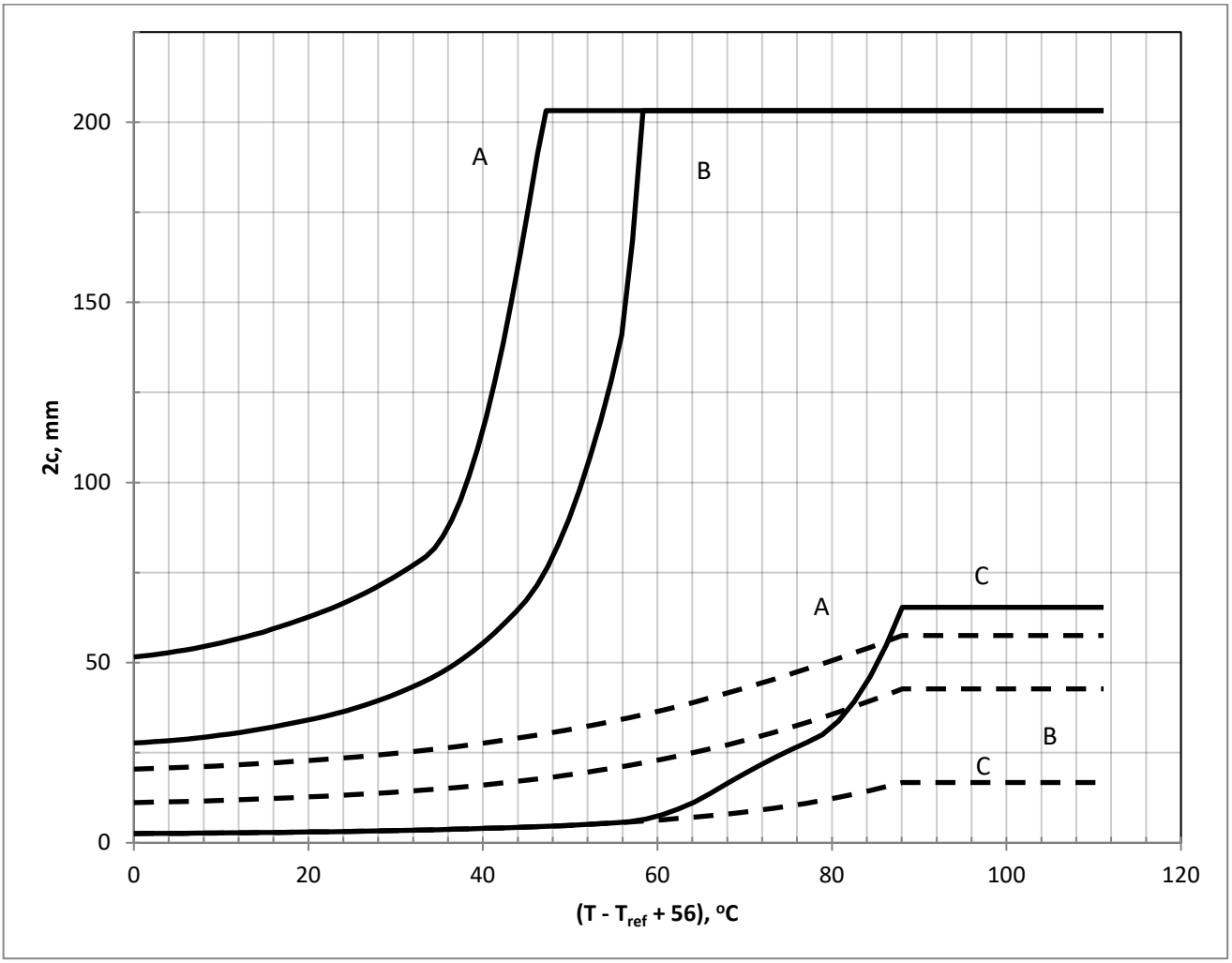

Notes:

1. Definition of Screening Curves (solid line ¼-t flaw, dashed line 1-t flaw):
   A – Allowable flaw size in base metal.
   B – Allowable flaw size in weld metal that has been subject to $PWHT$.
   C – Allowable flaw size in weld metal that has not been subject to $PWHT$.
2. Crack dimension for a 1-t and ¼-t flaw are shown in Annex 9B, Figures 9B.11 and 9B.15.
3. See paragraph 9.2.2(e)(1) for restrictions and limitations.
4. Guidelines for establishing the Reference Temperature, T_{ref}, are covered in paragraph 9.4.2.2(e).
5. The maximum permitted flaw length from this curve is $2c = 200\ mm$.

Figure 9.13M – Level 1 Assessment – Cylinder, Longitudinal Joint, Crack-Like Flaw Parallel to the Joint

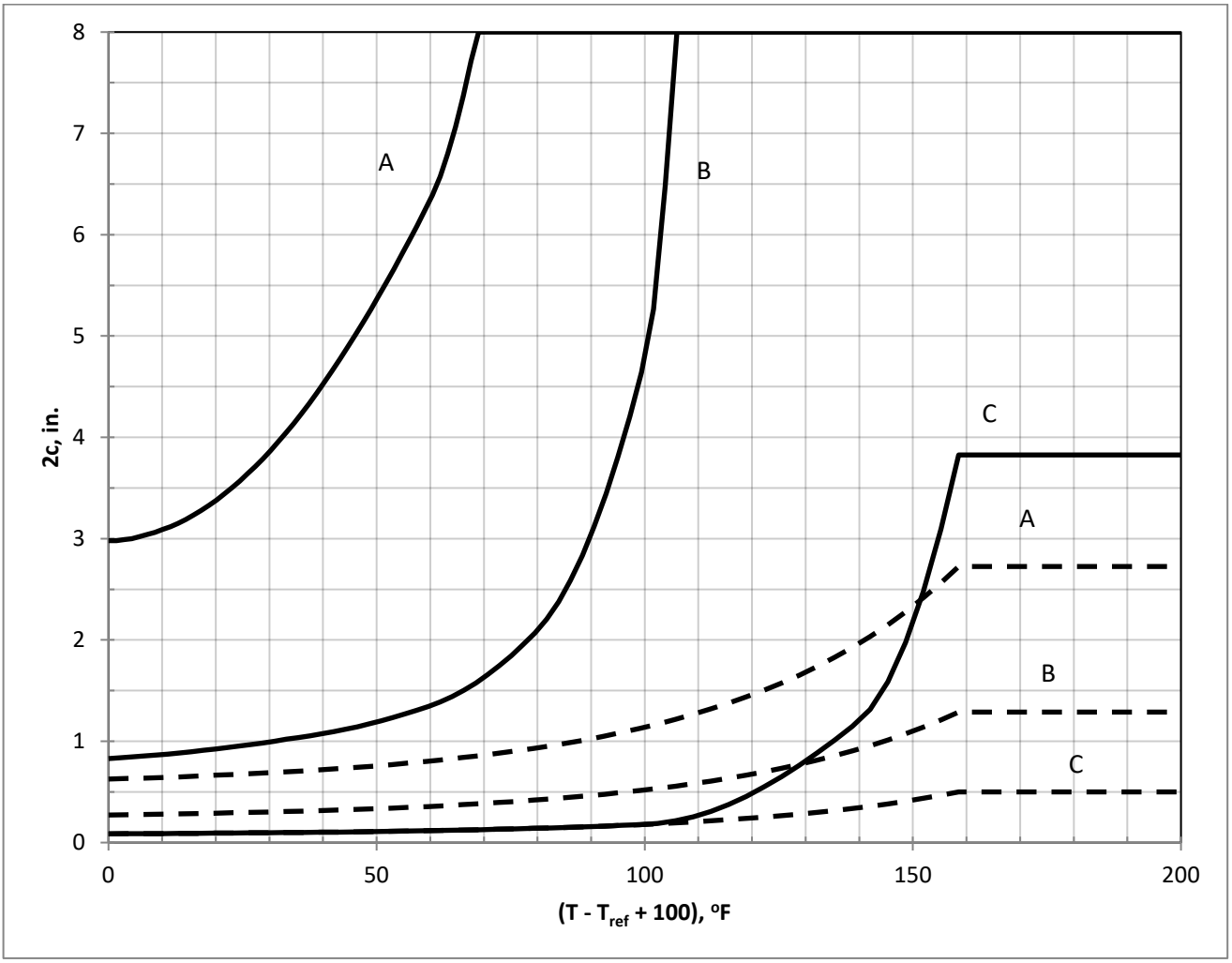

Notes:

1. Definition of Screening Curves (solid line ¼-t flaw, dashed line 1-t flaw):
   A – Allowable flaw size in base metal.
   B – Allowable flaw size in weld metal that has been subject to $PWHT$.
   C – Allowable flaw size in weld metal that has not been subject to $PWHT$.
2. Crack dimension for a 1-t and ¼-t flaw are shown in Annex 9B, Figures 9B.12 and 9B.16.
3. See paragraph 9.2.2(e)(1) for restrictions and limitations.
4. Guidelines for establishing the Reference Temperature, T_{ref}, are covered in paragraph 9.4.2.2(e).
5. The maximum permitted flaw length from this curve is $2c = 8\ in.$

Figure 9.14 – Level 1 Assessment – Cylinder, Longitudinal Joint, Crack-Like Flaw Perpendicular to the Joint

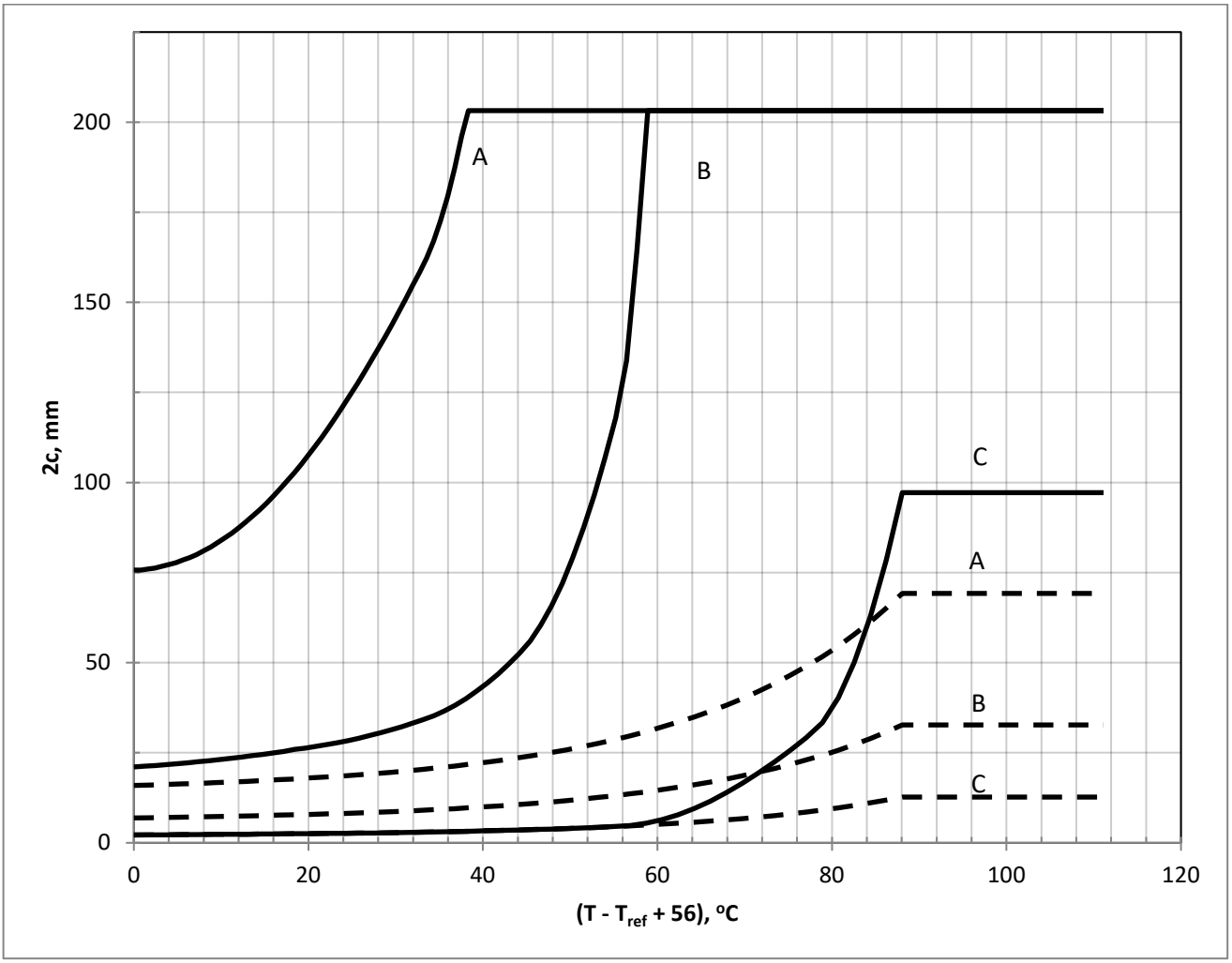

Notes:

1. Definition of Screening Curves (solid line ¼-t flaw, dashed line 1-t flaw):
   A – Allowable flaw size in base metal.
   B – Allowable flaw size in weld metal that has been subject to $PWHT$.
   C – Allowable flaw size in weld metal that has not been subject to $PWHT$.
2. Crack dimension for a 1-t and ¼-t flaw are shown in Annex 9B, Figures 9B.12 and 9B.16.
3. See paragraph 9.2.2(e)(1) for restrictions and limitations.
4. Guidelines for establishing the Reference Temperature, T_{ref}, are covered in paragraph 9.4.2.2(e).
5. The maximum permitted flaw length from this curve is $2c = 200\ mm$.

Figure 9.14M – Level 1 Assessment – Cylinder, Longitudinal Joint, Crack-Like Flaw Perpendicular to the Joint

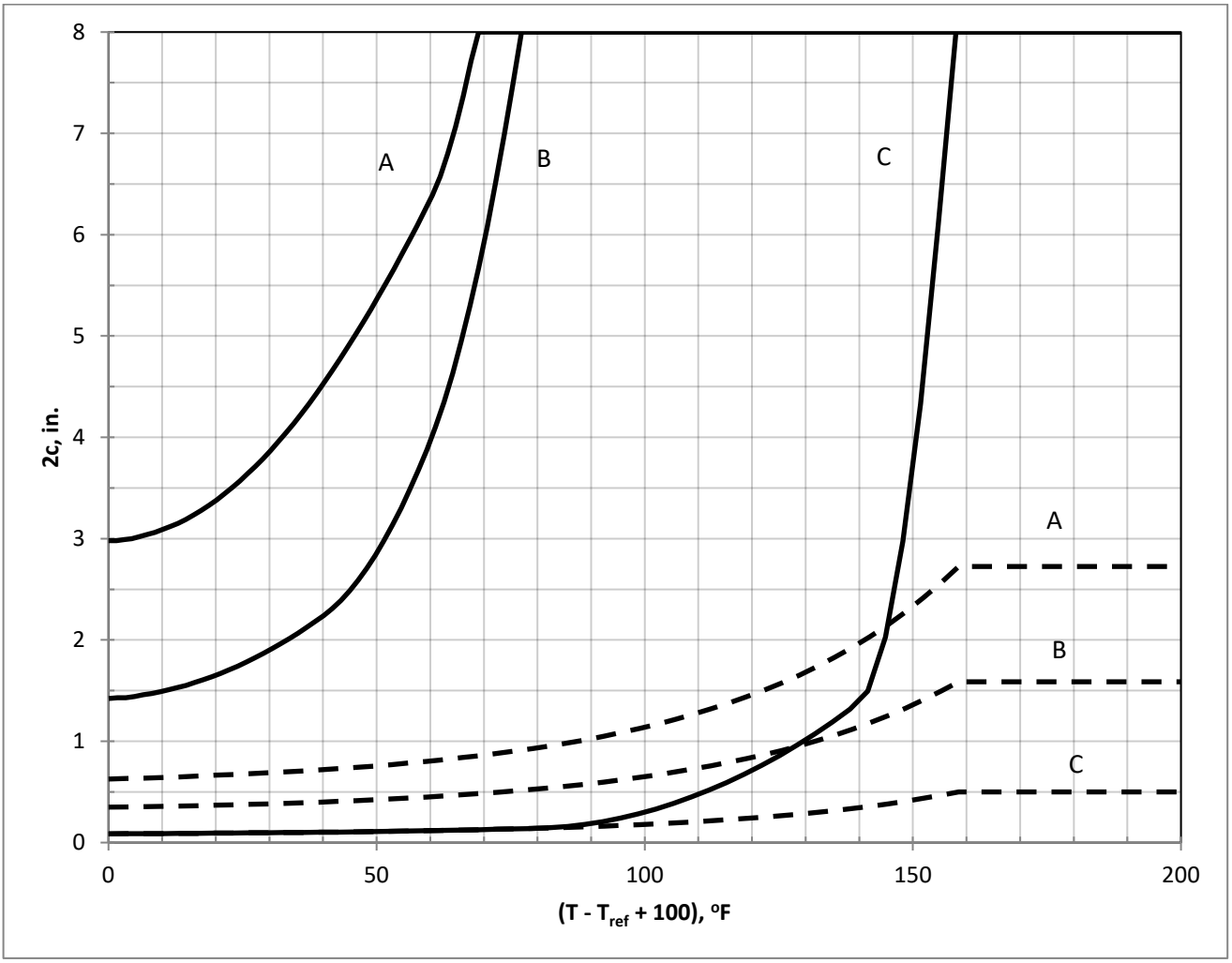

Notes:

1. Definition of Screening Curves (solid line ¼-t flaw, dashed line 1-t flaw):
   A – Allowable flaw size in base metal.
   B – Allowable flaw size in weld metal that has been subject to $PWHT$.
   C – Allowable flaw size in weld metal that has not been subject to $PWHT$.
2. Crack dimension for a 1-t and ¼-t flaw are shown in Annex 9B, Figures 9B.12 and 9B.16.
3. See paragraph 9.2.2(e)(1) for restrictions and limitations.
4. Guidelines for establishing the Reference Temperature, T_{ref}, are covered in paragraph 9.4.2.2(e).
5. The maximum permitted flaw length from this curve is $2c = 8\ in.$

Figure 9.15 – Level 1 Assessment – Cylinder, Circumferential Joint, Crack-Like Flaw Parallel to the Joint

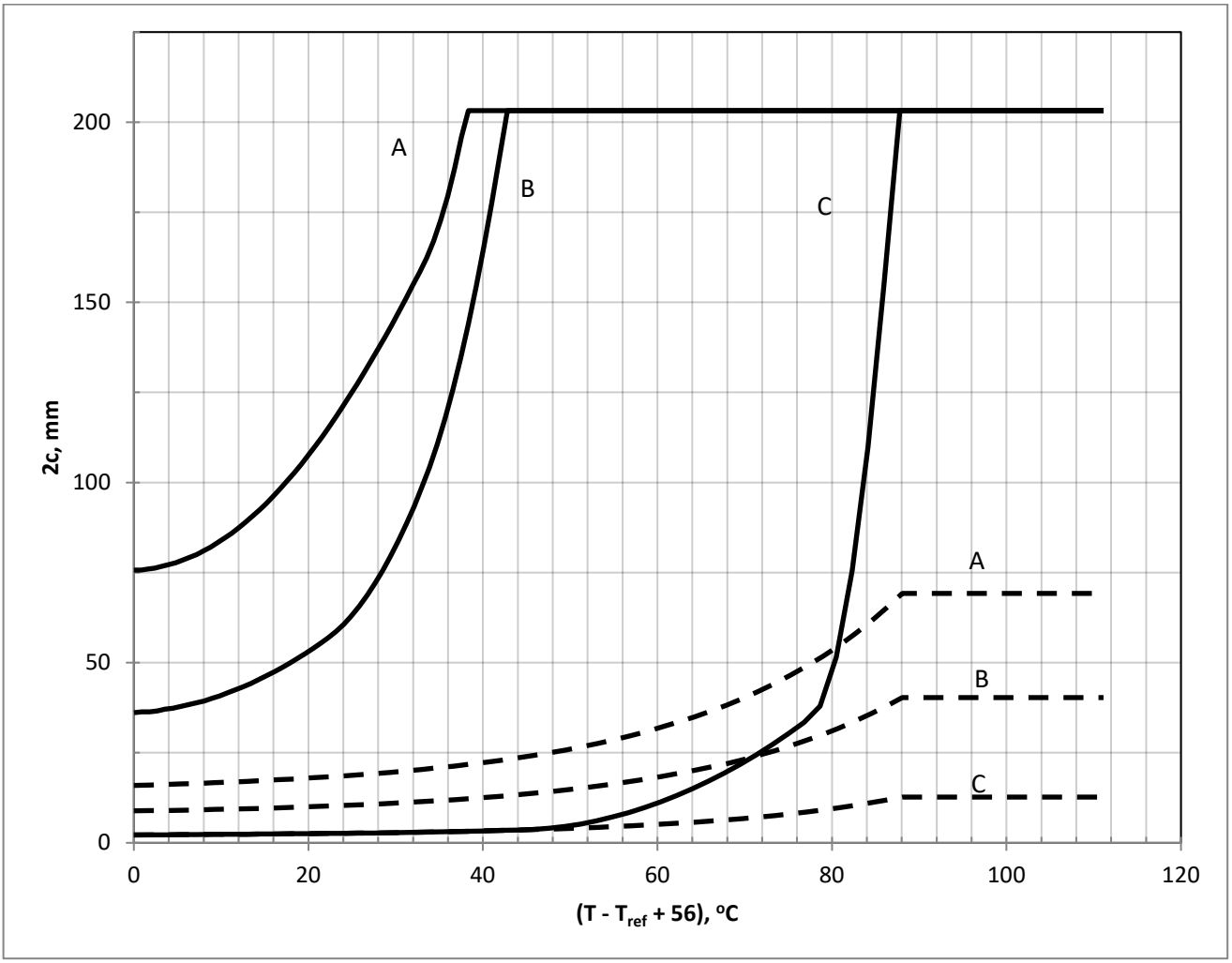

Notes:

1. Definition of Screening Curves (solid line ¼-t flaw, dashed line 1-t flaw):
   A – Allowable flaw size in base metal.
   B – Allowable flaw size in weld metal that has been subject to $PWHT$.
   C – Allowable flaw size in weld metal that has not been subject to $PWHT$.
2. Crack dimension for a 1-t and ¼-t flaw are shown in Annex 9B, Figures 9B.12 and 9B.16.
3. See paragraph 9.2.2(e)(1) for restrictions and limitations.
4. Guidelines for establishing the Reference Temperature, T_{ref}, are covered in paragraph 9.4.2.2(e).
5. The maximum permitted flaw length from this curve is $2c = 200\ mm$.

Figure 9.15M – Level 1 Assessment – Cylinder, Circumferential Joint, Crack-Like Flaw Parallel to the Joint

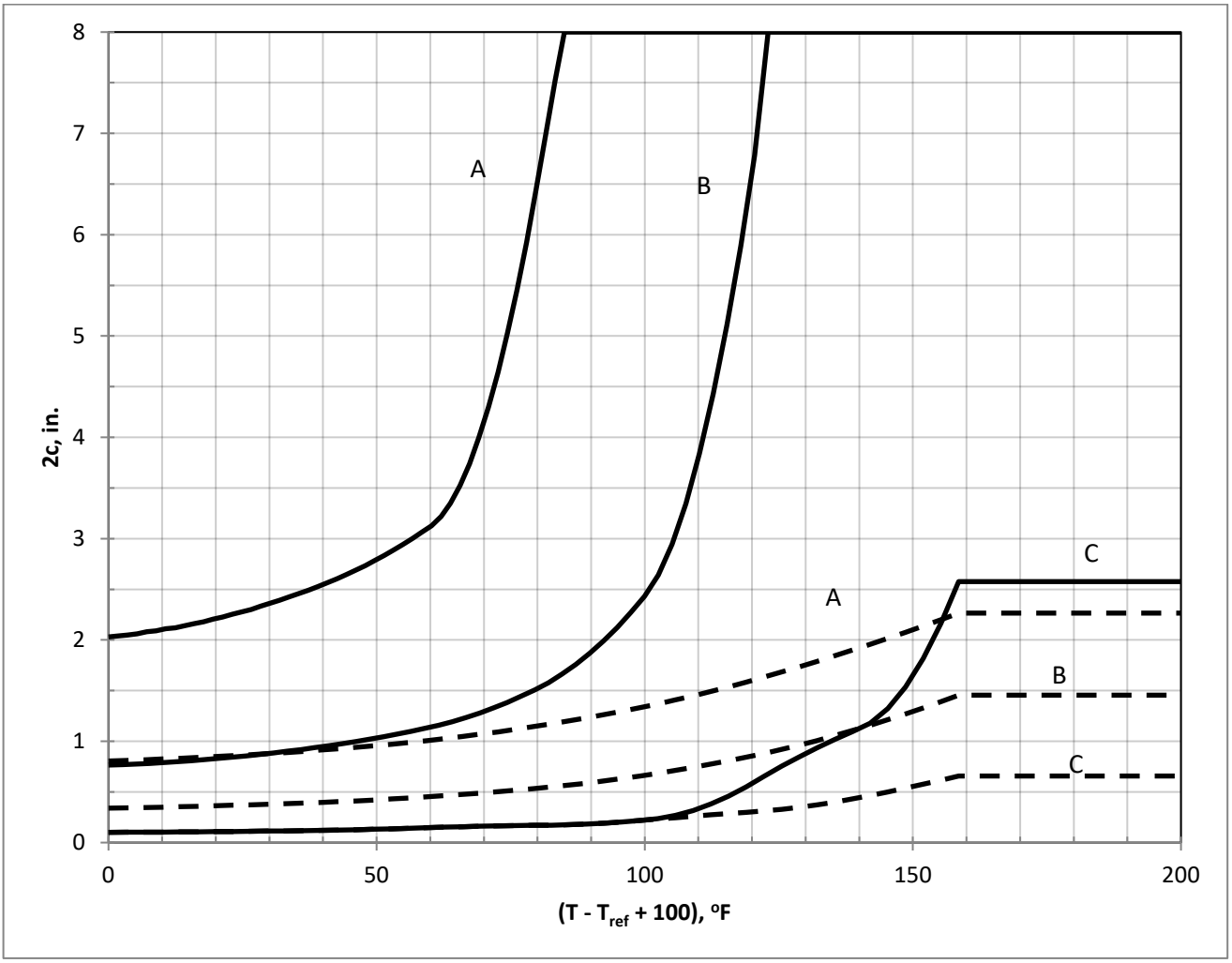

Notes:

1. Definition of Screening Curves (solid line ¼-t flaw, dashed line 1-t flaw):
   A – Allowable flaw size in base metal.
   B – Allowable flaw size in weld metal that has been subject to $PWHT$.
   C – Allowable flaw size in weld metal that has not been subject to $PWHT$.
2. Crack dimension for a 1-t and ¼-t flaw are shown in Annex 9B, Figures 9B.11 and 9B.15.
3. See paragraph 9.2.2(e)(1) for restrictions and limitations.
4. Guidelines for establishing the Reference Temperature, T_{ref}, are covered in paragraph 9.4.2.2(e).
5. The maximum permitted flaw length from this curve is $2c = 8\ in.$

Figure 9.16 – Level 1 Assessment – Cylinder, Circumferential Joint, Crack-Like Flaw Perpendicular to the Joint

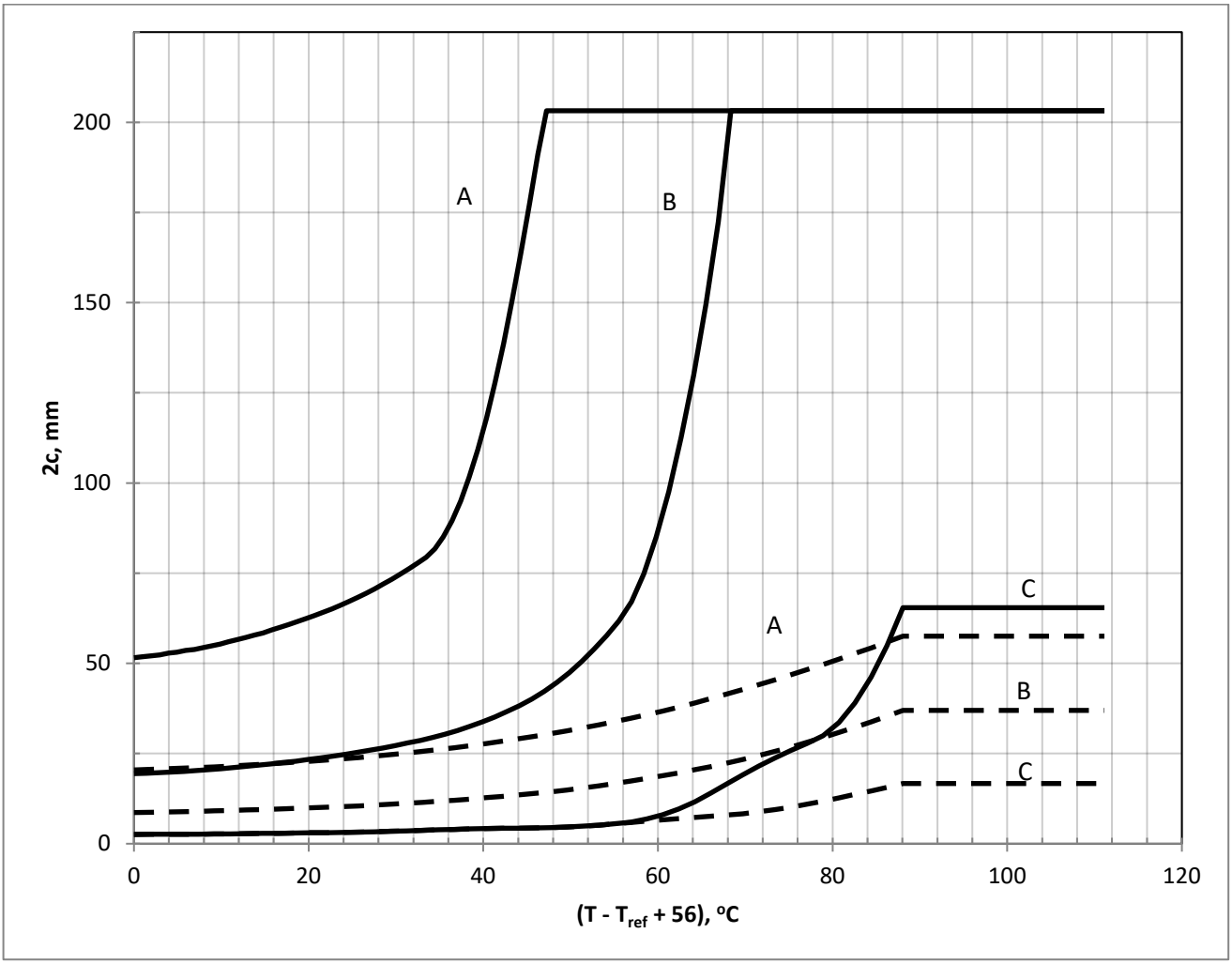

Notes:

1. Definition of Screening Curves (solid line ¼-t flaw, dashed line 1-t flaw):
   A – Allowable flaw size in base metal.
   B – Allowable flaw size in weld metal that has been subject to $PWHT$.
   C – Allowable flaw size in weld metal that has not been subject to $PWHT$.
2. Crack dimension for a 1-t and ¼-t flaw are shown in Annex 9B, Figures 9B.11 and 9B.15.
3. See paragraph 9.2.2(e)(1) for restrictions and limitations.
4. Guidelines for establishing the Reference Temperature, T_{ref}, are covered in paragraph 9.4.2.2(e).
5. The maximum permitted flaw length from this curve is $2c = 200\ mm$.

Figure 9.16M – Level 1 Assessment – Cylinder, Circumferential Joint, Crack-Like Flaw Perpendicular to the Joint

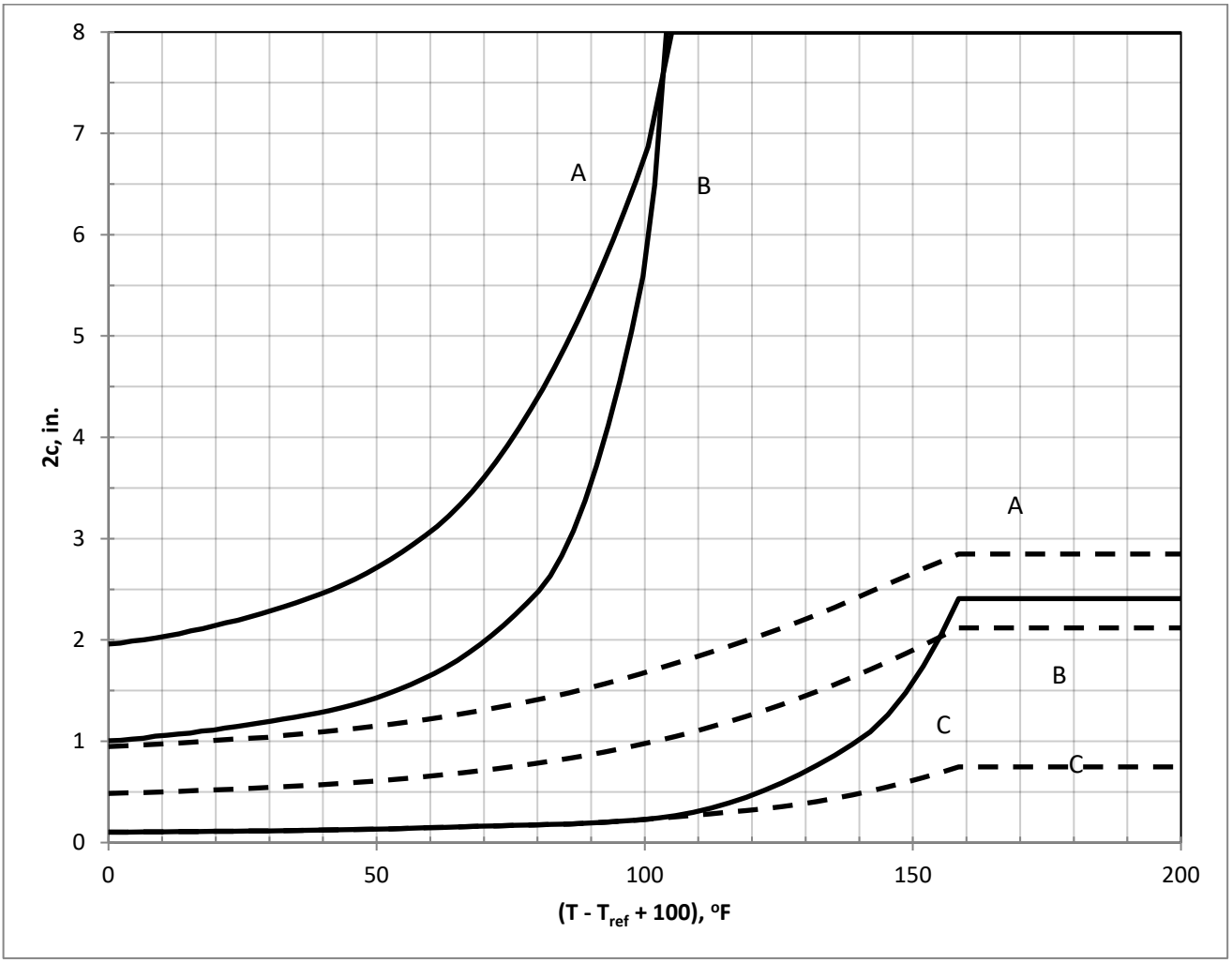

Notes:

1. Definition of Screening Curves (solid line ¼-t flaw, dashed line 1-t flaw):
   A – Allowable flaw size in base metal.
   B – Allowable flaw size in weld metal that has been subject to $PWHT$.
   C – Allowable flaw size in weld metal that has not been subject to $PWHT$.
2. Crack dimension for a 1-t and ¼-t flaw are shown in Annex 9B, Figures 9B.21 and 9B.23.
3. See paragraph 9.2.2(e)(1) for restrictions and limitations.
4. Guidelines for establishing the Reference Temperature, T_{ref}, are covered in paragraph 9.4.2.2(e).
5. The maximum permitted flaw length from this curve is $2c = 8\ in.$

Figure 9.17 – Level 1 Assessment – Sphere, Circumferential Joint, Crack-Like Flaw Parallel to the Joint

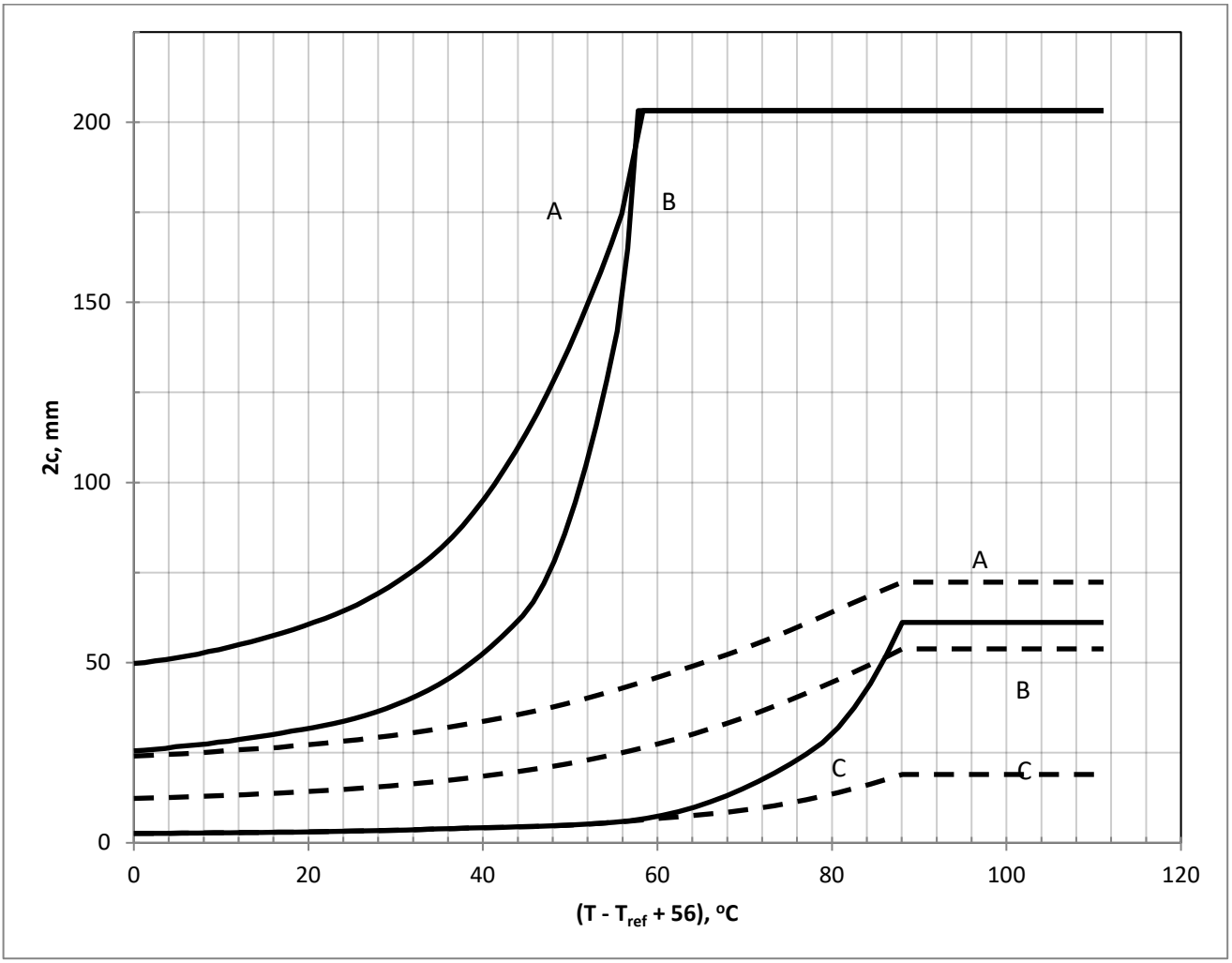

Notes:

1. Definition of Screening Curves (solid line ¼-t flaw, dashed line 1-t flaw):
   A – Allowable flaw size in base metal.
   B – Allowable flaw size in weld metal that has been subject to $PWHT$.
   C – Allowable flaw size in weld metal that has not been subject to $PWHT$.
2. Crack dimension for a 1-t and ¼-t flaw are shown in Annex 9B Figures 9B.21 and 9B.23.
3. See paragraph 9.2.2(e)(1) for restrictions and limitations.
4. Guidelines for establishing the Reference Temperature, T_{ref}, are covered in paragraph 9.4.2.2(e).
5. The maximum permitted flaw length from this curve is $2c = 200\ mm$.

Figure 9.17M– Level 1 Assessment – Sphere, Circumferential Joint, Crack-Like Flaw Parallel to the Joint

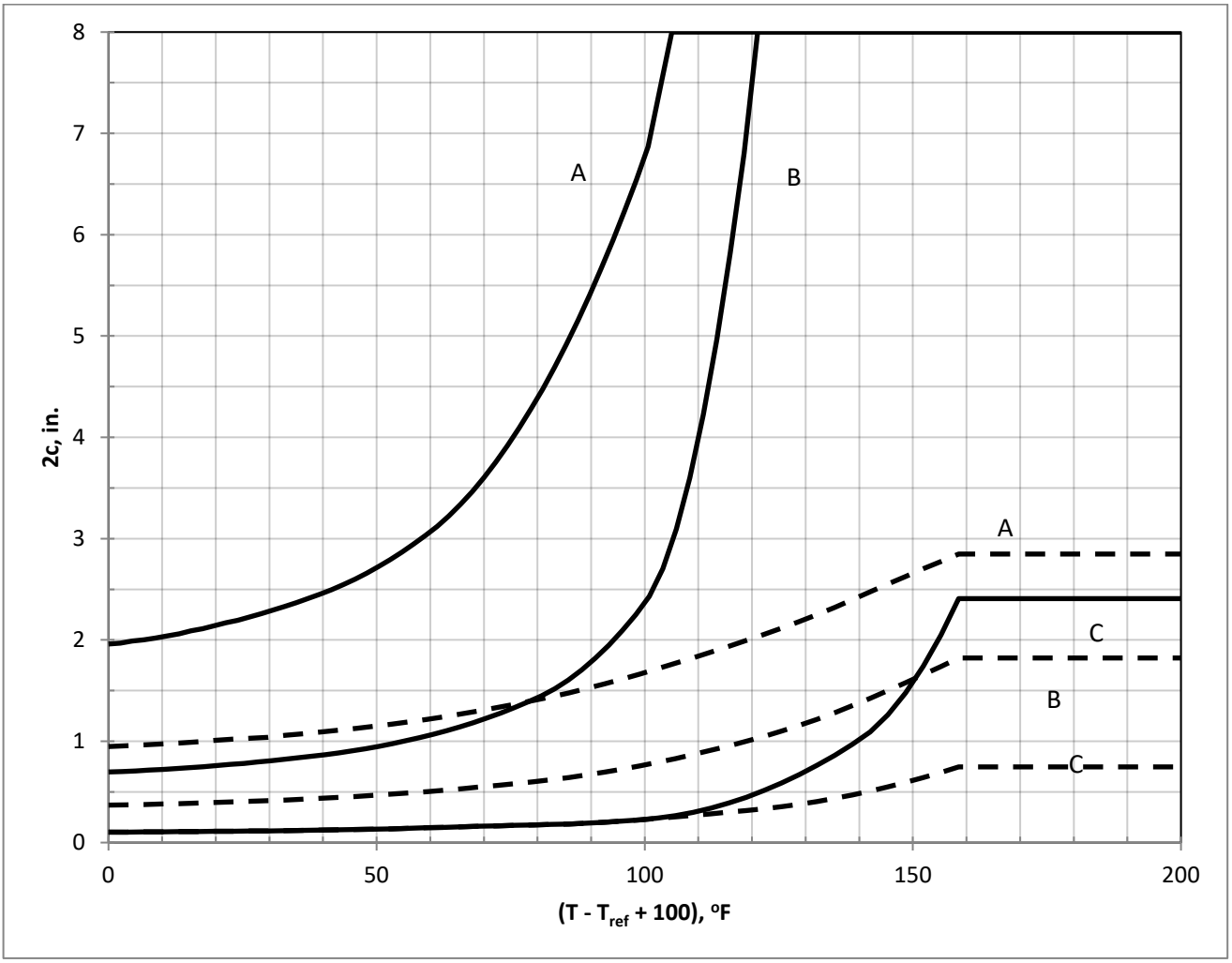

Notes:

1. Definition of Screening Curves (solid line ¼-t flaw, dashed line 1-t flaw):
   A – Allowable flaw size in base metal.
   B – Allowable flaw size in weld metal that has been subject to $PWHT$.
   C – Allowable flaw size in weld metal that has not been subject to $PWHT$.
2. Crack dimension for a 1-t and ¼-t flaw are shown in Annex 9B, Figures 9B.21 and 9B.23.
3. See paragraph 9.2.2(e)(1) for restrictions and limitations.
4. Guidelines for establishing the Reference Temperature, T_{ref}, are covered in paragraph 9.4.2.2(e).
5. The maximum permitted flaw length from this curve is $2c = 8\ in$.

Figure 9.18 – Level 1 Assessment – Sphere, Circumferential Joint, Crack-Like Flaw Perpendicular to the Joint

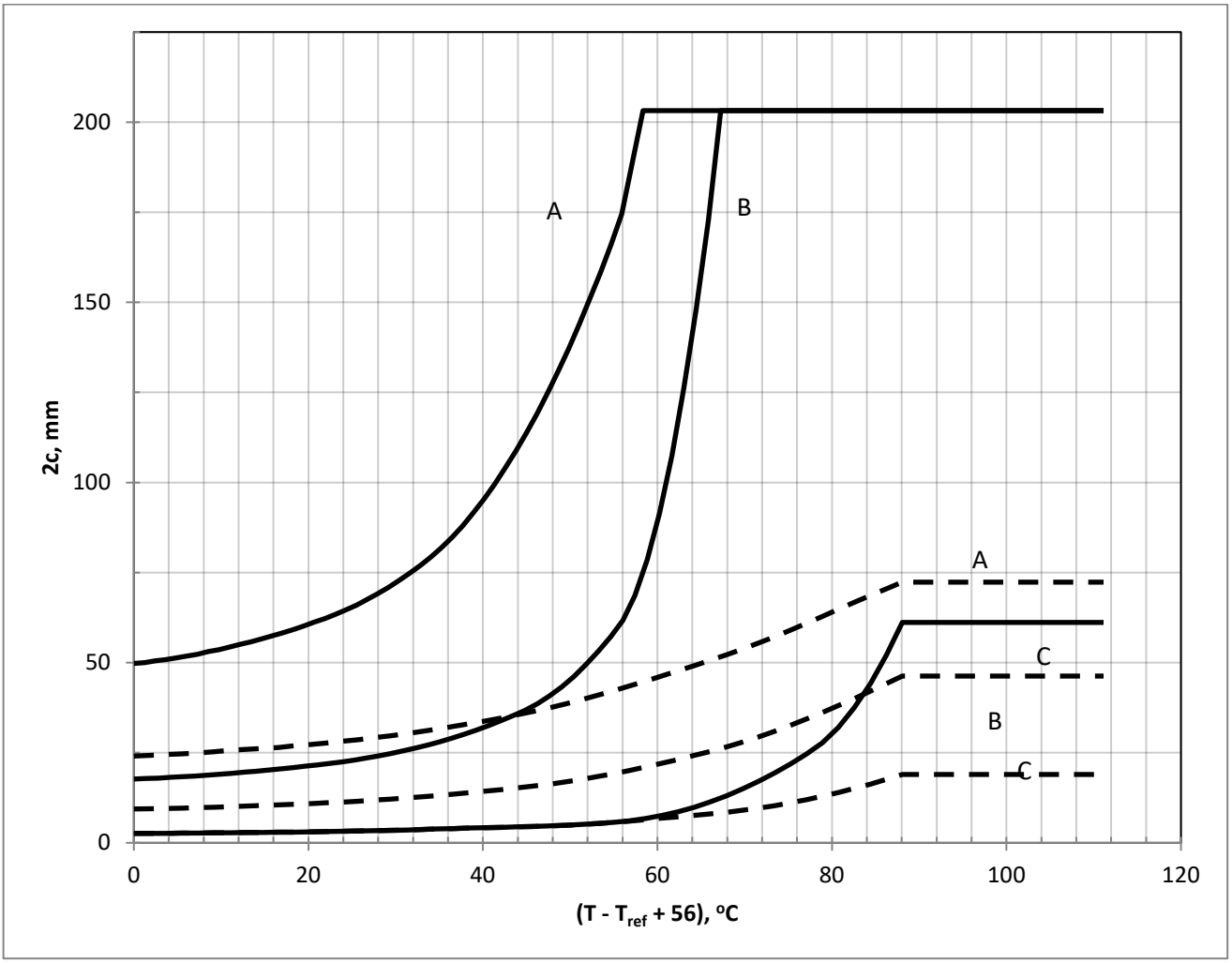

Notes:

1. Definition of Screening Curves (solid line ¼-t flaw, dashed line 1-t flaw):
   A – Allowable flaw size in base metal.
   B – Allowable flaw size in weld metal that has been subject to $PWHT$.
   C – Allowable flaw size in weld metal that has not been subject to $PWHT$.
2. Crack dimension for a 1-t and ¼-t flaw are shown in Annex 9B, Figures 9B.21 and 9B.23.
3. See paragraph 9.2.2(e)(1) for restrictions and limitations.
4. Guidelines for establishing the Reference Temperature, T_{ref}, are covered in paragraph 9.4.2.2(e).
5. The maximum permitted flaw length from this curve is $2c = 200\ mm$.

Figure 9.18M – Level 1 Assessment – Sphere, Circumferential Joint, Crack-Like Flaw Perpendicular to the Joint

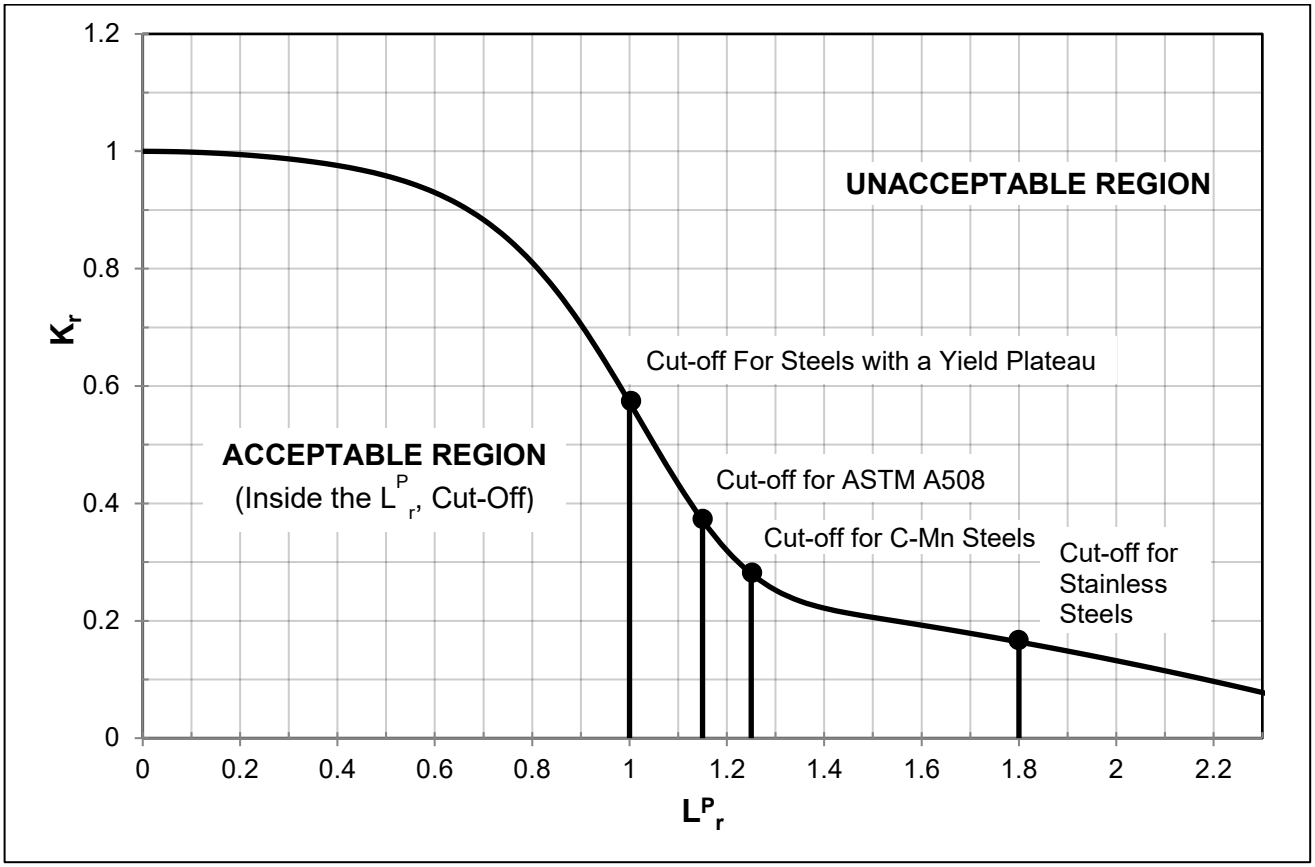

Notes:

1. The FAD is defined using the following equation:

$$K_r = \left(1 - 0.14\left(L_r^P\right)^2\right)\left(0.3 + 0.7\exp\left[-0.65\left(L_r^P\right)^6\right]\right) \qquad \left(for\ L_r^P \le L_{r(\max)}^P\right) \tag{9.22}$$

2. The extent of the FAD on the L_r^P axis is determined as follows:
   a) $L_{r(\max)}^P = 1.00$ for materials with yield point plateau (strain hardening exponent > 15),
   b) $L_{r(\max)}^P = 1.15$ for ASTM A508,
   c) $L_{r(\max)}^P = 1.25$ for C-Mn steels,
   d) $L_{r(\max)}^P = 1.80$ for austenitic stainless steels, and
   e) $L_{r(\max)}^P = \frac{\sigma_f}{\sigma_{ys}}$ for other materials where σ_f flow stress and σ_{ys} yield stress (see Annex 2E); the flow stress and yield stress are evaluated at the assessment temperature.
   f) $L_{r(\max)}^P = 1.0$ if the strain hardening characteristics of the material are unknown.
3. The value of $L_{r(\max)}^P$ may be increased for redundant components (see Annex 9C, paragraph 9C.2.5.2(b)).
4. If $L_{r(\max)}^P = 1.0$, then the FAD may be defined using following equation:

$$K_r = \left(1.0 - \left(L_r^P\right)^{2.5}\right)^{0.20} \tag{9.23}$$

Figure 9.19 – The Failure Assessment Diagram

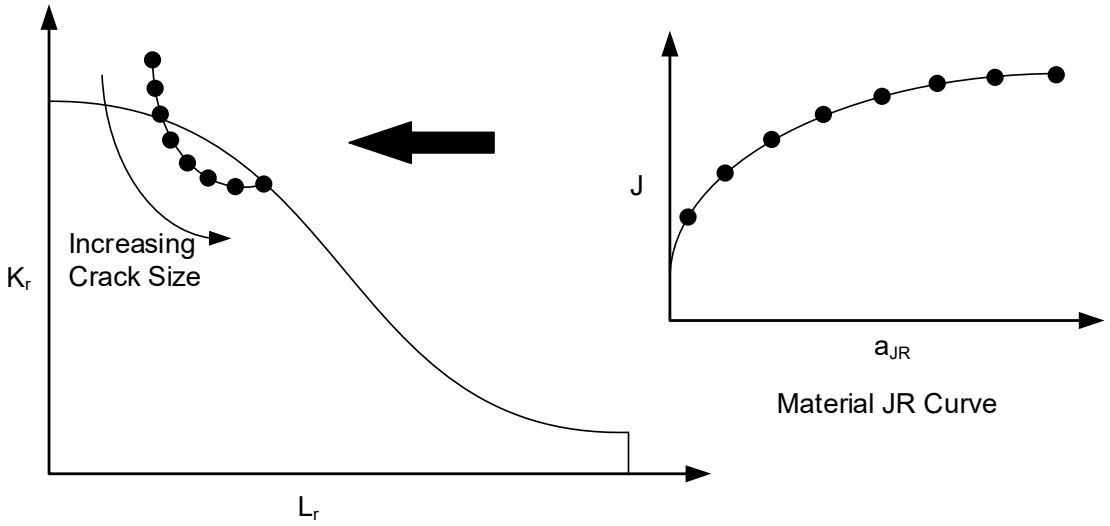

(a) Obtaining a Locus of Assessment Points from a JR-Curve

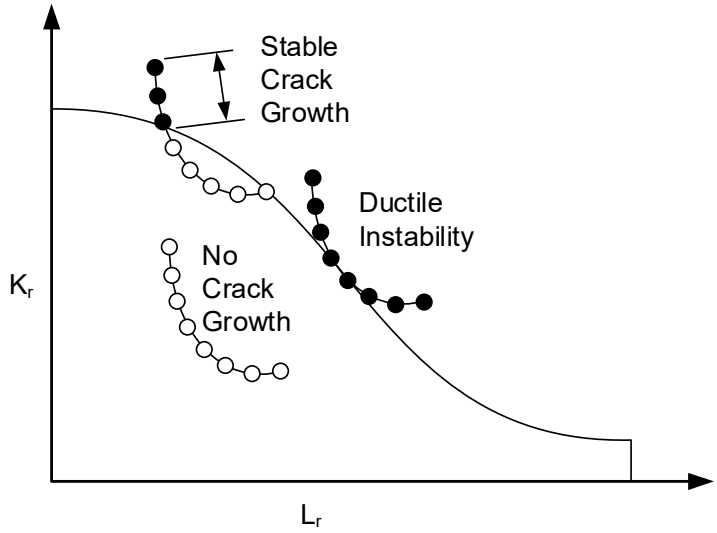

(b) Three Possible Outcomes of a Ductile Tearing Analysis

Figure 9.20 – Ductile Tearing Analysis

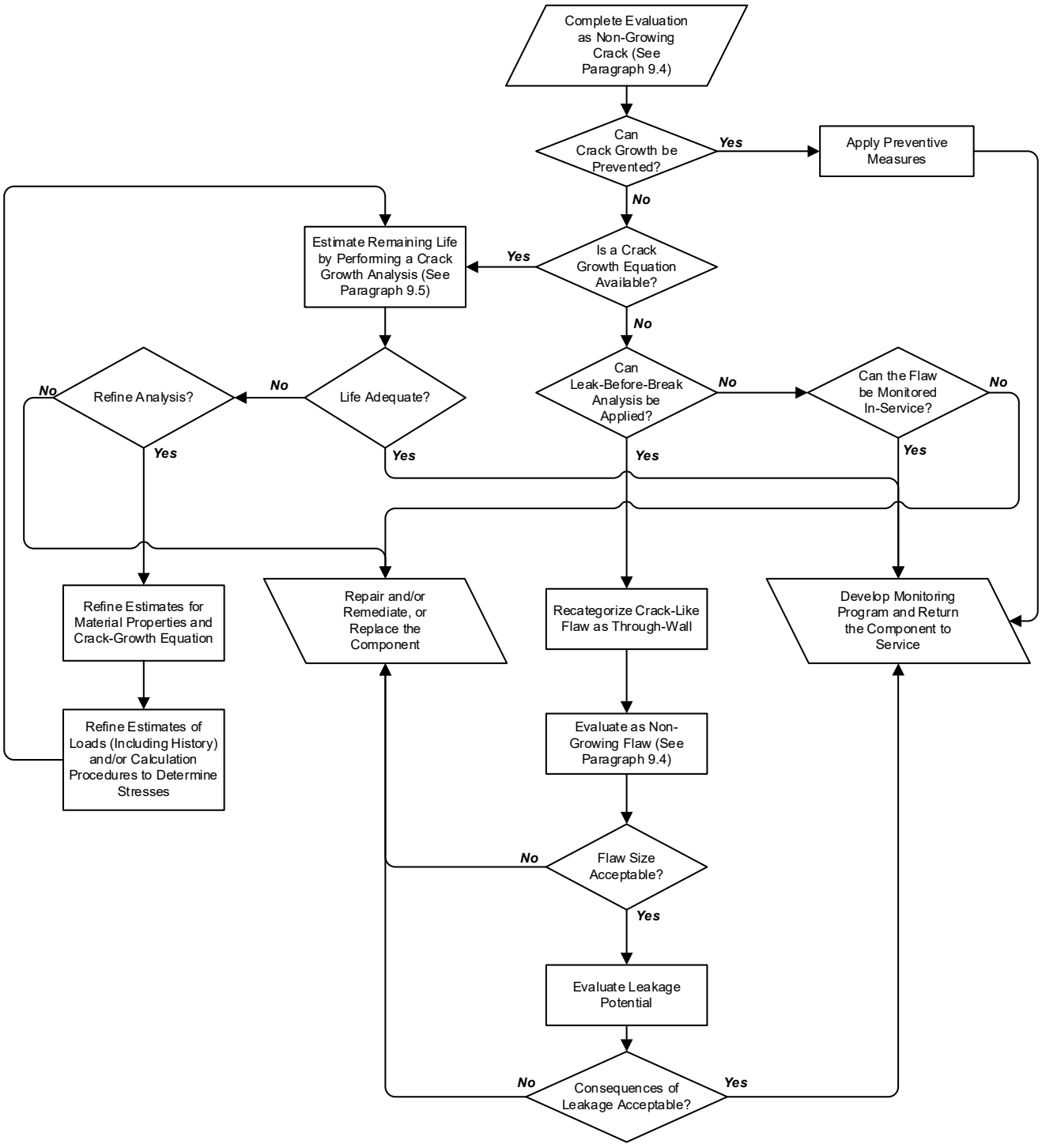

Figure 9.21 – Overview of the Assessment Procedures to Evaluate Growing Crack-Like Flaws

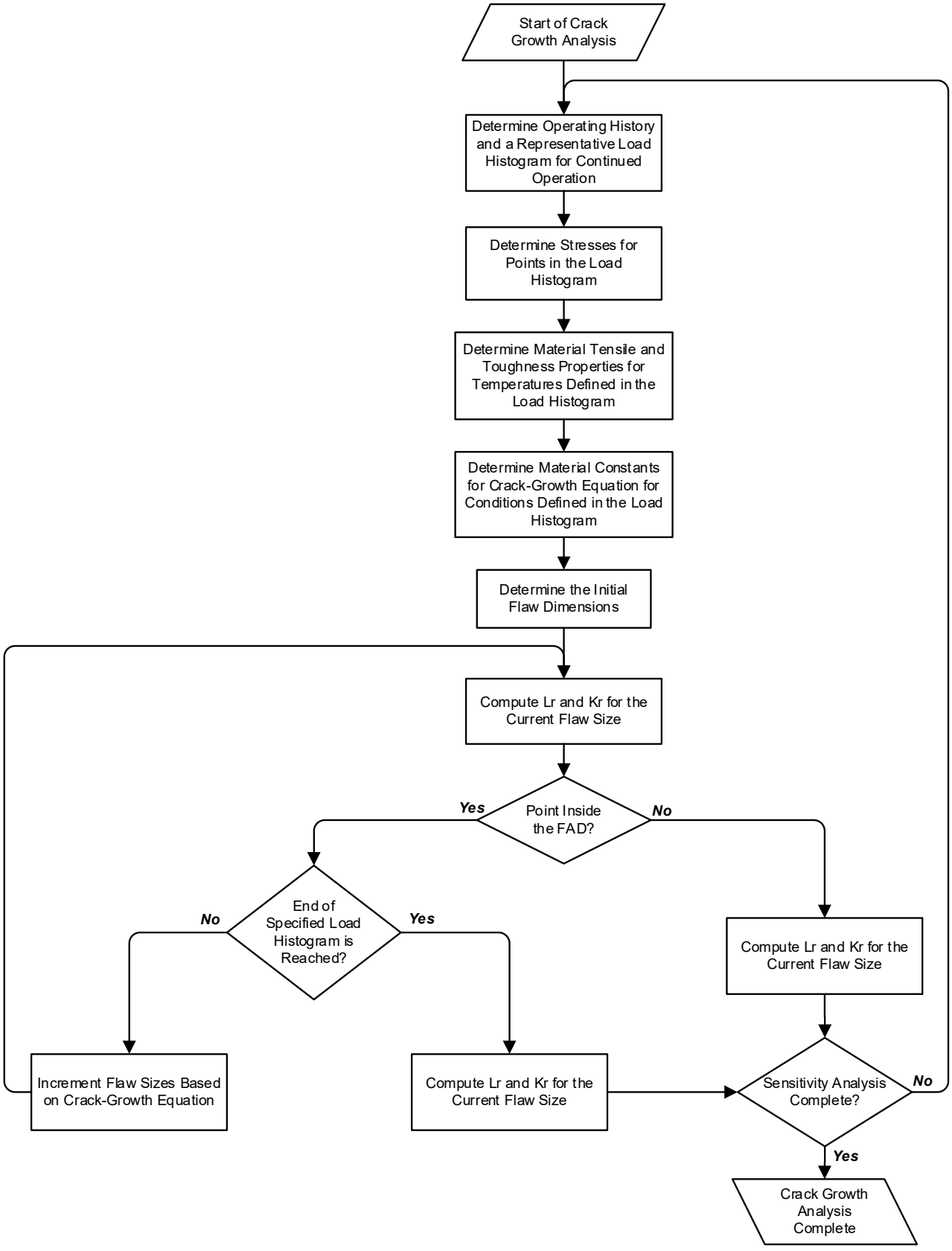

Figure 9.22 – Methodology for Crack Growth Analysis

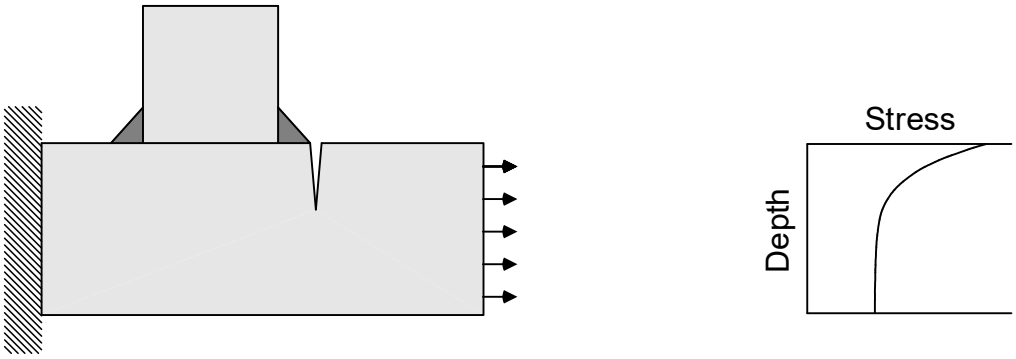

(a) Flaw at a Stress Raiser

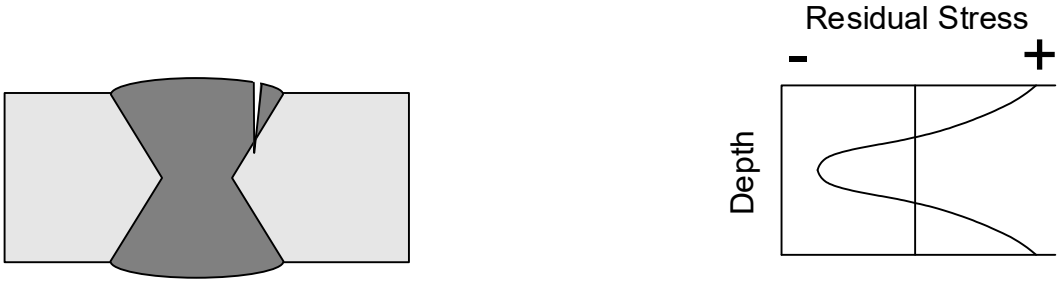

(b) Flaw Subject to High Residual Stresses

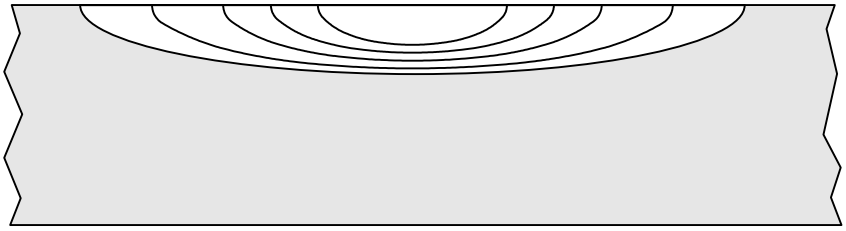

(c) Flaw Growth Predominantly in the Length Direction

Figure 9.23 – Leak-Before-Break for Flaws at or Near a Stress Concentration

[Intentionally Left Blank]

ANNEX 9A – TECHNICAL BASIS AND VALIDATION – ASSESSMENT OF CRACK-LIKE FLAWS

(INFORMATIVE)

CONTENTS

ANNEX 9A – TECHNICAL BASIS AND VALIDATION – ASSESSMENT OF CRACK-LIKE FLAWS..... 9A-1

9A.1 TECHNICAL BASIS AND VALIDATION..... 9A-1
9A.2 REFERENCES..... 9A-2

9A.1 Technical Basis and Validation

An overview of the assessment procedures in Part 9 for the evaluation of crack-like flaws is provided in reference [5]. The evaluation of crack-like flaws in Part 9 is based on the Failure Assessment Diagram (FAD) approach, see references [3] and [40]. This approach has gained wide acceptance throughout the world and has been adopted in a number of prominent codes and standards, including BS 7910 see reference [10], the R6 Method see reference [16], The Swedish Plant Inspectorate in reference [2], the Structural Integrity Assessment procedures for European Industry (SINTAP) see reference [43], and ASME B&PV Code, Section XI, Article H-4000. Although there are subtle differences among the FAD-based approaches in the various codes and standards, the overall concept is consistent throughout the world. A detailed comparison of various codified approaches for assessing crack-like flaws is provided in reference [40].

A FAD-based evaluation of a component with a crack-like flaw is described in Part 9 and entails computing a toughness ratio, K_r, and a load ratio, L_r. An assessment point with coordinates (K_r, L_r) is compared with the FAD curve, which represents the failure locus. The toughness ratio stems directly from linear elastic fracture mechanics in reference [3] and the load ratio provides a plasticity correction. A rigorously correct FAD curve for a given structural component with a crack can be derived from an elastic-plastic $J - integral$ solution of the cracked component, as described in Annex 9G and reference [3]. The Level 2 FAD curve in Part 9 is an approximation of the true elastic-plastic crack driving force. However, provided that the combined primary stresses are less than the yield strength, the outcome of a crack-like flaw assessment is insensitive to the shape of the FAD curve see reference [40].

The FAD-based approach has been extensively validated with burst tests and wide plate tests, see references [6], [11], [12], [13], [16], [38], and [49]. The approach is conservative, provided that a conservative estimate of the key input parameters (toughness, flaw size, primary stress, residual stress) is used. When assessment points are computed from the full-scale tests, such points fall outside of the FAD when conservative assumptions for input parameters are used. When mean estimates for input parameters are used, however, assessment points for full-scale tests fall both inside and outside of the FAD, with roughly a 50:50 split, see reference [4]. This indicates that the FAD method provides a good estimate of the mean failure conditions when all conservatism is removed from input parameters.

The uncertainty in the independent variables in a FAD analysis (i.e., stress, flaw size, and fracture toughness) may be accounted for by choosing conservative estimates for each of these parameters. Alternatively, mean values of these parameters may be used with Partial Safety Factors. The Partial Safety Factors in Part 9 are based on work reported in references [30], [45], [46], and [47].

9A.2 References

[1] Ainsworth, R.A., “The Treatment of Thermal and Residual Stresses in Fracture Assessments,” Engineering Fracture Mechanics, Vol. 24, No. 1, pp. 65-76, 1986.

[2] Anderson, P., Bergman, M., Brickstad, B., and Dahlberg, L., *A Procedure for Safety Assessment of Components with Cracks – Handbook*, 3rd Edition, SAQ/FoU-Report 96/08, SAQ Kontroll AB, Sweden, 1997.

[3] Anderson, T.L., *Fracture Mechanics – Fundamentals and Applications*, 3rd Edition, CRC Press, Boca Raton, Florida, 2005.

[4] Anderson, T.L., “Preliminary Validation of the MPC Fitness-for-Service Guidelines.” PVP Vol. 315, Fitness-for-Service and Decisions for Petroleum and Chemical Equipment, July 1995, pp. 123-129.

[5] Anderson, T.L. and Osage, D.A., “API 579: A Comprehensive Fitness-For-Service Guide,” International Journal of Pressure Vessels and Piping 77 (2000), pp 953-963.

[6] Prager, M., *Fitness-For-Service Evaluation Procedures for Operating Pressure Vessels, Tanks, and Piping in Refinery and Chemical Service*, FS-26, Consultants Report, MPC Program on Fitness-For-Service, WRC Bulletin 547, Welding Research Council, Inc., New York, NY, 2014.

[7] Bloom, J.M., “Deformation Plasticity Failure Assessment Diagram (DPFAD) for Materials with Non-Ramberg-Osgood Stress-Strain Curves,” Journal of Pressure Vessel Technology, American Society of Mechanical Engineers, Vol. 117, November 1995.

[8] Bloom, J.M., “Deformation Plasticity Failure Assessment Diagram (DPFAD) Approach / A Fitness-For-Purpose Fracture Mechanics Based Methodology for Use in the Petrochemical Industry,” PVP-Vol. 315, Fitness-for-Service and Decisions for Petroleum and Chemical Equipment, ASME, pp. 131-144, 1995.

[9] Bockrath, G. and Glassco, J., Fatigue and Fracture Mechanics of High Risk Parts – Application of LEFM & EMDM Theory, Chapman & Hall, New York, NY, 1997.

[10] BSI, Guide on Methods for Assessing the Acceptability of Flaws in Metallic Structures, BS 7910, British Standards Institute, 2013.

[11] Bhuyan, G.S., Sperling, E.J., Shen, G., Yin, H. and Rana, M.D., “Prediction of Failure Behavior of a Welded Pressure Vessel Containing Flaws During a Hydrogen Charged Burst Test,” Transactions of the ASME, Vol. 121, August 1999.

[12] Challenger, N.V., Phaal, R., and Garwood, S.J., “Fracture Mechanics Assessment of Industrial Pressure Vessel Failures”, International Journal of Pressure Vessels and Piping 61, 1995, pp 433-456.

[13] Challenger, N.V., Phaal, R., and Garwood, S.J., “Appraisal of PD6493:1991 Fracture Assessment Procedures, Part I: TWI Data”, TWI, Abington Hall, UK, June 1995.

[14] Dong, P., Rahman, S., Wilkowski, G., Brickstad, B., and Bergman, M., “Effects of Weld Residual Stresses on Crack Opening Area Analysis of Pipes for LBB Applications,” LBB-95; Specialist Meeting on Leak-Before-Break in Reactor Piping and Vessels, Lyon, France, October 1995.

[15] Dijkstra, O.D. and Straalen, J.J., van, “Fatigue Crack Growth Program FAFRAM (Fatigue Fracture Mechanics),” TNO Building and Construction Research, Report BI-91-051.

[16] EDF Energy Nuclear Generation Limited, Assessment of the Integrity of Structures Containing Defects, EDF Energy Nuclear Generation Limited R-6, Nuclear Electric, Revision 4, 2001.

[17] Ellyin, F., *Fatigue Damage Crack Growth and Life Prediction*, Chapman & Hall, Boundary Row, London 1997.

[18] Ewing, D.J.F., "Simple Methods for Predicting Gas Leakage Flows Through Cracks," Paper C376/047 In Proceedings of International Conference on Pipework Engineering and Operation, Institution of Mechanical Engineers, London, 21-22, Pp. 307-314, February 1989.

[19] Farahmand, B., Bockrath, G., and Glassco, J., Fatigue and Fracture Mechanics of High Risk Parts – Application of LEFM & FMDM Theory, Chapman Hall, New York, NY, 1997.

[20] Hazelton, W.S., "Technical Report on Material Selection and Processing Guidelines for BWR Coolant Pressure Boundary Piping (Draft Report)," NUREG -0313, Rev. 2, June 1986.

[21] Hooton, G.H. and Budden, P.J., "R6 Developments in the Treatment of Secondary Stresses," PVP-Vol. 304, ASME, 1995, pp 503-509.

[22] Kumar, V., German, M.D. and Shih, C.F., "An Engineering Approach for Elastic-Plastic Fracture Analysis," EPRI Report NP-1931, EPRI Palo Alto, CA, 1981.

[23] Langston, D.B., "A Reference Stress Approximation for Determining Crack Opening Displacements in Leak-Before-Break Calculations," TD/SID/REP/0112, Nuclear Electric Document, 1991.

[24] Langston, D.B., Haines, N.F., and Wilson, R., "Development of a Leak-Before-Break Procedure for Pressurized Components," CEGB, UK, pp. 287-292.

[25] Loushin, L.L., "Assessment of Structural Integrity in Pressure Vessels – Predictions and Verification," PVP Vol. 336, ASME, pp. 97-104, 1996.

[26] Liu, A.F., *Structural Life Assessment Methods*, ASM International, Materials Park, Ohio, 1998.

[27] Miller, A.G., "Elastic Crack Opening Displacements and Rotations in Through Cracks in Spheres and Cylinders Under Membrane and Bending Loading," Engineering Fracture Mechanics, Vol. 23, 1986.

[28] Milne, I., Ainsworth, R.A., Dowling, A.R. and Stewart, A.T., "Assessment of the Integrity of Structures Containing Defects," Int. J. Pres. Vessel & Piping, 32, 1988, pp. 3-104.

[29] Milne, I., Ainsworth, R.A., Dowling, A.R. and Stewart, A.T., "Background to and Validation of CEGB Report R/H/R6-Revision 3," Int. J. Pres. Vessel & Piping, 32, 1988, pp. 105-196.

[30] Osage, D.A., Shipley, K.S., Wirsching, P.H. and Mansour, A.E., "Application of Partial Safety Factors for Pressure Containing Equipment," PVP Vol. 411, Service Experience and Fitness-For-Service in Power and Petroleum Processing, ASME, 2000, pp. 121-142.

[31] Paris, P.C., and Johnson, R.E., "A Method of Application of Elastic-Plastic Fracture Mechanics to Nuclear Vessel Analysis," Elastic-Plastic Fracture: Second Symposium, Volume II-Fracture Resistance Curves and Engineering Applications, ASTM STP 803, 1983, pp. Ii-4-ii-40.

[32] Paul, D.D., Ahmad, J., Scott, P.M., Flanigan, L.F., and Wilkowski, G.M., "Evaluation and Refinement of Leak-Rate Estimation Models," NUREG/CR-5128, Rev. 1, June 1995.

[33] Phaal, R., "Non-unique Solutions in PD6493: 1991 Fracture Assessment Procedures," ASME PVP-Vol. 260, American Society of Mechanical Engineers, pp. 149-155, 1993.

[34] Popelar, C.H., "A Tearing Instability Analysis for Strain Hardening Materials," ASTM STP 833, 1984.

[35] Rahman, S., Brust, F., Ghadiali, N., Choi, Y.H., Krishnaswamy, P., Moberg, F., Brickstad, B., and Wilkowski, G., "Refinement and Evaluation of Crack Opening Area Analyses for Circumferential Through-Wall Cracks in Pipes," NUREG/CR-6300, 1995.

[36] Rahman, S., Ghadiali, Paul, D. and Wilkowski, G., "Probabilistic Pipe Fracture Evaluations for Leak-Rate-Detection Applications," NUREG/CR-6004, April 1995.

[37] SAQ/FoU, A Procedure for Safety Assessment of Components with Cracks – Handbook, SAQ/FoU-Report 96/08, 1997.

[38] Sattari-Farr, I. and Nilsson, F., *Validation of a Procedure for Safety Assessment of Cracks*, SA/FoU Report 91/19, 2nd Edition Revised, The Swedish Plant Inspectorate, 1991.

[39] Schaser, M.S. and Duffy, S.F., Material Specific Load Combination Factors for Option 2 FAD Curves, WRC Bulletin 544, Welding Research Council, Inc., New York, NY, 2014.

[40] Scott, P.M., Anderson, T.L., Osage, D.A., and Wilkowski, G.M., *A Review of Existing Fitness-For-Service Criteria for Crack-Like Flaws*, WRC Bulletin 430, Welding Research Council, Inc., New York, NY, April 1998.

[41] Sharples, J.K. and Bouchard, P.J., "Assessment of Crack Opening Area for Leak Rates," LBB-95; Specialist Meeting on Leak-Before-Break in Reactor Piping and Vessels, Lyon, France, October 1995.

[42] Smith, E., "The Opening of Through-Wall Cracks in BWR Coolant Lines Due to the Application of Severe Overloads," NUREG/CP-0051, August 1984.

[43] Webster, S. and Bannister, A., "Structural Integrity Assessment Procedure for Europe – of the SINTAP Programme Overview," Engineering Fracture Mechanics (67) 2000, pp. 481-514.

[44] Wilkowski, G., Scott, P., and Maxey, W., "Design and Optimization of Mechanical Crack Arrestors for Pipelines," NG-18 Report No. 134, American Gas Association, July 1983.

[45] Wirsching, P.H. and Mansour, A.E., "Incorporation of Structural Reliability methods into Fitness-For-Service Procedures," Mansour Engineering, Inc., Report to The Materials Properties Council, Inc., May 1998.

[46] Wirsching, P.H. and Mansour, A.E., "Incorporation of Structural Reliability methods into Fitness-For-Service Procedures," Mansour Engineering, Inc., Report to The Materials Properties Council, Inc., Supplement No. 1, April 1999.

[47] Wirsching, P.H. and Mansour, A.E., "Incorporation of Structural Reliability methods into Fitness-For-Service Procedures," Mansour Engineering, Inc., Report to The Materials Properties Council, Inc., Supplement No. 2, May 1999.

[48] Wuthrich, C., "Crack Opening Areas in Pressure Vessels and Pipes," Engineering Fracture Mechanics, Vol. 18, No. 5, pp. 1049-1057, 1983.

[49] Yin, H., and Bagnoli, D.L., "Case Histories Using Fitness-For-Service Methods," PVP-Vol. 288, Service Experience and Reliability Improvement: Nuclear, Fossil, and Petrochemical Plants, ASME, 1994.

[50] Dillstrom, et. al.," A combined deterministic and probabilistic procedure for safety assessment of components with cracks – Handbook", SSM Research Report 2008:01, Swedish Radiation Safety Authority, 2008.

ANNEX 9B – COMPENDIUM OF STRESS INTENSITY FACTOR SOLUTIONS

(NORMATIVE)

CONTENTS

ANNEX 9B – COMPENDIUM OF STRESS INTENSITY FACTOR SOLUTIONS 9B-1

9B.1 General 9B-1
9B.2 Stress Analysis 9B-2
9B.3 Stress Intensity Factor Solutions for Plates 9B-4
9B.4 Stress Intensity Factor Solutions for Plates with Holes 9B-15
9B.5 Stress Intensity Factor Solutions for Cylinders 9B-21
9B.6 Stress Intensity Factor Solutions for Spheres 9B-30
9B.7 Stress Intensity Factor Solutions for Elbows and Pipe Bends 9B-33
9B.8 Stress Intensity Factor Solutions for Nozzles and Piping Tees 9B-33
9B.9 Stress Intensity Factor Solutions for Ring-Stiffened Cylinders 9B-35
9B.10 Stress Intensity Factor Solutions for Sleeve Reinforced Cylinders 9B-36
9B.11 Stress Intensity Factor Solutions for Round Bars and Bolts 9B-36
9B.12 Stress Intensity Factor Solutions for Cracks at Fillet Welds 9B-39
9B.13 Stress Intensity Factor Solutions Cracks in Clad Plates and Shells 9B-41
9B.14 The Weight Function Method for Surface Cracks 9B-41
9B.15 Nomenclature 9B-45
9B.16 References 9B-50
9B.17 Tables 9B-54
9B.18 Figures 9B-225

9B.1 General

9B.1.1 Overview

This Annex contains stress intensity factor solutions for many crack geometries that are likely to occur in pressurized components. Stress intensity factor solutions are used in the assessment of crack-like flaws (see Part 9).

9B.1.2 Stress Intensity Factor Solutions

A summary of the stress intensity factor solutions is contained in Table 9B.1. These stress intensity factor solutions are recommended for most applications based on consideration of accuracy, range of applicability and convenience. However, additional cases and improved solutions are being produced for future incorporation into this Annex.

9B.1.3 Stress Intensity Factor Solutions – Approximation for Shells

The stress intensity factor solutions for plates can be utilized to approximate the solution for a curved shell (cylinder and sphere) by introduction of a surface correction or bulging factor (see paragraph 9B.2.3). This type of solution should only be utilized if a stress intensity factor equation is not listed in the sections covering shell type components.

9B.1.4 Stress Intensity Factor Identifier

An identifier has been assigned to each stress intensity factor solutions in this Annex (see Table 9B.1). This identifier is a set of alpha-numeric characters that uniquely identifies the component geometry, crack geometry,

and loading condition. The identifier can also be used to determine the associated reference stress solution to be used in an assessment of crack-like flaws (see Part 9). For example, if a flat plate with a through-wall crack subject to a membrane stress is being evaluated, the stress intensity factor solution to be used is KPTC, and the associated reference stress solution is RPTC. A listing of the reference stress solutions is provided in Table 9B.1.

9B.1.5 Alternate Sources for Stress Intensity Factor Solutions

Stress intensity factors not included in this Annex may be obtained from handbooks (see references [2], [14], [20], [21], and [28]) if the tabulated solutions correspond to the component and crack geometry, and the loading condition. Another source of stress intensity factors, J-integral and reference stress solutions is provided in references [44], [45], [46], [47], [48], [49], and [50]. Otherwise, the stress intensity factor should be computed using a numerical approach such as the finite element method.

9B.2 Stress Analysis

9B.2.1 Overview

9B.2.1.1 Stress Distribution Computation Requirements

A stress analysis using handbook or numerical techniques is required to compute the state of stress at the location of a crack. The stress distribution to be utilized in determining the stress intensity factor is based on the component of stress normal to the crack face. The distribution may be linear (made up of membrane and/or bending distributions) or highly non-linear based on the component geometry and loading conditions.

9B.2.1.2 Primary, Secondary and Residual Stress

The stress distribution normal to the crack face should be determined for the primary, secondary, and residual stress loading conditions based on the service requirements that the uncracked component geometry is subjected to.

9B.2.1.3 Multiple Operating Conditions

If the component is subject to different operating conditions, the stress distribution for each condition should be evaluated and a separate Fitness-For-Service Assessment should be performed for each condition.

9B.2.2 Stress Distributions

9B.2.2.1 Overview

The stress intensity factor solutions in this Annex are formulated in terms of the coefficients of a linear stress distribution (membrane and bending) or fourth order polynomial stress distribution, or in terms of a general stress distribution (weight functions). Therefore, if the stress intensity factor required for the assessment is written in terms of coefficients of a stress distribution, it is necessary to derive these coefficients from the results obtained from a stress analysis.

9B.2.2.2 General Stress Distribution

A general stress distribution through the wall thickness can be obtained from a two or three-dimensional elasticity solution (e.g., Lame solutions for a thick wall cylinder and sphere) or it can be determined using a numerical analysis technique such as the finite element method. In some cases, the stress distribution normal to the crack face may be highly non-linear.

a) Statically equivalent membrane and bending stress components can be determined from the general stress distribution using the following equations. The integration is performed along a line assuming a unit width.

$$\sigma_{ij,m} = \frac{1}{t}\int_0^t \sigma_{ij} dx \tag{9B.1}$$

$$\sigma_{ij,b} = \frac{6}{t^2}\int_0^t \sigma_{ij}\left(\frac{t}{2} - x\right) dx \tag{9B.2}$$

b) A general stress distribution can be used directly to determine a stress intensity factor by integration of this distribution with a suitable weight function. Weight functions are provided in this Annex for a limited number of component and crack geometries.

9B.2.2.3 Fourth Order Polynomial Stress Distribution

The fourth order polynomial stress distribution can be obtained by curve-fitting the general stress distribution. This distribution is utilized to obtain a more accurate representation of the stress intensity for a highly non-linear stress distribution. Many of the stress intensity factor solutions in this Annex have been developed based on a fourth order polynomial stress distribution.

a) The general form of the fourth order polynomial stress distribution is as follows:

$$\sigma(x) = \sigma_0 + \sigma_1\left(\frac{x}{t}\right) + \sigma_2\left(\frac{x}{t}\right)^2 + \sigma_3\left(\frac{x}{t}\right)^3 + \sigma_4\left(\frac{x}{t}\right)^4 \tag{9B.3}$$

b) The equivalent membrane and bending stress distributions for the fourth order polynomial stress distribution are:

$$\sigma_m = \sigma_0 + \frac{\sigma_1}{2} + \frac{\sigma_2}{3} + \frac{\sigma_3}{4} + \frac{\sigma_4}{5} \tag{9B.4}$$

$$\sigma_b = -\frac{\sigma_1}{2} - \frac{\sigma_2}{2} - \frac{9\sigma_3}{20} - \frac{6\sigma_4}{15} \tag{9B.5}$$

9B.2.2.4 Fourth Order Polynomial Stress Distribution with Net Section Bending Stress

This distribution is used to represent a through-wall fourth order polynomial stress and a net section or global bending stress applied to a circumferential crack in a cylindrical shell.

$$\sigma(x, x_g, y_g) = \sigma_0 + \sigma_1\left(\frac{x}{t}\right) + \sigma_2\left(\frac{x}{t}\right)^2 + \sigma_3\left(\frac{x}{t}\right)^3 + \sigma_4\left(\frac{x}{t}\right)^4 + \sigma_5\left(\frac{y_g}{R_i + t}\right) + \sigma_6\left(\frac{x_g}{R_i + t}\right) \tag{9B.6}$$

9B.2.2.5 Membrane and Through-Wall Bending Stress

The membrane and bending stress distributions are linear through the wall thickness and represent a common subset of the general stress distribution. These distributions occur in thin plate and shell structures and can be computed using handbook solutions or by using a numerical technique such as finite element analysis. If finite element analysis is utilized in a Fitness-For-Service Assessment, the results from plate and shell elements will directly yield membrane and bending stress distributions. The stress intensity factor solutions in this Annex can be used if a membrane and through-wall bending stress distribution is known. For the special case of weld

misalignment and shell out-of-roundness, the bending stress solution can be computed using the membrane stress solution and the following equation:

$$\sigma_b = \sigma_m R_b \tag{9B.7}$$

9B.2.3 Surface Correction Factors

9B.2.3.1 Definition

Surface correction or bulging factors are used to quantify the local increase in the state of stress at the location of a crack in a shell that occurs because of local bulging. The magnified state of stress is then used together with a reference stress solution for a plate with a similar crack geometry to determine the reference stress for the shell. Surface correction factors are typically only applied to the membrane part of the stress intensity solution because this represents the dominant part of the solution.

9B.2.3.2 Through-Wall and Surface Cracks

The surface correction factors for through-wall cracks in cylindrical and spherical shells subject to membrane stress loading are defined in Annex 9C, paragraph 9C.2.3.2. The surface correction factors for surface cracks can be approximated using the results obtained for a though-wall crack by using one of the methods discussed in Annex 9C, paragraph 9C.2.3.3. The surface correction factor based on net section collapse is recommended for use in this Annex.

9B.3 Stress Intensity Factor Solutions for Plates

9B.3.1 KPTC Plate – Through-Wall Crack, Through-Wall Membrane and Bending Stress (KPTC)

9B.3.1.1 The Mode I Stress Intensity Factor (References [1] and [35])

$$K_I = \left(\left(\sigma_m + p_c\right) + M_b \sigma_b\right)\sqrt{\pi\, c}\cdot f_w \tag{9B.8}$$

where,

$$M_b = \frac{0.302327 + 70.50193\psi + 110.305\psi^2}{1.0 + 110.960\psi + 98.7089\psi^2 + 0.753594\psi^3} \tag{9B.9}$$

$$\psi = \frac{t}{c\sqrt{10}} \tag{9B.10}$$

$$f_w = \left(\sec\left[\frac{\pi c}{2W}\right]\right)^{1/2} \tag{9B.11}$$

9B.3.1.2 Notes

a) See Table 9B.1 for the component and crack geometry.

b) Crack and geometry dimensional limits: $0.0 < c/W < 1.0$.

c) The membrane and bending stress, σ_m and σ_b, can be determined using stress equations based on strength of materials concepts.

9B.3.2 Plate – Surface Crack, Infinite Length, Through-Wall Fourth Order Polynomial Stress Distribution (KPSCL1)

9B.3.2.1 The Mode I Stress Intensity Factor (Reference [40])

$$K_I = \left[G_0\left(\sigma_0 + p_c\right) + G_1\sigma_1\left(\frac{a}{t}\right) + G_2\sigma_2\left(\frac{a}{t}\right)^2 + G_3\sigma_3\left(\frac{a}{t}\right)^3 + G_4\sigma_4\left(\frac{a}{t}\right)^4 \right]\sqrt{\pi a} \tag{9B.12}$$

9B.3.2.2 Notes:

a) See Figure 9B.2(b) for the component and crack geometry.

b) The coefficients of the stress distribution to be used are defined in paragraph 9B.2.2.3.

c) The influence coefficients G_0 through G_4 are given by the following equation where the constants C_0 through C_4 are provided in Table 9B.2.

$$G_i = C_0 + C_1\left(\frac{a}{t}\right)^2 + C_2\left(\frac{a}{t}\right)^4 + C_3\left(\frac{a}{t}\right)^6 + C_4\left(\frac{a}{t}\right)^8 \tag{9B.13}$$

d) Crack and geometry dimensional limits, $0.0 < a/t \leq 0.8$.

e) The solution presented is for the case of no restraint on the ends of the plate.

9B.3.3 Plate – Surface Crack, Infinite Length, Through-Wall Arbitrary Stress Distribution (KPSCL2)

9B.3.3.1 The Mode I Stress Intensity Factor (Reference [3])

The stress intensity factor can be determined using the weight function method (see paragraph 9B.14.3). The influence coefficients G_0 and G_1 required to compute M_1, M_2 and M_3 can be determined using paragraph 9B.3.2.2(c).

9B.3.3.2 Notes: see paragraph 9B.3.2.2.

9B.3.4 Plate – Surface Crack, Semi-Elliptical Shape, Through-wall Membrane and Bending Stress (KPSCE1)

9B.3.4.1 The Mode I Stress Intensity Factor (Reference [1])

$$K_I = \left(M_m\left(\sigma_m + p_c\right) + M_b\sigma_b\right)\sqrt{\frac{\pi a}{Q}} \tag{9B.14}$$

where,

$$Q = 1.0 + 1.464\left(\frac{a}{c}\right)^{1.65} \quad for \;\; a/c \leq 1.0 \tag{9B.15}$$

$$Q = 1.0 + 1.464\left(\frac{c}{a}\right)^{1.65} \quad for \;\; a/c > 1.0 \tag{9B.16}$$

The membrane correction factor is given by:

$$M_m = M_s\left(M_1 + M_2\left(\frac{a}{t}\right)^2 + M_3\left(\frac{a}{t}\right)^4\right) g \cdot f_\varphi \cdot f_w \tag{9B.17}$$

where,

$$M_s = 1.0 \tag{9B.18}$$

$$f_w = \left(\sec\left[\frac{\pi c}{2W} \cdot \sqrt{\frac{a}{t}} \right] \right)^{0.5} \tag{9B.19}$$

For $a/c \leq 1.0$:

$$M_1 = 1.13 - 0.09\left(\frac{a}{c}\right) \tag{9B.20}$$

$$M_2 = \frac{0.89}{0.2 + \left(\frac{a}{c}\right)} - 0.54 \tag{9B.21}$$

$$M_3 = 0.5 - \frac{1}{0.65 + \left(\frac{a}{c}\right)} + 14\left\{1 - \left(\frac{a}{c}\right)\right\}^{24} \tag{9B.22}$$

$$g = 1 + \left(0.1 + 0.35\left(\frac{a}{t}\right)^2\right)\left(1 - \sin[\varphi]\right)^2 \tag{9B.23}$$

$$f_\varphi = \left(\left(\frac{a}{c}\right)^2 \cos^2[\varphi] + \sin^2[\varphi]\right)^{0.25} \tag{9B.24}$$

For $a/c > 1.0$:

$$M_1 = \left(\frac{c}{a}\right)^{0.5}\left\{1 + 0.04\left(\frac{c}{a}\right)\right\} \tag{9B.25}$$

$$M_2 = 0.2\left(\frac{c}{a}\right)^4 \tag{9B.26}$$

$$M_3 = -0.11\left(\frac{c}{a}\right)^4 \tag{9B.27}$$

$$g = 1 + \left(0.1 + 0.35\left(\frac{c}{a}\right)\left(\frac{a}{t}\right)^2\right)\left(1 - \sin[\varphi]\right)^2 \tag{9B.28}$$

$$f_\varphi = \left(\left(\frac{c}{a}\right)^2 \sin^2[\varphi] + \cos^2[\varphi]\right)^{0.25} \tag{9B.29}$$

The bending correction factor is given by:

$$M_b = M_m H \tag{9B.30}$$

where,

$$H = H_1 + \left(H_2 - H_1\right)\sin^q\left[\varphi\right] \tag{9B.31}$$

$$H_2 = 1 + G_1\left(\frac{a}{t}\right) + G_2\left(\frac{a}{t}\right)^2 \tag{9B.32}$$

For $a/c \le 1.0$:

$$q = 0.2 + \left(\frac{a}{c}\right) + 0.6\left(\frac{a}{t}\right) \tag{9B.33}$$

$$H_1 = 1 - 0.34\left(\frac{a}{t}\right) - 0.11\left(\frac{a}{c}\right)\left(\frac{a}{t}\right) \tag{9B.34}$$

$$G_1 = -1.22 - 0.12\left(\frac{a}{c}\right) \tag{9B.35}$$

$$G_2 = 0.55 - 1.05\left(\frac{a}{c}\right)^{0.75} + 0.47\left(\frac{a}{c}\right)^{1.5} \tag{9B.36}$$

For $a/c > 1.0$:

$$q = 0.2 + \left(\frac{c}{a}\right) + 0.6\left(\frac{a}{t}\right) \tag{9B.37}$$

$$H_1 = 1 - \left(0.04 + 0.41\left(\frac{c}{a}\right)\right)\left(\frac{a}{t}\right) + \left(0.55 - 1.93\left(\frac{c}{a}\right)^{0.75} + 1.38\left(\frac{c}{a}\right)^{1.5}\right)\left(\frac{a}{t}\right)^2 \tag{9B.38}$$

$$G_1 = -2.11 + 0.77\left(\frac{c}{a}\right) \tag{9B.39}$$

$$G_2 = 0.55 - 0.72\left(\frac{c}{a}\right)^{0.75} + 0.14\left(\frac{c}{a}\right)^{1.5} \tag{9B.40}$$

9B.3.4.2 Notes:

a) See Figure 9B.2(a) for the component and crack geometry.

b) Crack and geometry dimensional limits:

1) $0.0 < a/t \le 0.8 \quad for \quad 0.0 < a/c \le 0.2$

2) $0.0 < a/t \le 1.0 \quad for \quad 0.2 < a/c \le 2.0$

3) $0.0 < a/c \le 2.0$

4) $0.0 < c/W < 1.0$

5) $0 \le \varphi \le \pi$

c) If $c >> a$, the solution approaches that of a plate with an edge crack (see Part 9, Figure 9.1(d)).

d) The solution presented can be used to determine a conservative estimate of the stress intensity factor for cylinders and spheres when $R_i/t > 10$. The following modifications are required:

1) A surface correction factor, M_s, should be used for longitudinal cracks or circumferential cracks in cylinders or circumferential cracks in spheres (see paragraph 9B.2.3).

2) The finite width correction factor should be set equal to one, $f_w = 1.0$.

3) For internal cracks, the pressure loading on the crack faces should be included in the membrane stress.

e) The stress intensity factor solution presented above may be overly conservative for finite width plates. A more accurate estimate of the stress intensity factor can be obtained by using the following finite width correction factor for the membrane stress in Equation 9B.18. The finite width correction factor for the bending stress is given by Equation 9B.40, (see reference [20]).

$$f_{wm} = f_b \left(\sec\left[\left(\frac{\pi c}{2W} \right) \cdot \sqrt{\left(\frac{a}{t} \right)\left(1 - 0.6\sin\left[\varphi\right]\right)} \right] \right)^{0.5} \tag{9B.41}$$

where,

$$f_b = 1 + 0.38\left(\frac{a}{c} \right)\left(\frac{a}{t} \right)\left(\frac{c}{W} \right)^2 \cos\left[\varphi\right] \tag{9B.42}$$

f) The stresses σ_m and σ_b can be determined using stress equations based on strength of materials concepts.

9B.3.5 Plate – Surface Cracks, Semi-Elliptical Shape, Through-Wall Fourth Order Polynomial Stress Distribution (KPSCE2)

9B.3.5.1 The Mode I Stress Intensity Factor (Reference [3])

$$K_I = \left[G_0\left(\sigma_0 + p_c\right) + G_1\sigma_1\left(\frac{a}{t} \right) + G_2\sigma_2\left(\frac{a}{t} \right)^2 + G_3\sigma_3\left(\frac{a}{t} \right)^3 + G_4\sigma_4\left(\frac{a}{t} \right)^4 \right] \sqrt{\frac{\pi a}{Q}} \cdot f_w \tag{9B.43}$$

9B.3.5.2 Notes:

a) See Figure 9B.2(a) for the component and crack geometry.

b) The coefficients of the stress distribution to be used are defined in paragraph 9B.2.2.3.

c) The influence coefficients G_0 through G_4 are given by the equations shown below. The constants for these equations are provided in Table 9B.3 for $0.2 \le a/c \le 1.0$. The expressions for the influence coefficients were developed by curve fitting the data provided in Tables A-3320-1 and A-3320-2 of Section XI, Division 1 of the ASME B&PV Code. The curve fit equations cover the full range of data within 3%.

For $\varphi = 0°$:

$$G_i = \frac{C_0 + C_2\left(\frac{a}{t} \right) + C_4\left(\frac{a}{2c} \right) + C_6\left(\frac{a}{t} \right)^2 + C_8\left(\frac{a}{2c} \right)^2 + C_{10}\left(\frac{a}{t} \right)\cdot\left(\frac{a}{2c} \right)}{1.0 + C_1\left(\frac{a}{t} \right) + C_3\left(\frac{a}{2c} \right) + C_5\left(\frac{a}{t} \right)^2 + C_7\left(\frac{a}{2c} \right)^2 + C_9\left(\frac{a}{t} \right)\cdot\left(\frac{a}{2c} \right)} \tag{9B.44}$$

For $\varphi = 90°$:

$$G_i = \left(\begin{array}{l} C_0 + C_1\left(\frac{a}{t}\right) + C_2 \ln\left[\frac{a}{2c}\right] + C_3\left(\frac{a}{t}\right)^2 + C_4\left(\ln\left[\frac{a}{2c}\right]\right)^2 + C_5\left(\frac{a}{t}\right)\cdot\left(\ln\left[\frac{a}{2c}\right]\right) + \\ C_6\left(\frac{a}{t}\right)^3 + C_7\left(\ln\left[\frac{a}{2c}\right]\right)^3 + C_8\left(\frac{a}{t}\right)\cdot\left(\ln\left[\frac{a}{2c}\right]\right)^2 + C_9\left(\frac{a}{t}\right)^2\cdot\left(\ln\left[\frac{a}{2c}\right]\right) \end{array} \right) \quad \text{(9B.45)}$$

d) If $a/c < 0.2$, the influence coefficients G_0 and G_1 are determined from the solution in paragraph 9B.3.4 using the equations shown below. The influence coefficients G_2, G_3, and G_4 can be computed using paragraph 9B.14.3 or 9B.14.4.

$$G_0 = \frac{M_m}{f_w} \quad \text{(9B.46)}$$

$$G_1 = \frac{t}{a}\left(\frac{M_m - M_b}{2}\right)\frac{1}{f_w} \quad \text{(9B.47)}$$

e) The following coefficients have been previously defined:

1) Q by Equation (9B.15) or (9B.16)

2) f_w by Equation (9B.19)

3) M_m by Equation (9B.17)

4) M_b by Equation (9B.30)

f) Crack and geometry dimensional limits:

1) $0.0 < a/t \leq 0.8$

2) $0.0 < a/c \leq 1.0$

3) $0.0 < c/W < 1.0$

4) $\varphi \leq \pi/2$; for $\pi/2 < \varphi \leq \pi$ $K_I(\varphi) = K_I(\pi - \varphi)$

g) See paragraph 9B.3.4.2(d) to determine M_s.

h) The solution in paragraph 9B.5.11 can be used for a flat plate by setting $t/R_i = 0$.

9B.3.6 Plate – Surface Crack, Semi-Elliptical Shape, Through-Wall Arbitrary Stress Distribution (KPSCE3)

9B.3.6.1 The Mode I Stress Intensity Factor (Reference [6])

$$K_I = \left[\int_0^a h(x,a)\,\sigma(x)\,dx\right] f_w \quad \text{(9B.48)}$$

The parameter $h(x,a)$ is a weight function, $\sigma(x)$ is the stress normal to the crack plane computed when the component is in the uncracked state, x is the through-thickness distance measured from the free surface that contains the crack, and f_w is the finite width correction factor given by Equation 9B.18.

The weight function at the deepest point of the crack $\varphi = \pi/2$:

$$h_{\varphi=90}(x,a) = \frac{2}{\sqrt{2\pi(a-x)}}\left[1 + M_1\left(1-\frac{x}{a}\right)^{1/2} + M_2\left(1-\frac{x}{a}\right) + M_3\left(1-\frac{x}{a}\right)^{3/2}\right] \quad (9B.49)$$

where Q is given by Equation (9B.15) or (9B.16) and,

$$M_1 = \frac{\pi}{\sqrt{2Q}}(4Y_0 - 6Y_1) - \frac{24}{5} \quad (9B.50)$$

$$M_2 = 3 \quad (9B.51)$$

$$M_3 = 2\left(\frac{\pi}{\sqrt{2Q}}Y_0 - M_1 - 4\right) \quad (9B.52)$$

$$Y_0 = B_0 + B_1\left(\frac{a}{t}\right)^2 + B_2\left(\frac{a}{t}\right)^4 \quad (9B.53)$$

$$B_0 = 1.10190 - 0.019863\left(\frac{a}{c}\right) - 0.043588\left(\frac{a}{c}\right)^2 \quad (9B.54)$$

$$B_1 = 4.32489 - 14.9372\left(\frac{a}{c}\right) + 19.4389\left(\frac{a}{c}\right)^2 - 8.52318\left(\frac{a}{c}\right)^3 \quad (9B.55)$$

$$B_2 = -3.03329 + 9.96083\left(\frac{a}{c}\right) - 12.582\left(\frac{a}{c}\right)^2 + 5.52318\left(\frac{a}{c}\right)^3 \quad (9B.56)$$

$$Y_1 = A_0 + A_1\left(\frac{a}{t}\right)^2 + A_2\left(\frac{a}{t}\right)^4 \quad (9B.57)$$

$$A_0 = 0.456128 - 0.114206\left(\frac{a}{c}\right) - 0.046523\left(\frac{a}{c}\right)^2 \quad (9B.58)$$

$$A_1 = 3.022 - 10.8679\left(\frac{a}{c}\right) + 14.94\left(\frac{a}{c}\right)^2 - 6.8537\left(\frac{a}{c}\right)^3 \quad (9B.59)$$

$$A_2 = -2.28655 + 7.88771\left(\frac{a}{c}\right) - 11.0675\left(\frac{a}{c}\right)^2 + 5.16354\left(\frac{a}{c}\right)^3 \quad (9B.60)$$

The weight function at the free surface of the crack ($\varphi = 0$):

$$h_{\varphi=0}(x,a) = \frac{2}{\sqrt{\pi x}}\left[1 + N_1\left(\frac{x}{a}\right)^{1/2} + N_2\left(\frac{x}{a}\right) + N_3\left(\frac{x}{a}\right)^{3/2}\right] \quad (9B.61)$$

where,

$$N_1 = \frac{\pi}{\sqrt{4Q}}\left(30F_1 - 18F_0\right) - 8 \tag{9B.62}$$

$$N_2 = \frac{\pi}{\sqrt{4Q}}\left(60F_0 - 90F_1\right) + 15 \tag{9B.63}$$

$$N_3 = -\left(1 + N_1 + N_2\right) \tag{9B.64}$$

$$F_0 = \alpha\left(\frac{a}{c}\right)^{\beta} \tag{9B.65}$$

$$\alpha = 1.14326 + 0.0175996\left(\frac{a}{t}\right) + 0.501001\left(\frac{a}{t}\right)^2 \tag{9B.66}$$

$$\beta = 0.458320 - 0.102985\left(\frac{a}{t}\right) - 0.398175\left(\frac{a}{t}\right)^2 \tag{9B.67}$$

$$F_1 = \gamma\left(\frac{a}{c}\right)^{\delta} \tag{9B.68}$$

$$\gamma = 0.976770 - 0.131975\left(\frac{a}{t}\right) - 0.484875\left(\frac{a}{t}\right)^2 \tag{9B.69}$$

$$\delta = 0.448863 - 0.173295\left(\frac{a}{t}\right) - 0.267775\left(\frac{a}{t}\right)^2 \tag{9B.70}$$

9B.3.6.2 Notes:

a) See Figure 9B.2(a) for the component and crack geometry.

b) Crack and geometry dimensional limits:

1) $0.0 < a/t \leq 0.8$

2) $0.1 < a/c \leq 1.0$

3) $0.0 < c/W < 1.0$

4) $\varphi \leq \pi/2 \quad for \quad \pi/2 < \varphi \leq \pi \quad K_I(\varphi) = K_I(\pi - \varphi)$

9B.3.7 Plate – Embedded Crack, Infinite Length, Through-Wall Fourth Order Polynomial Stress Distribution (KPECL)

9B.3.7.1 The Mode I Stress Intensity Factor (Reference [40])

$$K_I = \left[\begin{array}{l} G_0\left(\left(\sigma_0 + p_c\right) + \sigma_1\left(\frac{d_1}{t}\right) + \sigma_2\left(\frac{d_1}{t}\right)^2 + \sigma_3\left(\frac{d_1}{t}\right)^3 + \sigma_4\left(\frac{d_1}{t}\right)^4 \right) + \\ G_1\left(\sigma_1 + 2\sigma_2\left(\frac{d_1}{t}\right) + 3\sigma_3\left(\frac{d_1}{t}\right)^2 + 4\sigma_4\left(\frac{d_1}{t}\right)^3 \right)\left(\frac{a}{t}\right) + \\ G_2\left(\sigma_2 + 3\sigma_3\left(\frac{d_1}{t}\right) + 6\sigma_4\left(\frac{d_1}{t}\right)^2 \right)\left(\frac{a}{t}\right)^2 + \\ G_3\left(\sigma_3 + 4\sigma_4\left(\frac{d_1}{t}\right) \right)\left(\frac{a}{t}\right)^3 + \\ G_4\left(\sigma_4\right)\left(\frac{a}{t}\right)^4 \end{array} \right] \sqrt{\pi a} \qquad (9B.71)$$

9B.3.7.2 Notes:

a) See Figure 9B.3(b) for the component and crack geometry.

b) The coefficients of the stress distribution to be used are defined in paragraph 9B.2.2.3.

c) The influence coefficients G_1 through G_4 for Points A and B are provided in Table 9B.4.

d) Crack and geometry dimensional limits:

1) $0.1 \le d_1/t \le 0.9$

2) For $d_1/t > 0.5$ use $d_1/t = 1 - d_1/t$ to determine the influence coefficients G_1 through G_4 in Table 9B.4, and reverse the stress field for the analysis (see note below).

e) The datum for the stress distribution is at $d_1/t = 0.0$ for $d_1/t \le 0.5$ and at $\mathrm{d}_1/\mathrm{t} = 1.0$ for $d_1/t > 0.5$ (see Figure 9B.4).

f) The solution presented can be used for cylinders and spheres when $R_i/t \ge 5$. In this case, the finite width correction factor should be set to unity, or $f_w = 1.0$.

9B.3.8 Plate – Embedded Crack, Elliptical Shape, Through-Wall Membrane and Bending Stress (KPECE1)

9B.3.8.1 The Mode I Stress Intensity Factor (Reference [4])

$$K_I = \left(M_m \sigma_{me} + M_b \sigma_{be}\right)\sqrt{\frac{\pi a}{Q}} \qquad (9B.72)$$

where Q is given by Equation (9B.15) or (9B.16). The local membrane and bending stress components acting on the crack face (see Figure 9B.5) are given by the following equations.

$$\sigma_{me} = \left(\sigma_m + p_c\right) + \sigma_b\left(1 - \frac{2d_2}{t}\right) \qquad (9B.73)$$

$$\sigma_{be} = \sigma_b \left(\frac{2a}{t} \right) \tag{9B.74}$$

The membrane correction factor is given by:

$$M_m = H_\varphi f_\varphi f_w \tag{9B.75}$$

where f_w is given by Equation (9B.19), f_φ is given by Equation (9B.24) or (9B.29), and

$$H_\varphi = \frac{1}{2}\sin^2[\varphi] \cdot \left(H_{90}\left(1+\sin[\varphi]\right) + H_{270}\left(1-\sin[\varphi]\right)\right) + H_0 \cos^2[\varphi] \tag{9B.76}$$

with,

$$H_{90} = h_1(\alpha,\beta_1) \cdot h_3(\alpha,\beta_2) \tag{9B.77}$$

$$H_0 = h_2(\alpha,\beta_1) \cdot h_2(\alpha,\beta_2) \tag{9B.78}$$

$$H_{270} = h_3(\alpha,\beta_1) \cdot h_1(\alpha,\beta_2) \tag{9B.79}$$

$$h_1(\alpha,\beta_i) = 1 + \left(-0.04 + \frac{0.085}{0.34+\alpha} \right)\beta_i^2 + (0.05 - 0.03\alpha)\beta_i^4 \tag{9B.80}$$

$$h_2(\alpha,\beta_i) = 1 + \left(-0.03 + \frac{0.075}{0.3+\alpha} \right)\beta_i^2 + \left(0.08 - \frac{0.024}{0.1+\alpha} \right)\beta_i^4 \tag{9B.81}$$

$$h_3(\alpha,\beta_i) = 1 + \left(-0.06 + \frac{0.07}{0.25+\alpha} \right)\beta_i^2 + (0.643 - 0.343\alpha)\beta_i^4 \tag{9B.82}$$

$$\alpha = \frac{a}{c} \tag{9B.83}$$

$$\beta_1 = \frac{a}{d_1} \tag{9B.84}$$

$$\beta_2 = \frac{a}{d_2} \tag{9B.85}$$

The bending correction factor is:

$$M_b = -\left[0.5 + 0.2591\alpha^{1.5} - 0.09189\alpha^{2.5} \right] f_\varphi f_W f_\beta \sin[\varphi] \tag{9B.86}$$

where terms are defined above, and

$$f_\beta = \frac{f_{270} + f_{90}}{2} - \left(\frac{f_{270} - f_{90}}{2} \right)\sin[\varphi] \tag{9B.87}$$

$$f_{90} = 1 + \exp\left[-1.9249 - 3.9087\alpha^{0.5} + 4.1067\beta_2^{\,3} \right] \tag{9B.88}$$

$$f_{270} = 1 + \exp\left[-1.9249 - 3.9087\alpha^{0.5} + 4.1067\beta_1^{\,3} \right] \tag{9B.89}$$

9B.3.8.2 Notes:

a) See Figure 9B.3(a) for the component and crack geometry.

b) See Figure 9B.5 for the definition of the membrane and through-wall bending stress components.

c) See Figure 9B.6 for the sign convention of the bending stress.

d) Crack and geometry dimensional limits:

1) $\left(\frac{d_1-a}{t}\right) \geq 0.2 \qquad \left(when\ d_1 \leq \frac{t}{2}\right)$

2) $\left(\frac{d_2-a}{t}\right) \geq 0.2 \qquad \left(when\ d_2 \leq \frac{t}{2}\right)$

3) $0.20 \leq d_1/t \leq 0.80$

4) $0.0 < a/c < 1.0$

5) $0.0 < c/W < 1.0$

6) $-\pi/2 \leq \varphi \leq \pi/2$

e) The solution presented can be used for cylinders and spheres when $R_i/t \geq 5.0$. In this case, the finite width correction factor should be set to unity, $f_w = 1.0$.

9B.3.9 Plate – Embedded Crack, Elliptical Shape, Through-Wall Fourth Order Polynomial Stress Distribution (KPECE2)

9B.3.9.1 Mode I Stress Intensity Factor (Reference [40])

$$K_I = \left[\begin{array}{l} G_0\left((\sigma_0 + p_c) + \sigma_1\left(\frac{d_1}{t}\right) + \sigma_2\left(\frac{d_1}{t}\right)^2 + \sigma_3\left(\frac{d_1}{t}\right)^3 + \sigma_4\left(\frac{d_1}{t}\right)^4\right) + \\ G_1\left(\sigma_1 + 2\sigma_2\left(\frac{d_1}{t}\right) + 3\sigma_3\left(\frac{d_1}{t}\right)^2 + 4\sigma_4\left(\frac{d_1}{t}\right)^3\right)\left(\frac{a}{t}\right) + \\ G_2\left(\sigma_2 + 3\sigma_3\left(\frac{d_1}{t}\right) + 6\sigma_4\left(\frac{d_1}{t}\right)^2\right)\left(\frac{a}{t}\right)^2 + \\ G_3\left(\sigma_3 + 4\sigma_4\left(\frac{d_1}{t}\right)\right)\left(\frac{a}{t}\right)^3 + \\ G_4(\sigma_4)\left(\frac{a}{t}\right)^4 \end{array}\right] \sqrt{\frac{\pi a}{Q}} \cdot f_w \qquad (9B.90)$$

9B.3.9.2 Notes:

a) See Figure 9B.3(a) for the component and crack geometry.

b) The coefficients of the stress distribution to be used are defined in paragraph 9B.2.2.3.

c) The influence coefficients G_0 through G_4 for inside and outside surface cracks can be determined using the following equations.

$$G_0 = A_{0,0} + A_{0,1}\beta + A_{0,2}\beta^2 + A_{0,3}\beta^3 + A_{0,4}\beta^4 + A_{0,5}\beta^5 + A_{0,6}\beta^6 \quad (9B.91)$$

$$G_1 = A_{1,0} + A_{1,1}\beta + A_{1,2}\beta^2 + A_{1,3}\beta^3 + A_{1,4}\beta^4 + A_{1,5}\beta^5 + A_{1,6}\beta^6 \quad (9B.92)$$

$$G_2 = A_{2,0} + A_{2,1}\beta + A_{2,2}\beta^2 + A_{2,3}\beta^3 + A_{2,4}\beta^4 + A_{2,5}\beta^5 + A_{2,6}\beta^6 \quad (9B.93)$$

$$G_3 = A_{3,0} + A_{3,1}\beta + A_{3,2}\beta^2 + A_{3,3}\beta^3 + A_{3,4}\beta^4 + A_{3,5}\beta^5 + A_{3,6}\beta^6 \quad (9B.94)$$

$$G_4 = A_{4,0} + A_{4,1}\beta + A_{4,2}\beta^2 + A_{4,3}\beta^3 + A_{4,4}\beta^4 + A_{4,5}\beta^5 + A_{4,6}\beta^6 \quad (9B.95)$$

where,

$$\beta = \frac{2\varphi}{\pi} \quad (9B.96)$$

The parameters $A_{i,j}$ (i.e., the values from the row corresponding to G_i and column A_j) are provided in Table 9B.5 for $d_1/t = 0.25$ and $d_1/t = 0.50$.

d) The parameter Q is given by Equation (9B.15) or (9B.16), and f_w is given by Equation (9B.19).

e) Crack and geometry dimensional limits:

1) $0.1 \le d_1/t \le 0.9$

2) $0.125 < a/c \le 1.0$

3) $-\pi/2 \le \varphi \le \pi/2$

4) For $d_1/t > 0.5$ use $d_1/t = 1 - d_1/t$ to determine the influence coefficients G_1 through G_4 in Table 9B.5, and reverse the stress field for the analysis (see note below).

f) The datum for the stress distribution is at $d_1/t = 0.0$ for $d_1/t \le 0.5$ and at $d_1/t = 1.0$ for $d_1/t > 0.5$.

g) The solution presented can be used for cylinders and spheres when $R_i/t \ge 5$. In this case, the finite width correction factor should be set to unity, $f_w = 1.0$ (see Figure 9B.4).

9B.4 Stress Intensity Factor Solutions for Plates with Holes

9B.4.1 Plate with Hole – Through-Wall Single Edge Crack, Through-Wall Membrane and Bending Stress (KPHTC1)

9B.4.1.1 The Mode I Stress Intensity Factor (References [2] and [12])

$$K_I = M_m\{\sigma_m + p_c\}\sqrt{\pi c} + M_b\sigma_b\sqrt{\pi\left(R_h + c\right)} \quad (9B.97)$$

The membrane correction factor is given by:

$$M_m = F_1 + BF_2 \quad (9B.98)$$

$$F_1 = \frac{3.3583 + 6.33015\zeta + 3.80461\zeta^2}{1 + 4.012118\zeta + 5.317858\zeta^2} \quad (9B.99)$$

$$F_2 = \frac{-1.1186 + 0.534114\zeta - 0.0594921\zeta^2}{1 + 2.980567\zeta + 4.253003\zeta^2} \quad (9B.100)$$

and the bending correction factor is given by:

$$M_b = 0.4\left(\frac{19.252\zeta + 173.83\zeta^2 + 60.469\zeta^3}{1.0 + 49.254\zeta + 139.02\zeta^2 + 88.167\zeta^3 - 0.44324\zeta^4}\right) \quad (9B.101)$$

with,

$$\zeta = \frac{c}{R_h} \quad (9B.102)$$

9B.4.1.2 Notes:

a) See Figure 9B.7(a) for the component and crack geometry.

b) See Figure 9B.7(b) for the definition of B.

c) Crack and geometry dimensional limits: $\zeta \geq 0.0$; R_h << plate width.

d) The stresses σ_m and σ_b can be determined using stress equations based on strength of materials concepts.

9B.4.2 Plate with Hole – Through-Wall Double Edge Crack, Through-Wall Membrane and Bending Stress (KPHTC2)

9B.4.2.1 The Mode I Stress Intensity Factor (References [2] and [12])

$$K_I = M_m\left(\sigma_m + p_c\right)\sqrt{\pi c} + M_b\sigma_b\sqrt{\pi\left(R_h + c\right)} \quad (9B.103)$$

The membrane correction factor is given by:

$$M_m = F_1 + BF_2 \quad (9B.104)$$

$$F_1 = \frac{3.3633 + 3.6393\zeta + 0.680967\zeta^2}{1 + 3.54903\zeta + 0.652471\zeta^2} \quad (9B.105)$$

$$F_2 = \frac{-1.1152 + 0.176708\zeta - 0.0112175\zeta^2}{1 + 3.220917\zeta + 5.047662\zeta^2} \quad (9B.106)$$

The bending correction factor is given by:

$$M_b = 0.4\left(\frac{17.739\zeta + 105.05\zeta^2 + 128.16\zeta^3}{1.0 + 35.699\zeta + 95.850\zeta^2 + 130.02\zeta^3 - 0.15592\zeta^4}\right) \quad (9B.107)$$

with,

$$\zeta = \frac{c}{R_h} \quad (9B.108)$$

9B.4.2.2 Notes:

a) See Figure 9B.8(a) for the component and crack geometry.

b) See Figure 9B.8(b) for the definition of B.

c) Crack and geometry dimensional limits: $\zeta \geq 0.0$; R_h << plate width.

d) The stresses σ_m and σ_b can be determined using stress equations based on strength of materials concepts.

9B.4.3 Plate with Hole – Surface Crack in Hole, Semi-Elliptical Shape, Through-Wall Membrane Stress (KPHSC1)

9B.4.3.1 The Mode I Stress Intensity Factor (Reference [1])

$$K_I = M_m\left(\sigma_m + p_c\right)\sqrt{\frac{\pi a}{Q}} \tag{9B.109}$$

where Q is given by Equation (9B.15) or (9B.16), and the membrane correction factor is given by:

$$M_m = \left[M_1 + M_2\left(\frac{a}{t}\right)^2 + M_3\left(\frac{a}{t}\right)^4\right]\cdot g_1 \cdot g_2 \cdot g_3 \cdot f_\varphi \cdot f_w \tag{9B.110}$$

with,

$$M_2 = \frac{0.05}{0.11 + \left(\frac{a}{c}\right)^{1.5}} \tag{9B.111}$$

$$M_3 = \frac{0.29}{0.23 + \left(\frac{a}{c}\right)^{1.5}} \tag{9B.112}$$

$$g_1 = 1.0 - \frac{\left(\frac{a}{t}\right)^4\sqrt{2.6 - 2\left(\frac{a}{t}\right)}}{1.0 + 4\left(\frac{a}{c}\right)}\cdot\cos\left[\varphi\right] \tag{9B.113}$$

$$g_2 = \frac{1.0 + 0.358\zeta + 1.425\zeta^2 - 1.578\zeta^3 + 2.156\zeta^4}{1.0 + 0.08\zeta^2} \tag{9B.114}$$

$$\zeta = \frac{1.0}{1.0 + \left(\frac{c}{R_h}\right)\cos\left[0.9\varphi\right]} \tag{9B.115}$$

$$g_3 = 1.0 + 0.1\left(1 - \cos\left[\varphi\right]\right)^2\left(1 - \frac{a}{t}\right)^{10} \tag{9B.116}$$

In the following equation, set $n = 2$ for two cracks and $n = 1$ for one crack (see paragraph 9B.4.3.2(c)):

$$f_w = \left(\sec\left[\frac{\pi R_h}{2W}\right]\cdot\sec\left[\frac{\pi\left(2R_h + nc\right)}{4\left(W - c\right) + 2nc}\cdot\sqrt{\frac{a}{t}}\right]\right)^{0.5} \tag{9B.117}$$

For $a/c \le 1.0$, f_φ is given by Equation (9B.24) and,

$$M_1 = 1.0 \tag{9B.118}$$

For $a/c > 1.0$, f_φ is given by Equation (9B.29) and,

$$M_1 = \sqrt{\frac{c}{a}} \tag{9B.119}$$

9B.4.3.2 Notes:

a) See Figure 9B.9 for the component and crack geometry.

b) Crack and geometry dimensional limits:

1) $0.0 < a/t < 1.0$

2) $0.2 \le a/c \le 2.0$

3) $0.5 \le R_h/t \le 2.0$

4) $(R_h + c)/W < 0.5$

5) $-\pi/2 \le \varphi \le \pi/2$

c) The stress intensity factor solution provided is for two cracks. To estimate the stress intensity factor for one crack, the following equation can be used:

$$K_{1-crack} = \left(\sqrt{\frac{\frac{4}{\pi} + \frac{ac}{2tR_h}}{\frac{4}{\pi} + \frac{ac}{tR_h}}} \right) K_{2-crack} \tag{9B.120}$$

d) The membrane stress, σ_m, can be determined using stress equations based on strength of materials concepts.

9B.4.4 Plate with Hole, Corner Crack, Semi-Elliptical Shape, Through-Wall Membrane and Bending Stress (KPHSC2)

9B.4.4.1 The Mode I Stress Intensity Factor (Reference [1])

$$K_I = \left(M_m \left(\sigma_m + p_c \right) + M_b \sigma_b \right) \sqrt{\frac{\pi a}{Q}} \tag{9B.121}$$

where Q is given by Equation (9B.15) or (9B.16). The membrane correction factor is given by:

$$M_m = \left(M_1 + M_2 \left(\frac{a}{t} \right)^2 + M_3 \left(\frac{a}{t} \right)^4 \right) \cdot g_1 \cdot g_2 \cdot g_3 \cdot g_4 \cdot f_\varphi \cdot f_w \tag{9B.122}$$

where f_w is given by Equation 9B.116, and

$$g_2 = \frac{1.0 + 0.358\zeta + 1.425\zeta^2 - 1.578\zeta^3 + 2.156\zeta^4}{1.0 + 0.13\zeta^2} \tag{9B.123}$$

$$\zeta = \frac{1.0}{1.0 + \left(\frac{c}{R_h}\right)\cos\left[\mu\varphi\right]} \tag{9B.124}$$

$$\mu = 0.85 \tag{9B.125}$$

For $a/c \le 1.0$, f_φ is given by Equation (9B.24), and

$$M_1 = 1.13 - 0.09\left(\frac{a}{c}\right) \tag{9B.126}$$

$$M_2 = \frac{0.89}{0.2 + \left(\frac{a}{c}\right)} - 0.54 \tag{9B.127}$$

$$M_3 = 0.5 - \frac{1}{0.65 + \left(\frac{a}{c}\right)} + 14\left(1 - \left(\frac{a}{c}\right)\right)^{24} \tag{9B.128}$$

$$g_1 = 1 + \left(0.1 + 0.35\left(\frac{a}{t}\right)^2\right)\left(1 - \sin\left[\varphi\right]\right)^2 \tag{9B.129}$$

$$g_3 = \left[1 + 0.04\left(\frac{a}{c}\right)\right]\left[1 + 0.1\left(1 - \cos\left[\varphi\right]\right)^2\right]\left[0.85 + 0.15\left(\frac{a}{t}\right)^{0.25}\right] \tag{9B.130}$$

$$g_4 = 1 - 0.7\left[1 - \left(\frac{a}{t}\right)\right]\left[\left(\frac{a}{c}\right) - 0.2\right]\left[1 - \left(\frac{a}{c}\right)\right] \tag{9B.131}$$

For $a/c > 1.0$, f_φ is given by Equation (9B.29), and

$$M_1 = \left(\frac{c}{a}\right)^{0.5}\left(1 + 0.04\left(\frac{c}{a}\right)\right) \tag{9B.132}$$

$$M_2 = 0.2\left(\frac{c}{a}\right)^4 \tag{9B.133}$$

$$M_3 = -0.11\left(\frac{c}{a}\right)^4 \tag{9B.134}$$

$$g_1 = 1 + \left(0.1 + 0.35\left(\frac{c}{a}\right)\left(\frac{a}{t}\right)^2\right)\left(1 - \sin\left[\varphi\right]\right)^2 \tag{9B.135}$$

$$g_3 = \left[1.13 - 0.09\left(\frac{c}{a}\right)\right]\left[1 + 0.1\left(1 - \cos\left[\varphi\right]\right)^2\right]\left[0.85 + 0.15\left(\frac{a}{t}\right)^{0.25}\right] \tag{9B.136}$$

$$g_4 = 1.0 \tag{9B.137}$$

The bending correction factor is given by:

$$M_b = M_m H \tag{9B.138}$$

where M_m is evaluated using the above equations with,

$$\mu = 0.85 - 0.25\left(\frac{a}{t}\right)^{0.25} \tag{9B.139}$$

and,

$$H = H_1 + \left(H_2 - H_1\right)\sin^q\left[\varphi\right] \tag{9B.140}$$

$$H_1 = 1 + G_{11}\left(\frac{a}{t}\right) + G_{12}\left(\frac{a}{t}\right)^2 + G_{13}\left(\frac{a}{t}\right)^3 \tag{9B.141}$$

$$H_2 = 1 + G_{21}\left(\frac{a}{t}\right) + G_{22}\left(\frac{a}{t}\right)^2 + G_{23}\left(\frac{a}{t}\right)^3 \tag{9B.142}$$

For $a/c \leq 1.0$:

$$q = 0.2 + \left(\frac{a}{c}\right) + 0.6\left(\frac{a}{t}\right) \tag{9B.143}$$

$$G_{11} = -0.43 - 0.74\left(\frac{a}{c}\right) - 0.84\left(\frac{a}{c}\right)^2 \tag{9B.144}$$

$$G_{12} = 1.25 - 1.19\left(\frac{a}{c}\right) + 4.39\left(\frac{a}{c}\right)^2 \tag{9B.145}$$

$$G_{13} = -1.94 + 4.22\left(\frac{a}{c}\right) - 5.51\left(\frac{a}{c}\right)^2 \tag{9B.146}$$

$$G_{21} = -1.5 - 0.04\left(\frac{a}{c}\right) - 1.73\left(\frac{a}{c}\right)^2 \tag{9B.147}$$

$$G_{22} = 1.71 - 3.17\left(\frac{a}{c}\right) + 6.84\left(\frac{a}{c}\right)^2 \tag{9B.148}$$

$$G_{23} = -1.28 + 2.71\left(\frac{a}{c}\right) - 5.22\left(\frac{a}{c}\right)^2 \tag{9B.149}$$

For $a/c > 1.0$:

$$q = 0.2 + \left(\frac{c}{a}\right) + 0.6\left(\frac{a}{t}\right) \tag{9B.150}$$

$$G_{11} = -2.07 + 0.06\left(\frac{c}{a}\right) \tag{9B.151}$$

$$G_{12} = 4.35 + 0.16\left(\frac{c}{a}\right) \tag{9B.152}$$

$$G_{13} = -2.93 - 0.3\left(\frac{c}{a}\right) \tag{9B.153}$$

$$G_{21} = -3.64 + 0.37\left(\frac{c}{a}\right) \tag{9B.154}$$

$$G_{22} = 5.87 - 0.49\left(\frac{c}{a}\right) \tag{9B.155}$$

$$G_{23} = -4.32 + 0.53\left(\frac{c}{a}\right) \tag{9B.156}$$

9B.4.4.2 Notes:

a) See Figure 9B.10 for the component and crack geometry.

b) Crack and geometry dimensional limits:

1) $0.0 < a/t \leq 1.0 \qquad (for\ remote\ tension)$

2) $0.0 < a/t \leq 0.8 \qquad (for\ remote\ bending)$

3) $0.2 \leq a/c \leq 2.0$

4) $0.5 \leq R_h/t \leq 2.0$

5) $(R_h + c)/W < 0.5$

6) $\varphi \leq \pi/2\,;\quad for\quad \pi/2 < \varphi \leq \pi \quad K_I(\varphi) = K_I(\pi - \varphi)$

c) To estimate the stress intensity factor for one crack, use Equation 9B.119.

d) The membrane and bending stress, σ_m and σ_b, can be determined using stress equations based on strength of materials concepts.

9B.5 Stress Intensity Factor Solutions for Cylinders

9B.5.1 Cylinder – Through-Wall Crack, Longitudinal Direction, Through-Wall Membrane and Bending Stress (KCTCL)

9B.5.1.1 The Mode I Stress Intensity Factor (References [11] and [16])

Membrane and Bending Stress:

$$K_I = \left[\left(\sigma_m + p_c\right)G_0 + \sigma_b\left(G_0 - 2G_1\right)\right]\sqrt{\pi c} \tag{9B.157}$$

or

$$K_I = \left(\left(\sigma_0 + p_c\right)G_0 + \sigma_1 G_1\right)\sqrt{\pi c} \tag{9B.158}$$

Internal Pressure Only, crack face pressure loading is included:

$$K_I = \frac{pR_o}{t} G_p \sqrt{\pi c} \tag{9B.159}$$

9B.5.1.2 Notes:

a) See Figure 9B.11 for the component and crack geometry.

b) The influence coefficients G_0, G_1, and G_p are calculated using the following equations where the constants $A_1 \rightarrow A_6$ are provided in Table 9B.6 for K_I at the inside surface and in Table 9B.7 for the outside surface.

$$G_{0,1,p} = \frac{A_0 + A_1\lambda + A_2\lambda^2 + A_3\lambda^3}{1 + A_4\lambda + A_5\lambda^2 + A_6\lambda^3} \tag{9B.160}$$

$$\lambda = \frac{1.818c}{\sqrt{R_i t}} \tag{9B.161}$$

9B.5.2 Cylinder – Through-Wall Crack, Circumferential Direction, Through-Wall Membrane and Bending Stress (KCTCC1)

9B.5.2.1 The Mode I Stress Intensity Factor (References [11] and [16])

Membrane and Bending Stress:

$$K_I = \left[\left(\sigma_m + p_c \right) G_0 + \sigma_b \left(G_0 - 2G_1 \right) \right] \sqrt{\pi c} \tag{9B.162}$$

or

$$K_I = \left(\left(\sigma_0 + p_c \right) G_0 + \sigma_1 G_1 \right) \sqrt{\pi c} \tag{9B.163}$$

Internal Pressure Only, crack face pressure loading is included:

$$K_I = \frac{pR_o^2}{R_o^2 - R_i^2} \cdot G_0 \sqrt{\pi c} \tag{9B.164}$$

9B.5.2.2 Notes:

a) See Figure 9B.12 for the component and crack geometry.

b) The influence coefficients G_0 and G_1 are calculated using the following equations where the constants $A_1 \rightarrow A_6$ are provided in Table 9B.8 for inside diameter surface crack and in Table 9B.9 for outside diameter surface crack.

$$G_{0,1} = \frac{A_0 + A_1\lambda + A_2\lambda^2 + A_3\lambda^3}{1 + A_4\lambda + A_5\lambda^2 + A_6\lambda^3} \tag{9B.165}$$

$$\lambda = \frac{1.818c}{\sqrt{R_i t}} \tag{9B.166}$$

c) For internal pressure with a net section axial force,

$$\sigma_m = \frac{pR_i^2}{R_o^2 - R_i^2} + \frac{F}{\pi \left(R_o^2 - R_i^2 \right)} \tag{9B.167}$$

$$\sigma_b = 0.0 \tag{9B.168}$$

9B.5.3 Cylinder – Through-Wall Crack, Circumferential Direction, Pressure with Net Section Axial Force and Bending Moment (KCTCC2)

9B.5.3.1 The Mode I Stress Intensity Factor (Reference [16])

Membrane and Bending Stress:

$$K_I = \left[\left(\sigma_m + p_c \right) G_0 + \sigma_b \left(G_0 - 2G_1 \right) + \sigma_{gb} G_5 \right] \sqrt{\pi c} \tag{9B.169}$$

Internal Pressure Stress Plus Net Section Bending Only, crack face pressure loading is included:

$$K_I = \left[\frac{pR_o^2}{R_o^2 - R_i^2} G_0 + \sigma_{gb} G_5 \right] \sqrt{\pi c} \tag{9B.170}$$

9B.5.3.2 Notes:

a) See Figure 9B.12 for the component and crack geometry.

b) The influence coefficients G_0, G_1, and G_5 are calculated using the following equations where the constants $A_1 \rightarrow A_6$ are provided in Table 9B.8 for inside diameter surface crack and in Table 9B.9 for outside diameter surface crack.

$$G_{0,1,5} = \frac{A_0 + A_1\lambda + A_2\lambda^2 + A_3\lambda^3}{1 + A_4\lambda + A_5\lambda^2 + A_6\lambda^3} \tag{9B.171}$$

$$\lambda = \frac{1.818c}{\sqrt{R_i t}} \tag{9B.172}$$

c) For internal pressure with a net section axial force, and net-section bending moment.

$$\sigma_m = \frac{pR_i^2}{\left(R_o^2 - R_i^2 \right)} + \frac{F}{\pi \left(R_o^2 - R_i^2 \right)} \tag{9B.173}$$

$$\sigma_b = 0.0 \tag{9B.174}$$

$$\sigma_{gb} = \frac{MR_o}{0.25\pi \left(R_o^4 - R_i^4 \right)} \tag{9B.175}$$

9B.5.4 Cylinder – Surface Crack, Longitudinal Direction – Infinite Length, Internal Pressure (KCSCLL1)

9B.5.4.1 The Mode I Stress Intensity Factor (References [40], [53] and [54])

Inside Surface, crack face pressure loading is included:

$$K_I = \frac{pR_o^{\,2}}{R_o^{\,2} - R_i^{\,2}} \left[2G_0 - 2G_1 \left(\frac{a}{R_i} \right) + 3G_2 \left(\frac{a}{R_i} \right)^2 - 4G_3 \left(\frac{a}{R_i} \right)^3 + 5G_4 \left(\frac{a}{R_i} \right)^4 \right] \sqrt{\pi a} \tag{9B.176}$$

Outside Surface:

$$K_I = \frac{pR_i^2}{R_o^2 - R_i^2}\left[2G_0 + 2G_1\left(\frac{a}{R_o}\right) + 3G_2\left(\frac{a}{R_o}\right)^2 + 4G_3\left(\frac{a}{R_o}\right)^3 + 5G_4\left(\frac{a}{R_o}\right)^4\right]\sqrt{\pi a} \quad (9B.177)$$

9B.5.4.2 Notes:

a) See Figure 9B.13 for the component and crack geometry.

b) The influence coefficients G_0 through G_4 are provided in Table 9B.10.

c) Crack and geometry dimensional limits:

1) $0.0 \le a/t \le 0.8$

2) $0.001 \le t/R_i \le 3.0$

9B.5.5 Cylinder – Surface Crack, Longitudinal Direction – Infinite Length, Through-Wall Fourth Order Polynomial Stress Distribution (KCSCLL2)

9B.5.5.1 The Mode I Stress Intensity Factor (References [40], [53] and [54])

$$K_I = \left[G_0\left(\sigma_0 + p_c\right) + G_1\sigma_1\left(\frac{a}{t}\right) + G_2\sigma_2\left(\frac{a}{t}\right)^2 + G_3\sigma_3\left(\frac{a}{t}\right)^3 + G_4\sigma_4\left(\frac{a}{t}\right)^4\right]\sqrt{\pi a} \quad (9B.178)$$

9B.5.5.2 Notes:

a) See paragraph 9B.5.4.2.

b) The coefficients of the stress distribution to be used are defined in paragraph 9B.2.2.3.

9B.5.6 Cylinder – Surface Crack, Longitudinal Direction – Infinite Length, Through-Wall Arbitrary Stress Distribution (KCSCLL3)

9B.5.6.1 The Mode I Stress Intensity Factor

The stress intensity factor can be determined using the weight function method (see paragraph 9B.14.5). The influence coefficients G_0 and G_1 required to compute M_1, M_2, and M_3 can be determined using paragraph 9B.5.4.2(b).

9B.5.6.2 Notes: see paragraph 9B.5.4.2.

9B.5.7 Cylinder – Surface Crack, Circumferential Direction – 360 Degrees, Pressure with A Net Section Axial Force and Bending Moment (KCSCCL1)

9B.5.7.1 The Mode I Stress Intensity Factor

$$K_I = \left[G_0\left(\sigma_0 + p_c\right) + G_1\sigma_1\left(\frac{a}{t}\right)\right]\sqrt{\pi a} \quad (9B.179)$$

where for an inside surface crack,

$$\sigma_0 = \sigma_m - \sigma_b \quad (9B.180)$$

$$\sigma_1 = 2\sigma_b \quad (9B.181)$$

and for an outside surface crack,

$$\sigma_0 = \sigma_m + \sigma_b \tag{9B.182}$$

$$\sigma_1 = -2\sigma_b \tag{9B.183}$$

with,

$$\sigma_m = \frac{pR_i^2}{\left(R_o^2 - R_i^2\right)} + \frac{F}{\pi\left(R_o^2 - R_i^2\right)} + \frac{2M\left(R_o + R_i\right)}{\pi\left(R_o^4 - R_i^4\right)} \tag{9B.184}$$

$$\sigma_b = \frac{2M\left(R_o - R_i\right)}{\pi\left(R_o^4 - R_i^4\right)} \tag{9B.185}$$

9B.5.7.2 Notes:

a) See Figure 9B.14 for the component and crack geometry.

b) The influence coefficients G_0 and G_1 are provided in Table 9B.11.

c) Crack and geometry dimensional limits:

1) $0.0 \le a/t \le 0.8$

2) $0.001 \le t/R_i \le 3.0$

d) This solution represents the maximum stress intensity on the cross section at the location of maximum bending stress. The stress intensity factor at other locations can be determined by using the appropriate value of bending stress.

9B.5.8 Cylinder – Surface Crack, Circumferential Direction – 360 Degrees, Through-Wall Fourth Order Polynomial Stress Distribution (KCSCCL2)

9B.5.8.1 The Mode I Stress Intensity Factor (References [40], [53] and [54])

$$K_I = \left[G_0\left(\sigma_0 + p_c\right) + G_1\sigma_1\left(\frac{a}{t}\right) + G_2\sigma_2\left(\frac{a}{t}\right)^2 + G_3\sigma_3\left(\frac{a}{t}\right)^3 + G_4\sigma_4\left(\frac{a}{t}\right)^4 \right]\sqrt{\pi a} \tag{9B.186}$$

9B.5.8.2 Notes:

a) See paragraph 9B.5.7.2.

b) The coefficients of the stress distribution to be used are defined in paragraph 9B.2.2.3.

c) The influence coefficients G_0 through G_4 are provided in Table 9B.11.

9B.5.9 Cylinder – Surface Crack, Circumferential Direction – 360 Degrees, Through-Wall Arbitrary Stress Distribution (KCSCCL3)

9B.5.9.1 The Mode I Stress Intensity Factor

The stress intensity factor can be determined using the weight function method (see paragraph 9B.14.5). The influence coefficients G_0 and G_1 required to compute M_1, M_2, and M_3 can be determined using paragraph 9B.5.7.2(b).

9B.5.9.2 Notes: see paragraph 9B.5.7.2.

9B.5.10 Cylinder – Surface Crack, Longitudinal Direction – Semi-Elliptical Shape, Internal Pressure (KCSCLE1)

9B.5.10.1 The Mode I Stress Intensity Factor (References [40], [53] and [54])

Inside Surface, crack face pressure loading is included:

$$K_I = \frac{pR_o^2}{R_o^2 - R_i^2}\left[2G_0 - 2G_1\left(\frac{a}{R_i}\right) + 3G_2\left(\frac{a}{R_i}\right)^2 - 4G_3\left(\frac{a}{R_i}\right)^3 + 5G_4\left(\frac{a}{R_i}\right)^4\right]\sqrt{\frac{\pi a}{Q}} \quad (9B.187)$$

Outside Surface:

$$K_I = \frac{pR_i^2}{R_o^2 - R_i^2}\left[2G_0 + 2G_1\left(\frac{a}{R_o}\right) + 3G_2\left(\frac{a}{R_o}\right)^2 + 4G_3\left(\frac{a}{R_o}\right)^3 + 5G_4\left(\frac{a}{R_o}\right)^4\right]\sqrt{\frac{\pi a}{Q}} \quad (9B.188)$$

9B.5.10.2 Notes:

a) See Figure 9B.15 for the component and crack geometry.

b) The influence coefficients G_0 and G_1 for inside and outside surface cracks can be determined using the following equations:

$$G_0 = A_{0,0} + A_{0,1}\beta + A_{0,2}\beta^2 + A_{0,3}\beta^3 + A_{0,4}\beta^4 + A_{0,5}\beta^5 + A_{0,6}\beta^6 \quad (9B.189)$$

$$G_1 = A_{1,0} + A_{1,1}\beta + A_{1,2}\beta^2 + A_{1,3}\beta^3 + A_{1,4}\beta^4 + A_{1,5}\beta^5 + A_{1,6}\beta^6 \quad (9B.190)$$

where β is given by Equation (9B.95) and the parameters $A_{i,j}$ (i.e., the values from the row corresponding to G_i and column A_j) are provided in Table 9B.12 for an inside diameter crack and in Table 9B.13 for an outside diameter crack. The influence coefficients G_2, G_3, and G_4 can be computed using paragraph 9B.14.3 or 9B.14.4.

c) Q is determined using Equation (9B.14) or Equation (9B.16).

d) Crack and geometry dimensional limits:

1) $0.0 \le a/t \le 0.8$

2) $0.03125 \le a/c \le 2.0$

3) $\varphi \le \pi/2\,; \quad for \quad \pi/2 < \varphi \le \pi \quad K_I(\varphi) = K_I(\pi - \varphi)$

4) $0.0 \le t/R_i \le 3.0$

e) Influence coefficients are provided in Table 9B.12 and Table 9B.13 for values of $0.03125 \le a/c \le 2.0$. For long cracks where $a/c < 0.03125$, the influence coefficients can be determined by interpolation using the values in Table 9B.12 and Table 9B.13 and the following values for G_0 and G_1. The influence coefficients for the long flaw or infinite length solution (G_0^L and G_1^L) in these equations can be computed using Table 9B.10.

$$G_0 = G_0^L\left(\frac{2\varphi}{\pi}\right)^6 \quad (9B.191)$$

$$G_1 = G_1^L\left(\frac{2\varphi}{\pi}\right)^6 \quad (9B.192)$$

9B.5.11 Cylinder – Surface Crack, Longitudinal Direction – Semi-Elliptical Shape, Through-Wall Fourth Order Polynomial Stress Distribution (KCSCLE2)

9B.5.11.1 The Mode I Stress Intensity Factor (References [40], [53] and [54])

$$K_I = \left[G_0\left(\sigma_0 + p_c\right) + G_1\sigma_1\left(\frac{a}{t}\right) + G_2\sigma_2\left(\frac{a}{t}\right)^2 + G_3\sigma_3\left(\frac{a}{t}\right)^3 + G_4\sigma_4\left(\frac{a}{t}\right)^4 \right]\sqrt{\frac{\pi a}{Q}} \qquad (9B.193)$$

9B.5.11.2 Notes:

a) See paragraph 9B.5.10.2.

b) The coefficients of the stress distribution to be used are defined in paragraph 9B.2.2.3.

9B.5.12 Cylinder – Surface Crack, Longitudinal Direction – Semi-Elliptical Shape, Through-Wall Arbitrary Stress Distribution (KCSCLE3)

9B.5.12.1 The Mode I Stress Intensity Factor

The stress intensity factor can be determined using the weight function method (see paragraph 9B.14.5). The influence coefficients G_0 and G_1 required to compute M_1, M_2, and M_3 can be determined using paragraph 9B.5.10.2(b).

9B.5.12.2 Notes: see paragraph 9B.5.10.2.

9B.5.13 Cylinder – Surface Crack, Circumferential Direction – Semi-Elliptical Shape, Internal Pressure and Net-Section Axial Force (KCSCCE1)

9B.5.13.1 The Mode I Stress Intensity Factor (References [40], [53] and [54])

Inside Surface, crack face pressure loading is included:

$$K_I = G_0\left(\frac{pR_o^{\,2}}{R_o^{\,2} - R_i^{\,2}} + \frac{F}{\pi\left(R_o^{\,2} - R_i^{\,2}\right)}\right)\sqrt{\frac{\pi a}{Q}} \qquad (9B.194)$$

Outside Surface:

$$K_I = G_0\left(\frac{pR_i^{\,2}}{R_o^{\,2} - R_i^{\,2}} + \frac{F}{\pi\left(R_o^{\,2} - R_i^{\,2}\right)}\right)\sqrt{\frac{\pi a}{Q}} \qquad (9B.195)$$

9B.5.13.2 Notes:

a) See Figure 9B.16 for the component and crack geometry.

b) The influence coefficient, G_0, can be determined using paragraph 9B.5.14.2(b).

c) The parameter Q is given by Equation (9B.15) or (9B.16).

d) Crack and geometry dimensional limits are shown in paragraph 9B.5.14.2.

9B.5.14 Cylinder – Surface Crack, Circumferential Direction – Semi-Elliptical Shape, Through-Wall Fourth Order Polynomial Stress Distribution with a Net Section Bending Stress (KCSCCE2)

9B.5.14.1 The Mode I Stress Intensity Factor (References [40], [53] and [54])

$$K_I = \left[\begin{array}{l} G_0\left(\sigma_0 + p_c\right) + G_1\sigma_1\left(\frac{a}{t}\right) + G_2\sigma_2\left(\frac{a}{t}\right)^2 + \\ G_3\sigma_3\left(\frac{a}{t}\right)^3 + G_4\sigma_4\left(\frac{a}{t}\right)^4 + G_5\sigma_5 + G_6\sigma_6 \end{array} \right] \sqrt{\frac{\pi a}{Q}} \tag{9B.196}$$

9B.5.14.2 Notes:

a) See Figure 9B.16 for the component and crack geometry.

b) The influence coefficients G_0, G_1, G_5, and G_6 for inside and outside surface cracks can be determined using the following equations:

$$G_0 = A_{0,0} + A_{0,1}\beta + A_{0,2}\beta^2 + A_{0,3}\beta^3 + A_{0,4}\beta^4 + A_{0,5}\beta^5 + A_{0,6}\beta^6 \tag{9B.197}$$

$$G_1 = A_{1,0} + A_{1,1}\beta + A_{1,2}\beta^2 + A_{1,3}\beta^3 + A_{1,4}\beta^4 + A_{1,5}\beta^5 + A_{1,6}\beta^6 \tag{9B.198}$$

$$G_5 = A_{5,0} + A_{5,1}\beta + A_{5,2}\beta^2 + A_{5,3}\beta^3 + A_{5,4}\beta^4 + A_{5,5}\beta^5 + A_{5,6}\beta^6 \tag{9B.199}$$

$$G_6 = A_{6,0} + A_{6,1}\beta + A_{6,2}\beta^2 + A_{6,3}\beta^3 + A_{6,4}\beta^4 + A_{6,5}\beta^5 + A_{6,6}\beta^6 \tag{9B.200}$$

where β is given by Equation (9B.95) and the parameters $A_{i,j}$ (i.e., the values from the row corresponding to G_i and column A_j), are provided in Table 9B.14 for an inside diameter crack and in Table 9B.15 for an outside diameter crack. The influence coefficients G_2, G_3, and G_4 can be computed using paragraph 9B.14.3 or 9B.14.4.

c) The parameter Q is determined using Equation (9B.15) or (9B.16).

d) Crack and geometry dimensional limits:

1) $0.0 \le a/t \le 0.8$

2) $0.03125 \le a/c \le 2.0$

3) $G_0,\ G_1,\ G_2,\ G_3,\ G_4$: $\varphi \le \pi/2$; $for\quad \pi/2 < \varphi \le \pi \quad K_I(\varphi) = K_I(\pi - \varphi)$

4) $G_5,\ G_6$: $0 \le \varphi \le \pi$

5) $0.0 \le t/R_i \le 3.0$

e) Influence coefficients are provided in Table 9B.14 and Table 9B.15 for values of $0.03125 \le a/c \le 2.0$. For long cracks where $a/c < 0.03125$, the influence coefficients can be determined by interpolation using the values in Table 9B.14 and Table 9B.15 and the values for G_0 and G_1 computed using the equations in paragraph 9B.5.10.2. The influence coefficients for the long flaw or infinite length solution (G_0^L and G_1^L) in these equations can be computed using Table 9B.11.

f) The coefficients of the stress distribution to be used are defined in paragraph 9B.2.2.3.

g) The net-section bending stress about the x-axis and y-axis are computed as follows:

$$\sigma_5 = \frac{M_x R_o}{0.25\pi\left(R_o^4 - R_i^4\right)} \tag{9B.201}$$

$$\sigma_6 = \frac{M_y R_o}{0.25\pi\left(R_o^4 - R_i^4\right)} \tag{9B.202}$$

h) If the polynomial stress distribution has been derived from the most highly stressed location around the circumference using an analysis that include the net-section bending moments, then the terms with G_5 and G_6 do not need to be included in the calculation of the stress intensity factor using Equation (9B.196). It should be noted that this method will provide a conservative solution depending on the orientation of the crack with respect to the applied net-section bending moments.

9B.5.15 Cylinder – Surface Crack, Circumferential Direction – Semi-Elliptical Shape, Through-Wall Arbitrary Stress Distribution (KCSCCE3)

9B.5.15.1 The Mode I Stress Intensity Factor

The stress intensity factor can be determined using the weight function method (see paragraph 9B.14.5). The influence coefficients G_0 and G_1 required to compute M_1, M_2, and M_3 can be determined using paragraph 9B.5.14.2(b).

9B.5.15.2 Notes: see paragraph 9B.5.13.2.

9B.5.16 Cylinder – Embedded Crack, Longitudinal Direction – Infinite Length, Through-Wall Fourth Order Polynomial Stress Distribution (KCECLL)

9B.5.16.1 The Mode I Stress Intensity Factor solution in paragraph 9B.3.7 can be used.

9B.5.16.2 Notes:

a) See Figure 9B.17 for the component and crack geometry.

b) See paragraph 9B.3.7.

9B.5.17 Cylinder – Embedded Crack, Circumferential Direction – 360 Degrees, Through-Wall Fourth Order Polynomial Stress Distribution (KCECCL)

9B.5.17.1 The Mode I Stress Intensity Factor solution in paragraph 9B.3.7 can be used.

9B.5.17.2 Notes:

a) See Figure 9B.18 for the component and crack geometry.

b) See paragraph 9B.3.7.

9B.5.18 Cylinder – Embedded Crack, Longitudinal Direction – Elliptical Shape, Through-Wall Fourth Order Polynomial Stress Distribution (KCECLE)

9B.5.18.1 The Mode I Stress Intensity Factor solution in paragraph 9B.3.9 can be used.

9B.5.18.2 Notes:

a) See Figure 9B.19 for the component and crack geometry.

b) See paragraph 9B.3.9.2.

9B.5.19 Cylinder – Embedded Crack, Circumferential Direction – Elliptical Shape, Through-Wall Fourth Order Polynomial Stress Distribution (KCECCE)

9B.5.19.1 The Mode I Stress Intensity Factor solution in paragraph 9B.3.9 can be used.

9B.5.19.2 Notes:

a) See Figure 9B.20 for the component and crack geometry.

b) See paragraph 9B.3.9.2.

9B.6 Stress Intensity Factor Solutions for Spheres

9B.6.1 Sphere – Through-Wall Crack, Through-Wall Membrane and Bending Stress (KSTC)

9B.6.1.1 The Mode I Stress Intensity Factor (References [10] and [11])

Membrane and Bending Stress:

$$K_I = \left[\left(\sigma_m + p_c\right)G_0 + \sigma_b\left(G_0 - 2G_1\right)\right]\sqrt{\pi c} \tag{9B.203}$$

or

$$K_I = \left(\left(\sigma_0 + p_c\right)G_0 + \sigma_1 G_1\right)\sqrt{\pi c} \tag{9B.204}$$

Internal Pressure Only, crack face pressure loading is included:

$$K_I = \frac{pR_o^2}{R_o^2 - R_i^2} G_p \sqrt{\pi c} \tag{9B.205}$$

9B.6.1.2 Notes:

a) See Figure 9B.21 for the component and crack geometry.

b) The influence coefficients G_0, G_1, and G_p are calculated using the following equations where the constants $A_1 \rightarrow A_8$ are provided in Table 9B.16 for K_I at the inside diameter and in Table 9B.17 for K_I at the outside diameter.

$$G_{0,1,p} = A_0 + A_1\lambda + A_2\lambda^2 + A_3\lambda^3 + A_4\lambda^4 + A_5\lambda^5 + A_6\lambda^6 + A_7\lambda^7 + A_8\lambda^8 \tag{9B.206}$$

$$\lambda = \frac{1.818c}{\sqrt{R_i t}} \tag{9B.207}$$

9B.6.2 Sphere – Surface Crack, Circumferential Direction – 360 Degrees, Internal Pressure (KSSCCL1)

9B.6.2.1 The Mode I Stress Intensity Factor (Reference [40])

Inside Surface, crack face pressure loading is included:

$$K_I = \frac{pR_o^3}{R_o^3 - R_i^3}\left[1.5G_0 - 1.5G_1\left(\frac{a}{R_i}\right) + 3G_2\left(\frac{a}{R_i}\right)^2 - 5G_3\left(\frac{a}{R_i}\right)^3 + 7.5G_4\left(\frac{a}{R_i}\right)^4\right]\sqrt{\pi a} \tag{9B.208}$$

Outside Surface:

$$K_I = \frac{pR_i^3}{R_o^3 - R_i^3}\left[1.5G_0 + 1.5G_1\left(\frac{a}{R_o}\right) + 3G_2\left(\frac{a}{R_o}\right)^2 + 5G_3\left(\frac{a}{R_o}\right)^3 + 7.5G_4\left(\frac{a}{R_o}\right)^4\right]\sqrt{\pi a} \quad (9B.209)$$

9B.6.2.2 Notes:

a) See Figure 9B.22 for the component and crack geometry.

b) The influence coefficients G_0 through G_4 are provided in Table 9B.18.

c) Crack and geometry dimensional limits:

1) $0.0 < a/t \leq 0.8$

2) $0.001 < t/R_i \leq 0.3333$

9B.6.3 Sphere – Surface Crack, Circumferential Direction – 360 Degrees, Through-Wall Fourth Order Polynomial Stress Distribution (KSSCCL2)

9B.6.3.1 The Mode I Stress Intensity Factor (Reference [40])

$$K_I = \left[G_0(\sigma_0 + p_c) + G_1\sigma_1\left(\frac{a}{t}\right) + G_2\sigma_2\left(\frac{a}{t}\right)^2 + G_3\sigma_3\left(\frac{a}{t}\right)^3 + G_4\sigma_4\left(\frac{a}{t}\right)^4\right]\sqrt{\pi a} \quad (9B.210)$$

9B.6.3.2 Notes:

a) See paragraph 9B.6.2.2.

b) The coefficients of the stress distribution to be used are defined in paragraph 9B.2.2.3.

9B.6.4 Sphere – Surface Crack, Circumferential Direction – 360 Degrees, Through-Wall Arbitrary Stress Distribution (KSSCCL3)

9B.6.4.1 The Mode I Stress Intensity Factor (Reference [3])

The stress intensity factor can be determined using the weight function method (see paragraph 9B.14.5). The influence coefficients G_0 and G_1 required to compute M_1, M_2, and M_3 can be determined using paragraph 9B.6.2.2(b).

9B.6.4.2 Notes: see paragraph 9B.6.2.2.

9B.6.5 Sphere – Surface Crack, Circumferential Direction – Semi-Elliptical Shape, Internal Pressure (KSSCCE1)

9B.6.5.1 The Mode I Stress Intensity Factor (Reference [40])

Inside Surface, crack face pressure loading is included:

$$K_I = \frac{pR_o^3}{R_o^3 - R_i^3}\left[1.5G_0 - 1.5G_1\left(\frac{a}{R_i}\right) + 3G_2\left(\frac{a}{R_i}\right)^2 - 5G_3\left(\frac{a}{R_i}\right)^3 + 7.5G_4\left(\frac{a}{R_i}\right)^4\right]\sqrt{\frac{\pi a}{Q}} \quad (9B.211)$$

Outside Surface:

$$K_I = \frac{pR_i^3}{R_o^3 - R_i^3}\left[1.5G_0 + 1.5G_1\left(\frac{a}{R_o}\right) + 3G_2\left(\frac{a}{R_o}\right)^2 + 5G_3\left(\frac{a}{R_o}\right)^3 + 7.5G_4\left(\frac{a}{R_o}\right)^4\right]\sqrt{\frac{\pi a}{Q}} \quad (9B.212)$$

9B.6.5.2 Notes:

a) See Figure 9B.23 for the component and crack geometry.

b) The influence coefficients G_0 and G_1 for inside and outside surface cracks can be determined using the following equations:

$$G_0 = A_{0,0} + A_{0,1}\beta + A_{0,2}\beta^2 + A_{0,3}\beta^3 + A_{0,4}\beta^4 + A_{0,5}\beta^5 + A_{0,6}\beta^6 \quad (9B.213)$$

$$G_1 = A_{1,0} + A_{1,1}\beta + A_{1,2}\beta^2 + A_{1,3}\beta^3 + A_{1,4}\beta^4 + A_{1,5}\beta^5 + A_{1,6}\beta^6 \quad (9B.214)$$

where β is given by Equation (9B.96) and the parameters $A_{i,j}$ (i.e., the values from the row corresponding to G_i and column A_j) are provided in Table 9B.19 for inside diameter cracks and in Table 9B.20 for outside diameter cracks. The influence coefficients G_2, G_3, and G_4 can be calculated using paragraph 9B.14.3 or 9B.14.4.

c) The parameter Q is given by Equation (9B.15) or (9B.16).

d) Crack and geometry dimensional limits:

1) $0.0 \le a/t \le 0.8$

2) $0.03125 \le a/c \le 2.0$

3) $\varphi \le \pi/2\,; \quad for \;\; \pi/2 < \varphi \le \pi \;\; K_I(\varphi) = K_I(\pi - \varphi)$

4) $0.0 \le t/R_i \le 0.3333$

e) Influence coefficients are provided in Table 9B.19 and Table 9B.20 for values of $0.03125 \le a/c < 2.0$. For long cracks where $a/c < 0.03125$, the influence coefficients can be determined by interpolation using the values in Table 9B.19 and Table 9B.20 and the following values for G_0 and G_1 computed using the equations in paragraph 9B.5.10.2(e). The influence coefficients for the long flaw or infinite length solution (G_0^L and G_1^L) in these equations can be computed using Table 9B.18.

9B.6.6 Sphere – Surface Crack, Circumferential Direction – Semi-Elliptical Shape, Through-Wall Fourth Order Polynomial Stress Distribution (KSSCCE2)

9B.6.6.1 The Mode I Stress Intensity Factor (Reference [40])

$$K_I = \left[G_0(\sigma_0 + p_c) + G_1\sigma_1\left(\frac{a}{t}\right) + G_2\sigma_2\left(\frac{a}{t}\right)^2 + G_3\sigma_3\left(\frac{a}{t}\right)^3 + G_4\sigma_4\left(\frac{a}{t}\right)^4\right]\sqrt{\frac{\pi a}{Q}} \quad (9B.215)$$

9B.6.6.2 Notes:

a) See paragraph 9B.6.5.2.

b) The coefficients of the stress distribution to be used are defined in paragraph 9B.2.2.3.

9B.6.7 Sphere – Surface Crack, Circumferential Direction – Semi-Elliptical Shape, Through-Wall Arbitrary Stress Distribution (KSSCCE3)

9B.6.7.1 The Mode I Stress Intensity Factor (Reference [3])

The stress intensity factor can be determined using the weight function method (see paragraph 9B.14.5). The influence coefficients G_0 and G_1 required to compute M_1, M_2, and M_3 can be determined using paragraph 9B.6.5.2(b).

9B.6.7.2 Notes: see paragraph 9B.6.5.2.

9B.6.8 Sphere – Embedded Crack, Circumferential Direction – 360 Degrees, Through-Wall Fourth Order Polynomial Stress Distribution (KSECCL)

9B.6.8.1 The Mode I Stress Intensity Factor solution in paragraph 9B.3.7 can be used.

9B.6.8.2 Notes:

a) See Figure 9B.24 for the component and crack geometry.

b) See paragraph 9B.3.7.2.

9B.6.9 Sphere – Embedded Crack, Circumferential Direction – Elliptical Shape, Through-Wall Fourth Order Polynomial Stress Distribution (KSECCE)

9B.6.9.1 The Mode I Stress Intensity Factor solution in paragraph 9B.3.9 can be used.

9B.6.9.2 Notes:

a) See Figure 9B.25 for the component and crack geometry.

b) See paragraph 9B.3.9.2.

9B.7 Stress Intensity Factor Solutions for Elbows and Pipe Bends

The stress intensity factor solutions for cylinders can be used for elbows and pipe bends if the stress at the location of the crack is determined considering the bend geometry and applied loads. The net-section forces and moments applied to elbow, as well as internal pressure, should be considered when determining the stress at the crack location. Alternate stress intensity factor solutions for elbows are provided in reference [48].

9B.8 Stress Intensity Factor Solutions for Nozzles and Piping Tees

9B.8.1 Nozzle – Corner Crack, Radial Direction, Quarter-Circular Shape, Membrane Stress at the Corner (KNCC1)

9B.8.1.1 The Mode I Stress Intensity Factor (References [36] and [37])

$$K_I = M_f M_b \left(k_{ta} \sigma_{nom} + p_c \right) \frac{2\sqrt{\pi a}}{\pi} \tag{9B.216}$$

where,

$$M_f = 1.43 - 0.24\left(\sin\left[\varphi\right] + \cos\left[\varphi\right]\right) \tag{9B.217}$$

$$M_b = 1 + 0.15\left(\frac{a}{\sqrt{t^2 + t_n^2}} \right)^2 \tag{9B.218}$$

$$k_{ta} = 1 + \left(k_{tn} - 1\right)\left(1 + \frac{\pi a\left(\sin\left[\varphi\right] + \cos\left[\varphi\right]\right)}{2\left(d_n - t_n\right)}\right)^{-B} \tag{9B.219}$$

with,

$$B = 2 - 2\sqrt{\frac{t_n}{d_n}} \qquad (for\ nozzles\ in\ spherical\ shells) \tag{9B.220}$$

$$B = 2.7 - 2\sqrt{\frac{t_n}{d_n}} \qquad (for\ nozzles\ in\ cylindrical\ shells) \tag{9B.221}$$

$$B = 3.3 - 2\sqrt{\frac{t_n}{d_n}} \qquad (for\ nozzles\ in\ plates) \tag{9B.222}$$

9B.8.1.2 Notes:

a) See Figure 9B.26 (crack labeled G) and Figure 9B.27 for the component and crack geometry.

b) The parameter k_m is the theoretical stress concentration factor that can be used to compute the maximum stress at the corner of a nozzle, or

$$k_{tn} = \frac{\sigma_{\max}}{\sigma_{nom}} \tag{9B.223}$$

9B.8.2 Nozzle – Corner Crack, Radial Direction, Quarter-Circular Shape, Cubic Polynomial Stress at the Corner (KNCC)

9B.8.2.1 The Mode I Stress Intensity Factor (Reference [40])

$$K_I = \left[0.706\left(\sigma_0 + p_c\right) + 0.537\left(\frac{2a}{\pi}\right)\sigma_1 + 0.448\left(\frac{a^2}{2}\right)\sigma_2 + 0.393\left(\frac{4a^3}{3\pi}\right)\sigma_3\right]\sqrt{\pi a} \tag{9B.224}$$

9B.8.2.2 Notes:

a) See Figure 9B.26 (i.e., the crack labeled G) and Figure 9B.27 for the component and crack geometry.

b) Crack and geometry dimensional limits (see Figure 9B.27 for definitions of t and t_n):

1) $0.0 \le a/t \le 0.5$

2) $0.0 \le a/t_n \le 0.5$

3) $\varphi = \pi/4$

c) The coefficients of the stress distribution to be used are defined below:

$$\sigma(x) = \sigma_0 + \sigma_1 x + \sigma_2 x^2 + \sigma_3 x^3 \tag{9B.225}$$

9B.8.3 Surface Cracks at Nozzles – General Solution

The stress intensity factor solutions shown below can be used for surface cracks at nozzles if the stress distribution normal to the plane of the crack is determined based on the nozzle geometry and applied loads. The stress distribution normal to the plane of the crack, $\sigma(x)$, should be computed for the component in the uncracked state

considering the effects of the structural configuration and fillet weld geometry (see Figure 9B.33(b)). The net-section forces and moments applied to shell and nozzle, as well as internal pressure, should be considered when determining the stress distribution. The use of this method to compute the stress intensity factor will result in a conservative value as long as the geometry of the crack does not significantly reduce the stiffness of the cylinder-to-cylinder connection. If the geometry of the crack does result in a significant loss in stiffness, the resulting deformation will result in a higher value of the stress intensity factor. In these cases, an analysis of the cracked geometry is required to accurately determine the stress intensity factor.

a) Nozzle Neck or Branch (see Figure 9B.26)

   1) Crack A – Use KCTCC1, KCTCC2, KCSCCL3, KCSCCE3, KCECCL or KCECCE

   2) Crack B – Use KCTCL, KCSCLL3, KCSCLE3, KCECLL or KCECLE

b) Shell or Run Pipe (see Figure 9B.26)

   1) Crack D & F – Use KPTC, KPSCE3, KPECL, or KPECE2

   2) Crack E & C – Use KPTC, KPSCE3, KPECL, or KPECE2

   3) Crack G – Use KNCC1 or KNCC2

9B.9 Stress Intensity Factor Solutions for Ring-Stiffened Cylinders

9B.9.1 Ring-Stiffened Cylinder – Surface Crack at the Toe of One Fillet Weld, Circumferential Direction – 360 Degrees, Pressure Loading (KRCSCCL1)

9B.9.1.1 The Mode I Stress Intensity Factor (Reference [29])

$$K_I = pM_p^{1c}\sqrt{\pi a} \tag{9B.226}$$

9B.9.1.2 Notes:

a) See Figure 9B.28 for the component and crack geometry.

b) The coefficients, M_p^{1c}, are provided in Table 9B.21.

c) Crack and geometry dimensional limits:

   1) $0.2 \le a/t \le 0.8$

   2) $1.0 \le A_r/t \le 32.0$

   3) $10 \le R_i/t \le 300$, when $R_i/t < 10$ use $R_i/t = 10$ and when $R_i/t > 300$ use $R_i/t = 300$.

d) The effects of the fillet weld on the stress field at the location of the fillet weld are included in the solution; a magnification factor is not required.

e) This solution may be used for W, T, L, and I sections attached by fillet welds to the inside of the vessel when the vessel is subject to a positive internal pressure.

f) This solution may also be used for W, T, L, and I sections attached by fillet welds to the outside of the vessel when the vessel is subject to a partial or full vacuum. The results for this configuration and loading will be conservative because the membrane stress field in the vessel is compressive; the only tensile stress is a result of local through-wall bending at the ring to cylinder attachment location.

9B.9.2 Ring-Stiffened Cylinder – Surface Crack at the Toe of Both Fillet Welds, Circumferential Direction – 360 Degrees, Pressure Loading (KRCSCCL2)

9B.9.2.1 The Mode I Stress Intensity Factor (Reference [29])

$$K_I = pM_p^{2c}\sqrt{\pi a} \tag{9B.227}$$

9B.9.2.2 Notes:

a) See Figure 9B.28 for the component and crack geometry.

b) The coefficients, M_p^{2c}, are provided in Table 9B.21.

c) Refer to paragraph 9B.9.1.2 for other details regarding this solution.

9B.10 Stress Intensity Factor Solutions for Sleeve Reinforced Cylinders

The stress intensity factor solutions shown below can be used for surface cracks at sleeve-reinforced cylinders (see Figure 9B.29) if the stress distribution normal to the plane of the crack is determined based on the component geometry and applied loads. The stress distribution normal to the plane of the crack, $\sigma(x)$, should be computed for the component in the uncracked state considering the effects of the structural configuration and fillet weld geometry (see Figure 9B.33(b)). The net-section forces and moments applied to cylindrical shell, as well as internal pressure, should be considered when determining the stress distribution. The use of this method to compute the stress intensity factor will result in a conservative value as long as the geometry of the crack does not significantly reduce the stiffness of the sleeve-reinforced cylinder connection. If the geometry of the crack does result in a significant loss in stiffness, the resulting deformation will result in a higher value of the stress intensity factor. In these cases, an analysis of the cracked geometry is required to accurately determine the stress intensity factor.

a) Crack A – Use KCTCC1, KCTCC2, KCSCCL3, KCSCCE3, KCECCL or KCECCE

b) Crack B – Use KCTCL, KCSCLL3, KCSCLE3, KCECLL or KCECLE

9B.11 Stress Intensity Factor Solutions for Round Bars and Bolts

9B.11.1 Round Bar, Surface Crack – 360 Degrees, Through-Wall Membrane and Bending Stress (KBSCL)

9B.11.1.1 The Mode I Stress Intensity Factor (References [12] and [18])

$$K_I = \left(M_m\sigma_m + M_b\sigma_b\right)\sqrt{\pi a} \tag{9B.228}$$

where,

$$M_m = \frac{0.50}{\zeta^{1.5}}\left(1 + 0.5\zeta + 0.375\zeta^2 - 0.363\zeta^3 + 0.731\zeta^4\right) \tag{9B.229}$$

$$M_b = \frac{0.375}{\zeta^{2.5}}\left(1 + 0.5\zeta + 0.375\zeta^2 + 0.313\zeta^3 + 0.273\zeta^4 + 0.537\zeta^5\right) \tag{9B.230}$$

$$\zeta = 1 - \frac{a}{R_o} \tag{9B.231}$$

9B.11.1.2 Notes:

a) For the component and crack geometry see Figure 9B.30.

b) Crack geometry dimensional limits: $\zeta < 1.0$.

c) The membrane and bending stress, σ_m and σ_b, can be determined using the following equations:

$$\sigma_m = \frac{F_{bar}}{\pi R_o^2} \tag{9B.232}$$

$$\sigma_b = \frac{4M_{bar}}{\pi R_o^3} \tag{9B.233}$$

9B.11.2 Round Bar – Surface Crack, Straight Front, Through-Wall Membrane and Bending Stress (KBSCS)

9B.11.2.1 The Mode I Stress Intensity Factor (Reference [19])

$$K_I = \left(M_m\sigma_m + M_b\sigma_b\right)\sqrt{\pi a} \tag{9B.234}$$

where,

$$M_m = 0.926 - 1.771\zeta + 26.421\zeta^2 - 78.481\zeta^3 + 87.911\zeta^4 \tag{9B.235}$$

$$M_b = 1.04 - 3.64\zeta + 16.86\zeta^2 - 32.59\zeta^3 + 28.41\zeta^4 \tag{9B.236}$$

$$\zeta = \frac{a}{2R_o} \tag{9B.237}$$

9B.11.2.2 Notes:

a) For the component and crack geometry see Figure 9B.31.

b) Crack geometry dimensional limits: $0.0625 \le \zeta \le 0.625$.

c) The membrane and bending stress, σ_m and σ_b, can be determined using the following equations:

$$\sigma_m = \frac{F_{bar}}{\pi R_o^2} \tag{9B.238}$$

$$\sigma_b = \frac{4M_{bar}}{\pi R_o^3} \tag{9B.239}$$

9B.11.3 Round Bar, Surface Crack, Semi-Circular, Through-Wall Membrane and Bending Stress (KBSCC)

9B.11.3.1 The Mode I Stress Intensity Factor (Reference [12])

$$K_I = \left(M_m\sigma_m + M_b\sigma_b\right)\sqrt{\pi a} \tag{9B.240}$$

where,

$$M_m = g\left[0.752 + 2.02\zeta + 0.37\left(1 - \sin\left[\psi\right]\right)^3\right] \tag{9B.241}$$

$$M_b = g\left[0.923 + 0.199\left(1 - \sin\left[\psi\right]\right)^4\right] \tag{9B.242}$$

$$g = \frac{\frac{1.84}{\pi}\left(\frac{\tan[\psi]}{\psi}\right)^{0.5}}{\cos[\psi]} \tag{9B.243}$$

$$\zeta = \frac{a}{2R_o} \tag{9B.244}$$

$$\psi = \frac{\pi a}{4R_o} \tag{9B.245}$$

9B.11.3.2 Notes:

a) For the component and crack geometry see Figure 9B.31.

b) Crack geometry dimensional limits: $\zeta \leq 0.6$.

c) The membrane and bending stress, σ_m and σ_b, can be determined using stress Equations (9B.238) and (9B.239), respectively.

9B.11.4 Bolt, Surface Crack, Semi-Circular or Straight Front Shape, Membrane and Bending Stress (KBSC)

9B.11.4.1 The Mode I Stress Intensity Factor (Reference [17])

$$K_I = \left(M_m \sigma_m + M_b \sigma_b\right)\sqrt{\pi a} \tag{9B.246}$$

where,

$$M_m = 2.043e^{-31.332\zeta} + 0.6507 + 0.5367\zeta + 3.0469\zeta^2 - 19.504\zeta^3 + 45.647\zeta^4 \tag{9B.247}$$

$$M_b = 0.6301 + 0.03488\zeta - 3.3365\zeta^2 + 13.406\zeta^3 - 6.0021\zeta^4 \tag{9B.248}$$

$$\zeta = \frac{a}{2R_{th}} \tag{9B.249}$$

9B.11.4.2 Notes:

a) For the component and crack geometry see Figure 9B.32; the solution applies to a semi-circular or straight front surface crack.

b) Crack geometry dimensional limits: $0.004 \leq \zeta \leq 0.5$.

c) The solution provided is for UNF bolts. The solution for the bending stress does not include the effects of the thread.

d) The solution for the membrane stress can be used for round bars if the exponential term is set to zero.

e) The membrane and bending stress, σ_m and σ_b, can be determined using stress Equations (9B.237) and (9B.238), respectively.

9B.12 Stress Intensity Factor Solutions for Cracks at Fillet Welds

9B.12.1 Cracks at Fillet Welds – Surface Crack at a Tee Joint, Semi-Elliptical Shape, Through-Wall Membrane and Bending Stress (KFWSCE1)

9B.12.1.1 The Mode I Stress Intensity Factor (Reference [30])

$$K_I = \left(M_{km} M_m \left(\sigma_m + p_c\right) + M_{kb} M_b \sigma_b\right)\sqrt{\frac{\pi a}{Q}} \tag{9B.250}$$

where M_m and M_b are determined using the equations in paragraph 9B.3.4.1, and Q is determined using Equation (9B.15) or (9B.16).

The factors M_{km} and M_{kb} are given by the following equations using the appropriate parameters from Table 9B.22.

$$M_{km} = \max\left[\left(\left(F_1 - F_2\right)F_4 + F_2 + F_3\right),\ 1.0\right] \tag{9B.251}$$

$$M_{kb} = \max\left[\left(\left(F_1 - F_2\right)F_4 + F_2 + F_3\right),\ 1.0\right] \tag{9B.252}$$

where,

$$F_1 = 1.0 + P_1\left(\frac{r_w}{t}\right)^g \cdot \sin\left[\alpha\right]^h \cdot \left[1.0 - \exp\left(\left(P_6 + P_7\left(\frac{a}{c}\right)\right)\left(\frac{L}{t}\right)\right)\right] \cdot \left[1.0 + P_8\left(\frac{a}{c}\right)^{P_9}\right] \tag{9B.253}$$

$$g = P_2 + P_3\left(\frac{a}{c}\right) \tag{9B.254}$$

$$h = P_4 + P_5\left(\frac{a}{c}\right) \tag{9B.255}$$

$$F_2 = F_1\left[1.0 - P_{10} - P_{11}\left(\frac{a}{c}\right)\right] - P_{12} - P_{13}\left(\frac{a}{c}\right) \tag{9B.256}$$

$$F_3 = \left(\left[1.0 + P_{14}\left(\frac{a}{c}\right) + P_{15}\left(\frac{a}{c}\right)^2 + P_{16}\left(\frac{a}{c}\right)^3 + P_{17}\left(\frac{a}{c}\right)^4\right] \cdot \left[P_{18}\left(\frac{a}{t}\right) + P_{19}\left(\frac{a}{t}\right)^2 + P_{20}\left(\frac{a}{t}\right)^3 + P_{21}\left(\frac{a}{t}\right)^4\right]\right) \tag{9B.257}$$

For the deepest point of the crack (Point B):

$$F_4 = \left(\begin{array}{l} P_{22} \cdot \exp\left[-P_{23} \left(\frac{a}{t} \right)^{P_{24}} \right] + \\ P_{25} \left(\frac{a}{c} \right) \cdot \exp\left[-\left(\frac{a}{t} \right)^{P_{24}} \cdot \left(P_{23} + P_{26} \left(\frac{a}{c} \right) \right) \right] + \\ P_{27} \left(\frac{L}{t} \right) \cdot \exp\left[-\left(\frac{a}{t} \right)^{P_{24}} \cdot \left(P_{23} + P_{28} \left(\frac{L}{t} \right) \right) \right] + \\ P_{29} \left(\frac{t}{r_w} \right) \cdot \exp\left[-\left(\frac{a}{t} \right)^{P_{24}} \cdot \left(P_{23} + P_{30} \left(\frac{t}{r_w} \right) \right) \right] + \\ P_{31} \cdot \sin[\alpha] \cdot \exp\left[-\left(\frac{a}{t} \right)^{P_{24}} \cdot \left(P_{23} + P_{32} \cdot \sin[\alpha] \right) \right] \end{array} \right) \quad \text{(9B.258)}$$

For the surface point of the crack (Point A):

$$F_4 = \exp\left[-R \cdot \left(\frac{a}{t} \right)^{P_{22}} \right] + \left[P_{35} + P_{36} \left(\frac{a}{c} \right)^{P_{37}} \right] \cdot \left(\frac{a}{t} \right)^{P_{38}} \quad \text{(9B.259)}$$

$$R = \left(\begin{array}{l} P_{23} + P_{24} \left(\frac{a}{c} \right)^{P_{25}} + \left[P_{26} + P_{27} \left(\frac{a}{c} \right)^{P_{28}} \right] \left(\frac{L}{t} \right) + \\ \left[P_{29} + P_{30} \left(\frac{a}{c} \right)^{P_{31}} \right] \left(\frac{t}{r_w} \right) + \left[P_{32} + P_{33} \left(\frac{a}{c} \right)^{P_{34}} \right] \cdot \sin[\alpha] \end{array} \right) \quad \text{(9B.260)}$$

9B.12.1.2 Notes:

a) For the component and crack geometry see Figure 9B.33.

b) Crack and geometry dimensional limits:

1) $0.0 < a/t < 1.0$

2) $0.0 < a/c \leq 1.0$

3) $0.01 \leq r_w/t \leq 0.07$

4) $\pi/6 \leq \alpha \leq \pi/3$

5) $0.16 \leq L/t \leq 4.0$

c) The membrane and bending stress, σ_m and σ_b, can be determined using stress equations based on strength of materials concepts.

9B.12.2 Cracks at Fillet Welds in Tee Junctions– General Solution

The stress intensity factor solutions shown below can be used for surface cracks at tee junction fillet welds in pressure containing components (see Figure 9B.33) if the stress distribution normal to the plane of the crack is determined based on the tee junction geometry and applied loads. The stress distribution normal to the plane of the crack, $\sigma(x)$, should be computed for the component in the uncracked state considering the effects of the structural configuration and fillet weld geometry (see Figure 9B.33(b)). The use of this method to compute the stress intensity factor will result in a conservative value as long as the geometry of the crack does not significantly reduce the stiffness of the tee junction connection. If the geometry of the crack does result in a significant loss in stiffness, the resulting deformation will result in a higher value of the stress intensity factor. In these cases, an analysis of the cracked geometry is required to accurately determine the stress intensity factor.

a) Flat Plate Tee Junctions – Use KPTC, KPSCE3, KPECL, or KPECE2

b) Longitudinal Tee Junctions in Cylinders – Use KCTCL, KCSCLL3, KCSCLE3, KCECLL or KCECLE

c) Circumferential Tee Junctions in Cylinders – Use KCTCC1, KCTCC2, KCSCCL3, KCSCCE3, KCECCL or KCECCE

d) Circumferential Tee Junctions in Spheres – Use KSTC, KSSCCL3, KSECCL or KSECCE

9B.13 Stress Intensity Factor Solutions Cracks in Clad Plates and Shells

The stress intensity factor solutions in this Annex can be used to evaluate clad or weld overlayed plate and shell components if the modulus of elasticity between the clad or weld overlay is within 25% of the base material. If the difference between the elastic modulus is greater, the stress intensity factor should be computed numerically considering the actual properties of the materials. If the thermal expansion coefficients between the cladding and base material is different and the component is subject to a thermal load condition, a steep stress gradient will result at the cladding-to-base material interface. The weight function method (see paragraph 9B.14) should be used to compute the stress factor for this condition because it is the only method that can effectively capture the effects of the steep stress gradient.

a) Flat Plates – Use KPSCE3

b) Cylinders – KCSCLL3 or KCSCLE3

c) Spheres – Use KSSCCL3 or KSSCCE3

9B.14 The Weight Function Method for Surface Cracks

9B.14.1 Weight functions provide a means to infer stress intensity factors for nonuniform stress distributions. Consider a surface crack of depth a, subject to a normal stress $\sigma(x)$ that is an arbitrary function of x, where x is oriented in the crack depth direction and is measured from the free surface. The Mode I stress intensity factor for this case is given by the following equation where $h(x,a)$ is the weight function.

$$K_I = \int_0^a h(x,a)\,\sigma(x)\,dx \tag{9B.261}$$

For the deepest point of a semi-elliptical surface crack ($\varphi = \pi/2 \;\; or \;\; 90°$), the weight function can be represented by the following equation (see reference [32]) where M_1, M_2, and M_3 depend on the component geometry and crack size. This equation also applies to an infinitely long surface crack.

$$h_{90} = \frac{2}{\sqrt{2\pi(a-x)}}\left[1 + M_1\left(1-\frac{x}{a}\right)^{1/2} + M_2\left(1-\frac{x}{a}\right) + M_3\left(1-\frac{x}{a}\right)^{3/2}\right] \quad (9B.262)$$

For the surface point of the crack ($\varphi = 0$) the weight function can be represented by reference [32]:

$$h_0 = \frac{2}{\sqrt{\pi x}}\left[1 + N_1\left(\frac{x}{a}\right)^{1/2} + N_2\left(\frac{x}{a}\right) + N_3\left(\frac{x}{a}\right)^{3/2}\right] \quad (9B.263)$$

9B.14.2 The weight function coefficients M_I and N_I can be inferred from two reference stress intensity factor solutions. Normally, the K_I solutions for uniform and linear loading are used to derive the weight function coefficients. For a uniform stress, σ_0, the stress intensity factor is given by the following equation where G_0 is the influence coefficient, which depends on the component geometry and crack dimensions, and Q is given by Equation (9B.15) or (9B.16).

$$K_I = \sigma_0 G_0 \sqrt{\frac{\pi a}{Q}} \quad (9B.264)$$

For a linear stress distribution defined as:

$$\sigma(x) = \sigma_1\left(\frac{x}{t}\right) \quad (9B.265)$$

the Mode I stress intensity factor is given by the following expression,

$$K_I = \sigma_1 G_1\left(\frac{a}{t}\right)\sqrt{\frac{\pi a}{Q}} \quad (9B.266)$$

At the deepest point of the surface crack, the weight function coefficients are given by the following equations (see reference [33]) where the influence coefficients from the reference stress intensity factor solution, G_0 and G_1, are evaluated at $\varphi = \pi/2$.

$$M_1 = \frac{2\pi}{\sqrt{2Q}}(3G_1 - G_0) - \frac{24}{5} \quad (9B.267)$$

$$M_2 = 3 \quad (9B.268)$$

$$M_3 = \frac{6\pi}{\sqrt{2Q}}(G_0 - 2G_1) + \frac{8}{5} \quad (9B.269)$$

At the surface point of the surface crack, the weight function coefficients are given by the following equations (see reference [33]) where the influence coefficients from the reference stress intensity factor solution G_0, and G_1, are evaluated at $\varphi = 0$.

$$N_1 = \frac{3\pi}{\sqrt{Q}}(2G_0 - 5G_1) - 8 \quad (9B.270)$$

$$N_2 = \frac{15\pi}{\sqrt{Q}}(3G_1 - G_0) + 15 \quad (9B.271)$$

$$N_3 = \frac{3\pi}{\sqrt{Q}}\left(3G_0 - 10G_1\right) - 8 \tag{9B.272}$$

9B.14.3 The weight function coefficients defined above can be used to obtain a K_I solution for a polynomial stress distribution defined as:

$$\sigma(x) = \sigma_0 + \sigma_1\left(\frac{x}{t}\right) + \sigma_2\left(\frac{x}{t}\right)^2 + \sigma_3\left(\frac{x}{t}\right)^3 + \sigma_4\left(\frac{x}{t}\right)^4 \tag{9B.273}$$

The stress intensity solution is obtained by invoking the principle of superposition in summing contributions from each term in the polynomial.

$$K_I = \left[\sigma_0 G_0 + \sigma_1 G_1\left(\frac{a}{t}\right) + \sigma_2 G_2\left(\frac{a}{t}\right)^2 + \sigma_3 G_3\left(\frac{a}{t}\right)^3 + \sigma_4 G_4\left(\frac{a}{t}\right)^4\right]\sqrt{\frac{\pi a}{Q}} \tag{9B.274}$$

If the weight function coefficients M_I and N_I are known, it is possible to solve for the influence coefficients, G_i. This is accomplished by substituting Equation (9B.262) or Equation (9B.263) into Equation (9B.261) and integrating with the appropriate power-law stress distribution. The resulting expressions for G_i are given below (see reference [33]).

For the deepest point of a semi-elliptical surface crack ($\varphi = \pi/2$):

$$G_2 = \frac{\sqrt{2Q}}{\pi}\left(\frac{16}{15} + \frac{1}{3}M_1 + \frac{16}{105}M_2 + \frac{1}{12}M_3\right) \tag{9B.275}$$

$$G_3 = \frac{\sqrt{2Q}}{\pi}\left(\frac{32}{35} + \frac{1}{4}M_1 + \frac{32}{315}M_2 + \frac{1}{20}M_3\right) \tag{9B.276}$$

$$G_4 = \frac{\sqrt{2Q}}{\pi}\left(\frac{256}{315} + \frac{1}{5}M_1 + \frac{256}{3465}M_2 + \frac{1}{30}M_3\right) \tag{9B.277}$$

The above expressions can also be applied an infinitely long surface crack by setting $Q = 1.0$.

For the surface point of the crack ($\varphi = 0$):

$$G_2 = \frac{\sqrt{Q}}{\pi}\left(\frac{4}{5} + \frac{2}{3}N_1 + \frac{4}{7}N_2 + \frac{1}{2}N_3\right) \tag{9B.278}$$

$$G_3 = \frac{\sqrt{Q}}{\pi}\left(\frac{4}{7} + \frac{1}{2}N_1 + \frac{4}{9}N_2 + \frac{2}{5}N_3\right) \tag{9B.279}$$

$$G_4 = \frac{\sqrt{Q}}{\pi}\left(\frac{4}{9} + \frac{2}{5}N_1 + \frac{4}{11}N_2 + \frac{1}{3}N_3\right) \tag{9B.280}$$

9B.14.4 If the G_0 and G_1 influence coefficients are known for a given position along the crack front defined by the elliptic angle φ, then the complete K_I solution for a polynomial stress distribution defined by Equation (9B.273) can be determined by computing the G_2, G_3, and G_4 influence coefficients using the following equations and substituting the results into Equation (9B.274) (see Reference [34]). Note that if the K_I solution is required at $\varphi = \pi/2$ or $\varphi = 0$, then the G_2, G_3, and G_4 influence coefficients must be computed using the equations in paragraph 9B.14.3.

$$G_{21} = 108 + 180z + 576z^2 - 864z^3 + \left(1056 + 128M_1\right)\delta z^{2.5} \tag{9B.281}$$

$$G_{22} = M_3\left(45\eta + 54\eta z + 72\eta z^2 - 315\omega z^{2.5} + 144\eta z^3\right) \tag{9B.282}$$

$$G_2 = \frac{\sqrt{Q}}{945\pi}\left(G_{21} + G_{22}\right) \tag{9B.283}$$

$$G_{31} = 880 + 1232z + 2112z^2 + 7040z^3 - 11264z^4 + \left(13056 + 1280M_1\right)\delta z^{3.5} \tag{9B.284}$$

$$G_{32} = M_3\left(385\eta + 440\eta z + 528\eta z^2 + 704\eta z^3 - 3465\omega z^{3.5} + 1408\eta z^4\right) \tag{9B.285}$$

$$G_3 = \frac{\sqrt{Q}}{13860\pi}\left(G_{31} + G_{32}\right) \tag{9B.286}$$

$$G_{41} = \begin{pmatrix} 1820 + 2340z + 3328z^2 + 5824z^3 + 19968z^4 - \\ 33280z^5 + \left(37376 + 3072M_1\right)\delta z^{4.5} \end{pmatrix} \tag{9B.287}$$

$$G_{42} = M_3\left(819\eta + 909\eta z + 1040\eta z^2 + 1248\eta z^3 + 1664\eta z^4 - 9009\omega z^{4.5} + 3328\eta z^5\right) \tag{9B.288}$$

$$G_4 = \frac{\sqrt{Q}}{45045\pi}\left(G_{41} + G_{42}\right) \tag{9B.289}$$

where, (note that M_2 and M_4 are only used in paragraph 9B.14.5),

$$M_1 = \frac{-1050\pi G_1 + 105\pi G_0\left(3 + 7z\right) - 4\sqrt{Q}\left(35 - 70z + 35z^2 + 189\delta z^{0.5} + 61\delta z^{1.5}\right)}{\sqrt{Q}\left(168 + 152z\right)z^{0.5}\delta} \tag{9B.290}$$

$$M_2 = \frac{1}{3}\left(M_1 - 3\right) \tag{9B.291}$$

$$M_3 = \frac{2\left(-105\pi G_1 + 45\pi G_0 z + \sqrt{Q}\left(28 + 24z - 52z^2 + 44\delta z^{1.5}\right)\right)}{\sqrt{Q}\left(-21 + 2z + 19z^2\right)\eta} \tag{9B.292}$$

$$M_4 = \frac{\left(1 + M_3\eta\right)z}{z - 1} \tag{9B.293}$$

with,

$$z = \sin\varphi \tag{9B.294}$$

$$\delta = \sqrt{1 + z} \tag{9B.295}$$

$$\omega = \sqrt{1 - z} \tag{9B.296}$$

$$\eta = \sqrt{\frac{1}{z} - 1} \tag{9B.297}$$

The parameter Q is determined using Equation (9B.15) or (9B.16).

9B.14.5 The weight function method is recommended to compute the stress intensity factor for a through-wall arbitrary stress distribution. The stress distribution through the wall thickness of the component, $\sigma(x)$, can be evaluated using the finite element method. The weight function, $h(x,a)$, is evaluated as follows:

a) For $\varphi = \pi/2$ and all infinitely long cracks, evaluate the influence coefficients G_0 and G_1 for the applicable geometry at $\varphi = \pi/2$ and substitute the results into Equations (9B.267), (9B.268), and (9B.269) to determine M_1, M_2, and M_3, respectively. Substitute M_1, M_2, and M_3 into Equation (9B.262) to compute the weight function; note that for an infinitely long crack, $Q = 1$. The stress intensity factor is found by substituting the resulting equation into Equation (9B.261) and completing the integration.

b) For $\varphi = 0$, evaluate the influence coefficients G_0 and G_1 for the applicable geometry at $\varphi = 0$ and substitute the results into Equations (9B.270), (9B.271), and (9B.272) to determine N_1, N_2, and N_3, respectively. Substitute N_1, N_2, and N_3 into Equation (9B.263) to compute the weight function. The stress intensity factor is found by substituting the resulting equation into Equation (9B.261) and completing the integration.

c) For all other values of φ, evaluate the influence coefficients G_0 and G_1 for the applicable geometry at the angle φ and substitute the results into Equations (9B.290), (9B.291), (9B.292) and (9B.293) to determine M_1, M_2, M_3, and M_4, respectively. Substitute M_1, M_2, M_3, and M_4 into the following equations to determine the weight functions.

$$h_1(x,a) = \frac{\sqrt{\sin[\varphi]+1}}{\sqrt{\pi\left(a\sin[\varphi]-x\right)}}\left[1+M_1\left(1-\frac{x}{a\sin[\varphi]}\right)+M_2\left(1-\frac{x}{a\sin[\varphi]}\right)^2\right] \quad \text{(9B.298)}$$

$$h_2(x,a) = \frac{\sqrt{1-\sin[\varphi]}}{\sqrt{\pi\left(x-a\sin[\varphi]\right)}}\left[1+M_3\left(\frac{x}{a\sin[\varphi]}-1\right)^{1/2}+M_4\left(\frac{x}{a\sin[\varphi]}-1\right)\right] \quad \text{(9B.299)}$$

The stress intensity factor can be determined by substituting the resulting equations into the following equation and completing the integration.

$$K_I = \int_0^{a\sin[\varphi]} h_1(x,a)\sigma(x)dx + \int_{a\sin[\varphi]}^{a} h_2(x,a)\sigma(x)dx \quad \text{(9B.300)}$$

9B.14.6 Methods for performing the numerical integration of the weight function are provided in references [42] and [43].

9B.15 Nomenclature

A	parameters to compute the stress intensity factor.
A_{ij}	parameters to compute the stress intensity factor.
A_j	parameters to compute the stress intensity factor.
A_r	cross sectional area of a stiffening or tray support ring.
$A_0 \rightarrow A_6$	parameters to compute the stress intensity factor.
$A_{0,0} \rightarrow A_{6,6}$	parameters to compute the stress intensity factor.
a	crack depth parameter.

α fillet weld angle (degrees).

c crack length parameter.

B biaxial stress ratio.

$B_0 \rightarrow B_2$ parameters to compute the stress intensity factor.

β parameter to compute the stress intensity factor.

β_1 parameter to compute the stress intensity factor.

β_2 parameter to compute the stress intensity factor.

β_i parameter to compute the stress intensity factor.

$C_1 \rightarrow C_{10}$ parameters to compute the stress intensity factor.

d parameter to compute the stress intensity factor.

d_n mean nozzle diameter (see Figure 9B.27).

d_1 distance from plate surface to the center of an embedded elliptical crack (see Figure 9B.3).

d_2 distance from plate surface to the center of an embedded elliptical crack (see Figure 9B.3).

δ parameter to compute the stress intensity factor.

e parameter to compute the stress intensity factor.

η parameter to compute the stress intensity factor.

f_{90} parameter to compute the stress intensity factor at $\varphi = 90°$.

f_{270} parameter to compute the stress intensity factor at $\varphi = 270°$.

f_b parameter to compute the stress intensity factor.

f_B parameter to compute the stress intensity factor.

f_w finite width correction factor.

f_{wm} finite width correction factor for the membrane stress.

f_φ parameter to compute the stress intensity factor.

$F_0 \rightarrow F_3$ parameters to compute the stress intensity factor.

F_{bar} net-section axial force acting on a bar.

g parameter to compute the stress intensity factor.

$g_1 \rightarrow g_4$ parameters to compute the stress intensity factor.

$G_{0,1,p}$ parameter to compute the stress intensity factor.

$G_{0,1,5}$ parameter to compute the stress intensity factor.

$G_0 \rightarrow G_6$ influence coefficients to compute the stress intensity factor.

G_{11} parameter to compute the stress intensity factor.

G_{12} parameter to compute the stress intensity factor.

G_{13} parameter to compute the stress intensity factor.

G_{21} parameter to compute the stress intensity factor.

G_{22} parameter to compute the stress intensity factor.

G_{23} parameter to compute the stress intensity factor.

G_{31} parameter to compute the stress intensity factor.

G_{32} parameter to compute the stress intensity factor.

G_{41} parameter to compute the stress intensity factor.

G_{42} parameter to compute the stress intensity factor.

G_i parameter to compute the stress intensity factor.

G_p parameter to compute the stress intensity factor.

G_0^L parameter to compute the stress intensity factor.

G_1^L parameter to compute the stress intensity factor.

γ parameter to compute the stress intensity factor.

h parameter to compute the stress intensity factor.

$h_1 \rightarrow h_3$ parameters to compute the stress intensity factor.

h_φ parameter to compute the stress intensity factor.

H parameter to compute the stress intensity factor.

$H_0 \rightarrow H_2$ parameters to compute the stress intensity factor.

H_{90} parameter to compute the stress intensity factor.

H_{270} parameter to compute the stress intensity factor.

H_φ parameter to compute the stress intensity factor.

k_{ta} parameter to compute the stress intensity factor.

k_{tn} parameters to compute the stress intensity factor.

K_I Mode I stress intensity factor.

$K_{1-crack}$ parameters to compute the stress intensity factor.

$K_{2-crack}$ parameters to compute the stress intensity factor.

M resultant net section bending moment acting on a cylinder.

$M_1 \rightarrow M_3$ weight function coefficients to compute the stress intensity factor.

M_b bending stress correction factor to compute the stress intensity factor.

M_{bar} net-section bending moment acting on a bar.

M_{kb} parameter to compute the stress intensity factor.

M_{km} parameter to compute the stress intensity factor.

M_m membrane stress correction factor to compute the stress intensity factor.

M_s parameter to compute the stress intensity factor.

M_x net section bending moment about the x-axis acting on a cylinder.

M_y net section bending moment about the y-axis acting on a cylinder.

M_p^{1c} parameter to compute the stress intensity factor.

M_p^{2c} parameter to compute the stress intensity factor.

μ parameter to compute the stress intensity factor.

n parameter to compute the stress intensity factor.

$N_1 \rightarrow N_3$ weight function coefficients to compute the stress intensity factor.

p pressure.

p_c crack face pressure set $p_c = 0.0$ if pressure is not acting on the crack face.

$P_1 \rightarrow P_{38}$ parameters to compute the stress intensity factor.

ψ parameter to compute the stress intensity factor.

q parameter to compute the stress intensity factor.

Q parameter to compute the stress intensity factor.

R_b ratio of induced bending stress to the applied membrane stress (see Part 8, paragraphs 8.4.3.2, 8.4.3.3 and 8.4.3.4).

R_h hole radius.

R_i cylinder inside radius.

R_m cylinder mean radius.

R_o cylinder, round bar, or bolt outside radius, as applicable.

R_{th} root radius of a threaded bolt.

r_w root radius at the fillet weld.

σ stress.

σ_b through-wall bending stress component.

σ_{be} bending stress.

σ_{gb} global bending stress.

σ_{ij} stress component being evaluated.

$\sigma_{ij,m}$ equivalent membrane stress for a stress component.

$\sigma_{ij,b}$ equivalent bending stress for a stress component.

$\sigma_{\max}$ maximum stress at the nozzle corner where the crack is located.

σ_{nom} nominal membrane stress away from the nozzle corner; for a spherical or cylindrical shell the membrane stress perpendicular to the crack face away from the nozzle (i.e., hoop stress for a spherical shell or cylindrical shell with a radial corner crack aligned with the longitudinal axis), for a plate, the maximum membrane stress perpendicular to the crack face.

σ_m membrane stress component.

σ_{me} membrane stress.

σ_0 uniform coefficient for polynomial stress distribution.

σ_1 linear coefficient for polynomial stress distribution.

σ_2 quadratic coefficient for polynomial stress distribution.

σ_3 third order coefficient for polynomial stress distribution.

σ_4 fourth order coefficient for polynomial stress distribution.

σ_5 bending stress from the net section bending moment about the x-axis acting on a cylinder.

σ_6 bending stress from the net section bending moment about the y-axis acting on a cylinder.

t plate or shell thickness.

t_n nozzle thickness (see Figure 9B.27).

φ elliptic angle (see Figure 9B.2) for surface cracks in plates and shells, Figure 9B.3 for embedded flaws, and Figure 9B.10 for surface cracks at holes, and Figure 9B.27 for radial corner cracks at nozzles (radians).

W distance from the center of the flaw to the free edge of the plate (see Figure 9B.1).

ω parameter to compute the stress intensity factor.

x radial local coordinate originating at the internal surface of the component.

x_n Local coordinate for the stress distribution measured from the inside surface of the corner crack radius at an angle of $\varphi = \pi/4$ (see Figure 9B.27); note that this stress distribution is not normalized with the wall thickness (see paragraph 9B.2.2.3).

x_g global coordinate for definition of net section bending moment about the x-axis.

y_g global coordinate for definition of net section bending moment about the y-axis.

Y_0 parameter to compute the stress intensity factor.

Y_1 parameter to compute the stress intensity factor.

z parameter to compute the stress intensity factor.

ζ parameter to compute the stress intensity factor.

9B.16 References

[1] Newman, Jr., J.C., Raju, I.S., Stress Intensity Factor Equations for Cracks in Three-Dimensional Finite bodies Subject to Tension and Bending Loads, NASA Technical Memorandum 85793, April 1984.

[2] Rooke, DIP and Cartwright, D.J., *Compendium of Stress Intensity Factors*, Her Majesty's Stationary Office (HMSO), London, 1974.

[3] Cipolla, R.C., "Technical Basis for the Revised Stress Intensity Factor Equation for Surface Flaws in ASME Section XI Appendix A", PVP-Vol. 313-1, International Pressure Vessels and Piping Codes and Standards: Volume 1 – Current Applications, American Society of Mechanical Engineers, New York, NY, 1995, pp. 105-121.

[4] Anderson, T.L., Unpublished Work, 2005.

[5] Shen, G., and Glinka G. "Weight Functions for a Surface Semi-Elliptical Crack in a Finite Thickness Plate," Theoretical and Applied Fracture Mechanics, Vol 15, 1991, pp. 247-255.

[6] Vainshtok, V.A. and Varfolomeyev, I.V., "Stress Intensity Factor Equations for Part-Elliptical Cracks and Their Verification", Engineering Fracture Mechanics, Vol 34, 1989, pp. 125-136.

[7] Klecker, R., Brust, F.W., and Wilkowski, G., "NRC Leak Before Break Analysis Method for Circumferentially Through-Wall Cracked Pipes Under Axial Plus Bending Loads," NUREG/CR-4572, U.S. Nuclear Regulatory Commission, May 1986.

[8] Shin, C.S. and Wang, C.M. "Experimental Calibration of Stress Intensity Factors for Piping with Circumferential Through-Wall Crack," International Journal of Pressure Vessels and Piping, 60, 1994, pp. 285-296.

[9] Anderson, T.L., *Fracture Mechanics – Fundamentals and Applications*, 3rd Edition, CRC Press, Boca Raton, FL, 2005.

[10] Erdogen, F. and Kibler, J.J., "Cylindrical and Spherical Shells with Cracks," International Journal of Fracture Mechanics, 5, 1969, pp. 229-237.

[11] Folias, E.S., "On the Effect of Initial Curvature on Cracked Sheets," International Journal of Fracture Mechanics, Vol. 5, No. 4, December 1969, pp. 327-346.

[12] Murakami, Y., *Stress Intensity Factors Handbook*, Pergamon Press, Oxford, 1987, pp. 1356-1358.

[13] Eiber, R.J., Maxey, W.A., Duffy, A.R., and Atterbury, T.J., “Investigation of the Initiation and Extent of Ductile Pipe Rupture,” Battelle Report Task 17, June 1971.

[14] Fu, B., Haswell, J.V., Bettess, P., "Weld Magnification Factors for Semi-Elliptical Surface Cracks in Fillet Welded T-Butt Joints," International Journal of Fracture, 63, 1993, pp. 155-171.

[15] Brust, F.W. and Gilles, P., “Approximate Methods for Fracture Analysis of Tubular Members Subjected to Combined Tensile and Bending Loads,” Journal of Offshore Mechanics and Arctic Engineering, Vol. 116, November 1994.

[16] Green, D. and Knowles, J., “The Treatment of Residual Stress in Fracture Assessment of Pressure Vessels,” Journal of Pressure Vessel Technology, Vol. 116, American Society of Mechanical Engineers, November 1994, pp. 345-352.

[17] James, L.A., and Mills, W.J., “Review and Synthesis of Stress Intensity Factor Solutions Applicable to Cracks in Bolts,” Engineering Fracture Mechanics, Vol. 30, No. 5, 1988, pp. 641-654.

[18] Tada, H., Paris, P.C. and Irwin, G.R, “The Stress Analysis of Cracks Handbook – Second Edition,” Paris Productions Inc., St. Louis, MO, 1985.

[19] Sih, G.C., *Handbook of Stress Intensity Factors*, Institute of Fracture and Solid Mechanics, Lehigh University, Bethlehem, PA.

[20] Newman, J.C., Reuter, W.G., and Aveline Jr, C.R., “Stress and Fracture Analysis of the Surface Crack,” Fatigue and Fracture Mechanics: 30th Volume, ASTM STP 1360, K.L. Jerina and P.C. Paris, ASTM, Philadelphia, PA, 1999.

[21] Niu, X. and Glinka, G., “Theoretical and Experimental Analyses of Surface Fatigue Cracks in Weldments,” Surface-Crack Growth: Models, Experiments, and Structures, ASTM STP 1060, W.G. Reuter, J.H. Underwood, and J.C. Newman Jr., Eds., ASTM, Philadelphia, PA, 1990, pp. 390-413.

[22] Barsoum, R.S., Loomis, R.W., and Stewart, B.D., “Analysis of Through Cracks in Cylindrical Shells by the Quarter-Point Elements,” International Journal of Fracture, Vol. 15, No. 3, June 1979, pp. 259-280.

[23] Chell, G.G, “Application of the CEGB Failure Assessment Procedure, R6, to Surface Flaws,” Fracture Mechanics: Twenty-First Symposium, ASTM STP 1074, J.P. Gudas, J.A. Joyce, and E.M. Hackett, Eds., ASTM, Philadelphia, 1990, pp. 525-544.

[24] Kramer, G.S., Wilkowski, G.M., and Maxey, W.A., “Flaw Tolerance of Spiral Welded Pipe,” Battelle NG-18 Report No. 154, January 1987

[25] Kiefner, J.F. and Vieth, P.H., “Project PR 3-805, A Modified Criterion for Evaluating the Remaining Strength of Corroded Pipe,” Battelle Report to the Pipeline Committee of the American Gas Association, 1989.

[26] Fett, T., and Munz, D., *Stress Intensity Factors and Weight Functions*, Computational Mechanics Publications, Southampton, UK, 1997.

[27] France, C.F., Green, D., Sharples, J.K., and Chivers, T.C., “New Stress Intensity Factor and Crack Opening Area Solutions for Through-Wall Cracks in Pipes and Cylinders,” PVP-Vol. 350, Fatigue and Fracture, Vol. 1, American Society of Mechanical Engineers, New York, NY, 1997, pp. 143-195.

[28] Niu, X. and Glinka, G., “Stress-Intensity Factors for Semi-Elliptical Cracks in Welded Joints,” International Journal of Fracture, Vol. 40, Kluwer Academic Publishers, Netherlands, 1989, pp. 255-270.

[29] Brown, R.G., “Development of Elastic Stress Intensity Factor Solutions and Elastic-Plastic Failure Assessment Diagrams for Fillet Toe Cracks at Ring-Stiffened Cylindrical Shells,” Thesis, The University of Akron, Akron, OH, December 1996.

[30] HSE, “Development of Parametric Equations for MK-Factors for Semi-Elliptic Cracks in T-Butt Welds,” Offshore Technology Report – OTO 98 081, Health & Safety Executive, Research Admin, OSD, Bootle, Merseyside, August 1998.

[31] Forman, R.G., Hickman, J.C., and Shivakumer, V., “Stress Intensity Factors for Circumferential Through Cracks in Hollow Cylinders Subjected to Combined Tension and Bending Loads,” Engineering Fracture Mechanics, Vol 21, No. 3, 1985, pp. 563-571.

[32] Shen, G. and Glinka, G., “Determination of Weight Functions from Reference Stress Intensity Solutions.” Theoretical and Applied Fracture Mechanics, Vol. 15, 1991, pp. 237-245.

[33] Zheng, X.J., Kiciak, A., and Glinka, G., “Weight Functions and Stress Intensity Factors for Internal Surface Semi-Elliptical Crack in Thick-Walled Cylinder.” Engineering Fracture Mechanics, Vol. 58, 1997, pp. 207-221.

[34] Anderson, T.L., private communication to D.A. Osage, 1998.

[35] Sih, G.C., Mechanics of Fracture 3, Plates and Shells with Cracks, Noordhoff International Publishing Leydon, The Netherlands, 1977.

[36] Guozhong, C. and Qichao, H., “Stress Intensity Factors of Nozzle Corner Cracks,” Engineering Fracture Mechanics, Vol. 38, No. 1, pp. 27-35, 1991.

[37] Guozhong, C. and Qichao, H., “Approximate Stress-Intensity Factor Solutions for Nozzle Corner Cracks,” International Journal of Pressure Vessels and Piping, 42, pp. 75-96, 1990.

[38] Fife, A.B., Kobsa, I.R., Riccardella, P.C., and Watanabe, H.T., “Boiling Water Reactor Feedwater Nozzle/Spranger Interim Program Report,” NEDO-21480, 77NED125, Class I, General Electric, San Jose, CA, July 1977.

[39] Fife, A.B., Kobsa, I.R., Riccardella, P.C., and Watanabe, H.T., “Boiling Water Reactor Feedwater Nozzle/Spranger Interim Program Report,” NEDO-21480, 77NED125, Class I, General Electric, San Jose, CA, July 1977.

[40] Anderson, T.L., et. al, *Development of Stress Intensity Factor Solutions for Surface and Embedded Cracks in API 579*, WRC Bulletin 471, Welding Research Council, Inc., New York, NY, May 2002.

[41] Anderson, T.L., Stress Intensity and Crack Growth Opening Area Solutions for Through-Wall Cracks in Cylinders and Spheres, WRC Bulletin 478, Welding Research Council, Inc. New York, NY, January 2003.

[42] Anderson, T.L. and Glinka, G., “A Closed-Form Method for Integrating Weight Functions for Part-Through Cracks Subject to Mode I Loading,” Engineering Fracture Mechanics, Volume 73, Issue 15, October 2006, Pages 2153.

[43] Moftakhar, A.A. and Glinka, G., “Calculation of Stress Intensity Factors by Efficient Integration of Weight functions,” Engineering Fracture mechanics, Vol 43, No. 5, pp. 749-756, 1992.

[44] Ainsworth, R.,” Flaw analysis in the French RSE-M and RCC-MR code appendices,” International Journal of Pressure Vessels and Piping 84 (2007) 589.

[45] Marie, S., Chapuliot, S., Kayser, Y., Lacire, M.H., Drubay, B., Barthelet, B., Le Delliou, P., Rougier, V., Naudin, C., Gilles, P., Triay, M.," French RSE-M and RCC-MR code appendices for flaw analysis: Presentation of the fracture parameters calculation–Part I: General overview," International Journal of Pressure Vessels and Piping 84 (2007) 590–600.

[46] Marie, S., Chapuliot, S., Kayser, Y., Lacire, M.H., Drubay, B., Barthelet, B., Le Delliou, P., Rougier, V., Naudin, C., Gilles, P., Triay, M.," French RSE-M and RCC-MR code appendices for flaw analysis: Presentation of the fracture parameters calculation–Part II: Cracked plates," International Journal of Pressure Vessels and Piping 84 (2007) 601–613.

[47] Marie, S., Chapuliot, S., Kayser, Y., Lacire, M.H., Drubay, B., Barthelet, B., Le Delliou, P., Rougier, V., Naudin, C., Gilles, P., Triay, M.," French RSE-M and RCC-MR code appendices for flaw analysis: Presentation of the fracture parameters calculation–Part III: Cracked pipes," International Journal of Pressure Vessels and Piping 84 (2007) 614–658.

[48] Marie, S., Chapuliot, S., Kayser, Y., Lacire, M.H., Drubay, B., Barthelet, B., Le Delliou, P., Rougier, V., Naudin, C., Gilles, P., Triay, M., "French RSE-M and RCC-MR code appendices for flaw analysis: Presentation of the fracture parameters calculation–Part IV: Cracked elbows," International Journal of Pressure Vessels and Piping 84 (2007) 659–686.

[49] Marie, S., Chapuliot, S., Kayser, Y., Lacire, M.H., Drubay, B., Barthelet, B., Le Delliou, P., Rougier, V., Naudin, C., Gilles, P., Triay, M., "French RSE-M and RCC-MR code appendices for flaw analysis: Presentation of the fracture parameters calculation–Part V: Elements of validation," International Journal of Pressure Vessels and Piping 84 (2007) 687–696.

[50] RSE-M, *In-Service Inspection Rules for Mechanical Components of PWR Nuclear Islands*, French Association for Design, Construction and In-Service Inspection Rules for Nuclear Island Components, 1, place Jean Miller, 92084 La Défense cedex, France.

[51] Thorwald, G., Parietti, L., Fletcher, B., and Wright, J.E., "Development of Stress Intensity Factor Solutions for Internal Cracks in Thick-Walled Cylinder Vessels for ASME RFP-ASME ST-14-04," Project Number:13-GVT-105298, April 4, 2014.

[52] Wright, J.E., Parietti, L., Harris, J., Thorwald, G., and Anderson, T.," Summary Report: QA/QC of Existing KI Surface Crack Solutions in API 579 Annex C," Final Report: API Contract No. 2014-108341, September 19, 2014.

[53] Thorwald, G., Parietti, L., Fletcher, B. and Wright, J. "Stress Intensity Factor Solutions for Internal Cracks in Thick-Walled Cylinder Vessels," STP-PT-071, ASME Standards Technology LLC, 2014.

[54] Parietti, L. and Thorwald, G., "Stress Intensity K Factors for External Surface Cracks in Thick-Walled Cylinder Vessels," STP-PT-082, ASME Standards Technology LLC, 2017.

9B.17 Tables

Table 9B.1 – Summary of Stress Intensity Factor Solutions

Component Geometry	Crack Geometry	Crack Loading	Stress Intensity Factor Solution	Reference Stress Solution
Plate	Through-Wall Crack	Through-Wall Membrane and Bending Stress	KPTC (9B.3.1)	RPTC (9C.3.1)
	Surface Crack, Infinite Length	Through-Wall Fourth Order Polynomial Stress Distribution	KPSCL1 (9B.3.2)	RPSCL (9C.3.2)
	Surface Crack, Infinite Length	Through-Wall Arbitrary Stress Distribution	KPSCL2 (9B.3.3)	RPSCL (9C.3.3)
	Surface Crack, Semi-Elliptical Shape	Through-Wall Membrane and Bending Stress	KPSCE1 (9B.3.4)	RPSCE1 (9C.3.4)
	Surface Crack, Semi-Elliptical Shape	Through-Wall Fourth Order Polynomial Stress Distribution	KPSCE2 (9B.3.5)	RPSCE2 (9C.3.5)
	Surface Crack, Semi-Elliptical Shape	Through-Wall Arbitrary Stress Distribution	KPSCE3 (9B.3.6)	RPSCE3 (9C.3.6)
	Embedded Crack, Infinite Length	Through-Wall Fourth Order Polynomial Stress Distribution	KPECL (9B.3.7)	RPECL (9C.3.7)
	Embedded Crack, Elliptical Shape	Through-Wall Membrane and Bending Stress	KPECE1 (9B.3.8)	RPECE1 (9C.3.8)
	Embedded Crack, Elliptical Shape	Through-Wall Fourth Order Polynomial Stress Distribution	KPECE2 (9B.3.9)	RPECE2 (9C.3.9)
Plate with A Hole	Single Hole, Through-Wall Single Edge Crack	Through-Wall Membrane and Bending Stress	KPHTC1 (9B.4.1)	RPHTC1 (9C.4.1)
	Single Hole, Through-Wall Double Edge Crack	Through-Wall Membrane and Bending Stress	KPHTC2 (9B.4.2)	RPHTC2 (9C.4.2)
	Single Hole, Surface Crack, Semi-Elliptical Shape	Membrane Stress	KPHSC1 (9B.4.3)	RPHSC1 (9C.4.3)
	Single Hole, Corner Crack, Semi-Elliptical Shape	Through-Wall Membrane and Bending Stress	KPHSC2 (9B.4.4)	RPHSC2 (9C.4.4)

Table 9B.1 – Summary of Stress Intensity Factor Solutions

Component Geometry	Crack Geometry	Crack Loading	Stress Intensity Factor Solution	Reference Stress Solution
Cylinder	Through-Wall Crack, Longitudinal Direction	Through-Wall Membrane and Bending Stress	KCTCL (9B.5.1)	RCTCL (9C.5.1)
	Through-Wall Crack, Circumferential Direction	Through-Wall Membrane and Bending Stress	KCTCC1 (9B.5.2)	RCTCC1 (9C.5.2)
	Through-Wall Crack, Circumferential Direction	Pressure with a Net Section Axial Force and Bending Moment	KCTCC2 (9B.5.3)	RCTCC2 (9C.5.3)
	Surface Crack, Longitudinal Direction, Infinite Length	Internal Pressure (Lame Stress Distribution)	KCSCLL1 (9B.5.4)	RCSCLL1 (9C.5.4)
	Surface Crack, Longitudinal Direction, Infinite Length	Through-Wall Fourth Order Polynomial Stress Distribution	KCSCLL2 (9B.5.5)	RCSCLL2 (9C.5.5)
	Surface Crack, Longitudinal Direction, Infinite Length	Through-Wall Arbitrary Stress Distribution	KCSCLL3 (9B.5.6)	RCSCLL3 (9C.5.6)
	Surface Crack, Circumferential Direction, 360º	Pressure with Net Section Axial Force and Bending Moment	KCSCCL1 (9B.5.7)	RCSCCL1 (9C.5.7)
	Surface Crack, Circumferential Direction, 360º	Through-Wall Fourth Order Polynomial Stress Distribution & Net Section Bending Moments	KCSCCL2 (9B.5.8)	RCSCCL2 (9C.5.8)
	Surface Crack, Circumferential Direction, 360º	Through-Wall Arbitrary Stress Distribution	KCSCCL3 (9B.5.9)	RCSCCL3 (9C.5.9)
	Surface Crack, Longitudinal Direction, Semi-Elliptical Shape	Internal Pressure (Lame Stress Distribution)	KCSCLE1 (9B.5.10)	RCSCLE1 (9C.5.10)
	Surface Crack, Longitudinal Direction, Semi-Elliptical Shape	Through-Wall Fourth Order Polynomial Stress Distribution	KCSCLE2 (9B.5.11)	RCSCLE2 (9C.5.11)
	Surface Crack, Longitudinal Direction, Semi-Elliptical Shape	Through-Wall Arbitrary Stress Distribution	KCSCLE3 (9B.5.12)	RCSCLE3 (9C.5.12)
	Surface Crack, Circumferential Direction, Semi-Elliptical Shape	Internal Pressure (Lame Stress Distribution) with Net Section Axial Force	KCSCCE1 (9B.5.13)	RCSCCE1 (9C.5.13)
	Surface Crack, Circumferential Direction, Semi-Elliptical Shape	Through-Wall Fourth Order Polynomial Stress Distribution with Net Section Bending Moment	KCSCCE2 (9B.5.14)	RCSCCE2 (9C.5.14)
	Surface Crack, Circumferential Direction, Semi-Elliptical Shape	Through-Wall Arbitrary Stress Distribution	KCSCCE3 (9B.5.15)	RCSCCE3 (9C.5.15)
	Embedded Crack, Longitudinal Direction, Infinite Length	Through-Wall Fourth Order Polynomial Stress Distribution	KCECLL (9B.5.16)	RCECLL (9C.5.16)
	Embedded Crack, Circumferential Direction, 360º	Through-Wall Fourth Order Polynomial Stress Distribution	KCECCL (9B.5.17)	RCECCL (9C.5.17)
	Embedded Crack, Longitudinal Direction, Elliptical Shape	Through-Wall Fourth Order Polynomial Stress Distribution	KCECLE (9B.5.18)	RCECLE (9C.5.18)
	Embedded Crack, Circumferential Direction, Elliptical Shape	Through-Wall Fourth Order Polynomial Stress Distribution	KCECCE (9B.5.19)	RCECCE (9C.5.19)

Table 9B.1 – Summary of Stress Intensity Factor Solutions

Component Geometry	Crack Geometry	Crack Loading	Stress Intensity Factor Solution	Reference Stress Solution
Sphere	Through-Wall Crack	Through-Wall Membrane and Bending Stress	KSTC (9B.6.1)	RSTC (9C.6.1)
	Surface Crack, Circumferential Direction, 360º	Internal Pressure (Lame Stress Distribution)	KSSCCL1 (9B.6.2)	RSSCCL1 (9C.6.2)
	Surface Crack, Circumferential Direction, 360º	Through-Wall Fourth Order Polynomial Stress Distribution	KSSCCL2 (9B.6.3)	RSSCCL2 (9C.6.3)
	Surface Crack, Circumferential Direction, 360º	Through-Wall Arbitrary Stress Distribution	KSSCCL3 (9B.6.4)	RSSCCL3 (9C.6.4)
	Surface Crack, Circumferential Direction, Semi-Elliptical Shape	Internal Pressure (Lame Stress Distribution)	KSSCCE1 (9B.6.5)	RSSCCE1 (9C.6.5)
	Surface Crack, Circumferential Direction, Semi-Elliptical Shape	Through-Wall Fourth Order Polynomial Stress Distribution	KSSCCE2 (9B.6.6)	RSSCCE2 (9C.6.6)
	Surface Crack, Circumferential Direction, Semi-Elliptical Shape	Through-Wall Arbitrary Stress Distribution	KSSCCE3 (9B.6.7)	RSSCCE3 (9C.6.7)
	Embedded Crack, Circumferential Direction, 360º	Through-Wall Fourth Order Polynomial Stress Distribution	KSECCL (9B.6.8)	RSECCL (9C.6.8)
	Embedded Crack, Circumferential Direction, Elliptical Shape	Through-Wall Fourth Order Polynomial Stress Distribution	KSECCE (9B.6.9)	RSECCE (9C.6.9)
Elbow and Pipe Bend	General Solution	See Discussion in Paragraph 9B.7.	(9B.7)	(9C.7)
Nozzle or Piping Tee	Corner Cracks, Radial Direction, Quarter-Circular Shape	Membrane Stress	KNCC1 (9B.8.1)	RNCC1 (9C.8.1)
	Corner Cracks, Radial Direction, Quarter-Circular Shape	Cubic Polynomial Stress Distribution	KNCC2 (9B.8.2)	RNCC2 (9C.8.2)
	Surface Cracks at Nozzles – General Solution	See Discussion in Paragraph 9B.8.	(9B.8.3)	(9C.8.3)
Ring-Stiffened Cylinder	Surface Crack at the Toe of One Fillet Weld, Circumferential Direction – 360º	Pressure (Membrane and Bending Stress)	KRCSCCL1 (9B.9.1)	RRCSCCL1 (9C.9.1)
	Surface Crack at the Toe of Both Fillet Welds, Circumferential Direction – 360º	Pressure (Membrane and Bending Stress)	KRCSCCL2 (9B.9.2)	RRCSCCL2 (9C.9.2)

Table 9B.1 – Summary of Stress Intensity Factor Solutions

Component Geometry	Crack Geometry	Crack Loading	Stress Intensity Factor Solution	Reference Stress Solution
Sleeve Reinforced Cylinder	General Solution	See Discussion in Paragraph 9B.10.	(9B.10)	(9C.10)
Round Bar or Bolt	Round Bar, Surface Crack, 360º	Membrane and Bending Stress	KBSCL (9B.11.1)	RBSCL (9C.11.1)
	Round Bar, Surface Crack, Straight Front Shape	Membrane and Bending Stress	KBSCS (9B.11.2)	RBSCS (9C.11.2)
	Round Bar, Surface Crack, Semi-Circular Shape	Membrane and Bending Stress	KBSCC (9B.11.3)	RBSCC (9C.11.3)
	Bolt, Surface Crack, Semi-Elliptical or Straight Front Shape	Membrane and Bending Stress	KBSC (9B.11.4)	RBSC (9C.11.4)
Cracks at Fillet Welds	Surface Crack, Infinite Length	Membrane and Bending Stress	KFWSCE1 (9B.12.1)	RFWSCE1 (9C.12.1)
	Cracks at Fillet Welds in Tee Junctions in Pressurized Components - General Solution	See Discussion in Paragraph 9B.12.2	(9B.12.2)	(9C.12.1.3)
Cracks in Clad or Weld Overlayed Plate	General Solution	See Discussion in Paragraph 9B.13.	(9B.13)	(9C.13)

Table 9B.2 – Influence Coefficients for an Infinite Length Surface Crack in a Plate (1)

a/t	G_0	G_1	G_2	G_3	G_4
0.0	1.120000	0.682000	0.524500	0.440400	0.379100
0.1	1.180400	0.702800	0.535200	0.447300	0.383600
0.2	1.358700	0.773200	0.575300	0.474100	0.404300
0.4	2.099000	1.052600	0.728500	0.574100	0.479800
0.6	4.008200	1.745900	1.099800	0.812100	0.652600
0.8	11.827200	4.479200	2.524400	1.706900	1.275400
Influence Coefficients in Equation Form (2)					
Coefficient	C_0	C_1	C_2	C_3	C_4
G_0	1.1202	6.0061	-1.3891	7.9260	31.914
G_1	0.68109	2.3137	-0.71895	3.1140	10.702
G_2	0.52360	1.3006	-0.56913	2.1463	5.0660
G_3	0.43970	0.86873	-0.52507	1.7131	2.8443
G_4	0.37831	0.64919	-0.28777	0.87481	2.2063

Notes:

1. Interpolation may be used for intermediate values of a/t.
2. See paragraph 9B.3.2.2(c).

Table 9B.3 – Influence Coefficients for a Finite Length Surface Crack in a Plate

Coefficients C_0 Through C_5							
φ	G_i	C_0	C_1	C_2	C_3	C_4	C_5
0	G_0	0.27389	-0.79900	-0.26714	1.4761	3.7226	0.16033
	G_1	0.028002	-1.1022	-0.033521	0.22057	0.52258	0.10846
	G_2	0.012675	-1.1481	-0.015221	-0.082355	0.13759	0.041064
	G_3	7.3602e-3	-1.1544	-6.5361e-3	-0.36173	0.049133	0.044540
	G_4	4.9892e-3	-1.2132	-4.3696e-3	-0.46223	0.020326	0.068641
90	G_0	0.79807	0.041621	-0.55195	0.94721	-0.33668	0.52973
	G_1	0.82407	0.023018	0.14705	0.15481	0.048556	0.16795
	G_2	0.75607	1.8397e-3	0.28788	0.023688	0.12715	0.066900
	G_3	0.68582	-1.6499e-3	0.30738	-0.033522	0.13604	0.029992
	G_4	0.63097	8.4876e-3	0.30584	-0.067862	0.13547	0.025147
Coefficients C_6 Through C_{10}							
φ	G_i	C_6	C_7	C_8	C_9	C_{10}	---
0	G_0	0.64383	-1.7330	-2.5867	0.55987	-0.54503	---
	G_1	0.065941	-3.1077	-0.93098	2.4443	0.18878	---
	G_2	0.019569	-1.9848	-0.22151	2.9522	0.16896	---
	G_3	8.9574e-3	-1.4999	-0.081464	3.0826	0.10436	---
	G_4	4.1052e-3	-1.1912	-0.033493	3.2003	0.074990	---
90	G_0	-0.93391	-0.064536	0.28786	-0.22806	0.0	---
	G_1	-0.12109	7.2007e-3	0.093079	-0.094413	0.0	---
	G_2	0.012227	0.021628	0.041800	-0.051236	0.0	---
	G_3	0.072309	0.022755	0.022788	-0.030355	0.0	---
	G_4	0.092532	0.022520	0.015831	-0.029806	0.0	---

Table 9B.4 – Influence Coefficients for an Embedded Crack of Infinite Length in a Plate

d_1/t	a/d_1	Point A				
		G_0	G_1	G_2	G_3	G_4
0.1	0.20	1.037474	-0.525539	0.513530	-0.398121	0.385912
	0.40	1.063196	-0.512793	0.527960	-0.381408	0.393538
	0.60	1.124939	-0.511072	0.549082	-0.375003	0.405314
	0.80	1.292554	-0.539518	0.596937	-0.390045	0.431613
0.25	0.20	1.058534	-0.523445	0.525337	-0.391913	0.392771
	0.40	1.093824	-0.522160	0.533711	-0.391325	0.397355
	0.60	1.195165	-0.533388	0.561563	-0.398093	0.412760
	0.80	1.430213	-0.566890	0.625906	-0.415809	0.446381
0.5	0.20	1.069921	-0.675294	0.528362	-0.447519	0.394956
	0.40	1.172232	-0.721464	0.557197	-0.468248	0.411130
	0.60	1.375565	-0.809178	0.609550	-0.504208	0.437929
	0.80	1.912707	-1.049389	0.756235	-0.606419	0.514699
d_1/t	a/d_1	Point B				
		G_0	G_1	G_2	G_3	G_4
0.1	0.20	1.036385	0.500468	0.513132	0.373235	0.385696
	0.40	1.053488	0.529134	0.525443	0.399017	0.392261
	0.60	1.083573	0.543560	0.538003	0.413163	0.399621
	0.80	1.136074	0.537801	0.552329	0.410923	0.407874
0.25	0.20	1.057198	0.523110	0.525004	0.391746	0.392604
	0.40	1.084672	0.520354	0.531924	0.390650	0.396678
	0.60	1.144249	0.519696	0.548254	0.391129	0.405936
	0.80	1.239721	0.511818	0.573109	0.386992	0.418467
0.5	0.20	1.069921	0.675294	0.528362	0.447519	0.394956
	0.40	1.172232	0.721464	0.557197	0.468248	0.411130
	0.60	1.375565	0.809178	0.609550	0.504208	0.437929
	0.80	1.912707	1.049389	0.756235	0.606419	0.514699

Notes: Interpolation may be used for intermediate values of d_1/t and a/d_1.

Table 9B.5 – Influence Coefficients for an Embedded Crack of Finite Length in a Plate

a/c	d_1/t	a/d_1	G_i	A_0	A_1	A_2	A_3	A_4	A_5	A_6
0.125	0.1	0.2	G_0	0.453339	0.002579	2.377363	-0.009845	-3.608162	0.006526	1.809979
			G_1	5.857E-05	0.5078001	2.561E-05	0.3974088	-0.00063	-0.414078	0.0004351
			G_2	-0.001573	0.000157	0.964481	-0.000598	-0.358261	0.000320	-0.113455
			G_3	-5.64E-06	0.0013232	4.094E-05	1.0594535	-9.9E-05	-0.692845	2.883E-05
			G_4	-0.003972	0.000000	0.158606	-0.000020	0.975214	-0.000006	-0.768528
		0.4	G_0	0.466894	-0.000183	2.318151	-0.022260	-3.382581	0.014255	1.660507
			G_1	-7.98E-05	0.524491	-0.001379	0.3457247	-0.00389	-0.377892	0.0032573
			G_2	-0.002119	0.000261	0.984744	-0.005198	-0.381285	0.002939	-0.103774
			G_3	-4E-05	0.0040861	-0.000194	1.0562663	-0.00272	-0.692305	0.0019455
			G_4	-0.005178	0.000188	0.172885	-0.002378	0.963875	0.001210	-0.767266
		0.6	G_0	0.477274	-0.000129	2.365713	-0.090046	-3.281894	0.056426	1.567260
			G_1	-0.000273	0.5274077	-0.003353	0.3444216	-0.02502	-0.374755	0.0188494
			G_2	-0.002130	0.001859	1.000577	-0.023568	-0.366597	0.012765	-0.119386
			G_3	-0.000163	0.0041254	0.0009764	1.0602626	-0.0169	-0.694386	0.0112423
			G_4	-0.005726	0.001266	0.180947	-0.011073	0.971679	0.005175	-0.775605
		0.8	G_0	0.487714	0.010113	2.478118	-0.301636	-3.070704	0.173415	1.379379
			G_1	-0.001162	0.5179352	0.003687	0.3990023	-0.12955	-0.397981	0.0871266
			G_2	-0.000737	0.008895	1.001326	-0.082830	-0.263901	0.038980	-0.188657
			G_3	-0.000793	0.0008877	0.0112907	1.0760818	-0.0799	-0.697195	0.0487794
			G_4	-0.005154	0.005495	0.177660	-0.038930	1.021968	0.014325	-0.806620
0.125	0.25	0.2	G_0	0.402472	-0.050527	2.904407	0.255471	-4.947331	-0.281718	2.736348
			G_1	-0.002654	0.466214	-0.066963	0.459261	0.146976	-0.440574	-0.080979
			G_2	-0.002028	-0.011522	0.899724	-0.037831	-0.235939	0.058484	-0.195269
			G_3	0.001862	0.008824	-0.096953	0.958686	0.183063	-0.620891	-0.089157
			G_4	-0.003131	0.002178	0.153341	-0.082397	0.942617	0.092908	-0.762958
		0.4	G_0	0.423287	-0.031730	2.755031	0.106003	-4.356325	-0.113844	2.276538
			G_1	-0.004337	0.488376	-0.018798	0.445002	0.042130	-0.442372	-0.023399
			G_2	-0.000113	-0.012149	0.951095	-0.003645	-0.308412	0.015653	-0.149110
			G_3	0.000486	0.002651	-0.049583	1.025268	0.091154	-0.665949	-0.044010
			G_4	-0.002569	-0.001080	0.152314	-0.039286	0.982607	0.044717	-0.778851
		0.6	G_0	0.432989	-0.033577	2.872620	0.027125	-4.359993	-0.064021	2.235058
			G_1	-0.004351	0.486459	-0.027018	0.466641	0.031078	-0.455126	-0.013517
			G_2	0.001550	-0.011965	0.969643	-0.021303	-0.285069	0.024774	-0.171453
			G_3	0.000228	0.002766	-0.049174	1.036901	0.077402	-0.671945	-0.035391
			G_4	-0.001651	-0.000909	0.156156	-0.047470	1.008257	0.048482	-0.797691
		0.8	G_0	0.445542	-0.033047	3.041505	-0.234082	-4.127055	0.097677	2.009092
			G_1	-0.005232	0.488237	-0.017605	0.521073	-0.098628	-0.481469	0.071257
			G_2	0.003887	-0.004975	0.999241	-0.082000	-0.187212	0.044134	-0.245910
			G_3	-0.000904	-0.002210	-0.022680	1.092769	-0.025501	-0.702693	0.022851
			G_4	-0.000593	0.002201	0.155600	-0.064479	1.102858	0.042103	-0.860425

Table 9B.5 – Influence Coefficients for an Embedded Crack of Finite Length in a Plate

a/c	d_1/t	a/d_1	G_i	A_0	A_1	A_2	A_3	A_4	A_5	A_6
0.125	0.5	0.2	G_0	0.452208	-0.017180	2.496135	0.096821	-3.887236	-0.101879	2.006232
			G_1	0.000000	0.515985	-0.006471	0.418733	0.011986	-0.430803	-0.006741
			G_2	0.000137	-0.010747	0.903078	-0.035133	-0.235300	0.056911	-0.196866
			G_3	0.000000	0.005191	0.000427	1.086222	-0.001351	-0.709040	0.000756
			G_4	0.000042	-0.004570	0.184913	-0.033948	0.832546	0.037795	-0.665999
		0.4	G_0	0.460370	-0.014353	2.597565	0.086983	-3.930644	-0.094323	2.000952
			G_1	0.000000	0.514400	-0.000381	0.431274	0.000350	-0.438897	-0.000183
			G_2	0.000650	-0.011494	0.959328	0.003895	-0.301062	0.011214	-0.157400
			G_3	0.000000	0.004923	0.000370	1.088831	-0.000894	-0.710377	0.000399
			G_4	0.000265	-0.001303	0.151837	-0.022125	1.006405	0.027741	-0.796412
		0.6	G_0	0.470563	-0.014111	2.800145	0.085921	-3.915485	-0.093348	1.914262
			G_1	0.000000	0.511104	-0.000060	0.482732	-0.000416	-0.468649	0.000377
			G_2	0.002665	-0.011945	0.985090	0.005107	-0.243501	0.010583	-0.207033
			G_3	0.000000	0.004476	0.000652	1.106319	-0.001608	-0.718463	0.000880
			G_4	0.000610	-0.001640	0.158429	-0.034545	1.039227	0.042712	-0.820420
		0.8	G_0	0.481246	-0.013836	3.156476	0.084019	-3.534391	-0.091215	1.522475
			G_1	0.000000	0.495527	0.000335	0.688092	-0.000886	-0.571261	0.000469
			G_2	0.006111	-0.009234	1.017397	0.009922	-0.010110	0.001466	-0.376235
			G_3	0.000000	-0.002324	0.000564	1.190456	-0.000937	-0.751321	0.000289
			G_4	0.001439	-0.001644	0.150711	-0.020467	1.217097	0.026434	-0.936694
0.25	0.1	0.2	G_0	0.714697	0.001167	0.953383	-0.000623	-1.155770	-0.000063	0.487292
			G_1	0.0001178	0.6944657	0.0008962	0.1110875	-0.0015	-0.239918	0.000747
			G_2	0.037394	0.000196	1.024339	0.000237	-0.544663	-0.000239	0.007320
			G_3	-4.69E-06	0.0553272	0.0008538	1.0717715	-0.00118	-0.708304	0.0004599
			G_4	0.007400	0.000059	0.244037	0.000220	0.835392	-0.000164	-0.691443
		0.4	G_0	0.720390	-0.003207	0.971344	-0.004495	-1.172486	0.003565	0.492746
			G_1	-0.000306	0.6958178	-0.001132	0.1111092	0.000138	-0.240271	0.0003074
			G_2	0.038578	-0.000653	1.029789	-0.001011	-0.549975	0.000779	0.009142
			G_3	-0.000179	0.0558895	6.667E-05	1.0741125	-0.00084	-0.710034	0.0005104
			G_4	0.007885	-0.000285	0.246692	-0.000454	0.835724	0.000345	-0.692690
		0.6	G_0	0.733456	-0.011577	0.997438	-0.033163	-1.157522	0.022983	0.474860
			G_1	-0.001419	0.6942295	-0.005374	0.1208062	-0.00406	-0.247165	0.0046793
			G_2	0.040141	-0.002134	1.031069	-0.008717	-0.526401	0.005648	-0.009729
			G_3	-0.00062	0.0527525	-0.001938	1.0937201	-0.00303	-0.724647	0.0027423
			G_4	0.008386	-0.000853	0.241704	-0.004342	0.874998	0.002704	-0.723291
		0.8	G_0	0.757254	-0.025756	1.024336	-0.146935	-1.004243	0.089973	0.356990
			G_1	-0.004037	0.691387	-0.009454	0.1585973	-0.05812	-0.267008	0.0422383
			G_2	0.044036	-0.002861	1.040014	-0.044552	-0.503944	0.023692	-0.027120
			G_3	-0.001737	0.0540472	-0.001103	1.1054142	-0.03527	-0.733196	0.0235474
			G_4	0.008927	-0.000444	0.264009	-0.023174	0.845894	0.011089	-0.710276

Table 9B.5 – Influence Coefficients for an Embedded Crack of Finite Length in a Plate

a/c	d_1/t	a/d_1	G_i	A_0	A_1	A_2	A_3	A_4	A_5	A_6
0.25	0.25	0.2	G_0	0.537696	-0.025921	1.955145	0.120407	-2.938922	-0.125258	1.497329
			G_1	-0.000246	0.564125	-0.002740	0.343556	0.005187	-0.380079	-0.003435
			G_2	0.014281	0.000287	1.050888	-0.015054	-0.569580	0.016957	0.010362
			G_3	-0.000107	0.014103	0.000336	1.109461	-0.000465	-0.725386	-0.000354
			G_4	-0.000703	0.007998	0.251550	-0.055277	0.855937	0.063336	-0.739814
		0.4	G_0	0.547860	-0.027674	1.990139	0.108034	-2.971917	-0.117768	1.510431
			G_1	-0.000456	0.564074	-0.005148	0.343801	0.006167	-0.380055	-0.003335
			G_2	0.011184	0.000755	1.018531	-0.017088	-0.428454	0.018686	-0.087797
			G_3	-0.000212	0.014255	-0.000205	1.107599	-0.001989	-0.724060	0.001017
			G_4	-0.001173	0.005128	0.193131	-0.038389	1.010172	0.042987	-0.826030
		0.6	G_0	0.567565	-0.020461	1.969533	-0.009167	-2.705955	-0.016330	1.293079
			G_1	-0.001061	0.571398	-0.007944	0.342287	-0.010781	-0.382996	0.010056
			G_2	0.015595	0.000916	1.015394	-0.034520	-0.386367	0.029949	-0.118726
			G_3	-0.000456	0.016782	-0.001526	1.109613	-0.009983	-0.727432	0.007257
			G_4	0.000208	0.004933	0.203057	-0.044570	0.998683	0.046036	-0.819681
		0.8	G_0	0.576341	-0.040645	2.158031	-0.161776	-2.691429	0.064515	1.222566
			G_1	-0.003531	0.554035	-0.014173	0.424091	-0.087946	-0.426653	0.063971
			G_2	0.017718	-0.000648	1.042168	-0.079493	-0.354045	0.047244	-0.142868
			G_3	-0.001407	0.012543	0.000852	1.129475	-0.060002	-0.733130	0.039306
			G_4	0.001281	0.004904	0.217941	-0.065569	0.998171	0.050659	-0.817098
0.25	0.5	0.2	G_0	0.544046	-0.014364	1.959109	0.095272	-2.959061	-0.108774	1.512392
			G_1	0.000000	0.565516	-0.001180	0.341811	0.002349	-0.378954	-0.001650
			G_2	0.010169	0.002381	1.014622	-0.015806	-0.427709	0.018051	-0.087045
			G_3	0.000000	0.014335	0.001019	1.109745	-0.001143	-0.725493	0.000032
			G_4	0.000225	0.008198	0.254659	-0.052066	0.850805	0.060585	-0.736277
		0.4	G_0	0.556660	-0.014651	2.024524	0.097216	-3.011443	-0.111038	1.528937
			G_1	0.000000	0.566247	-0.001445	0.343967	0.003157	-0.380215	-0.002221
			G_2	0.014997	0.002695	1.004419	-0.017900	-0.387113	0.020447	-0.115022
			G_3	0.000000	0.014697	0.000740	1.109383	-0.000451	-0.725224	-0.000500
			G_4	0.000297	0.005454	0.193812	-0.036216	1.008950	0.041367	-0.824312
		0.6	G_0	0.581808	-0.008651	2.055696	0.049934	-2.712013	-0.053154	1.266472
			G_1	0.000000	0.574804	-0.000789	0.363279	0.000975	-0.395833	-0.000463
			G_2	0.018124	0.001634	1.042789	-0.009439	-0.409391	0.010048	-0.106126
			G_3	0.000000	0.017797	0.000904	1.120134	-0.002384	-0.733520	0.001419
			G_4	0.001852	0.005267	0.206731	-0.036055	1.009944	0.041703	-0.828698
		0.8	G_0	0.608273	-0.008227	2.345792	0.049047	-2.536023	-0.052853	1.042975
			G_1	0.000000	0.561954	-0.000788	0.539207	0.001266	-0.489579	-0.000686
			G_2	0.024349	0.002521	1.062774	-0.017745	-0.244333	0.020774	-0.230939
			G_3	0.000000	0.013542	0.000593	1.186767	-0.001749	-0.761495	0.001179
			G_4	0.004477	0.004744	0.222326	-0.033388	1.060651	0.039086	-0.862354

Table 9B.5 – Influence Coefficients for an Embedded Crack of Finite Length in a Plate

a/c	d_1/t	a/d_1	G_i	A_0	A_1	A_2	A_3	A_4	A_5	A_6
0.5	0.1	0.2	G_0	0.714697	0.001167	0.953383	-0.000623	-1.155770	-0.000063	0.487292
			G_1	0.0001178	0.6944657	0.0008962	0.1110875	-0.0015	-0.239918	0.000747
			G_2	0.037394	0.000196	1.024339	0.000237	-0.544663	-0.000239	0.007320
			G_3	-4.69E-06	0.0553272	0.0008538	1.0717715	-0.00118	-0.708304	0.0004599
			G_4	0.007400	0.000059	0.244037	0.000220	0.835392	-0.000164	-0.691443
		0.4	G_0	0.720390	-0.003207	0.971344	-0.004495	-1.172486	0.003565	0.492746
			G_1	-0.000306	0.6958178	-0.001132	0.1111092	0.000138	-0.240271	0.0003074
			G_2	0.038578	-0.000653	1.029789	-0.001011	-0.549975	0.000779	0.009142
			G_3	-0.000179	0.0558895	6.667E-05	1.0741125	-0.00084	-0.710034	0.0005104
			G_4	0.007885	-0.000285	0.246692	-0.000454	0.835724	0.000345	-0.692690
		0.6	G_0	0.733456	-0.011577	0.997438	-0.033163	-1.157522	0.022983	0.474860
			G_1	-0.001419	0.6942295	-0.005374	0.1208062	-0.00406	-0.247165	0.0046793
			G_2	0.040141	-0.002134	1.031069	-0.008717	-0.526401	0.005648	-0.009729
			G_3	-0.00062	0.0527525	-0.001938	1.0937201	-0.00303	-0.724647	0.0027423
			G_4	0.008386	-0.000853	0.241704	-0.004342	0.874998	0.002704	-0.723291
		0.8	G_0	0.757254	-0.025756	1.024336	-0.146935	-1.004243	0.089973	0.356990
			G_1	-0.004037	0.691387	-0.009454	0.1585973	-0.05812	-0.267008	0.0422383
			G_2	0.044036	-0.002861	1.040014	-0.044552	-0.503944	0.023692	-0.027120
			G_3	-0.001737	0.0540472	-0.001103	1.1054142	-0.03527	-0.733196	0.0235474
			G_4	0.008927	-0.000444	0.264009	-0.023174	0.845894	0.011089	-0.710276
0.5	0.25	0.2	G_0	0.717667	-0.020380	0.936510	0.057695	-1.153295	-0.056218	0.512093
			G_1	0.000134	0.723947	-0.006780	0.071199	0.008381	-0.217568	-0.004205
			G_2	0.035086	-0.001476	1.115370	-0.004442	-0.702698	0.006067	0.087912
			G_3	-0.000314	0.073308	0.002381	1.079510	-0.004861	-0.718140	0.001625
			G_4	0.002950	0.010332	0.287094	-0.071217	0.895005	0.082854	-0.796598
		0.4	G_0	0.730290	-0.015680	0.969475	0.043223	-1.201325	-0.047817	0.535517
			G_1	0.000220	0.726457	-0.006588	0.071565	0.007191	-0.218382	-0.003198
			G_2	0.041978	0.000008	1.088962	-0.011715	-0.643704	0.013340	0.051074
			G_3	-0.000330	0.074159	0.002652	1.079969	-0.005697	-0.718580	0.002201
			G_4	0.007325	0.008144	0.300095	-0.056601	0.830792	0.065468	-0.742353
		0.6	G_0	0.743860	-0.021962	1.005065	0.000002	-1.164803	-0.007235	0.483331
			G_1	-0.001394	0.711649	-0.010184	0.123002	0.005080	-0.252337	-0.000531
			G_2	0.042902	-0.001773	1.055272	-0.016718	-0.523410	0.015064	-0.026169
			G_3	-0.000737	0.058020	-0.001953	1.123562	-0.003418	-0.744614	0.002782
			G_4	0.008153	0.003902	0.251503	-0.034795	0.939929	0.035851	-0.790276
		0.8	G_0	0.760458	-0.048773	1.138436	-0.087284	-1.229980	0.034587	0.494763
			G_1	-0.005280	0.701105	-0.009052	0.189475	-0.067278	-0.291822	0.048830
			G_2	0.046198	-0.003951	1.076766	-0.053235	-0.515871	0.032111	-0.036005
			G_3	-0.002230	0.053570	0.000871	1.149157	-0.045224	-0.759029	0.030020
			G_4	0.010715	0.004107	0.251023	-0.057908	0.964621	0.048232	-0.808843

Table 9B.5 – Influence Coefficients for an Embedded Crack of Finite Length in a Plate

a/c	d_1/t	a/d_1	G_i	A_0	A_1	A_2	A_3	A_4	A_5	A_6
0.5	0.5	0.2	G_0	0.723987	-0.007139	0.955619	0.044991	-1.192714	-0.052151	0.535845
			G_1	0.000000	0.726564	-0.001605	0.070019	0.000591	-0.217340	-0.000287
			G_2	0.040720	0.001588	1.086529	-0.010068	-0.642235	0.011690	0.051144
			G_3	0.000000	0.074017	0.004101	1.080085	-0.006328	-0.718574	0.002099
			G_4	0.006760	0.008736	0.299516	-0.055454	0.830800	0.064516	-0.741818
		0.4	G_0	0.737303	-0.007298	0.992434	0.045879	-1.233273	-0.053050	0.551960
			G_1	0.000000	0.728397	-0.002109	0.072485	0.002030	-0.219508	-0.001176
			G_2	0.043920	0.001719	1.088827	-0.010917	-0.637685	0.012729	0.046100
			G_3	0.000000	0.074923	0.004527	1.080519	-0.007475	-0.719037	0.002846
			G_4	0.008774	0.008724	0.297714	-0.055392	0.835576	0.064431	-0.744573
		0.6	G_0	0.761395	-0.003760	1.051896	0.022076	-1.190796	-0.023822	0.486506
			G_1	0.000000	0.717045	-0.002967	0.131681	0.005004	-0.258490	-0.002813
			G_2	0.046659	0.001634	1.062532	-0.009691	-0.520306	0.010499	-0.031082
			G_3	0.000000	0.059948	0.000684	1.128646	-0.001600	-0.747943	0.000673
			G_4	0.010802	0.005183	0.249832	-0.030714	0.948557	0.033263	-0.795556
		0.8	G_0	0.801961	0.004280	1.253179	0.010431	-1.203325	-0.022751	0.437555
			G_1	0.000000	0.719005	0.011393	0.251467	-0.029449	-0.328034	0.018079
			G_2	0.054811	0.004299	1.094040	-0.015009	-0.474001	0.013135	-0.071147
			G_3	0.000000	0.059324	0.006812	1.183994	-0.016429	-0.778236	0.009714
			G_4	0.014771	0.006609	0.254211	-0.036096	0.997468	0.038652	-0.832479
1.0	0.1	0.2	G_0	0.997015	0.002272	-0.003260	-0.002969	0.006077	0.001445	-0.003279
			G_1	0.0003041	1.0345514	0.0008628	-0.423094	-0.00183	0.0473937	0.0010141
			G_2	0.067438	0.000505	1.277697	-0.000366	-1.003875	0.000119	0.247401
			G_3	3.694E-05	0.1526431	0.0012502	1.1129777	-0.00197	-0.770432	0.0008828
			G_4	0.015392	0.000209	0.385062	-0.000050	0.737408	-0.000018	-0.678470
		0.4	G_0	1.001919	-0.002820	-0.000186	0.000347	0.002072	0.000396	-0.001485
			G_1	-0.000194	1.036099	-0.000474	-0.423816	-8.5E-05	0.047516	0.0002371
			G_2	0.068391	-0.000591	1.280108	0.000073	-1.006202	0.000081	0.248204
			G_3	-0.000165	0.1531596	0.0006597	1.1152403	-0.00135	-0.772042	0.000648
			G_4	0.015780	-0.000262	0.386139	0.000040	0.739620	0.000030	-0.680471
		0.6	G_0	1.012755	-0.014234	0.008623	-0.002402	0.001257	0.004604	-0.004253
			G_1	-0.001492	1.0394698	-0.00346	-0.422808	0.000191	0.0462255	0.0011126
			G_2	0.070584	-0.003091	1.286666	-0.001234	-1.009755	0.001426	0.248393
			G_3	-0.000715	0.154303	-0.00065	1.1244011	-0.00155	-0.778162	0.0012577
			G_4	0.016561	-0.001372	0.389559	-0.000747	0.749817	0.000748	-0.688990
		0.8	G_0	1.035295	-0.044958	0.019907	-0.039550	0.059827	0.033096	-0.049943
			G_1	-0.004823	1.0421659	-0.016547	-0.399473	-0.01568	0.0319558	0.0162082
			G_2	0.075714	-0.009416	1.284485	-0.018607	-0.983455	0.012426	0.229440
			G_3	-0.002112	0.1562608	-0.005574	1.132651	-0.01341	-0.784041	0.0108586
			G_4	0.018564	-0.003881	0.390045	-0.011363	0.762197	0.006976	-0.699115

Table 9B.5 – Influence Coefficients for an Embedded Crack of Finite Length in a Plate

a/c	d_1/t	a/d_1	G_i	A_0	A_1	A_2	A_3	A_4	A_5	A_6
1.0	0.25	0.2	G_0	0.998584	-0.015684	-0.036382	0.016835	0.092538	-0.005774	-0.060056
			G_1	0.000250	1.052208	-0.007063	-0.426007	0.007622	0.046894	-0.003511
			G_2	0.063900	-0.005874	1.371599	0.019092	-1.170753	-0.020165	0.346043
			G_3	-0.000595	0.164589	0.005755	1.139653	-0.011252	-0.788627	0.004916
			G_4	0.008863	0.013112	0.408872	-0.091416	0.888747	0.107038	-0.856287
		0.4	G_0	1.015009	-0.007528	-0.030901	0.002447	0.081626	0.003224	-0.054949
			G_1	0.000819	1.057810	-0.005844	-0.429289	0.006556	0.047572	-0.003170
			G_2	0.072202	-0.003136	1.334405	0.009943	-1.090502	-0.010740	0.295820
			G_3	-0.000381	0.166856	0.005973	1.138556	-0.010985	-0.788519	0.004677
			G_4	0.015117	0.009818	0.432485	-0.066636	0.775413	0.077664	-0.761771
		0.6	G_0	1.025429	-0.018899	-0.024098	-0.001328	0.088452	0.008861	-0.064283
			G_1	-0.000546	1.056583	-0.009132	-0.425212	0.007313	0.044664	-0.002488
			G_2	0.075269	-0.005550	1.326501	0.007215	-1.074799	-0.007587	0.285693
			G_3	-0.000931	0.167496	0.004138	1.134758	-0.010558	-0.786476	0.004953
			G_4	0.016556	0.008581	0.430086	-0.067017	0.773639	0.077920	-0.759863
		0.8	G_0	1.042557	-0.064164	-0.020997	-0.026482	0.175951	0.035162	-0.131913
			G_1	-0.004758	1.051391	-0.032160	-0.395132	0.004437	0.028163	0.007076
			G_2	0.079656	-0.015330	1.317765	-0.011036	-1.043202	0.004666	0.266819
			G_3	-0.002593	0.167653	-0.005711	1.137499	-0.019303	-0.787576	0.014316
			G_4	0.018859	0.004686	0.426646	-0.079355	0.777681	0.084825	-0.760303
1.0	0.5	0.2	G_0	1.007335	0.000870	-0.032838	-0.005828	0.083483	0.006862	-0.055173
			G_1	0.000000	1.055473	-0.000686	-0.425363	-0.007413	0.043747	0.007607
			G_2	0.070700	-0.001362	1.333569	0.008830	-1.089365	-0.010341	0.295376
			G_3	0.000000	0.165942	0.007078	1.139476	-0.012172	-0.788841	0.005131
			G_4	0.014449	0.010548	0.432405	-0.066712	0.775486	0.077462	-0.761576
		0.4	G_0	1.020653	0.000802	-0.024712	-0.005325	0.069424	0.006308	-0.047845
			G_1	0.000000	1.059402	-0.000822	-0.426893	-0.006340	0.043580	0.006645
			G_2	0.073767	-0.001180	1.332171	0.007611	-1.083972	-0.008928	0.291070
			G_3	0.000000	0.167661	0.007030	1.138310	-0.012411	-0.788448	0.005386
			G_4	0.017079	0.010573	0.425339	-0.066981	0.787124	0.077776	-0.767555
		0.6	G_0	1.039108	0.000776	-0.005040	-0.005624	0.064248	0.006872	-0.052375
			G_1	0.000000	1.062759	-0.003182	-0.423205	0.000529	0.041231	0.001284
			G_2	0.078057	-0.001199	1.331264	0.007708	-1.079097	-0.008986	0.287330
			G_3	0.000000	0.170220	0.006127	1.135403	-0.010697	-0.787366	0.004307
			G_4	0.019181	0.010461	0.424202	-0.066392	0.785711	0.077226	-0.766443
		0.8	G_0	1.076678	0.001493	0.055210	-0.009915	0.119255	0.011779	-0.114726
			G_1	0.000000	1.077683	-0.006020	-0.374247	0.012880	0.014321	-0.010548
			G_2	0.086643	-0.001194	1.338314	0.007540	-1.043218	-0.008732	0.260265
			G_3	0.000000	0.177403	0.006432	1.156459	-0.012131	-0.800413	0.005542
			G_4	0.022932	0.010421	0.428579	-0.066205	0.798227	0.077073	-0.775999

Note: Interpolation may be used for intermediate values of a/c, d_1/t, and a/d_1.

Table 9B.6 – Influence Coefficients for a Longitudinal Through-Wall Crack in a Cylinder – Inside Surface

t/R_i	G_i	A_0	A_1	A_2	A_3	A_4	A_5	A_6
0.01 (1/100)	G_0	1.00762	-0.178500	0.161440	0.000000	-0.152520	0.058880	-0.003090
	G_1	0.0003	2.728940	0.424320	1.698480	13.87692	3.712580	0.073810
	G_p	1.01406	2.570610	1.040380	1.308630	2.148980	2.354210	-0.032420
0.01667 (1/60)	G_0	1.00764	0.013520	0.179410	0.000000	0.064370	0.024070	-0.001050
	G_1	0.00155	1.965340	0.176480	1.467290	9.452660	3.829850	0.018860
	G_p	1.0148	0.774270	0.451220	0.470680	0.635190	0.878590	-0.010450
0.05 (1/20)	G_0	1.00848	0.011360	0.194630	0.000000	0.073580	0.027420	-0.001140
	G_1	0.00382	0.784820	-0.285200	0.747730	1.890590	2.274800	-0.004600
	G_p	1.02776	0.014070	0.202280	0.000000	0.111820	0.023890	-0.000930
0.1 (1/10)	G_0	1.00856	0.149340	0.243300	0.000000	0.268710	0.009360	-0.000250
	G_1	0.00353	0.542290	-0.148882	0.419400	1.263990	1.193950	0.005930
	G_p	1.05546	0.166380	0.274280	0.000000	0.353440	0.007500	-0.000160
0.2 (1/5)	G_0	1.00475	0.107380	0.229090	0.000000	0.223980	0.012480	-0.000260
	G_1	0.00012	0.506470	0.246340	0.343420	3.059800	0.794490	0.018660
	G_p	1.096636	0.226909	0.315056	0.000000	0.473274	0.002693	0.000150
0.3333 (1/3)	G_0	1.00566	0.279910	0.286730	0.000000	0.483700	-0.012079	0.001377
	G_1	0.01447	0.179880	0.014630	0.000000	-0.029591	0.005410	0.000000
	G_p	1.12254	0.256880	0.371360	0.000000	0.569940	0.011600	-0.000096
1.0 (1/1)	G_0	0.9944	-0.095100	0.225710	0.000000	0.125240	0.029970	0.002957
	G_1	0.00359	0.137790	0.017440	0.000000	-0.065443	0.016350	0.000310
	G_p	1.32435	0.696980	0.400810	0.015540	1.302680	-0.089300	0.018523

Notes: Interpolation of the influence coefficients, G_i, may be used for intermediate values of R_i/t.

Table 9B.7 – Influence Coefficients for a Longitudinal Through-Wall Crack in a Cylinder – Outside Surface

t/R_i	G_i	A_0	A_1	A_2	A_3	A_4	A_5	A_6
0.01 (1/100)	G_0	1.004540	0.392250	0.086470	0.000000	-0.020700	0.030610	-0.000990
	G_1	0.999510	7.930100	4.196810	1.911150	9.117120	3.412640	0.503310
	G_p	0.999190	0.439200	-0.010021	0.000000	0.221300	-0.028073	0.000880
0.01667 (1/60)	G_0	1.004660	0.481660	0.168680	0.000000	0.124010	0.029580	-0.000250
	G_1	0.995030	2.659410	1.233980	0.250070	3.250500	0.526340	0.070820
	G_p	0.993200	0.767840	0.589870	0.000000	0.697560	0.074080	0.001593
0.05 (1/20)	G_0	0.996830	0.338140	0.091330	0.000000	-0.017405	0.027980	-0.000490
	G_1	0.992850	0.786010	0.490220	0.000000	1.020270	0.108660	0.001550
	G_p	0.980700	0.382500	0.206540	0.000000	0.148410	0.038930	0.000405
0.1 (1/10)	G_0	0.994730	0.510250	0.185410	0.000000	0.168770	0.030030	0.000233
	G_1	0.999220	1.713680	0.612070	0.075550	1.973850	0.142370	0.031160
	G_p	0.959540	0.494400	0.213340	0.000000	0.233840	0.032670	0.001154
0.2 (1/5)	G_0	0.995330	0.585820	0.211280	0.000000	0.230790	0.037440	-0.000130
	G_1	0.998190	0.665590	0.343860	0.000000	0.737420	0.097600	0.000330
	G_p	0.947910	0.478700	0.184790	0.000000	0.187160	0.043710	0.000000
0.3333 (1/3)	G_0	0.996150	1.422090	0.689830	0.000000	1.113750	0.085480	0.000444
	G_1	1.000870	0.928950	0.333800	0.000000	0.956970	0.087980	0.000130
	G_p	0.893150	-1.161606	1.758510	2.949500	-2.178423	4.097810	0.558077
1.0 (1/1)	G_0	0.987790	0.427250	0.048420	0.000000	0.053630	0.012170	0.000553
	G_1	0.998500	0.058340	0.016870	0.000000	-0.051282	0.010850	0.000220
	G_p	0.856150	0.357890	0.000900	0.000000	-0.009800	0.009160	-0.000060

Notes: Interpolation of the influence coefficients, G_i, may be used for intermediate values of R_i/t.

Table 9B.8 – Influence Coefficients for a Circumferential Through Wall Crack in a Cylinder – Inside Surface

t/R_i	G_i	A_0	A_1	A_2	A_3	A_4	A_5	A_6
0.01 (1/100)	G_0	0.993480	-0.047161	0.054090	0.000000	0.000380	-0.000680	0.000000
	G_1	0.029980	0.124380	0.000000	0.000000	-0.075550	0.001750	0.000000
	G_5	0.985590	-0.045610	0.051610	0.000000	-0.002030	-0.000410	0.000000
0.01667 (1/60)	G_0	0.983490	-0.020450	0.044819	0.000000	0.005920	-0.001050	0.000000
	G_1	0.031820	0.123290	0.000000	0.000000	-0.064940	0.001230	0.000000
	G_5	0.971070	-0.013090	0.046740	0.000000	0.020930	-0.001310	0.000000
0.05 (1/20)	G_0	0.973550	0.003040	0.084271	0.000000	0.113040	-0.014110	0.000399
	G_1	0.026150	0.140480	0.000000	0.000000	-0.066830	0.000870	0.000000
	G_5	0.933380	0.043860	0.055860	0.000000	0.106990	-0.013120	0.000417
0.1 (1/10)	G_0	0.943450	-0.023300	0.069755	0.000000	0.032420	0.007170	-0.000740
	G_1	0.025510	0.138400	-0.002950	0.000000	-0.065840	0.000400	0.000000
	G_5	0.867590	-0.171700	0.045540	0.000000	-0.207460	0.035710	-0.001580
0.2 (1/5)	G_0	0.892870	0.042440	0.048300	0.000000	0.062390	-0.010370	0.000000
	G_1	0.009880	0.154550	-0.085610	0.017910	-0.658110	0.177100	-0.010080
	G_5	0.766430	-0.113580	0.037070	0.000000	-0.181100	0.032760	-0.001890
0.3333 (1/3)	G_0	0.845290	-0.032400	0.028444	0.000000	-0.080250	-0.000280	0.000000
	G_1	0.005010	0.181600	0.015110	0.000000	0.248280	-0.055500	0.002400
	G_5	0.639210	-0.041000	0.000000	0.000000	-0.192540	0.009610	0.000000
1.0 (1/1)	G_0	0.684160	-0.042100	0.015715	0.000000	-0.167800	0.007820	0.000000
	G_1	-0.005310	0.100550	-0.004990	0.000000	-0.185520	0.009140	0.000000
	G_5	0.355650	0.007130	0.001360	0.000000	-0.182870	0.009290	0.000000

Notes: Interpolation of the influence coefficients, G_i, may be used for intermediate values of R_i/t.

Table 9B.9 – Influence Coefficients for a Circumferential Through Wall Crack in a Cylinder – Outside Surface

t/R_i	G_i	A_0	A_1	A_2	A_3	A_4	A_5	A_6
0.01 (1/100)	G_0	0.999190	0.439200	-0.010020	0.000000	0.221300	-0.028070	0.000880
	G_1	0.993970	1.590210	-0.060740	0.000000	2.031720	-0.212760	0.006006
	G_5	1.000000	0.276970	-0.022358	0.002353	0.063820	-0.011510	0.000697
0.01667 (1/60)	G_0	1.016350	0.098680	0.000000	0.000000	-0.045340	0.000760	0.000000
	G_1	0.990970	0.107330	0.023480	0.000000	0.216380	-0.006700	0.000077
	G_5	1.003060	-0.025740	0.004704	0.013164	-0.239280	0.070140	-0.000730
0.05 (1/20)	G_0	0.996070	0.069010	-0.005580	0.000000	-0.109370	0.004740	-0.000081
	G_1	0.987530	-0.008000	0.022790	0.000000	0.062310	-0.000900	0.000115
	G_5	1.004290	0.136840	-0.021254	0.000900	-0.041250	-0.005740	0.000393
0.1 (1/10)	G_0	1.009490	0.163660	-0.004640	0.000000	0.009750	-0.004170	0.000000
	G_1	0.986430	0.116390	0.002660	0.000000	0.167370	-0.012940	0.000000
	G_5	1.004690	0.074190	-0.000500	0.000000	-0.068590	0.013030	-0.000750
0.2 (1/5)	G_0	0.988400	0.047990	0.000000	0.000000	-0.068610	-0.000140	0.000000
	G_1	0.989020	-0.032660	0.009220	0.000000	0.014110	-0.005480	0.000000
	G_5	0.997760	-0.277760	0.030970	0.000000	-0.366350	0.056330	-0.002420
0.3333 (1/3)	G_0	0.962510	-0.022768	0.000000	0.000000	-0.146530	0.005950	0.000000
	G_1	0.990490	-0.143270	0.018590	0.000000	-0.104870	0.005070	0.000000
	G_5	1.004950	-0.013450	0.000000	0.000000	-0.062110	0.000000	0.000000
1.0 (1/1)	G_0	0.920180	-0.086731	0.000243	0.000000	-0.225570	0.014210	0.000000
	G_1	0.992110	0.319530	-0.042350	0.000000	0.490910	-0.140260	0.009044
	G_5	0.997020	0.250250	-0.043352	0.000000	0.309300	-0.086700	0.004725

Notes: Interpolation of the influence coefficients, G_i, may be used for intermediate values of R_i/t.

Table 9B.10 – Influence Coefficients for a Longitudinal Infinite Length Surface Crack in a Cylindrical Shell

t/R_i	a/t	Inside Surface					Outside Surface				
		G_0	G_1	G_2	G_3	G_4	G_0	G_1	G_2	G_3	G_4
0.001 (1/1000)	0	1.120000	0.682000	0.524500	0.440400	0.379075	1.120000	0.682000	0.524500	0.440400	0.379075
	0.2	1.362669	0.775768	0.577169	0.475763	0.405555	1.362492	0.775430	0.577078	0.475707	0.405320
	0.4	2.107481	1.059637	0.734602	0.578123	0.483688	2.106159	1.059018	0.734066	0.577700	0.483457
	0.6	4.023909	1.759944	1.112458	0.819725	0.660648	4.023909	1.759732	1.112458	0.819832	0.660479
	0.8	11.685450	4.447550	2.518103	1.697986	1.278424	11.909190	4.532179	2.565580	1.730506	1.301380
0.00333 (1/300)	0	1.120000	0.682000	0.524500	0.440400	0.379075	1.120000	0.682000	0.524500	0.440400	0.379075
	0.2	1.357654	0.772719	0.575074	0.474050	0.404119	1.357654	0.772836	0.575120	0.474050	0.404212
	0.4	2.098124	1.055171	0.731561	0.575621	0.481987	2.098131	1.055420	0.731740	0.575826	0.482184
	0.6	3.984819	1.744473	1.103460	0.813729	0.656089	3.988986	1.746621	1.104648	0.814588	0.656975
	0.8	11.431820	4.361182	2.474754	1.671906	1.260057	11.418040	4.356190	2.471838	1.670314	1.258819
0.01 (1/100)	0	1.120000	0.682000	0.524500	0.440400	0.379075	1.120000	0.682000	0.524500	0.440400	0.379075
	0.2	1.355721	0.772039	0.574618	0.473607	0.403962	1.355914	0.772205	0.574709	0.473663	0.404056
	0.4	2.088097	1.051685	0.729765	0.574481	0.481203	2.086534	1.050936	0.729261	0.574252	0.480917
	0.6	3.924228	1.722783	1.091988	0.806497	0.650855	3.923337	1.722585	1.091908	0.806497	0.650876
	0.8	10.554820	4.054112	2.314531	1.572029	1.189801	10.534910	4.046475	2.309298	1.569106	1.187672
0.01667 (1/60)	0	1.120000	0.682000	0.524500	0.440400	0.379075	1.120000	0.682000	0.524500	0.440400	0.379075
	0.2	1.353978	0.771359	0.574252	0.473441	0.403767	1.354559	0.771574	0.574391	0.473496	0.403822
	0.4	2.076759	1.047310	0.727245	0.572880	0.479971	2.075495	1.046684	0.726942	0.572615	0.479723
	0.6	3.857250	1.698243	1.078613	0.797885	0.644619	3.858610	1.698758	1.079099	0.798289	0.644759
	0.8	9.818255	3.796811	2.179989	1.488012	1.131273	9.814990	3.795084	2.177882	1.486756	1.130544
0.025 (1/40)	0	1.120000	0.682000	0.524500	0.440400	0.379075	1.120000	0.682000	0.524500	0.440400	0.379075
	0.2	1.351845	0.770679	0.573795	0.473108	0.403649	1.352815	0.770943	0.573978	0.473214	0.403667
	0.4	2.064088	1.042414	0.724534	0.571046	0.478588	2.058880	1.039137	0.721589	0.568690	0.477008
	0.6	3.780308	1.670205	1.063426	0.788181	0.637578	3.783314	1.671252	1.064248	0.788820	0.637814
	0.8	9.046439	3.526527	2.038831	1.400363	1.069409	9.072502	3.534701	2.042477	1.402231	1.070735
0.05 (1/20)	0	1.120000	0.682000	0.524500	0.440400	0.379075	1.120000	0.682000	0.524500	0.440400	0.379075
	0.2	1.345621	0.768292	0.572560	0.472331	0.402984	1.348153	0.769051	0.572972	0.472583	0.403085
	0.4	2.028188	1.028989	0.717256	0.566433	0.475028	2.028188	1.028734	0.717129	0.566281	0.474824
	0.6	3.573882	1.594673	1.023108	0.762465	0.618437	3.584289	1.598763	1.025243	0.763840	0.619628
	0.8	7.388754	2.946567	1.736182	1.211533	0.936978	7.522466	2.992945	1.760192	1.226597	0.947337
0.1 (1/10)	0	1.120000	0.682000	0.524500	0.440400	0.379075	1.120000	0.682000	0.524500	0.440400	0.379075
	0.2	1.332691	0.763153	0.569758	0.470495	0.401459	1.338976	0.765213	0.570770	0.471069	0.401850
	0.4	1.957764	1.002123	0.702473	0.556857	0.467621	1.964321	1.004607	0.703748	0.557628	0.468296
	0.6	3.223438	1.466106	0.953655	0.718048	0.585672	3.270363	1.483681	0.963144	0.724069	0.590347
	0.8	5.543784	2.300604	1.398958	1.000682	0.789201	5.839919	2.403771	1.452694	1.034485	0.812508

Table 9B.10 – Influence Coefficients for a Longitudinal Infinite Length Surface Crack in a Cylindrical Shell

t/R_i	a/t	Inside Surface					Outside Surface				
		G_0	G_1	G_2	G_3	G_4	G_0	G_1	G_2	G_3	G_4
0.2 (1/5)	0	1.120000	0.682000	0.524500	0.440400	0.379075	1.120000	0.682000	0.524500	0.440400	0.379075
	0.2	1.307452	0.753466	0.564298	0.466913	0.398757	1.324199	0.759716	0.567636	0.468987	0.400407
	0.4	1.833200	0.954938	0.676408	0.539874	0.454785	1.861734	0.964913	0.681357	0.542909	0.457058
	0.6	2.734052	1.287570	0.857474	0.656596	0.540720	2.864663	1.335823	0.883295	0.673156	0.553201
	0.8	3.940906	1.739955	1.106210	0.818230	0.661258	4.412961	1.903704	1.191550	0.871484	0.697846
0.3333 (1/3)	0	1.120000	0.682000	0.524500	0.440400	0.379075	1.120000	0.682000	0.524500	0.440400	0.379075
	0.2	1.276782	0.742170	0.558403	0.463081	0.359594	1.310620	0.755011	0.565121	0.467379	0.399359
	0.4	1.697454	0.903713	0.648337	0.521591	0.440820	1.768778	0.930197	0.662576	0.531192	0.447877
	0.6	2.343563	1.146104	0.781532	0.605006	0.505644	2.576840	1.231639	0.827059	0.637486	0.527420
	0.8	3.056124	1.430631	0.944773	0.717096	0.591403	3.652018	1.636477	1.051797	0.783771	0.636126
1.0 (1/1)	0	1.120000	0.682000	0.524500	0.440400	0.379075	1.120000	0.682000	0.524500	0.440400	0.379075
	0.2	1.158826	0.698680	0.534893	0.447408	0.391564	1.285334	0.746937	0.561622	0.464836	0.404029
	0.4	1.324233	0.763056	0.571186	0.471434	0.408975	1.580071	0.859440	0.624169	0.505814	0.433491
	0.6	1.552523	0.856392	0.625411	0.508045	0.435872	2.028996	1.029037	0.718030	0.567200	0.477607
	0.8	1.937307	1.039092	0.740258	0.589449	0.497688	2.781279	1.326331	0.887634	0.680511	0.560320
1.5 (1.5/1)	0	1.120000	0.682000	0.524500	0.440400	0.379075	1.120000	0.682000	0.524500	0.440400	0.379075
	0.2	1.095935	0.674192	0.521132	0.438343	0.385033	1.279295	0.744331	0.560077	0.463801	0.403292
	0.4	1.195441	0.714295	0.544247	0.453881	0.396420	1.538059	0.843482	0.615370	0.500116	0.429452
	0.6	1.363930	0.787606	0.588288	0.484241	0.419044	1.926480	0.991136	0.697431	0.553958	0.468249
	0.8	1.712406	0.960052	0.698716	0.563341	0.479524	2.637820	1.272779	0.858339	0.661590	0.546900
2.0 (2/1)	0	1.120000	0.682000	0.524500	0.440400	0.379075	1.120000	0.682000	0.524500	0.440400	0.379075
	0.2	1.050181	0.656452	0.511188	0.431805	0.380330	1.278540	0.743950	0.559845	0.463650	0.403192
	0.4	1.117793	0.684999	0.528081	0.443349	0.388885	1.520006	0.836545	0.611498	0.497580	0.427634
	0.6	1.260936	0.750026	0.567958	0.471166	0.409774	1.879787	0.973679	0.687848	0.547740	0.463816
	0.8	1.589273	0.916175	0.675351	0.548481	0.469075	2.566715	1.245025	0.842694	0.651267	0.539456
2.5 (2.5/1)	0	1.120000	0.682000	0.524500	0.440400	0.379075	1.120000	0.682000	0.524500	0.440400	0.379075
	0.2	1.015777	0.643173	0.503766	0.426933	0.376830	1.279489	0.744268	0.560012	0.463760	0.403275
	0.4	1.066260	0.665614	0.517390	0.436381	0.383896	1.512354	0.833585	0.609833	0.496480	0.426839
	0.6	1.195498	0.726062	0.554924	0.462733	0.403760	1.856524	0.964940	0.683035	0.544609	0.461578
	0.8	1.508842	0.886980	0.659542	0.538273	0.461798	2.523619	1.227606	0.832660	0.644550	0.534560
3.0 (3/1)	0	1.120000	0.682000	0.524500	0.440400	0.379075	1.120000	0.682000	0.524500	0.440400	0.379075
	0.2	0.989094	0.632923	0.498052	0.423189	0.374143	1.280960	0.744803	0.560300	0.463947	0.403410
	0.4	1.029530	0.651825	0.509783	0.431415	0.380334	1.509651	0.832519	0.609219	0.496062	0.426529
	0.6	1.149572	0.709114	0.545620	0.456656	0.399385	1.845007	0.960657	0.680705	0.543105	0.460501
	0.8	1.450839	0.865530	0.647735	0.530539	0.456213	2.494990	1.215762	0.825746	0.639874	0.531117

Note: Interpolation of the influence coefficients, G_i, may be used for intermediate values of t/R_i and a/t.

Table 9B.11 – Influence Coefficients for a Circumferential 360° Surface Crack in a Cylindrical Shell

t/R_i	a/t	Inside Surface					Outside Surface				
		G_0	G_1	G_2	G_3	G_4	G_0	G_1	G_2	G_3	G_4
0.001 (1/1000)	0	1.120000	0.682000	0.524500	0.440400	0.379075	1.120000	0.682000	0.524500	0.440400	0.379075
	0.2	1.322217	0.749276	0.557422	0.459379	0.392453	1.322614	0.749276	0.557516	0.459436	0.392373
	0.4	1.985705	0.991993	0.684695	0.537194	0.453928	1.988345	0.992918	0.685270	0.537439	0.454140
	0.6	3.550561	1.553001	0.979529	0.719751	0.589763	3.554007	1.554127	0.980154	0.720115	0.589975
	0.8	7.704234	2.997325	1.722909	1.174144	0.914488	7.714443	3.000386	1.724431	1.175261	0.914895
0.00333 (1/300)	0	1.120000	0.682000	0.524500	0.440400	0.379075	1.120000	0.682000	0.524500	0.440400	0.379075
	0.2	1.326772	0.756593	0.563926	0.464829	0.397395	1.327958	0.756940	0.564112	0.464942	0.397435
	0.4	1.963785	0.994898	0.692884	0.546635	0.460636	1.967788	0.996347	0.693830	0.547114	0.460995
	0.6	3.332548	1.491534	0.957864	0.713772	0.584192	3.340673	1.493877	0.959050	0.714507	0.584442
	0.8	6.166579	2.493763	1.483156	1.041092	0.819169	6.185694	2.499017	1.485806	1.042477	0.819550
0.01 (1/100)	0	1.120000	0.682000	0.524500	0.440400	0.379075	1.120000	0.682000	0.524500	0.440400	0.379075
	0.2	1.328921	0.764758	0.572095	0.471607	0.403497	1.332125	0.754093	0.552893	0.446495	0.394324
	0.4	1.899528	0.981795	0.692586	0.550532	0.463005	1.908312	0.972250	0.672981	0.524206	0.453612
	0.6	3.004384	1.379555	0.898565	0.673759	0.560242	3.023794	1.392928	0.914706	0.693364	0.567059
	0.8	4.812997	2.042848	1.263627	0.915957	0.729154	4.859478	2.057938	1.271054	0.920244	0.731930
0.01667 (1/60)	0	1.120000	0.682000	0.524500	0.440400	0.379075	1.120000	0.682000	0.524500	0.440400	0.379075
	0.2	1.318924	0.760855	0.569883	0.470144	0.402374	1.324190	0.750929	0.551104	0.445314	0.393380
	0.4	1.848413	0.962422	0.681854	0.543524	0.457730	1.862482	0.954704	0.663258	0.517887	0.448742
	0.6	2.813119	1.309799	0.861033	0.649812	0.542690	2.842912	1.326360	0.878647	0.670199	0.549981
	0.8	4.237503	1.841730	1.158696	0.850454	0.683358	4.298510	1.860923	1.167928	0.855764	0.686511
0.025 (1/40)	0	1.120000	0.682000	0.524500	0.440400	0.379075	1.120000	0.682000	0.524500	0.440400	0.379075
	0.2	1.308916	0.756949	0.567677	0.468679	0.401251	1.316699	0.747945	0.549407	0.444194	0.392491
	0.4	1.800221	0.944166	0.671752	0.536926	0.452764	1.820527	0.938621	0.654343	0.512094	0.444266
	0.6	2.649761	1.250285	0.829036	0.629406	0.527751	2.691258	1.270496	0.848362	0.650736	0.535620
	0.8	3.822034	1.696662	1.083009	0.803222	0.650398	3.900213	1.720900	1.094600	0.809896	0.654152
0.05 (1/20)	0	1.120000	0.682000	0.524500	0.440400	0.379075	1.120000	0.682000	0.524500	0.440400	0.379075
	0.2	1.286308	0.748129	0.562711	0.465393	0.398716	1.301318	0.741790	0.545907	0.441883	0.390643
	0.4	1.700591	0.906527	0.650941	0.523329	0.442578	1.738126	0.906946	0.636767	0.500662	0.435407
	0.6	2.354964	1.143036	0.771413	0.592683	0.500911	2.426798	1.172917	0.795410	0.616676	0.510449
	0.8	3.202288	1.480478	0.970278	0.732879	0.601399	3.326522	1.518951	0.988743	0.743640	0.607331
0.1 (1/10)	0	1.120000	0.682000	0.524500	0.440400	0.379075	1.120000	0.682000	0.524500	0.440400	0.379075
	0.2	1.254559	0.735816	0.555784	0.460810	0.395216	1.283010	0.734415	0.541694	0.439092	0.388405
	0.4	1.578769	0.860586	0.625575	0.506771	0.430190	1.646171	0.871503	0.617078	0.487850	0.425443
	0.6	2.054427	1.033913	0.712856	0.555383	0.473720	2.176175	1.080225	0.745040	0.584239	0.486420
	0.8	2.691796	1.302652	0.877596	0.675063	0.561238	2.895260	1.366730	0.908821	0.693565	0.571807

Table 9B.11 – Influence Coefficients for a Circumferential 360° Surface Crack in a Cylindrical Shell

t/R_i	a/t	Inside Surface					Outside Surface				
		G_0	G_1	G_2	G_3	G_4	G_0	G_1	G_2	G_3	G_4
0.2 (1/5)	0	1.120000	0.682000	0.524500	0.440400	0.379075	1.120000	0.682000	0.524500	0.440400	0.379075
	0.2	1.210829	0.718943	0.546312	0.454558	0.390464	1.263202	0.726351	0.537074	0.436025	0.385915
	0.4	1.437161	0.807345	0.596196	0.487609	0.415918	1.554170	0.835957	0.597311	0.474989	0.415406
	0.6	1.764286	0.928708	0.656426	0.519455	0.447584	1.966243	1.002411	0.702694	0.556948	0.466155
	0.8	2.272892	1.156841	0.801593	0.627635	0.528369	2.610699	1.265870	0.855722	0.660227	0.548031
0.3333 (1/3)	0	1.120000	0.682000	0.524500	0.440400	0.379075	1.120000	0.682000	0.524500	0.440400	0.379075
	0.2	1.169540	0.703965	0.537405	0.449080	0.386008	1.249224	0.720455	0.534174	0.434006	0.384331
	0.4	1.324079	0.764679	0.572698	0.472643	0.404510	1.495050	0.812809	0.584087	0.468236	0.408711
	0.6	1.564990	0.856347	0.617396	0.494415	0.429555	1.853386	0.960784	0.679981	0.542489	0.455252
	0.8	2.009679	1.065372	0.754056	0.598012	0.507836	2.500104	1.226225	0.834688	0.646925	0.538501
1.0 (1/1)	0	1.120000	0.682000	0.524500	0.440400	0.379075	1.120000	0.682000	0.524500	0.440400	0.379075
	0.2	1.053169	0.658654	0.512669	0.432896	0.381216	1.232973	0.725583	0.549530	0.457007	0.398605
	0.4	1.080814	0.673665	0.522499	0.439965	0.386602	1.429609	0.800092	0.590755	0.483843	0.417727
	0.6	1.201595	0.731350	0.558621	0.465436	0.405841	1.779493	0.934332	0.665826	0.533220	0.453295
	0.8	1.550424	0.905894	0.671003	0.546215	0.467733	2.593457	1.259538	0.852399	0.658163	0.544530
1.5 (1.5/1)	0	1.120000	0.682000	0.524500	0.440400	0.379075	1.120000	0.682000	0.524500	0.440400	0.379075
	0.2	0.999928	0.638332	0.501321	0.425408	0.375779	1.231001	0.724549	0.548801	0.456410	0.398071
	0.4	0.996737	0.641858	0.504882	0.428440	0.378318	1.428822	0.799833	0.590603	0.483722	0.417613
	0.6	1.092646	0.691085	0.536679	0.451259	0.395752	1.811186	0.946320	0.672404	0.537469	0.456304
	0.8	1.412219	0.856801	0.645041	0.529834	0.456303	2.757031	1.316829	0.882279	0.676781	0.557379
2.0 (2/1)	0	1.120000	0.682000	0.524500	0.440400	0.379075	1.120000	0.682000	0.524500	0.440400	0.379075
	0.2	0.960303	0.623235	0.492914	0.419883	0.371790	1.231398	0.724571	0.548748	0.456325	0.397966
	0.4	0.942151	0.621145	0.493395	0.420925	0.372918	1.435843	0.802596	0.592156	0.484737	0.418336
	0.6	1.025808	0.666248	0.523105	0.442473	0.389494	1.851603	0.961476	0.680693	0.542820	0.460100
	0.8	1.327371	0.826514	0.628977	0.519682	0.449210	2.920115	1.374001	0.912127	0.695398	0.570240
2.5 (2.5/1)	0	1.120000	0.682000	0.524500	0.440400	0.379075	1.120000	0.682000	0.524500	0.440400	0.379075
	0.2	0.929166	0.611376	0.486316	0.415552	0.368670	1.232576	0.724952	0.548925	0.456415	0.398008
	0.4	0.903373	0.606393	0.485205	0.415563	0.369067	1.444794	0.806090	0.594116	0.486024	0.419258
	0.6	0.980169	0.649222	0.513779	0.436430	0.385187	1.891474	0.976367	0.688822	0.548064	0.463819
	0.8	1.269478	0.805781	0.617961	0.512710	0.444336	3.073141	1.427641	0.940133	0.712870	0.582312
3.0 (3/1)	0	1.120000	0.682000	0.524500	0.440400	0.379075	1.120000	0.682000	0.524500	0.440400	0.379075
	0.2	0.903861	0.601739	0.480956	0.412036	0.366139	1.233992	0.725453	0.549184	0.456569	0.398105
	0.4	0.874241	0.595289	0.479035	0.411523	0.366163	1.453863	0.809615	0.596092	0.487321	0.420189
	0.6	0.946890	0.636771	0.506950	0.432000	0.382028	1.928454	0.990140	0.696330	0.552903	0.467250
	0.8	1.227317	0.790649	0.609910	0.507612	0.440770	3.214424	1.477147	0.965978	0.728993	0.593452

Note: Interpolation of the influence coefficients, G_i, may be used for intermediate values of t/R_i and a/t.

Table 9B.12 – Influence Coefficients for a Longitudinal Semi-Elliptical Surface Crack in a Cylinder – Inside Surface

t/R_i	a/c	a/t	G_i	A_0	A_1	A_2	A_3	A_4	A_5	A_6
0.0	0.03125	0	G_0	0.1965046	2.9373464	-5.2582823	7.4889153	-6.9282667	3.3673349	-0.6677966
			G_1	0.0051780	0.1750280	2.7718680	-4.6457154	4.6780502	-3.2768090	0.9840994
		0.2	G_0	0.2080760	3.0112422	-5.1048701	7.6348715	-6.8347547	2.7940766	-0.3882688
			G_1	0.0084834	0.2406767	2.4574292	-3.6452421	3.6142837	-2.8451814	0.9270638
		0.4	G_0	0.2357940	3.0822400	-3.5792100	3.9476890	1.9131590	-6.8872200	3.1896800
			G_1	0.0145140	0.4038000	1.6422700	-0.3906100	-0.6480700	-0.2940300	0.2514900
		0.6	G_0	0.2902240	3.6892050	-4.5739100	11.709890	-6.3750000	-5.8894100	4.2452400
			G_1	0.0208890	0.7016780	0.1631840	5.7072160	-8.2075800	3.4561120	-0.4454700
		0.8	G_0	0.5163550	2.5310830	14.712900	-43.621800	101.065700	-116.081000	46.190900
			G_1	0.0825460	0.4971770	4.6064810	-7.3326700	21.148620	-29.345100	12.491400
0.0	0.0625	0	G_0	0.2695332	2.1626001	-1.6551569	-1.2970208	4.5604304	-4.3163876	1.4010655
			G_1	0.0138667	0.1827458	2.5749608	-3.9044679	3.3556301	-2.1772209	0.6420134
		0.2	G_0	0.2845892	2.2264055	-1.4546190	-1.5760719	5.1131083	-4.9485443	1.6207574
			G_1	0.0199077	0.2210874	2.4642047	-3.5898625	3.1624039	-2.2403780	0.6965751
		0.4	G_0	0.3261480	2.5200870	-1.8847000	2.1798740	-1.4597100	-0.1886500	0.2393400
			G_1	0.0294120	0.3699370	1.9220850	-1.2071500	-0.4394000	0.2737550	-0.0395200
		0.6	G_0	0.4166330	3.1566470	-2.6248900	7.7325910	-9.6927800	3.6428700	-0.0892000
			G_1	0.0598460	0.4340740	2.6811560	-3.1936600	4.0753720	-4.6940200	1.8285500
		0.8	G_0	0.6540140	3.4231920	3.8158050	-4.1586900	3.4715330	-10.310400	6.6280000
			G_1	0.1214780	0.6975490	2.9718330	-1.3036500	-0.0754900	-3.0465100	2.1670000
0.0	0.125	0	G_0	0.4065238	0.7772483	3.8861644	-12.573943	16.760207	-11.014593	2.8706957
			G_1	0.0320270	0.1825342	2.2670449	-2.7076615	1.2088194	-0.3777430	0.0763155
		0.2	G_0	0.4242116	1.0089302	3.2973815	-12.159726	17.873386	-12.868668	3.6281712
			G_1	0.0429859	0.2033811	2.2563818	-2.8752160	1.8152558	-1.0512327	0.3181077
		0.4	G_0	0.4917770	1.6592320	-0.1080400	0.1793240	-2.7076100	3.3680620	-1.3489700
			G_1	0.0634270	0.3722500	1.6231670	-0.5306500	-2.0007400	1.8943780	-0.5880300
		0.6	G_0	0.6591820	1.8759140	1.0212600	-1.7698000	-0.5653600	1.2479960	-0.4376600
			G_1	0.1116040	0.4714500	1.7940590	-0.7557600	-1.4901700	1.0852180	-0.2113700
		0.8	G_0	0.9809330	1.8846320	4.8020780	-8.0580200	0.4447850	3.4772660	-1.0567500
			G_1	0.2039950	0.4800150	2.8822430	-2.5890100	-0.9683000	1.5372370	-0.3750200
0.0	0.25	0	G_0	0.6152816	-0.3348694	6.2955620	-15.590618	19.299508	-12.488107	3.3010035
			G_1	0.0703566	0.2828152	1.4036169	-0.6511596	-1.2076596	1.0318656	-0.2423741
		0.2	G_0	0.6385889	-0.3095132	6.5329787	-16.622882	21.056641	-13.850120	3.6988146
			G_1	0.0840059	0.1999367	1.8218113	-1.7756899	0.3757186	-0.0785358	0.0643386
		0.4	G_0	0.7390420	0.0548160	4.0842620	-7.5883100	5.4047530	-1.0146100	-0.3483400
			G_1	0.1164500	0.2479880	1.8282520	-1.7169900	0.1912120	0.1165770	-0.0186100
		0.6	G_0	0.9461210	-0.1858800	5.5867460	-9.8634900	5.9596870	0.1296440	-1.0026100
			G_1	0.1778050	0.2056680	2.0979210	-1.8039500	-0.5558700	1.1461400	-0.4206600
		0.8	G_0	1.2452110	-0.6921900	8.3260620	-14.948000	8.6936910	0.4755790	-1.3926600
			G_1	0.2585640	0.1548890	2.1170240	-0.4910000	-4.6146100	5.4550750	-1.9663300
0.0	0.5	0	G_0	0.8776607	-0.6729719	3.7721411	-6.5209060	6.3377934	-3.7028038	0.9872447
			G_1	0.1277541	0.4368502	0.4904522	1.0427434	-2.9631236	2.0826525	-0.5184313
		0.2	G_0	0.9003948	-0.8850488	5.2743239	-11.267523	13.890755	-9.6373584	2.8183906
			G_1	0.1404409	0.3215397	1.1010666	-1.0257556	0.6943940	-1.0793186	0.5410929
		0.4	G_0	1.0058060	-0.7322600	2.9951940	-1.9459200	-3.2613500	5.1424570	-2.0306200
			G_1	0.1740870	0.3051630	1.2070310	-0.6720500	-1.0651300	1.1445590	-0.3644800
		0.6	G_0	1.1826010	-1.1072500	3.9623640	-2.7781300	-4.3097300	7.2772750	-2.9648200
			G_1	0.2277120	0.1701170	1.5499470	-1.1051200	-0.8333700	1.1717060	-0.4194500
		0.8	G_0	1.3833380	-1.3900300	4.3755780	-3.7372600	-2.5403200	5.3036000	-2.0932400
			G_1	0.2820110	0.0839230	1.7258580	-1.5358100	-0.0635600	0.5006780	-0.1982200

Table 9B.12 – Influence Coefficients for a Longitudinal Semi-Elliptical Surface Crack in a Cylinder – Inside Surface

t/R_i	a/c	a/t	G_i	A_0	A_1	A_2	A_3	A_4	A_5	A_6
0.0	1.0	0	G0	1.1977992	-0.5244870	0.1498299	2.3284866	-5.1058499	4.3469049	-1.3487980
			G1	0.1870117	0.6987352	0.1316900	0.7269255	-2.5259384	2.1756251	-0.6540458
		0.2	G0	1.2263282	-1.1608467	4.4744783	-11.584231	17.811241	-14.408250	4.6998279
			G1	0.2154786	0.2441623	2.8107820	-7.6574580	11.171413	-9.0053693	2.9542871
		0.4	G0	1.2989480	-0.9978000	1.9479540	-1.3002700	-1.4940100	2.8306230	-1.2126000
			G1	0.2386246	0.1447774	3.3198992	-9.2456599	13.823512	-11.223715	3.6868232
		0.6	G0	1.3971180	-1.1348400	1.7918740	-0.4202600	-2.8679300	3.7685480	-1.4405000
			G1	0.2445870	0.5326670	0.5939690	-0.0361800	-2.0163100	2.2167010	-0.7782200
		0.8	G0	1.5117010	-1.3244800	1.7568350	-0.1337900	-2.8629300	3.2953270	-1.1412400
			G1	0.2704470	0.5113280	0.5357440	-0.0327300	-1.5570200	1.5570970	-0.5094600
0.0	2.0	0	G0	0.8150546	-0.5623828	1.4465771	-4.6778133	8.4192164	-7.9025932	2.9866351
			G1	0.1359146	0.0702340	3.5558581	-11.034445	16.967724	-14.126991	4.8706612
		0.2	G0	0.8463715	-1.0011024	4.0052312	-11.937181	19.189548	-16.039296	5.4674371
			G1	0.1395121	0.0753999	3.1895604	-9.5540932	14.214316	-11.649525	4.0073308
		0.4	G0	0.8570045	-1.0183085	3.9957306	-11.886878	19.152747	-16.047480	5.4801806
			G1	0.1436696	0.0544018	3.2816127	-9.8164232	14.610963	-11.942138	4.0907797
		0.6	G0	0.8839861	-1.0765270	4.0774087	-11.976171	19.173189	-15.996207	5.4501217
			G1	0.1504185	0.0478401	3.2579960	-9.6921199	14.370843	-11.736129	4.0258411
		0.8	G0	0.9033134	-0.9619755	2.8501500	-7.6366897	11.596116	-9.4828625	3.2550163
			G1	0.1458559	0.2313881	1.9882138	-5.5546045	7.4196069	-5.8965053	2.0855563
0.01 (1/100)	0.03125	0	G0	0.1965046	2.9373464	-5.2582823	7.4889153	-6.9282667	3.3673349	-0.6677966
			G1	0.0051780	0.1750280	2.7718680	-4.6457154	4.6780502	-3.2768090	0.9840994
		0.2	G0	0.2149558	2.4720875	-1.2147834	-4.1389650	10.539267	-9.6956094	3.1225660
			G1	0.0081814	0.2385252	2.4687702	-3.7439973	3.7704530	-2.9529315	0.9589542
		0.4	G0	0.2371100	3.0647320	-3.4513200	3.3917110	2.7324370	-7.4671300	3.3674100
			G1	0.0110140	0.4025030	1.6437570	-0.3727600	-0.8119700	-0.0858000	0.1781500
		0.6	G0	0.2921630	3.6926360	-4.6925300	11.901720	-7.7448000	-3.7999500	3.3544000
			G1	0.0226600	0.6715900	0.4388550	4.5930610	-6.5549400	2.3178280	-0.1251900
		0.8	G0	0.5243760	2.2524770	16.793480	-53.803200	114.103600	-119.702000	44.914100
			G1	0.0833680	0.4665890	4.7440270	-8.4336900	21.115630	-26.684500	10.785300
0.01 (1/100)	0.0625	0	G0	0.2695332	2.1626001	-1.6551569	-1.2970208	4.5604304	-4.3163876	1.4010655
			G1	0.0138667	0.1827458	2.5749608	-3.9044679	3.3556301	-2.1772209	0.6420134
		0.2	G0	0.3011924	1.7811106	0.8562316	-6.9529186	11.339236	-8.4567250	2.3835697
			G1	0.0198422	0.2079432	2.6052559	-4.3155521	4.6614903	-3.6113853	1.1602564
		0.4	G0	0.3321630	2.4901340	-1.5629300	0.0711970	3.2088600	-4.5926200	1.7583400
			G1	0.0275700	0.4338520	1.4670200	0.0742960	-2.3137100	1.6328580	-0.4232800
		0.6	G0	0.4174310	3.3955340	-4.5683700	12.806250	-16.603400	8.3551170	-1.3349400
			G1	0.0592490	0.4942840	2.2111170	-1.9453300	2.2241680	-3.3126700	1.4345200
		0.8	G0	0.6609890	3.4633420	2.8481190	-3.5483900	4.2900100	-10.609700	6.3367900
			G1	0.1233510	0.6910730	2.8678320	-1.6023100	0.5891520	-3.1647400	2.0037600
0.01 (1/100)	0.125	0	G0	0.4065238	0.7772483	3.8861644	-12.573943	16.760207	-11.014593	2.8706957
			G1	0.0320270	0.1825342	2.2670449	-2.7076615	1.2088194	-0.3777430	0.0763155
		0.2	G0	0.4140502	1.1388823	1.7096208	-6.0970813	7.5806259	-4.7412598	1.1879060
			G1	0.0486456	0.0159697	3.8996081	-9.0058939	12.464506	-9.7091690	2.9890898
		0.4	G0	0.4927230	1.5440820	0.6341780	-2.3645300	1.5071740	0.0175250	-0.3190500
			G1	0.0625230	0.3683750	1.6262050	-0.6018500	-1.8348700	1.7392560	-0.5338200
		0.6	G0	0.6457970	1.8450060	0.8248110	-1.2027800	-1.6161800	2.2686010	-0.8026800
			G1	0.1079430	0.4523420	1.7937000	-0.7530100	-1.6009900	1.2810970	-0.2997100
		0.8	G0	0.9331980	1.8484040	4.0610460	-6.4488400	-1.5508000	5.3526860	-1.8508400
			G1	0.1900180	0.4493580	2.8240480	-2.7063600	-0.5768000	1.3457950	-0.3958100

Table 9B.12 – Influence Coefficients for a Longitudinal Semi-Elliptical Surface Crack in a Cylinder – Inside Surface

t/R_i	a/c	a/t	G_i	A_0	A_1	A_2	A_3	A_4	A_5	A_6
0.01 (1/100)	0.25	0	G_0	0.6152816	-0.3348694	6.2955620	-15.590618	19.299508	-12.488107	3.3010035
			G_1	0.0703566	0.2828152	1.4036169	-0.6511596	-1.2076596	1.0318656	-0.2423741
		0.2	G_0	0.6241551	-0.2465111	7.0309527	-20.022042	27.911625	-19.682762	5.5162697
			G_1	0.0907721	0.1638762	2.5396012	-5.0799147	6.3011931	-4.8260624	1.4910341
		0.4	G_0	0.7353150	0.0335380	4.1529840	-7.8035600	5.7330000	-1.2513900	-0.2813800
			G_1	0.1163980	0.2222910	1.9859130	-2.2466100	1.0747840	-0.5982800	0.2057500
		0.6	G_0	0.9324150	-0.2341500	5.7957890	-10.643200	7.3266510	-0.9708400	-0.6676100
			G_1	0.1737550	0.1916590	2.1300350	-1.8831100	-0.4807900	1.1395430	-0.4345700
		0.8	G_0	1.2219490	-1.1415500	11.712920	-27.080700	29.834180	-16.937700	4.0600500
			G_1	0.2500840	0.0580650	2.8199190	-3.0313700	-0.1601400	1.7951480	-0.8296700
0.01 (1/100)	0.5	0	G_0	0.8776607	-0.6729719	3.7721411	-6.5209060	6.3377934	-3.7028038	0.9872447
			G_1	0.1277541	0.4368502	0.4904522	1.0427434	-2.9631236	2.0826525	-0.5184313
		0.2	G_0	0.9015490	-1.1113733	6.8843421	-16.342574	21.585452	-15.202444	4.3660359
			G_1	0.1484299	0.1541815	2.2768151	-4.5991695	5.8149262	-4.5777434	1.4654106
		0.4	G_0	0.9995660	-0.7280200	2.9776730	-1.9277500	-3.2709000	5.1505490	-2.0350400
			G_1	0.1726160	0.3087790	1.1425500	-0.3862200	-1.6344200	1.6645600	-0.5412700
		0.6	G_0	1.1705130	-1.1242900	4.0543560	-2.9851600	-4.1166400	7.2299430	-2.9791800
			G_1	0.2234860	0.1766680	1.5051550	-0.9863000	-0.9867500	1.2669540	-0.4418100
		0.8	G_0	1.3565360	-1.3769500	4.3964180	-3.8814500	-2.2095000	5.0187600	-2.0135800
			G_1	0.2754490	0.0635260	1.8760200	-1.9807100	0.6070780	0.0190700	-0.0683400
0.01 (1/100)	1.0	0	G_0	1.1977992	-0.5244870	0.1498299	2.3284866	-5.1058499	4.3469049	-1.3487980
			G_1	0.1870117	0.6987352	0.1316900	0.7269255	-2.5259384	2.1756251	-0.6540458
		0.2	G_0	1.2108906	-1.2118250	5.0003862	-13.525257	21.096357	-16.993711	5.4692793
			G_1	0.2135613	0.1822719	3.2508209	-9.1159303	13.526088	-10.816272	3.4876265
		0.4	G_0	1.2915440	-0.9860000	1.9198180	-1.2048700	-1.6920600	3.0190640	-1.2778100
			G_1	0.2335267	0.1351331	3.4108405	-9.6049414	14.454580	-11.727329	3.8372073
		0.6	G_0	1.3879210	-1.1637000	2.0681660	-1.2956400	-1.4973800	2.7147660	-1.1246500
			G_1	0.2442110	0.4839940	0.9407500	-1.1541500	-0.1848200	0.7462030	-0.3202300
		0.8	G_0	1.4955530	-1.3298700	1.9626990	-0.8242400	-1.7468100	2.4129690	-0.8712900
			G_1	0.2671290	0.4953350	0.6445810	-0.2740900	-1.3088000	1.4517080	-0.5006200
0.01 (1/100)	2.0	0	G_0	0.8150546	-0.5623828	1.4465771	-4.6778133	8.4192164	-7.9025932	2.9866351
			G_1	0.1359146	0.0702340	3.5558581	-11.034445	16.967724	-14.126991	4.8706612
		0.2	G_0	0.8108427	-0.9469615	4.0418669	-12.589699	20.713465	-17.423042	5.9097427
			G_1	0.1318838	0.0532545	3.3674428	-10.236137	15.430205	-12.636393	4.3051116
		0.4	G_0	0.8250898	-0.2999988	-0.8021829	3.4774334	-6.2776890	4.9519567	-1.3622968
			G_1	0.1346594	0.0300881	3.4841930	-10.598201	15.982963	-13.033343	4.4132933
		0.6	G_0	0.8505718	-0.3504564	-0.7638086	3.5152228	-6.4354105	5.1178036	-1.4187607
			G_1	0.1449083	0.0226142	3.4683252	-10.495830	15.799002	-12.901367	4.3816709
		0.8	G_0	0.9038677	-0.9803128	3.0688019	-8.3574085	12.791955	-10.493661	3.5981987
			G_1	0.1478039	0.0204313	3.4187237	-10.183273	14.776072	-11.479762	3.7099585
0.01667 (1/60)	0.03125	0	G_0	0.1965046	2.9373464	-5.2582823	7.4889153	-6.9282667	3.3673349	-0.6677966
			G_1	0.0051780	0.1750280	2.7718680	-4.6457154	4.6780502	-3.2768090	0.9840994
		0.2	G_0	0.2148671	2.4723189	-1.2180211	-4.1126757	10.496724	-9.6740573	3.1211775
			G_1	0.0080961	0.2401938	2.4502326	-3.6573824	3.5940475	-2.7881220	0.9010264
		0.4	G_0	0.2372950	3.0566010	-3.3944000	3.1477730	3.1530230	-7.7865200	3.4576600
			G_1	0.0106590	0.4095900	1.6083470	-0.3260900	-0.8035100	-0.1463900	0.2110000
		0.6	G_0	0.2937680	3.5870040	-3.8424000	8.4442010	-1.4600300	-8.9339200	4.9119300
			G_1	0.0220570	0.6740750	0.3474810	4.9629310	-7.3508700	3.1732170	-0.4659300
		0.8	G_0	0.4838350	3.1566150	8.8031170	-27.164800	69.601910	-82.479600	32.682600
			G_1	0.0716700	0.7084130	2.6085960	-1.4257400	9.3653570	-16.640500	7.3940300

Table 9B.12 – Influence Coefficients for a Longitudinal Semi-Elliptical Surface Crack in a Cylinder – Inside Surface

t/R_i	a/c	a/t	G_i	A_0	A_1	A_2	A_3	A_4	A_5	A_6
0.01667 (1/60)	0.0625	0	G_0	0.2695332	2.1626001	-1.6551569	-1.2970208	4.5604304	-4.3163876	1.4010655
			G_1	0.0138667	0.1827458	2.5749608	-3.9044679	3.3556301	-2.1772209	0.6420134
		0.2	G_0	0.2857109	2.0654488	-0.9893799	-1.3807471	2.8006402	-2.0206042	0.4892659
			G_1	0.0194914	0.2150005	2.5598171	-4.1817299	4.4576257	-3.4587288	1.1159282
		0.4	G_0	0.3287840	2.5921570	-2.4132600	3.0634190	-1.9525300	-0.3333000	0.4144600
			G_1	0.0280780	0.4276920	1.4973510	0.0288440	-2.3497300	1.7402640	-0.4758200
		0.6	G_0	0.4176850	3.4074150	-4.6753500	13.078590	-17.041300	8.7888280	-1.5084600
			G_1	0.0574660	0.5499100	1.7774590	-0.5099100	-0.1282100	-1.4365500	0.8552000
		0.8	G_0	0.6582530	3.5128870	2.2828230	-1.9924300	2.2310040	-8.6681700	5.4793000
			G_1	0.1225420	0.7046220	2.7569290	-1.4438200	0.6196850	-3.1640900	1.9357000
0.01667 (1/60)	0.125	0	G_0	0.4065238	0.7772483	3.8861644	-12.573943	16.760207	-11.014593	2.8706957
			G_1	0.0320270	0.1825342	2.2670449	-2.7076615	1.2088194	-0.3777430	0.0763155
		0.2	G_0	0.4141982	1.1344888	1.7439464	-6.2232541	7.7907137	-4.9072442	1.2389750
			G_1	0.0486813	0.0152024	3.9061790	-9.0327670	12.510777	-9.7464081	3.0006990
		0.4	G_0	0.4948480	1.4794440	1.1185270	-4.0444100	4.3282860	-2.2595600	0.3903500
			G_1	0.0625520	0.3656340	1.6407500	-0.6554600	-1.7474400	1.6670140	-0.5089000
		0.6	G_0	0.6409930	1.9652950	-0.1642100	2.2005520	-7.4218400	7.0583030	-2.3230500
			G_1	0.1083560	0.4453160	1.8399940	-0.9086700	-1.3774300	1.1373530	-0.2654300
		0.8	G_0	0.9356790	1.8738760	3.8946700	-6.0693900	-1.9444100	5.6896490	-2.0106100
			G_1	0.1916520	0.4524760	2.8002690	-2.6288800	-0.7144600	1.5221540	-0.4838500
0.01667 (1/60)	0.25	0	G_0	0.6152816	-0.3348694	6.2955620	-15.590618	19.299508	-12.488107	3.3010035
			G_1	0.0703566	0.2828152	1.4036169	-0.6511596	-1.2076596	1.0318656	-0.2423741
		0.2	G_0	0.6254105	-0.2756845	7.2372917	-20.717372	29.086839	-20.644329	5.8190829
			G_1	0.0900509	0.1754701	2.4653292	-4.8609065	5.9734789	-4.5843798	1.4212799
		0.4	G_0	0.7330250	0.0541030	4.0064310	-7.3694700	5.0627260	-0.7345100	-0.4373600
			G_1	0.1161040	0.2203390	2.0004310	-2.3056000	1.1713600	-0.6681400	0.2244900
		0.6	G_0	0.9210290	-0.0465700	4.4521870	-6.3769100	0.5403590	4.3048320	-2.2613700
			G_1	0.1702480	0.2497180	1.7270540	-0.6420800	-2.4041500	2.6026300	-0.8686500
		0.8	G_0	1.2047330	-0.7847600	8.9533120	-17.715200	14.218040	-4.3196500	0.1157300
			G_1	0.2472570	0.1171600	2.3652370	-1.4978600	-2.7028500	3.8489740	-1.4739500
0.01667 (1/60)	0.5	0	G_0	0.8776607	-0.6729719	3.7721411	-6.5209060	6.3377934	-3.7028038	0.9872447
			G_1	0.1277541	0.4368502	0.4904522	1.0427434	-2.9631236	2.0826525	-0.5184313
		0.2	G_0	0.8987625	-1.0615830	6.5352105	-15.173572	19.607233	-13.575646	3.8503478
			G_1	0.1492382	0.1399206	2.3632147	-4.8462524	6.1772411	-4.8415701	1.5410021
		0.4	G_0	0.9959920	-0.6970000	2.8073570	-1.4883600	-3.8580500	5.5420790	-2.1380800
			G_1	0.1731960	0.2880460	1.2897340	-0.8838700	-0.7861600	0.9618990	-0.3169700
		0.6	G_0	1.1640340	-1.0701100	3.7508010	-2.1976100	-5.1415900	7.8804140	-3.1390700
			G_1	0.2222510	0.1801650	1.4936230	-0.9830600	-0.9475900	1.2090310	-0.4178500
		0.8	G_0	1.3532210	-1.4106800	4.6621530	-4.7297600	-0.8479500	3.9686690	-1.7045800
			G_1	0.2729800	0.0878270	1.7214050	-1.5086900	-0.1139000	0.5633750	-0.2302700
0.01667 (1/60)	1.0	0	G_0	1.1977992	-0.5244870	0.1498299	2.3284866	-5.1058499	4.3469049	-1.3487980
			G_1	0.1870117	0.6987352	0.1316900	0.7269255	-2.5259384	2.1756251	-0.6540458
		0.2	G_0	1.2106055	-1.2105643	4.9943941	-13.508283	21.072293	-16.977692	5.4653669
			G_1	0.2138344	0.1777026	3.2716297	-9.1531646	13.549492	-10.812840	3.4815135
		0.4	G_0	1.2891190	-0.9709000	1.8325120	-0.9414100	-2.1003700	3.3316080	-1.3719500
			G_1	0.2133960	0.5774660	0.6071350	-0.1664100	-1.8486500	2.1386670	-0.7727600
		0.6	G_0	1.3851610	-1.1646000	2.1025010	-1.4262200	-1.2663500	2.5193910	-1.0614400
			G_1	0.2421130	0.5102400	0.7555890	-0.5305800	-1.2337100	1.5984880	-0.5866900
		0.8	G_0	1.4915010	-1.3274700	1.9683410	-0.7813900	-1.8938700	2.5733450	-0.9310100
			G_1	0.2653560	0.5038220	0.6296470	-0.3034500	-1.1613700	1.2707090	-0.4290900

Table 9B.12 – Influence Coefficients for a Longitudinal Semi-Elliptical Surface Crack in a Cylinder – Inside Surface

t/R_i	a/c	a/t	G_i	A_0	A_1	A_2	A_3	A_4	A_5	A_6
0.01667 (1/60)	2.0	0	G_0	0.8150546	-0.5623828	1.4465771	-4.6778133	8.4192164	-7.9025932	2.9866351
			G_1	0.1359146	0.0702340	3.5558581	-11.034445	16.967724	-14.126991	4.8706612
		0.2	G_0	0.8101916	-0.9412593	4.0126414	-12.507285	20.589007	-17.329107	5.8820015
			G_1	0.1322100	0.0467146	3.4045450	-10.328106	15.540798	-12.698847	4.3180540
		0.4	G_0	0.8245651	-0.3028365	-0.7600170	3.3001602	-5.9433064	4.6607966	-1.2672554
			G_1	0.1339511	0.0389739	3.4338823	-10.459900	15.789207	-12.900150	4.3776714
		0.6	G_0	0.8499410	-0.3556093	-0.7320158	3.4590456	-6.4089179	5.1364574	-1.4338641
			G_1	0.1450687	0.0152402	3.5174526	-10.643316	16.026897	-13.077077	4.4350680
		0.8	G_0	0.9019647	-0.9728613	3.0540609	-8.3490973	12.822350	-10.547233	3.6224835
			G_1	0.1471513	0.0263638	3.3848213	-10.079855	14.616140	-11.359881	3.6753008
0.05 (1/20)	0.03125	0	G_0	0.1965046	2.9373464	-5.2582823	7.4889153	-6.9282667	3.3673349	-0.6677966
			G_1	0.0051780	0.1750280	2.7718680	-4.6457154	4.6780502	-3.2768090	0.9840994
		0.2	G_0	0.2147553	2.4733297	-1.2474542	-4.0148844	10.325431	-9.5295230	3.0755621
			G_1	0.0081488	0.2377645	2.4723890	-3.7475362	3.7575353	-2.9323550	0.9509310
		0.4	G_0	0.2360970	3.0572780	-3.4936200	3.2721920	3.0580130	-7.6615500	3.3859300
			G_1	0.0102200	0.4124020	1.5384150	-0.0617800	-1.3675500	0.4323350	-0.0065400
		0.6	G_0	0.2861060	3.5905940	-4.3735000	9.6484880	-3.3065400	-7.0688300	4.1532600
			G_1	0.0198400	0.6562220	0.3810810	4.5714070	-6.6677400	2.8306200	-0.4505100
		0.8	G_0	0.4596930	2.6805760	10.718030	-36.889800	86.523190	-93.759400	35.081500
			G_1	0.0617560	0.6089050	2.8527370	-3.2715300	12.274680	-17.735900	7.2096800
0.05 (1/20)	0.0625	0	G_0	0.2695332	2.1626001	-1.6551569	-1.2970208	4.5604304	-4.3163876	1.4010655
			G_1	0.0138667	0.1827458	2.5749608	-3.9044679	3.3556301	-2.1772209	0.6420134
		0.2	G_0	0.2859329	2.0653053	-0.9905563	-1.4150031	2.8652343	-2.0661068	0.5016295
			G_1	0.0196037	0.2151084	2.5626289	-4.2011550	4.4798485	-3.4669351	1.1166928
		0.4	G_0	0.3300790	2.5687830	-2.2730100	2.4482290	-0.9061800	-1.1152300	0.6336900
			G_1	0.0272960	0.4545140	1.2940000	0.6585910	-3.3745900	2.5567530	-0.7249800
		0.6	G_0	0.4134110	3.3905790	-4.8820500	13.351920	-17.160600	9.1488940	-1.8015900
			G_1	0.0575670	0.5056840	2.0319140	-1.4822100	1.4954900	-2.5583400	1.1145400
		0.8	G_0	0.6264970	3.5543640	0.7919210	0.3194370	2.0824790	-8.6748200	4.8836700
			G_1	0.1126460	0.7058050	2.3784990	-0.9484300	0.6832120	-2.9086500	1.5439800
0.05 (1/20)	0.125	0	G_0	0.4065238	0.7772483	3.8861644	-12.573943	16.760207	-11.014593	2.8706957
			G_1	0.0320270	0.1825342	2.2670449	-2.7076615	1.2088194	-0.3777430	0.0763155
		0.2	G_0	0.4141745	1.1275356	1.7988949	-6.4537497	8.1885840	-5.2215937	1.3338255
			G_1	0.0487792	0.0133782	3.9204009	-9.0880489	12.590390	-9.7977291	3.0135889
		0.4	G_0	0.4917700	1.5480530	0.5402050	-2.1834600	1.2196150	0.2889000	-0.4136700
			G_1	0.0618810	0.3879900	1.4515410	-0.0167500	-2.8752400	2.6301310	-0.8213900
		0.6	G_0	0.6460050	1.8351450	0.8285700	-1.6608000	-0.4877600	1.3380790	-0.5504100
			G_1	0.1093030	0.4366540	1.9181290	-1.3212300	-0.5731700	0.4753220	-0.0675600
		0.8	G_0	0.9327440	1.9648060	3.1532800	-4.8291100	-1.9134300	5.1126320	-1.9475400
			G_1	0.1921390	0.4872100	2.5183370	-1.9746200	-1.3273800	2.0002740	-0.7177100
0.05 (1/20)	0.25	0	G_0	0.6152816	-0.3348694	6.2955620	-15.590618	19.299508	-12.488107	3.3010035
			G_1	0.0703566	0.2828152	1.4036169	-0.6511596	-1.2076596	1.0318656	-0.2423741
		0.2	G_0	0.6229529	-0.2485784	7.0430049	-20.131994	28.206025	-19.995012	5.6320877
			G_1	0.0905859	0.1617121	2.5472316	-5.1142004	6.3762462	-4.8989319	1.5167184
		0.4	G_0	0.7303090	0.0326040	4.1332170	-7.8985600	6.0159640	-1.5217600	-0.1897900
			G_1	0.1142170	0.2418060	1.8297700	-1.7682600	0.3018070	0.0205930	0.0144400
		0.6	G_0	0.9202510	-0.1540100	5.1619380	-8.8082400	4.5807010	1.1262150	-1.3066500
			G_1	0.1702680	0.2235180	1.8974360	-1.2399100	-1.4028300	1.8129880	-0.6307900
		0.8	G_0	1.2322960	-1.4426500	14.003620	-35.237500	44.199690	-28.746600	7.7018200
			G_1	0.2497100	0.1097790	2.4079700	-1.7073400	-2.2186700	3.4494480	-1.3726200

Table 9B.12 – Influence Coefficients for a Longitudinal Semi-Elliptical Surface Crack in a Cylinder – Inside Surface

t/R_i	a/c	a/t	G_i	A_0	A_1	A_2	A_3	A_4	A_5	A_6
0.05 (1/20)	0.5	0	G_0	0.8776607	-0.6729719	3.7721411	-6.5209060	6.3377934	-3.7028038	0.9872447
			G_1	0.1277541	0.4368502	0.4904522	1.0427434	-2.9631236	2.0826525	-0.5184313
		0.2	G_0	0.8998006	-1.1008716	6.7949974	-16.008148	20.985635	-14.692497	4.2008852
			G_1	0.1482707	0.1526809	2.2809119	-4.6071223	5.8286426	-4.5922291	1.4712639
		0.4	G_0	0.9875950	-0.6604200	2.5904420	-0.9060400	-4.6843400	6.1350420	-2.3065200
			G_1	0.1703150	0.3037660	1.2129670	-0.7351300	-0.9145500	0.9993630	-0.3136400
		0.6	G_0	1.1535210	-1.0846600	3.8853140	-2.6803400	-4.3200500	7.2246270	-2.9406900
			G_1	0.2189650	0.1820740	1.4974930	-1.0467100	-0.7825700	1.0459000	-0.3613100
		0.8	G_0	1.3387940	-1.3846800	4.5947460	-4.6182500	-0.8155300	3.8499650	-1.6650000
			G_1	0.2704200	0.0863940	1.7356660	-1.5215400	-0.1070200	0.5843010	-0.2509500
0.05 (1/20)	1.0	0	G_0	1.1977992	-0.5244870	0.1498299	2.3284866	-5.1058499	4.3469049	-1.3487980
			G_1	0.1870117	0.6987352	0.1316900	0.7269255	-2.5259384	2.1756251	-0.6540458
		0.2	G_0	1.2091906	-1.2119075	5.0112782	-13.553361	21.141961	-17.036849	5.4856225
			G_1	0.2131357	0.1842366	3.2319216	-9.0396511	13.389696	-10.704130	3.4528991
		0.4	G_0	1.2822600	-0.9719500	1.8928700	-1.1442300	-1.7968400	3.1176240	-1.3148300
			G_1	0.2313746	0.1294187	3.4578251	-9.7497871	14.680574	-11.902752	3.8908182
		0.6	G_0	1.3703740	-1.1028000	1.7930470	-0.4916100	-2.7326500	3.6494690	-1.4011700
			G_1	0.2379550	0.5278330	0.6693230	-0.2931400	-1.5654000	1.8255750	-0.6476900
		0.8	G_0	1.4740600	-1.2903000	1.9333060	-0.7538900	-1.8525600	2.4833110	-0.8912300
			G_1	0.2620950	0.4999820	0.6688010	-0.3352900	-1.2212800	1.3834660	-0.4801300
0.05 (1/20)	2.0	0	G_0	0.8150546	-0.5623828	1.4465771	-4.6778133	8.4192164	-7.9025932	2.9866351
			G_1	0.1359146	0.0702340	3.5558581	-11.034445	16.967724	-14.126991	4.8706612
		0.2	G_0	0.8405900	-0.9828964	3.9783944	-11.929139	19.232361	-16.107076	5.4985318
			G_1	0.1401448	0.0460755	3.3846820	-10.137821	15.107048	-12.328596	4.2110577
		0.4	G_0	0.8204618	-0.2806825	-0.8637066	3.6013842	-6.4111767	5.0203080	-1.3749797
			G_1	0.1422434	0.0527995	3.3104268	-9.9190612	14.794871	-12.107982	4.1496887
		0.6	G_0	0.8457322	-0.3595145	-0.6426755	3.1612151	-5.9385710	4.7719679	-1.3235536
			G_1	0.1488396	0.0406125	3.3249114	-9.9017635	14.712096	-12.020216	4.1204818
		0.8	G_0	0.8946607	-0.9436510	2.9530039	-8.0365810	12.297855	-10.128340	3.4958489
			G_1	0.1434305	0.2331398	2.0104442	-5.6212616	7.5252202	-5.9911091	2.1206547
0.1 (1/10)	0.03125	0	G_0	0.1965046	2.9373464	-5.2582823	7.4889153	-6.9282667	3.3673349	-0.6677966
			G_1	0.0051780	0.1750280	2.7718680	-4.6457154	4.6780502	-3.2768090	0.9840994
		0.2	G_0	0.2144509	2.4711734	-1.2860169	-3.9437101	10.258246	-9.4874515	3.0628400
			G_1	0.0080221	0.2380830	2.4576921	-3.7039504	3.6653669	-2.8375154	0.9161589
		0.4	G_0	0.2362020	3.0232830	-3.3746300	2.6514220	4.2691070	-8.6980100	3.7198100
			G_1	0.0103150	0.3971020	1.6371740	-0.4826500	-0.6416000	-0.1376700	0.1653300
		0.6	G_0	0.2803270	3.5106810	-4.3633000	9.2831770	-2.7203100	-7.4474300	4.2735200
			G_1	0.0176640	0.6383120	0.3362480	4.6736560	-7.0299900	3.3065000	-0.6400000
		0.8	G_0	0.4108450	2.7858000	7.1999900	-24.966400	63.838540	-72.490500	27.635600
			G_1	0.0459140	0.6441140	1.8109850	0.1500500	5.6303710	-11.329200	4.9191600
0.1 (1/10)	0.0625	0	G_0	0.2695332	2.1626001	-1.6551569	-1.2970208	4.5604304	-4.3163876	1.4010655
			G_1	0.0138667	0.1827458	2.5749608	-3.9044679	3.3556301	-2.1772209	0.6420134
		0.2	G_0	0.2852601	2.0623971	-0.9452314	-1.7155871	3.4690201	-2.5845388	0.6675616
			G_1	0.0195666	0.2161881	2.5579251	-4.2119758	4.4960423	-3.4714625	1.1164625
		0.4	G_0	0.3294820	2.5547280	-2.2095000	1.8316820	0.5378940	-2.4428800	1.0694100
			G_1	0.0290130	0.4029930	1.6912760	-0.7784700	-0.9590600	0.6513490	-0.1510800
		0.6	G_0	0.4058800	3.3662220	-5.1482900	13.513450	-16.655100	8.6671530	-1.7293500
			G_1	0.0569260	0.4451650	2.3945360	-2.9719000	4.1328030	-4.5775200	1.6727700
		0.8	G_0	0.5908720	3.5314460	-0.6929200	3.3140250	-0.2495400	-7.1101300	4.1118800
			G_1	0.1004430	0.7134420	1.8363740	0.1930190	-0.5388500	-1.7508700	0.9917100

Table 9B.12 – Influence Coefficients for a Longitudinal Semi-Elliptical Surface Crack in a Cylinder – Inside Surface

t/R_i	a/c	a/t	G_i	A_0	A_1	A_2	A_3	A_4	A_5	A_6
0.1 (1/10)	0.125	0	G_0	0.4065238	0.7772483	3.8861644	-12.573943	16.760207	-11.014593	2.8706957
			G_1	0.0320270	0.1825342	2.2670449	-2.7076615	1.2088194	-0.3777430	0.0763155
		0.2	G_0	0.4138525	1.1243780	1.7964950	-6.5013714	8.2843111	-5.2897626	1.3521056
			G_1	0.0488254	0.0124168	3.9238498	-9.1173502	12.630693	-9.8176804	3.0170051
		0.4	G_0	0.4900830	1.5797060	0.2456910	-1.4169300	0.1330550	1.0979610	-0.6544400
			G_1	0.0625190	0.3795970	1.5007820	-0.2215400	-2.5534400	2.4056210	-0.7613400
		0.6	G_0	0.6383460	1.8896790	0.1654880	0.1405470	-2.8887800	3.1374330	-1.1431800
			G_1	0.1078790	0.4418060	1.8093490	-1.0600900	-0.9104200	0.7835470	-0.1968000
		0.8	G_0	0.9106040	1.6778320	4.1741310	-7.6274100	2.6957210	2.3283330	-1.6172500
			G_1	0.1827830	0.5316620	2.0011150	-0.7238700	-2.5544000	2.7998200	-1.0318900
0.1 (1/10)	0.25	0	G_0	0.6152816	-0.3348694	6.2955620	-15.590618	19.299508	-12.488107	3.3010035
			G_1	0.0703566	0.2828152	1.4036169	-0.6511596	-1.2076596	1.0318656	-0.2423741
		0.2	G_0	0.6221458	-0.2652412	7.1236921	-20.415683	28.691172	-20.391119	5.7567350
			G_1	0.0893032	0.1771452	2.4437349	-4.8273884	5.9604631	-4.5972261	1.4308564
		0.4	G_0	0.7269240	0.0331400	4.0541080	-7.6758800	5.6254770	-1.1588100	-0.3180200
			G_1	0.1141390	0.2282720	1.9094300	-2.0571800	0.7745000	-0.3425200	0.1223300
		0.6	G_0	0.9136940	-0.1128200	4.7770370	-7.7684000	3.1756140	2.1324410	-1.6080500
			G_1	0.1690410	0.2367980	1.7775820	-0.9219600	-1.8420100	2.1429690	-0.7348800
		0.8	G_0	1.2285610	-1.3887200	13.423440	-33.608900	42.330360	-27.500000	7.2734400
			G_1	0.2605760	-0.1180300	4.1243640	-7.6919700	8.0993900	-4.9636300	1.2276300
0.1	0.5	0	G_0	0.8776607	-0.6729719	3.7721411	-6.5209060	6.3377934	-3.7028038	0.9872447
			G_1	0.1277541	0.4368502	0.4904522	1.0427434	-2.9631236	2.0826525	-0.5184313
		0.2	G_0	0.8939439	-1.0523498	6.4920812	-15.138217	19.688676	-13.725026	3.9161703
			G_1	0.1471464	0.1576874	2.2477033	-4.5209327	5.7119515	-4.5121924	1.4494557
		0.4	G_0	0.9797560	-0.6583400	2.5905960	-0.9807000	-4.5022900	5.9676820	-2.2512600
			G_1	0.1683280	0.3025050	1.2065640	-0.7030600	-0.9925300	1.0836790	-0.3460700
		0.6	G_0	1.1399170	-1.0507000	3.7096220	-2.2768200	-4.7650200	7.4625310	-2.9908600
			G_1	0.2156530	0.1890000	1.4447400	-0.8854600	-1.0301700	1.2393260	-0.4219600
		0.8	G_0	1.3104950	-1.0667900	2.8675320	-0.6020200	-5.1697700	6.1071010	-2.1308200
			G_1	0.2673520	0.1194700	1.5170160	-0.8642000	-1.0371700	1.2474400	-0.4452900
0.1 (1/10)	1.0	0	G_0	1.1977992	-0.5244870	0.1498299	2.3284866	-5.1058499	4.3469049	-1.3487980
			G_1	0.1870117	0.6987352	0.1316900	0.7269255	-2.5259384	2.1756251	-0.6540458
		0.2	G_0	1.2047909	-1.2012348	4.9676187	-13.426779	20.945504	-16.887172	5.4412264
			G_1	0.2119663	0.1873102	3.2105329	-8.9636386	13.261943	-10.603790	3.4231621
		0.4	G_0	1.2697440	-0.9183700	1.6384390	-0.4675200	-2.7367600	3.7616560	-1.4871500
			G_1	0.2313746	0.1294187	3.4578251	-9.7497871	14.680574	-11.902752	3.8908182
		0.6	G_0	1.3563790	-1.1020000	1.8638360	-0.5992700	-2.7466300	3.7780850	-1.4700900
			G_1	0.2338370	0.5347500	0.6371980	-0.1619900	-1.8137100	2.0426640	-0.7195100
		0.8	G_0	1.4582970	-1.3079100	2.2328620	-1.6002400	-0.6409600	1.6167600	-0.6502600
			G_1	0.2583450	0.5028090	0.6746630	-0.2815000	-1.3831100	1.5504100	-0.5408600
0.1 (1/10)	2.0	0	G_0	0.8150546	-0.5623828	1.4465771	-4.6778133	8.4192164	-7.9025932	2.9866351
			G_1	0.1359146	0.0702340	3.5558581	-11.034445	16.967724	-14.126991	4.8706612
		0.2	G_0	0.8389023	-0.9910627	4.0593253	-12.185366	19.630219	-16.411826	5.5902596
			G_1	0.1391760	0.0538372	3.3380006	-9.9908862	14.871100	-12.143930	4.1552336
		0.4	G_0	0.8168007	-0.2921048	-0.7346646	3.2014916	-5.8126583	4.5798416	-1.2477748
			G_1	0.1412816	0.0503888	3.3380869	-10.010705	14.949170	-12.238855	4.1935739
		0.6	G_0	0.8387058	-0.3482355	-0.6184382	3.0476208	-5.7528210	4.6253567	-1.2780857
			G_1	0.1473521	0.0388746	3.3532681	-9.9888648	14.848958	-12.132523	4.1580679
		0.8	G_0	0.8878357	-0.9627154	3.2133021	-8.8604927	13.568698	-11.103565	3.7915359
			G_1	0.1419379	0.2284659	2.0631482	-5.7641990	7.7262423	-6.1414207	2.1673189

Table 9B.12 – Influence Coefficients for a Longitudinal Semi-Elliptical Surface Crack in a Cylinder – Inside Surface

t/R_i	a/c	a/t	G_i	A_0	A_1	A_2	A_3	A_4	A_5	A_6
0.2 (1/5)	0.03125	0	G_0	0.1965046	2.9373464	-5.2582823	7.4889153	-6.9282667	3.3673349	-0.6677966
			G_1	0.0051780	0.1750280	2.7718680	-4.6457154	4.6780502	-3.2768090	0.9840994
		0.2	G_0	0.2190748	2.5203290	-2.0236870	-1.2734559	5.7568175	-5.8748904	1.9521817
			G_1	0.0082274	0.2471615	2.3678007	-3.4287724	3.2025223	-2.4520746	0.7939694
		0.4	G_0	0.2316580	3.0174340	-3.6739100	3.3486960	3.4951970	-8.3582900	3.7094000
			G_1	0.0132894	0.2678595	2.5665870	-4.0109437	5.6693993	-5.4751609	1.8921069
		0.6	G_0	0.2637180	3.3055520	-4.3385500	9.7328450	-4.9409500	-4.6514100	3.2218700
			G_1	0.0181909	0.3817362	2.1420212	-2.1977697	5.2001900	-7.0131972	2.7040967
		0.8	G_0	0.3497230	2.1192140	8.0739030	-27.587500	62.883920	-66.409000	24.306100
			G_1	0.0235580	0.5103500	1.5026960	1.4467780	1.4312900	-6.0350600	2.7698500
0.2 (1/5)	0.0625	0	G_0	0.2695332	2.1626001	-1.6551569	-1.2970208	4.5604304	-4.3163876	1.4010655
			G_1	0.0138667	0.1827458	2.5749608	-3.9044679	3.3556301	-2.1772209	0.6420134
		0.2	G_0	0.2852936	2.0689704	-1.0554851	-1.4836567	3.1890944	-2.3859114	0.6080571
			G_1	0.0197715	0.2169234	2.5536862	-4.2430898	4.5441255	-3.4924585	1.1187813
		0.4	G_0	0.3285480	2.4958610	-2.0243000	0.8619950	2.4744750	-4.0617200	1.5606500
			G_1	0.0361263	0.3182238	2.4231181	-3.6890071	4.2893407	-3.7603314	1.2600158
		0.6	G_0	0.3915700	3.2250850	-4.9945400	12.185590	-13.428900	5.6813190	-0.7529300
			G_1	0.0514191	0.4402715	2.1487271	-2.5959155	4.1080561	-4.8381973	1.8044669
		0.8	G_0	0.5261450	3.2405970	-1.3815100	4.1519310	0.5109400	-8.1414300	4.3185000
			G_1	0.0814479	0.6559984	1.5337156	0.4475435	0.0534894	-2.5096346	1.2137430
0.2 (1/5)	0.125	0	G_0	0.4065238	0.7772483	3.8861644	-12.573943	16.760207	-11.014593	2.8706957
			G_1	0.0320270	0.1825342	2.2670449	-2.7076615	1.2088194	-0.3777430	0.0763155
		0.2	G_0	0.4136013	1.1220276	1.7642454	-6.5135424	8.3634912	-5.3510304	1.3676362
			G_1	0.0490163	0.0123967	3.9211133	-9.1581812	12.709183	-9.8748627	3.0337707
		0.4	G_0	0.4909940	1.5098770	0.5876890	-2.8587400	2.8113040	-1.1202600	0.0293200
			G_1	0.0747677	0.0749203	3.9389068	-9.1864777	12.998452	-10.295081	3.1890105
		0.6	G_0	0.6249600	1.8325900	0.0013210	-0.0015000	-1.5020700	1.6414400	-0.6878100
			G_1	0.1105969	0.2637050	2.9884892	-5.4654500	6.9950075	-5.7793135	1.8496103
		0.8	G_0	0.8500710	1.9490000	1.0758800	-0.8402600	-2.2385800	3.1877320	-1.4499300
			G_1	0.1789668	0.2399490	3.8931390	-7.7610872	10.294824	-7.8565698	2.2277937
0.2 (1/5)	0.25	0	G_0	0.6152816	-0.3348694	6.2955620	-15.590618	19.299508	-12.488107	3.3010035
			G_1	0.0703566	0.2828152	1.4036169	-0.6511596	-1.2076596	1.0318656	-0.2423741
		0.2	G_0	0.6159056	-0.2050937	6.6909872	-19.186699	26.862981	-19.027126	5.3580488
			G_1	0.0891128	0.1702221	2.4720008	-4.9324186	6.1223136	-4.7123917	1.4632694
		0.4	G_0	0.7215670	0.0374900	3.9226910	-7.4222400	5.3541510	-0.9786100	-0.3710800
			G_1	0.1202781	0.1074802	2.4970523	-3.7079504	3.0213692	-1.8021829	0.4930615
		0.6	G_0	0.9048380	-0.1315600	4.6654820	-7.6840900	3.5404410	1.6663190	-1.4658800
			G_1	0.1803830	-0.0541023	3.7023114	-7.2913373	8.5546816	-5.9999118	1.7212304
		0.8	G_0	1.1866530	-0.8342800	8.7205780	-18.257500	18.406930	-8.8685700	1.4645500
			G_1	0.2633540	-0.1901259	4.3785426	-8.5606515	9.8591518	-6.4535782	1.6581104
0.2 (1/5)	0.5	0	G_0	0.8776607	-0.6729719	3.7721411	-6.5209060	6.3377934	-3.7028038	0.9872447
			G_1	0.1277541	0.4368502	0.4904522	1.0427434	-2.9631236	2.0826525	-0.5184313
		0.2	G_0	0.8858151	-1.0197403	6.2776913	-14.516668	18.732182	-12.986246	3.6925414
			G_1	0.1453215	0.1594771	2.2306775	-4.4869243	5.6738656	-4.4885955	1.4435985
		0.4	G_0	0.9688850	-0.6841400	2.7358770	-1.4201300	-3.8776500	5.5502200	-2.1443700
			G_1	0.1705287	0.1690974	1.9564466	-3.3798091	3.7905011	-3.0373612	1.0275733
		0.6	G_0	1.1240870	-1.0768400	3.8703920	-2.7987600	-3.8803000	6.7635310	-2.7860400
			G_1	0.2171748	0.0842974	2.2072273	-3.7731258	4.0998144	-3.1122546	1.0079677
		0.8	G_0	1.3125100	-1.3603100	4.4157580	-3.9151500	-1.6021800	4.3666690	-1.8710900
			G_1	0.2804807	-0.0036237	2.1078754	-2.5482535	1.5280380	-0.6890973	0.1306713

Table 9B.12 – Influence Coefficients for a Longitudinal Semi-Elliptical Surface Crack in a Cylinder – Inside Surface

t/R_i	a/c	a/t	G_i	A_0	A_1	A_2	A_3	A_4	A_5	A_6
0.2 (1/5)	1.0	0	G_0	1.1977992	-0.5244870	0.1498299	2.3284866	-5.1058499	4.3469049	-1.3487980
			G_1	0.1870117	0.6987352	0.1316900	0.7269255	-2.5259384	2.1756251	-0.6540458
		0.2	G_0	1.1957780	-1.1928788	4.9690673	-13.450328	20.984072	-16.917257	5.4506179
			G_1	0.2081893	0.2110738	3.0727215	-8.5670342	12.675874	-10.175528	3.3005282
		0.4	G_0	1.2499210	-0.8835300	1.5685020	-0.3587800	-2.8201600	3.7710640	-1.4756300
			G_1	0.2261821	0.1336704	3.4220588	-9.5448451	14.293730	-11.605247	3.8105474
		0.6	G_0	1.3280790	-1.0422100	1.7783590	-0.6033200	-2.4505600	3.3606510	-1.2970500
			G_1	0.2465393	0.1720577	2.9234104	-7.7004235	11.016864	-8.7581419	2.8432632
		0.8	G_0	1.4295430	-1.2362900	2.0609680	-0.9573800	-1.8135900	2.6148850	-0.9777200
			G_1	0.2736792	0.1461663	2.8913901	-7.2809390	10.022374	-7.6326797	2.3534796
0.2 (1/5)	2.0	0	G_0	0.8150546	-0.5623828	1.4465771	-4.6778133	8.4192164	-7.9025932	2.9866351
			G_1	0.1359146	0.0702340	3.5558581	-11.034445	16.967724	-14.126991	4.8706612
		0.2	G_0	0.8351796	-0.9975558	4.1493278	-12.445145	19.981918	-16.646781	5.6530002
			G_1	0.1380096	0.0562824	3.3282021	-9.9530116	14.806340	-12.097815	4.1444930
		0.4	G_0	0.8306994	-1.0237591	4.3698748	-13.269111	21.479545	-17.921928	6.0620530
			G_1	0.1376183	0.0406712	3.4210114	-10.313146	15.494157	-12.701908	4.3425313
		0.6	G_0	0.8558483	-1.0505654	4.3124794	-12.845362	20.558401	-17.096036	5.8004744
			G_1	0.1446670	0.0167777	3.5323058	-10.571235	15.816043	-12.923783	4.4101264
		0.8	G_0	0.8664408	-0.8724913	2.8280384	-7.6269457	11.393145	-9.2221390	3.1640805
			G_1	0.1390668	0.1865317	2.4237595	-7.0178287	9.8903995	-7.9357249	2.7360663
0.3333 (1/3)	0.03125	0	G_0	0.1965046	2.9373464	-5.2582823	7.4889153	-6.9282667	3.3673349	-0.6677966
			G_1	0.0051780	0.1750280	2.7718680	-4.6457154	4.6780502	-3.2768090	0.9840994
		0.2	G_0	0.2172042	2.5042847	-2.1152523	-1.0663053	5.5897238	-5.8369981	1.9620413
			G_1	0.0076407	0.2402259	2.3741989	-3.4818023	3.2921834	-2.5081221	0.8062819
		0.4	G_0	0.2213040	3.0865230	-5.3162800	10.104880	-9.4190500	3.0782450	-0.0751300
			G_1	0.0109040	0.2379070	2.7257150	-4.5589100	6.4148690	-5.9564800	2.0227340
		0.6	G_0	0.2326720	3.4536430	-7.5171600	21.602680	-27.456600	15.285850	-3.3080200
			G_1	0.0124870	0.2833310	2.5113570	-3.3810700	6.2551880	-7.1855300	2.6289150
		0.8	G_0	0.2431510	3.7925040	-9.4367000	34.625530	-49.585800	30.877910	-7.4781600
			G_1	0.0129250	0.3526240	1.9977450	-0.5838300	3.0764080	-5.7180400	2.2847340
0.3333 (1/3)	0.0625	0	G_0	0.2695332	2.1626001	-1.6551569	-1.2970208	4.5604304	-4.3163876	1.4010655
			G_1	0.0138667	0.1827458	2.5749608	-3.9044679	3.3556301	-2.1772209	0.6420134
		0.2	G_0	0.2844799	2.0640002	-1.1370689	-1.3784733	3.1901236	-2.4501643	0.6364234
			G_1	0.0196105	0.2162750	2.5422614	-4.2578287	4.5779897	-3.5058747	1.1186308
		0.4	G_0	0.3220940	2.4382140	-1.9837600	0.2441520	4.2246520	-5.9119800	2.2494420
			G_1	0.0302700	0.2690970	2.6242350	-4.3253900	5.2447410	-4.4149200	1.4273430
		0.6	G_0	0.3690150	2.8657790	-3.6714400	7.4894220	-5.1881800	-1.1502800	1.4278360
			G_1	0.0421480	0.3508870	2.4986830	-3.8769000	6.1282230	-6.2831600	2.2006960
		0.8	G_0	0.4274530	3.1943180	-5.0036400	17.183440	-22.134100	11.331200	-2.1369500
			G_1	0.0540340	0.4419180	2.1304980	-1.7669500	3.5006620	-4.6673800	1.6550060
0.3333 (1/3)	0.125	0	G_0	0.4065238	0.7772483	3.8861644	-12.573943	16.760207	-11.014593	2.8706957
			G_1	0.0320270	0.1825342	2.2670449	-2.7076615	1.2088194	-0.3777430	0.0763155
		0.2	G_0	0.4128225	1.1171748	1.7294667	-6.5703783	8.5967302	-5.5789250	1.4430231
			G_1	0.0491457	0.0109153	3.9207133	-9.2000295	12.768245	-9.8975712	3.0345710
		0.4	G_0	0.4999770	1.1122800	3.4080100	-12.831300	19.956770	-15.131900	4.4070790
			G_1	0.0655360	0.2653370	2.2964190	-3.1937600	2.6225790	-1.8132600	0.5497690
		0.6	G_0	0.6175010	1.2257330	4.0319720	-14.566200	24.320440	-19.886800	6.1066340
			G_1	0.0998390	0.2849510	2.6838120	-4.6127100	5.8013200	-4.8420000	1.5330940
		0.8	G_0	0.7920490	1.0127770	6.8668830	-21.954100	36.429260	-29.710200	9.0101920
			G_1	0.1476580	0.2244550	3.5532850	-7.2068400	10.474170	-8.3895400	2.3883100

Table 9B.12 – Influence Coefficients for a Longitudinal Semi-Elliptical Surface Crack in a Cylinder – Inside Surface

t/R_i	a/c	a/t	G_i	A_0	A_1	A_2	A_3	A_4	A_5	A_6
0.3333 (1/3)	0.25	0	G_0	0.6152816	-0.3348694	6.2955620	-15.590618	19.299508	-12.488107	3.3010035
			G_1	0.0703566	0.2828152	1.4036169	-0.6511596	-1.2076596	1.0318656	-0.2423741
		0.2	G_0	0.6151200	-0.2559286	6.9419508	-19.977395	28.061835	-19.892262	5.6000832
			G_1	0.0890045	0.1593445	2.5204791	-5.1000189	6.3764694	-4.8919376	1.5129735
		0.4	G_0	0.7305130	-0.3220800	6.3427310	-15.390600	18.411260	-11.349700	2.8193980
			G_1	0.1265635	0.1445088	2.2324974	-3.0386458	2.2662085	-1.4535727	0.4548018
		0.6	G_0	0.9124330	-0.7665200	9.1561340	-23.081300	29.896950	-19.945600	5.3119440
			G_1	0.1687760	0.1014170	2.6091130	-3.8884800	3.4192270	-2.2010400	0.6120270
		0.8	G_0	1.1626120	-1.3970900	12.596200	-31.856200	42.732810	-29.146600	7.7681640
			G_1	0.2450710	-0.1281000	3.9424300	-7.5372100	9.0064480	-6.0816100	1.5366290
0.3333 (1/3)	0.5	0	G_0	0.8776607	-0.6729719	3.7721411	-6.5209060	6.3377934	-3.7028038	0.9872447
			G_1	0.1277541	0.4368502	0.4904522	1.0427434	-2.9631236	2.0826525	-0.5184313
		0.2	G_0	0.8818313	-1.0917996	6.7441757	-15.991176	21.054792	-14.772037	4.2281725
			G_1	0.1441557	0.1424866	2.3284045	-4.7895448	6.1386818	-4.8362727	1.5452935
		0.4	G_0	0.9407980	-0.4985400	1.9170250	-0.0192500	-4.6370600	5.2166830	-1.8075400
			G_1	0.1711202	0.1668531	1.9267560	-3.2630245	3.5831509	-2.8636537	0.9729171
		0.6	G_0	1.1152890	-1.3442300	5.9458650	-10.097200	8.9327530	-4.0621300	0.7185930
			G_1	0.2163543	0.1549463	1.5248691	-1.5230688	0.7692177	-0.7731253	0.3699490
		0.8	G_0	1.2910080	-1.3463700	4.3601980	-3.7608100	-1.3364900	3.8436030	-1.6693300
			G_1	0.2617850	0.1512610	1.1793570	0.3568580	-2.8439400	2.6019470	-0.8740000
0.3333 (1/3)	1.0	0	G_0	1.1977992	-0.5244870	0.1498299	2.3284866	-5.1058499	4.3469049	-1.3487980
			G_1	0.1870117	0.6987352	0.1316900	0.7269255	-2.5259384	2.1756251	-0.6540458
		0.2	G_0	1.1843664	-1.1847612	4.9902280	-13.538735	21.119771	-17.017414	5.4794601
			G_1	0.2064638	0.1880635	3.2277985	-9.0382566	13.410536	-10.743271	3.4724686
		0.4	G_0	1.2310867	-1.2996546	5.3458402	-14.297856	22.283375	-18.132719	5.9308732
			G_1	0.2232606	0.1330441	3.4286845	-9.5400946	14.273538	-11.599332	3.8156481
		0.6	G_0	1.3016702	-1.3329884	4.6823879	-11.389326	16.885721	-13.394792	4.3283933
			G_1	0.2440755	0.1533295	3.0387623	-7.9723882	11.374712	-9.0179366	2.9233036
		0.8	G_0	1.4059990	-1.4844400	4.6015830	-9.7191000	12.979170	-9.5963900	2.9604700
			G_1	0.2547770	0.3338937	2.0367399	-5.9096868	9.5170399	-8.2252015	2.7607498
0.3333 (1/3)	2.0	0	G_0	0.8150546	-0.5623828	1.4465771	-4.6778133	8.4192164	-7.9025932	2.9866351
			G_1	0.1359146	0.0702340	3.5558581	-11.034445	16.967724	-14.126991	4.8706612
		0.2	G_0	0.8291377	-0.9895481	4.1798664	-12.600881	20.280744	-16.914774	5.7445745
			G_1	0.1367171	0.0546432	3.3517976	-10.030368	14.931862	-12.199484	4.1771813
		0.4	G_0	0.8281292	-1.0079708	4.3560940	-13.170690	21.184349	-17.624770	5.9654552
			G_1	0.1383911	0.0271839	3.5221879	-10.559706	15.796147	-12.905023	4.4038513
		0.6	G_0	0.8416824	-1.0386714	4.4633302	-13.408838	21.463769	-17.808130	6.0224184
			G_1	0.1432074	0.0086329	3.6113710	-10.774368	16.083937	-13.122391	4.4757876
		0.8	G_0	0.8492888	-0.8700518	3.1479406	-8.7543723	13.222524	-10.685678	3.6241547
			G_1	0.1360843	0.2203399	2.2144388	-6.1874959	8.3319395	-6.6071612	2.3172922
1.0 (1/1)	0.03125	0	G_0	0.1965046	2.9373464	-5.2582823	7.4889153	-6.9282667	3.3673349	-0.6677966
			G_1	0.0051780	0.1750280	2.7718680	-4.6457154	4.6780502	-3.2768090	0.9840994
		0.2	G_0	0.1887770	3.2460130	-7.9657120	15.803931	-18.601108	11.257414	-2.7708890
			G_1	0.0035310	0.2557830	2.2488600	-3.4182260	3.3729340	-2.6095290	0.8448730
		0.4	G_0	0.1936060	3.3256100	-9.3285050	23.269704	-32.015841	21.747820	-5.8692540
			G_1	0.0031910	0.2949310	1.8484630	-1.8812440	1.5093650	-1.6986400	0.6868650
		0.6	G_0	0.2027590	3.1972320	-8.5528700	24.163644	-35.834420	25.596244	-7.2230670
			G_1	0.0035920	0.3018150	1.6868040	-0.8209740	0.1147120	-0.9134420	0.4831660
		0.8	G_0	0.2144420	2.9332390	-6.2402450	19.707775	-31.405095	24.506206	-7.7838990
			G_1	0.0054130	0.2577100	1.9623290	-1.0564620	0.1832180	-0.0823050	-0.2325620

Table 9B.12 – Influence Coefficients for a Longitudinal Semi-Elliptical Surface Crack in a Cylinder – Inside Surface

t/R_i	a/c	a/t	G_i	A_0	A_1	A_2	A_3	A_4	A_5	A_6
1.0 (1/1)	0.0625	0	G_0	0.2695332	2.1626001	-1.6551569	-1.2970208	4.5604304	-4.3163876	1.4010655
			G_1	0.0138667	0.1827458	2.5749608	-3.9044679	3.3556301	-2.1772209	0.6420134
		0.2	G_0	0.2602710	2.5072370	-4.0196340	4.8604960	-3.1614410	0.5262740	0.1626390
			G_1	0.0140680	0.2618010	2.2080180	-3.3491570	3.0477360	-2.1577470	0.6622560
		0.4	G_0	0.2688020	2.6734540	-5.6446960	11.354033	-12.533332	6.4776680	-1.2817270
			G_1	0.0159260	0.2906450	2.0141960	-2.8616550	3.2482670	-2.9880670	1.0375950
		0.6	G_0	0.2798250	2.7173870	-6.5196150	17.301630	-23.167511	14.548473	-3.6124180
			G_1	0.0167090	0.3099060	1.7874040	-1.8952340	2.5146820	-3.0341200	1.1541790
		0.8	G_0	0.2958390	2.5709320	-5.8064300	18.880265	-28.546652	20.789752	-6.2493280
			G_1	0.0184130	0.2878740	1.8559320	-1.5905150	2.1014180	-2.1364600	0.5009230
1.0 (1/1)	0.125	0	G_0	0.4065238	0.7772483	3.8861644	-12.573943	16.760207	-11.014593	2.8706957
			G_1	0.0320270	0.1825342	2.2670449	-2.7076615	1.2088194	-0.3777430	0.0763155
		0.2	G_0	0.3892020	1.3031240	1.2426210	-7.6430130	12.601404	-9.5919880	2.7882590
			G_1	0.0357210	0.2481460	2.0826440	-2.9432810	2.2213120	-1.3865100	0.4111960
		0.4	G_0	0.4215680	1.3823700	0.7862470	-6.2768270	12.088434	-10.408977	3.2683420
			G_1	0.0469710	0.2600750	2.1211230	-3.2793580	3.4497760	-2.7324570	0.8673790
		0.6	G_0	0.4537450	1.3478430	0.7380390	-4.8590140	11.111854	-11.058568	3.7768470
			G_1	0.0546110	0.2388750	2.2799670	-3.8546110	5.4142280	-4.9049200	1.6068860
		0.8	G_0	0.4920000	1.1255500	1.6609330	-5.0325820	11.027984	-10.717680	3.3578350
			G_1	0.0614110	0.1664210	2.7612530	-5.2823370	8.4684220	-7.1584750	2.0083830
1.0 (1/1)	0.25	0	G_0	0.6152816	-0.3348694	6.2955620	-15.590618	19.299508	-12.488107	3.3010035
			G_1	0.0703566	0.2828152	1.4036169	-0.6511596	-1.2076596	1.0318656	-0.2423741
		0.2	G_0	0.5852570	-0.1000030	5.3861730	-14.481721	18.705926	-12.309007	3.2534580
			G_1	0.0724540	0.2056560	1.8919480	-2.3229410	1.2648190	-0.6502480	0.1954770
		0.4	G_0	0.6496920	-0.1878520	5.8413390	-15.672861	20.881370	-14.208984	3.8455090
			G_1	0.0973280	0.1668610	2.1152140	-2.9592280	2.3504650	-1.5298980	0.4550750
		0.6	G_0	0.7423520	-0.4978600	7.4225290	-19.524846	27.422578	-19.756959	5.5604290
			G_1	0.1265830	0.0720860	2.6494880	-4.4508230	5.0966590	-3.8637400	1.1526210
		0.8	G_0	0.8482320	-1.0301430	10.273454	-26.715328	39.521921	-29.403936	8.2660770
			G_1	0.1566560	-0.1005730	3.7205800	-7.6368800	10.814633	-8.2353200	2.2447720
1.0 (1/1)	0.5	0	G_0	0.8776607	-0.6729719	3.7721411	-6.5209060	6.3377934	-3.7028038	0.9872447
			G_1	0.1277541	0.4368502	0.4904522	1.0427434	-2.9631236	2.0826525	-0.5184313
		0.2	G_0	0.8223780	-0.6926820	4.1749310	-7.9388620	8.1437880	-4.5936300	1.0929220
			G_1	0.1187890	0.3291500	1.0684300	-0.6475430	-0.5247600	0.3663070	-0.0425330
		0.4	G_0	0.8714610	-0.7985800	4.4456080	-8.3111450	8.4837340	-4.7818110	1.1366370
			G_1	0.1400050	0.2762620	1.2050610	-0.8546340	-0.3238000	0.2554730	-0.0173390
		0.6	G_0	0.9849310	-1.1212490	5.6192930	-10.551055	11.336911	-6.7824610	1.6843950
			G_1	0.1799850	0.1599500	1.6390710	-1.7128890	0.8272690	-0.5646380	0.2024140
		0.8	G_0	1.1420050	-1.6597170	7.9007850	-15.439726	18.287019	-11.728046	2.9430680
			G_1	0.2328010	-0.0467300	2.6611540	-4.2325050	4.6610900	-3.2414360	0.8282060
1.0 (1/1)	1.0	0	G_0	1.1977992	-0.5244870	0.1498299	2.3284866	-5.1058499	4.3469049	-1.3487980
			G_1	0.1870117	0.6987352	0.1316900	0.7269255	-2.5259384	2.1756251	-0.6540458
		0.2	G_0	1.1185400	-0.7466120	2.2569970	-4.2923660	4.9732460	-3.1499340	0.8291370
			G_1	0.1679140	0.5576320	1.0788590	-2.1361180	1.8024530	-1.0315420	0.2739990
		0.4	G_0	1.1145190	-0.7542990	2.4059640	-4.7032890	5.5327610	-3.5380910	0.9367770
			G_1	0.1728850	0.5161020	1.2596510	-2.5441810	2.3216530	-1.3790280	0.3681920
		0.6	G_0	1.1735530	-0.9107720	3.0009520	-5.8521850	6.8037420	-4.2974970	1.1245860
			G_1	0.1962470	0.4424370	1.5387950	-3.0679190	2.9034670	-1.7325770	0.4560140
		0.8	G_0	1.2769660	-1.1593170	4.1356500	-8.2343020	9.8243940	-6.2987670	1.6318920
			G_1	0.2316340	0.3596110	1.9624090	-3.9342220	4.0485700	-2.4698850	0.6113770

Table 9B.12 – Influence Coefficients for a Longitudinal Semi-Elliptical Surface Crack in a Cylinder – Inside Surface

t/R_i	a/c	a/t	G_i	A_0	A_1	A_2	A_3	A_4	A_5	A_6
1.0 (1/1)	2.0	0	G_0	0.8150546	-0.5623828	1.4465771	-4.6778133	8.4192164	-7.9025932	2.9866351
			G_1	0.1359146	0.0702340	3.5558581	-11.034445	16.967724	-14.126991	4.8706612
		0.2	G_0	0.775542	-0.462170	0.928967	-1.913770	1.756740	-0.962982	0.359284
			G_1	0.097384	0.526486	0.559915	-1.023006	-0.438924	0.826732	-0.155968
		0.4	G_0	0.753133	-0.388979	0.888974	-2.082603	2.124123	-1.268587	0.454809
			G_1	0.094510	0.518909	0.656501	-1.304464	-0.040356	0.536911	-0.070183
		0.6	G_0	0.751738	-0.363300	0.947217	-2.348033	2.476364	-1.474385	0.500571
			G_1	0.097080	0.506094	0.751534	-1.522757	0.199706	0.411354	-0.045982
		0.8	G_0	0.763114	-0.328201	0.959728	-2.379355	2.427215	-1.397584	0.475059
			G_1	0.101836	0.514054	0.783355	-1.546819	0.186296	0.436725	-0.058225
1.5 (1.5/1)	0.03125	0	G_0	0.1965046	2.9373464	-5.2582823	7.4889153	-6.9282667	3.3673349	-0.6677966
			G_1	0.0051780	0.1750280	2.7718680	-4.6457154	4.6780502	-3.2768090	0.9840994
		0.2	G_0	0.1871480	3.2193230	-8.3547450	17.175306	-20.942694	13.168039	-3.3548220
			G_1	0.0030060	0.2554000	2.1744700	-3.2742650	3.1219380	-2.3757300	0.7702860
		0.4	G_0	0.1924970	3.1602870	-8.9552060	22.107565	-30.882925	21.558580	-5.9853310
			G_1	0.0026230	0.2827920	1.8022500	-1.8010740	1.0600520	-1.0743140	0.4426720
		0.6	G_0	0.2007990	2.9147360	-7.2825220	18.926376	-27.284947	19.422515	-5.5344220
			G_1	0.0034150	0.2633370	1.8589210	-1.6624560	1.1142900	-1.2854220	0.4955650
		0.8	G_0	0.2089150	2.6241930	-4.7336880	12.144243	-17.294853	13.150126	-4.3895340
			G_1	0.0054520	0.1974550	2.3605180	-3.0386650	3.3497840	-2.2295120	0.3139110
1.5 (1.5/1)	0.0625	0	G_0	0.2695332	2.1626001	-1.6551569	-1.2970208	4.5604304	-4.3163876	1.4010655
			G_1	0.0138667	0.1827458	2.5749608	-3.9044679	3.3556301	-2.1772209	0.6420134
		0.2	G_0	0.2559070	2.4769840	-4.3504330	5.8919370	-4.6070500	1.5228170	-0.1047370
			G_1	0.0130010	0.2543090	2.1712300	-3.3466990	3.1120910	-2.2150440	0.6794480
		0.4	G_0	0.2586610	2.5614580	-5.9014180	12.721828	-15.470208	9.1926230	-2.1678900
			G_1	0.0131400	0.2763000	1.9058070	-2.5549240	2.6325260	-2.4133820	0.8543080
		0.6	G_0	0.2656720	2.4734090	-5.9895820	16.084085	-22.645940	15.272607	-4.0948890
			G_1	0.0131630	0.2815210	1.7286740	-1.7149820	1.8204460	-2.1722910	0.8321520
		0.8	G_0	0.2775890	2.1933630	-4.1758210	13.096895	-20.086267	15.385136	-4.9778980
			G_1	0.0146580	0.2349820	1.9972960	-2.2158140	2.6615280	-2.1107110	0.3788710
1.5 (1.5/1)	0.125	0	G_0	0.4065238	0.7772483	3.8861644	-12.573943	16.760207	-11.014593	2.8706957
			G_1	0.0320270	0.1825342	2.2670449	-2.7076615	1.2088194	-0.3777430	0.0763155
		0.2	G_0	0.3818750	1.2835930	0.9980180	-7.0046230	11.895439	-9.2062130	2.7029670
			G_1	0.0343590	0.2418040	2.0501980	-2.9386520	2.2914760	-1.4565460	0.4323500
		0.4	G_0	0.3961210	1.3071730	0.4368370	-4.8889030	9.9277220	-8.8438190	2.8392680
			G_1	0.0399630	0.2368410	2.0641370	-3.1463250	3.3191750	-2.6636500	0.8534920
		0.6	G_0	0.4089220	1.2335480	0.3636820	-2.9736600	7.4102250	-7.8636990	2.7818630
			G_1	0.0421260	0.2101410	2.1800740	-3.5350670	4.8602020	-4.4375870	1.4650570
		0.8	G_0	0.4293380	0.9818900	1.4865920	-3.8063930	7.8389670	-7.3871220	2.1730080
			G_1	0.0448040	0.1401910	2.6357250	-4.9068160	7.7001560	-6.3988210	1.7452910
1.5 (1.5/1)	0.25	0	G_0	0.6152816	-0.3348694	6.2955620	-15.590618	19.299508	-12.488107	3.3010035
			G_1	0.0703566	0.2828152	1.4036169	-0.6511596	-1.2076596	1.0318656	-0.2423741
		0.2	G_0	0.5731260	-0.1026810	5.2348720	-14.166926	18.420386	-12.180789	3.2304300
			G_1	0.0702990	0.2007070	1.8692950	-2.3096600	1.2845320	-0.6705890	0.2010140
		0.4	G_0	0.6143650	-0.1925600	5.5595540	-14.837736	19.889910	-13.651961	3.7192640
			G_1	0.0883690	0.1573760	2.0664490	-2.8387660	2.2611150	-1.5113030	0.4566990
		0.6	G_0	0.6654280	-0.4603320	6.8976520	-17.926593	25.344704	-18.475562	5.2470810
			G_1	0.1046570	0.0712920	2.5490420	-4.1933050	4.8755320	-3.7949470	1.1474390
		0.8	G_0	0.7187580	-0.8684550	9.2364690	-23.834746	35.661603	-26.827229	7.5695330
			G_1	0.1188290	-0.0679130	3.4958570	-7.1384710	10.357177	-8.0270040	2.1959690

Table 9B.12 – Influence Coefficients for a Longitudinal Semi-Elliptical Surface Crack in a Cylinder – Inside Surface

t/R_i	a/c	a/t	G_i	A_0	A_1	A_2	A_3	A_4	A_5	A_6
1.5 (1.5/1)	0.5	0	G_0	0.8776607	-0.6729719	3.7721411	-6.5209060	6.3377934	-3.7028038	0.9872447
			G_1	0.1277541	0.4368502	0.4904522	1.0427434	-2.9631236	2.0826525	-0.5184313
		0.2	G_0	0.7999930	-0.6702080	4.0707980	-7.7423870	7.9267570	-4.4569440	1.0563660
			G_1	0.1136940	0.3275140	1.0561050	-0.6222870	-0.5586150	0.3946890	-0.0518860
		0.4	G_0	0.8340580	-0.7679320	4.3748960	-8.1995680	8.4148900	-4.7809860	1.1445190
			G_1	0.1316730	0.2685230	1.2319970	-0.9143400	-0.2371870	0.1907400	0.0010370
		0.6	G_0	0.9190840	-1.0556130	5.5921840	-10.647658	11.703544	-7.1783650	1.8163490
			G_1	0.1639280	0.1541250	1.7179280	-1.9278680	1.1814200	-0.8498530	0.2861980
		0.8	G_0	1.0300390	-1.4949880	7.8105150	-15.760033	19.464498	-12.940902	3.3317500
			G_1	0.2037050	-0.0326220	2.7728460	-4.6625480	5.5019510	-3.9548810	1.0376330
1.5 (1.5/1)	1.0	0	G_0	1.1977992	-0.5244870	0.1498299	2.3284866	-5.1058499	4.3469049	-1.3487980
			G_1	0.1870117	0.6987352	0.1316900	0.7269255	-2.5259384	2.1756251	-0.6540458
		0.2	G_0	1.0852720	-0.6957660	2.2172950	-4.3020260	5.0100220	-3.1731610	0.8335180
			G_1	0.1600320	0.5559860	1.1197960	-2.2372850	1.9209480	-1.1018790	0.2908130
		0.4	G_0	1.0677690	-0.6700770	2.3607410	-4.7941460	5.7101090	-3.6616170	0.9679420
			G_1	0.1628640	0.5114670	1.3435660	-2.7549090	2.5750130	-1.5331680	0.4059190
		0.6	G_0	1.1157850	-0.7876990	2.9678970	-6.1066660	7.2828380	-4.6617040	1.2265270
			G_1	0.1848650	0.4375840	1.6751360	-3.4351040	3.3829850	-2.0495000	0.5394720
		0.8	G_0	1.2068900	-0.9826140	4.1585140	-8.9187160	11.176646	-7.4049870	1.9577020
			G_1	0.2193180	0.3545180	2.1920070	-4.6216420	5.0632350	-3.2080740	0.8183490
1.5 (1.5/1)	2.0	0	G_0	0.8150546	-0.5623828	1.4465771	-4.6778133	8.4192164	-7.9025932	2.9866351
			G_1	0.1359146	0.0702340	3.5558581	-11.034445	16.967724	-14.126991	4.8706612
		0.2	G_0	0.7561570	-0.4113330	0.8922740	-1.9773740	1.9110700	-1.0892160	0.3972130
			G_1	0.0933630	0.5272230	0.5996590	-1.1437300	-0.2725070	0.7095340	-0.1221990
		0.4	G_0	0.7241860	-0.2955140	0.7740270	-2.0760430	2.2576180	-1.4080850	0.5016070
			G_1	0.0889820	0.5219580	0.7110940	-1.4830380	0.2133090	0.3549500	-0.0169870
		0.6	G_0	0.7176280	-0.2320270	0.7455130	-2.2314070	2.5330490	-1.5910440	0.5471650
			G_1	0.0911710	0.5123440	0.8122800	-1.7386130	0.5168220	0.1796240	0.0224790
		0.8	G_0	0.7269650	-0.1654350	0.7081360	-2.2629510	2.5901790	-1.6414820	0.5684870
			G_1	0.0967150	0.5207350	0.8694050	-1.8598470	0.6663950	0.0745500	0.0504730
2.0 (2/1)	0.03125	0	G_0	0.1965046	2.9373464	-5.2582823	7.4889153	-6.9282667	3.3673349	-0.6677966
			G_1	0.0051780	0.1750280	2.7718680	-4.6457154	4.6780502	-3.2768090	0.9840994
		0.2	G_0	0.1862430	3.1871860	-8.6163530	18.188665	-22.753444	14.696910	-3.8372360
			G_1	0.0026780	0.2562520	2.1051900	-3.1202060	2.8543730	-2.1321370	0.6915120
		0.4	G_0	0.1920990	3.0177060	-8.4884490	20.536080	-28.583790	20.061801	-5.6174020
			G_1	0.0024620	0.2700700	1.8131980	-1.9284640	1.1256460	-0.9743760	0.3773470
		0.6	G_0	0.1983990	2.7409340	-6.5746110	15.935994	-22.025830	15.297020	-4.3115820
			G_1	0.0033390	0.2394840	1.9724830	-2.2727940	2.0391010	-1.8617660	0.6305280
		0.8	G_0	0.2031130	2.4822360	-4.3202910	9.5883850	-12.002039	8.5599520	-2.9241860
			G_1	0.0051810	0.1730480	2.4959560	-3.8858380	4.8318130	-3.3353400	0.6305460
2.0 (2/1)	0.0625	0	G_0	0.2695332	2.1626001	-1.6551569	-1.2970208	4.5604304	-4.3163876	1.4010655
			G_1	0.0138667	0.1827458	2.5749608	-3.9044679	3.3556301	-2.1772209	0.6420134
		0.2	G_0	0.2524140	2.4488960	-4.6242740	6.8553650	-6.0831040	2.6044290	-0.4081730
			G_1	0.0121860	0.2500220	2.1254660	-3.2829480	3.0633290	-2.1881450	0.6736950
		0.4	G_0	0.2523970	2.4567070	-5.8696010	13.093788	-16.722829	10.577435	-2.6677870
			G_1	0.0115850	0.2671310	1.8321990	-2.3246290	2.1480750	-1.9489500	0.7009540
		0.6	G_0	0.2574010	2.2797210	-5.2623580	13.916127	-19.878743	13.753039	-3.8012160
			G_1	0.0114600	0.2599110	1.7415830	-1.7738130	1.6746070	-1.8524330	0.6909070
		0.8	G_0	0.2662910	1.9548690	-2.9564910	8.5694090	-12.795188	10.027274	-3.4753810
			G_1	0.0129120	0.2013170	2.1300020	-2.7866260	3.3951280	-2.4748490	0.4395870

Table 9B.12 – Influence Coefficients for a Longitudinal Semi-Elliptical Surface Crack in a Cylinder – Inside Surface

t/R_i	a/c	a/t	G_i	A_0	A_1	A_2	A_3	A_4	A_5	A_6
2.0 (2/1)	0.125	0	G_0	0.4065238	0.7772483	3.8861644	-12.573943	16.760207	-11.014593	2.8706957
			G_1	0.0320270	0.1825342	2.2670449	-2.7076615	1.2088194	-0.3777430	0.0763155
		0.2	G_0	0.3748730	1.2639710	0.7904890	-6.3714270	11.089171	-8.7055790	2.5790240
			G_1	0.0329740	0.2360890	2.0180140	-2.9029810	2.3012840	-1.4844670	0.4429370
		0.4	G_0	0.3781490	1.2493180	0.2447500	-3.9438800	8.2401310	-7.5012660	2.4462910
			G_1	0.0353370	0.2224590	2.0169060	-3.0046970	3.1104170	-2.5089710	0.8111170
		0.6	G_0	0.3821620	1.1526580	0.2952920	-2.2430110	5.5382370	-6.0193430	2.1625070
			G_1	0.0354260	0.1956370	2.1152900	-3.2992810	4.3790020	-3.9992790	1.3266410
		0.8	G_0	0.3949370	0.8871000	1.6486390	-4.0245560	7.3083980	-6.3274340	1.7120200
			G_1	0.0367850	0.1283150	2.5684690	-4.6806090	7.1443220	-5.8258650	1.5492980
2.0 (2/1)	0.25	0	G_0	0.6152816	-0.3348694	6.2955620	-15.590618	19.299508	-12.488107	3.3010035
			G_1	0.0703566	0.2828152	1.4036169	-0.6511596	-1.2076596	1.0318656	-0.2423741
		0.2	G_0	0.5618030	-0.1035380	5.0988920	-13.834804	18.062486	-11.989127	3.1886810
			G_1	0.0682240	0.1965170	1.8484400	-2.2815960	1.2768050	-0.6746000	0.2031190
		0.4	G_0	0.5849530	-0.1911790	5.3612680	-14.203101	19.045805	-13.116775	3.5843860
			G_1	0.0809390	0.1507230	2.0342940	-2.7447430	2.1665520	-1.4682140	0.4486100
		0.6	G_0	0.6118160	-0.4181520	6.5505680	-16.905352	23.894430	-17.478417	4.9807840
			G_1	0.0897990	0.0742610	2.4830030	-4.0277420	4.6950610	-3.6982770	1.1258740
		0.8	G_0	0.6407850	-0.7394080	8.5521120	-22.048286	33.082069	-24.941765	7.0306120
			G_1	0.0969020	-0.0414100	3.3411540	-6.8014460	9.9580220	-7.7663000	2.1232630
2.0 (2/1)	0.5	0	G_0	0.8776607	-0.6729719	3.7721411	-6.5209060	6.3377934	-3.7028038	0.9872447
			G_1	0.1277541	0.4368502	0.4904522	1.0427434	-2.9631236	2.0826525	-0.5184313
		0.2	G_0	0.7808210	-0.6481470	3.9820570	-7.5717910	7.7384130	-4.3424810	1.0271110
			G_1	0.1095090	0.3258980	1.0495910	-0.6078650	-0.5777140	0.4102660	-0.0569150
		0.4	G_0	0.8022710	-0.7320990	4.3103750	-8.1130780	8.3654180	-4.7826990	1.1512240
			G_1	0.1246280	0.2635460	1.2599510	-0.9801290	-0.1461210	0.1252090	0.0193550
		0.6	G_0	0.8642590	-0.9718420	5.4912950	-10.618665	11.869872	-7.3968370	1.8927400
			G_1	0.1502850	0.1572540	1.7654850	-2.0835480	1.4396750	-1.0536880	0.3453860
		0.8	G_0	0.9418280	-1.3072530	7.4965060	-15.531974	19.712631	-13.377824	3.4898520
			G_1	0.1800930	-0.0042500	2.7921390	-4.8612680	5.9465140	-4.3417630	1.1518700
2.0 (2/1)	1.0	0	G_0	1.1977992	-0.5244870	0.1498299	2.3284866	-5.1058499	4.3469049	-1.3487980
			G_1	0.1870117	0.6987352	0.1316900	0.7269255	-2.5259384	2.1756251	-0.6540458
		0.2	G_0	1.0569230	-0.6476300	2.1807510	-4.3311330	5.0910220	-3.2362090	0.8507590
			G_1	0.1536110	0.5538190	1.1636010	-2.3534050	2.0684520	-1.1965100	0.3151600
		0.4	G_0	1.0300060	-0.5858380	2.2773530	-4.8060360	5.8149950	-3.7533950	0.9942170
			G_1	0.1551260	0.5094730	1.4113730	-2.9400080	2.8110450	-1.6838480	0.4444420
		0.6	G_0	1.0683100	-0.6542190	2.8004260	-6.0398120	7.3697750	-4.7773480	1.2651390
			G_1	0.1753800	0.4426450	1.7504300	-3.6668490	3.6981780	-2.2615850	0.5960840
		0.8	G_0	1.1462360	-0.7799090	3.8903050	-8.8544090	11.517275	-7.8168230	2.0976050
			G_1	0.2074120	0.3687620	2.2982000	-5.0131860	5.6805960	-3.6723940	0.9519940
2.0 (2/1)	2.0	0	G_0	0.8150546	-0.5623828	1.4465771	-4.6778133	8.4192164	-7.9025932	2.9866351
			G_1	0.1359146	0.0702340	3.5558581	-11.034445	16.967724	-14.126991	4.8706612
		0.2	G_0	0.7389400	-0.3615380	0.8437490	-2.0110780	2.0338130	-1.1993770	0.4319790
			G_1	0.0899090	0.5283040	0.6347000	-1.2557710	-0.1127030	0.5943560	-0.0885320
		0.4	G_0	0.7002730	-0.2059430	0.6251970	-1.9668570	2.2617300	-1.4675680	0.5286020
			G_1	0.0846030	0.5263610	0.7486360	-1.6211710	0.4208860	0.1999990	0.0296600
		0.6	G_0	0.6904180	-0.1082490	0.4854150	-1.9171500	2.3152310	-1.5215830	0.5434940
			G_1	0.0865440	0.5217030	0.8372840	-1.8583160	0.7058700	0.0352600	0.0667980
		0.8	G_0	0.6981280	-0.0115610	0.3542570	-1.7803210	2.1994870	-1.4790330	0.5446590
			G_1	0.0924170	0.5337330	0.8900720	-1.9809530	0.8625850	-0.0758770	0.0966550

Table 9B.12 – Influence Coefficients for a Longitudinal Semi-Elliptical Surface Crack in a Cylinder – Inside Surface

t/R_i	a/c	a/t	G_i	A_0	A_1	A_2	A_3	A_4	A_5	A_6
2.5 (2.5/1)	0.03125	0	G_0	0.1965046	2.9373464	-5.2582823	7.4889153	-6.9282667	3.3673349	-0.6677966
			G_1	0.0051780	0.1750280	2.7718680	-4.6457154	4.6780502	-3.2768090	0.9840994
		0.2	G_0	0.1857440	3.1501810	-8.7718700	18.876054	-24.037777	15.813047	-4.1981080
			G_1	0.0024620	0.2567150	2.0482580	-2.9895930	2.6304520	-1.9284850	0.6245480
		0.4	G_0	0.1916320	2.9006620	-8.0688860	19.143584	-26.415141	18.500732	-5.1859770
			G_1	0.0024050	0.2591330	1.8351520	-2.0837920	1.3196860	-1.0439440	0.3779080
		0.6	G_0	0.1958000	2.6238780	-6.1523100	14.204867	-18.929996	12.806378	-3.5533230
			G_1	0.0032240	0.2249400	2.0323530	-2.6352560	2.6260590	-2.2581540	0.7333810
		0.8	G_0	0.1979980	2.3968770	-4.1796250	8.5687590	-9.7672150	6.5450920	-2.2549340
			G_1	0.0048620	0.1615050	2.5373410	-4.2541430	5.4940800	-3.8389940	0.7815340
2.5 (2.5/1)	0.0625	0	G_0	0.2695332	2.1626001	-1.6551569	-1.2970208	4.5604304	-4.3163876	1.4010655
			G_1	0.0138667	0.1827458	2.5749608	-3.9044679	3.3556301	-2.1772209	0.6420134
		0.2	G_0	0.2495760	2.4204110	-4.8308930	7.6716770	-7.4160590	3.6219260	-0.7024470
			G_1	0.0115540	0.2473680	2.0788480	-3.1902760	2.9538090	-2.1133250	0.6540410
		0.4	G_0	0.2479520	2.3584350	-5.6706510	12.829855	-16.820683	10.992456	-2.8676950
			G_1	0.0106020	0.2588410	1.7928860	-2.1927230	1.8414400	-1.6365650	0.5933490
		0.6	G_0	0.2512790	2.1304710	-4.5821940	11.752906	-16.756127	11.671124	-3.2684300
			G_1	0.0104480	0.2425830	1.7792800	-1.9172370	1.7559810	-1.7823800	0.6399450
		0.8	G_0	0.2575120	1.8032230	-2.1279290	5.3915830	-7.4871980	5.9449580	-2.2717190
			G_1	0.0118410	0.1786790	2.2328910	-3.2292330	4.0112620	-2.8463580	0.5291890
2.5	0.125	0	G_0	0.4065238	0.7772483	3.8861644	-12.573943	16.760207	-11.014593	2.8706957
			G_1	0.0320270	0.1825342	2.2670449	-2.7076615	1.2088194	-0.3777430	0.0763155
		0.2	G_0	0.3685050	1.2446800	0.6234320	-5.7943180	10.282331	-8.1658940	2.4373700
			G_1	0.0317050	0.2311310	1.9880370	-2.8507390	2.2701700	-1.4796410	0.4443650
		0.4	G_0	0.3647200	1.2008040	0.1718230	-3.3955360	7.1054830	-6.5224090	2.1448150
			G_1	0.0321260	0.2124340	1.9833230	-2.8867120	2.9072300	-2.3442520	0.7631890
		0.6	G_0	0.3636880	1.0902120	0.3781660	-2.1728690	4.8553400	-5.1372250	1.8293420
			G_1	0.0312410	0.1861530	2.0801130	-3.1535660	4.0343360	-3.6624150	1.2160450
		0.8	G_0	0.3720960	0.8223520	1.8978350	-4.7698880	7.9525070	-6.3800050	1.6254420
			G_1	0.0320290	0.1205900	2.5405200	-4.5805080	6.8144140	-5.4523610	1.4182810
2.5 (2.5/1)	0.25	0	G_0	0.6152816	-0.3348694	6.2955620	-15.590618	19.299508	-12.488107	3.3010035
			G_1	0.0703566	0.2828152	1.4036169	-0.6511596	-1.2076596	1.0318656	-0.2423741
		0.2	G_0	0.5513640	-0.1031960	4.9807880	-13.514392	17.681009	-11.765845	3.1359840
			G_1	0.0662870	0.1928840	1.8304400	-2.2477030	1.2530750	-0.6671240	0.2023610
		0.4	G_0	0.5608360	-0.1855330	5.2231160	-13.748194	18.394650	-12.672652	3.4658940
			G_1	0.0749650	0.1460730	2.0143950	-2.6794190	2.0884150	-1.4231420	0.4378620
		0.6	G_0	0.5730220	-0.3749280	6.3008620	-16.226249	22.884738	-16.737630	4.7728900
			G_1	0.0794450	0.0787400	2.4361670	-3.9152720	4.5488710	-3.5987530	1.0989970
		0.8	G_0	0.5890540	-0.6320750	8.0517490	-20.836556	31.285150	-23.571536	6.6291970
			G_1	0.0830520	-0.0204030	3.2297270	-6.5626130	9.6300540	-7.5203610	2.0510740
2.5 (2.5/1)	0.5	0	G_0	0.8776607	-0.6729719	3.7721411	-6.5209060	6.3377934	-3.7028038	0.9872447
			G_1	0.1277541	0.4368502	0.4904522	1.0427434	-2.9631236	2.0826525	-0.5184313
		0.2	G_0	0.7641350	-0.6263840	3.9047110	-7.4226330	7.5738980	-4.2448060	1.0029460
			G_1	0.1059990	0.3243810	1.0471780	-0.6016520	-0.5860160	0.4170780	-0.0591080
		0.4	G_0	0.7750140	-0.6920780	4.2400270	-8.0249580	8.3089080	-4.7728240	1.1533910
			G_1	0.1186170	0.2610560	1.2842080	-1.0414650	-0.0628360	0.0670260	0.0353280
		0.6	G_0	0.8191130	-0.8805800	5.3361650	-10.482028	11.876282	-7.4834910	1.9288670
			G_1	0.1389830	0.1653800	1.7895330	-2.1910300	1.6230050	-1.1956510	0.3858530
		0.8	G_0	0.8734990	-1.1262860	7.1029150	-15.081769	19.563489	-13.473806	3.5451920
			G_1	0.1616610	0.0263870	2.7751290	-4.9659700	6.2214550	-4.5835330	1.2229560

Table 9B.12 – Influence Coefficients for a Longitudinal Semi-Elliptical Surface Crack in a Cylinder – Inside Surface

t/R_i	a/c	a/t	G_i	A_0	A_1	A_2	A_3	A_4	A_5	A_6
2.5 (2.5/1	1.0	0	G_0	1.1977992	-0.5244870	0.1498299	2.3284866	-5.1058499	4.3469049	-1.3487980
			G_1	0.1870117	0.6987352	0.1316900	0.7269255	-2.5259384	2.1756251	-0.6540458
		0.2	G_0	1.0324520	-0.6011830	2.1409980	-4.3582800	5.1817540	-3.3127290	0.8731340
			G_1	0.1482970	0.5516790	1.2065340	-2.4724580	2.2262150	-1.3014010	0.3429840
		0.4	G_0	0.9985330	-0.5009460	2.1528470	-4.7143120	5.7955520	-3.7691560	1.0018110
			G_1	0.1488520	0.5106190	1.4584000	-3.0791030	2.9934080	-1.8019410	0.4749910
		0.6	G_0	1.0283220	-0.5169180	2.5383180	-5.7194220	7.1197050	-4.6641000	1.2417340
			G_1	0.1672010	0.4548210	1.7769250	-3.7792450	3.8544920	-2.3636660	0.6223050
		0.8	G_0	1.0942320	-0.5734050	3.4627400	-8.3267940	11.181782	-7.7328270	2.0956640
			G_1	0.1964770	0.3930970	2.3262100	-5.2012090	6.0026440	-3.9158460	1.0209590
2.5 (2.5/1)	2.0	0	G_0	0.8150546	-0.5623828	1.4465771	-4.6778133	8.4192164	-7.9025932	2.9866351
			G_1	0.1359146	0.0702340	3.5558581	-11.034445	16.967724	-14.126991	4.8706612
		0.2	G_0	0.7235680	-0.3127910	0.7840260	-2.0135440	2.1196690	-1.2881260	0.4617800
			G_1	0.0869170	0.5297760	0.6646520	-1.3566290	0.0355360	0.4852910	-0.0562090
		0.4	G_0	0.6801800	-0.1205960	0.4512540	-1.7698230	2.1434450	-1.4444650	0.5334980
			G_1	0.0810280	0.5320490	0.7700200	-1.7157760	0.5709570	0.0838880	0.0656720
		0.6	G_0	0.6682310	0.0054120	0.2033270	-1.4979710	1.9340030	-1.3319730	0.5051330
			G_1	0.0828040	0.5322990	0.8409160	-1.9152980	0.8038990	-0.0415310	0.0910030
		0.8	G_0	0.6746930	0.1266240	-0.0197870	-1.1652000	1.5729670	-1.1228530	0.4595140
			G_1	0.0887950	0.5480630	0.8831460	-2.0134080	0.9144120	-0.1069010	0.1040950
3.0 (3/1)	0.03125	0	G_0	0.1965046	2.9373464	-5.2582823	7.4889153	-6.9282667	3.3673349	-0.6677966
			G_1	0.0051780	0.1750280	2.7718680	-4.6457154	4.6780502	-3.2768090	0.9840994
		0.2	G_0	0.1854720	3.1105750	-8.8496190	19.310922	-24.898660	16.584729	-4.4532430
			G_1	0.0023170	0.2565300	2.0035860	-2.8882020	2.4603570	-1.7734860	0.5728710
		0.4	G_0	0.1909890	2.8041450	-7.7077130	17.979984	-24.578623	17.136021	-4.7948540
			G_1	0.0023710	0.2501920	1.8555810	-2.2184290	1.5150870	-1.1497460	0.3977250
		0.6	G_0	0.1932080	2.5383350	-5.8636290	13.087555	-16.958770	11.219450	-3.0666460
			G_1	0.0030890	0.2154910	2.0628360	-2.8470170	2.9732190	-2.4936190	0.7956080
		0.8	G_0	0.1935850	2.3360280	-4.0937180	7.9891660	-8.5296840	5.4357610	-1.8824050
			G_1	0.0045950	0.1542060	2.5544420	-4.4552010	5.8425860	-4.0949640	0.8588740
3.0 (3/1)	0.0625	0	G_0	0.2695332	2.1626001	-1.6551569	-1.2970208	4.5604304	-4.3163876	1.4010655
			G_1	0.0138667	0.1827458	2.5749608	-3.9044679	3.3556301	-2.1772209	0.6420134
		0.2	G_0	0.2472080	2.3905840	-4.9720610	8.3131070	-8.5268420	4.5002890	-0.9630730
			G_1	0.0110500	0.2453640	2.0360710	-3.0905990	2.8209630	-2.0179010	0.6278520
		0.4	G_0	0.2444330	2.2692400	-5.3946280	12.229002	-16.259335	10.822826	-2.8780790
			G_1	0.0099230	0.2509500	1.7765420	-2.1314410	1.6661040	-1.4397410	0.5221360
		0.6	G_0	0.2461280	2.0171870	-4.0110990	9.8729470	-13.914381	9.6618450	-2.7195070
			G_1	0.0097540	0.2287220	1.8217010	-2.0750740	1.9057040	-1.8048230	0.6257150
		0.8	G_0	0.2500930	1.7048220	-1.5641610	3.1415470	-3.6376450	2.9132180	-1.3557900
			G_1	0.0110900	0.1623440	2.3155670	-3.5860040	4.5240250	-3.1771650	0.6166940
3.0 (3/1)	0.125	0	G_0	0.4065238	0.7772483	3.8861644	-12.573943	16.760207	-11.014593	2.8706957
			G_1	0.0320270	0.1825342	2.2670449	-2.7076615	1.2088194	-0.3777430	0.0763155
		0.2	G_0	0.3627760	1.2255990	0.4957430	-5.2979490	9.5358830	-7.6394900	2.2937040
			G_1	0.0305720	0.2267660	1.9614760	-2.7921620	2.2151040	-1.4530790	0.4392390
		0.4	G_0	0.3540930	1.1589380	0.1775370	-3.1438440	6.4335240	-5.8778180	1.9344810
			G_1	0.0297610	0.2047140	1.9618870	-2.7988180	2.7360770	-2.1959850	0.7182120
		0.6	G_0	0.3496870	1.0422170	0.5205160	-2.4367920	4.8495510	-4.8427930	1.6795990
			G_1	0.0283480	0.1789660	2.0651280	-3.0774180	3.8074460	-3.4185580	1.1320990
		0.8	G_0	0.3551980	0.7796230	2.1412100	-5.6585150	9.0748680	-6.9595630	1.7298200
			G_1	0.0288630	0.1143000	2.5392970	-4.5790770	6.6750060	-5.2472820	1.3408860

Table 9B.12 – Influence Coefficients for a Longitudinal Semi-Elliptical Surface Crack in a Cylinder – Inside Surface

t/R_i	a/c	a/t	G_i	A_0	A_1	A_2	A_3	A_4	A_5	A_6
3.0 (3/1)	0.25	0	G_0	0.6152816	-0.3348694	6.2955620	-15.590618	19.299508	-12.488107	3.3010035
			G_1	0.0703566	0.2828152	1.4036169	-0.6511596	-1.2076596	1.0318656	-0.2423741
		0.2	G_0	0.5417740	-0.1021300	4.8807270	-13.221563	17.307959	-11.534801	3.0788490
			G_1	0.0645000	0.1896470	1.8157170	-2.2136400	1.2220480	-0.6530920	0.1997640
		0.4	G_0	0.5407990	-0.1764890	5.1230360	-13.424692	17.906727	-12.321021	3.3681240
			G_1	0.0701190	0.1429580	2.0019610	-2.6347540	2.0256560	-1.3802250	0.4262490
		0.6	G_0	0.5435050	-0.3316870	6.1046260	-15.750533	22.170554	-16.192318	4.6147910
			G_1	0.0718770	0.0837320	2.4013610	-3.8378080	4.4333730	-3.5072330	1.0717420
		0.8	G_0	0.5518140	-0.5393400	7.6581660	-19.972357	30.027081	-22.600886	6.3422920
			G_1	0.0735830	-0.0038460	3.1505930	-6.4081740	9.4024610	-7.3348060	1.9945030
3.0 (3/1)	0.5	0	G_0	0.8776607	-0.6729719	3.7721411	-6.5209060	6.3377934	-3.7028038	0.9872447
			G_1	0.1277541	0.4368502	0.4904522	1.0427434	-2.9631236	2.0826525	-0.5184313
		0.2	G_0	0.7493980	-0.6049330	3.8363260	-7.2925120	7.4313460	-4.1617390	0.9829080
			G_1	0.1029950	0.3229850	1.0478160	-0.6021740	-0.5855690	0.4172360	-0.0592530
		0.4	G_0	0.7513190	-0.6489120	4.1589930	-7.9202630	8.2277190	-4.7407140	1.1482170
			G_1	0.1134020	0.2607050	1.3026980	-1.0921650	0.0041630	0.0224460	0.0470640
		0.6	G_0	0.7816080	-0.7883740	5.1504150	-10.281252	11.790030	-7.4946860	1.9418320
			G_1	0.1295950	0.1758030	1.7998740	-2.2715600	1.7648080	-1.3022880	0.4152620
		0.8	G_0	0.8198030	-0.9619470	6.7048190	-14.603432	19.342110	-13.496749	3.5780390
			G_1	0.1472140	0.0544190	2.7532190	-5.0635130	6.4753390	-4.8012110	1.2865000
3.03.0 (3/1)	1.0	0	G_0	1.1977992	-0.5244870	0.1498299	2.3284866	-5.1058499	4.3469049	-1.3487980
			G_1	0.1870117	0.6987352	0.1316900	0.7269255	-2.5259384	2.1756251	-0.6540458
		0.2	G_0	1.0110600	-0.5558260	2.0945530	-4.3703350	5.2595950	-3.3847750	0.8952520
			G_1	0.1438240	0.5499280	1.2461170	-2.5859840	2.3804840	-1.4059820	0.3711750
		0.4	G_0	0.9716380	-0.4161580	1.9946130	-4.5289880	5.6538180	-3.7043420	0.9882270
			G_1	0.1435600	0.5145380	1.4861820	-3.1715230	3.1156690	-1.8800760	0.4949140
		0.6	G_0	0.9940750	-0.3824220	2.2293970	-5.2628860	6.6847350	-4.4228100	1.1828120
			G_1	0.1600490	0.4704520	1.7760170	-3.8255350	3.9226390	-2.4030370	0.6304980
		0.8	G_0	1.0496590	-0.3764990	2.9762360	-7.6040690	10.556149	-7.4320140	2.0299150
			G_1	0.1867120	0.4203210	2.3201450	-5.3058310	6.2080690	-4.0696470	1.0619810
3.0 (3/1)	2.0	0	G_0	0.8150546	-0.5623828	1.4465771	-4.6778133	8.4192164	-7.9025932	2.9866351
			G_1	0.1359146	0.0702340	3.5558581	-11.034445	16.967724	-14.126991	4.8706612
		0.2	G_0	0.7097660	-0.2651210	0.7141560	-1.9852530	2.1663010	-1.3523100	0.4854380
			G_1	0.0843020	0.5316670	0.6893550	-1.4446360	0.1684940	0.3855920	-0.0262520
		0.4	G_0	0.6630670	-0.0402430	0.2640300	-1.5141860	1.9365280	-1.3580590	0.5206620
			G_1	0.0780510	0.5384510	0.7797250	-1.7766660	0.6735050	0.0018470	0.0918760
		0.6	G_0	0.6498460	0.1072450	-0.0717320	-1.0600560	1.5098780	-1.1049810	0.4544390
			G_1	0.0797530	0.5421560	0.8388350	-1.9540010	0.8734420	-0.0940330	0.1068140
		0.8	G_0	0.6553890	0.2462780	-0.3627700	-0.5896640	0.9831970	-0.7818990	0.3750160
			G_1	0.0858250	0.5595750	0.8821940	-2.0645260	0.9934440	-0.1515770	0.1125270

Notes:

1. Interpolation of the influence coefficients, G_i, may be used for intermediate values of t/R_i, a/c, and a/t.
2. The value of the influence coefficients at the surface point of the crack defined by $\varphi = 0°$ are equal to: $G_i = A_0$.
3. The value of the influence coefficients at the deepest point of the crack defined by $\varphi = 90°$ are equal to $G_i = \sum_{n=0}^{6} A_n$.

Table 9B.13 – Influence Coefficients for a Longitudinal Semi-Elliptical Surface Crack in a Cylinder – Outside Surface

t/R_i	a/c	a/t	G_i	A_0	A_1	A_2	A_3	A_4	A_5	A_6
0.0	0.03125	0	G_0	0.1965046	2.9373464	-5.2582823	7.4889153	-6.9282667	3.3673349	-0.6677966
			G_1	0.0051780	0.1750280	2.7718680	-4.6457154	4.6780502	-3.2768090	0.9840994
		0.2	G_0	0.2080760	3.0112422	-5.1048701	7.6348715	-6.8347547	2.7940766	-0.3882688
			G_1	0.0084834	0.2406767	2.4574292	-3.6452421	3.6142837	-2.8451814	0.9270638
		0.4	G_0	0.2357940	3.0822400	-3.5792100	3.9476890	1.9131590	-6.8872200	3.1896800
			G_1	0.0145140	0.4038000	1.6422700	-0.3906100	-0.6480700	-0.2940300	0.2514900
		0.6	G_0	0.2902240	3.6892050	-4.5739100	11.709890	-6.3750000	-5.8894100	4.2452400
			G_1	0.0208890	0.7016780	0.1631840	5.7072160	-8.2075800	3.4561120	-0.4454700
		0.8	G_0	0.5163550	2.5310830	14.712900	-43.621800	101.06570	-116.08100	46.190900
			G_1	0.0825460	0.4971770	4.6064810	-7.3326700	21.148620	-29.345100	12.491400
0.0	0.0625	0	G_0	0.2695332	2.1626001	-1.6551569	-1.2970208	4.5604304	-4.3163876	1.4010655
			G_1	0.0138667	0.1827458	2.5749608	-3.9044679	3.3556301	-2.1772209	0.6420134
		0.2	G_0	0.2845892	2.2264055	-1.4546190	-1.5760719	5.1131083	-4.9485443	1.6207574
			G_1	0.0199077	0.2210874	2.4642047	-3.5898625	3.1624039	-2.2403780	0.6965751
		0.4	G_0	0.3261480	2.5200870	-1.8847000	2.1798740	-1.4597100	-0.1886500	0.2393400
			G_1	0.0294120	0.3699370	1.9220850	-1.2071500	-0.4394000	0.2737550	-0.0395200
		0.6	G_0	0.4166330	3.1566470	-2.6248900	7.7325910	-9.6927800	3.6428700	-0.0892000
			G_1	0.0598460	0.4340740	2.6811560	-3.1936600	4.0753720	-4.6940200	1.8285500
		0.8	G_0	0.6540140	3.4231920	3.8158050	-4.1586900	3.4715330	-10.310400	6.6280000
			G_1	0.1214780	0.6975490	2.9718330	-1.3036500	-0.0754900	-3.0465100	2.1670000
0.0	0.125	0	G_0	0.4065238	0.7772483	3.8861644	-12.573943	16.760207	-11.014593	2.8706957
			G_1	0.0320270	0.1825342	2.2670449	-2.7076615	1.2088194	-0.3777430	0.0763155
		0.2	G_0	0.4242116	1.0089302	3.2973815	-12.159726	17.873386	-12.868668	3.6281712
			G_1	0.0429859	0.2033811	2.2563818	-2.8752160	1.8152558	-1.0512327	0.3181077
		0.4	G_0	0.4917770	1.6592320	-0.1080400	0.1793240	-2.7076100	3.3680620	-1.3489700
			G_1	0.0634270	0.3722500	1.6231670	-0.5306500	-2.0007400	1.8943780	-0.5880300
		0.6	G_0	0.6591820	1.8759140	1.0212600	-1.7698000	-0.5653600	1.2479960	-0.4376600
			G_1	0.1116040	0.4714500	1.7940590	-0.7557600	-1.4901700	1.0852180	-0.2113700
		0.8	G_0	0.9809330	1.8846320	4.8020780	-8.0580200	0.4447850	3.4772660	-1.0567500
			G_1	0.2039950	0.4800150	2.8822430	-2.5890100	-0.9683000	1.5372370	-0.3750200
0.0	0.25	0	G_0	0.6152816	-0.3348694	6.2955620	-15.590618	19.299508	-12.488107	3.3010035
			G_1	0.0703566	0.2828152	1.4036169	-0.6511596	-1.2076596	1.0318656	-0.2423741
		0.2	G_0	0.6385889	-0.3095132	6.5329787	-16.622882	21.056641	-13.850120	3.6988146
			G_1	0.0840059	0.1999367	1.8218113	-1.7756899	0.3757186	-0.0785358	0.0643386
		0.4	G_0	0.7390420	0.0548160	4.0842620	-7.5883100	5.4047530	-1.0146100	-0.3483400
			G_1	0.1164500	0.2479880	1.8282520	-1.7169900	0.1912120	0.1165770	-0.0186100
		0.6	G_0	0.9461210	-0.1858800	5.5867460	-9.8634900	5.9596870	0.1296440	-1.0026100
			G_1	0.1778050	0.2056680	2.0979210	-1.8039500	-0.5558700	1.1461400	-0.4206600
		0.8	G_0	1.2452110	-0.6921900	8.3260620	-14.948000	8.6936910	0.4755790	-1.3926600
			G_1	0.2585640	0.1548890	2.1170240	-0.4910000	-4.6146100	5.4550750	-1.9663300
0.0	0.5	0	G_0	0.8776607	-0.6729719	3.7721411	-6.5209060	6.3377934	-3.7028038	0.9872447
			G_1	0.1277541	0.4368502	0.4904522	1.0427434	-2.9631236	2.0826525	-0.5184313
		0.2	G_0	0.9003948	-0.8850488	5.2743239	-11.267523	13.890755	-9.6373584	2.8183906
			G_1	0.1404409	0.3215397	1.1010666	-1.0257556	0.6943940	-1.0793186	0.5410929
		0.4	G_0	1.0058060	-0.7322600	2.9951940	-1.9459200	-3.2613500	5.1424570	-2.0306200
			G_1	0.1740870	0.3051630	1.2070310	-0.6720500	-1.0651300	1.1445590	-0.3644800
		0.6	G_0	1.1826010	-1.1072500	3.9623640	-2.7781300	-4.3097300	7.2772750	-2.9648200
			G_1	0.2277120	0.1701170	1.5499470	-1.1051200	-0.8333700	1.1717060	-0.4194500
		0.8	G_0	1.3833380	-1.3900300	4.3755780	-3.7372600	-2.5403200	5.3036000	-2.0932400
			G_1	0.2820110	0.0839230	1.7258580	-1.5358100	-0.0635600	0.5006780	-0.1982200

Table 9B.13 – Influence Coefficients for a Longitudinal Semi-Elliptical Surface Crack in a Cylinder – Outside Surface

t/R_i	a/c	a/t	G_i	A_0	A_1	A_2	A_3	A_4	A_5	A_6
0.0	1.0	0	G_0	1.1977992	-0.5244870	0.1498299	2.3284866	-5.1058499	4.3469049	-1.3487980
			G_1	0.1870117	0.6987352	0.1316900	0.7269255	-2.5259384	2.1756251	-0.6540458
		0.2	G_0	1.2263282	-1.1608467	4.4744783	-11.584231	17.811241	-14.408250	4.6998279
			G_1	0.2154786	0.2441623	2.8107820	-7.6574580	11.171413	-9.0053693	2.9542871
		0.4	G_0	1.2989480	-0.9978000	1.9479540	-1.3002700	-1.4940100	2.8306230	-1.2126000
			G_1	0.2386246	0.1447774	3.3198992	-9.2456599	13.823512	-11.223715	3.6868232
		0.6	G_0	1.3971180	-1.1348400	1.7918740	-0.4202600	-2.8679300	3.7685480	-1.4405000
			G_1	0.2445870	0.5326670	0.5939690	-0.0361800	-2.0163100	2.2167010	-0.7782200
		0.8	G_0	1.5117010	-1.3244800	1.7568350	-0.1337900	-2.8629300	3.2953270	-1.1412400
			G_1	0.2704470	0.5113280	0.5357440	-0.0327300	-1.5570200	1.5570970	-0.5094600
0.0	2.0	0	G_0	0.8150546	-0.5623828	1.4465771	-4.6778133	8.4192164	-7.9025932	2.9866351
			G_1	0.1359146	0.0702340	3.5558581	-11.034445	16.967724	-14.126991	4.8706612
		0.2	G_0	0.8463715	-1.0011024	4.0052312	-11.937181	19.189548	-16.039296	5.4674371
			G_1	0.1395121	0.0753999	3.1895604	-9.5540932	14.214316	-11.649525	4.0073308
		0.4	G_0	0.8570045	-1.0183085	3.9957306	-11.886878	19.152747	-16.047480	5.4801806
			G_1	0.1436696	0.0544018	3.2816127	-9.8164232	14.610963	-11.942138	4.0907797
		0.6	G_0	0.8839861	-1.0765270	4.0774087	-11.976171	19.173189	-15.996207	5.4501217
			G_1	0.1504185	0.0478401	3.2579960	-9.6921199	14.370843	-11.736129	4.0258411
		0.8	G_0	0.9033134	-0.9619755	2.8501500	-7.6366897	11.596116	-9.4828625	3.2550163
			G_1	0.1458559	0.2313881	1.9882138	-5.5546045	7.4196069	-5.8965053	2.0855563
0.01 (1/100)	0.03125	0	G_0	0.1965046	2.9373464	-5.2582823	7.4889153	-6.9282667	3.3673349	-0.6677966
			G_1	0.0051780	0.1750280	2.7718680	-4.6457154	4.6780502	-3.2768090	0.9840994
		0.2	G_0	0.2138782	2.4750252	-1.2287668	-4.0075659	10.335171	-9.5704005	3.0927956
			G_1	0.0075736	0.2344660	2.4810298	-3.7389842	3.7733192	-2.9707472	0.9655728
		0.4	G_0	0.2324070	3.0534560	-3.4791800	3.6288040	2.8534420	-7.8640400	3.5080100
			G_1	0.0090690	0.3929290	1.6585750	-0.4195300	-0.4687700	-0.4895200	0.3051300
		0.6	G_0	0.2702790	3.6742680	-5.4506000	14.673720	-9.6138800	-3.5469800	3.2402500
			G_1	0.0135480	0.6966430	-0.1423800	6.5888590	-8.9248900	3.9512840	-0.7275400
		0.8	G_0	0.4201630	3.2227600	6.0926870	-21.407000	81.165870	-105.68400	42.304800
			G_1	0.0451780	0.8660820	0.6788660	3.1439070	9.8824090	-22.058800	9.8817900
0.01	0.0625	0	G_0	0.2695332	2.1626001	-1.6551569	-1.2970208	4.5604304	-4.3163876	1.4010655
			G_1	0.0138667	0.1827458	2.5749608	-3.9044679	3.3556301	-2.1772209	0.6420134
		0.2	G_0	0.3009539	1.7912734	0.8670775	-6.9946825	11.455578	-8.5937165	2.4360990
			G_1	0.0194819	0.2065054	2.6293195	-4.3818393	4.7973348	-3.7470555	1.2084547
		0.4	G_0	0.3280520	2.5901900	-2.1894200	2.3456720	-0.3205300	-1.9618200	0.9696200
			G_1	0.0260390	0.4612930	1.2629800	0.8720110	-3.5821100	2.6029280	-0.7233600
		0.6	G_0	0.4103170	3.4373160	-4.7250300	14.025440	-17.047300	7.4350500	-0.8385600
			G_1	0.0550830	0.5361340	1.8981060	-0.6893400	0.8014830	-2.6604000	1.3066300
		0.8	G_0	0.6491600	3.5962240	2.0970240	2.6131640	0.5247410	-14.913300	9.6012600
			G_1	0.1176190	0.7527130	2.4225760	0.9070930	-1.0257200	-4.5224300	3.1016800
0.01	0.125	0	G_0	0.4065238	0.7772483	3.8861644	-12.573943	16.760207	-11.014593	2.8706957
			G_1	0.0320270	0.1825342	2.2670449	-2.7076615	1.2088194	-0.3777430	0.0763155
		0.2	G_0	0.4148168	1.1474441	1.7284441	-6.1319982	7.6187598	-4.7707753	1.1968314
			G_1	0.0483704	0.0169824	3.9147652	-9.0442049	12.537266	-9.7790670	3.0128034
		0.4	G_0	0.4972990	1.5382660	0.9543690	-3.4496900	3.4687010	-1.6986900	0.2430300
			G_1	0.0629740	0.3821060	1.5827310	-0.3922800	-2.1832500	2.0019660	-0.6135000
		0.6	G_0	0.6613540	1.9086020	0.9832580	-1.2632200	-1.3863400	1.7681160	-0.5715500
			G_1	0.1127330	0.4681870	1.8754590	-0.8796100	-1.2883700	0.8847250	-0.1438600
		0.8	G_0	0.9969100	1.9634260	4.8633420	-6.9046400	-1.5148200	4.2963280	-1.0385500
			G_1	0.2105360	0.4661310	3.2282240	-3.3926400	0.4841570	0.0394490	0.1974500

Table 9B.13 – Influence Coefficients for a Longitudinal Semi-Elliptical Surface Crack in a Cylinder – Outside Surface

t/R_i	a/c	a/t	G_i	A_0	A_1	A_2	A_3	A_4	A_5	A_6
0.01 (1/100)	0.25	0	G_0	0.6152816	-0.3348694	6.2955620	-15.590618	19.299508	-12.488107	3.3010035
			G_1	0.0703566	0.2828152	1.4036169	-0.6511596	-1.2076596	1.0318656	-0.2423741
		0.2	G_0	0.6260510	-0.2265274	6.9684962	-19.857860	27.709243	-19.572353	5.4946193
			G_1	0.0907270	0.1716775	2.5085021	-4.9758660	6.1431857	-4.7142903	1.4602442
		0.4	G_0	0.7427500	0.0470470	4.2013450	-7.9240300	5.9197900	-1.4176300	-0.2253900
			G_1	0.1183660	0.2202920	2.0681150	-2.5351300	1.5892970	-1.0403300	0.3487600
		0.6	G_0	0.9567890	-0.1725500	5.6362060	-9.8580500	5.8066120	0.2958180	-1.0611700
			G_1	0.1805700	0.2226460	2.0172020	-1.4629900	-1.1806500	1.6683430	-0.5867200
		0.8	G_0	1.3100100	-1.4349000	14.376600	-35.168100	42.221560	-26.611500	7.0832000
			G_1	0.2658870	0.2474310	1.4942640	1.7915740	-8.5849000	8.6773360	-2.9576800
0.01 (1/100)	0.5	0	G_0	0.8776607	-0.6729719	3.7721411	-6.5209060	6.3377934	-3.7028038	0.9872447
			G_1	0.1277541	0.4368502	0.4904522	1.0427434	-2.9631236	2.0826525	-0.5184313
		0.2	G_0	0.9074272	-1.0994201	6.7673813	-15.863097	20.705328	-14.454389	4.1256769
			G_1	0.1495038	0.1587994	2.2591841	-4.5394919	5.7148362	-4.4982384	1.4410683
		0.4	G_0	1.0125390	-0.7568900	3.1311310	-2.2752700	-2.8387900	4.8667220	-1.9590900
			G_1	0.1753200	0.3073370	1.1980380	-0.6340400	-1.1325100	1.1968380	-0.3793700
		0.6	G_0	1.1956150	-1.1378000	4.1718440	-3.3722900	-3.4456700	6.6512090	-2.7867200
			G_1	0.2292050	0.2061920	1.3306330	-0.4513200	-1.8161600	1.8921330	-0.6245200
		0.8	G_0	1.4139890	-1.4985700	5.0657640	-5.7703800	0.4973700	3.0329120	-1.4197400
			G_1	0.2896610	0.0882030	1.6827580	-1.3490500	-0.4354500	0.8253610	-0.3010300
0.01 (1/100)	1.0	0	G_0	1.1977992	-0.5244870	0.1498299	2.3284866	-5.1058499	4.3469049	-1.3487980
			G_1	0.1870117	0.6987352	0.1316900	0.7269255	-2.5259384	2.1756251	-0.6540458
		0.2	G_0	1.2219944	-1.2333687	5.0312977	-13.549512	21.104009	-16.993209	5.4694705
			G_1	0.2150830	0.1957502	3.1572284	-8.8200177	13.041658	-10.425024	3.3649964
		0.4	G_0	1.3069770	-1.0234600	2.0351750	-1.4790500	-1.2970400	2.7226080	-1.1890400
			G_1	0.2182770	0.5583990	0.7123630	-0.4628400	-1.4273700	1.8443680	-0.6917100
		0.6	G_0	1.4118930	-1.2128500	2.1731690	-1.4236900	-1.4877900	2.8257990	-1.1874200
			G_1	0.2486310	0.5073370	0.7680320	-0.6344600	-0.9874100	1.3617270	-0.5050000
		0.8	G_0	1.5327350	-1.4057100	2.1493270	-1.2998000	-1.0510400	1.8996060	-0.7187000
			G_1	0.2759430	0.4993180	0.5707200	-0.0960600	-1.5281700	1.5841410	-0.5294400
0.01 (1/100)	2.0	0	G_0	0.8150546	-0.5623828	1.4465771	-4.6778133	8.4192164	-7.9025932	2.9866351
			G_1	0.1359146	0.0702340	3.5558581	-11.034445	16.967724	-14.126991	4.8706612
		0.2	G_0	0.8182987	-0.9750326	4.0974302	-12.658801	20.765368	-17.441363	5.9109102
			G_1	0.1330319	0.0540205	3.3490248	-10.173407	15.321858	-12.541021	4.2720166
		0.4	G_0	0.8343927	-0.3351370	-0.7134755	3.3094161	-6.0713158	4.8139372	-1.3245293
			G_1	0.1361217	0.0308624	3.4638886	-10.533385	15.878401	-12.946378	4.3843584
		0.6	G_0	0.8600665	-0.3540640	-0.9003047	4.0339274	-7.2855701	5.7801566	-1.6177453
			G_1	0.1467987	0.0215030	3.4602749	-10.477254	15.776469	-12.882015	4.3737291
		0.8	G_0	0.9172330	-1.0076975	3.0568469	-8.2482710	12.624440	-10.377963	3.5671701
			G_1	0.1497781	0.0258058	3.3588241	-10.008896	14.518295	-11.284278	3.6504092
0.01667 (1/60)	0.03125	0	G_0	0.1965046	2.9373464	-5.2582823	7.4889153	-6.9282667	3.3673349	-0.6677966
			G_1	0.0051780	0.1750280	2.7718680	-4.6457154	4.6780502	-3.2768090	0.9840994
		0.2	G_0	0.2137018	2.4716292	-1.1955278	-4.1279147	10.564513	-9.7724089	3.1582282
			G_1	0.0074964	0.2331584	2.4891031	-3.7654612	3.8313393	-3.0295323	0.9870984
		0.4	G_0	0.2306780	3.0388050	-3.4728800	3.6385670	2.9071580	-7.9264700	3.5188400
			G_1	0.0109380	0.4020170	1.5438030	-0.0383700	-1.0428800	-0.0524400	0.1690900
		0.6	G_0	0.2647120	3.6557700	-5.5472500	14.585300	-8.9129600	-4.1661800	3.3668200
			G_1	0.0186290	0.6598410	0.0944350	5.5205580	-6.8688900	2.3000600	-0.2605800
		0.8	G_0	0.3916070	3.5824480	2.4629600	-10.937900	63.878550	-89.418500	36.130200
			G_1	0.0377860	0.9314520	-0.0349700	4.7321390	7.3105530	-18.985500	8.4478500

Table 9B.13 – Influence Coefficients for a Longitudinal Semi-Elliptical Surface Crack in a Cylinder – Outside Surface

t/R_i	a/c	a/t	G_i	A_0	A_1	A_2	A_3	A_4	A_5	A_6
0.01667 (1/60)	0.0625	0	G_0	0.2695332	2.1626001	-1.6551569	-1.2970208	4.5604304	-4.3163876	1.4010655
			G_1	0.0138667	0.1827458	2.5749608	-3.9044679	3.3556301	-2.1772209	0.6420134
		0.2	G_0	0.2852680	2.0769228	-0.9978735	-1.2931167	2.6484224	-1.9164331	0.4609809
			G_1	0.0189931	0.2154011	2.5632146	-4.1568147	4.4288027	-3.4553431	1.1186828
		0.4	G_0	0.3281130	2.3901810	-0.8095800	-1.4210300	4.8415630	-5.4354900	1.8791800
			G_1	0.0292320	0.3424400	2.1206150	-1.8136200	0.6498240	-0.6508300	0.2469300
		0.6	G_0	0.3983790	3.2298950	-3.5609200	11.585980	-14.538900	6.4780230	-0.8574500
			G_1	0.0533250	0.4541290	2.3964770	-2.0990900	2.9773820	-4.2600100	1.7406100
		0.8	G_0	0.6074810	3.5000360	1.9324190	4.0078860	-0.6767400	-14.170400	9.1300900
			G_1	0.1057170	0.7235000	2.3194730	1.3286790	-0.9833400	-4.8384300	3.1575700
0.01667 (1/60)	0.125	0	G_0	0.4065238	0.7772483	3.8861644	-12.573943	16.760207	-11.014593	2.8706957
			G_1	0.0320270	0.1825342	2.2670449	-2.7076615	1.2088194	-0.3777430	0.0763155
		0.2	G_0	0.4148376	1.1488796	1.7244494	-6.1093380	7.5825708	-4.7472976	1.1912448
			G_1	0.0483941	0.0166081	3.9196323	-9.0609034	12.573746	-9.8159555	3.0261057
		0.4	G_0	0.4991930	1.4929330	1.3181360	-4.6222100	5.4026230	-3.2510100	0.7215900
			G_1	0.0638630	0.3577190	1.7903870	-1.1250500	-0.8936300	0.9146490	-0.2640700
		0.6	G_0	0.6594470	1.9513050	0.7037310	-0.1328800	-3.1790500	3.0881030	-0.9571500
			G_1	0.1123460	0.4769800	1.8180370	-0.6167100	-1.6918000	1.1653880	-0.2229600
		0.8	G_0	0.9986260	2.0025290	4.7810950	-6.0706900	-2.3363000	4.2175710	-0.8170400
			G_1	0.2105640	0.5008290	3.0054380	-2.3954100	-1.0374800	1.0415670	-0.0534200
0.01667 (1/60)	0.25	0	G_0	0.6152816	-0.3348694	6.2955620	-15.590618	19.299508	-12.488107	3.3010035
			G_1	0.0703566	0.2828152	1.4036169	-0.6511596	-1.2076596	1.0318656	-0.2423741
		0.2	G_0	0.6300329	-0.2862567	7.3164619	-20.805174	29.055169	-20.534766	5.7677852
			G_1	0.0901070	0.1840622	2.4321564	-4.7467316	5.7958716	-4.4552013	1.3845027
		0.4	G_0	0.7457850	0.0066950	4.5171440	-8.9481000	7.5885640	-2.7405800	0.1792400
			G_1	0.1182950	0.2324830	1.9682530	-2.1456800	0.8739200	-0.4224000	0.1461600
		0.6	G_0	0.9598760	-0.1312600	5.3719100	-8.8692700	4.1076570	1.6665860	-1.4860300
			G_1	0.1817520	0.2311760	1.9819240	-1.3437900	-1.3528700	1.7795640	-0.6136800
		0.8	G_0	1.3010250	-0.8000000	9.5285520	-18.152100	13.249470	-3.0269200	-0.2860500
			G_1	0.2815970	0.0012600	3.4198490	-4.6353300	2.0735050	0.0924150	-0.2850300
0.01667 (1/60)	0.5	0	G_0	0.8776607	-0.6729719	3.7721411	-6.5209060	6.3377934	-3.7028038	0.9872447
			G_1	0.1277541	0.4368502	0.4904522	1.0427434	-2.9631236	2.0826525	-0.5184313
		0.2	G_0	0.9094180	-1.1229795	6.9181225	-16.309875	21.379833	-14.955815	4.2713814
			G_1	0.1505282	0.1451739	2.3390416	-4.7612919	6.0370436	-4.7336784	1.5092378
		0.4	G_0	1.0137270	-0.7517100	3.1226580	-2.2992700	-2.7311100	4.7379060	-1.9093200
			G_1	0.1760030	0.3062100	1.1968010	-0.5997200	-1.2268900	1.2973610	-0.4173000
		0.6	G_0	1.2008330	-1.1467100	4.2107140	-3.4130300	-3.4601300	6.6981550	-2.8074000
			G_1	0.2308490	0.2030300	1.3593140	-0.5530200	-1.6299900	1.7276510	-0.5695300
		0.8	G_0	1.4228920	-1.4437600	4.6822680	-4.5430000	-1.4261800	4.4784380	-1.8377400
			G_1	0.2948140	0.0607990	1.8702520	-1.9379200	0.5080380	0.0785840	-0.0704500
0.01667 (1/60)	1.0	0	G_0	1.1977992	-0.5244870	0.1498299	2.3284866	-5.1058499	4.3469049	-1.3487980
			G_1	0.1870117	0.6987352	0.1316900	0.7269255	-2.5259384	2.1756251	-0.6540458
		0.2	G_0	1.2229223	-1.2350945	5.0353697	-13.554987	21.107245	-16.993613	5.4693935
			G_1	0.2141793	0.2143843	3.0512609	-8.5440546	12.678058	-10.188549	3.3045727
		0.4	G_0	1.3069170	-0.9903600	1.7866620	-0.6452900	-2.7041200	3.8845890	-1.5614400
			G_1	0.2195930	0.5416490	0.8301860	-0.8579700	-0.7616300	1.3017760	-0.5219100
		0.6	G_0	1.4149780	-1.2145600	2.2099370	-1.6537800	-0.9621000	2.3118750	-1.0052600
			G_1	0.2492340	0.5158650	0.7022660	-0.4092700	-1.3769500	1.6896770	-0.6113900
		0.8	G_0	1.5405510	-1.4286100	2.2553870	-1.5994600	-0.6101900	1.5774700	-0.6256600
			G_1	0.2788740	0.4847010	0.6491960	-0.3234800	-1.1852500	1.3257010	-0.4524700

Table 9B.13 – Influence Coefficients for a Longitudinal Semi-Elliptical Surface Crack in a Cylinder – Outside Surface

t/R_i	a/c	a/t	G_i	A_0	A_1	A_2	A_3	A_4	A_5	A_6
0.01667 (1/60)	2.0	0	G_0	0.8150546	-0.5623828	1.4465771	-4.6778133	8.4192164	-7.9025932	2.9866351
			G_1	0.1359146	0.0702340	3.5558581	-11.034445	16.967724	-14.126991	4.8706612
		0.2	G_0	0.8182509	-0.9683874	4.0481966	-12.506099	20.531123	-17.266667	5.8604688
			G_1	0.1334825	0.0474146	3.3890896	-10.287120	15.485607	-12.657711	4.3047611
		0.4	G_0	0.8362279	-0.3571232	-0.5678228	2.8372219	-5.3004184	4.2029047	-1.1376264
			G_1	0.1356418	0.0411710	3.4054647	-10.380241	15.670811	-12.805065	4.3460700
		0.6	G_0	0.8628933	-0.3858659	-0.6981090	3.3951106	-6.2590966	4.9745741	-1.3727913
			G_1	0.1469324	0.0235743	3.4453527	-10.434511	15.714005	-12.835899	4.3600722
		0.8	G_0	0.9191929	-1.0122491	3.0710619	-8.2917080	12.689191	-10.419864	3.5764034
			G_1	0.1506695	0.0175076	3.4048063	-10.143058	14.721138	-11.435621	3.6945046
0.05 (1/20)	0.03125	0	G_0	0.1965046	2.9373464	-5.2582823	7.4889153	-6.9282667	3.3673349	-0.6677966
			G_1	0.0051780	0.1750280	2.7718680	-4.6457154	4.6780502	-3.2768090	0.9840994
		0.2	G_0	0.2126857	2.4579374	-1.1427912	-4.2121606	10.672531	-9.8506499	3.1779116
			G_1	0.0070880	0.2281639	2.4965869	-3.7556676	3.8111506	-3.0085539	0.9759280
		0.4	G_0	0.2274500	2.9794860	-3.2917300	3.1593030	3.6533720	-8.4864000	3.6768600
			G_1	0.0070090	0.3783660	1.6174000	-0.2661400	-0.6795200	-0.2841700	0.2120000
		0.6	G_0	0.2533640	3.6313610	-6.2242000	17.316250	-14.595100	1.3727100	1.3897900
			G_1	0.0073650	0.7111170	-0.6229600	8.0627590	-11.551800	6.5540000	-1.7339300
		0.8	G_0	0.3498690	3.6190920	0.1968900	-4.0412300	46.267320	-68.423400	27.621900
			G_1	0.0273550	0.8977570	-0.3675800	5.5541200	3.4269510	-12.911100	5.6559800
0.05 (1/20)	0.0625	0	G_0	0.2695332	2.1626001	-1.6551569	-1.2970208	4.5604304	-4.3163876	1.4010655
			G_1	0.0138667	0.1827458	2.5749608	-3.9044679	3.3556301	-2.1772209	0.6420134
		0.2	G_0	0.2848454	2.0654031	-0.9077591	-1.5276620	3.0161277	-2.2090336	0.5488481
			G_1	0.0187192	0.2128839	2.5716802	-4.1560222	4.4282009	-3.4585236	1.1185246
		0.4	G_0	0.3212960	2.3448030	-0.7426900	-1.4194200	5.0119970	-5.6810200	1.9536500
			G_1	0.0260960	0.3422190	2.0005180	-1.3336400	-0.0578300	-0.1230500	0.0775000
		0.6	G_0	0.3733960	3.1033220	-3.5889700	11.529910	-12.947400	4.6508610	-0.3427200
			G_1	0.0456010	0.3836560	2.5608530	-2.7553700	4.6129230	-5.6717900	2.1083700
		0.8	G_0	0.5226140	3.4234390	-0.6548100	9.7485540	-3.2235900	-13.877600	8.5410000
			G_1	0.0769380	0.7188470	1.2769760	3.5804480	-2.1787000	-4.2928600	2.6987400
0.05 (1/20)	0.125	0	G_0	0.4065238	0.7772483	3.8861644	-12.573943	16.760207	-11.014593	2.8706957
			G_1	0.0320270	0.1825342	2.2670449	-2.7076615	1.2088194	-0.3777430	0.0763155
		0.2	G_0	0.4152094	1.1478676	1.7621671	-6.1869855	7.6894963	-4.8377705	1.2221148
			G_1	0.0483124	0.0191548	3.9027693	-8.9811618	12.436651	-9.7095804	2.9940655
		0.4	G_0	0.4926390	1.5721320	0.6544250	-2.0393900	0.9779030	0.3354330	-0.4067600
			G_1	0.0627280	0.3528700	1.7990370	-1.0437500	-1.0428300	1.0290420	-0.3034100
		0.6	G_0	0.6429920	1.9132270	0.8599370	-0.1649600	-2.3392000	1.7431370	-0.4243800
			G_1	0.1057820	0.4826430	1.7091680	-0.0792900	-2.2797500	1.3984440	-0.2595000
		0.8	G_0	0.9533570	1.8590510	5.3300090	-6.3155200	0.9677320	-0.9493900	1.2538800
			G_1	0.1952550	0.4649740	3.0762920	-2.1340900	-0.3677000	-0.4107900	0.5626800
0.05 (1/20)	0.25	0	G_0	0.6152816	-0.3348694	6.2955620	-15.590618	19.299508	-12.488107	3.3010035
			G_1	0.0703566	0.2828152	1.4036169	-0.6511596	-1.2076596	1.0318656	-0.2423741
		0.2	G_0	0.6316981	-0.2961952	7.4180799	-21.116428	29.573759	-20.968968	5.9077913
			G_1	0.0906535	0.1788838	2.4733841	-4.8681054	5.9984214	-4.6244285	1.4384031
		0.4	G_0	0.7461440	0.0677980	4.1232100	-7.5000100	5.1211920	-0.7514200	-0.4390900
			G_1	0.1175070	0.2670220	1.7514510	-1.4364300	-0.2320500	0.4060910	-0.0954800
		0.6	G_0	0.9707830	-0.1536000	5.7123690	-9.6038400	5.1974000	0.7373360	-1.1792900
			G_1	0.1855560	0.2214630	2.0970730	-1.5522700	-1.0883500	1.5718930	-0.5495800
		0.8	G_0	1.3366720	-0.8115500	10.008990	-18.432900	13.074520	-2.9741300	-0.2298200
			G_1	0.2982610	-0.1094100	4.3991850	-7.5259600	6.7389080	-3.7449200	0.9458400

Table 9B.13 – Influence Coefficients for a Longitudinal Semi-Elliptical Surface Crack in a Cylinder – Outside Surface

t/R_i	a/c	a/t	G_i	A_0	A_1	A_2	A_3	A_4	A_5	A_6
0.05 (1/20)	0.5	0	G_0	0.8776607	-0.6729719	3.7721411	-6.5209060	6.3377934	-3.7028038	0.9872447
			G_1	0.1277541	0.4368502	0.4904522	1.0427434	-2.9631236	2.0826525	-0.5184313
		0.2	G_0	0.9094785	-1.0704029	6.5969031	-15.339481	19.891956	-13.831397	3.9381913
			G_1	0.1511354	0.1498618	2.3171901	-4.6991089	5.9510689	-4.6766956	1.4944878
		0.4	G_0	1.0187560	-0.7252200	2.9510620	-1.6965300	-3.7495300	5.5630180	-2.1679600
			G_1	0.1777910	0.3097340	1.1782720	-0.5207400	-1.3685100	1.4131580	-0.4534400
		0.6	G_0	1.2191680	-1.1624100	4.3039990	-3.4956600	-3.5264500	6.8389740	-2.8685000
			G_1	0.2368950	0.1990950	1.3665370	-0.4508000	-1.9303400	2.0355870	-0.6795900
		0.8	G_0	1.4670860	-1.4874600	4.9131560	-4.8217400	-1.4111900	4.6213220	-1.8973500
			G_1	0.3108650	0.0205500	2.1111910	-2.5101100	1.2177130	-0.3862800	0.0564600
0.05 (1/20)	1.0	0	G_0	1.1977992	-0.5244870	0.1498299	2.3284866	-5.1058499	4.3469049	-1.3487980
			G_1	0.1870117	0.6987352	0.1316900	0.7269255	-2.5259384	2.1756251	-0.6540458
		0.2	G_0	1.2267227	-1.2309827	4.9938199	-13.435866	20.942460	-16.881717	5.4396233
			G_1	0.2162188	0.2008041	3.1282931	-8.7575323	12.984058	-10.406989	3.3659724
		0.4	G_0	1.3146080	-1.0024200	1.8454760	-0.8744700	-2.2504400	3.4654690	-1.4164400
			G_1	0.2217160	0.5404660	0.8385940	-0.8990200	-0.6786400	1.2271190	-0.4969400
		0.6	G_0	1.4273930	-1.1722500	1.8107740	-0.2671700	-3.3078700	4.2258110	-1.6062100
			G_1	0.2553870	0.4839230	0.9022980	-1.0407000	-0.3630800	0.8909080	-0.3661900
		0.8	G_0	1.5669880	-1.4243900	2.0816990	-1.0406600	-1.4652500	2.2092880	-0.8044400
			G_1	0.2873270	0.4823500	0.6339350	-0.2953100	-1.2046800	1.3245420	-0.4469300
0.05 (1/20)	2.0	0	G_0	0.8150546	-0.5623828	1.4465771	-4.6778133	8.4192164	-7.9025932	2.9866351
			G_1	0.1359146	0.0702340	3.5558581	-11.034445	16.967724	-14.126991	4.8706612
		0.2	G_0	0.8410025	-1.0986979	4.6833289	-14.254400	23.077894	-19.117803	6.3907936
			G_1	0.1393039	0.0157399	3.5854198	-10.908384	16.465690	-13.405784	4.5256310
		0.4	G_0	0.8552595	-1.1713096	5.0505801	-15.423750	24.918773	-20.491114	6.7824876
			G_1	0.1433068	-0.0051111	3.7018421	-11.315879	17.126325	-13.897780	4.6633443
		0.6	G_0	0.8922163	-1.1791312	4.7085484	-14.194993	22.986733	-19.057873	6.3764561
			G_1	0.1531695	0.0011284	3.5772066	-10.858841	16.387974	-13.348661	4.5099477
		0.8	G_0	0.9462314	-1.6448744	7.4204133	-22.617661	35.895514	-28.367552	8.8839133
			G_1	0.1651920	-0.1064856	4.2963413	-13.173123	19.754851	-15.432417	4.9095345
0.1 (1/10)	0.03125	0	G_0	0.1965046	2.9373464	-5.2582823	7.4889153	-6.9282667	3.3673349	-0.6677966
			G_1	0.0051780	0.1750280	2.7718680	-4.6457154	4.6780502	-3.2768090	0.9840994
		0.2	G_0	0.2114908	2.4425792	-1.0853387	-4.3244076	10.821413	-9.9682430	3.2163776
			G_1	0.0066363	0.2226202	2.5052241	-3.7606471	3.8258183	-3.0282477	0.9830947
		0.4	G_0	0.2246500	2.9397340	-3.0871500	2.4310320	4.8690240	-9.5429900	4.0540600
			G_1	0.0148750	0.3763240	1.5876360	-0.2147600	-0.6979300	-0.3343000	0.2518400
		0.6	G_0	0.2495210	3.4159580	-4.9404800	13.042320	-8.3791000	-3.1660100	2.7863600
			G_1	0.0200470	0.6258430	-0.0433000	5.9592140	-8.1321500	3.8137330	-0.8504100
		0.8	G_0	0.3404240	2.7101300	5.4741060	-20.271800	65.828770	-78.807600	29.760500
			G_1	0.0306660	0.6856860	0.6916680	2.5535420	5.9341450	-13.208000	5.4184600
0.1 (1/10)	0.0625	0	G_0	0.2695332	2.1626001	-1.6551569	-1.2970208	4.5604304	-4.3163876	1.4010655
			G_1	0.0138667	0.1827458	2.5749608	-3.9044679	3.3556301	-2.1772209	0.6420134
		0.2	G_0	0.2834411	2.0560718	-0.8751298	-1.5432422	3.0228355	-2.2245268	0.5558294
			G_1	0.0182016	0.2072911	2.5921978	-4.2023608	4.5304917	-3.5646673	1.1564770
		0.4	G_0	0.3137750	2.3258560	-0.8579900	-0.9040300	4.2766520	-5.1745700	1.8051000
			G_1	0.0243570	0.3072050	2.1814360	-1.9816300	1.1663170	-1.1678700	0.4025600
		0.6	G_0	0.3600610	2.8884850	-2.6105300	8.0008110	-6.6659700	-0.3626000	1.1229800
			G_1	0.0371430	0.4201240	2.0068380	-1.0550900	2.0695720	-3.6421800	1.4368800
		0.8	G_0	0.4694430	3.3305190	-1.8346900	11.806850	-5.5419600	-10.763600	6.8425000
			G_1	0.0598490	0.7065030	0.7632970	4.4319820	-3.1569500	-2.8592200	1.8893100

Table 9B.13 – Influence Coefficients for a Longitudinal Semi-Elliptical Surface Crack in a Cylinder – Outside Surface

t/R_i	a/c	a/t	G_i	A_0	A_1	A_2	A_3	A_4	A_5	A_6
0.1 (1/10)	0.125	0	G_0	0.4065238	0.7772483	3.8861644	-12.573943	16.760207	-11.014593	2.8706957
			G_1	0.0320270	0.1825342	2.2670449	-2.7076615	1.2088194	-0.3777430	0.0763155
		0.2	G_0	0.4146617	1.1413375	1.8316706	-6.3486958	7.9232241	-5.0205478	1.2773760
			G_1	0.0480559	0.0160274	3.9258710	-9.0346145	12.528263	-9.7913648	3.0207677
		0.4	G_0	0.4883450	1.4676440	1.4043140	-4.4990000	5.3634750	-3.4240300	0.8052400
			G_1	0.0579240	0.3954930	1.4085140	0.3793750	-3.3794500	2.8735190	-0.8740400
		0.6	G_0	0.6140930	1.8274410	1.0767420	-0.6119200	-0.6954000	-0.1405600	0.2139800
			G_1	0.0956370	0.4497680	1.7875670	-0.2859900	-1.5203300	0.5472650	0.0260000
		0.8	G_0	0.8606090	1.8707420	3.9998690	-2.2213500	-1.4990000	-1.4366100	1.6902100
			G_1	0.1643640	0.4633370	2.6664580	-1.0454000	-0.4337900	-1.3064500	0.9429600
0.1 (1/10)	0.25	0	G_0	0.6152816	-0.3348694	6.2955620	-15.590618	19.299508	-12.488107	3.3010035
			G_1	0.0703566	0.2828152	1.4036169	-0.6511596	-1.2076596	1.0318656	-0.2423741
		0.2	G_0	0.6292130	-0.2336322	7.0478667	-19.982397	27.848411	-19.690368	5.5375234
			G_1	0.0904740	0.1857128	2.4363430	-4.7462460	5.8199075	-4.5017004	1.4053473
		0.4	G_0	0.7474850	0.0425110	4.3717980	-8.1944800	6.2538030	-1.6898700	-0.1427300
			G_1	0.1180950	0.2484880	1.9064220	-1.9057300	0.5526770	-0.2448400	0.1107400
		0.6	G_0	0.9661540	-0.1353200	5.7466490	-9.3625200	4.9078280	0.7588490	-1.1390900
			G_1	0.1830270	0.2407950	2.0333670	-1.2883400	-1.3714400	1.6503570	-0.5396800
		0.8	G_0	1.3341440	-0.9392800	11.458550	-22.447500	20.248040	-9.5095100	1.9907200
			G_1	0.2907130	0.0222280	3.5382670	-4.2976700	1.5378660	0.1623560	-0.1962600
0.1 (1/10)	0.5	0	G_0	0.8776607	-0.6729719	3.7721411	-6.5209060	6.3377934	-3.7028038	0.9872447
			G_1	0.1277541	0.4368502	0.4904522	1.0427434	-2.9631236	2.0826525	-0.5184313
		0.2	G_0	0.9130594	-1.0743549	6.5855208	-15.182614	19.523051	-13.484513	3.8207058
			G_1	0.1514847	0.1586198	2.2698801	-4.5668494	5.7721280	-4.5599113	1.4645610
		0.4	G_0	1.0280510	-0.7637100	3.1906790	-2.3185400	-2.8532900	4.8911910	-1.9674700
			G_1	0.1796830	0.3127760	1.1588480	-0.4062200	-1.6100500	1.6351940	-0.5292900
		0.6	G_0	1.2334260	-1.1348600	4.1411110	-2.7310000	-4.9657400	8.0561550	-3.2581700
			G_1	0.2434960	0.1656450	1.6261480	-1.2283300	-0.7166800	1.0912900	-0.3930600
		0.8	G_0	1.5039180	-1.5034000	5.1335790	-5.1827000	-1.0213400	4.2817510	-1.7636200
			G_1	0.3214900	0.0504200	1.9574280	-1.9407000	0.2832180	0.3023430	-0.1329900
0.1 (1/10)	1.0	0	G_0	1.1977992	-0.5244870	0.1498299	2.3284866	-5.1058499	4.3469049	-1.3487980
			G_1	0.1870117	0.6987352	0.1316900	0.7269255	-2.5259384	2.1756251	-0.6540458
		0.2	G_0	1.2309943	-1.2311243	4.9655300	-13.330137	20.774727	-16.757204	5.4042537
			G_1	0.2176088	0.1970437	3.1550798	-8.8500614	13.139627	-10.531333	3.4038623
		0.4	G_0	1.3231870	-0.9921100	1.6993240	-0.3237300	-3.2217300	4.2806730	-1.6779000
			G_1	0.2229300	0.5643960	0.6814060	-0.4239100	-1.4164100	1.7944570	-0.6675800
		0.6	G_0	1.4456210	-1.2064800	2.0156090	-1.0147800	-1.9519200	3.0609460	-1.2264900
			G_1	0.2588090	0.5174240	0.6565440	-0.2305700	-1.7170400	1.9972060	-0.7158800
		0.8	G_0	1.5973980	-1.4150900	1.8672670	-0.2830900	-2.7422700	3.2391740	-1.1212900
			G_1	0.2988890	0.4569940	0.7181120	-0.4164400	-1.2008400	1.4390610	-0.5091100
0.1 (1/10)	2.0	0	G_0	0.8150546	-0.5623828	1.4465771	-4.6778133	8.4192164	-7.9025932	2.9866351
			G_1	0.1359146	0.0702340	3.5558581	-11.034445	16.967724	-14.126991	4.8706612
		0.2	G_0	0.8430489	-1.1005326	4.6617449	-14.157253	22.899128	-18.964329	6.3406074
			G_1	0.1390871	0.0277092	3.5072974	-10.680541	16.126905	-13.155146	4.4523656
		0.4	G_0	0.8605308	-1.1997836	5.1936578	-15.844548	25.563051	-20.974259	6.9229799
			G_1	0.1443506	-0.0060804	3.7006839	-11.307283	17.100992	-13.865758	4.6492973
		0.6	G_0	0.9003490	-1.2107769	4.8455996	-14.595836	23.611401	-19.532572	6.5152373
			G_1	0.1545839	0.0063848	3.5329882	-10.721392	16.161920	-13.159436	4.4472006
		0.8	G_0	0.9554477	-1.6372153	7.2947649	-22.269116	35.425236	-28.048423	8.7975829
			G_1	0.1681089	-0.1082476	4.2889256	-13.154232	19.720738	-15.394068	4.8931181

Table 9B.13 – Influence Coefficients for a Longitudinal Semi-Elliptical Surface Crack in a Cylinder – Outside Surface

t/R_i	a/c	a/t	G_i	A_0	A_1	A_2	A_3	A_4	A_5	A_6
0.2 (1/5)	0.03125	0	G_0	0.1965046	2.9373464	-5.2582823	7.4889153	-6.9282667	3.3673349	-0.6677966
			G_1	0.0051780	0.1750280	2.7718680	-4.6457154	4.6780502	-3.2768090	0.9840994
		0.2	G_0	0.2114908	2.4425792	-1.0853387	-4.3244076	10.821413	-9.9682430	3.2163776
			G_1	0.0066363	0.2226202	2.5052241	-3.7606471	3.8258183	-3.0282477	0.9830947
		0.4	G_0	0.2200000	2.8881700	-3.0327900	2.7778770	3.3274220	-7.7404800	3.3939800
			G_1	0.0091060	0.3453610	1.7142900	-0.5311700	-0.3691000	-0.5118400	0.3025800
		0.6	G_0	0.2348060	3.2261810	-4.4851300	12.433050	-9.9964600	-0.2169700	1.5875600
			G_1	0.0145190	0.5102980	0.5788380	3.9687320	-5.3534000	1.8233690	-0.2307100
		0.8	G_0	0.2865680	2.4834660	4.1449600	-13.505800	45.152730	-55.423700	21.127000
			G_1	0.0206900	0.6400470	-0.0229200	6.0072670	-3.1147600	-3.7934800	2.1179200
0.2 (1/5)	0.0625	0	G_0	0.2695332	2.1626001	-1.6551569	-1.2970208	4.5604304	-4.3163876	1.4010655
			G_1	0.0138667	0.1827458	2.5749608	-3.9044679	3.3556301	-2.1772209	0.6420134
		0.2	G_0	0.2834411	2.0560718	-0.8751298	-1.5432422	3.0228355	-2.2245268	0.5558294
			G_1	0.0182016	0.2072911	2.5921978	-4.2023608	4.5304917	-3.5646673	1.1564770
		0.4	G_0	0.3052040	2.2875080	-0.9001700	-0.4660500	3.3131160	-4.3118300	1.5291400
			G_1	0.0212020	0.3013800	2.0904460	-1.6420300	0.6344910	-0.7559500	0.2745900
		0.6	G_0	0.3364570	2.8141420	-2.9703500	9.5644040	-9.9622400	2.7107940	0.1081600
			G_1	0.0315690	0.3510610	2.2422160	-1.9023800	3.3988860	-4.5777900	1.6874400
		0.8	G_0	0.4123650	2.9008610	-0.8830500	8.4174560	-2.8151000	-9.6909800	5.5666900
			G_1	0.0418770	0.6018790	0.8247160	3.9811330	-3.2906000	-1.5730100	1.1215000
0.2 (1/5)	0.125	0	G_0	0.4065238	0.7772483	3.8861644	-12.573943	16.760207	-11.014593	2.8706957
			G_1	0.0320270	0.1825342	2.2670449	-2.7076615	1.2088194	-0.3777430	0.0763155
		0.2	G_0	0.4146617	1.1413375	1.8316706	-6.3486958	7.9232241	-5.0205478	1.2773760
			G_1	0.0480559	0.0160274	3.9258710	-9.0346145	12.528263	-9.7913648	3.0207677
		0.4	G_0	0.4703850	1.5541910	0.5461170	-1.3287000	0.1961270	0.6156700	-0.4357400
			G_1	0.0532400	0.3675900	1.5616730	-0.1572400	-2.2528300	1.8144520	-0.5189800
		0.6	G_0	0.5699100	1.7741760	0.8463720	0.1611910	-0.9192500	-0.5062400	0.3641200
			G_1	0.0799060	0.4293480	1.7026530	-0.1213800	-1.2211100	0.0433470	0.1948200
		0.8	G_0	0.7433210	1.8172770	2.7976140	0.2753690	-1.4326200	-3.1035000	2.1815400
			G_1	0.1246100	0.4675080	2.0528940	0.3058490	-0.9948000	-1.4118400	0.9245700
0.2 (1/5)	0.25	0	G_0	0.6152816	-0.3348694	6.2955620	-15.590618	19.299508	-12.488107	3.3010035
			G_1	0.0703566	0.2828152	1.4036169	-0.6511596	-1.2076596	1.0318656	-0.2423741
		0.2	G_0	0.6292130	-0.2336322	7.0478667	-19.982397	27.848411	-19.690368	5.5375234
			G_1	0.0904740	0.1857128	2.4363430	-4.7462460	5.8199075	-4.5017004	1.4053473
		0.4	G_0	0.7429640	0.0378310	4.5014520	-8.4869900	6.8268360	-2.2638700	0.0578800
			G_1	0.1151780	0.2656350	1.7915450	-1.4270300	-0.2561800	0.3997230	-0.0925900
		0.6	G_0	0.9371100	-0.0255800	5.1408380	-7.0247800	1.5138460	3.0365680	-1.7628800
			G_1	0.1726810	0.2717190	1.8711170	-0.6546900	-2.1914600	2.1145170	-0.6484000
		0.8	G_0	1.2624900	-0.7577100	10.593400	-18.988200	16.245730	-7.7399600	1.7098800
			G_1	0.2602900	0.2432630	1.9870650	1.1808940	-6.9845000	6.5125760	-2.0745300
0.2 (1/5)	0.5	0	G_0	0.8776607	-0.6729719	3.7721411	-6.5209060	6.3377934	-3.7028038	0.9872447
			G_1	0.1277541	0.4368502	0.4904522	1.0427434	-2.9631236	2.0826525	-0.5184313
		0.2	G_0	0.9130594	-1.0743549	6.5855208	-15.182614	19.523051	-13.484513	3.8207058
			G_1	0.1514847	0.1586198	2.2698801	-4.5668494	5.7721280	-4.5599113	1.4645610
		0.4	G_0	1.0373150	-0.7658000	3.1866550	-2.0564900	-3.5112000	5.5279200	-2.1906800
			G_1	0.1827690	0.3016120	1.2494690	-0.6550800	-1.2174600	1.3119730	-0.4248500
		0.6	G_0	1.2483210	-1.1273200	4.2620860	-2.9342600	-4.6925200	7.8084440	-3.1741300
			G_1	0.2466090	0.1946990	1.4996030	-0.7717700	-1.4533500	1.6452820	-0.5551900
		0.8	G_0	1.5312830	-1.4214000	4.9906150	-4.3683700	-2.3611100	5.1413420	-1.9602900
			G_1	0.3312580	0.0718170	1.9412430	-1.7261000	-0.1198500	0.5699280	-0.1928500

Table 9B.13 – Influence Coefficients for a Longitudinal Semi-Elliptical Surface Crack in a Cylinder – Outside Surface

t/R_i	a/c	a/t	G_i	A_0	A_1	A_2	A_3	A_4	A_5	A_6
0.2 (1/5)	1.0	0	G_0	1.1977992	-0.5244870	0.1498299	2.3284866	-5.1058499	4.3469049	-1.3487980
			G_1	0.1870117	0.6987352	0.1316900	0.7269255	-2.5259384	2.1756251	-0.6540458
		0.2	G_0	1.2309943	-1.2311243	4.9655300	-13.330137	20.774727	-16.757204	5.4042537
			G_1	0.2176088	0.1970437	3.1550798	-8.8500614	13.139627	-10.531333	3.4038623
		0.4	G_0	1.3395810	-0.9995200	1.6152160	0.0782660	-3.9906500	4.9599370	-1.9049200
			G_1	0.2275940	0.5608710	0.6867250	-0.4215300	-1.4409800	1.8257330	-0.6796800
		0.6	G_0	1.4732900	-1.2085900	1.8254600	-0.1324400	-3.6681900	4.5929990	-1.7396900
			G_1	0.2660940	0.5279130	0.5952580	-0.0963000	-1.8423700	2.0313860	-0.7086300
		0.8	G_0	1.6447550	-1.4592200	1.9736270	-0.4261600	-2.6988600	3.2947350	-1.1534500
			G_1	0.3140820	0.4390350	0.8206310	-0.7553900	-0.6482700	0.9930760	-0.3665800
0.2 (1/5)	2.0	0	G_0	0.8150546	-0.5623828	1.4465771	-4.6778133	8.4192164	-7.9025932	2.9866351
			G_1	0.1359146	0.0702340	3.5558581	-11.034445	16.967724	-14.126991	4.8706612
		0.2	G_0	0.8536841	-1.0302392	4.0738131	-12.154325	19.629919	-16.443839	5.6017294
			G_1	0.1415607	0.0595042	3.2739576	-9.8453707	14.709899	-12.038154	4.1204970
		0.4	G_0	0.8704024	-1.0725850	4.1489689	-12.315492	19.879021	-16.632323	5.6546309
			G_1	0.1458020	0.0566824	3.2442161	-9.7698352	14.622301	-11.977784	4.1003749
		0.6	G_0	0.9098344	-1.0776714	3.7795127	-11.056320	17.894031	-15.112464	5.2038813
			G_1	0.1562757	0.0628573	3.1195301	-9.3277071	13.870685	-11.365405	3.9093291
		0.8	G_0	0.9473209	-1.0916848	3.2936932	-9.1104990	14.239343	-11.702777	3.9539503
			G_1	0.1579980	0.1971737	2.1502631	-6.2273300	8.6913835	-6.9646090	2.4150002
0.3333 (1/3)	0.03125	0	G_0	0.1965046	2.9373464	-5.2582823	7.4889153	-6.9282667	3.3673349	-0.6677966
			G_1	0.0051780	0.1750280	2.7718680	-4.6457154	4.6780502	-3.2768090	0.9840994
		0.2	G_0	0.2651746	2.0518539	-0.6576529	-2.2400914	4.0586003	-2.9557373	0.7509004
			G_1	0.0134241	0.2145035	2.4853811	-3.7294986	3.6634951	-2.8206848	0.9110972
		0.4	G_0	0.2068432	2.1289212	0.9488071	-7.9908119	17.527999	-16.818919	5.6744489
			G_1	0.0078550	0.1900840	2.9205940	-4.8299400	6.9364230	-6.4967600	2.2038400
		0.6	G_0	0.2176810	3.1796080	-4.8660500	13.825800	-14.215900	4.4304150	-0.0353400
			G_1	0.0077208	0.1777379	2.8308619	-4.4159417	8.8389790	-9.6804295	3.4134994
		0.8	G_0	0.2214280	3.4544570	-5.7728600	22.240290	-23.041500	5.5717540	0.9588560
			G_1	0.0086700	0.2576810	2.7260750	-3.5453100	10.980120	-13.837700	5.0393470
0.3333 (1/3)	0.0625	0	G_0	0.2695332	2.1626001	-1.6551569	-1.2970208	4.5604304	-4.3163876	1.4010655
			G_1	0.0138667	0.1827458	2.5749608	-3.9044679	3.3556301	-2.1772209	0.6420134
		0.2	G_0	0.2602402	1.9101229	0.6250582	-7.1510682	13.076057	-10.659369	3.2200458
			G_1	0.0149877	0.1955673	2.3230283	-2.9558560	2.2512432	-1.6085747	0.5105227
		0.4	G_0	0.2985878	1.4806070	4.0015159	-15.408972	26.416058	-21.963750	6.8318255
			G_1	0.0217550	0.2019200	2.8740480	-4.6530800	6.0952580	-5.4253400	1.7947570
		0.6	G_0	0.3248620	2.5827580	-1.7974700	4.6268000	-1.0563100	-4.8660300	2.6241440
			G_1	0.0274730	0.2394530	2.9636050	-4.8034000	8.6324210	-9.0423400	3.1584620
		0.8	G_0	0.3581590	2.8096210	-2.2342200	12.128880	-10.705600	-1.3607100	2.4982950
			G_1	0.0328400	0.3062750	2.7758730	-3.5996700	9.5233880	-11.672000	4.2059790
0.3333 (1/3)	0.125	0	G_0	0.4065238	0.7772483	3.8861644	-12.573943	16.760207	-11.014593	2.8706957
			G_1	0.0320270	0.1825342	2.2670449	-2.7076615	1.2088194	-0.3777430	0.0763155
		0.2	G_0	0.3882912	1.0609616	3.1532036	-10.997015	15.435099	-10.732447	2.9280131
			G_1	0.0361643	0.1993991	2.1521281	-2.4393155	1.2426343	-0.7115746	0.2338738
		0.4	G_0	0.4550911	0.6846515	5.9119227	-17.160497	24.468016	-17.877938	5.0878696
			G_1	0.0521360	0.2552780	2.3217540	-2.7072400	2.1186830	-1.7821100	0.6094100
		0.6	G_0	0.5489050	1.2094700	4.6400520	-12.898000	21.506680	-18.882700	6.1124270
			G_1	0.0713480	0.2757420	2.6582020	-3.5129500	4.7941620	-4.9393500	1.7461680
		0.8	G_0	0.6623640	1.1473380	6.6549140	-13.993000	24.090210	-23.773700	8.3646690
			G_1	0.0983440	0.2665520	3.1706930	-4.1673500	7.3879790	-8.2858400	2.9658590

Table 9B.13 – Influence Coefficients for a Longitudinal Semi-Elliptical Surface Crack in a Cylinder – Outside Surface

t/R_i	a/c	a/t	G_i	A_0	A_1	A_2	A_3	A_4	A_5	A_6
0.3333 (1/3)	0.25	0	G_0	0.6152816	-0.3348694	6.2955620	-15.590618	19.299508	-12.488107	3.3010035
			G_1	0.0703566	0.2828152	1.4036169	-0.6511596	-1.2076596	1.0318656	-0.2423741
		0.2	G_0	0.5813392	0.1754806	4.1064690	-9.6118175	10.697163	-6.3416068	1.5662906
			G_1	0.0754953	0.2165572	1.6757864	-1.2279181	-0.4611587	0.5138881	-0.0998820
		0.4	G_0	0.6898568	-0.0773270	5.4806293	-11.407142	11.633671	-6.3018895	1.3834825
			G_1	0.1094450	0.3008580	1.5214730	-0.4181100	-1.9095700	1.6678210	-0.4669100
		0.6	G_0	0.9181390	-0.5237900	9.0497720	-20.248100	24.464580	-16.157900	4.3547490
			G_1	0.1608860	0.2132020	2.3389990	-2.2357400	0.7909320	-0.5441000	0.2284680
		0.8	G_0	1.1608820	-0.7489100	10.891840	-20.643400	21.820600	-13.976200	3.9263300
			G_1	0.2308100	0.1303460	2.9946080	-2.6118400	0.5931240	-0.3660800	0.1958340
0.3333 (1/3)	0.5	0	G_0	0.8776607	-0.6729719	3.7721411	-6.5209060	6.3377934	-3.7028038	0.9872447
			G_1	0.1277541	0.4368502	0.4904522	1.0427434	-2.9631236	2.0826525	-0.5184313
		0.2	G_0	0.9073955	-0.8971202	5.6296095	-12.600224	16.002537	-11.129631	3.2028664
			G_1	0.1423042	0.1193355	2.5733770	-5.9665543	8.9660776	-7.7527147	2.6068720
		0.4	G_0	1.0227900	-0.4769800	1.8915950	0.6470380	-6.0011600	6.2817830	-2.1144300
			G_1	0.1805320	0.3494360	1.0799180	-0.3980200	-1.2385100	1.0681870	-0.2845100
		0.6	G_0	1.2558880	-1.3007200	5.9836960	-9.1319200	6.5768270	-2.0833900	0.1372010
			G_1	0.2408900	0.2961710	0.9788130	0.6485900	-3.2595400	2.6786820	-0.7609600
		0.8	G_0	1.5064650	-0.9515700	2.1848270	5.0110910	-17.165600	16.231510	-5.1671000
			G_1	0.3183620	0.3380430	0.2332610	3.8880520	-9.0315400	7.3427670	-2.1808400
0.3333 (1/3)	1.0	0	G_0	1.1977992	-0.5244870	0.1498299	2.3284866	-5.1058499	4.3469049	-1.3487980
			G_1	0.1870117	0.6987352	0.1316900	0.7269255	-2.5259384	2.1756251	-0.6540458
		0.2	G_0	1.2251938	-1.1088782	4.3783822	-11.902054	18.917314	-15.537073	5.0861925
			G_1	0.1967570	0.3750251	2.1938569	-6.3981104	9.8525023	-8.3093790	2.8070520
		0.4	G_0	1.3102610	-0.3521400	-1.8346200	8.5385630	-14.391600	11.108920	-3.2682300
			G_1	0.2225920	0.6936100	0.0198130	1.0770080	-3.0231700	2.5251620	-0.7509200
		0.6	G_0	1.4399700	-0.3693300	-2.7283100	11.493880	-18.862500	14.402850	-4.2113200
			G_1	0.2615940	0.6931840	-0.2579300	1.9715370	-4.3708500	3.5256390	-1.0416400
		0.8	G_0	1.6727600	-1.6027700	3.8701220	-8.1470100	11.569570	-9.1115900	2.9716790
			G_1	0.3252650	0.3406560	1.7824050	-4.4816900	6.1843940	-4.9886800	1.6486210
0.3333 (1/3)	2.0	0	G_0	0.8150546	-0.5623828	1.4465771	-4.6778133	8.4192164	-7.9025932	2.9866351
			G_1	0.1359146	0.0702340	3.5558581	-11.034445	16.967724	-14.126991	4.8706612
		0.2	G_0	0.8585767	-1.0507299	4.1528538	-12.361065	19.924151	-16.649393	5.6568794
			G_1	0.1410557	0.0851240	3.1023875	-9.3241192	13.898320	-11.411063	3.9302795
		0.4	G_0	0.8774308	-1.0721586	4.0656641	-12.050152	19.486315	-16.340345	5.5670727
			G_1	0.1466187	0.0740623	3.1240530	-9.4156798	14.080011	-11.557896	3.9707854
		0.6	G_0	0.9226380	-1.1036903	3.8099517	-11.072222	17.863569	-15.046439	5.1695991
			G_1	0.1587492	0.0714304	3.0474948	-9.1086668	13.518169	-11.073693	3.8126238
		0.8	G_0	0.9631792	-1.0845228	3.0958067	-8.4948235	13.327750	-11.030577	3.7571770
			G_1	0.1624555	0.1998637	2.1090767	-6.1178471	8.5262697	-6.8263049	2.3672889
1.0 (1/1)	0.03125	0	G_0	0.1965046	2.9373464	-5.2582823	7.4889153	-6.9282667	3.3673349	-0.6677966
			G_1	0.0051780	0.1750280	2.7718680	-4.6457154	4.6780502	-3.2768090	0.9840994
		0.2	G_0	0.185121	3.188854	-6.482680	12.192272	-14.288081	8.601706	-2.111614
			G_1	0.002218	0.232860	2.374893	-3.194681	2.780956	-2.182333	0.733360
		0.4	G_0	0.186114	3.287193	-6.563730	14.505569	-18.263240	11.201917	-2.777015
			G_1	0.002129	0.244419	2.316128	-2.628722	2.563704	-2.603491	0.963885
		0.6	G_0	0.188529	3.325573	-5.996440	15.350206	-19.372323	11.119877	-2.589131
			G_1	0.002421	0.243116	2.368197	-2.400275	3.363615	-4.068738	1.519781
		0.8	G_0	0.193403	3.286405	-4.711590	14.618870	-18.272045	10.744648	-3.083255
			G_1	0.003669	0.213041	2.638151	-2.681828	4.617077	-4.830043	1.364246

Table 9B.13 – Influence Coefficients for a Longitudinal Semi-Elliptical Surface Crack in a Cylinder – Outside Surface

t/R_i	a/c	a/t	G_i	A_0	A_1	A_2	A_3	A_4	A_5	A_6
1.0 (1/1)	0.0625	0	G_0	0.2695332	2.1626001	-1.6551569	-1.2970208	4.5604304	-4.3163876	1.4010655
			G_1	0.0138667	0.1827458	2.5749608	-3.9044679	3.3556301	-2.1772209	0.6420134
		0.2	G_0	0.254806	2.438464	-2.740803	2.446353	-0.875988	-0.687926	0.443576
			G_1	0.010465	0.233153	2.333591	-3.084952	2.518702	-1.890349	0.623018
		0.4	G_0	0.258618	2.576236	-3.094962	5.335968	-5.228664	1.823073	-0.096923
			G_1	0.010878	0.251163	2.286781	-2.688509	2.727195	-2.730801	0.999490
		0.6	G_0	0.266687	2.626036	-2.801017	7.246477	-8.149369	3.160303	-0.328226
			G_1	0.011508	0.261788	2.275605	-2.310747	3.341409	-4.089143	1.534823
		0.8	G_0	0.279917	2.544139	-1.352379	6.101193	-6.363617	2.135462	-0.577863
			G_1	0.013438	0.234425	2.564528	-2.758745	5.032575	-5.335732	1.569031
1.0 (1/1)	0.125	0	G_0	0.4065238	0.7772483	3.8861644	-12.573943	16.760207	-11.014593	2.8706957
			G_1	0.0320270	0.1825342	2.2670449	-2.7076615	1.2088194	-0.3777430	0.0763155
		0.2	G_0	0.388322	1.286602	2.053332	-8.581169	12.929838	-9.572280	2.754168
			G_1	0.030700	0.241330	2.153705	-2.590769	1.660060	-1.144276	0.384660
		0.4	G_0	0.408074	1.358016	2.369499	-8.562211	13.630668	-11.051005	3.394090
			G_1	0.034870	0.249348	2.279726	-2.807760	2.678116	-2.448695	0.858520
		0.6	G_0	0.434361	1.380693	2.944663	-8.351573	14.398774	-13.184658	4.362437
			G_1	0.039336	0.250796	2.450632	-3.161382	4.487216	-4.742839	1.684563
		0.8	G_0	0.473331	1.230496	4.682105	-10.876475	19.808960	-18.501541	5.890109
			G_1	0.045855	0.202062	3.017214	-4.823454	8.779062	-8.675663	2.746608
1.0 (1/1)	0.25	0	G_0	0.6152816	-0.3348694	6.2955620	-15.590618	19.299508	-12.488107	3.3010035
			G_1	0.0703566	0.2828152	1.4036169	-0.6511596	-1.2076596	1.0318656	-0.2423741
		0.2	G_0	0.615729	-0.067194	5.790334	-14.635175	18.282435	-11.915994	3.144657
			G_1	0.075431	0.228618	1.928275	-2.083113	0.875100	-0.476420	0.174582
		0.4	G_0	0.674497	-0.090521	6.569872	-16.059304	20.391703	-13.774825	3.744274
			G_1	0.091794	0.223343	2.158106	-2.489912	1.628560	-1.230448	0.428502
		0.6	G_0	0.759811	-0.239972	8.146341	-19.163030	25.452277	-18.373719	5.256740
			G_1	0.112785	0.197789	2.547677	-3.295084	3.354686	-2.991099	1.022499
		0.8	G_0	0.870119	-0.490355	10.419374	-23.472844	33.315741	-26.026024	7.835043
			G_1	0.138002	0.151077	3.121397	-4.538513	6.309718	-5.970779	1.973660
1.0 (1/1)	0.5	0	G_0	0.8776607	-0.6729719	3.7721411	-6.5209060	6.3377934	-3.7028038	0.9872447
			G_1	0.1277541	0.4368502	0.4904522	1.0427434	-2.9631236	2.0826525	-0.5184313
		0.2	G_0	0.913372	-0.735043	4.471574	-8.246856	8.320446	-4.717293	1.140654
			G_1	0.141033	0.343450	1.103703	-0.636195	-0.557657	0.346388	-0.023693
		0.4	G_0	1.015207	-0.819177	4.919757	-8.801732	8.658853	-4.835082	1.155029
			G_1	0.172015	0.326617	1.221840	-0.739579	-0.544412	0.364228	-0.032381
		0.6	G_0	1.174108	-0.982447	5.673358	-9.634007	9.126974	-5.036430	1.202715
			G_1	0.219163	0.296282	1.388126	-0.790142	-0.689149	0.499359	-0.073851
		0.8	G_0	1.398706	-1.364577	7.678071	-12.977835	12.357364	-6.859392	1.632145
			G_1	0.285589	0.171801	2.172638	-2.304679	0.996312	-0.452797	0.110046
1.0 (1/1)	1.0	0	G_0	1.1977992	-0.5244870	0.1498299	2.3284866	-5.1058499	4.3469049	-1.3487980
			G_1	0.1870117	0.6987352	0.1316900	0.7269255	-2.5259384	2.1756251	-0.6540458
		0.2	G_0	1.258829	-0.920383	2.464641	-4.643045	5.586619	-3.692533	1.007931
			G_1	0.204376	0.551618	1.038902	-2.136340	1.961327	-1.226688	0.345303
		0.4	G_0	1.358991	-1.000057	2.426376	-4.298265	5.004235	-3.246678	0.877984
			G_1	0.233727	0.546132	0.974941	-1.932976	1.666765	-1.014210	0.285017
		0.6	G_0	1.513798	-1.174129	2.592991	-4.334109	4.883126	-3.111444	0.837530
			G_1	0.278808	0.520717	0.939526	-1.754995	1.382899	-0.804174	0.226268
		0.8	G_0	1.722292	-1.472304	3.210428	-5.674377	6.979236	-4.950340	1.489916
			G_1	0.338285	0.461023	1.079305	-2.155003	2.109173	-1.450342	0.444958

Table 9B.13 – Influence Coefficients for a Longitudinal Semi-Elliptical Surface Crack in a Cylinder – Outside Surface

t/R_i	a/c	a/t	G_i	A_0	A_1	A_2	A_3	A_4	A_5	A_6
1.0 (1/1)	2.0	0	G_0	0.8150546	-0.5623828	1.4465771	-4.6778133	8.4192164	-7.9025932	2.9866351
			G_1	0.1359146	0.0702340	3.5558581	-11.034445	16.967724	-14.126991	4.8706612
		0.2	G_0	0.849913	-0.623478	0.993801	-1.666592	1.334505	-0.679852	0.286499
			G_1	0.114055	0.522567	0.443598	-0.722333	-0.788050	1.041518	-0.213190
		0.4	G_0	0.888847	-0.681988	0.956069	-1.405765	0.933773	-0.394995	0.208109
			G_1	0.123935	0.520367	0.390497	-0.579710	-0.970714	1.165073	-0.247663
		0.6	G_0	0.941188	-0.763541	0.916824	-1.073695	0.401173	0.006239	0.089259
			G_1	0.137170	0.516798	0.312866	-0.346017	-1.305150	1.420120	-0.327824
		0.8	G_0	1.002158	-0.820483	0.610344	0.027135	-1.168765	1.077598	-0.195853
			G_1	0.151742	0.526825	0.141814	0.139733	-1.967186	1.891335	-0.467090
1.5 (1.5/1)	0.03125	0	G_0	0.1965046	2.9373464	-5.2582823	7.4889153	-6.9282667	3.3673349	-0.6677966
			G_1	0.0051780	0.1750280	2.7718680	-4.6457154	4.6780502	-3.2768090	0.9840994
		0.2	G_0	0.184316	3.185155	-6.416255	12.046791	-14.275538	8.738850	-2.183521
			G_1	0.002013	0.230347	2.375843	-3.137204	2.600897	-1.998878	0.671756
		0.4	G_0	0.184814	3.260433	-6.215264	13.110697	-16.327198	10.012541	-2.490388
			G_1	0.001931	0.235164	2.368206	-2.719061	2.445339	-2.348690	0.859605
		0.6	G_0	0.186266	3.287464	-5.493228	12.836395	-15.634565	8.769382	-2.026212
			G_1	0.002280	0.226408	2.484911	-2.743251	3.420877	-3.756126	1.355909
		0.8	G_0	0.191146	3.204060	-3.742848	9.462399	-10.002877	5.397123	-1.873971
			G_1	0.004001	0.174807	2.957877	-3.844780	5.752158	-5.002880	1.230486
1.5 (1.5/1)	0.0625	0	G_0	0.2695332	2.1626001	-1.6551569	-1.2970208	4.5604304	-4.3163876	1.4010655
			G_1	0.0138667	0.1827458	2.5749608	-3.9044679	3.3556301	-2.1772209	0.6420134
		0.2	G_0	0.253290	2.432384	-2.700331	2.471102	-1.119732	-0.404040	0.344474
			G_1	0.009893	0.230422	2.326090	-3.003587	2.352958	-1.757793	0.585317
		0.4	G_0	0.255655	2.530458	-2.774915	4.458076	-4.467570	1.684671	-0.149831
			G_1	0.009796	0.243346	2.281730	-2.546274	2.265995	-2.248178	0.836391
		0.6	G_0	0.262267	2.527752	-2.052348	4.534908	-4.651024	1.251086	0.052376
			G_1	0.010197	0.243625	2.330894	-2.359678	2.926329	-3.438524	1.277687
		0.8	G_0	0.274290	2.369461	0.099091	0.075723	2.647639	-3.504190	0.668769
			G_1	0.012280	0.193341	2.809407	-3.538519	5.530894	-5.046760	1.308709
1.5 (1.5/1)	0.125	0	G_0	0.4065238	0.7772483	3.8861644	-12.573943	16.760207	-11.014593	2.8706957
			G_1	0.0320270	0.1825342	2.2670449	-2.7076615	1.2088194	-0.3777430	0.0763155
		0.2	G_0	0.386288	1.280467	2.090667	-8.562532	12.814964	-9.469762	2.724578
			G_1	0.029657	0.239008	2.150670	-2.542268	1.596761	-1.117368	0.381590
		0.4	G_0	0.400115	1.336465	2.405097	-8.395378	12.969802	-10.352825	3.160916
			G_1	0.031774	0.244066	2.247193	-2.631456	2.350692	-2.191296	0.785879
		0.6	G_0	0.419060	1.330162	3.066041	-8.484680	13.752128	-12.078859	3.905009
			G_1	0.034120	0.241769	2.394287	-2.898770	3.863367	-4.134184	1.481921
		0.8	G_0	0.450640	1.107318	5.318707	-13.164656	22.226266	-18.887038	5.545016
			G_1	0.038939	0.178025	3.047153	-4.891072	8.397487	-7.887477	2.369623
1.5 (1.5/1)	0.25	0	G_0	0.6152816	-0.3348694	6.2955620	-15.590618	19.299508	-12.488107	3.3010035
			G_1	0.0703566	0.2828152	1.4036169	-0.6511596	-1.2076596	1.0318656	-0.2423741
		0.2	G_0	0.615372	-0.065515	5.809641	-14.606558	18.215796	-11.880799	3.138708
			G_1	0.074698	0.229962	1.926585	-2.052209	0.841826	-0.470611	0.176804
		0.4	G_0	0.662416	-0.081773	6.514915	-15.788232	20.001912	-13.538879	3.688763
			G_1	0.086500	0.227179	2.125731	-2.375532	1.523831	-1.207143	0.431843
		0.6	G_0	0.726958	-0.216407	7.957721	-18.661309	24.880919	-18.044617	5.171054
			G_1	0.100550	0.205054	2.477465	-3.152103	3.307250	-3.042097	1.047174
		0.8	G_0	0.809636	-0.470411	10.327561	-23.997312	35.022219	-27.404207	8.132174
			G_1	0.117672	0.153798	3.101297	-4.814905	7.150848	-6.676981	2.144661

Table 9B.13 – Influence Coefficients for a Longitudinal Semi-Elliptical Surface Crack in a Cylinder – Outside Surface

t/R_i	a/c	a/t	G_i	A_0	A_1	A_2	A_3	A_4	A_5	A_6
1.5 (1.5/1)	0.5	0	G_0	0.8776607	-0.6729719	3.7721411	-6.5209060	6.3377934	-3.7028038	0.9872447
			G_1	0.1277541	0.4368502	0.4904522	1.0427434	-2.9631236	2.0826525	-0.5184313
		0.2	G_0	0.918760	-0.731705	4.461155	-8.157896	8.154855	-4.591132	1.104276
			G_1	0.142181	0.346826	1.093846	-0.591198	-0.631186	0.398937	-0.038268
		0.4	G_0	1.014734	-0.806287	4.926832	-8.766690	8.619895	-4.841968	1.164709
			G_1	0.170424	0.334969	1.215051	-0.709426	-0.569783	0.361184	-0.027134
		0.6	G_0	1.151961	-0.926971	5.590295	-9.448657	9.065317	-5.134747	1.251319
			G_1	0.209831	0.320543	1.345255	-0.693470	-0.738510	0.472814	-0.056995
		0.8	G_0	1.344390	-1.307328	7.957435	-14.256834	15.026217	-9.090496	2.246829
			G_1	0.266328	0.192432	2.270080	-2.739631	1.899766	-1.209805	0.319291
1.5 (1.5/1)	1.0	0	G_0	1.1977992	-0.5244870	0.1498299	2.3284866	-5.1058499	4.3469049	-1.3487980
			G_1	0.1870117	0.6987352	0.1316900	0.7269255	-2.5259384	2.1756251	-0.6540458
		0.2	G_0	1.269270	-0.926747	2.450385	-4.590910	5.520803	-3.653224	0.998752
			G_1	0.207128	0.552641	1.030480	-2.122401	1.952870	-1.226323	0.346278
		0.4	G_0	1.375650	-1.005464	2.400550	-4.206794	4.874890	-3.157636	0.853770
			G_1	0.237601	0.553017	0.945241	-1.865891	1.581884	-0.958034	0.269995
		0.6	G_0	1.529898	-1.163602	2.572592	-4.335524	4.967567	-3.218453	0.876237
			G_1	0.281949	0.536231	0.906808	-1.717306	1.371421	-0.816256	0.233496
		0.8	G_0	1.737002	-1.478165	3.530955	-6.973022	9.381206	-6.964274	2.110376
			G_1	0.341452	0.472790	1.153664	-2.548005	2.869377	-2.103032	0.651677
1.5 (1.5/1)	2.0	0	G_0	0.8150546	-0.5623828	1.4465771	-4.6778133	8.4192164	-7.9025932	2.9866351
			G_1	0.1359146	0.0702340	3.5558581	-11.034445	16.967724	-14.126991	4.8706612
		0.2	G_0	0.855544	-0.633346	0.990689	-1.634631	1.290258	-0.652614	0.280001
			G_1	0.115362	0.522373	0.436511	-0.708057	-0.799248	1.045258	-0.213580
		0.4	G_0	0.899631	-0.698248	0.933905	-1.296840	0.774931	-0.284849	0.177806
			G_1	0.126255	0.522508	0.363424	-0.511614	-1.057594	1.224395	-0.264591
		0.6	G_0	0.956020	-0.780211	0.864055	-0.883791	0.151258	0.165946	0.048131
			G_1	0.140261	0.522339	0.268634	-0.245630	-1.423882	1.497162	-0.349307
		0.8	G_0	1.021343	-0.839868	0.571171	0.097254	-1.115601	0.941571	-0.136834
			G_1	0.156211	0.531405	0.112872	0.151992	-1.911480	1.820393	-0.442582
2 (2/1)	0.03125	0	G_0	0.1965046	2.9373464	-5.2582823	7.4889153	-6.9282667	3.3673349	-0.6677966
			G_1	0.0051780	0.1750280	2.7718680	-4.6457154	4.6780502	-3.2768090	0.9840994
		0.2	G_0	0.183817	3.190141	-6.404381	12.027995	-14.359563	8.885385	-2.245389
			G_1	0.001926	0.229118	2.378913	-3.109083	2.499532	-1.891250	0.634664
		0.4	G_0	0.184160	3.251914	-6.019747	12.299556	-15.140288	9.231722	-2.288792
			G_1	0.001874	0.229989	2.405622	-2.795416	2.433543	-2.257482	0.817933
		0.6	G_0	0.185025	3.279455	-5.256690	11.563108	-13.649886	7.443417	-1.684608
			G_1	0.002242	0.218161	2.552444	-2.944665	3.510824	-3.661237	1.296263
		0.8	G_0	0.189573	3.190190	-3.412899	7.384079	-6.587833	3.139315	-1.338270
			G_1	0.004080	0.160315	3.088812	-4.322541	6.191462	-5.062445	1.184316
2 (2/1)	0.0625	0	G_0	0.2695332	2.1626001	-1.6551569	-1.2970208	4.5604304	-4.3163876	1.4010655
			G_1	0.0138667	0.1827458	2.5749608	-3.9044679	3.3556301	-2.1772209	0.6420134
		0.2	G_0	0.252448	2.433414	-2.689516	2.524077	-1.330543	-0.179648	0.267593
			G_1	0.009595	0.229567	2.319399	-2.944170	2.232762	-1.660824	0.557292
		0.4	G_0	0.254507	2.504975	-2.545742	3.787884	-3.747995	1.380155	-0.113186
			G_1	0.009338	0.239318	2.284590	-2.475733	2.015254	-1.980787	0.745002
		0.6	G_0	0.260573	2.477816	-1.588111	2.819232	-2.283418	-0.200328	0.394940
			G_1	0.009706	0.233960	2.373812	-2.421281	2.762152	-3.141390	1.157288
		0.8	G_0	0.271854	2.296694	0.811610	-2.957080	7.257252	-6.507686	1.389068
			G_1	0.011838	0.175439	2.924836	-3.887263	5.713223	-4.891194	1.195655

Table 9B.13 – Influence Coefficients for a Longitudinal Semi-Elliptical Surface Crack in a Cylinder – Outside Surface

t/R_i	a/c	a/t	G_i	A_0	A_1	A_2	A_3	A_4	A_5	A_6
2 (2/1)	0.125	0	G_0	0.4065238	0.7772483	3.8861644	-12.573943	16.760207	-11.014593	2.8706957
			G_1	0.0320270	0.1825342	2.2670449	-2.7076615	1.2088194	-0.3777430	0.0763155
		0.2	G_0	0.385244	1.277902	2.116594	-8.559753	12.754388	-9.414360	2.709228
			G_1	0.029082	0.237897	2.148968	-2.512087	1.557427	-1.101592	0.380342
		0.4	G_0	0.396455	1.326541	2.435886	-8.299013	12.527264	-9.868930	2.995677
			G_1	0.030255	0.242687	2.222371	-2.497910	2.097851	-1.990301	0.728675
		0.6	G_0	0.412667	1.302436	3.191425	-8.695131	13.488752	-11.462037	3.633573
			G_1	0.031797	0.239434	2.354123	-2.691984	3.376535	-3.670905	1.330592
		0.8	G_0	0.441614	1.043702	5.729282	-14.523178	23.512617	-18.992922	5.325051
			G_1	0.035993	0.171140	3.027231	-4.733296	7.780323	-7.123558	2.072234
2 (2/1)	0.25	0	G_0	0.6152816	-0.3348694	6.2955620	-15.590618	19.299508	-12.488107	3.3010035
			G_1	0.0703566	0.2828152	1.4036169	-0.6511596	-1.2076596	1.0318656	-0.2423741
		0.2	G_0	0.615397	-0.066314	5.839456	-14.641843	18.254930	-11.919328	3.152584
			G_1	0.074293	0.230222	1.930705	-2.048287	0.845516	-0.486068	0.183853
		0.4	G_0	0.656255	-0.075740	6.484539	-15.617332	19.728076	-13.355956	3.642522
			G_1	0.083628	0.229768	2.106178	-2.303216	1.451316	-1.184988	0.431647
		0.6	G_0	0.711262	-0.201332	7.849369	-18.315682	24.341573	-17.633459	5.048508
			G_1	0.094499	0.210035	2.433543	-3.041827	3.201758	-2.996266	1.037904
		0.8	G_0	0.782605	-0.460564	10.283615	-24.129380	35.258564	-27.325253	7.985350
			G_1	0.108363	0.156910	3.073152	-4.843272	7.255263	-6.691018	2.108915
2 (2/1)	0.5	0	G_0	0.8776607	-0.6729719	3.7721411	-6.5209060	6.3377934	-3.7028038	0.9872447
			G_1	0.1277541	0.4368502	0.4904522	1.0427434	-2.9631236	2.0826525	-0.5184313
		0.2	G_0	0.922532	-0.730699	4.461298	-8.110854	8.050518	-4.503858	1.077300
			G_1	0.142994	0.348797	1.088657	-0.561740	-0.684130	0.439705	-0.050299
		0.4	G_0	1.015035	-0.799312	4.939552	-8.766831	8.627855	-4.870363	1.177730
			G_1	0.169531	0.339974	1.213310	-0.697565	-0.574213	0.350034	-0.021074
		0.6	G_0	1.139643	-0.894057	5.537861	-9.334050	9.014844	-5.174226	1.272398
			G_1	0.204311	0.335213	1.318565	-0.635797	-0.767436	0.458348	-0.048112
		0.8	G_0	1.315050	-1.291944	8.202086	-15.229076	16.745919	-10.319619	2.524101
			G_1	0.255458	0.197858	2.359749	-3.085373	2.499094	-1.631376	0.412073
2 (2/1)	1.0	0	G_0	1.1977992	-0.5244870	0.1498299	2.3284866	-5.1058499	4.3469049	-1.3487980
			G_1	0.1870117	0.6987352	0.1316900	0.7269255	-2.5259384	2.1756251	-0.6540458
		0.2	G_0	1.276263	-0.928654	2.425219	-4.503400	5.388660	-3.556694	0.971288
			G_1	0.208947	0.554525	1.016847	-2.086479	1.903448	-1.191741	0.336644
		0.4	G_0	1.387164	-1.009504	2.385733	-4.154137	4.801173	-3.107119	0.840098
			G_1	0.240279	0.557502	0.926478	-1.824362	1.529570	-0.923380	0.260734
		0.6	G_0	1.540974	-1.159967	2.580554	-4.416389	5.156272	-3.391263	0.931638
			G_1	0.283941	0.546969	0.883818	-1.692805	1.365658	-0.824507	0.237811
		0.8	G_0	1.743113	-1.436305	3.448360	-6.982904	9.660351	-7.265219	2.198656
			G_1	0.340654	0.519463	0.958668	-2.087481	2.261394	-1.677544	0.528115
2 (2/1)	2.0	0	G_0	0.8150546	-0.5623828	1.4465771	-4.6778133	8.4192164	-7.9025932	2.9866351
			G_1	0.1359146	0.0702340	3.5558581	-11.034445	16.967724	-14.126991	4.8706612
		0.2	G_0	0.859353	-0.639193	0.984123	-1.599085	1.237097	-0.615546	0.269938
			G_1	0.116246	0.522528	0.430057	-0.692503	-0.817263	1.056307	-0.216427
		0.4	G_0	0.907007	-0.708775	0.916198	-1.217549	0.661203	-0.206523	0.156332
			G_1	0.127841	0.524094	0.344591	-0.464696	-1.117326	1.265231	-0.276270
		0.6	G_0	0.966075	-0.790014	0.820213	-0.741526	-0.027120	0.275480	0.020834
			G_1	0.142316	0.526518	0.237548	-0.178510	-1.499234	1.544221	-0.362234
		0.8	G_0	1.033509	-0.842482	0.493121	0.237477	-1.143199	0.854352	-0.089605
			G_1	0.158640	0.541374	0.060230	0.228912	-1.941684	1.803042	-0.430836

Table 9B.13 – Influence Coefficients for a Longitudinal Semi-Elliptical Surface Crack in a Cylinder – Outside Surface

t/R_i	a/c	a/t	G_i	A_0	A_1	A_2	A_3	A_4	A_5	A_6
2.5 (2.5)	0.03125	0	G_0	0.1965046	2.9373464	-5.2582823	7.4889153	-6.9282667	3.3673349	-0.6677966
			G_1	0.0051780	0.1750280	2.7718680	-4.6457154	4.6780502	-3.2768090	0.9840994
		0.2	G_0	0.183444	3.199596	-6.422436	12.078825	-14.497761	9.038508	-2.302152
			G_1	0.001887	0.228343	2.384046	-3.099658	2.445619	-1.828799	0.612191
		0.4	G_0	0.183765	3.250679	-5.904333	11.812501	-14.408678	8.732614	-2.155050
			G_1	0.001853	0.226912	2.431474	-2.848506	2.443648	-2.221701	0.799780
		0.6	G_0	0.184234	3.281586	-5.140124	10.899403	-12.608055	6.736571	-1.496977
			G_1	0.002214	0.214059	2.589481	-3.046237	3.544396	-3.603234	1.264639
		0.8	G_0	0.188392	3.197908	-3.324473	6.598755	-5.340667	2.352183	-1.151632
			G_1	0.004029	0.155917	3.131920	-4.465780	6.236356	-4.979185	1.143045
2.5 (2.5/1)	0.0625	0	G_0	0.2695332	2.1626001	-1.6551569	-1.2970208	4.5604304	-4.3163876	1.4010655
			G_1	0.0138667	0.1827458	2.5749608	-3.9044679	3.3556301	-2.1772209	0.6420134
		0.2	G_0	0.251899	2.437615	-2.693094	2.585700	-1.507845	-0.003070	0.208182
			G_1	0.009421	0.229388	2.314556	-2.901484	2.146220	-1.590598	0.536746
		0.4	G_0	0.254012	2.489415	-2.379965	3.293148	-3.167766	1.081907	-0.056920
			G_1	0.009110	0.236825	2.290024	-2.438631	1.870795	-1.825213	0.691604
		0.6	G_0	0.259776	2.450591	-1.292649	1.732248	-0.750743	-1.182894	0.641780
			G_1	0.009473	0.228480	2.402104	-2.458326	2.667535	-2.974973	1.091540
		0.8	G_0	0.270440	2.266674	1.166617	-4.475061	9.499801	-7.958250	1.748887
			G_1	0.011561	0.168280	2.968405	-3.986635	5.648062	-4.702266	1.117938
2.5 (2.5/1)	0.125	0	G_0	0.4065238	0.7772483	3.8861644	-12.573943	16.760207	-11.014593	2.8706957
			G_1	0.0320270	0.1825342	2.2670449	-2.7076615	1.2088194	-0.3777430	0.0763155
		0.2	G_0	0.384663	1.277033	2.136435	-8.566811	12.727903	-9.389030	2.702884
			G_1	0.028735	0.237340	2.148238	-2.492498	1.532310	-1.092683	0.380217
		0.4	G_0	0.394594	1.321356	2.462736	-8.239715	12.220739	-9.527499	2.877572
			G_1	0.029413	0.242560	2.204218	-2.397942	1.908557	-1.840422	0.686061
		0.6	G_0	0.409622	1.284876	3.301431	-8.894339	13.383426	-11.099699	3.467004
			G_1	0.030575	0.239125	2.325401	-2.533559	3.011120	-3.331759	1.221865
		0.8	G_0	0.437294	1.009803	5.977919	-15.261234	24.027669	-18.826864	5.133279
			G_1	0.034428	0.170872	2.987178	-4.502175	7.144780	-6.462467	1.842354
2.5 (2.5/1)	0.25	0	G_0	0.6152816	-0.3348694	6.2955620	-15.590618	19.299508	-12.488107	3.3010035
			G_1	0.0703566	0.2828152	1.4036169	-0.6511596	-1.2076596	1.0318656	-0.2423741
		0.2	G_0	0.615611	-0.068564	5.876234	-14.716634	18.358809	-12.002946	3.178561
			G_1	0.074069	0.229902	1.938052	-2.059174	0.868887	-0.512294	0.193183
		0.4	G_0	0.652911	-0.070685	6.463282	-15.488954	19.509680	-13.203103	3.602789
			G_1	0.081945	0.231799	2.092742	-2.250977	1.394776	-1.164288	0.430115
		0.6	G_0	0.702939	-0.188350	7.761673	-17.986916	23.755980	-17.155813	4.903291
			G_1	0.091139	0.214542	2.397243	-2.930525	3.051347	-2.897374	1.011401
		0.8	G_0	0.768697	-0.449129	10.211235	-23.920592	34.664269	-26.549447	7.650901
			G_1	0.103373	0.162129	3.026949	-4.715295	6.993910	-6.400747	1.991146
2.5 (2.5/1)	0.5	0	G_0	0.8776607	-0.6729719	3.7721411	-6.5209060	6.3377934	-3.7028038	0.9872447
			G_1	0.1277541	0.4368502	0.4904522	1.0427434	-2.9631236	2.0826525	-0.5184313
		0.2	G_0	0.925405	-0.731616	4.471464	-8.099602	7.997869	-4.449917	1.058505
			G_1	0.143627	0.349792	1.087210	-0.544051	-0.721795	0.471900	-0.060583
		0.4	G_0	1.015857	-0.795439	4.955212	-8.788170	8.668248	-4.918377	1.195647
			G_1	0.169085	0.343071	1.214971	-0.698492	-0.561795	0.329513	-0.012846
		0.6	G_0	1.132767	-0.870665	5.489081	-9.219404	8.925593	-5.161723	1.276347
			G_1	0.200980	0.345129	1.299407	-0.596200	-0.785258	0.445915	-0.041017
		0.8	G_0	1.298710	-1.289578	8.374998	-15.847276	17.685595	-10.850138	2.587584
			G_1	0.249121	0.197340	2.434467	-3.343382	2.883138	-1.848629	0.439847

Table 9B.13 – Influence Coefficients for a Longitudinal Semi-Elliptical Surface Crack in a Cylinder – Outside Surface

t/R_i	a/c	a/t	G_i	A_0	A_1	A_2	A_3	A_4	A_5	A_6
2.5 (2.5/1)	1.0	0	G_0	1.1977992	-0.5244870	0.1498299	2.3284866	-5.1058499	4.3469049	-1.3487980
			G_1	0.1870117	0.6987352	0.1316900	0.7269255	-2.5259384	2.1756251	-0.6540458
		0.2	G_0	1.281305	-0.928798	2.398643	-4.409085	5.237176	-3.439958	0.936634
			G_1	0.210243	0.556631	1.001780	-2.041925	1.835580	-1.140612	0.321636
		0.4	G_0	1.395762	-1.012974	2.378157	-4.127026	4.765460	-3.083804	0.834032
			G_1	0.242294	0.560582	0.913818	-1.797041	1.495320	-0.900481	0.254532
		0.6	G_0	1.549665	-1.162078	2.617463	-4.592160	5.497825	-3.682390	1.022477
			G_1	0.285352	0.556539	0.856485	-1.650577	1.330870	-0.809509	0.234814
		0.8	G_0	1.740405	-1.275340	2.537561	-4.431676	5.915260	-4.472444	1.365011
			G_1	0.334891	0.642412	0.247244	-0.047423	-0.795772	0.613602	-0.148998
2.5 (2.5/1)	2.0	0	G_0	0.8150546	-0.5623828	1.4465771	-4.6778133	8.4192164	-7.9025932	2.9866351
			G_1	0.1359146	0.0702340	3.5558581	-11.034445	16.967724	-14.126991	4.8706612
		0.2	G_0	0.862132	-0.643046	0.977353	-1.566126	1.184830	-0.576499	0.258643
			G_1	0.116897	0.522701	0.424937	-0.678476	-0.836705	1.070395	-0.220548
		0.4	G_0	0.912387	-0.715911	0.900375	-1.152978	0.570163	-0.144516	0.139509
			G_1	0.129001	0.525345	0.330472	-0.429895	-1.161259	1.295041	-0.284742
		0.6	G_0	0.973340	-0.795119	0.777879	-0.622157	-0.159838	0.344795	0.006808
			G_1	0.143761	0.530378	0.211730	-0.128108	-1.546185	1.566828	-0.367043
		0.8	G_0	1.040515	-0.814495	0.269682	0.741048	-1.635648	1.056751	-0.112083
			G_1	0.159141	0.567962	-0.084423	0.546320	-2.283229	1.980888	-0.466493
3 (3/1)	0.03125	0	G_0	0.1965046	2.9373464	-5.2582823	7.4889153	-6.9282667	3.3673349	-0.6677966
			G_1	0.0051780	0.1750280	2.7718680	-4.6457154	4.6780502	-3.2768090	0.9840994
		0.2	G_0	0.183142	3.211368	-6.455417	12.161009	-14.651499	9.181976	-2.351537
			G_1	0.001872	0.227742	2.391052	-3.103323	2.423686	-1.796792	0.599680
		0.4	G_0	0.183513	3.251910	-5.830150	11.501600	-13.936013	8.402556	-2.064365
			G_1	0.001843	0.224981	2.449524	-2.883923	2.455328	-2.206499	0.791327
		0.6	G_0	0.183702	3.286781	-5.080762	10.546551	-12.063968	6.369991	-1.398072
			G_1	0.002187	0.212028	2.609400	-3.091462	3.538008	-3.552750	1.243160
		0.8	G_0	0.187494	3.211646	-3.328841	6.371265	-5.040577	2.206727	-1.117011
			G_1	0.003931	0.155695	3.136961	-4.463766	6.118906	-4.844755	1.106976
3 (3/1)	0.0625	0	G_0	0.2695332	2.1626001	-1.6551569	-1.2970208	4.5604304	-4.3163876	1.4010655
			G_1	0.0138667	0.1827458	2.5749608	-3.9044679	3.3556301	-2.1772209	0.6420134
		0.2	G_0	0.251505	2.443076	-2.702545	2.644211	-1.651214	0.133274	0.163013
			G_1	0.009310	0.229435	2.311634	-2.871569	2.084858	-1.540746	0.522105
		0.4	G_0	0.253788	2.479416	-2.258966	2.931359	-2.724406	0.833600	-0.003410
			G_1	0.008984	0.235170	2.295402	-2.416637	1.781070	-1.729070	0.658714
		0.6	G_0	0.259335	2.435369	-1.100795	1.038238	0.229061	-1.822915	0.807820
			G_1	0.009338	0.225351	2.419062	-2.471284	2.592115	-2.863473	1.050189
		0.8	G_0	0.269492	2.255555	1.346372	-5.232093	10.545055	-8.612727	1.918617
			G_1	0.011346	0.166068	2.977216	-3.968303	5.474885	-4.506582	1.058789
3 (3/1)	0.125	0	G_0	0.4065238	0.7772483	3.8861644	-12.573943	16.760207	-11.014593	2.8706957
			G_1	0.0320270	0.1825342	2.2670449	-2.7076615	1.2088194	-0.3777430	0.0763155
		0.2	G_0	0.384319	1.277009	2.152071	-8.577009	12.717025	-9.377618	2.700566
			G_1	0.028510	0.237059	2.148050	-2.478948	1.515209	-1.087487	0.380637
		0.4	G_0	0.393563	1.318776	2.482892	-8.192465	11.988701	-9.271768	2.789076
			G_1	0.028897	0.242950	2.190022	-2.319799	1.762802	-1.726414	0.653816
		0.6	G_0	0.408070	1.272278	3.395628	-9.064693	13.342586	-10.869865	3.358090
			G_1	0.029858	0.239450	2.304238	-2.410452	2.733990	-3.080759	1.142811
		0.8	G_0	0.434987	0.990884	6.130310	-15.641141	24.115680	-18.517069	4.957879
			G_1	0.033475	0.173151	2.941916	-4.261616	6.564808	-5.911841	1.664399

Table 9B.13 – Influence Coefficients for a Longitudinal Semi-Elliptical Surface Crack in a Cylinder – Outside Surface

t/R_i	a/c	a/t	G_i	A_0	A_1	A_2	A_3	A_4	A_5	A_6
3 (3/1)	0.25	0	G_0	0.6152816	-0.3348694	6.2955620	-15.590618	19.299508	-12.488107	3.3010035
			G_1	0.0703566	0.2828152	1.4036169	-0.6511596	-1.2076596	1.0318656	-0.2423741
		0.2	G_0	0.615903	-0.071240	5.913565	-14.804158	18.485314	-12.102126	3.208693
			G_1	0.073945	0.229315	1.946665	-2.077022	0.901394	-0.543300	0.203516
		0.4	G_0	0.650951	-0.065130	6.438863	-15.362736	19.296125	-13.051053	3.562550
			G_1	0.080877	0.233784	2.080691	-2.204660	1.340499	-1.140070	0.426652
		0.6	G_0	0.698028	-0.173009	7.652069	-17.555767	22.976485	-16.517049	4.708637
			G_1	0.089058	0.219818	2.355831	-2.788305	2.831691	-2.736629	0.965584
		0.8	G_0	0.760777	-0.434999	10.101610	-23.465464	33.581563	-25.410509	7.228544
			G_1	0.100377	0.168715	2.968170	-4.501481	6.558589	-5.980828	1.842492
3 (3/1)	0.5	0	G_0	0.8776607	-0.6729719	3.7721411	-6.5209060	6.3377934	-3.7028038	0.9872447
			G_1	0.1277541	0.4368502	0.4904522	1.0427434	-2.9631236	2.0826525	-0.5184313
		0.2	G_0	0.927721	-0.734077	4.490784	-8.121851	7.998050	-4.434564	1.050624
			G_1	0.144151	0.350002	1.089497	-0.538932	-0.740380	0.490495	-0.067075
		0.4	G_0	1.016900	-0.793250	4.973102	-8.828964	8.744950	-4.994325	1.221928
			G_1	0.168895	0.344937	1.219752	-0.712142	-0.529605	0.295204	-0.000773
		0.6	G_0	1.128682	-0.848856	5.420969	-9.058890	8.780491	-5.118730	1.275788
			G_1	0.198871	0.352706	1.283825	-0.573117	-0.772783	0.407538	-0.025104
		0.8	G_0	1.289411	-1.294120	8.506556	-16.285868	18.298031	-11.132689	2.585888
			G_1	0.245426	0.190997	2.520463	-3.628440	3.301235	-2.091606	0.476155
3 (3/1)	1.0	0	G_0	1.1977992	-0.5244870	0.1498299	2.3284866	-5.1058499	4.3469049	-1.3487980
			G_1	0.1870117	0.6987352	0.1316900	0.7269255	-2.5259384	2.1756251	-0.6540458
		0.2	G_0	1.285157	-0.928199	2.373199	-4.316803	5.083796	-3.318708	0.900009
			G_1	0.211214	0.558843	0.985963	-1.992546	1.757365	-1.080319	0.303715
		0.4	G_0	1.402449	-1.015569	2.371906	-4.106893	4.740603	-3.067987	0.829870
			G_1	0.243842	0.563424	0.900771	-1.765908	1.452530	-0.869440	0.245489
		0.6	G_0	1.557104	-1.172949	2.708847	-4.950288	6.142465	-4.213040	1.185212
			G_1	0.286319	0.566755	0.818883	-1.581211	1.261642	-0.770743	0.224565
		0.8	G_0	1.726302	-0.929866	0.379370	1.991462	-3.887896	2.946602	-0.839760
			G_1	0.322018	0.886320	-1.261161	4.416832	-7.584188	5.723993	-1.656620
3 (3/1)	2.0	0	G_0	0.8150546	-0.5623828	1.4465771	-4.6778133	8.4192164	-7.9025932	2.9866351
			G_1	0.1359146	0.0702340	3.5558581	-11.034445	16.967724	-14.126991	4.8706612
		0.2	G_0	0.864248	-0.645272	0.967974	-1.527915	1.123775	-0.530054	0.245014
			G_1	0.117384	0.523199	0.418708	-0.659966	-0.864658	1.091576	-0.226834
		0.4	G_0	0.916461	-0.720297	0.881379	-1.084887	0.475648	-0.080998	0.122587
			G_1	0.129874	0.526645	0.317607	-0.398242	-1.200814	1.321215	-0.291951
		0.6	G_0	0.978875	-0.798541	0.748365	-0.570062	-0.156208	0.290952	0.033651
			G_1	0.144846	0.533261	0.197175	-0.124641	-1.501769	1.508253	-0.345201
		0.8	G_0	1.042042	-0.729579	-0.265310	2.047908	-3.159801	1.903248	-0.291006
			G_1	0.157084	0.627465	-0.414681	1.338731	-3.226914	2.531108	-0.592305

Notes:

1. Interpolation of the influence coefficients, G_i, may be used for intermediate values of t/R_i, a/c, and a/t.
2. The value of the influence coefficients at the surface point of the crack defined by $\varphi = 0°$ are equal to: $G_i = A_0$.
3. The value of the influence coefficients at the deepest point of the crack defined by $\varphi = 90°$ are equal to $G_i = \sum_{n=0}^{6} A_n$.

Table 9B.14 – Influence Coefficients for a Circumferential Semi-Elliptical Surface Crack in a Cylinder – Inside Surface

t/R_i	a/c	a/t	G_i	A_0	A_1	A_2	A_3	A_4	A_5	A_6
0.0	0.03125	0	G_0	0.1965046	2.9373464	-5.2582823	7.4889153	-6.9282667	3.3673349	-0.6677966
			G_1	0.0051780	0.1750280	2.7718680	-4.6457154	4.6780502	-3.2768090	0.9840994
			G_5	0.1965050	2.9373460	-5.2582820	7.4889150	-6.9282670	3.3673350	-0.6677970
			G_6	0.0000000	0.0000000	0.0000000	0.0000000	0.0000000	0.0000000	0.0000000
		0.2	G_0	0.2080760	3.0112422	-5.1048701	7.6348715	-6.8347547	2.7940766	-0.3882688
			G_1	0.0084834	0.2406767	2.4574292	-3.6452421	3.6142837	-2.8451814	0.9270638
			G_5	0.2080760	3.0112422	-5.1048701	7.6348715	-6.8347547	2.7940766	-0.3882688
			G_6	0.0000000	0.0000000	0.0000000	0.0000000	0.0000000	0.0000000	0.0000000
		0.4	G_0	0.2357940	3.0822400	-3.5792100	3.9476890	1.9131590	-6.8872200	3.1896800
			G_1	0.0145140	0.4038000	1.6422700	-0.3906100	-0.6480700	-0.2940300	0.2514900
			G_5	0.2357940	3.0822400	-3.5792100	3.9476890	1.9131590	-6.8872200	3.1896800
			G_6	0.0000000	0.0000000	0.0000000	0.0000000	0.0000000	0.0000000	0.0000000
		0.6	G_0	0.2902240	3.6892050	-4.5739100	11.709890	-6.3750000	-5.8894100	4.2452400
			G_1	0.0208890	0.7016780	0.1631840	5.7072160	-8.2075800	3.4561120	-0.4454700
			G_5	0.2902240	3.6892050	-4.5739100	11.709890	-6.3750000	-5.8894100	4.2452400
			G_6	0.0000000	0.0000000	0.0000000	0.0000000	0.0000000	0.0000000	0.0000000
		0.8	G_0	0.5163550	2.5310830	14.712900	-43.621800	101.06570	-116.08100	46.190900
			G_1	0.0825460	0.4971770	4.6064810	-7.3326700	21.148620	-29.345100	12.491400
			G_5	0.5163550	2.5310830	14.712900	-43.621800	101.06570	-116.08100	46.190900
			G_6	0.0000000	0.0000000	0.0000000	0.0000000	0.0000000	0.0000000	0.0000000
0.0	0.0625	0	G_0	0.2695332	2.1626001	-1.6551569	-1.2970208	4.5604304	-4.3163876	1.4010655
			G_1	0.0138667	0.1827458	2.5749608	-3.9044679	3.3556301	-2.1772209	0.6420134
			G_5	0.2695330	2.1626000	-1.6551570	-1.2970210	4.5604300	-4.3163880	1.4010660
			G_6	0.0000000	0.0000000	0.0000000	0.0000000	0.0000000	0.0000000	0.0000000
		0.2	G_0	0.2845892	2.2264055	-1.4546190	-1.5760719	5.1131083	-4.9485443	1.6207574
			G_1	0.0199077	0.2210874	2.4642047	-3.5898625	3.1624039	-2.2403780	0.6965751
			G_5	0.2845892	2.2264055	-1.4546190	-1.5760719	5.1131083	-4.9485443	1.6207574
			G_6	0.0000000	0.0000000	0.0000000	0.0000000	0.0000000	0.0000000	0.0000000
		0.4	G_0	0.3261480	2.5200870	-1.8847000	2.1798740	-1.4597100	-0.1886500	0.2393400
			G_1	0.0294120	0.3699370	1.9220850	-1.2071500	-0.4394000	0.2737550	-0.0395200
			G_5	0.3261480	2.5200870	-1.8847000	2.1798740	-1.4597100	-0.1886500	0.2393400
			G_6	0.0000000	0.0000000	0.0000000	0.0000000	0.0000000	0.0000000	0.0000000
		0.6	G_0	0.4166330	3.1566470	-2.6248900	7.7325910	-9.6927800	3.6428700	-0.0892000
			G_1	0.0598460	0.4340740	2.6811560	-3.1936600	4.0753720	-4.6940200	1.8285500
			G_5	0.4166330	3.1566470	-2.6248900	7.7325910	-9.6927800	3.6428700	-0.0892000
			G_6	0.0000000	0.0000000	0.0000000	0.0000000	0.0000000	0.0000000	0.0000000
		0.8	G_0	0.6540140	3.4231920	3.8158050	-4.1586900	3.4715330	-10.310400	6.6280000
			G_1	0.1214780	0.6975490	2.9718330	-1.3036500	-0.0754900	-3.0465100	2.1670000
			G_5	0.6540140	3.4231920	3.8158050	-4.1586900	3.4715330	-10.310400	6.6280000
			G_6	0.0000000	0.0000000	0.0000000	0.0000000	0.0000000	0.0000000	0.0000000

Table 9B.14 – Influence Coefficients for a Circumferential Semi-Elliptical Surface Crack in a Cylinder – Inside Surface

t/R_i	a/c	a/t	G_i	A_0	A_1	A_2	A_3	A_4	A_5	A_6
0.0	0.125	0	G_0	0.4065238	0.7772483	3.8861644	-12.573943	16.760207	-11.014593	2.8706957
			G_1	0.0320270	0.1825342	2.2670449	-2.7076615	1.2088194	-0.3777430	0.0763155
			G_5	0.4065240	0.7772480	3.8861640	-12.573943	16.760207	-11.014593	2.8706960
			G_6	0.0000000	0.0000000	0.0000000	0.0000000	0.0000000	0.0000000	0.0000000
		0.2	G_0	0.4242116	1.0089302	3.2973815	-12.159726	17.873386	-12.868668	3.6281712
			G_1	0.0429859	0.2033811	2.2563818	-2.8752160	1.8152558	-1.0512327	0.3181077
			G_5	0.4242116	1.0089302	3.2973815	-12.159726	17.873386	-12.868668	3.6281712
			G_6	0.0000000	0.0000000	0.0000000	0.0000000	0.0000000	0.0000000	0.0000000
		0.4	G_0	0.4917770	1.6592320	-0.1080400	0.1793240	-2.7076100	3.3680620	-1.3489700
			G_1	0.0634270	0.3722500	1.6231670	-0.5306500	-2.0007400	1.8943780	-0.5880300
			G_5	0.4917770	1.6592320	-0.1080400	0.1793240	-2.7076100	3.3680620	-1.3489700
			G_6	0.0000000	0.0000000	0.0000000	0.0000000	0.0000000	0.0000000	0.0000000
		0.6	G_0	0.6591820	1.8759140	1.0212600	-1.7698000	-0.5653600	1.2479960	-0.4376600
			G_1	0.1116040	0.4714500	1.7940590	-0.7557600	-1.4901700	1.0852180	-0.2113700
			G_5	0.6591820	1.8759140	1.0212600	-1.7698000	-0.5653600	1.2479960	-0.4376600
			G_6	0.0000000	0.0000000	0.0000000	0.0000000	0.0000000	0.0000000	0.0000000
		0.8	G_0	0.9809330	1.8846320	4.8020780	-8.0580200	0.4447850	3.4772660	-1.0567500
			G_1	0.2039950	0.4800150	2.8822430	-2.5890100	-0.9683000	1.5372370	-0.3750200
			G_5	0.9809330	1.8846320	4.8020780	-8.0580200	0.4447850	3.4772660	-1.0567500
			G_6	0.0000000	0.0000000	0.0000000	0.0000000	0.0000000	0.0000000	0.0000000
0.0	0.25	0	G_0	0.6152816	-0.3348694	6.2955620	-15.590618	19.299508	-12.488107	3.3010035
			G_1	0.0703566	0.2828152	1.4036169	-0.6511596	-1.2076596	1.0318656	-0.2423741
			G_5	0.6152820	-0.3348690	6.2955620	-15.590618	19.299508	-12.488107	3.3010030
			G_6	0.0000000	0.0000000	0.0000000	0.0000000	0.0000000	0.0000000	0.0000000
		0.2	G_0	0.6385889	-0.3095132	6.5329787	-16.622882	21.056641	-13.850120	3.6988146
			G_1	0.0840059	0.1999367	1.8218113	-1.7756899	0.3757186	-0.0785358	0.0643386
			G_5	0.6385889	-0.3095132	6.5329787	-16.622882	21.056641	-13.850120	3.6988146
			G_6	0.0000000	0.0000000	0.0000000	0.0000000	0.0000000	0.0000000	0.0000000
		0.4	G_0	0.7390420	0.0548160	4.0842620	-7.5883100	5.4047530	-1.0146100	-0.3483400
			G_1	0.1164500	0.2479880	1.8282520	-1.7169900	0.1912120	0.1165770	-0.0186100
			G_5	0.7390420	0.0548160	4.0842620	-7.5883100	5.4047530	-1.0146100	-0.3483400
			G_6	0.0000000	0.0000000	0.0000000	0.0000000	0.0000000	0.0000000	0.0000000
		0.6	G_0	0.9461210	-0.1858800	5.5867460	-9.8634900	5.9596870	0.1296440	-1.0026100
			G_1	0.1778050	0.2056680	2.0979210	-1.8039500	-0.5558700	1.1461400	-0.4206600
			G_5	0.9461210	-0.1858800	5.5867460	-9.8634900	5.9596870	0.1296440	-1.0026100
			G_6	0.0000000	0.0000000	0.0000000	0.0000000	0.0000000	0.0000000	0.0000000
		0.8	G_0	1.2452110	-0.6921900	8.3260620	-14.948000	8.6936910	0.4755790	-1.3926600
			G_1	0.2585640	0.1548890	2.1170240	-0.4910000	-4.6146100	5.4550750	-1.9663300
			G_5	1.2452110	-0.6921900	8.3260620	-14.948000	8.6936910	0.4755790	-1.3926600
			G_6	0.0000000	0.0000000	0.0000000	0.0000000	0.0000000	0.0000000	0.0000000

Table 9B.14 – Influence Coefficients for a Circumferential Semi-Elliptical Surface Crack in a Cylinder – Inside Surface

t/R_i	a/c	a/t	G_i	A_0	A_1	A_2	A_3	A_4	A_5	A_6
0.0	0.5	0	G_0	0.8776607	-0.6729719	3.7721411	-6.5209060	6.3377934	-3.7028038	0.9872447
			G_1	0.1277541	0.4368502	0.4904522	1.0427434	-2.9631236	2.0826525	-0.5184313
			G_5	0.8776610	-0.6729720	3.7721410	-6.5209060	6.3377930	-3.7028040	0.9872450
			G_6	0.0000000	0.0000000	0.0000000	0.0000000	0.0000000	0.0000000	0.0000000
		0.2	G_0	0.9003948	-0.8850488	5.2743239	-11.267523	13.890755	-9.6373584	2.8183906
			G_1	0.1404409	0.3215397	1.1010666	-1.0257556	0.6943940	-1.0793186	0.5410929
			G_5	0.9003948	-0.8850488	5.2743239	-11.267523	13.890755	-9.6373584	2.8183906
			G_6	0.0000000	0.0000000	0.0000000	0.0000000	0.0000000	0.0000000	0.0000000
		0.4	G_0	1.0058060	-0.7322600	2.9951940	-1.9459200	-3.2613500	5.1424570	-2.0306200
			G_1	0.1740870	0.3051630	1.2070310	-0.6720500	-1.0651300	1.1445590	-0.3644800
			G_5	0.9000590	-0.5476000	2.4416770	-1.2688500	-3.3815300	4.7868570	-1.8373900
			G_6	0.0000000	0.0000000	0.0000000	0.0000000	0.0000000	0.0000000	0.0000000
		0.6	G_0	1.1826010	-1.1072500	3.9623640	-2.7781300	-4.3097300	7.2772750	-2.9648200
			G_1	0.2277120	0.1701170	1.5499470	-1.1051200	-0.8333700	1.1717060	-0.4194500
			G_5	1.1826010	-1.1072500	3.9623640	-2.7781300	-4.3097300	7.2772750	-2.9648200
			G_6	0.0000000	0.0000000	0.0000000	0.0000000	0.0000000	0.0000000	0.0000000
		0.8	G_0	1.3833380	-1.3900300	4.3755780	-3.7372600	-2.5403200	5.3036000	-2.0932400
			G_1	0.2820110	0.0839230	1.7258580	-1.5358100	-0.0635600	0.5006780	-0.1982200
			G_5	1.3833380	-1.3900300	4.3755780	-3.7372600	-2.5403200	5.3036000	-2.0932400
			G_6	0.0000000	0.0000000	0.0000000	0.0000000	0.0000000	0.0000000	0.0000000
0.0	1.0	0	G_0	1.1977992	-0.5244870	0.1498299	2.3284866	-5.1058499	4.3469049	-1.3487980
			G_1	0.1870117	0.6987352	0.1316900	0.7269255	-2.5259384	2.1756251	-0.6540458
			G_5	1.1977990	-0.5244870	0.1498300	2.3284870	-5.1058500	4.3469050	-1.3487980
			G_6	0.0000000	0.0000000	0.0000000	0.0000000	0.0000000	0.0000000	0.0000000
		0.2	G_0	1.2263282	-1.1608467	4.4744783	-11.584231	17.811241	-14.408250	4.6998279
			G_1	0.2154786	0.2441623	2.8107820	-7.6574580	11.171413	-9.0053693	2.9542871
			G_5	1.2263282	-1.1608467	4.4744783	-11.584231	17.811241	-14.408250	4.6998279
			G_6	0.0000000	0.0000000	0.0000000	0.0000000	0.0000000	0.0000000	0.0000000
		0.4	G_0	1.2989480	-0.9978000	1.9479540	-1.3002700	-1.4940100	2.8306230	-1.2126000
			G_1	0.2386246	0.1447774	3.3198992	-9.2456599	13.823512	-11.223715	3.6868232
			G_5	1.2989480	-0.9978000	1.9479540	-1.3002700	-1.4940100	2.8306230	-1.2126000
			G_6	0.0000000	0.0000000	0.0000000	0.0000000	0.0000000	0.0000000	0.0000000
		0.6	G_0	1.3971180	-1.1348400	1.7918740	-0.4202600	-2.8679300	3.7685480	-1.4405000
			G_1	0.2445870	0.5326670	0.5939690	-0.0361800	-2.0163100	2.2167010	-0.7782200
			G_5	1.3971180	-1.1348400	1.7918740	-0.4202600	-2.8679300	3.7685480	-1.4405000
			G_6	0.0000000	0.0000000	0.0000000	0.0000000	0.0000000	0.0000000	0.0000000
		0.8	G_0	1.5117010	-1.3244800	1.7568350	-0.1337900	-2.8629300	3.2953270	-1.1412400
			G_1	0.2704470	0.5113280	0.5357440	-0.0327300	-1.5570200	1.5570970	-0.5094600
			G_5	1.5117010	-1.3244800	1.7568350	-0.1337900	-2.8629300	3.2953270	-1.1412400
			G_6	0.0000000	0.0000000	0.0000000	0.0000000	0.0000000	0.0000000	0.0000000

Table 9B.14 – Influence Coefficients for a Circumferential Semi-Elliptical Surface Crack in a Cylinder – Inside Surface

t/R_i	a/c	a/t	G_i	A_0	A_1	A_2	A_3	A_4	A_5	A_6
0.0	2.0	0	G_0	0.8150546	-0.5623828	1.4465771	-4.6778133	8.4192164	-7.9025932	2.9866351
			G_1	0.1359146	0.0702340	3.5558581	-11.034445	16.967724	-14.126991	4.8706612
			G_5	0.8150550	-0.5623830	1.4465770	-4.6778130	8.4192160	-7.9025930	2.9866350
			G_6	0.0000000	0.0000000	0.0000000	0.0000000	0.0000000	0.0000000	0.0000000
		0.2	G_0	0.8463715	-1.0011024	4.0052312	-11.937181	19.189548	-16.039296	5.4674371
			G_1	0.1395121	0.0753999	3.1895604	-9.5540932	14.214316	-11.649525	4.0073308
			G_5	0.8463715	-1.0011024	4.0052312	-11.937181	19.189548	-16.039296	5.4674371
			G_6	0.0000000	0.0000000	0.0000000	0.0000000	0.0000000	0.0000000	0.0000000
		0.4	G_0	0.8570045	-1.0183085	3.9957306	-11.886878	19.152747	-16.047480	5.4801806
			G_1	0.1436696	0.0544018	3.2816127	-9.8164232	14.610963	-11.942138	4.0907797
			G_5	0.8570045	-1.0183085	3.9957306	-11.886878	19.152747	-16.047480	5.4801806
			G_6	0.0000000	0.0000000	0.0000000	0.0000000	0.0000000	0.0000000	0.0000000
		0.6	G_0	0.8839861	-1.0765270	4.0774087	-11.976171	19.173189	-15.996207	5.4501217
			G_1	0.1504185	0.0478401	3.2579960	-9.6921199	14.370843	-11.736129	4.0258411
			G_5	0.8839861	-1.0765270	4.0774087	-11.976171	19.173189	-15.996207	5.4501217
			G_6	0.0000000	0.0000000	0.0000000	0.0000000	0.0000000	0.0000000	0.0000000
		0.8	G_0	0.9033134	-0.9619755	2.8501500	-7.6366897	11.596116	-9.4828625	3.2550163
			G_1	0.1458559	0.2313881	1.9882138	-5.5546045	7.4196069	-5.8965053	2.0855563
			G_5	0.9033134	-0.9619755	2.8501500	-7.6366897	11.596116	-9.4828625	3.2550163
			G_6	0.0000000	0.0000000	0.0000000	0.0000000	0.0000000	0.0000000	0.0000000
0.01 (1/100)	0.03125	0	G_0	0.1965046	2.9373464	-5.2582823	7.4889153	-6.9282667	3.3673349	-0.6677966
			G_1	0.0051780	0.1750280	2.7718680	-4.6457154	4.6780502	-3.2768090	0.9840994
			G_5	0.1945594	2.9082634	-5.2062198	7.4147673	-6.8596703	3.3339951	-0.6611852
			G_6	0.0000000	0.0000000	0.0000000	0.0000000	0.0000000	0.0000000	0.0000000
		0.2	G_0	0.2113693	2.4611847	-1.2555276	-3.9099693	10.168733	-9.4308428	3.0497093
			G_1	0.0068482	0.2344833	2.4101824	-3.4675608	3.2634711	-2.5230489	0.8210179
			G_5	0.2091661	2.4386755	-1.2400919	-3.8967307	10.151842	-9.4330385	3.0549558
			G_6	-0.0172100	-0.1521300	-0.1779700	1.9726870	-3.8338100	3.2472630	-1.0388400
		0.4	G_0	0.2291320	2.9276350	-3.0738200	2.7397460	2.9604660	-6.9798300	3.0083400
			G_1	0.0142030	0.2192850	2.0564800	-0.9489600	-1.5132300	1.9636370	-0.8532200
			G_5	0.2301040	2.6100030	-0.9176200	-4.6212100	15.609250	-17.451800	6.3333330
			G_6	-0.0150460	-0.1515480	0.4190890	-1.2072670	2.0290350	-1.3179820	0.2449160
		0.6	G_0	0.2623350	3.2092560	-3.2397400	8.5204270	-5.1220000	-3.7665800	2.8156500
			G_1	0.0248090	0.3513540	2.0700650	-0.5290600	0.0968000	-1.4958200	0.7241300
			G_5	0.2549450	3.0200540	-2.1778100	4.6517170	2.0776470	-10.061700	4.8888890
			G_6	-0.0814700	0.7240650	-11.914200	47.514510	-86.327200	74.653510	-24.569200
		0.8	G_0	0.3835990	1.7034980	12.805120	-35.291100	68.861500	-71.762500	27.102700
			G_1	0.0448690	0.0905890	5.0431910	-7.6013700	13.743680	-16.240200	6.5418600
			G_5	0.3481020	2.1573310	8.3171710	-20.490700	45.834380	-54.400000	22.000000
			G_6	-0.1363650	0.8255990	-8.0969840	10.864975	7.1092090	-19.508310	8.9002660

Table 9B.14 – Influence Coefficients for a Circumferential Semi-Elliptical Surface Crack in a Cylinder – Inside Surface

t/R_i	a/c	a/t	G_i	A_0	A_1	A_2	A_3	A_4	A_5	A_6
0.01 (1/100)	0.0625	0	G_0	0.2695332	2.1626001	-1.6551569	-1.2970208	4.5604304	-4.3163876	1.4010655
			G_1	0.0138667	0.1827458	2.5749608	-3.9044679	3.3556301	-2.1772209	0.6420134
			G_5	0.2668644	2.1411881	-1.6387693	-1.2841792	4.5152772	-4.2736515	1.3871941
			G_6	0.0000000	0.0000000	0.0000000	0.0000000	0.0000000	0.0000000	0.0000000
		0.2	G_0	0.2835264	2.0613640	-0.9368782	-1.5744499	3.1600245	-2.3327183	0.5899882
			G_1	0.0183834	0.2135060	2.5392469	-4.0904290	4.3065189	-3.3356302	1.0756474
			G_5	0.2808325	2.0498352	-0.9507559	-1.5219478	3.1086233	-2.3153897	0.5903314
			G_6	-0.0131300	-0.0756700	0.0857440	-0.1357400	0.5299420	-0.6651500	0.2740030
		0.4	G_0	0.3202080	2.5067530	-2.0649000	2.2278280	-0.8623600	-0.9432700	0.4956600
			G_1	0.0284060	0.2705840	1.9478260	-1.0579900	-0.9504800	1.1065000	-0.4544200
			G_5	0.3129040	2.4365950	-1.6600900	0.5673180	2.6075810	-4.3140000	1.7142860
			G_6	-0.0169490	0.0703960	-0.4886870	0.8510980	-0.5594650	0.2904380	-0.1440920
		0.6	G_0	0.3775210	3.2406620	-4.8245900	14.629680	-20.455900	12.075370	-2.7056900
			G_1	0.0496180	0.3348330	2.5241770	-2.7321800	3.1090090	-3.4203600	1.2509400
			G_5	0.3833880	2.7490360	-0.9162100	0.5336120	4.0711300	-8.2199700	3.7142860
			G_6	-0.0553810	0.2890290	-2.9240160	7.3178900	-7.6884650	3.7874410	-0.7302120
		0.8	G_0	0.5380920	2.7195780	4.0871740	-6.3008300	7.1473380	-10.827600	5.6152700
			G_1	0.0760440	0.4104780	3.1576040	-2.2896400	1.0207330	-2.3974500	1.3565500
			G_5	0.5039970	3.3050780	-0.9443300	10.766270	-20.957800	11.568260	-1.2903200
			G_6	-0.1220240	1.4824240	-11.677130	27.520060	-23.121698	2.7601930	3.1288300
0.01 (1/100)	0.125	0	G_0	0.4065238	0.7772483	3.8861644	-12.573943	16.760207	-11.014593	2.8706957
			G_1	0.0320270	0.1825342	2.2670449	-2.7076615	1.2088194	-0.3777430	0.0763155
			G_5	0.4024990	0.7695525	3.8476871	-12.449449	16.594264	-10.905538	2.8422733
			G_6	0.0000000	0.0000000	0.0000000	0.0000000	0.0000000	0.0000000	0.0000000
		0.2	G_0	0.4133004	1.1321686	1.8045358	-6.4250407	8.1265233	-5.1779761	1.3216183
			G_1	0.0478287	0.0131254	3.9210159	-9.0824041	12.609044	-9.8323116	3.0270205
			G_5	0.4085744	1.1502654	1.6207996	-5.8595868	7.2756359	-4.5530051	1.1438168
			G_6	-0.0219020	0.2358900	-1.0557450	1.2836690	0.4004010	-1.4438580	0.6076390
		0.4	G_0	0.4884630	1.5730830	0.6794250	-2.6942700	2.4688900	-1.0967700	0.1279400
			G_1	0.0721890	0.4196840	1.5725580	-0.5246000	-1.8820000	1.6181090	-0.4302300
			G_5	0.4804120	1.2808740	2.6986570	-9.6391400	14.039630	-10.260700	2.8888890
			G_6	-0.0216650	0.2362600	-1.0550020	1.2674570	0.4586870	-1.5213580	0.6415500
		0.6	G_0	0.6325650	1.9612380	0.2124640	1.0673660	-4.8520900	4.2428280	-1.2187600
			G_1	0.1171020	0.4578330	2.1168020	-1.8894800	0.5759570	-0.8442000	0.4875500
			G_5	0.6084410	1.5560570	2.7315980	-7.6163000	9.3971820	-6.7692300	2.0000000
			G_6	-0.0505070	0.4694550	-2.7933710	5.3874320	-3.3467640	-0.4227780	0.7601120
		0.8	G_0	0.9044670	1.6602910	5.4293610	-7.8741700	-1.3182900	5.4386470	-1.7533200
			G_1	0.1947050	0.4093530	3.3076490	-3.2250800	-0.4973400	1.2925110	-0.2919800
			G_5	0.8217350	1.6023680	4.7339870	-8.0546200	1.4068690	2.8512260	-1.1538500
			G_6	-0.1093090	1.9146030	-15.389770	49.115082	-74.961586	55.324734	-15.905227

Table 9B.14 – Influence Coefficients for a Circumferential Semi-Elliptical Surface Crack in a Cylinder – Inside Surface

t/R_i	a/c	a/t	G_i	A_0	A_1	A_2	A_3	A_4	A_5	A_6
0.01 (1/100)	0.25	0	G_0	0.6152816	-0.3348694	6.2955620	-15.590618	19.299508	-12.488107	3.3010035
			G_1	0.0703566	0.2828152	1.4036169	-0.6511596	-1.2076596	1.0318656	-0.2423741
			G_5	0.6091901	-0.3315535	6.2332297	-15.436255	19.108424	-12.364462	3.2683198
			G_6	0.0000000	0.0000000	0.0000000	0.0000000	0.0000000	0.0000000	0.0000000
		0.2	G_0	0.6246031	-0.2494174	7.0847353	-20.200719	28.227826	-19.960558	5.6093784
			G_1	0.0891236	0.1846386	2.4135204	-4.7013804	5.7368556	-4.4125580	1.3716268
			G_5	0.6161299	-0.2007834	6.8142686	-19.552840	27.443393	-19.500929	5.5094250
			G_6	-0.0541160	0.5971300	-2.1038670	2.5704450	-0.3120010	-1.2674590	0.5757640
		0.4	G_0	0.7329950	0.0996250	3.9573730	-7.2526600	4.9136700	-0.6649300	-0.4401500
			G_1	0.1244530	0.2438230	1.9426520	-2.0609400	0.6954550	-0.3004200	0.1292100
			G_5	0.7190360	-0.1450100	5.7680680	-13.467900	15.388650	-9.1789700	2.2222220
			G_6	-0.0206400	-0.1296000	0.8965700	-2.9862200	4.9277530	-3.8982200	1.2103470
		0.6	G_0	0.9335850	-0.0671400	4.9859720	-8.0099800	3.1444570	2.1751370	-1.5670900
			G_1	0.1861600	0.1872070	2.3208790	-2.4591900	0.4288930	0.3550800	-0.1581000
			G_5	0.8894260	-0.0854300	5.2732800	-9.6837700	6.7449300	-1.1691900	-0.4444400
			G_6	-0.0463100	-0.0874700	0.6337330	-2.4633100	4.4763150	-3.6982600	1.1853050
		0.8	G_0	1.2407050	-0.9832700	11.036350	-24.419000	25.074820	-13.247100	3.0448500
			G_1	0.2685320	0.0687020	2.9242790	-3.1935800	-0.0724900	1.6614580	-0.7248500
			G_5	1.1263020	-0.1935400	5.0577920	-4.8699400	-6.8200300	12.339280	-5.0000000
			G_6	-0.0921700	0.0037710	-0.1514300	0.1417710	0.1176790	0.1210370	-0.1406600
0.01 (1/100)	0.5	0	G_0	0.8776607	-0.6729719	3.7721411	-6.5209060	6.3377934	-3.7028038	0.9872447
			G_1	0.1277541	0.4368502	0.4904522	1.0427434	-2.9631236	2.0826525	-0.5184313
			G_5	0.8689713	-0.6663089	3.7347931	-6.4563426	6.2750426	-3.6661426	0.9774703
			G_6	0.0000000	0.0000000	0.0000000	0.0000000	0.0000000	0.0000000	0.0000000
		0.2	G_0	0.9002026	-1.0448586	6.4415960	-14.919959	19.300130	-13.414233	3.8224907
			G_1	0.1486748	0.1536960	2.2835405	-4.6118436	5.8374817	-4.6007501	1.4736264
			G_5	0.8967218	-1.1174698	6.9898115	-16.817521	22.611071	-16.255963	4.7757560
			G_6	-0.0224350	0.2340860	-0.7934310	0.9301460	-0.1266190	-0.3599330	0.1408310
		0.4	G_0	1.0063880	-0.7425700	3.1260260	-2.1867000	-3.0931200	5.1298930	-2.0520500
			G_1	0.1789440	0.3206900	1.1011660	-0.2780300	-1.7360100	1.6648710	-0.5147200
			G_5	0.9524140	-0.3624700	1.1644200	2.7118250	-9.3779500	9.0697680	-3.0000000
			G_6	-0.0457800	0.2901210	-1.3238400	2.8032230	-2.8108600	1.1635060	-0.0763800
		0.6	G_0	1.1876880	-1.1514600	4.3134430	-3.6414000	-3.2248100	6.5781370	-2.7782500
			G_1	0.2348560	0.1694010	1.5310330	-0.9297400	-1.2048400	1.4747130	-0.5037800
			G_5	1.1359920	-0.9448000	3.4128040	-1.8724600	-4.5753100	6.5909090	-2.5000000
			G_6	-0.0468900	0.1396290	-0.4115500	0.1517870	1.2863330	-2.0159700	0.8966670
		0.8	G_0	1.3768550	-1.1807900	3.4327750	-1.9675000	-3.7422900	5.2586230	-1.8511600
			G_1	0.2827170	0.2258060	0.9136330	0.4871590	-2.5046300	1.9013960	-0.5002900
			G_5	1.3394760	-1.4954100	5.6192840	-7.8528200	4.1462310	-0.0014000	-0.4666700
			G_6	-0.0491000	-0.0672300	0.3961180	-0.0658000	-1.5130700	2.1490470	-0.8499800

Table 9B.14 – Influence Coefficients for a Circumferential Semi-Elliptical Surface Crack in a Cylinder – Inside Surface

t/R_i	a/c	a/t	G_i	A_0	A_1	A_2	A_3	A_4	A_5	A_6
0.01 (1/100)	1.0	0	G_0	1.1977992	-0.5244870	0.1498299	2.3284866	-5.1058499	4.3469049	-1.3487980
			G_1	0.1870117	0.6987352	0.1316900	0.7269255	-2.5259384	2.1756251	-0.6540458
			G_5	1.1859396	-0.5192941	0.1483465	2.3054327	-5.0552970	4.3038663	-1.3354436
			G_6	0.0000000	0.0000000	0.0000000	0.0000000	0.0000000	0.0000000	0.0000000
		0.2	G_0	1.2067321	-1.7033309	8.4788390	-24.777373	38.683559	-29.873440	8.9989111
			G_1	0.2148016	0.0103054	4.4729009	-13.203805	19.861499	-15.242926	4.5969364
			G_5	1.2015675	-1.7750100	9.0214999	-26.633978	41.941806	-32.712927	9.9697884
			G_6	0.0016670	-0.0510880	0.2392280	-0.2578760	-0.4940620	1.1084580	-0.5456990
		0.4	G_0	1.3064660	-1.0152400	1.9350880	-0.8993700	-2.4736000	3.7825660	-1.5472100
			G_1	0.2235710	0.5338870	0.8263620	-0.7439300	-1.0125200	1.5328880	-0.6019500
			G_5	1.2517400	-0.7808000	1.3235020	-1.0210500	0.3224960	-0.1302300	0.1000000
			G_6	-0.0695000	0.6377210	-3.1510300	7.3922700	-8.6270500	4.7282640	-0.9106700
		0.6	G_0	1.4098990	-1.1943200	2.0682710	-0.9892900	-2.2245400	3.4010710	-1.3594400
			G_1	0.2530760	0.4979500	0.7711470	-0.5373400	-1.2119300	1.5653800	-0.5725000
			G_5	1.3465480	-0.8307100	0.6179530	1.6695920	-4.1552400	3.4418610	-1.0000000
			G_6	-0.0726000	0.6362230	-3.1015700	7.3056020	-8.6578800	4.9164400	-1.0262100
		0.8	G_0	1.5256800	-1.3415100	1.7834550	-0.0964700	-2.9501000	3.3412720	-1.1425600
			G_1	0.2815290	0.4575980	0.7882960	-0.6608400	-0.6979100	0.9575600	-0.3420100
			G_5	1.4505130	-0.9455100	0.4188330	2.2447860	-4.4641100	3.0139540	-0.6000000
			G_6	-0.0615400	0.2712860	-0.7398700	0.9603950	-0.3723600	-0.2362900	0.1783660
0.01 (1/100)	2.0	0	G_0	0.8150546	-0.5623828	1.4465771	-4.6778133	8.4192164	-7.9025932	2.9866351
			G_1	0.1359146	0.0702340	3.5558581	-11.034445	16.967724	-14.126991	4.8706612
			G_5	0.8069852	-0.5568149	1.4322545	-4.6314980	8.3358574	-7.8243495	2.9570644
			G_6	0.0000000	0.0000000	0.0000000	0.0000000	0.0000000	0.0000000	0.0000000
		0.2	G_0	0.8302318	-1.0537920	4.4849604	-13.681535	22.101428	-18.224902	6.0608442
			G_1	0.1359260	0.0420920	3.4125294	-10.351846	15.495515	-12.528053	4.2082167
			G_5	0.8480320	-1.4983161	7.5823511	-23.990117	39.865852	-33.470869	11.205087
			G_6	-0.0080970	0.1348050	-0.7140660	1.3153720	-0.3896700	-0.9981360	0.6542230
		0.4	G_0	0.8319520	-0.2882200	-0.9010500	3.7444010	-6.6020800	5.1512080	-1.4147000
			G_1	0.1383584	0.0278547	3.4704568	-10.542062	15.886092	-12.940522	4.3759927
			G_5	0.8560852	-1.5581979	7.9297434	-25.174918	42.077867	-35.552139	11.971236
			G_6	-0.0087500	0.0024420	0.0265390	-0.0760000	0.0506630	0.0276830	-0.0225900
		0.6	G_0	0.8587580	-0.3374500	-0.8921600	3.9094140	-7.0178900	5.5638580	-1.5595700
			G_1	0.1446303	0.0649644	3.1736270	-9.6071448	14.265975	-11.457141	3.8295030
			G_5	0.8805204	-1.4629959	6.9298534	-21.719290	35.917812	-29.984188	9.9790906
			G_6	-0.0119500	0.0130590	-0.0189400	-0.0124700	0.0793610	-0.0796600	0.0305960
		0.8	G_0	0.9123970	-0.9512000	2.8284570	-7.6354600	11.693170	-9.6165300	3.3094020
			G_1	0.1527108	0.0144266	3.5158698	-10.739376	15.998316	-12.610069	4.0831981
			G_5	0.9095908	-1.5365253	7.0754050	-21.927254	35.660007	-29.052725	9.3994559
			G_6	-0.0013200	-0.1153700	0.5804610	-0.9632700	0.0238800	1.2630520	-0.7874300

Table 9B.14 – Influence Coefficients for a Circumferential Semi-Elliptical Surface Crack in a Cylinder – Inside Surface

t/R_i	a/c	a/t	G_i	A_0	A_1	A_2	A_3	A_4	A_5	A_6
0.01667 (1/60)	0.03125	0	G_0	0.1965046	2.9373464	-5.2582823	7.4889153	-6.9282667	3.3673349	-0.6677966
			G_1	0.0051780	0.1750280	2.7718680	-4.6457154	4.6780502	-3.2768090	0.9840994
			G_5	0.1932836	2.8891928	-5.1720807	7.3661459	-6.8146889	3.3121328	-0.6568495
			G_6	0.0000000	0.0000000	0.0000000	0.0000000	0.0000000	0.0000000	0.0000000
		0.2	G_0	0.2107226	2.4486536	-1.2264604	-3.9760193	10.233171	-9.4520364	3.0496836
			G_1	0.0065380	0.2344969	2.3813083	-3.3550592	3.0827443	-2.3997909	0.7921590
			G_5	0.2063955	2.4043109	-1.2248880	-3.7768457	9.8578431	-9.1610116	2.9644987
			G_6	-0.0233860	-0.2565980	0.5389610	-1.1493680	1.8990440	-1.2165670	0.2090670
		0.4	G_0	0.2273500	2.8994780	-3.0702800	2.8459110	2.4358760	-6.3016400	2.7411400
			G_1	0.0189660	0.3037490	1.8836920	-0.6354500	-1.9172200	1.9671670	-0.6897400
			G_5	0.1945370	3.4390340	-9.0123200	25.942970	-38.952000	28.576390	-8.4444400
			G_6	-0.0743900	0.4483590	-9.4044900	38.831220	-70.525400	60.346370	-19.621700
		0.6	G_0	0.2595040	3.0460360	-2.3026600	5.1476090	-0.2504900	-7.0606900	3.7296200
			G_1	0.0257180	0.3727920	1.8347760	0.7184340	-1.9586500	-0.5017000	0.7219100
			G_5	0.2403820	2.8369760	-1.9677600	4.5458510	1.2275100	-8.5617300	4.2222220
			G_6	-0.0699260	-1.0245610	2.5586860	-8.4346200	15.170731	-10.826057	2.6247580
		0.8	G_0	0.3125960	3.1791700	-0.9308400	13.409610	-18.125500	3.2248090	2.4979200
			G_1	0.0367700	0.3553180	2.2611080	2.0125800	-1.6502800	-4.7043800	3.2604900
			G_5	0.3097830	1.8631470	8.1257570	-20.264800	43.972520	-50.000000	19.571430
			G_6	-0.1595320	0.0832100	-6.9477040	11.215244	1.0718880	-9.9117040	4.6272810
0.01667 (1/60)	0.0625	0	G_0	0.2695332	2.1626001	-1.6551569	-1.2970208	4.5604304	-4.3163876	1.4010655
			G_1	0.0138667	0.1827458	2.5749608	-3.9044679	3.3556301	-2.1772209	0.6420134
			G_5	0.2651144	2.1271475	-1.6280233	-1.2757584	4.4856689	-4.2456275	1.3780977
			G_6	0.0000000	0.0000000	0.0000000	0.0000000	0.0000000	0.0000000	0.0000000
		0.2	G_0	0.2829580	2.0531713	-0.9203782	-1.6053672	3.1800418	-2.3249558	0.5812694
			G_1	0.0182587	0.2137291	2.5327625	-4.0829513	4.3084495	-3.3473999	1.0827066
			G_5	0.2780593	2.0296062	-0.9496222	-1.4452190	2.9402537	-2.1624704	0.5394203
			G_6	-0.0225510	0.0272330	-0.4402790	0.8540010	-0.5328560	0.2460040	-0.1288840
		0.4	G_0	0.3177200	2.4789580	-2.0636800	2.3534080	-1.2687900	-0.4771100	0.3178800
			G_1	0.0379310	0.3225690	1.7647930	-0.7186000	-1.3796600	1.3640920	-0.4972600
			G_5	0.3081320	2.3588290	-1.4043700	-0.1304100	3.6134100	-5.0155600	1.9047620
			G_6	-0.0349600	-0.2394800	0.2252480	-0.0616800	0.6178930	-0.8596200	0.3526020
		0.6	G_0	0.3731390	3.0298410	-3.6957200	10.933370	-14.841000	8.0528590	-1.5849700
			G_1	0.0514370	0.3466610	2.5069820	-2.5319400	2.3055250	-2.5341400	0.9518700
			G_5	0.3401350	3.4619520	-7.6020900	24.312920	-36.614800	25.009010	-6.6666700
			G_6	-0.0732710	0.1153490	-2.6257100	6.7943630	-6.8870630	3.3544050	-0.6808330
		0.8	G_0	0.5126800	2.5746070	4.1006990	-6.7070900	7.1938800	-9.5294200	4.7148300
			G_1	0.0735390	0.3946950	3.2561800	-2.6515300	1.1069300	-1.9905100	1.1124200
			G_5	0.4933740	2.5442680	3.7776100	-5.6559200	6.3897230	-9.5947100	4.9032260
			G_6	-0.1353150	0.9140800	-9.2209120	21.912621	-17.958429	2.2107340	2.2578890

Table 9B.14 – Influence Coefficients for a Circumferential Semi-Elliptical Surface Crack in a Cylinder – Inside Surface

t/R_i	a/c	a/t	G_i	A_0	A_1	A_2	A_3	A_4	A_5	A_6
0.01667 (1/60)	0.125	0	G_0	0.4065238	0.7772483	3.8861644	-12.573943	16.760207	-11.014593	2.8706957
			G_1	0.0320270	0.1825342	2.2670449	-2.7076615	1.2088194	-0.3777430	0.0763155
			G_5	0.3998597	0.7645062	3.8224564	-12.367813	16.485450	-10.834026	2.8236354
			G_6	0.0000000	0.0000000	0.0000000	0.0000000	0.0000000	0.0000000	0.0000000
		0.2	G_0	0.4127878	1.1288265	1.8044046	-6.4152938	8.1001222	-5.1480835	1.3099846
			G_1	0.0477082	0.0127494	3.9215370	-9.0953666	12.638799	-9.8588153	3.0356787
			G_5	0.4051564	1.1427315	1.5835103	-5.7158859	7.0488009	-4.3781328	1.0910220
			G_6	-0.0257390	0.2239250	-1.0656070	1.3604470	0.3212500	-1.4129050	0.6046200
		0.4	G_0	0.4759910	1.6149290	0.0563100	-0.3881200	-1.8058600	2.7702150	-1.2288200
			G_1	0.0625368	0.2593641	2.1873520	-2.5516862	1.6083652	-1.1599244	0.3987083
			G_5	0.4717020	1.3107280	2.2107570	-7.7795000	10.750680	-7.4960600	2.0000000
			G_6	-0.0223500	-0.2105800	1.0960460	-3.6464900	6.5149560	-5.4848300	1.7532350
		0.6	G_0	0.6041080	1.7018390	1.2976620	-2.3454700	0.0435520	1.1629990	-0.5711700
			G_1	0.0872040	0.3767790	1.9214790	-0.9505800	-1.4252600	1.3537350	-0.4119700
			G_5	0.5935830	1.5018730	2.7019050	-7.3122800	8.7534260	-6.1481500	1.7777780
			G_6	-0.0632820	0.4081240	-2.6842580	5.2395720	-3.1385120	-0.5189860	0.7611220
		0.8	G_0	0.8018190	1.4311660	5.1378870	-7.5900400	-1.7258200	7.0870920	-2.9593700
			G_1	0.1409210	0.3131480	2.9222170	-2.2316000	-2.0494000	3.1817740	-1.2080000
			G_5	0.7692690	2.0175650	0.5872390	6.6193680	-23.272500	22.948860	-7.5000000
			G_6	-0.1237590	1.7115580	-14.359310	46.270554	-71.065247	52.964100	-15.407071
0.01667 (1/60)	0.25	0	G_0	0.6152816	-0.3348694	6.2955620	-15.590618	19.299508	-12.488107	3.3010035
			G_1	0.0703566	0.2828152	1.4036169	-0.6511596	-1.2076596	1.0318656	-0.2423741
			G_5	0.6051954	-0.3293793	6.1923561	-15.335034	18.983123	-12.283384	3.2468882
			G_6	0.0000000	0.0000000	0.0000000	0.0000000	0.0000000	0.0000000	0.0000000
		0.2	G_0	0.6229389	-0.2302666	6.9609935	-19.846329	27.701044	-19.565724	5.4918651
			G_1	0.0895535	0.1742480	2.4773249	-4.8948423	6.0340648	-4.6366707	1.4375883
			G_5	0.6114479	-0.1967060	6.7335744	-19.266510	26.945778	-19.076337	5.3693778
			G_6	-0.0564090	0.5906920	-2.0901230	2.5558090	-0.2933150	-1.2772490	0.5764810
		0.4	G_0	0.7230860	0.0763310	4.1369260	-8.0319300	6.3592360	-1.8637300	-0.0810400
			G_1	0.1028340	0.2539710	1.7163870	-1.3407600	-0.3668600	0.5645940	-0.1731400
			G_5	0.7005410	0.0839330	3.9999050	-7.5446700	5.5694900	-1.2943200	-0.2222200
			G_6	-0.0184500	-0.1333500	0.8293120	-2.5649100	4.1316010	-3.2421900	0.9979890
		0.6	G_0	0.9042470	-0.1856500	5.7291240	-10.550800	7.2888100	-0.9640900	-0.6920700
			G_1	0.1529590	0.2545430	1.6922640	-0.5535900	-2.4335400	2.5965280	-0.8797800
			G_5	0.8762120	-0.1312800	5.4835950	-10.309600	7.7457380	-1.9368700	-0.2222200
			G_6	-0.0323300	-0.0460700	0.3379100	-1.4409300	3.0261620	-2.8138300	0.9690880
		0.8	G_0	1.1316880	-0.4419800	6.7055250	-9.9538700	1.0924880	6.3974110	-3.2902800
			G_1	0.2221580	0.0260020	3.0773420	-3.8563700	1.2228800	0.7572230	-0.5598400
			G_5	1.0907520	-0.0093200	3.5712560	0.1162350	-14.914300	18.767860	-7.0000000
			G_6	-0.0379600	-0.0569500	0.4782960	-2.1563900	4.5710590	-4.2264200	1.4283640

Table 9B.14 – Influence Coefficients for a Circumferential Semi-Elliptical Surface Crack in a Cylinder – Inside Surface

t/R_i	a/c	a/t	G_i	A_0	A_1	A_2	A_3	A_4	A_5	A_6
0.01667 (1/60)	0.5	0	G_0	0.8776607	-0.6729719	3.7721411	-6.5209060	6.3377934	-3.7028038	0.9872447
			G_1	0.1277541	0.4368502	0.4904522	1.0427434	-2.9631236	2.0826525	-0.5184313
			G_5	0.8632731	-0.6619397	3.7103026	-6.4140059	6.2338948	-3.6421023	0.9710607
			G_6	0.0000000	0.0000000	0.0000000	0.0000000	0.0000000	0.0000000	0.0000000
		0.2	G_0	0.9018864	-1.0815324	6.6630598	-15.564973	20.271752	-14.141756	4.0363397
			G_1	0.1485414	0.1543040	2.2745789	-4.5728426	5.7593465	-4.5280704	1.4483622
			G_5	0.8878878	-1.0636710	6.6354133	-15.724941	20.876895	-14.895310	4.3591221
			G_6	-0.0240560	0.2342620	-0.7930600	0.9271080	-0.1130250	-0.3740260	0.1454300
		0.4	G_0	0.9932740	-0.6825600	2.8682700	-1.6035900	-3.8094000	5.5684300	-2.1598500
			G_1	0.1642050	0.3239630	1.1158550	-0.3663200	-1.5456100	1.5216710	-0.4853800
			G_5	0.9529570	-0.5373900	2.2996290	-0.7968700	-3.8415400	4.7720930	-1.7000000
			G_6	-0.0392000	0.2369810	-1.1181100	2.3926150	-2.3616400	0.9338270	-0.0444800
		0.6	G_0	1.1605830	-1.0763200	4.0197890	-3.0320900	-3.8705800	6.9112630	-2.8542800
			G_1	0.2139410	0.1922300	1.4906570	-1.0134500	-0.8145000	1.0597230	-0.3693500
			G_5	1.1232190	-0.9453400	3.4102860	-1.7964200	-4.7823700	6.8148880	-2.5869600
			G_6	-0.0322300	0.0915520	-0.2918800	0.0768490	1.1473990	-1.7748300	0.7831460
		0.8	G_0	1.3292370	-1.1615100	3.6535650	-2.8835300	-2.1241600	3.9940500	-1.5102100
			G_1	0.2555740	0.2241250	1.0529710	-0.0313700	-1.6192400	1.2592140	-0.3482200
			G_5	1.3186170	-1.4388800	5.2944210	-6.8009000	2.4762560	1.2996490	-0.8666700
			G_6	-0.0183200	-0.1070800	0.3822120	0.1708450	-1.9543600	2.4519870	-0.9252900
0.01667 (1/60)	1.0	0	G_0	1.1977992	-0.5244870	0.1498299	2.3284866	-5.1058499	4.3469049	-1.3487980
			G_1	0.1870117	0.6987352	0.1316900	0.7269255	-2.5259384	2.1756251	-0.6540458
			G_5	1.1781630	-0.5158889	0.1473738	2.2903151	-5.0221475	4.2756443	-1.3266866
			G_6	0.0000000	0.0000000	0.0000000	0.0000000	0.0000000	0.0000000	0.0000000
		0.2	G_0	1.2067109	-1.7065538	8.4979605	-24.835253	38.773155	-29.938748	9.0165829
			G_1	0.2151798	0.0025801	4.5248744	-13.370468	20.129832	-15.451386	4.6591613
			G_5	1.1935265	-1.7624606	8.9646344	-26.472241	41.691618	-32.517152	9.9089114
			G_6	0.0004290	-0.0477510	0.2303150	-0.2454810	-0.4980090	1.1046740	-0.5435480
		0.4	G_0	1.2939070	-0.9414400	1.6531910	-0.3354400	-2.9873500	3.9237560	-1.5227800
			G_1	0.2126570	0.5532720	0.7775530	-0.6949900	-0.9165800	1.3359110	-0.5126100
			G_5	1.2352820	-0.6784900	0.6678180	1.0594200	-3.0185000	2.4930230	-0.7000000
			G_6	-0.0594800	0.5291200	-2.6578000	6.2565790	-7.3052800	4.0245700	-0.7877100
		0.6	G_0	1.3919890	-1.1257400	1.8713870	-0.7440400	-2.1474300	3.0319020	-1.1729300
			G_1	0.2410950	0.5100520	0.7629270	-0.5721800	-1.0394000	1.3548150	-0.4949800
			G_5	1.3305680	-0.7687300	0.2917540	2.6225000	-5.5751700	4.4837210	-1.3000000
			G_6	-0.0589800	0.5290780	-2.6456800	6.3019950	-7.5575800	4.3779900	-0.9468200
		0.8	G_0	1.5025910	-1.3208600	1.9312100	-0.7670100	-1.6111100	2.1187910	-0.7381600
			G_1	0.2659580	0.4894100	0.6971000	-0.4857100	-0.8023900	0.9455810	-0.3278000
			G_5	1.4409720	-1.0211000	1.0122900	0.3944090	-1.5174900	0.7069770	0.1000000
			G_6	-0.0428700	0.1817060	-0.4353100	0.3506660	0.2052460	-0.4440300	0.1845920

Table 9B.14 – Influence Coefficients for a Circumferential Semi-Elliptical Surface Crack in a Cylinder – Inside Surface

t/R_i	a/c	a/t	G_i	A_0	A_1	A_2	A_3	A_4	A_5	A_6
0.01667 (1/60)	2.0	0	G_0	0.8150546	-0.5623828	1.4465771	-4.6778133	8.4192164	-7.9025932	2.9866351
			G_1	0.1359146	0.0702340	3.5558581	-11.034445	16.967724	-14.126991	4.8706612
			G_5	0.8016934	-0.5531636	1.4228626	-4.6011275	8.2811961	-7.7730423	2.9376738
			G_6	0.0000000	0.0000000	0.0000000	0.0000000	0.0000000	0.0000000	0.0000000
		0.2	G_0	0.8296376	-1.0437460	4.4199921	-13.483074	21.791644	-17.984029	5.9870082
			G_1	0.1357441	0.0451258	3.3972981	-10.320631	15.469959	-12.523598	4.2106689
			G_5	0.8422970	-1.4838582	7.5048455	-23.737340	39.436617	-33.106104	11.082670
			G_6	-0.0107800	0.1729480	-0.9051370	1.6854460	-0.5675240	-1.2190630	0.8440970
		0.4	G_0	0.8330510	-0.3136000	-0.7111000	3.1028630	-5.5335600	4.2965440	-1.1522500
			G_1	0.1386490	0.0238778	3.4915465	-10.596710	15.956852	-12.981046	4.3833101
			G_5	0.8502334	-1.5410277	7.8395219	-24.889211	41.608812	-35.164752	11.843785
			G_6	-0.0106700	0.0046110	0.0099130	0.0110280	-0.1252300	0.1847150	-0.0743700
		0.6	G_0	0.8601800	-0.3659600	-0.7108000	3.3562330	-6.1468900	4.8899160	-1.3568600
			G_1	0.1447870	0.0626517	3.1877176	-9.6465015	14.316634	-11.481536	3.8311770
			G_5	0.8767225	-1.4859068	7.0929349	-22.156518	36.504262	-30.362654	10.070615
			G_6	-0.0137600	0.0097030	0.0035010	-0.0347700	0.0516970	-0.0181900	0.0018220
		0.8	G_0	0.9130140	-0.9678700	2.9212000	-7.8705700	12.007920	-9.8246000	3.3624720
			G_1	0.1525958	0.0156732	3.5151883	-10.748640	16.017066	-12.616239	4.0802810
			G_5	0.9033272	-1.5238135	7.0480421	-21.856801	35.548564	-28.953022	9.3615973
			G_6	-0.0039000	-0.1111000	0.5786670	-0.9589900	0.0079690	1.2854910	-0.7981400
0.05 (1/20)	0.03125	0	G_0	0.1965046	2.9373464	-5.2582823	7.4889153	-6.9282667	3.3673349	-0.6677966
			G_1	0.0051780	0.1750280	2.7718680	-4.6457154	4.6780502	-3.2768090	0.9840994
			G_5	0.1871476	2.7974724	-5.0078876	7.1323000	-6.5983495	3.2069857	-0.6359971
			G_6	0.0000000	0.0000000	0.0000000	0.0000000	0.0000000	0.0000000	0.0000000
		0.2	G_0	0.2088527	2.4208010	-1.2059115	-3.9916735	10.186590	-9.3787430	3.0256184
			G_1	0.0055515	0.2359151	2.2714873	-2.9924979	2.5054847	-1.9490634	0.6549441
			G_5	0.1888984	2.1971707	-1.0372558	-3.4434858	9.1271458	-8.6616597	2.8410064
			G_6	-0.0623950	-0.7595440	1.1369060	-0.9471780	1.3406020	-0.7485480	0.0417860
		0.4	G_0	0.2339070	2.4866970	-0.3945000	-6.0377300	16.359450	-17.005100	6.0273300
			G_1	0.0156410	0.6614120	-0.8893200	8.0005790	-14.175100	10.019390	-2.7245400
			G_5	0.1673880	2.1612950	-2.2506700	3.7611730	-0.3508100	-3.8464100	1.9555560
			G_6	-0.1307900	-1.2357300	-1.7183400	13.994790	-27.356200	25.334110	-8.8878600
		0.6	G_0	0.2321560	3.2617860	-5.3526500	15.411070	-19.370700	9.7641860	-1.6839100
			G_1	0.0211950	0.2857910	2.5545540	-2.8774200	4.4712910	-5.3746700	2.0320100
			G_5	0.1288820	1.8063090	-2.3302600	8.5168820	-4.1140600	-4.8425900	3.0000000
			G_6	-0.1413800	-3.5684800	14.158750	-48.400400	86.154800	-68.333100	20.129870
		0.8	G_0	0.2646800	3.0895480	-2.7973700	16.180300	-26.132600	16.061620	-3.6341300
			G_1	0.0304540	0.3263940	1.7725930	3.2143820	-6.9108900	3.8177560	-0.8392400
			G_5	0.0800320	0.9383230	0.0482620	4.7846610	9.2012790	-20.880000	8.7142860
			G_6	-0.2457100	-2.4802500	0.1589000	-5.9846800	17.191700	-7.7771500	-0.8628100

Table 9B.14 – Influence Coefficients for a Circumferential Semi-Elliptical Surface Crack in a Cylinder – Inside Surface

t/R_i	a/c	a/t	G_i	A_0	A_1	A_2	A_3	A_4	A_5	A_6
0.05 (1/20)	0.0625	0	G_0	0.2695332	2.1626001	-1.6551569	-1.2970208	4.5604304	-4.3163876	1.4010655
			G_1	0.0138667	0.1827458	2.5749608	-3.9044679	3.3556301	-2.1772209	0.6420134
			G_5	0.2566981	2.0596191	-1.5763400	-1.2352581	4.3432667	-4.1108457	1.3343486
			G_6	0.0000000	0.0000000	0.0000000	0.0000000	0.0000000	0.0000000	0.0000000
		0.2	G_0	0.2802768	2.0413508	-0.9577520	-1.4564195	2.9169446	-2.1046670	0.5129783
			G_1	0.0171658	0.2157598	2.4727789	-3.9201614	4.1177933	-3.2563293	1.0723311
			G_5	0.2635526	1.9313264	-0.9120544	-1.2450163	2.5909773	-1.9333722	0.4853760
			G_6	-0.0490380	-0.1795280	-0.2454050	1.0625390	-0.7967470	0.3727910	-0.1617450
		0.4	G_0	0.3083410	2.3855850	-1.9218300	1.9803570	-1.0348400	-0.3750400	0.2365600
			G_1	0.0312820	0.3438540	1.7288400	-0.3368700	-2.3671700	2.0699200	-0.6086600
			G_5	0.2750280	2.1806580	-1.7967800	2.3832970	-1.4992300	-0.3630100	0.3333330
			G_6	-0.0890500	-0.6601200	0.5733550	0.4495970	-0.3843100	0.2417050	-0.1311800
		0.6	G_0	0.4011200	1.1955530	10.285170	-38.432200	67.857840	-57.992600	18.745000
			G_1	0.0423900	0.3548810	2.1404590	-1.3301800	0.7123500	-1.8956100	1.0072600
			G_5	0.2794130	2.7404610	-5.1200600	17.016710	-25.540900	17.136940	-4.5333300
			G_6	-0.1700610	-2.5508870	5.6011110	-17.785271	29.901886	-18.428740	3.4337990
		0.8	G_0	0.5058610	0.6109790	16.922960	-51.708500	81.151730	-66.073300	21.183300
			G_1	0.0609080	0.4408160	2.1634560	0.6206470	-3.8418100	1.9777360	-0.1831400
			G_5	0.3533810	1.7655490	3.4503590	-4.4932500	6.0530510	-8.4681500	3.8709680
			G_6	-0.2539510	-2.2330840	-0.1690700	-10.898011	25.769169	-11.742322	-0.4864810
0.05 (1/20)	0.125	0	G_0	0.4065238	0.7772483	3.8861644	-12.573943	16.760207	-11.014593	2.8706957
			G_1	0.0320270	0.1825342	2.2670449	-2.7076615	1.2088194	-0.3777430	0.0763155
			G_5	0.3871657	0.7402362	3.7011086	-11.975184	15.962102	-10.490089	2.7339962
			G_6	0.0000000	0.0000000	0.0000000	0.0000000	0.0000000	0.0000000	0.0000000
		0.2	G_0	0.4109456	1.1190116	1.7995105	-6.3821558	8.0421594	-5.1022908	1.2974798
			G_1	0.0473201	0.0067330	3.9647433	-9.3001823	13.031398	-10.195338	3.1437780
			G_5	0.3895573	1.0872270	1.5921659	-5.6384454	6.9313961	-4.2887233	1.0619525
			G_6	-0.0437360	0.1565020	-1.0313070	1.5105890	0.1664470	-1.3280550	0.5756200
		0.4	G_0	0.4680620	1.5180720	0.2614540	-0.8297400	-1.2785600	2.4640070	-1.1529200
			G_1	0.0526100	0.3455230	1.5293310	-0.1018700	-2.9746300	2.9400000	-0.9895200
			G_5	0.4431360	1.1850890	2.2362750	-7.6062200	10.527620	-7.4015700	2.0000000
			G_6	-0.0626000	-0.3093300	0.8619540	-2.4811300	4.9979170	-4.4640200	1.4572080
		0.6	G_0	0.5665160	1.5767920	1.2059820	-1.7776200	-1.2400200	2.5899110	-1.1423900
			G_1	0.0817480	0.3504140	2.0140820	-1.2364600	-1.2340500	1.4071190	-0.4663800
			G_5	0.5220930	1.4697450	1.3716660	-2.5367400	0.9215330	0.1851850	-0.2222200
			G_6	-0.0738600	-0.5319700	-0.7208000	8.0693990	-17.681500	16.815880	-5.8771600
		0.8	G_0	0.7146940	1.2725460	4.8660520	-7.4026300	-0.9288800	6.6483200	-3.0994700
			G_1	0.1242820	0.2617840	3.1204770	-3.0471900	-0.5955300	2.1074230	-0.9288200
			G_5	0.6587750	1.3060670	3.7931230	-4.5510100	-3.4868700	7.2543200	-2.9629600
			G_6	-0.1525200	-0.2139800	-1.2315300	2.6729460	0.8828610	-3.6394900	1.6817260

Table 9B.14 – Influence Coefficients for a Circumferential Semi-Elliptical Surface Crack in a Cylinder – Inside Surface

t/R_i	a/c	a/t	G_i	A_0	A_1	A_2	A_3	A_4	A_5	A_6
0.05 (1/20)	0.25	0	G_0	0.6152816	-0.3348694	6.2955620	-15.590618	19.299508	-12.488107	3.3010035
			G_1	0.0703566	0.2828152	1.4036169	-0.6511596	-1.2076596	1.0318656	-0.2423741
			G_5	0.5859829	-0.3189229	5.9957733	-14.848208	18.380484	-11.893435	3.1438124
			G_6	0.0000000	0.0000000	0.0000000	0.0000000	0.0000000	0.0000000	0.0000000
		0.2	G_0	0.6185825	-0.1889201	6.6630201	-18.947461	26.356152	-18.579782	5.2089411
			G_1	0.0888470	0.1766640	2.4509045	-4.8210542	5.9307746	-4.5640652	1.4174542
			G_5	0.5938754	-0.2661124	6.9889172	-20.068484	28.334612	-20.243019	5.7446666
			G_6	-0.0681120	0.5735220	-2.0883730	2.6098630	-0.3016110	-1.3119290	0.5925120
		0.4	G_0	0.7120460	0.0997300	3.7002710	-6.3957600	3.5324360	0.4713570	-0.8227100
			G_1	0.1024360	0.2393730	1.7991830	-1.6574200	0.1547970	0.1715920	-0.0598000
			G_5	0.6716500	-0.0268600	4.4154340	-8.9308000	8.0425260	-3.3808300	0.4444440
			G_6	-0.0437100	-0.1688200	0.9143180	-2.9907700	5.3160000	-4.4544200	1.4273980
		0.6	G_0	0.8701730	-0.2013500	5.4916110	-9.7304200	6.1268500	-0.1308800	-0.9428600
			G_1	0.1469610	0.2300010	1.8005340	-0.9098200	-1.9066500	2.2539830	-0.7998300
			G_5	0.8231710	-0.3648800	6.7247340	-14.567700	15.263370	-8.2323200	1.7777780
			G_6	-0.0748700	-0.0531400	0.1049720	-0.7885500	2.5097000	-2.6722100	0.9740960
		0.8	G_0	1.0661580	-0.6820000	8.2347200	-15.488000	11.384610	-2.4213500	-0.4876600
			G_1	0.2033950	0.1526570	2.0857100	-0.5861000	-4.0788400	4.9762720	-1.8710400
			G_5	0.9994820	-0.4571900	6.5754670	-10.481400	4.0268590	2.8928570	-2.0000000
			G_6	-0.1006100	-0.0290000	-0.0990100	-0.2568100	1.9597170	-2.3010900	0.8268150
0.05 (1/20)	0.5	0	G_0	0.8776607	-0.6729719	3.7721411	-6.5209060	6.3377934	-3.7028038	0.9872447
			G_1	0.1277541	0.4368502	0.4904522	1.0427434	-2.9631236	2.0826525	-0.5184313
			G_5	0.8358676	-0.6409257	3.5925152	-6.2103867	6.0359933	-3.5264800	0.9402333
			G_6	0.0000000	0.0000000	0.0000000	0.0000000	0.0000000	0.0000000	0.0000000
		0.2	G_0	0.8989180	-1.0427963	6.3805369	-14.662910	18.841814	-13.030293	3.6986806
			G_1	0.1482951	0.1559585	2.2564549	-4.5210175	5.6965240	-4.4932156	1.4409953
			G_5	0.8597078	-1.0466621	6.5257761	-15.496160	20.638594	-14.767469	4.3300207
			G_6	-0.0318180	0.2358030	-0.7996340	0.9487470	-0.1184270	-0.3787760	0.1467390
		0.4	G_0	0.9871950	-0.6970100	2.8922470	-1.6963800	-3.5365700	5.2595990	-2.0425800
			G_1	0.1641010	0.3116290	1.1745980	-0.5657200	-1.1954700	1.2303370	-0.3932700
			G_5	0.9152470	-0.5327500	2.2655200	-0.7412600	-3.8680300	4.7720930	-1.7000000
			G_6	-0.0548300	0.2201590	-1.0038000	2.1510600	-2.0964600	0.8311100	-0.0472500
		0.6	G_0	1.1416020	-1.0912600	4.0504810	-3.0974600	-3.6415200	6.6258570	-2.7429800
			G_1	0.2103960	0.1869600	1.4864060	-0.9635100	-0.9174600	1.1604050	-0.4073600
			G_5	1.0665520	-0.8887500	3.1626170	-1.2716000	-5.2179700	6.9104090	-2.5652200
			G_6	-0.0587900	0.1072110	-0.3228800	0.1376970	1.1227310	-1.7342600	0.7482830
		0.8	G_0	1.2858380	-1.0689700	3.0323820	-0.7046000	-5.5956800	6.6774710	-2.3334600
			G_1	0.2474970	0.2175330	1.1026400	-0.1675100	-1.3848400	1.0861840	-0.3080700
			G_5	1.2352800	-1.3022500	4.6326660	-4.9251900	-0.0373500	2.9824560	-1.3333300
			G_6	-0.0540900	-0.0927500	0.3897420	-0.0963800	-1.1396700	1.6443890	-0.6512400

Table 9B.14 – Influence Coefficients for a Circumferential Semi-Elliptical Surface Crack in a Cylinder – Inside Surface

t/R_i	a/c	a/t	G_i	A_0	A_1	A_2	A_3	A_4	A_5	A_6
0.05 (1/20)	1.0	0	G_0	1.1977992	-0.5244870	0.1498299	2.3284866	-5.1058499	4.3469049	-1.3487980
			G_1	0.1870117	0.6987352	0.1316900	0.7269255	-2.5259384	2.1756251	-0.6540458
			G_5	1.1407610	-0.4995114	0.1426952	2.2176067	-4.8627143	4.1399095	-1.2845695
			G_6	0.0000000	0.0000000	0.0000000	0.0000000	0.0000000	0.0000000	0.0000000
		0.2	G_0	1.2084687	-1.7294060	8.6186987	-25.175578	39.288339	-30.318733	9.1234045
			G_1	0.2163478	-0.0120989	4.6109160	-13.629267	20.529426	-15.746786	4.7419942
			G_5	1.1555075	-1.7008589	8.6393123	-25.454348	40.064649	-31.243623	9.5190147
			G_6	-0.0037710	-0.0489600	0.2447630	-0.2640320	-0.4864590	1.1025000	-0.5433790
		0.4	G_0	1.2913150	-0.9650100	1.8057540	-0.9174900	-1.8241900	2.8527550	-1.1595700
			G_1	0.2112910	0.5710160	0.6556010	-0.3623700	-1.3624500	1.6435020	-0.6006500
			G_5	1.1916900	-0.6676400	0.7450230	0.7992390	-2.5897600	2.1534890	-0.6000000
			G_6	-0.0691400	0.5307620	-2.6457900	6.2996400	-7.4455700	4.1740290	-0.8439300
		0.6	G_0	1.3852290	-1.1470100	1.9194050	-0.7144800	-2.2804400	3.1702690	-1.2274700
			G_1	0.2389740	0.5239180	0.6757630	-0.3719900	-1.2356100	1.4486510	-0.5158900
			G_5	1.2864450	-0.8387500	0.9039760	0.8524830	-2.8879500	2.4465120	-0.7000000
			G_6	-0.0758100	0.5692200	-2.8066600	6.7182820	-8.0668600	4.6803110	-1.0184900
		0.8	G_0	1.4894880	-1.3511400	2.1312770	-1.2578300	-0.8055500	1.4488030	-0.5327000
			G_1	0.2640980	0.4833400	0.7438410	-0.6804900	-0.3832900	0.5727370	-0.2136000
			G_5	1.3900720	-1.0885300	1.7049700	-1.5479000	1.3690280	-1.4232600	0.7000000
			G_6	-0.0635800	0.2164910	-0.5719900	0.7731070	-0.4185400	0.0227330	0.0417860
0.05 (1/20)	2.0	0	G_0	0.8150546	-0.5623828	1.4465771	-4.6778133	8.4192164	-7.9025932	2.9866351
			G_1	0.1359146	0.0702340	3.5558581	-11.034445	16.967724	-14.126991	4.8706612
			G_5	0.7762429	-0.5356029	1.3776924	-4.4550600	8.0183010	-7.5262791	2.8444143
			G_6	0.0000000	0.0000000	0.0000000	0.0000000	0.0000000	0.0000000	0.0000000
		0.2	G_0	0.8303757	-1.0498204	4.4477334	-13.542741	21.849163	-17.992876	5.9769347
			G_1	0.1354705	0.0543807	3.3359372	-10.128052	15.148588	-12.247389	4.1164665
			G_5	0.8151606	-1.4268649	7.2227537	-22.829526	37.909858	-31.815559	10.649474
			G_6	-0.0090960	0.1261280	-0.6706890	1.2469360	-0.3690640	-0.9602970	0.6306940
		0.4	G_0	0.8330780	-0.3084500	-0.7547200	3.2657440	-5.8159500	4.5465500	-1.2404700
			G_1	0.1377281	0.0408094	3.3855168	-10.277166	15.441270	-12.544940	4.2347369
			G_5	0.8233414	-1.4926311	7.6320418	-24.161868	40.274146	-33.946581	11.407910
			G_6	-0.0134800	-0.0043900	0.0592600	-0.1017500	0.0175090	0.0918390	-0.0489900
		0.6	G_0	0.8595130	-0.3581900	-0.7703600	3.5772760	-6.5251400	5.2235110	-1.4752700
			G_1	0.1441670	0.0764692	3.0963445	-9.3576065	13.828183	-11.044497	3.6744786
			G_5	0.8479635	-1.4134353	6.7655216	-21.067314	34.623427	-28.746902	9.5236582
			G_6	-0.0187500	0.0102610	0.0108250	-0.0443900	0.0620740	-0.0240800	0.0040530
		0.8	G_0	0.9118690	-0.9615800	2.8858030	-7.7145200	11.709760	-9.5193500	3.2371640
			G_1	0.1520131	0.0313966	3.4128759	-10.422563	15.464464	-12.118677	3.9007626
			G_5	0.8750218	-1.4693251	6.8784396	-21.216993	34.321483	-27.816896	8.9556168
			G_6	-0.0101100	-0.1069100	0.5613170	-0.9055800	-0.0257400	1.2574370	-0.7704300

Table 9B.14 – Influence Coefficients for a Circumferential Semi-Elliptical Surface Crack in a Cylinder – Inside Surface

t/R_i	a/c	a/t	G_i	A_0	A_1	A_2	A_3	A_4	A_5	A_6
0.1 (1/10)	0.03125	0	G_0	0.1965046	2.9373464	-5.2582823	7.4889153	-6.9282667	3.3673349	-0.6677966
			G_1	0.0051780	0.1750280	2.7718680	-4.6457154	4.6780502	-3.2768090	0.9840994
			G_5	0.1786409	2.6703146	-4.7802564	6.8081046	-6.2984246	3.0612136	-0.6070882
			G_6	0.0000000	0.0000000	0.0000000	0.0000000	0.0000000	0.0000000	0.0000000
		0.2	G_0	0.2073050	2.4043916	-1.2521489	-3.8112746	9.7691991	-8.9612397	2.8836220
			G_1	0.0043895	0.2579812	1.9801891	-2.0115020	0.9000182	-0.6939037	0.2816436
			G_5	0.1506071	1.8944151	-1.5339682	0.0383312	3.8549836	-5.2088399	1.9521928
			G_6	-0.1211200	-0.9625500	-2.4298600	15.998410	-29.266100	24.850920	-8.0696800
		0.4	G_0	0.2154860	2.8003500	-3.0453900	2.0532160	3.4108590	-6.8487000	2.9779500
			G_1	0.0178580	0.3079160	1.6813980	-0.0166100	-2.6394000	2.2074140	-0.6976200
			G_5	0.0618685	0.5599721	1.3932612	-3.1664766	12.223550	-14.947058	5.3365097
			G_6	-0.1830800	-2.4496400	2.8812760	-1.6867300	-0.6663700	5.6696970	-3.5651500
		0.6	G_0	0.2334930	2.7804350	-2.0696500	2.6579110	1.4535300	-5.8352000	2.8125900
			G_1	0.0205410	0.3888190	1.1499270	2.4877470	-5.7318100	3.6427850	-0.9172600
			G_5	-0.0478390	-1.1687890	4.7123230	-11.668796	35.914787	-38.382816	12.478830
			G_6	-0.5204160	2.9325180	-20.618744	20.746973	19.477781	-35.192654	13.184401
		0.8	G_0	0.2427700	2.8035350	-1.2713700	5.4620650	-6.1361900	1.5108850	0.0547000
			G_1	0.0304720	0.2067440	2.9709670	-3.2573400	4.9739790	-5.4464500	1.8285600
			G_5	-0.2096100	-1.0318800	-4.9809500	12.311260	10.127790	-15.473000	1.5969130
			G_6	-0.9534420	12.204386	-57.690628	61.528233	25.207428	-67.444443	27.160437
0.1 (1/10)	0.0625	0	G_0	0.2695332	2.1626001	-1.6551569	-1.2970208	4.5604304	-4.3163876	1.4010655
			G_1	0.0138667	0.1827458	2.5749608	-3.9044679	3.3556301	-2.1772209	0.6420134
			G_5	0.2450300	1.9660000	-1.5046882	-1.1791100	4.1458455	-3.9239891	1.2736964
			G_6	0.0000000	0.0000000	0.0000000	0.0000000	0.0000000	0.0000000	0.0000000
		0.2	G_0	0.2779608	2.0193256	-0.9275729	-1.5950891	3.1906437	-2.3502174	0.5991162
			G_1	0.0160185	0.2199692	2.3978435	-3.7534347	3.9341356	-3.1541845	1.0504548
			G_5	0.2419300	1.7627817	-0.7393570	-1.2164716	2.5994393	-2.1071979	0.5817704
			G_6	-0.0845470	-0.4374560	-0.1360350	1.8357670	-1.9350120	1.1367400	-0.3762580
		0.4	G_0	0.3011590	2.2369350	-1.2366000	-0.2270000	2.2512460	-2.8387200	1.0123400
			G_1	0.0201666	0.2827653	2.1695559	-2.9258419	3.5150238	-3.5336170	1.2986040
			G_5	0.2220849	1.6042375	-0.5613839	0.9851166	0.0274225	-1.6054790	0.7445933
			G_6	-0.1378000	-1.3643200	1.4106360	1.0971800	-2.9582600	3.4025980	-1.4500400
		0.6	G_0	0.3224330	2.7848890	-3.9933700	11.326780	-16.755000	10.978200	-2.7831100
			G_1	0.0410830	0.2313980	3.0577560	-4.8777100	6.3133550	-5.7918300	2.0004100
			G_5	0.1875036	1.1459365	0.9632276	-0.2360816	4.0646159	-7.1055726	2.8178537
			G_6	-0.2337900	-1.7348100	1.4149140	-2.0114000	6.7183760	-5.0399700	0.8866800
		0.8	G_0	0.4117650	1.7044180	7.4132840	-24.685800	41.662980	-35.936000	11.838500
			G_1	0.0609440	0.0592690	5.0648580	-10.833900	16.281600	-14.006400	4.5603700
			G_5	0.1284298	0.6557187	2.0158926	-0.7693775	9.0901536	-13.652912	4.9195995
			G_6	-0.3031900	-2.3426000	1.4260850	-4.5266500	13.114480	-7.8324800	0.4643600

Table 9B.14 – Influence Coefficients for a Circumferential Semi-Elliptical Surface Crack in a Cylinder – Inside Surface

t/R_i	a/c	a/t	G_i	A_0	A_1	A_2	A_3	A_4	A_5	A_6
0.1 (1/10)	0.125	0	G_0	0.4065238	0.7772483	3.8861644	-12.573943	16.760207	-11.014593	2.8706957
			G_1	0.0320270	0.1825342	2.2670449	-2.7076615	1.2088194	-0.3777430	0.0763155
			G_5	0.3695673	0.7065891	3.5328764	-11.430857	15.236552	-10.013266	2.6097236
			G_6	0.0000000	0.0000000	0.0000000	0.0000000	0.0000000	0.0000000	0.0000000
		0.2	G_0	0.4073632	1.1141359	1.7772808	-6.3608686	8.0436930	-5.1068311	1.2977650
			G_1	0.0463249	-0.0012662	4.0186652	-9.5730735	13.576928	-10.675057	3.3001718
			G_5	0.3672804	1.0342299	1.4947987	-5.2612250	6.4821928	-4.0450187	1.0109412
			G_6	-0.0690920	0.0713160	-1.0328520	1.8138710	-0.0862930	-1.2722490	0.5814380
		0.4	G_0	0.4570240	1.4083920	0.6887150	-2.2096300	0.8473750	0.9393130	-0.7335500
			G_1	0.0614672	0.0306071	4.1452838	-9.9995542	14.683048	-11.862862	3.7194167
			G_5	0.3967885	1.1376492	1.3272280	-3.7178419	4.3265950	-3.0093646	0.8528040
			G_6	-0.1162600	-0.3861300	0.1981140	0.1738100	1.2304200	-1.7726300	0.6726720
		0.6	G_0	0.5223070	1.5197230	1.2517870	-2.3805700	-0.1906100	1.9556200	-1.0072700
			G_1	0.0681380	0.3470990	1.8482480	-0.6958400	-1.9238800	1.7202440	-0.4798400
			G_5	0.4463316	1.1343342	1.5987945	-1.3817396	-0.9469882	1.1230761	-0.3362630
			G_6	-0.1798400	-0.5774800	-0.0079500	1.1466210	0.6354880	-1.6047100	0.5878760
		0.8	G_0	0.6294930	1.4366510	2.5517550	0.4151700	-14.348200	18.547370	-7.2502400
			G_1	0.0982030	0.3339670	2.3218800	-0.8035400	-3.5908200	4.2249730	-1.5661500
			G_5	0.5067261	0.8959043	2.5894421	3.3629236	-15.995588	16.491438	-5.7967706
			G_6	-0.2496000	-0.6660700	-1.9160800	7.6244820	-6.9942900	2.5337230	-0.3321600
0.1 (1/10)	0.25	0	G_0	0.6152816	-0.3348694	6.2955620	-15.590618	19.299508	-12.488107	3.3010035
			G_1	0.0703566	0.2828152	1.4036169	-0.6511596	-1.2076596	1.0318656	-0.2423741
			G_5	0.5593473	-0.3044264	5.7232382	-14.173289	17.545007	-11.352825	3.0009118
			G_6	0.0000000	0.0000000	0.0000000	0.0000000	0.0000000	0.0000000	0.0000000
		0.2	G_0	0.6203701	-0.2735697	7.1419540	-20.356869	28.489937	-20.172430	5.6739197
			G_1	0.0882439	0.1706464	2.4734911	-4.8946737	6.0398855	-4.6377769	1.4364040
			G_5	0.5619179	-0.2210541	6.4445349	-18.440179	25.960076	-18.524879	5.2543664
			G_6	-0.0833730	0.5360330	-2.0372090	2.5868910	-0.1578860	-1.5207340	0.6820320
		0.4	G_0	0.7051060	-0.0231600	4.3023810	-8.2775600	6.5937550	-1.9480200	-0.0820400
			G_1	0.1030370	0.2479400	1.7027470	-1.3246300	-0.4540100	0.6872710	-0.2195500
			G_5	0.6294410	-0.0696200	4.3250250	-8.6688000	7.8431060	-3.3350300	0.4444440
			G_6	-0.0809800	-0.1333100	0.4934000	-1.7465100	3.7729530	-3.4369900	1.1314340
		0.6	G_0	0.8272440	-0.1473300	4.8311860	-7.7180300	3.1488780	2.0824210	-1.5932300
			G_1	0.1412290	0.2010310	1.9839640	-1.5511200	-0.8183800	1.3484690	-0.5036100
			G_5	0.7434380	-0.3035400	5.9106100	-12.151600	11.934150	-5.9065700	1.1111110
			G_6	-0.1284100	-0.0539300	-0.1516800	-0.1596400	2.2505800	-2.8015900	1.0446610
		0.8	G_0	0.9848890	-0.5919300	7.5198620	-13.510100	8.8164640	-0.4816300	-1.1635500
			G_1	0.1816680	0.2057820	1.6810880	0.6978020	-6.0729600	6.5679730	-2.3864200
			G_5	0.8592330	0.0347720	2.7632420	1.7250280	-14.870100	17.491070	-6.5000000
			G_6	-0.1727300	-0.0102100	-0.5090200	0.5706760	2.0135520	-3.0636700	1.1714020

Table 9B.14 – Influence Coefficients for a Circumferential Semi-Elliptical Surface Crack in a Cylinder – Inside Surface

t/R_i	a/c	a/t	G_i	A_0	A_1	A_2	A_3	A_4	A_5	A_6
0.1 (1/10)	0.5	0	G_0	0.8776607	-0.6729719	3.7721411	-6.5209060	6.3377934	-3.7028038	0.9872447
			G_1	0.1277541	0.4368502	0.4904522	1.0427434	-2.9631236	2.0826525	-0.5184313
			G_5	0.7978736	-0.6117927	3.4292191	-5.9280964	5.7616300	-3.3661855	0.8974955
			G_6	0.0000000	0.0000000	0.0000000	0.0000000	0.0000000	0.0000000	0.0000000
		0.2	G_0	0.8973156	-1.0578646	6.4202252	-14.707694	18.854428	-13.015913	3.6898950
			G_1	0.1474310	0.1597183	2.2167686	-4.3932515	5.4975121	-4.3391504	1.3937659
			G_5	0.8192994	-0.9922420	6.1641760	-14.490390	19.139105	-13.615552	3.9753597
			G_6	-0.0430440	0.2417660	-0.8296330	1.0071940	-0.0903370	-0.4811070	0.1975610
		0.4	G_0	0.9797140	-0.7254800	2.9493190	-1.7803700	-3.3922500	5.1150450	-1.9900700
			G_1	0.1634700	0.3030870	1.1780260	-0.5382100	-1.2620000	1.2960220	-0.4171300
			G_5	0.8704930	-0.5506800	2.3089230	-0.9341600	-3.4657800	4.4325590	-1.6000000
			G_6	-0.0740800	0.2359400	-1.1185600	2.4582730	-2.4457400	1.0596080	-0.1154400
		0.6	G_0	1.1154070	-1.0657300	3.7727200	-2.1008700	-5.1931500	7.7858620	-3.0862200
			G_1	0.2048290	0.1913420	1.4364550	-0.8279000	-1.0808600	1.2687530	-0.4410400
			G_5	1.0037320	-0.9196900	3.4318250	-2.2468600	-3.4458400	5.4314890	-2.1087000
			G_6	-0.0889300	0.1269620	-0.4127300	0.2100800	1.3835970	-2.1123000	0.8933220
		0.8	G_0	1.2431440	-1.1153500	3.3984140	-1.6864300	-3.9663600	5.3741580	-1.9576100
			G_1	0.2383820	0.2082130	1.1743690	-0.3888200	-0.9823300	0.7689770	-0.2240300
			G_5	1.1409380	-1.1250400	3.7327740	-2.1506800	-4.1582500	6.0533330	-2.2666700
			G_6	-0.0964200	-0.0395100	0.1733090	0.2988850	-1.3297300	1.6351950	-0.6417300
0.1 (1/10)	1.0	0	G_0	1.1977992	-0.5244870	0.1498299	2.3284866	-5.1058499	4.3469049	-1.3487980
			G_1	0.1870117	0.6987352	0.1316900	0.7269255	-2.5259384	2.1756251	-0.6540458
			G_5	1.0889082	-0.4768064	0.1362091	2.1168064	-4.6416818	3.9517318	-1.2261800
			G_6	0.0000000	0.0000000	0.0000000	0.0000000	0.0000000	0.0000000	0.0000000
		0.2	G_0	1.2074332	-1.7377740	8.6237280	-25.122900	39.172348	-30.211985	9.0845561
			G_1	0.2154039	-0.0005543	4.5272627	-13.383481	20.173925	-15.484935	4.6634559
			G_5	1.1036486	-1.6181347	8.2081429	-24.114960	37.929125	-29.571408	9.0059756
			G_6	-0.0108580	-0.0329460	0.1737750	-0.1390550	-0.4552700	0.8873630	-0.4227350
		0.4	G_0	1.2859130	-0.9487500	1.6002530	-0.1814400	-2.9779600	3.7295100	-1.4241300
			G_1	0.2263929	0.2417342	2.6832302	-7.2978158	10.667447	-8.5251084	2.7415796
			G_5	1.1392380	-0.6650100	0.8422340	0.5045500	-2.1156100	1.7906980	-0.5000000
			G_6	-0.0770000	0.5142550	-2.5720700	6.1650010	-7.3245000	4.1561480	-0.8618300
		0.6	G_0	1.3753150	-1.1702100	2.0218150	-1.0181300	-1.5953100	2.4728220	-0.9798400
			G_1	0.2376410	0.5197520	0.6785190	-0.4124500	-1.0682900	1.2661940	-0.4553000
			G_5	1.2278340	-0.8558800	1.2069500	-0.0267600	-1.5232100	1.4046510	-0.4000000
			G_6	-0.0891700	0.5380320	-2.6437600	6.3949370	-7.7668300	4.6065810	-1.0398000
		0.8	G_0	1.4688630	-1.3084700	1.8356310	-0.1796200	-2.4202000	2.6048770	-0.8684600
			G_1	0.2596240	0.5185940	0.5077920	0.0042410	-1.3328100	1.2578320	-0.4221500
			G_5	1.3210180	-1.0737100	1.9343580	-2.1542600	2.3106990	-2.1488400	0.9000000
			G_6	-0.0851000	0.2200410	-0.5637000	0.7256100	-0.2530000	-0.1442400	0.1003900

Table 9B.14 – Influence Coefficients for a Circumferential Semi-Elliptical Surface Crack in a Cylinder – Inside Surface

t/R_i	a/c	a/t	G_i	A_0	A_1	A_2	A_3	A_4	A_5	A_6
0.1 (1/10)	2.0	0	G_0	0.8150546	-0.5623828	1.4465771	-4.6778133	8.4192164	-7.9025932	2.9866351
			G_1	0.1359146	0.0702340	3.5558581	-11.034445	16.967724	-14.126991	4.8706612
			G_5	0.7409591	-0.5112573	1.3150700	-4.2525573	7.6538327	-7.1841755	2.7151227
			G_6	0.0000000	0.0000000	0.0000000	0.0000000	0.0000000	0.0000000	0.0000000
		0.2	G_0	0.8298834	-1.0367874	4.3513354	-13.223826	21.319908	-17.547855	5.8279870
			G_1	0.1353367	0.1199528	2.8902835	-8.6472179	12.720573	-10.334998	3.5369914
			G_5	0.7789753	-1.3563946	6.8812447	-21.723632	36.036893	-30.217963	10.107456
			G_6	-0.0109630	0.1269130	-0.6713740	1.2490330	-0.3541110	-0.9907030	0.6459300
		0.4	G_0	0.8336540	-0.3330500	-0.6501700	3.0585860	-5.6171400	4.4906380	-1.2539900
			G_1	0.1405870	0.0669674	3.1921749	-9.5752272	14.211132	-11.510350	3.8996689
			G_5	0.7870987	-1.4187641	7.2712138	-22.901623	38.021413	-31.953295	10.715502
			G_6	-0.0151900	0.0158950	-0.0435700	0.1259000	-0.2066400	0.1827200	-0.0591100
		0.6	G_0	0.8590230	-0.3794700	-0.6620500	3.3021610	-6.1317800	4.9676950	-1.4192000
			G_1	0.1440687	0.1439522	2.6262653	-7.7509403	11.130715	-8.8604868	2.9920847
			G_5	0.8109444	-1.3410644	6.4943491	-20.143983	32.968174	-27.261393	8.9973210
			G_6	-0.0211000	0.0117120	-0.0131900	0.0464780	-0.0661000	0.0649330	-0.0227300
		0.8	G_0	0.9093260	-0.9654500	2.8959630	-7.6431200	11.484330	-9.2250600	3.1015570
			G_1	0.1479634	0.1791786	2.3828007	-6.9734350	9.8125456	-7.6664669	2.5487367
			G_5	0.8380323	-1.4012215	6.6971976	-20.575896	33.127834	-26.714540	8.5555764
			G_6	-0.0144800	-0.0979100	0.4954390	-0.7304000	-0.1978400	1.3085810	-0.7633900
1.0 (1/1)	0.03125	0	G_0	>360°	>360°	>360°	>360°	>360°	>360°	>360°
			G_1	>360°	>360°	>360°	>360°	>360°	>360°	>360°
			G_5	>360°	>360°	>360°	>360°	>360°	>360°	>360°
			G_6	>360°	>360°	>360°	>360°	>360°	>360°	>360°
		0.2	G_0	>360°	>360°	>360°	>360°	>360°	>360°	>360°
			G_1	>360°	>360°	>360°	>360°	>360°	>360°	>360°
			G_5	>360°	>360°	>360°	>360°	>360°	>360°	>360°
			G_6	>360°	>360°	>360°	>360°	>360°	>360°	>360°
		0.4	G_0	>360°	>360°	>360°	>360°	>360°	>360°	>360°
			G_1	>360°	>360°	>360°	>360°	>360°	>360°	>360°
			G_5	>360°	>360°	>360°	>360°	>360°	>360°	>360°
			G_6	>360°	>360°	>360°	>360°	>360°	>360°	>360°
		0.6	G_0	>360°	>360°	>360°	>360°	>360°	>360°	>360°
			G_1	>360°	>360°	>360°	>360°	>360°	>360°	>360°
			G_5	>360°	>360°	>360°	>360°	>360°	>360°	>360°
			G_6	>360°	>360°	>360°	>360°	>360°	>360°	>360°
		0.8	G_0	>360°	>360°	>360°	>360°	>360°	>360°	>360°
			G_1	>360°	>360°	>360°	>360°	>360°	>360°	>360°
			G_5	>360°	>360°	>360°	>360°	>360°	>360°	>360°
			G_6	>360°	>360°	>360°	>360°	>360°	>360°	>360°

Table 9B.14 – Influence Coefficients for a Circumferential Semi-Elliptical Surface Crack in a Cylinder – Inside Surface

t/R_i	a/c	a/t	G_i	A_0	A_1	A_2	A_3	A_4	A_5	A_6
0.2 (1/5)	0.0625	0	G_0	0.2695332	2.1626001	-1.6551569	-1.2970208	4.5604304	-4.3163876	1.4010655
			G_1	0.0138667	0.1827458	2.5749608	-3.9044679	3.3556301	-2.1772209	0.6420134
			G_5	0.2246108	1.8021667	-1.3792975	-1.0808508	3.8003583	-3.5969900	1.1675550
			G_6	0.0000000	0.0000000	0.0000000	0.0000000	0.0000000	0.0000000	0.0000000
		0.2	G_0	0.2746613	1.9926330	-0.9344868	-1.6006254	3.1712542	-2.2919293	0.5726679
			G_1	0.0154215	0.2148007	2.2991669	-3.1533248	2.5615750	-1.8272676	0.5911296
			G_5	0.1864580	1.3358788	-0.3565298	-0.6436695	1.7373083	-1.8574034	0.6055380
			G_6	-0.1420850	-0.9134530	0.5073540	1.1718630	-0.2639180	-0.5389720	0.1820820
		0.4	G_0	0.2905060	2.2613840	-2.0236600	2.2348690	-2.0384300	0.8480130	-0.1769400
			G_1	0.0144756	0.3060575	1.7690501	-1.9480031	2.1586426	-2.5707633	1.0419656
			G_5	0.0814338	0.4622342	0.9701344	-0.4170561	4.1954989	-6.6059029	2.5147927
			G_6	-0.2668900	-1.4913300	-2.2572300	13.963520	-23.281800	20.497450	-7.1637200
		0.6	G_0	0.3136790	2.2391710	-0.9686200	0.4644400	0.9116520	-2.1793200	0.9255600
			G_1	0.0185012	0.3155587	1.7412147	-0.9629640	0.4000714	-1.1702488	0.5577101
			G_5	-0.0515650	-0.7328410	2.8618300	-4.5953460	18.838778	-22.717566	7.8307830
			G_6	-0.3563400	1.0277720	-26.712600	94.035930	-163.57100	145.97540	-50.399100
		0.8	G_0	0.3307580	2.2665800	-0.1922100	0.2251110	0.2049680	-0.1791300	-0.4343900
			G_1	0.0244425	0.2650455	2.3621920	-2.3053317	2.2790075	-1.7977214	0.2912095
			G_5	-0.2289300	-0.7174000	-4.5793300	17.518560	-10.321900	2.8966740	-2.7936800
			G_6	-0.6610720	7.6071240	-40.963089	52.172005	2.7384000	-38.196888	17.299027
0.2 (1/5)	0.125	0	G_0	0.4065238	0.7772483	3.8861644	-12.573943	16.760207	-11.014593	2.8706957
			G_1	0.0320270	0.1825342	2.2670449	-2.7076615	1.2088194	-0.3777430	0.0763155
			G_5	0.3387700	0.6477067	3.2384700	-10.478286	13.966839	-9.1788275	2.3922467
			G_6	0.0000000	0.0000000	0.0000000	0.0000000	0.0000000	0.0000000	0.0000000
		0.2	G_0	0.4029371	1.0915242	1.8053108	-6.5056770	8.3443842	-5.3716087	1.3852674
			G_1	0.0452071	-0.0181395	4.1484326	-10.205731	14.812282	-11.740606	3.6414801
			G_5	0.3199265	0.9054968	1.2979152	-4.2860957	5.1801281	-3.2638264	0.8275216
			G_6	-0.1116150	-0.0781560	-1.0400430	2.3887150	-0.6732360	-1.0034070	0.5242030
		0.4	G_0	0.4333520	1.3570530	0.6442570	-1.6162700	-0.9947800	2.9604760	-1.4598700
			G_1	0.0541970	-0.0089757	4.3466655	-11.070580	16.815488	-13.712564	4.3164728
			G_5	0.2994313	0.8822012	0.9409687	-1.5062580	1.2907743	-1.1458133	0.3877044
			G_6	-0.2041000	-0.6628600	-0.0950100	2.3430480	-1.7270700	0.2829070	0.0630740
		0.6	G_0	0.4778330	1.6381280	-0.4449500	2.2452420	-6.0980400	5.5550270	-1.8235500
			G_1	0.0642112	0.0122041	4.5658760	-12.091301	19.452980	-16.480149	5.3023739
			G_5	0.2628298	0.6788669	1.0548894	1.1760094	-2.8340836	1.2008831	-0.1668244
			G_6	-0.3387500	-0.7171400	-2.0254800	7.4624010	-6.9186200	3.5122470	-0.9746500
		0.8	G_0	0.5678290	1.3699790	2.1829740	-2.2567200	-3.7602900	6.9941040	-3.1800000
			G_1	0.0780259	0.1849201	3.0922070	-4.8798214	5.5329482	-3.9782921	1.0031902
			G_5	0.2162607	0.1399392	3.8003479	-5.9198440	10.409525	-9.7649744	2.8601002
			G_6	-0.4437650	0.4896940	-10.579831	25.503460	-22.244274	7.8296060	-0.5675240

Table 9B.14 – Influence Coefficients for a Circumferential Semi-Elliptical Surface Crack in a Cylinder – Inside Surface

t/R_i	a/c	a/t	G_i	A_0	A_1	A_2	A_3	A_4	A_5	A_6
0.2 (1/5)	0.25	0	G_0	0.6152816	-0.3348694	6.2955620	-15.590618	19.299508	-12.488107	3.3010035
			G_1	0.0703566	0.2828152	1.4036169	-0.6511596	-1.2076596	1.0318656	-0.2423741
			G_5	0.5127350	-0.2790575	5.2463017	-12.992182	16.082923	-10.406756	2.7508358
			G_6	0.0000000	0.0000000	0.0000000	0.0000000	0.0000000	0.0000000	0.0000000
		0.2	G_0	0.6158704	-0.3044136	7.2958788	-20.842918	29.246345	-20.740650	5.8405190
			G_1	0.0860016	0.1750272	2.4176760	-4.7274150	5.7641284	-4.4067981	1.3617675
			G_5	0.5090451	-0.2459198	6.1850917	-17.727067	25.120721	-18.031279	5.1362957
			G_6	-0.0874650	0.2048870	-0.7877790	-0.1144930	3.4096200	-3.9775920	1.3587750
		0.4	G_0	0.6807090	-0.0181700	4.1010120	-7.7342100	5.7789710	-1.2781400	-0.3020800
			G_1	0.0977220	0.2345930	1.7571400	-1.5032200	-0.1782300	0.4680680	-0.1464000
			G_5	0.5474370	-0.1626600	4.5522900	-9.8670500	10.608220	-5.9592900	1.3333330
			G_6	-0.1429600	-0.1522700	0.3434280	-1.3869700	3.9981410	-4.1031700	1.4438050
		0.6	G_0	0.7643780	-0.1045600	4.6780500	-7.7826000	3.6090570	1.7154280	-1.5165200
			G_1	0.1231500	0.1987760	1.9756880	-1.5470200	-0.7898700	1.3021320	-0.4817700
			G_5	0.5889460	-0.0776600	3.9525530	-6.3655800	3.6415570	0.1212120	-0.6666700
			G_6	-0.2281500	-0.0472900	-0.6334600	1.2719350	1.1658530	-2.6941700	1.1652830
		0.8	G_0	0.9005030	-0.8174000	9.1343790	-18.318900	16.233020	-5.9092800	0.3336100
			G_1	0.1592400	0.1254450	2.2234910	-0.9907000	-3.2169100	4.2541320	-1.6800700
			G_5	0.6683370	-0.5392400	6.5084110	-10.972100	7.8124000	-1.5803600	-0.5000000
			G_6	-0.3136200	-0.0427800	-1.0031500	2.2762370	0.9773960	-3.3646700	1.4705920
0.2 (1/5)	0.5	0	G_0	0.8776607	-0.6729719	3.7721411	-6.5209060	6.3377934	-3.7028038	0.9872447
			G_1	0.1277541	0.4368502	0.4904522	1.0427434	-2.9631236	2.0826525	-0.5184313
			G_5	0.4388304	-0.3364859	1.8860705	-3.2604530	3.1688967	-1.8514019	0.4936224
			G_6	0.0000000	0.0000000	0.0000000	0.0000000	0.0000000	0.0000000	0.0000000
		0.2	G_0	0.8946047	-1.0880987	6.5367812	-14.977374	19.233142	-13.295577	3.7714422
			G_1	0.1468391	0.1494773	2.2541287	-4.4876841	5.6369940	-4.4388487	1.4200259
			G_5	0.7478801	-0.9261333	5.7417804	-13.425920	17.657798	-12.512022	3.6370309
			G_6	-0.0622140	0.2466480	-0.8549860	1.0627900	-0.0460670	-0.5911190	0.2472580
		0.4	G_0	0.9626500	-0.7111300	2.6613670	-0.7162500	-5.1454300	6.5075390	-2.4213200
			G_1	0.1614640	0.2974800	1.1660860	-0.5087200	-1.2726300	1.2871340	-0.4124100
			G_5	0.7806730	-0.4562300	1.7448190	0.5202550	-5.4270200	5.8139530	-2.0000000
			G_6	-0.1213700	0.4129990	-1.9995500	4.6351640	-5.0019800	2.4723590	-0.3976300
		0.6	G_0	1.0751750	-1.0983200	3.9916560	-2.7880300	-3.9548800	6.7235960	-2.7469000
			G_1	0.1954230	0.1962320	1.3895710	-0.6978800	-1.2117900	1.3183430	-0.4441600
			G_5	0.8810430	-0.8080000	3.0593790	-1.6390900	-3.7057000	5.2727270	-2.0000000
			G_6	-0.1479200	0.2002220	-0.6443400	0.5965410	1.5644630	-2.8569900	1.2880200
		0.8	G_0	1.1727800	-1.0890100	3.5149910	-1.9020000	-3.6889300	5.2643130	-1.9823400
			G_1	0.2227940	0.2349260	1.0309020	0.1224120	-1.7617400	1.3487430	-0.3982000
			G_5	0.9842910	-1.1276100	4.5985580	-5.5036800	1.9508470	0.9992980	-0.7333300
			G_6	-0.1671200	-0.0249100	0.2071610	0.6527170	-2.0799000	2.2037960	-0.7917400

Table 9B.14 – Influence Coefficients for a Circumferential Semi-Elliptical Surface Crack in a Cylinder – Inside Surface

t/R_i	a/c	a/t	G_i	A_0	A_1	A_2	A_3	A_4	A_5	A_6
0.2 (1/5)	1.0	0	G_0	1.1977992	-0.5244870	0.1498299	2.3284866	-5.1058499	4.3469049	-1.3487980
			G_1	0.1870117	0.6987352	0.1316900	0.7269255	-2.5259384	2.1756251	-0.6540458
			G_5	0.9981658	-0.4370725	0.1248583	1.9404058	-4.2548750	3.6224208	-1.1239983
			G_6	0.0000000	0.0000000	0.0000000	0.0000000	0.0000000	0.0000000	0.0000000
		0.2	G_0	1.2042139	-1.7184651	8.3974726	-24.297906	37.843150	-29.181362	8.7698916
			G_1	0.2141530	0.0177548	4.3818976	-12.940794	19.522869	-14.998781	4.5154005
			G_5	1.0104920	-1.4866607	7.5586755	-22.106442	34.708840	-27.030280	8.2196099
			G_6	-0.0226250	-0.0176200	0.1169620	-0.0423700	-0.3894120	0.6553310	-0.3004810
		0.4	G_0	1.2827300	-1.0376300	2.0196040	-1.2981600	-1.1540600	2.2233130	-0.9499300
			G_1	0.2239049	0.2463097	2.6203846	-7.1285809	10.498578	-8.4296199	2.7081472
			G_5	1.0436480	-0.6146200	0.7831210	0.6384640	-2.2283500	1.8139540	-0.5000000
			G_6	-0.1070200	0.6703990	-3.2584800	7.6913240	-8.8678600	4.7415690	-0.8699400
		0.6	G_0	1.3573590	-1.1704500	1.8759680	-0.3400600	-2.5386900	3.0522770	-1.1249500
			G_1	0.2339280	0.5254690	0.5931330	-0.1929100	-1.2290500	1.2994260	-0.4586100
			G_5	1.1254030	-0.9052000	1.9129080	-2.1369000	1.8300790	-1.2418600	0.4000000
			G_6	-0.1281700	0.6899310	-3.2765600	7.8600090	-9.3273600	5.2734440	-1.0912900
		0.8	G_0	1.4394340	-1.3098700	1.7771300	0.3860890	-3.3253800	3.2539520	-1.0700400
			G_1	0.2573740	0.4951230	0.6501790	-0.5490400	-0.1469600	0.1702270	-0.0718800
			G_5	1.1881780	-0.8564700	1.1754060	0.1918800	-1.2135200	0.4744190	0.1000000
			G_6	-0.1307600	0.3275810	-0.9451600	1.7563070	-1.5599400	0.5843160	-0.0323500
0.2 (1/5)	2.0	0	G_0	0.8150546	-0.5623828	1.4465771	-4.6778133	8.4192164	-7.9025932	2.9866351
			G_1	0.1359146	0.0702340	3.5558581	-11.034445	16.967724	-14.126991	4.8706612
			G_5	0.6792125	-0.4686525	1.2054808	-3.8981775	7.0160133	-6.5854942	2.4888625
			G_6	0.0000000	0.0000000	0.0000000	0.0000000	0.0000000	0.0000000	0.0000000
		0.2	G_0	0.8358198	-0.9924158	3.9768720	-11.895121	19.092328	-15.767916	5.2807657
			G_1	0.1359403	0.1029899	2.9965678	-8.9811709	13.214205	-10.645384	3.5992645
			G_5	0.7133337	-1.2206448	6.2110937	-19.560635	32.381152	-27.109103	9.0576036
			G_6	-0.0126410	0.1047460	-0.5669950	1.0875330	-0.3104870	-0.8897690	0.5826880
		0.4	G_0	0.8325100	-0.3194100	-0.7533800	3.3629820	-6.0395900	4.8258600	-1.3722100
			G_1	0.1390275	0.0874112	3.0561984	-9.1666723	13.520813	-10.858590	3.6501024
			G_5	0.7154977	-1.2303429	6.3379078	-19.902438	32.964781	-27.668674	9.2758719
			G_6	-0.0193200	-0.0131100	0.1021510	-0.1416000	0.0088670	0.1372810	-0.0742600
		0.6	G_0	0.8584020	-0.3933300	-0.6204500	3.2822090	-6.1804800	5.1102160	-1.5076600
			G_1	0.1440293	0.1448134	2.6171481	-7.7432148	11.073113	-8.6716926	2.8678919
			G_5	0.7385051	-1.1518575	5.6378202	-17.404615	28.376173	-23.390975	7.7010721
			G_6	-0.0312300	0.0232800	-0.0601000	0.1680520	-0.1758700	0.0935340	-0.0176600
		0.8	G_0	0.9059700	-0.9530400	2.7940290	-7.1938500	10.653830	-8.4054600	2.7741360
			G_1	0.1497196	0.1548492	2.5650135	-7.6154978	10.830952	-8.3100088	2.6668419
			G_5	0.7661965	-1.2226050	6.0077780	-18.334715	29.298571	-23.433628	7.4415387
			G_6	-0.0270400	-0.0979600	0.5106690	-0.7699900	-0.0498500	1.1091270	-0.6749600

Table 9B.14 – Influence Coefficients for a Circumferential Semi-Elliptical Surface Crack in a Cylinder – Inside Surface

t/R_i	a/c	a/t	G_i	A_0	A_1	A_2	A_3	A_4	A_5	A_6
0.3333 (1/3)	0.03125	0	G_0	>360°	>360°	>360°	>360°	>360°	>360°	>360°
			G_1	>360°	>360°	>360°	>360°	>360°	>360°	>360°
			G_5	>360°	>360°	>360°	>360°	>360°	>360°	>360°
			G_6	>360°	>360°	>360°	>360°	>360°	>360°	>360°
		0.2	G_0	>360°	>360°	>360°	>360°	>360°	>360°	>360°
			G_1	>360°	>360°	>360°	>360°	>360°	>360°	>360°
			G_5	>360°	>360°	>360°	>360°	>360°	>360°	>360°
			G_6	>360°	>360°	>360°	>360°	>360°	>360°	>360°
		0.4	G_0	>360°	>360°	>360°	>360°	>360°	>360°	>360°
			G_1	>360°	>360°	>360°	>360°	>360°	>360°	>360°
			G_5	>360°	>360°	>360°	>360°	>360°	>360°	>360°
			G_6	>360°	>360°	>360°	>360°	>360°	>360°	>360°
		0.6	G_0	>360°	>360°	>360°	>360°	>360°	>360°	>360°
			G_1	>360°	>360°	>360°	>360°	>360°	>360°	>360°
			G_5	>360°	>360°	>360°	>360°	>360°	>360°	>360°
			G_6	>360°	>360°	>360°	>360°	>360°	>360°	>360°
		0.8	G_0	>360°	>360°	>360°	>360°	>360°	>360°	>360°
			G_1	>360°	>360°	>360°	>360°	>360°	>360°	>360°
			G_5	>360°	>360°	>360°	>360°	>360°	>360°	>360°
			G_6	>360°	>360°	>360°	>360°	>360°	>360°	>360°
0.3333 (1/3)	0.0625	0	G_0	>360°	>360°	>360°	>360°	>360°	>360°	>360°
			G_1	>360°	>360°	>360°	>360°	>360°	>360°	>360°
			G_5	>360°	>360°	>360°	>360°	>360°	>360°	>360°
			G_6	>360°	>360°	>360°	>360°	>360°	>360°	>360°
		0.2	G_0	>360°	>360°	>360°	>360°	>360°	>360°	>360°
			G_1	>360°	>360°	>360°	>360°	>360°	>360°	>360°
			G_5	>360°	>360°	>360°	>360°	>360°	>360°	>360°
			G_6	>360°	>360°	>360°	>360°	>360°	>360°	>360°
		0.4	G_0	>360°	>360°	>360°	>360°	>360°	>360°	>360°
			G_1	>360°	>360°	>360°	>360°	>360°	>360°	>360°
			G_5	>360°	>360°	>360°	>360°	>360°	>360°	>360°
			G_6	>360°	>360°	>360°	>360°	>360°	>360°	>360°
		0.6	G_0	>360°	>360°	>360°	>360°	>360°	>360°	>360°
			G_1	>360°	>360°	>360°	>360°	>360°	>360°	>360°
			G_5	>360°	>360°	>360°	>360°	>360°	>360°	>360°
			G_6	>360°	>360°	>360°	>360°	>360°	>360°	>360°
		0.8	G_0	>360°	>360°	>360°	>360°	>360°	>360°	>360°
			G_1	>360°	>360°	>360°	>360°	>360°	>360°	>360°
			G_5	>360°	>360°	>360°	>360°	>360°	>360°	>360°
			G_6	>360°	>360°	>360°	>360°	>360°	>360°	>360°

Table 9B.14 – Influence Coefficients for a Circumferential Semi-Elliptical Surface Crack in a Cylinder – Inside Surface

t/R_i	a/c	a/t	G_i	A_0	A_1	A_2	A_3	A_4	A_5	A_6
0.3333 (1/3)	0.125	0	G_0	0.4065238	0.7772483	3.8861644	-12.573943	16.760207	-11.014593	2.8706957
			G_1	0.0320270	0.1825342	2.2670449	-2.7076615	1.2088194	-0.3777430	0.0763155
			G_5	0.3048930	0.5829360	2.9146230	-9.4304573	12.570155	-8.2609448	2.1530220
			G_6	0.0000000	0.0000000	0.0000000	0.0000000	0.0000000	0.0000000	0.0000000
		0.2	G_0	0.3975304	1.0704943	1.8409164	-6.7524995	8.8513103	-5.7966783	1.5167162
			G_1	0.0437487	-0.0379438	4.3032790	-10.979411	16.325212	-13.042939	4.0580042
			G_5	0.2598731	0.7431824	1.0817664	-3.0985122	3.7427052	-2.5608814	0.7055471
			G_6	-0.1560910	-0.1991580	-1.2102800	3.1753640	-1.1892930	-1.0207720	0.6068420
		0.4	G_0	0.4238500	1.1235390	2.5509630	-9.8789800	15.140340	-11.492500	3.3935110
			G_1	0.0497907	-0.0602976	4.7351023	-12.965424	20.468483	-16.831335	5.3096778
			G_5	0.1697435	0.5461098	0.3497346	1.7372481	-2.5772737	0.7601711	0.0073845
			G_6	-0.2516800	-0.8485800	-0.1616800	1.7778520	0.5757210	-1.6402700	0.5486370
		0.6	G_0	0.4556600	0.8736780	4.4545930	-13.785100	19.802200	-14.490000	4.1432600
			G_1	0.0541596	-0.0346110	4.8465458	-14.018203	23.536910	-20.054942	6.4399617
			G_5	0.0446172	0.0047650	1.3276798	-0.2022316	5.0799128	-8.1465781	3.0576874
			G_6	-0.2271900	-1.4977600	2.6245340	-13.151900	32.228690	-29.431700	9.4553330
		0.8	G_0	0.5070500	0.8103760	6.0448070	-18.725500	28.520740	-20.813300	5.5469780
			G_1	0.0626980	0.1915790	2.9204050	-4.4566900	4.6654090	-2.8958000	0.5196150
			G_5	-0.1081220	-0.3133160	0.2940120	2.0796550	8.4135110	-13.235033	4.3140810
			G_6	-0.5376350	3.5876730	-25.358362	45.712830	-26.722023	-0.9809940	4.2835110
0.3333 (1/3)	0.25	0	G_0	0.6152816	-0.3348694	6.2955620	-15.590618	19.299508	-12.488107	3.3010035
			G_1	0.0703566	0.2828152	1.4036169	-0.6511596	-1.2076596	1.0318656	-0.2423741
			G_5	0.4614615	-0.2511518	4.7216715	-11.692964	14.474631	-9.3660803	2.4757523
			G_6	0.0000000	0.0000000	0.0000000	0.0000000	0.0000000	0.0000000	0.0000000
		0.2	G_0	0.6083440	-0.2904124	7.0896330	-20.176785	28.205837	-19.948430	5.6066871
			G_1	0.0838285	0.1746451	2.3793286	-4.6232641	5.6071472	-4.2823544	1.3235074
			G_5	0.4499786	-0.1852406	4.4943031	-11.145785	14.081722	-9.4097438	2.5683214
			G_6	-0.1219890	0.2306280	-1.2120370	1.2196580	1.6286170	-2.7432500	1.0045930
		0.4	G_0	0.6526970	-0.4837600	7.6611730	-19.998400	26.417930	-17.968700	4.8913320
			G_1	0.0831650	0.2409880	1.6951000	-1.5385200	0.2695350	-0.1584300	0.1162410
			G_5	0.4292630	-0.3106000	5.3124130	-13.181800	17.490330	-12.245600	3.4183450
			G_6	-0.1386700	-0.6159000	1.3198340	-1.3713700	1.0283420	0.0952910	-0.3175300
		0.6	G_0	0.7317460	-0.3303400	5.5440620	-9.4951500	5.7237640	0.0933760	-0.9528500
			G_1	0.1080000	0.2765580	1.2250360	0.9782820	-4.7273400	4.2126330	-1.3066700
			G_5	0.4238890	-0.0841600	2.7845590	-2.2848200	-1.5056400	2.9519690	-1.2352400
			G_6	-0.3162700	0.0983480	-2.3401800	5.2319350	-2.9719700	-0.1371700	0.4353040
		0.8	G_0	0.8402820	-0.8949500	10.595930	-26.628500	34.904410	-23.479700	6.2376480
			G_1	0.1477640	0.0411330	3.1601870	-5.2967700	5.5402620	-3.5864300	0.8821650
			G_5	0.4212720	-0.4648100	5.9023420	-13.138900	18.981120	-14.760300	4.3338570
			G_6	-0.4127500	0.2305260	-3.9773100	9.4936830	-8.5226200	4.1775270	-0.9890500

Table 9B.14 – Influence Coefficients for a Circumferential Semi-Elliptical Surface Crack in a Cylinder – Inside Surface

t/R_i	a/c	a/t	G_i	A_0	A_1	A_2	A_3	A_4	A_5	A_6
0.3333 (1/3)	0.5	0	G_0	0.8776607	-0.6729719	3.7721411	-6.5209060	6.3377934	-3.7028038	0.9872447
			G_1	0.1277541	0.4368502	0.4904522	1.0427434	-2.9631236	2.0826525	-0.5184313
			G_5	0.6582458	-0.5047290	2.8291058	-4.8906795	4.7533448	-2.7771030	0.7404338
			G_6	0.0000000	0.0000000	0.0000000	0.0000000	0.0000000	0.0000000	0.0000000
		0.2	G_0	0.8895794	-1.1126308	6.5752022	-14.855752	18.769034	-12.769139	3.5706030
			G_1	0.1451309	0.1469326	2.2308775	-4.3705650	5.4139824	-4.2413440	1.3531815
			G_5	0.6658258	-0.7835355	4.8162796	-10.777119	13.753050	-9.6562727	2.8173218
			G_6	-0.0826750	0.2486620	-0.8714890	1.1120030	-0.0336570	-0.6328160	0.2623350
		0.4	G_0	0.9404760	-0.7171300	2.8683290	-1.9822900	-2.2272100	3.6257200	-1.3881800
			G_1	0.1574600	0.2822130	1.2690630	-0.9471000	-0.3659400	0.4292320	-0.1110700
			G_5	0.6852640	-0.5845700	2.7454920	-2.9660400	0.4623200	1.0854340	-0.5496200
			G_6	-0.1387000	0.0697930	-0.2841400	0.5371760	-0.0906000	-0.1401700	0.0466450
		0.6	G_0	1.0445780	-1.3803400	6.1955220	-10.014600	7.9838570	-2.9309700	0.2857320
			G_1	0.1787820	0.2882640	0.8060020	1.0425460	-3.7076700	3.0209080	-0.8866100
			G_5	0.7517630	-0.9610200	4.7115960	-7.5088500	6.2941800	-2.7984400	0.4781860
			G_6	-0.2099100	0.1853170	-0.7684100	1.1473110	0.1521720	-0.8435900	0.3371120
		0.8	G_0	1.0843000	-0.7460900	1.4321000	6.3082000	-19.305000	19.233000	-6.7012000
			G_1	0.2111800	0.1098200	1.8768000	-2.2163000	1.6060000	-1.0307000	0.2496700
			G_5	0.7720800	-0.5866300	2.0623000	1.3104000	-7.5437000	7.8678000	-2.7908000
			G_6	-0.1930800	0.3869550	-4.3698700	13.210980	-17.895400	12.239770	-3.3793400
0.3333 (1/3)	1.0	0	G_0	1.1977992	-0.5244870	0.1498299	2.3284866	-5.1058499	4.3469049	-1.3487980
			G_1	0.1870117	0.6987352	0.1316900	0.7269255	-2.5259384	2.1756251	-0.6540458
			G_5	0.8983493	-0.3933653	0.1123725	1.7463653	-3.8293875	3.2601788	-1.0115985
			G_6	0.0000000	0.0000000	0.0000000	0.0000000	0.0000000	0.0000000	0.0000000
		0.2	G_0	1.2012642	-1.7333005	8.3781140	-24.063822	37.374764	-28.763015	8.6237108
			G_1	0.2153060	-0.0149500	4.5588615	-13.461994	20.337566	-15.605137	4.6842087
			G_5	0.9105186	-1.1384184	5.4097849	-15.339953	24.188520	-19.160345	5.9427986
			G_6	-0.0345160	-0.0167840	0.1297610	-0.0527050	-0.3346670	0.5652860	-0.2567380
		0.4	G_0	1.2353020	-0.4554500	-1.3844300	7.7438190	-13.114500	9.9554010	-2.8936100
			G_1	0.2231273	0.2854589	2.2703165	-5.9312058	8.6225042	-7.0084921	2.2832798
			G_5	0.9136960	-0.2915800	-0.8322300	5.1393320	-8.6812300	6.4245520	-1.8094800
			G_6	-0.0911000	0.0616370	-0.1210900	0.3104310	-0.3007600	0.2039090	-0.0630300
		0.6	G_0	1.2948850	-0.5296600	-1.8164200	9.6512410	-16.061200	12.054080	-3.4771700
			G_1	0.2437058	0.2916478	1.9336493	-4.6996771	6.6474053	-5.3956082	1.7365158
			G_5	0.9663080	-0.3126800	-1.2238000	6.9796950	-11.736700	8.7605150	-2.5098100
			G_6	-0.1230600	0.0274730	0.1438200	-0.4241600	0.8313660	-0.6134200	0.1579830
		0.8	G_0	1.4110710	-1.5153300	3.6940490	-6.1586400	8.0493230	-6.3320300	2.0368880
			G_1	0.2576230	0.3718990	1.5321880	-3.5848900	5.2701160	-4.4872900	1.4628370
			G_5	1.0612560	-1.1039100	3.5230400	-6.9044200	9.8738080	-8.0508200	2.6221170
			G_6	-0.1788800	0.4037560	-2.0916400	6.1449500	-9.2086300	7.2003620	-2.2699200

Table 9B.14 – Influence Coefficients for a Circumferential Semi-Elliptical Surface Crack in a Cylinder – Inside Surface

t/R_i	a/c	a/t	G_i	A_0	A_1	A_2	A_3	A_4	A_5	A_6
0.3333 (1/3)	2.0	0	G_0	0.8150546	-0.5623828	1.4465771	-4.6778133	8.4192164	-7.9025932	2.9866351
			G_1	0.1359146	0.0702340	3.5558581	-11.034445	16.967724	-14.126991	4.8706612
			G_5	0.6112913	-0.4217873	1.0849328	-3.5083598	6.3144120	-5.9269448	2.2399763
			G_6	0.0000000	0.0000000	0.0000000	0.0000000	0.0000000	0.0000000	0.0000000
		0.2	G_0	0.8352781	-0.9846724	3.9006089	-11.598574	18.537951	-15.233685	5.0778570
			G_1	0.1352852	0.1228393	2.8607553	-8.5533030	12.496366	-10.010600	3.3741234
			G_5	0.6470104	-1.0551846	5.3220976	-16.632247	27.466509	-23.033790	7.7267507
			G_6	-0.0142710	0.0762410	-0.4315580	0.8690960	-0.2323740	-0.7815010	0.5099400
		0.4	G_0	0.8387535	-0.9644546	3.6234112	-10.614751	16.935822	-13.909712	4.6383496
			G_1	0.1391285	0.0994766	2.9628455	-8.8586428	12.949581	-10.264284	3.4057784
			G_5	0.6547443	-1.0753542	5.5609093	-17.311471	28.535555	-23.897683	8.0055284
			G_6	-0.0275500	0.0118070	-0.0132100	0.0962120	-0.1684500	0.1535230	-0.0523400
		0.6	G_0	0.8647141	-0.9933994	3.4972128	-9.9646125	15.605175	-12.506693	4.0588148
			G_1	0.1439330	0.1659077	2.4756770	-7.3335082	10.402275	-8.0129443	2.5997844
			G_5	0.6728344	-0.9405580	4.5855658	-13.905932	22.493373	-18.532141	6.1244287
			G_6	-0.0428500	0.0404420	-0.1589900	0.4421460	-0.4883600	0.2585730	-0.0509700
		0.8	G_0	0.8961065	-1.1484363	4.2826404	-12.236817	19.080943	-14.996807	4.7040118
			G_1	0.1518350	0.1503798	2.6001073	-7.7801582	11.113224	-8.4029371	2.6236987
			G_5	0.6973028	-0.9440042	4.5851930	-13.593268	21.493375	-17.216662	5.5090422
			G_6	-0.0425300	-0.0823600	0.4082940	-0.4782200	-0.3499100	1.2189920	-0.6742600
1.0 (1/1)	0.03125	0	G_0	0.4065238	0.7772483	3.8861644	-12.573943	16.760207	-11.014593	2.8706957
			G_1	0.0320270	0.1825342	2.2670449	-2.7076615	1.2088194	-0.3777430	0.0763155
			G_5	0.3048930	0.5829360	2.9146230	-9.4304573	12.570155	-8.2609448	2.1530220
			G_6	0.0000000	0.0000000	0.0000000	0.0000000	0.0000000	0.0000000	0.0000000
		0.2	G_0	0.196493	3.377334	-9.041602	17.693063	-20.695294	12.699726	-3.185109
			G_1	-0.000745	0.498196	0.980110	-0.502011	-0.655817	0.347143	-0.010599
			G_5	0.050763	-0.414714	2.188778	-2.801584	5.167600	-5.455342	1.838889
			G_6	-0.065484	-1.994233	5.264395	-9.596851	10.547575	-4.292014	0.134409
		0.4	G_0	>360°	>360°	>360°	>360°	>360°	>360°	>360°
			G_1	>360°	>360°	>360°	>360°	>360°	>360°	>360°
			G_5	>360°	>360°	>360°	>360°	>360°	>360°	>360°
			G_6	>360°	>360°	>360°	>360°	>360°	>360°	>360°
		0.6	G_0	>360°	>360°	>360°	>360°	>360°	>360°	>360°
			G_1	>360°	>360°	>360°	>360°	>360°	>360°	>360°
			G_5	>360°	>360°	>360°	>360°	>360°	>360°	>360°
			G_6	>360°	>360°	>360°	>360°	>360°	>360°	>360°
		0.8	G_0	>360°	>360°	>360°	>360°	>360°	>360°	>360°
			G_1	>360°	>360°	>360°	>360°	>360°	>360°	>360°
			G_5	>360°	>360°	>360°	>360°	>360°	>360°	>360°
			G_6	>360°	>360°	>360°	>360°	>360°	>360°	>360°

Table 9B.14 – Influence Coefficients for a Circumferential Semi-Elliptical Surface Crack in a Cylinder – Inside Surface

t/R_i	a/c	a/t	G_i	A_0	A_1	A_2	A_3	A_4	A_5	A_6
1.0 (1/1)	0.0625	0	G_0	0.6152816	-0.3348694	6.2955620	-15.590618	19.299508	-12.488107	3.3010035
			G_1	0.0703566	0.2828152	1.4036169	-0.6511596	-1.2076596	1.0318656	-0.2423741
			G_5	0.3076408	-0.1674347	3.1477810	-7.7953092	9.6497542	-6.2440535	1.6505017
			G_6	0.0000000	0.0000000	0.0000000	0.0000000	0.0000000	0.0000000	0.0000000
		0.2	G_0	0.5532170	0.0050000	5.0461120	-13.893308	18.383403	-12.420875	3.3644460
			G_1	0.0660190	0.1432040	2.2733860	-3.3708210	2.8831810	-1.9087910	0.5733580
			G_5	0.2212500	0.0127600	1.7074300	-2.9758760	3.0826040	-1.9821240	0.5111050
			G_6	-0.1680230	-0.2080990	-0.3914380	1.2264760	0.0644590	-0.8552860	0.3317690
		0.4	G_0	0.5542850	-0.0325720	5.1905180	-14.131699	18.821939	-12.851581	3.5085430
			G_1	0.0699330	0.1143180	2.3958230	-3.6444650	3.3378430	-2.2969570	0.6947610
			G_5	0.0554160	-0.0876360	0.9859450	-0.7494760	3.7727090	-5.3212110	1.9803790
			G_6	-0.2558240	-0.2471800	-1.1642670	1.6226710	1.0789640	-1.0380770	0.0035940
		0.6	G_0	0.6158850	-0.7001360	8.8279710	-23.714995	32.865831	-23.053009	6.3405370
			G_1	0.0827450	0.0515040	2.7004050	-4.4378380	4.8033830	-3.4867960	1.0139060
			G_5	-0.1335870	-0.1416500	0.0364640	-1.6021910	13.349263	-16.085695	5.3060660
			G_6	-0.2328840	0.0420070	-2.4218110	2.4417400	-3.1671030	7.5041470	-4.1676320
		0.8	G_0	>360°	>360°	>360°	>360°	>360°	>360°	>360°
			G_1	>360°	>360°	>360°	>360°	>360°	>360°	>360°
			G_5	>360°	>360°	>360°	>360°	>360°	>360°	>360°
			G_6	>360°	>360°	>360°	>360°	>360°	>360°	>360°
1.0 (1/1)	0.125	0	G_0	0.4065238	0.7772483	3.8861644	-12.573943	16.760207	-11.014593	2.8706957
			G_1	0.0320270	0.1825342	2.2670449	-2.7076615	1.2088194	-0.3777430	0.0763155
			G_5	0.3048930	0.5829360	2.9146230	-9.4304573	12.570155	-8.2609448	2.1530220
			G_6	0.0000000	0.0000000	0.0000000	0.0000000	0.0000000	0.0000000	0.0000000
		0.2	G_0	0.196493	3.377334	-9.041602	17.693063	-20.695294	12.699726	-3.185109
			G_1	-0.000745	0.498196	0.980110	-0.502011	-0.655817	0.347143	-0.010599
			G_5	0.050763	-0.414714	2.188778	-2.801584	5.167600	-5.455342	1.838889
			G_6	-0.065484	-1.994233	5.264395	-9.596851	10.547575	-4.292014	0.134409
		0.4	G_0	>360°	>360°	>360°	>360°	>360°	>360°	>360°
			G_1	>360°	>360°	>360°	>360°	>360°	>360°	>360°
			G_5	>360°	>360°	>360°	>360°	>360°	>360°	>360°
			G_6	>360°	>360°	>360°	>360°	>360°	>360°	>360°
		0.6	G_0	>360°	>360°	>360°	>360°	>360°	>360°	>360°
			G_1	>360°	>360°	>360°	>360°	>360°	>360°	>360°
			G_5	>360°	>360°	>360°	>360°	>360°	>360°	>360°
			G_6	>360°	>360°	>360°	>360°	>360°	>360°	>360°
		0.8	G_0	>360°	>360°	>360°	>360°	>360°	>360°	>360°
			G_1	>360°	>360°	>360°	>360°	>360°	>360°	>360°
			G_5	>360°	>360°	>360°	>360°	>360°	>360°	>360°
			G_6	>360°	>360°	>360°	>360°	>360°	>360°	>360°

Table 9B.14 – Influence Coefficients for a Circumferential Semi-Elliptical Surface Crack in a Cylinder – Inside Surface

t/R_i	a/c	a/t	G_i	A_0	A_1	A_2	A_3	A_4	A_5	A_6
1.0 (1/1)	0.25	0	G_0	0.6152816	-0.3348694	6.2955620	-15.590618	19.299508	-12.488107	3.3010035
			G_1	0.0703566	0.2828152	1.4036169	-0.6511596	-1.2076596	1.0318656	-0.2423741
			G_5	0.3076408	-0.1674347	3.1477810	-7.7953092	9.6497542	-6.2440535	1.6505017
			G_6	0.0000000	0.0000000	0.0000000	0.0000000	0.0000000	0.0000000	0.0000000
		0.2	G_0	0.5532170	0.0050000	5.0461120	-13.893308	18.383403	-12.420875	3.3644460
			G_1	0.0660190	0.1432040	2.2733860	-3.3708210	2.8831810	-1.9087910	0.5733580
			G_5	0.2212500	0.0127600	1.7074300	-2.9758760	3.0826040	-1.9821240	0.5111050
			G_6	-0.1680230	-0.2080990	-0.3914380	1.2264760	0.0644590	-0.8552860	0.3317690
		0.4	G_0	0.5542850	-0.0325720	5.1905180	-14.131699	18.821939	-12.851581	3.5085430
			G_1	0.0699330	0.1143180	2.3958230	-3.6444650	3.3378430	-2.2969570	0.6947610
			G_5	0.0554160	-0.0876360	0.9859450	-0.7494760	3.7727090	-5.3212110	1.9803790
			G_6	-0.2558240	-0.2471800	-1.1642670	1.6226710	1.0789640	-1.0380770	0.0035940
		0.6	G_0	0.6158850	-0.7001360	8.8279710	-23.714995	32.865831	-23.053009	6.3405370
			G_1	0.0827450	0.0515040	2.7004050	-4.4378380	4.8033830	-3.4867960	1.0139060
			G_5	-0.1335870	-0.1416500	0.0364640	-1.6021910	13.349263	-16.085695	5.3060660
			G_6	-0.2328840	0.0420070	-2.4218110	2.4417400	-3.1671030	7.5041470	-4.1676320
		0.8	G_0	>360°	>360°	>360°	>360°	>360°	>360°	>360°
			G_1	>360°	>360°	>360°	>360°	>360°	>360°	>360°
			G_5	>360°	>360°	>360°	>360°	>360°	>360°	>360°
			G_6	>360°	>360°	>360°	>360°	>360°	>360°	>360°
1.0 (1/1)	0.5	0	G_0	0.8776607	-0.6729719	3.7721411	-6.5209060	6.3377934	-3.7028038	0.9872447
			G_1	0.1277541	0.4368502	0.4904522	1.0427434	-2.9631236	2.0826525	-0.5184313
			G_5	0.4388304	-0.3364859	1.8860705	-3.2604530	3.1688967	-1.8514019	0.4936224
			G_6	0.0000000	0.0000000	0.0000000	0.0000000	0.0000000	0.0000000	0.0000000
		0.2	G_0	0.8588150	-1.1505680	6.2966200	-12.688489	14.144800	-8.6103180	2.1854770
			G_1	0.1256330	0.2587650	1.2669500	-0.8661530	-0.3093460	0.1907880	0.0150220
			G_5	0.4167790	-0.4634130	2.6373400	-4.3129710	3.7542040	-1.7965520	0.3468750
			G_6	-0.1324590	0.1728890	-0.9794030	2.4761070	-2.8715610	1.8728550	-0.5384790
		0.4	G_0	0.8805200	-1.4016620	7.1667530	-13.925667	15.011661	-8.8932810	2.2139520
			G_1	0.1348040	0.2057400	1.3039410	-0.5861710	-0.8644100	0.5855200	-0.0873070
			G_5	0.3701090	-0.4417510	2.3525090	-2.5527280	1.2083910	-0.2357170	-0.0478740
			G_6	-0.2518010	0.2523690	-1.2713390	1.7147270	0.4130870	-1.3092790	0.4520780
		0.6	G_0	0.9224310	-1.6634890	8.2940140	-15.798198	16.794604	-9.8012890	2.3851260
			G_1	0.1534350	0.1275230	1.5310370	-0.7372250	-0.8583320	0.6332240	-0.1188140
			G_5	0.2952280	-0.4342720	2.3264160	-2.4489470	2.8863140	-2.7708860	0.9028190
			G_6	-0.3525150	0.4096230	-2.2696340	2.8487460	0.5255160	-1.5989310	0.4371180
		0.8	G_0	1.0173120	-2.1660750	10.865217	-21.778875	25.306674	-15.495659	3.666350
			G_1	0.1939800	-0.0549670	2.3987660	-2.7120480	2.0130710	-1.1112710	0.1442770
			G_5	0.2155000	-0.4734570	2.3473370	-2.9742430	6.6372940	-6.7265580	1.9515050
			G_6	-0.4270850	0.5863830	-3.4732770	4.5516220	-1.6308310	1.2709000	-0.8777360

Table 9B.14 – Influence Coefficients for a Circumferential Semi-Elliptical Surface Crack in a Cylinder – Inside Surface

t/R_i	a/c	a/t	G_i	A_0	A_1	A_2	A_3	A_4	A_5	A_6
1.0 (1/1)	1.0	0	G0	1.1977992	-0.5244870	0.1498299	2.3284866	-5.1058499	4.3469049	-1.3487980
			G1	0.1870117	0.6987352	0.1316900	0.7269255	-2.5259384	2.1756251	-0.6540458
			G5	0.5988996	-0.2622435	0.0749149	1.1642433	-2.5529250	2.1734525	-0.6743990
			G6	0.0000000	0.0000000	0.0000000	0.0000000	0.0000000	0.0000000	0.0000000
		0.2	G0	1.1851680	-1.0992960	3.1805840	-5.678532	6.805073	-4.649857	1.303158
			G1	0.1854850	0.5422040	0.8564640	-1.554848	1.555252	-1.230298	0.390311
			G5	0.6014920	-0.4406990	1.2403130	-1.385155	0.736846	-0.096356	-0.061079
			G6	-0.0766940	0.0770970	-0.252314	0.584930	-0.585253	0.390523	-0.137938
		0.4	G0	1.2164150	-1.4028400	4.127932	-7.274444	8.998304	-6.515517	1.930765
			G1	0.1998200	0.4584380	1.042077	-2.049460	2.851224	-2.625849	0.890048
			G5	0.6171980	-0.5312910	1.749854	-2.209232	2.085857	-1.448441	0.425576
			G6	-0.1591580	0.1557710	-0.738026	2.296463	-3.399956	2.736813	-0.891522
		0.6	G0	1.2659220	-1.6617470	4.692820	-7.279671	8.253668	-5.923170	1.792086
			G1	0.2217270	0.3863870	1.061395	-1.741902	2.614214	-2.735439	0.992153
			G5	0.6315230	-0.6132890	2.075705	-2.230962	2.172165	-1.873904	0.639668
			G6	-0.2383560	0.1901270	-0.710806	0.840178	0.813463	-1.404429	0.510397
		0.8	G0	1.3563410	-1.9839650	5.564546	-7.611331	7.603290	-4.987116	1.371359
			G1	0.2613250	0.2807650	1.245979	-1.609410	2.364747	-2.484886	0.837423
			G5	0.6597780	-0.7444230	2.550643	-2.351869	2.439337	-2.278697	0.720555
			G6	-0.3173130	0.1789970	-0.732479	0.858558	0.220452	0.072857	-0.281343
1.0 (1/1)	2.0	0	G_0	0.8150546	-0.5623828	1.4465771	-4.6778133	8.4192164	-7.9025932	2.9866351
			G_1	0.1359146	0.0702340	3.5558581	-11.034445	16.967724	-14.126991	4.8706612
			G_5	0.4075273	-0.2811914	0.7232885	-2.3389066	4.2096082	-3.9512966	1.4933175
			G_6	0.0000000	0.0000000	0.0000000	0.0000000	0.0000000	0.0000000	0.0000000
		0.2	G_0	0.8191500	-0.5931060	1.0903880	-1.8353570	1.2731590	-0.1438910	-0.0750130
			G_1	0.1096810	0.5462320	0.3048620	-0.2825680	-1.6694950	2.1535120	-0.7330820
			G_5	0.4176450	-0.2188780	0.3863010	-0.2504610	-0.7513220	1.1688610	-0.4414390
			G_6	-0.0225190	0.0262460	-0.1212490	0.3992060	-0.5678040	0.4201750	-0.1319040
		0.4	G_0	0.8394950	-0.7297850	1.7020200	-3.5555770	4.1423710	-2.3606790	0.5388240
			G_1	0.1190770	0.5132440	0.4642960	-0.9878840	-0.2300000	1.0355160	-0.4569390
			G_5	0.4374170	-0.2298300	0.6760210	-0.9704160	0.2631730	0.4975540	-0.2939380
			G_6	-0.0471910	0.0376220	-0.1999980	0.6355000	-0.8006850	0.5288560	-0.1526420
		0.6	G_0	0.8647160	-0.8588720	2.2485390	-5.2431620	7.3577510	-5.2056610	1.4515070
			G_1	0.1306890	0.4721720	0.6853720	-2.0009110	1.9607260	-0.9129450	0.1465660
			G_5	0.4595140	-0.2427740	0.9498760	-1.7882310	1.8002930	-0.8593610	0.1324390
			G_6	-0.0726760	0.0431420	-0.3613230	1.3531400	-2.0533870	1.5862390	-0.4939430
		0.8	G_0	0.8987030	-0.9736490	2.6694460	-6.0938250	8.7462280	-6.3458830	1.7790820
			G_1	0.1452770	0.4441330	0.8173190	-2.5177670	3.1549300	-1.9659710	0.4458920
			G_5	0.4870630	-0.2663310	1.2807530	-2.5780820	3.1441270	-1.9614000	0.4422760
			G_6	-0.0984620	0.0418730	-0.5656400	2.1359290	-3.1667730	2.3444890	-0.6898820

Table 9B.14 – Influence Coefficients for a Circumferential Semi-Elliptical Surface Crack in a Cylinder – Inside Surface

t/R_i	a/c	a/t	G_i	A_0	A_1	A_2	A_3	A_4	A_5	A_6
1.5 (1.5/1)	0.03125	0	G_0	>360°	>360°	>360°	>360°	>360°	>360°	>360°
			G_1	>360°	>360°	>360°	>360°	>360°	>360°	>360°
			G_5	>360°	>360°	>360°	>360°	>360°	>360°	>360°
			G_6	>360°	>360°	>360°	>360°	>360°	>360°	>360°
		0.2	G_0	>360°	>360°	>360°	>360°	>360°	>360°	>360°
			G_1	>360°	>360°	>360°	>360°	>360°	>360°	>360°
			G_5	>360°	>360°	>360°	>360°	>360°	>360°	>360°
			G_6	>360°	>360°	>360°	>360°	>360°	>360°	>360°
		0.4	G_0	>360°	>360°	>360°	>360°	>360°	>360°	>360°
			G_1	>360°	>360°	>360°	>360°	>360°	>360°	>360°
			G_5	>360°	>360°	>360°	>360°	>360°	>360°	>360°
			G_6	>360°	>360°	>360°	>360°	>360°	>360°	>360°
		0.6	G_0	>360°	>360°	>360°	>360°	>360°	>360°	>360°
			G_1	>360°	>360°	>360°	>360°	>360°	>360°	>360°
			G_5	>360°	>360°	>360°	>360°	>360°	>360°	>360°
			G_6	>360°	>360°	>360°	>360°	>360°	>360°	>360°
		0.8	G_0	>360°	>360°	>360°	>360°	>360°	>360°	>360°
			G_1	>360°	>360°	>360°	>360°	>360°	>360°	>360°
			G_5	>360°	>360°	>360°	>360°	>360°	>360°	>360°
			G_6	>360°	>360°	>360°	>360°	>360°	>360°	>360°
1.5 (1.5/1)	0.0625	0	G_0	>360°	>360°	>360°	>360°	>360°	>360°	>360°
			G_1	>360°	>360°	>360°	>360°	>360°	>360°	>360°
			G_5	>360°	>360°	>360°	>360°	>360°	>360°	>360°
			G_6	>360°	>360°	>360°	>360°	>360°	>360°	>360°
		0.2	G_0	>360°	>360°	>360°	>360°	>360°	>360°	>360°
			G_1	>360°	>360°	>360°	>360°	>360°	>360°	>360°
			G_5	>360°	>360°	>360°	>360°	>360°	>360°	>360°
			G_6	>360°	>360°	>360°	>360°	>360°	>360°	>360°
		0.4	G_0	>360°	>360°	>360°	>360°	>360°	>360°	>360°
			G_1	>360°	>360°	>360°	>360°	>360°	>360°	>360°
			G_5	>360°	>360°	>360°	>360°	>360°	>360°	>360°
			G_6	>360°	>360°	>360°	>360°	>360°	>360°	>360°
		0.6	G_0	>360°	>360°	>360°	>360°	>360°	>360°	>360°
			G_1	>360°	>360°	>360°	>360°	>360°	>360°	>360°
			G_5	>360°	>360°	>360°	>360°	>360°	>360°	>360°
			G_6	>360°	>360°	>360°	>360°	>360°	>360°	>360°
		0.8	G_0	>360°	>360°	>360°	>360°	>360°	>360°	>360°
			G_1	>360°	>360°	>360°	>360°	>360°	>360°	>360°
			G_5	>360°	>360°	>360°	>360°	>360°	>360°	>360°
			G_6	>360°	>360°	>360°	>360°	>360°	>360°	>360°

Table 9B.14 – Influence Coefficients for a Circumferential Semi-Elliptical Surface Crack in a Cylinder – Inside Surface

t/R_i	a/c	a/t	G_i	A_0	A_1	A_2	A_3	A_4	A_5	A_6
1.5 (1.5/1)	0.125	0	G_0	0.4065238	0.7772483	3.8861644	-12.573943	16.760207	-11.014593	2.8706957
			G_1	0.0320270	0.1825342	2.2670449	-2.7076615	1.2088194	-0.3777430	0.0763155
			G_5	0.3387700	0.6477067	3.2384700	-10.478286	13.966839	-9.1788275	2.3922467
			G_6	0.0000000	0.0000000	0.0000000	0.0000000	0.0000000	0.0000000	0.0000000
		0.2	G_0	0.1877460	3.3666140	-9.1785680	17.900606	-20.873496	12.813742	-3.2176130
			G_1	-0.0017720	0.4888430	0.9814160	-0.5666390	-0.5690930	0.3173000	-0.0101010
			G_5	-0.0004620	-1.4645550	5.2095010	-10.576578	18.102884	-15.157836	4.3430190
			G_6	-0.0039240	-1.5298450	4.4763160	-10.662120	11.014719	-1.8253030	-1.4724760
		0.4	G_0	>360°	>360°	>360°	>360°	>360°	>360°	>360°
			G_1	>360°	>360°	>360°	>360°	>360°	>360°	>360°
			G_5	>360°	>360°	>360°	>360°	>360°	>360°	>360°
			G_6	>360°	>360°	>360°	>360°	>360°	>360°	>360°
		0.6	G_0	>360°	>360°	>360°	>360°	>360°	>360°	>360°
			G_1	>360°	>360°	>360°	>360°	>360°	>360°	>360°
			G_5	>360°	>360°	>360°	>360°	>360°	>360°	>360°
			G_6	>360°	>360°	>360°	>360°	>360°	>360°	>360°
		0.8	G_0	>360°	>360°	>360°	>360°	>360°	>360°	>360°
			G_1	>360°	>360°	>360°	>360°	>360°	>360°	>360°
			G_5	>360°	>360°	>360°	>360°	>360°	>360°	>360°
			G_6	>360°	>360°	>360°	>360°	>360°	>360°	>360°
1.5 (1.5/1)	0.25	0	G_0	0.6152816	-0.3348694	6.2955620	-15.590618	19.299508	-12.488107	3.3010035
			G_1	0.0703566	0.2828152	1.4036169	-0.6511596	-1.2076596	1.0318656	-0.2423741
			G_5	0.3076408	-0.1674347	3.1477810	-7.7953092	9.6497542	-6.2440535	1.6505017
			G_6	0.0000000	0.0000000	0.0000000	0.0000000	0.0000000	0.0000000	0.0000000
		0.2	G_0	0.5372600	-0.0095320	4.9894040	-13.790020	18.288571	-12.361561	3.3479260
			G_1	0.0622860	0.1355150	2.2532320	-3.3214620	2.8190710	-1.8601200	0.5588550
			G_5	0.1121500	-0.0255170	1.0621980	-1.2691310	1.9682390	-2.1205000	0.7390210
			G_6	-0.1776400	-0.1904600	-0.6898450	1.5816600	-0.0630220	-0.6557400	0.1950190
		0.4	G_0	0.5335140	-0.1357450	5.6886150	-15.846551	21.566821	-14.879862	4.0782790
			G_1	0.0658910	0.0785060	2.5206390	-4.0594950	3.9974960	-2.7741960	0.8246790
			G_5	-0.0960910	-0.2680870	0.5971130	-2.3141630	11.217411	-12.805323	4.1869020
			G_6	-0.1532600	-0.1938350	-0.7689420	-0.7290710	1.0914750	3.2076440	-2.4551200
		0.6	G_0	>360°	>360°	>360°	>360°	>360°	>360°	>360°
			G_1	>360°	>360°	>360°	>360°	>360°	>360°	>360°
			G_5	>360°	>360°	>360°	>360°	>360°	>360°	>360°
			G_6	>360°	>360°	>360°	>360°	>360°	>360°	>360°
		0.8	G_0	>360°	>360°	>360°	>360°	>360°	>360°	>360°
			G_1	>360°	>360°	>360°	>360°	>360°	>360°	>360°
			G_5	>360°	>360°	>360°	>360°	>360°	>360°	>360°
			G_6	>360°	>360°	>360°	>360°	>360°	>360°	>360°

Table 9B.14 – Influence Coefficients for a Circumferential Semi-Elliptical Surface Crack in a Cylinder – Inside Surface

t/R_i	a/c	a/t	G_i	A_0	A_1	A_2	A_3	A_4	A_5	A_6
1.5 (1.5/1)	0.5	0	G_0	0.8776607	-0.6729719	3.7721411	-6.5209060	6.3377934	-3.7028038	0.9872447
			G_1	0.1277541	0.4368502	0.4904522	1.0427434	-2.9631236	2.0826525	-0.5184313
			G_5	0.4388304	-0.3364859	1.8860705	-3.2604530	3.1688967	-1.8514019	0.4936224
			G_6	0.0000000	0.0000000	0.0000000	0.0000000	0.0000000	0.0000000	0.0000000
		0.2	G_0	0.8436160	-1.2186720	6.4749320	-12.772437	13.920327	-8.3075030	2.0765010
			G_1	0.1216220	0.2486950	1.2072890	-0.5692060	-0.7782250	0.5197600	-0.0735000
			G_5	0.3077780	-0.3470150	1.9527420	-2.6883900	1.8661520	-0.6854640	0.0755660
			G_6	-0.1540500	0.2129360	-1.1297190	1.9521930	-0.5735630	-0.7372730	0.4298770
		0.4	G_0	0.8474600	-1.5039700	7.5880430	-14.533094	15.316912	-8.8345200	2.1411830
			G_1	0.1259560	0.1897540	1.2376700	-0.1654000	-1.5921260	1.1319760	-0.2434700
			G_5	0.2048670	-0.2825200	1.5964370	-1.6043040	2.0459210	-2.1437900	0.7380250
			G_6	-0.2724300	0.3078980	-1.7531960	2.2251030	0.3608770	-1.1778820	0.3094960
		0.6	G_0	0.8792280	-1.8559460	9.3947030	-18.552392	20.554817	-12.358894	3.0518320
			G_1	0.1424390	0.0826260	1.6254650	-0.7687620	-0.8468500	0.6142880	-0.1193260
			G_5	0.0643590	-0.1954470	1.0374990	-1.6948330	6.8631740	-8.2226230	2.8072610
			G_6	-0.3293730	0.4542380	-2.6321670	2.1886930	1.4830830	-0.8673000	-0.2973430
		0.8	G_0	0.9691290	-2.5290450	13.106813	-28.695286	36.307054	-23.389376	5.6786220
			G_1	0.1816150	-0.1662170	2.8816330	-4.1652800	4.5555240	-2.9558390	0.5680170
			G_5	-0.0693110	-0.1853760	0.8225000	-4.9669610	18.150732	-17.929266	5.0525780
			G_6	-0.3121920	0.5635720	-3.5719260	4.6071040	-7.8054410	12.446179	-5.9278130
1.5 (1.5/1)	1.0	0	G_0	1.1977992	-0.5244870	0.1498299	2.3284866	-5.1058499	4.3469049	-1.3487980
			G_1	0.1870117	0.6987352	0.1316900	0.7269255	-2.5259384	2.1756251	-0.6540458
			G_5	0.9981658	-0.4370725	0.1248583	1.9404058	-4.2548750	3.6224208	-1.1239983
			G_6	0.0000000	0.0000000	0.0000000	0.0000000	0.0000000	0.0000000	0.0000000
		0.2	G_0	1.1767790	-1.1792990	3.3862400	-6.0301300	7.6841880	-5.7164500	1.7295200
			G_1	0.1850180	0.5164280	0.9251000	-1.9196150	2.6244510	-2.3927060	0.8118470
			G_5	0.4771910	-0.3549720	1.0629980	-1.1784280	0.8826090	-0.5231410	0.1406340
			G_6	-0.0934780	0.0859260	-0.3229380	1.0366460	-1.7033050	1.5756060	-0.5786670
		0.4	G_0	1.1946690	-1.5081560	4.2074550	-6.3032350	6.9540530	-4.9725190	1.5134360
			G_1	0.1967120	0.4361220	0.8994770	-1.4345260	2.2113000	-2.4456540	0.9111270
			G_5	0.4714760	-0.4265210	1.5014660	-1.5922220	1.5982090	-1.4461030	0.5068520
			G_6	-0.1882160	0.1517770	-0.5845380	0.7042650	0.6488940	-1.1634980	0.4317850
		0.6	G_0	1.2342000	-1.7924370	4.8504000	-5.9356390	5.1190450	-3.3583480	1.0412270
			G_1	0.2181590	0.3558900	0.8432980	-0.6189270	1.0600230	-1.8589740	0.8149020
			G_5	0.4534580	-0.5105100	1.9513880	-2.2250390	3.3751910	-3.6289990	1.3253900
			G_6	-0.2788880	0.1941950	-1.0859200	1.9982740	-1.5162390	1.3096280	-0.6212080
		0.8	G_0	1.3356880	-2.2383160	6.1917430	-6.7429100	4.5020220	-1.9803880	0.3277990
			G_1	0.2675930	0.1934480	1.1289280	-0.2891670	0.1853030	-0.9299710	0.3868010
			G_5	0.4467150	-0.6604910	2.2801380	-1.8406040	3.4227960	-3.9789140	1.3004170
			G_6	-0.3609490	0.1758460	-0.9439010	0.1354710	1.9712430	-0.5838580	-0.3942640

Table 9B.14 – Influence Coefficients for a Circumferential Semi-Elliptical Surface Crack in a Cylinder – Inside Surface

t/R_i	a/c	a/t	G_i	A_0	A_1	A_2	A_3	A_4	A_5	A_6
1.5 (1.5/1)	2.0	0	G_0	0.8150546	-0.5623828	1.4465771	-4.6778133	8.4192164	-7.9025932	2.9866351
			G_1	0.1359146	0.0702340	3.5558581	-11.034445	16.967724	-14.126991	4.8706612
			G_5	0.6792125	-0.4686525	1.2054808	-3.8981775	7.0160133	-6.5854942	2.4888625
			G_6	0.0000000	0.0000000	0.0000000	0.0000000	0.0000000	0.0000000	0.0000000
		0.2	G_0	0.8206090	-0.6260970	1.2171740	-2.1494640	1.8104050	-0.5203160	0.0003570
			G_1	0.1117490	0.5388720	0.3373700	-0.4804400	-1.2401410	1.8610540	-0.6869060
			G_5	0.3376320	-0.1703140	0.4194680	-0.5470220	-0.0344350	0.5030340	-0.2346000
			G_6	-0.0275590	0.0265540	-0.1343960	0.4446780	-0.6195270	0.4543560	-0.1423860
		0.4	G_0	0.8415970	-0.8029760	2.0644060	-4.7610910	6.5811550	-4.5673410	1.2476160
			G_1	0.1232560	0.4868550	0.6303610	-1.8557230	1.7183850	-0.7069030	0.0795790
			G_5	0.3562570	-0.1729060	0.7155570	-1.3638460	1.3579240	-0.6233200	0.0853210
			G_6	-0.0578900	0.0353740	-0.3005730	1.1477190	-1.8009330	1.4336390	-0.4562640
		0.6	G_0	0.8675200	-0.9389760	2.4670300	-5.5942130	8.2101600	-6.1290070	1.7682760
			G_1	0.1370090	0.4463770	0.7316230	-2.3887380	3.1984740	-2.1735990	0.5542510
			G_5	0.3754960	-0.1633230	0.7505330	-1.1341150	1.0430390	-0.4564260	0.0252130
			G_6	-0.0886610	0.0313410	-0.5218360	1.8734180	-2.5595050	1.7349240	-0.4681040
		0.8	G_0	0.9092960	-1.0919720	3.0500940	-6.8520530	10.495344	-8.2108710	2.4412760
			G_1	0.1577970	0.3968730	0.9237770	-3.1167710	4.9988640	-3.9082630	1.1083550
			G_5	0.4027050	-0.1943280	1.0602430	-1.8339650	2.5901090	-1.9760340	0.5121480
			G_6	-0.1193420	-0.0233800	-0.3417260	0.9608590	-0.4701750	-0.1274380	0.1226200
2.0 (2/1)	0.03125	0	G_0	>360°	>360°	>360°	>360°	>360°	>360°	>360°
			G_1	>360°	>360°	>360°	>360°	>360°	>360°	>360°
			G_5	>360°	>360°	>360°	>360°	>360°	>360°	>360°
			G_6	>360°	>360°	>360°	>360°	>360°	>360°	>360°
		0.2	G_0	>360°	>360°	>360°	>360°	>360°	>360°	>360°
			G_1	>360°	>360°	>360°	>360°	>360°	>360°	>360°
			G_5	>360°	>360°	>360°	>360°	>360°	>360°	>360°
			G_6	>360°	>360°	>360°	>360°	>360°	>360°	>360°
		0.4	G_0	>360°	>360°	>360°	>360°	>360°	>360°	>360°
			G_1	>360°	>360°	>360°	>360°	>360°	>360°	>360°
			G_5	>360°	>360°	>360°	>360°	>360°	>360°	>360°
			G_6	>360°	>360°	>360°	>360°	>360°	>360°	>360°
		0.6	G_0	>360°	>360°	>360°	>360°	>360°	>360°	>360°
			G_1	>360°	>360°	>360°	>360°	>360°	>360°	>360°
			G_5	>360°	>360°	>360°	>360°	>360°	>360°	>360°
			G_6	>360°	>360°	>360°	>360°	>360°	>360°	>360°
		0.8	G_0	>360°	>360°	>360°	>360°	>360°	>360°	>360°
			G_1	>360°	>360°	>360°	>360°	>360°	>360°	>360°
			G_5	>360°	>360°	>360°	>360°	>360°	>360°	>360°
			G_6	>360°	>360°	>360°	>360°	>360°	>360°	>360°

Table 9B.14 – Influence Coefficients for a Circumferential Semi-Elliptical Surface Crack in a Cylinder – Inside Surface

t/R_i	a/c	a/t	G_i	A_0	A_1	A_2	A_3	A_4	A_5	A_6
2.0 (2/1)	0.0625	0	G_0	>360°	>360°	>360°	>360°	>360°	>360°	>360°
			G_1	>360°	>360°	>360°	>360°	>360°	>360°	>360°
			G_5	>360°	>360°	>360°	>360°	>360°	>360°	>360°
			G_6	>360°	>360°	>360°	>360°	>360°	>360°	>360°
		0.2	G_0	>360°	>360°	>360°	>360°	>360°	>360°	>360°
			G_1	>360°	>360°	>360°	>360°	>360°	>360°	>360°
			G_5	>360°	>360°	>360°	>360°	>360°	>360°	>360°
			G_6	>360°	>360°	>360°	>360°	>360°	>360°	>360°
		0.4	G_0	>360°	>360°	>360°	>360°	>360°	>360°	>360°
			G_1	>360°	>360°	>360°	>360°	>360°	>360°	>360°
			G_5	>360°	>360°	>360°	>360°	>360°	>360°	>360°
			G_6	>360°	>360°	>360°	>360°	>360°	>360°	>360°
		0.6	G_0	>360°	>360°	>360°	>360°	>360°	>360°	>360°
			G_1	>360°	>360°	>360°	>360°	>360°	>360°	>360°
			G_5	>360°	>360°	>360°	>360°	>360°	>360°	>360°
			G_6	>360°	>360°	>360°	>360°	>360°	>360°	>360°
		0.8	G_0	>360°	>360°	>360°	>360°	>360°	>360°	>360°
			G_1	>360°	>360°	>360°	>360°	>360°	>360°	>360°
			G_5	>360°	>360°	>360°	>360°	>360°	>360°	>360°
			G_6	>360°	>360°	>360°	>360°	>360°	>360°	>360°
2.0 (2/1)	0.0125	0	G_0	>360°	>360°	>360°	>360°	>360°	>360°	>360°
			G_1	>360°	>360°	>360°	>360°	>360°	>360°	>360°
			G_5	>360°	>360°	>360°	>360°	>360°	>360°	>360°
			G_6	>360°	>360°	>360°	>360°	>360°	>360°	>360°
		0.2	G_0	>360°	>360°	>360°	>360°	>360°	>360°	>360°
			G_1	>360°	>360°	>360°	>360°	>360°	>360°	>360°
			G_5	>360°	>360°	>360°	>360°	>360°	>360°	>360°
			G_6	>360°	>360°	>360°	>360°	>360°	>360°	>360°
		0.4	G_0	>360°	>360°	>360°	>360°	>360°	>360°	>360°
			G_1	>360°	>360°	>360°	>360°	>360°	>360°	>360°
			G_5	>360°	>360°	>360°	>360°	>360°	>360°	>360°
			G_6	>360°	>360°	>360°	>360°	>360°	>360°	>360°
		0.6	G_0	>360°	>360°	>360°	>360°	>360°	>360°	>360°
			G_1	>360°	>360°	>360°	>360°	>360°	>360°	>360°
			G_5	>360°	>360°	>360°	>360°	>360°	>360°	>360°
			G_6	>360°	>360°	>360°	>360°	>360°	>360°	>360°
		0.8	G_0	>360°	>360°	>360°	>360°	>360°	>360°	>360°
			G_1	>360°	>360°	>360°	>360°	>360°	>360°	>360°
			G_5	>360°	>360°	>360°	>360°	>360°	>360°	>360°
			G_6	>360°	>360°	>360°	>360°	>360°	>360°	>360°

Table 9B.14 – Influence Coefficients for a Circumferential Semi-Elliptical Surface Crack in a Cylinder – Inside Surface

t/R_i	a/c	a/t	G_i	A_0	A_1	A_2	A_3	A_4	A_5	A_6
2.0 (2/1)	0.25	0	G_0	0.6152816	-0.3348694	6.2955620	-15.590618	19.299508	-12.488107	3.3010035
			G_1	0.0703566	0.2828152	1.4036169	-0.6511596	-1.2076596	1.0318656	-0.2423741
			G_5	0.3076408	-0.1674347	3.1477810	-7.7953092	9.6497542	-6.2440535	1.6505017
			G_6	0.0000000	0.0000000	0.0000000	0.0000000	0.0000000	0.0000000	0.0000000
		0.2	G_0	0.5230310	-0.0034300	4.8781900	-13.581021	18.065450	-12.217878	3.3084250
			G_1	0.0594020	0.1297560	2.2389200	-3.2921640	2.7799490	-1.8261960	0.5477370
			G_5	0.0316930	-0.0490320	0.4556670	0.2029610	1.1607840	-2.3288810	0.9202600
			G_6	-0.1588200	-0.2078160	-0.6054660	0.9276730	0.5688670	-0.4203210	-0.1043620
		0.4	G_0	>360°	>360°	>360°	>360°	>360°	>360°	>360°
			G_1	>360°	>360°	>360°	>360°	>360°	>360°	>360°
			G_5	>360°	>360°	>360°	>360°	>360°	>360°	>360°
			G_6	>360°	>360°	>360°	>360°	>360°	>360°	>360°
		0.6	G_0	>360°	>360°	>360°	>360°	>360°	>360°	>360°
			G_1	>360°	>360°	>360°	>360°	>360°	>360°	>360°
			G_5	>360°	>360°	>360°	>360°	>360°	>360°	>360°
			G_6	>360°	>360°	>360°	>360°	>360°	>360°	>360°
		0.8	G_0	>360°	>360°	>360°	>360°	>360°	>360°	>360°
			G_1	>360°	>360°	>360°	>360°	>360°	>360°	>360°
			G_5	>360°	>360°	>360°	>360°	>360°	>360°	>360°
			G_6	>360°	>360°	>360°	>360°	>360°	>360°	>360°
2.0 (2/1)	0.5	0	G_0	0.8776607	-0.6729719	3.7721411	-6.5209060	6.3377934	-3.7028038	0.9872447
			G_1	0.1277541	0.4368502	0.4904522	1.0427434	-2.9631236	2.0826525	-0.5184313
			G_5	0.4388304	-0.3364859	1.8860705	-3.2604530	3.1688967	-1.8514019	0.4936224
			G_6	0.0000000	0.0000000	0.0000000	0.0000000	0.0000000	0.0000000	0.0000000
		0.2	G_0	0.8299660	-1.2852680	6.7021900	-13.038291	13.947195	-8.1575160	2.0014940
			G_1	0.1180860	0.2378470	1.1674520	-0.3256670	-1.1959700	0.8327900	-0.1627080
			G_5	0.2284830	-0.2622160	1.4635930	-1.6013950	0.7823620	-0.1744680	-0.0226260
			G_6	-0.1618290	0.1382070	-0.6944400	0.7710550	0.7133080	-1.1190210	0.3524750
		0.4	G_0	0.8245610	-1.6271230	8.2516330	-16.049668	17.102002	-9.8951100	2.3925640
			G_1	0.1202460	0.1639650	1.2641410	-0.0440790	-1.8888250	1.3842360	-0.3212840
			G_5	0.0813220	-0.1502620	0.8475180	-0.8366060	3.3171700	-4.3109360	1.5405320
			G_6	-0.2573140	0.3045630	-1.8305850	1.6907690	1.1795710	-1.1601330	0.0729730
		0.6	G_0	0.8609610	-2.1023130	10.886247	-22.707845	26.425228	-16.356015	4.0906000
			G_1	0.1390780	0.0147340	1.8883340	-1.3732520	-0.0133220	0.0656510	0.0075140
			G_5	-0.0822530	-0.0675250	0.3583490	-3.7353100	15.141567	-16.060501	5.0360810
			G_6	-0.2351010	0.3604550	-2.1978990	1.2837550	-1.5176060	5.6728760	-3.3674260
		0.8	G_0	>360°	>360°	>360°	>360°	>360°	>360°	>360°
			G_1	>360°	>360°	>360°	>360°	>360°	>360°	>360°
			G_5	>360°	>360°	>360°	>360°	>360°	>360°	>360°
			G_6	>360°	>360°	>360°	>360°	>360°	>360°	>360°

Table 9B.14 – Influence Coefficients for a Circumferential Semi-Elliptical Surface Crack in a Cylinder – Inside Surface

t/R_i	a/c	a/t	G_i	A_0	A_1	A_2	A_3	A_4	A_5	A_6
2.0 (2/1)	1.0	0	G_0	1.1977992	-0.5244870	0.1498299	2.3284866	-5.1058499	4.3469049	-1.3487980
			G_1	0.1870117	0.6987352	0.1316900	0.7269255	-2.5259384	2.1756251	-0.6540458
			G_5	0.9981658	-0.4370725	0.1248583	1.9404058	-4.2548750	3.6224208	-1.1239983
			G_6	0.0000000	0.0000000	0.0000000	0.0000000	0.0000000	0.0000000	0.0000000
		0.2	G_0	1.1684530	-1.2585070	3.5279430	-5.7281070	6.7622570	-4.8681160	1.4500610
			G_1	0.1842740	0.4971500	0.8863610	-1.6758250	2.3326480	-2.2511380	0.7818420
			G_5	0.3920940	-0.3082200	1.0144020	-1.1644570	1.0183370	-0.7252250	0.2203410
			G_6	-0.1045090	0.1034900	-0.5379490	1.8429360	-3.0023320	2.5453970	-0.8468070
		0.4	G_0	1.1756370	-1.6091180	4.3312550	-5.4429200	4.8549020	-3.2105920	0.9894450
			G_1	0.1939300	0.4148800	0.7506560	-0.6964290	1.1923180	-1.8693060	0.7946840
			G_5	0.3655740	-0.3465940	1.2060660	-0.7425800	0.6355140	-0.9644920	0.4072180
			G_6	-0.2044080	0.0907420	-0.3211630	0.0829340	0.9098730	-0.5410640	-0.0171630
		0.6	G_0	1.2115270	-1.9531520	5.2040110	-5.0574660	2.2345640	-0.5984900	0.1312860
			G_1	0.2160920	0.3153030	0.6716000	0.5433680	-0.8981020	-0.4505530	0.4289850
			G_5	0.3182430	-0.4469350	1.6778140	-1.6543620	3.5036420	-4.2578910	1.5567750
			G_6	-0.2938460	0.1265600	-0.6483040	-0.3578200	2.5684500	-1.3478200	-0.0476580
		0.8	G_0	1.3236840	-2.5724680	7.4296210	-8.1088430	4.8737080	-1.4065580	-0.0770330
			G_1	0.2728460	0.0767560	1.2431330	0.3289470	-1.1072210	0.1430990	0.0246010
			G_5	0.2778880	-0.6806110	2.4439410	-3.6314780	8.8276540	-9.0860340	2.7929240
			G_6	-0.3647760	0.1905250	-1.1634880	-0.5289010	2.6594530	0.4073020	-1.2007620
2.0 (2/1)	2.0	0	G_0	0.8150546	-0.5623828	1.4465771	-4.6778133	8.4192164	-7.9025932	2.9866351
			G_1	0.1359146	0.0702340	3.5558581	-11.034445	16.967724	-14.126991	4.8706612
			G_5	0.6792125	-0.4686525	1.2054808	-3.8981775	7.0160133	-6.5854942	2.4888625
			G_6	0.0000000	0.0000000	0.0000000	0.0000000	0.0000000	0.0000000	0.0000000
		0.2	G_0	0.8220090	-0.6573050	1.3211640	-2.3835200	2.2476120	-0.8654190	0.0837280
			G_1	0.1138040	0.5313120	0.3635540	-0.6660590	-0.7827520	1.4925510	-0.5998280
			G_5	0.2839030	-0.1321360	0.3755980	-0.4917050	0.0057990	0.4159280	-0.2084330
			G_6	-0.0311120	0.0249870	-0.1298350	0.4140210	-0.5462970	0.3975560	-0.1280300
		0.4	G_0	0.8431730	-0.8668300	2.2754670	-5.1959420	7.4123430	-5.3232490	1.4802160
			G_1	0.1269720	0.4665950	0.6844680	-2.1836080	2.6144440	-1.5581290	0.3400780
			G_5	0.3008520	-0.1358360	0.6853590	-1.3332620	1.5256780	-0.8821160	0.1771800
			G_6	-0.0650110	0.0305470	-0.4108650	1.5855120	-2.4366030	1.8522060	-0.5545010
		0.6	G_0	0.8704980	-1.0359470	2.8000500	-6.3081210	9.6917160	-7.6547170	2.3161260
			G_1	0.1430250	0.4101650	0.8238710	-2.8739700	4.6188050	-3.6773280	1.0796420
			G_5	0.3171210	-0.1407400	0.7838550	-1.3410070	1.9059580	-1.5128840	0.4203580
			G_6	-0.0988910	-0.0177750	-0.2895770	0.7961280	-0.3432140	-0.1750190	0.1296260
		0.8	G_0	0.9207020	-1.2187090	3.3266570	-6.9200380	10.752025	-8.7612920	2.6934980
			G_1	0.1698530	0.3446940	0.9508500	-3.1852770	5.7428780	-4.9342150	1.5026470
			G_5	0.3432810	-0.2102620	1.1766120	-2.1868500	3.9367680	-3.5942370	1.1057150
			G_6	-0.1338270	-0.0933840	-0.3249220	1.4520770	-2.1708500	2.0700500	-0.7982220

Table 9B.14 – Influence Coefficients for a Circumferential Semi-Elliptical Surface Crack in a Cylinder – Inside Surface

t/R_i	a/c	a/t	G_i	A_0	A_1	A_2	A_3	A_4	A_5	A_6
2.5 (2.5/1)	0.03125	0	G_0	>360°	>360°	>360°	>360°	>360°	>360°	>360°
			G_1	>360°	>360°	>360°	>360°	>360°	>360°	>360°
			G_5	>360°	>360°	>360°	>360°	>360°	>360°	>360°
			G_6	>360°	>360°	>360°	>360°	>360°	>360°	>360°
		0.2	G_0	>360°	>360°	>360°	>360°	>360°	>360°	>360°
			G_1	>360°	>360°	>360°	>360°	>360°	>360°	>360°
			G_5	>360°	>360°	>360°	>360°	>360°	>360°	>360°
			G_6	>360°	>360°	>360°	>360°	>360°	>360°	>360°
		0.4	G_0	>360°	>360°	>360°	>360°	>360°	>360°	>360°
			G_1	>360°	>360°	>360°	>360°	>360°	>360°	>360°
			G_5	>360°	>360°	>360°	>360°	>360°	>360°	>360°
			G_6	>360°	>360°	>360°	>360°	>360°	>360°	>360°
		0.6	G_0	>360°	>360°	>360°	>360°	>360°	>360°	>360°
			G_1	>360°	>360°	>360°	>360°	>360°	>360°	>360°
			G_5	>360°	>360°	>360°	>360°	>360°	>360°	>360°
			G_6	>360°	>360°	>360°	>360°	>360°	>360°	>360°
		0.8	G_0	>360°	>360°	>360°	>360°	>360°	>360°	>360°
			G_1	>360°	>360°	>360°	>360°	>360°	>360°	>360°
			G_5	>360°	>360°	>360°	>360°	>360°	>360°	>360°
			G_6	>360°	>360°	>360°	>360°	>360°	>360°	>360°
2.5 (2.5/1)	0.0625	0	G_0	>360°	>360°	>360°	>360°	>360°	>360°	>360°
			G_1	>360°	>360°	>360°	>360°	>360°	>360°	>360°
			G_5	>360°	>360°	>360°	>360°	>360°	>360°	>360°
			G_6	>360°	>360°	>360°	>360°	>360°	>360°	>360°
		0.2	G_0	>360°	>360°	>360°	>360°	>360°	>360°	>360°
			G_1	>360°	>360°	>360°	>360°	>360°	>360°	>360°
			G_5	>360°	>360°	>360°	>360°	>360°	>360°	>360°
			G_6	>360°	>360°	>360°	>360°	>360°	>360°	>360°
		0.4	G_0	>360°	>360°	>360°	>360°	>360°	>360°	>360°
			G_1	>360°	>360°	>360°	>360°	>360°	>360°	>360°
			G_5	>360°	>360°	>360°	>360°	>360°	>360°	>360°
			G_6	>360°	>360°	>360°	>360°	>360°	>360°	>360°
		0.6	G_0	>360°	>360°	>360°	>360°	>360°	>360°	>360°
			G_1	>360°	>360°	>360°	>360°	>360°	>360°	>360°
			G_5	>360°	>360°	>360°	>360°	>360°	>360°	>360°
			G_6	>360°	>360°	>360°	>360°	>360°	>360°	>360°
		0.8	G_0	>360°	>360°	>360°	>360°	>360°	>360°	>360°
			G_1	>360°	>360°	>360°	>360°	>360°	>360°	>360°
			G_5	>360°	>360°	>360°	>360°	>360°	>360°	>360°
			G_6	>360°	>360°	>360°	>360°	>360°	>360°	>360°

Table 9B.14 – Influence Coefficients for a Circumferential Semi-Elliptical Surface Crack in a Cylinder – Inside Surface

t/R_i	a/c	a/t	G_i	A_0	A_1	A_2	A_3	A_4	A_5	A_6
2.5 (2.5/1)	0.125	0	G_0	>360°	>360°	>360°	>360°	>360°	>360°	>360°
			G_1	>360°	>360°	>360°	>360°	>360°	>360°	>360°
			G_5	>360°	>360°	>360°	>360°	>360°	>360°	>360°
			G_6	>360°	>360°	>360°	>360°	>360°	>360°	>360°
		0.2	G_0	>360°	>360°	>360°	>360°	>360°	>360°	>360°
			G_1	>360°	>360°	>360°	>360°	>360°	>360°	>360°
			G_5	>360°	>360°	>360°	>360°	>360°	>360°	>360°
			G_6	>360°	>360°	>360°	>360°	>360°	>360°	>360°
		0.4	G_0	>360°	>360°	>360°	>360°	>360°	>360°	>360°
			G_1	>360°	>360°	>360°	>360°	>360°	>360°	>360°
			G_5	>360°	>360°	>360°	>360°	>360°	>360°	>360°
			G_6	>360°	>360°	>360°	>360°	>360°	>360°	>360°
		0.6	G_0	>360°	>360°	>360°	>360°	>360°	>360°	>360°
			G_1	>360°	>360°	>360°	>360°	>360°	>360°	>360°
			G_5	>360°	>360°	>360°	>360°	>360°	>360°	>360°
			G_6	>360°	>360°	>360°	>360°	>360°	>360°	>360°
		0.8	G_0	>360°	>360°	>360°	>360°	>360°	>360°	>360°
			G_1	>360°	>360°	>360°	>360°	>360°	>360°	>360°
			G_5	>360°	>360°	>360°	>360°	>360°	>360°	>360°
			G_6	>360°	>360°	>360°	>360°	>360°	>360°	>360°
2.5 (2.5/1)	0.25	0	G_0	0.6152816	-0.3348694	6.2955620	-15.590618	19.299508	-12.488107	3.3010035
			G_1	0.0703566	0.2828152	1.4036169	-0.6511596	-1.2076596	1.0318656	-0.2423741
			G_5	0.3076408	-0.1674347	3.1477810	-7.7953092	9.6497542	-6.2440535	1.6505017
			G_6	0.0000000	0.0000000	0.0000000	0.0000000	0.0000000	0.0000000	0.0000000
		0.2	G_0	0.5157480	-0.0685670	5.2204410	-14.602858	19.536072	-13.238435	3.5866320
			G_1	0.0582110	0.1109290	2.3047860	-3.4564570	2.9769270	-1.9380620	0.5729910
			G_5	-0.0248510	-0.1079620	0.3053730	-0.1704640	3.4700070	-4.8921120	1.7636790
			G_6	-0.1287550	-0.1717190	-0.5881360	0.2936610	0.9132660	0.2780810	-0.5967810
		0.4	G_0	>360°	>360°	>360°	>360°	>360°	>360°	>360°
			G_1	>360°	>360°	>360°	>360°	>360°	>360°	>360°
			G_5	>360°	>360°	>360°	>360°	>360°	>360°	>360°
			G_6	>360°	>360°	>360°	>360°	>360°	>360°	>360°
		0.6	G_0	>360°	>360°	>360°	>360°	>360°	>360°	>360°
			G_1	>360°	>360°	>360°	>360°	>360°	>360°	>360°
			G_5	>360°	>360°	>360°	>360°	>360°	>360°	>360°
			G_6	>360°	>360°	>360°	>360°	>360°	>360°	>360°
		0.8	G_0	>360°	>360°	>360°	>360°	>360°	>360°	>360°
			G_1	>360°	>360°	>360°	>360°	>360°	>360°	>360°
			G_5	>360°	>360°	>360°	>360°	>360°	>360°	>360°
			G_6	>360°	>360°	>360°	>360°	>360°	>360°	>360°

Table 9B.14 – Influence Coefficients for a Circumferential Semi-Elliptical Surface Crack in a Cylinder – Inside Surface

t/R_i	a/c	a/t	G_i	A_0	A_1	A_2	A_3	A_4	A_5	A_6
2.5 (2.5/1)	0.5	0	G_0	0.8776607	-0.6729719	3.7721411	-6.5209060	6.3377934	-3.7028038	0.9872447
			G_1	0.1277541	0.4368502	0.4904522	1.0427434	-2.9631236	2.0826525	-0.5184313
			G_5	0.4388304	-0.3364859	1.8860705	-3.2604530	3.1688967	-1.8514019	0.4936224
			G_6	0.0000000	0.0000000	0.0000000	0.0000000	0.0000000	0.0000000	0.0000000
		0.2	G_0	0.8172450	-1.3481180	6.9572100	-13.448905	14.227621	-8.2045210	1.9842200
			G_1	0.1148620	0.2267720	1.1438510	-0.1392430	-1.5323520	1.0913480	-0.2375560
			G_5	0.1676440	-0.2134200	1.2608490	-1.5608540	1.5754380	-1.2549170	0.3906280
			G_6	-0.1693800	0.2608840	-1.5227800	2.7646470	-1.6485390	0.3020850	0.0131900
		0.4	G_0	0.8113640	-1.7862780	9.1974540	-18.482182	20.266938	-11.945319	2.9190070
			G_1	0.1175400	0.1261020	1.3831870	-0.1973060	-1.8138640	1.3972290	-0.3390450
			G_5	-0.0091710	-0.0618000	0.3306490	-1.0686930	6.2487680	-7.5772090	2.5797510
			G_6	-0.2205700	0.3008780	-1.8747490	1.5050700	0.3805010	0.8172900	-0.9088490
		0.6	G_0	0.9455360	-2.7554960	13.361923	-28.312165	33.368416	-20.645402	5.1212830
			G_1	0.1655170	-0.1638420	2.4551750	-2.5297460	1.3239690	-0.6723690	0.1491200
			G_5	-0.1608240	-0.0248280	0.6465500	-9.2023760	26.965082	-24.364996	6.6808210
			G_6	-0.0932520	0.1001720	-0.9054850	0.4358370	-8.7829790	17.697649	-8.4533110
		0.8	G_0	>360°	>360°	>360°	>360°	>360°	>360°	>360°
			G_1	>360°	>360°	>360°	>360°	>360°	>360°	>360°
			G_5	>360°	>360°	>360°	>360°	>360°	>360°	>360°
			G_6	>360°	>360°	>360°	>360°	>360°	>360°	>360°
2.5 (2.5/1)	1.0	0	G_0	1.1977992	-0.5244870	0.1498299	2.3284866	-5.1058499	4.3469049	-1.3487980
			G_1	0.1870117	0.6987352	0.1316900	0.7269255	-2.5259384	2.1756251	-0.6540458
			G_5	0.9981658	-0.4370725	0.1248583	1.9404058	-4.2548750	3.6224208	-1.1239983
			G_6	0.0000000	0.0000000	0.0000000	0.0000000	0.0000000	0.0000000	0.0000000
		0.2	G_0	1.1590900	-1.2957560	3.4373760	-4.9145300	5.3780360	-3.9256000	1.2178650
			G_1	0.1830380	0.4920840	0.7714040	-1.2761790	1.9387900	-2.1491980	0.7995210
			G_5	0.3289980	-0.2692330	0.9762170	-1.2887170	1.5668350	-1.3849150	0.4750060
			G_6	-0.1108660	0.1151040	-0.6332910	1.7513440	-2.1365770	1.3900580	-0.3751890
		0.4	G_0	1.1594010	-1.7109350	4.5228670	-4.8133080	2.9878570	-1.5098810	0.4541920
			G_1	0.1916070	0.3926920	0.6158680	0.0616640	0.0079450	-1.0829110	0.5986260
			G_5	0.2837100	-0.3141040	1.1864250	-0.9754530	1.6509220	-2.1305300	0.8211510
			G_6	-0.2156900	0.1527870	-0.7928160	0.8556940	0.4744150	-0.4701570	-0.0041710
		0.6	G_0	1.1966350	-2.1573060	5.9711390	-5.7101180	1.8020950	0.3427320	-0.2620330
			G_1	0.2155420	0.2582470	0.6472640	1.2501240	-2.2561150	0.5940990	0.1274930
			G_5	0.2100850	-0.4181950	1.4970410	-1.7402580	5.0032540	-5.9537880	2.0649740
			G_6	-0.2931230	0.1320870	-0.6892070	-1.2337590	4.0819130	-1.8442350	-0.1543160
		0.8	G_0	1.3215860	-2.9740500	9.2084560	-11.546556	8.5235570	-3.1467650	0.1275870
			G_1	0.2786360	-0.0645000	1.5788120	0.1569570	-1.2535680	0.4875250	-0.1697340
			G_5	0.1417100	-0.7037590	2.5254160	-5.9905080	15.439656	-14.727283	4.2310080
			G_6	-0.3391460	0.2596870	-1.5512270	-0.2491540	0.3598270	4.7600460	-3.2409580

Table 9B.14 – Influence Coefficients for a Circumferential Semi-Elliptical Surface Crack in a Cylinder – Inside Surface

t/R_i	a/c	a/t	G_i	A_0	A_1	A_2	A_3	A_4	A_5	A_6
2.5 (2.5/1)	2.0	0	G_0	0.8150546	-0.5623828	1.4465771	-4.6778133	8.4192164	-7.9025932	2.9866351
			G_1	0.1359146	0.0702340	3.5558581	-11.034445	16.967724	-14.126991	4.8706612
			G_5	0.6792125	-0.4686525	1.2054808	-3.8981775	7.0160133	-6.5854942	2.4888625
			G_6	0.0000000	0.0000000	0.0000000	0.0000000	0.0000000	0.0000000	0.0000000
		0.2	G_0	0.8233140	-0.6896340	1.4639210	-2.8708860	3.2948280	-1.8367130	0.3974910
			G_1	0.1158660	0.5207340	0.4273680	-1.0430740	0.1000730	0.7003940	-0.3589180
			G_5	0.2452760	-0.1095480	0.3915360	-0.6685110	0.4820900	-0.0619260	-0.0479060
			G_6	-0.0335840	0.0206590	-0.1342870	0.5163190	-0.8397390	0.7239840	-0.2523690
		0.4	G_0	0.8440940	-0.9190870	2.4185360	-5.5167990	8.2798820	-6.3126550	1.8495380
			G_1	0.1302880	0.4489600	0.7179050	-2.4818760	3.5820900	-2.5941690	0.7001700
			G_5	0.2601020	-0.1123300	0.6715530	-1.4149650	2.0058640	-1.4976410	0.4127260
			G_6	-0.0698080	0.0172330	-0.3980770	1.3423310	-1.6216030	0.9425130	-0.2111680
		0.6	G_0	0.8731990	-1.1266050	3.0382720	-6.5726730	10.284970	-8.4345410	2.6406220
			G_1	0.1484740	0.3764950	0.8514740	-3.0199380	5.3731900	-4.6398540	1.4497010
			G_5	0.2733380	-0.1524980	0.9421270	-1.9708270	3.5202730	-3.2168880	1.0315550
			G_6	-0.1062910	-0.0779050	-0.1203200	0.5822340	-0.6149490	0.6303610	-0.2922960
		0.8	G_0	0.9329520	-1.3609930	3.5941540	-6.6576470	10.081790	-8.3745020	2.6220510
			G_1	0.1814450	0.2851030	0.9497660	-2.9249950	5.6839010	-5.2106540	1.6534400
			G_5	0.2965610	-0.2368480	1.0450920	-1.3893000	3.0178630	-3.1545120	0.9995690
			G_6	-0.1450990	-0.1193010	-0.4039450	1.4203940	-1.9076310	1.9907130	-0.8341150
3.0 (3/1)	0.03125	0	G_0	>360°	>360°	>360°	>360°	>360°	>360°	>360°
			G_1	>360°	>360°	>360°	>360°	>360°	>360°	>360°
			G_5	>360°	>360°	>360°	>360°	>360°	>360°	>360°
			G_6	>360°	>360°	>360°	>360°	>360°	>360°	>360°
		0.2	G_0	>360°	>360°	>360°	>360°	>360°	>360°	>360°
			G_1	>360°	>360°	>360°	>360°	>360°	>360°	>360°
			G_5	>360°	>360°	>360°	>360°	>360°	>360°	>360°
			G_6	>360°	>360°	>360°	>360°	>360°	>360°	>360°
		0.4	G_0	>360°	>360°	>360°	>360°	>360°	>360°	>360°
			G_1	>360°	>360°	>360°	>360°	>360°	>360°	>360°
			G_5	>360°	>360°	>360°	>360°	>360°	>360°	>360°
			G_6	>360°	>360°	>360°	>360°	>360°	>360°	>360°
		0.6	G_0	>360°	>360°	>360°	>360°	>360°	>360°	>360°
			G_1	>360°	>360°	>360°	>360°	>360°	>360°	>360°
			G_5	>360°	>360°	>360°	>360°	>360°	>360°	>360°
			G_6	>360°	>360°	>360°	>360°	>360°	>360°	>360°
		0.8	G_0	>360°	>360°	>360°	>360°	>360°	>360°	>360°
			G_1	>360°	>360°	>360°	>360°	>360°	>360°	>360°
			G_5	>360°	>360°	>360°	>360°	>360°	>360°	>360°
			G_6	>360°	>360°	>360°	>360°	>360°	>360°	>360°

Table 9B.14 – Influence Coefficients for a Circumferential Semi-Elliptical Surface Crack in a Cylinder – Inside Surface

t/R_i	a/c	a/t	G_i	A_0	A_1	A_2	A_3	A_4	A_5	A_6
3.0 (3/1)	0.0625	0	G_0	>360°	>360°	>360°	>360°	>360°	>360°	>360°
			G_1	>360°	>360°	>360°	>360°	>360°	>360°	>360°
			G_5	>360°	>360°	>360°	>360°	>360°	>360°	>360°
			G_6	>360°	>360°	>360°	>360°	>360°	>360°	>360°
		0.2	G_0	>360°	>360°	>360°	>360°	>360°	>360°	>360°
			G_1	>360°	>360°	>360°	>360°	>360°	>360°	>360°
			G_5	>360°	>360°	>360°	>360°	>360°	>360°	>360°
			G_6	>360°	>360°	>360°	>360°	>360°	>360°	>360°
		0.4	G_0	>360°	>360°	>360°	>360°	>360°	>360°	>360°
			G_1	>360°	>360°	>360°	>360°	>360°	>360°	>360°
			G_5	>360°	>360°	>360°	>360°	>360°	>360°	>360°
			G_6	>360°	>360°	>360°	>360°	>360°	>360°	>360°
		0.6	G_0	>360°	>360°	>360°	>360°	>360°	>360°	>360°
			G_1	>360°	>360°	>360°	>360°	>360°	>360°	>360°
			G_5	>360°	>360°	>360°	>360°	>360°	>360°	>360°
			G_6	>360°	>360°	>360°	>360°	>360°	>360°	>360°
		0.8	G_0	>360°	>360°	>360°	>360°	>360°	>360°	>360°
			G_1	>360°	>360°	>360°	>360°	>360°	>360°	>360°
			G_5	>360°	>360°	>360°	>360°	>360°	>360°	>360°
			G_6	>360°	>360°	>360°	>360°	>360°	>360°	>360°
3.0 (3/1)	0.125	0	G_0	>360°	>360°	>360°	>360°	>360°	>360°	>360°
			G_1	>360°	>360°	>360°	>360°	>360°	>360°	>360°
			G_5	>360°	>360°	>360°	>360°	>360°	>360°	>360°
			G_6	>360°	>360°	>360°	>360°	>360°	>360°	>360°
		0.2	G_0	>360°	>360°	>360°	>360°	>360°	>360°	>360°
			G_1	>360°	>360°	>360°	>360°	>360°	>360°	>360°
			G_5	>360°	>360°	>360°	>360°	>360°	>360°	>360°
			G_6	>360°	>360°	>360°	>360°	>360°	>360°	>360°
		0.4	G_0	>360°	>360°	>360°	>360°	>360°	>360°	>360°
			G_1	>360°	>360°	>360°	>360°	>360°	>360°	>360°
			G_5	>360°	>360°	>360°	>360°	>360°	>360°	>360°
			G_6	>360°	>360°	>360°	>360°	>360°	>360°	>360°
		0.6	G_0	>360°	>360°	>360°	>360°	>360°	>360°	>360°
			G_1	>360°	>360°	>360°	>360°	>360°	>360°	>360°
			G_5	>360°	>360°	>360°	>360°	>360°	>360°	>360°
			G_6	>360°	>360°	>360°	>360°	>360°	>360°	>360°
		0.8	G_0	>360°	>360°	>360°	>360°	>360°	>360°	>360°
			G_1	>360°	>360°	>360°	>360°	>360°	>360°	>360°
			G_5	>360°	>360°	>360°	>360°	>360°	>360°	>360°
			G_6	>360°	>360°	>360°	>360°	>360°	>360°	>360°

Table 9B.14 – Influence Coefficients for a Circumferential Semi-Elliptical Surface Crack in a Cylinder – Inside Surface

t/R_i	a/c	a/t	G_i	A_0	A_1	A_2	A_3	A_4	A_5	A_6
3.0 (3/1)	0.25	0	G_0	0.6152816	-0.3348694	6.2955620	-15.590618	19.299508	-12.488107	3.3010035
			G_1	0.0703566	0.2828152	1.4036169	-0.6511596	-1.2076596	1.0318656	-0.2423741
			G_5	0.3076408	-0.1674347	3.1477810	-7.7953092	9.6497542	-6.2440535	1.6505017
			G_6	0.0000000	0.0000000	0.0000000	0.0000000	0.0000000	0.0000000	0.0000000
		0.2	G_0	0.5092630	-0.1116580	5.4386620	-15.263222	20.477375	-13.878474	3.7573240
			G_1	0.0574490	0.0961590	2.3532730	-3.5756360	3.1132730	-2.0094310	0.5874710
			G_5	-0.0598480	-0.1722580	0.3357990	-1.2969060	6.6887050	-7.7439470	2.5549460
			G_6	-0.0895140	-0.1355010	-0.4382920	-0.4499390	0.6696920	1.9138800	-1.4709220
		0.4	G_0	>360°	>360°	>360°	>360°	>360°	>360°	>360°
			G_1	>360°	>360°	>360°	>360°	>360°	>360°	>360°
			G_5	>360°	>360°	>360°	>360°	>360°	>360°	>360°
			G_6	>360°	>360°	>360°	>360°	>360°	>360°	>360°
		0.6	G_0	>360°	>360°	>360°	>360°	>360°	>360°	>360°
			G_1	>360°	>360°	>360°	>360°	>360°	>360°	>360°
			G_5	>360°	>360°	>360°	>360°	>360°	>360°	>360°
			G_6	>360°	>360°	>360°	>360°	>360°	>360°	>360°
		0.8	G_0	>360°	>360°	>360°	>360°	>360°	>360°	>360°
			G_1	>360°	>360°	>360°	>360°	>360°	>360°	>360°
			G_5	>360°	>360°	>360°	>360°	>360°	>360°	>360°
			G_6	>360°	>360°	>360°	>360°	>360°	>360°	>360°
3.0 (3/1)	0.5	0	G_0	0.8776607	-0.6729719	3.7721411	-6.5209060	6.3377934	-3.7028038	0.9872447
			G_1	0.1277541	0.4368502	0.4904522	1.0427434	-2.9631236	2.0826525	-0.5184313
			G_5	0.4388304	-0.3364859	1.8860705	-3.2604530	3.1688967	-1.8514019	0.4936224
			G_6	0.0000000	0.0000000	0.0000000	0.0000000	0.0000000	0.0000000	0.0000000
		0.2	G_0	0.8080000	-1.4173760	7.2776030	-14.069168	14.802654	-8.4479570	2.0183800
			G_1	0.1126130	0.2134570	1.1406690	-0.0019560	-1.8209540	1.3302010	-0.3097130
			G_5	0.1186730	-0.1587160	0.9299640	-0.9279380	1.2087210	-1.2829770	0.4427730
			G_6	-0.1638070	0.1593010	-0.9179970	0.9195590	0.8820790	-1.2093390	0.3300930
		0.4	G_0	0.8050380	-1.9402270	10.124940	-20.904894	23.415317	-13.960102	3.4270700
			G_1	0.1172350	0.0858800	1.5248990	-0.4209100	-1.6595420	1.3765470	-0.3537160
			G_5	-0.0712270	-0.0194620	0.1529210	-2.6473160	11.194896	-12.044855	3.8429080
			G_6	-0.1688550	0.2685760	-1.6711730	1.1409830	-1.3171800	4.2024080	-2.4554620
		0.6	G_0	>360°	>360°	>360°	>360°	>360°	>360°	>360°
			G_1	>360°	>360°	>360°	>360°	>360°	>360°	>360°
			G_5	>360°	>360°	>360°	>360°	>360°	>360°	>360°
			G_6	>360°	>360°	>360°	>360°	>360°	>360°	>360°
		0.8	G_0	>360°	>360°	>360°	>360°	>360°	>360°	>360°
			G_1	>360°	>360°	>360°	>360°	>360°	>360°	>360°
			G_5	>360°	>360°	>360°	>360°	>360°	>360°	>360°
			G_6	>360°	>360°	>360°	>360°	>360°	>360°	>360°

Table 9B.14 – Influence Coefficients for a Circumferential Semi-Elliptical Surface Crack in a Cylinder – Inside Surface

t/R_i	a/c	a/t	G_i	A_0	A_1	A_2	A_3	A_4	A_5	A_6
3.0 (3/1)	0.25	0	G_0	1.1977992	-0.5244870	0.1498299	2.3284866	-5.1058499	4.3469049	-1.3487980
			G_1	0.1870117	0.6987352	0.1316900	0.7269255	-2.5259384	2.1756251	-0.6540458
			G_5	0.9981658	-0.4370725	0.1248583	1.9404058	-4.2548750	3.6224208	-1.1239983
			G_6	0.0000000	0.0000000	0.0000000	0.0000000	0.0000000	0.0000000	0.0000000
		0.2	G_0	1.1509480	-1.3748120	3.6515840	-4.9127750	4.9631020	-3.5017310	1.0816400
			G_1	0.1821350	0.4719670	0.7543510	-1.0984850	1.7475320	-2.1061330	0.8114470
			G_5	0.2799420	-0.2220960	0.7201650	-0.3888320	0.0447350	-0.1429940	0.0799790
			G_6	-0.1143780	0.0905480	-0.3269890	0.1977480	0.9990440	-1.3431320	0.4975410
		0.4	G_0	1.1455860	-1.8169170	4.7962920	-4.4761490	1.5023990	-0.0194630	-0.0408080
			G_1	0.1897650	0.3678990	0.5097050	0.7678570	-1.1912060	-0.2203790	0.3655930
			G_5	0.2171140	-0.2808280	1.0155040	-0.6354660	1.6112380	-2.3274510	0.8915740
			G_6	-0.2153270	0.0793110	-0.4121900	-0.4203930	2.0797750	-1.0932910	-0.0182250
		0.6	G_0	1.1877880	-2.3608920	6.7810360	-6.6360260	1.7946990	1.0333440	-0.6080740
			G_1	0.2163410	0.1981580	0.6644170	1.8266490	-3.4982860	1.6306470	-0.1930330
			G_5	0.1220910	-0.4198910	1.5130330	-2.9403190	8.6566310	-9.3298940	3.0336740
			G_6	-0.2787010	0.1597080	-0.8236980	-1.6335990	4.2708700	-0.9358620	-0.7594130
		0.8	G_0	1.3384930	-3.4304130	11.322063	-16.277614	14.129577	-6.1705760	0.6414610
			G_1	0.2898230	-0.2295750	2.0920360	-0.6678940	-0.4630460	0.2577070	-0.2393760
			G_5	0.0369830	-0.7341970	2.8476580	-10.055329	24.817370	-21.872116	5.8472620
			G_6	-0.2872430	0.3450280	-1.9370900	1.0414520	-5.6386940	13.221166	-6.7455780
3.0 (3/1)	0.5	0	G_0	0.8150546	-0.5623828	1.4465771	-4.6778133	8.4192164	-7.9025932	2.9866351
			G_1	0.1359146	0.0702340	3.5558581	-11.034445	16.967724	-14.126991	4.8706612
			G_5	0.6792125	-0.4686525	1.2054808	-3.8981775	7.0160133	-6.5854942	2.4888625
			G_6	0.0000000	0.0000000	0.0000000	0.0000000	0.0000000	0.0000000	0.0000000
		0.2	G_0	0.8246410	-0.7315010	1.6888360	-3.6221930	4.7367520	-3.0931670	0.7915240
			G_1	0.1179610	0.5047760	0.5291810	-1.5299440	1.1409360	-0.2085010	-0.0831740
			G_5	0.2158830	-0.0845920	0.3149580	-0.4431140	0.1718160	0.1639890	-0.1217030
			G_6	-0.0356710	0.0234780	-0.2066250	0.8409900	-1.4499400	1.2472470	-0.4185760
		0.4	G_0	0.8454030	-0.9848660	2.6172730	-5.8458860	8.9166140	-6.9845610	2.0949390
			G_1	0.1335690	0.4256910	0.7599150	-2.7028200	4.3055420	-3.3897610	0.9817620
			G_5	0.2284750	-0.0907510	0.5426580	-0.9180460	1.2864860	-1.0039350	0.2704360
			G_6	-0.0733930	-0.0128630	-0.2081990	0.5097000	-0.0231240	-0.3822980	0.1913350
		0.6	G_0	0.8758580	-1.2098440	3.1645220	-6.2885230	9.7386540	-8.1872930	2.6296350
			G_1	0.1534910	0.3453510	0.8184490	-2.8291290	5.4187370	-4.9754020	1.6208130
			G_5	0.2376850	-0.1501270	0.7968190	-1.3259400	2.7140930	-2.7816080	0.9308800
			G_6	-0.1127800	-0.0711410	-0.4590290	1.7995550	-2.7209520	2.4743990	-0.9090510
		0.8	G_0	0.9461020	-1.5232270	3.9299210	-6.4121890	9.1262460	-7.5716110	2.3823030
			G_1	0.1926140	0.2163210	0.9661540	-2.5511090	5.2159180	-5.0477740	1.6492950
			G_5	0.2582160	-0.3144580	1.2066730	-1.6661360	3.9559860	-4.1958360	1.3395080
			G_6	-0.1509880	-0.1929920	-0.1522920	0.7298100	-1.4854300	2.4840460	-1.2315010

Notes:

1. Interpolation of the influence coefficients, G_i, may be used for intermediate values of t/R_i, a/c, and a/t.
2. The value of the influence coefficients at the surface point of the crack defined by $\varphi = 0°$ are equal to: $G_i = A_0$.
3. The value of the influence coefficients at the deepest point of the crack defined by $\varphi = 90°$ are equal to $G_i = \sum_{n=0}^{6} A_n$.

Table 9B.15 – Influence Coefficients for a Circumferential Semi-Elliptical Surface Crack in a Cylinder – Outside Surface

t/R_i	a/c	a/t	G_i	A_0	A_1	A_2	A_3	A_4	A_5	A_6
0.0	0.03125	0	G_0	0.1965046	2.9373464	-5.2582821	7.4889154	-6.9282665	3.3673348	-0.6677966
			G_1	0.0051779	0.1750280	2.7718679	-4.6457152	4.6780500	-3.2768089	0.9840994
			G_5	0.1965049	2.9373459	-5.2582821	7.4889149	-6.9282670	3.3673350	-0.6677970
			G_6	0.0000000	0.0000000	0.0000000	0.0000000	0.0000000	0.0000000	0.0000000
		0.2	G_0	0.2080760	3.0112421	-5.1048703	7.6348714	-6.8347549	2.7940766	-0.3882687
			G_1	0.0084834	0.2406767	2.4574291	-3.6452419	3.6142838	-2.8451814	0.9270638
			G_5	0.2080760	3.0112421	-5.1048703	7.6348714	-6.8347549	2.7940766	-0.3882687
			G_6	0.0000000	0.0000000	0.0000000	0.0000000	0.0000000	0.0000000	0.0000000
		0.4	G_0	0.2357939	3.0822401	-3.5792100	3.9476890	1.9131590	-6.8872199	3.1896800
			G_1	0.0145140	0.4038000	1.6422699	-0.3906100	-0.6480699	-0.2940300	0.2514899
			G_5	0.2357939	3.0822401	-3.5792100	3.9476890	1.9131590	-6.8872199	3.1896800
			G_6	0.0000000	0.0000000	0.0000000	0.0000000	0.0000000	0.0000000	0.0000000
		0.6	G_0	0.2902239	3.6892049	-4.5739102	11.7098903	-6.3750000	-5.8894100	4.2452402
			G_1	0.0208889	0.7016779	0.1631840	5.7072157	-8.2075796	3.4561119	-0.4454700
			G_5	0.2902239	3.6892049	-4.5739102	11.709890	-6.3750000	-5.8894100	4.2452402
			G_6	0.0000000	0.0000000	0.0000000	0.0000000	0.0000000	0.0000000	0.0000000
		0.8	G_0	0.5163549	2.5310831	14.7129001	-43.6217994	101.0656967	-116.081001	46.1908988
			G_1	0.0825460	0.4971770	4.6064810	-7.3326702	21.1486206	-29.345100	12.4913997
			G_5	0.5163549	2.5310831	14.712900	-43.6217994	101.065696	-116.081001	46.1908988
			G_6	0.0000000	0.0000000	0.0000000	0.0000000	0.0000000	0.0000000	0.0000000
0.0	0.0625	0	G_0	0.2695332	2.1626000	-1.6551568	-1.2970207	4.5604305	-4.3163876	1.4010654
			G_1	0.0138667	0.1827458	2.5749607	-3.9044678	3.3556301	-2.1772208	0.6420134
			G_5	0.2695330	2.1626000	-1.6551569	-1.2970210	4.5604300	-4.3163881	1.4010659
			G_6	0.0000000	0.0000000	0.0000000	0.0000000	0.0000000	0.0000000	0.0000000
		0.2	G_0	0.2845892	2.2264056	-1.4546190	-1.5760718	5.1131081	-4.9485445	1.6207573
			G_1	0.0199077	0.2210874	2.4642047	-3.5898623	3.1624038	-2.2403779	0.6965750
			G_5	0.2845892	2.2264056	-1.4546190	-1.5760718	5.1131081	-4.9485445	1.6207573
			G_6	0.0000000	0.0000000	0.0000000	0.0000000	0.0000000	0.0000000	0.0000000
		0.4	G_0	0.3261480	2.5200870	-1.8846999	2.1798739	-1.4597100	-0.1886499	0.2393400
			G_1	0.0294120	0.3699370	1.9220850	-1.2071499	-0.4393999	0.2737550	-0.0395199
			G_5	0.3261480	2.5200870	-1.8846999	2.1798739	-1.4597100	-0.1886499	0.2393400
			G_6	0.0000000	0.0000000	0.0000000	0.0000000	0.0000000	0.0000000	0.0000000
		0.6	G_0	0.4166330	3.1566469	-2.6248900	7.7325911	-9.6927795	3.6428699	-0.0891999
			G_1	0.0598459	0.4340740	2.6811559	-3.1936600	4.0753722	-4.6940197	1.8285499
			G_5	0.4166330	3.1566469	-2.6248900	7.7325911	-9.6927795	3.6428699	-0.0891999
			G_6	0.0000000	0.0000000	0.0000000	0.0000000	0.0000000	0.0000000	0.0000000
		0.8	G_0	0.6540140	3.4231920	3.8158050	-4.1586900	3.4715330	-10.310400	6.6280000
			G_1	0.1214779	0.6975489	2.9718329	-1.3036500	-0.0754899	-3.0465099	2.1670000
			G_5	0.6540140	3.4231920	3.8158050	-4.1586900	3.4715330	-10.310400	6.6280000
			G_6	0.0000000	0.0000000	0.0000000	0.0000000	0.0000000	0.0000000	0.0000000

Table 9B.15 – Influence Coefficients for a Circumferential Semi-Elliptical Surface Crack in a Cylinder – Outside Surface

t/R_i	a/c	a/t	G_i	A_0	A_1	A_2	A_3	A_4	A_5	A_6
0.0	0.125	0	G_0	0.4065238	0.7772483	3.8861644	-12.573943	16.760207	-11.014593	2.8706957
			G_1	0.0320270	0.1825342	2.2670449	-2.7076615	1.2088194	-0.3777430	0.0763155
			G_5	0.4065240	0.7772480	3.8861640	-12.573943	16.760207	-11.014593	2.8706960
			G_6	0.0000000	0.0000000	0.0000000	0.0000000	0.0000000	0.0000000	0.0000000
		0.2	G_0	0.4242116	1.0089302	3.2973815	-12.159726	17.873386	-12.868668	3.6281712
			G_1	0.0429859	0.2033811	2.2563818	-2.8752160	1.8152558	-1.0512327	0.3181077
			G_5	0.4242116	1.0089302	3.2973815	-12.159726	17.873386	-12.868668	3.6281712
			G_6	0.0000000	0.0000000	0.0000000	0.0000000	0.0000000	0.0000000	0.0000000
		0.4	G_0	0.4917770	1.6592320	-0.1080400	0.1793240	-2.7076100	3.3680620	-1.3489700
			G_1	0.0634270	0.3722500	1.6231670	-0.5306500	-2.0007400	1.8943780	-0.5880300
			G_5	0.4917770	1.6592320	-0.1080400	0.1793240	-2.7076100	3.3680620	-1.3489700
			G_6	0.0000000	0.0000000	0.0000000	0.0000000	0.0000000	0.0000000	0.0000000
		0.6	G_0	0.6591820	1.8759140	1.0212600	-1.7698000	-0.5653600	1.2479960	-0.4376600
			G_1	0.1116040	0.4714500	1.7940590	-0.7557600	-1.4901700	1.0852180	-0.2113700
			G_5	0.6591820	1.8759140	1.0212600	-1.7698000	-0.5653600	1.2479960	-0.4376600
			G_6	0.0000000	0.0000000	0.0000000	0.0000000	0.0000000	0.0000000	0.0000000
		0.8	G_0	0.9809330	1.8846320	4.8020780	-8.0580200	0.4447850	3.4772660	-1.0567500
			G_1	0.2039950	0.4800150	2.8822430	-2.5890100	-0.9683000	1.5372370	-0.3750200
			G_5	0.9809330	1.8846320	4.8020780	-8.0580200	0.4447850	3.4772660	-1.0567500
			G_6	0.0000000	0.0000000	0.0000000	0.0000000	0.0000000	0.0000000	0.0000000
0.0	0.25	0	G_0	0.6152816	-0.3348694	6.2955620	-15.590618	19.299508	-12.488107	3.3010035
			G_1	0.0703566	0.2828152	1.4036169	-0.6511596	-1.2076596	1.0318656	-0.2423741
			G_5	0.6152820	-0.3348690	6.2955620	-15.590618	19.299508	-12.488107	3.3010030
			G_6	0.0000000	0.0000000	0.0000000	0.0000000	0.0000000	0.0000000	0.0000000
		0.2	G_0	0.6385889	-0.3095132	6.5329787	-16.622882	21.056641	-13.850120	3.6988146
			G_1	0.0840059	0.1999367	1.8218113	-1.7756899	0.3757186	-0.0785358	0.0643386
			G_5	0.6385889	-0.3095132	6.5329787	-16.622882	21.056641	-13.850120	3.6988146
			G_6	0.0000000	0.0000000	0.0000000	0.0000000	0.0000000	0.0000000	0.0000000
		0.4	G_0	0.7390420	0.0548160	4.0842620	-7.5883100	5.4047530	-1.0146100	-0.3483400
			G_1	0.1164500	0.2479880	1.8282520	-1.7169900	0.1912120	0.1165770	-0.0186100
			G_5	0.7390420	0.0548160	4.0842620	-7.5883100	5.4047530	-1.0146100	-0.3483400
			G_6	0.0000000	0.0000000	0.0000000	0.0000000	0.0000000	0.0000000	0.0000000
		0.6	G_0	0.9461210	-0.1858800	5.5867460	-9.8634900	5.9596870	0.1296440	-1.0026100
			G_1	0.1778050	0.2056680	2.0979210	-1.8039500	-0.5558700	1.1461400	-0.4206600
			G_5	0.9461210	-0.1858800	5.5867460	-9.8634900	5.9596870	0.1296440	-1.0026100
			G_6	0.0000000	0.0000000	0.0000000	0.0000000	0.0000000	0.0000000	0.0000000
		0.8	G_0	1.2452110	-0.6921900	8.3260620	-14.948000	8.6936910	0.4755790	-1.3926600
			G_1	0.2585640	0.1548890	2.1170240	-0.4910000	-4.6146100	5.4550750	-1.9663300
			G_5	1.2452110	-0.6921900	8.3260620	-14.948000	8.6936910	0.4755790	-1.3926600
			G_6	0.0000000	0.0000000	0.0000000	0.0000000	0.0000000	0.0000000	0.0000000

Table 9B.15 – Influence Coefficients for a Circumferential Semi-Elliptical Surface Crack in a Cylinder – Outside Surface

t/R_i	a/c	a/t	G_i	A_0	A_1	A_2	A_3	A_4	A_5	A_6
0.0	0.5	0	G_0	0.8776607	-0.6729719	3.7721411	-6.5209060	6.3377934	-3.7028038	0.9872447
			G_1	0.1277541	0.4368502	0.4904522	1.0427434	-2.9631236	2.0826525	-0.5184313
			G_5	0.8776610	-0.6729720	3.7721410	-6.5209060	6.3377930	-3.7028040	0.9872450
			G_6	0.0000000	0.0000000	0.0000000	0.0000000	0.0000000	0.0000000	0.0000000
		0.2	G_0	0.9003948	-0.8850488	5.2743239	-11.267523	13.890755	-9.6373584	2.8183906
			G_1	0.1404409	0.3215397	1.1010666	-1.0257556	0.6943940	-1.0793186	0.5410929
			G_5	0.9003948	-0.8850488	5.2743239	-11.267523	13.890755	-9.6373584	2.8183906
			G_6	0.0000000	0.0000000	0.0000000	0.0000000	0.0000000	0.0000000	0.0000000
		0.4	G_0	1.0058060	-0.7322600	2.9951940	-1.9459200	-3.2613500	5.1424570	-2.0306200
			G_1	0.1740870	0.3051630	1.2070310	-0.6720500	-1.0651300	1.1445590	-0.3644800
			G_5	0.9000590	-0.5476000	2.4416770	-1.2688500	-3.3815300	4.7868570	-1.8373900
			G_6	0.0000000	0.0000000	0.0000000	0.0000000	0.0000000	0.0000000	0.0000000
		0.6	G_0	1.1826010	-1.1072500	3.9623640	-2.7781300	-4.3097300	7.2772750	-2.9648200
			G_1	0.2277120	0.1701170	1.5499470	-1.1051200	-0.8333700	1.1717060	-0.4194500
			G_5	1.1826010	-1.1072500	3.9623640	-2.7781300	-4.3097300	7.2772750	-2.9648200
			G_6	0.0000000	0.0000000	0.0000000	0.0000000	0.0000000	0.0000000	0.0000000
		0.8	G_0	1.3833380	-1.3900300	4.3755780	-3.7372600	-2.5403200	5.3036000	-2.0932400
			G_1	0.2820110	0.0839230	1.7258580	-1.5358100	-0.0635600	0.5006780	-0.1982200
			G_5	1.3833380	-1.3900300	4.3755780	-3.7372600	-2.5403200	5.3036000	-2.0932400
			G_6	0.0000000	0.0000000	0.0000000	0.0000000	0.0000000	0.0000000	0.0000000
0.0	1.0	0	G_0	1.1977992	-0.5244870	0.1498299	2.3284866	-5.1058499	4.3469049	-1.3487980
			G_1	0.1870117	0.6987352	0.1316900	0.7269255	-2.5259384	2.1756251	-0.6540458
			G_5	1.1977990	-0.5244870	0.1498300	2.3284870	-5.1058500	4.3469050	-1.3487980
			G_6	0.0000000	0.0000000	0.0000000	0.0000000	0.0000000	0.0000000	0.0000000
		0.2	G_0	1.2263282	-1.1608467	4.4744783	-11.584231	17.811241	-14.408250	4.6998279
			G_1	0.2154786	0.2441623	2.8107820	-7.6574580	11.171413	-9.0053693	2.9542871
			G_5	1.2263282	-1.1608467	4.4744783	-11.584231	17.811241	-14.408250	4.6998279
			G_6	0.0000000	0.0000000	0.0000000	0.0000000	0.0000000	0.0000000	0.0000000
		0.4	G_0	1.2989480	-0.9978000	1.9479540	-1.3002700	-1.4940100	2.8306230	-1.2126000
			G_1	0.2386246	0.1447774	3.3198992	-9.2456599	13.823512	-11.223715	3.6868232
			G_5	1.2989480	-0.9978000	1.9479540	-1.3002700	-1.4940100	2.8306230	-1.2126000
			G_6	0.0000000	0.0000000	0.0000000	0.0000000	0.0000000	0.0000000	0.0000000
		0.6	G_0	1.3971180	-1.1348400	1.7918740	-0.4202600	-2.8679300	3.7685480	-1.4405000
			G_1	0.2445870	0.5326670	0.5939690	-0.0361800	-2.0163100	2.2167010	-0.7782200
			G_5	1.3971180	-1.1348400	1.7918740	-0.4202600	-2.8679300	3.7685480	-1.4405000
			G_6	0.0000000	0.0000000	0.0000000	0.0000000	0.0000000	0.0000000	0.0000000
		0.8	G_0	1.5117010	-1.3244800	1.7568350	-0.1337900	-2.8629300	3.2953270	-1.1412400
			G_1	0.2704470	0.5113280	0.5357440	-0.0327300	-1.5570200	1.5570970	-0.5094600
			G_5	1.5117010	-1.3244800	1.7568350	-0.1337900	-2.8629300	3.2953270	-1.1412400
			G_6	0.0000000	0.0000000	0.0000000	0.0000000	0.0000000	0.0000000	0.0000000

Table 9B.15 – Influence Coefficients for a Circumferential Semi-Elliptical Surface Crack in a Cylinder – Outside Surface

t/R_i	a/c	a/t	G_i	A_0	A_1	A_2	A_3	A_4	A_5	A_6
0.0	2.0	0	G_0	0.8150546	-0.5623828	1.4465771	-4.6778133	8.4192164	-7.9025932	2.9866351
			G_1	0.1359146	0.0702340	3.5558581	-11.034445	16.967724	-14.126991	4.8706612
			G_5	0.8150550	-0.5623830	1.4465770	-4.6778130	8.4192160	-7.9025930	2.9866350
			G_6	0.0000000	0.0000000	0.0000000	0.0000000	0.0000000	0.0000000	0.0000000
		0.2	G_0	0.8463715	-1.0011024	4.0052312	-11.937181	19.189548	-16.039296	5.4674371
			G_1	0.1395121	0.0753999	3.1895604	-9.5540932	14.214316	-11.649525	4.0073308
			G_5	0.8463715	-1.0011024	4.0052312	-11.937181	19.189548	-16.039296	5.4674371
			G_6	0.0000000	0.0000000	0.0000000	0.0000000	0.0000000	0.0000000	0.0000000
		0.4	G_0	0.8570045	-1.0183085	3.9957306	-11.886878	19.152747	-16.047480	5.4801806
			G_1	0.1436696	0.0544018	3.2816127	-9.8164232	14.610963	-11.942138	4.0907797
			G_5	0.8570045	-1.0183085	3.9957306	-11.886878	19.152747	-16.047480	5.4801806
			G_6	0.0000000	0.0000000	0.0000000	0.0000000	0.0000000	0.0000000	0.0000000
		0.6	G_0	0.8839861	-1.0765270	4.0774087	-11.976171	19.173189	-15.996207	5.4501217
			G_1	0.1504185	0.0478401	3.2579960	-9.6921199	14.370843	-11.736129	4.0258411
			G_5	0.8839861	-1.0765270	4.0774087	-11.976171	19.173189	-15.996207	5.4501217
			G_6	0.0000000	0.0000000	0.0000000	0.0000000	0.0000000	0.0000000	0.0000000
		0.8	G_0	0.9033134	-0.9619755	2.8501500	-7.6366897	11.596116	-9.4828625	3.2550163
			G_1	0.1458559	0.2313881	1.9882138	-5.5546045	7.4196069	-5.8965053	2.0855563
			G_5	0.9033134	-0.9619755	2.8501500	-7.6366897	11.596116	-9.4828625	3.2550163
			G_6	0.0000000	0.0000000	0.0000000	0.0000000	0.0000000	0.0000000	0.0000000
0.01 (1/100)	0.03125	0	G_0	0.1965046	2.9373464	-5.2582823	7.4889153	-6.9282667	3.3673349	-0.6677966
			G_1	0.0051780	0.1750280	2.7718680	-4.6457154	4.6780502	-3.2768090	0.9840994
			G_5	0.1965046	2.9373464	-5.2582823	7.4889153	-6.9282667	3.3673349	-0.6677966
			G_6	0.0000000	0.0000000	0.0000000	0.0000000	0.0000000	0.0000000	0.0000000
		0.2	G_0	0.2116559	2.4625298	-1.2086946	-4.0808781	10.512452	-9.7505256	3.1574301
			G_1	0.0073553	0.2248471	2.5465614	-3.9586604	4.1543233	-3.2917455	1.0682038
			G_5	0.2117479	2.4669625	-1.2233443	-4.0356866	10.550152	-9.8518908	3.1982651
			G_6	-0.0150460	-0.1515480	0.4190890	-1.2072670	2.0290350	-1.3179820	0.2449160
		0.4	G_0	0.2267900	2.9874360	-3.3596600	3.3149040	3.3779620	-8.4920000	3.8326500
			G_1	0.0132270	0.4891340	1.4810220	-0.2505600	0.3517190	-2.2787900	1.1808200
			G_5	0.2294300	2.7425010	-1.7305900	-2.0047000	12.170560	-15.530100	6.0000000
			G_6	-0.0279300	-0.4216200	0.5326580	0.4761720	-2.2564800	2.9083470	-1.2111500
		0.6	G_0	0.2451630	3.4073570	-5.1754600	15.029690	-12.238400	-1.0593200	2.7584400
			G_1	0.0374510	0.7790480	-1.1197700	10.267710	-14.396700	7.1767130	-1.3237000
			G_5	0.2385960	3.3073170	-4.6399500	12.795250	-7.6318600	-5.3395100	4.2222220
			G_6	-0.0164590	-1.4702900	8.3251460	-27.317503	43.222664	-31.198496	8.4709110
		0.8	G_0	0.3001970	2.5133470	4.5572250	-10.605300	47.909900	-70.721400	30.714100
			G_1	0.0236690	0.4686529	2.5980287	-4.1635546	22.855996	-32.031979	12.632460
			G_5	0.2652400	3.0910960	-0.7764200	7.0895380	19.882670	-49.200000	24.285720
			G_6	-0.0789050	-0.7973820	3.7213660	-23.342093	50.937027	-44.347210	13.905159

Table 9B.15 – Influence Coefficients for a Circumferential Semi-Elliptical Surface Crack in a Cylinder – Outside Surface

t/R_i	a/c	a/t	G_i	A_0	A_1	A_2	A_3	A_4	A_5	A_6
0.01 (1/100)	0.0625	0	G_0	0.2695332	2.1626001	-1.6551569	-1.2970208	4.5604304	-4.3163876	1.4010655
			G_1	0.0138667	0.1827458	2.5749608	-3.9044679	3.3556301	-2.1772209	0.6420134
			G_5	0.2695332	2.1626001	-1.6551569	-1.2970208	4.5604304	-4.3163876	1.4010655
			G_6	0.0000000	0.0000000	0.0000000	0.0000000	0.0000000	0.0000000	0.0000000
		0.2	G_0	0.2843442	2.0632252	-0.8995815	-1.7002701	3.3771236	-2.5139267	0.6468602
			G_1	0.0193647	0.2110156	2.6078196	-4.3209835	4.6955691	-3.6663355	1.1845300
			G_5	0.2849763	2.0834845	-0.9850383	-1.4461643	3.0094661	-2.2550769	0.5742754
			G_6	-0.0169490	0.0703960	-0.4886870	0.8510980	-0.5594650	0.2904380	-0.1440920
		0.4	G_0	0.3234380	2.5413990	-2.0176200	1.6959050	0.9274120	-3.1662200	1.4358100
			G_1	0.0370330	0.4900840	1.6020220	-0.6385100	-0.7412100	-0.0710100	0.2447400
			G_5	0.3176740	2.5600660	-2.2743400	2.5573490	-0.3247200	-2.3422900	1.2380950
			G_6	-0.0279970	0.0585420	-1.0424680	3.0167250	-4.0103300	2.9378710	-0.9260650
		0.6	G_0	0.3905240	3.2576640	-4.3197100	12.918270	-15.947200	6.8514120	-0.5974600
			G_1	0.0592580	0.5014950	2.3544400	-2.2877200	3.5444420	-5.2408200	2.2860900
			G_5	0.3945880	2.9522020	-1.8265900	3.8511510	-0.2293500	-6.0328700	3.4285710
			G_6	-0.0477040	0.0487110	-1.0141000	0.9246810	2.6287790	-4.2774820	1.7419400
		0.8	G_0	0.5585480	3.0733050	2.7116060	0.1570170	1.1959110	-12.276100	8.1508500
			G_1	0.0998622	0.8721037	0.8806798	7.5243170	-12.931792	5.5339974	-0.1725691
			G_5	0.5311890	3.6060380	-1.6126300	14.376210	-21.813700	5.8796870	2.5806450
			G_6	-0.1319350	1.6593810	-12.837138	29.458530	-22.518377	-0.8027060	5.1521000
0.01 (1/100)	0.125	0	G_0	0.4065238	0.7772483	3.8861644	-12.573943	16.760207	-11.014593	2.8706957
			G_1	0.0320270	0.1825342	2.2670449	-2.7076615	1.2088194	-0.3777430	0.0763155
			G_5	0.4065238	0.7772483	3.8861644	-12.573943	16.760207	-11.014593	2.8706957
			G_6	0.0000000	0.0000000	0.0000000	0.0000000	0.0000000	0.0000000	0.0000000
		0.2	G_0	0.4141304	1.1377070	1.7925852	-6.3816121	8.0611916	-5.1373047	1.3130132
			G_1	0.0487218	0.0175251	3.9073870	-9.0112567	12.465726	-9.7159857	2.9937975
			G_5	0.4141387	1.1728917	1.5879788	-5.7380688	7.0270589	-4.3302414	1.0702122
			G_6	-0.0215100	0.2289000	-1.0183300	1.2001800	0.5002560	-1.5218740	0.6395240
		0.4	G_0	0.4884630	1.5730830	0.6794250	-2.6942700	2.4688900	-1.0967700	0.1279400
			G_1	0.0721890	0.4196840	1.5725580	-0.5246000	-1.8820000	1.6181090	-0.4302300
			G_5	0.4945010	1.2569410	3.1846440	-11.500300	17.519240	-13.417300	4.0000000
			G_6	-0.0326060	0.2599370	-1.2779750	1.6852560	0.2883000	-1.6417090	0.7272120
		0.6	G_0	0.6325650	1.9612380	0.2124640	1.0673660	-4.8520900	4.2428280	-1.2187600
			G_1	0.1171020	0.4578330	2.1168020	-1.8894800	0.5759570	-0.8442000	0.4875500
			G_5	0.6337930	1.7347580	2.0397750	-5.5002600	6.5478530	-5.1994300	1.7777780
			G_6	-0.0510510	0.4679150	-2.8026610	5.4927770	-3.6013470	-0.2141770	0.7157020
		0.8	G_0	0.9044670	1.6602910	5.4293610	-7.8741700	-1.3182900	5.4386470	-1.7533200
			G_1	0.1947050	0.4093530	3.3076490	-3.2250800	-0.4973400	1.2925110	-0.2919800
			G_5	0.8969920	1.8870180	4.1418380	-5.8086600	-1.6246200	3.6711750	-0.6923100
			G_6	-0.1196280	2.1647550	-17.369329	55.455597	-84.446342	61.931057	-17.624773

Table 9B.15 – Influence Coefficients for a Circumferential Semi-Elliptical Surface Crack in a Cylinder – Outside Surface

t/R_i	a/c	a/t	G_i	A_0	A_1	A_2	A_3	A_4	A_5	A_6
0.01 (1/100)	0.25	0	G_0	0.6152816	-0.3348694	6.2955620	-15.590618	19.299508	-12.488107	3.3010035
			G_1	0.0703566	0.2828152	1.4036169	-0.6511596	-1.2076596	1.0318656	-0.2423741
			G_5	0.6152816	-0.3348694	6.2955620	-15.590618	19.299508	-12.488107	3.3010035
			G_6	0.0000000	0.0000000	0.0000000	0.0000000	0.0000000	0.0000000	0.0000000
		0.2	G_0	0.6208898	-0.1664421	6.5968181	-18.807095	26.180692	-18.464818	5.1787192
			G_1	0.0903134	0.1796401	2.4581113	-4.8428461	5.9649997	-4.5970978	1.4302661
			G_5	0.6256175	-0.2460646	7.1786495	-20.690522	29.252069	-20.921801	5.9439866
			G_6	-0.0529280	0.5817080	-2.0439050	2.4908050	-0.3061320	-1.2173360	0.5545260
		0.4	G_0	0.7329950	0.0996250	3.9573730	-7.2526600	4.9136700	-0.6649300	-0.4401500
			G_1	0.1244530	0.2438230	1.9426520	-2.0609400	0.6954550	-0.3004200	0.1292100
			G_5	0.7324580	-0.0790000	5.2132460	-11.267200	11.336950	-5.7116200	1.1111110
			G_6	-0.0724760	0.7545830	-2.6909740	3.3377620	-0.4333620	-1.6647900	0.7776290
		0.6	G_0	0.9335850	-0.0671400	4.9859720	-8.0099800	3.1444570	2.1751370	-1.5670900
			G_1	0.1861600	0.1872070	2.3208790	-2.4591900	0.4288930	0.3550800	-0.1581000
			G_5	0.9308850	-0.2487900	6.4158440	-12.995000	11.662450	-4.8484800	0.6666670
			G_6	-0.0842130	0.8378360	-3.0789330	3.9428740	-0.4659710	-2.2536710	1.1097250
		0.8	G_0	1.2407050	-0.9832700	11.036350	-24.419000	25.074820	-13.247100	3.0448500
			G_1	0.2685320	0.0687020	2.9242790	-3.1935800	-0.0724900	1.6614580	-0.7248500
			G_5	1.2020050	-0.2413600	5.4364160	-5.7446000	-5.6959800	11.276780	-4.5000000
			G_6	-0.0450570	0.4286070	-2.4450330	5.2502870	-4.3532820	0.7113540	0.4546460
0.01 (1/100)	0.5	0	G_0	0.8776607	-0.6729719	3.7721411	-6.5209060	6.3377934	-3.7028038	0.9872447
			G_1	0.1277541	0.4368502	0.4904522	1.0427434	-2.9631236	2.0826525	-0.5184313
			G_5	0.8776607	-0.6729719	3.7721411	-6.5209060	6.3377934	-3.7028038	0.9872447
			G_6	0.0000000	0.0000000	0.0000000	0.0000000	0.0000000	0.0000000	0.0000000
		0.2	G_0	0.9005246	-1.0307386	6.3564034	-14.662730	18.900958	-13.111605	3.7340887
			G_1	0.1490274	0.1602062	2.2439024	-4.4879387	5.6373631	-4.4442698	1.4267720
			G_5	0.9044688	-1.0934309	6.8237929	-16.242399	21.630155	-15.453183	4.5238507
			G_6	-0.0216090	0.2225620	-0.7436250	0.8569840	-0.1124830	-0.3230500	0.1247120
		0.4	G_0	1.0063880	-0.7425700	3.1260260	-2.1867000	-3.0931200	5.1298930	-2.0520500
			G_1	0.1789440	0.3206900	1.1011660	-0.2780300	-1.7360100	1.6648710	-0.5147200
			G_5	0.9827660	-0.5544700	2.1195940	0.3228700	-6.2642600	7.0697670	-2.5000000
			G_6	-0.0330000	0.2558440	-1.2392500	2.7155410	-2.7845300	1.1748480	-0.0894600
		0.6	G_0	1.1876880	-1.1514600	4.3134430	-3.6414000	-3.2248100	6.5781370	-2.7782500
			G_1	0.2348560	0.1694010	1.5310330	-0.9297400	-1.2048400	1.4747130	-0.5037800
			G_5	1.1736920	-1.0985200	4.0914840	-3.4273500	-2.7996400	5.6581030	-2.3260900
			G_6	-0.0241400	0.1054660	-0.3692100	0.1480170	1.3452060	-2.2134300	1.0080860
		0.8	G_0	1.3768550	-1.1807900	3.4327750	-1.9675000	-3.7422900	5.2586230	-1.8511600
			G_1	0.2827170	0.2258060	0.9136330	0.4871590	-2.5046300	1.9013960	-0.5002900
			G_5	1.3852980	-1.4598800	4.8824450	-5.0567200	-0.7333900	3.9649120	-1.6666700
			G_6	-0.0069900	-0.1354100	0.5129600	-0.1715000	-1.4812600	2.0791380	-0.7969500

Table 9B.15 – Influence Coefficients for a Circumferential Semi-Elliptical Surface Crack in a Cylinder – Outside Surface

t/R_i	a/c	a/t	G_i	A_0	A_1	A_2	A_3	A_4	A_5	A_6
0.01 (1/100)	1.0	0	G_0	1.1977992	-0.5244870	0.1498299	2.3284866	-5.1058499	4.3469049	-1.3487980
			G_1	0.1870117	0.6987352	0.1316900	0.7269255	-2.5259384	2.1756251	-0.6540458
			G_5	1.1977992	-0.5244870	0.1498299	2.3284866	-5.1058499	4.3469049	-1.3487980
			G_6	0.0000000	0.0000000	0.0000000	0.0000000	0.0000000	0.0000000	0.0000000
		0.2	G_0	1.2163255	-1.2105406	4.9378591	-13.277329	20.674347	-16.657341	5.3664988
			G_1	0.2120446	0.2333067	2.9256445	-8.1389620	12.029482	-9.6839968	3.1519185
			G_5	1.2342990	-1.5314671	7.1783779	-20.802459	33.720887	-27.895912	9.1678853
			G_6	-0.0063570	0.0546490	-0.1675720	0.1767300	-0.0347210	-0.0153380	-0.0059650
		0.4	G_0	1.3064660	-1.0152400	1.9350880	-0.8993700	-2.4736000	3.7825660	-1.5472100
			G_1	0.2235710	0.5338870	0.8263620	-0.7439300	-1.0125200	1.5328880	-0.6019500
			G_5	1.2708350	-0.7002200	0.4078220	2.3529450	-5.6716200	5.0139540	-1.6000000
			G_6	-0.0551000	0.5974370	-3.0790700	7.3218950	-8.6144800	4.7584470	-0.9291300
		0.6	G_0	1.4098990	-1.1943200	2.0682710	-0.9892900	-2.2245400	3.4010710	-1.3594400
			G_1	0.2530760	0.4979500	0.7711470	-0.5373400	-1.2119300	1.5653800	-0.5725000
			G_5	1.3784730	-0.9308800	0.8922700	1.1776090	-3.7994200	3.4790700	-1.1000000
			G_6	-0.0532800	0.5783890	-2.9606800	7.0446380	-8.3727000	4.7445190	-0.9808900
		0.8	G_0	1.5256800	-1.3415100	1.7834550	-0.0964700	-2.9501000	3.3412720	-1.1425600
			G_1	0.2815290	0.4575980	0.7882960	-0.6608400	-0.6979100	0.9575600	-0.3420100
			G_5	1.4930550	-1.1540100	1.3584350	-0.4503500	-0.4058400	-0.0186000	0.3000000
			G_6	-0.0356300	0.1933460	-0.5365700	0.5289630	0.1260530	-0.5333200	0.2571630
0.01 (1/100)	2.0	0	G_0	0.8150546	-0.5623828	1.4465771	-4.6778133	8.4192164	-7.9025932	2.9866351
			G_1	0.1359146	0.0702340	3.5558581	-11.034445	16.967724	-14.126991	4.8706612
			G_5	0.8150546	-0.5623828	1.4465771	-4.6778133	8.4192164	-7.9025932	2.9866351
			G_6	0.0000000	0.0000000	0.0000000	0.0000000	0.0000000	0.0000000	0.0000000
		0.2	G_0	0.8305156	-1.0562168	4.5000068	-13.731088	22.186981	-18.304348	6.0907634
			G_1	0.1355569	0.0490656	3.3708754	-10.235299	15.333651	-12.425096	4.1851932
			G_5	0.8550171	-1.5076606	7.6119033	-24.094325	40.061917	-33.656957	11.274934
			G_6	-0.0073790	0.1254630	-0.6776960	1.2635280	-0.3727710	-0.9851780	0.6488970
		0.4	G_0	0.8365180	-0.3110000	-0.8673900	3.8166980	-6.9326300	5.5500280	-1.5710500
			G_1	0.1387820	0.0213261	3.5079466	-10.649233	16.059172	-13.095865	4.4331795
			G_5	0.8660112	-1.6018348	8.1519012	-25.857651	43.179547	-36.448593	12.261716
			G_6	-0.0053700	0.0119870	-0.0522000	0.0961370	-0.0717500	-0.0085200	0.0297200
		0.6	G_0	0.8647620	-0.3748400	-0.7702800	3.6933770	-6.8531100	5.5382040	-1.5740000
			G_1	0.1453037	0.0535496	3.2458818	-9.8284254	14.629459	-11.772523	3.9396898
			G_5	0.8903262	-1.4861418	7.0094321	-21.999673	36.426386	-30.440664	10.140504
			G_6	-0.0087300	0.0194820	-0.0907000	0.1566490	-0.0749200	-0.0574800	0.0556980
		0.8	G_0	0.9195010	-0.9913000	2.9513880	-7.8747300	11.960150	-9.7994600	3.3736570
			G_1	0.1530620	0.0091124	3.5469729	-10.839841	16.187023	-12.807490	4.1638505
			G_5	0.9218643	-1.5643932	7.1354779	-22.140328	36.077778	-29.456429	9.5508778
			G_6	-0.0021200	-0.1195900	0.5677590	-0.9385300	0.0050640	1.2720990	-0.7846800

Table 9B.15 – Influence Coefficients for a Circumferential Semi-Elliptical Surface Crack in a Cylinder – Outside Surface

t/R_i	a/c	a/t	G_i	A_0	A_1	A_2	A_3	A_4	A_5	A_6
0.01667 (1/60)	0.03125	0	G_0	0.1965046	2.9373464	-5.2582823	7.4889153	-6.9282667	3.3673349	-0.6677966
			G_1	0.0051780	0.1750280	2.7718680	-4.6457154	4.6780502	-3.2768090	0.9840994
			G_5	0.1965046	2.9373464	-5.2582823	7.4889153	-6.9282667	3.3673349	-0.6677966
			G_6	0.0000000	0.0000000	0.0000000	0.0000000	0.0000000	0.0000000	0.0000000
		0.2	G_0	0.2108342	2.4570800	-1.2157061	-4.0236499	10.416307	-9.6803603	3.1375768
			G_1	0.0071744	0.2169830	2.5959489	-4.1234042	4.4149777	-3.4775143	1.1164797
			G_5	0.2106227	2.4544929	-1.2190737	-3.9783189	10.457915	-9.7961980	3.1851951
			G_6	-0.0233720	-0.2625360	0.5660890	-1.2238920	2.0401900	-1.3756660	0.2817280
		0.4	G_0	0.2235430	2.9373900	-3.1994600	2.7809700	4.3738970	-9.3752900	4.1285200
			G_1	0.0153790	0.4262710	1.4374590	-0.0329200	0.1372970	-1.9720300	0.9767200
			G_5	0.2081430	3.1428470	-5.9452100	14.126020	-16.599400	8.7013890	-1.7777800
			G_6	-0.0494000	-0.5534600	0.2919720	1.5669970	-3.5734900	3.7883170	-1.4709400
		0.6	G_0	0.2315580	3.3152690	-5.3487100	15.866400	-14.268900	1.2426960	1.8259100
			G_1	0.0190830	0.6303640	-0.3898700	7.4202930	-10.418700	5.3450100	-1.2464600
			G_5	0.2185180	3.0724260	-4.3389400	12.251530	-6.9322100	-5.4074100	4.0000000
			G_6	-0.0431280	-1.8161870	8.6311060	-27.614206	43.137306	-29.957056	7.6761850
		0.8	G_0	0.2784200	1.6193770	13.249390	-52.219100	129.94510	-142.76800	54.258200
			G_1	0.0274250	-0.4708900	10.876180	-36.906200	79.258380	-78.743200	27.847000
			G_5	0.2018720	2.9940400	-3.6570500	15.285330	6.2359780	-34.960000	18.285720
			G_6	-0.0953020	-1.6854570	6.3336220	-27.809717	49.099262	-33.881794	8.0376910
0.01667 (1/60)	0.0625	0	G_0	0.2695332	2.1626001	-1.6551569	-1.2970208	4.5604304	-4.3163876	1.4010655
			G_1	0.0138667	0.1827458	2.5749608	-3.9044679	3.3556301	-2.1772209	0.6420134
			G_5	0.2695332	2.1626001	-1.6551569	-1.2970208	4.5604304	-4.3163876	1.4010655
			G_6	0.0000000	0.0000000	0.0000000	0.0000000	0.0000000	0.0000000	0.0000000
		0.2	G_0	0.2839701	2.0611223	-0.9023698	-1.6631113	3.3006585	-2.4507567	0.6281212
			G_1	0.0191537	0.2065367	2.6297112	-4.3764448	4.7735576	-3.7182062	1.1967908
			G_5	0.2845863	2.0778513	-0.9742253	-1.4550454	3.0154749	-2.2571717	0.5736301
			G_6	-0.0220090	0.0100440	-0.3065460	0.3744530	0.3410030	-0.5404890	0.1478000
		0.4	G_0	0.3212570	2.5165160	-2.0053400	1.8419650	0.5637890	-2.8167000	1.3130100
			G_1	0.0302880	0.4905940	1.3197410	0.4803190	-2.5162600	1.2803650	-0.1650100
			G_5	0.3153500	2.5119140	-2.0980700	2.0876390	0.4445220	-2.9646400	1.4285710
			G_6	-0.0352400	-0.2058200	-0.0717700	1.1031500	-1.6071400	1.1561240	-0.3393100
		0.6	G_0	0.3766880	3.1807610	-4.3574000	13.458080	-16.961900	7.7325420	-0.9039800
			G_1	0.0464920	0.5054590	1.8272520	-0.3010500	0.3199970	-2.6365000	1.4421600
			G_5	0.3498420	3.6756720	-8.5248700	27.663920	-40.188500	25.940540	-6.4000000
			G_6	-0.0645560	-0.2079890	-0.0562940	-1.9802090	7.4744930	-7.9086160	2.7486360
		0.8	G_0	0.5089370	2.8697610	2.3528320	1.8204240	-0.7866600	-10.843200	7.5884300
			G_1	0.0747990	0.5581130	2.4511290	0.7375290	-0.9973000	-4.1781700	2.9141700
			G_5	0.4963910	2.8883590	1.9568990	2.9262850	-1.2793200	-11.509500	8.0645160
			G_6	-0.1388700	0.6095490	-7.7130700	23.805260	-33.453600	23.682970	-6.7922600

Table 9B.15 – Influence Coefficients for a Circumferential Semi-Elliptical Surface Crack in a Cylinder – Outside Surface

t/R_i	a/c	a/t	G_i	A_0	A_1	A_2	A_3	A_4	A_5	A_6
0.01667 (1/60)	0.125	0	G_0	0.4065238	0.7772483	3.8861644	-12.573943	16.760207	-11.014593	2.8706957
			G_1	0.0320270	0.1825342	2.2670449	-2.7076615	1.2088194	-0.3777430	0.0763155
			G_5	0.4065238	0.7772483	3.8861644	-12.573943	16.760207	-11.014593	2.8706957
			G_6	0.0000000	0.0000000	0.0000000	0.0000000	0.0000000	0.0000000	0.0000000
		0.2	G_0	0.4141030	1.1370353	1.7918721	-6.3657982	8.0276077	-5.1090766	1.3043557
			G_1	0.0486343	0.0164272	3.9099112	-9.0029835	12.437460	-9.6860424	2.9828172
			G_5	0.4143081	1.1612439	1.6725006	-6.0389787	7.5553433	-4.7733918	1.2122682
			G_6	-0.0257390	0.2239250	-1.0656070	1.3604470	0.3212500	-1.4129050	0.6046200
		0.4	G_0	0.4860310	1.6014030	0.4174570	-1.7801100	0.9884490	0.0450910	-0.2110000
			G_1	0.0716230	0.3907820	1.7772010	-1.2379600	-0.5878700	0.4930510	-0.0604600
			G_5	0.4825390	1.5260960	1.0116470	-4.0246700	5.0139140	-3.3630800	0.8888890
			G_6	-0.0202900	-0.2224800	1.2564450	-4.3167000	7.7764130	-6.6030000	2.1296120
		0.6	G_0	0.6270060	1.9158750	0.3750140	0.7243790	-4.3115900	3.7865410	-1.0734300
			G_1	0.1097630	0.4925440	1.7137970	-0.4041900	-1.8971000	1.1354540	-0.1307000
			G_5	0.6308030	1.6413760	2.5244720	-6.8239600	8.5609730	-6.7236500	2.2222220
			G_6	-0.0654530	0.4089380	-2.7275000	5.4276500	-3.4503160	-0.3170070	0.7307650
		0.8	G_0	0.8834920	1.5499750	5.9525350	-9.3777300	1.6582560	2.6247130	-0.7903400
			G_1	0.1827450	0.4170240	3.0645390	-2.2689800	-1.8835600	2.2280410	-0.5460400
			G_5	0.8486090	2.5957920	-2.1629000	17.323570	-41.416700	36.306820	-11.000000
			G_6	-0.0526800	0.0313980	-0.9515500	1.6109290	0.6934160	-2.4678000	1.1362870
0.01667 (1/60)	0.25	0	G_0	0.6152816	-0.3348694	6.2955620	-15.590618	19.299508	-12.488107	3.3010035
			G_1	0.0703566	0.2828152	1.4036169	-0.6511596	-1.2076596	1.0318656	-0.2423741
			G_5	0.6152816	-0.3348694	6.2955620	-15.590618	19.299508	-12.488107	3.3010035
			G_6	0.0000000	0.0000000	0.0000000	0.0000000	0.0000000	0.0000000	0.0000000
		0.2	G_0	0.6268151	-0.2659538	7.2065345	-20.587488	28.869672	-20.486698	5.7761489
			G_1	0.0907196	0.1725963	2.5006366	-4.9586990	6.1276304	-4.7110563	1.4617796
			G_5	0.6251326	-0.2394193	7.1122784	-20.448049	28.825683	-20.563129	5.8286449
			G_6	-0.0564090	0.5906920	-2.0901230	2.5558090	-0.2933150	-1.2772490	0.5764810
		0.4	G_0	0.7331060	0.0986810	3.9472550	-7.1889400	4.7837550	-0.5451500	-0.4819600
			G_1	0.1237230	0.2464690	1.9255840	-2.0144800	0.6420620	-0.2712700	0.1223800
			G_5	0.7315800	-0.0604700	5.0518000	-10.721000	10.434690	-4.9906700	0.8888890
			G_6	-0.0146100	-0.1583700	1.0586750	-3.4445700	5.7766210	-4.7213100	1.5035680
		0.6	G_0	0.9330720	-0.0910200	5.1514030	-8.5062000	3.9372450	1.5522690	-1.3786200
			G_1	0.1835580	0.2173130	2.1201030	-1.8419100	-0.4959200	1.0292210	-0.3502900
			G_5	0.9242220	-0.1379100	5.6239620	-10.482500	7.7246490	-1.8459600	-0.2222200
			G_6	-0.0276100	-0.0847600	0.6326700	-2.4527000	4.7781310	-4.3193100	1.4735860
		0.8	G_0	1.2480880	-1.2667900	13.231880	-31.738500	37.283310	-23.122200	6.1251700
			G_1	0.2617530	0.1907690	1.9836910	0.0718510	-5.5586600	6.0836580	-2.0974100
			G_5	1.1785120	0.2633730	1.5798440	7.4390720	-27.718600	29.000000	-10.000000
			G_6	-0.0372000	0.0294390	-0.3454900	1.0579850	-1.3468700	0.8809930	-0.2388600

Table 9B.15 – Influence Coefficients for a Circumferential Semi-Elliptical Surface Crack in a Cylinder – Outside Surface

t/R_i	a/c	a/t	G_i	A_0	A_1	A_2	A_3	A_4	A_5	A_6
0.01667 (1/60)	0.5	0	G_0	0.8776607	-0.6729719	3.7721411	-6.5209060	6.3377934	-3.7028038	0.9872447
			G_1	0.1277541	0.4368502	0.4904522	1.0427434	-2.9631236	2.0826525	-0.5184313
			G_5	0.8776607	-0.6729719	3.7721411	-6.5209060	6.3377934	-3.7028038	0.9872447
			G_6	0.0000000	0.0000000	0.0000000	0.0000000	0.0000000	0.0000000	0.0000000
		0.2	G_0	0.9022613	-1.0595157	6.5513251	-15.271446	19.858891	-13.849252	3.9547586
			G_1	0.1492632	0.1564498	2.2690315	-4.5619815	5.7476801	-4.5263194	1.4510330
			G_5	0.9029354	-1.0732156	6.6901441	-15.831657	20.969482	-14.922494	4.3567685
			G_6	-0.0240560	0.2342620	-0.7930600	0.9271080	-0.1130250	-0.3740260	0.1454300
		0.4	G_0	1.0074290	-0.7627700	3.2930000	-2.7766500	-2.0930300	4.3235700	-1.8034700
			G_1	0.1810320	0.2833580	1.3218690	-0.8922400	-0.8601000	1.0459710	-0.3429800
			G_5	0.9858560	-0.6144600	2.5659140	-1.2397100	-3.5787400	4.8558140	-1.8000000
			G_6	-0.0338400	0.2387950	-1.1681400	2.5946840	-2.7007500	1.1765800	-0.1073300
		0.6	G_0	1.1851510	-1.1065900	4.0604300	-2.9480500	-4.2109900	7.2804210	-2.9762600
			G_1	0.2335280	0.1829380	1.4758450	-0.8294800	-1.2826600	1.4906960	-0.4992200
			G_5	1.1724980	-1.0832900	4.0212020	-3.3213400	-2.8475900	5.6324110	-2.3043500
			G_6	-0.0275600	0.1023610	-0.3536000	0.1087530	1.4111820	-2.2584400	1.0173030
		0.8	G_0	1.3763340	-1.1705800	3.4426520	-2.1143000	-3.3895100	4.9216180	-1.7364000
			G_1	0.2820140	0.2322400	0.9005230	0.4878420	-2.4663700	1.8500330	-0.4797300
			G_5	1.3815880	-1.3958500	4.5246880	-4.1377600	-1.9430100	4.7522810	-1.8666700
			G_6	-0.0123300	-0.1322000	0.4935200	-0.1065200	-1.5677300	2.1435930	-0.8183300
0.01667 (1/60)	1.0	0	G_0	1.1977992	-0.5244870	0.1498299	2.3284866	-5.1058499	4.3469049	-1.3487980
			G_1	0.1870117	0.6987352	0.1316900	0.7269255	-2.5259384	2.1756251	-0.6540458
			G_5	1.1977992	-0.5244870	0.1498299	2.3284866	-5.1058499	4.3469049	-1.3487980
			G_6	0.0000000	0.0000000	0.0000000	0.0000000	0.0000000	0.0000000	0.0000000
		0.2	G_0	1.2159041	-1.2019721	4.8943491	-13.164862	20.514432	-16.542122	5.3339888
			G_1	0.2138478	0.2009657	3.1365782	-8.7806790	13.020781	-10.439196	3.3770529
			G_5	1.2336102	-1.5324242	7.1847065	-20.827179	33.758570	-27.923695	9.1765536
			G_6	0.0004290	-0.0477510	0.2303150	-0.2454810	-0.4980090	1.1046740	-0.5435480
		0.4	G_0	1.3057270	-1.0008200	1.8572720	-0.6808000	-2.8231500	4.0709330	-1.6411400
			G_1	0.2250957	0.1870147	3.1086959	-8.6990069	12.827333	-10.126798	3.2062338
			G_5	1.2693430	-0.6672200	0.1805440	3.0628380	-6.8370600	5.9627910	-1.9000000
			G_6	-0.0555600	0.6002060	-3.0806100	7.2729560	-8.4525400	4.5719390	-0.8563900
		0.6	G_0	1.4097520	-1.1958700	2.1136310	-1.1728300	-1.9231000	3.1722290	-1.2928000
			G_1	0.2528090	0.4962060	0.8029830	-0.6609800	-1.0059000	1.4049960	-0.5248000
			G_5	1.3821790	-0.9982800	1.2826480	0.0761910	-2.2401100	2.3906980	-0.8000000
			G_6	-0.0539000	0.5709100	-2.9238200	6.9536840	-8.2458800	4.6543540	-0.9553500
		0.8	G_0	1.5261100	-1.3576900	1.9596150	-0.7444900	-1.8536800	2.4558510	-0.8665000
			G_1	0.2798340	0.4788400	0.6925290	-0.4412500	-0.9713700	1.1277000	-0.3828300
			G_5	1.4934890	-1.1805900	1.5372220	-1.0351600	0.5002050	-0.6976700	0.5000000
			G_6	-0.0364900	0.1772770	-0.4732300	0.4368740	0.1557290	-0.4866500	0.2265000

Table 9B.15 – Influence Coefficients for a Circumferential Semi-Elliptical Surface Crack in a Cylinder – Outside Surface

t/R_i	a/c	a/t	G_i	A_0	A_1	A_2	A_3	A_4	A_5	A_6
0.01667 (/1/60)	2.0	0	G_0	0.8150546	-0.5623828	1.4465771	-4.6778133	8.4192164	-7.9025932	2.9866351
			G_1	0.1359146	0.0702340	3.5558581	-11.034445	16.967724	-14.126991	4.8706612
			G_5	0.8150546	-0.5623828	1.4465771	-4.6778133	8.4192164	-7.9025932	2.9866351
			G_6	0.0000000	0.0000000	0.0000000	0.0000000	0.0000000	0.0000000	0.0000000
		0.2	G_0	0.8303718	-1.0537074	4.4841488	-13.682728	22.110765	-18.246611	6.0741015
			G_1	0.1357357	0.0454828	3.3938622	-10.305120	15.445864	-12.517992	4.2159592
			G_5	0.8545553	-1.5107503	7.6305267	-24.154355	40.161589	-33.739611	11.301885
			G_6	-0.0080940	0.1320720	-0.7037160	1.2969370	-0.3690340	-1.0141950	0.6605490
		0.4	G_0	0.8385880	-0.3494400	-0.6268500	3.1083630	-5.8624300	4.7444070	-1.3320400
			G_1	0.1388141	0.0199458	3.5199209	-10.693028	16.139831	-13.171184	4.4607143
			G_5	0.8648866	-1.5905958	8.0816882	-25.672324	42.927637	-36.279610	12.217855
			G_6	-0.0045600	0.0144990	-0.0770300	0.1717110	-0.1898700	0.0854060	-0.0001600
		0.6	G_0	0.8630510	-0.3484500	-0.9308100	4.1652080	-7.5678400	6.0687740	-1.7269300
			G_1	0.1454406	0.0490957	3.2762981	-9.9197082	14.771504	-11.888335	3.9781433
			G_5	0.8918880	-1.5257631	7.2468282	-22.705998	37.505258	-31.260474	10.386049
			G_6	-0.0086700	0.0226910	-0.1126100	0.2053490	-0.1206900	-0.0422900	0.0562240
		0.8	G_0	0.9207120	-1.0172500	3.1169740	-8.3590500	12.680850	-10.338100	3.5339560
			G_1	0.1532638	0.0041397	3.5793726	-10.934468	16.330683	-12.923367	4.2022735
			G_5	0.9223180	-1.5893812	7.2854088	-22.610593	36.827507	-30.047255	9.7335970
			G_6	-0.0038200	-0.1155400	0.5412020	-0.8878800	-0.0255700	1.2648840	-0.7732900
0.05 (1/20)	0.03125	0	G_0	0.1965046	2.9373464	-5.2582823	7.4889153	-6.9282667	3.3673349	-0.6677966
			G_1	0.0051780	0.1750280	2.7718680	-4.6457154	4.6780502	-3.2768090	0.9840994
			G_5	0.1965046	2.9373464	-5.2582823	7.4889153	-6.9282667	3.3673349	-0.6677966
			G_6	0.0000000	0.0000000	0.0000000	0.0000000	0.0000000	0.0000000	0.0000000
		0.2	G_0	0.2083391	2.4332249	-1.1884009	-3.9755311	10.292250	-9.5789402	3.1062164
			G_1	0.0065178	0.1974121	2.7143430	-4.4411003	4.8704764	-3.8110304	1.2146397
			G_5	0.1997427	2.3264369	-1.1013940	-3.6435752	9.8524559	-9.4316748	3.0993589
			G_6	-0.0625910	-0.7609300	1.1374040	-0.9700630	1.4330310	-0.8787870	0.1043810
		0.4	G_0	0.2126260	2.8183080	-3.0330200	2.7003490	3.8448090	-8.5201400	3.7625700
			G_1	0.0062779	0.1550679	3.1397907	-5.6725343	8.6311078	-7.9698086	2.6560323
			G_5	0.1703620	2.3140590	-2.5633700	3.7786360	2.0860560	-7.4455000	3.4222220
			G_6	-0.1152800	-1.7724100	2.7372250	-2.2958100	0.8232890	2.2788200	-1.6558300
		0.6	G_0	0.2218260	2.6845130	-1.0220600	-1.7085000	16.583430	-23.988200	9.7548700
			G_1	0.0035426	0.1135423	3.3308955	-6.2087481	12.547480	-12.941759	4.3992208
			G_5	0.1081350	2.2058260	-5.6718400	19.053640	-17.725100	4.2901230	0.2222220
			G_6	-0.1613800	-2.9385600	8.4224910	-27.306500	45.537000	-30.693100	7.1400850
		0.8	G_0	0.2334730	2.1926480	2.4092490	-4.8795600	23.225120	-33.519700	13.812200
			G_1	-0.0010039	0.0648251	3.6388741	-7.7669323	20.019952	-21.769540	7.4615512
			G_5	0.0181050	1.8710890	-7.9427300	26.287600	-14.291000	-7.0800000	4.5714290
			G_6	-0.1866490	-2.9656960	5.7981490	-22.657816	24.506548	5.1143480	-9.6122570

Table 9B.15 – Influence Coefficients for a Circumferential Semi-Elliptical Surface Crack in a Cylinder – Outside Surface

t/R_i	a/c	a/t	G_i	A_0	A_1	A_2	A_3	A_4	A_5	A_6
0.05 (1/20)	0.0625	0	G_0	0.2695332	2.1626001	-1.6551569	-1.2970208	4.5604304	-4.3163876	1.4010655
			G_1	0.0138667	0.1827458	2.5749608	-3.9044679	3.3556301	-2.1772209	0.6420134
			G_5	0.2695332	2.1626001	-1.6551569	-1.2970208	4.5604304	-4.3163876	1.4010655
			G_6	0.0000000	0.0000000	0.0000000	0.0000000	0.0000000	0.0000000	0.0000000
		0.2	G_0	0.2823254	2.0534799	-0.8811145	-1.6698150	3.3008195	-2.4575325	0.6309429
			G_1	0.0188087	0.1946355	2.6993220	-4.5348736	4.9477116	-3.7967993	1.2039837
			G_5	0.2797821	2.0418784	-0.9180277	-1.4895340	3.1041398	-2.3826466	0.6237899
			G_6	-0.0486790	-0.1891920	-0.1673130	0.7906470	-0.3121280	-0.0657460	-0.0034250
		0.4	G_0	0.3063080	2.5163740	-2.6301300	4.4511290	-4.0018200	0.9244040	0.1362300
			G_1	0.0257928	0.2227270	2.8558445	-4.6900594	6.1531628	-5.5334459	1.8695561
			G_5	0.2851800	2.5117860	-3.5047600	8.1394150	-10.199500	5.7808220	-1.3333300
			G_6	-0.0885600	-0.7138300	0.9058640	-0.5572300	1.0691100	-0.7296800	0.1143240
		0.6	G_0	0.3496580	2.2502050	1.2825590	-5.6176200	15.285390	-18.227200	7.0634600
			G_1	0.0277182	0.2448111	2.9531717	-3.9581805	6.6052497	-7.4653877	2.7783504
			G_5	0.2821840	2.8317890	-5.3474100	18.238870	-23.947400	12.697300	-2.4000000
			G_6	-0.1526900	-0.9075400	-0.3360500	3.1957760	-3.7192400	3.3890750	-1.4693400
		0.8	G_0	0.4354930	0.5803140	15.809350	-46.076600	82.663310	-77.844000	27.643100
			G_1	0.0176381	0.2811585	2.3799548	0.2769473	2.1722174	-6.8712443	3.3144284
			G_5	0.2913710	2.0067920	0.6126560	7.0477190	-2.6508000	-11.638500	7.5483870
			G_6	-0.2840000	0.0411220	-7.2462300	8.9246250	12.806090	-25.058600	10.816970
0.05 (1/20)	0.125	0	G_0	0.4065238	0.7772483	3.8861644	-12.573943	16.760207	-11.014593	2.8706957
			G_1	0.0320270	0.1825342	2.2670449	-2.7076615	1.2088194	-0.3777430	0.0763155
			G_5	0.4065238	0.7772483	3.8861644	-12.573943	16.760207	-11.014593	2.8706957
			G_6	0.0000000	0.0000000	0.0000000	0.0000000	0.0000000	0.0000000	0.0000000
		0.2	G_0	0.4141975	1.1355682	1.7964913	-6.3267923	7.9329008	-5.0287717	1.2797839
			G_1	0.0482613	0.0194124	3.8693280	-8.7975215	12.040298	-9.3437833	2.8723181
			G_5	0.4124603	1.1555788	1.6454564	-5.9059207	7.3388389	-4.6103126	1.1639931
			G_6	-0.0437600	0.1570090	-1.0325550	1.4917100	0.2508650	-1.4432340	0.6259590
		0.4	G_0	0.4854260	1.4708470	1.1375140	-3.9136300	4.4112120	-2.6701800	0.6201300
			G_1	0.0614100	0.3634290	1.7021770	-0.8033900	-1.2757100	1.0399430	-0.2466000
			G_5	0.4771150	1.3502680	1.9042120	-6.7349300	9.4785330	-6.9606300	2.0000000
			G_6	-0.0625500	-0.2867400	0.7272150	-2.0795100	4.4089060	-4.0660600	1.3587350
		0.6	G_0	0.5975400	1.7337620	1.0590410	-0.9381500	-1.4454000	1.2700200	-0.2491200
			G_1	0.0928190	0.4108880	1.9636550	-1.0589200	-0.6277300	0.0224880	0.2086300
			G_5	0.5842270	1.5377860	2.2724010	-5.3712700	6.6141750	-5.6410300	2.0000000
			G_6	-0.1216800	0.0383230	-2.5834000	8.8415970	-12.590200	9.0060030	-2.5906100
		0.8	G_0	0.7779550	1.3659070	5.9189090	-8.0788400	0.9424640	2.0346540	-0.4382700
			G_1	0.1414370	0.3351560	3.1427840	-2.4175800	-0.8165600	0.9132140	-0.1013800
			G_5	0.7510670	1.4270080	5.0667020	-6.3546600	0.2988000	1.1506170	0.1481480
			G_6	-0.1609000	-0.2162400	-1.2987300	2.6895960	1.3204280	-4.1914600	1.8573060

Table 9B.15 – Influence Coefficients for a Circumferential Semi-Elliptical Surface Crack in a Cylinder – Outside Surface

t/R_i	a/c	a/t	G_i	A_0	A_1	A_2	A_3	A_4	A_5	A_6
0.05 (1/20)	0.25	0	G_0	0.6152816	-0.3348694	6.2955620	-15.590618	19.299508	-12.488107	3.3010035
			G_1	0.0703566	0.2828152	1.4036169	-0.6511596	-1.2076596	1.0318656	-0.2423741
			G_5	0.6152816	-0.3348694	6.2955620	-15.590618	19.299508	-12.488107	3.3010035
			G_6	0.0000000	0.0000000	0.0000000	0.0000000	0.0000000	0.0000000	0.0000000
		0.2	G_0	0.6260632	-0.2355924	7.0084322	-19.936505	27.819799	-19.666590	5.5272065
			G_1	0.0907494	0.1737280	2.4989990	-4.9565466	6.1508242	-4.7530904	1.4807924
			G_5	0.6207464	-0.1740389	6.6462879	-18.975785	26.486146	-18.743280	5.2781587
			G_6	-0.0679890	0.5711840	-2.0794250	2.5966690	-0.2952400	-1.3108420	0.5915290
		0.4	G_0	0.7329360	0.0851660	3.9993920	-7.3274900	5.0490250	-0.7922300	-0.3978000
			G_1	0.1192830	0.2736740	1.7229450	-1.3700900	-0.3250300	0.4357600	-0.0817100
			G_5	0.7256530	-0.0593200	4.9453050	-10.464100	10.199980	-4.9143300	0.8888890
			G_6	-0.0425200	-0.1487000	0.8303450	-2.7784800	5.0546510	-4.3253300	1.4100300
		0.6	G_0	0.9247960	-0.1470300	5.5538350	-9.7985900	6.2555660	-0.4677600	-0.7143100
			G_1	0.1751020	0.2402440	1.9657640	-1.3682400	-1.1130700	1.4068600	-0.4424000
			G_5	0.9099290	-0.2582200	6.4177830	-13.249300	12.657030	-6.0202000	1.1111110
			G_6	-0.0729300	-0.0576300	0.1987110	-1.1582300	3.2150920	-3.3293900	1.2043850
		0.8	G_0	1.1968540	-0.7648200	9.5388220	-18.968400	16.307930	-6.5734600	1.0569200
			G_1	0.2507880	0.0646560	3.0320210	-3.5198100	0.7048460	0.8495480	-0.4370700
			G_5	1.1546950	-0.2482400	5.5468230	-5.9663300	-4.7348200	10.000000	-4.0000000
			G_6	-0.0999700	-0.0107700	-0.1792300	-0.0596600	1.7978730	-2.3389800	0.8907370
0.05 (1/20)	0.5	0	G_0	0.8776607	-0.6729719	3.7721411	-6.5209060	6.3377934	-3.7028038	0.9872447
			G_1	0.1277541	0.4368502	0.4904522	1.0427434	-2.9631236	2.0826525	-0.5184313
			G_5	0.8776607	-0.6729719	3.7721411	-6.5209060	6.3377934	-3.7028038	0.9872447
			G_6	0.0000000	0.0000000	0.0000000	0.0000000	0.0000000	0.0000000	0.0000000
		0.2	G_0	0.9024575	-1.0265565	6.3448697	-14.616034	18.788994	-12.994232	3.6905856
			G_1	0.1492827	0.1640885	2.2385342	-4.4987357	5.6810178	-4.4935522	1.4455306
			G_5	0.9059893	-1.1409542	7.1428296	-17.310642	23.384484	-16.840432	4.9473941
			G_6	-0.0317240	0.2339840	-0.7911240	0.9324040	-0.1062270	-0.3800660	0.1454050
		0.4	G_0	1.0049940	-0.7040200	2.9364040	-1.7198500	-3.7470300	5.6205220	-2.2024400
			G_1	0.1776020	0.3243230	1.0851530	-0.1989300	-1.9311900	1.8735070	-0.5938900
			G_5	0.9745420	-0.5075300	1.8740630	0.8245150	-6.8333300	7.4325590	-2.6000000
			G_6	-0.0532800	0.2868450	-1.3853900	3.1039090	-3.2363300	1.4406240	-0.1563900
		0.6	G_0	1.1816810	-1.0741600	3.9994710	-2.9800900	-3.9897100	7.0547810	-2.9051000
			G_1	0.2303560	0.1966400	1.4525790	-0.8304800	-1.2327600	1.4368850	-0.4815000
			G_5	1.1580110	-0.9930800	3.5342160	-2.0739000	-4.6145900	6.9433470	-2.6956500
			G_6	-0.0535700	0.1269210	-0.4300900	0.2393450	1.4467480	-2.4242500	1.0948900
		0.8	G_0	1.3657570	-1.0371100	2.8879690	-0.7595600	-5.1758900	6.1303710	-2.0679500
			G_1	0.2794450	0.2255490	1.0900980	-0.2597200	-1.1585800	0.7773970	-0.1447000
			G_5	1.3655410	-1.4063200	4.8813510	-5.6719000	0.7791320	2.5557890	-1.2000000
			G_6	-0.0492400	-0.1101500	0.4521470	-0.0943800	-1.3627200	1.8991630	-0.7348300

Table 9B.15 – Influence Coefficients for a Circumferential Semi-Elliptical Surface Crack in a Cylinder – Outside Surface

t/R_i	a/c	a/t	G_i	A_0	A_1	A_2	A_3	A_4	A_5	A_6
0.05 (1/20)	1.0	0	G_0	1.1977992	-0.5244870	0.1498299	2.3284866	-5.1058499	4.3469049	-1.3487980
			G_1	0.1870117	0.6987352	0.1316900	0.7269255	-2.5259384	2.1756251	-0.6540458
			G_5	1.1977992	-0.5244870	0.1498299	2.3284866	-5.1058499	4.3469049	-1.3487980
			G_6	0.0000000	0.0000000	0.0000000	0.0000000	0.0000000	0.0000000	0.0000000
		0.2	G_0	1.2190691	-1.2245353	5.0563228	-13.673288	21.292042	-17.129807	5.5105091
			G_1	0.2147079	0.1957634	3.1648328	-8.8299606	13.038660	-10.421992	3.3673069
			G_5	1.2323106	-1.5329918	7.1886225	-20.874850	33.839972	-27.983852	9.1956425
			G_6	-0.0035440	-0.0523620	0.2590590	-0.2857470	-0.4830820	1.1203680	-0.5539910
		0.4	G_0	1.3047890	-0.9921900	1.8925730	-0.9100700	-2.4222800	3.7609800	-1.5483900
			G_1	0.2235270	0.1965708	3.0378068	-8.4937162	12.539220	-9.9135650	3.1391235
			G_5	1.2659030	-0.7461000	0.7702550	1.0361650	-3.5093100	3.3395350	-1.1000000
			G_6	-0.0648600	0.6105630	-3.1269700	7.4646540	-8.7857700	4.8446300	-0.9422400
		0.6	G_0	1.4040090	-1.1188500	1.7571000	-0.2160400	-3.4338500	4.3876240	-1.6723000
			G_1	0.2516650	0.4932520	0.8559910	-0.7868600	-0.9283800	1.4229860	-0.5458900
			G_5	1.3698330	-0.9806800	1.3030750	-0.2859600	-1.4911100	1.7581400	-0.6000000
			G_6	-0.0683500	0.5865560	-2.9461100	6.9774480	-8.1882900	4.5482310	-0.9094800
		0.8	G_0	1.5229200	-1.3353800	2.0181060	-1.0374200	-1.5224000	2.3295770	-0.8591600
			G_1	0.2776610	0.4906660	0.6693060	-0.3281100	-1.3001900	1.4734990	-0.5029000
			G_5	1.4721020	-1.0128400	0.5606840	1.8012340	-3.9996100	2.8744190	-0.6000000
			G_6	-0.0559500	0.2195700	-0.6510100	0.9213840	-0.4641700	-0.0948500	0.1250260
0.05 (1/20)	2.0	0	G_0	0.8150546	-0.5623828	1.4465771	-4.6778133	8.4192164	-7.9025932	2.9866351
			G_1	0.1359146	0.0702340	3.5558581	-11.034445	16.967724	-14.126991	4.8706612
			G_5	0.8150546	-0.5623828	1.4465771	-4.6778133	8.4192164	-7.9025932	2.9866351
			G_6	0.0000000	0.0000000	0.0000000	0.0000000	0.0000000	0.0000000	0.0000000
		0.2	G_0	0.8314774	-1.0666453	4.5748028	-13.981706	22.606222	-18.657217	6.2084870
			G_1	0.1354322	0.0510718	3.3606358	-10.212501	15.321081	-12.446271	4.2036619
			G_5	0.8531681	-1.5115135	7.6197531	-24.136236	40.160863	-33.764166	11.318067
			G_6	-0.0089920	0.1254420	-0.6684330	1.2379590	-0.3507360	-0.9752040	0.6346010
		0.4	G_0	0.8364810	-0.3166000	-0.8197800	3.6598310	-6.6831400	5.3375150	-1.4963800
			G_1	0.1388577	0.0131108	3.5739271	-10.882306	16.486183	-13.496809	4.5805641
			G_5	0.8652411	-1.6446685	8.3920757	-26.621478	44.421021	-37.450368	12.580194
			G_6	-0.0075300	0.0157800	-0.0653600	0.1222650	-0.0886500	-0.0093700	0.0328670
		0.6	G_0	0.8629460	-0.3657900	-0.7831300	3.6718170	-6.7667900	5.4134900	-1.5137300
			G_1	0.1452917	0.0434537	3.3215942	-10.077069	15.070211	-12.191100	4.0976145
			G_5	0.8872276	-1.5214461	7.2033707	-22.690009	37.660813	-31.520822	10.507303
			G_6	-0.0129400	0.0225250	-0.0920100	0.1541220	-0.0464500	-0.0995900	0.0743410
		0.8	G_0	0.9186350	-1.0079400	3.1234490	-8.4794500	12.969650	-10.658800	3.6673810
			G_1	0.1533656	-0.0066478	3.6544321	-11.175413	16.760305	-13.339825	4.3620132
			G_5	0.9176926	-1.6105546	7.3753056	-22.943533	37.443783	-30.611265	9.9345712
			G_6	-0.0030500	-0.1191400	0.5628040	-0.8861500	-0.1023500	1.3745880	-0.8267100

Table 9B.15 – Influence Coefficients for a Circumferential Semi-Elliptical Surface Crack in a Cylinder – Outside Surface

t/R_i	a/c	a/t	G_i	A_0	A_1	A_2	A_3	A_4	A_5	A_6
0.1 (1/10)	0.03125	0	G_0	0.1965046	2.9373464	-5.2582823	7.4889153	-6.9282667	3.3673349	-0.6677966
			G_1	0.0051780	0.1750280	2.7718680	-4.6457154	4.6780502	-3.2768090	0.9840994
			G_5	0.1965046	2.9373464	-5.2582823	7.4889153	-6.9282667	3.3673349	-0.6677966
			G_6	0.0000000	0.0000000	0.0000000	0.0000000	0.0000000	0.0000000	0.0000000
		0.2	G_0	0.2062298	2.4111014	-1.1579831	-3.9618391	10.194552	-9.4698308	3.0669619
			G_1	0.0062688	0.1657744	2.9734268	-5.3001663	6.2503657	-4.8722734	1.5281608
			G_5	0.1707539	2.1495805	-1.7427511	-0.2523829	4.9976467	-6.3918133	2.3496098
			G_6	-0.1132000	-1.3780750	1.7708460	-0.7098550	1.0898820	-0.6591130	0.0017810
		0.4	G_0	0.2070540	2.7537250	-2.8761800	2.2271620	3.9733150	-8.0813400	3.4966400
			G_1	0.0114180	0.3847570	1.2716240	0.3967590	-1.1619600	-0.4328000	0.4535600
			G_5	0.1000570	0.3693550	5.3293420	-19.446200	42.939410	-41.629600	14.000000
			G_6	-0.1983100	-2.4680800	2.4220240	-0.3344800	-3.1190200	8.1947770	-4.4969100
		0.6	G_0	0.2083490	2.8416620	-3.5931900	9.5331750	-7.9036700	-0.4686300	1.6389100
			G_1	0.0179210	0.2958620	1.8278370	-0.7491300	2.2532060	-4.3480500	1.8406900
			G_5	-0.0243800	-1.0831350	5.8471220	-17.471939	47.872990	-47.687462	14.748522
			G_6	-0.7003980	5.3710890	-31.131767	35.464340	13.576927	-37.356426	14.794003
		0.8	G_0	0.2318420	2.0608840	3.3301360	-9.1692600	24.914970	-29.844100	11.474300
			G_1	0.0250440	0.3295030	1.3777280	1.7151740	-0.1612700	-3.4816300	1.6417600
			G_5	-0.1061790	-3.4134960	15.742338	-64.960976	145.911545	-123.324493	33.097134
			G_6	-1.2468150	16.314180	-74.739227	82.691963	20.063618	-72.719612	29.659088
0.1 (1/10)	0.0625	0	G_0	0.2695332	2.1626001	-1.6551569	-1.2970208	4.5604304	-4.3163876	1.4010655
			G_1	0.0138667	0.1827458	2.5749608	-3.9044679	3.3556301	-2.1772209	0.6420134
			G_5	0.2695332	2.1626001	-1.6551569	-1.2970208	4.5604304	-4.3163876	1.4010655
			G_6	0.0000000	0.0000000	0.0000000	0.0000000	0.0000000	0.0000000	0.0000000
		0.2	G_0	0.2806940	2.0374864	-0.8264929	-1.7807353	3.4872503	-2.6298524	0.6904449
			G_1	0.0183868	0.1812388	2.7703041	-4.6792926	5.1145222	-3.9051527	1.2343557
			G_5	0.2694368	1.9612473	-0.8397292	-1.3349670	2.9220021	-2.3881771	0.6601830
			G_6	-0.0842210	-0.4653830	0.0851980	1.0748480	-0.6388330	0.0605260	-0.0279550
		0.4	G_0	0.2914750	2.4030250	-2.1742700	3.0773360	-1.6736600	-1.0254100	0.7639500
			G_1	0.0189582	0.1692677	2.6058681	-3.5933205	4.0083771	-3.5825819	1.2144892
			G_5	0.2473869	1.7676353	-0.4026364	0.2114787	2.4100170	-4.1664108	1.5961656
			G_6	-0.1549900	-1.1945900	0.0000860	5.6600650	-10.284800	9.2054790	-3.2312900
		0.6	G_0	0.2964315	2.0324437	0.1308081	1.2861437	0.9477780	-4.5062364	2.0993887
			G_1	0.0288080	0.2379040	2.4807900	-2.1217300	2.8095710	-3.9330400	1.6059800
			G_5	0.1935424	1.1281848	1.9228156	-3.9287173	14.392040	-17.699290	6.2899615
			G_6	-0.2534700	-1.8722800	1.7439750	-3.6966400	9.2276760	-5.8967600	0.7475020
		0.8	G_0	0.3105210	2.1596820	0.7252700	4.2094560	-2.9669900	-4.8568700	3.3463100
			G_1	0.0552600	0.3259080	1.6878870	2.1616010	-3.0681200	-0.5893900	0.8396800
			G_5	0.0986230	0.9640790	-0.2969200	6.8734000	5.7201690	-19.387327	8.8759930
			G_6	-0.4195540	0.2357680	-11.714850	14.036224	10.723773	-19.820894	6.9692860

Table 9B.15 – Influence Coefficients for a Circumferential Semi-Elliptical Surface Crack in a Cylinder – Outside Surface

t/R_i	a/c	a/t	G_i	A_0	A_1	A_2	A_3	A_4	A_5	A_6
0.1 (1/10)	0.125	0	G_0	0.4065238	0.7772483	3.8861644	-12.573943	16.760207	-11.014593	2.8706957
			G_1	0.0320270	0.1825342	2.2670449	-2.7076615	1.2088194	-0.3777430	0.0763155
			G_5	0.4065238	0.7772483	3.8861644	-12.573943	16.760207	-11.014593	2.8706957
			G_6	0.0000000	0.0000000	0.0000000	0.0000000	0.0000000	0.0000000	0.0000000
		0.2	G_0	0.4130806	1.1359250	1.8126683	-6.3619008	7.9833472	-5.0681630	1.2910002
			G_1	0.0478518	0.0217848	3.8356845	-8.6007775	11.633103	-8.9788832	2.7517112
			G_5	0.4079083	1.1498064	1.5975285	-5.6900729	7.0055326	-4.3667746	1.0917928
			G_6	-0.0685020	0.0694090	-1.0205980	1.7915690	-0.0749590	-1.2699890	0.5791410
		0.4	G_0	0.4751460	1.4510040	1.0799110	-3.5387500	3.8108270	-2.2562200	0.5100700
			G_1	0.0507372	0.2672673	1.8729143	-1.2669216	-0.5238020	0.4880615	-0.0939352
			G_5	0.4529101	1.3061296	1.3684453	-3.6852104	4.2372131	-3.0306963	0.8716174
			G_6	-0.1164900	-0.4307100	0.4852870	-0.6401400	2.4648300	-2.7107700	0.9479970
		0.6	G_0	0.5473293	1.4394412	1.7927835	-0.9379253	-2.5499376	2.3507685	-0.6274414
			G_1	0.0742660	0.4355780	1.5411740	0.5590450	-3.5244300	2.5763870	-0.6659400
			G_5	0.5067973	1.3641876	1.3171498	1.2376984	-5.0238384	3.5282012	-0.8790585
			G_6	-0.2011600	-0.3635500	-1.6411400	6.4684860	-7.7232600	4.8110350	-1.3504200
		0.8	G_0	0.6313390	1.7303310	1.8669510	5.4830110	-18.749700	15.989820	-4.4518100
			G_1	0.0982930	0.3504230	2.4625830	0.3541020	-5.2317300	4.3173190	-1.1604400
			G_5	0.5294343	1.2641801	0.7660220	15.705514	-36.095888	29.203245	-8.6137828
			G_6	-0.3348500	-0.0513300	-3.5238900	2.5582000	14.748960	-22.917600	9.5205520
0.1 (1/10)	0.25	0	G_0	0.6152816	-0.3348694	6.2955620	-15.590618	19.299508	-12.488107	3.3010035
			G_1	0.0703566	0.2828152	1.4036169	-0.6511596	-1.2076596	1.0318656	-0.2423741
			G_5	0.6152816	-0.3348694	6.2955620	-15.590618	19.299508	-12.488107	3.3010035
			G_6	0.0000000	0.0000000	0.0000000	0.0000000	0.0000000	0.0000000	0.0000000
		0.2	G_0	0.6246869	-0.1990336	6.7819636	-19.242905	26.763081	-18.884677	5.3025074
			G_1	0.0907982	0.1745008	2.4998733	-4.9503710	6.1385868	-4.7449552	1.4786038
			G_5	0.6084341	0.0392000	5.1847656	-14.417451	19.401392	-13.395311	3.7145503
			G_6	-0.0839210	0.5447980	-2.0690200	2.6644150	-0.3136570	-1.3449380	0.6081850
		0.4	G_0	0.7326180	0.0366070	4.3380400	-8.4916000	7.1162860	-2.5538200	0.1732000
			G_1	0.1166070	0.2554820	1.8570560	-1.8477100	0.5584930	-0.3317600	0.1672700
			G_5	0.7095270	0.1328400	3.4099130	-5.3751600	1.9251720	1.6200170	-1.1111100
			G_6	-0.0801000	-0.1355000	0.5118230	-1.7399900	3.7294580	-3.4507000	1.1649940
		0.6	G_0	0.9058040	-0.1419600	5.5122770	-9.5617500	5.9764900	-0.3592700	-0.7266200
			G_1	0.1633120	0.2600410	1.8259160	-0.9386500	-1.7190000	1.8499160	-0.5803600
			G_5	0.8740860	-0.0414600	4.7396040	-7.6990800	3.8924480	0.6843440	-0.8888900
			G_6	-0.1301100	-0.0183300	-0.2843000	0.1701160	1.9935560	-2.8991100	1.1681810
		0.8	G_0	1.1362950	-0.6322700	8.9930590	-17.154200	13.986480	-5.2792000	0.7778800
			G_1	0.2267910	0.1761450	2.3523390	-1.3128900	-2.6788900	3.3719220	-1.1814200
			G_5	1.0830690	0.0257530	3.7725650	0.1269090	-14.114800	16.892860	-6.0000000
			G_6	-0.1689600	-0.0072400	-0.4675900	0.8092530	1.3871220	-2.5821300	1.0295540

Table 9B.15 – Influence Coefficients for a Circumferential Semi-Elliptical Surface Crack in a Cylinder – Outside Surface

t/R_i	a/c	a/t	G_i	A_0	A_1	A_2	A_3	A_4	A_5	A_6
0.1 (1/10)	0.5	0	G_0	0.8776607	-0.6729719	3.7721411	-6.5209060	6.3377934	-3.7028038	0.9872447
			G_1	0.1277541	0.4368502	0.4904522	1.0427434	-2.9631236	2.0826525	-0.5184313
			G_5	0.8776607	-0.6729719	3.7721411	-6.5209060	6.3377934	-3.7028038	0.9872447
			G_6	0.0000000	0.0000000	0.0000000	0.0000000	0.0000000	0.0000000	0.0000000
		0.2	G_0	0.9002023	-0.9702215	6.0536022	-13.882269	17.810396	-12.331265	3.5110491
			G_1	0.1495747	0.1634833	2.2505843	-4.5297851	5.7083424	-4.4995032	1.4438996
			G_5	0.8999997	-1.0136861	6.3084405	-14.786302	19.506612	-13.927996	4.0990080
			G_6	-0.0424730	0.2353750	-0.7985880	0.9626770	-0.1168940	-0.3848150	0.1473720
		0.4	G_0	1.0018170	-0.6526700	2.7525060	-1.5008000	-3.7179600	5.3983550	-2.0923200
			G_1	0.1773570	0.3012160	1.2765120	-0.8389800	-0.9008500	1.0771530	-0.3564800
			G_5	0.9665280	-0.4473900	1.5183180	1.6545410	-7.9008300	8.1581390	-2.8000000
			G_6	-0.0778300	0.3084970	-1.4829700	3.3510040	-3.5126300	1.6233420	-0.2094200
		0.6	G_0	1.1744170	-1.0266500	3.9235670	-3.0654300	-3.6018500	6.6578170	-2.7725400
			G_1	0.2255660	0.2202280	1.3847150	-0.6930400	-1.4302400	1.6013990	-0.5373200
			G_5	1.1441930	-0.9557800	3.4558090	-2.2783600	-3.9068700	6.2364950	-2.4565200
			G_6	-0.0885200	0.1578950	-0.5316000	0.4087900	1.4498400	-2.5408900	1.1444860
		0.8	G_0	1.3489390	-0.9235200	2.6704340	-0.6902900	-4.7097800	5.4725200	-1.8088900
			G_1	0.2731610	0.2563650	1.0548290	-0.2726400	-1.0807200	0.7012640	-0.1196200
			G_5	1.3439830	-1.3145200	4.6858860	-5.6761600	1.3418740	1.8498250	-0.9333300
			G_6	-0.0873500	-0.0886200	0.3878340	0.1649200	-1.6781300	2.1040180	-0.8026700
0.1 (1/10)	1.0	0	G_0	1.1977992	-0.5244870	0.1498299	2.3284866	-5.1058499	4.3469049	-1.3487980
			G_1	0.1870117	0.6987352	0.1316900	0.7269255	-2.5259384	2.1756251	-0.6540458
			G_5	1.1977992	-0.5244870	0.1498299	2.3284866	-5.1058499	4.3469049	-1.3487980
			G_6	0.0000000	0.0000000	0.0000000	0.0000000	0.0000000	0.0000000	0.0000000
		0.2	G_0	1.2189520	-1.2097738	5.0035806	-13.570604	21.154946	-17.035957	5.4883898
			G_1	0.2148545	0.1923835	3.2066624	-8.9783210	13.277850	-10.615434	3.4306144
			G_5	1.2348218	-1.5269201	7.1162363	-20.664373	33.524193	-27.770261	9.1475073
			G_6	-0.0092560	-0.0568710	0.2921860	-0.3315290	-0.4709780	1.1501860	-0.5729590
		0.4	G_0	1.3032840	-0.9801200	1.9396690	-1.2179000	-1.8798300	3.3323020	-1.4157700
			G_1	0.2260780	0.1891498	3.1559468	-8.8370736	12.955466	-10.205414	3.2420289
			G_5	1.2591380	-0.7390000	0.7251370	1.1755220	-3.9130200	3.8325580	-1.3000000
			G_6	-0.0778600	0.5780920	-2.8912800	6.8770170	-8.0159800	4.3504740	-0.8204600
		0.6	G_0	1.3998570	-1.0998500	1.8242350	-0.5517400	-3.0050500	4.1670200	-1.6320200
			G_1	0.2485370	0.5078860	0.8346190	-0.7374200	-1.0800000	1.5854580	-0.6001300
			G_5	1.3519740	-0.8505200	0.5388810	1.9241970	-5.0416900	4.6279070	-1.5000000
			G_6	-0.0912600	0.6323660	-3.1077800	7.4058900	-8.7302400	4.8882180	-0.9972000
		0.8	G_0	1.5124900	-1.2482100	1.8172430	-0.7418200	-1.9585100	2.7114870	-0.9820100
			G_1	0.2745170	0.4942760	0.7450050	-0.5511800	-1.1008400	1.4068690	-0.4942200
			G_5	1.4505080	-0.9441200	0.3685860	1.9679090	-4.1014600	2.9209300	-0.6000000
			G_6	-0.0843400	0.2453070	-0.6685400	0.9996230	-0.6106200	0.0423550	0.0762110

Table 9B.15 – Influence Coefficients for a Circumferential Semi-Elliptical Surface Crack in a Cylinder – Outside Surface

t/R_i	a/c	a/t	G_i	A_0	A_1	A_2	A_3	A_4	A_5	A_6
0.1 (1/10)	2.0	0	G_0	0.8150546	-0.5623828	1.4465771	-4.6778133	8.4192164	-7.9025932	2.9866351
			G_1	0.1359146	0.0702340	3.5558581	-11.034445	16.967724	-14.126991	4.8706612
			G_5	0.8150546	-0.5623828	1.4465771	-4.6778133	8.4192164	-7.9025932	2.9866351
			G_6	0.0000000	0.0000000	0.0000000	0.0000000	0.0000000	0.0000000	0.0000000
		0.2	G_0	0.8318082	-1.0744316	4.6367738	-14.199630	22.984826	-18.988399	6.3228538
			G_1	0.1359368	0.0389874	3.4384062	-10.446088	15.691611	-12.753307	4.3064449
			G_5	0.8564580	-1.5112769	7.5603932	-23.926791	39.860172	-33.596301	11.295662
			G_6	-0.0106640	0.1219130	-0.6449160	1.2065960	-0.3680280	-0.9134070	0.6033690
		0.4	G_0	0.8348640	-0.2936000	-0.9263100	3.9021310	-6.9762200	5.4984440	-1.5244400
			G_1	0.1393714	-0.0045032	3.6949749	-11.266421	17.130648	-14.059458	4.7767704
			G_5	0.8652730	-1.6261381	8.2098099	-26.112774	43.760418	-37.079714	12.518093
			G_6	-0.0145700	0.0176350	-0.0438700	0.0860730	-0.0635500	-0.0193900	0.0376720
		0.6	G_0	0.8612390	-0.3546400	-0.8071600	3.6751250	-6.7152100	5.3181550	-1.4639700
			G_1	0.1456764	0.0206678	3.4832840	-10.595840	15.947484	-12.963085	4.3682056
			G_5	0.8854193	-1.5303165	7.1553070	-22.472768	37.311145	-31.322730	10.487317
			G_6	-0.0216900	0.0302850	-0.0929100	0.1801340	-0.1065400	-0.0528800	0.0635980
		0.8	G_0	0.9156630	-0.9908500	3.0995250	-8.5396400	13.206200	-10.984000	3.8193200
			G_1	0.1530811	-0.0218691	3.7692054	-11.555637	17.436930	-13.982208	4.6031925
			G_5	0.9068474	-1.5066824	6.5832667	-20.426436	33.519921	-27.720880	9.1309784
			G_6	-0.0130600	-0.1144100	0.5959870	-0.9610000	-0.0207700	1.3396050	-0.8263400
0.2 (1/5)	0.03125	0	G_0	>360°	>360°	>360°	>360°	>360°	>360°	>360°
			G_1	>360°	>360°	>360°	>360°	>360°	>360°	>360°
			G_5	>360°	>360°	>360°	>360°	>360°	>360°	>360°
			G_6	>360°	>360°	>360°	>360°	>360°	>360°	>360°
		0.2	G_0	>360°	>360°	>360°	>360°	>360°	>360°	>360°
			G_1	>360°	>360°	>360°	>360°	>360°	>360°	>360°
			G_5	>360°	>360°	>360°	>360°	>360°	>360°	>360°
			G_6	>360°	>360°	>360°	>360°	>360°	>360°	>360°
		0.4	G_0	>360°	>360°	>360°	>360°	>360°	>360°	>360°
			G_1	>360°	>360°	>360°	>360°	>360°	>360°	>360°
			G_5	>360°	>360°	>360°	>360°	>360°	>360°	>360°
			G_6	>360°	>360°	>360°	>360°	>360°	>360°	>360°
		0.6	G_0	>360°	>360°	>360°	>360°	>360°	>360°	>360°
			G_1	>360°	>360°	>360°	>360°	>360°	>360°	>360°
			G_5	>360°	>360°	>360°	>360°	>360°	>360°	>360°
			G_6	>360°	>360°	>360°	>360°	>360°	>360°	>360°
		0.8	G_0	>360°	>360°	>360°	>360°	>360°	>360°	>360°
			G_1	>360°	>360°	>360°	>360°	>360°	>360°	>360°
			G_5	>360°	>360°	>360°	>360°	>360°	>360°	>360°
			G_6	>360°	>360°	>360°	>360°	>360°	>360°	>360°

Table 9B.15 – Influence Coefficients for a Circumferential Semi-Elliptical Surface Crack in a Cylinder – Outside Surface

t/R_i	a/c	a/t	G_i	A_0	A_1	A_2	A_3	A_4	A_5	A_6
0.2 (1/5)	0.0625	0	G_0	0.2695332	2.1626001	-1.6551569	-1.2970208	4.5604304	-4.3163876	1.4010655
			G_1	0.0138667	0.1827458	2.5749608	-3.9044679	3.3556301	-2.1772209	0.6420134
			G_5	0.2695332	2.1626001	-1.6551569	-1.2970208	4.5604304	-4.3163876	1.4010655
			G_6	0.0000000	0.0000000	0.0000000	0.0000000	0.0000000	0.0000000	0.0000000
		0.2	G_0	0.2774908	2.0262553	-0.8133105	-1.7375464	3.4202878	-2.6009946	0.6867850
			G_1	0.0179837	0.1529136	2.9576751	-5.1711648	5.7849984	-4.3571052	1.3519411
			G_5	0.2399928	1.8100037	-0.7426186	-1.4325636	4.3104695	-4.4371558	1.4878002
			G_6	-0.1338400	-1.0002800	0.8073470	0.6262070	0.6560130	-1.7063600	0.7509160
		0.4	G_0	0.2781441	2.1182907	-0.8573663	-0.6940178	4.1137120	-5.3210542	1.9749190
			G_1	0.0170279	0.1270926	3.0978063	-5.1503505	6.6321310	-5.7118949	1.8626268
			G_5	0.1376850	0.8752836	0.9229982	-1.1394534	6.2867597	-8.7023069	3.1746372
			G_6	-0.2668900	-1.4913300	-2.2572300	13.963520	-23.281800	20.497450	-7.1637200
		0.6	G_0	0.2698597	2.1631441	-1.0979827	2.5533805	1.1045698	-5.3720025	2.4755770
			G_1	0.0093374	0.1071110	3.0699264	-4.8291996	8.1014107	-8.2339838	2.8377620
			G_5	0.0387421	0.0943716	-3.8239057	18.474536	-15.996194	3.4545316	-0.2379488
			G_6	-0.5162980	2.8230530	-22.077059	29.947357	2.3949620	-22.020474	9.4596610
		0.8	G_0	0.2674593	2.0433452	0.0155220	2.7277592	1.5017795	-6.3715518	2.5965143
			G_1	0.0038165	0.0595955	3.3820597	-5.9553893	12.305288	-12.483753	4.0394895
			G_5	-0.1637740	-2.1522890	8.4315250	-31.959866	87.248184	-84.943283	26.083073
			G_6	-0.9471640	10.467512	-54.115318	68.373581	0.2221720	-43.533421	19.528240
0.2 (1/5)	0.125	0	G_0	0.4065238	0.7772483	3.8861644	-12.573943	16.760207	-11.014593	2.8706957
			G_1	0.0320270	0.1825342	2.2670449	-2.7076615	1.2088194	-0.3777430	0.0763155
			G_5	0.4065238	0.7772483	3.8861644	-12.573943	16.760207	-11.014593	2.8706957
			G_6	0.0000000	0.0000000	0.0000000	0.0000000	0.0000000	0.0000000	0.0000000
		0.2	G_0	0.4117875	1.1385881	1.7784942	-6.1639923	7.6448761	-4.8213505	1.2226378
			G_1	0.0470699	0.0295648	3.7396060	-8.1204493	10.711888	-8.1991643	2.5060356
			G_5	0.3971461	1.1200570	1.5332235	-5.2800357	6.4550368	-4.0686358	1.0314054
			G_6	-0.0989900	-0.3971800	0.6515250	-1.4711400	3.9895020	-4.1519400	1.4782250
		0.4	G_0	0.4492521	1.2970887	1.6394114	-4.6101707	5.5388028	-3.8995510	1.1013127
			G_1	0.0584564	0.0847062	3.5928149	-7.0140416	8.9104748	-6.9581901	2.1577698
			G_5	0.3925974	1.1782321	1.0536644	-1.8881185	1.8376671	-1.6477686	0.5450371
			G_6	-0.2041000	-0.6628600	-0.0950100	2.3430480	-1.7270700	0.2829070	0.0630740
		0.6	G_0	0.4881660	1.6507400	0.2050560	2.1433950	-4.5291500	2.1963290	-0.2168300
			G_1	0.0566450	0.3309960	1.9818650	-0.9123500	-0.4442300	-0.4525300	0.4199700
			G_5	0.3466423	1.0235299	0.7336500	4.0764251	-7.4318993	3.9119364	-0.7633649
			G_6	-0.3387500	-0.7171400	-2.0254800	7.4624010	-6.9186200	3.5122470	-0.9746500
		0.8	G_0	0.5121250	1.5704480	2.4143130	0.2498080	-4.3262900	2.1073350	-0.0575300
			G_1	0.0561240	0.3465660	2.3212940	-0.6279400	-1.0469300	-0.2889500	0.4244900
			G_5	0.2408720	0.4224221	3.5982027	-0.5713316	4.0453456	-9.4061812	4.1654423
			G_6	-0.4674500	-1.1687700	0.4132170	-10.223100	34.719670	-34.908100	11.634500

Table 9B.15 – Influence Coefficients for a Circumferential Semi-Elliptical Surface Crack in a Cylinder – Outside Surface

t/R_i	a/c	a/t	G_i	A_0	A_1	A_2	A_3	A_4	A_5	A_6
0.2 (1/5)	0.25	0	G_0	0.6152816	-0.3348694	6.2955620	-15.590618	19.299508	-12.488107	3.3010035
			G_1	0.0703566	0.2828152	1.4036169	-0.6511596	-1.2076596	1.0318656	-0.2423741
			G_5	0.6152816	-0.3348694	6.2955620	-15.590618	19.299508	-12.488107	3.3010035
			G_6	0.0000000	0.0000000	0.0000000	0.0000000	0.0000000	0.0000000	0.0000000
		0.2	G_0	0.6271377	-0.2298482	7.0204766	-19.981373	27.955848	-19.841412	5.6004795
			G_1	0.0907652	0.1775295	2.5002998	-4.9548232	6.1690007	-4.7911060	1.4984781
			G_5	0.6267188	-0.2150752	5.9244999	-15.141684	19.361210	-12.962335	3.5399114
			G_6	-0.0730300	-0.1039500	0.3779340	-1.4730700	3.4257760	-3.3001300	1.1464610
		0.4	G_0	0.7243940	0.0982170	3.8649050	-6.8572100	4.4474240	-0.4646900	-0.4610600
			G_1	0.1116160	0.2421110	1.9598510	-2.2366400	1.2671380	-0.9068300	0.3367200
			G_5	0.6870350	0.0387870	3.9170980	-7.1437000	5.1449910	-1.1416500	-0.2222200
			G_6	-0.1429600	-0.1522700	0.3434280	-1.3869700	3.9981410	-4.1031700	1.4438050
		0.6	G_0	0.8591310	0.0156500	4.8410810	-7.6957700	3.5329350	1.1471070	-1.0891600
			G_1	0.1506290	0.2414840	2.0792750	-1.7964600	-0.2806200	0.6982770	-0.2306800
			G_5	0.7980120	-0.1517600	5.6710930	-11.201800	10.646550	-5.3611100	1.1111110
			G_6	-0.2281500	-0.0472900	-0.6334600	1.2719350	1.1658530	-2.6941700	1.1652830
		0.8	G_0	1.0109730	-0.1571000	7.0684530	-11.622100	6.4274650	-0.2949400	-0.5470500
			G_1	0.1949920	0.1486120	2.9915130	-3.4528600	0.9912030	0.3037770	-0.2056700
			G_5	0.8870610	0.3775580	2.2456250	3.9607610	-17.744100	18.035720	-6.0000000
			G_6	-0.3136200	-0.0427800	-1.0031500	2.2762370	0.9773960	-3.3646700	1.4705920
0.2 (1/5)	0.5	0	G_0	0.8776607	-0.6729719	3.7721411	-6.5209060	6.3377934	-3.7028038	0.9872447
			G_1	0.1277541	0.4368502	0.4904522	1.0427434	-2.9631236	2.0826525	-0.5184313
			G_5	0.8776607	-0.6729719	3.7721411	-6.5209060	6.3377934	-3.7028038	0.9872447
			G_6	0.0000000	0.0000000	0.0000000	0.0000000	0.0000000	0.0000000	0.0000000
		0.2	G_0	0.9018630	-0.9538496	5.9919622	-13.738556	17.612623	-12.191476	3.4725648
			G_1	0.1495608	0.1733747	2.2120339	-4.4335931	5.5703879	-4.4014805	1.4175068
			G_5	0.8989059	-0.9882804	6.1271579	-14.287453	18.780450	-13.406411	3.9549546
			G_6	-0.0705200	0.2567410	-1.2495900	2.8677950	-3.0504600	1.4356940	-0.1896600
		0.4	G_0	1.0019030	-0.6556300	2.8775410	-1.9787200	-3.0003900	4.9257760	-1.9790600
			G_1	0.1738940	0.3355690	1.1270520	-0.4578300	-1.4623100	1.5065800	-0.4867600
			G_5	0.9505460	-0.4598500	1.7330080	0.5011690	-5.6648600	6.2604660	-2.2000000
			G_6	-0.1213700	0.4129990	-1.9995500	4.6351640	-5.0019800	2.4723590	-0.3976300
		0.6	G_0	1.1589040	-0.9119700	3.6019430	-2.5613200	-4.0414800	6.8676550	-2.8162900
			G_1	0.2195810	0.2504100	1.3344200	-0.6342900	-1.5137700	1.6844020	-0.5678100
			G_5	1.1041200	-0.8565000	3.1614520	-2.0800900	-3.6322300	5.7885380	-2.2826100
			G_6	-0.1479200	0.2002220	-0.6443400	0.5965410	1.5644630	-2.8569900	1.2880200
		0.8	G_0	1.3175280	-0.7714200	2.5794970	-1.1653400	-3.4376600	4.2682690	-1.4121500
			G_1	0.2602210	0.3199750	0.9492120	-0.1839400	-1.1009900	0.6684550	-0.0987300
			G_5	1.2740170	-1.1637300	4.5095380	-6.0754300	2.7026250	0.4828070	-0.4666700
			G_6	-0.1671200	-0.0249100	0.2071610	0.6527170	-2.0799000	2.2037960	-0.7917400

Table 9B.15 – Influence Coefficients for a Circumferential Semi-Elliptical Surface Crack in a Cylinder – Outside Surface

t/R_i	a/c	a/t	G_i	A_0	A_1	A_2	A_3	A_4	A_5	A_6
0.2 (1/5)	1.0	0	G_0	1.1977992	-0.5244870	0.1498299	2.3284866	-5.1058499	4.3469049	-1.3487980
			G_1	0.1870117	0.6987352	0.1316900	0.7269255	-2.5259384	2.1756251	-0.6540458
			G_5	1.1977992	-0.5244870	0.1498299	2.3284866	-5.1058499	4.3469049	-1.3487980
			G_6	0.0000000	0.0000000	0.0000000	0.0000000	0.0000000	0.0000000	0.0000000
		0.2	G_0	1.2208938	-1.2041917	5.0334698	-13.741887	21.435583	-17.257339	5.5625096
			G_1	0.2144977	0.2060705	3.1319639	-8.7325400	12.853217	-10.282493	3.3370053
			G_5	1.2350971	-1.5079685	6.9553573	-20.208191	32.816115	-27.245603	9.0067094
			G_6	-0.0828200	0.6613920	-3.3269100	7.7832260	-8.6558500	4.1418630	-0.5209000
		0.4	G_0	1.2974480	-0.8978500	1.5464860	-0.0684400	-3.8891500	5.0715000	-1.9856700
			G_1	0.2279963	0.2557041	2.7316895	-7.3765941	10.510743	-8.3256498	2.7071280
			G_5	1.2392890	-0.7267700	0.7939140	0.5894400	-2.7996000	2.9069770	-1.0000000
			G_6	-0.1070200	0.6703990	-3.2584800	7.6913240	-8.8678600	4.7415690	-0.8699400
		0.6	G_0	1.3902670	-1.0526700	1.8671080	-0.9437600	-2.5011700	3.9208390	-1.5891100
			G_1	0.2440310	0.5137240	0.8974300	-0.8785500	-1.0881800	1.7286490	-0.6657300
			G_5	1.3181210	-0.7998800	0.4938380	1.5489800	-4.2573600	3.9953490	-1.3000000
			G_6	-0.1281700	0.6899310	-3.2765600	7.8600090	-9.3273600	5.2734440	-1.0912900
		0.8	G_0	1.4978360	-1.1640500	1.8344600	-1.1167700	-1.6062200	2.6731730	-1.0165300
			G_1	0.2690770	0.5138280	0.7713690	-0.5894800	-1.2981100	1.6877650	-0.5889500
			G_5	1.4113850	-0.9874900	1.0715580	-0.7321800	0.2206270	-0.3814000	0.4000000
			G_6	-0.1307600	0.3275810	-0.9451600	1.7563070	-1.5599400	0.5843160	-0.0323500
0.2 (1/5)	2.0	0	G_0	0.8150546	-0.5623828	1.4465771	-4.6778133	8.4192164	-7.9025932	2.9866351
			G_1	0.1359146	0.0702340	3.5558581	-11.034445	16.967724	-14.126991	4.8706612
			G_5	0.8150546	-0.5623828	1.4465771	-4.6778133	8.4192164	-7.9025932	2.9866351
			G_6	0.0000000	0.0000000	0.0000000	0.0000000	0.0000000	0.0000000	0.0000000
		0.2	G_0	0.8319739	-1.0737151	4.6490836	-14.283121	23.181415	-19.212560	6.4181218
			G_1	0.1367829	0.0195825	3.5727027	-10.883865	16.435739	-13.397326	4.5265031
			G_5	0.8587201	-1.5078217	7.4605134	-23.602425	39.397717	-33.324166	11.250246
			G_6	-0.0013600	0.0067490	-0.0078600	0.0154990	-0.0227600	0.0006890	0.0090320
		0.4	G_0	0.8306360	-0.2783600	-0.9579000	3.8962200	-6.8631100	5.3033590	-1.4257900
			G_1	0.1414167	-0.0083138	3.7265323	-11.341965	17.307508	-14.334310	4.9200146
			G_5	0.8651941	-1.6414372	8.2119118	-26.195706	44.070198	-37.499897	12.710196
			G_6	-0.0204200	0.0175040	-0.0184100	0.0563730	-0.0617800	0.0082410	0.0185040
		0.6	G_0	0.8556570	-0.3568100	-0.6900000	3.2047690	-5.8960900	4.5761710	-1.1943900
			G_1	0.1450802	0.0389886	3.3678594	-10.170959	15.319892	-12.658323	4.3602413
			G_5	0.8781226	-1.5169522	6.9468106	-21.892973	36.571741	-30.949926	10.451527
			G_6	-0.0301300	0.0314260	-0.0707200	0.1957270	-0.1994100	0.0478270	0.0252810
		0.8	G_0	0.9091900	-1.0214700	3.4711980	-9.9203800	15.637600	-13.142700	4.5753490
			G_1	0.1478586	0.0682866	3.1625977	-9.5415913	14.299739	-11.806182	4.0649234
			G_5	0.8923217	-1.4448983	6.0075154	-18.631958	30.794580	-25.802121	8.6362697
			G_6	-0.0234000	-0.1198900	0.6560330	-0.9660400	-0.2436600	1.6734190	-0.9764600

Table 9B.15 – Influence Coefficients for a Circumferential Semi-Elliptical Surface Crack in a Cylinder – Outside Surface

t/R_i	a/c	a/t	G_i	A_0	A_1	A_2	A_3	A_4	A_5	A_6
0.3333 (1/3)	0.03125	0	G_0	>360°	>360°	>360°	>360°	>360°	>360°	>360°
			G_1	>360°	>360°	>360°	>360°	>360°	>360°	>360°
			G_5	>360°	>360°	>360°	>360°	>360°	>360°	>360°
			G_6	>360°	>360°	>360°	>360°	>360°	>360°	>360°
		0.2	G_0	>360°	>360°	>360°	>360°	>360°	>360°	>360°
			G_1	>360°	>360°	>360°	>360°	>360°	>360°	>360°
			G_5	>360°	>360°	>360°	>360°	>360°	>360°	>360°
			G_6	>360°	>360°	>360°	>360°	>360°	>360°	>360°
		0.4	G_0	>360°	>360°	>360°	>360°	>360°	>360°	>360°
			G_1	>360°	>360°	>360°	>360°	>360°	>360°	>360°
			G_5	>360°	>360°	>360°	>360°	>360°	>360°	>360°
			G_6	>360°	>360°	>360°	>360°	>360°	>360°	>360°
		0.6	G_0	>360°	>360°	>360°	>360°	>360°	>360°	>360°
			G_1	>360°	>360°	>360°	>360°	>360°	>360°	>360°
			G_5	>360°	>360°	>360°	>360°	>360°	>360°	>360°
			G_6	>360°	>360°	>360°	>360°	>360°	>360°	>360°
		0.8	G_0	>360°	>360°	>360°	>360°	>360°	>360°	>360°
			G_1	>360°	>360°	>360°	>360°	>360°	>360°	>360°
			G_5	>360°	>360°	>360°	>360°	>360°	>360°	>360°
			G_6	>360°	>360°	>360°	>360°	>360°	>360°	>360°
0.3333 (1/3)	0.0625	0	G_0	>360°	>360°	>360°	>360°	>360°	>360°	>360°
			G_1	>360°	>360°	>360°	>360°	>360°	>360°	>360°
			G_5	>360°	>360°	>360°	>360°	>360°	>360°	>360°
			G_6	>360°	>360°	>360°	>360°	>360°	>360°	>360°
		0.2	G_0	>360°	>360°	>360°	>360°	>360°	>360°	>360°
			G_1	>360°	>360°	>360°	>360°	>360°	>360°	>360°
			G_5	>360°	>360°	>360°	>360°	>360°	>360°	>360°
			G_6	>360°	>360°	>360°	>360°	>360°	>360°	>360°
		0.4	G_0	>360°	>360°	>360°	>360°	>360°	>360°	>360°
			G_1	>360°	>360°	>360°	>360°	>360°	>360°	>360°
			G_5	>360°	>360°	>360°	>360°	>360°	>360°	>360°
			G_6	>360°	>360°	>360°	>360°	>360°	>360°	>360°
		0.6	G_0	>360°	>360°	>360°	>360°	>360°	>360°	>360°
			G_1	>360°	>360°	>360°	>360°	>360°	>360°	>360°
			G_5	>360°	>360°	>360°	>360°	>360°	>360°	>360°
			G_6	>360°	>360°	>360°	>360°	>360°	>360°	>360°
		0.8	G_0	>360°	>360°	>360°	>360°	>360°	>360°	>360°
			G_1	>360°	>360°	>360°	>360°	>360°	>360°	>360°
			G_5	>360°	>360°	>360°	>360°	>360°	>360°	>360°
			G_6	>360°	>360°	>360°	>360°	>360°	>360°	>360°

Table 9B.15 – Influence Coefficients for a Circumferential Semi-Elliptical Surface Crack in a Cylinder – Outside Surface

t/R_i	a/c	a/t	G_i	A_0	A_1	A_2	A_3	A_4	A_5	A_6
0.3333 (1/3)	0.125	0	G0	0.4065238	0.7772483	3.8861644	-12.573943	16.760207	-11.014593	2.8706957
			G1	0.0320270	0.1825342	2.2670449	-2.7076615	1.2088194	-0.3777430	0.0763155
			G5	0.4065238	0.7772483	3.8861644	-12.573943	16.760207	-11.014593	2.8706957
			G6	0.0000000	0.0000000	0.0000000	0.0000000	0.0000000	0.0000000	0.0000000
		0.2	G0	0.4099613	1.1334144	1.8167755	-6.1933976	7.6194214	-4.7676610	1.1972653
			G1	0.0462103	0.0340256	3.6705315	-7.7292467	9.9287487	-7.5175409	2.2859463
			G5	0.3781184	1.0782386	1.3896969	-4.4300255	5.1708948	-3.2094344	0.8003934
			G6	-0.1440800	-0.5237500	0.4347310	-0.2173300	2.3742060	-3.1240500	1.2002700
		0.4	G0	0.4533770	1.0766900	3.5058010	-11.549900	17.918540	-14.316700	4.4298660
			G1	0.0523522	0.0848838	3.4278771	-6.1023514	7.1456705	-5.4439258	1.6695382
			G5	0.3133139	0.9747113	0.6917682	0.6225195	-1.5943871	0.3406017	0.0734211
			G6	-0.2907100	-0.8909900	-0.1971000	2.5029520	-0.4154300	-1.2933500	0.5846360
		0.6	G0	0.4709970	0.7906930	6.3141400	-17.458100	26.655280	-21.459500	6.6178750
			G1	0.0462130	0.1791657	2.8322826	-3.4762634	3.7158317	-3.6187167	1.3051475
			G5	0.1771076	0.3899173	2.3204598	-1.4538642	6.0522140	-9.3757919	3.6701943
			G6	-0.4185600	-1.1827300	-0.9627800	2.7897690	1.8354460	-2.5019400	0.4407850
		0.8	G0	0.4435980	1.2520030	3.3031060	-2.6255800	2.8823370	-4.6559200	1.9668050
			G1	0.0347263	0.1941740	2.8167869	-2.0526330	2.2452322	-3.3744831	1.3721332
			G5	-0.0186530	-0.0008300	1.6033700	2.8965590	7.6443440	-17.212490	7.2772780
			G6	-0.4254840	0.9613640	-18.455093	34.953655	-17.226433	-3.3806720	3.5785980
0.3333 (1/3)	0.25	0	G_0	0.6152816	-0.3348694	6.2955620	-15.590618	19.299508	-12.488107	3.3010035
			G_1	0.0703566	0.2828152	1.4036169	-0.6511596	-1.2076596	1.0318656	-0.2423741
			G_5	0.6152816	-0.3348694	6.2955620	-15.590618	19.299508	-12.488107	3.3010035
			G_6	0.0000000	0.0000000	0.0000000	0.0000000	0.0000000	0.0000000	0.0000000
		0.2	G_0	0.6247110	-0.1841775	6.7646437	-19.122556	26.490065	-18.633480	5.2176726
			G_1	0.0902680	0.1863897	2.4580412	-4.8000656	5.9136117	-4.5969548	1.4420194
			G_5	0.6188062	-0.2124520	5.8656185	-14.966741	19.138738	-12.819133	3.5001285
			G_6	-0.1133700	0.0386090	-0.7483700	1.8940110	-1.3915000	0.2087770	0.1118400
		0.4	G_0	0.7285570	-0.1787800	5.9836260	-13.655900	15.406530	-9.1372500	2.2140220
			G_1	0.1068720	0.2817480	1.6735290	-1.1790200	-0.6310000	0.7077640	-0.1838800
			G_5	0.6544370	-0.1552600	5.2209810	-11.650100	13.030050	-7.7164200	1.8592460
			G_6	-0.2193000	0.0425450	-1.3544600	3.7675290	-3.2851000	1.1023660	-0.0535800
		0.6	G_0	0.8443080	-0.5795400	9.6687260	-23.049300	28.167150	-18.272400	4.8614220
			G_1	0.1391010	0.2003860	2.4182470	-2.4894900	0.4710610	0.2306300	-0.0993900
			G_5	0.7034360	-0.4721000	7.8058200	-17.653700	21.157630	-13.776400	3.6887940
			G_6	-0.3396100	0.0377040	-1.9404100	5.1897370	-3.6971200	0.3704200	0.3792770
		0.8	G_0	0.9520760	-0.1754800	7.5423420	-13.331500	11.885240	-6.9538200	2.0803610
			G_1	0.1701480	0.2848700	2.1734480	-1.0215800	-1.7757000	1.4765150	-0.2998500
			G_5	0.7201900	-0.1035200	5.4180790	-7.7404000	5.9504530	-4.0595900	1.5230280
			G_6	-0.4790200	0.0451970	-2.0762300	3.9884540	1.1847190	-4.8004700	2.1373500

Table 9B.15 – Influence Coefficients for a Circumferential Semi-Elliptical Surface Crack in a Cylinder – Outside Surface

t/R_i	a/c	a/t	G_i	A_0	A_1	A_2	A_3	A_4	A_5	A_6
0.3333 (1/3)	0.5	0	G_0	0.8776607	-0.6729719	3.7721411	-6.5209060	6.3377934	-3.7028038	0.9872447
			G_1	0.1277541	0.4368502	0.4904522	1.0427434	-2.9631236	2.0826525	-0.5184313
			G_5	0.8776607	-0.6729719	3.7721411	-6.5209060	6.3377934	-3.7028038	0.9872447
			G_6	0.0000000	0.0000000	0.0000000	0.0000000	0.0000000	0.0000000	0.0000000
		0.2	G_0	0.9066169	-1.0098809	6.4500448	-15.276412	20.122076	-14.176827	4.0826731
			G_1	0.1492778	0.1842512	2.1734412	-4.3450372	5.4492142	-4.3195528	1.3970909
			G_5	0.8914928	-0.9078192	5.6229793	-12.889289	16.743862	-11.930113	3.5383034
			G_6	-0.0731700	-0.0019200	0.1112140	-0.3517100	0.7595710	-0.6537100	0.2097210
		0.4	G_0	0.9745940	-0.2537500	0.9422670	2.4134430	-8.0311500	7.6591860	-2.5119400
			G_1	0.1677910	0.3861730	0.9608550	-0.2805400	-1.3649300	1.1990170	-0.3335200
			G_5	0.9236760	-0.3872800	1.4642830	0.6726050	-5.2981700	5.6675470	-1.9567300
			G_6	-0.1336400	-0.0061900	0.2483910	-0.7804100	1.6547940	-1.4364400	0.4535040
		0.6	G_0	1.1489090	-0.9628100	4.7197790	-7.2385800	4.7190150	-0.8600300	-0.2218800
			G_1	0.2074750	0.3710920	0.7536550	0.8750530	-3.5617500	3.0181320	-0.8916700
			G_5	1.0605150	-0.9384600	4.2401570	-6.3570900	3.8804030	-0.3727100	-0.3571700
			G_6	-0.2088100	0.1861540	-0.5969000	1.1076490	-0.1339800	-0.7782600	0.4241420
		0.8	G_0	1.2919860	-0.5742900	1.7855010	2.6509560	-11.664400	11.851350	-3.9241400
			G_1	0.2520800	0.4019340	0.4065200	2.4606020	-6.6673200	5.7443690	-1.7758300
			G_5	1.1599780	-0.5682200	1.3649980	3.1291180	-11.561500	11.451800	-3.7613000
			G_6	-0.2744400	0.1898780	-0.4285700	0.7415200	0.4312720	-1.1716300	0.5119770
0.3333 (1/3)	1.0	0	G_0	1.1977992	-0.5244870	0.1498299	2.3284866	-5.1058499	4.3469049	-1.3487980
			G_1	0.1870117	0.6987352	0.1316900	0.7269255	-2.5259384	2.1756251	-0.6540458
			G_5	1.1977992	-0.5244870	0.1498299	2.3284866	-5.1058499	4.3469049	-1.3487980
			G_6	0.0000000	0.0000000	0.0000000	0.0000000	0.0000000	0.0000000	0.0000000
		0.2	G_0	1.2220417	-1.2014542	5.0931939	-14.015936	21.882198	-17.611726	5.6790779
			G_1	0.2144011	0.2076611	3.1479697	-8.7880102	12.919129	-10.335990	3.3611678
			G_5	1.2320744	-1.5110742	6.9601667	-20.284073	32.929016	-27.327658	9.0387452
			G_6	-0.0490800	-0.0266200	0.3507710	-1.0858100	1.7945020	-1.4605800	0.4768160
		0.4	G_0	1.2493780	-0.1807200	-2.1512500	9.0872720	-15.619500	12.451940	-3.7683100
			G_1	0.2277520	0.2442248	2.8502573	-7.7013661	10.911804	-8.6055298	2.8003299
			G_5	1.1860660	-0.1633600	-2.5846400	10.208460	-17.192400	13.660050	-4.1506700
			G_6	-0.0847200	-0.0130400	0.4450670	-1.3612100	2.2705210	-1.8636500	0.6070300
		0.6	G_0	1.3282800	-0.1805500	-2.6139900	10.483400	-17.872600	14.215520	-4.2781900
			G_1	0.2244930	0.7671250	-0.4475100	2.7627880	-6.2712500	5.3388310	-1.6303400
			G_5	1.2510160	-0.2335300	-2.7704000	10.674610	-17.843000	14.118660	-4.2549700
			G_6	-0.1229000	0.0987760	-0.0510800	0.0753380	0.2033960	-0.3948100	0.1912830
		0.8	G_0	1.4785910	-1.2353000	3.6180340	-8.2725500	10.979570	-8.0343800	2.5668670
			G_1	0.2647100	0.4116600	1.8029290	-4.2515600	5.0019550	-3.7691200	1.2975750
			G_5	1.3832810	-1.3901800	4.0196220	-10.087000	14.697690	-11.393300	3.7011250
			G_6	-0.1828100	0.6153590	-3.1104800	9.4475170	-14.736200	11.582900	-3.6163100

Table 9B.15 – Influence Coefficients for a Circumferential Semi-Elliptical Surface Crack in a Cylinder – Outside Surface

t/R_i	a/c	a/t	G_i	A_0	A_1	A_2	A_3	A_4	A_5	A_6
0.3333 (1/3)	2.0	0	G_0	0.8150546	-0.5623828	1.4465771	-4.6778133	8.4192164	-7.9025932	2.9866351
			G_1	0.1359146	0.0702340	3.5558581	-11.034445	16.967724	-14.126991	4.8706612
			G_5	0.8150546	-0.5623828	1.4465771	-4.6778133	8.4192164	-7.9025932	2.9866351
			G_6	0.0000000	0.0000000	0.0000000	0.0000000	0.0000000	0.0000000	0.0000000
		0.2	G_0	0.8331327	-1.0983961	4.8310919	-14.895078	24.214240	-20.089273	6.7122349
			G_1	0.1374607	0.0008167	3.6998791	-11.290852	17.125293	-14.000885	4.7362430
			G_5	0.8590462	-1.4944677	7.2901818	-23.037515	38.516128	-32.701232	11.093104
			G_6	-0.0046700	0.0180740	-0.0638400	0.1222610	-0.0829200	-0.0216300	0.0327160
		0.4	G_0	0.8283100	-0.2747400	-0.9278400	3.7320330	-6.5492300	4.9873730	-1.2999200
			G_1	0.1426112	-0.0204439	3.8267365	-11.671861	17.925207	-14.972682	5.1786686
			G_5	0.8690036	-1.7119175	8.5353824	-27.203901	45.752326	-38.936187	13.200079
			G_6	-0.0276200	0.0342780	-0.0751100	0.1858580	-0.1916200	0.0577570	0.0164540
		0.6	G_0	0.8508740	-0.3486600	-0.6430600	2.9213950	-5.3199000	3.9848080	-0.9604400
			G_1	0.1448686	0.0284442	3.4562322	-10.447804	15.869466	-13.299505	4.6445600
			G_5	0.8707662	-1.5022966	6.7207535	-21.298542	35.863052	-30.637128	10.444495
			G_6	-0.0400200	0.0397750	-0.0574200	0.1528560	-0.1187200	-0.0270400	0.0505700
		0.8	G_0	0.9042450	-1.0486000	3.8207860	-11.291000	18.161500	-15.468300	5.4125140
			G_1	0.1453857	0.0854754	3.0581116	-9.1833308	13.836217	-11.703621	4.1461877
			G_5	0.8788989	-1.4042484	5.5584708	-17.279835	28.790156	-24.426973	8.2965772
			G_6	-0.0362200	-0.1136800	0.6936160	-1.0067200	-0.3158000	1.8522520	-1.0734500
1.0 (1/1)	0.03125	0	G_0	>360°	>360°	>360°	>360°	>360°	>360°	>360°
			G_1	>360°	>360°	>360°	>360°	>360°	>360°	>360°
			G_5	>360°	>360°	>360°	>360°	>360°	>360°	>360°
			G_6	>360°	>360°	>360°	>360°	>360°	>360°	>360°
		0.2	G_0	>360°	>360°	>360°	>360°	>360°	>360°	>360°
			G_1	>360°	>360°	>360°	>360°	>360°	>360°	>360°
			G_5	>360°	>360°	>360°	>360°	>360°	>360°	>360°
			G_6	>360°	>360°	>360°	>360°	>360°	>360°	>360°
		0.4	G_0	>360°	>360°	>360°	>360°	>360°	>360°	>360°
			G_1	>360°	>360°	>360°	>360°	>360°	>360°	>360°
			G_5	>360°	>360°	>360°	>360°	>360°	>360°	>360°
			G_6	>360°	>360°	>360°	>360°	>360°	>360°	>360°
		0.6	G_0	>360°	>360°	>360°	>360°	>360°	>360°	>360°
			G_1	>360°	>360°	>360°	>360°	>360°	>360°	>360°
			G_5	>360°	>360°	>360°	>360°	>360°	>360°	>360°
			G_6	>360°	>360°	>360°	>360°	>360°	>360°	>360°
		0.8	G_0	>360°	>360°	>360°	>360°	>360°	>360°	>360°
			G_1	>360°	>360°	>360°	>360°	>360°	>360°	>360°
			G_5	>360°	>360°	>360°	>360°	>360°	>360°	>360°
			G_6	>360°	>360°	>360°	>360°	>360°	>360°	>360°

Table 9B.15 – Influence Coefficients for a Circumferential Semi-Elliptical Surface Crack in a Cylinder – Outside Surface

t/R_i	a/c	a/t	G_i	A_0	A_1	A_2	A_3	A_4	A_5	A_6
1.0 (1/1)	0.0625	0	G_0	0.2695332	2.1626001	-1.6551569	-1.2970208	4.5604304	-4.3163876	1.4010655
			G_1	0.0138667	0.1827458	2.5749608	-3.9044679	3.3556301	-2.1772209	0.6420134
			G_5	0.2695332	2.1626001	-1.6551569	-1.2970208	4.5604304	-4.3163876	1.4010655
			G_6	0.0000000	0.0000000	0.0000000	0.0000000	0.0000000	0.0000000	0.0000000
		0.2	G_0	0.247757	2.511528	-3.360426	4.053683	-2.892102	0.661436	0.052018
			G_1	0.008798	0.225308	2.366204	-3.198590	2.661117	-1.932026	0.609342
			G_5	0.011614	-0.241994	2.029974	-0.881880	6.011700	-9.252675	3.503553
			G_6	-0.232852	-2.795556	5.125727	-8.758967	11.713588	-5.102963	0.049416
		0.4	G_0	>360°	>360°	>360°	>360°	>360°	>360°	>360°
			G_1	>360°	>360°	>360°	>360°	>360°	>360°	>360°
			G_5	>360°	>360°	>360°	>360°	>360°	>360°	>360°
			G_6	>360°	>360°	>360°	>360°	>360°	>360°	>360°
		0.6	G_0	>360°	>360°	>360°	>360°	>360°	>360°	>360°
			G_1	>360°	>360°	>360°	>360°	>360°	>360°	>360°
			G_5	>360°	>360°	>360°	>360°	>360°	>360°	>360°
			G_6	>360°	>360°	>360°	>360°	>360°	>360°	>360°
		0.8	G_0	>360°	>360°	>360°	>360°	>360°	>360°	>360°
			G_1	>360°	>360°	>360°	>360°	>360°	>360°	>360°
			G_5	>360°	>360°	>360°	>360°	>360°	>360°	>360°
			G_6	>360°	>360°	>360°	>360°	>360°	>360°	>360°
1.0 (1/1)	0.125	0	G_0	0.4065238	0.7772483	3.8861644	-12.573943	16.760207	-11.014593	2.8706957
			G_1	0.0320270	0.1825342	2.2670449	-2.7076615	1.2088194	-0.3777430	0.0763155
			G_5	0.4065238	0.7772483	3.8861644	-12.573943	16.760207	-11.014593	2.8706957
			G_6	0.0000000	0.0000000	0.0000000	0.0000000	0.0000000	0.0000000	0.0000000
		0.2	G_0	0.409839	0.865110	5.194634	-19.027492	29.748805	-22.618492	6.672461
			G_1	0.033588	0.203603	2.494891	-3.766022	3.444365	-2.437597	0.754064
			G_5	0.299849	0.842519	1.473313	-3.994471	6.206978	-5.369094	1.698818
			G_6	-0.259341	-0.826076	-1.153719	6.919820	-8.326430	4.846767	-1.199104
		0.4	G_0	0.428252	0.516646	7.678538	-25.031224	40.129628	-31.856532	9.693451
			G_1	0.030030	0.191561	2.625685	-3.748247	4.046931	-3.454566	1.149637
			G_5	0.003803	0.116787	1.087918	0.676268	5.743929	-10.574666	4.268672
			G_6	-0.440682	-0.821534	-4.207636	13.128939	-15.200336	11.636560	-4.095609
		0.6	G_0	0.345592	0.450129	7.280712	-20.851656	36.762671	-32.234625	10.304173
			G_1	-0.002149	0.137029	2.658398	-3.233150	5.036300	-5.516540	1.947561
			G_5	-0.357604	-0.764569	-0.166214	3.379018	15.505212	-24.771002	8.762189
			G_6	-0.388085	-0.770944	-4.200932	4.711123	-6.678571	16.889332	-9.566777
		0.8	G_0	>360°	>360°	>360°	>360°	>360°	>360°	>360°
			G_1	>360°	>360°	>360°	>360°	>360°	>360°	>360°
			G_5	>360°	>360°	>360°	>360°	>360°	>360°	>360°
			G_6	>360°	>360°	>360°	>360°	>360°	>360°	>360°

Table 9B.15 – Influence Coefficients for a Circumferential Semi-Elliptical Surface Crack in a Cylinder – Outside Surface

t/R_i	a/c	a/t	G_i	A_0	A_1	A_2	A_3	A_4	A_5	A_6
1.0 (1/1)	0.25	0	G_0	0.6152816	-0.3348694	6.2955620	-15.590618	19.299508	-12.488107	3.3010035
			G_1	0.0703566	0.2828152	1.4036169	-0.6511596	-1.2076596	1.0318656	-0.2423741
			G_5	0.6152816	-0.3348694	6.2955620	-15.590618	19.299508	-12.488107	3.3010035
			G_6	0.0000000	0.0000000	0.0000000	0.0000000	0.0000000	0.0000000	0.0000000
		0.2	G_0	0.642203	-0.591017	9.407568	-26.226017	36.409149	-25.675756	7.218564
			G_1	0.078493	0.177371	2.330308	-3.464707	2.962435	-1.968066	0.592190
			G_5	0.597175	-0.189487	5.008770	-11.161526	11.798820	-5.962328	1.009192
			G_6	-0.205419	0.146389	-2.243008	6.434774	-6.973531	3.500426	-0.657197
		0.4	G_0	0.716921	-0.671910	10.581040	-28.785449	39.785482	-28.136590	7.918208
			G_1	0.098922	0.182456	2.554512	-3.835006	3.397113	-2.316700	0.702704
			G_5	0.526799	0.056523	3.278685	-5.527425	5.514782	-3.664674	1.036028
			G_6	-0.409426	0.298796	-4.137143	11.535049	-12.197372	6.092473	-1.179321
		0.6	G_0	0.772005	-0.557388	11.132743	-28.559682	39.226360	-28.451164	8.241971
			G_1	0.112555	0.231377	2.699926	-3.658122	3.087772	-2.331284	0.776799
			G_5	0.370724	0.263209	2.357866	-1.490640	1.511231	-2.953498	1.372598
			G_6	-0.600582	0.397934	-5.699708	15.169907	-15.275139	7.587635	-1.577963
		0.8	G_0	0.780413	-0.173354	10.848313	-23.187026	30.543124	-23.653595	7.382764
			G_1	0.110836	0.346095	2.730669	-2.344297	1.081502	-1.390964	0.645274
			G_5	0.128573	0.501983	1.925075	1.527162	1.152650	-7.191812	3.758399
			G_6	-0.766888	0.369485	-6.610261	14.691242	-9.580139	1.675853	0.221636
1.0 (1/1)	0.50	0	G_0	0.8776607	-0.6729719	3.7721411	-6.5209060	6.3377934	-3.7028038	0.9872447
			G_1	0.1277541	0.4368502	0.4904522	1.0427434	-2.9631236	2.0826525	-0.5184313
			G_5	0.8776607	-0.6729719	3.7721411	-6.5209060	6.3377934	-3.7028038	0.9872447
			G_6	0.0000000	0.0000000	0.0000000	0.0000000	0.0000000	0.0000000	0.0000000
		0.2	G_0	0.895170	-0.745369	4.991207	-10.772758	12.818511	-8.330682	2.252615
			G_1	0.133206	0.368555	1.052939	-0.577089	-0.802806	0.676996	-0.152642
			G_5	0.857575	-0.657613	3.859075	-5.815975	2.702688	1.091876	-1.012435
			G_6	-0.130280	0.145817	-0.622182	1.445699	-1.230356	0.432131	-0.038434
		0.4	G_0	0.980306	-0.758597	5.362770	-11.571932	13.258488	-8.163748	2.097123
			G_1	0.159022	0.366166	1.223342	-1.051170	-0.281608	0.410020	-0.097312
			G_5	0.900766	-0.541544	3.245547	-6.472677	7.199266	-4.184981	0.897910
			G_6	-0.259540	0.288675	-1.208585	3.025827	-2.839288	1.112566	-0.116170
		0.6	G_0	1.113120	-0.750256	6.040810	-14.499960	18.926659	-13.396328	3.926543
			G_1	0.197796	0.371590	1.366604	-1.254617	-0.377874	0.666404	-0.193564
			G_5	0.935033	-0.559150	2.730464	0.819428	-13.454191	17.775072	-7.146293
			G_6	-0.387632	0.415403	-1.612910	4.289826	-4.322402	1.886297	-0.264422
		0.8	G_0	1.280489	-0.589927	5.881083	-11.951889	11.510151	-5.933053	1.389378
			G_1	0.245759	0.428715	1.362974	-0.810840	-1.703275	1.905925	-0.573148
			G_5	0.970075	-0.060126	1.053885	0.829069	-3.987165	2.842479	-0.452050
			G_6	-0.518779	0.542636	-2.000866	5.598763	-5.721481	2.349674	-0.246534

Table 9B.15 – Influence Coefficients for a Circumferential Semi-Elliptical Surface Crack in a Cylinder – Outside Surface

t/R_i	a/c	a/t	G_i	A_0	A_1	A_2	A_3	A_4	A_5	A_6
1.0 (1/1)	1.0	0	G_0	1.1977992	-0.5244870	0.1498299	2.3284866	-5.1058499	4.3469049	-1.3487980
			G_1	0.1870117	0.6987352	0.1316900	0.7269255	-2.5259384	2.1756251	-0.6540458
			G_5	1.1977992	-0.5244870	0.1498299	2.3284866	-5.1058499	4.3469049	-1.3487980
			G_6	0.0000000	0.0000000	0.0000000	0.0000000	0.0000000	0.0000000	0.0000000
		0.2	G_0	1.216988	-0.884321	2.937341	-6.400540	7.830685	-5.009303	1.330252
			G_1	0.187037	0.610481	0.792272	-1.104000	-0.275137	0.812769	-0.307562
			G_5	1.182886	-0.835082	2.174227	-3.937059	3.613834	-1.384165	0.105864
			G_6	-0.076840	0.117823	-0.376402	1.029985	-1.287340	0.780511	-0.185806
		0.4	G_0	1.267648	-0.867212	2.971680	-6.610152	7.694060	-4.606490	1.177332
			G_1	0.199251	0.626331	0.703413	-0.529063	-1.682994	2.074106	-0.680039
			G_5	1.203098	-0.824141	1.496227	-0.962097	-2.391329	3.970122	-1.624243
			G_6	-0.151378	0.227897	-0.664339	1.889576	-2.430470	1.473029	-0.341702
		0.6	G_0	1.346752	-0.855553	2.861587	-6.257117	6.610069	-3.566047	0.893401
			G_1	0.219786	0.625261	0.725340	-0.507528	-1.851573	2.078951	-0.586744
			G_5	1.249657	-0.882507	1.802534	-4.396143	6.497793	-5.146725	1.687030
			G_6	-0.223726	0.332083	-0.837231	2.461713	-3.241110	1.945461	-0.434041
		0.8	G_0	1.452767	-0.837935	2.467001	-4.490136	2.796140	-0.426842	0.067437
			G_1	0.244401	0.631729	0.656894	0.004686	-2.970157	2.823204	-0.694572
			G_5	1.299952	-0.969162	2.328826	-6.998699	10.534412	-7.746337	2.285366
			G_6	-0.295422	0.443427	-0.971428	2.972785	-4.060981	2.453585	-0.538396
1.0 (1/1)	2.0	0	G_0	0.8150546	-0.5623828	1.4465771	-4.6778133	8.4192164	-7.9025932	2.9866351
			G_1	0.1359146	0.0702340	3.5558581	-11.034445	16.967724	-14.126991	4.8706612
			G_5	0.8150546	-0.5623828	1.4465771	-4.6778133	8.4192164	-7.9025932	2.9866351
			G_6	0.0000000	0.0000000	0.0000000	0.0000000	0.0000000	0.0000000	0.0000000
		0.2	G_0	0.820072	-0.533658	0.890602	-1.724605	1.638909	-1.139743	0.518042
			G_1	0.103873	0.548918	0.341865	-0.367842	-1.318218	1.260911	-0.190080
			G_5	0.795584	-0.521223	0.438534	-0.374874	-0.372261	0.479771	-0.032278
			G_6	-0.023871	0.050547	-0.194357	0.575648	-0.822423	0.595134	-0.176444
		0.4	G_0	0.829623	-0.557437	1.072062	-2.500268	3.120638	-2.572894	1.056904
			G_1	0.104690	0.534923	0.453443	-0.766164	-0.501827	0.344661	0.194263
			G_5	0.795840	-0.602703	0.590105	-1.049967	1.040653	-0.827483	0.415867
			G_6	-0.046402	0.091402	-0.303591	0.907021	-1.303663	0.926164	-0.265611
		0.6	G_0	0.843470	-0.577584	1.166860	-3.086424	4.458407	-4.027290	1.641687
			G_1	0.106668	0.514932	0.595145	-1.334138	0.722947	-1.011313	0.747720
			G_5	0.799070	-0.667599	0.598364	-1.332764	1.868519	-1.681591	0.723190
			G_6	-0.068334	0.134480	-0.393677	1.198434	-1.790210	1.302523	-0.377049
		0.8	G_0	0.862215	-0.614692	1.329916	-3.928620	6.255639	-5.888609	2.365042
			G_1	0.109085	0.486801	0.815164	-2.237327	2.620300	-2.994293	1.516129
			G_5	0.807039	-0.741798	0.593287	-1.506023	2.410195	-2.234824	0.921269
			G_6	-0.089734	0.179142	-0.452674	1.393734	-2.171409	1.624931	-0.477047

Table 9B.15 – Influence Coefficients for a Circumferential Semi-Elliptical Surface Crack in a Cylinder – Outside Surface

t/R_i	a/c	a/t	G_i	A_0	A_1	A_2	A_3	A_4	A_5	A_6
1.5 (1.5/1)	0.03125	0	G_0	>360°	>360°	>360°	>360°	>360°	>360°	>360°
			G_1	>360°	>360°	>360°	>360°	>360°	>360°	>360°
			G_5	>360°	>360°	>360°	>360°	>360°	>360°	>360°
			G_6	>360°	>360°	>360°	>360°	>360°	>360°	>360°
		0.2	G_0	>360°	>360°	>360°	>360°	>360°	>360°	>360°
			G_1	>360°	>360°	>360°	>360°	>360°	>360°	>360°
			G_5	>360°	>360°	>360°	>360°	>360°	>360°	>360°
			G_6	>360°	>360°	>360°	>360°	>360°	>360°	>360°
		0.4	G_0	>360°	>360°	>360°	>360°	>360°	>360°	>360°
			G_1	>360°	>360°	>360°	>360°	>360°	>360°	>360°
			G_5	>360°	>360°	>360°	>360°	>360°	>360°	>360°
			G_6	>360°	>360°	>360°	>360°	>360°	>360°	>360°
		0.6	G_0	>360°	>360°	>360°	>360°	>360°	>360°	>360°
			G_1	>360°	>360°	>360°	>360°	>360°	>360°	>360°
			G_5	>360°	>360°	>360°	>360°	>360°	>360°	>360°
			G_6	>360°	>360°	>360°	>360°	>360°	>360°	>360°
		0.8	G_0	>360°	>360°	>360°	>360°	>360°	>360°	>360°
			G_1	>360°	>360°	>360°	>360°	>360°	>360°	>360°
			G_5	>360°	>360°	>360°	>360°	>360°	>360°	>360°
			G_6	>360°	>360°	>360°	>360°	>360°	>360°	>360°
1.5 (1.5/1)	0.0625	0	G_0	0.2695332	2.1626001	-1.6551569	-1.2970208	4.5604304	-4.3163876	1.4010655
			G_1	0.0138667	0.1827458	2.5749608	-3.9044679	3.3556301	-2.1772209	0.6420134
			G_5	0.2695332	2.1626001	-1.6551569	-1.2970208	4.5604304	-4.3163876	1.4010655
			G_6	0.0000000	0.0000000	0.0000000	0.0000000	0.0000000	0.0000000	0.0000000
		0.2	G_0	0.244309	2.466376	-3.157444	3.645765	-2.264582	0.132711	0.218572
			G_1	0.007399	0.212887	2.387620	-3.171574	2.627572	-1.931601	0.612685
			G_5	-0.067669	-1.030374	3.259752	-2.287097	9.982790	-13.492740	4.806477
			G_6	-0.221174	-2.673058	4.713841	-10.105322	13.492672	-4.184595	-1.024783
		0.4	G_0	>360°	>360°	>360°	>360°	>360°	>360°	>360°
			G_1	>360°	>360°	>360°	>360°	>360°	>360°	>360°
			G_5	>360°	>360°	>360°	>360°	>360°	>360°	>360°
			G_6	>360°	>360°	>360°	>360°	>360°	>360°	>360°
		0.6	G_0	>360°	>360°	>360°	>360°	>360°	>360°	>360°
			G_1	>360°	>360°	>360°	>360°	>360°	>360°	>360°
			G_5	>360°	>360°	>360°	>360°	>360°	>360°	>360°
			G_6	>360°	>360°	>360°	>360°	>360°	>360°	>360°
		0.8	G_0	>360°	>360°	>360°	>360°	>360°	>360°	>360°
			G_1	>360°	>360°	>360°	>360°	>360°	>360°	>360°
			G_5	>360°	>360°	>360°	>360°	>360°	>360°	>360°
			G_6	>360°	>360°	>360°	>360°	>360°	>360°	>360°

Table 9B.15 – Influence Coefficients for a Circumferential Semi-Elliptical Surface Crack in a Cylinder – Outside Surface

t/R_i	a/c	a/t	G_i	A_0	A_1	A_2	A_3	A_4	A_5	A_6
1.5 (1.5/1)	0.125	0	G_0	0.4065238	0.7772483	3.8861644	-12.573943	16.760207	-11.014593	2.8706957
			G_1	0.0320270	0.1825342	2.2670449	-2.7076615	1.2088194	-0.3777430	0.0763155
			G_5	0.4065238	0.7772483	3.8861644	-12.573943	16.760207	-11.014593	2.8706957
			G_6	0.0000000	0.0000000	0.0000000	0.0000000	0.0000000	0.0000000	0.0000000
		0.2	G_0	0.934128	4.697086	-17.361149	27.237992	-20.847359	6.191749	0.934128
			G_1	0.203449	2.501921	-3.755076	3.443494	-2.461267	0.766651	0.203449
			G_5	0.448914	3.087923	-7.070942	9.411067	-6.757007	1.768642	0.448914
			G_6	-0.931483	-1.454120	8.187521	-10.115515	6.349177	-1.734557	-0.931483
		0.4	G_0	0.491419	7.607231	-24.366627	39.524989	-31.792549	9.738286	0.491419
			G_1	0.185848	2.537753	-3.281802	3.464665	-3.143065	1.074491	0.185848
			G_5	-0.074904	-0.824725	8.001586	-2.888848	-5.843260	3.077302	-0.074904
			G_6	-0.824346	-4.361047	11.400758	-12.679390	11.797668	-4.899369	-0.824346
		0.6	G_0	0.360003	6.732286	-20.285509	40.250788	-37.078281	11.923697	0.360003
			G_1	-1.360254	10.319252	-23.701078	34.942503	-27.251486	8.060240	-1.360254
			G_5	-1.123870	-1.516707	2.967728	25.407465	-34.543476	10.974648	-1.123870
			G_6	-0.521150	-3.812601	-1.530481	-5.157112	27.353115	-16.105408	-0.521150
		0.8	G_0	>360°	>360°	>360°	>360°	>360°	>360°	>360°
			G_1	>360°	>360°	>360°	>360°	>360°	>360°	>360°
			G_5	>360°	>360°	>360°	>360°	>360°	>360°	>360°
			G_6	>360°	>360°	>360°	>360°	>360°	>360°	>360°
1.5 (1.5/1)	0.25	0	G_0	0.6152816	-0.3348694	6.2955620	-15.590618	19.299508	-12.488107	3.3010035
			G_1	0.0703566	0.2828152	1.4036169	-0.6511596	-1.2076596	1.0318656	-0.2423741
			G_5	0.6152816	-0.3348694	6.2955620	-15.590618	19.299508	-12.488107	3.3010035
			G_6	0.0000000	0.0000000	0.0000000	0.0000000	0.0000000	0.0000000	0.0000000
		0.2	G_0	0.643234	-0.519794	8.840914	-24.342219	33.579698	-23.696622	6.691108
			G_1	0.078321	0.189997	2.265215	-3.257390	2.657137	-1.758057	0.536719
			G_5	0.572518	-0.263719	6.141599	-15.135805	17.718445	-9.894333	1.956311
			G_6	-0.244765	0.152225	-2.449150	6.917711	-7.153994	3.327685	-0.547192
		0.4	G_0	0.711073	-0.493332	9.505373	-25.346688	34.719186	-24.623729	6.978427
			G_1	0.097626	0.196166	2.554600	-3.797668	3.353763	-2.318730	0.712440
			G_5	0.469463	-0.419338	6.676024	-14.716328	17.504519	-10.858870	2.556001
			G_6	-0.471585	0.289235	-4.421912	12.292908	-12.811850	6.407745	-1.281585
		0.6	G_0	0.738419	-0.349896	10.620221	-27.271195	38.655595	-29.198179	8.742946
			G_1	0.102578	0.272682	2.618383	-3.217368	2.519548	-2.075710	0.742662
			G_5	0.240392	0.025666	2.388526	2.640792	-8.215843	6.151896	-1.793005
			G_6	-0.662228	0.328048	-5.941392	15.545000	-15.135962	7.548923	-1.680522
		0.8	G_0	0.633272	0.191366	9.635282	-17.860726	24.478675	-21.439248	7.261653
			G_1	0.062674	0.463875	2.260488	-0.191016	-1.688785	-0.031327	0.419193
			G_5	-0.149711	0.897143	-2.080685	16.226423	-19.459345	6.057525	0.368673
			G_6	-0.831514	0.260178	-6.970555	13.466600	-5.018823	-1.991211	1.085739

Table 9B.15 – Influence Coefficients for a Circumferential Semi-Elliptical Surface Crack in a Cylinder – Outside Surface

t/R_i	a/c	a/t	G_i	A_0	A_1	A_2	A_3	A_4	A_5	A_6
1.5 (1.5/1)	0.50	0	G_0	0.8776607	-0.6729719	3.7721411	-6.5209060	6.3377934	-3.7028038	0.9872447
			G_1	0.1277541	0.4368502	0.4904522	1.0427434	-2.9631236	2.0826525	-0.5184313
			G_5	0.8776607	-0.6729719	3.7721411	-6.5209060	6.3377934	-3.7028038	0.9872447
			G_6	0.0000000	0.0000000	0.0000000	0.0000000	0.0000000	0.0000000	0.0000000
		0.2	G_0	0.983478	-0.637437	4.745461	-9.947368	11.204734	-7.005326	1.877543
			G_1	0.159305	0.391583	1.148714	-0.834729	-0.661140	0.712346	-0.183603
			G_5	0.873224	-0.661696	4.923891	-11.791861	13.948271	-7.710853	1.444908
			G_6	-0.307576	0.323756	-1.289001	3.259921	-3.000563	1.102352	-0.085449
		0.4	G_0	1.120359	-0.671356	6.499562	-16.370106	21.575812	-15.059969	4.311617
			G_1	0.199440	0.411780	1.331732	-1.172688	-0.592782	0.844440	-0.234067
			G_5	0.888202	-0.120639	-0.400064	9.105764	-22.074089	20.388943	-6.698464
			G_6	-0.453128	0.470675	-1.847450	5.224087	-5.613451	2.650393	-0.426860
		0.6	G_0	1.298817	-0.183319	4.438347	-7.676958	5.059233	-1.594927	0.356679
			G_1	0.251006	0.507020	1.258388	-0.380135	-2.599679	2.550437	-0.704912
			G_5	0.896163	-0.379211	4.951513	-9.579768	7.326591	-1.864988	-0.156262
			G_6	-0.597760	0.573901	-1.980767	5.831218	-5.876313	2.158679	-0.105614
		0.8	G_0	0.896742	-0.723168	4.970579	-10.820133	12.922809	-8.406209	2.273033
			G_1	0.133509	0.378231	1.025672	-0.531811	-0.833924	0.667254	-0.138491
			G_5	0.853533	-0.568458	3.141223	-4.171455	1.482985	0.950411	-0.669691
			G_6	-0.155570	0.168085	-0.709073	1.665531	-1.406535	0.468225	-0.028228
1.5 (1.5/1)	1.0	0	G_0	1.1977992	-0.5244870	0.1498299	2.3284866	-5.1058499	4.3469049	-1.3487980
			G_1	0.1870117	0.6987352	0.1316900	0.7269255	-2.5259384	2.1756251	-0.6540458
			G_5	1.1977992	-0.5244870	0.1498299	2.3284866	-5.1058499	4.3469049	-1.3487980
			G_6	0.0000000	0.0000000	0.0000000	0.0000000	0.0000000	0.0000000	0.0000000
		0.2	G_0	1.217809	-0.860622	2.868641	-6.259973	7.555429	-4.750153	1.246484
			G_1	0.186734	0.617158	0.770903	-0.999736	-0.528553	1.044189	-0.377516
			G_5	1.176882	-0.765000	1.467445	-1.146847	-1.628867	3.199765	-1.399288
			G_6	-0.091576	0.132498	-0.394281	1.083396	-1.335176	0.786422	-0.179343
		0.4	G_0	1.268002	-0.814545	2.844085	-6.329234	7.105454	-4.079007	1.023942
			G_1	0.198158	0.647266	0.620156	-0.243836	-2.191515	2.425091	-0.750887
			G_5	1.191112	-0.718965	0.814378	0.251373	-2.760564	3.096456	-1.037188
			G_6	-0.180045	0.264250	-0.715443	2.064619	-2.666524	1.595044	-0.359277
		0.6	G_0	1.347624	-0.764540	2.703343	-5.984825	6.014451	-3.113648	0.816716
			G_1	0.218449	0.644734	0.706644	-0.379585	-2.204115	2.303890	-0.599527
			G_5	1.228937	-0.871353	1.917320	-5.234064	7.697250	-5.674633	1.693182
			G_6	-0.265435	0.391695	-0.909937	2.769403	-3.749861	2.272171	-0.504897
		0.8	G_0	1.458000	-0.627682	1.659737	-2.665548	0.644863	0.344716	0.187250
			G_1	0.243250	0.678287	0.492849	0.473512	-3.551262	2.838634	-0.505125
			G_5	1.260266	-0.967693	2.795534	-7.534121	8.183348	-3.364214	0.284941
			G_6	-0.347949	0.519695	-0.973242	3.101215	-4.364920	2.624754	-0.555997

Table 9B.15 – Influence Coefficients for a Circumferential Semi-Elliptical Surface Crack in a Cylinder – Outside Surface

t/R_i	a/c	a/t	G_i	A_0	A_1	A_2	A_3	A_4	A_5	A_6
1.5 (1.5/1)	2.0	0	G_0	0.8150546	-0.5623828	1.4465771	-4.6778133	8.4192164	-7.9025932	2.9866351
			G_1	0.1359146	0.0702340	3.5558581	-11.034445	16.967724	-14.126991	4.8706612
			G_5	0.8150546	-0.5623828	1.4465771	-4.6778133	8.4192164	-7.9025932	2.9866351
			G_6	0.0000000	0.0000000	0.0000000	0.0000000	0.0000000	0.0000000	0.0000000
		0.2	G_0	0.819435	-0.528462	0.879297	-1.744264	1.737595	-1.291108	0.591296
			G_1	0.103374	0.547820	0.357172	-0.431293	-1.169658	1.075091	-0.107267
			G_5	0.793164	-0.529666	0.419197	-0.322203	-0.432511	0.507169	-0.034484
			G_6	-0.028315	0.056066	-0.202357	0.599888	-0.849730	0.604994	-0.176348
		0.4	G_0	0.828020	-0.549839	1.083638	-2.692100	3.618497	-3.147098	1.294347
			G_1	0.103627	0.530280	0.507724	-1.000148	0.013483	-0.229694	0.429132
			G_5	0.790611	-0.617111	0.574791	-1.112962	1.291431	-1.114043	0.525202
			G_6	-0.055114	0.106023	-0.329168	0.993856	-1.448051	1.033471	-0.295749
		0.6	G_0	0.840949	-0.571295	1.252843	-3.683858	5.798729	-5.405785	2.164704
			G_1	0.105141	0.502777	0.727283	-1.907060	1.927853	-2.257699	1.226569
			G_5	0.790837	-0.687727	0.631696	-1.732733	2.835524	-2.602511	1.036609
			G_6	-0.081083	0.159278	-0.424910	1.307167	-2.001868	1.476853	-0.429328
		0.8	G_0	0.859385	-0.613837	1.532800	-5.125289	8.758127	-8.288419	3.221896
			G_1	0.107398	0.462912	1.060175	-3.309948	4.804572	-5.139206	2.301687
			G_5	0.794138	-0.734263	0.388965	-1.393586	2.920660	-3.001593	1.228697
			G_6	-0.106325	0.214844	-0.476064	1.481993	-2.403679	1.841543	-0.545415
2.0 (2/1)	0.03125	0	G_0	>360°	>360°	>360°	>360°	>360°	>360°	>360°
			G_1	>360°	>360°	>360°	>360°	>360°	>360°	>360°
			G_5	>360°	>360°	>360°	>360°	>360°	>360°	>360°
			G_6	>360°	>360°	>360°	>360°	>360°	>360°	>360°
		0.2	G_0	>360°	>360°	>360°	>360°	>360°	>360°	>360°
			G_1	>360°	>360°	>360°	>360°	>360°	>360°	>360°
			G_5	>360°	>360°	>360°	>360°	>360°	>360°	>360°
			G_6	>360°	>360°	>360°	>360°	>360°	>360°	>360°
		0.4	G_0	>360°	>360°	>360°	>360°	>360°	>360°	>360°
			G_1	>360°	>360°	>360°	>360°	>360°	>360°	>360°
			G_5	>360°	>360°	>360°	>360°	>360°	>360°	>360°
			G_6	>360°	>360°	>360°	>360°	>360°	>360°	>360°
		0.6	G_0	>360°	>360°	>360°	>360°	>360°	>360°	>360°
			G_1	>360°	>360°	>360°	>360°	>360°	>360°	>360°
			G_5	>360°	>360°	>360°	>360°	>360°	>360°	>360°
			G_6	>360°	>360°	>360°	>360°	>360°	>360°	>360°
		0.8	G_0	>360°	>360°	>360°	>360°	>360°	>360°	>360°
			G_1	>360°	>360°	>360°	>360°	>360°	>360°	>360°
			G_5	>360°	>360°	>360°	>360°	>360°	>360°	>360°
			G_6	>360°	>360°	>360°	>360°	>360°	>360°	>360°

Table 9B.15 – Influence Coefficients for a Circumferential Semi-Elliptical Surface Crack in a Cylinder – Outside Surface

t/R_i	a/c	a/t	G_i	A_0	A_1	A_2	A_3	A_4	A_5	A_6
2.0 (2/1)	0.0625	0	G_0	0.2695332	2.1626001	-1.6551569	-1.2970208	4.5604304	-4.3163876	1.4010655
			G_1	0.0138667	0.1827458	2.5749608	-3.9044679	3.3556301	-2.1772209	0.6420134
			G_5	0.2695332	2.1626001	-1.6551569	-1.2970208	4.5604304	-4.3163876	1.4010655
			G_6	0.0000000	0.0000000	0.0000000	0.0000000	0.0000000	0.0000000	0.0000000
		0.2	G_0	2.495049	-3.487719	4.840795	-4.040595	1.385195	-0.134425	2.495049
			G_1	0.199326	2.416546	-3.185959	2.678518	-2.004195	0.638991	0.199326
			G_5	-1.852411	6.009866	-9.102339	21.088995	-21.909464	7.032883	-1.852411
			G_6	-2.535124	4.628582	-11.953745	15.463749	-3.422560	-1.986421	-2.535124
		0.4	G_0	>360°	>360°	>360°	>360°	>360°	>360°	>360°
			G_1	>360°	>360°	>360°	>360°	>360°	>360°	>360°
			G_5	>360°	>360°	>360°	>360°	>360°	>360°	>360°
			G_6	>360°	>360°	>360°	>360°	>360°	>360°	>360°
		0.6	G_0	>360°	>360°	>360°	>360°	>360°	>360°	>360°
			G_1	>360°	>360°	>360°	>360°	>360°	>360°	>360°
			G_5	>360°	>360°	>360°	>360°	>360°	>360°	>360°
			G_6	>360°	>360°	>360°	>360°	>360°	>360°	>360°
		0.8	G_0	>360°	>360°	>360°	>360°	>360°	>360°	>360°
			G_1	>360°	>360°	>360°	>360°	>360°	>360°	>360°
			G_5	>360°	>360°	>360°	>360°	>360°	>360°	>360°
			G_6	>360°	>360°	>360°	>360°	>360°	>360°	>360°
2.0 (2/1)	0.125	0	G_0	0.4065238	0.7772483	3.8861644	-12.573943	16.760207	-11.014593	2.8706957
			G_1	0.0320270	0.1825342	2.2670449	-2.7076615	1.2088194	-0.3777430	0.0763155
			G_5	0.4065238	0.7772483	3.8861644	-12.573943	16.760207	-11.014593	2.8706957
			G_6	0.0000000	0.0000000	0.0000000	0.0000000	0.0000000	0.0000000	0.0000000
		0.2	G_0	0.403671	0.953985	4.788497	-17.979409	28.647710	-22.195487	6.652757
			G_1	0.032467	0.208078	2.476581	-3.654324	3.305165	-2.378477	0.747152
			G_5	0.237826	0.303551	2.607992	-3.731791	3.674248	-2.537343	0.594392
			G_6	-0.319569	-1.040926	-1.322684	7.857416	-9.379192	5.833343	-1.626588
		0.4	G_0	0.375386	0.552242	6.880293	-21.777542	36.104206	-29.679867	9.193728
			G_1	0.012627	0.176960	2.461409	-2.884253	3.027434	-2.957622	1.038923
			G_5	-0.211156	-0.672257	0.896684	4.024819	4.244158	-11.590322	4.614143
			G_6	-0.411726	-0.886423	-3.789361	7.919580	-8.022952	10.383710	-5.194411
		0.6	G_0	>360°	>360°	>360°	>360°	>360°	>360°	>360°
			G_1	>360°	>360°	>360°	>360°	>360°	>360°	>360°
			G_5	>360°	>360°	>360°	>360°	>360°	>360°	>360°
			G_6	>360°	>360°	>360°	>360°	>360°	>360°	>360°
		0.8	G_0	>360°	>360°	>360°	>360°	>360°	>360°	>360°
			G_1	>360°	>360°	>360°	>360°	>360°	>360°	>360°
			G_5	>360°	>360°	>360°	>360°	>360°	>360°	>360°
			G_6	>360°	>360°	>360°	>360°	>360°	>360°	>360°

Table 9B.15 – Influence Coefficients for a Circumferential Semi-Elliptical Surface Crack in a Cylinder – Outside Surface

t/R_i	a/c	a/t	G_i	A_0	A_1	A_2	A_3	A_4	A_5	A_6
2.0 (2/1)	0.25	0	G_0	0.6152816	-0.3348694	6.2955620	-15.590618	19.299508	-12.488107	3.3010035
			G_1	0.0703566	0.2828152	1.4036169	-0.6511596	-1.2076596	1.0318656	-0.2423741
			G_5	0.6152816	-0.3348694	6.2955620	-15.590618	19.299508	-12.488107	3.3010035
			G_6	0.0000000	0.0000000	0.0000000	0.0000000	0.0000000	0.0000000	0.0000000
		0.2	G_0	0.644901	-0.520151	8.984654	-25.081396	35.169072	-25.200078	7.208586
			G_1	0.078472	0.188951	2.315210	-3.451959	3.008918	-2.057087	0.632547
			G_5	0.552343	-0.215641	5.869658	-13.727943	14.498444	-6.690732	0.806327
			G_6	-0.270114	0.162003	-2.660832	7.560643	-7.900853	3.771564	-0.659927
		0.4	G_0	0.708230	-0.481973	10.001095	-27.536860	38.979180	-28.396869	8.215713
			G_1	0.096826	0.213382	2.508375	-3.615957	3.086004	-2.148692	0.670914
			G_5	0.425687	-0.196560	3.679836	-2.903585	-2.272016	4.424191	-1.943944
			G_6	-0.507491	0.288696	-4.805064	13.631496	-14.749922	7.891444	-1.746237
		0.6	G_0	0.710168	-0.249490	10.021922	-23.913354	32.613019	-24.387461	7.258058
			G_1	0.091842	0.310703	2.490269	-2.577811	1.586499	-1.510822	0.610236
			G_5	0.101299	0.432677	1.167085	2.398617	-1.100307	-3.739478	2.198523
			G_6	-0.702710	0.339768	-6.231491	15.263008	-13.173098	5.558127	-1.051481
		0.8	G_0	0.460782	0.650182	7.368339	-9.320670	13.574515	-15.734917	6.187175
			G_1	0.007358	0.577315	1.725194	2.093667	-4.591023	1.377486	0.197229
			G_5	-0.332955	0.535391	-0.724945	14.890208	-17.525185	4.069720	0.998219
			G_6	-0.881593	0.084862	-6.910293	11.487902	-0.180830	-5.296292	1.695338
2.0 (2/1)	0.5	0	G_0	0.8776607	-0.6729719	3.7721411	-6.5209060	6.3377934	-3.7028038	0.9872447
			G_1	0.1277541	0.4368502	0.4904522	1.0427434	-2.9631236	2.0826525	-0.5184313
			G_5	0.8776607	-0.6729719	3.7721411	-6.5209060	6.3377934	-3.7028038	0.9872447
			G_6	0.0000000	0.0000000	0.0000000	0.0000000	0.0000000	0.0000000	0.0000000
		0.2	G_0	0.898006	-0.708281	4.964654	-10.874859	13.021276	-8.474461	2.291230
			G_1	0.133920	0.380123	1.053640	-0.670154	-0.573202	0.441053	-0.063929
			G_5	0.851484	-0.537869	2.953335	-4.069142	2.074902	0.034983	-0.294659
			G_6	-0.172305	0.184486	-0.783857	1.884721	-1.660577	0.608594	-0.058619
		0.4	G_0	0.988868	-0.611897	4.935197	-11.143346	13.756121	-9.376212	2.686712
			G_1	0.160419	0.397915	1.204781	-1.061381	-0.305994	0.438966	-0.098551
			G_5	0.850924	-0.565679	4.158315	-7.731637	4.700313	1.365704	-1.761789
			G_6	-0.338468	0.348927	-1.372766	3.555641	-3.367668	1.304910	-0.127128
		0.6	G_0	1.133755	-0.538422	5.653084	-12.581715	13.923038	-8.176993	2.032520
			G_1	0.202815	0.440499	1.261605	-0.843488	-1.316754	1.484798	-0.431488
			G_5	0.849968	-0.069906	1.343760	-1.184919	0.118486	-0.368374	0.396096
			G_6	-0.495592	0.511954	-1.951133	5.498686	-5.707081	2.434968	-0.287480
		0.8	G_0	1.320717	-0.043912	5.156075	-10.916628	10.972936	-6.903365	2.205768
			G_1	0.256591	0.573514	1.131253	0.118589	-3.508726	3.135079	-0.802789
			G_5	0.848206	0.098670	0.632586	7.318856	-21.969851	21.288313	-7.012517
			G_6	-0.646440	0.597990	-2.114737	6.617607	-7.002899	2.750062	-0.198201

Table 9B.15 – Influence Coefficients for a Circumferential Semi-Elliptical Surface Crack in a Cylinder – Outside Surface

t/R_i	a/c	a/t	G_i	A_0	A_1	A_2	A_3	A_4	A_5	A_6
2.0 (2/1)	1.0	0	G_0	1.1977992	-0.5244870	0.1498299	2.3284866	-5.1058499	4.3469049	-1.3487980
			G_1	0.1870117	0.6987352	0.1316900	0.7269255	-2.5259384	2.1756251	-0.6540458
			G_5	1.1977992	-0.5244870	0.1498299	2.3284866	-5.1058499	4.3469049	-1.3487980
			G_6	0.0000000	0.0000000	0.0000000	0.0000000	0.0000000	0.0000000	0.0000000
		0.2	G_0	1.218534	-0.845119	2.824572	-6.168247	7.371567	-4.577082	1.191116
			G_1	0.186586	0.621632	0.755873	-0.926404	-0.703472	1.201403	-0.424248
			G_5	1.174192	-0.783461	1.672492	-1.988049	-0.116965	1.913706	-0.977747
			G_6	-0.101362	0.143627	-0.417102	1.162574	-1.448288	0.860074	-0.197590
		0.4	G_0	1.269512	-0.779909	2.761399	-6.144328	6.715548	-3.739290	0.930554
			G_1	0.198046	0.653032	0.635397	-0.306066	-2.101713	2.310490	-0.689329
			G_5	1.186510	-0.753833	1.314848	-2.380365	2.726539	-1.952217	0.673764
			G_6	-0.198910	0.287802	-0.735748	2.136243	-2.752614	1.617861	-0.351996
		0.6	G_0	1.352910	-0.693363	2.345919	-4.703960	3.626191	-1.195959	0.277190
			G_1	0.218422	0.666409	0.594177	0.078894	-3.054549	2.911874	-0.734521
			G_5	1.210770	-0.818645	1.970500	-6.057953	9.050650	-6.450074	1.814528
			G_6	-0.292769	0.431906	-0.928747	2.839062	-3.827600	2.252012	-0.470683
		0.8	G_0	1.469948	-0.576148	1.929694	-4.483673	4.545563	-3.595386	1.687504
			G_1	0.244554	0.685341	0.591036	-0.015629	-2.440050	1.505846	0.077572
			G_5	1.234619	-0.846149	2.011291	-3.957121	0.238591	4.254626	-2.327353
			G_6	-0.381574	0.574578	-0.995862	3.309023	-4.842983	2.989497	-0.649145
2.0 (2/1)	2.0	0	G_0	0.8150546	-0.5623828	1.4465771	-4.6778133	8.4192164	-7.9025932	2.9866351
			G_1	0.1359146	0.0702340	3.5558581	-11.034445	16.967724	-14.126991	4.8706612
			G_5	0.8150546	-0.5623828	1.4465771	-4.6778133	8.4192164	-7.9025932	2.9866351
			G_6	0.0000000	0.0000000	0.0000000	0.0000000	0.0000000	0.0000000	0.0000000
		0.2	G_0	0.819045	-0.525260	0.873864	-1.766595	1.822345	-1.410010	0.646434
			G_1	0.103057	0.546891	0.369004	-0.480904	-1.055277	0.936446	-0.046843
			G_5	0.791409	-0.533255	0.398655	-0.291840	-0.415713	0.443800	-0.000710
			G_6	-0.031259	0.059835	-0.207486	0.615621	-0.868503	0.612810	-0.176846
		0.4	G_0	0.827253	-0.546276	1.102491	-2.867149	4.042184	-3.612309	1.480127
			G_1	0.103021	0.526251	0.551630	-1.189796	0.424505	-0.674787	0.606846
			G_5	0.787293	-0.629238	0.597469	-1.299976	1.736295	-1.546495	0.676465
			G_6	-0.060870	0.116382	-0.347756	1.058887	-1.562290	1.123060	-0.322185
		0.6	G_0	0.840071	-0.570913	1.337019	-4.194349	6.899480	-6.498881	2.567444
			G_1	0.104359	0.493291	0.824310	-2.331766	2.818589	-3.168079	1.571706
			G_5	0.786357	-0.707723	0.668295	-2.023112	3.528411	-3.273780	1.270016
			G_6	-0.089477	0.176372	-0.441043	1.363766	-2.124745	1.582744	-0.461542
		0.8	G_0	0.858904	-0.619034	1.702378	-6.057041	10.627234	-10.006984	3.812187
			G_1	0.106637	0.441967	1.261125	-4.158405	6.458577	-6.694246	2.850570
			G_5	0.786106	-0.746891	0.397980	-1.790126	3.920114	-3.899015	1.504538
			G_6	-0.117268	0.242207	-0.510527	1.623058	-2.734187	2.149863	-0.646318

Table 9B.15 – Influence Coefficients for a Circumferential Semi-Elliptical Surface Crack in a Cylinder – Outside Surface

t/R_i	a/c	a/t	G_i	A_0	A_1	A_2	A_3	A_4	A_5	A_6
2.5 (2.5/1)	0.03125	0	G_0	>360°	>360°	>360°	>360°	>360°	>360°	>360°
			G_1	>360°	>360°	>360°	>360°	>360°	>360°	>360°
			G_5	>360°	>360°	>360°	>360°	>360°	>360°	>360°
			G_6	>360°	>360°	>360°	>360°	>360°	>360°	>360°
		0.2	G_0	>360°	>360°	>360°	>360°	>360°	>360°	>360°
			G_1	>360°	>360°	>360°	>360°	>360°	>360°	>360°
			G_5	>360°	>360°	>360°	>360°	>360°	>360°	>360°
			G_6	>360°	>360°	>360°	>360°	>360°	>360°	>360°
		0.4	G_0	>360°	>360°	>360°	>360°	>360°	>360°	>360°
			G_1	>360°	>360°	>360°	>360°	>360°	>360°	>360°
			G_5	>360°	>360°	>360°	>360°	>360°	>360°	>360°
			G_6	>360°	>360°	>360°	>360°	>360°	>360°	>360°
		0.6	G_0	>360°	>360°	>360°	>360°	>360°	>360°	>360°
			G_1	>360°	>360°	>360°	>360°	>360°	>360°	>360°
			G_5	>360°	>360°	>360°	>360°	>360°	>360°	>360°
			G_6	>360°	>360°	>360°	>360°	>360°	>360°	>360°
		0.8	G_0	>360°	>360°	>360°	>360°	>360°	>360°	>360°
			G_1	>360°	>360°	>360°	>360°	>360°	>360°	>360°
			G_5	>360°	>360°	>360°	>360°	>360°	>360°	>360°
			G_6	>360°	>360°	>360°	>360°	>360°	>360°	>360°
2.5 (2.5/1)	0.0625	0	G_0	0.2695332	2.1626001	-1.6551569	-1.2970208	4.5604304	-4.3163876	1.4010655
			G_1	0.0138667	0.1827458	2.5749608	-3.9044679	3.3556301	-2.1772209	0.6420134
			G_5	0.2695332	2.1626001	-1.6551569	-1.2970208	4.5604304	-4.3163876	1.4010655
			G_6	0.0000000	0.0000000	0.0000000	0.0000000	0.0000000	0.0000000	0.0000000
		0.2	G_0	0.236934	2.397311	-2.975954	3.478131	-1.954255	-0.211817	0.333398
			G_1	0.004615	0.187374	2.439765	-3.202290	2.742030	-2.086810	0.667886
			G_5	-0.149468	-1.880229	4.937598	-6.882432	20.785297	-23.236427	7.591803
			G_6	-0.179772	-2.297543	4.052476	-12.288204	15.596411	-1.946504	-2.940197
		0.4	G_0	>360°	>360°	>360°	>360°	>360°	>360°	>360°
			G_1	>360°	>360°	>360°	>360°	>360°	>360°	>360°
			G_5	>360°	>360°	>360°	>360°	>360°	>360°	>360°
			G_6	>360°	>360°	>360°	>360°	>360°	>360°	>360°
		0.6	G_0	>360°	>360°	>360°	>360°	>360°	>360°	>360°
			G_1	>360°	>360°	>360°	>360°	>360°	>360°	>360°
			G_5	>360°	>360°	>360°	>360°	>360°	>360°	>360°
			G_6	>360°	>360°	>360°	>360°	>360°	>360°	>360°
		0.8	G_0	>360°	>360°	>360°	>360°	>360°	>360°	>360°
			G_1	>360°	>360°	>360°	>360°	>360°	>360°	>360°
			G_5	>360°	>360°	>360°	>360°	>360°	>360°	>360°
			G_6	>360°	>360°	>360°	>360°	>360°	>360°	>360°

Table 9B.15 – Influence Coefficients for a Circumferential Semi-Elliptical Surface Crack in a Cylinder – Outside Surface

t/R_i	a/c	a/t	G_i	A_0	A_1	A_2	A_3	A_4	A_5	A_6
2.5 (2.5/1)	0.125	0	G_0	0.4065238	0.7772483	3.8861644	-12.573943	16.760207	-11.014593	2.8706957
			G_1	0.0320270	0.1825342	2.2670449	-2.7076615	1.2088194	-0.3777430	0.0763155
			G_5	0.4065238	0.7772483	3.8861644	-12.573943	16.760207	-11.014593	2.8706957
			G_6	0.0000000	0.0000000	0.0000000	0.0000000	0.0000000	0.0000000	0.0000000
		0.2	G_0	0.407435	0.864218	5.363353	-19.480826	30.678020	-23.562820	7.012419
			G_1	0.032373	0.204850	2.497989	-3.687878	3.354679	-2.423736	0.762053
			G_5	0.195170	0.572974	0.609996	1.540704	-2.185503	0.211700	0.204128
			G_6	-0.337159	-1.019014	-1.778750	9.037863	-10.796230	6.825377	-1.930287
		0.4	G_0	0.356604	0.461819	7.110410	-21.994654	36.674930	-30.314911	9.387500
			G_1	0.004506	0.170241	2.378834	-2.515485	2.647775	-2.808888	1.011679
			G_5	-0.296263	-0.392805	-1.872826	10.889576	-2.249825	-8.978096	4.211162
			G_6	-0.394221	-0.753066	-4.432755	8.418486	-9.547796	13.422059	-6.715129
		0.6	G_0	>360°	>360°	>360°	>360°	>360°	>360°	>360°
			G_1	>360°	>360°	>360°	>360°	>360°	>360°	>360°
			G_5	>360°	>360°	>360°	>360°	>360°	>360°	>360°
			G_6	>360°	>360°	>360°	>360°	>360°	>360°	>360°
		0.8	G_0	>360°	>360°	>360°	>360°	>360°	>360°	>360°
			G_1	>360°	>360°	>360°	>360°	>360°	>360°	>360°
			G_5	>360°	>360°	>360°	>360°	>360°	>360°	>360°
			G_6	>360°	>360°	>360°	>360°	>360°	>360°	>360°
2.5 (2.5/1)	0.25	0	G_0	0.6152816	-0.3348694	6.2955620	-15.590618	19.299508	-12.488107	3.3010035
			G_1	0.0703566	0.2828152	1.4036169	-0.6511596	-1.2076596	1.0318656	-0.2423741
			G_5	0.6152816	-0.3348694	6.2955620	-15.590618	19.299508	-12.488107	3.3010035
			G_6	0.0000000	0.0000000	0.0000000	0.0000000	0.0000000	0.0000000	0.0000000
		0.2	G_0	0.646174	-0.525424	9.143771	-25.765392	36.470175	-26.329628	7.573289
			G_1	0.078937	0.186120	2.344789	-3.517002	3.077901	-2.091296	0.638082
			G_5	0.548920	-0.308881	5.989992	-12.676971	11.245064	-3.316572	-0.390119
			G_6	-0.287623	0.164338	-2.772689	7.877572	-8.189482	3.886825	-0.676411
		0.4	G_0	0.712553	-0.562743	10.642420	-29.095698	40.939718	-29.625359	8.509887
			G_1	0.096786	0.215408	2.542044	-3.657096	3.127104	-2.186810	0.684258
			G_5	0.368824	0.244610	1.182995	2.753019	-7.324268	5.592899	-1.598399
			G_6	-0.535174	0.339161	-5.208002	14.399722	-15.120214	7.738258	-1.610395
		0.6	G_0	0.673012	-0.052397	9.024902	-20.384584	27.657097	-21.252682	6.484488
			G_1	0.080887	0.339128	2.389818	-2.030676	0.788381	-1.037417	0.502752
			G_5	0.039407	-0.015935	3.486568	-2.293297	4.009482	-6.367896	2.615585
			G_6	-0.725779	0.257981	-6.074530	14.465792	-11.617932	4.586692	-0.890490
		0.8	G_0	0.307204	0.872562	6.321009	-4.379749	7.588667	-13.236204	5.936393
			G_1	0.033723	-0.860076	11.482194	-27.595887	42.604798	-35.731934	11.531278
			G_5	-0.515062	1.009484	-3.275712	20.084518	-18.595024	-0.328811	3.582715
			G_6	-0.936841	0.098565	-7.667915	10.713270	4.560637	-9.685005	2.916137

Table 9B.15 – Influence Coefficients for a Circumferential Semi-Elliptical Surface Crack in a Cylinder – Outside Surface

t/R_i	a/c	a/t	G_i	A_0	A_1	A_2	A_3	A_4	A_5	A_6
2.5 (2.5/1)	0.50	0	G_0	0.8776607	-0.6729719	3.7721411	-6.5209060	6.3377934	-3.7028038	0.9872447
			G_1	0.1277541	0.4368502	0.4904522	1.0427434	-2.9631236	2.0826525	-0.5184313
			G_5	0.8776607	-0.6729719	3.7721411	-6.5209060	6.3377934	-3.7028038	0.9872447
			G_6	0.0000000	0.0000000	0.0000000	0.0000000	0.0000000	0.0000000	0.0000000
		0.2	G_0	0.899031	-0.697102	4.961208	-10.916128	13.091583	-8.521083	2.303200
			G_1	0.134286	0.380995	1.076627	-0.769726	-0.402630	0.304386	-0.021679
			G_5	0.850471	-0.537452	3.016722	-4.676394	3.576189	-1.422912	0.202655
			G_6	-0.184102	0.192797	-0.806902	1.931565	-1.649948	0.547475	-0.028412
		0.4	G_0	0.994094	-0.601777	5.144509	-12.164603	15.683333	-11.022270	3.214187
			G_1	0.161844	0.403289	1.211076	-1.039873	-0.435212	0.593030	-0.154843
			G_5	0.842569	-0.539916	3.410377	-3.414484	-4.590003	9.930612	-4.627675
			G_6	-0.359862	0.360096	-1.372917	3.549918	-3.244142	1.118792	-0.048366
		0.6	G_0	1.144867	-0.387060	4.766777	-9.403235	8.413263	-3.752685	0.697106
			G_1	0.205938	0.465678	1.204730	-0.630049	-1.734590	1.813714	-0.518768
			G_5	0.826107	-0.191919	3.526355	-9.707863	14.630972	-11.817173	3.816637
			G_6	-0.523912	0.516213	-1.845082	5.151293	-4.963991	1.689914	-0.020071
		0.8	G_0	1.343716	0.050212	5.305349	-10.616317	9.319625	-5.227032	1.692441
			G_1	0.261626	0.617556	1.082777	0.405235	-4.088326	3.474133	-0.832308
			G_5	0.793608	0.616477	-1.658844	12.042666	-25.485199	20.959295	-6.052388
			G_6	-0.681961	0.630248	-2.187510	6.744433	-6.611061	1.914347	0.195155
2.5 (2.5/1)	1.0	0	G_0	1.1977992	-0.5244870	0.1498299	2.3284866	-5.1058499	4.3469049	-1.3487980
			G_1	0.1870117	0.6987352	0.1316900	0.7269255	-2.5259384	2.1756251	-0.6540458
			G_5	1.1977992	-0.5244870	0.1498299	2.3284866	-5.1058499	4.3469049	-1.3487980
			G_6	0.0000000	0.0000000	0.0000000	0.0000000	0.0000000	0.0000000	0.0000000
		0.2	G_0	1.219167	-0.834186	2.793795	-6.103070	7.238777	-4.452091	1.151366
			G_1	0.186514	0.624839	0.744777	-0.872216	-0.831339	1.315235	-0.457742
			G_5	1.172784	-0.822997	2.097229	-3.712884	3.063501	-0.838495	-0.071605
			G_6	-0.108320	0.151805	-0.434674	1.225038	-1.541382	0.923788	-0.214331
		0.4	G_0	1.271327	-0.755291	2.702747	-6.012492	6.438983	-3.504852	0.869469
			G_1	0.198219	0.655969	0.652358	-0.360901	-2.034420	2.233664	-0.648422
			G_5	1.183583	-0.776499	1.586568	-3.712243	5.314290	-4.183114	1.386732
			G_6	-0.212326	0.306959	-0.768599	2.258853	-2.943335	1.741557	-0.380471
		0.6	G_0	1.357558	-0.613278	1.904938	-3.366416	1.535739	0.255287	-0.072777
			G_1	0.218785	0.684682	0.500470	0.404414	-3.576632	3.211988	-0.770651
			G_5	1.201684	-0.870960	2.617870	-8.252692	12.017151	-8.193296	2.173949
			G_6	-0.311746	0.458354	-0.925071	2.855357	-3.865436	2.245866	-0.454139
		0.8	G_0	1.482378	-0.559720	2.279296	-6.301756	8.153310	-7.058144	2.960963
			G_1	0.246605	0.682650	0.705529	-0.518781	-1.347879	0.259993	0.602443
			G_5	1.224340	-0.807651	1.435728	-0.869255	-6.448674	10.352286	-4.313798
			G_6	-0.404988	0.615050	-1.013029	3.475179	-5.233278	3.291023	-0.726416

Table 9B.15 – Influence Coefficients for a Circumferential Semi-Elliptical Surface Crack in a Cylinder – Outside Surface

t/R_i	a/c	a/t	G_i	A_0	A_1	A_2	A_3	A_4	A_5	A_6
2.5 (2.5/1)	2.0	0	G_0	0.8150546	-0.5623828	1.4465771	-4.6778133	8.4192164	-7.9025932	2.9866351
			G_1	0.1359146	0.0702340	3.5558581	-11.034445	16.967724	-14.126991	4.8706612
			G_5	0.8150546	-0.5623828	1.4465771	-4.6778133	8.4192164	-7.9025932	2.9866351
			G_6	0.0000000	0.0000000	0.0000000	0.0000000	0.0000000	0.0000000	0.0000000
		0.2	G_0	0.818791	-0.523110	0.871045	-1.787122	1.892158	-1.503663	0.688853
			G_1	0.102839	0.546140	0.378159	-0.519539	-0.966804	0.830855	-0.001362
			G_5	0.790362	-0.543421	0.454176	-0.528874	0.046036	0.028998	0.139182
			G_6	-0.033354	0.062623	-0.211489	0.628124	-0.884534	0.620775	-0.177991
		0.4	G_0	0.826879	-0.544522	1.121725	-3.016588	4.391971	-3.986572	1.626705
			G_1	0.102644	0.522883	0.587041	-1.342809	0.752881	-1.024406	0.744444
			G_5	0.784884	-0.629984	0.539157	-1.153944	1.555009	-1.432874	0.648070
			G_6	-0.064940	0.123110	-0.351769	1.068626	-1.577669	1.130393	-0.322541
		0.6	G_0	0.839882	-0.572545	1.409921	-4.611690	7.779709	-7.355043	2.877251
			G_1	0.103909	0.485474	0.903847	-2.682689	3.548002	-3.899965	1.844356
			G_5	0.782397	-0.690467	0.417175	-1.245746	2.336109	-2.363317	0.995519
			G_6	-0.095420	0.188874	-0.451092	1.401343	-2.215040	1.664782	-0.487400
		0.8	G_0	0.859297	-0.624851	1.831157	-6.745372	11.962337	-11.190216	4.204363
			G_1	0.106237	0.426193	1.405590	-4.754746	7.584638	-7.723315	3.204929
			G_5	0.780634	-0.757415	0.400018	-2.001873	4.403633	-4.261393	1.587867
			G_6	-0.124997	0.261395	-0.523253	1.681075	-2.904270	2.319604	-0.702764
3.0 (3/1)	0.03125	0	G_0	>360°	>360°	>360°	>360°	>360°	>360°	>360°
			G_1	>360°	>360°	>360°	>360°	>360°	>360°	>360°
			G_5	>360°	>360°	>360°	>360°	>360°	>360°	>360°
			G_6	>360°	>360°	>360°	>360°	>360°	>360°	>360°
		0.2	G_0	>360°	>360°	>360°	>360°	>360°	>360°	>360°
			G_1	>360°	>360°	>360°	>360°	>360°	>360°	>360°
			G_5	>360°	>360°	>360°	>360°	>360°	>360°	>360°
			G_6	>360°	>360°	>360°	>360°	>360°	>360°	>360°
		0.4	G_0	>360°	>360°	>360°	>360°	>360°	>360°	>360°
			G_1	>360°	>360°	>360°	>360°	>360°	>360°	>360°
			G_5	>360°	>360°	>360°	>360°	>360°	>360°	>360°
			G_6	>360°	>360°	>360°	>360°	>360°	>360°	>360°
		0.6	G_0	>360°	>360°	>360°	>360°	>360°	>360°	>360°
			G_1	>360°	>360°	>360°	>360°	>360°	>360°	>360°
			G_5	>360°	>360°	>360°	>360°	>360°	>360°	>360°
			G_6	>360°	>360°	>360°	>360°	>360°	>360°	>360°
		0.8	G_0	>360°	>360°	>360°	>360°	>360°	>360°	>360°
			G_1	>360°	>360°	>360°	>360°	>360°	>360°	>360°
			G_5	>360°	>360°	>360°	>360°	>360°	>360°	>360°
			G_6	>360°	>360°	>360°	>360°	>360°	>360°	>360°

Table 9B.15 – Influence Coefficients for a Circumferential Semi-Elliptical Surface Crack in a Cylinder – Outside Surface

t/R_i	a/c	a/t	G_i	A_0	A_1	A_2	A_3	A_4	A_5	A_6
3.0 (3/1)	0.0625	0	G_0	0.2695332	2.1626001	-1.6551569	-1.2970208	4.5604304	-4.3163876	1.4010655
			G_1	0.0138667	0.1827458	2.5749608	-3.9044679	3.3556301	-2.1772209	0.6420134
			G_5	0.2695332	2.1626001	-1.6551569	-1.2970208	4.5604304	-4.3163876	1.4010655
			G_6	0.0000000	0.0000000	0.0000000	0.0000000	0.0000000	0.0000000	0.0000000
		0.2	G_0	0.232797	2.408139	-3.195721	4.323159	-3.264773	0.771071	0.035246
			G_1	0.003581	0.175540	2.472642	-3.269614	2.890415	-2.230988	0.713746
			G_5	-0.161758	-2.344199	6.960485	-13.222033	31.655401	-31.632271	9.910460
			G_6	-0.160464	-2.141958	3.817228	-12.874300	15.523235	-0.189679	-3.977852
		0.4	G_0	>360°	>360°	>360°	>360°	>360°	>360°	>360°
			G_1	>360°	>360°	>360°	>360°	>360°	>360°	>360°
			G_5	>360°	>360°	>360°	>360°	>360°	>360°	>360°
			G_6	>360°	>360°	>360°	>360°	>360°	>360°	>360°
		0.6	G_0	>360°	>360°	>360°	>360°	>360°	>360°	>360°
			G_1	>360°	>360°	>360°	>360°	>360°	>360°	>360°
			G_5	>360°	>360°	>360°	>360°	>360°	>360°	>360°
			G_6	>360°	>360°	>360°	>360°	>360°	>360°	>360°
		0.8	G_0	>360°	>360°	>360°	>360°	>360°	>360°	>360°
			G_1	>360°	>360°	>360°	>360°	>360°	>360°	>360°
			G_5	>360°	>360°	>360°	>360°	>360°	>360°	>360°
			G_6	>360°	>360°	>360°	>360°	>360°	>360°	>360°
3.0 (3/1)	0.125	0	G_0	0.4065238	0.7772483	3.8861644	-12.573943	16.760207	-11.014593	2.8706957
			G_1	0.0320270	0.1825342	2.2670449	-2.7076615	1.2088194	-0.3777430	0.0763155
			G_5	0.4065238	0.7772483	3.8861644	-12.573943	16.760207	-11.014593	2.8706957
			G_6	0.0000000	0.0000000	0.0000000	0.0000000	0.0000000	0.0000000	0.0000000
		0.2	G_0	0.407240	0.881898	5.132923	-18.428025	28.723110	-21.913626	6.486562
			G_1	0.032015	0.208373	2.472138	-3.581163	3.189646	-2.306871	0.729262
			G_5	0.168313	0.572771	0.711969	0.337033	1.375201	-3.583373	1.567646
			G_6	-0.347676	-1.034024	-1.909452	9.353003	-11.180316	7.225214	-2.105167
		0.4	G_0	0.336414	0.500329	6.522439	-19.908727	33.826848	-28.416141	8.847111
			G_1	-0.002117	0.158436	2.355133	-2.387438	2.657041	-2.950807	1.069227
			G_5	-0.330079	-0.820162	0.193235	4.028705	10.139735	-19.057772	7.163984
			G_6	-0.371296	-0.757652	-4.121877	6.304007	-7.191635	13.428007	-7.292659
		0.6	G_0	>360°	>360°	>360°	>360°	>360°	>360°	>360°
			G_1	>360°	>360°	>360°	>360°	>360°	>360°	>360°
			G_5	>360°	>360°	>360°	>360°	>360°	>360°	>360°
			G_6	>360°	>360°	>360°	>360°	>360°	>360°	>360°
		0.8	G_0	>360°	>360°	>360°	>360°	>360°	>360°	>360°
			G_1	>360°	>360°	>360°	>360°	>360°	>360°	>360°
			G_5	>360°	>360°	>360°	>360°	>360°	>360°	>360°
			G_6	>360°	>360°	>360°	>360°	>360°	>360°	>360°

Table 9B.15 – Influence Coefficients for a Circumferential Semi-Elliptical Surface Crack in a Cylinder – Outside Surface

t/R_i	a/c	a/t	G_i	A_0	A_1	A_2	A_3	A_4	A_5	A_6
3.0 (3/1)	0.25	0	G_0	0.6152816	-0.3348694	6.2955620	-15.590618	19.299508	-12.488107	3.3010035
			G_1	0.0703566	0.2828152	1.4036169	-0.6511596	-1.2076596	1.0318656	-0.2423741
			G_5	0.6152816	-0.3348694	6.2955620	-15.590618	19.299508	-12.488107	3.3010035
			G_6	0.0000000	0.0000000	0.0000000	0.0000000	0.0000000	0.0000000	0.0000000
		0.2	G_0	0.647084	-0.528532	9.262426	-26.251039	37.346864	-27.055721	7.797888
			G_1	0.079159	0.190235	2.317997	-3.403834	2.871308	-1.918756	0.583446
			G_5	0.542212	-0.219623	4.784004	-7.727555	2.464825	3.831226	-2.584167
			G_6	-0.300599	0.171738	-2.911559	8.319340	-8.758313	4.257839	-0.775900
		0.4	G_0	0.711934	-0.500330	10.129381	-26.905306	36.979476	-26.342991	7.475923
			G_1	0.096269	0.227009	2.499063	-3.471185	2.828967	-1.975194	0.625987
			G_5	0.331240	0.301230	1.559593	-0.117142	-0.530005	-0.973855	0.653302
			G_6	-0.553321	0.333968	-5.217353	14.144399	-14.297375	6.954299	-1.361273
		0.6	G_0	0.640343	-0.020839	9.338531	-21.402223	30.144240	-23.933646	7.464794
			G_1	0.069994	0.365553	2.295054	-1.559691	0.148839	-0.699161	0.438978
			G_5	-0.027353	0.238961	0.714585	8.204041	-13.008048	6.535464	-1.168343
			G_6	-0.744808	0.240870	-6.311386	14.791185	-11.539640	4.444598	-0.878999
		0.8	G_0	0.167922	1.197860	4.428925	2.638901	-1.274556	-8.695864	5.128669
			G_1	0.121329	-2.626898	20.610111	-50.113245	72.939443	-56.737009	17.329902
			G_5	-0.634688	0.787310	-1.813778	15.830370	-9.981714	-8.552686	6.373093
			G_6	-0.985620	0.041683	-7.721091	7.471664	13.275793	-17.102539	5.018599
3.0 (3/1)	0.50	0	G_0	0.8776607	-0.6729719	3.7721411	-6.5209060	6.3377934	-3.7028038	0.9872447
			G_1	0.1277541	0.4368502	0.4904522	1.0427434	-2.9631236	2.0826525	-0.5184313
			G_5	0.8776607	-0.6729719	3.7721411	-6.5209060	6.3377934	-3.7028038	0.9872447
			G_6	0.0000000	0.0000000	0.0000000	0.0000000	0.0000000	0.0000000	0.0000000
		0.2	G_0	0.899888	-0.688287	4.957977	-10.944747	13.138705	-8.550607	2.310352
			G_1	0.134596	0.381806	1.091509	-0.830201	-0.307469	0.234016	-0.001334
			G_5	0.850191	-0.553797	3.189651	-5.494405	5.184900	-2.812129	0.642088
			G_6	-0.192992	0.202184	-0.853746	2.077002	-1.834135	0.659078	-0.054908
		0.4	G_0	0.998690	-0.592855	5.287802	-12.822303	16.848923	-11.966725	3.504084
			G_1	0.163046	0.413322	1.166128	-0.854790	-0.804290	0.916474	-0.257871
			G_5	0.835402	-0.444105	2.327560	0.956101	-12.307252	16.125980	-6.484058
			G_6	-0.375866	0.378947	-1.482100	3.981929	-3.957598	1.674551	-0.216428
		0.6	G_0	1.155278	-0.299271	4.456842	-8.519395	7.126406	-2.931453	0.519386
			G_1	0.208975	0.477062	1.235816	-0.724860	-1.620698	1.711485	-0.473769
			G_5	0.812100	-0.334569	5.077700	-14.300287	20.594437	-15.309299	4.543179
			G_6	-0.544486	0.521086	-1.807819	5.102059	-4.831253	1.508893	0.055902
		0.8	G_0	1.358743	0.258158	4.347345	-6.687381	2.079421	0.571776	0.002718
			G_1	0.265039	0.664440	0.975181	0.842547	-4.831924	3.901920	-0.882703
			G_5	0.757720	0.603741	0.477189	2.123710	-6.185174	3.756816	-0.307392
			G_6	-0.707859	0.641524	-2.174056	6.725723	-6.289503	1.377131	0.430632

Table 9B.15 – Influence Coefficients for a Circumferential Semi-Elliptical Surface Crack in a Cylinder – Outside Surface

t/R_i	a/c	a/t	G_i	A_0	A_1	A_2	A_3	A_4	A_5	A_6
3.0 (3/1)	1.0	0	G_0	1.1977992	-0.5244870	0.1498299	2.3284866	-5.1058499	4.3469049	-1.3487980
			G_1	0.1870117	0.6987352	0.1316900	0.7269255	-2.5259384	2.1756251	-0.6540458
			G_5	1.1977992	-0.5244870	0.1498299	2.3284866	-5.1058499	4.3469049	-1.3487980
			G_6	0.0000000	0.0000000	0.0000000	0.0000000	0.0000000	0.0000000	0.0000000
		0.2	G_0	1.219715	-0.826112	2.771565	-6.056398	7.142432	-4.361354	1.122749
			G_1	0.186482	0.627255	0.736214	-0.830453	-0.928983	1.401471	-0.482895
			G_5	1.170143	-0.778305	1.657095	-1.980794	-0.165226	1.973126	-0.994580
			G_6	-0.113517	0.158179	-0.449035	1.274862	-1.614380	0.972432	-0.226624
		0.4	G_0	1.273132	-0.736722	2.657894	-5.911180	6.229734	-3.332182	0.826590
			G_1	0.198474	0.658339	0.661161	-0.381917	-2.025233	2.212453	-0.629425
			G_5	1.181243	-0.784638	1.691609	-4.277567	6.388563	-5.064320	1.652247
			G_6	-0.222319	0.322060	-0.800708	2.387451	-3.163373	1.905923	-0.426423
		0.6	G_0	1.362440	-0.565511	1.708499	-2.933598	1.059299	0.377648	-0.014046
			G_1	0.219423	0.695278	0.460264	0.523260	-3.723559	3.212568	-0.720344
			G_5	1.195219	-0.896080	2.891668	-8.870137	12.149021	-7.610339	1.814716
			G_6	-0.325787	0.482102	-0.961986	3.037835	-4.226598	2.538868	-0.541320
		0.8	G_0	1.493776	-0.552029	2.571585	-7.756467	10.993048	-9.768668	3.956321
			G_1	0.248437	0.683650	0.770085	-0.859648	-0.519801	-0.741575	1.033950
			G_5	1.213776	-0.649866	0.034696	4.279867	-15.331769	17.391764	-6.392768
			G_6	-0.422230	0.647202	-1.044534	3.699807	-5.744789	3.722471	-0.854438
3.0 (3/1)	2.0	0	G_0	0.8150546	-0.5623828	1.4465771	-4.6778133	8.4192164	-7.9025932	2.9866351
			G_1	0.1359146	0.0702340	3.5558581	-11.034445	16.967724	-14.126991	4.8706612
			G_5	0.8150546	-0.5623828	1.4465771	-4.6778133	8.4192164	-7.9025932	2.9866351
			G_6	0.0000000	0.0000000	0.0000000	0.0000000	0.0000000	0.0000000	0.0000000
		0.2	G_0	0.818616	-0.521582	0.869584	-1.805350	1.950267	-1.579292	0.722536
			G_1	0.102683	0.545509	0.385622	-0.551150	-0.895017	0.746502	0.034559
			G_5	0.789471	-0.544741	0.435198	-0.475383	-0.022934	0.069549	0.130848
			G_6	-0.034930	0.065059	-0.217685	0.650285	-0.920559	0.647741	-0.185778
		0.4	G_0	0.826702	-0.543653	1.139311	-3.141996	4.679831	-4.289729	1.743975
			G_1	0.102395	0.520080	0.615877	-1.467343	1.018310	-1.303877	0.853387
			G_5	0.783584	-0.650183	0.695348	-1.838576	2.884726	-2.613762	1.040876
			G_6	-0.067988	0.128554	-0.357448	1.086668	-1.610184	1.154633	-0.329039
		0.6	G_0	0.839999	-0.574809	1.471198	-4.951538	8.485961	-8.032164	3.119156
			G_1	0.103650	0.478524	0.972922	-2.983256	4.161300	-4.502719	2.065060
			G_5	0.779726	-0.693194	0.393994	-1.334706	2.694973	-2.764783	1.143293
			G_6	-0.099864	0.199472	-0.468196	1.467681	-2.355636	1.790445	-0.527892
		0.8	G_0	0.860011	-0.629880	1.926018	-7.246794	12.902993	-11.991946	4.459634
			G_1	0.105999	0.414572	1.507646	-5.167247	8.338036	-8.392425	3.429546
			G_5	0.776885	-0.773059	0.466970	-2.388405	5.133531	-4.809737	1.729769
			G_6	-0.130757	0.275729	-0.526799	1.700814	-2.991658	2.413368	-0.733926

Notes:

1. Interpolation of the influence coefficients, G_i, may be used for intermediate values of t/R_i, a/c, and a/t.
2. The value of the influence coefficients at the surface point of the crack defined by $\varphi = 0°$ are equal to: $G_i = A_0$.
3. The value of the influence coefficients at the deepest point of the crack defined by $\varphi = 90°$ are equal to $G_i = \sum_{n=0}^{6} A_n$.

Table 9B.16 – Influence Coefficients for a Circumferential Through Wall Crack in a Sphere – Inside Surface

t/R_i	G_i	A_0	A_1	A_2	A_3	A_4
0.01 (1/100)	G_0	0.996176140	-0.136758833	0.287370688	-0.021281327	0.001614339
	G_1	0.044812392	0.259340393	0.002323025	0.015757981	-0.001236315
	G_p	1.004221696	-0.167942026	0.292305595	-0.022174673	0.001329751
0.01667 (1/60)	G_0	0.991485916	-0.123995291	0.258774210	-0.003234973	-0.003037501
	G_1	0.044449377	0.329870565	-0.080013831	0.043185458	-0.004430561
	G_p	1.007412943	-0.122314488	0.207938107	0.027876580	-0.011026831
0.05 (1/20)	G_0	0.972086762	-0.160593405	0.322770004	-0.046962649	0.009841309
	G_1	0.005444054	0.500718442	-0.407095219	0.257589713	-0.064153363
	G_p	1.016842538	-0.124612983	0.192323868	0.029228099	-0.010429496
0.1 (1/10)	G_0	0.942279944	-0.099201862	0.204585843	0.024467655	-0.009996340
	G_1	0.002573686	0.205082631	0.057545268	0.002773726	-0.000044775
	G_p	1.003333955	-0.099987188	0.145978848	0.052933686	-0.016655808
0.2 (1/5)	G_0	0.906931687	-0.135342636	0.113534642	0.245624518	-0.167632893
	G_1	0.001981728	0.195681690	0.078164645	-0.006180974	0.000733825
	G_p	1.031155982	-0.675755928	1.239084081	-0.741013347	0.250332573
0.3333 (1/3)	G_0	0.852357575	0.022535087	-0.543973921	1.124441452	-0.716813516
	G_1	-0.001766453	0.265994715	-0.214958095	0.279847270	-0.134380666
	G_p	1.037606706	-1.065302487	2.222552179	-1.657623100	0.630449841
t/R_i	G_i	A_5	A_6	A_7	A_8	---
0.01 (1/100)	G_0	-0.000042228	0.000000000	0.000000000	0.000000000	---
	G_1	0.000032495	0.000000000	0.000000000	0.000000000	---
	G_p	-0.000003796	-0.000001208	0.000000000	0.000000000	---
0.01667 (1/60)	G_0	0.000453864	-0.000017696	0.000000000	0.000000000	---
	G_1	0.000151378	0.000000000	0.000000000	0.000000000	---
	G_p	0.001260660	-0.000044986	0.000000000	0.000000000	---
0.05 (1/20)	G_0	-0.001237926	0.000082018	-0.000002120	0.000000000	---
	G_1	0.008073071	-0.000494471	0.000011706	0.000000000	---
	G_p	0.001403746	-0.000083815	0.000001882	0.000000000	---
0.1 (1/10)	G_0	0.001470499	-0.000092852	0.000002178	0.000000000	---
	G_1	0.000004322	0.000000000	0.000000000	0.000000000	---
	G_p	0.002250674	-0.000138201	0.000003223	0.000000000	---
0.2 (1/5)	G_0	0.052005435	-0.008216050	0.000637070	-0.000019115	---
	G_1	0.000000000	0.000000000	0.000000000	0.000000000	---
	G_p	-0.042638069	0.003496156	-0.000109049	0.000000000	---
0.3333 (1/3)	G_0	0.228690564	-0.038335412	0.003210444	-0.000105495	---
	G_1	0.032990268	-0.003923423	0.000177997	0.000000000	---
	G_p	-0.119933248	0.010997535	-0.000385651	0.000000000	---

Note: Interpolation may be used for intermediate values of R_i/t.

Table 9B.17 – Influence Coefficients for a Circumferential Through Wall Crack in a Sphere – Inside Surface

t/R_i	G_i	A_0	A_1	A_2	A_3	A_4
0.01 (1/100)	G_0	1.000081599	0.373644366	0.191913526	-0.067372381	0.009174932
	G_1	0.988670046	-0.084224131	0.181255625	-0.038122523	0.002831900
	G_p	0.990490873	0.379074327	0.117700970	-0.033786795	0.002265847
0.01667 (1/60)	G_0	0.993366131	0.400052320	0.137082159	-0.039414298	0.003414265
	G_1	0.990851836	-0.141604651	0.258638595	-0.066265614	0.006355895
	G_p	0.999261355	0.352070288	0.140730133	-0.046550905	0.004654802
0.05 (1/20)	G_0	0.994548744	0.264794870	0.328273330	-0.156754808	0.035235794
	G_1	0.999613246	-0.168935301	0.384213423	-0.175389720	0.040401774
	G_p	0.996575908	0.311883656	0.125315390	-0.036745174	0.002252144
0.1 (1/10)	G_0	0.996187434	0.214400912	0.348804428	-0.167469117	0.040060365
	G_1	0.999493403	-0.008575611	0.123480901	-0.032176781	0.003701792
	G_p	0.975810822	0.380142341	0.011074721	0.017934230	-0.011467369
0.2 (1/5)	G_0	0.995213839	0.014598654	0.815870555	-0.616813158	0.241781646
	G_1	1.002745997	-0.078220201	0.229674431	-0.087645986	0.015431840
	G_p	0.951843702	0.586803756	-0.442871291	0.328892014	-0.112749517
0.3333 (1/3)	G_0	0.994134590	-0.111105053	1.066365098	-0.901784563	0.398023204
	G_1	0.999438036	-0.054656134	0.318788668	-0.294466264	0.158987833
	G_p	0.932521476	0.711948724	-0.770560233	0.584183910	-0.209919538
t/R_i	G_i	A_5	A_6	A_7	A_8	---
0.01 (1/100)	G_0	-0.000594291	0.000014130	0.000000000	0.000000000	---
	G_1	-0.000072325	0.000000000	0.000000000	0.000000000	---
	G_p	-0.000047279	0.000000000	0.000000000	0.000000000	---
0.01667 (1/60)	G_0	-0.000107359	0.000000000	0.000000000	0.000000000	---
	G_1	-0.000210459	0.000000000	0.000000000	0.000000000	---
	G_p	-0.000211522	0.000003441	0.000000000	0.000000000	---
0.05 (1/20)	G_0	-0.004290880	0.000260114	-0.000006143	0.000000000	---
	G_1	-0.004958385	0.000301935	-0.000007156	0.000000000	---
	G_p	0.000123218	-0.000023892	0.000000908	0.000000000	---
0.1 (1/10)	G_0	-0.005671383	0.000460140	-0.000019943	0.000000360	---
	G_1	-0.000238211	0.000006200	0.000000000	0.000000000	---
	G_p	0.001989205	-0.000155782	0.000004675	0.000000000	---
0.2 (1/5)	G_0	-0.053716832	0.006690865	-0.000434417	0.000011398	---
	G_1	-0.001330949	0.000042881	0.000000000	0.000000000	---
	G_p	0.018687574	-0.001498727	0.000046390	0.000000000	---
0.3333 (1/3)	G_0	-0.099327539	0.013916145	-0.001018574	0.000030207	---
	G_1	-0.048834246	0.008271172	-0.000719616	0.000025055	---
	G_p	0.037632809	-0.003303607	0.000112568	0.000000000	---

Note: Interpolation may be used for intermediate values of R_i/t.

Table 9B.18 – Influence Coefficients for a Circumferential 360° Surface Crack in a Spherical Shell

t/R_i	a/t	Inside Surface					Outside Surface				
		G_0	G_1	G_2	G_3	G_4	G_0	G_1	G_2	G_3	G_4
0.001 (1/1000)	0	1.120000	0.682000	0.524500	0.440400	0.379075	1.120000	0.682000	0.524500	0.440400	0.379075
	0.05	1.024082	0.601169	0.459493	0.387539	0.333594	1.020798	0.602390	0.461317	0.389214	0.335227
	0.1	0.982026	0.555537	0.420873	0.355007	0.305499	0.980903	0.554875	0.420499	0.355007	0.305194
	0.2	0.969389	0.484180	0.351367	0.294234	0.250941	0.969389	0.484342	0.351591	0.294144	0.251071
	0.4	1.584413	0.640551	0.375023	0.262572	0.253033	1.586151	0.641165	0.375198	0.262821	0.253176
	0.6	2.990095	1.039894	0.508081	0.285484	0.291371	2.993602	1.040903	0.508425	0.285546	0.291477
	0.8	6.751458	2.106236	0.886556	0.388222	0.392172	6.760196	2.108414	0.887591	0.388560	0.392167
0.00333 (1/300)	0	1.120000	0.682000	0.524500	0.440400	0.379075	1.120000	0.682000	0.524500	0.440400	0.379075
	0.05	1.070867	0.635287	0.486127	0.408884	0.351531	1.067923	0.637431	0.488495	0.411111	0.353835
	0.1	1.075365	0.625130	0.475100	0.399249	0.342505	1.075365	0.624542	0.474658	0.398986	0.342035
	0.2	1.133792	0.611639	0.451255	0.374918	0.320027	1.134948	0.611982	0.451429	0.375058	0.320071
	0.4	1.746727	0.796624	0.510245	0.378227	0.345428	1.752724	0.808879	0.528579	0.401085	0.354033
	0.6	3.051466	1.234450	0.721692	0.496415	0.434741	3.059194	1.236715	0.722661	0.496943	0.435008
	0.8	5.772142	2.124837	1.136853	0.715883	0.602916	5.789161	2.129462	1.138928	0.716981	0.603212
0.01 (1/100)	0	1.120000	0.682000	0.524500	0.440400	0.379075	1.120000	0.682000	0.524500	0.440400	0.379075
	0.05	1.098440	0.655289	0.501637	0.421894	0.362018	1.097580	0.655129	0.501846	0.422044	0.362062
	0.1	1.112300	0.654809	0.498490	0.417996	0.358862	1.114656	0.655369	0.498700	0.418247	0.358839
	0.2	1.208823	0.673259	0.500433	0.414909	0.354317	1.212723	0.674660	0.501219	0.415415	0.354658
	0.4	1.775773	0.870581	0.593351	0.462736	0.398785	1.786084	0.874039	0.595117	0.463840	0.399489
	0.6	2.860047	1.249167	0.783061	0.572346	0.484799	2.879549	1.255034	0.785848	0.573872	0.485592
	0.8	4.638121	1.877737	1.107159	0.768207	0.632040	4.684553	1.891310	1.113538	0.771869	0.633612
0.01667 (1/60)	0	1.120000	0.682000	0.524500	0.440400	0.379075	1.120000	0.682000	0.524500	0.440400	0.379075
	0.05	1.103967	0.660076	0.505804	0.425190	0.364742	1.104537	0.660076	0.505596	0.425066	0.364628
	0.1	1.123564	0.664117	0.505907	0.424102	0.364056	1.127294	0.665538	0.506736	0.424720	0.364446
	0.2	1.226490	0.690153	0.514444	0.426569	0.364299	1.232890	0.692392	0.515615	0.427307	0.364810
	0.4	1.756462	0.875239	0.600383	0.468847	0.406373	1.772076	0.884482	0.610136	0.479525	0.410645
	0.6	2.712860	1.220200	0.783173	0.582943	0.491062	2.742675	1.229196	0.787404	0.585487	0.492297
	0.8	4.126269	1.735804	1.057964	0.755031	0.620864	4.178392	1.750103	1.064146	0.758412	0.621879
0.025 (1/40)	0	1.120000	0.682000	0.524500	0.440400	0.379075	1.120000	0.682000	0.524500	0.440400	0.379075
	0.05	1.106720	0.662931	0.508081	0.427061	0.366476	1.108710	0.663406	0.508287	0.427159	0.366458
	0.1	1.129154	0.669390	0.510348	0.427798	0.367156	1.134717	0.671581	0.511580	0.428533	0.367796
	0.2	1.233528	0.699216	0.522388	0.433221	0.370142	1.243062	0.702548	0.524143	0.434370	0.370900
	0.4	1.727851	0.875389	0.607334	0.478073	0.412216	1.750478	0.886408	0.616977	0.487689	0.416505
	0.6	2.575276	1.185079	0.773736	0.583393	0.490483	2.616709	1.197704	0.779703	0.586830	0.492296
	0.8	3.748132	1.624554	1.013576	0.737098	0.607492	3.814046	1.642621	1.021248	0.741180	0.608762

Table 9B.18 – Influence Coefficients for a Circumferential 360° Surface Crack in a Spherical Shell

t/R_i	a/t	Inside Surface					Outside Surface				
		G_0	G_1	G_2	G_3	G_4	G_0	G_1	G_2	G_3	G_4
0.05 (1/20)	0	1.120000	0.682000	0.524500	0.440400	0.379075	1.120000	0.682000	0.524500	0.440400	0.379075
	0.05	1.109939	0.666405	0.510964	0.429585	0.368611	1.115692	0.667977	0.511785	0.429951	0.368718
	0.1	1.132866	0.675010	0.515361	0.432069	0.370909	1.143927	0.679194	0.517596	0.433524	0.372045
	0.2	1.232890	0.707311	0.530660	0.440666	0.376746	1.251895	0.713993	0.534207	0.442923	0.378290
	0.4	1.654952	0.864381	0.612924	0.489863	0.417989	1.694893	0.877783	0.619735	0.494049	0.420723
	0.6	2.313398	1.108205	0.743888	0.572346	0.481359	2.384504	1.130006	0.754394	0.578425	0.484579
	0.8	3.170440	1.445533	0.935159	0.698728	0.579813	3.277447	1.475174	0.948252	0.705919	0.582125
0.1 (1/10)	0	1.120000	0.682000	0.524500	0.440400	0.379075	1.120000	0.682000	0.524500	0.440400	0.379075
	0.05	1.108615	0.667506	0.512195	0.430804	0.369757	1.123378	0.671737	0.514240	0.431826	0.370189
	0.1	1.129154	0.676718	0.517697	0.434370	0.373018	1.151243	0.684964	0.522238	0.437260	0.375197
	0.2	1.214669	0.706198	0.532683	0.443396	0.379499	1.252314	0.719666	0.539728	0.447812	0.382744
	0.4	1.548235	0.833006	0.600820	0.485289	0.414232	1.622130	0.858289	0.613780	0.493332	0.419680
	0.6	2.033355	1.018225	0.702908	0.551016	0.465383	2.152844	1.055420	0.720965	0.561704	0.471242
	0.8	2.688413	1.290690	0.862710	0.659519	0.552344	2.865317	1.341520	0.885964	0.672615	0.557628
0.2 (1/5)	0	1.120000	0.682000	0.524500	0.440400	0.379075	1.120000	0.682000	0.524500	0.440400	0.379075
	0.05	1.103301	0.666719	0.512400	0.431194	0.370190	1.124218	0.677493	0.519316	0.436202	0.374625
	0.1	1.115127	0.673609	0.516886	0.434249	0.373337	1.156245	0.688402	0.524943	0.439534	0.376947
	0.2	1.177157	0.695982	0.528877	0.441915	0.378829	1.249587	0.722068	0.542782	0.450731	0.385211
	0.4	1.415271	0.789345	0.580161	0.474188	0.405897	1.546794	0.834422	0.603652	0.488737	0.415653
	0.6	1.758950	0.926020	0.657926	0.525343	0.446501	1.953068	0.987620	0.688199	0.543506	0.456957
	0.8	2.297752	1.162919	0.801303	0.624584	0.528260	2.574511	1.243062	0.837873	0.645142	0.537022
0.3333 (1/3)	0	1.120000	0.682000	0.524500	0.440400	0.379075	1.120000	0.682000	0.524500	0.440400	0.379075
	0.05	1.094572	0.664481	0.512071	0.430731	0.369999	1.133297	0.680394	0.520747	0.436776	0.374992
	0.1	1.093356	0.667271	0.513708	0.432827	0.372573	1.160379	0.689942	0.525766	0.440225	0.378198
	0.2	1.137977	0.684117	0.523336	0.439239	0.376944	1.253402	0.725103	0.548614	0.454180	0.387225
	0.4	1.326360	0.753316	0.562372	0.463844	0.398192	1.503800	0.820848	0.598058	0.486976	0.414096
	0.6	1.574222	0.863314	0.626650	0.510734	0.433284	1.845450	0.950648	0.670079	0.533337	0.448895
	0.8	2.058835	1.084679	0.763446	0.602847	0.513638	2.448941	1.201019	0.817044	0.632677	0.528476

Note: Interpolation of the influence coefficients, G_i, may be used for intermediate values of t/R_i and a/t.

Table 9B.19 – Influence Coefficients for a Circumferential Semi-Elliptical Surface Crack in a Sphere – Inside Surface

t/R_i	a/c	a/t	G_i	A_0	A_1	A_2	A_3	A_4	A_5	A_6
0.0	0.03125	0.0	G_0	0.1965046	2.9373464	-5.2582823	7.4889153	-6.9282667	3.3673349	-0.6677966
			G_1	0.0051780	0.1750280	2.7718680	-4.6457154	4.6780502	-3.2768090	0.9840994
		0.2	G_0	0.2080760	3.0112422	-5.1048701	7.6348715	-6.8347547	2.7940766	-0.3882688
			G_1	0.0084834	0.2406767	2.4574292	-3.6452421	3.6142837	-2.8451814	0.9270638
		0.4	G_0	0.2357940	3.0822400	-3.5792100	3.9476890	1.9131590	-6.8872200	3.1896800
			G_1	0.0145140	0.4038000	1.6422700	-0.3906100	-0.6480700	-0.2940300	0.2514900
		0.6	G_0	0.2902240	3.6892050	-4.5739100	11.709890	-6.3750000	-5.8894100	4.2452400
			G_1	0.0208890	0.7016780	0.1631840	5.7072160	-8.2075800	3.4561120	-0.4454700
		0.8	G_0	0.5163550	2.5310830	14.712900	-43.621800	101.06570	-116.08100	46.190900
			G_1	0.0825460	0.4971770	4.6064810	-7.3326700	21.148620	-29.345100	12.491400
0.0	0.0625	0.0	G_0	0.2695332	2.1626001	-1.6551569	-1.2970208	4.5604304	-4.3163876	1.4010655
			G_1	0.0138667	0.1827458	2.5749608	-3.9044679	3.3556301	-2.1772209	0.6420134
		0.2	G_0	0.2845892	2.2264055	-1.4546190	-1.5760719	5.1131083	-4.9485443	1.6207574
			G_1	0.0199077	0.2210874	2.4642047	-3.5898625	3.1624039	-2.2403780	0.6965751
		0.4	G_0	0.3261480	2.5200870	-1.8847000	2.1798740	-1.4597100	-0.1886500	0.2393400
			G_1	0.0294120	0.3699370	1.9220850	-1.2071500	-0.4394000	0.2737550	-0.0395200
		0.6	G_0	0.4166330	3.1566470	-2.6248900	7.7325910	-9.6927800	3.6428700	-0.0892000
			G_1	0.0598460	0.4340740	2.6811560	-3.1936600	4.0753720	-4.6940200	1.8285500
		0.8	G_0	0.6540140	3.4231920	3.8158050	-4.1586900	3.4715330	-10.310400	6.6280000
			G_1	0.1214780	0.6975490	2.9718330	-1.3036500	-0.0754900	-3.0465100	2.1670000
0.0	0.125	0.0	G_0	0.4065238	0.7772483	3.8861644	-12.573943	16.760207	-11.014593	2.8706957
			G_1	0.0320270	0.1825342	2.2670449	-2.7076615	1.2088194	-0.3777430	0.0763155
		0.2	G_0	0.4242116	1.0089302	3.2973815	-12.159726	17.873386	-12.868668	3.6281712
			G_1	0.0429859	0.2033811	2.2563818	-2.8752160	1.8152558	-1.0512327	0.3181077
		0.4	G_0	0.4917770	1.6592320	-0.1080400	0.1793240	-2.7076100	3.3680620	-1.3489700
			G_1	0.0634270	0.3722500	1.6231670	-0.5306500	-2.0007400	1.8943780	-0.5880300
		0.6	G_0	0.6591820	1.8759140	1.0212600	-1.7698000	-0.5653600	1.2479960	-0.4376600
			G_1	0.1116040	0.4714500	1.7940590	-0.7557600	-1.4901700	1.0852180	-0.2113700
		0.8	G_0	0.9809330	1.8846320	4.8020780	-8.0580200	0.4447850	3.4772660	-1.0567500
			G_1	0.2039950	0.4800150	2.8822430	-2.5890100	-0.9683000	1.5372370	-0.3750200
0.0	0.25	0.0	G_0	0.6152816	-0.3348694	6.2955620	-15.590618	19.299508	-12.488107	3.3010035
			G_1	0.0703566	0.2828152	1.4036169	-0.6511596	-1.2076596	1.0318656	-0.2423741
		0.2	G_0	0.6385889	-0.3095132	6.5329787	-16.622882	21.056641	-13.850120	3.6988146
			G_1	0.0840059	0.1999367	1.8218113	-1.7756899	0.3757186	-0.0785358	0.0643386
		0.4	G_0	0.7390420	0.0548160	4.0842620	-7.5883100	5.4047530	-1.0146100	-0.3483400
			G_1	0.1164500	0.2479880	1.8282520	-1.7169900	0.1912120	0.1165770	-0.0186100
		0.6	G_0	0.9461210	-0.1858800	5.5867460	-9.8634900	5.9596870	0.1296440	-1.0026100
			G_1	0.1778050	0.2056680	2.0979210	-1.8039500	-0.5558700	1.1461400	-0.4206600
		0.8	G_0	1.2452110	-0.6921900	8.3260620	-14.948000	8.6936910	0.4755790	-1.3926600
			G_1	0.2585640	0.1548890	2.1170240	-0.4910000	-4.6146100	5.4550750	-1.9663300
0.0	0.5	0.0	G_0	0.8776607	-0.6729719	3.7721411	-6.5209060	6.3377934	-3.7028038	0.9872447
			G_1	0.1277541	0.4368502	0.4904522	1.0427434	-2.9631236	2.0826525	-0.5184313
		0.2	G_0	0.9003948	-0.8850488	5.2743239	-11.267523	13.890755	-9.6373584	2.8183906
			G_1	0.1404409	0.3215397	1.1010666	-1.0257556	0.6943940	-1.0793186	0.5410929
		0.4	G_0	1.0058060	-0.7322600	2.9951940	-1.9459200	-3.2613500	5.1424570	-2.0306200
			G_1	0.1740870	0.3051630	1.2070310	-0.6720500	-1.0651300	1.1445590	-0.3644800
		0.6	G_0	1.1826010	-1.1072500	3.9623640	-2.7781300	-4.3097300	7.2772750	-2.9648200
			G_1	0.2277120	0.1701170	1.5499470	-1.1051200	-0.8333700	1.1717060	-0.4194500
		0.8	G_0	1.3833380	-1.3900300	4.3755780	-3.7372600	-2.5403200	5.3036000	-2.0932400
			G_1	0.2820110	0.0839230	1.7258580	-1.5358100	-0.0635600	0.5006780	-0.1982200

Table 9B.19 – Influence Coefficients for a Circumferential Semi-Elliptical Surface Crack in a Sphere – Inside Surface

t/R_i	a/c	a/t	G_i	A_0	A_1	A_2	A_3	A_4	A_5	A_6
0.0	1.0	0.0	G_0	1.1977992	-0.5244870	0.1498299	2.3284866	-5.1058499	4.3469049	-1.3487980
			G_1	0.1870117	0.6987352	0.1316900	0.7269255	-2.5259384	2.1756251	-0.6540458
		0.2	G_0	1.2263282	-1.1608467	4.4744783	-11.584231	17.811241	-14.408250	4.6998279
			G_1	0.2154786	0.2441623	2.8107820	-7.6574580	11.171413	-9.0053693	2.9542871
		0.4	G_0	1.2989480	-0.9978000	1.9479540	-1.3002700	-1.4940100	2.8306230	-1.2126000
			G_1	0.2386246	0.1447774	3.3198992	-9.2456599	13.823512	-11.223715	3.6868232
		0.6	G_0	1.3971180	-1.1348400	1.7918740	-0.4202600	-2.8679300	3.7685480	-1.4405000
			G_1	0.2445870	0.5326670	0.5939690	-0.0361800	-2.0163100	2.2167010	-0.7782200
		0.8	G_0	1.5117010	-1.3244800	1.7568350	-0.1337900	-2.8629300	3.2953270	-1.1412400
			G_1	0.2704470	0.5113280	0.5357440	-0.0327300	-1.5570200	1.5570970	-0.5094600
0.0	2.0	0.0	G_0	0.8150546	-0.5623828	1.4465771	-4.6778133	8.4192164	-7.9025932	2.9866351
			G_1	0.1359146	0.0702340	3.5558581	-11.034445	16.967724	-14.126991	4.8706612
		0.2	G_0	0.8463715	-1.0011024	4.0052312	-11.937181	19.189548	-16.039296	5.4674371
			G_1	0.1395121	0.0753999	3.1895604	-9.5540932	14.214316	-11.649525	4.0073308
		0.4	G_0	0.8570045	-1.0183085	3.9957306	-11.886878	19.152747	-16.047480	5.4801806
			G_1	0.1436696	0.0544018	3.2816127	-9.8164232	14.610963	-11.942138	4.0907797
		0.6	G_0	0.8839861	-1.0765270	4.0774087	-11.976171	19.173189	-15.996207	5.4501217
			G_1	0.1504185	0.0478401	3.2579960	-9.6921199	14.370843	-11.736129	4.0258411
		0.8	G_0	0.9033134	-0.9619755	2.8501500	-7.6366897	11.596116	-9.4828625	3.2550163
			G_1	0.1458559	0.2313881	1.9882138	-5.5546045	7.4196069	-5.8965053	2.0855563
0.01 (1/100)	0.03125	0.0	G_0	0.1965046	2.9373464	-5.2582823	7.4889153	-6.9282667	3.3673349	-0.6677966
			G_1	0.0051780	0.1750280	2.7718680	-4.6457154	4.6780502	-3.2768090	0.9840994
		0.2	G_0	0.2054741	2.5611013	-2.9596332	3.1954661	-2.6645031	1.2439888	-0.3032678
			G_1	0.0054195	0.2246517	2.4896120	-3.8089914	3.8104646	-2.9072861	0.9224626
		0.4	G_0	0.2294240	2.9738130	-3.3635100	3.3893400	2.1700680	-6.5149000	2.9153700
			G_1	0.0154010	0.2512660	1.9593420	-0.8526500	-1.4031000	1.6657830	-0.7008700
		0.6	G_0	0.2674970	3.1773150	-2.7738500	6.3229130	-1.1128000	-6.8512500	3.6651000
			G_1	0.0165544	0.4538318	1.5394249	0.5061319	0.6658622	-3.7799579	1.8704652
		0.8	G_0	0.3747330	2.0063460	10.399280	-28.789300	59.058120	-62.102200	23.033300
			G_1	0.0434670	0.1280210	4.7021650	-6.7931300	12.190040	-13.929700	5.3401500
0.01 (1/100)	0.0625	0.0	G_0	0.2695332	2.1626001	-1.6551569	-1.2970208	4.5604304	-4.3163876	1.4010655
			G_1	0.0138667	0.1827458	2.5749608	-3.9044679	3.3556301	-2.1772209	0.6420134
		0.2	G_0	0.2759680	2.0225739	-0.6996063	-2.1721721	3.8653975	-2.7105955	0.6601162
			G_1	0.0166925	0.2164200	2.5114777	-4.0903645	4.4164183	-3.4801215	1.1319557
		0.4	G_0	0.3202990	2.5245970	-2.1779500	2.4733910	-1.2325400	-0.6552000	0.4148000
			G_1	0.0279540	0.2953030	1.7740760	-0.5112500	-1.8441100	1.8025300	-0.6586400
		0.6	G_0	0.3823290	3.2747250	-4.8976100	14.499560	-20.205300	11.981390	-2.7101200
			G_1	0.0411270	0.3611160	2.3656710	-2.1931200	2.0455880	-2.4365800	0.9174400
		0.8	G_0	0.5540600	2.8620620	3.5774670	-5.4505700	6.1537190	-9.4586500	4.8515500
			G_1	0.0836030	0.4318770	3.2512220	-2.7789000	1.7943750	-2.7518800	1.3433300
0.01 (1/100)	0.125	0.0	G_0	0.4065238	0.7772483	3.8861644	-12.573943	16.760207	-11.014593	2.8706957
			G_1	0.0320270	0.1825342	2.2670449	-2.7076615	1.2088194	-0.3777430	0.0763155
		0.2	G_0	0.4048264	1.1578449	1.6197884	-5.7295006	6.9227475	-4.2148411	1.0309624
			G_1	0.0464705	0.0041545	4.0262527	-9.5703182	13.562839	-10.666035	3.2973390
		0.4	G_0	0.4791840	1.3870110	1.5742300	-5.0231600	5.7521780	-3.4899500	0.8181900
			G_1	0.0511420	0.2534930	1.9906620	-1.3981400	-0.6794600	0.9027200	-0.3071400
		0.6	G_0	0.6096530	1.7754120	0.7329590	0.2126290	-5.2166300	6.0034300	-2.2092100
			G_1	0.0912660	0.2790100	2.6496090	-3.3562600	2.5558220	-1.8436100	0.5793000
		0.8	G_0	0.8402230	1.5177340	5.2378910	-8.4186300	-0.2464500	5.9346420	-2.6149000
			G_1	0.1513260	0.3150260	3.0469360	-2.6913700	-1.2904100	2.5995700	-1.0407500

Table 9B.19 – Influence Coefficients for a Circumferential Semi-Elliptical Surface Crack in a Sphere – Inside Surface

t/R_i	a/c	a/t	G_i	A_0	A_1	A_2	A_3	A_4	A_5	A_6
0.01 (1/100)	0.25	0.0	G_0	0.6152816	-0.3348694	6.2955620	-15.590618	19.299508	-12.488107	3.3010035
			G_1	0.0703566	0.2828152	1.4036169	-0.6511596	-1.2076596	1.0318656	-0.2423741
		0.2	G_0	0.6001162	0.1425199	4.5757413	-12.857132	17.390660	-12.106120	3.3854502
			G_1	0.0826855	0.2816842	1.7854964	-2.9045659	3.1646698	-2.6210713	0.8899897
		0.4	G_0	0.7214580	0.1033650	3.9806460	-7.6039800	5.7251550	-1.3917500	-0.2178800
			G_1	0.1022410	0.2585340	1.6925330	-1.2923900	-0.4045500	0.5652840	-0.1652700
		0.6	G_0	0.8959000	0.0229790	4.2765850	-6.0386200	0.2589510	4.3815880	-2.2677400
			G_1	0.1546700	0.2341080	1.8505670	-1.1247800	-1.4402800	1.7689870	-0.6143800
		0.8	G_0	1.0846360	0.6183170	-1.7905600	20.153400	-50.372100	48.289670	-16.326200
			G_1	0.2163400	0.1783190	1.8690990	0.2361760	-5.3445000	5.7549830	-2.0155900
0.01 (1/100)	0.5	0.0	G_0	0.8776607	-0.6729719	3.7721411	-6.5209060	6.3377934	-3.7028038	0.9872447
			G_1	0.1277541	0.4368502	0.4904522	1.0427434	-2.9631236	2.0826525	-0.5184313
		0.2	G_0	0.8843656	-0.8825526	5.4237760	-11.876360	14.769862	-10.169874	2.9324829
			G_1	0.1435544	0.2047681	1.9196249	-3.4935583	4.1718932	-3.4276657	1.1625408
		0.4	G_0	0.9897010	-0.6737700	2.9314480	-2.0870300	-2.7294800	4.5595390	-1.8183600
			G_1	0.1647140	0.3010190	1.2635350	-0.8087200	-0.8819100	1.0349150	-0.3461100
		0.6	G_0	1.1473540	-0.8992000	3.2669790	-2.0093700	-3.6942100	5.5965600	-2.1518600
			G_1	0.2127700	0.2268860	1.4293980	-1.0538200	-0.6404000	0.8730140	-0.2917800
		0.8	G_0	1.3239080	-1.0764400	3.1315630	-1.3594100	-4.3926100	5.6756190	-2.0025500
			G_1	0.2534620	0.2515530	0.8944120	0.4182770	-2.2677700	1.7287360	-0.4840800
0.01 (1/100)	1.0	0.0	G_0	1.1977992	-0.5244870	0.1498299	2.3284866	-5.1058499	4.3469049	-1.3487980
			G_1	0.1870117	0.6987352	0.1316900	0.7269255	-2.5259384	2.1756251	-0.6540458
		0.2	G_0	1.2070754	-1.2221997	5.1111900	-13.966446	22.144836	-18.212527	5.9900420
			G_1	0.2126878	0.1592439	3.4016275	-9.6610590	14.631958	-11.939360	3.9249291
		0.4	G_0	1.2866950	-0.9149800	1.6025020	-0.4064800	-2.6297800	3.5109270	-1.3680900
			G_1	0.2348060	0.1500424	3.2918536	-9.1682940	13.723214	-11.151448	3.6625083
		0.6	G_0	1.3875130	-1.1342100	1.9912280	-1.1972200	-1.3615400	2.3898410	-0.9730700
			G_1	0.2384520	0.5247780	0.6991270	-0.4392000	-1.1781000	1.4236780	-0.5076100
		0.8	G_0	1.4863980	-1.2449000	1.6321080	-0.1886400	-2.0854400	2.2312950	-0.7176800
			G_1	0.2607040	0.5186780	0.5832820	-0.3285000	-0.7939400	0.7881120	-0.2472200
0.01 (1/100)	2.0	0.0	G_0	0.8150546	-0.5623828	1.4465771	-4.6778133	8.4192164	-7.9025932	2.9866351
			G_1	0.1359146	0.0702340	3.5558581	-11.034445	16.967724	-14.126991	4.8706612
		0.2	G_0	0.8004572	-0.9423051	3.8677945	-11.733659	19.085447	-16.027877	5.4594536
			G_1	0.1279139	0.0638427	3.2498718	-9.8213966	14.739825	-12.074165	4.1253194
		0.4	G_0	0.8282738	-0.2914582	-0.8469581	3.5453417	-6.2544427	4.8659458	-1.3264716
			G_1	0.1412848	0.0553372	3.2844423	-9.8782715	14.769556	-12.077829	4.1273126
		0.6	G_0	0.8574827	-0.3584410	-0.7392613	3.4427023	-6.2878270	4.9979448	-1.3881873
			G_1	0.1482679	0.0191704	3.4720530	-10.498316	15.789419	-12.865211	4.3570473
		0.8	G_0	0.9080987	-0.9400711	2.7958615	-7.5701151	11.657561	-9.6444073	3.3336215
			G_1	0.1513719	0.0242499	3.4636042	-10.591832	15.792927	-12.472688	4.0477749
0.01667 (1/60)	0.03125	0.0	G_0	0.1965046	2.9373464	-5.2582823	7.4889153	-6.9282667	3.3673349	-0.6677966
			G_1	0.0051780	0.1750280	2.7718680	-4.6457154	4.6780502	-3.2768090	0.9840994
		0.2	G_0	0.2052101	2.5533693	-2.9267157	3.0534719	-2.4121435	1.0357930	-0.2362885
			G_1	0.0052759	0.2286923	2.4404265	-3.6371264	3.5390118	-2.7186132	0.8760317
		0.4	G_0	0.2189337	3.1279004	-5.3775994	11.531042	-12.856477	6.2795553	-1.1577653
			G_1	0.0114659	0.2526547	2.5727508	-3.7773155	5.1638660	-5.1014550	1.8020600
		0.6	G_0	0.2636630	3.0068190	-1.7595700	2.2584030	5.4483910	-11.617400	4.9994800
			G_1	0.0264910	0.3382800	2.1916910	-0.7796200	0.6936340	-2.5355000	1.2872700
		0.8	G_0	0.3210130	2.8196340	2.3419320	-1.8680300	11.537550	-20.523200	9.1151800
			G_1	0.0459550	0.3427560	2.3730470	0.8057490	0.7883340	-5.8950700	3.1843100

Table 9B.19 – Influence Coefficients for a Circumferential Semi-Elliptical Surface Crack in a Sphere – Inside Surface

t/R_i	a/c	a/t	G_i	A_0	A_1	A_2	A_3	A_4	A_5	A_6
0.01667 (1/60)	0.0625	0.0	G_0	0.2695332	2.1626001	-1.6551569	-1.2970208	4.5604304	-4.3163876	1.4010655
			G_1	0.0138667	0.1827458	2.5749608	-3.9044679	3.3556301	-2.1772209	0.6420134
		0.2	G_0	0.2755463	2.0190847	-0.7102131	-2.1466612	3.8346488	-2.6931885	0.6576969
			G_1	0.0166594	0.2184216	2.4941038	-4.0488103	4.3570043	-3.4386099	1.1217193
		0.4	G_0	0.3189630	2.5036380	-2.1918000	2.5893110	-1.5926000	-0.2460600	0.2646500
			G_1	0.0288524	0.2884400	2.3985840	-3.2802142	3.5681601	-3.2862980	1.1551067
		0.6	G_0	0.3798610	3.1009390	-3.9959800	11.503410	-15.719300	8.9415330	-1.9392700
			G_1	0.0445670	0.3566430	2.5396620	-2.7728300	2.6905830	-2.7764600	1.0050600
		0.8	G_0	0.5255960	2.8068730	2.7604390	-3.3079300	2.6131920	-5.3475400	2.9814200
			G_1	0.0798310	0.4515320	3.0733190	-2.3711000	0.9991140	-1.7909000	0.9239300
0.01667 (1/60)	0.125	0.0	G_0	0.4065238	0.7772483	3.8861644	-12.573943	16.760207	-11.014593	2.8706957
			G_1	0.0320270	0.1825342	2.2670449	-2.7076615	1.2088194	-0.3777430	0.0763155
		0.2	G_0	0.4044209	1.1520573	1.6383619	-5.7992049	7.0395445	-4.3026142	1.0557168
			G_1	0.0463551	0.0048175	4.0171926	-9.5540173	13.544104	-10.652816	3.2935742
		0.4	G_0	0.4742270	1.4486540	0.9441430	-2.7830300	1.8682280	-0.2627600	-0.2064200
			G_1	0.0684887	0.0711241	3.9201925	-8.9540416	12.651466	-10.126277	3.1705597
		0.6	G_0	0.6007740	1.7794800	0.4132540	1.2838500	-7.0074700	7.5056630	-2.6984600
			G_1	0.0919660	0.2738720	2.6953680	-3.5387900	2.7558210	-1.9110000	0.5789800
		0.8	G_0	0.8236880	1.4243800	5.4504410	-9.3568100	1.7122670	4.4942090	-2.3085900
			G_1	0.1501480	0.3110770	3.0739110	-2.9209300	-0.8651500	2.3593210	-1.0179600
0.01667 (1/60)	0.25	0.0	G_0	0.6152816	-0.3348694	6.2955620	-15.590618	19.299508	-12.488107	3.3010035
			G_1	0.0703566	0.2828152	1.4036169	-0.6511596	-1.2076596	1.0318656	-0.2423741
		0.2	G_0	0.6006412	0.1200883	4.6889410	-13.147636	17.760233	-12.331467	3.4379468
			G_1	0.0823805	0.2845653	1.7595773	-2.8182477	3.0142764	-2.4926028	0.8479623
		0.4	G_0	0.7168180	0.1385890	3.6456880	-6.4571300	3.8053530	0.1619780	-0.7025200
			G_1	0.1180703	0.1215398	2.4566849	-3.4891053	2.6628686	-1.5512395	0.4242018
		0.6	G_0	0.8876110	0.0006320	4.3344170	-6.2527900	0.6754690	4.0262590	-2.1571000
			G_1	0.1534930	0.2234680	1.9335370	-1.4780100	-0.7810300	1.2056120	-0.4326300
		0.8	G_0	1.0714710	0.5124440	-1.0787600	17.590810	-45.713000	44.368040	-15.098000
			G_1	0.2165780	0.0967650	2.4940140	-1.9755700	-1.5151400	2.6158670	-1.0374400
0.01667 (1/60)	0.5	0.0	G_0	0.8776607	-0.6729719	3.7721411	-6.5209060	6.3377934	-3.7028038	0.9872447
			G_1	0.1277541	0.4368502	0.4904522	1.0427434	-2.9631236	2.0826525	-0.5184313
		0.2	G_0	0.8797856	-0.8189753	5.0106624	-10.648831	12.938939	-8.8379105	2.5566038
			G_1	0.1429203	0.2118953	1.8692102	-3.3358064	3.9194259	-3.2278570	1.1008228
		0.4	G_0	0.9858350	-0.6539200	2.7563870	-1.4880900	-3.7182700	5.3443380	-2.0581100
			G_1	0.1752744	0.1759213	1.9448935	-3.3090927	3.6614977	-2.9372114	0.9971908
		0.6	G_0	1.1386810	-0.8767800	3.1183900	-1.5659500	-4.3491900	6.0771430	-2.2920100
			G_1	0.2098120	0.2475400	1.3012030	-0.6895000	-1.1717600	1.2614220	-0.4043400
		0.8	G_0	1.3083680	-1.0202700	2.7808040	-0.2523900	-6.0662600	6.9210510	-2.3716800
			G_1	0.2498370	0.2674650	0.7878510	0.7536720	-2.7696800	2.0998750	-0.5937600
0.01667 (1/60)	1.0	0.0	G_0	1.1977992	-0.5244870	0.1498299	2.3284866	-5.1058499	4.3469049	-1.3487980
			G_1	0.1870117	0.6987352	0.1316900	0.7269255	-2.5259384	2.1756251	-0.6540458
		0.2	G_0	1.2056440	-1.2177859	5.0817914	-13.869274	21.990752	-18.094492	5.9547617
			G_1	0.2121530	0.1654877	3.3487320	-9.4747450	14.317893	-11.685705	3.8460630
		0.4	G_0	1.2854180	-0.9345000	1.7077280	-0.6641200	-2.2863700	3.2735540	-1.3019700
			G_1	0.2341252	0.1481234	3.3101935	-9.2393973	13.855454	-11.264661	3.6985698
		0.6	G_0	1.3804330	-1.0926500	1.7268520	-0.3443200	-2.7397100	3.4824740	-1.3117200
			G_1	0.2377410	0.5177690	0.7425160	-0.5650700	-0.9866000	1.2847770	-0.4700800
		0.8	G_0	1.4791920	-1.2508200	1.7403820	-0.5515300	-1.4528000	1.7023130	-0.5518600
			G_1	0.2596210	0.5100840	0.6508110	-0.5404300	-0.4458500	0.5142900	-0.1661100

Table 9B.19 – Influence Coefficients for a Circumferential Semi-Elliptical Surface Crack in a Sphere – Inside Surface

t/R_i	a/c	a/t	G_i	A_0	A_1	A_2	A_3	A_4	A_5	A_6
0.01667 (1/60)	2.0	0.0	G_0	0.8150546	-0.5623828	1.4465771	-4.6778133	8.4192164	-7.9025932	2.9866351
			G_1	0.1359146	0.0702340	3.5558581	-11.034445	16.967724	-14.126991	4.8706612
		0.2	G_0	0.8000774	-0.9446252	3.8893952	-11.802689	19.194938	-16.111926	5.4842920
			G_1	0.1277364	0.0659659	3.2316806	-9.7467461	14.591103	-11.934479	4.0760751
		0.4	G_0	0.8278456	-0.3064661	-0.7104847	3.0736923	-5.4721608	4.2460084	-1.1379080
			G_1	0.1412063	0.0537972	3.2925671	-9.8930279	14.775749	-12.067699	4.1195287
		0.6	G_0	0.8563095	-0.3647863	-0.6828579	3.2780595	-6.0457187	4.8229046	-1.3386430
			G_1	0.1478074	0.0209242	3.4681015	-10.494533	15.786300	-12.857397	4.3516213
		0.8	G_0	0.9071520	-0.9586397	2.9370213	-7.9787493	12.257472	-10.076715	3.4546072
			G_1	0.1508950	0.0261778	3.4556040	-10.564756	15.743394	-12.423987	4.0289121
0.05 (`1/20)	0.03125	0.0	G_0	0.1965046	2.9373464	-5.2582823	7.4889153	-6.9282667	3.3673349	-0.6677966
			G_1	0.0051780	0.1750280	2.7718680	-4.6457154	4.6780502	-3.2768090	0.9840994
		0.2	G_0	0.2063002	2.4348208	-1.6792669	-2.0521935	6.7328132	-6.5230628	2.1312083
			G_1	0.0046542	0.2627118	2.0457223	-2.3629875	1.5974738	-1.2915665	0.4682223
		0.4	G_0	0.2223780	2.8577860	-3.2804700	3.2986700	1.3072070	-5.0730500	2.3355800
			G_1	0.0166560	0.3647680	1.5986630	-0.8164400	0.8155950	-2.1386000	1.0593800
		0.6	G_0	0.2428340	2.9680040	-2.7123500	4.2276280	1.9716580	-8.4856900	4.0759500
			G_1	0.0217110	0.4843760	0.7385220	3.7350680	-7.3827500	4.9965730	-1.4675300
		0.8	G_0	0.2902570	2.3196210	4.2465490	-13.689800	31.500160	-34.075400	12.499100
			G_1	0.0274960	0.2852170	2.3927440	-0.4558000	0.7192520	-2.5606000	1.0195300
0.05 (1/20)	0.0625	0.0	G_0	0.2695332	2.1626001	-1.6551569	-1.2970208	4.5604304	-4.3163876	1.4010655
			G_1	0.0138667	0.1827458	2.5749608	-3.9044679	3.3556301	-2.1772209	0.6420134
		0.2	G_0	0.2737872	2.0048135	-0.7265377	-2.1376005	3.8183170	-2.6580856	0.6426073
			G_1	0.0159227	0.2244459	2.4125747	-3.8360214	4.0737272	-3.2611907	1.0825973
		0.4	G_0	0.3132520	2.4121650	-1.9883100	1.7361320	-0.2765900	-1.1091800	0.4834300
			G_1	0.0243370	0.3319760	1.8759790	-0.8794800	-1.6338700	1.6356670	-0.5085300
		0.6	G_0	0.3487740	2.9277140	-3.9144400	10.759540	-15.166200	9.7091670	-2.5697200
			G_1	0.0369750	0.3228750	2.4958380	-2.7866100	3.2162240	-3.7181600	1.4702100
		0.8	G_0	0.4409800	2.4409310	2.1913290	-4.0767400	5.8623460	-6.4414300	2.3701600
			G_1	0.0518150	0.3919640	2.4879240	-1.1766000	-0.0382500	-0.7649400	0.3544400
0.05 (1/20)	0.125	0.0	G_0	0.4065238	0.7772483	3.8861644	-12.573943	16.760207	-11.014593	2.8706957
			G_1	0.0320270	0.1825342	2.2670449	-2.7076615	1.2088194	-0.3777430	0.0763155
		0.2	G_0	0.4023356	1.1416026	1.6015250	-5.7067883	6.9115457	-4.2052659	1.0280524
			G_1	0.0461385	-0.0013993	4.0568875	-9.7684931	13.957243	-11.003908	3.4062359
		0.4	G_0	0.4731020	1.4598250	0.6686580	-2.4313900	1.4392340	0.3170760	-0.4982700
			G_1	0.0539600	0.3468750	1.5149680	-0.1187500	-2.9767700	2.9842000	-1.0116100
		0.6	G_0	0.5768930	1.6736950	0.5839020	-0.4166100	-2.9284700	3.8129030	-1.5216800
			G_1	0.0873860	0.3718430	1.9316280	-1.1754100	-1.1865200	1.3307430	-0.4408300
		0.8	G_0	0.7476330	1.5255190	3.4911010	-5.9067000	0.6609760	3.8597640	-2.1647600
			G_1	0.1350910	0.3555410	2.6415380	-2.4037300	-0.4893400	1.6644630	-0.8079800
0.05 (1/20)	0.25	0.0	G_0	0.6152816	-0.3348694	6.2955620	-15.590618	19.299508	-12.488107	3.3010035
			G_1	0.0703566	0.2828152	1.4036169	-0.6511596	-1.2076596	1.0318656	-0.2423741
		0.2	G_0	0.5995216	0.0745184	4.9157036	-13.844652	18.839744	-13.140826	3.6737383
			G_1	0.0813168	0.2876417	1.7176699	-2.7024974	2.8342997	-2.3477094	0.8026856
		0.4	G_0	0.7102380	0.0439840	3.9902400	-7.4695900	5.3742220	-1.0152600	-0.3583400
			G_1	0.1036140	0.2398990	1.7711840	-1.5881000	0.0239240	0.2836080	-0.0909500
		0.6	G_0	0.8668440	-0.1853500	5.2094010	-9.0092600	5.1296440	0.6287600	-1.1777900
			G_1	0.1484450	0.2501360	1.6315370	-0.4506700	-2.5744500	2.7430720	-0.9382000
		0.8	G_0	1.0904790	-0.8801900	9.5612400	-20.310000	20.023580	-9.4224700	1.5940800
			G_1	0.2092240	0.2051490	1.6130080	0.9488890	-6.5225500	6.9995060	-2.5512200

Table 9B.19 – Influence Coefficients for a Circumferential Semi-Elliptical Surface Crack in a Sphere – Inside Surface

t/R_i	a/c	a/t	G_i	A_0	A_1	A_2	A_3	A_4	A_5	A_6
0.05 (1/20)	0.5	0.0	G_0	0.8776607	-0.6729719	3.7721411	-6.5209060	6.3377934	-3.7028038	0.9872447
			G_1	0.1277541	0.4368502	0.4904522	1.0427434	-2.9631236	2.0826525	-0.5184313
		0.2	G_0	0.8775005	-0.8675711	5.2847489	-11.413044	14.009496	-9.5615193	2.7437562
			G_1	0.1415696	0.2121724	1.8544551	-3.2969631	3.8715613	-3.1962335	1.0916526
		0.4	G_0	0.9746810	-0.6764800	2.7817250	-1.4704600	-3.7922100	5.4145200	-2.0805200
			G_1	0.1609320	0.3221510	1.0828040	-0.2783200	-1.6569600	1.5946140	-0.5042700
		0.6	G_0	1.1219930	-1.0618100	3.8706440	-2.6144100	-4.3263600	7.1328260	-2.8953300
			G_1	0.2049110	0.2110230	1.3108450	-0.4293200	-1.7417300	1.7933410	-0.5985300
		0.8	G_0	1.2840520	-1.3687200	4.7660190	-4.9287800	-0.3916900	3.5649270	-1.6220800
			G_1	0.2543300	0.0523300	2.0496430	-2.5303100	1.5985850	-0.7631200	0.1387500
0.05 (1/20)	1.0	0.0	G_0	1.1977992	-0.5244870	0.1498299	2.3284866	-5.1058499	4.3469049	-1.3487980
			G_1	0.1870117	0.6987352	0.1316900	0.7269255	-2.5259384	2.1756251	-0.6540458
		0.2	G_0	1.2002994	-1.2236777	5.1305529	-13.994650	22.171398	-18.221125	5.9865275
			G_1	0.2108241	0.1630844	3.3655746	-9.5404779	14.447016	-11.795107	3.8786410
		0.4	G_0	1.2775500	-0.9717200	1.9465790	-1.3327300	-1.2496000	2.4601150	-1.0533700
			G_1	0.2271050	0.1554666	3.2762813	-9.2008474	13.878254	-11.301080	3.7032258
		0.6	G_0	1.3630880	-1.1355900	2.0377550	-1.1421700	-1.5764700	2.6001810	-1.0483700
			G_1	0.2340870	0.5037420	0.8243890	-0.7879300	-0.6213500	0.9879850	-0.3791600
		0.8	G_0	1.4588610	-1.2829700	1.9411540	-0.5400700	-2.1595700	2.6385470	-0.9299900
			G_1	0.2575880	0.4907760	0.7196260	-0.4754300	-0.8587700	1.0287600	-0.3729500
0.05 (1/20)	2.0	0.0	G_0	0.8150546	-0.5623828	1.4465771	-4.6778133	8.4192164	-7.9025932	2.9866351
			G_1	0.1359146	0.0702340	3.5558581	-11.034445	16.967724	-14.126991	4.8706612
		0.2	G_0	0.7973196	-0.9381424	3.8909617	-11.830984	19.234526	-16.118679	5.4755183
			G_1	0.1274597	0.0631239	3.2547584	-9.8153123	14.686785	-11.990357	4.0857813
		0.4	G_0	0.8219489	-0.2688351	-0.9012045	3.6405439	-6.3491321	4.9311895	-1.3509729
			G_1	0.1368187	0.0344331	3.4352335	-10.428022	15.682372	-12.738140	4.2956725
		0.6	G_0	0.8502963	-0.3657363	-0.5930920	2.9905584	-5.6109214	4.5263371	-1.2674956
			G_1	0.1462277	0.0307414	3.4084485	-10.285583	15.400473	-12.485259	4.2107194
		0.8	G_0	0.8970583	-0.9194808	2.8028991	-7.5318379	11.471860	-9.3822670	3.2124529
			G_1	0.1489320	0.0377374	3.4059416	-10.404290	15.449222	-12.125448	3.9093420
0.1 (1/10)	0.03125	0.0	G_0	0.1965046	2.9373464	-5.2582823	7.4889153	-6.9282667	3.3673349	-0.6677966
			G_1	0.0051780	0.1750280	2.7718680	-4.6457154	4.6780502	-3.2768090	0.9840994
		0.2	G_0	0.2056151	2.3876240	-1.2594709	-3.9600494	10.263090	-9.4728811	3.0615394
			G_1	0.0055285	0.2220479	2.2722444	-2.9582870	2.2834250	-1.6416281	0.5311764
		0.4	G_0	0.2092293	2.9825394	-4.9329850	8.8533505	-8.2951024	2.9215984	-0.1801457
			G_1	0.0086354	0.2230926	2.5017267	-3.5679613	4.2965576	-3.9848117	1.3716472
		0.6	G_0	0.2156946	3.3194024	-6.7127312	17.752305	-22.219396	12.305863	-2.6343514
			G_1	0.0095494	0.2722523	2.2990303	-2.5229292	3.9759245	-4.8178097	1.8171860
		0.8	G_0	0.2106541	4.0693503	-12.314028	43.297719	-67.899601	49.749656	-14.453951
			G_1	0.0052008	0.5131981	0.2825660	5.8237240	-9.7973928	6.2698867	-1.7971248
0.1 (1/10)	0.0625	0.0	G_0	0.2695332	2.1626001	-1.6551569	-1.2970208	4.5604304	-4.3163876	1.4010655
			G_1	0.0138667	0.1827458	2.5749608	-3.9044679	3.3556301	-2.1772209	0.6420134
		0.2	G_0	0.2734455	1.9681289	-0.6332429	-2.4507798	4.3416872	-3.0780568	0.7761721
			G_1	0.0152751	0.2288569	2.3378606	-3.6783066	3.9024648	-3.1657268	1.0624553
		0.4	G_0	0.3069420	2.2661960	-1.4011000	-0.1823600	2.5876020	-3.1790500	1.0989000
			G_1	0.0170970	0.3974880	1.2707560	0.7398430	-3.5913300	2.7604580	-0.7723900
		0.6	G_0	0.3252810	2.9110250	-5.0383200	13.339660	-17.918400	11.117430	-2.8068700
			G_1	0.0321510	0.2670050	2.7738640	-4.2188800	5.4231930	-4.8925100	1.5974400
		0.8	G_0	0.4029060	2.5130770	-0.8265200	2.0036310	0.8442140	-4.1326900	1.7303900
			G_1	0.0410260	0.4369650	1.6388160	0.3340340	-1.6643000	0.8372800	-0.3914600

Table 9B.19 – Influence Coefficients for a Circumferential Semi-Elliptical Surface Crack in a Sphere – Inside Surface

t/R_i	a/c	a/t	G_i	A_0	A_1	A_2	A_3	A_4	A_5	A_6
0.1 (1/10)	0.125	0.0	G_0	0.4065238	0.7772483	3.8861644	-12.573943	16.760207	-11.014593	2.8706957
			G_1	0.0320270	0.1825342	2.2670449	-2.7076615	1.2088194	-0.3777430	0.0763155
		0.2	G_0	0.3993741	1.1157939	1.7168739	-6.1865447	7.7474504	-4.8620610	1.2242468
			G_1	0.0455353	-0.0135463	4.1419231	-10.167325	14.710359	-11.641060	3.6088361
		0.4	G_0	0.4617530	1.4622820	0.2156210	-0.8812900	-1.3328400	2.7878940	-1.3388300
			G_1	0.0536630	0.3276020	1.6209140	-0.4541700	-2.5278500	2.6497620	-0.8945800
		0.6	G_0	0.5380720	1.6213820	0.4653070	-0.5397900	-2.4739000	3.7359840	-1.6506700
			G_1	0.0753350	0.3637430	1.7925290	-0.8305100	-1.4751600	1.3895700	-0.4213100
		0.8	G_0	0.6628870	1.4047270	2.7816950	-4.1401700	-0.3587800	4.2499960	-2.4267700
			G_1	0.1086010	0.3364230	2.3178370	-1.7185200	-0.6824300	1.5432330	-0.8117800
0.1 (1/10)	0.25	0.0	G_0	0.6152816	-0.3348694	6.2955620	-15.590618	19.299508	-12.488107	3.3010035
			G_1	0.0703566	0.2828152	1.4036169	-0.6511596	-1.2076596	1.0318656	-0.2423741
		0.2	G_0	0.5946315	0.1630558	4.1726937	-11.442887	15.001336	-10.166362	2.7840781
			G_1	0.0799165	0.3122584	1.5121304	-2.0502690	1.8012664	-1.5552403	0.5688688
		0.4	G_0	0.7002690	-0.0112900	4.0839410	-7.7072400	5.6977540	-1.1953700	-0.3271800
			G_1	0.1044360	0.2092790	1.9497990	-2.2166900	1.0304150	-0.4828700	0.1377200
		0.6	G_0	0.8327810	-0.1429600	4.6335640	-7.4550200	3.1278560	1.9985630	-1.5759000
			G_1	0.1447420	0.2143310	1.8268530	-1.1379500	-1.4219100	1.8413810	-0.6692300
		0.8	G_0	1.0408980	-1.0572400	10.765920	-25.160500	29.563410	-17.485000	4.0117800
			G_1	0.2090000	-0.0738100	3.7135650	-6.3740300	6.0799340	-3.2263400	0.5888100
0.1 (1/10)	0.5	0.0	G_0	0.8776607	-0.6729719	3.7721411	-6.5209060	6.3377934	-3.7028038	0.9872447
			G_1	0.1277541	0.4368502	0.4904522	1.0427434	-2.9631236	2.0826525	-0.5184313
		0.2	G_0	0.8763580	-0.8696069	5.2444797	-11.291330	13.885305	-9.5329867	2.7563560
			G_1	0.1414533	0.2149777	1.8065139	-3.1255644	3.5946509	-2.9851198	1.0299591
		0.4	G_0	0.9628790	-0.7184100	2.9189220	-1.8029700	-3.2999000	5.0465790	-1.9741800
			G_1	0.1596580	0.3006910	1.1779510	-0.5684100	-1.1982000	1.2462930	-0.4026600
		0.6	G_0	1.0967370	-1.1070900	4.0513750	-3.0267600	-3.6936500	6.6464720	-2.7585600
			G_1	0.1997760	0.1953150	1.3974000	-0.7646900	-1.0876900	1.2196840	-0.4138900
		0.8	G_0	1.2424830	-1.3001900	4.2941430	-3.2969300	-2.7560400	5.3099170	-2.1723700
			G_1	0.2473640	0.0819390	1.8270490	-1.8506300	0.6823350	-0.1218100	-0.0558100
0.1 (1/10)	1.0	0.0	G_0	1.1977992	-0.5244870	0.1498299	2.3284866	-5.1058499	4.3469049	-1.3487980
			G_1	0.1870117	0.6987352	0.1316900	0.7269255	-2.5259384	2.1756251	-0.6540458
		0.2	G_0	1.2005677	-1.2230016	5.0985217	-13.837672	21.890898	-17.988267	5.9105357
			G_1	0.2113782	0.1664234	3.3274422	-9.4052634	14.236208	-11.632675	3.8277229
		0.4	G_0	1.2638600	-0.9614100	1.8822030	-1.1747600	-1.3442200	2.4305450	-1.0245000
			G_1	0.2282186	0.1489274	3.2665130	-9.0686011	13.608451	-11.071798	3.6294031
		0.6	G_0	1.3385050	-1.0805500	1.6851940	0.0595880	-3.4485600	4.0132490	-1.4715700
			G_1	0.2286090	0.5343970	0.6085790	-0.1308700	-1.5964100	1.7241660	-0.6053000
		0.8	G_0	1.4306440	-1.2636300	1.9100820	-0.1800600	-2.8031200	3.1532600	-1.1039200
			G_1	0.2524840	0.5095760	0.6303900	-0.2703000	-1.0026900	1.0556480	-0.3754900
0.1 (1/10)	2.0	0.0	G_0	0.8150546	-0.5623828	1.4465771	-4.6778133	8.4192164	-7.9025932	2.9866351
			G_1	0.1359146	0.0702340	3.5558581	-11.034445	16.967724	-14.126991	4.8706612
		0.2	G_0	0.8037855	-0.9092929	3.7353895	-11.416378	18.639255	-15.682327	5.3485818
			G_1	0.1286222	0.0914525	3.0868205	-9.2893804	13.840605	-11.320690	3.8796337
		0.4	G_0	0.8174447	-0.2826820	-0.7753340	3.3044722	-5.9069786	4.6666813	-1.2969702
			G_1	0.1396265	0.0763945	3.1512330	-9.3939695	13.870673	-11.246516	3.8300230
		0.6	G_0	0.8412020	-0.3463883	-0.6219701	3.0678735	-5.7507939	4.6839414	-1.3382006
			G_1	0.1457296	0.0728417	3.1174048	-9.2123878	13.483161	-10.858611	3.6845393
		0.8	G_0	0.8871849	-0.9132745	2.8983617	-7.7749672	11.739486	-9.4660625	3.1911523
			G_1	0.1406352	0.2552970	1.8998084	-5.2594318	6.8575162	-5.2828773	1.8237938

Table 9B.19 – Influence Coefficients for a Circumferential Semi-Elliptical Surface Crack in a Sphere – Inside Surface

t/R_i	a/c	a/t	G_i	A_0	A_1	A_2	A_3	A_4	A_5	A_6
0.2 (1/5)	0.0625	0.0	G_0	0.2695332	2.1626001	-1.6551569	-1.2970208	4.5604304	-4.3163876	1.4010655
			G_1	0.0138667	0.1827458	2.5749608	-3.9044679	3.3556301	-2.1772209	0.6420134
		0.2	G_0	0.2737585	2.0989557	-1.3366600	-2.0216133	5.7609793	-5.3164212	1.7002530
			G_1	0.0172389	0.1931788	2.4328584	-3.5131947	2.8778096	-1.8716576	0.5553443
		0.4	G_0	0.2942695	1.6309557	1.9282841	-10.599320	19.044288	-15.839499	4.9002661
			G_1	0.0197789	0.1838190	2.5736443	-4.1164538	4.6841392	-3.8087419	1.2237021
		0.6	G_0	0.3582710	1.1316670	8.9981080	-39.164000	74.850940	-66.338200	21.892300
			G_1	0.0252680	0.5624700	-0.0774500	5.6321440	-11.573200	9.2788790	-2.9259400
		0.8	G_0	0.3499740	2.2914350	-0.2831900	-2.4992200	9.7923300	-11.123300	3.7094100
			G_1	0.0264840	0.4051970	1.5865810	-0.3364900	-0.3696500	0.1769020	-0.3491600
0.2 (1/5)	0.125	0.0	G_0	0.4065238	0.7772483	3.8861644	-12.573943	16.760207	-11.014593	2.8706957
			G_1	0.0320270	0.1825342	2.2670449	-2.7076615	1.2088194	-0.3777430	0.0763155
		0.2	G_0	0.4084458	0.9728544	2.9451362	-11.032946	16.077444	-11.435539	3.1901555
			G_1	0.0385061	0.2062311	2.1039263	-2.6035551	1.5672811	-0.9370389	0.3033573
		0.4	G_0	0.4430160	1.3487560	0.6778660	-2.4532700	1.0000460	1.1820340	-0.8966900
			G_1	0.0452250	0.3516930	1.3572720	0.1641320	-3.1358400	2.8585510	-0.8900400
		0.6	G_0	0.4939730	1.6106370	-0.4741100	1.0725300	-2.4838600	2.2320220	-0.8679600
			G_1	0.0599710	0.4327900	1.0944060	0.8406750	-3.5251900	2.8446460	-0.8879300
		0.8	G_0	0.5703130	1.5331780	0.1960790	1.6381490	-5.1731200	6.2059300	-2.9109200
			G_1	0.0836110	0.3426920	1.8504940	-1.1043800	-0.5459400	1.3182020	-0.8771200
0.2 (1/5)	0.25	0.0	G_0	0.6152816	-0.3348694	6.2955620	-15.590618	19.299508	-12.488107	3.3010035
			G_1	0.0703566	0.2828152	1.4036169	-0.6511596	-1.2076596	1.0318656	-0.2423741
		0.2	G_0	0.6133907	-0.2635319	5.9754897	-15.245175	19.397444	-12.868262	3.4777552
			G_1	0.0815379	0.1197957	2.3185388	-3.4598086	2.9385877	-1.8712161	0.5393793
		0.4	G_0	0.6835090	-0.0762400	4.1822090	-8.0663800	6.2903700	-1.5521400	-0.2711800
			G_1	0.1004930	0.2132070	1.8019670	-1.6633100	-0.0824400	0.5789510	-0.2348900
		0.6	G_0	0.7811640	-0.1443900	4.5779910	-7.7709400	4.0234850	1.3759920	-1.4785900
			G_1	0.1308160	0.2114970	1.7861730	-1.1092300	-1.3132500	1.7043170	-0.6271500
		0.8	G_0	0.9516200	-1.0914200	10.564350	-24.138600	28.221470	-16.194300	3.3940700
			G_1	0.1855060	-0.0949900	3.7286180	-6.5150900	6.8116510	-3.9697800	0.7915400
0.2 (1/5)	0.5	0.0	G_0	0.8776607	-0.6729719	3.7721411	-6.5209060	6.3377934	-3.7028038	0.9872447
			G_1	0.1277541	0.4368502	0.4904522	1.0427434	-2.9631236	2.0826525	-0.5184313
		0.2	G_0	0.8742248	-0.9052377	5.2670077	-11.045503	13.195491	-8.8422731	2.5138892
			G_1	0.1403924	0.2163568	1.7349237	-2.8428627	3.1113750	-2.5977594	0.9110634
		0.4	G_0	0.9401030	-0.7451800	2.9664560	-1.9749400	-2.8932700	4.6449810	-1.8344300
			G_1	0.1555140	0.2970190	1.1574570	-0.5681000	-1.0965000	1.1098090	-0.3486700
		0.6	G_0	1.0537880	-1.1093600	4.0579950	-3.1632500	-3.1381200	6.0141240	-2.5319500
			G_1	0.1922940	0.1879200	1.3801410	-0.6746200	-1.2045000	1.2997450	-0.4403500
		0.8	G_0	1.1884610	-1.2911700	4.2898150	-3.0135200	-3.0823600	5.6399870	-2.3739300
			G_1	0.2380870	0.1010080	1.6081810	-1.0026700	-0.6465600	0.9578210	-0.4255000
0.2 (1/5)	1.0	0.0	G_0	1.1977992	-0.5244870	0.1498299	2.3284866	-5.1058499	4.3469049	-1.3487980
			G_1	0.1870117	0.6987352	0.1316900	0.7269255	-2.5259384	2.1756251	-0.6540458
		0.2	G_0	1.2019274	-1.2495893	5.1046981	-13.602601	21.368497	-17.519717	5.7503733
			G_1	0.2123063	0.1600851	3.3211697	-9.3446295	14.144479	-11.559200	3.7991746
		0.4	G_0	1.2422470	-0.9714600	1.8852790	-0.9908600	-1.6585700	2.6485320	-1.0881700
			G_1	0.2218584	0.1625068	3.1510566	-8.7140941	13.119255	-10.711408	3.5113447
		0.6	G_0	1.3046120	-1.0790500	1.7356360	0.0128460	-3.1861400	3.6339400	-1.3238800
			G_1	0.2222060	0.5241130	0.6543980	-0.3228700	-1.0897200	1.2192770	-0.4395200
		0.8	G_0	1.3908420	-1.2477800	1.9896800	-0.1664500	-2.7059000	2.9650450	-1.0478600
			G_1	0.2488650	0.5058520	0.6232410	-0.2059600	-0.9627500	0.9695670	-0.3598300

Table 9B.19 – Influence Coefficients for a Circumferential Semi-Elliptical Surface Crack in a Sphere – Inside Surface

t/R_i	a/c	a/t	G_i	A_0	A_1	A_2	A_3	A_4	A_5	A_6
0.2 (1/5)	2.0	0.0	G_0	0.8150546	-0.5623828	1.4465771	-4.6778133	8.4192164	-7.9025932	2.9866351
			G_1	0.1359146	0.0702340	3.5558581	-11.034445	16.967724	-14.126991	4.8706612
		0.2	G_0	0.8250975	-0.9438687	3.8105923	-11.470951	18.537512	-15.482925	5.2571666
			G_1	0.1356047	0.0746798	3.1854379	-9.5353120	14.124071	-11.450020	3.8901899
		0.4	G_0	0.8139942	-0.3159698	-0.4999519	2.5090342	-4.7632356	3.9015300	-1.1103420
			G_1	0.1380121	0.0952916	3.0412294	-9.0460679	13.258399	-10.660849	3.6064159
		0.6	G_0	0.8300414	-0.3394132	-0.5415102	2.8491907	-5.4748640	4.5771074	-1.3522891
			G_1	0.1429879	0.0961143	2.9878547	-8.7967602	12.736287	-10.120997	3.3946646
		0.8	G_0	0.8729867	-0.8783754	2.8952584	-7.7169371	11.500786	-9.0803442	2.9911160
			G_1	0.1400092	0.2554510	1.9392782	-5.3577221	6.9103675	-5.1468324	1.7079398
0.3333 (1/3)	0.125	0.0	G_0	0.4065238	0.7772483	3.8861644	-12.573943	16.760207	-11.014593	2.8706957
			G_1	0.0320270	0.1825342	2.2670449	-2.7076615	1.2088194	-0.3777430	0.0763155
		0.2	G_0	0.4020000	0.9853595	2.7043980	-10.513668	15.464532	-11.026411	3.0760461
			G_1	0.0372110	0.2063396	2.0679496	-2.5708822	1.5350316	-0.8956604	0.2859264
		0.4	G_0	0.4353513	1.0074059	2.9587394	-11.549309	18.119891	-13.752999	4.0097223
			G_1	0.0491893	0.1999997	2.2616203	-3.1204287	2.5261383	-1.7193112	0.5223301
		0.6	G_0	0.6536134	-0.3960714	3.9021296	1.1836114	-14.440087	16.822912	-6.2583556
			G_1	0.0893580	0.2902339	-0.1501292	7.0452471	-14.749314	11.977710	-3.6847679
		0.8	G_0	0.5730046	-0.2848721	11.935635	-34.590748	49.744679	-33.654577	8.2066323
			G_1	0.0918762	-0.2872288	5.8672732	-13.319779	17.442403	-11.198133	2.4320312
0.3333 (1/3)	0.25	0.0	G_0	0.6152816	-0.3348694	6.2955620	-15.590618	19.299508	-12.488107	3.3010035
			G_1	0.0703566	0.2828152	1.4036169	-0.6511596	-1.2076596	1.0318656	-0.2423741
		0.2	G_0	0.6051739	-0.2720363	5.8549634	-14.849672	18.753613	-12.354730	3.3228649
			G_1	0.0797227	0.1133642	2.3119122	-3.4664732	2.9490005	-1.8638300	0.5327646
		0.4	G_0	0.7512788	-1.7015711	13.690661	-35.526023	47.428484	-32.325665	8.8198002
			G_1	0.1009842	0.0938557	2.2987210	-3.1266301	2.3590792	-1.4947249	0.4568768
		0.6	G_0	0.8342864	-1.9526111	15.450960	-40.564748	55.579185	-38.728413	10.698090
			G_1	0.1312765	-0.0059848	2.9477834	-4.8816998	5.1202114	-3.5854913	1.0355862
		0.8	G_0	0.8805576	-1.3233844	12.321751	-32.489275	46.108417	-32.487421	8.6957482
			G_1	0.1723697	-0.1621971	4.0976228	-8.5360647	11.331973	-8.0070418	2.0432026
0.3333 (1/3)	0.5	0.0	G_0	0.8776607	-0.6729719	3.7721411	-6.5209060	6.3377934	-3.7028038	0.9872447
			G_1	0.1277541	0.4368502	0.4904522	1.0427434	-2.9631236	2.0826525	-0.5184313
		0.2	G_0	0.8637041	-0.9579411	5.5193636	-11.685961	14.029918	-9.3776725	2.6483366
			G_1	0.1375681	0.2020794	1.7847423	-2.9704902	3.2909875	-2.7216072	0.9438583
		0.4	G_0	1.0748010	-3.1343180	15.652793	-35.787158	45.096152	-29.974302	8.1420931
			G_1	0.1585619	0.1298599	1.7627391	-2.4097712	2.4267576	-2.2345607	0.8527975
		0.6	G_0	1.1434265	-3.2071828	16.049409	-36.939714	47.156679	-31.706900	8.6657124
			G_1	0.1911418	0.0566092	1.9186548	-2.2593205	1.6495597	-1.3251807	0.4935857
		0.8	G_0	1.1547897	-1.8109612	8.1002548	-15.155969	17.051101	-10.542865	2.6030956
			G_1	0.2421556	-0.0724574	2.5190224	-3.7734438	4.0569536	-2.9162745	0.7860745
0.3333 (1/3)	1.0	0.0	G_0	1.1977992	-0.5244870	0.1498299	2.3284866	-5.1058499	4.3469049	-1.3487980
			G_1	0.1870117	0.6987352	0.1316900	0.7269255	-2.5259384	2.1756251	-0.6540458
		0.2	G_0	1.1875625	-1.2432639	5.0281758	-13.245081	20.748463	-17.004471	5.5764820
			G_1	0.2082564	0.1715823	3.2203073	-9.0303758	13.686914	-11.208961	3.6846903
		0.4	G_0	1.4876625	-4.5324977	19.641221	-46.607296	62.182534	-43.493509	12.383858
			G_1	0.2385240	-0.0937573	4.2543566	-11.186814	16.198364	-12.669420	3.9990332
		0.6	G_0	1.5000661	-4.1947739	17.489127	-40.328659	52.861248	-36.481471	10.252286
			G_1	0.2511561	-0.0152239	3.5438994	-8.7733020	12.271038	-9.4722234	2.9534289
		0.8	G_0	1.3390263	-1.3241238	3.2298761	-4.6387878	5.7003012	-4.6556451	1.5695068
			G_1	0.2576932	0.3305364	1.4832349	-3.0035476	4.2515862	-3.7224290	1.2347530

Table 9B.19 – Influence Coefficients for a Circumferential Semi-Elliptical Surface Crack in a Sphere – Inside Surface

t/R_i	a/c	a/t	G_i	A_0	A_1	A_2	A_3	A_4	A_5	A_6
0.3333 (1/3)	2.0	0.0	G_0	0.8150546	-0.5623828	1.4465771	-4.6778133	8.4192164	-7.9025932	2.9866351
			G_1	0.1359146	0.0702340	3.5558581	-11.034445	16.967724	-14.126991	4.8706612
		0.2	G_0	0.8183590	-0.9202621	3.7119207	-11.153624	17.978556	-14.963095	5.0641776
			G_1	0.1336155	0.0946846	3.0589552	-9.1310235	13.436743	-10.839985	3.6743713
		0.4	G_0	0.8271021	-0.9666760	3.9511559	-11.593058	18.251495	-14.828350	4.9121211
			G_1	0.1363643	0.1116181	2.9365323	-8.6680634	12.529636	-9.9279173	3.3204599
		0.6	G_0	0.8340322	-0.9307282	3.6181955	-10.368517	16.099398	-12.941929	4.2608708
			G_1	0.1413107	0.1037118	2.9507169	-8.6545394	12.400986	-9.6678730	3.1751898
		0.8	G_0	0.8474108	-0.8443446	2.9324673	-7.7308789	11.239031	-8.5582060	2.7123537
			G_1	0.1412033	0.2357192	2.1073932	-5.8766063	7.6722573	-5.5747592	1.7604674

Notes:

1. Interpolation of the influence coefficients, G_i, may be used for intermediate values of t/R_i, a/c, and a/t.
2. The value of the influence coefficients at the surface point of the crack defined by $\varphi = 0°$ are equal to: $G_i = A_0$.
3. The value of the influence coefficients at the deepest point of the crack defined by $\varphi = 90°$ are equal to $G_i = \sum_{n=0}^{6} A_n$.

Table 9B.20 – Influence Coefficients for a Circumferential Semi-Elliptical Surface Crack in a Sphere – Outside Surface

t/R_i	a/c	a/t	G_i	A_0	A_1	A_2	A_3	A_4	A_5	A_6
0.0	0.03125	0.0	G_0	0.1965046	2.9373464	-5.2582823	7.4889153	-6.9282667	3.3673349	-0.6677966
			G_1	0.0051780	0.1750280	2.7718680	-4.6457154	4.6780502	-3.2768090	0.9840994
		0.2	G_0	0.2080760	3.0112422	-5.1048701	7.6348715	-6.8347547	2.7940766	-0.3882688
			G_1	0.0084834	0.2406767	2.4574292	-3.6452421	3.6142837	-2.8451814	0.9270638
		0.4	G_0	0.2357940	3.0822400	-3.5792100	3.9476890	1.9131590	-6.8872200	3.1896800
			G_1	0.0145140	0.4038000	1.6422700	-0.3906100	-0.6480700	-0.2940300	0.2514900
		0.6	G_0	0.2902240	3.6892050	-4.5739100	11.709890	-6.3750000	-5.8894100	4.2452400
			G_1	0.0208890	0.7016780	0.1631840	5.7072160	-8.2075800	3.4561120	-0.4454700
		0.8	G_0	0.5163550	2.5310830	14.712900	-43.621800	101.06570	-116.08100	46.190900
			G_1	0.0825460	0.4971770	4.6064810	-7.3326700	21.148620	-29.345100	12.491400
0.0	0.0625	0.0	G_0	0.2695332	2.1626001	-1.6551569	-1.2970208	4.5604304	-4.3163876	1.4010655
			G_1	0.0138667	0.1827458	2.5749608	-3.9044679	3.3556301	-2.1772209	0.6420134
		0.2	G_0	0.2845892	2.2264055	-1.4546190	-1.5760719	5.1131083	-4.9485443	1.6207574
			G_1	0.0199077	0.2210874	2.4642047	-3.5898625	3.1624039	-2.2403780	0.6965751
		0.4	G_0	0.3261480	2.5200870	-1.8847000	2.1798740	-1.4597100	-0.1886500	0.2393400
			G_1	0.0294120	0.3699370	1.9220850	-1.2071500	-0.4394000	0.2737550	-0.0395200
		0.6	G_0	0.4166330	3.1566470	-2.6248900	7.7325910	-9.6927800	3.6428700	-0.0892000
			G_1	0.0598460	0.4340740	2.6811560	-3.1936600	4.0753720	-4.6940200	1.8285500
		0.8	G_0	0.6540140	3.4231920	3.8158050	-4.1586900	3.4715330	-10.310400	6.6280000
			G_1	0.1214780	0.6975490	2.9718330	-1.3036500	-0.0754900	-3.0465100	2.1670000
0.0	0.125	0.0	G_0	0.4065238	0.7772483	3.8861644	-12.573943	16.760207	-11.014593	2.8706957
			G_1	0.0320270	0.1825342	2.2670449	-2.7076615	1.2088194	-0.3777430	0.0763155
		0.2	G_0	0.4242116	1.0089302	3.2973815	-12.159726	17.873386	-12.868668	3.6281712
			G_1	0.0429859	0.2033811	2.2563818	-2.8752160	1.8152558	-1.0512327	0.3181077
		0.4	G_0	0.4917770	1.6592320	-0.1080400	0.1793240	-2.7076100	3.3680620	-1.3489700
			G_1	0.0634270	0.3722500	1.6231670	-0.5306500	-2.0007400	1.8943780	-0.5880300
		0.6	G_0	0.6591820	1.8759140	1.0212600	-1.7698000	-0.5653600	1.2479960	-0.4376600
			G_1	0.1116040	0.4714500	1.7940590	-0.7557600	-1.4901700	1.0852180	-0.2113700
		0.8	G_0	0.9809330	1.8846320	4.8020780	-8.0580200	0.4447850	3.4772660	-1.0567500
			G_1	0.2039950	0.4800150	2.8822430	-2.5890100	-0.9683000	1.5372370	-0.3750200
0.0	0.25	0.0	G_0	0.6152816	-0.3348694	6.2955620	-15.590618	19.299508	-12.488107	3.3010035
			G_1	0.0703566	0.2828152	1.4036169	-0.6511596	-1.2076596	1.0318656	-0.2423741
		0.2	G_0	0.6385889	-0.3095132	6.5329787	-16.622882	21.056641	-13.850120	3.6988146
			G_1	0.0840059	0.1999367	1.8218113	-1.7756899	0.3757186	-0.0785358	0.0643386
		0.4	G_0	0.7390420	0.0548160	4.0842620	-7.5883100	5.4047530	-1.0146100	-0.3483400
			G_1	0.1164500	0.2479880	1.8282520	-1.7169900	0.1912120	0.1165770	-0.0186100
		0.6	G_0	0.9461210	-0.1858800	5.5867460	-9.8634900	5.9596870	0.1296440	-1.0026100
			G_1	0.1778050	0.2056680	2.0979210	-1.8039500	-0.5558700	1.1461400	-0.4206600
		0.8	G_0	1.2452110	-0.6921900	8.3260620	-14.948000	8.6936910	0.4755790	-1.3926600
			G_1	0.2585640	0.1548890	2.1170240	-0.4910000	-4.6146100	5.4550750	-1.9663300
0.0	0.5	0.0	G_0	0.8776607	-0.6729719	3.7721411	-6.5209060	6.3377934	-3.7028038	0.9872447
			G_1	0.1277541	0.4368502	0.4904522	1.0427434	-2.9631236	2.0826525	-0.5184313
		0.2	G_0	0.9003948	-0.8850488	5.2743239	-11.267523	13.890755	-9.6373584	2.8183906
			G_1	0.1404409	0.3215397	1.1010666	-1.0257556	0.6943940	-1.0793186	0.5410929
		0.4	G_0	1.0058060	-0.7322600	2.9951940	-1.9459200	-3.2613500	5.1424570	-2.0306200
			G_1	0.1740870	0.3051630	1.2070310	-0.6720500	-1.0651300	1.1445590	-0.3644800
		0.6	G_0	1.1826010	-1.1072500	3.9623640	-2.7781300	-4.3097300	7.2772750	-2.9648200
			G_1	0.2277120	0.1701170	1.5499470	-1.1051200	-0.8333700	1.1717060	-0.4194500
		0.8	G_0	1.3833380	-1.3900300	4.3755780	-3.7372600	-2.5403200	5.3036000	-2.0932400
			G_1	0.2820110	0.0839230	1.7258580	-1.5358100	-0.0635600	0.5006780	-0.1982200

Table 9B.20 – Influence Coefficients for a Circumferential Semi-Elliptical Surface Crack in a Sphere – Outside Surface

t/R_i	a/c	a/t	G_i	A_0	A_1	A_2	A_3	A_4	A_5	A_6
0.0	1.0	0.0	G_0	1.1977992	-0.5244870	0.1498299	2.3284866	-5.1058499	4.3469049	-1.3487980
			G_1	0.1870117	0.6987352	0.1316900	0.7269255	-2.5259384	2.1756251	-0.6540458
		0.2	G_0	1.2263282	-1.1608467	4.4744783	-11.584231	17.811241	-14.408250	4.6998279
			G_1	0.2154786	0.2441623	2.8107820	-7.6574580	11.171413	-9.0053693	2.9542871
		0.4	G_0	1.2989480	-0.9978000	1.9479540	-1.3002700	-1.4940100	2.8306230	-1.2126000
			G_1	0.2386246	0.1447774	3.3198992	-9.2456599	13.823512	-11.223715	3.6868232
		0.6	G_0	1.3971180	-1.1348400	1.7918740	-0.4202600	-2.8679300	3.7685480	-1.4405000
			G_1	0.2445870	0.5326670	0.5939690	-0.0361800	-2.0163100	2.2167010	-0.7782200
		0.8	G_0	1.5117010	-1.3244800	1.7568350	-0.1337900	-2.8629300	3.2953270	-1.1412400
			G_1	0.2704470	0.5113280	0.5357440	-0.0327300	-1.5570200	1.5570970	-0.5094600
0.0	2.0	0.0	G_0	0.8150546	-0.5623828	1.4465771	-4.6778133	8.4192164	-7.9025932	2.9866351
			G_1	0.1359146	0.0702340	3.5558581	-11.034445	16.967724	-14.126991	4.8706612
		0.2	G_0	0.8463715	-1.0011024	4.0052312	-11.937181	19.189548	-16.039296	5.4674371
			G_1	0.1395121	0.0753999	3.1895604	-9.5540932	14.214316	-11.649525	4.0073308
		0.4	G_0	0.8570045	-1.0183085	3.9957306	-11.886878	19.152747	-16.047480	5.4801806
			G_1	0.1436696	0.0544018	3.2816127	-9.8164232	14.610963	-11.942138	4.0907797
		0.6	G_0	0.8839861	-1.0765270	4.0774087	-11.976171	19.173189	-15.996207	5.4501217
			G_1	0.1504185	0.0478401	3.2579960	-9.6921199	14.370843	-11.736129	4.0258411
		0.8	G_0	0.9033134	-0.9619755	2.8501500	-7.6366897	11.596116	-9.4828625	3.2550163
			G_1	0.1458559	0.2313881	1.9882138	-5.5546045	7.4196069	-5.8965053	2.0855563
0.01 (1/100)	0.03125	0.0	G_0	0.1965046	2.9373464	-5.2582823	7.4889153	-6.9282667	3.3673349	-0.6677966
			G_1	0.0051780	0.1750280	2.7718680	-4.6457154	4.6780502	-3.2768090	0.9840994
		0.2	G_0	0.2077867	2.2749380	0.1405830	-8.1883567	16.585201	-14.085844	4.3580585
			G_1	0.0058829	0.2123600	2.6447168	-4.3435807	4.7836038	-3.7532574	1.1949871
		0.4	G_0	0.2228150	2.9734920	-3.4283200	3.3930740	3.7873140	-9.1100500	4.0601300
			G_1	0.0112870	0.4802660	1.4073800	0.0510890	-0.0972200	-1.8992500	1.0371600
		0.6	G_0	0.2282140	3.5166310	-6.8236400	20.411300	-20.304700	5.6194120	0.3783500
			G_1	0.0183830	0.7773130	-1.4752300	11.278750	-15.823300	8.6430980	-1.9893500
		0.8	G_0	0.2615290	2.7339220	1.5901460	-6.4403200	48.322670	-70.868000	29.356500
			G_1	0.0220870	0.8779500	-2.0000400	11.244490	-3.7584200	-9.8042500	5.5705000
0.01 (1/100)	0.0625	0.0	G_0	0.2695332	2.1626001	-1.6551569	-1.2970208	4.5604304	-4.3163876	1.4010655
			G_1	0.0138667	0.1827458	2.5749608	-3.9044679	3.3556301	-2.1772209	0.6420134
		0.2	G_0	0.2769613	2.0258789	-0.6462394	-2.3171130	4.1211301	-2.9457279	0.7405852
			G_1	0.0177280	0.2145484	2.5823250	-4.3171184	4.8055429	-3.8182428	1.2440577
		0.4	G_0	0.3198770	2.5511570	-2.0536700	1.7976150	1.0661150	-3.4940800	1.5768700
			G_1	0.0352270	0.5096780	1.4381240	-0.0647700	-1.5756000	0.5058010	0.0840900
		0.6	G_0	0.3724790	3.3785840	-5.5275400	17.226590	-21.828900	10.689630	-1.6511000
			G_1	0.0528640	0.5448000	1.8813540	-0.5637400	1.1153130	-3.5764200	1.8037600
		0.8	G_0	0.5171860	3.0210280	1.8715830	3.6003150	1.4454340	-16.702800	10.241500
			G_1	0.0816830	0.6467690	2.0872710	2.2894120	-2.1269000	-4.5735100	3.3312900
0.01 (1/100)	0.125	0.0	G_0	0.4065238	0.7772483	3.8861644	-12.573943	16.760207	-11.014593	2.8706957
			G_1	0.0320270	0.1825342	2.2670449	-2.7076615	1.2088194	-0.3777430	0.0763155
		0.2	G_0	0.4061772	1.1680061	1.5950075	-5.6041264	6.7047751	-4.0556730	0.9877657
			G_1	0.0474966	0.0088231	4.0171999	-9.5055990	13.434246	-10.567935	3.2711539
		0.4	G_0	0.4850880	1.4332010	1.5839620	-5.0901000	6.1655090	-4.1166300	1.1040100
			G_1	0.0731420	0.3638050	1.8984620	-1.4040100	-0.4493800	0.3771280	-0.0065100
		0.6	G_0	0.6328180	1.9450870	0.3228000	1.9973750	-7.5429500	6.9968300	-2.2307700
			G_1	0.1186200	0.4314880	2.3144430	-2.1725900	0.7855010	-0.9041900	0.4760100
		0.8	G_0	0.9239180	1.7165070	5.8526200	-7.9882200	-0.8312700	4.0567570	-1.0070400
			G_1	0.2017510	0.4407840	3.3328700	-2.8052100	-1.1192100	1.4485860	-0.2278300

Table 9B.20 – Influence Coefficients for a Circumferential Semi-Elliptical Surface Crack in a Sphere – Outside Surface

t/R_i	a/c	a/t	G_i	A_0	A_1	A_2	A_3	A_4	A_5	A_6
0.01 (1/100)	0.25	0.0	G_0	0.6152816	-0.3348694	6.2955620	-15.590618	19.299508	-12.488107	3.3010035
			G_1	0.0703566	0.2828152	1.4036169	-0.6511596	-1.2076596	1.0318656	-0.2423741
		0.2	G_0	0.6034886	0.1249569	4.7121854	-13.217504	17.879255	-12.438871	3.4748076
			G_1	0.0832497	0.2943416	1.7190774	-2.6924810	2.8266885	-2.3624724	0.8135845
		0.4	G_0	0.7329190	0.1074600	4.0675530	-7.6739500	5.6676310	-1.3115800	-0.2299100
			G_1	0.1240140	0.2681570	1.8177580	-1.6805900	0.1395580	0.0835500	0.0274100
		0.6	G_0	0.9370040	0.0230720	4.5541080	-6.4470500	0.4628380	4.3635300	-2.2615500
			G_1	0.1861970	0.2475700	1.9590760	-1.2692500	-1.4877100	1.8549340	-0.6173600
		0.8	G_0	1.2073610	0.2919720	1.0067710	12.275230	-38.970100	39.620240	-13.603400
			G_1	0.2727130	0.1608730	2.1939320	-0.2432300	-5.2756800	5.8457490	-1.9946000
0.01 (1/100)	0.5	0.0	G_0	0.8776607	-0.6729719	3.7721411	-6.5209060	6.3377934	-3.7028038	0.9872447
			G_1	0.1277541	0.4368502	0.4904522	1.0427434	-2.9631236	2.0826525	-0.5184313
		0.2	G_0	0.8872475	-0.8816683	5.4321461	-11.914421	14.854353	-10.257839	2.9661420
			G_1	0.1439007	0.2201219	1.8303174	-3.2294108	3.7691815	-3.1256488	1.0743502
		0.4	G_0	1.0045010	-0.7016800	3.0089200	-1.9772600	-3.2633100	5.1698220	-2.0441700
			G_1	0.1806240	0.3006750	1.2260040	-0.5849200	-1.3514400	1.4305690	-0.4612300
		0.6	G_0	1.1836260	-0.9309300	3.2905090	-1.6010900	-4.8402800	6.7524960	-2.5536700
			G_1	0.2368250	0.2146190	1.4242410	-0.8414500	-1.1900400	1.3808530	-0.4493600
		0.8	G_0	1.3992290	-1.1131100	2.9649560	-0.3065100	-6.5225200	7.4276460	-2.4919100
			G_1	0.2922820	0.2075630	1.0263870	0.1996680	-2.0883700	1.5772350	-0.3978900
0.01 (1/100)	1.0	0.0	G_0	1.1977992	-0.5244870	0.1498299	2.3284866	-5.1058499	4.3469049	-1.3487980
			G_1	0.1870117	0.6987352	0.1316900	0.7269255	-2.5259384	2.1756251	-0.6540458
		0.2	G_0	1.2100415	-1.2196778	5.0851813	-13.887803	22.015976	-18.111977	5.9617039
			G_1	0.2140206	0.1547905	3.4287820	-9.7373187	14.739129	-12.020076	3.9511125
		0.4	G_0	1.3056570	-0.9840700	1.8094060	-0.6734700	-2.5826300	3.7122980	-1.4919000
			G_1	0.2232750	0.5449490	0.7738700	-0.6566600	-1.0193200	1.4561880	-0.5611700
		0.6	G_0	1.4183740	-1.2135500	2.1993510	-1.4933300	-1.2218900	2.4847680	-1.0514900
			G_1	0.2551250	0.5019830	0.7547510	-0.5639900	-1.0363700	1.3526400	-0.4940600
		0.8	G_0	1.5326420	-1.3065800	1.5838410	0.2543670	-3.0285100	3.0930990	-0.9974000
			G_1	0.2830950	0.4811650	0.6674890	-0.5045900	-0.6068900	0.6856470	-0.2173300
0.01 (1/100)	2.0	0.0	G_0	0.8150546	-0.5623828	1.4465771	-4.6778133	8.4192164	-7.9025932	2.9866351
			G_1	0.1359146	0.0702340	3.5558581	-11.034445	16.967724	-14.126991	4.8706612
		0.2	G_0	0.8028980	-0.9650666	3.9970040	-12.122017	19.696606	-16.510345	5.6097792
			G_1	0.1301047	0.0878063	3.0990196	-9.3341391	13.946577	-11.459553	3.9447497
		0.4	G_0	0.8356296	-0.3224289	-0.7985231	3.5989904	-6.5651593	5.2488556	-1.4769852
			G_1	0.1402778	0.0513398	3.3153847	-10.032609	15.088369	-12.371071	4.2273204
		0.6	G_0	0.8661064	-0.3731907	-0.7988330	3.7602432	-6.9074912	5.5440593	-1.5664796
			G_1	0.1500634	0.0351369	3.3528083	-10.075993	15.097091	-12.363741	4.2277521
		0.8	G_0	0.9207020	-0.9736206	2.8107240	-7.4869514	11.444939	-9.4620056	3.2859159
			G_1	0.1497823	0.1241355	2.7412325	-8.1567935	11.844592	-9.4737292	3.1871348
0.01667 (1/60)	0.03125	0.0	G_0	0.1965046	2.9373464	-5.2582823	7.4889153	-6.9282667	3.3673349	-0.6677966
			G_1	0.0051780	0.1750280	2.7718680	-4.6457154	4.6780502	-3.2768090	0.9840994
		0.2	G_0	0.2072100	2.2706177	0.1180275	-8.0757534	16.419765	-13.978696	4.3309594
			G_1	0.0056314	0.2083374	2.6523526	-4.3557964	4.7921966	-3.7396344	1.1821048
		0.4	G_0	0.2187800	2.9201170	-3.2541400	2.7790300	4.9355160	-10.096300	4.3752100
			G_1	0.0097590	0.3943140	1.5573730	-0.5245700	1.0871590	-2.7010000	1.1644800
		0.6	G_0	0.2221170	3.2864290	-5.6165700	15.962040	-13.285800	0.6263510	1.7133900
			G_1	0.0094710	0.6041920	-0.2782800	6.3200750	-7.7901100	3.2903430	-0.7791200
		0.8	G_0	0.2135000	3.4928720	-5.7522600	17.914470	2.5583030	-28.453500	14.547300
			G_1	0.0113070	0.7637710	-1.1723500	8.1834960	-3.4020600	-4.7874200	2.3849100

Table 9B.20 – Influence Coefficients for a Circumferential Semi-Elliptical Surface Crack in a Sphere – Outside Surface

t/R_i	a/c	a/t	G_i	A_0	A_1	A_2	A_3	A_4	A_5	A_6
0.01667 (1/60)	0.0625	0.0	G_0	0.2695332	2.1626001	-1.6551569	-1.2970208	4.5604304	-4.3163876	1.4010655
			G_1	0.0138667	0.1827458	2.5749608	-3.9044679	3.3556301	-2.1772209	0.6420134
		0.2	G_0	0.2766818	2.0225220	-0.6355478	-2.3051909	4.0699208	-2.8921145	0.7209720
			G_1	0.0174385	0.2100226	2.6007574	-4.3532124	4.8533251	-3.8493461	1.2507471
		0.4	G_0	0.3147650	2.5291720	-2.0919000	2.1143120	0.5588770	-3.1232700	1.4632900
			G_1	0.0279520	0.4902460	1.2476560	0.8350840	-3.0553800	1.6809190	-0.2943900
		0.6	G_0	0.3554270	3.1691060	-4.7808200	15.069000	-17.990700	7.6081440	-0.7807800
			G_1	0.0396470	0.4761990	1.8210230	-0.2332000	0.8740410	-3.4309000	1.7059100
		0.8	G_0	0.4441620	2.8737710	0.2861520	8.2262140	-3.4495800	-13.232100	8.8135400
			G_1	0.0514840	0.5532200	1.6197540	3.3442680	-2.5539000	-4.3338700	3.0434300
0.01667 (1/60)	0.125	0.0	G_0	0.4065238	0.7772483	3.8861644	-12.573943	16.760207	-11.014593	2.8706957
			G_1	0.0320270	0.1825342	2.2670449	-2.7076615	1.2088194	-0.3777430	0.0763155
		0.2	G_0	0.4064707	1.1624907	1.6426210	-5.7433231	6.9198224	-4.2203447	1.0363847
			G_1	0.0473528	0.0100264	4.0034731	-9.4376443	13.307126	-10.460898	3.2369598
		0.4	G_0	0.4821610	1.4369770	1.5439830	-4.8198600	5.6391460	-3.6557100	0.9473000
			G_1	0.0716470	0.3226950	2.1748350	-2.3167400	1.1718590	-1.0086300	0.4403100
		0.6	G_0	0.6240930	1.8391850	1.0572030	-0.2916400	-3.4030700	3.3740640	-1.0492000
			G_1	0.1102270	0.4453490	2.0731700	-1.1859400	-0.7675400	0.2583820	0.1253900
		0.8	G_0	0.8805760	1.7866630	4.9018830	-3.9261500	-6.4686100	7.4680620	-1.8176000
			G_1	0.1837080	0.4424260	3.1186980	-1.8691400	-2.0596300	1.6779760	-0.1873200
0.01667 (1/60)	0.25	0.0	G_0	0.6152816	-0.3348694	6.2955620	-15.590618	19.299508	-12.488107	3.3010035
			G_1	0.0703566	0.2828152	1.4036169	-0.6511596	-1.2076596	1.0318656	-0.2423741
		0.2	G_0	0.6023257	0.1545741	4.5360513	-12.711785	17.157905	-11.940369	3.3414681
			G_1	0.0835309	0.2906933	1.7444852	-2.7644188	2.9354101	-2.4449975	0.8380360
		0.4	G_0	0.7331250	0.0894980	4.3048780	-8.5018200	7.0726920	-2.4545500	0.1249100
			G_1	0.1237180	0.2606840	1.8820280	-1.8520000	0.3848460	-0.0889900	0.0727300
		0.6	G_0	0.9357390	0.0600830	4.4065180	-5.8388500	-0.5866500	5.1893780	-2.5117500
			G_1	0.1846200	0.2541920	1.9652450	-1.3196500	-1.2886700	1.5996390	-0.5141500
		0.8	G_0	1.2001780	0.5721990	-0.8532500	18.991280	-50.389900	48.780140	-16.417100
			G_1	0.2722260	0.1802680	2.1304200	0.0968830	-5.8603400	6.2649050	-2.1059800
0.01667 (1/60)	0.5	0.0	G_0	0.8776607	-0.6729719	3.7721411	-6.5209060	6.3377934	-3.7028038	0.9872447
			G_1	0.1277541	0.4368502	0.4904522	1.0427434	-2.9631236	2.0826525	-0.5184313
		0.2	G_0	0.8861552	-0.8475972	5.2281796	-11.342469	14.043389	-9.6947405	2.8144567
			G_1	0.1437180	0.2270616	1.7877516	-3.0976685	3.5596526	-2.9618029	1.0245128
		0.4	G_0	1.0082480	-0.7456300	3.3510180	-3.0347700	-1.6027300	3.8799180	-1.6527200
			G_1	0.1796900	0.3205770	1.1071750	-0.2040000	-1.9598000	1.9027500	-0.6035800
		0.6	G_0	1.1877360	-0.9200100	3.2830680	-1.5231900	-5.0470300	6.9575050	-2.6253200
			G_1	0.2384060	0.2050470	1.5138910	-1.1176800	-0.7473400	1.0264950	-0.3388600
		0.8	G_0	1.4129910	-1.1463200	3.3006820	-1.3233100	-4.9730900	6.2362190	-2.1281100
			G_1	0.2966970	0.1915670	1.1787620	-0.3009000	-1.2516400	0.8833770	-0.1739600
0.01667 (1/60)	1.0	0.0	G_0	1.1977992	-0.5244870	0.1498299	2.3284866	-5.1058499	4.3469049	-1.3487980
			G_1	0.1870117	0.6987352	0.1316900	0.7269255	-2.5259384	2.1756251	-0.6540458
		0.2	G_0	1.2109353	-1.2177397	5.0743805	-13.865698	21.990202	-18.097614	5.9594076
			G_1	0.2130552	0.1755510	3.3026352	-9.3689236	14.181057	-11.600284	3.8274381
		0.4	G_0	1.3107300	-1.0156000	1.9707500	-1.0039900	-2.2721700	3.6010860	-1.4904600
			G_1	0.2235330	0.5550130	0.6959270	-0.3676800	-1.5233900	1.8742770	-0.6944500
		0.6	G_0	1.4219950	-1.1738900	1.9016680	-0.4274700	-3.0901900	4.0467930	-1.5502100
			G_1	0.2575680	0.4881880	0.8193810	-0.6793500	-0.9509600	1.3387320	-0.5011100
		0.8	G_0	1.5441710	-1.3325300	1.7019960	0.0066410	-2.7889800	2.9926440	-0.9845900
			G_1	0.2855800	0.4863980	0.6356880	-0.4253800	-0.6903700	0.7139070	-0.2145800

Table 9B.20 – Influence Coefficients for a Circumferential Semi-Elliptical Surface Crack in a Sphere – Outside Surface

t/R_i	a/c	a/t	G_i	A_0	A_1	A_2	A_3	A_4	A_5	A_6
0.01667 (1/60)	2.0	0.0	G_0	0.8150546	-0.5623828	1.4465771	-4.6778133	8.4192164	-7.9025932	2.9866351
			G_1	0.1359146	0.0702340	3.5558581	-11.034445	16.967724	-14.126991	4.8706612
		0.2	G_0	0.8028351	-0.9568446	3.9434949	-11.975192	19.497930	-16.382699	5.5792085
			G_1	0.1279559	0.0702782	3.2025280	-9.6672580	14.491084	-11.886655	4.0727789
		0.4	G_0	0.8380589	-0.3513714	-0.6291162	3.1142671	-5.8512931	4.7228055	-1.3233607
			G_1	0.1419656	0.0558979	3.2758482	-9.8563050	14.756640	-12.102671	4.1493773
		0.6	G_0	0.8665287	-0.3612175	-0.8863819	4.0316038	-7.3391614	5.8802748	-1.6679659
			G_1	0.1509178	0.0382471	3.3253185	-9.9492109	14.852138	-12.164336	4.1704975
		0.8	G_0	0.9224303	-0.9753725	2.8158522	-7.5259514	11.536233	-9.5573301	3.3229496
			G_1	0.1476854	0.1915534	2.2701951	-6.5794718	9.2487344	-7.4444819	2.5829071
0.05 (1/20)	0.03125	0.0	G_0	0.1965046	2.9373464	-5.2582823	7.4889153	-6.9282667	3.3673349	-0.6677966
			G_1	0.0051780	0.1750280	2.7718680	-4.6457154	4.6780502	-3.2768090	0.9840994
		0.2	G_0	0.2033833	2.5286342	-1.8283974	-2.6930570	9.3707942	-9.5463774	3.2538037
			G_1	0.0049452	0.1952030	2.6898536	-4.3708930	4.7450394	-3.6789217	1.1613232
		0.4	G_0	0.2089810	2.8283000	-3.1998500	3.1505100	3.4039130	-8.3689700	3.7588300
			G_1	0.0080440	0.2694800	1.9433080	-0.3471100	-2.3907600	2.4438430	-0.9810100
		0.6	G_0	0.2055460	3.1555140	-5.5955300	15.954450	-15.825500	4.1143530	0.5020900
			G_1	0.0082470	0.3030350	1.9668890	-1.9390600	6.1885430	-8.7757300	3.4765000
		0.8	G_0	0.2369010	2.2074040	2.8793440	-8.9851400	32.279360	-41.393400	16.253700
			G_1	0.0090710	0.5351660	-0.0295000	5.5371600	-3.5366700	-2.5110100	1.5982100
0.05 (1/20)	0.0625	0.0	G_0	0.2695332	2.1626001	-1.6551569	-1.2970208	4.5604304	-4.3163876	1.4010655
			G_1	0.0138667	0.1827458	2.5749608	-3.9044679	3.3556301	-2.1772209	0.6420134
		0.2	G_0	0.2777401	2.0228942	-0.3762730	-3.9243880	7.6606230	-6.2555801	1.8583009
			G_1	0.0167530	0.1966749	2.6687417	-4.4807588	4.9742054	-3.8877324	1.2453071
		0.4	G_0	0.2949710	2.4263270	-1.9374800	1.8505470	1.3048900	-3.9403500	1.7452900
			G_1	0.0204430	0.2543760	2.4978040	-3.4240000	4.3019290	-4.0825600	1.3571300
		0.6	G_0	0.2932040	2.9237900	-4.9116200	15.281750	-17.518100	7.3210470	-0.8963700
			G_1	0.0226050	0.2234740	2.8903570	-3.8473800	6.1195550	-6.2676700	2.0574300
		0.8	G_0	0.3122360	2.4798240	-1.4430000	9.7299330	-3.1601800	-10.668500	6.2696700
			G_1	0.0313670	0.3920770	1.1522490	3.1467290	-1.8541600	-2.8779900	1.6154400
0.05 (1/20)	0.125	0.0	G_0	0.4065238	0.7772483	3.8861644	-12.573943	16.760207	-11.014593	2.8706957
			G_1	0.0320270	0.1825342	2.2670449	-2.7076615	1.2088194	-0.3777430	0.0763155
		0.2	G_0	0.4060953	1.1644812	1.6385609	-5.6458829	6.7482434	-4.1123639	1.0134083
			G_1	0.0467212	0.0112075	3.9795496	-9.2799411	13.005505	-10.210942	3.1584278
		0.4	G_0	0.4637710	1.6245020	0.4824070	-1.9574400	1.8537600	-1.0826800	0.2160800
			G_1	0.0559820	0.3663650	1.7297660	-0.8434800	-0.9789500	0.6140790	-0.0788100
		0.6	G_0	0.5549300	1.8055790	0.9321470	-0.3578800	-0.5307800	-0.8350500	0.6371000
			G_1	0.0767100	0.4575490	1.5658320	0.4829420	-2.5380200	1.0860880	-0.0526300
		0.8	G_0	0.6787290	1.7207550	3.5024190	-0.7988100	-2.6258600	-1.5230200	2.0523400
			G_1	0.1083820	0.4007860	2.5476580	-0.5622500	-0.9045000	-1.2453500	1.0278300
0.05 (1/20)	0.25	0.0	G_0	0.6152816	-0.3348694	6.2955620	-15.590618	19.299508	-12.488107	3.3010035
			G_1	0.0703566	0.2828152	1.4036169	-0.6511596	-1.2076596	1.0318656	-0.2423741
		0.2	G_0	0.6336200	-0.2241448	6.0145553	-15.177593	19.245817	-12.833947	3.4982967
			G_1	0.0857951	0.1479275	2.2281138	-3.0764070	2.3359025	-1.4641332	0.4360045
		0.4	G_0	0.7210140	0.2079740	3.8695370	-7.2148900	5.1589060	-1.0561100	-0.2846700
			G_1	0.1159200	0.2797270	1.8006830	-1.5262400	-0.0969100	0.2472200	-0.0259400
		0.6	G_0	0.9203340	-0.0146700	5.6709480	-9.9731200	6.6568860	-1.0393900	-0.4792100
			G_1	0.1729310	0.2700710	1.9969270	-1.2725900	-1.2286900	1.3793560	-0.4054400
		0.8	G_0	1.2153540	-0.4744400	9.0911160	-15.761900	10.345020	-2.2431500	-0.0760500
			G_1	0.2558270	0.1978370	2.4511390	-0.7909400	-4.1058800	4.5470700	-1.5064400

Table 9B.20 – Influence Coefficients for a Circumferential Semi-Elliptical Surface Crack in a Sphere – Outside Surface

t/R_i	a/c	a/t	G_i	A_0	A_1	A_2	A_3	A_4	A_5	A_6
0.05 (1/20)	0.5	0.0	G_0	0.8776607	-0.6729719	3.7721411	-6.5209060	6.3377934	-3.7028038	0.9872447
			G_1	0.1277541	0.4368502	0.4904522	1.0427434	-2.9631236	2.0826525	-0.5184313
		0.2	G_0	0.8960862	-0.8110788	4.9563363	-10.433624	12.562793	-8.5356654	2.4644908
			G_1	0.1473772	0.2208319	1.8261603	-3.1801479	3.6631029	-3.0395570	1.0501901
		0.4	G_0	1.0097830	-0.6874900	3.2330140	-2.5544100	-2.5969400	4.7905890	-1.9612600
			G_1	0.1799730	0.3053860	1.2909090	-0.7459300	-1.1007400	1.2104980	-0.3861300
		0.6	G_0	1.2068900	-1.0128100	3.9596390	-2.3313200	-5.6495000	8.6313880	-3.4362100
			G_1	0.2394390	0.1895050	1.5832110	-1.0518100	-0.9937500	1.2574080	-0.4225600
		0.8	G_0	1.4575620	-1.3492700	4.9831730	-4.9881500	-1.4061800	4.6648170	-1.8907900
			G_1	0.3110330	0.0849830	1.9084200	-1.7754200	0.0212320	0.4653100	-0.1625300
0.05 (1/20)	1.0	0.0	G_0	1.1977992	-0.5244870	0.1498299	2.3284866	-5.1058499	4.3469049	-1.3487980
			G_1	0.1870117	0.6987352	0.1316900	0.7269255	-2.5259384	2.1756251	-0.6540458
		0.2	G_0	1.2317647	-1.2668535	5.2719942	-14.375480	22.713640	-18.634068	6.1234149
			G_1	0.2185075	0.1721631	3.3030368	-9.3243704	14.064573	-11.498670	3.7993477
		0.4	G_0	1.3280650	-1.0067200	1.8840770	-0.4718700	-3.3649000	4.5608980	-1.8016300
			G_1	0.2288730	0.5425330	0.7718760	-0.5272300	-1.2930700	1.6853270	-0.6337000
		0.6	G_0	1.4498840	-1.2061500	2.1605180	-1.0888200	-2.2230600	3.4522760	-1.3820700
			G_1	0.2647910	0.4868560	0.8402780	-0.6830900	-0.9740800	1.3518340	-0.5012700
		0.8	G_0	1.5986470	-1.4400100	2.2795920	-1.2360400	-1.6646800	2.6100510	-0.9686900
			G_1	0.3004770	0.4631460	0.7203190	-0.3884500	-1.1395400	1.2722420	-0.4237800
0.05 (1/2)	2.0	0.0	G_0	0.8150546	-0.5623828	1.4465771	-4.6778133	8.4192164	-7.9025932	2.9866351
			G_1	0.1359146	0.0702340	3.5558581	-11.034445	16.967724	-14.126991	4.8706612
		0.2	G_0	0.8261869	-0.9760945	3.9159333	-11.828914	19.270954	-16.254170	5.5646493
			G_1	0.1343782	0.0647996	3.2358020	-9.7518926	14.621269	-12.017040	4.1281758
		0.4	G_0	0.8404268	-0.3327374	-0.7716352	3.4961782	-6.3579059	5.0391431	-1.3957126
			G_1	0.1443070	0.0426802	3.3560498	-10.087084	15.121007	-12.419980	4.2634049
		0.6	G_0	0.8721260	-0.3774122	-0.8225068	3.8259304	-6.9952612	5.5798197	-1.5623326
			G_1	0.1521311	0.0386765	3.3191844	-9.9331613	14.859339	-12.233733	4.2193345
		0.8	G_0	0.9313062	-1.0113444	2.9977317	-8.1240616	12.547051	-10.425995	3.6200006
			G_1	0.1491534	0.2059118	2.1482404	-6.1418067	8.5120738	-6.9013685	2.4416991
0.1 (1/10)	0.03125	0.0	G_0	0.1965046	2.9373464	-5.2582823	7.4889153	-6.9282667	3.3673349	-0.6677966
			G_1	0.0051780	0.1750280	2.7718680	-4.6457154	4.6780502	-3.2768090	0.9840994
		0.2	G_0	0.2137025	1.4325421	4.1167565	-19.216759	33.344440	-26.945303	8.2464142
			G_1	0.0052475	0.1259041	2.6736467	-4.5590793	5.2686292	-4.1357154	1.3041985
		0.4	G_0	0.1979150	1.9340145	1.4781131	-9.2801878	19.142396	-17.924063	6.0232196
			G_1	0.0040005	0.1461665	2.5347969	-3.8021141	5.3553730	-5.2227792	1.8176331
		0.6	G_0	0.1860194	2.5432457	-2.3392398	6.5940454	-5.3262654	-0.8960931	1.3680747
			G_1	0.0020990	0.1774103	2.3394685	-2.7383263	5.4523448	-6.6666842	2.4847314
		0.8	G_0	0.1754774	2.9957430	-5.6326095	23.665960	-34.288886	21.521790	-5.5542454
			G_1	0.0002774	0.1921685	2.1887636	-1.5273413	5.0483569	-7.1411578	2.5874760
0.1 (1/10)	0.0625	0.0	G_0	0.2695332	2.1626001	-1.6551569	-1.2970208	4.5604304	-4.3163876	1.4010655
			G_1	0.0138667	0.1827458	2.5749608	-3.9044679	3.3556301	-2.1772209	0.6420134
		0.2	G_0	0.2890499	0.9219896	6.0096997	-21.937629	33.946446	-25.339866	7.3108326
			G_1	0.0147811	0.1328586	2.5982425	-3.8907259	3.5562726	-2.4471215	0.7260215
		0.4	G_0	0.2873059	1.3052621	4.6012131	-17.084571	28.947144	-23.791473	7.3353113
			G_1	0.0155072	0.1448568	2.6766011	-3.9466405	4.8914663	-4.4048681	1.4680245
		0.6	G_0	0.2809744	1.7401393	2.2988686	-7.7235391	17.385265	-18.152842	6.3604835
			G_1	0.0126043	0.1465942	2.7615205	-4.0810736	7.2809390	-7.7678947	2.7177283
		0.8	G_0	0.2695106	1.9636065	1.2283002	-0.8213441	9.9420209	-15.935439	6.3440991
			G_1	0.0084372	0.1053328	3.0865264	-5.1047572	11.797139	-12.904792	4.3973960

Table 9B.20 – Influence Coefficients for a Circumferential Semi-Elliptical Surface Crack in a Sphere – Outside Surface

t/R_i	a/c	a/t	G_i	A_0	A_1	A_2	A_3	A_4	A_5	A_6
0.1 (1/10)	0.125	0.0	G_0	0.4065238	0.7772483	3.8861644	-12.573943	16.760207	-11.014593	2.8706957
			G_1	0.0320270	0.1825342	2.2670449	-2.7076615	1.2088194	-0.3777430	0.0763155
		0.2	G_0	0.4043512	1.1681039	1.6434561	-5.5687394	6.5838903	-3.9846901	0.9756456
			G_1	0.0458647	0.0143495	3.9367213	-9.0232258	12.498287	-9.7735425	3.0170109
		0.4	G_0	0.4325510	1.7019350	-0.0540700	-0.2710400	-0.2974000	0.1894200	-0.0856700
			G_1	0.0452780	0.3334410	1.8205130	-1.1453300	-0.2249300	-0.0767900	0.1196500
		0.6	G_0	0.4662460	1.8462810	0.1188260	1.8951460	-2.2287300	-0.6467800	0.7465300
			G_1	0.0515130	0.3627920	1.9453630	-0.8198300	0.0320510	-1.0330000	0.5409500
		0.8	G_0	0.5004200	1.5655730	2.1869090	2.2008540	-2.1879200	-4.1459300	2.8744500
			G_1	0.0509260	0.3210580	2.0764570	0.5519790	-0.7578200	-2.1663300	1.3044300
0.1 (1/10)	0.25	0.0	G_0	0.6152816	-0.3348694	6.2955620	-15.590618	19.299508	-12.488107	3.3010035
			G_1	0.0703566	0.2828152	1.4036169	-0.6511596	-1.2076596	1.0318656	-0.2423741
		0.2	G_0	0.6350228	-0.2119641	5.9568028	-14.916184	18.776502	-12.456735	3.3832587
			G_1	0.0856903	0.1511286	2.2237294	-3.0557324	2.3214261	-1.4731351	0.4439542
		0.4	G_0	0.6987930	0.3447790	3.4424380	-6.0517700	3.6043320	-0.0452500	-0.5532900
			G_1	0.1077030	0.2651880	2.0013730	-2.2123900	1.2433410	-0.9817400	0.3852200
		0.6	G_0	0.8589440	0.2633150	4.5097920	-6.4207300	1.9301370	1.8839450	-1.2009200
			G_1	0.1525220	0.2760100	2.0850880	-1.4562900	-0.6710600	0.7275950	-0.1720400
		0.8	G_0	1.0845520	-0.2782000	9.0855350	-15.543200	12.287140	-5.7702200	1.4420300
			G_1	0.2113300	0.2542150	2.3848150	-0.4194600	-3.8790000	3.6488360	-1.0778800
0.1 (1/10)	0.5	0.0	G_0	0.8776607	-0.6729719	3.7721411	-6.5209060	6.3377934	-3.7028038	0.9872447
			G_1	0.1277541	0.4368502	0.4904522	1.0427434	-2.9631236	2.0826525	-0.5184313
		0.2	G_0	0.9089240	-0.9470277	5.8122694	-12.939505	16.332513	-11.352074	3.2913303
			G_1	0.1487903	0.2149757	1.8829219	-3.3561626	3.9304025	-3.2399641	1.1093948
		0.4	G_0	1.0029850	-0.5759600	2.9821620	-1.8309800	-3.8190200	5.7887660	-2.2760500
			G_1	0.1771680	0.3219970	1.2553580	-0.4865100	-1.6480100	1.6936600	-0.5453300
		0.6	G_0	1.2064040	-0.9321800	4.1240170	-2.7832100	-5.1249600	8.3127460	-3.3621500
			G_1	0.2383680	0.2030160	1.6282540	-0.9652900	-1.3505200	1.6296530	-0.5561200
		0.8	G_0	1.4594660	-1.1444900	4.7732460	-4.1451600	-2.9602200	5.8139350	-2.1977000
			G_1	0.3122420	0.1024290	2.0857110	-2.0834200	0.2839790	0.3119550	-0.1176700
0.1 (1/10)	1.0	0.0	G_0	1.1977992	-0.5244870	0.1498299	2.3284866	-5.1058499	4.3469049	-1.3487980
			G_1	0.1870117	0.6987352	0.1316900	0.7269255	-2.5259384	2.1756251	-0.6540458
		0.2	G_0	1.2380657	-1.2701768	5.2914711	-14.476169	22.897148	-18.796156	6.1822911
			G_1	0.2194837	0.1768071	3.2996872	-9.3618333	14.167089	-11.612517	3.8461643
		0.4	G_0	1.3427420	-1.0146600	2.0436160	-0.7478200	-3.1748800	4.5270860	-1.8145100
			G_1	0.2328790	0.5209850	0.9293030	-0.9415700	-0.6268200	1.1262530	-0.4527700
		0.6	G_0	1.4757130	-1.2047200	2.2963490	-1.2790300	-2.2758700	3.6916080	-1.4981600
			G_1	0.2721640	0.4674680	0.9709180	-0.9130500	-0.7725000	1.2665250	-0.4901300
		0.8	G_0	1.6389960	-1.3600900	2.0178020	-0.3744100	-3.2533700	3.9560490	-1.3889300
			G_1	0.3141930	0.4470660	0.8433550	-0.6042100	-0.9836700	1.2289950	-0.4219000
0.1 (1/10)	2.0	0.0	G_0	0.8150546	-0.5623828	1.4465771	-4.6778133	8.4192164	-7.9025932	2.9866351
			G_1	0.1359146	0.0702340	3.5558581	-11.034445	16.967724	-14.126991	4.8706612
		0.2	G_0	0.8297052	-0.9932212	3.9945197	-12.078107	19.703504	-16.637981	5.6988875
			G_1	0.1348860	0.0624776	3.2528748	-9.8245409	14.775725	-12.179089	4.1921695
		0.4	G_0	0.8458749	-0.3594010	-0.6577823	3.1889098	-5.9152513	4.6977129	-1.2859128
			G_1	0.1452270	0.0359473	3.4048512	-10.271104	15.480348	-12.777595	4.4006315
		0.6	G_0	0.8760954	-0.3601463	-0.9648929	4.2085152	-7.5094681	5.8890448	-1.6240482
			G_1	0.1537017	0.0238822	3.4227047	-10.295342	15.522205	-12.858919	4.4503340
		0.8	G_0	0.9390036	-1.0262914	3.0604601	-8.3936234	13.086182	-10.973664	3.8361075
			G_1	0.1509371	0.1981818	2.1987908	-6.3405515	8.9157835	-7.3314460	2.6167416

Table 9B.20 – Influence Coefficients for a Circumferential Semi-Elliptical Surface Crack in a Sphere – Outside Surface

t/R_i	a/c	a/t	G_i	A_0	A_1	A_2	A_3	A_4	A_5	A_6
0.2 (1/5)	0.0625	0.0	G_0	0.2695332	2.1626001	-1.6551569	-1.2970208	4.5604304	-4.3163876	1.4010655
			G_1	0.0138667	0.1827458	2.5749608	-3.9044679	3.3556301	-2.1772209	0.6420134
		0.2	G_0	0.2846891	0.9259643	5.9103335	-21.460325	33.126452	-24.702238	7.1191407
			G_1	0.0133598	0.1259805	2.6073541	-3.8908359	3.6033838	-2.5215410	0.7547302
		0.4	G_0	0.2766488	1.6110281	2.3516100	-10.341186	18.921547	-16.540412	5.3013624
			G_1	0.0118367	0.1575003	2.5745703	-3.6857687	4.6301169	-4.2961611	1.4533059
		0.6	G_0	0.2689968	1.9034093	0.6472840	-2.3491353	8.1436603	-10.667333	4.1167079
			G_1	0.0087301	0.1497819	2.6774334	-3.9694008	7.0437495	-7.5002452	2.6245395
		0.8	G_0	0.2554783	2.0468462	-0.0822131	3.4213664	0.6981926	-6.5421021	2.9676454
			G_1	0.0045719	0.1110321	2.9583143	-5.0077730	11.197636	-11.755968	3.8272846
0.2 (1/5)	0.125	0.0	G_0	0.4065238	0.7772483	3.8861644	-12.573943	16.760207	-11.014593	2.8706957
			G_1	0.0320270	0.1825342	2.2670449	-2.7076615	1.2088194	-0.3777430	0.0763155
		0.2	G_0	0.4014872	1.1741907	1.5646730	-5.0362060	5.5615994	-3.1453683	0.7160267
			G_1	0.0443453	0.0224028	3.8206837	-8.4139316	11.339663	-8.7979577	2.7081857
		0.4	G_0	0.3823340	1.7459190	-0.0828300	-0.5504300	1.0904920	-1.5202200	0.5548400
			G_1	0.0316780	0.3226130	1.5266340	0.6253550	-3.9114300	3.3310290	-1.0507400
		0.6	G_0	0.3795700	1.9588500	-1.1419500	4.1575230	-2.7423400	-1.7343300	1.2469000
			G_1	0.0220180	0.4043780	1.1228810	1.4114680	-2.2682000	0.0447910	0.3250500
		0.8	G_0	0.3743020	1.7350230	-0.3704600	7.0142130	-6.6994400	0.1724090	0.6283300
			G_1	0.0075720	0.4255330	0.6869830	3.4008880	-3.5933800	0.2812360	0.1435500
0.2 (1/5)	0.25	0.0	G_0	0.6152816	-0.3348694	6.2955620	-15.590618	19.299508	-12.488107	3.3010035
			G_1	0.0703566	0.2828152	1.4036169	-0.6511596	-1.2076596	1.0318656	-0.2423741
		0.2	G_0	0.6359717	-0.1946895	5.9248092	-14.774025	18.556654	-12.309769	3.3437575
			G_1	0.0852188	0.1622272	2.1678098	-2.8437025	1.9809989	-1.2197689	0.3704304
		0.4	G_0	0.6548070	0.4906810	3.4735670	-6.8787000	5.9955580	-2.6086300	0.3784600
			G_1	0.0918840	0.3012510	1.8673950	-1.7219200	0.7157350	-0.7857800	0.3675700
		0.6	G_0	0.7367620	0.5329010	4.0652760	-5.6789800	2.7020960	-0.0771700	-0.3437600
			G_1	0.1127050	0.3293460	1.9238500	-0.8550500	-1.1357300	0.7270230	-0.1169400
		0.8	G_0	0.8235610	0.0496050	8.0660590	-12.067200	10.889570	-7.8621300	2.6614300
			G_1	0.1336310	0.1468590	3.2572260	-2.8593100	1.4996830	-1.7545100	0.7932100
0.2 (1/5)	0.5	0.0	G_0	0.8776607	-0.6729719	3.7721411	-6.5209060	6.3377934	-3.7028038	0.9872447
			G_1	0.1277541	0.4368502	0.4904522	1.0427434	-2.9631236	2.0826525	-0.5184313
		0.2	G_0	0.9111832	-0.8704236	5.4253176	-11.903328	14.866815	-10.312652	3.0008184
			G_1	0.1497822	0.2268838	1.8393043	-3.2327001	3.7365317	-3.0918831	1.0662371
		0.4	G_0	0.9872480	-0.4453000	3.1245470	-2.4761100	-2.8171500	5.0194640	-2.0491500
			G_1	0.1679190	0.3768860	1.1273070	-0.0344600	-2.3343800	2.1644560	-0.6727400
		0.6	G_0	1.1816730	-0.7620000	4.3929080	-3.4235600	-4.4982000	7.9816110	-3.3045700
			G_1	0.2253530	0.2659600	1.5824750	-0.6755000	-1.8341300	1.9429500	-0.6350900
		0.8	G_0	1.4137870	-0.9166800	5.7849410	-6.8719200	1.0910810	2.4108090	-1.0690500
			G_1	0.2953760	0.1751530	2.2894570	-2.3905100	0.6532250	-0.1021700	0.0564000
0.2 (1/5)	1.0	0.0	G_0	1.1977992	-0.5244870	0.1498299	2.3284866	-5.1058499	4.3469049	-1.3487980
			G_1	0.1870117	0.6987352	0.1316900	0.7269255	-2.5259384	2.1756251	-0.6540458
		0.2	G_0	1.2459636	-1.2684630	5.3227950	-14.672901	23.252766	-19.096733	6.2858919
			G_1	0.2223172	0.1610842	3.4145518	-9.6936477	14.621415	-11.929534	3.9388987
		0.4	G_0	1.3688960	-1.0440800	2.5361260	-1.8901400	-1.7813900	3.6257870	-1.5804900
			G_1	0.2392750	0.5323640	0.8557990	-0.4613200	-1.4868900	1.7868370	-0.6475000
		0.6	G_0	1.5187010	-1.1782100	2.5603360	-1.6965000	-2.2170100	3.9633910	-1.6481800
			G_1	0.2836700	0.4844930	0.9316080	-0.5572500	-1.4804500	1.8386220	-0.6623700
		0.8	G_0	1.7061150	-1.2868800	2.2454580	-0.7754000	-3.3317500	4.3578560	-1.5589200
			G_1	0.3325930	0.4674090	0.8587280	-0.3981100	-1.5912000	1.7969810	-0.6017500

Table 9B.20 – Influence Coefficients for a Circumferential Semi-Elliptical Surface Crack in a Sphere – Outside Surface

t/R_i	a/c	a/t	G_i	A_0	A_1	A_2	A_3	A_4	A_5	A_6
0.2 (1/5)	2.0	0.0	G_0	0.8150546	-0.5623828	1.4465771	-4.6778133	8.4192164	-7.9025932	2.9866351
			G_1	0.1359146	0.0702340	3.5558581	-11.034445	16.967724	-14.126991	4.8706612
		0.2	G_0	0.8328850	-0.9992018	4.0086624	-12.151398	19.883977	-16.849142	5.7890893
			G_1	0.1355167	0.0583355	3.2799736	-9.9261053	14.984541	-12.404007	4.2843881
		0.4	G_0	0.8514779	-0.3260458	-0.8924282	3.7884421	-6.6921368	5.1564980	-1.3771960
			G_1	0.1471213	0.0328202	3.4336651	-10.388789	15.742019	-13.094220	4.5426268
		0.6	G_0	0.8852158	-0.3912028	-0.7878178	3.5577693	-6.3491249	4.8462272	-1.2556058
			G_1	0.1565145	-0.0057907	3.6253156	-10.968973	16.711109	-13.958826	4.8532715
		0.8	G_0	0.9511352	-1.0642903	3.3097711	-9.3699961	14.892041	-12.642730	4.4397097
			G_1	0.1534693	0.1916966	2.2421706	-6.5009981	9.2612620	-7.7751453	2.8260643
0.3333 (1/3)	0.125	0.0	G_0	0.4065238	0.7772483	3.8861644	-12.573943	16.760207	-11.014593	2.8706957
			G_1	0.0320270	0.1825342	2.2670449	-2.7076615	1.2088194	-0.3777430	0.0763155
		0.2	G_0	0.3999453	1.1378099	1.8837409	-5.9120772	6.9147328	-4.2124418	1.0410171
			G_1	0.0432523	0.0215395	3.7904607	-8.1289447	10.763741	-8.3129980	2.5551138
		0.4	G_0	0.4296335	1.0041041	3.8959378	-12.057383	18.412611	-14.408772	4.3022733
			G_1	0.0397925	0.1879821	2.4341024	-2.9044672	2.6267076	-2.3395968	0.8089253
		0.6	G_0	0.4270492	0.9372419	4.6774304	-12.816229	22.136585	-19.630950	6.3060701
			G_1	0.0324591	0.1435626	2.7929483	-3.9397629	5.9961920	-6.0796339	2.0851337
		0.8	G_0	0.3995502	0.7593599	5.9836408	-15.132435	30.500061	-29.316818	9.5533887
			G_1	0.0161665	0.0491796	3.4935697	-6.7094610	13.737725	-13.713995	4.4513954
0.3333 (1/3)	0.25	0.0	G_0	0.6152816	-0.3348694	6.2955620	-15.590618	19.299508	-12.488107	3.3010035
			G_1	0.0703566	0.2828152	1.4036169	-0.6511596	-1.2076596	1.0318656	-0.2423741
		0.2	G_0	0.6381645	-0.2547494	6.5598868	-16.785781	21.683987	-14.680561	4.0404689
			G_1	0.0852630	0.1512639	2.2794720	-3.1334300	2.3872418	-1.5138985	0.4543945
		0.4	G_0	0.7229440	-0.1327500	5.9623940	-13.044300	14.489110	-8.6605800	2.1226270
			G_1	0.1014390	0.3149520	1.5304960	-0.5374400	-1.5532000	1.2896360	-0.3327000
		0.6	G_0	0.8056090	-0.5534700	10.013880	-23.141800	29.129710	-19.917800	5.5198320
			G_1	0.1214770	0.2249700	2.3876170	-2.0864300	0.3425960	-0.1442200	0.1042080
		0.8	G_0	0.8320670	0.2103690	5.3637430	-5.4363900	4.4211560	-5.5005100	2.5690920
			G_1	0.1229720	0.4233740	1.3543830	1.8448010	-4.2606800	1.6752550	0.0117770
0.3333 (1/3)	0.5	0.0	G_0	0.8776607	-0.6729719	3.7721411	-6.5209060	6.3377934	-3.7028038	0.9872447
			G_1	0.1277541	0.4368502	0.4904522	1.0427434	-2.9631236	2.0826525	-0.5184313
		0.2	G_0	0.9167822	-0.8329923	5.2670130	-11.483170	14.269534	-9.8883620	2.8823826
			G_1	0.1519046	0.2243972	1.8954464	-3.4222778	4.0428864	-3.3359097	1.1424959
		0.4	G_0	1.0084180	-0.2094500	0.8034380	3.1162370	-9.2606100	8.5893620	-2.7802200
			G_1	0.1751170	0.4253180	0.8135250	0.2323860	-2.1952900	1.8341110	-0.5239700
		0.6	G_0	1.2023400	-0.8461300	4.4196170	-5.8060400	2.2669380	0.9670340	-0.7423700
			G_1	0.2222170	0.4177690	0.6748910	1.2429340	-4.1524200	3.4107350	-0.9888200
		0.8	G_0	1.3694060	-0.2562400	0.7922660	6.8643940	-18.758400	17.024640	-5.3342900
			G_1	0.2738310	0.5220650	0.0389670	3.9695460	-9.2012700	7.5724070	-2.2613100
0.3333 (1/3)	1.0	0.0	G_0	1.1977992	-0.5244870	0.1498299	2.3284866	-5.1058499	4.3469049	-1.3487980
			G_1	0.1870117	0.6987352	0.1316900	0.7269255	-2.5259384	2.1756251	-0.6540458
		0.2	G_0	1.2554619	-1.2705280	5.3824723	-14.954811	23.731001	-19.481595	6.4118814
			G_1	0.2245665	0.1648418	3.4055159	-9.6584362	14.530510	-11.851660	3.9206556
		0.4	G_0	1.3026300	-0.1578200	-2.5260000	10.182540	-17.165300	13.533850	-4.0656700
			G_1	0.2187120	0.7561160	-0.2289500	1.9239160	-4.7376100	4.0820740	-1.2574500
		0.6	G_0	1.4126140	-0.0936900	-3.3743500	12.583770	-20.843800	16.338280	-4.8785500
			G_1	0.2479600	0.8009420	-0.6180700	3.1142740	-6.6660300	5.5667210	-1.6809600
		0.8	G_0	1.5053276	-0.4119768	0.8465948	-6.1807564	14.714118	-14.632260	5.3209771
			G_1	0.3021350	0.4630840	1.5275970	-3.6089400	4.0734720	-3.0503100	1.0770470

Table 9B.20 – Influence Coefficients for a Circumferential Semi-Elliptical Surface Crack in a Sphere – Outside Surface

t/R_i	a/c	a/t	G_i	A_0	A_1	A_2	A_3	A_4	A_5	A_6
0.3333 (1/3)	2.0	0.0	G_0	0.8150546	-0.5623828	1.4465771	-4.6778133	8.4192164	-7.9025932	2.9866351
			G_1	0.1359146	0.0702340	3.5558581	-11.034445	16.967724	-14.126991	4.8706612
		0.2	G_0	0.8376294	-1.0150330	4.0796464	-12.398254	20.340898	-17.278075	5.9462878
			G_1	0.1365429	0.0531598	3.3094628	-10.022244	15.161783	-12.584481	4.3568636
		0.4	G_0	0.8578558	-0.3356978	-0.8868820	3.7430432	-6.5595632	4.9671659	-1.2850147
			G_1	0.1173823	0.5937733	-0.0584056	0.7822906	-2.9803324	2.5765209	-0.6281954
		0.6	G_0	0.8935993	-0.4091679	-0.6966760	3.1316414	-5.4783764	3.9792295	-0.9268708
			G_1	0.1252608	0.5771663	-0.0010861	0.6133328	-2.6701696	2.2230706	-0.4717927
		0.8	G_0	0.9611381	-1.0777619	3.4192395	-10.046519	16.437777	-14.263452	5.0697660
			G_1	0.1520218	0.1854095	2.5856063	-7.9036293	11.911110	-10.256157	3.7281358

Notes:

1. Interpolation of the influence coefficients, G_i, may be used for intermediate values of t/R_i, a/c, and a/t.
2. The value of the influence coefficients at the surface point of the crack defined by $\varphi = 0°$ are equal to: $G_i = A_0$.
3. The value of the influence coefficients at the deepest point of the crack defined by $\varphi = 90°$ are equal to $G_i = \sum_{n=0}^{6} A_n$.

Table 9B.21 – Coefficients for One and Two Cracks at the Toe of a Fillet Weld of a Ring Stiffened Cylinder Subject to Internal Pressure

R_i/t	A_r/t	a/t	M_p^{1c}	M_p^{2c}
10 (10/1)	1	0.1	11.106	10.707
		0.2	10.428	9.564
		0.4	11.463	9.438
		0.6	13.562	10.255
		0.8	16.369	12.590
	2	0.1	12.717	12.261
		0.2	11.659	10.689
		0.4	12.328	10.134
		0.6	14.174	10.736
		0.8	16.691	12.900
	4	0.1	15.156	14.644
		0.2	13.452	12.425
		0.4	13.474	11.326
		0.6	14.740	11.640
		0.8	16.789	13.533
	8	0.1	16.514	15.941
		0.2	14.560	13.486
		0.4	14.041	12.001
		0.6	14.854	12.083
		0.8	16.423	13.613
	16	0.1	17.276	16.862
		0.2	14.826	14.080
		0.4	13.902	12.488
		0.6	14.359	12.526
		0.8	15.789	13.970
	32	0.1	17.649	17.440
		0.2	14.860	14.532
		0.4	13.486	12.956
		0.6	13.607	12.938
		0.8	14.808	14.193

Table 9B.21 – Coefficients for One and Two Cracks at the Toe of a Fillet Weld of a Ring Stiffened Cylinder Subject to Internal Pressure

R_i/t	A_r/t	a/t	M_p^{1c}	M_p^{2c}
20 (20/1)	1	0.1	19.269	18.769
		0.2	18.759	17.561
		0.4	22.239	18.858
		0.6	28.552	21.683
		0.8	36.175	26.663
	2	0.1	22.159	21.552
		0.2	21.068	19.680
		0.4	24.104	20.277
		0.6	30.009	22.710
		0.8	36.920	27.288
	4	0.1	27.603	26.846
		0.2	25.406	23.693
		0.4	27.389	23.099
		0.6	32.190	24.732
		0.8	37.716	28.528
	8	0.1	31.262	30.328
		0.2	28.564	26.601
		0.4	29.584	25.029
		0.6	33.343	25.978
		0.8	37.377	27.814
	16	0.1	34.441	33.532
		0.2	30.598	28.778
		0.4	30.707	26.632
		0.6	33.518	27.214
		0.8	36.815	29.750
	32	0.1	36.535	35.879
		0.2	31.740	30.526
		0.4	30.505	28.082
		0.6	31.891	25.247
		0.8	34.014	30.330

Table 9B.21 – Coefficients for One and Two Cracks at the Toe of a Fillet Weld of a Ring Stiffened Cylinder Subject to Internal Pressure

R_i/t	A_r/t	a/t	M_p^{1c}	M_p^{2c}
30 (30/1)	1	0.1	27.137	26.548
		0.2	26.846	25.383
		0.4	33.060	28.564
		0.6	44.379	34.219
		0.8	58.493	42.370
	2	0.1	30.669	30.098
		0.2	30.063	28.385
		0.4	35.781	30.696
		0.6	46.776	35.734
		0.8	59.767	43.291
	4	0.1	38.831	37.948
		0.2	36.414	34.273
		0.4	40.976	34.996
		0.6	50.576	38.833
		0.8	61.329	45.094
	8	0.1	44.710	43.574
		0.2	41.641	39.072
		0.4	44.887	38.289
		0.6	52.987	40.955
		0.8	61.249	45.531
	16	0.1	50.589	49.352
		0.2	45.798	43.140
		0.4	47.902	41.291
		0.6	54.624	43.252
		0.8	61.231	47.163
	32	0.1	54.929	53.818
		0.2	48.707	46.566
		0.4	48.797	44.041
		0.6	53.038	45.271
		0.8	56.949	48.127

Table 9B.21 – Coefficients for One and Two Cracks at the Toe of a Fillet Weld of a Ring Stiffened Cylinder Subject to Internal Pressure

R_i/t	A_r/t	a/t	M_p^{1c}	M_p^{2c}
50 (50/1)	1	0.1	42.373	41.659
		0.2	42.679	40.812
		0.4	54.728	48.412
		0.6	77.789	61.044
		0.8	108.432	77.271
	2	0.1	47.993	47.208
		0.2	47.448	45.328
		0.4	59.055	51.864
		0.6	81.723	63.725
		0.8	111.144	78.974
	4	0.1	60.278	59.142
		0.2	57.556	54.808
		0.4	67.696	59.067
		0.6	88.740	68.963
		0.8	113.738	81.561
	8	0.1	70.395	69.008
		0.2	66.013	62.587
		0.4	75.063	65.135
		0.6	94.910	73.402
		0.8	116.860	83.943
	16	0.1	81.194	79.428
		0.2	74.987	71.097
		0.4	82.216	71.569
		0.6	99.803	78.017
		0.8	117.931	86.566
	32	0.1	90.505	88.764
		0.2	82.141	78.609
		0.4	86.581	77.296
		0.6	99.968	82.189
		0.8	112.846	89.028

Table 9B.21 – Coefficients for One and Two Cracks at the Toe of a Fillet Weld of a Ring Stiffened Cylinder Subject to Internal Pressure

R_i/t	A_r/t	a/t	M_p^{1c}	M_p^{2c}
100 (100/1)	1	0.1	79.179	78.162
		0.2	81.194	78.532
		0.4	108.832	99.108
		0.6	164.902	134.456
		0.8	252.502	178.701
	2	0.1	88.154	87.030
		0.2	88.966	86.077
		0.4	116.236	105.308
		0.6	173.060	140.138
		0.8	259.063	182.328
	4	0.1	108.924	107.511
		0.2	106.530	102.873
		0.4	132.464	119.117
		0.6	187.884	150.595
		0.8	264.764	187.021
	8	0.1	128.327	126.560
		0.2	123.176	118.394
		0.4	148.108	132.338
		0.6	203.026	161.154
		0.8	274.309	192.685
	16	0.1	151.741	149.243
		0.2	143.372	137.502
		0.4	166.274	147.919
		0.6	218.889	173.102
		0.8	282.962	199.688
	32	0.1	174.828	171.926
		0.2	162.498	156.236
		0.4	182.044	163.057
		0.6	228.983	184.588
		0.8	280.464	205.977

Table 9B.21 – Coefficients for One and Two Cracks at the Toe of a Fillet Weld of a Ring Stiffened Cylinder Subject to Internal Pressure

R_i/t	A_r/t	a/t	M_p^{1c}	M_p^{2c}
200 (200/1)	1	0.1	150.420	148.849
		0.2	156.308	152.523
		0.4	216.593	201.874
		0.6	347.722	293.750
		0.8	587.259	419.471
	2	0.1	164.425	162.944
		0.2	168.545	164.634
		0.4	228.814	212.712
		0.6	361.852	304.020
		0.8	601.956	427.103
	4	0.1	198.318	196.602
		0.2	197.859	193.131
		0.4	257.233	237.679
		0.6	390.600	325.449
		0.8	619.002	437.690
	8	0.1	232.986	230.791
		0.2	228.011	221.767
		0.4	287.511	263.983
		0.6	423.357	348.986
		0.8	640.233	450.670
	16	0.1	279.311	276.031
		0.2	269.046	263.426
		0.4	326.872	298.360
		0.6	463.529	378.446
		0.8	670.028	468.110
	32	0.1	330.530	326.493
		0.2	313.114	303.480
		0.4	369.008	335.703
		0.6	502.465	409.708
		0.8	685.282	485.817

Table 9B.21 – Coefficients for One and Two Cracks at the Toe of a Fillet Weld of a Ring Stiffened Cylinder Subject to Internal Pressure

R_i/t	A_r/t	a/t	M_p^{1c}	M_p^{2c}
300 (300/1)	1	0.1	219.626	217.842
		0.2	229.605	224.306
		0.4	322.659	304.104
		0.6	532.144	460.036
		0.8	955.006	691.338
	2	0.1	238.716	237.289
		0.2	246.132	241.842
		0.4	340.143	320.429
		0.6	553.121	475.768
		0.8	976.452	703.323
	4	0.1	282.843	281.077
		0.2	284.925	279.572
		0.4	378.344	354.437
		0.6	594.759	507.204
		0.8	1006.246	720.786
	8	0.1	330.278	327.755
		0.2	326.495	319.091
		0.4	421.111	392.473
		0.6	644.305	543.771
		0.8	1047.281	743.266
	16	0.1	397.141	393.356
		0.2	386.084	376.539
		0.4	480.278	444.954
		0.6	708.066	591.154
		0.8	1098.128	772.214
	32	0.1	475.863	471.069
		0.2	454.952	443.355
		0.4	547.772	505.320
		0.6	778.832	645.850
		0.8	1140.055	804.194

Note: Interpolation may be used for intermediate values of R_i/t, A_r/t, and a/t.

Table 9B.22 – Parameters for Mk-Factors – Surface Crack at Tee Joint, Semi-Elliptical Shape, Through-Wall Membrane and Bending Stress

Function	Parameter	Deepest point of the crack (Point B)		Surface point of the crack (Point A)	
		M_{km}	M_{kb}	M_{km}	M_{kb}
F_1	P_1	1.04424	1.19137	0.47722	0.52011
	P_2	-0.09627	-0.14198	-0.46228	-0.36027
	P_3	0.03790	0.038086	0.19046	0.12547
	P_4	0.54616	0.86676	0.39777	0.54940
	P_5	-0.12508	-0.24951	0.22176	-0.098759
	P_6	-2.43313	-2.03967	-3.25447	-2.80066
	P_7	-0.07251	0.20231	-0.63489	-0.71090
	P_8	0.18353	0.40094	2.85835	1.50561
	P_9	0.87051	0.94855	1.95878	1.86540
F_2	P_{10}	0.99924	1.00095	0.40489	0.96775
	P_{11}	0.04125	0.10217	0.34526	-0.21496
	P_{12}	-0.75765	-0.95780	-0.29917	-0.82377
	P_{13}	-0.000426	-0.075004	-0.77810	-0.25998
F_3	P_{14}	-0.05692	-0.68779	41.72046	-8.77203
	P_{15}	1.19362	-8.67636	-78.8175	24.27778
	P_{16}	-1.43325	16.16166	34.10390	-28.1240
	P_{17}	0.61335	-8.14948	2.73640	11.4415
	P_{18}	1.05721	-0.152293	0.030034	2.64087
	P_{19}	-2.4052	-0.148843	-0.13126	-10.4940
	P_{20}	2.61759	1.77150	0.11538	12.8098
	P_{21}	-0.98207	-1.27776	0.040551	-5.98773
F_4	P_{22}	1.06748	1.78291	0.53107	0.78365
	P_{23}	7.74090	8.37239	0.26223	-0.24718
	P_{24}	0.47714	0.41021	-0.24730	1.55530
	P_{25}	-0.21542	-0.95097	12.2781	0.049054
	P_{26}	-1.08081	1.64652	-0.059328	0.040332
	P_{27}	-0.002871	3.52508	-0.002740	-0.000146
	P_{28}	0.89122	31.9326	1.04175	-2.41618
	P_{29}	0.008454	0.000011	0.050788	0.002455
	P_{30}	0.14155	0.010084	-0.039354	0.013053
	P_{31}	0.48533	0.93093	1.39315	0.57026
	P_{32}	-2.12357	-2.52809	-10.8442	0.40172
	P_{33}	---	---	16.6945	0.35095
	P_{34}	---	---	0.12542	0.55589
	P_{35}	---	---	-1.39604	0.047656
	P_{36}	---	---	1.21456	0.042067
	P_{37}	---	---	0.69694	1.07535
	P_{38}	---	---	0.42960	-0.48462

9B.18 Figures

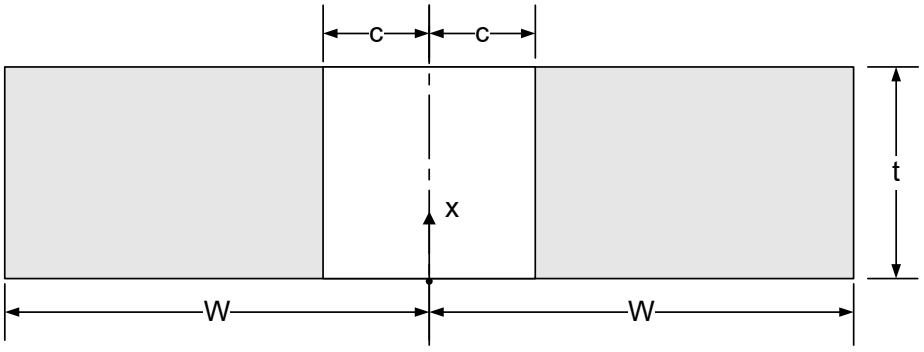

Figure 9B.1 – Plate – Through Wall Crack

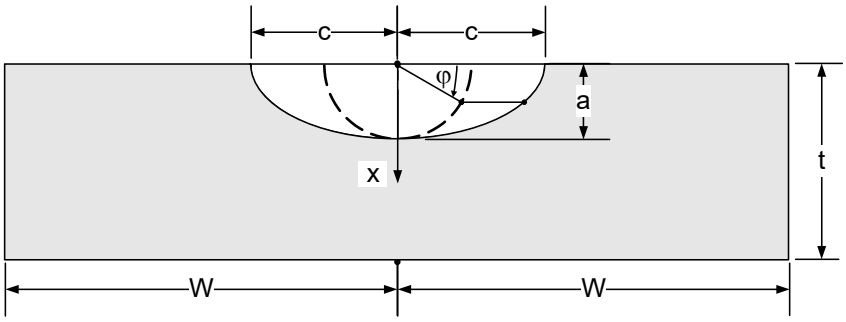

(a) Finite Length Surface Crack

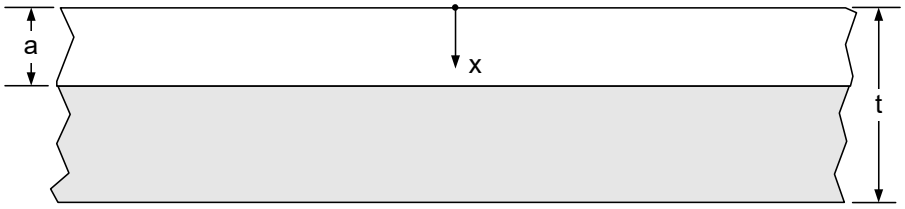

(b) Infinitely Long Surface Crack (c>>a)

Figure 9B.2 – Plate – Surface Crack, Semi-Elliptical Shape

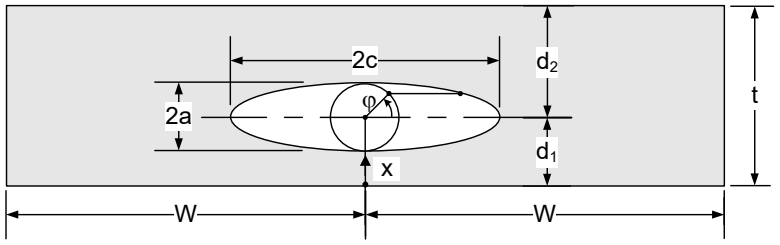

(a) Finite Length Embedded Crack

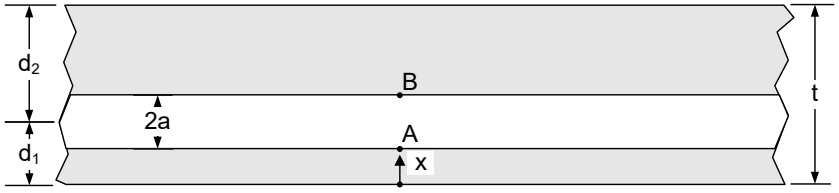

(b) Infinitely Long Embedded Crack (c>>a)

Figure 9B.3 – Plate – Embedded Crack, Elliptical Shape

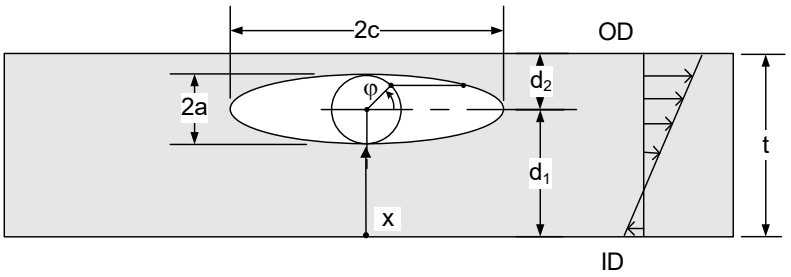

a) Actual Embedded Flaw ($d_1/t>0.5$)

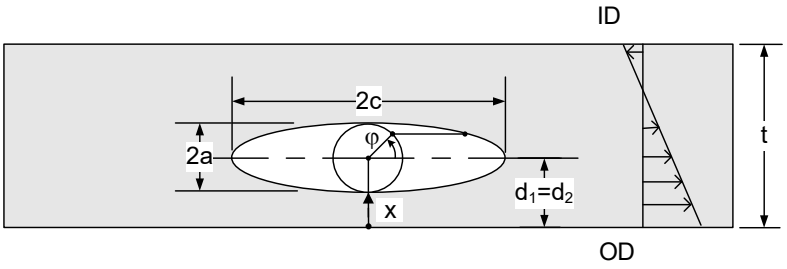

b) Re-characterization of an Embedded Flaw with
Reversed Stress Field

Figure 9B.4 – Plate – Embedded Crack Re-Characterization

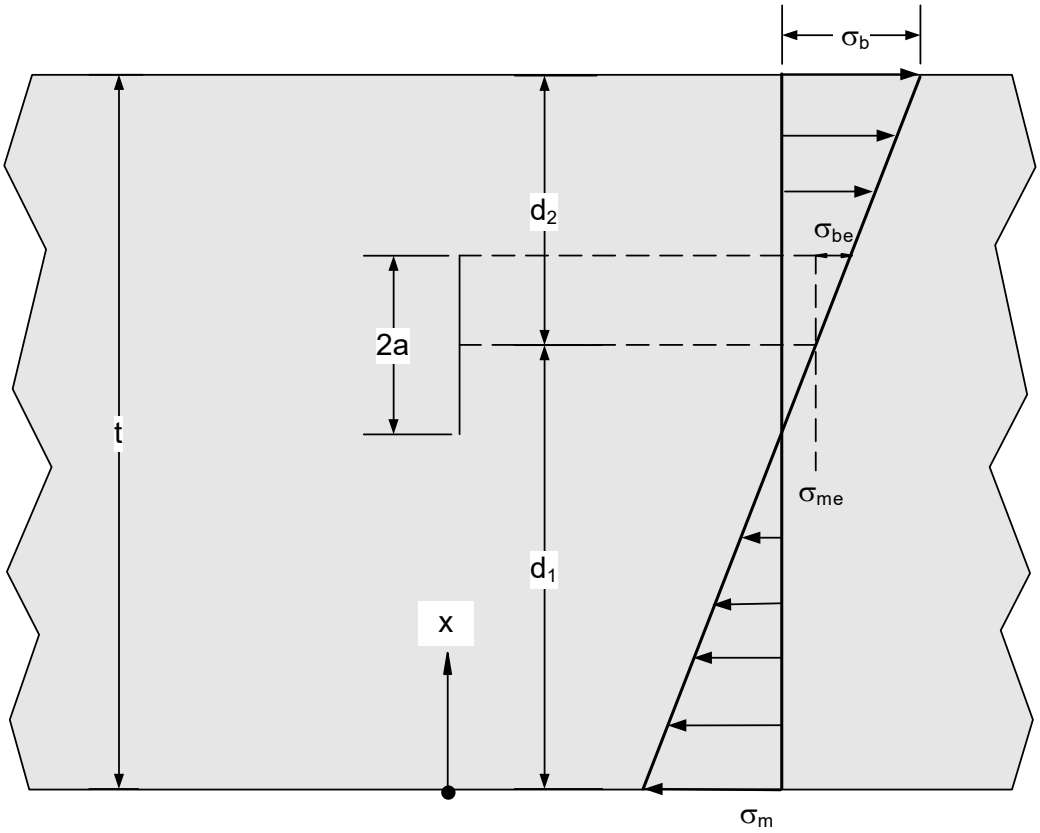

Note: The membrane and bending stress acting on the crack face can be computed using the equations in paragraph 9B.3.7.1.

Figure 9B.5 – Plate – Embedded Crack, Definition of Membrane and Bending Stress

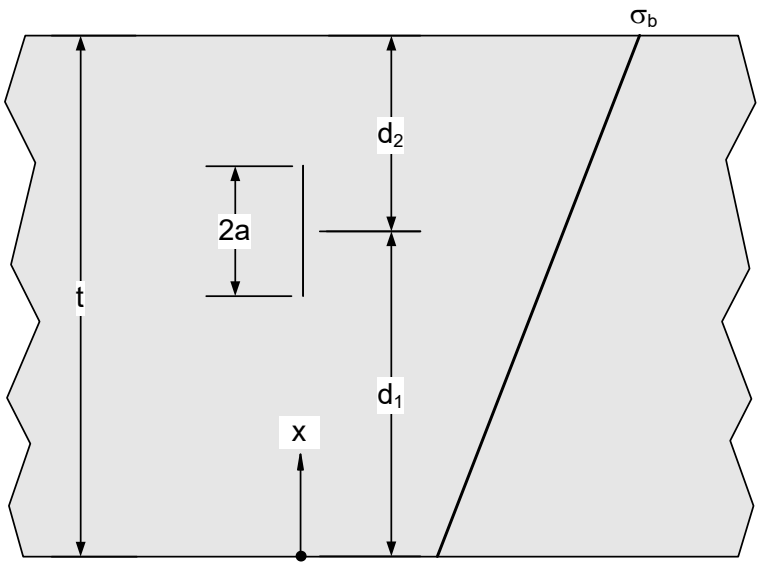

(a) Positive σ_b

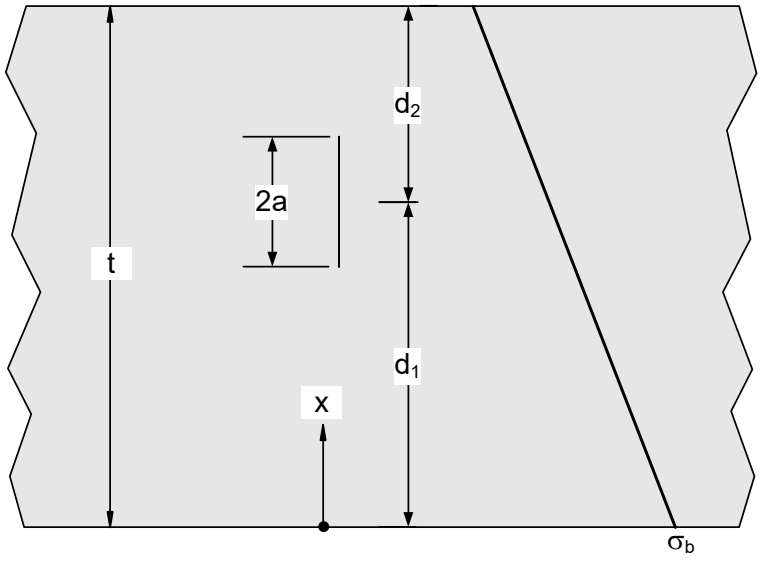

(b) Negative σ_b

Figure 9B.6 – Plate – Embedded Cracks, Sign Convention for Bending Stress Distribution

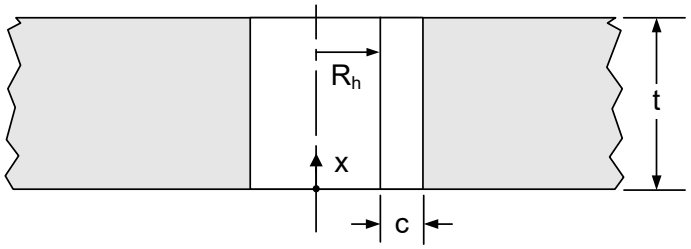

(a) Through-Wall Single Edge Crack

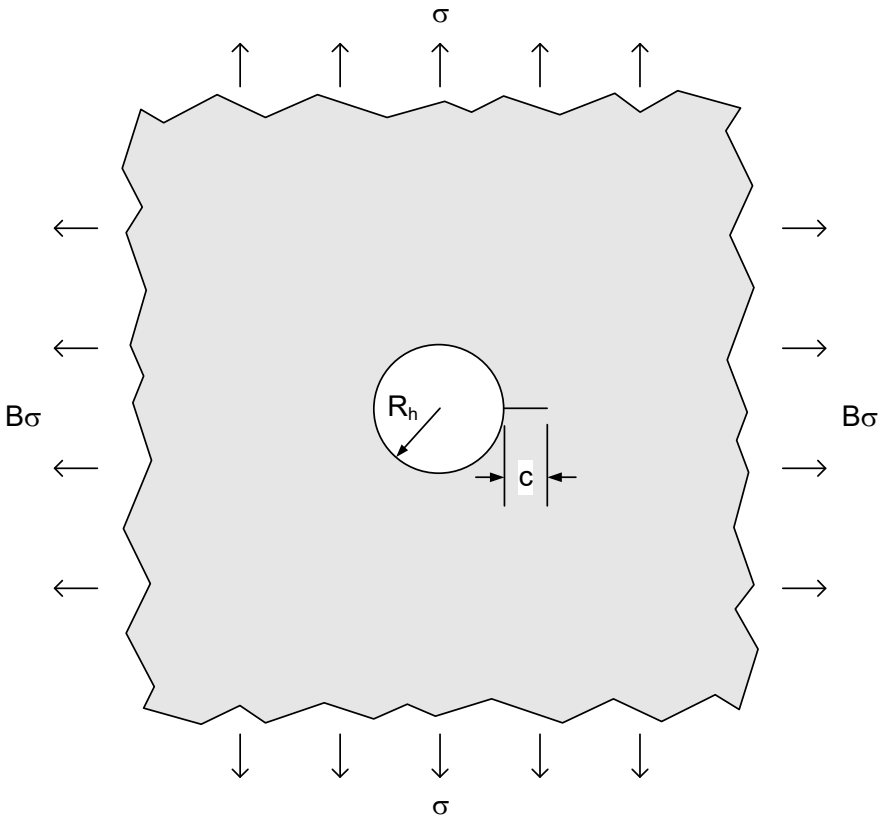

(b) Biaxial Loading

Figure 9B.7 – Plate With Hole – Through-wall Single Edge Crack

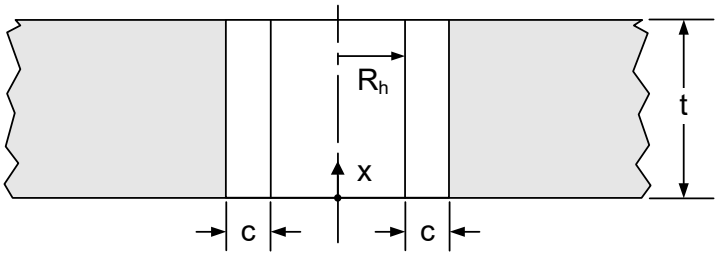

(a) Through-Wall Double Edge Crack

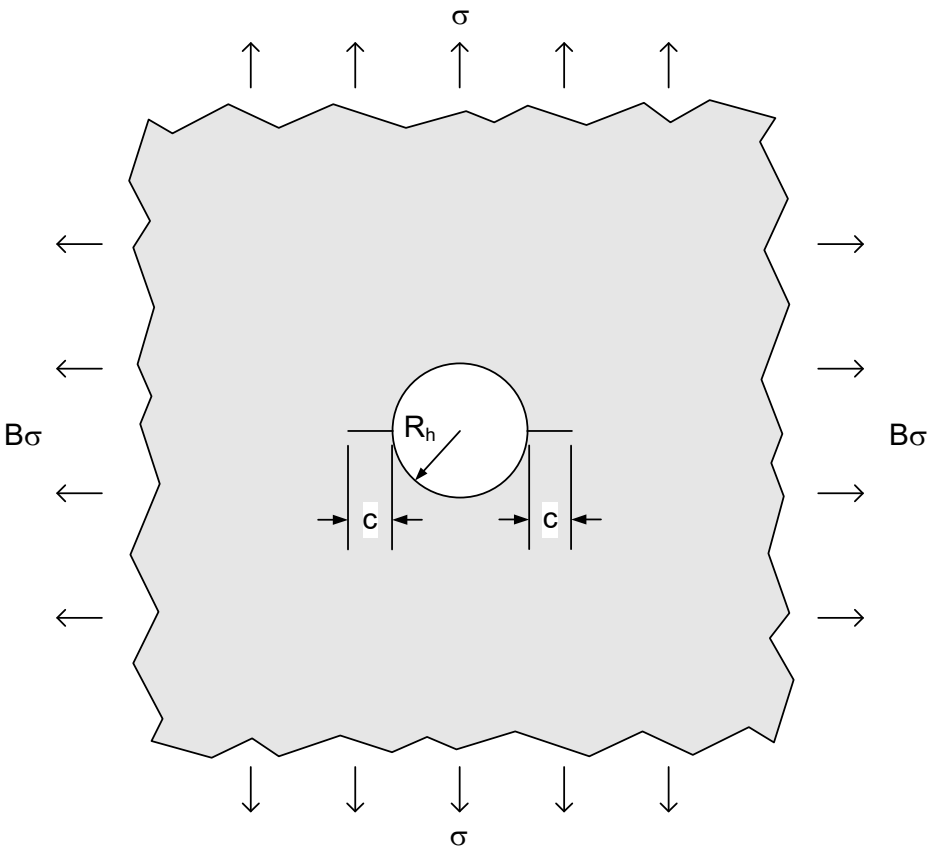

(b) Biaxial Loading

Figure 9B.8 – Plate With Hole – Through-wall Double Edge Crack

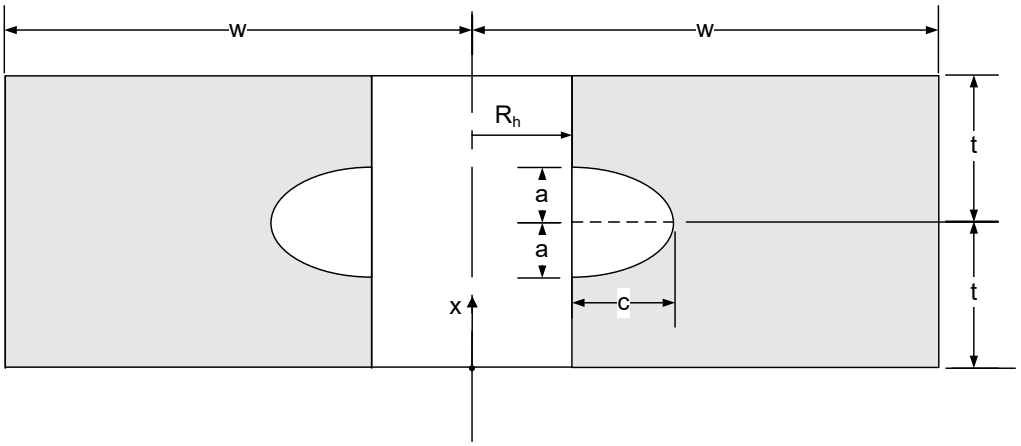

Figure 9B.9 – Plate With Hole – Surface Crack, Semi-Elliptical Shape

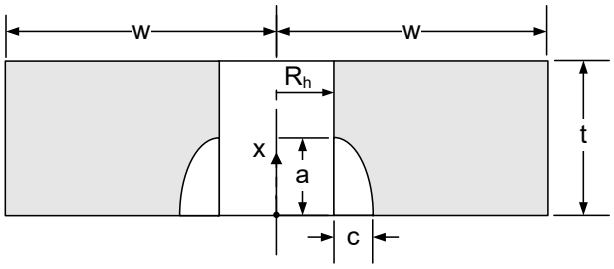

(a) Crack Geometry

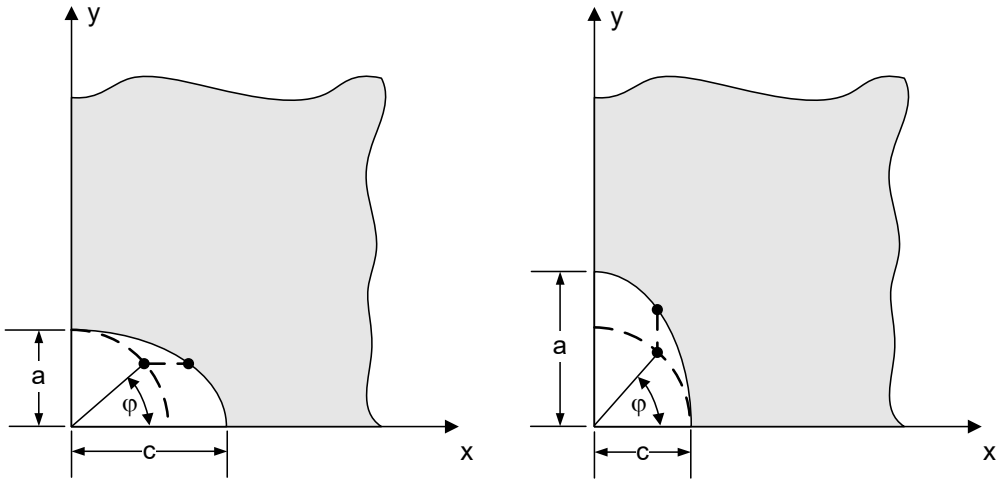

(a) $a/c \leq 1$ (b) $a/c > 1$

(b) Coordinate System Used to Define the Parametric Angle

Figure 9B.10 – Plate With Hole – Corner Crack, Semi-Elliptical Shape

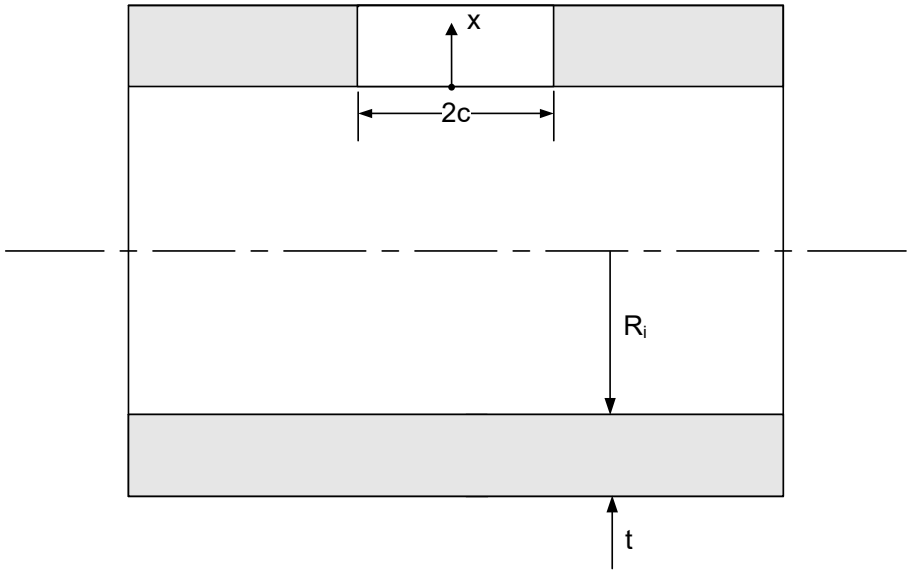

Figure 9B.11 – Cylinder – Through-wall Crack, Longitudinal Direction

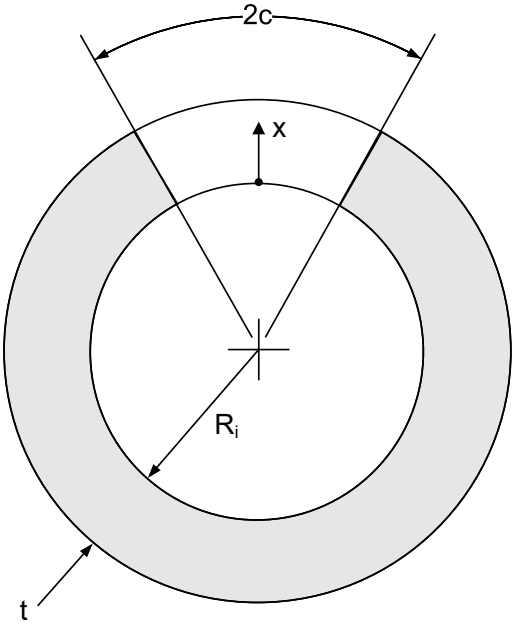

Figure 9B.12 – Cylinder – Through-wall Crack, Circumferential Direction

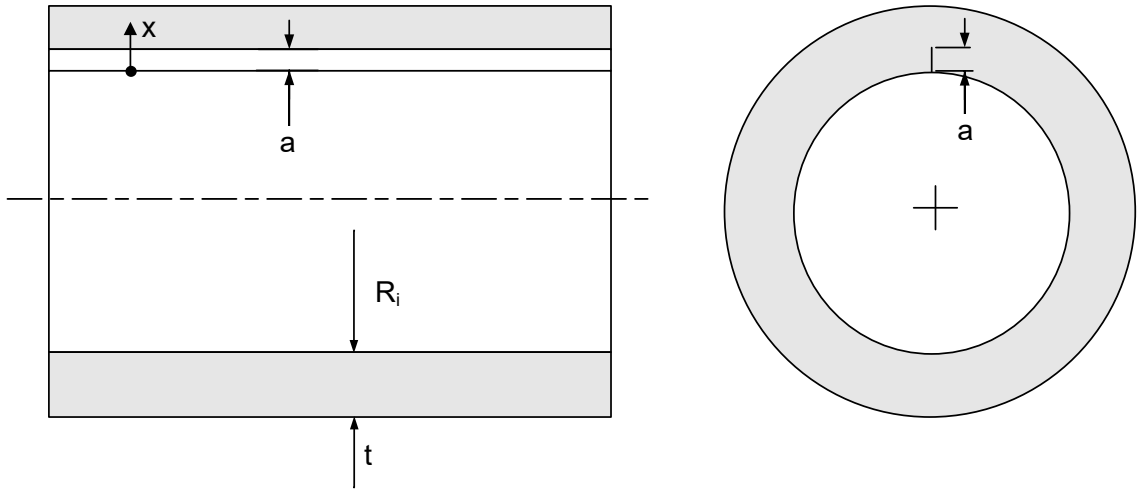

(a) Inside Surface

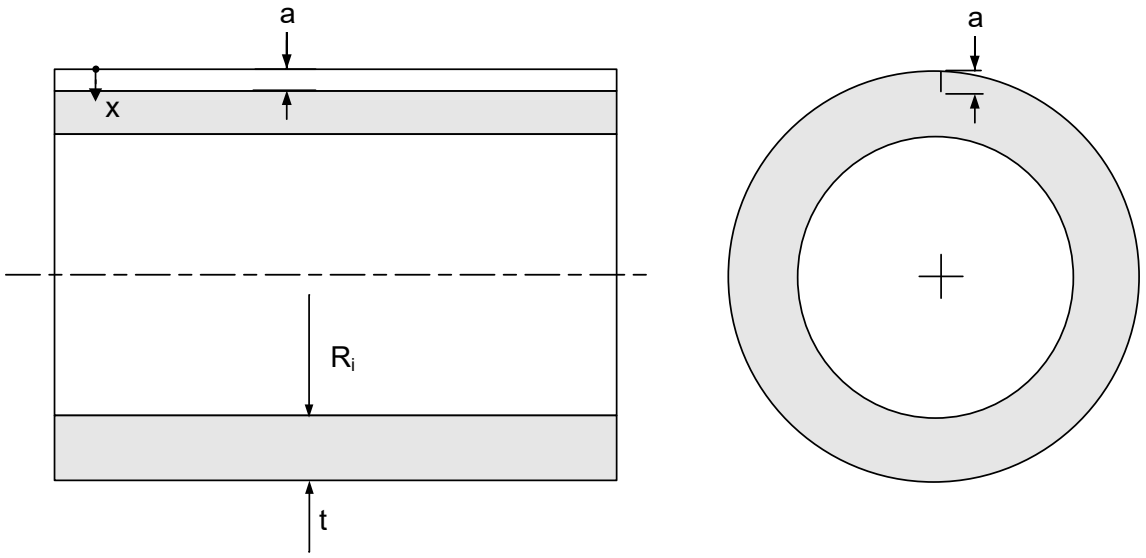

(b) Outside Surface

Figure 9B.13 – Cylinder – Surface Crack, Longitudinal Direction, Infinite Length

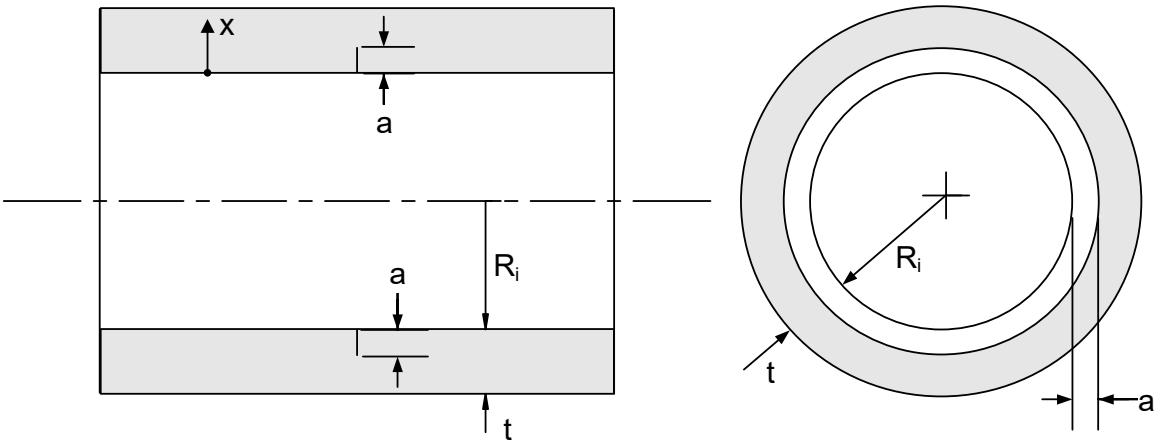

(a) Inside Surface

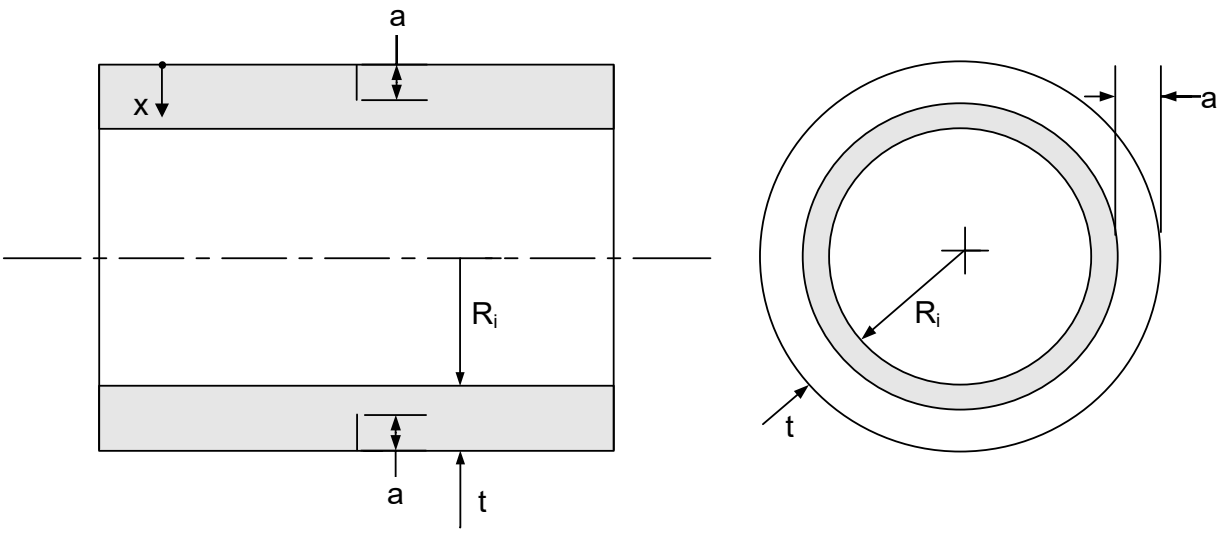

(b) Outside Surface

Figure 9B.14 – Cylinder – Surface Crack, Circumferential Direction, 360 Degrees

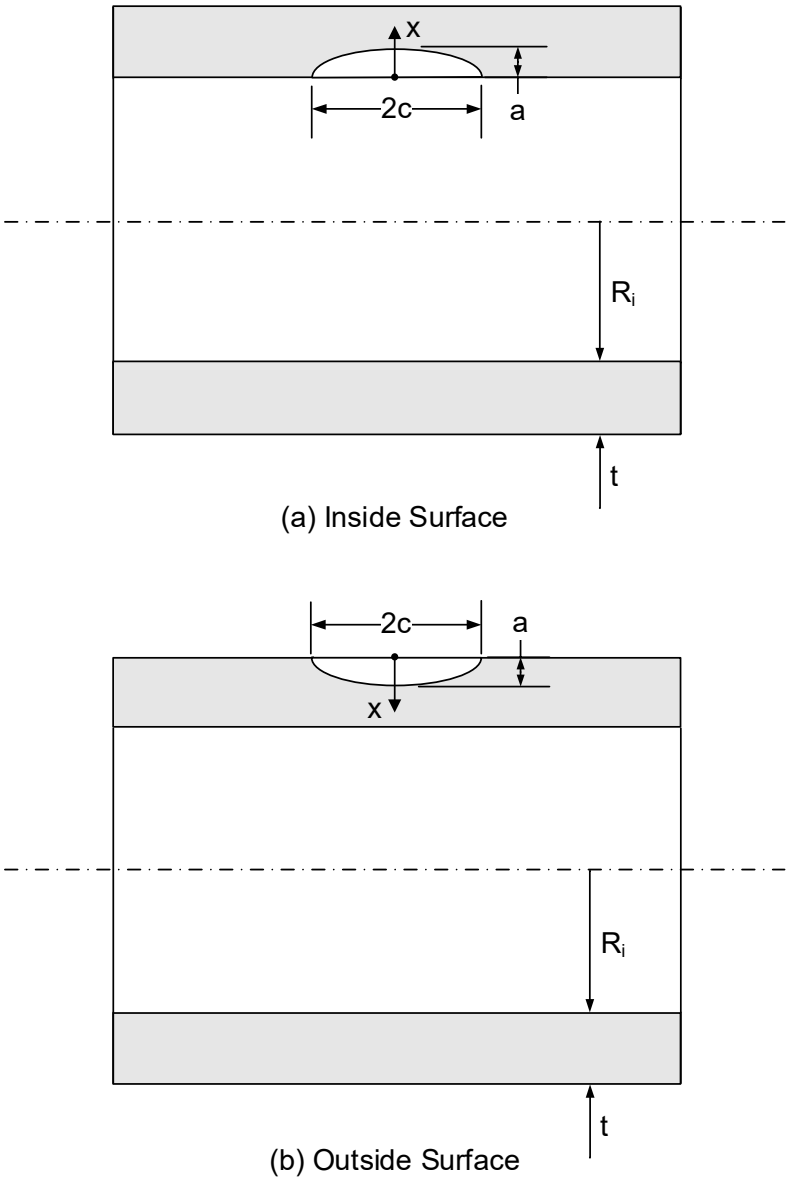

Figure 9B.15 – Cylinder – Surface Crack, Longitudinal Direction – Semi-Elliptical Shape

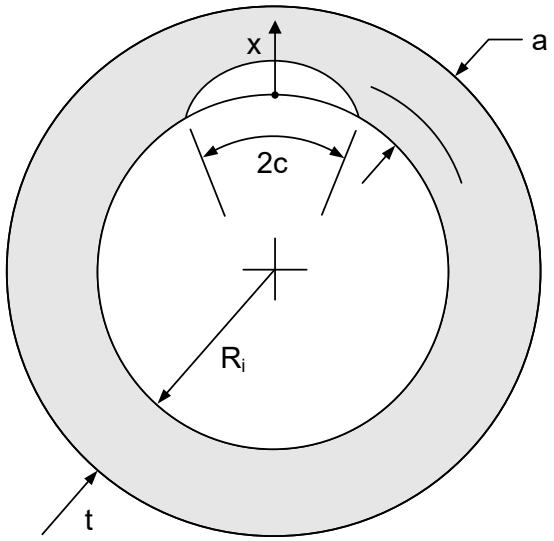

(a) Inside Surface

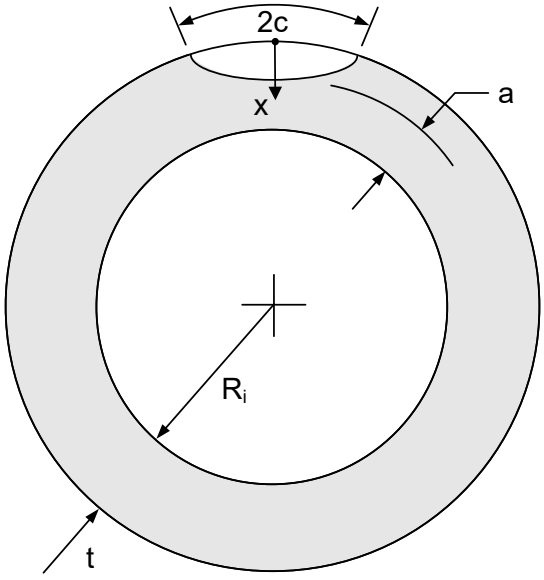

(b) Outside Surface

Figure 9B.16 – Cylinder – Surface Crack, Circumferential Direction, Semi-Elliptical Shape

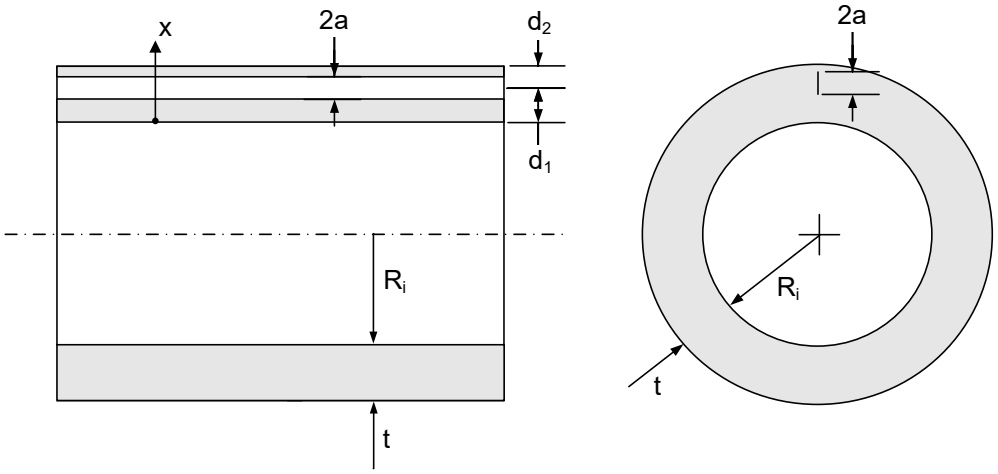

Figure 9B.17 – Cylinder – Embedded Crack, Longitudinal Direction, Infinite Length

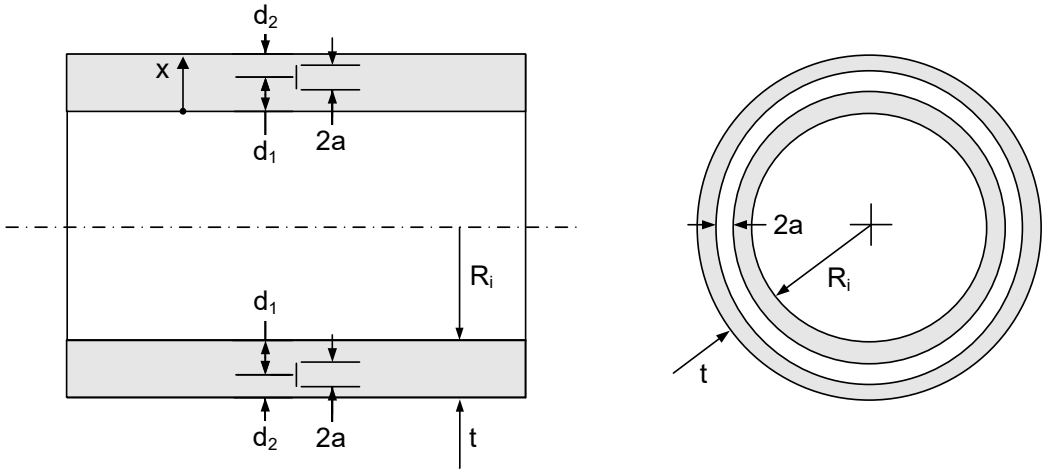

Figure 9B.18 – Cylinder – Embedded Crack, Circumferential Direction – 360 Degrees

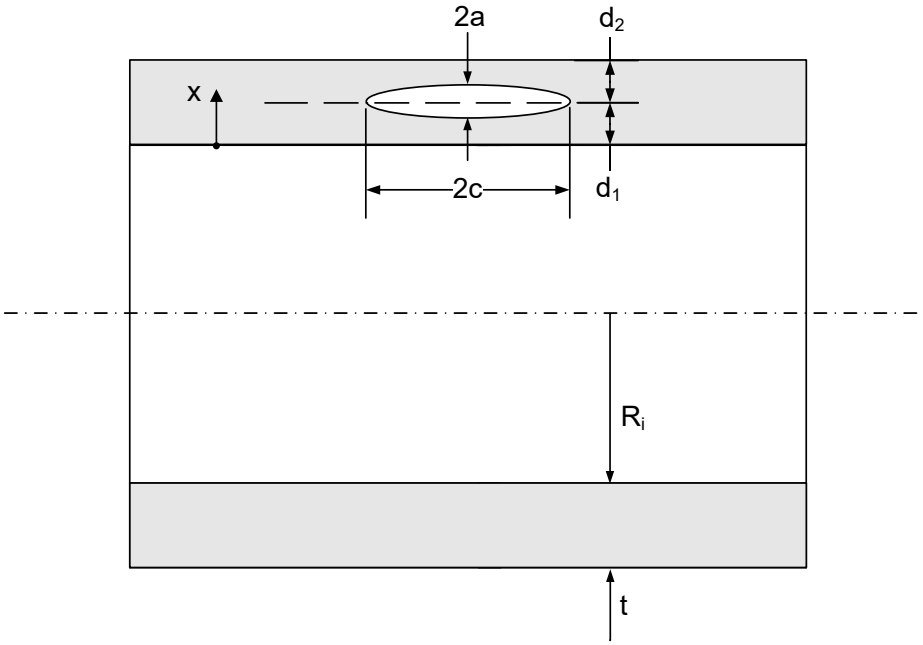

Figure 9B.19 – Cylinder – Embedded Crack, Longitudinal Direction, Elliptical Shape

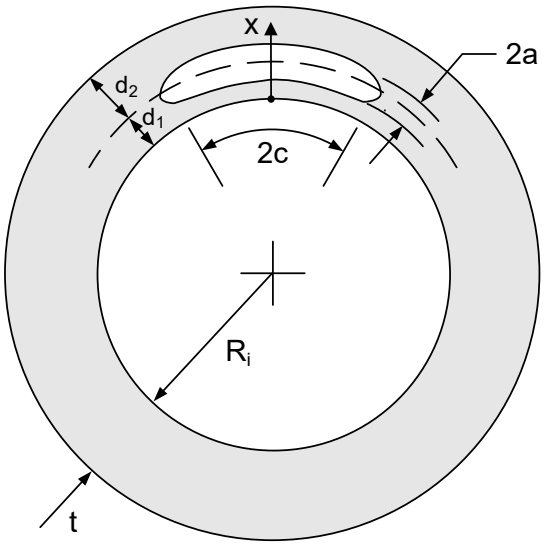

Figure 9B.20 – Cylinder – Embedded Crack, Circumferential Direction, Elliptical Shape

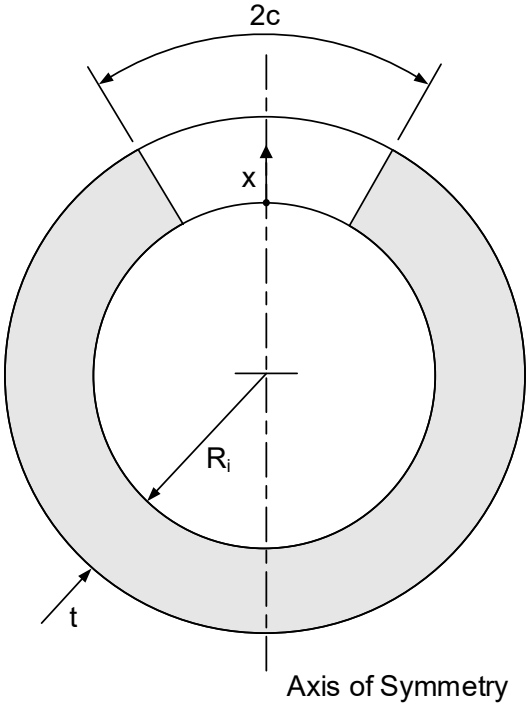

Figure 9B.21 – Sphere – Through-wall Crack

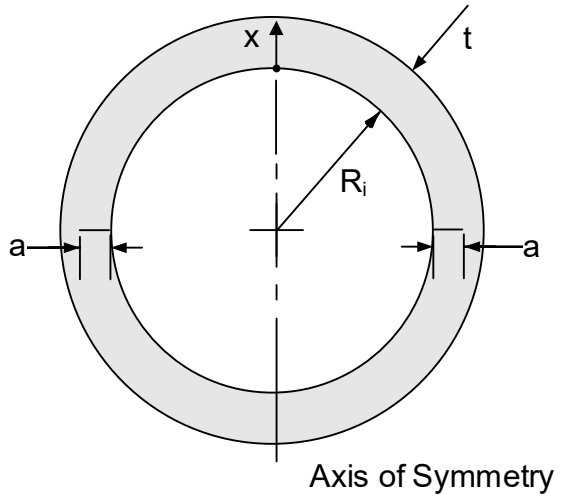

(a) Inside Surface

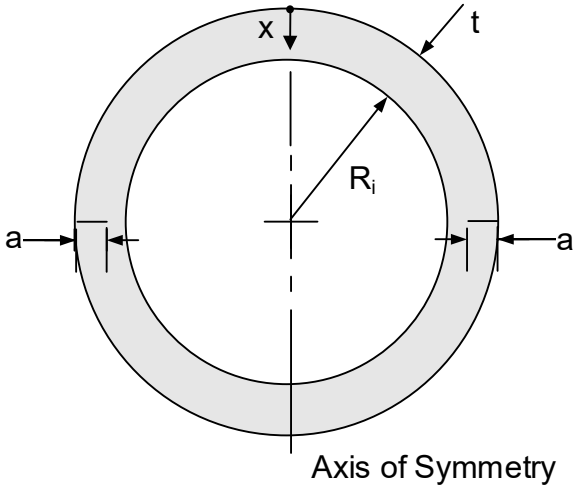

(b) Outside Surface

Figure 9B.22 – Sphere – Surface Crack, Circumferential Direction, 360 Degrees

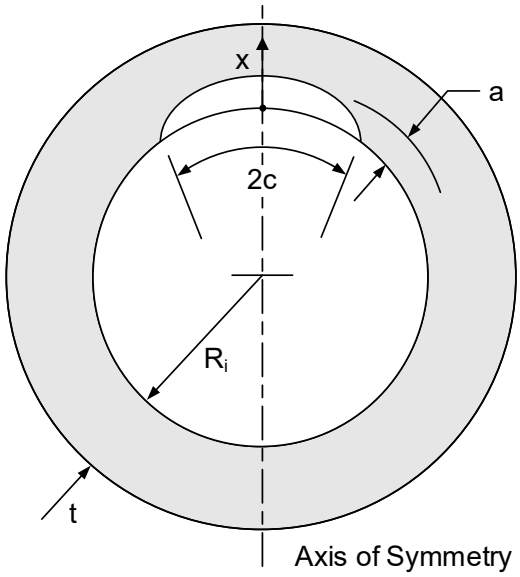

(a) Inside Surface

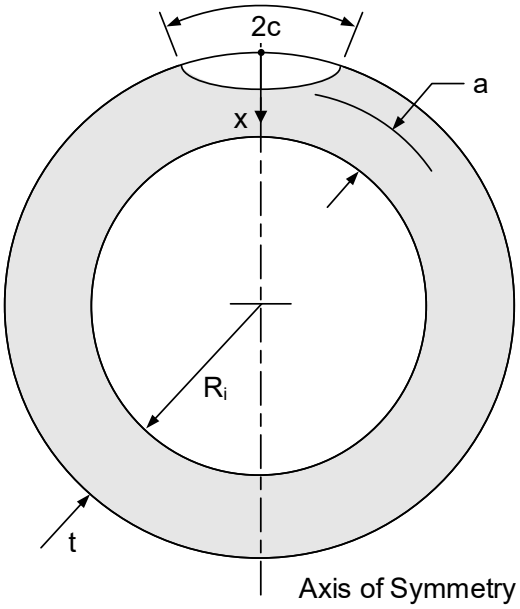

(b) Outside Surface

Figure 9B.23 – Sphere – Surface Crack, Circumferential Direction, Semi-Elliptical Shape

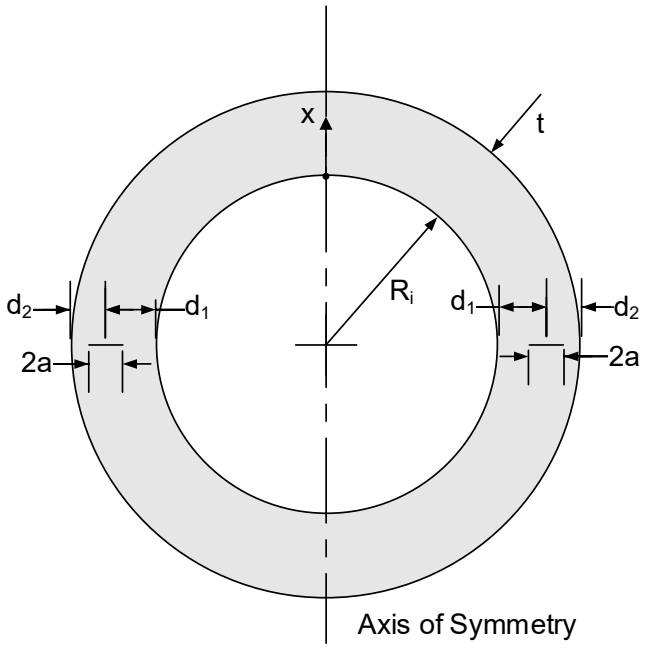

Figure 9B.24 – Sphere – Embedded Crack, Circumferential Direction, 360 Degrees

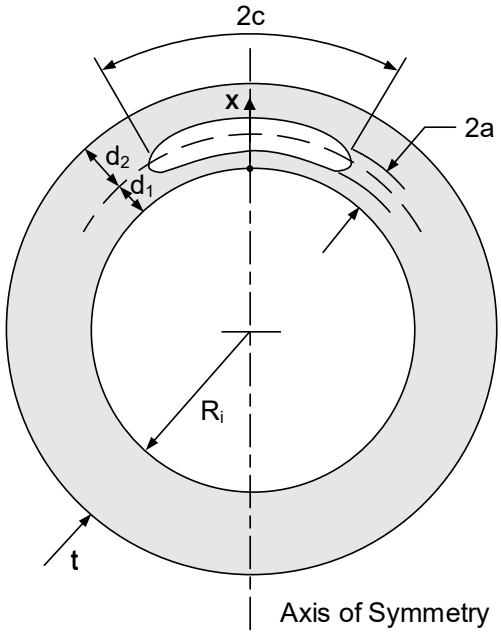

Figure 9B.25 – Sphere – Embedded Crack, Circumferential Direction, Elliptical Shape

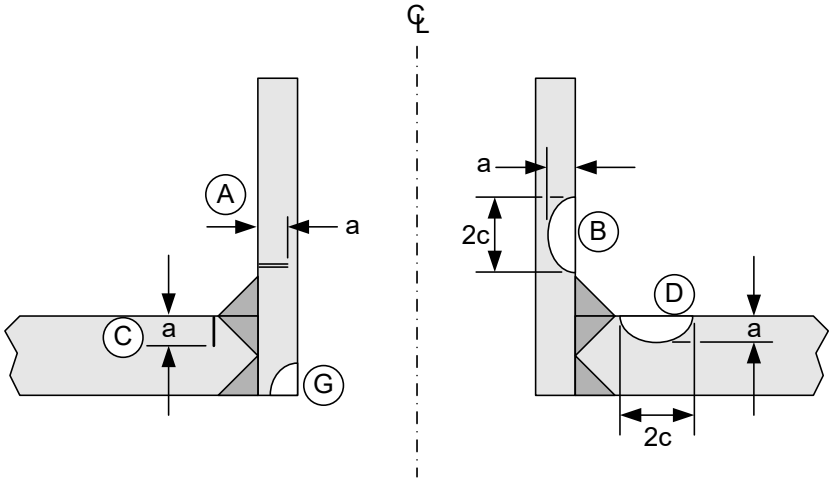

(a) Nozzle or Branch Connection

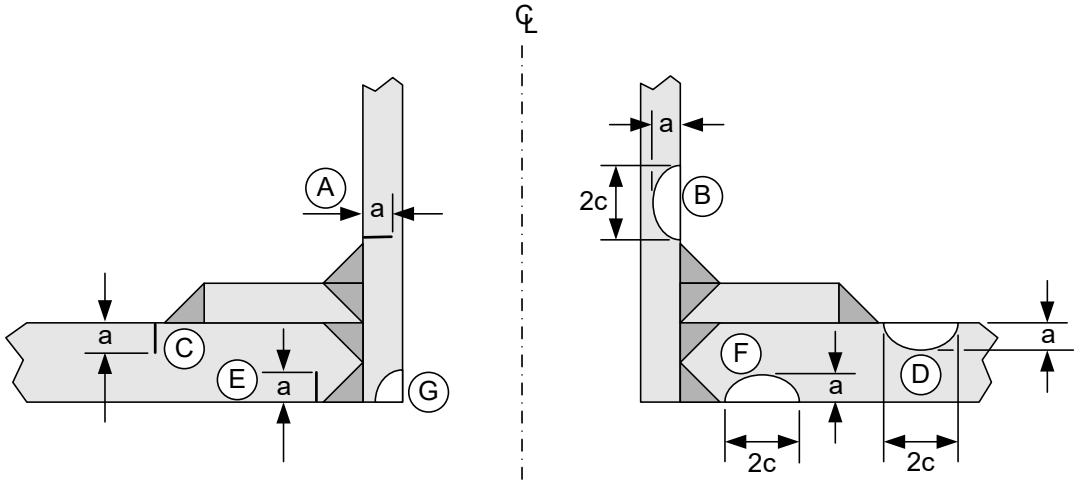

(b) Nozzle or Branch Connection with a Reinforcing Pad

Figure 9B.26 – Cracks At Nozzles And Piping Branch Connections

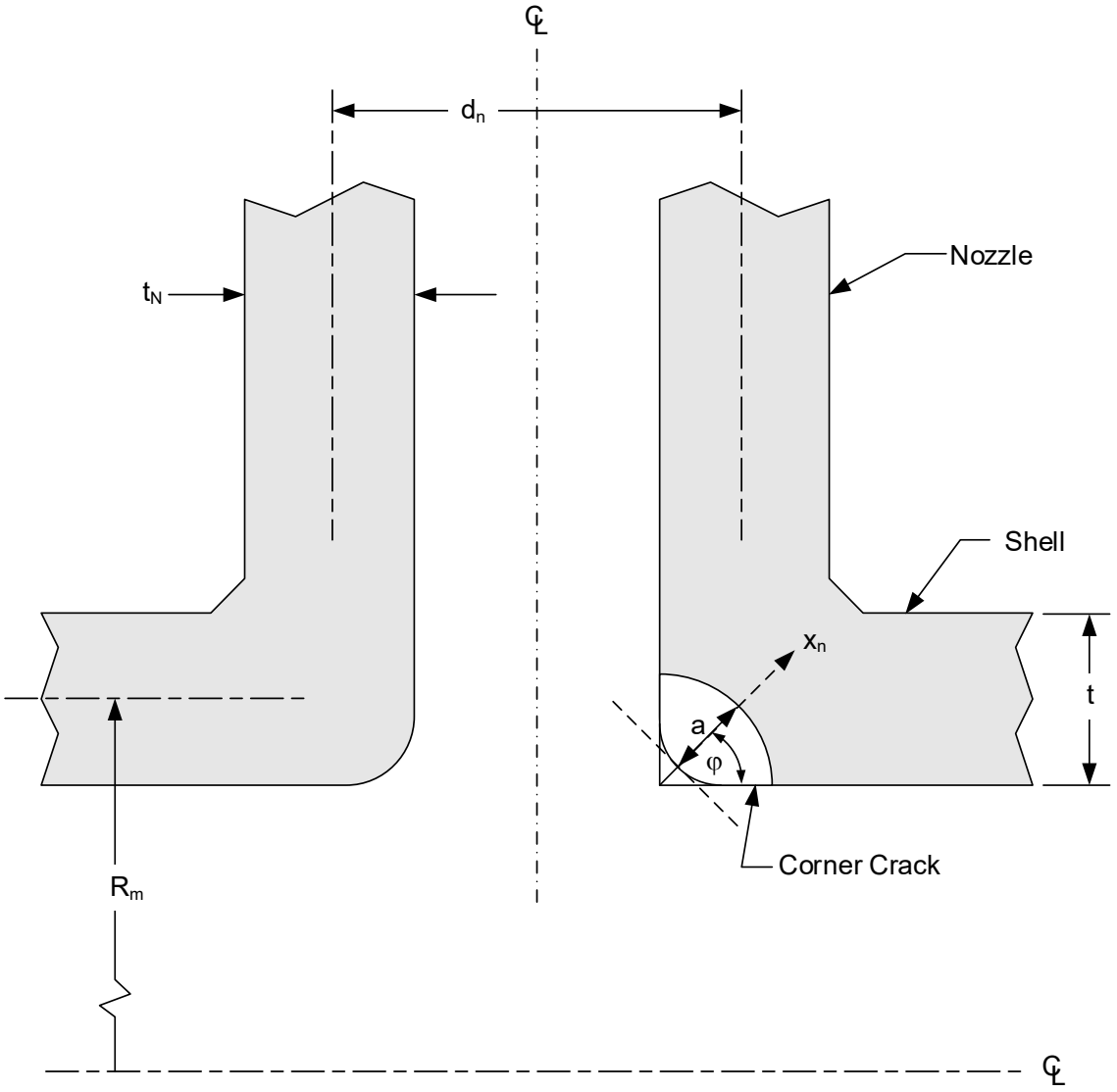

Figure 9B.27 – Nozzle Corner Cracks

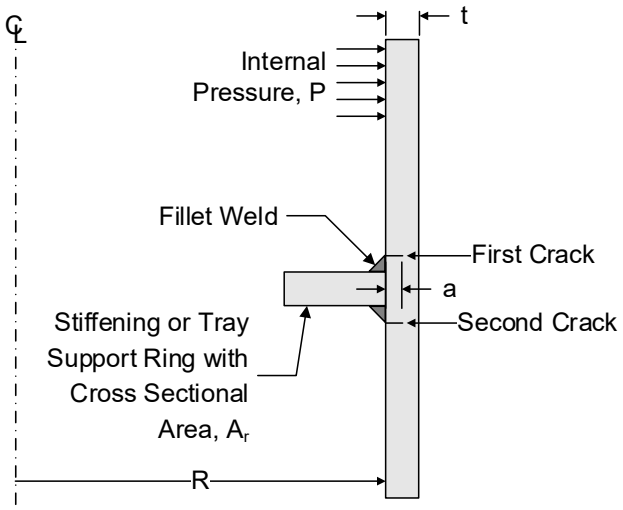

(a) Internal Ring, Internal Pressure

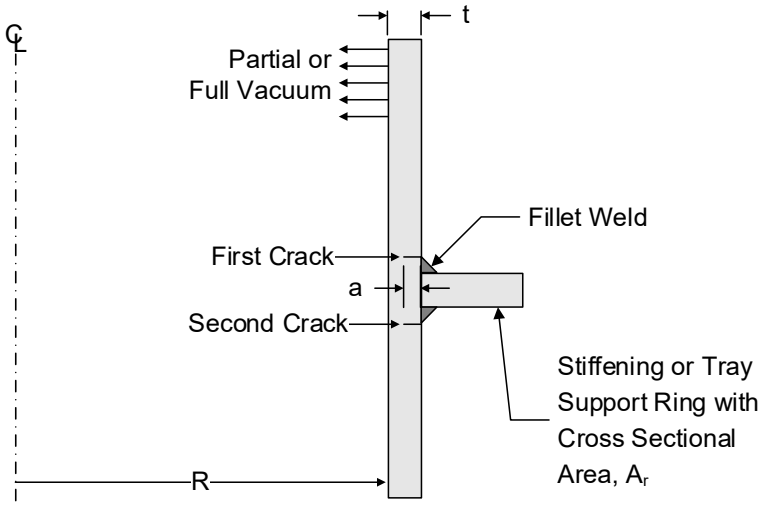

(b) External Ring, Partial or Full Vacuum

Figure 9B.28 – Ring Stiffened Cylinders – Edge Cracks At Fillet Welds

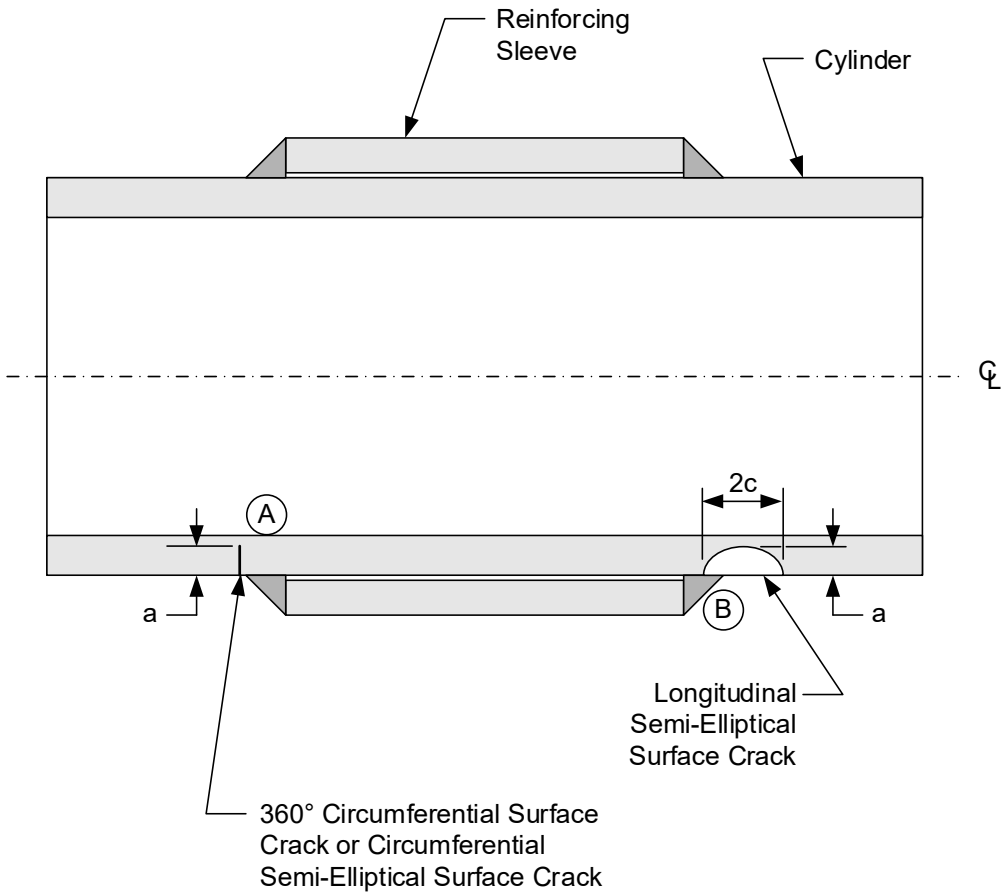

Figure 9B.29 – Cracks At Sleeve Reinforced Cylinders

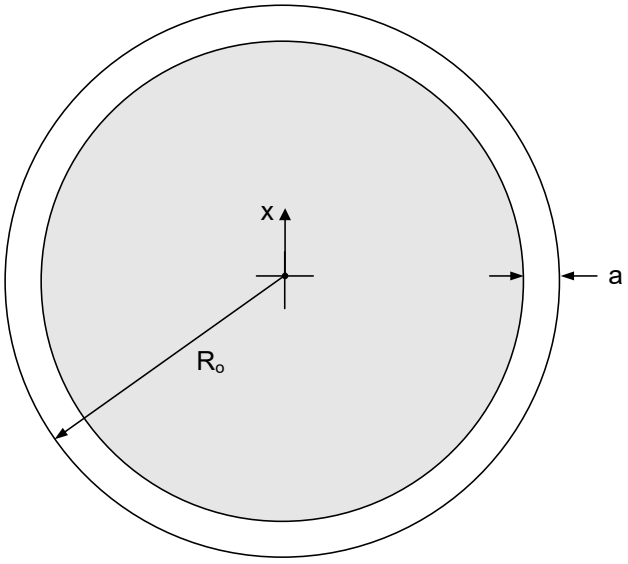

Figure 9B.30 – Round Bar – Surface Crack, 360 Degrees

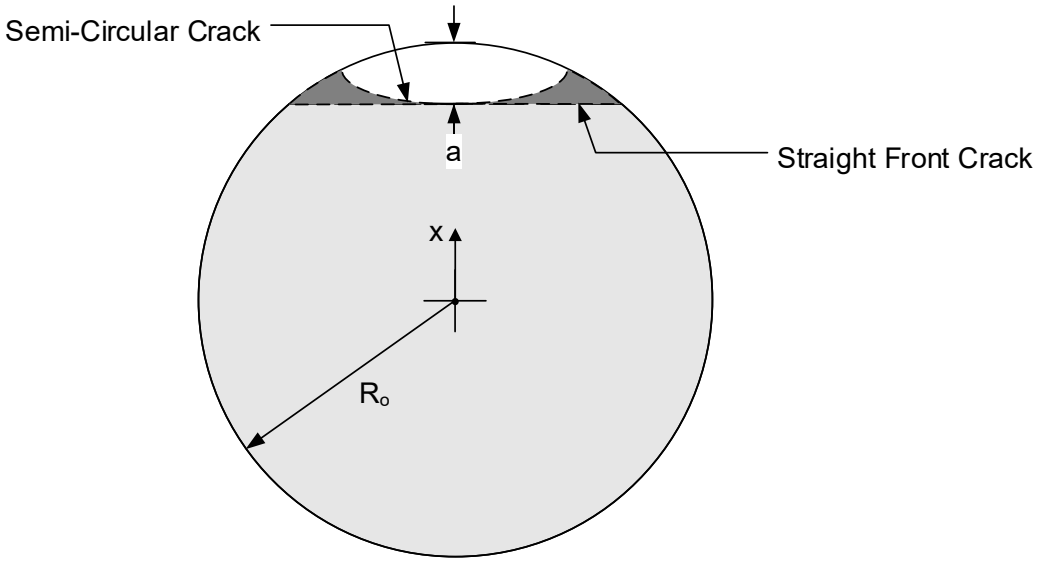

Figure 9B.31 – Round Bar – Surface Crack

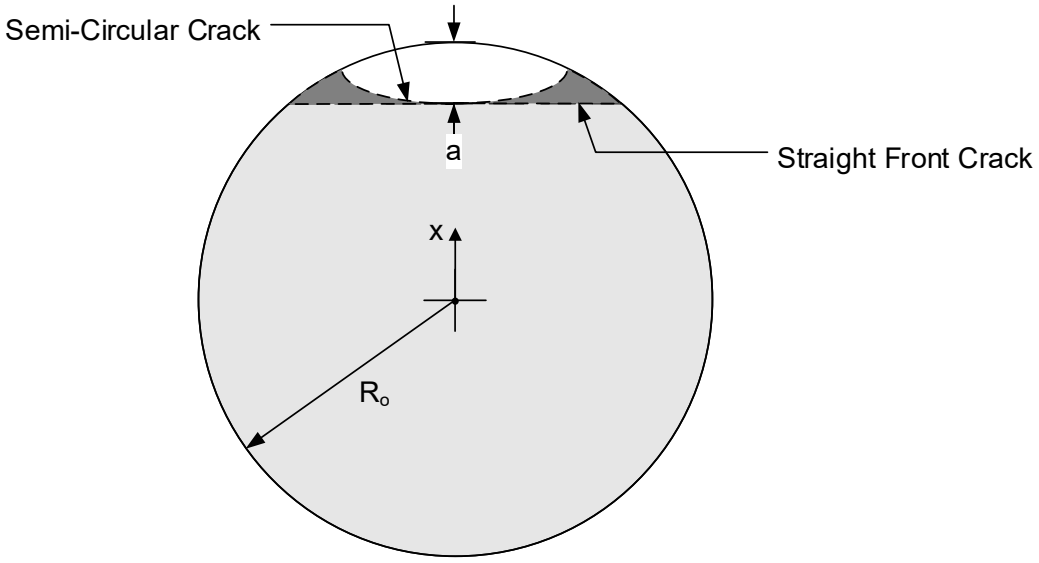

Figure 9B.32 – Bolt – Surface Crack

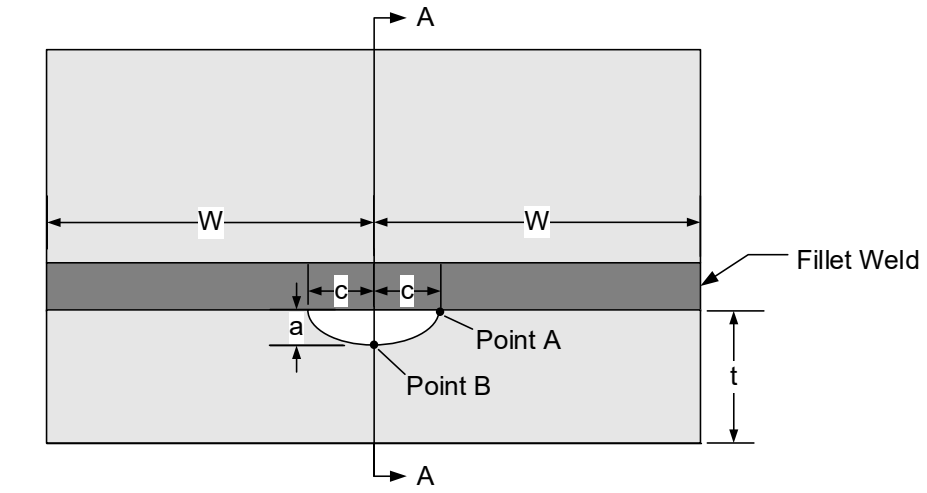

(a) Tee-Joint -- End View

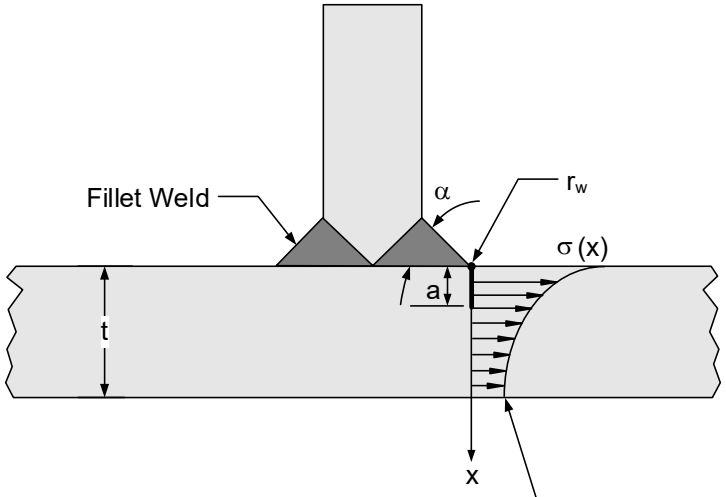

(b) Section A-A

Stress distribution at the location of the crack acting normal to the crack plane determine based on the structural configuration including the effects of the fillet weld geometry

Figure 9B.33 – Crack At Fillet Weld – Surface Crack, Semi-Elliptical Shape

ANNEX 9C – COMPENDIUM OF REFERENCE STRESS SOLUTIONS FOR CRACK-LIKE FLAWS

(NORMATIVE)

CONTENTS

ANNEX 9C – COMPENDIUM OF REFERENCE STRESS SOLUTIONS FOR CRACK-LIKE FLAWS 9C-1
9C.1 General 9C-1
9C.2 Stress Analysis 9C-2
9C.3 Reference Stress Solutions for Plates 9C-9
9C.4 Reference Stress Solutions for Plates with Holes 9C-12
9C.5 Reference Stress Solutions for Cylinders 9C-13
9C.6 Reference Stress Solutions for Spheres 9C-22
9C.7 Reference Stress Solutions for Elbows and Pipe Bends 9C-23
9C.8 Reference Stress Solutions for Nozzles and Piping Tees 9C-24
9C.9 Reference Stress Solutions for Ring-Stiffened Cylinders 9C-25
9C.10 Reference Stress Solutions for Sleeve Reinforced Cylinders 9C-25
9C.11 Reference Stress Solutions for Round Bars and Bolts 9C-25
9C.12 Reference Stress Solutions for Cracks at Fillet Welds 9C-27
9C.13 Reference Stress Solutions for Cracks in Clad Plates and Shells 9C-27
9C.14 Reference Stress Solutions for Cracks in Heavy Wall Cylinders $1 \leq t/Ri \leq 3$ 9C-27
9C.15 Nomenclature 9C-28
9C.16 References 9C-31
9C.17 Tables 9C-33
9C.18 Figures 9C-45

9C.1 General

9C.1.1 Overview

This Annex contains reference stress solutions for many crack geometries that are likely to occur in pressurized components. Reference stress solutions are used in the assessment of crack-like flaws (see Part 9).

9C.1.2 ASME B&PV Code, Section VIII, Division 2 (VIII-2)

Some of stress analysis concepts and methods in this Annex are based on ASME B&PV Code, Section VIII, Division 2 (VIII-2), Part 5, and reference to VIII-2 is made directly.

9C.1.3 Reference Stress Solutions

A summary of the reference stress solutions in this Annex is contained in Annex 9B, Table 9B.1. These reference stress solutions are recommended for most applications based on consideration of accuracy, range of applicability, and convenience.

9C.1.4 Reference Stress Solutions – Approximations for Shells

The reference stress solutions for plates can be used to approximate the solutions for cylinders and spheres by introducing a surface correction (Folias or bulging) factor. This is an approximation that is supported by experimental results.

9C.1.5 Reference Stress Solutions Identifier

An identifier has been assigned to each reference stress solution in this Annex (see Annex 9B, Table 9B.1). This identifier consists of a series of alpha-numeric characters that uniquely identifies the component geometry, crack geometry, and loading condition. The identifier is used to determine the associated stress intensity factor solution to be used in an assessment of crack-like flaws (see Part 9). For example, if a flat plate with a through-wall crack subject to a membrane stress and/or bending stress is being evaluated, the reference stress solution is RPTC and the associated stress intensity factor solution is KPTC.

9C.1.6 Reference Stress Solutions Not Included in the Compendium

Reference stress solutions not included in this Annex may be obtained from publications (for example see references [1] and [2]) if the tabulated solutions correspond to the component and crack geometry, and the loading condition. Another source of reference stress solutions is provided in references [19], [20], [21], [22], [23], [24], and [25]. Otherwise, the reference stress should be computed using a numerical approach such as the finite element method.

9C.2 Stress Analysis

9C.2.1 Overview

9C.2.1.1 A stress analysis using handbook or numerical techniques is required to compute the state of stress at the location of a crack. The stress distribution to be utilized in determining the stress intensity factor is based on the component of stress normal to the crack face. The distribution may be linear (made up of membrane and/or bending distributions) or highly non-linear depending on the component geometry and loading conditions.

9C.2.1.2 The stress distribution normal to the crack face resulting from primary loads should be determined based on service loading conditions and the uncracked component geometry. If the component is subject to different operating conditions, the stress distribution should be evaluated, and a separate Fitness-For-Service assessment should be performed for each condition.

9C.2.1.3 In this Annex, the variable P is used in place of σ to signify that the stress distributions used to determine the reference stress and the L_r ratio for the assessment of a crack-like flaw using the FAD (see Part 9) are categorized as primary stress (see VIII-2, Part 5).

9C.2.2 Stress Distributions

9C.2.2.1 Overview

The reference stress solutions in this Annex are formulated in terms of the coefficients of a linear stress distribution (membrane and bending stress). Therefore, it is necessary to derive these coefficients from the results obtained from a stress analysis.

9C.2.2.2 General Stress Distribution

A stress distribution through the wall thickness at the location of a crack-like flaw can be determined using a handbook solution or a numerical analysis technique such as the finite element method. In some cases, the stress distribution normal to the crack face may be highly non-linear. Statically equivalent membrane and bending stress components can be determined from the general stress distribution using the following equations: the integration is performed along a line assuming a unit width (see VIII-2, Part 5).

$$P_{ij,m} = \frac{1}{t}\int_0^t P_{ij}\,dx \tag{9C.1}$$

$$P_{ij,b} = \frac{6}{t^2}\int_0^t P_{ij}\left(\frac{t}{2} - x\right)dx \tag{9C.2}$$

9C.2.2.3 Fourth Order Polynomial Stress Distribution

The fourth order polynomial stress distribution can be obtained by curve-fitting a general stress distribution to obtain the coefficients of the best-fit fourth order polynomial. The equivalent membrane and bending stress distributions for use in the reference stress solutions in this Annex, can be obtained directly from the coefficients of this polynomial.

a) The general form of the fourth order polynomial stress distribution is as follows:

$$P(x) = P_0 + P_1\left(\frac{x}{t}\right) + P_2\left(\frac{x}{t}\right)^2 + P_3\left(\frac{x}{t}\right)^3 + P_4\left(\frac{x}{t}\right)^4 \tag{9C.3}$$

b) The equivalent membrane and bending stress distributions for the fourth order polynomial stress distribution are:

$$P_m = P_0 + \frac{P_1}{2} + \frac{P_2}{3} + \frac{P_3}{4} + \frac{P_4}{5} \tag{9C.4}$$

$$P_b = -\frac{P_1}{2} - \frac{P_2}{2} - \frac{9P_3}{20} - \frac{6P_4}{15} \tag{9C.5}$$

9C.2.2.4 Fourth Order Polynomial Stress Distribution with Net Section Bending Stress

This distribution is used to represent a through-wall fourth order polynomial stress and a net section or global bending stress applied to a circumferential crack in a cylindrical shell.

$$P(x, x_g, y_g) = P_0 + P_1\left(\frac{x}{t}\right) + P_2\left(\frac{x}{t}\right)^2 + P_3\left(\frac{x}{t}\right)^3 + P_4\left(\frac{x}{t}\right)^4 + P_5\left(\frac{x_g}{R_i + t}\right) + P_6\left(\frac{y_g}{R_i + t}\right) \tag{9C.6}$$

9C.2.2.5 Membrane and Through-Wall Bending Stress Distribution

The membrane and bending stress distribution are linear through the wall thickness and represents a common subset of the general stress distribution (see paragraph 9C.2.2.2). Attributes of this stress distribution are discussed in Annex 9B, paragraph 9B.2.2.5. The components of this stress distribution can be used directly in the reference stress solutions in this Annex.

9C.2.3 Surface Correction Factor for Shells

9C.2.3.1 Overview

A surface correction (also referred to as the Folias or bulging factor) is used to quantify the local increase in the state of stress at the location of a crack in a shell type structure that occurs because of local bulging. The magnified state of stress is then used together with a reference stress solution for a plate with similar crack geometry to determine the reference stress for the shell. Surface correction factors are typically only applied to the membrane part of the reference stress because this represents the dominant part of the solution.

9C.2.3.2 Surface Correction Factors for Through-wall Cracks

The surface correction factors for through-wall cracks in cylindrical and spherical shells subject to membrane stress loading are shown below. The surface correction factors are normally defined in terms of a single shell parameter, λ, given by the following Equation (9C.7). However, recent work indicates that the surface correction factors for cylindrical shells are also a function of the shell radius-to-thickness ratio, (see reference [9]).

$$\lambda = \frac{1.818c}{\sqrt{R_i t}} \tag{9C.7}$$

a) Cylindrical shell – Longitudinal through-wall crack

1) Data fit from references [10] and [11] (recommended for use in all assessments):

$$M_t = \left(\frac{1.02 + 0.4411\lambda^2 + 0.006124\lambda^4}{1.0 + 0.02642\lambda^2 + 1.533(10^{-6})\lambda^4} \right)^{0.5} \tag{9C.8}$$

2) Approximate expression from references [12] and [13]:

$$M_t = \left(1 + 0.3797\lambda^2 - 0.001236\lambda^4\right)^{0.5} \qquad for \;\; \lambda \le 9.1 \tag{9C.9}$$

$$M_t = 0.01936\lambda^2 + 3.3 \qquad for \;\; \lambda > 9.1 \tag{9C.10}$$

3) Upper bound expression from reference [14]:

$$M_t = \left(1 + 0.4845\lambda^2\right)^{0.5} \tag{9C.11}$$

4) A general expression for membrane stress and pressure loading is given by Equations (9C.12) and (9C.13), respectively, where the coefficients G_0 and G_p are calculated using the equations in Annex 9B, paragraph 9B.5.1. These equations include an R_i/t ratio dependency that may be significant.

$$M_t = G_0 \qquad membrane\ stress \tag{9C.12}$$

$$M_t = G_p \qquad pressure\ loading \tag{9C.13}$$

b) Cylindrical shell – Circumferential through-wall crack

1) Data fit from reference [15] (recommended for use in all assessments):

$$M_t = \left(\frac{1.0078 + 0.10368\lambda^2 + 3.7894(10^{-4})\lambda^4}{1.0 + 0.021979\lambda^2 + 1.5742(10^{-6})\lambda^4} \right)^{0.5} \tag{9C.14}$$

2) The general expression for membrane stress and pressure loading is given by Equations (9C.12) and (9C.13) where the coefficients G_0 and G_p are calculated using the equations in Annex 9B, paragraph 9B.5.2.

c) Spheres – Circumferential through-wall crack

1) Data fit from references [10] and [11] (recommended for use in all assessments):

$$M_t = \frac{1.0005 + 0.49001\lambda + 0.32409\lambda^2}{1.0 + 0.50144\lambda - 0.011067\lambda^2} \tag{9C.15}$$

2) Approximate expression (see reference [16]):

$$M_t = \left(1 + 0.427\lambda^2 + 0.00666\lambda^3\right)^{0.5} \tag{9C.16}$$

3) A general expression for membrane stress and pressure loading is given by Equations (9C.12) and (9C.13), respectively, where the coefficients G_0 and G_p are calculated using the equations in Annex 9B, paragraph 9B.6.1.

9C.2.3.3 Surface Correction Factors for Surface Cracks

The surface correction factors for surface cracks can be approximated using the results obtained for a through-wall crack by using one of the following methods. In all these methods, the equations for M_t are provided in paragraph 9C.2.3.2.

a) Cylindrical or Spherical Shell – The following is an empirical equation which does not produce consistent results when the crack approaches a through-wall configuration (see reference [14]). The factor C in the equation is used to define a model for the cross sectional area of the surface crack to be included in the analysis. A value of $C = 1.0$ corresponds to a rectangular model and a value of $C = 0.67$ is used to model a parabolic shape. Experimental results indicate that a value of $C = 0.85$ provides an optimum fit to the data (see references [7] and [8]). The results from this equation are usually associated with a local limit load solution; the superscript L in the following equation designates a local limit load solution.

$$M_s^L = \frac{1 - C\left(\frac{a}{t}\right)\left(\frac{1}{M_t}\right)}{1 - C\left(\frac{a}{t}\right)} \tag{9C.17}$$

b) Cylindrical or Spherical Shell – Equation (9C.18) is based on a lower bound limit load solution and produces a consistent result as the crack approaches a through-wall configuration (see reference [17]).

1) In the following equation, the term $M_t(\lambda_a)$ signifies that M_t is evaluated using the equations cited for a through-wall crack with the λ_a shell parameter as opposed to the λ shell parameter (compare Equation (9C.7) with Equation (9C.19)). The results from this equation are usually associated with a net section limit load solution; the superscript NS in the following equation designates a net section limit load solution.

$$M_s^{NS} = \frac{1}{1 - \frac{a}{t} + \frac{a}{t}\left(\frac{1}{M_t(\lambda_a)}\right)} \tag{9C.18}$$

where,

$$\lambda_a = \frac{1.818c}{\sqrt{R_t a}} \tag{9C.19}$$

2) In reference [17], the crack area is idealized as an equivalent rectangle with an area equal to the elliptical crack area. In this paragraph, this approximation is not used, and the area chosen to evaluate M_t is a rectangular area based on the crack depth and the full length of the crack. If desired, the equivalent elliptical area approximation can be introduced into the assessment by multiplying the a/t term in Equation (9C.18) by $\pi/4$, or:

$$M_s^{NS} = \frac{1}{1 - \frac{a}{t}\left(\frac{\pi}{4}\right) + \frac{a}{t}\left(\frac{\pi}{4}\right)\left(\frac{1}{M_t(\lambda_a)}\right)} \tag{9C.20}$$

3) Equation (9C.18) is written in terms of the component thickness and maximum depth of the flaw. If the flaw shape is characterized by a nonuniform thickness profile, Equation (9C.18) can be written in terms of areas as follows:

$$M_s^{NS} = \frac{1}{1 - \frac{A}{A_o} + \frac{A}{A_o}\left(\frac{1}{M_t(\lambda_a)}\right)} \tag{9C.21}$$

c) The results from Equations (9C.17) and (9C.18) are approximately the same for flaws up to $a/t \leq 0.5$. Above this value, the use of Equation (9C.17) to compute M_s will produce values that significantly exceed those obtained using Equation (9C.18). This will result in conservatism in the computation of the stress intensity ratio, K_r, if the stress intensity factor is a function of M_s, and the load ratio, L_r, in the FAD assessment for a given material toughness and yield stress. Experimental results indicate that Equation (9C.18) produces consistent results for $a/t > 0.5$. Therefore, Equation (9C.18) is recommended for use to compute the stress intensity factor (numerator in K_r) and reference stress (numerator in L_r) unless additional conservatism is desired in the assessment. In summary, the following values can be used to compute the surface correction factor:

$$M_s = M_s^L \qquad \textit{assessment based on local ligament criteria} \tag{9C.22}$$

$$M_s = M_s^{NS} \qquad \textit{assessment based on net section collapse (recommended)} \tag{9C.23}$$

9C.2.4 Load Ratio and Reference Stress

9C.2.4.1 Load Ratio

The load ratio is the horizontal coordinate on the failure assessment diagram (see Part 9), and is defined as:

$$L_r = \frac{P_l}{P_{ly}} \tag{9C.24}$$

alternatively, the load ratio can be written in terms of a reference stress:

$$L_r = \frac{\sigma_{ref}}{\sigma_{ys}} \tag{9C.25}$$

with,

$$\sigma_{ref} = \left(\frac{P_l}{P_{ly}} \right) \sigma_{ys} \tag{9C.26}$$

9C.2.4.2 Reference Stress Solutions

This Annex contains reference stress solutions for selected crack-like flaw geometries. The reference stress solution in paragraph 9C.2.4.1 can be converted into a yield load solution by rearranging Equation (9C.26). The limit load can be inferred by replacing the yield strength with an appropriate flow stress (see Annex 2E).

9C.2.5 Plastic Collapse in the Assessment of Crack-Like Flaws

9C.2.5.1 The position of an assessment point (K_r, L_r) on the FAD represents a particular combination of flaw size, stresses, and material properties. This point can be used to demonstrate whether the flaw is acceptable, and an associated in-service margin can be computed based on the location of this point. If the flaw is unacceptable, the location of the assessment point on the FAD can indicate the type of failure that would be expected.

a) The failure assessment diagram can be divided into three zones as illustrated in Figure 9C.1. If the assessment point lies in Zone 1, the predicted failure mode is predominantly fracture controlled and could be associated with brittle fracture. If the assessment point lies in Zone 3, the predicted failure mode is collapse controlled with extensive yielding resulting in large deformations in the component. If the assessment point lies in a Zone 2 the predicted failure mode is elastic-plastic fracture.

b) The significance of the L_r parameter in a FAD assessment can be described in terms of crack-tip plasticity. If fracture occurs under elastic plastic conditions, the K_r value defined by the failure assessment line at the corresponding L_r value represents the elastic component of the crack driving force. The limiting value of K_r reduces from unity as L_r increases. Thus $(1 - K_r)$ represents the enhancement of the crack driving force due to plasticity. Therefore, the value of the L_r parameter represents a measure of the crack tip plasticity if the L_r parameter is less than the maximum permitted or cut-of value (see paragraph 9C.2.5.2(b)).

9C.2.5.2 The value of L_r depends on the type of plastic collapse load solution utilized in the assessment.

a) Plastic collapse solutions can be defined in three ways:

1) *Local Collapse* – Plastic collapse of the remaining ligament adjacent to the flaw being assessed. The reference stress solutions shown for plates in paragraphs 9C.3 and 9C.4 are based on a local collapse solution. The reference stress solutions shown for cylinders and spheres that utilize the plate ligament equations (see paragraph 9C.3) with a surface correction factor, M_s, based on a local limit load (see paragraph 9C.2.3.3, and Annex 9B paragraph 9B.2.3.2) are also considered to be local collapse solutions.

2) *Net Section Collapse* – Plastic collapse of the structural section containing the flaw. The reference stress solutions shown for cylinders and spheres that do not utilize the plate ligament formulas of paragraph 9C.3 are net section collapse solutions. In addition, the reference stress solutions shown for

cylinders and spheres which utilize the plate ligament equations (see paragraph 9C.3) with a surface correction factor, M_s, based on a global limit load (see paragraph 9C.2.3.3) are also considered to be net section collapse solutions. The reference stress solutions for bars and bolts in paragraph 9C.11 are net section collapse solutions.

3) *Gross Collapse* – Plastic collapse of the structure by unconstrained or gross straining throughout the structure. This occurs when a plastic collapse mechanism is formed in the structure and may be unaffected by the presence of the crack.

b) It is acceptable to use the local plastic collapse solution to determine the reference stress when computing the value of L_r. However, this may be excessively conservative for redundant structures. If the structure or component has degrees of redundancy, plasticity at the cracked ligament may be contained by the surrounding structure until conditions for gross collapse are reached. In such cases, it may be possible to use more appropriate estimates of L_r based on modified lower bound collapse solutions that are based on the response of the entire structure. For this approach to be adopted, it is essential to confirm by analysis that the plasticity at the cracked section is contained sufficiently by the remaining structure, so that the use of the standard assessment diagram gives conservative results. In ferritic steels, care must also be exercised to ensure that local constraint conditions are not sufficient to induce brittle fracture by a cleavage mechanism. Where global collapse can be shown to occur after the attainment of $L_{r(\max)}$, the $L_{r(cut-off)}$ can be extended to the value relating to global collapse as described.

c) If the assessment point falls outside the acceptable region, then recategorization of the flaw being evaluated can be undertaken and a reassessment made (see Part 9). In general, the recategorization procedures described in Part 9 will only be effective if the assessment point falls within the elastic plastic fracture controlled zone or beyond $L_{r(\max)}$ (in the collapse controlled zone).

9C.2.5.3 The reference stress solutions in this Annex are based on the assessment of a single flaw. Multiple flaws which interact should be recategorized according to Part 9. However, multiple flaws that do not interact according to Part 9 may still affect the plastic collapse conditions, and allowances should be made to the collapse solutions to accommodate these effects.

9C.2.5.4 It is recommended that a gross collapse assessment be performed to ensure that the applied stresses derived for local conditions do not cause failure of the structure in other regions.

a) In many cases a simple calculation can be performed to identify the highest applied stress condition that will result in the attainment of the flow strength on a significant cross section. In certain structures, gross collapse may occur in regions away from the flaw being assessed because of thinned areas, or where design conditions result in yielding of the general structure prior to collapse of the local regions.

b) To facilitate understanding of the relative importance of local, net section and gross collapse loads, it is useful to calculate the minimum collapse load for regions away from the cracked section, as well as that involving the cracked section and determining the parameter for both conditions. The minimum ratio of the gross collapse load for regions away from the cracked section to the local or net section collapse load at the cracked section represents a maximum value or cut-off on the $L_r - axis$. The cut-off limit may be less than one and in such cases the assessment diagram is effectively restricted by this cut-off. The failure assessment diagram is generally limited at higher values of L_r to a cut-off at $L_{r(\max)}$ that is based on material properties rather than structural behavior. In displacement controlled applications, the assessment diagram may be extended beyond the $L_{r(\max)}$ limit to the structural cut-off limit.

9C.3 Reference Stress Solutions for Plates

9C.3.1 Plate – Through-Wall Crack, Through-Wall Membrane and Bending Stress (RPTC)

9C.3.1.1 The Reference Stress is (Reference [3]):

$$\sigma_{ref} = \frac{P_b + \left(P_b^2 + 9P_m^2\right)^{0.5}}{3\left(1-\alpha\right)} \tag{9C.27}$$

where,

$$\alpha = \frac{c}{W} \tag{9C.28}$$

9C.3.1.2 Notes:

a) See Annex 9B, Figure 9B.1 for the component and crack geometry.

b) See paragraph 9C.2.2.3 for determination of P_m and P_b.

9C.3.2 Plate – Surface Crack, Infinite Length, Through-Wall Fourth Order Polynomial Stress Distribution (RPSCL1)

9C.3.2.1 The Reference Stress is given by Equation (9C.31) with the following definition of α:

$$\alpha = \frac{a}{t} \tag{9C.29}$$

9C.3.2.2 Notes:

a) See Annex 9B, Figure 9B.2(b) for the component and crack geometry.

b) See paragraph 9C.2.3.3 for determination of P_m and P_b.

9C.3.3 Plate – Surface Crack, Infinite Length, Through-wall Arbitrary Stress Distribution (RPSCL2)

9C.3.3.1 Reference Stress in paragraph 9C.3.2 can be used.

9C.3.3.2 Notes: see paragraph 9C.3.2.2.

9C.3.4 Plate – Surface Crack, Semi-Elliptical Shape, Through-wall Membrane and Bending Stress (RPSCE1)

9C.3.4.1 The Reference Stress is (References [3] and [18]):

a) With bending restraint:

$$\sigma_{ref} = \frac{gP_b + \left[\left(gP_b\right)^2 + 9P_m^2\left(1-\alpha\right)^2\right]^{0.5}}{3\left(1-\alpha\right)^2} \tag{9C.30}$$

b) With negligible bending restraint (e.g., pin-jointed):

$$\sigma_{ref} = \frac{P_b + 3P_m\alpha + \left[\left(P_b + 3P_m\alpha\right)^2 + 9P_m^2\left(1-\alpha\right)^2\right]^{0.5}}{3\left(1-\alpha\right)^2} \tag{9C.31}$$

where,

$$g = 1 - 20\left(\frac{a}{2c}\right)^{0.75}\alpha^3 \tag{9C.32}$$

$$\alpha = \frac{\frac{a}{t}}{1+\frac{t}{c}} \qquad for \quad W \geq (c+t) \tag{9C.33}$$

$$\alpha = \left(\frac{a}{t}\right)\left(\frac{c}{W}\right) \qquad for \quad W < (c+t) \tag{9C.34}$$

9C.3.4.2 Notes:

a) See Annex 9B, Figure 9B.2(a) for the component and crack geometry.

b) See paragraph 9C.2.2.3 for determination of P_m and P_b.

c) The normal bending restraint solution can be obtained by setting $g = 1.0$, (see reference [18]).

d) If $a > c$, compute g based on $a/2c = 0.5$.

e) In Equation (9C.31) (i.e., pin-jointed or bending restraint is not considered) the assumption is that P_m contributes to the bending moment due to the movement of the neutral axis away from the mid-thickness because of the presence of the flaw. In Equation (9C.30) (i.e., bending restraint is considered) the assumption is that this additional bending moment is carried externally. The bending restraint solution may be used without further justification if the surface of the crack is small compared to the uncracked surface and the crack depth is less than the half thickness. The pin-joint solution, which is more conservative than the bending restraint solution, should be selected if there is uncertainty in the restraint condition (see reference [3]).

9C.3.5 Plate – Surface Cracks, Semi-Elliptical Shape, Through-Wall Fourth Order Polynomial Stress Distribution (RPSCE2)

9C.3.5.1 The Reference Stress in paragraph 9C.3.4 can be used.

9C.3.5.2 Notes: see paragraph 9C.3.4.2.

9C.3.6 Plate – Surface Crack, Semi-Elliptical Shape, Through-wall Arbitrary Stress Distribution (RPSCE3)

9C.3.6.1 The Reference Stress in paragraph 9C.3.4 can be used.

9C.3.6.2 Notes: see paragraph 9C.3.4.2.

9C.3.7 Plate – Embedded Crack, Infinite Length, Through-Wall Fourth Order Polynomial Stress Distribution (RPECL)

9C.3.7.1 The Reference Stress is (Reference [3]):

$$\sigma_{ref} = \frac{P_b + 3P_m\alpha + \left[\left(P_b + 3P_m\alpha\right)^2 + 9P_m^2\left(\left(1-\alpha\right)^2 + \frac{4d\alpha}{t}\right)\right]^{0.5}}{3\left[\left(1-\alpha\right)^2 + \frac{4d\alpha}{t}\right]} \tag{9C.35}$$

where,

$$d = d_1 - a \tag{9C.36}$$

$$\alpha = \frac{2a}{t} \tag{9C.37}$$

9C.3.7.2 Notes:

a) See Annex 9B, Figure 9B.3(b) for the component and crack geometry.

b) See paragraph 9C.2.2.3 for determination of P_m and P_b.

9C.3.8 Plate – Embedded Crack, Elliptical Shape, Through-Wall Membrane and Bending Stress (RPECE1)

9C.3.8.1 The Reference Stress is given by Equation (9C.35) with following definitions of d and α:

$$d = d_1 - a \tag{9C.38}$$

$$\alpha = \frac{\frac{2a}{t}}{1+\frac{t}{c}} \qquad for \quad W \geq \left(c+t\right) \tag{9C.39}$$

$$\alpha = \left(\frac{2a}{t}\right)\left(\frac{c}{W}\right) \qquad for \quad W < \left(c+t\right) \tag{9C.40}$$

9C.3.8.2 Notes:

a) See Annex 9B, Figure 9B.3(a) for the component and crack geometry.

b) See paragraph 9C.2.2.3 for determination of P_m and P_b.

9C.3.9 Plate – Embedded Crack, Elliptical Shape, Through-Wall Fourth-Order Polynomial Stress Distribution (RPECE2)

9C.3.9.1 The Reference Stress in paragraph 9C.3.8.1 can be used.

9C.3.9.2 Notes:

a) See Annex 9B, Figure 9B.3(a) for the component and crack geometry.

b) See paragraph 9C.2.2.3 for determination of P_m and P_b.

9C.4 Reference Stress Solutions for Plates with Holes

9C.4.1 Plate with Hole – Through-Wall Single Edge Crack, Through-Wall Membrane and Bending Stress (RPHTC1)

9C.4.1.1 The Reference Stress is given by Equation (9C.27) with the following definition of α:

$$\alpha = \frac{ct}{t\left(c+t\right)} \tag{9C.41}$$

9C.4.1.2 Notes:

a) See Annex 9B, Figure 9B.7(a) for the component and crack geometry.

b) See paragraph 9C.2.2.3 for determination of P_m and P_b.

9C.4.2 Plate with Hole – Through-Wall Double Edge Crack, Through-Wall Membrane and Bending Stress (RPHTC2)

9C.4.2.1 The Reference Stress is given by Equation (9C.27) with the following definition of α:

$$\alpha = \frac{2ct}{t\left(2c+t\right)} \tag{9C.42}$$

9C.4.2.2 Notes:

a) See Annex 9B, Figure 9B.8(a) for the component and crack geometry.

b) See paragraph 9C.2.2.3 for determination of P_m and P_b.

9C.4.3 Plate with Hole – Surface Crack, Semi-Elliptical Shape, Through-Wall Membrane Stress (RPHSC1)

9C.4.3.1 The Reference Stress is:

$$\sigma_{ref} = \frac{3P_m\alpha + \left[\left(3P_m\alpha\right)^2 + 9P_m^2\left(\left(1-\alpha\right)^2 + \frac{4d\alpha}{t}\right)\right]^{0.5}}{3\left[\left(1-\alpha\right)^2 + \frac{4d\alpha}{t}\right]} \tag{9C.43}$$

where,

$$d = t - c \tag{9C.44}$$

$$\alpha = \frac{\frac{2c}{t}}{1+\frac{t}{a}} \tag{9C.45}$$

9C.4.3.2 Notes:

a) See Annex 9B, Figure 9B.9 for the component and crack geometry.

b) See paragraph 9C.2.2.3 for determination of P_m.

9C.4.4 Plate with Hole, Corner Crack, Semi-Elliptical Shape, Through-Wall Membrane and Bending Stress (RPHSC2)

9C.4.4.1 The Reference Stress is given by Equation (9C.27) with the following definition of α:

$$\alpha = \frac{2ac}{t\left(2a+t\right)} \tag{9C.46}$$

9C.4.4.2 Notes:

a) See Annex 9B, Figure 9B.10 for the component and crack geometry.

b) See paragraph 9C.2.2.3 for determination of P_m and P_b.

9C.5 Reference Stress Solutions for Cylinders

9C.5.1 Cylinder – Through-Wall Crack, Longitudinal Direction, Through-Wall Membrane and Bending Stress (RCTCL)

9C.5.1.1 The Reference Stress is (References [1] and [3])

$$\sigma_{ref} = \frac{P_b + \left(P_b^2 + 9\left(M_t \cdot P_m\right)^2\right)^{0.5}}{3} \tag{9C.47}$$

9C.5.1.2 Notes:

a) See Annex 9B, Figure 9B.11 for the component and crack geometry.

b) See paragraph 9C.2.2.3 for determination of P_m and P_b. For internal pressure loading:

$$P_m = \frac{pR_i}{t} \tag{9C.48}$$

$$P_b = \frac{p}{2} \qquad \textit{for an internal crack} \tag{9C.49}$$

$$P_b = \frac{-p}{2} \qquad \textit{for an external crack} \tag{9C.50}$$

c) See paragraph 9C.2.3 to determine M_t for a through-wall crack in a cylinder.

9C.5.2 Cylinder – Through-Wall Crack, Circumferential Direction, Through-Wall Membrane and Bending Stress (RCTCC1)

9C.5.2.1 The Reference Stress is (Reference [2]):

$$\sigma_{ref} = \frac{P_b + \left[P_b^2 + 9\left(Z \cdot P_m \cdot \left(1-\alpha\right)^2\right)^2\right]^{0.5}}{3\left(1-\alpha\right)^2} \tag{9C.51}$$

where,

$$Z = \frac{\pi\left(R_o^2 - R_i^2\right)}{\left(2-\tau\right)R_o t\left(2\psi - \theta\right)} \tag{9C.52}$$

$$\tau = \frac{t}{R_o} \tag{9C.53}$$

$$\psi = \arccos\left[\frac{\sin\left[\theta\right]}{2}\right] \tag{9C.54}$$

$$\theta = \frac{c}{R_m} \tag{9C.55}$$

$$\alpha = \frac{c}{\pi R_m} \tag{9C.56}$$

9C.5.2.2 Notes:

a) See Annex 9B, Figure 9B.12 for the component and crack geometry.

b) See paragraph 9C.2.2.3 for determination of P_m and P_b.

c) For an internal pressure with a net section axial force, P_m shall be replaced by $U \cdot P_{m,eq}$ where $P_{m,eq}$ is shown below and U is defined in paragraph 9C.5.13.1.

$$\sigma_{ml} = \frac{pR_i^2}{R_o^2 - R_i^2} + \frac{F}{\pi\left(R_o^2 - R_i^2\right)} \tag{9C.57}$$

$$\sigma_{mc} = \frac{pR_i}{t} \tag{9C.58}$$

$$P_{m,eq} = \sqrt{\frac{\left(\sigma_{mc} - \sigma_{ml}\right)^2 + \sigma_{mc}^2 + \sigma_{ml}^2}{2}} \tag{9C.59}$$

$$P_b = 0.0 \tag{9C.60}$$

9C.5.3 Cylinder – Through-Wall Crack, Circumferential Direction, Pressure with a Net Section Axial Force and Bending Moment (RCTCC2)

9C.5.3.1 The Reference Stress is (Reference [4]):

$$\sigma_{ref} = \left[\frac{M}{2\sigma_{ys}R_m^2 t\left(2\cos\left[\beta\right] - \sin\left[\theta\right]\right) - 2pR_m^3\cos\left[\beta\right]}\right]\sigma_{ys} + \sigma_{ref}^{9C.5.2} \tag{9C.61}$$

where, $\sigma_{ref}^{9C.5.2}$ is the reference stress from paragraph 9C.5.2, and

$$\beta = \frac{\sigma_{ys} R_m t\theta + \frac{F}{2}}{2\sigma_{ys} R_m t - pR_m^2} \tag{9C.62}$$

$$\theta = \frac{c}{R_m} \tag{9C.63}$$

9C.5.3.2 Notes:

a) See Annex 9B, Figure 9B.12 for the component and crack geometry.

b) If the net-section bending moment is zero, the solution in paragraph 9C.5.2 shall be used.

9C.5.4 Cylinder – Surface Crack, Longitudinal Direction – Infinite Length, Internal Pressure (RCSCLL1)

9C.5.4.1 The Reference Stress (References [1] and [3]):

$$\sigma_{ref} = \frac{P_b + \left[P_b^2 + 9\left(M_s \cdot P_m \cdot (1-\alpha)^2 \right)^2 \right]^{0.5}}{3(1-\alpha)^2} \tag{9C.64}$$

where,

$$M_s = \frac{1.0}{1.0-\alpha} \tag{9C.65}$$

$$\alpha = \frac{a}{t} \tag{9C.66}$$

9C.5.4.2 Notes:

a) See Annex 9B, Figure 9B.13 for the component and crack geometry.

b) See paragraph 9C.5.1.2(b) for determination of P_m and P_b.

c) See paragraph 9C.14 for heavy wall cylinder reference stress solutions.

9C.5.5 Cylinder – Surface Crack, Longitudinal Direction – Infinite Length, Through-Wall Fourth Order Polynomial Stress Distribution (RCSCLL2)

9C.5.5.1 The Reference Stress in paragraph 9C.5.4 can be used.

9C.5.5.2 Notes: see paragraph 9C.5.4.2.

9C.5.6 Cylinder – Surface Crack, Longitudinal Direction – Infinite Length, Through-wall Arbitrary Stress Distribution (RCSCLL3)

9C.5.6.1 The Reference Stress in paragraph 9C.5.4 can be used.

9C.5.6.2 Notes: see paragraph 9C.5.4.2.

9C.5.7 Cylinder – Surface Crack, Circumferential Direction – 360 Degrees, Pressure with a Net Section Axial Force and Bending Moment (RCSCCL1)

9C.5.7.1 The Reference Stress is (Reference [5]):

$$\sigma_{ref} = \frac{M_r}{2} + \left(N_r^2 + \frac{M_r^2}{4} \right)^{0.5} \tag{9C.67}$$

where,

$$N_r = U \cdot \sqrt{\frac{\left(\sigma_{mc} - \Sigma_{ml}\right)^2 + \sigma_{mc}^2 + \Sigma_{ml}^2}{2}} \tag{9C.68}$$

$$U = 1.3807 - 0.2978\left(\frac{a}{t}\right) + \left\{0.003\left(\frac{a}{t}\right) - 0.0154\right\}\left(\frac{R_i}{t}\right) \qquad for\ 2 \le R_i/t \le 20 \tag{9C.69}$$

When using Equations (9C.67) through (9C.69) note the following:

- For $R_i/t > 20$, use the value of U at $R_i/t = 20$.
- For $1 < R_i/t < 2$ and pressure loading only, interpolate between σ_{ref} obtained in paragraph 9C.14 and σ_{ref} at $R_i/t = 2$.

For an inside surface crack:

$$\Sigma_{ml} = \frac{\sigma_{ml}\left[R_o^2 - R_i^2\right]}{\left[R_o^2 - \left(R_i + a\right)^2\right]} \tag{9C.70}$$

$$M_r = P_{bg}\frac{3\pi}{16}\left[\frac{R_o^4 - R_i^4}{R_o^4 - R_i\left(R_i + a\right)^3}\right] \tag{9C.71}$$

For an outside surface crack:

$$\Sigma_{ml} = \frac{\sigma_{ml}\left[R_o^2 - R_i^2\right]}{\left[\left(R_o - a\right)^2 - R_i^2\right]} \tag{9C.72}$$

$$M_r = P_{bg}\frac{3\pi}{16}\left[\frac{R_o^4 - R_i^4}{R_o\left(R_o - a\right)^3 - R_i^4}\right] \tag{9C.73}$$

9C.5.7.2 Notes:

a) See Annex 9B, Figure 9B.14 for the component and crack geometry.

b) σ_{ml}, σ_{mc} and P_{bg} are determined using the following equations:

$$\sigma_{ml} = \frac{pR_i^2}{R_o^2 - R_i^2} + \frac{F}{\pi\left(R_o^2 - R_i^2\right)} \tag{9C.74}$$

$$\sigma_{mc} = \frac{pR_i}{t} \tag{9C.75}$$

$$P_{bg} = \frac{MR_o}{0.25\pi\left(R_o^4 - R_i^4\right)} \tag{9C.76}$$

c) See paragraph 9C.14 for heavy wall cylinder reference stress solutions.

9C.5.8 Cylinder – Surface Crack, Circumferential Direction – 360 Degrees, Through-Wall Fourth Order Polynomial Stress Distribution (RCSCCL2)

9C.5.8.1 The Reference Stress is (Reference [2]):

$$\sigma_{ref} = \frac{P_b + \left[P_b^2 + 9\left(U \cdot \Sigma_m \left(1-\alpha\right)^2\right)^2\right]^{0.5}}{3\left(1-\alpha\right)^2} \tag{9C.77}$$

where,

$$\Sigma_m = \sqrt{\frac{\left(\sigma_{mc} - Z \cdot P_m\right)^2 + \sigma_{mc}^2 + \left(Z \cdot P_m\right)^2}{2}} \tag{9C.78}$$

$$Z = \left[1 - \alpha\left(\frac{2 - 2\tau + \alpha\tau}{2 - \tau}\right)\right]^{-1} \tag{9C.79}$$

$$\tau = \frac{t}{R_o} \tag{9C.80}$$

$$\alpha = \frac{a}{t} \tag{9C.81}$$

$$\sigma_{mc} = \frac{pR_i}{t} \qquad \textit{with an internal pressure} \tag{9C.82}$$

$$\sigma_{mc} = 0 \qquad \textit{otherwise} \tag{9C.83}$$

$$U = 1.3807 - 0.2978\left(\frac{a}{t}\right) + \left\{0.003\left(\frac{a}{t}\right) - 0.0154\right\}\left(\frac{R_i}{t}\right) \qquad \text{For } 2 \le R_i / t \le 20 \tag{9C.84}$$

When using Equations (9C.77) through (9C.84) note the following:

- For $R_i/t > 20$, use the value of U at $R_i/t = 20$.
- For $R_i/t = 1$, σ_{ref} shall be calculated in accordance with paragraph 9C.5.13 with $2c = 2\pi R_i$ for internal crack, and $2c = 2\pi R_o$ for external crack.
- For $1 < R_i/t < 2$, interpolate between σ_{ref} at $R_i/t = 1$ and σ_{ref} at $R_i/t = 2$.

9C.5.8.2 Notes:

a) See Annex 9B, Figure 9B.14 for the component and crack geometry.

b) See paragraph 9C.2.2.3 for determination of P_m and P_b.

c) See paragraph 9C.14 for heavy wall cylinder reference stress solutions.

9C.5.9 Cylinder – Surface Crack, Circumferential Direction – 360 Degrees, Through-wall Arbitrary Stress Distribution (RCSCCL3)

9C.5.9.1 The Reference Stress in paragraph 9C.5.8 can be used.

9C.5.9.2 Notes: see paragraph 9C.5.8.2.

9C.5.10 Cylinder – Surface Crack, Longitudinal Direction – Semi-Elliptical Shape, Internal Pressure (RCSCLE1)

9C.5.10.1 The Reference Stress is (References [3] and [6]):

$$\sigma_{ref} = \frac{gP_b + \left[\left(gP_b \right)^2 + 9\left(M_s \cdot P_m \cdot \left(1-\alpha \right)^2 \right)^2 \right]^{0.5}}{3\left(1-\alpha \right)^2} \tag{9C.85}$$

where g is given by Equation (9C.32) with the following definition of α:

$$\alpha = \frac{\frac{a}{t}}{1+\frac{t}{c}} \tag{9C.86}$$

9C.5.10.2 Notes:

a) See Annex 9B, Figure 9B.15 for the component and crack geometry.

b) See paragraph 9C.5.1.2(b) for determination of P_m and P_b.

c) See paragraph 9C.2.3 to determine M_s for a surface crack in a cylinder.

9C.5.11 Cylinder – Surface Crack, Longitudinal Direction – Semi-Elliptical Shape, Through-Wall Fourth Order Polynomial Stress Distribution (RCSCLE2)

9C.5.11.1 The Reference Stress in paragraph 9C.5.10 can be used.

9C.5.11.2 Notes: see paragraph 9C.5.10.2.

9C.5.12 Cylinder – Surface Crack, Longitudinal Direction – Semi-Elliptical Shape, Through-wall Arbitrary Stress Distribution (RCSCLE3)

9C.5.12.1 The Reference Stress in paragraph 9C.5.10 can be used.

9C.5.12.2 Notes: see paragraph 9C.5.10.2.

9C.5.13 Cylinder – Surface Crack, Circumferential Direction – Semi-Elliptical Shape, Internal Pressure and Net-Section Axial Force (RCSCCE1)

9C.5.13.1 The Reference Stress is (Reference [2]):

$$\sigma_{ref} = \frac{P_b + \left[P_b^2 + 9\left(U \cdot Z \cdot P_{m,eq} \cdot \left(1-\alpha \right)^2 \right)^2 \right]^{0.5}}{3\left(1-\alpha \right)^2} \tag{9C.87}$$

where,

$$\sigma_{ml} = \frac{pR_i^2}{R_o^2 - R_i^2} + \frac{F}{\pi\left(R_o^2 - R_i^2\right)} + P_m \tag{9C.88}$$

$$\sigma_{mc} = \frac{pR_i}{t} \tag{9C.89}$$

$$P_{m,eq} = \sqrt{\frac{\left(\sigma_{mc} - \sigma_{ml}\right)^2 + \sigma_{mc}^2 + \sigma_{ml}^2}{2}} \tag{9C.90}$$

$$Z = \left[\frac{2\psi}{\pi} - \frac{x\theta}{\pi}\left(\frac{2 - 2\tau + x\tau}{2 - \tau}\right)\right]^{-1} \tag{9C.91}$$

$$\psi = \arccos\left[A\sin\left[\theta\right]\right] \tag{9C.92}$$

$$\alpha = \frac{\frac{a}{t}}{1 + \frac{t}{c}} \tag{9C.93}$$

$$A = x\left[\frac{(1-\tau)(2 - 2\tau + x\tau) + (1 - \tau + x\tau)^2}{2\left(1 + (2-\tau)(1-\tau)\right)}\right] \tag{9C.94}$$

$$\tau = \frac{t}{R_o} \tag{9C.95}$$

$$x = \frac{a}{t} \tag{9C.96}$$

$$\theta = \frac{\pi c}{4R_i} \qquad \textit{for an internal crack} \tag{9C.97}$$

$$\theta = \frac{\pi c}{4R_o} \qquad \textit{for an external crack} \tag{9C.98}$$

$$U = 1.3068 - 0.495\left(\frac{a}{t}\right) + \left\{0.055\left(\frac{a}{t}\right) - 0.026\right\}\left(\frac{R_i}{t}\right) \qquad \textit{for } 2 \le R_i / t \le 20 \tag{9C.99}$$

$$U = 1.601 - 0.550\left(\frac{a}{t}\right) \qquad \textit{for } R_i / t = 1 \tag{9C.100}$$

When using Equations (9C.87) through (9C.100) note the following:

- For $R_i/t > 20$, use the value of U at $R_i/t = 20$.
- For $1 < R_i/t < 2$, interpolate U between values at $R_i/t = 1$ and at $R_i/t = 2$.

9C.5.13.2 Notes:

a) See Annex 9B, Figure 9B.16 for the component and crack geometry.

b) The solution for an applied pressure and axial force is based on the equivalent membrane stress. This solution can be used for any other applied through-wall stress distribution if paragraph 9C.2.2.3 is used to determine of P_m and P_b.

c) See paragraph 9C.14 for heavy wall cylinder reference stress solutions.

9C.5.14 Cylinder – Surface Crack, Circumferential Direction – Semi-Elliptical Shape, Through-Wall Fourth Order Polynomial Stress Distribution with a Net Section Bending Stress (RCSCCE2)

9C.5.14.1 The Reference Stress is (Reference [2]):

If $(\theta + \beta) \le \pi$, then

$$\sigma_{ref} = \frac{M}{2R_m^2 t\left(2\sin[\beta] - \left(\frac{a}{t}\right)\sin[\theta]\right)} + \sigma_{ref}^{9C.5.13} \tag{9C.101}$$

where, $\sigma_{ref}^{9C.5.13}$ is the reference stress from paragraph 9C.5.13, and

$$\beta = \frac{\pi}{2}\left[1 - \left(\frac{\theta}{\pi}\right)\left(\frac{a}{t}\right) - \frac{P_{m,eq}}{\sigma_{ys}}\right] \tag{9C.102}$$

$$\theta = \frac{\pi c}{4R_i} \qquad \textit{for an internal crack} \tag{9C.103}$$

$$\theta = \frac{\pi c}{4R_o} \qquad \textit{for an external crack} \tag{9C.104}$$

If $(\theta + \beta) > \pi$, then

$$\sigma_{ref} = \frac{M}{2R_m^2 t\left(2 - \frac{a}{t}\right)\sin[\beta]} + \sigma_{ref}^{9C.5.13} \tag{9C.105}$$

where, $\sigma_{ref}^{9C.5.13}$ is the reference stress from paragraph 9C.5.13, and

$$\beta = \frac{\pi\left(1 - \frac{a}{t} - \frac{P_{m,eq}}{\sigma_{ys}}\right)}{2 - \frac{a}{t}} \tag{9C.106}$$

9C.5.14.2 Notes:

a) See Annex 9B, Figure 9B.16 for the component and crack geometry.

b) See paragraph 9C.2.2.3 for determination of P_m.

c) If the net section bending moment is zero, the solution in paragraph 9C.5.13 can be used with $F = 0.0$ and P_m is equal to the value determined in subparagraph b above.

d) See paragraph 9C.14 for heavy wall cylinder reference stress solutions.

9C.5.15 Cylinder – Surface Crack, Circumferential Direction – Semi-Elliptical Shape, Through-wall Arbitrary Stress Distribution (RCSCCE3)

9C.5.15.1 The Reference Stress in paragraph 9C.5.13.1 can be used.

9C.5.15.2 Notes:

a) See Annex 9B, Figure 9B.16 for the component and crack geometry.

b) See paragraph 9C.2.2.3 for determination of P_m and P_b.

9C.5.16 Cylinder – Embedded Crack, Longitudinal Direction – Infinite Length, Through-Wall Fourth Order Polynomial Stress Distribution (RCECLL)

9C.5.16.1 The Reference Stress in paragraph 9C.3.7.1 can be used.

9C.5.16.2 Notes:

a) See Annex 9B, Figure 9B.17 for the component and crack geometry.

b) See paragraph 9C.2.2.3 for determination of P_m and P_b.

9C.5.17 Cylinder – Embedded Crack, Circumferential Direction – 360 Degrees, Through-Wall Fourth Order Polynomial Stress Distribution (RCECCL)

9C.5.17.1 The Reference Stress in paragraph 9C.3.7.1 can be used.

9C.5.17.2 Notes:

a) See Annex 9B, Figure 9B.18 for the component and crack geometry.

b) See paragraph 9C.2.2.3 for determination of P_m and P_b.

c) See paragraph 9C.5.2.2(c) for an internal pressure with a net section axial force.

9C.5.18 Cylinder – Embedded Crack, Longitudinal Direction – Elliptical Shape, Through-Wall Fourth Order Polynomial Stress Distribution (RCECLE)

9C.5.18.1 The Reference Stress is given by Equation (9C.35) with the following definitions for d and α:

$$d = d_1 - a \tag{9C.107}$$

$$\alpha = \frac{\frac{2a}{t}}{1+\frac{t}{c}} \tag{9C.108}$$

9C.5.18.2 Notes:

a) See Annex 9B, Figure 9B.19 for the component and crack geometry.

b) See paragraph 9C.2.2.3 for determination of P_m and P_b.

9C.5.19 Cylinder – Embedded Crack, Circumferential Direction – Elliptical Shape, Through-Wall Fourth Order Polynomial Stress Distribution (RCECCE)

9C.5.19.1 The Reference Stress in paragraph 9C.5.18.1 can be used.

9C.5.19.2 Notes:

a) See Annex 9B, Figure 9B.20 for the component and crack geometry.

b) See paragraph 9C.2.2.3 for determination of P_m and P_b.

c) See paragraph 9C.5.2.2(c) for an internal pressure with a net section axial force.

9C.6 Reference Stress Solutions for Spheres

9C.6.1 Sphere – Through-Wall Crack, Through-Wall Membrane and Bending Stress (RSTC)

9C.6.1.1 The Reference Stress solution in paragraph 9C.5.1.1 can be used.

9C.6.1.2 Notes:

a) See Annex 9B, Figure 9B.21 for the component and crack geometry.

b) See paragraph 9C.2.2.3 for determination of P_m and P_b. For internal pressure loading only:

$$P_m = \frac{pR_i^2}{R_o^2 - R_i^2} \tag{9C.109}$$

$$P_b = \frac{pR_o^3}{R_o^3 - R_i^3}\left[\frac{3}{4}\left(\frac{t}{R_i}\right) - \frac{3}{2}\left(\frac{t}{R_i}\right)^2 + \frac{9}{4}\left(\frac{t}{R_i}\right)^3\right] \tag{9C.110}$$

c) See paragraph 9C.2.3.2 to determine M_t for a through-wall crack in a sphere.

9C.6.2 Sphere – Surface Crack, Circumferential Direction – 360 Degrees, Internal Pressure (RSSCCL1)

9C.6.2.1 The Reference Stress in paragraph 9C.5.4.1 can be used.

9C.6.2.2 Notes:

a) See Annex 9B, Figure 9B.22 for the component and crack geometry.

b) See paragraph 9C.2.2.3 for determination of P_m and P_b.

c) See paragraph 9C.2.3.3 to determine M_s for a surface crack in a sphere.

9C.6.3 Sphere – Surface Crack, Circumferential Direction – 360 Degrees, Through-Wall Fourth Order Polynomial Stress Distribution (RSSCCL2)

9C.6.3.1 The Reference Stress in paragraph 9C.5.4.1 can be used.

9C.6.3.2 Notes: see paragraph 9C.6.2.2.

9C.6.4 Sphere – Surface Crack, Circumferential Direction – 360 Degrees, Through-wall Arbitrary Fourth Order Polynomial Stress Distribution (RSSCCL3)

9C.6.4.1 The Reference Stress in paragraph 9C.5.4.1 can be used.

9C.6.4.2 Notes: see paragraph 9C.6.2.2.

9C.6.5 Sphere – Surface Crack, Circumferential Direction – Semi-Elliptical Shape, Internal Pressure (RSSCCE1)

9C.6.5.1 The Reference Stress in paragraph 9C.5.10.1 can be used.

9C.6.5.2 Notes:

a) See Annex 9B, Figure 9B.23 for the component and crack geometry.

b) See paragraph 9C.6.1.2(b) for determination of P_m and P_b.

c) See paragraph 9C.2.3.3 to determine M_s for a surface crack in a sphere.

9C.6.6 Sphere – Surface Crack, Circumferential Direction – Semi-Elliptical Shape, Through-Wall Fourth Order Polynomial Stress Distribution (RSSCCE2)

9C.6.6.1 The Reference Stress in paragraph 9C.5.10.1 can be used.

9C.6.6.2 Notes: see paragraph 9C.6.5.2.

9C.6.7 Sphere – Surface Crack, Circumferential Direction – Semi-Elliptical Shape, Through-wall Arbitrary Stress Distribution (RSSCCE3)

9C.6.7.1 The Reference Stress in paragraph 9C.5.10.1 can be used.

9C.6.7.2 Notes: see paragraph 9C.6.5.2.

9C.6.8 Sphere – Embedded Crack, Circumferential Direction – 360 Degrees, Through-Wall Fourth Order Polynomial Stress Distribution (RSECCL)

9C.6.8.1 The Reference Stress in paragraph 9C.3.7.1 can be used.

9C.6.8.2 Notes:

a) See Annex 9B, Figure 9B.24 for the component and crack geometry.

b) See paragraph 9C.2.2.3 for determination of P_m and P_b.

9C.6.9 Sphere – Embedded Crack, Circumferential Direction – Elliptical Shape, Through-Wall Fourth Order Polynomial Stress Distribution (RSECCE)

9C.6.9.1 The Reference Stress in paragraph 9C.3.8.1 can be used.

9C.6.9.2 Notes:

a) See Annex 9B, Figure 9B.25 for the component and crack geometry.

b) See paragraph 9C.2.2.3 for determination of P_m and P_b.

9C.7 Reference Stress Solutions for Elbows and Pipe Bends

The reference stress solutions for cylinders can be used for elbows and pipe bends if the equivalent membrane and bending stress at the location of the crack is determined considering the bend geometry and applied loads. A discussion regarding the stress analysis for elbows is provided in Annex 9B, paragraph 9B.7. Alternate reference stress solutions for elbows are provided in reference [23].

9C.8 Reference Stress Solutions for Nozzles and Piping Tees

9C.8.1 Nozzle – Corner Crack, Radial Direction, Quarter-Circular Shape, Membrane Stress at the Corner (RNCC1)

9C.8.1.1 The Reference Stress is (Reference [2]):

$$\sigma_{ref} = P_m \left(\frac{2.5t_n^2 + (q - r_n)t}{2.5t_n^2 + (q - r_n)t - 0.25\pi a^2} \right) \tag{9C.111}$$

where,

$$q = \max\left[2r_n, (r_n + t_n + t) \right] \tag{9C.112}$$

$$r_n = \frac{d_n - t_n}{2} \tag{9C.113}$$

9C.8.1.2 Notes:

a) See Annex 9B, Figure 9B.26 (crack labeled G) and Annex 9B, Figure 9B.27 for the component and crack geometry.

b) P_m is the primary membrane stress at the nozzle, the effects of the stress concentration are neglected in the calculation of the reference stress because this stress is localized.

9C.8.2 Nozzle – Corner Crack, Radial Direction, Quarter-Circular Shape, Cubic Polynomial Stress Distribution (RNCC2)

9C.8.2.1 The Reference Stress is computed using equations in paragraph 9C.8.1.1 with an equivalent membrane stress.

9C.8.2.2 Notes:

a) See Annex 9B, Figure 9B.26 (crack labeled G) and Annex 9B, Figure 9B.27 for the component and crack geometry.

b) See paragraph 9C.2.2.3 for determination of P_m.

9C.8.3 Surface Cracks at Nozzles – General Solution

The reference stress solutions shown below can be used for nozzles if the equivalent membrane and bending stress at the location of the crack is determined considering the nozzle geometry and applied loads. A discussion regarding the stress analysis for nozzles is provided in Annex 9B, paragraph 9B.8.

a) Nozzle Neck or Branch (see Annex 9B, Figure 9B.26)

   1) Crack A – Use RCTCC1, RCTCC2, RCSCCL3, RCSCCE3, RCECCL or RCECCE

   2) Crack B – Use RCTCL, RCSCLL3, RCSCLE3, RCECLL or RCECLE

b) Shell or Run Pipe (see Annex 9B, Figure 9B.26)

   1) Crack D & F – Use RPTC, RPSCE3, RPECL, or RPECE2

   2) Crack E & C – Use RPTC, RPSCE3, RPECL, or RPECE2

   3) Crack G – Use the solutions in paragraph 9C.8

9C.9 Reference Stress Solutions for Ring-Stiffened Cylinders

9C.9.1 Ring-Stiffened Cylinder – Internal Ring, Surface Crack at the Toe of One Fillet Weld, Circumferential Direction – 360 Degrees, Pressure Loading (RRCSCCL1)

9C.9.1.1 The Reference Stress in paragraph 9C.5.8.1 can be used with an equivalent membrane and bending stress.

9C.9.1.2 Notes:

a) See Annex 9B, Figure 9B.28 for the component and crack geometry.

b) The equivalent membrane stress, P_m, and bending stress, P_b, based on the stress results at the inside and outside surface are:

$$P_m = \frac{\sigma_{s,ID} + \sigma_{s,OD}}{2} \tag{9C.114}$$

$$P_b = \frac{\left|\sigma_{s,ID} - \sigma_{s,OD}\right|}{2} \tag{9C.115}$$

9C.9.2 Ring-Stiffened Cylinder – Internal Ring, Surface Crack at the Toe of Both Fillet Welds, Circumferential Direction – 360 Degrees, Pressure Loading (RRCSCCL2)

9C.9.2.1 The Reference Stress in paragraph 9C.5.8.1 can be used with an equivalent membrane and bending stress.

9C.9.2.2 Notes: see paragraph 9C.9.1.2.

9C.10 Reference Stress Solutions for Sleeve Reinforced Cylinders

The reference stress solutions shown below can be used for sleeve reinforced cylinders (see Annex 9B, Figure 9B.29) if the stress at the location of the crack is determined considering the actual component geometry and applied loads. A discussion regarding the stress analysis is provided for sleeve reinforced cylinders in Annex 9B, paragraph 9B.10.

a) Crack A – Use RCTCC1, RCTCC2, RCSCCL3, RCSCCE3, RCECCL or RCECCE

b) Crack B – Use RCTCL, RCSCLL3, RCSCLE3, RCECLL or RCECLE

9C.11 Reference Stress Solutions for Round Bars and Bolts

9C.11.1 Round Bar, Surface Crack – 360 Degrees, Membrane and Bending Stress (RBSCL)

9C.11.1.1 The Reference Stress is:

$$\sigma_{ref} = \frac{M_r}{2} + \left(N_r^2 + \frac{M_r^2}{4} \right)^{0.5} \tag{9C.116}$$

where,

$$N_r = \frac{P_m R_o^2}{\left(R_o - a\right)^2} \tag{9C.117}$$

$$M_r = P_{bg}\frac{3\pi}{16}\left[\frac{R_o^4}{R_o\left(R_o - a\right)^3}\right] \tag{9C.118}$$

9C.11.1.2 Notes:

a) See Annex 9B, Figure 9B.30 for the component and crack geometry.

b) The primary membrane and global bending stresses are computed using the following equations:

$$P_m = \frac{F}{\pi R_o^2} \tag{9C.119}$$

$$P_{bg} = \frac{4M}{\pi R_o^3} \tag{9C.120}$$

9C.11.2 Round Bar – Surface Crack, Straight Front, Membrane and Bending Stress (RBSCS)

9C.11.2.1 The Reference Stress is (Reference [6]):

$$\sigma_{ref} = \frac{\pi P_m}{\frac{\pi}{2} + \frac{\sin\left[2\beta\right]}{2} + \beta} + \frac{3\pi P_{bg}}{16\omega} \tag{9C.121}$$

where,

$$\beta = \arcsin\left[\frac{R_o - a}{R_o}\right] \tag{9C.122}$$

$$\omega = 1.0002 - 3.9927\left(\frac{a}{2R_o}\right)^{1.5} + 5.8491\left(\frac{a}{2R_o}\right)^{2.5} - 2.8550\left(\frac{a}{2R_o}\right)^{3} \tag{9C.123}$$

9C.11.2.2 Notes:

a) For the component and crack geometry see Annex 9B, Figure 9B.31.

b) The primary membrane and global bending stresses can be determined using the equations in paragraph 9C.11.1.2(b).

9C.11.3 Round Bar – Surface Crack, Semi-Circular, Membrane and Bending Stress (RBSCC)

9C.11.3.1 The Reference Stress in paragraph 9C.11.2.1 can be used.

9C.11.3.2 Notes:

a) See Annex 9B, Figure 9B.31 for the component and crack geometry.

b) The semi-elliptical flaw is evaluated as an equivalent to a straight front flaw.

9C.11.4 Bolt, Surface Crack, Semi-Circular or Straight Front Shape, Membrane and Bending Stress (RBSC)

9C.11.4.1 The Reference Stress in paragraph 9C.11.2.1 can be used by replacing R_o with R_{th}.

9C.11.4.2 Notes:

a) See Annex 9B, Figure 9B.32 for the component and crack geometry.

b) The solution applies to a semi-circular or straight front surface crack.

9C.12 Reference Stress Solutions for Cracks at Fillet Welds

9C.12.1 Cracks at Fillet Welds – Surface Crack at a Tee Joint, Semi-Elliptical Shape, Through-Wall Membrane and Bending Stress (RFWSCE1)

9C.12.1.1 The Reference Stress in paragraph 9C.3.4.1 can be used with an equivalent membrane and bending stress.

9C.12.1.2 Notes:

a) See Annex 9B, Figure 9B.33 for the component and crack geometry.

b) See paragraph 9C.2.2.3 for determination of P_m and P_b.

9C.12.1.3 Cracks at Fillet Welds of Tee Junctions in Pressurized Components – General Solution

The reference stress solutions shown below can be used for cracks at tee junction fillet welds in pressure containing components (see Annex 9B, Figure 9B.33) if the stress at the location of the crack is determined considering the actual component geometry and applied loads. A discussion regarding the stress analysis is provided in Annex 9B, paragraph 9B.12.

a) Flat Plate Tee Junctions – Use RPTC, RPSCE3, RPECL, or RPECE2

b) Longitudinal Tee Junctions in Cylinders – Use RCTCL, RCSCLL3, RCSCLE3, RCECLL or RCECLE

c) Circumferential Tee Junctions in Cylinders – Use RCTCC1, RCTCC2, RCSCCL3, RCSCCE3, RCECCL or RCECCE

d) Circumferential Tee Junctions in Spheres – Use RSTC, RSSCCL3, RSECCL or RSECCE

9C.13 Reference Stress Solutions for Cracks in Clad Plates and Shells

The reference stress solutions in this Annex can be used to evaluate clad or weld overlayed plate and shell components. A discussion regarding the stress analysis for clad and weld overlayed plate and shell components is provided in Annex 9B, paragraph 9B.13.

9C.14 Reference Stress Solutions for Cracks in Heavy Wall Cylinders $1 \le t/R_i \le 3$

9C.14.1 The Reference Stress is Reference [28]:

$$\sigma_{ref} = F_{ref} \cdot p \qquad \text{(9C.124)}$$

The parameter F_{ref} is given in Tables 9C.1, 9C.2, 9C.3, or 9C.4 based on the surface crack geometry type and orientation, and p is the internal pressure. The parameter F_{ref} includes the pressure load on the crack face for an inside surface and zero pressure on the crack faces for an outside surface crack.

9C.14.2 Notes

a) The crack type and orientation covered are:

1) Table 9C.1 – Infinite Length Axial Crack in a Cylinders, inside and outside surface.

2) Table 9C.2 – Semi-Elliptical Axial Surface Crack in a Cylinders, inside and outside surface.

3) Table 9C.3 – 360° Circumferential Surface Crack in a Cylinder, inside and outside surface.

4) Table 9C.4 – Semi-Elliptical Circumferential Surface Crack in a Cylinders, inside and outside surface.

b) The crack geometries are shown in Annex 9B.

1) Figure 9B.13 – Infinite Length Axial Crack in a Cylinders, inside and outside surface.

2) Figure 9B.15 – Semi-Elliptical Axial Surface Crack in a Cylinders, inside and outside surface.

3) Figure 9B.14 – 360° Circumferential Surface Crack in a Cylinder, inside and outside surface.

4) Figure 9B.16 – Semi-Elliptical Circumferential Surface Crack in a Cylinders, inside and outside surface

9C.15 Nomenclature

A	cross-sectional area of the flaw.
A_o	cross-sectional area of the component computed for the flaw length.
a	crack depth parameter.
α	reference stress parameter.
β	reference stress parameter.
c	crack length parameter.
C	surface correction factor parameter.
d	reference stress parameter.
d_1	distance from plate surface to the center of an embedded elliptical crack (see Annex 9B, Figure 9B.3).
F	net section axial force acting on a cylinder.
F_{ref}	reference stress geometry factor for heavy wall cylinders.
g	is a reference stress bending parameter.
G_p	influence coefficient.
G_0	influence coefficient
K_r	toughness ratio, y-axis parameter on the FAD.
L_r	load ratio, x-axis parameter on the FAD.
$L_{r(\max)}$	maximum value of the load ratio.
$L_{r(cut-off)}$	cut-off value for the load ratio based on the material.

λ shell parameter used to determine the surface correction factors.

λ_a shell parameter used to determine the surface correction factors.

M resultant net-section bending moment acting on a cylinder.

M_r bending moment.

M_s surface correction factor for a surface crack.

M_t correction factor for a through-wall crack.

M_s^L surface correction factor for a through-wall crack.

M_s^{NS} surface correction factor for a through-wall crack.

N_r force.

ω reference stress parameter.

P primary stress.

P_b through-wall primary bending stress component.

P_{bg} primary net-section bending stress.

P_l generalized loading parameter, such as applied stress, bending moment, or pressure.

P_m primary membrane stress component.

$P_{m,eq}$ primary membrane stress component based on equivalent stress.

P_{ij} primary stress component being evaluated.

$P_{ij,b}$ equivalent primary bending stress for a stress component.

$P_{ij,m}$ equivalent primary membrane stress for a stress component.

P_{ly} value of the generalized loading parameter evaluated for the component with a crack-like flaw at the yield stress.

P_0 uniform coefficient for polynomial primary stress distribution.

P_1 linear coefficient for polynomial primary stress distribution.

P_2 quadratic coefficient for polynomial primary stress distribution.

P_3 third order coefficient for polynomial primary stress distribution.

P_4 fourth order coefficient for polynomial primary stress distribution.

P_5 net-section primary bending stress about the x-axis.

P_6 net-section primary bending stress about the y-axis.

p pressure.

Φ plasticity interaction factor.

ψ reference stress parameter.

q nozzle reinforcement zone.

r_n nozzle radius.

R_i cylinder inside radius.

R_m cylinder mean radius.

R_o cylinder, round bar, or bolt outside radius, as applicable.

R_{th} root radius of a threaded bolt.

σ stress.

σ_{mc} circumferential membrane stress.

σ_{ml} longitudinal membrane stress.

σ_{ref} reference stress.

$\sigma_{ref}^{9C.5.2}$ reference stress per paragraph 9C.5.2.

$\sigma_{ref}^{9C.5.13}$ reference stress per paragraph 9C.5.13.

σ_{ys} yield stress (see Annex 2E).

$\sigma_{s,ID}$ surface stress on the inside diameter.

$\sigma_{s,OD}$ surface stress on the outside diameter.

Σ_m membrane stress based on equivalent stress.

Σ_{ml} longitudinal membrane stress function.

t plate or shell thickness.

t_n nozzle thickness (see Annex 9B, Figure 9B.27).

τ reference stress parameter.

θ half-angle of the crack.

U reference stress parameter for circumferential cracks to account for pressure loading.

W distance from the center of the flaw to the free edge of the plate.

x radial local coordinate originating at the internal surface of the component or a reference stress parameter.

x_g global coordinate for definition of net section bending moment about the x-axis.

y_g global coordinate for definition of net section bending moment about the y-axis.

Z reference stress parameter.

9C.16 References

[1] Miller, A.G., “Review of Limit Loads of Structures Containing Defects,” International Journal of Pressure Vessels & Piping, Vol. 32, 1988.

[2] Zahoor, A., *Ductile Fracture Handbook*, Electric Power Research Institute, Palo Alto, CA, 1989.

[3] Willoughby, A.A. and Davey, T.G., “Plastic Collapse in Part-Wall Flaws in Plates,” Fracture Mechanics: Perspectives and Directions (Twentieth Symposium), ASTM STP 1020, R.P. Wei and R.P. Gangloff, Eds., American Society for Testing and Materials, Philadelphia, 1989, pp. 390-409.

[4] Bamford, W.H., Landerman, E.I., and Diaz, E., “Thermal Analysis of Cast Stainless Steel, and its Impact on Piping Integrity,” Circumferential Cracks in Pressure vessels and Piping – Vol. II, ASME PVP – Vol. 95, G.M. Wilkowski, American Society of Mechanical Engineers, 1984, pp. 137-172.

[5] Bergman, M., Bjorn, B., Dahlberg, L., Nilsson, F., and Sattari-Far, I., “A Procedure for Safety Assessment of Components with Cracks – Handbook,” SA/FoU-Report 91/01, The Swedish Plant Inspectorate, Stockholm, Sweden, December 1991.

[6] BSI, “Draft Revision to PD6493 Fracture Assessment”, TWI, March 1996.

[7] Kiefner, J.F. and Vieth, P.H., “Project PR 3-805, A Modified Criterion for Evaluating the Remaining Strength of Corroded Pipe,” Battelle Report to the Pipeline Committee of the American Gas Association, 1989.

[8] Stephens, 9C.R., Krishnaswamy, P, Mohan, R., Osage, 9C.A., Sims, J.R., and Wilkowski, G., “A Review of Analysis Methods and Acceptance Criteria for Local Thinned Areas in Piping and Piping Components,” 1997 Pressure Vessels and Piping Conference, Orlando, FL, July 1997.

[9] Green, 9C. and Knowles, J., “The Treatment of Residual Stress in Fracture Assessment of Pressure Vessels,” ASME, *Journal of Pressure Vessel Technology*, Vol. 116, November 1994, pp. 345-352.

[10] Folias, E.S., “On the Effect of Initial Curvature on Cracked Sheets,” *International Journal of Fracture Mechanics*, Vol. 5, No. 4, December 1969, pp. 327-346.

[11] Sih, G.C., “Handbook of Stress Intensity Factors,” Institute of Fracture and Solid Mechanics, Lehigh University, Bethlehem, PA.

[12] Kramer, G.S., Wilkowski, G.M., and Maxey, W.A., “Flaw Tolerance of Spiral Welded Pipe,” Battelle NG-18 Report No. 154, January 1987.

[13] Kiefner, J.F. and Vieth, P.H., “Project PR 3-805, A Modified Criterion for Evaluating the Remaining Strength of Corroded Pipe,” Battelle Report to the Pipeline Committee of the American Gas Association, 1989.

[14] Eiber, R.J., Maxey, W.A., Duffy, A.R., and Atterbury, T.J., “Investigation of the Initiation and Extent of Ductile Pipe Rupture,” Battelle Report Task 17, June 1971.

[15] Murakami, Y., “Stress Intensity Factors Handbook,” Pergamon Press, Oxford, 1987, pp. 1356-1358.

[16] Tada, H., Paris, P.C. and Irwin, G.R, “The Stress Analysis of Cracks Handbook – Second Edition,” Paris Productions Inc., St. Louis, MO, 1985.

[17] Chell, G.G., “Application of the CEGB Failure Assessment Procedure, R6, to Surface Flaws,” Fracture Mechanics: Twenty-First Symposium, ASTM STP 1074, J.P. Gudas, J.A. Joyce, and E.M. Hackett, Eds., American Society for Testing and Materials, Philadelphia, 1990, pp. 525-544.

[18] Sattari-Far, I., “Finite Element Analysis of Limit Loads for Surface Cracks in Plates*,” Int. J. Pres. Ves. & Pipin*g, 57, 1994, pp. 237-243.

[19] Ainsworth, R.,” Flaw analysis in the French RSE_M and RCC-MR code appendices,” International Journal of Pressure Vessels and Piping 84 (2007) 589.

[20] Marie, S., Chapuliot, S., Kayser, Y., Lacire, M.H., Drubay, B., Barthelet, B., Le Delliou, P., Rougier, V., Naudin, C., Gilles, P., Triay, M., “French RSE-M and RCC-MR code appendices for flaw analysis: Presentation of the fracture parameters calculation–Part I: General overview,” International Journal of Pressure Vessels and Piping 84 (2007) 590–600.

[21] Marie, S., Chapuliot, S., Kayser, Y., Lacire, M.H., Drubay, B., Barthelet, B., Le Delliou, P., Rougier, V., Naudin, C., Gilles, P., Triay, M., “French RSE-M and RCC-MR code appendices for flaw analysis: Presentation of the fracture parameters calculation–Part II: Cracked plates,” International Journal of Pressure Vessels and Piping 84 (2007) 601–613.

[22] Marie, S., Chapuliot, S., Kayser, Y., Lacire, M.H., Drubay, B., Barthelet, B., Le Delliou, P., Rougier, V., Naudin, C., Gilles, P., Triay, M., “French RSE-M and RCC-MR code appendices for flaw analysis: Presentation of the fracture parameters calculation–Part III: Cracked pipes,” International Journal of Pressure Vessels and Piping 84 (2007) 614–658.

[23] Marie, S., Chapuliot, S., Kayser, Y., Lacire, M.H., Drubay, B., Barthelet, B., Le Delliou, P., Rougier, V., Naudin, C., Gilles, P., Triay, M., “French RSE-M and RCC-MR code appendices for flaw analysis: Presentation of the fracture parameters calculation–Part IV: Cracked elbows,” International Journal of Pressure Vessels and Piping 84 (2007) 659–686.

[24] Marie, S., Chapuliot, S., Kayser, Y., Lacire, M.H., Drubay, B., Barthelet, B., Le Delliou, P., Rougier, V., Naudin, C., Gilles, P., Triay, M., “French RSE-M and RCC-MR code appendices for flaw analysis: Presentation of the fracture parameters calculation–Part V: Elements of validation,” International Journal of Pressure Vessels and Piping 84 (2007) 687–696.

[25] RSE-M, *In-Service Inspection Rules for Mechanical Components of PWR Nuclear Islands*, French Association for Design, Construction and In-Service Inspection Rules for Nuclear Island Components, 1, place Jean Miller, 92084 La Défense cedex, France.

[26] Ishizaki, Y. and Thorwald, G., “Significance of Ms and Validation of Reference Stress Solutions for Crack Like Flaws: Part 1,” PVP2020-21085, Proceedings of the ASME 2020, Pressure Vessels & Piping Conference, PVP2020, July 20-24, 2020, Virtual, Online

[27] Ishizaki, Y., Thorwald, G., and Yonekawa, F., “Significance of Ms and Validation of Reference Stress Solutions for Crack Like Flaws: Part 2,” PVP2020-21086, Proceedings of the ASME 2020, Pressure Vessels & Piping Conference, PVP2020, July 20-24, 2020, Virtual, Online.

[28] Thorwald, G., “Reference Stress Solutions for Thick-Wall Cylinders,” Quest Integrity Report 275040, November 2020, ASME Standards Technology project STLLC-0174.

9C.17 Tables

Table 9C.1 – Reference Stress Geometry Factor – Infinite Length Axial Crack in a Cylinder

t/R_i	a/c	Internal Crack	External Crack
		F_{ref}	F_{ref}
1	0.2	1.461	1.588
1	0.4	1.915	1.951
1	0.6	2.916	2.746
1	0.8	5.941	5.096
1.5	0.2	1.087	1.284
1.5	0.4	1.425	1.465
1.5	0.6	2.193	1.978
1.5	0.8	4.578	3.588
2	0.2	0.789	1.158
2	0.4	1.182	1.249
2	0.6	1.823	1.589
2	0.8	3.847	2.766
2.5	0.2	0.694	1.082
2.5	0.4	1.034	1.144
2.5	0.6	1.600	1.360
2.5	0.8	3.394	2.273
3	0.2	0.631	1.027
3	0.4	0.931	1.074
3	0.6	1.462	1.218
3	0.8	3.074	1.933

Table 9C.2 – Reference Stress Geometry Factor – Semi-Elliptical Axial Surface Crack in a Cylinder

t/R_i	a/c	a/t	Internal Crack	External Crack
			F_{ref}	F_{ref}
1	0.03125	0.2	1.514	1.554
1	0.03125	0.4	1.885	1.916
1	0.03125	0.6	2.806	2.654
1	0.03125	0.8	5.760	4.900
1	0.0625	0.2	1.499	1.545
1	0.0625	0.4	1.805	1.903
1	0.0625	0.6	2.703	2.628
1	0.0625	0.8	5.595	4.772
1	0.125	0.2	1.383	1.539
1	0.125	0.4	1.700	1.846
1	0.125	0.6	2.400	2.503
1	0.125	0.8	5.096	4.335
1	0.25	0.2	1.271	1.517
1	0.25	0.4	1.490	1.715
1	0.25	0.6	1.953	2.188
1	0.25	0.8	3.853	3.362
1	0.5	0.2	1.226	1.475
1	0.5	0.4	1.327	1.610
1	0.5	0.6	1.569	1.861
1	0.5	0.8	2.322	2.376
1	1	0.2	1.208	1.435
1	1	0.4	1.264	1.502
1	1	0.6	1.375	1.624
1	1	0.8	1.651	1.813
1	2	0.2	1.213	1.443
1	2	0.4	1.247	1.465
1	2	0.6	1.337	1.510
1	2	0.8	1.433	1.577
1.5	0.03125	0.2	1.022	1.229
1.5	0.03125	0.4	1.395	1.440
1.5	0.03125	0.6	2.089	1.929
1.5	0.03125	0.8	4.393	3.473
1.5	0.0625	0.2	1.027	1.230

Table 9C.2 – Reference Stress Geometry Factor – Semi-Elliptical Axial Surface Crack in a Cylinder

t/R_i	a/c	a/t	Internal Crack	External Crack
			F_{ref}	F_{ref}
1.5	0.0625	0.4	1.340	1.437
1.5	0.0625	0.6	2.038	1.919
1.5	0.0625	0.8	4.314	3.409
1.5	0.125	0.2	0.971	1.239
1.5	0.125	0.4	1.223	1.414
1.5	0.125	0.6	1.875	1.860
1.5	0.125	0.8	3.990	3.179
1.5	0.25	0.2	0.927	1.230
1.5	0.25	0.4	1.090	1.343
1.5	0.25	0.6	1.497	1.695
1.5	0.25	0.8	3.161	2.656
1.5	0.5	0.2	0.921	1.201
1.5	0.5	0.4	0.978	1.285
1.5	0.5	0.6	1.179	1.470
1.5	0.5	0.8	1.911	1.919
1.5	1	0.2	0.921	1.181
1.5	1	0.4	0.929	1.217
1.5	1	0.6	1.022	1.304
1.5	1	0.8	1.316	1.490
1.5	2	0.2	0.920	1.177
1.5	2	0.4	0.938	1.193
1.5	2	0.6	1.012	1.231
1.5	2	0.8	1.101	1.309
2	0.03125	0.2	0.827	1.099
2	0.03125	0.4	1.136	1.214
2	0.03125	0.6	1.736	1.562
2	0.03125	0.8	3.707	2.710
2	0.0625	0.2	0.825	1.100
2	0.0625	0.4	1.093	1.220
2	0.0625	0.6	1.721	1.557
2	0.0625	0.8	3.631	2.667
2	0.125	0.2	0.807	1.100
2	0.125	0.4	0.991	1.211

Table 9C.2 – Reference Stress Geometry Factor – Semi-Elliptical Axial Surface Crack in a Cylinder

t/R_i	a/c	a/t	Internal Crack	External Crack
			F_{ref}	F_{ref}
2	0.125	0.6	1.610	1.531
2	0.125	0.8	3.379	2.527
2	0.25	0.2	0.807	1.101
2	0.25	0.4	0.889	1.172
2	0.25	0.6	1.303	1.429
2	0.25	0.8	2.730	2.200
2	0.5	0.2	0.792	1.087
2	0.5	0.4	0.814	1.146
2	0.5	0.6	0.999	1.268
2	0.5	0.8	1.663	1.669
2	1	0.2	0.814	1.070
2	1	0.4	0.814	1.100
2	1	0.6	0.841	1.154
2	1	0.8	1.133	1.332
2	2	0.2	0.798	1.062
2	2	0.4	0.814	1.074
2	2	0.6	0.848	1.105
2	2	0.8	0.933	1.196
2.5	0.03125	0.2	0.752	1.028
2.5	0.03125	0.4	0.979	1.106
2.5	0.03125	0.6	1.543	1.343
2.5	0.03125	0.8	3.257	2.239
2.5	0.0625	0.2	0.752	1.027
2.5	0.0625	0.4	0.947	1.110
2.5	0.0625	0.6	1.526	1.342
2.5	0.0625	0.8	3.191	2.208
2.5	0.125	0.2	0.779	1.023
2.5	0.125	0.4	0.873	1.104
2.5	0.125	0.6	1.419	1.322
2.5	0.125	0.8	2.977	2.109
2.5	0.25	0.2	0.779	1.025
2.5	0.25	0.4	0.765	1.076
2.5	0.25	0.6	1.162	1.261

Table 9C.2 – Reference Stress Geometry Factor – Semi-Elliptical Axial Surface Crack in a Cylinder

t/R_i	a/c	a/t	Internal Crack	External Crack
			F_{ref}	F_{ref}
2.5	0.25	0.8	2.432	1.888
2.5	0.5	0.2	0.752	1.017
2.5	0.5	0.4	0.765	1.061
2.5	0.5	0.6	0.898	1.150
2.5	0.5	0.8	1.490	1.525
2.5	1	0.2	0.752	1.005
2.5	1	0.4	0.772	1.028
2.5	1	0.6	0.752	1.071
2.5	1	0.8	1.010	1.237
2.5	2	0.2	0.759	0.997
2.5	2	0.4	0.772	1.006
2.5	2	0.6	0.746	1.027
2.5	2	0.8	0.765	1.124
3	0.03125	0.2	0.759	0.980
3	0.03125	0.4	0.882	1.043
3	0.03125	0.6	1.408	1.201
3	0.03125	0.8	2.943	1.921
3	0.0625	0.2	0.728	0.979
3	0.0625	0.4	0.860	1.045
3	0.0625	0.6	1.380	1.203
3	0.0625	0.8	2.879	1.898
3	0.125	0.2	0.752	0.974
3	0.125	0.4	0.796	1.040
3	0.125	0.6	1.278	1.190
3	0.125	0.8	2.689	1.825
3	0.25	0.2	0.752	0.971
3	0.25	0.4	0.740	1.019
3	0.25	0.6	1.053	1.145
3	0.25	0.8	2.210	1.667
3	0.5	0.2	0.728	0.969
3	0.5	0.4	0.740	1.006
3	0.5	0.6	0.823	1.072
3	0.5	0.8	1.371	1.403

Table 9C.2 – Reference Stress Geometry Factor – Semi-Elliptical Axial Surface Crack in a Cylinder

t/R_i	a/c	a/t	Internal Crack	External Crack
			F_{ref}	F_{ref}
3	1	0.2	0.728	0.961
3	1	0.4	0.740	0.980
3	1	0.6	0.716	1.016
3	1	0.8	0.894	1.180
3	2	0.2	0.734	0.955
3	2	0.4	0.740	0.963
3	2	0.6	0.711	0.976
3	2	0.8	0.711	1.072

Table 9C.3 – Reference Stress Geometry Factor – 360° Circumferential Surface Crack in a Cylinder

t/R_i	a/c	Internal Crack	External Crack
		F_{ref}	F_{ref}
1	0.2	1.163	1.398
1	0.4	1.202	1.533
1	0.6	1.442	1.796
1	0.8	3.367	2.626
1.5	0.2	0.904	1.123
1.5	0.4	0.904	1.215
1.5	0.6	1.114	1.414
1.5	0.8	2.750	1.992
2	0.2	0.792	1.006
2	0.4	0.800	1.067
2	0.6	0.941	1.215
2	0.8	2.429	1.667
2.5	0.2	0.759	0.941
2.5	0.4	0.759	0.987
2.5	0.6	0.848	1.088
2.5	0.8	2.229	1.467
3	0.2	0.728	0.903
3	0.4	0.734	0.937
3	0.6	0.777	1.012
3	0.8	2.103	1.332

Table 9C.4 – Reference Stress Geometry Factor – Semi-Elliptical Circumferential Surface Crack in a Cylinder

t/R_i	a/c	a/t	Internal Crack	External Crack
			F_{ref}	F_{ref}
1	0.03125	0.2	NA	NA
1	0.03125	0.4	NA	NA
1	0.03125	0.6	NA	NA
1	0.03125	0.8	NA	NA
1	0.0625	0.2	NA	1.381
1	0.0625	0.4	NA	NA
1	0.0625	0.6	NA	NA
1	0.0625	0.8	NA	NA
1	0.125	0.2	1.172	1.379
1	0.125	0.4	NA	1.485
1	0.125	0.6	NA	1.711
1	0.125	0.8	NA	NA
1	0.25	0.2	1.175	1.376
1	0.25	0.4	1.196	1.437
1	0.25	0.6	1.273	1.572
1	0.25	0.8	NA	1.922
1	0.5	0.2	1.190	1.362
1	0.5	0.4	1.181	1.407
1	0.5	0.6	1.220	1.468
1	0.5	0.8	1.793	1.564
1	1	0.2	1.180	1.353
1	1	0.4	1.189	1.385
1	1	0.6	1.194	1.411
1	1	0.8	1.289	1.427
1	2	0.2	1.221	1.341
1	2	0.4	1.200	1.356
1	2	0.6	1.205	1.369
1	2	0.8	1.219	1.381
1.5	0.03125	0.2	NA	NA
1.5	0.03125	0.4	NA	NA
1.5	0.03125	0.6	NA	NA

Table 9C.4 – Reference Stress Geometry Factor – Semi-Elliptical Circumferential Surface Crack in a Cylinder

t/R_i	a/c	a/t	Internal Crack	External Crack
			F_{ref}	F_{ref}
1.5	0.03125	0.8	NA	NA
1.5	0.0625	0.2	NA	1.119
1.5	0.0625	0.4	NA	NA
1.5	0.0625	0.6	NA	NA
1.5	0.0625	0.8	NA	NA
1.5	0.125	0.2	0.904	1.121
1.5	0.125	0.4	NA	1.191
1.5	0.125	0.6	NA	1.369
1.5	0.125	0.8	NA	NA
1.5	0.25	0.2	0.904	1.118
1.5	0.25	0.4	0.911	1.166
1.5	0.25	0.6	NA	1.275
1.5	0.25	0.8	NA	1.581
1.5	0.5	0.2	0.904	1.122
1.5	0.5	0.4	0.907	1.156
1.5	0.5	0.6	0.932	1.202
1.5	0.5	0.8	1.830	1.276
1.5	1	0.2	0.904	1.107
1.5	1	0.4	0.906	1.131
1.5	1	0.6	0.913	1.156
1.5	1	0.8	1.079	1.174
1.5	2	0.2	0.904	1.102
1.5	2	0.4	0.906	1.109
1.5	2	0.6	0.909	1.121
1.5	2	0.8	0.930	1.129
2	0.03125	0.2	NA	NA
2	0.03125	0.4	NA	NA
2	0.03125	0.6	NA	NA
2	0.03125	0.8	NA	NA
2	0.0625	0.2	NA	1.010
2	0.0625	0.4	NA	NA

Table 9C.4 – Reference Stress Geometry Factor – Semi-Elliptical Circumferential Surface Crack in a Cylinder

t/R_i	a/c	a/t	Internal Crack	External Crack
			F_{ref}	F_{ref}
2	0.0625	0.6	NA	NA
2	0.0625	0.8	NA	NA
2	0.125	0.2	NA	1.006
2	0.125	0.4	NA	1.051
2	0.125	0.6	NA	NA
2	0.125	0.8	NA	NA
2	0.25	0.2	0.792	1.001
2	0.25	0.4	NA	1.040
2	0.25	0.6	NA	1.121
2	0.25	0.8	NA	1.386
2	0.5	0.2	0.792	1.007
2	0.5	0.4	0.792	1.032
2	0.5	0.6	0.815	1.065
2	0.5	0.8	NA	1.134
2	1	0.2	0.792	0.994
2	1	0.4	0.792	1.009
2	1	0.6	0.792	1.030
2	1	0.8	1.072	1.047
2	2	0.2	0.792	0.990
2	2	0.4	0.792	0.994
2	2	0.6	0.792	1.003
2	2	0.8	0.814	1.012
2.5	0.03125	0.2	NA	NA
2.5	0.03125	0.4	NA	NA
2.5	0.03125	0.6	NA	NA
2.5	0.03125	0.8	NA	NA
2.5	0.0625	0.2	NA	0.955
2.5	0.0625	0.4	NA	NA
2.5	0.0625	0.6	NA	NA
2.5	0.0625	0.8	NA	NA
2.5	0.125	0.2	NA	0.947

Table 9C.4 – Reference Stress Geometry Factor – Semi-Elliptical Circumferential Surface Crack in a Cylinder

t/R_i	a/c	a/t	Internal Crack	External Crack
			F_{ref}	F_{ref}
2.5	0.125	0.4	NA	0.975
2.5	0.125	0.6	NA	NA
2.5	0.125	0.8	NA	NA
2.5	0.25	0.2	0.752	0.944
2.5	0.25	0.4	NA	0.968
2.5	0.25	0.6	NA	1.030
2.5	0.25	0.8	NA	1.256
2.5	0.5	0.2	0.752	0.939
2.5	0.5	0.4	0.752	0.962
2.5	0.5	0.6	0.752	0.984
2.5	0.5	0.8	NA	1.050
2.5	1	0.2	0.752	0.931
2.5	1	0.4	0.752	0.943
2.5	1	0.6	0.746	0.960
2.5	1	0.8	1.148	0.974
2.5	2	0.2	0.746	0.928
2.5	2	0.4	0.746	0.933
2.5	2	0.6	0.746	0.939
2.5	2	0.8	0.746	0.945
3	0.03125	0.2	NA	NA
3	0.03125	0.4	NA	NA
3	0.03125	0.6	NA	NA
3	0.03125	0.8	NA	NA
3	0.0625	0.2	NA	0.920
3	0.0625	0.4	NA	NA
3	0.0625	0.6	NA	NA
3	0.0625	0.8	NA	NA
3	0.125	0.2	NA	0.912
3	0.125	0.4	NA	0.928
3	0.125	0.6	NA	NA
3	0.125	0.8	NA	NA

Table 9C.4 – Reference Stress Geometry Factor – Semi-Elliptical Circumferential Surface Crack in a Cylinder

t/R_i	a/c	a/t	Internal Crack	External Crack
			F_{ref}	F_{ref}
3	0.25	0.2	0.722	0.908
3	0.25	0.4	NA	0.924
3	0.25	0.6	NA	0.970
3	0.25	0.8	NA	1.163
3	0.5	0.2	0.722	0.902
3	0.5	0.4	0.722	0.917
3	0.5	0.6	NA	0.934
3	0.5	0.8	NA	0.992
3	1	0.2	0.722	0.897
3	1	0.4	0.722	0.904
3	1	0.6	0.716	0.916
3	1	0.8	1.236	0.928
3	2	0.2	0.722	0.895
3	2	0.4	0.722	0.896
3	2	0.6	0.716	0.901
3	2	0.8	0.716	0.908

9C.18 Figures

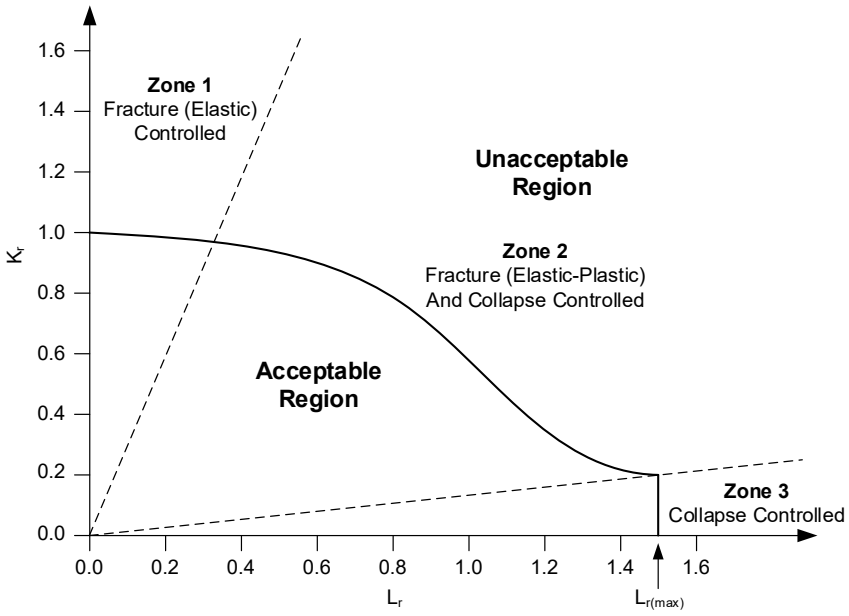

Figure 9C.1 – Failure Regions on the Failure Assessment Diagram

[Intentionally Left Blank]

ANNEX 9D – RESIDUAL STRESSES IN A FITNESS-FOR-SERVICE EVALUATION

(NORMATIVE)

CONTENTS

ANNEX 9D – RESIDUAL STRESSES IN A FITNESS-FOR-SERVICE EVALUATION 9D-1

9D.1 GENERAL 9D-2
9D.1.1 Scope 9D-2
9D.1.2 Crack Driving Force Associated with Residual Stress 9D-2
9D.2 APPLICABILITY AND LIMITATIONS 9D-2
9D.2.1 Residual Stress Solutions for In-Service and New Welded Joints 9D-2
9D.2.2 Technical Basis 9D-3
9D.2.3 Applicable Materials 9D-3
9D.2.4 Weld Joint Geometry 9D-3
9D.2.5 Residual Stress Distributions 9D-3
9D.2.6 Residual Stress Distribution Reference Point 9D-3
9D.2.7 Use of Alternative Residual Stress Solutions 9D-3
9D.2.8 Residual Stress Distributions from Welding Simulation 9D-3
9D.3 DATA REQUIREMENTS AND DEFINITION OF VARIABLES 9D-4
9D.3.1 Required Data 9D-4
9D.3.2 Optional Data 9D-4
9D.3.3 Yield Strength in Residual Stress Calculations 9D-4
9D.4 RESIDUAL STRESS DISTRIBUTION MODIFYING FACTORS 9D-4
9D.4.1 Post Weld Heat Treatment 9D-4
9D.4.2 Pressure Tests 9D-5
9D.5 FULL PENETRATION CIRCUMFERENTIAL WELDS IN PIPING & PRESSURE VESSEL CYLINDRICAL SHELLS 9D-5
9D.5.1 Residual Stress Perpendicular to the Weld Seam (Circumferential Flaw) 9D-5
9D.5.2 Residual Stress Parallel to the Weld Seam (Longitudinal Flaw) 9D-6
9D.5.3 Technical Basis 9D-7
9D.6 FULL PENETRATION LONGITUDINAL WELDS IN PIPING & PRESSURE VESSEL CYLINDRICAL SHELLS 9D-7
9D.6.1 Residual Stress Perpendicular to the Weld Seam (Longitudinal Flaw) 9D-7
9D.6.2 Residual Stress Parallel to the Weld Seam (Circumferential Flaw) 9D-7
9D.6.3 Technical basis 9D-8
9D.7 FULL PENETRATION CIRCUMFERENTIAL WELDS IN SPHERES AND PRESSURE VESSEL HEADS 9D-8
9D.7.1 Residual Stress Perpendicular to the Weld Seam (Circumferential Flaw) 9D-8
9D.7.2 Residual Stress Parallel to the Weld Seam (Meridional Flaw) 9D-8
9D.7.3 Technical Basis 9D-8
9D.8 FULL PENETRATION MERIDIONAL (SEAM) WELDS IN SPHERES AND PRESSURE VESSEL HEADS 9D-9
9D.8.1 Residual Stress Perpendicular to the Weld Seam (Meridional Flaw) 9D-9
9D.8.2 Residual Stress Parallel to the Weld Seam (Circumferential Flaw) 9D-9
9D.8.3 Technical Basis 9D-9
9D.9 FULL PENETRATION WELDS IN STORAGE TANKS 9D-9
9D.10 FULL PENETRATION WELDS AT CORNER JOINTS (NOZZLES OR PIPING BRANCH CONNECTIONS) 9D-9
9D.10.1 Corner Joint, Set-In Nozzle Weld (See Figure 9D.7 and Figure 9D.8, Weld Joint A) 9D-9
9D.10.1.1 Residual Stress Perpendicular to the Weld Seam (See Figure 9D.9) 9D-9
9D.10.1.2 Residual Stress Parallel to the Weld Seam (See Figure 9D.9) 9D-10
9D.10.2 Corner Joint, Set-On Nozzle Weld (See Figure 9D.7 and Figure 9D.8, Weld Joint B) 9D-10
9D.10.2.1 Residual Stress Perpendicular to the Weld Seam 9D-10
9D.10.2.2 Residual Stress Parallel to the Weld Seam 9D-11
9D.10.3 Reinforcing Pad Shell Fillet Weld (See Figure 9D.7 and Figure 9D.8, Weld Joint C) 9D-11
9D.10.3.1 Residual Stress Perpendicular to the Weld Seam 9D-11

9D.10.3.2 Residual Stress Parallel to the Weld Seam 9D-11
9D.10.4 Piping Branch Connection (See Figure 9D.11) *9D-11*
9D.10.4.1 Residual Stress Perpendicular to the Weld Seam (See Figure 9D.11) 9D-11
9D.10.4.2 Residual Stress Parallel to the Weld Seam (see Figure 9D.11) 9D-12
9D.10.5 Technical Basis *9D-12*
9D.11 FULL PENETRATION AND FILLET WELDS AT A TEE JOINT 9D-13
9D.11.1 Main Plate (See Figure 9D.12, Figure 9D.13 and Figure 9D.15) *9D-13*
9D.11.1.1 Residual Stress Perpendicular to the Weld Seam 9D-13
9D.11.1.2 Residual Stress Parallel to the Weld Seam 9D-13
9D.11.2 Stay Plate (See Figure 9D.12, Figure 9D.14 and Figure 9D.15) *9D-14*
9D.11.2.1 Residual Stress Perpendicular to the Weld 9D-14
9D.11.2.2 Residual Stress Parallel to the Weld Seam 9D-14
9D.11.3 Technical Basis *9D-14*
9D.12 REPAIR WELDS 9D-15
9D.12.1 Residual Stress Perpendicular to the Weld *9D-15*
9D.12.2 Residual Stress Parallel to the Weld Seam *9D-15*
9D.12.3 Technical Basis *9D-15*
9D.13 WELDING SIMULATION-BASED STRESS DISTRIBUTIONS 9D-16
9D.13.1 General *9D-16*
9D.13.2 Description of Simplified Method *9D-16*
9D.13.3 Simulation References *9D-17*
9D.14 NOMENCLATURE 9D-18
9D.15 REFERENCES 9D-19
9D.16 TABLES 9D-23
9D.17 FIGURES 9D-25

9D.1 General

9D.1.1 Scope

Guidance for determining the magnitude and distribution of residual stresses at a welded joint is provided in this Annex. The residual stress distribution is required as input to perform a Fitness-For-Service Assessment of a component containing a crack-like flaw at or near a weld joint (see Part 9).

9D.1.2 Crack Driving Force Associated with Residual Stress

The information from this Annex is used to compute the crack driving force associated with the residual stresses and serves as input data for determination of the plasticity interaction factor, Φ, (see Part 9), which quantifies the crack driving force that occurs under situations of combined loading (i.e., primary, secondary, and residual stress).

9D.2 Applicability and Limitations

9D.2.1 Residual Stress Solutions for In-Service and New Welded Joints

The methodology provided herein applies to welded joints located in equipment that has been in-service, as well as to new construction. Residual stress distributions are provided for the following weld joint configurations:

a) Full Penetration Welds in Piping and Pressure Vessel Cylindrical Shells (see paragraphs 9D.4 and 9D.6).

b) Full Penetration Welds in Spheres and Pressure Vessel Heads (see paragraphs 9D.7 and 9D.8).

c) Full Penetration Welds in Storage Tanks (see paragraph 9D.9).

d) Full Penetration and Fillet Welds at Corner Joints (see paragraph 9D.10).

e) Full Penetration Fillet Welds at Tee Joints (see paragraph 9D.11).

f) Repair Welds (see paragraph 9D.12).

9D.2.2 Technical Basis

The residual stress distributions presented in this Annex are based on a literature survey of published results, supplemented with numerical analysis. A comprehensive review of past editions of API 579-1/ASME FFS-1 (see references [1] and [2]) and other relevant standards and practices (see references [3], [4], and [5]) as well as the available technical basis documents (see references [6] through [20]) was performed. The recommended stress distributions presented here are judged to reflect the most accurate or defensible guidance from these sources at this time. Due to the scatter in the reported results and recommended guidance, and the uncertainty inherent to residual stresses due to welding, the residual stress distributions in this Annex reflect an upper bound solution.

9D.2.3 Applicable Materials

Currently, this Annex applies to ferritic and stainless steel weldments. If no distinction is made as to the material of construction for a particular stress profile, then it may be applied for either material.

9D.2.4 Weld Joint Geometry

The residual stress distribution can be affected by the weld joint geometry. Currently, the bounding solutions presented in this Annex apply for both single V-Type and double V-Type joints.

9D.2.5 Residual Stress Distributions

The residual stress distributions in this Annex are provided through the wall thickness. The residual stress in the plane of the component diminishes with increasing distance from the weld joint, which is also given in this Annex. The effects of this reduced residual stress may be used in the assessment.

9D.2.6 Residual Stress Distribution Reference Point

The equations for the residual stress distributions provided in this Annex are referenced from the side opposite of the widest weld groove width, or from the side opposite of the last weld pass (typically the inside surface). In some cases, the term “inside surface” (or “outside surface”) is used for simplicity; however, the preceding definition applies in all cases with the exception of piping branch connection and plate tee welds, which are referenced from the weld toe (outside surface).

9D.2.7 Use of Alternative Residual Stress Solutions

Results from the literature, testing, experimental analysis, or numerical analysis may be used to determine the residual stress at a welded joint as an alternative to the solutions provided in this Annex. For example, residual stresses measured in the field using the depth-controlled hole drilling method can be used to determine the residual stress on the surface of a component. All assumptions used to determine the residual stress distribution by this alternative means should be documented with the assessment results. Residual stress distributions from a single literature source should not be used unless specific information is available to confirm their accuracy.

9D.2.8 Residual Stress Distributions from Welding Simulation

Welding simulation of a specific joint may also be utilized to assess the through-wall and attenuation behavior at a specific location. The results of any welding simulation should be conservatively interpreted with respect to flaw position within the simulated stress field, and overall stress magnitude. Guidance on welding simulation as it applies to developing conservative residual stress distributions are given in paragraph 9D.13.

9D.3 Data Requirements and Definition of Variables

9D.3.1 Required Data

The following data are required to estimate the residual stress field caused by a welded joint:

a) The material specification,

b) The material specified minimum or actual yield strength,

c) The wall thickness of the component,

d) The type of weld (i.e., girth or circumferential joint, longitudinal seam, repair weld, or attachment weld), and

e) The weld joint configuration (e.g., butt joint, corner joint, fillet weld).

9D.3.2 Optional Data

The following data, if available, may be used to refine the estimate of the residual stress field caused by a welded joint:

a) The heat input used to make the weld,

b) Whether the weld has been subject to post weld heat treatment in accordance with the original construction code, and

c) Whether the weld has been subject to a pressure test in accordance with the original construction code.

9D.3.3 Yield Strength in Residual Stress Calculations

In order to estimate the magnitude of the residual stress distribution at a weld joint, an estimate of the actual yield strength of the material must be made. If actual data do not exist or cannot be determined, Equations (9D.1) or (9D.2) may be used to estimate the magnitude of the yield strength. If the actual value of the yield strength is known, then it may be used in the assessment. The elevation of the effective yield strength above the specified minimum yield strength accounts for the typical elevation of actual properties above minimum requirements. The properties of the base material should be used to determine the specified minimum yield strength. Weld metal properties typically include work hardening effects due to the welding process itself; this work hardening is considered conservative relative to the overall flaw assessment procedure contained in this procedure.

$$\sigma_{ys}^{r} = \sigma_{ys} + 69\,\text{MPa} \tag{9D.1}$$

$$\sigma_{ys}^{r} = \sigma_{ys} + 10\,\text{ksi} \tag{9D.2}$$

9D.4 Residual Stress Distribution Modifying Factors

9D.4.1 Post Weld Heat Treatment

a) Residual stress distributions are provided in this Annex for the as-welded conditions. If the weld is known to have been subject to Post Weld Heat Treatment ($PWHT$) per the original construction code, then the following uniform residual stresses may be assumed:

1) Residual Stress Perpendicular to the Weld Seam for Uniform $PWHT$:

$$\sigma^{r}(x) = 0.2\sigma_{ys}^{r} \tag{9D.3}$$

2) Residual Stress Parallel to the Weld Seam for Uniform $PWHT$:

$$\sigma^r(x) = 0.3\sigma^r_{ys} \tag{9D.4}$$

b) These recommendations are based on a uniform $PWHT$ temperature applied to the component and are intended to be a conservative bound to data reported in references such as references [21], [22], and [23]. Uncontrolled and/or local $PWHT$ may result in significantly higher residual stresses. Discussions on the effect of local $PWHT$ can be found in references [24], [25], and [26]. If the type of $PWHT$ cannot be established, the residual stress distribution for the as-welded condition shall be used in the assessment. If the weld joint is in a component operating in the creep range (i.e., long-term operation), then the residual stress based on the $PWHT$ condition may be used in the assessment. The effects of test pressure and $PWHT$ shall be evaluated separately, not in combination.

9D.4.2 Pressure Tests

A reduction in residual stress resulting from pressure tests (such a hydrotest or proof test) after welding may be used if the effect can be quantified. The amount of stress reduction is dependent on the test conditions and geometry. In general, a more uniform reduction is obtained in piping as compared to pressure vessels which have more complex geometries. Consideration should also be given to whether the flaw was present before or after the pressure test. Annex O of reference [4] provides a discussion of these effects but is recommended to be used with caution when applied to vessels. The effects of test pressure and $PWHT$ shall be evaluated separately, not in combination.

9D.5 Full Penetration Circumferential Welds in Piping & Pressure Vessel Cylindrical Shells

9D.5.1 Residual Stress Perpendicular to the Weld Seam (Circumferential Flaw)

a) Heat Input – The recommended distributions perpendicular or transverse to the weld seam (see Figure 9D.1) depend on the linear heat input, $\dot{q}$, used to make the weld that is given by Equations (9D.5) and (9D.6). This definition does not include the welding arc efficiency, η, consistent with the implementation in reference [3]. The linear heat input is then divided by the weldment thickness, t, to differentiate between low, medium and high heat input conditions, each with a corresponding transverse residual stress distribution, as shown below in Equations (9D.7), (9D.8), and (9D.9). Note that the most conservative distribution is the low heat input case, which corresponds physically to thick sections, or very low heat input (and subsequently many passes for a given weldment thickness), which would not be typical of most process equipment. This distribution can always be used as a conservative bound on the effect of weld residual stress in a component. The heat input used in an assessment should be established from the original welding procedure. If the heat input is not known, an average value from Table 9D.1 may be used.

$$\dot{q} = \frac{I \cdot V}{u} \qquad \left(amps,\ volts,\ \frac{mm}{sec},\ \frac{J}{mm} \right) \tag{9D.5}$$

$$\dot{q} = 0.06 \cdot \frac{I \cdot V}{u} \qquad \left(amps,\ volts,\ \frac{in}{min},\ \frac{kJ}{in} \right) \tag{9D.6}$$

b) Through-Thickness Residual Stress Distribution – The residual stress distribution for this category of weld made remote from all geometric discontinuities can be approximated using Equations (9D.7), (9D.8), and (9D.9), and illustrated in Figure 9D.2. The local coordinate x for the stress distribution through the wall

thickness is measured from the side opposite of the widest weld groove width or last pass (typically the inside surface). This distribution applies within $1.0t$ of the weld centerline (in either direction).

1) For high heat input $\left(\frac{\dot{q}}{t} > 120\frac{J}{mm^2}\left(77.4\frac{kJ}{in^2}\right)\right)$ ferritic and austenitic stainless steels welds:

$$\sigma^r(x) = \sigma^r_{ys}\left[1.00 - 0.22\left(\frac{x}{t}\right) - 3.06\left(\frac{x}{t}\right)^2 + 1.88\left(\frac{x}{t}\right)^3\right] \quad (9D.7)$$

For medium heat input $\left(120\frac{J}{mm^2}\left(77.4\frac{kJ}{in^2}\right) \geq \frac{\dot{q}}{t} > 50\frac{J}{mm^2}\left(32.3\frac{kJ}{in^2}\right)\right)$ ferritic steels welds:

$$\sigma^r(x) = \sigma^r_{ys}\left[1.00 - 4.43\left(\frac{x}{t}\right) + 13.53\left(\frac{x}{t}\right)^2 - 16.93\left(\frac{x}{t}\right)^3 + 7.03\left(\frac{x}{t}\right)^4\right] \quad (9D.8)$$

2) For low heat input $\left(\frac{\dot{q}}{t} \leq 50\frac{J}{mm^2}\left(32.3\frac{kJ}{in^2}\right)\right)$ ferritic and medium/low heat input austenitic stainless steels welds:

$$\sigma^r(x) = \sigma^r_{ys}\left[1.00 - 6.80\left(\frac{x}{t}\right) + 24.30\left(\frac{x}{t}\right)^2 - 28.68\left(\frac{x}{t}\right)^3 + 11.18\left(\frac{x}{t}\right)^4\right] \quad (9D.9)$$

c) Residual Stress Attenuation – The through-thickness residual stress distribution may be varied with distance from the weld centerline (y) as follows (see Figure 9D.3). Equations (9D.12) and (9D.13) are intended to capture the transverse stress reversal that can occur for thinner sections. This can cause outside surface tensile stresses away from the weld, even while the weld stresses are predicted to be compressive.

1) From 0.0 to $1.0w$:

$\sigma^r(x)$ from Equations (9D.7), (9D.8), and (9D.9) (9D.10)

2) For thicknesses greater than 9.525 mm (0.375 inch):

$\sigma^r(x)$ linearly decreasing to 0 from $1.0w$ to $2.0\sqrt{rt}$ (9D.11)

3) For thicknesses less than or equal to 9.525 mm (0.375 inch):

$\sigma^r(x)$ linearly varying to $-0.5\sigma^r(x)$ from $1.0w$ to $2.0w$ (9D.12)

$\sigma^r(x)$ linearly varying from $-0.5\sigma^r(x)$ to 0 from $2.0w$ to $2.0\sqrt{rt}$ (9D.13)

9D.5.2 Residual Stress Parallel to the Weld Seam (Longitudinal Flaw)

a) Through-Thickness Residual Stress Distribution – The residual stress distribution for this category of weld made remote from all geometric discontinuities can be approximated using Equation (9D.14) through (9D.19). The local coordinate x for the stress distribution through the wall thickness is measured from the side opposite of the widest weld groove width or last pass (typically the inside surface). This distribution applies within $1.0w$ of the weld centerline (in either direction).

$$\sigma^r(x) = \sigma^r_i + \left(\sigma^r_o - \sigma^r_i\right)\left(\frac{x}{t}\right) \quad (9D.14)$$

with,

$$\sigma_o^r = \sigma_{ys}^r \tag{9D.15}$$

and,

$$\sigma_i^r = \sigma_{ys}^r \qquad \left(for\ t \le 15\,mm\ (0.59\,in.)\right) \tag{9D.16}$$

$$\sigma_i^r = \sigma_{ys}^r \left[1.0 - 0.0143\left(t^* - 15\right)\right] \qquad \left(for 15\,mm\ (0.59\,in.) < t \le 85\,mm\ (3.35\,in.)\right) \tag{9D.17}$$

$$\sigma_i^r = 0.0 \qquad \left(for\ t > 85\,mm\ (3.35\,in.)\right) \tag{9D.18}$$

where,

$$t^* = t \cdot C_{ul} \tag{9D.19}$$

b) Residual Stress Attenuation – The through-thickness residual stress distribution may be decreased with distance from the weld centerline (y) as follows (see Figure 9D.3):

$\sigma^r(x)$ Equations (9D.14) through (9D.19) from 0.0 to $1.0w$ (9D.20)

$\sigma^r(x)$ linearly decreasing to 0 from $1.0w$ to $1.5w$: (9D.21)

9D.5.3 Technical Basis

The residual stress distributions for cylinder girth (butt) welds (see Figure 9D.1) are taken from the recommendations of the R6 Procedure Reference [3], the basis for which can be found in references [16], [17], [6], and [20], among others.

9D.6 Full Penetration Longitudinal Welds in Piping & Pressure Vessel Cylindrical Shells

9D.6.1 Residual Stress Perpendicular to the Weld Seam (Longitudinal Flaw)

a) Through-Thickness Residual Stress Distribution – The residual stress distribution for this category of weld made remote from all geometric discontinuities can be approximated using Equation (9D.22) or Figure 9D.4. The local coordinate x for the stress distribution through the wall thickness is measured from the side opposite of the widest weld groove width or last pass (typically the inside surface). This distribution applies within $1.0w$ of the weld centerline (in either direction).

$$\sigma^r(x) = \sigma_{ys}^r \left[1.230 - 9.269\left(\frac{x}{t}\right) + 17.641\left(\frac{x}{t}\right)^2 - 8.660\left(\frac{x}{t}\right)^3\right] \tag{9D.22}$$

b) Residual Stress Attenuation – The through-thickness residual stress distribution may be decreased with distance from the weld centerline (y) as follows (see Figure 9D.5):

$\sigma^r(x)$ Equation (9D.22) from 0.0 to $1.0w$ (9D.23)

$\sigma^r(x)$ linearly decreasing to 0 from $1.0w$ to $2.0w$ (9D.24)

9D.6.2 Residual Stress Parallel to the Weld Seam (Circumferential Flaw)

a) Through-Thickness Residual Stress Distribution – The residual stress distribution for this category of weld made remote from all geometric discontinuities can be approximated using Equation (9D.25). The local

coordinate x for the stress distribution through the wall thickness is measured from the side opposite of the widest weld groove width or last pass (typically the inside surface). This distribution applies within $1.0w$ of the weld centerline (in either direction).

$$\sigma^r(x) = \sigma^r_{ys} \tag{9D.25}$$

b) Residual Stress Attenuation – The through-thickness residual stress distribution may be decreased with distance from the weld centerline (y) as follows:

$\sigma^r(x)$ Equation (9D.25) from 0.0 to $1.0w$ (9D.26)

$\sigma^r(x)$ linearly decreasing to 0 from $1.0w$ to $1.5w$ (9D.27)

9D.6.3 Technical basis

The residual stress distributions for cylinder longitudinal (seam) welds (see Figure 9D.1), are taken from the recommendations of the BS7910 Procedure (see reference [4]). Note that the transverse stress functional form given here has been refitted to start from the inside surface but is otherwise identical to the stress distribution recommended in reference [4]. Unlike cylinder girth welds, there are relatively few cases that make up the supporting experimental database, and all cases are for thicknesses greater than 50.8 mm (2 inches), (see reference [16]).

9D.7 Full Penetration Circumferential Welds in Spheres and Pressure Vessel Heads

9D.7.1 Residual Stress Perpendicular to the Weld Seam (Circumferential Flaw)

a) Through-Thickness Residual Stress Distribution – The residual stress distribution for this category of weld remote from all geometric discontinuities can be approximated using the equations in paragraph 9D.5.1(b), (see Figure 9D.6).

b) Residual Stress Attenuation – The residual stress distribution for this category of weld remote from all geometric discontinuities can be approximated using the equations in paragraph 9D.5.1(c), replacing r by r_c.

c) The heat input used in an assessment should be established from the original welding procedure. If the heat input is not known, an average may be estimated from Table 9D.1.

9D.7.2 Residual Stress Parallel to the Weld Seam (Meridional Flaw)

a) Through-Thickness Residual Stress Distribution – The residual stress distribution for this category of weld can be approximated using the equations in paragraph 9D.5.2(a).

b) Residual Stress Attenuation – The residual stress attenuation for this category of weld remote from all geometric discontinuities can be approximated using the equations in paragraph 9D.5.2(b).

9D.7.3 Technical Basis

Very little experimental or numerical data exists for welds in spheres; nonetheless, practical experience suggests that circumferential residual stresses in spheres and heads are comparable to residual stresses in circumferential (girth) welds in cylindrical shells, but with consideration given to the position of the weld within the sphere or head through r_c (see Figure 9D.6).

9D.8 Full Penetration Meridional (Seam) Welds in Spheres and Pressure Vessel Heads

9D.8.1 Residual Stress Perpendicular to the Weld Seam (Meridional Flaw)

a) Through-Thickness Residual Stress Distribution – The residual stress distribution for this category can be approximated using the equations in paragraph 9D.6.1(a), (see Figure 9D.6).

b) Residual Stress Attenuation – The residual stress distribution for this category of weld made remote from all geometric discontinuities can be approximated using the equations in paragraph 9D.6.1(b).

9D.8.2 Residual Stress Parallel to the Weld Seam (Circumferential Flaw)

a) Through-Thickness Residual Stress Distribution – The residual stress distribution for this category can be approximated using paragraph 9D.6.2(a), (see Figure 9D.6).

b) Residual Stress Attenuation – The residual stress distribution for this category of weld made remote from all geometric discontinuities can be approximated using the equations in paragraph 9D.6.2(b).

9D.8.3 Technical Basis

Very little experimental or numerical data exists for welds in spheres. Nonetheless, practical experience suggests that meridional residual stresses in spheres and heads are comparable to residual stresses in longitudinal (seam) welds in cylindrical shells.

9D.9 Full Penetration Welds in Storage Tanks

The residual stress distributions provided for the longitudinal (seam) weld joint in piping and pressure vessel cylindrical shells in paragraph 9D.6 may be used for all shell course weld joints (both vertical and horizontal welds) in storage tanks.

9D.10 Full Penetration Welds at Corner Joints (Nozzles or Piping Branch Connections)

9D.10.1 Corner Joint, Set-In Nozzle Weld (See Figure 9D.7 and Figure 9D.8, Weld Joint A)

9D.10.1.1 Residual Stress Perpendicular to the Weld Seam (See Figure 9D.9)

a) Through-Thickness Residual Stress Distribution – The residual stress distribution for this category of weld made remote from all other geometric discontinuities can be approximated using Equation (9D.28). The local coordinate x for the stress distribution through the wall thickness is measured from the side opposite of the widest weld groove width or last pass (typically the inside surface). This distribution applies to both the shell and nozzle neck thickness. This distribution also applies from the weld centerline to the nozzle corner (in both the shell and nozzle), and within $1.0t_s$ of the weld centerline moving into the shell or nozzle neck.

$$\sigma^r(x) = \sigma^r_{ys}\left[1.00 - 16.0\left(\frac{x}{t}\right)^2 + 32.0\left(\frac{x}{t}\right)^3 - 16.0\left(\frac{x}{t}\right)^4\right] \tag{9D.28}$$

b) Residual Stress Attenuation – The through-thickness residual stress distribution may be decreased with distance from the weld centerline (y) as follows (see Figure 9D.10):

1) Shell:

$\sigma^r(x)$ Equation (9D.28) from nozzle bore to $1.0t_s$ past nozzle outside surface (9D.29)

$\sigma^r(x)$ linearly decreasing to 0 from $1.0t_s$ to L_s past nozzle outside surface (9D.30)

The parameter L_s is defined as a function of shell radius to thickness ratio:

$$L_s = 6.0t_s \qquad \left(for\ \frac{r_s}{t_s} \le 5 \right) \tag{9D.31}$$

$$L_s = t_s \left[6.237 - 0.0474 \left(\frac{r_s}{t_s} \right) \right] \qquad \left(for\ 5 < \frac{r_s}{t_s} \le 100 \right) \tag{9D.32}$$

$$L_s = 1.5t_s \qquad \left(for\ \frac{r_s}{t_s} > 100 \right) \tag{9D.33}$$

2) Nozzle Neck:

$\sigma^r(x)$ Equation (9D.28) from nozzle bore to $1.0t_s$ past shell outside surface (9D.34)

$\sigma^r(x)$ linearly decreasing to 0 from $1.0t_s$ to $1.5t_s$ past shell outside surface (9D.35)

9D.10.1.2 Residual Stress Parallel to the Weld Seam (See Figure 9D.9)

a) Through-Thickness Residual Stress Distribution – The residual stress distribution for this category of weld made remote from all geometric discontinuities can be approximated using Equation (9D.36). The local coordinate x for the stress distribution through the wall thickness is measured from the side opposite of the widest weld groove width or last pass (typically the inside surface). This distribution applies within $1.0t_s$ of the weld centerline (in either direction).

$$\sigma^r(x) = \sigma^r_{ys} \tag{9D.36}$$

b) Residual Stress Attenuation – The through-thickness residual stress distribution may be decreased with distance from the weld centerline (y) as follows:

1) Shell:

$\sigma^r(x)$ Equation (9D.36) from nozzle bore to $1.0t_s$ past nozzle outside surface (9D.37)

$\sigma^r(x)$ linearly decreasing to 0 from $1.0t_s$ to $1.5t_s$ past nozzle outside surface (9D.38)

2) Nozzle Neck:

$\sigma^r(x)$ Equation (9D.36) from nozzle bore to $1.0t_s$ past shell outside surface (9D.39)

$\sigma^r(x)$ linearly decreasing to 0 from $1.0t_s$ to $1.5t_s$ past shell outside surface (9D.40)

9D.10.2 Corner Joint, Set-On Nozzle Weld (See Figure 9D.7 and Figure 9D.8, Weld Joint B)

9D.10.2.1 Residual Stress Perpendicular to the Weld Seam

a) Through-Thickness Residual Stress Distribution – The residual stress distributions provided in Equation (9D.28) may be used for this configuration.

b) Residual Stress Attenuation – The through-thickness residual stress distribution may be decreased with distance from the weld centerline (y) as follows (see Figure 9D.10):

1) Shell: The stress attenuation from the equations in paragraph 9D.10.1.1(b) may be used.

2) Nozzle Neck:

$\sigma^r(x)$ Equation (9D.28) from nozzle bore to $1.0t_n$ past shell outside surface (9D.41)

$\sigma^r(x)$ linearly decreasing to 0 from $1.0t_n$ to $6.0t_n$, past shell outside surface (9D.42)

9D.10.2.2 Residual Stress Parallel to the Weld Seam

a) Through-Thickness Residual Stress Distribution – The residual stress distributions provided in the equations in paragraph 9D.10.2(a) may be used for this configuration.

b) Residual Stress Attenuation – The through-thickness residual stress distribution may be decreased with distance from the weld centerline (y) according to the equations in paragraph 9D.10.1.2(b).

9D.10.3 Reinforcing Pad Shell Fillet Weld (See Figure 9D.7 and Figure 9D.8, Weld Joint C)

9D.10.3.1 Residual Stress Perpendicular to the Weld Seam

a) Through-Thickness Residual Stress Distribution – The residual stress distributions provided in Equation (9D.28) may be used for this configuration. This residual stress distribution may be overly conservative for thick shell sections; therefore, alternatively, the guidance for tee joint welds (main plate) in paragraph 9D.11.1 may be used for shell thicknesses greater than 25.4 mm (1 inch).

b) Residual Stress Attenuation – The through-thickness residual stress distribution may be decreased with distance from the weld centerline (y) as follows (both towards and away from the nozzle centerline), (see Figure 9D.10):

$\sigma^r(x)$ Equation (9D.28) from 0.0 to $1.0w$ (9D.43)

$\sigma^r(x)$ linearly decreasing to 0 from $1.0w$ to $2.0w$ (9D.44)

The total residual stress under the pad should be the sum of the (attenuated) stress from both the corner joint weld (Weld Joint A or B) and reinforcing pad outer fillet weld (Weld Joint C).

9D.10.3.2 Residual Stress Parallel to the Weld Seam

a) Through-Thickness Residual Stress Distribution – The residual stress distributions provided in Equation (9D.36) may be used for this configuration. This residual stress distribution may be overly conservative for thick shell sections; therefore, alternatively, the guidance for tee joint welds (main plate) in paragraph 9D.11.2 may be used for shell thicknesses greater than 25.4 mm (1 inch).

b) Residual Stress Attenuation – The through-thickness residual stress distribution may be decreased with distance from the weld centerline (y) according to the equations in paragraph 9D.10.1.2(b).

9D.10.4 Piping Branch Connection (See Figure 9D.11)

9D.10.4.1 Residual Stress Perpendicular to the Weld Seam (See Figure 9D.11)

a) Through-Thickness Residual Stress Distribution – The residual stress distribution for this category of weld made remote from all other geometric discontinuities can be approximated using Equations (9D.45) and (9D.46). The local coordinate x for the stress distribution through the wall thickness is measured from the toe of the fillet weld (the outside surface). This distribution applies through the run pipe thickness; in lieu of information, it may also be applied to the branch pipe, with caution. This distribution applies from the weld centerline to the branch corner, and within $1.0w$ of the branch outside surface, moving into the run pipe.

$$\sigma^r(x) = \sigma^r_{ys}\left(\begin{array}{l} 0.97 + 2.327\left(\frac{x}{t}\right) - 24.125\left(\frac{x}{t}\right)^2 + \\ 42.485\left(\frac{x}{t}\right)^3 - 21.087\left(\frac{x}{t}\right)^4 \end{array}\right) \qquad \left(for\ \ ferritic\ steels\right) \qquad (9D.45)$$

$$\sigma^r(x) = \sigma^r_{ys} \qquad \left(for\ austenitic\ stainless\ steels\right) \qquad (9D.46)$$

b) Residual Stress Attenuation – The through-thickness residual stress distribution may be decreased with distance from the weld (y) according to paragraph 9D.10.1.1(b) or 9D.10.2.1(b), as appropriate.

9D.10.4.2 Residual Stress Parallel to the Weld Seam (see Figure 9D.11)

a) Through-Thickness Residual Stress Distribution – The residual stress distribution for this category of weld made remote from all other geometric discontinuities can be approximated using Equations (9D.47) and (9D.48). The local coordinate x for the stress distribution through the wall thickness is measured from the toe of the fillet weld (the outside surface). This distribution applies through the run pipe thickness; in lieu of information, it may also be applied to the branch pipe, with caution. This distribution applies from the weld centerline to the branch corner, and within $1.0w$ of the branch outside surface, moving into the run pipe.

$$\sigma^r(x) = \sigma^r_{ys}\left(\begin{array}{l} 1.025 + 3.478\left(\frac{x}{t}\right) - 27.861\left(\frac{x}{t}\right)^2 + \\ 45.788\left(\frac{x}{t}\right)^3 - 21.799\left(\frac{x}{t}\right)^4 \end{array}\right) \qquad \left(for\ ferritic\ steels\right) \qquad (9D.47)$$

$$\sigma^r(x) = \sigma^r_{ys} \qquad \left(for\ austenitic\ stainless\ steels\right) \qquad (9D.48)$$

b) Residual Stress Attenuation – The through-thickness residual stress distribution may be decreased with distance from the weld (y) according to the equations of paragraph 9D.10.1.2(b) or 9D.10.2.2(b) as appropriate.

9D.10.5 Technical Basis

Recommendations for nozzle weld residual stress distributions are given for corner joint set-in and set-on configurations, both with and without a reinforcing pad (see Figure 9D.8, Weld Joint A and Weld Joint B). The (reinforcing) nozzle fillet weld shown in Figure 9D.8 is considered part of the basic corner joint in all cases. Nozzle guidance is based on review of an extensive numerical study documented in reference [12]. Through-wall stresses in both the nozzle neck and shell show negligible difference between the set-in and set-on configurations (see reference [12]) and so are treated the same here. Nozzle neck stress attenuation is demonstrated to be different for the set-on nozzle case, and this is addressed. The corner joint (set-in or set-on) residual stress distributions are assumed to be unaffected by the reinforcing pad attachments, in lieu of other information. In this case, the basic stress distribution given in this paragraph should be applied through the reinforcing pad (at the nozzle), and through the shell itself, separately. An additional through-wall stress location is given at the outer pad to shell fillet weld attachment (see Figure 9D.8, Weld Joint C).

Stress distributions are also given for piping branch connections, and are taken directly from the R6 Guidance (see reference [3]) that is based on a compendium of experimentally measured distributions for pipe-to-plate, pipe t-node and pipe y-node connections (see reference [16]). Stress attenuation is assumed to follow the nozzle

corner joint recommendations of this document, which are obtained from inspection of the results in reference [12].

9D.11 Full Penetration and Fillet Welds at a Tee Joint

9D.11.1 Main Plate (See Figure 9D.12, Figure 9D.13 and Figure 9D.15)

9D.11.1.1 Residual Stress Perpendicular to the Weld Seam

a) Through-Thickness Residual Stress Distribution – The residual stress distribution for this category of weld made remote from all other geometric discontinuities can be approximated using Equations (9D.49) through (9D.57). The local coordinate x for the stress distribution through the wall thickness is measured from the toe of the fillet weld (the outside surface). This distribution applies from the base of the stay plate extending $1.5t$ into the main plate, in either direction.

$$\sigma^r(x) = \sigma_i^r - 3.636\left(\sigma_i^r - \sigma_m^r\right)\left(\frac{x}{t}\right) \qquad \left(for\ 0 \le \frac{x}{t} \le 0.275\right) \tag{9D.49}$$

$$\sigma^r(x) = \sigma_m^r + \left(\sigma_o^r - \sigma_m^r\right)\left(1.379\frac{x}{t} - 0.379\right) \qquad \left(for\ 0.275 < \frac{x}{t} \le 1.0\right) \tag{9D.50}$$

with,

$$\sigma_i^r = \sigma_{ys}^r \tag{9D.51}$$

$$\sigma_m^r = \sigma_{ys}^r \qquad \left(for\ t \le 6.35\,mm\ (0.25\,in.)\right) \tag{9D.52}$$

$$\sigma_m^r = \sigma_{ys}^r\left(1.340 - 0.0536t^*\right) \qquad \left(for\ 6.35\,mm\ (0.25\,in.) < t \le 25\,mm\ (0.984\,in.)\right) \tag{9D.53}$$

$$\sigma_m^r = 0.0 \qquad \left(for\ t > 25\,mm\ (0.984\,in.)\right) \tag{9D.54}$$

$$\sigma_o^r = \sigma_{ys}^r \qquad \left(for\ t \le 6.35\,mm\ (0.25\,in.)\right) \tag{9D.55}$$

$$\sigma_o^r = \sigma_{ys}^r\left(1.170 - 0.0268t^*\right) \qquad \left(for\ 6.35\,mm\ (0.25\,in.) < t \le 25\,mm\ (0.984\,in.)\right) \tag{9D.56}$$

$$\sigma_o^r = 0.5 \cdot \sigma_{ys}^r \qquad \left(for\ t > 25\,mm\ (0.984\,in.)\right) \tag{9D.57}$$

where t^* is given by Equation (9D.19).

b) Residual Stress Attenuation – The through-thickness residual stress distribution may be decreased with distance from the plate face (y) as follows (see Figure 9D.15):

$\sigma^r(x)$ Equations (9D.49) or (9D.50) from 0.0 to $1.5t$ (9D.58)

$\sigma^r(x)$ linearly decreasing to 0 from $1.5t$ to $2.0t$ (9D.59)

9D.11.1.2 Residual Stress Parallel to the Weld Seam

a) Through-Thickness Residual Stress Distribution – The residual stress distribution for this category can be approximated using paragraph 9D.11.1.1(a).

b) Residual Stress Attenuation – The through-thickness residual stress distribution may be decreased with distance from the weld centerline (y) according to paragraph 9D.11.1.1(b).

9D.11.2 Stay Plate (See Figure 9D.12, Figure 9D.14 and Figure 9D.15)

9D.11.2.1 Residual Stress Perpendicular to the Weld

a) Through-Thickness Residual Stress Distribution – The residual stress distribution for this category of weld made remote from all other geometric discontinuities can be approximated using Equations (9D.60) through (9D.63). The local coordinate x for the stress distribution through the wall thickness is measured from the toe of the fillet weld (the outside surface). This distribution applies from the base of the stay plate extending $1.5t$ upwards into the plate. Note that for $\beta = 1$ the nozzle corner joint distribution is returned. In all cases the stay plate equations are a family of fourth order polynomials whose coefficients vary only with stay plate thickness, t.

$$\sigma^r(x) = \sigma^r_{ys}\left[1.00 - \beta\left(16.0\left(\frac{x}{t}\right)^2 - 32.0\left(\frac{x}{t}\right)^3 + 16.0\left(\frac{x}{t}\right)^4\right)\right] \tag{9D.60}$$

and,

$$\beta = 0.0 \qquad \left(for\ t \le 6.35\,mm\ (0.25\,in.)\right) \tag{9D.61}$$

$$\beta = 0.0536t^* - 0.340 \qquad \left(for\ 6.35\,mm\ (0.25\,in.) < t \le 25\,mm\ (0.984\,in.)\right) \tag{9D.62}$$

$$\beta = 1.0 \qquad \left(for\ t > 25\,mm\ (0.984\,in.)\right) \tag{9D.63}$$

where t^* is given by Equation (9D.19).

b) The through-thickness residual stress distribution may be decreased with distance from the weld centerline (y) according to paragraph 9D.11.1.1(b).

9D.11.2.2 Residual Stress Parallel to the Weld Seam

a) Through-Thickness Residual Stress Distribution – The residual stress distribution for this category can be approximated using paragraph 9D.11.2.1(a).

b) Residual Stress Attenuation – The through-thickness residual stress distribution may be decreased with distance from the weld centerline (y) according to paragraph 9D.11.1.2(b).

9D.11.3 Technical Basis

Residual stress distributions for full penetration and fillet welds at thick plate-to-plate tee joints are taken from the experimental work and recommendations of reference [27]. Thick is defined here to be all thicknesses greater than 25.4 mm (1 inch). This data is in good agreement with the measured residual stress data in reference [16] as well. Therefore stress attenuation guidance is taken from reference [16], since reference [27] does not include this information. The parallel (longitudinal) stress distribution is recommended here to be the same as the perpendicular (transverse) stress recommendation given in reference [27], based on a comparison of both data sets. This assumption is corroborated by comparison of the piping branch connection parallel and perpendicular recommendations (see Figure 9D.1), which are nearly identical.

In both references [16] and [27] experimental results correspond to plate thicknesses between 25 mm (0.984 inch) and 100 mm (3.937 inches). Thinner plates could be expected to have a more uniform stress distribution through-thickness, as reflected in the guidance in references [1] and [3], as well as limited literature studies (references [28] through [31]). Therefore, plates 6.35 mm (0.25 inch) and thinner are specified here to have a uniform yield

level tensile stress through-thickness. A linear transition between the two profiles discussed here is then assumed, as given in Equations (9D.60) through (9D.63).

9D.12 Repair Welds

9D.12.1 Residual Stress Perpendicular to the Weld

a) Through-Thickness Residual Stress Distribution – The residual stress distribution for this category of weld made remote from all other geometric discontinuities can be approximated using Equations (9D.64) and (9D.65). Note that this distribution is referenced to the position of the repair, such that the through-thickness origin always corresponds to the last pass of the repair weld. Additionally, this distribution assumes that the repair is of sufficient depth to dominate the through-thickness distribution, such that the original distribution need not be considered. For shallow repairs, or for flaws on the side of the section opposite of the repair, the original recommended stress distribution should be considered, modified by yield over the (shallow) repair depth. The local coordinate x for the stress distribution through the wall thickness is measured from the surface corresponding to the last pass of the repair.

$$\sigma^r = \sigma^r_{ys} \qquad \left(for\ \frac{x}{t} \le \frac{t_w}{t} \right) \tag{9D.64}$$

$$\sigma^r = \sigma^r_{ys} \left(\frac{1.0}{1.0 - \frac{t_w}{t}} \right) \left(1.0 - \frac{x}{t} \right) \qquad \left(for\ \frac{t_w}{t} < \frac{x}{t} \le 1.0 \right) \tag{9D.65}$$

a) Residual Stress Attenuation – The through-thickness residual stress distribution may be decreased with distance from the weld centerline (y) according to the guidance for the original weld joint and configuration (e.g., girth, seam).

9D.12.2 Residual Stress Parallel to the Weld Seam

a) Through-Thickness Residual Stress Distribution – The residual stress distribution for this category can be approximated using paragraph 9D.12.1(a).

b) Residual Stress Attenuation – The through-thickness residual stress distribution may be decreased with distance from the weld centerline (y) according to the guidance for the original weld joint and configuration (e.g., girth, seam).

9D.12.3 Technical Basis

The recommended guidance for repair welds presented here is a simplified version of the procedure in reference [4]. This guidance applies to partial-thickness repair welds of all lengths and configurations, where the repair depth is denoted by t_w (see Figure 9D.16), in a section of overall thickness t. A residual stress distribution of uniform yield is assumed over the entire repair depth (t_w), which linearly attenuates to zero over the remaining thickness, in both the perpendicular (transverse) and parallel (longitudinal) directions.

9D.13 Welding Simulation-Based Stress Distributions

9D.13.1 General

Finite Element Methods for simulation of stresses due to welding are becoming mature, simplified, appropriate for determining stress profiles for FFS Assessment, and practical to apply in certain situations. Such situations may arise due to the simplified nature of the residual stress distributions, which will inevitably be overly-conservative for some cases. Correspondingly, simulation may be used to help judge the conservatism for a specific joint and flaw location. Any welding simulation applied to FFS activities should employ established verification and validation (V&V) guidance; specifically, the guidance of reference [32].

Simplified methods are appropriate for determining the shape of through-wall stress distributions, and their attenuation behavior. The trends obtained should always be referenced to the nominal yield strength, σ_{ys}^{r}, consistent with the bounding stress distributions of this Annex. Simulation should not generally be used with the intent of justifying stress distributions with maximum values lower than σ_{ys}^{r}, due to the inherent uncertainty in the welding process, material properties, and employed simulation methods and models. If such an approach is pursued in certain exceptional situations, then an accompanying experimental program is typically required, such as illustrated in reference [33].

If the simplified method described in the next section is used for generating residual stress trends (and not magnitudes), a substantial portion of the generally required validation (comparison to actual behavior) is alleviated. Enough validation shall be performed to ensure that the generated results are suitable in the experience of the analyst (for example, comparison to similar published results, or comparison to the distributions recommended in this Annex at common locations); however, specific experimental results are not generally required. Verification (which ensures that the mathematical model is functioning correctly), (see reference [32]) is always required.

9D.13.2 Description of Simplified Method

The following simplified method can be used to determine stress distribution shapes and attenuation behavior in pressure vessel and piping components. This approximate method should not be used when accurate stress magnitudes or local stress details are desired. In these cases, advanced material models and simulation techniques are required, typically including three-dimensional traveling torch methods as shown in references [33] and [34] that illustrate the required analysis complexity when trying to accurately predict the residual stresses in even relatively simple configurations. Note that even simplified simulation requires proficiency in non-linear thermal-stress finite element analysis and should be pursued with caution.

The simplified method for determining the residual stress distribution in a welded joint consists of the following:

a) Two-dimensional (2D) axisymmetric or generalized plane strain finite element analysis: while 2D welding simulation is not generally valid, it has been shown to generate useful trends (see for example references [32], [35], [36], and [37]) which is the goal of simulation in this Annex.

b) Material properties: material properties corresponding to austenitic stainless steel may be assumed, irrespective of the actual material(s) properties. It should be understood that stress distributions generated in this way may deviate significantly from typical distributions of non-austenitic stainless steels, due to solid state phase transformations and related phenomena. However, this assumption should give reasonably conservative stress profiles (see references [38]) while eliminating the complexity of solid state phase transformations, which is a very significant analysis simplification.

c) Uniform assigned temperature thermal analysis: the critical input to any (arc) welding simulation is the power transferred to the work piece through the welding arc. In general welding simulation, this input must be

known, and reaction fluxes from the simulation verified to balance the applied power input (see references [32] and [35]). The most direct way to apply the welding power in a simulation is through distributed power density models (FEA heat flux). A comprehensive discussion of such approaches is provided in references [32] and [39]. However, these approaches also typically require special programming to implement. The conjugate to a heat flux implementation is an assigned temperature. In 2D simulation, this approach is easy to implement and consists of ramping the edge of the weld pass being introduced up to the (initial high) temperature of the weld pass itself, and then removing any temperature assignment conditions and allowing the transient conduction solution to develop. The welding power does not need to be known in this case, though to achieve equivalent heat inputs typical of actual welding processes, a preheat time of several seconds and an assigned temperature greater than the metal melting temperature are required (see references [35] and [40]). This method, when implemented correctly, also gives meaningful prediction of residual stress trends as shown in reference [41], and is therefore recommended due to its simplicity.

d) Use of a cutoff temperature: High temperature material properties can be required for an advanced welding simulation, spanning the range from room temperature to beyond the melting temperature. Typically, properties approaching the melting temperature are unknown, and existing standard models are inadequate to capture the actual material response (see reference [32]). A convenient solution is to impose a cutoff temperature in the mechanical analysis, above which stress and strain are not calculated. The weld metal is defined as stress free at the cutoff temperature (it shrinks as it cools), and the temperature history is filtered with a simple subroutine to reset any (thermal analysis) temperatures greater than the cutoff temperature equal to the cutoff temperature. A cutoff temperature of $0.8T_m$ (melt temperature in degrees Kelvin) is typically used. Above $0.8T_m$ high temperature phenomena (such as rapid stress relaxation and dynamic recrystallization) dominate the material response and stresses that would be modeled in finite element analysis at these temperatures would have no physical meaning (see references [32], [39], [41], and [35]). The cutoff temperature is also used as an annealing temperature where any accumulated hardening (equivalent plastic strain) is reset to zero. If a cutoff temperature is not used, or if higher cutoff temperatures are employed, extreme care should be exercised in specification of the material properties and models in the high temperature range, since they can have a profound effect on the final stress results in some cases.

e) Isotropic hardening metal plasticity with annealing: the choice of hardening model has a profound effect on the simulation results obtained. It has recently been identified as one of the most critical inputs, with complex models generally required for accurate residual stress prediction (see references [34], and [35] through [45]). However, the simplest metal plasticity model, isotropic hardening, can still give meaningful trends. This can be deduced by inspection of the stress result trends in references [34], and [35] through [45]. A multiple backstress non-linear kinematic hardening model should be considered as a more accurate simulation option, even for the simplified method, but must be implemented with care (see reference [35]). In all cases, accumulated equivalent plastic strain that exists in the solution must be reset to zero when the melting (or cutoff) temperature is reached.

Further details on this simplified method can be found in references [35] and [40].

9D.13.3 Simulation References

A number of references exist for welding simulation, and can be consulted for further background, or guidance on more advanced techniques. In addition to references [36], [39], and [41], references [46] through [50] also provide

valuable information. These references address the full range of advanced simulation topics, including solid state phase transformations typical of carbon and low allow steels.

9D.14 Nomenclature

C_{ul} unit's conversion constant: equal to 1.0 if the thickness is expressed in mm and 25.4 if the thickness is expressed in inches.

I welding current used.

ID inside diameter or internal surface.

L_s transverse stress attenuation distance in the shell.

OD outside diameter or external surface.

$\dot{q}$ linear heat input to the weld.

r mean radius of the pipe, cylindrical, or spherical shell, as applicable.

r_s mean radius of the pipe, cylindrical, or spherical shell, as applicable, for corner joint calculations.

r_c chord length of the spherical shell.

t nominal wall thickness of the component.

t_n wall thickness of the nozzle.

t_s wall thickness of the shell.

t_1 wall thickness of the main plate.

t_2 wall thickness of the stay plate.

t_w repair weld depth.

u welding travel speed.

V welding voltage used.

w weld width.

x local coordinate defined through the wall thickness of the component to define the residual stress distribution.

y local coordinate defined along the surface of the component to define the residual stress distribution.

β thickness-dependent residual stress scaling factor.

η welding arc efficiency.

σ_{ys} specified minimum yield strength.

σ_{ys}^{r} magnitude of the effective yield strength to be used to estimate the residual stress at a welded joint.

σ^{r} residual stress distribution either through thickness or along surface.

σ_i^r residual stress at the inner surface.

σ_o^r residual stress at the outer surface.

σ_m^r residual stress at the interior (for plate tee joint welds).

9D.15 References

[1] API 579-1/ASME FFS-1, *Fitness-For-Service*, 2nd Edition, The American Petroleum Institute, 2007.

[2] API Recommend Practice 579 (API RP 579), *Fitness-For-Service*, 1st Edition, The American Petroleum Institute, 2000.

[3] EDF Energy Nuclear Generation Limited, *Assessment of the Integrity of Structures Containing Defects*, EDF Energy Nuclear Generation Limited R-6, Nuclear Electric, Revision 4, 2001.

[4] BS7910. Guidance on Methods for Assessing the Acceptability of Flaws in Metallic Structures. British Standards Institute, London, UK. 2005.

[5] FITNET Fitness-For-Service (FFS) – Procedure (Volume 1) ISBN 978-3-940923-00-4, Koçak, M., Webster, S., Janosch, J.J., Ainsworth, R.A., Koers, R. and FITNET Fitness-For-Service (FFS) – Annex (Volume 2) ISBN 978-3-940923-01-1, Koçak, M., Hadley, I., Szavai, S., Tkach, Y., Taylor, N., both printed by GKSS Research Center, Geesthacht, 2008.

[6] Sharples, J., P. Gill, L. Wei and S. Bate, 2011, "Revised Guidance on Residual Stresses in BS7910," PVP2011-57071, ASME 2011 Pressure Vessels and Piping Conference, ASME, New York.

[7] Michaleris, P., M. Kirk, and K. Laverty, 1996, "Incorporation of Residual Stresses into Fracture Assessment Models," Final Report, EWI Project No. J7412, submitted to the Materials Properties Council, New York.

[8] Koppenhoefer, K.C., Z. Feng, and W. Cheng, 1998, "Incorporation of Residual Stresses Caused by Welding into Fracture Assessment Procedures," Final Report, EWI Project No. 40568-CSP, MPC No. FS-II-5, submitted to the Materials Properties Council, New York.

[9] Mohr, W.C., P. Michaleris and M.T. Kirk, 1996, "An Improved Treatment of Residual Stresses in Flaw Assessment of Pipes and Pressure Vessels Fabricated from Ferritic Steels," *ASME 1996 Pressure Vessels and Piping Conference*, ASME, New York.

[10] Mohr, W.C., 1996, "Internal Surface Residual Stresses in Girth Butt-Welded Pipes," Residual Stresses in Design, Fabrication, Assessment and Repair," PVP-Vol. 327. ASME, New York.

[11] Michaleris, P., 1996, "Residual Stress Distributions for Multi-Pass Welds in Pressure Vessel and Piping Components," *ASME 1996 Pressure Vessels and Piping Conference*, ASME, New York.

[12] Dong, P., Z. Cao, and J.K. Hong, 2007, "Final PVRC Residual Stress and Local PWHT JIP on Investigation of Weld Residual Stresses and Local Post-Weld Heat Treatment," submitted to PVRC JIP Sponsors, Center for Welded Structures Research, Battelle Laboratories, Columbus, OH.

[13] Dong, P., and J.K. Hong, 2002, "Recommendations for Determining Residual Stresses in Fitness-For-Service Assessment," WRC Bulletin 476, Welding Research Council, Inc., New York, NY.

[14] Dong, P., and J.K. Hong, 2007, "On the Residual Stress Profiles in New API 579/ASME FFS-1 Appendix E," Welding in the World, Doc. IIW-1803-07, The International Institute of Welding, France.

[15] Cao, Z., 2007, “Weld Residual Stress Distribution Characterization of Pipe Girth/Seam Welds – Technical Details for The Appendix E of API 579,” Center for Welded Structures Research, Battelle Laboratories, Columbus, OH.

[16] Bate, S.K., Green, D. and Buttle, D., “A Review of Residual Stress Distributions in Welded Joints for the Defect Assessment of Offshore Structures,” Health and Safety Executive – Offshore Technology Report OTH 482, 1997.

[17] Scaramangas, A. and R.F.D. Porter Goff, 1985, “Residual Stresses in Cylinder Girth Butt Welds,” OTC 5024, 17th Annual Offshore Technology Conference, Houston, TX.

[18] Scaramangas, A., “Residual Stresses in Girth Butt Welded Pipes,” Ph.D. dissertation, Cambridge University, May 1984.

[19] Bouchard, P.J., 2007, “Validated residual stress profile for fracture assessments of stainless steel pipe girth welds,” International Journal of Pressure Vessels and Piping (84), pp. 195–222.

[20] Zhang, Y.-H., S. Smith, L. Wei, and C. Johnston, 2012, “Residual stress measurements and modeling,” Submitted to the Health and Safety Executive, TWI Ltd., Cambridge, UK.

[21] Stout, R.D., *Postweld Heat Treatment of Pressure Vessel Steels,* WRC Bulletin 302, Welding Research Council, Inc., New York, NY, 1985.

[22] Chen, P.S., Herman, W.A., and Pense, A.W., *Relaxation Stresses in Pressure Vessels*, WRC Bulletin 302, Welding Research Council, Inc., New York, NY, 1985.

[23] Zhou, R.J., Pense, A.W., Basehore, M.L., and Lyons, D.H., *A Study of Residual Stresses in Pressure Vessel Steels*, WRC Bulletin 302, Welding Research Council, Inc., New York, NY, 1985.

[24] McEnerney, J.W., and Dong, P., *Recommended Practices for Local Heating of Welds in Pressure Vessels*, WRC Bulletin 452, Welding Research Council, Inc., New York, NY, 2000.

[25] Murakawa, H., Wang, J., Hao, L., and Horii, Y., *Suitable Heating Conditions in Local Post Weld Heat Treatment*, WRC Bulletin 485, Welding Research Council, Inc., New York, NY, 2003.

[26] Burdekin, F.M., “Local Stress Relief of Circumferential Butt Welds in Cylinders,” British Welding Journal, September 1963, pp. 483-490.

[27] Wimpory, R.C., May, P.S., O’Dowd, N.P., Webster, G.A., Smith, D.J., and Kingston, E., “Measurement of Residual Stresses in T-Plate Weldments,” Journal of Strain Analysis, Vol. 38, No. 4, pp. 349-365, 2003.

[28] Kassab, R.K., Champilaud, H. Van Lê, N., Lanteigne, J., and Thomas, M., “Experimental and Finite Element Analysis of a T-Joint Welding,” Journal of Mechanical Engineering and Automation, Vol. 2, pp. 411-421, 2012.

[29] Barsoum, Z. and Lundbäck, A., “Simplified FE Welding Simulation of Fillet Welds – 3D Effects on the Formation Residual Stresses,” Engineering Failure Analysis, Vol. 16, pp. 2281-2289, 2009.

[30] Teng, T.-L., Fung, C.-P., Chang, P.-H., and Yang, W.-C., “Analysis of Residual Stresses and Distortions in T-Joint Fillet Welds,” International Journal of Pressure Vessel and Piping, Vol. 78, pp. 523-538, 2001.

[31] Andersen, L.F., “Residual Stresses and Deformations in Steel Structures,” Ph.D. dissertation, Technical University of Denmark, December 2000.

[32] AWS A9.5:2013, “Guide for Verification and Validation in Computational Weld Mechanics,” American

Welding Society, USA, 2013.

[33] Smith, M.C. et al, “Review of the NeT Task Group 1 Single Weld Bead on Plate Benchmark Round Robin,” EDF Energy Report E/REP/BBGB/0074/GEN/11, Revision 0, October 2011. EDF Energy, UK.

[34] Muransky, O., Hamelin, C., Smith, M., Bendeich, P., and Edwards, L., “The Effect of Plasticity Theory on Predicted Residual Stress Fields in Numerical Weld Analyses,” Journal of Computational Material Science, Vol. 54, pp. 125-134, 2012.

[35] Dewees, D.J., P.E. Prueter, S.R. Kummari, R.G. Brown, K.J. Smith, T.L. Thome, C.H. Panzarella, M.F.P. Bifano, and D.A. Osage, *Development of Revised Weld Residual Stress Guidance for Fitness-For-Service Assessments in API 579-1/ASME FFS-1,* Welding Research Council, Inc., New York, NY, 2014.

[36] Radaj, D., Welding Residual Stresses and Distortion: Calculation and Measurement, Germany, DVS Verlag, 2003.

[37] Ku, F.H., and S.S. Tang, 2012, “Investigative Study of 2-D vs. 3-D Weld Residual Stress Analyses of the NRC Phase II Mockup,” PVP2012-78760, *ASME 2012 Pressure Vessels and Piping Conference*, ASME, New York.

[38] McDill, J.M.J., Oddy, A.S., Goldak, J.A., and Bennison, S., “Technical Note: Finite Element Analysis of Weld Distortion in Carbon and Stainless Steels,” Journal of Strain Analysis, Vol. 25, No. 1, pp. 51-53, 1990.

[39] Goldak, J.A., and Akhlaghi, M., *Computational Welding Mechanics*, Springer, New York, 2005.

[40] Dewees, D., “Comparison of Heat Input Methods in Welding Residual Stress Analysis,” PVP2012-78574, ASME 2012 Pressure Vessels and Piping Conference, ASME, New York.

[41] Lindgren, L.E., Computational Welding Mechanics: Thermomechanical and Microstructural Simulations, CRC Press, Boca Raton, USA and Woodhead Publishing Ltd., Cambridge, England, 2007.

[42] Rathbun, H., L.F. Fredette, P.M. Scott, A.A. Csontos and D.L. Rudland, 2011, “NRC Welding Residual Stress Validation Program International Round Robin Program and Findings,” PVP2011-57642, *ASME 2011 Pressure Vessels and Piping Conference*, ASME, New York.

[43] Joosten, M.M. and M.S. Gallegillo, 2012, “A Study of the Effect of Hardening Model in the Prediction of Welding Residual Stress,” PVP2012-78055, *ASME 2012 Pressure Vessels and Piping Conference*, ASME, New York.

[44] Smith, M.C. et al, 2010, “The Impact of Key Simulation Variables on Predicted Residual Stresses in Pressurizer Nozzle Dissimilar Metal Weld Mock-Ups. Part 2 – Comparison of Simulation and Measurements,” PVP2010-26025, *ASME 2010 Pressure Vessels and Piping Conference*, ASME, New York.

[45] Kerr, M., and H. Rathbun, 2012, “Summary of Finite Element (FE) Sensitivity Studies Conducted in Support of the NRC/EPRI Welding Residual Stress (WRS) Program,” PVP2012-78883, *ASME 2012 Pressure Vessels and Piping Conference*, ASME, New York.

[46] Lindgren, L.E., Modeling for Residual Stresses and Deformations Due to Welding - Knowing What is Not Necessary to Know, Editors: Cerjak, H. & Bhadeshia, H. K. D. H., Mathematical Modeling of Weld Phenomena 6: 491–518.

[47] Lindgren, L.E., “Finite Element Modelling and Simulation of Welding, Part 1 Increased Complexity,” Journal of Thermal Stresses Vol. 24, pp. 141–192, 2001.

[48] Lindgren, L.E., “Finite Element Modelling and Simulation of Welding, Part 2 Improved Material Modeling,” Journal of Thermal Stresses, Vol. 24, pp. 195–231, 2001.

[49] Lindgren, L.E., “Finite Element Modelling and Simulation of Welding, Part 3 Efficiency and Integration,” Journal of Thermal Stresses, Vol. 24, pp. 305–334, 2001.

[50] Processes and Mechanisms of Welding Residual Stress and Distortion, Z. Feng, ed. Woodhead Publishing Limited, Cambridge, England. 2005.

9D.16 Tables

Table 9D.1 – Heat Input Based on Welding Process

Welding Process	Heat Input (KJ/in)			
	Ferritic Steels		Stainless Steel	
	Average	Upper Bound	Average	Upper Bound
SMAW (1)	28.7	46.7	23.9	33.8
SAW (2)	31.0	49.3	27.4	48.8
GTAW (3)	12.7	25.4	12.7	24.0
GMAW (4)	9.9	18.3	9.9	18.3

Notes:

1. Based on 1/8 inch electrode, 6 in/min (0.1 in/sec) travel speed, for carbon steel: average 115A-25V, upper bound 180A-26V, for stainless steel: average 95A-25V, upper bound 130A-26V.
2. Based on 5/32 inch electrode, 35 in/min (0.58 in/sec) travel speed, for carbon steel: average 600A-30V, upper bound 800A-36V, for stainless steel: average 500A-32V, upper bound 750A-38V.
3. Based on 3/32 inch electrode, 6 in/min (0.1 in/sec) travel speed, for carbon steel: average 90A-14V, upper bound 160A-16V, for stainless steel: average 90A-14V, upper bound 150A-16V.
4. Based on 0.035 inch electrode, 12 in/min (0.2 in/sec) travel speed, for carbon steel: average 110A-18V, upper bound 175A-21V, for stainless steel: average 100A-20V, upper bound 160A-23V.

Table 9D.1M – Heat Input Based on Welding Process

Welding Process	Heat Input (J/mm)			
	Ferritic Steels		Stainless Steel	
	Average	Upper Bound	Average	Upper Bound
SMAW (1)	1130	1840	940	1330
SAW (2)	1220	1940	1080	1920
GTAW (3)	500	1000	500	944
GMAW (4)	390	720	390	720

Notes:

1. Based on 3.2 mm electrode, 152 mm/min (2.5 mm/sec) travel speed, for carbon steel: average 115A-25V, upper bound 180A-26V, for stainless steel: average 95A-25V, upper bound 130A-26V.
2. Based on 4 mm electrode, 889 mm/min (15 mm/sec) travel speed, for carbon steel: average 600A-30V, upper bound 800A-36V, for stainless steel: average 500A-32V, upper bound 750A-38V.
3. Based on 2.3 mm electrode, 152 mm/min (2.5 mm/sec) travel speed, for carbon steel: average 90A-14V, upper bound 160A-16V, for stainless steel: average 90A-14V, upper bound 150A-16V.
4. Based on 0.9 mm electrode, 305 mm/min (5 mm/sec) travel speed, for carbon steel: average 110A-18V, upper bound 175A-21V, for stainless steel: average 100A-20V, upper bound 160A-23V.

9D.17 Figures

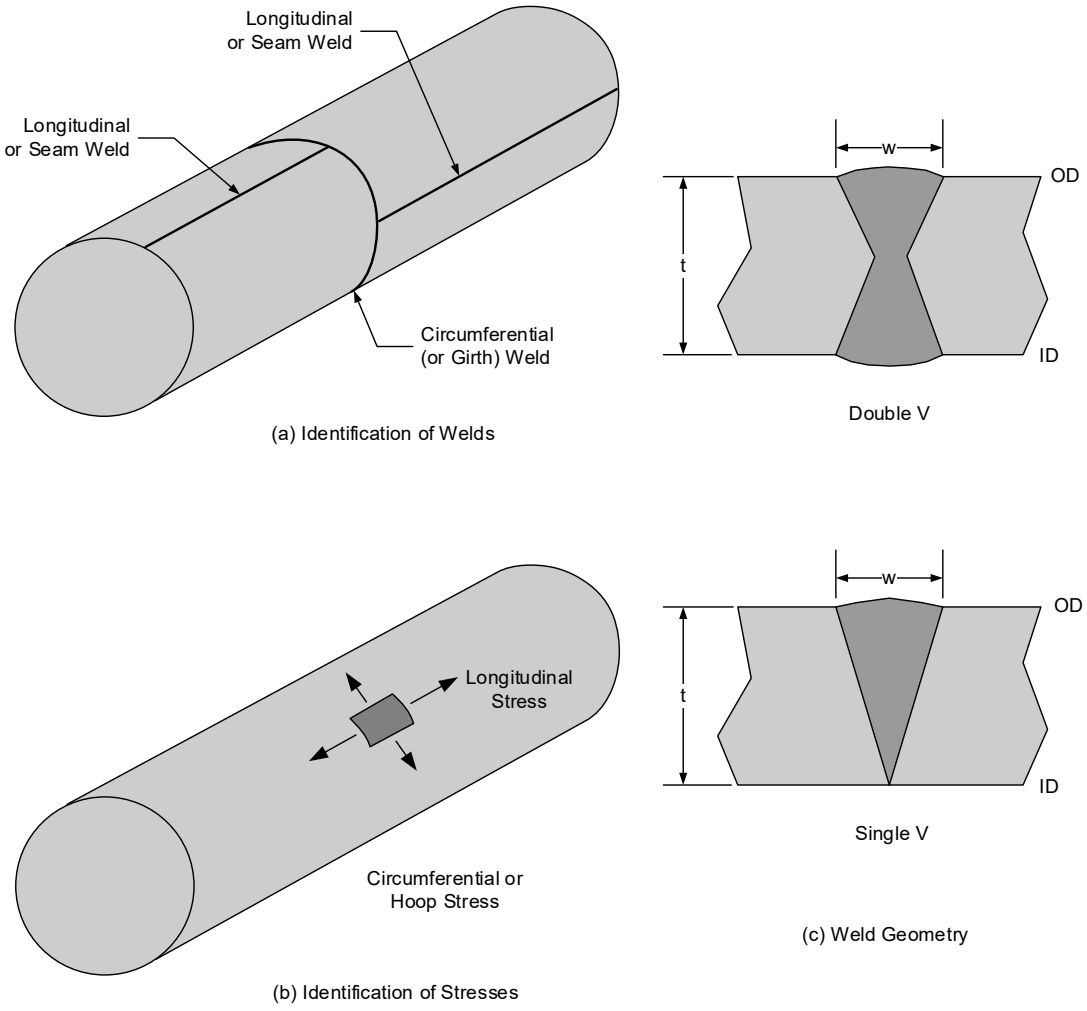

Definition of Stress Directions		
Weld Seam	**Stress Component Perpendicular to the Weld Seam**	**Stress Component Parallel to the Weld Seam**
Longitudinal	Circumferential (Hoop) Stress	Longitudinal Stress
Circumferential (Girth)	Longitudinal Stress	Circumferential (Hoop) Stress

Figure 9D.1 – Weld Locations and Stress Directions in a Cylindrical Shell

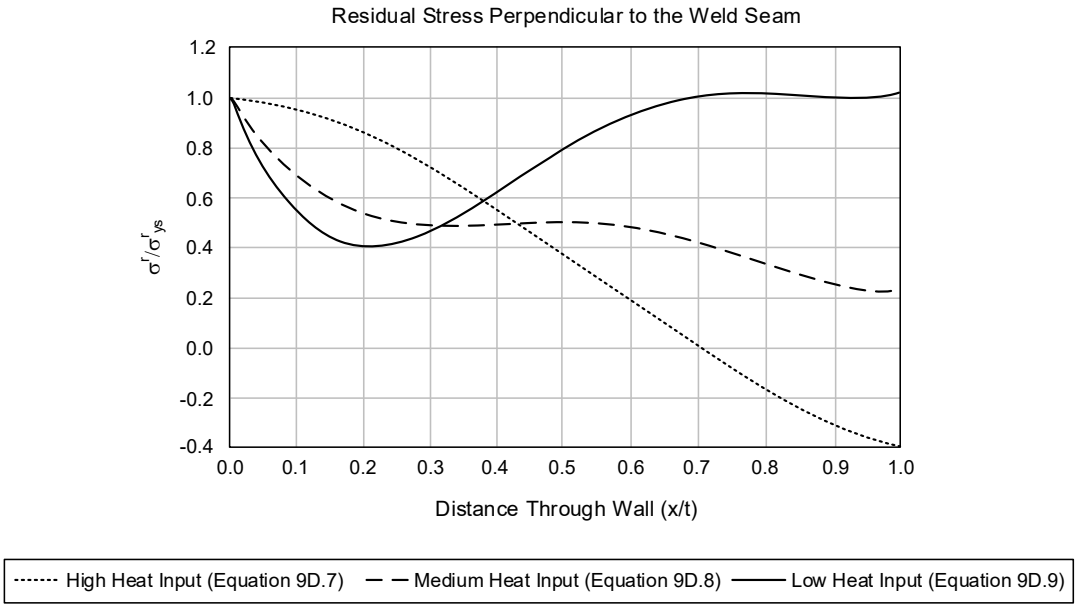

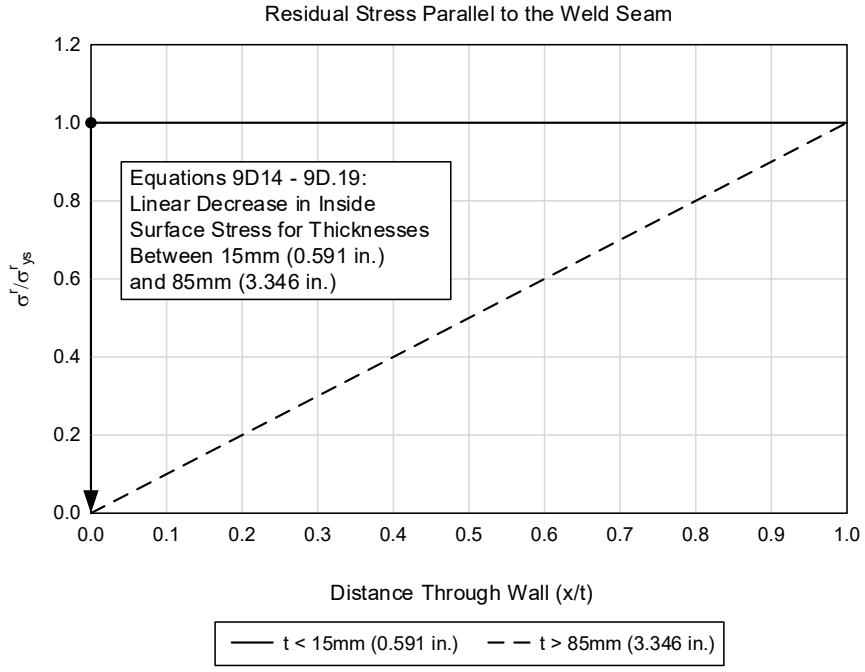

Figure 9D.2 – Residual Stress Through-Wall Distributions for Full Penetration Circumferential Welds in Piping and Pressure Vessel Cylindrical Shells

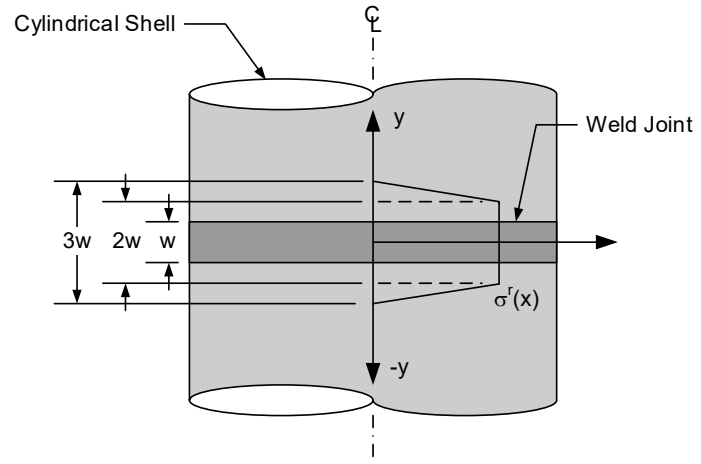

Variation of Stress
Parallel to Weld

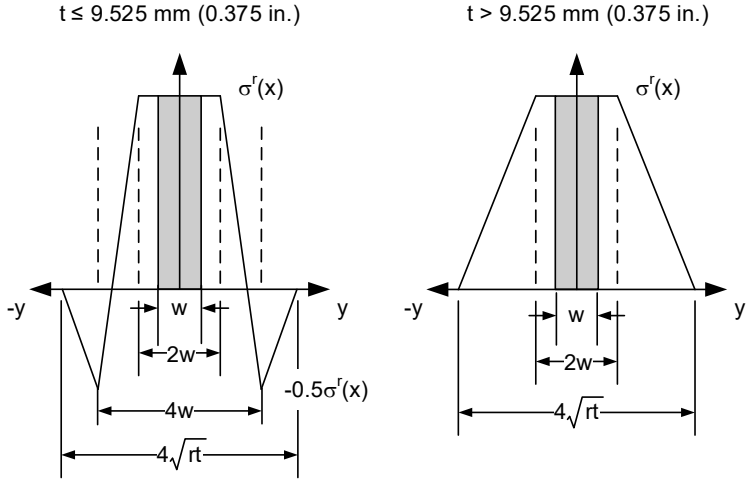

Variation of Stress
Perpendicular to Weld

Figure 9D.3 – Residual Stress Variation for Full Penetration Circumferential Welds in Piping and Pressure Vessel Cylindrical Shells with Distance from Weld Centerline

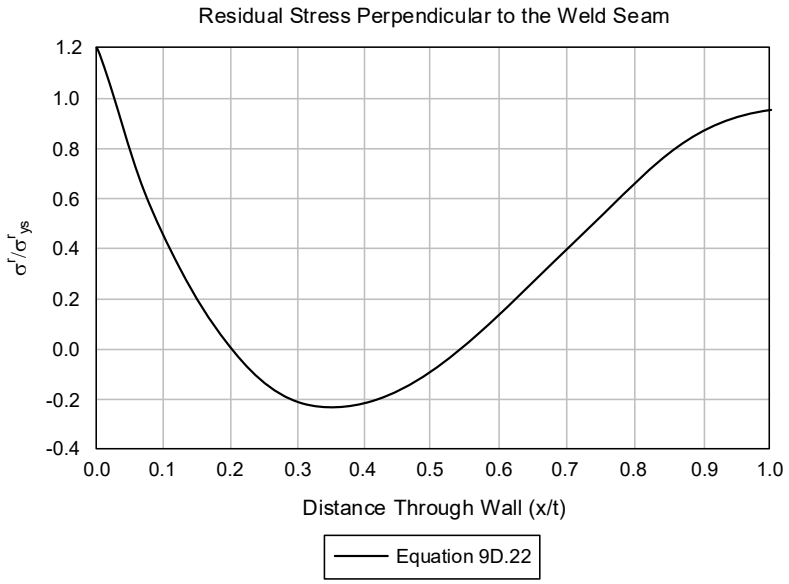

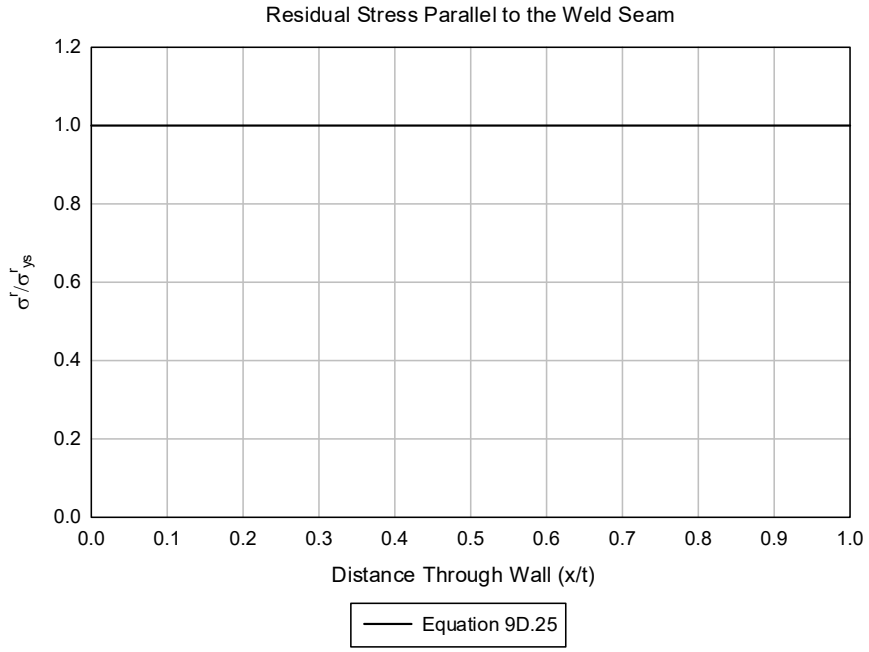

Figure 9D.4 – Residual Stress Through-Wall Distributions for Full Penetration Longitudinal Welds in Piping and Pressure Vessel Cylindrical Shells with Distance from Weld Centerline

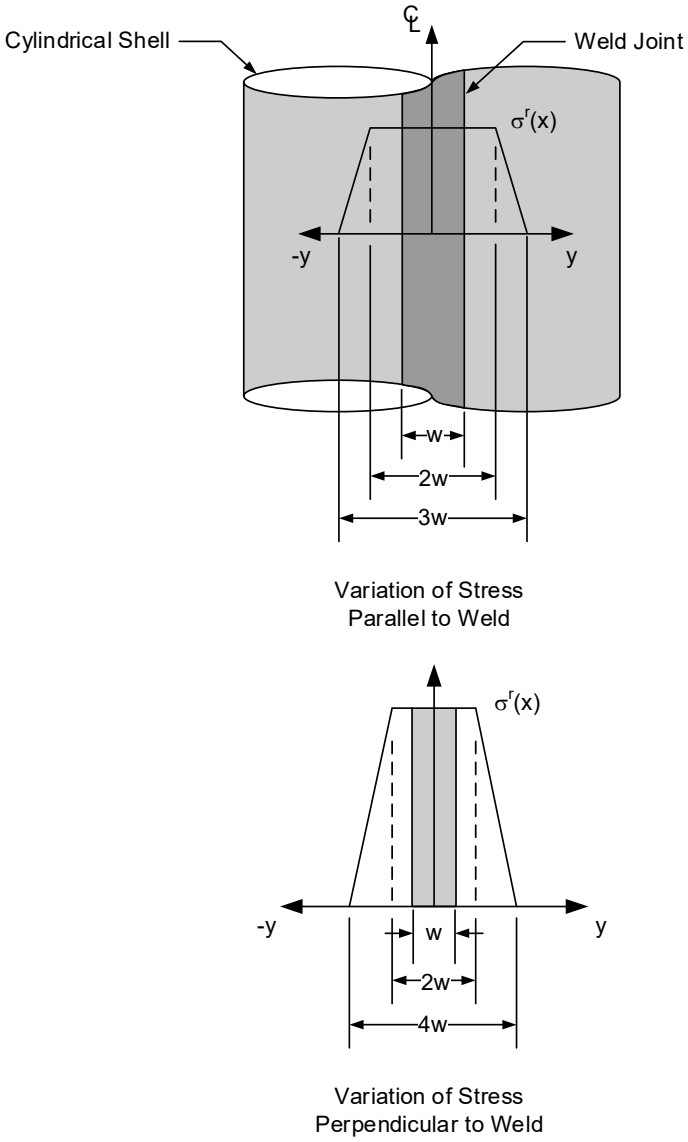

Figure 9D.5 – Residual Stress Variation for Full Penetration Longitudinal Welds in Piping and Pressure Vessel Cylindrical Shells with Distance from Weld Centerline

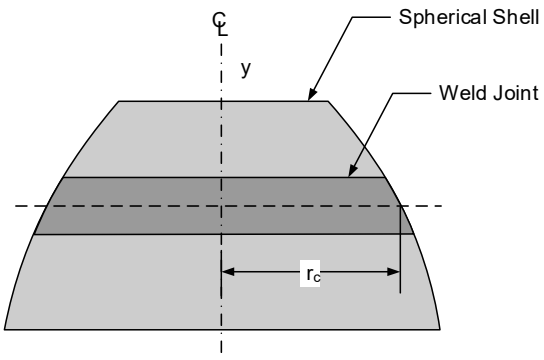

(a) Illustration of Chord Length, r_c

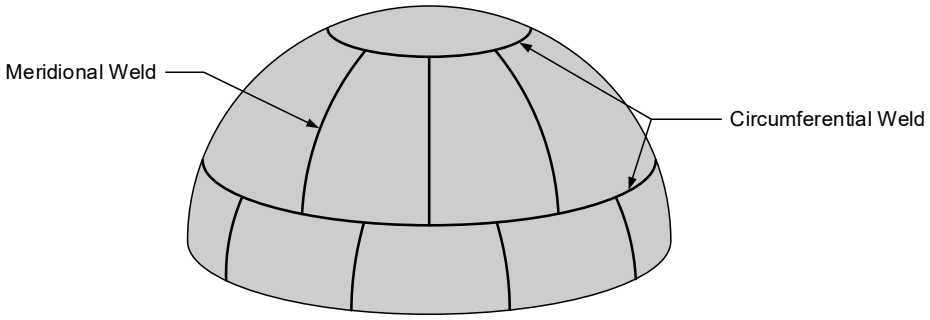

(b) Identification of Welds

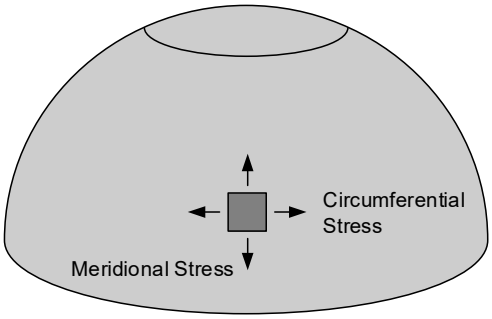

(c) Identification of Stresses

Definition of Stress Directions		
Weld Seam	**Stress Component Perpendicular to the Weld Seam**	**Stress Component Parallel to the Weld Seam**
Meridional	Circumferential Stress	Meridional Stress
Circumferential (Girth)	Meridional Stress	Circumferential Stress

Figure 9D.6 – Weld Locations and Stress Directions in a Spherical Shell or Formed Head

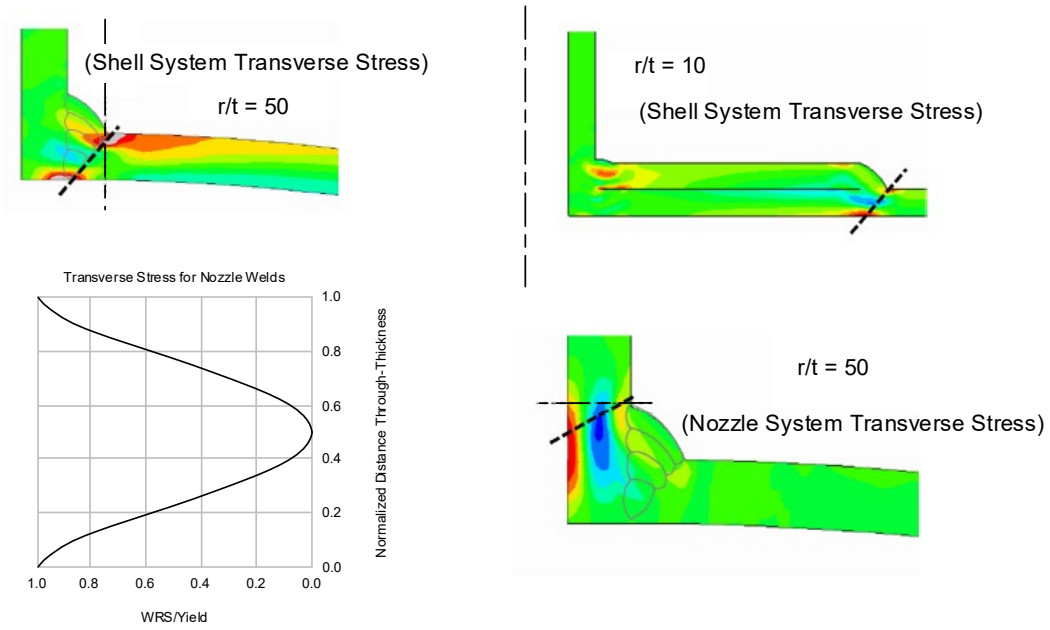

(a) Illustration of Profile Basis for Transverse Stress

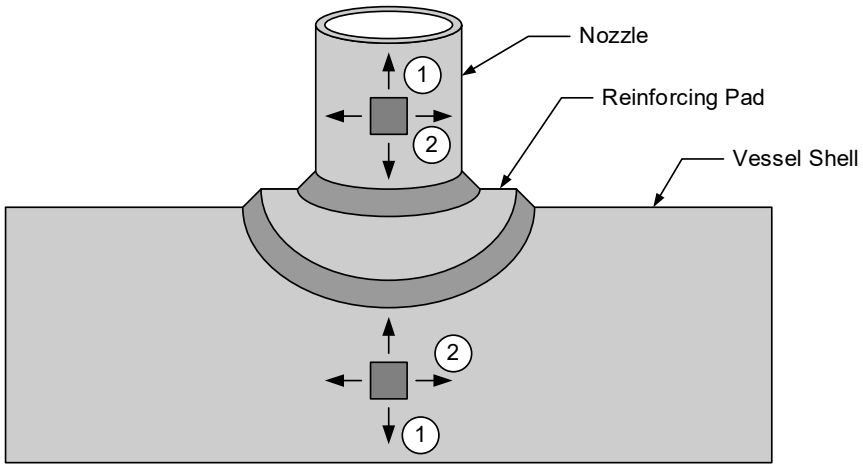

(1) - Stress Perpendicular to the Weld Direction (2) - Stress Parallel to the Weld Direction

(b) Identification of Stresses

Figure 9D.7 – Corner Joint (Nozzle Attachment) Illustration and Stress Direction Definitions

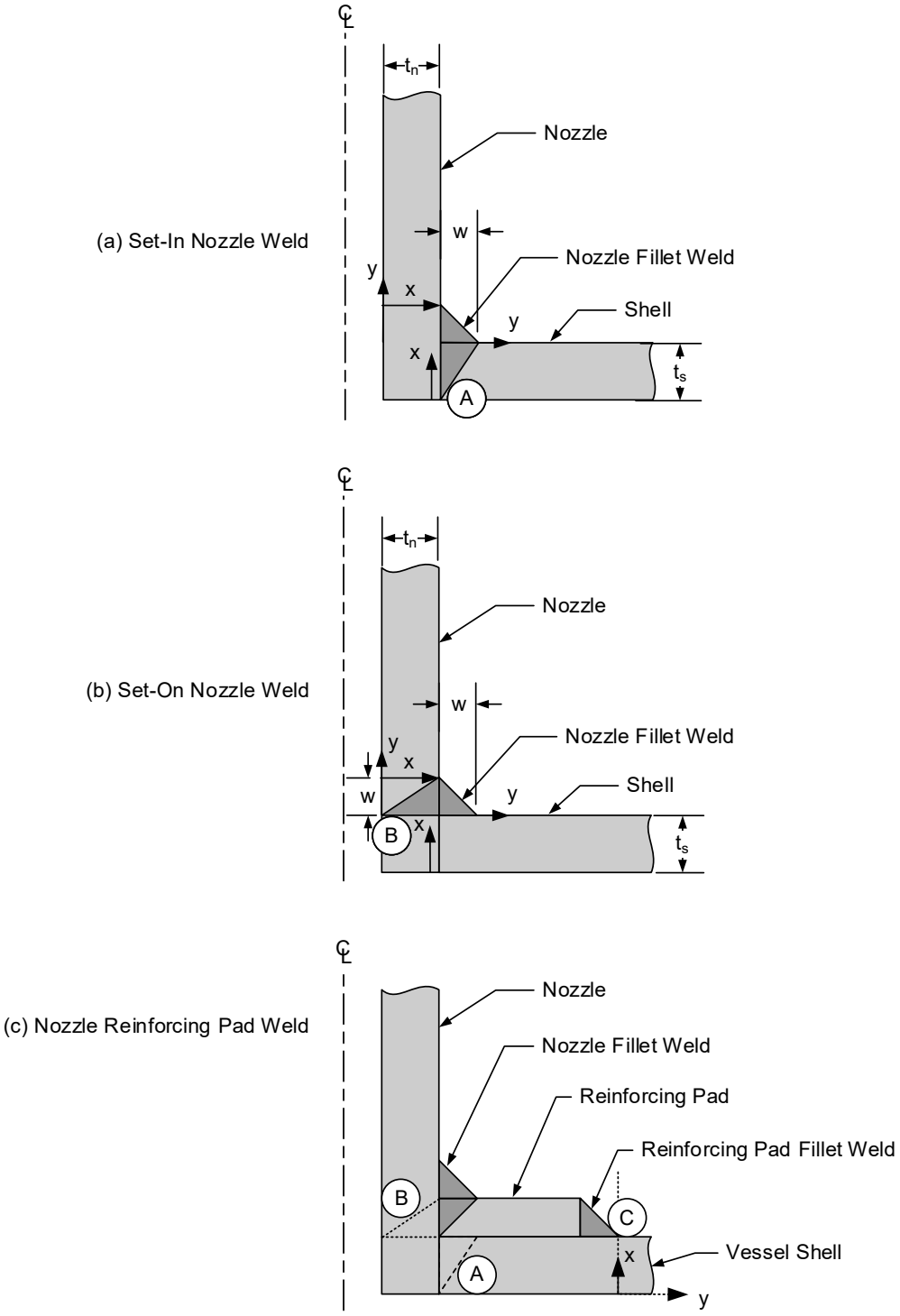

Figure 9D.8 – Corner Joint (Nozzle Attachment) Weld Locations

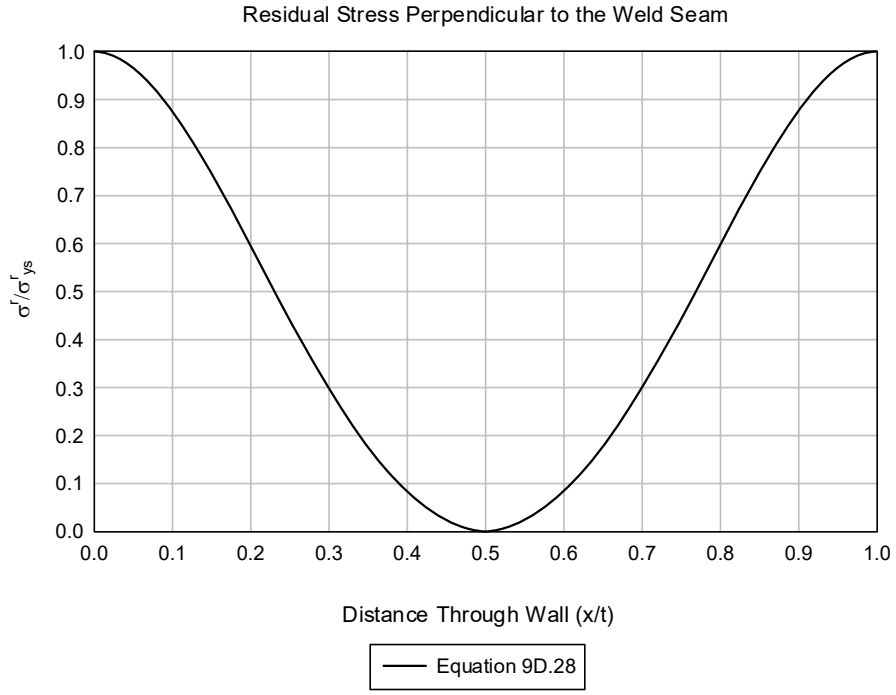

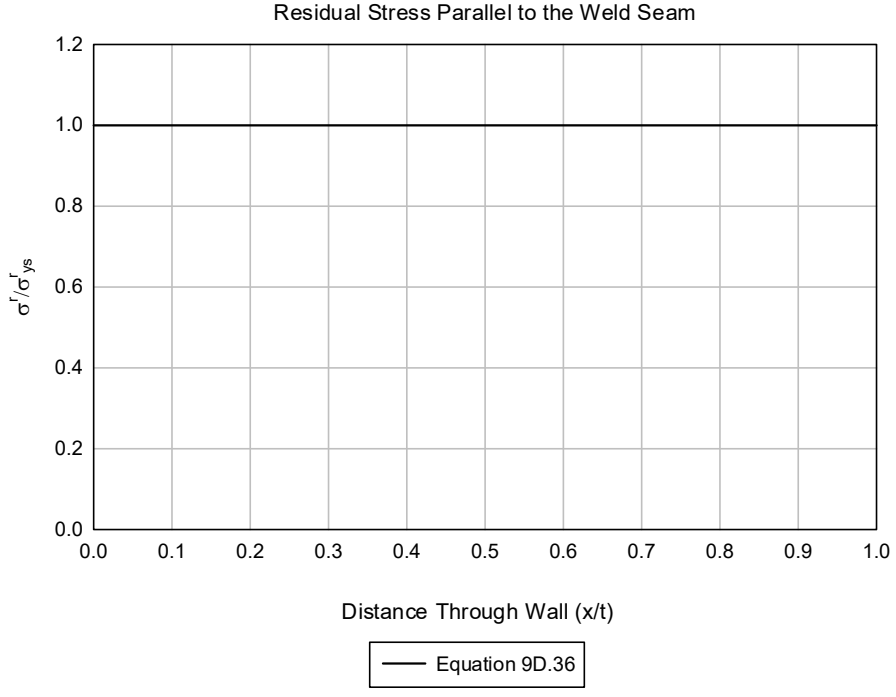

Figure 9D.9 – Residual Stress Through-Wall Distributions for Corner Joint Weld Locations

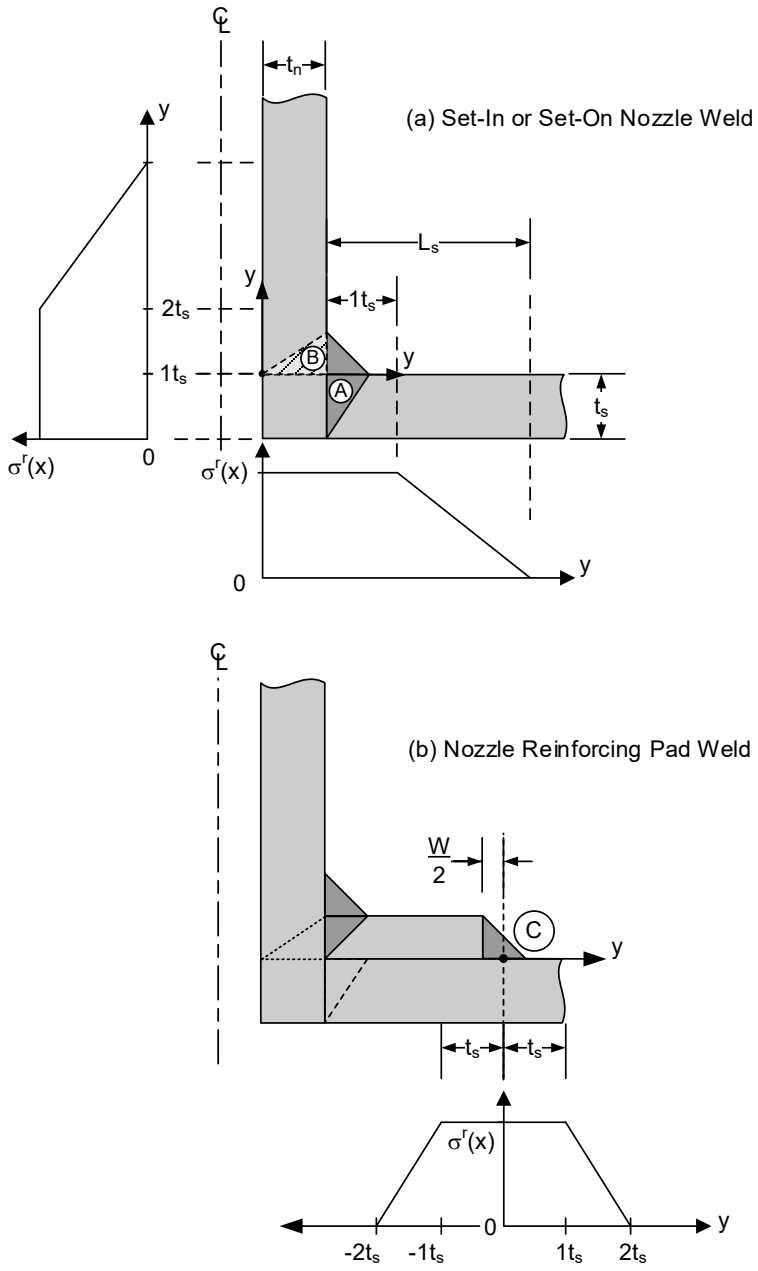

Figure 9D.10 – Variation of Stress Distribution Perpendicular to the Weld for Corner Joint Weld Locations with Distance from Weld Centerline

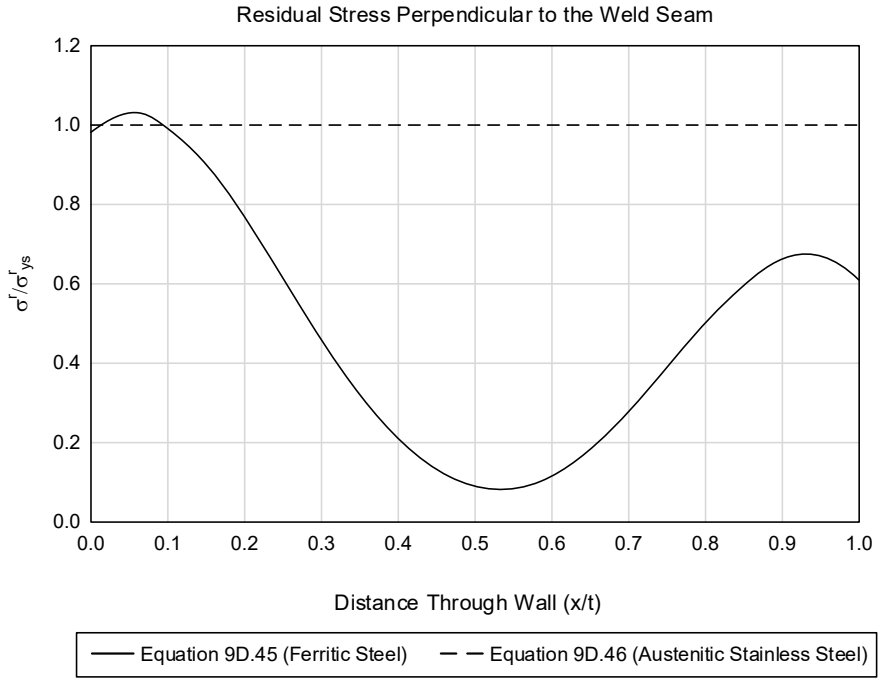

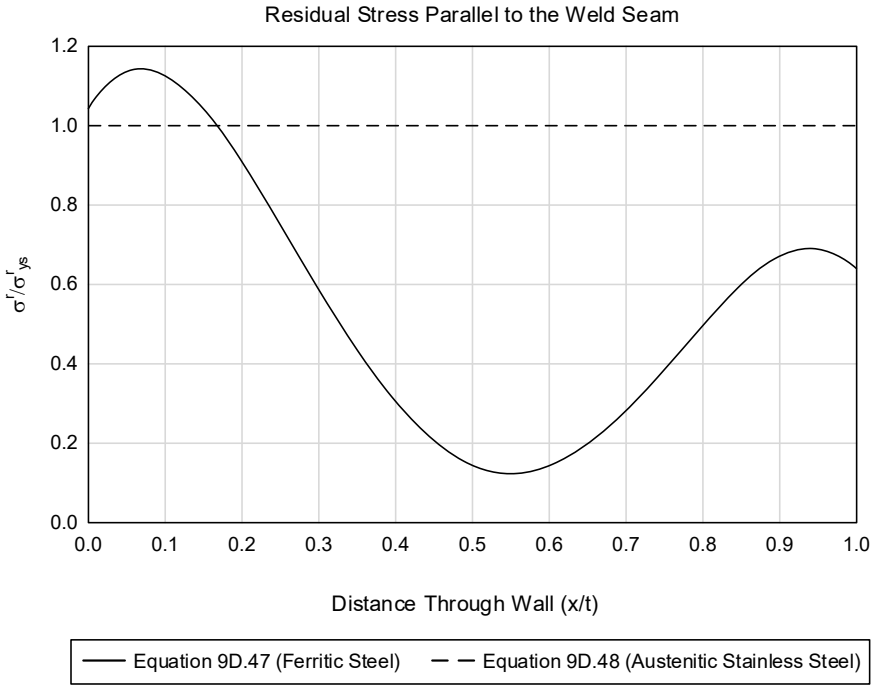

Figure 9D.11 – Residual Stress Through-Wall Distributions for Piping Branch Connections

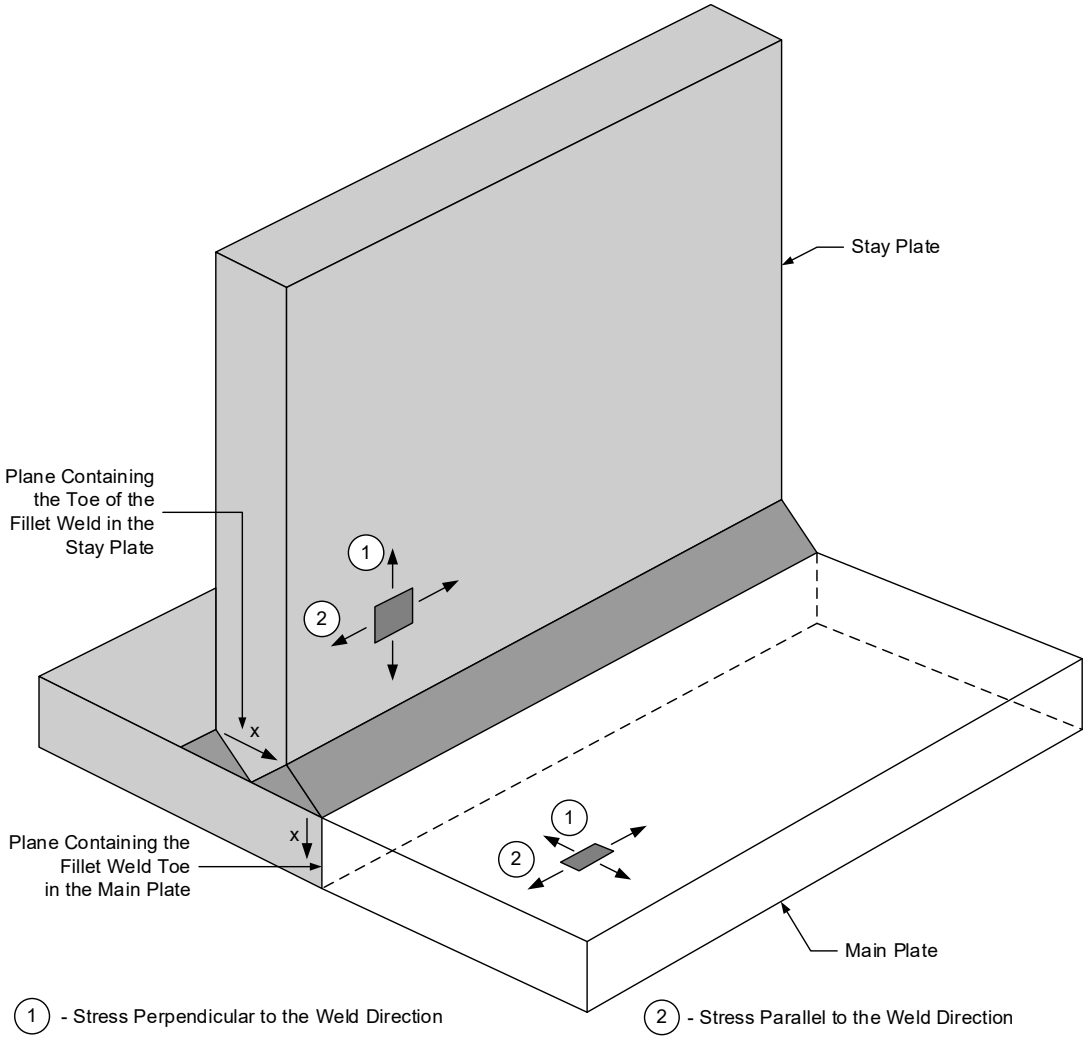

Figure 9D.12 – Weld Locations and Stress Directions in a Tee Joint

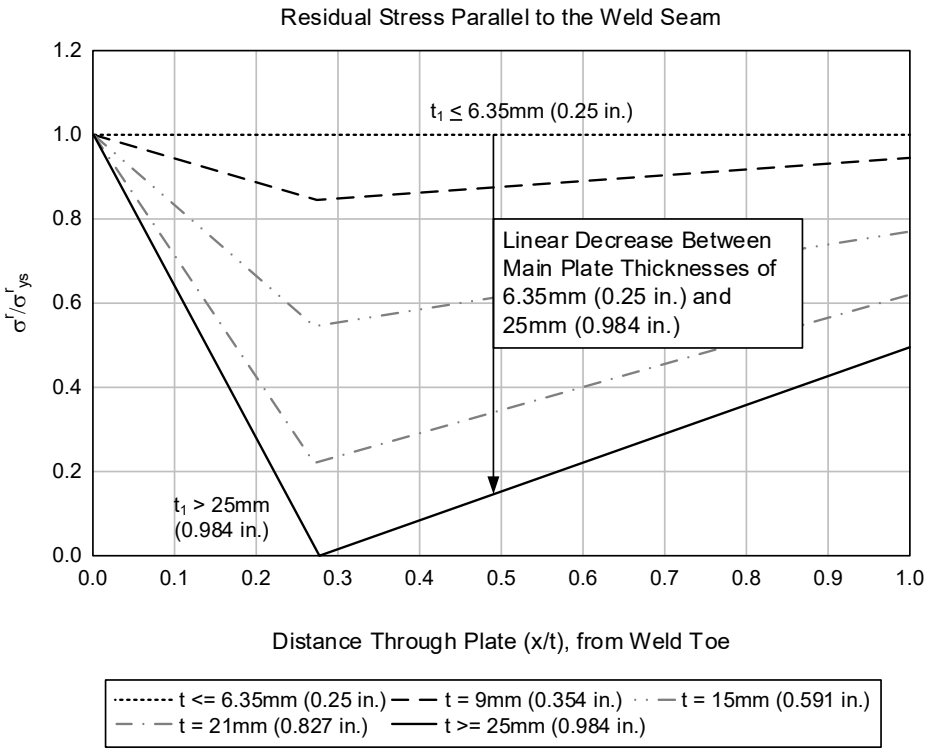

Figure 9D.13 – Residual Stress Through-Wall Distributions for Fillet Welds at a Tee Joint – Main Plate

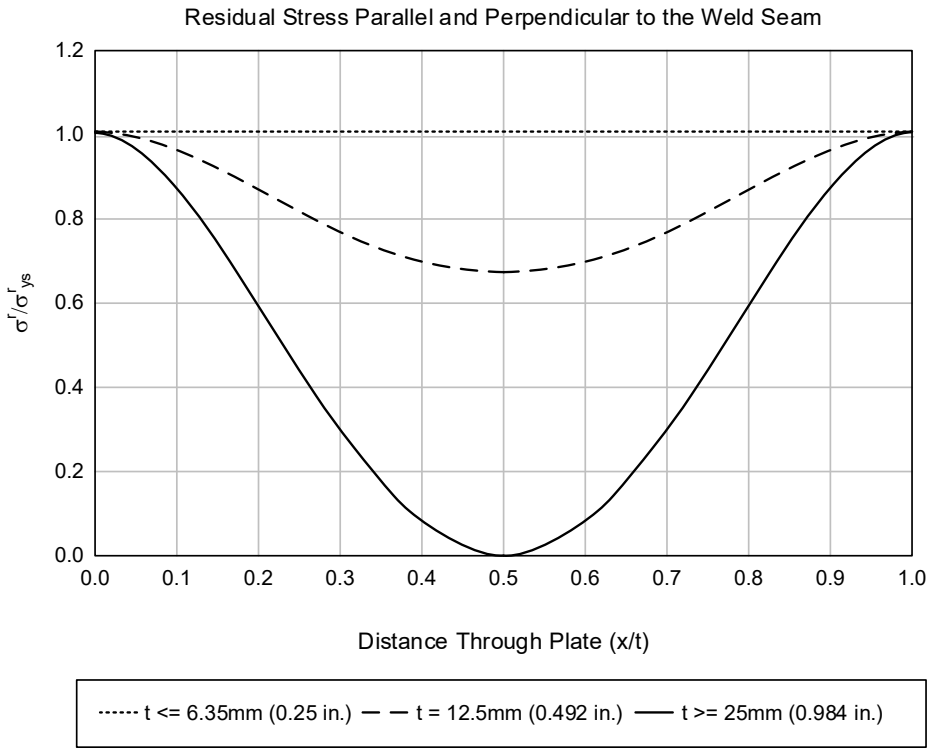

Figure 9D.14 – Residual Stress Through-Wall Distributions for Fillet Welds at a Tee Joint – Stay Plate

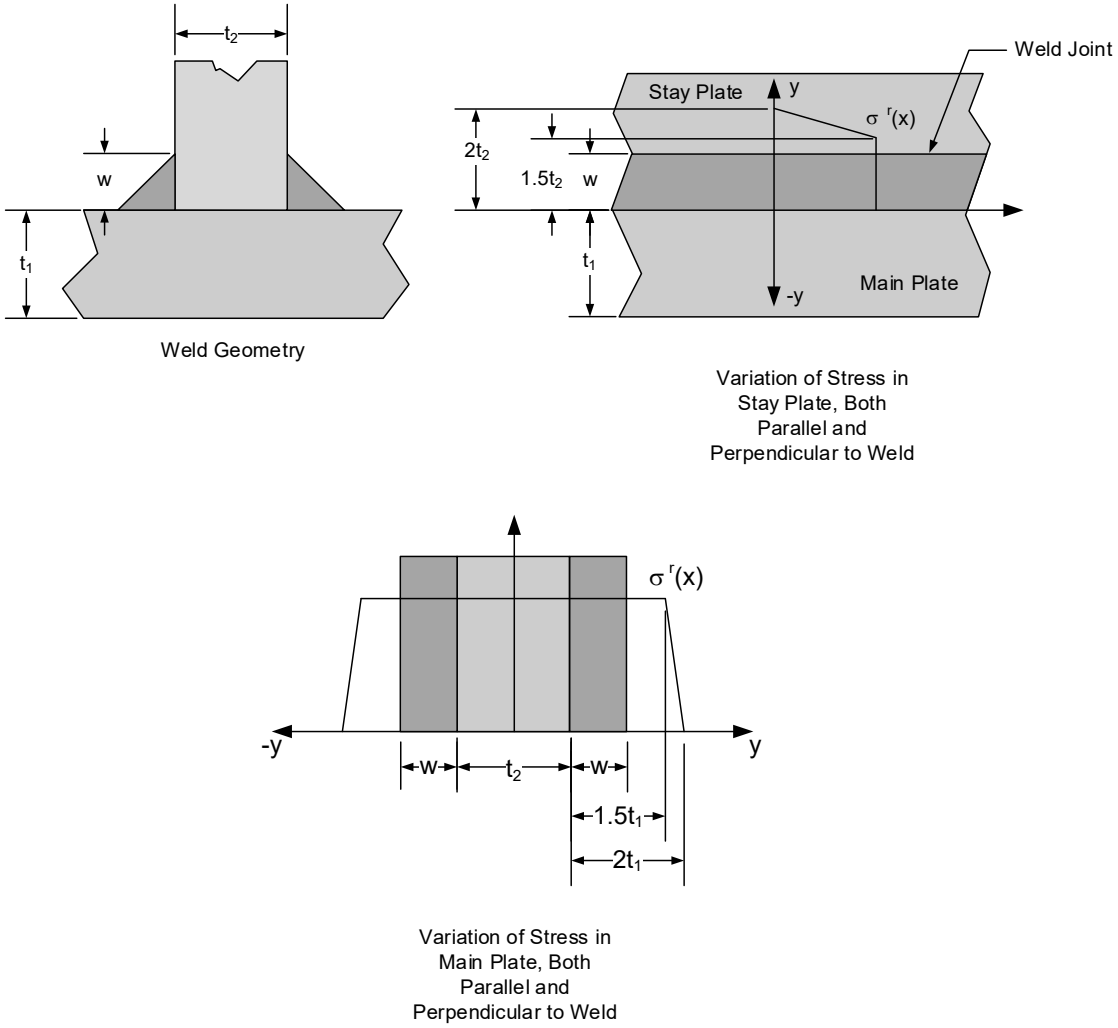

Figure 9D.15 – Residual Stress Variation for Fillet Welds at a Tee Joint with Distance from Weld Centerline

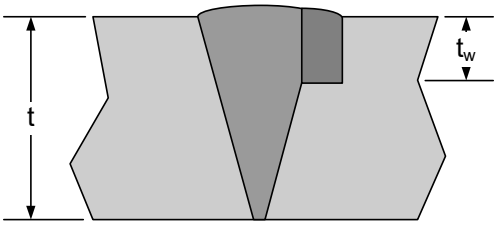

Weld Geometry

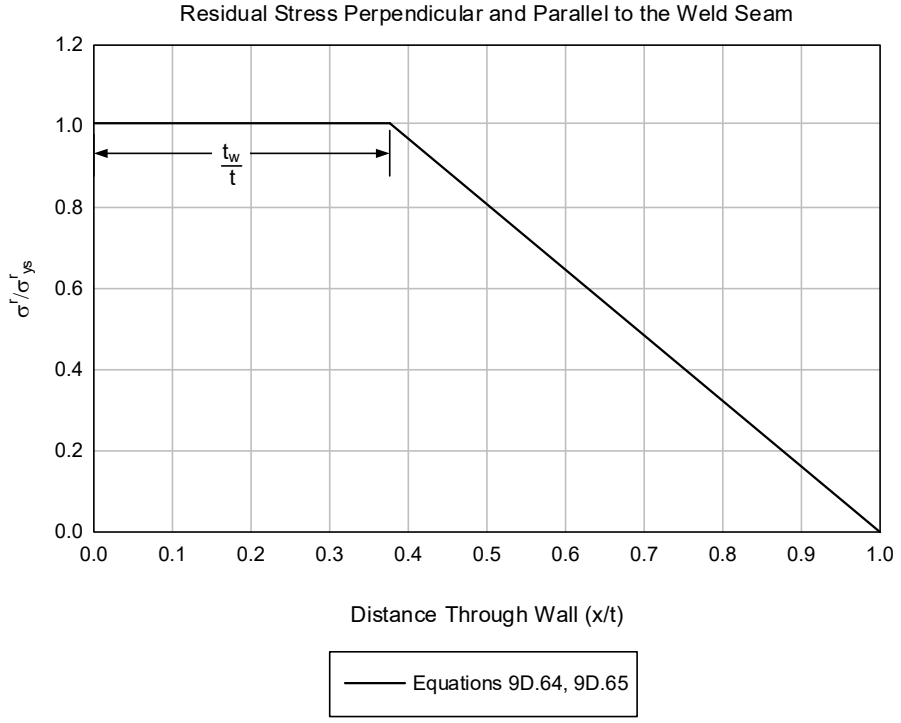

Figure 9D.16 – Residual Stress Through-Wall Distributions for Repair Welds

ANNEX 9E – CRACK OPENING AREAS

(NORMATIVE)

CONTENTS

ANNEX 9E – CRACK OPENING AREAS 9E-1

9E.1 INTRODUCTION 9E-1
9E.1.1 Scope 9E-1
9E.1.2 Overview of Crack Opening Area Calculations 9E-1
9E.2 CRACK OPENING AREAS (COA) FOR CYLINDERS AND SPHERES 9E-2
9E.2.1 Longitudinal Cracks in Cylinders 9E-2
9E.2.2 Circumferential Cracks in Cylinders 9E-3
9E.2.3 Meridional Cracks in Spheres 9E-4
9E.2.4 Plasticity Correction for the COA 9E-5
9E.2.5 Nomenclature 9E-5
9E.2.6 References 9E-6
9E.2.7 Tables 9E-7

9E.1 Introduction

9E.1.1 Scope

The equations for the Crack Opening Areas (COA) in this Annex have been derived for both elastic and plastic conditions for cylinders and spheres with membrane and/or bending stresses based on reference [1]. Alternative methods to compute the COA are covered in references [2], [3], [4], [5], and [6].

9E.1.2 Overview of Crack Opening Area Calculations

9E.1.2.1 The solutions for cylinders and spheres effectively assume that the cracks are in the center of an infinite body and away from structural discontinuities. For most geometries this will be a reasonable approximation. However, if the crack is close to a major structural discontinuity (e.g., a pipe nozzle intersection) then local stress effects will influence the COA. The COA solutions in this Annex may be used to estimate the COA at a structural discontinuity if the membrane and bending stresses are computed using a stress analysis model that considers the structural discontinuity.

9E.1.2.2 Mean material properties should be used to provide a best estimate of the COA. These properties should be relevant to the expected condition of the component; time dependent changes in properties, such as degradation, relaxation and redistribution processes must be taken into consideration. The variation in material properties at welds, the influence of the weld preparation angle, and the presence of residual welding stresses may affect the COA.

9E.1.2.3 Through-wall bending stresses can induce elastic crack face rotations that reduce the effective crack opening area. If complete crack closure occurs, a LBB analysis cannot be justified. Significant local through-wall bending stresses may be present in thick wall shells subject to internal pressure or shells subject to membrane and bending stresses associated with geometric discontinuities and/or thermal gradients. The COA solutions in this Annex can be used to determine the taper associated with the through-wall crack by computing the COA on the inside and outside surface. Typically, other models used to determine the COA provide solutions at the shell

mid-surface position, and do not account for the crack taper resulting from through-wall bending loads. A method to account for crack taper is discussed in reference [7].

9E.1.2.4 The effects on crack face rotations due to welding residual stresses should be evaluated (see reference [8]).

9E.1.2.5 The orientation of the net-section bending moment with respect to the through-wall crack should be considered when determining the COA in a cylindrical shell. The orientation of the net-section bending moment may cause an asymmetric crack opening, partial crack closure, or complete crack closure if the crack is located entirely on the compressive side of the shell section.

9E.2 Crack Opening Areas (COA) for Cylinders and Spheres

9E.2.1 Longitudinal Cracks in Cylinders

9E.2.1.1 For internal pressure, the crack opening area is given by:

$$COA = H_p\left(\frac{pR_o}{t}\right)\left(\frac{2\pi c^2}{E}\right) \tag{9E.1}$$

The parameter H_p for inside and outside surface is given in Table 9E.1 and Table 9E.2, respectively. The limiting values of the parameter H_p for inside and outside surfaces are:

$$\lim_{c\to 0}[H_{p(OD)}] = \left(\frac{R_o^{\,2}+R_i^{\,2}}{R_o^{\,2}-R_i^{\,2}}\right)\left(\frac{t}{R_o}\right) \tag{9E.2}$$

$$\lim_{c\to 0}\left[H_{p(ID)}\right] = \left(\frac{2R_o^{\,2}}{R_o^{\,2}-R_i^{\,2}}\right)\left(\frac{t}{R_o}\right) \tag{9E.3}$$

9E.2.1.2 For a uniform and linear through-wall stress distribution, the crack opening area is given by the following equation where σ_0 and σ_1 are determined in accordance with Annex 9B.

$$COA = \left(H_0\sigma_0 + H_1\sigma_1\right)\cdot\frac{2\pi c^2}{E} \tag{9E.4}$$

In terms of a membrane and bending stress, Equation (9E.4) can be written as:

$$COA = \left(\sigma_m H_0 + \sigma_b\left(H_0 - 2H_1\right)\right)\cdot\frac{2\pi c^2}{E} \tag{9E.5}$$

The parameters H_0 and H_1 for the inside and outside surface are given in Table 9E.1 and Table 9E.2, respectively. The limiting values of the parameters H_0 and H_1 for inside and outside surfaces are:

$$\lim_{c\to 0}\left[H_{0(ID)}\right] = 1 \tag{9E.6}$$

$$\lim_{c\to 0}\left[H_{0(OD)}\right] = 1 \tag{9E.7}$$

$$\lim_{c\to 0}\left[H_{1(OD)}\right] = 1 \tag{9E.8}$$

$$\lim_{c\to 0}\left[H_{1(ID)}\right]=0 \tag{9E.9}$$

9E.2.2 Circumferential Cracks in Cylinders

9E.2.2.1 For internal pressure, the crack opening area is given by:

$$COA=H_0\left(\frac{pR_o^{\,2}}{R_o^{\,2}-R_i^{\,2}}\right)\left(\frac{2\pi c^2}{E}\right) \tag{9E.10}$$

The parameter H_0 for inside and outside surface is given in Table 9E.3 and Table 9E.4, respectively. The limiting values of the parameter H_p for inside and outside surfaces are:

$$\lim_{c\to 0}\left[H_{0(OD)}\right]=1 \tag{9E.11}$$

$$\lim_{c\to 0}\left[H_{0(ID)}\right]=\left(\frac{R_i}{R_o}\right)^2 \tag{9E.12}$$

9E.2.2.2 For a uniform and linear through-wall stress distribution, the crack opening area is given by the following equation where σ_0 and σ_1 are determined in accordance with Annex 9B.

$$COA=\left(H_0\sigma_0+H_1\sigma_1\right)\cdot\frac{2\pi c^2}{E} \tag{9E.13}$$

In terms of a membrane and bending stress, Equation (9E.13) can be written as:

$$COA=\left(\sigma_m H_0+\sigma_b\left(H_0-2H_1\right)\right)\cdot\frac{2\pi c^2}{E} \tag{9E.14}$$

The parameters H_0 and H_1 for the inside and outside surface are given in Table 9E.3 and Table 9E.4, respectively. The limiting values of the parameters H_0 and H_1 for inside and outside surfaces are:

$$\lim_{c\to 0}\left[H_{0(OD)}\right]=1 \tag{9E.15}$$

$$\lim_{c\to 0}\left[H_{0(ID)}\right]=\left(\frac{R_i}{R_o}\right)^2 \tag{9E.16}$$

$$\lim_{c\to 0}\left[H_{1(OD)}\right]=1 \tag{9E.17}$$

$$\lim_{c\to 0}\left[H_{1(ID)}\right]=0 \tag{9E.18}$$

9E.2.2.3 For the global bending moment, the crack opening area is:

$$COA=H_5\left[\frac{M_x R_o}{\frac{\pi}{4}\left(R_o^{\,4}-R_i^{\,4}\right)}\right]\left(\frac{2\pi c^2}{E}\right) \tag{9E.19}$$

The parameter H_5 for inside and outside surface is given in Table 9E.3 and Table 9E.4, respectively. The limiting values of the parameter H_5 for inside and outside surfaces are:

$$\lim_{c\to 0}\left[H_{5(OD)}\right]=1 \tag{9E.20}$$

$$\lim_{c\to 0}\left[H_{5(ID)}\right]=\left(\frac{R_i}{R_o}\right)^3 \tag{9E.21}$$

9E.2.3 Meridional Cracks in Spheres

9E.2.3.1 For internal pressure, the crack opening area is given by:

$$COA=H_p\left(\frac{pR_o^{\,2}}{R_o^{\,2}-R_i^{\,2}}\right)\left(\frac{2\pi c^2}{E}\right) \tag{9E.22}$$

The parameter H_p for inside and outside surface is given in Table 9E.5 and Table 9E.6, respectively. The limiting values of the parameter H_p for inside and outside surfaces are:

$$\lim_{c\to 0}\left[H_{p(OD)}\right]=\left(\frac{R_o^{\,3}+0.5R_i^{\,3}}{R_o^{\,3}-R_i^{\,3}}\right)\left(\frac{R_o^{\,2}-R_i^{\,2}}{R_o^{\,2}}\right) \tag{9E.23}$$

$$\lim_{c\to 0}\left[H_{p(ID)}\right]=\frac{1.5R_i^{\,2}\left(R_o^{\,2}-R_i^{\,2}\right)}{R_o\left(R_o^{\,3}-R_i^{\,3}\right)} \tag{9E.24}$$

9E.2.3.2 For a uniform and linear through-wall stress distribution, the crack opening area is given by the following equation where σ_0 and σ_1 are determined in accordance with Annex 9B.

$$COA=\left(H_0\sigma_0+H_1\sigma_1\right)\cdot\frac{2\pi c^2}{E} \tag{9E.25}$$

In terms of a membrane and bending stress, Equation (9E.25) can be written as:

$$COA=\left(\sigma_m H_0+\sigma_b\left(H_0-2H_1\right)\right)\cdot\frac{2\pi c^2}{E} \tag{9E.26}$$

The parameters H_0 and H_1 for the inside and outside surface are given in Table 9E.5 and Table 9E.6, respectively. The limiting values of the parameters H_0 and H_1 for inside and outside surfaces are given by the following equations:

$$\lim_{c\to 0}\left[H_{0(OD)}\right]=1 \tag{9E.27}$$

$$\lim_{c\to 0}\left[H_{0(ID)}\right]=\left(\frac{R_i}{R_o}\right)^2 \tag{9E.28}$$

$$\lim_{c\to 0}\left[H_{1(OD)}\right]=1 \tag{9E.29}$$

$$\lim_{c\to 0}\left[H_{1(ID)}\right]=0 \tag{9E.30}$$

9E.2.4 Plasticity Correction for the COA

The crack opening areas in paragraph 9E.2 are based on linear elastic fracture mechanics. For elastic-plastic conditions, the crack opening areas in paragraph 9E.2 shall be modified as follows:

$$COA = \gamma_p \cdot COA_{elastic} \tag{9E.31}$$

The plasticity modifier, γ_p, is determined using the following equation:

$$\gamma_p = 1.008 - 0.33015\left(L_r\right)^2 + 5.53696\left(L_r\right)^4 - 3.96974\left(L_r\right)^6 + 2.00844\left(L_r\right)^8 \tag{9E.32}$$

The above equation is valid for $0 \le L_r \le 1.2$. The load ratio L_r is computed using the procedures in Part 9.

9E.2.5 Nomenclature

$A_1 \rightarrow A_8$ crack opening area parameter.

c half-length of the crack.

COA crack opening area corrected for plasticity.

$COA_{elastic}$ elastically calculated crack opening area.

E modulus of elasticity.

γ_p plasticity correction factor for the crack opening area.

H_p pressure loading crack parameter for determining the COA.

H_0 membrane stress crack parameter for determining the COA.

H_1 through-wall bending stress crack parameter for determining the COA.

H_5 net-section bending stress crack parameter for determining the COA.

$H_{p,0,1}$ notation to indicate the calculation of H_p, H_0, and H_1.

$H_{p(ID)}$ H_p parameter for the inside surface of the shell.

$H_{p(OD)}$ H_p parameter for the outside surface of the shell.

$H_{0(ID)}$ H_0 parameter for the inside surface of the shell.

$H_{0(OD)}$ H_0 parameter for the outside surface of the shell.

$H_{1(ID)}$ H_1 parameter for the inside surface of the shell.

$H_{1(OD)}$ H_1 parameter for the outside surface of the shell.

$H_{5(ID)}$ H_5 parameter for the inside surface of the shell.

$H_{5(OD)}$ H_5 parameter for the outside surface of the shell.

L_r load ratio.

λ through-wall crack shell parameter.

M_x net-section bending moment about the x-axis acting on a cylinder (see Annex 9B).

p pressure.

R_i inside radius.

R_o outside radius.

σ_b through-wall bending stress component.

σ_m membrane stress component.

σ_0 uniform coefficient for polynomial stress distribution.

σ_1 linear coefficient for polynomial stress distribution.

t shell thickness.

9E.2.6 References

[1] Anderson, T.L., Stress Intensity and Crack Growth Opening Area Solutions for Through-wall Cracks in Cylinders and Spheres, WRC Bulletin 478, Welding Research Council, Inc., January 2003.

[2] Langston, D.B., "A Reference Stress Approximation for Determining Crack Opening Displacements in Leak-Before-Break Calculations," TD/SID/REP/0112, Nuclear Electric Document, 1991.

[3] Paul, D.D., Ahmad, J., Scott, P.M., Flanigan, L.F. and Wilkowski, G.M., "Evaluation and Refinement of Leak-Rate Estimation Models," NUREG/CR-5128, Rev. 1, June 1995.

[4] Rahman, S., Brust, F., Ghadiali, N., Choi, Y.H., Krishnaswamy, P., Moberg, F., Brickstad, B. and Wilkowski, G., "Refinement and Evaluation of Crack Opening Area Analyses for Circumferential Through-Wall Cracks in Pipes," NUREG/CR-6300, 1995.

[5] Scott, P.M., Anderson, T.L., Osage, D.A., and Wilkowski, G.M., *Review of Existing Fitness-For-Service Criteria for Crack-Like Flaws*, WRC Bulletin 430, Welding Research Council, Inc., 1998.

[6] Sharples, J.K. and Bouchard, P.J., "Assessment of Crack Opening Area for Leak Rates," LBB95; Specialist Meeting on Leak-Before-Break in Reactor Piping and Vessels, Lyon, France, October 1995.

[7] Miller, A.G., "Elastic Crack Opening Displacements and Rotations in Through Cracks in Spheres and Cylinders Under Membrane and Bending Loading," Engineering Fracture Mechanics, Vol. 23, 1986.

[8] Dong, P., Rahman, S., Wilkowski, G., Brickstad, B., Bergman, M., "Effects of Weld Residual Stresses on Crack Opening Area Analysis of Pipes for LBB Applications," LBB95; Specialist Meeting on Leak-Before-Break in Reactor Piping and Vessels, Lyon, France, October 1995.

9E.2.7 Tables

Table 9E.1 – Fitting Coefficients for Non-Dimensional COA for a Through-Wall Axial Crack in a Cylinder – Inside Surface

$H_{p,0,1}$	$\frac{R_i}{t}$	A_0	A_1	A_2	A_3	A_4	A_5	A_6	A_7
H_p	1	1.3285E+00	-2.0500E-02	2.9616E-01	7.1300E-03	6.0958E-01	-4.5900E-02	5.0461E-03	0.0000E+00
	3	1.1325E+00	6.3690E-01	3.1021E-01	0.0000E+00	1.1955E+00	-2.3526E-01	1.5132E-02	0.0000E+00
	5	1.0939E+00	-1.3430E-01	2.6375E-01	0.0000E+00	1.4787E-01	-3.7400E-03	7.2150E-05	0.0000E+00
	10	1.0561E+00	-1.0080E-01	2.5285E-01	0.0000E+00	1.2380E-01	-4.3000E-03	1.0480E-04	0.0000E+00
	20	1.0309E+00	-9.9600E-02	2.2706E-01	0.0000E+00	6.4060E-02	8.6700E-04	-8.8150E-05	0.0000E+00
	60	1.0253E+00	-1.0020E-01	2.0975E-01	0.0000E+00	2.2530E-02	5.1530E-03	-2.9210E-04	0.0000E+00
	100	1.0118E+00	-1.5890E-01	1.7653E-01	0.0000E+00	-1.1020E-01	2.7880E-02	-1.5922E-03	0.0000E+00
H_0	1	1.0006E+00	-1.4839E-01	2.2231E-01	0.0000E+00	2.0398E-01	-3.4400E-03	1.6426E-03	0.0000E+00
	3	1.0102E+00	-1.0250E-01	2.3144E-01	0.0000E+00	1.3604E-01	-4.3400E-03	2.3506E-04	0.0000E+00
	5	1.0096E+00	-1.6138E-01	2.0773E-01	0.0000E+00	8.1700E-03	1.1710E-02	-5.4290E-04	0.0000E+00
	10	1.0080E+00	-9.0320E-02	2.3175E-01	0.0000E+00	8.8590E-02	-1.4300E-03	1.5395E-05	0.0000E+00
	20	1.0086E+00	-1.0869E-01	2.1726E-01	0.0000E+00	3.5190E-02	4.7500E-03	-2.6170E-04	0.0000E+00
	60	1.0062E+00	-8.0880E-02	2.2574E-01	0.0000E+00	6.0020E-02	6.7000E-04	-1.0720E-04	0.0000E+00
	100	1.0057E+00	-6.8770E-02	2.3517E-01	0.0000E+00	6.5400E-02	1.6000E-03	-2.4480E-04	0.0000E+00
H_1	1	0.0000E+00	2.9294E-01	3.0686E-01	1.5597E-01	3.0619E+00	9.9880E-02	1.0369E-02	2.0034E-03
	3	0.0000E+00	4.5779E-01	6.0330E-02	2.5004E-01	1.7604E+00	4.4082E-01	-2.5522E-02	1.0270E-03
	5	0.0000E+00	5.0958E-01	-1.5290E-01	3.6275E-01	7.9176E-01	1.0117E+00	-8.6835E-02	3.2753E-03
	10	0.0000E+00	8.3007E-01	6.2430E-02	3.6629E-01	3.0214E+00	3.3320E-01	-1.0162E-02	2.3810E-04
	20	0.0000E+00	1.1904E+00	5.4410E-02	5.3063E-01	4.1730E+00	5.5928E-01	-3.2950E-02	1.1460E-03
	60	0.0000E+00	2.2472E+00	2.2038E-01	6.3774E-01	8.5083E+00	-4.8485E-01	9.6235E-02	-3.9870E-03
	100	0.0000E+00	3.0857E+00	3.4730E-01	3.1003E-01	1.2352E+01	-3.5319E+00	5.4458E-01	-2.7082E-02

Notes:

1. H_p, H_0, and H_1 are computed as a function of c, R_i, t, and the coefficients in this table using the following equations.

$$H_{p,0,1} = \frac{A_0 + A_1\lambda + A_2\lambda^2 + A_3\lambda^3}{1 + A_4\lambda + A_5\lambda^2 + A_6\lambda^3 + A_7\lambda^4}$$

where,

$$\lambda = \frac{1.818c}{\sqrt{R_i t}}$$

2. For $R_i/t > 100$, use $R_i/t = 100$ for determining H_p, H_0, and H_1.

Table 9E.2 – Fitting Coefficients for Non-Dimensional COA for a Through-Wall Axial Crack in a Cylinder – Outside Surface

$H_{p,0,1}$	$\frac{R_i}{t}$	A_0	A_1	A_2	A_3	A_4	A_5	A_6	A_7
H_p	1	8.4566E-01	3.2057E-01	5.3890E-02	0.0000E+00	-5.8500E-02	6.2480E-03	1.6910E-04	0.0000E+00
	3	8.9368E-01	3.3349E+00	8.4789E-01	7.2986E-01	2.8505E+00	3.9278E-01	-5.7363E-03	0.0000E+00
	5	9.2511E-01	9.9959E+00	2.5503E+00	2.3599E+00	9.5370E+00	1.0363E+00	-1.2140E-02	0.0000E+00
	10	9.7884E-01	2.2825E-01	1.6445E-01	0.0000E+00	-1.0300E-02	5.2870E-03	-1.6050E-04	0.0000E+00
	20	9.8548E-01	1.5869E-01	1.6186E-01	0.0000E+00	-5.8600E-02	1.2954E-02	-5.3460E-04	0.0000E+00
	60	9.9507E-01	2.7326E-01	3.0251E-01	0.0000E+00	1.5427E-01	-7.5700E-03	1.9570E-04	0.0000E+00
	100	9.9156E-01	5.6846E-01	5.0043E-01	0.0000E+00	5.0579E-01	-4.9210E-02	2.0737E-03	0.0000E+00
H_0	1	1.0008E+00	4.0232E+00	9.3771E-01	4.4196E-01	3.2624E+00	1.0241E-01	9.4544E-03	1.9540E-03
	3	1.0000E+00	4.7679E+00	1.5757E+00	1.3700E+00	3.8236E+00	1.2494E+00	-7.5746E-02	2.8130E-03
	5	1.0011E+00	8.6861E-01	8.0009E-01	9.0884E-01	2.1182E-01	1.4194E+00	-1.2576E-01	4.7020E-03
	10	1.0115E+00	2.1754E-01	1.6257E-01	0.0000E+00	-1.6400E-02	5.9600E-03	-1.8540E-04	0.0000E+00
	20	1.0109E+00	1.2351E-01	1.5247E-01	0.0000E+00	-8.7500E-02	1.6830E-02	-7.0310E-04	0.0000E+00
	60	1.0083E+00	2.7650E-01	2.8587E-01	0.0000E+00	1.3697E-01	-6.8300E-03	1.9226E-04	0.0000E+00
	100	1.0075E+00	5.8706E-01	4.4485E-01	0.0000E+00	4.6436E-01	-5.1030E-02	2.3824E-03	0.0000E+00
H_1	1	1.0016E+00	4.7767E+00	2.0223E-01	4.3078E-01	4.2867E+00	2.7910E-01	7.5547E-03	3.5696E-03
	3	1.0004E+00	5.7661E+00	1.7726E+00	1.5125E+00	5.2299E+00	3.3364E+00	-2.1697E-01	7.5483E-03
	5	1.0000E+00	2.8753E+00	1.6731E+00	1.0874E+00	2.6982E+00	2.9318E+00	-2.4959E-01	9.2830E-03
	10	1.0041E+00	1.3792E-01	3.0920E-01	0.0000E+00	4.8762E-01	-2.4170E-02	6.0590E-04	0.0000E+00
	20	1.0044E+00	4.4300E-01	4.5137E-01	0.0000E+00	1.0648E+00	-9.2470E-02	3.3787E-03	0.0000E+00
	60	9.9975E-01	2.8059E+00	9.1254E-01	4.1162E-01	4.2700E+00	1.6323E-01	-9.1160E-05	0.0000E+00
	100	1.0001E+00	3.1285E+00	1.2271E+00	2.5375E-01	5.0417E+00	-2.3327E-01	1.7392E-02	0.0000E+00

Notes:

1. H_p, H_0, and H_1 are computed as a function of c, R_i, t, and the coefficients in this table using the following equations.

$$H_{p,0,1} = \frac{A_0 + A_1\lambda + A_2\lambda^2 + A_3\lambda^3}{1 + A_4\lambda + A_5\lambda^2 + A_6\lambda^3 + A_7\lambda^4}$$

where,

$$\lambda = \frac{1.818c}{\sqrt{R_i t}}$$

2. For $R_i/t > 100$, use $R_i/t = 100$ for determining H_p, H_0, and H_1.

Table 9E.3 – Fitting Coefficients for Non-Dimensional COA for a Through-Wall Circumferential Crack in a Cylinder – Inside Surface

$H_{p,0,1}$	$\frac{R_i}{t}$	A_0	A_1	A_2	A_3	A_4	A_5
H_p	1	2.5679E-01	-7.6590E-02	8.0900E-03	-3.9071E-01	5.4545E-02	-2.5887E-03
	3	5.7995E-01	-9.5710E-02	1.9180E-02	-1.8178E-01	1.3878E-02	-5.1270E-04
	5	7.1328E-01	-2.9910E-02	2.8760E-02	4.5300E-04	-1.2001E-02	4.6022E-04
	10	8.4104E-01	-2.8570E-02	4.2970E-02	3.1681E-02	-7.7060E-03	1.2773E-04
	20	9.1639E-01	-1.2106E-01	4.1570E-02	-1.0001E-01	3.2437E-03	-2.8080E-05
	60	9.7316E-01	-5.3280E-02	4.0970E-02	-8.0600E-03	-4.7620E-03	1.5812E-04
	100	9.8234E-01	-9.1150E-02	3.5500E-02	-7.6050E-02	1.4295E-03	9.2293E-06
H_0	1	8.9000E-04	3.1810E-02	-2.2300E-03	-2.1446E-01	1.1953E-02	0.0000E+00
	3	3.4300E-03	1.6963E-01	1.8504E-02	6.6176E-01	-1.3716E-01	6.3978E-03
	5	4.9200E-03	3.1458E-01	6.7112E-02	1.5293E+00	-2.3140E-01	8.3724E-03
	10	5.3490E-02	9.6620E-02	0.0000E+00	-8.9140E-02	1.7150E-03	0.0000E+00
	20	7.8390E-02	-1.3060E-02	4.3040E-03	-8.3850E-02	1.6960E-03	0.0000E+00
	60	7.7190E-02	1.0374E-01	0.0000E+00	-9.3820E-02	2.3390E-03	0.0000E+00
	100	7.3460E-02	1.0618E-01	0.0000E+00	-1.0334E-01	2.8380E-03	0.0000E+00
H_1	1	1.2750E-01	1.3160E-03	-1.2000E-04	-2.0852E-01	1.1501E-02	0.0000E+00
	3	4.2775E-01	-1.7090E-02	1.0353E-02	-9.9150E-02	9.2990E-04	0.0000E+00
	5	5.8083E-01	-9.3130E-02	1.5425E-02	-2.1415E-01	2.2591E-02	-9.5390E-04
	10	7.5405E-01	-4.1230E-02	3.5941E-02	-2.6160E-02	3.3975E-03	-3.3130E-04
	20	8.6656E-01	-8.1980E-02	2.9441E-02	-8.9350E-02	2.4262E-03	-7.7230E-06
	60	9.5446E-01	-4.5710E-02	4.2358E-02	7.3090E-03	-5.8760E-03	1.8060E-04
	100	9.7167E-01	-6.4890E-02	4.0249E-02	-2.8960E-02	-3.8160E-03	1.6380E-04

Notes:

1. H_0, H_1, and H_5 are computed as a function of c, R_i, t, and the coefficients in this table using the following equations.

$$H_{0,1,5} = \frac{A_0 + A_1\lambda + A_2\lambda^2}{1 + A_3\lambda + A_4\lambda^2 + A_5\lambda^3}$$

where,

$$\lambda = \frac{1.818c}{\sqrt{R_i t}}$$

2. For $R_i/t > 100$, use $R_i/t = 100$ for determining H_0, H_1, and H_5.

Table 9E.4 – Fitting Coefficients for Non-Dimensional COA for a Through-Wall Circumferential Crack in a Cylinder – Outside Surface

$H_{p,0,1}$	$\frac{R_i}{t}$	A_0	A_1	A_2	A_3	A_4	A_5
H_p	1	9.9891E-01	-5.3550E-02	2.5360E-02	-2.8100E-02	-2.2115E-02	1.6721E-03
	3	9.9970E-01	1.5021E-01	8.7700E-03	1.0150E-01	-4.1762E-02	2.2694E-03
	5	9.9545E-01	6.9580E-02	1.2140E-02	-2.4630E-02	-1.1780E-02	6.0617E-04
	10	1.0047E+00	3.3570E-02	1.5700E-02	-7.4960E-02	1.1228E-03	-1.5110E-05
	20	1.0135E+00	-2.1130E-02	2.4020E-02	-1.2421E-01	5.4938E-03	-8.3540E-05
	60	1.0020E+00	-3.4100E-02	5.9000E-04	-1.8029E-01	1.1321E-02	-2.4220E-04
	100	1.0001E+00	1.3090E-02	7.0500E-03	-1.3201E-01	6.0185E-03	-8.9900E-05
H_0	1	1.0204E+00	-1.9110E-01	4.4396E-02	1.3990E-02	-1.9467E-02	1.0366E-03
	3	1.0225E+00	1.2294E-01	1.2724E-02	4.4502E-01	-1.0201E-01	4.9602E-03
	5	1.0099E+00	2.6856E-01	1.5057E-02	6.3403E-01	-1.1177E-01	4.4571E-03
	10	9.8708E-01	1.7136E-01	4.5114E-02	4.9503E-01	-5.7289E-02	1.4503E-03
	20	9.9143E-01	-3.5580E-01	3.6745E-02	-5.3770E-02	5.7210E-03	-2.8500E-04
	60	9.7469E-01	8.2480E-02	4.9754E-02	3.8322E-01	-4.3263E-02	1.1589E-03
	100	9.9100E-01	1.0069E+00	6.1993E-02	1.8451E+00	-2.2699E-01	6.9875E-03
H_1	1	1.0044E+00	-2.1929E-01	4.0998E-02	-1.6870E-01	2.1505E-02	-1.2516E-03
	3	9.9290E-01	5.0980E-02	1.3548E-02	5.6730E-02	-2.4037E-02	9.9160E-04
	5	9.9190E-01	-1.6194E-01	1.9518E-02	-2.3093E-01	2.4630E-02	-1.0109E-03
	10	9.9715E-01	5.2434E-02	2.3549E-02	-2.1830E-02	-2.3400E-04	-1.2520E-04
	20	1.0027E+00	-1.6640E-02	1.3537E-02	-1.2529E-01	5.6843E-03	-8.8230E-05
	60	9.9920E-01	-2.0840E-02	5.0330E-03	-1.5207E-01	8.6274E-03	-1.7380E-04
	100	9.9936E-01	1.9795E-01	2.6089E-02	8.4923E-02	-1.8846E-02	6.5230E-04

Notes:

1. H_0, H_1, and H_5 are computed as a function of c, R_i, t, and the coefficients in this table using the following equations.

$$H_{0,1,5} = \frac{A_0 + A_1\lambda + A_2\lambda^2}{1 + A_3\lambda + A_4\lambda^2 + A_5\lambda^3}$$

where,

$$\lambda = \frac{1.818c}{\sqrt{R_i t}}$$

2. For $R_i/t > 100$, use $R_i/t = 100$ for determining H_0, H_1, and H_5.

Table 9E.5 – Fitting Coefficients for Non-Dimensional COA for a Through-Wall Meridional Crack in a Sphere – Inside Surface

$H_{p,0,1}$	$\frac{R_i}{t}$	A_0	A_1	A_2	A_3	A_4	A_5	A_6	A_7	A_8
H_p	3	6.3820E-01	5.2320E-01	-2.1590E+00	2.8049E+00	-1.6082E+00	4.8428E-01	-7.8246E-02	6.3921E-03	-2.0640E-04
	5	7.5650E-01	3.6733E-01	-1.3556E+00	1.6151E+00	-8.0953E-01	2.1603E-01	-3.1080E-02	2.2633E-03	-6.4980E-05
	10	8.6265E-01	1.8085E-01	-3.2998E-01	2.9748E-01	-7.0830E-02	8.8890E-03	-5.2107E-04	1.2029E-05	0.0000E+00
	20	9.3328E-01	3.7654E-01	-1.3090E+00	1.6340E+00	-7.8345E-01	1.8948E-01	-2.3612E-02	1.4482E-03	-3.4460E-05
	60	9.7959E-01	4.4481E-02	-1.5300E-02	1.5209E-01	-3.3080E-02	3.5060E-03	-1.1791E-04	0.0000E+00	0.0000E+00
	100	9.8904E-01	-2.4740E-02	1.3751E-01	5.7876E-02	-8.2800E-03	8.2800E-04	-2.0828E-05	0.0000E+00	0.0000E+00
H_0	3	5.5951E-01	5.9326E-01	-2.1874E+00	2.8054E+00	-1.6045E+00	4.8297E-01	-7.8045E-02	6.3775E-03	-2.0600E-04
	5	6.9651E-01	4.5017E-01	-1.4391E+00	1.6642E+00	-8.2580E-01	2.1915E-01	-3.1424E-02	2.2834E-03	-6.5470E-05
	10	8.3787E-01	-1.9300E-02	1.1321E-01	-1.5380E-02	3.1976E-02	-8.9500E-03	1.1625E-03	-6.9610E-05	1.5908E-06
	20	9.1363E-01	3.8633E-01	-1.3057E+00	1.6258E+00	-7.7882E-01	1.8830E-01	-2.3461E-02	1.4388E-03	-3.4240E-05
	60	9.7615E-01	1.0130E-01	-8.9080E-02	1.7366E-01	-3.0280E-02	1.9610E-03	0.0000E+00	0.0000E+00	0.0000E+00
	100	9.8823E-01	8.9840E-03	9.8248E-02	7.3648E-02	-1.1120E-02	1.0640E-03	-2.8430E-05	0.0000E+00	0.0000E+00
H_1	3	4.0800E-03	5.1657E-01	-1.1727E+00	1.3634E+00	-7.4432E-01	2.1677E-01	-3.3997E-02	2.6922E-03	-8.3880E-05
	5	4.2850E-03	5.6616E-01	-9.6738E-01	9.6474E-01	-4.5722E-01	1.1864E-01	-1.6803E-02	1.2119E-03	-3.4580E-05
	10	6.5070E-03	5.3228E-01	-4.1931E-01	2.3174E-01	-5.0090E-02	5.8649E-03	-3.3100E-04	7.4162E-06	0.0000E+00
	20	2.1112E-02	6.4770E-01	-5.9407E-01	3.4358E-01	-8.0100E-02	9.8780E-03	-5.8880E-04	1.3688E-05	0.0000E+00
	60	2.2701E-02	9.1335E-01	-9.5929E-01	5.3652E-01	-1.1614E-01	1.1010E-02	-3.5870E-04	0.0000E+00	0.0000E+00
	100	1.7394E-02	8.1190E-01	-6.3608E-01	2.9564E-01	-4.9270E-02	3.6997E-03	-9.4170E-05	0.0000E+00	0.0000E+00

Notes:

1. H_p, H_0, and H_1 are computed as a function of c, R_i, t, and the coefficients in this table using the following equations.

$$H_{p,0,1} = A_o + A_1\lambda + A_2\lambda^2 + A_3\lambda^3 + A_4\lambda^4 + A_5\lambda^5 + A_6\lambda^6 + A_7\lambda^7 + A_8\lambda^8$$

where,

$$\lambda = \frac{1.818c}{\sqrt{R_i t}}$$

2. For $R_i/t > 100$, use $R_i/t = 100$ for determining H_p, H_0, and H_1.

Table 9E.6 – Fitting Coefficients for Non-Dimensional COA for a Through-Wall Meridional Crack in a Sphere – Outside Surface

$H_{p,0,1}$	$\frac{R_i}{t}$	A_0	A_1	A_2	A_3	A_4	A_5	A_6	A_7	A_8
H_p	3	9.1492E-01	1.4629E+00	-3.5770E+00	4.3639E+00	-2.4612E+00	7.3545E-01	-1.1832E-01	9.6396E-03	-3.1070E-04
	5	9.3705E-01	1.1282E+00	-2.0467E+00	2.1926E+00	-1.0661E+00	2.8028E-01	-4.0008E-02	2.9006E-03	-8.3070E-05
	10	9.6831E-01	4.9451E-01	-3.5850E-02	3.5690E-02	2.4577E-02	-8.5900E-03	1.1958E-03	-7.3770E-05	1.7134E-06
	20	9.8208E-01	8.1052E-01	-1.3304E+00	1.6135E+00	-7.7555E-01	1.8861E-01	-2.3603E-02	1.4521E-03	-3.4630E-05
	60	9.9722E-01	5.2138E-01	-1.4522E-01	1.9683E-01	-4.1820E-02	4.3080E-03	-1.4379E-04	0.0000E+00	0.0000E+00
	100	1.0001E+00	3.5564E-01	1.3783E-01	4.0415E-02	-4.4100E-03	5.2700E-04	-1.2930E-05	0.0000E+00	0.0000E+00
H_0	3	9.9959E-01	1.4933E+00	-3.7141E+00	4.4908E+00	-2.5169E+00	7.4877E-01	-1.2010E-01	9.7641E-03	-3.1430E-04
	5	1.0044E+00	1.1086E+00	-2.0715E+00	2.2219E+00	-1.0785E+00	2.8300E-01	-4.0332E-02	2.9207E-03	-8.3570E-05
	10	1.0133E+00	4.6529E-01	-2.3780E-02	3.3565E-02	2.4623E-02	-8.5500E-03	1.1897E-03	-7.3410E-05	1.7056E-06
	20	1.0075E+00	8.2707E-01	-1.4411E+00	1.7429E+00	-8.3913E-01	2.0397E-01	-2.5511E-02	1.5686E-03	-3.7390E-05
	60	1.0080E+00	4.3694E-01	-2.0270E-02	1.1892E-01	-1.9150E-02	1.2980E-03	0.0000E+00	0.0000E+00	0.0000E+00
	100	1.0067E+00	3.4149E-01	1.4671E-01	3.6530E-02	-3.8000E-03	5.0700E-04	-1.4040E-05	0.0000E+00	0.0000E+00
H_1	3	1.0012E+00	2.7649E-01	-1.0546E+00	1.3698E+00	-7.4319E-01	2.0942E-01	-3.1154E-02	2.2851E-03	-6.3660E-05
	5	1.0023E+00	1.3664E-01	-7.0664E-01	9.6719E-01	-5.0371E-01	1.3677E-01	-1.9867E-02	1.4556E-03	-4.1970E-05
	10	1.0074E+00	-2.8973E-01	4.2467E-01	-1.7623E-01	6.0568E-02	-1.1265E-02	1.1763E-03	-6.2404E-05	1.3198E-06
	20	1.0077E+00	-4.5888E-01	6.5971E-01	-2.7309E-01	7.1320E-02	-9.1840E-03	5.8770E-04	-1.4413E-05	0.0000E+00
	60	9.9121E-01	-6.6101E-01	9.6480E-01	-4.0660E-01	8.8452E-02	-8.0150E-03	2.5722E-04	0.0000E+00	0.0000E+00
	100	9.8931E-01	-6.1407E-01	7.7232E-01	-2.4905E-01	4.3340E-02	-3.0320E-03	7.5979E-05	0.0000E+00	0.0000E+00

Notes:

1. H_p, H_0, and H_1 are computed as a function of c, R_i, t, and the coefficients in this table using the following equations.

$$H_{p,0,1} = A_o + A_1\lambda + A_2\lambda^2 + A_3\lambda^3 + A_4\lambda^4 + A_5\lambda^5 + A_6\lambda^6 + A_7\lambda^7 + A_8\lambda^8$$

where,

$$\lambda = \frac{1.818c}{\sqrt{R_i t}}$$

2. For $R_i/t > 100$, use $R_i/t = 100$ for determining H_p, H_0, and H_1.

ANNEX 9F – MATERIAL PROPERTIES FOR CRACK-LIKE FLAWS

(NORMATIVE)

CONTENTS

ANNEX 9F – MATERIAL PROPERTIES FOR CRACK-LIKE FLAWS 9F-1

9F.1 GENERAL 9F-2
9F.2 CHARPY V-NOTCH IMPACT ENERGY 9F-3
9F.2.1 Definition 9F-3
9F.2.2 Charpy V-Notch (CVN) Test 9F-3
9F.2.3 Charpy V-Notch Transition Curve 9F-5
9F.2.4 Charpy Transition Curves and ASME Division 1 and 2 Toughness Exemption Curves 9F-6
9F.2.4.1 Section VIII, Divisions 1 and 2 Toughness Requirements 9F-6
9F.2.4.2 Charpy Transition Curve for Toughness Exemption 9F-6
9F.2.4.3 Reference Temperature Determination 9F-7
9F.2.4.4 Reference Temperature for Part 9, Level 1 Assessments 9F-7
9F.2.4.5 Reference Temperature for Part 12 Assessments of Gouges and Dent-Gouge Combinations 9F-7
9F.3 FRACTURE TOUGHNESS 9F-8
9F.3.1 Definition 9F-8
9F.3.2 Fracture Toughness Parameters 9F-8
9F.3.3 Fracture Toughness Testing 9F-9
9F.3.3.1 Obtaining Samples for Toughness Testing 9F-9
9F.3.3.2 Fracture Toughness Tests 9F-9
9F.3.3.3 JR-Curve 9F-10
9F.3.4 Fracture Toughness Estimation from Charpy V-Notch Data 9F-10
9F.3.5 ASME B&PV Code, Section VIII Division 1 and 2 Fracture Toughness 9F-10
9F.4 FRACTURE TOUGHNESS ESTIMATION FOR AN FFS ASSESSMENT 9F-11
9F.4.1 Introduction 9F-11
9F.4.2 ASME Section XI Fracture Toughness 9F-11
9F.4.2.1 Indexing Procedure for Fracture Toughness Determination 9F-11
9F.4.2.2 Lower Bound Toughness Based on ASME Section XI Reference Curves 9F-12
9F.4.3 Fracture Toughness Master Curve 9F-12
9F.4.3.1 Overview 9F-12
9F.4.3.2 Determining the Master Curve Reference Transition Temperature $T0$ 9F-13
9F.4.3.3 Fracture Toughness Prediction Using the Master Curve 9F-17
9F.4.3.4 Determining the Master Curve Reference Transition Temperature T_0 for Modern Cr-Mo Steels 9F-18
9F.4.4 Upper Shelf Fracture Toughness 9F-18
9F.4.4.1 Overview 9F-18
9F.4.4.2 Fracture Toughness Prediction 9F-18
9F.4.5 Dynamic and Crack Arrest Fracture Toughness 9F-19
9F.4.5.1 Overview 9F-19
9F.4.5.2 Dynamic Fracture Toughness Prediction 9F-19
9F.4.5.3 Arrest Fracture Toughness Prediction 9F-20
9F.4.6 Fracture Toughness for Materials Subject to In-Service Degradation 9F-21
9F.4.6.1 Service Environment Effects on Fracture Toughness 9F-21
9F.4.6.2 Hydrogen Effects on Fracture Toughness and Flaw Assessment 9F-21
9F.4.6.3 Overview of Metallurgical Embrittlement that Reduces Ductility and Fracture Toughness 9F-22
9F.4.7 Aging Effects on the Fracture Toughness of Cr-Mo Steels 9F-23
9F.4.7.1 Overview 9F-23
9F.4.7.2 Effect of Tramp Elements on the Fracture Toughness of 1.25Cr-0.5Mo 9F-23
9F.4.7.3 Effect of Tramp Elements on the Fracture Toughness of 2.25Cr-1Mo 9F-24
9F.4.8 Fracture Toughness of Electroslag Welds in 2.25Cr-1Mo Vessels 9F-25
9F.4.9 Fracture Toughness as a Function of Temperature for Ferritic Materials 9F-26
9F.4.10 The Effect of Warm Pre-stress on Fracture Toughness 9F-26
9F.4.10.1 Introduction 9F-26
9F.4.10.2 Benefits 9F-26
9F.4.10.3 Procedure 9F-26

9F.4.10.4 Conditions to be Satisfied 9F-27
9F.4.11 Fracture Toughness Estimation for Brittle Fracture Assessments 9F-27
9F.4.12 Fracture Toughness of Austenitic Stainless Steel 9F-28
9F.4.13 Ductile Tearing Assessment Using a JR-curve 9F-28
9F.5 MATERIAL DATA FOR CRACK GROWTH CALCULATIONS 9F-28
9F.5.1 Categories of Crack Growth 9F-28
9F.5.1.1 Crack Growth by Fatigue 9F-28
9F.5.1.2 Crack Growth by Stress Corrosion Cracking (SCC) 9F-29
9F.5.1.3 Crack Growth by Hydrogen Assisted Cracking (HAC) 9F-29
9F.5.1.4 Crack Growth by Corrosion Fatigue 9F-29
9F.5.2 Fatigue Crack Growth Equations 9F-30
9F.5.2.1 Overview 9F-30
9F.5.2.2 Paris Equation 9F-30
9F.5.2.3 Modified Paris Equation for Welded Joints 9F-31
9F.5.2.4 Walker Equation 9F-31
9F.5.2.5 Trilinear and Bilinear Equations 9F-32
9F.5.2.6 Modified Forman Equation 9F-32
9F.5.2.7 NASGRO Equation 9F-33
9F.5.2.8 Collipriest Equation 9F-33
9F.5.2.9 ASME B&PV Code, Section VIII, Division 3 ..... 9F-33
9F.5.3 Fatigue Crack Growth Data 9F-34
9F.5.3.1 Sources for Crack Growth Data 9F-34
9F.5.3.2 ASME B&PV Code, Section VIII, Division 3 ..... 9F-34
9F.5.3.3 ASME B&PV Code, Section XI 9F-34
9F.5.3.4 AFCEN Code, RSE-M 9F-34
9F.5.3.5 Barsom Original Crack Growth Data 9F-34
9F.5.3.6 Crack Growth Data for Welds 9F-34
9F.5.3.7 BS 7910 Crack Growth Data for Screening 9F-35
9F.5.3.8 BS 7910 Bilinear Crack Growth Data 9F-35
9F.5.3.9 Crack Growth Data for Pipeline Steels 9F-35
9F.5.3.10 NASGRO Crack Growth Data 9F-36
9F.5.4 Hydrogen Assisted Crack Growth 9F-36
9F.5.4.1 ASME B31.12 ..... 9F-36
9F.5.4.2 ASME B&PV Code, Section VIII, Division 3 ..... 9F-36
9F.5.5 Stress Corrosion Crack (SCC) Growth Equations 9F-36
9F.5.6 Stress Corrosion Crack Growth Data 9F-37
9F.5.7 Conversion of Units for Crack Growth Data 9F-37
9F.5.7.1 Cyclic Crack Growth Conversion Method 9F-37
9F.5.7.2 Time-Dependent Crack Growth Conversion Method 9F-37
9F.6 NOMENCLATURE 9F-38
9F.7 REFERENCES 9F-43
9F.8 TABLES 9F-46
9F.9 FIGURES 9F-59

9F.1 General

The information in this Annex is intended to provide guidance on determining fracture toughness for use in an FFS Assessment of crack-like flaws. Deterministic approaches based on the ASME Section XI Fracture Toughness lower bound equations and the Master Curve for the transition region are provided. A probabilistic approach is also provided based on the Master Curve. The fracture toughness relationship consistent with the toughness rules in the ASME Code, Section VIII, Divisions 1 and 2 are also provided for use with Level 3 brittle fracture assessments.

The Fitness-For-Service Assessment procedures in this Standard cover situations involving flaws commonly encountered in pressure vessels, piping and tankage that have been exposed to service for long periods of time. Therefore, when selecting material properties for an assessment, care shall be taken to evaluate these properties in terms of equipment that has been in-service; the properties used in the assessment should reflect any change

or degradation, including aging, resulting from the service environment or past operation. Guidelines for estimating fracture toughness for materials subject to in-service degradation are also provided in this Annex.

9F.2 Charpy V-Notch Impact Energy

9F.2.1 Definition

The Charpy impact test, also known as the Charpy V-notch test, is a standardized high strain-rate test which determines the amount of energy absorbed by a material during fracture. This absorbed energy is a measure of a given material's notch toughness and is used to determine the temperature-dependent ductile-brittle transition. It is widely used in industry to evaluate the toughness of a material on a comparative basis, since it is easy to prepare and conduct and results can be obtained quickly and at low cost compared to standard fracture toughness tests (see paragraph 9F.3).

9F.2.2 Charpy V-Notch (CVN) Test

The US standard for CVN testing is ASTM Standard E23. The Charpy specimen is a rectangular bar with cross section measurements of 10 mm x 10 mm and length between end supports of 40 mm. A notch 2 mm deep is machined opposite the impact point with a 0.25 mm notch radius. The axis of the notch is usually oriented in the through-thickness direction with respect to the original material placement. When a component is less than 10 mm thick, “sub-size” specimens are used.

a) The thickness of the CVN specimen can influence both the absorbed energy and the transition temperature as described below.

   1) Effect on Absorbed Energy – The reduced cross-sectional area of a sub-size CVN specimen may reduce its ability to absorb energy. The absorbed energy values for sub-size CVN specimens will be less than that characteristic of standard size CVN specimens when both specimens are tested at the same temperature and both specimens are on the upper shelf or lower shelf (100% shear or 0% shear, respectively). However, the reverse trend is often observed in the transition region due to the constraint-induced temperature shift described in (2) below.

   2) Effect on Transition Temperature – The reduced wall thickness of sub-size CVN specimens reduce the triaxial constraint against plastic flow in comparison with that characteristic of a standard size CVN specimen. This reduced level of constraint makes cleavage fracture less likely to occur in a sub-size CVN specimen than in a standard size CVN specimen when both are tested at the same temperature. Therefore, the fracture mode transition will occur at lower temperatures in sub-sized CVN specimens than in standard CVN size specimens of the same material.

b) For plate materials used in pressure vessels, piping and tankage, the following equations may be used for the energy and temperature shift (see reference [1]).

$$C_{V-std} = C_{V-ss}\left(\frac{t_{std}}{t_{ss}}\right) \qquad \left(for\ \ t_{ss} \le t_{std}\right) \tag{9F.1}$$

$$TT_{std} = TT_{ss} + T_{shift} \tag{9F.2}$$

with,

$$T_{shift} = 51.4 \cdot \ln\left[2\left(\frac{t_{ss}}{10}\right)^{0.25} - 1\right] \qquad \left({}^{o}C,\ mm\right) \tag{9F.3}$$

$$T_{shift} = 92.52 \cdot \ln\left[2\left(2.54 \cdot t_{ss}\right)^{0.25} - 1\right] \qquad \left({}^{o}F,\ in\right) \tag{9F.4}$$

c) For pipeline materials (e.g., API 5L), the following procedure has been used to correlate the impact energies obtained from sub-size and full-size Charpy specimens. The expressions were derived from statistical analysis of data from tests on plain carbon and low alloy steels reported in reference [2]. The correlation is not exact because Charpy test data often exhibits scatter, particularly in the transition region. In addition, the use of the correlation may be inappropriate for materials that do not exhibit impact toughness behavior typical of plain carbon and low alloy steels. Note that in the following calculation procedure, the units for the Charpy impact energy are ft-lbs, thickness is in inches, and temperature is in degrees Fahrenheit.

1) STEP 1 – Determine C_A and C_B parameters based upon the size of the Charpy specimen from the following table.

Charpy Specimen Size	1/4	1/3	1/2	2/3	Full
C_A	22	28	36	41	50
C_B	19	24	30	32	33

2) STEP 2 – Obtain the following four quantities from the sub-size specimen (denoted with a subscript "ss") Charpy energy transition curve: C_{V-ss}, $C_{V-US-ss}$, SA_{ss} and T_{c-ss}. If only two or three of the quantities are available, the unknown quantities can be determined from the following equations. If only one of the quantities is known, the transformation cannot be performed.

$$SA_{ss} = 1.1\left(\frac{C_{V-ss}}{C_{V-US-ss}} - 0.1\right) \tag{9F.5}$$

$$C_{V-US-ss} = \frac{C_{V-ss}}{0.9 \cdot SA_{ss} + 0.1} \tag{9F.6}$$

$$SA_{ss} = \left(1 + \exp\left[-\left\{\frac{\left(T - T_{c-ss}\right) + C_A}{C_B}\right\}\right]\right)^{-1} \tag{9F.7}$$

$$T_{c-ss} = T - C_B \cdot \ln\left[\frac{SA_{ss}}{1 - SA_{ss}}\right] + C_A \tag{9F.8}$$

3) STEP 3 – Calculate the full-size specimen 85% Shear Area Transition Temperature (SATT).

$$T_c = T_{c-ss} + 66 \cdot \left(t_{NWT}\right)^{0.55} \cdot \left(\left(t_{ss}\right)^{-0.7} - \left(t_{std}\right)^{-0.7}\right) \tag{9F.9}$$

4) STEP 4 – Calculate the shear area of the full-size specimen using the following equation.

$$SA = \left(1 + \exp\left[-\left\{\frac{\left(T - T_c\right) + 50}{33}\right\}\right]\right)^{-1} \tag{9F.10}$$

5) STEP 5 – Calculate the upper shelf impact energy for the full-size specimen using the following equation.

$$C_{V-US} = C_{V-US-ss}\left(\frac{t_{std}}{t_{ss}}\right) \tag{9F.11}$$

6) STEP 6 – Calculate the impact energy for the full size specimen using the Equation (9F.12). Note that if C_{V-ss} is on the lower shelf or SA_{ss} is less than five percent, and $t_{ss} < t_c$, then the impact energy for the full size specimen can be computed using Equation (9F.13).

$$C_V = C_{V-US}\left(0.9 \cdot SA + 0.1\right) \tag{9F.12}$$

$$C_V = C_{V-ss}\left(\frac{t_{std}}{t_{ss}}\right) \tag{9F.13}$$

9F.2.3 Charpy V-Notch Transition Curve

CVN data may be curve-fit to the hyperbolic tangent equation shown below to determine the relationship between the Charpy impact energy and temperature. The characteristics of this equation are shown in Figure 9F.1(a). A typical curve-fit to CVN data is shown in Figure 9F.1(b).

$$C_v = A + B\tanh\left[\frac{(T-D)}{C}\right] \tag{9F.14}$$

where,

$$A = \frac{C_{V-US} + C_{V-LS}}{2} \tag{9F.15}$$

$$B = \frac{C_{V-US} - C_{V-LS}}{2} \tag{9F.16}$$

An alternate form of Equation (9F.14) can be written using Equations (9F.15) and (9F.16).

$$C_V = \left(\frac{C_{V-US} - C_{V-LS}}{2}\right) \cdot \left(1 + \tanh\left[\frac{(T-D)}{C}\right]\right) + C_{V-LS} \tag{9F.17}$$

In exponential form, Equation (9F.16) becomes:

$$C_V = \frac{\left(C_{V-US} - C_{V-LS}\right) \cdot \exp\left[\frac{2(T-D)}{C}\right]}{1 + \exp\left[\frac{2(T-D)}{C}\right]} + C_{V-LS} \tag{9F.18}$$

Using Equation (9F.18), the equations to find the temperature for a given value of C_V are:

$$T = D + \frac{C}{2} \cdot \ln\left[\frac{C_V - C_{V-LS}}{C_{V-US} - C_V}\right] \qquad \left(for\ C_V \neq C_{V-LS}\ and\ C_V \neq C_{V-US}\right) \tag{9F.19}$$

$$T = D + \frac{C}{2} \cdot \ln\left[\frac{\varepsilon_{CVN}}{1 - \varepsilon_{CVN}}\right] \qquad \left(for\ C_V = C_{V-LS}\right) \tag{9F.20}$$

$$T = D + \frac{C}{2} \cdot \ln\left[\frac{1-\varepsilon_{CVN}}{\varepsilon_{CVN}}\right] \qquad \left(for\ C_V = C_{V-US}\right) \tag{9F.21}$$

9F.2.4 Charpy Transition Curves and ASME Division 1 and 2 Toughness Exemption Curves

9F.2.4.1 Section VIII, Divisions 1 and 2 Toughness Requirements

The ASME Codes, Section VIII, Divisions 1 and 2 have toughness requirements for materials of construction based on the design conditions for a pressure vessel. A variation of these toughness requirements has also been adopted by the ASME B31.3 Piping Code. The toughness requirements in the ASME Code are established based on toughness exemption curves. These curves and the ASME procedures for their use have been implemented in Part 3 of this standard.

a) In the development of the ASME Code toughness rules, Charpy transition curves and an associated fracture toughness model were developed for four toughness categories of materials designated A, B, C, and D. Category D represent materials with the highest expected toughness, Category A materials have the lowest expected toughness, and categories B and C represent materials with intermediate expected toughness values.

b) A material is assigned to a toughness category based on expected toughness and strength. In this assignment, the expected toughness is typically based on heat treatment and grain size.

c) The Charpy transition curve model is based on the hyperbolic tangent function described in paragraph 9F.2.3 and the associated fracture toughness model is described in paragraph 9F.3.5.

d) The Charpy transition curve model is used to establish a reference temperature for use in estimating fracture toughness for an FFS Assessment (see paragraph 9F.4).

9F.2.4.2 Charpy Transition Curve for Toughness Exemption

The Charpy Transition Curve consistent with the ASME Section VIII, Division 1 and 2 toughness exemption curves may be determined using Equation (9F.18) in combination with the following equations.

$$C_{V-US} = \frac{\left(0.290\sqrt{3}\sigma_{msys} - 27\right)^2}{0.535\sigma_{msys}} + \frac{\sigma_{msys}}{101.7} \qquad \left(J,\ MPa\right) \tag{9F.22}$$

$$C_{V-US} = \frac{\left(2\sqrt{3}\sigma_{msys} - 27\right)^2}{5\sigma_{msys}} + \frac{\sigma_{msys}}{20} \qquad \left(ft-lbs,\ ksi\right) \tag{9F.23}$$

$$C_{V-LS} = \left(\frac{K_{Id-LS}}{14.155}\right)^2 \qquad \left(J,\ MPa\sqrt{m}\right) \tag{9F.24}$$

$$C_{V-LS} = \left(\frac{K_{Id-LS}}{15}\right)^2 \qquad \left(ft-lbs,\ ksi\sqrt{in}\right) \tag{9F.25}$$

$$K_{Id-LS} = 29.7MPa\sqrt{m} \quad \left(27\,ksi\sqrt{in}\right) \tag{9F.26}$$

$$D = \begin{pmatrix} 45.6^{\circ}C & \left(114^{\circ}F\right) & for\ ASME\ Exemption\ Curve\ A \\ 24.4^{\circ}C & \left(76^{\circ}F\right) & for\ ASME\ Exemption\ Curve\ B \\ 3.3^{\circ}C & \left(38^{\circ}F\right) & for\ ASME\ Exemption\ Curve\ C \\ -11.1^{\circ}C & \left(12^{\circ}F\right) & for\ ASME\ Exemption\ Curve\ D \end{pmatrix} \tag{9F.27}$$

$$C = 36.7^{\circ}C \quad \left(66^{\circ}F\right) \tag{9F.28}$$

9F.2.4.3 Reference Temperature Determination

A reference temperature, or the expected temperature for an associated Charpy Energy value, consistent with the ASME Section VIII, Division 1 and 2 toughness exemption curves, T_{ref}, may be established for a material using Equation (9F.29) in combination with Equations (9F.22) through (9F.28). If the reference temperature is used to estimate a fracture toughness, then the value of C_V should be set at 20 Joules (15 ft-lbs) for carbon steels and 27 Joules (20 ft-lbs) for low alloy steels. Values of T_{ref} are shown in Part 9, Table 9.2 for materials assigned to the A, B, C and D Exemption Curves (see Part 3, Table 3.2).

$$T_{ref} = D + \frac{C}{2} \cdot \ln\left[\frac{C_V - C_{V-LS}}{C_{V-US} - C_V}\right] \tag{9F.29}$$

9F.2.4.4 Reference Temperature for Part 9, Level 1 Assessments

The reference temperatures required for a Part 9, Level 1 Assessment are provided in Part 9, Table 9.2. These temperatures are determined with the following equations.

$$T_{20\ Joules} = D + \frac{C}{4} \cdot \ln\left[\frac{20 - C_{V-LS}}{C_{V-US} - 20}\right] \qquad \left({}^{o}C, J\right) \tag{9F.30}$$

$$T_{15\ ft-lbs} = D + \frac{C}{4} \cdot \ln\left[\frac{15 - C_{V-LS}}{C_{V-US} - 15}\right] \qquad \left({}^{o}F, ft-lbs\right) \tag{9F.31}$$

$$T_{27\ Joules} = D + \frac{C}{4} \cdot \ln\left[\frac{27 - C_{V-LS}}{C_{V-US} - 27}\right] \qquad \left({}^{o}C, J\right) \tag{9F.32}$$

$$T_{20\ ft-lbs} = D + \frac{C}{4} \cdot \ln\left[\frac{20 - C_{V-LS}}{C_{V-US} - 20}\right] \qquad \left({}^{o}F, ft-lbs\right) \tag{9F.33}$$

The parameter D is determined from Equation (9F.27), the parameter C is determined from Equation (9F.68) or (9F.69), the lower shelf Charpy energy, C_{V-LS}, is determined from Equation (9F.61), and the upper shelf energy, C_{V-US}, is determined from Equation (9F.64) through (9F.67). Due to the uncertainty in the estimate of the C parameter from Equation (9F.68) or (9F.69), a safety margin of 2.0 on the slope of the Charpy-temperature curve has been incorporated into the above expressions.

9F.2.4.5 Reference Temperature for Part 12 Assessments of Gouges and Dent-Gouge Combinations

The reference temperatures required for a Part 12, Level 1 Assessment are provided in Part 12, Table 12.2. These temperatures are determined with the following equations.

$$T_{40\,Joules} = D + \frac{C}{4} \cdot \ln\left[\frac{40 - C_{V-LS}}{C_{V-US} - 40}\right] \qquad \left({}^{o}C, J\right) \tag{9F.34}$$

$$T_{30\,ft-lbs} = D + \frac{C}{4} \cdot \ln\left[\frac{30 - C_{V-LS}}{C_{V-US} - 30}\right] \qquad \left({}^{o}F, ft-lbs\right) \tag{9F.35}$$

The parameter D is determined from Equation (9F.27), the parameter C is determined from Equation (9F.68) or (9F.69), and the lower shelf Charpy energy, C_{V-LS}, is determined from Equation (9F.61), and the upper shelf energy, C_{V-US}, is determined from Equation (9F.64) through (9F.67). Due to the uncertainty in the estimate of the C parameter from Equation (9F.69), a safety margin of 2.0 on the slope of the Charpy-temperature curve has been incorporated into the above expressions.

9F.3 Fracture Toughness

9F.3.1 Definition

The fracture toughness of a material measures its ability to resist crack initiation and propagation. Several fracture toughness parameters are available, including critical stress intensity factor (K_{IC}), the critical value of the J-lintegral (J_{crit}), and the critical crack tip opening displacement $CTOD$ or δ_{crit}. Any one of these parameters can be used for a Fitness-For-Service Assessment of a component containing crack-like flaws.

9F.3.2 Fracture Toughness Parameters

For most materials and structures covered by this Standard, it is possible to measure toughness only in terms of J and $CTOD$; valid K_{IC} data can only be obtained for brittle materials or thick sections. It is possible, however, to infer "equivalent" K_{IC} values from J and $CTOD$ data by exploiting the relationships among these three parameters under plane strain linear elastic conditions. A fracture mechanics analysis may be expressed in terms of any one of the three parameters based on the relationships shown below (see reference [3]).

a) An equivalent K_{IC}, denoted as K_{JC}, can be computed from J_{crit} using Equation (9F.36)

$$K_{JC} = \sqrt{\frac{J_{crit} \cdot E_{yT}}{1 - \nu^2}} \tag{9F.36}$$

b) An approximate relationship between the J-integral and $CTOD$ is given by Equation (9F.37).

$$J_{crit} = m_{CTOD} \cdot \sigma_{fT} \cdot \delta_{crit} \tag{9F.37}$$

c) By combining the above equations, the equivalent K_{IC} value, or $K_{\delta C}$, computed from $CTOD$ data is given by Equation (9F.38).

$$K_{\delta C} = \sqrt{\frac{m_{CTOD} \cdot \sigma_{fT} \cdot \delta_{crit} \cdot E_{yT}}{1 - \nu^2}} \tag{9F.38}$$

In Equations (9F.37) and (9F.38), the flow stress may be determined using the following equation.

$$\sigma_{fT} = \frac{\sigma_{ysT} + \sigma_{utsT}}{2} \tag{9F.39}$$

9F.3.3 Fracture Toughness Testing

9F.3.3.1 Obtaining Samples for Toughness Testing

Ideally, fracture toughness tests should be heat specific, which necessitates removing specimens from the material under consideration. This can be accomplished in one of three ways:

a) Removal of a Sample from a Component Currently In-service for Testing – Removal of a material sample from a component is an extreme step, but it is often the only way to obtain heat-specific fracture toughness data for a given structure. The value of component specific toughness data should be assessed versus the potential problems that may result from the procedure required to repair the region where the sample was obtained.

b) Removal of a Sample from a Retired Component in a Similar Service and Testing – Testing material from a retired component (preferably one that was fabricated from the same material heat) is beneficial because such data provide a relative indication of the toughness of similar vessels. However, these data shall be used with caution because a material's fracture toughness data can have significant heat-to-heat variations, and data from one component may not be necessarily applicable to another.

c) Testing a Plate That Was Welded at the Time of Fabrication – A test weldment will not normally be available for components that have been in service for some time; however, a plate can be produced at the time of fabrication for a new component. The steel in a test plate should come from the same heat as the material used in the actual structure, and it should be welded according to the same procedure and with the same batch of consumables as the structure. If possible, the same welders and equipment should be used for the test plate and structure, and the plate should also have the same $PWHT$ as the structure. Finally, the weld joint should be subject to the same operating conditions if these conditions cause embrittlement.

9F.3.3.2 Fracture Toughness Tests

The following items should be noted if testing of a sample is to be performed to determine the fracture toughness of a material for a Fitness-For-Service Assessment.

a) Test methods for measurement of the K, J, and $CTOD$ fracture toughness parameters are covered in ASTM 1820.

b) A test method to determine the reference temperature, T_0, for ferritic steels in the transition region is covered in ASTM E1921 (see paragraph 9F.4.3).

c) It is recommended that a minimum of three specimens be tested for each condition and temperature. If additional test results are available, the equivalent to the minimum of three tests may be used (see Table 9F.1). If more than ten tests are available, the data may be fitted to the Master Curve (see paragraph 9F.3.4). Another option, which is described in references [4] and [5], and involves fitting a distribution to the data, allows a characteristic value to be determined for the lower 20% percentile with 90% confidence.

d) Currently, an ASTM Standard covering fracture toughness testing of weldments does not exist. A procedure to test weldments is provided by ISO 15653:2018.

e) The results from a fracture toughness test can vary significantly. The fracture toughness Master Curve approach can be used to quantify this variation in the ductile-brittle transition region of carbon and low-alloy steels.

f) The fracture toughness of a material tends to decrease with increasing crack tip triaxiality. Standard laboratory specimens used to determine a material's fracture toughness are usually highly constrained.

Therefore, laboratory fracture toughness tests usually underestimate the fracture toughness of structural components of equivalent thickness that contain crack-like flaws, and flaw assessments based on standard fracture toughness data tend to be conservative.

9F.3.3.3 JR-Curve

A measure of the fracture tearing resistance as a function of the amount of stable ductile tearing is provided by determination of a JR-curve. Testing methods for the determination of JR-curves are covered in ASTM E1820. It should be noted that a JR-curve might significantly change depending on loading rate; therefore, dynamic JR-curve data should be used in the assessment of components under dynamic loading conditions.

9F.3.4 Fracture Toughness Estimation from Charpy V-Notch Data

In many instances, Charpy V-notch data are the only available measurements of toughness. The Charpy test provides an indication of fracture toughness rather than a direct measurement. Many correlations between Charpy energy and fracture toughness have been published over the years and are summarized in references [6] and [7]. Most of these correlations were developed with limited data, and no information was provided on the statistical variance of fracture toughness estimates. In some cases, correlations developed in the 1970s, when fracture toughness testing was in its infancy, have been shown to be unreliable when applied to the large amount of toughness data that is available today.

Recommendations for estimating fracture toughness for use in an FFS Assessment using Charpy data that are based on the latest technology are provided in paragraph 9F.4. For carbon and low-alloy steels, the recommended procedures for estimating fracture toughness from Charpy V-notch data are provided in paragraphs 9F.4.2 for lower bound estimates, paragraph 9F.4.3 for estimates in the transition region, and paragraph 9F.4.4 for estimates in the upper shelf region.

9F.3.5 ASME B&PV Code, Section VIII Division 1 and 2 Fracture Toughness

The dynamic and static fracture toughness consistent with the ASME Section VIII, Division 1 and 2 toughness exemption curves is given by Equations (9F.40) though (9F.43) where the parameters D and C are determined using Equations (9F.27) and (9F.28), respectively (see reference [8]).

$$K_{Id} = 0.1594\sigma_{msys}\left(\sqrt{3}+\left(\sqrt{3}-\frac{186.16}{\sigma_{msys}}\right)\cdot\tanh\left[\frac{T-D}{C}\right]\right) \qquad \left(MPa\sqrt{m},\ MPa,\ ^{\circ}C\right) \qquad (9F.40)$$

$$K_{Id} = \sigma_{msys}\left(\sqrt{3}+\left(\sqrt{3}-\frac{27}{\sigma_{msys}}\right)\cdot\tanh\left[\frac{T-D}{C}\right]\right) \qquad \left(ksi\sqrt{in},\ ksi,\ ^{\circ}F\right) \qquad (9F.41)$$

$$K_{IC} = 0.1594\sigma_{msys}\left(\sqrt{3}+\left(\sqrt{3}-\frac{186.16}{\sigma_{msys}}\right)\cdot\tanh\left[\frac{T-(D-41.67)}{C}\right]\right) \qquad \left(MPa\sqrt{m},\ MPa,\ ^{\circ}C\right) \qquad (9F.42)$$

$$K_{IC} = \sigma_{msys}\left(\sqrt{3}+\left(\sqrt{3}-\frac{27}{\sigma_{msys}}\right)\cdot\tanh\left[\frac{\left(T-\left(D-75\right)\right)}{C}\right]\right) \qquad \left(ksi\sqrt{in},\ ksi,\ ^{\circ}F\right) \qquad (9F.43)$$

9F.4 Fracture Toughness Estimation for an FFS Assessment

9F.4.1 Introduction

The fracture toughness input to the FFS analysis should come from test data for the specific material of interest (see paragraph 9F.3.3). In practice, however, heat-specific fracture toughness data are usually not available for an existing component. Consequently, alternative means are often employed to obtain conservative estimates of fracture toughness. Methods for obtaining conservative estimates of fracture toughness for use in an FFS Assessment are provided in this paragraph.

9F.4.2 ASME Section XI Fracture Toughness

9F.4.2.1 Indexing Procedure for Fracture Toughness Determination

When fracture toughness data are not available, an indexing procedure based on a reference temperature can provide a conservative lower-bound estimate of fracture toughness for a ferritic material (i.e., carbon and low alloy steels).

a) The basic premise behind the approach is illustrated schematically in Figure 9F.2. Various ferritic steels, as well as different heats of the same steel, exhibit toughness-temperature curves with similar shapes, but with ductile-brittle transitions at different temperatures. When the fracture toughness is plotted against a temperature relative to a reference transition temperature, these data tend to collapse onto a common trend, albeit with more scatter than in individual data sets. This additional scatter reflects the fact that the indexing temperature removes most, but not all, of the heat-to-heat variation in the fracture toughness curves.

b) The indexing approach was originally developed for nuclear reactor pressure vessel steels, and this methodology is included in Section XI of the ASME Boiler and Pressure Vessel Code. The reference temperature utilized is termed the RT_{NDT}. The RT_{NDT} is defined as the maximum of the nil-ductility transition temperature established by a drop weight test, and the temperature from a Charpy test where the specimen exhibits at least 0.89 mm (35 mils) of lateral expansion and not less than 68 Joules (50 ft-lbs) absorbed energy minus 33°C (60°F).

c) In the late 1960s and early 1970s, a large fracture toughness data set was collected for multiple heats of low alloy pressure vessel steels and was plotted against relative temperature. Two curves were then drawn below the data. The K_{IC} curve is a lower envelope to all the fracture toughness tests loaded at quasi-static rates. The K_{IR} curve is a lower envelope to all data that include quasi-static initiation, dynamic initiation, and crack arrest toughness results. The K_{IC} and K_{IR} reference, or *Million Dollar*, curves are shown in Figure 9F.3. The equations for these curves are shown below.

$$K_{IC} = 36.5 + 3.084\exp\left[0.036\left(T - T_{ref} + 56\right)\right] \qquad \left(MPa\sqrt{m},\ ^{\circ}C\right) \qquad (9F.44)$$

$$K_{IC} = 33.2 + 2.806\exp\left[0.02\left(T - T_{ref} + 100\right)\right] \qquad \left(ksi\sqrt{in},\ ^{\circ}F\right) \qquad (9F.45)$$

and,

$$K_{IR} = 29.5 + 1.344\exp\left[0.0260\left(T - T_{ref} + 89\right)\right] \qquad \left(MPa\sqrt{m},\ ^{\circ}C\right) \qquad (9F.46)$$

$$K_{IR} = 26.8 + 1.223\exp\left[0.0144\left(T - T_{ref} + 160\right)\right] \qquad \left(ksi\sqrt{in},\ ^{\circ}F\right) \qquad (9F.47)$$

d) Although the ASME Section XI reference curves were originally developed for nuclear grade pressure vessel steels, they have also been validated for carbon steel plates and weldments, as well as several heats of 2.25Cr-1Mo steel (see references [9] and [10]).

e) The equations for K_{IC} and K_{IR}, and the curves in Figure 9F.3, should be truncated as follows unless data are available that indicate higher maximum upper shelf toughness.

1) $110\ MPa\sqrt{m}\ \left(100\ ksi\sqrt{in}\right)$ shall be used for materials with an unknown chemistry.

2) $220\ MPa\sqrt{m}\ \left(200\ ksi\sqrt{in}\right)$ may be used for low sulfur carbon steels (0.01 percent or less), for $\bar{X}$ controlled 1.25Cr-0.5Mo steels where $\bar{X} \leq 12$ (see paragraph 9F.4.7.2), or for J controlled 2.25Cr-1Mo steels where $J \leq 120$ (see paragraph 9F.4.7.3).

9F.4.2.2 Lower Bound Toughness Based on ASME Section XI Reference Curves

A recommended procedure for determining lower bound fracture toughness for a ferritic material based on ASME Section XI Reference Curves is shown below.

a) STEP 1 – If the RT_{NDT} is known, this value can be used as T_{ref}; therefore, proceed to STEP 4. Otherwise proceed to STEP 2.

b) STEP 2 – Based on the material specification, determine the ASME Exemption Curve using Part 3, Table 3.2.

c) STEP 3 – Determine the reference temperature using paragraph 9F.2.4.3.

d) STEP 4 – Compute K_{IC} using Equations (9F.44) or (9F.45), or K_{IR} using Equations (9F.46) or (9F.47), as applicable. The truncations described in paragraph 9F.4.2.1(e) shall be applied.

9F.4.3 Fracture Toughness Master Curve

9F.4.3.1 Overview

The Fracture Toughness Master Curve (Master Curve) is used to model the lower shelf and transition region for ferritic materials. The Master Curve was developed to enable prediction of fracture toughness in the transition region including a model of uncertainty due to scatter in fracture toughness data.

A review of the micro-mechanisms of cleavage fracture indicates that cleavage toughness data tend to be highly scattered, especially in the transition region. Because of this substantial scatter, data should be treated statistically rather than deterministically. That is, a given steel does not have a single value of toughness at a particular temperature in the transition region; rather, the material has a toughness distribution. Testing numerous specimens to obtain a statistical distribution can be expensive and time consuming. The Fracture Toughness Master Curve has been developed to simplify this process for ferritic steels and has been standardized in ASTM E1921.

Research over the past 30-years into the fracture of ferritic steels in the ductile-brittle transition region has led to two important conclusions:

- Scatter in fracture toughness data in the transition region follows a characteristic statistical distribution that is the same for all ferritic steels.
- The shape of the fracture toughness versus temperature curve in the transition range is virtually identical for all ferritic steels. The only significant difference between steels is the absolute position of this curve on the temperature axis.

The term Fracture Toughness Master Curve was coined (see references [1] and [3]) to describe these two characteristics of steel. ASTM E1921 outlines a fracture toughness test method that is based on the Master Curve concept. Due to the idiosyncrasies of the micro-mechanism of cleavage fracture (see reference [3]), the fracture toughness at a fixed temperature in the transition region follows a 3-parameter Weibull distribution with a slope of four. The cumulative probability for this distribution is expressed as follows.

$$P_f = 1 - \exp\left[-\frac{B}{25}\left(\frac{K_{Jc} - K_{\min}}{K_0 - K_{\min}} \right)^4 \right] \qquad \left(mm,\ MPa\sqrt{m} \right) \tag{9F.48}$$

$$P_f = 1 - \exp\left[-B\left(\frac{K_{Jc} - K_{\min}}{K_0 - K_{\min}} \right)^4 \right] \qquad \left(in,\ ksi\sqrt{in} \right) \tag{9F.49}$$

In API 579-1/ASME FFS-1 the threshold toughness $(K_{\min})$ in Equations (9F.48) and (9F.49) is set equal to $20\ MPa\sqrt{m}$ $(18.2\ ksi\sqrt{in})$, and the cumulative distribution function is given by the equations shown below. Note that the thickness (i.e., crack front length) L is accounted for in these equations.

$$P_f = 1 - \exp\left[-\frac{L}{25}\left(\frac{K_{Jc} - 20}{K_0 - 20} \right)^4 \right] \qquad \left(mm,\ MPa\sqrt{m} \right) \tag{9F.50}$$

$$P_f = 1 - \exp\left[-L\left(\frac{K_{Jc} - 18.2}{K_0 - 18.2} \right)^4 \right] \qquad \left(in,\ ksi\sqrt{in} \right) \tag{9F.51}$$

The temperature dependence of the median fracture toughness in the transition region can be estimated using the following equation. Note that at $T = T_0$, the median fracture toughness is $100\ MPa\sqrt{m}$ $(91\ ksi\sqrt{in})$ for a 25.4 mm (1-inch) crack front length (L) (or a 1-inch fracture toughness specimen).

$$K_{Jc(median)} = 30 + 70\exp\left[0.0190\left(T - T_0 \right) \right] \qquad \left(MPa\sqrt{m}, {}^{\circ}C \right) \tag{9F.52}$$

$$K_{Jc(median)} = 27 + 64\exp\left[0.0106\left(T - T_0 \right) \right] \qquad \left(ksi\sqrt{in}, {}^{\circ}F \right) \tag{9F.53}$$

The Fracture Toughness Master Curve for ferritic steels is shown in Figure 9F.4. By combining Equations (9F.50) and (9F.51) with Equations (9F.52) and (9F.53), a median $(P_f = 0.50)$, upper bound $(P_f = 0.95)$ and lower-bound $(P_f = 0.05)$ fracture toughness as a function of temperature may be inferred if the reference transition temperature (T_0) is known (see paragraph 9F.4.3.3). Note that the fracture toughness may be established for any value of the cumulative probability that satisfies $0 < P_f < 1$.

The inherent fracture toughness of a material can be affected by the service environment. For example, temperature exposure can produce temper embrittlement in some materials and hydrogen can diffuse into the steel and can result in an apparent loss of fracture toughness. In these cases, a lower fracture toughness that accounts for the loss of toughness resulting from the service environment shall be accounted for. The loss of toughness from the service environment may be accounted for by shifting the Master Curve along the temperature axis to a higher temperature, i.e., shifting the Master Curve to the right (see Figure 9F.4).

9F.4.3.2 Determining the Master Curve Reference Transition Temperature T_0

The option used to determine the reference transition temperature (T_0) depends on the available toughness data. Four options are outlined below. Note in these procedures subsize CVN data are corrected to full-size values

(see paragraph 9F.2.2(c)) to compute T_0.

a) OPTION A – If CVN data are not available, a fracture toughness reference temperature (T_0) consistent with the VIII-1 and VIII-2 toughness exemption curves may be established using the following procedure.

1) STEP 1 – Determine the ASME exemption curve designation A, B, C and D Exemption Curves based on the material of construction (see Part 3).

2) STEP 2 – Determine the fracture toughness reference temperature (T_0).

i) For low sulfur carbon steels (0.01% or less):

$$T_0 = C_{T_0} + 0.0958\sigma_{ysA} \qquad \left(MPa,\ ^{o}C\right) \tag{9F.54}$$

$$T_0 = C_{T_0} + 1.1899\sigma_{ysA} \qquad \left(ksi,\ ^{o}F\right) \tag{9F.55}$$

where,

$$C_{T_0} = \begin{pmatrix} -18.9\,^{\circ}C & \left(-2.0\,^{\circ}F\right) & for\ ASME\ Exemption\ Curve\ A \\ -40.1\,^{\circ}C & \left(-40.2\,^{\circ}F\right) & for\ ASME\ Exemption\ Curve\ B \\ -61.2\,^{\circ}C & \left(-78.2\,^{\circ}F\right) & for\ ASME\ Exemption\ Curve\ C \\ -75.6\,^{\circ}C & \left(-104.1\,^{\circ}F\right) & for\ ASME\ Exemption\ Curve\ D \end{pmatrix} \tag{9F.56}$$

ii) For high sulfur carbon steels (greater than 0.01%)

$$T_0 = C_{T_0} + 0.1021\sigma_{ysA} \qquad \left(MPa,\ ^{o}C\right) \tag{9F.57}$$

$$T_0 = C_{T_0} + 1.2629\sigma_{ysA} \qquad \left(ksi,\ ^{o}F\right) \tag{9F.58}$$

where,

$$C_{T_0} = \begin{pmatrix} -14.8\,^{\circ}C & \left(+5.4\,^{\circ}F\right) & for\ ASME\ Exemption\ Curve\ A \\ -36.0\,^{\circ}C & \left(-32.8\,^{\circ}F\right) & for\ ASME\ Exemption\ Curve\ B \\ -57.1\,^{\circ}C & \left(-70.8\,^{\circ}F\right) & for\ ASME\ Exemption\ Curve\ C \\ -71.4\,^{\circ}C & \left(-96.5\,^{\circ}F\right) & for\ ASME\ Exemption\ Curve\ D \end{pmatrix} \tag{9F.59}$$

Equations (9F.54) through (9F.59) incorporate an upward temperature shift above the mean T_0 estimate of 1.5 standard deviations, which is equal to 27°C (48.6°F). The development of the above equations is provided in WRC Bulletin 562 (see reference [11]).

b) OPTION B – If CVN data are available at one or more temperatures with impact energies different from 28 J (20 ft-lbs), but there are insufficient data to fit a transition curve, the following procedure may be used to estimate the 28 J (20 ft-lbs) reference temperature, i.e., $T_{28\ Joules}$ $\left(T_{20\ ft-lbs}\right)$. It is noted that using this option with CVN energies less than 13.5 J (10 ft-lbs) may result in inaccurate estimations for the 28 J (20 ft-lbs) reference temperature. In addition, this option has not been validated for steels with upper-shelf Charpy energies above 200 J (147 ft-lbs).

1) STEP 1 – Calculate the average full-size Charpy impact energy (C_V) at the test temperature (TC_V). If data are available at more than one temperature, choose the temperature at which the average Charpy impact energy is closest to 28 J (20 ft-lbs).

2) STEP 2 – Estimate the full-size lower shelf CVN impact energy (C_{V-LS}) . If direct measurements of lower shelf CVN energy are not available, it can be estimated using Equation (9F.60) or (9F.61).

$$C_{V-LS} = 2.50 + \left(\frac{\sigma_{ysA}}{460}\right)^2 \qquad (J, MPa) \qquad \text{(9F.60)}$$

$$C_{V-LS} = 1.84 + 0.738\left(\frac{\sigma_{ysA}}{66.7}\right)^2 \qquad (ft-lbs, ksi) \qquad \text{(9F.61)}$$

3) STEP 3 – Estimate the full-size upper shelf Charpy impact energy (C_{V-US}).

i) If direct measurements of upper shelf toughness are not available, it may be estimated if the percent shear area (SA) is included in the Charpy test report (see reference [1]).

I) Ferritic Materials:

$$C_{V-US} = \frac{C_V}{0.05 + 0.95\left(\frac{SA}{100}\right)^{0.72}} \qquad \text{(9F.62)}$$

II) Austenite-Ferrite Duplex Materials:

$$C_{V-US} = \frac{C_V}{0.05 + 0.95\left(\frac{SA}{100}\right)^{2}} \qquad \text{(9F.63)}$$

ii) If the percent shear is not available, a conservative value for the upper shelf Charpy impact energy may be estimated as follows.

I) For low sulfur carbon steels (0.01% or less):

$$C_{V-US} = 200\ J \qquad \text{(9F.64)}$$

$$C_{V-US} = 147.6\ ft-lbs \qquad \text{(9F.65)}$$

II) For high sulfur carbon steels (greater than 0.01%):

$$C_{V-US} = 100\ J \qquad \text{(9F.66)}$$

$$C_{V-US} = 73.8\ ft-lbs \qquad \text{(9F.67)}$$

4) STEP 4 – Estimate the hyperbolic tangent fitting parameter (C) using the following equations (see reference [11]).

$$C = 34^{\circ}C + \frac{\sigma_{ysA}}{35.1} - \frac{C_{V-US}}{14.3} \qquad (^{\circ}C, MPa, J) \qquad \text{(9F.68)}$$

$$C = 61^{\circ}F + \frac{\sigma_{ysA}}{2.83} - \frac{C_{V-US}}{5.86} \qquad (^{\circ}F, ksi, ft-lbs) \qquad \text{(9F.69)}$$

5) STEP 5 – Determine $T_{28\ Joules}\ (T_{20\ ft-lbs})$ if $C_{V-LS} < C_V < C_{V-US}$ use the following equations.

$$T_{28Joules} = TC_V - \beta C \cdot \ln\left[\frac{(C_V - C_{V-LS})\cdot(C_{V-US} - 28)}{(28 - C_{V-LS})\cdot(C_{V-US} - C_V)}\right] \qquad (^{\circ}C, J) \qquad \text{(9F.70)}$$

$$T_{20\,ft-lbs} = TC_V - \beta C \cdot \ln\left[\frac{(C_V - C_{V-LS})\cdot(C_{V-US} - 20)}{(20 - C_{V-LS})\cdot(C_{V-US} - C_V)}\right] \qquad (^{\circ}F,\ ft-lbs) \qquad \text{(9F.71)}$$

where,

- $\beta = 0.25 \quad if \quad C_V \geq T_{28\ Joules}\ (T_{20\ ft-lbs})$.
- $\beta = 1.0 \quad if \quad C_V < T_{28\ Joules}\ (T_{20\ ft-lbs})$.

These β factors ensure that the extrapolation to the $T_{28\ Joules}\ (T_{20\ ft-lbs})$ reference temperature is conservative. There is a significant degree of uncertainty in the C parameter when it is estimated from Equation (9F.68) or (9F.69). If a hyperbolic tangent function has been fit to Charpy data, such that C is known, then $\beta = 0.5$.

If only upper-shelf Charpy data are available, a conservative estimate of the $T_{28\ Joules}\ (T_{20\ ft-lbs})$ reference temperature can be inferred from the following equations:

$$T_{28Joules} = TC_{V-US} - \left(\frac{C}{4}\right)\cdot\ln\left[\frac{19\cdot(C_{V-US} - 28)}{28}\right] \qquad (^{\circ}C, J) \qquad \text{(9F.72)}$$

$$T_{20\,ft-lbs} = TC_{V-US} - \left(\frac{C}{4}\right)\cdot\ln\left[\frac{19\cdot(C_{V-US} - 20)}{20}\right] \qquad (^{\circ}F,\ ft-lbs) \qquad \text{(9F.73)}$$

Where TC_{V-US} is the minimum test temperature.

6) STEP 6 – Determine the Master Curve reference transition temperature (T_0) using Equation (9F.74) or (9F.75).

c) OPTION C – If sufficient Charpy data are available to fit a transition curve, or if sufficient data are available at multiple temperatures to interpolate the 28 J (20 ft-lbs) transition temperature, then set the reference transition temperature $T_{28\ Joules}\ (T_{20\ ft-lbs})$ equal to the temperature at which the mean full-size Charpy data energy is equal to 28 J (20 ft-lbs). The hyperbolic tangent equation is recommended for fitting Charpy versus temperature data (see paragraph 9F.2.3). Based on $T_{28\ Joules}\ (T_{20\ ft-lbs})$, C_{V-US}, and σ_{ysA}, the Master Curve reference transition temperature (T_0) may be determined using the equations shown below. This option has not been validated for steels with upper-shelf Charpy energies above 200 J (147 ft-lbs).

$$T_0 = T_{28\ Joules} - 79^{o}C + \frac{\sigma_{ysA}}{9\ MPa\cdot{}^{o}C^{-1}} - \frac{C_{V-US}}{59\ J\cdot{}^{o}C^{-1}} + \Delta T_0 \qquad (^{o}C, MPa, J) \qquad \text{(9F.74)}$$

$$T_0 = T_{20\,ft-lbs} - 142^{o}F + \frac{\sigma_{ysA}}{0.725\ ksi\cdot{}^{o}F^{-1}} - \frac{C_{V-US}}{24.2\ ft-lbs\cdot{}^{o}F^{-1}} + \Delta T_0 \qquad (^{o}F, ksi, ft-lbs) \qquad \text{(9F.75)}$$

where ΔT_0 is a temperature shift on T_0. For a Level 2 Assessment, set ΔT_0 to +18°C (+32.4°F), which corresponds to one standard deviation on the T_0 estimate from the Charpy reference temperature. For a Level 3 probabilistic assessment, ΔT_0 may be treated as a random variable with a mean value of 0°C (0°F) and a standard deviation of ±18°C (±32.4°F).

d) OPTION D – If direct fracture toughness measurements in the ductile-brittle transition range are available, these data are used to compute the Master Curve reference transition temperature (T_0). If a valid (T_0) value is obtained from testing in accordance with ASTM Standard E1921, then this value should be used directly. Alternatively, if three (3) fracture toughness tests have been performed at a fixed test temperature (T) in the transition region, then the following procedure can be followed.

1) STEP 1 – Using the lowest of the three measured fracture toughness values, convert the critical J or $CTOD$ value to K_{Jc} using the following equations.

$$K_{Jc} = \sqrt{\frac{J_{crit} \cdot E_{yT}}{1-\nu^2}} \tag{9F.76}$$

$$K_{\delta c} = \sqrt{\frac{m_{CTOD} \cdot \sigma_{fT} \cdot E_{yT} \cdot \delta_{crit}}{1-\nu^2}} \tag{9F.77}$$

where,

$$\sigma_{fT} = \frac{\sigma_{ysT} + \sigma_{utsT}}{2} \tag{9F.78}$$

And the subscript T in the material properties refers the test temperature in this case.

2) STEP 2 – If the specimen thickness (B) is greater than or less than 25 mm (1-inch), adjust the K_{mat} value from STEP 1 using the following equations.

$$K_{mat(25mm)} = 20 + \left(K_{mat(B)} - 20\right)\left(\frac{B}{25}\right)^{0.25} \qquad \left(MPa\sqrt{m},\, mm\right) \tag{9F.79}$$

$$K_{mat(1in)} = 18.2 + \left(K_{mat(B)} - 18.2\right)\left(\frac{B}{1.0}\right)^{0.25} \qquad \left(ksi\sqrt{in},\, in\right) \tag{9F.80}$$

3) STEP 3 – Determine T_0 from the following equations.

$$T_0 = T - \left(\frac{1}{0.0190}\right) \cdot \ln\left[\frac{K_{mat(25mm)} - 30}{70}\right] \qquad \left(^{\circ}C,\, MPa\sqrt{m}\right) \tag{9F.81}$$

$$T_0 = T - \left(\frac{1}{0.0106}\right) \cdot \ln\left[\frac{K_{mat(1in)} - 27}{64}\right] \qquad \left(^{\circ}F,\, ksi\sqrt{in}\right) \tag{9F.82}$$

9F.4.3.3 Fracture Toughness Prediction Using the Master Curve

A fracture toughness prediction at an assessment temperature corresponding to a cumulative probability of failure, P_f, can be established using following procedure.

a) STEP 1 – Determine Master Curve index temperature (T_0) using paragraph 9F.4.3.2.

b) STEP 2 – Determine a cumulative probability (P_f) to use in the assessment. Note that the recommended cumulative probability to represent a lower bound estimate is $P_f = 0.05$, corresponding to a 5% lower bound.

c) STEP 3 – Determine the parameter L, for a surface or embedded flaw:

$$L = \min\left[2c,\, 100\,mm\ (4\,in)\right] \tag{9F.83}$$

d) STEP 4 – Determine the fracture toughness in the transition region $\left(K_{mat-TR} = K_{Jc}\right)$ at the assessment temperature T using Equations (9F.84) or (9F.85).

$$K_{Jc} = 20 + \left(11 + 77\exp\left[0.0190\left(T - T_0\right)\right]\right)\left(\ln\left[\frac{1}{1-P_f}\right]\cdot\left(\frac{25}{L}\right)\right)^{0.25} \quad \left(MPa\sqrt{m}, {}^{\circ}C, mm\right) \qquad (9F.84)$$

$$K_{Jc} = 18.2 + \left(9.9 + 70.1\exp\left[0.0106\left(T - T_0\right)\right]\right)\left(\ln\left[\frac{1}{1-P_f}\right]\cdot\left(\frac{1}{L}\right)\right)^{0.25} \quad \left(ksi\sqrt{in}, {}^{\circ}F, in\right) \qquad (9F.85)$$

9F.4.3.4 Determining the Master Curve Reference Transition Temperature T_0 for Modern Cr-Mo Steels

Modern Cr-Mo steels that are constructed to the API 934-A, API 934-C, or API 934-E standards are made to higher toughness requirements (e.g., 54 Joules (40 ft-lbs)) compared to typical carbon and low alloy steels. Therefore, establishing the Master Curve index temperature (T_0) using ASME exemption curve designation A, B, C and D (see paragraph 9F.4.3.2, Option A) will be conservative. In such cases, T_0 may be estimated using paragraph 9F.4.3.2, Option B with the known values of Charpy impact energies or the minimum toughness requirements of the specific API 934 standard.

9F.4.4 Upper Shelf Fracture Toughness

9F.4.4.1 Overview

The Master Curve is used to model the lower shelf and the ductile-brittle transition region as described in paragraph 9F.4.3. However, the Master Curve is unsuitable as a model for the upper shelf because Equations (9F.84) and (9F.85) increase without bound with increasing temperature. Therefore, a model for the upper shelf is required to limit the Master Curve toughness prediction. Two options are provided for the upper shelf fracture toughness model.

a) Option A is based on another empirical relationship developed by Wallin that relates the upper shelf Charpy impact energy to the J-integral at 1 mm of ductile tearing, J_{1mm}. The upper shelf fracture toughness is determined using $J_{crit} = 0.7J_{1mm}$, (see reference [1]).

b) Option B is based on the upper bound provided in paragraph 9F.4.2.1(e).

9F.4.4.2 Fracture Toughness Prediction

The following two options, applicable to carbon and low-allow steels, are provided to estimate the fracture toughness for the upper shelf (K_{mat-US}). Note in these procedures subsize CVN data should be corrected to full-size values (see paragraph 9F.2.2(c)).

a) OPTION A – In the Wallin J-integral Correlation the upper shelf Charpy impact energy is correlated with the J-integral at 1 mm (0.039-inch) of ductile tearing (J_{1mm}). This correlation has a 17% Coefficient of Variation (COV) on the J_{1mm} estimate. Note that if this model is used for the upper shelf, K_{mat-US} will be a function of temperature because E_y is a function of temperature.

1) Median correlation:

$$J_{1\text{ mm}} = 0.74\left(C_{V-US}\right)^{1.28} \quad \left(kJ/m^2, J\right) \qquad (9F.86)$$

$$J_{1\text{ mm}} = 6.248\left(C_{V-US}\right)^{1.28} \quad \left(in-lbs/in^2, ft-lb\right) \qquad (9F.87)$$

2) 5% Lower-Bound correlation:

$$J_{1\,\mathrm{mm}} = 0.53\left(C_{V-US}\right)^{1.28} \qquad \left(kJ/m^2,\ J\right) \tag{9F.88}$$

$$J_{1\,\mathrm{mm}} = 4.482\left(C_{V-US}\right)^{1.28} \qquad \left(in-lbs/in^2,\ ft-lbs\right) \tag{9F.89}$$

The upper shelf fracture toughness (K_{mat-US}) can be determined using Equation (9F.76) with $J_{crit} = 0.7J_{1mm}$:

$$K_{mat-US} = K_{Jc} = \sqrt{\frac{J_{crit} \cdot E_{yT}}{1-v^2}} \tag{9F.90}$$

b) OPTION B – The following estimates from paragraph 9F.4.2.1(e) may be used for the upper shelf fracture toughness (K_{mat-US}).

1) Equation (9F.91) should be used for materials with an unknown chemistry.

$$K_{mat-US} = 110\ MPa\sqrt{m}\ \left(100\ ksi\sqrt{in}\right) \tag{9F.91}$$

2) Equation (9F.92) may be used for low sulfur carbon steels (0.01 percent or less), for 1.25Cr-0.5Mo with $\bar{X} \leq 15$ (see paragraph 9F.4.7.2) and for 2.25Cr-1Mo steels with $J \leq 150$ (see paragraph 9F.4.7.3).

$$K_{mat-US} = 220\ MPa\sqrt{m}\ \left(200\ ksi\sqrt{in}\right) \tag{9F.92}$$

9F.4.5 Dynamic and Crack Arrest Fracture Toughness

9F.4.5.1 Overview

When a material is subject to a rapidly applied load or a rapidly propagating crack, the response of that material may be drastically different from the quasi-static case. When rapid loading or unstable crack propagation are likely to occur in practice, it is important to properly estimate the material properties in an assessment. The dynamic fracture toughness and the crack-arrest toughness are two important material properties for many applications. The dynamic fracture toughness is a measure of the resistance of a material to the onset of crack propagation under rapid loading, while the crack-arrest toughness quantifies the ability of a material to stop a rapidly propagating crack. In the latter case, the crack may initiate under either dynamic or quasi-static conditions, but unstable propagation is generally a dynamic phenomenon. Dynamic fracture problems are often complicated by inertia effects, material rate dependence, and reflected stress waves.

9F.4.5.2 Dynamic Fracture Toughness Prediction

A procedure to estimate the dynamic fracture toughness (K_{1d}) in terms of the Fracture Toughness Master Curve is shown below. The dynamic fracture toughness can be determined using the Master Curve by shifting the reference transition temperature (T_0) for static loading (see Figure 9F.5 and reference [1]).

a) STEP 1 – Determine Master Curve index temperature (T_0) using paragraph 9F.4.3.2.

b) STEP 2 – Estimate the Zener-Hollomon type parameter using the equations shown below.

$$\Gamma = 1.78 \cdot \exp\left[\left(\frac{T_0 + 273.15}{194}\right)^{1.9} + \left(\frac{\sigma_{ysA}}{44.2}\right)^{0.37}\right] \qquad \left({}^{\circ}C,\ MPa\right) \tag{9F.93}$$

$$\Gamma = 1.78 \cdot \exp\left[\left(\frac{T_0 + 459.67}{349}\right)^{1.9} + \left(\frac{\sigma_{ysA}}{6.41}\right)^{0.37}\right] \qquad \left(^{\circ}F,\ ksi\right) \qquad \text{(9F.94)}$$

c) STEP 3 – Estimate the temperature shift from the loading rate in the elastic range, as characterized by the stress intensity factor rate, $\dot{K}_I$. The quasi-static loading rate, $\dot{K}_{I-static}$, may be set to $1\ MPa\sqrt{m}/\sec\ \left(0.91\ ksi\sqrt{in}/sec\right)$.

$$\Delta T_s = \frac{\left(T_0 + 273.15\right) \cdot \ln\left[\dfrac{\dot{K}_{1-dynamic}}{\dot{K}_{1-static}}\right]}{\Gamma - \ln\left[\dfrac{\dot{K}_{1-dynamic}}{\dot{K}_{1-static}}\right]} \qquad \left(^{o}C\right) \qquad \text{(9F.95)}$$

$$\Delta T_s = \frac{\left(T_0 + 459.67\right) \cdot \ln\left[\dfrac{\dot{K}_{1-dynamic}}{\dot{K}_{1-static}}\right]}{\Gamma - \ln\left[\dfrac{\dot{K}_{1-dynamic}}{\dot{K}_{1-static}}\right]} \qquad \left(^{o}F\right) \qquad \text{(9F.96)}$$

d) STEP 4 – Determine the index temperature for estimating the dynamic fracture toughness (T_0^D).

$$T_0^{\ D} = T_0 + \Delta T_s \qquad \text{(9F.97)}$$

e) STEP 5 – Determine the fracture toughness using $T_0 = T_0^D$ in conjunction with paragraph 9F.4.3.3.

9F.4.5.3 Arrest Fracture Toughness Prediction

The crack arrest toughness (K_{IR}) can be determined using the Master Curve by shifting the index temperature (T_0) for static loading (see Figure 9F.5 and reference [1]).

a) STEP 1 – Determine the Master Curve index temperature (T_0) using paragraph 9F.4.3.2.

b) STEP 2 – Determine the temperature shift between the quasi-static toughness and the arrest toughness (ΔT_s) using the equations shown below. If the steel contains a high Nickel content (Ni > 1%), this may be accounted for when calculating the temperature shift.

1) Without Nickel effect (Ni ≤ 1%):

$$\Delta T_s = \exp\left[5.25 - \left(\frac{T_0 + 273.15}{162.6}\right) + \left(\frac{\sigma_{ysA}}{1897.4}\right)\right] \qquad \left(^{\circ}C,\ MPa\right) \qquad \text{(9F.98)}$$

$$\Delta T_s = 1.8 \cdot \exp\left[5.25 - \left(\frac{T_0 + 459.67}{292.7}\right) + \left(\frac{\sigma_{ysA}}{275.1}\right)\right] \qquad \left(^{\circ}F,\ ksi\right) \qquad \text{(9F.99)}$$

2) With Nickel effect (Ni > 1%):

$$\Delta T_s = \exp\left[5.48 - \left(\frac{T_0 + 273.15}{172.0}\right) + \left(\frac{\sigma_{ysA}}{27000}\right) - \left(\frac{\%\text{Ni}}{4.3}\right)\right] \qquad \left(^{\circ}C,\ MPa,\%\right) \qquad \text{(9F.100)}$$

$$\Delta T_s = 1.8 \cdot \exp\left[5.48 - \left(\frac{T_0 + 459.67}{309.6}\right) + \left(\frac{\sigma_{ysA}}{3916.0}\right) - \left(\frac{\%\text{Ni}}{4.3}\right)\right] \qquad \left(^{\circ}F,\ ksi,\%\right) \qquad \text{(9F.101)}$$

c) STEP 3 – Determine the index temperature for estimating the arrest fracture toughness $\left(T_0^A\right)$.

$$T_0^A = T_0 + \Delta T_s \tag{9F.102}$$

d) STEP 4 – Determine the fracture toughness using $T_0 = T_0^A$ in conjunction with paragraph 9F.4.3.3.

9F.4.6 Fracture Toughness for Materials Subject to In-Service Degradation

9F.4.6.1 Service Environment Effects on Fracture Toughness

The inherent fracture toughness of a material can be affected by the service environment. For example, hydrogen can diffuse into the steel and can result in an apparent loss of fracture toughness. Temperature exposure can produce embrittlement, such as strain aging, temper embrittlement, 885-embrittlement, and sigma phase embrittlement. In these cases, a lower fracture toughness that accounts for the loss of toughness resulting from the service environment shall be used in the assessment.

9F.4.6.2 Hydrogen Effects on Fracture Toughness and Flaw Assessment

Hydrogen dissolved in ferritic steel can significantly reduce the apparent fracture toughness of a material. Fracture initiation is enhanced when hydrogen diffuses to the tip of a crack. If rapid unstable crack propagation begins, however, diffusing hydrogen cannot keep pace with the growing crack; therefore, the resistance to rapid crack propagation increases with increasing rate and the rate slows to establish equilibrium between the growth rate and the hydrogen delivery rate. In other words, the toughness corresponding to initiation of fast fracture in a hydrogen-charged steel will not fall below the arrest toughness because the ability of atomic hydrogen to affect toughness is limited by diffusion rates to the crack tip. The arrest toughness lower bound does not protect against subcritical hydrogen-driven growth, which may continue at an equilibrium rate governed by diffusion kinetics and other factors.

If the hydrogen concentration is less than or equal to 1 ppm, then the hydrogen effects on fracture toughness is negligible.

a) Fracture Toughness – To account for the loss in fracture toughness when the hydrogen concentration is greater than 1 ppm, a material dependent temperature shift or the use of the arrest toughness is used. If actual fracture toughness data is available, it may be used in the assessment.

1) For 2.25Cr-1Mo – An upper limit for temperature shift is shown below, reference [12]. The temperature shift calculated using the equations below is added to T_0, that is determined from paragraphs 9F.4.3.2, 9F.4.7.2 or 9F.4.7.3, as applicable. This temperature shift is based on data for 2.25 Cr – 1 Mo steels. Steels with lower alloy content and yield strength < 690 MPa (100 ksi) are likely less susceptible to hydrogen embrittlement, which translates to a lower $T_{Shift}^{\mathrm{H_2}}$ than indicated above. An alternative temperature shift may be used if data are available for the material of interest.

$$T_{Shift}^{H_2} = 50^\circ C \tag{9F.103}$$

$$T_{Shift}^{H_2} = 90^\circ F \tag{9F.104}$$

2) For 2.25Cr-1Mo-V – Hydrogen does not affect the fracture toughness of this material; therefore, a temperature shift is not required for T_0 that is determined from paragraphs 9F.4.3.2, 9F.4.7.2 or 9F.4.7.3, as applicable).

$$T_{Shift}^{H_2} = 0^\circ C \tag{9F.105}$$

$$T_{Shift}^{H_2} = 0^{\circ} F \tag{9F.106}$$

3) Carbon Steels and Low Chrome Alloys that are not Defined Above – A temperature shift cannot be accurately defined for these materials because of the lack of test data. Therefore, the arrest toughness in terms of the Master Curve shall be used as a conservative estimate or lower bound of the resistance of a ferritic steel containing dissolved hydrogen to rapid unstable crack propagation. Note, the arrest toughness does not provide a threshold against subcritical crack growth. A procedure to estimate arrest toughness in terms of the Fracture Toughness Master Curve is provided in paragraph 9F.4.5.3.

b) Flaw Assessment – The assessment of flaws in hydrogen charged materials should be treated with extreme caution. The above procedure does not take account of the following two factors.

1) If a material remains in a hydrogen-charging environment in service, the cracks may grow by what is known as subcritical crack growth. Consequently, a flaw that is acceptable at its current size may grow to a critical size over time. If the applied K is above the threshold stress intensity for crack growth, the flaw will grow until the crack driving force exceeds the arrest toughness, at which time unstable fracture will occur.

2) Long exposure to hydrogen may produce irreversible damage (e.g., micro-cracks) in the material. The apparent toughness could fall below the arrest toughness in such cases.

9F.4.6.3 Overview of Metallurgical Embrittlement that Reduces Ductility and Fracture Toughness

There are several types of metallurgical embrittlement listed below that can reduce the ductility and fracture properties of carbon, alloy, and stainless steels below the original fracture toughness.

a) Brief descriptions of the types of embrittlement currently encountered in industry are described below.

1) Strain Age Embrittlement of Carbon and Carbon/Molybdenum Steels – occurs in the plastic zone at the tip of a crack or at a strain concentration. It most typically occurs when a weld is made near a crack, causing the material near the crack tip to be strained and heated in the 149°C (300°F) to 260°C (500°F) range. Steels with an aluminum content greater than 0.015 wt % (i.e., killed steels) are not susceptible, and PWHT alleviates the problem for susceptible steels.

2) Loss of Toughness with Aging of 1.25Cr-0.5Mo Steel – can occur in steels that have been in service in the 371°C (700°F) to 593°C (1100°F) temperature range. Embrittlement is thought to be related to carbide formation and/or the level of tramp element impurities (i.e., As, P, Sb, and Sn) present in the steel. Factors such as heat treatment condition and microstructure play a role. In many cases, older steels usually are more susceptible than newer generation steels. Toughness may be affected up to 149°C (300°F). In general, steels are more susceptible the higher the carbon content and steels above 0.15 wt % carbon are most susceptible. Although the correlation is not strong, the loss of toughness for 1.25Cr-0.5Mo has been correlated to the $\bar{X}$ factor (see paragraph 9F.4.7.2).

3) Temper Embrittlement of 2.25Cr-1Mo Steel – can occur in steels that have been in service in the 343°C (650°F) to 593°C (1100°F) temperature range. Embrittlement is related to the level of tramp element impurities (i.e., Mn, P, Si, and Sn) present in the steel, and to the heat treatment condition and microstructure. In many cases, older steels usually are more susceptible than newer generation steels. Toughness may be affected up to 149°C (300°F) and more. The degree of susceptibility for 2.25Cr-1Mo has been correlated to the J factor for base metal and $\bar{X}$ factor for weld metal (see paragraph 9F.4.7.3).

4) 885 (°F) Embrittlement of Ferritic or Duplex Stainless Steels – can occur if a ferritic or duplex stainless steel is subjected to the temperature range of 299°C (570°F) to 349°C (660°F). The material toughness for 885 embrittled steels is affected up to 149°C (300°F).

5) Sigma Phase Embrittlement of Austenitic Stainless Steels – sigma phase can form in austenitic stainless steels that contain ferrite in welds and are subject to heat treatment in the 649°C (1200°F) to 760°C (1400°F) temperature range, or irrespective of ferrite content if subjected to a 593°C (1100°F) to 816°C (1500°F) temperature range for prolonged periods. Toughness is affected most at ambient temperatures but is affected even at operating temperatures.

b) If a material has experienced embrittlement because of the service environment, the toughness can be extremely low. To ascertain the toughness, samples may be removed and tests, such as CVN, could be conducted on the material to estimate the toughness. Otherwise, the toughness values may be used based on the relative degree of embrittlement.

9F.4.7 Aging Effects on the Fracture Toughness of Cr-Mo Steels

9F.4.7.1 Overview

The effect of embrittlement due to service conditions on the fracture toughness may be estimated for certain Cr-Mo steels based on chemistry. The transition reference temperature (T_0) is used to characterize the extent of the embrittlement.

a) If the toughness calculated using the following temper embrittlement analyses is higher than predicted by the methods in paragraphs 9F.4.3 and 9F.4.4 for a non-embrittled steel, then the temper embrittlement has no effect on the fracture toughness.

b) If the fracture toughness predicted by the following temper embrittlement analyses is lower than that predicted by the methods in paragraphs 9F.4.3 and 9F.4.4, then temper embrittlement may affect the fracture toughness and the lower value of the estimated fracture toughness should be used in the assessment.

9F.4.7.2 Effect of Tramp Elements on the Fracture Toughness of 1.25Cr-0.5Mo

A procedure to determine the fracture toughness for 1.25Cr-0.5Mo including the effects of temper embrittlement is shown below. The technical background for this procedure is provided in references [11]–[12]).

a) STEP 1 – Determine the value of the chemistry parameter $\bar{X}$.

1) If the tramp elements, weight percent of phosphorous $(\%P)$, antimony $(\%Sb)$, tin $(\%Sn)$, and arsenic $(\%As)$, are known, $\bar{X}$ is determined from the following equation. Note that samples may be obtained to determine the tramp elements required to determine $\bar{X}$.

$$\bar{X} = \left(10 \cdot \%P + 5 \cdot \%Sb + 4 \cdot \%Sn + \%As\right) \cdot 100 \qquad \text{(9F.107)}$$

2) If the tramp elements are not known, a conservative value of $\bar{X} = 35$ shall be used.

b) STEP 2 – Determine the Fracture Appearance Transition Temperature $(FATT)$ based on a material chemistry parameter $\bar{X}$ as shown below. This correlation applies to both weld metal and base metal in the case of 1.25Cr-0.5Mo steel. This correlation only considers the effect of tramp elements on toughness. This prediction may be non-conservative if severe carbide embrittlement is possible. In such a case, a higher estimated $FATT$ should be used.

$$FATT\big|_{\substack{upper\\bound}} = -87.355 + 11.437\bar{X} - 0.14712\bar{X}^2 \qquad \left(^{\circ}C\right) \tag{9F.108}$$

$$FATT\big|_{\substack{upper\\bound}} = -125.239 + 20.5866\bar{X} - 0.26480\bar{X}^2 \qquad \left(^{\circ}F\right) \tag{9F.109}$$

c) STEP 3 – Determine the reference transition temperature (T_0) using the following equations.

$$T_0 = FATT\big|_{\substack{upper\\bound}} - 50^{\circ}C \qquad \left(^{\circ}C\right) \tag{9F.110}$$

$$T_0 = FATT\big|_{\substack{upper\\bound}} - 90^{\circ}F \qquad \left(^{\circ}F\right) \tag{9F.111}$$

d) STEP 4 – Determine the fracture toughness using paragraph 9F.4.3.3.

9F.4.7.3 Effect of Tramp Elements on the Fracture Toughness of 2.25Cr-1Mo

Two procedures are provided to determine the fracture toughness for 2.25Cr-1Mo including the effects of temper embrittlement. The first procedure for base metal uses the chemistry parameter J and the second procedure for weld metal uses the chemistry parameter $\bar{X}$. Note that $\bar{X}$ is only applicable to weld metal in the case of 2.25Cr-1Mo steel. The technical background for this procedure is provided in reference [12].

a) Chemistry Parameter J (base metal):

1) STEP 1 – Determine the value of the chemistry parameter J.

i) If the tramp elements, weight percent of manganese ($\%Mn$), silicon ($\%Si$), phosphorous ($\%P$), and tin ($\%Sn$), are available, J is determined from the following equation. Note that samples may be obtained to determine the tramp elements required to determine J.

$$J = \left(\%Mn + \%Si\right) \cdot \left(\%P + \%Sn\right) \cdot 10000 \tag{9F.112}$$

ii) If the tramp elements are not known, a conservative value of J may be determined as follows based on the vintage of the material.

- Post 1990 – $J = 50$
- 1975 - 1990 – $J = 146$
- Prior to 1975 – $J = 230$

2) STEP 2 – Determine the Fracture Appearance Transition Temperature ($FATT$) based on a material chemistry parameter J from STEP 1. Note, this prediction may be non-conservative if severe carbide embrittlement is possible. In such a case, a higher estimated $FATT$ should be used.

$$FATT = \begin{cases} -30^{o}C & J \le 50 \\ 0.8333J - 71.667 & 50 < J < 230 \\ 120^{o}C & J \ge 230 \end{cases} \qquad \left(^{o}C\right) \tag{9F.113}$$

$$FATT = \begin{cases} -22^{o}F & J \le 50 \\ 1.50J - 97.0 & 50 < J < 230 \\ 248^{o}F & J \ge 230 \end{cases} \qquad \left(^{o}F\right) \tag{9F.114}$$

3) STEP 3 – Determine the reference transition temperature (T_0) using the following equations.

$$T_0 = FATT - 50^\circ C \qquad \left(^\circ C\right) \qquad \text{(9F.115)}$$

$$T_0 = FATT - 90^\circ F \qquad \left(^\circ F\right) \qquad \text{(9F.116)}$$

4) STEP 4 – Determine the fracture toughness using paragraph 9F.4.3.3.

b) Chemistry Parameter $\bar{X}$ (weld metal):

1) STEP 1 – Determine the value of the chemistry parameter $\bar{X}$.

i) If the tramp elements, weight percent of phosphorous $(\%P)$, antimony $(\%Sb)$, tin $(\%Sn)$, and arsenic $(\%As)$, are known, $\bar{X}$ is determined from the following equation. Note that samples may be obtained to determine the tramp elements required to determine $\bar{X}$.

$$\bar{X} = \left(10 \cdot \%P + 5 \cdot \%Sb + 4 \cdot \%Sn + \%As\right) \cdot 100 \qquad \text{(9F.117)}$$

ii) If tramp elements for the weld metal are unknown, assume the weld metal is no worse than the base metal and calculate T_0 using the guidance from paragraph 9F.4.7.3(a).

2) STEP 2 – Determine the Fracture Appearance Transition Temperature $(FATT)$ based on a material chemistry parameter $\bar{X}$ as shown below. This correlation applies to both weld metal and base metal. This correlation only considers the effect of tramp elements on toughness. This prediction may be non-conservative if severe carbide embrittlement is possible. In such a case, a higher estimated $FATT$ should be used.

$$FATT = \begin{cases} -30^o C & \bar{X} \le 10 \\ 11.538\bar{X} - 145.385 & 10 < \bar{X} < 23 \\ 120^o C & \bar{X} \ge 23 \end{cases} \qquad \left(^o C\right) \qquad \text{(9F.118)}$$

$$FATT = \begin{cases} -22^o F & \bar{X} \le 10 \\ 20.769\bar{X} - 229.692 & 10 < \bar{X} < 23 \\ 248^o F & \bar{X} \ge 23 \end{cases} \qquad \left(^o F\right) \qquad \text{(9F.119)}$$

3) STEP 3 – Determine the reference transition temperature (T_0) using the following equations.

$$T_0 = FATT\Big|_{\substack{upper \\ bound}} - 50^\circ C \qquad \left(^\circ C\right) \qquad \text{(9F.120)}$$

$$T_0 = FATT\Big|_{\substack{upper \\ bound}} - 90^\circ F \qquad \left(^\circ F\right) \qquad \text{(9F.121)}$$

4) STEP 4 – Determine the fracture toughness using paragraph 9F.4.3.3.

9F.4.8 Fracture Toughness of Electroslag Welds in 2.25Cr-1Mo Vessels

For reactors with electroslag welds the temperature at which the toughness is reported to be 54 J (40 ft-lbs) may be up to 170°C (340°F) (see reference [14]), or

$$T_{54 Joules} = 170^o C \qquad \text{(9F.122)}$$

$$T_{40\,ft-lbs} = 340^o F \qquad \text{(9F.123)}$$

Assuming $T_{54J} = FATT - 7°C$ $\left(T_{40\,ft-lbs} = FATT - 12.6°F\right)$ (see reference [14]), the temperature for an expected Charpy impact energy of 28 Joules (20 ft-lbs) may be estimated by:

$$T_{28Joules} = \left(FATT - 7^{\circ}C\right) - 0.26 \cdot \left(26.3^{\circ}C + \frac{\sigma_{msys}}{35.1}\right) \qquad \left(^{o}C,\ MPa\right) \qquad \text{(9F.124)}$$

$$T_{20\,ft-lbs} = \left(FATT - 12.6^{\circ}F\right) - 0.26 \cdot \left(47.34^{\circ}F + \frac{\sigma_{msys}}{2.828}\right) \qquad \left(^{o}F,\ ksi\right) \qquad \text{(9F.125)}$$

The reference transition temperature (T_0) is determined using Equations (9F.74) and (9F.75).

9F.4.9 Fracture Toughness as a Function of Temperature for Ferritic Materials

The fracture toughness curve as a function of temperature is created by capping the transition region toughness with an upper shelf toughness value as shown in Equation (9F.126). In this equation, K_{mat-TR} is determined using paragraph 9F.4.3.3, 9F.4.7.2 and 9F.4.7.3, as applicable. The upper shelf toughness K_{mat-US} is determined using paragraph 9F.4.4.

$$K_{mat} = \min\left[K_{mat-TR},\ K_{mat-US}\right] \qquad \text{(9F.126)}$$

9F.4.10 The Effect of Warm Pre-stress on Fracture Toughness

9F.4.10.1 Introduction

The Warm Pre-stress (WPS) effect describes the effect of a prior loading on the subsequent effective fracture toughness. When a crack is loaded to some crack driving force parameter value (K, J or CTOD) that is lower than the fracture toughness at the temperature in question, the effect will be an effective increase in fracture toughness if the specimen is re-loaded at a lower temperature at which the prior loading exceeds the original fracture toughness. The WPS does not affect the material's fracture toughness directly. It alters the stress field around the crack and this way produces an apparent increase of toughness. Loading transients that can lead to a WPS situation are shown in Figure 9F.6. The technical basis for accounting for warm prestress effects on fracture toughness is based on reference [1].

9F.4.10.2 Benefits

The greatest benefit in terms of maximizing the fracture toughness at failure, K_f, is given by the LCF transient, and the least is achieved by the LUCF transient with full unloading. Intermediate forms of transient, where partial unloading occurs prior to re-loading to failure, and where the temperature and loads, including pressure, are simultaneously reduced, give benefits lying between these two limits.

9F.4.10.3 Procedure

A procedure for quantifying the effect of the WPS on K_f for a given structural geometry and flaw dimensions is shown below.

a) STEP 1 – Determine K_{1-WPS} stress intensity factor corresponding to temperature and pressure at the WPS (see Figure 9F.6).

b) STEP 2 – Determine the stress intensity factor at the unloaded condition, K_2 (see Figure 9F.6).

c) STEP 3 – Determine the stress intensity factor decrement due to the unload, $K_{1-WPS} - K_2$. The decrement is independent of the magnitude of any system or residual stresses and depends on the contribution due to the varying load only.

d) STEP 4 – Evaluate the fracture toughness, K_{mat}, of the material at the assessment time, but neglecting the effects of the WPS.

e) STEP 5 – Evaluate the stress intensity factor at failure from the following equations.

$$K_2 = K_{1-WPS} \qquad \left(if\ K_2 \geq K_{1-WPS} - K_{mat}\right) \qquad (9F.127)$$

$$K_f = 0.15 \cdot K_{mat} + \sqrt{K_{mat} \cdot \left(K_{1-WPS} - K_2\right)} + K_2 \qquad \left(if\ K_f > K_{mat}\right) \qquad (9F.128)$$

$$K_f = K_{mat} \qquad \left(if\ K_f \leq K_{mat}\right) \qquad (9F.129)$$

9F.4.10.4 Conditions to be Satisfied

For a WPS argument to be made according to the procedure of this section, the following conditions shall be met (see references [4] and [15]):

a) The failure mechanism at the service condition should be transgranular cleavage or intergranular brittle fracture.

b) The flow properties of the material should increase between the WPS and the service failure condition; this might be due to a decrease in temperature or due to in-service hardening.

c) There should be no significant sub-critical crack growth between WPS and the service failure condition. The amount of any such crack growth should be much less than the extent of the residual plastic zone following unloading.

d) The stress intensity factor due to the WPS loading, K_{1-WPS}, exceeds the fracture toughness at the reload condition, K_{mat}.

e) Small-scale yielding conditions hold at the pre-load. There is evidence that, for increasing preloads, the benefits on the apparent reload fracture toughness lessen. Indeed, in the limit of extensive plasticity, the toughness might be reduced compared to its value in the absence of the WPS.

f) The preload and reload should be in the same direction; that is, both tensile and both compressive at the crack tip. A compressive preload followed by a tensile reload may reduce the apparent fracture toughness.

9F.4.11 Fracture Toughness Estimation for Brittle Fracture Assessments

The following toughness estimation procedures may be used for brittle fracture analysis performed in accordance Part 3, Level 3 Assessments for carbon and low alloy steels.

a) Paragraph 9F.3.5 – ASME B&PV Code, Section VIII Division 1 and 2 Fracture Toughness

b) Paragraph 9F.4.2 – ASME Section XI Fracture Toughness – Lower Bound

c) Paragraph 9F.4.3 – Assessing Fracture Toughness Carbon and Low Alloys Steels – Transition Region

d) Paragraph 9F.4.4 – Assessing Fracture Toughness Carbon and Low Alloys Steels – Upper Shelf

e) Paragraph 9F.4.5 – Dynamic Fracture or Arrest Toughness

f) Paragraph 9F.4.6 – Fracture Toughness for Materials Subject to In-Service Degradation

g) Paragraph 9F.4.7 – Aging Effects on the Fracture Toughness of Cr-Mo Steels

h) Paragraph 9F.4.8 – Fracture Toughness of Electroslag Welds in 2.25Cr-1Mo Vessels

i) Paragraph 9F.4.10 – The Effect of Warm Pre-Stress on Fracture Toughness

9F.4.12 Fracture Toughness of Austenitic Stainless Steel

In most cases, austenitic stainless steels do not experience a ductile-brittle transition like ferritic steels. The fracture toughness is usually high, even at low temperatures, provided the material has not experienced degradation in toughness because of exposure to the environment. However, a toughness transition may occur in austenitic stainless steels with high ferrite content, i.e., castings or in the embrittled condition.

If specific information on the fracture toughness is not available, the values in Table 9F.2 may be used in an assessment provided the material has not experienced significant thermal degradation and does not exhibit a transition region (see reference [16]).

9F.4.13 Ductile Tearing Assessment Using a JR-curve

Data for JR curves are provided in Table 9F.3 and may be used if the material has not experienced degradation from environmental effects (see reference [17]).

Alternatively, the following equations may be used to determine a JR Curve for a material that has not experienced degradation from environmental effects (see paragraph 9F.4.4.2(a)).

$$J_R = J_{1\text{ mm}}\left(\Delta a\right)^m \qquad \left(kJ/m^2,\ mm\right) \tag{9F.130}$$

$$J_R = J_{1\text{ mm}}\left(\frac{\Delta a}{0.039}\right)^m \qquad \left(in-lbs/in^2,\ in\right) \tag{9F.131}$$

A conservative estimate (15th percentile) of the exponent m in the above equations can be determined from the upper-shelf Charpy energy as shown below.

$$m = 0.432\left(\frac{CVN}{100}\right)^{0.256} - \frac{\sigma_{ys}}{4664} + 0.03 \qquad \left(J,\ MPa\right) \tag{9F.132}$$

$$m = 0.432\left(\frac{CVN}{73.7}\right)^{0.256} - \frac{\sigma_{ys}}{676} + 0.03 \qquad \left(ft-lbs,\ ksi\right) \tag{9F.133}$$

9F.5 Material Data for Crack Growth Calculations

9F.5.1 Categories of Crack Growth

9F.5.1.1 Crack Growth by Fatigue

Crack growth by fatigue occurs when a component is subject to time varying loads that result in cyclic stresses. Each increment of crack extension correlates to a certain increment of stress cycles. Linear Elastic Fracture Mechanics (LEFM) has been validated to relate the crack growth per cycle to the applied stress intensity factor range through a fatigue crack growth model. The simplest and most common form of fatigue crack growth model is the Paris Equation (see paragraph 9F.5.2.2). More advanced forms of fatigue crack growth models that take explicit account of such factors as stress ratio, ranges of ΔK, effects of a threshold stress intensity factor, ΔK_{th}, and plasticity-induced crack closure are available for certain materials and environments. These models should

be considered in an assessment based on the applied loading, crack configuration, and service environment. The variation of fatigue crack growth rate with cyclic stresses which produce a range of ΔK and the associated fracture mechanisms are shown in Figure 9F.7. An overview of the fatigue crack growth models and available data are provided in paragraphs 9F.5.2 and 9F.5.3, respectively.

9F.5.1.2 Crack Growth by Stress Corrosion Cracking (SCC)

Stress corrosion cracking results from the combination of a corrosive environment, a static applied or residual tensile stress, and a susceptible material. In the presence of these elements, the passivation, re-passivation, and metal dissolution that occur locally at the crack tip are altered such that when the crack tip stress intensity factor exceeds a critical threshold value, SCC will initiate and grow for the specified condition. Active SCC usually accelerates initially until it attains an approximately uniform velocity that is independent of the stress intensity factor, but may be dependent on duration (time), material, temperature, and specific environmental factors. The different type of relationships between crack velocity and stress intensity factor that can occur during stress corrosion cracking are shown in Figure 9F.8(a) for two different environments. The difference in the relationship between the crack velocity and applied stress intensity factor should be noted. An overview of the stress corrosion crack growth models and available data are provided in paragraph 9F.5.4 and 9F.5.5, respectively.

9F.5.1.3 Crack Growth by Hydrogen Assisted Cracking (HAC)

This covers a broad range of crack growth mechanisms that are associated with absorbed hydrogen in the metal. This includes hydrogen embrittlement, Hydrogen Induced Cracking (HIC), Stress-Oriented Hydrogen Induced Cracking (SOHIC), and sulfide stress cracking. In contrast to the other failure mechanisms, HAC susceptibility is highest at ambient and moderate temperatures and low strain rates.

a) HAC occurs when hydrogen is absorbed by a material during a corrosion process, or by exposure to high-temperature and/or high-pressure hydrogen gas, and diffuses to a pre-existing flaw as atomic hydrogen, and stresses are applied, including residual stresses, to the flaw. The crack will continue to propagate at an increasing subcritical velocity until fracture occurs as long as the stress intensity factor resulting from the applied and residual stresses exceeds a critical threshold value, K_{th}, and a critical concentration of atomic hydrogen is maintained in the vicinity of the crack tip either by continuous absorption of hydrogen from the external surface, or by redistribution of internal lattice hydrogen and internal sources such as hydrogen traps in the material. The rapid, hydrogen accelerated propagation condition is dictated by the value of the material toughness in the presence of absorbed hydrogen at the crack tip. This toughness is designated as K_{IC-H}.

b) Within a LEFM methodology, a HAC crack growth model can be determined from test specimens that relate the crack growth rate to the combined applied and residual stress intensity factor, the material/environment constants, and loading (strain) rate. A simple form of the HAC crack growth curve is shown in Figure 9F.8(b). A typical crack growth model for HAC is shown in paragraph 9F.5.5.2.

9F.5.1.4 Crack Growth by Corrosion Fatigue

The synergistic effect of combined SCC or HAC with fatigue under cyclic loading in an aggressive environment can produce significantly higher crack growth per cycle compared to an inert environment where SCC or HAC is absent. This interaction can be very complicated and makes development of a simple crack growth model difficult.

a) Corrosion fatigue crack propagation typically exhibits the three basic types of crack growth rate behavior shown in Figure 9F.9.

1) True Corrosion Fatigue (TCF) – describes the behavior when fatigue crack growth rates are enhanced by the presence of aggressive environment at levels of applied K below K_{IC} (see Figure 9F.9(a)). This behavior is characteristic of materials that do not exhibit stress corrosion (i.e., $K_{ISCC} = K_{IC}$).

2) Stress Corrosion Fatigue (SCF) – describes corrosion under cyclic loading that occurs whenever the stress intensity in the cycle is greater than K_{ISCC}. This is characterized by a plateau in crack growth (see Figure 9F.9(b)) like that observed in stress-corrosion cracking.

3) Combination TCF and SCF – this is the most common type of corrosion fatigue behavior (see Figure 9F.9(c)) which is characterized by stress-corrosion fatigue above K_{ISCC}, superimposed on true corrosion fatigue at all stress intensity levels.

b) Equations that describe corrosion fatigue behavior are available for limited stress intensity ranges and material/environment combinations. Therefore, it is advisable to establish and use upper bound crack growth models for such cases.

9F.5.2 Fatigue Crack Growth Equations

9F.5.2.1 Overview

a) Fatigue crack growth equations that have been used are summarized below. A complete discussion of all aspects of these crack growth models is beyond the scope of this Standard. Further information on fatigue crack growth models can be found in references [18]–[22].

a) Although experimental data suggest the presence of a threshold condition for fatigue crack growth, fatigue cracking in actual structures with residual stresses may not exhibit fatigue threshold behavior and this should be considered in an analysis.

9F.5.2.2 Paris Equation

a) The Paris Equation is the simplest of the fatigue crack growth models (see Figure 9F.7). The Paris Equation has the form shown below. Note that in this model, the crack growth rate is independent of the load ratio.

$$\frac{da}{dN} = C\left(\Delta K\right)^n \tag{9F.134}$$

b) The Paris Equation may also be used in conjunction with a threshold value ΔK_{th}. The crack growth rate is given by Equation (9F.135) above the threshold value and Equation (9F.136) at or below the threshold values.

$$\frac{da}{dN} = C\left(\Delta K\right)^n \qquad \left(for\ \Delta K > \Delta K_{th}\right) \tag{9F.135}$$

$$\frac{da}{dN} = 0.0 \qquad \left(for\ \Delta K \le \Delta K_{th}\right) \tag{9F.136}$$

c) The Paris Equation may also be adjusted for temperature and used in conjunction with a threshold value ΔK_{th} using the ratio E_y/E_{yT}. The crack growth rate is given by Equation (9F.137) above the threshold value and Equation (9F.138) at or below the threshold value.

$$\frac{da}{dN} = C\left(R_E \cdot \Delta K\right)^n \qquad \left(for\ \Delta K > \Delta K_{th}\right) \tag{9F.137}$$

$$\frac{da}{dN} = 0.0 \qquad \left(for\ \Delta K \le \Delta K_{th}\right) \tag{9F.138}$$

where,

$$R_E = \max\left[\frac{E_y}{E_{yT}}, 1.0\right] \tag{9F.139}$$

9F.5.2.3 Modified Paris Equation for Welded Joints

a) The crack growth rate is given by Equation (9F.140) above the threshold value ΔK_{th} and Equation (9F.141) at or below the threshold value (see reference [24]).

$$\frac{da}{dN} = C\left(\Delta K^n - \Delta K_{th}{}^n\right) \qquad \left(for\ \Delta K > \Delta K_{th}\right) \tag{9F.140}$$

$$\frac{da}{dN} = 0.0 \qquad \left(for\ \Delta K \le \Delta K_{th}\right) \tag{9F.141}$$

b) Equation (9F.140) may also be adjusted for temperature and used in conjunction with a threshold value of ΔK_{th}. The crack growth rate is given by Equation (9F.142) above the threshold value ΔK_{th} and Equation (9F.143) below the threshold values.

$$\frac{da}{dN} = C\left(\left(R_E \cdot \Delta K\right)^n - \left(\Delta K_{th}\right)^n\right) \qquad \left(for\ \Delta K > \Delta K_{th}\right) \tag{9F.142}$$

$$\frac{da}{dN} = 0.0 \qquad \left(for\ \Delta K \le \Delta K_{th}\right) \tag{9F.143}$$

where R_E is given by Equation (9F.139).

9F.5.2.4 Walker Equation

a) The Walker Equation is a simple but significant generalization of the Paris Equation. The Walker Equation has the form:

$$\frac{da}{dN} = C\left(\Delta K_{eff}\right)^n \qquad \left(for\ \Delta K > \Delta K_{th}\right) \tag{9F.144}$$

where,

$$\Delta K_{eff} = \frac{\Delta K}{(1-R)^m} \tag{9F.145}$$

$$R = \frac{K_{\min}}{K_{\max}} \tag{9F.146}$$

b) The Walker Equation is the same as the Paris Equation except that ΔK is replaced by an effective value, ΔK_{eff}, that is now dependent on the load ratio. Therefore, while the Paris Equation is only dependent on ΔK, the Walker Equation is dependent on both ΔK and R. The appearance of R in the Walker Equation results in larger crack growth rates being predicted for larger values of R, even if ΔK is held constant. This behavior is intuitive and is also supported by experimental data for numerous metals. The effects of ΔK and $K_{\max}$ are more clearly seen by writing ΔK_{eff} in the following way:

$$\Delta K_{eff} = \Delta K^{(1-m)} K_{\max}^{m} \tag{9F.147}$$

or

$$\Delta K_{eff} = (1-R)^{(1-m)} K_{\max} \tag{9F.148}$$

c) The parameter m controls the relative importance of ΔK and $K_{\max}$ on ΔK_{eff}, and thus on the crack growth rate. If $m = 0.0$, then $\Delta K_{eff} = \Delta K$ and the Walker Equation simplifies to the Paris Equation. If $m = 1.0$, then the crack growth rate is dependent only on $K_{\max}$. The parameter m allows the load ratio dependence of the Walker Equation to be adjusted to fit available experimental data. As a result of this additional parameter, the Walker Equation parameters are more difficult to determine than the Paris Equation parameters.

9F.5.2.5 Trilinear and Bilinear Equations

a) The Trilinear and Bilinear Equations reflect another approach to generalization of the Paris Equation. The Trilinear Equation is a combination of three Paris Equations as shown below. The value of ΔK to be used is dependent on the specified transition stress intensity factors, $\Delta K_{tran,1}$ and $\Delta K_{tran,2}$. Note that in the Trilinear Equations, different crack growth rates are predicted at $\Delta K_{tran,1}$ and $\Delta K_{tran,2}$.

$$\frac{da}{dN} = C_1 (\Delta K)^{n_1} \qquad \left(for\ \Delta K_{th} < \Delta K < \Delta K_{tran,1} \right) \tag{9F.149}$$

$$\frac{da}{dN} = C_2 (\Delta K)^{n_2} \qquad \left(for\ \Delta K_{tran,1} < \Delta K < \Delta K_{tran,2} \right) \tag{9F.150}$$

$$\frac{da}{dN} = C_3 (\Delta K)^{n_3} \qquad \left(for\ \Delta K \geq \Delta K_{tran,2} \right) \tag{9F.151}$$

b) The Bilinear Equation is a special case of the Trilinear Equation in that only two Paris equation models are used with a single transition stress intensity factor $\Delta K_{tran,1}$.

9F.5.2.6 Modified Forman Equation

a) The Modified Forman Equation is a general crack growth model and can be used to represent the state of crack growth across the full regime of crack propagation (see references [20]–[21]). The form of the Modified Forman Equation is:

$$\frac{da}{dN} = C(\Delta K)^{n} \cdot \frac{(1-R)^{m} \left(1 - \frac{\Delta K_{th}}{\Delta K}\right)^{p}}{\left(1 - \frac{K_{\max}}{K_{IC}}\right)^{q}} \tag{9F.152}$$

b) The Modified Forman Equation is like the Walker Equation in that there is a $(1-R)^m$ factor. However, the constant m in the Modified Forman Equation is not the same as in the Walker Equation due to the term appearing in the numerator, and due to the $(1-R)^m$ term not being raised to the n power. If p and q are set to zero, then this law becomes equivalent to the Walker Equation with,

$$m_F = -m_w \cdot n \tag{9F.153}$$

c) The terms with the p and q exponents allow the law to accurately represent da/dN versus ΔK data in the low growth rate (threshold) region, in the mid-range region, and in the high growth rate region, i.e., $K_{\max}$

approaching K_{IC}, as shown in Figure 9F.6. The exponents p and q are in the range of zero to unity and are typically equal. With such values, the factor with the p exponent tends to affect the behavior of the law primarily in the threshold region, while the factor with the q exponent tends to affect the behavior primarily near load levels close to K_{IC}. It should be clear that the p and q exponents have no physical significance, the only real basis for their choice is in making the law fit actual crack growth data.

9F.5.2.7 NASGRO Equation

a) The NASGRO Equation represents the most general crack growth model, and except for special purpose models, is the one that would best represent the state of the art in fatigue crack growth relationships (see references [20]–[21]. This model also incorporates the effects of fatigue crack closure. The form of the NASGRO Equation is:

$$\frac{da}{dN} = C\left(\Delta K\right)^n \cdot \frac{\left(1-f\right)^n \left(1-\frac{\Delta K_{th}}{\Delta K}\right)^p}{\left(1-R\right)^n \left(1-\frac{\Delta K}{\left(1-R\right)K_{IC}}\right)^q} \tag{9F.154}$$

b) Details regarding the NASGRO Equation and associated material data, typically for materials used in the aircraft industry, may be found in references [20]–[21].

9F.5.2.8 Collipriest Equation

a) The Collipriest Equation was an early attempt at addressing the shortcomings of the Paris and Walker Equations in terms of representing behavior in the threshold and large ΔK regions of the da/dN versus ΔK plot. The Collipriest Equation tries to compensate for the lack of non-linear behavior of the simpler models without introducing additional parameters.

$$\frac{da}{dN} = C\left(\Delta K_{th} \cdot K_{IC}\right)^{\frac{n}{2}} \cdot \exp\left[\left(\frac{n}{2}\right) \cdot \ln\left[\frac{K_{IC}}{\Delta K_{th}}\right] \cdot a \cdot \tanh\left[\frac{\ln\left[\frac{\left(\Delta K\right)^2}{\Delta K_{th}\left(1-R\right)K_{IC}}\right]}{\ln\left[\frac{\left(1-R\right)K_{IC}}{\Delta K_{th}}\right]}\right]\right] \tag{9F.155}$$

b) Details on the Collipriest model can be found in reference [23].

c) The material parameters of the Collipriest model are the same as for the Paris Equation. This does not imply, however, that one can simply substitute Paris Equation parameters into the Collipriest Equation without verifying that the resulting model provides a reasonable representation of actual material behavior.

9F.5.2.9 ASME B&PV Code, Section VIII, Division 3

Division 3, Section KD-430 provides crack growth rate equations and parameters to be used for high pressure vessels typically constructed to Division 3 or vessels that are constructed to other codes but within the scope of Division 3. For example, Division 3 crack growth equations can be used for pressure vessels with design pressures generally above 10 ksi (70 MPa). Another example is pressure vessel manufactured by inducing beneficial residual stresses using processes such as autofrettage. The crack growth equations in Division 3 are similar to the Paris Equation. The primary differences are in the inclusion of a multiplier which is a function of the ratio of stress intensity factors, R, and the inclusion of residual stress intensity in the calculation of R.

9F.5.3 Fatigue Crack Growth Data

9F.5.3.1 Sources for Crack Growth Data

When possible, fatigue crack growth data should be evaluated from test results on similar materials and in similar environments since this can greatly affect the crack growth rate. Sources for fatigue crack growth data, da/dN versus ΔK , for various materials and service environments may be found in the literature. However, data from the literature should be evaluated to ensure the loading and environmental conditions are applicable to the component being evaluated.

9F.5.3.2 ASME B&PV Code, Section VIII, Division 3

The ASME B&PV Code, Section VIII, Division 3 contains crack growth models and model parameters for the materials of construction shown below. These crack growth models and model parameters shall be used when evaluating vessels constructed to Division 3 or vessels that are constructed to other codes but within the scope of Division 3.

a) Low alloy steels, $\sigma_{ys} \leq 621\ MPa\ \ (90\ ksi)$

b) High strength alloy steels, $\sigma_{ys} > 621\ MPa\ \ (90\ ksi)$

c) Martensitic Precipitation-hardened steels

d) Austenitic stainless steels

e) Aluminum alloys

9F.5.3.3 ASME B&PV Code, Section XI

The ASME B&PV Code, Section XI contains crack growth models and model parameters for nuclear components for the following materials of construction and environment combinations.

a) Ferritic steel in air and light water reactor

b) Austenitic stainless steel in air and water environments

9F.5.3.4 AFCEN Code, RSE-M

The AFCEN Code, RSE-M contains crack growth models and model parameters for nuclear components for the following materials of construction and environment combinations.

a) Ferritic steel in air, pressurized water reactor, and void

b) Austenitic stainless steel in air, pressurized water reactor, and void

c) Nickel alloy Ni-Cr-Fe in air and pressurized water reactor

9F.5.3.5 Barsom Original Crack Growth Data

The fatigue crack growth constants in Table 9F.4 may be used with the Paris Equation, (see paragraph 9F.5.2.2) in FFS Assessments. These constants correspond to the historical values developed by Barsom (see reference [22]) and represent an upper bound.

9F.5.3.6 Crack Growth Data for Welds

The fatigue crack growth constants in Table 9F.5 may be used with the Paris Equation (see paragraph 9F.5.2.2) in FFS Assessments. These constants are based on data determined from crack propagation testing of as-welded

joints in steel components (see reference [24]). Constants are provided for a 99.5% confidence limit and mean and are applicable both for ferritic and for austenitic steels at constant amplitude or random loadings.

9F.5.3.7 BS 7910 Crack Growth Data for Screening

The fatigue crack growth constants in Table 9F.6 may be used with the Paris Equation (see paragraph 9F.5.2.2), in FFS Assessments (see reference [4]). These constants are valid for materials with yield strengths less than or equal to $600\ MPa\ (87\ ksi)$ and are intended for preliminary screening calculations that can be compared with calculations based on fatigue design rules for welded steels where the slope of the S-N fatigue curve is typically equal to 3. These constants correspond to the upper bounds to the equations in paragraph 9F.5.3.8 with a slope of three and will result in a more conservative estimate of crack growth.

9F.5.3.8 BS 7910 Bilinear Crack Growth Data

Fatigue crack growth parameters for use with the Paris Bilinear Equation (see paragraph 9F.5.2.4) are provided in Table 9F.7 for different steels and service environments including marine environments with and without cathodic protection (see reference [4]). Threshold values are shown in Table 9F.8 (see reference [21]). The upper bound (mean +2σ, corresponding to 97.7% probability of survival) values for $R \geq 0.5$ are recommended to be used in assessments concerned with flaws in welded joints in the as-welded condition (see reference [4]).

9F.5.3.9 Crack Growth Data for Pipeline Steels

a) The fatigue crack growth equations shown below can be used for pipeline steels (e.g., API 5L) at ambient temperatures in crude oil service (see reference [25]). These correlations represent mean values.

$$\left.\frac{da}{dN}\right|_l = C_l\left(\Delta K + B \cdot R\right)^{n_l} \quad \left(for\ \Delta K_{th} < \Delta K < \Delta K_{tran}\right)\ \left(mm/cycle,\ MPa\sqrt{m}\right) \tag{9F.156}$$

$$\left.\frac{da}{dN}\right|_u = C_u\left(\Delta K + B \cdot R\right)^{n_u} \quad \left(for\ \Delta K \geq \Delta K_{tran}\right) \qquad \left(mm/cycle,\ MPa\sqrt{m}\right) \tag{9F.157}$$

The parameters B and ΔK_{tran} are computed using the following equations.

$$B = 4.0 \tag{9F.158}$$

$$\Delta K_{tran} = \left(\frac{C_l}{C_u}\right)^{\left(\frac{1}{n_u - n_l}\right)} \tag{9F.159}$$

The parameters to use in the above equations are based on the service environment.

1) For sour crude oil (with H_2S); in Equations (9F.160) and (9F.162) the parameter C_{H_2S} is the concentration of H_2S in ppm.

$$C_l = 7.12\left(10^{-16}\right) \cdot C_{H_2S} + 3.40\left(10^{-13}\right) \tag{9F.160}$$

$$n_l = 6.40 \tag{9F.161}$$

$$C_u = 2.50\left(10^{-11}\right) \cdot C_{H_2S} + 1.48\left(10^{-7}\right) \tag{9F.162}$$

$$n_u = 2.72 \tag{9F.163}$$

$$\Delta K_{th} = 6\ MPa\sqrt{m} \tag{9F.164}$$

2) For sweat crude oil (without H_2S):

$$C_l = 1.48\left(10^{-11}\right) \quad (9F.165)$$

$$n_l = 4.80 \quad (9F.166)$$

$$C_u = 4.00\left(10^{-7}\right) \quad (9F.167)$$

$$n_u = 1.90 \quad (9F.168)$$

$$\Delta K_{th} = 8\ MPa\sqrt{m} \quad (9F.169)$$

b) Additional crack growth data for pipeline materials from API RP 1176 is shown in Table 9F.9.

9F.5.3.10 NASGRO Crack Growth Data

Fatigue crack growth parameters for use with the NASGRO Equation (see paragraph 9F.5.2.6) are given in reference [20] for different materials and service environments.

9F.5.4 Hydrogen Assisted Crack Growth

9F.5.4.1 ASME B31.12

The following equation from ASME B31.12, paragraph PL-3.7.1.b.2 may be used to estimate fatigue crack growth in carbon steels in gaseous hydrogen in pipeline service up to 20 MPa (3000 psi), references [26]–[27]. This equation is applicable for $R < 0.5$ where R is given by Equation (9F.146).

$$\frac{da}{dN} = a_1 \Delta K^{b_1} + \left[\left(a_2 \Delta K^{b_2}\right)^{-1} + \left(a_3 \Delta K^{b_3}\right)^{-1}\right]^{-1} \quad (9F.170)$$

In the above equation, the SI units of da/dN are mm/cycle with ΔK, $K_{\min}$, and $K_{\max}$ in $MPa\sqrt{m}$. In US Customary units, the units of da/dN are in/cycle with ΔK, $K_{\min}$, and $K_{\max}$ in $ksi\sqrt{in}$. The constants for this equation are provided in Table 9F.10.

9F.5.4.2 ASME B&PV Code, Section VIII, Division 3

Division 3, Article KD-10 provides procedures for testing to determine fatigue crack growth constants in hydrogen. In lieu of testing for fatigue crack growth rates in hydrogen environments for pressure vessels meeting some criteria specified in ASME BP&V Code Case 2938, this Code Case may be utilized for performing fatigue crack growth calculations.

9F.5.5 Stress Corrosion Crack (SCC) Growth Equations

Within the LEFM methodology, a Stress Corrosion Crack (SCC) growth equation can be experimentally determined which relates the crack growth rate to the stress intensity factor (K), the material, service environment, and time. This crack growth model can subsequently be used to characterize the crack growth behavior in equipment under a similar combination of stress, material, and service environment to that used in the experiment. An overview of stress corrosion crack growth models is provided in references [18] and [19]. Examples of SCC crack growth models that have been used are shown below.

a) The following three equations have been used to model SCC. In Equation (9F.171), the crack growth rate is a function of the stress intensity factor and associated constants. In Equation (9F.172) the crack growth rate

is a function of time and associated constants, and in Equation (9F.173) the crack growth rate is a constant and independent of the stress intensity factor and time.

$$\frac{da}{dt} = D_1 \left(K\right)^{n_1} \qquad \left(for\ K_{th} \le K \le K_{IC}\right) \tag{9F.171}$$

$$\frac{da}{dt} = D_2 \left(t\right)^{n_2} \qquad \left(for\ K_{th} \le K \le K_{IC}\right) \tag{9F.172}$$

$$\frac{da}{dt} = D_3 \qquad \left(for\ K_{th} \le K \le K_{IC}\right) \tag{9F.173}$$

b) The following equation is a typical crack growth model for Hydrogen Assisted Crack Growth (HAC).

$$\frac{da}{dt} = D\left(K\right)^{n} \qquad \left(for\ K_{th} \le K \le K_{IC-H}\right) \tag{9F.174}$$

9F.5.6 Stress Corrosion Crack Growth Data

When possible, stress corrosion crack growth data should be evaluated from test results in a similar environment since this can greatly affect the crack growth rate. Sources for stress corrosion crack growth data, da/dt, for various materials and service environments may be found in the literature. However, data from the literature should be evaluated to ensure the loading and environmental conditions are applicable to the component being evaluated. An overview of crack growth mechanisms and rates for several cracking mechanisms commonly observed in materials utilized for petroleum refinery applications is included in reference [28].

9F.5.7 Conversion of Units for Crack Growth Data

9F.5.7.1 Cyclic Crack Growth Conversion Method

The cyclic crack growth equation, i.e., Paris law, is given by:

$$\frac{da}{dN} = C \cdot \Delta K^{n} \tag{9F.175}$$

The units and value of C depend on those used to measure da/dN and ΔK, and on the value of the exponent, n. If C is known in one set of units, C_A, then the corresponding value for another set of units, C_B is given by:

$$C_B = C_A \cdot \left(\frac{F_A}{\left(F_B\right)^{n}} \right) \tag{9F.176}$$

The parameter F_A is the conversion factor for da/dN from the first to the second unit system; and F_B is the conversion factor for ΔK from the first to the second unit system.

9F.5.7.2 Time-Dependent Crack Growth Conversion Method

A time-dependent growth equation is:

$$\frac{da}{dt} = C \cdot K^{n} \tag{9F.177}$$

The units and value of C depend on those used to measure da/dt and K, and on the value of the exponent, n. If C is known in one set of units, C_A, then the corresponding value for another set of units, C_B is given by:

$$C_B = C_A \cdot \left(\frac{F_A}{(F_B)^n} \right) \tag{9F.178}$$

The parameter F_A is the conversion factor for da/dt from the first to the second unit system; and F_B is the conversion factor for K from the first to the second unit system.

9F.6 Nomenclature

a crack depth in the case of a surface crack. Half depth of a buried crack.

A hyperbolic tangent curve fit coefficient.

β Multiplying factor on the hyperbolic tangent fitting coefficient C to ensure that the extrapolation to the 28 Joules (20 ft-lbs) reference temperature is conservative.

B hyperbolic tangent curve fit coefficient, the cyclic crack growth model constant or specimen thickness for the Master Curve, as applicable.

c crack half- length in the case of buried, surface and through-wall flaws. Crack length for a corner crack.

C hyperbolic tangent curve fit coefficient, crack growth modeling constant, or the constant for the Master Fatigue Curve, as applicable.

C_A & C_B parameters for estimating the impact energy of subsize Charpy specimens, or conversion factors for crack growth equations, as applicable.

C_l material parameter for crack growth modeling.

$C_{T_{20-ft-lbs}}$ constant to determine 20 ft-lbs reference temperature as a function of σ_{ysA}.

$C_{T_{28.Joules}}$ constant to determine 28 Joules reference temperature as a function of σ_{ysA}.

C_{T_0} constant to determine Master Curve reference transition temperature (T_0) as a function of σ_{ysA}.

C_u material parameter for crack growth modeling.

C_R parameter for J-Integral equation used in a ductile tearing analysis.

C_V CVN value.

C_{V-ss} CVN energy value for the sub-size specimen.

C_{V-std} CVN energy value for the standard size specimen.

C_{V-LS} Lower shelf value of CVN energy.

C_{V-US} Upper shelf value of CVN energy.

C_{V-ss} Charpy impact energy at the test temperature for the sub-size specimen.

$C_{V-US-ss}$ Charpy upper shelf impact energy for the sub-size specimen.

$C_1 \rightarrow C_3$ material parameters for a fatigue crack growth model.

D hyperbolic tangent curve fit coefficient or stress corrosion crack growth coefficient, as applicable.

$D_1 \rightarrow D_3$ material parameters for a stress corrosion crack growth model.

ΔT_0 temperature shift on the estimation of the Master Curve index temperature, T_0 from the Charpy reference temperature, $T_{28\ Joules}$ or $T_{20\ ft-lbs}$.

ΔT_s temperature shift for dynamic to static fracture toughness prediction.

da/dt crack growth rate.

da/dN increment of crack growth for a given cycle.

δ_{crit} critical CTOD value.

E_y Young's Modulus at ambient temperature.

E_{yT} Young's Modulus at the temperature of interest.

ε_{CVN} tolerance to determine the temperature of the upper and lower shelf for the Charpy V-notch transition curve modeled using the hyperbolic tangent function, a value of $\varepsilon_{CVN} = 0.005$ is recommended.

$FATT$ fracture appearance transition temperature note that the temperature is in centigrade for this correlation.

f parameter which reflects the amount of plasticity-induced crack closure that is present in the material.

F_A crack growth factor.

F_B crack growth factor.

Γ Zener-Hollomon type parameter to compute the static to dynamic temperature shift for toughness estimation.

h exponent for the Master Fatigue Curve.

J elastic plastic driving force parameter or the material chemistry parameter used to determine the Fracture Appearance Transition Temperature ($FATT$) for 2.25Cr-1Mo.

J_{crit} critical J-Integral value.

J_i J -Integral required for initiation of crack extension in a tearing analysis.

J_{1mm} J -Integral at 1 mm of ductile tearing.

J_R J -Integral value in a ductile tearing analysis

K elastic crack driving force parameter, stress intensity factor, or a parameter in the MPC stress-strain curve model, as applicable.

$\dot{K}$ stress intensity factor rate.

ΔK $K_{\max} - K_{\min}$; if $\Delta K > \Delta K_{th}$ crack growth occurs; otherwise, if $\Delta K \leq \Delta K_{th}$ crack growth does not occur, or $da/dN = 0.0$.

ΔK_{eff} effective ΔK.

K_f fracture toughness at failure based on the warm prestress effect.

K_I applied mode I stress intensity factor.

K_{IC} plane-strain fracture toughness.

K_{IC-H} material fracture toughness measured in the hydrogen charging environment.

K_{Id} dynamic plane-strain fracture toughness.

K_{Id-LS} lower shelf dynamic plane-strain fracture toughness consistent with ASME Section VIII, Division 1 and 2 Exemptions Curves.

K_{IR} arrest fracture toughness.

$K_{\delta c}$ equivalent fracture toughness derived from $CTOD$ data.

K_{IH} threshold fracture toughness value for a hydrogen environment.

K_{ISCC} threshold fracture toughness value for stress corrosion cracking.

K_{Jc} fracture toughness established by converting J_{crit} to an equivalent K.

$K_{Jc(median)}$ median fracture toughness.

K_{mat} material fracture toughness for the transition region and upper shelf.

K_{mat-TR} material fracture toughness for the transition region.

K_{mat-US} material fracture toughness for the upper shelf.

$K_{mat(B)}$ material fracture toughness of a specimen with a thickness B.

$K_{mat(1in)}$ material fracture toughness for 1-inch thickness plate.

$K_{mat(25mm)}$ material fracture toughness for 25 mm thickness plate.

K_{max} maximum stress intensity for a given cycle.

K_{min} minimum stress intensity for a given cycle.

ΔK_{th} threshold stress intensity factor.

K_{th} threshold stress intensity factor for the material and environment, above which measurable crack extension will occur.

ΔK_{tran} transition ΔK used to determine the constants in the Bilinear crack growth model.

$\Delta K_{tran,1}$ first transition ΔK used to determine the constants in the Trilinear crack growth model.

$\Delta K_{tran,2}$ second transition ΔK used to determine the constants in the Trilinear crack growth model.

K_0 Weibull mean toughness that corresponds to the 63rd percentile fracture toughness ($P_f = 0.63$ when $K_{Jc} = K_0$).

K_{mat}^{mean} mean value of fracture toughness.

L crack length used in the Master Curve Model; for a surface crack L can be approximated as the total crack length, for an embedded crack L can be approximated as twice the total crack length, and for a through-wall crack L can be approximated as twice the component thickness.

m material parameter for crack growth or ductile tearing modeling.

m_{CTOD} conversion constant, 1.4 can be used in the absence of more reliable information.

m_F constant for the Modified Forman Equation.

m_w constant for the Walker Equation.

n material parameter for crack growth modeling.

n_l material parameter for crack growth modeling.

n_R parameter for J-Integral equation used in a ductile tearing analysis.

n_u material parameter for crack growth modeling.

$n_1 \rightarrow n_3$ material/environment constants for crack growth modeling.

p material parameter for Forman and NASGRO Crack Growth Models.

P_f cumulative probability of failure for use with the fracture toughness Master Curve.

$\%As$ weight percent Arsenic.

$\%Mn$ weight percent Manganese.

$\%Ni$ weight percent Nickel.

$\%P$ weight percent Phosphorous.

$\%Sb$ weight percent Antimony.

$\%Si$ weight percent Silicon.

$\%Sn$ weight percent Tin.

q material parameter for Forman and NASGRO Crack Growth Models.

R $K_{\min}/K_{\max}$ ratio of the minimum to maximum applied stress intensity factors.

R_E E_y/E_{yT} ratio of Young's modulus at room temperature to Young's modulus at the temperature of interest.

R_{HT} parameter used to compute the expected temperature for an associated Charpy energy value for materials with an ASME Exemption Curve.

RT_{NDT} maximum of the nil-ductility transition temperature established by a drop weight test, and the temperature from a Charpy test where the specimen exhibits at least 0.89 mm (35 mils) of lateral expansion and not less than 68 Joules (50 ft-lbs) absorbed energy minus 33°C (60°F).

SA shear area for a full-size Charpy specimen, expressed as percent divided by 100, or the shear area for the full-size specimen at the test temperature for the sub-size specimen expressed as percent.

SA_{ss} shear area for the sub-size specimen at the test temperature for the sub-size specimen expressed as percent.

σ_{fT} flow stress at the temperature of interest.

σ_{ysA} actual yield strength at ambient temperature. It can be estimated by adding 69 MPa (10 ksi) to σ_{msys}.

σ_{ysT} yield strength at the temperature of interest.

σ_{msys} minimum specified yield strength at ambient temperature.

σ_{utsT} ultimate tensile strength at the temperature of interest.

T Temperature.

T_c 85% SATT for the full-size specimen.

T_{c-ss} 85% Shear Area Transition Temperature (SATT) for the sub-size specimen.

T_{corr} temperature correction.

T_{ref} reference temperature.

T_{ref}^{D} reference temperature after adjustment for rate dependent loading.

T_{shift} temperature shift (temperature at the midpoint between the lower and upper shelf impact energies).

T_0 reference transition temperature.

T_0^A reference transition temperature for estimating the arrest fracture toughness.

T_0^D reference transition temperature after adjustment for rate dependent loading.

$T_{28\,Joules}$ temperature corresponding to 28 Joules.

$T_{54\,Joules}$ temperature corresponding to 54 Joules.

$T_{20\,ft-lbs}$ predicted temperature at 20 ft-lbs.

$T_{Shift}^{H_2}$ temperature shift in Master Curve due to hydrogen effects.

TT_{std} transition temperature for the standard size CVN specimen (temperature at the midpoint between the lower and upper shelf impact energies).

TT_{ss} transition temperature for the sub-size CVN specimen (temperature at the midpoint between the lower and upper shelf impact energies).

t_c component thickness.

t_{ss} thickness of sub-sized CVN specimen.

t_{std} thickness of standard size CVN specimen.

t_{NWT} nominal wall thickness of the pipe.

ν Poisson's ratio.

$\overline{X}$ material chemistry parameter used to determine the Fracture Appearance Transition Temperature ($FATT$) for 1.25Cr-0.5Mo.

9F.7 References

[1] Wallin, K., Fracture Toughness of Engineering Materials, EMAS Publishing, UK, 2011.

[2] McNicol, R.C., "Correlation of Charpy Test Results for Standard and Nonstandard Size Specimens," Welding Research Supplement, WRC 385-s, September 1965.

[3] Anderson, T.L., Fracture Mechanics – Fundamentals and Applications, 2nd Edition, CRC Press, Boca Raton, FL, 2005.

[4] BSI, Guide on Methods for Assessing the Acceptability of Flaws in Structures, BS 7910, British Standards Institute, 2019.

[5] Pisarski, H.G., "Treatment of Fracture Toughness data for Engineering Critical Assessment (ECA)," Weld World (2017) 61:723-732.

[6] Roberts, R. and Newton, C., Interpretive Report on Small Scale Test Correlations with KIc Data, WRC Bulletin 265, Welding Research Council, Inc., New York, NY, February 1981.

[7] Phaal, R., Macdonald, K.A., and Brown, P.A., Correlations Between Fracture Toughness and Charpy Impact Energy, Report from the Co-operative Research Programme for Industrial Members Only, TWI Report 504/1994, The Welding Institute, Cambridge, U.K., 1994.

[8] Prager, M., Osage, D.A., Staats, J. and B. Macejko, Development of Material Fracture Toughness Rules for ASME B&PV Code Section VIII, Division 2, WRC Bulletin 528, Welding Research Council, Inc., New York, NY.

[9] Prager, M., Fitness-For-Service Evaluation Procedures for Operating Pressure Vessels, Tanks, and Piping in Refinery and Chemical Service, FS-26, Consultants Report, MPC Program on Fitness-For-Service, WRC Bulletin 547, Welding Research Council, Inc., New York, NY, 2014.

[10] Iwadate, T., "Pressurization Temperature of Pressure Vessels Made of Cr-Mo Steels," PVP-Vol. 288, ASME, 1994, pg. 155-163.

[11] Osage, D.A., Spring, D.W., Anderson, T.L., Kummari, S.R., Prueter, P.E. and Wallin, K.R.W., Recommendations for Establishing the Minimum Pressurization Temperature (MPT) for Equipment, 2nd Edition, WRC Bulletin 562, Welding Research Council, Inc., New York, NY.

[12] Gangloff, R.P. and Anderson, T.L.," The Effects of Hydrogen for Establishing a Minimum Pressurization Temperature (MPT) for Heavy Wall Steel Reactor Vessels," API TR 934-F Part 4, First Edition (2018), American Petroleum Institute, Washington, D.C.

[13] Iwadate, T., Tanaka, Y., and Takemata, "Prediction of Fracture Toughness Kic Transition Curves of Pressure Vessel Steels from Charpy V-Notch Impact Test Results," Journal of Pressure Vessel technology, ASME, November 1994, Vol. 116, pp. 353-358.

[14] Pillot, S., Chauvy, C., Corre, S., Coudreuse, L., Gingell, A., Héritier, D., and Toussaint, P., "Effect of temper and hydrogen embrittlement on mechanical properties of 2,25Cr-1Mo steel grades e Application to Minimum Pressurizing Temperature (MPT) issues. Part II: Vintage reactors & MPT determination," International Journal of Pressure Vessels and Piping 110 (2013) 17 – 23.

[15] Budden, P.J. and Connors, D.C., "Assessment of Load History Effects on Fracture," ECF 15 Stockholm, Sweden, Aug 11-13, 2004 "Advanced Fracture Mechanics for Life and Safety Assessments."

[16] Mills, W.J., "Fracture Toughness of Austenitic Stainless Steels and Their Welds," ASM Handbook, Volume 19; Fatigue and Fracture, p 733-756, 1996.

[17] Zahoor, A., "Ductile Fracture Handbook Review – Volume 3," Electric Power Research Institute, Palo Alto, CA, 1991.

[18] Liu, A.F., Structural Life Assessment Methods, ASM International, Materials Park, OH, 1998.

[19] Ellyrin, F., Fatigue Damage Crack Growth and Life Prediction, Chapman & Hall, Boundary Row, London, U.K., 1997.

[20] NASA, "Derivation of Crack Growth Properties of Materials for NASA/FLAGRO 2.0," Volumes I, II, and III, JSC-26254, National Aeronautics and Space Administration, Houston, TX, 1994.

[21] NASA, "Fatigue Crack Growth Computer Program NASGRO Version 3.00," Revision B, JSC-22267B, National Aeronautics and Space Administration, Houston, TX, September 1998.

[22] Barsom, J.M., Fatigue Behavior of Pressure-Vessel Steels, WRC Bulletin 194, Welding Research Council, Inc., New York, NY, May 1974.

[23] Collipriest, J.E., "An Experimentalist's View of the Surface Flaw Problem", The Surface Crack: Physical Problems and Computational Solutions, American Society of Mechanical Engineers, 1972, pp. 43-61.

[24] Ohta, A., Maeda, Y., Kosuge, M., Machida, S., Yoshinari, H., "Fatigue Crack Propagation curve for Design of Welded Structures," Transactions of the Japan Welding Society, Vol 20, No. 1, April 1989.

[25] Vosikovsky, O., Macecek, M. and Ross, D.J., "Allowable Defect Sizes in a Sour Crude Oil Pipeline for Corrosion Fatigue Conditions," International Journal of Pressure Vessels & Piping, 13, pp. 197-226, 1983.

[26] Slifka, A.J., Drexler, E.S., Amaro, R.L., Hayden, L.E., Stalheim, D.G., Lauria, D.S., Hrabe, N.W., "Fatigue measurement of pipeline steels for the application of transporting gaseous hydrogen," ASME Journal of Pressure Vessel Technology, 140 (1), 2018, pp. 011407-1 to 011407-12.

[27] Amaro, R.L., White, R.M., Looney, C.P., Drexler, E.S., Slifka, A.J., "Development of a model for hydrogen-assisted fatigue crack growth in pipeline steel," ASME Journal of Pressure Vessel Technology, 140 (2),2018, pp. 021403-1 to 021403-13.

[28] Cayard, M.S. and Kane, R.D., “Fitness-For-Service Methodologies for the Assessment of Equipment Containing Corrosion Induced Damage,” Plenary Lecture at the 2nd NACE Latin American Region Corrosion Congress, Rio de Janeiro, Brazil, September 1996.

[29] Iwadate, T., Watanabe, J. and Tanaka, Y., “Prediction of the Remaining Life of High-Temperature/Pressure Reactors made of Cr-Mo Steels,” Transactions of the ASME, Vol. 107, August 1985, pp. 230 – 238.

[30] Wada, Y., Kayano, R., Hasegawa, T. and Inoue, H., “Hydrogen Embrittle Testing of Aging Vessel Steels Using Thick Specimens, Proceeding ICPVT-10, July 7-10, Vienna, Austria.

[31] Barsom, J. and Rolfe, S., Fracture and Fatigue Control in Structures: Applications of Fracture Mechanics, 3rd Edition, ASTM, West Conshohocken, PA, 1999.

[32] Vosikovsky, O., “Fatigue Crack Growth in an X-65 Line Pipe Steel at Low Cyclic Frequency in Aqueous Environments,” Journal of Engineering Materials and Technology, Vol. 97, No. 4, pp 298-304, October 1975.

[33] Vosikovsky, O., “Fatigue Crack Growth in an X-65 Line Pipe Steel in Sour Crude Oil,” NACE Corrosion, Vol. 32, No. 12, pp 472-475, December 1976.

[34] Andreason, D.H. and Vitovec, F.H., “The Effect of Temperature on Fatigue Crack Propagation in Linepipe Steel,” Metallurgical Transactions, Vol. 5, pp. 1779-1783, August 1974.

[35] Keller, J., Somerday, B. and San Marchi, C., “Hydrogen Embrittlement in Structural Steels,” DOE Hydrogen and Fuel Cells Program, FY2011 Annual Progress Report.

[36] San Marchi, C., et al., “Fracture and Fatigue of Commercial Grade API Pipeline Steels in Gaseous Hydrogen,” Proceedings of the ASME 2010 Pressure Vessel & Piping Division, PVP2010-25825, 2010.

[37] Stahlheim, D. et al., “Microstructure and Mechanical Property Performance of Commercial Grade API Pipeline Steels in High Pressure Gaseous Hydrogen,” Proceedings of the 8th International Pipeline Conference, IPC2010-31301, 2010.

[38] Lambert, S.B., et al., “Mechanical Factor Affecting Stress Corrosion Crack Growth Rates in Buried Pipelines,” International Pipeline Conference, IPC2000-0165, 2000.

9F.8 Tables

Table 9F.1 – Equivalent to the Minimum of Three Tests

Number of Fracture Toughness Tests	Equivalent to The Minimum of Three Tests
$3 \rightarrow 5$	Lowest value
$6 \rightarrow 10$	Second Lowest Value
$11 \rightarrow 15$	Third Lowest Value
$16 \rightarrow 20$	Fourth Lowest Value
$21 \rightarrow 25$	Fifth Lowest Vale
$26 \rightarrow 30$	Sixth Lowest Value

Notes:

1. Test results are assumed to be similar, i.e., all specimens test the same microstructure, all fail by brittle fracture, or all represent ductile behavior for the same crack extension. Specimens are also assumed to have a thickness representative of the component thickness.
2. If only three results are available and the minimum toughness is less than 70% of the average of three K values (half the average of three J values), or if the maximum toughness is more than 140% of the average of three K values (twice the average of three J values), scatter is considered excessive and additional test data are necessary.
3. The minimum of three tests represents the median (50^{th} percentile) of the fracture toughness distribution with 87.5% confidence. In other words, the minimum of three represents the median fracture toughness with high confidence; there is 12.5% chance that it can be lower. Another way of interpreting the minimum of three is that it represents the 20th percentile of the distribution with 50% confidence. Therefore, there is 50% chance that the 20^{th} percentile is overestimated when only three tests are conducted, (see references [4]-[5]).
4. The "Equivalent to the Minimum of Three Tests" approach is intended to maintain the same level of conservatism in the fracture assessment as implied by the lowest of three fracture toughness test results, when more than three results are available. However, using results from only a small number of fracture toughness tests (where final fracture is by cleavage) and applying the "Equivalent to the Minimum of Three Tests" approach, although simple, may not provide sufficiently reliable results for high integrity applications (see reference [4]). A more reliable approach for determining a lower bound estimate of fracture toughness with high confidence requires that more tests be conducted.

Table 9F.2 – J_c (1) and dJ/da values for Austenitic Stainless Steels (see reference [16])

Alloy	Condition (2)	Temperature (3) $(°F)$	Mean J_c $(in-lbs/in^2)$	Lower Bound (3) J_c $(in-lbs/in^2)$	Mean dJ/da (ksi)	Lower Bound (4) dJ/da (ksi)
Types 304, 308, 309, 316, 321, 347	Wrought	32 – 257	3840	1224	508.8	102
	GTA Weld		2808	1096.8	679.2	241.2
	SA Weld		838.8	384	261.6	120
	Wrought	752 – 1022	2400	552	457.2	132
	GTA Weld		1668	1028.4	534	186

Notes:

1. K_{JC} may be determined using Equation (9F.36)
2. GTA is gas –Tungsten Arc, SA is Submerged Arc
3. Linear interpolation may be used for temperature between 257°F and 752°F.
4. Lower bound indicates 90/95% lower bound for tolerance limits bracketing 90% of the total population at a 95% confidence level.

Table 9F.2M – J_c (1) and dJ/da values for Austenitic Stainless Steels (see reference [16])

Alloy	Condition (2)	Temperature (3) $(°C)$	Mean J_c (kJ/m^2)	Lower Bound (3) J_c (kJ/m^2)	Mean dJ/da (MPa)	Lower Bound (4) dJ/da (MPa)
Types 304, 308, 309, 316, 321, 347	Wrought	0 – 125	672	215	292	59
	GTA Weld		492	192	390	139
	SA Weld		147	67	150	72
	Wrought	400 – 550	421	96	263	79
	GTA Weld		293	180	307	107

Notes:

1. K_{JC} may be determined using Equation (9F.36)
2. GTA is gas –Tungsten Arc, SA is Submerged Arc
3. Linear interpolation may be used for temperature between 125°C and 400°C.
4. Lower bound indicates 90/95% lower bound for tolerance limits bracketing 90% of the total population at a 95% confidence level.

Table 9F.3 – JR Tearing Resistance Curve Data (see reference [17])

Material	Temperature $(°F)$	Thickness (in)	J_i $(in-lbs/in^2)$	C_R $(in-lbs/in^2)/in^{n_T}$	n_R
Generic CS-1	550	1.0	350	1808	0.277
Generic CS-2	550	1.0	600	2563	0.274
Generic CS-3	550	1.0	1050	5400	0.344
T 304 SS	75	1.0	6500	32758	0.519
Generic SS/SMAW	550	1.0	990	6033	0.391
Generic SS/SAW	550	1.0	650	4448	0.431
A508 Cl3	550	1.378	446	3443	0.329
A106 Gr B (NPS 8 inch Pipe)	120	0.54	2900	13008	0.334
TP 304 SS (NPS 4 inch pipe)	75	0.34	8000	33642	0.435

Notes:

1. The values in this table represent typical values for the stated temperature and wall thickness, actual values should be used when available.
2. The equation for the JR curve is $J_R = C_R(\Delta a)^{n_R}$.

Table 9F.3M – JR Tearing Resistance Curve Data (see reference [17])

Material	Temperature $(°C)$	Thickness (mm)	J_i (KJ/m^2)	C_R $(KJ/m^2)/mm^{n_T}$	n_R
Generic CS-1	288	25	61	129	0.277
Generic CS-2	288	25	105	185	0.274
Generic CS-3	288	25	184	311	0.344
T 304 SS	24	25	1138	1070	0.519
Generic SS/SMAW	288	25	173	298	0.391
Generic SS/SAW	288	25	114	193	0.431
A508 Cl3	288	35	78	208	0.329
A106 Gr B (NPS 8 inch Pipe)	49	14	508	773	0.334
TP 304 SS (NPS 4 inch pipe)	24	9	1401	1443	0.435

Notes:

1. The values in this table represent typical values for the stated temperature and wall thickness, actual values should be used when available.
2. The equation for the JR curve is $J_R = C_R(\Delta a)^{n_R}$.

Table 9F.4 – Constants for Paris Crack Growth Equations from Barsom – Upper Bound Data (see reference [22])

Material and Service	C	N	Threshold ΔK_{th}	Comments
For martensitic steels with a yield strength from 80 ksi to 300 ksi at room temperature in air or other non-aggressive environments	6.60E-9	2.25	$6.37(1-0.85R)$	Use Equations (9F.135) and (9F.136)
For ferritic-pearlite steels at room temperature in air or other non-aggressive environments	3.6E-10	3	$6.37(1-0.85R)$	Use Equations (9F.135) and (9F.136)
For austenitic stainless steels at room temperature in air or other non-aggressive environments	3.00E-10	3.25	$6.37(1-0.85R)$	Use Equations (9F.135) and (9F.136)
Note: Units: $da/dN - in/cycle,\ \Delta K\ and\ \Delta K_{th} - ksi\sqrt{in}$				

Table 9F.4M – Constants for Paris Crack Growth Equations from Barsom – Upper Bound Data (see reference [22])

Material and Service	C	n	Threshold ΔK_{th}	Comments
For martensitic steels with a yield strength from 552 MPa to 2068 MPa at room temperature in air or other non-aggressive environments	1.36E-7	2.25	$7.0(1-0.85R)$	Use Equations (9F.135) and (9F.136)
For ferritic-pearlite steels at room temperature in air or other non-aggressive environments	6.89E-9	3	$7.0(1-0.85R)$	Use Equations (9F.135) and (9F.136)
For austenitic stainless steels at room temperature in air or other non-aggressive environments	5.61E-9	3.25	$7.0(1-0.85R)$	Use Equations (9F.135) and (9F.136)
Note: Units: $da/dN - mm/cycle,\ \Delta K\ and\ \Delta K_{th} - MPa\sqrt{m}$				

Table 9F.5 – Constants for Crack Growth Equations for Welded Joints (see reference [24])

Material and Service	C	N	Threshold ΔK_{th}	Comments
Upper bound data (99.5% probability of survival) for steels in air or other non-corrosive environment	1.33E-09	2.75	1.82	Use Equations (9F.140) and (9F.141)
Mean data (50% probability of survival) for steels in air or other non-corrosive environment.	7.40E-10	2.75	2.18	Use Equations (9F.140) and (9F.141)
Note: Units: $da/dN - in/cycle,\ \Delta K\ and\ \Delta K_{th} - ksi\sqrt{in}$				

Table 9F.5M – Constants for Crack Growth Equations for Welded Joints (see reference [24])

Material and Service	C	n	Threshold ΔK_{th}	Comments
Upper bound data (99.5% probability of survival) for steels in air or other non-corrosive environment	2.60E-08	2.75	2.00	Use Equations (9F.140) and (9F.141)
Mean data (50% probability of survival) for steels in air or other non-corrosive environment	1.45E-08	2.75	2.45	Use Equations (9F.140) and (9F.141)
Note: Units: $da/dN - mm/cycle,\ \Delta K\ and\ \Delta K_{th} - MPa\sqrt{m}$				

Table 9F.6 – Constants for Paris Crack Growth Equations from BS 7910 for Screening – Upper Bound Data (see reference [4])

Material and Service	C	n	Threshold ΔK_{th}	Comments
For ferritic and austenitic steels in air or other non-aggressive service environments at temperatures up to 212°F	8.61E-10	3	1.8	Use Equations (9F.137) and (9F.138)
For ferritic and austenitic steels in air or other non-aggressive service environments at temperatures operating between 212°F and 1112°F with cyclic frequencies greater than or equal to 1 Hz:	8.61E-10	3	1.8	Use Equations (9F.137) and (9F.138)
For ferritic steels operating in a marine environment with cathodic protection, at temperatures up to 68°F	3.80E-9	3	1.8	Use Equations (9F.135) and (9F.136)
For ferritic steels operating in a marine environment without cathodic protection, at temperatures up to 68°F	3.80E-9	3	0.0	Use Equations (9F.135) and (9F.136)
Note: Units: $da/dN - in/cycle,\ \Delta K\ and\ \Delta K_{th} - ksi\sqrt{in}$				

Table 9F.6M – Constants for Paris Crack Growth Equations from BS 7910for Screening– Upper Bound Data (see reference [4])

Material and Service	C	n	Threshold ΔK_{th}	Comments
For ferritic and austenitic steels in air or other non-aggressive service environments at temperatures up to 100°C	1.65E-8	3	2.0	Use Equations (9F.135) and (9F.136)
For ferritic and austenitic steels in air or other non-aggressive service environments at temperatures operating between 100°C and 600°C with cyclic frequencies greater than or equal to 1 Hz:	1.65E-8	3	2.0	Use Equations (9F.137) and (9F.138)
For ferritic steels operating in a marine environment with cathodic protection, at temperatures up to 20°C	7.27E-8	3	2.0	Use Equations (9F.135) and (9F.136)
For ferritic steels operating in a marine environment without cathodic protection, at temperatures up to 20°C	7.27E-8	3	0.0	Use Equations (9F.135) and (9F.136)
Note: Units: $da/dN - mm/cycle,\ \Delta K\ and\ \Delta K_{th} - MPa\sqrt{m}$				

Table 9F.7 – Two Stage Paris Crack Growth Constants from BS 7910 – Upper Bound Data (Mean +2σ, Corresponding to 97.7% Probability of Survival (see reference [4])

$R = \frac{K_{min}}{K_{max}}$	Stage A			Stage B			Stage A/Stage B Transition Point	
	C_1 $Mean$	C_1 $Mean + 2\sigma$	n_1	C_2 $Mean$	C_2 $Mean + 2\sigma$	n_2	$Mean$	$Mean + 2\sigma$
Steel in Air (2)								
$R < 0.5$	1.79E-15	6.45E-15	8.16	4.29E-10	7.31E-10	2.88	10.45	9.07
$R \geq 0.5$	1.37E-11	5.97E-11	5.1	6.32E-10	1.39E-09	2.88	5.64	4.14
Steel Freely Corroding in a Marine Environment (3)								
$R < 0.5$	2.20E-10	6.27E-10	3.42	5.04E-07	7.65E-07	1.3	38.45	28.58
$R \geq 0.5$	3.94E-10	1.26E-09	3.42	1.15E-06	1.51E-06	1.11	31.60	21.53
Steel in a Marine Environment with Cathodic Protection at -850mV (Ag/AgCl) (3)								
$R < 0.5$	1.79E-15	6.45E-15	8.16	2.64E-09	6.76E-09	2.67	13.30	12.49
$R \geq 0.5$	1.37E-11	5.97E-11	5.1	3.07E-09	1.03E-08	2.67	9.30	8.35
Steel in a Marine Environment with Cathodic Protection at -1100mV (Ag/AgCl) (3)								
$R < 0.5$	1.79E-15	6.45E-15	8.16	3.12E-07	5.23E-07	1.4	16.58	14.79
$R \geq 0.5$	1.37E-11	5.97E-11	5.1	2.97E-07	5.77E-07	1.4	14.88	11.94

Notes:

1. Units: $da/dN - in/cycle,\ \Delta K\ and\ \Delta K_{th} - ksi\sqrt{in}.$
2. Steels (ferritic, austenitic, or duplex ferritic-austenitic) with yield strengths ≤ 101 ksi operating in air or other non-corrosive environment at temperatures up to 212°F.
3. Steels (excluding austenitic and duplex stainless steels) with yield strengths ≤ 87 ksi operating in marine environments at temperatures up to 70°F.

Table 9F.7M – Two Stage Paris Crack Growth Constants from BS 7910 – Upper Bound Data (Mean +2σ, Corresponding to 97.7% Probability of Survival (see reference [4])

$R = \frac{K_{min}}{K_{max}}$	Stage A			Stage B			Stage A/Stage B Transition Point	
	C_1 $Mean$	C_1 $Mean + 2\sigma$	n_1	C_2 $Mean$	C_2 $Mean + 2\sigma$	n_2	$Mean$	$Mean + 2\sigma$
Steel in Air (2)								
$R < 0.5$	2.10E-14	7.59E-14	8.16	8.32E-09	1.41E-08	2.88	11.48	9.96
$R \geq 0.5$	2.14E-10	9.38E-10	5.1	1.22E-08	2.70E-08	2.88	6.20	4.55
Steel Freely Corroding in a Marine Environment (3)								
$R < 0.5$	4.05E-09	1.15E-08	3.42	1.13E-05	1.72E-05	1.3	42.25	31.40
$R \geq 0.5$	7.24E-09	2.32E-08	3.42	2.62E-05	3.46E-05	1.11	34.72	23.65
Steel in a Marine Environment with Cathodic Protection at -850mV (Ag/AgCl) (3)								
$R < 0.5$	2.10E-14	7.59E-14	8.16	5.22E-08	1.34E-07	2.67	14.61	13.72
$R \geq 0.5$	2.14E-10	9.38E-10	5.1	6.07E-08	2.04E-07	2.67	10.21	9.17
Steel in a Marine Environment with Cathodic Protection at -1100mV (Ag/AgCl) (3)								
$R < 0.5$	2.10E-14	7.59E-14	8.16	6.94E-06	1.16E-05	1.4	18.21	16.25
$R \geq 0.5$	2.14E-10	9.38E-10	5.1	6.61E-06	1.28E-05	1.4	16.35	13.12

Notes:

1. Units: $da/dN - mm/cycle,\ \Delta K\ and\ \Delta K_{th} - MPa\sqrt{m}.$
2. Steels (ferritic, austenitic, or duplex ferritic-austenitic) with yield strengths ≤ 700 MPa operating in air or other non-corrosive environment at temperatures up to 100°C.
3. Steels (excluding austenitic and duplex stainless steels) with yield strengths ≤ 600 MPa operating in marine environments at temperatures up to 20°C.

Table 9F.8– Threshold Values for Use with Crack Growth Constants in Table 9F.7 (see reference [4])

Material	Environment	Threshold ΔK_{th}
Steels including austenitic stainless steels	Air or other nonaggressive environments up to 212°F	1.8
Steels excluding austenitic stainless steels	Marine with cathodic protection up to 70°F	1.8
Steels including austenitic stainless steels	Marine Unprotected	0.0
Note: Units: $\Delta K_{th} - ksi\sqrt{in}$		

Table 9F.8M – Threshold Values for Use with Crack Growth Constants in Table 9F.7M (see reference [4])

Material	Environment	Threshold ΔK_{th}
Steels including austenitic stainless steels	Air or other non-aggressive environments up to 100°C	2.0
Steels excluding austenitic stainless steels	Marine with cathodic protection up to 20°C	2.0
Steels including austenitic stainless steels	Marine Unprotected	0.0
Note: Units: $\Delta K_{th} - MPa\sqrt{m}$		

Table 9F.9 – Sampling of Line Pipe Fatigue Crack Growth Parameter from API RP 1176 – Upper Bound Data

Source	Application	C	n
Barsom & Rolfe, reference [31]	Typical Ferrite-Pearlite Steels	3.60E-10	3
Vosikovsky, reference [32]	X65 in Aqueous Environments	5.20E-10	2.82
Vosikovsky, reference [33]	X65 In Air, $\Delta K < 18\ ksi\sqrt{in}$	6.8E-11	3.5
	X65 In Air, $\Delta K \geq 18\ ksi\sqrt{in}$	2.7E-09	2.5
	X65 Sweat Crude, $\Delta K < 31\ ksi\sqrt{in}$	1.4E-12	4.8
	X65 Sweat Crude, $\Delta K \geq 31\ ksi\sqrt{in}$	3.8E-08	1.9
	X65 Sour Crude, $\Delta K < 23\ ksi\sqrt{in}$	7.3E-14	6.4
	X65 Sour Crude, $\Delta K \geq 23\ ksi\sqrt{in}$	8.9E-09	2.7
Andreason & Vitovec, reference [34]	Grade B	2.15E-13	5.4
Keller et al. (DOE), reference [35]	X52	4.30E-11	3.77
San Marchi et al. reference [36] & Stahlheim et al. reference [37]	TMCP	1.34E-13	3.5
Wintage Line Pipe, early 1950s	Youngstown DC-ERW	1.12E-10	3.31
	Kaiser SSAW	1.51-11	4.01
	A.O. Smith	2.33E-11	3.89
Lambert et al. reference [38]	X60 fatigue Component of SCC lab testing with SCC Crack Growth Rate of 0.00365 in/yr	1.53E-14	3.97
Maxey	10 inch and 12 inch OD X52 ERW (In Air)	2.12E-11	4.0
Maxey	10 inch and 12 inch OD X52 ERW Pipes (NaCl environment at Free Corrosion Potential)	8.33E-11	3.60

Note: Units: $da/dN - in/cycle,\ \Delta K - ksi\sqrt{in}$

Table 9F.9M – Sampling of Line Pipe Fatigue Crack Growth Parameter from API RP 1176 – Upper Bound Data

Source	Application	C	n
Barsom & Rolfe, reference [31]	Typical Ferrite-Pearlite Steels	6.89E-09	3
Vosikovsky, reference [32]	X65 in Aqueous Environments	1.01E-08	2.82
Vosikovsky, reference [33]	X65 In Air, $\Delta K < 20\ MPa\sqrt{m}$	1.24E-09	3.5
	X65 In Air, $\Delta K \geq 20\ MPa\sqrt{m}$	5.42E-08	2.5
	X65 Sweat Crude, $\Delta K < 34\ MPa\sqrt{m}$	2.26E-11	4.8
	X65 Sweat Crude, $\Delta K \geq 34\ MPa\sqrt{m}$	8.07E-07	1.9
	X65 Sour Crude, $\Delta K < 25\ MPa\sqrt{m}$	1.01E-12	6.4
	X65 Sour Crude, $\Delta K \geq 25\ MPa\sqrt{m}$	1.75E-07	2.7
Andreason & Vitovec reference [34]	Grade B	3.28E-12	5.4
Keller et al. (DOE), reference [35]	X52	7.66E-10	3.77
San Marchi et al. reference [36] & Stahlheim et al. reference [37]	TMCP	2.45E-12	3.5
Wintage Line Pipe, early 1950s	Youngstown DC-ERW	2.08E-09	3.31
	Kaiser SSAW	2.63E-10	4.01
	A.O. Smith	4.10E-10	3.89
Lambert et al. reference [38]	X60 fatigue Component of SCC lab testing with SCC Crack Growth Rate of 0.0927 mm/yr	2.67E-13	3.97
Maxey	250 mm and 300 mm OD X52 ERW (In Air)	3.69E-10	4.0
Maxey	250 mm and 300 mm OD X52 ERW Pipes (NaCl environment at Free Corrosion Potential)	1.51E-09	3.60

Note: Units: $da/dN - mm/cycle,\ \Delta K - MPa\sqrt{m}$

Table 9F.10 – Hydrogen Assisted Crack Growth Data – Upper Bound Data (see references [26]-[27])

Material Constant	Value – US Customary Units
a_1	2.1746E-10
b_1	3.2106
a_2	2.9637E-12
b_2	6.4822
a_3	2.7018E-09
b_3	3.6147
Note: Units: $da/dN - in/cycle$, $\Delta K - ksi\sqrt{in}$	

Table 9F.10M – Hydrogen Assisted Crack Growth Data – Upper Bound Data (see references [26]-[27])

Material Constant	Value – SI Units
a_1	4.0812E-09
b_1	3.2106
a_2	4.0862E-11
b_2	6.4822
a_3	4.8810E-08
b_3	3.6147
Note: Units: $da\ /\ dN - \ mm\ /\ cycle, \Delta K - MPa\sqrt{m}$	

9F.9 Figures

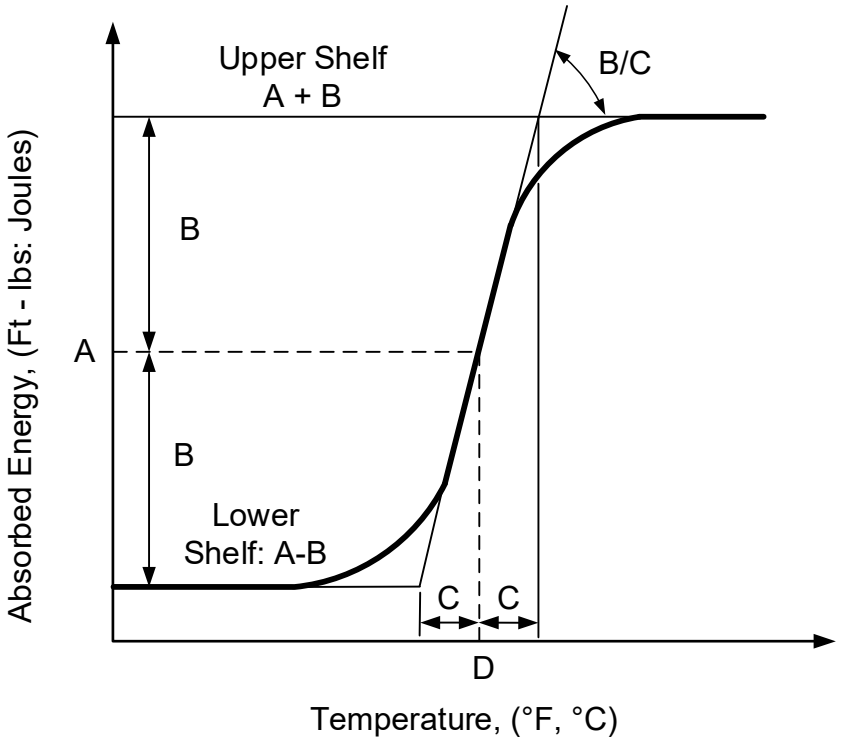

(a) Characteristics of the Hyperbolic Tangent Function

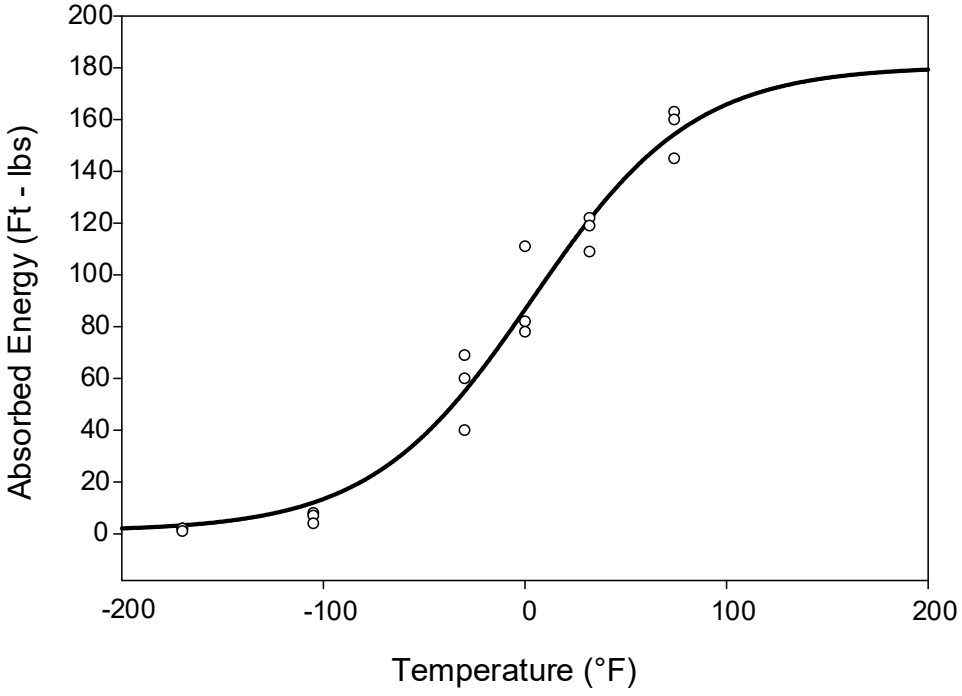

(b) Typical Hyperbolic Tangent Function Curve Fit to CVN data

Figure 9F.1 – Curve Fitting of Charpy Data

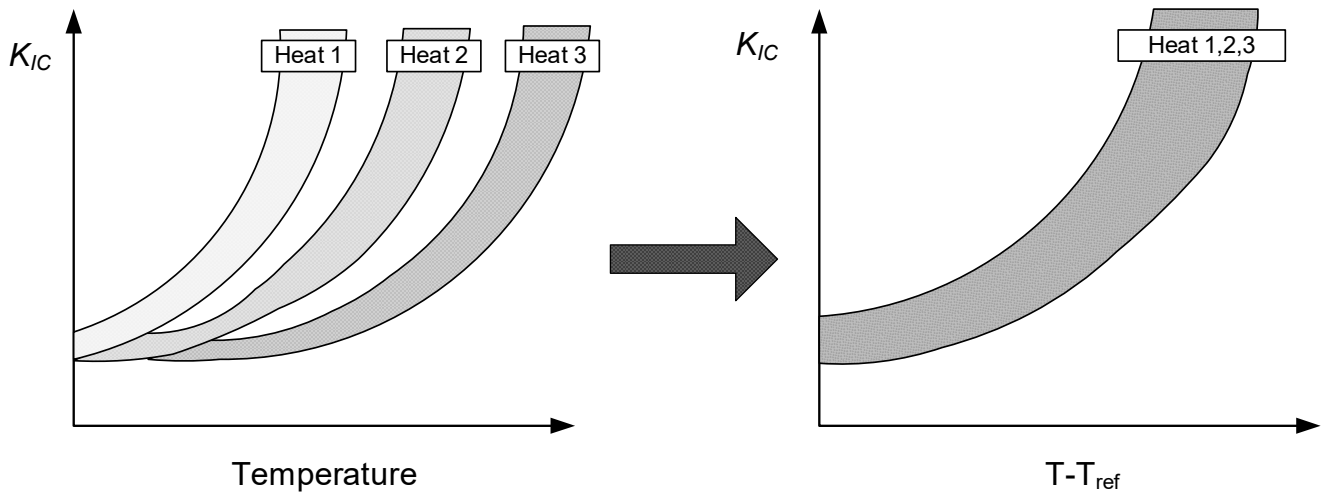

Figure 9F.2 – Fracture Toughness Indexing Approach

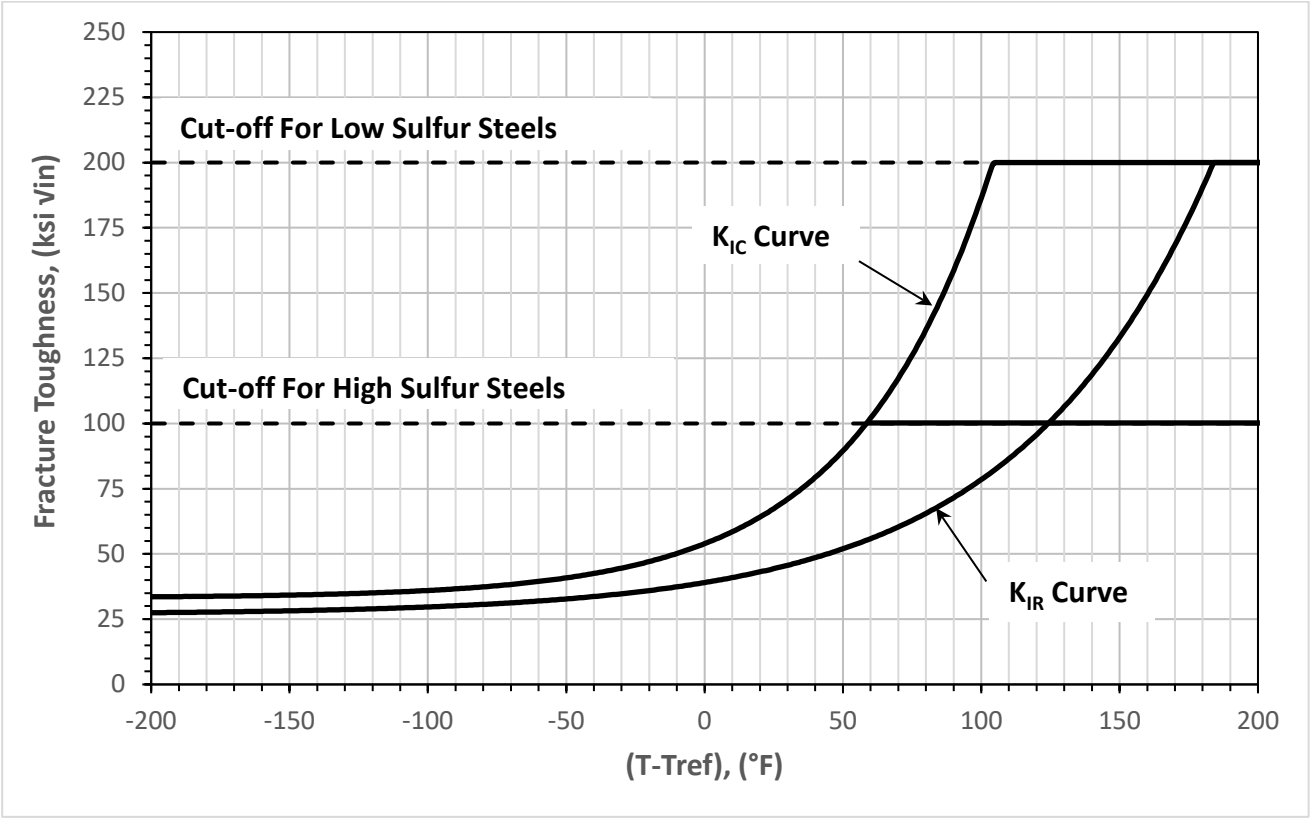

Figure 9F.3 – Lower-Bound Fracture Toughness Curves for Ferritic Steels

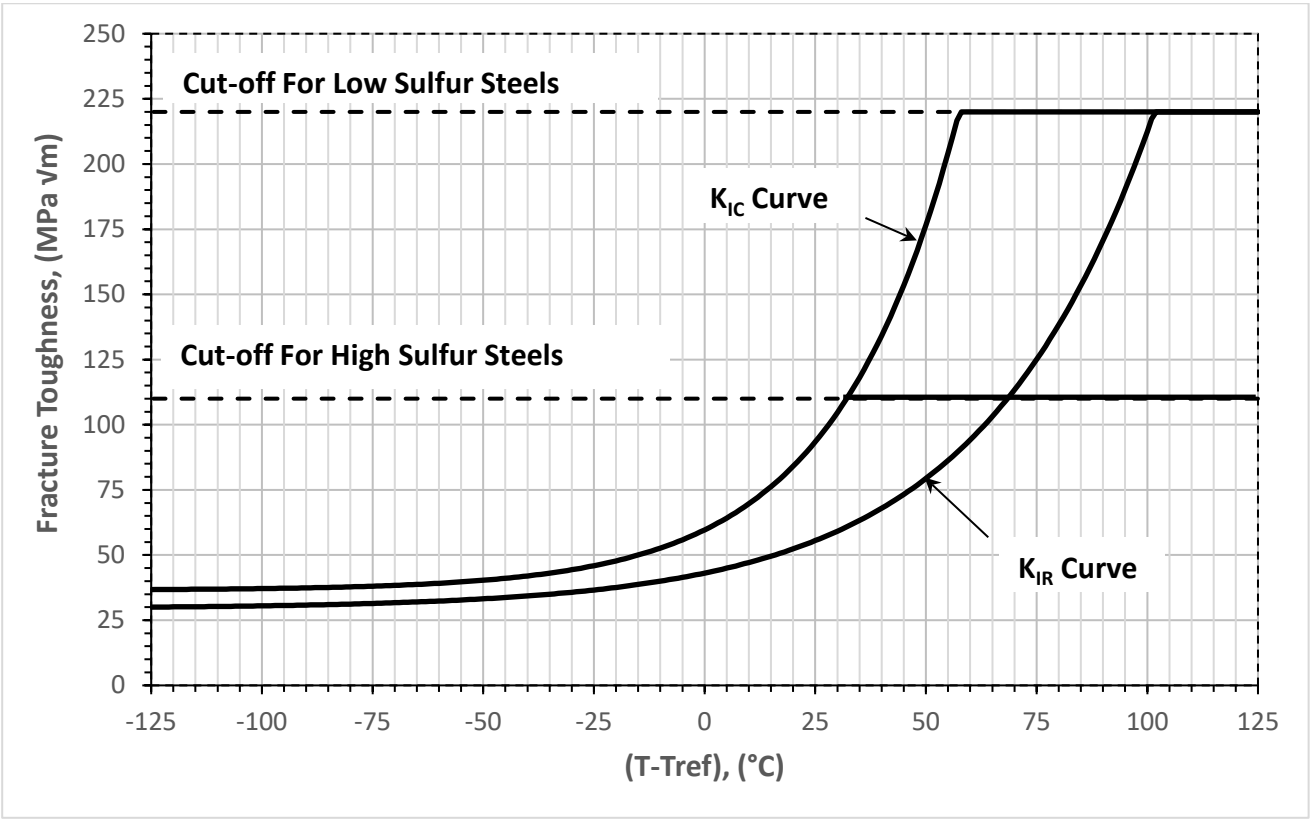

Figure 9F.3M – Lower-Bound Fracture Toughness Curves for Ferritic Steels

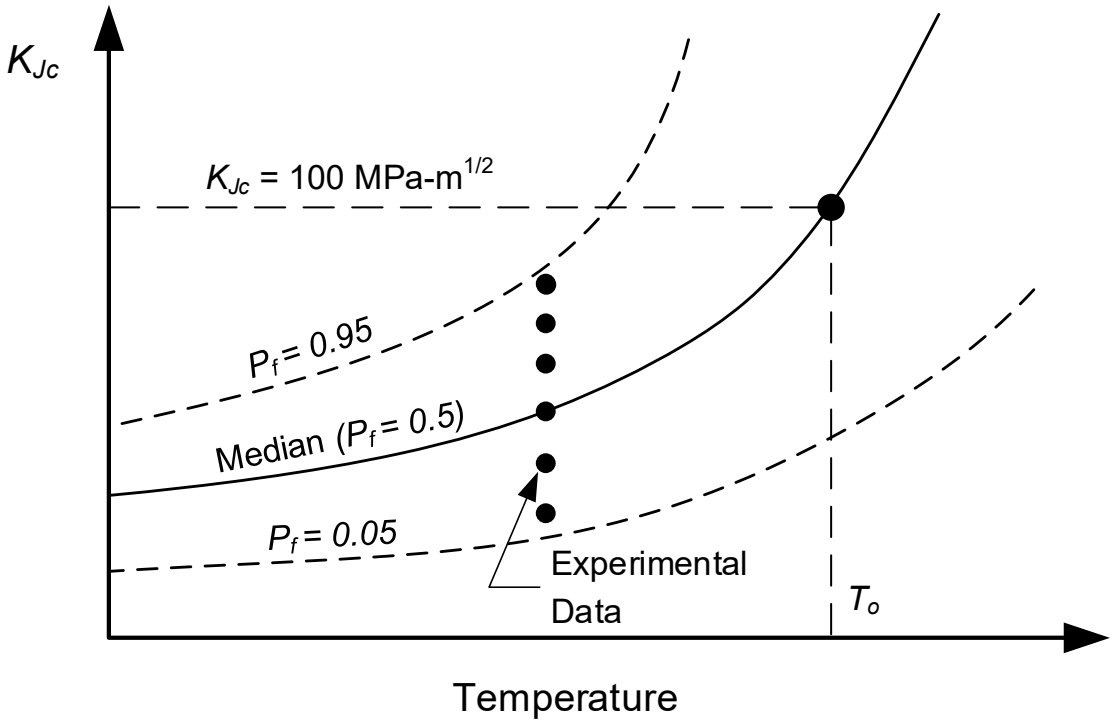

Figure 9F.4 – The Fracture Toughness Master Curve

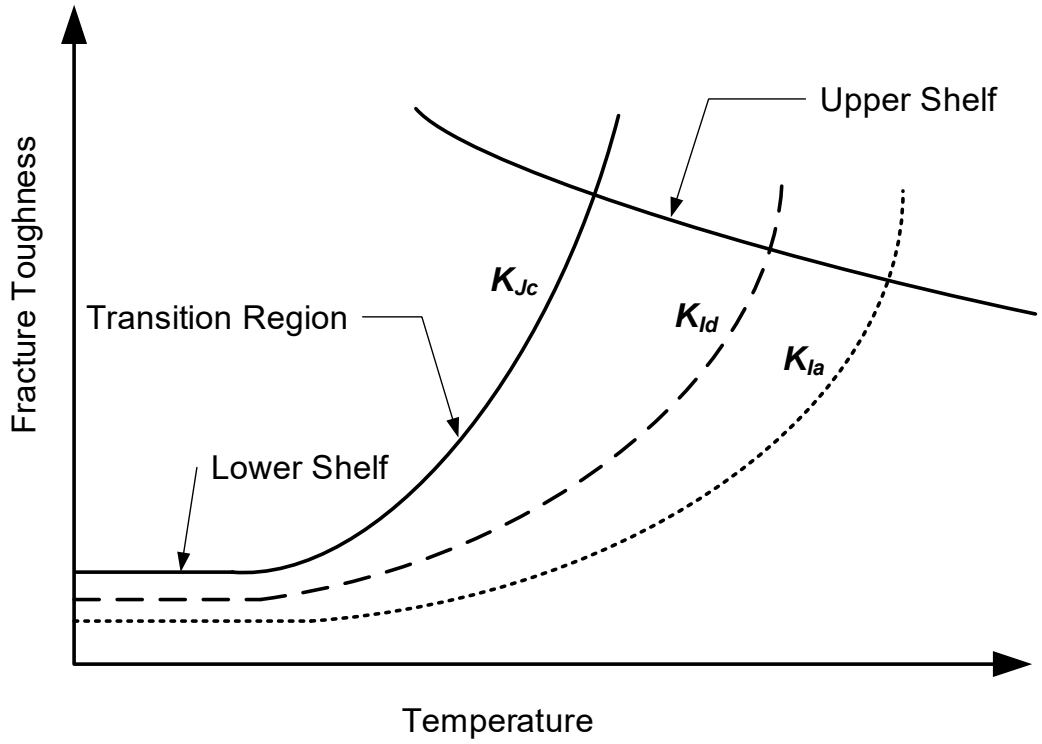

Figure 9F.5 – The Fracture Toughness Master Curve (K_{Jc}) Dynamic Curve (K_{1d}) and Arrest Curve (K_{1a})

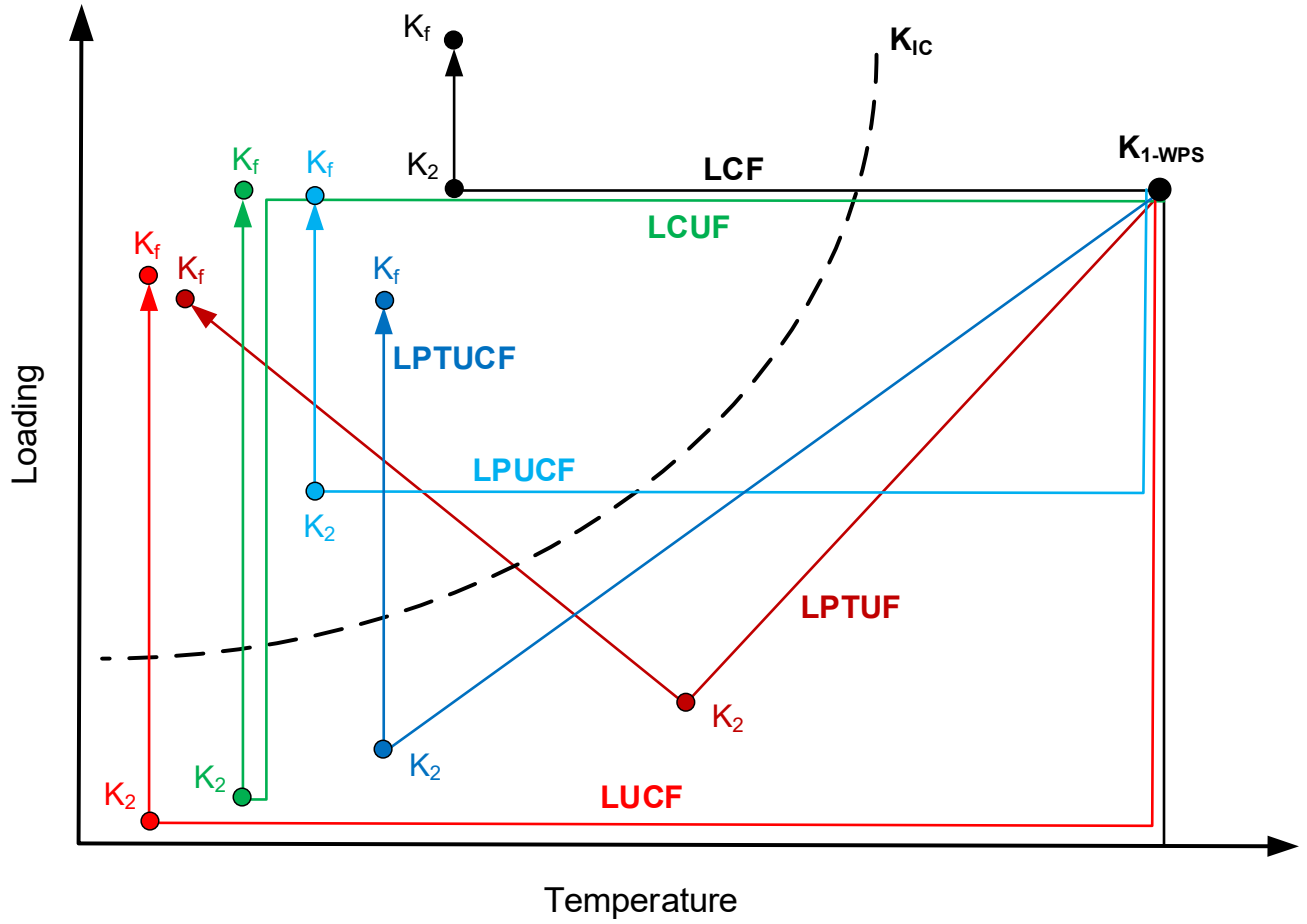

Notes

1. LCF – Load Cool Fracture
2. LUCF – Load Unload Cool Fracture
3. LCUF – Load Cool Unload Fracture
4. LPUCF – Load Partial Unload Cool Fracture
5. LPTUF – Load Partial Transient Unload Fracture
6. LPTUCF – Load Partial Transient Unload Cool Fracture

Figure 9F.6 – The Principal and Possible Transients of the Warm Prestress (WPS) Effect

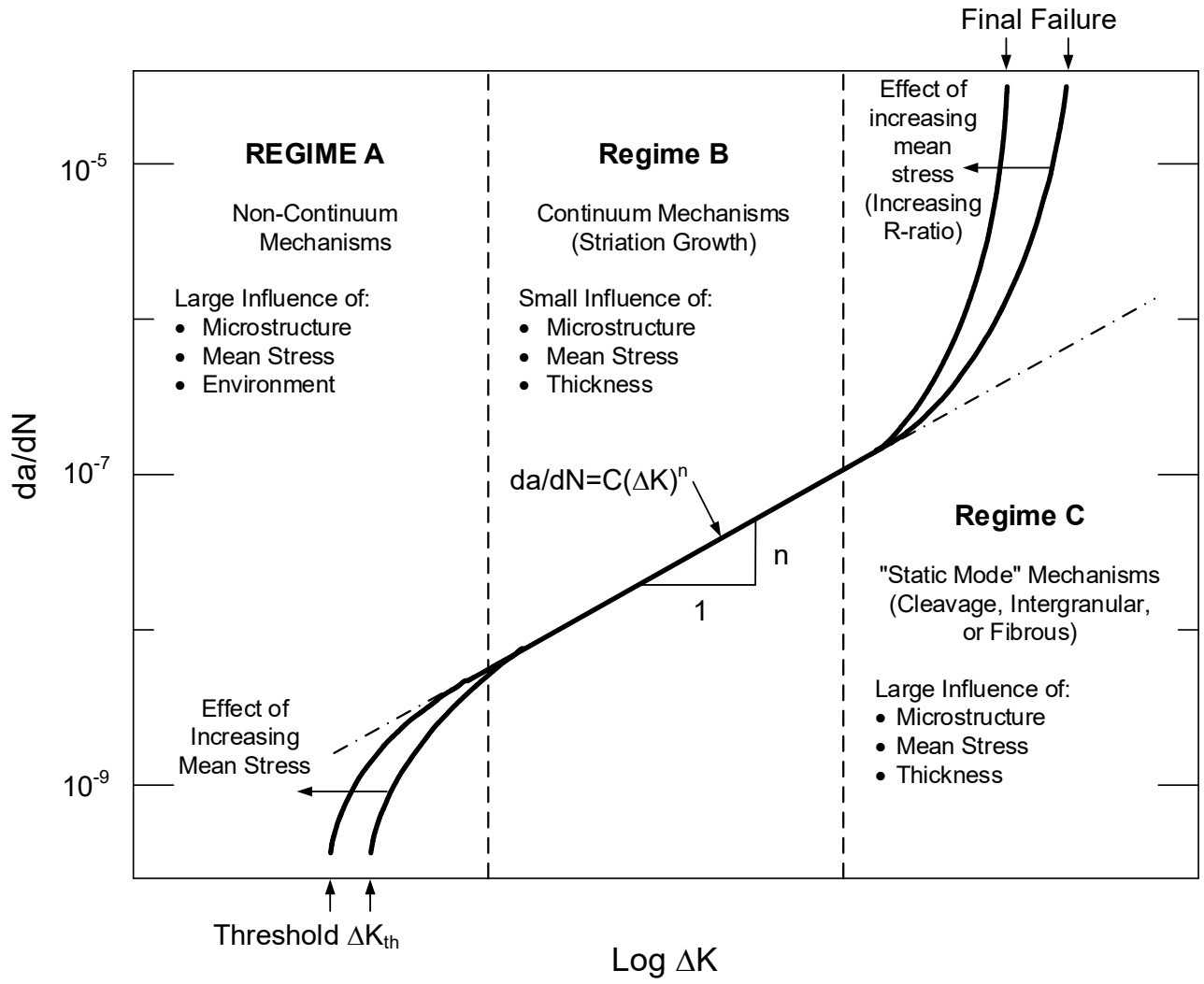

Figure 9F.7 – Crack Growth Behavior – Fatigue

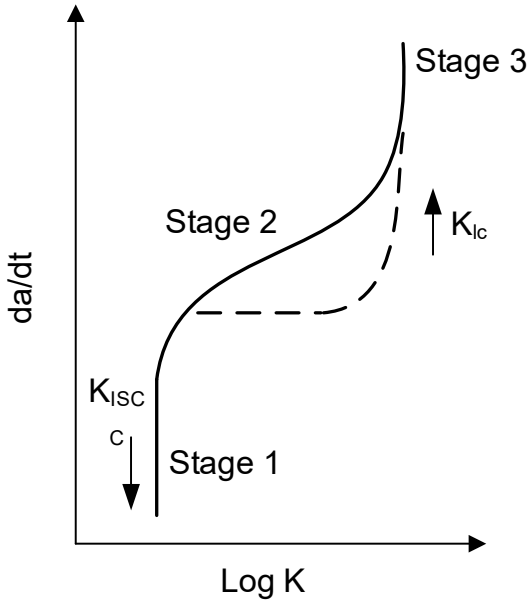

(a) Crack Growth Rate and Stress Intensity Factor Relationship for Two Enviornments

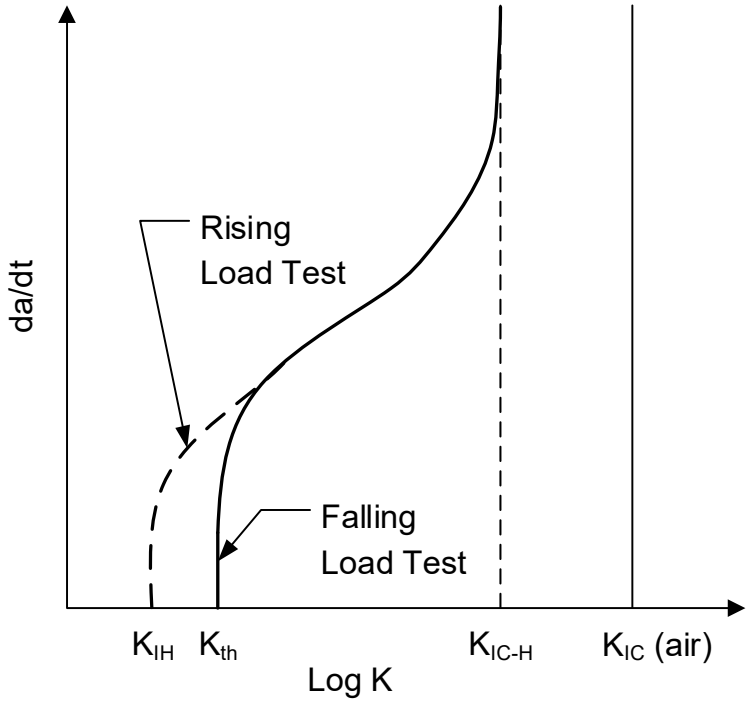

(b) Hydrogen Assisted Crack (HAC) Growth Curve

Figure 9F.8 – Crack Growth Behavior – Stress Corrosion Cracking and HAC

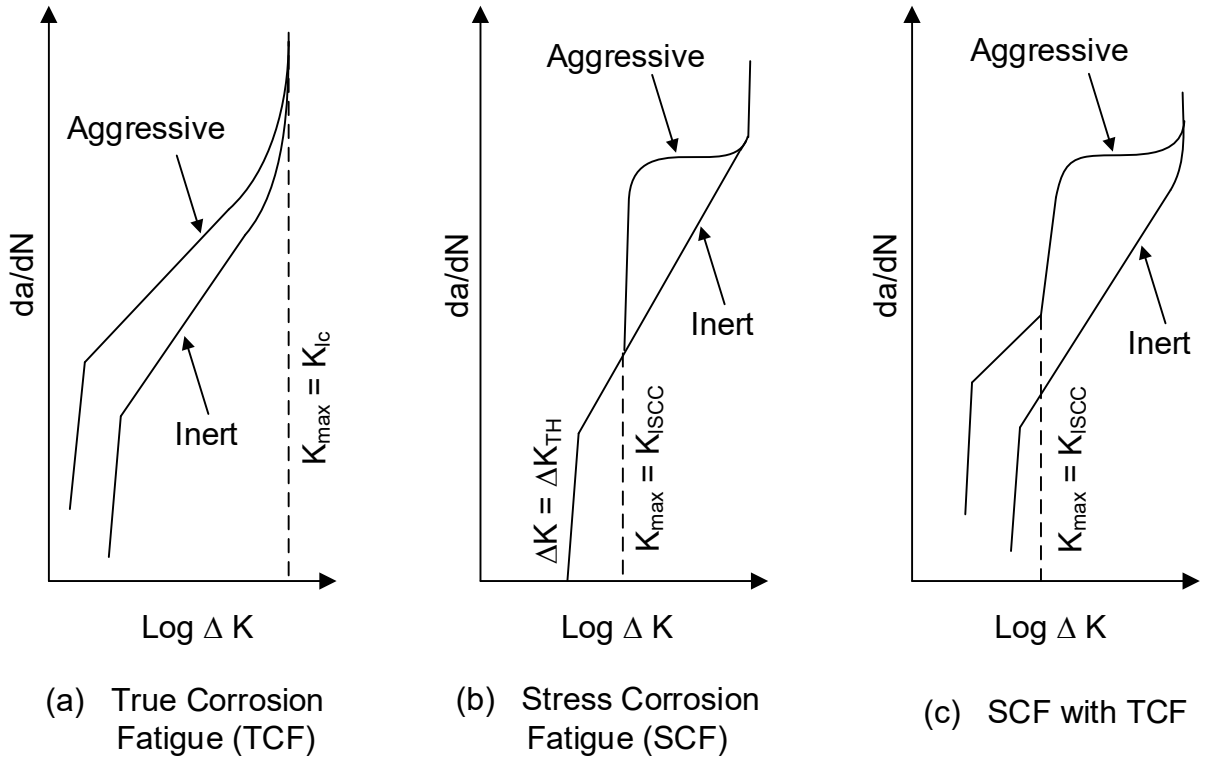

Figure 9F.9 – Crack Growth Behavior – Corrosion Fatigue

ANNEX 9G – STRESS ANALYSIS FOR CRACK-LIKE FLAWS

(NORMATIVE)

CONTENTS

ANNEX 9G – STRESS ANALYSIS FOR CRACK-LIKE FLAWS 9G-1

9G.1 GENERAL REQUIREMENTS 9G-1
9G.1.1 Scope 9G-1
9G.1.2 ASME B&PV Code, Section VIII, Division 2 (VIII-2) 9G-2
9G.1.3 FAD-Based Assessment Procedure 9G-2
9G.1.4 Assessment Using Stress Analysis Results – Uncracked Configuration 9G-2
9G.1.5 Assessment Using Stress Analysis Results – Crack Incorporated into the Model 9G-2
9G.1.6 Assessment of Growing Cracks 9G-2
9G.1.7 Numerical Analysis 9G-2
9G.1.8 Applicable Loads and Load Case Combinations 9G-2
9G.2 STRESS ANALYSIS OF THE UN-CRACKED CONFIGURATION 9G-3
9G.2.1 Overview 9G-3
9G.2.2 Categorization and Linearization of Stress Results 9G-3
9G.2.3 Fitting Stress Results to a Polynomial 9G-3
9G.2.4 The Weight Function Method 9G-3
9G.3 FINITE ELEMENT ANALYSIS OF COMPONENTS WITH CRACKS 9G-4
9G.3.1 Overview 9G-4
9G.3.2 Output Quantity 9G-4
9G.3.3 Mesh Design 9G-4
9G.3.4 Crack Tip Modeling Approaches 9G-4
9G.3.5 Focused Mesh Approach 9G-4
9G.3.6 Finite Radius Approach 9G-5
9G.3.7 Small Strain vs. Large Strain Analysis 9G-6
9G.3.8 Convergence 9G-6
9G.3.9 Initial and Thermal Strains 9G-7
9G.3.10 Modeling Procedure 9G-7
9G.4 FAD-BASED METHOD FOR NON-GROWING CRACKS 9G-8
9G.4.1 Overview 9G-8
9G.4.2 Assessment Procedure 9G-8
9G.5 DRIVING FORCE METHOD FOR NON-GROWING CRACKS 9G-10
9G.5.1 Overview 9G-10
9G.5.2 Assessment Procedure 9G-10
9G.6 ASSESSMENT OF GROWING CRACKS 9G-11
9G.6.1 Crack Growth Models 9G-11
9G.6.2 Crack Parameter Solutions 9G-11
9G.6.3 Determination of a Remaining Life 9G-11
9G.6.4 Crack Growth Using Numerical Methods 9G-11
9G.7 NOMENCLATURE 9G-11
9G.8 REFERENCES 9G-12
9G.9 FIGURES 9G-14

9G.1 General Requirements

9G.1.1 Scope

The analytical methods contained within this Annex can be used for stress analysis when performing a Fitness-For-Service (FFS) Assessment of a component with a crack-like flaw operating below the creep regime.

Assessment procedures for crack-like flaws operating in the creep regime are provided in Part 10. The determination of the creep regime for a material may be determined using Part 4, Table 4.1, or Part 10.

9G.1.2 ASME B&PV Code, Section VIII, Division 2 (VIII-2)

Some of stress analysis concepts and methods in this Annex are based on ASME B&PV Code, Section VIII, Division 2 (VIII-2), Part 5, and reference to VIII-2 is made directly.

9G.1.3 FAD-Based Assessment Procedure

The Level 2 FAD-based assessment procedures in Part 9 have been developed to make maximum use of existing solutions for crack driving force (i.e., stress intensity factor and reference stress solutions in Annex 9B and Annex 9C, respectively). Even in cases where a rigorous closed form solution has not been tabulated, it is often possible to use existing solutions to generate reasonable approximations of the case at hand. The weight function method, for example, enables stress intensity factor solutions to be derived for arbitrary through-wall stress distributions. There are other instances where the problem is sufficiently complex that it is appropriate to perform a detailed stress analysis where the crack-like flaw is explicitly included in the numerical model.

9G.1.4 Assessment Using Stress Analysis Results – Uncracked Configuration

A stress analysis of the component is required to evaluate a crack-like flaw in a component using the Level 2 or Level 3 Assessment procedures in this standard. Guidelines for using the results from a stress analysis for these assessments where the crack is not included in the stress analysis model are provided in paragraph 9G.2.

9G.1.5 Assessment Using Stress Analysis Results – Crack Incorporated into the Model

The Level 3 Assessment procedures provide an option to incorporate a crack-like flaw directly into a stress analysis. Guidelines for performing a stress analysis using the finite element method where the crack is incorporated into the model are provided in paragraph 9G.3. Note that other numerical techniques to evaluate cracks in components such as the boundary element method or mesh-less methods may also be used. The specific details of the analysis and the way in which the results are used depend on the application. Two alternative approaches for assessing non-growing cracks are given in paragraphs 9G.4 and 9G.5.

9G.1.6 Assessment of Growing Cracks

Guidelines for the assessment of growing cracks are addressed in paragraph 9G.6.

9G.1.7 Numerical Analysis

The assessment methods in this Annex are based on the use of results obtained from a detailed stress analysis of a component. Depending on the loading condition, a thermal analysis to determine the temperature distribution and resulting thermal stresses may also be required. Recommendations for stress analysis are provided in Annex 2C, Annex 2D and VIII-2, Part 5.

9G.1.8 Applicable Loads and Load Case Combinations

All applicable applied loads on the component shall be considered when performing an FFS Assessment. Supplemental loads shall be considered in addition to the applied pressure in the form of applicable load cases. If any of the loads vary with time, a loading histogram shall be developed to show the time variation of each specific load. An overview on applicable loads and load case combinations that need to be considered in an FFS Assessment is provided in Annex 2C, Annex 2D and VIII-2, Part 5.

9G.2 Stress Analysis of the Un-Cracked Configuration

9G.2.1 Overview

Stress analysis results based on an un-cracked configuration may be used in a crack-like flaw assessment. The approach entails post-processing the stress values in such a way as to tie into the existing K_I and σ_{ref} solutions in Annex 9B and Annex 9C, respectively. This approach is best suited to cases where the geometry can be approximated by simple shapes that are addressed in Annex 9B and Annex 9C (e.g., flat plate, cylindrical shell, spherical shell). The stress distribution may either be uniform or non-uniform through the wall thickness at the location of the crack. Several examples are listed below:

a) Cylindrical or spherical shell under pressure loading,

b) Cylindrical shell with an internal attachment, which creates a local peak stress,

c) Thermal shock on the inside of a pressure vessel, which creates a highly non-uniform thermal stress distribution, and

d) Seam weld with a non-uniform through-wall weld residual stress distribution, obtained from Annex 9D or from a multi-pass weld simulation.

9G.2.2 Categorization and Linearization of Stress Results

Membrane and bending stresses normal to the plane of the crack can be used with several of the K_I and σ_{ref} solutions in Annex 9B and Annex 9C. These stresses can be obtained by stress linearization of the stress components through the wall thickness with the same orientation using the methods in Annex 2D. The linearization may be performed based on the crack location within the wall thickness (see Figure 9G.1) or the section thickness (see Figure 9G.2). Linearization simply operates on the given total stress values and is not the same as categorization of the resulting membrane and bending stresses as primary, secondary, or peak. Stress categorization typically involves consideration of both the load type and the location within the component. Methods for both stress categorization and linearization are provided in VIII-2, Part 5.

The linearization method is not recommended for K_I estimation when the stress distribution is highly non-uniform because significant errors can occur, and more accurate methods are available, (see paragraphs 9G.3 and 9G.4 below). The reference stress is controlled by the development of net-section plasticity, so it is less sensitive to local peak stresses. Therefore, an accurate reference stress may be determined from the membrane and bending stresses derived from the linearization of stress results.

9G.2.3 Fitting Stress Results to a Polynomial

If the stress distribution normal to the flaw can be represented by a polynomial (4th degree or lower), then the K_I solutions in Annex 9B may be used if a component geometry and crack geometry can be found to model the actual cracked configuration. Note that a linear approximation of the through-wall stress distribution is merely a special case of the polynomial approach. As is the case with the linearization method, a polynomial fit of the stress distribution can be performed locally at the flaw location or through the entire cross section.

9G.2.4 The Weight Function Method

In many cases, a simple polynomial expression does not provide a good fit to stress analysis results. In these cases, it is preferable to use the weight function approach. The weight function method (see Annex 9B) may be used to compute K_I for an arbitrary through-wall variation of stress normal to the crack plane. The disadvantage of the weight function method is that numerical integration is required.

9G.3 Finite Element Analysis of Components with Cracks

9G.3.1 Overview

General guidelines for numerical analysis of components with cracks are provided in this paragraph. A step-by-step modeling procedure based on these guidelines is provided in paragraph 9G.3.10. Additional considerations are discussed in paragraphs 9G.4 and 9G.5. Incorporating one or more cracks into a finite element model is considered a Level 3 approach and should be undertaken only by individuals with suitable qualifications. An overview of the background, requirements and limitations of modern numerical fracture mechanics analysis is provided in reference [1].

9G.3.2 Output Quantity

Finite element analysis of components with cracks may be used to determine the J-integral (or equivalently K_I in the case of bulk elastic material response) and the crack tip opening displacement (CTOD). For cases where the required conditions for J-integral validity could be violated (large deformation, non-proportional loading, kinematic hardening plasticity with multiple load cycles, etc.), (see reference [2]), the CTOD provides a generally valid crack deformation parameter. For such cases however, the tie between any (single) crack tip parameter and fracture is less clear, and results obtained by comparing numerical results with separately measured toughness values should be used with caution. Further discussion and references can be found in the following paragraphs.

9G.3.3 Mesh Design

The suggested, but not mandatory, mesh design for the crack tip region is a focused “spider web” mesh that has elements concentrated at the crack tip (see Figure 9G.3 and Figure 9G.4). This is the most efficient way to structure the mesh for defining successive contour integral domains. In some commercial Finite Element Analysis (FEA) programs, this type of construction is essentially required for defining unique domains for all requested contours. This mesh design is not necessarily required for CTOD analysis, though it often is efficient to use such an approach, and this design also allows possible simultaneous determination of the J-integral. The treatment of the first ring of elements within the spider web mesh is the subject of the next section.

9G.3.4 Crack Tip Modeling Approaches

In either two-dimensional (2D) or three-dimensional (3D) analysis, there are two primary crack tip modeling approaches: focused mesh and finite radius. Both methods can be used to determine the J -integral or CTOD, although special considerations are discussed in paragraph 9G.3.7. In all cases, modeling of the crack tip (singular) behavior only enhances convergence of the numerical result and is not necessarily required for a valid solution. Convergence of results is discussed further in paragraph 9G3.8.

9G.3.5 Focused Mesh Approach

In this approach, standard finite elements are manipulated to create specific stress versus position behavior within the element. Standard four-sided elements are collapsed along one edge or face in three dimensions (see Figure 9G.3 and Figure 9G.4) to create a three-sided shape with coincident nodes. The coincident nodes represent the crack tip position, and elements manipulated in this way are referred to singular elements since the collapsing of the edge or face creates a stress singularity at the coincident nodes that mimics the infinite stress predicted at the crack tip in traditional LEFM. The specific stress versus position behavior is dictated by the problem (elastic vs. elastic-plastic) and is determined by the element order (linear or quadratic), mid-side node positioning (if quadratic

elements are used) and the assigned behavior of the initially coincident nodes under load (tied versus free). The options for modeling are as follows:

a) For Linear-Elastic Analysis:

1) Quadratic elements: Coincident nodes at the crack tip are tied together and the mid-side nodes are moved from the ½ point position to the ¼ point position (towards the crack tip). This generates a $1/\sqrt{r}$ stress vs. position behavior along all theta rays within the first ring of (collapsed/singular) elements.

2) Linear Elements: Coincident nodes at the crack tip are again tied together, and the singular field is approximated by the linear displacement field. A substantially finer mesh, relative to use of quadratic elements, may be required to obtain a converged solution.

b) For Elastic-Plastic Analysis:

1) Quadratic elements: Coincident nodes at the crack tip are not tied together and the mid-side nodes are left at the ½ point position. This generates a $1/r$ stress versus position behavior along all theta rays within the first ring of (collapsed/singular) elements.

2) Linear Elements: Coincident nodes at the crack tip are not tied together, and the singular field is approximated by the linear displacement field. A substantially finer mesh may be required, although linear elements can avoid common elastic-plastic element problems such as volumetric locking.

3) This last elastic-plastic case is referred to as a blunted notch approach, since the initially coincident nodes are allowed to move apart under load and has been used (with small strain analysis) to determine the majority of J -CTOD relationships in the literature (see reference [3]).

c) Tools to implement the focused mesh approach into commercial finite element packages are available directly in many FEA programs, as well as through after-market products.

9G.3.6 Finite Radius Approach

In this approach, conventional elements are used and a finite radius at the crack tip is modeled (see Figure 9G.5). This results in an initial offset of the crack faces; a “keyhole” mesh, which is created by removing the first ring of collapsed elements from a focused “spider web” mesh, can also be used, but is less desirable than a mesh with a finite crack tip radius. This approach is often associated with large strain analysis (see paragraph 9G3.7) when very accurate crack tip region stresses, and strains are desired for large scale yielding conditions. The required radius depends on the subsequent deformation: the initial crack tip radius should be three to five times smaller than the tip radius in the deformed state to remove any dependence of the solution on the assumed initial radius. This requires an iterative approach, and for small CTOD values (moderate, but still local yield level loading), can be extremely difficult to obtain due to numerical precision difficulties in defining unique nodal positions. Appropriate mesh refinement along the crack radius is also required and is problem dependent. Note this approach is described for completeness but is really needed only for research studies that require refined values of the large-deformation strain-stress fields over distances of less than five times the CTOD from the crack front. This approach is not needed for typical FFS engineering assessments.

9G.3.7 Small Strain vs. Large Strain Analysis

Small strain analysis bases element stiffness on the original configuration of the element, while large strain analysis updates the stiffness behavior of each element as it deforms through the course of loading. This difference is often negligible for structures or components under meaningful loading conditions.

Large strain analysis is not recommended for use with the focused mesh approach that is expected to be the standard analysis method for FFS Assessments. This is due to likely convergence problems as elements may distort to the point of inverting if their shape is updated throughout the solution. However, its use is not precluded, though in the case that a converged solution can be obtained, results should be checked to ensure that local element distortions, if present, are not affecting the solution quantity of interest. Large strain analysis is typically associated with the Finite Radius Approach (see paragraph 9G.3.6) and similarly is only important when deformations and strains extremely close to the crack tip are of interest (as in research studies). In this case, consideration of the effect of deformation on the stiffness behavior of the near-tip elements can be important and should be considered (see reference [1]).

9G.3.8 Convergence

Numerical fractures mechanics is an extremely powerful tool for determination of contour integrals for many practical applications. Surprisingly coarse meshes can be used to obtain converged contour integral (J or K_I) solutions, (see reference [1]). In this sense, convergence refers to successive contours moving away from the crack tip giving consistent (J or K_I) values. Convergence is often rapidly obtained for linear elastic (small scale yielding) conditions, such that configurations that involve complex geometry not well-represented by the standard solution available in Annex 9B, but straightforward loading (such as internal pressure, or external forces and moments) can be rapidly and rigorously analyzed. This is particularly true with the automation of the Extended Finite Element Method (XFEM) in commercial FEA programs, where no complex mesh design is necessary, as described in paragraph 9G.3.3, but only geometric definition of the flaw itself in the structure is required. This method is currently limited to the linear elastic small scale yielding case, though inclusion of plastic material behavior in the model constitutive behavior may not be prohibited by the FEA program. This last point is a caution, and the user and theory manuals for the FEA program should always be consulted when performing any computational fracture mechanics analysis.

When non-linear material behavior is included in the analysis (i.e., plasticity), convergence of results becomes much more difficult, even without the initial or thermal strain considerations discussed in paragraph 9G3.9. A J-integral solution under non-uniform plastic straining generally requires that the contour domain be increased in size (so that yielded regions are increasingly enclosed by the defined contours) until convergence is obtained. This can be particularly challenging for shallower cracks and may require elongated (or egg-shaped) contours be defined so that the entire thickness can be contained in the contour region if necessary. This is not necessary for CTOD determination, but on the other hand, very refined meshes are generally required near the crack tip in this case, with either the focused or finite radius mesh techniques (see reference [4]). A mesh convergence study is likely required for CTOD determination, where the CTOD is typically defined as the crack tip opening (displacement of crack faces) at the original crack tip, or alternately as the crack face perpendicular displacement at lines oriented at 45 degrees to the crack face (see reference [1] and see Figure 9G.6). More than one element along the crack sidewall before the CTOD determination point is likely required to alleviate initially singular element distortion and achieve convergence.

9G.3.9 Initial and Thermal Strains

The standard form of the J -integral does not consider thermal strains and has been shown to lead to path-dependent values or non-convergence of J, as originally discussed in reference [2]. However, by replacing the total strain with the sum of the mechanical and thermal strains, an additional term is generated (relative to the basic definition) and path-independence is restored (see references [5] and [6]). This is demonstrated in detail in reference [7] for the widely used Domain Integral implementation of J, and is implemented automatically in most commercial programs (though the specific user and theory manuals should always be consulted by the user).

Evaluation of contour integrals in simulated residual stress (WRS) fields also often leads to path dependence or non-convergence of the J -integral. The common assumption is that path independence may also be restored for the WRS problem by treating the initial stresses and strains due to welding (in the un-cracked plate) as equivalent to a thermal stress-strain field, (see references [8], [9], and [10]). This formulation has been demonstrated to restore convergence of the J -integral, but as discussed in paragraph 9G.3.2, caution should be used when comparing this value to separately measured standard toughness values, as the tie with fracture when using this modified contour integral definition is less-established for weld residual stress and strain fields. Note that the CTOD does not require any corrections, but the caution about comparison to standard toughness values still applies.

Finally note that if a J -integral approach is ultimately used in relating WRS to flaw driving force, additional corrections may be needed to account for non-proportional loading that could occur during welding and stress and strain redistribution as the flaw is allowed to open. This subject is treated in detail in reference [8].

9G.3.10 Modeling Procedure

a) STEP 1 – Develop a finite element model of the component, including all relevant geometry and flaw characteristics. Consideration of the sensitivity of the solution to the position within the simulated stress field should be given, and appropriate safety factors applied to account for uncertainty.

b) STEP 2 – Define all relevant loading conditions including pressure, supplemental loads, temperature distributions, and residual stresses (see paragraph 9G.3.8 and Annex 9D). Crack face tractions should also be applied where appropriate. Note that with the FAD-based method (paragraph 9G.4), primary loads must be considered separately from secondary and residual stresses.

c) STEP 3 – Define the appropriate material properties. An elastic-plastic finite element analysis requires a stress-strain curve for the material of interest. Standard computational fracture mechanics analysis results (as described in this Annex) are most valid when a basic isotropic (linear or non-linear) hardening plasticity model is used. In cases where complex cyclic loading is present (for example, weld residual stress, followed by thermal and mechanical cycling that cause local reversed yielding), a cyclic hardening (e.g., kinematic, or combined/mixed kinematic-isotropic) model is most appropriate for determining instantaneous stresses and strains, but the tie with separately measured toughness values is less clear.

d) STEP 4 – Perform the finite element analysis and evaluate the results (J -Integral or K_I). The type of results and evaluation procedure depend on the application (see paragraph 9G.3.4). Specific guidance on results evaluation is given in paragraph 9G4.2 and paragraph 9G.5.2.

9G.4 FAD-Based Method for Non-Growing Cracks

9G.4.1 Overview

This procedure entails the determination of stress intensity factor and reference stress solutions, as well as the FAD curve, for the configuration of interest and then applying the Level 2 Assessment in Part 9. The FAD method requires that loads (or stresses) be categorized as primary, secondary, or residual. If more than one primary load is present (e.g., the component is subject to both a membrane and bending stress), the FAD method assumes that these loads are applied simultaneously. If the primary loads are out of phase with one another (e.g., if the membrane stress is applied first, followed by the bending stress), the FAD approach is not strictly valid. The J driving force method described in paragraph 9G.5 is better suited to such situations.

9G.4.2 Assessment Procedure

The following steps describe the determination of a J -based FAD curve for the configuration of interest, followed by an assessment in accordance with the Level 2 procedure in Part 9.

a) STEP 1 – Categorize all loads as primary, secondary, or residual. It is important to recognize that stresses that are labeled as secondary in the original construction code may not behave as such in a crack-like flaw analysis. The two questions below can be used to determine whether a particular load should be categorized as primary or secondary. When in doubt, the load should be treated as primary.

   1) Could the load, if its magnitude were sufficiently high, contribute to overload, rupture, or buckling of the component? If the answer is yes, then the load is primary. Thermal expansion loads could lead to rupture or buckling of a piping system, despite these loads being classified as secondary by the construction code.

   2) Will the stress in question relax if there is net-section yielding in the vicinity of the crack? If so, the stress can be classified as secondary/residual. Weld residual stresses relax with local plastic flow, but long-range thermal expansion loads may not.

b) STEP 2 – Construct an elastic-plastic finite element model of the configuration of interest (see paragraph 9G.3). Include only the primary loading in the model.

c) STEP 3 – During the finite element analysis, gradually increase the applied primary load(s) and compute the J -integral at each step. If there is more than one primary load, they should be applied proportionately. For example, for combined membrane and bending stress, a constant σ_b^P/σ_m^P ratio should be maintained throughout the analysis. Make sure that there are several output steps at low loads where plastic strains are negligible, and that there are several output steps in the fully plastic regime. Specifying the appropriate load values to define the FAD curve may require some trial and error.

d) STEP 4 – At each output step, convert the J -integral to the equivalent stress intensity factor using the following relationship:

$$K_J = \sqrt{\frac{JE_y}{1-\nu^2}} \tag{9G.1}$$

e) STEP 5 – Infer the elastic K_I^P solution for the configuration of interest from the initial slope of the K_J versus applied stress plot (see Figure 9G.7(a)). Note that the deviation from a linear response in this figure is a result of plasticity effect, which are shown on the FAD diagram in Figure 9G.7(b). Alternatively, perform a separate elastic finite element analysis on the configuration of interest.

f) STEP 6 – Compute the vertical coordinate of the FAD, K_r, at each load step as follows:

$$K_r = \frac{K_I^P}{K_J} \tag{9G.2}$$

g) STEP 7 – Determine the reference stress solution for the configuration of interest and compute the horizontal coordinate of the FAD, L_r, at each K_r value.

1) The load ratio is defined follows:

$$L_r = \frac{\sigma_{ref}}{\sigma_{ys}} \tag{9G.3}$$

2) The K_r at which $L_r = 1$ is given by:

$$K_r\big|_{L_r=1} = \left[1 + \frac{0.002E_y}{\sigma_{ys}} + \frac{1}{2}\left(1 + \frac{0.002E_y}{\sigma_{ys}}\right)^{-1}\right]^{-0.5} \tag{9G.4}$$

3) From the K_r values determined in STEP 6, determine the applied stress at which Equation (9G.4) is satisfied. The reference stress is related to the applied primary stress as follows.

$$\sigma_{ref} = F_{ref} \cdot \sigma^P \tag{9G.5}$$

The parameter F_{ref} is the reference stress geometry factor, which is given by:

$$F_{ref} = \frac{\sigma_{ys}}{\sigma^P\big|_{L_r=1}} \tag{9G.6}$$

h) STEP 8 – Plot K_r versus L_r, using the maximum load ratio (material dependent) specified in, Part 9, Figure 9.19. This is the FAD curve (see Figure 9G.7(c)).

i) STEP 9 – Compute L_r for the operating loads from Equations (9G.3) and (9G.5).

j) STEP 10 – Compute K_I^P for the operating loads using the elastic solution determined in STEP 5.

k) STEP 11 – Compute K_I^{SR} corresponding to the secondary and residual stresses. Unless the through-wall distribution of secondary and residual stresses is the same as the primary stresses, the elastic solution from STEP 5 is not applicable. Consequently, another elastic solution is needed. This can be accomplished by re-using the finite element model created in STEP 2. The crack tip elements should be modified for use with an elastic material model (see paragraph 9G.3.5(a)). There are two common methods for inferring K_I^{SR} from elastic finite element analysis:

1) Method 1 – Apply the secondary and residual normal stress distribution as a crack face traction and compute the resulting stress intensity factor. To use this approach, however, the crack face mesh must be sufficiently refined to capture the stress gradients. Errors will result if the traction varies significantly across an element face.

2) Method 2 – If the flaw of interest is a part-through surface crack, the weight function method (see Annex 9B) may be used to compute K_I^{SR}. The weight function coefficients can be inferred from reference K_I solutions for uniform and linear crack face pressure. These reference solutions can be obtained from the finite element model of the component of interest. Unlike Method 1 above, which entails applying

the secondary and residual stress directly as a crack-face traction, the weight function method does not require a high degree of crack face refinement to compute K_I^{SR} in the case of steep stress gradients.

l) STEP 12 – Compute the plasticity interaction factor, Φ, according to the procedure outlined in Part 9.

m) STEP 13 – Compute the toughness ratio as follows:

$$K_r = \frac{K_I^P + \Phi K_I^{SR}}{K_{mat}} \tag{9G.7}$$

n) STEP 14 – Plot the point (L_r, K_r) (from STEPs 9 and 13, respectively) on the FAD curve determined in STEP 8.

o) STEP 15 – Evaluate the results. Note that Partial Safety Factors (PSFs) were not prescribed in the above assessment. Uncertainty in the independent variables of the assessment (i.e., load, fracture toughness and flaw size) may be introduced in a variety of manners depending on the application. Examples are given below.

1) For a deterministic Fitness-For-Service Assessment of a known crack-like flaw, the flaw size in the finite element analysis may be adjusted by a PSF. Additional PSFs can then be applied to other input parameters in STEPs 9 and 13.

2) For a probabilistic assessment, STEPs 9 to 14 may be repeated numerous times in a Monte Carlo analysis. To address uncertainty in flaw size, however, the finite element analysis would have to be performed for a range of flaw dimensions.

3) To predict the results of a burst test or to quantify the critical conditions for a failure, the above assessment could be applied deterministically without adjusting the input values with PSFs.

9G.5 Driving Force Method for Non-Growing Cracks

9G.5.1 Overview

The FAD method suffers from several limitations, even if an elastic-plastic finite element solution for the configuration of interest is available. The FAD approach requires stress classification. Moreover, when multiple primary loads are present, they are assumed to increase and decrease in phase with one another. Direct evaluation of the J -integral from an elastic-plastic finite element analysis and comparison with the fracture toughness avoids these difficulties and limitations. Stress classification is unnecessary, and the approach is sufficiently general to handle any load history.

9G.5.2 Assessment Procedure

The J -integral driving force method is described below. As with the J -based FAD approach in paragraph 9G.4, the procedure that follows does not incorporate an explicit safety margin. It is the responsibility of the analyst to use these results in a prudent manner.

a) STEP 1 – Construct an elastic-plastic finite element model of the configuration of interest (see paragraph 9G.3).

b) STEP 2 – Impose loading that is initially present in the component, such as weld residual stresses.

Guidelines for determining a residual stress distribution from a welding simulation are provided in Annex 9D. In all cases, the computed residual stresses can then be mapped onto a mesh that contains a crack. The crack should not be allowed to open until after the mapping is complete.

c) STEP 3 – Impose the loads in the sequence they occur in service and evaluate the J -integral at each load step. It may be appropriate to take the model through multiple operating cycles to determine if there is ratcheting in the J -integral. The loading history might also include a hydro test, or a process upset, depending on the scenario that is being evaluated.

d) STEP 4 – Convert the applied J -integral at each load step to K_J using Equation (9G.1). Compare the crack driving force to the fracture toughness, K_{mat}.

e) STEP 5 – Analyze the structure containing the explicitly modeled flaw under primary loading only to demonstrate protection against plastic collapse. This step replaces the plastic collapse check embedded in the reference stress and FAD-based assessment approach for the un-cracked structure analysis as described in paragraph 9G.4. Any plastic collapse analysis method and corresponding acceptance criteria allowed in Annex 2C, paragraph 2C.2 may be used.

9G.6 Assessment of Growing Cracks

9G.6.1 Crack Growth Models

Examples of crack growth models for various mechanisms are provided in Annex 9F. The rate of growth of a crack-like flaw can usually be correlated to a fracture mechanics driving force parameter. Fatigue and environmental cracking are typically correlated to the applied stress intensity factor, while creep crack growth is a function of a time-dependent parameter defined as C_t. The latter parameter can be estimated from K_I and σ_{ref}.

9G.6.2 Crack Parameter Solutions

Solutions for K_I and σ_{ref} for a range of geometries are listed in Annex 9B and Annex 9C, respectively. When the solutions are not available for the geometry of interest, they can be obtained from finite element analysis. An elastic analysis of the cracked component is sufficient to determine K_I, but an elastic-plastic analysis is required to infer σ_{ref}. The procedure outlined in STEPs 1 through 7 of paragraph 9G.4.2 should be followed when computing σ_{ref} for a given application.

9G.6.3 Determination of a Remaining Life

Remaining life prediction is normally accomplished by integrating the crack growth expression from an initial crack size to a final size. The latter may be based on a failure criterion, such as the assessment point (L_r, K_r) falling outside of the FAD curve, or on a practical crack growth limit (e.g., crack growth through the wall, resulting in a leak).

9G.6.4 Crack Growth Using Numerical Methods

It is also possible to model a growing crack in a finite element model. Such an analysis requires special modeling capabilities that involve continuous updating of the model to account for crack growth.

9G.7 Nomenclature

a radius of hot spot or heated area within a plate or the depth of a crack-like flaw at a weld toe, as applicable. C_t time-dependent crack growth parameter.

E_y Young's modulus at the assessment temperature.

F_{ref} reference stress geometry factor.

J total J solution for the specific flaw and loading condition being evaluated.

K_r equivalent stress ratio.

K_I stress intensity factor.

K_I^P stress intensity factor associated with primary stress.

K_I^{SR} stress intensity factor associated with secondary and residual stress.

K_J stress intensity factor derived from J -integral.

K_{mat} material fracture toughness.

L_r load ratio.

ν Poisson's ratio.

Φ plasticity interaction factor.

r distance from the crack tip.

σ stress.

σ_{ref} reference stress.

σ_{ys} yield strength of material at the assessment temperature.

σ^P generalized stress from primary loads.

σ_b^P primary bending stress.

σ_m^P primary membrane stress.

σ_1 principal stress in the 1-direction.

σ_2 principal stress in the 2-direction.

t minimum wall thickness in the region under consideration, or the thickness of the component, as applicable.

9G.8 References

[1] Anderson, T.L., *Fracture Mechanics – Fundamentals and Applications*, 3rd Edition, CRC Press, Boca Raton, FL, 2005.

[2] Rice, J.R., "Discussion: The Path-Dependence of the J-Contour Integral by G.G. Chell and P.T. Heald," *International Journal of Fracture*, Vol. 11, (1975), pp. 352-353.

[3] Kirk, M.T., and R.H. Dodds, Jr., 1992, NUREG/CR-5969; "J and CTOD Estimation Equations for Shallow Cracks in Single Edge Notch Bend Specimens," Naval Surface Warfare Center, Annapolis Detachment, Carderock Division.

[4] Dewees, D.J., R.H. Dodds Jr., 2013, “Comparison of Flaw Driving Force Estimates in Simulated Weld Residual Stress Fields,” PVP2013-97410, *ASME 2013 Pressure Vessels and Piping Conference,* ASME, New York.

[5] Shih, C.F., Moran, B., and Nakamura, T., “Energy Release Rate Along a Three-Dimensional Crack Front in a Thermally Stressed Body.” *International Journal of Fracture*, Vol. 30, 1986, pp. 79-102.

[6] Ainsworth, R. A. *et al*, “Fracture Behavior in the Presence of Thermal Strains,” *I Mech E Proc Tolerance of Flaws in Pressurized Components*, London, May 1978, pp. 171-178.

[7] Matos, C.G., and R. H. Dodds Jr., “Modeling the Effects of Residual Stress on Defects in the Welds of Steel Frame Connections,” *Engineering Structures*, Vol. 22, (2000), pp. 1103-1120.

[8] Lei, Y. *et al*, “Fracture Mechanics Analysis of a Crack in a Residual Stress Field,” *International Journal of Fracture*, Vol. 106, (2000), pp. 195-216.

[9] Lewis, S.J. *et al*, “A Comparison of 2D and 3D Fracture Assessments in the Presence of Residual Stress,” PVP2007-26264, *Proceedings of the ASME 2007 Pressure Vessels and Piping Conference*, San Antonio, Texas, July 2007.

[10] Dewees, D.J., R.H. Dodds Jr., P.E. Prueter and D.A. Osage, 2012, “Three-Dimensional Analysis of Crack Driving Force in Simulated Weld Residual Stress Fields,” *9th International Trends in Welding Research Conference*, Hilton Chicago/Indian Lakes Resort, ASM International, Materials Park, OH.

9G.9 Figures

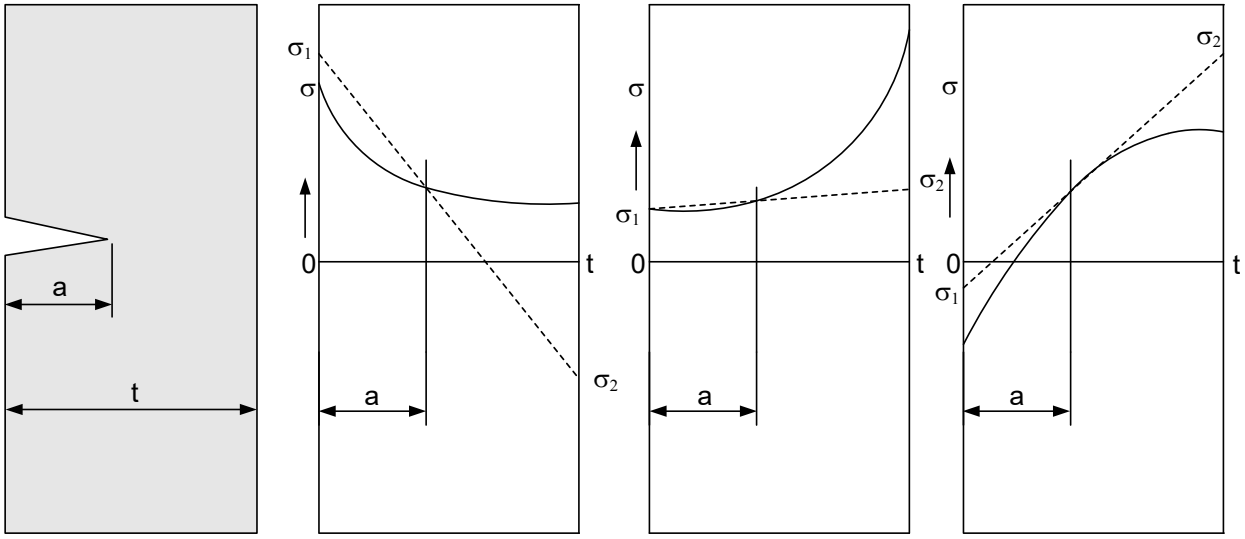

(a) Linearization Over the Defect - Surface Flaw

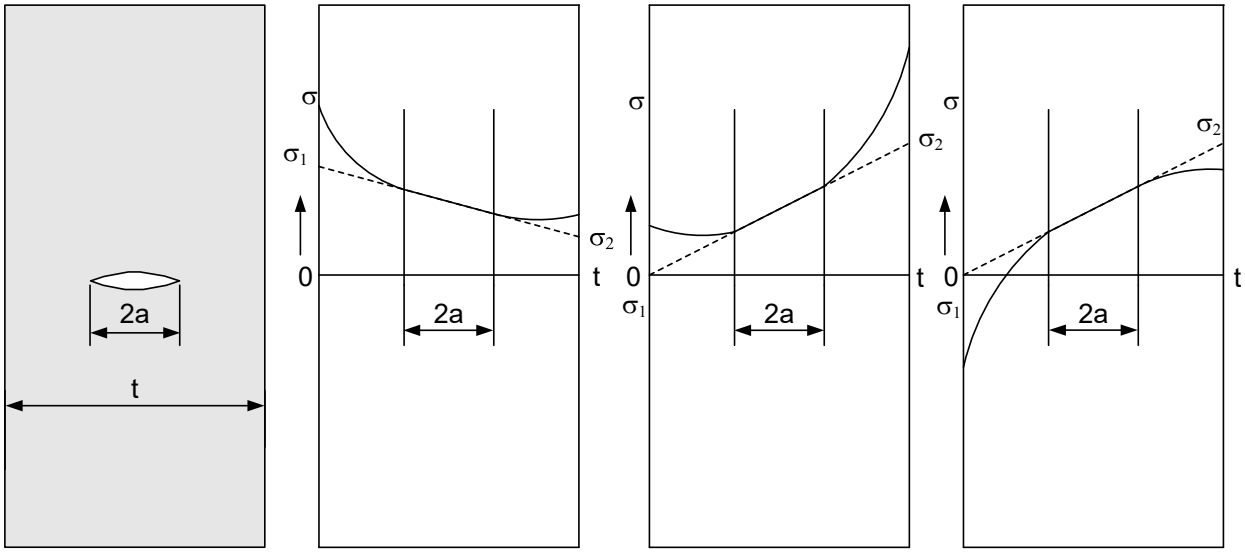

(b) Linearization Over the Defect - Embedded Flaw

Figure 9G.1 – Stress Linearization Based on the Defect

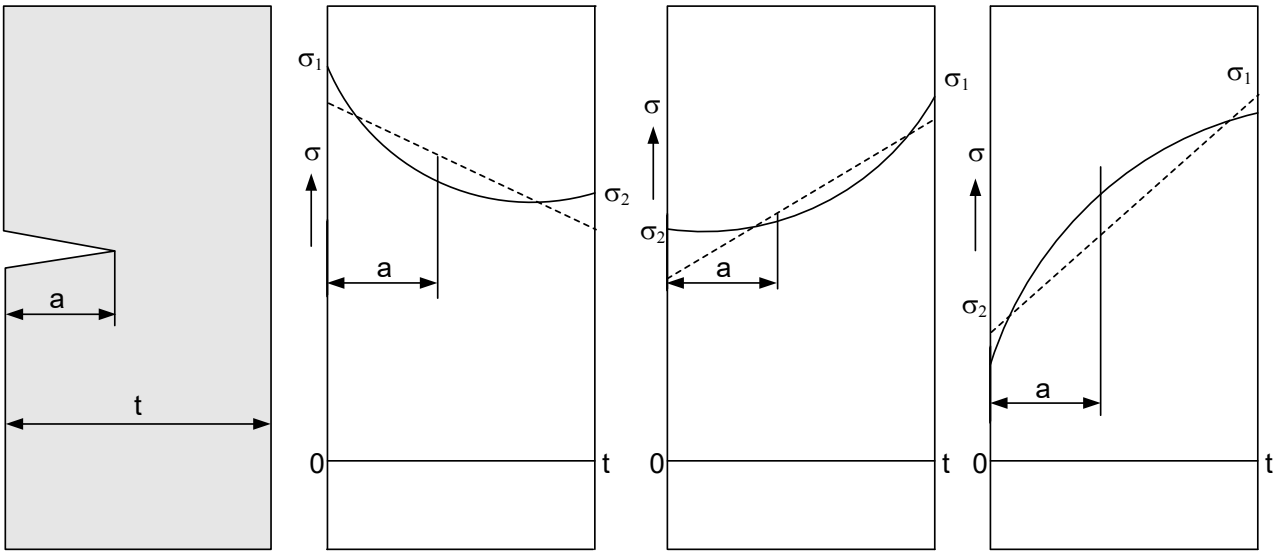

(a) Linearization Over the Cross Section - Surface Flaw

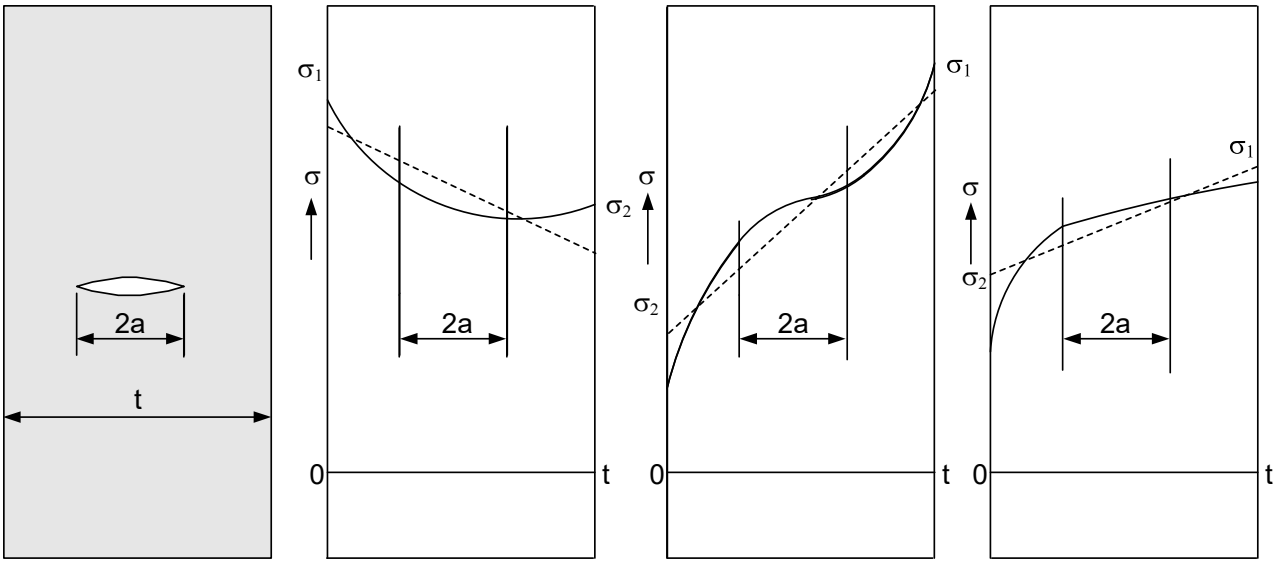

(b) Linearization Over the Cross Section - Embedded Flaw

Figure 9G.2 – Stress Linearization Based on the Cross Section

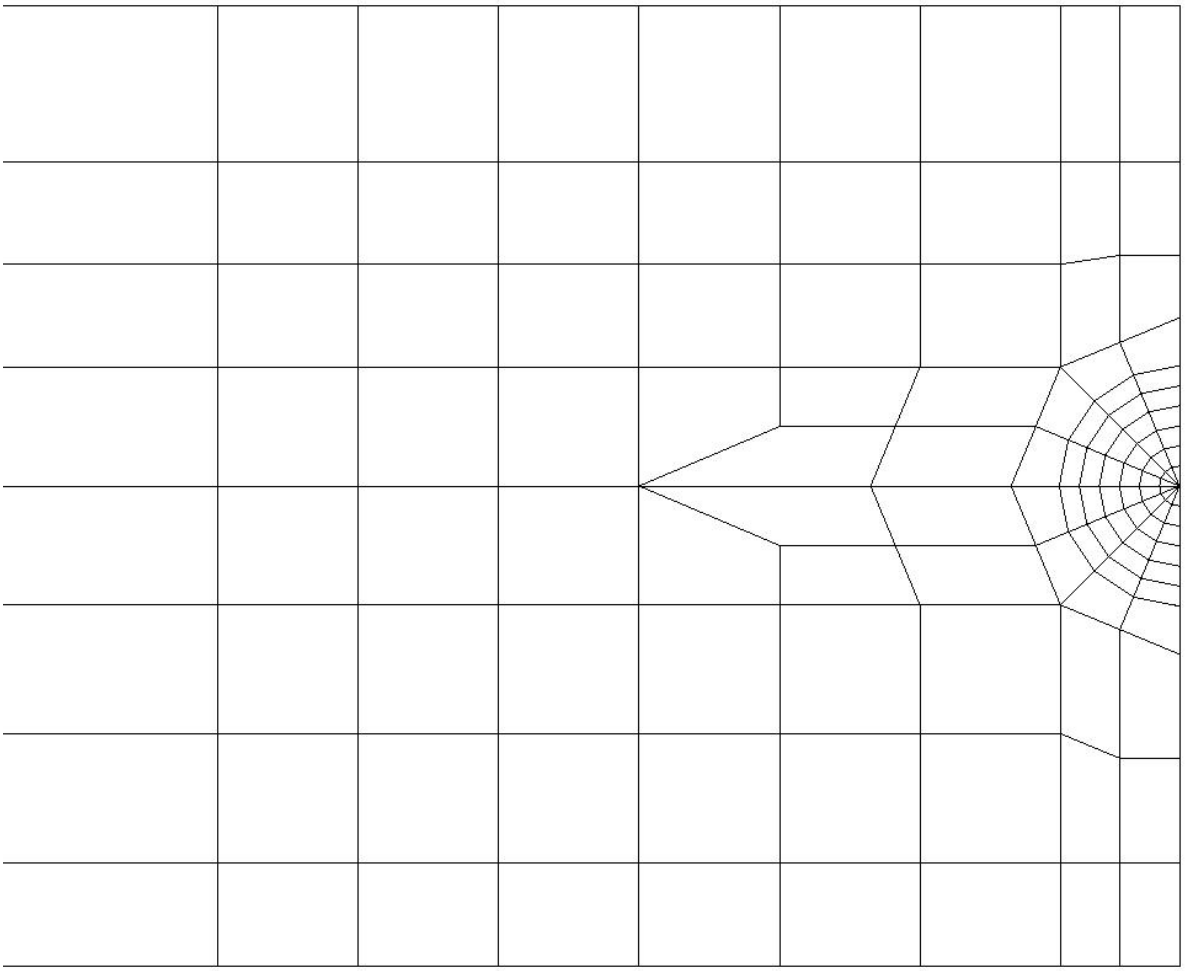

Figure 9G.3 – Focused or *Spider Web* Mesh with Elements Concentrated at the Crack Tip

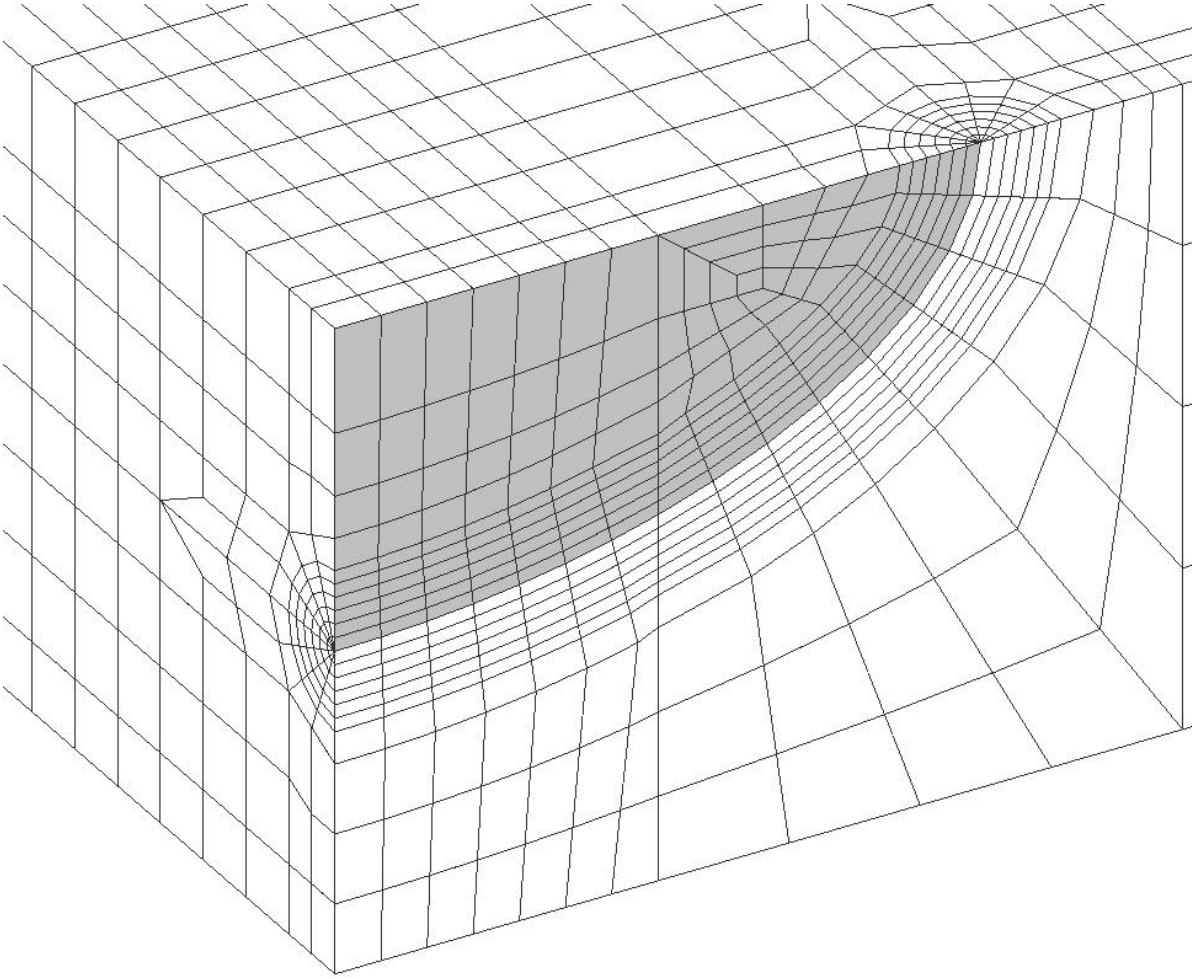

Figure 9G.4 – Typical 3D Finite Model of a Surface Crack

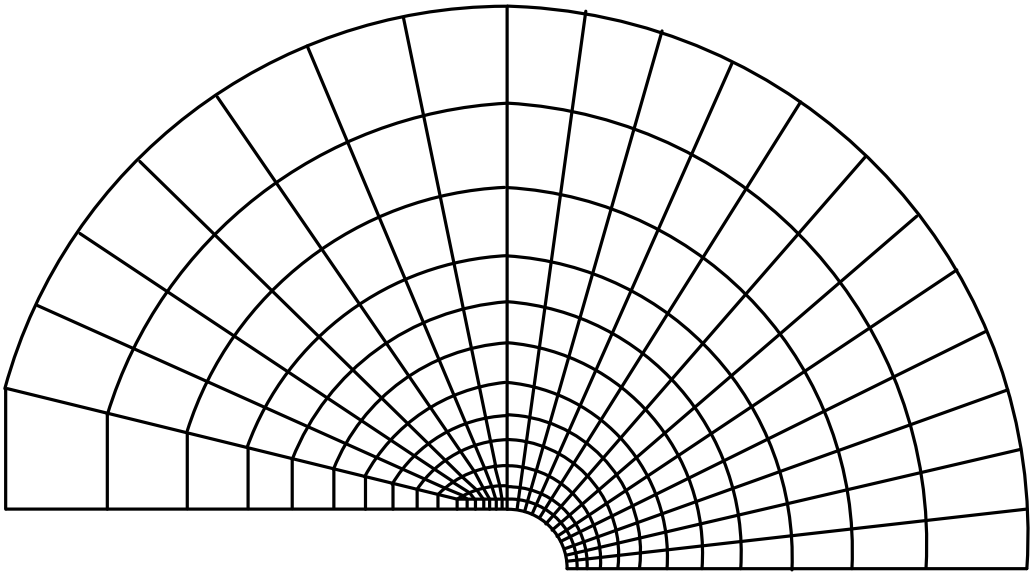

Figure 9G.5 – Illustration of Finite Radius Approach Mesh

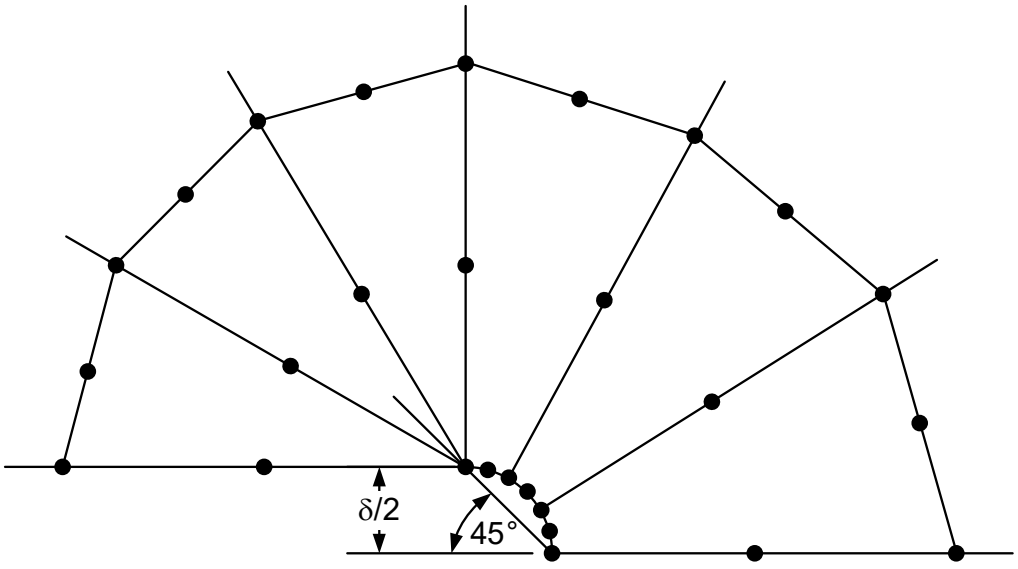

Figure 9G.6 – Illustration of CTOD Determination

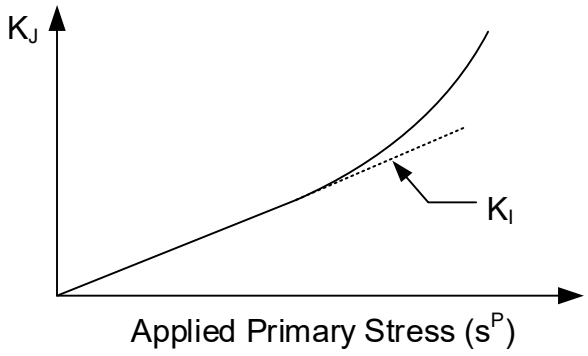

(a) Crack Driving Force (K_J) Versus Primary Stress

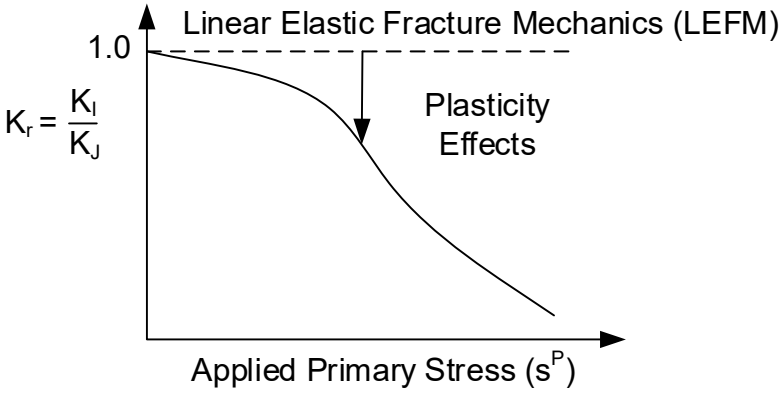

(b) Definition Of The Vertical Axis Of The FAD

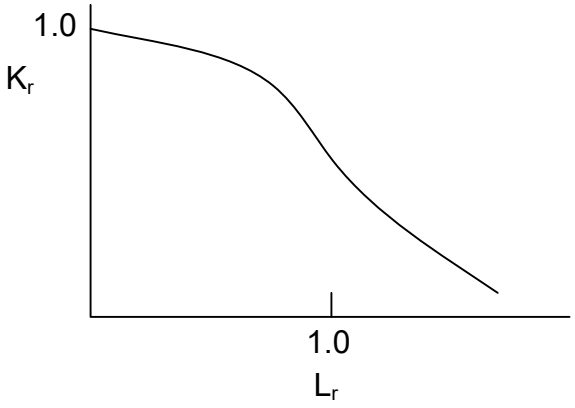

(c) Normalizing The Horizontal Axis With L_r

Figure 9G.7 – Derivation of a J-Based FAD Curve

[Intentionally Left Blank]

ANNEX 9H – CONSTRAINT EFFECTS FOR SURFACE FLAWS IN CARBON AND LOW-ALLOY STEEL COMPONENTS IN THE DUCTILE-BRITTLE TRANSITION REGION

(NORMATIVE)

CONTENTS

ANNEX 9H – CONSTRAINT EFFECTS FOR SURFACE FLAWS IN CARBON AND LOW-ALLOY STEEL COMPONENTS IN THE DUCTILE-BRITTLE TRANSITION REGION 9H-1

9H.1 GENERAL 9H-1
9H.1.1 Overview 9H-1
9H.1.2 Applicability and Limitations of the Procedure 9H-1
9H.1.3 Fracture Toughness Estimation Procedure 9H-2
9H.2 NOMENCLATURE 9H-3
9H.3 REFERENCES 9H-5
9H.4 TABLES 9H-6
9H.5 FIGURES 9H-11

9H.1 General

9H.1.1 Overview

This Annex contains a procedure to incorporate constraint effects for surface flaws in a Level 2 FFS Assessment. The primary benefit of accounting for constraint effect in a Part 9 assessment comes from a downward shift in the Master Curve index temperature for fracture toughness in the transition region, reference [1].

The Part 9 Level 2 Failure Assessment Diagram (FAD) procedure to assess crack-like flaws entails plotting an assessment point on the FAD. Unstable fracture is driven primarily by the dimensionless toughness ratio, K_r, which is the y coordinate of the assessment point. The numerator of K_r is a function of the elastic stress intensity factors due to primary, secondary, and residual stresses, while the denominator is the fracture toughness, K_{mat}.

In this Annex, a procedure to adjust K_{mat} for constraint effects for carbon and low-alloy steels in the ductile-brittle transition region is provided. Annex 9I contains a companion procedure for computing the numerator of K_r for the special case of brittle fracture in the transition region.

9H.1.2 Applicability and Limitations of the Procedure

The following is a summary of the applicability and limitations for Annex 9H:

- The assessment procedures in this Annex are applicable only to carbon and low-alloy steel components that operate in the ductile-brittle transition region. Weld overlay and clad components are excluded.
- The procedure shall only be applied to surface-breaking crack-like flaws.
- The procedure shall not be used when the primary and secondary/residual stresses across the flaw plane cannot be accurately represented with a membrane and bending stress obtained through linearization of the stress profile over the interval $x = 0$ to $x = a$, as shown in Figure 9H.1. Note that in the case of a nonlinear

stress profile, the through wall local membrane and bending components obtained by linearizing over the crack plane will differ from the membrane and bending components that result from linearizing over the full cross section. The linearization is performed over the interval $x = 0$ to $x = a$ to minimize errors. The procedure in this Annex is not applicable to nonlinear stress profiles where linearizing over the crack plane results in a poor approximation of the stresses acting on the flaw plane.

- The procedure shall only be used for the assessment of brittle fracture. Local crack-growth is dependent on local (i.e., $\phi = 0$ or $\phi = \pi/2$) crack driving force and local constraint and should not be evaluated using this Annex.

9H.1.3 Fracture Toughness Estimation Procedure

a) STEP 1 – Given the crack dimensions and stress profiles determined in the Part 9 Level 2 Assessment, resolve the primary, secondary, and residual stresses into membrane and bending components by linearizing the stress profile over the interval $x = 0$ to $x = a$, as shown in Figure 9H.1. Calculate the through thickness membrane, $\sigma_m^{P,S,R}$, and bending, $\sigma_b^{P,S,R}$, components of the primary, secondary, and residual stresses using Equations (9H.1) and (9H.2), respectively.

$$\sigma_m^{P,S,R} = \frac{\sigma(0)^{P,S,R} \cdot \left(2 - \frac{t}{a}\right) + \left(\frac{t}{a}\right) \cdot \sigma(a)^{P,S,R}}{2} \tag{9H.1}$$

$$\sigma_b^{P,S,R} = \frac{\sigma(0)^{P,S,R} - \sigma(a)^{P,S,R}}{2} \cdot \left(\frac{t}{a}\right) \tag{9H.2}$$

b) STEP 2 – Determine the component geometry and the crack dimensions. Obtain the non-dimensional T-stress parameters, τ_m and τ_b, from Tables 9H.1 through 9H.5, as applicable. If the value of τ_m or τ_b is less than -1, set it equal to -1.

c) STEP 3 – Calculate the T-stress due to primary loads with Equation (9H.3).

$$T_\sigma^P = \tau_m \sigma_m^P + \tau_b \sigma_b^P \tag{9H.3}$$

d) STEP 4 – Calculate the T-stress due to secondary and residual loads with Equations (9H.4), (9H.5), and (9H.6).

$$T_\sigma^S = \tau_m \sigma_m^S + \tau_b \sigma_b^S \tag{9H.4}$$

$$T_\sigma^R = \tau_m \sigma_m^R + \tau_b \sigma_b^R \tag{9H.5}$$

$$T_\sigma^{SR} = \max\left[\left(T_\sigma^S + T_\sigma^R\right),\ -0.4\sigma_{YS}\right] \tag{9H.6}$$

e) STEP 5 – Calculate the combined T-stress for primary, secondary, and residual loads with Equation (9H.7).

$$T_\sigma = T_\sigma^P + T_\sigma^{SR} \tag{9H.7}$$

f) STEP 6 – Determine the Master Curve index temperature, T_o, using the procedures in Annex 9F, Paragraph 9F.4.3.2.

g) STEP 7 – Calculate the T_o temperature shift from Equation (9H.8) or (9H.10). Then calculate the constraint-modified Master Curve index temperature, T_o^{CM}, using Equation (9H.12).

$$\Delta T_o = \frac{T_\sigma}{10\ \text{MPa}/^o\text{C}} \qquad T_\sigma < 0 \qquad \left(^\circ\text{C, MPa}\right) \tag{9H.8}$$

$$\Delta T_o = 0 \qquad T_\sigma \geq 0 \qquad \left(^o C,\ \text{MPa}\right) \tag{9H.9}$$

$$\Delta T_o = \frac{T_\sigma}{0.806\ \text{ksi}/^o\text{F}} \qquad T_\sigma < 0 \qquad \left(^o\text{F, ksi}\right) \tag{9H.10}$$

$$\Delta T_o = 0 \qquad T_\sigma \geq 0 \qquad \left(^o\text{F, ksi}\right) \tag{9H.11}$$

$$T_o^{CM} = T_o + \Delta T_o \tag{9H.12}$$

h) STEP 8 – At the metal temperature of interest, calculate the median toughness for a 25 mm (1-inch) crack front from Equation (9H.13) or (9H.14).

$$K_{median(25\ \text{mm})} = 30 + 70\exp\left[0.019\left(T - T_o^{CM}\right)\right] \qquad \left(^\circ\text{C, MPa}\sqrt{\text{m}}\right) \tag{9H.13}$$

$$K_{median(1\ \text{in})} = 27 + 64\exp\left[0.0106\left(T - T_o^{CM}\right)\right] \qquad \left(^o\text{F, ksi}\sqrt{\text{in}}\right) \tag{9H.14}$$

i) STEP 9 – Calculate the crack front length for a semi-elliptical flaw, L, using Equation (9H.15).

$$L = \min\left[2c, 100\,mm\ (4\,in)\right] \tag{9H.15}$$

j) STEP 10 – At the metal temperature of interest, calculate the toughness corresponding to a cumulative probability, P_f, and a crack front length, L, from Equation (9H.16) or (9H.17). The recommended cumulative probability to represent a lower-bound estimate is $P_f = 0.05$, corresponding to a 5% lower bound. Other P_f values may be used if justified by the circumstances.

$$K_{mat}(P_f, L) = 20 + \left(K_{median(25\ \text{mm})} - 20\right)\left[\left(\frac{25}{L}\right)\frac{\ln\left(\frac{1}{1-P_f}\right)}{\ln(2)}\right]^{0.25} \qquad \left(\text{mm, MPa}\sqrt{\text{m}}\right) \tag{9H.16}$$

$$K_{mat}(P_f, L) = 18 + \left(K_{median(1\ \text{in})} - 18\right)\left[\left(\frac{1}{L}\right)\frac{\ln\left(\frac{1}{1-P_f}\right)}{\ln(2)}\right]^{0.25} \qquad \left(\text{in, ksi}\sqrt{in}\right) \tag{9H.17}$$

9H.2 Nomenclature

a depth of a surface crack.

c half-length of a semi-elliptical crack.

ΔT_o shift in the Master Curve index temperature due to constraint loss.

K_{mat} fracture toughness used in an FFS Assessment.

K_{median} median fracture toughness for a 1-inch (25 mm) crack front.

K_r toughness ratio in the FAD method.

L crack length for a surface flaw.

P_f cumulative probability of failure for use with the fracture toughness Master Curve.

σ uniaxial stress.

$\sigma_b^{P,S,R}$ through-wall bending stress components for the primary, secondary, and residual stresses inferred from linearizing stress profile over the interval $x = 0$ to $x = a$.

$\sigma_m^{P,S,R}$ through-wall membrane stress components for the primary, secondary, and residual stresses inferred from linearizing stress profile over the interval $x = 0$ to $x = a$.

σ_{YS} yield strength at the temperature of interest.

σ_b^P applied through-wall primary bending stresses.

σ_m^P applied through-wall primary membrane stress.

σ_b^R applied through-wall residual bending stresses.

σ_m^R applied through-wall residual membrane stresses.

σ_b^S applied through-wall secondary bending stresses.

σ_m^S applied through-wall secondary membrane stresses.

t wall thickness or plate thickness.

T metal temperature of interest.

T_o Master Curve index transition temperature.

T_o^{CM} Constraint-modified T_o.

T_σ T-stress.

T_σ^P T-stress due to primary stress.

T_σ^S T-stress due to secondary stress.

T_σ^R T-stress due to residual stress.

T_σ^{SR} T-stress due to secondary and residual stresses.

τ nondimensional T-stress, normalized by applied stress.

τ_b nondimensional bending T-stress parameter, normalized by applied bending stress.

τ_m nondimensional membrane T-stress parameter, normalized by applied membrane stress.

x crack depth parameter.

9H.3 References

[1] Anderson, T.L., Constraint Effects on Fracture Toughness in Ductile-Brittle Transition Region, WRC Bulletin 577, Welding Research Council, Inc., Shaker Heights, OH, 2019.

9H.4 Tables

Table 9H.1 – Dimensionless T-Stress Solutions for Surface Cracks in a Flat Plate

c/a	a/t	Membrane Stress (τ_m)	Through Wall Bending Stress (τ_b)
1	0	-0.5313	-0.5313
	0.2	-0.5348	-0.2102
	0.4	-0.5512	0.1024
	0.6	-0.6105	0.3972
	0.8	-0.8103	0.7093
2	0	-0.4970	-0.4970
	0.2	-0.5056	-0.1742
	0.4	-0.5366	0.1352
	0.6	-0.6232	0.4290
	0.8	-0.8807	0.7710
4	0	-0.5029	-0.5029
	0.2	-0.5210	-0.1849
	0.4	-0.5600	0.1246
	0.6	-0.6042	0.4582
	0.8	-0.7732	0.8809
8	0	-0.5117	-0.5117
	0.2	-0.5420	-0.2027
	0.4	-0.5718	0.1175
	0.6	-0.5141	0.5160
	0.8	-0.4186	1.0735
16	0	-0.5209	-0.5209
	0.2	-0.5639	-0.2216
	0.4	-0.5817	0.1103
	0.6	-0.3976	0.5817
	0.8	0.2067	1.3620
32	0	-0.5348	-0.5348
	0.2	-0.5894	-0.2431
	0.4	-0.6017	0.0961
	0.6	-0.3047	0.6313
	0.8	1.0813	1.7365

Table 9H.2 – Dimensionless T-Stress Solutions for Axial External Surface Cracks in a Cylindrical Shell

c/a	a/t	Membrane Stress (τ_m)			Through Wall Bending Stress (τ_b)		
		$t/R_i = 0.01$	$t/R_i = 0.05$	$t/R_i = 0.2$	$t/R_i = 0.01$	$t/R_i = 0.05$	$t/R_i = 0.2$
1	0.2	-0.5353	-0.5323	-0.5258	-0.2106	-0.2081	-0.2023
	0.4	-0.5496	-0.5472	-0.5358	0.1035	0.1055	0.1144
	0.6	-0.6096	-0.6069	-0.5980	0.3978	0.3994	0.4053
	0.8	-0.8088	-0.8078	-0.8134	0.7094	0.7074	0.6983
2	0.2	-0.5074	-0.5011	-0.4913	-0.1757	-0.1702	-0.1616
	0.4	-0.5359	-0.5313	-0.5167	0.1358	0.1393	0.1505
	0.6	-0.6232	-0.6221	-0.6251	0.4289	0.4293	0.4275
	0.8	-0.8815	-0.8937	-0.9729	0.7694	0.7598	0.7147
4	0.2	-0.5247	-0.5156	-0.5067	-0.1878	-0.1802	-0.1724
	0.4	-0.5614	-0.5589	-0.5515	0.1243	0.1255	0.1315
	0.6	-0.6073	-0.6225	-0.6681	0.4561	0.4467	0.4198
	0.8	-0.7773	-0.8469	-1.1264	0.8767	0.8397	0.7065
8	0.2	-0.5423	-0.5383	-0.5287	-0.2030	-0.1995	-0.1911
	0.4	-0.5747	-0.5805	-0.5788	0.1155	0.1115	0.1135
	0.6	-0.5244	-0.5703	-0.6589	0.5095	0.4826	0.4330
	0.8	-0.4188	-0.6207	-1.1302	1.0698	0.9737	0.7494
16	0.2	-0.5659	-0.5620	-0.5491	-0.2231	-0.2198	-0.2086
	0.4	-0.5902	-0.5995	-0.5882	0.1045	0.0982	0.1072
	0.6	-0.4210	-0.4979	-0.5966	0.5678	0.5247	0.4705
	0.8	0.2372	-0.1785	-0.8823	1.3696	1.1836	0.8771
32	0.2	-0.5941	-0.5890	-0.5686	-0.2469	-0.2425	-0.2252
	0.4	-0.6177	-0.5890	-0.5911	0.0855	0.1151	0.1042
	0.6	-0.3505	-0.4327	-0.5437	0.6057	0.5608	0.4971
	0.8	1.1076	0.4043	-0.6486	1.7375	1.4331	0.9714

Table 9H.3 – Dimensionless T-Stress Solutions for Axial Internal Surface Cracks in a Cylindrical Shell

c/a	a/t	Membrane Stress (τ_m)			Through Wall Bending Stress (τ_b)		
		$t/R_i = 0.01$	$t/R_i = 0.05$	$t/R_i = 0.2$	$t/R_i = 0.01$	$t/R_i = 0.05$	$t/R_i = 0.2$
1	0.2	-0.5360	-0.5378	-0.5468	-0.2112	-0.2129	-0.2209
	0.4	-0.5515	-0.5572	-0.5756	0.1020	0.0978	0.0837
	0.6	-0.6128	-0.6225	-0.6560	0.3959	0.3900	0.3698
	0.8	-0.8167	-0.8407	-0.9125	0.7070	0.6980	0.6707
2	0.2	-0.5069	-0.5106	-0.5237	-0.1753	-0.1786	-0.1900
	0.4	-0.5384	-0.5466	-0.5766	0.1339	0.1278	0.1057
	0.6	-0.6293	-0.6491	-0.7162	0.4255	0.4142	0.3755
	0.8	-0.9014	-0.9639	-1.1407	0.7628	0.7381	0.6679
4	0.2	-0.5229	-0.5269	-0.5405	-0.1863	-0.1900	-0.2018
	0.4	-0.5633	-0.5727	-0.6113	0.1228	0.1154	0.0875
	0.6	-0.6164	-0.6558	-0.7713	0.4513	0.4290	0.3636
	0.8	-0.8309	-0.9847	-1.3337	0.8564	0.7917	0.6486
8	0.2	-0.5416	-0.5472	-0.5612	-0.2024	-0.2072	-0.2194
	0.4	-0.5749	-0.5886	-0.6354	0.1153	0.1055	0.0722
	0.6	-0.5410	-0.6115	-0.7659	0.5007	0.4611	0.3758
	0.8	-0.5680	-0.8698	-1.3513	1.0081	0.8793	0.6839
16	0.2	-0.5649	-0.5698	-0.5852	-0.2224	-0.2265	-0.2398
	0.4	-0.5875	-0.6060	-0.6536	0.1063	0.0933	0.1123
	0.6	-0.4495	-0.5443	-0.7031	0.5526	0.5007	0.4148
	0.8	-0.1013	-0.5118	-1.1024	1.2274	1.0552	0.8088
32	0.2	-0.5926	-0.5987	-0.6170	-0.2457	-0.2509	-0.2662
	0.4	-0.6142	-0.6345	-0.6814	0.0879	0.0741	0.0425
	0.6	-0.3835	-0.4760	-0.6631	0.5884	0.5393	0.4375
	0.8	0.6143	0.0967	-0.8572	1.5372	1.3185	0.9082

Table 9H.4 – Dimensionless T-Stress Solutions for Circumferential External Surface Cracks in a Cylindrical Shell

c/a	a/t	Membrane Stress (τ_m)			Through Wall Bending Stress (τ_b)		
		$t/R_i = 0.01$	$t/R_i = 0.05$	$t/R_i = 0.2$	$t/R_i = 0.01$	$t/R_i = 0.05$	$t/R_i = 0.2$
1	0.2	-0.5241	-0.5338	-0.5246	-0.2035	-0.2091	-0.2026
	0.4	-0.5512	-0.5516	-0.5418	0.1024	0.1037	0.1092
	0.6	-0.6112	-0.6071	-0.5894	0.3969	0.3974	0.3968
	0.8	-0.8115	-0.8099	-0.8061	0.7078	0.7042	0.6883
2	0.2	-0.5036	-0.5051	-0.5012	-0.1727	-0.1735	-0.1700
	0.4	-0.5384	-0.5371	-0.5380	0.1341	0.1355	0.1371
	0.6	-0.6277	-0.9200	-0.6614	0.4266	0.1365	0.4096
	0.8	-0.8885	0.6317	-1.0142	0.7667	2.2994	0.6965
4	0.2	-0.5186	-0.5218	-0.5202	-0.1834	-0.1853	-0.1831
	0.4	-0.5625	-0.5678	-0.5851	0.1230	0.1199	0.1096
	0.6	-0.6141	-0.6472	-0.7465	0.4524	0.4338	0.3785
	0.8	-0.8016	-0.9226	-1.2785	0.8664	0.8062	0.6363
8	0.2	-0.5423	-0.5434	-0.5462	-0.2030	-0.2037	-0.2054
	0.4	-0.5762	-0.5890	-0.6250	0.1145	0.1062	0.0832
	0.6	-0.5377	-0.6230	-0.8289	0.5022	0.4533	0.3385
	0.8	-0.5147	-0.8957	-1.6845	1.0255	0.8444	0.4889
16	0.2	-0.5643	-0.5655	-0.5679	-0.2218	-0.2226	-0.2240
	0.4	-0.5895	-0.6102	-0.6562	0.1050	0.0912	0.0620
	0.6	-0.4564	-0.6317	-0.9199	0.5472	0.4473	0.2917
	0.8	-0.1194	-1.0178	-2.0486	1.2048	0.7943	0.3676
32	0.2	-0.5898	-0.5895	---	-0.2434	-0.2429	---
	0.4	-0.6141	-0.6389	---	0.0876	0.0712	---
	0.6	-0.4358	-0.6968	---	0.5555	0.4109	---
	0.8	0.1180	-1.2557	---	1.2902	0.7014	---

Table 9H.5 – Dimensionless T-Stress Solutions for Circumferential Internal Surface Cracks in a Cylindrical Shell

c/a	a/t	Membrane Stress (τ_m)			Through Wall Bending Stress (τ_b)		
		$t/R_i = 0.01$	$t/R_i = 0.05$	$t/R_i = 0.2$	$t/R_i = 0.01$	$t/R_i = 0.05$	$t/R_i = 0.2$
1	0.2	-0.5296	-0.5314	-0.5368	-0.2066	-0.2080	-0.2126
	0.4	-0.5465	-0.5498	-0.5611	0.1042	0.1021	0.0941
	0.6	-0.6116	-0.6183	-0.6432	0.3966	0.3931	0.3796
	0.8	-0.8183	-0.8367	-0.9017	0.7058	0.6999	0.6778
2	0.2	-0.5110	-0.5064	-0.5113	-0.1780	-0.1750	-0.1795
	0.4	-0.5408	-0.5401	-0.5520	0.1335	0.1323	0.1222
	0.6	-0.6266	-0.6387	-0.6778	0.4267	0.4189	0.3932
	0.8	-0.8965	-0.9466	-1.0874	0.7638	0.7403	0.6751
4	0.2	-0.5208	-0.5203	-0.5202	-0.1846	-0.1845	-0.1852
	0.4	-0.5572	-0.5609	-0.5699	0.1250	0.1230	0.1139
	0.6	-0.6140	-0.6427	-0.7244	0.4519	0.4335	0.3800
	0.8	-0.8284	-0.9812	-1.3169	0.8545	0.7809	0.6209
8	0.2	-0.5417	-0.5391	-0.5351	-0.2025	-0.2006	-0.1978
	0.4	-0.5718	-0.5741	-0.5907	0.1171	0.1147	0.0998
	0.6	-0.5432	-0.6241	-0.7900	0.4983	0.4488	0.3462
	0.8	-0.6104	-1.0184	-1.6274	0.9831	0.7903	0.5108
16	0.2	-0.5621	-0.5584	-0.5506	-0.2201	-0.2171	-0.2113
	0.4	-0.5827	-0.5907	-0.6190	0.1093	0.1026	0.0796
	0.6	-0.4743	-0.6387	-0.8646	0.5363	0.4392	0.3068
	0.8	-0.3550	-1.1466	-1.8402	1.1021	0.7408	0.4440
32	0.2	-0.5865	-0.5805	---	-0.2408	-0.2359	---
	0.4	-0.6052	-0.6200	---	0.0933	0.0819	---
	0.6	-0.4614	-0.6954	---	0.5407	0.4076	---
	0.8	-0.2164	-1.2909	---	1.1527	0.6874	---

9H.5 Figures

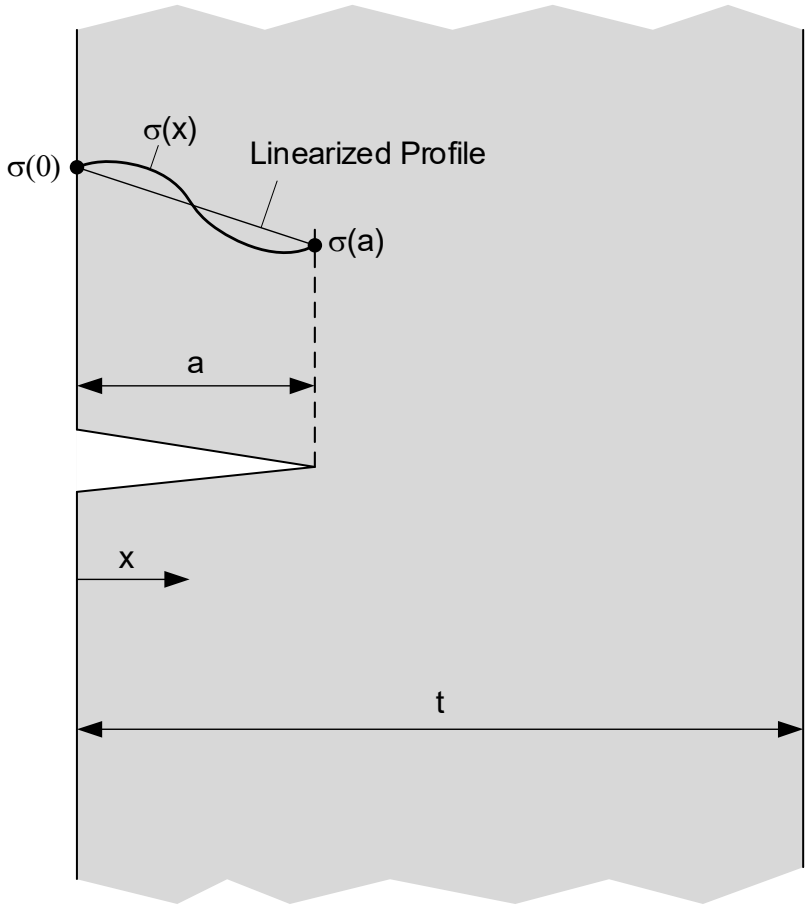

Figure 9H.1 – Linearization of a Stress Profile Over the Crack Plane ($x = 0$ to $x = a$).

[Intentionally Left Blank]

ANNEX 9I – ALTERNATIVE ESTIMATE OF MODE I STRESS INTENSITY FACTORS FOR FFS ASSESSMENTS IN THE DUCTILE-BRITTLE TRANSITION REGION

(NORMATIVE)

CONTENTS

ANNEX 9I – ALTERNATIVE ESTIMATE OF MODE I STRESS INTENSITY FACTORS FOR FFS ASSESSMENTS IN THE DUCTILE-BRITTLE TRANSITION REGION 9I-1

9I.1 GENERAL 9I-1
9I.1.1 Overview 9I-1
9I.1.2 Applicability and Limitations of the Procedure 9I-1
9I.1.3 Alternative Estimate of Mode I Stress Intensity Factors for K_r Determination 9I-2
9I.2 NOMENCLATURE 9I-3
9I.3 REFERENCES 9I-4
9I.4 FIGURES 9I-5

9I.1 General

9I.1.1 Overview

This Annex contains an alternative method to compute the numerator in the toughness ratio, K_r, in a Part 9 Level 2 FFS Assessment. The benefit of this alternative method is a reduction in the level of conservatism in the K_r calculation, as K_I^P and K_I^{SR} correspond to integrated values over the crack front rather than peak values, reference [1]. This method applies exclusively to FFS assessments of brittle fracture in the transition region.

This Annex can be used as a companion to Annex 9H. This Annex results in a reduction in conservatism in the numerator of K_r, while the Annex 9H adjustment to the fracture toughness, K_{mat}, due to constraint effects reduces the conservatism in the denominator of K_r.

9I.1.2 Applicability and Limitations of the Procedure

The following is a summary of the applicability and limitations for Annex 9I:

- The procedure shall only be applied to surface-breaking semi-elliptical crack-like flaws.
- The procedure shall only be used for the assessment of brittle fracture in carbon and low-alloy steels in the ductile-brittle transition region. Weld overlay and clad components are excluded.
- The procedure in paragraph 9I.1.3.1 shall not be used when the primary and secondary/residual stresses across the flaw plane cannot be accurately represented with a membrane and bending stress obtained through linearization of the stress profile over the interval $x = 0$ to $x = a$, as shown in Figure 9I.1. Note that in the case of a nonlinear stress profile, the through wall local membrane and bending components obtained by linearizing over the crack plane will differ from the membrane and bending components that result from linearizing over the full cross section. The linearization is performed over the interval $x = 0$ to $x = a$ to minimize errors. The procedure in paragraph 9I.1.3.2 may be used for general nonlinear stress profiles where linearizing over the crack plane results in a poor approximation of the stresses acting on the flaw plane.

- The procedure shall only be used to assess initiation of brittle fracture. Local crack-growth is dependent on local (i.e., $\varphi = 0$ or $\varphi = \pi/2$) crack driving force and local constraint and should not be evaluated using this Annex.

9I.1.3 Alternative Estimate of Mode I Stress Intensity Factors for K_r Determination

9I.1.3.1 Through-Wall Membrane and Bending Stress

For a through-wall membrane and bending stresses (linearized stress profiles), the average stress intensity over the crack front can be determined using the closed form equations shown below.

a) STEP 1 – Given the crack dimensions and stress profiles determined in the Part 9 Level 2 assessment, resolve the primary and secondary plus residual stresses into through-wall membrane and bending components by linearizing the stress profile over the interval $x = 0$ to $x = a$, as shown in Figure 9I.1. Calculate the through thickness membrane, $\sigma_m^{P,SR}$, and bending, $\sigma_b^{P,SR}$, components of the primary and secondary plus residual stresses using Equations (9I.1) and (9I.2), respectively.

$$\sigma_m^{P,SR} = \frac{\sigma(0)^{P,SR} \cdot \left(2 - \frac{t}{a}\right) + \left(\frac{t}{a}\right) \cdot \sigma(a)^{P,SR}}{2} \tag{9I.1}$$

$$\sigma_b^{P,SR} = \frac{\sigma(0)^{P,SR} - \sigma(a)^{P,SR}}{2} \cdot \left(\frac{t}{a}\right) \tag{9I.2}$$

b) STEP 2 – For the geometry and flaw size of interest, obtain the appropriate functions for the influence coefficients $G_0(\beta)$ and $G_1(\beta)$ from Annex 9B.

c) STEP 3 – Determine average influence coefficients by integrating the influence coefficient functions over the crack front.

$$\bar{G}_o = \int_0^1 G_o(\beta) d\beta \tag{9I.3}$$

$$\bar{G}_1 = \int_0^1 G_1(\beta) d\beta \tag{9I.4}$$

If the influence coefficient functions are 6-degree polynomials, the above integrals have the following closed-form solutions due to the polynomial form of $G_i(\beta)$.

$$G_o(\beta) = \sum_{i=0}^{6} A_{i,o} \beta^i \tag{9I.5}$$

$$G_1(\beta) = \sum_{i=0}^{6} A_{i,1} \beta^i \tag{9I.6}$$

$$\bar{G}_o = \int_0^1 G_o(\beta) d\beta = \int_0^1 \sum_{i=0}^{6} A_{i,o} \beta^i = \sum_{i=0}^{6} \frac{A_{i,o}}{i+1} \tag{9I.7}$$

$$\bar{G}_1 = \int_0^1 G_1(\beta) d\beta = \int_0^1 \sum_{i=0}^{6} A_{i,1} \beta^i = \sum_{i=0}^{6} \frac{A_{i,1}}{i+1} \tag{9I.8}$$

where

$$\beta = \frac{2\varphi}{\pi} \tag{9I.9}$$

If required, use the integrated average values from Annex 9B tables, $\bar{G}_n(a/t,\ a/c,\ t/R_i)$ for interpolation.

d) STEP 4 – Compute the influence coefficient for bending from $\bar{G}_0$ and $\bar{G}_1$ with Equation (9I.10).

$$\bar{G}_b = \bar{G}_o - 2\bar{G}_1\left(\frac{a}{t}\right) \tag{9I.10}$$

e) STEP 5 – Compute the Mode I stress intensity factors for primary and secondary/residual stresses.

$$\bar{K}_I^P = \left(\bar{G}_o\sigma_m^P + \bar{G}_b\sigma_b^P\right)\sqrt{\frac{\pi a}{Q}} \tag{9I.11}$$

$$\bar{K}_I^{SR} = \left(\bar{G}_o\sigma_m^{SR} + \bar{G}_b\sigma_b^{SR}\right)\sqrt{\frac{\pi a}{Q}} \tag{9I.12}$$

9I.1.3.2 Through-Wall Arbitrary Stress Distributions

For stress distributions other than through-wall membrane and bending stress, closed form solutions are not readily available. In cases where linearizing over the crack plane results in a poor approximation of the stresses acting on the flaw plane, average stress intensity can be determined by numerically integrating stress intensity over the crack front. The general integral equations are shown below.

$$\bar{K}_I^P = \int_0^2 K_I^P(\beta)d\beta \quad \text{or} \quad \int_0^\pi K_I^P(\varphi)d\varphi \tag{9I.13}$$

$$\bar{K}_I^{SR} = \int_0^2 K_I^{SR}(\beta)d\beta \quad \text{or} \quad \int_0^\pi K_I^{SR}(\varphi)d\varphi \tag{9I.14}$$

The stress intensity at a position along the crack front defined by β or φ may be determined using Annex 9B, paragraphs 9B.14.4 or 9B.14.5.

9I.2 Nomenclature

a depth of a surface crack.

$A_{i,o}$ crack parameter from Annex 9B for uniform crack face loading.

$A_{i,1}$ crack parameter from Annex 9B for linear crack face loading.

β normalized parametric angle along an elliptical crack.

c half-length of a semi-elliptical crack.

G_i stress intensity influence coefficients.

$\bar{G}_b$ average influence coefficient for bending.

G_o stress intensity influence coefficient for uniform crack face loading.

$\overline{G}_o$ G_0 averaged over the crack front.

G_1 stress intensity influence coefficient for linear crack face loading.

$\overline{G}_1$ G_1 averaged over the crack front.

K_{mat} fracture toughness used in an FFS Assessment.

K_r toughness ratio in the FAD method.

K_I^P Model I stress intensity factor for primary stresses.

K_I^{SR} Mode I stress intensity factor for secondary/residual stresses.

$\overline{K}_I^P$ Model I stress intensity factor for primary stresses integrated over crack front.

$\overline{K}_I^{SR}$ Mode I stress intensity factor for secondary/residual stresses integrated over crack front.

φ parametric angle along the crack front.

$\sigma_b^{P,SR}$ primary and secondary plus residual through-wall bending stresses inferred from linearizing stress profile over the interval $x = 0$ to $x = a$.

$\sigma_m^{P,SR}$ primary and secondary plus residual through-wall membrane stresses inferred from linearizing stress profile over the interval $x = 0$ to $x = a$.

σ_b^P applied primary bending stresses.

σ_m^P applied primary membrane stress.

σ_b^{SR} applied secondary and residual bending stresses.

σ_m^{SR} applied secondary and residual membrane stresses.

t wall thickness or plate thickness.

x crack depth parameter.

9I.3 References

[1] Anderson, T.L., Constraint Effects on Fracture Toughness in Ductile-Brittle Transition Region, WRC Bulletin 577, Welding Research Council, Inc., Shaker Heights, OH, 2019.

9I.4 Figures

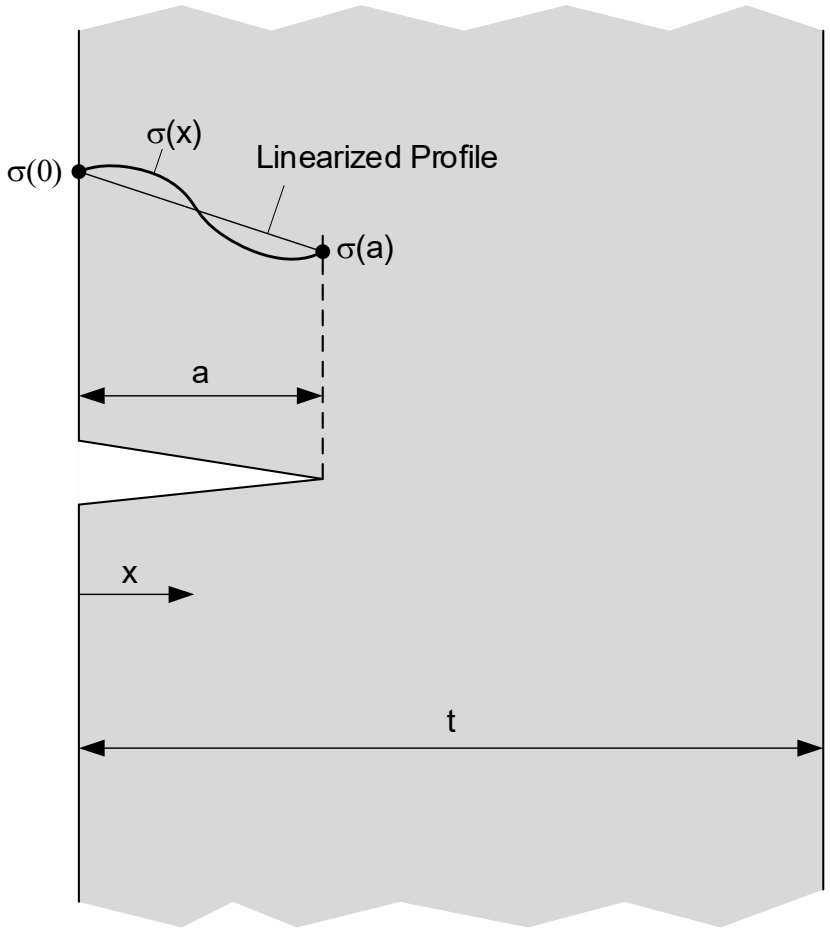

Figure 9I.1 – Linearization of a stress profile over the crack plane ($x = 0$ to $x = a$).

[Intentionally Left Blank]

ANNEX 9J – DETERMINATION OF THE MINIMUM ALLOWABLE TEMPERATURE (MAT) USING A LEVEL 2 FRACTURE MECHANICS APPROACH CONSISTENT WITH PARTS 3 AND 9

(NORMATIVE)

CONTENTS

ANNEX 9J – DETERMINATION OF THE MINIMUM ALLOWABLE TEMPERATURE (MAT) USING A LEVEL 2 FRACTURE MECHANICS APPROACH CONSISTENT WITH PARTS 3 AND 9 ..... 9J-1

9J.1 INTRODUCTION 9J-1
9J.2 PROCEDURE TO DETERMINE THE MAT 9J-1
9J.2.1 General Procedure 9J-1
9J.2.2 Simplified Procedure 9J-3
9J.3 REQUIRED MODIFICATIONS FOR HYDROGEN SERVICE 9J-4
9J.3.1 Overview 9J-4
9J.3.2 2.25 Cr – 1 Mo 9J-4
9J.3.3 2.25 Cr – 1 Mo - V 9J-5
9J.3.4 Carbon Steel and Other Low-Chrome Alloys 9J-5
9J.4 MAT ENVELOPE 9J-6
9J.5 NOMENCLATURE 9J-6
9J.6 REFERENCES 9J-7
9J.7 TABLES 9J-8
9J.8 FIGURES 9J-11

9J.1 Introduction

This Annex provides a procedure to determine the Minimum Allowable Temperature (MAT) using a Level 2 fracture mechanics approach that is consistent with Parts 3 and 9. In this Annex, the MAT is defined as the lowest (coldest) permissible metal temperature for a pressurized component for a given material, stress state (i.e., pressure and other applied loadings), and flaw size based on its resistance to brittle fracture. It may be a single temperature, or an envelope of allowable operating temperatures as a function of pressure. Modifications to the procedure to determine the MAT are provided for materials in hydrogen environments. Note that subcritical crack growth in hydrogen environments is considered to be negligible when using these procedures to detemine the MAT.

9J.2 Procedure to Determine the MAT

9J.2.1 General Procedure

A procedure to determine the MAT for a pressurized component for a given material, stress state (i.e., pressure and other applied loadings), and flaw size based on its resistance to brittle fracture using the Level 2 FAD approach described in Part 9, paragraph 9.4.3.2 is shown below.

a) STEP 1 – Determine the pressure and supplemental loading combinations to be evaluated (see Part 9, paragraph 9.4.3.2, STEP 1).

b) STEP 2 – Determine the stress distributions at the location of the flaw based on the applied loads in STEP 1 and classify the stresses as primary, secondary, and residual (see Part 9, paragraph 9.4.3.2, STEP 2).

c) STEP 3 – Assume a reference flaw.

1) A reference flaw with a depth equal to the minimum of 25% of the nominal wall thickness or 25mm (1-inch), and a length equal to six times this depth represents a conservative assumption and may be used.

2) A smaller postulated reference flaw may be used based on the level of Non-Destructive Examination (NDE) performed at the time of component fabrication. Note that additional in-service NDE may be considered in establishing a reference flaw.

3) If repairs to the component have been made, care should be exercised in establishing a reference flaw because many brittle fractures of pressurized components have been associated with repaired regions. NDE of the repair area may be warranted to justify the size of the reference flaw.

d) STEP 4 – Estimate the Master Curve reference transition temperature, T_0 for the material of construction (see Annex 9F, paragraph 9F.4.3.2). If appropriate, account for the effects of in-service toughness degradation (see Annex 9F, paragraph 9F.4.6) and aging effects (see Annex 9F, paragraph 9F.4.7).

e) STEP 5 – Assume an initial value for assessment temperature, T_{assume}.

f) STEP 6 – Determine the yield strength at the assumed temperature T_{assume}, $\sigma_{ys}(T_{assume})$.

g) STEP 7 – Determine the fracture toughness at the assumed temperature, $K_{mat}(T_{assume})$. Constraint effects per Annex 9H may be included in the determination of $K_{mat}(T_{assume})$.

h) STEP 8 – Compute the reference stress for primary stresses, σ_{ref}^{P}, based on the primary stress distribution and flaw size from STEP 2 and STEP 3, respectively, and the reference stress solutions in Annex 9C.

i) STEP 9 – Compute the Load Ratio or the abscissa of the FAD using the reference stress for primary loads from STEP 8 and the yield strength from STEP 6.

$$L_r^P = \frac{\sigma_{ref}^P}{\sigma_{ys}(T_{assume})} \tag{9J.1}$$

j) STEP 10 – Compute the stress intensity factor attributed to the primary loads, K_I^P, using the primary stress distribution and flaw size from STEP 2 and STEP 3, respectively, and the stress intensity factor solutions in Annex 9B. Annex 9I may be used to determine the stress intensity factor. If $K_I^P < 0.0$, then set $K_I^P = 0.0$.

k) STEP 11 – Compute the stress intensity factor attributed to secondary and residual stresses, K_I^{SR}, using the secondary and residual stress distributions and flaw size from STEP 2 and STEP 3, respectively, and the stress intensity factor solutions in Annex 9B. Annex 9I may be used to determine the stress intensity factor. If $K_I^{SR} < 0.0$, then set $K_I^{SR} = 0.0$. The value of K_I^{SR} should be determined at the same location along the crack front as that used to determine K_I^P.

l) STEP 12 – Compute the plasticity interaction factor, Φ (see Part 9, paragraph 9.4.3.2, STEP 10).

m) STEP 13 – Determine toughness ratio or ordinate of the FAD Assessment point where K_I^P is the applied stress intensity factor due to the primary stress distribution from STEP 10, K_I^{SR} is the applied stress intensity factor due to the secondary and residual stress distributions from STEP 11, $K_{mat}(T_{assume})$ is the material toughness from STEP 7, and Φ is the plasticity correction factor from STEP 12.

$$K_r = \frac{K_I^P + \Phi K_I^{SR}}{K_{mat}(T_{assume})} \tag{9J.2}$$

n) STEP 14 – Evaluate results; the FAD Assessment point for the current flaw size and operating conditions (i.e., stress levels) is defined as (K_r, L_r^P) where K_r is from STEP 13 and L_r^P is from STEP 9.

- If the FAD Assessment point (K_r, L_r^P) is on the FAD envelope (see Part 9, Figure 9.19); then, $MAT = T_{assume}$ and the analysis is complete.
- If the FAD Assessment point (K_r, L_r^P) is in the acceptable region of the FAD envelope (see Part 9, Figure 9.19); then, assume a lower (i.e., colder) value for T_{assume} and return to STEP 5.
- If the FAD Assessment point (K_r, L_r^P) is in the unacceptable region of the FAD envelope (see Part 9, Figure 9.19); then, assume a higher (i.e., warmer) value for T_{assume} and return to STEP 5.

9J.2.2 Simplified Procedure

9J.2.2.1 Limitations

The simplified procedure is subject to the following limitations:

- Applicable only to carbon and low alloy steels without austenitic stainless-steel clad lining or weld overlay and no dissimilar welds.
- Applicable only to equipment governed by pressure loading, i.e., Type A components per Part 4, Table 4.2. Supplemental loading (including weight, wind, thermal transients, piping expansion stress, etc.) are negligible even at low pressures.
- Applicable to pressure vessels and piping components with a thickness less than or equal to 38 mm (1.5-inches) in the as-welded and $PWHT$ condition, and components with a thickness greater than 38 mm (1.5-inches) that have been subject to $PWHT$ at the time of construction.
- Applicable to components that have not been subject to a repair.

9J.2.2.2 Procedure

A simplified procedure that will provide a conservative estimate of the MAT for pressurized components is shown below.

a) STEP 1 – Estimate the Master Curve reference transition temperature, T_0, for the material of construction (see Annex 9F, paragraph 9F.4.3.2). If appropriate, account for the effects of in-service toughness degradation (see Annex 9F, paragraph 9F.4.6) and aging effects (see Annex 9F, paragraph 9F.4.7). Modifications for the effects of hydrogen are provided in paragraph 9J.3. Do not use Annex 9H to adjust T_0 for constraint effects.

b) STEP 2 – Assume an initial value for assessment temperature, T_{assume}.

c) STEP 3 – Calculate the yield pressure, p_y, at T_{assume}.

$$p_y = \frac{\sigma_{ys}(T_{assume})t}{R_i} \tag{9J.3}$$

d) STEP 4 – Determine the allowable pressure p from Figure 9J.1 or 9J.2, as appropriate, using T_0 from STEP 1, $T = T_{assume}$ from STEP 2, and p_y from STEP 3. The equations for the curves in Figures 9J.1 and 9J.2 are provided in Tables 9J.1 and 9J.2, respectively.

1) If $t \leq 38\ mm\ (1.5\ inches)$ for the as-welded or $PWHT$ condition, use Figure 9J.1.

2) If $t > 38\ mm\ (1.5\ inches)$ for the $PWHT$ condition at the time of construction, use Figure 9J.2.

3) If $\sigma_{ys}(T_{ambient}) \leq 275\ MPa\ (40\ ksi)$, use the pressure – temperature curve for $\sigma_{ys} = 275\ MPa\ (40\ ksi)$.

4) If $275\ MPa\ (40\ ksi) < \sigma_{ys}(T_{ambient}) \leq 450\ MPa\ (65\ ksi)$, use the pressure – temperature curve for $\sigma_{ys} = 450\ MPa\ (65\ ksi)$.

e) STEP 5 – Evaluate the allowable pressure from STEP 4.

1) If $p =$ the desired pressure, then $MAT = T_{assume}$.

2) If $p <$ the desired pressure, increase T_{assume} and return to STEP 3.

3) If $p >$ the desired pressure, decrease T_{assume} and return to STEP 3.

9J.3 Required Modifications for Hydrogen Service

9J.3.1 Overview

A hydrogen environment has a detrimental effect on the fracture toughness of most carbon and low alloy steels. Therefore, modifications of the MAT derived from the General and Simplified procedures in paragraph 9J.2 are required. These modifications are only required for components in hydrogen service with a dissolved bulk hydrogen concentration greater than 1 ppm (see Annex 9F, paragraph 9F.4.6.2).

9J.3.2 2.25 Cr – 1 Mo

A procedure for determining the MAT in paragraph 9J.2 requires the following modification.

a) STEP 1 – Given the maximum operating temperature, T_{op}, and the hydrogen partial pressure, p_{H_2} at the $MAWP$, calculate the dissolved hydrogen concentration at the ID surface:

$$c_{surface} = 3.3620\sqrt{p_{H_2}}\exp\left[\frac{-3{,}257.0}{T_{op} + 273.15^{o}C}\right] \qquad \left(ppm, {}^{o}C, kPa\right) \tag{9J.4}$$

$$c_{surface} = 8.8278\sqrt{p_{H_2}}\exp\left[\frac{-5{,}862.7}{T_{op} + 459.67^{o}F}\right] \qquad \left(ppm, {}^{o}F, psi\right) \tag{9J.5}$$

b) STEP 2 – If weld overlay or cladding is present on the ID surface, compute the hydrogen concentration, c_H, at the ID interface with the 2.25Cr–1Mo steel by adjusting for the thickness of the weld overlay, t_w. Otherwise, $c_H = c_{surface}$.

$$c_H = c_{surface}\left(1 - \left(3.396 \cdot 10^{-2}\right)t_w + \left(8.027 \cdot 10^{-4}\right)t_w^2\right) \qquad \left(ppm, mm\right) \tag{9J.6}$$

$$c_H = c_{surface}\left(1 - 0.8626 t_w + 0.5179 t_w^2\right) \qquad \left(ppm, in\right) \tag{9J.7}$$

c) STEP 3 – If $c_H > 1\ ppm$ proceed to STEP 4. Otherwise, the fracture toughness is not influenced by dissolved hydrogen, the MAT is computed using the General or Simplified procedure in paragraph 9J.2.1 or 9J.2.2, respectively, and the remaining steps of this procedure are not required.

d) STEP 4 – Estimate the fracture appearance transition temperature for the thermally exposed material of construction, $(FATT_{thermal})$.

1) If possible, infer $FATT_{thermal}$ from Charpy testing on service-exposed or step-cooled material.

2) If Charpy data are not available but chemistry data exist, refer to Annex 9F paragraph 9F4.7.3 for a procedure to estimate $FATT_{thermal}$ from the J or $\bar{X}$ factor for base metal or weld metal, respectively.

3) If neither Charpy nor chemistry data are available, use the appropriate default $FATT_{thermal}$ in Table 9J.1 that corresponds to the vintage of the material.

e) STEP 5 – Perform either the General or Simplified procedure in paragraph 9J.2.1 or 9J.2.2, respectively, to infer the minimum pressurization temperature for fast fracture, $T_{fracture} = MAT$. In this calculation, define the index transition temperature, T_0, as given by Equation (9J.8), Note the effects of temper embrittlement have been included (refer to Annex 9F, paragraphs 9F.4.6.2 and 9F.4.7.3):

$$T_0 = FATT_{thermal} \tag{9J.8}$$

f) STEP 6 – Determine the appropriate T_{IH} curve in Figure 9J.3 to apply based on the $FATT_{thermal}$ determined in STEP 4, where T_{IH} is the critical temperature for stable hydrogen crack growth.

1) For $FATT_{thermal} \leq -30℃\ (-22℉)$ use the low $FATT$ curve.

2) For $-30℃ < FATT_{thermal} \leq 50℃\ (122℉)$ use the medium $FATT$ curve.

3) For $FATT_{thermal} > 50℃\ (122℉)$ use the high $FATT$ curve.

g) STEP 7 – Estimate T_{IH} from Figure 9J.3. Equations for the three curves in Figure 9J.3 are provided in Table 9J.4.

h) STEP 8 – Determine the MAT as follows.

1) For pressure greater than or equal to 20% of the $MAWP$ (see Figure 9J.4):

$$MAT = \max\left[T_{fracture}, T_{IH}\right] \tag{9J.9}$$

2) For pressures less than 20% of the $MAWP$ (see Figure 9J.5):

$$MAT = T_{fracture} \tag{9J.10}$$

9J.3.3 2.25 Cr – 1 Mo - V

Modification of the procedure in paragraph 9J.2 for components in hydrogen service is not required; therefore, the MAT may be determined directly from paragraph 9J.2.

9J.3.4 Carbon Steel and Other Low-Chrome Alloys

As indicated in Annex 9F, paragraph 9F.4.6.2(a)(3), the effects of hydrogen cannot be defined for these materials because of the lack of test data. To facilitate an FFS Assessment, the arrest toughness may be used as an estimate or lower bound of the resistance of a ferritic steel containing dissolved hydrogen to rapid unstable crack propagation. The arrest toughness is defined in Annex 9F, paragraph 9F.4.5.3. In the general procedure, use

$T_0 = T_0^A$ in STEP 4 of paragraph 9J.2.1, and for the Simplified procedure use $T_0 = T_0^A$ in STEP 1 of paragraph 9J.2.2.

9J.4 MAT Envelope

The procedures in paragraphs 9J.2 and 9J.3 provide a value of MAT for a single pressure. An envelope of MAT versus pressure can be obtained by assuming a range of pressures (i.e., from low to high) and performing the procedure in paragraph 9J.2 and 9J.3 for each pressure.

For 2.25 Cr-1 Mo steel in hydrogen service, Figure 9J.4 schematically illustrates the MAT-envelope that incorporates both fast fracture and stable hydrogen cracking. The MAT is established in accordance with paragraph 9J.3.2(h).

9J.5 Nomenclature

$FATT$	fracture appearance transition temperature.
K_I^P	stress intensity factor based on primary stresses.
K_I^{SR}	stress intensity factor based on secondary and residual stresses.
$K_{mat}(T_{assume})$	value of the material fracture toughness evaluated at the assumed temperature T_{assume}.
K_r	toughness ratio.
L_r^P	load ratio based on primary stress.
MAT	the Minimum Allowable Temperature.
$MAWP$	the Maximum Allowable Working Pressure.
p	allowable pressure.
p_{H_2}	partial pressure of hydrogen at the $MAWP$.
Φ	plasticity correction factor.
R_i	inside radius.
σ_{ys}	yield strength evaluated at the temperature T (see Annex 2E).
$\sigma_{ys}(T_{assume})$	yield strength evaluated at the assumed temperature T_{assume} (see Annex 2E).
σ_{ref}^P	reference stress based on the primary stress.
t	wall thickness.
T_0	reference transition temperature.
T_0^A	reference transition temperature for estimating the arrest fracture toughness.
$T_{ambient}$	ambient temperature.
T_{assume}	assumed temperature to compute the MAT.

$T_{fracture}$ MAT for fast fracture in 2.25 Cr-1 Mo steel.

T_{IH} critical temperature below which 2.25 Cr-1 Mo steel is susceptible to stable hydrogen cracking.

T_{op} maximum operating temperature.

9J.6 References

[1] Gangloff, R.P. and Anderson, T.L., ”The Effects of Hydrogen for Establishing a Minimum Pressurization Temperature (MPT) for Heavy Wall Steel Reactor Vessels,” API TR 934-F Part 4, First Edition (2018), American Petroleum Institute, Washington, DC.

[2] Anderson, T.L. and Brown, G.W. An Engineering Approach for Determining Minimum Pressurization Temperature (MPT) in Heavy-Wall 2.25 Cr -1 Mo Steel Reactors in Hydrogen Service, WRC Bulletin 563, Welding Research Council, Inc., Shaker Heights, OH.

9J.7 Tables

Table 9J.1 – Fitting Coefficients for the Pressure – Temperature Curves in Figure 9J.1.

Curve	B_0	B_1	B_2	B_3	B_4
$\sigma_{ys} = 40\ ksi$ $PWHT$	6.28126E-01	4.22251E-03	4.07734E-06	-6.75003E-08	-2.00675E-10
$\sigma_{ys} = 40\ ksi$ As-welded (No $PWHT$)	7.70625E-02	-1.46551E-02	3.61847E-04	-1.60742E-06	0.00000E+00
$\sigma_{ys} = 65\ ksi$ $PWHT$	3.34523E-01	4.47966E-03	1.96830E-05	-4.78297E-08	-5.35081E-10
$\sigma_{ys} = 65\ ksi$ As-welded (No $PWHT$)	-2.97096E+00	-3.98014E-02	-9.93226E-05	0.00000E+00	0.00000E+00
Note: $\frac{p}{p_y} = B_0 + B_1\tau + B_2\tau^2 + B_3\tau^3 + B_4\tau^4 \quad where\ \tau = T - T_0$ (°F)					

Table 9J.1M – Fitting Coefficients for the Pressure – Temperature Curves in Figure 9J.1M.

Curve	B_0	B_1	B_2	B_3	B_4
$\sigma_{ys} = 275\ MPa$ $PWHT$	6.28126E-01	7.60052E-03	1.32106E-05	-3.93662E-07	-2.10660E-09
$\sigma_{ys} = 275\ MPa$ As-welded (No $PWHT$)	-6.32880E-01	2.41735E-02	2.30348E-05	-9.92085E-07	0.00000E+00
$\sigma_{ys} = 450\ MPa$ $PWHT$	3.34523E-01	8.06339E-03	6.37729E-05	-2.78943E-07	-5.61707E-09
$\sigma_{ys} = 450\ MPa$ As-welded (No $PWHT$)	-1.32523E+00	2.80488E-02	-7.35359E-05	0.00000E+00	0.00000E+00
Note: $\frac{p}{p_y} = B_0 + B_1\tau + B_2\tau^2 + B_3\tau^3 + B_4\tau^4 \quad where\ \tau = T - T_0$ (°C)					

Table 9J.2 – Fitting Coefficients for the Pressure – Temperature Curves in Figure 9J.2.

Curve	B_0	B_1	B_2	B_3	B_4
$\sigma_{ys} = 40\ ksi$ $PWHT$	1.86890E-01	3.14304E-03	1.99641E-05	1.22569E-08	-4.72030E-10
$\sigma_{ys} = 65\ ksi$ $PWHT$	5.02378E-03	2.41483E-03	-1.83894E-05	4.67607E-07	-1.59364E-09
Note: $\frac{p}{p_y} = B_0 + B_1\tau + B_2\tau^2 + B_3\tau^3 + B_4\tau^4 \quad where\ \tau = T - T_0$ (°F)					

Table 9J.2M – Fitting Coefficients for the Pressure – Temperature Curves in Figure 9J.2M.

Curve	B_0	B_1	B_2	B_3	B_4
$\sigma_{ys} = 275\ MPa$ $PWHT$	1.86890E-01	5.65748E-03	6.46838E-05	7.14823E-08	-4.95518E-09
$\sigma_{ys} = 450\ MPa$ $PWHT$	5.02378E-03	4.34670E-03	-5.95816E-05	2.72708E-06	-1.67294E-08
Note: $\frac{p}{p_y} = B_0 + B_1\tau + B_2\tau^2 + B_3\tau^3 + B_4\tau^4 \quad where\ \tau = T - T_0$ (°C)					

Table 9J.3 – Default $FATT$ Values when Charpy or Chemistry Data are Not Available.

Vintage of 2.25 Cr–1 Mo Steel	$FATT$ for $T_{fracture}$ Analysis	T_{IH} Curve in Figure 9J.3
Post 1990	-30 °C (-22 °F)	Low $FATT$
1975 – 1990	50 °C (122 °F)	Medium $FATT$
Prior to 1975	120 °C (248 °F)	High $FATT$

Table 9J.4 – Fitting Constants for the T_{IH} Curves in Figure 9J.3

Material	A_0	A_1	A_2	A_3	A_4
Low $FATT$	-22.869	135.89	-55.092	11.638	-0.9099
Medium $FATT$	30.885	176.10	-70.111	+14.757	-1.152
High $FATT$	62.947	203.22	-79.965	+16.796	-1.310
Note: $T_{IH} = A_0 + A_1 C_H + A_2 {C_H}^2 + A_3 {C_H}^3 + A_4 {C_H}^4 \quad (ppm, °F)$					

Table 9J.4M – Fitting Constants for T_{IH} Curves in Figure 9J.3M

Material	A_0	A_1	A_2	A_3	A_4
Low $FATT$	-30.483	75.493	-30.607	6.4655	-0.5055
Medium $FATT$	-0.6196	97.834	-38.951	8.198	-0.640
High $FATT$	17.193	112.9	-44.425	9.3309	-0.7278
Note: $T_{IH} = A_0 + A_1 C_H + A_2 {C_H}^2 + A_3 {C_H}^3 + A_4 {C_H}^4 \quad (ppm, °C)$					

9J.8 Figures

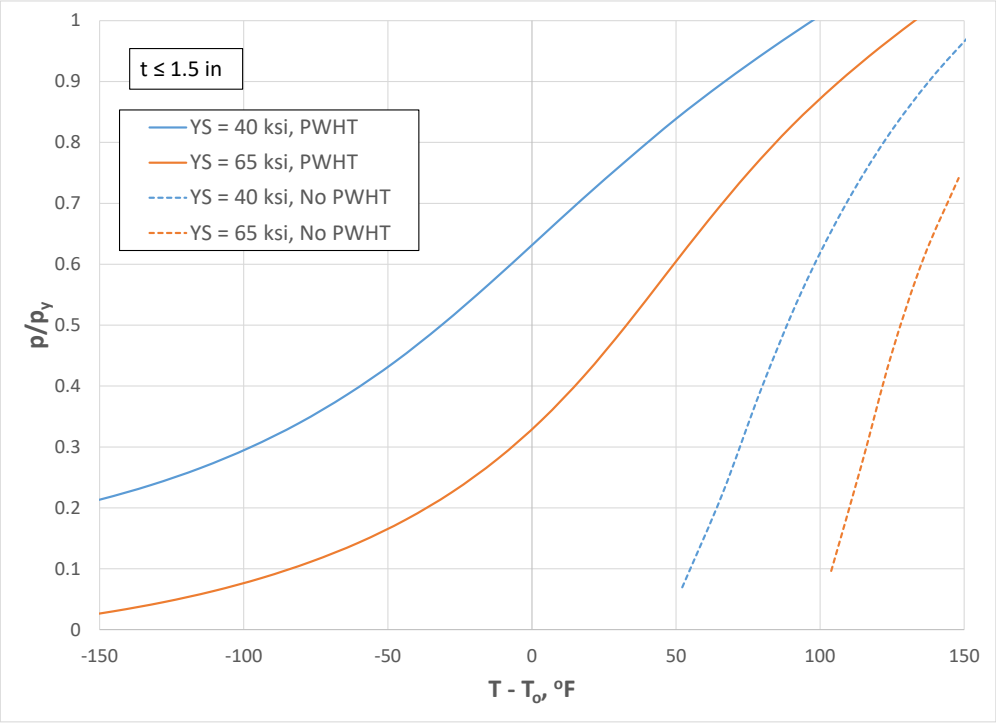

Figure 9J.1 – Pressure-Temperature Curves for Fast Fracture with Wall Thickness ≤ 1.5 inches.

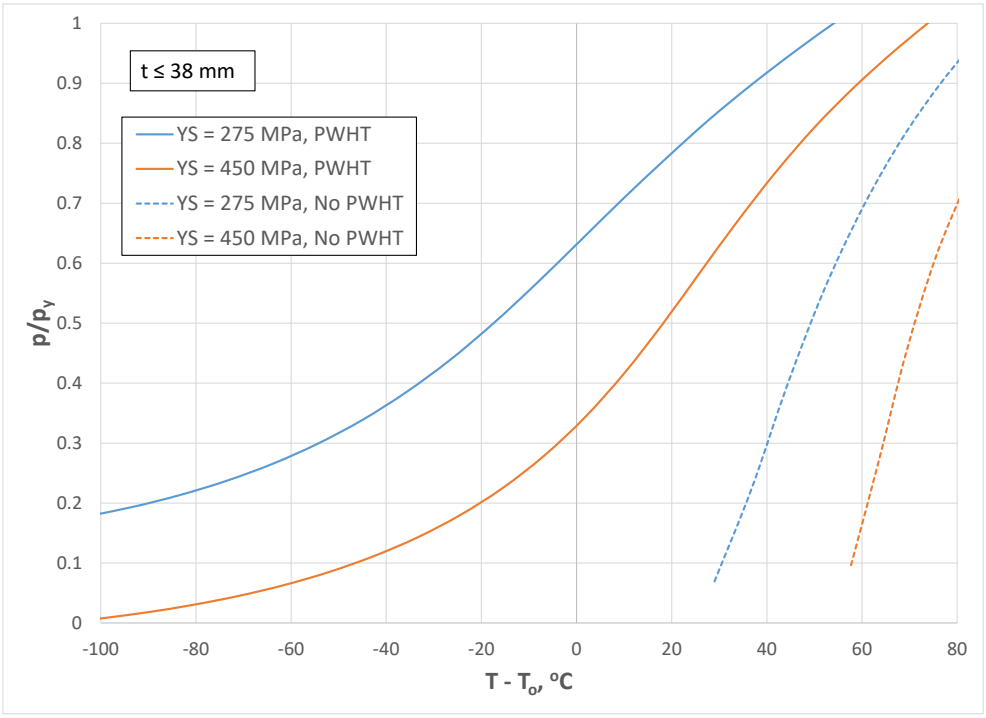

Figure 9J.1M – Pressure-Temperature Curves for Fast Fracture with Wall Thickness ≤ 38 mm.

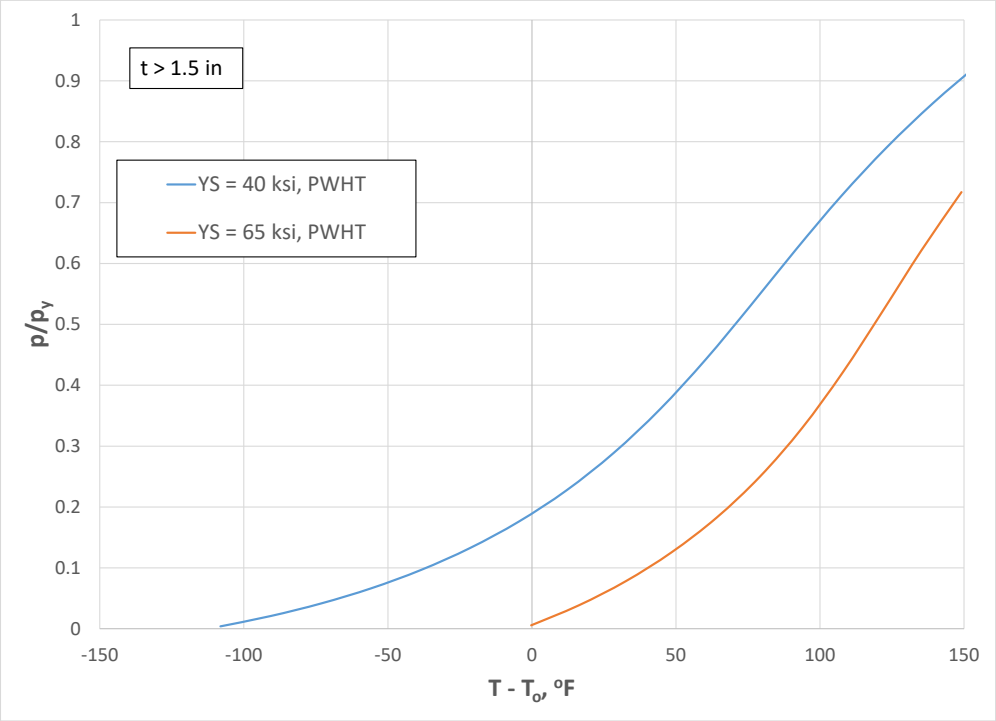

Figure 9J.2 – Pressure-Temperature Curves for Fast Fracture with Wall Thickness > 1.5 inches.

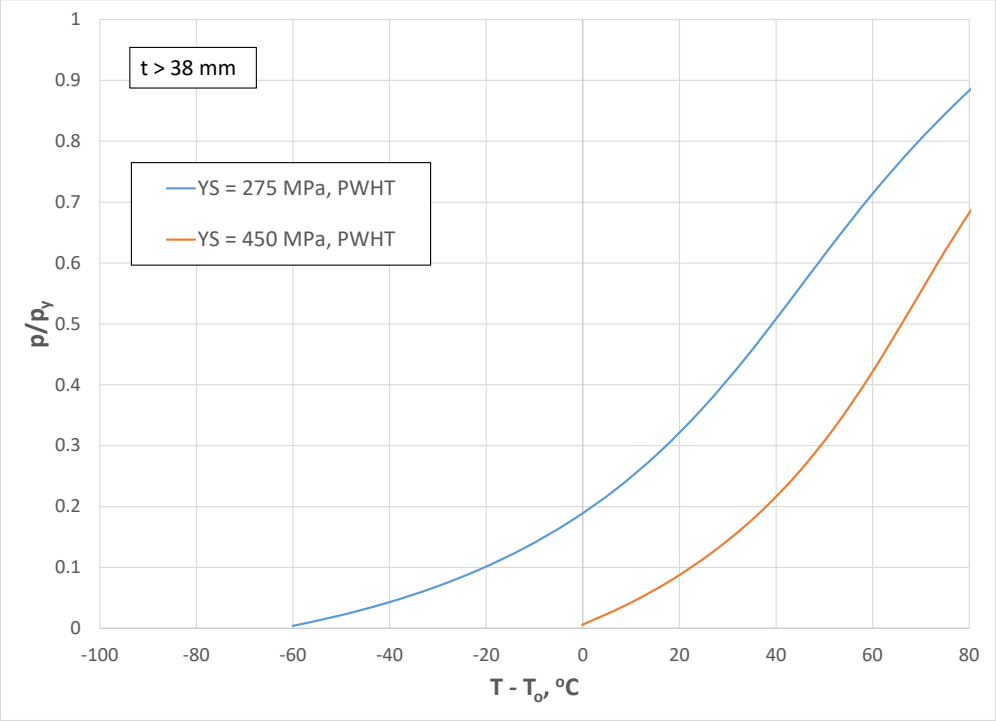

Figure 9J.2M – Pressure-Temperature Curves for Fast Fracture with Wall Thickness > 38 mm.

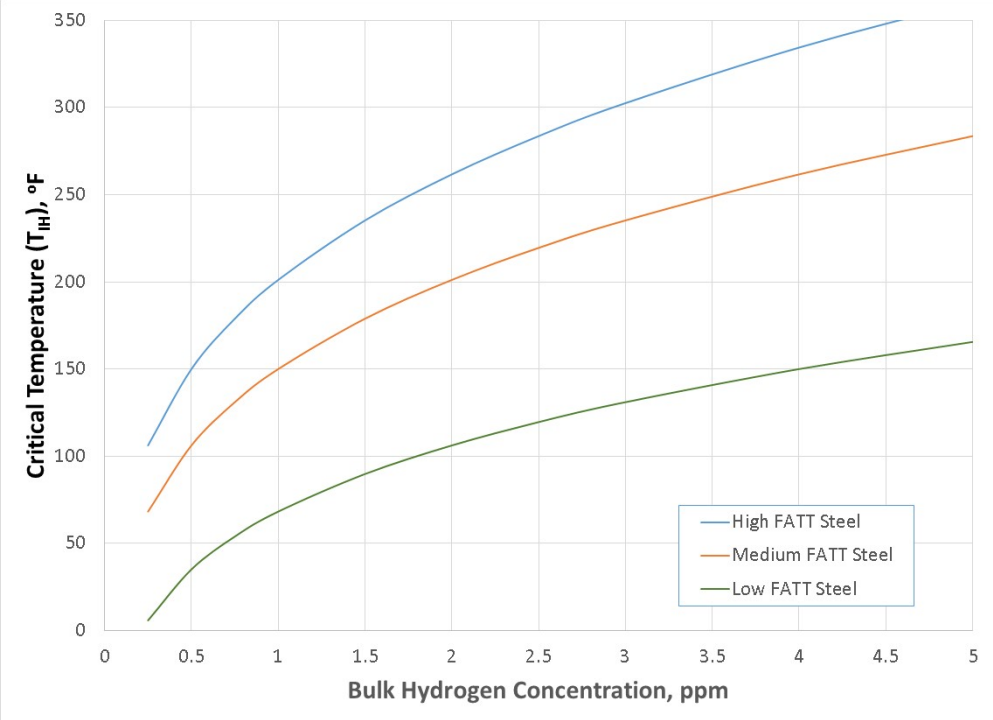

Figure 9J.3 – Critical Temperature for Stable Hydrogen Cracking in 2.25 Cr - 1 Mo Steel, T_{IH}.

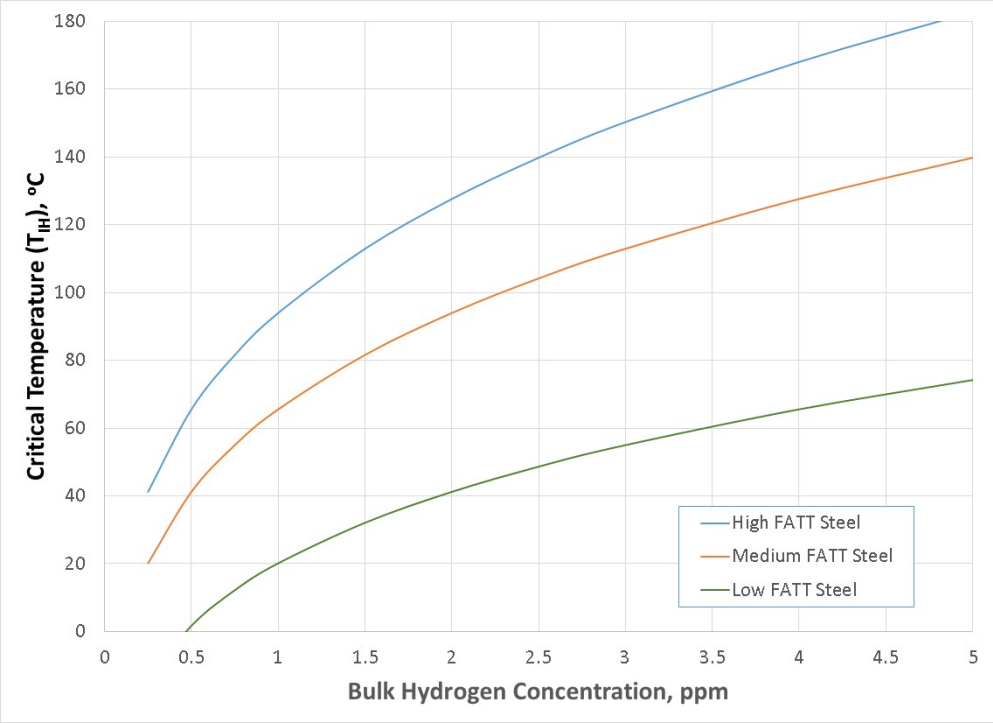

Figure 9J.3M – Critical Temperature for Stable Hydrogen Cracking In 2.25 Cr - 1 Mo Steel, T_{IH}.

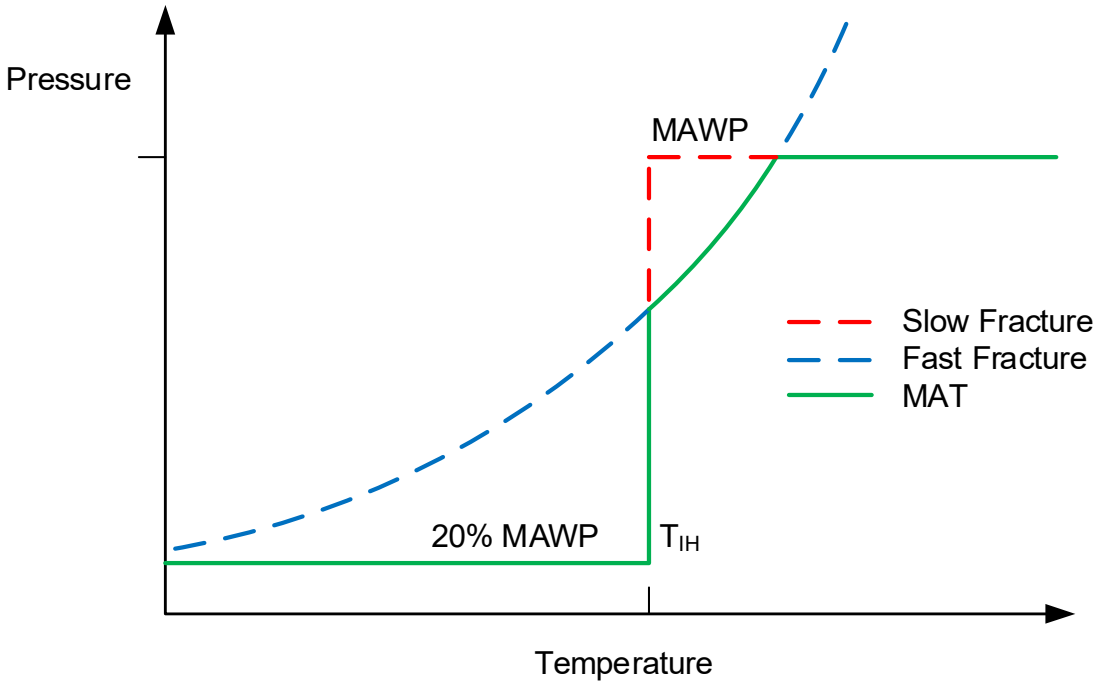

Figure 9J.4 – Schematic MAT Envelop for 2.25 Cr - 1 Mo Steel in Hydrogen Service with Pressures Greater Than or Equal to 20% of the $MAWP$

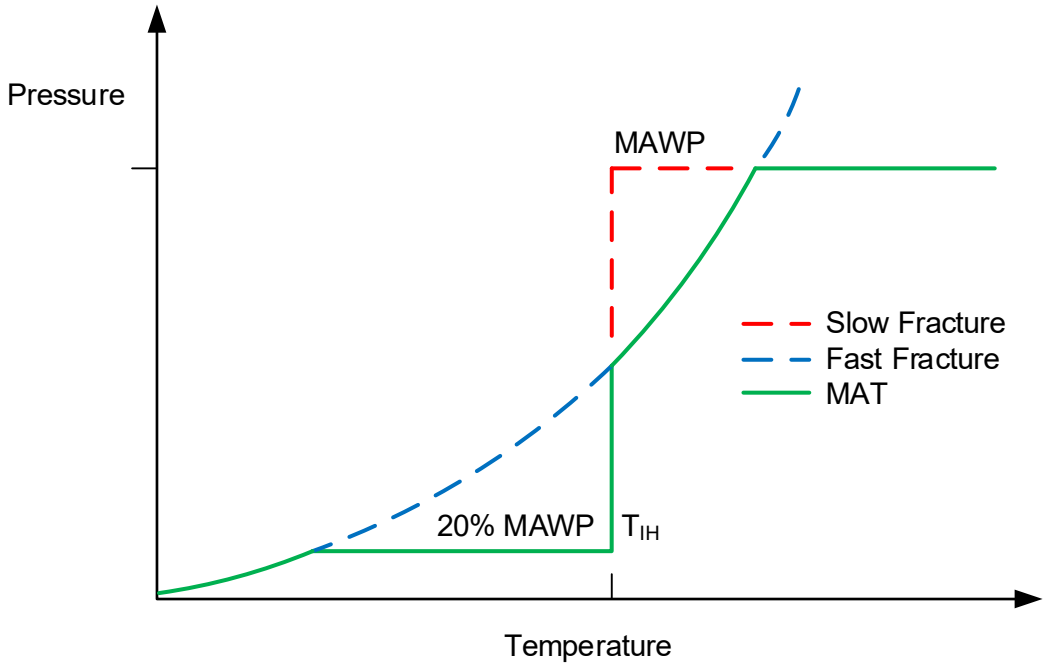

Figure 9J.5 – Schematic MAT Envelop for 2.25 Cr - 1 Mo Steel in Hydrogen Service with Pressures Less Than 20% of the $MAWP$ where Fast Fracture Governs

PART 10 – ASSESSMENT OF COMPONENTS OPERATING IN THE CREEP RANGE

CONTENTS

PART 10 – ASSESSMENT OF COMPONENTS OPERATING IN THE CREEP RANGE 10-1

10.1 GENERAL 10-2
10.1.1 FFS Procedures and Temperature Limits 10-2
10.1.2 Remaining Life of Components with and without Crack-Like Flaws 10-2
10.2 APPLICABILITY AND LIMITATIONS OF THE PROCEDURE 10-2
10.2.1 Suitability for Service and Remaining Life 10-2
10.2.2 Applicability and Limitations 10-2
10.2.3 Recommendations for Life Predictions Exceeding 35 Years 10-4
10.3 DATA REQUIREMENTS 10-4
10.3.1 General 10-4
10.3.2 Original Equipment Design Data 10-4
10.3.3 Maintenance and Operational History 10-4
10.3.4 Required Data for an FFS Assessment – Loads and Stresses 10-5
10.3.5 Required Data for an FFS Assessment – Material Properties 10-6
10.3.6 Required Data for an FFS Assessment – Damage Characterization 10-7
10.3.7 Recommendation for Inspection Technique and Sizing Requirements 10-8
10.4 ASSESSMENT TECHNIQUES AND ACCEPTANCE CRITERIA 10-10
10.4.1 Overview 10-10
10.4.2 Level 1 Assessment 10-11
10.4.3 Level 2 Assessment 10-12
10.4.4 Level 3 Assessment 10-13
10.5 REMAINING LIFE ASSESSMENT 10-13
10.5.1 Overview 10-13
10.5.2 Creep Rupture Life 10-15
10.5.3 Creep-Fatigue Interaction 10-22
10.5.4 Creep Crack Growth 10-22
10.5.5 Creep Buckling 10-27
10.5.6 Creep-Fatigue Assessment of Ferritic-Austenitic Dissimilar Weld Joints 10-29
10.5.7 Microstructural Approach 10-32
10.6 REMEDIATION 10-34
10.6.1 Components with and without a Crack-Like Flaw 10-34
10.6.2 Components with a Crack-Like Flaw 10-34
10.7 IN-SERVICE MONITORING 10-34
10.8 DOCUMENTATION 10-34
10.8.1 General 10-34
10.8.2 Assumptions Used in the Assumption 10-34
10.8.3 Documentation for Life Assessment 10-34
10.8.4 Supplemental Documentation for Creep Crack Growth 10-35
10.8.5 Supplemental Documentation for Microstructural Approaches 10-35
10.9 NOMENCLATURE 10-36
10.10 REFERENCES 10-43
10.11 TABLES 10-44
10.12 FIGURES 10-51

10.1 General

10.1.1 FFS Procedures and Temperature Limits

Fitness-For-Service (FFS) Assessment procedures for pressurized components operating in the creep range are provided in this Part. The temperature above which creep needs to be evaluated can be established using a Level 1 Assessment. The procedures in this Part can be used to qualify a component for continued operation or for re-rating. A flow chart for the assessment procedures for components operating in the creep range is shown in Figure 10.1.

10.1.2 Remaining Life of Components with and without Crack-Like Flaws

The FFS Assessment procedure for components operating in the creep range requires an estimate of remaining life. Assessment procedures for determining a remaining life are provided for components with and without a crack-like flaw subject to steady-state and cyclic operating conditions. If the component contains a crack-like flaw, and is not operating in the creep range, then Part 9 can be used for the FFS Assessment.

10.2 Applicability and Limitations of the Procedure

10.2.1 Suitability for Service and Remaining Life

The assessment procedures in this Part can be used to determine the suitability for continued operation and the remaining life of a component operating in the creep range. The use of these procedures is not normally required for equipment designed to a recognized code or standard that is operating within the original design parameters. Conditions that may warrant a FFS evaluation for components operating in the creep range include:

a) Operational upsets that result in an operating temperature and pressure, or other loading conditions that may result in creep damage and were not included in the original design.

b) Metal loss in the component beyond that provided for in the original design; metal loss in this category will result in component stress above those originally considered in the original design.

c) Component weldments that have significantly different properties in the weld metal, Heat Affected Zone (HAZ), and base metal. Examples include 1.25Cr-0.5Mo, 2.25Cr-1Mo and 9Cr-1Mo-V.

d) Stress concentration regions in the components that were not accounted for in the original design. Examples include out-of-roundness or peaking in longitudinal seam welds, notch-like locations such as transition regions with a slope greater than 1:3, and bulges that have occurred in service.

e) Fire damage that can result in a short time heating event.

f) The discovery of a crack-like flaw; both initial fabrication and service induced crack-like flaws should be evaluated.

g) The discovery of an LTA, pitting damage, weld misalignment, out-of-roundness, bulge, dent, or dent-gouge combination that can result in localized creep strain accumulation and subsequent cracking. Both initial fabrication and service-induced flaws should be evaluated.

10.2.2 Applicability and Limitations

Specific details pertaining to the applicability and limitations of each of the assessment procedures are discussed below.

10.2.2.1 The Level 1 Assessment procedures apply only if all the following conditions are satisfied:

a) The original design criteria were in accordance with Part 2, paragraph 2.2.2.

b) The component has not been subject to fire damage or another overheating event that has resulted in a significant change in shape such as sagging or bulging, or excessive metal loss from scaling.

c) The material meets or exceeds the respective minimum hardness and carbon content shown in Table 10.1.

d) The component does not contain:

1) An LTA or groove-like flaw,

2) Pitting damage,

3) Blister, HIC, or SOHIC damage,

4) Weld misalignment, out-of-roundness, or bulge that exceed the original design code tolerances,

5) A dent or dent-gouge combination,

6) A crack-like flaw, or

7) Microstructural abnormality such as graphitization, sigma phase formation, carburization, or hydrogen attack.

10.2.2.2 The Level 2 Assessment procedures apply only if all the following conditions are satisfied:

a) The original design criteria were in accordance with Part 2, paragraph 2.2.2.

b) A history of the operating conditions and documentation of future operating conditions for the component are available.

c) The component has been subject to less than or equal to 50 cycles of operation including startup and shutdown conditions, or less than that specified in the original design.

d) The component does not contain any of the flaws listed in paragraph 10.2.2.1(d).

10.2.2.3 A Level 3 Assessment should be performed when the Level 1 and 2 methods cannot be applied due to applicability and limitations of the procedure or when the results obtained indicate that the component is not suitable for continued service.

a) Conditions that typically require a Level 3 Assessment include the following.

1) Advanced stress analysis techniques are required to define the state of stress because of complicated geometry and/or loading conditions.

2) The component is subject to cyclic operation (see paragraph 10.2.2.2(c)).

3) The component contains a flaw listed in paragraph 10.2.2.1(d). A detailed assessment procedure is provided for a crack-like flaw; however, this procedure cannot be used to evaluate crack-like flaws that are caused by stress corrosion, oxide wedging, or similar environmental phenomena.

b) The Level 3 Assessment procedures, except for the procedure for the evaluation of dissimilar metal welds, can be used to evaluate components that contain the flaw types in paragraph 10.2.2.1(d). A separate procedure is provided to evaluate components with crack-like flaws.

c) The assessment procedure provided for dissimilar metal welds is only applicable to 2.25Cr - 1Mo to austenitic stainless steel welds made with stainless steel or nickel-based filler metals. An alternative assessment procedure for this material and other materials that are not currently covered may be used.

10.2.2.4 To perform an evaluation to any of the assessment levels, the material properties for the temperature and stress conditions the component is subject to must be available. For a Level 1 Assessment, the required material properties are included in the material screening curves (see paragraph 10.4.2). For the Level 2 and Level 3 Assessments, the required material properties are included for many commonly used materials in Annex 10B.

10.2.2.5 The Level 1 and Level 2 Assessment procedures include a limitation on the minimum thickness. The limitation on minimum thickness is to guard against potential inadequacy in inspection method capabilities to accurately characterize excessively thinned areas. If the limitation on minimum thickness is not satisfied, a Level 3 Assessment may be performed. Future inspection frequency shall be established based on a detailed investigation of all applicable damage mechanisms and inspection results shall be appropriately validated (see Part 4, paragraph 4.3.4.6).

10.2.3 Recommendations for Life Predictions Exceeding 35 Years

The creep constants contained in this Part are based on laboratory testing covering a wide range of materials, stresses, temperatures, and durations. The longest test durations vary by material but are typically in the range of 50,000 hours to 250,000 hours. Therefore, creep damage and rupture life predictions for longer times represent extrapolation relative to known response. Caution is advised when total life predictions exceed approximately 300,000 hours or 35 years, and the predictions should be treated as increasingly approximate. Additionally, these long times typically correspond to lower stresses and temperatures, where damage at the microstructural level can occur with very little accompanying bulk strain or deformation. Due to reasons such as extrapolation of test data, little or no visible deformation at failure, non-destructive examination and material testing are recommended as an essential part of life management for operating durations greater than 35 years.

10.3 Data Requirements

10.3.1 General

10.3.1.1 The Level 1 Assessment is a screening criterion based on the original design of the component, the past and future planned operating conditions. This assessment can be performed based on the following information.

a) Original Equipment Design Data (see paragraph 10.3.2).

b) Maintenance and Operating History (see paragraph 10.3.3).

10.3.1.2 Significant input data are required to perform a Level 2 or Level 3 Assessment. Details regarding the required data are discussed in paragraphs 10.3.2 through 10.3.6. The accuracy of these data and stress conditions will determine the accuracy of the assessment in this Part.

10.3.2 Original Equipment Design Data

An overview of the original equipment data required for an assessment is provided in Part 2, paragraph 2.3.1.

10.3.3 Maintenance and Operational History

10.3.3.1 An overview of the maintenance and operational history required for an assessment is provided in Part 2, paragraph 2.3.2.

10.3.3.2 The definition of the operating history is required in perform an FFS Assessment of a component operating in the creep range.

a) The component operating history and future operational conditions are required to perform a remaining life assessment. This information should include an accurate description of operating temperatures, pressures, supplemental loads, and the corresponding time period for all significant events. These events include start-ups, normal operation, upset conditions, and shutdowns. Past operating history may not be required as described in paragraph 10.3.5.2.

b) If an accurate history cannot be generated, then an approximate history shall be developed based on information obtained from plant personnel. This information shall include a description of all assumptions made and include a discussion of the accuracy in establishing points on the history. A sensitivity analysis (see paragraph 10.5.1.4) shall be included in the FFS Assessment to determine and evaluate the effects of the assumptions made to develop the operating history.

c) If past operating conditions are not known or estimated operating conditions have a significant amount of uncertainty, a material test can be performed whereby the creep damage associated with past operation can be evaluated in terms of a material parameter (see paragraph 10.3.5.2).

d) When creating the history, the history to be used in the assessment shall be based on the actual sequence of operation.

10.3.4 Required Data for an FFS Assessment – Loads and Stresses

10.3.4.1 A stress analysis is required for a Level 2 or Level 3 Assessment.

a) Level 1 Assessment – Nominal stresses are required. The nominal stresses may be computed using code equations (see Annex 2C).

b) Level 2 and Level 3 Assessments – stress analysis may be performed using the following methods.

   1) Handbook solutions may be used if these solutions accurately represent the component geometry and loading condition.

   2) Reference stress solutions that include the effects of stress re-distribution during creep may be used in the assessment if these solutions accurately represent the material creep response, component geometry, and loading conditions.

   3) Numerical analysis techniques such as the finite element method can be used to determine the stress state at major structural discontinuities or at the location of a flaw (e.g., crack-like flaw or LTA) where creep damage or creep crack growth is normally manifested. In these cases, it is recommended that this analysis includes the effects of plasticity and creep to account for the redistribution of stresses that occurs in the creep range. This is particularly important because the stresses at major structural discontinuities relax to magnitudes that are significantly less than those computed using an elastic stress calculation. Since the stress results are used directly in the assessment procedure and the remaining life from this procedure is sensitive to the magnitude of stress, the results from an elastic analysis will typically over-estimate the creep damage and result in a conservative estimate of remaining life.

   4) Guidelines for computing stresses for a tube or elbow in a Level 2 Assessment are provided in paragraph 10.5.2.5.

10.3.4.2 Stress calculations shall be performed for all points included in the load history (see paragraph 10.3.3.2) that will be used in the assessment.

10.3.4.3 The stress analysis performed for all assessment levels shall include the effects of service-induced wall thinning (e.g., oxidation).

10.3.4.4 Additional information regarding stress analysis for a component containing a crack-like flaw is provided in Part 9, paragraph 9.3.4.2.

10.3.4.5 Component temperatures used in an assessment should be based on the operating temperatures considering the following.

a) Heat transfer analysis considering thermal conductivity, fluid film coefficients, and transient effects.

b) Insulating effects of scale, other corrosion products, or process products left on the component surfaces.

c) The influence of the process environment on local overheating or cooling.

10.3.5 Required Data for an FFS Assessment – Material Properties

10.3.5.1 An overview of the material data required to perform a remaining life assessment is provided in Annex 10B and summarized below. The material data presented in Annex 10B are from the MPC Project Omega data that are based on a strain-rate approach, and the creep rupture life data from API Std 530. Both types of data can be used in the Level 2 or Level 3 Assessment procedures to determine a remaining life. The Project Omega data is required in a Level 3 creep buckling analysis. Material data applicable to service exposed materials from other sources may be used in a Level 3 Assessment.

a) MPC Project Omega Data – data are provided in terms of a damage parameter and strain-rate parameter, a method is suggested to account for minimum and average properties.

b) Creep Rupture Data – data are provided for minimum and average properties in terms of the Larson-Miller Parameter.

10.3.5.2 As previously described, a precise description of the component operating history and future operational conditions is required to perform a remaining life assessment. The future planned operating conditions can be readily defined; however, many times an adequate description of the past operating history cannot be made. To address this problem, the MPC Project Omega Program has developed a testing protocol to evaluate material parameters required for a remaining life assessment. The required tests necessitate removal of a material sample from a location in the component subject to the highest creep damage. This location is typically associated with the highest temperature and/or stress location. When an Omega Test is performed on a material sample from the component, the Omega material parameters are determined, and these parameters include the effects of creep damage associated with past operation. Therefore, by performing an Omega test, the remaining life problem is “shifted” such that the operating conditions up to the time of the test do not need to be evaluated to determine a remaining life (see Figure 10.2). This feature of the MPC Omega Method provides a means to accurately account for creep damage from past operation without having to know how the component was operated.

10.3.5.3 The material data from the MPC Project Omega Program (see Annex 10B) can be used directly to model creep behavior in an inelastic finite element analysis by implementing the equation shown below. This equation provides a strain-hardening relationship for the creep strain rate, i.e., the current creep strain rate is a function of the current stress, and temperature, and accumulated creep strain, and can be used with finite element computer programs that utilize either an explicit or implicit time integration algorithm for solution of the creep problem. Note

that this creep constitutive relationship will need to be implemented in a customized user-subroutine. However, most of the finite element programs that have creep analysis capability provide this option.

$$\dot{\varepsilon}_c = \dot{\varepsilon}_{co} \exp\left[\Omega_m \varepsilon_c\right] \tag{10.1}$$

10.3.5.4 If the component contains a crack-like flaw, parameters for the creep-crack growth equation is required (see Annex 10B). In addition, the fracture toughness is also required because an evaluation of the flaw using the Failure Assessment Diagram (FAD) based assessment procedures of Part 9 is required. It should be noted that although unstable crack growth is unlikely at elevated temperature, it may be a possibility during the start-up or shutdown phase of the cycle. In addition, the FAD Assessment is required to place a limit on the plastic collapse of a component containing a crack-like flaw.

10.3.6 Required Data for an FFS Assessment – Damage Characterization

10.3.6.1 General requirements for all components

a) It shall be verified that the component material conformed to the original specification for the material of construction or does so now.

b) The remaining sound wall thickness and the extent of corrosion/erosion shall be determined on all surfaces of the component.

c) The existence of flaws or damage described in paragraph 10.2.2.1(d) shall be determined. If a flaw is found, the extent of the damage shall be documented in accordance with the applicable Parts of this Standard.

d) Local variations in the operating conditions shall be identified. These may result from hot spots, coolant flow patterns, furnace or heater firing condition, etc. Local variations in operating conditions may result in a localized increased rate of wall thinning.

e) Any unusual loading conditions resulting from missing or damaged supports, dead weight loads, etc., shall be noted, and considered in the stress analysis (see paragraph 10.3.4).

f) The allowable creep damage D_c^{allow} shall be specified. If information is not available for the specific material being evaluated, then $D_c^{allow} = 0.8$ shall be used for Level 1 and $D_c^{allow} = 1.0$ shall be used for Level 2.

g) Environmental interaction such as carburization, decarburization, hydrogen attack, etc., shall be considered and noted accordingly.

h) Where appropriate and based on the observed metal loss or known reaction rates and the time-temperature history, future reaction rates shall be appropriately accounted for in the assessment.

   1) Where rates of future reactions are not reaction-product thickness limited, the reaction rate may be fit to a form shown in Equation (10.2) based on measurements or literature.

$$R_r = Ae^{-Q/RT} \tag{10.2}$$

   2) Where the rate of material thickness change is dependent on the thickness of the reaction product, the reaction rate may be fit to a form shown in Equation (10.3) based on measurements or literature.

$$R_r = B \cdot t^{1/2} \cdot e^{-Q/RT} \tag{10.3}$$

i) If a Level 2 or 3 Assessment is performed, then the grain size, carbon content, and heat treatment conditions should be considered.

j) If a Level 2 or 3 Assessment is performed for a weldment, then the following information should be considered.

1) The weld joint geometry.

2) Composition of the deposit, especially carbon and oxygen contents, and tramp elements and possible resulting embrittlement.

3) Welding process used during fabrication.

4) The effect of creep rate mismatch between the base metal and weld metal or HAZ on the remaining life.

5) The stress concentration at the toe of the weld.

6) The effect of radial (offset) and angular (peaking) misalignment at the weld joint, shell out-of-roundness, and other geometrical imperfections on the remaining life (see Part 8).

7) Inspection records.

8) Post weld heat treatment originally used at the time of construction.

9) Repair history including subsequent $PWHT$ information.

10) Residual stress effects.

11) The effects of precipitates in welds or inclusions on void formation that may result in a reduction in the remaining life.

10.3.6.2 Supplemental requirements for a component with a crack-like flaw

a) A determination should be made whether the crack-like indication is an original fabrication flaw or service damage induced. If the origin of the crack-like indication cannot be established, then it shall be classified as a service-induced flaw.

b) If a crack-like flaw is in the vicinity of a weld, the location of the flaw, in the heat affected zone, at the fusion line, or in the deposit shall be recorded. In addition, the crack-like flaw length and depth, and location from the surface for an embedded flaw shall be established in accordance with Part 9.

10.3.7 Recommendation for Inspection Technique and Sizing Requirements

10.3.7.1 General requirements for all components

Inspection should be performed to establish the component condition and any detectable damage.

a) Wall Thinning – straight beam Ultrasonic Thickness examination (UT).

b) Crack-Like Flaws (see Part 9, paragraph 9.3.7 for additional information).

1) Surface Cracks – The crack length, angle relative to the principal stress direction (see Part 9, Figure 9.2) and distance to other surface cracks may be determined using Magnetic Particle (MT) or Dye Penetrant (PT) examination technique. The depth and angle of the flaw relative to the surface (see Part 9, Figure 9.4) is typically determined using angle beam ultrasonic thickness (UT) examination technique.

2) Embedded Cracks – The crack depth, length, angle, and distance to other surface breaking or embedded cracks are typically determined using angle beam Ultrasonic Thickness (UT) examination technique (e.g., Time-Of-Flight-Diffraction (TOFD) or pulse echo techniques). The calibration settings may need to be more sensitive than are used for new construction weld quality inspections.

c) Bulging – the extent of the bulge shall be measured from a reference plane.

d) Hardness Measurements – may be taken in the field, although measurements made in the laboratory on samples of material in service are more reliable. For measurements in the field, the removal of about 0.5mm (0.02-inch) of material from the surface is recommended. All evidence of oxidation, sulfidation, carburization, nitriding, and decarburization must be removed. All measurements shall be performed in conjunction with the use of calibration blocks in the range of hardness expected.

e) Tube Diameter or Circumference Measurements – Calipers can be used to determine the diameter of a fired heater or boiler tube at orthogonal directions; however, a better method is to measure the circumference of the tube with a strap (flexible measuring tape).

1) Strap measurements should be taken at the highest heat flux areas of tubes. This type of measurement can be related to the swelling and creep in the tube, although complexities arise when there is external oxidation on the tube surface, or the tube has ovalized in service due to non-uniform circumferential heating. Therefore, in certain cases, strap measurements are not considered to be a quantitative measure of strain but are instead performed to provide an indication of overheating or a qualitative measure of creep damage.

2) Strap measurements taken at defined locations on new tubes (baseline measurements) and subsequently at different points in time can provide an indication of creep damage if ovalization or other damage has not occurred.

3) Another way to determine that severe bulging and creep damage has not occurred is to use a set of no-go gauges preset at a given percent (%) strain (for example 2%) that can easily be slipped over the tube and slid along the tube length. The location and extent of uneven bulging should be recorded.

4) The level of acceptable strain varies greatly amongst the tube materials and the operating conditions. For heater tubes made of HK alloys, the amount of strain at failure can be as low as 0.5%, so there are limitations to using strapping as a stand-alone method for deciding on when tube replacement is warranted.

10.3.7.2 Nondestructive material examination by means of replication is a metallographic examination method that exposes and replicates the microstructure of the surface material.

a) Method – Portable equipment is typically used for the examination. Surface preparation is conducted by progressive grinding to remove scale, surface carburization, and other surface material. After final grinding, the surface must be polished in the following ways: electrolytic polishing or mechanical polishing using polishing discs and diamond paste (i.e., particle size of 1μ to 7μ). After polishing, the surface must be cleaned thoroughly and dried. It is particularly important to thoroughly clean the surface after electro-polishing to prevent corrosion on the newly polished surface by the aggressive electrolyte. A strip of acetate tape is softened in a solvent and pressed against the polished surface. Once the tape dries it is removed and can be viewed under the optical or electron microscope when vapor deposit coated with carbon or gold.

b) Application – The replication method can be used for the examination of all metallic materials. Replication is typically used to establish microstructure of the materials and to determine if cavities or cracks are present. This method is restricted to relatively small areas for examination; however, many replicas can be taken to ensure coverage of a large area. Replication can be used as a follow-up to other detection methods such as magnetic particle or eddy current. Surface cracks can be identified at a much earlier stage using the

replication method than with other NDE methods. This early detection allows time to plan repairs and/or replacements thus avoiding unscheduled repairs.

c) Flaw Detection – Because each type of crack has specific characteristics, a damage type determination is usually possible with this method. If further evaluation is desired for metallurgical and microstructural components, such as carbides, cavities, etc., replicas can be coated with a reflective, conductive material and studied in a scanning electron microscope.

d) Limitations – The replication method can only be used on surfaces that are readily accessible. The surface conditions must be exposed, dry, and at ambient temperature, between about -18°C to 32°C (0°F to 90°F).

10.3.7.3 As an alternative to replication, small samples can be removed from the component to determine composition as well as microstructure. However, it should be noted that repair of this area may be required unless the region can be qualified for continued operation with a Level 3 Assessment.

10.3.7.4 Supplemental requirements for a component with a crack-like flaw

a) Detection and sizing of crack-like flaws originating in creep service requires validation and qualification of procedures and personnel. Service-induced cracks may not be good planar reflectors, and they may not be located in regions easily accessed by shear wave.

b) Surface cracks may be characterized by magnetic particle, dye penetrant, eddy current, or ultrasonic examination, or by replication. Subsurface cracks may be characterized using UT. If crack-like indications are found, the location, length, position relative to surface, and extent must be determined. Position relative to a weld or discontinuity must be recorded.

c) Automated TOFD can be effectively used for rapid screening of aligned clusters of small cavities. High frequency composite transducers may be used for detection of low levels of aligned cavitation. Focus beam transducers may be used for early stage damage characterization, provided the signal responses have been characterized and validated.

10.4 Assessment Techniques and Acceptance Criteria

10.4.1 Overview

The FFS Assessment procedures used to evaluate the remaining life of a component operating in the creep range are described below. The three assessment levels used to evaluate creep damage are based on the data and details required for the analysis, whether the component contains a crack-like flaw, the degree of complexity required for a given situation, and the perceived risk (see API RP 580 or API RP 581).

a) Level 1 Assessments are used to evaluate a single operating condition in the creep range based on a comparison with specified time-temperature-stress limits. Both time-dependent and time-independent behaviors are considered. In addition, a check on material properties in terms of hardness or carbon content and a visual examination of the component is made to evaluate the potential for creep damage based on component distortion and material characteristics such as discoloration or scaling.

b) Level 2 Assessments are used to evaluate multiple operating conditions for components operating in the creep regime that satisfy the requirements of paragraph 10.2.2.2. A creep damage rule is used to evaluate the creep damage from each operating condition. The stress analysis for the assessment may be based on closed form stress solutions, reference stress solutions, or solutions obtained from finite element analysis.

c) Level 3 Assessments can be used to evaluate those cases that do not meet the requirements of Level 1 or Level 2 Assessments. A detailed stress analysis is required to evaluate creep damage, creep-fatigue damage, creep crack growth, and creep buckling. In addition, a separate procedure is provided to perform a creep-fatigue assessment of a dissimilar-weld joint.

10.4.2 Level 1 Assessment

10.4.2.1 The Level 1 Assessment for a component subject to a single operating condition in the creep range is provided below.

a) STEP 1 – Determine the material of construction for the component and establish the metallurgical requirements and Level 1 screening curve (see Table 10.1). If the material of construction is not present or does not satisfy the metallurgical requirements in Table 10.1, go to paragraph 10.4.2.3.

b) STEP 2 – Determine the maximum operating temperature, pressure, and service time for the condition being evaluated. If the component contains a welded joint that is loaded in the stress direction that governs the minimum required wall thickness, then 14ºC (25ºF) shall be added to the maximum operating temperature to determine the assessment temperature. Otherwise, the assessment temperature is the maximum operating temperature. If the assessment temperature is greater than the temperature on the x-axis of the screening curve, go to paragraph 10.4.2.3.

c) STEP 3 – Determine the wall thickness of the component at the end of the operating condition including the effects of corrosion and erosion. If the wall thickness is less than t_{lim} defined by Equation (10.4), go to paragraph 10.4.2.3.

$$t_{\lim} = \min\left[0.9t_{nom},\ 2.5\,mm\left(0.10\,inches\right)\right] \tag{10.4}$$

d) STEP 4 – Determine the nominal stress of the component for the operating condition defined in STEP 2 and wall thickness in STEP 3, and the corroded geometry of the component using the construction code equations for wall thickness, i.e., solve for the component nominal stress given the geometry, pressure, and other loads, as applicable (see Annex 2C).

e) STEP 5 – Determine the permissible time for operation based on the screening curve from STEP 1, assessment temperature from STEP 2, the nominal stress from STEP 4. If the point defined by the temperature and the nominal stress is above the time-independent curve (i.e., black line) in the Screening Curve, go to paragraph 10.4.2.3.

f) STEP 6 – If the permissible time for operation from STEP 5 exceeds the service time for the component from STEP 2, then the component is acceptable per the Level 1 Assessment procedure. Otherwise, go to paragraph 10.4.2.3.

10.4.2.2 The Level 1 Assessment for a component subject to multiple operating conditions in the creep range is shown below.

a) STEP 1 – Determine the material of construction for the component and establish the metallurgical requirements and Level 1 screening curve (see Table 10.1). If the material of construction is not present or does not satisfy the metallurgical requirements in Table 10.1, go to paragraph 10.4.2.3.

b) STEP 2 – Determine the maximum number of operating conditions N.

c) STEP 3 – For each operating condition $n \leq N$:

1) STEP 3.1 – Determine the pressure, temperature, and service time, ${}^{n}t$,for each design or operating condition. If the component contains a weld joint that is loaded in the stress direction that governs the minimum required wall thickness calculation, then 14ºC (25ºF) shall be added to the operating temperature to determine the assessment temperature. Otherwise, the operating temperature is the assessment temperature. If the assessment temperature is greater than the temperature on the x-axis of the screening curve, go to paragraph 10.4.2.3.

2) STEP 3.2 – Determine the wall thickness of the component at the end of the current operating condition including the effects of corrosion and erosion. If the wall thickness is less than t_{lim} define by Equation (10.4) go to paragraph 10.4.2.3. If future operation is included in the assessment, then an estimate of future corrosion or erosion estimate is required.

3) STEP 3.3 – Determine the nominal stress of the component based on the pressure from STEP 3.1, the wall thickness from STEP 3.2, and the corroded geometry of the component using the construction code equations for wall thickness, i.e., solve for the component nominal stress given the geometry, pressure, and other loads, as applicable (see Annex 2C).

4) STEP 3.4 – Determine the permissible time at temperature, ${}^{n}L$, using the screening curve from STEP 1, temperature from STEP 3.1, nominal stress from STEP 3.3, i.e., enter the screening with temperature and stress and determine the time. Logarithmic interpolation shall be used for points that lie between lines of constant time. If the point defined by the temperature and nominal stress is above the time-independent curve (i.e., black line) in the Screening Curve, go to paragraph 10.4.2.3.

5) STEP 3.5 – Compute the creep damage ${}^{n}D_c$ using Equation (10.5)

$$ {}^{n}D_c = \frac{{}^{n}t}{{}^{n}L} \tag{10.5}$$

d) STEP 4 – Compute the creep damage for total number of operating conditions, N, using Equation (10.6).

$$ D_c^{total} = \sum_{n=1}^{N} {}^{n}D_c \tag{10.6}$$

e) STEP 5 – If the total creep damage determined from STEP 4 satisfies Equation (10.7), then the component is acceptable per the Level 1 Assessment procedure. Otherwise, go to paragraph 10.4.2.3.

$$ D_c^{total} \le 0.80 \tag{10.7}$$

10.4.2.3 If the component does not meet the Level 1 Assessment requirements, then the following, or combinations thereof, can be considered:

a) Rerate, repair, or replace the component.

b) Adjust the future operating condition(s), the corrosion allowance, or both.

c) Conduct a Level 2 or a Level 3 Assessment.

10.4.3 Level 2 Assessment

10.4.3.1 The Level 2 Assessment procedure shall be performed in accordance with paragraph 10.5.2.3. The temperature of the component used in the assessment is assumed to be uniform for each specific time step.

10.4.3.2 If the component does not meet the Level 2 Assessment requirements, then the following, or combinations thereof, can be considered:

a) Rerate, repair, or replace the component.

b) Adjust the future operating conditions, the corrosion allowance, or both; note that this does not apply if $D_c^{total} > D_c^{allow}$ based on the current operating time.

c) Conduct a Level 3 Assessment.

10.4.4 Level 3 Assessment

10.4.4.1 The Level 3 Assessment procedures are covered in paragraph 10.5. Except for the procedure for the evaluation of dissimilar metal welds, these procedures can also be used to evaluate a component containing one or more of the flaws listed in paragraph 10.2.2.1(d). If the flaw is volumetric (i.e., LTA, pitting damage, weld misalignment, out-of-roundness, bulge, dent, or dent-gouge combination), then the stress analysis model used to evaluate the remaining life shall include the flaw so that localized stresses and strains are accounted for. These stress results are then directly used in the assessment. If the component contains a crack-like flaw, then the stress analysis used for remaining life can be based on an uncracked body analysis. The effects of the crack are accounted for in the assessment procedure.

10.4.4.2 If the component does not meet the Level 3 Assessment requirements, then the following, or combinations thereof, can be considered:

a) Rerate, repair, replace, or retire the component.

b) Adjust the future operating conditions, the corrosion allowance, or both; note that this does not apply if $D_c^{total} > D_c^{allow}$ based on the current operating time.

10.5 Remaining Life Assessment

10.5.1 Overview

10.5.1.1 A remaining life calculation is required for all components operating in the creep range. The assessment procedures in paragraph 10.4 are limited to components that are not subject to significant cyclic operation and/or components that do not contain crack-like flaws.

10.5.1.2 The assessment procedures described in this paragraph provide the best estimate of the structural integrity of a component operating at elevated temperature. Five assessment procedures are provided.

a) *Creep Rupture Life* – The assessment procedure is given in paragraph 10.5.2, and is applicable to components that are subject to steady-state operation in the creep range which do not have crack-like flaws.

b) *Creep-Fatigue Interaction* – The assessment procedure is given in paragraph 10.5.2, and is used in conjunction with the information in paragraph 10.5.3. This procedure is applicable to components that are subject to cyclic operation in the creep range which do not have crack-like flaws.

c) *Creep Crack Growth* – The assessment procedure is given in paragraph 10.5.4, and is applicable to components that are subject to either steady-state or cyclic operation in the creep range which contain crack-like flaws.

d) *Creep Buckling* – The assessment procedure is given in paragraph 10.5.5, and can be used to determine the time at which a component in the creep range may be subject to structural instability due to a compressive stress field. The procedure can be used for a component both with and without a crack-like flaw.

e) *Creep-Fatigue Assessment of Dissimilar-Weld Joint* – The assessment procedure is given in paragraph 10.5.6, and is applicable to 2.25Cr–1Mo and 2.25Cr–1Mo-V to austenitic stainless steel dissimilar weld joints made with stainless steel or nickel-based filler metals. This procedure is applicable to components that are subject to cyclic operation in the creep range that do not have crack-like flaws. For other types of dissimilar weld joints or for dissimilar weld joints with crack-like flaws, the procedures described above can be used for the assessment. In these cases, the thermal expansion and creep rate differences between the base materials and the weldment shall be considered in the stress analysis.

f) *Microstructural Approaches* – Because of limited applicability and uncertainty of microstructural approaches, these types of assessments are normally used to supplement other techniques. A description of the recognized microstructural approaches is given in paragraph 10.5.7.

10.5.1.3 The recognized assessment procedures listed below may be used as an alternative to the procedures in paragraph 10.5.1.2. Other assessment procedures may be used if the technology used adequately addresses the damage mechanism, a remaining life can be determined, and adequate documentation is provided that discloses all the assumptions used in the assessment.

a) EDF Energy R-5 (see Part 1, Table 1.1).

b) BS 7910 (see Part 1, Table 1.1).

c) EPRI *Remaining-Life of Boiler Pressure Parts-Crack Growth Studies* (see Annex 10A, reference [8]).

d) WRC Bulletin 440 *A Synthesis of the Fracture Assessment methods Proposed in the French RCC-MR Code for High Temperature* (see Annex 10A, reference [10]).

e) ASME Code, Section III, Division 5 (see Part 1, Table 1.1).

f) VGB-S-517-00-2014-11-DE-EN Guidelines for rating the microstructural composition and creep rupture damage of creep-resistant steel for high pressure pipelines and boiler components and their weld connections (see Annex 10A, reference [29]).

10.5.1.4 A sensitivity analysis, (see Part 2, paragraph 2.4.3.1) should be performed as part of the assessment regardless of the method chosen.

a) The assessment procedures in this Part do not contain recommendations for in-service margins that should be applied to the remaining life calculation. It is recommended that the margin be placed on the remaining life prediction rather than the independent variables of the solution (i.e., time in service, applied stress, temperature, etc.).

b) Remaining life estimates in the creep range are sensitive to materials data, applied stresses, and corresponding temperature. Therefore, sensitivity studies should be performed to evaluate the effects of these variables on the remaining life prediction.

c) Confidence may be gained in the assessment by using a sensitivity analysis when it is possible to demonstrate that small changes in the independent variables do not lead to dramatic reductions in the estimated remaining life of a component. Further confidence is gained when the predictions at the end of an appropriate inspection period indicate that creep damage, or crack growth in the case of a component containing a flaw, is not accelerating in such a way as to lead to imminent failure.

d) Sensitivity analyses should consider the effects of different assumptions on the assessment results. For example, there may be uncertainties in the service loading conditions including temperature and associated

time in-service; the extrapolation of materials data to service conditions; the nature, size, and shape of the crack-like flaw; and other input variables.

10.5.2 Creep Rupture Life

10.5.2.1 The following analysis procedure can be utilized to evaluate a component operating in the creep range using the results from a stress analysis. The assessment is based on the stresses and strains at a point and through the wall thickness in the component, and the associated operating time and temperature. If an inelastic analysis is used to evaluate the effects of creep, then a material model is required to compute the creep strains in the component as a function of stress, temperature, and accumulated creep strain, strain hardening model (see paragraph 10.3.5.3) or time hardening model. If the computed stresses exceed the yield strength of the material at temperature, plasticity should also be included in the material model.

10.5.2.2 The assessment procedure in this paragraph provides a systematic approach for evaluating the creep damage for each operating cycle that is applied to the component. The total creep damage is computed as the sum of the creep damages calculated for each cycle.

10.5.2.3 A procedure to determine the creep damage based upon the results of a stress analysis is shown below. This procedure is based on computation of stresses at discrete times during the load history. The stresses may be based on elastic analysis, or inelastic analysis considering the effects of creep relaxation.

a) STEP 1 – Determine a load history based on past operation and future planned operation. The load history should include all significant operating loads and events that are applied to the component. If there is cyclic operation, the load history should be divided into operating cycles as shown in Figure 10.33. Define M as the total number of operating cycles. Note that it is important that the loading conditions in the history be analyzed in the same order as the actual sequence of operations even if this entails breaking a loading condition into two or more analysis steps.

b) STEP 2 – For the current operating cycle m, determine the total cycle time, ${}^{m}t$, and divide the cycle into a number of time increments, ${}^{n}t$ as shown in Figure 10.34. Define N as the total number of time increments in operating cycle m.

   1) The time increments used to model the operating cycle should be small enough to capture all significant variations in the operating cycle. The smaller the time increment, the more accurate the remaining life predication.

   2) If the component is subject to corrosion or erosion, the time increments should be set small enough to capture changes in the wall thickness.

c) STEP 3 – Determine the wall thickness of the component for the time increment ${}^{n}t$ including the effects of corrosion and erosion. If the wall thickness is less than t_{lim} define by Equation (10.4), go to STEP 13.

d) STEP 4 – Determine the assessment temperature, ${}^{n}T$, for the time increment ${}^{n}t$.

e) STEP 5 – Determine the stress components, ${}^{n}\sigma_{ij}$, for the time increment ${}^{n}t$.

   1) Equations for the principal stresses for cylindrical and spherical shells subject to pressure loading are shown in Table 10.2. Stress calculations for tubes and elbows are discussed in paragraph 10.5.2.5.

   2) The principal stresses can also be computed using a finite element analysis.

f) STEP 6 – Determine if the component has adequate protection against plastic collapse.

1) If the stress components are determined from an elastic analysis, determine the primary load reference stress using Equation (10.8) and check that the criterion in Equation (10.9) or Equation (10.10) is satisfied. The value of the yield strength, σ_{ys} in this equation is evaluated at temperature ${}^{n}T$ at time increment ${}^{n}t$. If the criterion in Equations (10.9) or Equation (10.10) is satisfied, proceed to STEP 7, otherwise, proceed to STEP 13.

$$ {}^{n}\sigma_{ref}^{p} = \frac{{}^{n}P_b + \left({}^{n}P_b^2 + 9 \cdot {}^{n}P_L^2 \right)^{0.5}}{3} \tag{10.8} $$

$$ {}^{n}\sigma_{ref}^{p} \le \sigma_{ys} \qquad \left(for\ austenitic\ stainless\ steels\ \&\ nickel-based\ alloys \right) \tag{10.9} $$

$$ {}^{n}\sigma_{ref}^{p} \le 0.74 \cdot \sigma_{ys} \qquad \left(for\ all\ other\ materials \right) \tag{10.10} $$

2) If the stress components are based on an inelastic analysis that includes plasticity and creep, protection against plastic collapse can be determined by a limit load or plastic collapse solution in accordance with Annex 2D.

g) STEP 7 – Determine the principal stresses, ${}^{n}\sigma_1$, ${}^{n}\sigma_2$, ${}^{n}\sigma_3$ and the effective stress, ${}^{n}\sigma_e$, using Equation (10.11) for the time increment ${}^{n}t$.

$$ {}^{n}\sigma_e = \frac{1}{\sqrt{2}} \left[\left({}^{n}\sigma_1 - {}^{n}\sigma_2 \right)^2 + \left({}^{n}\sigma_1 - {}^{n}\sigma_3 \right)^2 + \left({}^{n}\sigma_2 - {}^{n}\sigma_3 \right)^2 \right]^{0.5} \tag{10.11} $$

h) STEP 8 – Determine a remaining life at the stress level ${}^{n}\sigma_e$ and temperature ${}^{n}T$ for time increment ${}^{n}t$ by utilizing creep rupture data for the material and designate this value as ${}^{n}L$, note that the units of ${}^{n}L$ are in hours.

1) If MPC Project Omega Data are used in the assessment (see Annex 10B) then the time to rupture is given by Equation (10.12). If a weld is being analyzed in a Level 2 Assessment, then $\Delta_{\Omega}^{sr} = -0.5$. In a Level 3 Assessment, an alternate value may be assigned based on the weld material composition and other factors.

$$ {}^{n}L = \frac{1}{\dot{\varepsilon}_{co}\Omega_m} \tag{10.12} $$

where,

$$ \log_{10}\left[\dot{\varepsilon}_{co} \right] = -\left[\left(A_o + \Delta_{\Omega}^{sr} \right) + \left[\frac{A_1 + A_2 S_l + A_3 S_l^2 + A_4 S_l^3}{T_{refa} + {}^{n}T} \right] \right] \tag{10.13} $$

$$ T_{refa} = 460 \qquad \left(for\ {}^{o}F \right) \tag{10.14} $$

$$ T_{refa} = 273 \qquad \left(for\ {}^{o}C \right) \tag{10.15} $$

$$ \Omega_m = \Omega_n^{\delta_{\Omega}+1} + \alpha_{\Omega} \cdot n_{BN} \tag{10.16} $$

$$ \Omega_n = \max\left[\left(\Omega - n_{BN} \right),\ 3.0 \right] \tag{10.17} $$

$$\log_{10}[\Omega] = \left[\left(B_o + \Delta_{\Omega}^{cd} \right) + \left(\frac{B_1 + B_2 S_l + B_3 S_l^2 + B_4 S_l^3}{T_{refa} + {}^{n}T} \right) \right] \tag{10.18}$$

$$\delta_{\Omega} = \beta_{\Omega} \left(\frac{{}^{n}\sigma_1 + {}^{n}\sigma_2 + {}^{n}\sigma_3}{{}^{n}\sigma_e} - 1.0 \right) \tag{10.19}$$

$$n_{BN} = -\left(\frac{A_2 + 2A_3 S_l + 3A_4 S_l^2}{T_{refa} + {}^{n}T} \right) \tag{10.20}$$

$$S_l = \log_{10}\left[{}^{n}\sigma_e \right] \tag{10.21}$$

2) If creep rupture data are provided in terms of the Larson-Miller parameter, (see Annex 10B, paragraph 10B.2.2), then the time to rupture is given by the equation shown below.

$$\log_{10}\left[{}^{n}L \right] = \frac{1000 \cdot LMP({}^{n}S_{eff})}{\left(T_{refa} + {}^{n}T \right)} - C_{LMP} \tag{10.22}$$

where T_{refa} is defined in Equation (10.14) or Equation (10.15),

$${}^{n}S_{eff} = {}^{n}\sigma_e \cdot \exp\left[0.24 \left(\frac{J_1}{S_s} - 1 \right) \right] \tag{10.23}$$

$$J_1 = {}^{n}\sigma_1 + {}^{n}\sigma_2 + {}^{n}\sigma_3 \tag{10.24}$$

$$S_s = \left({}^{n}\sigma_1^2 + {}^{n}\sigma_2^2 + {}^{n}\sigma_3^2 \right)^{0.5} \tag{10.25}$$

3) Other expressions for creep rupture life that is a function of temperature and stress, and stress measures to determine creep damage, i.e., effective stress, may be used for specific materials if test results or documentation is available.

4) Note that the in-service margin in the remaining life assessment is introduced when determining the time to rupture based on material data, ${}^{n}L$. If MPC Project Omega Data are used in the assessment per subparagraph 1) above, then the time to rupture may be adjusted using the Δ_{Ω}^{sr} and Δ_{Ω}^{cd} to model minimum or expected time to rupture. If creep rupture data are provided in terms of the Larson-Miller parameter per subparagraph 2) above, then the minimum or average time to rupture may be used. If other expressions for creep rupture are used in the assessment per subparagraph 3) above, then appropriate margins shall be assigned based on the material model.

i) STEP 9 – Repeat STEPs 3 through 8 for each time increment ${}^{n}t$ in the m^{th} operating cycle to determine the rupture time, ${}^{n}L$, for each increment.

j) STEP 10 – Compute the accumulated creep damage for all points in the m^{th} cycle using Equation (10.26). In this equation, ${}^{n}t$ is defined as the time increment where the component is subject to a stress level ${}^{n}\sigma_e$ at a corresponding operating temperature ${}^{n}T$, and ${}^{n}L$ is the permissible life at this temperature based on material data.

$${}^{m}D_c = \sum_{n=1}^{N} \frac{{}^{n}t}{{}^{n}L} \tag{10.26}$$

k) STEP 11 – Repeat STEPs 2 through 10 for each of the operating cycles defined in STEP 1.

l) STEP 12 – Compute the total creep damage for all cycles of operation.

$$D_c^{total} = \sum_{m=1}^{M} {}^{m}D_c \le D_c^{allow} \tag{10.27}$$

m) STEP 13 – The creep damage prediction is complete for this location in the component. The allowable creep damage in Equation (10.28) may be used unless an alternative value can be justified.

$$D_c^{allow} = 1.0 \tag{10.28}$$

1) If the minimum wall thickness criterion is not satisfied then the component is not acceptable for continued operation, refer to paragraph 10.4.3.2 or 10.4.4.2, as applicable, for recommended actions.

2) If the criterion for protection against plastic collapse for any point in the operating history is not satisfied, then the component is not acceptable for continued operation, refer to paragraph 10.4.3.2 or 10.4.4.2, as applicable, for recommended actions.

3) If the total creep damage, D_c^{total}, is less than or equal to the allowable creep damage, D_c^{allow}, then the component is acceptable for continued operation. The remaining life for operation is determined by analyzing additional load cycles and determining the time when $D_c^{total} = D_c^{allow}$.

4) If the total creep damage, D_c^{total}, is greater than the allowable creep damage, D_c^{allow}, then the life of the component is limited to the time corresponding to $D_c^{total} = D_c^{allow}$. If this time is less than the current operating time refer to paragraph 10.4.3.2 or 10.4.4.2, as applicable, for recommended actions.

n) STEP 14 – In addition to satisfying the damage criterion in STEP 13, if the stress components are based on an inelastic analysis that includes plasticity and creep, a limit on the total accumulated inelastic strains should be set to a value that will not limit the operability of the component. The suggested limits for the accumulated strains are given in Table 10.3.

10.5.2.4 As an alternative to the procedure in paragraph 10.5.2.3, an inelastic analysis including the effects of creep may be performed based on the procedure shown below. This procedure is defined in terms of integral equations as opposed to the discrete steps provided in the procedure of paragraph 10.5.2.3. The integral equation procedure is more suitable for implementation into numerical software that provide user subroutine support for creep modeling.

a) The inelastic analysis shall be based on the history defined in paragraph 10.5.2.3(a) using one of the Options shown below.

1) Option 1 – Protection against ratcheting may be demonstrated using an elastic analysis in lieu of an inelastic analysis. To evaluate protection against ratcheting, the following limit shall be satisfied.

$$P_L + P_b + Q \le \left(S_h + S_{yc}\right) \tag{10.29}$$

2) Option 2 – An approximate ratcheting analysis may be performed, based on establishing elastic shakedown at all points in the structure. If this option is chosen, a conservative load history shall be used based on the most extreme conditions of stress and temperature. A minimum of two complete cycles shall be computed, including a hold time of a minimum of one year, for the purpose of establishing the effects of creep relaxation. During the last computed cycle, a state of linear elasticity must be demonstrated throughout the cycle. If this criterion is not achieved, a full inelastic analysis using the

actual time dependent thermal and mechanical loading histories shall be performed as per Option 3 below.

3) Option 3 – If it is elected not to perform a simplified analysis as per Option 1 or 2, or if such an analysis is carried out and fails to demonstrate elastic shakedown according to the criterion stated in Option 1 or 2, then a full inelastic analysis shall be performed using the actual time dependent thermal and mechanical loading histories, including all operating cycles and their associated hold times. This analysis shall be continued for all cycles defined in the load history including their associated hold times. This analysis may demonstrate shakedown to a stable state, or a steady ratchet deformation. In either case, the strain limits in paragraph g) below shall be satisfied.

b) In Options 1 and 2, a simplified history may be used if elastic action is demonstrated throughout the cycle for the most serve loading condition. If this condition cannot be satisfied, Option 3 is provided which requires a complete inelastic analysis of a load history. In Option 3, the complete history is analyzed using inelastic analysis to evaluate creep damage and the total accumulated inelastic strains. An elastic-perfectly-plastic stress-strain curve is used for the stabilized cyclic stress-strain curve, which will produce a conservative result for plastic strains. Shakedown is not required because a limit is placed on total accumulated inelastic strains, similar to ASME Section III, Subsection NH, paragraph T1310.

c) Unless specific data are available, an elastic-perfectly plastic stress-strain curve using the yield strength at the operating temperature and the following creep rate shall be used in the inelastic analysis. The strain rate to be used in the inelastic analysis, i.e. creep model shall be determined using Equations (10.30) through (10.42).

$$\dot{\varepsilon}_c = \frac{\dot{\varepsilon}_{oc}}{1 - D_c} \tag{10.30}$$

$$\log_{10}\left[\dot{\varepsilon}_{oc}\right] = -\left[\left(A_o + \Delta_{\Omega}^{sr}\right) + \left(\frac{A_1 + A_2 S_l + A_3 S_l^2 + A_4 S_l^3}{T_{refa} + T}\right)\right] \tag{10.31}$$

$$T_{refa} = 460 \qquad \left(for\ \ ^{o}F\right) \tag{10.32}$$

$$T_{refa} = 273 \qquad \left(for\ \ ^{o}C\right) \tag{10.33}$$

$$S_l = \log_{10}\left[\sigma_e\right] \tag{10.34}$$

$$\sigma_e = \frac{1}{\sqrt{2}}\left[\left(\sigma_1 - \sigma_2\right)^2 + \left(\sigma_1 - \sigma_3\right)^2 + \left(\sigma_2 - \sigma_3\right)^2\right]^{0.5} \tag{10.35}$$

$$D_c = \int_0^t \dot{D}_c dt \le 1.0 \tag{10.36}$$

$$\dot{D}_c = \Omega_m \cdot \dot{\varepsilon}_{oc} \tag{10.37}$$

$$\Omega_m = \Omega_n^{\delta_{\Omega}+1} \tag{10.38}$$

$$\Omega_n = \max\left[\left(\Omega - n_{BN}\right),\ 3.0\right] \tag{10.39}$$

$$\log_{10}[\Omega] = \left[\left(B_o + \Delta_{\Omega}^{cd} \right) + \left(\frac{B_1 + B_2 S_l + B_3 S_l^2 + B_4 S_l^3}{T_{refa} + T} \right) \right] \tag{10.40}$$

$$n_{BN} = -\left(\frac{A_2 + 2A_3 S_l + 3A_4 S_l^2}{T_{refa} + T} \right) \tag{10.41}$$

$$\delta_{\Omega} = \beta_{\Omega} \left(\frac{\sigma_1 + \sigma_2 + \sigma_3}{\sigma_e} - 1.0 \right) \tag{10.42}$$

d) Primary creep is not included in the model described above. Primary creep at the effective stresses typically associated with construction code designs is extremely small and does not contribute to life shortening creep damage in a significant way. In addition, at high stresses, the Omega model, while not treating primary behavior explicitly does predict accelerated creep rates and assigns damage to the relaxation associated with this creep. This treatment of relaxation is more conservative than letting primary creep relax without damage. It is recognized that high principal stresses occur at discontinuities. For these multiaxial situations, the effective stresses are reduced, and significant primary creep does not occur.

e) Inelastic analysis is required to be performed, for selected locations experiencing the most extreme conditions of stress and temperature, to determine the creep life. Sufficient locations are required to be selected for analysis to ensure that the most critical conditions have been considered. The creep life is defined as the time in which the inelastic analysis produces an accumulated creep damage such that $D_c \approx D_c^{allow}$ where D_c^{allow} is given by Equation (10.28). The remaining life is defined as the creep life minus the time in actual operation.

f) Strains at local discontinuities are accounted for in the inelastic analysis, the creep damage calculation, and the creep-fatigue calculation. The shakedown requirement essentially ensures small plastic strains during fatigue, and this requirement is imposed at a point.

g) Based on the time, temperature, and load history and the results of the inelastic analysis, the following criteria are required to be satisfied.

1) The creep damage at all locations shall be such that $D_c \leq D_c^{allow}$ where D_c^{allow} is given by Equation (10.28).

2) The equivalent total accumulated inelastic strain should not exceed the values shown in Table 10.3.

3) For materials with a specified minimum yield strength of greater than 345 MPa (50 ksi), the creep damage in weldments and adjacent base material located within a distance of 25 mm (1 inch) measured from the weld bevel should be $D_c = D_c^{allow}/2$ where D_c^{allow} is given by Equation (10.28). This supplemental check for weldments and adjacent base material is recommended for high strength materials because compliance with the total accumulated strain criterion in (2) above is not sufficient to preclude failure from creep damage.

10.5.2.5 Fired heater and boiler tubes may be evaluated as a special case of the procedure in paragraph 10.5.2.3 if the pressure is approximately constant and temperature is approximately uniform around the circumference of the tube during operation.

a) *Stress Calculations* – recommendations for stress calculations are shown below.

1) Thin Wall Tubes and Elbows Subject to Pressure and Supplemental Loads – For thin wall heater tubes with an outside diameter to thickness ratio greater than six, the thin wall equations for a cylinder based on the mean diameter in Table 10.2 may be used in the assessment. The creep rupture life, life fraction, and cumulative life fraction are evaluated at the equivalent stress. For a straight section of tube, the Lorenz factor is equal to 1.0. The term t_{sl} can be set to zero if the longitudinal stress due to supplementary loads, e.g., weight, is negligible. The resulting stress components for these conditions for the n^{th} operating period are shown below.

$$ {}^{n}\sigma_1 = {}^{n}\sigma_{mean} = \frac{PD_{mean}}{2t_{comp}} \tag{10.43} $$

$$ {}^{n}\sigma_2 = 0.5 \cdot {}^{n}\sigma_{mean} \tag{10.44} $$

$$ {}^{n}\sigma_3 = 0.0 \tag{10.45} $$

$$ {}^{n}\sigma_e = 0.866 \cdot {}^{n}\sigma_{mean} \tag{10.46} $$

2) Thin or Thick Wall Tubes Subject to Pressure – For thin or thick wall heater, the reference stress solutions in Table 10.2 may be used in the assessment. The creep rupture life, life fraction, and cumulative life fraction are evaluated at the reference stress.

3) Thick Wall Tube and Elbow Subject to Pressure – For thick wall heater tubes with an outside diameter to thickness ratio less than six, the steady-state creep solutions in Table 10.2 may be used in the assessment. The creep rupture life, life fraction, and cumulative life fraction are evaluated at the equivalent stress that is computed at the outer diameter, mid-wall, and inner diameter by setting the variable r to R_o, R_{mean}, and R_i, respectively. A realistic value of the Bailey-Norton coefficient n_{BN} shall be used in the stress calculation. This coefficient is a function of the material type, stress, and temperature. An approach that can be used in the stress calculation to arrive at a suitable Bailey-Norton coefficient is to assume a value for n_{BN}, compute σ_1, σ_2, and σ_3, and iterate until a converged value of n_{BN} is obtain using Equation (10.20). Note that although the stresses at the inner surface are typically higher than those at the outside surface, the metal temperature at the outside surface may be higher, and this may result in a corresponding higher value of creep damage on the outside surface. An alternate reasonable approach that can be used is to compute the stress at the mid-wall location and use the outer wall tube metal temperature in the creep damage calculation.

b) *Determination of Rupture Life* – After the stress components for the n^{th} operating period are computed, the corresponding rupture life, ${}^{n}L$, can be obtained using the MPC Project Omega Method or the Larson-Miller based method (see paragraph 10.5.2.3(g)). In the Larson-Miller method, if a thin wall tube is subject to only internal pressure, then the stress for the tube for the n^{th} operating period given by Equation (10.47) reduces to:

$$ {}^{n}S_{eff} = 0.94 \cdot {}^{n}\sigma_{mean} \tag{10.47} $$

c) *Life Fraction* – After the rupture life ${}^{n}L$ for the n^{th} operating period are computed, the life faction for time period n^{th} is determined using Equation (10.48).

$$ {}^{n}D_c = \frac{{}^{n}t}{{}^{n}L} \tag{10.48} $$

d) *Cumulative Life Fraction* The tube life is assumed to be consumed when the cumulative life fraction used for all operating period exceeds D_c^{allow}, where D_c^{allow} is given by Equation (10.28). Note that this is similar to the procedure currently used in API Std 530.

$$D_c^{total} = \sum_{n=1}^{N} {}^{n}D_c \le D_c^{allow} \tag{10.49}$$

10.5.3 Creep-Fatigue Interaction

10.5.3.1 If there are significant cyclic operations during the operating period, then the effects of combined creep and fatigue damage shall be evaluated. The combination of creep and fatigue damage may be evaluated using the following procedure.

a) STEP 1 – Evaluate the creep and fatigue damage independently. If the assessment procedure in paragraph 10.5.2 is used to evaluate the creep part of the damage, then Equation (10.50) shall be used for the creep damage. If the assessment procedure in Part 14 is used, then Equation (10.51) shall be used for the fatigue damage.

$$D_c = \sum_{m=1}^{M} {}^{m}D_c \tag{10.50}$$

$$D_f = \sum_{m=1}^{M} \frac{{}^{m}n}{{}^{m}N} \tag{10.51}$$

b) STEP 2 – Determine the acceptable material envelope for creep-fatigue damage based on Figure 10.35 and the material of construction.

c) STEP 3 – Plot the point defined by D_f and D_c calculated in STEP 1 on Figure 10.35 based on the applicable acceptable material envelope for creep-fatigue damage developed in STEP 2. If the point lies on or below the envelope, the component is acceptable for continued operation. If the point lies outside of the envelope, the component is unacceptable for continued operation.

d) STEP 4 – In addition to satisfying the damage criterion in paragraph 10.5.3.1, a limit on the total accumulated inelastic strains should be set to a value that will not limit the operability of the component (see paragraph 10.5.2.3(m)).

10.5.3.2 In lieu of the procedure given in paragraph 10.5.3.1, ASME Code Case 2605 may be used to evaluate creep-fatigue damage for components constructed from 2.25Cr-1Mo-V.

10.5.4 Creep Crack Growth

10.5.4.1 The following analysis procedure can be utilized to evaluate a component operating in the creep range with a crack-like flaw using the results from a stress analysis. The assessment is based on the stresses and strains at a point and through the wall thickness in the component, and the associated operating time and temperature. If an inelastic analysis is used to evaluate the effects of creep, then a material model is required to compute the creep strains in the component as a function of stress, temperature, and accumulated creep strain, strain hardening model (see paragraph 10.3.5.3) or time hardening model. If the computed stresses exceed the yield strength of the material at temperature, plasticity should also be included in the material model.

10.5.4.2 A procedure to determine creep crack growth based upon the results of a stress analysis is shown below.

a) STEP 1 – Determine a load history based on past operation and future planned operation. The load history should include all significant operating loads and events that are applied to the component. If there is cyclic operation, the load history should be divided into operating cycles. Note that it is important that the loading conditions in the history be analyzed in the same order as the actual sequence of operations even if this entails breaking a loading condition into two of more analysis steps.

b) STEP 2 – Determine the material properties; yield strength, tensile strength, Young's Modulus, fracture toughness (see Part 9, paragraph 9.3.5), and creep properties (see Annex 10B). The yield and tensile strength should be established using nominal values, i.e., minimum specified per the material specification if actual values are unknown, and the toughness should be based on the mean value (see Part 9, Table 9.2, Note 6).

c) STEP 3 – Determine the past damage in the material ahead of the crack prior to cracking, D_{bc}. During this time period, it has been verified that a crack was not present.

1) If the component is not in cyclic operation, then the damage prior to cracking is the creep damage computed using the procedure in paragraph 10.5.2. The creep damage is computed using Equation (10.52) where M_{bc} is the total number of operating cycles before the onset of cracking.

$$D_{bc} = \sum_{m=1}^{M_{bc}} {}^{m}D_{c} \tag{10.52}$$

2) If the component is subject to cyclic operation, then the damage prior to cracking is the creep-fatigue damage computed using the procedure in paragraph 10.5.2 in conjunction with paragraph 10.5.3.1. The creep-fatigue damage is computed using Equation (10.53) where M_{bc} is the total number of operating cycles before the onset of cracking.

$$D_{bc} = \sum_{m=1}^{M_{bc}} {}^{m}D_{c} + \sum_{m=1}^{M_{bc}} \frac{{}^{m}n}{{}^{m}N} \tag{10.53}$$

d) STEP 4 – Determine the past damage, in the material ahead of the crack for the period corresponding to the last time it was verified that a crack was not present and the time that the crack was found. The damage, ${}^{0}D_{ac}$,is calculated with a crack present during this entire period as follows.

1) Determine the crack-like flaw dimensions from inspection data and designate these values, a_0 and c_0. The crack-like flaw should be categorized using the procedure in Part 9, paragraph 9.3.6.2.

2) The creep damage ahead of the crack, ${}^{0}D_{ac}$, for the time period is computed using the procedure in paragraph 10.5.2 with the following modification:

i) The reference stress, ${}^{n}\sigma_{ref}^{P}$, in STEP 5 of paragraph 10.5.2.3 is determined using Annex 9C based on the crack-like flaw dimensions a_0 and c_0, and the stress distribution for time increment ${}^{n}t$.

ii) If the MPC Project Omega Creep Data are used for the determination of the remaining life for time increment ${}^{n}t$, then Equation (10.21) is replaced by Equation (10.54).

$$S_l = \log_{10}\left[{}^{n}\sigma_{ref}^{P}\right] \tag{10.54}$$

iii) The creep damage is computed using Equation (10.55) where M_{ac} is the total number of operating cycles for this period of time.

$$ {}^{0}D_{ac} = \sum_{m=1}^{M_{ac}} {}^{m}D_{c} \tag{10.55} $$

e) STEP 5 – Initialize the initial flaw dimension sizes and the starting time for the cycle:

$$ {}^{i=1}a = a_o \tag{10.56} $$

$$ {}^{i=1}c = c_o \tag{10.57} $$

$$ {}^{i=0}t = 0.0 \tag{10.58} $$

f) STEP 6 – For the current operating cycle m, determine the total cycle time, ${}^{m}t$, and divide the cycle into several time periods. Designate the time at the end of each time period ${}^{i}t$. Note that sufficient time periods should be evaluated based on the loading history, and the desired accuracy of the final results. A sensitivity analysis may need to be performed to evaluate the number of time periods required to achieve the desired accuracy.

g) STEP 7 – Determine the temperature, ${}^{i}T$, and compute the stress components ${}^{i}\sigma_{ij}$ through the wall of the component containing the crack-like flaw at time ${}^{i}t$.

h) STEP 8 – Determine the reference stress, ${}^{i}\sigma_{ref}$, at time ${}^{i}t$ using Annex 9C based on the crack-like flaw dimensions ${}^{i}a$ and ${}^{i}c$, and the corresponding stress distribution.

i) STEP 9 – Determine if the components have adequate protection against plastic collapse. If the criterion in Equation (10.9) or Equation (10.10) is satisfied, then proceed to STEP 10, otherwise proceed to STEP 22.

j) STEP 10 – Perform a FAD Assessment at time ${}^{i}t$ using the procedures in Part 9 based on the crack-like flaw dimensions ${}^{i}a$ and ${}^{i}c$, and the corresponding stress and temperature distribution. If the resulting FAD point is outside of the FAD failure envelope, go to STEP 22; otherwise, go to STEP 11. Note that the FAD Assessment at elevated temperatures will essentially result in a plastic collapse check because the fracture toughness will be on the upper shelf. However, at lower temperatures in the history, unstable crack growth may occur because of a reduction in the material fracture toughness.

k) STEP 11 – Determine the damage in the material ahead of the crack, ${}^{i}D_{ac}$, at time ${}^{i}t$ based on the crack-like flaw dimensions ${}^{i}a$ and ${}^{i}c$, and the corresponding stress and temperature distribution.

$$ {}^{i}D_{ac} = {}^{i-1}D_{ac} + \frac{\left({}^{i}t - {}^{i-1}t\right)}{{}^{i}L_{ac}} \tag{10.59} $$

1) If MPC Project Omega Creep Data are used in the assessment, then ${}^{i}L_{ac}$ is evaluated using Equation (10.60) where the parameters Ω_m and $\dot{\varepsilon}_{co}$ are determined using Equations (10.13) through (10.21) with S_l given by Equation (10.61).

$$ {}^{i}L_{ac} = \frac{1}{\Omega_m \dot{\varepsilon}_{co}} \tag{10.60} $$

$$ S_l = \log_{10}\left[{}^{i}\sigma_{ref}\right] \tag{10.61} $$

2) If creep rupture data are provided in terms of the Larson-Miller parameter (see Annex 10B) then ${}^{i}L_{ac}$ can be computed using Equation (10.22). Other expressions for creep rupture data that are a function of time and stress level may also be used.

l) STEP 12 – Determine if the damage ahead of the crack is acceptable. The allowable creep damage in Equation (10.28) may be used unless an alternative value can be justified. If the criterion in Equation (10.62) is satisfied, then proceed to STEP 13, otherwise proceed to STEP 22.

$$D_{bc} + {}^{i}D_{ac} \le D_c^{allow} \tag{10.62}$$

m) STEP 13 – Determine the reference strain rate, ${}^{i}\dot{\varepsilon}_{ref}$, at time ${}^{i}t$ based on the crack-like flaw dimensions, ${}^{i}a$ and ${}^{i}c$, and the corresponding stress and temperature distribution using Equation (10.13) evaluated at the reference stress, or $S_l = \log_{10}[\,{}^{i}\sigma_{ref}]$.

n) STEP 14 – Determine the stress intensity factor at the deepest point, $K_I^{90}({}^{i}a,\ {}^{i}c)$, and surface point, $K_I^{0}({}^{i}a,\ {}^{i}c)$, of the flaw at time ${}^{i}t$ based on the crack-like flaw dimensions ${}^{i}a$ and ${}^{i}c$, and the corresponding stress and temperature distribution using Annex 9B.

o) STEP 15 – Determine the crack driving force at the deepest point, $C_t^{90}({}^{i}a,\ {}^{i}c)$, and surface point, $C_t^{0}({}^{i}a,\ {}^{i}c)$, of the flaw at time ${}^{i}t$ based on the crack-like flaw dimensions ${}^{i}a$ and ${}^{i}c$, and the corresponding stress and temperature distribution using the equations shown below.

$$C_t^{90}({}^{i}a,{}^{i}c) = C^{*90}({}^{i}a,{}^{i}c)\cdot\left[\left(\frac{t_{relax}^{90}({}^{i}a,{}^{i}c)}{{}^{i}t}\right)^{\left(\frac{n_{BN}-3}{n_{BN}-1}\right)}+1\right] \tag{10.63}$$

$$C^{*90}({}^{i}a,{}^{i}c) = \left(\frac{{}^{i}\dot{\varepsilon}_{ref}}{1-D_{bc}-{}^{i}D_{ac}}\right)\frac{\left(K_I^{90}({}^{i}a,{}^{i}c)\right)^2}{{}^{i}\sigma_{ref}} \tag{10.64}$$

$$t_{relax}^{90}({}^{i}a,{}^{i}c) = \frac{0.91\cdot\left(K_I^{90}({}^{i}a,{}^{i}c)\right)^2}{(n_{BN}+1)\cdot E_y\cdot C^{*90}({}^{i}a,{}^{i}c)} \tag{10.65}$$

$$C_t^{0}({}^{i}a,{}^{i}c) = C^{*0}({}^{i}a,{}^{i}c)\cdot\left[\left(\frac{t_{relax}^{0}({}^{i}a,{}^{i}c)}{{}^{i}t}\right)^{\left(\frac{n_{BN}-3}{n_{BN}-1}\right)}+1\right] \tag{10.66}$$

$$C^{*0}({}^{i}a,{}^{i}c) = \left(\frac{{}^{i}\dot{\varepsilon}_{ref}}{1-D_{bc}-{}^{i}D_{ac}}\right)\frac{\left(K_I^{0}({}^{i}a,{}^{i}c)\right)^2}{{}^{i}\sigma_{ref}} \tag{10.67}$$

$$t_{relax}^{0}({}^{i}a,{}^{i}c) = \frac{0.91\cdot\left(K_I^{0}({}^{i}a,{}^{i}c)\right)^2}{(n_{BN}+1)\cdot E_y\cdot C^{*0}({}^{i}a,{}^{i}c)} \tag{10.68}$$

p) STEP 16 – Compute the crack growth rates at time ${}^{i}t$ using Equations (10.69) and (10.70) based on the crack-like flaw dimensions ${}^{i}a$ and ${}^{i}c$, and the corresponding stress and temperature distribution.

$$\frac{{}^{i}da}{dt} = H_c\cdot\left(C_t^{90}({}^{i}a,{}^{i}c)\right)^{\mu} \tag{10.69}$$

$$\frac{{}^{i}dc}{dt} = H_c \cdot \left(C_t^0 ({}^{i}a, {}^{i}c) \right)^{\mu} \tag{10.70}$$

1) If MPC Project Omega creep data are used in the assessment, the constants for the creep crack growth equation are given by Equations (10.71) and (10.72). The units of measure for use in these equations are in, ksi, and °F, the corresponding crack growth rate is computed in in/hr. In Equations (10.71) and (10.72) the parameters Ω and n_{BN} are evaluated using Equation (10.18) and (10.20), respectively, with S_l computed using Equation (10.61).

$$H_c = \frac{\Omega}{500} \tag{10.71}$$

$$\mu = \frac{n_{BN}}{n_{BN} + 1} \tag{10.72}$$

2) Alternatively, the constants for the creep crack growth equations used in Equations (10.69) and (10.70) can be determined using Annex 10B.

q) STEP 17 – Compute the time step for integration at time t_i using Equation (10.73). An explicit time integration algorithm is used in this procedure. A suggested value for the explicit time integration parameter is $C_{intg} = 0.005$. A different value may be used based on the specific application. A sensitivity analysis should be used to qualify this value because it is a function of the creep strain rate and crack driving force.

$$\Delta t = \frac{C_{intg} \cdot t_c}{\max\left[\frac{{}^{i}da}{dt}, \frac{{}^{i}dc}{dt} \right]} \tag{10.73}$$

r) STEP 18 – Update the flaw dimensions ${}^{i}a$ and ${}^{i}c$, and the accumulated time in the cycle, ${}^{i}t$.

$${}^{i}a = {}^{i}a + \frac{{}^{i}da}{dt} \cdot \Delta t \tag{10.74}$$

$${}^{i}c = {}^{i}c + \frac{{}^{i}dc}{dt} \cdot \Delta t \tag{10.75}$$

$${}^{i}t = {}^{i}t + \Delta t \tag{10.76}$$

s) STEP 19 – If the current time in the cycle is less than the total time of the cycle, ${}^{i}t < {}^{m}t$, then go to STEP 5 to continue to grow the crack. Otherwise, proceed to STEP 20.

t) STEP 20 – If the component is subject to cyclic loading, then increment the crack size to account for crack growth from fatigue using the equations shown below. Otherwise, proceed to STEP 21.

$${}^{i}a = {}^{i}a + \frac{{}^{m}da}{dN} \tag{10.77}$$

$${}^{i}c = {}^{i}c + \frac{{}^{m}dc}{dN} \tag{10.78}$$

where,

$$\frac{^{m}da}{dN} = H_f \cdot \left({}^{m}\Delta K_{eff}^{90} \cdot \frac{E_{amb}}{E_T} \right)^{\lambda} \tag{10.79}$$

$${}^{m}\Delta K_{eff}^{90} = q_0 \cdot \left({}^{m}K_{I,\max}^{90} - {}^{m}K_{I,\min}^{90} \right) \tag{10.80}$$

$$\frac{^{m}dc}{dN} = H_f \cdot \left({}^{m}\Delta K_{eff}^{0} \cdot \frac{E_{amb}}{E_T} \right)^{\lambda} \tag{10.81}$$

$${}^{m}\Delta K_{eff}^{0} = q_0 \cdot \left({}^{m}K_{I,\max}^{0} - {}^{m}K_{I,\min}^{0} \right) \tag{10.82}$$

The parameter, q_0, is computed using the following equations where $K_{I,\min}$ and $K_{I,\max}$ are evaluated at the $0°$ and $90°$ positions, respectively. The effects of the R-ratio on crack growth given by Equation (10.85) may also be evaluated using an alternative method based on the applicability and availability of crack growth models.

$$q_0 = 1 \qquad R \geq 0 \tag{10.83}$$

$$q_0 = \frac{1 - 0.5R}{1 - R} \qquad R \leq 0 \tag{10.84}$$

where,

$$R = \frac{K_{I,\min}}{K_{I,\max}} \tag{10.85}$$

u) STEP 21 – If this is the last cycle in the history, go to STEP 22. Otherwise, go to STEP 6 to continue to grow the crack based on the next cycle of operation.

v) STEP 22 – The crack growth prediction is complete for a location in the component. If another location is to be evaluated, go to STEP 3. If this is the last location in the component, evaluate the crack growth results.

1) If the points on the FAD predicted during crack growth are all within the FAD failure envelope, protection against plastic collapse is adequate, and the damage ahead of the crack is acceptable, then the component with the crack-like flaw is acceptable for future operation. The remaining life shall be determined by analyzing additional load cycles and determining the minimum time at which the FAD Assessment point lies on the FAD envelope, the protection against plastic collapse is no longer adequate, or the damage ahead of the crack becomes unacceptable.

2) If protection against plastic collapse is not adequate, the damage ahead of the crack is unacceptable, or a point on the FAD predicted during crack growth lies on or outside the FAD failure envelope, then the life of the component is limited to the minimum time corresponding to these criteria. If this time is less than the current operating time, the component should be repaired or replaced.

10.5.5 Creep Buckling

10.5.5.1 The in-service margin for protection against collapse from buckling shall be satisfied to avoid buckling of components with a compressive stress field under applied design loads.

a) Time-Independent Buckling – Time-Independent Buckling shall be evaluated in accordance with Annex 2D.

b) Time-Dependent Buckling – To protect against load-controlled creep buckling, it shall be demonstrated that instability does not occur within the total operational time for a load history obtained by multiplying the specified loadings in paragraph 10.3.3.2 by an in-service margin equal to 1.5. An in-service margin of 1.0 may be used for purely strain-controlled buckling because strain-controlled loads are reduced concurrently with resistance of the structure to buckling when creep is significant.

1) Load-controlled buckling is characterized by continued application of an applied load in the post-buckling regime, leading to failure, e.g., collapse of a tube under external pressure. Strain-controlled buckling is characterized by the immediate reduction of strain induced load upon initiation of buckling, and by the self-limiting nature of the resulting deformations. The in-service margin applicable to load-controlled buckling shall be used for the combination of load-controlled and strain-controlled loads for conditions under which load-controlled and strain-controlled buckling interact or significant elastic follow-up occurs.

2) The effects of original fabrication tolerances, geometrical imperfections, and other flaw types, as applicable, shall be considered in determining the critical buckling time.

3) Material properties that may be used in the calculation including isochronous stress-strain curves are provided in Annex 10B.

4) If a numerical analysis is performed to determine the buckling load for a component, all possible buckling mode shapes shall be considered in determining the minimum buckling load for the component (see Annex 2D).

10.5.5.2 The rules for external pressure and compressive stress design in Annex 2B may be used if the strain rate computed using Equation (10.86) based on the membrane stress for the most severe combination of applied loads that results in compressive stress and a value of $D_c = 0.25$ satisfy Equation (10.86). Note that satisfaction of this equation implies minimal creep at the imposed stress and temperature condition being evaluated. Therefore, the time-independent rules for external pressure and compressive stress evaluation may be used directly.

$$\dot{\varepsilon}_c \le 3(10)^{-8}\frac{1}{hr} \tag{10.86}$$

10.5.5.3 The following analysis method may be used to estimate the critical time for creep buckling in the creep range. The cylindrical shell cannot contain a major structural discontinuity. If the cylindrical shell contains a major structural discontinuity, then the critical time should be determined using a numerical analysis similar to that described in paragraph 10.5.5.1. In addition, the stress at the applied load adjusted by the in-service margin should be less than 50% of the minimum specified yield strength at the assessment temperature. If the stress is above this value, then primary creep may be a concern and the critical time for creep buckling may be underestimated.

a) The critical time for creep buckling for components subject to a constant loading condition and temperature can be determined using the following procedure.

1) STEP 1 – Based on the loading history, determine the applied loads, P^L or σ_e^L, and temperature, T, for the assessment.

2) STEP 2 – Determine the elastic buckling load, P^{cr}, based on the applied loading condition including the effects of imperfections, for example see Annex 2D. If the buckling load is a function of more than one load type, e.g., pressure and applied axial force, then compute the stress components and effective stress, σ_e^{cr}, for all the load types at the critical buckling load.

3) STEP 3 – Multiply all loads in the applied loading condition by an in-service margin equal to 1.5 and determine the stress components and effective stress, σ_e.

4) STEP 4 – Determine the effective critical creep strain at the onset of elastic-plastic buckling.

$$\varepsilon_{ce}^{cr} = \frac{\sigma_e}{E_y} \cdot \frac{2(1+\nu)}{3} \cdot (Q-1) \tag{10.87}$$

where,

$$Q = \frac{P^{cr}}{P^{L}} \tag{10.88}$$

or depending on the applied loads,

$$Q = \frac{\sigma_e^{cr}}{\sigma_e} \tag{10.89}$$

5) STEP 5 – Determine the critical time for creep buckling using Equation (10.90). The parameters Ω_m and $\dot{\varepsilon}_{co}$ in Equation (10.90) are evaluated using Equations (10.13) through (10.21), and Equation (10.11).

$$t^{cr} = \frac{1-\exp\left[-\varepsilon_{ce}^{cr}\Omega_m\right]}{\dot{\varepsilon}_{co}\Omega_m} \tag{10.90}$$

b) The critical time for creep buckling for components subject to varying loads and temperatures can be estimated using the procedure described in paragraph 10.5.5.3(a) for each loading period and the equation shown below. Note that in this equation, the critical time for creep buckling is implicitly defined and can be determined by an iterative procedure.

$$\int_{o}^{t^{cr}} \frac{\varepsilon_{ce}^{cr}\left(P^{L}(t), T(t)\right)}{t^{cr}\left(P^{L}(t), T(t)\right)} dt = \varepsilon_{ce}^{cr}\left(P^{L}(t^{cr}),\ T(t^{cr})\right) \tag{10.91}$$

10.5.5.4 In lieu of the procedure in paragraph 10.5.5.3, the critical time for creep buckling may be estimated by using the allowable compressive stress rules in Annex 2D with a time-dependent tangent modulus evaluated using Annex 10B. This assessment is considered to be a conservative estimate of the time for creep buckling because the compressive stress rules in Annex 2D account for imperfections.

10.5.6 Creep-Fatigue Assessment of Ferritic-Austenitic Dissimilar Weld Joints

10.5.6.1 The metallurgical characteristics of the damage observed in both service and laboratory test samples indicate that creep rupture is the dominant failure mode for Dissimilar Metal Welds (DMW). However, it has also been observed that temperature cycling contributes significantly to damage and can cause failure even when primary stress levels are relatively low. Therefore, a creep-fatigue assessment procedure is required as part of a remaining life calculation. In the assessment of DMW, a creep-fatigue interaction equation is provided to evaluate damage caused by thermal mismatch, sustained primary stresses, and cyclic secondary loads.

10.5.6.2 The damage mechanism of concern is creep damage in the Heat-Affected Zone (HAZ) on the ferritic steel side of the DMW. Damage in this region is expected to occur first because the creep resistance of the material, at the temperatures of interest, is much lower than that of the austenitic base metal or the commonly used filler metals, i.e., stainless steel or nickel-based. The general macroscopic appearance of many failures

suggests that failure occurs by a relatively low ductility process and the final fracture surface may show evidence of the weld bead contours. However, detailed examination has shown that failure can occur by one of the following two modes of damage.

a) Mode I – Inter-granular cracking which occurs along prior austenite grain boundaries within the ferritic HAZ adjacent (1 to 2 grains) to the weld metal interface. This mode occurs for DMWs made with austenitic stainless filler metal and sometimes for DMWs made with nickel-based filler metal. The initial inter-granular voiding or cracking develops within the wall of the component and does not normally initiate either at the inside or outside surfaces. Failure occurs by crack link-up and propagation to the surfaces.

b) Mode II – Interfacial voiding in which voids and cracking occur along a planar array of coarse globular carbides that form along the ferritic HAZ to weld metal interface. This mode occurs only for DMWs made with nickel-based filler metal, but failure may be accompanied by some Mode I cracking. The initial interfacial voiding again starts from within the wall of the component. Final failure occurs by void link-up and crack propagation to the surfaces.

10.5.6.3 The assessment procedure in this paragraph provides a systematic approach for evaluating the creep-fatigue Mode I and Mode II damage for operating cycles that are applied to a DMW in a component.

10.5.6.4 The Mode I creep-fatigue damage based on the results of a stress analysis can be computed using the assessment procedure shown below. This mode of failure is only applicable to a DMW made with stainless steel or nickel-based filler metal. Note that the damage equations in this assessment procedure were developed in US Customary Units; therefore, the units of the parameters that must be used in the assessment procedure are shown within parentheses in the nomenclature.

a) STEP 1 – Determine a load history based on past operation and future planned operation. The load history should include all significant operating loads and events that are applied to the component. If there is cyclic operation, the load history should be divided into operating cycles as shown in Figure 10.33. Define M as the total number of different types of loading cycles and N is the total number of steady-state loading durations.

b) STEP 2 – Determine the intrinsic creep-fatigue damage created by the differential thermal expansion between the filler and the base materials using Equation (10.92).

$$D_{Ic}^{I} = \sum_{j=1}^{M} k_1 \cdot n_j \cdot \left(\varepsilon_j^T\right)^{\gamma} + \sum_{i=1}^{N} k_2 \cdot t_i \cdot \left(\sigma_i^T\right)^{\beta} \cdot 10^{f(T_i)} \tag{10.92}$$

where the constants in Equation (10.92) are defined in Table 10.4, and:

$$\varepsilon_j^T = \Delta\alpha_j \cdot \Delta T_j \tag{10.93}$$

$$\sigma_i^T = \frac{E_i \cdot \Delta\alpha_i \left(T_i - 70\right)}{2} \tag{10.94}$$

c) STEP 3 – Determine the primary load creep-fatigue damage created by primary loads, i.e., pressure and dead weight, using Equation (10.95).

$$D_{Pc}^{I} = \sum_{i=1}^{N} k_3 \cdot t_i \cdot \left(\sigma_i^P\right)^{\beta} \cdot 10^{f(T_i)} \tag{10.95}$$

where the constants in Equation (10.95) are defined in Table 10.4.

d) STEP 4 – Determine the secondary load creep-fatigue damage created by secondary load, i.e., thermal expansion and discontinuity stresses as applicable, using Equation (10.96).

$$D_{Sc}^{I} = \sum_{j=1}^{M} k_4 \cdot n_j \cdot \left(\varepsilon_j^S\right)^{\gamma} + \sum_{i=1}^{N} k_5 \cdot t_i \cdot \left(\sigma_i^S\right)^{\beta} \cdot 10^{f(T_i)} \tag{10.96}$$

where the constants in Equation (10.96) are defined in Table 10.4, and:

$$\varepsilon_j^s = \frac{\sigma_j^S}{E_j} \tag{10.97}$$

e) STEP 5 – Determine the total creep-fatigue damage for Mode I using Equation (10.98).

$$D_c^I = D_{Ic}^I + D_{Pc}^I + D_{Sc}^I \tag{10.98}$$

f) STEP 6 – Determine the total creep-fatigue damage for Mode I acceptance criteria using Equation (10.99).

$$D_c^I \le 1.0 \tag{10.99}$$

10.5.6.5 The Mode II creep-fatigue damage based upon the results of a stress analysis can be computed using the assessment procedure shown below. This mode of failure is only applicable to a DMW made with nickel-based filler metal. Note that the damage equations in this assessment procedure were developed in US Customary Units; therefore, the units of the parameters that must be used in the assessment procedure are shown within parentheses in the nomenclature.

a) STEP 1 – The Mode II damage is computed using the history in paragraph 10.5.6.4(a). For the calculation, the history is subdivided into segments each representing a different level of either applied load or operating temperature and its associated time duration (see Figure 10.33).

b) STEP 2 – Determine the primary load creep-fatigue damage created by primary loads, i.e. pressure and dead weight, using Equation (10.100).

$$D_{Pc}^{II} = \sum_{i=1}^{N} k_3 \cdot t_i \cdot \left(\frac{\sigma_i^P}{1 - k_6 \cdot 10^{g(T_i)} \cdot \left(TW_i + 0.5t_i\right)^{1/3}} \right)^{\beta} \cdot 10^{f(T_i)} \tag{10.100}$$

where the constants in Equation (10.100) are defined in Table 10.5, and:

$$TW_i = \overline{t}_i \qquad when\ \overline{t}_i \le MT_i \tag{10.101}$$

$$TW_i = 2 \cdot MT_i - \overline{t}_i \qquad when\ MT_i < \overline{t}_i \le 2 \cdot MT_i \tag{10.102}$$

$$TW_i = 0.0 \qquad when\ \overline{t}_i > 2 \cdot MT_i \tag{10.103}$$

$$\overline{t}_i = \sum_{k=1}^{(i-1)} t_k \cdot 10^b \tag{10.104}$$

$$b = 25665 \cdot \left[\frac{1}{\left(T_i + 460\right)} - \frac{1}{\left(T_k + 460\right)} \right] \tag{10.105}$$

$$MT_i = 10^c \tag{10.106}$$

$$c = \left[\frac{38500}{(T_i + 460)} - 20 \right] \tag{10.107}$$

c) STEP 3 – Determine the secondary load creep-fatigue damage created by secondary load, i.e., thermal expansion and discontinuity stresses as applicable, using Equation (10.108).

$$D_{Sc}^{II} = \sum_{j=1}^{M} k_4 \cdot n_j \cdot (\varepsilon_j^S)^{\gamma} + \sum_{i=1}^{N} k_5 \cdot t_i \cdot \left(\frac{\sigma_i^S}{1 - k_6 \cdot 10^{g(T_i)} \cdot (TW_i + 0.5T_i)^{1/3}} \right)^{\beta} \cdot 10^{f(T_i)} \tag{10.108}$$

where the constants in Equation (10.108) are defined in Table 10.5, and TW_i is evaluated in STEP 2 above, and:

$$\varepsilon_j^S = \frac{\sigma_j^S}{E_j} \tag{10.109}$$

d) STEP 4 – Determine the total creep-fatigue damage for Mode II using Equation (10.110).

$$D_c^{II} = D_{Pc}^{II} + D_{Sc}^{II} \tag{10.110}$$

e) STEP 5 – Determine the total creep-fatigue damage for Mode II acceptance criteria using Equation (10.111).

$$D_c^{II} \le 1.0 \tag{10.111}$$

10.5.7 Microstructural Approach

10.5.7.1 Microstructural Approach Overview

a) Because of limited applicability and uncertainty of microstructural approaches, they are normally used in conjunction with one another and to supplement other techniques. Decisions are usually not made based on a single set of microstructural observations. For example, hardness reduction combined with evidence of cavity coalescence in a material with very coarse grain in a region of high triaxiality or cyclic service may support the finding of advanced damage.

b) Widespread availability, low cost and convenience of microstructural techniques make them a common component of the Fitness-For-Service approach. All critical areas should be sampled, and a database of results should be maintained. Changes over time in hardness, appearance, void size, or population should be taken as indications of time dependent damage. Thus, microstructural softening occurs in many materials without contributing to the damage rate.

10.5.7.2 Microstructural approaches have been used to estimate the remaining life of a component. The following procedures are recognized.

a) *Hardness Changes* – For certain alloys, tensile strength and hardness are believed to correlate with remaining life. For many other situations, hardness may bear no relation to status with respect to creep damage. However, the absence of a hardness change during service may indicate that the service exposure is unlikely to have caused significant creep damage.

1) Materials for which hardness is above a reference level indicates that the material is suitable for continued service at nominal design stress levels and temperatures below those indicated in Table 10.6, absent any flaws, etc.

2) Materials shown in Table 10.7, if known not to have changed in hardness after extended service, are unlikely to have suffered significant creep damage, and are suitable for future service if the future service conditions are not more severe than the past service conditions. The initial hardness readings must be known with certainty to use the information in Table 10.7.

b) *Creep Cavity Evaluation* – Some engineering alloys exhibit creep cavities as precursors to crack initiation and failure. Many alloys do not exhibit such a characteristic. The time to the appearance of detectable creep cavities depend upon stress state, heat treatment, grain size, material cleanliness, embrittlement, and other factors. The numbers, size, and spacing of cavities reported depends on the microscopic techniques, sample preparation, void size, and observer experience.

1) Certain circumstances may warrant the development of a calibration curve applicable to specific materials where cavity size and spacing are desired to be used for life assessment. Absent such an application specific calibration curve, the following guidelines may be used.

i) No detectable cavities indicating less than 10% life consumption.

- High Strength Cr-Mo Alloys (UTS > 110 ksi).
- High Strength Cr-Mo-V Alloys (UTS > 100 ksi).
- Submerged arc welds.
- Coarse grain heat affected zones in the above.

ii) The presence of multiple cavities of character greater than 1.5μ on most grain boundaries normal to the principal stress or linked cavities appearing as microcracks or fissures is indicative that creep damage exceeds 50% in the area under examination.

2) Sample preparation must be adequate for detection and sizing of cavities by optical and/or electron microscopic techniques.

3) Examinations may be made on shadowed replicas or samples removed from the section of interest. The area to be studied should be free of environmentally caused damage such as oxide penetration. Areas particularly susceptible to cavitation damage include.

i) Coarse grain base metal adjacent to weld fusion line in Cr-Mo and Cr-Mo-V alloys.

ii) Fine grain regions of heat affected zone in base metal or weld metal when surrounded by relatively higher strength material.

iii) Material located in region of high stress concentration in higher strength alloys. Examples include the dovetail of a turbine blade, sharp notches, and changes in the component cross section.

iv) Materials containing regions of coarse precipitate particles such as stigmatized stainless steels or other high alloy materials.

c) *Optical Metallography* – Some guidance as to the creep resistance of materials or the damage state may be obtained from optical microscopy. This information may be useful in modifying the referenced Omega method based strain rate and Omega coefficient equations provided in Annex 10B. Aside from the cavitation issues noted above, the effects on strain rate and the Omega parameter are shown in Table 10.8.

10.6 Remediation

10.6.1 Components with and without a Crack-Like Flaw

For components that do not contain a crack-like flaw, if the component does not satisfy the creep damage criterion within the required service life, or if the sensitivity analysis indicates unacceptable results, then remedial action is required. One of the following may be considered.

a) Change in Service Parameters – a change in service parameters (load, temperature, service life) may be made and the assessment repeated either to demonstrate acceptance or to estimate at what time replacement will be necessary.

b) Use of Thermal Linings – conversion of existing hot-wall pressure vessel and piping systems to a cold wall design that utilizes a thermal lining, i.e., refractory, has been performed. In these cases, the thermal lining is designed to reduce the metal temperature to a value below the creep range thereby preventing future creep damage.

10.6.2 Components with a Crack-Like Flaw

For components containing a crack-like flaw, if failure by excessive crack growth is indicated within the required service life, or if the sensitivity analysis indicates unacceptable results, then remedial action is required, such as repair of the component by removing the flaw. Alternatively, a change in service parameters such as load, temperature, and desired service life may be made, and the assessment repeated either to demonstrate acceptance or to estimate at what time repair will be necessary. Finally, it may be possible to obtain data on the material used in the component to remove conservatism in the assessment resulting from the use of bounding data.

10.7 In-Service Monitoring

The most effective tool for in-service monitoring of equipment subject to creep damage is to monitor the temperature and pressure. This information can be used to update the creep remaining life calculation to determine if continued operation is acceptable.

10.8 Documentation

10.8.1 General

The documentation of the FFS Assessment should include the information cited in Part 2, paragraph 2.8. Additional documentation requirements are essential because of the complexity associated with the assessment. This information should be permanently stored with the equipment record files.

10.8.2 Assumptions Used in the Assumption

All assumptions used in the assessment procedures should be documented. In addition, all departures from the procedures in this Part should be reported and separately justified. A separate statement should be made about the significance of potential failure mechanisms remote from the defective areas, if applicable.

10.8.3 Documentation for Life Assessment

The following information shall be documented; the applicable assessment levels are shown within parentheses.

a) *Assessment Level* – Any deviations or modifications used at a given level of analysis (Levels 1, 2, and 3).

b) *Loading Conditions* – A load history showing the historical and assumed future start-up, normal, upset, and shut-down conditions should be reported (Levels 1, 2, and 3). In addition, any additional loads and stresses considered in the assessment (e.g., stresses from supplement loads, thermal gradients, and residual stresses (Levels 2 and 3).

c) *Stress Analysis Results* – The stress analysis method (handbook, finite-element, or other numerical techniques) and categorization of stress results if required (Levels 1, 2, and 3).

d) *Material Properties* – The material specification of the component; yield strength, ultimate tensile stress, fracture toughness, and creep properties should be reported including whether the data were obtained by direct testing, or indirect means together with the source of the data. If testing is performed to determine material properties, the test results should be included in the documentation. In addition, a description of the process environment including its effect on material properties. If cyclic loads are present, a description of the creep-fatigue interaction rules should be documented (Levels 2 and 3).

e) *Sensitivity Analysis* – A listing of the input parameters used to perform sensitivity studies (e.g., time in service, loads, material properties, flaw size, etc.); the results of each individual study should be summarized (Levels 2 and 3).

10.8.4 Supplemental Documentation for Creep Crack Growth

The following additional information should be documented if a creep crack growth assessment has been performed as part of a Level 3 Assessment.

a) *Characterization of Flaw* – For components with cracks, the flaw location, shape, and size; NDE method used for flaw sizing and allowance for sizing errors; and whether re-characterization of the flaw was required (see Part 9).

b) *Partial Safety Factors* – A list of the Partial Safety Factors used in the FAD analysis; a technical summary should be provided if alternative factors are utilized in the assessment.

c) *Reference Stress Solution* – The source of the reference stress solutions, e.g., handbook solution or finite-element analysis, used in the assessment including whether the local and/or global collapse was considered.

d) *Stress Intensity Factor Solution* – The source of stress intensity factor solutions, e.g., handbook solution or finite-element analysis, used in the assessment.

e) *Failure Assessment Diagram (FAD)* – whether the Part 9, Level 2 FAD, a material specific curve, including the source and validity of stress-strain data, or a curve derived from J-analysis is used in the assessment.

f) *Material Properties* – the source and complete description of the creep strain rate and other data used to determine a remaining life should be included.

g) *Creep Crack Growth Equation* – the equation and associated constants used to model creep crack growth, and for components subject to cyclic operation, the equation and associated constants used to model the fatigue crack growth should be summarized, i.e., from technical publication or laboratory measurements.

10.8.5 Supplemental Documentation for Microstructural Approaches

If microstructural approaches are used as part of the assessment, all examination results shall be included in the documentation. If a Creep Cavity Evaluation is made in accordance with paragraph 10.5.7.2(b), then the

examination results, cavity sizing procedure and results, and the calibration curve applicable to specific to the component material shall be included in the documentation.

10.9 Nomenclature

a_0 initial crack-like flaw depth.

${}^{i}a$ depth of the crack-like flaw for the i^{th} time step.

A is a reaction rate parameter.

$A_1 \rightarrow A_4$ material coefficients for the MPC Project Omega strain-rate-parameter (see Annex 10B).

α_Ω triaxiality parameter based on the state of stress for MPC Project Omega Life Assessment Model.

= 3.0 – pressurized sphere or formed head,

= 2.0 – pressurized cylinder or cone,

= 1.0 – for all other components and stress states,

= 0.0 – for all components and stress states when geometric nonlinearity (large displacement) is used in the computational method.

B reaction rate parameter.

$B_1 \rightarrow B_4$ material coefficients for the MPC Project Omega Omega-parameter (see Annex 10B) or parameters to determine creep damage in a bimetallic weld.

β constant used in the assessment of a DMW.

β_Ω MPC Project Omega parameter to 0.33.

β_1 parameter for creep-fatigue interaction.

β_2 parameter for creep-fatigue interaction.

c_0 initial crack-like flaw half-length.

${}^{i}c$ half-length of the existing flaw for the i^{th} time step.

C_F creep damage fraction used in creep-fatigue interaction.

C_{intg} explicit time integration parameter.

$C^{*90}({}^{i}a, {}^{i}c)$ crack driving force associated with global steady-state creep at the deepest point of the crack.

$C^{*0}({}^{i}a, {}^{i}c)$ crack driving force associated with global steady-state creep at the surface point of the crack.

C_{LMP} Larson Miller Constant (see Annex 10B).

$C_t^{90}({}^{i}a, {}^{i}c)$ total crack driving force for creep crack growth at the deepest point of the crack including transient and steady-state creep effects.

$C_t^{0}({}^{i}a, {}^{i}c)$ total crack driving force for creep crack growth at the surface point of the crack including transient and steady-state creep effects.

D_c creep damage.

$\dot{D}_c$ creep damage rate.

D_f fatigue damage.

D_{cm} creep damage based material parameter used in creep-fatigue interaction.

D_{fm} fatigue damage based material parameter used in creep-fatigue interaction.

D_{ac}^{i} local creep damage after the crack initiates, the damage is computed using the reference stress (see Annex 9C) considering the post-crack loading history.

D_{ac} local creep damage after the crack initiates, the damage is computed using the reference stress (see Annex 9C) considering the post-crack loading history for the i^{th} time step.

D_{bc} local creep damage before the initiation of the crack, the damage is computed using the net section stress considering the pre-crack loading history.

D_{mean} mean diameter of a cylinder or sphere.

D_c^{allow} allowable creep damage.

D_{Ic}^{I} Mode I intrinsic creep-fatigue damage created by differential thermal expansion between the filler and based metal, used in the assessment of a DMW.

D_{Pc}^{I} Mode I creep-fatigue damage created by primary loads, used in the assessment of a DMW.

D_{Sc}^{I} Mode I creep-fatigue damage created by secondary loads, used in the assessment of a DMW.

D_c^{I} Mode I total creep-fatigue damage, used in the assessment of a DMW.

D_{Pc}^{II} Mode II creep-fatigue damage created by primary loads, used in the assessment of a DMW.

D_{Sc}^{II} Mode II creep-fatigue damage created by secondary loads, used in the assessment of a DMW.

D_c^{II} Mode II total creep-fatigue damage used in the assessment of a DMW.

${}^{n}D_c$ creep damage for the n^{th} time period.

${}^{0}D_{ac}$ past damage in the material ahead of the crack for the period corresponding to the last time it was verified that a crack was not present and the time that the crack was found.

D_c^{total} total creep damage considering all operating cycles.

D_{cf}^{total} total creep-fatigue damage considering all operating cycles.

$\Delta\alpha_j$ differential value of the coefficient of thermal expansion between the filler and base metal associated with the temperatures used to define ΔT_j. $\Delta\alpha_j$ is calculated at the minimum and maximum temperatures of the cycle maximum value shall be used in the analysis.

Δt time step.

ΔT_j mean wall cyclic temperature range for the j^{th} loading condition, used in the assessment of a DMW ($°F$).

${}^{m}\Delta\sigma_s$ maximum range of axial secondary stress due to applied net-section forces and moments.

Δ_{Ω}^{cd} adjustment factor for creep ductility in the Project Omega Model, a range of $+0.3$ for brittle behavior and -0.3 for ductile behavior can be used.

Δ_{Ω}^{sr} adjustment factor for creep strain rate to account for the material scatter band in the Project Omega Model, a range of -0.5 for the bottom of the scatter band to $+0.5$ for the top of the scatter band can be used.

$\frac{{}^{i}da}{dt}$ crack growth rate for the deepest point of a surface flaw for the i^{th} time step.

$\frac{{}^{m}da}{dN}$ increment of fatigue crack growth for the deepest point of a surface flaw for the m^{th} cycle.

$\frac{{}^{i}dc}{dt}$ crack growth rate for the surface point of a surface flaw for the i^{th} time step.

$\frac{{}^{m}dc}{dN}$ increment of fatigue crack growth for the surface point of a surface flaw for the m^{th} cycle.

δ_{Ω} MPC Project Omega parameter.

E_y Young's Modulus evaluated at the mean temperature of the cycle.

${}^{n}E_y$ Young's Modulus for the loading history for the n^{th} time increment.

E_{amb} Young's modulus at ambient temperature.

E_T Young's modulus at the assessment temperature.

E_i mean value of Young's Modulus for the i^{th} steady-state loading condition, used in the assessment of a DMW (psi).

E_j mean value of Young's Modulus for the j^{th} cycle loading type, used in the assessment of a DMW (psi).

ε_c accumulated creep strain.

ε_{ce}^{cr} critical effective creep strain at the onset of elastic creep buckling.

$\dot{\varepsilon}_c$ creep strain rate.

$\dot{\varepsilon}_{co}$ initial creep strain rate at the start of the time period being evaluated based on the stress state and temperature (see Annex 10B); note, the units of measure for computing this parameter must be ksi and °F.

${}^{i}\dot{\varepsilon}_{ref}$ uniaxial strain rate evaluated at the reference stress for the i^{th} time step.

$^{n}\dot{\varepsilon}_{ref}$ uniaxial strain rate evaluated at the reference stress for the n^{th} time increment.

ε_j^S cyclic secondary strain range for the j^{th} loading cycle type, used in the assessment of a DMW (psi).

ε_j^T cyclic differential thermal expansion strain range for the j^{th} loading cycle type, used in the assessment of a DMW (psi).

f exponent in the creep-fatigue damage calculation.

$f(T_i)$ function used in the assessment of a DMW.

γ constant used in the assessment of a DMW.

$g(T_i)$ function used in the assessment of a DMW.

H_c coefficient for the creep crack growth model.

H_f coefficient for the fatigue crack growth model.

j operating condition number or cycle, as applicable.

J total number of operating conditions or cycles, as applicable.

J_1 term used to compute $^{n}S_{eff}$.

K total number of operating cycles.

K_{bc} total number of operating cycles before the initiation of the crack.

$K_{I,\max}$ maximum value of the stress intensity.

$K_{I,\min}$ minimum value of the stress intensity.

$K_I^0(^ia, ^ic)$ applied Mode I stress intensity factor at the surface point of a surface crack (see Annex 9B).

$K_I^{90}(^ia, ^ic)$ applied Mode I stress intensity factor at the deepest point of a surface crack (see Annex 9B).

$^{m}\Delta K_{eff}^0$ effective range of the cyclic applied mode I stress intensity factor at the surface point of a surface crack that occurs in the m^{th} cycle.

$^{m}K_{I,\max}^0$ maximum value of the cyclic applied Mode I stress intensity factor at the surface point of a surface crack that occurs in the m^{th} cycle (see Annex 9B).

$^{m}K_{I,\min}^0$ minimum value of the cyclic applied Mode I stress intensity factor at the surface point of a surface crack that occurs in the m^{th} cycle (see Annex 9B).

$^{m}\Delta K_{eff}^{90}$ effective range of the cyclic applied Mode I stress intensity factor at the deepest point of a surface crack that occurs in the m^{th} cycle.

$^{m}K_{I,\max}^{90}$ maximum value of the cyclic applied Mode I stress intensity factor at the deepest point of a surface crack that occurs in the m^{th} cycle (see Annex 9B).

$^{m}K_{I,\min}^{90}$ minimum value of the cyclic applied Mode I stress intensity factor at the deepest point of a surface crack that occurs in the m^{th} cycle (see Annex 9B).

k current operating cycle.

$k_1 \rightarrow k_6$ constants used in the evaluation of a DMW.

L_f Lorentz Factor (see Annex 2B).

L_r load ratio based on primary stress.

^{n}L rupture time for the loading history for the n^{th} time increment or operating condition.

$LMP(^{n}S_{eff})$ Larson-Miller parameter at stress S_{eff}^{n}.

$^{i}L_{ac}$ rupture time for the loading history after initiation of the crack applied for time increment ^{i}t computed using the reference stress.

λ exponent in the fatigue crack growth equation.

m current operating cycle number.

M total number of operating cycles, or the total number of different types of loading cycles used in the assessment of DMW.

M_{ac} is the total number of operating cycles for the period of time under consideration.

MT_i time parameter for the i^{th} steady-state loading condition, used in the evaluation of a DMW (hour).

M_{bc} total number of operating cycles before the onset of cracking.

μ exponent in the creep crack growth equation.

n the n[th] operating condition defined.

N total number of time increments in an operating cycle, or the total number of steady-state loading conditions used in the assessment of DMW.

^{m}N number of allowable cycles determined from a fatigue curve for the m^{th} cycle.

^{m}n number of applications of the m^{th} cycle.

n_j total number of fatigue cycles for the j^{th} loading cycle type in the assessment of a DMW.

n_{BN} Bailey-Norton coefficient $(n_{BN} = -d\log\dot{\varepsilon}_c/d\log\sigma)$ evaluated at the reference stress in the current load increment, used in the MPC Project Omega Life Assessment Model.

ν Poisson's ratio.

P pressure inside of a cylinder or sphere.

P_L primary local membrane stress (see Annex 2C).

P_b primary bending stress (see Annex 2C).

$^{n}P_b$ primary bending stress (see Annex 2C) for the n^{th} time increment.

$^{n}P_{L}$ primary local membrane stress (see Annex 2C) for the n^{th} time increment.

P^{L} generalized applied loading parameter.

$P^{L}(t)$ generalized applied loading parameter as a function of time.

P^{cr} critical buckling load associated with the generalized loading parameter.

Q secondary equivalent stress resulting from operation loads for the cycle under consideration, the loading parameter for a creep buckling analysis, or the activation energy, as applicable.

r radial coordinate in a cylinder or sphere at the location where the stress is being computed.

R universal gas constant.

R_{c} creep damage rate.

R_{i} inside radius of a cylinder or sphere.

R_{mean} mean radius of a cylinder or sphere.

R_{o} outside radius of a cylinder or sphere.

R_{r} reaction rate.

S_{h} allowable stress at the maximum temperature for the cycle under consideration.

S_{l} log base 10 of the effective stress.

S_{s} term used to compute $^{n}S_{eff}$.

S_{yc} yield strength at the minimum temperature for the cycle under consideration.

$^{n}S_{eff}$ effective stress used to compute the remaining life in terms of the Larson-Miller parameter for the n^{th} time increment.

σ_{e} effective stress.

σ_{m} meridional stress in a cylinder or sphere stress.

σ_{mean} mean stress for a cylinder subject to internal pressure.

σ_{c} circumferential stress in a cylinder or sphere.

σ_{r} radial stress in a cylinder or sphere stress.

σ_{ys} yield strength at the assessment temperature (see Annex 2D).

σ_{e}^{cr} critical effective stress associated with the generalized loading parameter at the critical buckling load.

σ_{1} principal stress.

σ_{2} principal stress.

σ_{3} principal stress.

$^{i}\sigma_{ij}$ applied stress components for the i^{th} time step.

$^{i}\sigma_{ref}$ reference stress for the i^{th} time step (see Annex 9C).

$^{n}\sigma_{e}$ effective stress for the n^{th} time increment.

$^{n}\sigma_{ij}$ applied stress components for the n^{th} time increment.

$^{n}\sigma_{mean}$ mean stress for a cylinder subject to internal pressure based on the mean diameter equation for the n^{th} time increment.

$^{n}\sigma_{p}$ axial primary stress due to pressure and applied net-section forces and moments for the n^{th} time increment.

$^{n}\sigma_{ref}$ reference stress for the n^{th} time increment (see Annex 9C).

$^{n}\sigma_{s}$ axial secondary stress due to applied net-section forces and moments for the n^{th} time increment.

$^{n}\sigma_{1}$ principal stress for the n^{th} time increment.

$^{n}\sigma_{2}$ principal stress for the n^{th} time increment.

$^{n}\sigma_{3}$ principal stress for the n^{th} time increment.

σ_{i}^{P} primary stress for the i^{th} steady-state loading condition, used in the assessment of a DMW (psi).

σ_{i}^{S} secondary stress for the i^{th} steady-state loading condition, typically the stress caused by axial thermal expansion, used in the assessment of a DMW (psi).

σ_{i}^{T} differential thermal expansion stress for the i^{th} steady-state loading condition, used in the assessment of a DMW (psi).

σ_{j}^{S} cyclic secondary stress range for the j^{th} loading cycle type, used in the assessment of a DMW (psi).

t time.

$t_{\lim}$ limiting thickness.

t_{nom} nominal thickness of the component.

t_{i} time duration of the i^{th} steady-state loading condition, in the assessment of a DMW (hour).

$\overline{t_{i}}$ time parameter for the i^{th} steady-state loading condition, in the assessment of a DMW (hour).

t_{c} component thickness adjusted for metal loss and future corrosion allowance, as applicable.

t_{sl} thickness required for supplemental loads (see Annex 2C).

t_{ac} accumulated creep time in the solution.

T temperature.

$T(t)$ temperature as a function of time.

T_i temperature for the i^{th} steady-state loading condition, used in the assessment of a DMW (°F).

TW_i time parameter for the i^{th} steady-state loading condition, used in the evaluation of a DMW.

${}^{i}T$ temperature for the i^{th} time step.

${}^{n}T$ temperature for the n^{th} time increment.

t_{comp} component thickness adjusted for metal loss and corrosion allowance as required.

$t_{relax}^{90}({}^{i}a, {}^{i}c)$ relaxation term in the crack driving force associated with the deepest point of the crack for the i^{th} time step.

$t_{relax}^{0}({}^{i}a, {}^{i}c)$ relaxation term in the crack driving force associated with the surface point of the crack for the i^{th} time step.

${}^{i}T$ cumulative time at the end of the i^{th} time period in the m^{th} cycle.

${}^{m}t$ total time in the m^{th} cycle.

${}^{n}t$ time increment or operating condition load duration for use in the damage calculation.

t^{cr} critical time at the onset of elastic-creep buckling.

Y_{B31} coefficient from ASME B31 Piping codes used for determining the pipe wall thickness (see Annex 2B).

Ω uniaxial Omega damage parameter (see Annex 10B); note, the units of measure for computing this parameter must be ksi and °F.

Ω_m multiaxial Omega damage parameter (see Annex 10B).

Ω_n adjusted uniaxial Omega damage parameter.

10.10 References

References for this Part are provided in Annex 10A – Technical Basis and Validation – Assessment of Components Operating in the Creep Range.

10.11 Tables

Table 10.1 – Metallurgical Requirements

Material	Brinell Hardness	Minimum Carbon Content	Level 1 Screening Curve Figure
Carbon Steel $\sigma_{uts}^{min} \leq 379\ MPa\ (55\ ksi)$	95	---	10.3
Carbon Steel $\sigma_{uts}^{min} = 413\ MPa\ (60\ ksi)$	95	---	10.4
Carbon Steel $\sigma_{uts}^{min} = 448\ MPa\ (65\ ksi)$	100	---	10.5
Carbon Steel $\sigma_{uts}^{min} = 483\ MPa\ (70\ ksi)$	100	---	10.6
Carbon Steel $\sigma_{uts}^{min} \geq 517\ MPa\ (75\ ksi)$	100	---	10.7
Carbon Steel – Graphitized	100	---	10.8
C-0.5Mo	110	---	10.9
1.25Cr-0.5Mo – Normalized & Tempered	130	---	10.10
1.25Cr-0.5Mo – Annealed	120	---	10.11
2.25Cr-1Mo – Normalized & Tempered	140	---	10.12
2.25Cr-1Mo – Annealed	130	---	10.13
2.25Cr-1Mo – Quenched & Tempered	150	---	10.14
2.25Cr-1Mo-V & 3Cr-1Mo-V	180	---	10.15
5Cr-0.5Mo	130	---	10.16
9Cr-1Mo	140	---	10.17
9Cr-1Mo-V	180	---	10.18
10.5Cr-V (Alloy 115 UNSK91060)	180		10.19
12 Cr	180	---	10.20
AISI Type 304 & 304H	---	0.04	10.21
AISI Type 316 & 316H	---	0.04	10.22

Table 10.1 – Metallurgical Requirements

Material	Brinell Hardness	Minimum Carbon Content	Level 1 Screening Curve Figure
AISI Type 321	---	0.04	10.23
AISI Type 321H	---	0.04	10.24
AISI Type 347	---	0.04	10.25
AISI Type 347H	---	0.04	10.26
Type 347 LN (UNS S34751)	---	0.002-0.020 (1)	10.27
Type 347 AP Advanced (UNS S34752)	---	0.002-0.020 (1)	10.28
Alloy 800	---	0.03	10.29
Alloy 800H	---	0.04	10.30
Alloy 800HT	---	0.05	10.31
HK-40	---	0.30	10.32

Note: 1) Values provided represent the acceptable range of carbon content.

Table 10.2 – Stress Equations for Cylindrical and Spherical Shells

Geometry	Stress Equations
Cylinder or Elbow – Elastic Stress Solution Based on Mean Diameter	$\sigma_1 = \sigma_c = \frac{PD_{mean}}{2t_{comp}} \cdot L_f$ $\sigma_2 = \sigma_m = \frac{PD_{mean}}{4\left(t_{comp} - t_{sl}\right)}$ $\sigma_3 = \sigma_r = 0.0$
Cylinder – Reference Stress Solution	$\sigma_1 = \sigma_c = \frac{P\left(1 - \ln\left[R_{r2}\right]\right)}{\ln\left[R_{r1}\right]}$ $\sigma_2 = \sigma_m = \frac{P\left(1 - 2\ln\left[R_{r2}\right]\right)}{2\ln\left[R_{r1}\right]}$ $\sigma_3 = \sigma_r = \frac{-P\left(\ln\left[R_{r2}\right]\right)}{\ln\left[R_{r1}\right]}$ $R_{r1} = \frac{R_o}{R_i}$ $R_{r2} = \frac{R_o}{r}$
Cylinder or Elbow – Steady-State Creep Solution	$\sigma_1 = \sigma_c = C\left[1 + \left(\frac{2 - n_{BN}}{n_{BN}}\right)\left(\frac{R_o}{r}\right)^{\left(\frac{2}{n_{BN}}\right)}\right] \cdot L_f$ $\sigma_2 = \sigma_m = C\left[1 + \left(\frac{1 - n_{BN}}{n_{BN}}\right)\left(\frac{R_o}{r}\right)^{\left(\frac{2}{n_{BN}}\right)}\right]$ $\sigma_3 = \sigma_r = C\left[1 - \left(\frac{R_o}{r}\right)^{\left(\frac{2}{n_{BN}}\right)}\right]$ $C = \frac{P}{\left[\left(\frac{R_o}{R_i}\right)^{\left(\frac{2}{n_{BN}}\right)} - 1\right]}$
Sphere – Elastic Stress Solution Based on Mean Diameter	$\sigma_1 = \sigma_c = \frac{PD_{mean}}{4t_{comp}}$ $\sigma_2 = \sigma_m = \sigma_c$ $\sigma_3 = \sigma_r = 0.0$

Table 10.2 – Stress Equations for Cylindrical and Spherical Shells

Geometry	Stress Equations
Sphere – Reference Stress Solution	$\sigma_1 = \sigma_c = \frac{P\left(2 - 3\ln\left[R_{r2}\right]\right)}{3\ln\left[R_{r1}\right]}$ $\sigma_2 = \sigma_m = \sigma_c$ $\sigma_3 = \sigma_r = \frac{-P\left(\ln\left[R_{r2}\right]\right)}{\ln\left[R_{r1}\right]}$ $R_{r1} = \frac{R_o}{R_i}$ $R_{r2} = \frac{R_o}{r}$
Sphere – Steady-State Creep Solution	$\sigma_1 = \sigma_c = C\left[1 + \left(\frac{3 - 2n_{BN}}{2n_{BN}}\right)\left(\frac{R_o}{r}\right)^{\left(\frac{3}{n_{BN}}\right)}\right]$ $\sigma_2 = \sigma_m = C\left[1 + \left(\frac{3 - 2n_{BN}}{2n_{BN}}\right)\left(\frac{R_o}{r}\right)^{\left(\frac{3}{n_{BN}}\right)}\right]$ $\sigma_3 = \sigma_r = C\left[1 - \left(\frac{R_o}{r}\right)^{\left(\frac{3}{n_{BN}}\right)}\right]$ $C = \frac{P}{\left[\left(\frac{R_o}{R_i}\right)^{\left(\frac{3}{n_{BN}}\right)} - 1\right]}$

Notes:

1. The above equations do not include the effect of metal loss or future corrosion allowance. The inside radius, outside radius, and wall thickness should be adjusted accordingly based on service experience.
2. For a cylinder, the Lorentz Factor is $L_f = 1.0$, for an elbow, L_f can be evaluated using Annex 2C, paragraph 2C.5.5.
3. The thick wall stress equations are provided in terms of the Bailey-Norton creep exponent, n_{BN}. This form of the equations will account for the stress redistribution that occurs in the creep range. The elastic solution or Lame equations can be obtained by setting $n_{BN} = 1.0$.

Table 10.3 – Accumulated Inelastic Strain Criterion

Type of Stress	Accumulated Inelastic Strain	
	Weld and HAZ	Other Parts
Membrane	0.5%	1.0%
Membrane plus Bending	1.25%	2.5%
Local (at any point)	2.5%	5.0%

Table 10.4 – Constants for DMW Mode I Creep-Fatigue Damage

Name of Constant	Type of Filler Metal	
	Stainless Steel	Nickel-Base
k_1	6.8E-4	0.0
k_2	2.5E-10	0.0
k_3	2.4E-7	1.6E-7
k_4	1.0E-2	1.0E-2
k_5	5.5E-10	5.5E-10
γ	0.2	0.2
β	2.7	2.7
$f(T_i)$	$13.26 - \frac{31032}{(T_i + 460)}$	$13.26 - \frac{31032}{(T_i + 460)}$

Table 10.5 – Constants for DMW Mode II Creep-Fatigue Damage for Nickel-base Filler Metals

Name of Constant	Value
k_3	6.8E-8
k_4	1.6E-3
k_5	8.9E-9
k_6	0.65
γ	0.2
β	2.7
$f(T_i)$	$13.26 - \frac{31032}{(T_i + 460)}$
$g(T_i)$	$4.0 - \frac{8555}{(T_i + 460)}$

Table 10.6 – Reference Hardness and Temperature Criterion

Material	Reference Hardness, HB	Temperature (˚F)
2.25Cr+Mo, Q+T	190	825
2.25Cr-1Mo-V, Q+T	200	875
3Cr-1Mo-V, Q+T	200	850
9Cr-1Mo-V	200	1075
12Cr-2Mo-V	200	1100

Table 10.6M – Reference Hardness and Temperature Criterion

Material	Reference Hardness, HB	Temperature (˚C)
2.25Cr+Mo, Q+T	190	440
2.25Cr-1Mo-V, Q+T	200	470
3Cr-1Mo-V, Q+T	200	455
9Cr-1Mo-V	200	580
12Cr-2Mo-V	200	595

Table 10.7 – Temperature Criterion for No Change in Hardness During Service that Indicates Creep Damage is Unlikely

Material	Temperature (˚F)
1.25Cr-0.5Mo, Q+T or N+T	850
2.25Cr-1Mo, Q+T or N+T	900
3Cr-1Mo, Q+T or N+T	900
9Cr-1Mo-V	1050
Rotor Steels	875

Table 10.7M – Temperature Criterion for No Change in Hardness During Service that Indicates Creep Damage is Unlikely

Material	Temperature (˚C)
1.25Cr-0.5Mo, Q+T or N+T	455
2.25Cr-1Mo, Q+T or N+T	480
3Cr-1Mo, Q+T or N+T	480
9Cr-1Mo-V	565
Rotor Steels	470

Table 10.8 – Trends of The MPC Project Omega Strain Rate and Omega Parameter with Microstructure

Microstructure	Strain Rate	Omega
Coarse Grain	Decreases	Increases
Fine Grain	Increases	Decreases
Nodular Graphite	Increases	---
Sigma Formation	---	Increases
Spherodized Carbides	Increases	---
Decarburization	Increases	---
Carburization	Decreases	Increases
Nitriding	Decreases	Increases

10.12 Figures

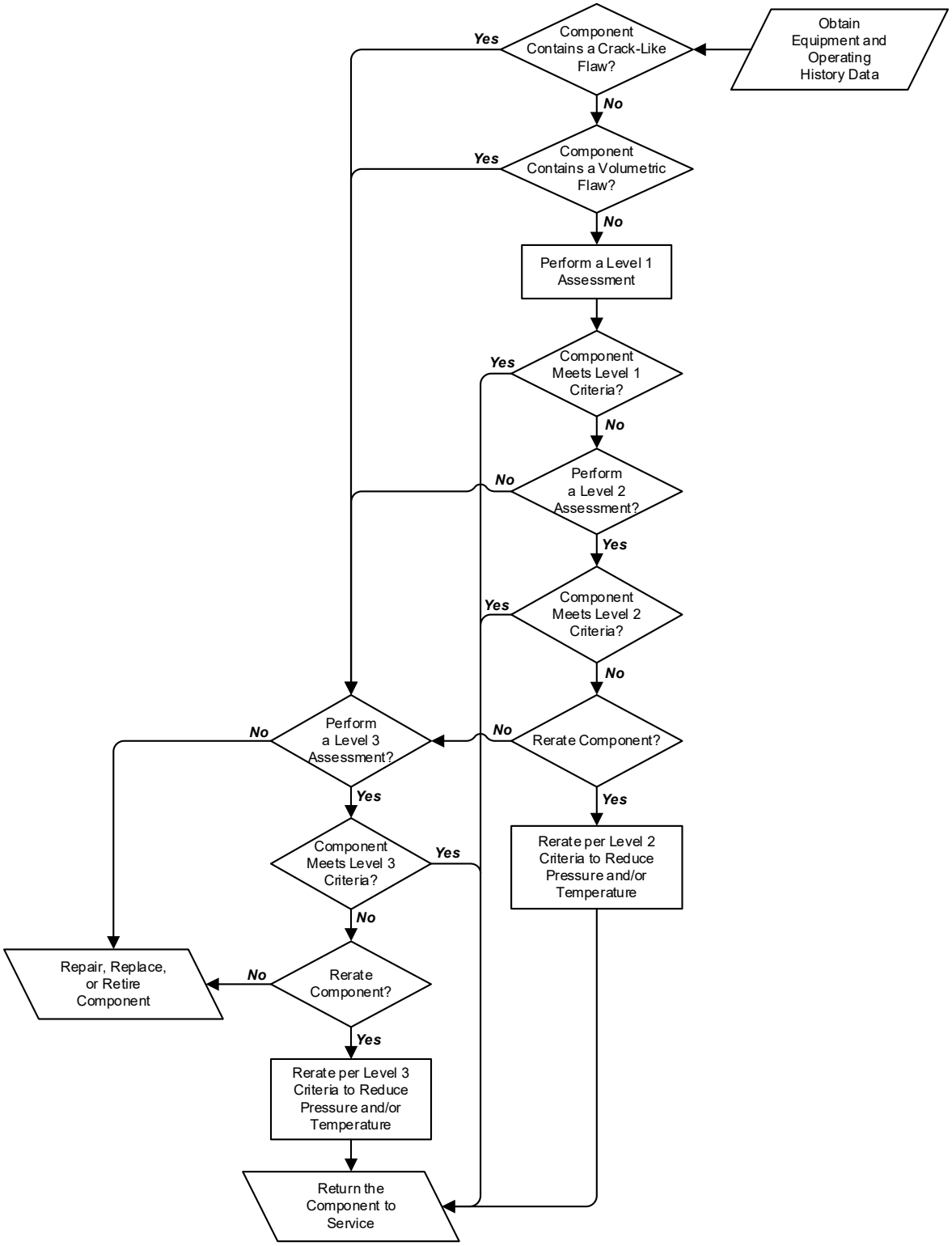

Figure 10.1 – Overview of the Assessment Procedures to Evaluate a Component in the Creep Range

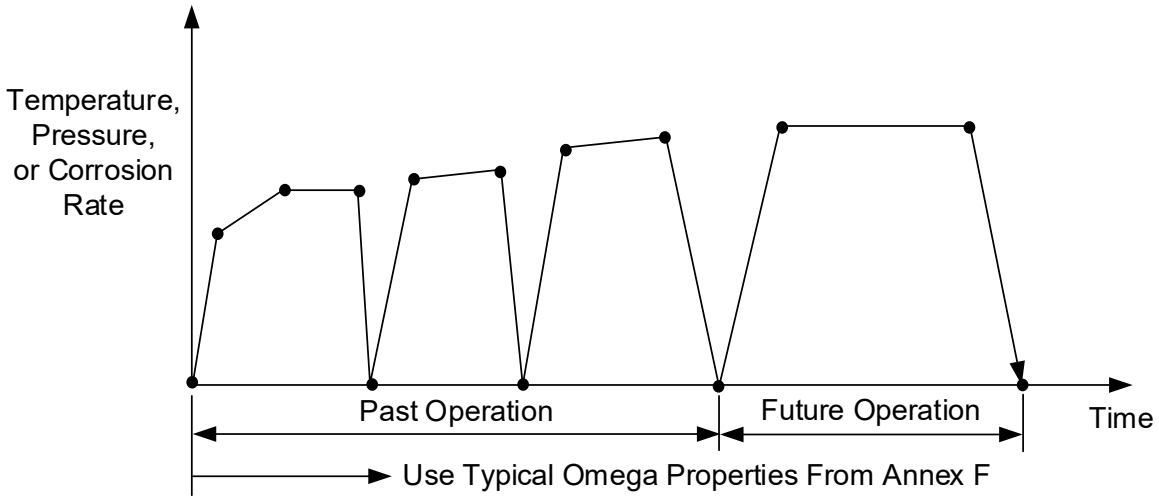

(a) Operating Histogram Showing Past and Future Operation

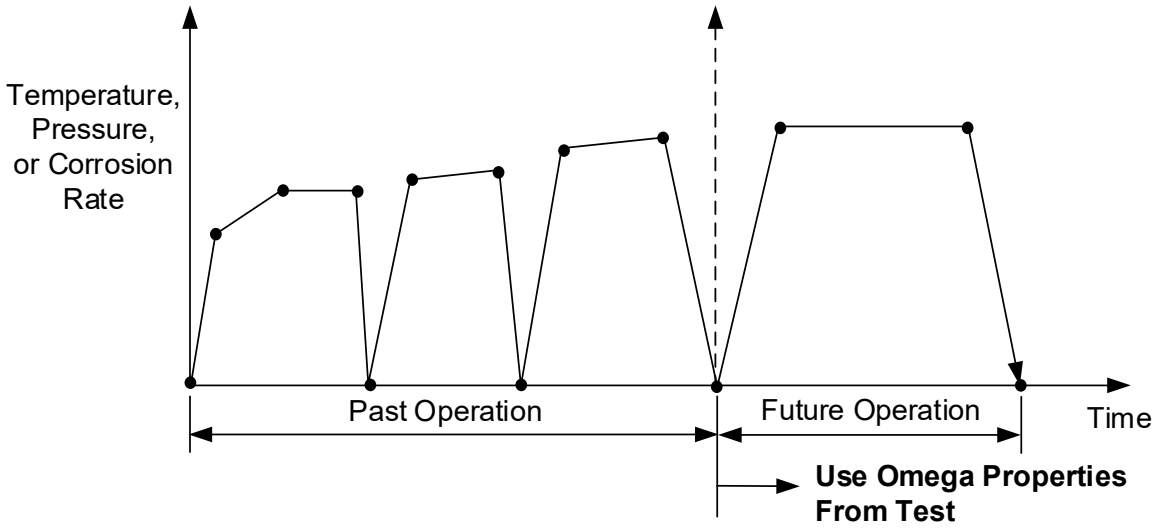

(b) Operating Histogram "Shifted" Based On MPC Project Omega Test

Figure 10.2 – Shifting of the Operating History Based on MPC Project Omega Testing

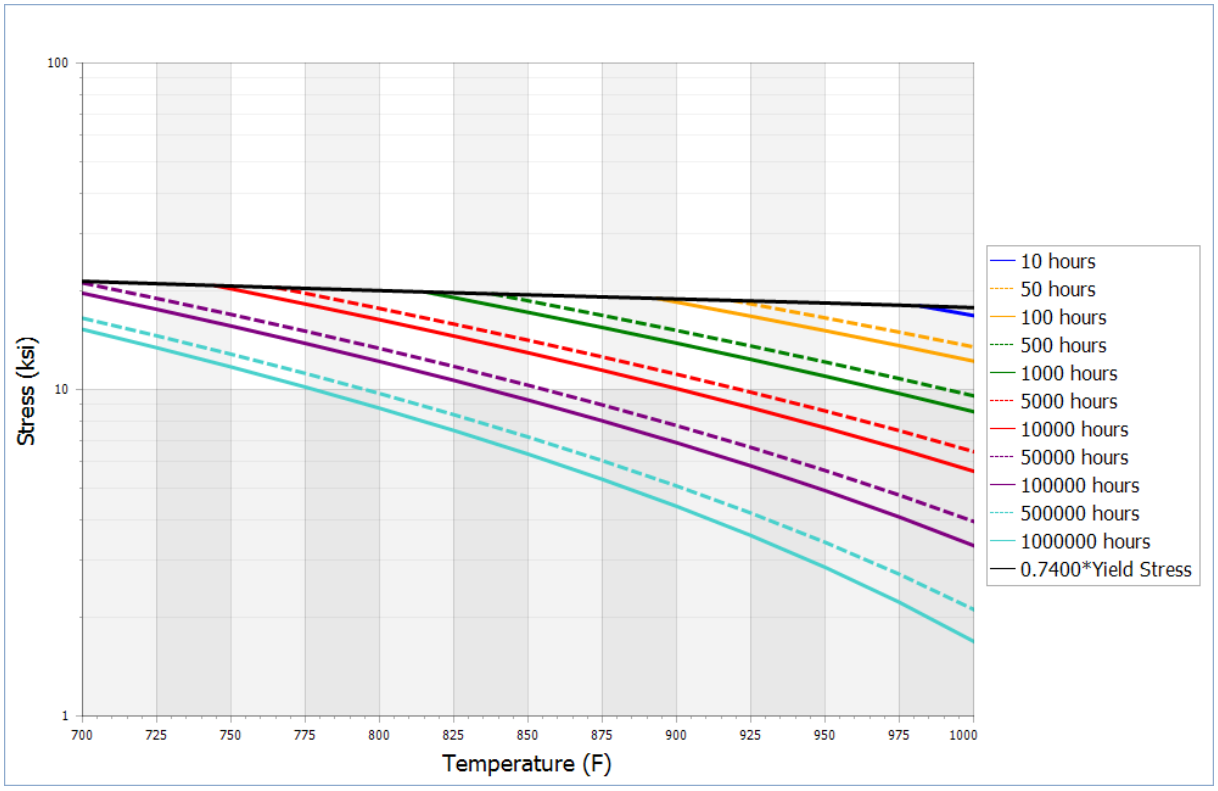

Figure 10.3 – Level 1 Screening Curve for Carbon Steel – $\sigma_{uts}^{min} < 60\ ksi$

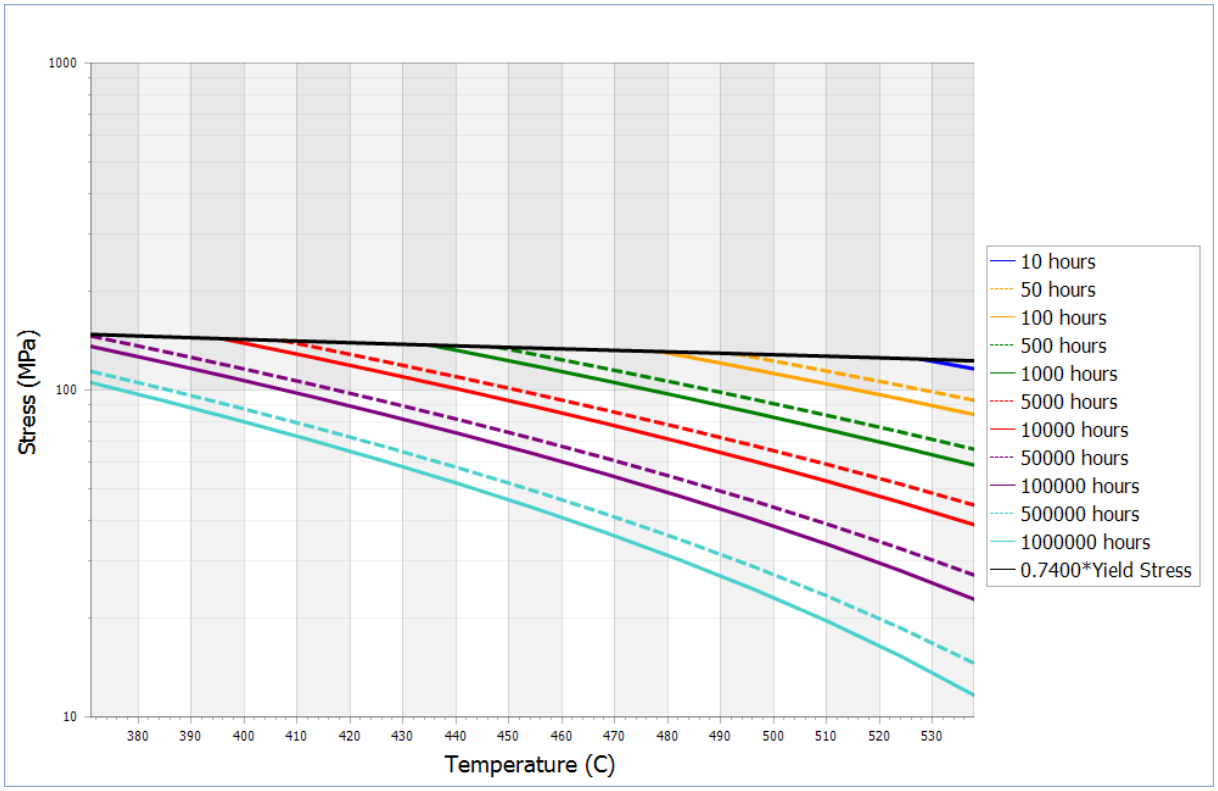

Figure 10.3M – Level 1 Screening Curve for Carbon Steel – $\sigma_{uts}^{min} < 413\ MPa$

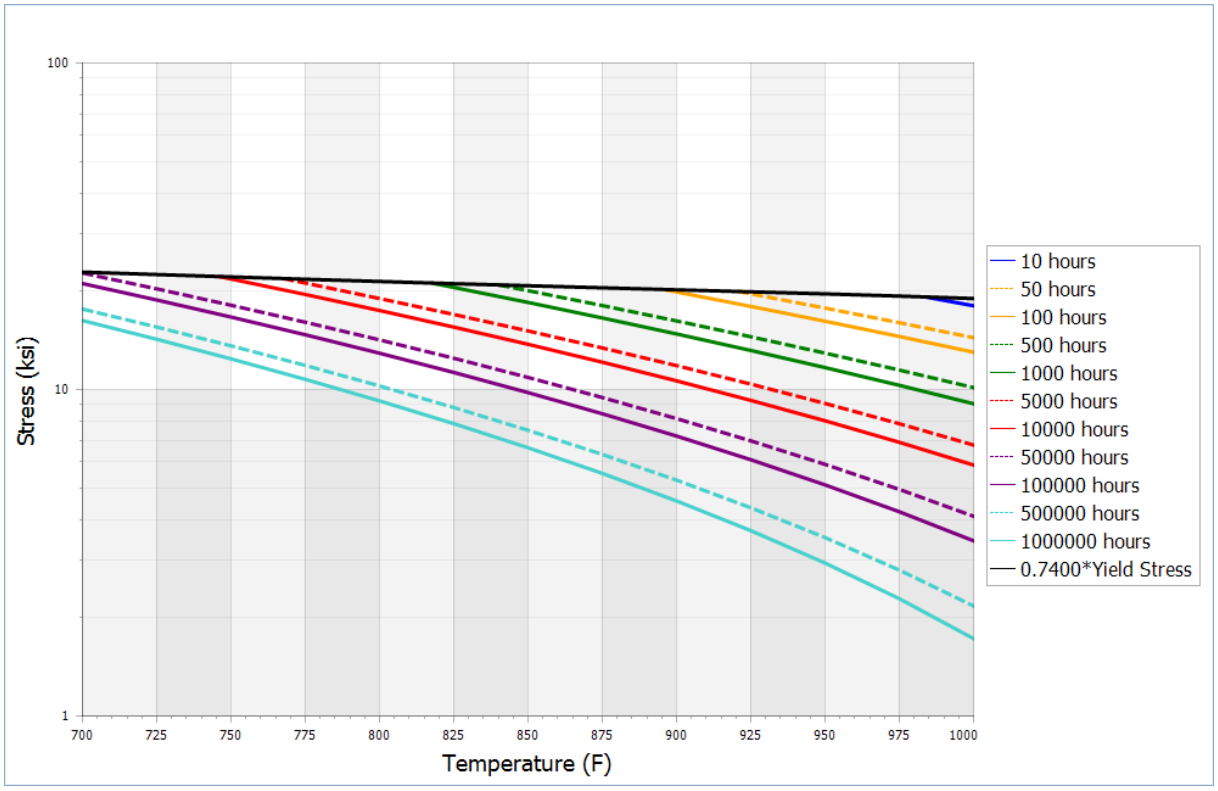

Figure 10.4 – Level 1 Screening Curve for Carbon Steel – $60\ ksi \leq \sigma_{uts}^{min} < 65\ ksi$

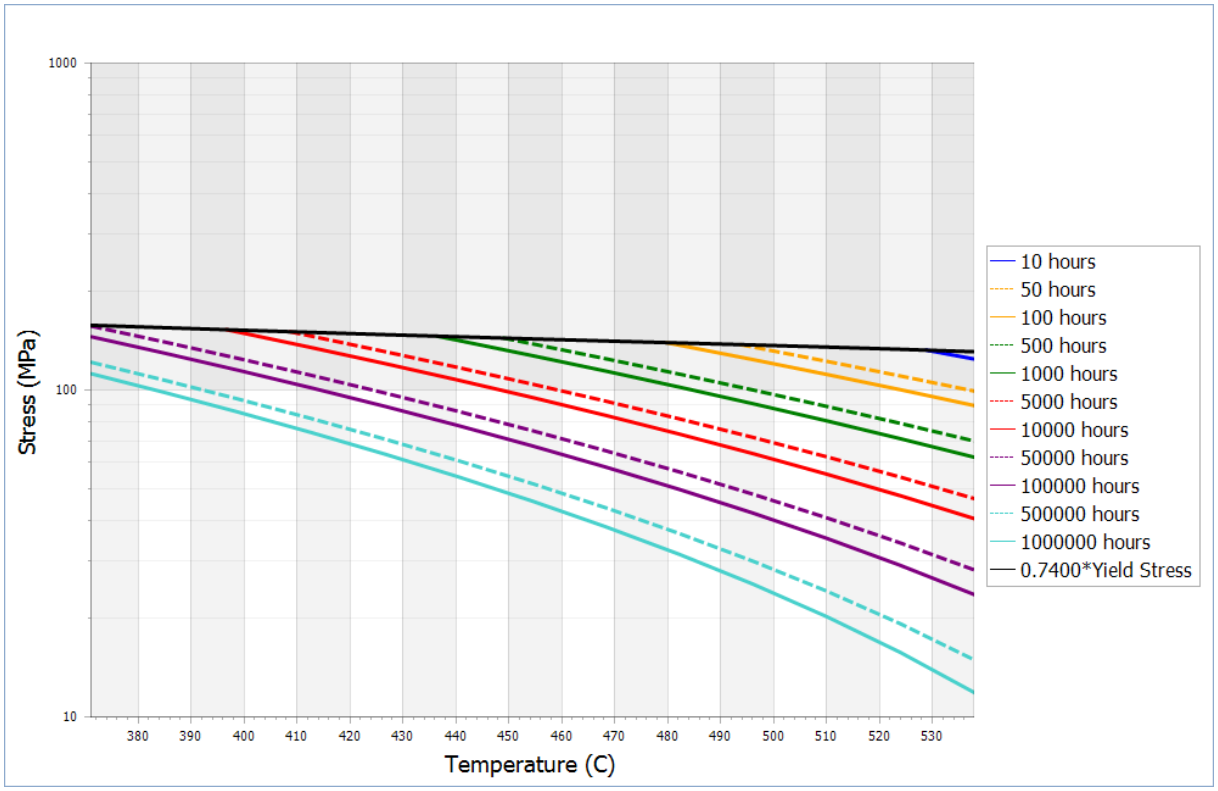

Figure 10.4M – Level 1 Screening Curve for Carbon Steel – $413\ MPa \leq \sigma_{uts}^{min} < 448\ MPa$

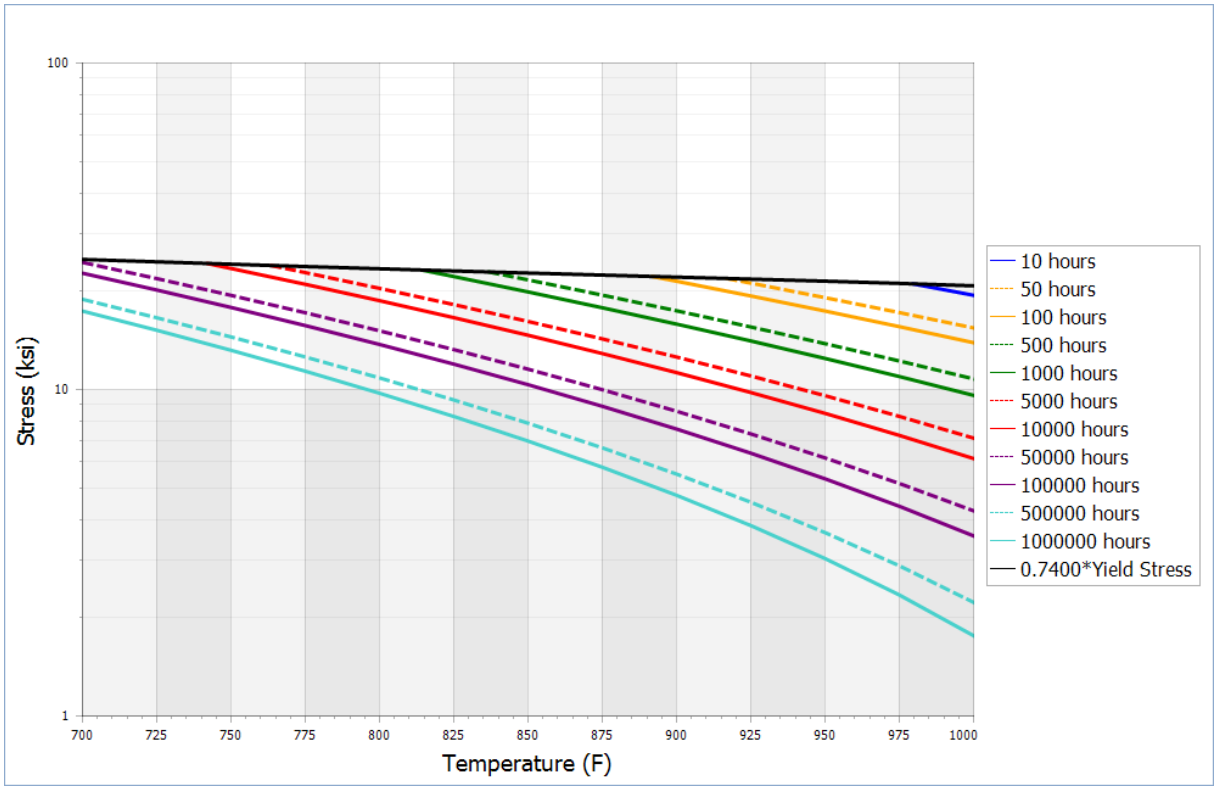

Figure 10.5 – Level 1 Screening Curve for Carbon Steel – $65\ ksi \leq \sigma_{uts}^{min} < 70\ ksi$

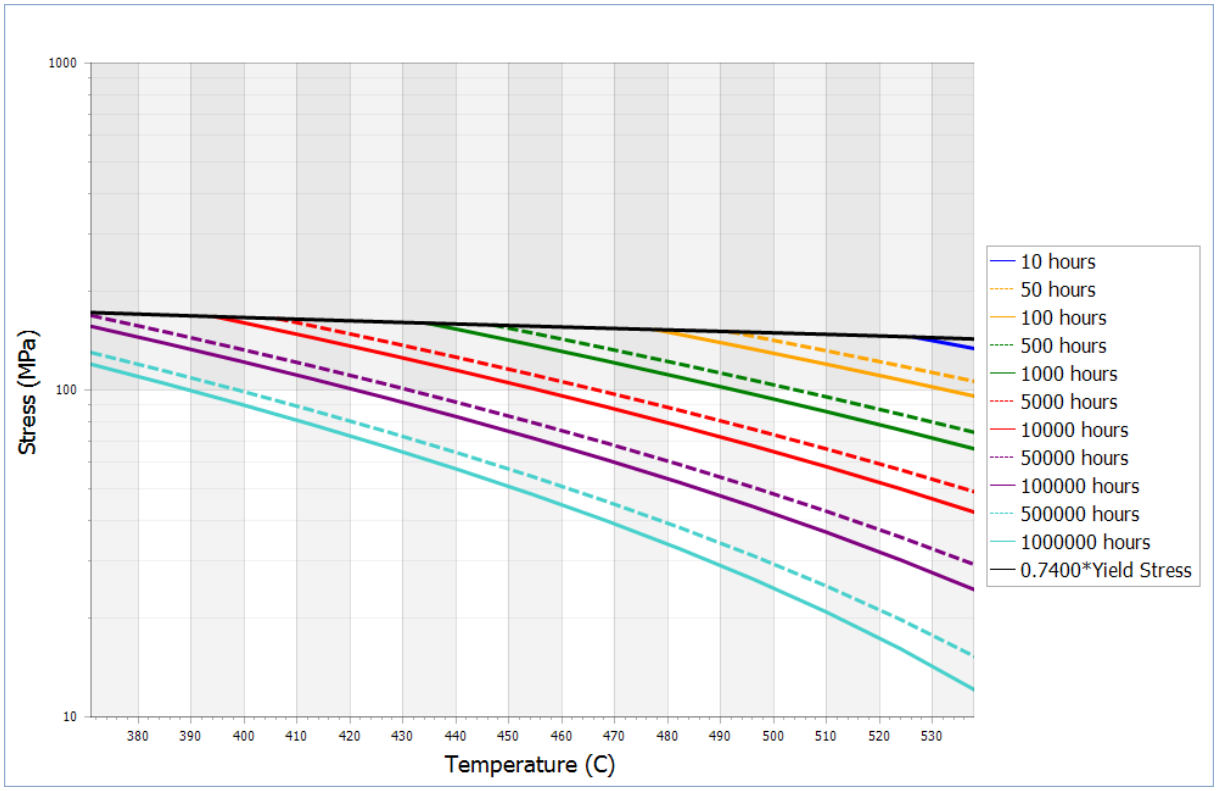

Figure 10.5M – Level 1 Screening Curve for Carbon Steel – $448\ MPa \leq \sigma_{uts}^{min} < 483\ MPa$

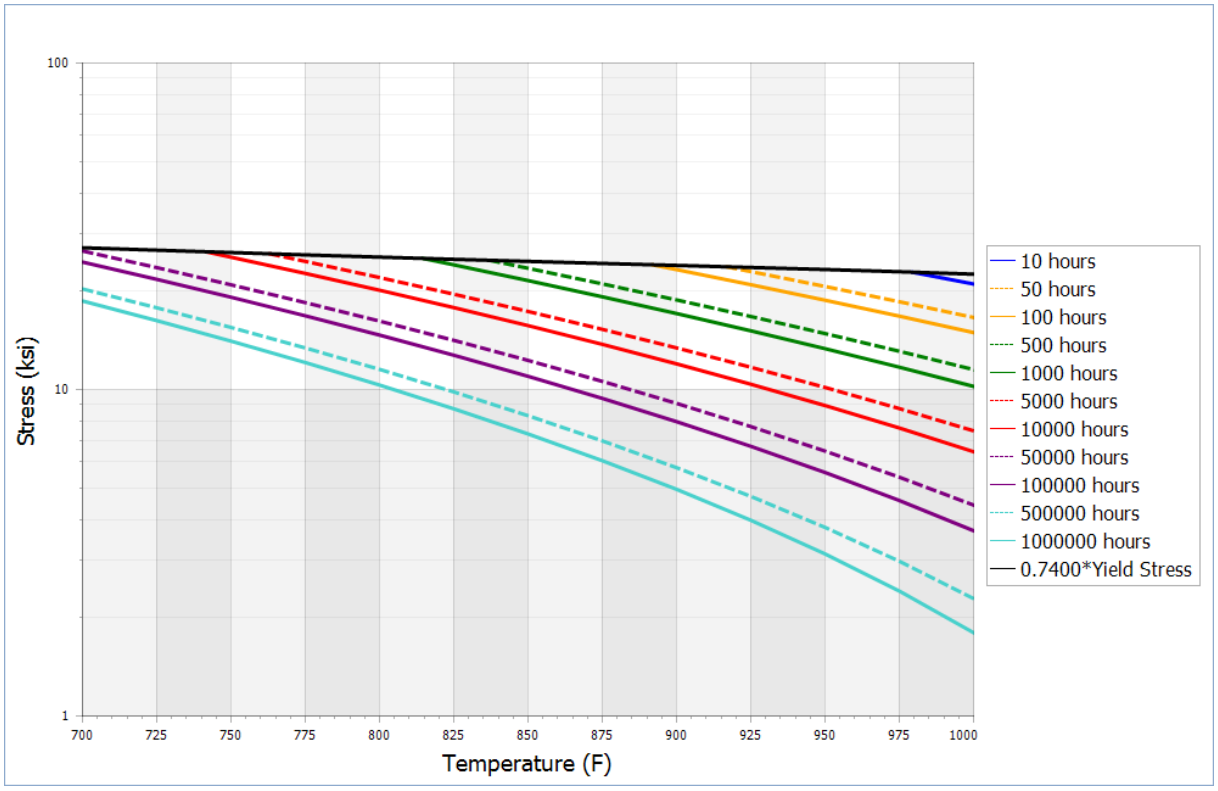

Figure 10.6 – Level 1 Screening Curve for Carbon Steel – $70\ ksi \leq \sigma_{uts}^{min} < 75\ ksi$

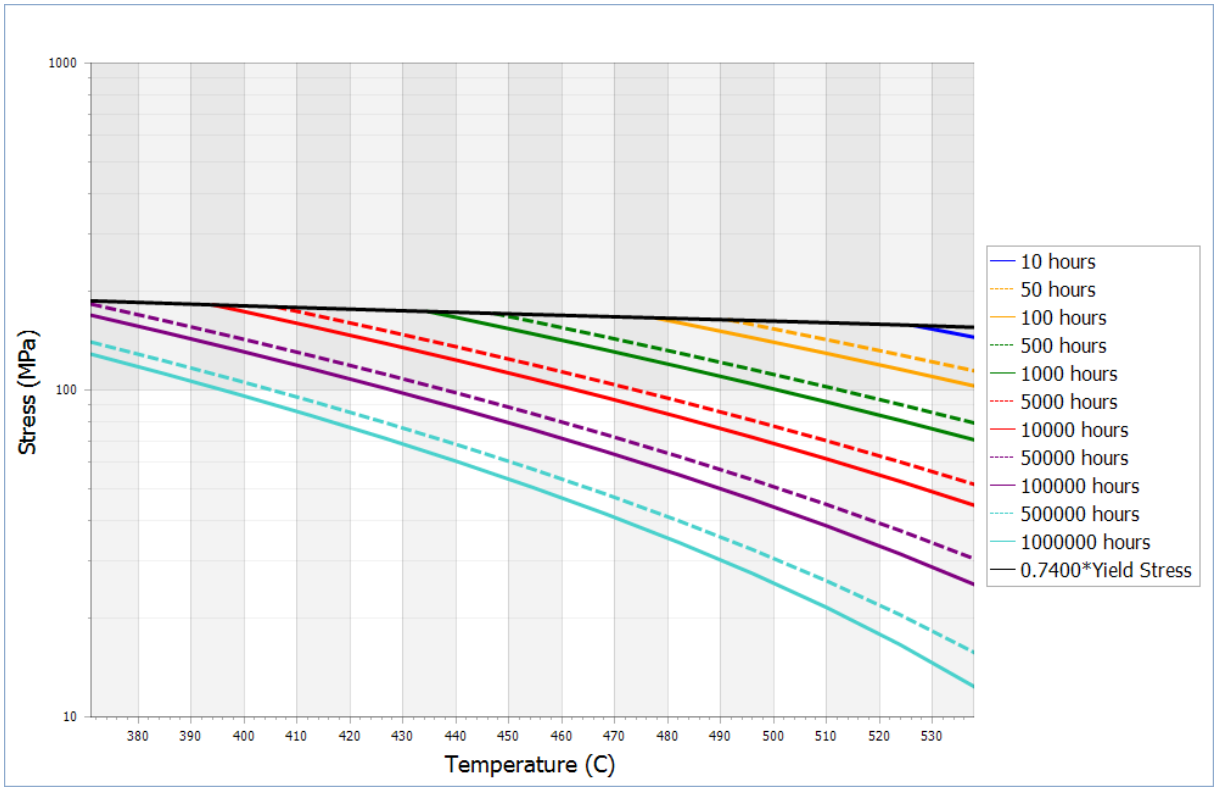

Figure 10.6M – Level 1 Screening Curve for Carbon Steel – $483\ MPa \leq \sigma_{uts}^{min} < 517\ MPa$

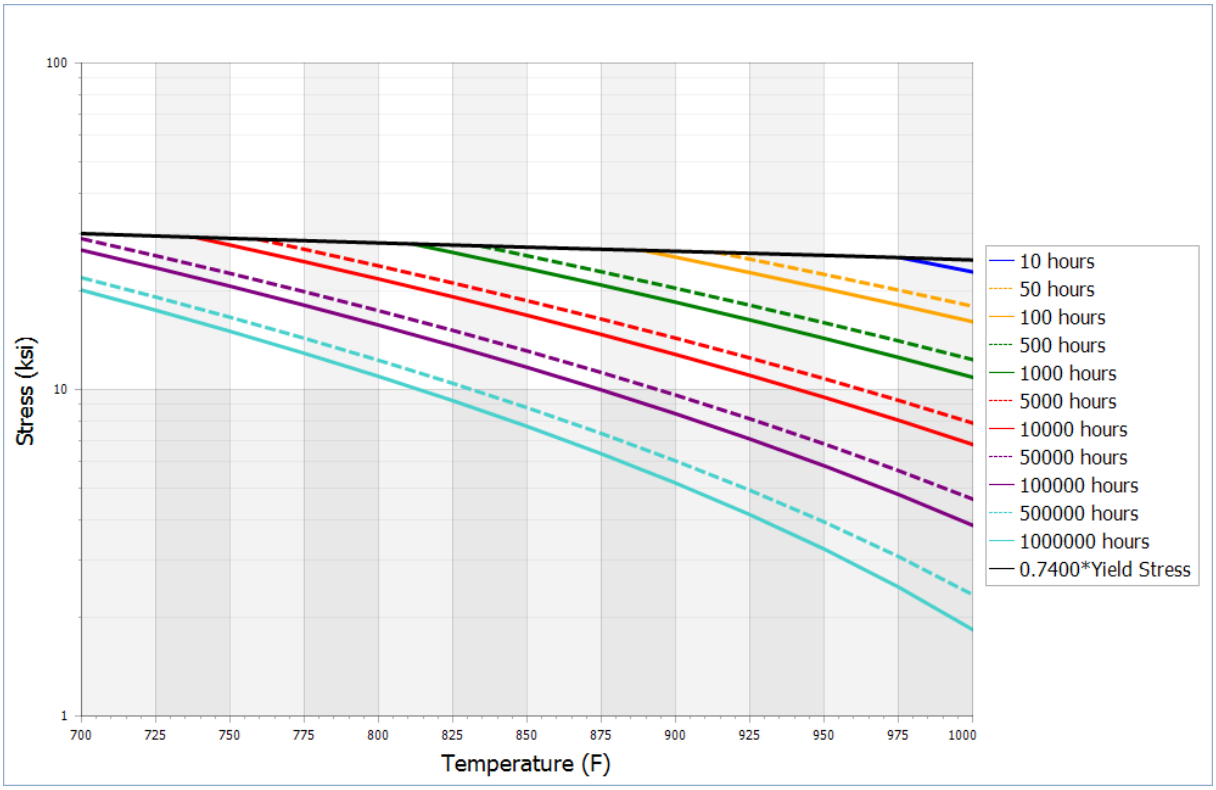

Figure 10.7 – Level 1 Screening Curve for Carbon Steel – $\sigma_{uts}^{min} \geq 75\ ksi$

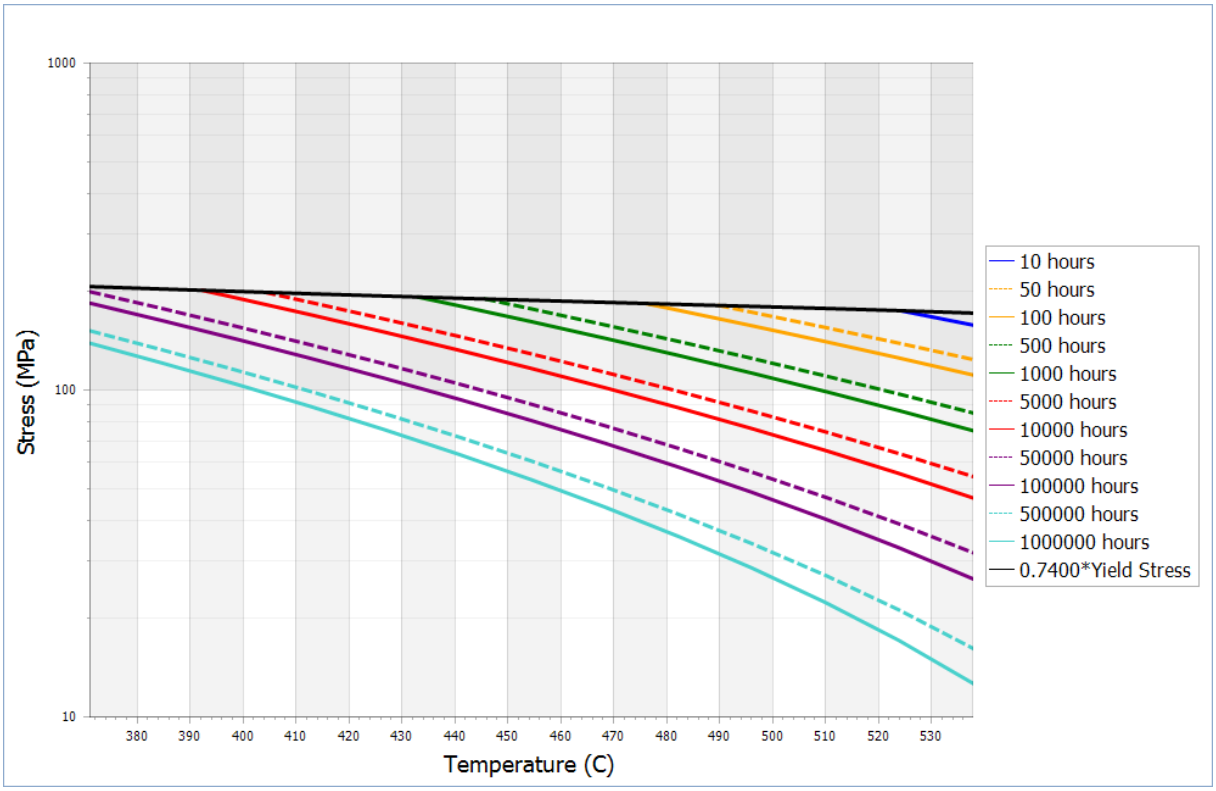

Figure 10.7M – Level 1 Screening Curve for Carbon Steel – $\sigma_{uts}^{min} \geq 517\ MPa$

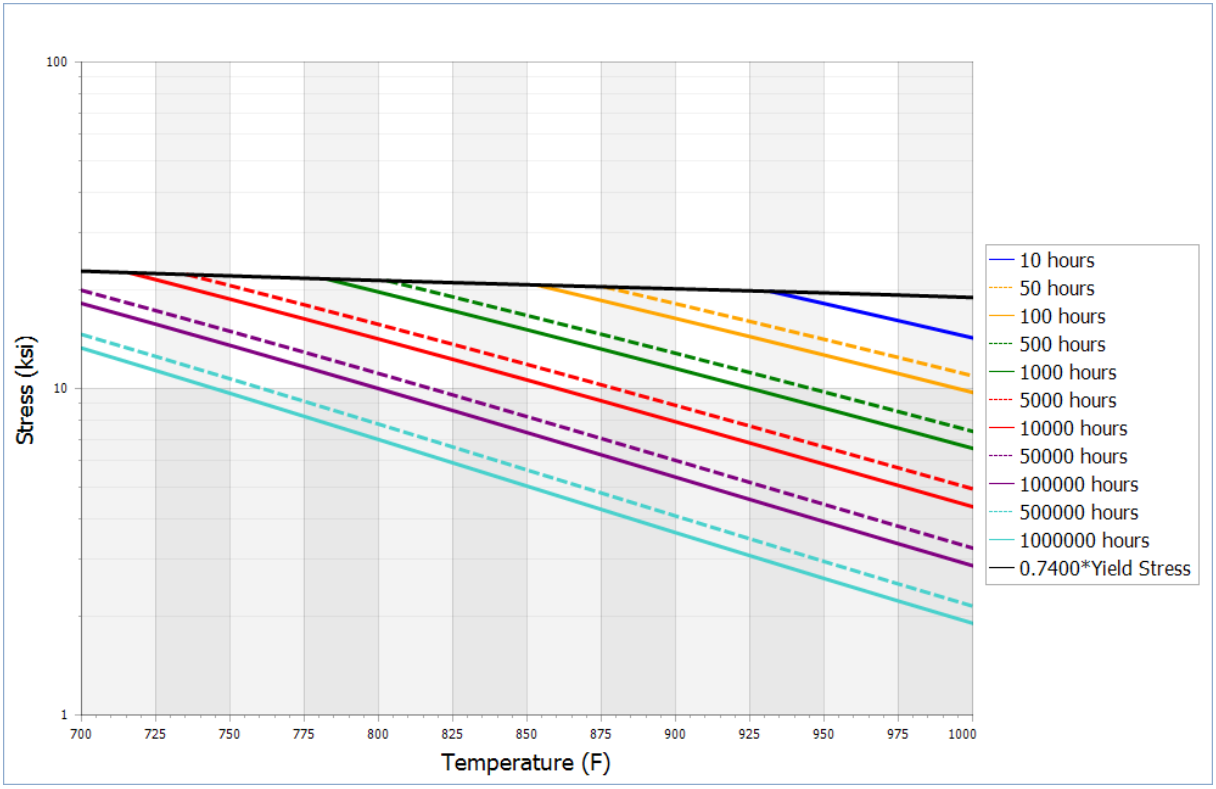

Figure 10.8 – Level 1 Screening Curve for Carbon Steel (Graphitized)

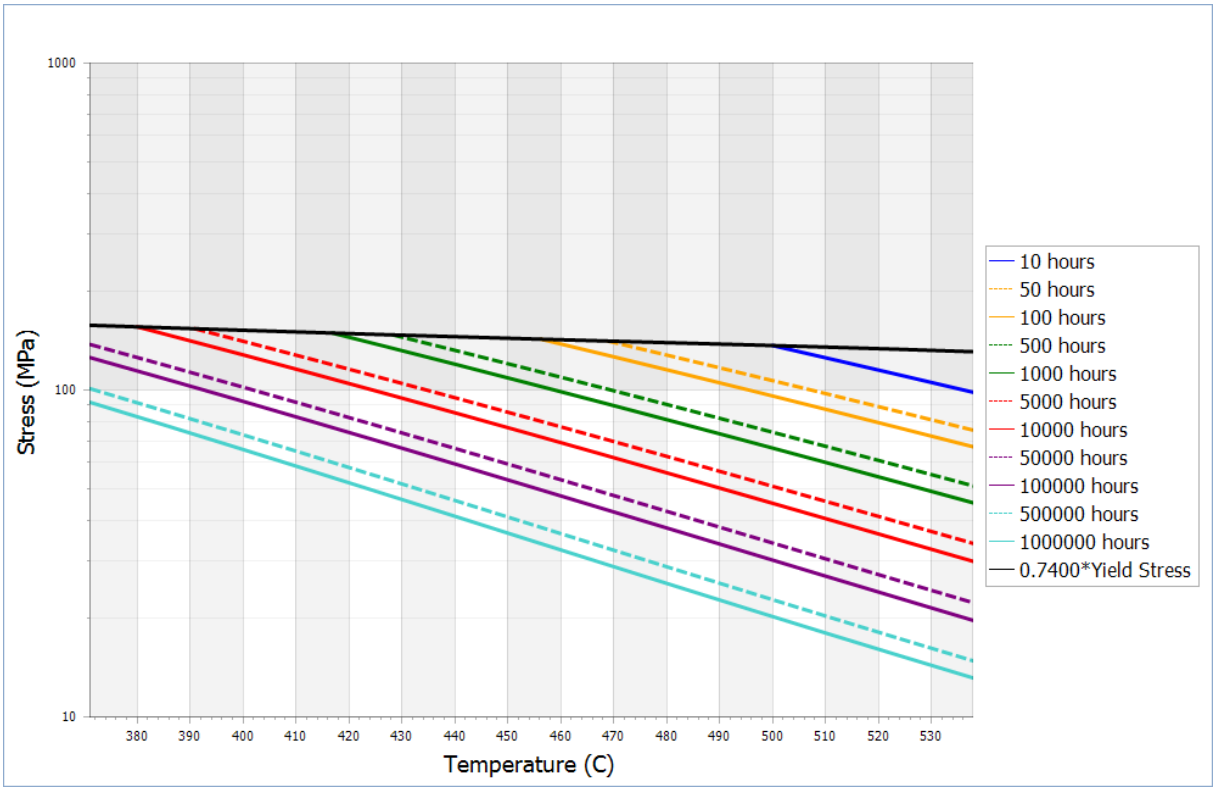

Figure 10.8M – Level 1 Screening Curve for Carbon Steel (Graphitized)

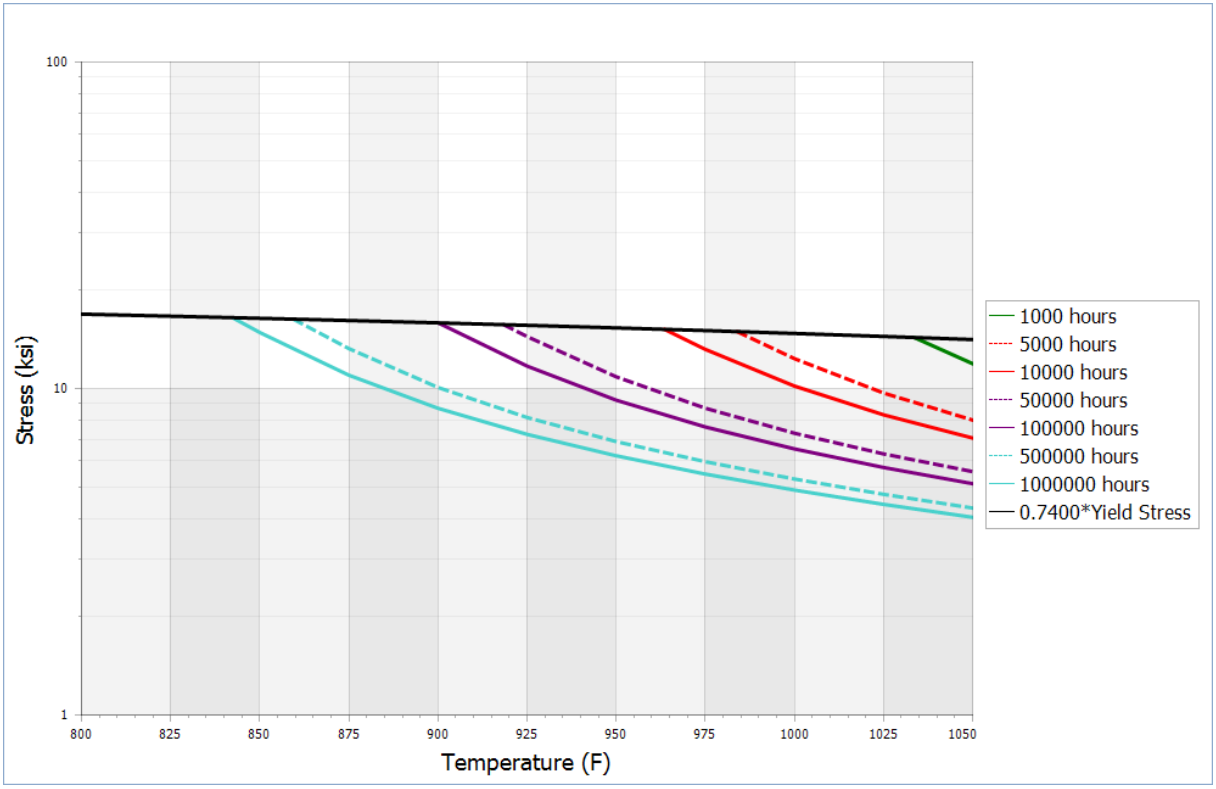

Figure 10.9 – Level 1 Screening Curve for C–0.5Mo

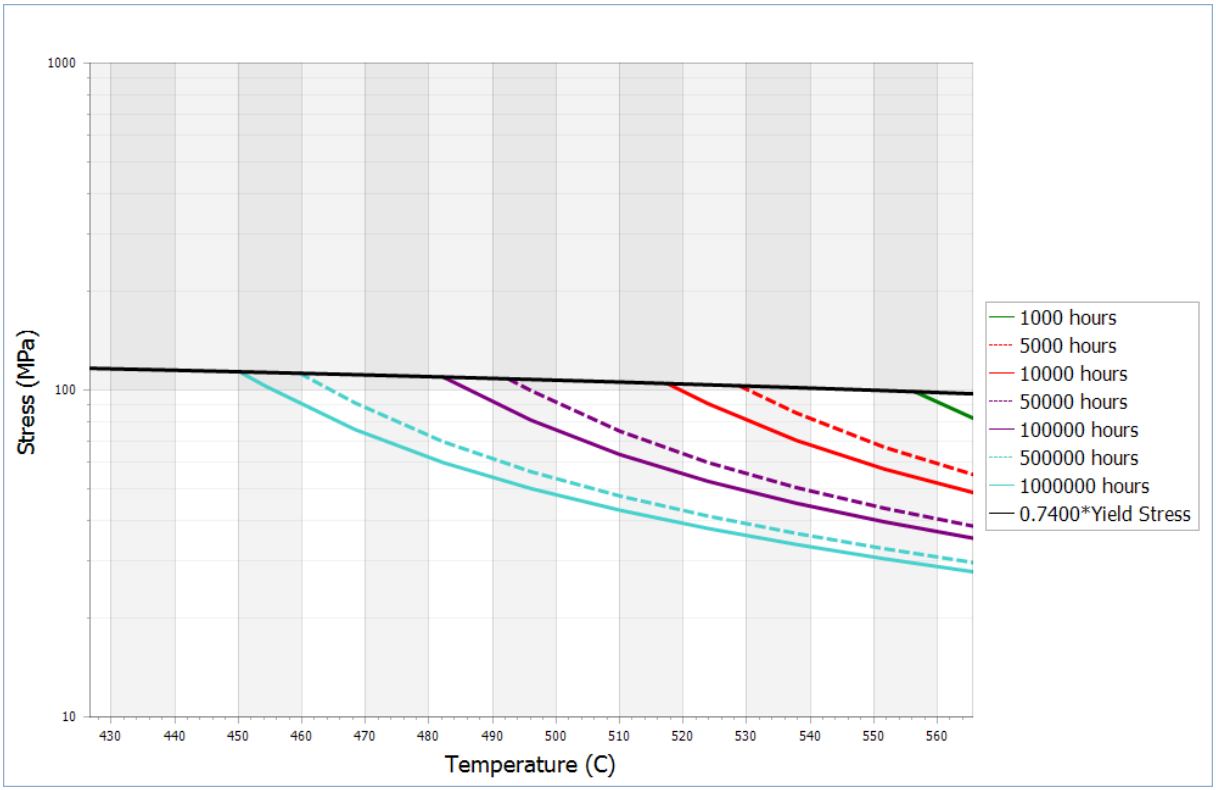

Figure 10.9M – Level 1 Screening Curve for C–0.5Mo

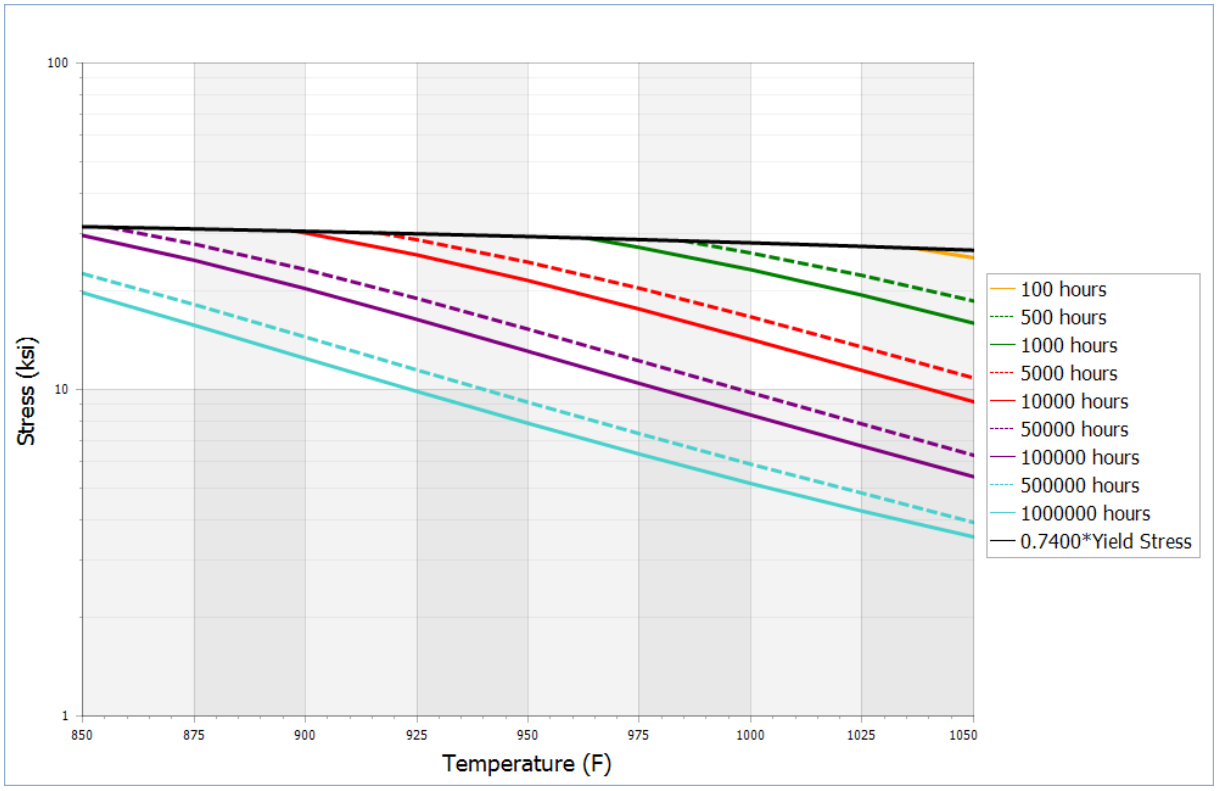

Figure 10.10 – Level 1 Screening Curve for 1.25Cr–0.5Mo (NT)

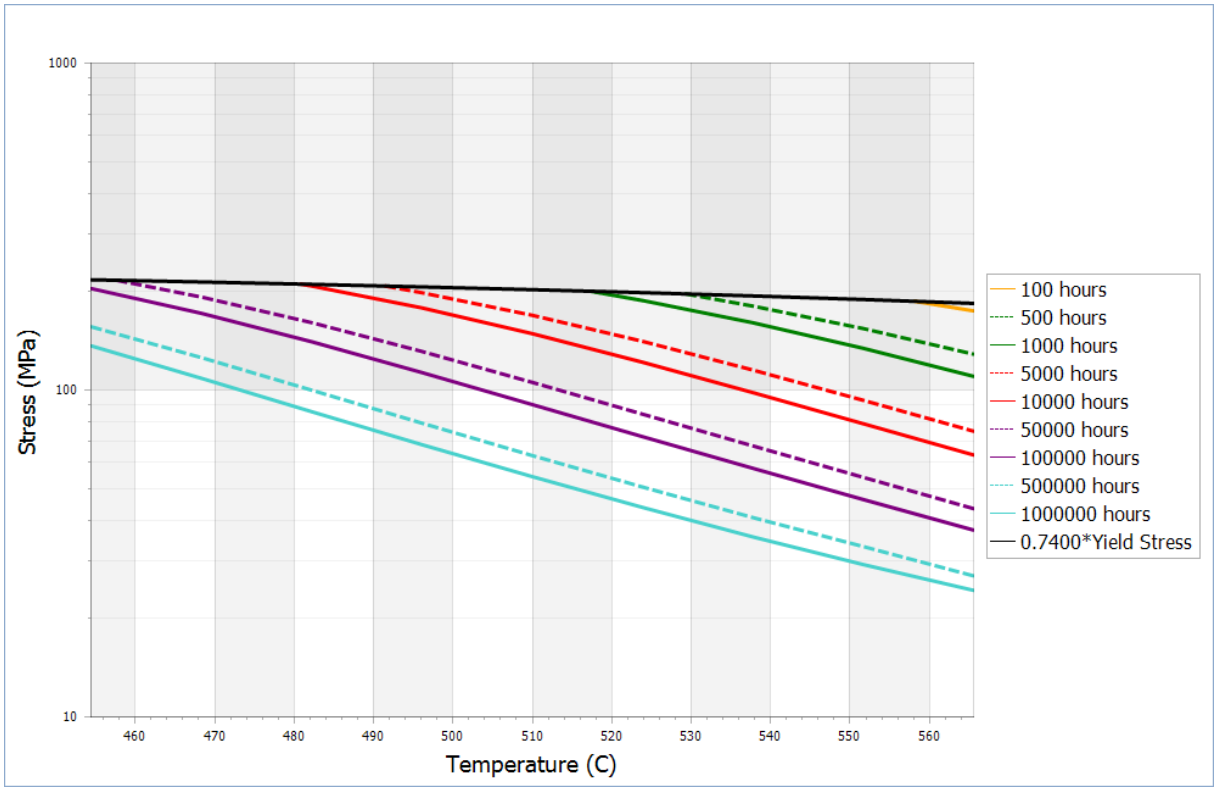

Figure 10.10M – Level 1 Screening Curve for 1.25Cr–0.5Mo (NT)

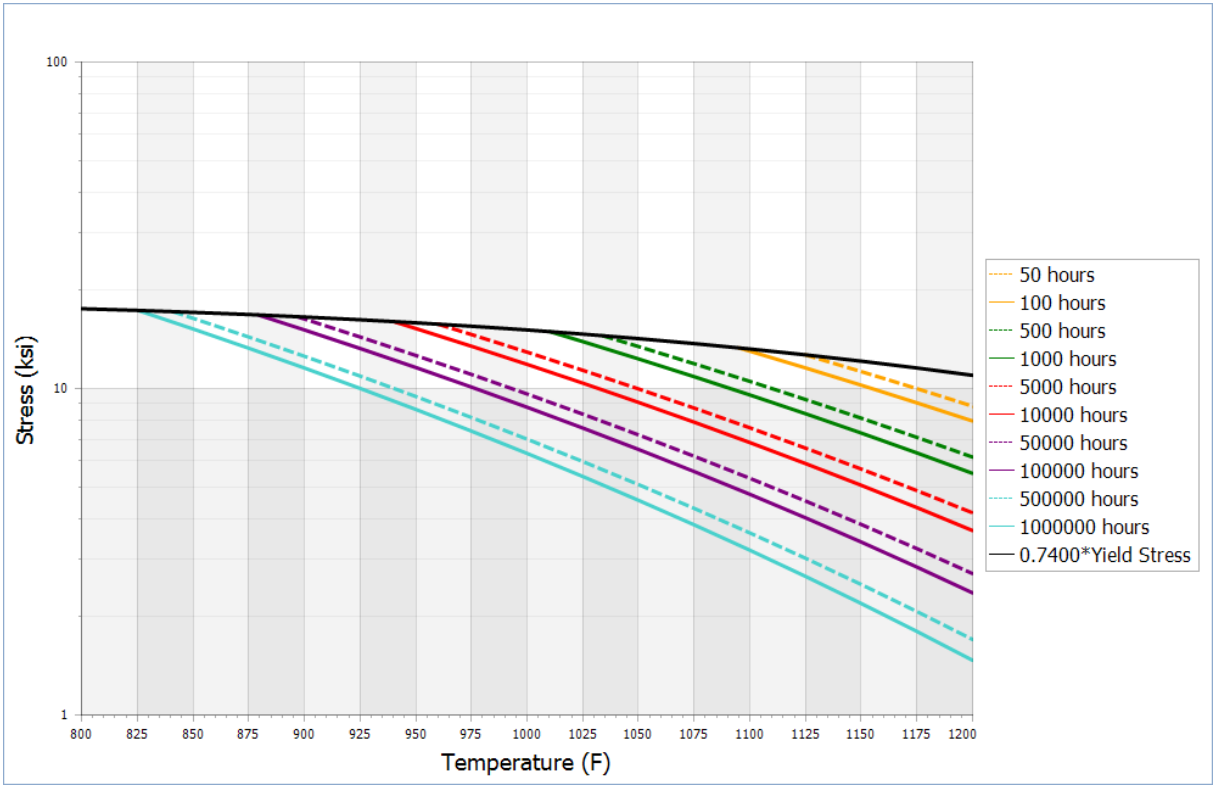

Figure 10.11 – Level 1 Screening Curve for 1.25Cr–0.5Mo (Annealed)

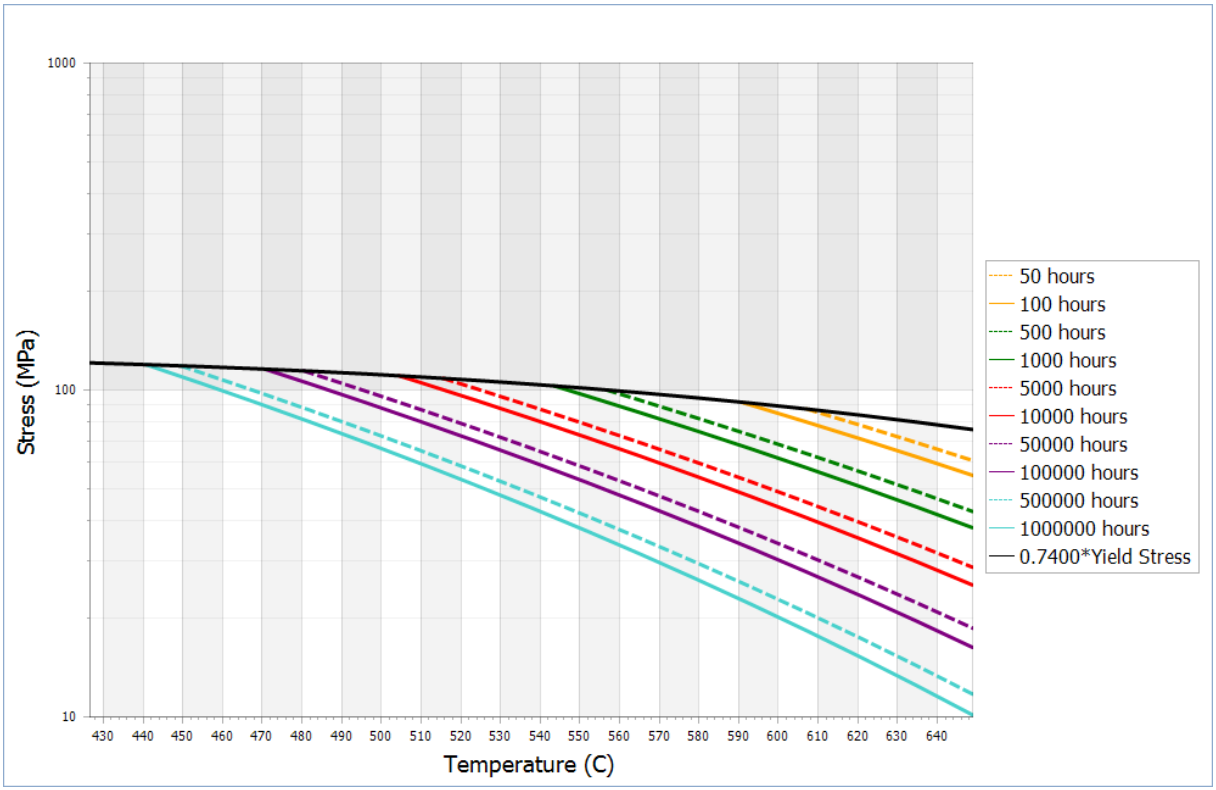

Figure 10.11M – Level 1 Screening Curve for 1.25Cr–0.5Mo (Annealed)

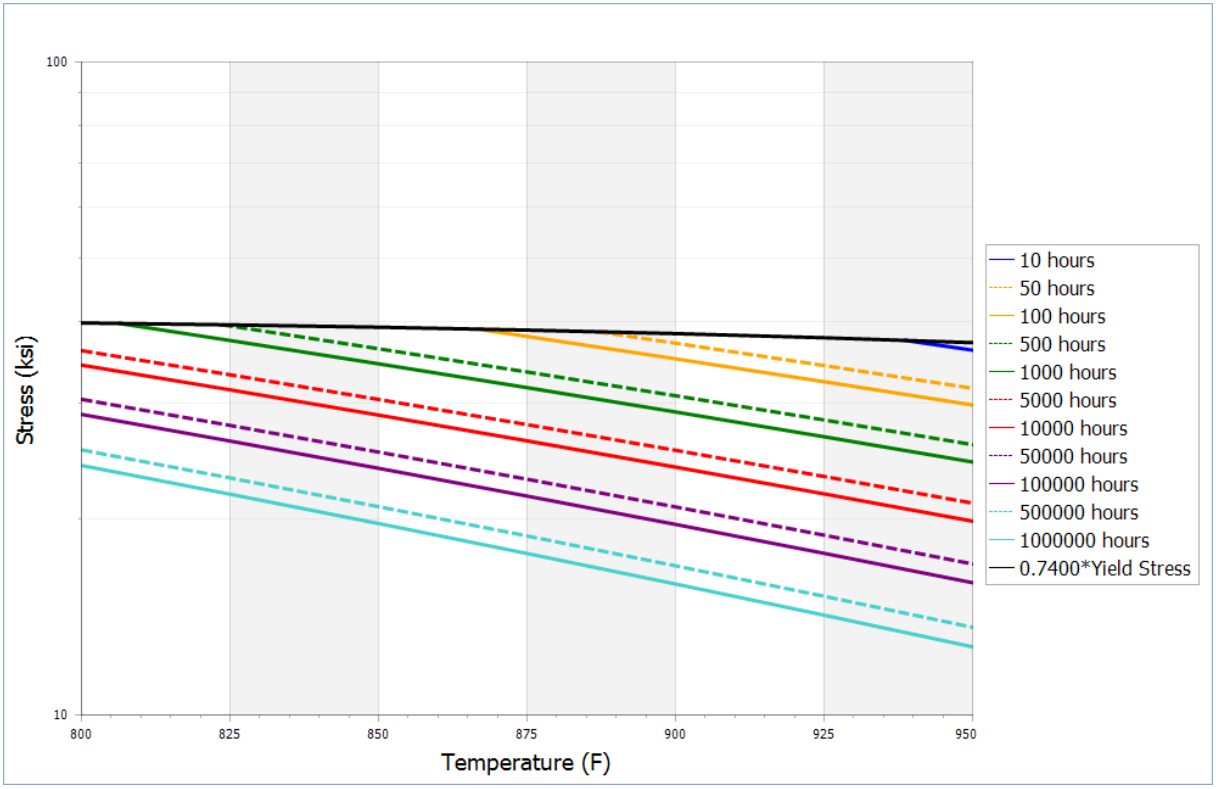

Figure 10.12 – Level 1 Screening Curve for 2.25Cr–1Mo (NT)

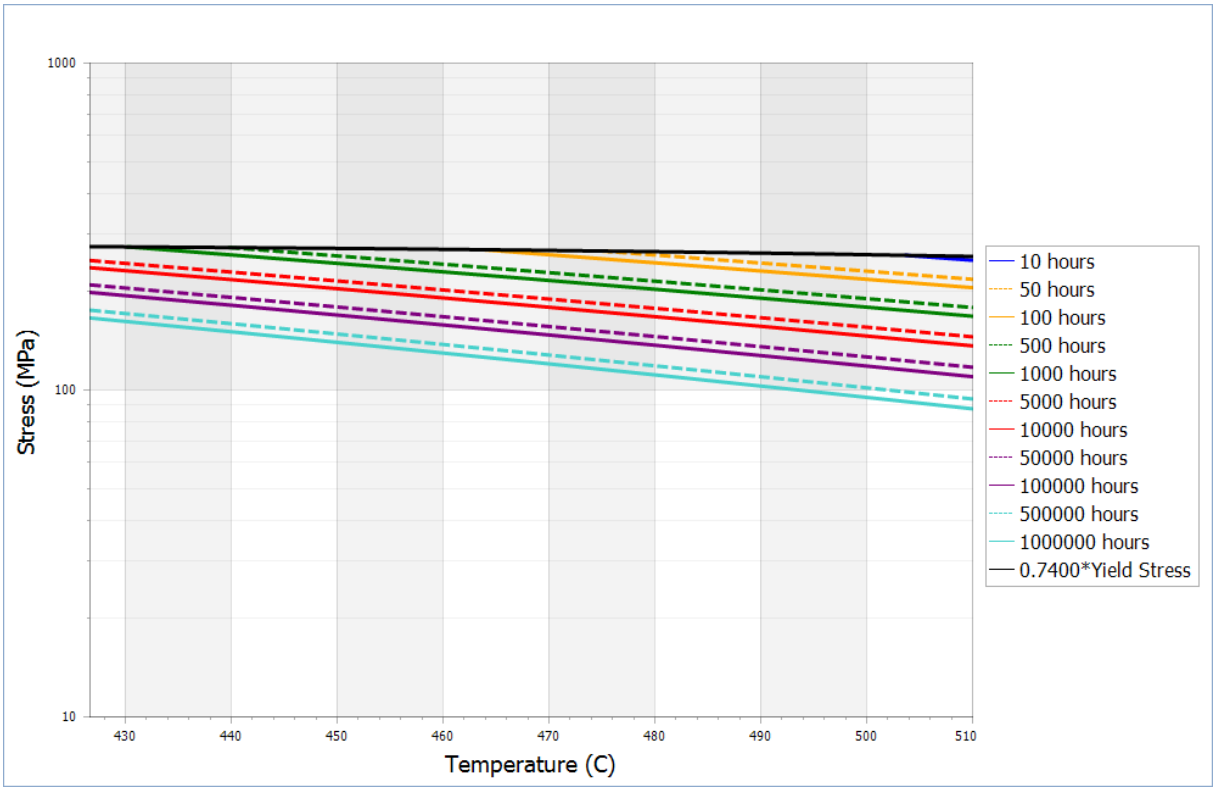

Figure 10.12M – Level 1 Screening Curve for 2.25Cr–1Mo (NT)

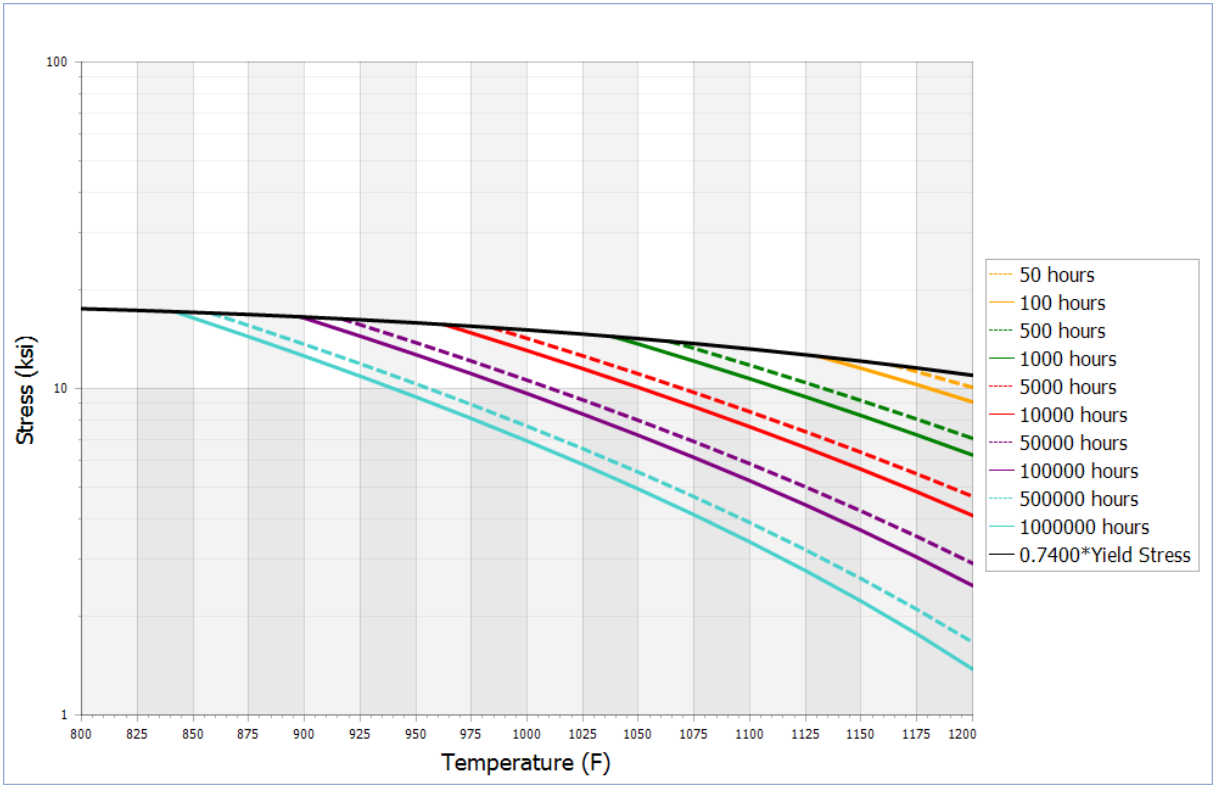

Figure 10.13 – Level 1 Screening Curve for 2.25Cr–1Mo (Annealed)

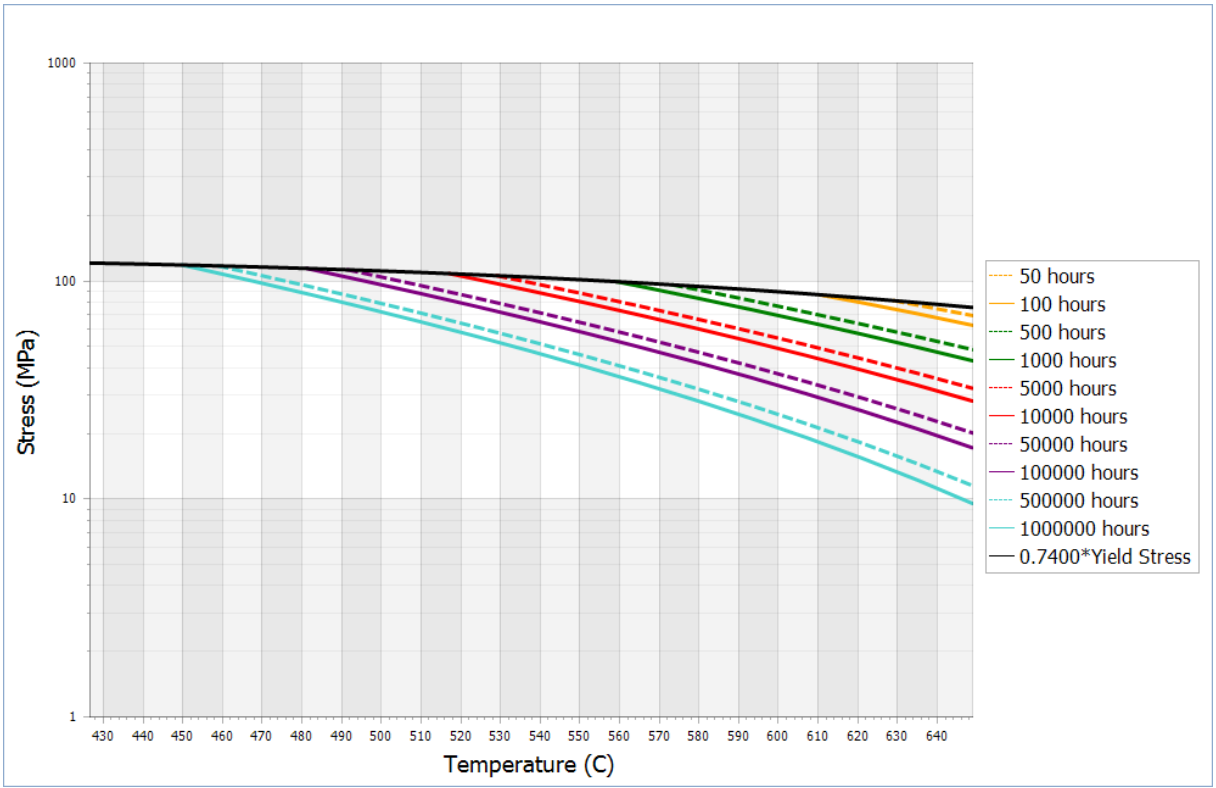

Figure 10.13M – Level 1 Screening Curve for 2.25Cr–1Mo (Annealed)

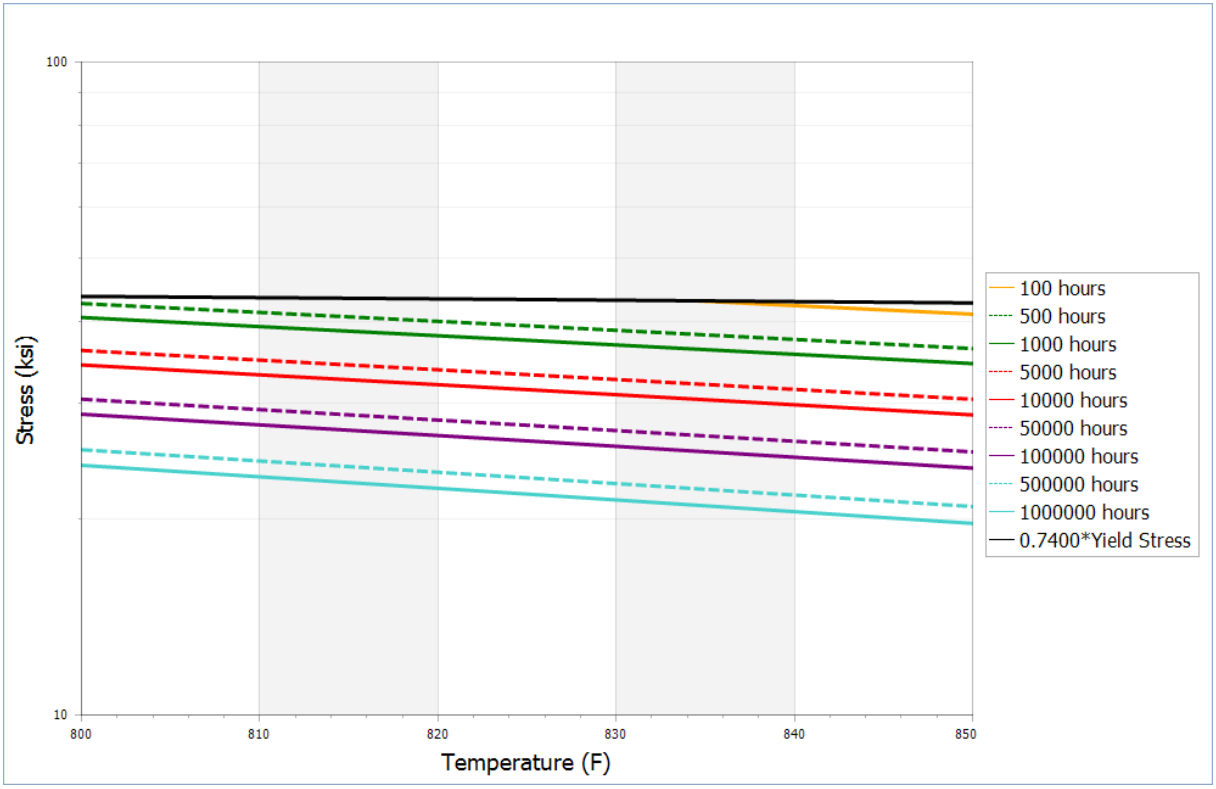

Figure 10.14 – Level 1 Screening Curve for 2.25Cr–1Mo (QT)

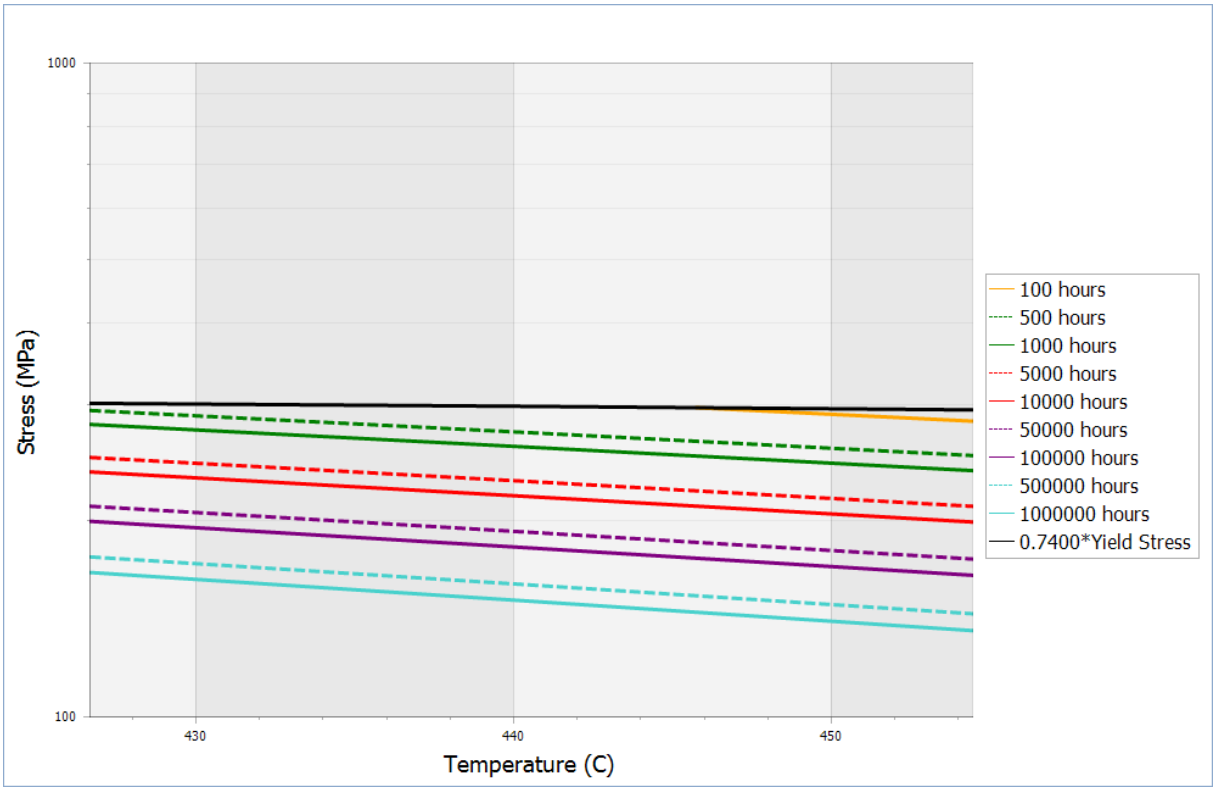

Figure 10.14M – Level 1 Screening Curve for 2.25Cr–1Mo (QT)

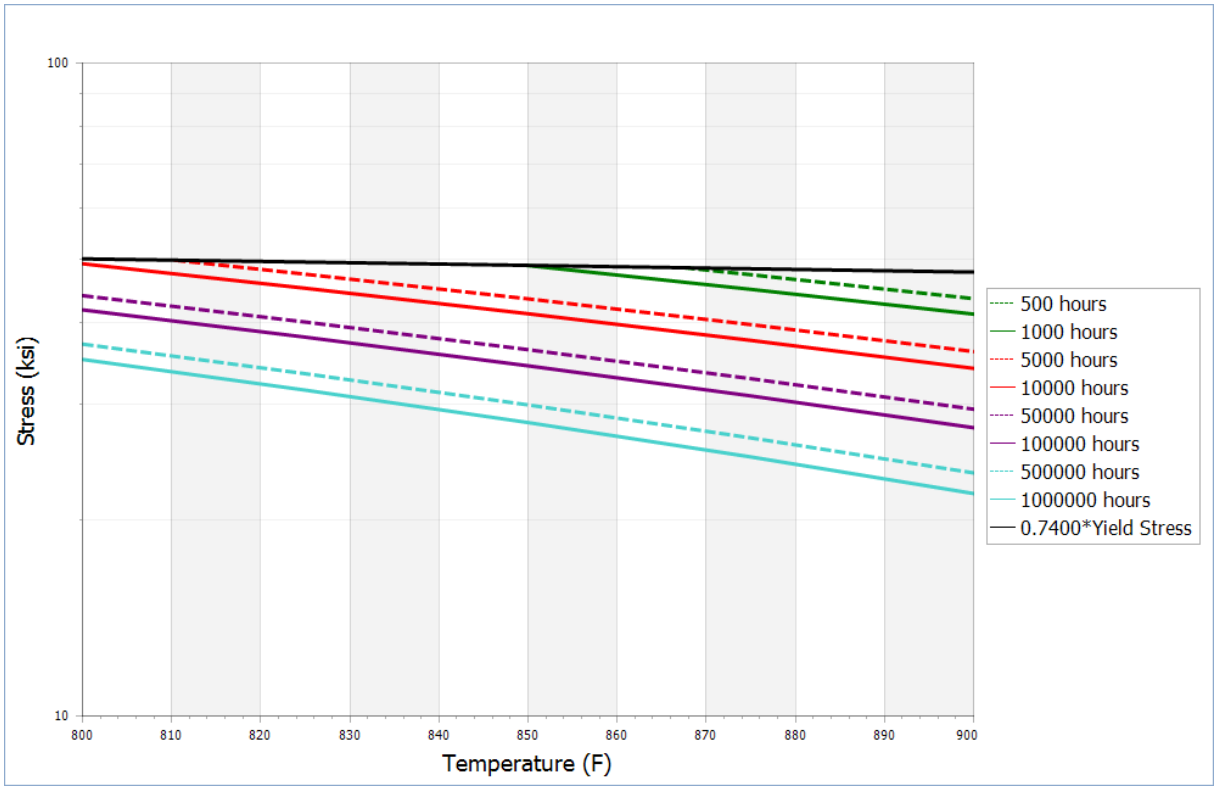

Figure 10.15 – Level 1 Screening Curve for 2.25Cr–1Mo–V

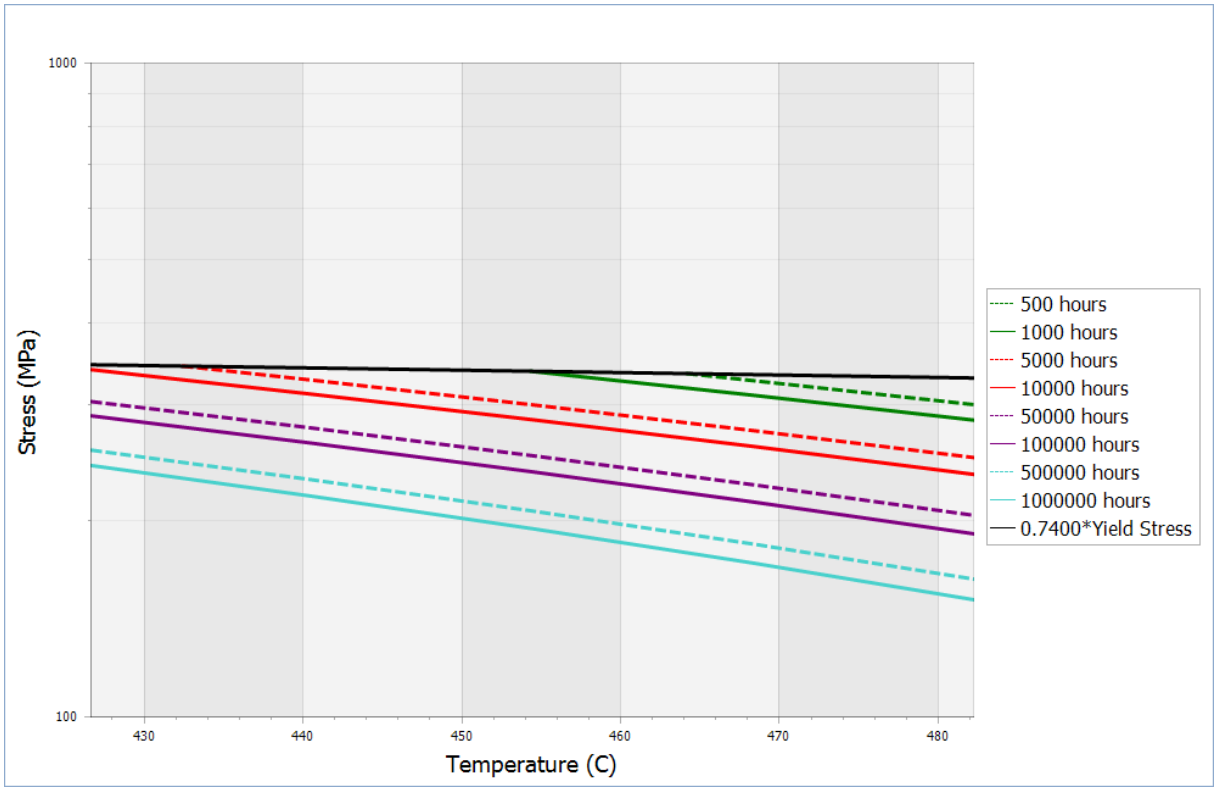

Figure 10.15M – Level 1 Screening Curve for 2.25Cr–1Mo–V

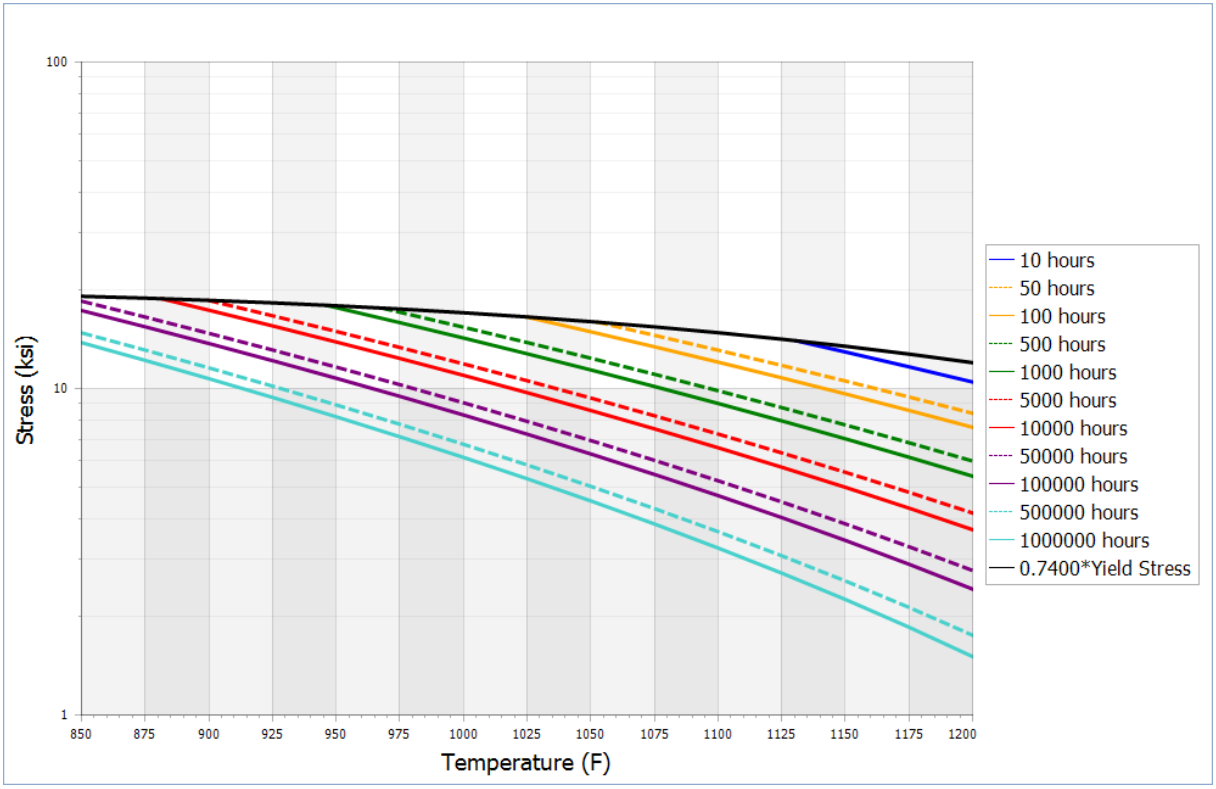

Figure 10.16 – Level 1 Screening Curve for 5Cr–0.5Mo

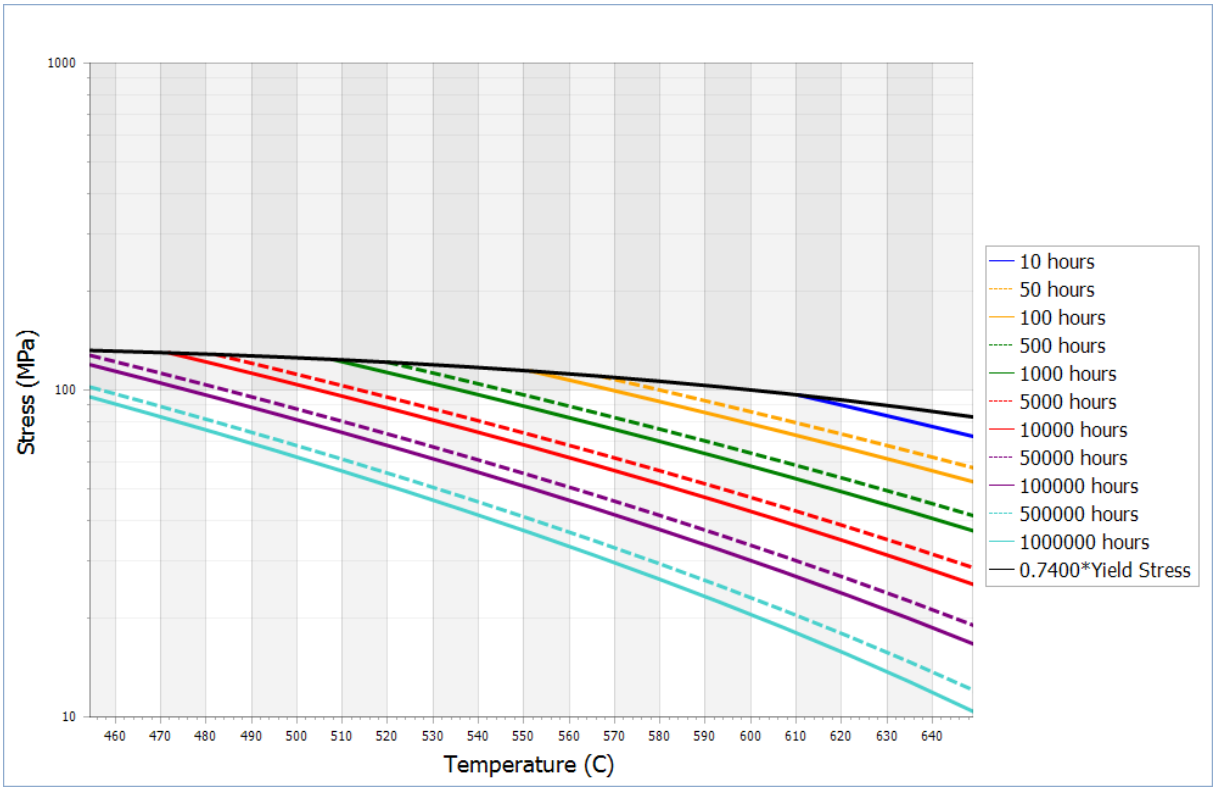

Figure 10.16M – Level 1 Screening Curve for 5Cr–0.5Mo

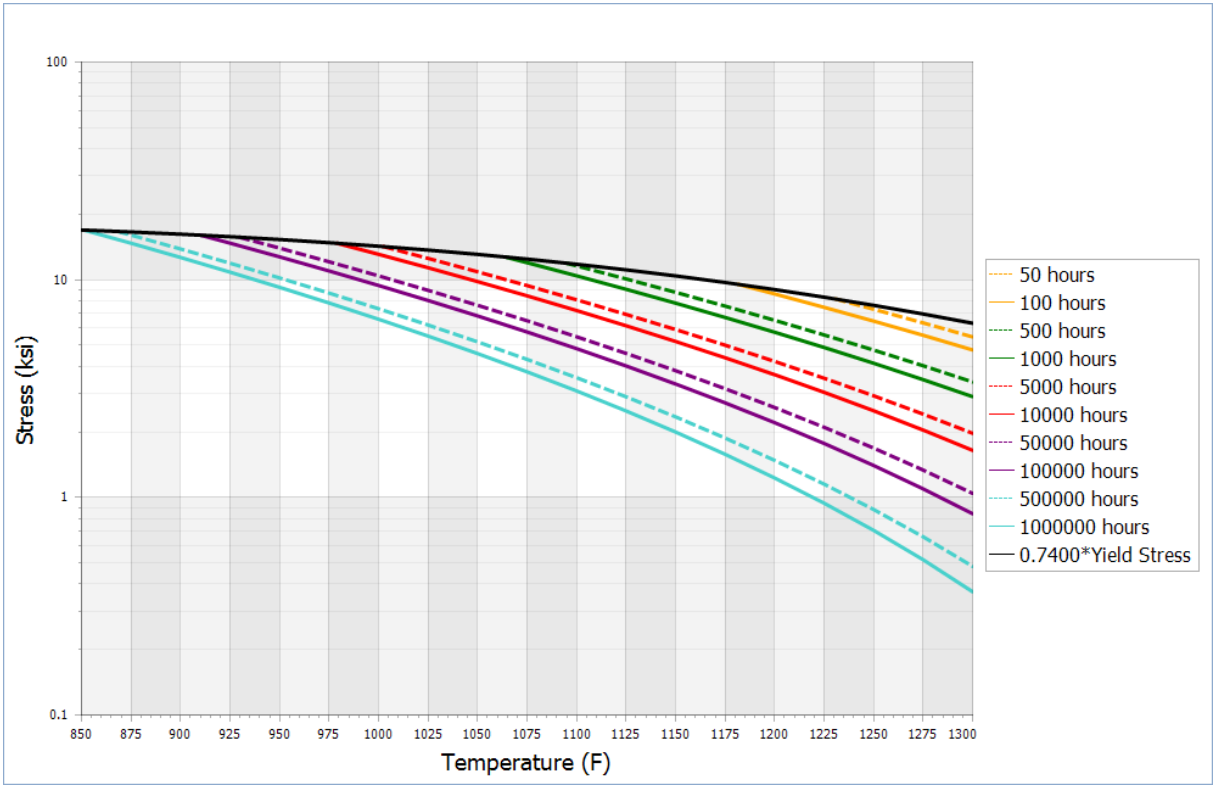

Figure 10.17 – Level 1 Screening Curve for 9Cr–1Mo

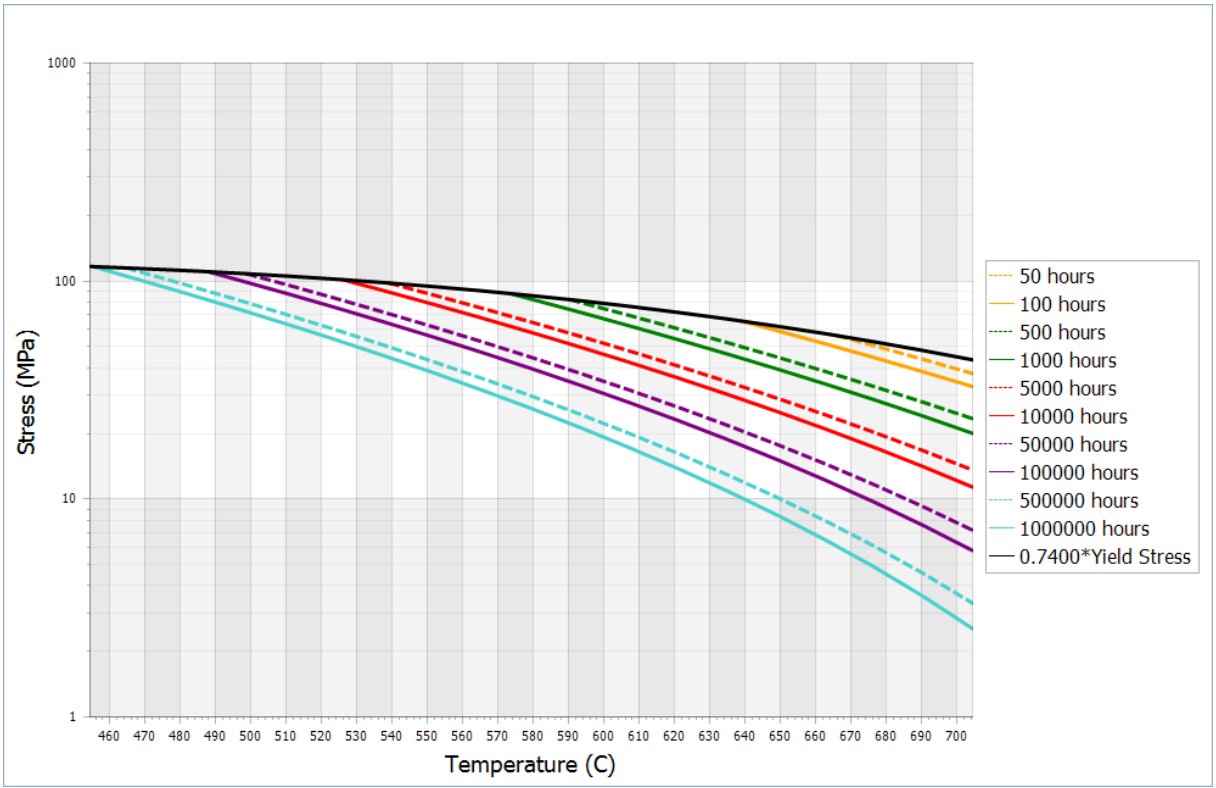

Figure 10.17M – Level 1 Screening Curve for 9Cr–1Mo

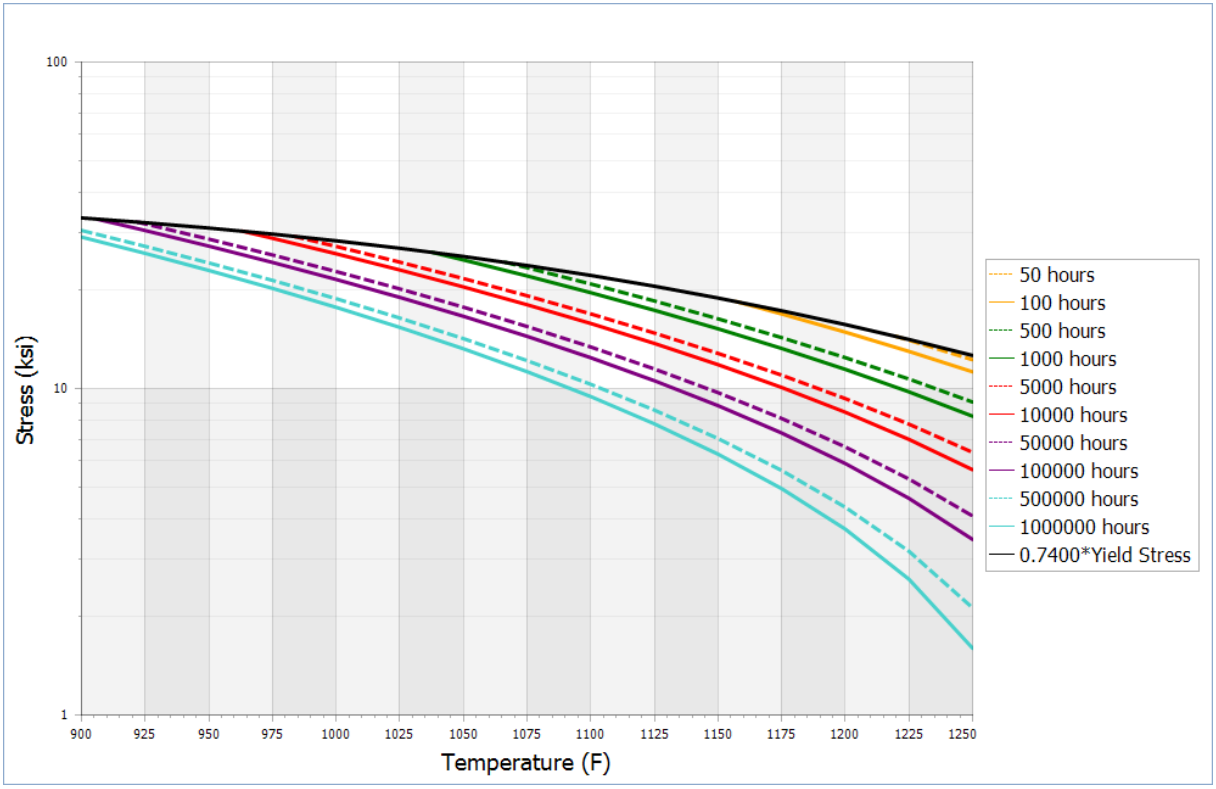

Figure 10.18 – Level 1 Screening Curve for 9Cr–1Mo–V

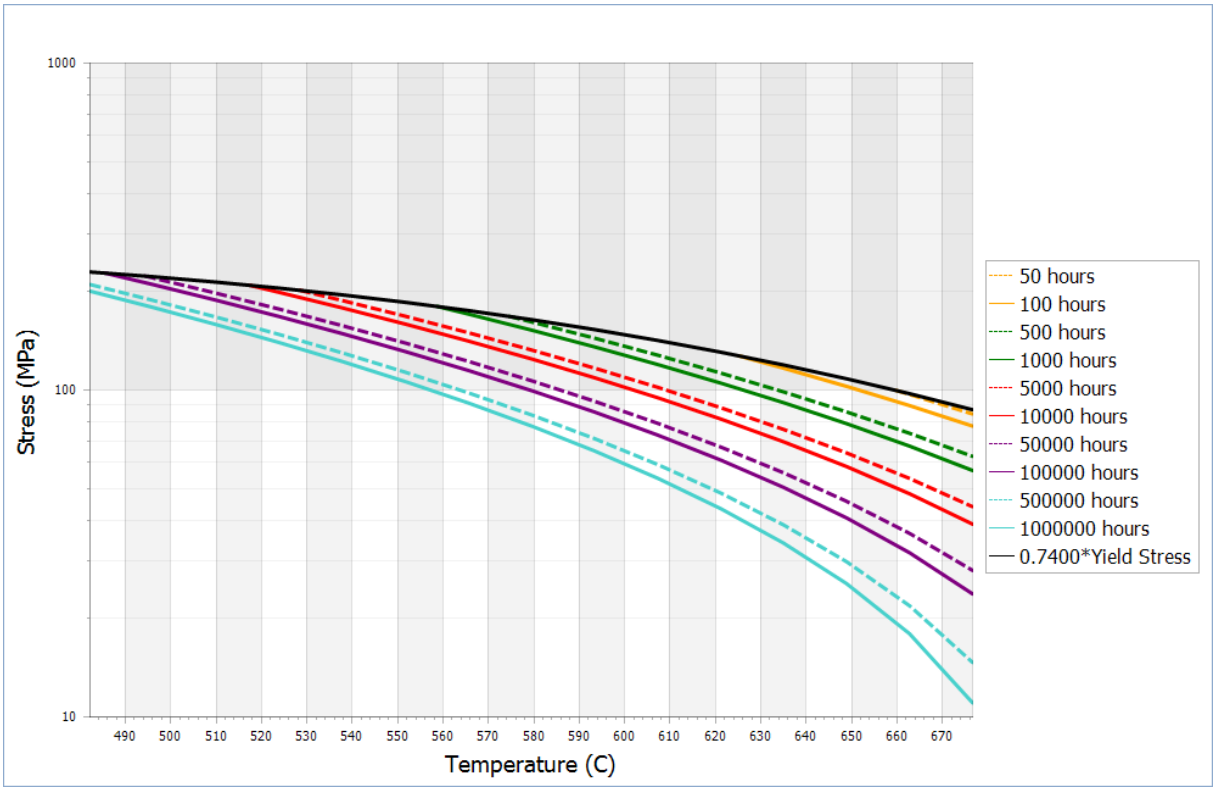

Figure 10.18M – Level 1 Screening Curve for 9Cr–1Mo–V

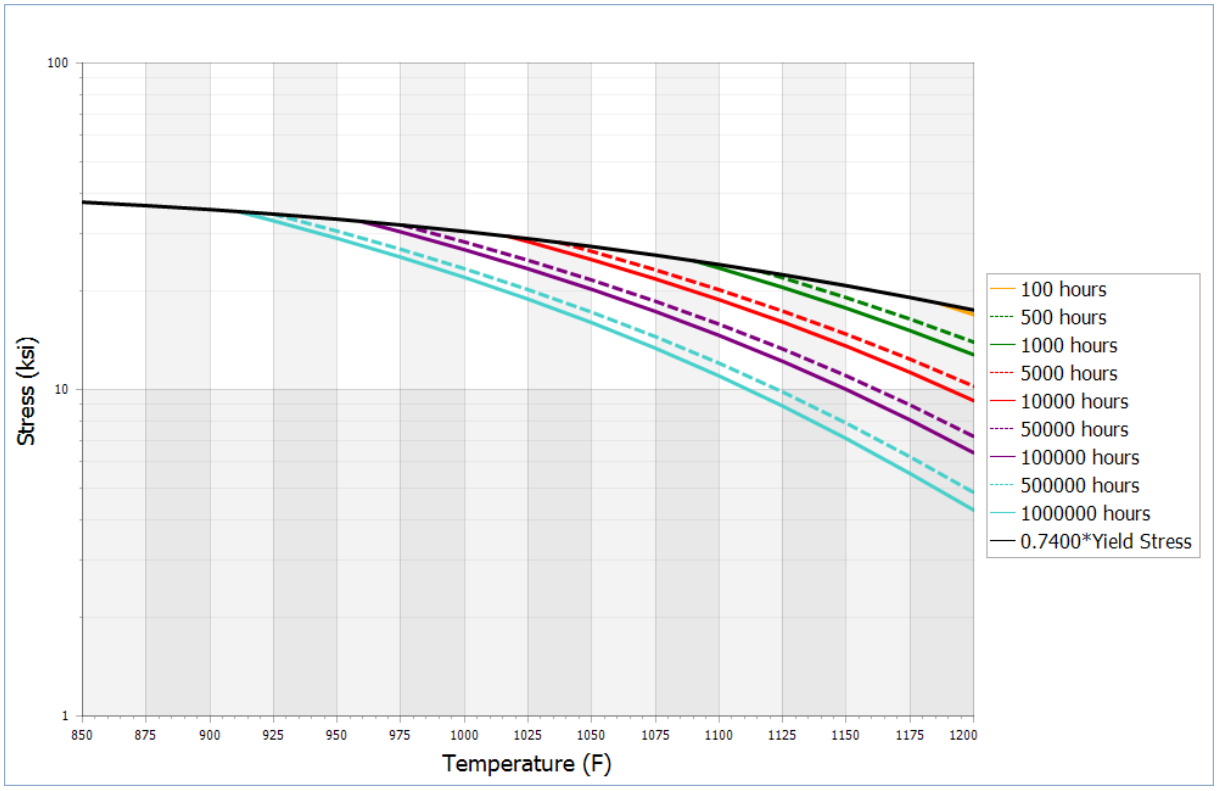

Figure 10.19 – Level 1 Screening Curve for 10.5Cr–V (Alloy 115 UNSK91060)

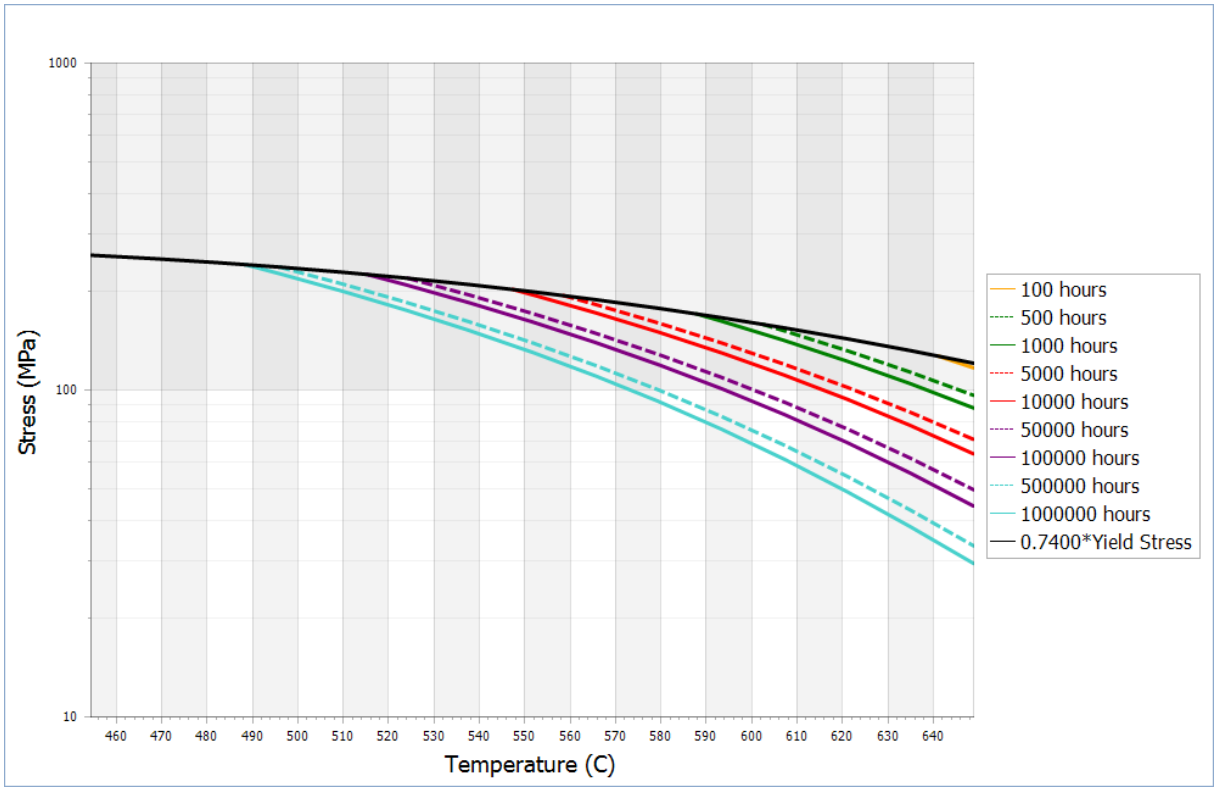

Figure 10.19M – Level 1 Screening Curve for 10.5Cr–V (Alloy 115 UNSK91060)

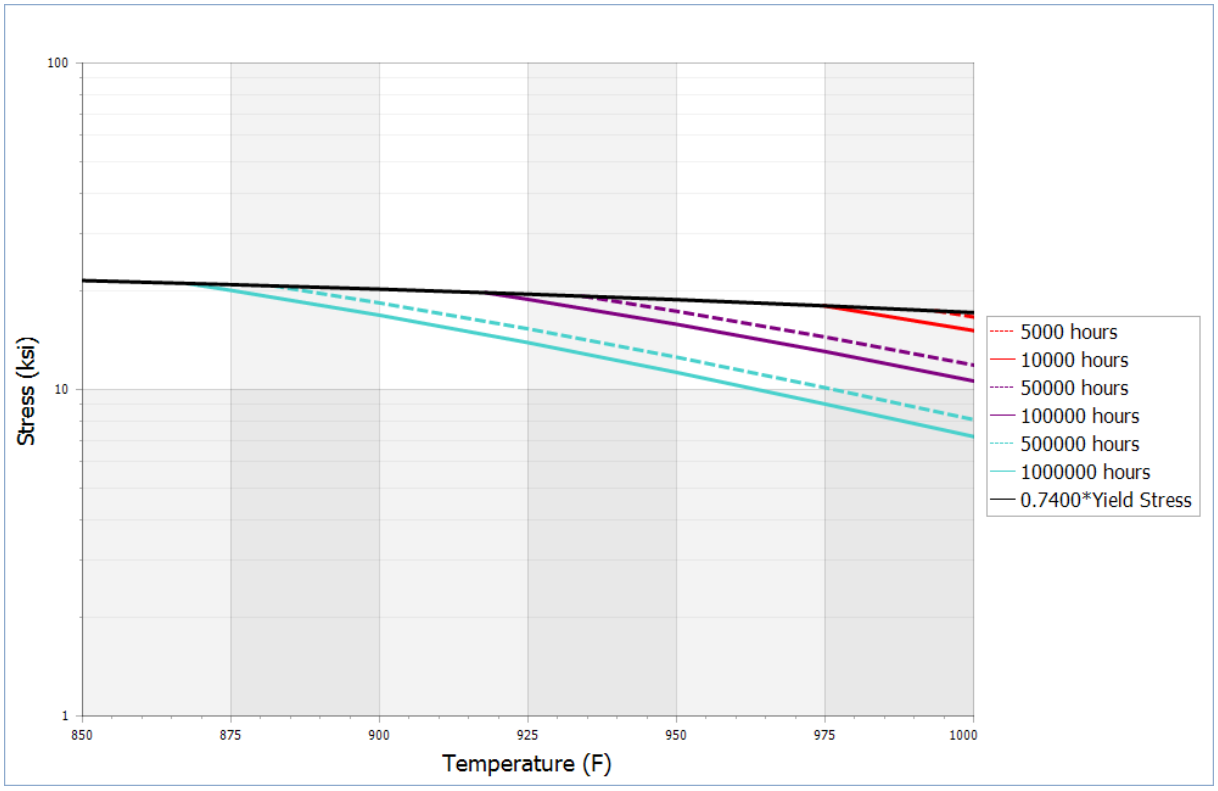

Figure 10.20 – Level 1 Screening Curve for 12Cr

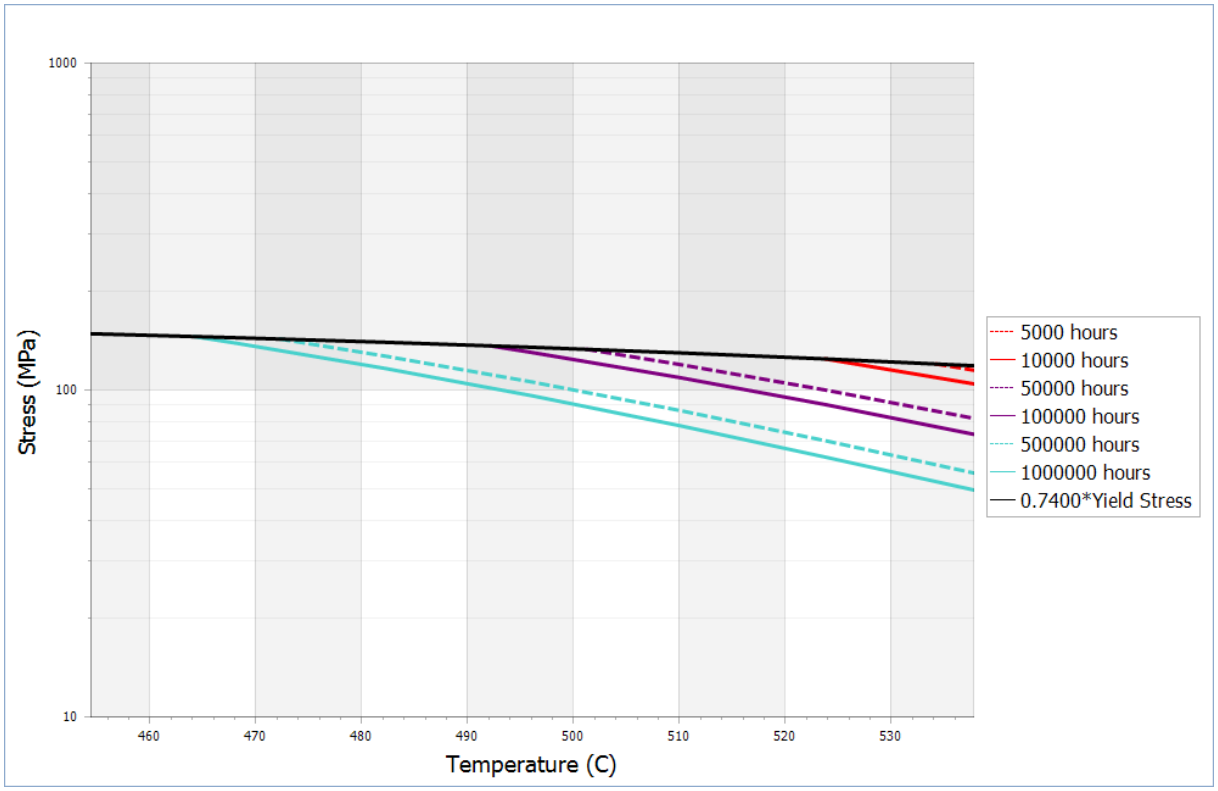

Figure 10.20M – Level 1 Screening Curve for 12Cr

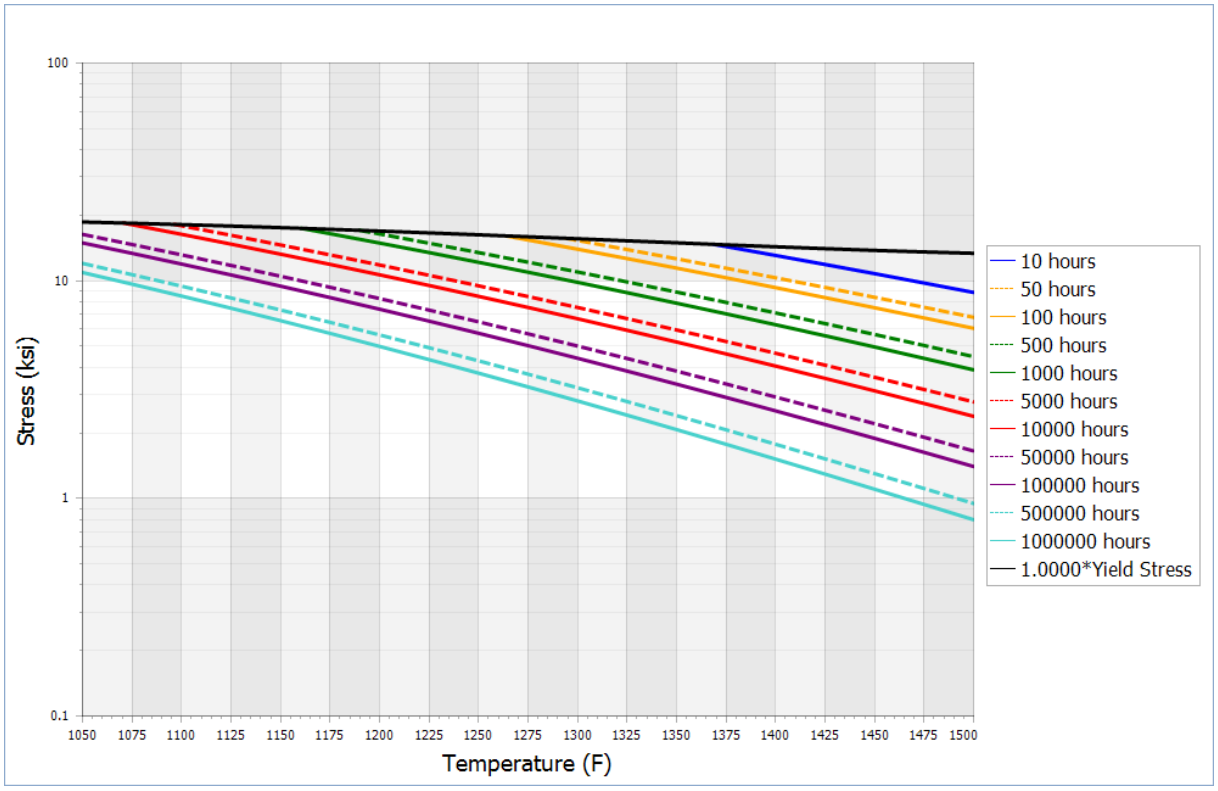

Figure 10.21 – Level 1 Screening Curve for Type 304 and 304H SS

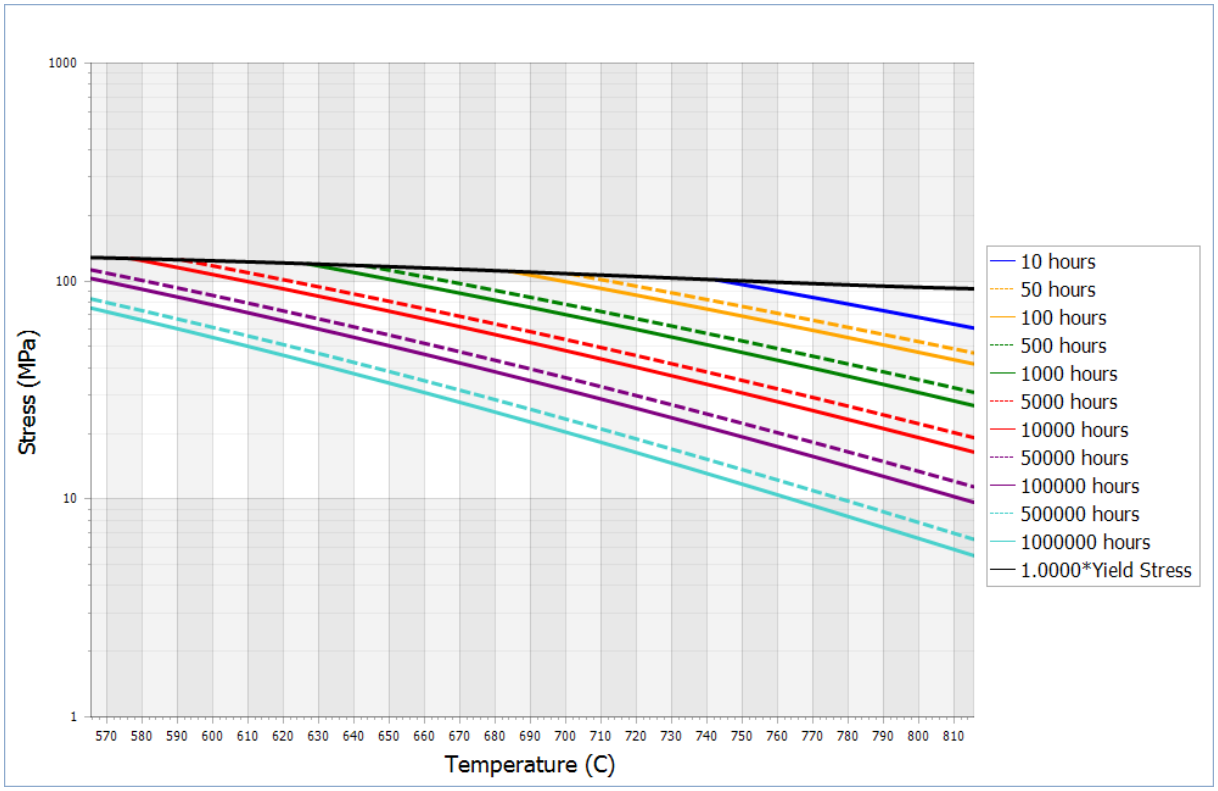

Figure 10.21M – Level 1 Screening Curve for Type 304 and 304H SS

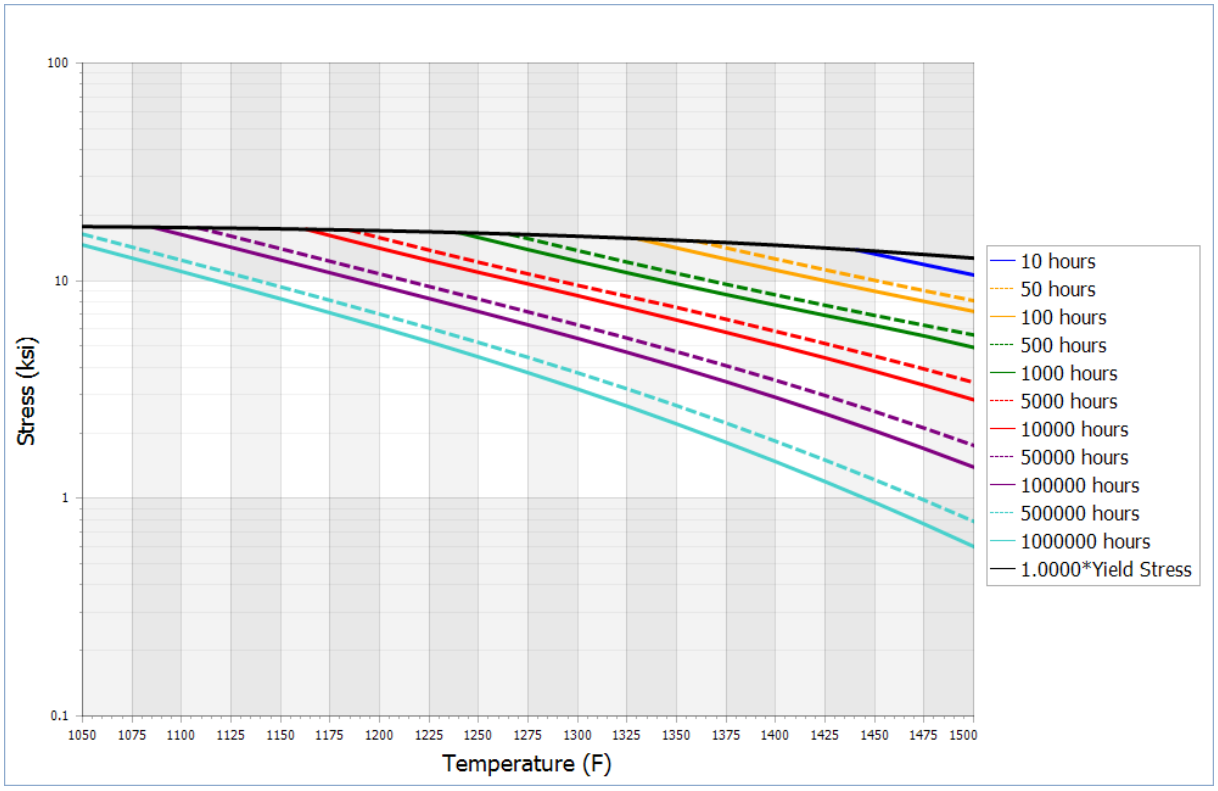

Figure 10.22 – Level 1 Screening Curve for Type 316 and 316H SS

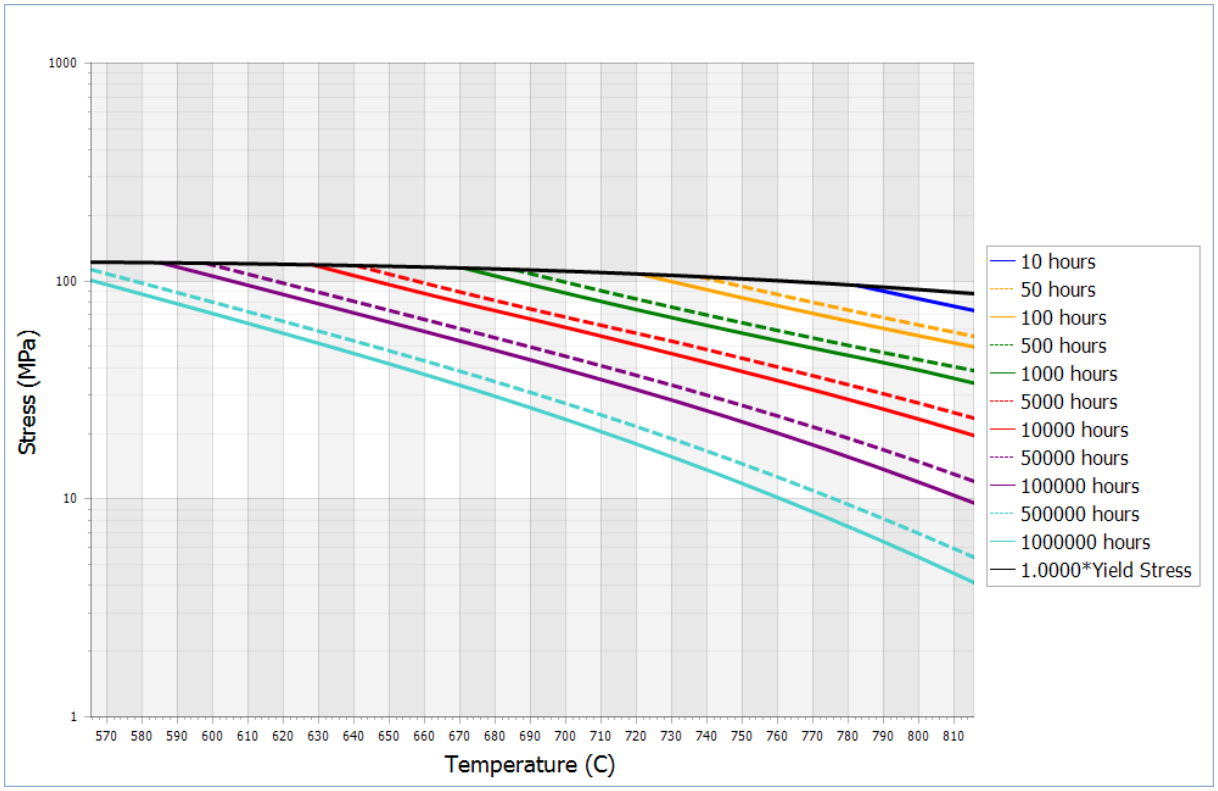

Figure 10.22M – Level 1 Screening Curve for Type 316 and 316H SS

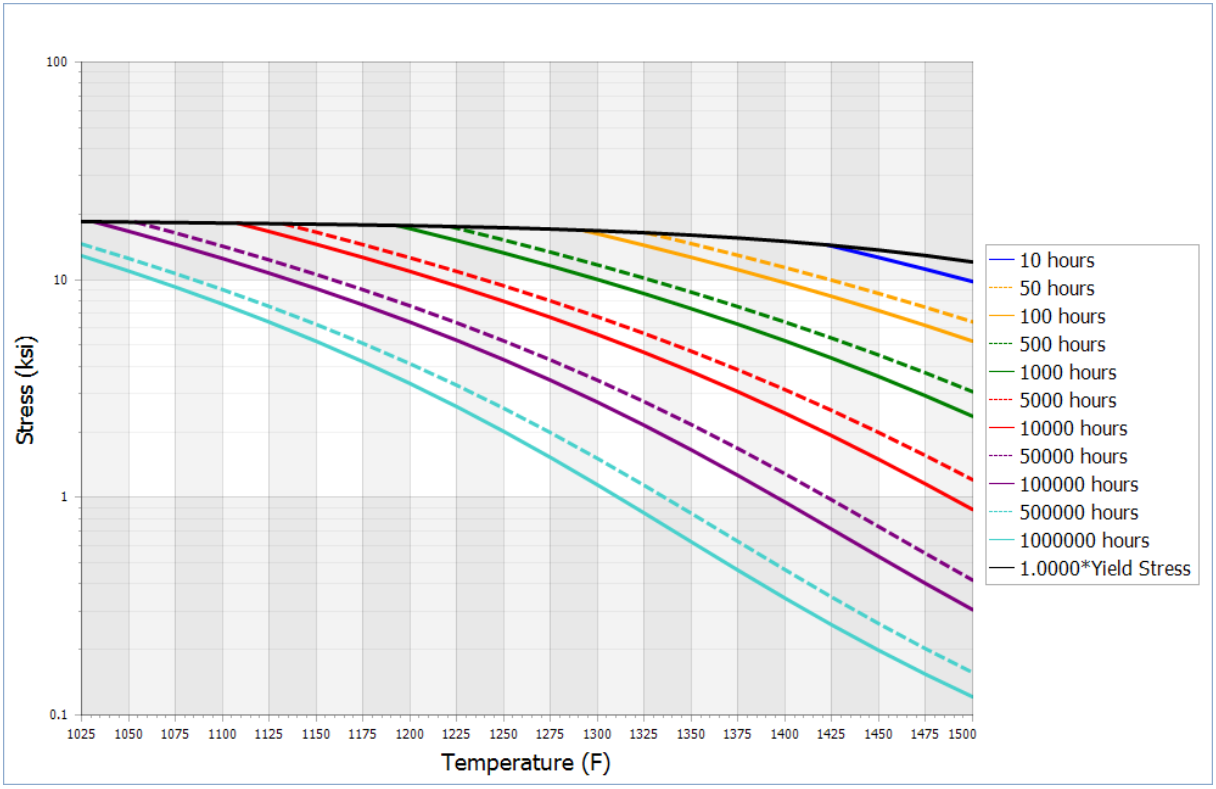

Figure 10.23 – Level 1 Screening Curve for Type 321 SS

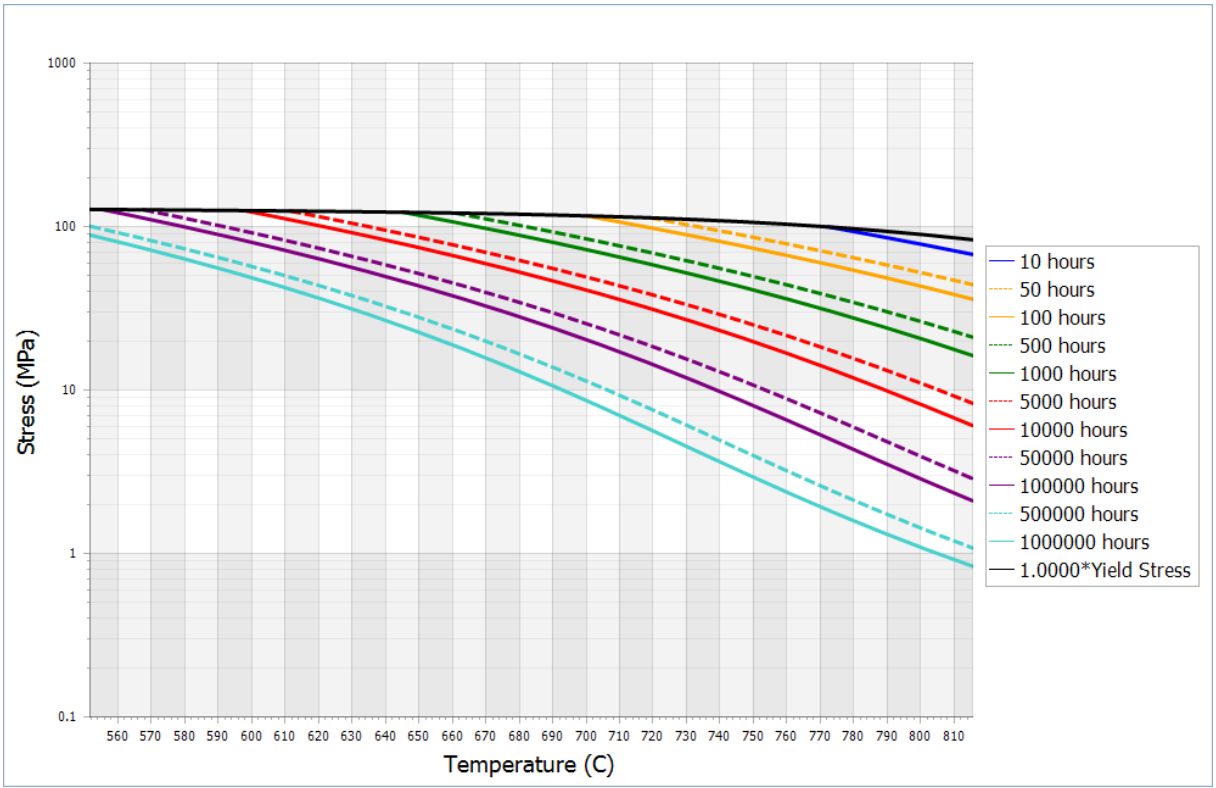

Figure 10.23M – Level 1 Screening Curve for Type 321 SS

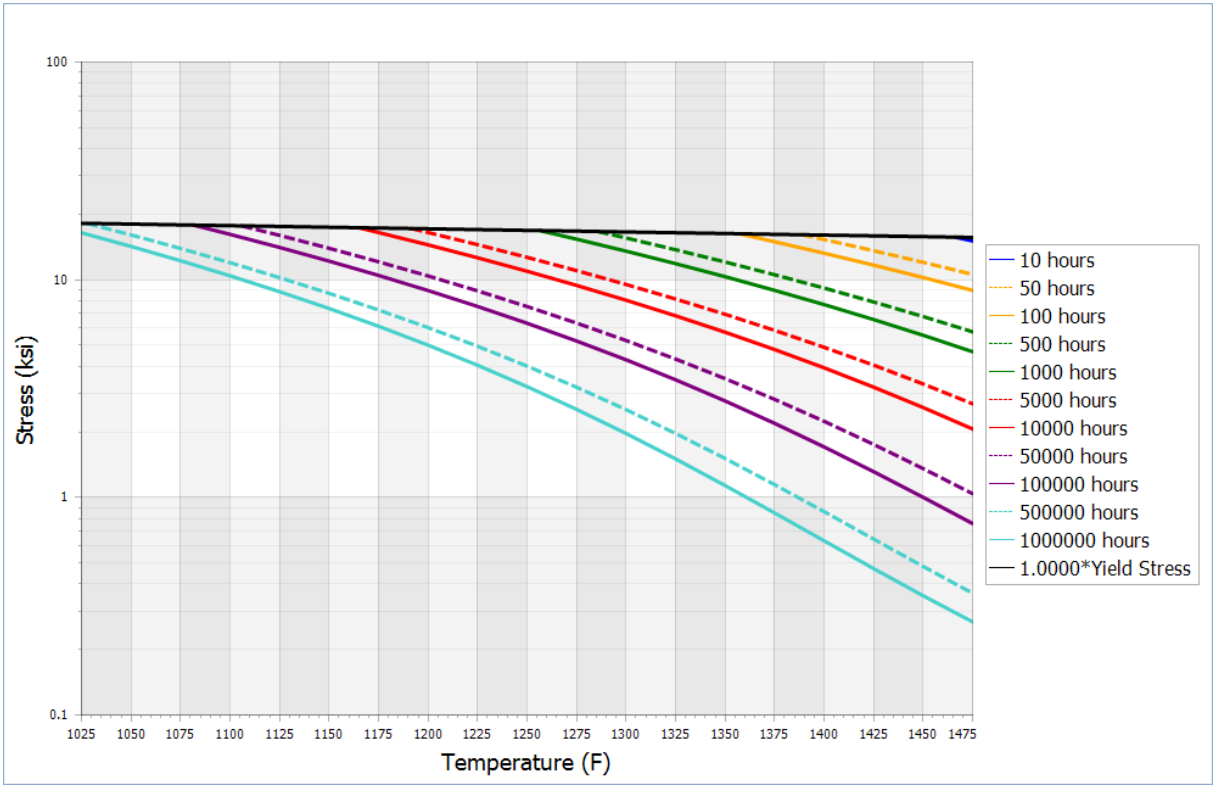

Figure 10.24 – Level 1 Screening Curve for Type 321H SS

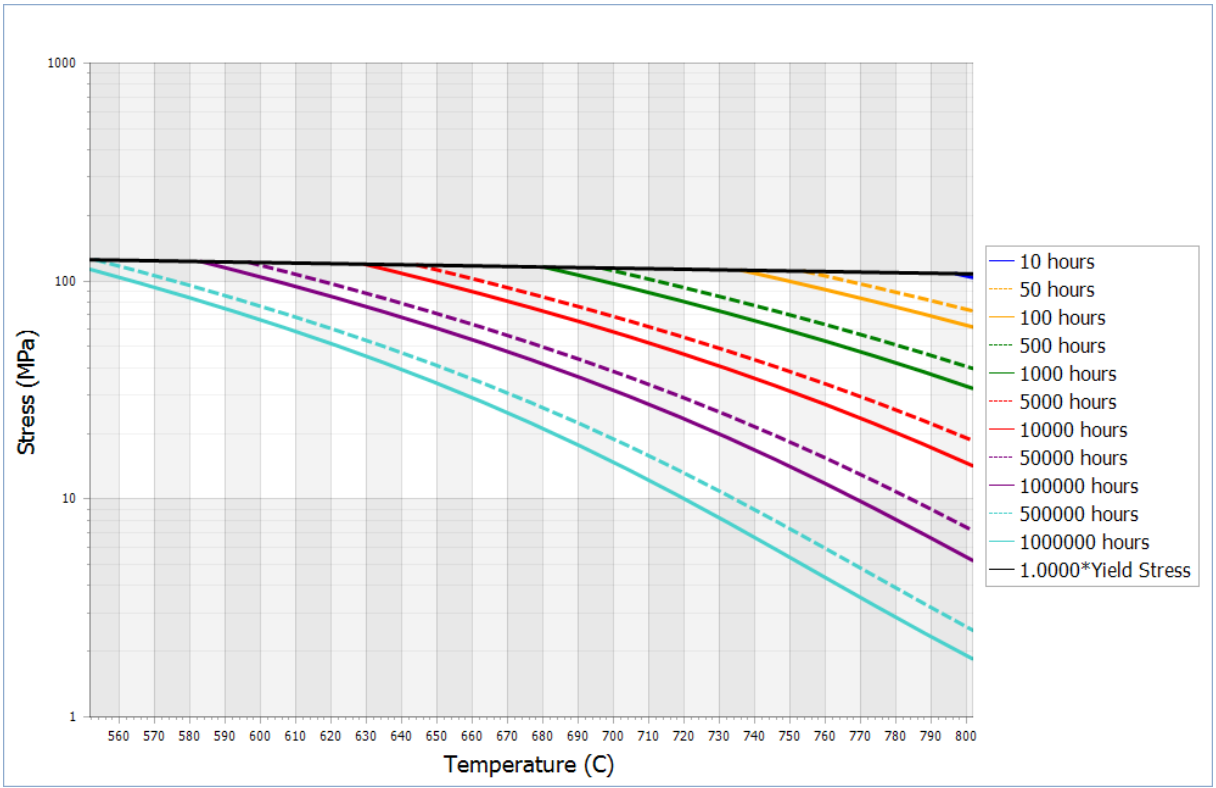

Figure 10.24M – Level 1 Screening Curve for Type 321H SS

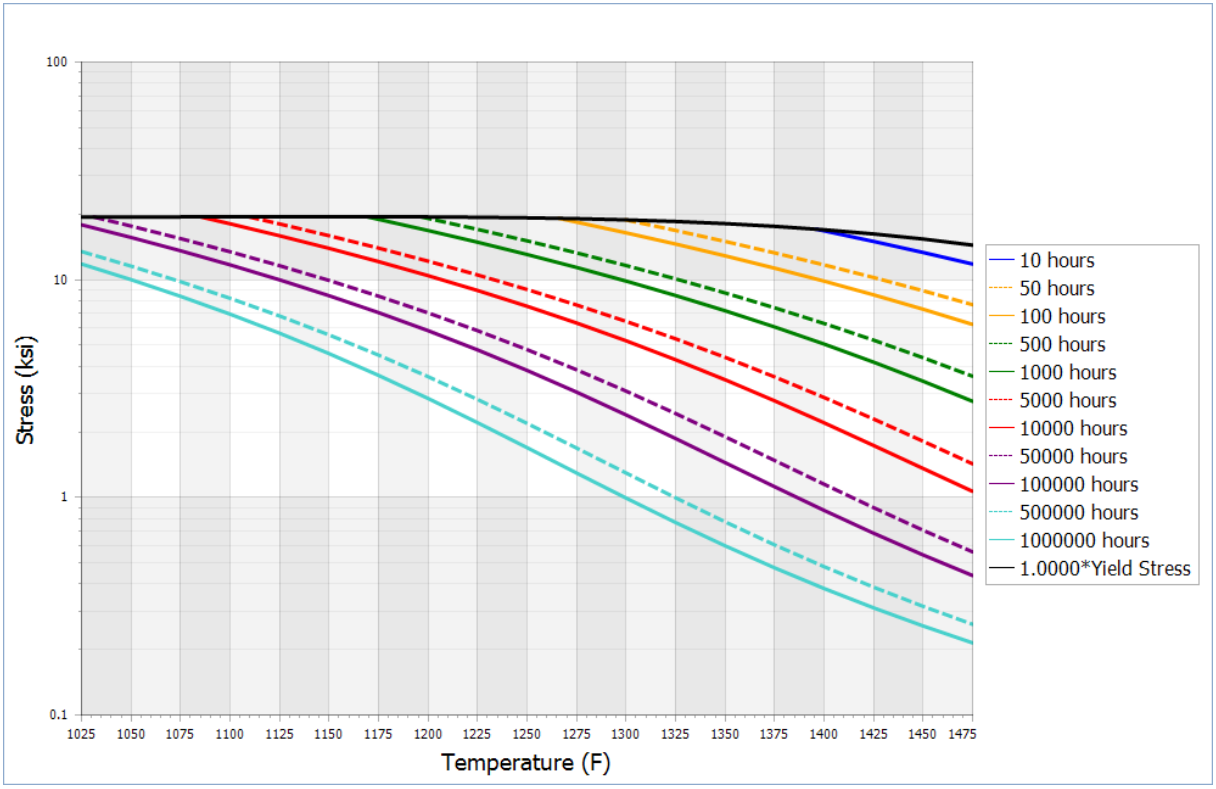

Figure 10.25 – Level 1 Screening Curve for Type 347 SS

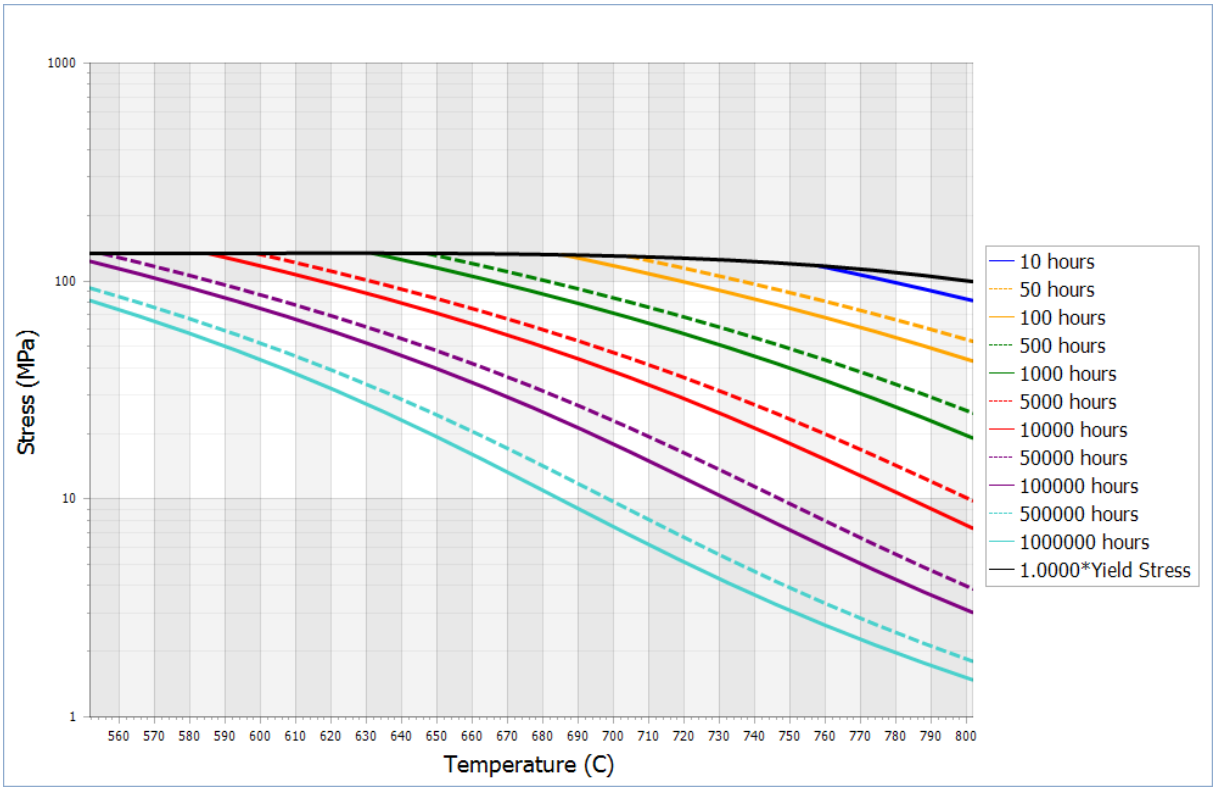

Figure 10.25M – Level 1 Screening Curve for Type 347 SS

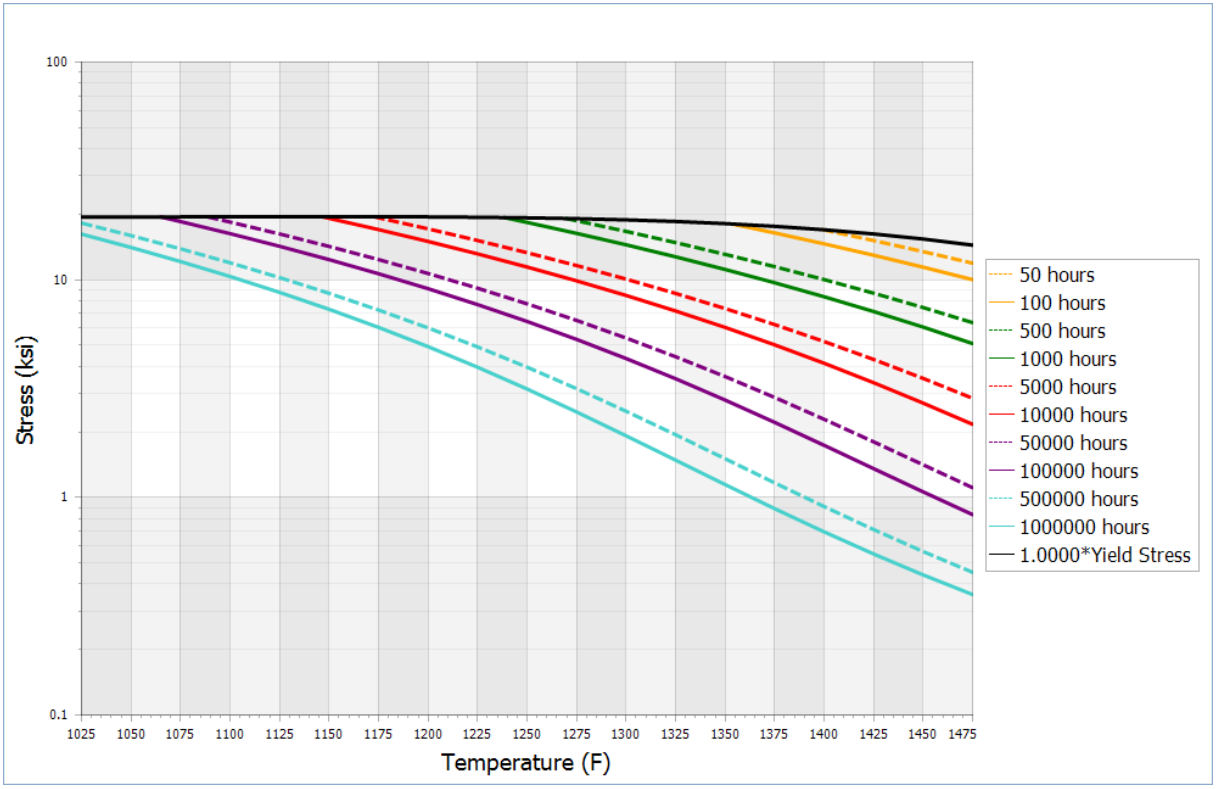

Figure 10.26 – Level 1 Screening Curve for Type 347H SS

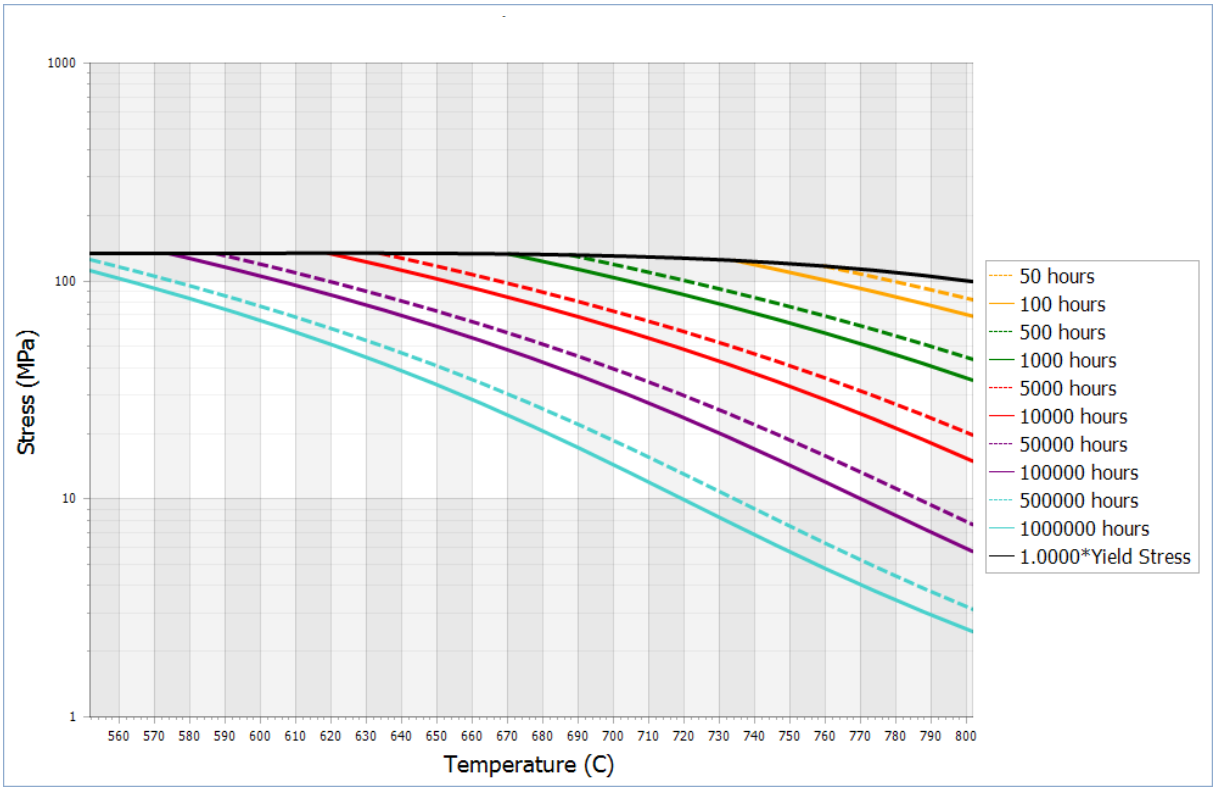

Figure 10.26M – Level 1 Screening Curve for Type 347H SS

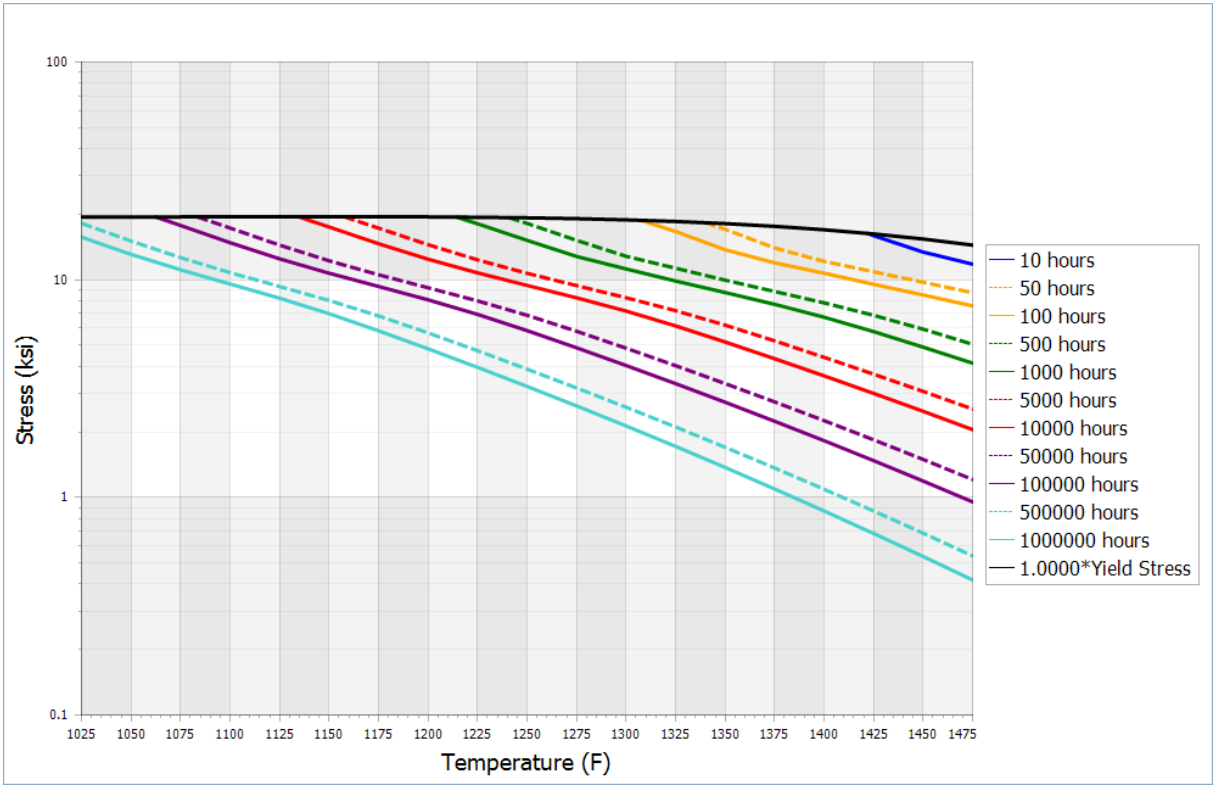

Figure 10.27 – Level 1 Screening Curve for Type 347LN SS (UNS S34751)

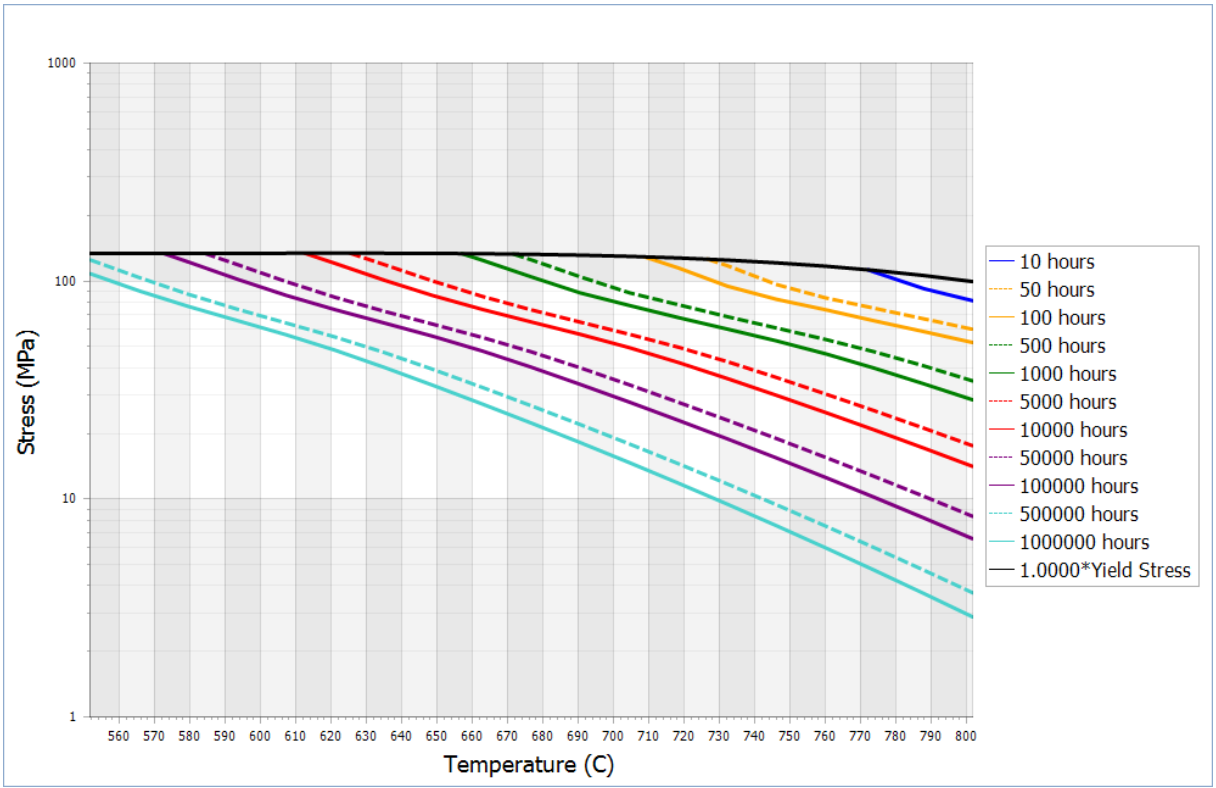

Figure 10.27M – Level 1 Screening Curve for Type 347LN SS (UNS S34751)

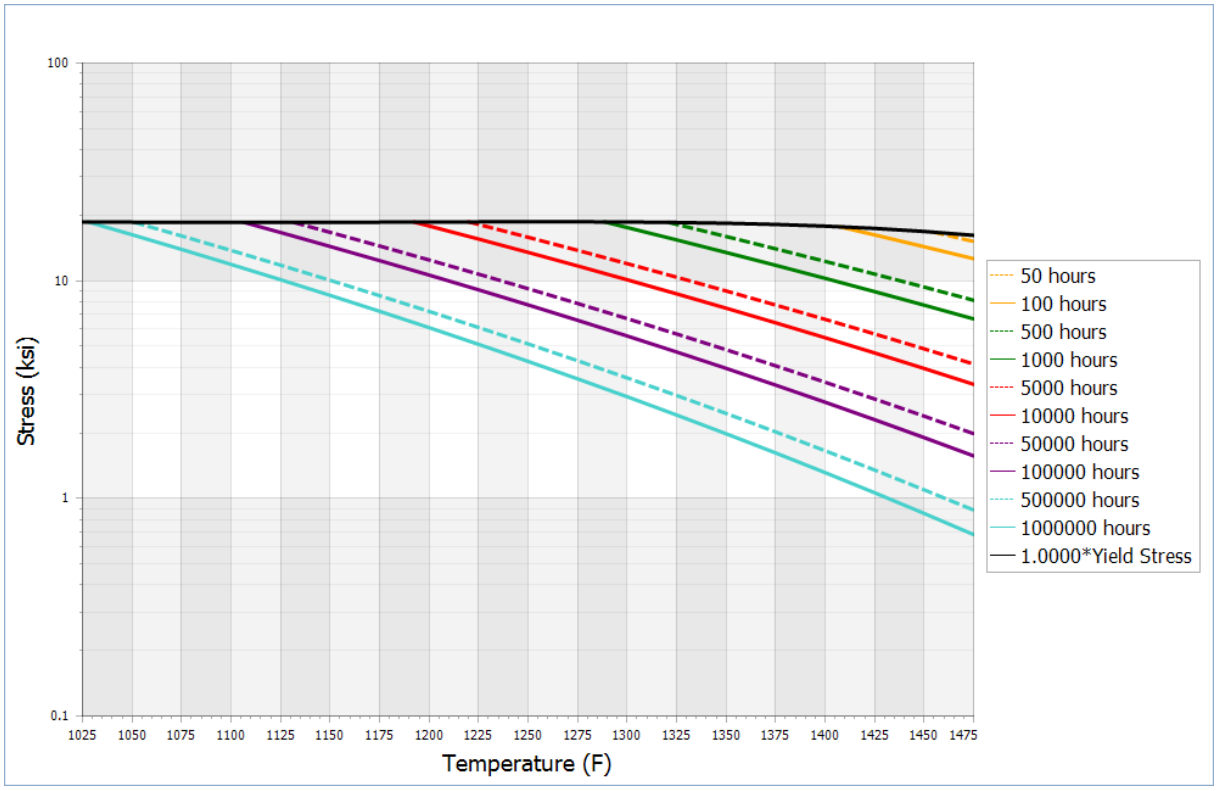

Figure 10.28 – Level 1 Screening Curve for Type 347AP Advanced SS (UNS S34751)

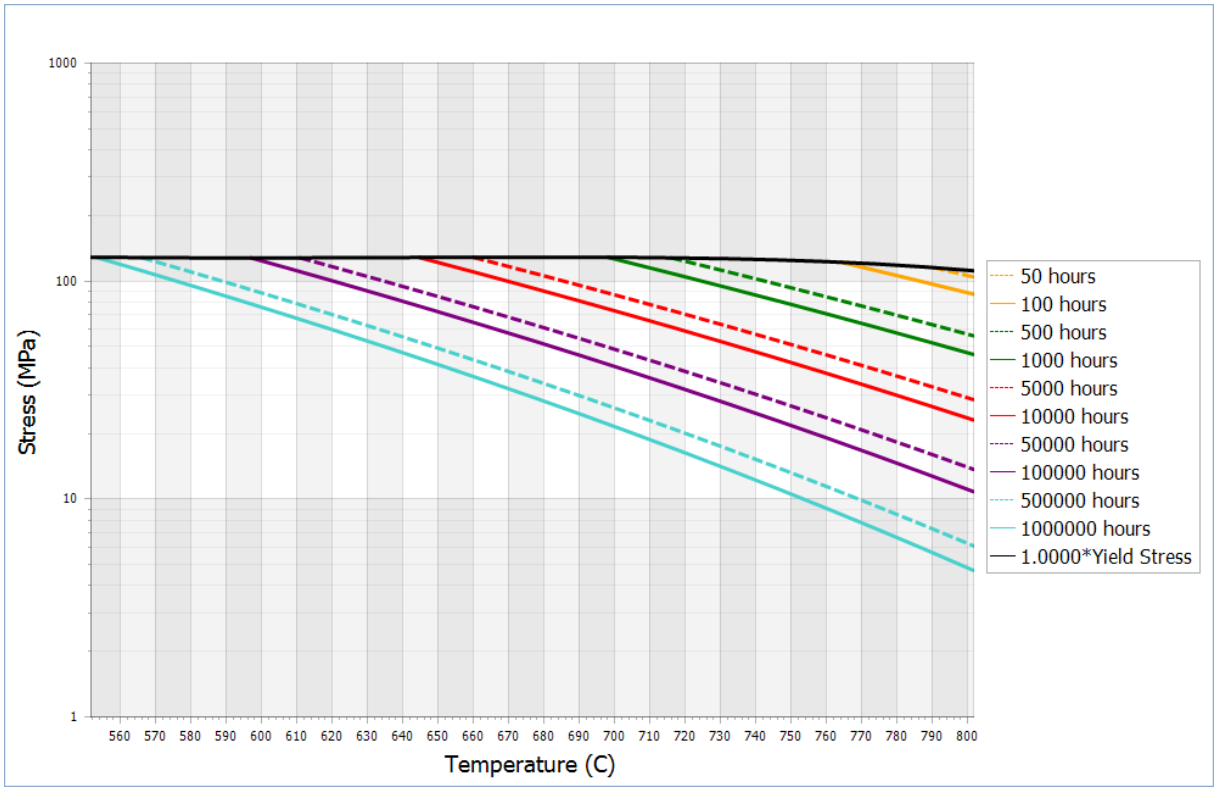

Figure 10.28M – Level 1 Screening Curve for Type 347AP Advanced SS (UNS S34751)

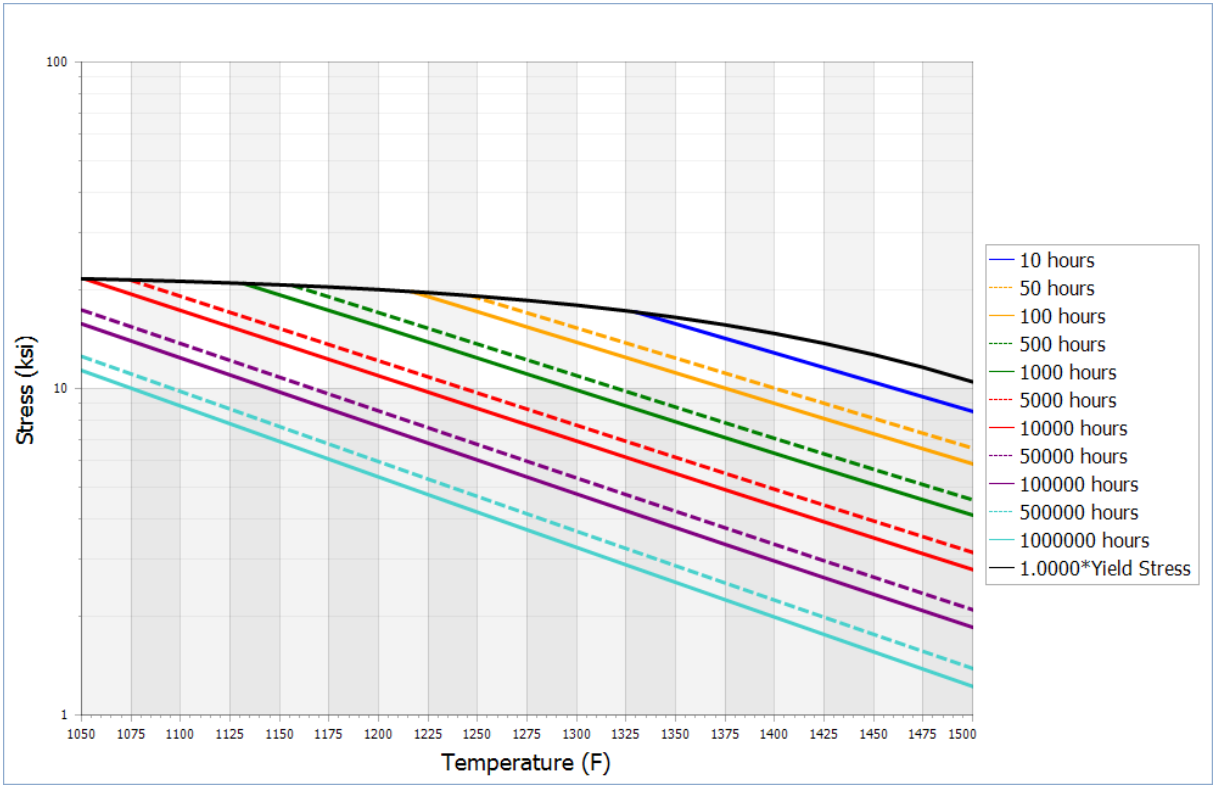

Figure 10.29 – Level 1 Screening Curve for Alloy 800

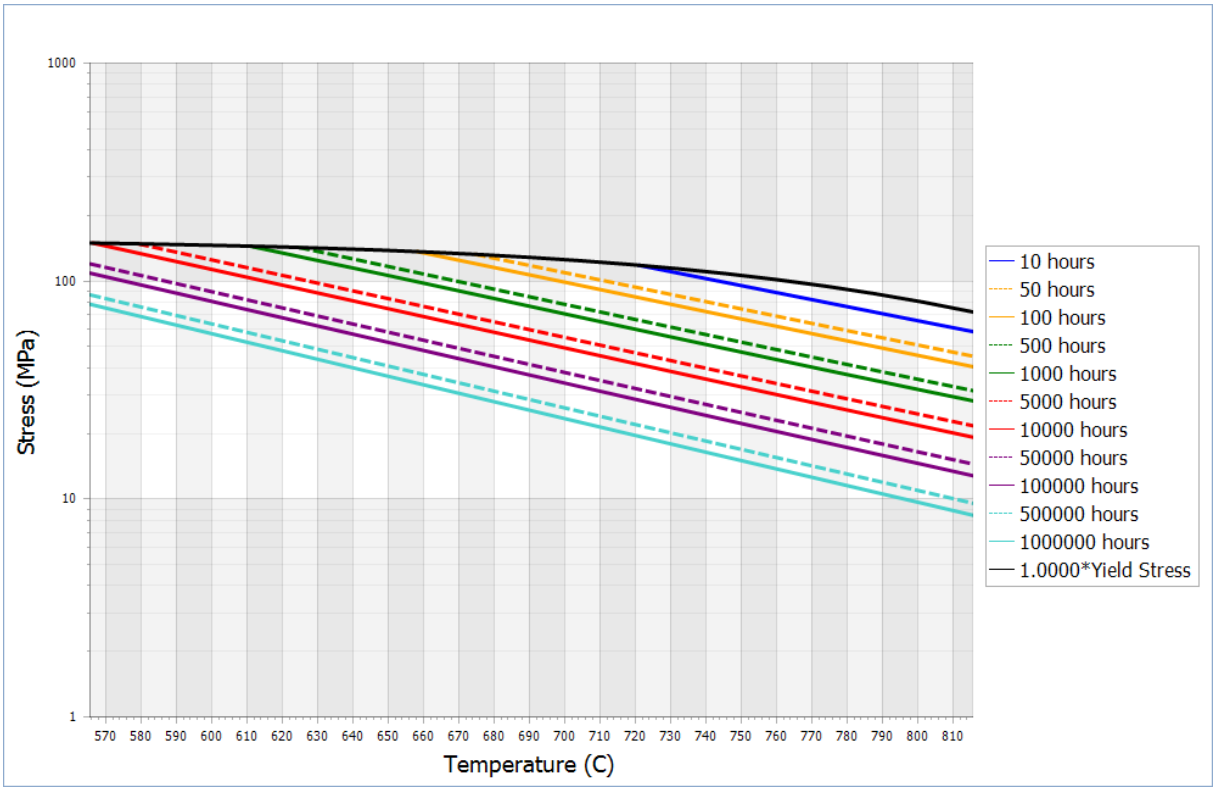

Figure 10.29M – Level 1 Screening Curve for Alloy 800

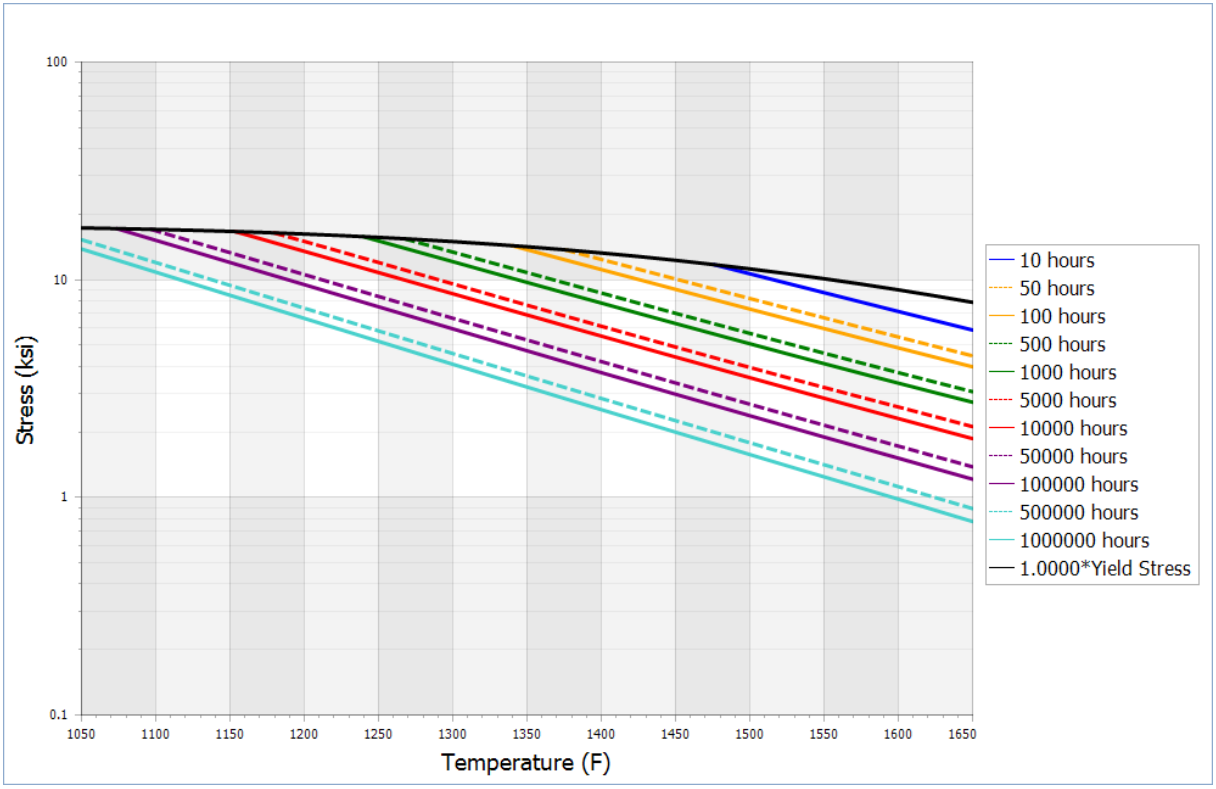

Figure 10.30 – Level 1 Screening Curve for Alloy 800H

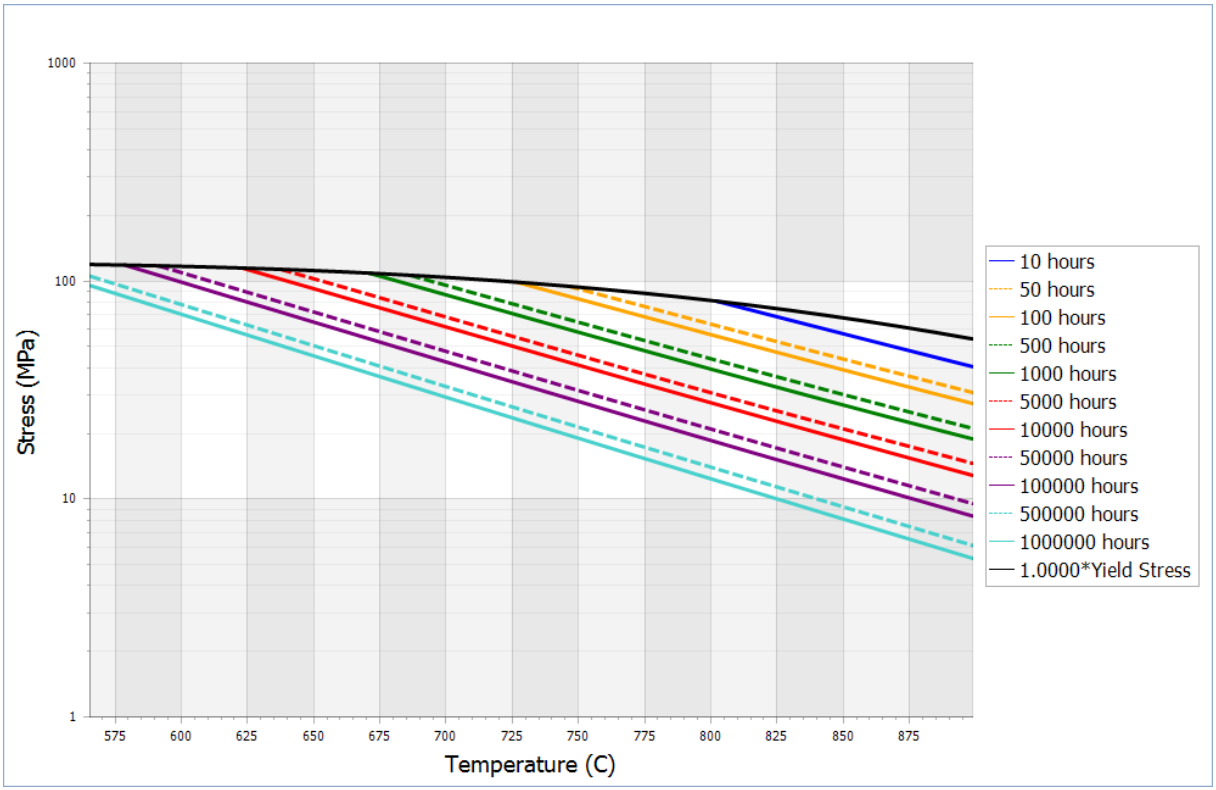

Figure 10.30M – Level 1 Screening Curve for Alloy 800H

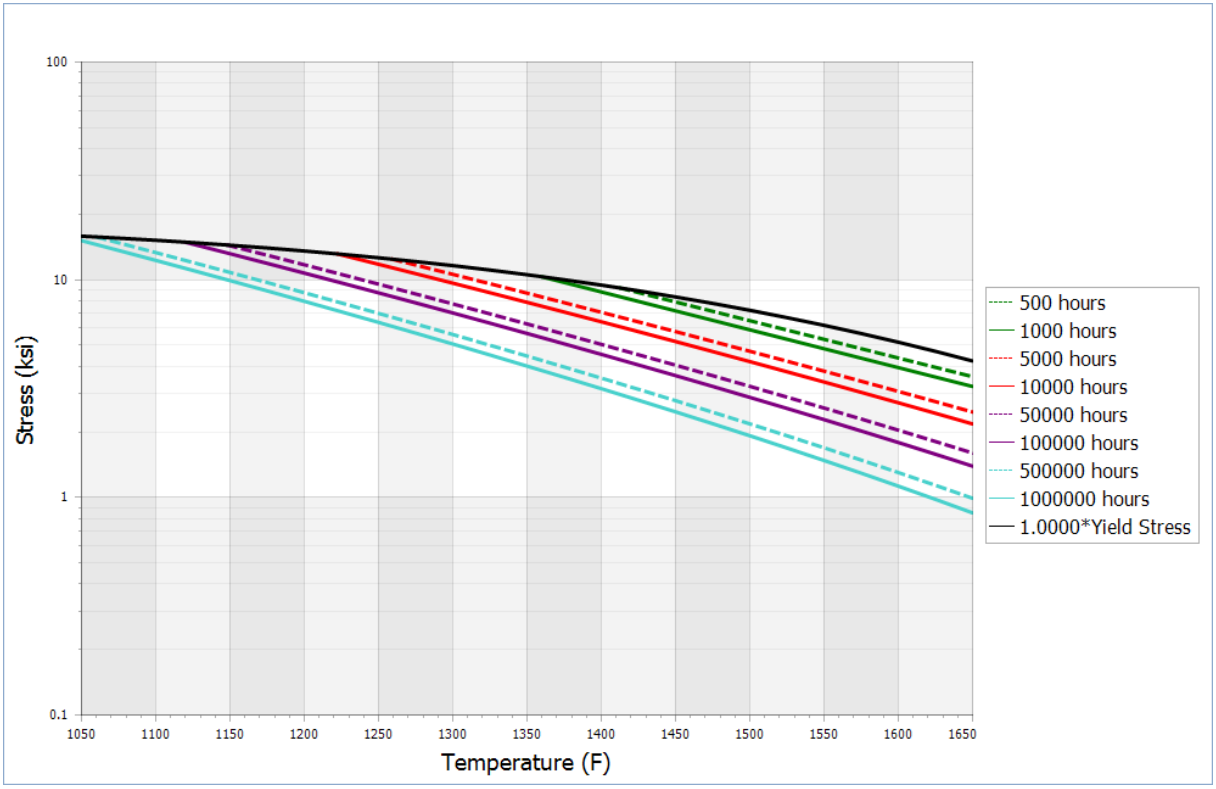

Figure 10.31 – Level 1 Screening Curve for Alloy 800HT

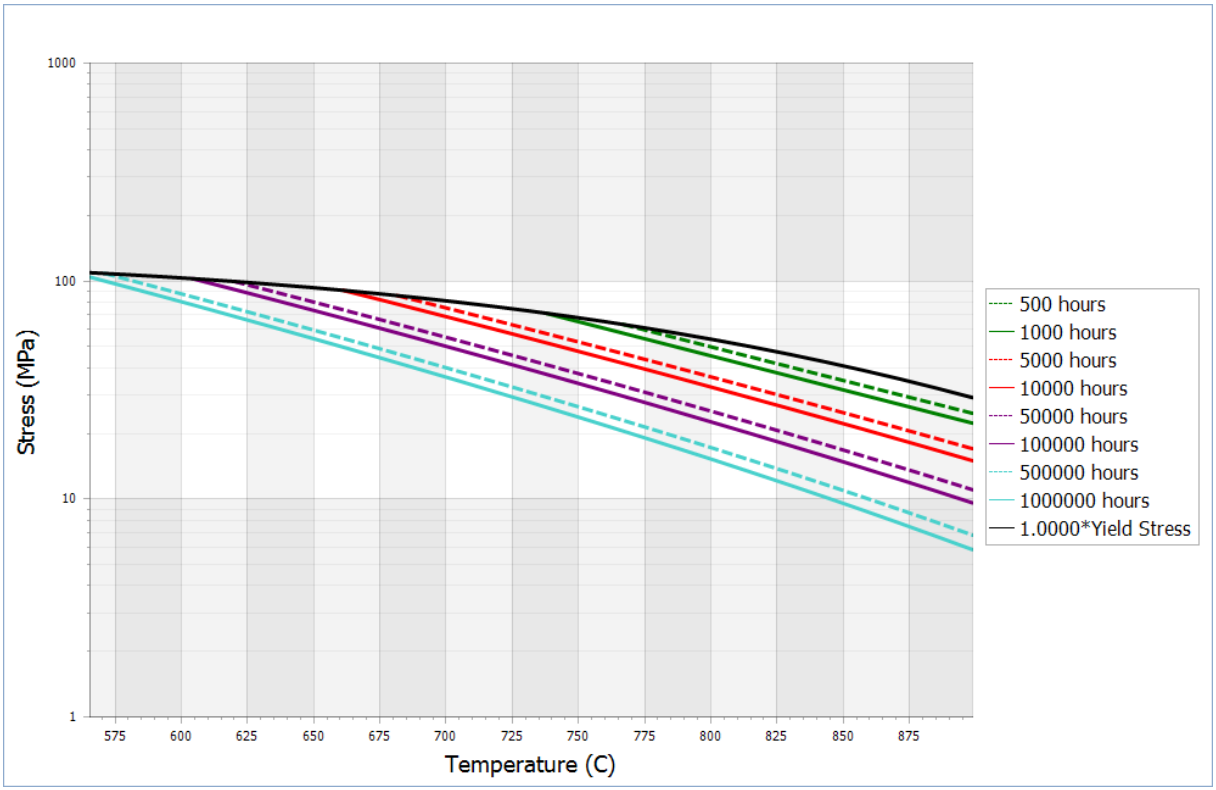

Figure 10.31M – Level 1 Screening Curve for Alloy 800HT

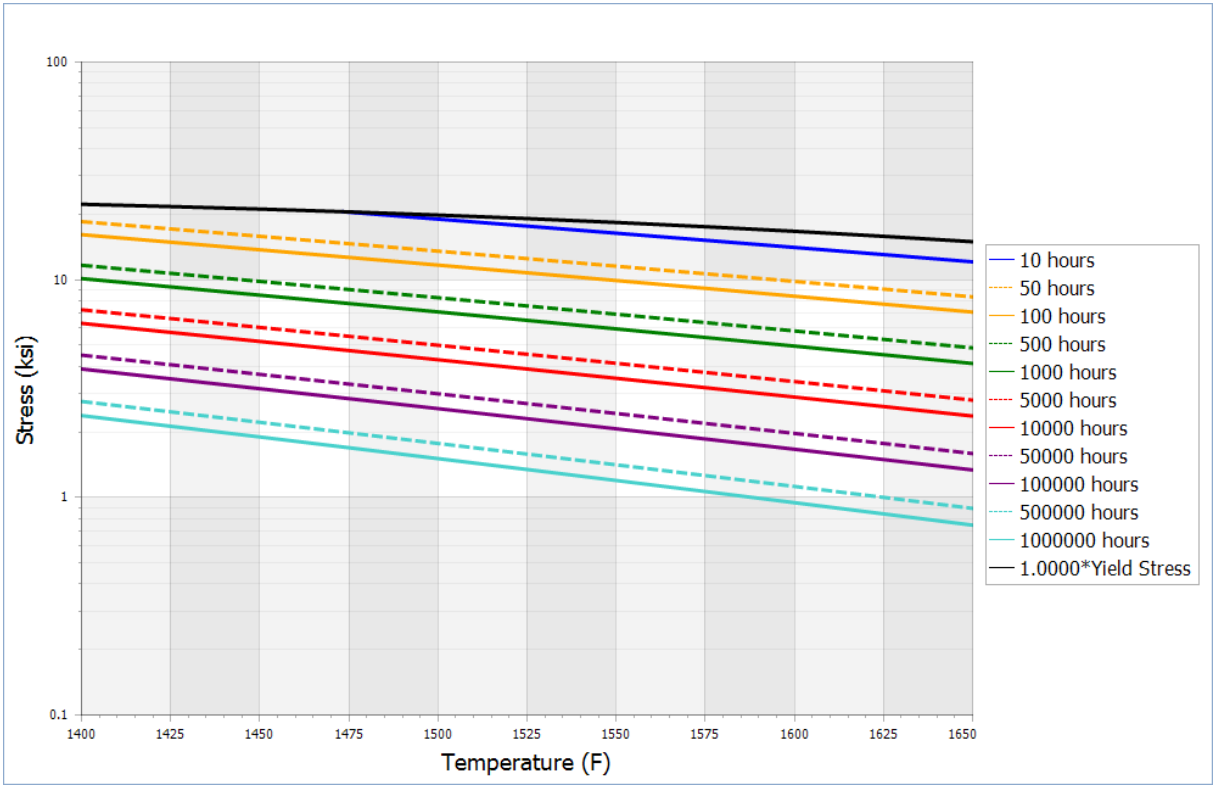

Figure 10.32 – Level 1 Screening Curve for Alloy HK–40

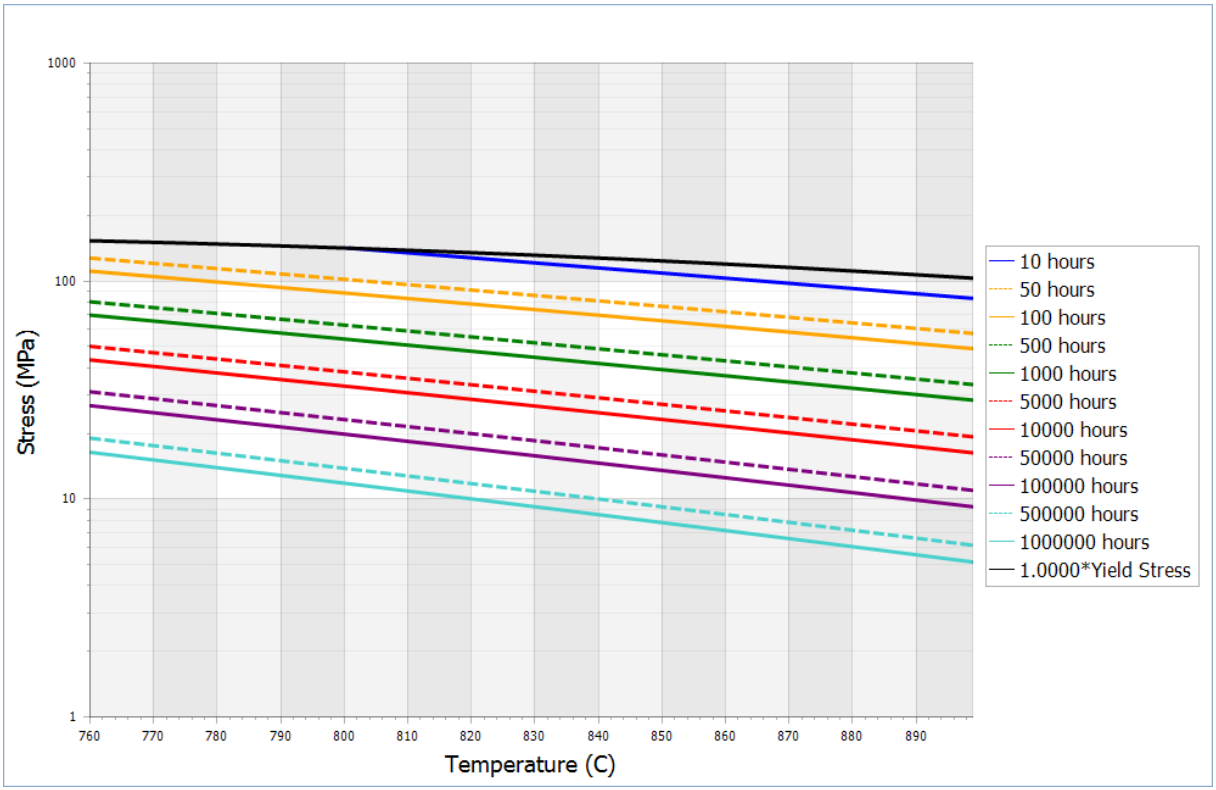

Figure 10.32M – Level 1 Screening Curve for Alloy HK–40

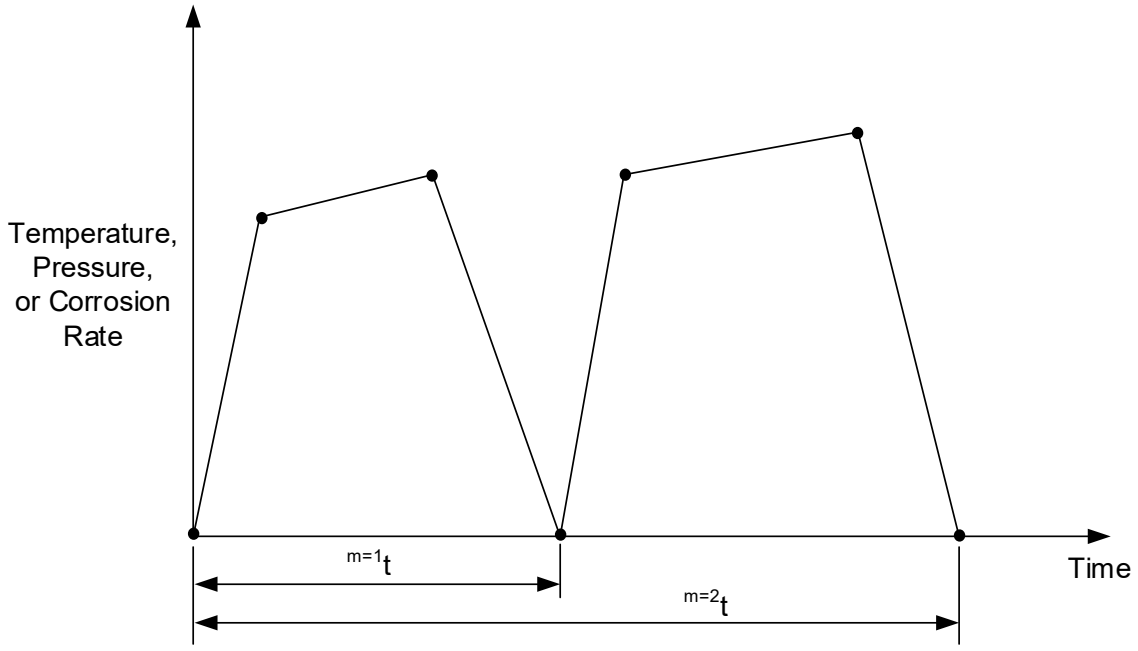

Figure 10.33 – Definition of Multiple Cycles in a Load History

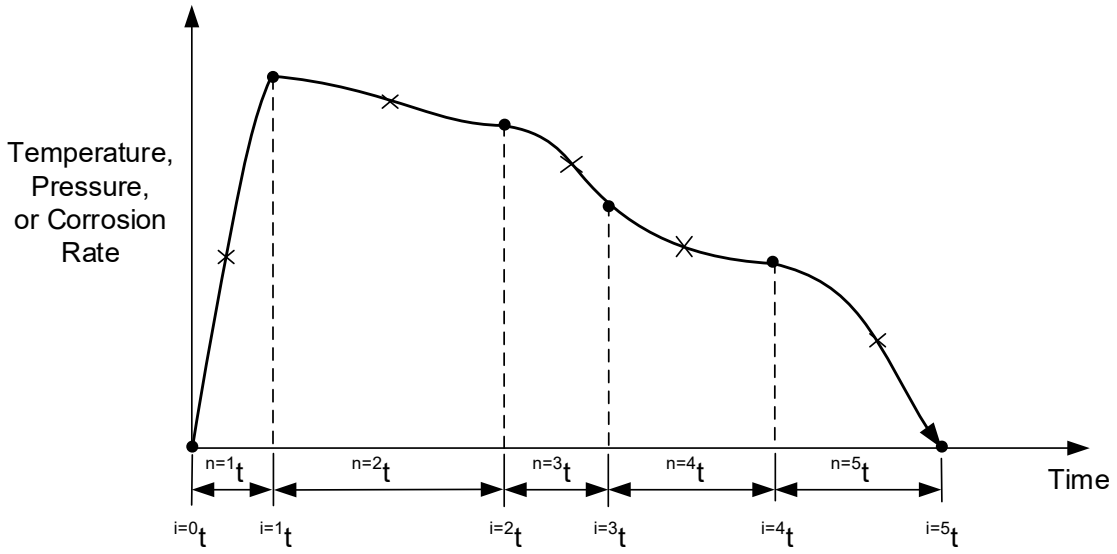

(a) Actual Parameter Variation

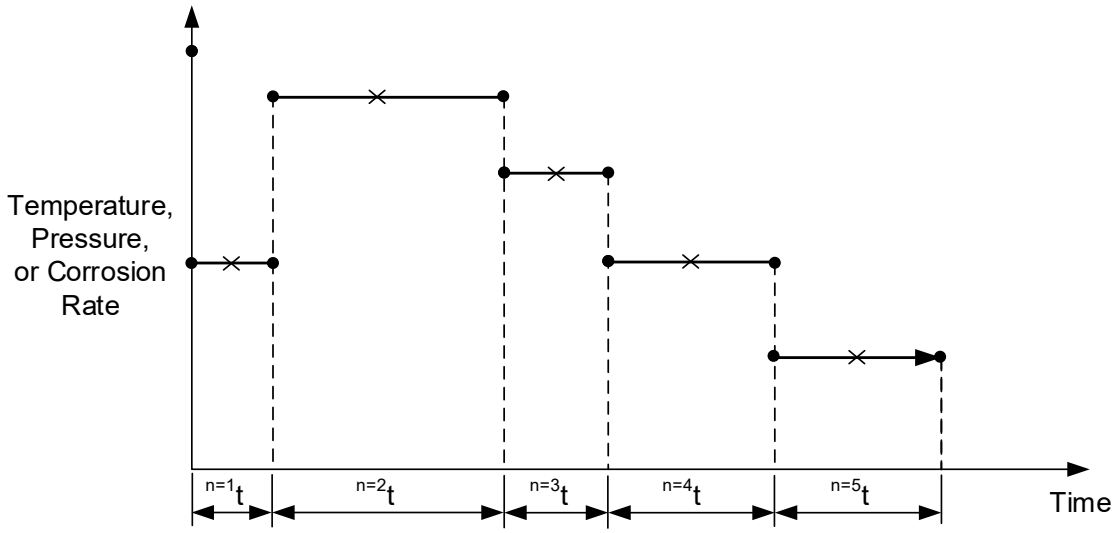

(b) Idealized Parameter Variation Using Average Values Of Parameters

Figure 10.34 – Modeling of Time Increments in a Cycle for a Remaining Life Calculation

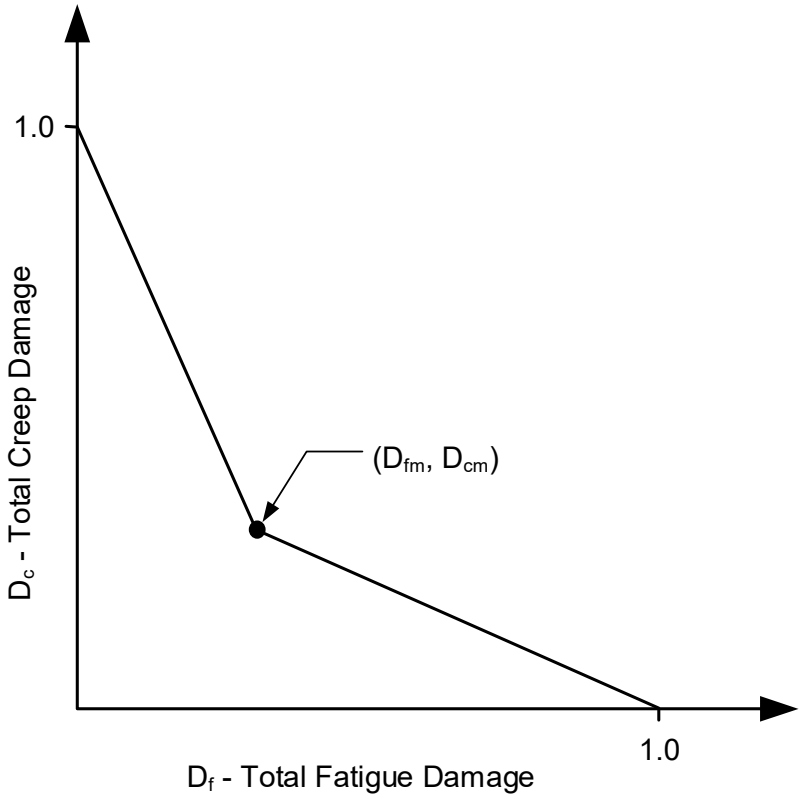

Material Parameters to Define the Acceptable Creep-Fatigue Envelope		
Material	D_{fm}	D_{cm}
Carbon Steels	0.15	0.15
Low Alloy Steels	0.15	0.15
9Cr – 1Mo-V	0.10	0.02
Type 304 SS	0.30	0.30
Type 316 SS	0.30	0.30
Alloy 800H	0.15	0.15

Figure 10.35 – Creep Fatigue Damage Acceptance Criterion

[Intentionally Left Blank]

ANNEX 10A – TECHNICAL BASIS AND VALIDATION – ASSESSMENT OF COMPONENTS OPERATING IN THE CREEP RANGE

(INFORMATIVE)

CONTENTS

ANNEX 10A – TECHNICAL BASIS AND VALIDATION – ASSESSMENT OF COMPONENTS OPERATING IN THE CREEP RANGE 10A-1

10A.1 TECHNICAL BASIS AND VALIDATION 10A-1
10A.2 TECHNICAL BASIS AND VALIDATION REFERENCES 10A-1
10A.3 ADDITIONAL REFERENCES 10A-3

10A.1 Technical Basis and Validation

The elevated temperature life assessment methods in Part 10 are based on traditional concepts, such as linear life summing rules, and recognize the material properties and documented approaches developed by MPC under the heading of the Omega Method. The original and most complete exposition of the Omega Method is found in reference [1]. It has been summarized in other papers by Prager et. al. in references [2] and [3], Zamrik, et. al. in reference [4], and Dyson in reference [5]. The Omega Method is widely reported by industrial and academic investigators in literature in Japan by Prager and many others in references [6], [7], [8], [9], [10], [11], and also by the European Creep Collaborative Committee in reference [12]. The method evolved from examination of experimental data that was then converted to parametric expressions for ease of use and extrapolation as described in reference [1]. Application to complex geometries, creep crack growth and other complex stress states, especially for tubular components, was first reported in reference [13]. The parametric approaches applied in the Omega Method are also used for generation of ASME code allowable stresses at elevated temperatures and material modeling as reported in references [14] and [15], respectively. The techniques were applied to life assessment as an alternative to the methods in API Std 530 starting about 1988, well before the publication of reference [1], and have been in use since then by the petroleum and power industries. Case histories using the Omega Method for assessment of components may be found in references [16], [17], [18], and [19].

The technical basis for the creep crack growth method in Part 10 is described in references [3] and [20]. Additional technical basis and validation are provided in references [21], [22] and [23]. International approaches that were also reviewed during the development of Part 10 are provided in references [24] and [25].

The technical basis for creep buckling is provided in references [26] and [27].

The technical basis for creep-fatigue assessment of dissimilar welds is provided in reference [28].

10A.2 Technical Basis and Validation References

[1] Prager, M., “Development of the MPC Project Omega Method for Life Assessment in the Creep Range,” PVP-Vol. 288, ASME, 1994, pp. 401-421.

[2] Prager, M., “Damage Evaluation and Remaining Life Assessment in High Temperature Structural Components by the Omega Method,” Proceedings of 7th Workshop on the Ultra Steel, Ultra Steel: Requirements from New Design of Constructions, June 24 and 25, 2003, pages 150-158.

[3] Prager, M., and Osage, D., “Special Topics in Elevated Temperature Life Applications Including Assessment Rules for API 579,”, PVP-Vol. 411, Service Experience and Fitness-For-Service in Power and Petroleum Processing, ASME, 2000, pages 91-104.

[4] Zamrik, S.Y. and Annigeri, R., “Creep Damage Models for Elevated Temperature Design,” Proc. ICPVT-10 July 7-10, 2004.

[5] Dyson, B., “Use of CDM in Materials Modeling and Component Creep Life Prediction,” ASME, Journal of Pressure Vessel Technology, Vol. 122, August 2000, pages 281-296.

[6] Prager, M., “The Omega Method – An Effective Method for Life and Damage Prediction in Creep Tests and Service,” Oikawa (eds.), Strength of Materials, Japan Institute of Metals, 1994, pp. 571-574.

[7] Endo, T., Park, K.S. and Masuyama, F. “Creep Modeling and Life Evaluation of Long-Term Aged Modified 9 Cr-1Mo Steel,” Symposium on Integrity and Failures in Industry, Milan, Italy, Sept. 1-Oct. 1, 1999, organised by the Italian Group on Fracture and ENEL Research (Milan - I) Editors: V. Bicego, A. Nitta, J. W. H. Price and R. Viswanathan. ISBN 1 901537 15 3 (1999).

[8] Endo, T., and Shi, J., “Factors Affecting the Creep Rate and Creep Life of a 2.25Cr-1Mo Steel Under Constant Load,” Strength of Materials, Oikawa et al. ed., ICSMA 10 Sendai, The Japan Institute for Metals, 1994, pp 665-668.

[9] Osage, D.A., Shipley, K.S., Wirsching, P.H. and Mansour, A.E., “Application of Partial Safety Factors for Pressure Containing Equipment,” PVP Vol. 411, Service Experience and Fitness-For-Service in Power and Petroleum Processing, ASME, 2000, pp. 121-142.

[10] Prager, M. and Masuyama, F., “Examination of the Effects of Materials Variables in Advanced Alloys by Studying Creep Deformation Behavior,” Strength of Materials, Oikawa et al. ed., ICSMA 10 Sendai, The Japan Institute for Metals, 1994, pp 575-578.

[11] Yokobori Jr. A.T. and Prager M., “Proposal for a new Concept on Creep Fracture Remnant Life for a Pre-cracked Specimen”, Materials at High Temperatures, 16(3), 1999. pp 137-141.

[12] Merckling G., “The European Creep Collaborative Committee,” International Symposium on NIMS Creep Data Sheet, National Institute for Materials Science in Japan, March 16, 2004, pp.25-52.

[13] Buchheim, G.M., Osage, D.A., Brown, R.G., and Dobis, J.D., “Failure Investigation of a Low Chrome Long-Seam Weld in a High-Temperature Refinery Piping System,” PVP-Vol. 288, ASME, 1994, pp. 363-386.

[14] Prager, M., “Generation of Isochronous Creep, Tubing Life and Crack Growth Curves Using the MPC Omega Method, Structural Integrity,” NDE, Risk and Material Performance for Petroleum, process and Power, PVP-Vol. 336, ASME, 1996, pp. 303-322.

[15] Prager, M., “Proposed Implementation of Criteria for Assignment of Allowable Stresses in the Creep Range,” ASME Journal of Pressure Vessel Technology, May, 1996, Vol. 335, pp. 273-293.

[16] Ibarra, S. and Konet, R.R., “Life Assessment of 1 1/4Cr-1/2Mo Steel Catalytic Reformer Furnace Tubes Using the MPC Omega Method,” PVP-Vol. 288, Service Experience and Reliability Improvement: Nuclear, Fossil, and Petrochemical Plants, ASME 1994, pages 387-400.

[17] Kim, D.S. and Mead, H.E., “Remaining Life Assessment of Refinery Heater Tubes,” PVP-Vol. 388, Fracture, Design Analysis of Pressure Vessels, Heat Exchangers, Piping Components, and Fitness-For-Service, ASME, 1999, pages 361-366.

[18] Klehn, R. and Laughlin, C.A., “Chevron’s Experience Using Omega Method Creep Tests for Life Assessment of Refinery Equipment,” PVP-Vol. 288, Service Experience and Reliability Improvement: Nuclear, Fossil, and Petrochemical Plants, ASME 1994, pages 345-350.

[19] Prager, M. and Ibarra, S., “Approaches to Long Term Life prediction of Furnace and Boiler Tubes,” Fitness For Adverse Environments in Petroleum and Power Equipment, PVP-Vol. 359, ASME, 1997, pp. 339-352.

[20] Scott, P.M., Anderson, T.L., Osage, D.A., and Wilkowski, G.M., *A Review of Existing Fitness-For-Service Criteria for Crack-Like Flaws*, WRC Bulletin 430, Welding Research Council, Inc., New York, NY, April 1998.

[21] Saxena, A. and Yoon, D., *Creep Crack Growth Assessment of Defects in High Temperature Components*, WRC Bulletin 483, Welding Research Council, Inc., New York, NY, 2003.

[22] Webster, G.A. and Ainsworth, R.A., *High Temperature Component Life Assessment*, Chapman & Hall, London, U.K., 1994.

[23] Saxena, A., *Nonlinear Fracture Mechanics for Engineers*, CRC Press, Boca Raton, FL, 1998.

[24] Moulin, D., Drubay, B. and Laiarinandrasana, L., “A Synthesis of the Fracture Assessment Methods Proposed in the French RCC-MR Code for High Temperature,” WRC Bulletin 440, Welding Research Council, Inc., New York, NY, 1999.

[25] Nuclear Electric, Assessment Procedure for High Temperature Response of Structures, Nuclear Electric R-5, Nuclear Electric, Issue 3, 2003.

[26] Chern, J.M., “A Simplified Approach to the Prediction of Creep Buckling Time in Structures,” PVP-PB-029, Simplified Methods in Pressure Vessel Analysis, ASME, 1978.

[27] Kraus, H., Creep Analysis, John Wiley & Sons, New York, NY, 1980.

[28] Ryder, R.H. and Dahms, C.F., *Design Criteria for Dissimilar Metal Welds*, WRC Bulletin 350, Welding Research Council, Inc., New York, NY, January 1990.

10A.3 Additional References

[1] Anderson, T.L., Fracture Mechanics – Fundamentals and Applications, 3rd Edition, CRC Press, Boca Raton, FL, 2005.

[2] Buchheim, G.M., Becht, C., Nikbin, K.M, Dimopolos, V., Webster, G.A., and Smith D.J., “Influence of Aging on High-Temperature Creep Crack Growth in Type 304H Stainless Steel,” Nonlinear Fracture Mechanics, ASTM STP 995, Volume 1, The American Society of Testing and Materials, PA, 1988, pp. 153-172.

[3] Hashimoto, K., Tokuno, K., Hamada, K., Tsuchida, Y., and Prager, M., “Creep Embrittlement of V-Modified 2.25 Cr-1Mo Steels.” ASME PVP (Vol. 299, pp. 81–88). Presented at the Serviceability of Petroleum, Process, and Power Equipment, American Society of Mechanical Engineers, 1992.

[4] Huddleston, R.L., “Assessment of an Improved Multiaxial Strength Theory Based on Creep Rupture Data for Inconel 600,” PVP-Vol. 262, High-Temperature and Time-Dependent Failure, ASME, 1993.

[5] Imgram, A., Ibarra, S., and Prager, M., “A Vanadium Modified 2-1/4Cr-1Mo Steel with Superior Performance in Creep and Hydrogen Service,” ASME PVP (Vol. 201, pp. 1–28), Presented at the New Alloys for Pressure Vessels and Piping, American Society of Mechanical Engineers, 1990.

[6] Law, P.K. and Saxena, A., “Remaining Life Estimation of Boiler Pressure Parts–Crack Growth Studies,” ERPI CS-4688, Electric Power Research Institute, Palo A lot, CA, July 1886.

[7] Leyda, W. E., and Prager, M., “Data Requirements and Procedures for the Evaluation and Analysis of Stress Rupture Data,” Materials Property Data: Applications and Access, MPD-1, PVP-111 (pp. 97 – 104), New York, NY, American Society of Mechanical Engineers, 1986.

[8] Lundin, C. D., Liu, P., and Prager, M., “Creep Behavior of Weld Heat Affected Zone Regions for Modified 9Cr-lMo Steel (Changes in Microstructure 2),” Proceedings of the 7th International Conference on Creep and Fatigue at Elevated Temperatures (pp. 379–382), Japan Society of Mechanical Engineers, 2001.

[9] Lundin, C., Zhou, G., and Prager, M., “Cryo-Cracking: A Technique for Creep Damage Assessment in High Temperature Components,” Materials at High Temperatures, 15(3-4), 167–173, 1998.

[10] Lundin, C., Zhou, G., and Prager, M., “Failure Modes of Welded Steam Piping,” ASME PVP (Vol. 380, pp. 331–344), Presented at Fitness-for-Service Evaluations in Petroleum and Fossil Power Plants. American Society of Mechanical Engineers, 1998.

[11] Lundin, Carl, and Prager, M., “A New Approach to Investigation into Type IV Cracking Susceptibility,” ASME PVP (Vol. 380, pp. 345–354), Presented at Fitness-for-Service Evaluations in Petroleum and Fossil Power Plants. American Society of Mechanical Engineers, 1998.

[12] McClung, R.C., Chell, G.G., Lee, Y.D., Russell, D.A., and Orient, G.E., “Development of a Practical Methodology for Elastic-Plastic and Fully Plastic Fatigue Crack Growth,” NASA/CR-1999-209428, Marshall Space Flight Center, Alabama, USA, 1999.

[13] Nikbin, K.M., Smith, D.J., and Webster, G.A., “An Engineering Approach to the Prediction of Creep Crack Growth,” Journal of Engineering Materials and Technology, Vol. 108, The American Society of Mechanical Engineers, pp. 186-191, April 1986.

[14] Prager, M., “The Omega Method: An Effective Method for Life and Damage Prediction in Creep Tests and Service,” Strength of materials: fundamental physical aspects of the strength of crystalline materials SCMA 10 (pp. 571 – 574). Presented at the ISCMA 10: Proceedings of the 10th International Conference, Sendai, Japan: Japan Institute of Metals, 1994.

[15] Prager, M., “Modeling Multiaxial Creep and Damage for Application to Pressure Vessels and Piping,” Presented at the Inelasticity and Damage in Solids Subject to Microstructural Change, St. John’s, Newfoundland: Memorial University of Newfoundland, 1997.

[16] Prager, M., “Damage Evaluation and Remaining Life Assessment in High Temperature Structural Components by the Omega Method,” Chotekko Wakusshopu, 7, 150–158, 2003.

[17] Prager, M., “The Omega Method–An Engineering Approach to Life Assessment,” Journal of Pressure Vessel Technology, 122, 273, 2000.

[18] Prager, M, “Progress in Analysis of Fatigue and Stress Rupture,” Journal of Pressure Vessel Technology, 107, 99, 1985.

[19] Prager, M., “Dissimilar-Weld Failure Analysis and Development Program: Volume 3, Accelerated Discriminatory Tests: Final Report (No. EPRI-CS-4252-Vol.3),” Metal Properties Council, Inc.

[20] Prager, M., Cox, T.B., and Wada, T., Enhanced and Modified Materials for Higher Temperatures and Pressures, Welding Research Council, Inc., WRC Bulletin 524, 1–22, New York, NY 2009.

[21] Prager, M., and Ibarra, S. J., “Analytical Treatment of Damage in Creeping Components,” ASME PVP (Vol. 380, pp. 381–386), Presented at the Fitness-for-Service Evaluations in Petroleum and Fossil Power Plants, American Society of Mechanical Engineers, 1988.

[22] Prager, M., Manson, S. S., and Muralidharan, U., “Analysis of Creep-Rupture Data for Five Multiheat Alloys by the Minimum-Commitment Method Using Double Heat-Term-Centering Technique: Final Report,” (No. EPRI-CS-3171) (p. 65), Metal Properties Council, Inc.; Case Western Reserve University, 1983.

[23] Prager, M., “Extend Low Chrome Fatigue Design,” STP-PT-027, ASME Standards Technology, LLC, The American Society of Mechanical Engineers, New York, NY, 2009.

[24] Saxena, A., Han, J., and Banerji, K, “Creep Crack Growth Behavior in Power Plant Boiler and Steam Pipe Steels,” Journal of Pressure Vessel Technology, The American Society of Mechanical Engineers, Vol. 110, pp. 137-146, May 1988.

[25] Sullivan, D., Prager, M., and Lundin, C., “Performance of Welded Seam Piping - Fact and Fiction,” ASME PVP (Vol. 380, pp. 371–374), Presented at the Fitness-for-Service Evaluations in Petroleum and Fossil Power Plants, American Society of Mechanical Engineers, 1998.

[26] Viswanathan, R., “Damage Mechanisms and Life Assessment of High-Temperature Components, ASM International, Metals Park, Ohio, 1989.

[27] Webster, G.A., “Lifetime Estimates of Cracked High Temperature Components,” International Journal of Pressure Vessels & Piping, 50, pp. 133-145, 1992.

[28] Yokobori, A. T., and Prager, M., “Proposal of a New Concept on Creep Fracture Remnant Life for a Precracked Specimen,” Materials at High Temperatures, 16(3), 137–141, 1999.

[29] *VGB-S-517-00-2014-11-DE-EN,* Guidelines for rating the microstructural composition and creep rupture damage of creep-resistant steel for high pressure pipelines and boiler components and their weld connections, VGB Service, ISBN: 978-3-86875-812-2.

[Intentionally Left Blank]

ANNEX 10B – MATERIAL DATA FOR CREEP ANALYSIS

(NORMATIVE)

CONTENTS

ANNEX 10B – MATERIAL DATA FOR CREEP ANALYSIS 10B-1

10B.1 GENERAL 10B-1
10B.2 CREEP RUPTURE DATA 10B-1
10B.2.1 MPC Project Omega 10B-1
10B.2.2 API Std 530, 6th Edition, September 2008 ..... 10B-3
10B.2.3 WRC Bulletin 541 ..... 10B-3
10B.3 TANGENT AND SECANT MODULUS 10B-4
10B.4 CREEP STRAIN-RATE DATA 10B-5
10B.5 ISOCHRONOUS STRESS-STRAIN CURVES 10B-5
10B.6 CREEP REGIME FATIGUE CURVES (CRACK INITIATION) 10B-6
10B.7 CREEP CRACK GROWTH DATA 10B-6
10B.8 NOMENCLATURE 10B-7
10B.9 REFERENCES 10B-9
10B.9.1 Technical References – High Temperature Assessment 10B-9
10B.9.2 Creep Rupture Strength and Creep Strain Rate Data 10B-10
10B.9.3 Creep Crack Growth Data 10B-12
10B.10 TABLES 10B-14
10B.11 FIGURES 10B-59

10B.1 General

The information in this Annex is intended to provide guidance on the materials information required for the Fitness-For-Service (FFS) Assessment of creep damage. Specific materials data are provided for many of the creep damage assessment methods; however, some of the materials data are provided in terms of references to published sources. To include, and keep up to date, all the property information required by the assessment methods in this Standard would be prohibitive. This is especially true for properties that are affected by the service environment.

The Fitness-For-Service Assessment procedures in Part 10 cover situations involving creep damage and flaws commonly encountered in pressure vessels and piping that have been exposed to service for long periods of time. Therefore, when selecting materials properties for an analysis, care must be taken to evaluate these properties in terms of equipment that has been in-service; the properties used in the assessment should reflect any change or degradation, including aging, resulting from the service environment or past operation.

10B.2 Creep Rupture Data

10B.2.1 MPC Project Omega

The assessment techniques developed under the Materials Properties Council (MPC) Project Omega program provide a methodology for estimating the remaining life of a component operating in the creep regime that has been extensively used in the refining and petrochemical industry. The MPC Project Omega Method is an assessment procedure documented in the public domain with a proven record and associated property relations covering a wide range of materials used in the refining and petrochemical industry. In this methodology, a strain-rate parameter and multi-axial damage parameter (Omega) are used to predict the rate of strain

accumulation, creep damage accumulation, and remaining time to failure as a function of stress state and temperature.

a) The remaining life of a component, L, for a given stress state and temperature can be computed using the following equations. In these equations, stress is in units of ksi (MPa), temperature is in degrees Fahrenheit (degrees Celsius), and the remaining life and time are in hours.

$$L = \frac{1}{\dot{\varepsilon}_{co}\Omega_m} \tag{10B.1}$$

where,

$$\log_{10}\left[\dot{\varepsilon}_{co}\right] = -\left[\left(A_0 + \Delta_{\Omega}^{sr}\right) + \left(\frac{A_1 + A_2 S_l + A_3 S_l^2 + A_4 S_l^3}{T_{refa} + T}\right)\right] \tag{10B.2}$$

$$\Omega_m = \Omega_n^{\delta_{\Omega}+1} + \alpha_{\Omega} n_{BN} \tag{10B.3}$$

$$\Omega_n = \max\left[\left(\Omega - n_{BN}\right),\ 3.0\right] \tag{10B.4}$$

$$\log_{10}\left[\Omega\right] = \left[\left(B_0 + \Delta_{\Omega}^{cd}\right) + \left(\frac{B_1 + B_2 S_l + B_3 S_l^2 + B_4 S_l^3}{T_{refa} + T}\right)\right] \tag{10B.5}$$

$$\delta_{\Omega} = \beta_{\Omega} \cdot \left(\frac{\sigma_1 + \sigma_2 + \sigma_3}{\sigma_e} - 1.0\right) \tag{10B.6}$$

$$n_{BN} = -\left(\frac{A_2 + 2A_3 S_l + 3A_4 S_l^2}{T_{refa} + T}\right) \tag{10B.7}$$

$$T_{refa} = 460.0 \quad for\ ^{o}F \tag{10B.8}$$

$$T_{refa} = 273.0 \quad for\ ^{o}C \tag{10B.9}$$

$$S_l = \log_{10}\left[\sigma_e\right] \tag{10B.10}$$

$$\sigma_e = \frac{1}{\sqrt{2}}\left[\left(\sigma_1 - \sigma_2\right)^2 + \left(\sigma_1 - \sigma_3\right)^2 + \left(\sigma_2 - \sigma_3\right)^2\right]^{1/2} \tag{10B.11}$$

b) The coefficients for Equations (10B.2), (10B.5), and (10B.7) for different materials are provided in Table 10B.1.

c) The MPC Project Omega Model for creep currently does not include the effects of primary creep. The effects of primary creep may be important depending on the material, magnitude of applied stress, and exposure temperature. The effects of primary creep may be taken as negligible when the stress from the applied load is less than or equal to 50% of the minimum yield strength at the assessment temperature.

d) The strain rate that may be used in the inelastic analysis (i.e., creep model used with a finite element program) is given by Equations (10B.12), (10B.13), and (10B.14). All other variables are defined in subparagraph (a) above.

$$\dot{\varepsilon}_c = \frac{\dot{\varepsilon}_{co}}{1 - D_c} \tag{10B.12}$$

$$D_c = \int_0^t \dot{D}_c dt \tag{10B.13}$$

$$\dot{D}_c = \dot{\varepsilon}_{co} \Omega_m \tag{10B.14}$$

e) The creep rupture as a function of stress and temperature is shown in Figure 10B.1 to 10B.30. A factor of two has been applied to the average creep rupture life computed using the MPC Project Omega coefficients in Table 10B.1 is included in these plots. In addition, the minimum ultimate tensile stress, and 0.74 times the minimum yield strength for carbon steel and low alloy or the minimum yield strength for high alloy and nickel based alloys are also shown on each plot. The yield strength and ultimate tensile strength for all carbon steel strength levels (excluding Carbon Steel Graphitized), 1.25Cr-0.5Mo (NT), 2.25Cr-1Mo (NT), 2.25Cr-1Mo (QT), and 2.25Cr-1Mo-V are taken from the ASME B&PV Code, Section II, Part D. The yield strength and ultimate tensile strength for all other materials are taken from Annex 2E, Table 2E.7.

10B.2.2 API Std 530, 6th Edition, September 2008

API Std 530 is the API Standard used for the design of fired heater tubes in the refining and petrochemical industry. This standard contains creep rupture data that may be used to evaluate the remaining life of a component operating in the creep regime.

The 6th Edition of this standard was the last edition before the re-evaluation of the data for all materials performed by the Materials Properties Council. This re-evaluation effort led to the creation of WRC Bulletin 541. The data in the 7th Edition of API Std 530 are based on WRC Bulletin 541, 2nd Edition.

a) Minimum and average creep rupture data are typically expressed in terms of the Larson-Miller parameter that combines the time to rupture and temperature into a single variable. The Larson-Miller parameter and the time to rupture are computed using Equations (10B.15) and (10B.16).

$$LMP(\sigma) = (T + 460)\left(C_{LMP} + \log_{10}[L]\right)10^{-3} \qquad for\ ^oF \tag{10B.15}$$

$$\log_{10}[L] = \frac{1000 \cdot LMP(\sigma)}{(T + 460)} - C_{LMP} \qquad for\ ^oF \tag{10B.16}$$

b) The Larson-Miller parameter as a function of stress, $LMP(\sigma)$, which appears in Equations (10B.15) and, (10B.16) for different materials are provided in Table 10B.2. Note that only U.S. Customary units may be used with this table.

c) The limiting design metal temperature for use with the materials in API Std 530, 6th Edition are shown in Table 10B.3.

10B.2.3 WRC Bulletin 541

The purpose of WRC Bulletin 541 was to gather new mechanical property data that reflects modern steel making practices for alloys currently produced and used for petroleum refinery heater applications, and to analyze these new data using modern parametric data analysis methods to derive equations suitable for incorporation into API Std 530.

a) The materials data presented in WRC Bulletin 541 were obtained from materials produced more recently than those used in preparing prior editions of API Std 530. The data for this project were gathered by the MPC and include test results for materials produced and tested at facilities outside of the United States (US). The data collections for prior editions of API Std 530 were limited to US sources. The new data for each alloy were evaluated using modern parametric analysis methods and the results compared graphically to the previously published properties. The coefficients for the polynomials resulting from the regression analysis of the newer materials are presented in tabular form in this document to facilitate computer implementation for design and life assessment.

b) The material data required for a design calculation in accordance with API Std 530 are the yield strength, ultimate tensile strength, stress-rupture exponent, and minimum and average stress rupture properties as described using Larson-Miller Parameter equations. This information is used to obtain the time-independent or elastic allowable stress and the time-dependent or rupture allowable stresses used in determining the required wall thickness of a fired heater tube or bend for a specified service life and temperature.

c) A series of examples is provided to illustrate application of the analytical equations used to represent the properties.

d) The final sections of this bulletin provide in tabular and graphical form the yield strength, ultimate tensile strength, and the minimum and average stress rupture properties. Comparisons of the properties determined under this project with those in the prior edition of API Std 530 are also provided.

e) In WRC 541, the Larson-Miller Parameter and the time to rupture are computed using Equations (10B.8), (10B.9), (10B.15), and (10B.16).

$$LMP(\sigma) = \left(T + T_{refa}\right)\left(C_{LMP} + \log_{10}\left[L\right]\right) \tag{10B.17}$$

$$\log_{10}\left[L\right] = \frac{LMP(\sigma)}{\left(T + T_{refa}\right)} - C_{LMP} \tag{10B.18}$$

f) The Larson-Miller Parameter as a function of stress, $LMP(\sigma)$, which appears in the above Equations for different materials are provided in Table B10.4. Note that for minimum properties, the minimum value of the Larson-Miller constant should be used for C_{LMP}, and for average properties the average value of the Larson-Miller constant should be used for C_{LMP}.

g) The elastic allowable stress factor, creep rupture design allowable stress factor, and applicable temperature range for use with the materials in WRC Bulletin 541 3rd Edition are shown in Table 10B.5.

10B.3 Tangent and Secant Modulus

The secant modulus and the tangent modulus can be determined using the MPC Project Omega data.

a) The secant modulus is computed using Equation (10B.19).

$$E_s = \frac{\sigma}{\varepsilon_e + \varepsilon_p + \varepsilon_c} \tag{10B.19}$$

where,

$$\varepsilon_e = \frac{\sigma}{E_y} \tag{10B.20}$$

$$\varepsilon_p = \gamma_1 + \gamma_2 \tag{10B.21}$$

$$\varepsilon_c = -\frac{1}{\Omega}\ln\left[1 - \dot{\varepsilon}_{co}\Omega t\right] \tag{10B.22}$$

Equations for γ_1 and γ_2 are provided in Annex 2E.

b) The tangent modulus is computed using Equations (10B.23) or (10B.24).

$$E_t = \left\{\frac{\partial \varepsilon_t}{\partial \sigma}\right\}^{-1} = \left\{\frac{\partial\left(\varepsilon_e + \varepsilon_p + \varepsilon_c\right)}{\partial \sigma}\right\}^{-1} \tag{10B.23}$$

or

$$E_t = \frac{1}{\frac{1}{E_y} + \frac{\partial \varepsilon_p}{\partial \sigma} + D_5 + D_6} \tag{10B.24}$$

where,

$$D_5 = -\varepsilon_c \cdot \left(\frac{B_2 + 2B_3 \cdot S_l + 3B_4 \cdot S_l^2}{\sigma \cdot \left(T + T_{refa}\right)}\right) \tag{10B.25}$$

$$D_6 = \frac{\dot{\varepsilon}_{co} t \cdot \left(\left(B_2 - A_2\right) + 2\left(B_3 - A_3\right) \cdot S_l + 3\left(B_4 - A_4\right) \cdot S_l^2\right)}{\sigma \cdot \left(T + T_{refa}\right) \cdot \left(1 - \dot{\varepsilon}_{c0}\Omega t\right)} \tag{10B.26}$$

$$\frac{\partial \varepsilon_p}{\partial \sigma_t} = D_1 + D_2 + D_3 + D_4 \tag{10B.27}$$

In the above equations, T_{refa} and S_l are computed using Equations (10B.8), (10B.9), and (10B.10). Equations for γ_1, γ_2, D_1, D_2, D_3, and D_4 are provided in Annex 2E.

10B.4 Creep Strain-Rate Data

The creep strain rate can be determined using the MPC Project Omega data. The parameters for this equation are defined in paragraph 10B.2.1.

$$\dot{\varepsilon}_c = \dot{\varepsilon}_{co} \exp\left[\Omega_m \varepsilon_c\right] \tag{10B.28}$$

Other sources for creep strain rate data are provided in paragraph 10B.9.2.

10B.5 Isochronous Stress-Strain Curves

Isochronous stress-strain curves may be calculated using Equation (10B.29) obtained by using the MPC Project Omega expressions in paragraph 10B.2.1. Since ε_e and ε_p are functions of the material of construction, stress and temperature, and ε_c is a function of the material of construction, stress, temperature and time (see

Equations (10B.20) and (10B.2)), the specification of a time of interest yields a closed form equation for an isochronous stress-strain curve, or:

$$\varepsilon_t(t) = \varepsilon_e + \varepsilon_p + \varepsilon_c(t) \tag{10B.29}$$

The elastic strain, ε_e, is given by Equation (10B.20), the plastic strain, ε_p, is given by Equation (10B.21), and $\varepsilon_c(t)$ is the creep strain, evaluated using Equation (10B.22).

Other sources for isochronous stress-strain curves for various materials for components operating in the creep regime are provided in paragraph 10B.9.2. Isochronous stress-strain curves may be required to evaluate the remaining life of a component operating in the creep regime. These curves are particularly useful in evaluating the creep buckling potential of a component.

10B.6 Creep Regime Fatigue Curves (Crack Initiation)

For temperatures in the creep range, the allowable number of cycles is provided for the materials shown below in terms of a polynomial function.

a) Materials – The equations, data, and plots for fatigue curves is described below.

- Type 304 SS – Table 10B.6, Table 10B.11 and Figure 10B.31, respectively.
- Type 316 SS – Table 10B.7, Table 10B.12 and Figure 10B.32, respectively.
- Alloy 800H – Table 10B.8, Table 10B.13 and Figure 10B.33, respectively.
- 2.25Cr-1Mo – Table 10B.9, Table 10B.14 and Figure 10B.34, respectively.
- 9Cr-1Mo-V – Table 10B.10, Table 10B.15 and Figure 10B.35, respectively.

b) Sources for fatigue curves (crack initiation) for various materials for components operating in the creep regime are provided in paragraph 10B.9.3.

10B.7 Creep Crack Growth Data

Crack growth data may be required to evaluate the remaining life of a component operating in the creep regime containing a crack. The creep crack growth rate can be correlated to the creep fracture mechanics parameter C^* using Equation (10B.30). The parameters C_t or $C(t)$ can also be used in this equation.

$$\frac{da}{dt} = D_{cc} \cdot (C^*)^{n_{cc}} \tag{10B.30}$$

If the crack driving force is in terms of C^*, then Equations (10B.31), (10B.32), and (10B.33) may be used to estimate the crack growth for a wide range of materials where da/dt is in m/hour, C^* is in MPa-m/hour, and ε_f^* is in percentage strain (see EDF Nuclear Energy R-5).

$$\frac{da}{dt} = \frac{0.3\left(C^*\right)^{0.85}}{\varepsilon_f^*} \qquad (plane\ stress) \tag{10B.31}$$

$$\frac{da}{dt} = \frac{0.03\left(C^*\right)^{0.85}}{\varepsilon_{fLB}^*} \qquad (plane\ stress - Lower\ Bound\ Data) \tag{10B.32}$$

$$\frac{da}{dt} = \frac{15\left(C^*\right)^{0.85}}{\varepsilon_f^*} \qquad (plane\ strain) \tag{10B.33}$$

The above equations have been used for remaining life assessment for high temperature components. However, the fracture strain in this model can be difficult to estimate for an in-service component where only limited materials data are available. In addition, the model does not provide a means to consider prior and ongoing damage in the material where the crack will grow. Another creep crack growth relationship, based on MPC Project Omega Methodology that has been used is shown in Equation (10B.34). The parameters and use of this equation are fully described in Part 10.

$$\frac{da}{dt} = \frac{\Omega}{500} \cdot \left(C_t\right)^{\frac{n_{BN}}{n_{BN}+1}} \tag{10B.34}$$

Data sources for creep crack growth data for C^* and other measures of the crack driving force, C_t or $C(t)$, are provided in paragraph 10B.9.3. The C_t parameter is used in Part 10, paragraph 10.5.4.

10B.8 Nomenclature

$A_0 \rightarrow A_5$ curve-fit coefficients for the Yield strength data, the MPC Project Omega creep strain rate parameter, or the Larson Miller Parameter, as applicable.

α_Ω parameter based on the state-of-stress for MPC Project Omega Life Assessment Model.

= 3.0 – pressurized sphere or formed head,

= 2.0 – pressurized cylinder or cone,

= 1.0 – for all other components and stress states,

= 0.0 – for all components and stress states when geometric nonlinearity (large displacement) is used in the computational method.

$B_0 \rightarrow B_5$ curve-fit coefficients for the MPC Project Omega parameter, as applicable.

β_Ω Prager factor equal to 0.33, for MPC Project Omega Life Assessment Model.

$C_1 \rightarrow C_{11}$ curve-fit coefficients for high temperature fatigue data.

C^* crack driving force associated with global steady-state creep.

C_{LMP} Larson Miller Constant.

C_t crack driving force related to the expansion of the creep zone.

$C(t)$ crack driving force related to the expansion of the creep zone.

$D_1 \rightarrow D_6$ constants to compute the tangent modulus.

$\dot{D}_c$ creep damage rate.

Δ_Ω^{cd} adjustment factor for creep ductility in the Project Omega Model; a range of $+0.3$ for brittle behavior and -0.3 for ductile behavior can be used.

Δ_{Ω}^{sr} adjustment factor for creep strain rate to account for the material scatter band in the Project Omega Model; a range of -0.5 for the bottom of the scatter band to $+0.5$ for the top of the scatter band can be used.

$\frac{da}{dt}$ crack growth rate.

δ_{Ω} damage parameter exponent for MPC Project Omega Life Assessment Model.

E_s secant Modulus.

E_t tangent Modulus.

E_y Young's Modulus at the temperature of interest.

ε_e elastic strain.

ε_c creep strain.

$\dot{\varepsilon}_c$ creep strain rate.

$\varepsilon_c(t)$ creep strain as a function of time.

ε_p plastic strain.

ε_r strain range.

ε_t total true strain.

$\varepsilon_t(t)$ total true strain as a function of time.

$\dot{\varepsilon}_{co}$ initial or reference creep strain rate at the start of the time period being evaluated based on stress state and temperature.

ε_f^* creep ductility based on the state of stress at the crack tip, may be taken to be equal to the uniaxial creep ductility at the reference stress.

ε_{fLB}^* lower bound value for ε_f^*.

γ_1 true strain in the micro-strain region of the stress-strain curve (see Annex 2E).

γ_2 true strain in the macro-strain region of the stress-strain curve (see Annex 2E).

L rupture life (hours).

$LMP(\sigma)$ Larson-Miller Parameter as a function of stress.

N allowable number of cycles.

n_{BN} Bailey Norton coefficient evaluated at the reference stress in the current load increment, use in the MPC Project Omega Life Assessment Model.

Ω Omega uniaxial damage parameter.

Ω_m Omega multiaxial damage parameter.

Ω_n minimum value of the Omega uniaxial damage parameter.

S_l stress parameter.

σ stress or the standard deviation, as applicable.

σ_e effective stress.

σ_1 principal stress.

σ_2 principal stress.

σ_3 principal stress.

T temperature.

T_{refa} reference temperature.

t time.

10B.9 References

10B.9.1 Technical References – High Temperature Assessment

[1] Buchheim, G.M., Osage, D.A., Brown, R.G., and Dobis, J.D., “Failure Investigation of a Low Chrome Long-Seam Weld in a High-Temperature Refinery Piping System,” PVP-Vol. 288, ASME, 1994, pp. 363-386.

[2] Dyson, B., “Use of CDM in Materials Modeling and Component Creep Life Prediction,” ASME, Journal of Pressure Vessel Technology, Vol. 122, August 2000, pages 281-296.

[3] Ibarra, S. and Konet, R.R., “Life Assessment of 1 1/4Cr-1/2Mo Steel Catalytic Reformer Furnace Tubes Using the MPC Omega Method,” PVP-Vol. 288, Service Experience and Reliability Improvement: Nuclear, Fossil, and Petrochemical Plants, ASME 1994, pages 387-400.

[4] Kim, D.S. and Mead, H.E., “Remaining Life Assessment of Refinery Heater Tubes,” PVP-Vol. 388, Fracture, Design Analysis of Pressure Vessels, Heat Exchangers, Piping Components, and Fitness-For-Service, ASME, 1999, pages 361-366.

[5] Klehn, R. and Laughlin, C.A., “Chevron’s Experience Using Omega Method Creep Tests for Life Assessment of Refinery Equipment,” PVP-Vol. 288, Service Experience and Reliability Improvement: Nuclear, Fossil, and Petrochemical Plants, ASME 1994, pages 345-350.

[6] Prager, M. and Ibarra, S., “Approaches to Long Term Life prediction of Furnace and Boiler Tubes,” Fitness for Adverse Environments in Petroleum and Power Equipment, PVP-Vol. 359, ASME, 1997, pp. 339-352.

[7] Prager, M., “Development of the MPC Project Omega Method for Life Assessment in the Creep Range,” PVP-Vol. 288, ASME, 1994, pp. 401-421.

[8] Prager, M., “The Omega Method – An Effective Method for Life and Damage Prediction in Creep Tests and Service,” Oikawa (eds.), Strength of Materials, Japan Institute of Metals, 1994, pp. 571-574.

[9] Prager, M., “Proposed Implementation of Criteria for Assignment of Allowable Stresses in the Creep Range,” ASME Journal of Pressure Vessel Technology, May 1996, Vol. 335, pp. 273-293.

[10] Prager, M., “Generation of Isochronous Creep, Tubing Life and Crack Growth Curves Using the MPC Omega Method, Structural Integrity,” NDE, Risk and Material Performance for Petroleum, Process and Power, PVP-Vol. 336, ASME, 1996, pp. 303-322.

[11] Prager, M. and Ibarra, S., “Approaches to Long Term Life Prediction of Furnace and Boiler Tubes,”, PVP-Vol. 359, Fitness for Adverse Environments in Petroleum and Power Equipment, ASME 1997, pages 339-352.

[12] Prager, M., and Osage, D., “Special Topics in Elevated Temperature Life Applications Including Assessment Rules for API 579,”, PVP-Vol. 411, Service Experience and Fitness-For-Service in Power and Petroleum Processing, ASME, 2000, pages 91-104.

[13] Prager, M., “Damage Evaluation and Remaining Life Assessment in High Temperature Structural Components by the Omega Method,” Proceedings of 7th Workshop on the Ultra Steel, Ultra Steel: Requirements from New Design of Constructions, June 24 and 25, 2003, pages 150-158.

10B.9.2 Creep Rupture Strength and Creep Strain Rate Data

[1] ASM, *Atlas of Creep and Stress-Rupture Curves*, ASM International, Metals Park, OH, 1988.

[2] ASME, Subsection NH – Class 1 Components in Elevated Temperature Service, ASME Code Section III, Division 1, ASME, New York, NY.

[3] ASTM, “An Evaluation of the Elevated Temperature Tensile and Creep-Rupture Properties of Wrought,” ASTM Data Series DS 11S1, American Society for Testing Materials, Philadelphia, PA, 1970.

[4] ASTM, “An Evaluation of the Yield, Tensile, Creep, and Rupture Strengths of Wrought 304, 316, 321, and 347 Stainless Steels at Elevated-Temperatures,” ASTM Data Series DS 5S2, American Society for Testing Materials, Philadelphia, PA, 1969.

[5] ASTM, “Elevated-Temperature Properties of Carbon Steels,” ASTM Special Technical Publication No. 180, American Society for Testing Materials, Philadelphia, Pa., 1955.

[6] ASTM, “Evaluation of the Elevated Temperature Tensile and Creep-Rupture Properties of 1/2 Cr – 1/2 Mo, 1 Cr – 1/2 Mo, and 1 1/4 Cr – 1/2 Mo-Si Steels,” ASTM Data Series DS 50, American Society for Testing Materials, Philadelphia, PA, 1973.

[7] ASTM, “Evaluation of the Elevated-Temperature Tensile and Creep Rupture Properties of 3 to 9 Percent Chromium-Molybdenum Steels,” ASTM Data Series DS 58, American Society for Testing Materials, Philadelphia, PA, 1971.

[8] ASTM, “Evaluations of the Elevated Temperature Tensile and Creep-Rupture Properties of C-Mo, Mn-Mo and Mn-Mo-Ni Steels,” ASTM Data Series DS 47, American Society for Testing Materials, Philadelphia, PA, 1971.

[9] ASTM, “Evaluations of the Elevated-Temperature Tensile and Creep Rupture Properties of 12 to 27 Percent Chromium Steels,” ASTM Data Series DS 59, American Society for Testing Materials, Philadelphia, PA, 1980.

[10] ASTM, “Report on Elevated-Temperature Properties of Chromium Steels (12 to 27 percent),” ASTM Special Technical Publication No. 228, American Society for Testing Materials, Philadelphia, PA, 1958.

[11] ASTM, “Report on Elevated-Temperature Properties of Stainless Steels,” ASTM Special Technical Publication No. 124, American Society for Testing Materials, Philadelphia, PA, 1952.

[12] ASTM, “Supplemental report on the Elevated-Temperature Properties of Chromium-Molybdenum Steels,” ASTM Data series DS 6S1, American Society for Testing Materials, Philadelphia, PA, 1966.

[13] ASTM, “Supplemental Report on the Elevated-Temperature Properties of Chromium-Molybdenum Steels (AN Evaluation of 2 1/4 Cr – 1Mo Steel),” ASTM Data series DS 6S2, American Society for Testing Materials, Philadelphia, PA, 1971.

[14] ASTM, “Supplemental Report on the Elevated-Temperature Properties of Chromium-Molybdenum Steels,” ASTM Special Technical Publication No. 151, American Society for Testing Materials, Philadelphia, PA, 1953.

[15] ASTM, “The Elevated-Temperature Properties of Weld-Deposited Metal and Weldments,” ASTM Special Technical Publication No. 226, American Society for Testing Materials, Philadelphia, PA, 1958.

[16] Atkins, D.F. and Schwartzbat, H., “Stress-Rupture Behavior of Welded and Decarburized Tubular 2 1/4 Cr – 1 Mo Steel,” MPC-7, The American Society of Mechanical Engineers, New York, NY, 1978, pp. 205-223.

[17] Blackburn, L.D., “Isochronous Stress-Strain Curves for Austenitic Stainless Steels," The Generation of Isochronous Stress-Strain Curves, American Society of Mechanical Engineers, New York, NY, 1972.

[18] Booker, M.K., “An Analytical Treatment of the Creep and Creep-Rupture Behavior of Alloy 800H,” MPC-7, The American Society of Mechanical Engineers, New York, NY, 1978, pp. 1-27.

[19] Booker, M.K., “Use of Generalized Regression Models for the Analysis of Stress-Rupture Data,” Characterization of Materials for Service at Elevated Temperatures,” MPC-7, The American Society of Mechanical Engineers, New York, NY, 1978, pp. 459-499.

[20] Ellis, F.V., “Time-Temperature Parameter Based Incremental Creep Equation for Finite Element Analysis,” MPC-7, The American Society of Mechanical Engineers, New York, NY, 1978, pp. 29-49.

[21] Jaske, C.E., “Consideration of Experimental Techniques Used in the Development of Long-Term Properties of Pressure Vessel and Piping Alloys,” MPC-7, The American Society of Mechanical Engineers, New York, NY, 1978, pp. 129-144.

[22] MEP, “High Temperature Design Data for Ferritic Pressure Vessel Steels,” The Creep of Steels Working Party of the Institute of Mechanical Engineers, Mechanical Engineering Publications, Ltd, London.

[23] Panzarella, C.H, Gassama, E., Cochran, J.D., and Osage D.A., *The Valid Stress Range for the MPC Omega Model in API 579-1/ASME FFS-1 2016 and the Creep Rupture Model in WRC 541*, WRC Bulletin 554, The Welding Research Council, Inc., New York, NY, 2019.

[24] Prager, M., Osage, D.A., Panzarella, C.H., Sutton, N.G., O’Brien, I., and Baldesberger, L.A., *Evaluation of Material Strength Data for Use in API Std 530*, WRC Bulletin 541 3rd Edition, Welding Research Council, Inc., New York, NY, 2013.

[25] Sikka, V.K., Booker, M.K., and Brinkman, C.R., “Relationships Between Short-And Long-Term Mechanical Properties of Several Austenitic Stainless Steels,” MPC-7, The American Society of Mechanical Engineers, New York, NY, 1978, pp. 51-82.

[26] Schill, T.V. and Bassfor, T.H., “Extrapolation of Incoloy Alloy 800 Creep-Rupture Data at 500°C to 650°C,” MPC-7, The American Society of Mechanical Engineers, New York, NY, 1978, pp. 95-105.

[27] USS, Steels for Elevated Temperature Service, United States Steel Corporation.

[28] Van Echo, J.A., and Roach, D.B., “Investigation of Mechanical, Physical, and Creep Rupture Properties of Reformer Materials,” Battelle Technical Report on Materials for Steam Reformer Furnaces, Battelle, Columbus, OH, 1973.

[29] Warke, R.W., “A Review of High Temperature Performance Trends and Design Rules for Cr-Mo Steel Weldments,” EPRI, Palo Alto, CA, 1998, TR-110807.

10B.9.3 Creep Crack Growth Data

[1] BSI, Guide on Methods for Assessing the Acceptability of Flaws in Structures, BS 7910, British Standards Institute.

[2] Buchheim, G.M., Becht, C., Nikbin, K.M, Dimopolos, V., Webster, G.A., and Smith D.J., “Influence of Aging on High-Temperature Creep Crack Growth in Type 304H Stainless Steel,” Nonlinear Fracture Mechanics, ASTM STP 995, Volume 1, The American Society of Testing and Materials, PA, 1988, pp. 153-172.

[3] Dimopulos, V., Nikbin, K.M., and Webster, G.A., “Influence of Cyclic to Mean Load Ratio on Creep/Fatigue Crack Growth,” Metallurgical Transactions A, Volume 19A, pp. 873-880, May 1988.

[4] Hollstein, T and Voss, B., “Experimental Determination of the High-Temperature Crack Growth Behavior of Incoloy 800H,” Nonlinear Fracture Mechanics, ASTM STP 995, Volume 1, The American Society of Testing and Materials, PA, 1988, pp. 195-213.

[5] Konosu, S. and Maeda, K., “Creep Embrittlement Susceptibility and Creep Crack Growth Behavior in Low-Alloy Steels: An Assessment of the Effects of Residual Impurity Elements and Postweld Heat Treatment Condition on Creep Ductility and Crack Growth,” Nonlinear Fracture Mechanics, ASTM STP 995, Volume 1, The American Society of Testing and Materials, PA, 1988, pp. 127-152.

[6] Liaw, P.K., Rao, G.V., and Burke, M.G., “Creep Fracture Behavior of 2 1/4 Cr – 1 Mo Welds from a 31-Year-Old Fossil Power Plant,” Materials Science and Engineering, A131, pp. 187-201, 1991.

[7] Liaw, P.K., Saxena, A., and Schaefer, J., “Estimating Remaining Life of Elevated-Temperature Steam Pipes-Part I. Materials Properties,” Engineering Fracture Mechanics, Vol. 32, No. 5, pp. 675-708, 1989.

[8] Nikbin, K.M., Smith, D.J., and Webster, G.A., “An Engineering Approach to the Prediction of Creep Crack Growth,” Journal of Engineering Materials and Technology, Vol. 108, The American Society of Mechanical Engineers, pp. 186-191, April 1986.

[9] Sadananda, K. and Shahinian, P, “Effect of Specimen Thickness on Crack Growth Behavior in Alloy 718 Under Creep and Fatigue Conditions,” MPC-7, The American Society of Mechanical Engineers, New York, NY, 1978, pp. 107-127.

[10] Saxena, A., Han, J., and Banerji, K, “Creep Crack Growth Behavior in Power Plant Boiler and Steam Pipe Steels,” Journal of Pressure Vessel Technology, The American Society of Mechanical Engineers, Vol. 110, pp. 137-146, May 1988.

[11] Webster, G.A., “Lifetime Estimates of Cracked High Temperature Components,” International Journal of Pressure Vessels & Piping, 50, pp. 133-145, 1992.

[12] Austin, T.S.P. and Webster, G.A., “Application of a Creep-Fatigue Crack Growth Model to Type 316 Stainless Steel”, ESIS Publication 15, Behavior of Defects at High Temperatures, Mechanical Engineering Publications Limited, London, 1993.

[13] Okazaki, M., Hashimoto, M., and Mochizuki, T., “Creep-Fatigue Strength of Long-Term Post-Service 2 1/4 Cr – 1 Mo Steel and Remaining Life Estimation,” Journal of Pressure Vessel Technology, Vol. 119, The American Society of Mechanical Engineers, pp. 549-555, 1991.

10B.10 Tables

Table 10B.1 – MPC Project Omega Creep Data (ksi, °F).

Material	Notes	Strain Rate Parameter – $\dot{\varepsilon}_{co}$		Omega Parameter – Ω	
Carbon Steel $\sigma_{uts}^{min} \leq 55$	• See Notes 1, 2, and 3	A_0	-1.600000E+01	B_0	-1.000000E+00
		A_1	3.519286E+04	B_1	3.124493E+03
		A_2	-3.310228E+03	B_2	-4.807777E+01
		A_3	-2.132352E+03	B_3	-5.389615E+02
		A_4	-4.578665E+02	B_4	1.749835E+02
Carbon Steel $\sigma_{uts}^{min} = 60$	• See Notes 1, 2, and 3	A_0	-1.600000E+01	B_0	-1.000000E+00
		A_1	3.524034E+04	B_1	3.171972E+03
		A_2	-3.275595E+03	B_2	-1.267951E+02
		A_3	-2.037106E+03	B_3	-4.437148E+02
		A_4	-4.222948E+02	B_4	1.439052E+02
Carbon Steel $\sigma_{uts}^{min} = 65$	• See Notes 1, 2, and 3	A_0	-1.600000E+01	B_0	-1.000000E+00
		A_1	3.528787E+04	B_1	3.219497E+03
		A_2	-3.241766E+03	B_2	-2.063161E+02
		A_3	-1.940557E+03	B_3	-3.471664E+02
		A_4	-3.872131E+02	B_4	1.123369E+02
Carbon Steel $\sigma_{uts}^{min} = 70$	• See Notes 1, 2, and 3	A_0	-1.600000E+01	B_0	-1.000000E+00
		A_1	3.533558E+04	B_1	3.267211E+03
		A_2	-3.209096E+03	B_2	-2.869956E+02
		A_3	-1.842527E+03	B_3	-2.491363E+02
		A_4	-3.526338E+02	B_4	8.026620E+01
Carbon Steel $\sigma_{uts}^{min} \geq 75$	• See Notes 1, 2, and 3	A_0	-1.600000E+01	B_0	-1.000000E+00
		A_1	3.538350E+04	B_1	3.315135E+03
		A_2	-3.177710E+03	B_2	-3.689600E+02
		A_3	-1.742836E+03	B_3	-1.494446E+02
		A_4	-3.186231E+02	B_4	4.762685E+01

Table 10B.1 – MPC Project Omega Creep Data (ksi, °F)

Material	Notes	Strain Rate Parameter – $\dot{\varepsilon}_{co}$		Omega Parameter – Ω	
Carbon Steel – Graphitized	• See Notes 1 and 2	A_0	-1.680000E+01	B_0	-1.000000E+00
		A_1	3.806000E+04	B_1	3.060000E+03
		A_2	-9.165000E+03	B_2	1.350000E+02
		A_3	1.200000E+03	B_3	-7.600000E+02
		A_4	-6.000000E+02	B_4	2.470000E+02
C-0.5Mo	• See Notes 1 and 2	A_0	-1.950000E+01	B_0	-1.300000E+00
		A_1	6.100000E+04	B_1	4.500000E+03
		A_2	-4.900000E+04	B_2	2.000000E+03
		A_3	3.300000E+04	B_3	-4.500000E+03
		A_4	-8.000000E+03	B_4	2.000000E+03
1.25Cr-0.5Mo – N&T	• See Notes 1 and 2 • Use only below 538 ºC (1000 ºF)	A_0	-2.335000E+01	B_0	-4.400000E+00
		A_1	6.207000E+04	B_1	1.451000E+04
		A_2	-4.752000E+04	B_2	-2.467100E+04
		A_3	4.380000E+04	B_3	2.938400E+04
		A_4	-1.479000E+04	B_4	-1.063000E+04
1.25Cr-0.5Mo – Annealed	• See Notes 1 and 2	A_0	-2.350000E+01	B_0	-2.650000E+00
		A_1	5.278700E+04	B_1	6.287000E+03
		A_2	-5.965500E+03	B_2	1.534500E+03
		A_3	-2.621000E+03	B_3	-1.871000E+03
		A_4	-3.840000E+02	B_4	1.660000E+02
2.25Cr-1Mo – N&T	• See Notes 1 and 2 • Use only below 510 ºC (950 ºF)	A_0	-2.156000E+01	B_0	-1.120000E+00
		A_1	5.552600E+04	B_1	5.040000E+03
		A_2	-1.098590E+04	B_2	-4.359000E+02
		A_3	-1.560170E+03	B_3	-2.175170E+03
		A_4	-7.386000E+01	B_4	1.136140E+03

Table 10B.1 – MPC Project Omega Creep Data (ksi, °F)

Material	Notes	Strain Rate Parameter – $\dot{\varepsilon}_{co}$		Omega Parameter – Ω	
2.25Cr-1Mo – Annealed	• See Notes 1 and 2	A_0	-2.186000E+01	B_0	-1.850000E+00
		A_1	5.166900E+04	B_1	7.195000E+03
		A_2	-7.597400E+03	B_2	-2.358000E+03
		A_3	-2.131000E+03	B_3	-1.274000E+02
		A_4	-1.993000E+02	B_4	5.620000E+01
2.25Cr-1Mo – Q&T	• See Notes 1 and 2 • Use only below 510 ºC (950 ºF)	A_0	-2.156000E+01	B_0	-1.120000E+00
		A_1	5.553000E+04	B_1	5.044000E+03
		A_2	-1.100580E+04	B_2	-4.558000E+02
		A_3	-1.544000E+03	B_3	-2.159000E+03
		A_4	-7.221000E+01	B_4	1.137790E+03
2.25Cr-1Mo – V	• See Notes 1 and 2 • Use only below 510 ºC (950 ºF)	A_0	-2.500000E+01	B_0	-2.520000E+00
		A_1	5.221050E+04	B_1	5.797600E+03
		A_2	-9.367000E+02	B_2	-3.648000E+02
		A_3	-1.814000E+03	B_3	-2.282000E+02
		A_4	-1.171000E+03	B_4	2.949000E+02
5Cr-0.5Mo	• See Notes 1 and 2	A_0	-2.240000E+01	B_0	-1.400000E+00
		A_1	5.166870E+04	B_1	5.019240E+03
		A_2	-7.597370E+03	B_2	-1.207620E+03
		A_3	-2.131000E+03	B_3	2.213200E+02
		A_4	-1.992700E+02	B_4	8.943000E+01
9Cr-1Mo	• See Notes 1 and 2	A_0	-2.255000E+01	B_0	-2.050000E+00
		A_1	5.147300E+04	B_1	6.410800E+03
		A_2	-7.027300E+03	B_2	-1.426600E+03
		A_3	-1.718000E+03	B_3	-6.900000E+01
		A_4	-1.406000E+02	B_4	8.380000E+01

Table 10B.1 – MPC Project Omega Creep Data (ksi, °F)

Material	Notes	Strain Rate Parameter – $\dot{\varepsilon}_{co}$		Omega Parameter – Ω	
9Cr-1Mo – V	• See Notes 1 and 2	A_0	-3.400000E+01	B_0	-2.000000E+00
		A_1	7.328500E+04	B_1	7.185000E+03
		A_2	-3.428000E+03	B_2	-1.231720E+03
		A_3	-3.433000E+03	B_3	-4.492800E+02
		A_4	-1.146170E+03	B_4	2.052200E+02
10.5Cr-V (Alloy 115) UNS K91060	• See Notes 1 and 2	A_0	-3.732000E+01	B_0	-1.963000E+00
		A_1	8.496750E+04	B_1	9.403300E+03
		A_2	-2.140980E+04	B_2	-8.867700E+03
		A_3	1.623600E+04	B_3	1.003100E+04
		A_4	-7.606000E+03	B_4	-3.876900E+03
12 Cr	• See Notes 1 and 2	A_0	-3.029000E+01	B_0	-3.298000E+00
		A_1	6.711000E+04	B_1	6.508000E+03
		A_2	-2.109300E+04	B_2	3.016000E+03
		A_3	1.455600E+04	B_3	-2.784000E+03
		A_4	-5.884000E+03	B_4	4.800000E+02
Type 304 & 304H	• See Notes 1 and 2	A_0	-1.917000E+01	B_0	-3.400000E+00
		A_1	5.376240E+04	B_1	1.125000E+04
		A_2	-1.344240E+04	B_2	-5.635800E+03
		A_3	3.162600E+03	B_3	3.380400E+03
		A_4	-1.685200E+03	B_4	-9.936000E+02
Type 316 & 316H	• See Notes 1 and 2	A_0	-1.890000E+01	B_0	-4.163000E+00
		A_1	5.726150E+04	B_1	1.717626E+04
		A_2	-1.865600E+04	B_2	-1.321600E+04
		A_3	3.866860E+03	B_3	4.973798E+03
		A_4	-2.671640E+02	B_4	-6.736400E+01

Table 10B.1 – MPC Project Omega Creep Data (ksi, °F)

Material	Notes	Strain Rate Parameter – $\dot{\varepsilon}_{co}$		Omega Parameter – Ω	
Type 321	• See Notes 1 and 2	A_0	-1.900000E+01	B_0	-3.400000E+00
		A_1	4.942500E+04	B_1	1.062500E+04
		A_2	-7.417000E+03	B_2	-3.217000E+03
		A_3	1.240000E+03	B_3	1.640000E+03
		A_4	-1.290000E+03	B_4	-4.900000E+02
Type 321H	• See Notes 1 and 2	A_0	-1.840000E+01	B_0	-3.400000E+00
		A_1	4.942500E+04	B_1	1.062500E+04
		A_2	-7.417000E+03	B_2	-3.217000E+03
		A_3	1.240000E+03	B_3	1.640000E+03
		A_4	-1.290000E+03	B_4	-4.900000E+02
Type 347	• See Notes 1 and 2	A_0	-1.830000E+01	B_0	-3.500000E+00
		A_1	4.714000E+04	B_1	1.000000E+04
		A_2	-5.434000E+03	B_2	-8.000000E+02
		A_3	5.000000E+02	B_3	-1.000000E+02
		A_4	-1.128000E+03	B_4	1.000000E+02
Type 347H	• See Notes 1 and 2	A_0	-1.770000E+01	B_0	-3.650000E+00
		A_1	4.714000E+04	B_1	1.000000E+04
		A_2	-5.434000E+03	B_2	-8.000000E+02
		A_3	5.000000E+02	B_3	-1.000000E+02
		A_4	-1.128000E+03	B_4	1.000000E+02
Type 347LN UNS S34751	• See Notes 1 and 2	A_0	-1.680664E+01	B_0	-4.000000E-01
		A_1	1.067725E+05	B_1	6.488220E+04
		A_2	-1.448239E+05	B_2	-1.391989E+05
		A_3	1.004320E+05	B_3	1.010732E+05
		A_4	-2.401329E+04	B_4	-2.384369E+04

Table 10B.1 – MPC Project Omega Creep Data (ksi, °F)

Material	Notes	Strain Rate Parameter – $\dot{\varepsilon}_{co}$		Omega Parameter – Ω	
Type 347 AP Advanced UNS S34752	• See Notes 1 and 2	A_0	-1.432000E+01	B_0	-5.500000E-01
		A_1	4.356980E+04	B_1	5.584300E+03
		A_2	-6.471400E+03	B_2	-1.163200E+03
		A_3	-2.949000E+02	B_3	4.087300E+02
		A_4	-4.480000E+00	B_4	1.113900E+02
Alloy 800	• See Notes 1 and 2	A_0	-1.940000E+01	B_0	-3.600000E+00
		A_1	5.554800E+04	B_1	1.125000E+04
		A_2	-1.587700E+04	B_2	-5.635000E+03
		A_3	3.380000E+03	B_3	3.380000E+03
		A_4	-9.930000E+02	B_4	-9.930000E+02
Alloy 800H	• See Notes 1 and 2	A_0	-1.880000E+01	B_0	-3.600000E+00
		A_1	5.554800E+04	B_1	1.125000E+04
		A_2	-1.587700E+04	B_2	-5.635000E+03
		A_3	3.380000E+03	B_3	3.380000E+03
		A_4	-9.930000E+02	B_4	-9.930000E+02
Alloy 800HT	• See Notes 1 and 2	A_0	-2.025000E+01	B_0	-3.400000E+00
		A_1	5.944500E+04	B_1	1.119500E+04
		A_2	-1.412300E+04	B_2	-4.848500E+03
		A_3	4.142000E+01	B_3	1.556000E+03
		A_4	-4.050000E-02	B_4	8.242000E+01

Table 10B.1 – MPC Project Omega Creep Data (ksi, °F)

Material	Notes	Strain Rate Parameter – $\dot{\varepsilon}_{co}$		Omega Parameter – Ω	
HK-40	• See Notes 1 and 2	A_0	-1.480000E+01	B_0	-4.400000E+00
		A_1	4.725200E+04	B_1	1.300000E+04
		A_2	-8.684000E+03	B_2	-4.000000E+02
		A_3	-4.060000E+02	B_3	-1.800000E-01
		A_4	-6.330000E+00	B_4	3.004000E-01

Notes:

1) Coefficients in this table are estimates of the typical material behavior (center of scatter band) based on the MPC Project Omega Materials data from service-aged materials at design stress levels.
2) The coefficients in this table are intended to describe material behavior in the range of the ASME Code design allowable stress for a given material at a specified temperature. These coefficients may be used to estimate the stress relaxation resulting from creep over a similar stress range.
3) σ_{UTS}^{min} is the minimum specified ultimate tensile strength at room temperature.

Table 10B.1M – MPC Project Omega Creep Data (MPa, °C).

Material	Notes	Strain Rate Parameter – $\dot{\varepsilon}_{co}$		Omega Parameter – Ω	
Carbon Steel $\sigma_{uts}^{min} \leq 379$	• See Notes 1, 2, and 3	A_0	-1.600000E+01	B_0	-1.000000E+00
		A_1	2.041067E+04	B_1	1.490383E+03
		A_2	-3.888827E+02	B_2	6.804895E+02
		A_3	-5.447574E+02	B_3	-5.439680E+02
		A_4	-2.543703E+02	B_4	9.721306E+01
Carbon Steel $\sigma_{uts}^{min} = 413$	• See Notes 1, 2, and 3	A_0	-1.600000E+01	B_0	-1.000000E+00
		A_1	2.044647E+04	B_1	1.600815E+03
		A_2	-4.166975E+02	B_2	5.115982E+02
		A_3	-5.415552E+02	B_3	-4.476203E+02
		A_4	-2.346082E+02	B_4	7.994735E+01
Carbon Steel $\sigma_{uts}^{min} = 448$	• See Notes 1, 2, and 3	A_0	-1.600000E+01	B_0	-1.000000E+00
		A_1	2.048334E+04	B_1	1.712316E+03
		A_2	-4.467459E+02	B_2	3.404734E+02
		A_3	-5.369449E+02	B_3	-3.498646E+02
		A_4	-2.151184E+02	B_4	6.240938E+01
Carbon Steel $\sigma_{uts}^{min} = 483$	• See Notes 1, 2, and 3	A_0	-1.600000E+01	B_0	-1.000000E+00
		A_1	2.052159E+04	B_1	1.825205E+03
		A_2	-4.794071E+02	B_2	1.667357E+02
		A_3	-5.308094E+02	B_3	-2.505836E+02
		A_4	-1.959077E+02	B_4	4.459233E+01
Carbon Steel $\sigma_{uts}^{min} \geq 517$	• See Notes 1, 2, and 3	A_0	-1.600000E+01	B_0	-1.000000E+00
		A_1	2.056140E+04	B_1	1.939644E+03
		A_2	-5.149966E+02	B_2	-9.930231E+00
		A_3	-5.229561E+02	B_3	-1.495848E+02
		A_4	-1.770129E+02	B_4	2.645936E+01

Table 10B.1M – MPC Project Omega Creep Data (MPa, °C)

Material	Notes	Strain Rate Parameter – $\dot{\varepsilon}_{co}$		Omega Parameter – Ω	
Carbon Steel – Graphitized	• See Notes 1 and 2	A_0	-1.680000E+01	B_0	-1.000000E+00
		A_1	2.607917E+04	B_1	1.259338E+03
		A_2	-6.912806E+03	B_2	1.072531E+03
		A_3	1.505186E+03	B_3	-7.674130E+02
		A_4	-3.333330E+02	B_4	1.372220E+02
C-0.5Mo	• See Notes 1 and 2	A_0	-1.950000E+01	B_0	-1.300000E+00
		A_1	7.222599E+04	B_1	-8.445560E+02
		A_2	-6.734277E+04	B_2	7.647419E+03
		A_3	2.951359E+04	B_3	-5.295063E+03
		A_4	-4.444444E+03	B_4	1.111111E+03
1.25Cr-0.5Mo – N&T	• See Notes 1 and 2 • Use only below 538 ºC (1000 ºF)	A_0	-2.335000E+01	B_0	-4.400000E+00
		A_1	7.857368E+04	B_1	3.451366E+04
		A_2	-8.453968E+04	B_2	-5.353966E+04
		A_3	4.500283E+04	B_3	3.118021E+04
		A_4	-8.216667E+03	B_4	-5.905556E+03
1.25Cr-0.5Mo – Annealed	• See Notes 1 and 2	A_0	-2.350000E+01	B_0	-2.650000E+00
		A_1	3.120707E+04	B_1	1.992720E+03
		A_2	-1.322206E+03	B_2	2.790216E+03
		A_3	-9.194590E+02	B_3	-1.271435E+03
		A_4	-2.133330E+02	B_4	9.222200E+01
2.25Cr-1Mo – N&T	• See Notes 1 and 2 • Use only below 510 ºC (950 ºF)	A_0	-2.156000E+01	B_0	-1.120000E+00
		A_1	3.538025E+04	B_1	1.781266E+03
		A_2	-4.736240E+03	B_2	3.115806E+03
		A_3	-7.635390E+02	B_3	-2.796219E+03
		A_4	-4.103300E+01	B_4	6.311890E+02

Table 10B.1M – MPC Project Omega Creep Data (MPa, °C)

Material	Notes	Strain Rate Parameter – $\dot{\varepsilon}_{co}$		Omega Parameter – Ω	
2.25Cr-1Mo – Annealed	• See Notes 1 and 2	A_0	-2.186000E+01	B_0	-1.850000E+00
		A_1	3.147707E+04	B_1	5.027509E+03
		A_2	-2.468902E+03	B_2	-1.125445E+03
		A_3	-9.053610E+02	B_3	-1.493190E+02
		A_4	-1.107220E+02	B_4	3.122200E+01
2.25Cr-1Mo – Q&T	• See Notes 1 and 2 • Use only below 510 ºC (950 ºF)	A_0	-2.156000E+01	B_0	-1.120000E+00
		A_1	3.539752E+04	B_1	1.798534E+03
		A_2	-4.760427E+03	B_2	3.091619E+03
		A_3	-7.568620E+02	B_3	-2.789542E+03
		A_4	-4.011700E+01	B_4	6.321060E+02
2.25Cr-1Mo – V	• See Notes 1 and 2 • Use only below 510 ºC (950 ºF)	A_0	-2.500000E+01	B_0	-2.520000E+00
		A_1	2.911717E+04	B_1	3.205108E+03
		A_2	-2.026610E+02	B_2	3.554580E+02
		A_3	6.289840E+02	B_3	-5.388370E+02
		A_4	-6.507110E+02	B_4	1.638140E+02
5Cr-0.5Mo	• See Notes 1 and 2	A_0	-2.240000E+01	B_0	-1.400000E+00
		A_1	3.147688E+04	B_1	3.408189E+03
		A_2	-2.468850E+03	B_2	-7.723020E+02
		A_3	-9.054030E+02	B_3	-2.026000E+00
		A_4	-1.107060E+02	B_4	4.968300E+01
9Cr-1Mo	• See Notes 1 and 2	A_0	-2.255000E+01	B_0	-2.050000E+00
		A_1	3.124471E+04	B_1	4.171728E+03
		A_2	-2.468179E+03	B_2	-6.300670E+02
		A_3	-7.579510E+02	B_3	-1.554460E+02
		A_4	-7.811100E+01	B_4	4.655600E+01

Table 10B.1M – MPC Project Omega Creep Data (MPa, °C)

Material	Notes	Strain Rate Parameter – $\dot{\varepsilon}_{co}$		Omega Parameter – Ω	
9Cr-1Mo – V	• See Notes 1 and 2	A_0	-3.400000E+01	B_0	-2.000000E+00
		A_1	4.134523E+04	B_1	4.322741E+03
		A_2	-4.910700E+01	B_2	-2.521200E+01
		A_3	-3.054130E+02	B_3	-5.364010E+02
		A_4	-6.367610E+02	B_4	1.140110E+02
10.5Cr-V (Alloy 115) UNS K91060	• See Notes 1 and 2	A_0	-3.732000E+01	B_0	-1.963000E+00
		A_1	6.601171E+04	B_1	1.454345E+04
		A_2	-3.593500E+04	B_2	-1.881580E+04
		A_3	1.964982E+04	B_3	1.099097E+04
		A_4	-4.225560E+03	B_4	-2.153830E+03
12 Cr	• See Notes 1 and 2	A_0	-3.029000E+01	B_0	-3.298000E+00
		A_1	5.472248E+04	B_1	9.658680E+02
		A_2	-3.217519E+04	B_2	4.831865E+03
		A_3	1.630974E+04	B_3	-2.217482E+03
		A_4	-3.268889E+03	B_4	2.666670E+02
Type 304 & 304H	• See Notes 1 and 2	A_0	-1.917000E+01	B_0	-3.400000E+00
		A_1	3.791740E+04	B_1	1.052130E+04
		A_2	-1.238937E+04	B_2	-7.444834E+03
		A_3	4.112120E+03	B_3	3.266587E+03
		A_4	-9.362220E+02	B_4	-5.520000E+02
Type 316 & 316H	• See Notes 1 and 2	A_0	-1.890000E+01	B_0	-4.163000E+00
		A_1	4.210070E+04	B_1	1.766389E+04
		A_2	-1.428023E+04	B_2	-1.205519E+04
		A_3	2.521626E+03	B_3	2.857364E+03
		A_4	-1.484240E+02	B_4	-3.742400E+01

Table 10B.1M – MPC Project Omega Creep Data (MPa, °C)

Material	Notes	Strain Rate Parameter – $\dot{\varepsilon}_{co}$		Omega Parameter – Ω	
Type 321	• See Notes 1 and 2	A_0	-1.900000E+01	B_0	-3.400000E+00
		A_1	3.182039E+04	B_1	8.202508E+03
		A_2	-6.787544E+03	B_2	-3.889400E+03
		A_3	2.491705E+03	B_3	1.595902E+03
		A_4	-7.166670E+02	B_4	-2.722220E+02
Type 321H	• See Notes 1 and 2	A_0	-1.840000E+01	B_0	-3.400000E+00
		A_1	3.182039E+04	B_1	8.202508E+03
		A_2	-6.787544E+03	B_2	-3.889400E+03
		A_3	2.491705E+03	B_3	1.595902E+03
		A_4	-7.166670E+02	B_4	-2.722220E+02
Type 347	• See Notes 1 and 2	A_0	-1.830000E+01	B_0	-3.500000E+00
		A_1	2.928506E+04	B_1	5.856415E+03
		A_2	-4.806587E+03	B_2	-2.340900E+02
		A_3	1.854193E+03	B_3	-1.953090E+02
		A_4	-6.266670E+02	B_4	5.555600E+01
Type 347H	• See Notes 1 and 2	A_0	-1.770000E+01	B_0	-3.650000E+00
		A_1	2.928506E+04	B_1	5.856415E+03
		A_2	-4.806587E+03	B_2	-2.340900E+02
		A_3	1.854193E+03	B_3	-1.953090E+02
		A_4	-6.266670E+02	B_4	5.555600E+01
Type 347 LN UNS S34751	• See Notes 1 and 2	A_0	-1.680664E+01	B_0	-4.000000E-01
		A_1	1.738794E+05	B_1	1.481833E+05
		A_2	-2.021692E+05	B_2	-1.994429E+05
		A_3	8.935494E+04	B_3	8.947416E+04
		A_4	-1.334073E+04	B_4	-1.324650E+04

Table 10B.1M – MPC Project Omega Creep Data (MPa, °C)

Material	Notes	Strain Rate Parameter – $\dot{\varepsilon}_{co}$		Omega Parameter – Ω	
Type 347 AP Advanced UNS S34752	• See Notes 1 and 2	A_0	-1.432000E+01-	B_0	-5.500000E-01
		A_1	2.710638E+04	B_1	3.767430E+03
		A_2	-3.325720E+03	B_2	-8.965000E+02
		A_3	-1.575700E+02	B_3	7.140000E+01
		A_4	-2.490000E+00	B_4	6.188000E+01
Alloy 800	• See Notes 1 and 2	A_0	-1.940000E+01	B_0	-3.600000E+00
		A_1	3.990174E+04	B_1	1.052057E+04
		A_2	-1.313331E+04	B_2	-7.443314E+03
		A_3	3.265527E+03	B_3	3.265527E+03
		A_4	-5.516670E+02	B_4	-5.516670E+02
Alloy 800H	• See Notes 1 and 2	A_0	-1.880000E+01	B_0	-3.600000E+00
		A_1	3.990174E+04	B_1	1.052057E+04
		A_2	-1.313331E+04	B_2	-7.443314E+03
		A_3	3.265527E+03	B_3	3.265527E+03
		A_4	-5.516670E+02	B_4	-5.516670E+02
Alloy 800HT	• See Notes 1 and 2	A_0	-2.025000E+01	B_0	-3.400000E+00
		A_1	3.962031E+04	B_1	9.058896E+03
		A_2	-7.884749E+03	B_2	-4.046733E+03
		A_3	2.306800E+01	B_3	7.492600E+02
		A_4	-2.300000E-02	B_4	4.578900E+01

Table 10B.1M – MPC Project Omega Creep Data (MPa, °C)

Material	Notes	Strain Rate Parameter – $\dot{\varepsilon}_{co}$		Omega Parameter – Ω	
HK-40	• See Notes 1 and 2	A_0	-1.480000E+01	B_0	-4.400000E+00
		A_1	3.013998E+04	B_1	7.408391E+03
		A_2	-4.453597E+03	B_2	-2.217020E+02
		A_3	-2.167090E+02	B_3	-5.200000E-01
		A_4	-3.517000E+00	B_4	1.670000E-01

Notes:

1) Coefficients in this table are estimates of the typical material behavior (center of scatter band) based on the MPC Project Omega Materials data from service-aged materials at design stress levels.
2) The coefficients in this table are intended to describe material behavior in the range of the ASME Code design allowable stress for a given material at a specified temperature. These coefficients may be used to estimate the stress relaxation resulting from creep over a similar stress range.
3) σ_{UTS}^{min} is the minimum specified ultimate tensile strength at room temperature.

Table 10B.2 – Minimum and Average Larson-Miller Parameters as a Function of Stress Based on API STD 530, 6th Edition, September 2008 (see Table 10B.3 for Temperature Limits)

Material	Equation (3)	Parameters	Minimum Larson-Miller Parameter – LMP_m	Average Larson-Miller Parameter – LMP_a
Low Carbon Steel (Figure F.1) A161 A192	1	A_0	3.9472132E+01	3.9793713E+01
		A_1	-1.7555884E-01	-1.5443414E-01
		A_2	0.0000000E+00	0.0000000E+00
		A_3	-2.5495581E+00	-2.6260065E+00
		C_{LMP}	20.0	20.0
Medium Carbon Steel (Figure F.2) A53 Grade B A106 Grade B A210 Grade A-1	1	A_0	4.0588307E+01	4.1406114E+01
		A_1	-1.7712679E-01	-9.4412373E-02
		A_2	0.0000000E+00	0.0000000E+00
		A_3	0.0000000E+00	0.0000000E+00
		C_{LMP}	20.0	20.0
C-0.5Mo (Figure F.3) A 161 T1 A 209 T1 A 335 P1	1	A_0	4.0572407E+01	4.1235292E+01
		A_1	4.6810884E-02	3.7759486E-02
		A_2	-1.7428803E-03	-1.1188817E-03
		A_3	-2.4287545E+00	-2.4403636E+00
		C_{LMP}	20.0	20.0
1.25Cr-0.5Mo (Figure F.4) A 213 T11 A 335 P11 A 200 T11	1	A_0	4.1444290E+01	4.2605250E+01
		A_1	-1.6608091E-03	0.0000000E+00
		A_2	0.0000000E+00	0.0000000E+00
		A_3	-2.5842632E+00	-2.6236052E+00
		C_{LMP}	20.0	20.0
2.25Cr-1Mo (Figure F.5) A 213 T22 A 335 P22 A 200 T22	2	A_0	4.3981719E+01	4.3494159E+01
		A_1	-8.4656117E-01	-6.0165638E-01
		A_2	-4.0483005E+01	-2.8040471E+01
		A_3	2.6236081E-01	2.0644229E-01
		A_4	1.5373650E+01	1.0982290E+01
		A_5	4.9673781E-02	2.8393767E-02
		A_6	6.6049429E-01	3.6067024E-01
		C_{LMP}	20.0	20.0

Table 10B.2 – Minimum and Average Larson-Miller Parameters as a Function of Stress Based on API STD 530, 6th Edition, September 2008 (see Table 10B.3 for Temperature Limits)

Material	Equation (3)	Parameters	Minimum Larson-Miller Parameter – LMP_m	Average Larson-Miller Parameter – LMP_a
3Cr-1Mo (Figure F.6) A 213 T5 A 335 P5 A 200 T5	1	A_0	4.4051838E+01	4.4786113E+01
		A_1	0.0000000E+00	0.0000000E+00
		A_2	0.0000000E+00	0.0000000E+00
		A_3	-3.4764953E+00	-3.5012470E+00
		C_{LMP}	20.0	20.0
5Cr-0.5Mo (Figure F.7) A 213 T5 A 335 P5 A 200 T5	1	A_0	4.4060307E+01	4.5561570E+01
		A_1	0.0000000E+00	0.0000000E+00
		A_2	0.0000000E+00	0.0000000E+00
		A_3	-3.8832654E+00	-3.9292158E+00
		C_{LMP}	20.0	20.0
5Cr-0.5Mo-Si (Figure F.8) A 213 T5b A 335 P5b	1	A_0	4.3412435E+01	4.5193964E+01
		A_1	6.0084603E-04	0.0000000E+00
		A_2	0.0000000E+00	0.0000000E+00
		A_3	-4.0873944E+00	-4.0637419E+00
		C_{LMP}	20.0	20.0
7Cr-0.5Mo (Figure F.9) A 213 T7 A 335 P7 A 200 T7	1	A_0	4.4585981E+01	4.5795478E+01
		A_1	0.0000000E+00	0.0000000E+00
		A_2	0.0000000E+00	0.0000000E+00
		A_3	-4.4159080E+00	-4.4250128E+00
		C_{LMP}	20.0	20.0
9Cr-1Mo (Figure F.10) A 213 T9 A 335 P9 A 200 T9	1	A_0	4.3440090E+01	4.4713375E+01
		A_1	0.0000000E+00	0.0000000E+00
		A_2	0.0000000E+00	0.0000000E+00
		A_3	-3.1274348E+00	-3.1087353E+00
		C_{LMP}	20.0	20.0

Table 10B.2 – Minimum and Average Larson-Miller Parameters as a Function of Stress Based on API STD 530, 6th Edition, September 2008 (see Table 10B.3 for Temperature Limits)

Material	Equation (3)	Parameters	Minimum Larson-Miller Parameter – LMP_m	Average Larson-Miller Parameter – LMP_a
9Cr-1Mo-V (Figure F.11) A 213 T91 A 335 P91 A 200 T91	2	A_0	5.8775488E+01	6.0293151E+01
		A_1	6.3030427E-01	2.9164576E-01
		A_2	4.3080961E+01	2.0624046E+01
		A_3	-4.2138473E-02	8.1446975E-03
		A_4	-5.8181139E+00	-1.3816921E+00
		A_5	1.3056690E-03	1.2791388E-04
		A_6	2.8215429E-01	6.5750485E-02
		C_{LMP}	30.0	30.0
Type 304 & 304H (Figure F.12) A 213 Type 304 & 304H A 271 Type 304 & 304H A 312 Type 304 & 304H A 376 Type 304 & 304H	1	A_0	4.1604481E+01	4.3167974E+01
		A_1	0.0000000E+00	0.0000000E+00
		A_2	0.0000000E+00	0.0000000E+00
		A_3	-4.1590309E+00	-4.1576784E+00
		C_{LMP}	15. 0	15.0
Type 316 & 316H (Figure F.13) A 213 Type 316 & 316H A 271 Type 316 & 316H A 312 Type 316 & 316H A 376 Type 316 & 316H	1	A_0	4.0727285E+01	4.1474655E+01
		A_1	0.0000000E+00	0.0000000E+00
		A_2	0.0000000E+00	0.0000000E+00
		A_3	-3.3777142E+00	-3.3744962E+00
		C_{LMP}	15.0	15.0
Type 316L (Figure F.14) A 213 Type 316L A 312 Type 316L	1	A_0	4.0013821E+01	4.0734498E+01
		A_1	0.0000000E+00	-3.7185119E-03
		A_2	0.0000000E+00	0.0000000E+00
		A_3	-3.2795068E+00	-3.2327975E+00
		C_{LMP}	15.0	15.0
Type 321 (Figure F.15) A 213 Type 321 A 271 Type 321 A 312 Type 321 A 376 Type 321	1	A_0	3.7886814E+01	3.9898092E+01
		A_1	0.0000000E+00	0.0000000E+00
		A_2	0.0000000E+00	0.0000000E+00
		A_3	-3.1045579E+00	-3.1231396E+00
		C_{LMP}	15.0	15.0

Table 10B.2 – Minimum and Average Larson-Miller Parameters as a Function of Stress Based on API STD 530, 6th Edition, September 2008 (see Table 10B.3 for Temperature Limits)

Material	Equation (3)	Parameters	Minimum Larson-Miller Parameter – LMP_m	Average Larson-Miller Parameter – LMP_a
Type 321H (Figure F.16) A 213 Type 321H A 271 Type 321H A 312 Type 321H A 376 Type 321H	1	A_0	4.0463845E+01	4.2128555E+01
		A_1	0.0000000E+00	0.0000000E+00
		A_2	0.0000000E+00	0.0000000E+00
		A_3	-3.8251065E+00	-3.8415837E+00
		C_{LMP}	15.0	15.0
Type 347 & 347H (Figure F.17) A 213 Type 347 & 347H A 271 Type 347 & 347H A 312 Type 347 & 347H A 376 Type 347 & 347H	1	A_0	4.0978191E+01	4.1681564E+01
		A_1	0.0000000E+00	0.0000000E+00
		A_2	0.0000000E+00	0.0000000E+00
		A_3	-3.3967083E+00	-3.3844260E+00
		C_{LMP}	15.0	15.0
Alloy 800H (Figure F.18) B407 Alloy 800H	1	A_0	4.2984876E+01	4.3972044E+01
		A_1	1.0453205E-02	1.1049396E-02
		A_2	0.0000000E+00	0.0000000E+00
		A_3	-4.4907290E+00	-4.4942889E+00
		C_{LMP}	15.0	15.0
HK-40 (Figure F.19) A608 Grade HK-40	1	A_0	4.4347806E+01	4.5201670E+01
		A_1	-2.0236623E-01	-1.6593352E-01
		A_2	0.0000000E+00	0.0000000E+00
		A_3	-3.7794033E+00	-3.8011626E+00
		C_{LMP}	15.0	15.0

Notes:

1) Data for the minimum and average Larson-Miller parameters in this table are from Figures 4-A thru 4-S of API STD 530 *Calculation of Heater Tube Thickness in Petroleum Refineries*.
2) Units for the equations in this table are as follows: σ are in ksi.
3) Equations 1 and 2 for $LMP(\sigma)$ are as follows: σ is in ksi:

   Equation 1: $LMP(\sigma) = A_0 + A_1\sigma + A_2\sigma^2 + A_3 \ln \sigma$

   Equation 2: $LMP(\sigma) = \frac{A_0 + A_2\sigma^{0.5} + A_4\sigma + A_6\sigma^{1.5}}{1 + A_1\sigma^{0.5} + A_3\sigma + A_5\sigma^{1.5}}$
4) LMP_m is the minimum Larson-Miller parameter based on minimum stress to rupture data.
5) LMP_a is the average Larson-Miller parameter based on average stress to rupture data.

Table 10B.3 – Limiting Design Metal Temperature for Heater-Tube Alloys, API STD 530, 6th Edition, September 2008

Materials	Type or Grade	Limiting Design Metal Temperature		Lower Critical Temperature	
		(˚C)	(˚F)	(˚C)	(˚F)
Carbon Steel	B	540	1000	720	1325
C-½Mo	T1 or P1	595	1100	720	1325
1¼Cr-½Mo	T11 or P11	595	1100	775	1430
2¼Cr-1Mo	T22 or P22	650	1200	805	1480
3Cr-1Mo	T21 or P21	650	1200	815	1500
5Cr-½Mo	T5 or P5	650	1200	820	1510
5Cr-½Mo-Si	T5b or P5b	705	1300	845	1550
7Cr-½Mo	T7 or P7	705	1300	825	1515
9Cr-1Mo	T9 or P9	705	1300	825	1515
9Cr-1Mo-V	T91 or P91	650 (See Note Below)	1200 (See Note Below)	830	1525
18Cr-8Ni	304 or 304H	815	1500	---	---
16Cr-12Ni-2Mo	316 or 316H	815	1500	---	---
16Cr-12Ni-2Mo	316L	815	1300	---	---
18Cr-10Ni-Ti	321 or 321H	815	1500	---	---
18Cr-10Ni-Nb	347 or 347H	815	1500	---	---
Ni-Fe-Cr	Alloy 800H/800HT	985 (See Note Below)	1800 (See Note Below)	---	---
25Cr-20Ni	HK40	1010 (See Note Below)	1850 (See Note Below)	---	---

Note: This is the upper limit on the reliability of the rupture strength data; however, these materials are commonly used for heater tubes at higher temperatures in applications where the internal pressure is so low that rupture strength does not govern the design.

Table 10B.4 – Minimum and Average Larson-Miller Parameters as a Function of Stress (ksi, °F) from WRC 541 3rd Edition

Material (Case, Note 1)	Parameter	Larson-Miller Constant and Parameter vs. Stress: Minimum Properties (C_{min})	Larson-Miller Constant and Parameter vs. Stress: Average Properties (C_{avg})
Low Carbon Steel	Temperature Range (˚F)	700-1000	
	C	18.15	17.7
	A_0	3.5107000E+04	
	A_1	-3.6580000E+03	
	A_2	-1.8080000E+03	
	A_3	-2.9790000E+02	
Medium Carbon Steel	Temperature Range (˚F)	700-1000	
	C	15.6	15.15
	A_0	3.2068370E+04	
	A_1	-3.3755550E+03	
	A_2	-1.5933910E+03	
	A_3	-3.0000000E+02	
C-0.5 Mo	Temperature Range (˚F)	700-1050	
	C	19.0078	18.725
	A_0	3.8792100E+04	
	A_1	-4.9502240E+03	
	A_2	0	
	A_3	0	
1.25Cr-0.5Mo	Temperature Range (˚F)	800-1200	
	C	22.0548	21.55
	A_0	4.6355000E+04	
	A_1	-6.9535500E+03	
	A_2	-3.3195000E+02	
	A_3	-5.2800000E+00	

Table 10B.4 – Minimum and Average Larson-Miller Parameters as a Function of Stress (ksi, °F) from WRC 541 3rd Edition

Material (Case, Note 1)	Parameter	Larson-Miller Constant and Parameter vs. Stress: Minimum Properties (C_{min})	Larson-Miller Constant and Parameter vs. Stress: Average Properties (C_{avg})
2.25Cr-1Mo	Temperature Range (˚F)	800-1200	
	C	19.566	18.918
	A_0	4.3946400E+04	
	A_1	-8.3900000E+03	
	A_2	0	
	A_3	0	
3Cr-1Mo	Temperature Range (˚F)	800-1200	
	C	15.7852	15.3811
	A_0	3.7264510E+04	
	A_1	-7.9439300E+03	
	A_2	0	
	A_3	0	
5Cr-0.5Mo	Temperature Range (˚F)	800-1200	
	C	16.0258	15.5893
	A_0	3.7264510E+04	
	A_1	-7.9439300E+03	
	A_2	0	
	A_3	0	
5Cr-0.5Mo-Si	Temperature Range (˚F)	800-1200	
	C	16.0258	15.5893
	A_0	3.7264510E+04	
	A_1	-7.9439300E+03	
	A_2	0	
	A_3	0	

Table 10B.4 – Minimum and Average Larson-Miller Parameters as a Function of Stress (ksi, °F) from WRC 541 3rd Edition

Material (Case, Note 1)	Parameter	Larson-Miller Constant and Parameter vs. Stress: Minimum Properties (C_{min})	Larson-Miller Constant and Parameter vs. Stress: Average Properties (C_{avg})
7Cr-0.5Mo	Temperature Range (˚F)	900-1200	
	C	20.4375	19.6206
	A_0	4.5219510E+04	
	A_1	-1.0217000E+04	
	A_2	5.2679960E+00	
	A_3	-6.3855690E+00	
9Cr-1Mo	Temperature Range (˚F)	900-1300	
	C	20.946	20.50
	A_0	4.506215E+04	
	A_1	-5.600730E+03	
	A_2	-1.649030E+03	
	A_3	-2.243810E+02	
9Cr-1Mo-V	Temperature Range (˚F)	900-1300	
	C	23.45	23.11
	A_0	5.256770E+04	
	A_1	-1.091480E+04	
	A_2	6.383600E+03	
	A_3	-3.316400E+03	
Alloy 115 (10.5Cr-V)	Temperature Range (˚F)	950-1250	
	C	25.95	25.66
	A_0	5.7037900E+04	
	A_1	-8.6688000E+03	
	A_2	3.6993000E+03	
	A_3	-2.4936000E+03	

Table 10B.4 – Minimum and Average Larson-Miller Parameters as a Function of Stress (ksi, °F) from WRC 541 3rd Edition

Material (Case, Note 1)	Parameter	Larson-Miller Constant and Parameter vs. Stress: Minimum Properties (C_{min})	Larson-Miller Constant and Parameter vs. Stress: Average Properties (C_{avg})
Type 304L SS	Temperature Range (˚F)	900-1500	
	C	18.2879	17.55
	A_0	4.6184000E+04	
	A_1	-8.5083000E+03	
	A_2	-1.3117600E+03	
	A_3	-6.7414000E+01	
Type 304/304H SS	Temperature Range (˚F)	1000-1500	
	C	16.1459	15.522
	A_0	4.3539460E+04	
	A_1	-9.7318000E+03	
	A_2	0	
	A_3	0	
Type 316L SS	Temperature Range (˚F)	900-1500	
	C	15.7401	15.2
	A_0	4.1503500E+04	
	A_1	-6.2210000E+03	
	A_2	-1.4945000E+03	
	A_3	-1.1969000E+02	
Type 316/316H SS	Temperature Range (˚F)	1000-1500	
	C	16.7641	16.3099
	A_0	4.4933830E+04	
	A_1	-9.4286740E+03	
	A_2	0	
	A_3	0	

Table 10B.4 – Minimum and Average Larson-Miller Parameters as a Function of Stress (ksi, °F) from WRC 541 3rd Edition

Material (Case, Note 1)	Parameter	Larson-Miller Constant and Parameter vs. Stress: Minimum Properties (C_{min})	Larson-Miller Constant and Parameter vs. Stress: Average Properties (C_{avg})
Type 317L SS	Temperature Range (˚F)	900-1500	
	C	15.7401	15.2
	A_0	4.1504000E+04	
	A_1	-6.2210000E+03	
	A_2	-1.4945000E+03	
	A_3	-1.1970000E+02	
Type 321 SS	Temperature Range (˚F)	900-1500	
	C	13.325	12.8
	A_0	3.5718000E+04	
	A_1	-5.6930000E+03	
	A_2	-7.0010000E+02	
	A_3	-2.8700000E+01	
Type 321H SS	Temperature Range (˚F)	900-1500	
	C	15.294	14.7596
	A_0	4.0548170E+04	
	A_1	-6.5741510E+03	
	A_2	-8.8665870E+02	
	A_3	-3.9861400E+01	
Type 347 SS	Temperature Range (˚F)	900-1500	
	C	14.889	14.25
	A_0	3.7960000E+04	
	A_1	-7.1172160E+03	
	A_2	3.1133520E+03	
	A_3	-2.3000000E+03	

Table 10B.4 – Minimum and Average Larson-Miller Parameters as a Function of Stress (ksi, °F) from WRC 541 3rd Edition

Material (Case, Note 1)	Parameter	Larson-Miller Constant and Parameter vs. Stress: Minimum Properties (C_{min})	Larson-Miller Constant and Parameter vs. Stress: Average Properties (C_{avg})
Type 347H SS	Temperature Range (˚F)	900-1500	
	C	14.17	13.65
	A_0	3.9536020E+04	
	A_1	-1.2225330E+04	
	A_2	6.7502400E+03	
	A_3	-2.8722460E+03	
Type 347LN SS (UNS S34751)	Temperature Range (˚F)	900-1282	
	C	16.6233	16.4067
	A_0	4.189031E+04	
	A_1	-5.625046E+03	
	A_2	-6.412536E+02	
	A_3	-1.696062E+02	
Advanced 347AP SS (UNS S34752)	Temperature Range (˚F)	900–1500	
	C	17.99	17.67
	A_0	4.7040400E+04	
	A_1	-6.4035000E+03	
	A_2	-1.0761000E+03	
	A_3	-6.0280000E+01	
Alloy 800	Temperature Range (˚F)	900-1500	
	C	17.0054	16.5088
	A_0	4.3171030E+04	
	A_1	-8.1470000E+03	
	A_2	0	
	A_3	0	

Table 10B.4 – Minimum and Average Larson-Miller Parameters as a Function of Stress (ksi, °F) from WRC 541 3rd Edition

Material (Case, Note 1)	Parameter	Larson-Miller Constant and Parameter vs. Stress: Minimum Properties (C_{min})	Larson-Miller Constant and Parameter vs. Stress: Average Properties (C_{avg})
Alloy 800H	Temperature Range (˚F)	1000-1650	
	C	16.564	16.0423
	A_0	4.5996670E+04	
	A_1	-1.0291740E+04	
	A_2	-2.7922200E+02	
	A_3	-2.5252000E+00	
Alloy 800HT)	Temperature Range (˚F)	900-1800	
	C	13.6067	13.2341
	A_0	4.0112700E+04	
	A_1	-9.0816690E+03	
	A_2	0	
	A_3	0	
HK-40	Temperature Range (˚F)	1400-1850	
	C	10.8565	10.4899
	A_0	3.4136600E+04	
	A_1	-7.7469630E+03	
	A_2	-8.7554600E+02	
	A_3	-3.2984000E+01	

Note: The Equation for $LMP(\sigma)$ is: $LMP(\sigma) = A_0 + A_1 \cdot \log_{10}[\sigma] + A_2 \cdot (\log_{10}[\sigma])^2 + A_3 \cdot (\log_{10}[\sigma])^3$

Table 10B.4M – Minimum and Average Larson-Miller Parameters as a Function of Stress (MPa, °C) from WRC Bulletin 541 3rd Edition

Material (Case, Note 1)	Parameter	Larson-Miller Constant and Parameter vs. Stress: Minimum Properties (C_{min})	Larson-Miller Constant and Parameter vs. Stress: Average Properties (C_{avg})
Low Carbon Steel	Temperature Range (˚C)	371-538	
	C	18.15	17.7
	A_0	2.0599281E+04	
	A_1	-6.9682690E+02	
	A_2	-5.8811980E+02	
	A_3	-1.6550000E+02	
Medium Carbon Steel	Temperature Range (˚C)	371-538	
	C	15.6	15.15
	A_0	1.8864096E+04	
	A_1	-7.4232249E+02	
	A_2	-4.6595773E+02	
	A_3	-1.6666667E+02	
C-0.5 Mo	Temperature Range (˚C)	371-566	
	C	19.0078	18.725
	A_0	2.3857198E+04	
	A_1	-2.7501244E+03	
	A_2	0	
	A_3	0	
1.25Cr-0.5Mo	Temperature Range (˚C)	427-649	
	C	22.0548	21.55
	A_0	2.8864110E+04	
	A_1	-3.5599970E+03	
	A_2	-1.7703800E+02	
	A_3	-2.9330000E+00	

Table 10B.4M – Minimum and Average Larson-Miller Parameters as a Function of Stress (MPa, °C) from WRC Bulletin 541 3rd Edition

Material (Case, Note 1)	Parameter	Larson-Miller Constant and Parameter vs. Stress: Minimum Properties (C_{min})	Larson-Miller Constant and Parameter vs. Stress: Average Properties (C_{avg})
2.25Cr-1Mo	Temperature Range (˚C)	427-649	
	C	19.566	18.918
	A_0	2.8323097E+04	
	A_1	-4.6611111E+03	
	A_2	0	
	A_3	0	
3Cr-1Mo	Temperature Range (˚C)	427-649	
	C	15.7852	15.3811
	A_0	2.4403137E+04	
	A_1	-4.4132944E+03	
	A_2	0	
	A_3	0	
5Cr-0.5Mo	Temperature Range (˚C)	427-649	
	C	16.0258	15.5893
	A_0	2.4403137E+04	
	A_1	-4.4132944E+03	
	A_2	0	
	A_3	0	
5Cr-0.5Mo-Si	Temperature Range (˚C)	427-649	
	C	16.0258	15.5893
	A_0	2.4403137E+04	
	A_1	-4.4132944E+03	
	A_2	0	
	A_3	0	

Table 10B.4M – Minimum and Average Larson-Miller Parameters as a Function of Stress (MPa, °C) from WRC Bulletin 541 3rd Edition

Material (Case, Note 1)	Parameter	Larson-Miller Constant and Parameter vs. Stress: Minimum Properties (C_{min})	Larson-Miller Constant and Parameter vs. Stress: Average Properties (C_{avg})
7Cr-0.5Mo	Temperature Range (˚C)	482-649	
	C	20.4375	19.6206
	A_0	2.9885713E+04	
	A_1	-5.6885026E+03	
	A_2	1.1850862E+01	
	A_3	-3.5475383E+00	
9Cr-1Mo	Temperature Range (˚C)	482-704	
	C	20.946	20.5
	A_0	2.70729453E+04	
	A_1	-18380780E+03	
	A_2	-6.025482E+02	
	A_3	-1.246561E+02	
9Cr-1Mo-V	Temperature Range (˚C)	482-704	
	C	23.45	23.11
	A_0	3.7868927E+04	
	A_1	-1.5897896E+04	
	A_2	8.1813029E+03	
	A_3	-1.8424444E+03	
Alloy 115 (10.5Cr-V)	Temperature Range (˚C)	510-677	
	C	25.95	25.66
	A_0	3.7987270E+04	
	A_1	-1.1182000E+04	
	A_2	5.5398530E+03	
	A_3	-1.3853300E+03	

Table 10B.4M – Minimum and Average Larson-Miller Parameters as a Function of Stress (MPa, °C) from WRC Bulletin 541 3rd Edition

Material (Case, Note 1)	Parameter	Larson-Miller Constant and Parameter vs. Stress: Minimum Properties (C_{min})	Larson-Miller Constant and Parameter vs. Stress: Average Properties (C_{avg})
Type 304L SS	Temperature Range (˚C)	482-816	
	C	18.2879	17.55
	A_0	2.9131000E+04	
	A_1	-3.5836822E+03	
	A_2	-6.3454240E+02	
	A_3	-3.7452200E+01	
Type 304/304H SS	Temperature Range (˚C)	538-816	
	C	16.1459	15.522
	A_0	2.8722088E+04	
	A_1	-5.4065556E+03	
	A_2	0	
	A_3	0	
Type 316L SS	Temperature Range (˚C)	482-816	
	C	15.7401	15.2
	A_0	2.5410938E+04	
	A_1	-2.2039633E+03	
	A_2	-6.6300720E+02	
	A_3	-6.6494400E+01	
Type 316/316H SS	Temperature Range (˚C)	538-816	
	C	16.7641	16.3099
	A_0	2.9355529E+04	
	A_1	-5.2381522E+03	
	A_2	0	
	A_3	0	

Table 10B.4M – Minimum and Average Larson-Miller Parameters as a Function of Stress (MPa, °C) from WRC Bulletin 541 3rd Edition

Material (Case, Note 1)	Parameter	Larson-Miller Constant and Parameter vs. Stress: Minimum Properties (C_{min})	Larson-Miller Constant and Parameter vs. Stress: Average Properties (C_{avg})
Type 317L SS	Temperature Range (˚C)	482-816	
	C	15.7401	15.2
	A_0	2.5411219E+04	
	A_1	-2.2039750E+03	
	A_2	-6.6299320E+02	
	A_3	-6.6500000E+01	
Type 321 SS	Temperature Range (˚C)	482-816	
	C	13.325	12.8
	A_0	2.2231311E+04	
	A_1	-2.5441355E+03	
	A_2	-3.4883530E+02	
	A_3	-1.5944400E+01	
Type 321H SS	Temperature Range (˚C)	482-816	
	C	15.294	14.7596
	A_0	2.5256000E+04	
	A_1	-2.8729289E+03	
	A_2	-4.3688060E+02	
	A_3	-2.2145200E+01	
Type 347 SS	Temperature Range (˚C)	482-816	
	C	14.889	14.25
	A_0	2.6373880E+04	
	A_1	-9.5499515E+03	
	A_2	4.9439628E+03	
	A_3	-1.2777778E+03	

Table 10B.4M – Minimum and Average Larson-Miller Parameters as a Function of Stress (MPa, °C) from WRC Bulletin 541 3rd Edition

Material (Case, Note 1)	Parameter	Larson-Miller Constant and Parameter vs. Stress: Minimum Properties (C_{min})	Larson-Miller Constant and Parameter vs. Stress: Average Properties (C_{avg})
Type 347H SS	Temperature Range (˚C)	482-816	
	C	14.17	13.65
	A_0	3.1237102E+04	
	A_1	-1.6446827E+04	
	A_2	7.7641880E+03	
	A_3	-1.5956922E+03	
Type 347LN SS (UNS S34751)	Temperature Range (˚C)	482-694	
	C	16.6233	16.4067
	A_0	2.5697897E+04	
	A_1	-2.7263280E+03	
	A_2	-1.1921765E+02	
	A_3	-9.4225667E+01	
Advanced 347AP SS (UNS S34752)	Temperature Range (˚C)	482-816	
	C	17.99	17.67
	A_0	2.8716030E+04	
	A_1	-2.6255300E+03	
	A_2	-5.1359000E+02	
	A_3	-3.3490000E+01	
Alloy 800	Temperature Range (˚C)	482-816	
	C	17.0054	16.5088
	A_0	2.7779136E+04	
	A_1	-4.5261111E+03	
	A_2	0	
	A_3	0	

Table 10B.4M – Minimum and Average Larson-Miller Parameters as a Function of Stress (MPa, °C) from WRC Bulletin 541 3rd Edition

Material (Case, Note 1)	Parameter	Larson-Miller Constant and Parameter vs. Stress: Minimum Properties (C_{min})	Larson-Miller Constant and Parameter vs. Stress: Average Properties (C_{avg})
Alloy 800H	Temperature Range (˚C)	538-899	
	C	16.564	16.0423
	A_0	3.0239807E+04	
	A_1	-5.4604448E+03	
	A_2	-1.5159430E+02	
	A_3	-1.4029000E+00	
Alloy 800HT	Temperature Range (˚C)	482-982	
	C	13.6067	13.2341
	A_0	2.6515473E+04	
	A_1	-5.0453717E+03	
	A_2	0	
	A_3	0	
HK-40	Temperature Range (˚C)	760-1010	
	C	10.8565	10.4899
	A_0	2.2242452E+04	
	A_1	-3.5267854E+03	
	A_2	-4.4031830E+02	
	A_3	-1.8324400E+01	

Note: The Equation for $LMP(\sigma)$ is: $LMP(\sigma) = A_0 + A_1 \cdot \log_{10}[\sigma] + A_2 \cdot (\log_{10}[\sigma])^2 + A_3 \cdot (\log_{10}[\sigma])^3$

Table 10B.5 – Elastic Allowable Stress Factor, Creep Rupture Design Allowable Stress Factor, and Applicable Temperature Range from WRC Bulletin 541 3rd Edition

Material	F_{ed} (1)	F_{cr} (2)	Applicable Temperature Range (°F)		Applicable Temperature Range (°C)	
			Minimum	Maximum	Minimum	Maximum
Low Carbon Steel	2/3	1.0	70	1000	21	538
Medium Carbon Steel	2/3	1.0	70	1000	21	538
C-0.5Mo	2/3	1.0	70	1050	21	566
1.25Cr-0.5Mo	2/3	1.0	70	1200	21	649
2.25Cr-1Mo	2/3	1.0	70	1200	21	649
3Cr-1Mo	2/3	1.0	70	1200	21	649
5Cr-0.5Mo	2/3	1.0	70	1200	21	649
5Cr-0.5Mo-Si	2/3	1.0	70	1200	21	649
7Cr-0.5Mo	2/3	1.0	70	1200	21	649
9Cr-1Mo	2/3	1.0	70	1300	21	704
9Cr-1Mo-V	2/3	1.0	70	1300	21	704
Alloy 115 (10.5Cr-V)	2/3	1.0	70	1250	21	677
Type 304L SS	0.9	0.8	70	1500	21	816
Type 304/304H SS	0.9	1.0	70	1500	21	816
Type 316L SS	0.9	0.8	70	1500	21	816
Type 316/316H SS	0.9	1.0	70	1500	21	816
Type 317L SS	0.9	0.8	70	1500	21	816
Type 321 SS	0.9	1.0	70	1500	21	816
Type 321H SS	0.9	1.0	70	1500	21	816
Type 347 SS	0.9	1.0	70	1500	21	816
Type 347H SS	0.9	1.0	70	1500	21	816
Type 347LN SS (UNS S34751)	0.9	1.0	70	1282	21	694

Table 10B.5 – Elastic Allowable Stress Factor, Creep Rupture Design Allowable Stress Factor, and Applicable Temperature Range from WRC Bulletin 541 3rd Edition

Material	F_{ed} (1)	F_{cr} (2)	Applicable Temperature Range (°F)		Applicable Temperature Range (°C)	
			Minimum	Maximum	Minimum	Maximum
Advanced 347AP SS (UNS S34752)	0.9	1.0	70	≤1300	21	≤704
	0.9	0.8	>1300	1500	>704	816
Alloy 800	0.9	1.0	70	1500	21	816
Alloy 800H	0.9	1.0	70	1650	21	899
Alloy 800HT	0.9	1.0	70	1800	21	982
HK-40	0.9	1.0	70	1850	21	1010

Note:

1) Elastic Design Factor - Factor to be applied to the elastic allowable stress.

2) Creep Rupture Design Factor – Factor to be applied to the creep rupture allowable stress.

Table 10B.6 – Fatigue Coefficients and Equation for High Temperature Assessments – 304 SS

Coefficients	100 °F (38 °C)	800 °F (427 °C)	900 °F (482 °C)	1000 °F (538 °C)
C_1	6.682000000000E+01	-6.922535206597E+01	-9.177396533851E+01	-1.407824306721E+02
C_2	-1.808045000000E+02	1.870409067488E+02	2.415802396018E+02	3.465757937423E+02
C_3	2.126471178198E+02	-2.183090375556E+02	-2.756058534750E+02	-3.704744677706E+02
C_4	-1.420180000000E+02	1.463306483440E+02	1.807492522698E+02	2.276914339687E+02
C_5	5.998925466474E+01	-6.221016661101E+01	-7.533489785682E+01	-8.906670373671E+01
C_6	-1.679136680000E+01	1.754778555797E+01	2.087456438624E+01	2.320575364733E+01
C_7	3.164939141700E+00	-3.330677247555E+00	-3.899691007484E+00	-4.085140312527E+00
C_8	-3.981738700000E-01	4.207396511975E-01	4.857447813127E-01	4.806374888657E-01
C_9	3.212280491675E-02	-3.391175980874E-02	-3.867024367242E-02	-3.623353293943E-02
C_{10}	-1.506115524149E-03	1.577613601045E-03	1.779643631767E-03	1.583075495657E-03
C_{11}	3.126657285393E-05	-3.222364314922E-05	-3.601090787392E-05	-3.048832983874E-05
Coefficients	**1100 °F (593 °C)**	**1200 °F (649 °C)**	**1300 °F (704 °C)**	---
C_1	-2.042032334174E+02	1.728900000000E+02	-8.563000000000E+00	---
C_2	4.809976080127E+02	-3.837630328300E+02	5.654091629247E+00	---
C_3	-4.941149847598E+02	3.730450964166E+02	7.528396818171E+00	---
C_4	2.927118346967E+02	-2.086158480821E+02	-1.078665400000E+01	---
C_5	-1.107405286370E+02	7.450765208948E+01	6.019627872462E+00	---
C_6	2.798964741838E+01	-1.778151122043E+01	-1.906172290000E+00	---
C_7	-4.791807739551E+00	2.875843569240E+00	3.758688604888E-01	---
C_8	5.492975119756E-01	-3.116986694169E-01	-4.709601554156E-02	---
C_9	-4.039482278860E-02	2.169928702521E-02	3.651822144815E-03	---
C_{10}	1.722695539990E-03	-8.774114415764E-04	-1.599628188356E-04	---
C_{11}	-3.238724775094E-05	1.566912115112E-05	3.028614999610E-06	---

Note: The equation for the number of cycles as a function of strain range is:

$$\log_{10}[N] = \left(C_1 + C_2X^2 + C_3X^4 + C_4X^6 + C_5X^8 + C_6X^{10} + C_7X^{12} + C_8X^{14} + C_9X^{16} + C_{10}X^{18} + C_{11}X^{20}\right)$$

$$X = \log_{10}[\varepsilon_r]$$

Table 10B.7 – Fatigue Coefficients and Equation for High Temperature Assessments – 316 SS

Coefficients	100 °F (38 °C)	800 °F (427 °C)	900 °F (482 °C)
C_1	3.756660335078E+03	1.696799417205E+03	4.086914613504E+03
C_2	1.592779424697E+04	7.117235545101E+03	1.585187013812E+04
C_3	2.920906153473E+04	1.292837742289E+04	2.664439146761E+04
C_4	3.025765358048E+04	1.328526685271E+04	2.534735199084E+04
C_5	1.936703738846E+04	8.449655992480E+03	1.492838569514E+04
C_6	7.843897299528E+03	3.406370836655E+03	5.574015072905E+03
C_7	1.963454226495E+03	8.501649388438E+02	1.288712044862E+03
C_8	2.777973678321E+02	1.201274530019E+02	1.687078078194E+02
C_9	1.701465025863E+01	7.359321516750E+00	9.576813460129E+00
Coefficients	**1000 °F (538 °C)**	**1200 °F (649 °C)**	**1300° F (704 °C)**
C_1	1.331846040610E+03	1.331846040610E+03	4.007643000000E+03
C_2	4.764117571658E+03	4.764117571658E+03	1.545931921815E+04
C_3	7.383260434289E+03	7.383260434289E+03	2.569786059066E+04
C_4	6.475761875335E+03	6.475761875335E+03	2.406862480912E+04
C_5	3.517580454802E+03	3.517580454802E+03	1.390459931525E+04
C_6	1.212153441556E+03	1.212153441556E+03	5.077090302913E+03
C_7	2.589355680215E+02	2.589355680215E+02	1.144941947709E+03
C_8	3.137472167913E+01	3.137472167913E+01	1.458740219008E+02
C_9	1.652852250448E+00	1.652852250448E+00	8.043306600599E+00

Note: The equation for the number of cycles as a function of strain range is:

$$\log_{10}[N] = C_1 + C_2X + C_3X^2 + C_4X^3 + C_5X^4 + C_6X^5 + C_7X^6 + C_8X^7 + C_9X^8$$

$$X = \log_{10}[\varepsilon_r]$$

Table 10B.8 – Fatigue Coefficients and Equation for High Temperature Assessments – Alloy 800H

Coefficients	800 °F (427 °C)	1000 °F (538 °C)	1200 °F (649 °C)	1400 °F (760 °C)
Limit	$\varepsilon_r < 6.44E-03$	$\varepsilon_r < 4.33E-03$	$\varepsilon_r < 3.27E-03$	$\varepsilon_r < 3.09E-03$
C_1	1.369130975874E+01	3.506080003431E+00	8.863380630917E+00	-3.541370000000E+01
C_2	-2.947970542760E+01	-6.254164422454E+00	-1.471390556734E+01	5.675935996944E+01
C_3	2.639286314596E+01	5.316554276289E+00	1.051803024975E+01	-3.655700975779E+01
C_4	-1.190231511065E+01	-2.167029629668E+00	-3.790375250617E+00	1.236806692243E+01
C_5	2.930722864314E+00	4.873668308290E-01	7.534766996363E-01	-2.297267634238E+00
C_6	-3.745088532665E-01	-5.770217011065E-02	-7.865936138117E-02	2.218803914061E-01
C_7	1.945527891104E-02	2.830720301110E-03	3.387392578519E-03	-8.689665366861E-03
Limit	$\varepsilon_r \geq 6.44E-03$	$\varepsilon_r \geq 4.33E-03$	$\varepsilon_r \geq 3.27E-03$	$\varepsilon_r \geq 3.09E-03$
C_1	-2.431713857388E+03	-7.393159500000E+04	-3.063619603784E+05	2.680710201263E+03
C_2	2.536664379803E+03	6.777870313392E+04	2.512484536663E+05	-1.457767073667E+03
C_3	-1.093340416139E+03	-2.581805322732E+04	-8.568028508483E+04	2.411334310976E+02
C_4	2.495198697832E+02	5.230303126333E+03	1.555259054596E+04	3.332764145740E+00
C_5	-3.180337712301E+01	-5.942986069292E+02	-1.584932777281E+03	-5.188233875076E+00
C_6	2.147339060124E+00	3.590964940577E+01	8.597990265892E+01	5.460895054959E-01
C_7	-6.002051298816E-02	-9.013827850027E-01	-1.939824461940E+00	-1.829426162456E-02

Note: The equation for the number of cycles as a function of strain range is:

$$\log_{10}[N] = C_1 + C_2X^2 + C_3X^4 + C_4X^6 + C_5X^8 + C_6X^{10} + C_7X^{12}$$

$$X = \log_{10}[\varepsilon_r]$$

Table 10B.9 – Fatigue Coefficients and Equation for High Temperature Assessments – 2.25Cr-1Mo

Coefficients	800 °F (427 °C)	900 °F (482 °C)	1100 °F (593 °C)
Limit	$\boldsymbol{\varepsilon_r < 4.00E-03}$	$\boldsymbol{\varepsilon_r < 3.90E-03}$	$\boldsymbol{\varepsilon_r < 3.90E-03}$
C_1	-4.925003714199E+01	-9.423700000000E+00	-9.423700000000E+00
C_2	-1.382619814024E+02	-2.024118576578E+01	-2.024118576578E+01
C_3	-1.513629821072E+02	-1.476141768336E+01	-1.476141768336E+01
C_4	-8.242945617717E+01	-4.815228303502E+00	-4.815228303502E+00
C_5	-2.227163205250E+01	-5.708571657640E-01	-5.708571657640E-01
C_6	-2.393262815762E+00	0.000000000000E+00	0.000000000000E+00
Limit	$\boldsymbol{\varepsilon_r \geq 4.00E-03}$	$\boldsymbol{\varepsilon_r \geq 3.90E-03}$	$\boldsymbol{\varepsilon_r \geq 3.90E-03}$
C_1	-1.980700261879E+04	-6.496375804637E+03	-6.496375804637E+03
C_2	-3.755619232512E+04	-1.187539434143E+04	-1.187539434143E+04
C_3	-2.845311287534E+04	-8.674644370236E+03	-8.674644370236E+03
C_4	-1.076735096820E+04	-3.166226102325E+03	-3.166226102325E+03
C_5	-2.035264885156E+03	-5.775226441315E+02	-5.775226441315E+02
C_6	-1.537347158075E+02	-4.212282904136E+01	-4.212282904136E+01

Note:

1) The equation for the number of cycles as a function of strain range is:

$$\log_{10}[N] = \left(C_1 + C_2 X + C_3 X^2 + C_4 X^3 + C_5 X^4 + C_6 X^5\right)^2$$

$$X = \log_{10}[\varepsilon_r]$$

2) The fatigue curves for 900 °F (482 °C) and 1100 °F (593 °C) are the same.

Table 10B.10 – Fatigue Coefficients and Equation for High Temperature Assessments – 9Cr-1Mo-V

Coefficients	1000 °F (538 °C)
Limit	$\boldsymbol{\varepsilon_r < 3.90E-03}$
C_1	3.045631374530E+01
C_2	-4.821668374173E+01
C_3	3.161374489920E+01
C_4	-1.075109586133E+01
C_5	2.025544996789E+00
C_6	-2.007277670313E-01
C_7	8.204242728788E-03
Limit	$\boldsymbol{3.90E-03 \le \varepsilon_r \le 1.70E-03}$
C_1	-4.197857000000E+02
C_2	2.432283800000E+02
C_3	-5.203999600000E+01
C_4	4.902054700000E+00
C_5	-1.706950800000E-01
C_6	0.000000000000E+00
C_7	0.000000000000E+00
Limit	$\boldsymbol{\varepsilon_r > 1.70E-03}$
C_1	-6.149578186318E+05
C_2	2.853892854734E+05
C_3	-3.520683491606E+04
C_4	-2.961976957850E+03
C_5	1.089428132565E+03
C_6	-9.423388402745E+01
C_7	2.773964071903E+00

Note: The equation for the number of cycles as a function of strain range is:

$$\log_{10}[N] = C_1 + C_2X^2 + C_3X^4 + C_4X^6 + C_5X^8 + C_6X^{10} + C_7X^{12}$$

$$X = \log_{10}[\varepsilon_r]$$

Table 10B.11 – Data for High Temperature Fatigue Curves in Table 10B.5 – Type 304 SS

Number of Cycles	Strain Range at Temperature (Cyclic Strain Rate 1.0E-3 in/in/sec or mm/mm/sec)						
	100 °F (38 °C)	800 °F (427 °C)	900 °F (482 °C)	1000 °F (538 °C)	1100 °F (593 °C)	1200 °F (649 °C)	1300 °F (704 °C)
1.0E+01	5.10E-02	5.00E-02	4.65E-02	4.25E-02	3.82E-02	3.35E-02	2.97E-02
2.0E+01	3.60E-02	3.45E-02	3.15E-02	2.84E-02	2.50E-02	2.17E-02	1.86E-02
4.0E+01	2.63E-02	2.46E-02	2.22E-02	1.97E-02	1.70E-02	1.46E-02	1.23E-02
1.0E+02	1.80E-02	1.64E-02	1.46E-02	1.28E-02	1.10E-02	9.30E-03	7.70E-03
2.0E+02	1.42E-02	1.25E-02	1.10E-02	9.60E-03	8.20E-03	6.90E-03	5.70E-03
4.0E+02	1.13E-02	9.65E-03	8.45E-03	7.35E-03	6.30E-03	5.25E-03	4.43E-03
1.0E+03	8.45E-03	7.25E-03	6.30E-03	5.50E-03	4.70E-03	3.85E-03	3.33E-03
2.0E+03	6.70E-03	5.90E-03	5.10E-03	4.50E-03	3.80E-03	3.15E-03	2.76E-03
4.0E+03	5.45E-03	4.85E-03	4.20E-03	3.73E-03	3.20E-03	2.63E-03	2.30E-03
1.0E+04	4.30E-03	3.85E-03	3.35E-03	2.98E-03	2.60E-03	2.15E-03	1.85E-03
2.0E+04	3.70E-03	3.30E-03	2.90E-03	2.56E-03	2.26E-03	1.87E-03	1.58E-03
4.0E+04	3.20E-03	2.87E-03	2.54E-03	2.24E-03	1.97E-03	1.62E-03	1.38E-03
1.0E+05	2.72E-03	2.42E-03	2.13E-03	1.88E-03	1.64E-03	1.40E-03	1.17E-03
2.0E+05	2.40E-03	2.15E-03	1.90E-03	1.67E-03	1.45E-03	1.23E-03	1.05E-03
4.0E+05	2.15E-03	1.92E-03	1.70E-03	1.50E-03	1.30E-03	1.10E-03	9.40E-04
1.0E+06	1.90E-03	1.69E-03	1.49E-03	1.30E-03	1.12E-03	9.80E-04	8.40E-04

Table 10B.12 – Data for High Temperature Fatigue Curves in Table 10B.6 – Type 316 SS

Number of Cycles	Strain Range at Temperature (Cyclic Strain Rate 1.0E-3 in/in/sec or mm/mm/sec)					
	100 °F (38 °C)	800 °F (427 °C)	900 °F (482 °C)	1000 °F (538 °C)	1200 °F (649 °C)	1300 °F (704 °C)
1.0E+01	5.07E-02	4.38E-02	3.78E-02	3.18E-02	3.18E-02	2.14E-02
2.0E+01	3.57E-02	3.18E-02	2.51E-02	2.08E-02	2.08E-02	1.49E-02
4.0E+01	2.60E-02	2.33E-02	1.81E-02	1.48E-02	1.48E-02	1.05E-02
1.0E+02	1.77E-02	1.59E-02	1.23E-02	9.74E-03	9.74E-03	7.11E-03
2.0E+02	1.39E-02	1.25E-02	9.61E-03	7.44E-03	7.44E-03	5.51E-03
4.0E+02	1.10E-02	9.56E-03	7.61E-03	5.74E-03	5.74E-03	4.31E-03
1.0E+03	8.18E-03	7.16E-03	5.71E-03	4.24E-03	4.24E-03	3.28E-03
2.0E+03	6.43E-03	5.81E-03	4.66E-03	3.39E-03	3.39E-03	2.68E-03
4.0E+03	5.18E-03	4.76E-03	3.81E-03	2.79E-03	2.79E-03	2.26E-03
1.0E+04	4.03E-03	3.76E-03	3.01E-03	2.21E-03	2.21E-03	1.86E-03
2.0E+04	3.43E-03	3.16E-03	2.56E-03	1.86E-03	1.86E-03	1.62E-03
4.0E+04	2.93E-03	2.73E-03	2.21E-03	1.61E-03	1.61E-03	1.44E-03
1.0E+05	2.45E-03	2.26E-03	1.82E-03	1.36E-03	1.36E-03	1.21E-03
2.0E+05	2.13E-03	1.96E-03	1.59E-03	1.21E-03	1.21E-03	1.08E-03
4.0E+05	1.88E-03	1.73E-03	1.39E-03	1.09E-03	1.09E-03	9.54E-04
1.0E+06	1.63E-03	1.51E-03	1.18E-03	9.63E-04	9.63E-04	8.34E-04

Table 10B.13 – Data for High Temperature Fatigue Curves in Table 10B.5 – 800H

Number of Cycles	Strain Range at Temperature (Cyclic Strain Rate 1.0E-3 in/in/sec or mm/mm/sec)			
	800 °F (427 °C)	1000 °F (538 °C)	1200 °F (649 °C)	1400 °F (760 °C)
1.0E+01	5.00E-02	4.24E-02	3.41E-02	2.84E-02
2.0E+01	3.62E-02	2.74E-02	2.20E-02	1.83E-02
4.0E+01	2.70E-02	1.85E-02	1.48E-02	1.23E-02
1.0E+02	1.84E-02	1.16E-02	9.32E-03	7.74E-03
2.0E+02	1.42E-02	8.49E-03	6.78E-03	5.62E-03
4.0E+02	1.13E-02	6.60E-03	5.33E-03	4.69E-03
1.0E+03	8.41E-03	5.15E-03	4.17E-03	3.88E-03
2.0E+03	6.85E-03	4.54E-03	3.66E-03	3.49E-03
3.0E+03	6.44E-03	4.33E-03	3.47E-03	3.09E-03
4.0E+03	5.72E-03	4.09E-03	3.27E-03	2.70E-03
1.0E+04	4.52E-03	2.93E-03	2.34E-03	2.12E-03
2.0E+04	3.92E-03	2.43E-03	1.97E-03	1.83E-03
4.0E+04	3.43E-03	2.12E-03	1.75E-03	1.64E-03
1.0E+05	2.88E-03	1.94E-03	1.55E-03	1.49E-03
2.0E+05	2.54E-03	1.86E-03	1.47E-03	1.40E-03
4.0E+05	2.29E-03	1.78E-03	1.40E-03	1.32E-03
1.0E+06	2.00E-03	1.69E-03	1.31E-03	1.22E-03

Table 10B.14 – Data for High Temperature Fatigue Curves in Table 10B.6 – 2.25Cr-1Mo

Number of Cycles	Strain Range at Temperature (Cyclic Strain Rate 1.0E-3 in/in/sec or mm/mm/sec)		
	800 °F (427 °C)	900 °F (482 °C)	1100 °F (593 °C)
1.0E+01	5.60E-02	4.00E-02	4.00E-02
4.0E+01	2.30E-02	1.63E-02	1.63E-02
1.0E+02	1.30E-02	9.70E-03	9.70E-03
2.0E+02	9.40E-03	7.00E-03	7.00E-03
4.0E+02	7.00E-03	5.60E-03	5.60E-03
1.0E+03	5.20E-03	4.20E-03	4.20E-03
2.0E+03	4.40E-03	3.90E-03	3.90E-03
4.0E+03	4.00E-03	3.50E-03	3.50E-03
1.0E+04	3.20E-03	2.65E-03	2.65E-03
2.0E+04	2.60E-03	2.15E-03	2.15E-03
4.0E+04	2.30E-03	1.82E-03	1.82E-03
1.0E+05	1.95E-03	1.58E-03	1.58E-03
2.0E+05	1.73E-03	1.42E-03	1.42E-03
4.0E+05	1.55E-03	1.30E-03	1.30E-03
1.0E+06	1.37E-03	1.18E-03	1.18E-03

Table 10B.15 – Data for High Temperature Fatigue Curves in Table 10B.7 – 9Cr-1Mo-V

Number of Cycles	Strain Range at Temperature (Cyclic Strain Rate 1.0E-3 in/in/sec or mm/mm/sec)
	1000 °F (538 °C)
1.0E+01	2.80E-02
2.0E+01	1.90E-02
4.0E+01	1.38E-02
1.0E+02	9.50E-03
2.0E+02	7.50E-03
4.0E+02	6.20E-03
1.0E+03	5.00E-03
2.0E+03	4.40E-03
4.0E+03	3.90E-03
1.0E+04	2.90E-03
2.0E+04	2.40E-03
4.0E+04	2.10E-03
1.0E+05	1.90E-03
2.0E+05	1.76E-03
4.0E+05	1.70E-03
1.0E+06	1.63E-03
2.0E+06	1.55E-03
4.0E+06	1.48E-03
1.0E+07	1.40E-03
2.0E+07	1.32E-03
4.0E+07	1.25E-03
1.0E+08	1.20E-03

10B.11 Figures

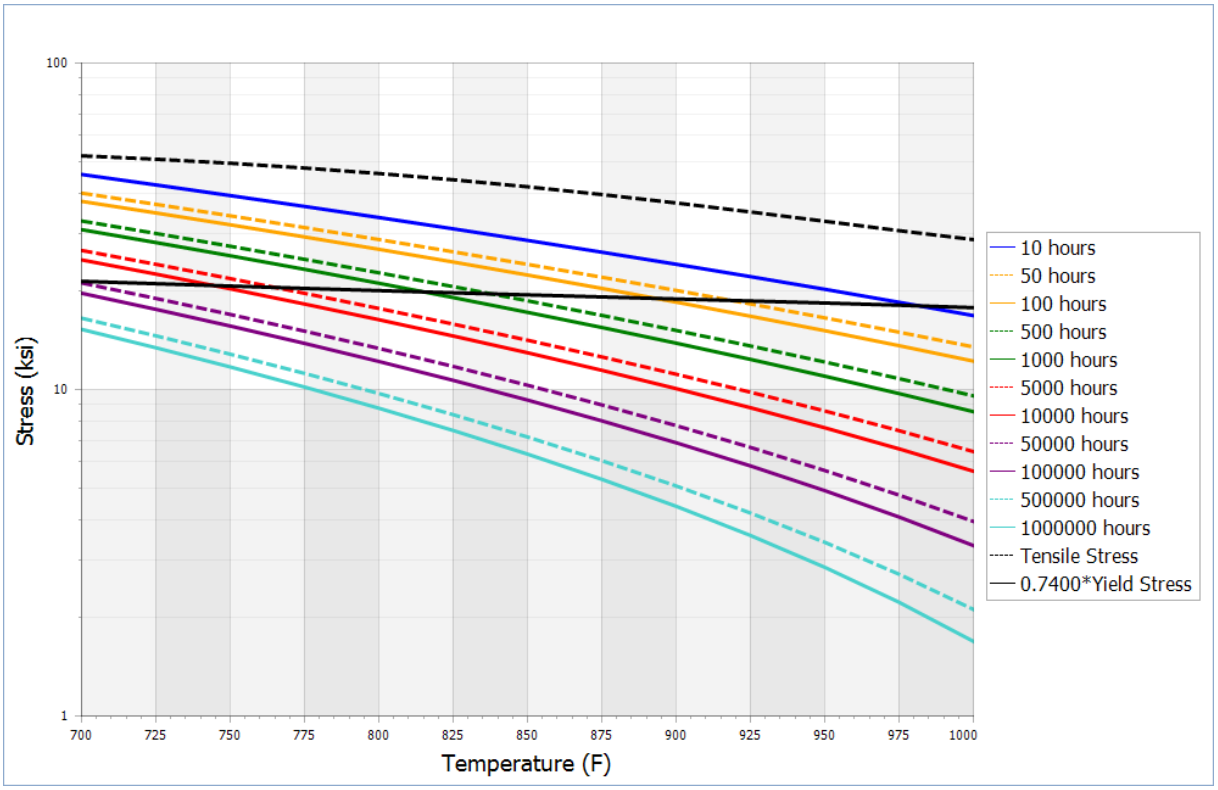

Figure 10B.1 – Level 1 Screening Curve for Carbon Steel – $\sigma_{uts}^{min} < 60\ ksi$

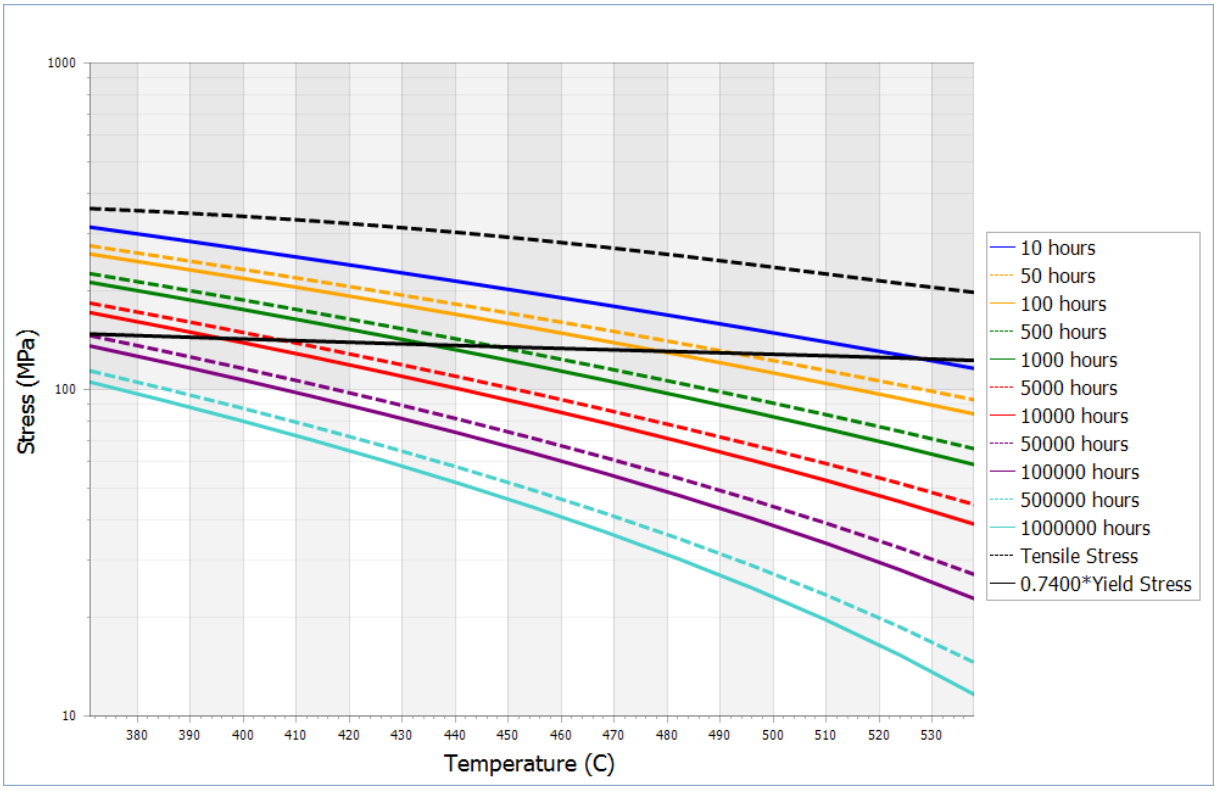

Figure 10B.1M – Level 1 Screening Curve for Carbon Steel – $\sigma_{uts}^{min} < 413\ MPa$

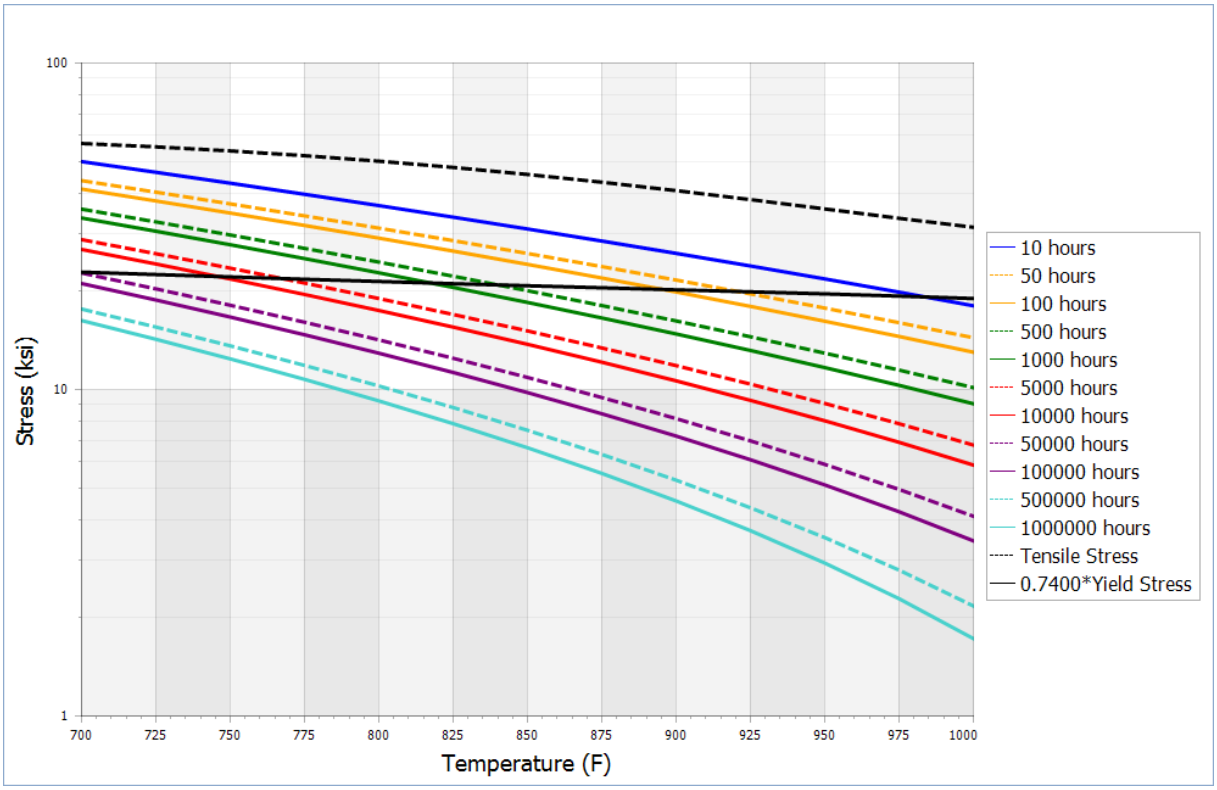

Figure 10B.2 – Level 1 Screening Curve for Carbon Steel – $60\ ksi \leq \sigma_{uts}^{min} < 65\ ksi$

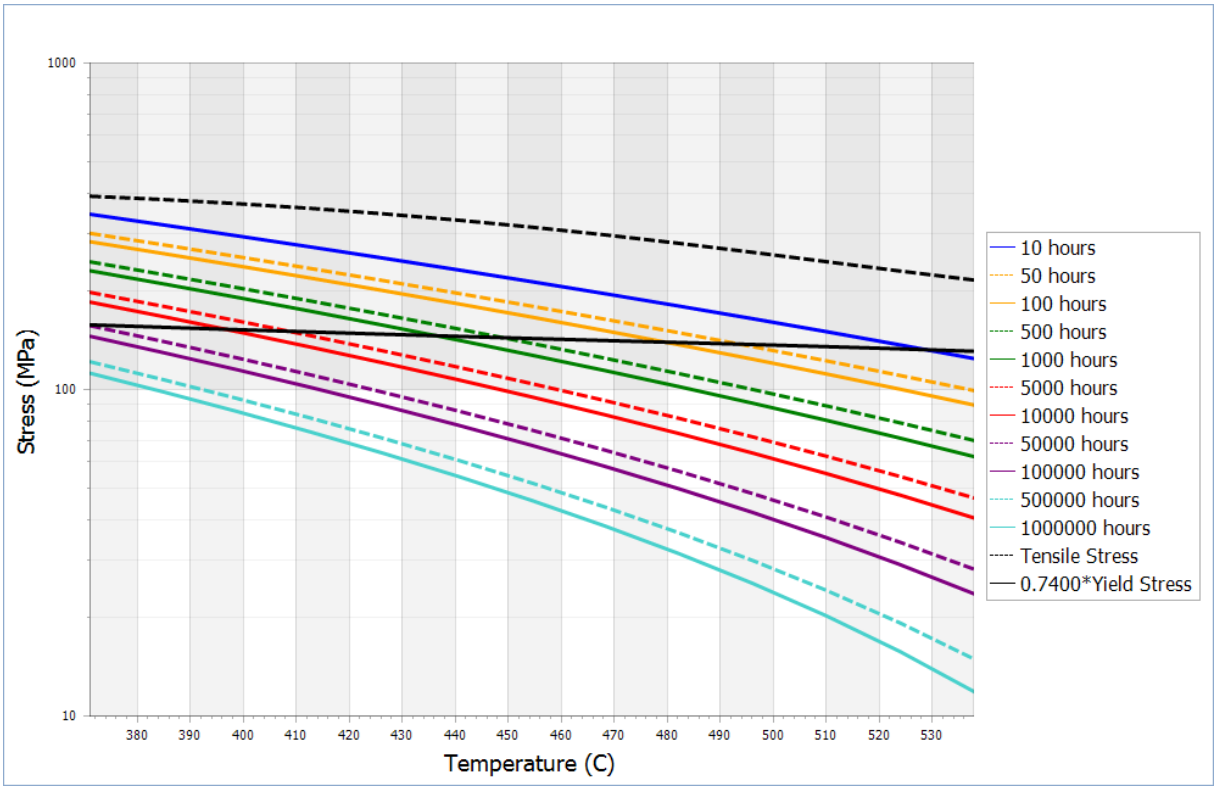

Figure 10B.2M – Level 1 Screening Curve for Carbon Steel – $413\ MPa \leq \sigma_{uts}^{min} < 448\ MPa$

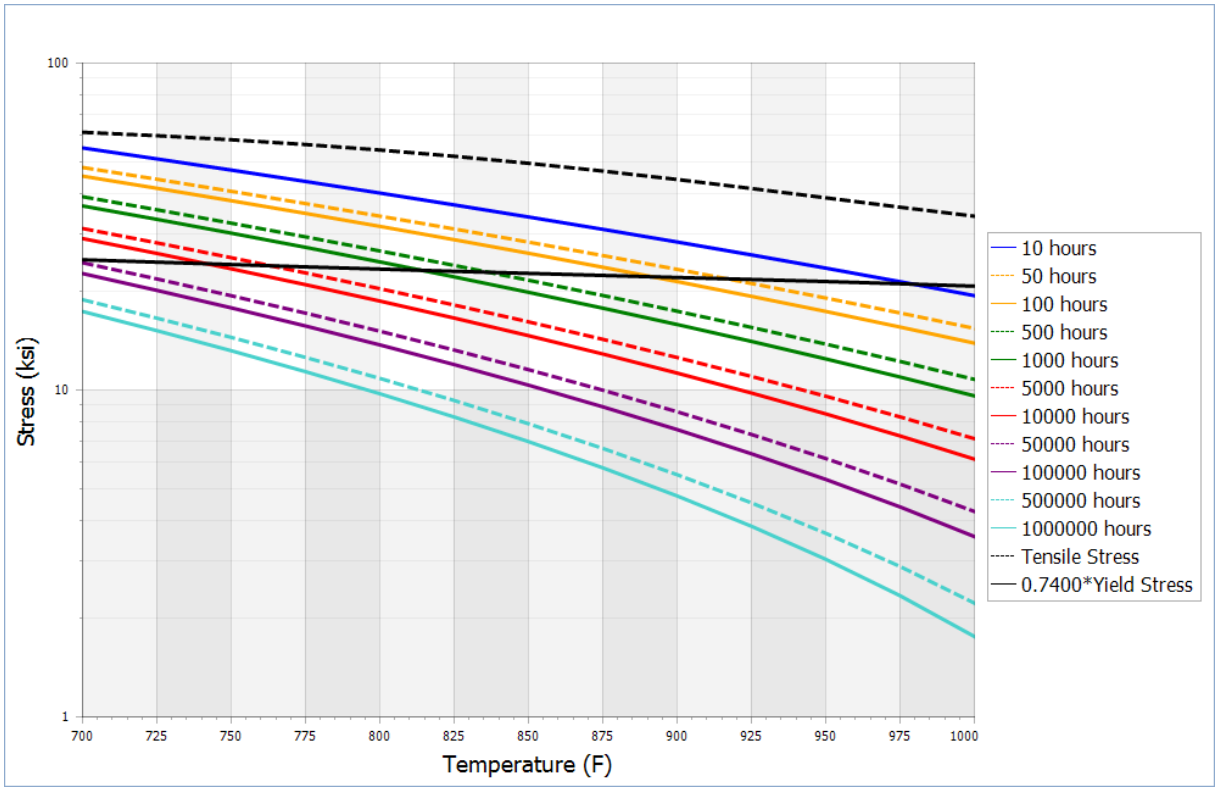

Figure 10B.3 – Level 1 Screening Curve for Carbon Steel – $65\ ksi \leq \sigma_{uts}^{min} < 70\ ksi$

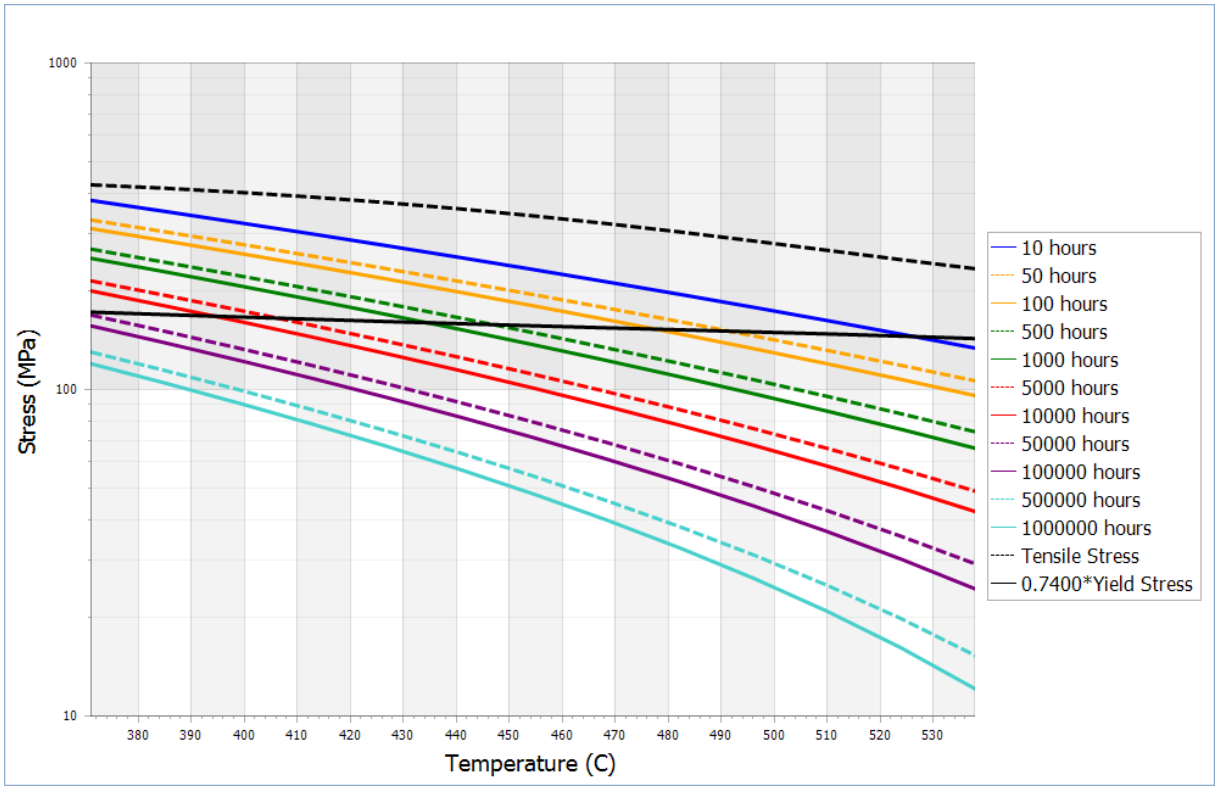

Figure 10B.3M – Level 1 Screening Curve for Carbon Steel – $448\ MPa \leq \sigma_{uts}^{min} < 483\ MPa$

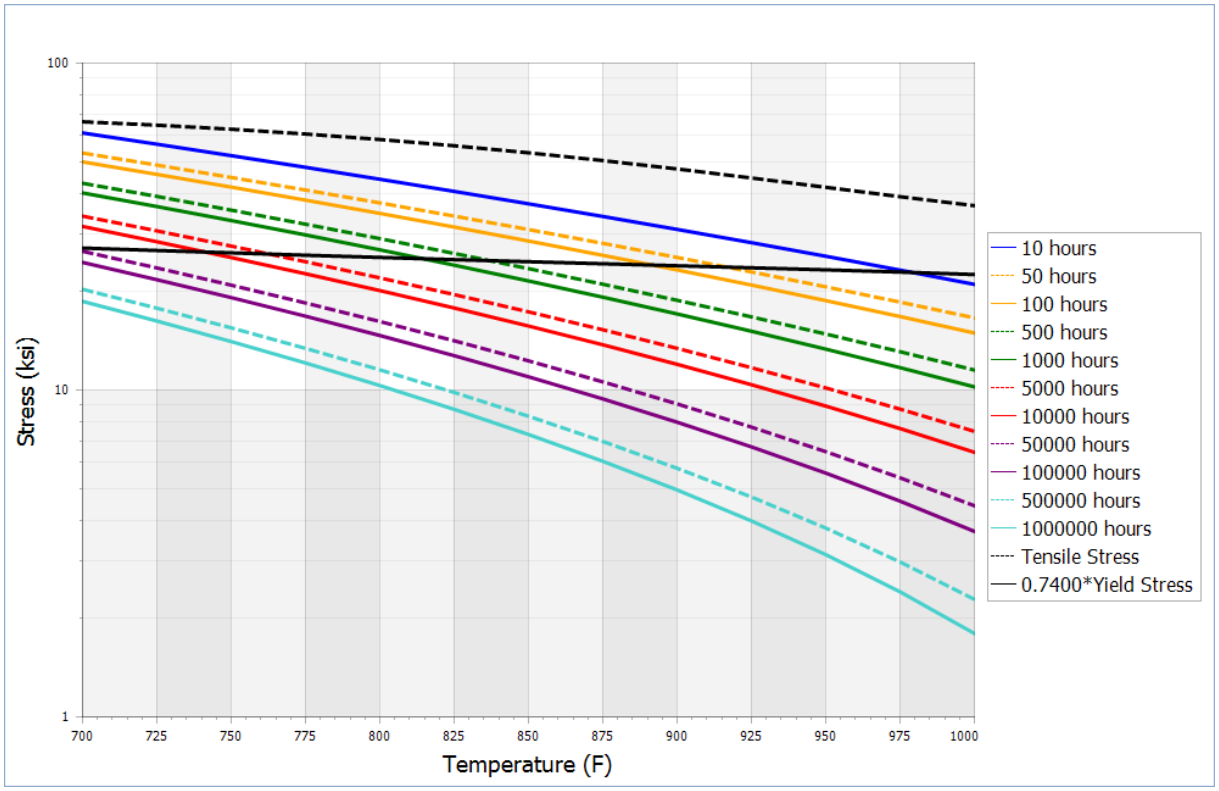

Figure 10B.4 – Level 1 Screening Curve for Carbon Steel – $70\ ksi \leq \sigma_{uts}^{min} < 75\ ksi$

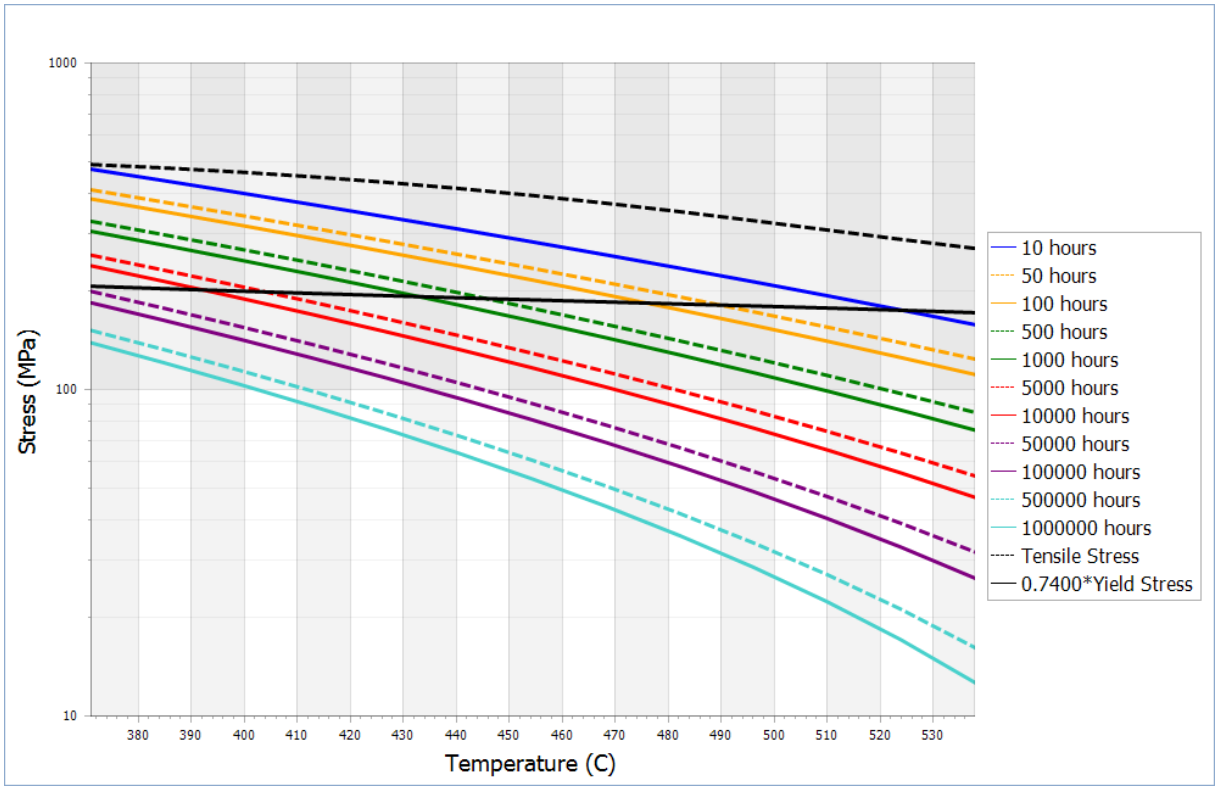

Figure 10B.4M – Level 1 Screening Curve for Carbon Steel – $483\ MPa \leq \sigma_{uts}^{min} < 517\ MPa$

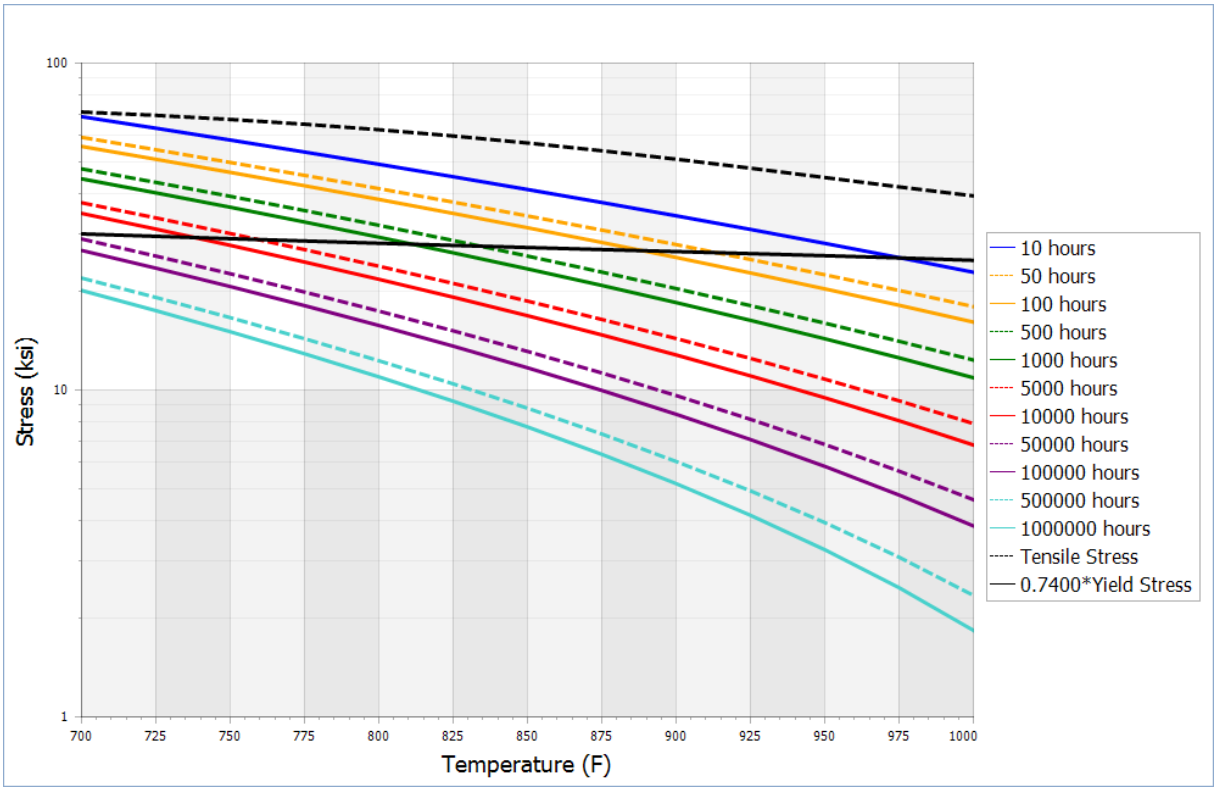

Figure 10B.5 – Level 1 Screening Curve for Carbon Steel – $\sigma_{uts}^{min} \geq 75$

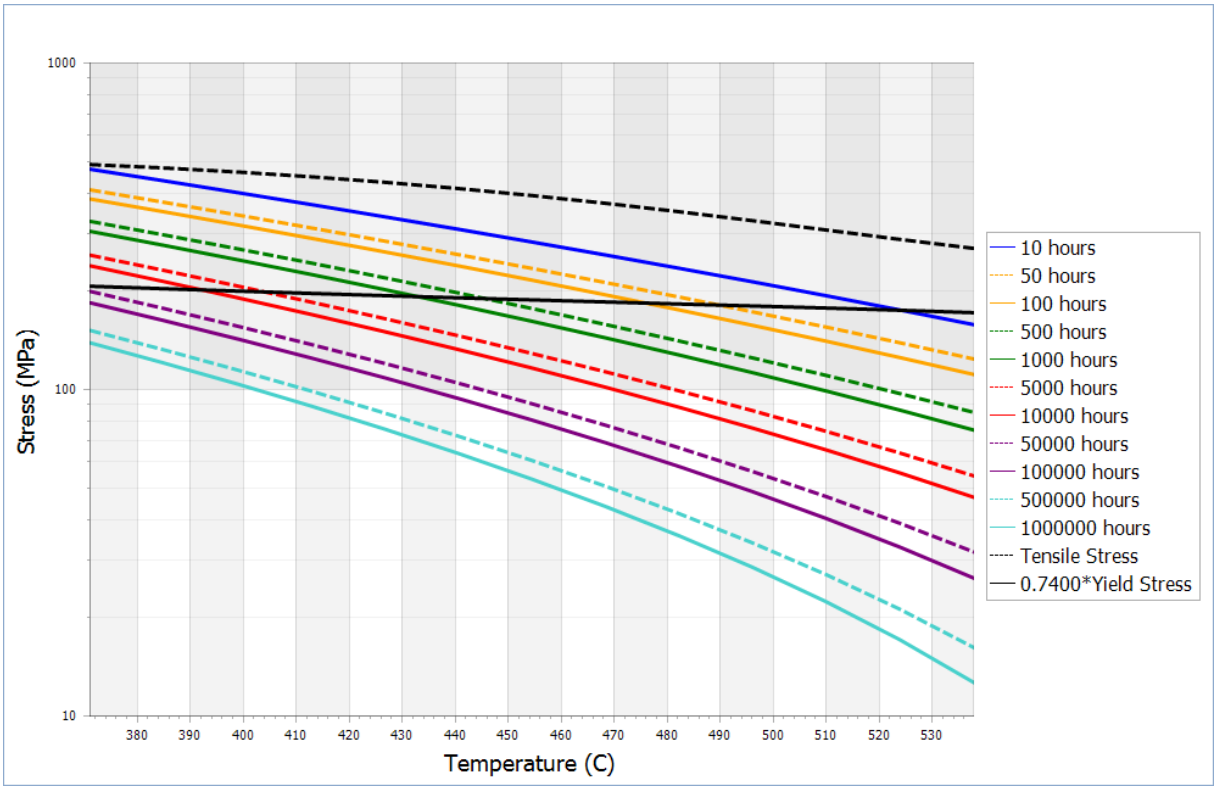

Figure 10B.5M – Level 1 Screening Curve for Carbon Steel – $\sigma_{uts}^{min} \geq 517\ MPa$

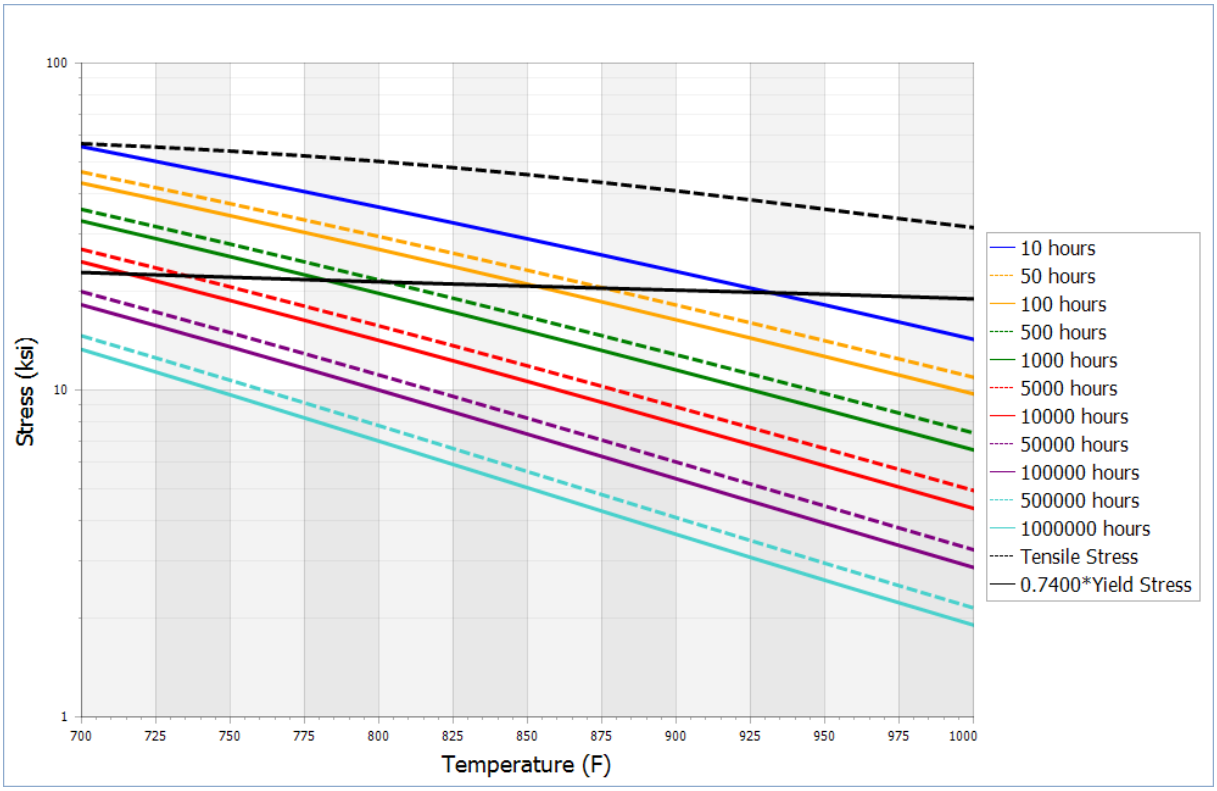

Figure 10B.6 – Level 1 Screening Curve for Carbon Steel (Graphitized)

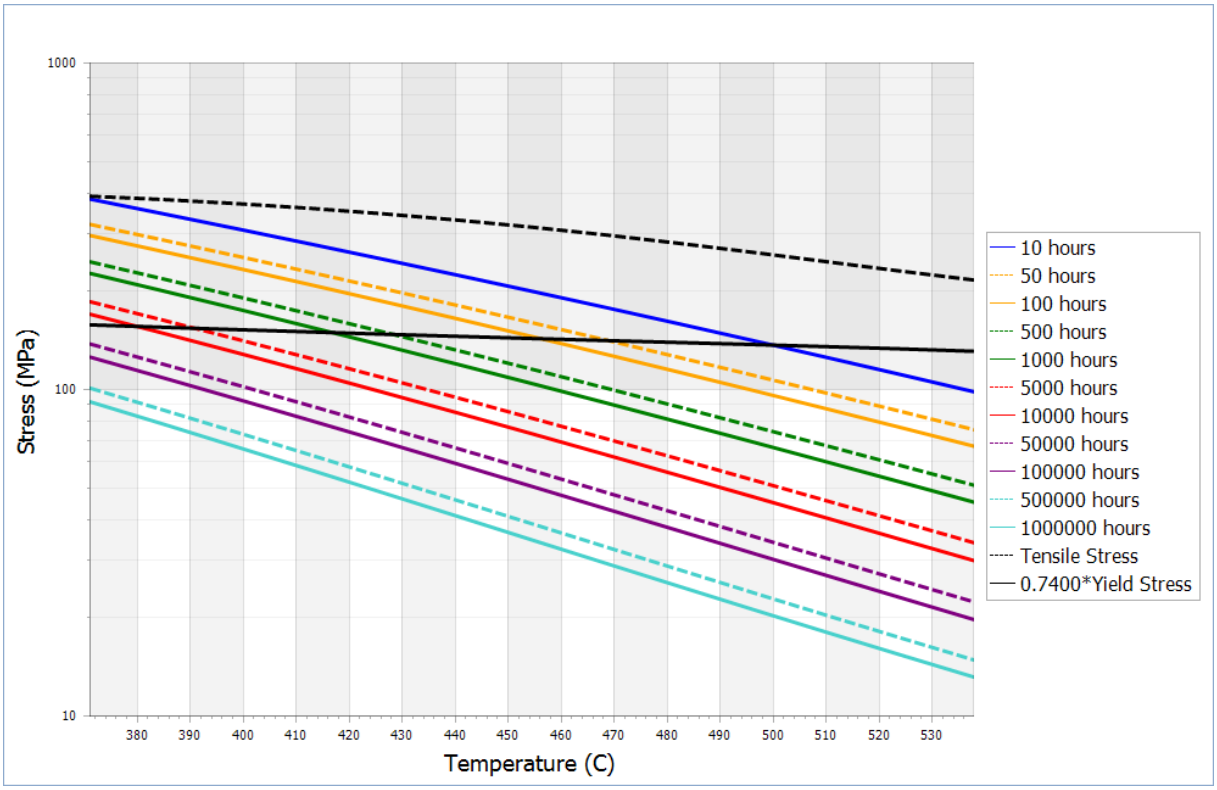

Figure 10B.6M – Level 1 Screening Curve for Carbon Steel (Graphitized)

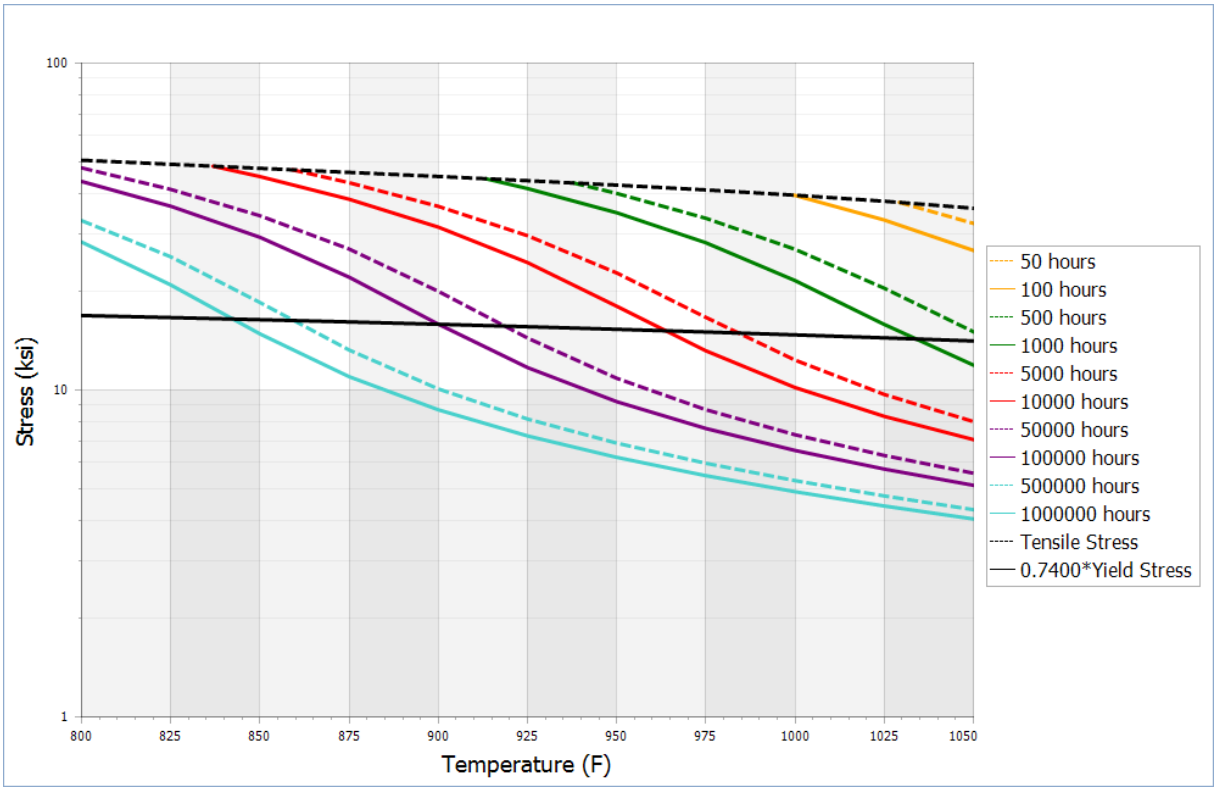

Figure 10B.7 – Level 1 Screening Curve for C–0.5Mo

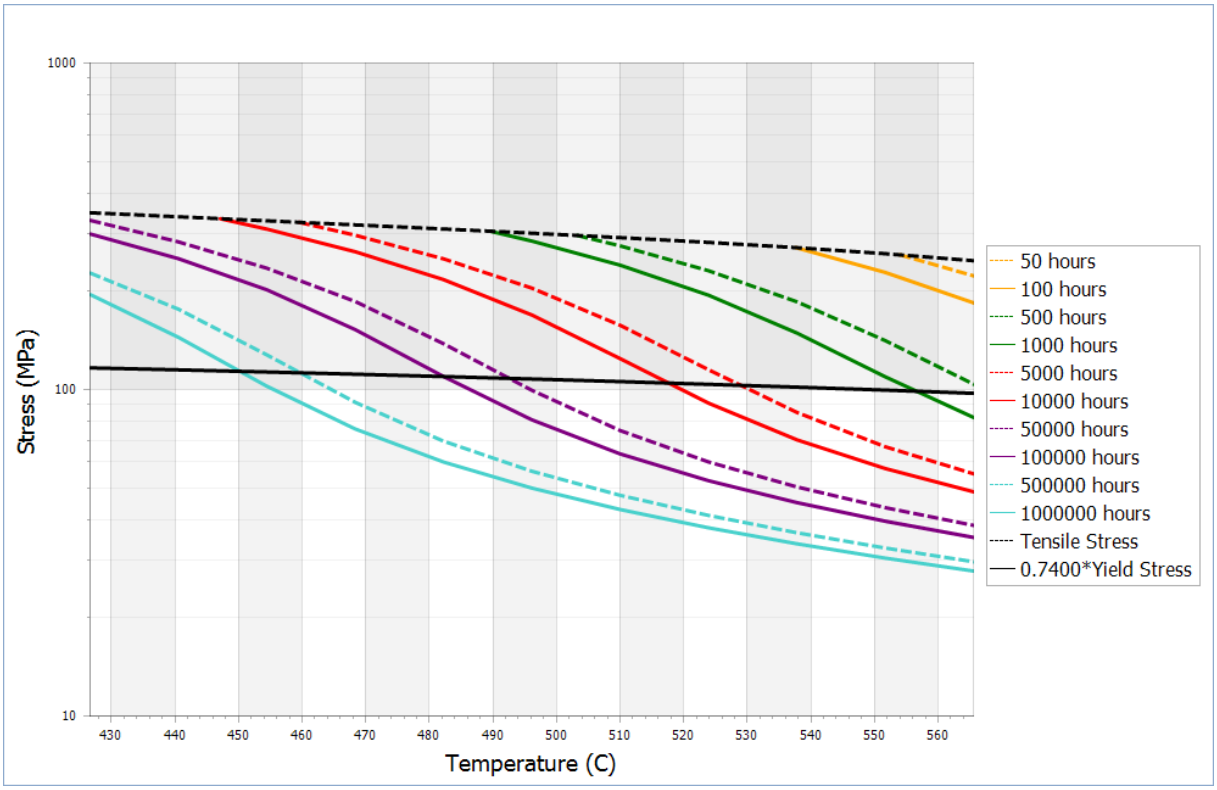

Figure 10B.7M – Level 1 Screening Curve for C–0.5Mo

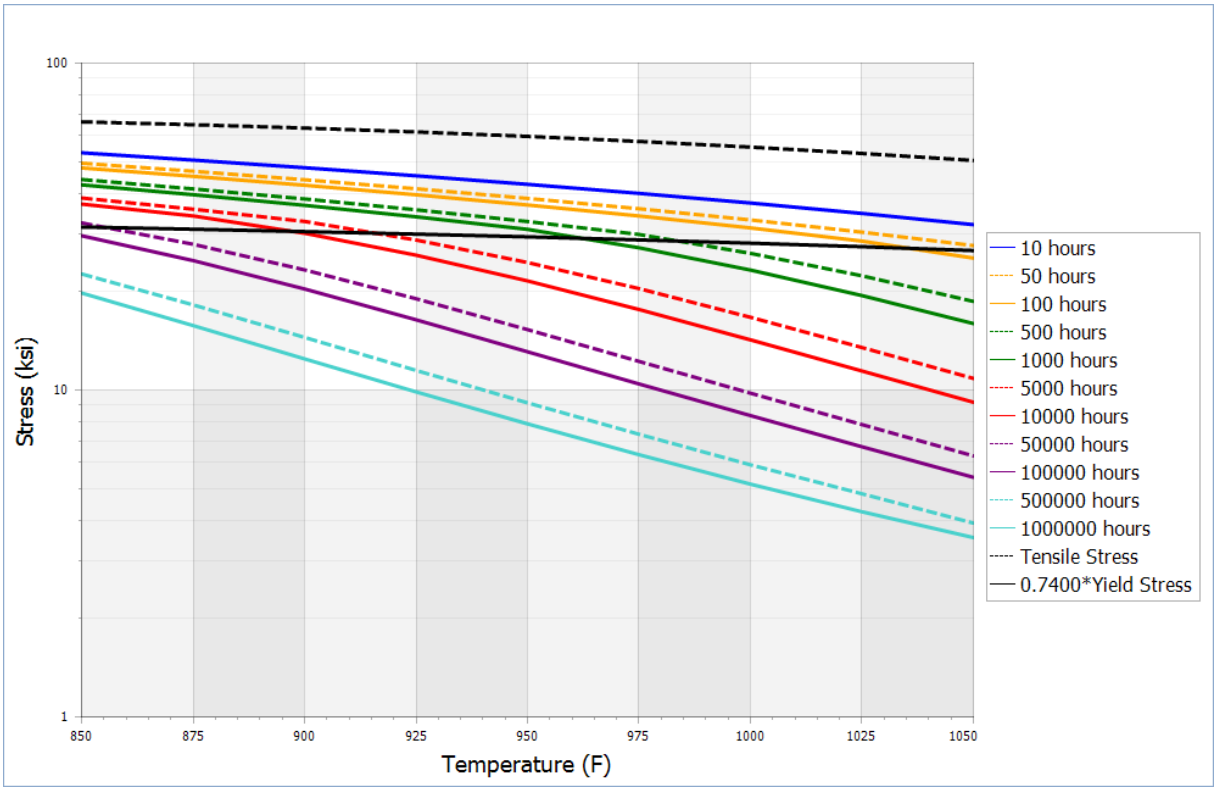

Figure 10B.8 – Level 1 Screening Curve for 1.25Cr–0.5Mo (NT)

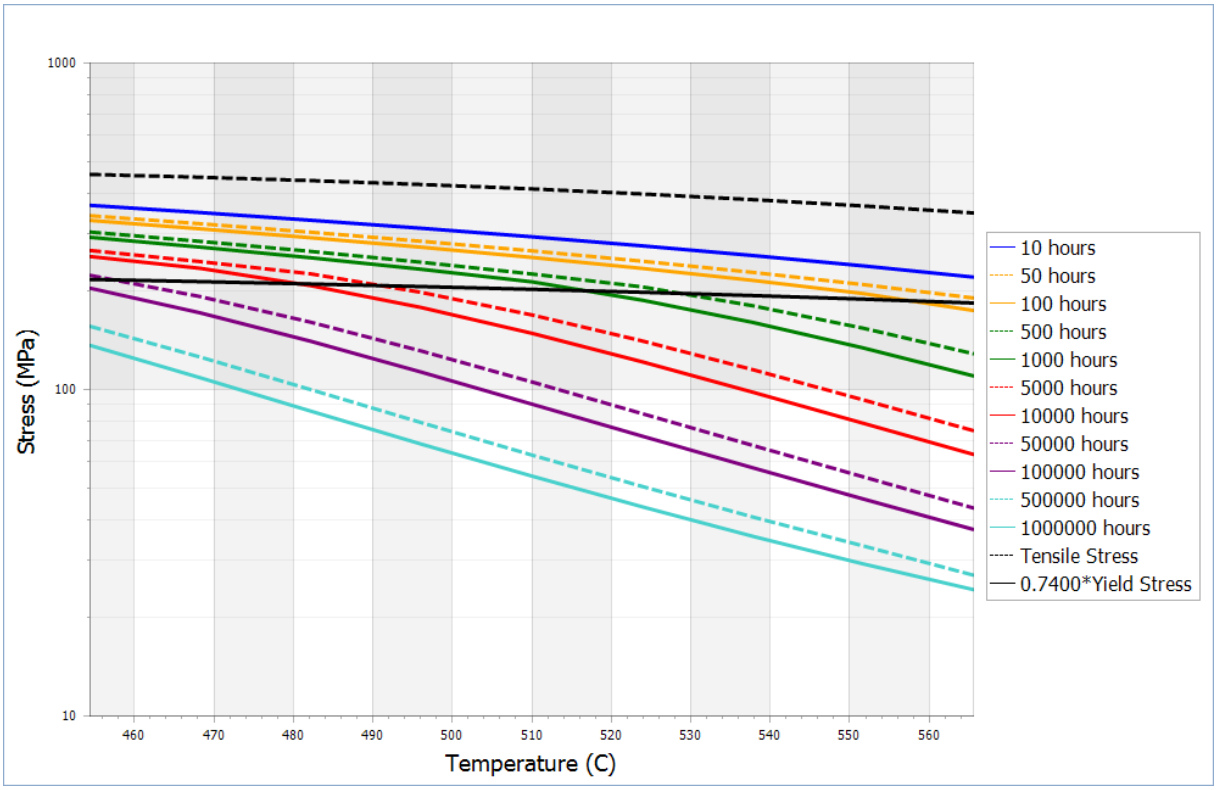

Figure 10B.8M – Level 1 Screening Curve for 1.25Cr–0.5Mo (NT)

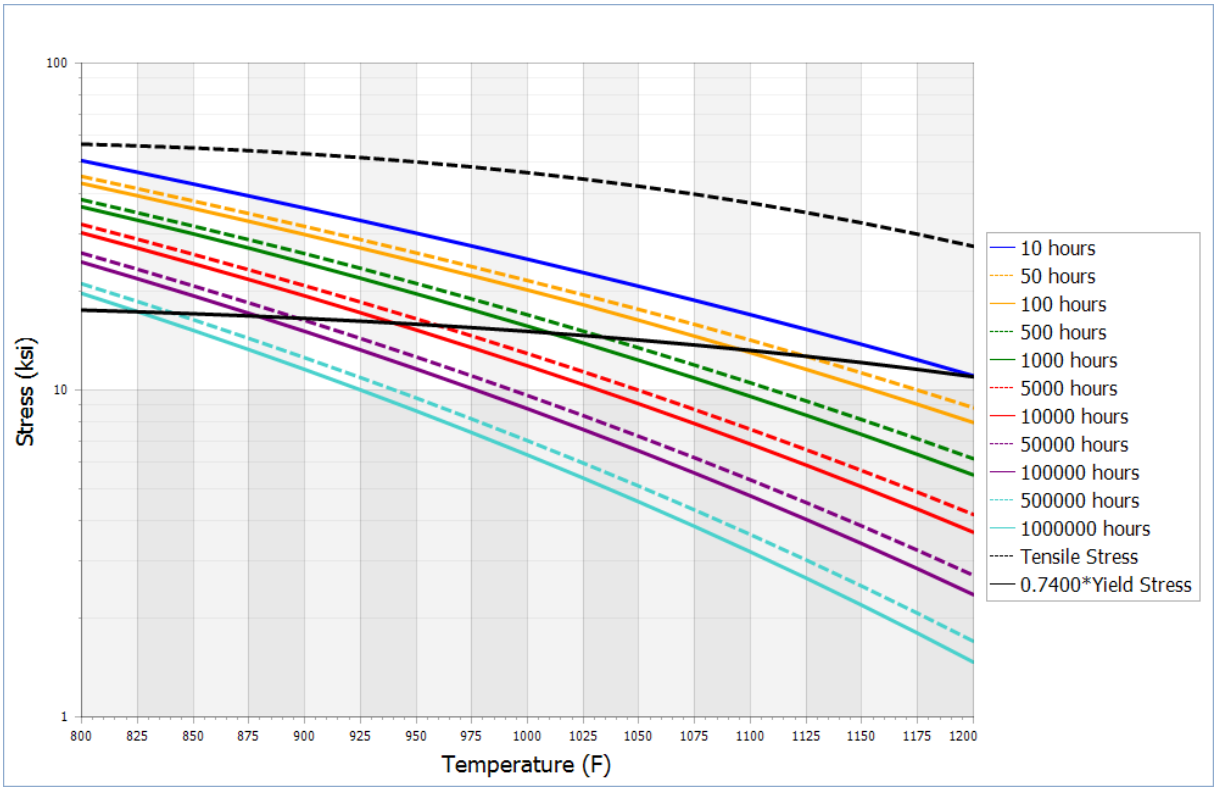

Figure 10B.9 – Level 1 Screening Curve for 1.25Cr–0.5Mo (Annealed)

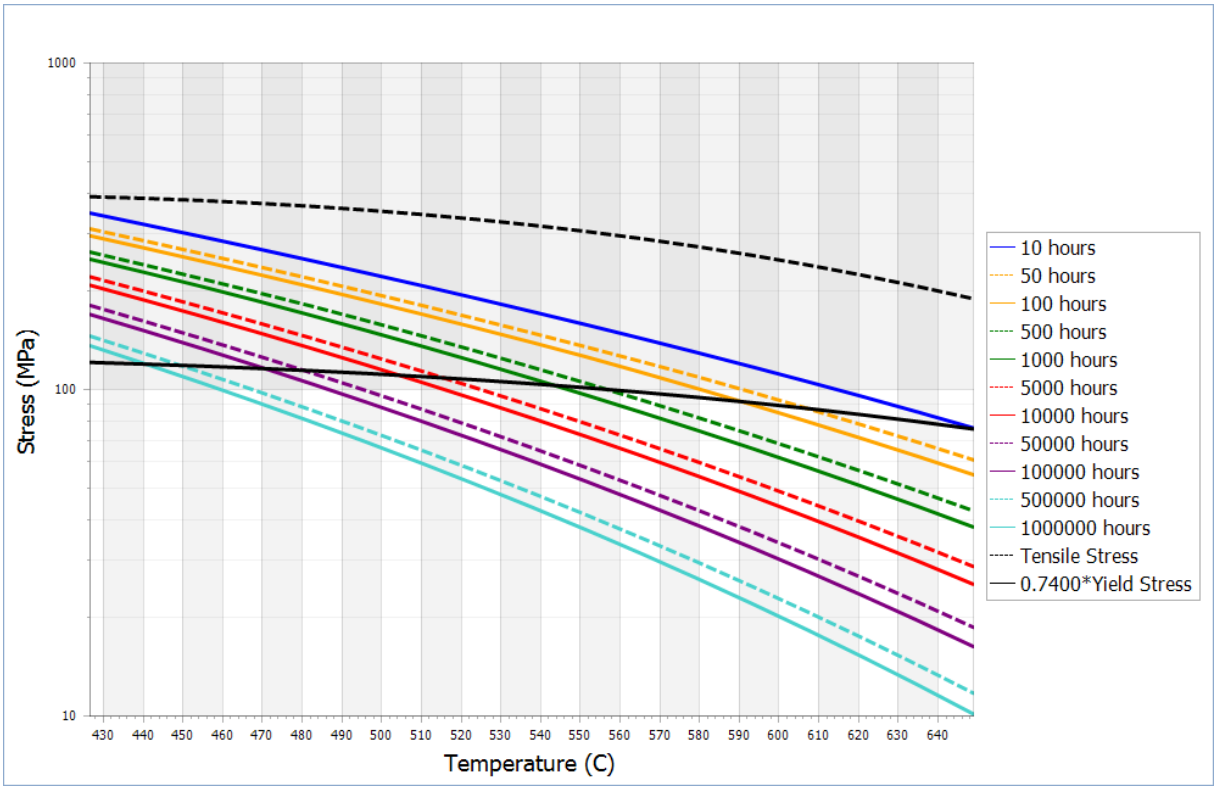

Figure 10B.9M – Level 1 Screening Curve for 1.25Cr–0.5Mo (Annealed)

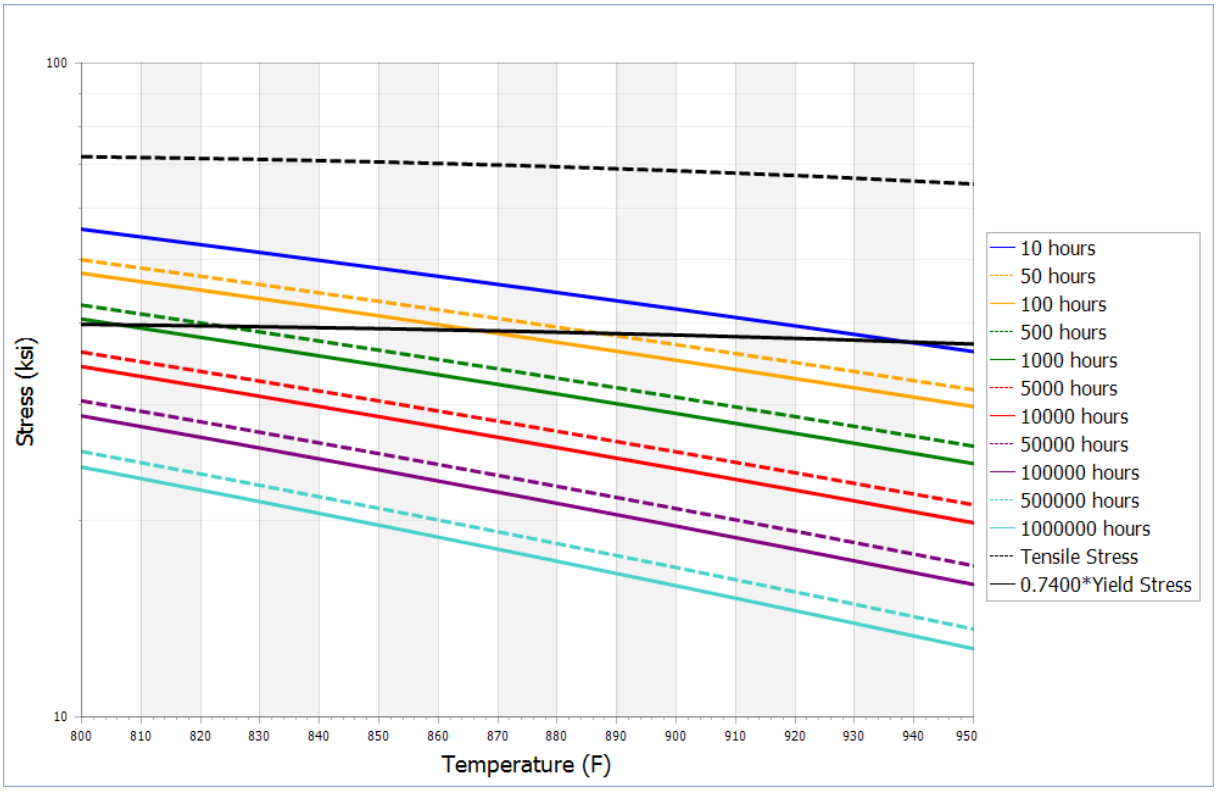

Figure 10B.10 – Level 1 Screening Curve for 2.25Cr–1Mo (NT)

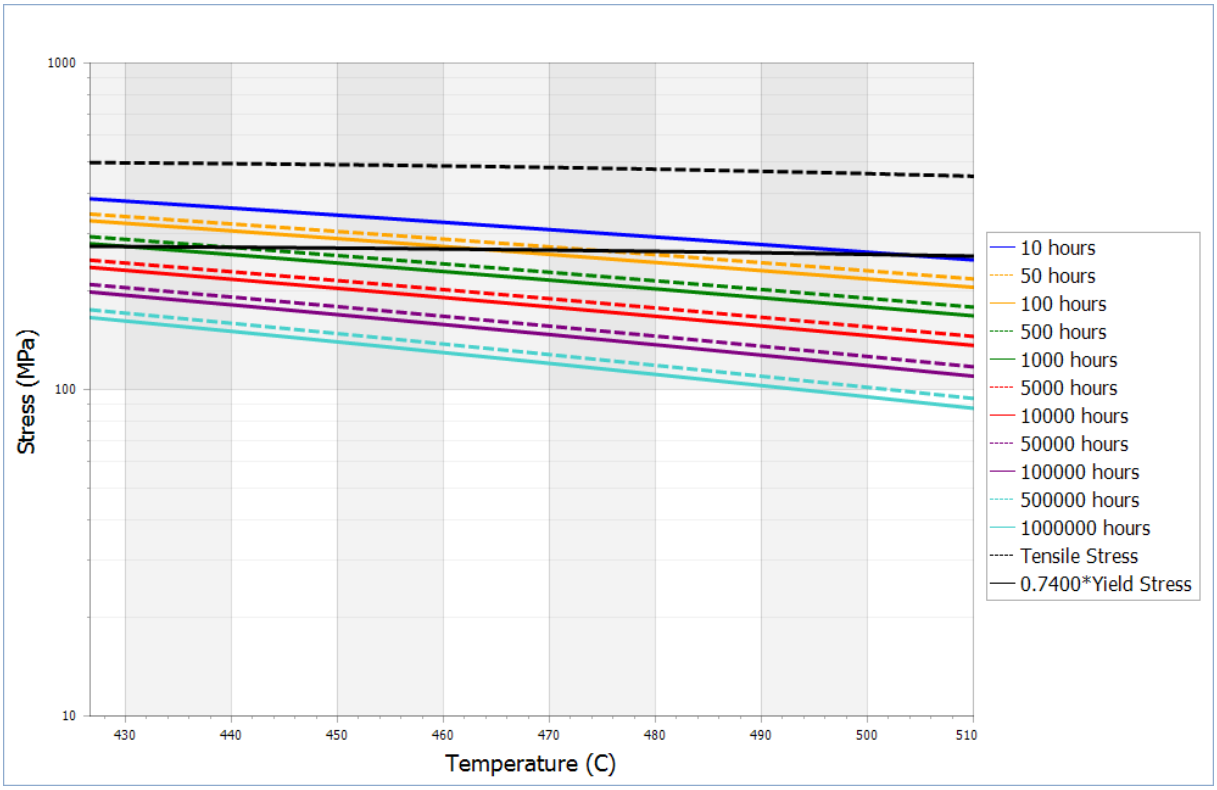

Figure 10B.10M – Level 1 Screening Curve for 2.25Cr–1Mo (NT)

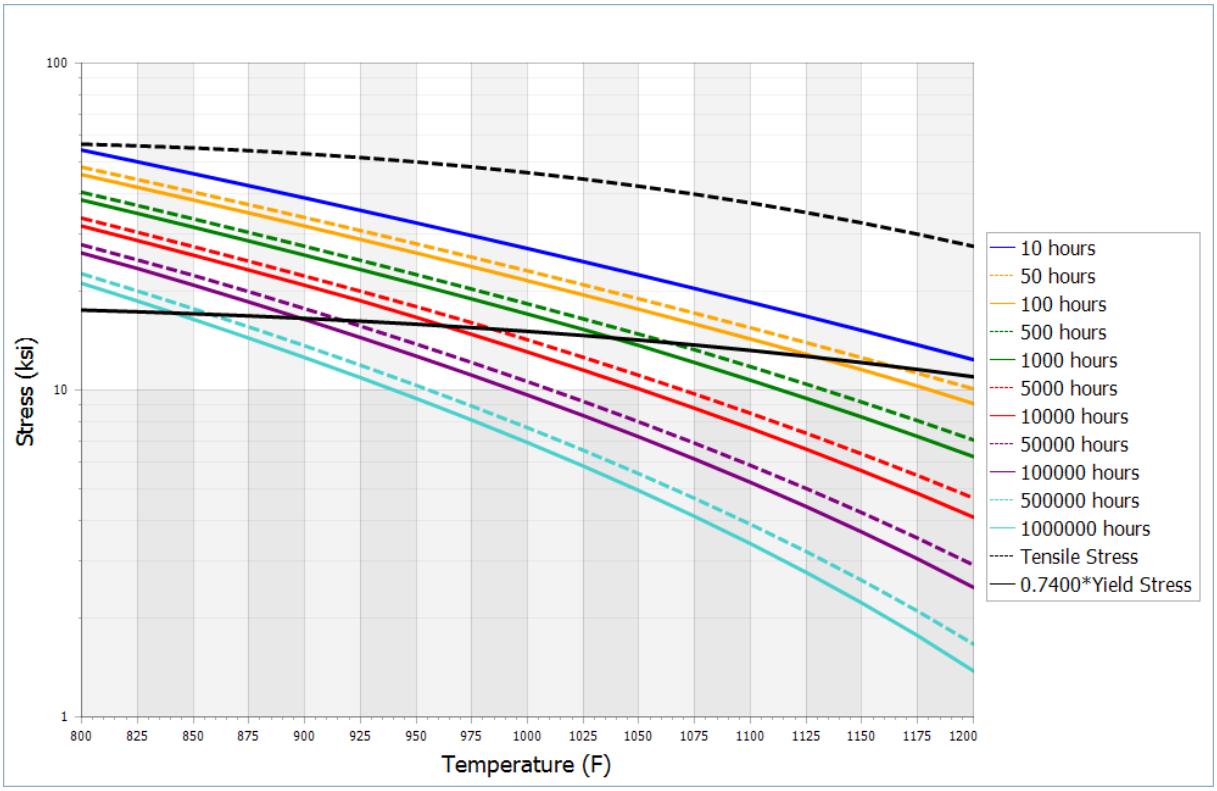

Figure 10B.11 – Level 1 Screening Curve for 2.25Cr–1Mo (Annealed)

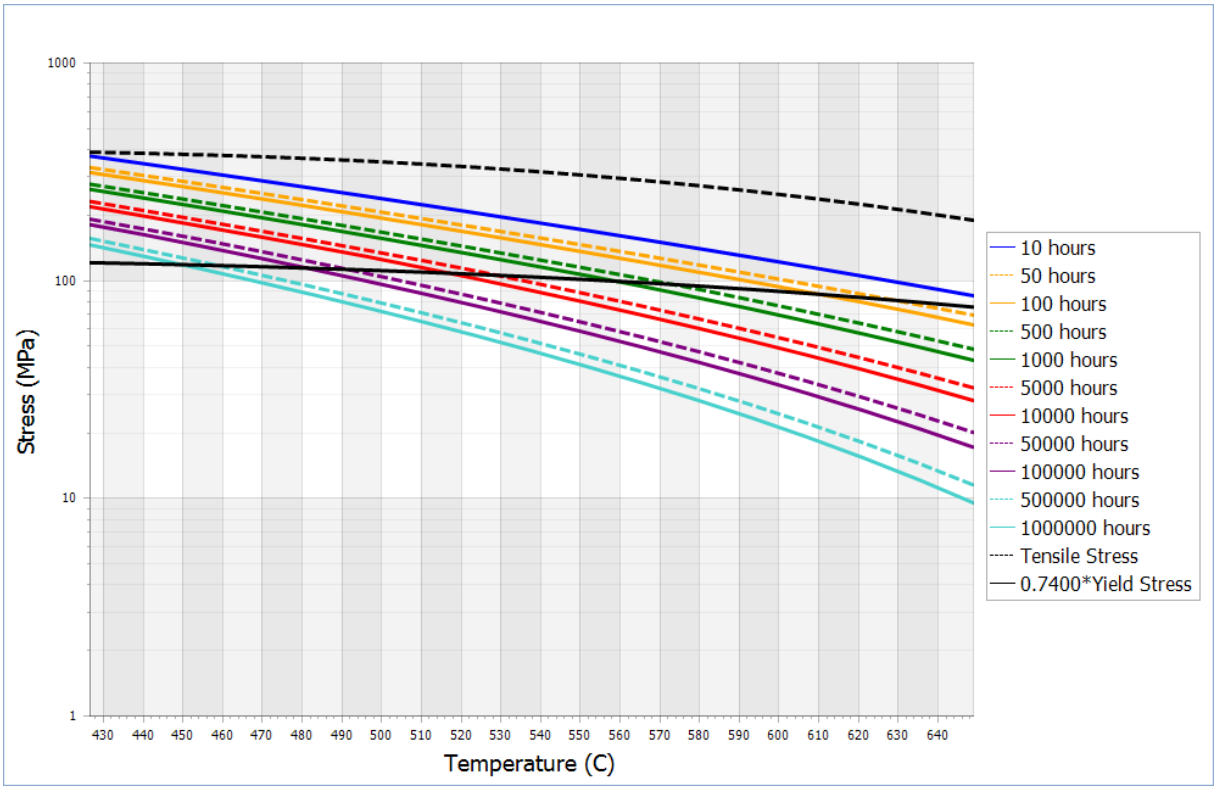

Figure 10B.11M – Level 1 Screening Curve for 2.25Cr–1Mo (Annealed)

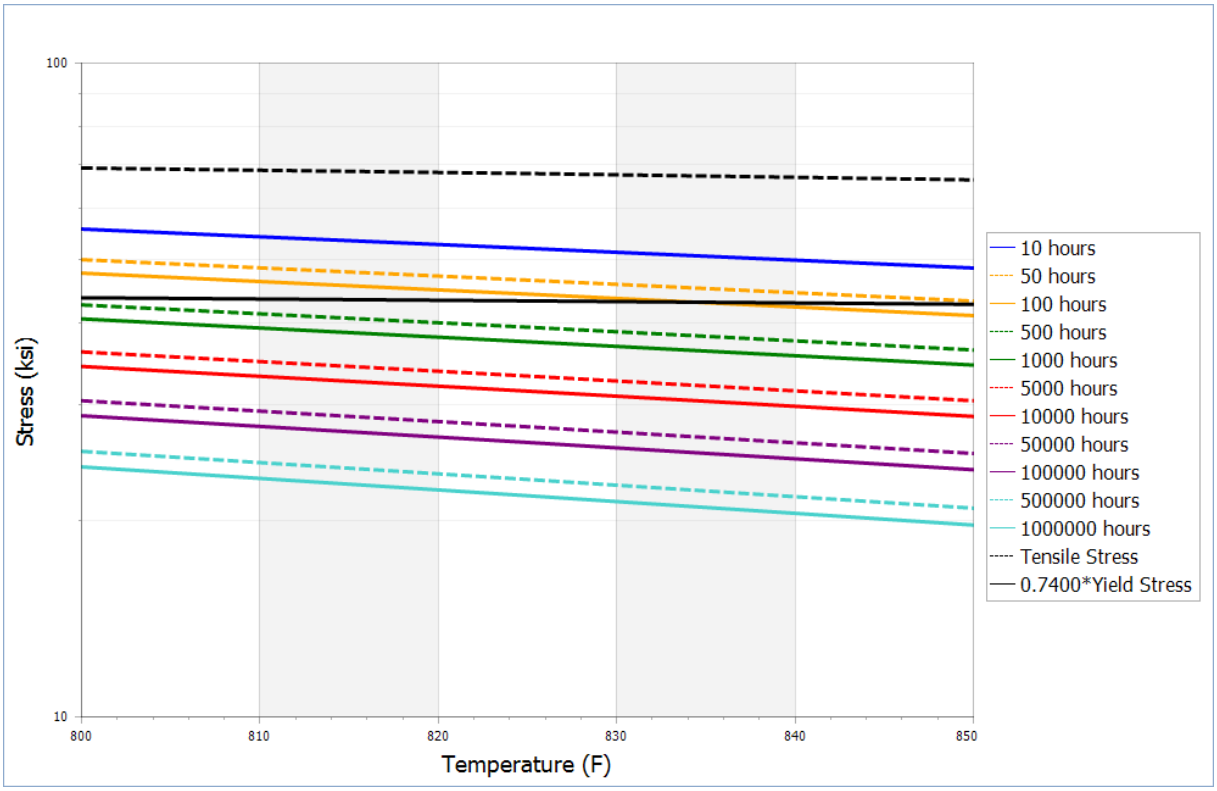

Figure 10B.12 – Level 1 Screening Curve for 2.25Cr–1Mo (QT)

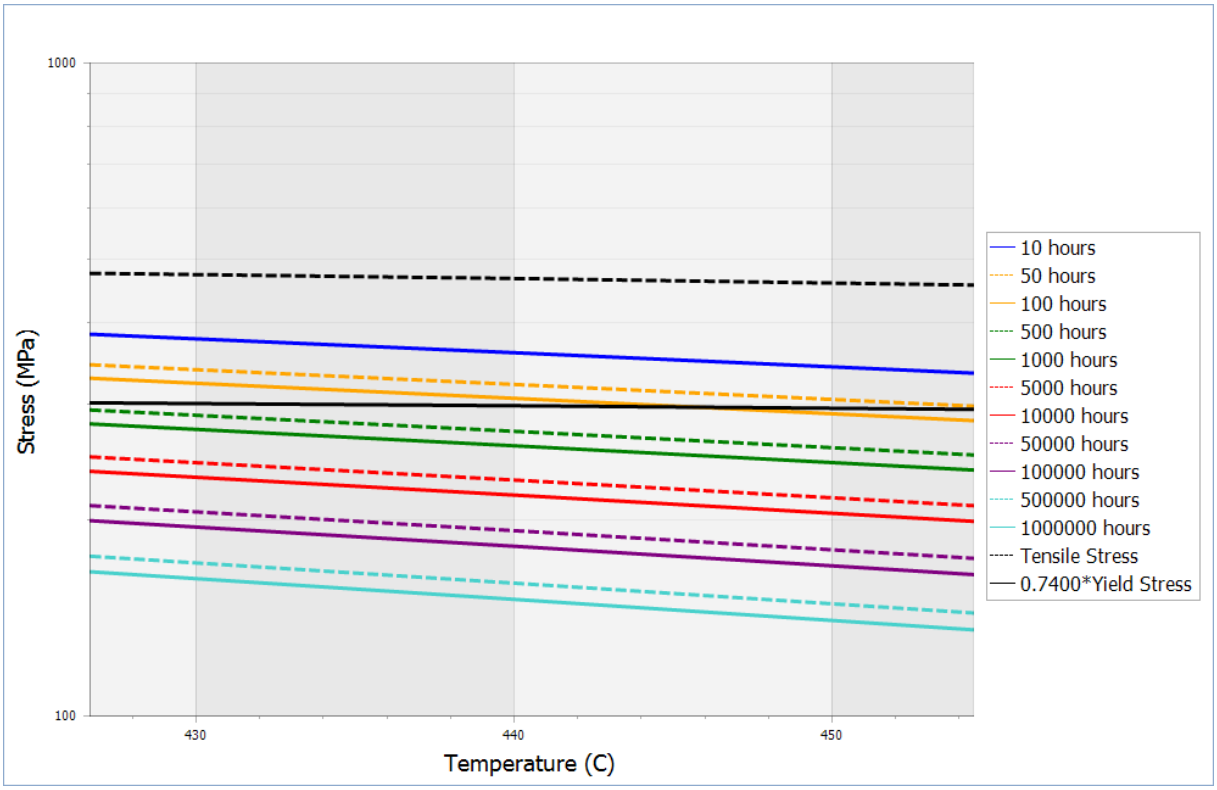

Figure 10B.12M – Level 1 Screening Curve for 2.25Cr–1Mo (QT)

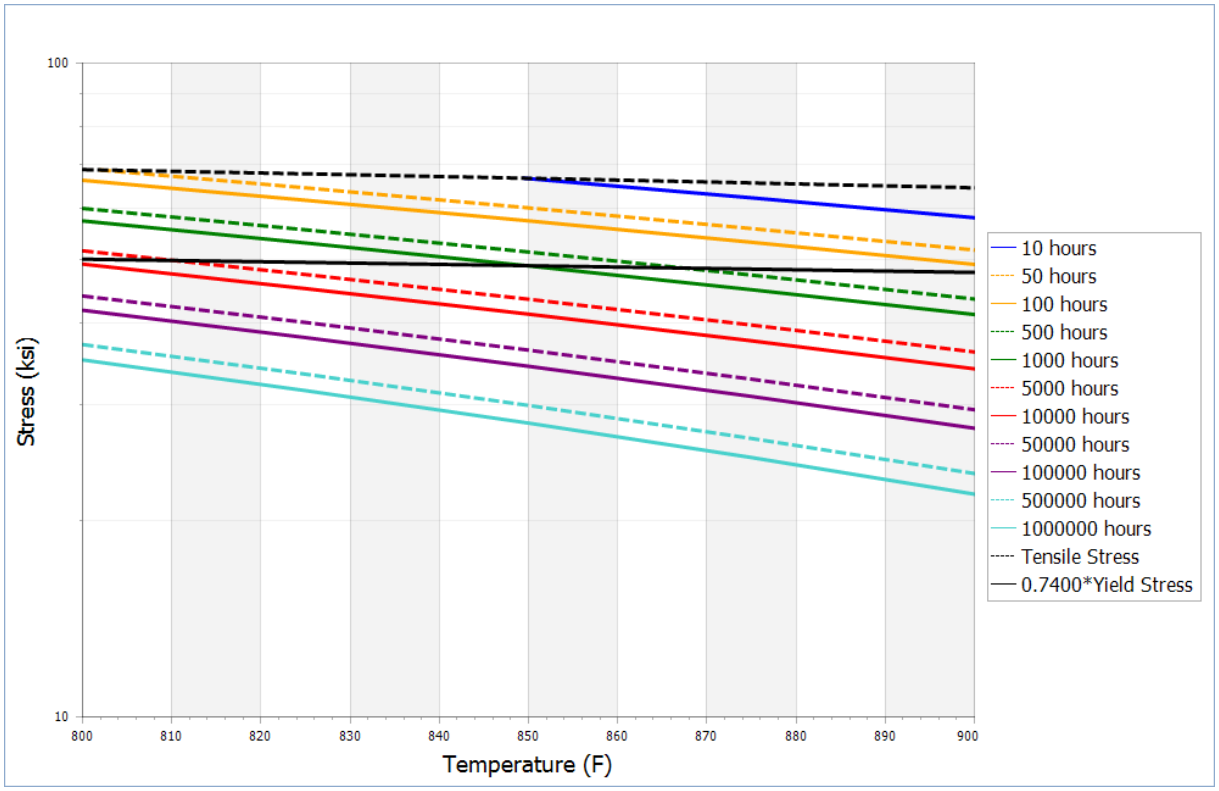

Figure 10B.13 – Level 1 Screening Curve for 2.25Cr–1Mo–V

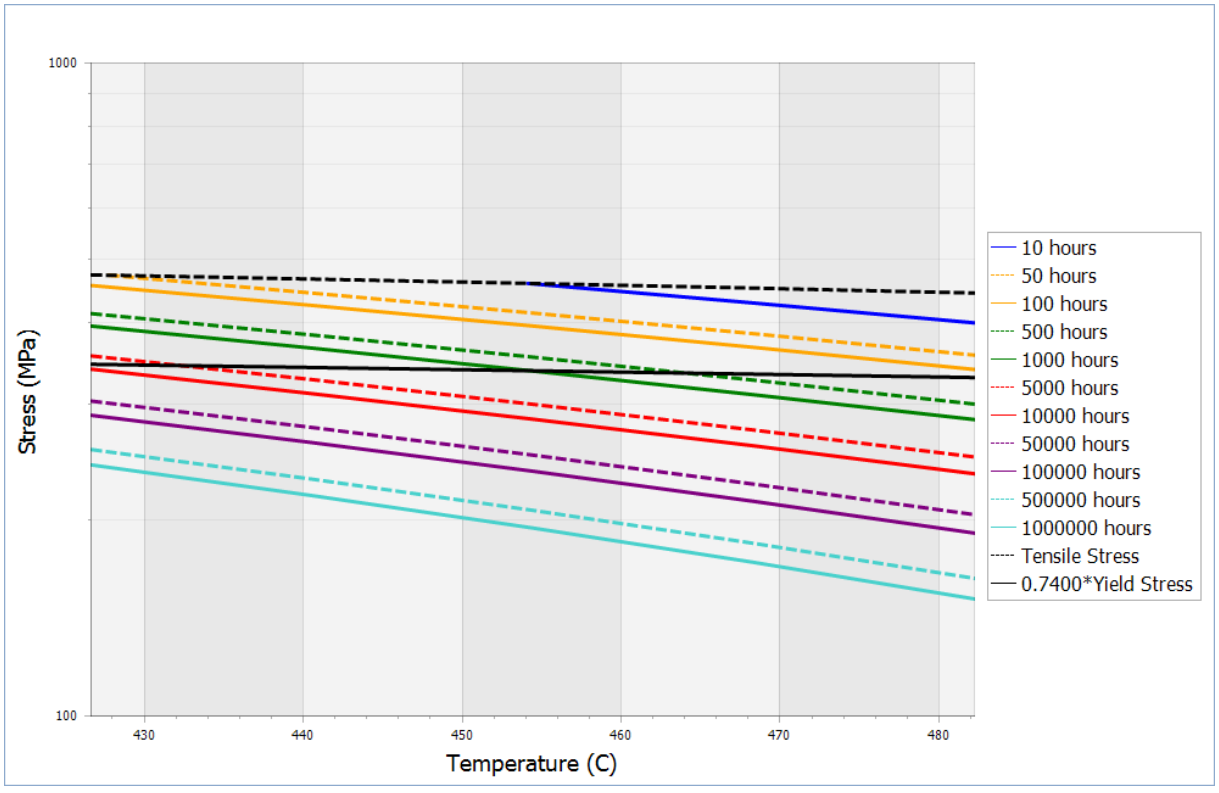

Figure 10B.13M – Level 1 Screening Curve for 2.25Cr–1Mo–V

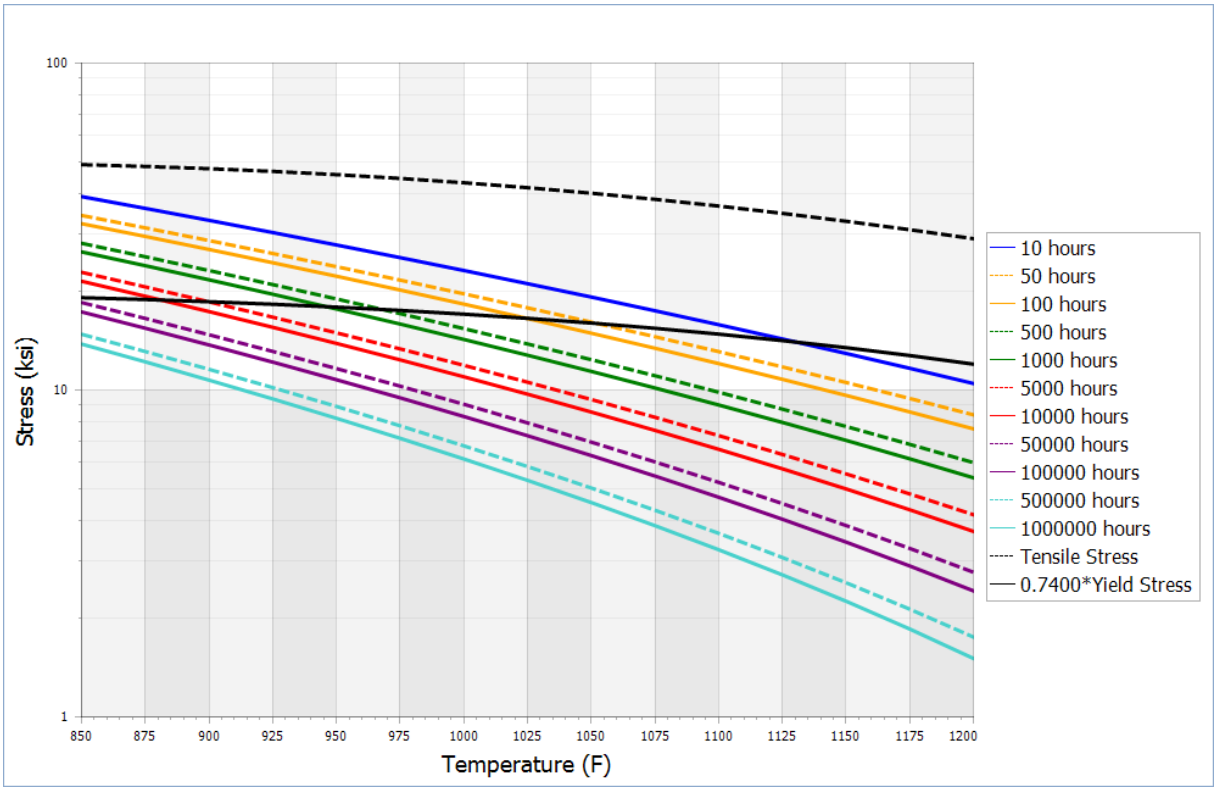

Figure 10B.14 – Level 1 Screening Curve for 5Cr–0.5Mo

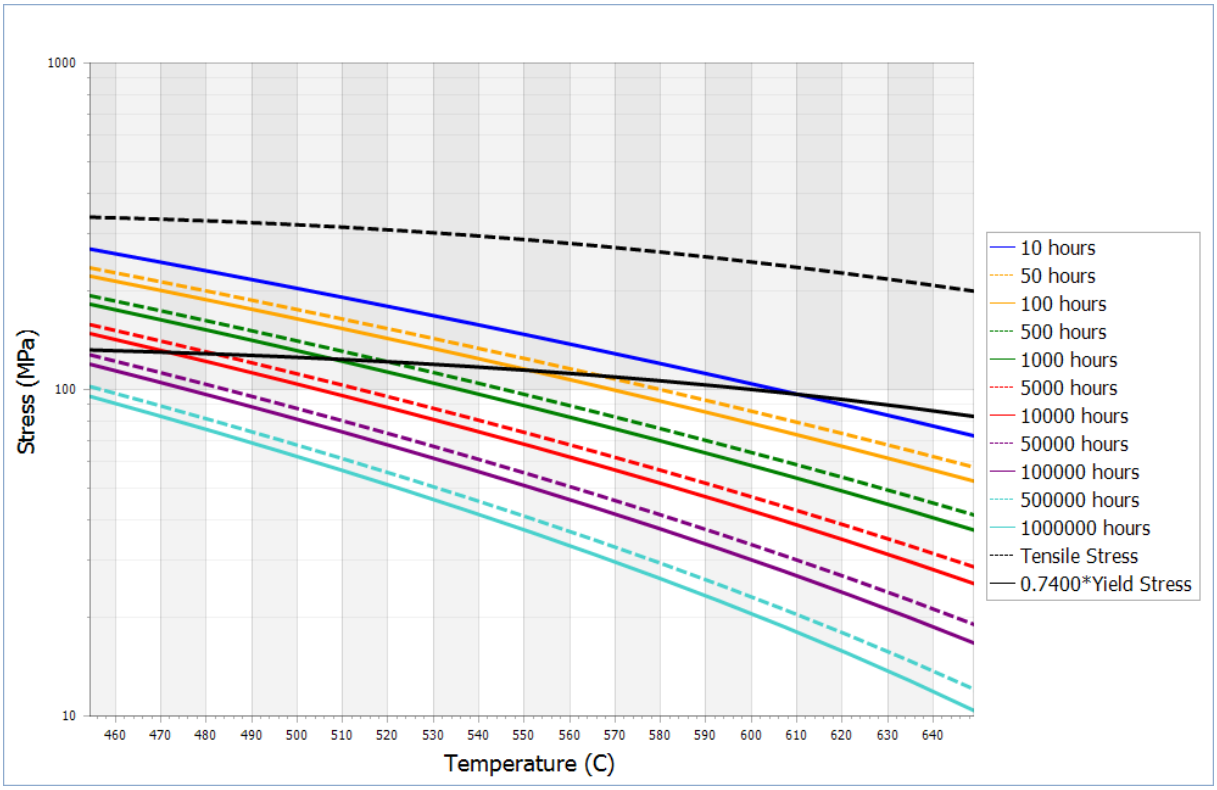

Figure 10B.14M – Level 1 Screening Curve for 5Cr–0.5Mo

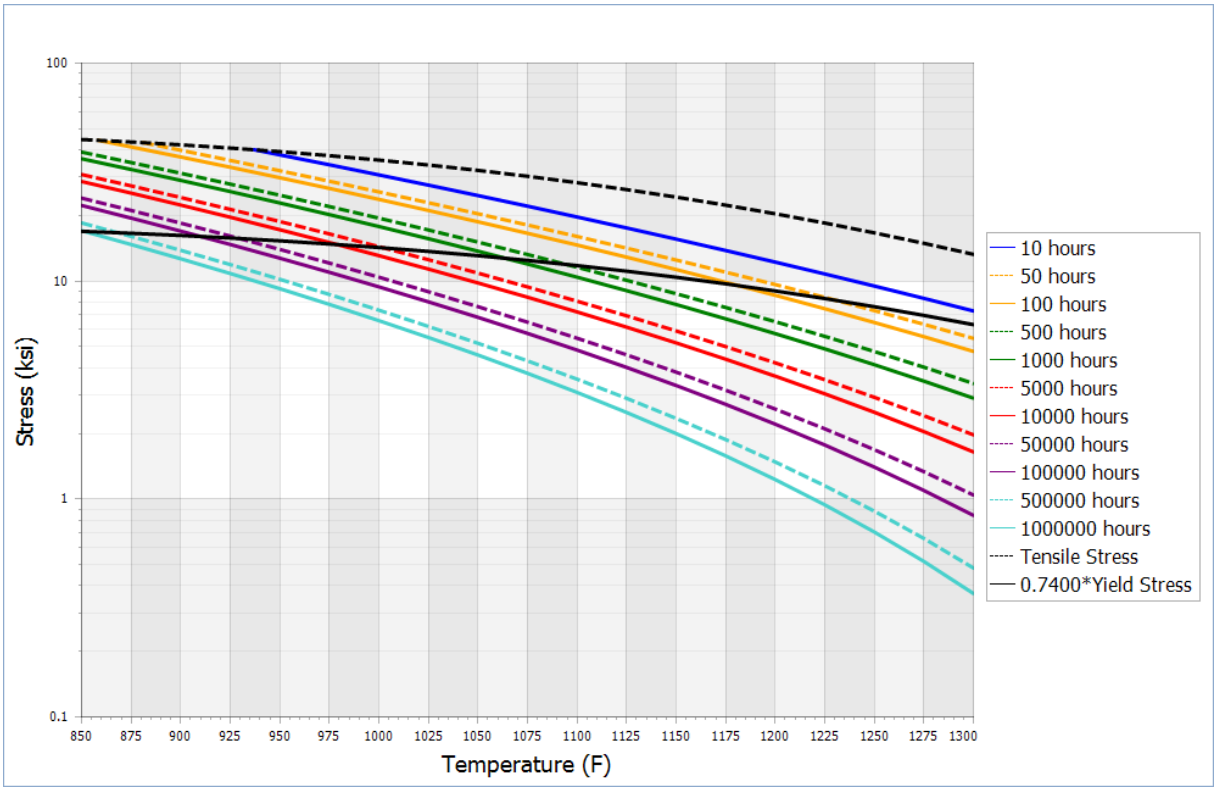

Figure 10B.15 – Level 1 Screening Curve for 9Cr–1Mo

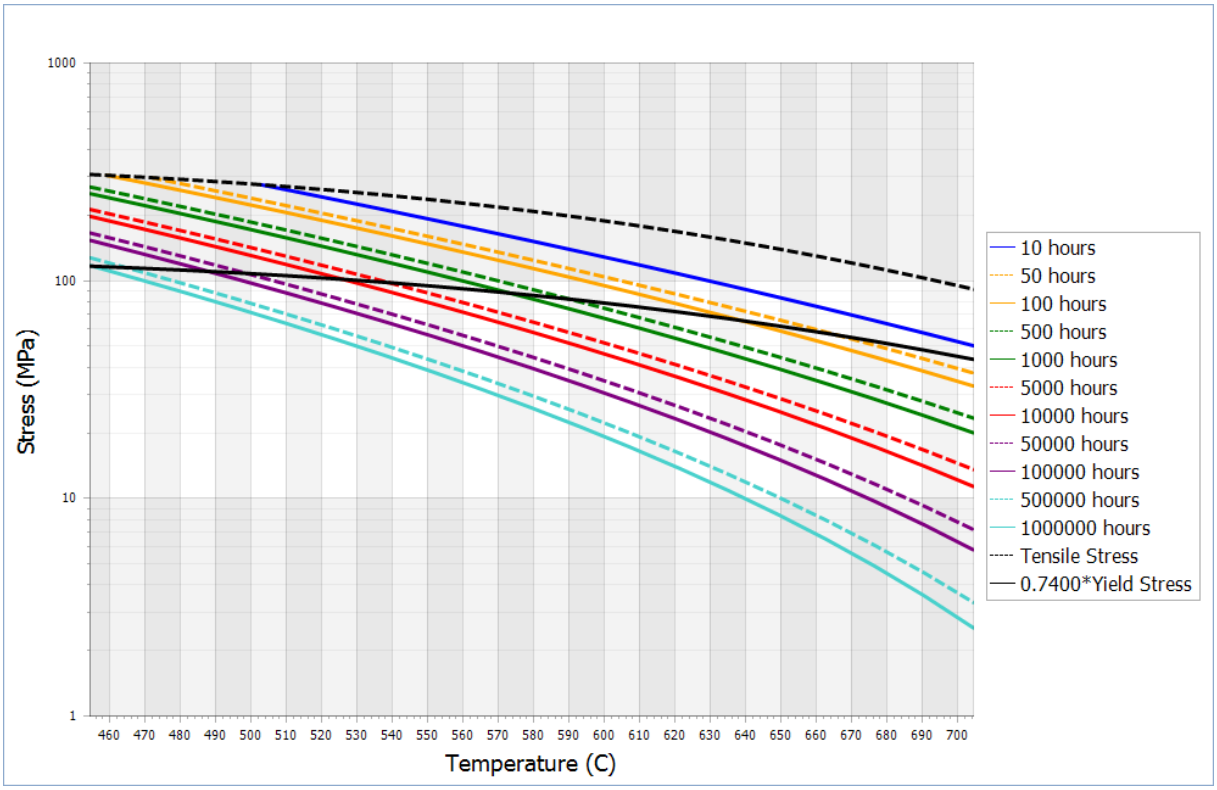

Figure 10B.15M – Level 1 Screening Curve for 9Cr–1Mo

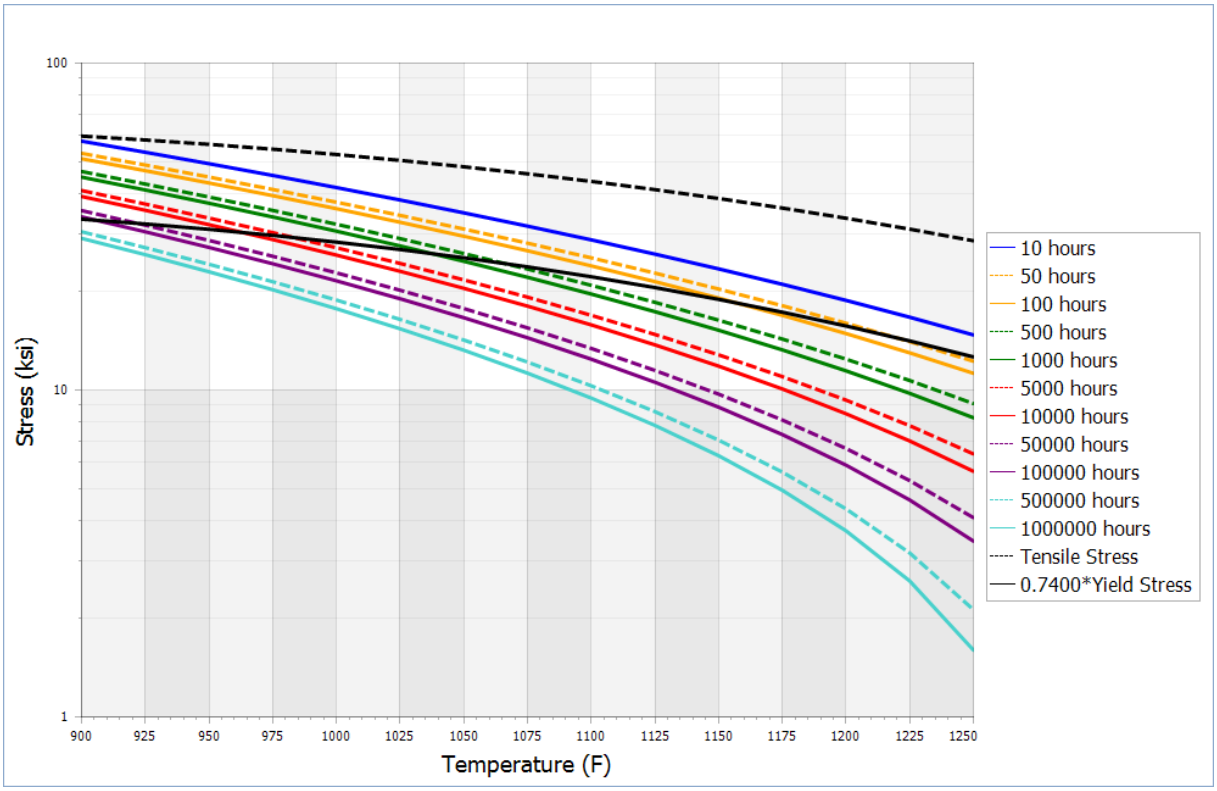

Figure 10B.16 – Level 1 Screening Curve for 9Cr–1Mo–V

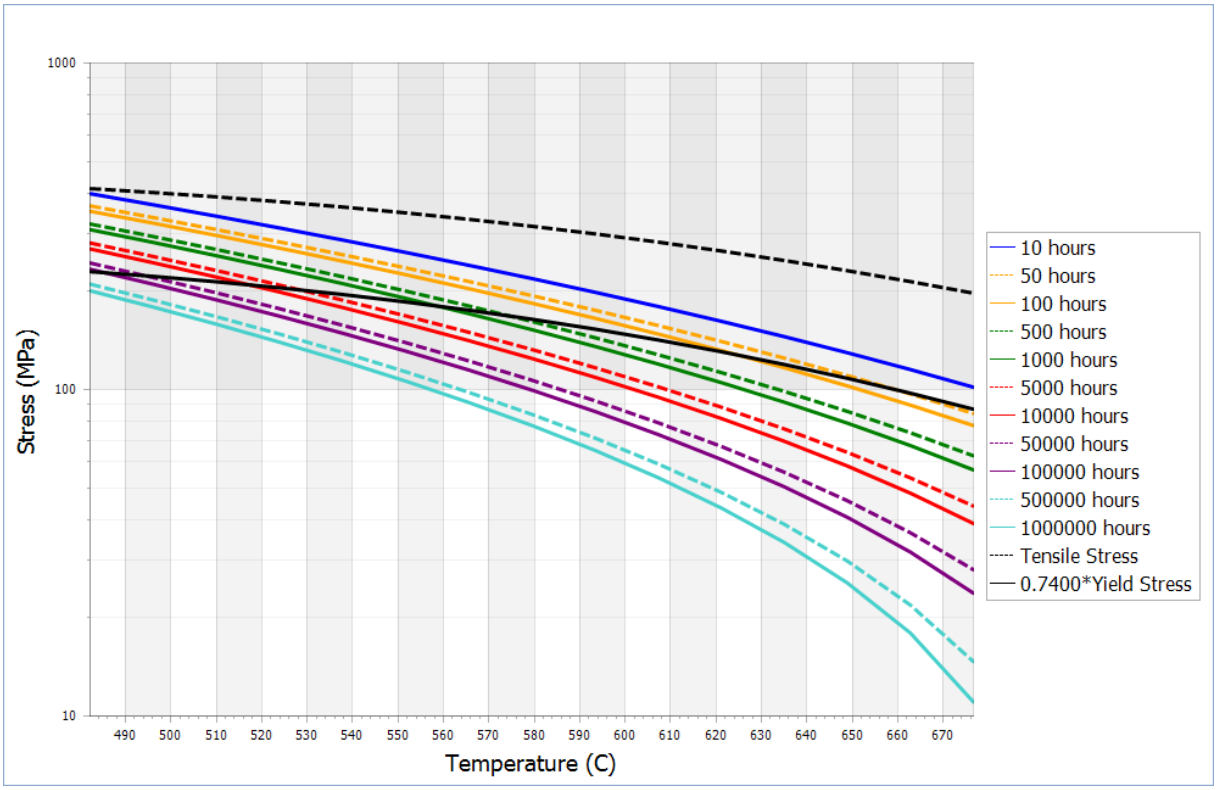

Figure 10B.16M – Level 1 Screening Curve for 9Cr–1Mo–V

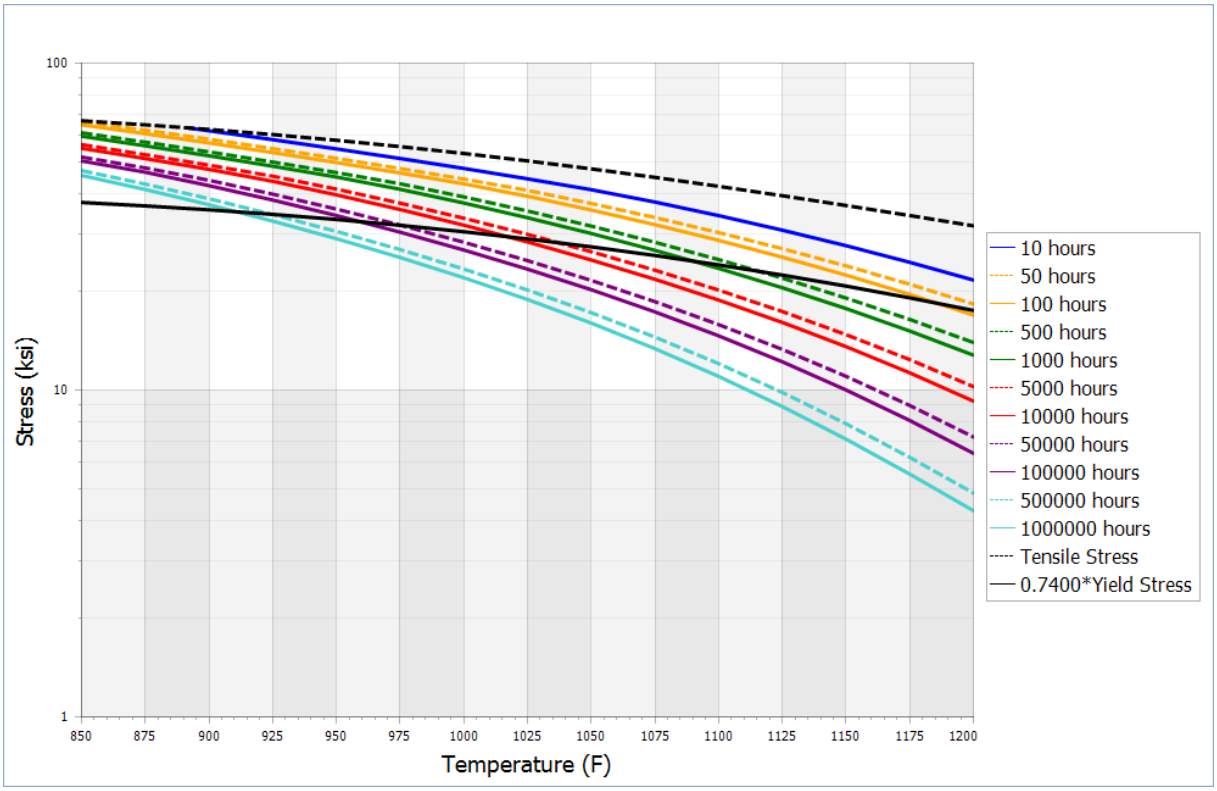

Figure 10B.17 – Level 1 Screening Curve for 10.5Cr–V (Alloy 115 UNSK91060)

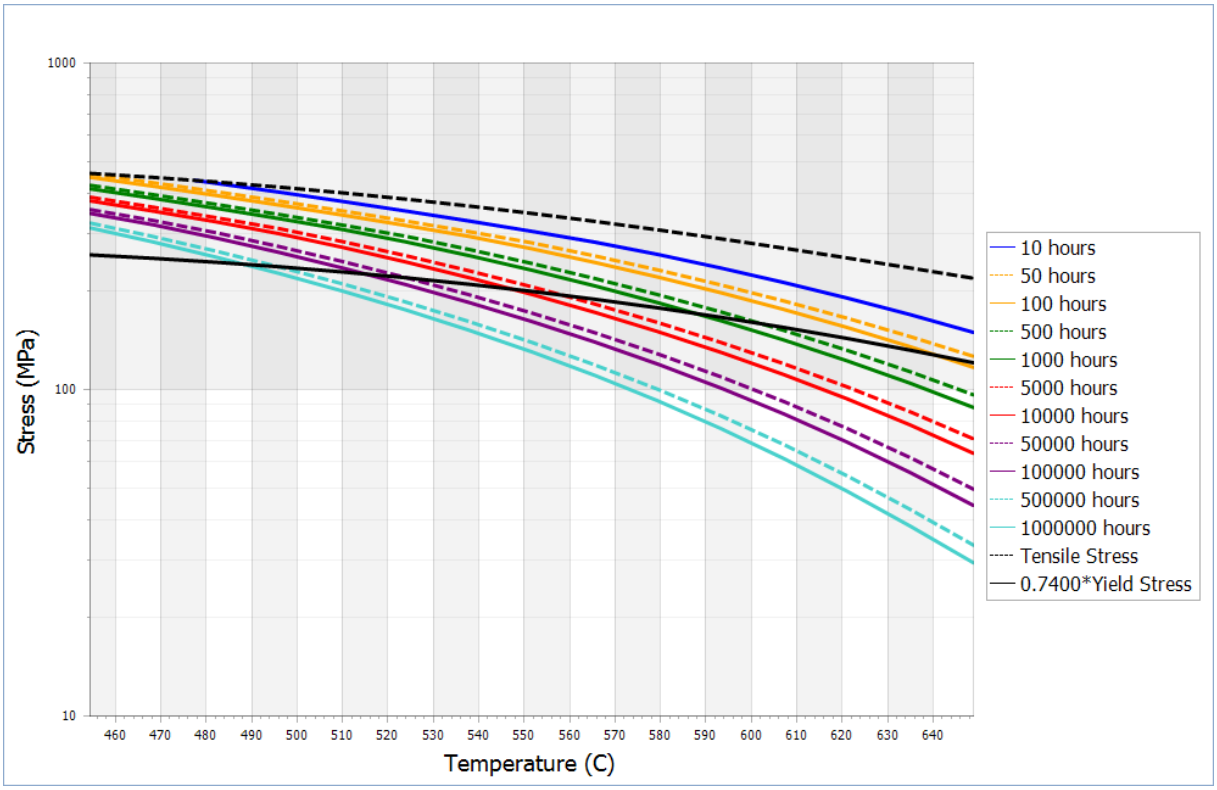

Figure 10B.17M – Level 1 Screening Curve for 10.5Cr–V (Alloy 115 UNSK91060)

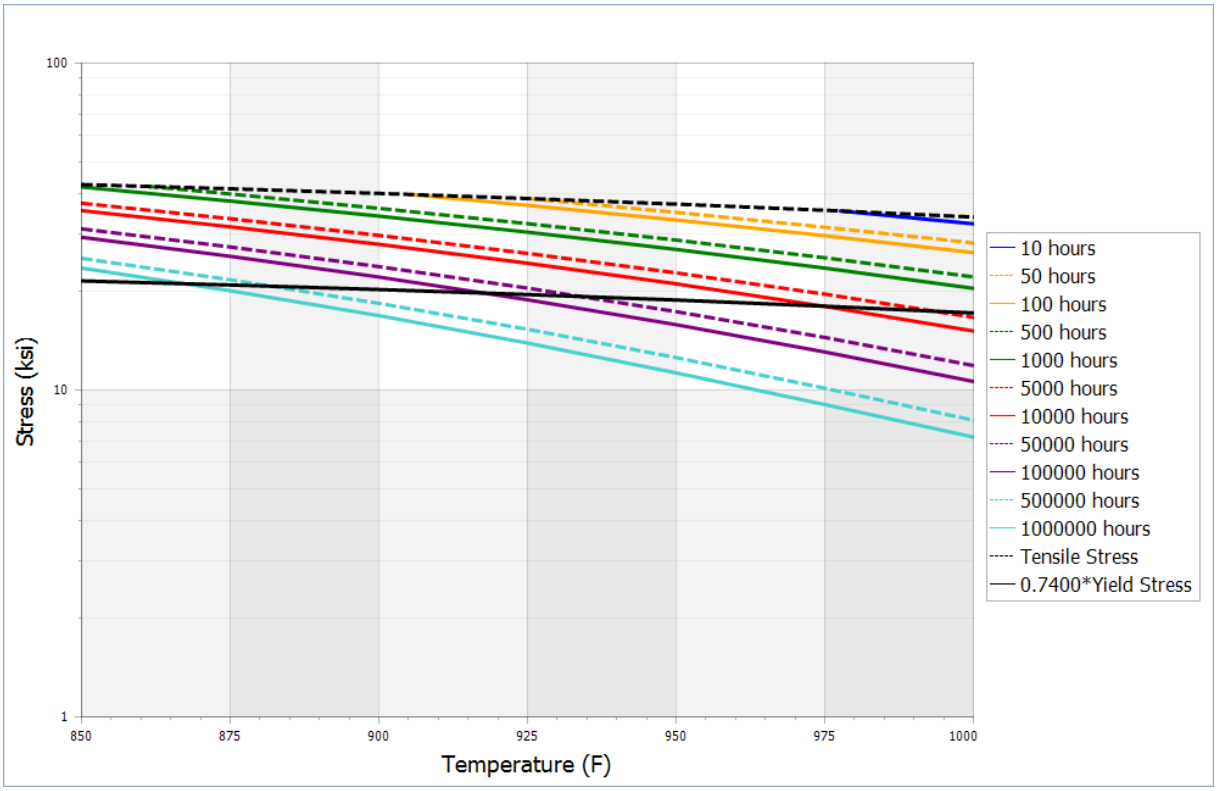

Figure 10B.18 – Level 1 Screening Curve for 12Cr

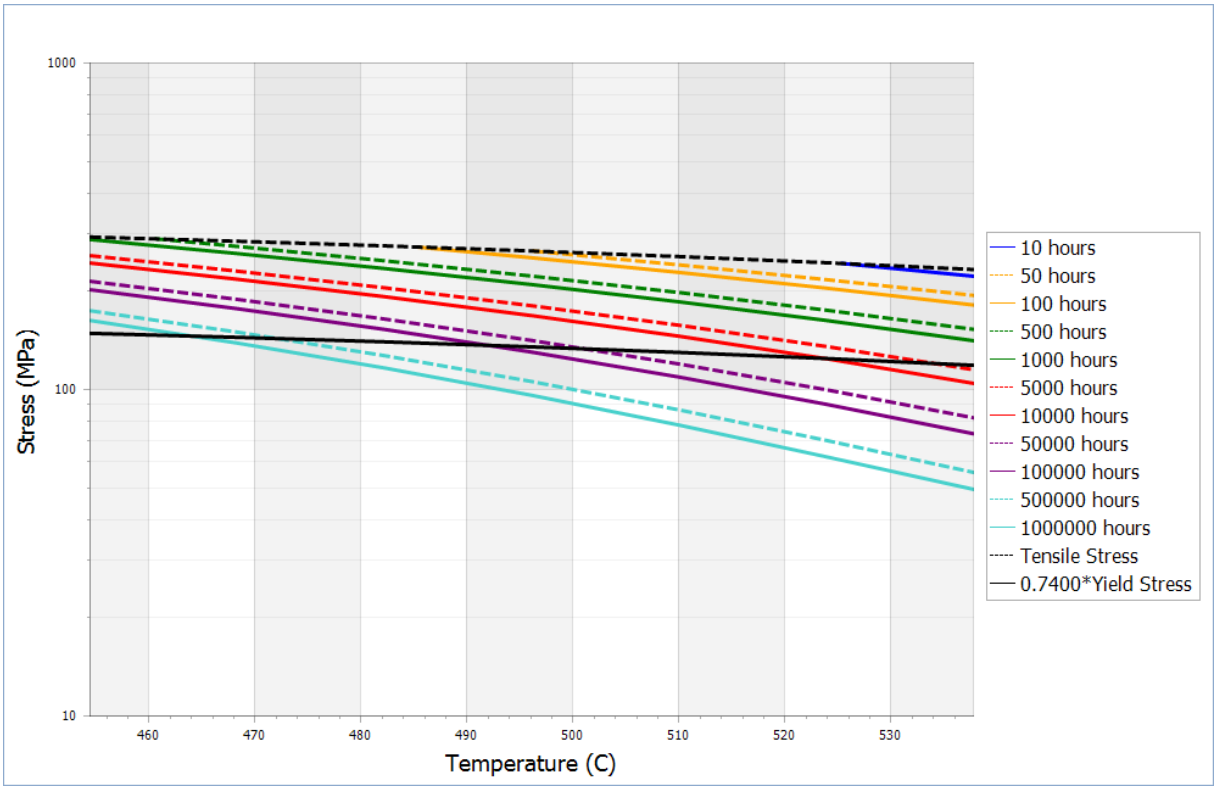

Figure 10B.18M – Level 1 Screening Curve for 12Cr

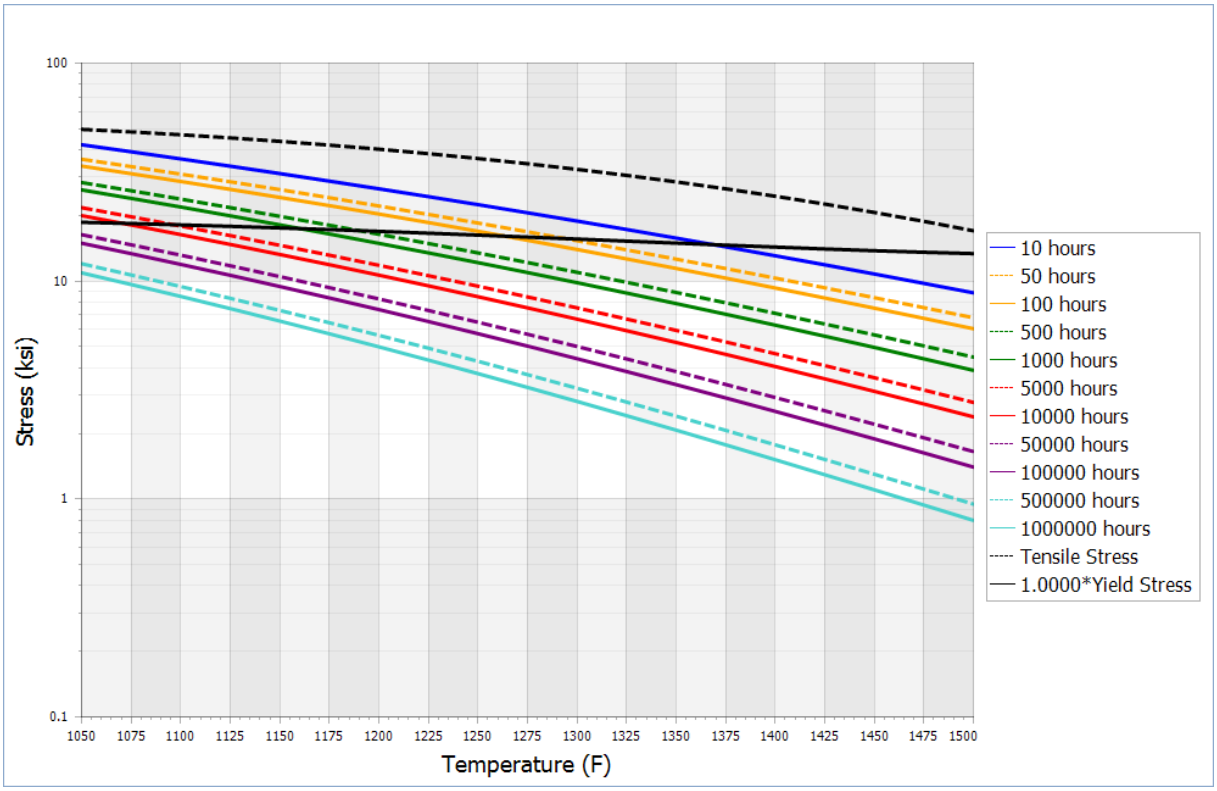

Figure 10B.19 – Level 1 Screening Curve for Type 304 and 304H SS

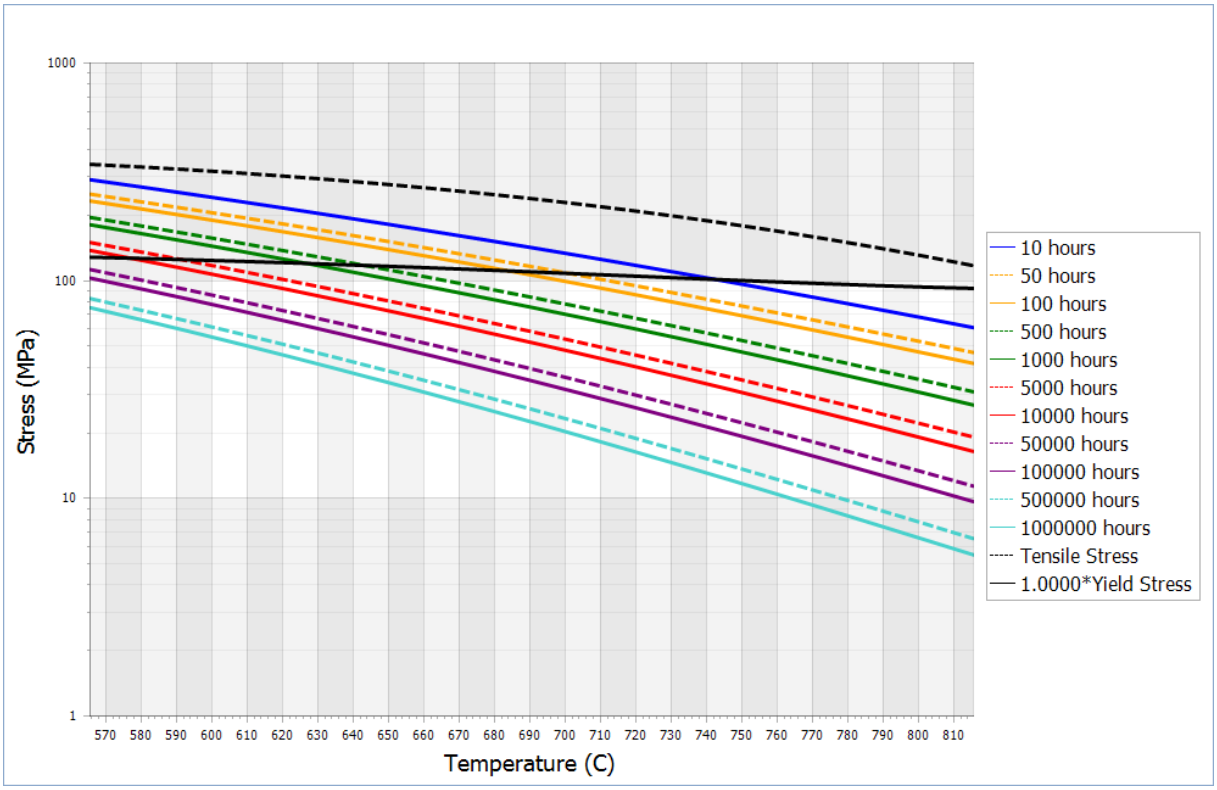

Figure 10B.19M – Level 1 Screening Curve for Type 304 and 304H SS

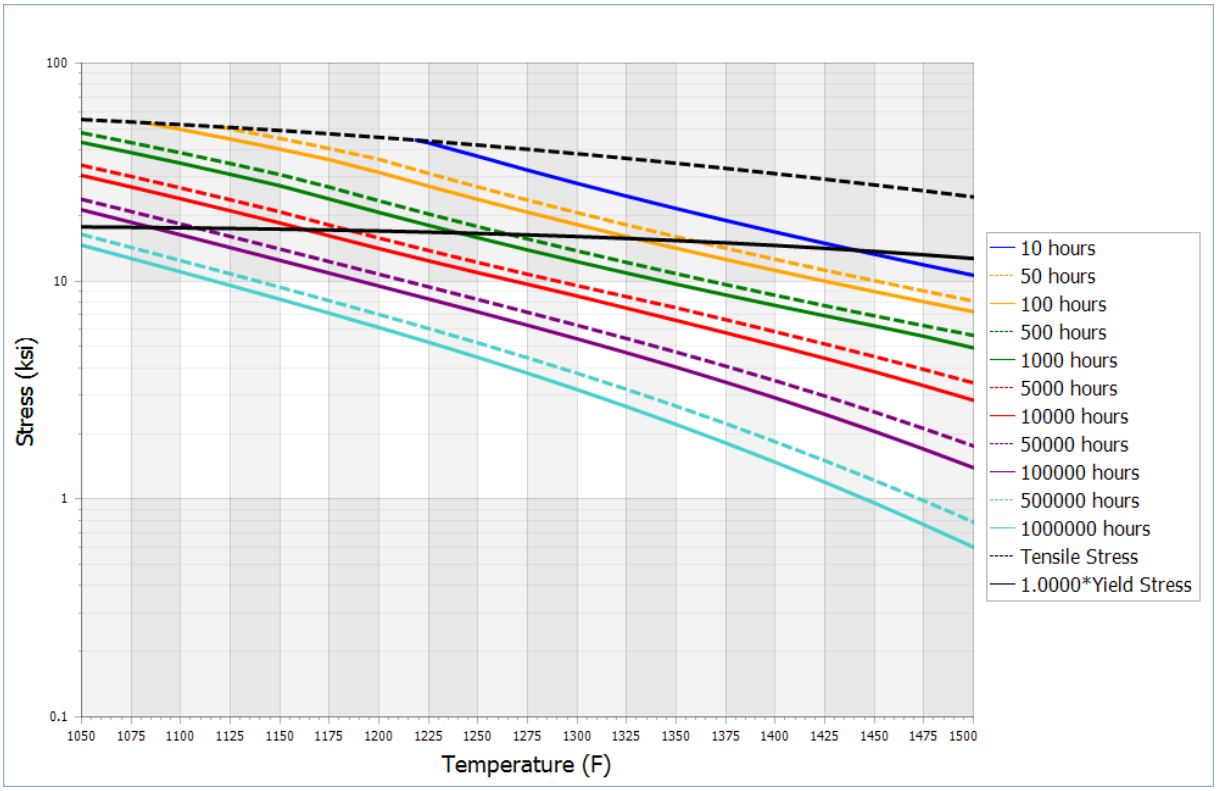

Figure 10B.20 – Level 1 Screening Curve for Type 316 and 316H SS

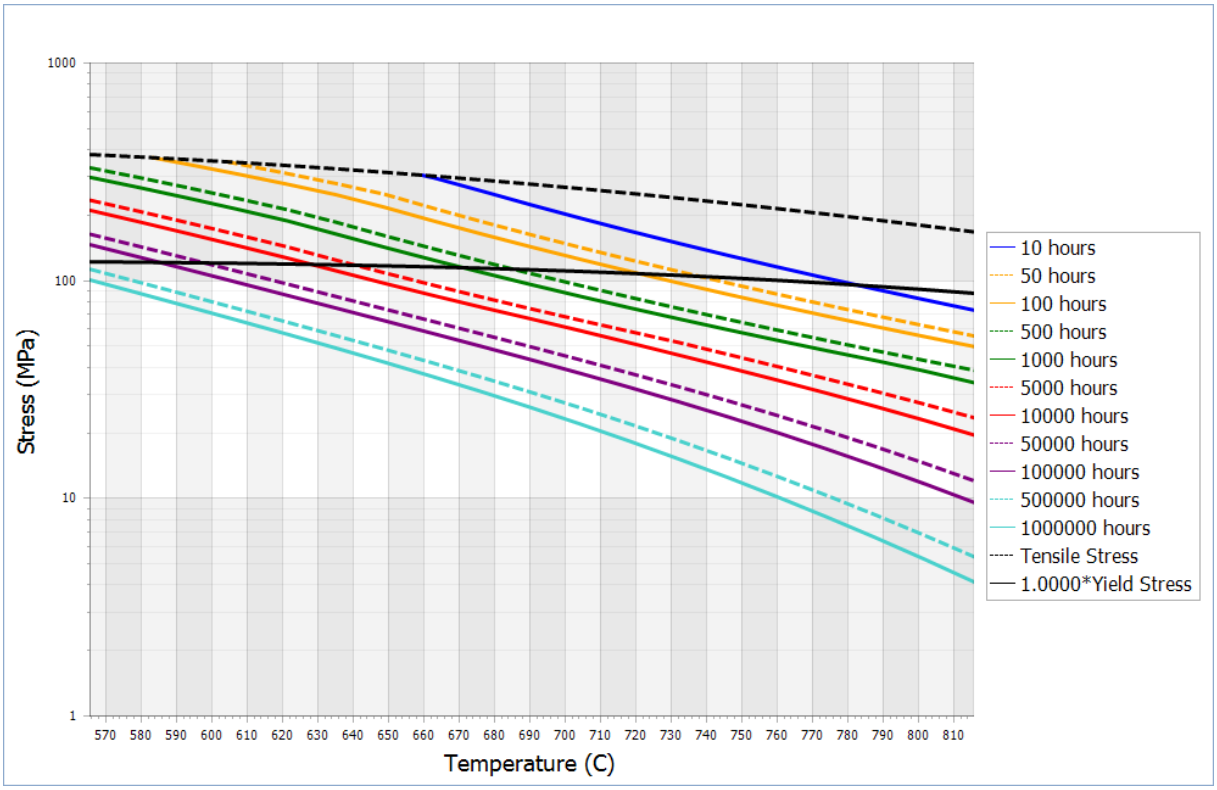

Figure 10B.20M – Level 1 Screening Curve for Type 316 and 316H SS

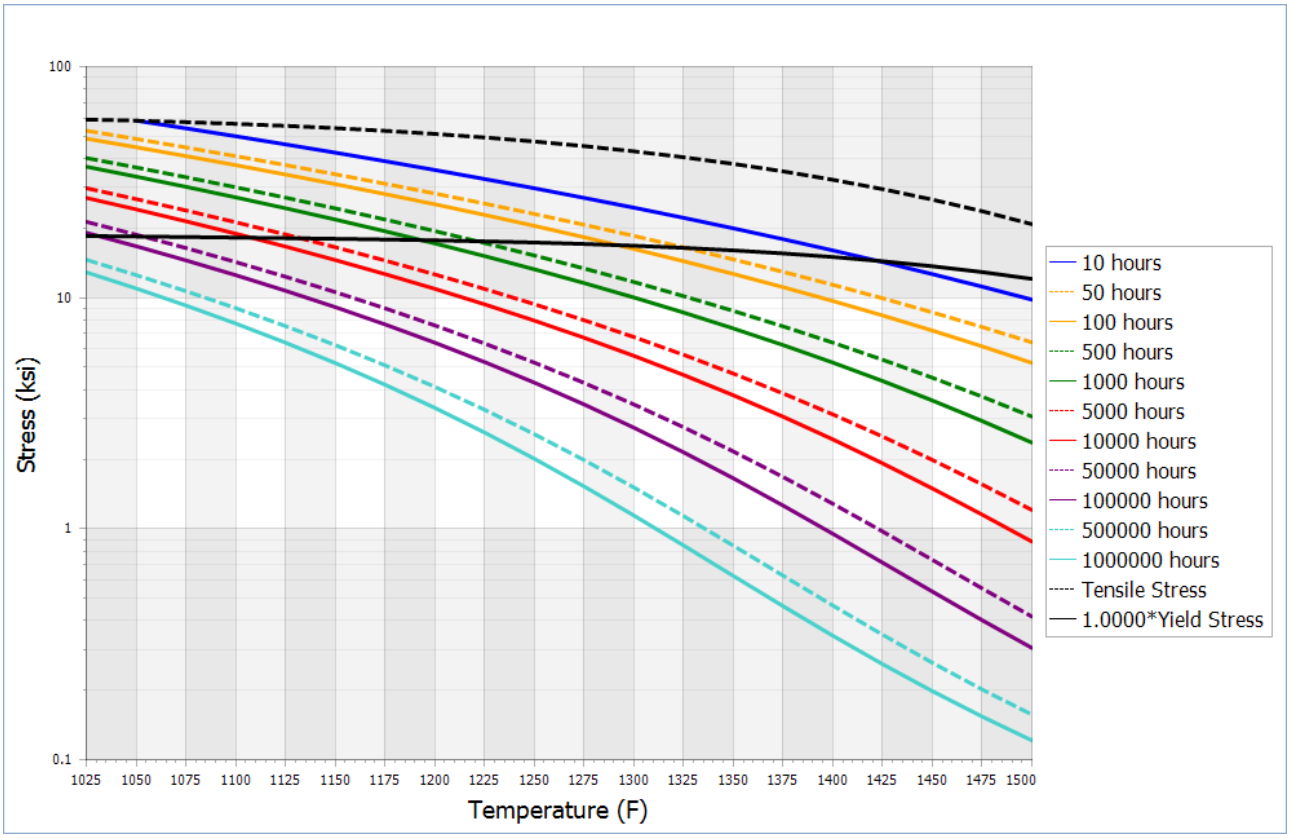

Figure 10B.21 – Level 1 Screening Curve for Type 321 SS

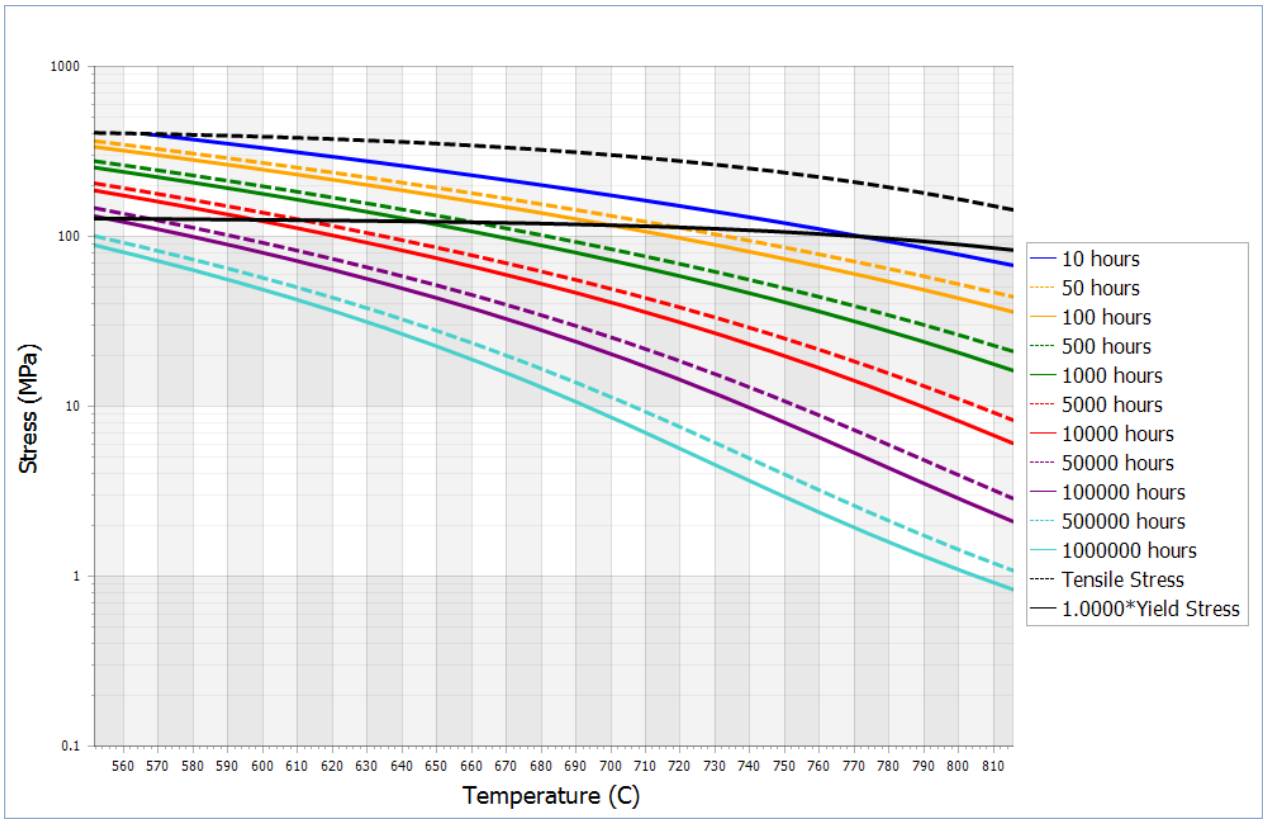

Figure 10B.21M – Level 1 Screening Curve for Type 321 SS

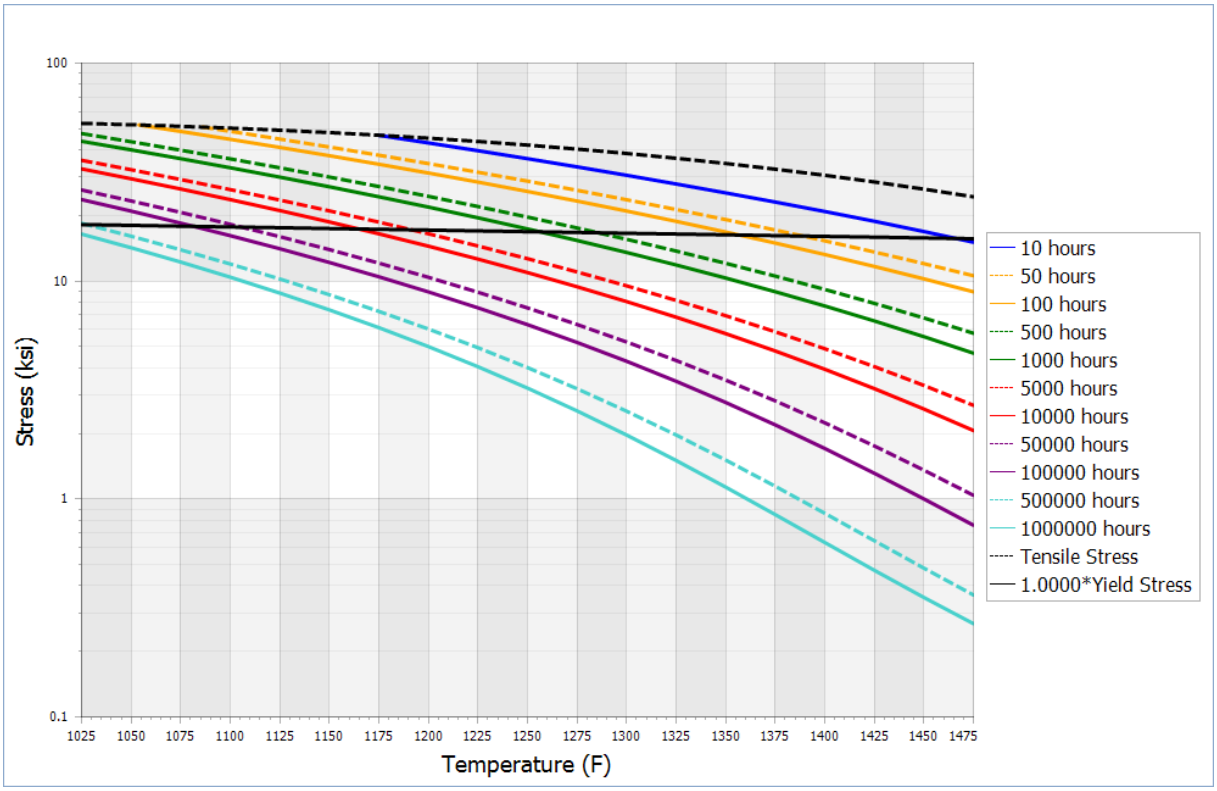

Figure 10B.22 – Level 1 Screening Curve for Type 321H SS

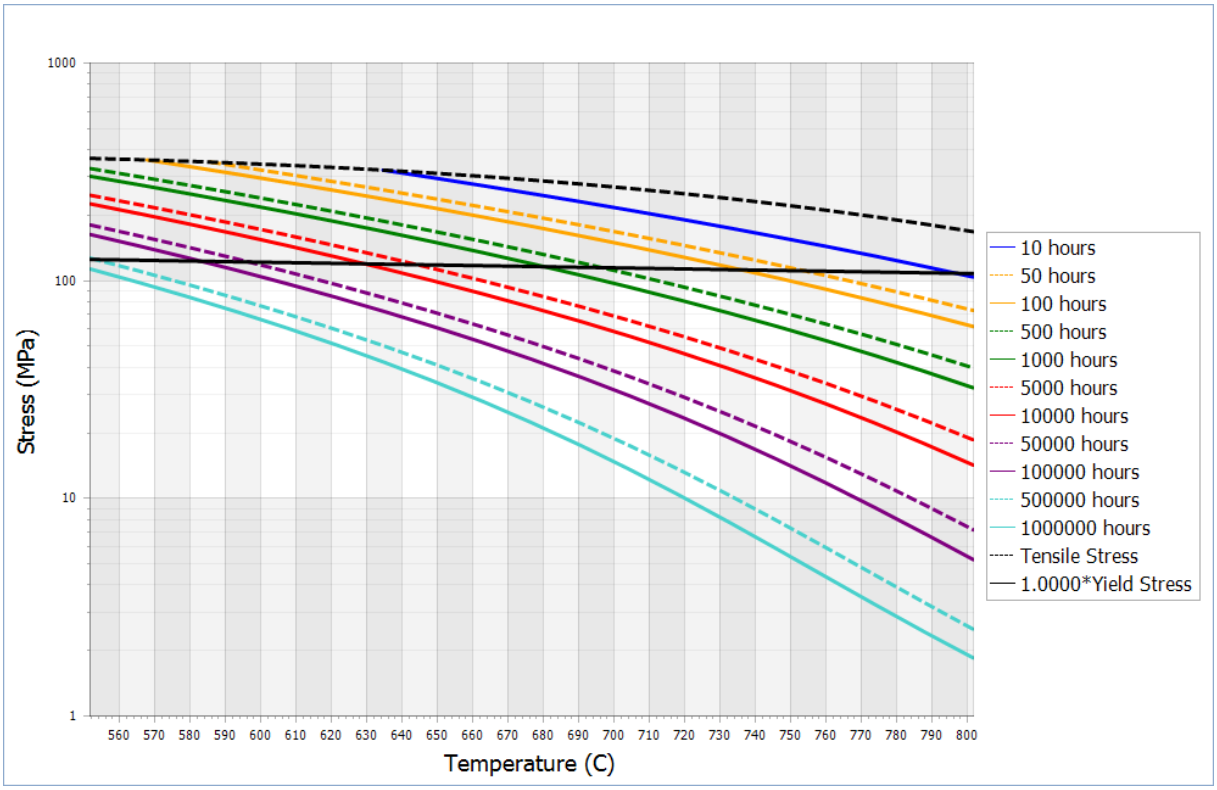

Figure 10B.22M – Level 1 Screening Curve for Type 321H SS

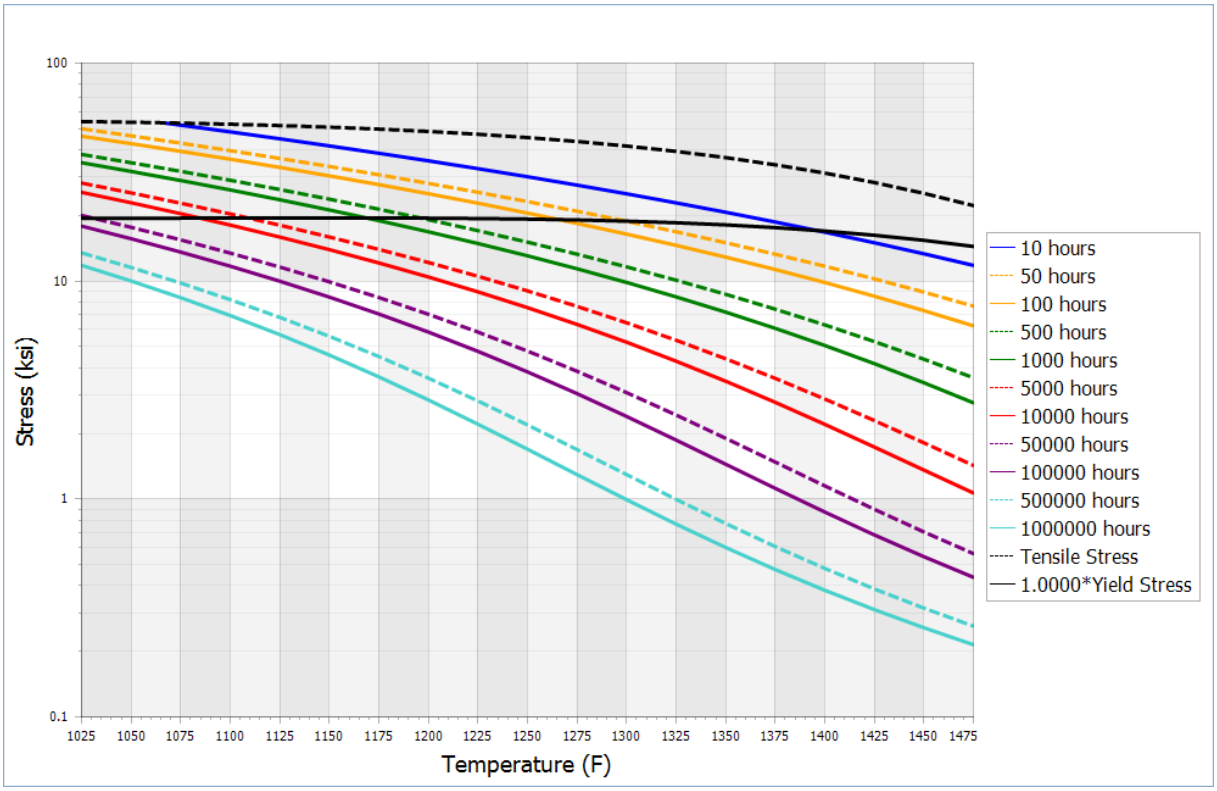

Figure 10B.23 – Level 1 Screening Curve for Type 347 SS

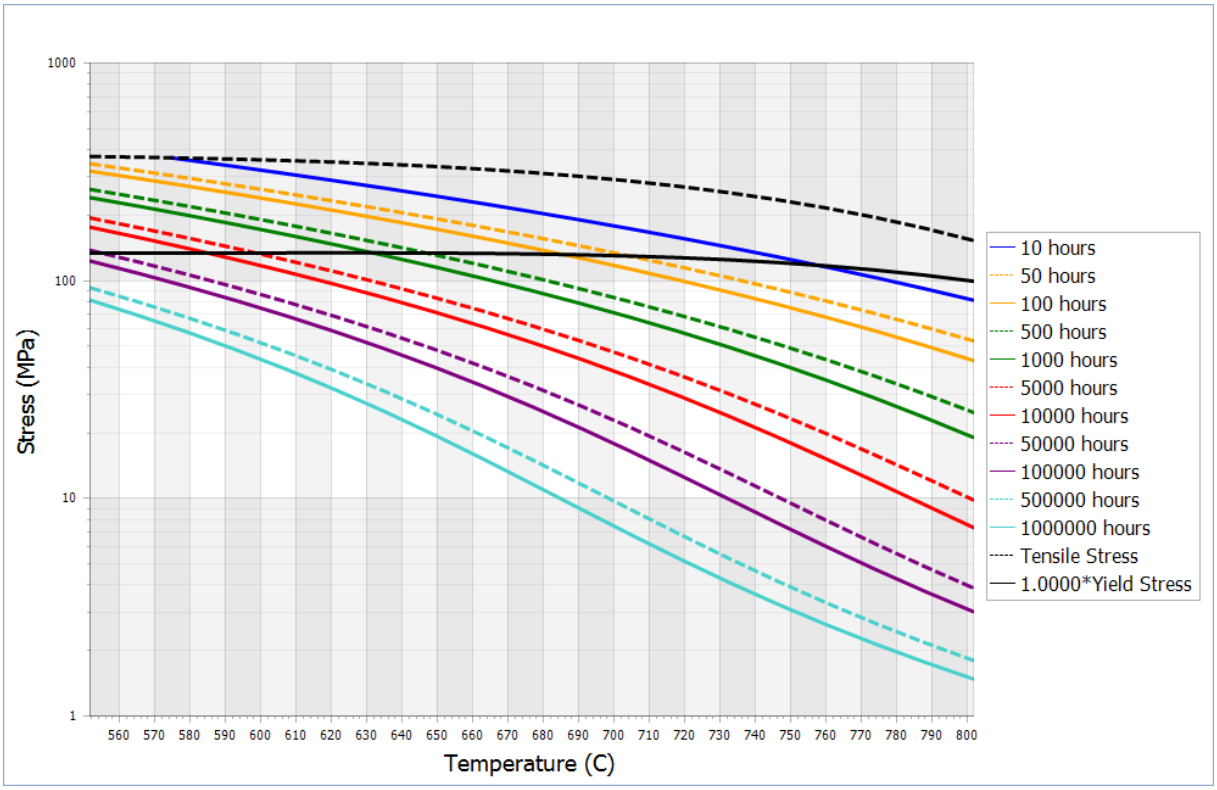

Figure 10B.23M – Level 1 Screening Curve for Type 347 SS

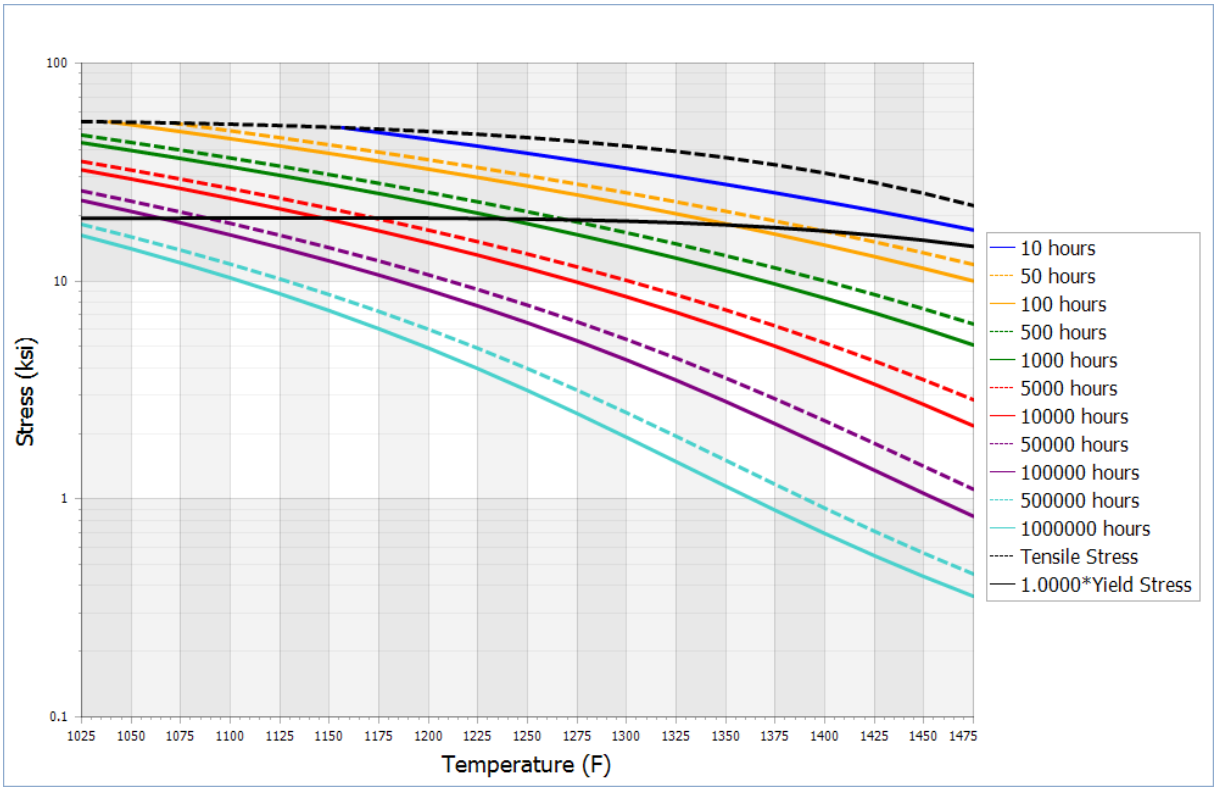

Figure 10B.24 – Level 1 Screening Curve for Type 347H SS

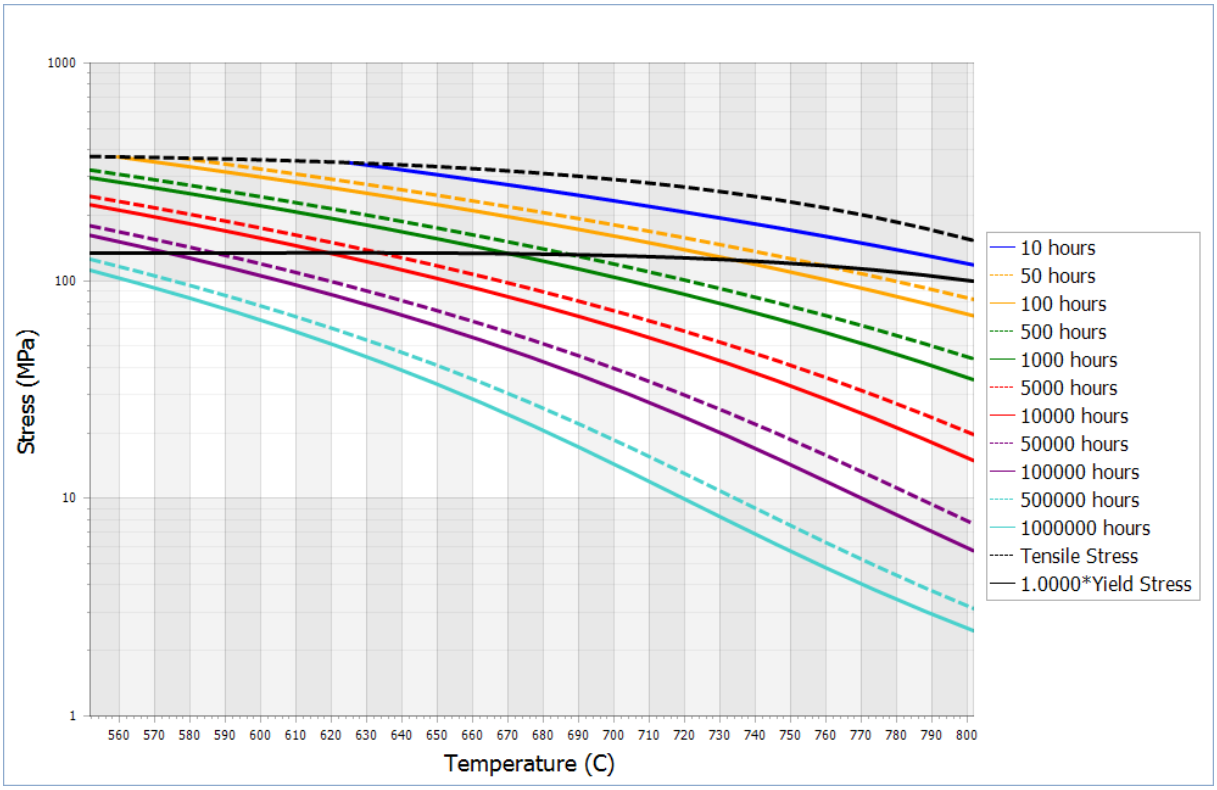

Figure 10B.24M – Level 1 Screening Curve for Type 347H SS

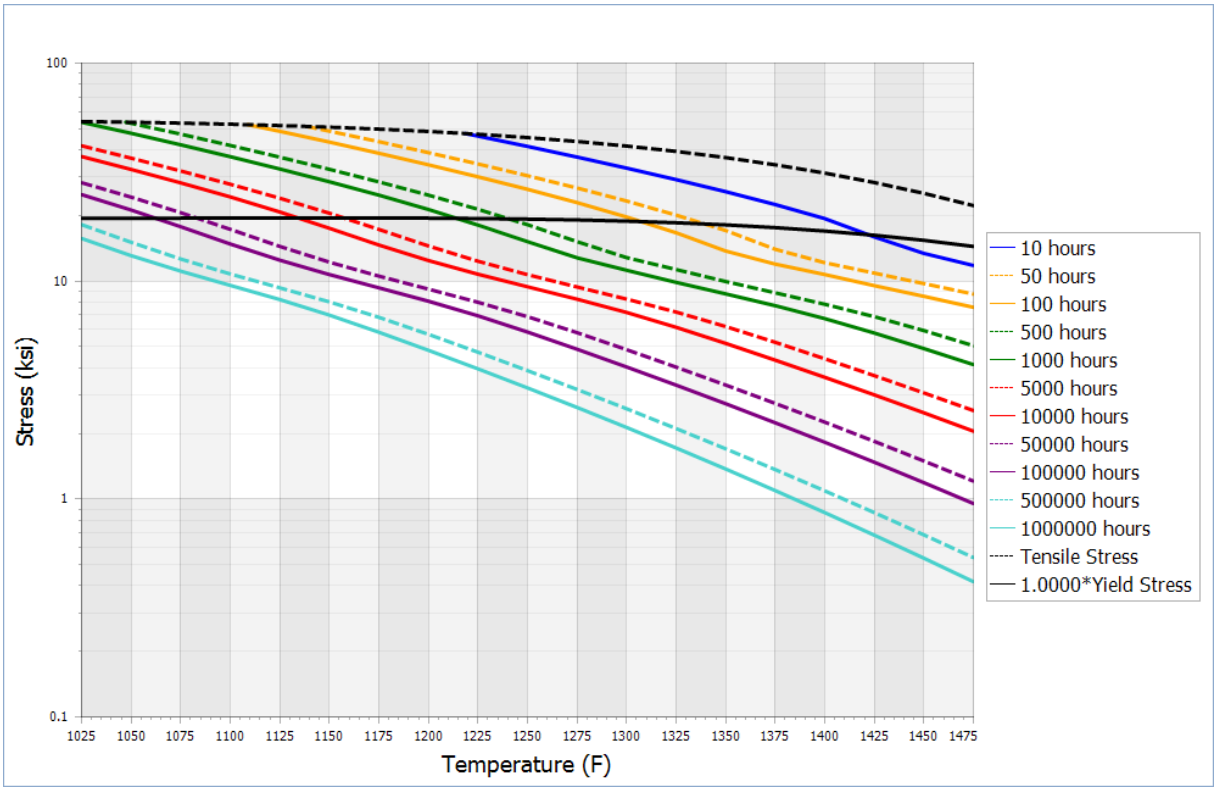

Figure 10B.25 – Level 1 Screening Curve for Type 347LN SS (UNS S34751)

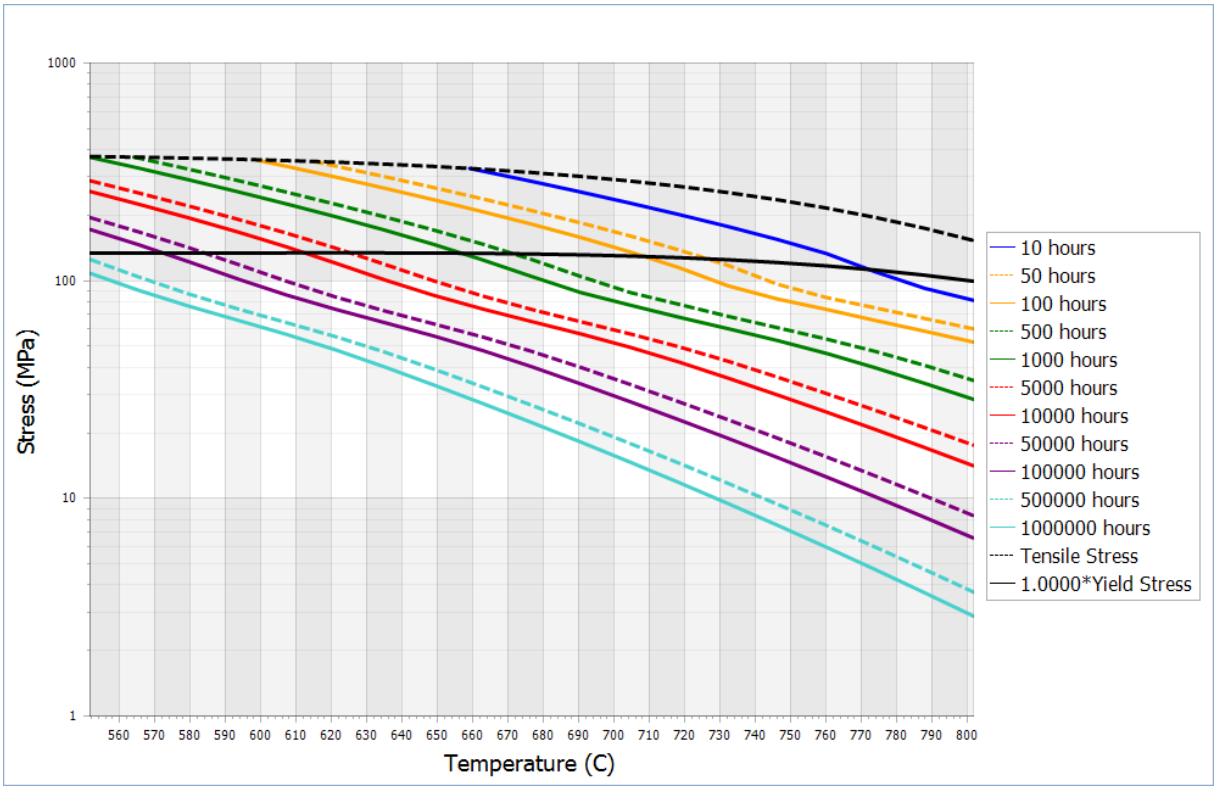

Figure 10B.25M – Level 1 Screening Curve for Type 347LN SS (UNS S34751)

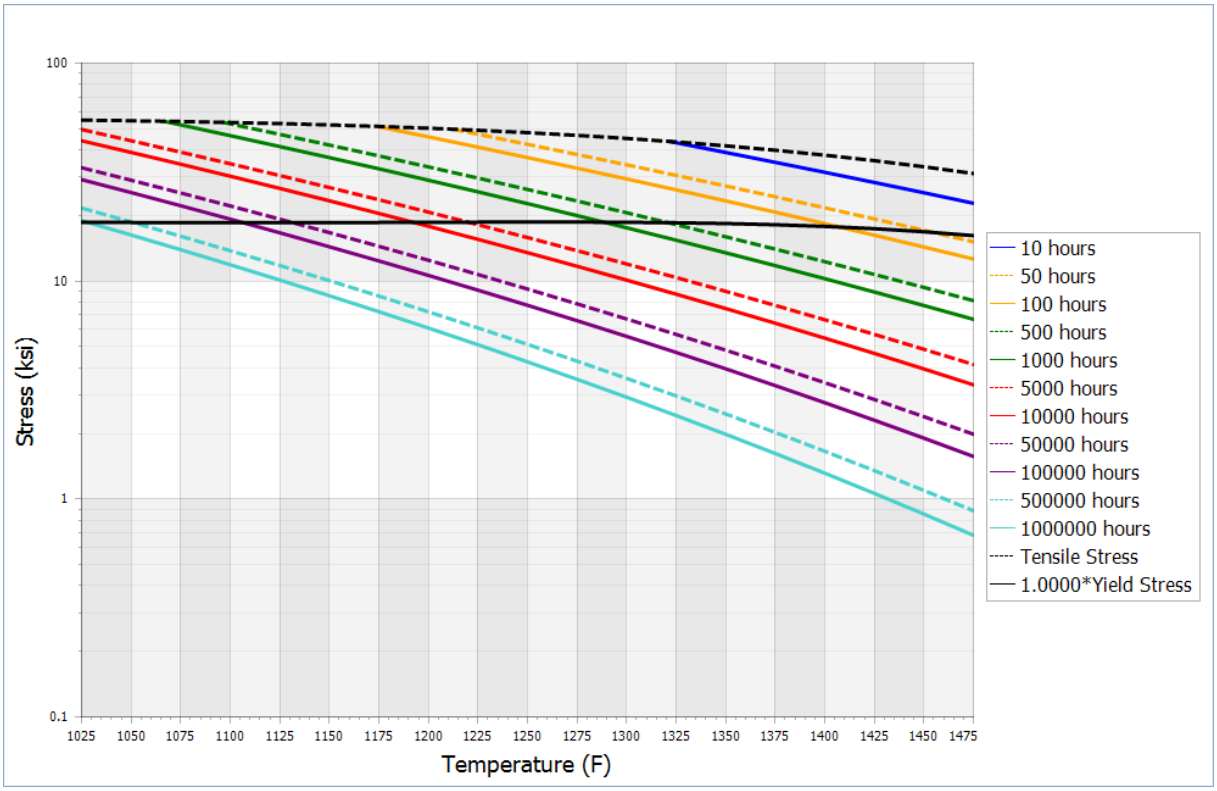

Figure 10B.26 – Level 1 Screening Curve for Type 347AP Advanced SS (UNS S34751)

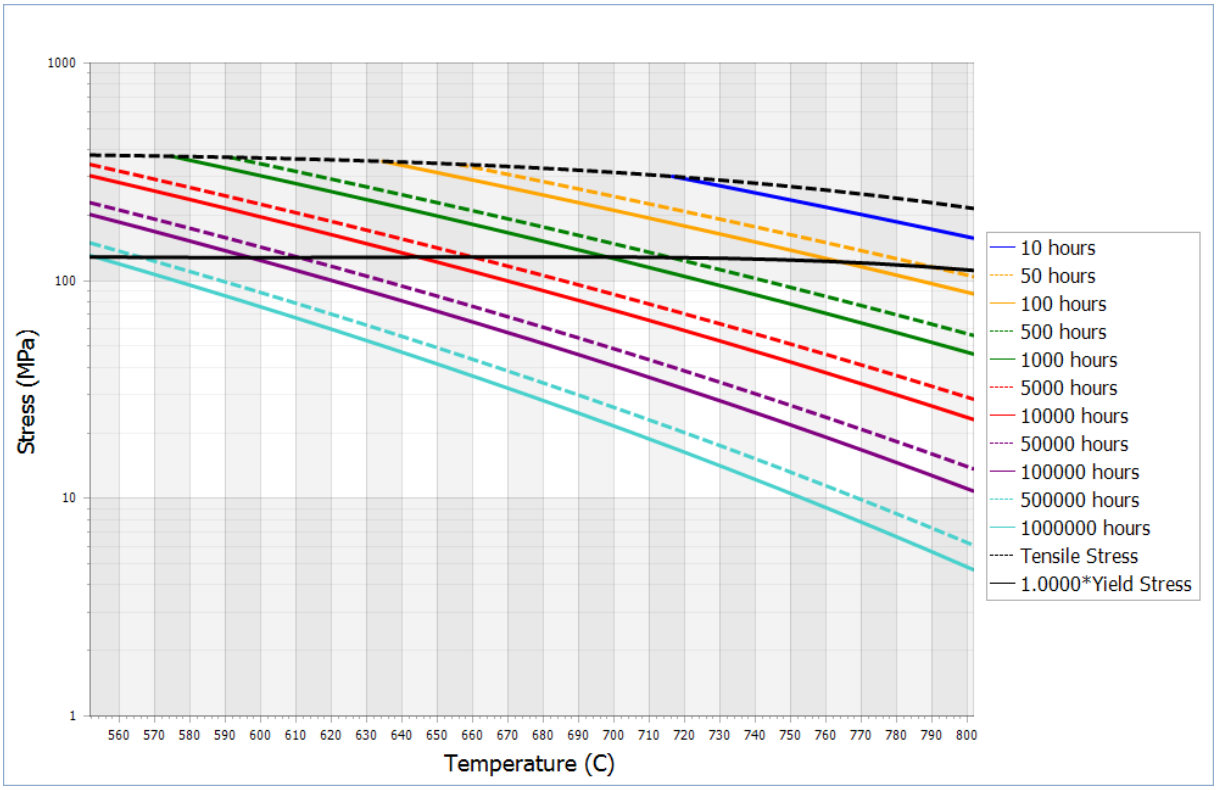

Figure 10B.26M – Level 1 Screening Curve for Type 347AP Advanced SS (UNS S34751)

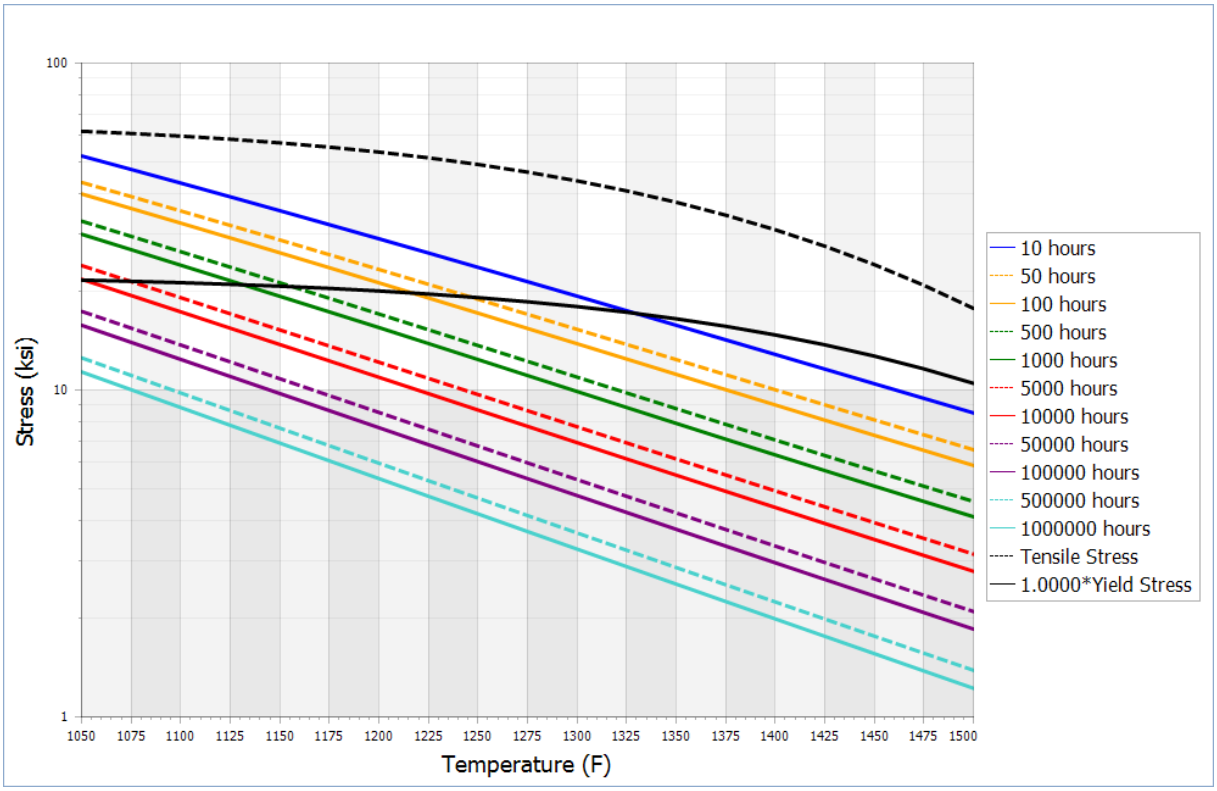

Figure 10B.27 – Level 1 Screening Curve for Alloy 800

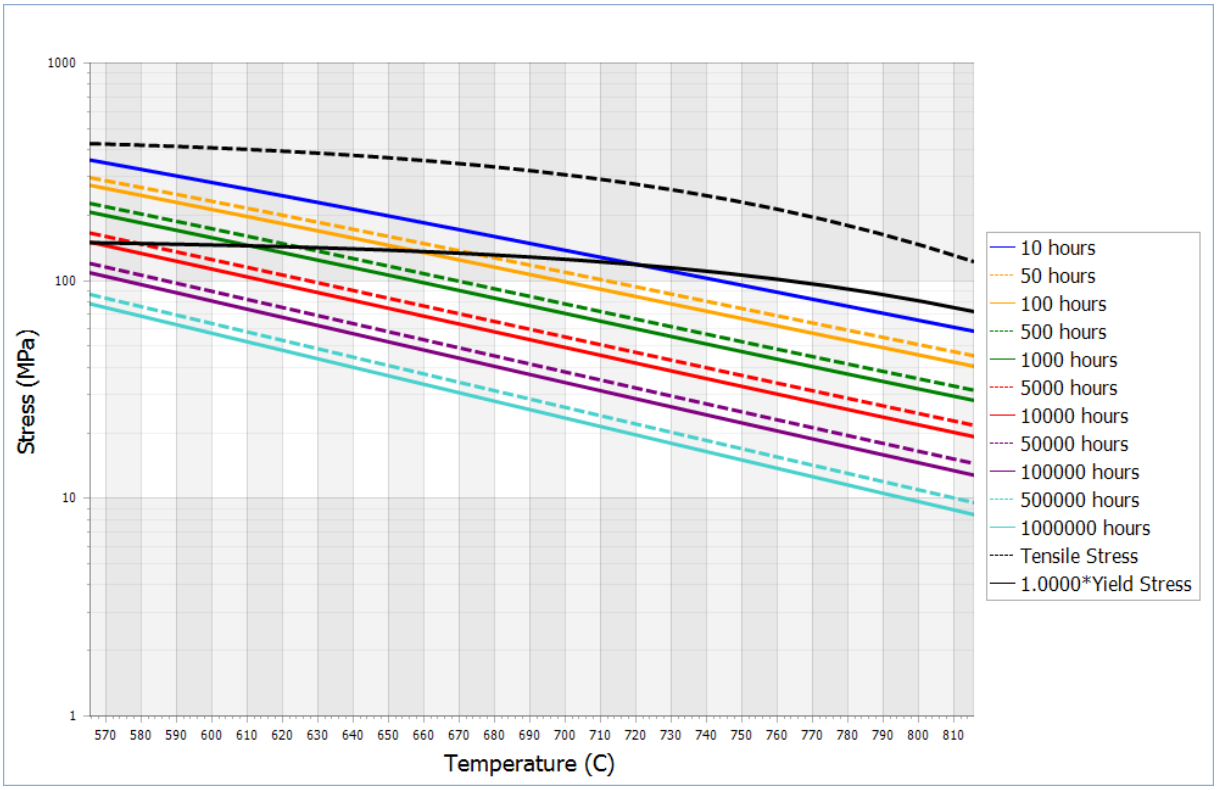

Figure 10B.27M – Level 1 Screening Curve for Alloy 800

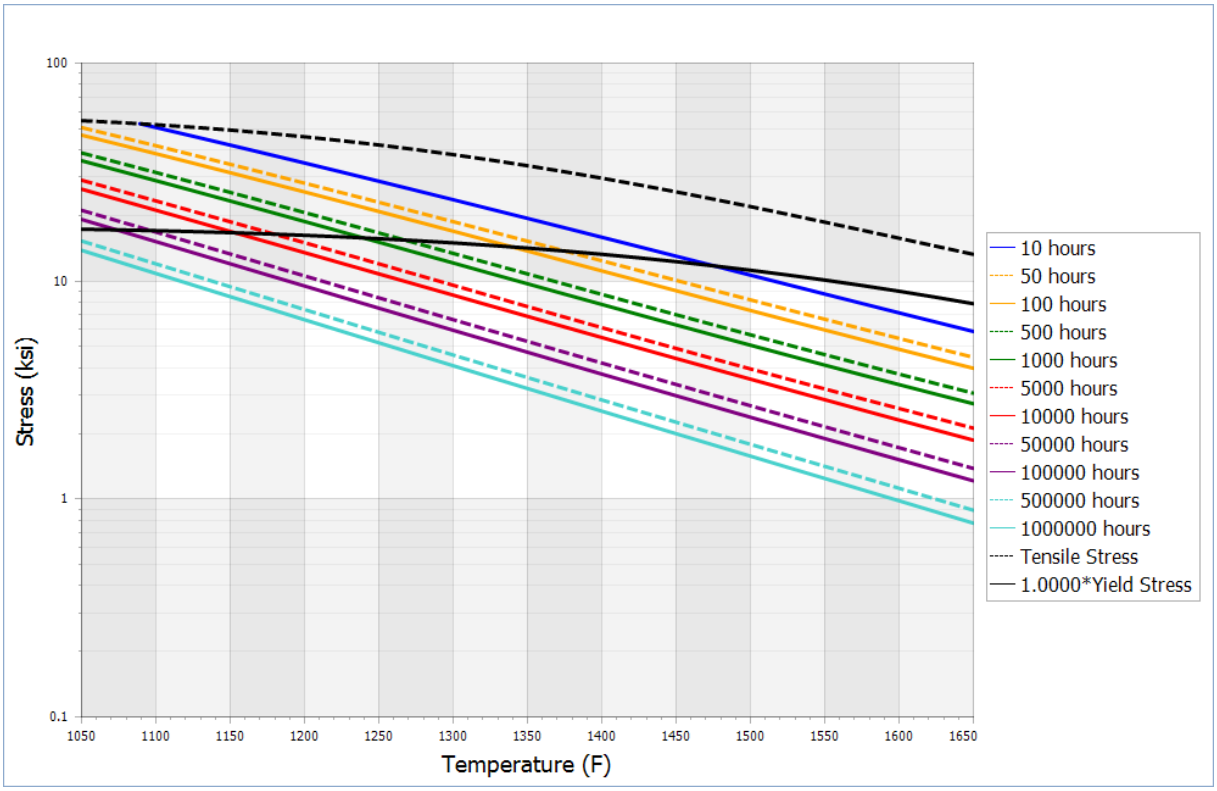

Figure 10B.28 – Level 1 Screening Curve for Alloy 800H

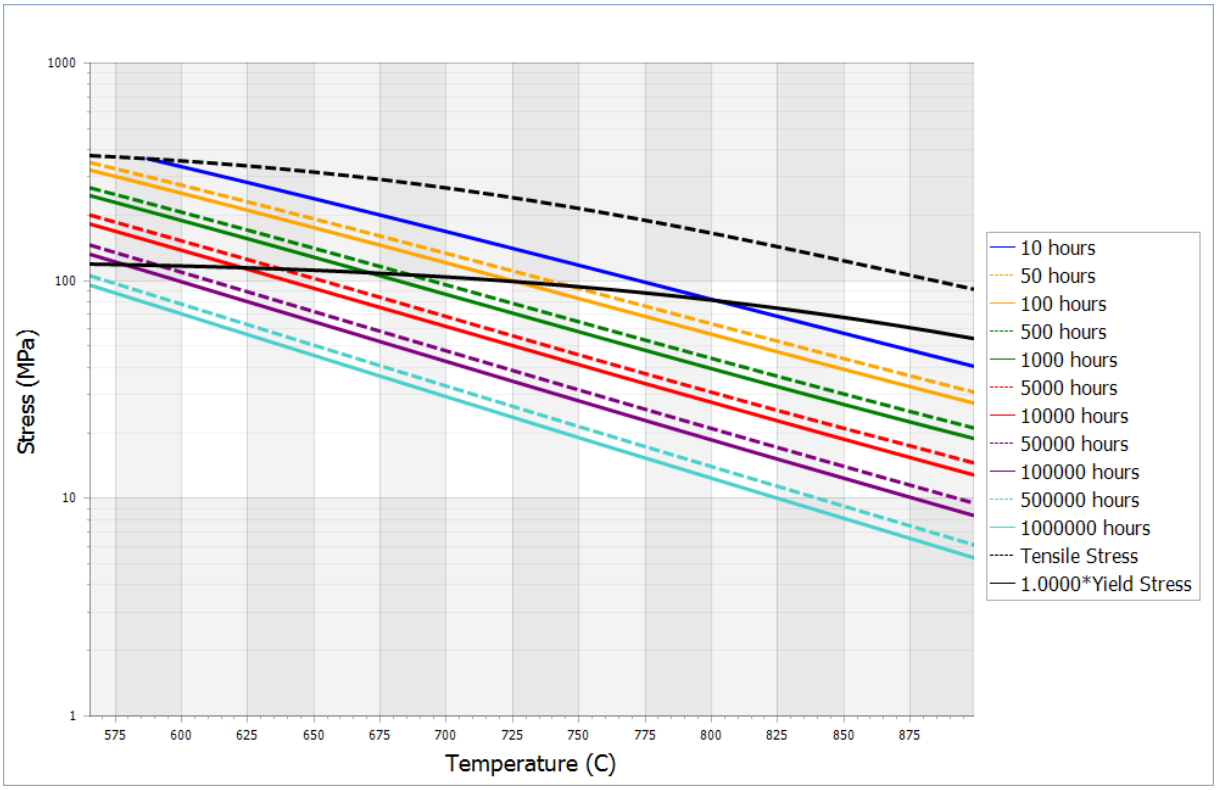

Figure 10B.28M – Level 1 Screening Curve for Alloy 800H

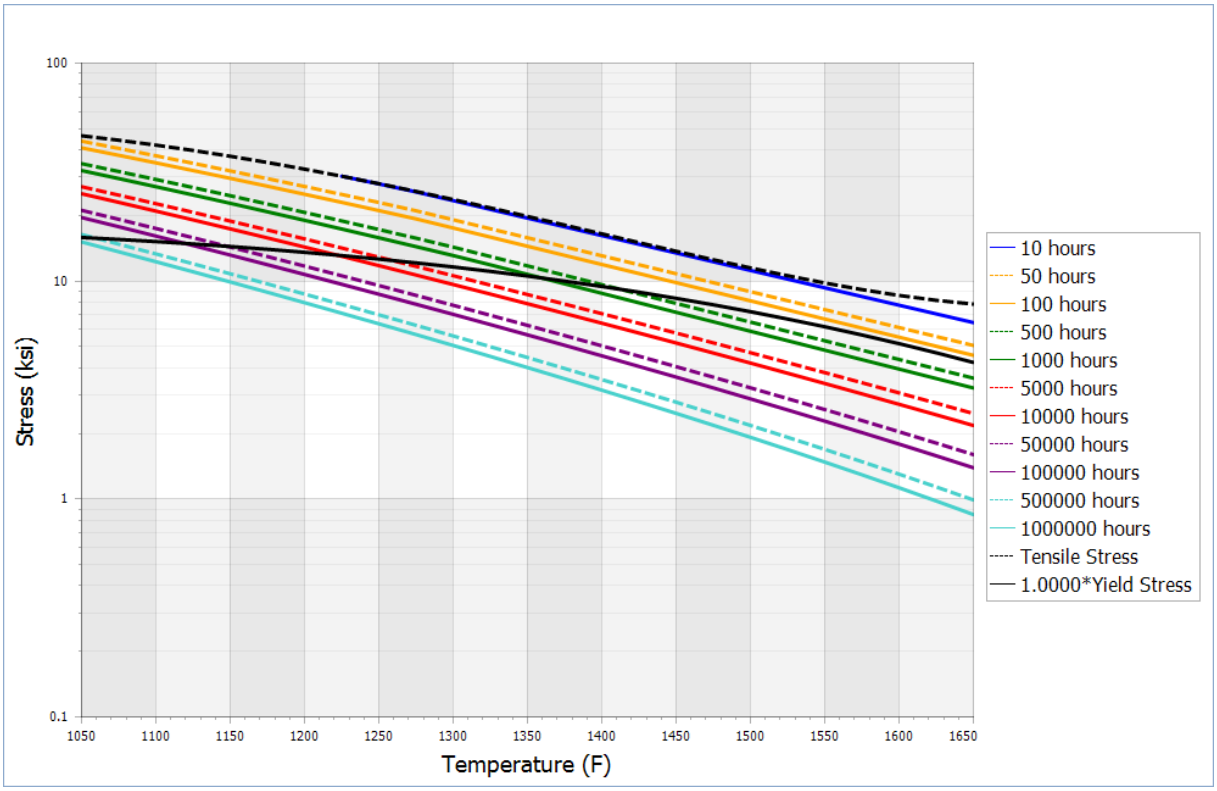

Figure 10B.29 – Level 1 Screening Curve for Alloy 800HT

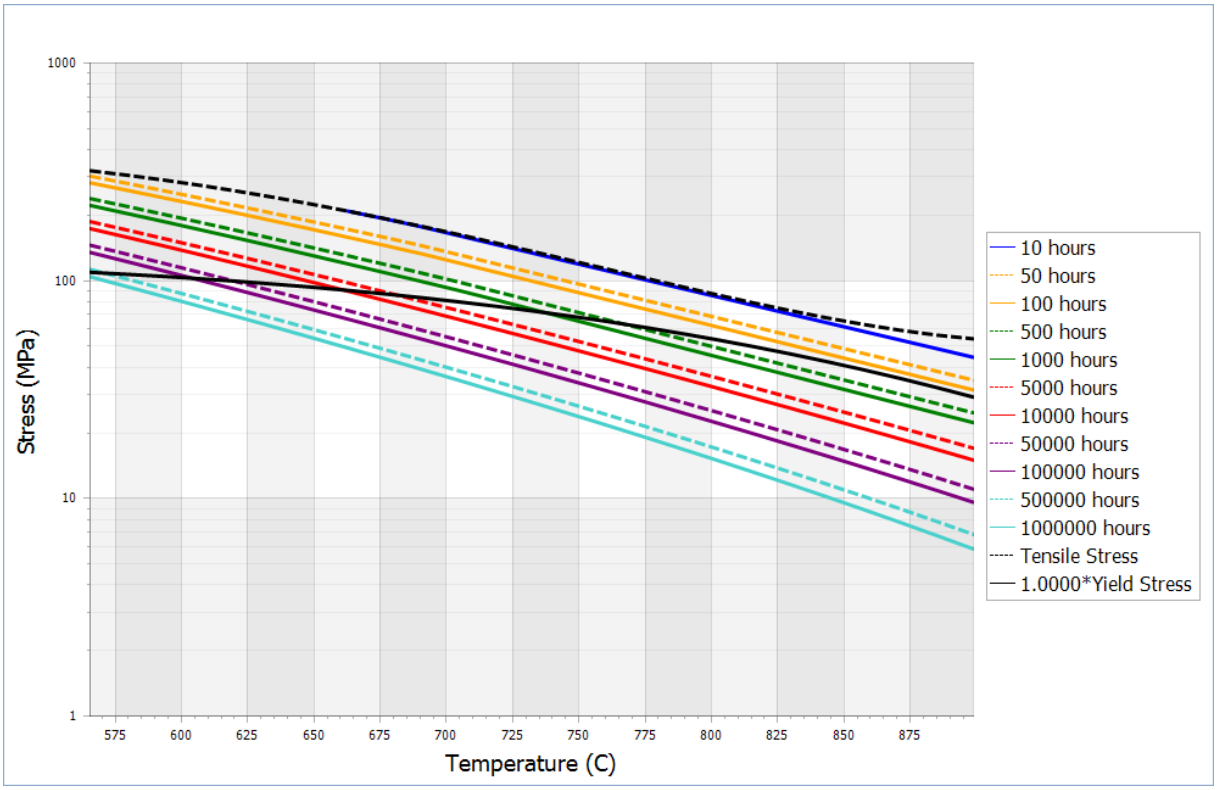

Figure 10B.29M – Level 1 Screening Curve for Alloy 800HT

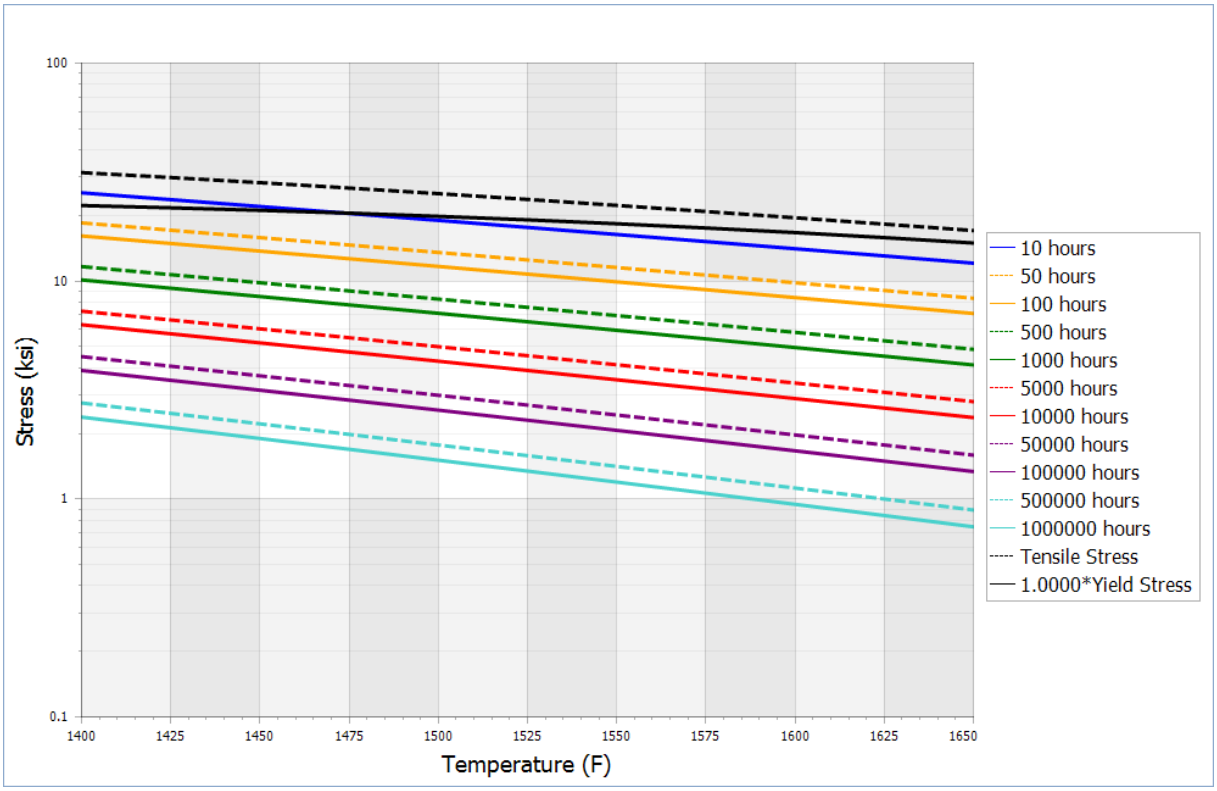

Figure 10B.30 – Level 1 Screening Curve for Alloy HK–40

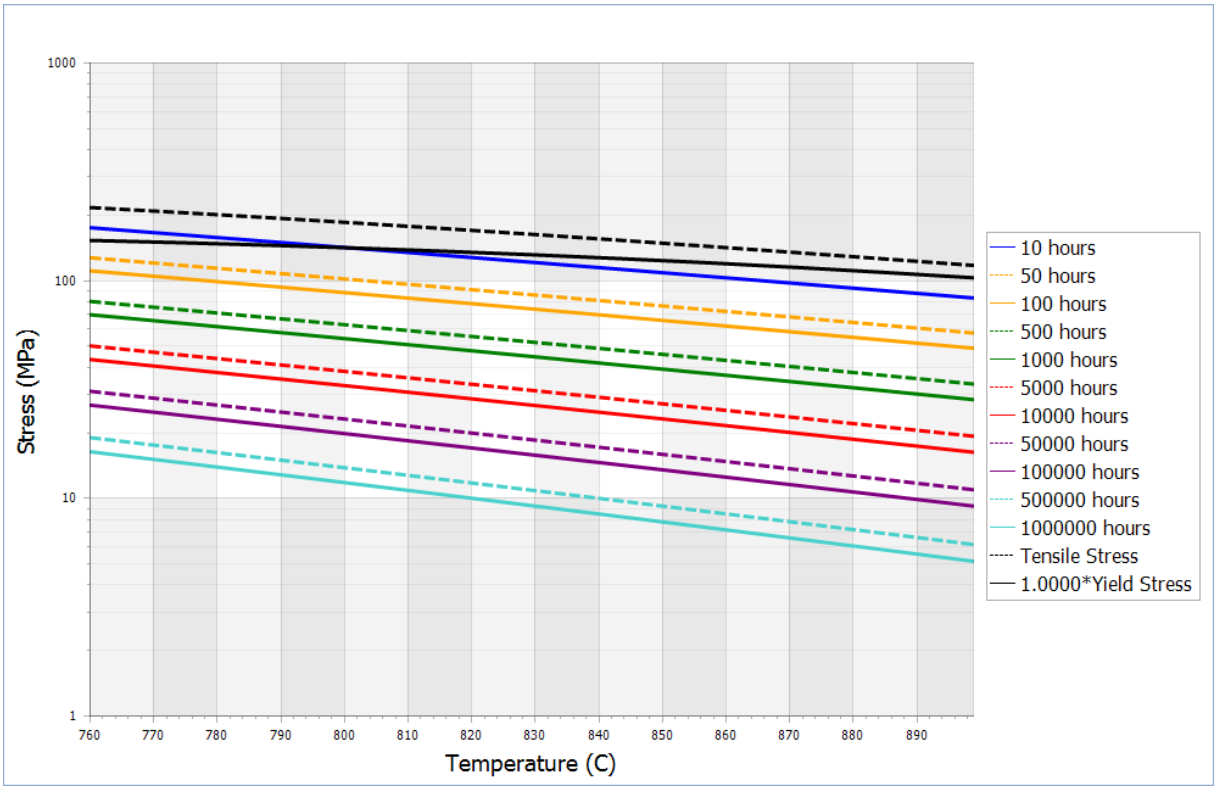

Figure 10B.30M – Level 1 Screening Curve for Alloy HK–40

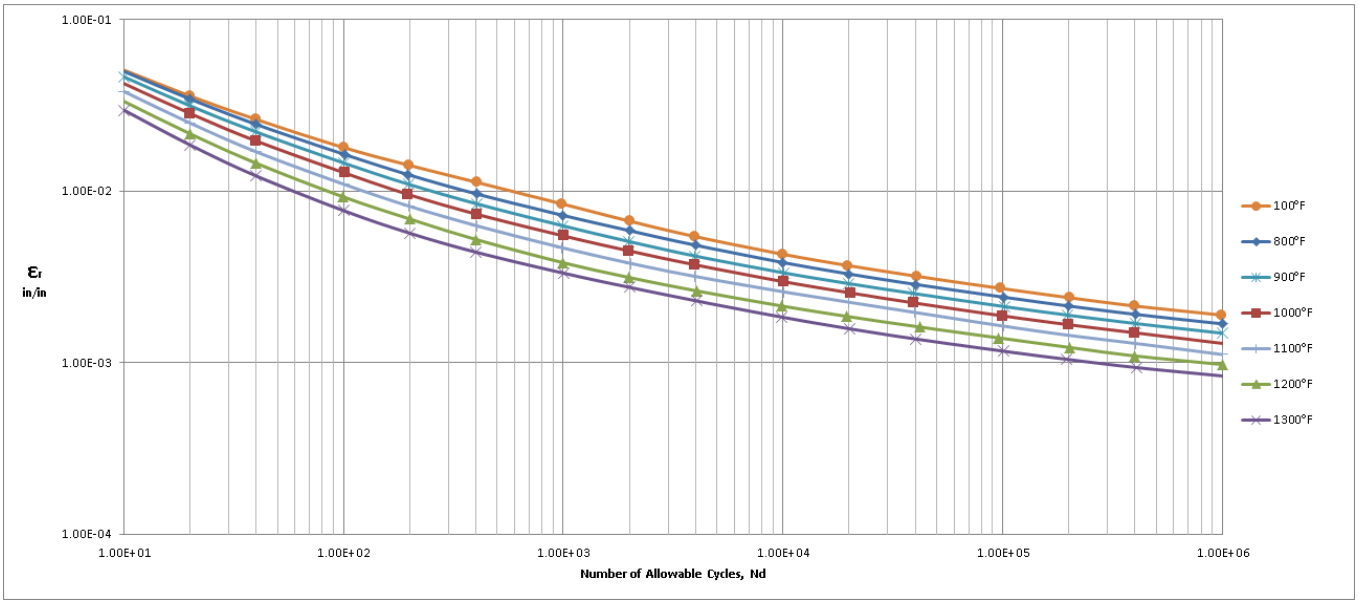

Figure 10B.31 – Fatigue Strain Range – 304 SS

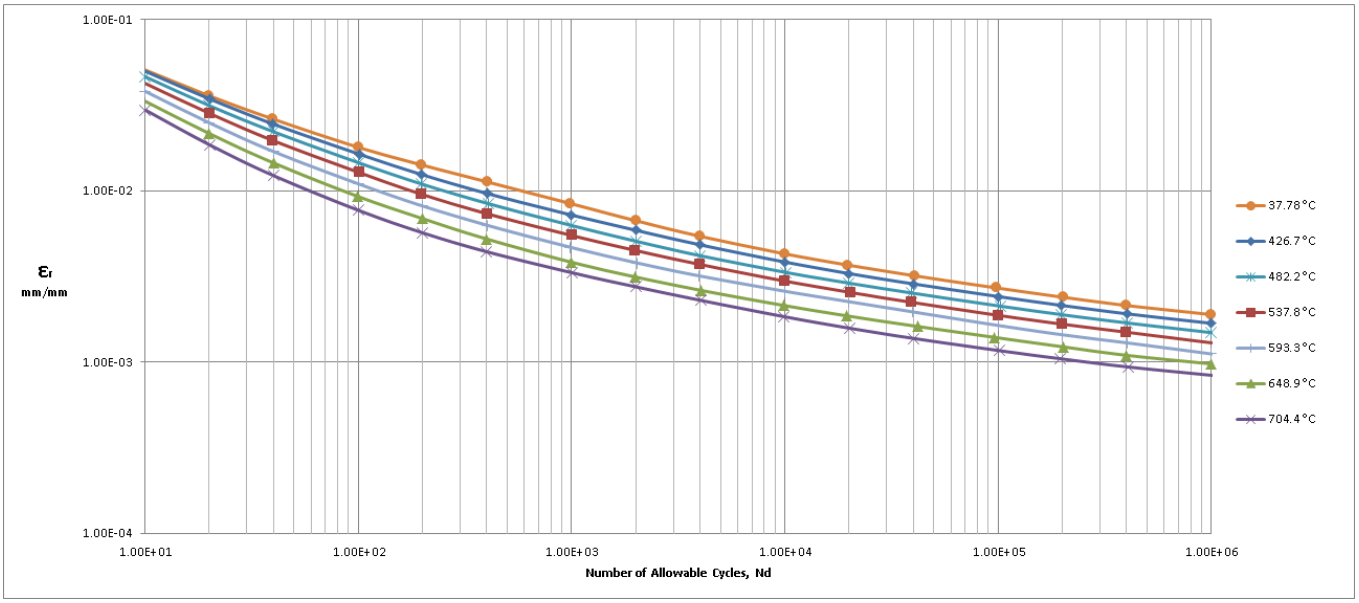

Figure 10B.31M – Fatigue Strain Range – 304 SS

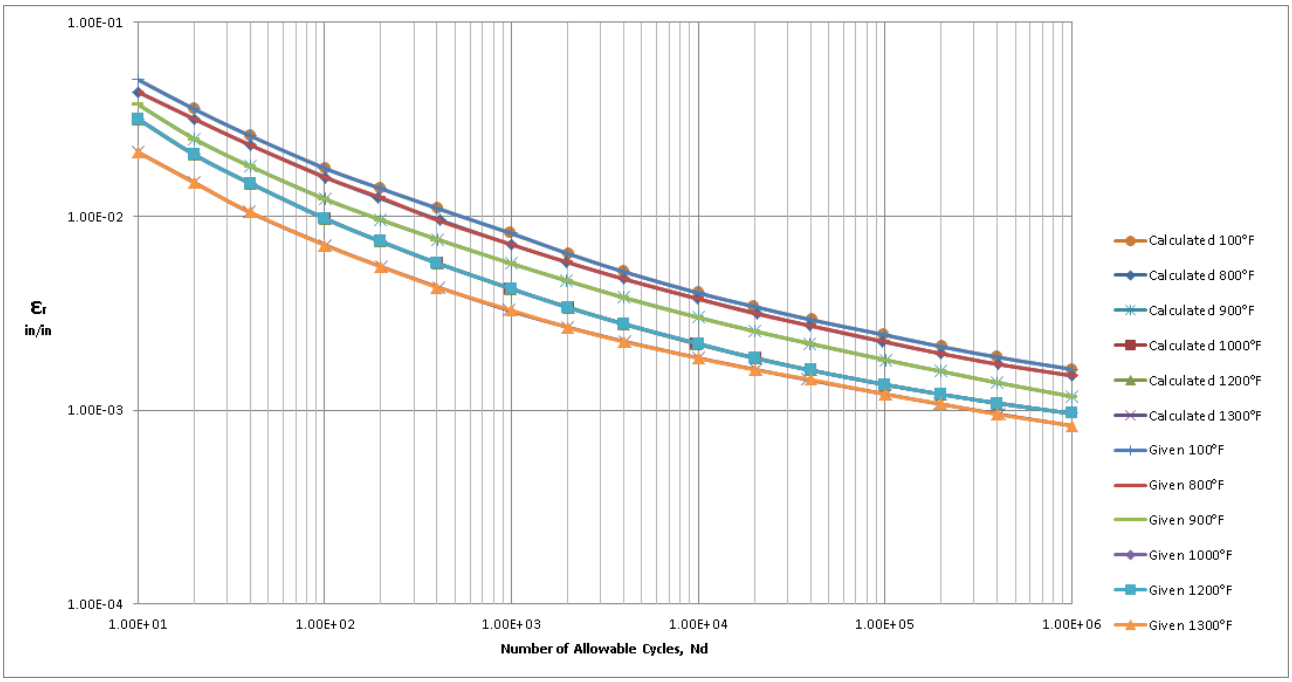

Figure 10B.32 – Fatigue Strain Range – 316 SS

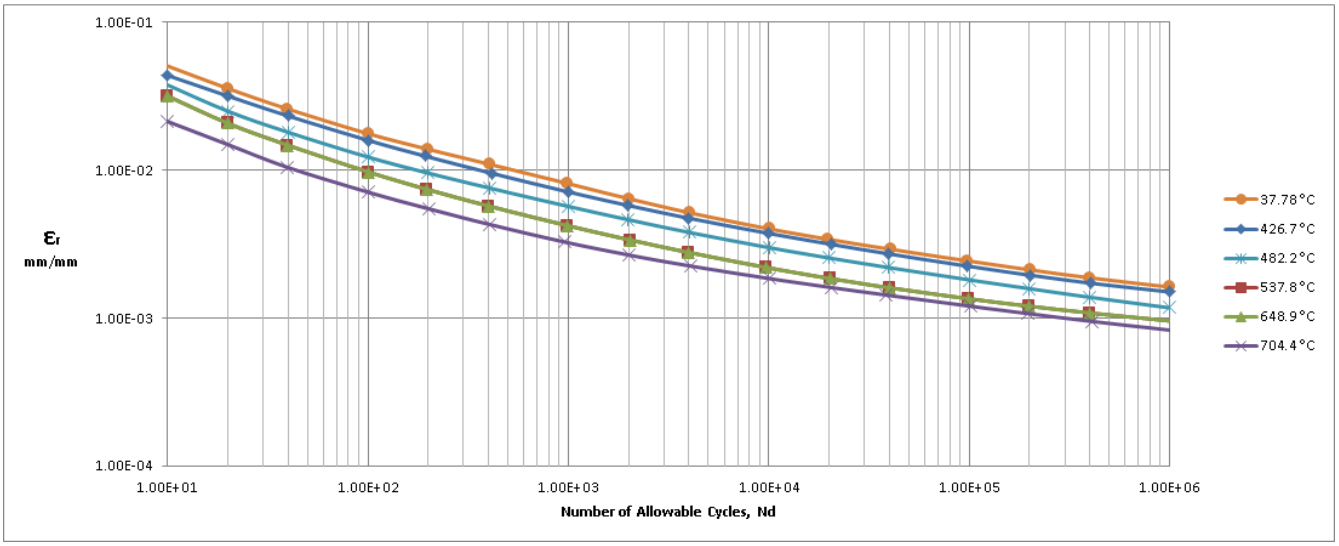

Figure 10B.32M – Fatigue Strain Range – 316 SS

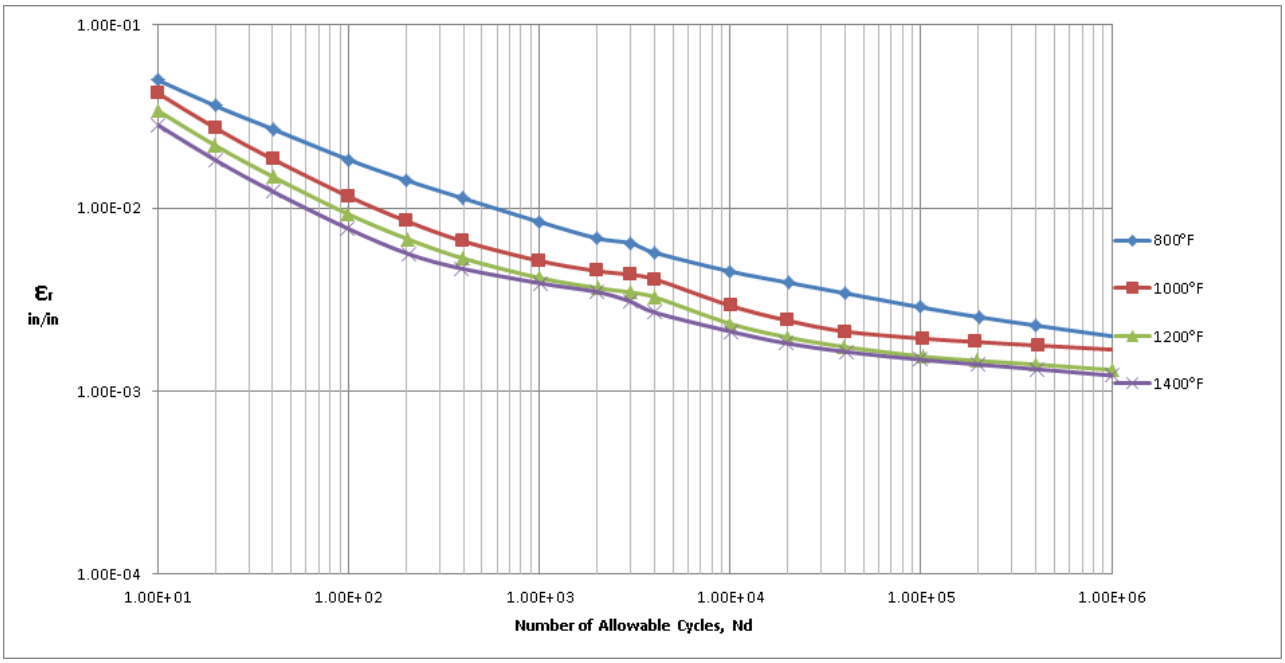

Figure 10B.33 – Fatigue Strain Range – Alloy 800H

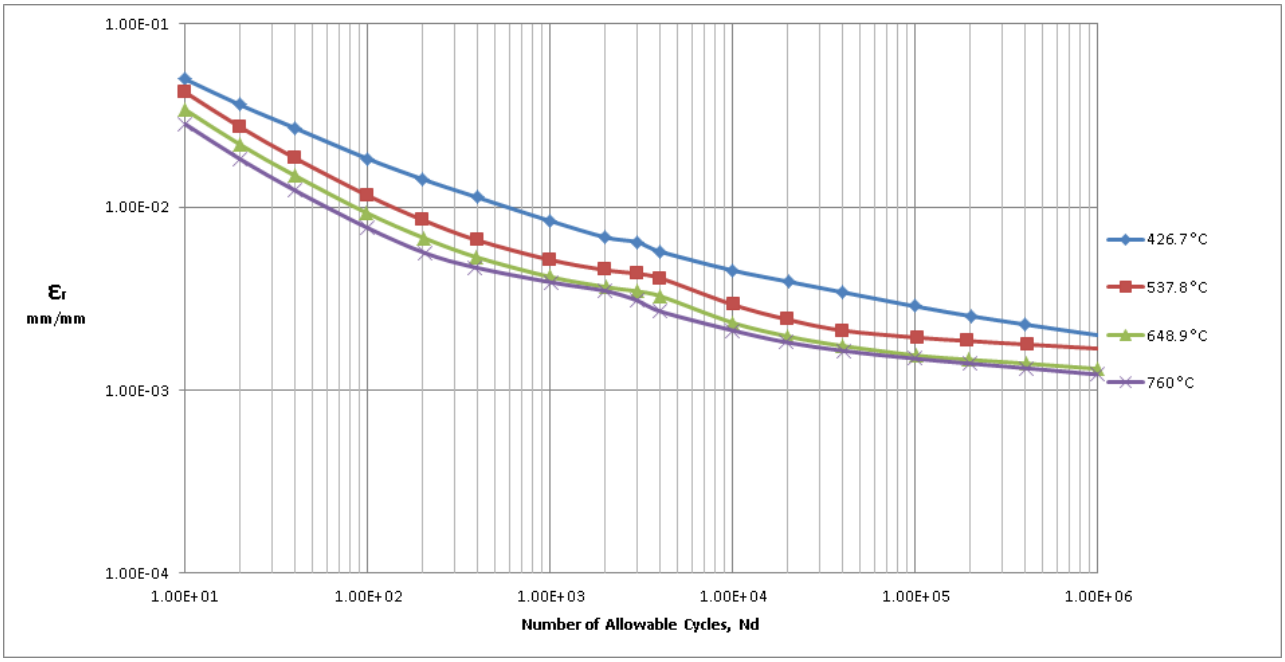

Figure 10B.33M – Fatigue Strain Range – Alloy 800H8

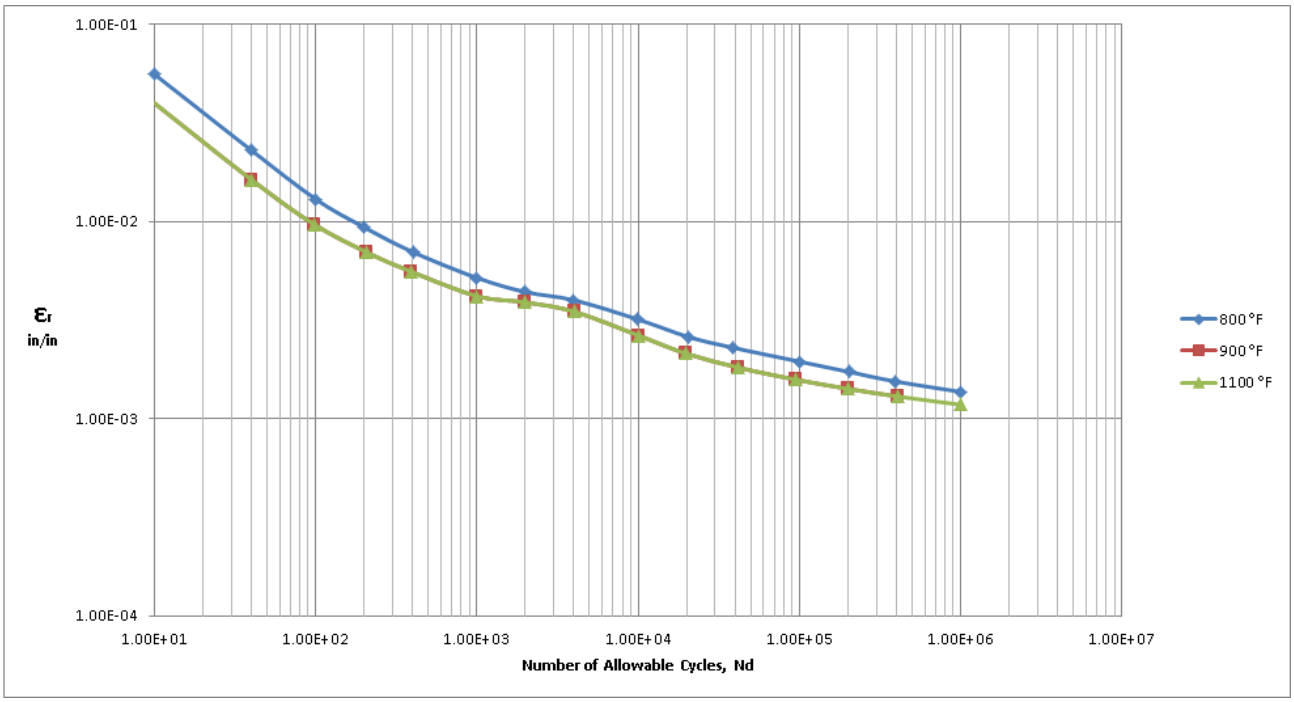

Figure 10B.34 – Fatigue Strain Range – 2.25Cr-1Mo

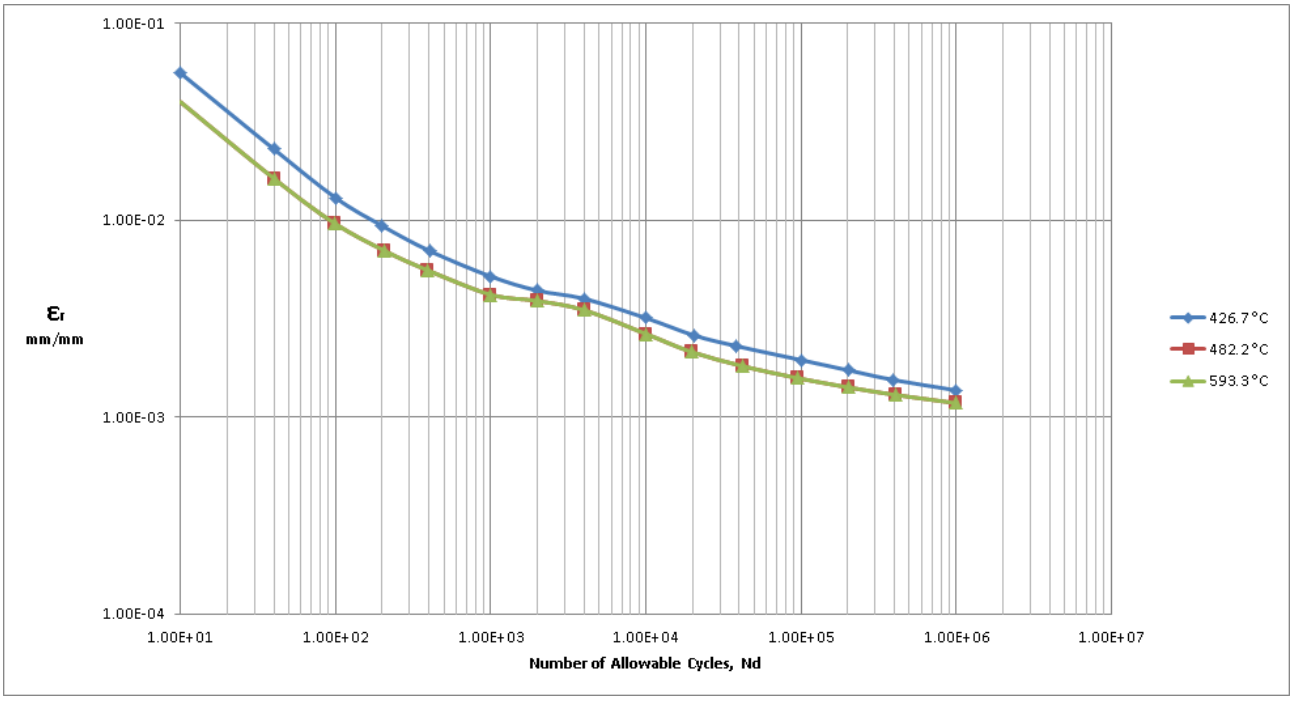

Figure 10B.34M – Fatigue Strain Range – 2.25Cr-1Mo

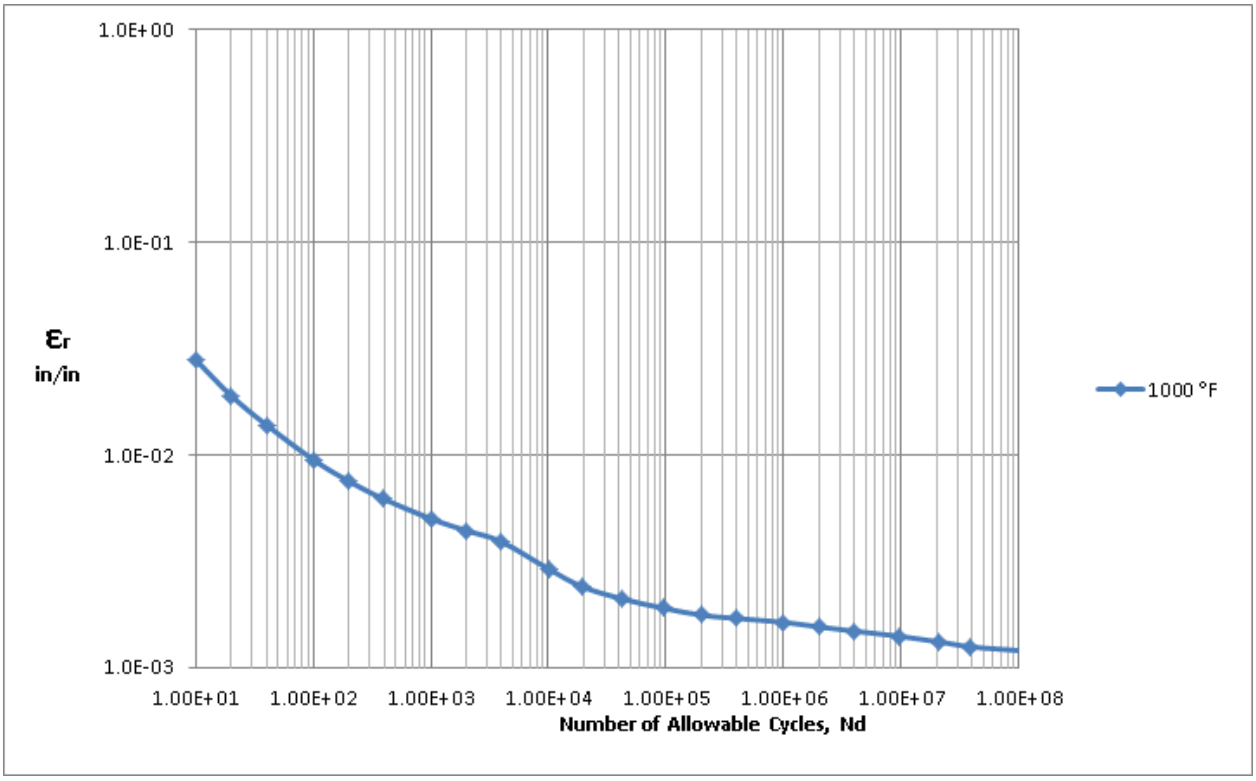

Figure 10B.35 – Fatigue Strain Range – 9Cr-1Mo-V

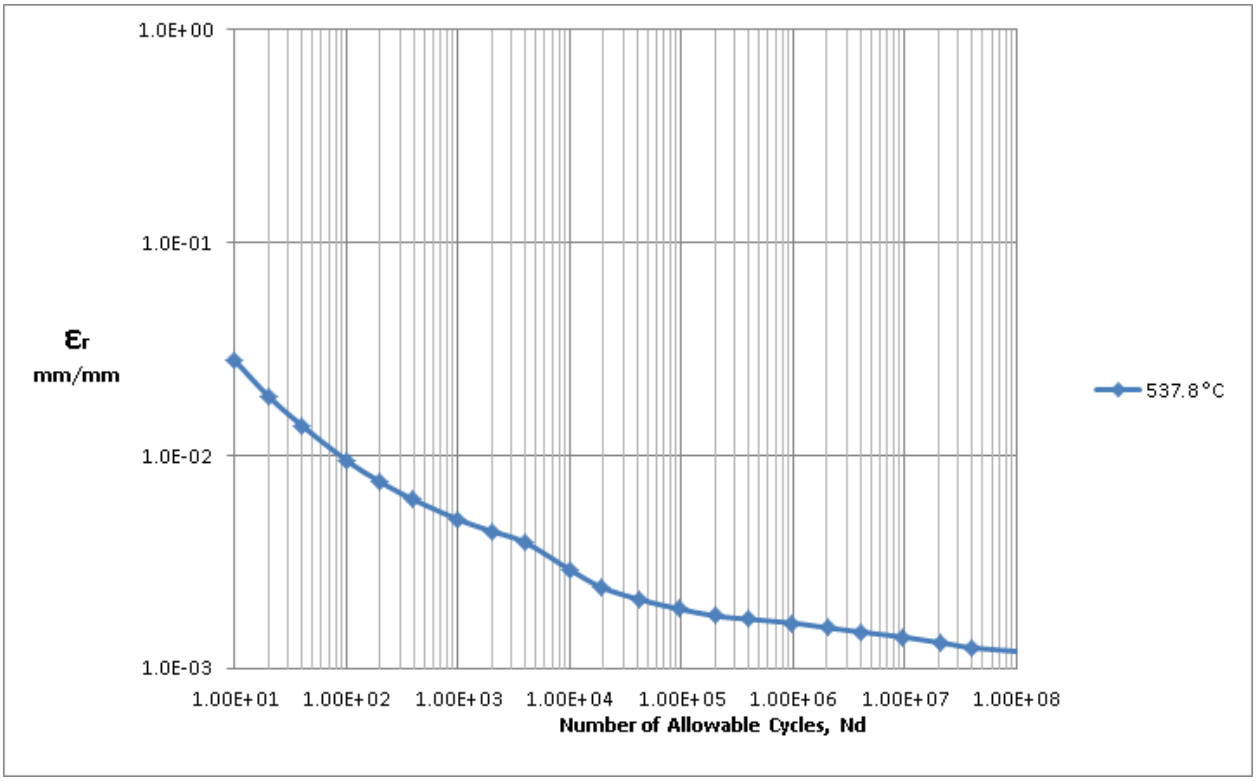

Figure 10B.35M – Fatigue Strain Range – 9Cr-1Mo-V

[Intentionally Left Blank]

PART 11 – ASSESSMENT OF FIRE DAMAGE

CONTENTS

PART 11 – ASSESSMENT OF FIRE DAMAGE 11-1

11.1 GENERAL 11-1
11.1.1 Assessment of Fire Damage 11-1
11.1.2 Assessment of Process Upsets 11-1
11.1.3 Guidelines and Assessment Flowchart 11-2
11.1.4 Forms of Fire Damage 11-2
11.1.5 Alternative Methods for Equipment Not Suitable for Operation 11-2
11.2 APPLICABILITY AND LIMITATIONS OF THE PROCEDURE 11-2
11.2.1 Equipment and Components Covered by the Assessment Procedure 11-2
11.2.2 Equipment and Components Not Covered by the Assessment Procedure 11-2
11.3 DATA REQUIREMENTS 11-3
11.3.1 Original Equipment Design Data 11-3
11.3.2 Maintenance and Operational History 11-3
11.3.3 Required Data/Measurements for an FFS Assessment 11-3
11.3.4 Recommendations for Inspection Techniques and Sizing Requirements 11-7
11.4 ASSESSMENT TECHNIQUES AND ACCEPTANCE CRITERIA 11-8
11.4.1 Overview 11-8
11.4.2 Level 1 Assessment 11-9
11.4.3 Level 2 Assessment 11-9
11.4.4 Level 3 Assessment 11-11
11.5 REMAINING LIFE ASSESSMENT 11-12
11.5.1 Thinning and Crack-Like Flaw Damage 11-12
11.5.2 Creep Damage 11-12
11.6 REMEDIATION 11-12
11.6.1 Techniques 11-12
11.6.2 Need for Repair or Replacement 11-12
11.7 IN-SERVICE MONITORING 11-12
11.8 DOCUMENTATION 11-12
11.8.1 General 11-12
11.8.2 Heat Exposure Zones 11-13
11.8.3 Record Retention 11-13
11.9 NOMENCLATURE 11-13
11.10 REFERENCES 11-13
11.11 TABLES 11-14
11.12 FIGURES 11-38

11.1 General

11.1.1 Assessment of Fire Damage

Fitness-For-Service (FFS) Assessment procedures for evaluating pressure vessels, piping and tanks subjected to flame impingement and the radiant heat of a fire are covered in this Part. These assessment procedures address the visually observable structural degradation of components and the less apparent degradation of mechanical properties, such as strength, ductility, and toughness.

11.1.2 Assessment of Process Upsets

This Part provides FFS procedures for pressurized components (i.e., internal and/or external pressure) that are potentially damaged by exposure to a fire. Typically, this is due to a plant fire external to the component.

However, these procedures are just as applicable for process upsets due to a chemical reaction within process vessels.

11.1.3 Guidelines and Assessment Flowchart

Guidelines are given to assist in the identification of components that require an FFS evaluation before being returned to service. Some of these guidelines can assist in rerating components that have experienced changes in mechanical properties due to exposure to a fire. A flow chart for the assessment procedure for components subject to fire damage or overheating due to a process upset is shown in Figure 11.1.

11.1.4 Forms of Fire Damage

The general forms of damage that should be considered include:

a) Mechanical distortion and structural damage,

b) Degradation of mechanical properties,

c) Degradation of metallurgical microstructure,

d) Degradation in corrosion resistance and susceptibility to environmental cracking and creep damage,

e) Presence of crack-like flaws in the pressure boundary, and

f) Residual stress changes.

11.1.5 Alternative Methods for Equipment Not Suitable for Operation

If the results of the FFS evaluation indicate that the equipment is not suitable to operate at design conditions, then one of the following methods may be used.

a) A new maximum allowable working pressure, $MAWP$, (or tank maximum fill height, MFH), maximum design temperature, and/or minimum design metal temperature may be established using the appropriate evaluation procedures contained in other Parts of this standard.

b) Defective sections of the equipment may be repaired or replaced.

c) The equipment may be retired from service.

11.2 Applicability and Limitations of the Procedure

11.2.1 Equipment and Components Covered by the Assessment Procedure

This Part includes procedures that may be used to identify and evaluate components subject to fire damage or overheating due to a process upset. The pressurized equipment covered in this Part includes all pressure boundary components of pressure vessels, piping, and shell courses of storage tanks.

11.2.2 Equipment and Components Not Covered by the Assessment Procedure

The following equipment and components are not specifically addressed in this Part. However, useful information on fire damage may be derived from the guidelines in this Part.

a) FFS procedures for fixed and floating roofs and bottom plates of storage tanks are covered in Part 2 of API-653.

b) Structural steel, ladders and platforms are usually distorted during a fire. This Part does not address such non-pressure containing components although information concerning non-pressure components may be

helpful in assessing pressurized components. The distortion of equipment external attachments such as ladders, pipe supports, and platforms does not necessarily mean that the pressure envelope of the equipment is no longer suitable for continued service. The process fluid inside the vessel could have served as a cooling medium during the fire, thus preventing degradation of the material's mechanical properties.

c) Instrumentation and wiring are generally destroyed in and around the area affected by a fire. The assessment of instrumentation and wiring are not addressed in this Part.

d) External insulation and paint are generally affected and, in most cases, destroyed in and around the area affected by the fire. This Part does not address assessment of paint or insulation, but observation of their damage may be used in the evaluation of pressurized components.

11.3 Data Requirements

11.3.1 Original Equipment Design Data

An overview of the original equipment data required for an assessment is provided in Part 2, paragraph 2.3.1.

11.3.2 Maintenance and Operational History

An overview of the maintenance and operational history required for an assessment is provided in Part 2, paragraph 2.3.2.

11.3.3 Required Data/Measurements for an FFS Assessment

11.3.3.1 Fire Damage Evidence

a) Evidence of fire damage may be collected both during the course of a fire and after the fire is extinguished. The objective of collecting such evidence is twofold:

   1) to determine the cause(s) of the fire, and

   2) to assess the nature and extent of damage so that equipment may be returned to service.

b) Since an accidental fire is a random event, extensive data collection during an accidental fire is seldom possible. However, alert observers can learn significant facts about fires in progress that can help to determine the appropriate boundaries of potential damage.

c) Industrial plant fires take many different forms. Some are confined to a rather small area while others are widespread or may have multiple fire sites or sources. The investigator must be alert to such possible variations when studying the fire scene. Flame patterns are often irregular and there may be equipment farther from the flame source that are more severely damaged than equipment closer to the source, because of wind direction, heat flow, insulation differences, fire monitors, etc.

d) Although each fire investigation is unique, data should normally be collected to determine:

   1) The temperature extremes to which various components were exposed.

   2) The nature of the fuel.

   3) The location of ignition source or sources.

   4) The exposure time to relatively high temperatures.

   5) The cooling rate.

e) Of the items in (d) above, the first three may typically be obtained without difficulty. The exposure time to relatively high temperatures can often be deduced from logbooks and fire department records. An estimate of the cooling rate is the most difficult to determine and may only be qualitative for materials that respond to thermal treatment. During the collection of the data listed in (d), information should be gathered from multiple pieces of equipment and in some cases from several components of the same piece of equipment.

f) Where circumstances and manpower permit, a video recording of a fire in progress can be an extremely useful tool for analyzing the nature and extent of fire damage. A fire in progress is always dangerous and could be unpredictable. Video recording a fire in progress should be supervised by the fire marshal or incident commander in control of the scene. However, when video recording evidence is available, it could be possible to deduce the nature of the fuel, the fire's progression from its ignition source, and temperature extremes from visual evidence in the recording.

g) The initial damage investigation at the fire scene should be thoroughly documented with photographs for later study. Debriefing of plant personnel should occur as soon as possible after the fire is extinguished. Video recording of the site after the fire offers an excellent technique for recording the overview of the fire-damaged area.

11.3.3.2 Record of the Fire Incident

A record of the fire incident including, but not limited to, the following should be developed to help identify the equipment that needs to be evaluated before being returned to service.

a) A plot plan of the area showing the location of the equipment.

b) The locations of the primary and secondary fire sources, and wind direction during the incident should be shown on the plot plan.

c) The duration of the incident.

d) The nature of the reactants (fuel) producing the flame in order to estimate flame temperatures and the compatibility of the reactants with the equipment.

e) The temperature, pressure, and relief valve release data for the equipment prior to and during the incident. Note that in many instances, computer storage of process operating conditions is retained for a limited time; therefore, this information should be retrieved as soon as possible.

f) The location, flow directions and the type of water used by fire monitors and hoses to control the incident.

11.3.3.3 Heat Exposure Zones

The Heat Exposure Zone should be defined for each pressure vessel, tank and piping circuit exposed to fire, in order to determine the components that would require an assessment. A description of Heat Exposure Zones is provided in Table 11.1.

a) A Heat Exposure Zone is established for a component based on the maximum exposure temperature incurred during the fire. This temperature is typically established after the fire is extinguished and is based on field observations and knowledge of the degradation associated with each exposure zone. The concept of a Heat Exposure Zone implies a physical region that was exposed to a certain temperature range. This zone may be limited to only a portion of the equipment affected. The assignment of the Heat Exposure Zone helps to screen pieces of equipment or components. However, adjacent components could have been exposed to different levels of heat and therefore suffered varying degree of damage, because one of

the components was insulated or fireproofed while the other was not. The goal is to establish the Heat Exposure Zone or Zones for the pressure boundary. In the case of completely insulated or fireproofed equipment, the Heat Exposure Zone may be less than that for unprotected components. The Heat Exposure Zone may also be affected by the orientation of horizontal vessels and the shrouding of adjacent equipment.

b) A wide range of temperature-indicating observations may be used to categorize fire-damaged equipment into appropriate Heat Exposure Zones. The basis for these observations is knowledge of the changes of state that take place in materials as temperature increases. Oxidation of polymers and metals, scale formation on metals, melting points, boiling points, and solid-state phase changes are all possible temperature indicators if properly interpreted. Knowledge of the forms of degradation, and an overview of some observations associated with fire damage that can be used to deduce the temperature range to which a component was exposed are shown in Tables 11.2 through 11.5. Additional information pertaining to temperature indications that can be used to establish a Heat Exposure Zone are provided in Table 11.6. Temperature indicators based on a knowledge of the damage a component has sustained when subject to a fire are provided in Table 11.7. There are other observations and temperature indicators that might be used to define a Heat Affected Zone that are not included in these tables.

c) The highest Heat Exposure Zone for a component exposed to more than one fire zone shall be used in the assessment, unless there is a distinct reason to allow for separate assessments, such as with heat exchangers. The component should be assigned to the next most severe fire zone if the information gathered during the investigation is insufficient to adequately categorize a component in a specific zone. As described in paragraph 11.3.3.3(a), adjacent components could have been exposed to various degrees of heat because of shrouding and differences in insulation and fireproofing. Caution should be exercised before categorizing equipment or components. For example, it may not be appropriate to categorize all parts of an insulated vessel completely into a low Heat Exposure Zone, since flanges, piping, and other appurtenances that are not insulated could have suffered damage and therefore should be assigned to a higher Heat Exposure Zone. The default categorization of these insulated components should be similar to that of adjacent uninsulated components.

d) Knowledge of the source of the fire can assist in the determination of a Heat Exposure Zone. The damage from fire and its extreme heat usually extends outward from the fuel source and upward (see Figures 11.2 and 11.3). Exceptions are in the cases of high-pressure fuel sources, where a flame jet or torch can be highly directional.

e) Temperatures associated with the fire can also be determined using instrument readings taken during the course of the fire. If a video recording is available, temperatures may be estimated based on radiation colors observed on steel surfaces during the fire. Radiation colors corresponding to a range of different temperatures are given in Table 11.8.

f) Knowledge of the nature of the fuel in a fire and the ignition source could be useful in establishing a Heat Exposure Zone.

   1) If the source of the fire is known, the fuel being consumed will often be obvious based on known flammable products in the area. However, this is not always the case, and observers on the scene may be able to characterize the fuel based on the color of the smoke (see Table 11.9).

   2) Ignition sources in refinery and petrochemical plants include electrical sparks, open flames, and exposed hot surfaces. Flammable mixtures of organic vapors and air typically exhibit an autoignition

temperature above which the mixture will ignite without a spark or additional energy source. For example, a hot surface with a temperature in excess of the autoignition temperature could be an ignition source. Autoignition temperatures for typical gases and liquids are shown in Table 11.10 and Table 11.11.

11.3.3.4 Degradation Associated with Heat Exposure

A specific inspection plan should be developed for each component subject to fire damage, based on first assigning a Heat Exposure Zone (see paragraph 11.3.3.3) and then taking into account the following forms of degradation associated with heat exposure as listed in Table 11.6:

a) Softening, sagging (plastic deformation) and over aging of aluminum alloys.

b) Softening and sagging (plastic deformation) of copper alloys.

c) Hardening and/or tempering of heat treatable steels (e.g., ASTM A193 B7 stud bolts).

d) Grain growth, degradation in corrosion resistance and susceptibility to environmental cracking, softening, sagging (plastic deformation), hardening or loss of toughness of carbon and low alloy steels.

e) Short term creep and creep rupture.

f) Spheroidization of carbon steels after long periods of exposure.

g) Stress relieving of stainless steels and nickel alloys (e.g., resulting in tube roll leaks in heat exchangers).

h) Sensitization of stainless steels.

i) Halide contamination of austenitic stainless steel or other austenitic alloy surfaces, especially under wet insulation or if salt water is used for fire-fighting.

j) Liquid metal corrosion or cracking, such as caused by molten zinc dripping on austenitic stainless steel.

k) Incipient melting of alloys (e.g., localized melting of low melting point segregation and eutectics).

l) Excessive oxidation of metals leading to wall loss, particularly if the fire or overheat incident exceeds many hours.

m) Deterioration of gaskets and valve packing.

n) Damage to coating systems, especially coatings applied for under insulation corrosion protection.

o) High residual stresses due to distortion, restraint, and loss of supports.

p) Cracking of metals due to distortion and restraint, for example, restraint of cooler internal components cracking attachment welds.

q) Embrittlement of some grades of steels when cooled through critical temperature ranges.

r) Formation of a cast iron structure due to carburization and localized melting of the carbon rich alloy (most likely in furnace tubes processing hydrocarbons).

11.3.3.5 The typical material degradation and appearance of the microstructure that may occur in carbon steel, low alloy steels, and stainless steel are shown in Table 11.12. These degradations shall be considered in the judgment to reuse the components with fire damage. Normally, components subject to high temperatures during a fire do not experience significant creep damage because the time at temperature is short and significant creep strains and associated damage cannot accumulate. Therefore, this mechanism is not included

in Table 11.12. In cases that the exposure time is long enough and/or temperature is high enough such that creep damage is no longer negligible, the creep damage and the associated remaining life should be evaluated according to Part 10. A Level 1 Assessment per Part 10 should be considered as a screening procedure to determine if creep damage should be considered.

11.3.3.6 Data and Measurements for Components Subject to Heat Exposure

Collection of the following data and measurements should be considered for components assigned to a Heat Exposure Zone where mechanical property changes and dimensional changes can occur:

a) Diametrical and circumferential variations of cylindrical vessels.

b) Dimension profiles of vertical and horizontal vessels.

c) Straightness of shell and piping sections.

d) Nozzle orientations.

e) Vertical plumb measurements.

f) Hardness tests of the base metal and welds.

g) Removal of coupons for mechanical testing.

h) Wall thickness measurements of pressure containing components.

i) In-situ metallography and microstructure replication.

j) Surface crack detection techniques such as magnetic particle and dye penetrant examination.

k) Surface condition of equipment with respect to scale formation, melting, coating damage, insulation condition, and weather barrier construction and condition.

11.3.3.7 Evaluation of Mechanical Properties for Components Subject to Heat Exposure

a) Components susceptible to changes in mechanical properties at exposure temperature should be evaluated to determine if the material has retained the necessary strength and toughness properties stipulated in the original construction code. The effects of temperature on mechanical properties of various metals are included in Table 11.6. If mechanical properties have been degraded, the actual strength and toughness properties shall be determined (or estimated) in order to rerate the affected component. In this context, components include:

   1) Pressure Vessels: shell sections, heads, nozzle necks, flanges, vessel supports.

   2) Piping Systems: pipe sections, elbows, tees, reducers, flanges, and piping supports.

   3) Tankage: tank shell courses and nozzle necks.

b) Metallurgical investigation and mechanical testing are helpful aids in assessing the effect of elevated temperature exposure to metals during a fire event. Guidelines for conducting metallographic analysis as well as mechanical testing in a fire damage assessment are provided in Annex 11B.

11.3.4 Recommendations for Inspection Techniques and Sizing Requirements

11.3.4.1 Shell dimensional profiles should be taken for equipment subjected to fire damage. Dimensional profiles of vertical vessels can be obtained by dropping a reference vertical line from the top of the vessel and measuring the bulges and dents of the shell sections relative to this vertical line at appropriate increments. An

example on how to measure a profile for a vertical vessel is illustrated in Figures 11.4 and 11.5. Dimensional profiles of horizontal drums can be taken in a similar way using a horizontal level. Laser scan or laser mapping can also be used to obtain more accurate dimensional profiles of pressurized equipment distorted during a fire event, especially in those cases where large components suffered distortions at several locations and/or when access to perform manual profiling is an issue. Additional methods to determine shell distortions using field measurement techniques are covered in Part 8.

11.3.4.2 Evaluation of the impact of relatively high temperature exposure to the microstructure of the material and its mechanical properties may be needed to determine if equipment or a component involved in a fire event can be returned to service or reused. Annex 11B provides guidelines for metallographic evaluation and mechanical testing including removal of samples when needed.

11.3.4.3 Other inspection techniques, such as magnetic particle testing, dye penetrant testing, and ultrasonic testing may be needed based on the observed or suspected deterioration mode (see paragraph 11.3.3.4).

11.3.4.4 Leak testing of mechanical equipment subject to fire damage in Heat Exposure Zones IV and higher should be considered prior to returning the equipment to service. The types of equipment included are:

a) Flanged connections.

b) Threaded connections which are not seal-welded.

c) Valves (i.e., both shell and closure test per API 598 should be considered).

d) Gaskets and packing.

e) Heat exchanger tube sheet rolled joints.

11.4 Assessment Techniques and Acceptance Criteria

11.4.1 Overview

An overview of the assessment levels is provided in Figure 11.1.

a) The Level 1 Assessment procedure is a screening criterion where the acceptability for continued service is based on the Heat Exposure Zone and the material of construction. The screening criteria are conservative, and calculations are not required to establish suitability for continued service.

b) The Level 2 Assessment procedure determines the structural integrity of a component by evaluating the material strength of a fire-damaged component. Assessment procedures include evaluation methods for flaws and damage incurred during the fire (e.g., local thin areas, crack-like flaws, and shell distortions) and a means to rerate the components. These assessment procedures are typically applied to components subject to a Heat Exposure Zone of V and higher, or when dimensional changes are noted during a visual inspection. Replication or in-situ field metallography and field hardness testing may be utilized in a Level 2 Assessment.

c) The Level 3 Assessment procedures may be utilized if the current material strength of the component established using the Level 2 Assessment procedures result in an unacceptable evaluation. Replication or in-situ field metallography, hardness testing, and the removal and testing of material samples may be utilized in a Level 3 Assessment, together with a detailed stress analysis.

11.4.2 Level 1 Assessment

11.4.2.1 The objective of this Level 1 Assessment is to gather and document the observations and data used to justify assigning a Heat Exposure Zone to each component. Components do not need a further assessment of mechanical properties if they are assigned to an acceptable Heat Exposure Zone, and there is no mechanical damage or dimensional deviation. The Heat Exposure Zone levels for the materials of construction that are acceptable per a Level 1 Assessment are shown in Table 11.13. Alloys in this table might be susceptible to loss of corrosion resistance and/or environmental cracking at the Heat Exposure Zone levels satisfying the Level 1 Assessment criteria, and this shall be taken into consideration during the assessment.

11.4.2.2 Gasket inspections and leak checking of flange joints should be included in a startup check list for components passing a Level 1 Assessment.

11.4.2.3 Protective coating damage can occur for some components that satisfy the Level 1 acceptance criteria. Protective coatings required for external or internal corrosion resistance must be repaired prior to startup.

11.4.2.4 If the component does not meet the Level 1 Assessment requirements, then the following, or combinations thereof, may be considered:

a) Repair, replace or retire the component,

b) Conduct a Level 2 or Level 3 Assessment, or

c) Rerate the component.

11.4.3 Level 2 Assessment

11.4.3.1 Pressurized components that do not pass a Level 1 Assessment may be evaluated for continued service using a Level 2 Assessment. This evaluation should consider the degradation modes described in paragraph 11.3.3.4.

11.4.3.2 An overview of the Level 2 Assessment procedure is provided in Figure 11.6.

a) The first step in the assessment is to conduct dimensional checks on pressure components. The dimensional checks generally take the following forms; overall out-of-plumb or sagging of the component(s) and localized shell distortion. As listed below, the forms of overall out-of-plumbness or sagging are dependent on equipment type whereas local shell distortions such as bulges are common for all equipment types:

   1) Ovality or out-of-roundness,

   2) Sagging or bowing of horizontal vessels,

   3) Vertical deviations (out-of-plumbness), and

   4) Bulges.

b) Hardness testing is used to estimate the approximate tensile strength of a fire exposed component made of carbon and/or low alloy steel. The information is subsequently used with the rerating procedures in this document to establish an acceptable $MAWP$ (or tank maximum fill height, MFH). Further evaluation is required to assess specific damage from localized thinning, shell distortions and creep.

c) Components that experience dimensional changes provide insight into the additional evaluations that are required. This insight is based on the observation that carbon steel equipment does not experience a

significant reduction in short term high temperature strength properties that would result in a dimension change (i.e., out-of-plumb, sagging or bulging) until a temperature in excess of 425°C (800°F) is reached.

11.4.3.3 The following procedure may be used to evaluate a pressurized component constructed of carbon or low alloy steels for continued operation if the mechanical strength properties are suspected to have been degraded by the fire exposure.

a) STEP 1 – If the component is fabricated from carbon steel, low alloy steel, or stainless steel, perform a hardness test on the component (see Annex 11B) and convert the resulting hardness value into an estimated ultimate tensile strength using Annex 2E, Table 2E.1. If the component is fabricated from other high alloy, nickel based or non-ferrous materials, an alternative method is usually required to determine an acceptable material strength level for an FFS Assessment. Additional materials evaluation may need to be performed depending on the observed severity of damage and future service requirements, including in-situ field metallography to determine the condition of the material in a component. Guidelines for this type of evaluation are provided in Figure 11.7, paragraph 11.3.3.6, and Annex 11B.

b) STEP 2 – Determine an allowable stress for the fire damaged component based on the estimated ultimate tensile stress determined in STEP 1 using Equation (11.1). In this equation, the parameter C_{ism} is the in-service margin. The in-service margin may be taken equal to the design margin used on the ultimate tensile strength in the original construction code. If this value is not known, a value of $C_{ism} = 4.0$ may be used if inspections and engineering assessments demonstrate a level of integrity comparable to that of an established construction code.

$$S_{afd} = \min\left[\left\{\left(\frac{S_{uts}^{ht}}{C_{ism}}\right)\cdot\left(\frac{S_{aT}}{S_{aA}}\right)\right\},\ \{S_{aT}\}\right] \tag{11.1}$$

c) STEP 3 – Perform the necessary $MAWP$ calculations using the value of allowable stress determined in STEP 2 and the equations in Annex 4A.

d) STEP 4 – If additional forms of damage are present, the $MAWP$ should be further modified using the applicable Parts in this document:

1) General thinning – Part 4.
2) Local thinning – Part 5.
3) Pitting – Part 6.
4) HIC, SOHIC and blister damage – Part 7.
5) Shell distortions including out-of-roundness and bulges – Part 8.
6) Crack-like flaws – Part 9.
7) Dents, gouges, and dent-gouge combinations – Part 12.
8) Laminations – Part 13.

e) STEP 5 – Evaluate creep damage of the component using Part 10. Normally, components subject to high temperatures during a fire do not experience significant creep damage because the exposure time at temperature is relatively short and significant creep strain and associated damage cannot accumulate.

11.4.3.4 Other effects that should be considered in the assessment include the following:

a) Internal attachments that may have been subject to large thermal gradients during a fire should be inspected for cracks on the component surface and at the attachment weld. This inspection is especially important for internal components fabricated from materials with a coefficient of thermal expansion significantly different from that of the shell (e.g., austenitic stainless steel internal attachment support welded to a carbon or low alloy steel shell).

b) Pressure components being rerated because of the reduction in mechanical properties should be assessed if there is a plausible reason to expect a change in the corrosion resistance or susceptibility to environmental cracking in the service which the vessel will be exposed (the future corrosion allowance may need to be increased).

11.4.3.5 The beneficial effects of $PWHT$ (stress relief) may have been compromised because of heat exposure. Pressurized components that were subjected to $PWHT$ in accordance with the original construction code (i.e., based on the material and thickness at the weld joint) or for service conditions (e.g., carbon steel subject to caustic SCC, in wet H_2S service, or any other degradation mechanism) should be evaluated to ascertain whether the benefits of the $PWHT$ have been compromised:

a) For carbon steel, the issue is usually on relief of residual stresses, but sometimes also on tempering hard zones in the microstructure or on improved toughness. Distortion and/or quenching in fire-fighting efforts can leave the component with higher residual stresses that could lead to service related cracking.

b) For low alloy steels, the issue is usually on retaining mechanical properties. The original $PWHT$ was conducted to temper a hard microstructure and/or to improve toughness. Heat exposure can lead to a very hard/brittle microstructure in the component that if left in place can lead to premature failure.

11.4.3.6 If the component does not meet the Level 2 Assessment requirements, then the following, or combinations thereof, may be considered:

a) Repair, replace or retire the component,

b) Adjust the future corrosion allowance, FCA, by applying remediation techniques (see Part 4, paragraph 4.6),

c) Adjust the weld joint efficiency factor, E, by conducting additional examination and repeat the assessment (see Part 4, paragraph 4.4.2.2(c)), and/or

d) Conduct a Level 3 Assessment.

11.4.4 Level 3 Assessment

11.4.4.1 A Level 3 Assessment of a fire damaged component may be performed if the component does not satisfy the Level 1 or Level 2 Assessment criteria. A Level 3 Assessment is usually performed for the following reasons.

a) The $MAWP$ (or MFH) calculations associated with a Level 2 Assessment cannot be used to adequately represent the current condition of the component. If the component is severely deformed or shell distortions are located in the region of a major structural discontinuity, then a stress analysis technique from Annex 2C may be utilized for the assessment.

b) The current strength of the material established from a hardness test taken on the material surface approximates the actual tensile strength of the material that in some cases could be conservative, resulting

in a reduction of the $MAWP$ (or MFH). In such cases, testing on material samples can be performed to develop a better estimate of the strength of the material. Guidelines for material sample removal, metallurgical investigation, and evaluation of mechanical properties are given in Annex 11B.

11.4.4.2 A Level 3 Assessment of a known fire-damaged component shall be conducted if an increase in the original $MAWP$ (or temperature) is required. A representative sample of the base metal and weld should be tested to establish an acceptable allowable stress value for use in the rerating calculations. Estimates of changes in mechanical properties based only on hardness measurements and microstructure shall not be used to increase the allowable stress value of a component subject to fire damage.

11.5 Remaining Life Assessment

11.5.1 Thinning and Crack-Like Flaw Damage

The applicable Parts of this document may be used to assess remaining life for the damage mechanisms cited in paragraph 11.4.3.3.

11.5.2 Creep Damage

Creep damage and the associated remaining life may be calculated using the assessment procedures of Part 10.

11.6 Remediation

11.6.1 Techniques

Remediation techniques for the damage mechanisms cited in paragraph 11.4.3.3 are covered in the applicable Parts of this document.

11.6.2 Need for Repair or Replacement

In general, badly distorted components should be repaired or replaced. However, if a component cannot be repaired or replaced because of physical limitations or extended replacement schedules, then temporary supports and reinforcement can be added to help reduce stresses associated with the deformed condition. For example, the increased bending stress resulting from out-of-plumbness of a process tower may be acceptable if some form of support is introduced to minimize bending stresses associated with non-pressure loadings such as wind and seismic loads. Note that added supports should be designed to accommodate thermal expansion of the equipment.

11.7 In-Service Monitoring

Recommendations for in-service monitoring for the damage mechanisms cited in paragraph 11.4.3.3 are covered in the applicable Parts of this document.

11.8 Documentation

11.8.1 General

The documentation of the FFS Assessment shall include the information cited in Part 2, paragraph 2.8.

11.8.2 Heat Exposure Zones

Information used to assign the Heat Exposure Zones, video recording and photographic materials to define the extent of the affected area and visual damage, measurements to quantify component distortions, metallurgical and mechanical property changes to quantify the degree of material deterioration, calculations for the $MAWP$ (or MFH), and remaining life calculations should be documented.

11.8.3 Record Retention

All documentation including the calculations used to determine the FFS of a pressurized component should be kept with the inspection records for the component or piece of equipment in the Owner-User inspection department.

11.9 Nomenclature

C_{ism} in-service margin.

FCA future corrosion allowance.

S_{afd} allowable stress for a fire damaged material.

S_{aA} allowable stress of the original design code or standard at the ambient temperature when the hardness tests are taken.

S_{aT} allowable stress of the original design code or standard at the specified design temperature.

S_{uts}^{ht} Ultimate tensile strength based on the results from a hardness test.

11.10 References

References for this Part are provided in Annex 11A – Technical Basis and Validation – Assessment of Fire Damage.

11.11 Tables

Table 11.1 – Description of Heat Exposure Zones to Evaluate Fire Damage (1)

Heat Exposure Zone	Description	Thermal Effects on Materials in the Fire Zone
I	Ambient temperature during fire event, no fire exposure	No damaging effects
II	Ambient to 65°C (150°F); smoke and water exposure	No damaging effects
III	65°C to 205°C (150°F to 400°F); light heat exposure	Table 11.2
IV	> 205°C to 425°C (>400°F to 800°F); moderate heat exposure	Table 11.3
V	> 425°C to 730°C (>800°F to 1350°F); heavy heat exposure	Table 11.4
VI	> 730°C (>1350°F); severe heat exposure	Table 11.5
Note: An overview of the damage that is likely to occur in each fire zone is provided in Table 11.6.		

Table 11.2 – Guidelines for Observing Fire Damage – Thermal Effects on Materials Heat Exposure Zone III, 65°C to 205°C (150°F to 400°F)

Temperature (1)		Materials of Construction	Forms or Usage	Thermal Effects
°C	°F			
90	200	Vinyl coatings (3), (4), (5)	Paints on tanks, structural steel, etc.	Begins to melt, flow, and bubble; may burn
150	300	Alkyd coatings (6)	Paints on tanks, structural steel, etc.	Color change visible; surface crazing
400	750	Inorganic zinc silicate (10)	Paints on tanks, structural steel, etc.	Begins to melt, flow, and bubble; may burn
205	400	Epoxies & polyurethanes (11)	Paints on tanks, structural steel, etc.	Color change visible; blistering and charring
190	375	UHMW HD Polyethylene (7)	Pipe	Softening and melting
175	350	Elastomers, neoprene (2), (8)	Hose, diaphragms, gaskets	Softening, melting; some burning / charring
180	360	Lead / tin solder	Electrical equipment connectors	Melts
260	500	Baked phenolic (9)	Fiberglass mat binder, micarta tank linings	Surface discoloration; blistering
205	400	Acrylic mastic	Weatherproof coating for insulation	"Mud" cracking; charring

Notes:

1. The temperatures listed in this table are the lower limits of temperature where significant damage is observed. Similar effects may occur at higher temperatures in shorter times.
2. Effects of heat vary greatly due to formation of an elastomer and end product. Do not attempt to be too specific based on observations of elastomer condition.
3. The term vinyl can mean two different things when it comes to paint. Solution vinyls are single package paints with polymeric resin dissolved in strong hydrocarbon solvent. The other type of vinyl is like latex house paint; these water based paints are typically vinyl acrylic, but they may also be vinyl acetate and other polymer types.
4. Solution vinyl coatings (thermoplastics) have a maximum continuous service temperature of about 60°C to 65°C (140°F to 150°F) and soften in the 65°C to 80°C (150°F to 180°F) range; above 90°C (200°F) these coatings will begin to melt and flow, (giving up HCl as a by-product.) They may blister but are generally not good candidates for burning and charring. The significant halogen content stifles burning initially. This will occur with some bubbling which may be a little different than blistering.
5. Vinyl latex paints are also thermoplastic paints, but these do not generally contain chlorine or other halogens. Above 90°C (200°F) these materials will begin to melt and flow much like solution vinyls, but they burn differently.
6. Alkyd's thermoset and as such they have much better temperature resistance than do the vinyls. Alkyds can handle 105°C to 120°C (225°F to 250°F) continuously for months or years. A good alkyd can handle 150°C (300°F) for several hours. The first symptoms of heat/oxidation damage are yellowing and surface crazing. Different colors mean different pigments and color changes could be important.
7. UHMW and HD polyethylene used as pipe, has a temperature rating of 65°C to 70°C (150°F to 160°F) depending on commodity and pressure. The softening temperature is about 125°C (260°F); it takes some time at temperatures well above 150°C (300°F) to cause appreciable melting. Consider that HDPE pipe is welded at 205°C to 260°C (400°F to 500°F), depending on the technique.
8. Neoprene has a dry temperature rating of 150°C to 175°C (300°F to 350°F) depending on formulation specifics. Flame and heat aging/air oxidation resistance are very good for rubber. Neoprene is a type of chlorinated rubber and so it resists burning.
9. Baked phenolics thermoset, typically are bake cured in the 165°C to 205°C (325°F to 400°F) range. Phenolics are typically red, brown, or black initially, so a color change may be difficult to observe. While this generic class may degrade over a range of temperature, the materials would need to be at temperatures close to 260°C (500°F) before major degradation would be observed.
10. For zinc silicate primers, the silicate binders can handle up to about 540°C (1000°F). However, the metallic zinc pigment can be impacted above the melting point near 400°C (750°F).
11. Epoxies and polyurethanes can typically withstand temperatures to about 150°C (300°F) with no significant impact. These paints may begin to blister and/or char once the temperature exceeds 205°C (400°F). As with the alkyd paints, color changes may occur. For example, a common yellow finish color is obtained with hydrated ferric oxide and as the coating gets hot the water of hydration is driven off and the coating starts to turn pink.

Table 11.3 – Guidelines for Observing Fire Damage – Thermal Effects on Materials Heat Exposure Zone IV, Greater than 205°C to 425°C (Greater than 400°F to 800°F)

Temperature (1)		Material of Construction	Forms or Usage	Thermal Effects
(°C)	(°F)			
205	400	Tempered aluminum alloys	Pipe and tanks of T6 or other temper	Reduced strength (check hardness & electrical conductivity)
230+	450+	Wood – various	Various	Charring, burns
260	500	Steel – machined or polished	Machinery or instrument parts	Develops blue temper color
270	520	Babbitt (2) -- lead based	Sleeve bearings	Melts
280	540	Copper -- cold drawn, bright annealed	Instrument and condenser tubing	Softens, sags, grain coarsening occurs
330	623	Lead (soft)	Lining in pipe and tanks	Melts
390	730	Zinc/aluminum die casting	Small valve handles and instrument parts	Melts
420	790	Zinc	Galvanized coating for steel structures	Melts

Notes:
1. The temperatures listed in this table are the lower limits of temperature where significant damage is observed. Similar effects may occur at higher temperatures in shorter times.
2. Trade Name.

Table 11.4 – Guidelines for Observing Fire Damage – Thermal Effects on Materials Heat Exposure Zone V, Greater than 425°C to 730°C (Greater than 800°F to 1350°F)

Temperature (1)		Material of Construction	Forms or Usage	Thermal Effects
(°C)	(°F)			
480	900	Quenched and Tempered Steels	Springs, fasteners, 4140, etc., (particularly socket head cap screws)	Tempering to lower strength
510	950	Glass	Light bulbs	Distort and melt
540	1000	18-8 Stainless Steel	Vessels, piping etc.	Sensitized (carbide PPT) and reduced corrosion resistance
595	1100	Steel	Vessels and piping	Thermal distortion and creep, some heat scale
620	1150	Precipitation Hardened Stainless Steel	Machinery and valves	Overages -- reduced strength
650	1200	Steel	Vessels, piping, structures	Rapid oxidation -- thick black scale
655	1215	Aluminum	Tanks, piping, accessories	Melts
695	1285	Glass	Windows	Melts
705	1300	Copper	Tubing, pipe, vessels	Rapid oxidation -- black
710	1310	Glass	Pyrex (2) – pipe, sight glass	Melts
730	1350	Silver Solder	Brazed joints on accessories	Melts (may start at lower temperature)

Notes:

1. The temperatures listed in this table are the lower limits of temperature where significant damage is observed. Similar effects may occur at higher temperatures in shorter times.
2. Trade Name.

Table 11.5 – Guidelines for Observing Fire Damage – Thermal Effects on Materials Heat Exposure Zone VI, Greater than 730°C (Greater than 1350°F)

Temperature (1), (2)		Material of Construction	Forms or Usage	Thermal Effects
(°C)	(°F)			
760	1400	Steel	Vessels and piping	Iron carbide (cementite) spheroidizes
815	1500	Steel	All forms -- low alloy most susceptible	Austenitizes -- slow cool equals anneal, fast quench turns hard and brittle
905	1660	Zinc	Galvanizing on steel	Oxidizes to white powder or vaporizes
980	1800	Cellular glass	Thermal insulation	Melts
1095	2000	Copper	Tubing, pipe, etc.	Melts
1305	2385	Alloy C-276	Vessels, pipe	Melts
1400	2550	316 SS – cast	Pumps, valves	Melts
1455	2650	316 SS – wrought	Vessels, pipe	Melts
1515	2760	Steel	Various	Melts
1685	3065	Titanium	Vessels, pipe, etc.	Melts

Notes:

1. The temperatures listed in this table are the lower limits of temperature where significant damage is observed. Similar effects may occur at higher temperatures in shorter times. Temperatures shown are those in which significant damage begins to occur to the material of construction listed.
2. The temperatures listed in this table are the lower temperatures where heat effects begin. Similar effects may occur at higher temperatures in shorter times.

Table 11.6 – Guidelines for Assessing Fire Damage Effects Description of The Types of Damage That May Occur in the Heat Exposure Zone Categories

Heat Exposure Zone	Temperature Range	Heat/Temperature Effects	Observations and Conclusions
ZONE I No evidence of heat, flame, or smoke contact	AMBIENT	Equipment clean. Paint, plastic, and elastomer items unaffected.	• No damage, acceptable to operate.
ZONE II Smoke and water contact but no heat exposure	AMBIENT to 65°C (150°F)	Equipment dirty, sooty, and wet. No effects on paint, elastomer, or plastic items.	• No damage to major equipment. Water and smoke may have damaged insulation, insulation jackets and delicate mechanisms or electronics (1). • Smoke or fumes from burning chlorinated compounds, i.e., PVC, will release chlorine or HCl, can damage electronics or contaminate insulation (2). • Wet by water/Just sooty in general. • Paint colors unchanged. • Elastomer kept flexible without hardening. • Coatings show no change in color. • Power cables retained continuity. • Synthetic resins show no change in color.
ZONE III Light heat exposure	Over 65°C (150°F) to 205°C (400°F)	Vinyl and alkyd paints blistered, paints darkened to black, elastomers hardened or charred, plastics charred or melted, lead-tin solder melts.	• No damage to major equipment. Some damage to non-metallics. Check packing and gaskets for heat effects (3). • Electrical wiring and electronic components damaged (4). • Belts on machinery drives need replacing. • Check for chlorine or HCl contact from burning organic chlorides (2). • Solder shows deflection, distortion, and/or traces of melting. • Aluminum alloy/Copper alloy shows deflection, distortion, and/or traces of melting. • Paint colors changed, burned, blackened, or cracked. • Elastomer shows hardening, carburization, or traces of melting. • Coatings show change in colors, bulging, or burned. • Power cables show lost continuity/dielectric damaged or breakdown. • Synthetic resins show deflection, distortion, and/or traces of melting. • PTFE gaskets damaged (check by disassembling flanged joints)

Table 11.6 – Guidelines for Assessing Fire Damage Effects Description of The Types of Damage That May Occur in the Heat Exposure Zone Categories

Heat Exposure Zone	Temperature Range	Heat/Temperature Effects	Observations and Conclusions
ZONE IV Medium heat exposure	Over 205°C (400°F) to 425°C (800°F)	Organic coatings blistered or burned off. Plastics and rubber melted or charred. Insulation on electric wiring destroyed.	• Severe general damage to ancillary equipment such as electrical wiring, circuit boards and motors. • All gaskets and packing shall be replaced except those made from metallic, spiral or graphite.
		Springs will be tempered and softened. Valves, gauges out of calibration.	• Springs in pressure relief valves, check valves etc., will be tempered out of calibration. Rupture discs may also be affected by heat and should be replaced (5).
		Cold drawn copper alloys lose strength. Solution annealed copper alloys are less affected.	• Roll joints in heat exchangers might be affected. Sagging tubing joints on instrument tubing might leak. Consult mechanical engineers about copper alloy pressure components if loss of copper alloy strength is observed (6).
		Aluminum alloys may experience considerable loss in strength due to over-aging and recrystallization. Distortion of aluminum alloys may occur.	• Aluminum equipment often requires replacement (6).
		Structural steels, stainless steels, solution annealed nickel alloys, non-heat treated titanium and zirconium alloys generally are not affected.	• Usually can be returned to service (7).
		Possibility of liquid metal embrittlement begins and may affect the integrity of equipment.	• Refurbish susceptible metallic items that have had molten metal dripped on them by repairing damaged areas (by welding and/or grinding) and inspecting for cracking (8).

Table 11.6 – Guidelines for Assessing Fire Damage Effects Description of The Types of Damage That May Occur in the Heat Exposure Zone Categories

Heat Exposure Zone	Temperature Range	Heat/Temperature Effects	Observations and Conclusions
ZONE V Severe heat exposure. Direct exposure to flames, no impingement. This is the most important area of fire damage effects. Major equipment has been exposed to severe radiant heat, but not enough to destroy it.	Over 425°C (800°F) to 730°C (1350°F)	Nonmetals destroyed or consumed. Aluminum, pyre, and some silver solders melting.	• All ancillary equipment and small piping, tubing, copper materials should be replaced. Concentrate on major equipment. • All gaskets and packing shall be replaced.
		The cold-rolled tube ends in heat exchangers may be stress relieved causing leaks.	• Major equipment, including pressure vessels, heat exchangers and rotating equipment should be cleaned, inspected and pressure tested. (9)
		Heat-treated or cold-worked metals may be softened. Check springs on pressure relief valves. Check A193-B7 stud bolts in flanges for softening. Check for localized heating and stressing of steel equipment in critical service.	• In areas of highest temperature, replace all B7 bolts. [Note (10)] Pressurized components may need metallurgical sampling to determine exact degree of effects by high-temperature exposure. (13)
		Long exposure to these temperatures may affect grain structure, properties and corrosion resistance of steels and stainless steels.	• Vessel, piping, and tankage components, and associated structural steel supports, that are warped or distorted may require repair or replacement. Regular carbon stainless steels are sensitized, may need replacing (10), (11), (12).
		Steel starting to oxidize, the thicker the scale the hotter the temperature.	• Remove oxide scale and determine amount of physical damage (13).
		Copper tubing oxidizing to black scale, softened and distorted.	• Replace copper tubing which has black oxide scale.

Table 11.6 – Guidelines for Assessing Fire Damage Effects Description of The Types of Damage That May Occur in the Heat Exposure Zone Categories

Heat Exposure Zone	Temperature Range	Heat/Temperature Effects	Observations and Conclusions
ZONE VI Extreme heat exposure, indicating vicinity of fire source or flame impingement	Over 730°C (1350°F)	Copper and copper alloys destroyed or melted.	• Almost all copper alloys will have to be scrapped. Critical equipment that was protected by insulation, water spray or fire proofing construction will have to be thoroughly inspected and tested.
		Heavily scaled steel may be distorted due to thermal stresses.	• Check areas of severe oxidation (13).
		Grain growth in fine grained steels.	• Possibility of liquid metal embrittlement cracking (LME) is greatest at these temperatures. Check areas exposed to molten metal for LME (8). • Check piping and vessels in low-temperature service for increase in grain size and loss of toughness. (14).
		Steel that is water quenched may harden and lose ductility. All heat-treated or cold-worked materials may have altered properties.	• Check bolting, vessels, and piping components for metallurgical changes (10), (11), and (12).

Notes:

1. Equipment heavily contaminated with smoke and water will require cleaning. Consider the potential effect of chloride-bearing fire water as a source of external stress-corrosion cracking or corrosion under insulation during service at a later date.
2. Consumption of organic chlorides (e.g., vinyl chloride or polyvinyl chloride (PVC)) in the fire may generate chlorine, HCl, or both. These gaseous products will be carried by the smoke and water spray onto the surrounding equipment. If so, decontamination, neutralizing, cleaning, and testing will be required to ensure that HCl corrosion has not and will not damage the equipment. If the fire water has carried acid chlorides onto stainless equipment, rapid external stress corrosion cracking failures could result from further service. A chloride spot check of uninsulated stainless equipment should reveal whether or not decontamination is required.
3. Temperatures in the range of 65°C to 205°C (150°F to 400°F) may begin to melt, char, harden, or change the color of paints, coatings, plastic tubing, and elastomers. Such changes will normally signal the need for replacement or re-coating of such organic components. Flange gaskets, O-ring seals, valve packing, and so forth should be checked for possible deterioration. These items are largely confined, so their deterioration may not be evident on first inspection.
4. As temperatures approach 205°C (400°F) electrical motors may be damaged due to the thermal decomposition of wiring and electrical insulation. Lead-tin solders begin to melt in this temperature range, breaking some electrical connections.
5. Steels of extremely high hardness (tool steels, springs, etc.) are tempered in this temperature range so accidental fire exposure may lower their hardness. Rupture disks, pressure relief valve springs, and pressure gauges may all be out of calibration due to exposure in the 205°C to 425°C (400°F to 800°F) range.

   Since the early 1980s, counterfeit bolts and cap screws have been used in some components and many of these bolts do not meet the strength and alloy requirements of ASTM or Society of Automotive Engineers (SAE) standards. Such substandard bolts may lose substantial strength at temperatures where ASTM or SAE standard fasteners are unaffected. For example, SAE low alloy steel with boron additions (and plain carbon steel) has been substituted for SAE grade 8 low alloy steel cap screws. These substandard cap screws will lose substantial strength if exposed to temperatures in excess of about 315°C (600°F) while standard SAE grade 8 cap screws would be completely unaffected by such exposure. Therefore, investigators should be alert to the possibility of lowered strength on flange connections and valve bonnets due to low-temperature tempering of such substandard bolting alloys.
6. Cold-drawn copper and copper alloys lose significant strength due to annealing and recrystallization in the range of 205°C to 425°C (400°F to 800°F). Roll joints in heat exchangers are commonly affected; leak testing and re-rolling will often be necessary. Sagging and deformation of copper instrument tubing will be observed, and tubing joints will often leak.

   Solution-annealed copper alloys suffer relatively little from exposure in the 205°C to 425°C (400°F to 800°F) range; pressurized components should be checked to determine if any observed loss of strength affects the structural integrity.

   Aluminum alloy equipment may suffer considerable loss of strength due to over-aging and recrystallization in the 205°C to 425°C (400°F to 800°F) range. The large thermal expansion of aluminum may cause widespread warping and tensile failures as well. Aluminum equipment exposed in this temperature range will often require replacement.
7. Low carbon structural steels, stainless steels, solution-annealed nickel alloys, non-heat-treated titanium and zirconium alloys are largely unaffected by exposure in the 205°C to 425°C (400°F to 800°F) range and may often be returned to service with no serious damage.
8. Contact of molten tin, lead, zinc, and their alloys with structural alloys may seriously affect the integrity of equipment due to liquid

Table 11.6 – Guidelines for Assessing Fire Damage Effects Description of The Types of Damage That May Occur in the Heat Exposure Zone Categories

Heat Exposure Zone	Temperature Range	Heat/Temperature Effects	Observations and Conclusions
			metal embrittlement (LME). Threshold temperatures and times for cracking are not well established although susceptible combinations of low-melting alloys and structural alloys have been documented (see Annex 11A, reference [5]). There is a possibility of LME in the temperature range 205°C to 425°C (400°F to 800°F); however, the risk of serious damage gets worse as temperatures go up in heat exposure Zones V and VI. If a low-melting alloy has dripped onto a structural item, refurbishment should include a careful and thorough removal of the low-melting alloy and a careful check for intergranular cracking.
			9. The onset of many severe metallurgical effects that affect vessel integrity and future service occurs in the range of 425°C to 730°C (800°F to 1350°F). Therefore, equipment exposed in this temperature range will require extra attention from the materials engineer and inspection team. Spheroidization or tempering of carbon and low alloy steels may significantly lower the strength of the materials used in the construction of pressurized components. If there is evidence of such metallurgical change, tests should be performed on samples removed from the equipment in question to ensure that the properties still meet specification. Stress relief of stainless steel and nickel alloys will begin in this temperature range. In the absence of thermal distortion or sensitization, such stress relief is not a cause for concern. However, rolled joints in shell and tube heat exchangers will often relax and leak, requiring resealing. Table 11.12 summarizes typical material degradation and appearance in the microstructure that may occur in carbon steel, low alloy steels, and stainless steel as a consequence of exposure to this range of temperatures.
			10. The normal tempering temperature is approximately 595°C (1100°F) for AISI alloy 4140 stud bolts. These bolts are commonly used in processing plants to ASTM specification A193 Grade B7. If the fire exposes such bolts to temperatures in excess of approximately 665°C (1225°F), the bolts will be softened below their required minimum strength level. Bolts with low strength may yield on re-torquing, producing leaks during unit restart. Low carbon steel used for piping and structures will be relatively unaffected by exposure for short times at temperatures in the range 425°C to 730°C (800°F to 1350°F); long-term exposure may lead to strength loss by spheroidization. Scaling due to oxidation in air begins on carbon steels in this temperature range. The scale itself is essentially equivalent to the mill scale often encountered on newly delivered steel products. The problems of dealing with such heat scale are similar to the problems of dealing with mill scale; such scale may promote pitting and localized attack in service and makes a poor anchor for protective coatings. For these reasons, the heat scale should be removed, as mill scale is, by abrasive blasting.
			11. Radiant heating or uneven heat flux to a portion of a vessel or pipe can cause severe residual stresses to develop during thermal expansion and contraction. If the various temperature indicators point to localized metal temperatures more than 540°C (1100°F), potentially harmful residual stresses should be considered in an FFS Assessment. A field stress relief may be needed to reduce uneven or undesirable residual stresses.
			12. Sensitization of austenitic stainless steels and other austenitic alloys may occur on exposure to temperatures above 425°C (800°F) and is normally most severe at temperatures around 675°C (1250°F). A sensitized austenitic stainless steel will lose considerable corrosion resistance in many environments; depending on the service such sensitized materials may not be suitable for further use. The mechanical properties of AISI Type 300 stainless steels are not significantly reduced by sensitization.
			13. Oxidation of low carbon steel occurs rapidly above 730°C (1350°F) resulting in heavy scale build-up. Damage may be less than it appears initially since the volume of scale is from seven to 20 times greater than that of the metal from which it formed. Heavily scaled parts should be cleaned of scale, checked for thickness, grain structure, and hardness to facilitate decisions regarding reuse. After exposure to temperatures in excess of 730°C (1350°F), hardenable steels may exhibit a wide range of hardness, toughness and grain structure depending on exposure temperature and cooling rate. If exposure at temperatures in excess of 730°C (1350°F) is followed by rapid cooling steels may show extremely high hardness and low toughness. Such hardened material is extremely prone to delayed brittle fracture or hydrogen-assisted cracking and therefore must be identified and removed prior to returning the equipment to service.
			14. The grain growth that occurs in carbon steels exposed to temperatures above about 815°C (1500°F) is extremely detrimental to toughness. Common structural steels such as ASTM A53 show a gradual coarsening of the grain as temperatures increase; above about 955°C (1750°F), the grain size may be large enough to raise the ductile-to-brittle transition temperature well above the ambient temperature. Fine-grained low-temperature steels such as ASTM A516 and A333 tend to show grain coarsening more abruptly over a narrow range of temperatures beginning at about 1040°C (1900°F). The primary concern for the presence of such coarse grains is the severe loss in toughness. It is seldom practical to refine the grain size of grain-coarsened steels in the field. In some circumstances, a normalization treatment in a heat-treating shop may be used to restore original grain size and toughness.

Table 11.7 – Temperature Indicators That Can Be Used to Categorize Fire Damaged Components

Temperature Indicators	Description
Melting, Charring and Ignition	Melting points make excellent temperature indicators, since a piece of melted equipment is easy to identify, and the melting ranges of alloys are largely unaffected by time. Only eutectic alloy compositions have a true melting point; all other alloys melt across a range of temperatures (e.g., the lead-based Babbitt frequently used for sliding bearings in pumps and compressors has a solidus temperature of 240°C (465°F), and a liquidus temperature of 270°C (520°F)). The liquidus temperatures for a wide variety of processing plant materials are shown in Table 11.14. Ignition of wood is affected by species, temperature, and time. The ignition temperature for some types of woods is shown in Table 11.15. Glass will melt at high temperature and will crack if subjected to even moderately high cooling rates. Consequently, the condition of sight glasses, flow meters, gauge faces, and other glass items may give useful indications of temperature and cooling rates. Glasses are non-crystalline even at room temperature; their transition to liquid is somewhat different from that of metal alloys. As the temperature of glass increases, it reaches a point where it begins to soften. Higher temperatures produce lower hardness and lower shear strength until, at the "working temperature," the glass is essentially a syrupy liquid. The softening point and working temperatures of many glasses are shown in Table 11.16. The discoloration and charring of some organic materials such as polyurethane foam, phenolics resin, and acrylic resins are also largely controlled by temperature.
Oxidation of Metals	The onset of high-temperature scaling on carbon steels or stainless steel exposed to air is largely temperature controlled. Below a certain temperature (approximately 540°C (1000°F) for carbon steels, and 845°C (1550°F) for 18Cr-8Ni stainless steels), essentially no high-temperature oxidation will be observed. Above that threshold temperature, a significant oxide scale may form, even in the short-term exposures (15 minutes to several hours) characteristic of accidental fires. The friable nature and logarithmic growth curve of some high-temperature oxides make time or temperature estimates from oxides thickness difficult to interpret. The presence of scale itself is, however, indicative of temperatures at least as high as the threshold. The scaling temperatures for a variety of common processing plant materials are shown in Table 11.17.
Tempering of Steels	In the range of 205°C to 480°C (400°F to 900°F), cold-worked and heat-treated steels of high hardness begin to lose strength. Bearing assemblies, springs, aircraft-grade fasteners, and other items are affected. The reduction in hardness may be used to estimate time and temperature of exposure based on the tempering curves of the alloy in question. One of the more common bolting materials in processing plants is ASTM A193 Grade B7. Its response to heat exposure is fairly well known and can be used to help assess the heat to which adjacent piping or vessels were subjected. Different tempering temperatures produce different characteristic colors on clean steel surfaces such as pump shafts. (Temper colors will not develop on painted steel or rusty surfaces.) The temper colors commonly observed on steel as a function of temperature are shown in Tables 11.18(a) and (b). A picture with samples heated at different temperatures for 10 and 30 minutes exposures and then cooled in the air is shown in Table 11.18(b) for reference.

Table 11.7 – Temperature Indicators That Can Be Used to Categorize Fire Damaged Components

Temperature Indicators	Description
Grain Growth of Carbon Steel	General purpose carbon steels such as ASTM A53 show a gradual coarsening of the grains as the temperature is increased above the austenitizing temperature. Exposure above about 930°C (1700°F) produces very large grains. The effect of temperature on grain growth of carbon steel is shown in Figure 11.8. Fine-grained carbon steels of high toughness are used for low-temperature service; typical specifications included ASME SA 333 for pipe and SA 350 for flanges. The fine grain size is produced by deoxidizing practice (usually aluminum additions), normalizing, and cooling at a controlled rate. Steels made to fine-grained practice (ASTM 333, 516, etc.) show little grain coarsening between the austenitizing temperature and 1030°C (1900°F). Between 1030°C to 1095°C (1900°F to 2000°F), the grain size increases dramatically.
Grain Growth in Copper and Associated Alloys	In the range of 205°C to 425°C (400°F to 800°F), copper and copper alloys will soften and begin to show grain growth. Laboratory determination of hardness and grain size, when compared with equipment not exposed to the fire, may be useful for estimating the time and temperature of exposure. The effect of temperature on grain growth of cold-drawn, commercially pure copper is shown in Figure 11.9. The effects of temperature on grain size and hardness of cold-drawn admiralty brass are shown in Figures 11.10 and 11.11, respectively.
Spheroidization of Carbon Steel	Long-term (several hours) exposure to temperatures in the range of 650°C to 730°C (1200°F to 1350°F) may spheroidizes carbon steel if the cooling rate is slow. Spheroidization reduces the strength of the steel.
Sensitization of Austenitic Stainless Steels	The well-known sensitization reaction of austenitic stainless steels can be a useful temperature indicator. In the temperature range of 425°C to 900°C (800°F to 1650°F) chromium carbide precipitation in the grain boundaries leaves a distinctive ditching pattern when these alloys are examined metallographically using the ASTM A262 practice A test. Much of the chromium-nickel austenitic stainless steel produced in recent years is of the low carbon variety, to avoid sensitization during welding. Such low carbon stainless steel may still be sensitized during accidental fires if the time of exposure exceeds approximately 10 hours (See Figure 11.12).
Distortion of Structural Steel	Gross plastic deformation of low carbon steel I-beams, channel sections, and other structural members is sometimes observed if the temperature is high enough to reduce the yield stress below the applied stress. Above 760 °C (1400 °F), the yield stress of carbon steel has dropped to only 26 MPa (3750 psi) and gross plastic flow is possible at relatively low stress levels (see Figure 11.13). Therefore, the presence of structural steel grossly deformed by a fire is indicative of temperatures of 760°C (1400°F) or above.
Softening of Aluminum Alloys	Aluminum alloys rapidly lose strength above about 150°C (300°F), (see Figure 11.14). Sagging or warping of aluminum piping for fittings is suggestive of temperatures at least that high.
Stress Relief of Austenitic Stainless Steel and Nickel Alloys	Exposure to temperatures above about 480°C (900°F) for more than 15 to 30 minutes will begin to produce significant stress relief of many austenitic stainless steels and nickel alloys. Observations involving stress relief of stainless items include leaking joints in rolled-in heat exchanger tubes, leaking fittings on swaged instrument tubing joints, and softened bourdon tubes on pressure gauges.

Table 11.8 – Temperature of Steel Based on the Visible Radiation Spectrum

Radiation Color During a Fire	Approximate Temperature	
	(°C)	(°F)
Black	540	1000
Faint Dark Red	590	1100
Cherry Red (Dark)	650	1200
Cherry Red (Medium)	700	1300
Red	760	1400
Light Red	815	1500
Reddish-Orange	870	1600
Orange	930	1700
Orange To Pale Orange-Lemon	980	1800
Orange To Pale Orange-Lemon	1040	1900
Orange To Pale Orange-Lemon	1090	2000
Lemon	1150	2100
Light Lemon	1205	2200
Yellow	1260	2300
Light Yellow	1315	2400
Yellowish-Grey: "White"	1370	2500

Table 11.9 – Color of Smoke from Fuel Burned in Air

Fuel	Color of Smoke
Hay/Vegetable Compounds	White
Phosphorus	White
Benzene	White to gray
Nitro-Cellulose	Yellow to Brownish Yellow
Sulfur	Yellow to Brownish Yellow
Sulfuric Acid, Nitric Acid, Hydrochloric Acid	Yellow to Brownish Yellow
Gunpowder	Yellow to Brownish Yellow
Chlorine Gas	Greenish Yellow
Wood	Gray to Brown
Paper	Gray to Brown
Cloth	Gray to Brown
Iodine	Violet
Cooking Oil	Brown
Naphtha	Brown to Black
Lacquer Thinner	Black
Turpentine	Black
Acetone	Black
Kerosene	Black
Gasoline	Black
Lubricating Oil	Black
Rubber	Black
Tar	Black
Coal	Black
Foamed Plastic	Black
Butadiene	Black

Table 11.10 – Ignition Temperature of Gases

Gas	Temperature	
	(°C)	(°F)
Ammonia (Anhydrous)	650	1200
Butane	405	760
Carbon Monoxide	610	1130
Ethane	515	960
Ethylene	490	915
Hydrogen	400	750
Hydrogen Sulfide	260	500
Methane	540	1005
Natural Gas	480-630	900-1170
Propane	450	840
Propylene	460	860

Table 11.11 – Ignition Temperature of Liquids

Liquid	Flash Point (1)		Autoignition Temperature (2)	
	(°C)	(°F)	(°C)	(°F)
Castor Oil	230	450	450	840
Corn Oil	255	490	395	740
Creosote Oil	75	165	335	635
Denatured Alcohol	15	60	400	750
Ethyl Alcohol, Ethanol	15	55	365	690
Ethyl Ether	-45	-50	160	320
Fuel Oil No. 1	40-75	100-165	210	410
Fuel Oil No. 2	44-90	110-190	255	495
Fuel Oil No. 3	45-110	110-230	260	500
Fuel Oil No. 4	55-65	130-150	265	505
Fuel Oil No. 5	55-65	130-150	NA	NA
Fuel Oil No. 6	65	150	405	765
Gasoline	-45	-45	255	495
Glycerin	160	320	365	690
Kerosene	40-75	100-165	210	410
Lacquer	-20-25	0-80	NA	NA
Linseed Oil	220	430	345	650
Methyl Alcohol	10	50	385	725
Methyl Ethyl Ketene	-5	20	515	960
Naphtha, Safety Solvent	40-60	100-140	235	455
Naphthalene	80	175	525	980
Olive Oil	225	440	345	650
Peanut Oil	280	540	445	835
Soybean Oil	280	540	445	835
Toluene	5	40	480	895
Tong Oil	290	550	455	855
Turpentine	35	95	255	490
Xylem	25-30	80-90	465-530	865-985

Notes:

1. Flash Point – The lowest temperature at which a liquid exposed to air gives off sufficient vapor to form a flammable mixture near the surface of the liquid.
2. Autoignition – The lowest temperature required to cause a self-sustaining combustion, without initiation by a spark or flame, of a flammable material when its vapor is mixed with air in a flammable concentration.

Table 11.12 – Typical Material Degradation and Damage That May Occur in Carbon Steel, Low Alloys Steels, and Stainless Steels due to Heat Exposure During Fire

Degradation of Material	Potential Failure Mode	Appearances in Microstructure	Aspects to be Considered for Reuse
Reduction in Tensile Strength or Softening	Ductile Failure	Grain Coarsening Spheroidization of Carbides	Decrease of Hardness
Reduction in Toughness	Brittle Failure	Hardened Microstructure	Decrease of Impact Energy Increase of Hardness
Decrease of Corrosion Resistance	Corrosion Metal Loss	Sensitization at Grain Boundary and Intergranular Corrosion	Operating Environment
	Stress Corrosion Cracking	Sensitization	Operating Environment, especially for Polythionic Acid or Humid Environment
		Hardened microstructure	Operating Environment, especially for Hydrogen Embrittlement, Sulfide, Amine, Alkali, Liquid Ammonia, CO-CO_2-H_2O Environment

Table 11.13 – Heat Exposure Levels for Materials of Construction Which Satisfy the Level 1 Assessment Criteria

Materials	Typical ASTM Specifications for Pressurized Components	Heat Exposure Zone Levels Which Satisfy the Level 1 Assessment Criteria
Carbon Steels	A36, A53, A105, A106, A131, A139, A181, A216, A234, A266, A283, A285, A333, A350, A352, A420, A515, A516, A537, A671, A672, API 5L	I, II, III, IV
Low Alloy Steels	A182, A217, A234, A335, A336, A387, A691	I, II, III, IV
Austenitic Stainless Steels (1)	A312, A358, A240, A403, A351	I, II, III, IV
Alloy 20	B366, B462, B463, B464, B729, B744	I, II, III, IV
Alloy 400	B127, B164, B165, B366, B564, A494	I, II, III
Duplex Stainless Steels (2) Alloy 2205 Alloy 2507	A182, A240, A789, A790, A815 (UNS S31803, UNS J92205) (2507 – UNS S39275)	I, II
Alloy 800, 800H	B163, B366, B407, B409, B564	I, II, III, IV
Alloy 825	B163, B366, B423, B424, B704, B705	I, II, III, IV
Alloy 600	B163, B168, B366, B564	I, II, III, IV
Alloy 625	B167, B366, B443, B444, B564, A494	I, II, III, IV
Alloy C-276	B366, B575, B622	I, II, III, IV
Copper Alloys	B68, B96, B111, B169, B171, B395, B584	I, II
Aluminum Alloys	B209, B210, B241, B247	I, II
Precipitation Hardened Alloy Steels (3)	17-4PH, 17-7PH	I, II, III

Notes:

1. If the austenitic stainless steel components are insulated, are not coated for under insulation stress corrosion cracking protection, and normally operate between 50°C and 175°C (120°F and 350°F), then preventative maintenance may be required to assure that halide contamination of the insulated surfaces has not occurred. The concern in this case is halide induced stress corrosion cracking of contaminated insulated surfaces after the equipment is returned to service.
2. Above 315°C (600°F), Duplex alloys will undergo a loss of toughness with time and temperature. In addition, severe loss in ductility (sigma phase formation) with short term exposure to 595°C and 925°C (1100°F and 1700°F) can also occur.
3. Precipitation hardened alloys may experience a loss in toughness when heated above 260°C (500°F), and slowly cooled.

Table 11.14 – Melting Points of Metals and Alloys

Material	UNS Number	Melting Point (1)	
		(°C)	(°F)
Commercially Pure Aluminum	A91050	655	1215
Aluminum Alloy	A96061	650	1205
Red Brass	C23000	1025	1880
Yellow Brass	C26800	930	1710
Admiralty Brass	C44300	940	1720
Naval Brass	C46400	900	1650
70/30 Copper Nickel	C71500	1240	2260
Silicon Bronze (2)	C87200	915	1680
Tin Bronze (2)	C90300	1000	1830
2.52% Carbon Gray Iron (2)	F11701	1295	2360
Ductile Iron (2)	F32800	1160	2120
0.15% Carbon Steel	G10150	1525	2780
CA15 (2)	J91150	1510	2750
CD-4Mcu (2)	--	1480	2695
CF-8 (2)	J92600	1425	2595
CF-8M (2)	J92900	1400	2550
CK-20 (2)	J94202	1425	2595
CN-7M (2)	--	1455	2650
1 ¼ Cr – ½ Mo	K11597	1510	2750
2 ¼ Cr – 1 Mo	K21590	1515	2760
5 Cr – ½ Mo	K41545	1510	2755
9 Cr – 1 Mo	K90941	1500	2730
Nickel 200	N02200	1445	2635
Alloy 400 (Model (3))	N04400	1350	2460
Alloy K-500 (Model (3))	N05500	1350	2460
Alloy X (Hostelry (3))	N06002	1315	2400
Alloy G (Hostelry (3))	N06007	1345	2450
Alloy 600 (Inconel (3))	N06600	1415	2580

Table 11.14 – Melting Points of Metals and Alloys

Material	UNS Number	Melting Point (1)	
		(°C)	(°F)
Alloy 601 (Inconel (3))	N06601	1370	2495
Alloy 625 (Inconel (3))	N06625	1350	2460
Alloy 718 (Inconel (3))	N07718	1335	2435
Alloy X-750 (Inconel (3))	N07750	1425	2600
Alloy 20 (20Cb3 (3))	N08020	1425	2600
Alloy 800 (Incoloy (3))	N08800	1385	2525
Alloy 801 (Incoloy (3))	N08801	1385	2525
Alloy 825 (Incoloy (3))	N08825	1400	2550
Alloy 925 (Incoloy (3))	N09925	1365	2490
Alloy C-276 (Hastelloy (3))	N10276	1315	2400
Alloy B-2 (Hastelloy (3))	N10665	1380	2520
17-4 PH	S17400	1440	2625
Type 304	S30400	1450	2640
Type 310	S31000	1450	2640
Type 316	S31600	1400	2550
Type 321	S32100	1425	2595
Type 347	S34700	1425	2595
Titanium Grade 2	R50400	1705	3100
Stellite 6 (3)	W73006	1355	2470
Copper (4)	--	1085	1980
Gold (4)	--	1065	1945
Iron (4)	--	1535	2795
Lead (4)	--	330	620
Magnesium (4)	--	650	1200
Tin (4)	--	230	450
Silver (4)	--	960	1760
Zinc (4)	--	420	790
Zirconium (4)	--	1850	3365

Table 11.14 – Melting Points of Metals and Alloys

Material	UNS Number	Melting Point (1)	
		(°C)	(°F)
95/5 Lead-Tin Solder	54320	310	595
97.5/2.5 Lead-Silver Solder (5)	--	305	580
Lead Babbitt – Alloy 7 (6)	--	270	515

Notes:
1. Pure metals melt at a specific temperature. Metal alloys melt over a temperature range. The temperature shown for alloys is the liquidus temperature; that is, the temperature at which the alloy is completely liquid. The temperature at which the alloy begins to melt (solidus temperature) is somewhat lower.
2. Casting.
3. Trade Name.
4. Pure element.
5. ASTM Alloy Grade 2.5S.
6. ASTM B23.

Table 11.15 – Ignition Temperature of Wood

Type of Wood	Approximate Ignition Temperature	
	(°C)	(°F)
Douglas Fir	260	500
Paper Birch	200	400
Spruce	260	500
Western Red Cedar	190	380
White Oak	200	400
White Pine	260	500

Note: The ordinary ignition temperature of wood is between 230°C and 430°C (450°F and 800°F). The values in the table represent average ignition temperatures for selected wood types.

Table 11.16 – Properties of Commercial Glass

Glass Code	Glass type	Principal Use	Thermal Expansion Coefficient ($°C^{-1}$)	Modulus of Elasticity (MPa)	Thermal Shock Resistance			Thermal Stress Resistance (°C)	Softening Point (°C)	Working Point (°C)
					1/8 inch Thick (°C)	1/4 inch Thick (°C)	1/2 inch Thick (°C)			
0010	Potash-soda lead	Lamp tubing	$91(10)^{-7}$	$6.21(10^4)$	65	50	35	19	625	970
0041	Potash-soda-lead	Thermometers	$84(10)^{-7}$	--	70	60	40	19	650	--
0080	Soda-line	Lamp bulbs	$92(10)^{-7}$	$6.76(10^4)$	65	50	35	17	695	1000
0120	Potash-soda-lead	Lamp tubing	$89(10)^{-7}$	--	65	50	35	17	630	975
1710	Hard lime	Cooking utensils	$42(10)^{-7}$	$8.76(10^4)$	135	115	75	29	915	1200
1770	Soda-lime	General	$82(10)^{-7}$	--	70	60	40	19	710	--
2405	Hard red	General	$43(10)^{-7}$	--	135	115	75	36	800	--
2475	Soft-red	Neon signs	$91(10)^{-7}$	--	65	50	35	17	695	--
3321	Hard green sealing	Sealing	$40(10)^{-7}$	--	135	115	75	39	780	--
4407	Soft green	Signal ware	$90(10)^{-7}$	--	65	50	35	17	695	--
6720	Opal	General	$80(10)^{-7}$	--	70	60	40	19	775	--
6750	Opal	Lighting ware	$87(10)^{-7}$	--	65	50	35	18	670	--
6810	Opal	Lighting ware	$69(10)^{-7}$	--	85	70	45	23	770	--
7050	Borosilicate	Series sealing	$46(10)^{-7}$	--	125	100	70	34	705	--
7052	Borosilicate	Kovar sealing	$46(10)^{-7}$	--	125	100	70	34	710	1115
7070	Borosilicate	Low-loss electrical	$32(10)^{-7}$	$4.68(10^4)$	180	150	100	70	---	1100
7250	Borosilicate	Baking Ware	$36(10)^{-7}$	---	160	130	90	43	775	---
7340	Borosilicate	Gauge Glass	$67(10)^{-7}$	$7.93(10^4)$	85	70	45	20	785	---
7720	Borosilicate	Electrical	$36(10)^{-7}$	$6.55(10^4)$	160	130	90	45	755	1110
7740	Borosilicate	General	$32(10)^{-7}$	$6.76(10^4)$	180	150	100	48	820	1220
7760	Borosilicate	Electrical	$34(10)^{-7}$	$6.27(10^4)$	160	130	90	51	780	1210
7900	96% Silica	High Temperature	$8(10)^{-7}$	$6.69(10^4)$	1250	1000	750	200	1500	---
7910	96% Silica	Ultraviolet Transmission	$8(10)^{-7}$	$6.69(10^4)$	1250	1000	750	200	1500	---
7911	96% Silica	Ultraviolet Transmission	$8(10)^{-7}$	$6.69(10^4)$	1250	1000	750	200	1500	---
8870	High Lead	Sealing or Electrical	$91(10)^{-7}$	$5.24(10^4)$	65	50	35	22	580	---
9700	---	Ultraviolet Transmission	$37(10)^{-7}$	---	150	120	80	42	805	1195
9741	---	Ultraviolet Transmission	$39(10)^{-7}$	---	150	120	80	40	705	---

Table 11.17 – Scaling Temperatures of Alloys in Air

Alloy Designation	Composition	Scaling Temperature	
		(°C)	(°F)
Carbon Steel	Fe-0.10C	480	900
Low Alloy Steel	1-1/4Cr-1/2Mo	620	1150
Low Alloy Steel	2-1/4Cr-1Mo	620	1150
Low-Alloy Steel	5Cr-0.5Mo	620	1150
Low Alloy Steel	7Cr-1Mo	650	1200
Low Alloy Steel	9Cr-1Mo	675	1250
Type 410 Stainless Steel	12Cr	760	1400
Type 430 Stainless Steel	17Cr	845	1550
Type 442 Stainless Steel	21Cr	955	1750
Type 446 Stainless Steel	27Cr	1040	1900
Type 304 Stainless Steel Type 321 Stainless Steel Type 347 Stainless Steel	18Cr-8Ni 18Cr-10Ni-Ti 18Cr-10Ni-Cb	900	1650
Type 309 Stainless Steel	23Cr-12Ni	1095	2000
Type 310 Stainless Steel	25Cr-20Ni	1150	2100
Type 316 Stainless Steel	18Cr-8Ni-2Mo	900	1650
Duplex 2205 Duplex 2507	22Cr-5Ni-3Mo 25Cr-7Ni-4Mo	1040	1900
Alloy 600 Alloy 625	72Ni-15Cr-8Fe 60Ni-22Cr-9Mo-3.5Cb	1040	1900
Alloy 800 Alloy 825	33Ni-42Fe-21Cr 42Ni-Fe-21.5Cr-3Mo-2.3Cu	1040	1900
N-155	Fe-based superalloy	1040	1900
S-816	Co-based superalloy	980	1800
M-252	Ni-based superalloy	980	1800
HS-21	Co-based superalloy Cr-based superalloy Ni-based superalloy Cu-based superalloy	1150 900 790 455	2100 1650 1450 850
Brass	70Cu-30Zn	705	1300
Alloy B-2	Ni-based superalloy	760	1400
Alloy C-276	Ni-based superalloy	1150	2100
Alloy X	Ni-based superalloy	1205	2200
HW HT	12Cr-60Ni-bal Fe 15Cr-66Ni-bal Fe	1120 1150	2050 2100
HX	17Cr-66Ni-bal Fe	1150	2100

Note:

1. The temperature below which the oxidation rate is negligible. Negligible is often defined as less than 3 g weight gain per square meter (0.002 g weight gain per square inch) per hour.

Table 11.18(a) – Tempering Colors of Steel

Temper Color	Approximate Temperature	
	(°C)	(°F)
Pale Yellow	190	380
Straw Yellow	215-225	420-440
Yellowish-Brown	240-250	460-480
Bluish-Purple	260-280	500-540
Violet	280-295	540-560
Pale Blue	295-305	560-580
Blue	315-340	600-640

Table 11.18(b) – Tempering Colors of Steel by Experimental Exposure

Temper	200°C (392°F)	250°C (482°F)	300°C (572°F)	350°C (662°F)	400°C (752°F)
10 min AC	Silver	Silver Gray	Yellow Brown	Dark Grey	Blue
30 min AC	Silver Gray	Yellow Brown	Bluish-Purple	Blue	Yellow Ocher

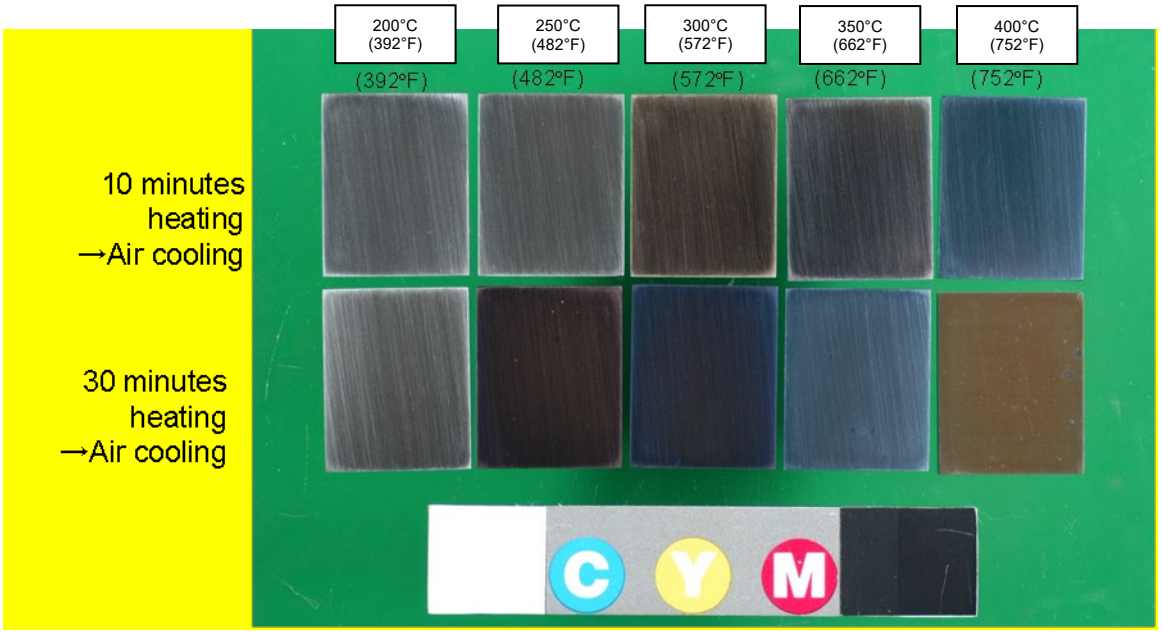

Notes:

1. Material: ASTM A36.
2. Temper Color varies depending on the exposed temperature and duration. Longer thermal exposure will make the change of color clear.
3. Reference colors are C Cyan; Y: Yellow; M: Magenta.

11.12 Figures

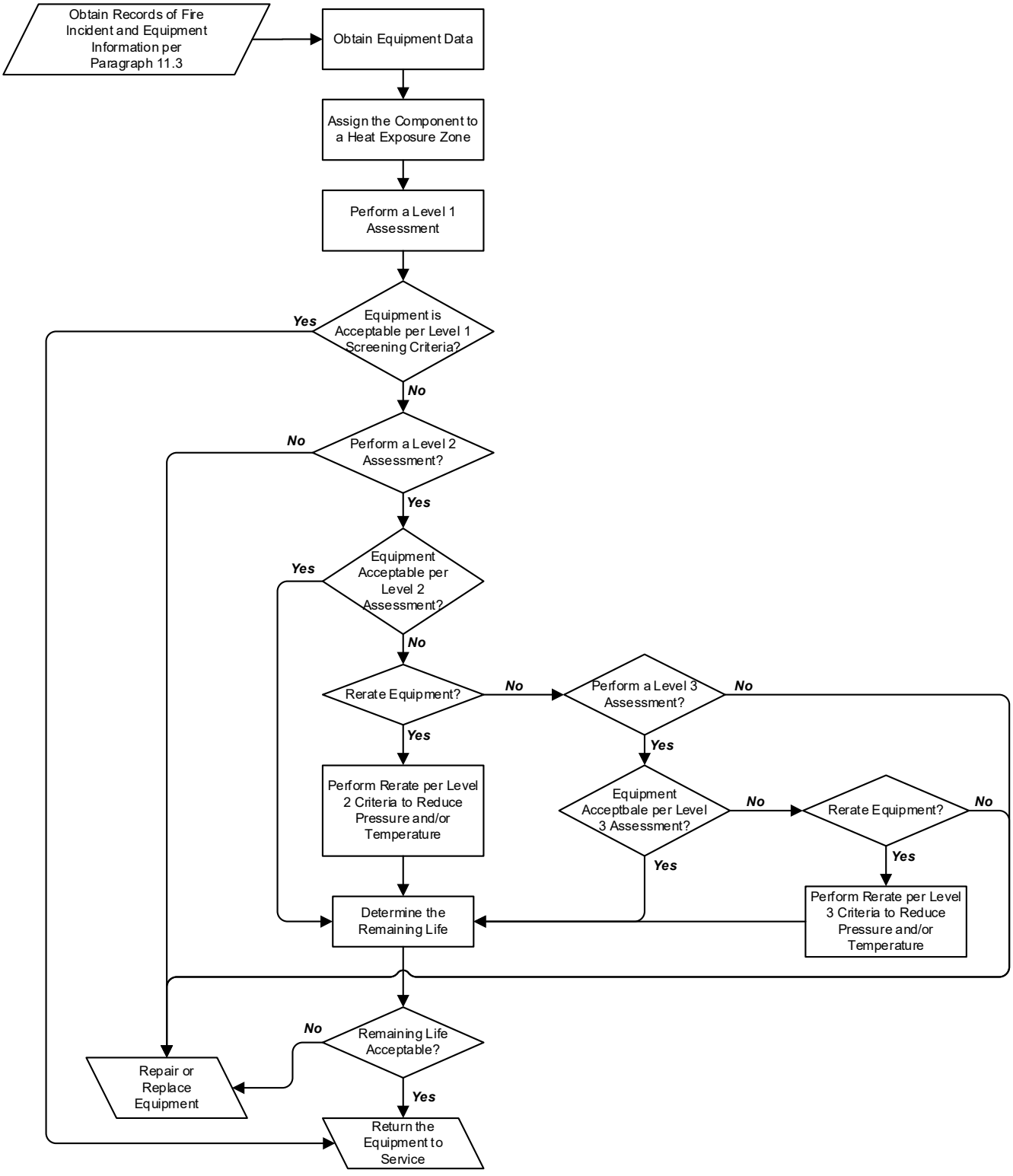

Figure 11.1 – Overview of the Procedure to Evaluate a Component with Fire Damage

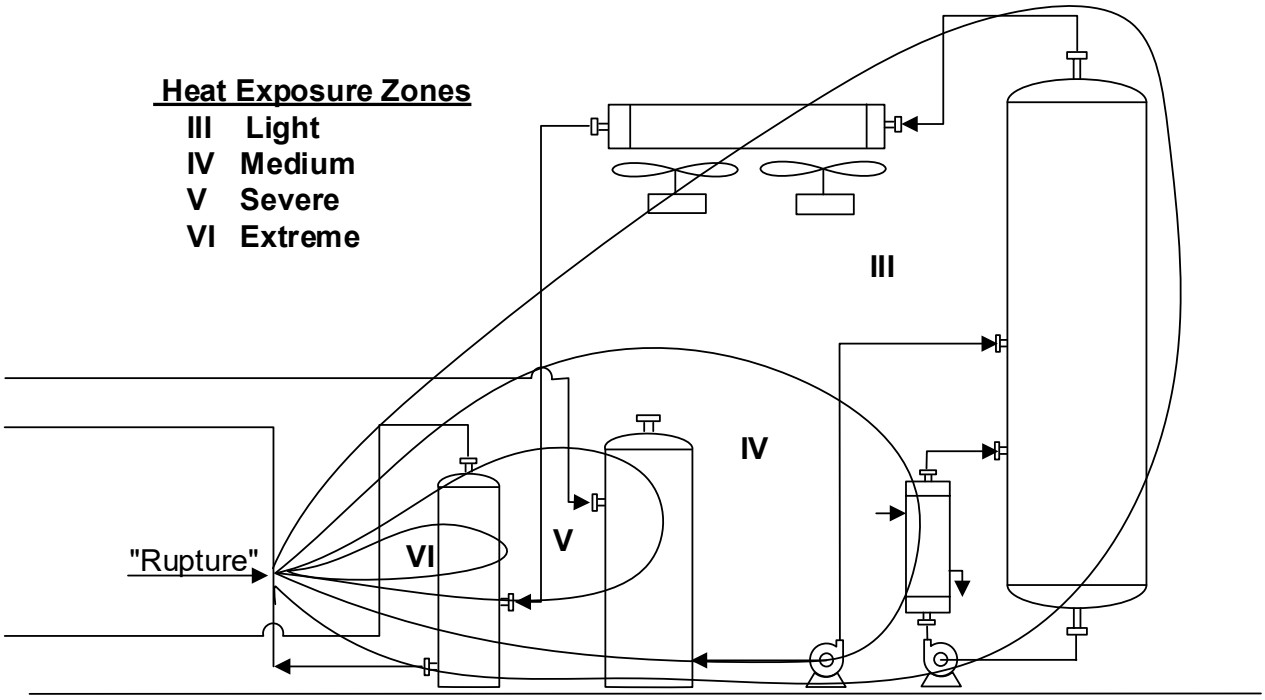

Note: See Table 11.6 for definitions of the Heat Exposure Zones.

Figure 11.2 – Idealized Representation of Plant Equipment Exposed to Different Fire (Heat) Zones III through VI

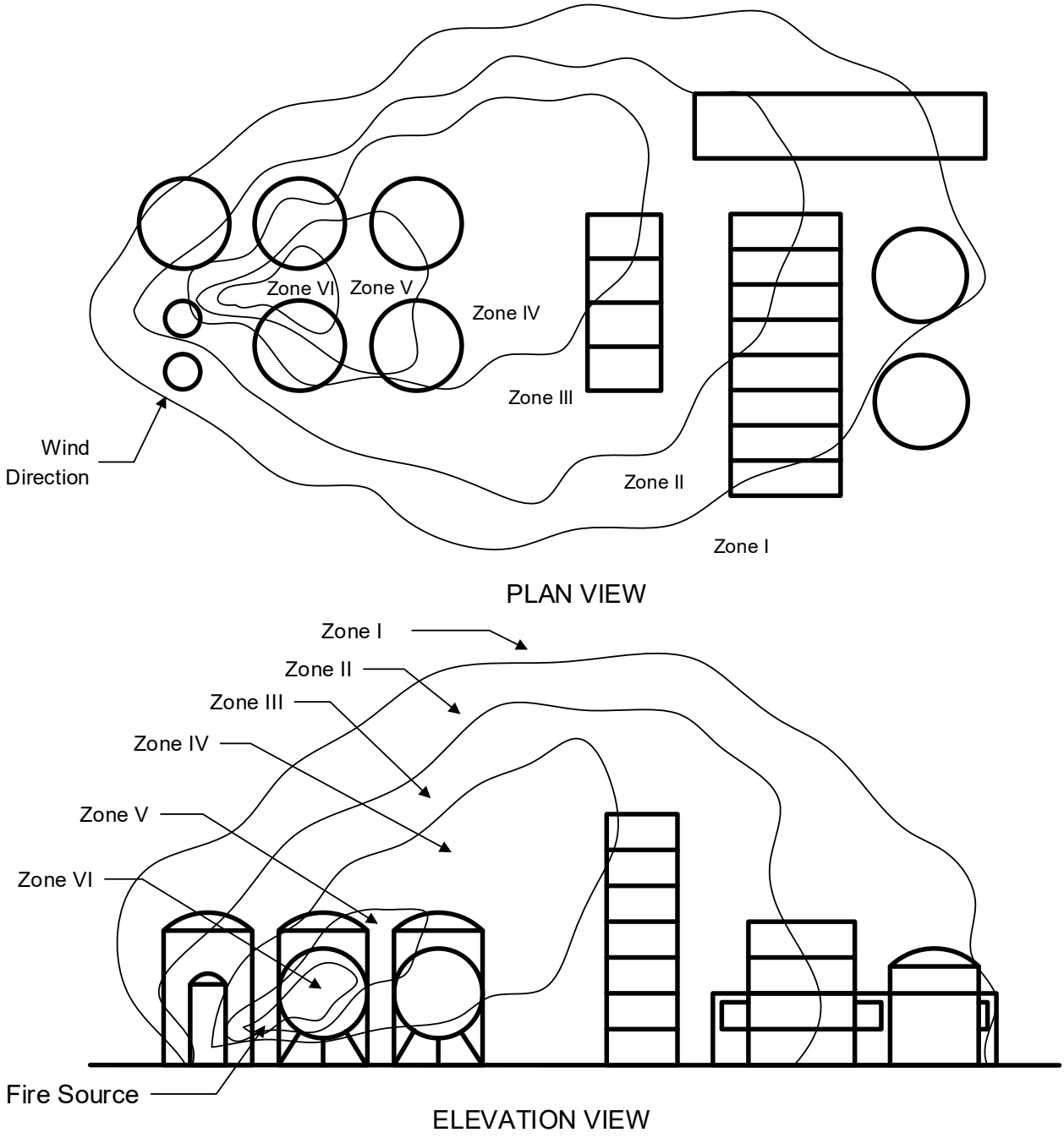

Note: See Table 11.6 for definitions of the Heat Exposure Zones.

Figure 11.3 – Idealized Fire (Heat) Pattern and Equipment Exposure with Zones I through VI Shown

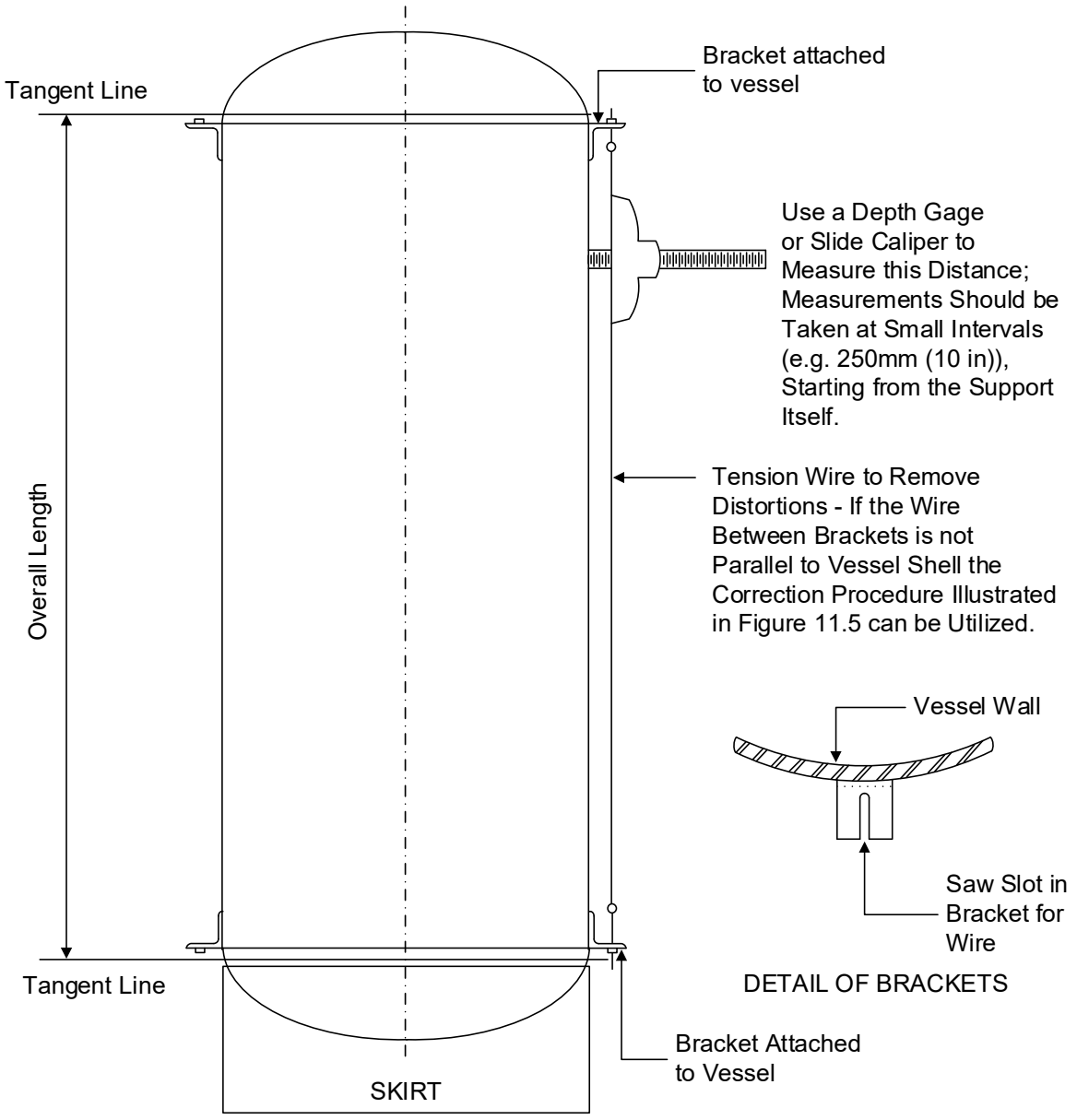

Figure 11.4 – Sketch Illustrating the Procedure for Measuring the Vertical Shell Profile to Detect Vessel Distortion

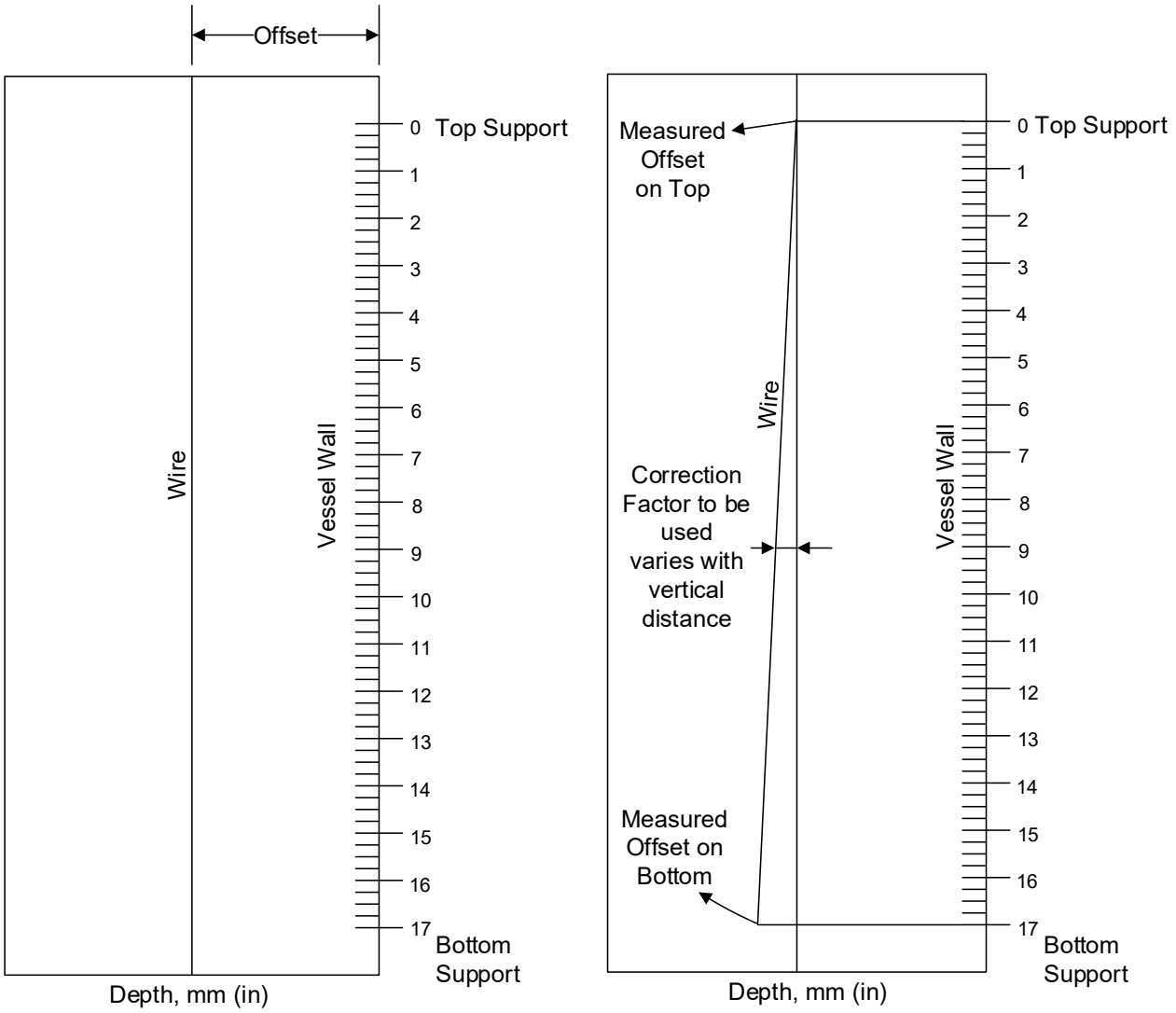

Note: The correction factor is applied to the offset measurements to account for a non-vertical datum (vertical wire used as a reference line)

Figure 11.5 – Illustration of Vertical Wire Offset for Measuring Profile for the Ideal Situation and When the String is Not Parallel to the Vessel

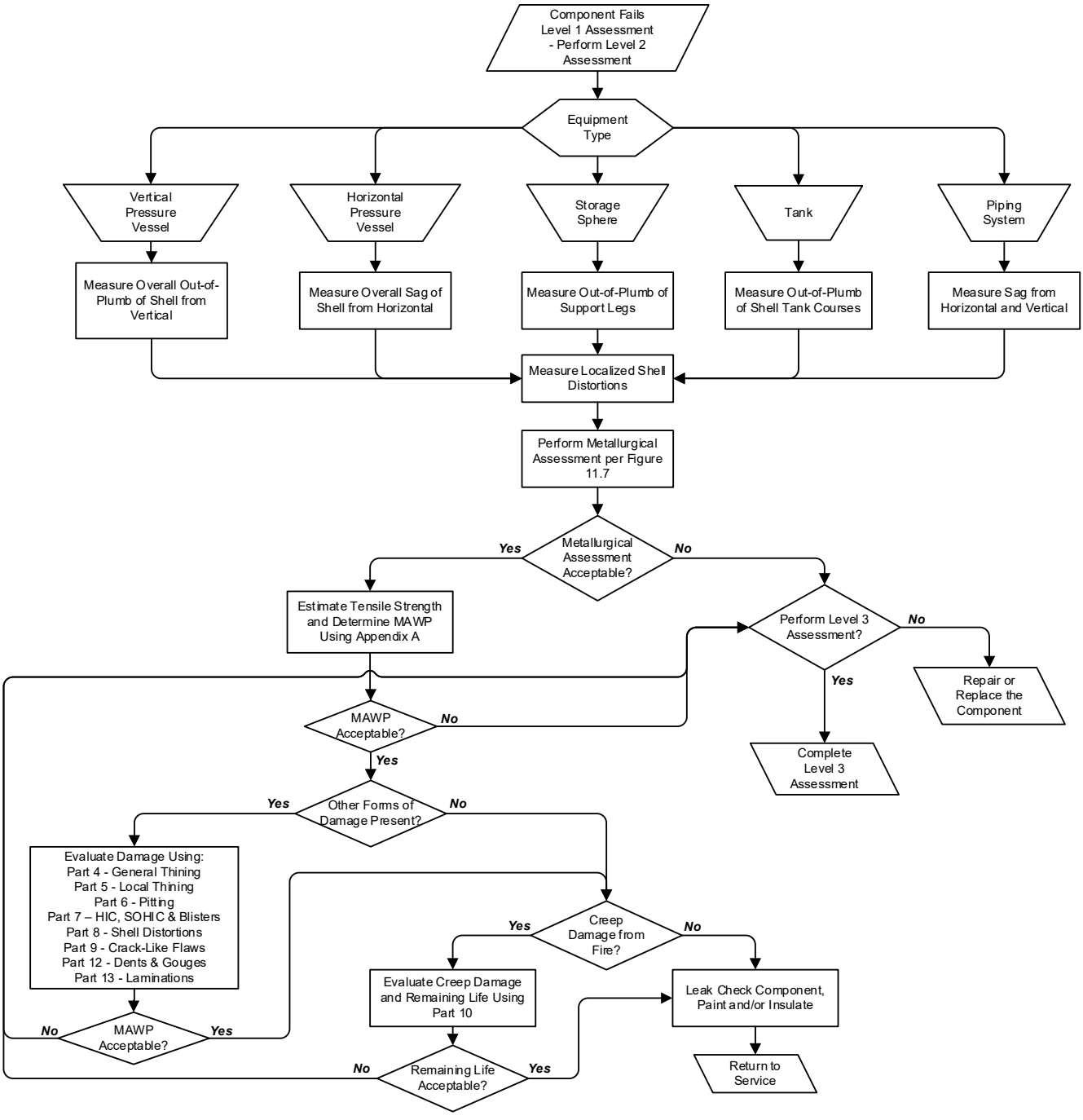

Figure 11.6 – Level 2 Assessment Procedure for Fire Damage

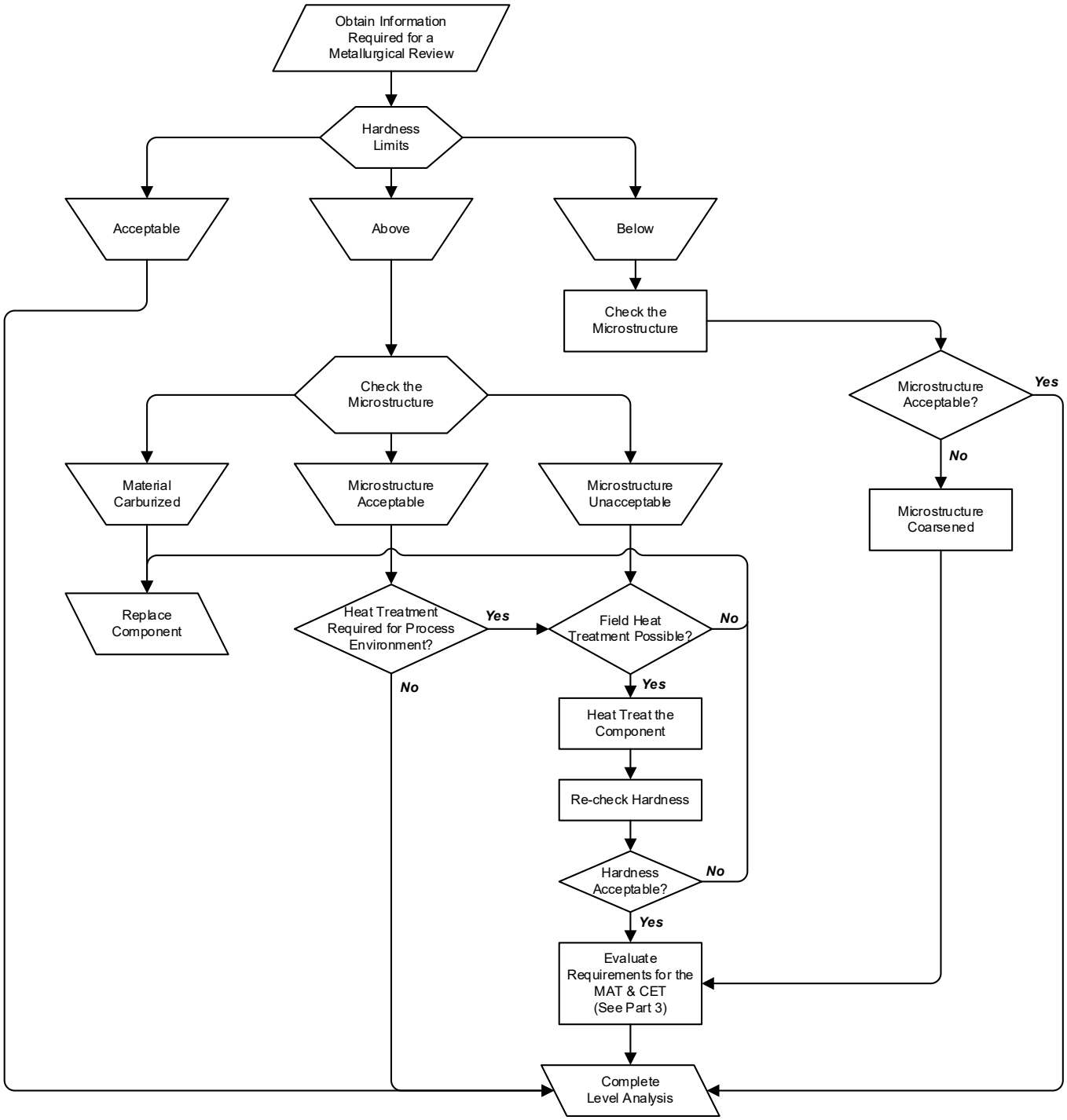

Figure 11.7 – Flow Diagram for Metallurgical Assessment of Fire Damage to Carbon and Low Alloy Steels

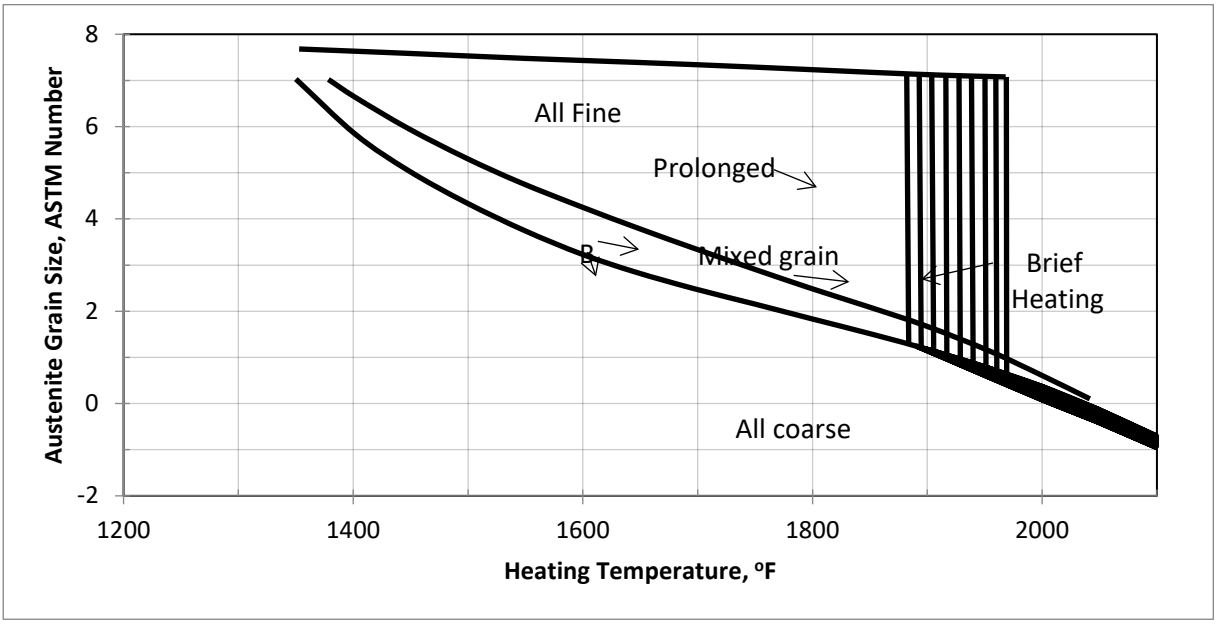

Notes:

1) Curve A – killed steel with a fine austenitic grain size (e.g., ASTM A 516).
2) Curve B – killed steel with a coarse austenitic grain size (e.g., ASTM A 515).

Figure 11.8 – Coarsening Behavior of Carbon Steels as a Function of Temperature (From: ASM Metals Handbook, 1948, ASM International)

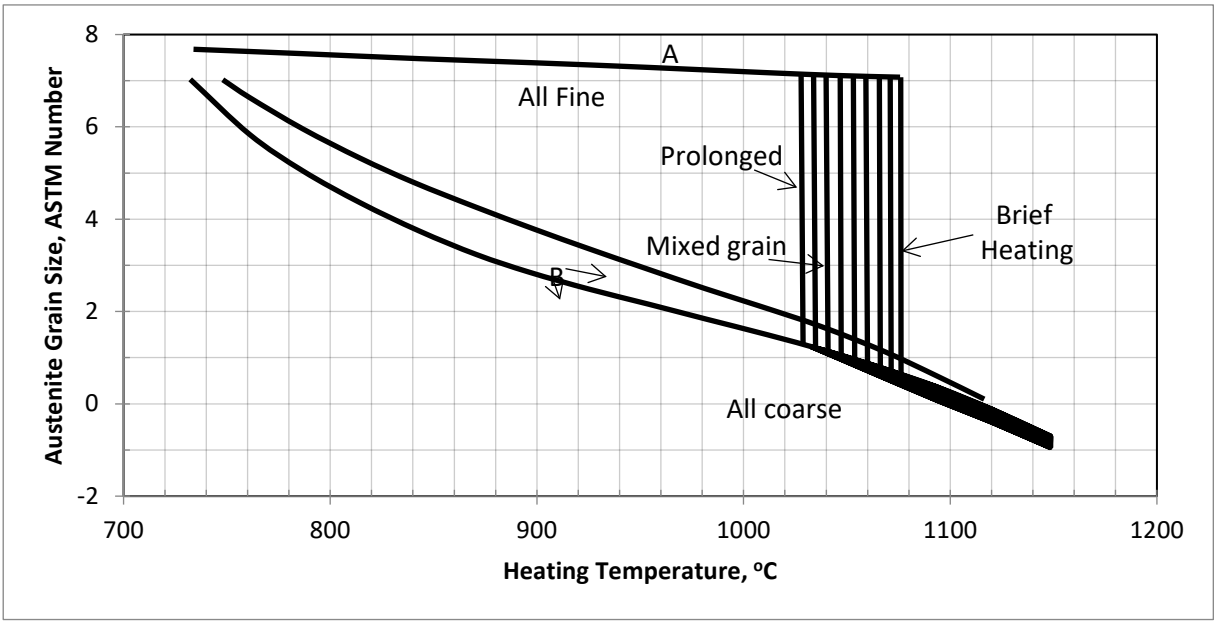

Notes:

1) Curve A – killed steel with a fine austenitic grain size (e.g., ASTM A 516).
2) Curve B – killed steel with a coarse austenitic grain size (e.g., ASTM A 515).

Figure 11.8M – Coarsening Behavior of Carbon Steels as a Function of Temperature (From: ASM Metals Handbook, 1948, ASM International)

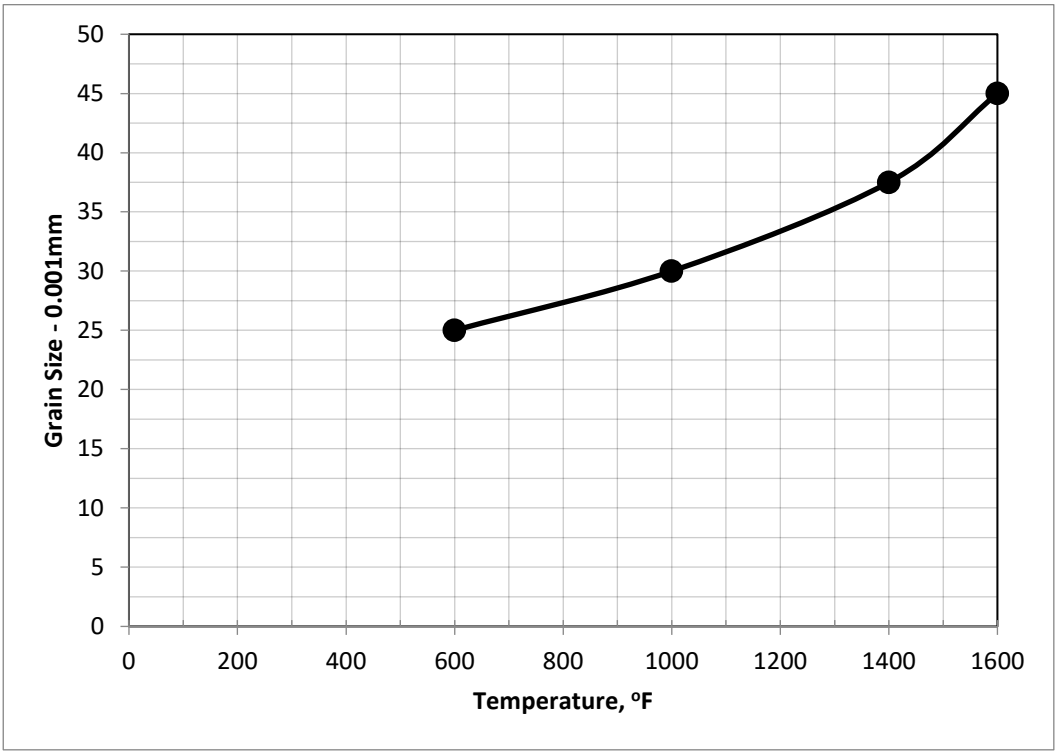

Figure 11.9 – Effect of Heat on the Grain Size of Copper

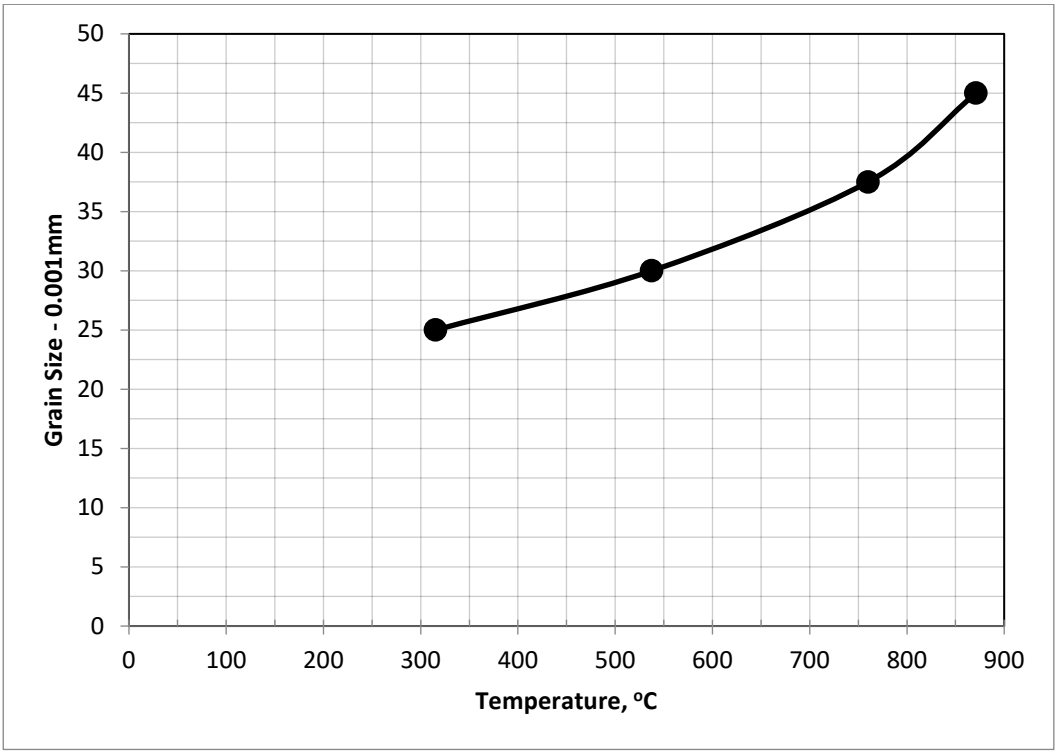

Figure 11.9M – Effect of Heat on the Grain Size of Copper

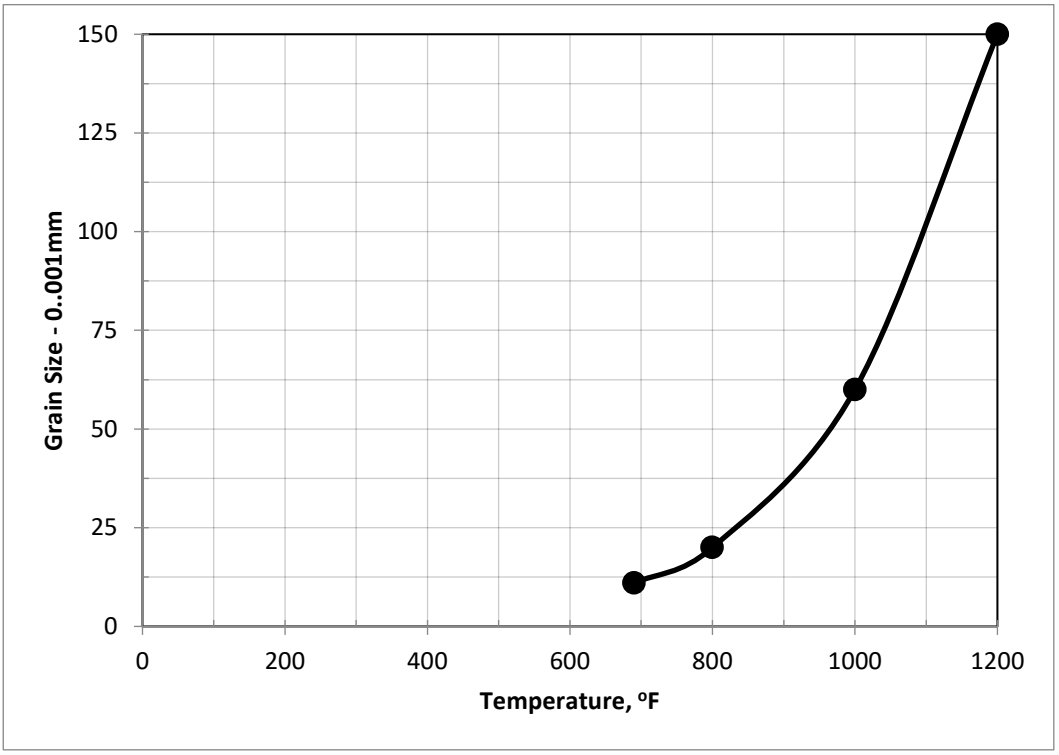

Figure 11.10 – Effect of Heat on the Grain Size of Admiralty Brass Tubing Cold Drawn 50%

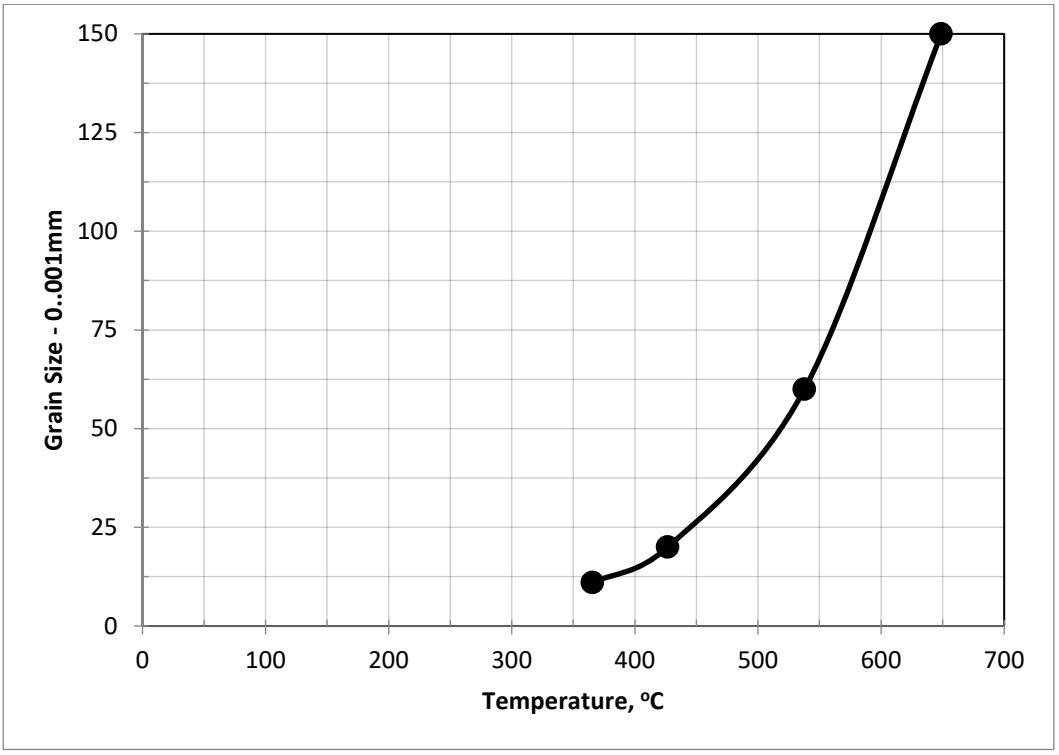

Figure 11.10M – Effect of Heat on the Grain Size of Admiralty Brass Tubing Cold Drawn 50%

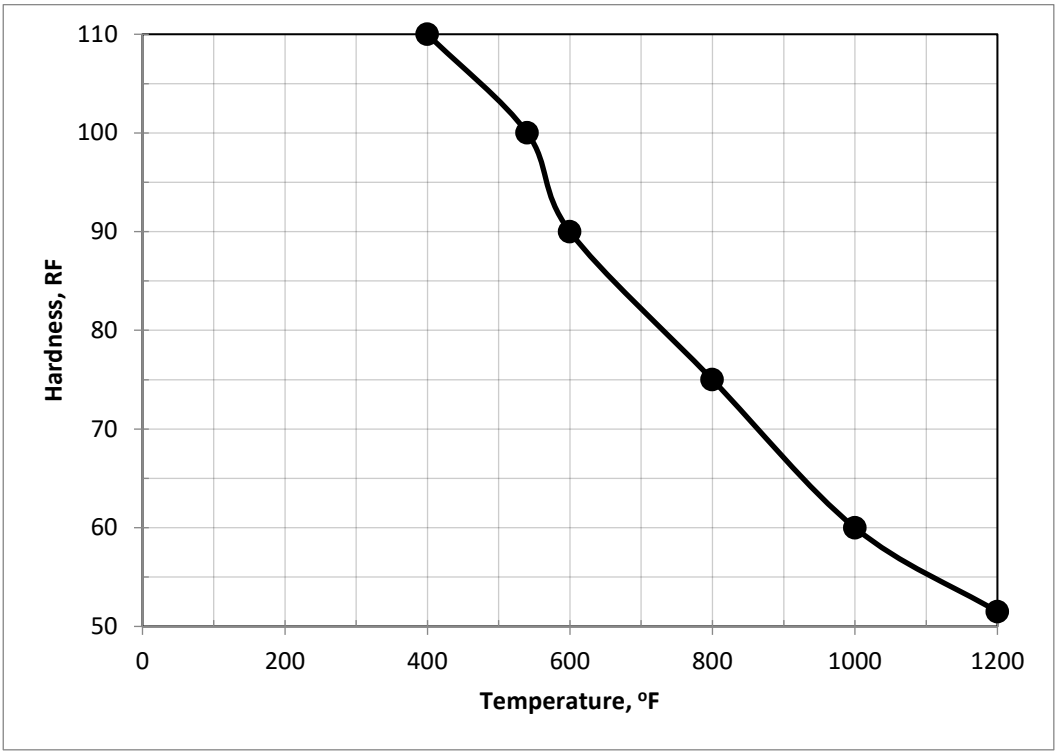

Figure 11.11 – Effect of Heat (Based on a One Hour Exposure) on the Hardness of Admiralty Brass Tubing Cold Drawn 50%

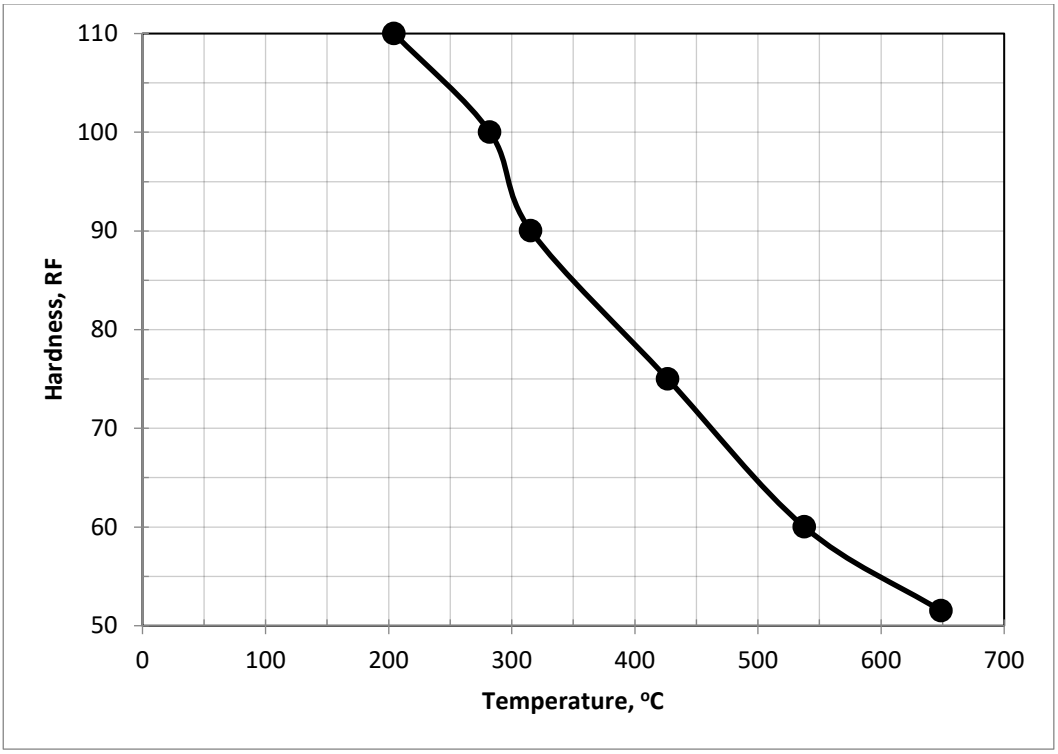

Figure 11.11M – Effect of Heat (Based on a One Hour Exposure) on the Hardness of Admiralty Brass Tubing Cold Drawn 50%

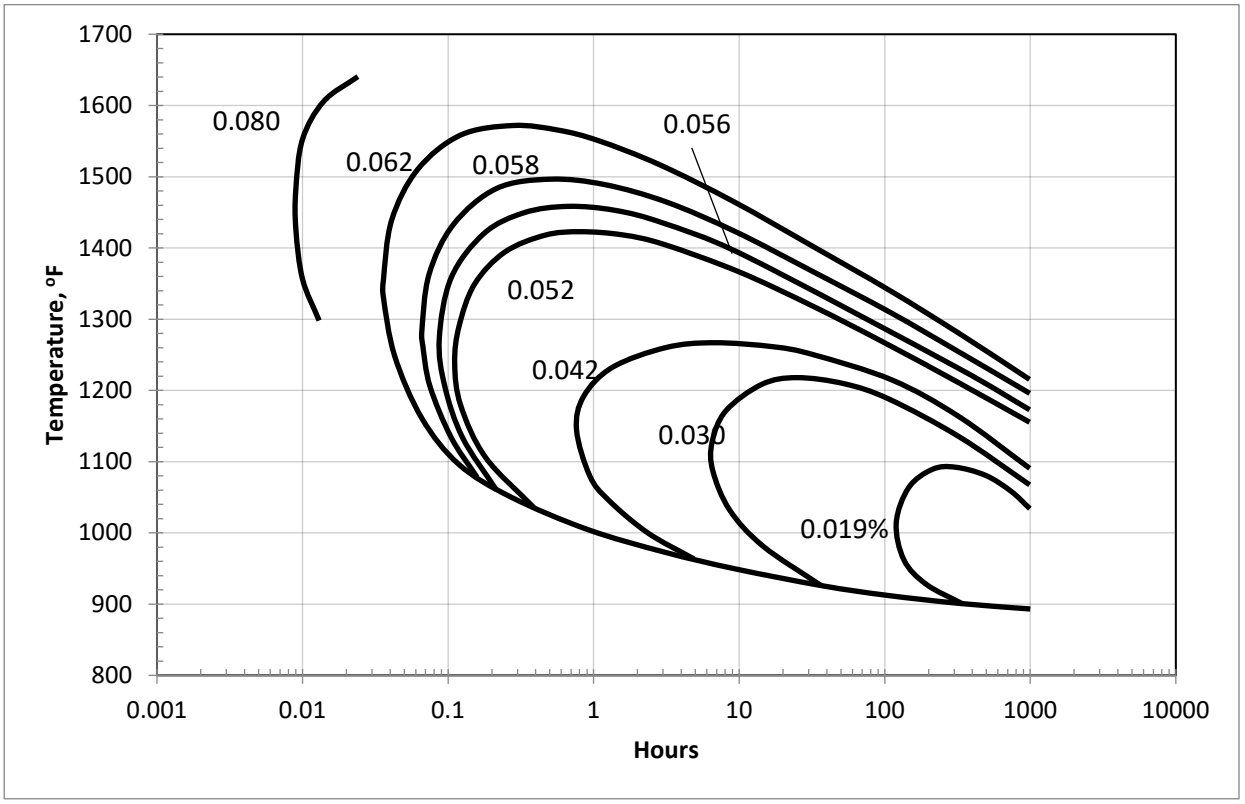

Notes:

1) The time required for formation of carbide precipitation in stainless steels with various carbon contents is shown in the above graph. Carbide precipitation forms in the areas to the right of the various carbon-content curves.

2) Within the time periods applicable to welding, chromium-nickel stainless steels with 0.05% or less carbon would be quite free from grain boundary precipitation.

3) The figure is from *Stainless Steels for Acetic Acid Service*, American Iron and Steel Institute, 1977.

Figure 11.12 – Sensitization of Type 300 Series Stainless Steels

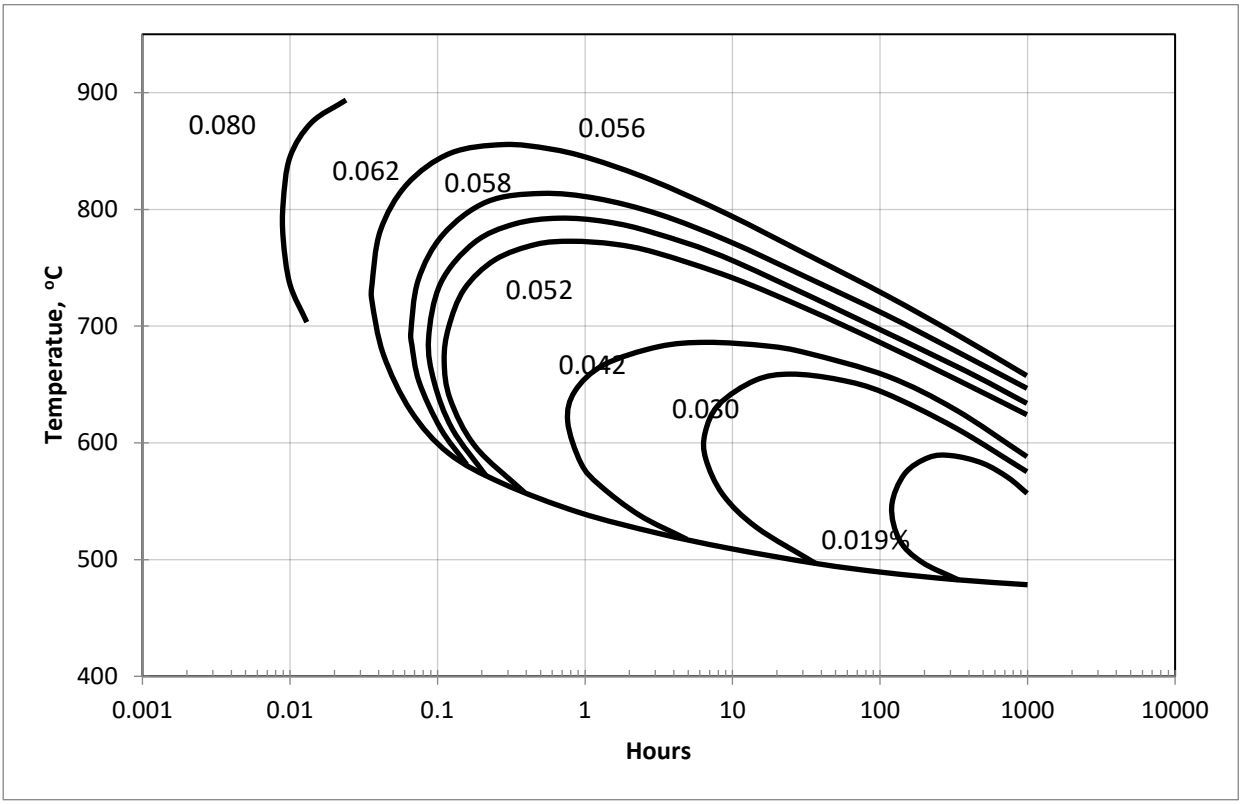

Notes:

1) The time required for formation of carbide precipitation in stainless steels with various carbon contents is shown in the above graph. Carbide precipitation forms in the areas to the right of the various carbon-content curves.

2) Within the time periods applicable to welding, chromium-nickel stainless steels with 0.05% or less carbon would be quite free from grain boundary precipitation.

3) The figure is from *Stainless Steels for Acetic Acid Service*, American Iron and Steel Institute, 1977.

Figure 11.12M – Sensitization of Type 300 Series Stainless Steels

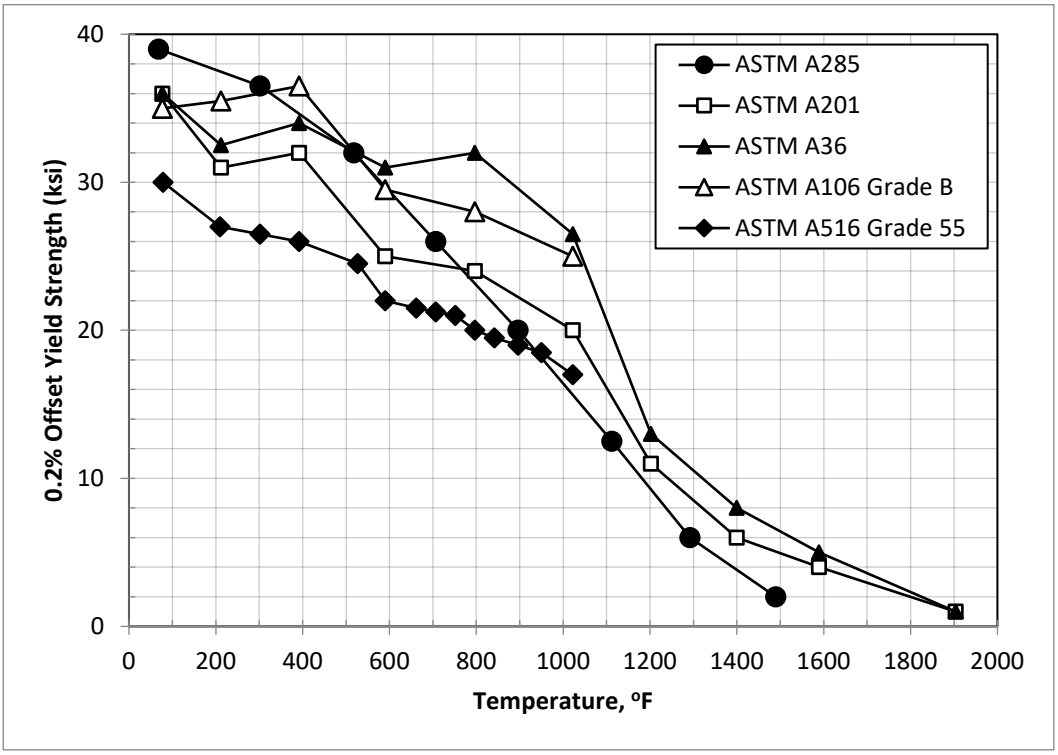

Figure 11.13 – High Temperature Yield Strengths of Some Low Carbon Steels

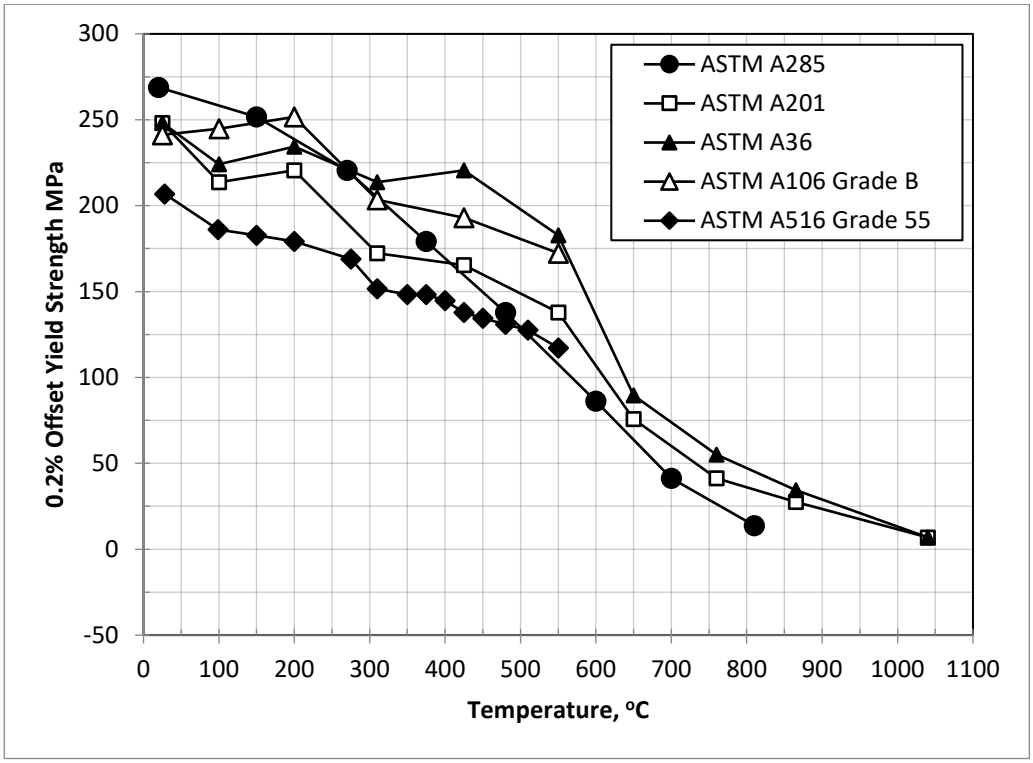

Figure 11.13M – High Temperature Yield Strengths of Some Low Carbon Steels

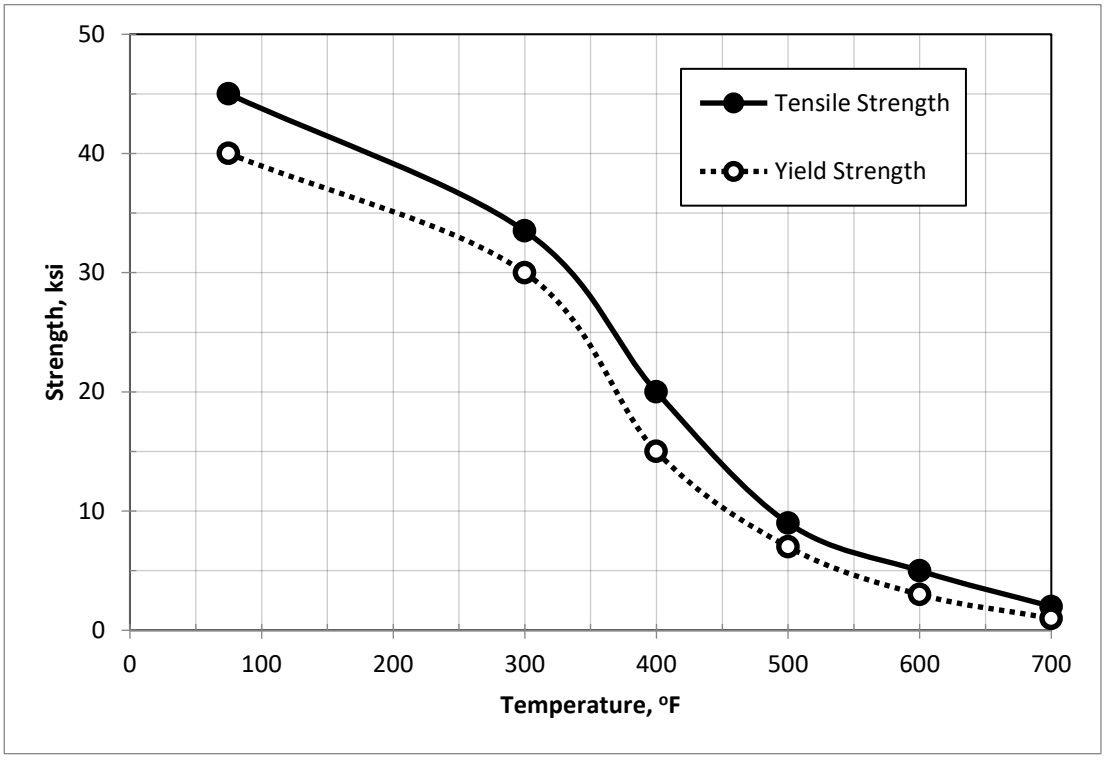

Figure 11.14 – Effect of Heat Exposure on the Strength of Aluminum Alloy 6061-T6

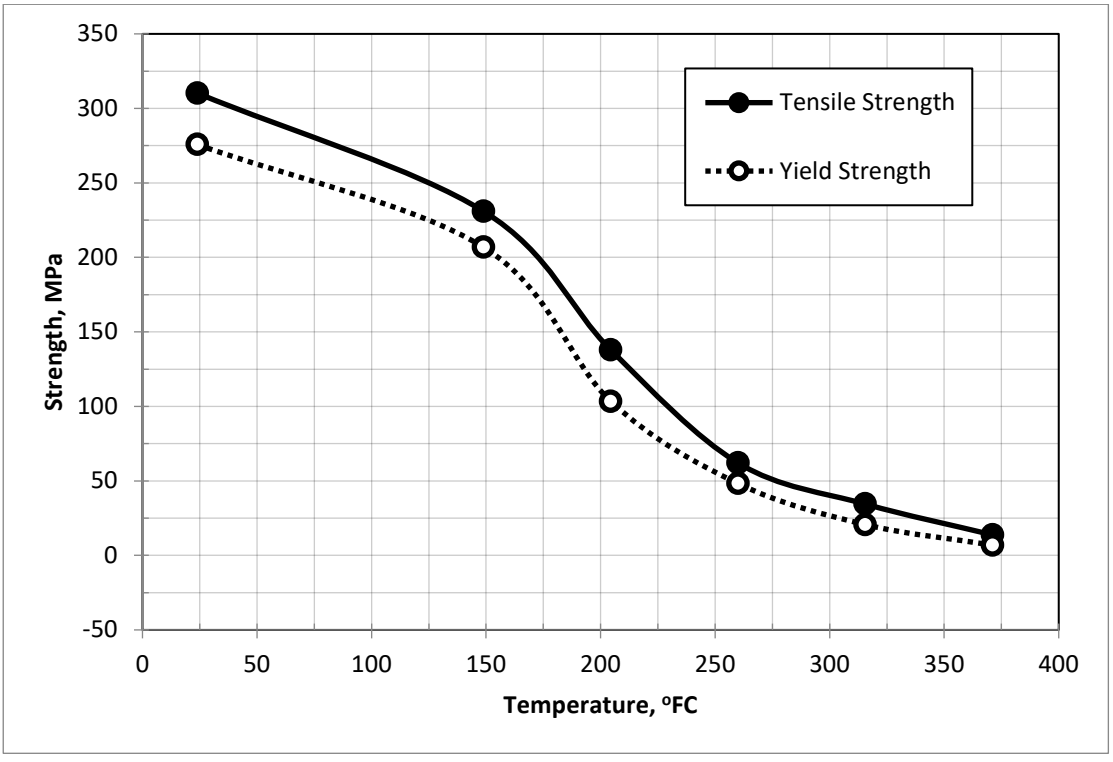

Figure 11.14M – Effect of Heat Exposure on the Strength of Aluminum Alloy 6061-T6

ANNEX 11A – TECHNICAL BASIS AND VALIDATION – ASSESSMENT OF FIRE DAMAGE

(INFORMATIVE)

CONTENTS

ANNEX 11A – TECHNICAL BASIS AND VALIDATION – ASSESSMENT OF FIRE DAMAGE 11A-1

11A.1 TECHNICAL BASIS AND VALIDATION 11A-1
11A.2 REFERENCES 11A-1

11A.1 Technical Basis and Validation

The basic principles used to develop the assessment procedures in Part 11 for fire damage are provided in references [1] and [2]. These principles are combined with the relevant assessment procedures from the other Parts of this standard (i.e., Part 4 for the assessment of thinning, Part 9 for the assessment of crack-like flaws, and Part 10 for the assessment of creep damage) to provide an overall evaluation procedure for fire damage.

11A.2 References

[1] ASM, “Powder Metallurgy,” Metals Handbook, Volume 7, 8th Edition, American Society of Materials, pg. 133, 1972.

[2] ASM, “Properties and Selection: Iron and Steels,” Metals Handbook, Volume 1, 9th Edition, American Society of Materials, pg. 204, 1978.

[3] Hau, J.L., "Assessment of Fire Damage to Pressure Vessels in a Refinery Unit", Corrosion, pp 420-437, Vol. 49, No.5, 1993.

[4] McIntyre, D.R. and Ashbaugh, W.G., “Guidelines for Assessing Fire and Explosions Damage,” MTI Publication No. 30, Materials Technology Institute of the Chemical Process Industries, Inc., 1st Edition, 1990.

[5] McIntyre, D.R., “Damage Assessment: Investigating Fires, Explosions and Storm Damage in Chemical Plants,” MTI Publication No. 30, 2nd Edition, Materials Technology Institute, Inc., 2012.

[6] McIntyre, D.R. and Dillon C.P., “Guidelines for Preventing Stress-Corrosion Cracking in the Chemical Process Industries,” MTI Publication No. 15, Materials Technology Institute of the Chemical Process Industries, Inc., 1990.

[7] Treseder, ed., *Corrosion Engineer's Reference Book*, National Association of Corrosion Engineers, Houston, TX, p. 177, 1980.

[8] Wilson, A.D., Roper, C.R., Orie, K.E., and Fletcher, F.B., Properties and Behavior of Modern A 387 Cr-Mo Steels, PVP-Vol. 239, Serviceability of Petroleum, Process, and Power Equipment, Book No. G00674 – 1992.

[9] Orie, Kenneth E. and Upitis, Elmar, The Effect of Post Weld Heat Treatment and Notch Toughness on Welded Joints and on Normalized Base-Metal Properties of A-516 Steel, WRC Bulletin 481, Welding Research Council, Inc., New York, NY, March 2005.

[10] Hau, J.L., “Understanding the Microstructure of Overheated Carbon Steel,” Materials Performance, November 2004.

[11] Keyser, C. A., *Basic Engineering Metallurgy*, Prentice-hall, Inc., pp.175-181, 2nd Edition 1959.

[12] ASME PCC-2, Repair of Pressure Equipment and Piping, latest edition.

[13] ASTM E1351-01, 2006, “Standard Practice for Production and Evaluation of Field Metallographic Replicas.”

[14] ISO 3057:1998, “Non-destructive testing – Metallographic replica techniques of surface examination.”

ANNEX 11B – METALLURGICAL INVESTIGATION AND EVALUATION OF MECHANICAL PROPERTIES IN FIRE DAMAGE ASSESSMENT

(INFORMATIVE)

CONTENTS

ANNEX 11B – METALLURGICAL INVESTIGATION AND EVALUATION OF MECHANICAL PROPERTIES IN FIRE DAMAGE ASSESSMENT 11B-1

11B.1 GENERAL 11B-2
11B.1.1 Metallurgical Investigations 11B-2
11B.1.2 Materials Covered 11B-2
11B.1.3 Change in material properties from Fire Damage 11B-2
11B.2 APPLICABILITY AND LIMITATIONS OF THE PROCEDURE 11B-2
11B.3 SPECIFIC RESPONSIBILITIES AND QUALIFICATIONS 11B-2
11B.3.1 Overview 11B-2
11B.3.2 Field Assessment Team 11B-2
11B.3.3 Laboratory Assessment Team 11B-3
11B.4 EVALUATION TECHNIQUES 11B-3
11B.5 FIELD ASSESSMENT TECHNIQUES 11B-3
11B.5.1 Field Hardness Testing 11B-3
11B.5.2 In-situ Metallography or Replication 11B-4
11B.5.3 Positive Material Identification 11B-4
11B.6 LABORATORY ASSESSMENT TECHNIQUES 11B-5
11B.6.1 Coupon or Sample Removal 11B-5
11B.6.2 Metallurgical Mounts and Mechanical Testing Specimens 11B-5
11B.7 WORK PROCEDURE 11B-5
11B.7.1 STEP 1 – Select Equipment and Component Subject to Analysis 11B-5
11B.7.2 STEP 2 – Select Sampling Technique(s) 11B-6
11B.7.3 STEP 3 – Perform In-situ Metallography or Replica Evaluation 11B-6
11B.7.4 STEP 4 – Take Field Hardness Readings 11B-6
11B.7.5 STEP 5 – Remove Samples for Laboratory Analysis and Mechanical Testing (Optional) 11B-7
11B.8 GUIDANCE FOR METALLOGRAPHIC ANALYSIS AND MECHANICAL TESTING INTERPRETATION 11B-7
11B.8.1 Overview 11B-7
11B.8.2 Reduction in Tensile Strength 11B-7
11B.8.3 Reduction in Toughness 11B-7
11B.8.4 Decrease of Corrosion Resistance 11B-8
11B.8.5 Consideration for Reuse 11B-8
11B.8.6 Heat Treatment 11B-8
11B.9 EXAMPLE OF METALLOGRAPHY ANALYSIS AND HARDNESS TESTING RESULTS 11B-8
11B.9.1 Overview 11B-8
11B.9.2 Samples 11B-9
11B.9.3 Test Sequence 11B-9
11B.9.4 Test Results – Metallography 11B-9
11B.9.5 Test Results – Hardness 11B-10
11B.10 FIGURES 11B-11

11B.1 General

11B.1.1 Metallurgical Investigations

Guidelines for carrying out the metallurgical investigations and mechanical testing to assess the degradation of materials exposed to elevated temperatures during a fire event are provided in this Annex.

11B.1.2 Materials Covered

The metallurgical investigations and mechanical testing are intended to cover metallic materials in process units, specifically carbon steel, low alloy steels, and stainless steels. These procedures may be used for high alloy metals, if the owner/user and/or investigator have data on the specific alloy being evaluated.

11B.1.3 Change in material properties from Fire Damage

Investigations based on metallography and mechanical testing are conducted to understand the changes in the mechanical properties that could occur in the metal exposed to elevated temperatures during a fire event. Investigation techniques described in this Annex include replication or in-situ field metallography evaluation, laboratory metallographic evaluation, hardness testing, tensile testing, impact testing, etc. Material degradation shall not be evaluated based on the information of metallurgical investigations only, and other methods of evaluation shall be considered to obtain a better understanding of the conditions of the material after being exposed to a fire event.

11B.2 Applicability and Limitations of the Procedure

Procedures in this Annex are applicable to the following materials of the pressure containing components.

- Carbon steels; normalized, annealed, tempered, or cold worked.
- Low alloy steels; normalized, annealed, tempered, or cold worked.
- Stainless steels.

11B.3 Specific Responsibilities and Qualifications

11B.3.1 Overview

In addition to the responsibilities and qualifications for engineers and inspectors outlined in Part 1, paragraphs 1.4.2 and 1.4.3, the members of the team performing the investigation shall comply with the following requirements.

11B.3.2 Field Assessment Team

a) Membership – Members of the team performing the field evaluation shall include technicians/inspectors and engineers.

b) Technicians and Inspectors – Technicians and inspectors participating in the field assessment shall be trained and experienced in tasks related to the in-situ metallographic analysis such as grinding, polishing, etching, replication, and photomicrography, as well as field hardness testing. Technicians and inspectors shall be qualified and have the appropriate tools to remove samples for mechanical testing and laboratory metallographic analysis. Technicians/inspectors shall understand the operation and precision of the tools used to remove samples and shall follow guidance provided by engineers regarding minimum and maximum sample sizes and locations of sample removal.

c) Engineers – Engineers responsible for the selection of the sample's sizes and the locations of sample removal shall understand the limitations and impact of removing samples from components that might be reused after fire assessment and are also responsible for coordinating any Fitness-For-Service (FFS) Assessment to be conducted before sample removal if putting the component back in service without repair after sample removal is intended. If repairing the component after sample removal is intended, the engineers shall coordinate the preparation of weld repair procedures of the area affected. Engineers involved in the interpretation of field assessment results shall have the expertise in material assessment technology including metallography, hardness testing, etc.

11B.3.3 Laboratory Assessment Team

When samples or in-situ metallographic replicas are taken to a laboratory for a more detailed analysis, technicians and engineers shall comply with the following requirements.

a) Technicians – Technicians conducting the sample handling, specimen preparation, metallography analysis and mechanical testing shall be trained and experienced in metallographic analysis, material characterization, and mechanical testing.

b) Engineers – Engineers involved in the interpretation shall have the expertise in material assessment technology including metallography, hardness testing, tensile testing, toughness testing, etc.

11B.4 Evaluation Techniques

Field and laboratory evaluation techniques and tests may be used to evaluate the condition of the material in a pressurized equipment or component affected by a fire event. Field and laboratory techniques commonly used are described in paragraphs 11B.5 and 11B.6.

11B.5 Field Assessment Techniques

11B.5.1 Field Hardness Testing

a) Hardness testing can be used to determine the changes in tensile strength of carbon and low alloy steels, and changes in other material properties such as toughness and ductility. For example, hardness can be measured in areas of a carbon steel pressure vessel known to be in Heat Exposure Zones I through IV (see Part 11, paragraph 11.3.3.3). These results should be compared to hardness measurements obtained in areas suspected of being exposed to higher temperatures, Zones V and VI.

b) Hardness testing is primarily used to estimate tensile strength, and changes in tensile strength. Either substantial increases or decreases in tensile strength are of concern to an FFS Assessment. Steels exposed to fires at temperatures below the lower critical temperature (approximately 720°C (1325°F) for carbon steels) may suffer reductions in tensile strength below their original specification limits, requiring de-rating or replacement. Steels exposed to fires at temperatures above the lower critical temperature may, depending on cooling rate and duration of exposure, have phase transformations which can increase tensile strength and hardness and reduce toughness. Hardness testing is often most useful when conducted on a grid pattern, which will give the size of areas heated above the lower critical temperature compared to surrounding areas tempered to lower hardness. Toughness cannot be inferred directly from hardness. Significant increases in hardness often signal significant decreases in toughness. Reductions in hardness are usually accompanied by some increase in toughness. However, phase transformations which result in mixed microstructures may show little or no change in hardness yet have reduced toughness. Similarly, long term exposure to temperatures above the grain coarsening temperature, followed by slow cooling, may yield a

structure with relatively low hardness but increased ductile-to-brittle transition temperature due to grain growth. Consequently, the potential for degradation in toughness should be assessed by other methods, such as field metallography and mechanical testing of appropriate samples. Hardness correlates best with ultimate tensile strength. Estimates of yield strength based on hardness, using some assumed ratio of yield-to-tensile strength, may be in error by a significant margin.

c) Surface preparation is critical for accurate field hardness measurements, especially when microscopic tests, such as Vickers, are used rather than a portable indentation type of hardness tester. When making field hardness measurements, at least 0.5 mm (0.02 inch) of metal surface should be removed because of oxide scale and surface carburization or decarburization.

11B.5.2 In-situ Metallography or Replication

a) Nondestructive material examination by means of replication is a metallographic examination method that exposes (or replicates) the microstructure of the surface material.

   1) Method – Portable equipment is typically used for the examination. Surface preparation requires grinding, sanding, and polishing by mechanical or electrolytic means to a mirror finish, followed by etching. The surface can be viewed directly, or a replica can be taken by means of a solvent softened acetate strip applied to the surface. Coating the strip with carbon or gold enhances the features.

   2) Application – Replication is typically used for the evaluation of microstructures and characterization of crack-like flaws. Creep damage can be identified at a much earlier stage using the replication method than with other NDE methods.

   3) Flaw Detection – Because each type of crack has specific characteristics, the damage mechanism causing the cracking may be determined using this method.

   4) Limitations – The replication method can only be used on surfaces that are readily accessible and at metal or ambient temperatures between about -18°C to 32°C (0°F to 90°F).

b) In-situ metallography or replication should be performed on surfaces of components having significantly divergent hardness values or where a certain microstructure is required, such as having a normalized microstructure in carbon steel equipment for notch toughness requirements. In-situ metallography or replication should also be performed in areas shielded from the thermal effects of the fire. These two sets of microstructures should be compared and interpreted by an experienced material engineer. Proper attention to field procedures is imperative for proper replicas.

c) In-situ metallography can be helpful in assessing components if replicas can be obtained from both a fire affected zone and an unaffected zone of the same component. In-situ metallography can also be helpful in assessing sensitized austenitic stainless steel or other alloy microstructures.

11B.5.3 Positive Material Identification

The use of incorrect materials or alloys in a piece of equipment or location, especially in piping circuits operating in aggressive service (corrosion or environmental cracking) can be the cause of a fire. The use of Positive Material Identification (PMI) techniques could be helpful during a fire assessment in determining, with a quick test in the field, if failure or rupture of the suspected component where the fire ignited is associated with the incorrect use of an alloy.

11B.6 Laboratory Assessment Techniques

11B.6.1 Coupon or Sample Removal

a) If hardness readings and in-situ field metallography are inconclusive, then consideration should be given to coupon removal from the component for destructive testing and evaluation. Destructive evaluation might include metallographic examination of the fire side surface and in a through-thickness direction, as well as mechanical tests such tensile, bending, impact, toughness, and other tests.

b) There are several options available for removal of coupons or samples to be evaluated in the laboratory as part of the investigation. Among these options, the following are the most commonly used:

   1) Plate Sample – a piece of plate with full thickness cut from the affected zone; the use of this option requires repair using a butt-welded insert plate.

   2) Boat Sample – a small piece in the shape of a boat hull that in most cases is cut without affecting the full thickness of the cut location; the use of this option requires weld repair due to the notch at its corners.

   3) Partial-Hemisphere Sample – a small piece in the shape of a partial hemisphere cut with custom machines; use of this option may or may not require weld repair depending upon the component thickness, operating condition, and sample dimensions.

c) Samples have to be large enough to provide enough material for metallurgical investigation and mechanical testing. Sample(s) size and location(s) of removal shall be discussed with the owner/user before removal. If it is the intent to remove samples without weld repair, an FFS Assessment is mandatory before the removal to demonstrate that the component will be fit for the continued operation without repair. For equipment that are exposed to relatively high operating stresses or are in cyclic service, the use of insert plates may cause premature cracking at or adjacent to the butt welds. In such cases, proper engineering assessment shall be made prior to obtaining plate samples.

d) If weld repair of the component after sample removal is intended, a weld repair procedure for the areas where the samples are to be removed shall be prepared before removal.

e) ASME PCC-2 provides guidance on repairs after sample removal as well as information on metal sample removal.

11B.6.2 Metallurgical Mounts and Mechanical Testing Specimens

a) Metallographic mounts shall be prepared in those samples selected for microstructure investigation, and they may include base metal, heat affected zone, and weld metal.

b) Mechanical testing may include tensile test, bending test, impact test, toughness test and hardness in cross section; other mechanical tests might be included, based on the type of alloy and the expected damage due to elevated temperature exposure during fire.

c) Reduced size specimens should be considered when there is a limited amount of material for testing.

11B.7 Work Procedure

11B.7.1 STEP 1 – Select Equipment and Component Subject to Analysis

The following points should be considered in selecting the parts to be evaluated with metallographic analysis.

a) Material – Metallurgical analysis is carried out to investigate the effects of heat exposure to the part concerned. The base metal of the component subject to the assessment should be analyzed, not weld metal or HAZ. In order to compare, the reference microstructure, data should be taken from another location in the component or in a similar component that is obviously unaffected by the heat exposure. Since the microstructure may be different depending on the raw material and the manufacturing process, even in materials categorized as same type, it is advisable to take a reference sample at a location with the same specification, otherwise as similar as possible.

b) Heat Exposure Zone – Select the equipment or component that has been exposed to the highest temperature in each heat exposure zone and pick the location(s) to be analyzed (potentially affected by highest temperatures during fire event).

c) Cooling Rates – Clarify the effects of cooling rates on the parts due to fire-fighting water by checking both the quenched part and the gradually cooled part that have been exposed to similar temperature levels.

11B.7.2 STEP 2 – Select Sampling Technique(s)

Select sampling technique(s) for the metallurgical analysis, either replication, sample removal on affected component or a combination. Sample removal allows collecting metallography data not only from the surface but also along the thickness direction. It also allows measuring actual mechanical properties by tensile test, impact test, bending test, etc. However, repair welding and the related heat treatment, in some cases, may be difficult for the component where the sample would be taken from. Therefore, weldability and other issues related to weld repair shall be considered before removing samples.

11B.7.3 STEP 3 – Perform In-situ Metallography or Replica Evaluation

The procedure of the replica inspection should be as follows.

a) Preparation – Remove oxide scale and carburized/decarburized surface layer by rough grinding. Depth of the grinding must be at least 0.5 mm (0.02 inch), but it should be kept as minimum as possible. Then polish the ground surface to smooth out and clean. In cases where several replicas have to be taken the use of electrolytic polishing to expedite polishing process should be considered.

b) Etching – Etch the polished surface using an appropriate etchant. In case of carbon steels or low alloy steels, 2-5% Nital is a suitable standard etchant, but in some cases Villela's may be needed for 5Cr and 9Cr alloy steels. Aquaregia or Chromic Acid is used for stainless steels. Electropolishing with 10% Oxalic Acid is often carried out to evaluate the sensitization of austenitic stainless steel.

c) Production of Replica – The replica film, normally a cellulose acetate tape softened with acetone solvent; is pressed against the surface to replicate the metal surface to the film. To protect the produced replicas, they should be kept dry and free of dust. Identify each replica with location and type of etchant information.

d) Observation – The produced replicas can be examined in the Light Optical Microscope or the Scanning Electron Microscope. Take photomicrographs as needed and document field metallography observations.

11B.7.4 STEP 4 – Take Field Hardness Readings

When performing the field hardness test, the following should be considered:

a) Ensure a good surface preparation before taking hardness reading.

b) Take at least five readings at each location. If one location includes base metal, heat affected zone, and weld, take five readings at each zone.

c) When hardness testing is performed at replica locations, use the same identification for both the replicas and the readings for future analysis.

11B.7.5 STEP 5 – Remove Samples for Laboratory Analysis and Mechanical Testing (Optional)

When it is necessary to remove samples to enhance investigation, the following should be considered:

a) Mark sample location based on discussion with owner/user or the team of consultants performing the assessment.

b) Record sample locations: photographs are recommended for this purpose.

c) Make sure that all provisions have been taken regarding type of samples, repair procedure after removal, FFS Assessment if repair is not expected, etc.

d) Use appropriate tools approved by the owner/user, these tools should be calibrated and approved by site safety personnel.

e) Identify each sample for tracking in the laboratory.

f) Prepare the sample for shipping and handling.

11B.8 Guidance for Metallographic Analysis and Mechanical Testing Interpretation

11B.8.1 Overview

The following paragraphs may be used as a guidance to evaluate the degradation of materials based on the metallographic analysis. The following guidance should be considered in the investigation of the effects of temperature exposure of carbon steel and low alloy steel during a fire event. An example of a typical case of metallographic analysis and hardness testing is provided in paragraph 11B.9.

11B.8.2 Reduction in Tensile Strength

Tensile strength may be reduced due to heat exposure when the softened microstructure or spheroidization is observed in the metallography as shown in Figures 11B.4(a) and 11B.8(a). Note that the changes in appearance of microstructure and the reduction of tensile strength for the cold formed or work hardened materials differ from those for the materials not subject to cold work.

11B.8.3 Reduction in Toughness

Embrittlement would be suspected when an increase in hardness above normal limits is observed, as well as when a hardened microstructure like martensite, such as those shown in Figures 11B.4(c) and 11B.8(c), is found. In this case, further investigation should be performed by impact testing, allowing quantification of the degrees of embrittlement. Since the cooling rates in fires are different depending upon the location through the wall thickness, the quenched microstructure may be present at the surface layer only. When the hardened microstructure is found at the surface after fire, it is recommended to carry out grinding and metallographic analysis at the slightly deeper layer from the surface to evaluate the embrittlement at the core of the component.

11B.8.4 Decrease of Corrosion Resistance

a) Carbon Steel

- In cases where the measured hardness is less than the specified value and a softened microstructure is observed, the risk of Stress Corrosion Cracking (SCC) would generally decrease. However, when a reduction in tensile strength is observed, further evaluation might be required.
- In cases where the measured hardness is greater than the specified value and a hardened microstructure is observed, there is a potential of an increase in the sensitivity to SCC. If it is the case, appropriate measures such as heat treatment, grind out, or repair should be considered to protect against possible failure.

b) Stainless Steel

- A short term heat exposure might cause sensitization. Sensitization can be detected by etching the component with a 10% Oxalic Acid. Once sensitization is found, the exposed temperature and the exposure time can be estimated by guidelines provided in Table 11.7 and Figure 11.12 of Part 11.
- Note that the sensitization should not always be the reason to disregard the reuse of the components subject to fire. Stainless steel is often utilized as the material for elevated temperatures even if the operating temperature is in the sensitization temperature range. Thus, considerations on reuse would depend on whether the operating environment is corrosive or not.

11B.8.5 Consideration for Reuse

Based on paragraphs 11B.8.2, 11B8.3, and 11B8.4, if it is concluded that the damage due to heat exposure is unacceptable, even in the case where the heat degraded part is limited to a local area, the pressure equipment under evaluation including the damaged components would be considered no longer fit for continued operation. However, in the case where the reduction in tensile strength of a part is expected, the area where strength reduction is expected can be treated as the equivalent metal loss and the acceptance of the reuse of the component may be evaluated according to the assessment of metal loss in Part 5. Finite element analysis may be required to evaluate the stress in the component. In this case, it is required to ensure that the extent of degraded material is precisely identified. In cases where the reduction in toughness or corrosion resistance of the component is suspected, it is unacceptable to reuse even if the heat degraded part is limited to a small local area because cracks or further damage may initiate and extend to the undamaged part.

11B.8.6 Heat Treatment

Material degradation due to heat exposure might be reversed by applying heat treatment identical to the original one used during manufacturing, though most of the heat treatments cannot be applicable in practice because of problems associated with thermal stresses or the difficulty of control at heat treatment temperatures. If the heat treatment is applied to the damaged part, the purpose and effect of the heat treatment should be analyzed in advance by simulation and it should be validated during fire investigation by using metallographic analysis and hardness measurements of that part.

11B.9 Example of Metallography Analysis and Hardness Testing Results

11B.9.1 Overview

This section shows results of metallographic analysis and hardness tests on samples made of carbon steel and low alloy steel after an overheat event. The objective was to present typical changes in microstructure and

hardness values of these materials, after exposure to simulate levels of heat exposure and cooling rates during a fire event. Metallographic analyses and hardness tests were performed on specimens in the as-new condition as well as specimens heated and cooled. This work was performed in a project coordinated by the Standardizing FFS Assessment Committee organized by Petroleum Association of Japan, PAJ and Japan Petrochemical Industry Association, JPIA.

11B.9.2 Samples

a) Carbon steel, ASTM specification A515 Grade 60.

b) Low alloy steel 1.25Cr-0.5Mo, ASTM specification A387 Grade 11 Class 2.

11B.9.3 Test Sequence

a) Electric muffle furnace heated up to the specified temperatures of 1000°C (1832°F) and 738°C (1360°F).

b) Specimen in the as-new condition kept at the specified temperature for 1hr.

c) Cool down using different quenching/cooling media, water, air and furnace.

d) After cooled down, a surface layer of about 0.5 mm (0.02 inch) was removed by a grinding and polishing to #320 grit surface.

e) Polished to a surface roughness of #800 - #1000 by a grinder or emery paper. Polishing was done in different directions against grinding mark from the preceding stage to remove these polishing marks completely. Final buff polishing was done by alumina particles with 1-3μm or diamond particles and removed abrasive powders and dusts completely.

f) Etched in 5% Nital etchant.

g) Metallographic analysis was done by light optical microscope.

h) Micro Vickers hardness test was carried out by 1000 gf of force applied for 30 seconds.

11B.9.4 Test Results – Metallography

a) Specimens exposed to 1000°C (1832°F)

- A515 Grade 60: furnace cooled specimen shows grain growth. Widmanstätten microstructure is observed in air cooled specimen. Martensite microstructure is exhibited by water quenched specimen.
- A387 Grade 11 Class 2: furnace cooled specimen shows the change in microstructure to ferrite and pearlite. No change can be observed in the microstructure of the air cooled specimen. Martensite microstructure is exhibited by water quenched specimen, as observed in A515 Grade 60.

b) Specimens exposed to 738°C (1360°F)

- A515 Grade 60: all specimens (air and furnace cooled, and water quenched) show slight pearlite decomposition, with no significant difference in microstructure regarding type of cooling media used.
- A387 Grade 11 Class 2: changes in microstructure are not observable in any of the specimens (air and furnace cooled, and water quenched).

11B.9.5 Test Results – Hardness

a) Specimens exposed to 1000°C (1832°F)

- A515 Grade 60: when comparing to the as-new material a decrease in hardness is observed in the furnace cooled specimen due to annealing. Hardness does not vary in the air cooled specimen. Significant increase in hardness is observed in the water quenched specimen.
- A387 Grade 11 Class 2: when comparing to the as-new material a decrease in hardness is observed in the furnace cooled specimen due to annealing. Air cooling makes the hardness increased significantly. Increase of hardness in water quenched specimen is significant and much more than carbon steel because of the high hardenability of this low alloy steel.

b) Specimens exposed to 738°C (1360°F)

- A515 Grade 60: when comparing to the as-new material water quenched specimen shows a slight increase in hardness. Air and furnace cooled specimens show no significant change in the hardness.
- A387 Grade 11 Class 2: changes in hardness are not significant in any of the specimens (air and furnace cooled, and water quenched).

11B.10 Figures

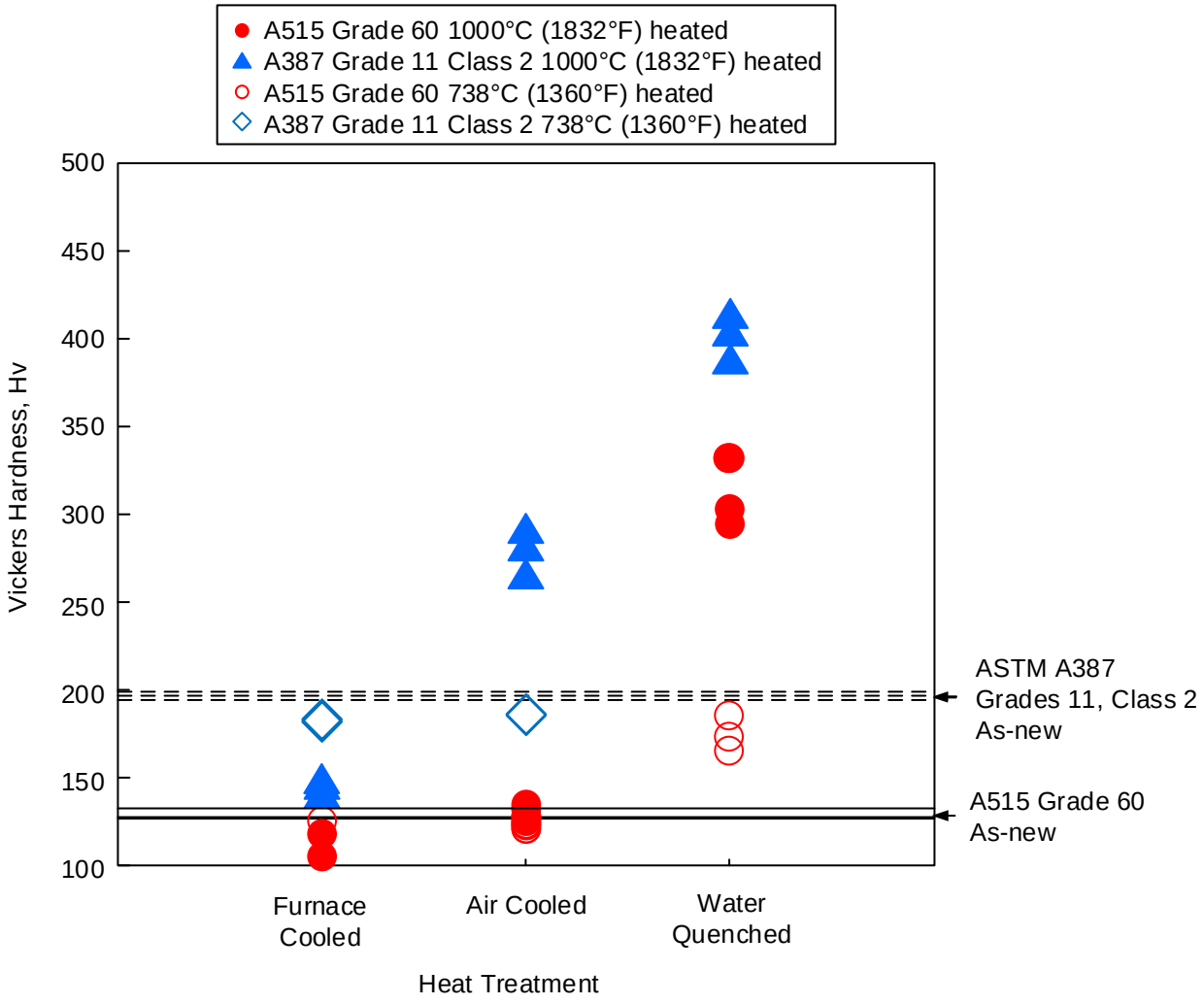

Figure 11B.1 – Vickers Hardness in Heated Specimens

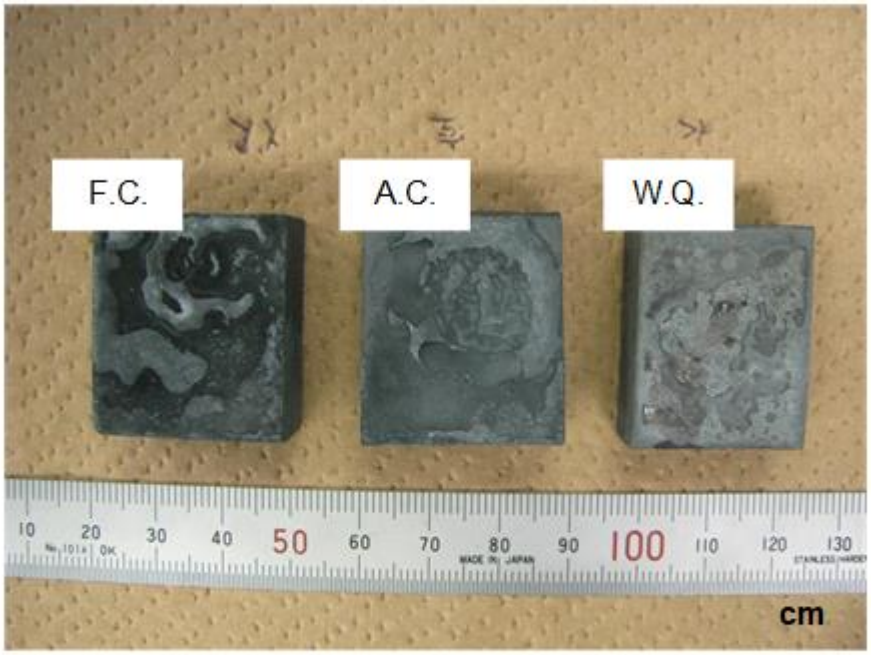

1832°F-1h Heated Specimens

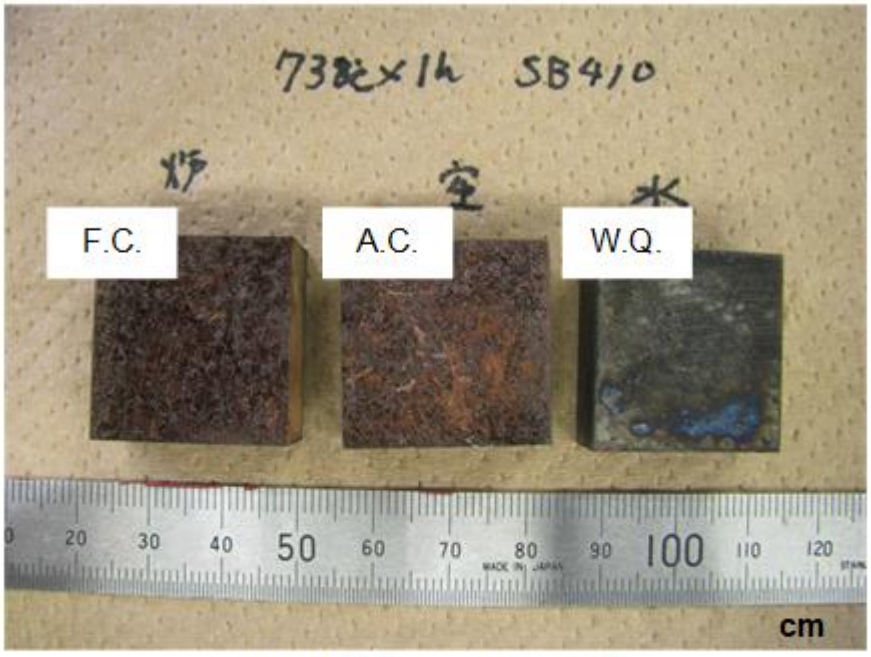

1360°F-1h Heated Specimens

F.C. – Furnace Cooled, A.C. – Air Cooled, W.Q. – Water Quenched

Figure 11B.2 – Appearance of ASTM A515 Grade 60 Heated Specimens

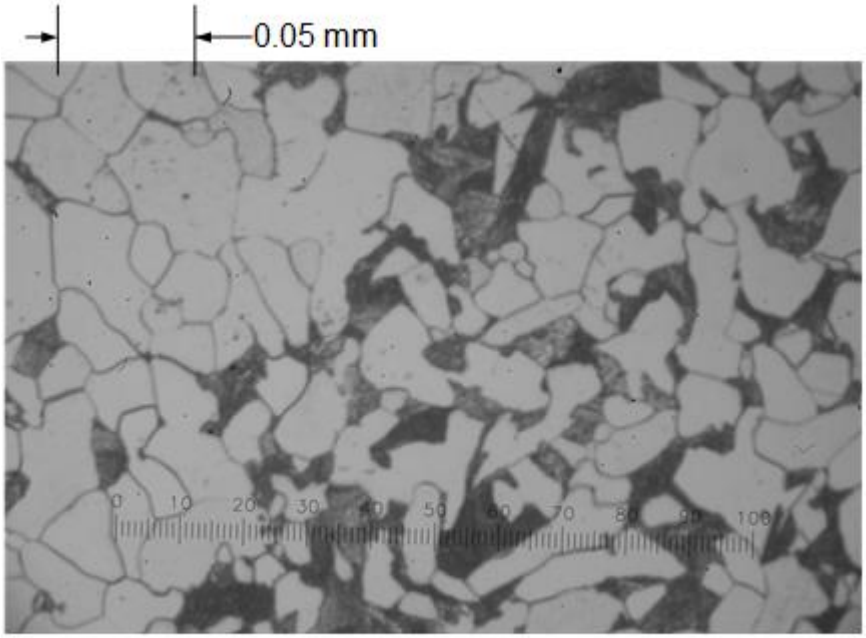

200X

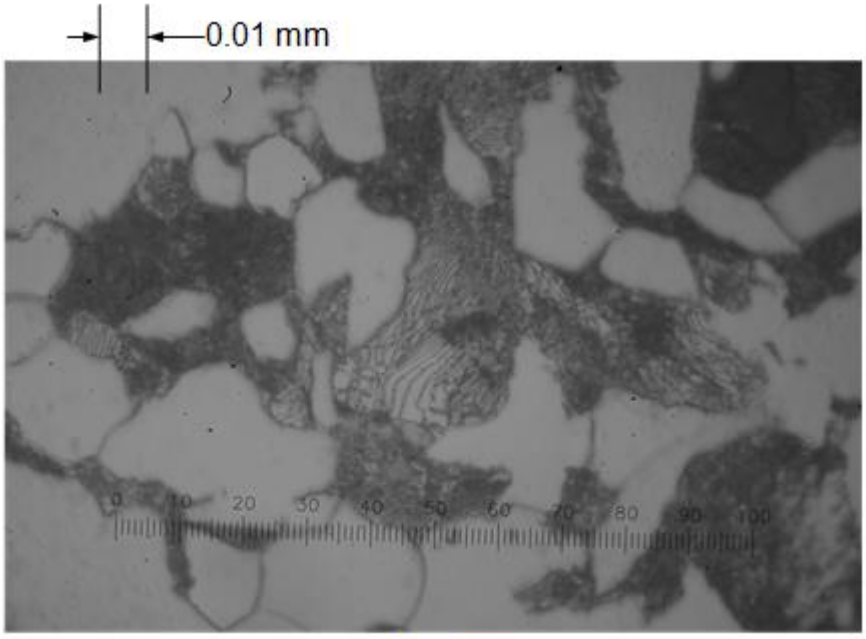

Higher Magnification

Figure 11B.3 – Microstructure of ASTM A515 Grade 60 Specimens – As-New Condition

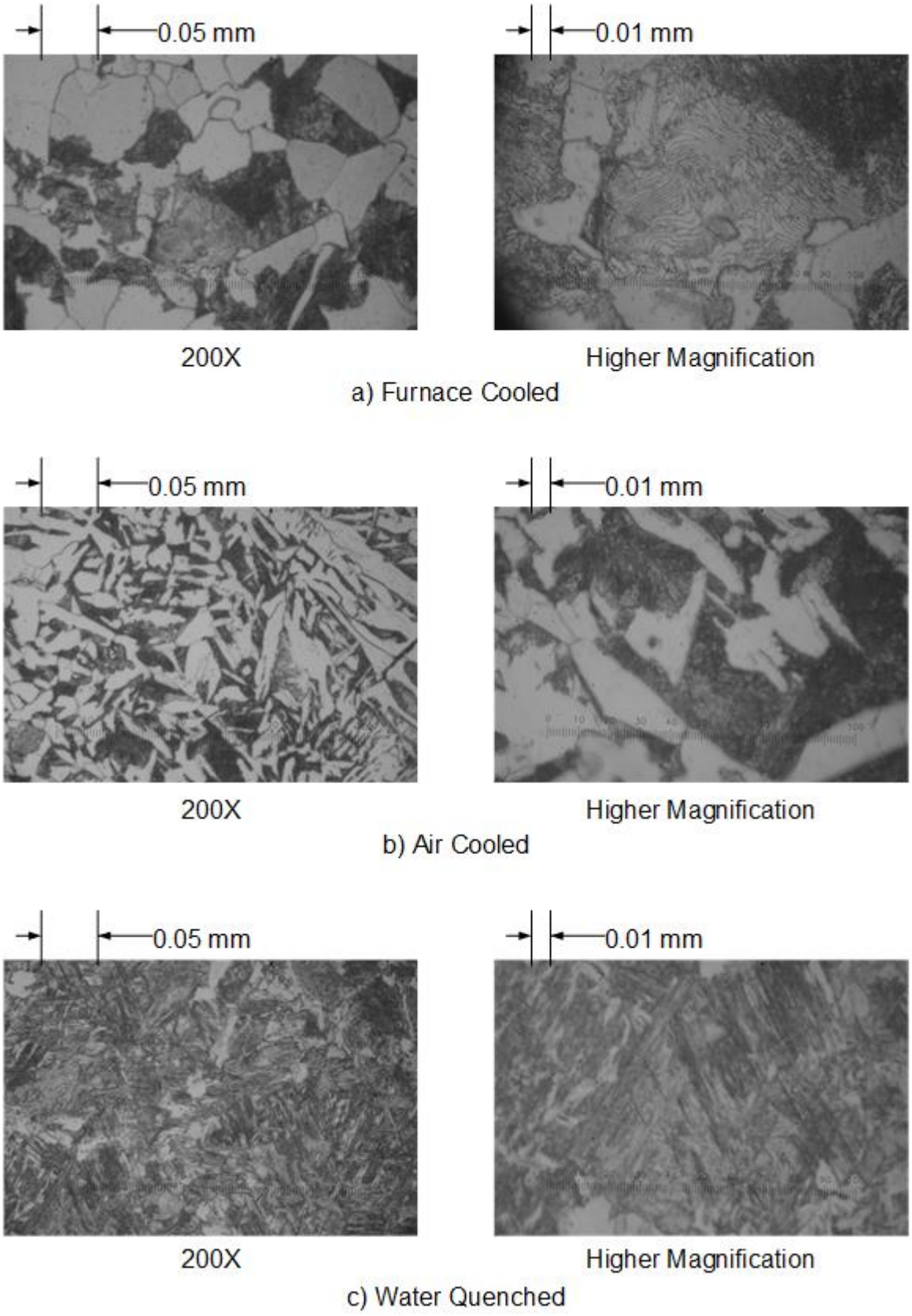

Figure 11B.4 – Microstructure of ASTM A515 Grade 60 Specimens - 1hr Heated at 1000ºC (1832ºF)

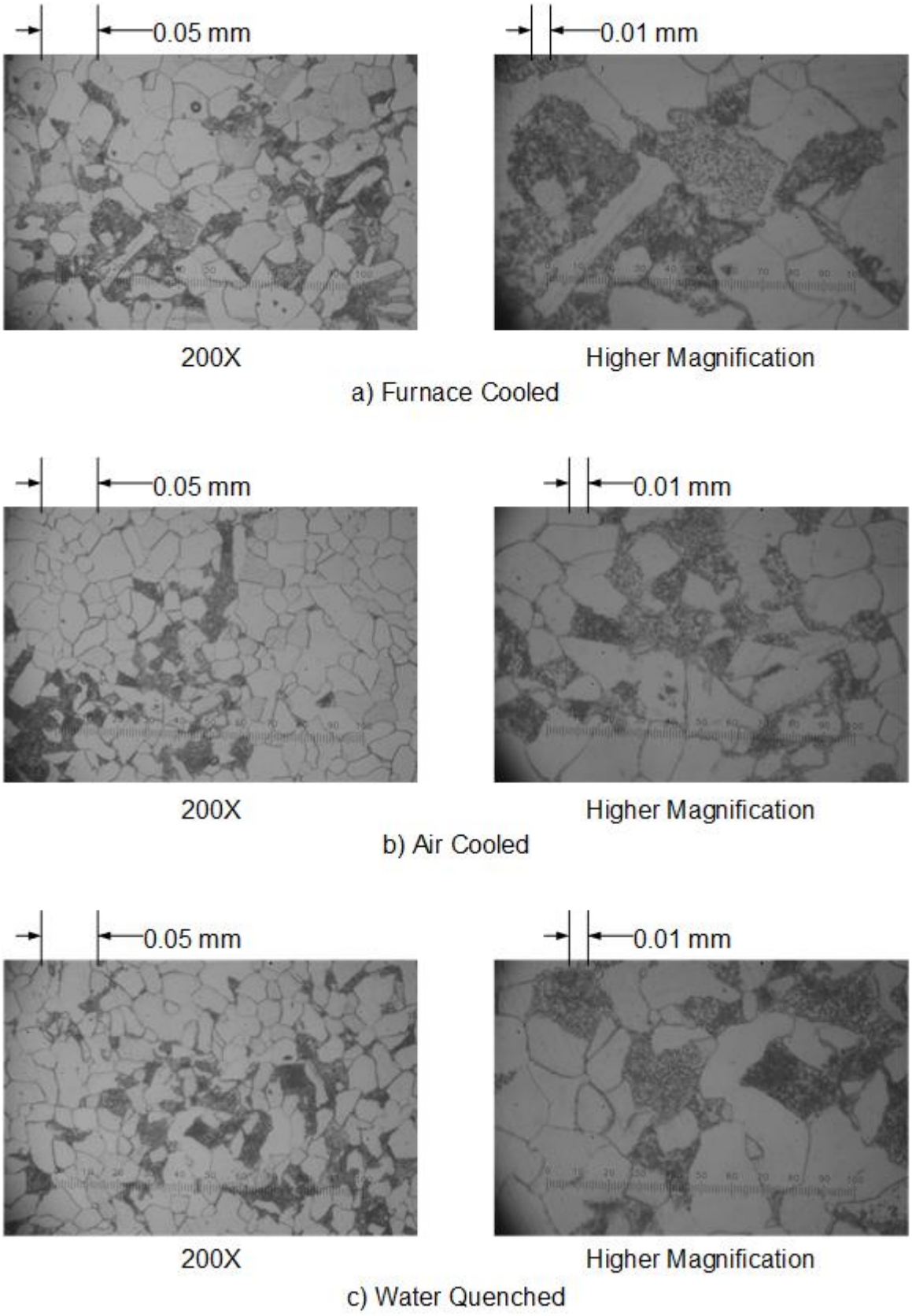

Figure 11B.5 – Microstructure of ASTM A515 Grade 60 Specimens - 1hr Heated 738ºC (1360ºF)

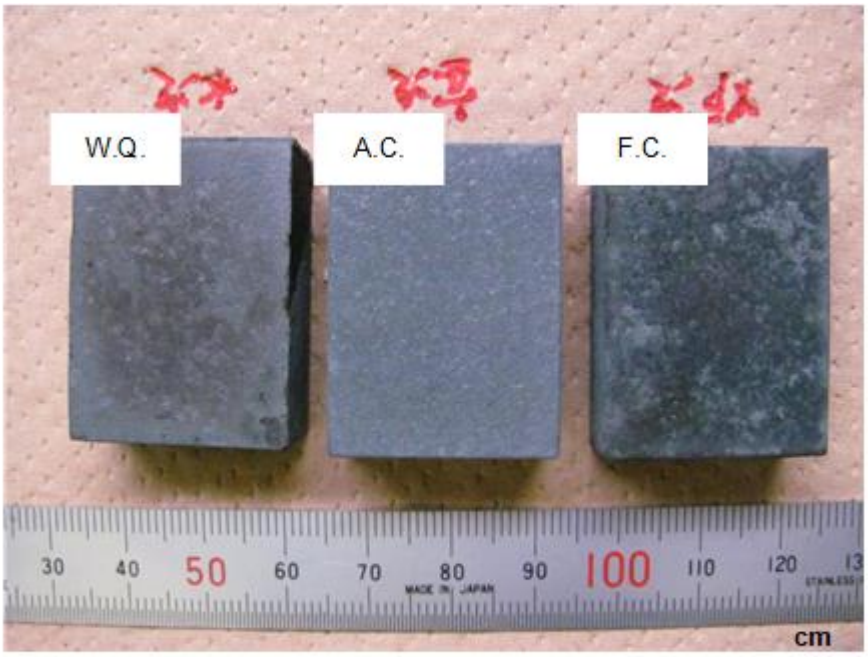

1832°F-1h Heated Specimens

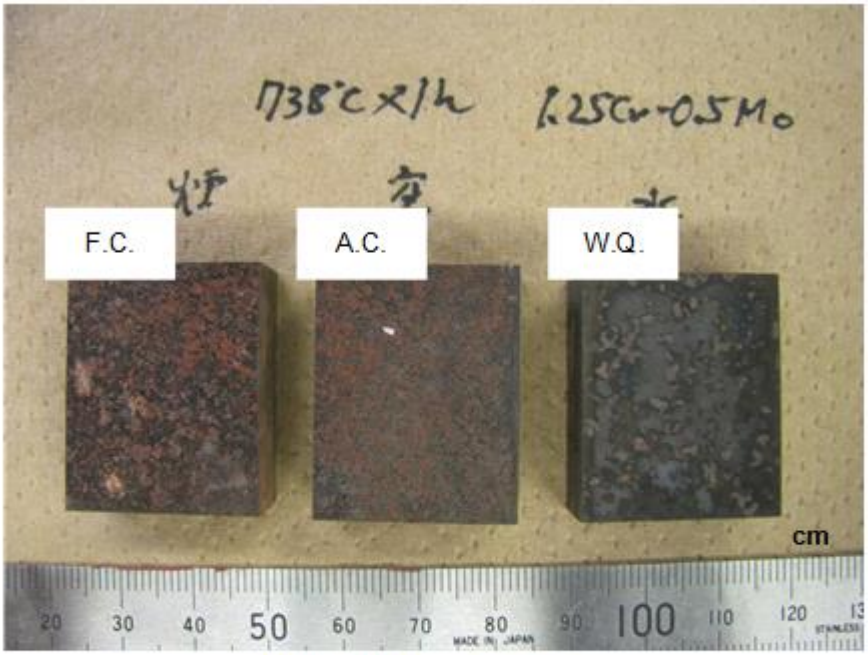

1360°F-1h Heated Specimens

F.C. – Furnace Cooled, A.C. – Air Cooled, W.Q. – Water Quenched

Figure 11B.6 – Appearance of ASTM A387 Grade 11 Class 2 Heated Specimens

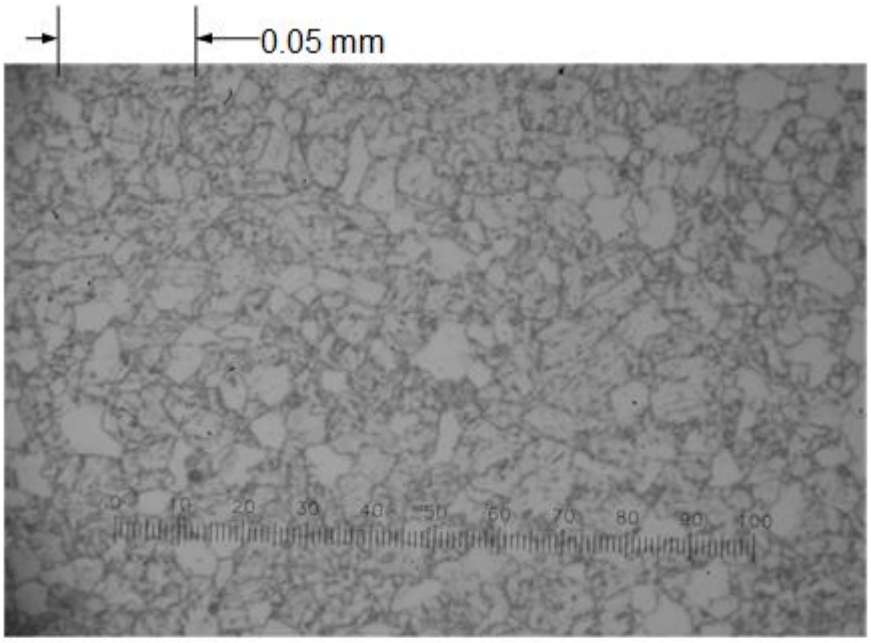

200X

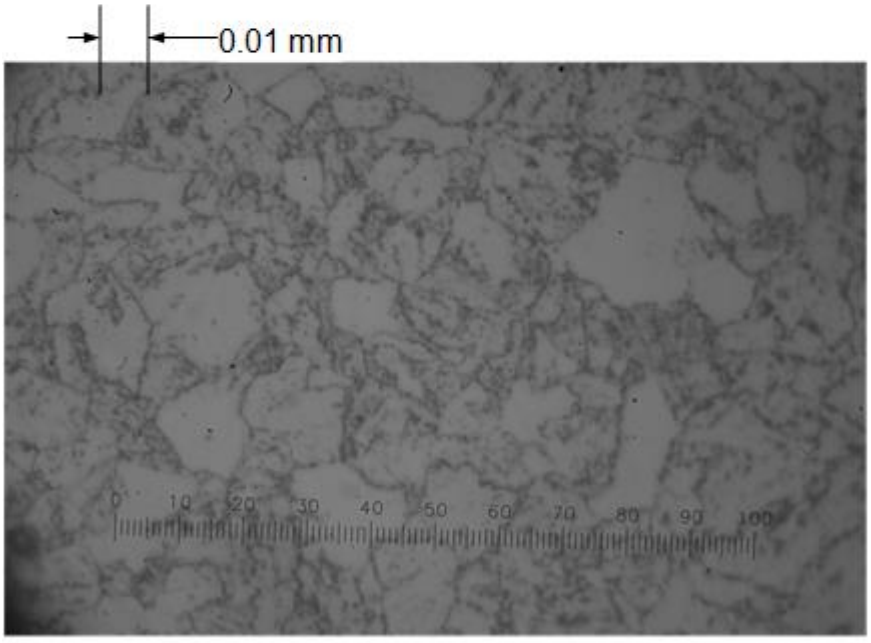

Higher Magnification

Figure 11B.7 – Microstructure of ASTM A387 Grade 11 Class 2 Specimens – As-New Condition

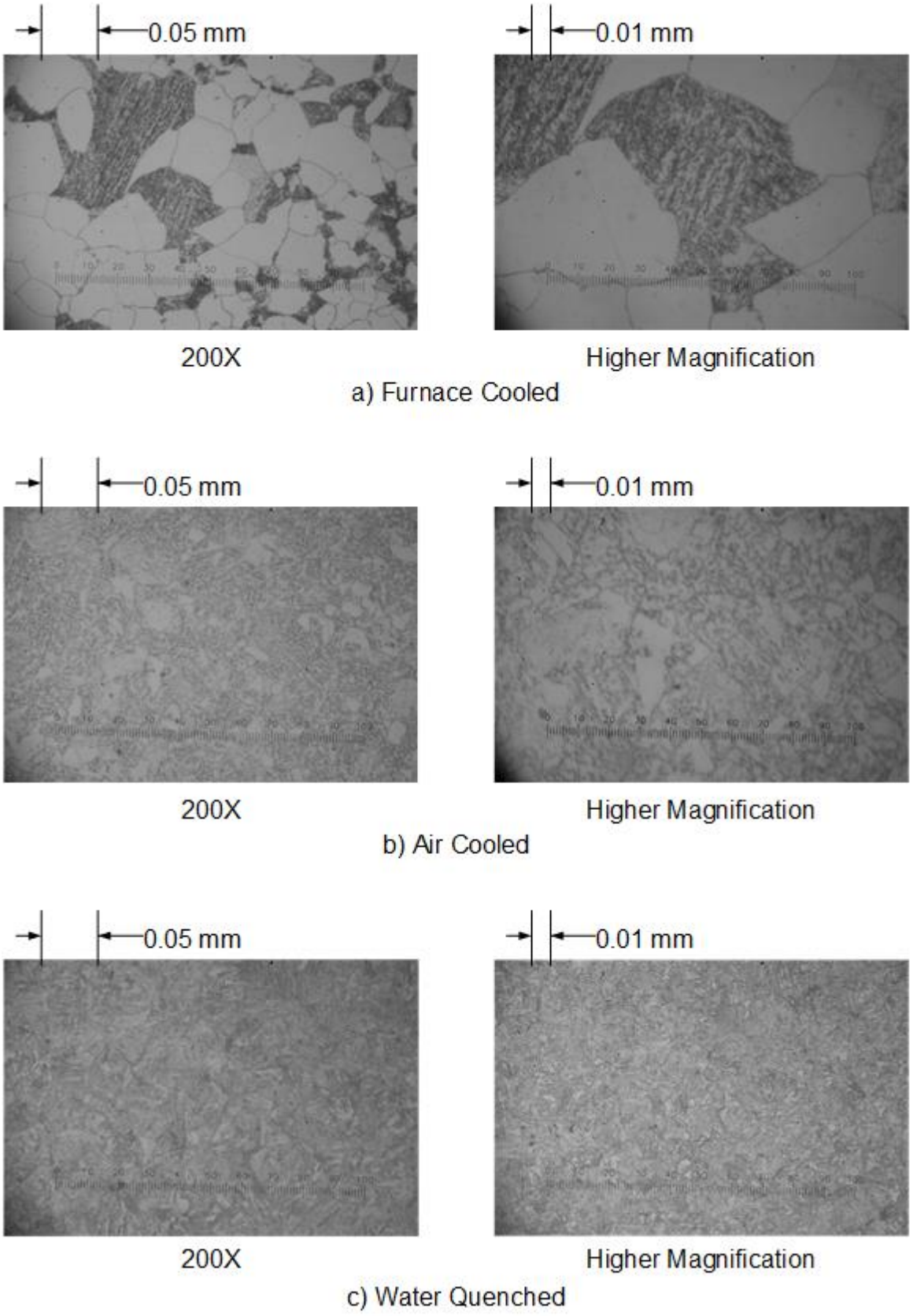

Figure 11B.8 – Microstructure of ASTM A387 Grade 11 Cl 2 Specimens - 1hr Heated At 1000ºC (1832ºF)

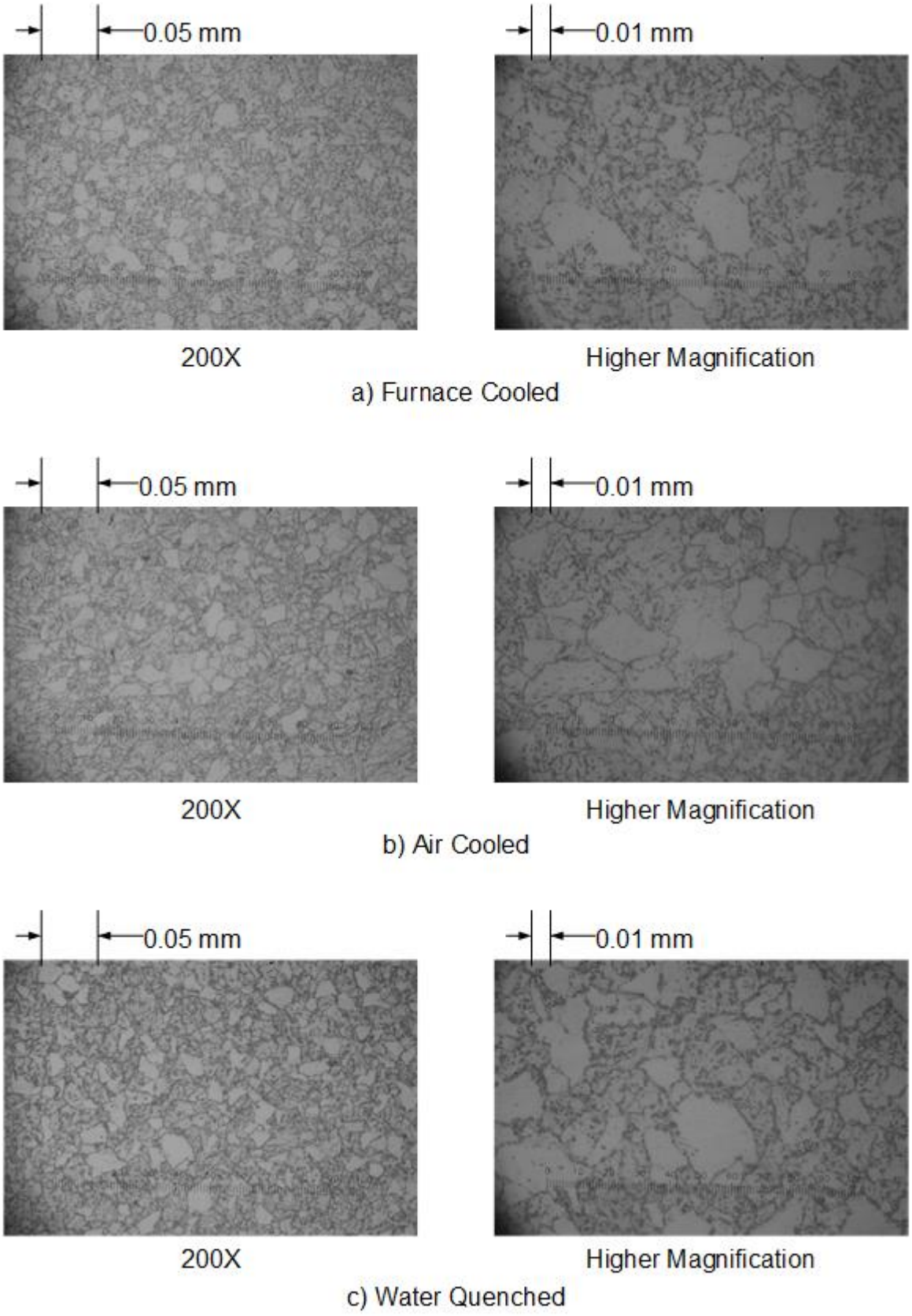

Figure 11B.9 – Microstructure of ASTM A387 Grade 11 Cl 2 Specimens - 1hr Heated At 738ºC (1360ºF)

[Intentionally Left Blank]

PART 12 – ASSESSMENT OF DENTS, GOUGES, AND DENT-GOUGE COMBINATIONS

CONTENTS

PART 12 – ASSESSMENT OF DENTS, GOUGES, AND DENT-GOUGE COMBINATIONS 12-1

12.1 GENERAL 12-1
12.1.1 Assessment Procedures for Dents, Gouges and Dent-Gouge Combinations 12-1
12.1.2 Assessment Procedures for LTAs, Grooves, and Other Shell Distortions 12-2
12.2 APPLICABILITY AND LIMITATIONS OF THE PROCEDURE 12-2
12.2.1 Overview 12-2
12.2.2 Calculation of the MAWP and Coincident Temperature 12-2
12.2.3 Limitations Based on Flaw Type 12-2
12.2.4 Limitations Based on Temperature 12-2
12.2.5 Applicability of the Level 1 and Level 2 Assessment Procedures 12-3
12.2.6 Applicability of the Level 3 Assessment Procedure 12-4
12.3 DATA REQUIREMENTS 12-4
12.3.1 Original Equipment Design Data 12-4
12.3.2 Maintenance and Operational History 12-4
12.3.3 Required Data/Measurements for an FFS Assessment 12-4
12.3.4 Recommendations for Inspection Technique and Sizing Requirements 12-7
12.4 ASSESSMENT TECHNIQUES AND ACCEPTANCE CRITERIA 12-7
12.4.1 Overview 12-7
12.4.2 Level 1 Assessment 12-8
12.4.3 Level 2 Assessment 12-10
12.4.4 Level 3 Assessment 12-13
12.5 REMAINING LIFE ASSESSMENT 12-14
12.5.1 Categories of Remaining Life Assessment 12-14
12.5.2 Requirements for a Level 3 Assessment 12-14
12.6 REMEDIATION 12-14
12.6.1 Flaw Severity and Evaluation of Material Condition 12-14
12.6.2 Reinforcement of Dents, Gouges and Dent-Gouge Combinations 12-14
12.6.3 Use of General Corrosion Remediation Methods 12-14
12.7 IN-SERVICE MONITORING 12-15
12.7.1 Requirements for In-Service Monitoring 12-15
12.7.2 Visual Inspection and Field Measurements of Distortion 12-15
12.8 DOCUMENTATION 12-15
12.8.1 Requirements 12-15
12.8.2 Inspection and Field Measurements 12-15
12.9 NOMENCLATURE 12-15
12.10 REFERENCES 12-17
12.11 TABLES 12-18
12.12 FIGURES 12-21

12.1 General

12.1.1 Assessment Procedures for Dents, Gouges and Dent-Gouge Combinations

Fitness-For-Service (FFS) Assessment procedures for pressurized components containing dents, gouges, or dent-gouge combinations resulting from mechanical damage are provided in this Part. The procedures can be used to qualify a component for continued operation or for determining a reduced maximum allowable working

pressure. A flow chart for the assessment procedures for components containing dents, gouges, or dent-gouge combinations is shown in Figure 12.1.

12.1.2 Assessment Procedures for LTAs, Grooves, and Other Shell Distortions

Assessment procedures for metal loss categorized as a locally thin area or a groove are covered in Part 5, and assessment procedures for other shell distortions such as weld misalignment, out-of-roundness, and bulges are covered in Part 8.

12.2 Applicability and Limitations of the Procedure

12.2.1 Overview

The procedures in this Part can be used to evaluate components with dents, gouges, or dent-gouge combinations resulting from mechanical damage as defined below.

a) Dent – An inward deviation of a cross-section of a shell member from an ideal shell geometry that is characterized by a small local radius or notch (see Figure 12.2). When the local radius of curvature (in any direction) of the sharpest part of the dent is less than or equal to five times the wall thickness, the dent is defined as a kinked dent.

b) Gouge – An elongated local removal and/or relocation of material from the surface of a component caused by mechanical means that results in a reduction in wall thickness; the length of a gouge is much greater than the width and the material may have been cold worked in the formation of the flaw. The gouge may occur on the inside or outside of the component. The geometry of a gouge is similar to that of a groove, (see Part 5, Figures 5.3 and 5.4). Gouges are caused by mechanical damage and often have a work hardened layer of material because of the gouging process (e.g., gouging of a section of pipe by mechanical equipment during the excavation of a pipeline). Gouges are frequently associated with dents due to the nature of mechanical damage.

c) Dent-Gouge Combination – A dent with a gouge present in the deformed region (see Figure 12.3).

12.2.2 Calculation of the MAWP and Coincident Temperature

Calculation methods are provided to determine acceptable $MAWP$ and coincident temperature if the acceptance criteria in this Part are not satisfied. For pressurized components, the calculation methods can be used to find a reduced maximum allowable working pressure ($MAWP_r$).

12.2.3 Limitations Based on Flaw Type

Unless otherwise specified, this Part is limited to the evaluation of dents, gouges, or dent-gouge combinations. General or uniform corrosion is considered in the assessment procedures. Other flaw types shall be evaluated in accordance with Part 2, Table 2.1.

12.2.4 Limitations Based on Temperature

The assessment procedures only apply to components that are not operating in the creep range; the design temperature is less than or equal to the value in Part 4, Table 4.1. A materials engineer should be consulted regarding the creep range temperature limit for materials not listed in this table.

12.2.5 Applicability of the Level 1 and Level 2 Assessment Procedures

12.2.5.1 The Level 1 or 2 Assessment procedures in this Part apply only if all the following conditions are satisfied.

a) Dents and Dent-Gouge Combinations

1) The original design criteria were in accordance with a recognized code or standard (see Part 1, paragraphs 1.2.2 or 1.2.3).

2) The material is considered to have sufficient material toughness. If there is uncertainty regarding the material toughness, then a Part 3 assessment should be performed. If the component is subject to embrittlement during operation due to temperature and/or the process environment (e.g., hydrogen embrittlement), a Level 3 Assessment should be performed. Temperature and/or process conditions that result in material embrittlement are discussed in Annex 2B. One other factor that is unique to dents and gouges is that cold work may be produced by the deformation. This cold worked area may be more susceptible to some forms of mechanical and environmental cracking.

3) The component satisfies the following requirements.

i) The component is a cylindrical shell with a geometry that satisfies Equations (12.1), (12.2) and (12.3).

$$168\ mm(6.625\ in) \le D_o \le 1050\ mm(42\ in) \tag{12.1}$$

$$5\ mm(0.20\ in) \le t_{rd} \le 19\ mm(0.75\ in) \tag{12.2}$$

$$23.6 \le D_o / t_{rd} \le 80.0 \tag{12.3}$$

ii) The component is subject only to internal pressure (i.e., supplemental loads are assumed to be negligible).

iii) The component material is carbon steel with Specified Minimum Yield Strength ($SMYS$) that satisfies Equation (12.4) and an Ultimate Tensile Strength (UTS) that satisfies Equation (12.5). The limit on SMYS only applies to the static assessment of dent-gouge combinations, and the limit on UTS only applies to the fatigue assessment of dents and dent-gouge combinations.

$$SMYS \le 482\ MPa(70\ ksi) \tag{12.4}$$

$$UTS \le 711\ MPa(103\ ksi) \tag{12.5}$$

iv) The radius of curvature (in any direction) of the sharpest part of the dent satisfies Equation (12.6).

$$r_d > 5t_{rd} \tag{12.6}$$

4) The assessment procedures only apply to isolated dents and dent-gouge combinations. In this context, isolated dents are defined as dents spaced at least two times the limit established by L_{msd}.

5) For dent-gouge combinations, the gouge orientation shall be longitudinal (i.e., in the axial direction). Circumferentially-oriented gouges in dent-gouge combinations require a Level 3 Assessment.

b) Gouges – If the material toughness satisfies the assessment criterion, the Level 1 and Level 2 Assessment procedures of Part 5 (including the applicability and limitations of the Part 5 assessment procedures) shall be used.

12.2.5.2 The Level 1 Assessment procedures are applicable if the component is not in cyclic service. If the component is subject to less than 150 cycles (i.e., pressure and/or temperature variations including operational changes and start-ups and shut-downs) throughout its previous operating history and future planned operating conditions or satisfies the cyclic service screening procedure in Part 14, then the component is not in cyclic service. In a Level 2 Assessment, if the component is in cyclic pressure service and a fatigue analysis is provided, then the permissible number of cycles shall be determined. Note that if the pressure cycles are complex, or other forms of cyclic stress are present, a Level 3 Assessment is required.

12.2.6 Applicability of the Level 3 Assessment Procedure

A Level 3 Assessment can be performed when the Level 1 and 2 Assessment procedures do not apply, or when these assessment levels produce conservative results (i.e., would not permit operation at the current design conditions). Examples include but are not limited to the following.

a) Type A, B, or C Components (see Part 4, paragraph 4.2.5) with a geometry that does not satisfy the Level 1 and 2 requirements.

b) The component loading conditions include internal pressure, external pressure, supplemental loads, thermal loads, or any combination thereof.

c) The component material does not satisfy the Level 1 and 2 requirements.

d) Components with a design based on proof testing, e.g., piping tee or reducer produced in accordance with ASME B16.9 where the design may be based on proof testing.

e) Components in cyclic service where the cyclic stresses are a result of complex pressure cycles or other load cycles, i.e., supplemental loads and thermal loads.

f) Components operating in the creep range.

g) Components with closely spaced dents, gouges, and/or dent-gouge combinations.

h) Dent-gouge combinations with gouges oriented in any direction other than longitudinal (i.e., axial).

12.3 Data Requirements

12.3.1 Original Equipment Design Data

An overview of the original equipment data required for an assessment is provided in Part 2, paragraph 2.3.1. This data can be entered in the form provided in Part 2, Table 2.2, and Table 12.1 for each component under evaluation.

12.3.2 Maintenance and Operational History

An overview of the maintenance and operational history required for an assessment is provided in Part 2, paragraph 2.3.2.

12.3.3 Required Data/Measurements for an FFS Assessment

12.3.3.1 The required data and measurements for assessment of a dent are listed below.

a) *Dent Depth in the Pressurized Condition*, d_{dp}, *or Unpressurized Condition*, d_{d0} – The maximum depth of the dent in the pressurized and the unpressurized condition shall be determined. These values may be measured directly. The Owner-User should consider the risk before increasing the pressure from the current level to

measure the depth of the dent in the pressurized condition. Alternatively, if the operating pressure is greater than or equal to 70% of the $MAWP$, then the relationship between the dent depth in the pressurized condition and the dent depth in the unpressurized condition is given by Equation (12.7). Otherwise, the dent depth in the pressurized condition shall be assumed to be equal to the dent depth in the unpressurized condition, or $d_{dp} = d_{p0}$.

$$d_{dp} = 0.70 d_{d0} \tag{12.7}$$

b) *Minimum Specified Ultimate Tensile Strength*, σ_{uts} – The minimum specified ultimate tensile strength may be determined based on the material specification. If the material specification is unknown, then $\sigma_{uts} = 414\ MPa\ (60\ ksi)$ may be used in the assessment. This information is required for Level 2 and Level 3 Assessments.

c) *Cyclic Pressure Components*, P_{max} and P_{min} – If the component is in cyclic pressure service that can be represented by a maximum and minimum pressure, the maximum and minimum pressures of the cycle shall be determined. This information is required for a Level 2 Assessment and may be required for a Level 3 Assessment.

d) *Dent Spacing to Weld Joints, L_w – M*easurements should be made to determine the spacing between the edge of the dent and the nearest weld joint. This information should be detailed and provided on an inspection sketch.

e) *Dent Spacing to Major Structural Discontinuities, L_{msd} – M*easurements should be made to determine the spacing between the edge of the dent and the nearest major structural discontinuity. This information should be detailed and provided on an inspection sketch.

12.3.3.2 The required data and measurements for assessment of a gouge are listed below.

a) *Gouge Dimensions* – The flaw dimensions of the gouge shall be determined using the methods described for a groove in Part 5.

b) *Temperature Corresponding to 40 Joules (30 ft-lbs) of CVN impact energy of a full size specimen* – The Level 1 and Level 2 Assessment of Part 5 may be used if one of the following is true.

1) The component is operating at or above the temperature that corresponds to 40 Joules (30 ft-lbs) of CVN impact energy of a full-size specimen. This can be verified using actual CVN impact energy data, if available, or estimated per Table 12.2 based on material temperature exemption curves and minimum specified yield strength.

2) The gouge is formed by a process that results in a work hardened layer, and the gouge is subsequently dressed to remove this layer and any other defects to obtain a smooth profile.

c) *Material Temperature Exemption Curve* – This data is only required if the temperature that corresponds to 40 Joules (30 ft-lbs) of CVN impact energy of a full-size specimen is estimated based on the material specification and the minimum specified yield strength. Material Temperature Exemption Curves are provided in Part 3, Table 3.2.

d) *Minimum Specified Yield Strength*, σ_{ys} – This data is only required if the temperature that corresponds to 40 Joules (30 ft-lbs) of CVN impact energy of a full-size specimen is estimated based on the material specification and the minimum specified yield strength.

e) *Gouge Spacing to Major Structural Discontinuities,* L_{msd} – *M*easurements should be made to determine the spacing between the edge of the gouge and the nearest major structural discontinuity. This information should be detailed and provided on an inspection sketch.

12.3.3.3 The required data and measurements for assessment of a dent-gouge combination are listed below.

a) *Dent Depth in the Pressurized Condition*, d_{dp}, *or Unpressurized Condition*, d_{d0} – The maximum depth of the dent in the pressurized or the unpressurized condition shall be measured (see paragraph 12.3.3.1(a)).

b) *Gouge Depth* d_g – The maximum depth of the gouge shall be determined using the methods described for a groove in Part 5.

c) *Minimum Specified Yield Strength*, σ_{ys} – The minimum specified yield strength may be determined based on the material specification.

d) *Minimum Specified Ultimate Tensile Strength*, σ_{uts} – The minimum specified ultimate tensile strength may be determined based on the material specification. If the material specification is unknown, then $\sigma_{uts} = 414\ MPa\ (60\ ksi)$ may be used in the assessment. This information is required for Level 2 and Level 3 Assessments.

e) *Cyclic Pressure Components*, P_{max} and P_{min} – If the component is in cyclic pressure service that can be represented by a maximum and minimum pressure, the maximum and minimum pressures of the cycle shall be determined. This information is required for a Level 2 Assessment and may be required for a Level 3 Assessment.

f) *Dent-gouge Combination Spacing to Weld Joints,* L_w – *M*easurements should be made to determine the spacing between the edge of the dent-gouge combination and the nearest weld joint. This information should be detailed and provided on an inspection sketch.

g) *Dent-gouge Combination Spacing to Major Structural Discontinuities,* L_{msd} – *M*easurements should be made to determine the spacing between the edge of the dent-gouge combination and the nearest major structural discontinuity. This information should be detailed and provided on an inspection sketch.

h) *Charpy V-notch impact energy of a 2/3 sub-size specimen* $CVN_{2/3}$ – If only the Charpy V-notch impact energy of a full-size specimen is known then the procedures of Annex 9F, paragraph 9F.2.2 can be used to calculate $CVN_{2/3}$.

i) *Temperature Corresponding to 40 Joules (30 ft-lbs) of* CVN *impact energy of a full size specimen*. This can be verified using actual *CVN* impact energy data, if available, or estimated per Table 12.2 based on material temperature exemption curves and minimum specified yield strength.

j) *Material Temperature Exemption Curve* – This data is only required if the temperature that corresponds to 40 Joules (30 ft-lbs) of CVN impact energy of a full-size specimen is estimated based on the material specification and the minimum specified yield strength. Material Temperature Exemption Curves are provided in Part 3, Table 3.2.

12.3.3.4 The information required to perform a Level 3 Assessment is dependent on the analysis method utilized. In most cases, stress analysis in accordance with Annex 2D and Part 14, as applicable, will be performed. The stress analysis will typically require a complete description of the geometry, material properties, and loading condition including pressure, supplemental, and thermal loads.

12.3.4 Recommendations for Inspection Technique and Sizing Requirements

12.3.4.1 The maximum depth of the dent may be established using a straight edge along the axis of the cylinder and measuring the offset in the region of the dent. Note that numerous measurements should be taken to establish the dent profile in the axial and circumferential directions if a Level 3 Assessment is to be performed. Only the maximum dent depth is used in the Level 1 and 2 Assessments. The complete dent profile may be used in a Level 3 Assessment.

12.3.4.2 The gouge dimensions may be obtained in accordance with Part 4 and Part 5.

12.3.4.3 The flaw size of the dent-gouge combination may be established using the methods described above.

12.3.4.4 For dents within the weld band region (as defined in Annex 2C, paragraph 2C.2.5), surface examination (e.g., MT or PT) and volumetric examination (e.g., UTSW, PAUT, or TOFD) shall be performed to confirm no cracking or other flaws exist in or near the weld. If crack-like flaws or defects are identified, a Level 3 Assessment is required.

12.3.4.5 The surface of all dents, gouges, and dent-gouge combinations shall be inspected for potential crack-like defects using applicable NDE techniques (e.g., MT or PT). If crack-like flaws or defects are identified, a Level 3 Assessment is required.

12.4 Assessment Techniques and Acceptance Criteria

12.4.1 Overview

12.4.1.1 An overview of the assessment levels for the evaluation of a dent is provided below.

a) The Level 1 Assessment acceptability criterion is based on limiting the maximum dent depth in the component to a percentage of the component's outside diameter when the component is not subject to cyclic loading.

b) The Level 2 Assessment follows the Level 1 Assessment procedure but includes a fatigue analysis to evaluate the effects of cyclic pressure loading.

c) The Level 3 Assessment rules are intended to evaluate dents in complex geometries subject to general loading conditions. A Level 3 Assessment is also required for materials other than carbon steel. Numerical stress analysis techniques are utilized in a Level 3 Assessment.

12.4.1.2 An overview of the assessment levels for the evaluation of a gouge is provided below.

a) The Level 1 and Level 2 Assessment procedures are based on the Level 1 and Level 2 Assessment procedures of Part 5, respectively, if the material has a CVN impact energy greater than 40 Joules (30 ft-lbs) or if the gouge is dressed to remove the work hardened layer, which may have been formed during the gouging process. If the material CVN impact energy is unknown, the temperature at which the material can be expected to have a CVN impact energy greater than 40 Joules (30ft-lbs) is provided.

b) Level 3 Assessment rules are intended to evaluate gouges in complex geometries subject to general loading conditions. Numerical stress analysis techniques are utilized in a Level 3 Assessment.

12.4.1.3 An overview of the assessment levels for the evaluation of a dent-gouge combination is provided below.

a) A screening curve is provided in the Level 1 Assessment procedure to determine the acceptability criterion for continued operation based on the ratio of the dent depth to cylinder outside diameter and the ratio of the gouge depth to wall thickness for components not subject to cyclic loading.

b) Level 2 Assessment is limited to dent-gouge combinations in carbon steel cylindrical shells located away from structural discontinuities. A remaining strength factor approach is utilized to determine an acceptable $MAWP$ based on the dent depth and gouge depth. In addition, a fatigue assessment to evaluate the effects of cyclic pressure loading is provided.

c) Level 3 Assessment rules are intended to evaluate dent-gouge combinations in complex geometries subject to general loading conditions. A Level 3 Assessment is also required for materials other than carbon steel. Numerical stress analysis techniques are utilized in a Level 3 Assessment.

12.4.2 Level 1 Assessment

12.4.2.1 Dent Assessment Procedure

The Level 1 Assessment procedure for determining the acceptability of a dent is shown below.

a) STEP 1 – Determine the parameters in paragraph 12.3.3.1 together with D, D_o, FCA, either t_{rd} or t_{nom} and $LOSS$.

b) STEP 2 – Determine the wall thickness to be used in the assessment, t_c, using Equation (12.8) or Equation (12.9), as applicable.

$$t_c = t_{nom} - LOSS - FCA \tag{12.8}$$

$$t_c = t_{rd} - FCA \tag{12.9}$$

c) STEP 3 – If Equation (12.10) is satisfied, proceed to STEP 4. Otherwise, the Level 1 Assessment is not satisfied.

$$L_{msd} \geq 1.8\sqrt{Dt_c} \tag{12.10}$$

d) STEP 4 – If Equation (12.11) or Equation (12.12) is satisfied, proceed to STEP 5. Otherwise, the Level 1 Assessment is not satisfied.

$$d_{dp} \leq 0.07D_o \qquad for\ L_w \geq \max\left[2t_c,\ 25\,mm\ (1\ in)\right] \tag{12.11}$$

$$d_{dp} \leq 0.04D_o \qquad for\ L_w < \max\left[2t_c,\ 25\,mm\ (1\ in.)\right] \tag{12.12}$$

e) STEP 5 – Determine the $MAWP$ for the component (see Annex 2C, paragraph 2C.2) using the thickness from STEP 2. If the $MAWP$ is greater than or equal to the equipment design pressure or equipment $MAWP$, then the component is acceptable for continued operation. Otherwise, the Level 1 Assessment is not satisfied.

12.4.2.2 Gouge Assessment Procedure

The Level 1 Assessment procedure for determining the acceptability of a gouge is as shown below.

a) STEP 1 – Determine the minimum operating temperature and the parameters in paragraph 12.3.3.2.

b) STEP 2 – Determine the CVN impact energy for the material at the minimum operating temperature. If greater than 40 Joules (30ft-lbs) or if the surface of the gouge is dressed to remove the work hardened layer, then proceed to STEP 3. Otherwise, the Level 1 Assessment is not satisfied. Note that if the CVN impact energy of the material is unknown, the temperature at which the material can be expected to have a CVN impact energy greater than 40 Joules (30ft-lbs) may be obtained from Table 12.2 if an ASME Exemption Curve and the minimum specified yield strength for the material are known. Alternatively, Annex 9F,

paragraph 9F.2 may be used to estimate the temperature at which the material can be expected to have a CVN impact energy greater than 40 Joules (30ft-lbs).

c) STEP 3 – The gouge shall be evaluated using the Level 1 Assessment procedures in Part 5.

12.4.2.3 Dent-Gouge Combination Assessment Procedure

The Level 1 Assessment procedure for determining the acceptability of a dent-gouge combination is as shown below.

a) STEP 1 – Determine the parameters in paragraph 12.3.3.3 together with D, D_o, FCA, $LOSS$, g_r (see Part 5, Figure 5.3), and either t_{rd} or t_{nom}.

b) STEP 2 – Determine the wall thickness to be used in the assessment, t_c, using Equation (12.8) or Equation (12.9), and t_{mm} using Equation (12.13) or Equation (12.14).

$$t_{mm} = t_{rd} - d_g \tag{12.13}$$

$$t_{mm} = t_{nom} - LOSS - d_g \tag{12.14}$$

c) STEP 3 – Determine the remaining thickness ratio.

$$R_t = \frac{t_{mm} - FCA}{t_c} \tag{12.15}$$

d) STEP 4 – If the following requirements are satisfied, proceed to STEP 5. Otherwise, the Level 1 Assessment procedure is not satisfied.

$$t_{mm} - FCA \geq \max\left[0.2t_{nom},\ 2.5\ mm\ (0.10\ inches)\right] \qquad for\ Pressure\ Vessels \tag{12.16}$$

$$t_{mm} - FCA \geq \max\left[0.2t_{nom},\ 1.3\ mm\ (0.05\ inches)\right] \qquad for\ Piping \tag{12.17}$$

$$L_{msd} \geq 1.8\sqrt{Dt_c} \tag{12.18}$$

$$L_w \geq \max\left[2t_c,\ 25\,mm\ (1\ inch)\right] \tag{12.19}$$

$$\frac{g_r}{(1-R_t)t_c} \geq 0.5 \tag{12.20}$$

e) STEP 5 – Determine the circumferential stress, σ_m^C, for the component (see Annex 2C, paragraph 2C.2) using t_c from STEP 2.

f) STEP 6 – Determine the gouge depth to wall thickness ratio, d_g/t_c, and the dent depth to component diameter ratio, d_{dp}/D_o. Enter these data with the circumferential stress, σ_m^C, determined in STEP 5 on Figure 12.4. If the point defined by the intersection of these values is on or below the curve in this figure that corresponds to the circumferential stress in terms of the minimum specified yield strength for the component and the component is not in cyclic service, proceed to STEP 7. Otherwise, the Level 1 Assessment is not satisfied.

g) STEP 7 – Determine the $MAWP$ for the component (see Annex 2C, paragraph 2C.2) using t_c from STEP 2. If the $MAWP$ is greater than or equal to the equipment design pressure or equipment $MAWP$, then the component is acceptable for continued operation. Otherwise, the Level 1 Assessment is not satisfied.

12.4.2.4 If the component does not meet the Level 1 Assessment requirements, then the following, or combinations thereof, shall be considered:

a) Rerate, repair, or replace the component.

b) Adjust the FCA by applying remediation techniques (see Part 4, paragraph 4.6).

c) Conduct a Level 2 or Level 3 Assessment.

12.4.3 Level 2 Assessment

12.4.3.1 Dent Assessment Procedure

The Level 2 Assessment procedure for determining the acceptability of a dent is as shown below.

a) STEP 1 – Complete STEPs 1 through 5 of the Level 1 Assessment procedure in paragraph 12.4.2.1. If all the criteria are satisfied, proceed to STEP 2. Otherwise, the Level 2 Assessment is not satisfied.

b) STEP 2 – If the component is not subject to pressure cycles, the component is acceptable for continued operation and the assessment is complete. If the component is subject to pressure cycles, then determine the acceptable number of cycles as shown below.

1) STEP 2.1 – Determine the circumferential stresses, $\sigma^{C}_{m,max}$ and $\sigma^{C}_{m,min}$, based on P_{max} and P_{min}, respectively, for the component (see Annex 2C, paragraph 2C.2) using t_c from paragraph 12.4.2.1(b).

2) STEP 2.2 – Determine the acceptable number of cycles. If the acceptable number of cycles is greater than or equal to the sum of the past and future anticipated number of cycles, then the component is acceptable for continued operation at the specified conditions. Otherwise, the Level 2 Assessment is not satisfied.

$$N_c = \frac{1000}{\alpha_c M_u}\left[\frac{\left(\sigma_{uts} - U_0\right)}{2\sigma_A K_s}\right]^{4.292} \tag{12.21}$$

$$M_u = 1.0 \qquad for\ L_w \geq \max\left[2t_c,\ 25\,mm\ (1\ in.)\right] \tag{12.22}$$

$$M_u = 10.0 \qquad for\ L_w < \max\left[2t_c,\ 25\,mm\ (1\,in.)\right] \tag{12.23}$$

$$\sigma_A = \frac{\sigma_{uts}}{2}\left[B\left(4 + B^2\right)^{0.5} - B^2\right] \tag{12.24}$$

$$B = \frac{\dfrac{\sigma_a}{\sigma_{uts}}}{\left[1 - \dfrac{\sigma_a}{\sigma_{uts}}\left(\dfrac{1+R}{1-R}\right)\right]^{0.5}} \tag{12.25}$$

$$\sigma_a = \frac{\sigma^{C}_{m,max} - \sigma^{C}_{m,min}}{2} \tag{12.26}$$

$$R = \frac{\sigma^{C}_{m,\min}}{\sigma^{C}_{m,\max}} \tag{12.27}$$

$$K_s = \max\left[2.871\sqrt{K_d},\ 1.0\right] \qquad \left(\sqrt{mm}\right) \tag{12.28}$$

$$K_s = \max\left[14.469\sqrt{K_d},\ 1.0\right] \qquad \left(\sqrt{in}\right) \tag{12.29}$$

$$K_d = d_{d0}\left(\frac{t_{rd}}{D_o}\right) \tag{12.30}$$

12.4.3.2 Gouge Assessment Procedure

The Level 2 Assessment procedure for determining the acceptability of a gouge is as shown below.

a) STEP 1 – Determine the minimum operating temperature and the parameters in paragraph 12.3.3.2.

b) STEP 2 – Determine the CVN impact energy for the material at the minimum operating temperature. If the CVN impact energy is greater than 40 Joules (30ft-lbs) or if the surface of the gouge is dressed to remove the work hardened layer and any other defects to obtain a smooth profile, then proceed to STEP 3. Otherwise, the Level 2 Assessment is not satisfied. Note that if the CVN impact energy of the material is unknown, the temperature at which the material can be expected to have a CVN impact energy greater than 40 Joules (30ft-lbs) may be obtained from Table 12.2 if an ASME Exemption Curve and the minimum specified yield strength for the material are known. Alternatively, Annex 9F, paragraph 9F.2 may be used to estimate the temperature at which the material can be expected to have a CVN impact energy greater than 40 Joules (30ft-lbs).

c) STEP 3 – The gouge shall be evaluated using the Level 2 Assessment procedures in Part 5.

12.4.3.3 Dent-Gouge Combination Assessment Procedure

The Level 2 Assessment procedure for determining the acceptability of a dent-gouge combination is as shown below.

a) STEP 1 – Determine the parameters in paragraph 12.3.3.3 together with D, D_o, FCA, either t_{rd} or t_{nom}, and $LOSS$.

b) STEP 2 – Determine the wall thickness to be used in the assessment, t_c, using Equations (12.8) or (12.9), and t_{mm} using Equations (12.13) or (12.14).

c) STEP 3 – If the requirements in paragraph 12.4.2.3(d) are satisfied, then proceed to STEP 4. Otherwise, the Level 2 Assessment is not satisfied.

d) STEP 4 – If Equations (12.11) or (12.12) are satisfied, and Equation (12.31) is satisfied, then proceed to STEP 5. Otherwise, the Level 2 Assessment is not satisfied.

$$d_g \le 0.66 t_c \tag{12.31}$$

e) STEP 5 – Determine the $MAWP$ for the component (see Annex 2C, paragraph 2C.2) using t_c from STEP 2. If the $MAWP$ is greater than or equal to the equipment design pressure or equipment $MAWP$ proceed to STEP 6. Otherwise, the Level 2 Assessment is not satisfied.

f) STEP 6 – Determine Remaining Strength Factor (RSF) for the dent-gouge combination.

$$RSF = \frac{2}{\pi}\arccos\left[\exp\left[\frac{-C_1 \cdot C_3}{C_2^2}\right]\right] \cdot \left(1 - \frac{d_g}{t_c}\right) \tag{12.32}$$

$$C_1 = \frac{1.5\pi E_y U_1}{\overline{\sigma}^2 \cdot A_{CVN,2/3} \cdot d_g} \tag{12.33}$$

$$C_2 = Y_1\left(1 - \frac{1.8d_{d0}}{D_o}\right) + Y_2\left(\frac{10.2d_{d0}}{2t_c}\right) \tag{12.34}$$

$$C_3 = \exp\left[\frac{\ln(U_2 \cdot CVN_{2/3}) - 1.9}{0.57}\right] \tag{12.35}$$

$$\overline{\sigma} = 1.15 \cdot \sigma_{ys}\left(1 - \frac{d_g}{t_c}\right) \tag{12.36}$$

$$Y_1 = 1.12 - 0.23\left(\frac{d_g}{t_c}\right) + 10.6\left(\frac{d_g}{t_c}\right)^2 - 21.7\left(\frac{d_g}{t_c}\right)^3 + 30.4\left(\frac{d_g}{t_c}\right)^4 \tag{12.37}$$

$$Y_2 = 1.12 - 1.39\left(\frac{d_g}{t_c}\right) + 7.32\left(\frac{d_g}{t_c}\right)^2 - 13.1\left(\frac{d_g}{t_c}\right)^3 + 14.0\left(\frac{d_g}{t_c}\right)^4 \tag{12.38}$$

g) STEP 7 – If $RSF \geq RSF_a$, then the dent-gouge combination is acceptable for operation at the $MAWP$ determined in STEP 5. If $RSF < RSF_a$, then the dent-gouge combination is acceptable for operation at a reduced $MAWP$ ($MAWP_r$) computed using the equations in Part 2, paragraph 2.4.2.2. The $MAWP$ from STEP 5 shall be used in this calculation. See paragraph 2.4.2.2(e) to determine the acceptability of the equipment for continued operation.

h) STEP 8 – If the component is not subject to pressure cycles, then the component is acceptable for continued operation and the assessment is complete. If the component is subject to pressure cycles, then determine the acceptable number of cycles using the procedure in paragraph 12.4.3.1(b) with M_u set equal to 100.0. If all the following additional criteria are satisfied, the component is acceptable for continued operation for the calculated number of cycles. Otherwise, the Level 2 Assessment is not satisfied.

1) $d_{do} \leq 0.04D_o$ or $d_{dp} \leq 0.028D_o$

2) $d_g \leq 0.20t_c$

3) The CVN impact energy for the material at the minimum operating temperature shall be greater than 40 Joules (30ft-lbs) or the surface of the gouge shall be dressed to remove the work hardened layer. Note that if the CVN impact energy of the material is unknown, the temperature at which the material can be expected to have a CVN impact energy greater than 40 Joules (30ft-lbs) may be obtained from Table 12.2 if an ASME Exemption Curve and the minimum specified yield strength for the material are known. Alternatively, Annex 9F, paragraph 9F.2 may be used to estimate the temperature at which the material can be expected to have a *CVN* impact energy greater than 40 Joules (30ft-lbs).

12.4.3.4 If the component does not meet the Level 2 Assessment requirements (see Part 2, paragraph 2.4.2.2(e)), then the following, or combinations thereof, shall be considered:

a) Rerate, repair, or replace the component.

b) Adjust the FCA by applying remediation techniques (see Part 4, paragraph 4.6).

c) Conduct a Level 3 Assessment.

12.4.4 Level 3 Assessment

12.4.4.1 The Level 3 Assessment procedures for dents, gouges, and dent-gouge combinations involve the evaluation of potential failure modes based on component geometry, material of construction, loading conditions, and operating temperature range.

a) The failure modes listed below shall be considered for dents, gouges, and dent-gouge combinations where the toughness is sufficient to ensure plastic behavior.

   1) Plastic Collapse (see Annex 2D, paragraph 2D.2).

   2) Local Failure (see Annex 2D, paragraph 2D.3).

   3) Collapse from Buckling (see Annex 2D, paragraph 2D.4).

   4) Fatigue Damage or Ratcheting (see Part 14).

   5) Creep or Creep-Fatigue Damage (see Part 10).

b) The failure modes listed in paragraph 12.4.4.1(a) and those shown below shall be considered for gouges and dent-gouge combinations with insufficient toughness to ensure plastic behavior.

   1) Crack Stability and Crack Growth (see Part 9).

   2) Creep Crack Stability and Crack Growth (see Part 10).

12.4.4.2 The numerical stress analysis should be performed considering the material as well as geometric non-linearity to account for the effect of pressure stiffening on the dent and re-rounding of the shell that occurs under pressure loading.

12.4.4.3 The stress analysis used in the assessment should simulate the deformation process that causes the damage to determine the magnitude of permanent plastic strain developed. To simulate the distortion process, an analysis that includes geometric and material non-linearity as well as the contact interaction between the original undeformed shell structure and the contacting body may be performed. The contacting component may be explicitly modeled as a deformable body or as a simple rigid surface. The analysis should include applicable loadings to develop the final distorted configuration of the shell structure.

12.4.4.4 If a kink or sharp bend exists in a shell, shell theory will not provide an accurate estimate of the stress state. In this case, a continuum model is recommended in the stress analysis described in paragraph 12.4.4.3.

12.4.4.5 For gouges and dent-gouge combinations that are evaluated using the crack-like flaw assessment procedures in Part 9 or Part 10, as applicable, the equivalent crack depth may be taken as the gouge depth and the equivalent crack length may be taken as the gouge length.

12.4.4.6 If the component is operating in the creep range, stresses due to localized geometric irregularities may not sufficiently relax with time due to the surrounding compliance of the component. In this case, creep strains can accumulate and may result in significant creep damage or cracking. The assessment of components that contain dents, gouges, or dent-gouge combinations requires an approach using a stress analysis that incorporates a material model for creep that includes the effects of triaxiality.

A Level 3 Assessment may be performed using guidance from other applicable Codes or Standards (e.g., API RP 1183, etc.) so long as the alternative procedures adequately address the applicable damage mechanisms, a remaining life can be determined, and adequate documentation is provided that discloses all the assumptions used in the assessment.

12.5 Remaining Life Assessment

12.5.1 Categories of Remaining Life Assessment

A remaining life assessment of components with a dent, gouge, or dent-gouge combination generally consists of one of the following three categories:

a) *Metal Loss Resulting from A Corrosive/Erosive Environment* – In this case, adequate protection from a corrosive/erosive environment can be established by setting an appropriate value for the future corrosion allowance. The remaining life as a function of time can be established using the $MAWP$ Approach described in Part 4, paragraph 4.5.2.

b) *Cyclic Loading* – The Level 2 Assessment procedures include a fatigue evaluation for dents and dent-gouge combinations. A Level 3 Assessment is required for a fatigue analysis of a gouge. If a Level 3 Assessment is performed, the fatigue analysis may be based on the S-N approach described in Part 14 or a fracture mechanics approach described in Part 9. The remaining life can be established by combining the results from this analysis with the operational history of the component.

c) *High Temperature Operation* – If the component is operating in the creep regime, the assessment procedures in Part 10 should be utilized to determine a remaining life.

12.5.2 Requirements for a Level 3 Assessment

If the component's operation is not within one of the above categories, a detailed Level 3 analysis should be performed to determine the remaining life of the component.

12.6 Remediation

12.6.1 Flaw Severity and Evaluation of Material Condition

A dent or dent-gouge combination represents a very severe flaw type because it is difficult to establish the condition (strength and ductility) at the location of maximum deformation. Therefore, unless the condition of the material can be adequately evaluated, repair or replacement of the component is recommended.

12.6.2 Reinforcement of Dents, Gouges and Dent-Gouge Combinations

Dents, gouges, and dent-gouge combinations may be reinforced using stiffening plates and lap patches depending on the geometry, temperature, and loading conditions. The reinforcement, if utilized, should be designed using the principles and allowable stresses of the original construction code. Cylindrical shell sections that are out-of-round can be brought to within original fabrication tolerances or to a shape that reduces the local stress to within acceptable limits by mechanical means. Hydraulic jacks have been used successfully to alter the out-of-round shape of stiffened cylindrical shells. The design of the jacking arrangement and loads should be carefully established and monitored during the shaping process to minimize the potential for damage to the shell and attachments.

12.6.3 Use of General Corrosion Remediation Methods

The remediation methods for general corrosion provided in Part 4, paragraph 4.6 is applicable to local metal loss near dents, gouges, and dent-gouge combinations. Because of the localized damage pattern, it may be necessary in some cases to fill deep areas of metal loss with substances such as caulking before the application of a lining.

12.7 In-Service monitoring

12.7.1 Requirements for In-Service Monitoring

The shell distortion associated with dents, gouges, and dent-gouge combinations do not normally require in-service monitoring unless one or more of the following are true.

a) An unusually corrosive environment exists, and future corrosion allowance cannot be adequately estimated,

b) The component is subject to a cyclic operation and the load history cannot be adequately established, or

c) The component is operating in the creep range.

12.7.2 Visual Inspection and Field Measurements of Distortion

If in-service monitoring is performed, it usually entails visual inspection and field measurements of the component's distortion at regular intervals. The type of measurements made depends on the procedure utilized in the assessment.

12.8 Documentation

12.8.1 Requirements

The documentation of the FFS Assessment should include the information cited in Part 2, paragraph 2.8.

12.8.2 Inspection and Field Measurements

Inspection data including all field measurements associated with the dent, gouge, or dent-gouge combination, should be recorded, and included in the documentation. A sample data sheet is provided in Table 12.1 for this purpose. A sketch, photograph, or both showing the location and orientation of the dent, gouge, or dent-gouge combination on the component is also recommended.

12.9 Nomenclature

$A_{CVN,2/3}$ fracture area of a 2/3 Charpy specimen; $A_{CVN,2/3} = 53.33\ mm^2\ (0.083\ in^2)$.

α_c Uncertainty factor for the fatigue life prediction. For a confidence level of 95%, α_c shall be set equal to 6.42.

CVN Charpy V-notch impact energy of a full-size specimen.

$CVN_{2/3}$ Charpy V-notch impact energy of a 2/3 sub-size specimen.

C_{ul} conversion factor, $C_{ul} = 1.0$ if d_{d0} is in millimeters and $C_{ul} = 25.4$ if d_{d0} is in inches.

C_1 parameter used to compute the RSF for a dent-gouge combination.

C_2 parameter used to compute the RSF for a dent-gouge combination.

C_3 parameter used to compute the RSF for a dent-gouge combination.

d_g maximum depth of the gouge.

d_{dp} depth of the dent measured when the component is pressurized.

d_{d0} depth of the dent measured when the component is not pressurized.

D inside diameter of the cylinder.

D_o outside diameter of the cylinder.

E_y modulus of elasticity.

g_r the radius at the base of the gouge in a dent-gouge combination.

FCA future corrosion allowance.

$LOSS$ amount of uniform metal loss at the time of the assessment.

K_d stress concentration parameter associated with a dent that is used to compute N_c.

L_{msd} distance to the nearest major structural discontinuity.

L_w distance to the nearest weld joint.

$MAWP$ maximum allowable working pressure of the undamaged component.

MFH maximum fill height of the undamaged component.

M_u constant; $M_u = 1.0, 10.0, \ or \ 100.0$ per the applicable procedure.

N_c permissible number of pressure cycles.

P_{max} maximum pressure for cyclic pressure operation.

P_{min} minimum pressure for cyclic pressure operation.

RSF computed remaining strength factor.

RSF_a allowable remaining strength factor (see Part 2, paragraph 2.4.2.2).

r_d radius at the base of the dent.

R_t remaining thickness ratio.

σ_a cyclic circumferential membrane stress amplitude.

σ_A adjusted cyclic circumferential membrane stress amplitude.

σ_m^C circumferential membrane stress in the cylinder.

$\sigma_{m,max}^C$ circumferential membrane stress associated with P_{max}.

$\sigma_{m,min}^C$ circumferential membrane stress associated with P_{min}.

σ_{ys} minimum specified yield strength.

σ_{uts} minimum specified ultimate tensile strength.

$\bar{\sigma}$ flow stress at the gouge in a dent-gouge combination.

t_c wall thickness in the future corroded condition.

t_{mm} minimum remaining thickness determined at the time of the assessment.

t_{nom} nominal or furnished thickness of the component adjusted for mill undertolerance, as applicable.

t_{rd} uniform thickness away from the damage established by thickness measurements at the time of the assessment.

U_0 constant; $U_0 = 50$ if σ_{uts} is in MPa $U_0 = 7.25$ if σ_{uts} is in ksi.

U_1 conversion factor; $U_1 = 113.0$ if E_y and $\bar{\sigma}$ are in MPa, $A_{CVN,2/3}$ is in mm^2, and d_{do} is in mm, and $U_1 = 1.0$ if E_y and $\bar{\sigma}$ are in psi, $A_{CVN,2/3}$ is in in^2, and d_{do} is in inches.

U_2 conversion factor; $U_2 = 0.738$ for units of $Joules$, and $U_2 = 1.0$ for units of $ft - lbs$.

Y_1 parameter used to compute the RSF for a dent-gouge combination.

Y_2 parameter used to compute the RSF for a dent-gouge combination.

12.10 References

References for this Part are provided in Annex 12A Technical Basis and Validation – Assessment of Dents, Gouges, and Dent-Gouge Combinations.

12.11 Tables

Table 12.1 – Data Required for the Assessment of Dents, Gouges, and Dent-Gouge Combinations

Use this form to summarize the data obtained from a field inspection.

Equipment Identification: _____
Equipment Type: _____ Pressure Vessel _____ Storage Tank _____ Piping Component
Component Type & Location: _____

_____

Data Required for A Level 1 And Level 2 Assessment

General Data
Outside Diameter: _____
Nominal Wall Thickness t_{nom}, or Thickness Reading t_{rd}: _____
Metal Loss $LOSS$: _____
Future Corrosion Allowance FCA: _____
Distance to the Nearest Weld Joint L_w: _____
Distance to the Nearest Major Structural Discontinuity L_{msd}: _____

Specific Data for Dents
Dent Depth d_{dp}: _____
Minimum Specified Ultimate Tensile Strength σ_{uts}: _____
Maximum and Minimum Pressure P_{max} and P_{min} (cyclic operation only): _____

Specific Data for Gouges
Temperature Corresponding to a CVN of 40 J (30 ft-lbs): _____
ASME Exemption Curve: _____
Minimum Specified Yield Strength σ_{ys}: _____
Gouge Depth d_g: _____
Gouge Length: _____
Gouge Width: _____

Specific Data for Dent-Gouge Combinations
Dent Depth d_{dp}: _____
Gouge Depth d_g: _____
Minimum Specified Ultimate Tensile Strength σ_{uts}: _____
Charpy V-notch impact energy of a 2/3 sub-size specimen $CVN_{2/3}$: _____
Maximum and Minimum Pressure P_{max} and P_{min} (cyclic operation only): _____

Table 12.2 – Minimum Temperature Where the Expected Value of the Charpy Impact Energy (CVN) is Above 40 Joules or 30 ft-lbs

Minimum Specified Yield Strength (MSYS) (ksi)	ASME Exemption Curve			
	A (°F)	B (°F)	C (°F)	D (°F)
30	106.9	68.9	30.9	4.9
32	106.9	68.9	30.9	4.9
34	106.8	68.8	30.8	4.8
36	106.7	68.7	30.7	4.7
38	106.6	68.6	30.6	4.6
40	106.5	68.5	30.5	4.5
42	106.4	68.4	30.4	4.4
44	106.3	68.3	30.3	4.3
46	106.2	68.2	30.2	4.2
48	106.0	68.0	30.0	4.0
50	105.9	67.9	29.9	3.9
52	105.8	67.8	29.8	3.8
54	105.7	67.7	29.7	3.7
56	105.6	67.6	29.6	3.6
58	105.5	67.5	29.5	3.5
60	105.4	67.4	29.4	3.4
62	105.3	67.3	29.3	3.3
64	105.2	67.2	29.2	3.2
66	105.0	67.0	29.0	3.0
68	104.9	66.9	28.9	2.9
70	104.8	66.8	28.8	2.8
72	104.7	66.7	28.7	2.7
74	104.5	66.5	28.5	2.5
76	104.4	66.4	28.4	2.4
78	104.3	66.3	28.3	2.3
80	104.2	66.2	28.2	2.2

Note: The transition temperatures in this table are determined using Annex 9F, paragraph 9F.2.4.5.

Table 12.2M – Minimum Temperature Where the Expected Value of the Charpy Impact Energy (CVN) is Above 40 Joules or 30 ft-lbs

Minimum Specified Yield Strength (MSYS) (MPa)	ASME Exemption Curve			
	A (ºC)	B (ºC)	C (ºC)	D (ºC)
200	41.4	20.2	-0.8	-15.3
210	41.4	20.2	-0.9	-15.3
220	41.4	20.2	-0.9	-15.3
230	41.3	20.1	-0.9	-15.4
240	41.3	20.1	-1.0	-15.4
250	41.2	20.0	-1.0	-15.5
260	41.2	20.0	-1.1	-15.5
270	41.2	20.0	-1.1	-15.5
280	41.1	19.9	-1.2	-15.6
290	41.1	19.9	-1.2	-15.6
300	41.0	19.8	-1.2	-15.7
310	41.0	19.8	-1.3	-15.7
320	40.9	19.7	-1.3	-15.8
330	40.9	19.7	-1.4	-15.8
340	40.9	19.7	-1.4	-15.8
360	40.8	19.6	-1.5	-15.9
380	40.7	19.5	-1.6	-16.0
400	40.6	19.4	-1.7	-16.1
420	40.5	19.3	-1.8	-16.2
440	40.4	19.2	-1.9	-16.3
460	40.3	19.1	-2.0	-16.4
480	40.2	19.0	-2.1	-16.5
500	40.1	18.9	-2.2	-16.6
520	40.0	18.8	-2.3	-16.7
540	39.9	18.7	-2.4	-16.8
560	39.7	18.5	-2.5	-17.0

Note: The transition temperatures in this table are determined using Annex 9F, paragraph 9F.2.4.5.

12.12 Figures

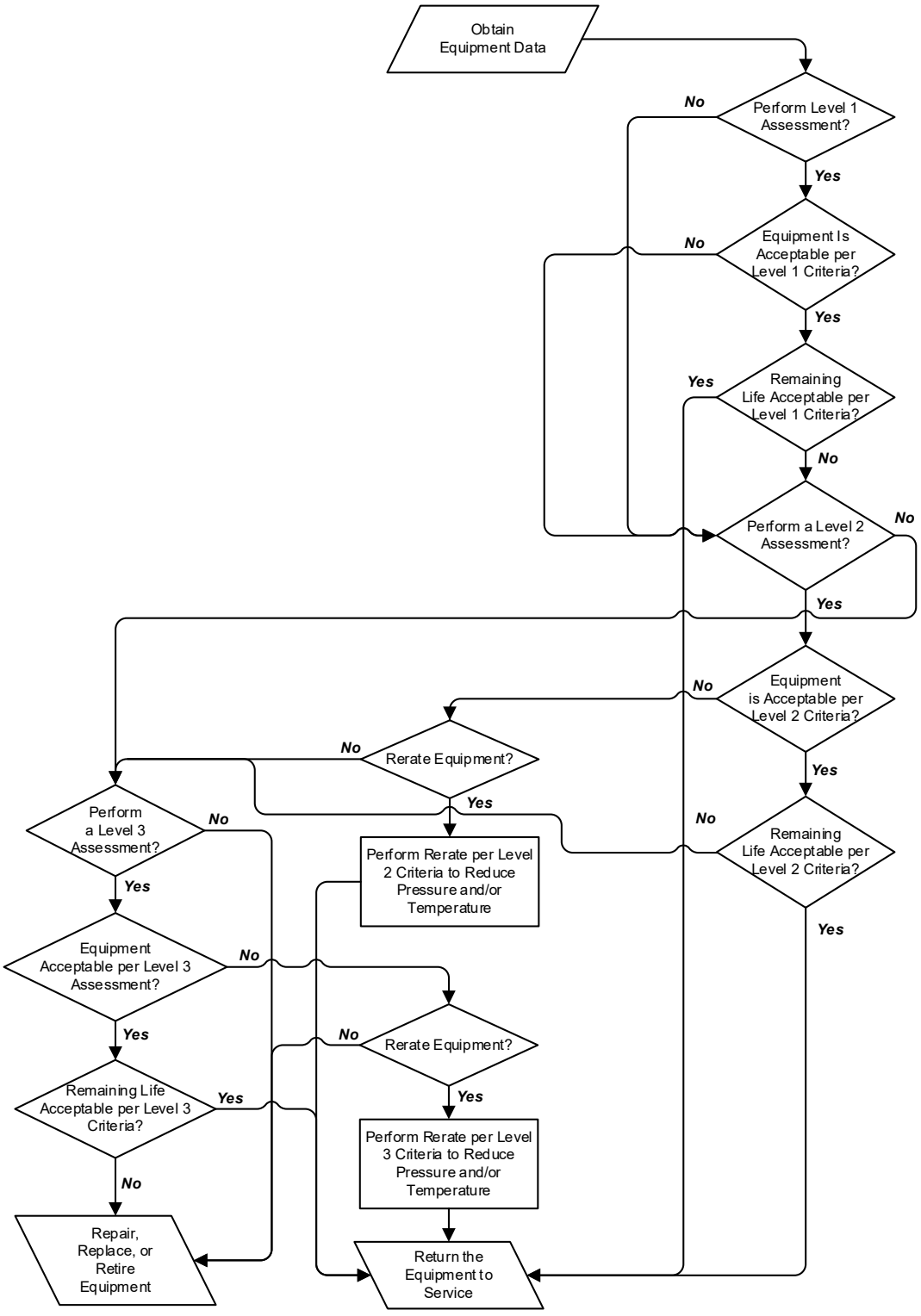

Figure 12.1 – Overview of the Assessment Procedures to Evaluate a Component with a Dent, Gouge, or Dent-Gouge Combination

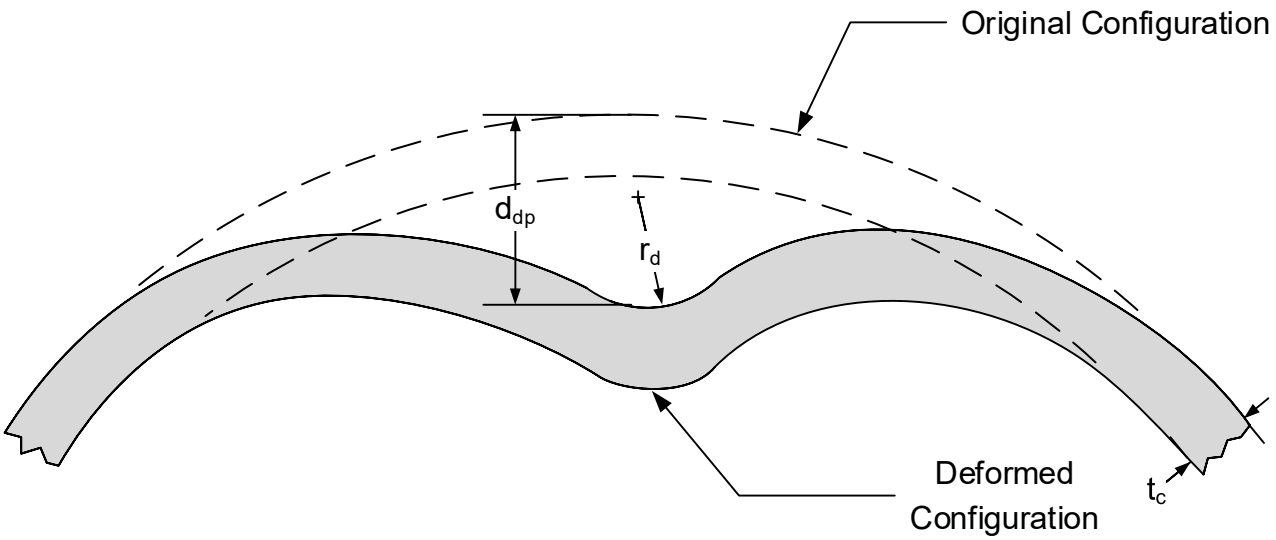

Figure 12.2 – Dent Dimensions

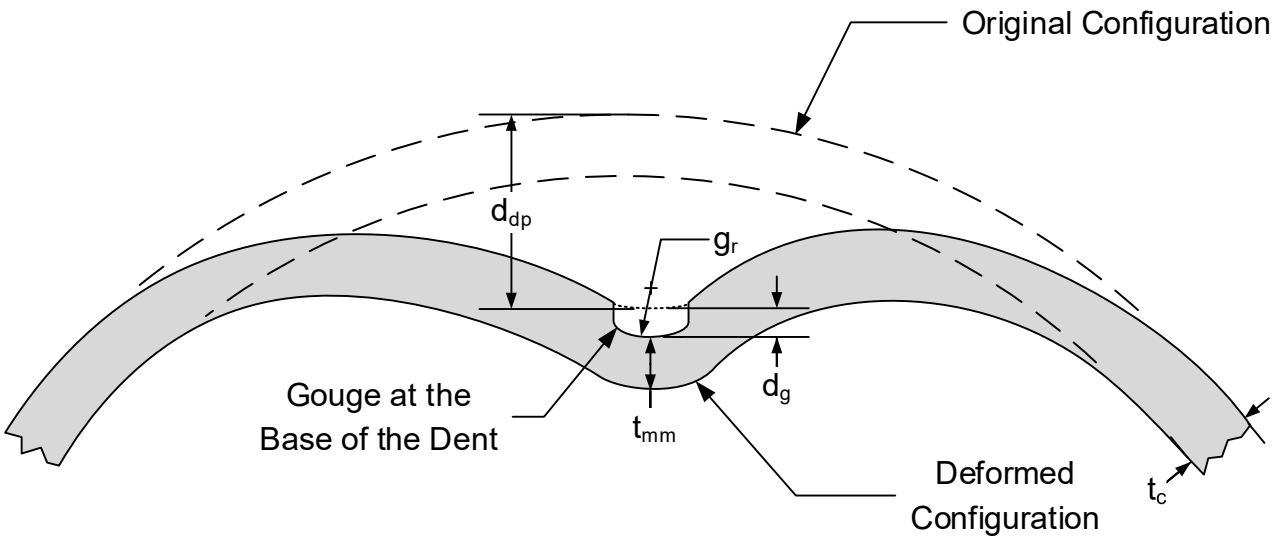

Figure 12.3 – Dent-Gouge Dimensions

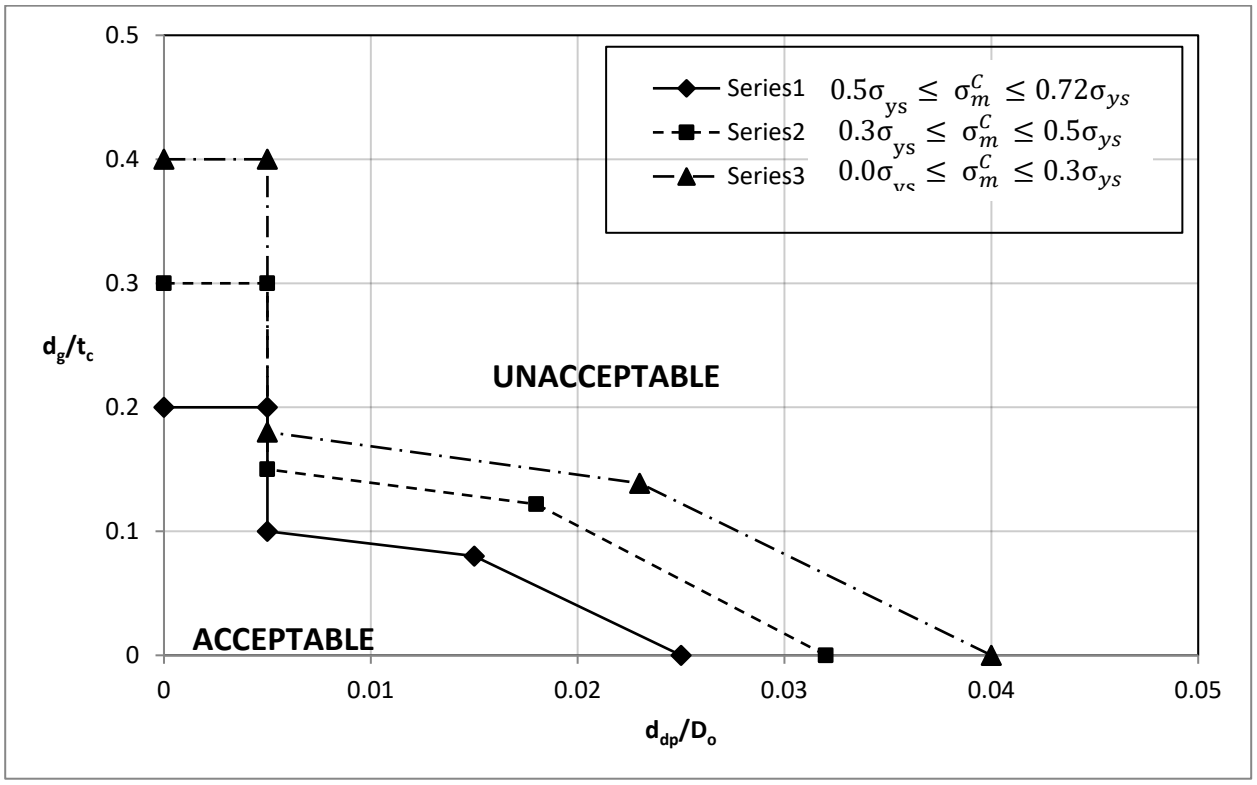

Data Points for Interaction Diagram for Determining the Acceptability of a Dent-Gouge Combination					
$0.0\sigma_{ys} \leq \sigma_m^C < 0.3\sigma_{ys}$		$0.3\sigma_{ys} \leq \sigma_m^C < 0.5\sigma_{ys}$		$0.5\sigma_{ys} \leq \sigma_m^C < 0.72\sigma_{ys}$	
d_{dp}/D_o	d_g/t_c	d_{dp}/D_o	d_g/t_c	d_{dp}/D_o	d_g/t_c
0.0000	0.4000	0.0000	0.3000	0.0000	0.2000
0.0050	0.4000	0.0050	0.3000	0.0050	0.2000
0.0050	0.1800	0.0050	0.1500	0.0050	0.1000
0.0230	0.1387	0.0180	0.1219	0.0150	0.0800
0.0400	0.0000	0.0320	0.0000	0.0250	0.0000

Figure 12.4 – Interaction Diagram for Determining the Acceptability of a Dent-Gouge Combination

ANNEX 12A – TECHNICAL BASIS AND VALIDATION – ASSESSMENT OF DENTS, GOUGES, AND DENT-GOUGE COMBINATIONS

(INFORMATIVE)

CONTENTS

ANNEX 12A – TECHNICAL BASIS AND VALIDATION – ASSESSMENT OF DENTS, GOUGES, AND DENT-GOUGE COMBINATIONS 12A-1

12A.1 TECHNICAL BASIS AND VALIDATION 12A-1
12A.2 REFERENCES 12A-1

12A.1 Technical Basis and Validation

The technical basis and validation of the assessment procedures in Part 12 for dents, gouges and dent-gouge combinations are provided in reference [1]-[2]. Additional information can be found in references [3]-[25].

12A.2 References

[1] Roovers, P., Bood, R., Galli, M., Marewski, U., Steiner, M. and Zarea, M., "EPRG Methods for Assessing the Tolerance and Resistance of Pipelines to External Damage," Pipeline Technology, Volume II, R. Denys (Editor), Elsevier Science B.V., 2000.

[2] PDAM, *Pipeline Defect Assessment Manual*, Edition 2, Penspen, 3 Water Lane, Richmond upon Thames, Surrey TW9 1TJ, October 2016.

[3] Alexander, C., and Keifner, J., "Effects of Smooth and Rock Dents on Liquid Petroleum Pipelines", API Publication 1156, November 1997.

[4] Alexander, C. and Keifner, J., "Effects of Smooth and Rock Dents on Liquid Petroleum Pipelines – Phase II", API Publication 1156 – Addendum, October 1999.

[5] Cairns, A., and Hopkins, P., "A Statistical Analysis of Data from Burst Tests on Pipe Containing Dent/Flaw Combinations", ERS R.2381, October 1981.

[6] Corder, I. and Chatain, P., "EPRG Recommendations for the Assessment of the Resistance of Pipelines to External Damage", Paper Number 12.

[7] Corder, I. and Chatain, P., "Towards EPRG Recommendations for the Assessment of the Tolerance and Resistance of Pipelines to External Damage", Paper Number 13.

[8] Cosham, A. and Hopkins, P., "The Pipeline Defect Assessment Manual', IPC02-27067, Proceedings of IPC 2002, International Pipeline Conference, 29 September - 3 October 2002; Calgary, Alberta, Canada.

[9] Eiber, R., and others, "The Effects of Dents on the Failure Characteristics of Line Pipe", Battelle Columbus Report to A.G.A. NG-18, A.G.A. Catalog No. L51403, May 1981.

[10] Eiber, Robert J. and Leis, Brains N., "Line Pipe Resistance to Outside Force", Paper Number 14.

[11] Shannon, R.W.E., "The Failure Behavior of Linepipe Flaws", International Journal of Pressure Vessel and Piping, pp. 243-255, 1974.

[12] Fowler, J. R., and Ayers, R. R., “Acceptability of Plain Dents for Offshore Pipelines”, Paper 35, Proceedings of the PRC/EPRG Ninth Biennial Joint Technical Meeting on Line Pipe Research, Houston, TX, May 1993.

[13] Fowler, J.R., Alexander, C.R., Kovach, P.J., and Connelly, L.M., “Cyclic Pressure Fatigue Life of Pipelines with Plain Dents, Dents with Gouges, and Dents with Welds”, AGA Catalog No. L51705, AGA, June 1994.

[14] Hopkins, P., Jones, D.G. and Clyne, A.J., “The Significance of Dents and Defects in Transmission Pipelines”, IMechE, C376/049, 1989.

[15] Lancaster, E.R. and Palmer, S.C., “Experimental Study of Strains Caused by Pressurization of Pipes with Dents”, Proceedings of the Fourth (1994) International Offshore and Polar Engineering Conference, Osaka, Japan, April 10-15, 1994, Pages 110-117.

[16] Jiao, Guoyang, Sotbert, T., and Bruschi, R., “Probabilistic Assessment of the Wall Thickness Requirement for Pressure Containment of Offshore Pipelines”, 1992 OMAE – Volume V-a, Pipeline Technology, ASME 1992, Pages 249-255.

[17] Jones, D.G., “The Significance of Mechanical Damage in Pipelines”, Presented at A.G.A./EPRG Linepipe Research Seminar, Duisburg, W. Germany, ERS E291, September 1981.

[18] Kiefner, John F., “Review and Critique of Dent Acceptability Criteria for Offshore Pipelines”, Contract No. PR 218-9119, AGA Report, June 30, 1992.

[19] Maxey, W.A., “Topical Report on Outside Force Flaw Behavior”, NG-18 Report 162, Task No. SI-1.1-79, AGA, August 15, 1986.

[20] Maxey, W.A., “Outside Force Flaw Behavior”, 7th Symposium on Line Pipe Research, Houston, Texas, Paper 14, October 1986.

[21] MSL Engineering Limited, “Appraisal and Development of Pipeline Defect Assessment Methodologies”, Minerals Management Service, US Department of the Interior, Washington, D.C., Contract No. 1435-01-CT-99-50001, DOC REF CH109R001, Rev 0, June 2000.

[22] Oguchi, N. and Hagiwara, N., “Fatigue Behavior of Line Pipes Subjected to Severe Mechanical Damage”, Journal of Pressure Vessel Technology, Vol 121, ASME, November 1999, Pages 369-374.

[23] Osage, D.A., Krishnaswamy, P., Stephens, D.R., Scott, P., Janelle, J., Mohan, R., and Wilkowski, G.M., *Technologies for the Evaluation of Non-Crack-Like Flaws in Pressurized Components – Erosion/Corrosion, Pitting, Blisters, Shell Out-Of-Roundness, Weld Misalignment, Bulges and Dents*, WRC Bulletin 465, Welding Research Council, Inc., September 2001.

[24] Spiekhout, J., Gresnight, A.M., Koning, C., and Wildschut, H., “Calculation Models for the Evaluation of the Resistance Against Mechanical Damage of Pipelines”, 3R International, 25, Jahrgang, Heft, 4 April 1986, pages 198-203.

[25] Wang, K.C. and Smith, E.D., “The Effect of Mechanical Damage on Fracture Initiation in Linepipe Part I – Dents”, Metals Technology Laboratories, Report MTL 88-11(TR), January 1982.

[26] Wang, K.C. and Smith, E.D., “The Effect of Mechanical Damage on Fracture Initiation in Linepipe Part II – Gouges”, Metals Technology Laboratories, Report MTL 88-16(TR), March 1988.

[27] Wang, K.C. and Smith, E.D., “The Effect of Mechanical Damage on Fracture Initiation in Linepipe Part III – Gouge in a Dent”, Metals Technology Laboratories, Report PMRL 85-69, December 1985.

PART 13 – ASSESSMENT OF LAMINATIONS

CONTENTS

PART 13 – ASSESSMENT OF LAMINATIONS 13-1

13.1 GENERAL 13-1
13.1.1 Assessment Procedures for Laminations 13-1
13.1.2 Definition of Laminations 13-2
13.1.3 Laminations in Hydrogen Charging Service 13-2
13.1.4 Detection of Laminations 13-2
13.1.5 Acceptance of Laminations 13-2
13.2 APPLICABILITY AND LIMITATIONS OF THE PROCEDURE 13-2
13.2.1 Applicability and Limitations of the Assessments Procedures for Laminations 13-2
13.2.2 Calculation of MAWP and Coincident Temperature 13-2
13.2.3 Limitations Based on Temperature 13-2
13.2.4 Limitations Based on Flaw Type 13-3
13.2.5 Applicability of the Level 1 and Level 2 Assessment Procedures 13-3
13.2.6 Applicability of the Level 3 Assessment 13-3
13.3 DATA REQUIREMENTS 13-4
13.3.1 Original Equipment Design Data 13-4
13.3.2 Maintenance and Operational History 13-4
13.3.3 Required Data/Measurements for an FFS Assessment 13-4
13.3.4 Recommendations for Inspection Technique and Sizing Requirements 13-5
13.4 ASSESSMENT TECHNIQUES AND ACCEPTANCE CRITERIA 13-5
13.4.1 Overview 13-5
13.4.2 Level 1 Assessment 13-5
13.4.3 Level 2 Assessment 13-6
13.4.4 Level 3 Assessment 13-7
13.5 REMAINING LIFE ASSESSMENT 13-7
13.6 REMEDIATION 13-7
13.7 IN-SERVICE MONITORING 13-7
13.8 DOCUMENTATION 13-7
13.8.1 General 13-7
13.8.2 Documentation of Flaw Size and Conditions 13-8
13.8.3 Documentation of Flaw Growth 13-8
13.9 NOMENCLATURE 13-8
13.10 REFERENCES 13-8
13.11 TABLES 13-9
13.12 FIGURES 13-10

13.1 General

13.1.1 Assessment Procedures for Laminations

Fitness-For-Service (FFS) Assessment procedures for pressurized components with laminations, excluding HIC or SOHIC damage, are provided in this Part. The assessment procedures for laminations are shown in the flow chart contained in Figure 13.1.

13.1.2 Definition of Laminations

Laminations are a plane of non-fusion in the interior of a steel plate that results from the steel manufacturing process and exist on one or more planes in the equipment. Laminations cause no bulging of the metal surface, have no cracking in the through thickness direction, and are not linked.

13.1.3 Laminations in Hydrogen Charging Service

Laminations in equipment in a hydrogen charging environment shall be evaluated using the techniques in Part 7. An example of a hydrogen charging environment that results in HIC and SOHIC is wet H_2S service (see API 571). Laminations not in hydrogen charging environment can be evaluated using this Part.

13.1.4 Detection of Laminations

Laminations are usually detected using ultrasonic examination inspection methods. Laminations affect welding, interfere with ultrasonic examination of welds, and reduce the strength of the plate when the plate is subjected to bending stresses, compressive stresses, or through thickness stresses. Laminations also result in voids to trap hydrogen in components that are in wet hydrogen sulfide service, which may result in blisters.

13.1.5 Acceptance of Laminations

Laminations may not be objectionable if the laminations are parallel to the plate surface, the component is subjected only to tensile membrane stresses from internal pressure, and the laminations are away from structural discontinuities where local bending stresses occur.

13.2 Applicability and Limitations of the Procedure

13.2.1 Applicability and Limitations of the Assessments Procedures for Laminations

The FFS Assessment procedures described below may be used to evaluate the acceptability of laminations subject to the limitations in this Part. The assessment procedures include analysis methods for laminations that are parallel to the surface of the plate or that have a through-thickness component (i.e., the lamination is not parallel to the surface of the plate).

13.2.2 Calculation of MAWP and Coincident Temperature

Calculation methods are provided to determine acceptable $MAWP$ and coincident temperature if the acceptance criteria in this Part are not satisfied. For pressurized components, the calculation methods can be used to find a reduced maximum allowable working pressure. The calculation methods can be used to determine a reduced maximum fill height for tank components (i.e., shell courses).

13.2.3 Limitations Based on Temperature

The assessment procedures only apply to components that are not operating in the creep range (e.g., the design temperature is less than or equal to the value in Part 4, Table 4.1). A Materials Engineer should be consulted regarding the creep range temperature limit for materials not listed in this table. In the creep range, the lamination shall be evaluated using the Level 3 Assessment method in Part 10.

13.2.4 Limitations Based on Flaw Type

a) Unless otherwise specified, this Part is limited to the evaluation of laminations. Other flaw types shall be evaluated in accordance with Part 2, Table 2.1.

b) Part 13 Assessment procedures do not apply if any of the following criteria are satisfied:

   1) If the lamination exhibits evidence of an associated surface bulge, it shall be characterized as a blister and evaluated using the assessment procedure of Part 7.

   2) The component is in hydrogen charging service. Components with laminations in hydrogen service shall be evaluated using Part 7.

c) If the lamination has a through-wall linear indication, it shall be evaluated as an equivalent crack-like flaw using the assessment procedure of Part 9 as directed by the Level 1 and Level 2 Assessment procedures of this Part.

13.2.5 Applicability of the Level 1 and Level 2 Assessment Procedures

The Level 1 and 2 Assessment procedures for laminations apply only if all the following criteria are satisfied:

a) The original design criteria were in accordance with a recognized code or standard (see Part 1, paragraphs 1.2.2 or 1.2.3).

b) The material is considered to have sufficient material toughness. If there is uncertainty regarding the material toughness, then a Part 3 Assessment should be performed. If the component is subject to embrittlement during operation due to temperature and/or the process environment, a Level 3 Assessment should be performed. Temperature and/or process conditions that result in material embrittlement are discussed in Annex 2B.

c) The component is not in cyclic service, or the component is in cyclic service and adjacent laminations (see Equation (13.1)) are in the same plane and there is no indication of through thickness cracking. If the component is subject to less than 150 cycles (i.e., pressure and/or temperature variations including operational changes and start-ups and shut-downs) throughout its previous operating history and future planned operation or satisfies the cyclic service screening procedure in Part 14, paragraph 14.4.2, then the component is not in cyclic service.

d) The following limitations on component types and applied loads are satisfied:

   1) Level 1 Assessment – Type A components (see Part 4, paragraph 4.2.5) subject to internal pressure.

   2) Level 2 Assessment – Type A and Type B Class 1 components (see Part 4, paragraph 4.2.5) subject to internal pressure, supplemental loads, or any combination thereof.

13.2.6 Applicability of the Level 3 Assessment

A Level 3 Assessment for laminations can be performed when the requirements of paragraph 13.2.5 are not satisfied.

13.3 Data Requirements

13.3.1 Original Equipment Design Data

An overview of the original equipment data required for an assessment is provided in Part 2, paragraph 2.3.1. These data can be entered in the form provided in Part 2, Table 2.2, and Table 13.1 for each component under evaluation.

13.3.2 Maintenance and Operational History

An overview of the maintenance and operational history required for an assessment is provided in Part 2, paragraph 2.3.2.

13.3.3 Required Data/Measurements for an FFS Assessment

13.3.3.1 The required data and measurements for a lamination are shown below. This information should be recorded in Table 13.1. In addition, the creation of a sketch at the time of the inspection showing the information in this paragraph is recommended.

a) Lamination Dimensions – The largest dimensions in the longitudinal and circumferential direction, s and c, respectively, shall be recorded.

b) Lamination Height – The lamination height, L_h, shall be recorded.

c) Lamination-to-Lamination Spacing, L_s – Measurements should be made to determine the edge-to-edge spacing between laminations. This information should be detailed and provided on an inspection sketch. If there are multiple laminations in close proximity to one another, the size of the lamination to be used in the assessment is established considering the effects of neighboring laminations using the criterion for local metal loss described in Part 5 (Figure 5.2). In addition, if the distance between two adjacent laminations (measured edge-to-edge) is less than or equal to two times the corroded plate thickness, t_c, the laminations shall be combined and evaluated as a single lamination.

d) Lamination Minimum Measured Wall Thickness, t_{mm} – This is the smallest distance from either surface to the lamination (see Figure 13.2) modified by the future corrosion allowance (FCA) as required.

e) Lamination Spacing to Weld Joints, L_w – Measurements shall be made to determine the spacing of laminations from weld joints. This information is important because if the lamination is close to a weld, through-wall cracking may occur. This information should be detailed and provided on an inspection sketch. A lamination is considered located at a weld seam if it lies within 25 mm (1 inch) or twice the plate thickness from the edge of the weld, whichever is greater (see Figure 13.3). Laminations close to weld seams can propagate along the weld fusion line or in the heat affected zone in the through-thickness direction, particularly if the welds were not originally subject to post weld heat treatment. Therefore, laminations at weld seams should be monitored in-service.

f) Lamination Spacing to Major Structural Discontinuities, L_{msd} – Measurements shall be made to determine the location of the lamination with respect to major structural discontinuities. This information should be detailed and provided on an inspection sketch.

g) Lamination Cracking – The lamination shall be examined to determine if there are any cracks extending from the plane of the lamination in the through-thickness direction.

13.3.4 Recommendations for Inspection Technique and Sizing Requirements

13.3.4.1 Laminations are usually discovered during an in-service inspection/monitoring UT examination. If any visual observation of surface bulging on either the inside or the outside of the equipment is recorded, then the lamination shall be categorized as a blister and evaluated in accordance with Part 7.

13.3.4.2 Ultrasonic examination can be used to determine the depth of the lamination and remaining plate thickness at the lamination location.

13.4 Assessment Techniques and Acceptance Criteria

13.4.1 Overview

13.4.1.1 The assessment procedures of this Part shall be followed to evaluate the lamination even when the lamination is located within the region of the specified corrosion/erosion allowance.

13.4.1.2 An overview of the assessment levels for laminations is provided in Figure 13.1.

a) The Level 1 Assessment procedure is a screening criterion for laminations based on: the lamination size, orientation relative to the surface, structural discontinuities, spacing of the lamination to weld joints, and other laminations.

b) The Level 2 Assessment procedure can be used to evaluate laminations in a Type A and a Type B class component subject to internal pressure, supplemental loads, or any combination thereof.

c) The Level 3 Assessment procedures are intended to evaluate situations that do not satisfy the Level 1 or Level 2 Assessment procedures. Detailed stress analysis techniques are normally required in a Level 3 assessment.

13.4.2 Level 1 Assessment

13.4.2.1 The following procedure shall be used to determine the acceptability of a lamination in a Type A component subject to internal pressure:

a) STEP 1 – Determine the information in paragraph 13.3.3.1.

b) STEP 2 – If there are two or more laminations on the same plane and the spacing does not satisfy Equation (13.1), then the laminations shall be combined into a single larger lamination in the assessment with new dimensions of s and c adjusted accordingly. If there are two or more laminations at different depths in the wall thickness of the component and the spacing does not satisfy Equation (13.1), then the group of laminations shall be evaluated as equivalent HIC damage using the assessment methodology in Part 7. In applying this criterion, the spacing shall be measured parallel to the wall thickness.

$$L_s > 2t_c \tag{13.1}$$

c) STEP 3 – If the distance between the source of localized bending stress or nearest structural discontinuity and the lamination satisfies Equation (13.2), proceed to STEP 4, otherwise the lamination is not acceptable per the Level 1 Assessment procedure.

$$L_{msd} \geq 1.8\sqrt{Dt_c} \tag{13.2}$$

d) STEP 4 – If Equation (13.3) is satisfied, proceed to STEP 5; otherwise, evaluate the through-thickness component of the lamination as a crack-like flaw using the Level 1 Assessment methodology in Part 9. In

this evaluation, the crack depth shall be equal to $2a = L_h$ and the crack length shall be equal to $2c = \max[s, c]$.

$$L_h \le 0.09 \max\left[s,\ c\right] \quad \text{and} \quad L_h \le \min\left[\frac{t_c}{3},\ 13\ mm\ (0.5\ in)\right] \tag{13.3}$$

e) STEP 5 – Determine the wall thickness to be used in the assessment using Equation (13.4) or Equation (13.5), as applicable.

$$t_c = t_{nom} - LOSS - FCA \tag{13.4}$$

$$t_c = t_{rd} - FCA \tag{13.5}$$

f) STEP 6 – If all the following conditions are satisfied, proceed to STEP 7; otherwise, the lamination is not acceptable per the Level 1 Assessment procedure.

1) There is no indication of through-thickness cracking.

2) The lamination is not surface breaking in accordance with Equation 13.6.

$$t_{mm} \ge 0.10 t_c \tag{13.6}$$

3) The distance between the edge of the lamination and the nearest weld seam satisfies Equation (13.7).

$$L_w \ge \max\left[2t_c,\ 25\ mm\ (1.0\ in)\right] \tag{13.7}$$

g) STEP 7 – Determine the $MAWP$ for the component (see Annex 2C) using the thickness from STEP 5. The component with the lamination is acceptable for operation at this calculated $MAWP$.

13.4.2.2 If the component does not meet the Level 1 Assessment requirements, then the following, or combinations thereof, can be considered:

a) Rerate, repair, or replace the component.

b) Conduct a Level 2 or Level 3 Assessment.

13.4.3 Level 2 Assessment

13.4.3.1 The following procedure shall be used to determine the acceptability of a lamination in a Type A and a Type B Class 1 component subject to internal pressure, supplemental loads, or any combination thereof.

a) STEP 1 – see paragraph 13.4.2.1 STEP 1.

b) STEP 2 – see paragraph 13.4.2.1 STEP 2.

c) STEP 3 – see paragraph 13.4.2.1 STEP 3.

d) STEP 4 – see paragraph 13.4.2.1 STEP 4.

e) STEP 5 – see paragraph 13.4.2.1 STEP 5.

f) STEP 6 – If all the following conditions are satisfied, proceed to STEP 7; otherwise, the lamination is not acceptable per the Level 2 Assessment procedure.

1) There is no indication of through-thickness cracking.

2) The lamination is not surface breaking in accordance with Equation (13.6).

3) If the distance between the edge of the lamination and the nearest weld seam satisfies Equation (13.7), proceed to STEP 7. Laminations that do not satisfy the spacing criteria may be acceptable if it is confirmed that though-thickness cracking does not occur and there is no indication of cracking in the direction towards the inside or outside surface. An in-service monitoring system should be developed to monitor for lamination cracking while the component is in service.

g) STEP 7 – Determine the $MAWP$ for the component (see Annex 2C) using the thickness from STEP 5. The component with the lamination is acceptable for operation at this calculated $MAWP$.

13.4.3.2 If the component does not meet the Level 2 Assessment requirements, then the following, or combinations thereof, can be considered:

a) Rerate, repair, or replace the component.

b) Conduct a Level 3 Assessment.

13.4.4 Level 3 Assessment

A Level 3 Assessment for laminations consists of performing a detailed stress analysis using the techniques and acceptance criteria provided in Annex 2D. Components subject to external pressure or other loads that result in compressive stresses require continuity through the full thickness to avoid loss of buckling strength. Laminations in components originally designed to resist compressive stresses require a careful evaluation by a competent pressure vessel engineer to ensure that the component has adequate margin against the buckling mode of failure.

13.5 Remaining Life Assessment

A remaining life evaluation is typically not required for shell components under internal pressure loads (i.e., membrane tensile loads) because there is no loss of strength and no associated effect on the internal inspection interval except for the special inspection requirements for in-service monitoring. A remaining life may be required for laminations subject to compressive stresses or bending stresses, or for laminations in components subject to cyclic loads.

13.6 Remediation

Laminations meeting acceptance criteria of any assessment require no further remediation. If the lamination is in hydrogen service, then the remediation provided in Part 7 may be used. If the plate material is severely damaged and cannot be accepted per the assessment procedures, it should be repaired or replaced.

13.7 In-Service Monitoring

Laminations in components in hydrogen charging or other services that may lead to growth of the lamination shall be monitored to determine if there is growth or through-wall cracking occurring (see Part 7, paragraph 7.7). If the lamination is found to grow or cracks are detected during monitoring, then the lamination shall be re-evaluated.

13.8 Documentation

13.8.1 General

The documentation of the FFS Assessment shall include the information cited in Part 2, paragraph 2.8.

13.8.2 Documentation of Flaw Size and Conditions

The location, size, spacing and condition of existing laminations should be recorded along with the results of the assessments performed. A sample data sheet is provided in Table 13.1 for this purpose.

13.8.3 Documentation of Flaw Growth

If lamination growth is detected during the monitoring process, the physical dimensions and location of the lamination should be recorded along with the time between measurements. In addition, the associated operating conditions and process stream constituents should be recorded to permit an evaluation of the hydrogen-charging environment relative to the operation of the equipment. This information may be valuable in determining suitable process changes in the operation of the equipment, if possible, to mitigate further damage.

13.9 Nomenclature

$2a$	depth of through-wall embedded crack associated with a lamination.
c	lamination dimension in the circumferential direction.
$2c$	length of through-wall embedded crack associated with a lamination.
D	inside diameter of the component corrected for $LOSS$ and FCA as applicable.
FCA	future corrosion allowance to account for uniform metal loss, or future corrosion allowance to account for uniform metal loss away from damage area.
L_h	lamination height.
L_{msd}	spacing to the nearest major structural discontinuity or a source of localized bending stress
L_s	lamination-to-lamination spacing.
L_w	spacing to the nearest weld joint.
$LOSS$	amount of uniform metal loss at the time of inspection, or uniform metal loss away from the damage area at the time of the inspection.
$MAWP$	Maximum Allowable Working Pressure.
s	lamination dimension in the longitudinal direction.
t_c	corroded wall thickness, allowing for future corrosion loss.
t_{mm}	minimum measured thickness modified by the future corrosion allowance (FCA) as required.
t_{nom}	nominal or furnished thickness of the component adjusted for mill undertolerance as applicable.
t_{rd}	uniform thickness away from the lamination location established by thickness measurements at the time of the assessment.

13.10 References

References for this Part are provided in Annex 13A – Technical Basis and Validation – Assessment of Laminations.

13.11 Tables

Table 13.1 – Size, Location, Condition, And Spacing for Laminations

Enter the data obtained from a field inspection on this form.

Inspection Date: _____

Equipment Identification: _____

Equipment Type: _____ Pressure Vessel _____ Storage Tank _____ Piping Component

Component Type & Location: _____

_____

t_{nom}: _____

$LOSS$: _____

FCA: _____

t_{rd}: _____

Data Required for Level 1 And Level 2 Assessment					
Lamination Identification					
Dimension s (1)					
Dimension c (1)					
Lamination Height L_h (1)					
Edge-To-Edge Spacing to the nearest lamination L_s (2)					
Minimum Measured Thickness t_{mm} (1)					
Spacing to the Nearest Weld Joint L_w (2)					
Spacing to the Nearest Major Structural Discontinuity L_{msd}					
Through-Wall Cracking (Yes/No)					

Notes:
1. See Figure 13.2.
2. See Figure 13.3.

13.12 Figures

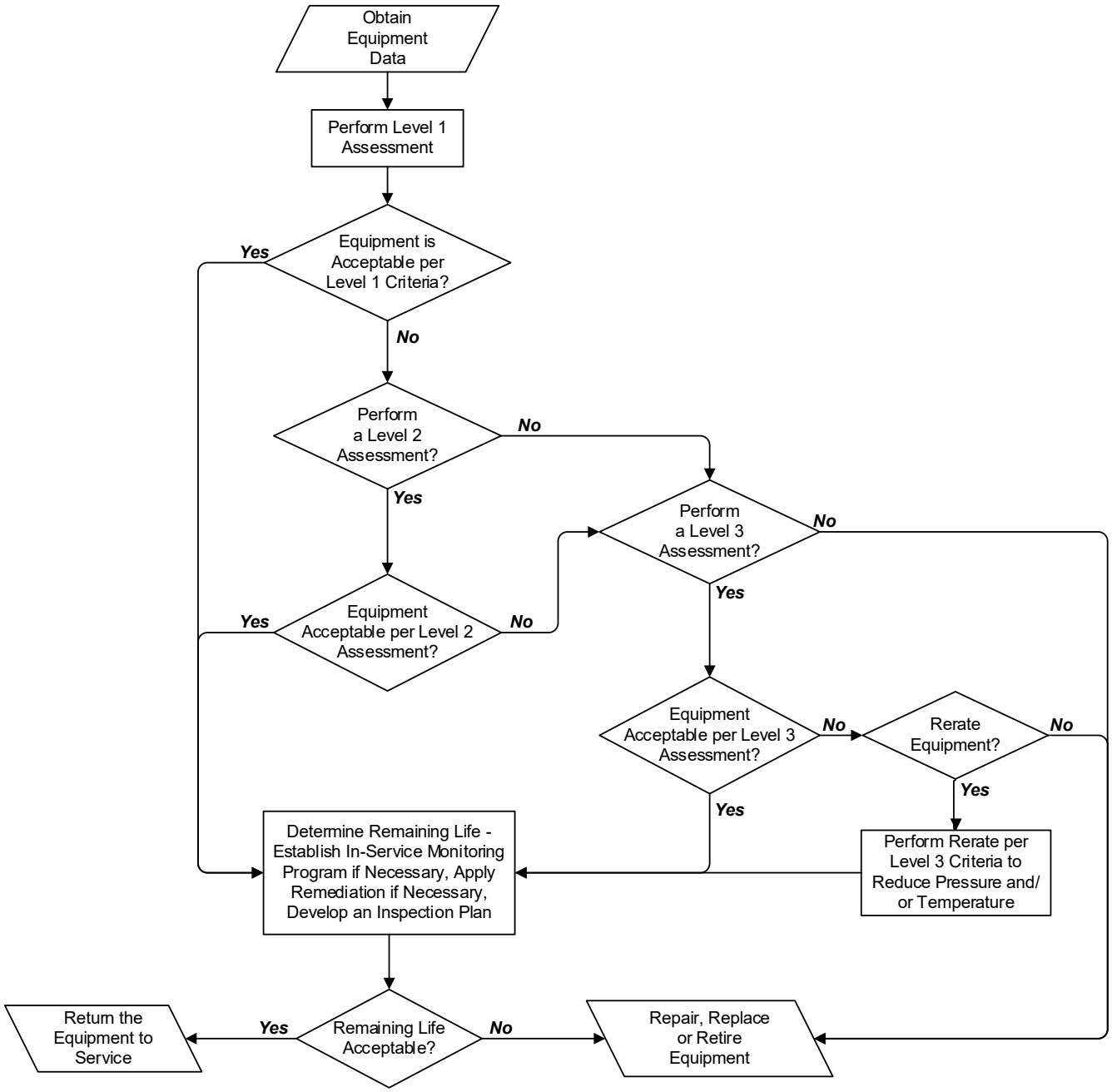

Figure 13.1 – Overview of the Assessment Procedure to Evaluate a Component with Laminations

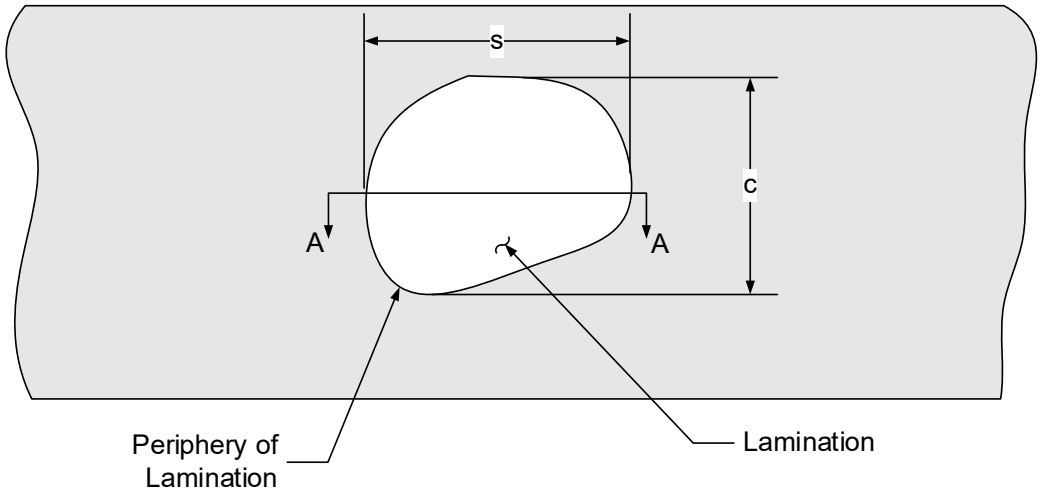

Lamination Plan View

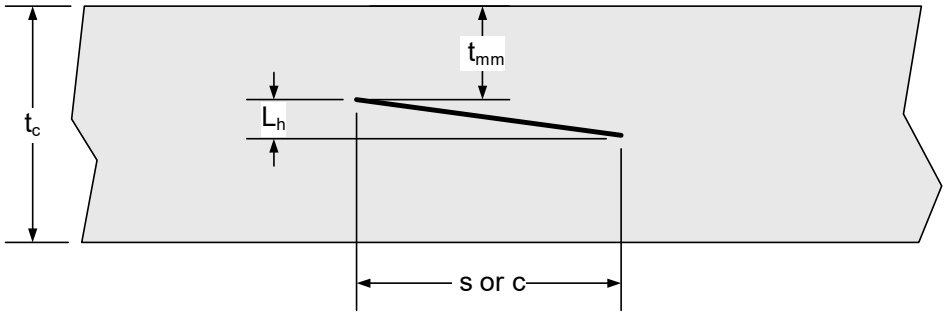

Section A-A
Cross Section of Lamination

Figure 13.2 – Typical Lamination

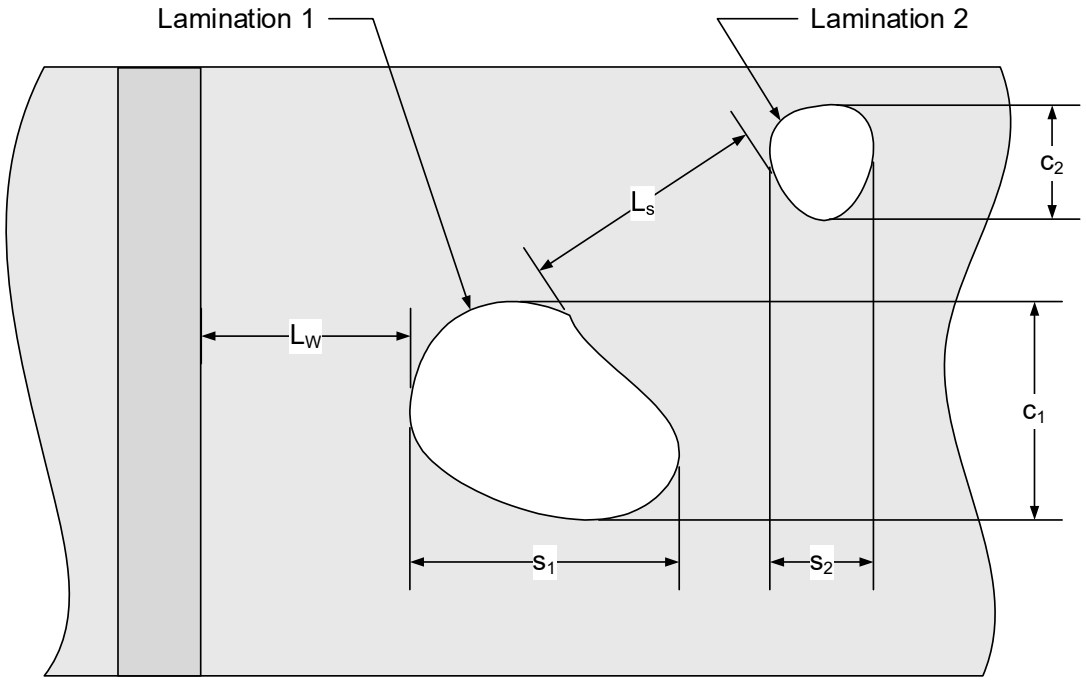

a) Planar View of Laminations Close to a Weld Seam and to Other Laminations

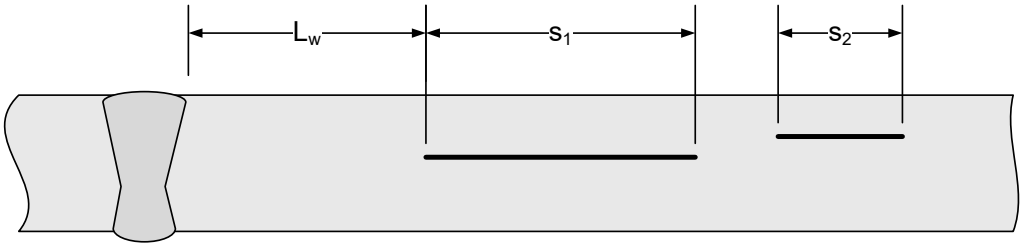

b) Cross Sectional View of Laminations Close to a Weld Seam and to Other Laminations

Figure 13.3 – Weld Joint Spacing and Multiple Laminations

ANNEX 13A – TECHNICAL BASIS AND VALIDATION – ASSESSMENT OF LAMINATIONS

(INFORMATIVE)

CONTENTS

ANNEX 13A – TECHNICAL BASIS AND VALIDATION – ASSESSMENT OF LAMINATIONS 13A-1

13A.1 TECHNICAL BASIS AND VALIDATION 13A-1
13A.2 REFERENCES 13A-1

13A.1 Technical Basis and Validation

The technical basis of the assessment procedures in Part 13 for laminations is provided in references [1] and [2].

13A.2 References

[1] Buchheim, G.M., “Fitness-For-Service Hydrogen Blistering and lamination Assessment Rules in API 579,” PVP Vol. 411, Service Experience and Fitness-For-Service in Power and Petroleum Processing, ASME, 2000, pp. 177-190.

[2] Osage, D.A., Krishnaswamy, P., Stephens, D.R., Scott, P., Janelle, J., Mohan, R., and Wilkowski, G.M., Technologies for the Evaluation of Non-Crack-Like Flaws in Pressurized Components – Erosion/Corrosion, Pitting, Blisters, Shell Out-Of-Roundness, Weld Misalignment, Bulges and Dents, WRC Bulletin 465, Welding Research Council, Inc., New York, NY, September 2001.

[Intentionally Left Blank]

PART 14 – ASSESSMENT OF FATIGUE DAMAGE

CONTENTS

PART 14 – ASSESSMENT OF FATIGUE DAMAGE 14-1

14.1 GENERAL 14-2
14.1.1 Assessment Procedures for Fatigue Damage 14-2
14.1.2 Damage Tolerance 14-2
14.1.3 Fatigue Evaluation in the Creep Range 14-2
14.1.4 Fatigue Evaluation and Crack-Like Flaws 14-2
14.1.5 ASME B&PV Code, Section VIII, Division 2 (VIII-2) 14-3
14.1.6 Use of Fatigue Curves in Performing Assessments 14-3
14.1.7 Adjustment for Mean Stress 14-3
14.1.8 Ratcheting 14-3
14.2 APPLICABILITY AND LIMITATIONS OF THE PROCEDURE 14-3
14.2.1 Applicability and Limitations of the Assessment Procedures 14-3
14.2.2 Calculation of MAWP and Coincident Temperature 14-3
14.2.3 Limitations Based on Temperature 14-4
14.2.4 Limitations Based on Flaw Type 14-4
14.2.5 Applicability of the Level 1 and Level 2 Assessment Procedures 14-4
14.2.6 Applicability of the Level 3 Assessment 14-4
14.3 DATA REQUIREMENTS 14-5
14.3.1 Original Equipment Design Data 14-5
14.3.2 Maintenance and Operational History 14-5
14.3.3 Required Data/Measurements for an FFS Assessment 14-5
14.3.4 Recommendations for Inspection Technique and Sizing Requirements 14-5
14.4 ASSESSMENT TECHNIQUES AND ACCEPTANCE CRITERIA 14-6
14.4.1 Overview 14-6
14.4.2 Level 1 Assessment 14-6
14.4.2.1 Overview 14-6
14.4.2.2 Method A – Fatigue Screening Based on Experience with Comparable Equipment 14-7
14.4.2.3 Method B – Fatigue Screening 14-7
14.4.2.4 Method C – Fatigue Screening 14-8
14.4.2.5 Method D – Fatigue Screening, Welded Joints 14-10
14.4.2.6 Level 1 Assessment Results 14-12
14.4.3 Level 2 Assessment 14-12
14.4.3.1 Overview 14-12
14.4.3.2 Method A – Fatigue Assessment Using Elastic Stress Analysis and Equivalent Stresses 14-13
14.4.3.3 Method B – Fatigue Assessment Using Elastic-Plastic Stress Analysis and Equivalent Strain 14-17
14.4.3.4 Method C – Fatigue Assessment of Welds Using the Equivalent Structural Stress 14-19
14.4.3.5 Ratcheting Assessment – Elastic Stress Analysis 14-23
14.4.3.6 Ratcheting Assessment – Elastic-Plastic Stress Analysis 14-25
14.4.3.7 Ratcheting Assessment – Non-Integral Connections 14-26
14.4.3.8 Level 2 Assessment Results 14-26
14.4.4 Level 3 Assessment 14-26
14.4.4.1 Overview 14-26
14.4.4.2 Method A – Elastic Stress Analysis and Critical Plane Approach 14-27
14.4.4.3 Method B – Elastic-Plastic Stress Analysis and Critical Plane Approach 14-28
14.4.4.4 Method C – Recognized Codes and Standards 14-29
14.5 REMAINING LIFE ASSESSMENT 14-29
14.5.1 Included in Level 2 and Level 3 Assessments 14-29
14.5.2 Loading Time History 14-29
14.6 REMEDIATION 14-29
14.6.1 Overview 14-29
14.6.2 Removal or Reduction of the Driving Energy Source or Forces. 14-30

14.6.3 Alteration of Component Constraint, Mechanical Design, or Weld Quality *14-30*
14.6.4 Reduction of Temperature Differentials or Gradients *14-31*
14.7 IN-SERVICE MONITORING 14-31
14.8 DOCUMENTATION 14-31
14.8.1 General *14-31*
14.8.2 Assessment Level *14-31*
14.8.3 Loading Time History *14-31*
14.8.4 Material Properties *14-32*
14.8.5 Stress Analysis Results *14-32*
14.8.6 Assessment Results *14-32*
14.8.7 Remaining Life Assessment *14-32*
14.8.8 Remediation Methods *14-32*
14.8.9 In-Service Monitoring *14-32*
14.9 NOMENCLATURE 14-32
14.10 REFERENCES 14-41
14.11 TABLES 14-42
14.12 FIGURES 14-65

14.1 General

14.1.1 Assessment Procedures for Fatigue Damage

Fitness-For-Service (FFS) Assessment procedures for evaluating fatigue damage in components subject to cyclic operation below the creep range that do not contain crack-like flaws, HIC, step-wise indications, and/or SOHIC are covered in this Part. The component may also contain volumetric flaws such as thinning, pitting damage, and weld misalignment. The evaluation for fatigue damage is made based on the number of historical and estimated future applied cycles of a stress or strain range at a point in the component that may result in crack initiation. The technical background for the assessment procedures is provided in Annex 14A.

14.1.2 Damage Tolerance

A damage tolerance approach is used in Part 14 to determine if the component is acceptable for continued operation. In a damage tolerance approach, an analysis is performed that may justify an increase in the loading magnitude and the number of future operating cycles when compared to the original design conditions. To determine acceptability for continued operation, the past loading time history (i.e., cycles and loading magnitude) plus the planned future loading time history shall be adequate for total time under evaluation (i.e., the fatigue damage fraction for the component shall not exceed unity for the specified component life.) Examples where an FFS Assessment of fatigue damage may be used include components subject to the original design basis mechanical and/or thermal cycles (i.e., number of cycles and magnitude of loads), components subject to significant or unanticipated vibration, or components subject to slug flow or fluid surge.

14.1.3 Fatigue Evaluation in the Creep Range

If the component under evaluation is in the creep range, the fatigue evaluation shall be performed using a creep-fatigue assessment (see Part 10, paragraph 10.5.3).

14.1.4 Fatigue Evaluation and Crack-Like Flaws

If the component under evaluation has a crack-like flaw and is below the creep range, or has HIC or SOHIC damage, the fatigue evaluation shall be performed using a subcritical crack growth assessment, see Part 9, paragraph 9.5.1. If the component under evaluation has a crack-like flaw and is in the creep range, the fatigue evaluation shall be performed using a creep crack growth assessment, see Part 10, paragraph 10.5.4.

14.1.5 ASME B&PV Code, Section VIII, Division 2 (VIII-2)

The stress analysis concepts and methods in this Part are based on ASME B&PV Code, Section VIII, Division 2 (VIII-2), Part 5.

14.1.6 Use of Fatigue Curves in Performing Assessments

Fatigue curves are presented in two forms: fatigue curves that are based on smooth bar test specimens and fatigue curves that are based on test specimens that include weld details with quality consistent with the fabrication and inspection requirements for pressure containing equipment. The fatigue curves to be used with this Part are contained in Annex 14B. Selection of the fatigue curve to use shall consider the following:

a) Smooth bar fatigue curves may be used for components with or without welds. The welded joint curves shall only be used for welded joints.

b) The smooth bar fatigue curves are applicable up to the maximum number of cycles given on the curves. The welded joint fatigue curves do not exhibit an endurance limit and are acceptable for all cycles.

14.1.7 Adjustment for Mean Stress

Stresses and strains produced by any load or thermal condition that does not vary during the cycle need not be considered in a fatigue analysis if the fatigue curves utilized in the evaluation are adjusted for mean stresses and strains. The design fatigue curves based on smooth bar test specimens are adjusted for the maximum possible effect of mean stress and strain; therefore, an adjustment for mean stress effects is not required. The welded joint fatigue curves are based on welded test specimens and include explicit adjustments for thickness and mean stress effects.

14.1.8 Ratcheting

Under certain combinations of steady state and cyclic loadings there is a possibility of ratcheting. Ratcheting is a progressive incremental inelastic deformation or strain that can occur in a component subjected to variations of mechanical stress, thermal stress, or both. Ratcheting is produced by a sustained or cyclic load acting over the full cross section of a component, in combination with a strain controlled cyclic load or temperature distribution that is alternately applied and removed. Ratcheting results in a cyclic straining of the material, which can result in failure by fatigue and at the same time produces cyclic incremental growth of a structure, which could ultimately lead to collapse. Assessment procedures for protection against ratcheting for components operating below the creep range are included in this Part. For ratcheting of components operating in the creep range, see Part 10, paragraph 10.5.2.4.

14.2 Applicability and Limitations of the Procedure

14.2.1 Applicability and Limitations of the Assessment Procedures

Fitness-For-Service (FFS) Assessment procedures for evaluating fatigue damage in components subject to cyclic operation below the creep range that do not contain crack-like flaws are covered in this Part. The component may contain volumetric flaws such as thinning, pitting damage, and weld misalignment.

14.2.2 Calculation of MAWP and Coincident Temperature

The fatigue assessment procedures in this part are formulated in terms of an applied stresses defined using a loading time history. The $MAWP$ or reduced $MAWP$, as applicable, may be determined implicitly by directly

including the stress from pressure in the assessment. The same procedure can be used to determine a maximum fill height for tank components (i.e., shell courses in flat bottom storage tanks).

14.2.3 Limitations Based on Temperature

The assessment procedures only apply to components that are not operating in the creep range, e.g., the design temperature is less than or equal to the value in Part 4, Table 4.1. A Materials Engineer should be consulted regarding the creep range temperature limit for materials not listed in this table.

14.2.4 Limitations Based on Flaw Type

a) The component may contain volumetric damage from general thinning, local thinning, pitting and/or weld misalignment. In these cases, the remaining strength factor will be required for a Level 1 Assessment and the local stresses resulting from the volumetric damage will be required in a Level 2 Assessment.

b) The component does not contain a crack-like flaw.

c) For a Level 1 or Level 2 Assessment the component does not contain a dent, gouge, or dent-gouge combination.

d) The component does not contain HIC, step-wise cracking, or SOHIC damage.

14.2.5 Applicability of the Level 1 and Level 2 Assessment Procedures

The Level 1 and 2 Assessment procedures apply only if all the following criteria are satisfied:

a) The original design criteria were in accordance with a recognized code or standard, see Part 1, paragraphs 1.2.2 or 1.2.3.

b) A loading time history can be established in accordance with paragraph 14.3.3.

c) The stresses, and strains for Method B in Level 2, in the component, including the effects of flaws permitted by paragraph 14.2.4, can be determined at each point in the loading time history.

d) A fatigue curve for the component's material of construction can be determined using Annex 14B.

e) The component material is considered to have sufficient toughness. If there is uncertainty regarding the material toughness, then a Part 3 assessment should be performed. If the component is subject to embrittlement during operation because of temperature and/or the process environment, a Level 3 Assessment should be performed. Temperature and/or process conditions that result in material embrittlement are discussed in Annex 2B.

14.2.6 Applicability of the Level 3 Assessment

The Level 3 Assessment may be used to determine the fatigue life for all components, with or without welds. A loading time history is required and may be established in accordance with paragraph 14.3.3 and stresses and strains in the component, including the effects of flaws permitted by paragraph 14.2.4, can be determined at each point in the loading time history. The Level 3 Assessment procedure is consistent with modern fatigue analysis methods employed in numerical fatigue evaluation and durability software applications designed to post process results directly from a finite element analysis. Examples where the Level 3 Assessment may be used include the following:

a) Geometrically complex components subject to complicated transient loading from pressure and/or thermal effects where post-processing of results from a finite element program is desired.

b) Components subject to nonproportional loading.

c) Components subject to loading where the sequence of loads may influence the fatigue life.

14.3 Data Requirements

14.3.1 Original Equipment Design Data

An overview of the original equipment data required for an assessment is provided in Part 2, paragraph 2.3.1. These data can be entered in the form provided in Part 2, Table 2.2 for each component under evaluation.

14.3.2 Maintenance and Operational History

An overview of the maintenance and operational history required for an assessment is provided in Part 2, paragraph 2.3.2.

14.3.3 Required Data/Measurements for an FFS Assessment

A loading history shall be developed to show the time variation of each specific load.

a) The loading history shall include all significant operating temperatures, pressures, supplemental loads, and the corresponding cycles or time periods for all significant events that are applied to the component. Significant loads and events are described as part of the Level 1 Assessment. The following shall be considered in developing the loading history.

   1) The number of cycles associated with each event during the operation life; these events shall include start-ups, normal operation, upset conditions, and shutdowns.

   2) Vibration measurements, as applicable.

   3) The history to be used in the assessment shall be based on the past and anticipated sequence of operation.

   4) Applicable loadings such as pressure, temperature, supplemental loads such as weight, support displacements, and nozzle reaction loadings.

   5) The sequential relationship between the applied loadings during the time history.

b) If an accurate loading time history cannot be generated, then an approximate loading time history shall be developed based on information obtained from the owner. This information shall include a description of all assumptions made and include a discussion of the accuracy in establishing points on the loading time history. A sensitivity analysis (see Part 2, paragraph 2.4.3) shall be included in the FFS Assessment to determine and evaluate the effects of the assumptions made to develop the operating history.

14.3.4 Recommendations for Inspection Technique and Sizing Requirements

Prior to crack initiation, non-destructive methods to detect fatigue damage are not generally available. Fatigue cracking typically first appears at the component surface. Depending on the accessibility, component materials of construction and crack-like flaw physical characteristics, dye-penetrant, magnetic particle, eddy current, radiographic, or ultrasonic examination may be used to determine the presence of fatigue induced cracking. For components with volumetric or geometric damage, the inspection recommendations in Part 4, Part 5, Part 6, and Part 8 should be considered.

14.4 Assessment Techniques and Acceptance Criteria

14.4.1 Overview

An overview of the assessment levels for fatigue damage is provided in Figure 14.1.

a) The Level 1 Assessment procedure is a fatigue screening criterion that may be used to determine if a detailed fatigue analysis is required. The fatigue screening procedures are based on VIII-2, Part 5 with customization for in-service components. An overview of the Level 1 Assessment procedure is shown in Figure 14.2.

b) The Level 2 Assessment procedure for fatigue is based on VIII-2, Part 5 with customization for in-service components. A loading time history covering past and future operation is derived showing the cyclic nature of all applied loadings including thermal gradients. Primary, secondary, and peak stresses are computed based on VIII-2, and load pairs are defined for each cycle so that a stress or strain amplitude may be computed. The allowable number of cycles for the stress and strain amplitude is determined from a fatigue curve in Annex 14B. For variable amplitude loading, the Palmgren-Miner cumulative damage model is used to determine the total fatigue damage for the specified history. An overview of the Level 2 Assessment procedure is shown in Figure 14.3.

c) The Level 3 Assessment procedures are included to provide modern fatigue evaluation technology used in post-processing software typically associated with commercial finite element software. In addition, the Level 3 Assessment includes the effects of nonproportional loading and load sequence effects on fatigue life.

14.4.2 Level 1 Assessment

14.4.2.1 Overview

The Level 1 Assessment procedure is a fatigue screening criterion that may be used to determine if a detailed fatigue analysis is required. An overview of the Level 1 Assessment Method is shown in Figure 14.2.

a) The fatigue screening Methods to determine the need for fatigue analysis are described below. If any one of the screening Methods is satisfied, then a fatigue analysis is not required as part of the FFS Assessment.

   1) Method A – Experience with comparable equipment operating under similar conditions, see paragraph 14.4.2.2.

   2) Method B – Screening based on materials of construction (limited applicability), construction details, loading history, and smooth bar fatigue curve data, see paragraph 14.4.2.3.

   3) Method C – Screening based on the materials of construction (unlimited applicability), construction details, loading history, and smooth bar fatigue curve data, see paragraph 14.4.2.4.

   4) Method D – Screening based on the materials of construction (unlimited applicability), construction details, loading history, and welded joint fatigue curve data, see paragraph 14.4.2.5.

b) The fatigue exemption in accordance with this paragraph is performed on a component or part basis. One component (integral) may be exempt, while another component (non-integral) is not exempt. If any one component is not exempt, then a fatigue evaluation shall be performed for that component. If the specified number of cycles is greater than 10^6 cycles, then the screening criteria are not applicable and a fatigue analysis using the Level 2 or Level 3 Assessment procedures is required.

14.4.2.2 Method A – Fatigue Screening Based on Experience with Comparable Equipment

If successful experience over a sufficient time frame (greater than or equal to the intended design life of a given component) is obtained with comparable equipment subject to a similar loading time history, then a fatigue analysis is not required as part of the FFS Assessment. When evaluating experience with comparable equipment operating under similar conditions as related to the design and service contemplated, the possible harmful effects of the following features shall be evaluated.

a) Components with a flaw characterized by a Remaining Strength Factor determined in accordance with Part 5, Part 6, Part 7, Part 8, or Part 12,

b) The use of non-integral construction, such as the use of pad type reinforcements or fillet welded attachments, as opposed to integral construction,

c) The use of pipe threaded connections, particularly for pipe outside diameters more than 70 mm (2.75 inches),

d) The use of stud bolted attachments,

e) The use of partial penetration welds,

f) Major thickness changes between adjacent members, and

g) Attachments and nozzles in the knuckle region of formed heads.

14.4.2.3 Method B – Fatigue Screening

The following procedure may only be used for steel components with materials of construction that have a specified minimum tensile strength that is less than or equal to 552 MPa (80 ksi).

a) STEP 1 – Determine a loading time history as defined in paragraph 14.3.3. The loading time history should include all cyclic operating loads and events that are applied to the component and consider both past and future planned operation.

b) STEP 2 – Based on the loading time history in STEP 1, determine the historical and estimated future number of full-range pressure cycles including startup and shutdown, and designate this value as $N_{\Delta FP}$.

c) STEP 3 – Based on the loading time history in STEP 1, determine the historical and estimated future number of operating pressure cycles in which the range of pressure variation exceeds 20% of the design pressure for integral construction or 15% of the design pressure for non-integral construction, and designate this value as $N_{\Delta PO}$. Examples of significant operating pressure cycles for both integral and non-integral construction are provided in Figure 14.4. Pressure cycles in which the pressure variation does not exceed these percentages of the design pressure (or equipment $MAWP$ or reduced $MAWP$, as applicable) and pressure cycles caused by changes in atmospheric conditions do not need to be considered in this evaluation.

d) STEP 4 – Based on the loading time history in STEP 1, determine the effective number of changes in metal temperature difference between any two adjacent points within the component, ΔT_E, and designate this value as $N_{\Delta TE}$. The effective number of changes in metal temperature is determined by multiplying the number of changes in metal temperature difference of a certain magnitude by the factor given in Table 14.1, and by adding the resulting numbers for all temperature differences. In calculating the temperature difference between adjacent points, conductive heat transfer shall be considered only through welded or integral cross sections with no allowance for conductive heat transfer across un-welded contact surfaces, e.g., a vessel shell and reinforcing pad. Temperature cycles caused by changes in atmospheric conditions do not need to be considered in this evaluation.

1) For surface temperature differences, points are adjacent if they are within the distance L computed as follows:

   i) For shells and dished heads in the meridional or circumferential directions,

$$L = 2.5\sqrt{Rt} \tag{14.1}$$

   ii) For flat plates,

$$L = 3.5 \cdot R_{HS} \tag{14.2}$$

2) For through-the-thickness temperature differences, adjacent points are defined as any two points on a line normal to any surface in the component.

Examples of adjacent points on a cylindrical shell are provided in Figure 14.5 and examples of adjacent points near a nozzle-to-head junction are shown in Figure 14.6. Additionally, examples of adjacent points near ring-to-shell junctions and support skirt-to-shell junctions are given in Figure 14.7 and Figure 14.8, respectively. Finally, examples of adjacent points on a flat head or plate are provided in Figure 14.9. These figures are intended to offer examples of adjacent points on typical pressure vessel component geometries. They are not intended to show all possible combinations of adjacent points that shall be considered for this fatigue screening procedure, nor are they intended to bound all possible geometric configurations.

e) STEP 5 – Based on the loading time history in STEP 1, determine the number of temperature cycles for components involving welds between materials having different coefficients of thermal expansion that causes the value of $(\alpha_1 - \alpha_2) \cdot \Delta T$ to exceed 0.00034, and designate this value as $N_{\Delta T\alpha}$. An example of a significant temperature cycle for adjacent components with different thermal expansion properties is provided in Figure 14.10.

f) STEP 6 – If the expected number of operating cycles from STEPs 2, 3, 4 and 5 satisfies the criterion in Table 14.2, then the Level 1 Assessment criterion is satisfied. If this criterion is not satisfied, then use of an alternative Level 1 Method or a Level 2 or Level 3 Assessment is required.

14.4.2.4 Method C – Fatigue Screening

The following procedure may be used for materials with a designated smooth bar fatigue curve in Annex 14B. Note that in this procedure:

- $N[S_{alt}]$ is defined as a function to determine the number of cycles from the applicable smooth bar fatigue curve evaluated at the alternating stress amplitude S_{alt}. This function is used in STEPs 3 through 8.
- S_{as} is the value of the stress amplitude evaluated at $(10)^6$ cycles using the same smooth bar fatigue curve from Annex 14B for the material being evaluated. S_{as} is used in STEPs 4, 6, 7, and 8.

a) STEP 1 – Determine a loading time history as defined in paragraph 14.3.3. The loading time history should include all cyclic operating loads and events that are applied to the component and consider both past and future planned operation.

b) STEP 2 – Determine K_{fc} and H_c based on the type of construction (see Table 14.3). If the component contains a flaw, then the parameter K_{fc} shall be divided by the RSF calculated per the applicable flaw assessment procedures in this standard. The adjusted value of K_{fc} shall be subsequently used in the following steps of this procedure.

c) STEP 3 – Based on the loading time history in STEP 1, determine the design number of full-range pressure cycles including startup and shutdown, $N_{\Delta FP}$. Calculate the damage associated with the full-range pressure cycles, D_{FP}.

$$D_{FP} = \frac{N_{\Delta FP}}{N\left[\frac{3S \cdot K_{fc} \cdot H_c}{2}\right]} \tag{14.3}$$

d) STEP 4 – Based on the loading time history in STEP 1, determine the maximum range of pressure fluctuation during normal operation, excluding startups and shutdowns, ΔP_N, and the corresponding number of significant cycles, $N_{\Delta P}$. Significant pressure fluctuation cycles are defined as cycles where the pressure range exceeds $2P \cdot S_{as}/(3S \cdot K_{fc} \cdot H_c)$. An example of a significant pressure fluctuation cycle for this step is given in Figure 14.11. Calculate the damage associated with ΔP_N, D_{PN}.

$$D_{PN} = \frac{N_{\Delta P}}{N\left[\frac{\Delta P_N \cdot 3S \cdot K_{fc} \cdot H_c}{2P}\right]} \tag{14.4}$$

e) STEP 5 – Based on the loading time history in STEP 1, determine the maximum range of temperature difference between any two adjacent points during startup and shutdown operation, ΔT_N, where ΔT_N is either ΔT_A or ΔT_T, and the corresponding number of cycles, $N_{\Delta TN}$. Calculate the damage associated with ΔT_N, D_{TN}.

$$D_{TN} = \frac{N_{\Delta TN}}{N\left[\frac{\left(2E_{ym} \cdot \alpha \cdot \Delta T_N\right) \cdot K_{fc} \cdot H_c}{2}\right]} \tag{14.5}$$

f) STEP 6 – Based on the loading time history in STEP 1, determine the maximum range of temperature difference between any two adjacent points, ΔT_R, where ΔT_R is either ΔT_A or ΔT_T during normal operation, excluding startups and shutdowns, and the corresponding number of significant cycles, $N_{\Delta TR}$. Significant temperature difference cycles for this step are defined as cycles where the temperature range exceeds $S_{as}/(E_{ym} \cdot \alpha \cdot K_{fc} \cdot H_c)$. Calculate the damage associated with ΔT_R, D_{TR}. An example of a significant temperature difference cycle for this step is provided in Figure 14.12.

$$D_{TR} = \frac{N_{\Delta TR}}{N\left[\frac{\left(2E_{ym} \cdot \alpha \cdot \Delta T_R\right) \cdot K_{fc} \cdot H_c}{2}\right]} \tag{14.6}$$

g) STEP 7 –Based on the loading time history in STEP 1, determine the maximum range of temperature difference between any two adjacent points for components involving welds between materials having different coefficients of thermal expansion during normal operation, ΔT_M, and the corresponding number of significant cycles, $N_{\Delta TM}$. Significant temperature difference cycles for this step are defined as cycles where the temperature range exceeds $S_{as}/\left(\left(E_{y1}\alpha_1 - E_{y2}\alpha_2\right) \cdot K_{fc} \cdot H_c\right)$. The fatigue curve that results in the lowest significant temperature difference and lowest number of cycles for the two materials shall be used. Calculate the damage associated with ΔT_M, D_{TM}. An example of a significant temperature difference cycle for this step is rendered in Figure 14.13.

$$D_{TM} = \frac{N_{\Delta TM}}{N\left[\frac{2\Delta T_m \left(E_{y1}\alpha_1 - E_{y2}\alpha_2\right)\cdot K_{fc}\cdot H_c}{2}\right]} \tag{14.7}$$

h) STEP 8 – Based on the loading time history in STEP 1, determine the equivalent stress range computed from the specified full range of mechanical loads, excluding pressure but including piping reactions, ΔS_{ML}, and the corresponding number of significant cycles, $N_{\Delta S}$. As shown in Figure 14.14, significant mechanical load range cycles for this step are defined as cycles where the stress range exceeds $2\,S_{as}/\left(K_{fc}\cdot H_c\right)$. Calculate the damage associated with ΔS_{ML},

$$D_{ML} = \frac{N_{\Delta S_{ML}}}{N\left[\frac{\Delta S_{ML}\cdot K_{fc}\cdot H_c}{2}\right]} \tag{14.8}$$

i) STEP 9 – If the sum of the damage D_f, satisfies Equation (14.9), then a detailed fatigue analysis of the component is not required.

$$D_f = D_{FP} + D_{PN} + D_{TN} + D_{TR} + D_{TM} + D_{ML} \le 1.0 \tag{14.9}$$

14.4.2.5 Method D – Fatigue Screening, Welded Joints

The following procedure may be used for fatigue screening of welded joints for materials with a designated welded joint fatigue curve in Annex 14B. Note that in this procedure:

- $N[\Delta S_{ess}]$ is defined as a function to determine the number of cycles from the applicable welded joint fatigue curve evaluated at the equivalent structural stress range ΔS_{ess} (see Annex 14B, paragraph 14B.4.2). In this calculation, the minus 3-sigma fatigue curve coefficients shall be used. This function is used in STEPs 3 through 8.
- S_{as} is the value of the stress amplitude evaluated at $(10)^6$ cycles using a smooth bar fatigue curve from Annex 14B for the material being evaluated. S_{as} is used in STEPs 4, 5, 7, and 8.
- $\Delta S_{ess}[\Delta\sigma]$ is defined as a function to compute the equivalent structural stress range, ΔS_{ess}, as a function of the applied stress range, $\Delta\sigma$, and is given by Equations (14.10) and (14.11). This function is used in STEPs 3 through 8.

$$\Delta S_{ess}\left[\Delta\sigma\right] = \frac{\Delta\sigma}{0.4079} \qquad \left(MPa\right) \tag{14.10}$$

$$\Delta S_{ess}\left[\Delta\sigma\right] = \frac{\Delta\sigma}{0.8341} \qquad \left(ksi\right) \tag{14.11}$$

a) STEP 1 – Determine a loading time history as defined in paragraph 14.3.3. The loading time history should include all cyclic operating loads and events that are applied to the component and consider both past and future planned operation.

b) STEP 2 – Determine K_{fc} and H_c based on the type of construction (see Table 14.3). If the component contains a flaw, then the parameter K_{fc} shall be divided by the RSF calculated per the applicable flaw assessment procedures in this standard. The adjusted value of K_{fc} shall be subsequently used in the following steps of this procedure.

c) STEP 3 – Based on the loading time history in STEP 1, determine the design number of full-range pressure cycles including startup and shutdown, $N_{\Delta FP}$. Calculate the damage associated with the full-range pressure cycles, D_{FP}.

$$D_{FP} = \frac{N_{\Delta FP}}{N\left[\Delta S_{ess}\left[3S \cdot K_{fc} \cdot H_c\right]\right]} \tag{14.12}$$

d) STEP 4 – Based on the loading time history in STEP 1, determine the maximum range of pressure cycles during normal operation, excluding startups and shutdowns, ΔP_N, and the corresponding number of significant cycles, $N_{\Delta P}$. Significant pressure cycles are defined as cycles where the pressure range exceeds $2P \cdot S_{as}/\left(3S \cdot K_{fc} \cdot H_c\right)$. An example of a significant pressure cycle for this step is given in Figure 14.11. Calculate the damage associated with ΔP_N.

$$D_{PN} = \frac{N_{\Delta P}}{N\left[\Delta S_{ess}\left[\frac{\Delta P_N \cdot 3S \cdot K_{fc} \cdot H_c}{P}\right]\right]} \tag{14.13}$$

e) STEP 5 – Based on the loading time history in STEP 1, determine the maximum range of temperature difference between any two adjacent points during startup and shutdown operation, ΔT_N, where ΔT_N is either ΔT_A or ΔT_T, and the corresponding number of cycles, $N_{\Delta TN}$. Calculate the damage associated with ΔT_N, D_{TN}.

$$D_{TN} = \frac{N_{\Delta TN}}{N\left[\Delta S_{ess}\left[\left(\left(2E_{ym} \cdot \alpha \cdot \Delta T_N\right) \cdot K_{fc} \cdot H_c\right)\right]\right]} \tag{14.14}$$

f) STEP 6 – Based on the loading time history in STEP 1, determine the maximum range of temperature difference between any two adjacent points, ΔT_R, where ΔT_R is either ΔT_A or ΔT_T during normal operation, excluding startups and shutdowns, and the corresponding number of significant cycles, $N_{\Delta TR}$. Significant temperature difference cycles for this step are defined as cycles where the temperature range exceeds $S_{as}/\left(E_{ym} \cdot \alpha \cdot K_{fc} \cdot H_c\right)$. Calculate the damage associated with ΔT_R, D_{TR}. An example of a significant temperature difference cycle for this step is provided in Figure 14.12.

$$D_{TR} = \frac{N_{\Delta TR}}{N\left[\Delta S_{ess}\left[\left(2E_{ym} \cdot \alpha \cdot \Delta T_R\right) \cdot K_{fc} \cdot H_c\right]\right]} \tag{14.15}$$

g) STEP 7 – Based on the loading time history in STEP 1, determine the maximum range of temperature difference between any two adjacent points for components involving welds between materials having different coefficients of thermal expansion during normal operation, ΔT_M, and the corresponding number of significant cycles, $N_{\Delta TM}$. Significant temperature difference cycles for this step are defined as cycles where the temperature range exceeds $S_{as}/\left(\left(E_{y1}\alpha_1 - E_{y2}\alpha_2\right) \cdot K_{fc} \cdot H_c\right)$. The fatigue curve that results in the lowest significant temperature difference and lowest number of cycles for the two materials shall be used. Calculate the damage associated with ΔT_M, D_{TM}. An example of a significant temperature difference cycle for this step is rendered in Figure 14.13.

$$D_{TM} = \frac{N_{\Delta TM}}{N\left[\Delta S_{ess}\left[2\Delta T_m\left(E_{y1}\alpha_1 - E_{y2}\alpha_2\right) \cdot K_{fc} \cdot H_c\right]\right]} \tag{14.16}$$

h) STEP 8 – Based on the loading time history in STEP 1, determine the equivalent stress range computed from the specified full range of mechanical loads, excluding pressure but including piping reactions, ΔS_{ML}, and the corresponding number of significant cycles, $N_{\Delta S}$. As shown in Figure 14.14, significant mechanical load range cycles for this step are defined as cycles where the stress range exceeds $2\,S_{as}/\left(K_{fc}\cdot H_c\right)$. Calculate the damage associated with ΔS_{ML},

$$D_{ML} = \frac{N_{\Delta S}}{N\left[\Delta S_{ess}\left[\Delta S_{ml}\cdot K_{fc}\cdot H_c\right]\right]} \tag{14.17}$$

i) STEP 9 – If the sum of the damage D_f, satisfies Equation (14.18), then a detailed fatigue analysis of the component is not required.

$$D_f = D_{FP} + D_{PN} + D_{TN} + D_{TR} + D_{TM} + D_{ML} \le 1.0 \tag{14.18}$$

14.4.2.6 Level 1 Assessment Results

If the component does not meet the Level 1 Assessment requirements, then the following, or combinations thereof, can be considered:

a) Conduct a Level 2 or Level 3 Assessment.

b) Rerate or repair the component. Note that the accumulated component fatigue damage may need to be monitored.

c) Replace the component.

14.4.3 Level 2 Assessment

14.4.3.1 Overview

a) Three fatigue assessment methods are provided and are summarized below. An Overview of the Level 2 Assessment procedures is shown in Figure 14.3.

1) Method A – Fatigue Assessment Using Elastic Stress Analysis and Equivalent Stresses. In this method, the fatigue damage and remaining life is computed based on effective total equivalent stress obtained from a linear elastic stress analysis, and a smooth bar fatigue curve, see paragraph 14.1.5.

2) Method B – Fatigue Assessment Using Elastic-Plastic Stress Analysis and Equivalent Strain. In this method, the fatigue damage and remaining life is computed based on an effective strain range obtained from an elastic-plastic stress analysis, and a smooth bar fatigue curve, see paragraph 14.1.5.

3) Method C – Fatigue Assessment of Welds Using the Equivalent Structural Stress. In this method, the fatigue damage and remaining life is computed based on an equivalent structural stress range parameter obtained from a linear elastic stress analysis, and a welded joint fatigue curve, see paragraph 14.1.5.

b) In addition to the fatigue damage and remaining life methods, two methods are provided to evaluate the propensity for ratcheting, see paragraph 14.1.8. A ratcheting assessment for non-integral connections is also provided.

1) Elastic Stress Analysis – The protection against ratcheting is evaluated using an elastic analysis with conservative assumptions to approximate the effects of steady-state and cyclic loading conditions.

2) Elastic-Plastic Stress Analysis – The protection against ratcheting is evaluated using an elastic-plastic analysis by directly simulating the plastic strain accumulation from steady-state and cyclic loading conditions.

14.4.3.2 Method A – Fatigue Assessment Using Elastic Stress Analysis and Equivalent Stresses

14.4.3.2.1 Overview

a) The effective total equivalent stress amplitude is used to evaluate the fatigue damage for results obtained from a linear elastic stress analysis. The controlling stress for the fatigue evaluation is the primary plus secondary plus peak equivalent stress amplitude that is defined as one-half of the primary plus secondary plus peak stress equivalent stress range, $(P_L + P_b + Q + F)$, calculated for each cycle in the loading history, see Figure 14.15 and Annex 2D. The primary plus secondary plus peak stress equivalent stress range is the equivalent stress, derived from the highest value across the thickness of a section, of the combination of all primary, secondary, and peak stresses produced by specified operating pressures and other mechanical loads and by general and local thermal effects and including the effects of gross and local structural discontinuities, see VIII-2, Part 5.

b) Two options are provided to determine the primary plus secondary plus peak stress equivalent stress range.

1) OPTION 1 – The local thermal stress range is not separated from the total stress range and any stress concentration factors (SCF), fatigue strength reduction factors (K_f) and fatigue penalty factors are applied to the total stress range directly.

2) OPTION 2 – The local thermal stress range is separated from the total stress range. Stress concentration factors (SCF) and/or fatigue strength reduction factors (K_f) are applied to the range of equivalent primary plus secondary plus peak stress minus the local thermal stress range. The plastic Poisson's ratio adjustment factor (K_v) is applied to the local thermal stress range.

c) If the range of primary plus secondary plus peak equivalent stress exceeds S_{PS}, then a simplified elastic-plastic evaluation based on the results of elastic stress analysis in combination with a fatigue penalty factor is required.

d) A flow diagram for the Method A Fatigue calculation procedure is shown in Figure 14.16.

14.4.3.2.2 Assessment Procedure

The following procedure can be used to evaluate protection against failure due to cyclic loading for a component based on the effective total equivalent stress amplitude.

a) STEP 1 – Determine a loading time history as defined in paragraph 14.3.3. The loading time history should include all significant operating loads and events that are applied to the component and consider both past and future planned operation.

b) STEP 2 – Perform an elastic stress analysis of the component based on the loading time history from STEP 1. The stress tensor shall be determined at each location in the component at each point identified in the loading time history.

c) STEP 3 – Determine the cyclic stress ranges at the location under consideration based on the elastic stress analysis in STEP 2 and the cycle counting methods in Annex 14C. Define the total number of cyclic stress ranges in the loading time history as M.

d) STEP 4 – Perform the following for each cyclic stress range in the loading time history: $k \leq M$.

1) STEP 4.1 – Obtain the stress tensor at the start and end of the k^{th} cycle counted in STEP 3, ${}^{m}\sigma_{ij,k}$ and ${}^{n}\sigma_{ij,k}$. If the peak stress is calculated using a stress concentration factor and/or fatigue strength reduction factor, then compute the linearized component membrane plus bending values, ${}^{m}\sigma_{ij,k}^{MB}$ and ${}^{n}\sigma_{ij,k}^{MB}$.

2) STEP 4.2 – Calculate the equivalent primary plus secondary plus peak stress range for the k^{th} cycle from STEP 4.1. Two OPTIONS are permitted.

   i) OPTION 1: The local thermal stress range is not separated from the total stress range prior to applying fatigue penalty factor, $K_{e,k}$.

      I) Calculate the stress range tensor, $\Delta\sigma_{ij,k}$, using Table 14.4.

      II) Calculate the equivalent stress range:

$$\Delta S_{P,k} = \frac{1}{\sqrt{2}}\left[\begin{array}{l}\left(\Delta\sigma_{11,k}-\Delta\sigma_{22,k}\right)^2+\left(\Delta\sigma_{11,k}-\Delta\sigma_{33,k}\right)^2+\\ \left(\Delta\sigma_{22,k}-\Delta\sigma_{33,k}\right)^2+6\left(\Delta\sigma_{12,k}^2+\Delta\sigma_{13,k}^2+\Delta\sigma_{23,k}^2\right)\end{array}\right]^{0.5} \tag{14.19}$$

   ii) OPTION 2: The local thermal stress range is separated from the total stress range prior to applying fatigue penalty factor, $K_{e,k}$.

      I) Determine the local thermal stress from $\sigma_{ij,k}$ at the start and end of the cycle and designate these values as ${}^{m}\sigma_{ij,k}^{LT}$ and ${}^{n}\sigma_{ij,k}^{LT}$, respectively. An alternative method for determining ${}^{m}\sigma_{ij,k}^{LT}$ and ${}^{n}\sigma_{ij,k}^{LT}$ is provided in paragraph 14.4.3.2.3.

      II) Calculate the equivalent local thermal stress range using Equation (14.20).

$$\Delta S_{LT,k} = \frac{1}{\sqrt{2}}\left[\begin{array}{l}\left(\Delta\sigma_{11,k}^{LT}-\Delta\sigma_{22,k}^{LT}\right)^2+\left(\Delta\sigma_{11,k}^{LT}-\Delta\sigma_{33,k}^{LT}\right)^2+\\ \left(\Delta\sigma_{22,k}^{LT}-\Delta\sigma_{33,k}^{LT}\right)^2+\\ 6\left(\left(\Delta\sigma_{12,k}^{LT}\right)^2+\left(\Delta\sigma_{13,k}^{LT}\right)^2+\left(\Delta\sigma_{23,k}^{LT}\right)^2\right)\end{array}\right]^{0.5} \tag{14.20}$$

      where,

$$\Delta\sigma_{ij,k}^{LT} = {}^{m}\sigma_{ij,k}^{LT} - {}^{n}\sigma_{ij,k}^{LT} \tag{14.21}$$

      III) Calculate the total minus local thermal stress range tensor, $\Delta\sigma_{ij,k}$, using Table 14.4.

      IV) Calculate the range of equivalent primary plus secondary plus peak stress minus the local thermal stress range using Equation (14.22).

$$\Delta S_{P-LT,k} = \frac{1}{\sqrt{2}}\left[\begin{array}{l}\left(\Delta\sigma_{11,k}-\Delta\sigma_{22,k}\right)^2+\left(\Delta\sigma_{11,k}-\Delta\sigma_{33,k}\right)^2+\\ \left(\Delta\sigma_{22,k}-\Delta\sigma_{33,k}\right)^2+6\left(\Delta\sigma_{12,k}^2+\Delta\sigma_{13,k}^2+\Delta\sigma_{23,k}^2\right)\end{array}\right]^{0.5} \tag{14.22}$$

3) STEP 4.3 – Calculate the effective alternating equivalent stress amplitude for the k^{th} cycle using the results from STEP 4.2.

i) For OPTION 1:

$$S_{alt,k} = \frac{K_{e,k} \cdot \Delta S_{P,k}}{2} \tag{14.23}$$

ii) For OPTION 2:

$$S_{alt,k} = \frac{K_{e,k} \cdot \Delta S_{P-LT,k} + K_{v,k} \cdot \Delta S_{LT,k}}{2} \tag{14.24}$$

The fatigue penalty factor, $K_{e,k}$, in Equations (14.23) and (14.24) is evaluated using the following equations where the parameters m and n are determined from Table 14.7, and S_{PS} and $\Delta S_{n,k}$ are defined in paragraph 14.4.3.5.1. An alternative method for determining $K_{e,k}$ is provided in paragraph 14.4.3.2.4.

$$K_{e,k} = 1.0 \qquad \left(for \;\; \Delta S_{n,k} \le S_{PS}\right) \tag{14.25}$$

$$K_{e,k} = 1.0 + \frac{(1-n)}{n(m-1)}\left(\frac{\Delta S_{n,k}}{S_{PS}} - 1\right) \qquad \left(for \;\; S_{PS} < \Delta S_{n,k} < mS_{PS}\right) \tag{14.26}$$

$$K_{e,k} = \frac{1}{n} \qquad \left(for \;\; \Delta S_{n,k} \ge mS_{PS}\right) \tag{14.27}$$

The Poisson's correction factor, $K_{v,k}$ in Equation (14.24) is computed using Equation (14.28). Note that the Poisson's correction factor is not required for OPTION 1 because the fatigue penalty factor, $K_{e,k}$, is applied to the entire stress range including $\Delta S_{LT,k}$. This is typically conservative since $K_{e,k} \ge K_{v,k}$.

$$K_{v,k} = \frac{(1-\nu)}{(1-\nu_p)} \tag{14.28}$$

where,

$$\nu_p = \max\left[0.5 - 0.2\left(\frac{S_{y,k}}{S_{a,k}}\right), \quad \nu\right] \tag{14.29}$$

4) STEP 4.4 – If $K_{e,k} > 1.0$ and the material of construction for the component satisfies $YS/UTS \le 0.80$; then, proceed to STEP 4.5. Otherwise, Method A cannot be used for the fatigue assessment.

5) STEP 4.5 – Determine the permissible number of cycles, N_k, for the alternating equivalent stress amplitude computed in STEP 4.3 using a fatigue curve based on the materials of construction in Annex 14B for the k^{th} cycle.

6) STEP 4.6 – Calculate the fatigue damage for the k^{th} cycle using Equation (14.30) where the actual number of repetitions of the k^{th} cycle is n_k.

$$D_{f,k} = \frac{n_k}{C_H \cdot N_k} \tag{14.30}$$

e) STEP 5 – Calculate the accumulated fatigue damage using Equation (14.31). The location in the component is acceptable for continued operation if this equation is satisfied.

$$D_f = \sum_{k=1}^{M} D_{f,k} \le 1.0 \tag{14.31}$$

f) STEP 6 – Repeat STEPs 4 and 5 for each point in the component subject to a fatigue evaluation.

14.4.3.2.3 Alternative Method for Computing the Local Thermal Stress

It may be difficult to calculate the local thermal stress from stress distributions obtained from numerical methods. If this is the case, the procedure below can be used to calculate the local thermal membrane and bending stresses due to a non-linear temperature distribution. This method is based on calculating a thermal stress difference range associated with the linearized temperature distribution along the stress classification line. Consistent with this approach, consider the distribution of the temperature obtained from a numerical method as a function of the local through thickness direction.

The temperature distribution can be separated into three parts.

a) A constant temperature equal to the average of the temperature distribution,

$$T_{avg} = \frac{1}{t}\int_0^t T dx \tag{14.32}$$

b) The linearly varying portion of the temperature distribution,

$$T_b = \frac{6}{t^2}\int_0^t T\left(\frac{t}{2} - x\right) dx \tag{14.33}$$

c) The non-linear portion of the temperature distribution,

$$T_p = \max\left[\left(T\big|_{x=0} - \left(T_{avg} + T_b\right)\right),\ \left(T\big|_{x=t} - \left(T_{avg} + T_b\right)\right)\right] \tag{14.34}$$

By assuming full constraint of the differential expansion of the cross-section, the associated local thermal stress parallel to the surface may be calculated as given below where T_p is given by Equation (14.34).

$$\sigma_{ij,k}^{LT} = \frac{-E_{ya,k} \cdot \alpha_{a,k} \cdot T_p}{1-\nu} \qquad \left(for\ i = j = 1,2\right) \tag{14.35}$$

$$\sigma_{ij,k}^{LT} = 0 \qquad \left(for\ i \ne j\ and\ i = j = 3\right) \tag{14.36}$$

Using Equations (14.35) and (14.36), determine the local thermal component stress ranges at the start and end of the cycle and designate this quantity as ${}^{m}\sigma_{ij,k}^{LT}$ and ${}^{n}\sigma_{ij,k}^{LT}$, respectively.

14.4.3.2.4 Alternative Method for Computing the Fatigue Penalty Factor

The fatigue penalty factor, $K_{e,k}$, in paragraph 14.4.3.2.2, STEP 4.3 may be calculated using Equation (14.37) based on the results of an elastic analysis and elastic-plastic analysis. In Equation (14.37), the numerator is evaluated using the results from an elastic-plastic analysis and the denominator is evaluated using the results from an elastic analysis.

$$K_{e,k} = \frac{\left(\Delta\varepsilon_{peq,k}\right)_{Elastic-Plastic\ Analysis}}{\left(\Delta\varepsilon_{e,k}\right)_{Elastic\ Analysis}} \tag{14.37}$$

where,

$$\Delta\varepsilon_{peq,k} = \frac{\sqrt{2}}{3}\left[\begin{array}{l}\left(\Delta p_{11,k} - \Delta p_{22,k}\right)^2 + \left(\Delta p_{22,k} - \Delta p_{33,k}\right)^2 + \\ \left(\Delta p_{33,k} - \Delta p_{11,k}\right)^2 + C_\gamma \cdot \left(\Delta p_{12,k}^2 + \Delta p_{23,k}^2 + \Delta p_{31,k}^2\right)\end{array}\right]^{0.5} \tag{14.38}$$

$$\Delta p_{ij,k} = {}^{m}p_{ij,k} - {}^{n}p_{ij,k}$$

$$\Delta\varepsilon_{e,k} = \frac{1}{\sqrt{2}\left(1+\nu\right)}\left[\begin{array}{l}\left(\Delta e_{11,k} - \Delta e_{22,k}\right)^2 + \left(\Delta e_{22,k} - \Delta e_{33,k}\right)^2 + \\ \left(\Delta e_{33,k} - \Delta e_{11,k}\right)^2 + C_\gamma \cdot \left(\Delta e_{12,k}^2 + \Delta e_{23,k}^2 + \Delta e_{31,k}^2\right)\end{array}\right]^{0.5} \tag{14.39}$$

$$\Delta e_{ij,k} = {}^{m}e_{ij,k} - {}^{n}e_{ij,k}$$

14.4.3.3 Method B – Fatigue Assessment Using Elastic-Plastic Stress Analysis and Equivalent Strain

14.4.3.3.1 Overview

a) An effective strain range is used to evaluate the fatigue damage based on the results from an elastic-plastic stress analysis. This analysis is performed for the complete loading time history using a cyclic plasticity algorithm with kinematic hardening. The effective strain range is subsequently calculated for each cycle identified using a multiaxial cycle counting procedure. For simple loading time histories, the Twice Yield Method may be used in lieu of a cycle-by-cycle analysis.

b) For the calculation of the stress range and strain range of a cycle at a point in the component, a stabilized cyclic stress-strain curve and other material properties shall be used that correspond to the cycle being evaluated for each material of construction (i.e., material properties shall be evaluated at the temperature corresponding to a point in the cycle). The cyclic curve may be that obtained by test for the material, or for a material which is known to have more conservative cyclic behavior than the material that is specified. Cyclic stress-strain curves are provided in Annex 14B for different materials as a function of temperature. Other cyclic stress-strain curves may be used that are known to be either more accurate for the application or lead to more conservative results.

c) A flow diagram for the Method B Fatigue calculation procedure is shown in Figure 14.17.

14.4.3.3.2 Assessment Procedure

The following procedure can be used to evaluate protection against failure due to cyclic loading using elastic-plastic stress analysis.

a) STEP 1 – Determine a loading time history as defined in paragraph 14.3.3. The loading time history should include all significant operating loads and events that are applied to the component and consider both past and future planned operation.

b) STEP 2 – Perform an elastic-plastic stress analysis of the component based on the loading time history from STEP 1. The material model used in the elastic-plastic analysis shall incorporate a cyclic plasticity algorithm with kinematic hardening. The stress tensor and plastic strain tensor shall be determined at each location in the component at each point identified in the loading time history.

c) STEP 3 – Determine the cyclic strain ranges at the location under consideration based on the elastic-plastic stress analysis in STEP 2 and the cycle counting methods in Annex 14C. Define the total number of cyclic strain ranges in the loading time history as M.

d) STEP 4 – Perform the following for each cyclic stress range in the loading time history: $k \leq M$.

1) STEP 4.1 – Obtain the elastic strain tensor and plastic strain tensor at the start and end of the of the k^{th} cycle counted in STEP 3, ${}^{m}e_{ij,k}$ and ${}^{n}e_{ij,k}$, and ${}^{m}p_{ij,k}$ and ${}^{n}p_{ij,k}$, respectively.

2) STEP 4.2 – Calculate the equivalent elastic strain range tensor, $\Delta\varepsilon_{e,k}$, for the k^{th} using Equation (14.39).

3) STEP 4.3 – Calculate the plastic strain range tensor, $\Delta\varepsilon_{peq,k}$, for the k^{th} cycle using Equation (14.38).

4) STEP 4.4 – Calculate the total equivalent effective strain range for the k^{th} cycle using Equation (14.40).

$$\Delta\varepsilon_{eff,k} = \Delta\varepsilon_{e,k} + \Delta\varepsilon_{peq,k} \tag{14.40}$$

5) STEP 4.5 – Calculate the effective alternating equivalent stress for the k^{th} cycle using Equation (14.41).

$$S_{alt,k} = \frac{E_{ya,k} \cdot \Delta\varepsilon_{eff,k}}{2} \tag{14.41}$$

6) STEP 4.6 – Determine the permissible number of cycles, N_k, for the alternating equivalent stress computed in STEP 4.5 using a fatigue curve based on the materials of construction in Annex 14B for the k^{th} cycle.

7) STEP 4.7 – Calculate the fatigue damage for the k^{th} cycle using Equation (14.42) where the actual number of repetitions of the k^{th} cycle is n_k.

$$D_{f,k} = \frac{n_k}{C_H \cdot N_k} \tag{14.42}$$

e) STEP 5 – Calculate the accumulated fatigue damage using Equation (14.43). The location in the component is acceptable for continued operation if this equation is satisfied.

$$D_f = \sum_{k=1}^{M} D_{f,k} \leq 1.0 \tag{14.43}$$

f) STEP 6 – Repeat STEPs 3 through 5 for each point in the component subject to a fatigue evaluation.

14.4.3.3.3 The Twice Yield Method

a) The Twice Yield Method is an elastic-plastic stress analysis performed in a single loading step, based on a specified stabilized cyclic stress range-strain curve and a specified load range representing a cycle. Stress and strain ranges are the direct output from this analysis. This method is performed in the same manner as a monotonic elastic-plastic analysis and does not require cycle-by-cycle analysis of unloading and reloading. Therefore, the Twice Yield Method can be used with an analysis program that does not have a cyclic plasticity algorithm with kinematic hardening.

b) The Twice Yield Method is based on Masing's hypothesis that states that the stabilized hysteresis loop branch may be obtained by doubling the basic material cyclic stress-strain curve.

c) In the Twice Yield Method, the loading at the start point of the cycle is zero and the loading at the end point is the load determined from the loading time history. Therefore, a formal cycle counting process is not used

and the load range associated with the maximum strain range needs to be deduced from the loading time history.

d) The cyclic stress range-strain range curve or hysteresis loop stress-strain curve, see Annex 14B, is used in the monotonic elastic-plastic analysis. For thermal loading, the loading range in the Twice-Yield Method may be applied by specifying the temperature field at the start point for the cycle as an initial condition and applying the temperature field at the end point for the cycle in a single loading step.

e) The stress tensor and plastic strain tensor are output directly from the elastic-plastic analysis and processed in accordance with paragraph 14.4.3.3.2, STEP 4 and STEP 5.

14.4.3.4 Method C – Fatigue Assessment of Welds Using the Equivalent Structural Stress

14.4.3.4.1 Overview

a) An equivalent structural stress range parameter is used to evaluate the fatigue damage from the results obtained from a linear elastic stress analysis. The controlling stress for the fatigue evaluation is the structural stress that is a function of the membrane and bending stresses normal to the hypothetical crack plane. This method is recommended for evaluation of welded joints that have not been machined to a smooth profile. Weld joints with controlled smooth profiles may be evaluated using paragraphs 14.4.3.2 or 14.4.3.3.

b) Fatigue cracks at pressure vessel welds are typically located at the toe of a weld. For as-welded joints and weld joints subject to post weld heat treatment, the expected orientation of a fatigue crack is along the weld toe in the through-thickness direction, and the structural stress normal to the expected crack is the stress measure used to correlate fatigue life data. For fillet welded components, fatigue cracking may occur at the toe of the fillet weld or the weld throat, and both locations shall be considered in the assessment. It is difficult to accurately predict fatigue life at the weld throat due to variability in throat dimension, which is a function of the depth of the weld penetration. It is recommended to perform sensitivity analysis where the weld throat dimension is varied.

c) If thermal transients result in a through-thickness stress difference at any time that is greater than the steady state difference, the number of design cycles shall be determined as the smaller of the number of cycles for the base metal established using Method A or Method B, and for the weld established using Method C.

A flow diagram for the Method C Fatigue calculation procedure is shown in Figure 14.18.

14.4.3.4.2 Assessment Procedure

The following procedure can be used to evaluate protection against failure due to cyclic loading using the equivalent structural stress range. This procedure shall be performed along the weld joint at two locations on the hypothetical crack plane, the first point corresponding to the location of maximum tensile bending stress and the second point corresponding to the location of the maximum compressive bending stress.

a) STEP 1 – Determine a loading time history as defined in paragraph 14.3.3. The loading time history should include all significant operating loads and events that are applied to the component and consider both past and future planned operation.

b) STEP 2 – Perform an elastic stress analysis of the component based on the loading time history from STEP 1. The stress tensor shall be determined at each hypothetical crack plane in the component at each point identified in the loading time history. Note that the normal and shear stresses on the hypothetical crack plane used in this procedure are computed from the stress tensor.

c) STEP 3 – Determine the cyclic stress ranges at the location under consideration based on the elastic stress analysis in STEP 2 and the cycle counting methods in Annex 14C. Define the total number of cyclic stress ranges in the loading time history as M.

d) STEP 4 – Perform the following for each cyclic stress range in the loading time history: $k \leq M$.

1) STEP 4.1 – Determine the elastic membrane and bending stresses normal to the assumed hypothetical crack plane at the start and end points for the k^{th} cycle counted in STEP 3. Using these data, calculate the bending stress range, and the maximum, minimum, and mean stress for the k^{th} cycle. The algebraic signs of the stresses shall be used in all the calculations.

$$\Delta\sigma^{e}_{b,k} = \left| {}^{m}\sigma^{e}_{b,k} - {}^{n}\sigma^{e}_{b,k} \right| \tag{14.44}$$

$$\sigma_{max,k} = \max\left[\left({}^{m}\sigma^{e}_{m,k} + {}^{m}P_{c,k} + {}^{m}\sigma^{e}_{b,k} \right),\ \left({}^{n}\sigma^{e}_{m,k} + {}^{n}P_{c,k} + {}^{n}\sigma^{e}_{b,k} \right) \right] \tag{14.45}$$

$$\sigma_{min,k} = \min\left[\left({}^{m}\sigma^{e}_{m,k} + {}^{m}P_{c,k} + {}^{m}\sigma^{e}_{b,k} \right),\ \left({}^{n}\sigma^{e}_{m,k} + {}^{n}P_{c,k} + {}^{n}\sigma^{e}_{b,k} \right) \right] \tag{14.46}$$

$$\sigma_{mean,k} = \frac{\sigma_{max,k} + \sigma_{min,k}}{2} \tag{14.47}$$

2) STEP 4.2 – Calculate the elastic structural stress range $\Delta\sigma^{e}_{k}$ for the k^{th} cycle using Equation (14.48).

$$\Delta\sigma^{e}_{k} = \sigma_{max,k} - \sigma_{min,k} \tag{14.48}$$

3) STEP 4.3 – Calculate the elastic structural strain range $\Delta\varepsilon^{e}_{k}$ for the k^{th} cycle using Equation (14.49).

$$\Delta\varepsilon^{e}_{k} = \frac{\Delta\sigma^{e}_{k}}{E_{ya,k}} \tag{14.49}$$

4) STEP 4.4 – Calculate the pseudo-elastic structural strain range, $\Delta\varepsilon_{k}$ for the k^{th} cycle by solving the nonlinear algebraic Equation (14.50).

$$\Delta\varepsilon_{k} = \frac{\Delta\sigma^{e}_{k} \cdot \Delta\varepsilon^{e}_{k}}{E_{ya,k} \cdot \Delta\varepsilon_{k}} + 2\left(\frac{\Delta\sigma_{k}}{2K_{css} \cdot \Delta\varepsilon_{k}} \right)^{\frac{1}{n_{css}}} \tag{14.50}$$

Note that Equation (14.50) is derived from Neuber's rule expressed by Equation (14.51), see Annex 14C, and a model for the material hysteresis loop stress-strain curve given by Equation (14.52), see Annex 14B (i.e., Equation (14.50) is derived by substituting Equation(14.51) in Equation (14.52)).

$$\Delta\sigma_{k} \cdot \Delta\varepsilon_{k} = \Delta\sigma^{e}_{k} \cdot \Delta\varepsilon^{e}_{k} \tag{14.51}$$

$$\Delta\varepsilon_{k} = \frac{\Delta\sigma_{k}}{E_{ya,k}} + 2\left(\frac{\Delta\sigma_{k}}{2K_{css}} \right)^{\frac{1}{n_{css}}} \tag{14.52}$$

5) STEP 4.5 – Calculate the pseudo-elastic structural stress range $\Delta\sigma_{k}$ for the k^{th} cycle using Equation (14.53).

$$\Delta\sigma_{k} = E_{ya,k} \cdot \Delta\varepsilon_{k} \tag{14.53}$$

6) STEP 4.6 – Calculate the equivalent structural stress range parameter $\Delta S_{ess,k}$ for the k^{th} cycle using Equation (14.54).

$$\Delta S_{ess,k} = \frac{\Delta\sigma_k}{t_{ess}^{\left(\frac{2-m_{ss}}{2m_{ss}}\right)} \cdot I^{\frac{1}{m_{ss}}} \cdot f_{M,k}} \tag{14.54}$$

where,

$$m_{ss} = 3.6 \tag{14.55}$$

$$t_{ess} = 16\ mm\ (0.625\ in.) \qquad \left(for\ t \le 16\ mm\ (0.625\ in.)\right) \tag{14.56}$$

$$t_{ess} = t \qquad \left(for\ 16\ mm\ (0.625\ in.) < t < 150\ mm\ (6\ in.)\right) \tag{14.57}$$

$$t_{ess} = 150\ mm\ (6\ in.) \qquad \left(for\ t \ge 150\ mm\ (6\ in.)\right) \tag{14.58}$$

$$I^{\frac{1}{m_{ss}}} = \frac{1.23 - 0.364R_{b,k} - 0.17R_{b,k}^2}{1.007 - 0.306R_{b,k} - 0.178R_{b,k}^2} \tag{14.59}$$

$$R_{b,k} = \frac{\Delta\sigma_{b,k}^e}{\Delta\sigma_k^e} \tag{14.60}$$

$$R_k = \frac{\sigma_{min,k}}{\sigma_{max,k}} \tag{14.61}$$

If $\sigma_{mean,k} \ge 0.5S_{y,k}$, $\sigma_{\max,k} \ne 0$, $R_k > 0$, and $\Delta\sigma_k^e \le 2S_{y,k}$ are all true, then

$$f_{M,k} = \left(1 - R_k\right)^{\frac{1}{m_{ss}}} \tag{14.62}$$

Otherwise

$$f_{M,k} = 1.0 \tag{14.63}$$

Note that in Equation (14.54), for SI Units, the thickness, t, stress range, $\Delta\sigma_k$, and the equivalent structural stress range parameter, $\Delta S_{ess,k}$, are in mm, MPa, and $MPa/(mm)^{(2-m_{ss})/2m_{ss}}$, respectively. For US Customary Units, the thickness, t, stress range, $\Delta\sigma_k$, and the equivalent structural stress range parameter, $\Delta S_{ess,k}$, are in $inches$, ksi, and $ksi/(inches)^{(2-m_{ss})/2m_{ss}}$, respectively.

7) STEP 4.7 – Determine the permissible number of cycles, N_k, based on the equivalent structural stress range parameter for the k^{th} cycle computed in STEP 4.6 using the fatigue curve based on the materials of construction in Annex 14B.

8) STEP 4.8 – Calculate the fatigue damage for the k^{th} cycle using Equation (14.64) where the actual number of repetitions of the k^{th} cycle is n_k.

$$D_{f,k} = \frac{n_k}{N_k} \tag{14.64}$$

e) STEP 5 – Compute the accumulated fatigue damage using Equation (14.65). The location along the weld joint is suitable for continued operation if this equation is satisfied.

$$D_f = \sum_{k=1}^{M} D_{f,k} \le 1.0 \tag{14.65}$$

14.4.3.4.3 Assessment Procedure Modifications

The assessment procedure in paragraph 14.4.3.4.2 may be modified as shown below.

a) Multiaxial Fatigue – If the structural shear stress range is not negligible, i.e., $\Delta\tau_k^e > \Delta\sigma_k/3$, a modification should be made when computing the equivalent structural stress range. Two conditions need to be considered:

1) If $\Delta\sigma_k$ and $\Delta\tau_k^e$ are out of phase, the equivalent structural stress range $\Delta S_{ess,k}$ in Equation (14.54) is be replaced by:

$$\Delta S_{ess,k} = \frac{1}{F(\delta)}\left[\left(\frac{\Delta\sigma_k}{t_{ess}^{\left(\frac{2-m_{ss}}{2m_{ss}}\right)} \cdot I^{\frac{1}{m_{ss}}} \cdot f_{M,k}}\right)^2 + 3\left(\frac{\Delta\tau_k^e}{t_{ess}^{\left(\frac{2-m_{ss}}{2m_{ss}}\right)} \cdot I_\tau^{\frac{1}{m_{ss}}}}\right)^2\right]^{0.5} \tag{14.66}$$

where,

$$I_\tau^{\frac{1}{m_{ss}}} = \frac{1.23 - 0.364R_{b\tau,k} - 0.17R_{b\tau,k}^2}{1.007 - 0.306R_{b\tau,k} - 0.178R_{b\tau,k}^2} \tag{14.67}$$

$$\Delta\tau_{b,k}^e = \left|{}^m\tau_{b,k}^e - {}^n\tau_{b,k}^e\right| \tag{14.68}$$

$$\tau_{max,k} = \max\left[\left({}^m\tau_{m,k}^e + {}^m\tau_{b,k}^e\right),\ \left({}^n\tau_{m,k}^e + {}^n\tau_{b,k}^e\right)\right] \tag{14.69}$$

$$\tau_{min,k} = \min\left[\left({}^m\tau_{m,k}^e + {}^m\tau_{b,k}^e\right),\ \left({}^n\tau_{m,k}^e + {}^n\tau_{b,k}^e\right)\right] \tag{14.70}$$

$$\Delta\tau_k^e = \tau_{max,k} - \tau_{min,k} \tag{14.71}$$

$$R_{b\tau,k} = \frac{\Delta\tau_{b,k}^e}{\Delta\tau_k^e} \tag{14.72}$$

In Equation (14.66), $F(\delta)$ is a function of the out-of-phase angle, δ, between $\Delta\sigma_k$ and $\Delta\tau_k^e$ if both loading modes can be described by sinusoidal functions, or:

$$F(\delta) = \frac{1}{\sqrt{2}}\left[1 + \left[1 - \frac{12\cdot\Delta\sigma_k^2\cdot\left(\Delta\tau_k^e\right)^2\cdot\sin^2[\delta]}{\left(\Delta\sigma_k^2 + 3\left(\Delta\tau_k^e\right)^2\right)^2}\right]^{0.5}\right]^{0.5} \tag{14.73}$$

A conservative approach is to ignore the out-of-phase angle and recognize the existence of a minimum possible value for $F(\delta)$ in Equation (14.73) given by:

$$F(\delta) = \frac{1}{\sqrt{2}} \tag{14.74}$$

2) If $\Delta\sigma_k$ and $\Delta\tau_k^e$ are in-phase the equivalent structural stress range $\Delta S_{ess,k}$ is given by Equation (14.66) with $F(\delta) = 1.0$.

b) Weld Quality – If a defect exists at the toe of a weld that can be characterized as a crack-like flaw, i.e. undercut, and this defect exceeds the value permitted by the applicable construction code, then a reduction in fatigue life may be calculated by substituting the value of $I^{1/m_{ss}}$ in Equation (14.59) with the value given by Equation (14.75). In this equation, a is the depth of the crack-like flaw at the weld toe. Equation (14.75) is valid only when $a/t \le 0.1$. If $a/t > 0.1$, then a crack growth analysis in accordance with Part 9 is recommended.

$$I^{\frac{1}{m_{ss}}} = \frac{1.229 - 0.365R_{b,k} + 0.789\left(\frac{a}{t}\right) - 0.17R_{b,k}^2 + 13.771\left(\frac{a}{t}\right)^2 + 1.243R_{b,k}\left(\frac{a}{t}\right)^3}{1 - 0.302R_{b,k} + 7.115\left(\frac{a}{t}\right) - 0.178R_{b,k}^2 + 12.903\left(\frac{a}{t}\right)^2 - 4.091R_{b,k}\left(\frac{a}{t}\right)^3} \tag{14.75}$$

14.4.3.5 Ratcheting Assessment – Elastic Stress Analysis

14.4.3.5.1 Elastic Ratcheting Analysis Method

a) If the primary plus secondary equivalent stress range, $\Delta S_{n,k}$, satisfies Equation (14.76), then ratcheting will not occur and shakedown behavior is predicted.

$$\Delta S_{n,k} \le S_{PS} \tag{14.76}$$

c) The primary plus secondary equivalent stress range, $\Delta S_{n,k}$, is the equivalent stress range, derived from the highest value across the thickness of a section, of the combination of linearized general or local primary membrane stress plus primary bending stress plus secondary stress $(P_L + P_b + Q)$, produced by specified operating pressure and other specified mechanical loads and by general thermal effects. The effects of gross structural discontinuities but not of local structural discontinuities (stress concentrations) shall be included.

d) The maximum range of this equivalent stress is limited to S_{PS}. In the determination of the maximum primary plus secondary equivalent stress range, it may be necessary to consider the effects of multiple cycles where the total stress range may be greater than the stress range of any of the individual cycles. In this case, the value of S_{PS} may vary with the specified cycle, or combination of cycles, being considered since the temperature extremes may be different in each case. Therefore, care shall be exercised to assure that the applicable value of S_{PS} for each cycle, or combination of cycles, is used.

e) The allowable limit on the primary plus secondary stress range, S_{PS}, is determined as shown in Equation (14.77). In this equation, the material parameters are denoted as $(S_{UTS,k}, S_k, S_{y,k})$ to indicate that the constants are average values at the highest and lowest temperatures of the k^{th} cycle.

$$S_{PS} = \min\left[S_{UTS,k},\ \max\left[3S_k,\ 2S_{y,k}\right]\right] \tag{14.77}$$

14.4.3.5.2 Elastic Ratcheting Analysis Using the Bree Diagram

If Equation (14.76) is not satisfied, then the ratcheting assessment may be performed using the Bree Diagram. The use of the Bree Diagram permits alternating plasticity for the primary plus secondary equivalent stress range to occur in conjunction with an applied fatigue penalty factor, $K_{e,k}$ (see paragraph 14.4.3.2.2, STEPs 4.3 and 4.4). The procedure for evaluating ratcheting using the Bree Diagram is shown below. This procedure considers four loading types and can only be used with a linear primary and secondary stress range.

a) STEP 1 – Determine the type of loading. The four loading types are shown below. If the loading type does not match any of these four types, then proceed to paragraph 14.4.3.6.

1) Cyclic Load Type A – Fixed primary membrane stress and cyclic secondary stress (see Table 14.8 and Figure 14.19).

2) Cyclic Load Type B – Cyclic primary membrane stress and cyclic secondary stress that are in-phase (see Table 14.9 and Figure 14.20).

3) Cyclic Load Type C – Cyclic primary membrane stress and cyclic secondary stress that are out-of-phase (see Table 14.10 and Figure 14.21).

4) Cyclic Load Type D – Cyclic primary membrane stress and fixed secondary stress (see Table 14.11 and Figure 14.22).

b) STEP 2 – If the Cyclic Load Type is D, then ratcheting cannot occur and the assessment procedure is completed.

c) STEP 3 – Determine the yield strength at the off-load condition, typically the lowest temperature of the cycle, $S_{y-off\ load}$, and at the on-load condition, typically the highest temperature of the cycle, $S_{y-on\ load}$.

$$R_y = \frac{S_{y-on\ load}}{S_{y-off\ load}} \tag{14.78}$$

d) STEP 4 – Determine the ratio of the primary membrane stress to the yield strength at the lowest temperature of the cycle.

$$X = \left(\frac{P_m}{S_{y-off\ load}} \right) \tag{14.79}$$

Note: At structural discontinuities:

$$X = \left(\frac{P_L}{S_{y-off\ load}} \right) \tag{14.80}$$

e) STEP 5 – Determine the ratio of the secondary stress to the yield strength at the lowest average temperature of the cycle.

$$Y = \left(\frac{Q}{S_{y-off\ load}} \right) \tag{14.81}$$

f) STEP 6 – Based on the Cyclic Load Type from STEP 1, the R_y parameter from STEP 3, and the X and Y parameters from STEPs 4 and 5, respectively, determine the location of the point defined by the X and Y coordinates on the Bree Diagram.

1) If the location of the point is within the E, S1, or S2 regions, then ratcheting will not occur and shakedown behavior is predicted.

2) If the point falls within the P1, P2, or P3 regions, then cyclic plasticity is predicted for the primary plus secondary equivalent stress range and a penalty factor, $K_{e,k}$ (see paragraph 14.4.3.2.2, STEPs 4.3 and 4.4), is introduced into the fatigue analysis.

3) If the point falls within the ratcheting regions R1, R2 or R3, then ratcheting behavior is predicted.

Note: The definition of the regions in the Bree diagram are as follows:

- E – Elastic Region
- S1 – Shakedown Region 1
- S2 – Shakedown Region 2
- P1 – Cyclic Plasticity Region 1
- P2 – Cyclic Plasticity Region 2
- P3 – Cyclic Plasticity Region 3
- R1 – Ratcheting Region 1
- R2 – Ratcheting Region 2
- R3 – Ratcheting Region 3

g) STEP 7 – If ratcheting behavior is predicted from STEP 6, then the elastic-plastic ratcheting analysis in paragraph 14.4.3.6 may be used for the assessment of ratcheting.

14.4.3.6 Ratcheting Assessment – Elastic-Plastic Stress Analysis

14.4.3.6.1 Overview

The protection against ratcheting is evaluated using an elastic-plastic analysis by directly simulating the steady-state and cyclic loading conditions. If protection against ratcheting is satisfied, it may be assumed that progression of the stress-strain hysteresis loop along the strain axis cannot be sustained under cyclic loading; therefore, the hysteresis loop will stabilize. A separate check for plastic shakedown to alternating plasticity is not required.

14.4.3.6.2 Assessment Procedure

The following assessment procedure can be used to evaluate protection against ratcheting using elastic-plastic analysis.

a) STEP 1 – Develop a numerical model of the component including all relevant geometry characteristics. The model used for the analysis shall be selected to accurately represent the component geometry, boundary conditions, and applied loads.

b) STEP 2 – Define all relevant loads and applicable load cases (see Annex 2D).

c) STEP 3 – An elastic-perfectly plastic material model shall be used in the analysis. The von Mises yield function and associated flow rule shall be utilized. The yield strength defining the plastic limit shall be the minimum specified yield strength at temperature. The effects of non-linear geometry shall be considered in the analysis.

d) STEP 4 – Perform an elastic-plastic analysis for the applicable loading from STEP 2 for several repetitions of a loading event or, if more than one event is applied, of multiple events that are selected to produce the highest likelihood of ratcheting. If there is uncertainty relating to determination of the loading events that produce the highest likelihood of ratcheting, a sensitivity study is recommended.

e) STEP 5 – The ratcheting criteria below should be evaluated after application of a minimum of three complete repetitions of the cycle. Additional cycles may need to be applied to demonstrate convergence. If any one of the following conditions is met, the ratcheting criteria are satisfied. If any of the criteria shown below are satisfied, the component will not be subject to ratcheting during service.

1) There is no plastic action (i.e., zero plastic strains incurred) in the component.

2) There is an elastic core in the primary-load-bearing boundary of the component.

3) There is not a permanent change in the overall dimensions of the component under cyclic loading conditions. This can be demonstrated by developing a plot of relevant component dimensions versus time between the last and the next to the last cycles.

14.4.3.7 Ratcheting Assessment – Non-Integral Connections

Screwed-on caps, screwed-in plugs, shear ring closures, and breech lock closures are examples of non-integral connections that are subject to failure by bell-mouthing or other types of progressive deformation. If any combination of applied loads produces yielding, such joints are subject to ratcheting because the mating members may become loose at the end of each complete operating cycle and may start the next cycle in a new relationship with each other, with or without manual manipulation. Additional distortion may occur in each cycle so that interlocking parts, such as threads, can eventually lose engagement. Therefore, primary plus secondary equivalent stresses that produce slippage between the parts of a non-integral connection in which disengagement could occur because of progressive distortion, shall be limited to the minimum specified yield strength at temperature, S_y, or evaluated using the procedure in paragraph 14.4.3.5.2.

14.4.3.8 Level 2 Assessment Results

If the component does not meet the Level 2 Assessment requirements, then the following, or combinations thereof, can be considered:

a) Conduct a Level 3 Assessment.

b) Rerate or repair the component. Note that the accumulated component fatigue damage may need to be monitored.

c) Replace the component.

14.4.4 Level 3 Assessment

14.4.4.1 Overview

a) The Level 3 Assessment determines allowable fatigue cycles for a component and loading history using a multiaxial strain-life equation with a mean stress correction, see Figure 14.23 and Figure 14.24, respectively, in combination with a critical plane approach. The critical plane approach resolves the stress-strain state at a given point on several candidate planes. Fatigue damage is calculated on each candidate plane using the strain-life equation, and the plane with the maximum damage identifies the critical plane and the overall fatigue damage for the given point.

b) The results from an elastic stress analysis or elastic-plastic stress analysis may be used in combination with a critical plane approach, see paragraphs 14.4.4.2 and 14.4.4.3, respectively. If an elastic analysis is used, the elastic strains are corrected for cyclic plasticity using a multiaxial Neuber correction, see Annex 14C, based on a cyclic stress strain curve, see Annex 14B. If an elastic-plastic analysis is performed, see paragraph 14.4.3.3, strain results are post-processed directly.

c) The complexity of post-processing required in the critical plane approach is justified because this method shows improved correlation with fatigue test results as compared to the Method A and Method B in Level 2.

d) The use of other recognized codes and standards for fatigue evaluate is permitted in Method C.

14.4.4.2 Method A – Elastic Stress Analysis and Critical Plane Approach

The following procedure may be used to evaluate protection against failure due to cyclic loading for a component the results from an elastic stress analysis in combination with a critical plane approach. A flow diagram for the fatigue damage calculation based on a multiaxial strain-life equation in combination with a critical plane approach is shown in Figure 14.25. A detailed description of the procedure including software routines is provided in Annex 14C.

a) STEP 1 – Determine a loading time history as defined in paragraph 14.3.3. The loading time history should include all significant operating loads and events that are applied to the component and consider both past and future planned operation.

b) STEP 2 – Perform an elastic stress analysis of the component based on the loading time history from STEP 1. The stress tensor shall be determined at each location in the component at each point identified in the loading time history. In the elastic stress analysis, the loadings may be analyzed independently and assigned sequences in, or by, post-processing.

c) STEP 3 – Correct the stress and strain tensor for plasticity using a multiaxial plasticity Neuber correction, see Annex 14C, paragraph 14C.2.2.

d) STEP 4 – Select a candidate critical plane and calculate the maximum shear strain and associated normal strain on the candidate plane for all points in the load time history using the results from STEP 3.

e) STEP 5 – Determine the cyclic stress and strain ranges at the location under consideration based on the elastic stress analysis in STEP 2 and the cycle counting methods in Annex 14C. Define the total number of cyclic stress ranges in the loading time history as M.

f) STEP 6 – Perform the following for each cyclic stress range in the loading time history: $k \leq M$.

1) STEP 6.1 – Calculate the maximum shear strain range, $\Delta\gamma_{\max,k}$, and the associated normal strain range, $\Delta\varepsilon_N$, on the current candidate plane.

2) STEP 6.2 – Determine the permissible number of reversals (half-cycles), $N_{f,k}$, for each cycle identified in STEP 5 using the Brown-Miller strain-life equation, Equation (14.82).

$$\frac{\Delta\gamma_{\max,k}}{2}+\frac{\Delta\varepsilon_{N,k}}{2}=1.65\left(\frac{\sigma'_{f,k}-\sigma_{N-mean,k}}{E_{ya,k}}\right)\left(2N_{f,k}\right)^{b_k}+1.75\varepsilon'_{f,k}\left(2N_{f,k}\right)^{c_k} \quad (14.82)$$

In Equation (14.82), the strain-life equation parameters are denoted as $\left(\sigma'_{f,k},\ \varepsilon'_{f,k},\ b_k,\ c_k\right)$ to indicate that the constants are average values at the highest and lowest temperatures of the k^{th} cycle (see Annex 14B). Equation (14.82) directly incorporates both the elastic and elastic-plastic Poisson's ratio; therefore, a further correction is not required. Note that if the strain-life equation constants have been determined from data or a fatigue curve that already includes the effect of mean stress, the following version of the Brown-Miller equation is recommended:

$$\frac{\Delta\gamma_{\max,k}}{2}+\frac{\Delta\varepsilon_{N,k}}{2}=1.65\left(\frac{\sigma'_{f,k}}{E_{ya,k}}\right)\left(2N_{f,k}\right)^{b_k}+1.75\varepsilon'_{f,k}\left(2N_{f,k}\right)^{c_k} \quad (14.83)$$

The effect of this change is illustrated in Figure 14.24 by the dashed line corresponding to mean stress-shifted elastic region slope. Other strain-life equations may be used depending on the availability of model parameters for the material and temperatures being evaluated.

3) STEP 6.3 – Determine the fatigue damage for the k^{th} cycle, where the actual number of repetitions of the k^{th} cycle is n_k using Equation (14.84). In computing the fatigue damage for the k^{th} cycle, consideration should be given to the effects of size, surface finish, environment and other factors that may affect the fatigue life. Guidance on fatigue knockdown factors or a margin on cycles, f_{ND}, to account for these affects are provided in Table 14.12. The fatigue knockdown factor should always be greater than or equal to one.

$$D_{f,k} = \frac{n_k}{\left(\frac{N_{f,k}}{f_{ND}}\right)} \qquad \left(f_{ND} \geq 1.0\right) \tag{14.84}$$

g) STEP 7 – Compute the accumulated fatigue damage for the loading time history identified in STEP 1 using Equation (14.85). The location in the component is acceptable for continued operation if this equation is satisfied.

$$D_f = \sum_{k=1}^{M} D_{f,k} \leq 1.0 \tag{14.85}$$

h) STEP 8 – Go to STEP 4 and evaluate the next candidate critical plane. If all critical planes have been evaluated, proceed to STEP 8.

i) STEP 9 – Determine the maximum fatigue damage for all critical planes.

j) STEP 10 – Repeat STEPs 3 through 8 for each location that is subject to a fatigue evaluation.

14.4.4.3 Method B – Elastic-Plastic Stress Analysis and Critical Plane Approach

The following procedure may be used to evaluate protection against failure due to cyclic loading for a component using the results from an elastic-plastic stress analysis in combination with a critical plane approach.

a) STEP 1 – Determine a loading time history as defined in paragraph 14.3.3. The loading time history should include all significant operating loads and events that are applied to the component and consider both past and future planned operation.

b) STEP 2 – Perform an elastic-plastic stress analysis of the component based on the loading time history from STEP 1. The elastic and plastic strain tensor shall be determined at each location in the component at each point identified in the loading time history. The loading shall be analyzed in the sequence corresponding to the loading time history in STEP 1.

c) STEP 3 – Select a candidate critical plane and calculate the maximum shear strain and associated normal strain on the candidate plane for all points in the load time history using the results from STEP 2.

d) STEP 4 – Determine the cyclic strain ranges at the location under consideration based on the elastic-plastic stress analysis in STEP 2 and the cycle counting methods in Annex 14C. Define the total number of cyclic stress ranges in the loading time history as M.

e) STEP 5 – Perform the following for each cyclic stress range in the loading time history: $k \leq M$, and perform STEPs 6.1 through 6.3 of paragraph 14.4.4.2.

f) STEP 6 – Compute the accumulated fatigue damage for the loading time history identified in STEP 1 using Equation (14.86). The location in the component is acceptable for continued operation if this equation is satisfied.

$$D_f = \sum_{k=1}^{M} D_{f,k} \leq 1.0 \tag{14.86}$$

g) STEP 7 – Go to STEP 3 and evaluate the next candidate critical plane. If all critical planes have been evaluated, proceed to STEP 8.

h) STEP 8 – Determine the maximum fatigue damage for all critical planes.

i) STEP 9 – Repeat STEPs 3 through 8 for each location that is subject to a fatigue evaluation.

14.4.4.4 Method C – Recognized Codes and Standards

a) Fatigue assessment methods from recognized codes and standards may be used. The assumptions and technical basis of these methods shall be reviewed to ensure their applicability to the materials of construction and the loading time history being evaluated.

   1) A remaining life assessment is implicitly included in the Level 2 and Level 3 Assessment procedures. If the component is subject to corrosion, the fatigue assessment procedures in Level 2 and Level 3 shall be modified to include the effects of metal loss.

   2) If the loading time history is unknown or uncertain, alternate loading time histories that bound the operating conditions of the component should be evaluated using the Level 2 or Level 3 Assessment procedures. This sensitivity analysis on the loading time history shall be included in the assessment results.

14.5 Remaining Life Assessment

14.5.1 Included in Level 2 and Level 3 Assessments

A remaining life assessment is implicitly included in the Level 2 and Level 3 Assessment procedures. If the component is subject to corrosion, the fatigue assessment procedures in Level 2 and Level 3 shall be modified to include the effects of metal loss.

14.5.2 Loading Time History

If the loading time history is unknown or uncertain, alternate loading time histories that bound the operating conditions of the component should be evaluated using the Level 2 or Level 3 Assessment procedures. This sensitivity analysis on the loading time history shall be included in the assessment results.

14.6 Remediation

14.6.1 Overview

Remediation of fatigue should consider the origin of fatigue. Remediation may also depend on component or equipment geometry and whether other damage types are present (e.g., weld misalignment or bulges). The major sources of energy that may contribute to fatigue include:

a) Periodic Mechanical

b) Acoustic

c) Pulsation

d) Slug Flow

e) Vortex Shedding

f) Hydraulic Transients

g) Periodic or Transient Pressure

h) Periodic or Transient Thermal

Table 14.13 contains a description of the energy source and the characteristics (magnitude and frequency) of vibration or stresses that may result in fatigue. Figures 14.22 to 14.29 illustrate some of the concepts involved. Methods to remediate fatigue discussed herein include:

a) Removal or reduction of the driving energy source

b) Changes to the constraint or restraint of the equipment or its components

c) In the case of thermally-induced fatigue, reduction of the temperature differentials or gradients.

14.6.2 Removal or Reduction of the Driving Energy Source or Forces.

Removal or reduction of the driving energy source, when possible, is one of the most effective methods to remediate fatigue. Table 14.14 provides a discussion for each of the energy sources, their applicability, and methods of removing or reducing the driving energy source as a remediation technique. The applicability of this remediation is often restricted by the limits on the ability to make changes to process parameters.

14.6.3 Alteration of Component Constraint, Mechanical Design, or Weld Quality

Due to the limit on changes to process parameters, it is not always possible to remove or reduce the driving energy or forces. In many such cases changes to the constraint, the mechanical design, or the weld quality, particularly surface treatments, can be used to limit the stress or to alter the natural frequency of the components away from the driving energy frequency. Table 14.15 provides a discussion for each of the energy sources, their applicability, and methods of altering component constraint or mechanical design changes as a remediation technique.

a) The two major types of constraint available are rigid or flexible. These constraints limit displacements in a different manner. Rigid constraints are usually stiffer than the vibrating component and apply a force to the component that reduces all displacements to small values. Figure 14.48 shows a rigid strut with ball joints to permit lateral displacement. Figure 14.49 shows two-plane gussets at small bore connections such as vents or drains, typically used downstream of rotating or reciprocal machinery. Flexible constraints consist of force-displacement types (e.g., springs) or force-velocity types (e.g., viscous dampers). Figure 14.50 shows a typical viscous snubber. The application of the type of constraint often depends on the component thermal loading. Since constraint of thermal displacements can also lead to fatigue, the flexible type of constraints may be more suitable for remediating fatigue in components that could experience fatigue from non-thermal and thermal energy sources.

b) The constraint forces can often be estimated through structural modeling, with the constraint modeled explicitly or implicitly by restricting displacements at the attachment location. Where constraint is used to alter the structural natural frequency, the constraint should seek to obtain a ratio of natural frequency to the driving frequency of less than 0.75 or greater than 1.4. To avoid fatigue at the constraint location, best practice calls for attaching the constraint using non-welded clamps, or pads welded to the component that distribute the load so that the stresses in the attachment welds are low.

c) Table 14.5 shows the effect of surface treatment, and Table 14.6 the effect of weld inspection on preventing fatigue at welds. For welded locations these are applicable regardless of the energy source.

14.6.4 Reduction of Temperature Differentials or Gradients

In some cases where thermal differentials or gradients produce stresses that lead to fatigue, isolation of the components using insulation, thermal sleeves, or reduction in mechanical stiffness may remediate the fatigue. This is a special application of reduction of the driving force. In some cases, (e.g., piping systems subject to fluid induced vibration), thermal and mechanical fatigue may both be present and need consideration. Table 14.16 provides a discussion for each of the energy sources, of the applicability and methods of thermal fatigue remediation techniques.

14.7 In-Service Monitoring

Where uncertainty exists regarding the remaining life of a component subjected to the potential for fatigue damage, or the effectiveness of a remediation action, in-service monitoring may be required. The methods typically available for in-service monitoring are shown below. A brief description of each method appears in Table 14.17. The applicability and effectiveness of each of these monitoring methods as they relate to the type of energy causing the fatigue appears in Table 14.18.

a) Visual Inspection

b) Accelerometers

c) Proximity Probes

d) Strain Gauges

e) Periodic UT, PT, MT, or Eddy Current examination

f) Thermocouples

g) Pressure Gauges or Pressure Transducers

14.8 Documentation

14.8.1 General

The documentation of the FFS Assessment should include the information cited in Part 2, paragraph 2.8. Additional documentation requirements are essential because of the complexity associated with the assessment. This information should be permanently stored with the equipment record files.

14.8.2 Assessment Level

The assessment level shall be identified. In addition, any deviations, modifications, and assumptions used in the assessment shall be documented.

14.8.3 Loading Time History

The loading time history showing the historical and assumed future start-up, normal, upset, and shut-down conditions should be reported. In addition, any additional loads and stresses considered in the assessment, e.g., stresses from supplement loads, thermal gradients, and residual stresses.

14.8.4 Material Properties

The material specification for the component shall be identified. Material properties included in the analysis shall be documented including:

a) Physical properties, e.g., Young's Modulus, expansion coefficient, thermal conductivity, and thermal diffusivity as a function of temperature,

b) Strength parameters, yield strength and ultimate tensile stress as a function of temperature,

c) Cyclic stress-strain curve as a function of temperature, and

d) Fatigue curve or fatigue curve parameters as a function of temperature.

14.8.5 Stress Analysis Results

The stress analysis method used to compute the stress results shall be documented.

14.8.6 Assessment Results

For the Level 1 Assessment, the results of the screening assessment shall be documented. For the Level 2 and Level 3 the total number of cycles and the remaining life shall be documented. Factors used in determining the alternating stress, (e.g., the fatigue strength reduction factor), as part of the calculation of the permitted number of cycles shall be recorded.

14.8.7 Remaining Life Assessment

If the loading time history is unknown or uncertain, the sensitivity analysis on the loading time history shall be documented.

14.8.8 Remediation Methods

The incorporation of any remediation methods and the effects on the remaining life assessment shall be documented.

14.8.9 In-Service Monitoring

If an in-service monitoring system is instituted, then the following documentation should be kept with the equipment files:

a) Specification for the system,

b) Procedures for installation of the system,

c) System validation and calibration,

d) Procedures for recording data,

e) All data readings while the component is in-service, and

f) Analysis results based on in-service data to justify continued operation of the component.

14.9 Nomenclature

a the depth of a flaw at a weld toe.

α average of the thermal expansion coefficient values for the material at two adjacent points.

α_1 thermal expansion coefficient for material 1 at the assessment temperature.

α_2 thermal expansion coefficient for material 2 at the assessment temperature.

$\alpha_{a,k}$ average of the thermal expansion coefficient values for the material at the highest and lowest temperatures of the k^{th} cycle.

b_k strain-life equation parameter for the k^{th} cycle.

β angle for reaction force from slug flow.

C_γ coefficient in elastic and plastic effective strain equations. $C = 1.5$ if shear strains are engineering strain values and $C = 6.0$ is the shear strains are tensor values.

C_H $C_H = 0.5$ if the cycles counted with the cycle counting method correspond to half-cycles, i.e., the Wang-Brown Cycle Counting (WBCC) method (see Annex 14C, paragraph 14C.4). $C_H = 1.0$ if the cycles counted with the cycle counting method correspond to full-cycles, i.e., the Rainflow Cycle Counting (RFC) methods (see Annex 14C, paragraph 14C.3).

c_k strain-life equation parameter for the k^{th} cycle.

C_m parameter in the backstress equation.

C_D drag coefficient.

C_L lift coefficient.

D diameter.

D_f cumulative fatigue damage.

$D_{f,k}$ fatigue damage for the k^{th} cycle.

D_{FP} damage associated with the full-range pressure cycles.

D_{ML} damage associated with the mechanical loads, excluding pressure but including piping reactions.

D_{PN} damage associated with the pressure fluctuation cycles during normal operation.

D_{TM} damage associated with the temperature differences for components having different coefficients of thermal expansion.

D_{TN} damage associated with the temperature differences during startup and shutdown.

D_{TR} damage associated with the temperature differences during normal operation.

$\Delta\varepsilon$ total strain range.

$\Delta\varepsilon_k$ pseudo elastic strain range at the point under evaluation for the k^{th} cycle.

$\Delta\varepsilon_N$ normal strain range on the critical plane.

$\Delta\varepsilon_{N,k}$ normal strain range on the critical plane for the k^{th} cycle.

$\Delta\varepsilon_k^e$ elastically calculated structural strain range at the point under evaluation for the k^{th} cycle.

$\Delta\varepsilon_{t,k}$ equivalent strain range for the k^{th} cycle, computed using the total strain less the free thermal strain.

$\Delta\varepsilon_{peq,k}$ equivalent plastic strain range for the k^{th} loading condition or cycle.

$\Delta\varepsilon_{eff,k}$ effective strain range for the k^{th} cycle.

$\Delta\gamma_N$ shear strain range on the critical plane.

$\Delta\gamma_{\max,k}$ maximum shear strain range on the critical plane for the k^{th} cycle.

$\Delta e_{ij,k}$ change in elastic strain range components at the point under evaluation for the k^{th} loading condition or cycle. Note that the shear strains typically output from a finite element analysis are engineering strains (i.e., not tensor strains).

$\Delta p_{ij,k}$ change in plastic strain range components at the point under evaluation for the k^{th} loading condition or cycle. Note that the shear strains typically output from a finite element analysis are engineering strains (i.e., not tensor strains).

ΔP_N maximum design range of pressure associated with $N_{\Delta P}$.

ΔS_{ij} total stress tensor increment.

ΔS_{ij}^{e} elastic stress tensor increment.

$\Delta S_{n,k}$ primary plus secondary equivalent stress range.

$\Delta S_{P,k}$ range of primary plus secondary plus peak equivalent stress for the k^{th} cycle.

$\Delta S_{P-LT,k}$ range of equivalent primary plus secondary plus peak stress minus the local thermal stress for the k^{th} cycle.

$\Delta S_{LT,k}$ local thermal equivalent stress for the k^{th} cycle.

ΔS_{ess} equivalent structural stress range.

$\Delta S_{ess,k}$ equivalent structural stress range for the k^{th} cycle.

ΔS_{ML} linearized equivalent stress range computed from the specified full range of mechanical loads, excluding pressure but including piping reactions.

ΔT operating temperature range.

ΔT_A maximum range of temperature difference between any two adjacent points of the component.

ΔT_{AB} temperature difference between any two adjacent points of the component at a given point in time.

ΔT_T twice the difference between the maximum and minimum temperature for the defined cycle. Note, using the difference between the maximum and minimum temperatures for the defined cycle is a more conservative assumption; however, it simplifies the calculation if ΔT_A is used.

ΔT_E change in metal temperature difference between any two adjacent points of the component.

ΔT_M maximum range of temperature difference between any two adjacent points during normal operation for components fabricated from different materials of construction. ΔT_N maximum range of temperature difference between any two adjacent points of the component during startup and shutdown.

ΔT_R maximum range of temperature difference between any two adjacent points of the component during normal operation, excluding startups and shutdowns.

$\Delta\sigma_i$ stress range associated with the principal stress in the i^{th}-direction.

$\Delta\sigma_{ij}$ total stress tensor range.

$\Delta\sigma_{ij}^{e}$ elastic stress tensor range.

$\Delta\sigma_k$ pseudo elastic stress range at the point under evaluation for the k^{th} cycle.

$\Delta\sigma_k^e$ elastically calculated structural stress range at the point under evaluation for the k^{th} cycle.

$\Delta\sigma_{b,k}^e$ elastically calculated structural bending stress range at the point under evaluation for the k^{th} cycle.

$\Delta\sigma_{ij,k}$ stress tensor range at the point under evaluation for the k^{th} cycle.

$\Delta\sigma_{ij,k}^{LT}$ local thermal stress tensor range at the point under evaluation for the k^{th} cycle.

$\Delta\sigma_{m,k}^e$ elastically calculated structural membrane stress range at the point under evaluation for the k^{th} cycle.

$\Delta\tau_k^e$ elastically calculated structural shear stress range at the point under evaluation for the k^{th} cycle.

$\Delta\tau_{m,k}^e$ elastically calculated bending component of the structural shear stress range at the point under evaluation for the k^{th} cycle.

$\Delta\tau_{m,k}^e$ elastically calculated membrane component of the structural shear stress range at the point under evaluation for the k^{th} cycle.

ΔV change in velocity.

δ out-of-phase angle between $\Delta\sigma_k$ and $\Delta\tau_k$ for the k^{th} cycle.

${}^{m}e_{ij,k}$ elastic strain tensor at the location under evaluation at time point ${}^{m}t$ for the k^{th} cycle.

${}^{n}e_{ij,k}$ elastic strain tensor at the location under evaluation at time point ${}^{n}t$ for the k^{th} cycle.

E_t Young's modulus of the tube at the assessment temperature.

E_y Young's modulus at the assessment temperature.

$E_{ya,k}$ average of the modulus of elasticity values for the material at the highest and lowest temperatures of the k^{th} cycle.

E_{y1} Young's Modulus of material 1 at the assessment temperature.

E_{y2} Young's Modulus of material 2 at the assessment temperature.

E_{ym} average of the Young's Modulus values for the material at two adjacent points.

ε_{ij} total strain tensor.

ε_{ij}^{e} elastic strain tensor.

ε_{ij}^{ep} elastic plus plastic or total strain tensor.

$\varepsilon'_{f,k}$ strain-life equation parameter for the k^{th} cycle.

f frequency.

$f_{M,k}$ mean stress correction factor for the k^{th} cycle.

F force.

$F(\delta)$ a fatigue modification factor based on the out-of-phase angle between $\Delta\sigma_k$ and $\Delta\tau_k$.

H_c stress concentration factor to adjust the stress for a nozzle connection in a head or toriconical shell transition, used in the Method C fatigue screening, see Table 14.3.

I correction factor used in the structural stress evaluation.

f_{ND} fatigue knockdown factor.

I_τ correction factor used in the structural shear stress evaluation.

K bulk modulus.

K_f fatigue strength reduction factor used to compute the cyclic stress amplitude or range.

K_{fc} fatigue strength reduction factor used in the Method C fatigue screening, see Table 14.3.

K_{css} parameter for the cyclic stress-strain curve.

$K_{e,k}$ fatigue penalty factor for the k^{th} cycle.

$K_{v,k}$ plastic Poisson's ratio adjustment factor for the local thermal and thermal bending stresses for the k^{th} cycle.

L length between points used in the fatigue screening analysis or the length of a pipe, as applicable.

M total number of stress ranges at a point derived from the cycle counting procedure, or the applied net-section bending moment, as applicable.

m material constant used for the fatigue knock-down factor in the simplified elastic-plastic analysis.

m_{ss} exponent used in a fatigue analysis based on the structural stress.

m_2 strain hardening exponent.

μ dynamic viscosity.

n material constant used for the fatigue knock-down factor in the simplified elastic-plastic analysis; a parameter to compute the deviation from a true circle; a harmonic number.

n_k actual number of repetitions of the k^{th} cycle.

n_{css} material parameter for the cyclic stress-strain curve model.

N number of cycles.

N_f number of cycles to failure.

$N_{f,k}$ number of cycles to failure for the k^{th} cycle.

N_k permissible number of cycles for the k^{th} cycle.

$N_{\Delta FP}$ design number of full-range pressure cycles including startup and shutdown.

$N_{\Delta P}$ number of significant cycles associated with ΔP_N.

$N_{\Delta PO}$ expected number of operating pressure cycles in which the range of pressure variation exceeds 20% of the design pressure for integral construction or 15% of the design pressure for non-integral construction.

$N_{\Delta S}$ number of significant cycles associated with ΔS_{ML}.

$N_{\Delta TE}$ number of cycles associated with ΔT_E.

$N_{\Delta TM}$ number of significant cycles associated with ΔT_M.

$N_{\Delta TN}$ number of significant cycles associated with ΔT_N.

$N_{\Delta TR}$ number of significant cycles associated with ΔT_R.

$N[S_{alt}]$ a function to determine the number of cycles from the applicable smooth bar fatigue curve evaluated at stress amplitude S_a.

$N[\Delta S_{ess}]$ a function to determine the number of cycles from the applicable smooth bar fatigue curve evaluated at the equivalent structural stress range, ΔS_{ess}.

ν Poisson's ratio.

ν_p Poisson's ratio adjusted for plasticity.

$p_{ij,k}$ plastic strain tensor for the k^{th} cycle.

${}^m p_{ij,k}$ plastic strain tensor at the location under evaluation at time point ${}^m t$ for the k^{th} cycle.

${}^n p_{ij,k}$ plastic strain tensor at the location under evaluation at time point ${}^n t$ for the k^{th} cycle.

P component design pressure, $MAWP$ or reduced $MAWP$. Note that the pressure used to determine the fatigue damage is based on the actual or operating pressure defined in the loading time-history.

P_b primary bending equivalent stress.

$^{n}P_{c,k}$ crack face pressure at time ^{n}t for the k^{th} cycle for use in the Method C fatigue analysis. If the weld toe undercut is on a surface subject to pressure loading, then this value is equal to the pressure from the load history. If the weld toe undercut is on a surface not subject to pressure loading, then this value is set to zero. If the pressure is zero, then the crack face pressure is zero.

$^{m}P_{c,k}$ crack face pressure at time ^{m}t for the k^{th} cycle for use in the Method C fatigue analysis. If the weld toe undercut is on a surface subject to pressure loading, then this value is equal to the pressure from the load history. If the weld toe undercut is on a surface not subject to pressure loading, then this value is set to zero. If the pressure is zero, then the crack face pressure is zero.

P_L local primary membrane equivalent stress.

P_m general primary membrane equivalent stress.

Q secondary bending equivalent stress.

R inside radius measured normal to the surface from the mid-wall of the shell to the axis of revolution, or the ratio of the minimum stress in the k^{th} cycle to the maximum stress in the k^{th} cycle, as applicable.

R_y ratio of $S_{y-on\ load}$ to $S_{y-off\ load}$.

ρ fluid density.

R_{HS} radius of hot spot or heated area within a plate.

R_b bend radius.

R_k stress ratio for the k^{th} cycle.

$R_{b,k}$ ratio of the bending stress to the membrane plus bending stress.

$R_{b\tau,k}$ ratio of the bending component of the shear stress to the membrane plus bending component of the shear stress.

RSF computed remaining strength factor.

S allowable membrane stress from the applicable construction code at the design temperature; or the computed equivalent stress; or the elastic section modulus of full shell cross section, as applicable.

$S_{ess}\left[\Delta\sigma\right]$ a function to compute the equivalent structural stress range as a function of the applied stress range.

S_k average of the allowable membrane stress values for the material at the highest and lowest temperatures during the operational cycle.

$S_{a,k}$ value of alternating stress amplitude obtained from the applicable design fatigue curve for the specified number of cycles of the k^{th} cycle.

S_{alt} alternating equivalent stress amplitude.

$S_{alt,k}$ alternating equivalent stress amplitude for the k^{th} cycle.

S_{as} stress amplitude from the applicable smooth bar design fatigue curve (see Annex 14B) evaluated at 10^6 cycles.

S_n Strouhal number.

S_{PS} allowable limit on the primary plus secondary stress range.

$S_{y-off\ load}$ yield strength at the unloaded condition.

$S_{y-on\ load}$ yield strength at the loaded condition.

$S_{y,k}$ average of the minimum specified yield strength values for the material at the highest and lowest temperatures during the operational cycle.

$S_{UTS,k}$ average of the ultimate tensile strength values for the material at the highest and lowest temperatures during the operational cycle.

SCF_{ij} stress concentration value for each stress component.

σ_e von Mises stress.

$\sigma_{e,k}$ von Mises stress for the k^{th} loading condition.

$\sigma_{max,k}$ maximum stress in the k^{th} cycle.

$\sigma_{mean,k}$ mean stress in the k^{th} cycle.

$\sigma_{min,k}$ minimum stress in the k^{th} cycle.

σ_{ys} yield strength of material at the assessment temperature.

$\sigma_{ij,k}$ stress tensor at the point under evaluation for the k^{th} cycle.

$\sigma'_{f,k}$ strain-life equation parameter for the k^{th} cycle.

σ_b^p bending stress from primary loads.

σ_m^p membrane stress from primary loads.

$\sigma_{ij,k}^{LT}$ stress tensor due to local thermal stress at the location and time point under evaluation for the k^{th} cycle.

${}^m\sigma_{ij,k}$ stress tensor at the location under evaluation at time point ${}^m t$ for the k^{th} cycle.

${}^n\sigma_{ij,k}$ stress tensor at the location under evaluation at time point ${}^n t$ for the k^{th} cycle.

${}^m\sigma_{ij,k}^{LT}$ stress tensor due to local thermal stress at the location under evaluation at time point ${}^m t$ for the k^{th} cycle.

${}^{n}\sigma_{ij,k}^{LT}$ stress tensor due to local thermal stress at the location under evaluation at time point ${}^{n}t$ for the k^{th} cycle.

${}^{m}\sigma_{ij,k}^{MB}$ linearized membrane plus bending stress components at the location under evaluation at time point ${}^{m}t$ for the k^{th} cycle.

${}^{n}\sigma_{ij,k}^{MB}$ linearized membrane plus bending stress components at the location under evaluation at time point ${}^{n}t$ for the k^{th} cycle.

${}^{m}\sigma_{b,k}^{e}$ elastically calculated bending stress normal to the hypothetical crack plane at the location under evaluation at time point ${}^{m}t$ for the k^{th} cycle.

${}^{n}\sigma_{b,k}^{e}$ elastically calculated bending stress normal to the hypothetical crack plane at the location under evaluation at time point ${}^{n}t$ for the k^{th} cycle.

${}^{m}\sigma_{m,k}^{e}$ elastically calculated membrane stress normal to the hypothetical crack plane at the location under evaluation at time point ${}^{m}t$ for the k^{th} cycle.

${}^{n}\sigma_{m,k}^{e}$ elastically calculated membrane stress normal to the hypothetical crack plane at the location under evaluation at time point ${}^{n}t$ for the k^{th} cycle.

$\sigma_{1,k}$ principal stress in the 1-direction for the k^{th} loading condition.

$\sigma_{2,k}$ principal stress in the 2-direction for the k^{th} loading condition.

$\sigma_{3,k}$ principal stress in the 3-direction for the k^{th} loading condition.

t thickness of the component.

t_{ess} equivalent structural stress effective thickness.

T temperature.

T_{avg} average temperature.

T_b linear portion of temperature distribution.

T_p nonlinear portion of temperature distribution.

$T_{max,k}$ maximum temperature in the k^{th} cycle.

${}^{m}\tau_{b,k}^{e}$ elastically calculated bending component of shear stress parallel to the hypothetical crack plane at the location under evaluation at time point ${}^{m}t$ for the k^{th} cycle.

${}^{n}\tau_{b,k}^{e}$ elastically calculated bending component of shear stress parallel to the hypothetical crack plane at the location under evaluation at time point ${}^{n}t$ for the k^{th} cycle.

${}^{m}\tau_{m,k}^{e}$ elastically calculated membrane component shear stress parallel to the hypothetical crack plane at the location under evaluation at time point ${}^{m}t$ for the k^{th} cycle.

$^{n}\tau^{e}_{m,k}$ elastically calculated membrane component shear stress parallel to the hypothetical crack plane at the location under evaluation at time point ^{n}t for the k^{th} cycle.

θ bend angle.

V velocity.

X ratcheting parameter.

Y ratcheting parameter.

14.10 References

References for this Part are provided in Annex 14A – *Technical Basis and Validation – Assessment of Fatigue Damage*.

14.11 Tables

Table 14.1 – Temperature Factors for Fatigue Screening Criteria for Method B

Metal Temperature Differential		Temperature Factor for Fatigue Screening Criteria
°C	°F	
28 or less	50 or less	0
29 to 56	51 to 100	1
57 to 83	101 to 150	2
84 to 139	151 to 250	4
140 to 194	251 to 350	8
195 to 250	351 to 450	12
Greater than 250	Greater than 450	20

Notes:

1. If the weld metal temperature differential is unknown or cannot be established, a value of 20 shall be used.
2. As an example, illustrating the use of this table, consider a component subject to metal temperature differentials for the following number of thermal cycles.

Temperature Differential	Temperature Factor Based on Temperature Differential	Number of Thermal Cycles
28°C (50°F)	0	1000
50°C (90°F)	1	250
222°C (400°F)	12	5

The effective number of thermal cycles due to changes in metal temperature is:

$$N_{\Delta TE} = 1000(0) + 250(1) + 5(12) = 310\ cycles$$

Table 14.2 – Fatigue Screening Criteria for Method B

Construction Type	Description	Permissible Number of Cycles
Integral Construction	Attachments and nozzles in the knuckle region of formed heads	$N_{\Delta FP} + N_{\Delta PO} + N_{\Delta TE} + N_{\Delta T\alpha} \leq 350$
	All other components that do not contain a flaw	$N_{\Delta FP} + N_{\Delta PO} + N_{\Delta TE} + N_{\Delta T\alpha} \leq 1000$
Non-integral construction (1)	Attachments and nozzles in the knuckle region of formed heads	$N_{\Delta FP} + N_{\Delta PO} + N_{\Delta TE} + N_{\Delta T\alpha} \leq 60$
	All other components that do not contain a flaw	$N_{\Delta FP} + N_{\Delta PO} + N_{\Delta TE} + N_{\Delta T\alpha} \leq 400$
Components with a flaw that are characterized by a Remaining Strength Factor, RSF , determined in accordance with Parts Part 5, Part 6, Part 7, Part 8, or Part 12		$N_{\Delta FP} + N_{\Delta PO} + N_{\Delta TE} + N_{\Delta T\alpha} \leq 150$

Notes:

1. Examples of non-integral attachments are screwed-on caps, screwed-in plugs, fillet welded attachments, shear ring closures, and breech lock closures.

Table 14.3 – Fatigue Screening Criteria Factors for Methods C and D

Factor	Fatigue Screening Method	Description	Factor
K_{fc}	C	Integral Welded	Per Tables 14.5 and 14.6 But with a maximum value of 3.0
		Integral Non-welded	1.0
		Non-integral	3.0
	D	Welded Joints	1.0
H_c	C and D	Attachments and nozzles in the knuckle region of formed head or toriconical shell transition.	1.35
		All other attachments	1.0

Table 14.4 – Calculation of the Stress Tensor Range

Description	OPTION 1 Total Stress Range Tensor	OPTION 2 The Total Stress Range Tensor Minus the Local Thermal Stress Range Tensor
If all sources of peak stress are explicitly accounted for in the stress analysis model; use OPTION 1 for elastic-plastic analysis.	$\Delta\sigma_{ij,k} = \left({}^{m}\sigma_{ij,k} - {}^{n}\sigma_{ij,k} \right)$	$\Delta\sigma_{ij,k} = \left({}^{m}\sigma_{ij,k} - {}^{n}\sigma_{ij,k} \right) - \Delta\sigma_{ij,k}^{LT}$
For the case of a well-defined geometric Stress Concentration Factor (SCF) not at a weld location that is not accounted for in the stress analysis model; note $SCF_{ij} \geq 1.0$.	$\Delta\sigma_{ij,k} = SCF_{ij} \cdot \left({}^{m}\sigma_{ij,k} - {}^{n}\sigma_{ij,k} \right)$	$\Delta\sigma_{ij,k} = SCF_{ij} \cdot \left({}^{m}\sigma_{ij,k}^{MB} - {}^{n}\sigma_{ij,k}^{MB} \right)$
These equations are used for welded locations where the stress concentration factor effects are explicitly included in the stress analysis model while notch effects are not included. A fatigue strength reduction factor, K_f, shall be included. Recommended values for fatigue strength reduction factors for welds are provided in Table 14.5 and Table 14.6. If other values of the fatigue strength reduction factors are used, they shall be applied to the stress consistent with their derivation.	$\Delta\sigma_{ij,k} = K_f \cdot \left({}^{m}\sigma_{ij,k} - {}^{n}\sigma_{ij,k} \right)$	$\Delta\sigma_{ij,k} = K_f \cdot \left({}^{m}\sigma_{ij,k}^{MB} - {}^{n}\sigma_{ij,k}^{MB} \right)$
The fatigue strength reduction and stress concentration effects are present but are not included in the stress analysis model. These equations may be used at welded and non-welded locations. The value of $K_f \cdot SCF$ may be limited to 5.0 unless a higher value is indicated by test data or experience. Other recognized methods may be used if their combination of method and resistance may be shown to be in accordance with the design margins of the applicable construction code.	$\Delta\sigma_{ij,k} = K_f \cdot SCF_{ij} \cdot \left({}^{m}\sigma_{ij,k} - {}^{n}\sigma_{ij,k} \right)$	$\Delta\sigma_{ij,k} = K_f \cdot SCF_{ij} \cdot \left({}^{m}\sigma_{ij,k}^{MB} - {}^{n}\sigma_{ij,k}^{MB} \right)$

Table 14.5 – Weld Surface Fatigue Strength Reduction Factors

Weld Condition	Surface Condition	Quality Levels (see Table 14.6)						
		1	2	3	4	5	6	7
Full penetration	Machined	1.0	1.5	1.5	2.0	2.5	3.0	4.0
	As-welded	1.2	1.6	1.7	2.0	2.5	3.0	4.0
Partial Penetration	Final Surface Machined	N/A	1.5	1.5	2.0	2.5	3.0	4.0
	Final Surface As-welded	N/A	1.6	1.7	2.0	2.5	3.0	4.0
	Root	N/A	1.5	N/A	N/A	N/A	3.0	4.0
Fillet	Toe machined	N/A	N/A	1.5	N/A	2.5	3.0	4.0
	Toe as-welded	N/A	N/A	1.7	N/A	2.5	3.0	3.0 - 4.0
	Root	N/A	N/A	N/A	N/A	N/A	3.0	4.0

Table 14.6 – Weld Surface Fatigue Strength Reduction Factors

Fatigue-Strength-Reduction Factor	Quality Level	Definition
1.0	1	Machined or ground weld that receives a full volumetric examination, and a surface that receives MT/PT examination and a VT examination
1.2	1	As-welded weld that receives a full volumetric examination, and a surface that receives MP/PT and VT examination
1.5	2	Machined or ground weld that receives a partial volumetric examination, and a surface that receives MT/PT examination and VT examination
1.6	2	As-welded weld that receives a partial volumetric examination, and a surface that receives MP/PT and VT examination
1.5	3	Machined or ground weld surface that receives MT/PT examination and a VT examination (visual), but the weld receives no volumetric examination inspection
1.7	3	As-welded weld surface that receives MT/PT examination and a VT examination (visual), but the weld receives no volumetric examination inspection
2.0	4	Weld has received a partial or full volumetric examination, and the surface has received VT examination, but no MT/PT examination
2.5	5	VT examination only of the surface; no volumetric examination nor MT/PT examination
3.0	6	Volumetric examination only
4.0	7	Weld backsides that are non-definable and/or receive no examination

Notes:

1. Volumetric examination is RT or UT in accordance with the applicable construction code.
2. MT/PT examination is magnetic particle or liquid penetrant examination in accordance with the applicable construction code.
3. VT examination is visual examination in accordance with the applicable construction code.
4. See WRC Bulletin 432 for further information.

Table 14.7 – Fatigue Penalty Factors for Elastic Fatigue Analysis

Material	$K_{e,k}$ (1)		$T_{max,k}$ (2)	
	m	n	(°C)	(°F)
Low alloy steel	2.0	0.2	371	700
Martensitic stainless steel	2.0	0.2	371	700
Carbon steel	3.0	0.2	371	700
Austenitic stainless steel	1.7	0.3	427	800
Nickel-chromium-iron	1.7	0.3	427	800
Nickel-copper	1.7	0.3	427	800

Notes:

1. Fatigue penalty factor.
2. The fatigue penalty factor should only be used if all the following are satisfied:
   - The component is not subject to thermal ratcheting, and
   - The maximum temperature in the cycle is within the table listed value for the material.

Table 14.8 – Regions, Boundaries and Ratchet Strains for the Bree Diagram for Load Case A – Fixed Primary Load and a Cycling Secondary Load with Different Yield Stresses in the On-Load and Off-Load Condition, Equation Boundaries for the Regions Given with Respect to the Off-Load Yield Stress $\left(\boldsymbol{X = (P_m \ or \ P_L)/S_{y-off\ load},\ Y = Q/S_{y-off\ load},\ R_y = S_{y-on\ load}/S_{y-off\ load}}\right)$.

Ratcheting Boundary Equation (see Figure 14.19)

$XY = R_y \qquad for\ X \le X_{int} \qquad where\ X_{int} = 1 - \frac{1}{1+R_y}$

$Y = \left(\sqrt{R_y - X} + \sqrt{1 - X}\right)^2 \quad for\ X > X_{int}$

Region	Boundary Equations	Ratchet Strain ($E\varepsilon_R/\sigma_y^{off}$)
E	Below $X + Y = R_y$	N/A
S1	Above $X + Y = R_y$ Below $Y(R_y - X) = R_y^2$ Below $Y = \left(\sqrt{R_y - X} + \sqrt{1 - X}\right)^2$	N/A
S2	Above $Y(R_y - X) = R_y^2$ Below $Y = R_y + 1$	N/A
P1	Above $Y = R_y + 1$ Below $XY = R_y$	N/A
R1	Above $Y = \left(\sqrt{R_y - X} + \sqrt{1 - X}\right)^2$ Below $Y(R_y - X) = R_y^2$	$2Y - 2\sqrt{Y(R_y - X)} - 2\sqrt{Y(1 - X)}$
R2	Above $Y(1 - X) = 1$ Above $XY = R_y$	$\frac{XY}{R_y} + XY - R_y - 1$
R3	Above $Y(1 - X) = 1$ Below $Y(R_y - X) = R_y^2$	$XY - 1 - Y + 2\sqrt{Y(R_y - X)}$

Note: X_{int} is defined at the point in common with Regions S_1, S_2, P_1, R_1, R_2, and R_3 (see Figure 14.19).

Table 14.9 – Regions, Boundaries and Ratchet Strains for the Bree Diagram for Load Case B – In-phase Primary and Secondary Load Cycling with Different Yield Stresses in the On-load and Off-Load Conditions, Equation Boundaries for the Regions Given with Respect to the Off-load Yield Stress $\left(\boldsymbol{X = (P_m \ or \ P_L)/S_{y-off\ load},\ Y = Q/S_{y-off\ load},\ R_y = S_{y-on\ load}/S_{y-off\ load}}\right)$.

Ratcheting Boundary Equation (see Figure 14.20)

$XY = R_y(1 + R_y) \qquad for\ X \le X_{int} \qquad where\ \frac{X_{int}}{R_y - X_{int}} = \frac{R_y(1+R_y)}{R_y^2}$

$\frac{1}{4}\left(2 + 4R_y - Y - \frac{1}{Y}\right) = X \qquad for\ X > X_{int}$

Region	Equation Boundaries	Ratchet Strain ($E\varepsilon_R/\sigma_y^{off}$)
E	Below $X + Y = R_y$	N/A
S1	Above $X + Y = R_y$ Below $Y(R_y - X) = R_y^2$ Below $X + Y = 1 + R_y$	N/A
S2	Above $Y(R_y - X) = R_y^2$ Below $X + Y = 1 + R$	N/A
P1	Above $X + Y = 1 + R$ Below $Y(R_y - X) = R_y^2$ Below $\frac{1}{4}\left(2 + 4R_y - Y - \frac{1}{Y}\right) = X$	N/A
P2	Above $Y(1 + R_y - X) = (1 + R_y)^2$ Below $XY = R_y(1 + R_y)$	N/A
P3	Above $X + Y = 1 + R_y$ Above $Y(R_y - X) = R_y^2$ Below $Y(1 + R_y - X) = (1 + R_y)^2$	N/A
R1	Above $\frac{1}{4}\left(2 + 4R_y - Y - \frac{1}{Y}\right) = X$ Below $Y(R_y - X) = R_y^2$	$Y - 1 - 2\sqrt{Y(R - X)}$
R2	Above $Y(R_y - X) = R_y^2$ Above $XY = R_y(1 + R_y)$	$\frac{XY}{R_y} - R_y - 1$

Note: X_{int} is defined at the point in common with Regions P_1, P_2, P_3, R_1, and R_2 (see Figure 14.20).

Table 14.10 – Regions, Boundaries and Ratchet Strains for the Bree Diagram for Load Case C – Out-of-phase Primary and Secondary Load Cycling with Different Yield Stresses in the On-load and Off-load Condition, Equation Boundaries for the Regions Given with Respect to the Off-load Yield Stress $\left(\boldsymbol{X = (P_m \ or \ P_L)/S_{y-off\ load}},\ \boldsymbol{Y = Q/S_{y-off\ load}},\ \boldsymbol{R_y = S_{y-on\ load}/S_{y-off\ load}}\right)$.

Ratcheting Boundary Equation (see Figure 14.21)		
$XY = 1 + R_y \quad for\ X \le X_{int} \quad where\ \frac{X_{int}}{1-X_{int}} = 1 + R_y$		
$\frac{1}{4}\left(4 + 2R_y - Y - \frac{R_y^2}{Y}\right) = X \quad for\ X > X_{int}$		
Region	**Equation Boundaries**	**Ratchet Strain ($E\varepsilon_R/\sigma_y^{off}$)**
E	Below $Y = R_y$	N/A
S1	Above $Y = R_y$ Below $X + Y = 1 + R_y$	N/A
P1	Above $X + Y = 1 + R_y$ Below $Y(1 + R_y - X) = \left(1 + R_y\right)^2$ Below $\frac{1}{4}\left(4 + 2R_y - Y - \frac{R_y^2}{Y}\right) = X$	N/A
P2	Above $Y(1 + R_y - X) = \left(1 + R_y\right)^2$ Below $XY = 1 + R_y$	N/A
R1	Above $\frac{1}{4}\left(4 + 2R_y - Y - \frac{R_y^2}{Y}\right) = X$ Below $Y(1 - X) = 1$	$Y - R_y - 2\sqrt{Y(1-X)}$
R2	Above $Y(1 - X) = 1$ Above $XY = 1 + R_y$	$XY - R_y - 1$

Note: X_{int} is defined at the point in common with Regions P_1, P_2, R_1, and R_2 (see Figure 14.21).

Table 14.11 – Regions, Boundaries, and Ratchet Strains for the Bree Diagram for Load Case D – Cyclic Primary Load and a Fixed Secondary Load with Different Yield Stresses in the On-Load and Off-Load Conditions, Equation Boundaries for the Regions Given with Respect to On-Load Yield Stress (see Figure 14.22)

$X = (P_m \text{ or } P_L)/S_{y-off\ load}$, $Y = Q/S_{y-off\ load}$,

Region	Equation Boundaries	Ratchet Strain
E	Below $X + Y = 1$	N/A
S1	Above $X + Y = 1$ Below $\sqrt{Y(1-X)} + \frac{X}{2} = 1$	N/A
P1	Above $\sqrt{Y(1-X)} + \frac{X}{2} = 1$ Below $Y(1-X) = 1$	N/A
P2	Above $Y(1-X) = 1$	N/A

Table 14.12 – Fatigue Life Knockdown Factors

Item	ASME	PVRC Working Group on S-N Data		PVRC Working Group on Evaluation Methods	
		Best Estimate of Margin Needed	Conservative Estimate of Margin Needed	Best Estimate of Margin Needed	Conservative Estimate of Margin Needed
Size Effect	2.5	1	1.2	1.0	1.2
Surface Finish	4 (1)	1.5	2	1.0	1.5
Data Scatter	2	2	2.5	2.0	2.5
Environmental Effects	4 (1)	2.5	4	---	---
Loading time history Effects	NC	1	1	1.0	2.5
Multi-Axial Stress Field	---	---	---	1.0	1.3
Product	20	7.5	24	2.0	14.6

Notes:

1. Surface finish and environmental combined with a margin of 4.
2. From WRC Bulletin 487, Table 1.

Table 14.13 – Energy Source Driving Fatigue

Source	Description	Magnitude	Frequency
Periodic Mechanical, see Figure 14.26	Usually associated with the attachment of machinery to the equipment component. Examples include unbalanced shafts in pumps, and mixers attached to vessel or tank nozzles.	Magnitude will depend on the power of the machinery and the relative mass of the exciting machinery and the excited equipment.	Usually related to a harmonic of the machinery operating rotational speed in revolutions per minute (rpm): $f = \frac{n \cdot rpm}{60}\ hertz$
Acoustically Induced, see Figure 14.27	Results from the conversion of pressure energy to other forms, mainly noise but also heat. Typically associated with pressure reduction and turbulence at valves or orifices.	Consists of relatively small magnitude (through thickness) bending of the component wall in a bi-axial pattern that depends on component geometry.	Vibration frequency is broad-band, usually in the range of 300 - 2000 Hz.
Pulsation, see Figure 14.28 through Figure 14.30	Pulsations typically result from energy sources such as reciprocating pumps and compressors. May also occur from the blade passing frequency in centrifugal pumps. The pulsation consists of a periodic pressure increase, usually above a mean pressure in the component that propagates as a wave downstream and may interact with the conveying component.	This pulsation creates forces in the component (usually a piping system) that are the product of the pulsation magnitude and the component area. These forces typically interact with the conveying component at changes in flow direction and may cause standing waves to occur. Large magnitudes may accompany acoustic resonance when the pulsation frequency is close to the acoustic natural frequency of the conveying component.	Input energy is usually related to a harmonic of the machinery operating rotational speed in revolutions per minute (rpm), see above. The interaction from standing waves (i.e., acoustic resonance) depends on the length of the path, the speed of sound in the flow medium, and the end conditions (open or closed) of the ends of the path. Acoustic natural frequencies are given by either: $f = \frac{n \cdot c}{2L}\ or\ f = \frac{(2n-1) \cdot c}{4L}$
Slug Flow, see Figure 14.31	Results from a two-phase flow regime where the phases separate to form “pockets” that alternate in the longitudinal (i.e., flow) direction. The higher volumetric flow of the vapor phase governs the flow velocity. Most flow momentum, however, is from the denser liquid/solid phase. Examples of slug flow occur downstream of furnaces and in FCCU transfer piping.	Results in forces at each directional change of flow. The force magnitude can be determined from Newton’s second law, $F = ma$, where “m” is the mass of the liquid/solid and “a” depends on the time rate of change of the liquid/solid velocity vector. Results in a force proportional to the liquid/solid density and the velocity magnitude squared.	Slug flow may be periodic or transient and depends on phase densities, mass flow rate and orientation of the component (usually piping). It is periodic if the alternating pockets are uniformly spaced in time and space. If the formation of the alternating pockets occurs only occasionally, the result will be a transient (though often large magnitude) force.

Table 14.13 – Energy Source Driving Fatigue

Source	Description	Magnitude	Frequency
Vortex Shedding, see Figure 14.32	Vortex shedding consists of periodic pulsations resulting from the separation of flow (liquid or vapor) around a solid object or surface. The presence of vortex shedding forces depends on the flow's Reynold's number, $R_E = \frac{\rho V D}{\mu}$ As Figure 14.32(a) shows, not all flow regimes result in alternating vortex shedding forces. Vortex shedding may cause either an external or internal pulsation. The effects of Internal pulsations are like those from machinery such as pumps or compressors. Alternating pulsation forces on an object may result in rigid body vibration of the object that causes the flow separation. Examples include vibration of towers and stacks (external) and pulsations at valve internals or pressure/temperature sensors projected into the flow path.	The magnitude of the forces will depend on the shape of the object, the angle of attack of the flow, and the flow velocity. The magnitude can be estimated from drag and lift coefficients, C_D and C_L respectively, as published in documents related to flow and turbulence.	The frequency of vortex shedding is given by the equation: $f = \frac{S_n \cdot V}{D}$ Values of Strouhal number, S_n, depend on the density of the fluid, the shape and size of the component in the flow path, and the velocity of the fluid flow. For cylinders in air S_n is usually taken as 0.2. The forces developed by the shedding vortices alternate at the vortex shedding frequency, resulting in vibration whose magnitude depends on the alternating vortex shedding frequency and its relation to the structural natural frequency of the object.
Hydraulic Hammer, see Figure 14.33	Hydraulic hammer results from the conversion of kinetic energy to potential energy (pressure). Its name derives from the sound that is typically associated with the movement of the conveying component from fluid-structure interaction. Typical causes of hydraulic hammer include rapid valve closure, relief valve discharge into a liquid filled line, pump startup or pump trip and sudden steam pocket collapse.	The force magnitude equals the pressure change times the flow area of the conveying component. The pressure change depends on the fluid density and compressibility (bulk modulus), and the compliance of the conveying component. A conservative force estimate is given by the equation: $F = \rho \cdot A_{pipe} \cdot \Delta V \cdot c$ $c = \sqrt{\frac{K}{\rho} \cdot \frac{1}{\left(1 + \left(\frac{K}{E}\right)\left(\frac{D}{t}\right)\right)}}$	In many cases, the phenomenon of hydraulic hammer is one that is transient. An example of periodic hydraulic hammer would be the dosing of a process flow by liquid injection where the valve controlling the injection fluid cycles from open to close on a timed basis. In such a case the frequency of the hydraulic pressure and flow matches that of the cycling valve.

Table 14.13 – Energy Source Driving Fatigue

Source	Description	Magnitude	Frequency
Periodic Pressure	The periodic or transient pressures referenced here are those that occur when the equipment is put into service or the operating pressure changes significantly. Examples are pressure swing absorbers, cyclic regeneration, and tanks undergoing filling and emptying. Such pressure changes cause corresponding stress changes that can lead to fatigue.	The cyclic stresses generated are typically proportional to the cyclic pressures. Fatigue usually results at locations of structural discontinuity or stress risers at welds. If stresses significantly exceed yield, ratcheting may occur.	The frequency is totally dependent on the operational frequency. For complicated operational conditions, a rainfall approach may be necessary.
Periodic or Transient Thermal	Thermal energy can result in fatigue due to the stresses generated when thermal expansion is constrained. This may occur due to external constraint (e.g., constraint of piping system expansion), from differing temperatures between adjacent regions of a component (e.g., thermal gradients during the filling or quenching of delayed coke drums), from differential expansion due to differing expansion coefficients (e.g., stainless steel internals connected to a carbon or low alloy steel pressure boundary), or from some combination of these factors. They may also occur due to rapid local changes in the process and metal temperature at thermal mix points.	The stresses generated by periodic or transient thermal energy can be estimated by considering the continuity of displacements that must exist in a structure, vessel, piping system etc. The displacements result from the effects of the material properties, $E_y \; and \; \alpha$, the geometry of components (i.e., area, moment of inertia, etc.), and the differential temperature or temperature gradients all as a function of time. The temperature gradients will depend on heat transfer characteristics including material thermal conductivity, convection, radiation, and thermal diffusivity.	The frequency is totally dependent on the operational frequency. For complicated operational conditions, a rainfall approach may be necessary. In the case of thermal mix points, computational fluid dynamics has shown that the rapid changes of temperature can result in high cycle fatigue local to the process side metal surface.

Table 14.14 – Remediation by Removal or Reduction of Energy Source

Source	Discussion of Remediation
Periodic Mechanical	The forces associated with mechanical energy depend on such factors as the power supplied by the source (usually machinery), the eccentricity of shaft(s), misalignment between the driver and the machine, or in the case of mixers, free vibration of the shaft near the mixing components. Of these, the supplied power is usually the most difficult to alter. The other factors can be changed through such actions as: • Machining the shaft to remove eccentricities, • Ensuring proper alignment between driving and driven shafts, • Constraining the free vibration of the shaft near the mixing components (e.g., paddles) through an end bearing attached to the containing vessel or tank, see Figure 14.34.
Acoustically Induced, see Figure 14.35 through Figure 14.38	The energy involved with acoustically induced fatigue results from conversion of fluid pressure upstream of a pressure reduction device to other forms of energy, mainly noise but also some heat. The fatigue most often is associated with constant flow valves/orifices in vapor service. The noise will usually be accompanied by significant turbulence. Remediation by energy reduction usually consists of one of the following: • Dividing the flow into two or more flow paths to reduce turbulence. • Use of “low noise” pressure reduction valves that convert the pressure energy to heat. • Multistage pressure reduction where each stage takes part of the energy conversion with an accompanying reduction in noise and turbulence at each.
Pulsation, see Figure 14.39 and Figure 14.40	Energy input is in the form of pressure pulsations at the discharge end of a compressor or pump. The effect is more prevalent with reciprocating, positive displacement devices. Remediation of the pulsating energy is accomplished using: • Pulsation bottles whose internals are designed to filter the pulsation out of the flow. • Side branch resonators that adsorb the pulsation energy at a particular frequency. • Detuning the downstream piping’s natural frequency away from the driving (pulsation) frequency.
Slug Flow, see Figure 14.41 and Figure 14.42	The most effective way to remediate the energy associated with slug flow is to avoid flow regimes that give rise to the slugs forming. Since slug flow is most often associated with piping systems, this can sometimes be controlled by selection of pipe size to change the flow velocity or pipe orientation. The phenomenon may also occur in fluidized bed reactors and regenerators. Such energy results from the fluidized bed turbulence and is difficult to control.
Vortex Shedding, see Figure 14.43 and Figure 14.44	The energy source that results in vortex shedding energy may be difficult to control directly. Methods sometime employed are to shield the structure from the energy (e.g., bundle shields or flow deflectors at the inlet nozzles in shell-and-tube heat exchangers) or change the shape of the component that sees the energy (e.g., strakes on tall thin towers or stacks).

Table 14.14 – Remediation by Removal or Reduction of Energy Source

Source	Discussion of Remediation
Hydraulic Hammer, see Figure 14.45 through Figure 14.47	The energy that causes hydraulic hammer comes from the conversion between kinetic and potential forms of energy associated with the liquids change in velocity (i.e., stopping or starting flow) in a piping system. The effects of the energy on fatigue/vibration can be accomplished by: • Reducing the rapidity of the velocity change (i.e., fluid acceleration or deceleration). This is done by controlling (slowing) valve opening/closing or stroking the valve (changing it from linear to stepped opening) or starting pumps against an initially closed valve. • Removal of the energy through pressure relief valves/rupture discs/accumulators with the hydraulic hammer event occurs and valve closure cannot be easily controlled.
Periodic Pressure	Remediation of energy that drives fatigue in this case can only be changed by a change in the magnitude, usually not a practical solution unless it is acceptable from a process standpoint.
Periodic/Transient Thermal	Remediation in some cases is possible by either reducing temperature (usually not acceptable from a process standpoint) or by reducing the rapidity of the heat-up/cool down to reduce thermal gradients/differentials that drive thermal fatigue.

Table 14.15 – Remediation by Constraint or Design Changes

Source	Discussion of Remediation
Periodic Mechanical	If the energy causing fatigue cannot be removed or reduced, constraint of the system may be used. Since for this type of energy the fatigue stress is almost always directly proportional to the displacements, the goal is to reduce the maximum displacements where they occur. The type of constraint should consider the guidance provided in paragraph 14.6.3. For vessels or piping attached to rotating equipment, consider two plane gusseting, see Figure 14.49, for small bore connections for a distance of $20D$ from the source.
Acoustically Induced	Due to the nature of the vibration causing fatigue, constraint of the component is usually ineffective. Constraint, if non-axisymmetric may be counter-productive since its attachment may locally increase stresses and lead to fatigue. Usually, design changes, either to the system to reduce the sound power magnitude, see Table 14.13, or by lowering the stress by increasing component thickness is required.
Pulsation	If pulsation energy cannot be abated by a method described in Table 14.13, constraints may be added to the component to limit displacements and stresses caused by the pulsation forces. The pulsation forces should be estimated as the pulsation pressure magnitude times the flow area of the component conveying the pressure pulse. If structural resonance is present (or suspected), constraint may also be used to alter the component structural natural frequency away from the energy source frequency. If acoustic resonance exists, a redesign to detune the component may be necessary since acoustic resonance can lead to large dynamic load factors.
Slug Flow	If pulsation energy cannot be abated by a method described in Table 14.13, constraints may be added to the component to limit displacements and stresses caused by the pulsation forces. The slug force, F, acts at an angle that bisects the change in direction β and may be estimated by application of Newton's Second Law: $$F = \rho \cdot (DV)^2 \cdot \cos[0.5\beta]$$ Since the force is an impulse, it is recommended to double this magnitude or determine the dynamic load factor by comparing the load duration to the structural natural period [Biggs].
Vortex Shedding	Vortex shedding usually results in fatigue when either the fluid velocity is periodic in magnitude or when the vortex shedding frequency matches (i.e., is resonant to) that of the structure. If the vortices cannot be abated, either constraints or a design change can be applied. Constraint for vortex shedding from external flow past the component experiencing fatigue usually is done to alter the structural natural frequency away from the vortex shedding frequency (e.g., change the spacing of tube supports/baffles in a heat exchanger). For vortex shedding from internal flow past a protrusion into the flow (e.g., process thermal or pressure sensor) or a recess, the resultant vortex shedding will create pulsations in the process flow. Refer to Pulsation above for the design of external constraints in such a case. Alternatively, for both external and internal flow the components may be redesigned by changing their shape or size to avoid the vortex shedding (e.g., using strakes on a stack, see Figure 14.44.)

Table 14.15 – Remediation by Constraint or Design Changes

Source	Discussion of Remediation
Hydraulic Hammer	If the magnitude (or frequency in cases involving periodic flow) of the hydraulic hammer energy cannot be abated, the usual approach is to provide sufficient constraint to resist the forces from the pressure wave(s). The forces can be estimated by first calculating the pressure force resulting from the change in flow velocity using the equation in Table 14.13. Alternatively, a commercially available hydraulic flow computer program may be used to determine the pressure wave magnitude more accurately prior to multiplying by the flow area. Due to the impulsive nature of the hydraulic hammer forces the force may be multiplied by two and applied statically in a piping stress analysis, or if desired, the force-versus time may be determined, and the force applied in a loading time history to the structure.
Periodic Pressure	Constraints are usually not effective for remediating fatigue from this type of energy, except in the case of geometric irregularities, see Part 8. More often, remediation occurs using design changes that reduce local stresses from the applied pressure loads at structural discontinuities.
Periodic/Transient Thermal	Constraints are usually ineffective in remediating thermal fatigue, and sometimes may be a contributing cause. Remediation of the thermal fatigue usually involves some type of design change to reduce thermal gradients between components or locations in the same component (see Table 14.16.)

Table 14.16 – Remediation by Insulation or Thermal Isolation

Source	Discussion of Remediation
Periodic Mechanical	Not applicable
Acoustically Induced	Not Applicable
Pulsation	Not Applicable
Slug Flow	Not Applicable
Vortex Shedding	Not Applicable
Hydraulic Hammer	Not Applicable
Periodic Pressure	Not Applicable
Periodic/Transient Thermal	Remediation of fatigue by periodic or transient thermally induced stresses can be accomplished by use of thermal Isolation, or by providing sufficient flexibility so as not to constrain thermal displacements. Thermal insulation consists of a thermal barrier between the process fluid and the metal undergoing expansion/contraction. An example of this is the refractory lining installed in high temperature equipment, e.g., reformers, FCCU units. Often the refractory serves more than one purpose. It lowers the metal temperature, thus allowing higher allowable stresses while at the same time reducing thermal displacements and the stresses that accompany them when constrained. Another application of thermal insulation is a hot box, see Figure 14.51, as used in high temperature equipment such as coke drums and other equipment where the hot process fluid must contact the metal. The hot box helps to convey thermal energy to the support skirt of the vessel through stagnant air conduction and radiation thus reducing thermal gradients along the skirt. Thermal isolation, such as the use of thermal sleeves, see Figure 14.52, or thermal insulation, see Figures 14.53 and Figure 14.54, has as its goal the reduction of thermal differentials between different equipment components. An example is that of an alloy nozzle designed for high temperatures intersecting refractory lined vessel. The thermal sleeve, often containing some insulation, reduces the temperature difference, and thus the thermal stresses, at the junction of the components. Providing flexibility in the equipment reduces the amount of constraint on the thermal expansion, and thus the thermal stresses. It is often used in piping systems using pipe loops, offsets, and sometimes the use of expansion joints. A difficulty may exist in high temperature piping systems subject to fatigue from some other source in that added flexibility may increase the propensity for fatigue from increase vibratory stresses.

Table 14.17 – Description of In-Service Monitoring Methods

Method	Description
Visual	Operators or Inspectors periodically observe the equipment or component to detect displacements that can lead to fatigue. Can also be done using a camera installed to monitor the displacements. Inspectors may also periodically observe locations of suspected cracking (e.g., branch connections/nozzles subject to periodic mechanical or thermal loads).
Accelerometers	Accelerometers are transducers that convert the time rate of change of the velocity of a component to an electrical signal. The accelerometers measure motion in a particular direction, at the location of their attachment to the component/equipment. Accelerometers typically attach to the component using magnetic force (for ferrous materials only) or may be bonded to the component or attached by clamping. Accelerometers are used to monitor rotating equipment for vibration. Accelerometers provide data in the time domain. Using filters and Fourier transforms, information in the frequency domain may be obtained as well. Accelerometers may be, piezoelectric, piezoresistive or capacitive. For applications where the driving energy or structural natural frequency or frequencies exceed two hertz, any of the three may be used. However, applications where the frequencies of interest may be below two hertz, the capacitive type is recommended as experience has shown that the others produce numerical inaccuracy/false data below two hertz. Since they contain electronics, accelerometers have a limited temperature range. Most start to be inaccurate if the electronics' temperature exceeds 250°F (120°C) for more than a few minutes. For measurements of high temperature components, the accelerometer must either be insulated from the thermal energy or cooled in some manner. This requirement may limit their application. The data measured by accelerometers must be integrated twice to obtain the displacements that are useful in evaluating the potential for fatigue forces. These integrations may lead to numerical inaccuracy that may require signal conditioning. Once obtained the displacements may be used to estimate forces and stresses in the component.
Proximity Probe	Proximity probes consist of devices that measure the displacements directly with or without contact to the component. Examples of such devices are Linear Variable Displacement Transducers (LVDT) and lasers. Since they measure displacements directly, they do not suffer from the potential for numerical inaccuracy associated with needing to integrate the signal. Both types of devices produce an electric signal. The LDVT attaches directly to the component whose motion is being measured, often by bonding and measures motion by use of the motion of an extension of the attached rod through a coil, producing an AC electric signal. Laser devices use light send/receive transducers to measure displacement and are not attached to the component. Both devices require a reference frame that is stationary relative to the component whose motion is being measured. This may produce difficulties when the energy driving the fatigue also causes vibration of structural platforms from which the measurements are being made. Due to their more robust nature or the fact that they do not require a direct attachment, proximity probes may be used for measurements of components that operate at more extreme temperature ranges. Like with accelerometers, the data from proximity probes may be converted from the time domain to the frequency domain to obtain information regarding the driving energy and/or structural response frequency leading to fatigue.

Table 14.17 – Description of In-Service Monitoring Methods

Method	Description
Strain Gauge	Strain gauges attach to the component being monitored using an adhesive or welding. The strain gauge consists of a fine wire, coiled in a plane. The surface of the component causes the coiled wire to change length. When an electrical current is applied to the wire, the change in length results in a change in resistance that can be measured and correlated to the strain in the component. The strain can then be related to the state of stress causing fatigue. As with the other sensors, the data from strain gauges may be recorded for post processing. Strain gauges are used more for monitoring over a longer time period and are usually attached to the component when it is not undergoing motion as the device needs calibration. While some thermal limitations may exist in using strain gauges, they can directly measure both mechanical and thermal strain.
Periodic Inspection with UT, PT, MT, or Eddy Current Examination	In addition to visual inspection (VT) the Inspector may apply other inspection techniques such as UT, PT, MT, or Eddy Current examination to detect the initiation or growth of fatigue cracks.
Thermocouple	Thermocouples are widely used in the process industry for temperature measurement of process streams. They consist of two wires of differing thermo-electrical properties in contact with one another. The application of heat energy results in a current that can be measured and related to the temperature of the device. When multiple thermocouples are applied, they can be used to measure thermal gradients. These gradients may then be used with thermo-structural models to determine full-field thermal gradients and thermal stresses in the component caused by these gradients. An example of the use of thermo-couples for such a purpose is monitoring of the skin temperature of coke drums and their support skirts during the drums heat up-soak-quench cycle.
Pressure Gauge or Pressure Transducers	Like thermocouples, pressure gauges or Pressure Transducers are widely used in the process industry for controlling aspects of the process. Pressure gauges usually consist of “static” type or “dynamic” type. The static type uses a coiled tube that changes shape (uncoils) as it is pressurized. It cannot measure rapidly changing pressures (although most have a feature that allows the maximum attained pressure within the gauge’s range to be visually observed). The “dynamic” type typically uses a small thin membrane with a strain gauge attached. As the pressure increases the membrane displaces causing strain to occur. By calibration, the strain can be related to the applied pressure. Such devices can react to pressure changes rapidly. Pressure transducers or sensors typically use a force collector (such a diaphragm, piston, bourdon tube, or bellows) to measure strain (or deflection) due to applied force (pressure) over an area. Pressure ranges and response times are available to characterize transient flow regimes such as acoustically induced, pulsation, or slug flow. Like with thermocouples, the measurement of the pressure in time can be related through structural models to the stress in the component or equipment. An example where such data may be useful is in pressure swing absorbers.

Table 14.18 – Applicability and Use of In-Service Monitoring Methods

Source	Visual	Accelerometers	Proximity Probes	Strain Gauges	Thermocouples	Pressure Gauges or Pressure Transducers
Periodic Mechanical	Effective in detecting vibration or displacements	Effective in measuring vibration or displacements	Effective in measuring vibration or displacements	May be used, usually not cost effective	Not Applicable	Not Applicable
Acoustically Induced	May be used, vibration magnitude usually small and frequency high	May be used, usually not cost effective due to number required	May be used, usually not cost effective due to number required	Install near locations of discontinuities	Not Applicable	Not Applicable
Pulsation	Effective in detecting vibration or displacements	Effective in measuring vibration or displacements	Effective in measuring vibration or displacements	May be used, usually not cost effective	Not Applicable	May be used, must be capable of measuring dynamic pressures
Slug Flow	Effective in detecting vibration or displacements	Effective in measuring vibration or displacements	Effective in measuring vibration or displacements	May be used, usually not cost effective	Not Applicable	Pressure gauges are not applicable, pressure transducers may be used
Vortex Shedding	Effective in detecting vibration or displacements	Effective in measuring vibration or displacements	Effective in measuring vibration or displacements	May be used, usually not cost effective	Not Applicable	Not Applicable
Hydraulic Hammer	Effective in detecting vibration or displacements	Effective in measuring vibration or displacements	Effective in measuring vibration or displacements	May be used, usually not cost effective	Not Applicable	Pressure gauges are not applicable, pressure transducers may be used
Periodic Pressure	Not Applicable	Not Applicable	Not Applicable	May be used, strain values are proportional to pressure. Install away from and near discontinuity	Not Applicable	May be used in conjunction with stress analysis to monitor pressure stresses
Periodic & Transient Thermal	Not Applicable	Not Applicable	Not Applicable	Not Applicable	Install as required to measure thermal gradients or differentials. Use along with stress analysis to monitor thermal stresses	Not Applicable

14.12 Figures

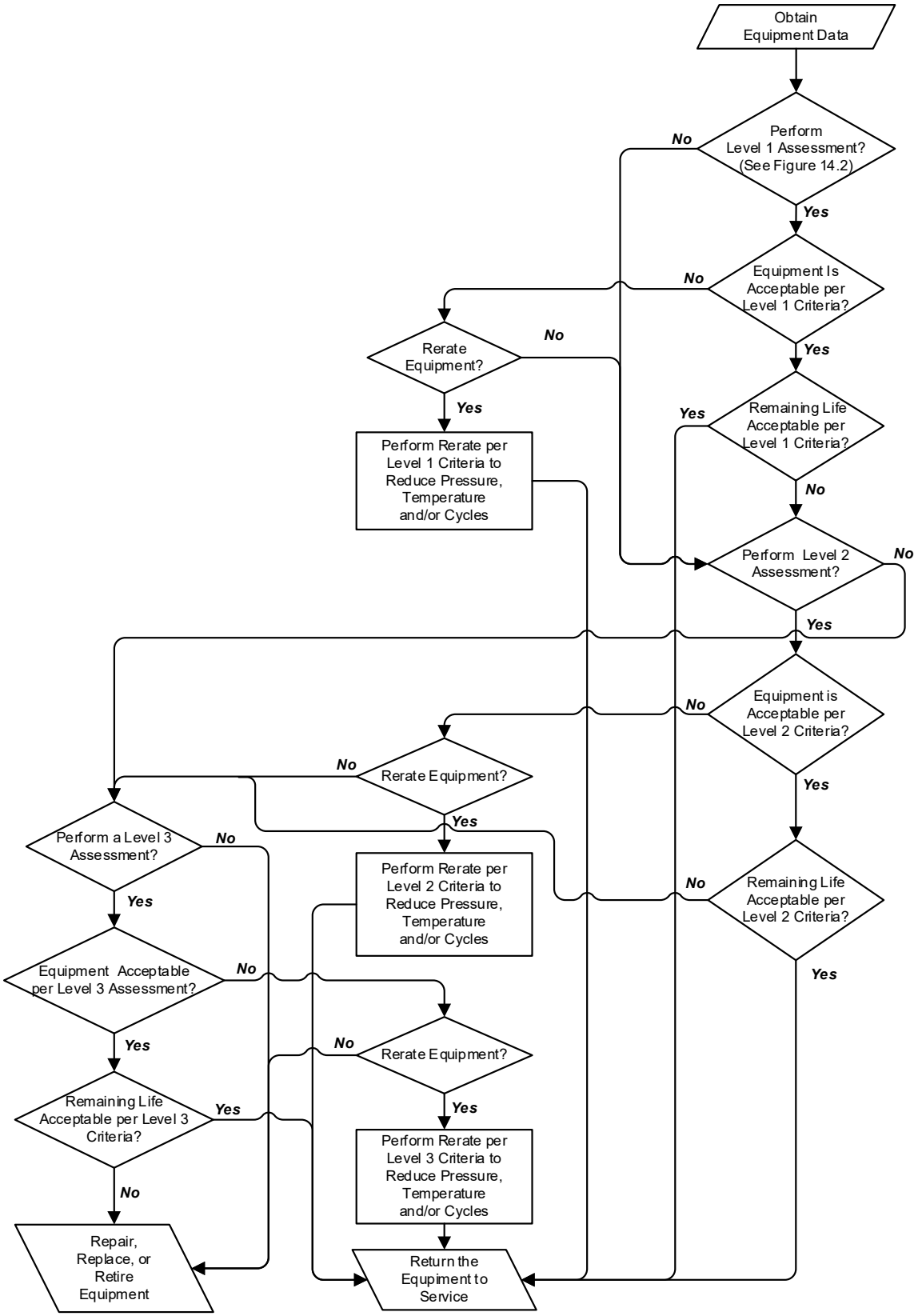

Figure 14.1 – Overview of the Assessment Procedure to Evaluate a Component Subject to Fatigue

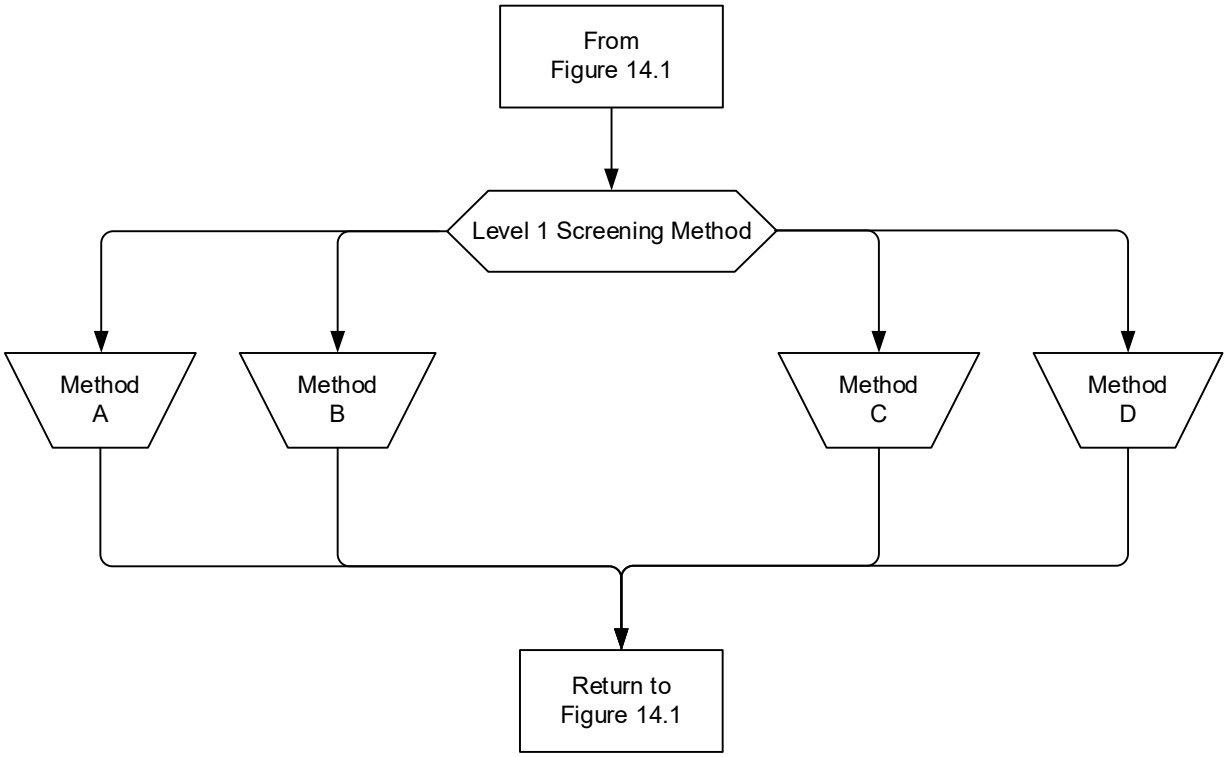

Figure 14.2 – Level 1 Assessment – Fatigue Screening Methods

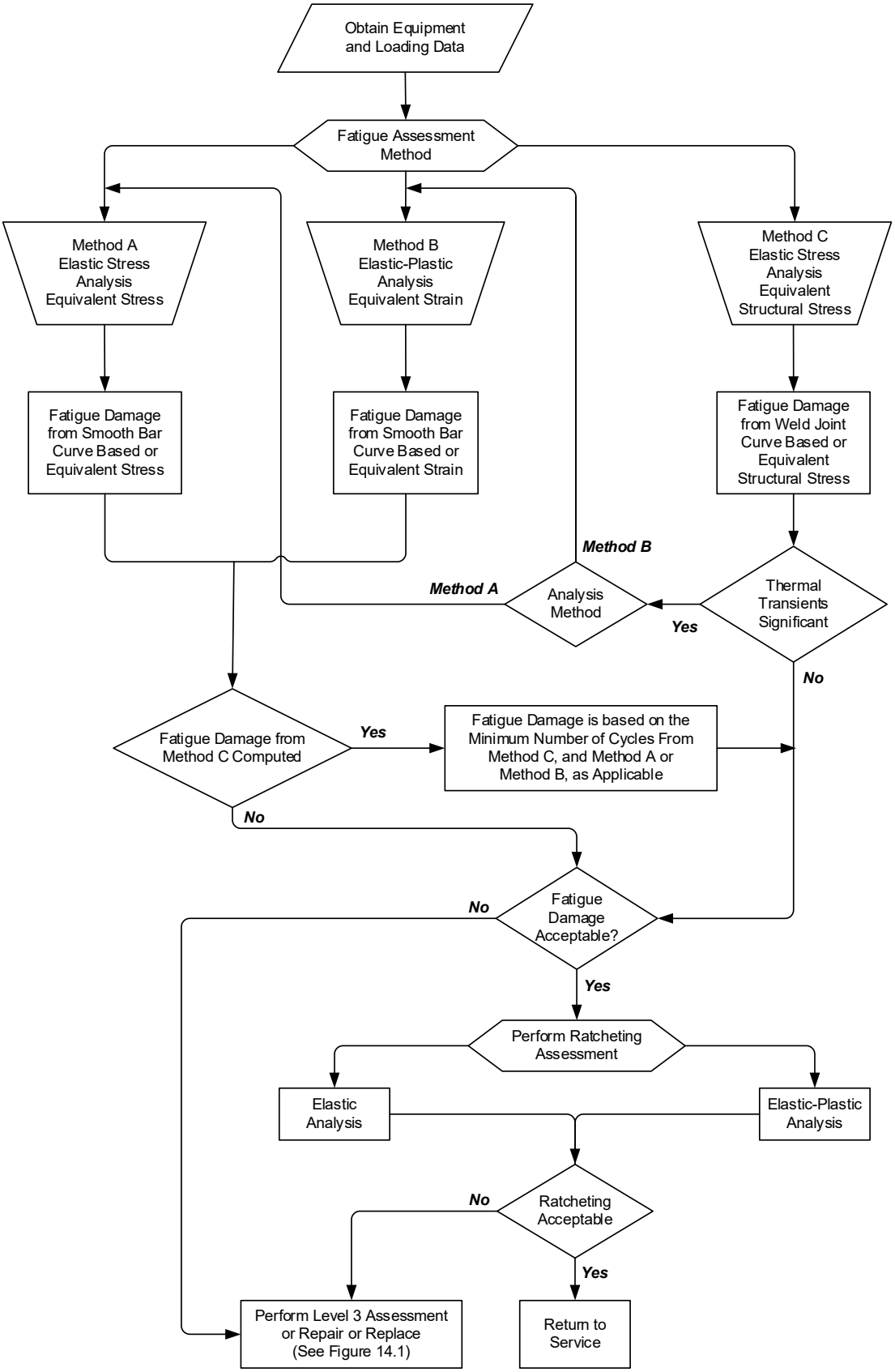

Figure 14.3 – Level 2 Fatigue Analysis Assessment Methods

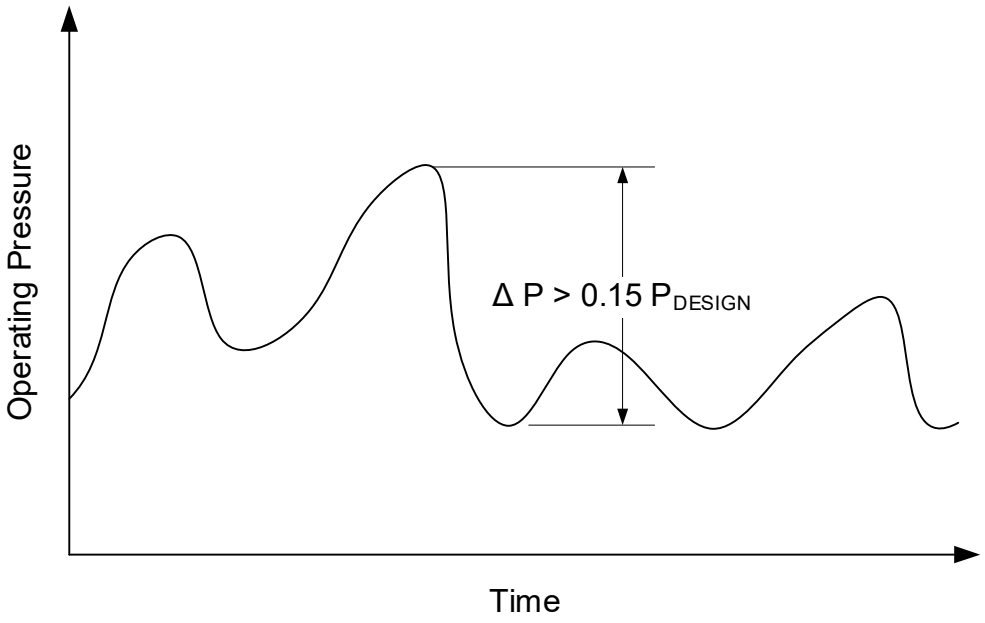

Non-Integral Construction

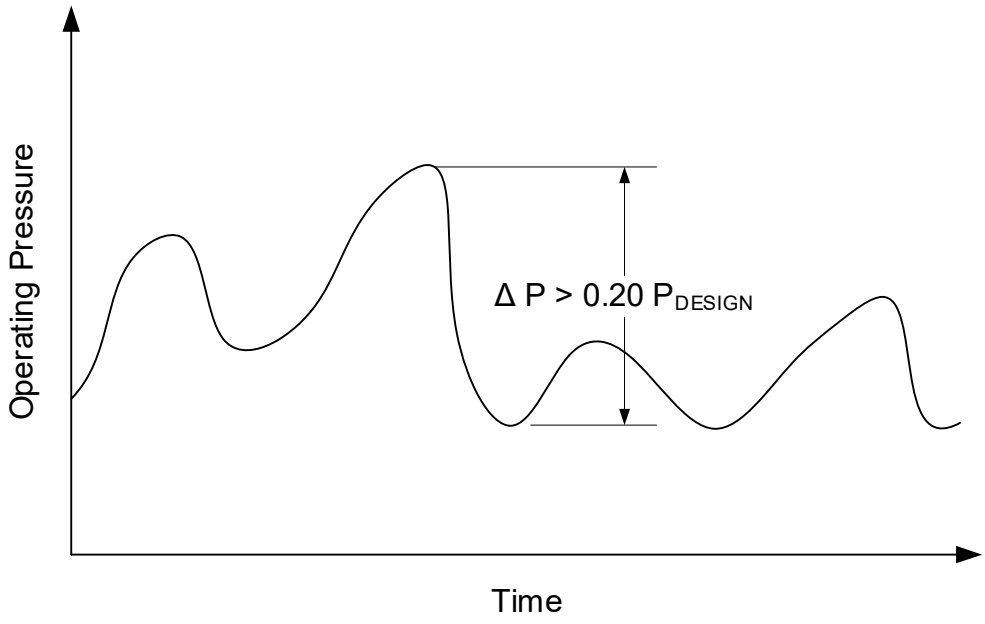

Integral Construction

Figure 14.4 – Examples of Significant Operating pressure Cycles (Integral and Non-Integral Construction) for Fatigue Screening Method B, STEP 3

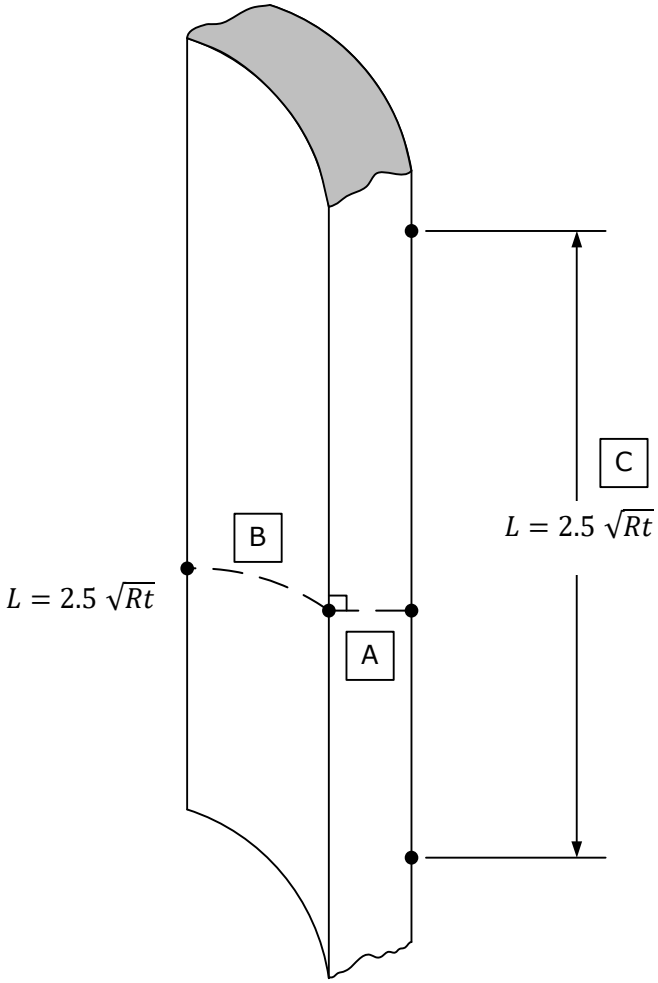

A: Through-Thickness Temperature Difference (Radial Direction)

B: Surface Temperature Difference (Circumferential Direction)

C: Surface Temperature Difference (Meridional Direction)

Figure 14.5 – Examples of Adjacent Points on a Cylindrical Shell for Fatigue Screening Method B, STEP 4

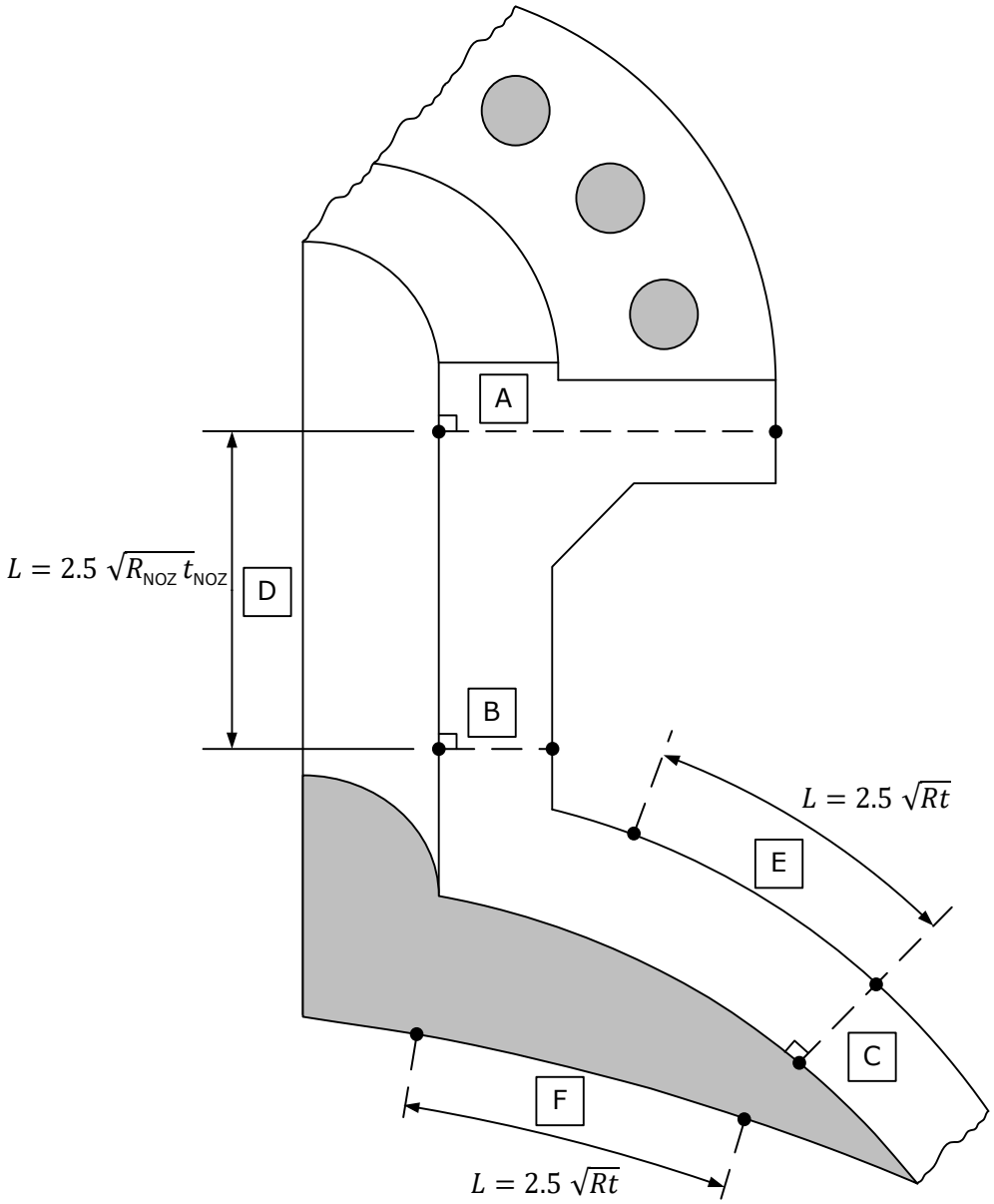

A,B,C: Through-Thickness Temperature Difference (Radial Direction)

D,E: Surface Temperature Difference (Meridional Direction)

F: Surface Temperature Difference (Circumferential Direction)

Figure 14.6 – Examples of Adjacent Points Near a Nozzle-to-Head Junction for Fatigue Screening Method B, STEP 4

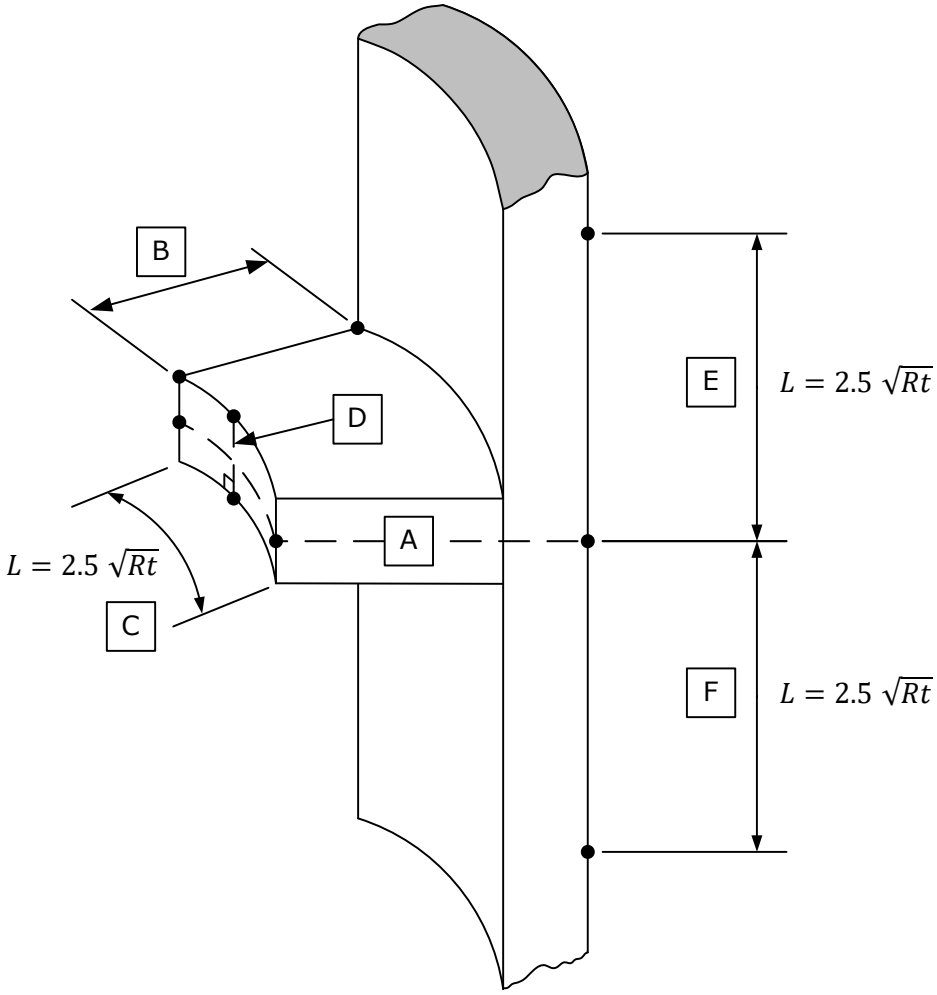

A,B: Through-Thickness Temperature Difference (Radial Direction)

C: Surface Temperature Difference (Circumferential Direction)

D,E,F: Surface Temperature Difference (Meridional Direction)

Figure 14.7 – Examples of Adjacent Points Near an Integral Ring-to-Shell Junction for Fatigue Screening Method B, STEP 4

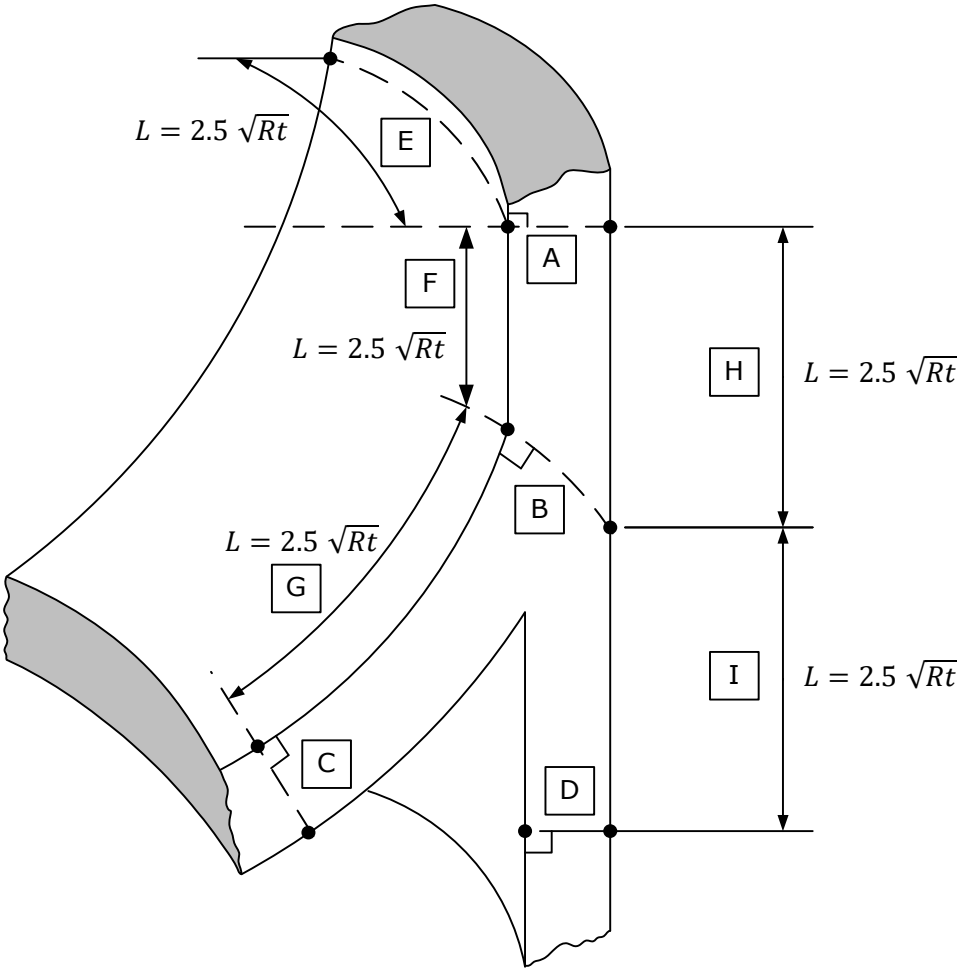

A,B,C,D: Through-Thickness Temperature Difference

E: Surface Temperature Difference (Circumferential Direction)

F,G,H,I: Surface Temperature Difference (Meridional Direction)

Figure 14.8 – Examples of Adjacent Points Near a Head-to-Skirt Junction for Fatigue Screening Method B, STEP 4

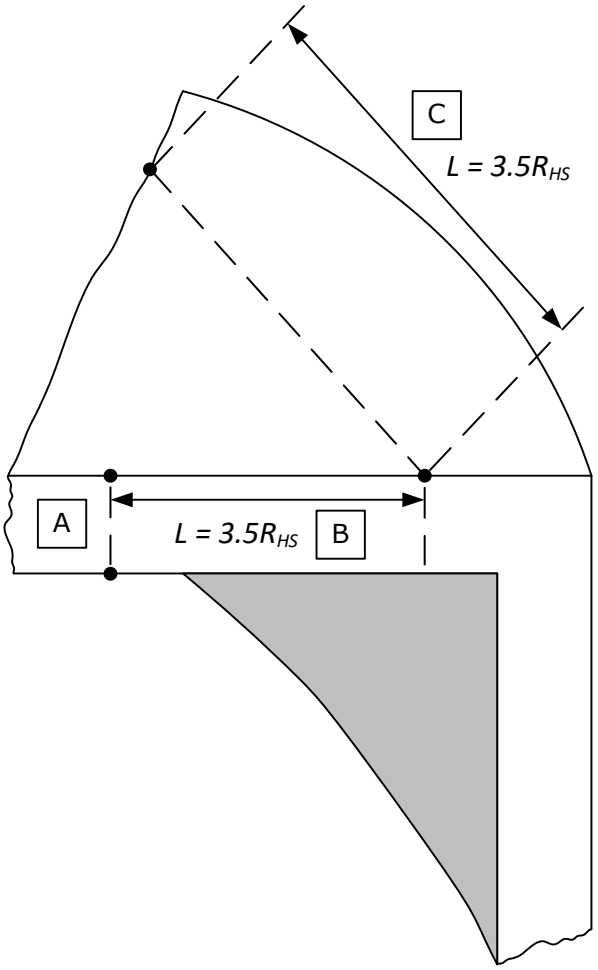

A: Through-Thickness Temperature Difference

B,C: Surface Temperature Difference (Any Direction on Plane of Surface)

Figure 14.9 – Examples of Adjacent Points on a Plate for Fatigue Screening Method B, STEP 4

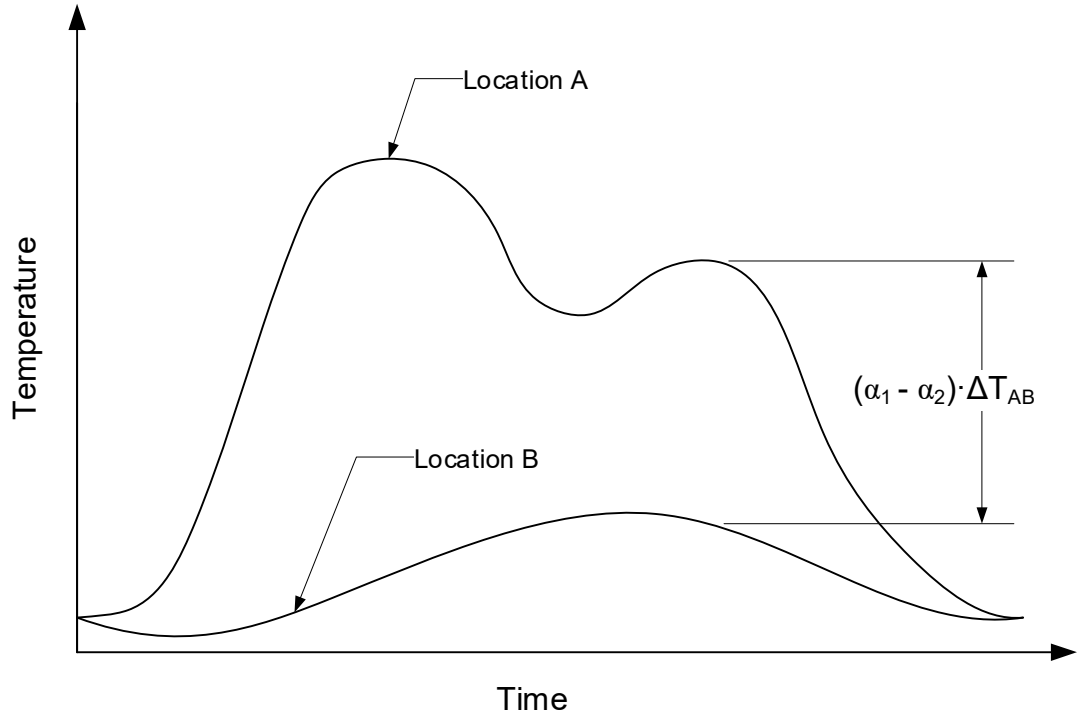

Note: Calculation of Temperature Difference $(\alpha_1 - \alpha_2)\cdot\Delta T_{AB}$ Between Two Points A and B as a Function of Time

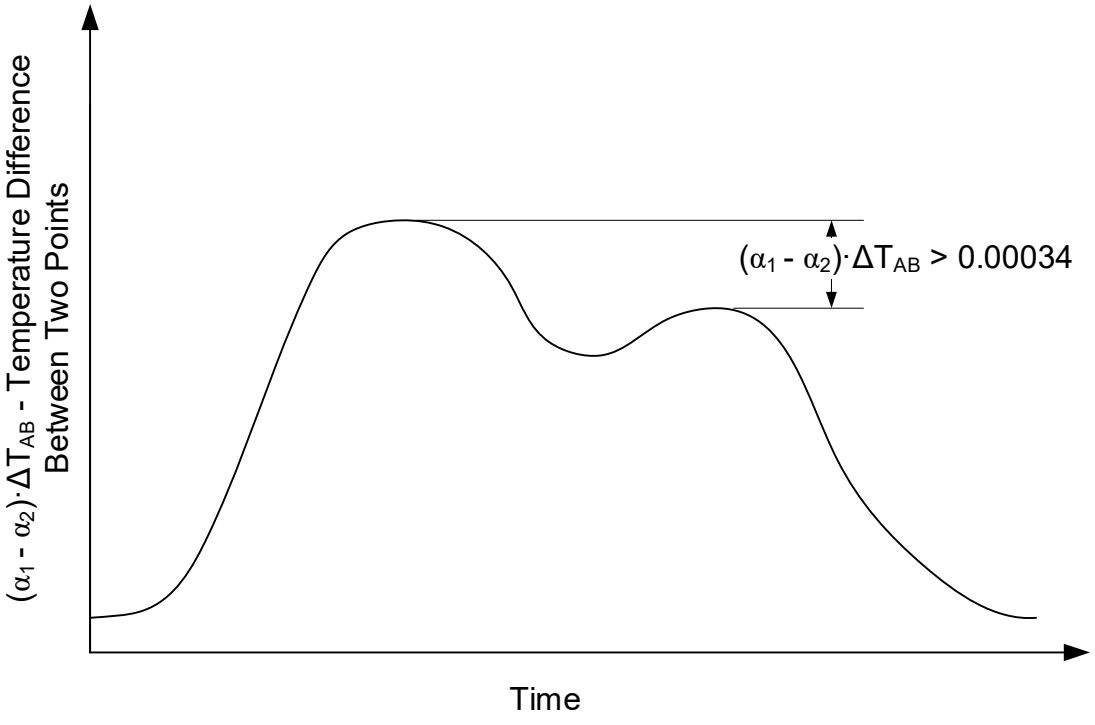

Figure 14.10 – Example of a Significant Temperature Cycle for Fatigue Screening Method B, STEP 5

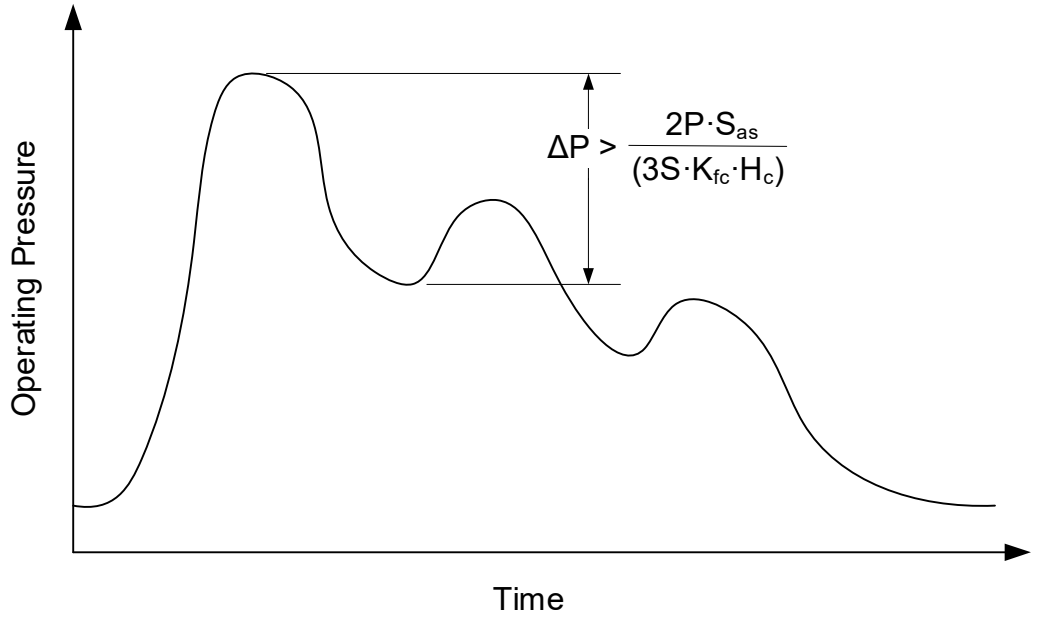

Figure 14.11 – Example of a Significant Pressure Cycle for Fatigue Screening Methods C and D, STEP 4

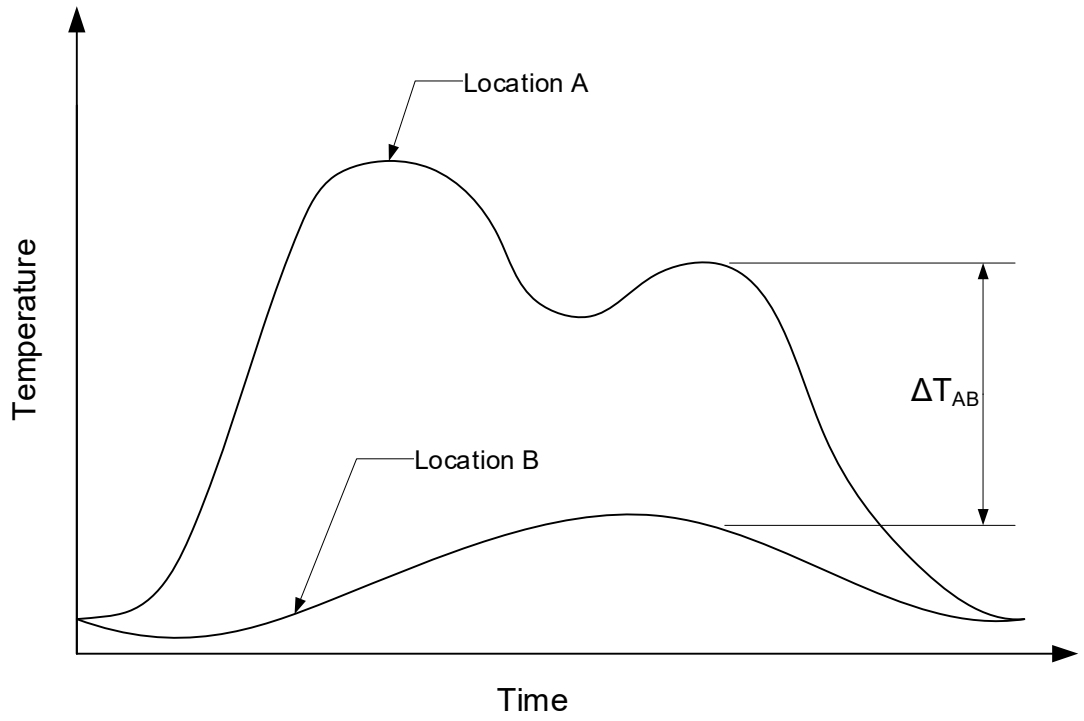

Note: Calculation of Temperature Difference ΔT_{AB} Between Two Points A and B as a Function of Time

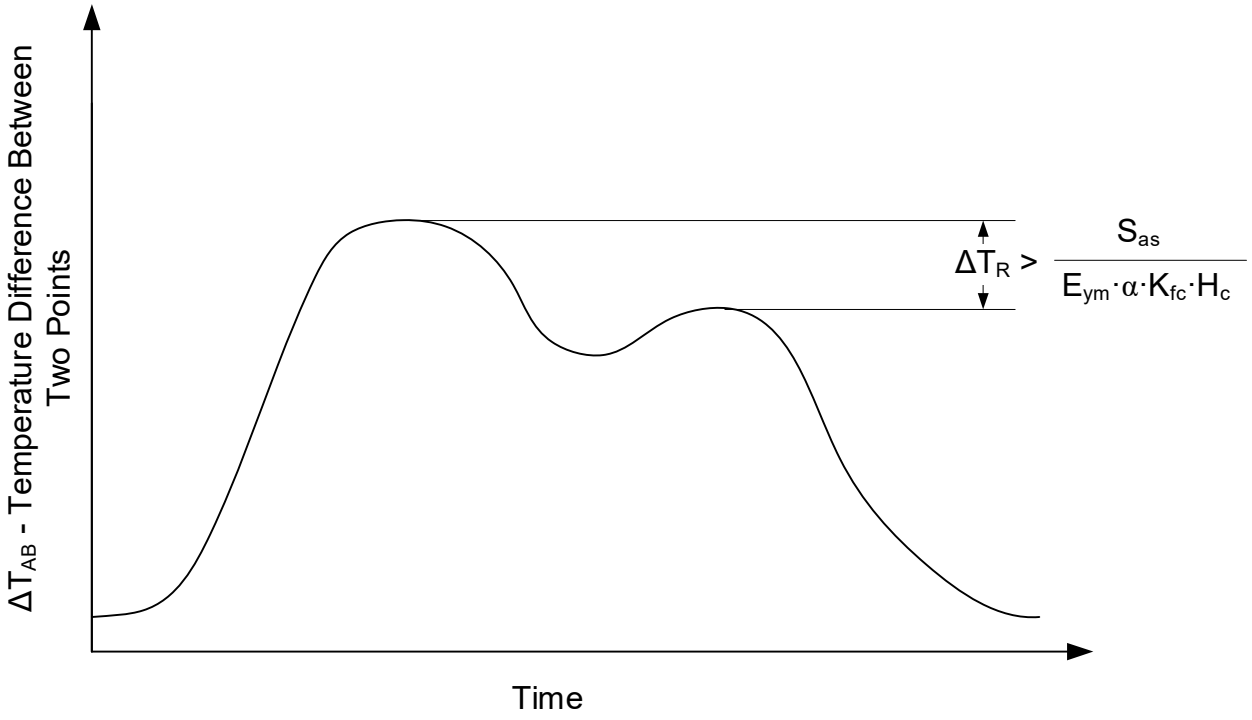

Figure 14.12 – Example of a Significant Temperature Difference Cycle for Fatigue Screening Methods C and D, STEP 6

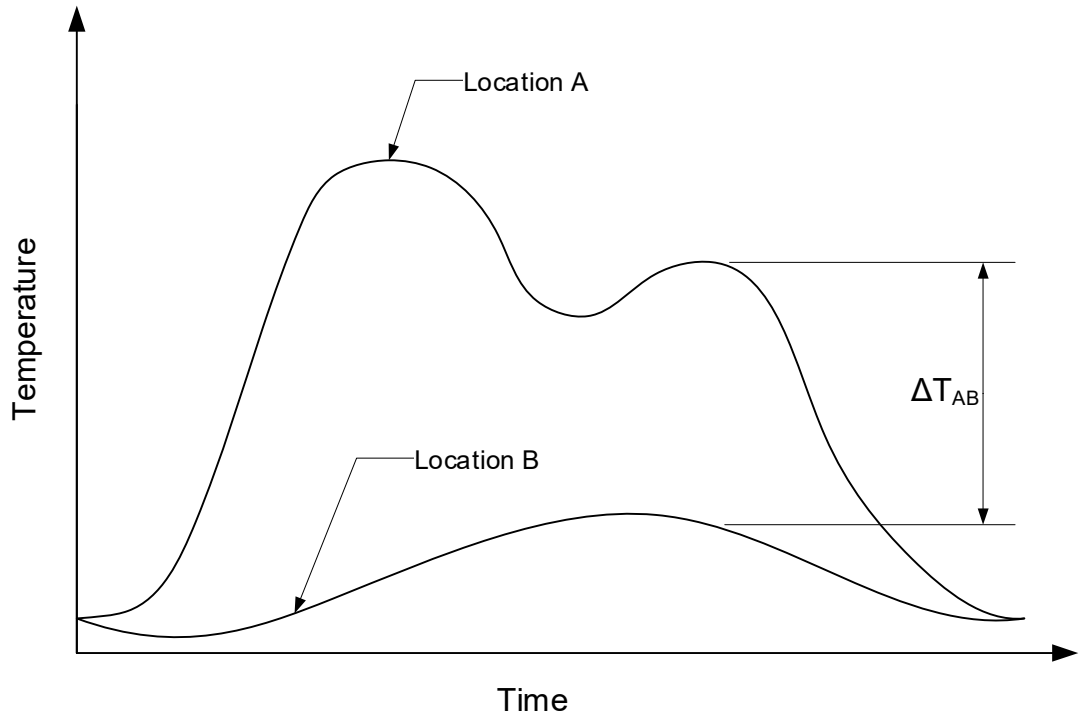

Note: Calculation of Temperature Difference ΔT_{AB} Between Two Points A and B as a Function of Time

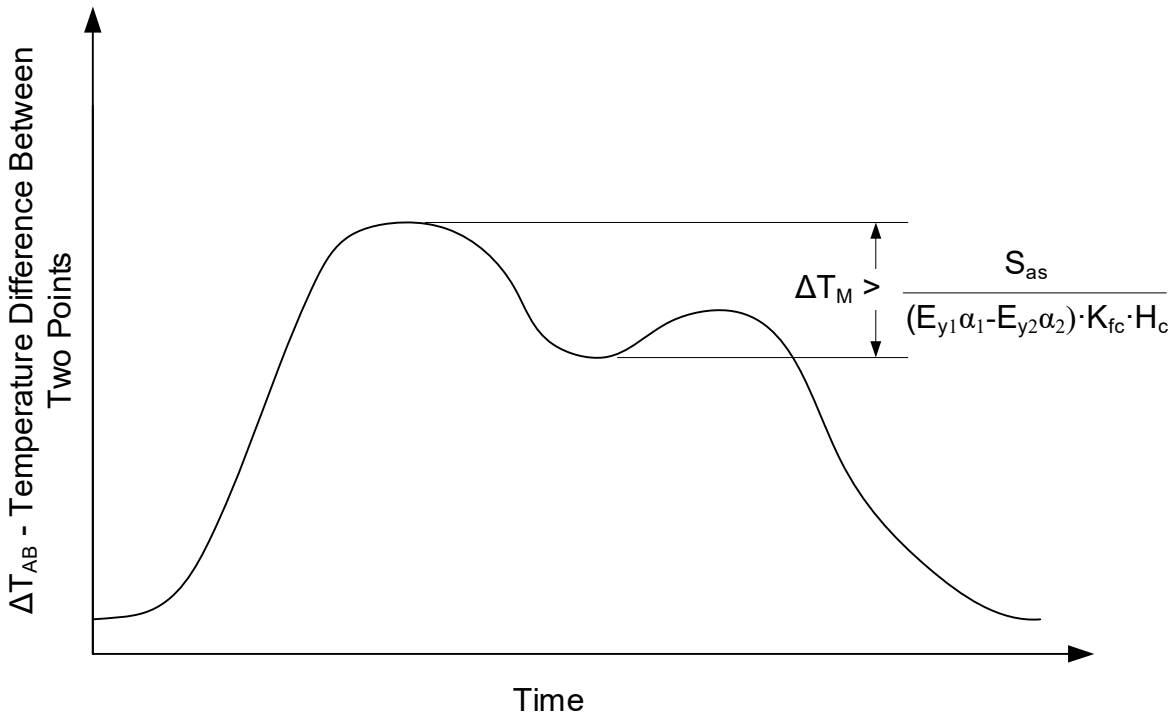

Figure 14.13 – Example of a Significant Temperature Difference Cycle for Fatigue Screening Methods C and D, STEP 7

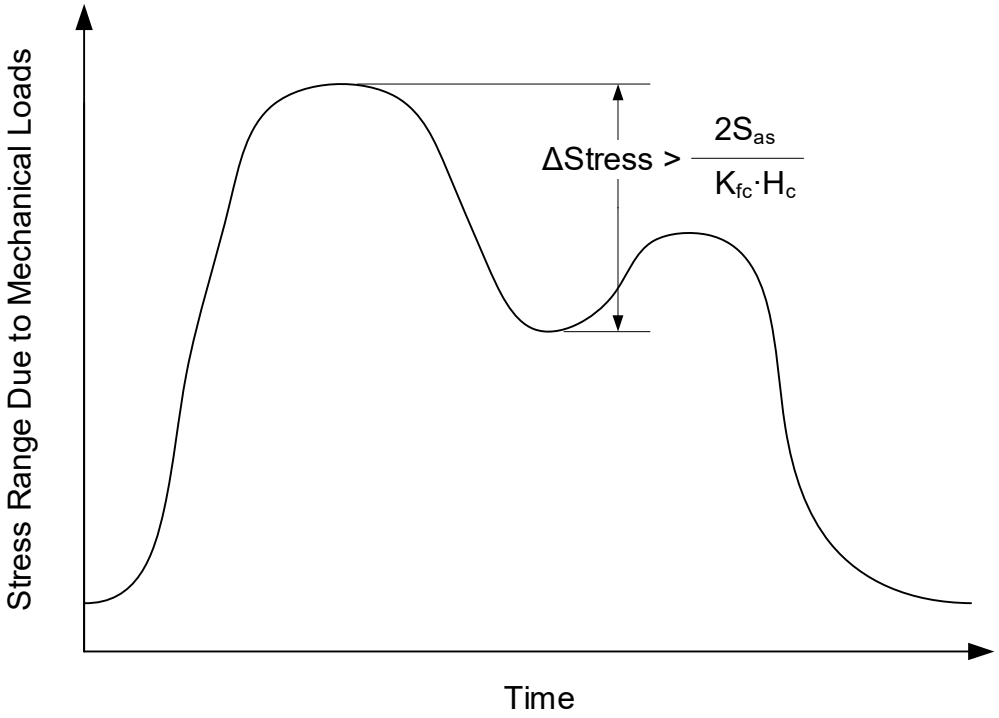

Figure 14.14 – Example of a Significant Mechanical Load Range Cycle for Fatigue Screening Methods C and D, STEP 8

Stress Category	Primary			Secondary Membrane plus Bending	Peak
	General Membrane	Local Membrane	Bending		
Description (see Annex 2D and VIII-2, Part 5)	Average primary stress across solid section. Excludes discontinuities and concentrations. Produced only by mechanical loads.	Average stress across any solid section. Considers discontinuities but not concentrations. Produced only by mechanical loads.	Component of primary stress proportional to distance from centroid of solid section. Excludes discontinuities and concentrations. Produced only by mechanical loads.	Self-equilibrating stress necessary to satisfy continuity of structure. Occurs at structural discontinuities. Can be caused by mechanical load or by differential thermal expansion. Excludes local stress concentrations.	1. Increment added to primary or secondary stress by a concentration (notch). 2. Certain thermal stresses which may cause fatigue but not distortion of vessel shape.
Symbol	P_m	P_L	P_b	Q	F

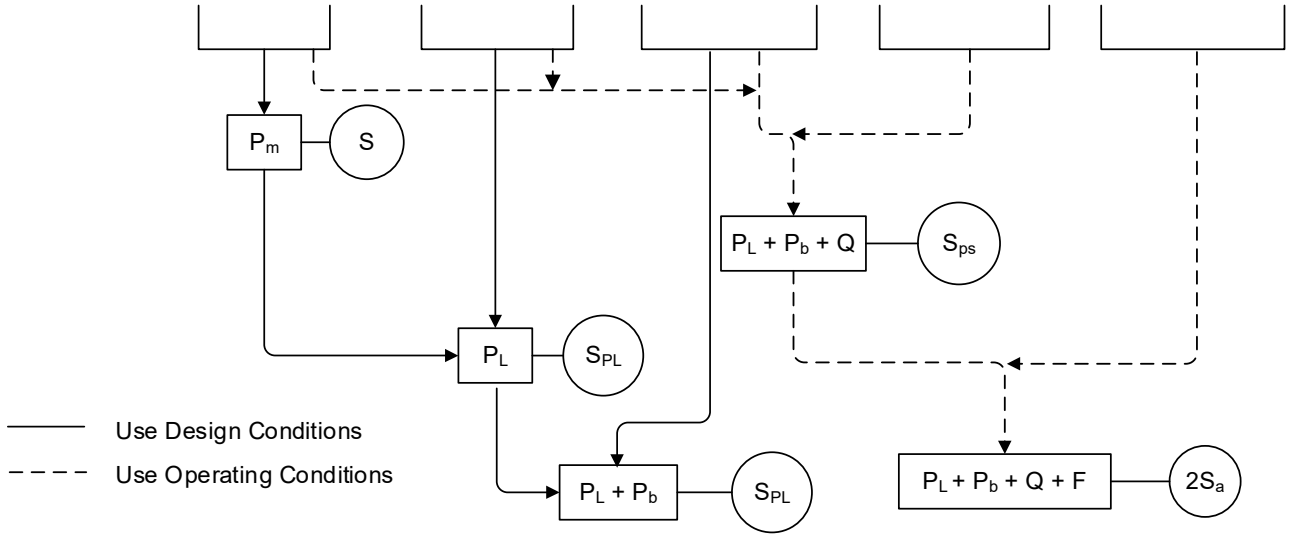

Figure 14.15 – Stress Categories and Limits of Equivalent Stress

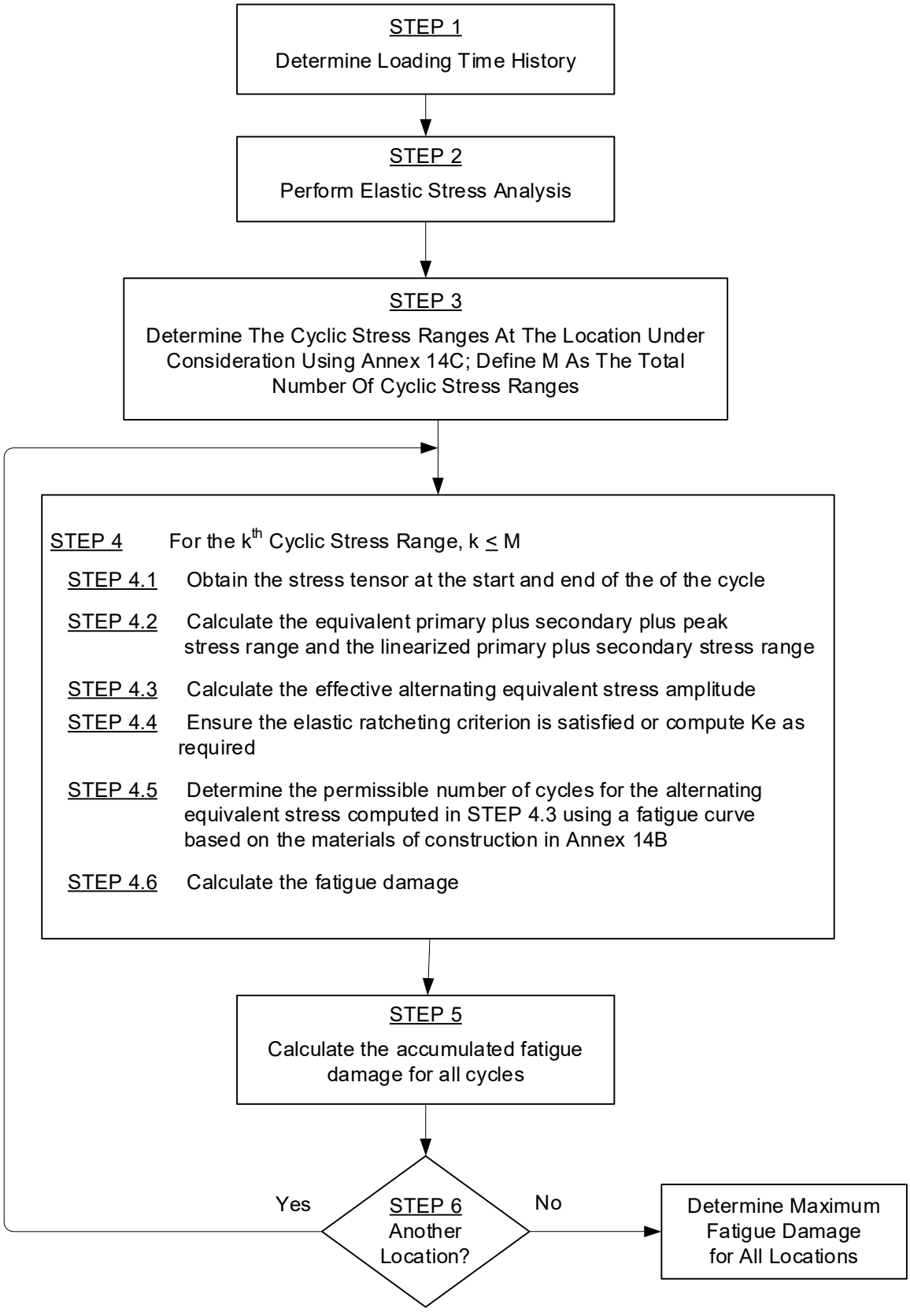

Figure 14.16 – Level 2, Method A Fatigue Assessment Method

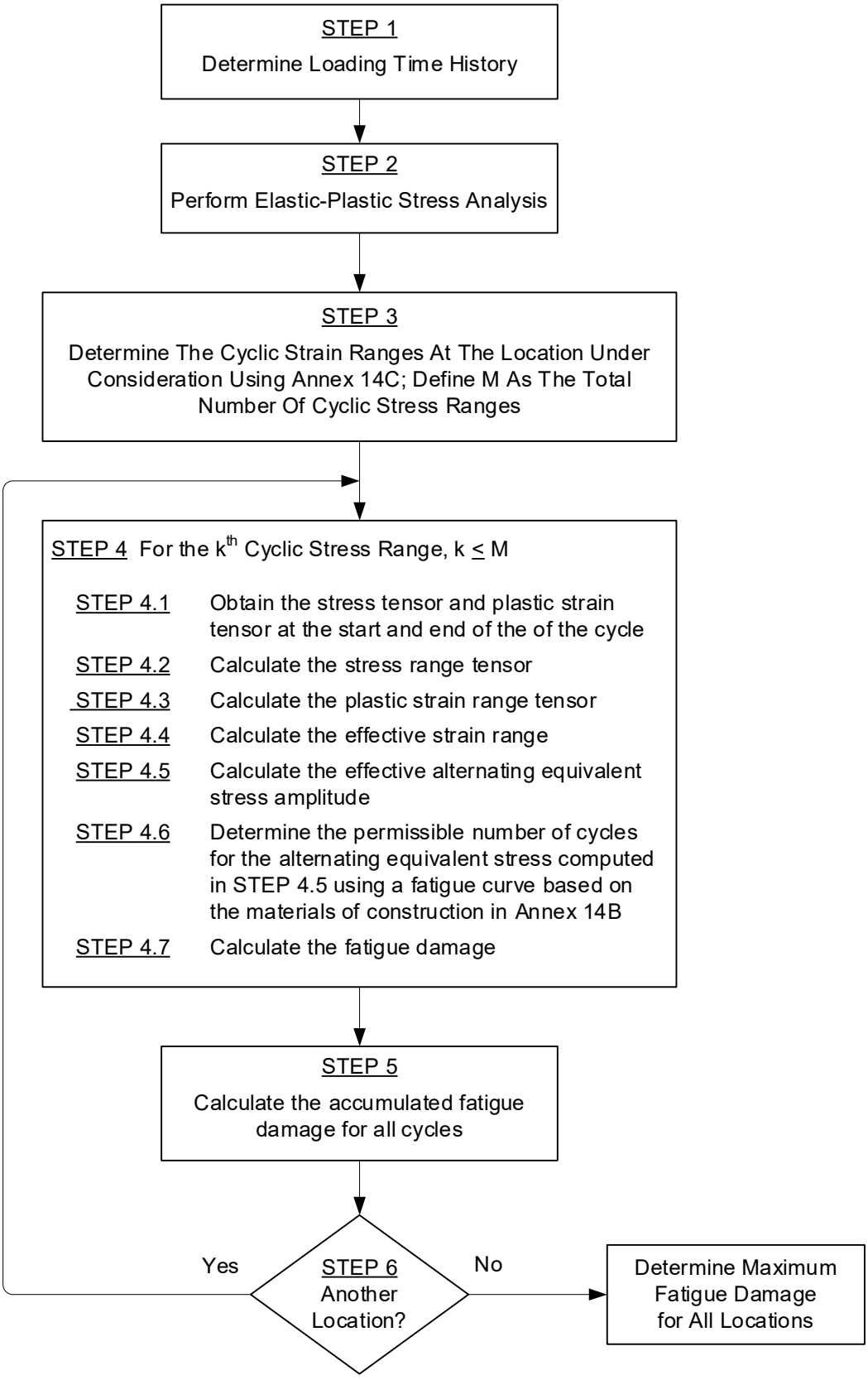

Figure 14.17 – Level 2, Method B Fatigue Assessment Method

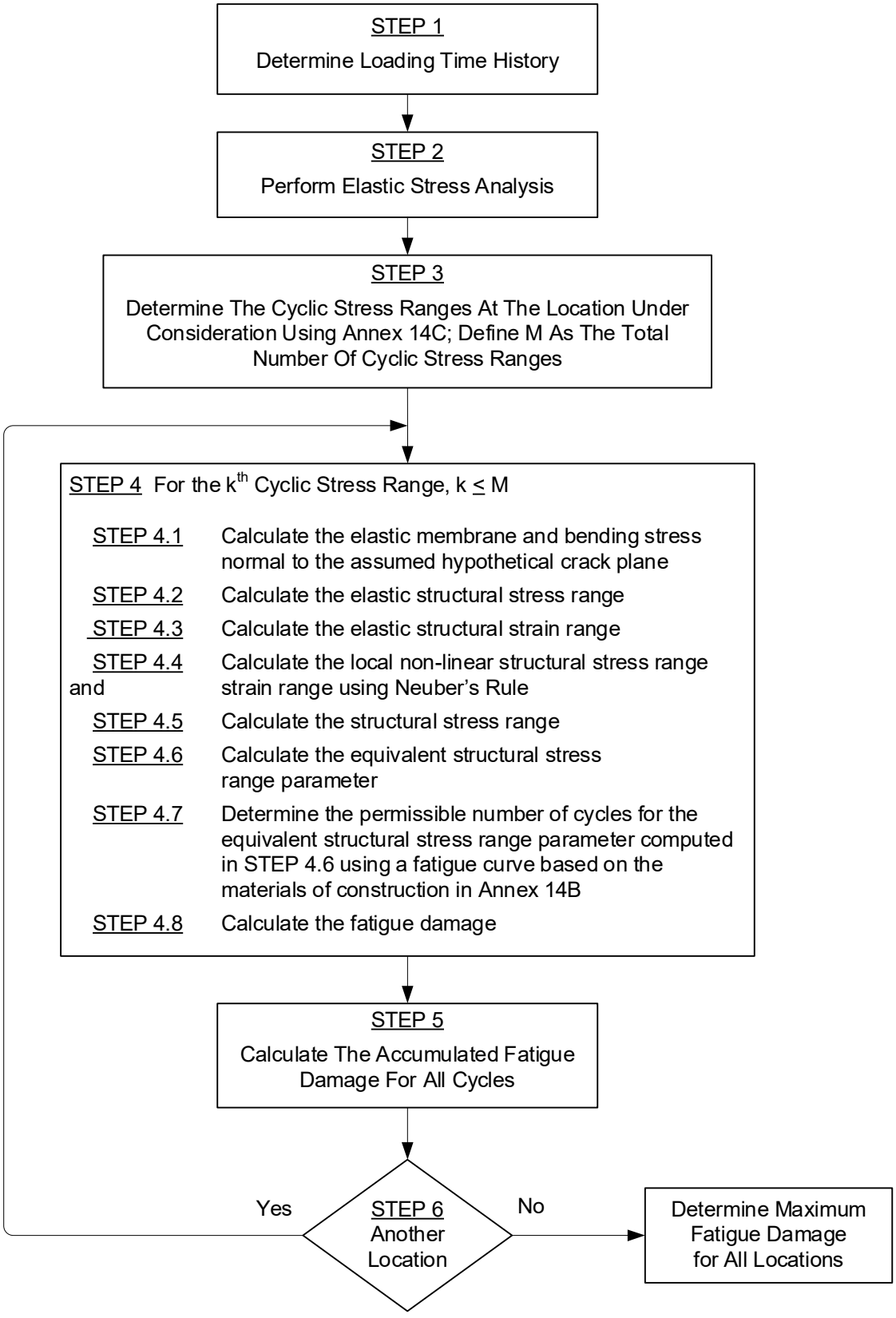

Figure 14.18 – Level 2, Method C Fatigue Assessment Method

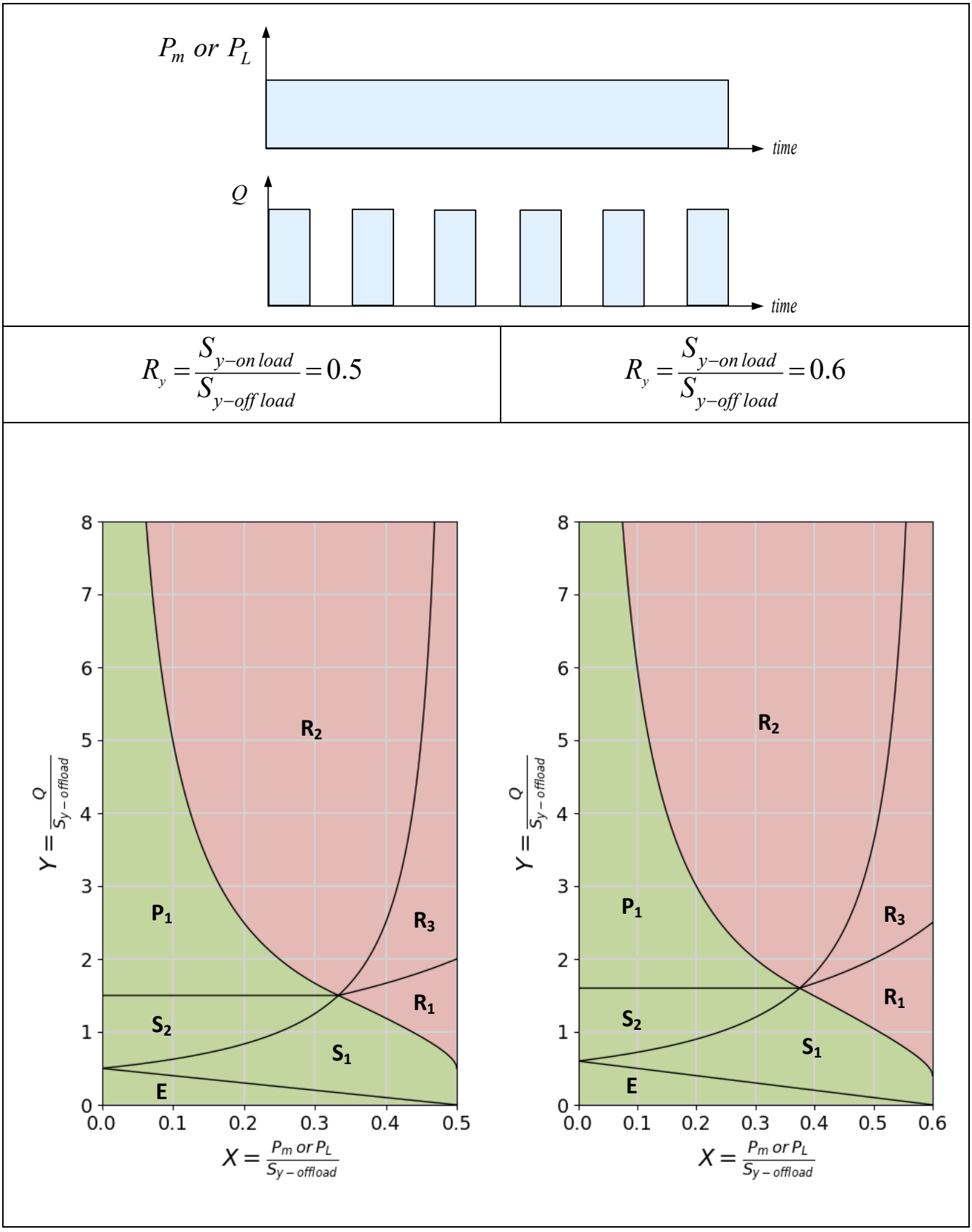

Figure 14.19 – Bree Diagram for Load Case A – Fixed Primary Load and a Cyclic Secondary Load with Different Yield Stresses in the On-Load and Off-Load Condition

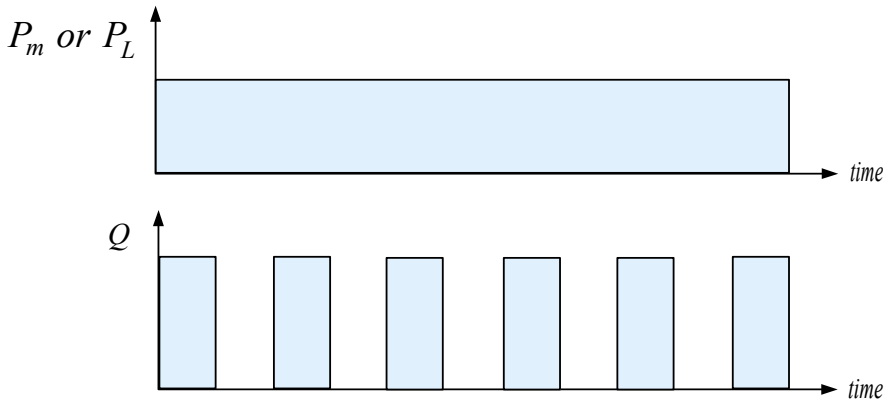

$R_y = \frac{S_{y-on\,load}}{S_{y-off\,load}} = 0.7$	$R_y = \frac{S_{y-on\,load}}{S_{y-off\,load}} = 0.8$

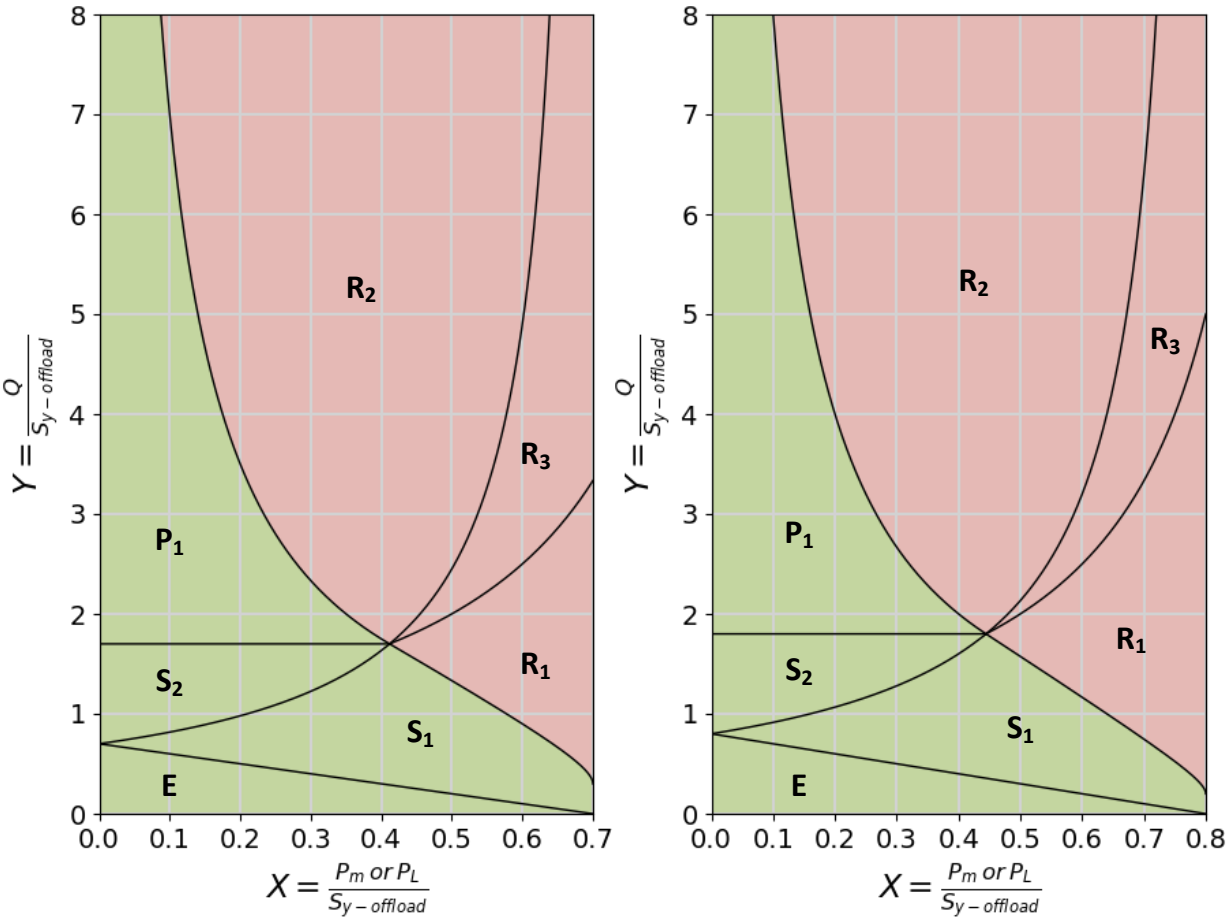

Figure 14.19 – Bree Diagram for Load Case A – Fixed Primary Load and a Cyclic Secondary Load with Different Yield Stresses in the On-Load and Off-Load Condition (Continued)

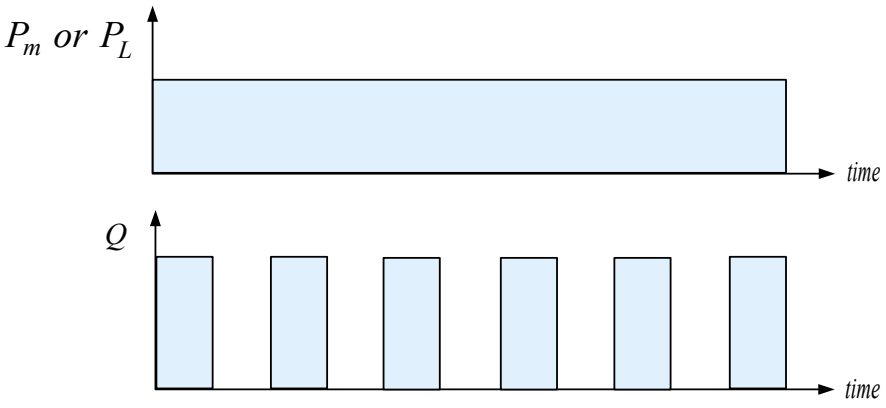

$R_y = \frac{S_{y-on\ load}}{S_{y-off\ load}} = 0.9$	$R_y = \frac{S_{y-on\ load}}{S_{y-off\ load}} = 1.0$

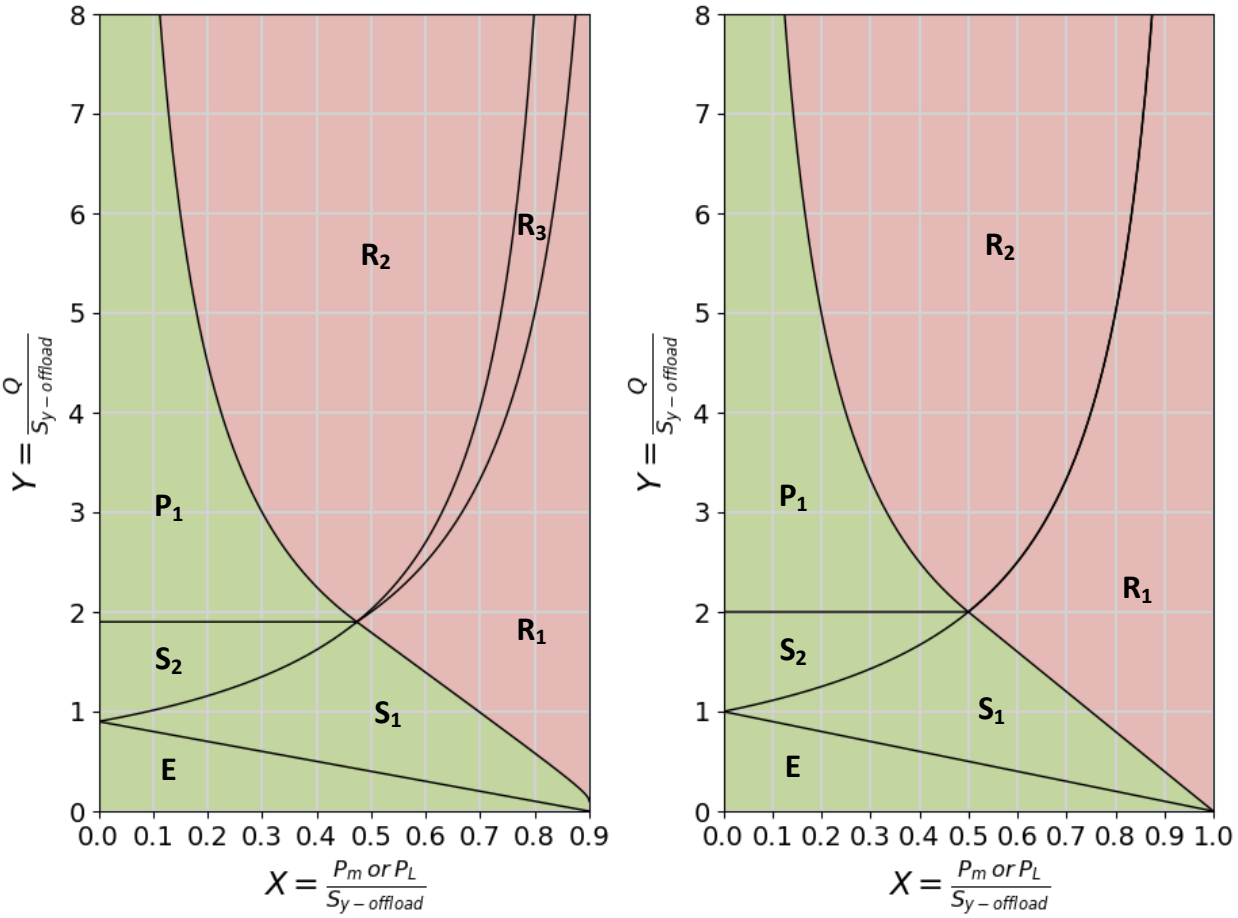

Figure 14.19 – Bree Diagram for Load Case A – Fixed Primary Load and a Cyclic Secondary Load with Different Yield Stresses in the On-Load and Off-Load Condition (Continued)

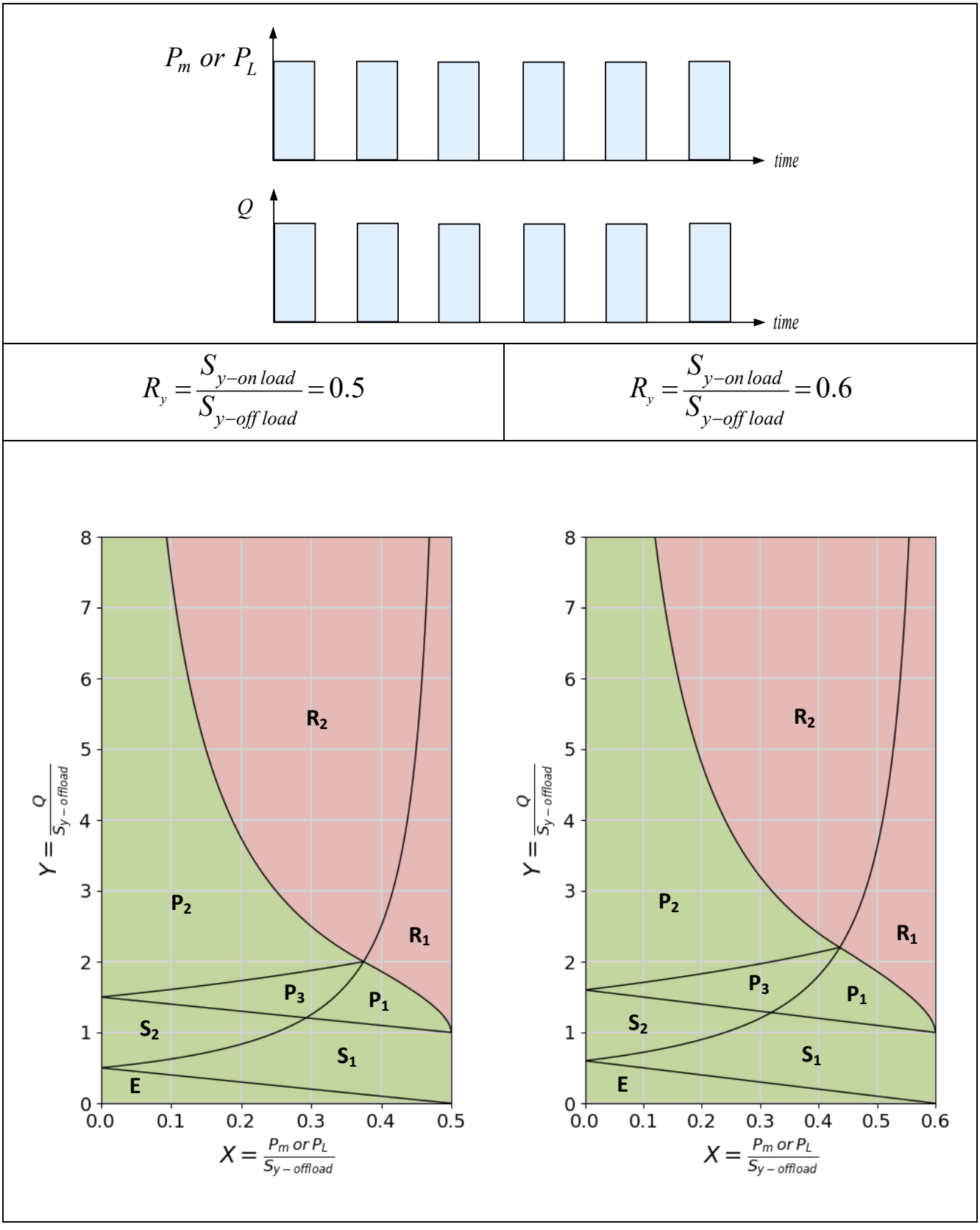

Figure 14.20 – Bree Diagram for Load Case B – Cyclic Primary Load and a Cyclic Secondary Load that are in Phase with Different Yield Stresses in the On-Load and Off-Load Condition

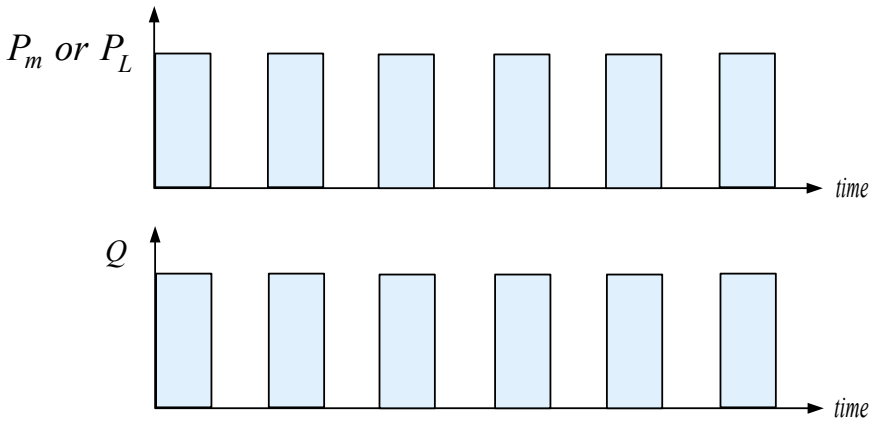

$R_y = \frac{S_{y-on\ load}}{S_{y-off\ load}} = 0.7$	$R_y = \frac{S_{y-on\ load}}{S_{y-off\ load}} = 0.8$

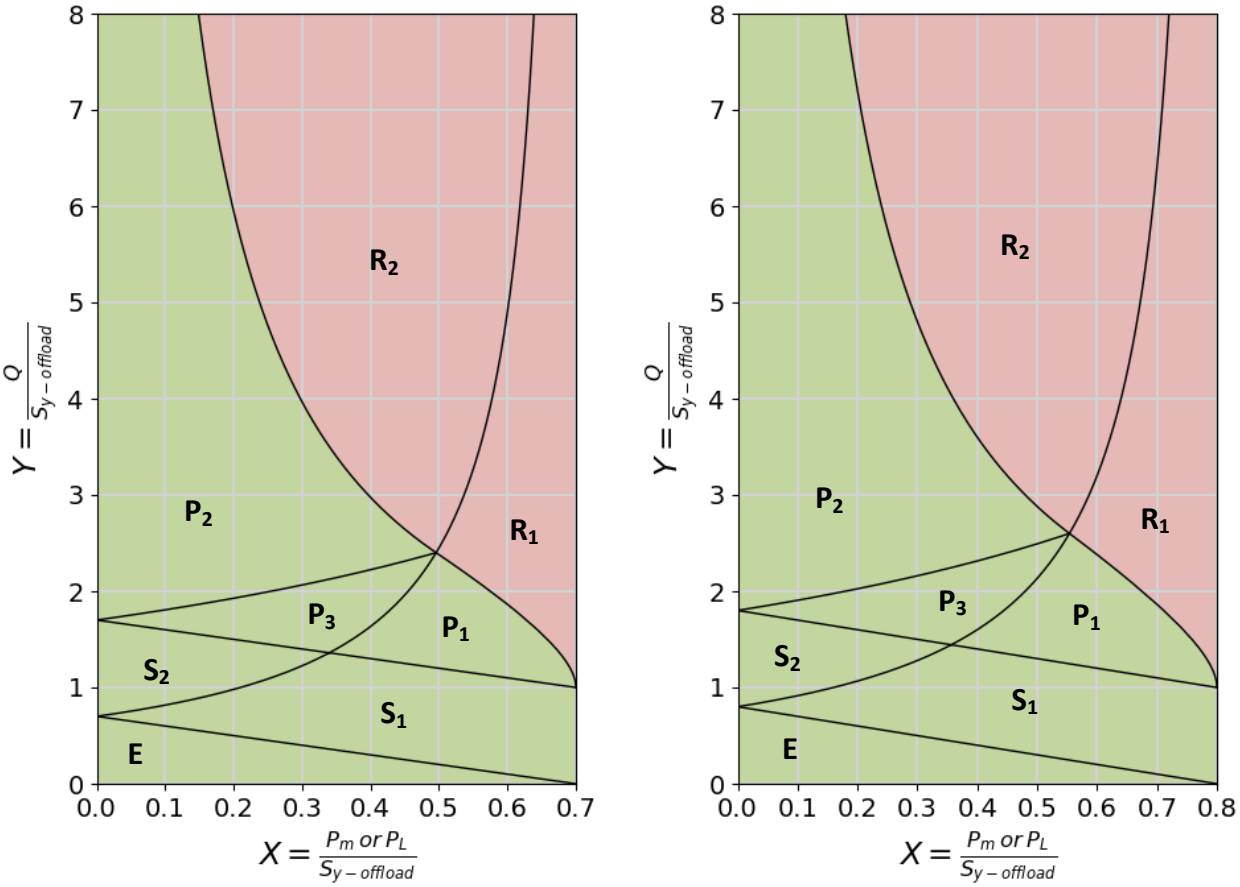

Figure 14.20 – Bree Diagram for Load Case B – Cyclic Primary Load and a Cyclic Secondary Load that are in Phase with Different Yield Stresses in the On-Load and Off-Load Condition (Continued)

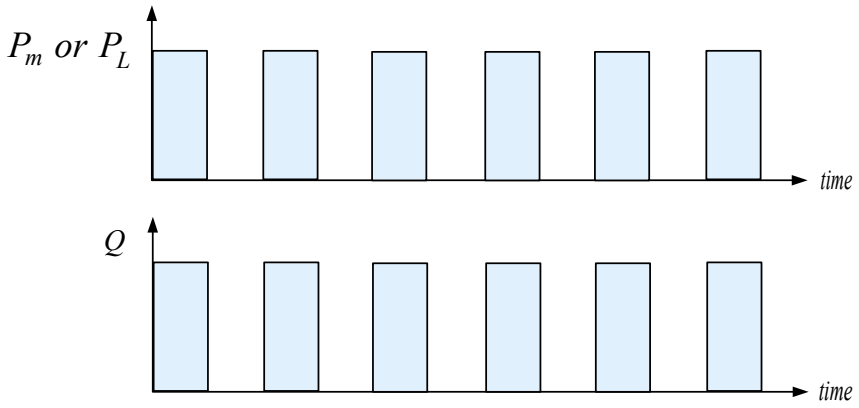

$R_y = \frac{S_{y-on\ load}}{S_{y-off\ load}} = 0.9$	$R_y = \frac{S_{y-on\ load}}{S_{y-off\ load}} = 1.0$

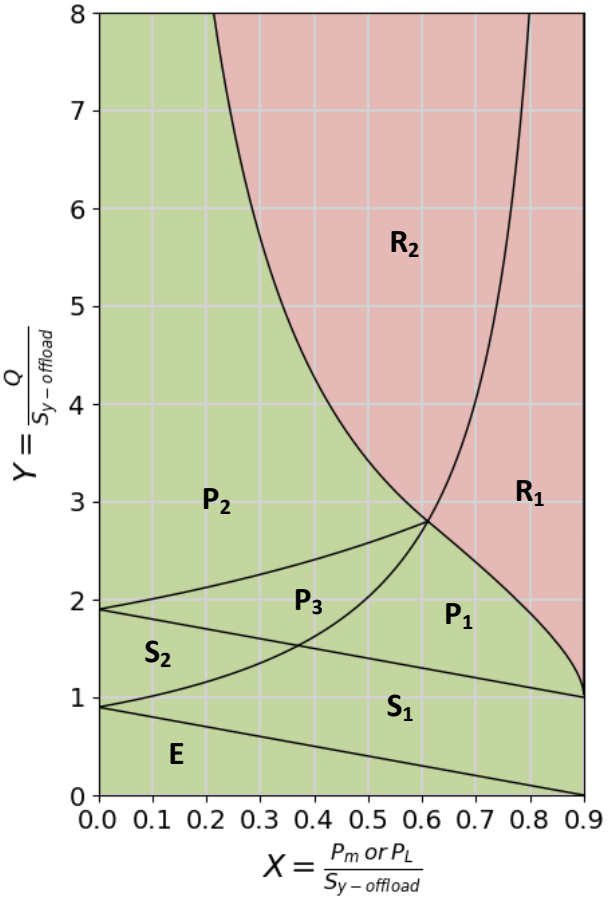

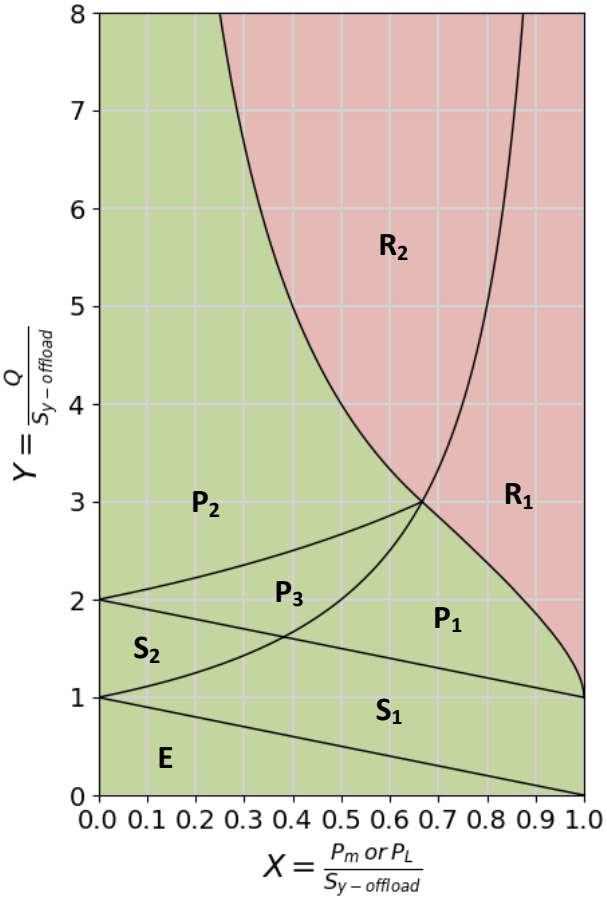

Figure 14.20 – Bree Diagram for Load Case B – Cyclic Primary Load and a Cyclic Secondary Load that are in Phase with Different Yield Stresses in the On-Load and Off-Load Condition (Continued)

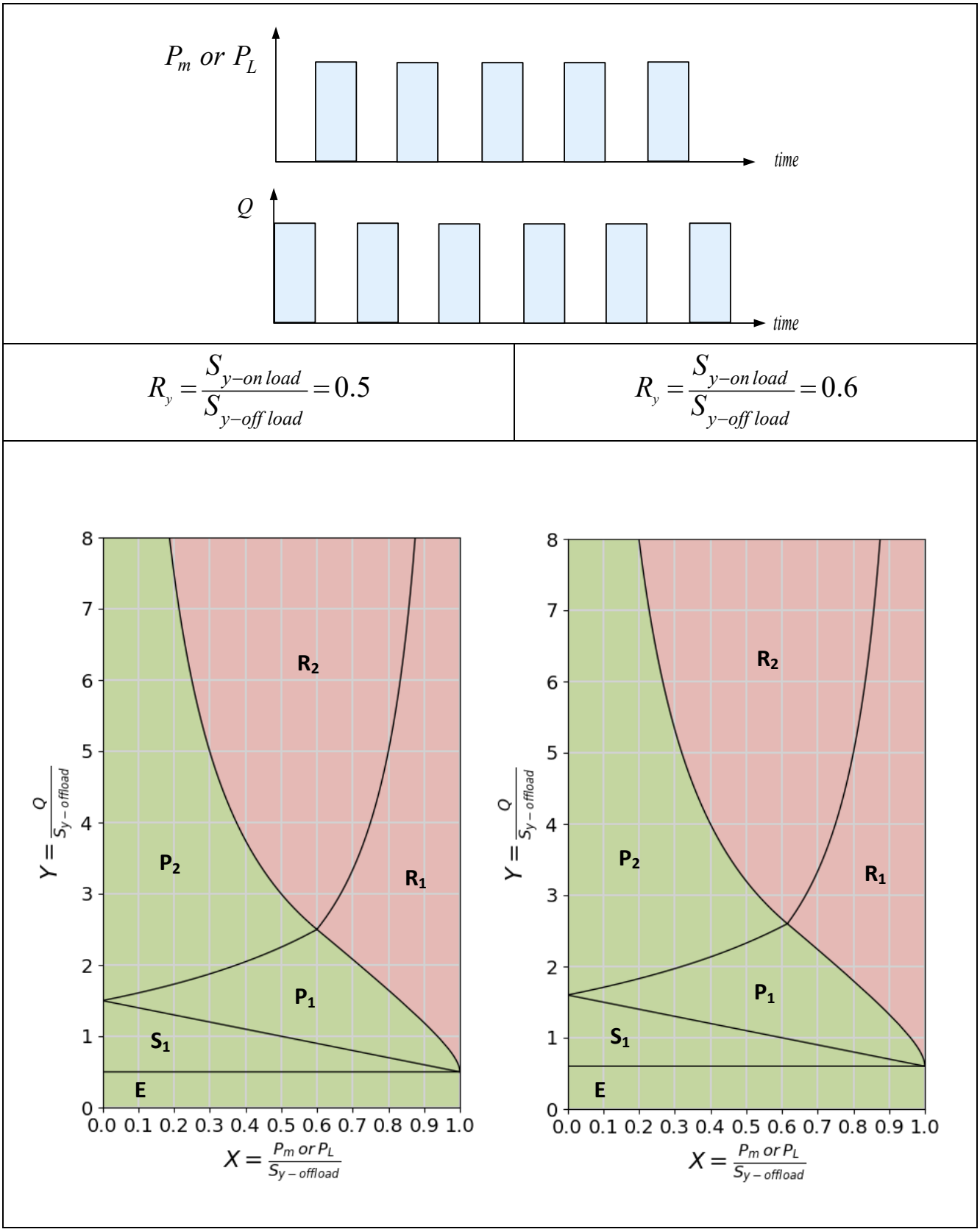

Figure 14.21 – Bree Diagram for Load Case C – Cyclic Primary Load and a Cyclic Secondary Load that are Out of Phase with Different Yield Stresses in the On-Load and Off-Load Condition

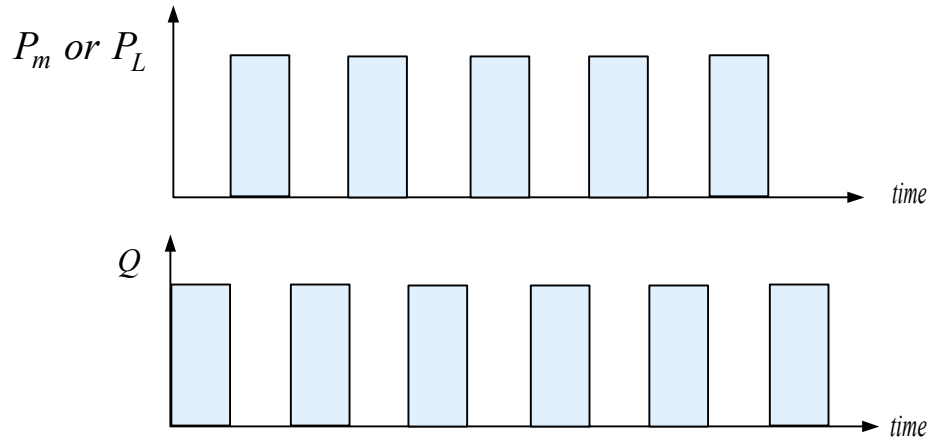

$R_y = \frac{S_{y-on\ load}}{S_{y-off\ load}} = 0.7$	$R_y = \frac{S_{y-on\ load}}{S_{y-off\ load}} = 0.8$

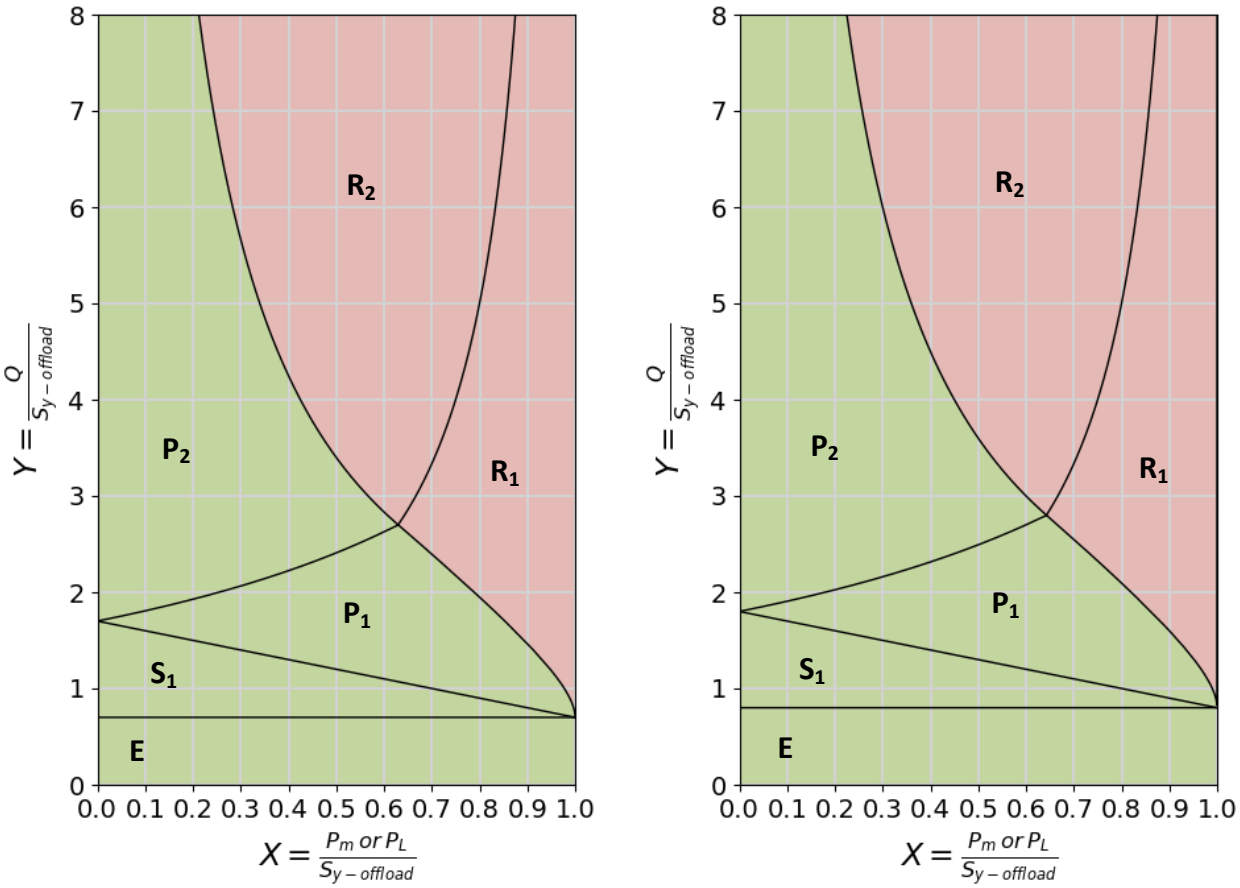

Figure 14.21 – Bree Diagram for Load Case C – Cyclic Primary Load and a Cyclic Secondary Load that are Out of Phase with Different Yield Stresses in the On-Load and Off-Load Condition (Continued)

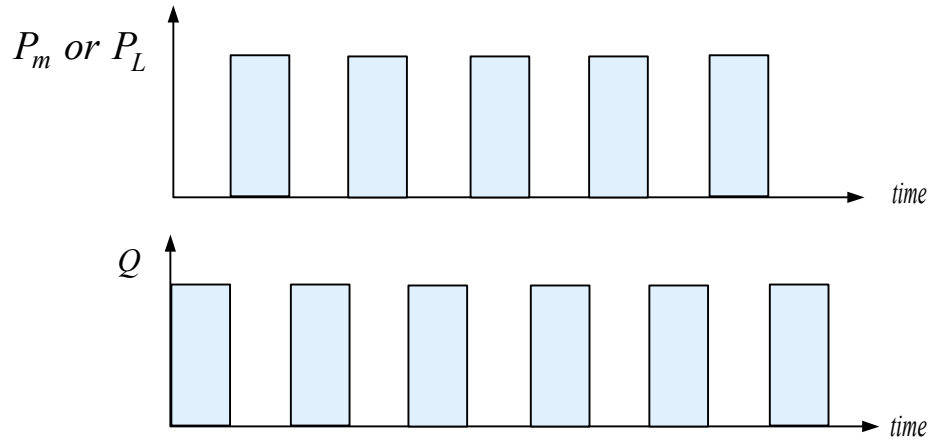

$R_y = \frac{S_{y-on\ load}}{S_{y-off\ load}} = 0.9$	$R_y = \frac{S_{y-on\ load}}{S_{y-off\ load}} = 1.0$

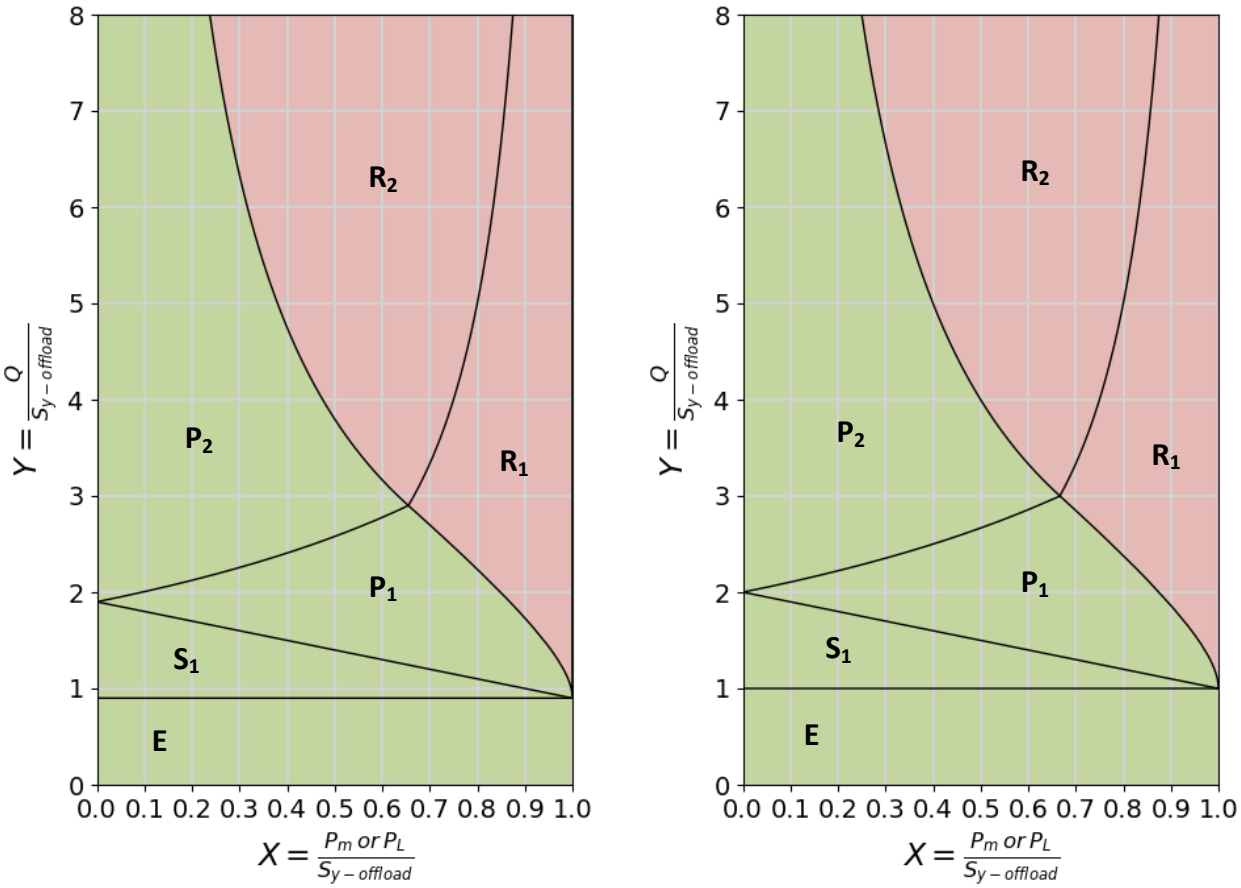

Figure 14.21 – Bree Diagram for Load Case C – Cyclic Primary Load and a Cyclic Secondary Load that are Out of Phase with Different Yield Stresses in the On-Load and Off-Load Condition (Continued)

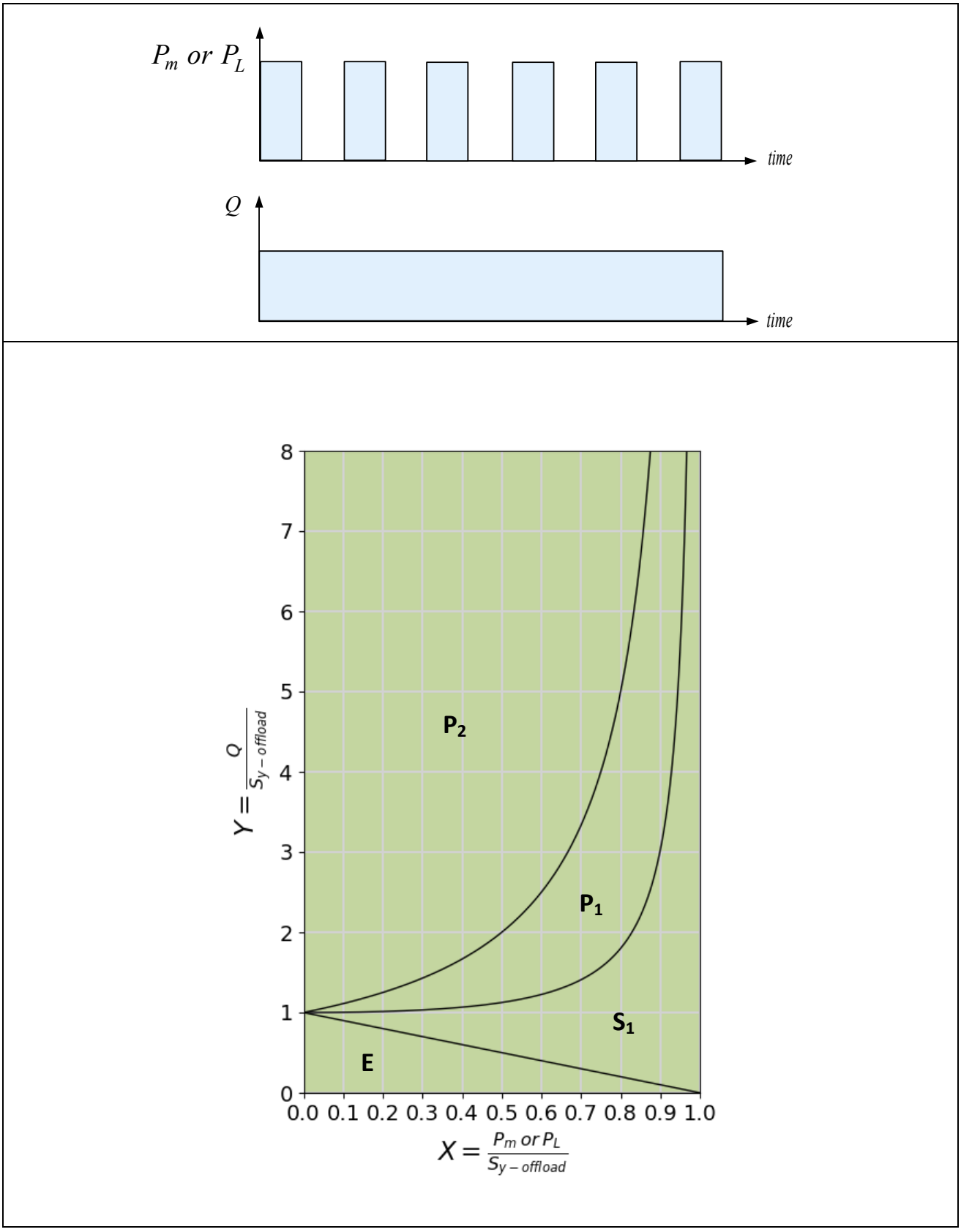

Figure 14.22 – Bree Diagram for Load Case D – Cyclic Primary Load and a Fixed Secondary Load with Different Yield Stresses in the On-Load and Off-Load Condition

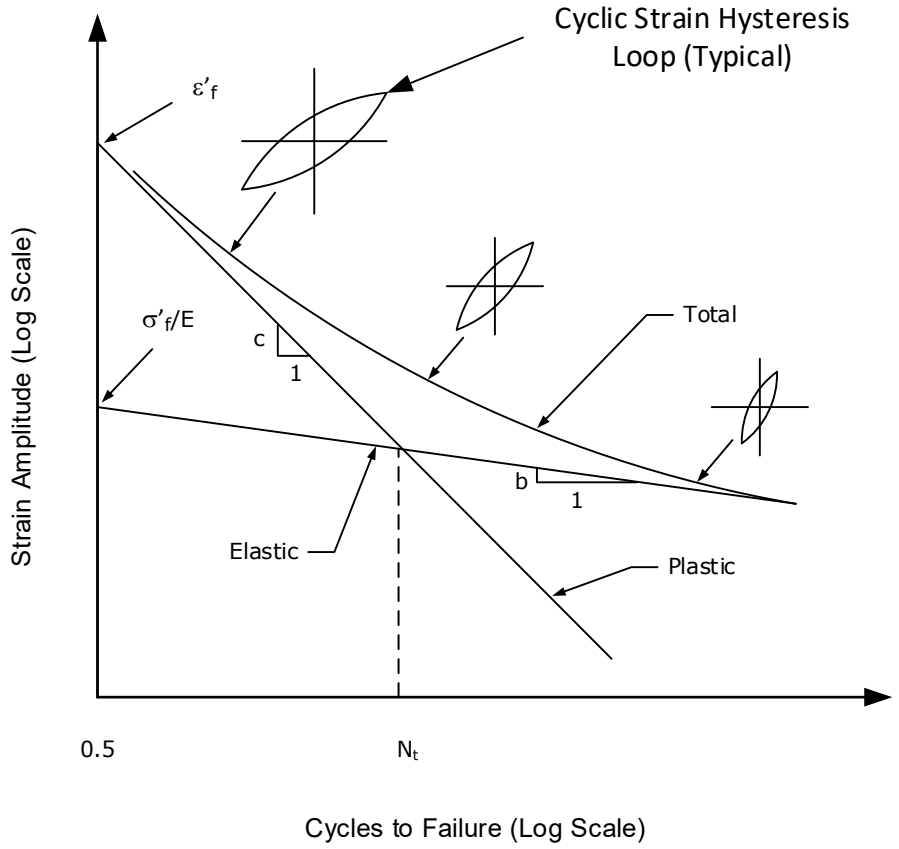

Figure 14.23 – Multiaxial Strain-Life Approach

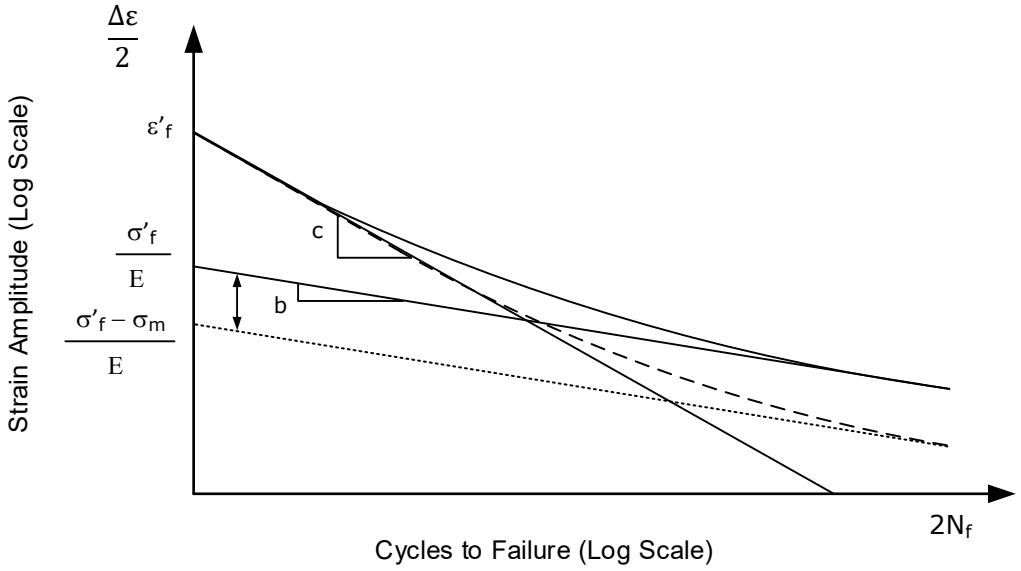

Figure 14.24 – Morrow mean Stress Correction

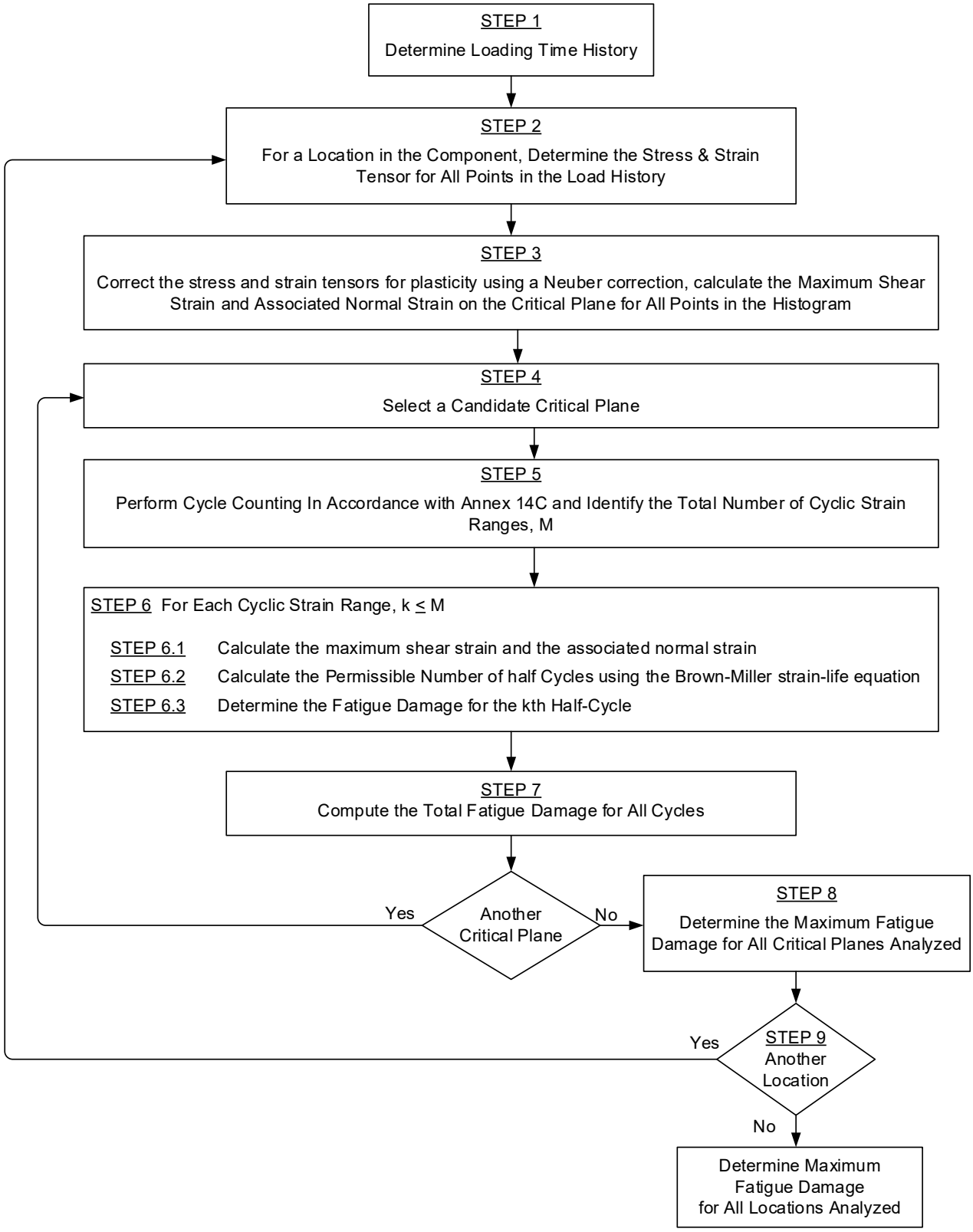

Figure 14.25 – Level 3 Method A Fatigue Damage Calculation Based on a Multiaxial Strain-Life Equation in Combination with a Critical Plane Approach

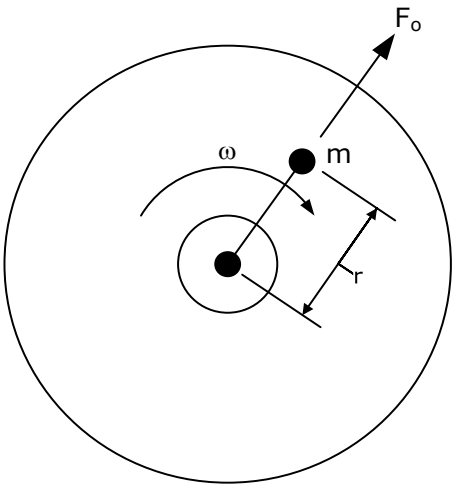

$F_o = mr\omega^2 \sin[\omega t]$

Where:
F_o = Unbalanced Harmonic Force, lb
m = Rotating Mass, lb-sec^2/in
r = Eccentricity, in
ω = Operating Speed, rad/sec
t = time

(a) Unbalanced Force in Rotating Equipment

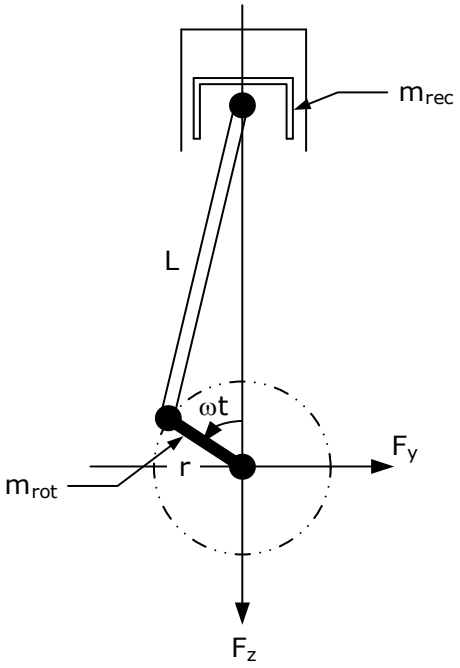

$F_y = m_{rot}\, r\omega^2 \sin[\omega t]$
$F_z = (m_{rec} + m_{rot})\, r\omega^2 \cos[\omega t] + m_{rec} \frac{r^2}{L} \omega^2 \cos[2\omega t]$

Where:
r = Crank Radius
L = Connecting Rod Length

(b) Total Forces in a Single Cylinder Reciprocating Machine

Figure 14.26 – Unbalanced Forces in Rotating Equipment (See Table 14.13)

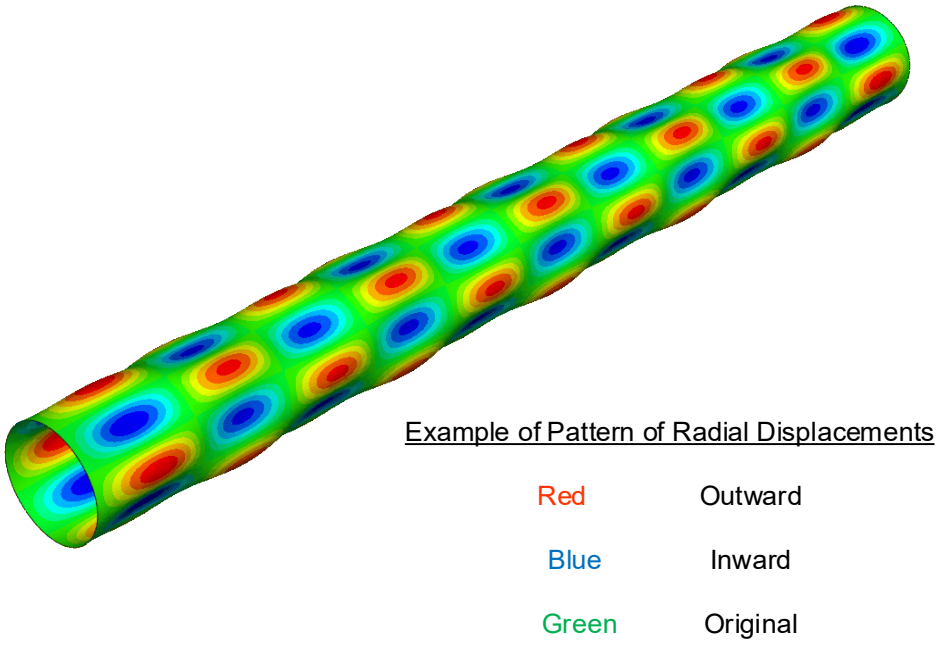

Figure 14.27 – Example of Pattern of Radial Displacements from Acoustic Vibration (See Table 14.13)

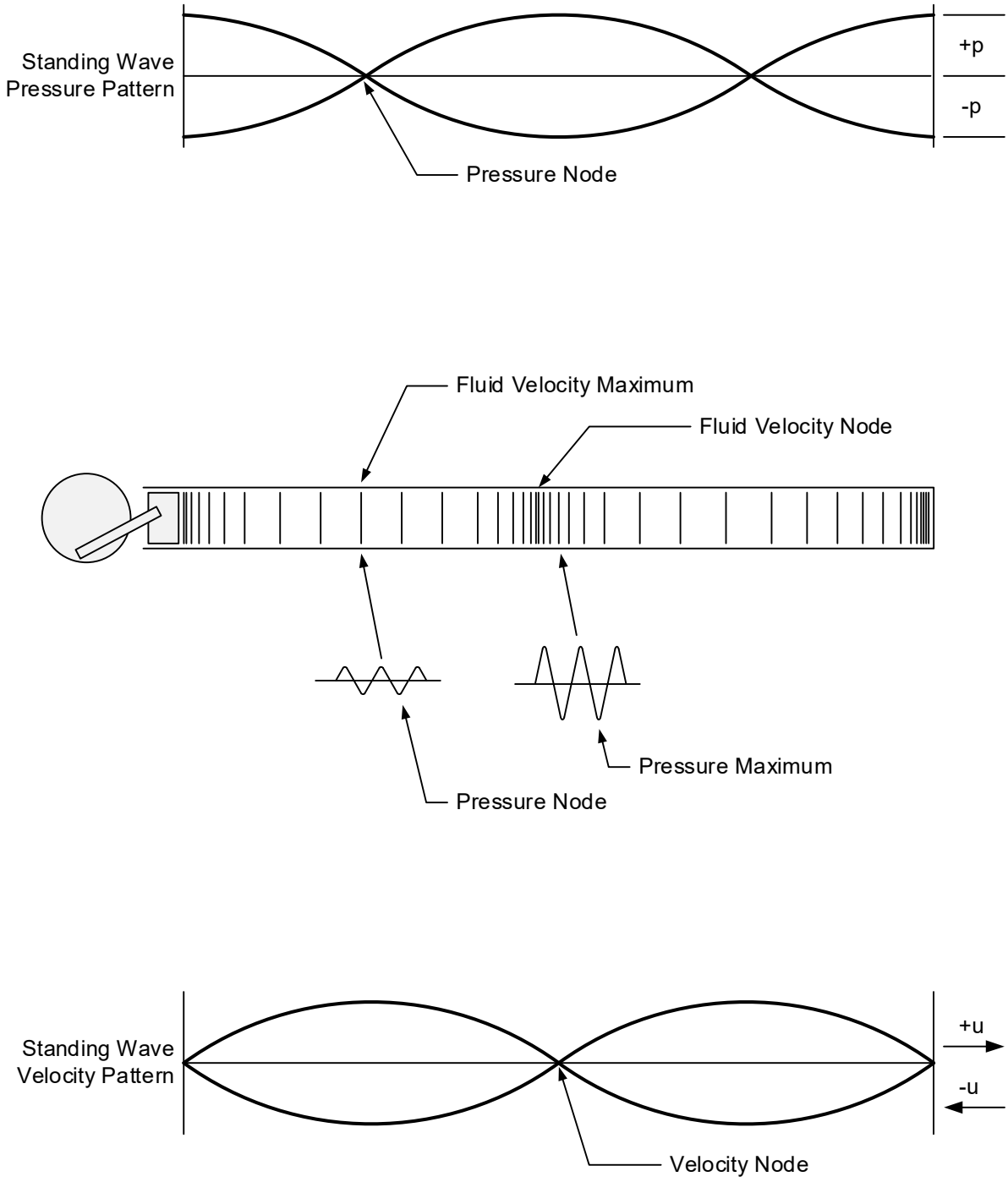

Figure 14.28 – Pulsation and Standing Wave Patterns Due to Acoustical Propagation in a Closed Pipe – Standing Waves in Piping Systems (See Table 14.13)

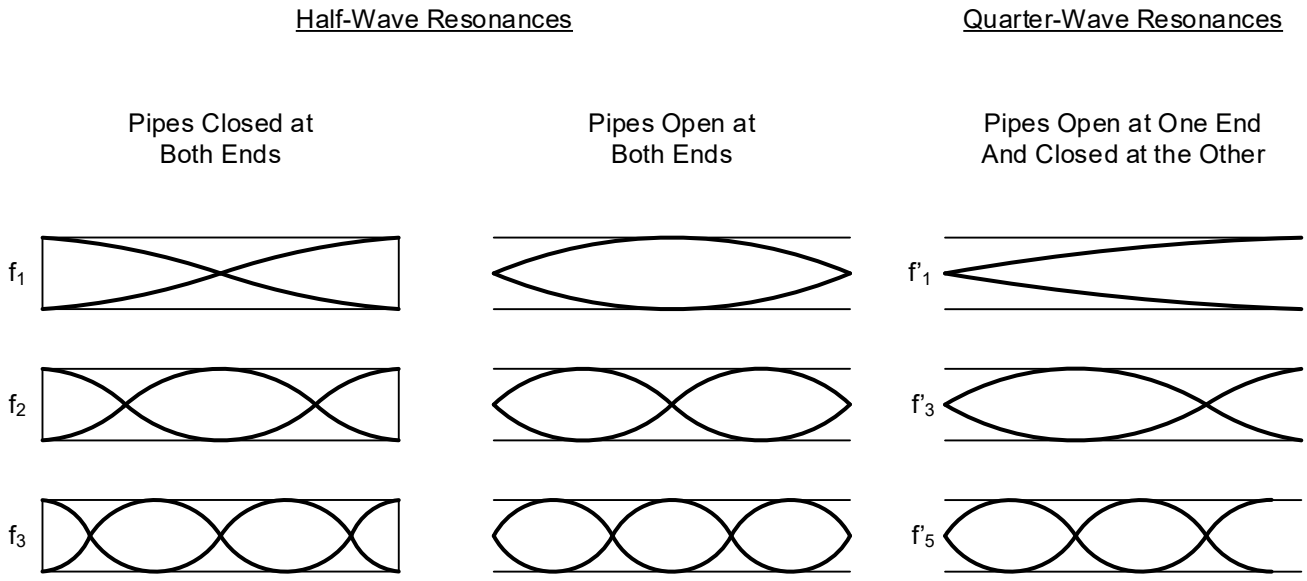

$$f = \frac{nc}{2L}$$

f_1 = 0.5 wave
f_2 = 1.0 wave
f_3 = 1.5 wave

$$f' = \frac{(2n-1)\,c}{4L}$$

f'_1 = 0.25 wave
f'_2 = 0.75 wave
f'_3 = 1.25 wave

Where:
f = Acoustic Natural Frequency, Hz
c = Acoustic Velocity
L = Length
n = Integers, 1,2,3, ...

Figure 14.29 – Pulsation and Standing Wave Patterns Due to Acoustical Propagation in Pipe – Half-Wave and Quarter Wave Resonances (See Table 14.13)

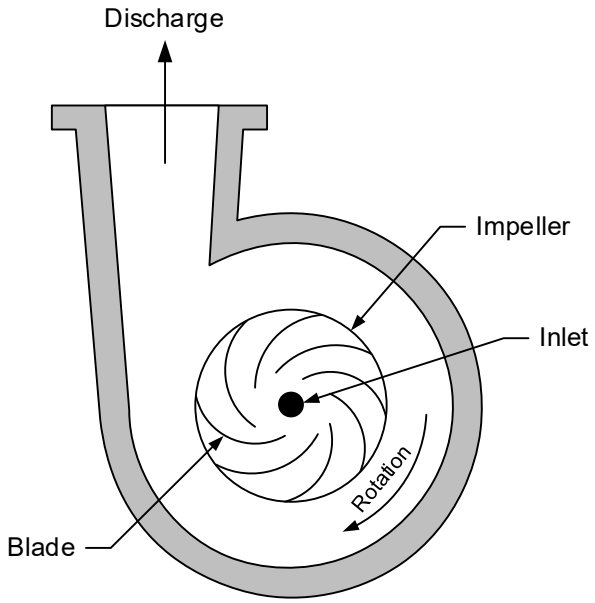

(a) Pump with Volute Casing

Primary Frequency for Both Centrifugal Pumps and Compressors can Include:

$$(1)\ f = \frac{nN}{60}$$

$$(2)\ f = \frac{nBN}{60}$$

$$(3)\ f = \frac{nVN}{60}$$

Where:

n = Integers, 1,2,3 (nodes)
N = Speed, rpm
B = Number of Impeller Blades
V = Number of Vane Diffusers

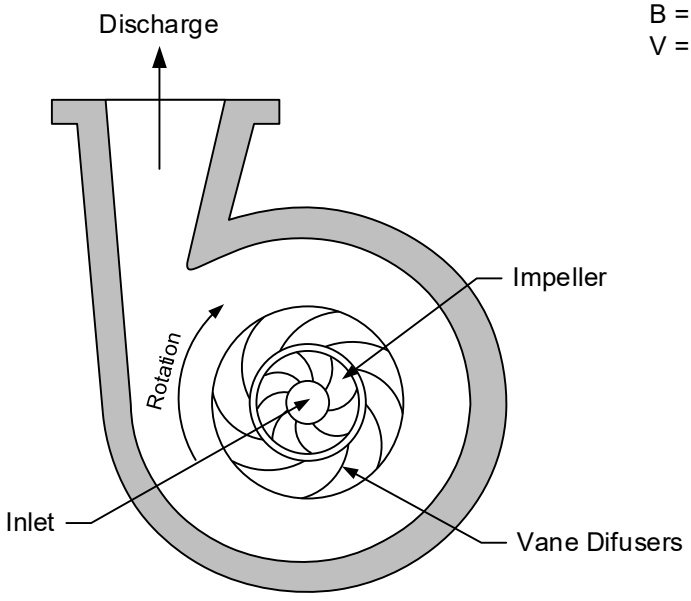

(b) Compressor with Vaned Diffuser

Figure 14.30 – Centrifugal Pump and Compressor Pulsations (See Table 14.13)

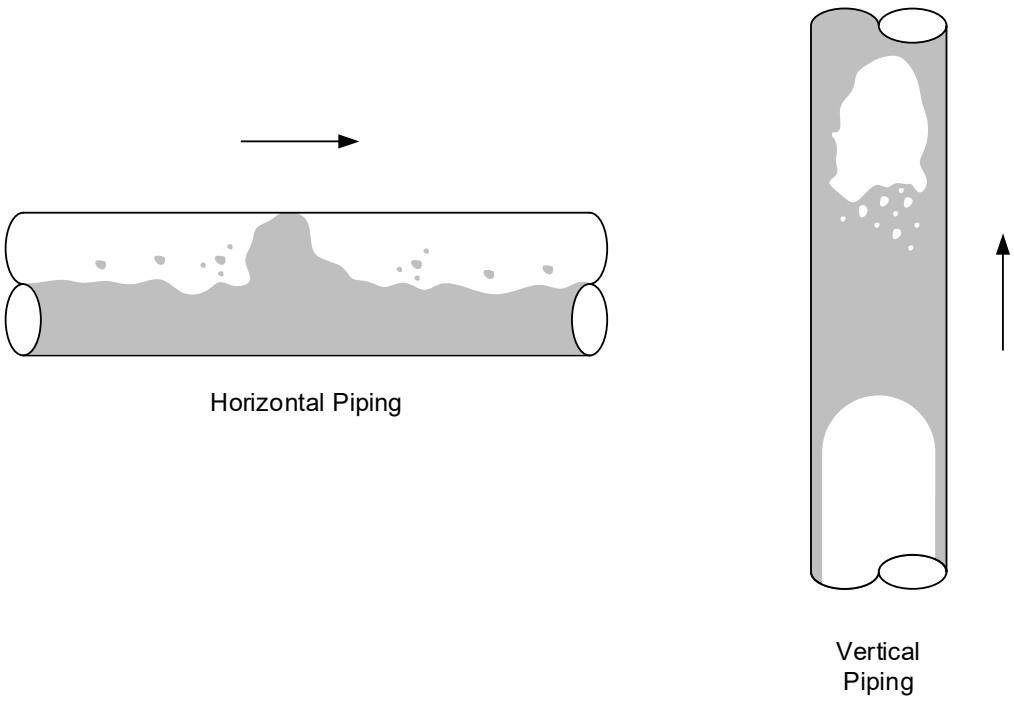

(a) Slug Flow in Horizontal and Vertical Piping

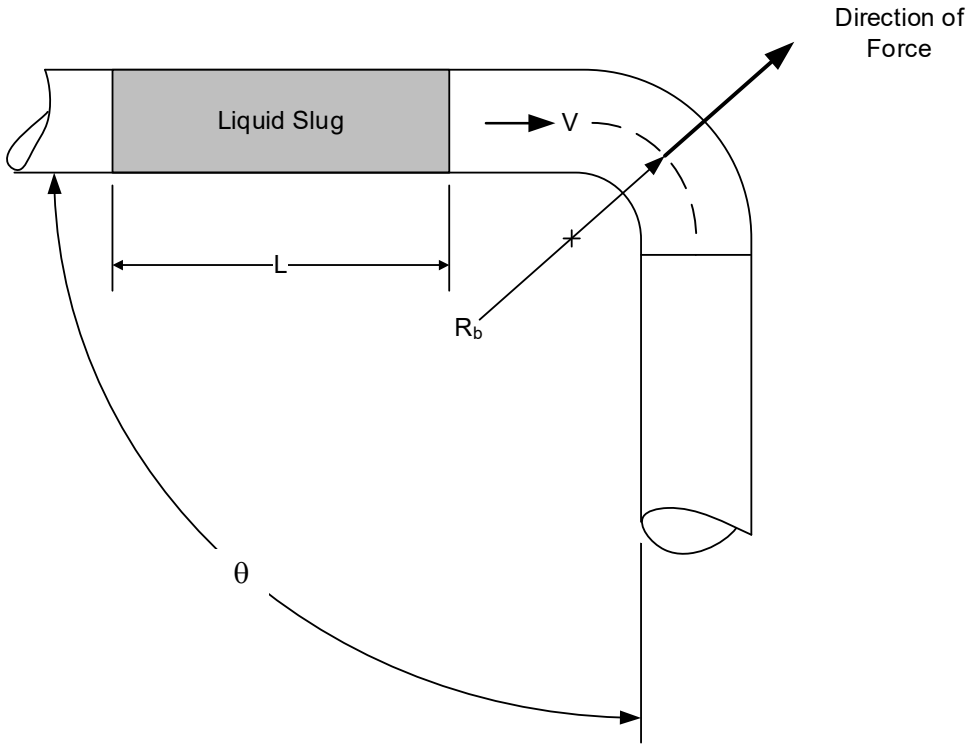

(b) Reaction Force at Change of Direction Locations

Figure 14.31 – Slug Flow (See Table 14.13)

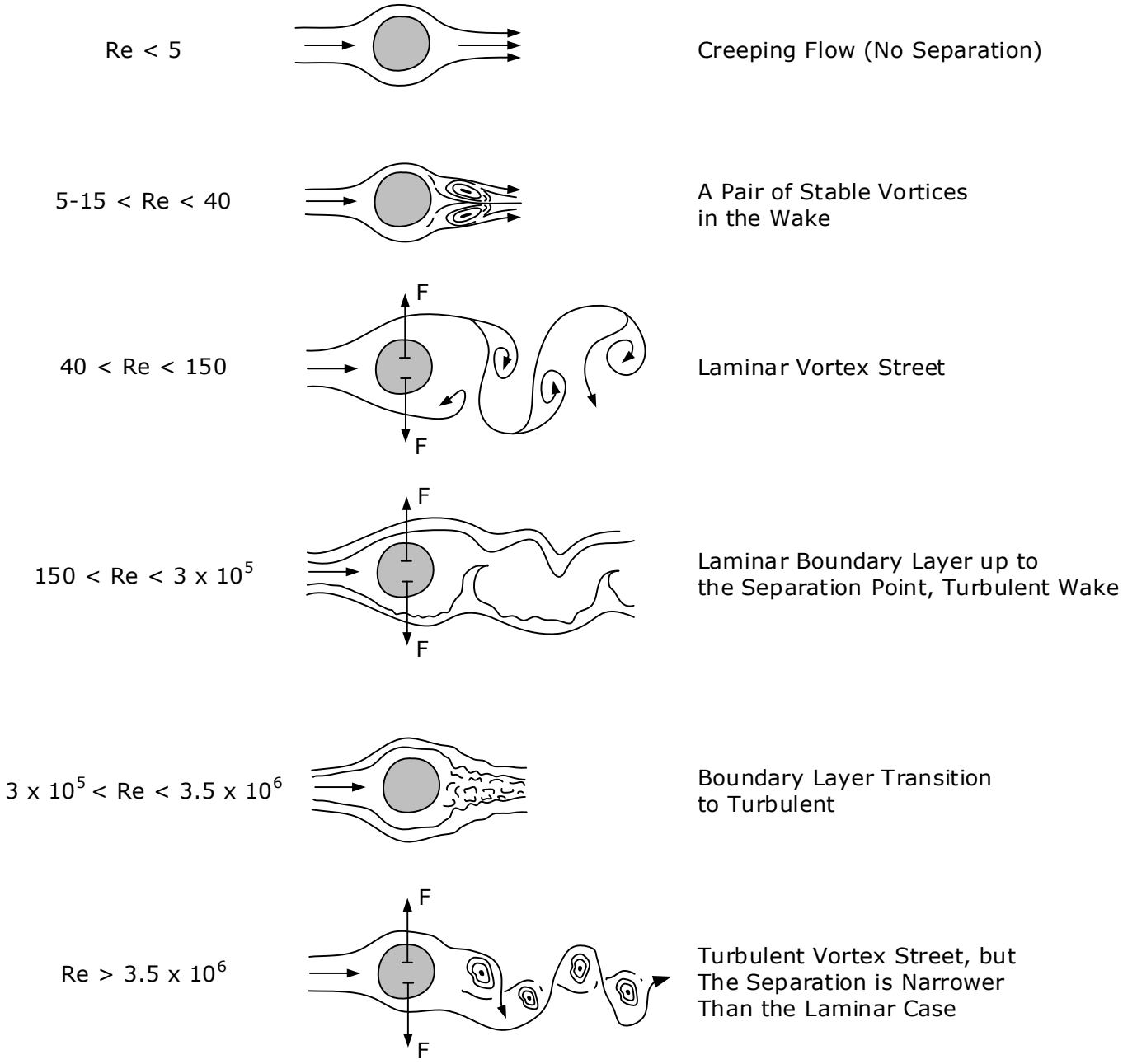

Note: Force F is an Alternating Force at Vortex Shedding Frequency f

(a) Vortex Shedding Around a Structure

Figure 14.32 – Vortex Shedding (See Table 14.13)

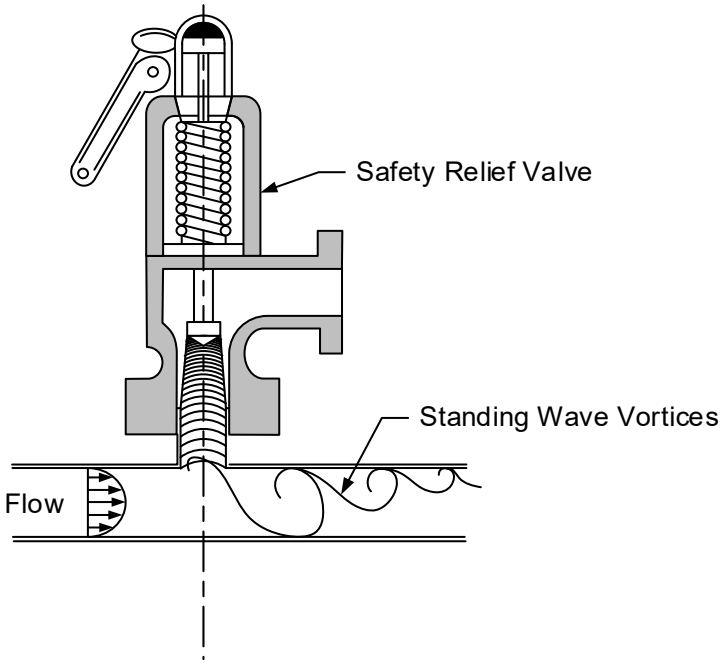

(b) Standing Wave Vortex in a Piping System

Figure 14.32 – Vortex Shedding (See Table 14.13) (Continued)

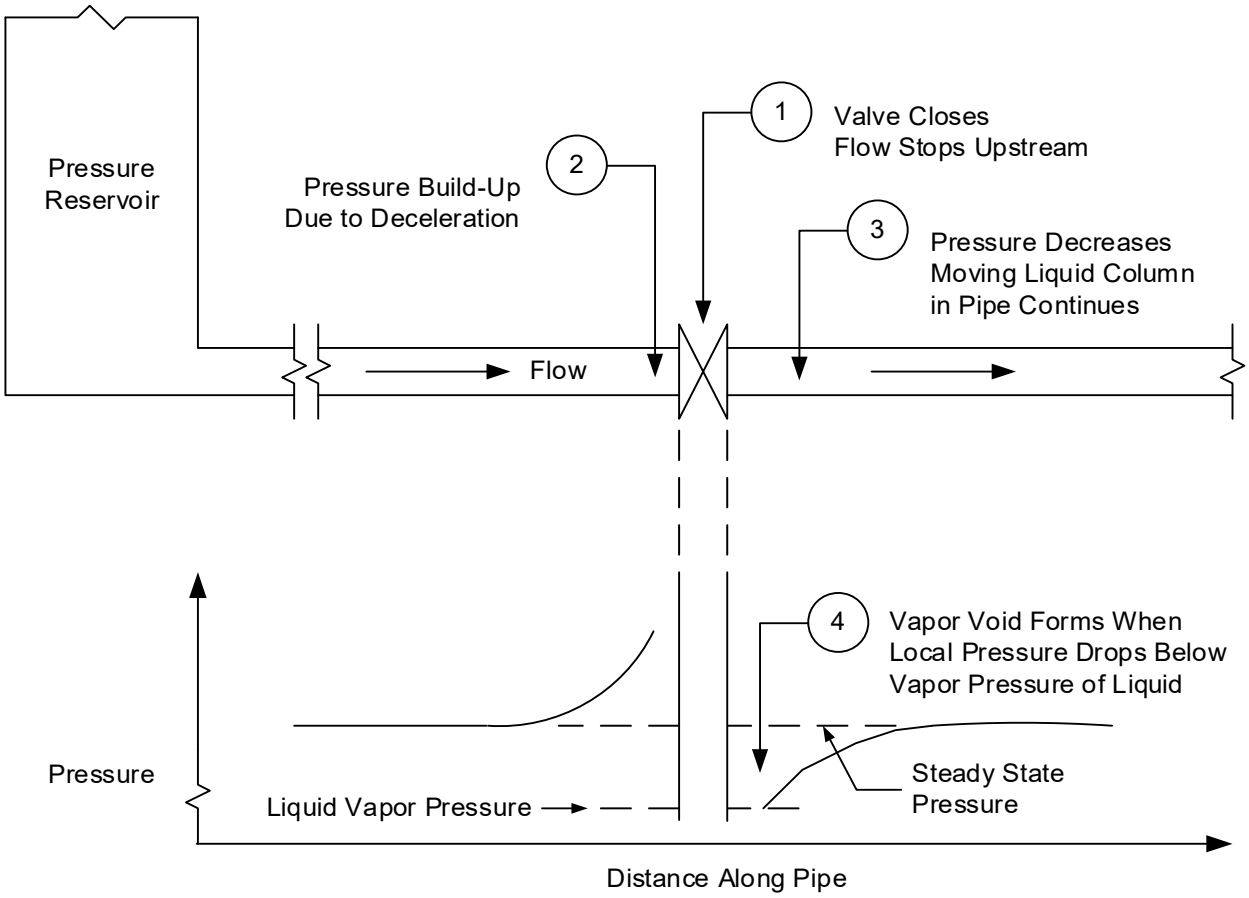

Figure 14.33 – Hydraulic Hammer from Valve Closure (See Table 14.13)

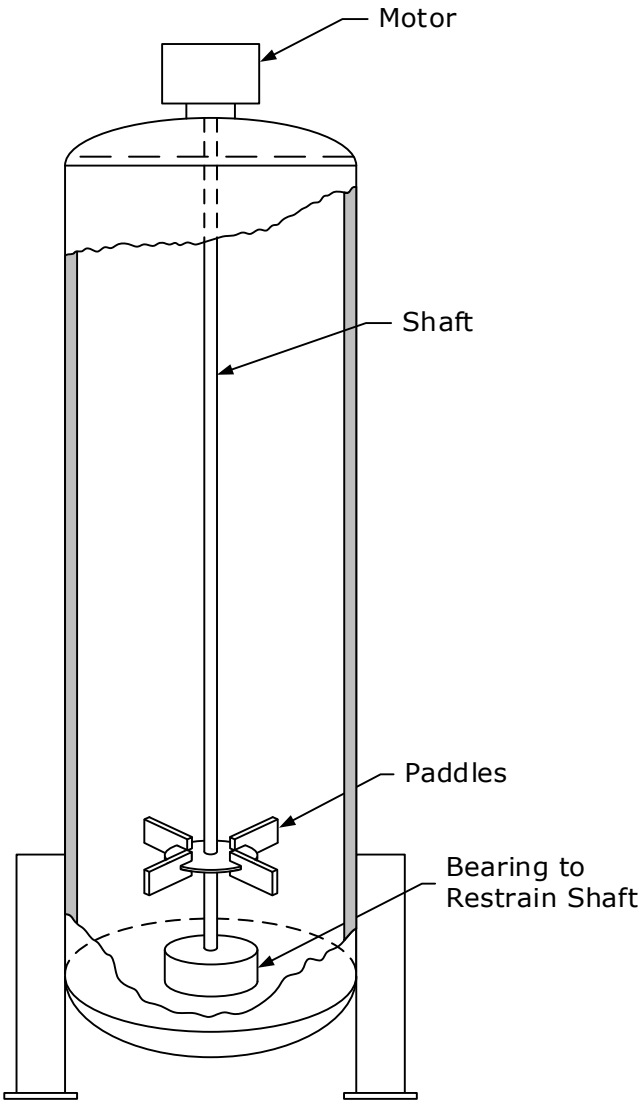

Figure 14.34 – Constraint of Impeller in Mixing Tank (See Table 14.14)

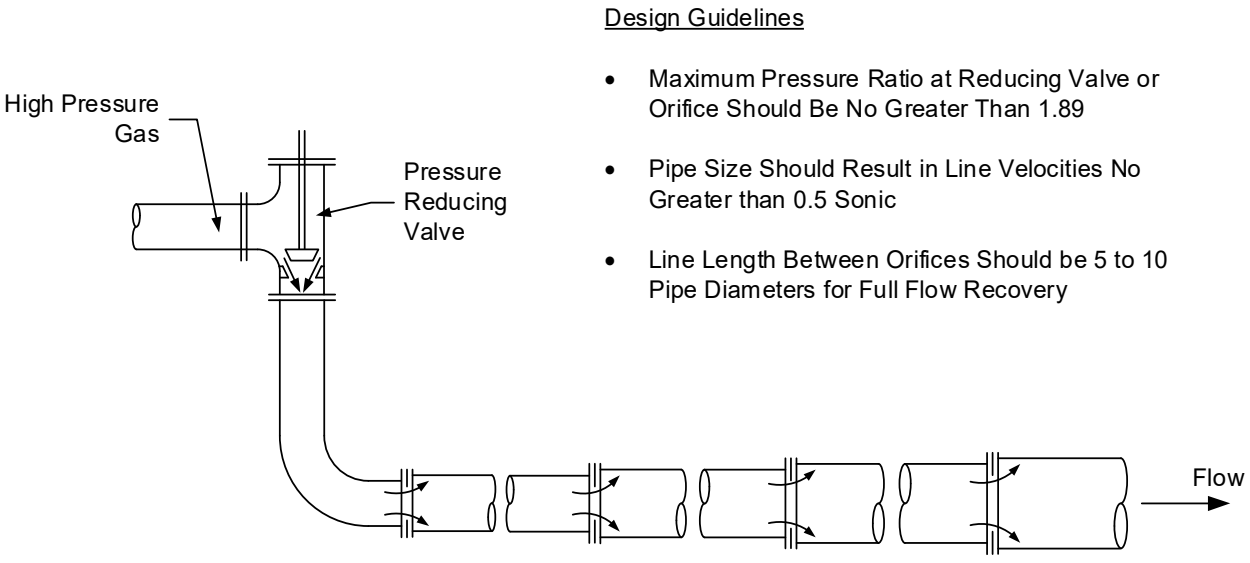

(a) Multi-Stage Orifices

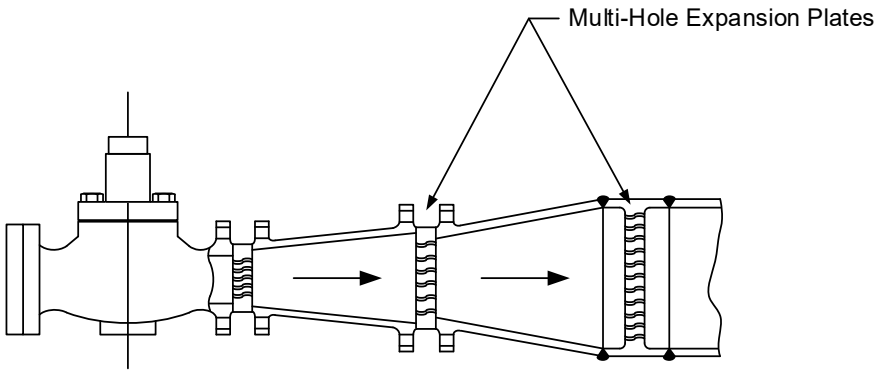

(b) Multi-Hole Exapnsion Plates

Figure 14.35 – Multi-Staged Restriction Orifices and Multi-Port Expansion Plates (See Table 14.14)

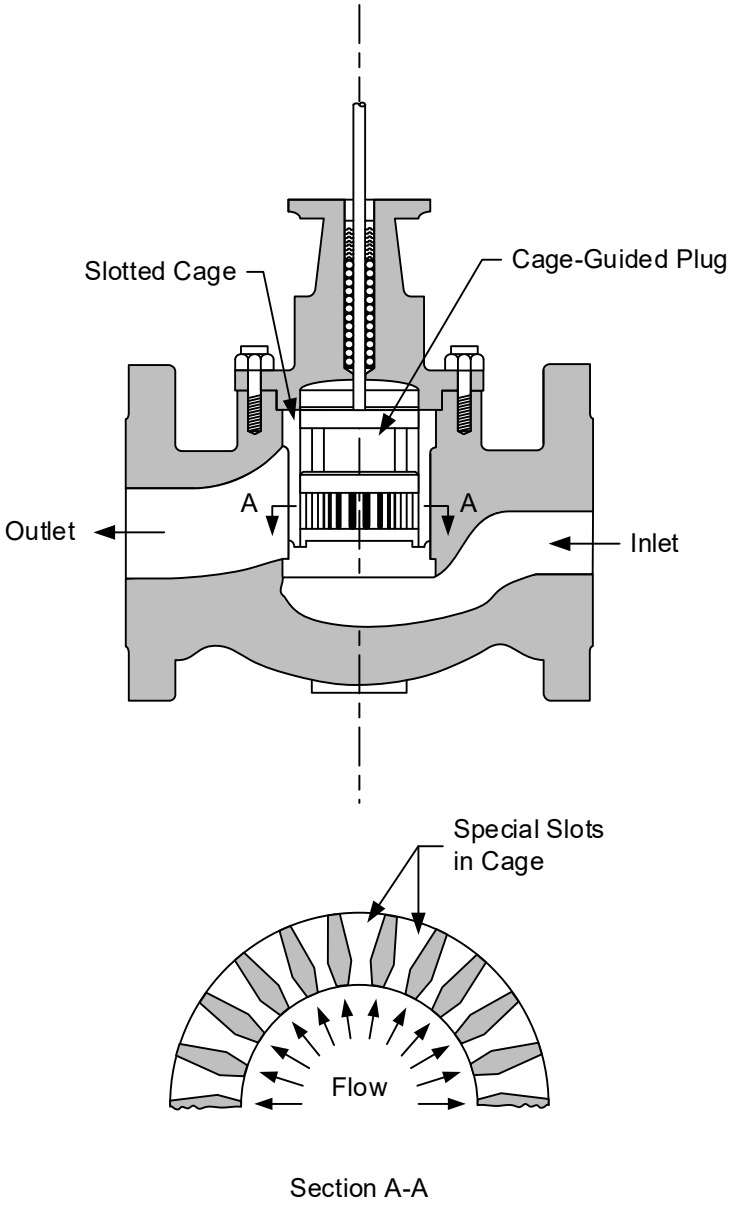

Figure 14.36 – Low Noise Control Valves – Control Valve with Whisper Trim (See Table 14.14)

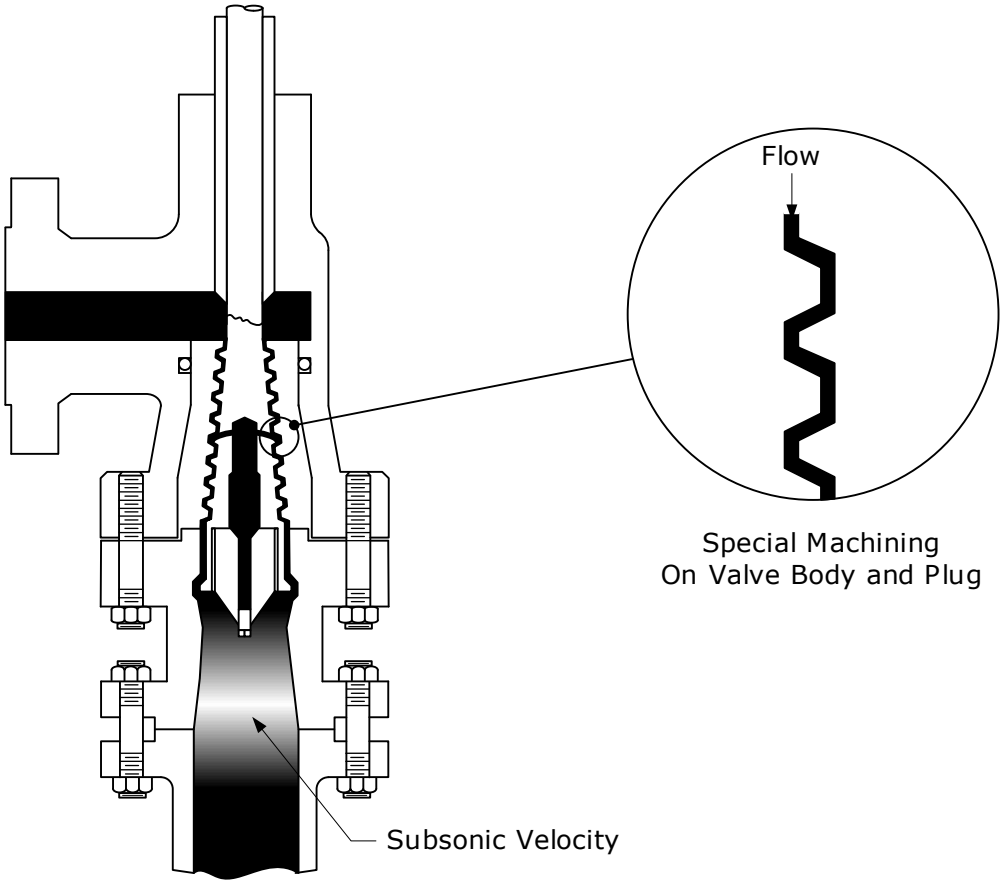

Figure 14.37 – Low Noise Control Valves – Staged Trim Low Noise Control Valve (See Table 14.14)

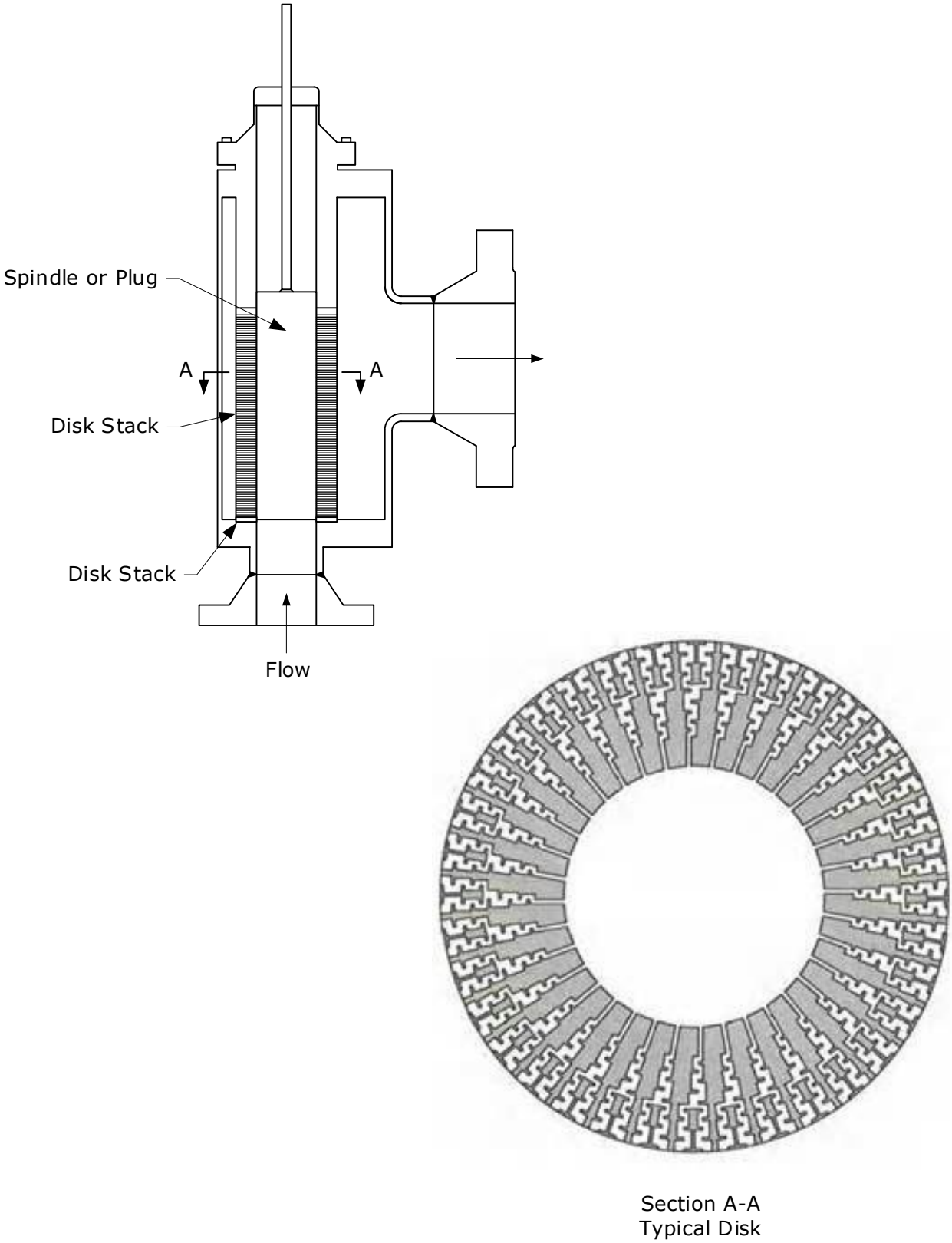

Figure 14.38 – Low Noise Control Valves – Labyrinth-Disk Type Low Noise Valve (See Table 14.14)

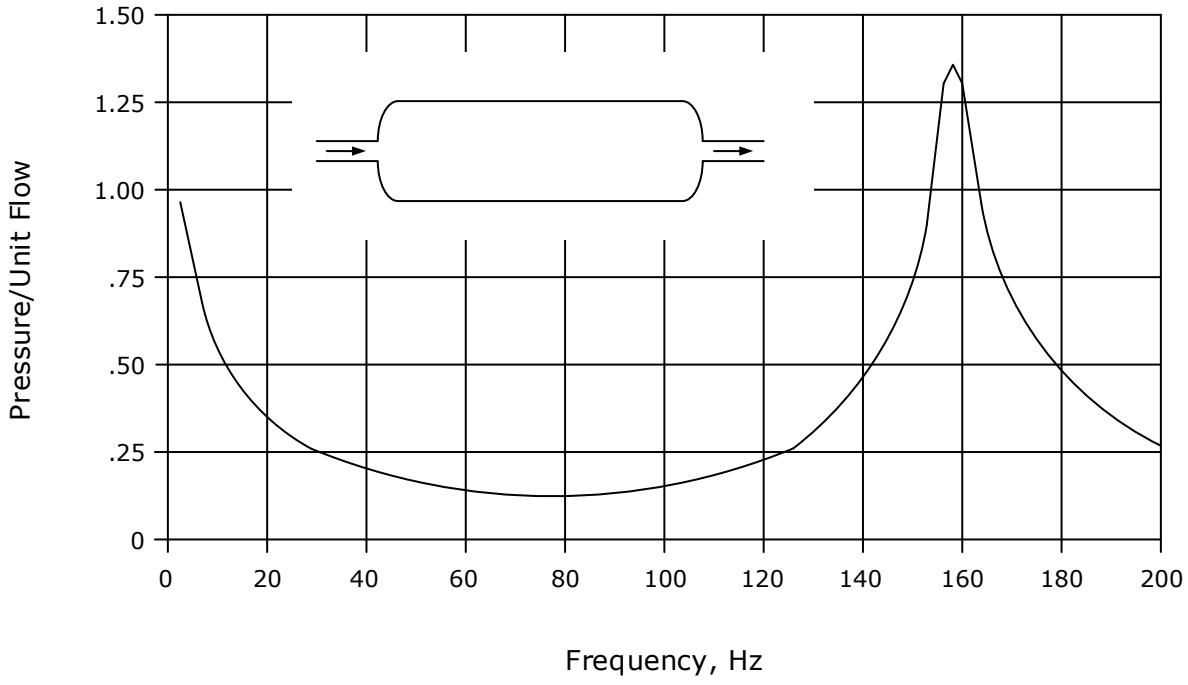

Figure 14.39 – Surge Bottle Attenuation (See Table 14.14)

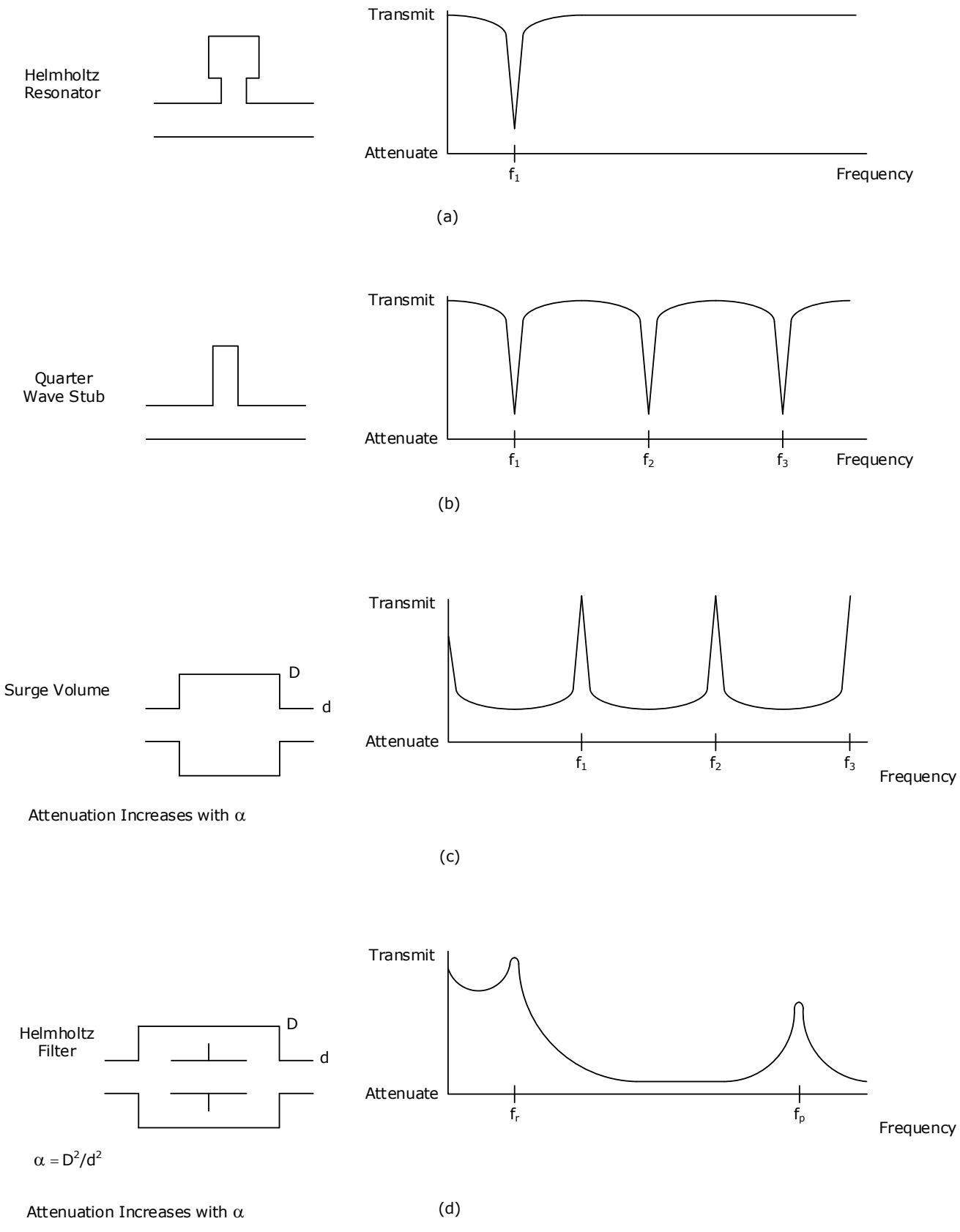

Figure 14.40 – Attenuation Characteristics of Common Acoustic Components (See Table 14.14)

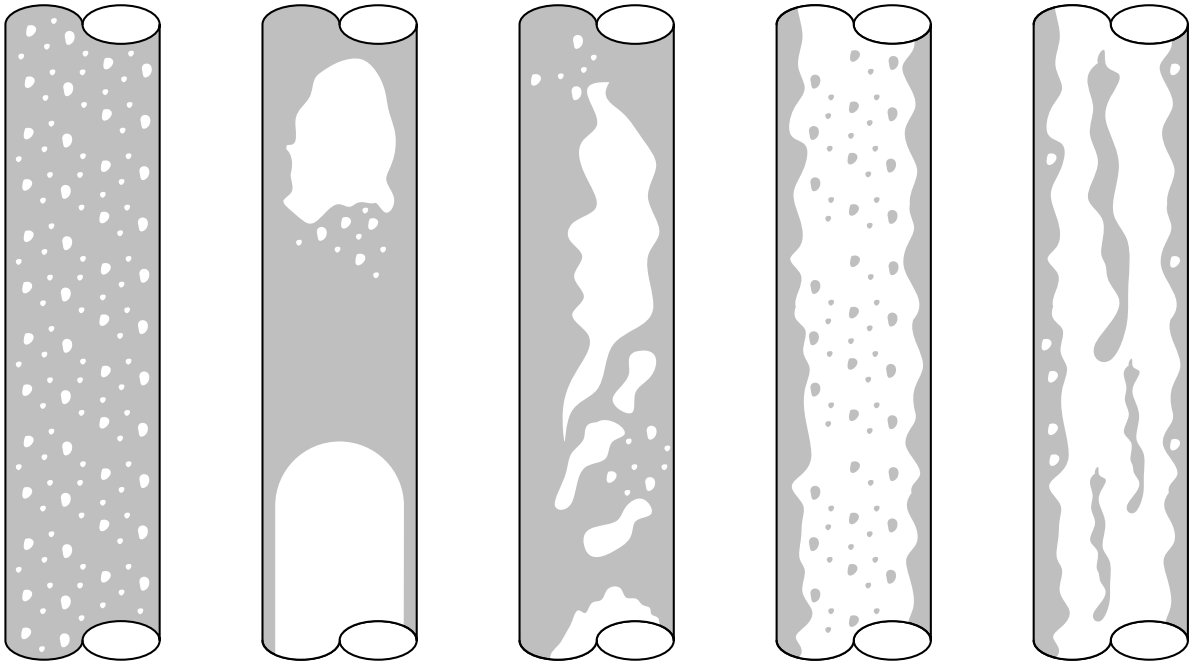

Vertical Upflow	Description
Bubble Flow	There is a continuous liquid phase, and the gas phase is dispersed as bubbles within the liquid continuum. The bubbles travel with a complex motion within the flow, may be coalescing and are generally of non-uniform size
Plug Flow	This flow pattern, which in vertical systems is often referred to as slug flow, occurs when the bubble size tends toward that of the channel diameter, and characteristic bullet-shaped bubbles are formed. A thin film of liquid surrounds a bubble, which is often called a Taylor bubble. The liquid between the Taylor bubbles often contain a dispersion of smaller bubbles.
Churn Flow	At higher gas velocities, the Taylor bubbles in plug flow break down into an unstable pattern in which there is a churning or oscillatory motion of liquid. This flow occurs more predominantly in large-bore pipes and tubes and may not be as important in narrow-bore pipes and tubes where the region of churn flow is small. Churn flow with its characteristic oscillations, is an important pattern covering a wide range of flowrates. At the lower range of gas flowrate, it may be regarded as a breaking-up of plug flow with an occasional bridging across the pipe by the liquid phase. At the higher range of gas flowrate, it may be considered as a degenerate form of annular flow with the direction of the film flow changing and very large waves being formed on the interface. (In this range, the term semi-annular flow has sometimes been used.)
Annular Flow and Wispy Annular Flow	This configuration is characterized by liquid traveling as a film on the channel walls, and gas flowing through the center. Part of the liquid can be carried as drops in the central gas core. In fact, for certain flowrates, most of the liquid travels as drops leading to the term “mist flow”. However, only in heat transfer systems where the walls can become too hot to be wetted is there flow with no liquid film. Interchange of liquid occurs between the film and the drops. Under some circumstances, bubbles of gas can be entrained in the liquid film. At very high liquid flowrates, liquid concentrations in the gas core are so high that “wisps” are observed instead of droplets. This is the wispy-annular flow defined in certain flow-pattern maps.

Figure 14.41 – Two-Phase Flow Patterns – Vertical Upflow, From Daniels, Lawrence, “Dealing with Two-Phase Flow,” Chem. Eng., 102, 6, pp. 70-78, June 1995 (See Table 14.14)

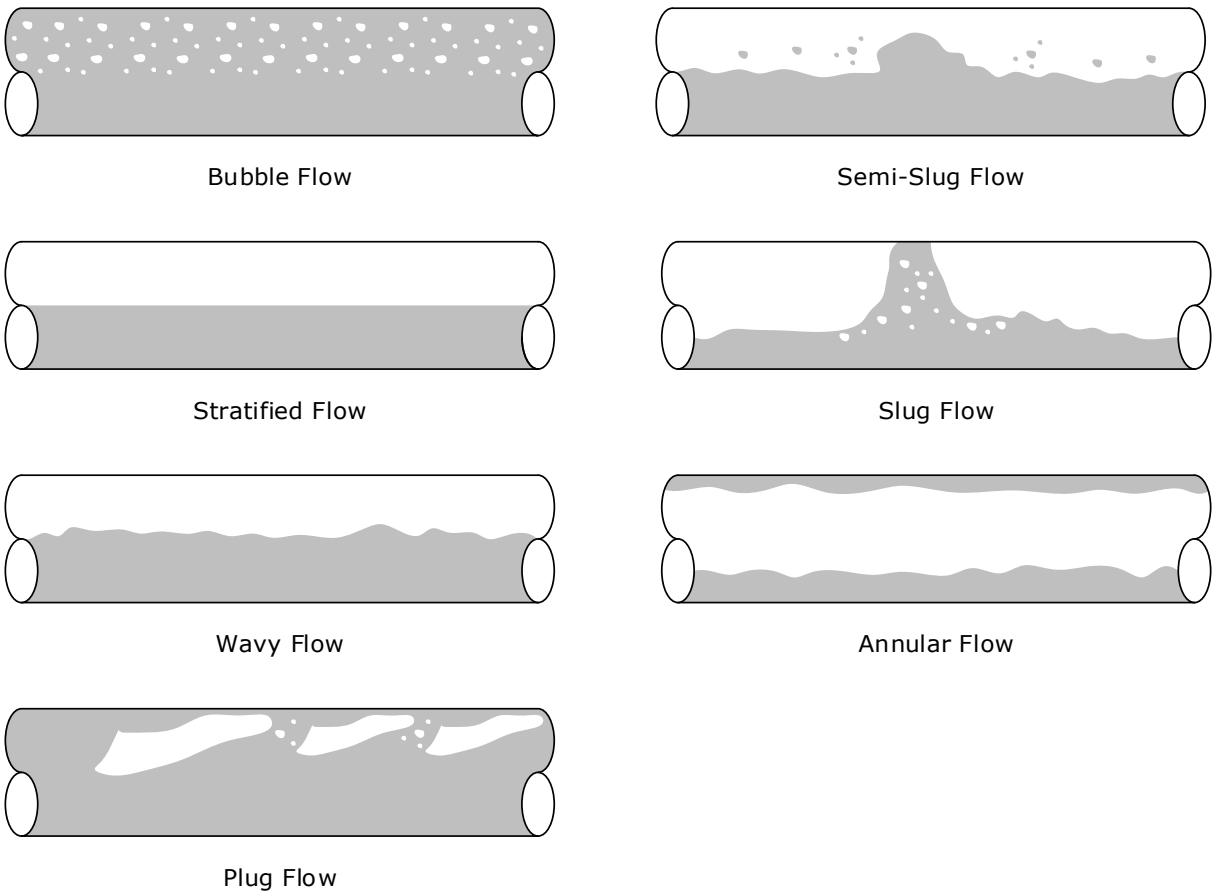

Horizontal Flow	Description Note: When gravity acts perpendicularly to the pipe axis, separation of the phases can occur. This increases the possible flow patterns that may exist in a piping system.
Bubble Flow	This, like the equivalent pattern in vertical flow, consists of gas bubbles dispersed in a liquid continuum. However, except at very high liquid velocities when the intensity of the turbulence is enough to disperse the bubbles about the cross section, gravity tends to cause bubbles to accumulate in the upper part of the pipe.
Stratified Flow	In this flow pattern, liquid flows in the lower part of the pipe with the gas above it. The interface is smooth.
Wavy Flow	An increase of gas velocity causes waves to form on the interface of stratified flow.
Plug flow	This flow pattern is characterized by bullet-shaped gas bubbles as seen in vertical flow. However, here they travel along the top of the pipe
Slug Flow	This flow pattern, like plug flow, is intermittent. The gas bubbles are bigger, while the liquid slugs contain many smaller bubbles. When the slugs are highly aerated, the term, “frothy surges,” has been used in the literature. Some researchers have used the term “semi-slug” to describe cases where the surges do not fill the pipe completely. However, this might be more correctly considered as part of wavy flow.
Annular Flow	A continuous gas core with a wall film characterizes this flow pattern. As with the equivalent pattern in vertical flow, liquid can be entrained as drops in the gas core. Gravity causes the film to be thicker on the bottom of the pipe but as the gas velocity is increased, the film becomes more uniform around the circumference.

Figure 14.42 – Two-Phase Flow Patterns – Horizontal flow, From Daniels, Lawrence, “Dealing with Two-Phase Flow,” Chem. Eng., 102, 6, pp. 70-78, June 1995 (See Table 14.14)

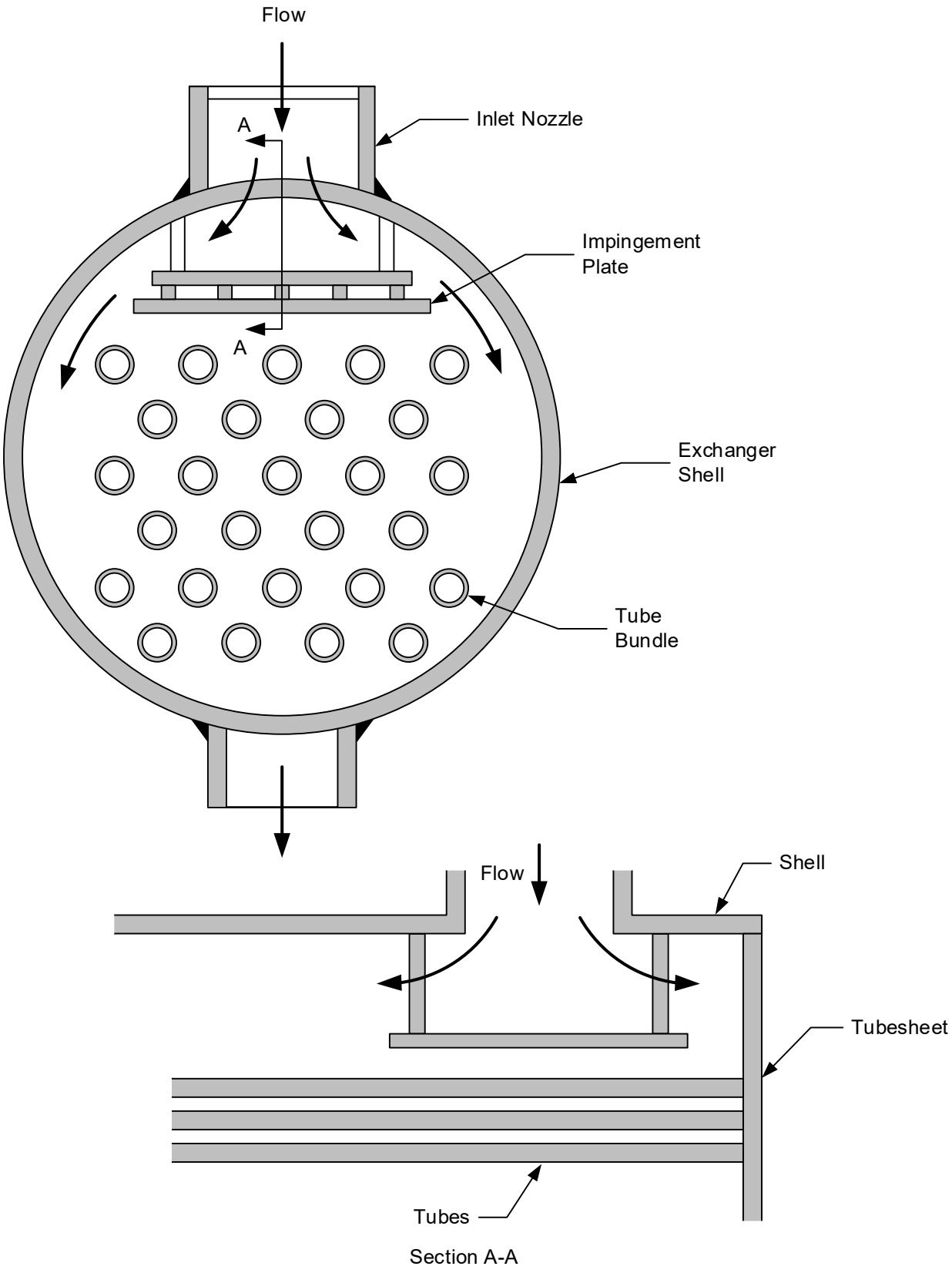

Figure 14.43 – Heat Exchanger Inlet Baffle (See Table 14.14)

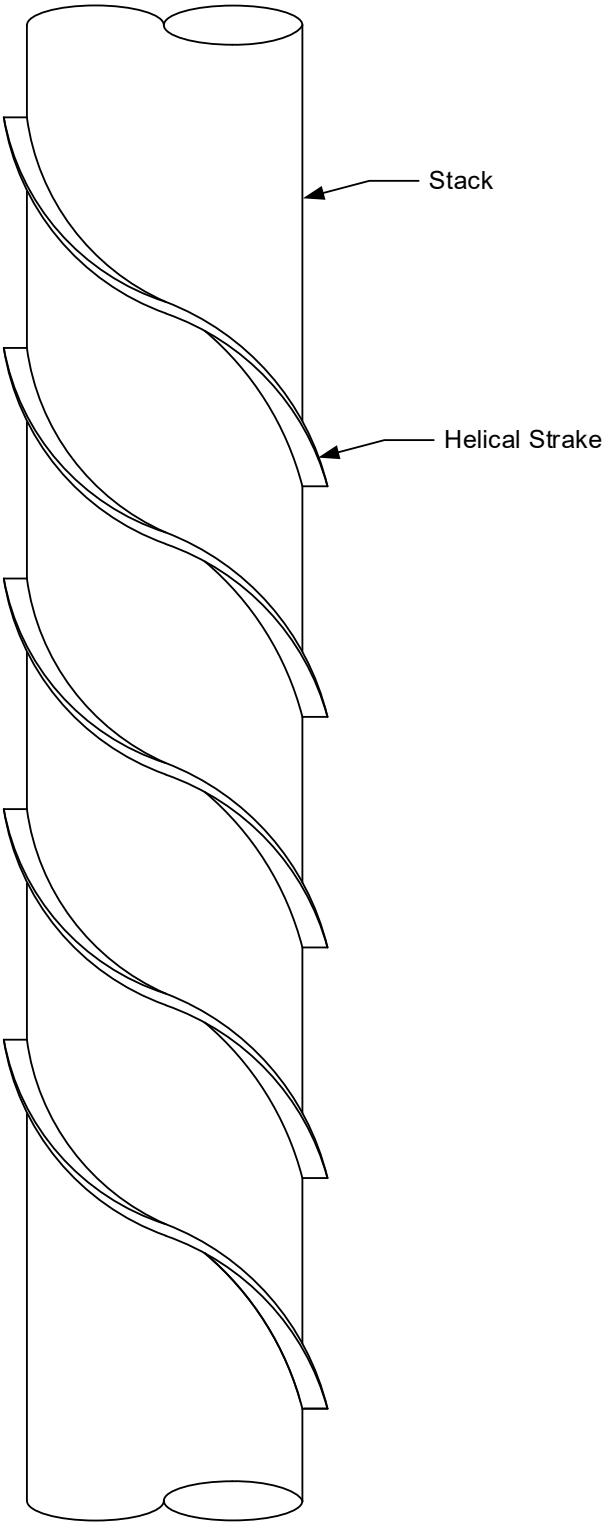

Figure 14.44 – Helical Strakes on a Stack (See Table 14.14)

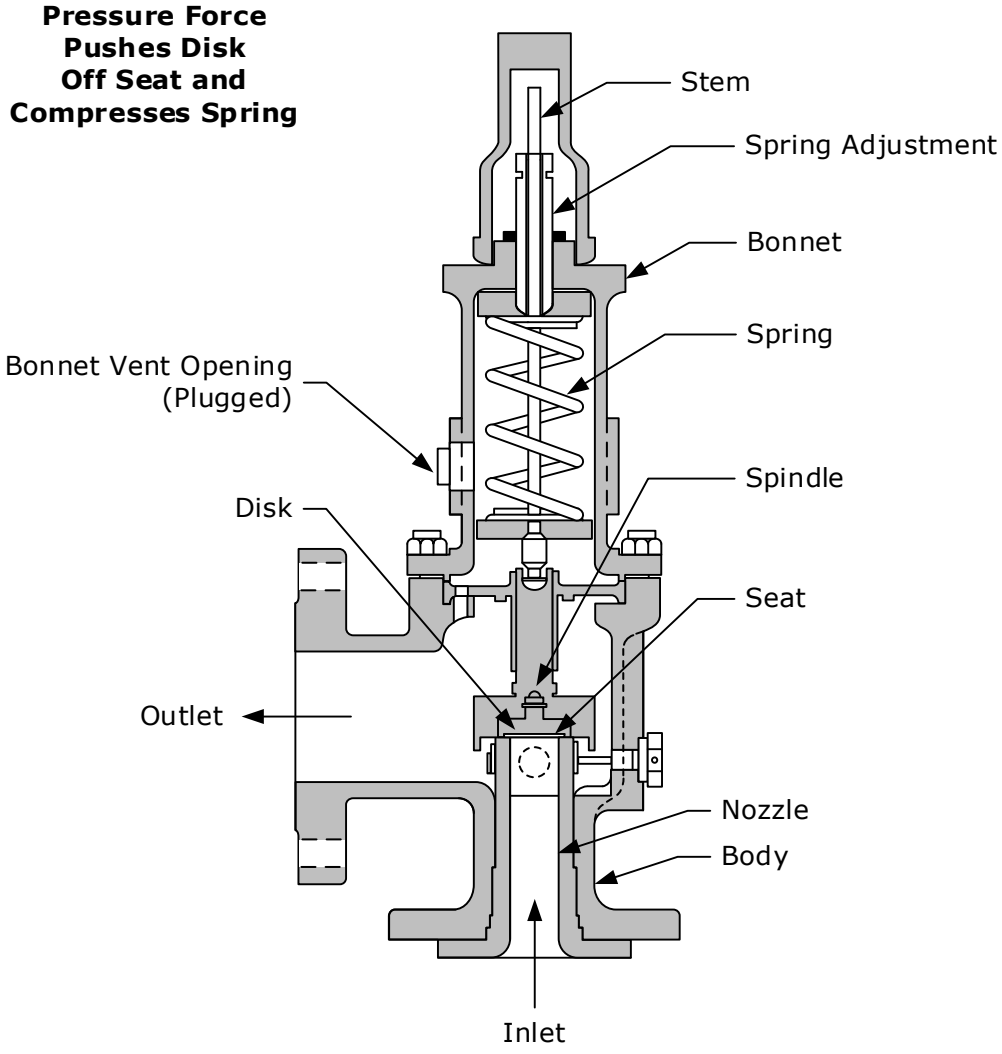

Figure 14.45 – Pressure Relief Valve (See Table 14.14)

Figure 14.46 – Rupture Disks (See Table 14.14)

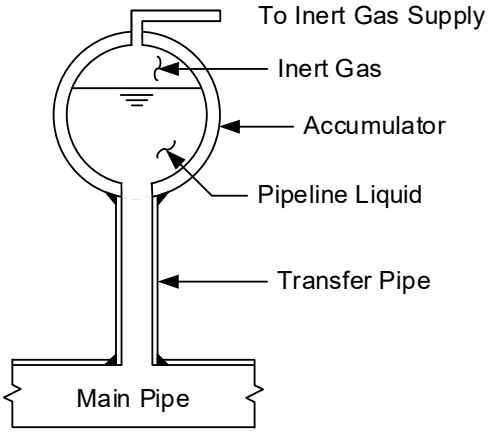

(a) Conventional

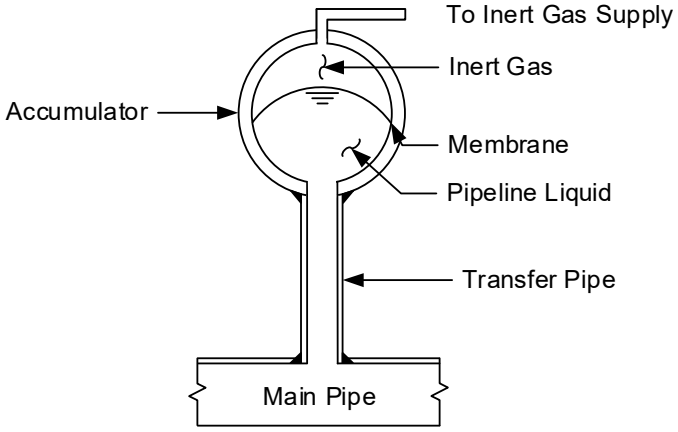

(b) With Membrane

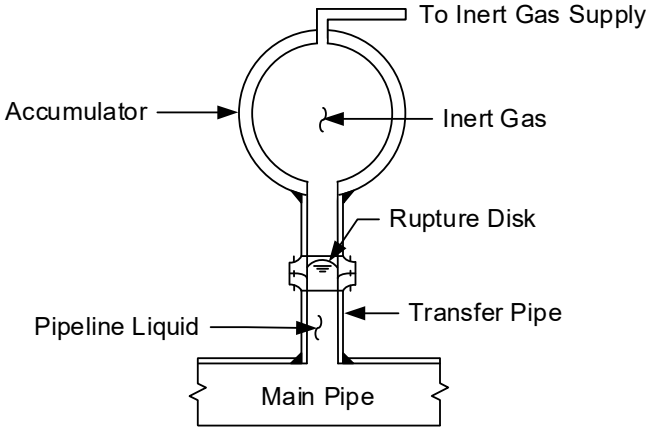

(c) With Rupture Disk

Figure 14.47 – Accumulators (See Table 14.14)

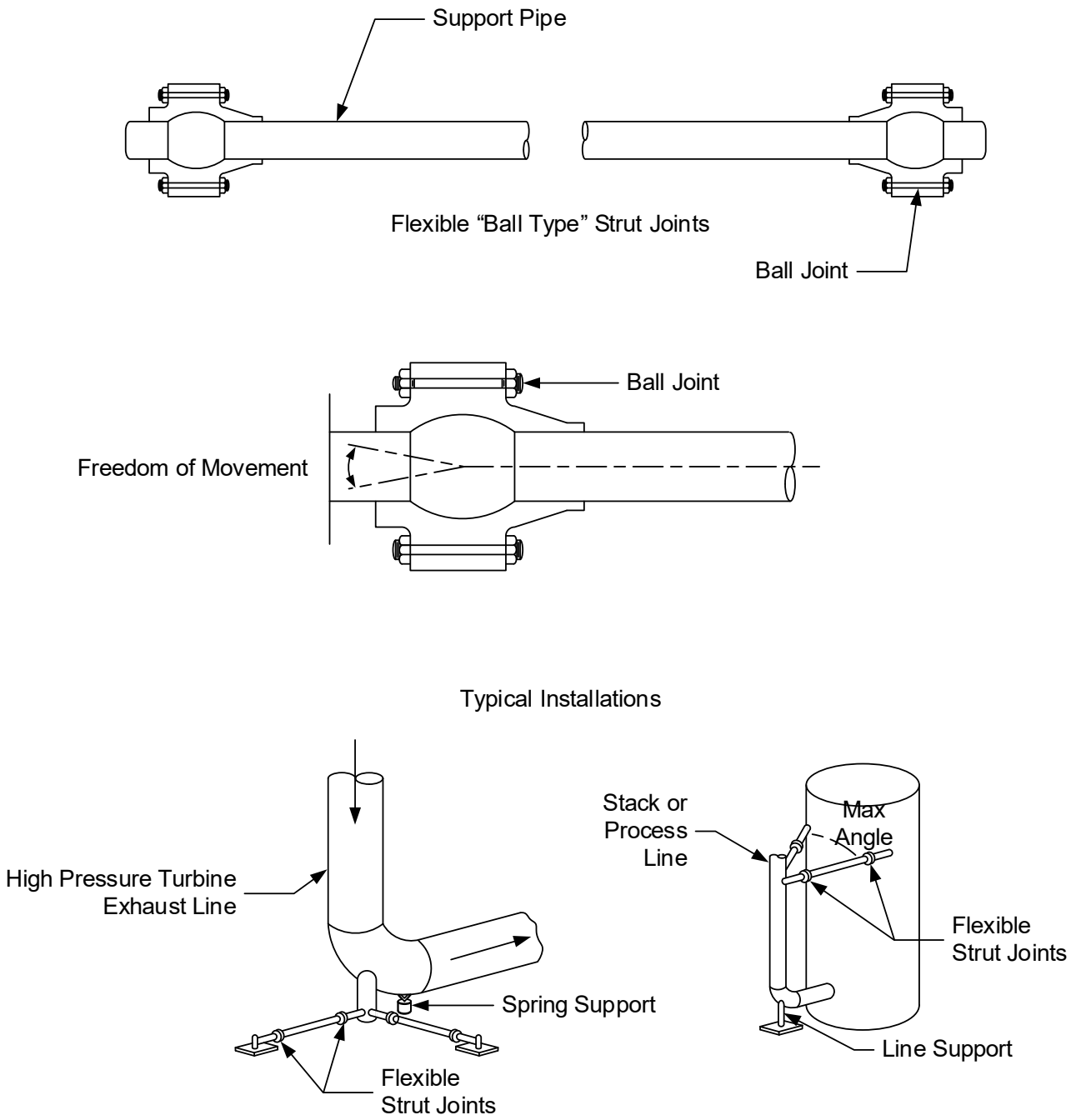

Figure 14.48 – Typical Ball-Type Vibration Strut (See Table 14.15)

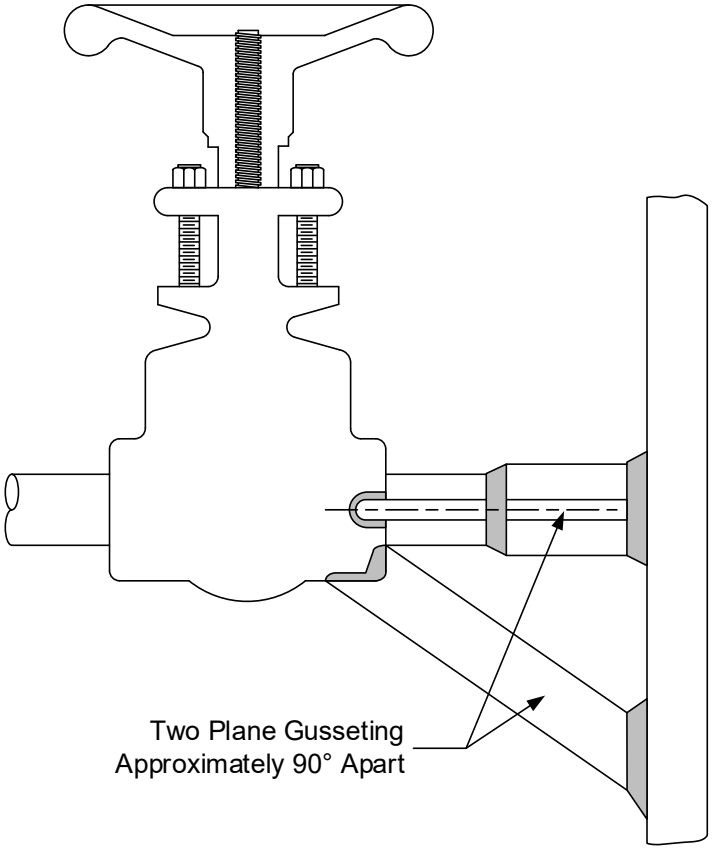

Figure 14.49 – Typical Two-Plane Gusset Detail for Small Bore Piping Connections (See Table 14.15)

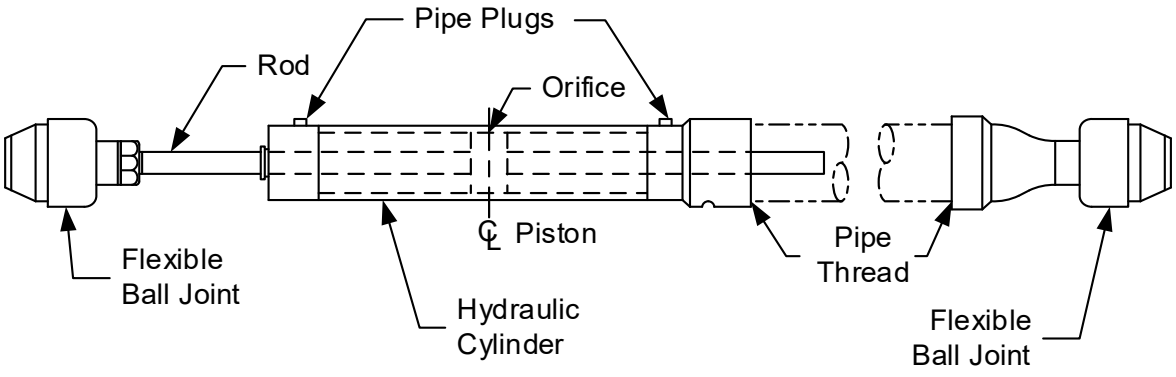

Figure 14.50 – Typical Hydraulic Snubber

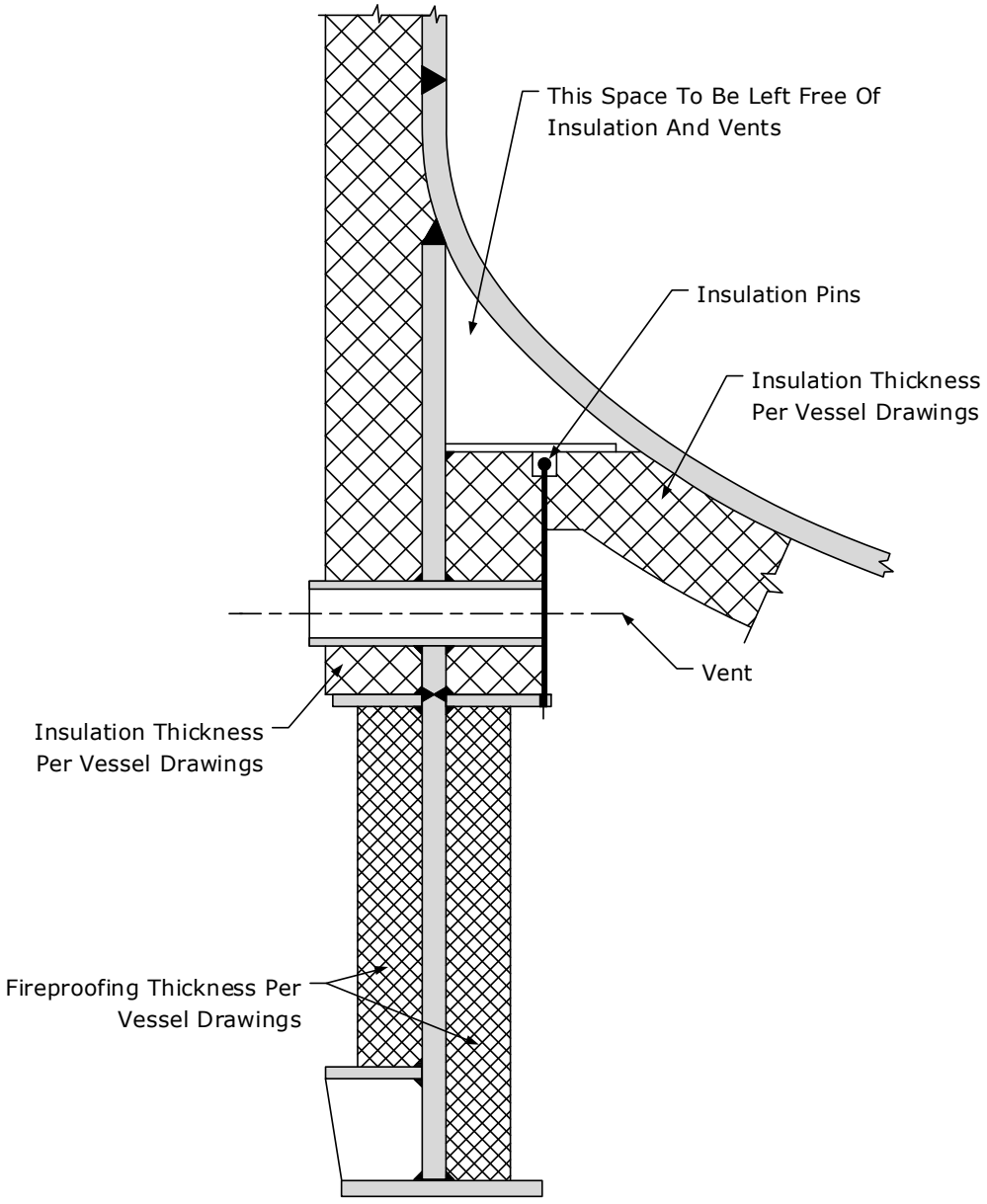

Figure 14.51 – Typical Hot-Box Detail (See Table 14.16)

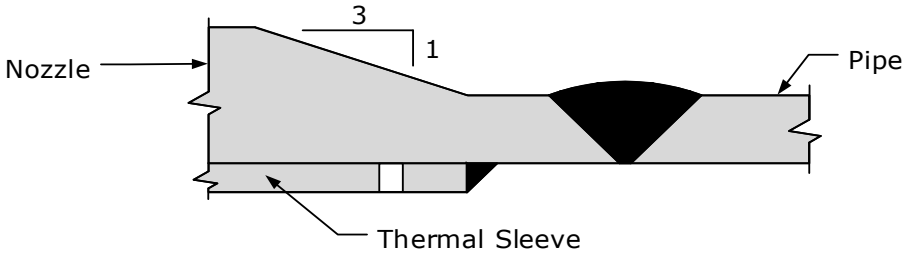

Figure 14.52 – Typical Thermal Sleeve Detail with No Insulation (See Table 14.16)

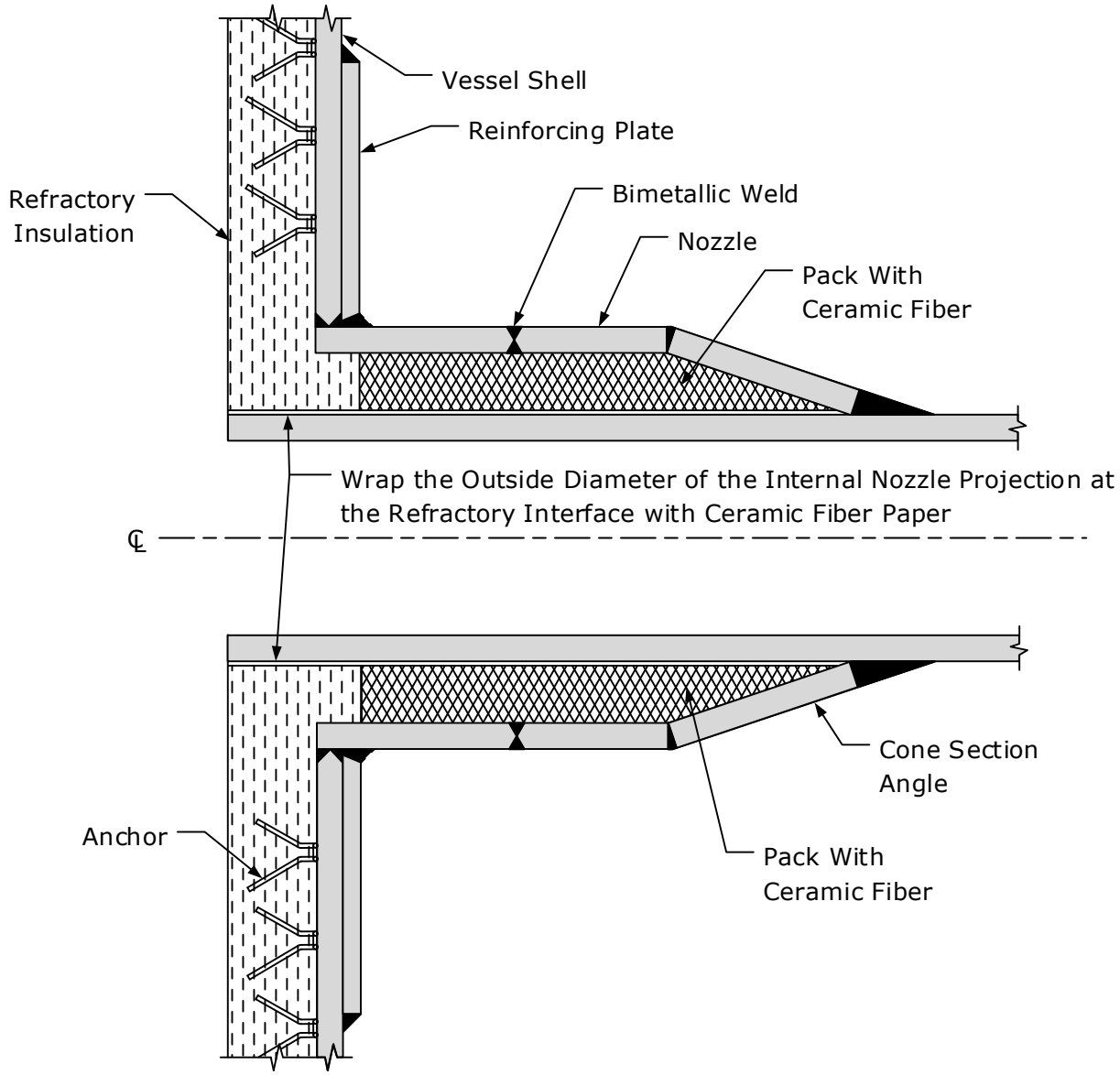

Figure 14.53 – Typical Hot Piping to Cold Vessel Wall Transition (See Table 14.16)

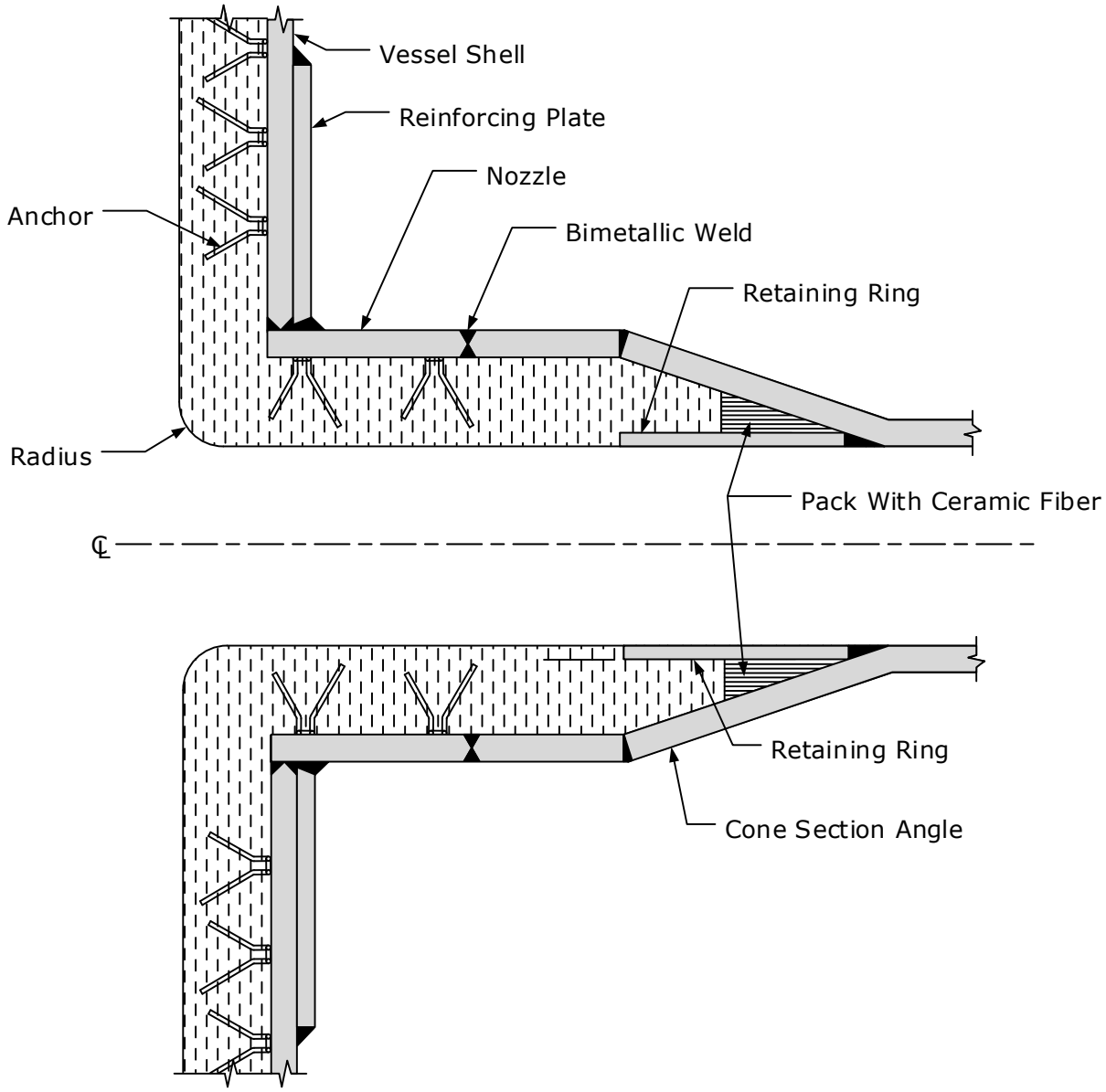

Figure 14.54 – Typical Hot Piping to Cold Vessel Wall Transition (See Table 14.16) – Alternative Detail

ANNEX 14A – TECHNICAL BASIS AND VALIDATION – ASSESSMENT OF FATIGUE DAMAGE

(INFORMATIVE)

CONTENTS

ANNEX 14A – TECHNICAL BASIS AND VALIDATION – ASSESSMENT OF FATIGUE DAMAGE 14A-1

14A.1 TECHNICAL BASIS AND VALIDATION 14A-1
14A.2 REFERENCES 14A-1

14A.1 Technical Basis and Validation

An overview of the fatigue methods used in Part 14 is provided in reference [1]. The technical background to the Level 1 and Level 2 Assessment procedures in Part 14 for the evaluation of fatigue is provided in reference [2]. Additional background information on the Level 2, Method C fatigue assessment of welds using the equivalent structural stress is provided in references [3] and [4].

The technical background for the fatigue screening Method C is provided in references [21] and [22].

The fatigue method present in Level 3 is documented in references [5] through [15].

The technical background for the ratcheting assessment based on elastic stress analysis using the Bree diagram is provided in references [23] and [24].

Remediation and in-service monitoring techniques for fatigue are included in references [16] through [20].

14A.2 References

[1] Osage, D.A "Fatigue Assessment for In-Service Components – A New Part for API 579-1/ASME FFS-1 Fitness-For-Service," 6th Fatigue Design Conference, Fatigue Design 1015, Procedia Engineering, PROENG27760, Elsevier Ltd., 2016.

[2] Osage, D.A and Sowinski, J.C., *ASME Section VIII Division 2 Criteria and Commentary*, PTB-1-2013, ASME New York, NY, 2013.

[3] Dong, P., Hong, J.K, Osage, D.A., Dewees, D. and Prager, M., The Master S-N Curve Method: An Implementation for Fatigue Evaluation of Welded Components in the ASME B&PV Code, Section VIII, Division 2, and API 579-1/ASME FFS-1, WRC Bulletin 523, Welding Research Council, Inc., New York, NY.

[4] Dong, P, Hong, J.K, Osage, D.A., and Prager, M., *Master S-N Curve Method for Fatigue Evaluation of Welded Components*, WRC Bulletin 474, Welding Research Council, Inc., New York, NY.

[5] Stenta, A., Gassama, E., Panzarella, C., Cochran, J. and Osage, D.A., *Standardization of Fatigue Methods for Use in API 579-1/ASME FFS-1*, WRC Bulletin 550, Welding Research Council, Inc., New York, NY, 2015.

[6] Dewees, D.J., 2010, "Application of Elastic-Plastic Design Data in the New ASME B&PV Code Section VIII Division 2," PVP2010-25641, pp. 99-109, ASME 2010 Pressure Vessels and Piping Conference, ASME, New York.

[7] Kalnins, A., J. Rudolph, and A. Willuweit, 2013, “Using the Nonlinear Kinematic Hardening Material Model of Chaboche for Elastic-Plastic Ratcheting Analysis,” PVP2013-98150, ASME 2013 Pressure Vessels and Piping Conference, ASME, New York.

[8] Draper, J., Modern Metal Fatigue Analysis, EMAS Publishing, Warrington, UK, 2008.

[9] Suresh, S., Fatigue of Materials, 2nd Edition, Cambridge University Press, New York, 1998.

[10] Buczynski, A. and G. Glinka, "An Analysis of Elastic-Plastic Strains and Stresses in Notched Bodies Subjected to Cyclic Non-Proportional Loading Paths," European Structural Integrity Society, Volume 31, Elsevier 2003, pgs. 265-283.

[11] Bannantine, J.A., Comer, J.J. and Handrock, J.L., Fundamentals of Metal Fatigue Analysis, Upper Saddle River, NJ: Prentice Hall, 1997.

[12] Dowling, N.E., Mechanical Behavior of Materials: Engineering Methods for Deformation, Fracture, and Fatigue, 4th edition, Prentice Hall, Upper Saddle River, NJ.

[13] Stephens, R.I., Fatemi, A., Stephens, R.R. and Fuchs, H., *Metal Fatigue in Engineering*, 2nd ed., John Wiley & Sons, 2000.

[14] Socie, D.F. and Marquis, G.B., *Multiaxial Fatigue*, Society of Automotive Engineers, Inc., 1999.

[15] Lee, Y, Barkey, M.E., and Kang, H., Metal Fatigue Analysis Handbook, Practical Problem-Solving Techniques for Computer Aided Engineering, Elsevier, Inc., 2012.

[16] Marshall, Rebekkah, Two-Phase Flow Patterns, Chemical Engineering, November 2006, p. 55

[17] SGA-PCRC Seminar on Controlling the Effects of Pressure Transients in Piping Systems, Report 160, presented by Southwest Research Institute, November 7-9, 1979 (at San Antonio, TX).

[18] Carucci, V.A. and Mueller, R.T., 1982, “Acoustically Induced Piping Vibration in High Capacity Pressure Reducing Systems,” ASME PVP Paper 82-WA/PVP-8.

[19] Eisinger, F.L.,1997, “Designing Piping Systems Against Acoustically Induced Structural Fatigue,” Journal of Pressure Vessel Technology, Vol. 119, August 1997, pg. 379-383.

[20] Energy Institute, Guidelines for the Avoidance of Vibration Induced Fatigue Failure in Process Pipework, 2nd edition, January 2008.

[21] Kirkpatrick, K., Johnson, C.R., and Adin Mann III, J.,”Method B Fatigue Screening In ASME BPV Code, Section VIII, Division 2”, PVP2019-93812, Proceedings of the ASME 2019, Pressure Vessels and Piping Conference, PVP2019, July 14-19, 2019, San Antonio, Texas.

[22] Langer BF, “Design-stress Basis for Pressure Vessels,” Pressure Vessel and Piping: Design and Analysis, A Decade of Progress, Volume 1, Analysis, ASME, 1972, pp. 84-94.

[23] Spring, D.W., Panzarella, C. and Osage, D.A., “Revisiting the Bree Diagram”, PVP2016-63635, Proceedings of the 2016 ASME Pressure Vessels & Piping Conference, PVP2016, July 17-21, 2016, Vancouver, BC, Canada.

[24] Spring, D.W., Panzarella, C. and Osage, D.A., *Revisiting the Bree Diagram: Derivation with Temperature Dependent Properties*, WRC Bulletin 575, Welding Research Council, Inc., New York, NY.

ANNEX 14B – MATERIAL PROPERTIES FOR FATIGUE ANALYSIS

(NORMATIVE)

CONTENTS

ANNEX 14B – MATERIAL PROPERTIES FOR FATIGUE ANALYSIS 14B-1

14B.1 SMOOTH BAR DESIGN FATIGUE CURVES – ASME CODE, SECTION VIII, DIVISION 2 ..... 14B-1
14B.1.1 Temperature Correction 14B-1
14B.1.2 Interpolation 14B-1
14B.1.3 Design Fatigue Curves Based on Testing in Air 14B-1
14B.1.4 Design Fatigue Curve Models 14B-2
14B.1.5 Computation of Allowable Cycles 14B-4
14B.2 SMOOTH BAR DESIGN FATIGUE CURVES – MEAN CURVE WITH EXPLICIT MARGINS 14B-4
14B.3 UNIFORM MATERIAL LAW 14B-5
14B.4 WELDED JOINT FATIGUE CURVES – ASME CODE, SECTION VIII, DIVISION 2 ..... 14B-5
14B.4.1 Fatigue Curve Models 14B-5
14B.4.2 Computation of Allowable Cycles 14B-5
14B.5 NOMENCLATURE 14B-6
14B.6 REFERENCES 14B-8
14B.7 TABLES 14B-10
14B.8 FIGURES 14B-17

14B.1 Smooth Bar Design Fatigue Curves – ASME Code, Section VIII, Division 2

14B.1.1 Temperature Correction

When using the design fatigue curves, the calculated stress amplitude, S_a, shall be corrected for temperature by the ratio of modulus of elasticity of the given fatigue curve to the value used in the stress analysis. The equations used to correct S_a for the temperature effects are provided in Table 14B.1 for the smooth bar fatigue curves included in this Annex. The temperature corrected stress amplitude, S_{ac}, is then used to enter the smooth bar fatigue curves to determine the number of allowable cycles, N.

14B.1.2 Interpolation

The fatigue curve values may be interpolated as follows:

- Carbon, Low Alloy, Series 4xx, High Alloy Steels and High Tensile Strength Steels for temperatures not exceeding 371°C (700°F), the fatigue curve values may be interpolated for intermediate values of the ultimate tensile strength.
- For Wrought 70-30 Copper-Nickel for temperatures not exceeding 371°C (700°F), the fatigue curve values may be interpolated for intermediate values of the minimum specified yield strength.

14B.1.3 Design Fatigue Curves Based on Testing in Air

The design fatigue curves in this paragraph are from the ASME Code, Section VIII, Division 2, Annex 3F and are based on fatigue tests conducted in air.

14B.1.4 Design Fatigue Curve Models

Equations for smooth bar fatigue curves for different materials are provided below. The equations for the fatigue curves were developed using U.S. Customary units. However, consistent use of SI units for values of S_a and E_T when computing the parameter Y will produce the correct number of cycles, N, see paragraph 14B.1.3.

a) Carbon, Low Alloy, Series 4xx, High Alloy Steels, and High Tensile Strength Steels for temperatures not exceeding 371°C (700°F). The fatigue curve values may be interpolated for intermediate values of the ultimate tensile strength.

$$Y = \log_{10}\left[28.3E3\left(\frac{S_a}{E_T}\right)\right] \tag{14B.1}$$

1) For $\sigma_{uts} \le 552\ MPa\ (80\ ksi)$, (see Figure 14B.1), and for $48\ MPa\ (7\ ksi) \le S_a \le 3999\ MPa\ (580\ ksi)$.

$$X = \left(\begin{array}{l} -4706.5245 + \\ 1813.6228 \cdot Y + \dfrac{6785.5644}{Y} - \\ 368.12404 \cdot Y^2 - \dfrac{5133.7345}{Y^2} + \\ 30.708204 \cdot Y^3 + \dfrac{1596.1916}{Y^3} \end{array}\right) \qquad \left(10^Y \ge 20\right) \tag{14B.2}$$

$$X = \left(\frac{38.1309 - 60.1705 \cdot Y^2 + 25.0352 \cdot Y^4}{1 + 1.80224 \cdot Y^2 - 4.68904 \cdot Y^4 + 2.26536 \cdot Y^6}\right) \qquad \left(10^Y < 20\right) \tag{14B.3}$$

2) For $\sigma_{uts} = 793 - 896\ MPa\ (115 - 130\ ksi)$, (see Figure 14B.2), and for $77.2\ MPa\ (11.2\ ksi) \le S_a \le 2896\ MPa\ (420\ ksi)$.

$$X = \frac{5.37689 - 5.25401 \cdot Y + 1.14427 \cdot Y^2}{1 - 0.960816 \cdot Y + 0.291399 \cdot Y^2 - 0.0562968 \cdot Y^3} \qquad \left(10^Y \ge 43\right) \tag{14B.4}$$

$$X = \frac{-9.41749 + 14.7982 \cdot Y - 5.94 \cdot Y^2}{1 - 3.46282 \cdot Y + 3.63495 \cdot Y^2 - 1.21849 \cdot Y^3} \qquad \left(10^Y < 43\right) \tag{14B.5}$$

b) Series 3xx High Alloy Steels, Nickel-Chromium-Iron Alloy, Nickel-Iron-Chromium Alloy, and Nickel-Copper Alloy for temperatures not exceeding 427°C (800°F), (see Figure 14B.3), and for $93.7\ MPa\ (13.6\ ksi) \le S_a \le 6000\ MPa\ (870\ ksi)$.

$$Y = \log_{10}\left[28.3E3\left(\frac{S_a}{E_T}\right)\right] \tag{14B.6}$$

$$X = \left(\frac{17.0181 - 19.8713 \cdot Y + 4.21366 \cdot Y^2}{1 - 0.1720606 \cdot Y - 0.633592 \cdot Y^2}\right) \qquad \left(10^Y \ge 14.4\right) \tag{14B.7}$$

$$X = \frac{1}{\left(-0.331096 + \dfrac{4.3261 \cdot \ln[Y]}{Y^2}\right)} \qquad \left(10^Y < 14.4\right) \tag{14B.8}$$

c) Wrought 70-30 Copper-Nickel for temperatures not exceeding 371°C (700°F). The fatigue curve values may be interpolated for intermediate values of the minimum specified yield strength.

$$Y = \log_{10}\left[20.0E3 \cdot \left(\frac{S_a}{E_T}\right)\right] \tag{14B.9}$$

1) For: $\sigma_{ys} \le 134\ MPa\ (18\ ksi)$, (see Figure 14B.4), and for $83\ MPa\ (12\ ksi) \le S_a \le 1793\ MPa\ (260\ ksi)$.

$$X = -2.632 + \frac{0.1186}{\ln[Y]} + \frac{15.12 \cdot \ln[Y]}{Y^2} + \frac{7.087}{Y^2} \tag{14B.10}$$

2) For: $\sigma_{ys} = 207\ MPa\ (30\ ksi)$, (see Figure 14B.5), and for $62\ MPa\ (9\ ksi) \le S_a \le 1793\ MPa\ (260\ ksi)$.

$$X = 8.580044 - 1.889784 \cdot Y - \frac{8.261383 \cdot \ln[Y]}{Y} \qquad \left(10^Y \ge 24.5\right) \tag{14B.11}$$

$$X = 5.89029 - 0.2280247 \cdot Y - \frac{6.649501 \cdot \ln[Y]}{Y} \qquad \left(10^Y < 24.5\right) \tag{14B.12}$$

3) For: $\sigma_{ys} = 310\ MPa\ (45\ ksi)$, (see Figure 14B.6), and for $34\ MPa\ (5\ ksi) \le S_a \le 1793\ MPa\ (260\ ksi)$.

$$X = \left(\begin{array}{l} -884.9989 + \frac{8936.214}{Y} - \frac{36034.88}{Y^2} + \\ \frac{72508.69}{Y^3} - \frac{72703.36}{Y^4} + \frac{29053.66}{Y^5} \end{array}\right) \qquad \left(10^Y \ge 46\right) \tag{14B.13}$$

$$X = \left(\begin{array}{l} -17.50197 + \frac{109.168}{Y} - \frac{236.7921}{Y^2} + \\ \frac{257.9938}{Y^3} - \frac{137.1654}{Y^4} + \frac{28.55546}{Y^5} \end{array}\right) \qquad \left(10^Y < 46\right) \tag{14B.14}$$

d) Nickel-Chromium-Molybdenum-Iron, Alloys X, G, C-4, and C-276 for temperatures not exceeding 427°C (800°F), (see Figure 14B.7), and for $103\ MPa\ (15\ ksi) \le S_a \le 4881\ MPa\ (708\ ksi)$.

$$Y = \log_{10}\left[28.3E3\left(\frac{S_a}{E_T}\right)\right] \tag{14B.15}$$

$$X = \frac{-42.08579 + 12.514054 \cdot Y}{1 - 4.3290016 \cdot Y + 0.60540862 \cdot Y^2} \qquad \left(10^Y \ge 35.9\right) \tag{14B.16}$$

$$X = \frac{9.030556 - 8.1906623 \cdot Y}{1 - 0.36077181 \cdot Y - 0.47064984 \cdot Y^2} \qquad \left(10^Y < 35.9\right) \tag{14B.17}$$

e) High strength bolting for temperatures not exceeding 371°C (700°F).

$$Y = \log_{10}\left[30.0E3 \cdot \left(\frac{S_a}{E_T}\right)\right] \tag{14B.18}$$

1) For a Maximum Nominal Stress $\leq 2.7S$, (see Figure 14B.8), and for $93\ MPa\ (13.5\ ksi) \leq S_a \leq 7929\ MPa\ (1150\ ksi)$.

$$X = \left(\begin{array}{l} 3.75565644 - \dfrac{75.58638}{Y} + \dfrac{403.70774}{Y^2} - \\ \dfrac{830.40346}{Y^3} + \dfrac{772.53426}{Y^4} - \dfrac{267.75105}{Y^5} \end{array} \right) \tag{14B.19}$$

2) For a Maximum Nominal Stress $> 2.7S$, (see Figure 14B.9) and for $37\ MPa\ (5.3\ ksi) \leq S_a \leq 7929\ MPa\ (1150\ ksi)$.

$$X = \left(\begin{array}{l} -9.0006161 + \dfrac{51.928295}{Y} - \dfrac{86.121576}{Y^2} + \\ \dfrac{73.1573}{Y^3} - \dfrac{29.945507}{Y^4} + \dfrac{4.7332046}{Y^5} \end{array} \right) \tag{14B.20}$$

14B.1.5 Computation of Allowable Cycles

The number of cycles, N, can be computed from Equation (14B.21) based on the parameter X calculated for the applicable material. The computed number of cycles, N, shall not exceed the maximum number of cycles computed using Equation (14B.21) or as determined using Figure 14B.1 through Figure 14B.9.

$$N = 10^X \tag{14B.21}$$

14B.2 Smooth Bar Design Fatigue Curves – Mean Curve with Explicit Margins

The recommended procedure for computing the permissible number of cycles, N,for an alternating stress, S_a, with a mean stress correction based on S_{mean}, explicit margins on stress and cycles, and temperature effect is shown below. The procedure given below permits the actual value of mean stress to be used when determining the permissible number of cycles.

a) STEP 1 – Based on the material of construction, obtain A, B, C, E_{yrt}, σ_{ys} and σ_{uts} from Table 14B.2. If in-house fatigue data is available, the user may obtain their own A, B, and C by curve-fitting the Langer model and by defining E_{yrt}, σ_{ys} and σ_{uts} for the test material at the test temperature.

b) STEP 2 – Define S_a, S_{mean}, and E_T for the loading cycle of interest.

c) STEP 3 – Define the margin on cycles, M_N, (20 is used in VIII-2) and the margin on stress, M_S, (2 is used in VIII-2).

d) STEP 4 – Calculate the temperature correction factor.

$$f_{MT} = \frac{E_{yrt}}{E_T} \tag{14B.22}$$

e) STEP 5 – Calculate the stress amplitude adjusted for the mean stress and explicit margin on stress.

$$S^*_{a,S} = \frac{M_S \cdot f_{MT} \cdot S_a}{1 - \dfrac{f_{MT} \cdot S_{mean}}{\sigma_{uts}}} \qquad for \quad M_S \cdot f_{MT} \cdot S_a < \sigma_{ys} \tag{14B.23}$$

$$S^*_{a,S} = M_S \cdot f_{MT} \cdot S_a \qquad for \quad M_S \cdot f_{MT} \cdot S_a \geq \sigma_{ys} \tag{14B.24}$$

f) STEP 6 – Calculate the stress amplitude adjusted for mean stress. Note, the explicit margin on cycles is incorporated into Equation (14B.27), not Equations (14B.25) and (14B.26).

$$S_a^* = \frac{f_{MT} \cdot S_a}{1 - \frac{f_{MT} \cdot S_{mean}}{\sigma_{uts}}} \qquad for \qquad f_{MT} \cdot S_a < \sigma_{ys} \tag{14B.25}$$

$$S_a^* = f_{MT} \cdot S_a \qquad for \qquad f_{MT} \cdot S_a \geq \sigma_{ys} \tag{14B.26}$$

g) STEP 7 – If $S_a^* > B$ and $S_{a,S}^* > B$, compute the permissible number of cycles using Equation (14B.27). Otherwise, proceed to STEP 8.

$$N = \min \left[\frac{1}{M_N} \left(\frac{A}{S_a^* - B} \right)^{1/C} , \left(\frac{A}{S_{a,S}^* - B} \right)^{1/C} \right] \tag{14B.27}$$

h) STEP 8 – The permissible number of cycles is in the Very High Cycle (VHC) region of the fatigue curve that is not covered by the model. Therefore, the permissible number of cycles cannot be determined.

14B.3 Uniform Material Law

Baumel and Seeger developed a Uniform Material Law (see references [6]-[12]) for estimating the mean cyclic stress-strain curve and consistent mean strain-life properties for plain carbon and low to medium alloy steels, and for aluminum and titanium alloys. The method is shown in Annex 2E, Table 2E.10 and shown in Table 14B.4 for convenience. The Uniform Material Law provides generally satisfactory agreement with measured material properties and may on occasion provide an exceptional correlation. It is the general method recommended for estimating cyclic stress-strain curves and strain life properties when actual data for a specific material are not provided in the form of a correlation or actual data points.

14B.4 Welded Joint Fatigue Curves – ASME Code, Section VIII, Division 2

14B.4.1 Fatigue Curve Models

Welded joint fatigue curves are provided to evaluate welded joints for the following materials and associated temperature limits.

a) Ferritic and Stainless Steels and Nonferrous Alloys, see Figure 14B.10, including:

1) Carbon, Low Alloy, Series 4xx, High Alloy Steels, and High Tensile Strength Steels for temperatures not exceeding 371°C (700°F).

2) Series 3xx High Alloy Steels, Nickel-Chromium-Iron Alloy, Nickel-Iron-Chromium Alloy, and Nickel-Copper Alloy for temperatures not exceeding 427°C (800°F).

3) Wrought 70 Copper-Nickel for temperatures not exceeding 371°C (700°F).

4) Nickel-Chromium-Molybdenum-Iron, Alloys X, G, C-4, and C-276 for temperatures not exceeding 427°C (800°F).

b) Aluminum Alloys for temperatures not exceeding 120°C (250°F), see Figure 14B.11.

14B.4.2 Computation of Allowable Cycles

The number of allowable cycles for the welded joint fatigue curve shall be computed as follows.

a) The number of allowable cycles, N, can be computed from Equation (14B.28) based on the equivalent structural stress range parameter, $\Delta S_{ess,k}$, determined in accordance with Part 14, paragraph 14.4.3.4. The constants C and h for use in Equation (14B.28) are provided in Table 14B.5. The Lower 95% Prediction Interval (-2σ) shall be used unless another value can be justified. The prediction interval used to establish the fatigue curve shall be documented as part of the assessment.

$$N = \frac{f_I}{f_E}\left(\frac{f_{MT}\cdot C}{\Delta S_{ess,k}}\right)^{\frac{1}{h}} \tag{14B.28}$$

b) If a fatigue improvement method is performed that exceeds the fabrication requirements of the code of construction, a fatigue improvement factor, f_I, may be taken greater than 1.0 using the applicable equation shown below. The fatigue improvement method and factor shall be documented as part of the FFS Assessment.

1) For burr grinding.

$$f_I = 1.0 + 2.5\cdot(10)^q \tag{14B.29}$$

2) For TIG dressing.

$$f_I = 1.0 + 2.5\cdot(10)^q \tag{14B.30}$$

3) For hammer peening.

$$f_I = 1.0 + 4.0\cdot(10)^q \tag{14B.31}$$

4) In the above equations, the parameter q is given by the following equation.

$$q = -0.0016\cdot\left(\frac{\Delta S_{ess,k}}{C_{usm}}\right)^{1.6} \tag{14B.32}$$

c) The fatigue cycles given by Equation (14B.22) accounts for the effects of environment other than ambient air that may cause corrosion or sub-critical crack propagation. The environmental modification factor, f_E, is typically a function of the fluid environment, loading frequency, temperature, and material variables such as grain size and chemical composition. The range of $1.0 \le f_E \le 4.0$ may be used depending on the severity of the material and environmental interaction. The environmental modification factor, f_E, shall be specified in the assessment.

d) A temperature adjustment is required to the fatigue curve for materials other than carbon steel and/or for temperatures above 21°C (70°F). The temperature adjustment factor is given by Equation (14B.27).

$$f_{MT} = \frac{E_T}{E_A} \tag{14B.33}$$

14B.5 Nomenclature

a parameter used in the Uniform Material Law.

A smooth bar fatigue curve parameter.

b fatigue strength exponent, Basquin's exponent, in the Uniform Material Law.

B smooth bar fatigue curve parameter.

c fatigue strength exponent, Coffin-Manson exponent, Uniform Material Law.

C smooth bar or welded joint fatigue curve parameter.

C_{usm} conversion factor, $C_{usm} = 1.0$ for units of stress in ksi and $C_{usm} = 14.148299$ for units of stress in MPa.

E_A modulus of elasticity of carbon steel or aluminum, as applicable, at ambient temperature or 21°C (70°F).

E_T average of the modulus of elasticity values for the material at the highest and lowest temperature points of the cycle.

E_y modulus of elasticity at the temperature of interest.

E_{yrt} modulus of elasticity at room temperature or 21°C (70°F).

ε_{tr} total strain range.

ε_f^* fatigue ductility coefficient in the Uniform Material Law.

f_E environmental correction factor to the welded joint fatigue curve.

f_I fatigue improvement method correction factor to the welded joint fatigue curve.

f_{MT} material and temperature correction factor to the welded joint fatigue curve.

h welded joint fatigue curve exponent.

K_{css} material parameter for the cyclic stress-strain curve model in accordance with the Uniform Material Law.

q parameter used to determine the effect equivalent structural stress range on the fatigue improvement factor.

M_N smooth bar fatigue curve margin applied to cycles, 20 is used in the ASME Code, Section VIII, Division 2.

M_S smooth bar fatigue curve margin applied to the applied stress, 2 is used in the ASME Code, Section VIII, Division 2.

N number of allowable cycles.

N_f number of cycles to failure in accordance with the Uniform Material Law.

n_{css} material parameter for the cyclic stress-strain curve model in accordance with the Uniform Material Law.

S average of the allowable stress values for the material at the highest and lowest temperature points of the cycle.

S_a computed stress amplitude from Part 14.

S_a^* stress amplitude adjusted for mean stress and the ratio of the modulus of elasticity at room temperature to average of the modulus of elasticity values for the material at the highest and lowest temperature points of the cycle.

$S_{a,S}^*$ stress amplitude adjusted for mean stress, margin on stress, and the ratio of the modulus of elasticity at room temperature to average of the modulus of elasticity values for the material at the highest and lowest temperature points of the cycle.

S_{ac} temperature corrected stress amplitude.

$\Delta S_{ess,k}$ computed equivalent structural stress range parameter from Part 14.

σ_r applied stress range.

σ_{ys} average of the minimum specified yield strength values for the material at the highest and lowest temperature points of the cycle being evaluated.

σ_{uts} average of the minimum specified ultimate tensile strength values for the material at the highest and lowest temperature points of the cycle being evaluated.

σ_f^* fatigue strength coefficient.

X exponent used to compute the permissible number of cycles.

Y stress amplitude temperature correction factor used to compute X.

14B.6 References

[1] Osage, D.A. and Sowinski, J.C., *ASME Section VIII - Division 2 Criteria and Commentary*, ASME PTB-1-2013, American Society of Mechanical Engineers, New York, NY, 2013.

[2] J. Keisler, O.K. Chopra, and W.J. Shack, “Fatigue Strain-Life Behavior of Carbon and Low-Alloy Steels, Austenitic Stainless Steels, and Alloy 600 in LWR Environments,” NUREG/CR-6335 and ANL-95/15.

[3] Jaske, C.E. and O’Donnell, W.J., “Fatigue Design Criteria for Pressure Vessel Alloys,” Journal of Pressure Vessel Technology, Transactions of the ASME, November 1977.

[4] Yahr, G.T., “Fatigue Design Curves for 6061-T6 Aluminum,” Journal of Pressure Vessel Technology, May 1997, Vol. 119.

[5] Gross, M.R and Schwab, R. C., “Fatigue Properties of Nonferrous Alloys for Heat Exchangers, Pumps, and Piping,” Assignment 86 108, MEL R&D Report 232/66, May 1966.

[6] Bäumel, A. and Seeger, T., *Materials data for cyclic loading, Supplement 1*, Elsevier Amsterdam, 1990.

[7] Boller, C. and Seeger, T., Materials data for cyclic loading, Part A – Unalloyed steels, Elsevier, Amsterdam, 1987.

[8] Boller, C. and Seeger, T., *Materials data for cyclic loading*, Part B – Low-alloy steels, Elsevier, Amsterdam, 1987.

[9] Boller, C. and Seeger, T., *Materials data for cyclic loading*, Part C – High-alloy steels, Elsevier, Amsterdam, 1987.

[10] Boller, C. and Seeger, T., *Materials data for cyclic loading, Part D*, Elsevier, Amsterdam, 1987.

[11] Boller, C. and Seeger, T., *Materials data for cyclic loading, Part E*, Elsevier, Amsterdam, 1987.

[12] Korkmaz, S., Uniform Material Law: Extension to High-Strength Steel, VDM Publishing, Germany, 2010.

14B.7 Tables

Table 14B.1 – Smooth Bar Fatigue Curve Stress Amplitude Correction Equations

Fatigue Curve	Temperature Corrected Stress Amplitude, S_{ac}	
	Units of Stress in MPa	Units of Stress in ksi
Figure 14B.1	$S_{ac} = 195.0E3\left(\frac{S_a}{E_T}\right)$	$S_{ac} = 28.3E3\left(\frac{S_a}{E_T}\right)$
Figure 14B.2		
Figure 14B.3		
Figure 14B.4	$S_{ac} = 138.0E3\left(\frac{S_a}{E_T}\right)$	$S_{ac} = 20.0E3\left(\frac{S_a}{E_T}\right)$
Figure 14B.5		
Figure 14B.6		
Figure 14B.7	$S_{ac} = 195.0E3\left(\frac{S_a}{E_T}\right)$	$S_{ac} = 28.3E3\left(\frac{S_a}{E_T}\right)$
Figure 14B.8	$S_{ac} = 206.0E3\left(\frac{S_a}{E_T}\right)$	$S_{ac} = 30.0E3\left(\frac{S_a}{E_T}\right)$
Figure 14B.9		

Table 14B.2 – Smooth Bar Fatigue Curve Parameters

Material	A (ksi)	B (ksi)	C	E_{yrt} (ksi)	σ_{ys} (ksi)	σ_{uts} (ksi)	Temp Limit (ºF)	Ref
Carbon Steels	8664	21.645	0.5	28300	40	80	700	1,2
Low Alloy Steels (Mn-Mo, Mn-Mo, Ni)	7139	38.5	0.5	28300	70	100	700	1.2
Austenitic Stainless Steels	8415	43.5	0.5	28300	44	94	800	1,2
Series 3xx High Alloy Steels, Nickel-Chromium-Iron Alloy, Nickel-Iron-Chromium Alloy, and Nickel-Copper Alloy	9058	33.05	0.5	28300	44	94	800	3
Types 304, 310, 316, 347 and 348	9081	31.59	0.5	28300	44	94	800	3
Alloy 800	8557	38.5	0.5	27600	44	94	800	3
Alloy 600	10393	39.2	0.5	31700	44	94	800	3
Alloy 718	9195	62.7	0.5	29800	44	94	700	3
6061-T6 Aluminum	2100	14.0	0.5	10000	38	42	300	5
Gun Metal, As-cast (MIL-M-16576) (1)	1016	6.0	0.35	15000	15.6	36	120	5
Valve Bronze, As-cast (MIL-B-16541) (1)	403	6.0	0.32	14000	15.8	28	120	5
Ni-Al Bronze, As-Cast (MIL-B-21230 Alloy 1) (1)	5570	29.0	0.49	13000	42.1	97.3	120	5
Ni-Al Bronze, Forged, Annealed (QQ- B-679 comp 2) (1)	3530	35.0	0.42	17000	51.8	103.3	120	5
Superaton 40, Cast, As-cast (MIL-B- 21230 Alloy 2) (1)	3900	25	0.44	18000	43.4	85.4	120	5
70-30 Cupronickel, Cast, As-cast (MIL-C-20159) (1)	2800	13.0	0.45	18000	48.1	79.2	120	5
70-30 Cupronickel, Wrought, Annealed (MIL-C-15726) (1)	1900	20.0	0.35	22000	20.2	58.5	120	5
90-10 Cupronickel, Wrought, Hard (MIL-C-15726), (1)	2300	20.0	0.42	20000	46	53.8	120	5
Cufenloy 40, wrought, Annealed (1)	10000	25.0	0.58	24000	22.4	70.3	120	5
Cufenloy 40, Wrought, DSR (1)	1400	20.0	0.34	20000	68.4	79	120	5
Cupronickel-707, Wrought, Annealed (1)	2400	23.0	0.39	22000	51	81.6	120	5
Monel E, Cast, As-cast (QQ-N-288) (1)	2510	16.0	0.42	23000	27	59.5	700	5
Monel, Wrought, Annealed (MIL-N- 894 Class A) (1)	21000	33.0	0.61	26000	33.1	83.6	700	5

Note:

1. See Table 14B.3 for material properties

Table 14B.2M – Smooth Bar Fatigue Curve Parameters

Material	A (MPa)	B (MPa)	C	E_{yrt} (GPa)	σ_{ys} (MPa)	σ_{uts} (MPa)	Temp Limit (ºC)	Ref
Carbon Steels	59736.1	149.2	0.5	195.1217	275.8	551.6	371	1,2
Low Alloy Steels (Mn-Mo, Mn-Mo, Ni)	49221.7	265.4	0.5	195.1217	482.6	689.5	371	1.2
Austenitic Stainless Steels	58019.4	299.9	0.5	195.1217	303.4	648.1	427	1,2
Series 3xx High Alloy Steels, Nickel-Chromium-Iron Alloy, Nickel-Iron-Chromium Alloy, and Nickel-Copper Alloy	62452.7	227.8	0.5	195.1217	303.4	648.1	427	3
Types 304, 310, 316, 347 and 348	62611.3	217.8	0.5	195.1217	303.4	648.1	427	3
Alloy 800	58998.5	265.4	0.5	190.2954	303.4	648.1	427	3
Alloy 600	71657.2	270.3	0.5	218.5639	303.4	648.1	427	3
Alloy 718	63397.3	432.3	0.5	205.4638	303.4	648.1	371	3
6061-T6 Aluminum	14479.0	96.5	0.5	68.9476	262.0	289.6	149	5
Gun Metal, As-cast (MIL-M-16576) (1)	7005.1	41.4	0.35	103.4214	107.6	248.2	49	5
Valve Bronze, As-cast (MIL-B-16541) (1)	2778.6	41.4	0.32	96.5266	108.9	193.1	49	5
Ni-Al Bronze, As-Cast (MIL-B-21230 Alloy 1) (1)	38403.8	199.9	0.49	89.6319	290.3	670.9	49	5
Ni-Al Bronze, Forged, Annealed (QQ- B-679 comp 2) (1)	24338.5	241.3	0.42	117.2109	357.1	712.2	49	5
Superaton 40, Cast, As-cast (MIL-B- 21230 Alloy 2) (1)	26889.6	172.4	0.44	124.1057	299.2	588.8	49	5
70-30 Cupronickel, Cast, As-cast (MIL-C-20159) (1)	19305.3	89.6	0.45	124.1057	331.6	546.1	49	5
70-30 Cupronickel, Wrought, Annealed (MIL-C-15726) (1)	13100.0	137.9	0.35	151.6847	139.3	403.3	49	5
90-10 Cupronickel, Wrought, Hard (MIL-C-15726), (1)	15857.9	137.9	0.42	137.8952	317.2	370.9	49	5
Cufenloy 40, wrought, Annealed (1)	68947.6	172.4	0.58	165.4742	154.4	484.7	49	5
Cufenloy 40, Wrought, DSR (1)	9652.7	137.9	0.34	137.8952	471.6	544.7	49	5
Cupronickel-707, Wrought, Annealed (1)	16547.4	158.6	0.39	151.6847	351.6	562.6	49	5
Monel E, Cast, As-cast (QQ-N-288) (1)	17305.8	110.3	0.42	158.5795	186.2	410.2	371	5
Monel, Wrought, Annealed (MIL-N- 894 Class A) (1)	144789.9	227.5	0.61	179.2637	228.2	576.4	371	5

Note:

1. See Table 14B.3 for material properties

Table 14B.3 – Material Properties of Nonferrous Alloys (see Reference [5])

Material	Chemical Composition (%)									σ_{ys} (ksi)	σ_{uts} (ksi)
	Cu	Ni	Fe	Mn	Zn	Al	Sn	Si	Other		
Gun Metal, As-cast (MIL-M-16576)	87.2	0.7	0.02	-	3.5	-	8.4	-	-	15.6	36.0
Valve Bronze, As-cast (MIL-B-16541)	88.5	0.5	0.01	-	3.8	-	5.6	-	Pb-1.6	15.8	28.0
Ni-Al Bronze, As-Cast (MIL-B-21230 Alloy 1)	80.1	5.2	3.7	0.7	-	10.3	-	-	P-0.01	42.1	97.3
Ni-Al Bronze, Forged, Annealed (QQ-B-679 comp 2)	81.2	4.5	2.8	0.9	-	10.6	Nil	-	-	51.8	103.3
Superaton 40, Cast, As-cast (MIL-B-21230 Alloy 2)	74.6	2.2	3.3	12.5	-	7.4	-	-	-	43.4	85.4
70-30 Cupronickel, Cast, As-cast (MIL-C-20159)	66.8	30.4	0.5	1.25	-	-	-	0.5	-	48.1	79.2
70-30 Cupronickel, Wrought, Annealed (MIL-C-15726)	68.6	29.6	0.6	0.9	0.2	-	-	-	Cb-0.5	20.2	58.5
90-10 Cupronickel, Wrought, Hard (MIL-C-15726)	88.0	10	1.3	0.6	0.04	-	-	-	-	49/6	53.8
Cufenloy 40, wrought, Annealed	55.0	Rem	2.2	1.4	0.06	0.01	0.01	-	Pb<0.02	22.4	70.3
Cufenloy 40, Wrought, DSR	55.0	Rem	2.2	1.4	0.06	0.01	0.01	-	Pb-0.01 As-0.01	68.4	79.0
Cupronickel-707, Wrought, Annealed	54.1	29.6	5.4	0.8	0.11	-	<0.05	0.02	Pb-0.01 As-0.01	51.0	81.6
Monel E, Cast, As-cast (QQ-N-288)	30.2	63.1	2.2	0.9	-	-	-	1.6	c-0.01	27.0	59.5
Monel, Wrought, Annealed (MIL-N-894 Class A)	32.7	65.0	0.9	1.0	-	0.02	-	-	Cb-1.6	33.1	83.6

Table 14B.3M – Material Properties of Nonferrous Alloys (see Reference [5])

Material	Chemical Composition (%)									σ_{ys} (MPa)	σ_{uts} (MPa)
	Cu	Ni	Fe	Mn	Zn	Al	Sn	Si	Other		
Gun Metal, As-cast (MIL-M-16576)	87.2	0.7	0.02	-	3.5	-	8.4	-	-	107.6	248.2
Valve Bronze, As-cast (MIL-B-16541)	88.5	0.5	0.01	-	3.8	-	5.6	-	Pb-1.6	108.9	193.1
Ni-Al Bronze, As-Cast (MIL-B-21230 Alloy 1)	80.1	5.2	3.7	0.7	-	10.3	-	-	P-0.01	290.3	670.9
Ni-Al Bronze, Forged, Annealed (QQ-B-679 comp 2)	81.2	4.5	2.8	0.9	-	10.6	Nil	-	-	357.1	712.2
Superaton 40, Cast, As-cast (MIL-B-21230 Alloy 2)	74.6	2.2	3.3	12.5	-	7.4	-	-	-	299.2	588.8
70-30 Cupronickel, Cast, As-cast (MIL-C-20159)	66.8	30.4	0.5	1.25	-	-	-	0.5	-	331.6	546.1
70-30 Cupronickel, Wrought, Annealed (MIL-C-15726)	68.6	29.6	0.6	0.9	0.2	-	-	-	Cb-0.5	139.3	403.3
90-10 Cupronickel, Wrought, Hard (MIL-C-15726)	88.0	10	1.3	0.6	0.04	-	-	-	-	342.0	370.9
Cufenloy 40, wrought, Annealed	55.0	Rem	2.2	1.4	0.06	0.01	0.01	-	Pb<0.02	154.4	484.7
Cufenloy 40, Wrought, DSR	55.0	Rem	2.2	1.4	0.06	0.01	0.01	-	Pb-0.01 As-0.01	471.6	544.7
Cupronickel-707, Wrought, Annealed	54.1	29.6	5.4	0.8	0.11	-	<0.05	0.02	Pb-0.01 As-0.01	351.6	562.6
Monel E, Cast, As-cast (QQ-N-288)	30.2	63.1	2.2	0.9	-	-	-	1.6	c-0.01	186.2	410.2
Monel, Wrought, Annealed (MIL-N-894 Class A)	32.7	65.0	0.9	1.0	-	0.02	-	-	Cb-1.6	228.2	576.4

Table 14B.4 – Uniform Material Law for Estimating the Mean Cyclic Stress-Strain Curve and Mean Strain-Life Properties

Parameter	Plain Carbon and Low to Medium Alloy Steels	Aluminum and Titanium Alloys
n_{css}	0.15	0.11
K_{css}	$1.65\sigma_{uts}$	$1.61\sigma_{uts}$
σ_f'	$1.5\sigma_{uts}$	$1.67\sigma_{uts}$
ε_f'	$0.59 \cdot a$	0.35
B	-0.087	-0.095
c	-0.58	-0.69

Cyclic Stress-Strain Curve – Mean Curve:

$$\varepsilon_{tr} = \frac{\sigma_r}{E_y} + 2\left[\frac{\sigma_r}{2K_{css}}\right]^{\frac{1}{n_{css}}}$$

Strain-Life Equation – Mean Curve:

$$\frac{\varepsilon_{tr}}{2} = \frac{\sigma_f'}{E_y}\left(2N_f\right)^b + \varepsilon_f'\left(2N_f\right)^c$$

where,

$$a = 1.0 \qquad \left(for \quad \frac{\sigma_{uts}}{E_y} < 0.003\right)$$

$$a = 1.375 - 125.0\left(\frac{\sigma_{uts}}{E_y}\right) \qquad \left(for \quad \frac{\sigma_{uts}}{E_y} \geq 0.003\right)$$

Table 14B.5 – Coefficients for the Welded Joint Fatigue Curves

Statistical Basis	Ferritic, Stainless, and Nonferrous Alloy Steels		Aluminum	
	C	h	C	h
Mean Curve	1408.7	0.31950	247.04	0.27712
Upper 68% Prediction Interval $(+1\sigma)$	1688.3	0.31950	303.45	0.27712
Lower 68% Prediction Interval (-1σ)	1175.4	0.31950	201.12	0.27712
Upper 95% Prediction Interval $(+2\sigma)$	2023.4	0.31950	372.73	0.27712
Lower 95% Prediction Interval (-2σ)	980.8	0.31950	163.73	0.27712
Upper 99% Prediction Interval $(+3\sigma)$	2424.9	0.31950	457.84	0.27712
Lower 99% Prediction Interval (-3σ)	818.3	0.31950	133.29	0.27712

Note: In U.S. Customary Units, the equivalent structural stress range parameter, $\Delta S_{ess,k}$, and the structural stress effective thickness, t_{ess}, are in $ksi/(inches)^{(2-m_{ss})/2m_{ss}}$ and $inches$, respectively.

Table 14B.5M – Coefficients for the Welded Joint Fatigue Curves

Statistical Basis	Ferritic, Stainless, and Nonferrous Alloy Steels		Aluminum	
	C	h	C	h
Mean Curve	19930.2	0.31950	3495.13	0.27712
Upper 68% Prediction Interval $(+1\sigma)$	23885.8	0.31950	4293.19	0.27712
Lower 68% Prediction Interval (-1σ)	16629.7	0.31950	2845.42	0.27712
Upper 95% Prediction Interval $(+2\sigma)$	28626.5	0.31950	5273.48	0.27712
Lower 95% Prediction Interval (-2σ)	13875.7	0.31950	2316.48	0.27712
Upper 99% Prediction Interval $(+3\sigma)$	34308.1	0.31950	6477.60	0.27712
Lower 99% Prediction Interval (-3σ)	11577.9	0.31950	1885.87	0.27712

Note: In SI Units, the equivalent structural stress range parameter, $\Delta S_{ess,k}$, and the structural stress effective thickness, t_{ess}, are in $MPa/(mm)^{(2-m_{ss})/2m_{ss}}$ and mm, respectively.

14B.8 Figures

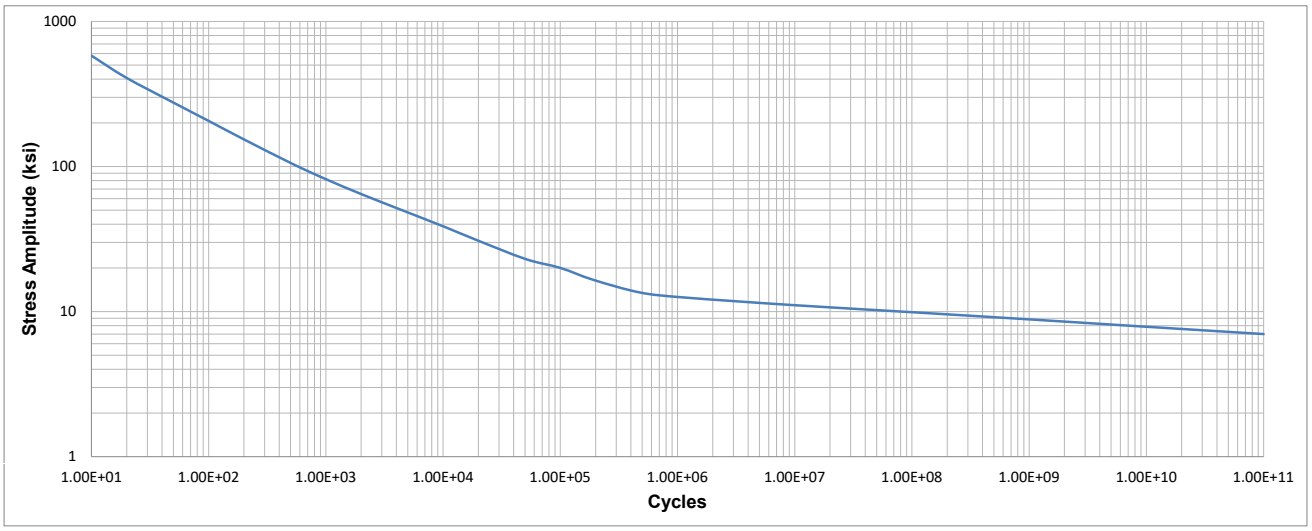

Figure 14B.1 – Fatigue Curve for Carbon, Low Alloy, Series 4XX, High Alloy Steels, and High Tensile Strength Steels for Temperatures not Exceeding 700°F – $\sigma_{uts} \leq 80\ ksi$

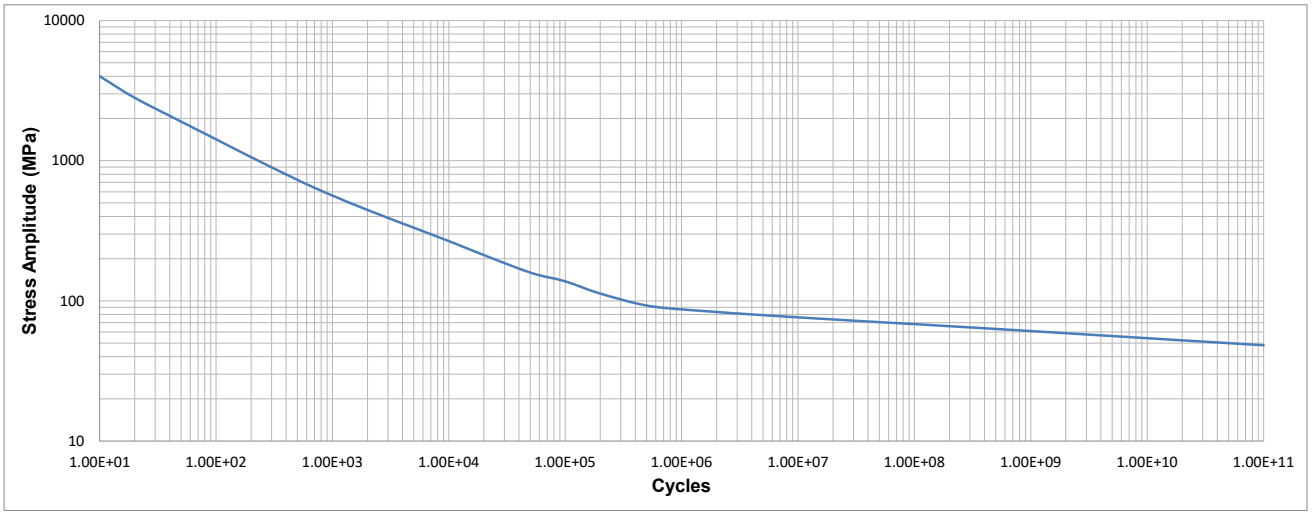

Figure 14B.1M – Fatigue Curve for Carbon, Low Alloy, Series 4XX, High Alloy Steels, and High Tensile Strength Steels for Temperatures not Exceeding 371°C – $\sigma_{uts} \leq 552\ MPa$

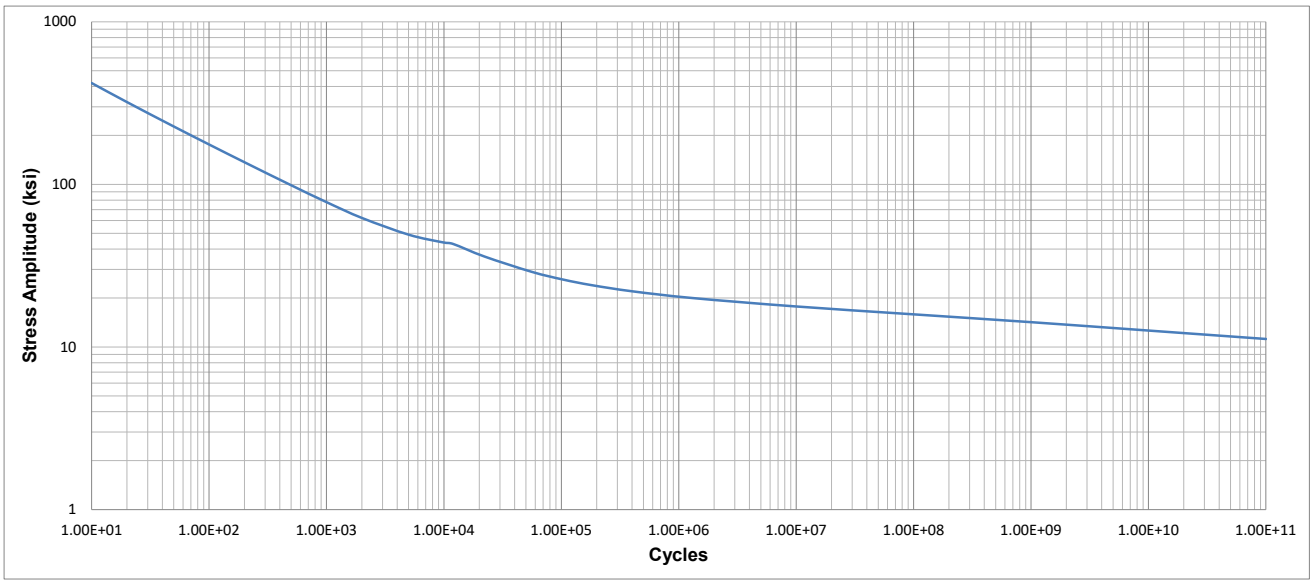

Figure 14B.2 – Fatigue Curve for Carbon, Low Alloy, Series 4XX, High Alloy Steels, and High Tensile Strength Steels for Temperatures not Exceeding 700°F – $\sigma_{uts} = 115 - 130\ ksi$

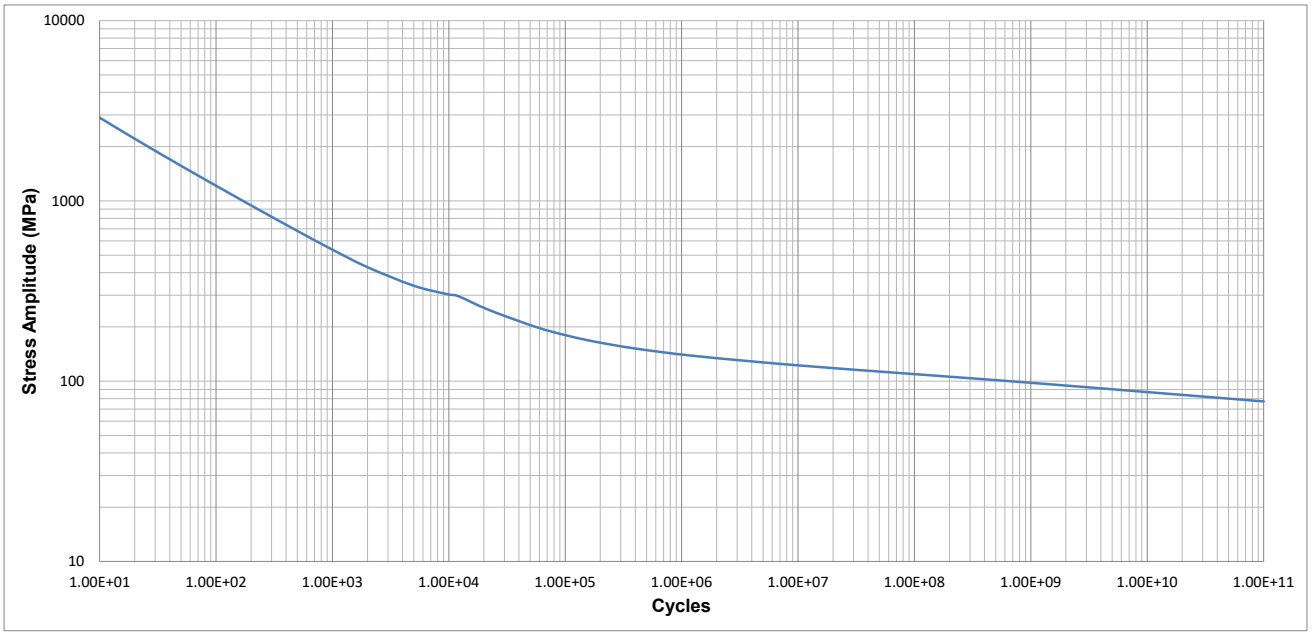

Figure 14B.2M – Fatigue Curve for Carbon, Low Alloy, Series 4XX, High Alloy Steels, and High Tensile Strength Steels for Temperatures not Exceeding 371°C – $\sigma_{uts} = 793 - 892\ MPa$

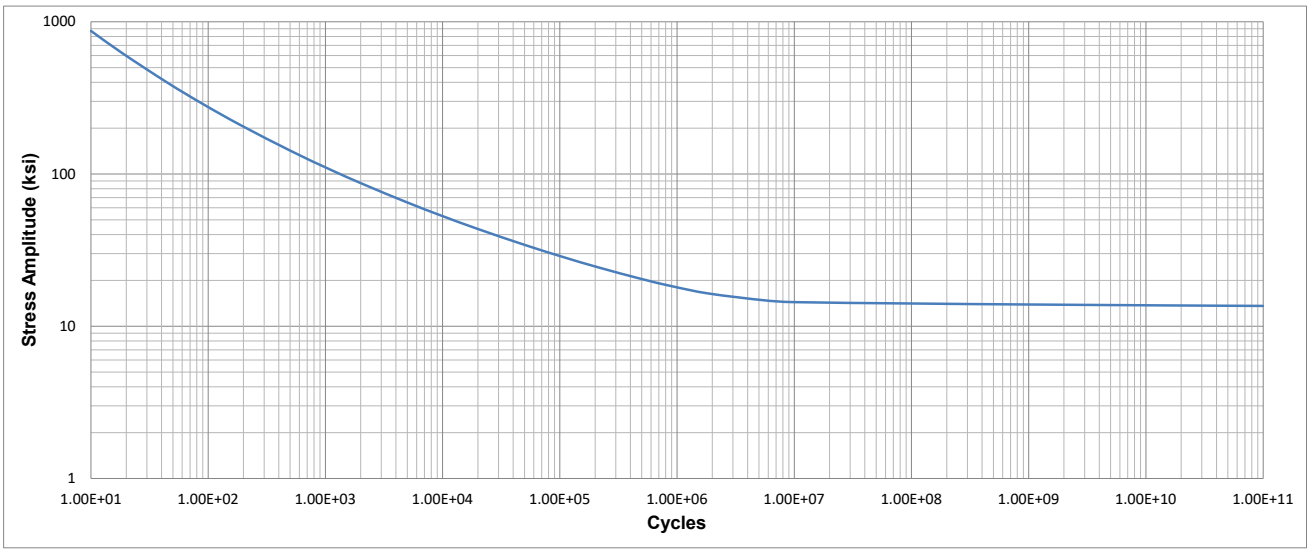

Figure 14B.3 – Fatigue Curve for Series 3xx High Alloy Steels, Nickel-Chromium-Iron Alloy, Nickel-Iron-Chromium Alloy, and Nickel-Copper Alloy for Temperatures not Exceeding 800°F

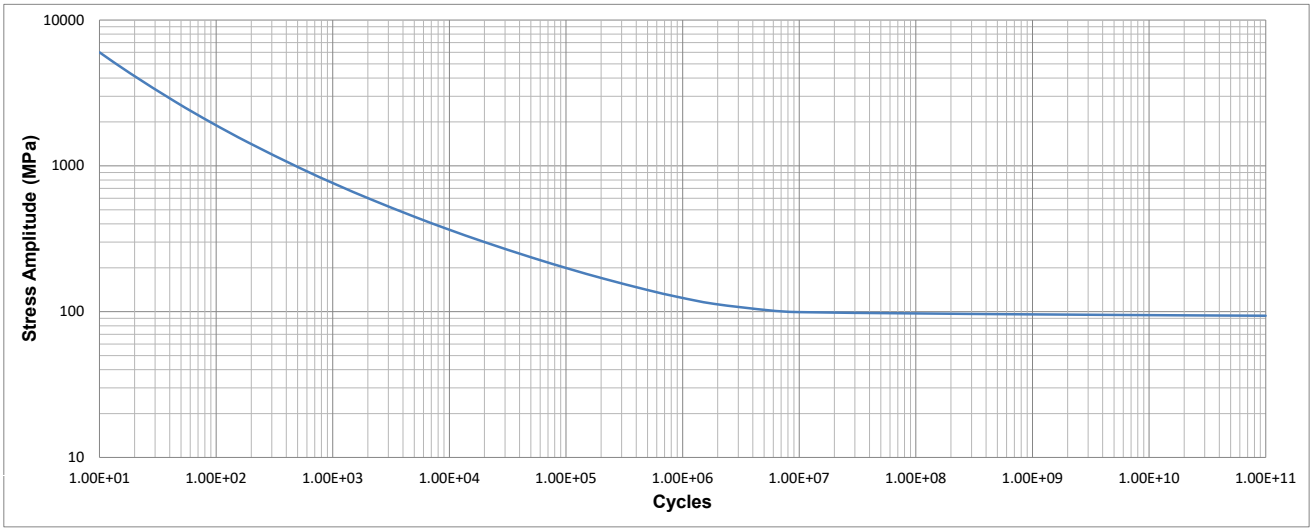

Figure 14B.3M – Fatigue Curve for Series 3xx High Alloy Steels, Nickel-Chromium-Iron Alloy, Nickel-Iron-Chromium Alloy, and Nickel-Copper Alloy for Temperatures not Exceeding 427°C

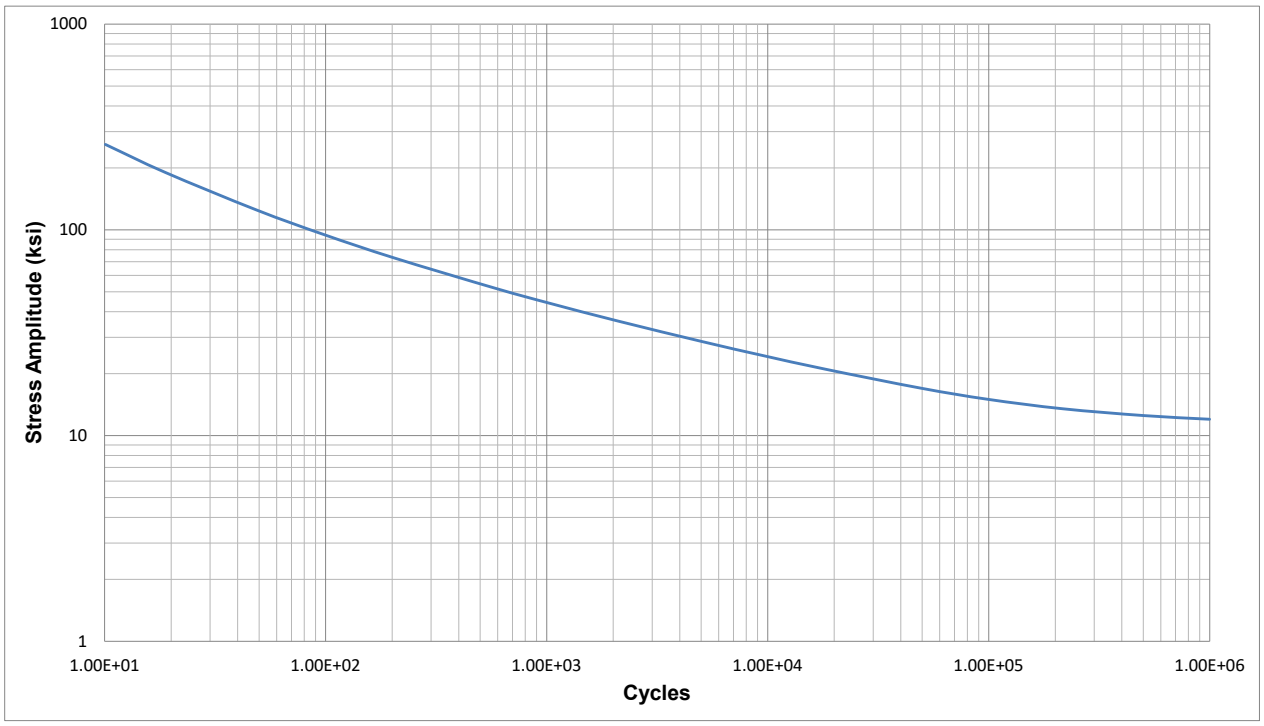

Figure 14B.4 – Fatigue Curve for Wrought 70 Copper-Nickel for Temperatures Not Exceeding 700°F – $\sigma_{ys} \leq 18\ ksi$

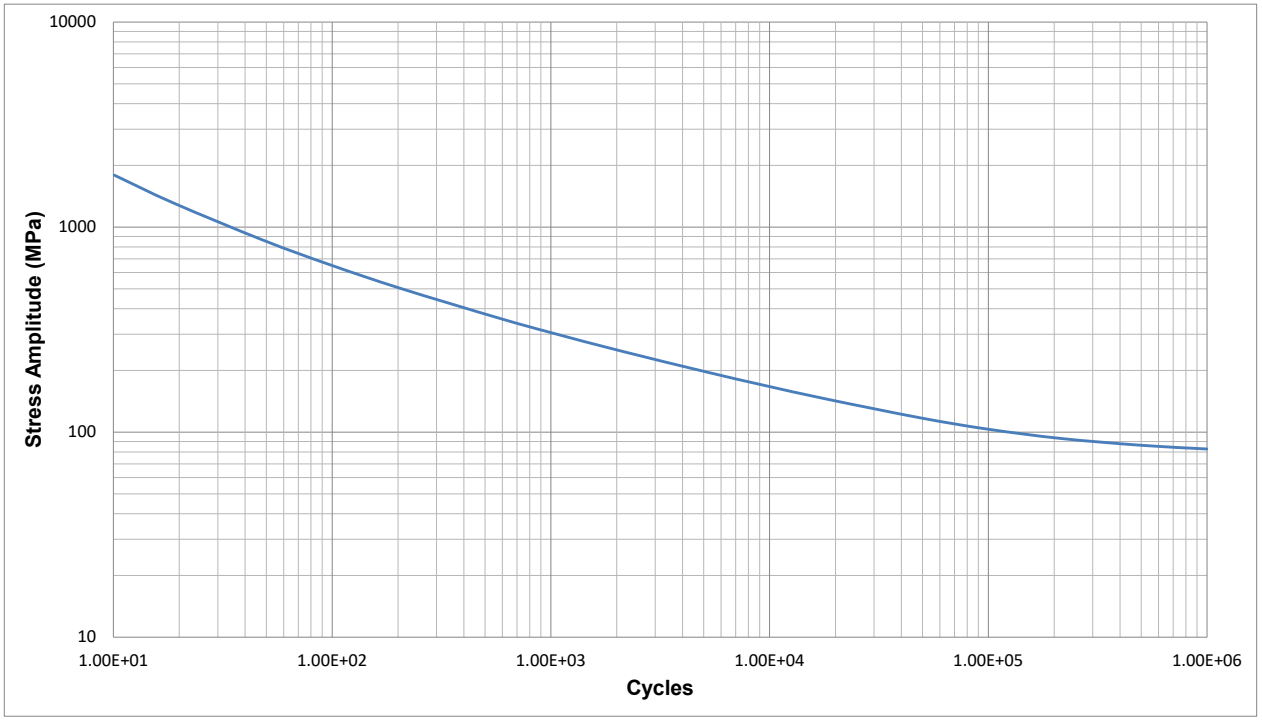

Figure 14B.4M – Fatigue Curve for Wrought 70 Copper-Nickel for Temperatures Not Exceeding 371°C – $\sigma_{ys} \leq 134\ MPa$

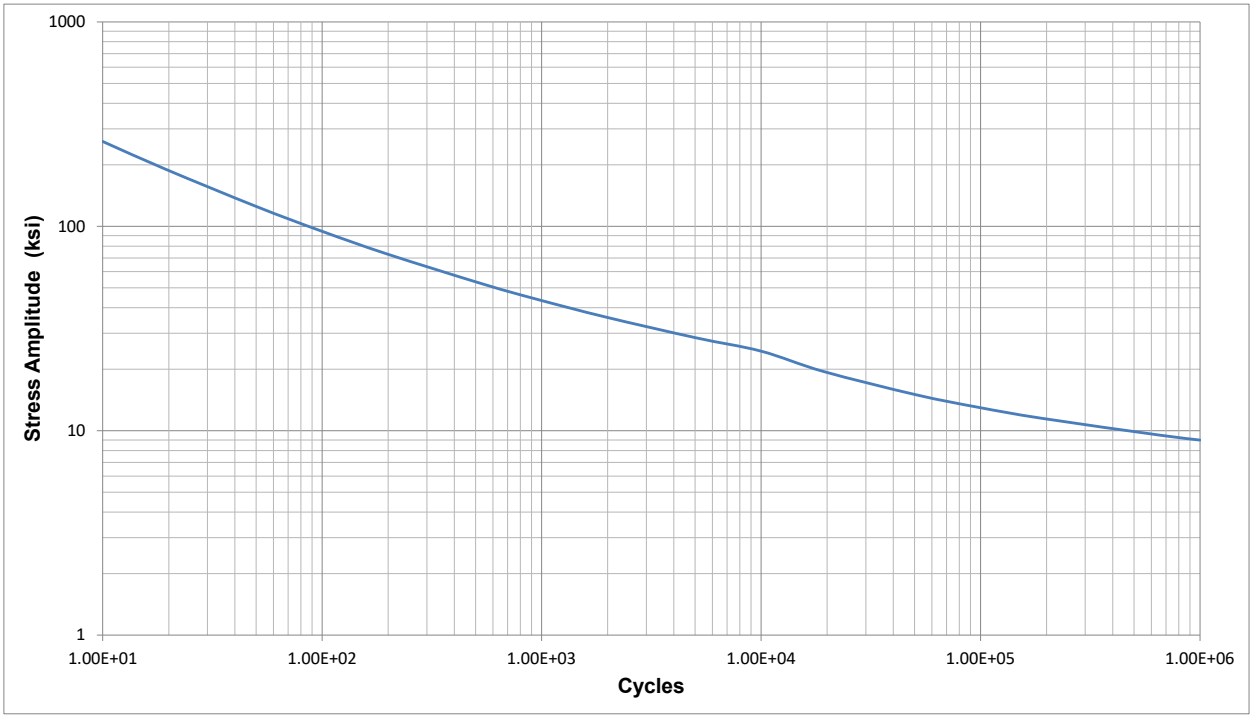

Figure 14B.5 – Fatigue Curve for Wrought 70 Copper-Nickel for Temperatures Not Exceeding 700°F – $\sigma_{ys} = 30\ ksi$

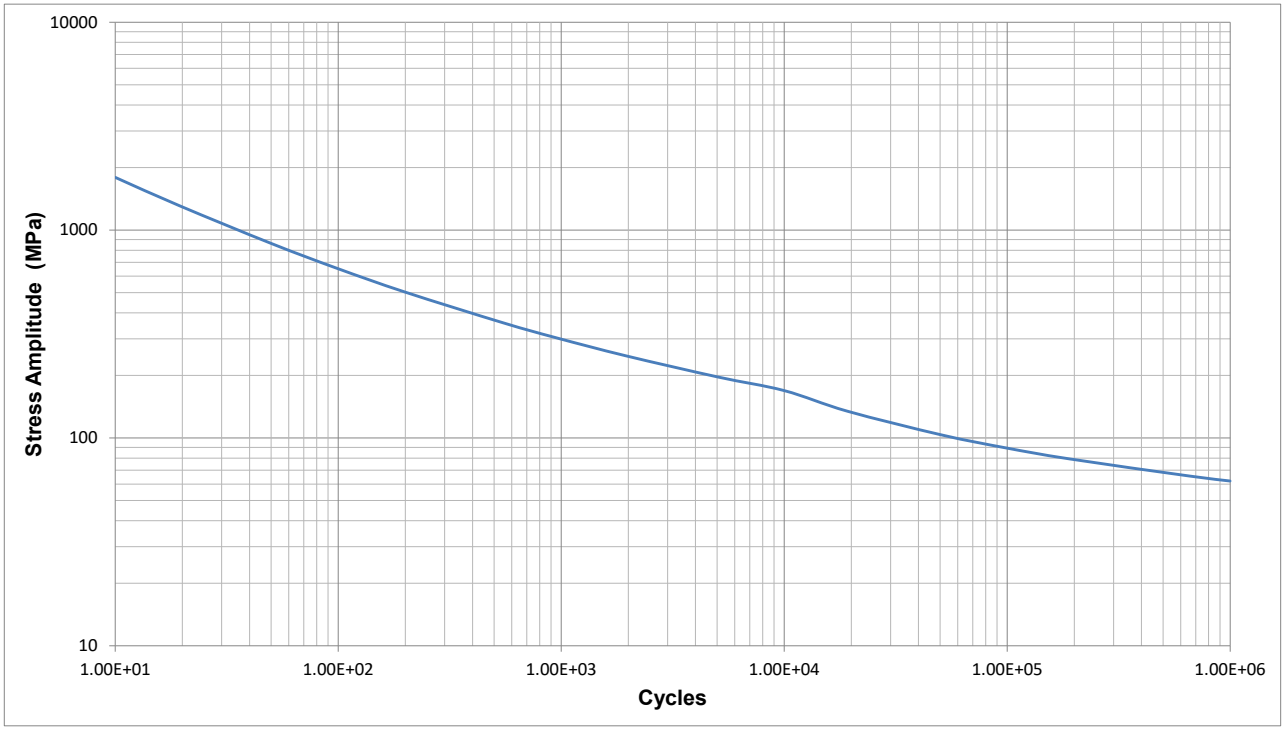

Figure 14B.5M – Fatigue Curve for Wrought 70 Copper-Nickel for Temperatures Not Exceeding 371°C – $\sigma_{ys} = 207\ MPa$

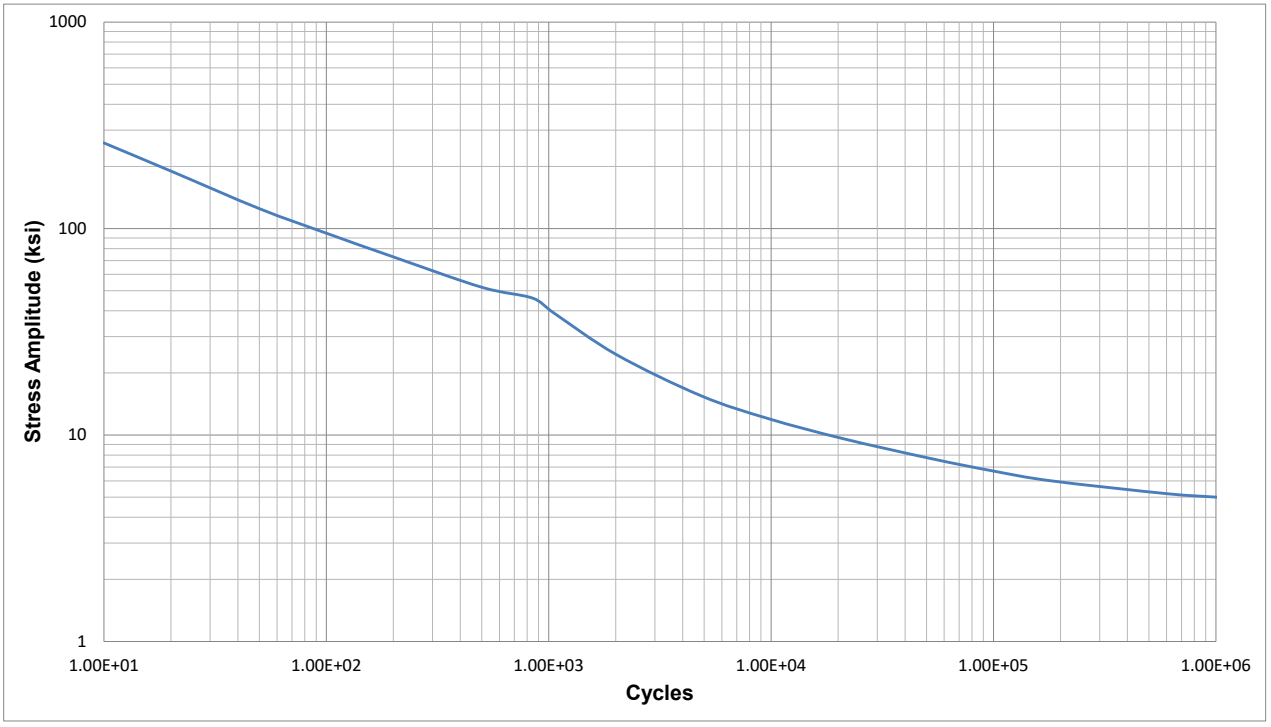

Figure 14B.6 – Fatigue Curve for Wrought 70 Copper-Nickel for Temperatures Not Exceeding 700°F – $\sigma_{ys} = 45\ ksi$

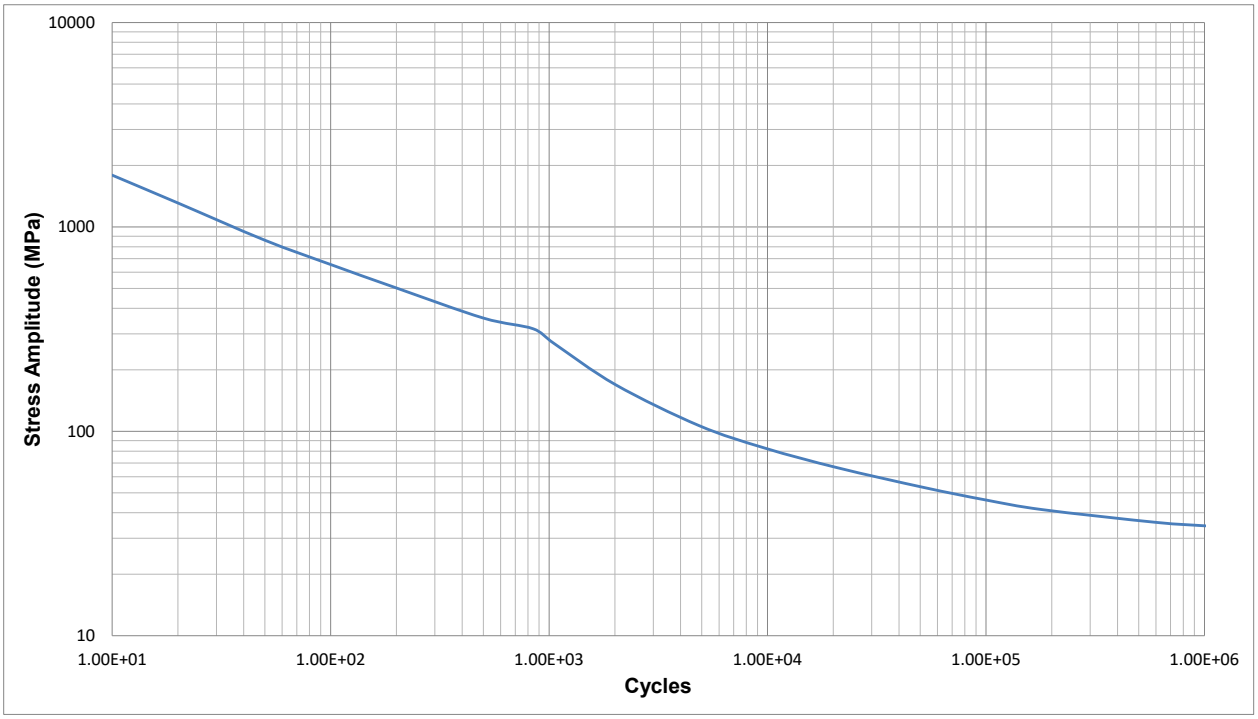

Figure 14B.6M – Fatigue Curve for Wrought 70 Copper-Nickel for Temperatures Not Exceeding 371°C – $\sigma_{ys} = 310\ MPa$

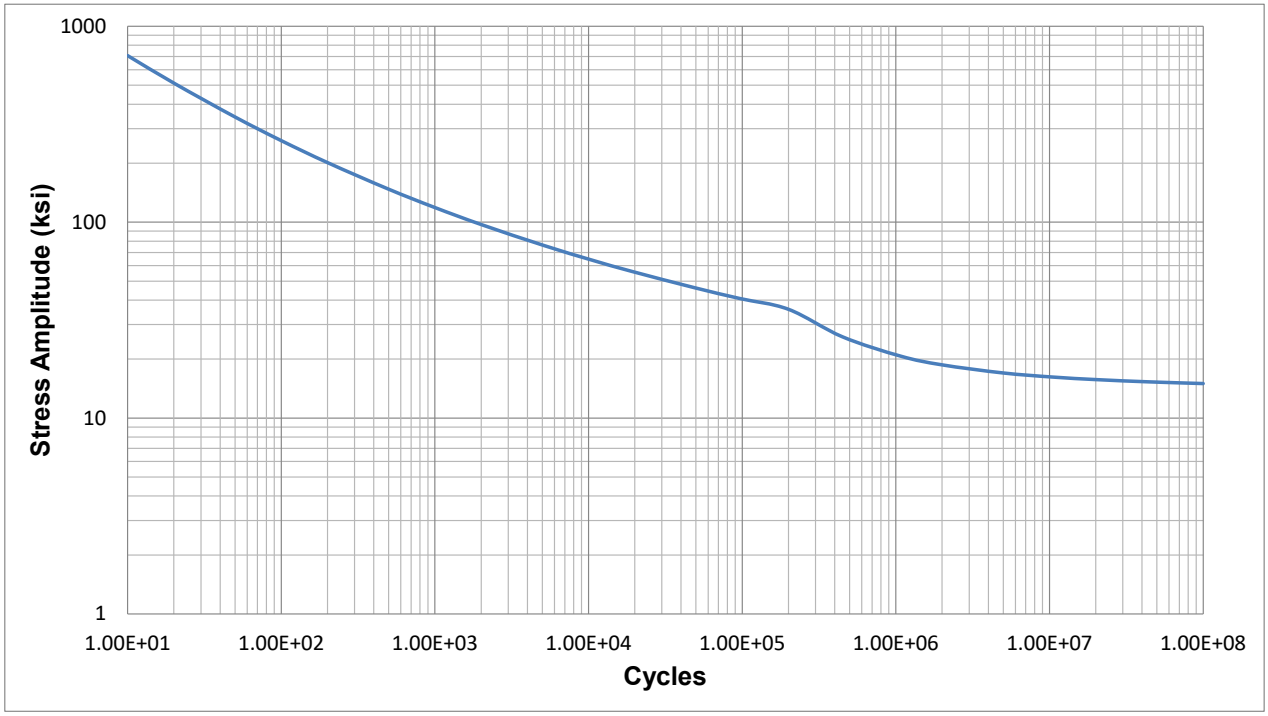

Figure 14B.7 – Fatigue Curve for Nickel-Chromium-Molybdenum-Iron, Alloys X, G, C-4, and C-276 for Temperatures Not Exceeding 800°F

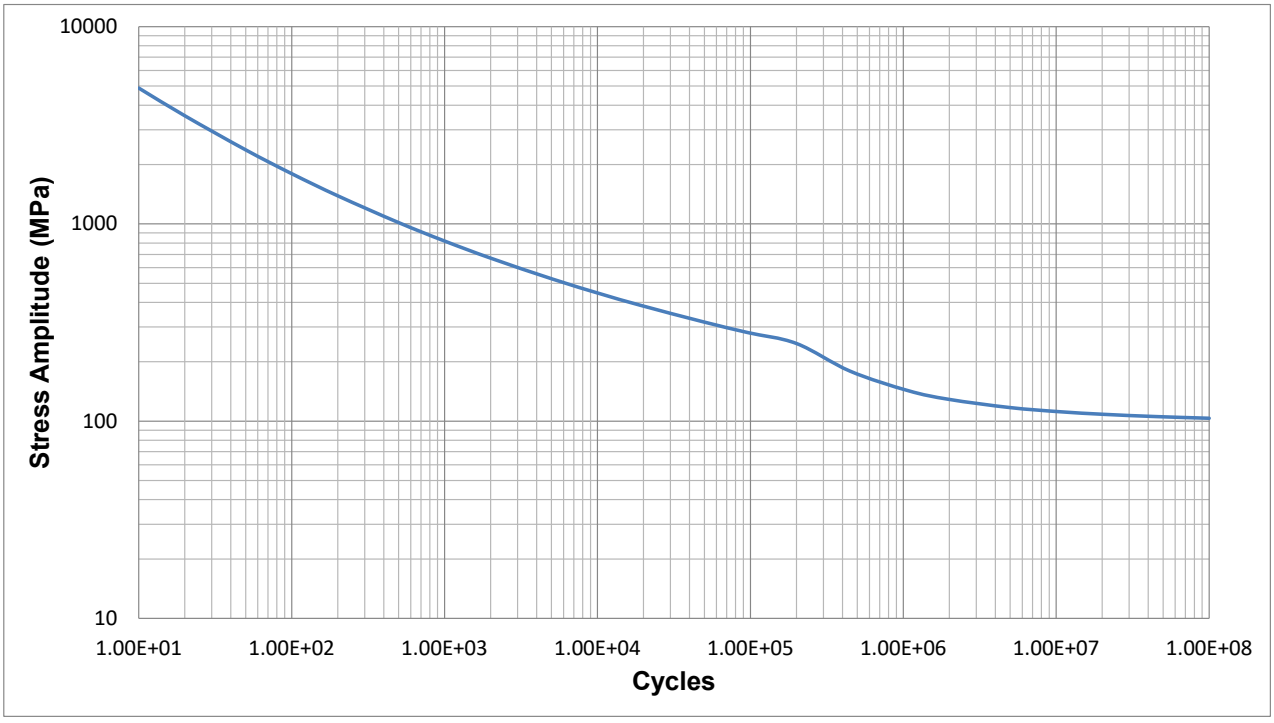

Figure 14B.7M – Fatigue Curve for Nickel-Chromium-Molybdenum-Iron, Alloys X, G, C-4, and C-276 for Temperatures Not Exceeding 427°C

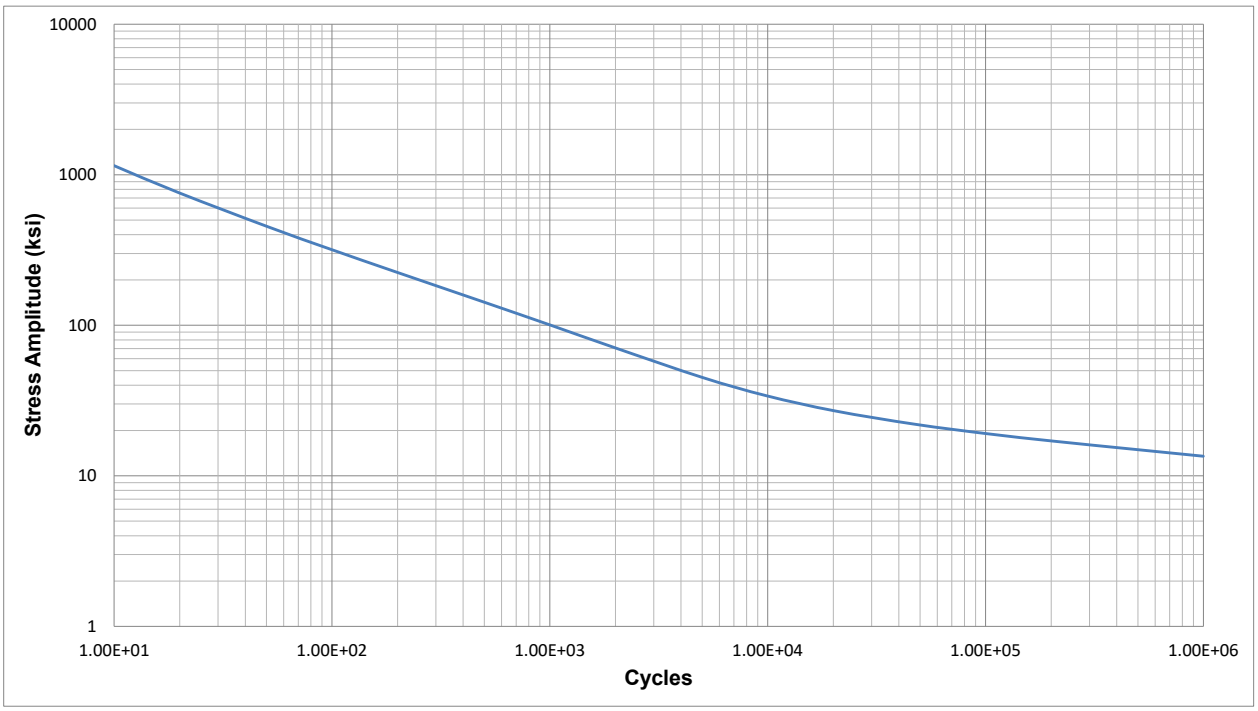

Figure 14B.8 – Fatigue Curve for High Strength Bolting for Temperatures Not Exceeding 700°F – Maximum Nominal Stress $\leq 2.7S$

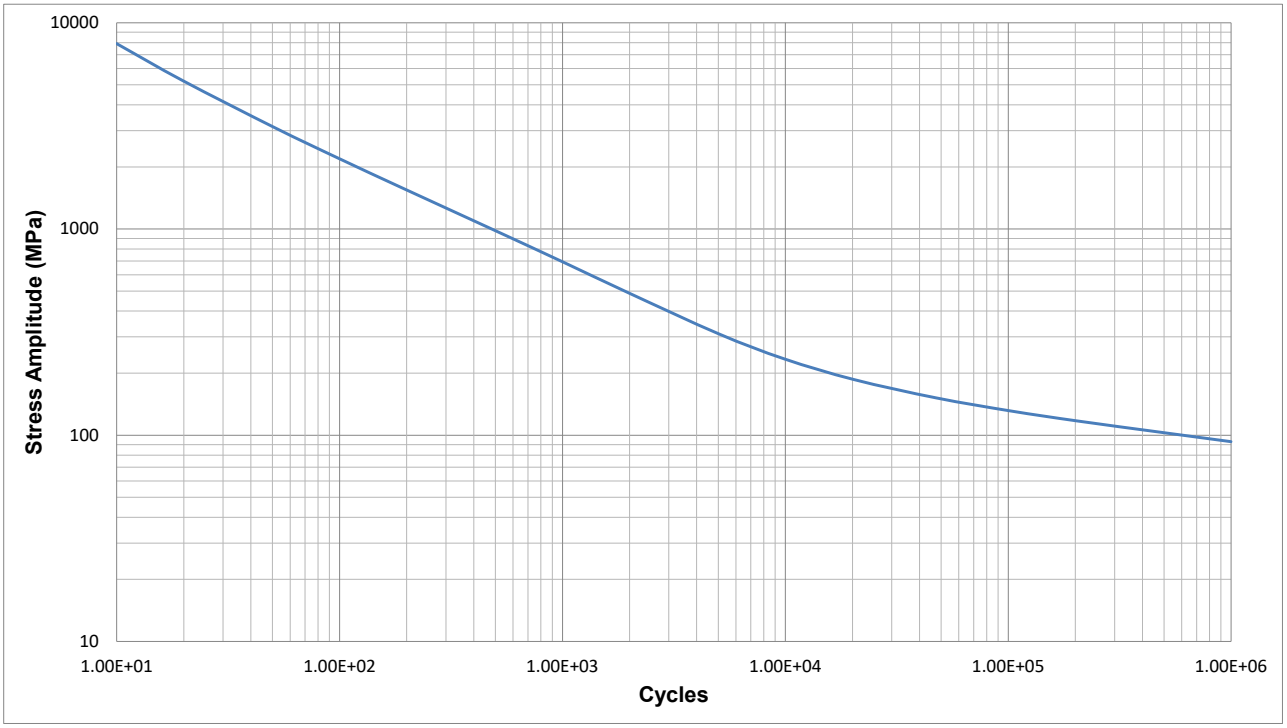

Figure 14B.8M – Fatigue Curve for High Strength Bolting for Temperatures Not Exceeding 371°C – Maximum Nominal Stress $\leq 2.7S$

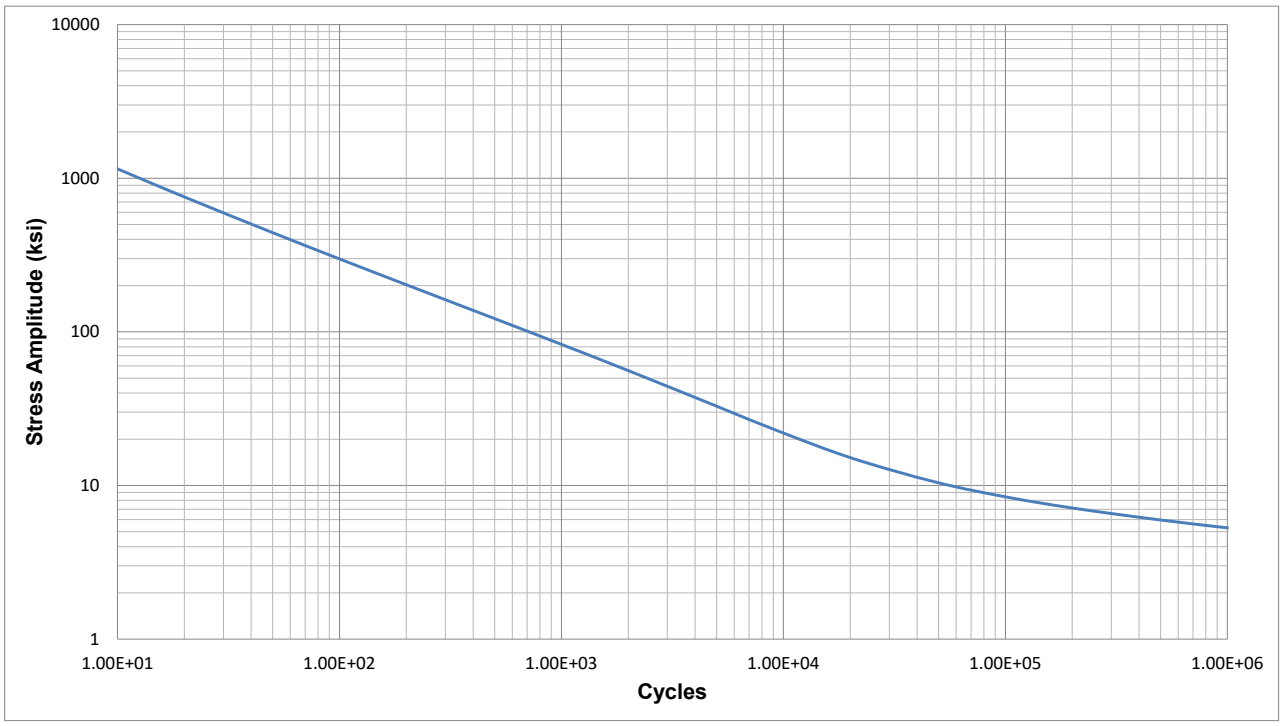

Figure 14B.9 – Fatigue Curve for High Strength Bolting for Temperatures Not Exceeding 700°F – Maximum Nominal Stress $> 2.7S$

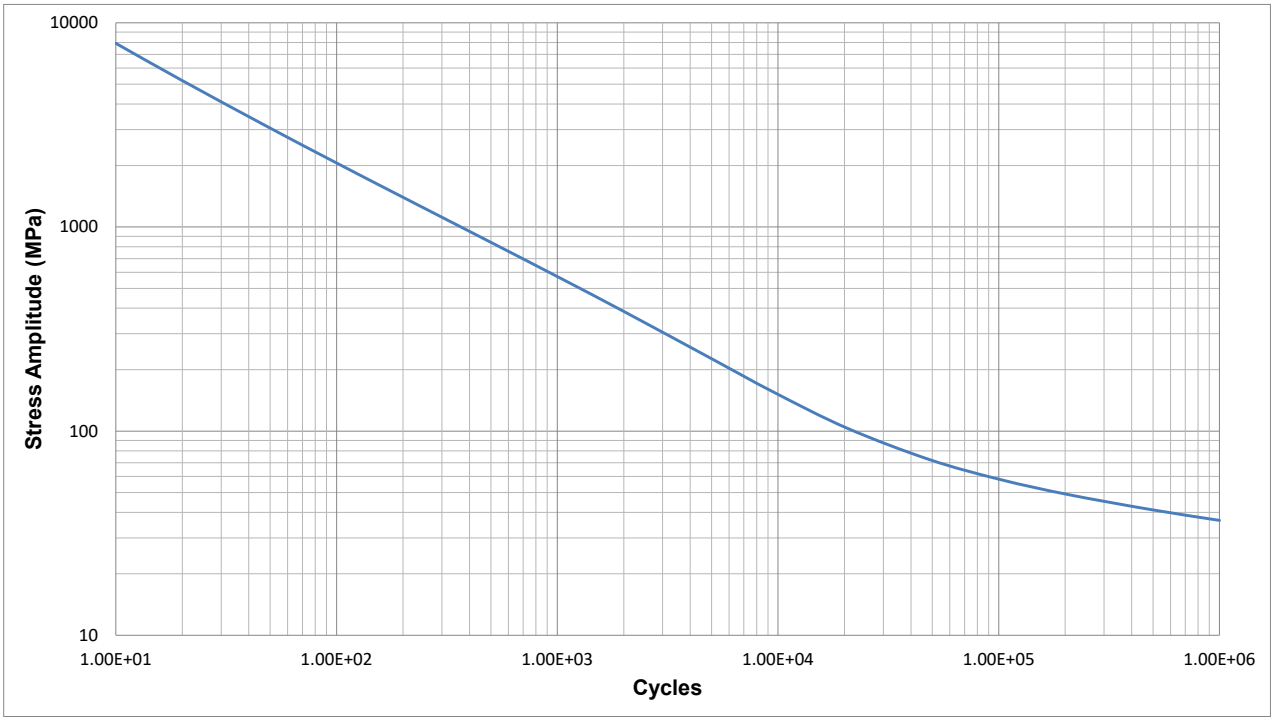

Figure 14B.9M – Fatigue Curve for High Strength Bolting for Temperatures Not Exceeding 371°C – Maximum Nominal Stress $> 2.7S$

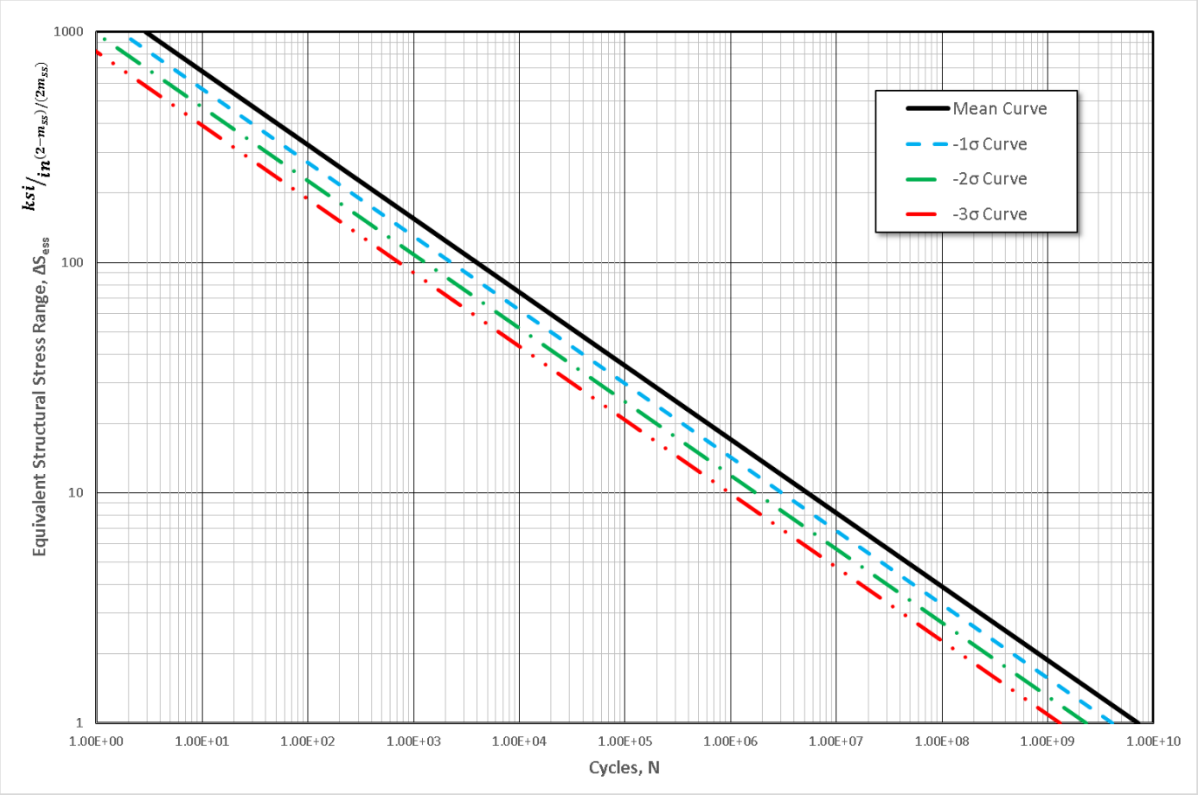

Figure 14B.10 – Welded Joint Fatigue Curve for Ferritic and Stainless Steels, and Nonferrous Alloys

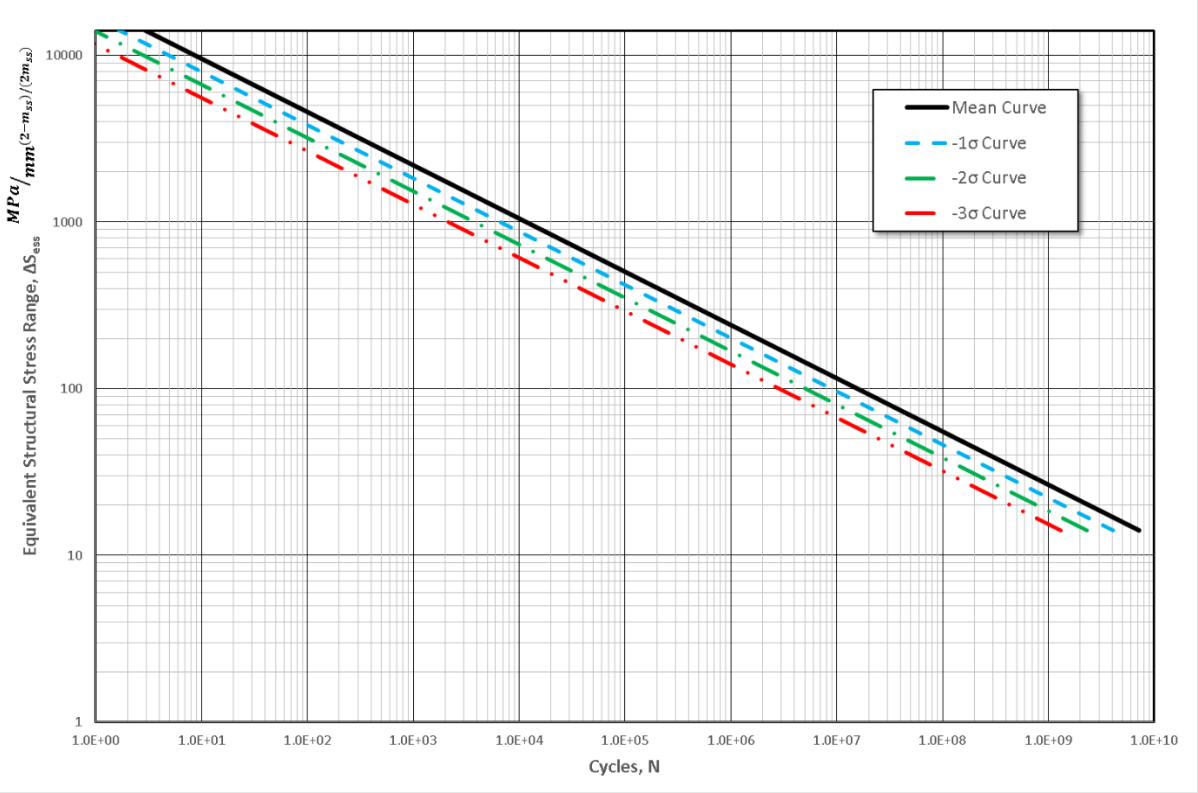

Figure 14B.10M – Welded Joint Fatigue Curve for Ferritic and Stainless, and Nonferrous Alloys

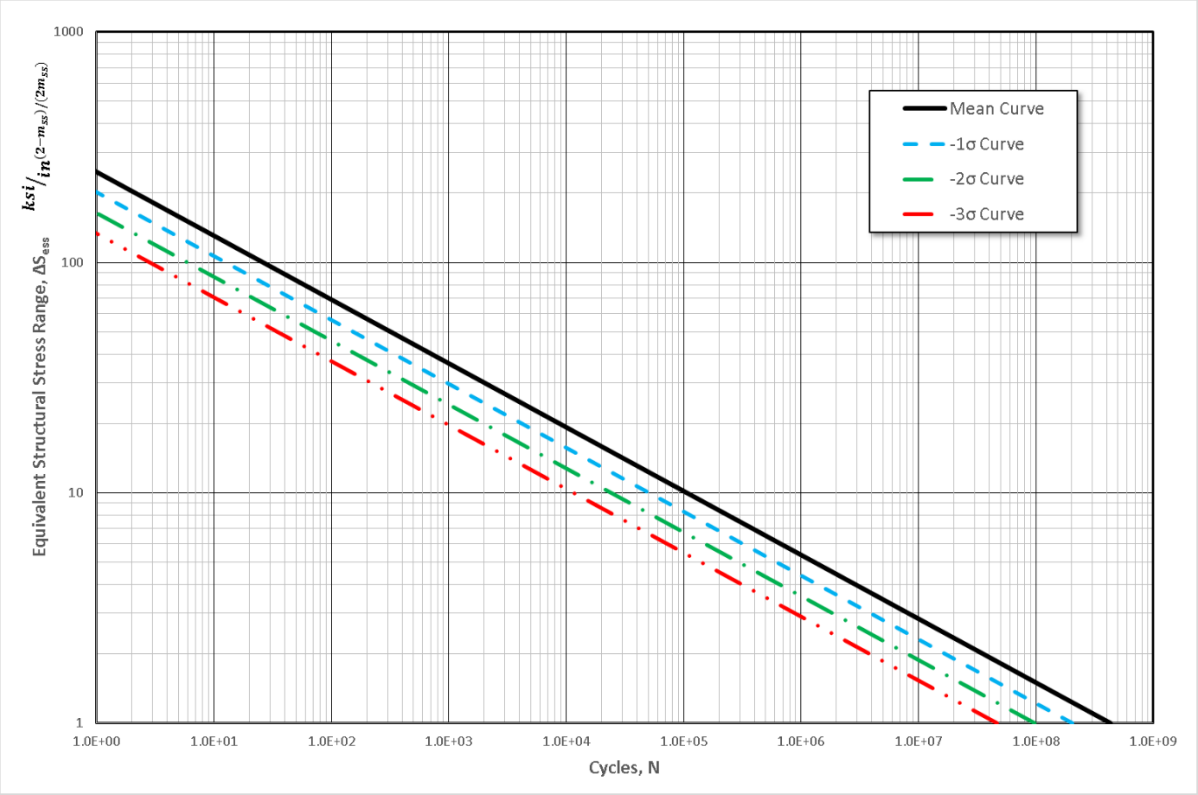

Figure 14B.11 – Welded Joint Fatigue Curves for Aluminum Alloys

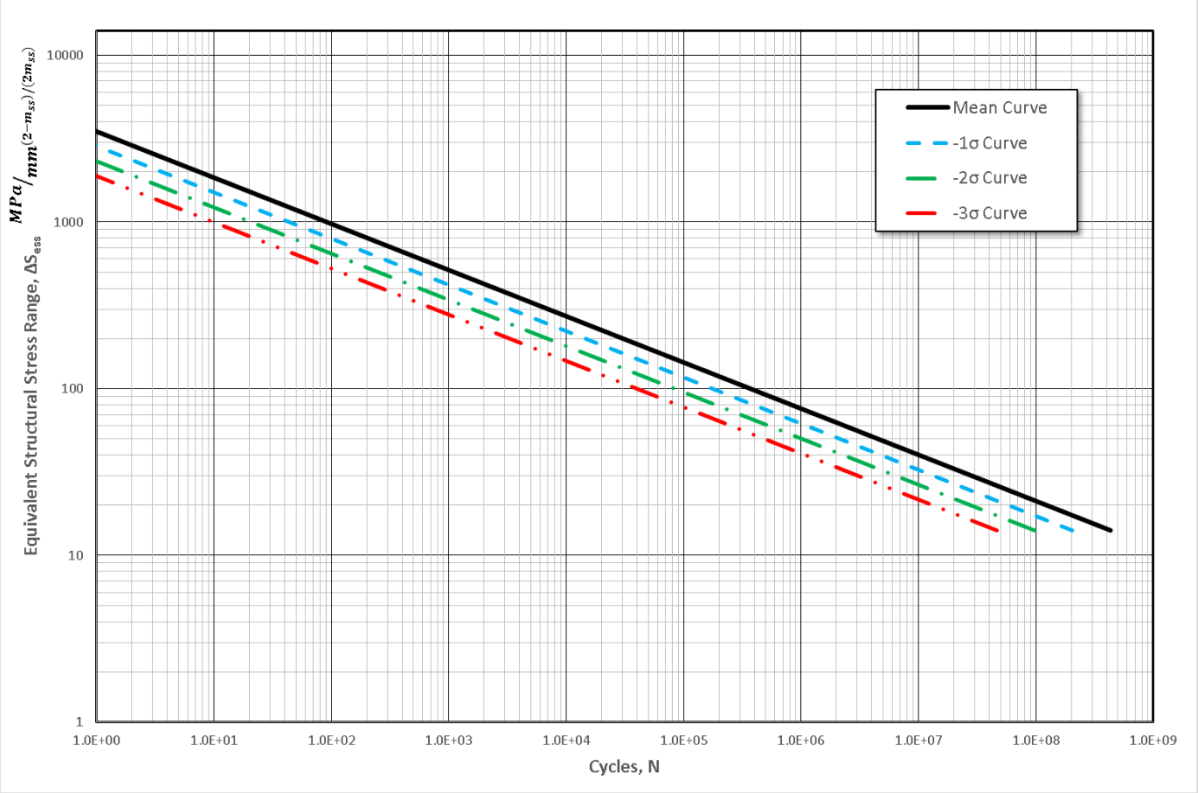

Figure 14B.11M – Welded Joint Fatigue Curves for Aluminum Alloys

[Intentionally Left Blank]

ANNEX 14C – PLASTICITY CORRECTION AND CYCLE COUNTING FOR FATIGUE ANALYSIS

(NORMATIVE)

CONTENTS

ANNEX 14C – PLASTICITY CORRECTION AND CYCLE COUNTING FOR FATIGUE ANALYSIS 14C-1

14C.1 INTRODUCTION 14C-1
14C.1.1 Cycle Counting 14C-1
14C.1.2 Plasticity Correction 14C-1
14C.1.3 Definitions 14C-2
14C.1.4 Histogram Development 14C-3
14C.2 PLASTICITY CORRECTION 14C-3
14C.2.1 Uniaxial Plasticity Correction 14C-3
14C.2.2 Multiaxial Plasticity Correction 14C-3
14C.3 UNIAXIAL CYCLE COUNTING 14C-9
14C.3.1 Rainflow Cycle Counting – With Reordering 14C-9
14C.3.2 Additional Rainflow Cycle Counting – Without Reordering 14C-10
14C.4 MULTIAXIAL CYCLE COUNTING 14C-10
14C.4.1 Wang-Brown Cycle Counting 14C-10
14C.4.2 Critical Plane Cycle Counting 14C-15
14C.5 NOMENCLATURE 14C-18
14C.6 REFERENCES 14C-24
14C.7 FIGURES 14C-25

14C.1 Introduction

14C.1.1 Cycle Counting

Cycle counting procedures are required to perform fatigue assessments of variable amplitude stress or strain time histories. These procedures are used to break down the loading history into individual cycles or reversals that can be evaluated using the fatigue assessment rules in Part 14. Different approaches are required depending on whether the input stress or strain history has only a single component (uniaxial) or multiple components (multiaxial). One uniaxial cycle counting method is presented in Paragraph 14C.3.1, and two multiaxial cycle counting methods are presented in Paragraph 14C.4. For each method a step-by-step procedure is included in the main text along with a corresponding flowchart in Paragraph 14C.7. Guidance as to which algorithm to select depending on the level and method chosen in Part 14 is illustrated in the flowchart shown in Figure 14C.1. Additional documentation, in-depth analyses, and demonstration algorithms implemented in the programming language Python are provided in WRC Bulletin 550 [1].

14C.1.2 Plasticity Correction

If the actual elastic-plastic loading history is known, it can be used directly in the appropriate cycle counting method. However, for modern Finite Element Analysis (FEA) fatigue assessments it is typically more efficient to obtain elastic FEA stress/strain results first and then post-process the elastic data to correct for local plasticity effects using a method such as Neuber's rule, see references [2], [3], and [4]. The resulting elastic-plastic loading history is then used in the cycle counting procedure. A uniaxial plasticity correction procedure is described in Paragraph 14C.2.1 and a multiaxial plasticity correction procedure is included in Paragraph 14C.2.2. The

multiaxial procedure is an incremental Neuber's rule with a combined isotropic and kinematic hardening law. For additional details on the plasticity correction implementation, case specific examples, and in-depth discussions, refer to WRC Bulletin 550 [1].

14C.1.3 Definitions

The definitions used in this Annex are listed below.

a) Cycle – A cycle is a relationship between stress and strain that is established by the specified loading at a particular location in a vessel or component. More than one stress-strain cycle may be produced at any location, either within an event or in transition between two events, and the accumulated fatigue damage of the stress-strain cycles determines the adequacy for the specified operation at that location. This determination shall be made with respect to the stabilized stress-strain cycle. For uniaxial loadings the cycles are defined by closed stress-strain hysteresis loops. For multiaxial loadings the cycles are defined as half-cycles or reversals, as hysteresis visualizations are not easily obtained for multiaxial loads.

b) Event – The loading time history may include one or more events that produce fatigue damage. Each event consists of loading components specified at a number of time points over some time period and is repeated a specified number of times. For example, an event may be the startup, shutdown, upset condition, or any other cyclic action. The sequence of multiple events may be specified or random.

c) Bauschinger Effect – In most metals, plastic deformation in the tensile or compressive direction will affect subsequent plastic response in the reverse direction. A material that is pulled in tension, for example, shows a reduction in compressive strength. This effect is known as the Bauschinger effect, Figure 14C.2.

d) Isotropic Hardening – During plastic deformation, isotropic hardening describes the uniform expansion of the yield surface in all directions in the stress space (see Figure 14C.3(a)).

e) Kinematic Hardening – A hardening rule in which the yield surface only translates in stress space (see Figure 14C.3(b)) but does not change size. This is represented by a fixed elastic range of twice the initial yield strength and captures the Bauschinger effect. The yield surface translation coordinates in space define the back stress, which in uniaxial loading is just the stress past the yield stress.

f) Combined Isotropic-Kinematic Hardening – Involves both translation and expansion of the yield surface during plastic deformation (see Figure 14C.3(c)). This model will capture the Bauschinger effect as well as allowing increases in strength beyond the initial yield strength and is more representative of actual material behavior than either isotropic or kinematic hardening alone. This model is used in the multiaxial plasticity correction method in Paragraph 14C.2.2.

g) Uniaxial Loading – A loading history where the variation of stress or strain over time can be represented by a single parameter. Uniaxial loads are cycle counted using the Rainflow Algorithm that is defined in Paragraph 14C.3.1.

h) Proportional Loading – If the orientations of the principal axes are fixed during cyclic loading, the loading is called proportional. An example of proportional loading is a nozzle in a pressure vessel subject to internal pressure and an external bending moment vector that does not change direction with each cycle. A visual interpretation of a proportional loading history is shown in Figure 14C.4 Consider the loading path; 1→2, 2→3, 3→4, 4→5, 5→6, and 6→1. Throughout this loading path the directions of principal stresses do not change, i.e., the loading path occurs along a linear path with the origin at zero.

i) Multiaxial Loading – A loading history where the variation in time of loading, stress, or strain cannot be represented by a single parameter. Multiaxial loading can represent proportional or non-proportional loading. A stress/strain tensor is used to contain the components of the multiaxial load at each time history point. Multiaxial loads are cycle counted using the two techniques defined in Paragraph 14C.4.

j) Non-Proportional Loading – If the orientations of the principal axes are not fixed during cyclic loading, the loading is called non-proportional. An example of non-proportional loading is a nozzle in a pressure vessel subject to internal pressure and an external bending moment vector that changes direction with each cycle. A visual interpretation of a proportional vs. non-proportional loading history is shown in Figure 14C.4. Consider the loading path; 1→2, 2→3, 3→4, 4→5, 5→6, and 6→1. Throughout this loading path the directions of principal stresses change, i.e., the loading path is not along a linear path for all cycles with an origin at zero.

k) Peak – The point at which the first derivative of the loading history changes sign from positive to negative.

l) Valley – The point at which the first derivative of the loading history changes sign from negative to positive.

14C.1.4 Histogram Development

The loading histogram should include all significant operating loads and events that are applied to the component, see Part 14. If local plasticity effects have not been accounted for, the methods in Paragraph 14C.2 should be used to correct the loading history prior to cycle counting. The counting method may also require filtering of the data to include only reversal points (peaks and valleys) and/or reorder the data to begin/end with the absolute maximum loading point. The following should be considered in developing the loading histogram.

a) The number of repetitions of each event during the operation life.

b) The sequence of events during the operation life, if applicable.

c) Applicable loadings such as pressure, temperature, supplemental loads such as weight, support displacements, and nozzle reaction loadings.

d) The sequential relationship between the applied loadings during the time history.

14C.2 Plasticity Correction

14C.2.1 Uniaxial Plasticity Correction

For uniaxial stress states, the cyclic stress-strain curve is used along with Neuber's rule to obtain the elastic-plastic stress/strain histories from the purely elastic stress/strain histories. Note that if a Level 2 Method C Assessment (Fatigue Assessment of Welds Using the Equivalent Structural Stress) is being performed, plasticity effects are accounted for as part of the procedure defined in Part 14, Paragraph 14.4.3.4.2, and only the uniaxial Rainflow cycle counting procedure is performed, using the elastic stress history (see Paragraph 14C.3).

14C.2.2 Multiaxial Plasticity Correction

14C.2.2.1 For multiaxial stress states (either proportional or non-proportional), the general, incremental, multiaxial Neuber's rule is used to estimate the N_{EP} desired elastic-plastic stress and strain components, ${}^{q}\sigma_{ij}$ and ${}^{q}\varepsilon_{ij}$ at times ${}^{q}t$, $qe = 1, 2, \ldots, N_{EP}$, from the N_E purely elastic stress and strain components, ${}^{qe}\sigma^{e}_{ij}$ and ${}^{qe}\varepsilon^{e}_{ij}$ with $qe = 1, 2, \ldots, N_E$, along with an appropriate cyclic plasticity model, see references [3] through [11]. The elastic values are typically obtained by running a linear elastic Finite Element Analysis (FEA). The cyclic plasticity model used in this procedure is a combined isotropic and multiple back stress non-linear kinematic hardening

model, where the total back stress is the sum of n individual back stresses. For illustration, $n = 4$ back stresses are assumed in the procedure.

14C.2.2.2 If a Level 2 Method A Assessment is being performed, cycle count the elastic stress-based loading history first using the Wang Brown Algorithm in Paragraph 14C.4.1 and then refer to Part 14, Paragraph 14.4.3.2.2 for plasticity correction after cycle counting. In a Level 2 Method B Assessment (Part 14, Paragraph 14.4.3.3.2), it is assumed that the elastic-plastic history is already incorporated into the FEA results for the strain-based approach. If the elastic-plastic history is not provided for the Level 2 Method B Assessment or a Level 3 Assessment is being performed, then multiaxial plasticity correction should be used prior to cycle counting.

14C.2.2.3 A visual representation of the Neuber plasticity correction is shown in Figure 14C.5. A flowchart for the multiaxial Neuber's rule plasticity correction procedure is shown in Figure 14C.6. A step-by-step procedure for plasticity correction prior to cycle counting is shown below. An example that demonstrates the use of this algorithm is included in WRC Bulletin 550 [1].

a) STEP 1 – Run an appropriate linear elastic FEA analysis to obtain the elastic stress history at the location of interest and the times indexed by $qe = 1, 2, \ldots, N_E$. These points are indicated by the red squares in Figure 14C.7. If the elastic strain history is known use Hooke's law to obtain the elastic stress history.

b) STEP 2 – Initialize the time indices to $q = 1$ and $qe = 1$, corresponding to the first point in the loading history.

c) STEP 3 – Assume the first point in the loading history is within the elastic regime, and the actual stresses and strains for this first point are set equal to the corresponding elastic values for $i = 1,2,3$ and $1 \le j \le i$ (the other stress and strain components are obtained by making use of the symmetry of the stress and strain tensors, namely that ${}^{q}\sigma_{ij} = {}^{q}\sigma_{ji}$ and ${}^{q}\varepsilon_{ij} = {}^{q}\varepsilon_{ji}$). The elastic strain is obtained from the elastic stress by using Hooke's law.

$$ {}^{q}\sigma_{ij} = {}^{qe}\sigma^{e}_{ij} \tag{14C.1} $$

$$ {}^{q}\varepsilon_{ij} = {}^{qe}\varepsilon^{e}_{ij} = \frac{1}{E}\left((1+\nu)\cdot {}^{qe}\sigma^{e}_{ij} - \nu\cdot\delta_{ij}\cdot\left({}^{qe}\sigma^{e}_{11} + {}^{qe}\sigma^{e}_{22} + {}^{qe}\sigma^{e}_{33}\right)\right) \tag{14C.2} $$

d) STEP 4 – Calculate the corresponding elastic, deviatoric stress.

$$ S_{ij} = {}^{qe}\sigma^{e}_{ij} - \frac{1}{3}\cdot\delta_{ij}\cdot\left({}^{qe}\sigma^{e}_{11} + {}^{qe}\sigma^{e}_{22} + {}^{qe}\sigma^{e}_{33}\right) \tag{14C.3} $$

e) STEP 5 – Assume there is no initial kinematic hardening.

$$ \alpha^{k}_{ij} = 0 \qquad \text{for } k = 1\ldots n \tag{14C.4} $$

$$ \alpha_{ij} = \sum_{k=1}^{n}\alpha^{k}_{ij} = 0 \tag{14C.5} $$

$$ a^{k}_{ij} = {}^{qe}\alpha^{e}_{ij} - \frac{1}{3}\cdot\delta_{ij}\cdot\left({}^{qe}\alpha^{e}_{11} + {}^{qe}\alpha^{e}_{22} + {}^{qe}\alpha^{e}_{33}\right) = 0 \qquad \text{for } k = 1\ldots n \tag{14C.6} $$

$$ a_{ij} = \sum_{k=1}^{n} a^{k}_{ij} = 0 \tag{14C.7} $$

f) STEP 6 – Assume there is no initial isotropic hardening.

$$r = 0 \tag{14C.8}$$

g) STEP 7 – Consider the next point in the purely elastic loading history.

$$qe = qe + 1 \tag{14C.9}$$

h) STEP 8 – Calculate the change in the elastic stress and strain between the current and previous elastic points.

$$\Delta\sigma_{ij}^{e} = {}^{qe}\sigma_{ij}^{e} - {}^{qe-1}\sigma_{ij}^{e} \tag{14C.10}$$

$$\Delta\varepsilon_{ij}^{e} = \frac{1}{E}\left(\left(1+\nu\right)\cdot\Delta\sigma_{ij}^{e} - \nu\cdot\delta_{ij}\cdot\left(\Delta\sigma_{11}^{e} + \Delta\sigma_{22}^{e} + \Delta\sigma_{33}^{e}\right)\right) \tag{14C.11}$$

i) STEP 9 – Calculate the increment in deviatoric stress between the current and previous elastic points.

$$\Delta S_{ij} = \Delta\sigma_{ij}^{e} - \frac{1}{3}\cdot\delta_{ij}\cdot\left(\Delta\sigma_{11}^{e} + \Delta\sigma_{22}^{e} + \Delta\sigma_{33}^{e}\right) \tag{14C.12}$$

j) STEP 10 – Calculate the trial deviatoric stress using this increment.

$$S_{ij}^{T} = S_{ij} + \Delta S_{ij} \tag{14C.13}$$

k) STEP 11 – Evaluate the yield function f using the trial deviatoric stress computed in STEP 10.

$$f = \left[\frac{3}{2}\cdot\begin{pmatrix}\left(S_{11}^{T} - a_{11}\right)^{2} + \left(S_{22}^{T} - a_{22}\right)^{2} + \left(S_{33}^{T} - a_{33}\right)^{2} + \\ 2\cdot\left(S_{12}^{T} - a_{12}\right)^{2} + 2\cdot\left(S_{13}^{T} - a_{13}\right)^{2} + 2\cdot\left(S_{23}^{T} - a_{23}\right)^{2}\end{pmatrix}\right]^{0.5} - \sigma_{0} - r \tag{14C.14}$$

l) STEP 12 – If $f \leq 0$, (elastic loading), update the stress and strain values elastically at the current time by adding the elastic increments to the previous stress and strain values and set S to its trial value.

$$q = q + 1 \tag{14C.15}$$

$${}^{q}\sigma_{ij} = {}^{q-1}\sigma_{ij} + \Delta\sigma_{ij}^{e} \tag{14C.16}$$

$${}^{q}\varepsilon_{ij} = {}^{q-1}\varepsilon_{ij} + \Delta\varepsilon_{ij}^{e} \tag{14C.17}$$

$$S_{ij} = S_{ij}^{T} \tag{14C.18}$$

After this, if $qe < N_E$, return to STEP 7 and continue with the next time point. Otherwise, go to STEP 24.

m) STEP 13 – If $f > 0$ (plastic loading), subdivide the stress range between $qe - 1$ and qe into N_{EI} sufficiently small, equally-spaced increments and denote the linearly interpolated stress and strain at these intermediate points by ${}^{qi}\tilde{\sigma}_{ij}^{e}$ and ${}^{qi}\tilde{\varepsilon}_{ij}^{e}$, $qi = 1, \ldots, N_{EI}$. These interpolated points are denoted by the black circles in Figure 14C.7.

$$qi = 1 \tag{14C.19}$$

$$\Delta\sigma_{ij}^{e} = \frac{{}^{qe}\sigma_{ij}^{e} - {}^{qe-1}\sigma_{ij}^{e}}{N_{EI}} \tag{14C.20}$$

$$\Delta\varepsilon_{ij}^{e} = \frac{1}{E}\left((1+\nu)\cdot\Delta\sigma_{ij}^{e} - \nu\cdot\delta_{ij}\cdot(\Delta\sigma_{11}^{e} + \Delta\sigma_{22}^{e} + \Delta\sigma_{33}^{e})\right) \tag{14C.21}$$

$${}^{1}\tilde{\sigma}_{ij}^{e} = {}^{qe-1}\sigma_{ij}^{e} \tag{14C.22}$$

$${}^{1}\tilde{\varepsilon}_{ij}^{e} = {}^{qe-1}\varepsilon_{ij}^{e} \tag{14C.23}$$

n) STEP 14 – Obtain the elastic stresses and strains at the next intermediate point.

$$qi = qi + 1 \tag{14C.24}$$

$$q = q + 1 \tag{14C.25}$$

$${}^{qi}\tilde{\sigma}_{ij}^{e} = {}^{qi-1}\tilde{\sigma}_{ij}^{e} + \Delta\sigma_{ij}^{e} \tag{14C.26}$$

$${}^{qi}\tilde{\varepsilon}_{ij}^{e} = {}^{qi-1}\tilde{\varepsilon}_{ij}^{e} + \Delta\varepsilon_{ij}^{e} \tag{14C.27}$$

o) STEP 15 – Calculate the elastic deviatoric stress increments.

$$\Delta S_{ij} = \Delta\sigma_{ij}^{e} - \frac{1}{3}\cdot\delta_{ij}\cdot\left(\Delta\sigma_{11}^{e} + \Delta\sigma_{22}^{e} + \Delta\sigma_{33}^{e}\right) \tag{14C.28}$$

p) STEP 16 – Calculate the trial deviatoric stresses.

$$S_{ij}^{T} = S_{ij} + \Delta S_{ij} \tag{14C.29}$$

q) STEP 17 – Evaluate the yield function f using the trial deviatoric stress computed in STEP 16.

$$f = \left[\frac{3}{2}\cdot\begin{pmatrix}\left(S_{11}^{T} - a_{11}\right)^{2} + \left(S_{22}^{T} - a_{22}\right)^{2} + \left(S_{33}^{T} - a_{33}\right)^{2} + \\ 2\cdot\left(S_{12}^{T} - a_{12}\right)^{2} + 2\cdot\left(S_{13}^{T} - a_{13}\right)^{2} + 2\cdot\left(S_{23}^{T} - a_{23}\right)^{2}\end{pmatrix}\right]^{0.5} - \sigma_{0} - r \tag{14C.30}$$

r) STEP 18 – If $f \le 0$, (purely elastic loading), then update the stress and strain values at the current time by adding the elastic increments to the previous stress and strain values and set S to its trial value.

$${}^{q}\sigma_{ij} = {}^{q-1}\sigma_{ij} + \Delta\sigma_{ij}^{e} \tag{14C.31}$$

$${}^{q}\varepsilon_{ij} = {}^{q-1}\varepsilon_{ij} + \Delta\varepsilon_{ij}^{e} \tag{14C.32}$$

$$S_{ij} = S_{ij}^{T} \tag{14C.33}$$

After this, if $qi < N_{EI}$, then return to STEP 14 and continue with the next intermediate point. Otherwise, if $qi \ge N_{EI}$, go to STEP 24.

s) STEP 19 – If $f > 0$ (plastic loading), obtain the 12 unknown stress and strain increments $\Delta\sigma_{ij}$ and $\Delta\varepsilon_{ij}$, for $i = 1,2,3$ with $1 \le j \le i$ by solving the following system of 12 non-linear equations represented by Equations (14C.34) and (14C.35) for these same values of i and j, using a non-linear system of equations solver. The coefficients c_1, c_2, c_3, c_4, γ_1, γ_2, γ_3, γ_4, $\overline{a}_4$, b and Q are material-specific parameters. Chaboche [6]

and Krishna [10] provide some material-specific methods for obtaining these parameters. If isotropic hardening is not desired, then set $b = r = 0$.

$$\Delta\varepsilon_{ij} = \frac{1}{E}\left((1+\nu)\cdot\Delta\sigma_{ij} - \nu\cdot\delta_{ij}\cdot\left(\Delta\sigma_{11}+\Delta\sigma_{22}+\Delta\sigma_{33}\right)\right) + \frac{3}{2}\cdot\frac{d\lambda}{\sigma_{eq}}\cdot\left(S_{ij}-a_{ij}\right) \tag{14C.34}$$

$${}^{qi-1}\tilde{\sigma}^{e}_{ij}\cdot\Delta\varepsilon^{e}_{ij} + {}^{qi-1}\tilde{\varepsilon}^{e}_{ij}\cdot\Delta\sigma^{e}_{ij} = {}^{q-1}\sigma_{ij}\cdot\Delta\varepsilon_{ij} + {}^{q-1}\varepsilon_{ij}\cdot\Delta\sigma_{ij} \tag{14C.35}$$

These make use of the following functional definitions:

$$S_{ij} = {}^{q-1}\sigma_{ij} - \frac{1}{3}\cdot\delta_{ij}\cdot\left({}^{q-1}\sigma_{11} + {}^{q-1}\sigma_{22} + {}^{q-1}\sigma_{33}\right) \tag{14C.36}$$

$$\sigma_{eq} = \left[\frac{3}{2}\cdot\left(\begin{array}{l}\left(S_{11}-a_{11}\right)^2+\left(S_{22}-a_{22}\right)^2+\left(S_{33}-a_{33}\right)^2+\\ \quad 2\left(S_{12}-a_{12}\right)^2+2\left(S_{13}-a_{13}\right)^2+2\left(S_{23}-a_{23}\right)^2\end{array}\right)\right]^{0.5} \tag{14C.37}$$

$$d\lambda = \max\left[\frac{1.5}{H\cdot\sigma_{eq}}\left(\begin{array}{l}\left(S_{11}-a_{11}\right)\cdot\Delta\sigma_{11}+\left(S_{22}-a_{22}\right)\cdot\Delta\sigma_{22}+\\ \left(S_{33}-a_{33}\right)\cdot\Delta\sigma_{33}+2\left(S_{12}-a_{12}\right)\cdot\Delta\sigma_{12}+\\ 2\left(S_{13}-a_{13}\right)\cdot\Delta\sigma_{13}+2\left(S_{23}-a_{23}\right)\cdot\Delta\sigma_{23}\end{array}\right),\ 0\right] \tag{14C.38}$$

$$H = H_1 + H_2 + H_3 + H_4 + b\cdot\left(Q-r\right) \tag{14C.39}$$

$$H_k = c_k - \frac{3}{2}\cdot\frac{\gamma_k}{\Phi_r\cdot\sigma_{eq}}\left[\left(\begin{array}{l}\left(S_{11}-a_{11}\right)\cdot a^k_{11}+\left(S_{22}-a_{22}\right)\cdot a^k_{22}+\\ \left(S_{33}-a_{33}\right)\cdot a^k_{33}+2\left(S_{12}-a_{12}\right)\cdot a^k_{12}+\\ 2\left(S_{13}-a_{13}\right)\cdot a^k_{13}+2\left(S_{23}-a_{23}\right)\cdot a^k_{23}\end{array}\right)\right] \quad \text{for } k = 1,2,3 \tag{14C.40}$$

$$H_4 = c_4 - \frac{3}{2}\cdot\frac{\gamma_4}{\Phi_r\cdot\sigma_{eq}}\left[\left(\begin{array}{l}\left(S_{11}-a_{11}\right)\cdot a^4_{11}+\left(S_{22}-a_{22}\right)\cdot a^4_{22}+\\ \left(S_{33}-a_{33}\right)\cdot a^4_{33}+2\left(S_{12}-a_{12}\right)\cdot a^4_{12}+\\ 2\left(S_{13}-a_{13}\right)\cdot a^4_{13}+2\left(S_{23}-a_{23}\right)\cdot a^4_{23}\end{array}\right)\right]\cdot g_4 \tag{14C.41}$$

$$\Phi_r = 1 + \frac{r}{\sigma_0} \tag{14C.42}$$

$$a^4_{eq} = \left[\frac{3}{2}\cdot\left(\begin{array}{l}\left(\frac{2}{3}\alpha^4_{11}-\frac{1}{3}(\alpha^4_{22}+\alpha^4_{33})\right)^2+\left(\frac{2}{3}\alpha^4_{22}-\frac{1}{3}(\alpha^4_{11}+\alpha^4_{33})\right)^2+\\ \left(\frac{2}{3}\alpha^4_{33}-\frac{1}{3}(\alpha^4_{11}+\alpha^4_{22})\right)^2+2\left(\alpha^4_{12}\right)^2+2\left(\alpha^4_{13}\right)^2+2\left(\alpha^4_{23}\right)^2\end{array}\right)\right]^{0.5} \tag{14C.43}$$

$$g_4 = \max\left[1-\frac{\overline{a}_4}{a^4_{eq}},\ 0\right] \tag{14C.44}$$

t) STEP 20 – Update the stress, strain, and deviatoric stress using the results obtained in STEP 19.

$$^{q}\sigma_{ij} = {}^{q-1}\sigma_{ij} + \Delta\sigma_{ij} \tag{14C.45}$$

$$^{q}\varepsilon_{ij} = {}^{q-1}\varepsilon_{ij} + \Delta\varepsilon_{ij} \tag{14C.46}$$

$$\Delta S_{ij} = \Delta\sigma_{ij} - \frac{1}{3}\cdot\delta_{ij}\cdot\left(\Delta\sigma_{11} + \Delta\sigma_{22} + \Delta\sigma_{33}\right) \tag{14C.47}$$

$$S_{ij} = S_{ij} + \Delta S_{ij} \tag{14C.48}$$

u) STEP 21 – Update the back stresses using a modified Chaboche kinematic hardening rule.

$$\alpha_{ij} = \alpha_{ij} + \Delta\alpha_{ij} \tag{14C.49}$$

$$\alpha_{ij}^{k} = \alpha_{ij}^{k} + \Delta\alpha_{ij}^{k} \qquad \text{for } k = 1,2,3,4 \tag{14C.50}$$

$$a_{ij} = \alpha_{ij} - \frac{1}{3}\delta_{ij}\cdot\left(\alpha_{11} + \alpha_{22} + \alpha_{33}\right) \tag{14C.51}$$

$$a_{ij}^{k} = \alpha_{ij}^{k} - \frac{1}{3}\delta_{ij}\cdot\left(\alpha_{11}^{k} + \alpha_{22}^{k} + \alpha_{33}^{k}\right) \qquad \text{for } k = 1,2,3,4 \tag{14C.52}$$

where,

$$\Delta\alpha_{ij} = \Delta\alpha_{ij}^{1} + \Delta\alpha_{ij}^{2} + \Delta\alpha_{ij}^{3} + \Delta\alpha_{ij}^{4} \tag{14C.53}$$

$$\Delta\alpha_{ij}^{k} = \frac{2}{3}c_k\cdot\Delta\varepsilon_{ij}^{p} - \frac{\gamma_k}{\Phi_r}\cdot\alpha_{ij}^{k}\cdot dp \qquad \text{for } k = 1,2,3 \tag{14C.54}$$

$$\Delta\alpha_{ij}^{4} = \frac{2}{3}c_4\cdot\Delta\varepsilon_{ij}^{p} - \frac{\gamma_4}{\Phi_r}\cdot\alpha_{ij}^{4}\cdot dp\cdot g_4 \tag{14C.55}$$

$$\Delta\varepsilon_{ij}^{p} = \Delta\varepsilon_{ij} - \Delta\varepsilon_{ij}^{e} \tag{14C.56}$$

$$\Delta\varepsilon_{ij}^{e} = \frac{1}{E}\left(\left(1+\nu\right)\cdot\Delta\sigma_{ij} - \nu\cdot\delta_{ij}\cdot\left(\Delta\sigma_{11} + \Delta\sigma_{22} + \Delta\sigma_{33}\right)\right) \tag{14C.57}$$

$$dp = \left[\frac{2}{3}\cdot\left(\left(\Delta\varepsilon_{11}^{p}\right)^2 + \left(\Delta\varepsilon_{22}^{p}\right)^2 + \left(\Delta\varepsilon_{33}^{p}\right)^2 + 2\left(\Delta\varepsilon_{12}^{p}\right)^2 + 2\left(\Delta\varepsilon_{13}^{p}\right)^2 + 2\left(\Delta\varepsilon_{23}^{p}\right)^2\right)\right]^{0.5} \tag{14C.58}$$

v) STEP 22 – Update the isotropic yield stress hardening function r if isotropic hardening is desired and the material parameters b and Q are known.

$$r = r + b\cdot(Q - r)\cdot dp \tag{14C.59}$$

Otherwise, set $r = 0$ for kinematic hardening only.

w) STEP 23 – If $qi < N_{EI}$, return to STEP 14. Otherwise, continue with STEP 24.

x) STEP 24 – If $qe < N_E$, return to STEP 7. Otherwise, the plasticity correction algorithm is complete.

14C.3 Uniaxial Cycle Counting

14C.3.1 Rainflow Cycle Counting – With Reordering

14C.3.1.1 The Rainflow Cycle Counting (RCC) method (ASTM Standard No. E1049 three point method) is recommended to determine the time points representing individual cycles for situations where the variation of stress or strain over time can be represented by a single parameter, see references [12], [13], and [14]. The RCC method is not applicable for non-proportional loading, which is addressed by two multiaxial methods in Paragraph 14C.4 instead. The RCC method is used for the Level 2 Method C Assessment in Part 14, Paragraph 14.4.3.4.2. Cycles counted with the Rainflow method correspond to closed stress-strain hysteresis loops, with each loop representing a single cycle.

14C.3.1.2 A step-by-step procedure for the RCC algorithm is shown below for an arbitrary loading history (stress or strain). The flowchart associated with this procedure is shown in Figure 14C.8. An example that demonstrates the use of this algorithm is included in WRC Bulletin 550 [1]. In addition, this bulletin provides many comparative literature examples and explores the limitations and applications of each algorithm.

a) STEP 1 – Obtain the original, uniaxial loading history in terms of stress or strain at the position of interest, represented as a list of times and associated stress or strain values at those times. If the sequence of events is unknown, the worst case sequence should be chosen.

b) STEP 2 – Reorder the loading history to begin and end with the absolute maximum peak or valley by shifting the data appropriately, assuming the input data is periodic. This is accomplished by moving the portion of the data including and after the maximum point to the beginning of the data array, followed by the portion of the data from the original starting position up to the maximum.

c) STEP 3 – Filter the reordered loading history from STEP 2 to remove all of the points that lie between successive peaks and valleys. The filtered loading history must contain only reversal peaks and valleys (intermediate points between peaks and valleys must be removed). Denote the filtered, reordered stresses and strains by either ${}^{q}\sigma$ (for stress) or ${}^{q}\varepsilon$ (for strain), where $q = 1, \ldots, N_{LH}$. N_{LH} is the number of points in the loading history.

d) STEP 4 – Initialize the number of cycles to zero by setting $M = 0$.

e) STEP 5 – If $N_{LH} \geq 3$, proceed to STEP 6. Otherwise, proceed to STEP 12.

f) STEP 6 – Initialize the time index to $q = 3$.

g) STEP 7 – If $q \leq N_{LH}$, proceed to STEP 8. Otherwise, go to STEP 11.

h) STEP 8 – Form the loading ranges X and Y as follows if the loading history is in terms of stress.

$$X = \left| {}^{q}\sigma - {}^{q-1}\sigma \right| \tag{14C.60}$$

$$Y = \left| {}^{q-1}\sigma - {}^{q-2}\sigma \right| \tag{14C.61}$$

or as follows if the loading history is in terms of strain.

$$X = \left| {}^{q}\varepsilon - {}^{q-1}\varepsilon \right| \tag{14C.62}$$

$$Y = \left| {}^{q-1}\varepsilon - {}^{q-2}\varepsilon \right| \tag{14C.63}$$

i) STEP 9 – Compare the absolute values of ranges X and Y.

1) If $X < Y$, set $q = q + 1$ and go back to STEP 7.
2) If $X \geq Y$, go to STEP 10.

j) STEP 10 – Increment the number of cycles by one, $M = M + 1$. If the loading history is in terms of stress, set the stress range of the M^{th} cycle to $\Delta\sigma_M = Y$. If the loading history is in terms of strain, set the strain range of the M^{th} cycle to $\Delta\varepsilon_M = Y$.

k) STEP 11 – Form a new loading history (sequence of ${}^{q}\sigma$ or ${}^{q}\varepsilon$) by removing all the points from the previous loading history that corresponded to the start and end points of the previously identified cycle. Reset the value of N_{LH} to the total number of remaining points in this new loading history. Using this new loading history, return to STEP 5 and continue.

l) STEP 12 – The final list of M cycles is obtained with stress or strain ranges given by $\Delta\sigma_k$ or $\Delta\varepsilon_k$, $k = 1, \ldots M$.

14C.3.1.3 Using the recorded cycle count data obtained by using the RCC method, a fatigue damage assessment is performed in accordance with Part 14, Paragraph 14.4.3.4.2 for a Level 2 Method C Assessment. Additional uniaxial damage assessment models are included in WRC Bulletin 550 [1] for comparison, demonstration, and validation purposes.

14C.3.2 Additional Rainflow Cycle Counting – Without Reordering

An additional Rainflow algorithm as shown in reference [12] that does not require reordering of the loading history is also available for comparison of the simulated cycles, see WRC Bulletin 550 [1].

14C.4 Multiaxial Cycle Counting

14C.4.1 Wang-Brown Cycle Counting

14C.4.1.1 The Wang-Brown Cycle Counting (WBCC) method is a six-dimensional, multiaxial Rainflow count that is recommended to determine the time points representing individual half cycles for situations where the variation in time of loading, stress, or strain cannot be represented by a single parameter, see references [15], [16], and [17]. The WBCC method is applicable for non-proportional loading and is used in Part 14, Paragraph 14.4.3.2.2 for Level 2 Method A (Stress-Based) and Paragraph 14.4.3.3.2 for Level 2 Method B (Strain-Based) Assessments. Cycles counted with the WBCC method correspond to half-cycles, as each loading and unloading event is counted separately.

14C.4.1.2 The WBCC algorithm takes as input a sequence of N_{LH} loading history values indexed by $q = 1, \ldots, N_{LH}$. For each value of q, the stress and/or the strain may be specified, depending on whether a strain-based or stress-based approach is desired. The WBCC algorithm counts the N_{TP} total paths that have been identified (also referred to as half-cycles or reversals), indexed by the path number $p = 1, \ldots, N_{TP}$. For each path p, a list of ordered indices $Q_{p,k}$ for the $k = 1, \ldots, N_p$ points belonging to that path is determined as the final output of this algorithm. From this list of $Q_{p,k}$ values, stress or strain ranges for each path can be determined after the path counting algorithm is completed rather than happening within the path counting algorithm itself as other investigators have proposed.

14C.4.1.3 Each point on a path may correspond to one of the original loading history points, or it may be an interpolated point that lies between two of those existing points. If the k^{th} point corresponds exactly to an original point in the loading history, then the value of $Q_{p,k}$ is simply the integer value of q corresponding to that original point. If the k^{th} point is newly created by interpolating between two existing points, then the value of $Q_{p,k}$ is a real number (not an integer) that lies between the two integer values of $q_B = \text{int}\left[Q_{p,k}\right]$ and $q_A = q_B + 1$, which

do correspond to points in the original loading history. The difference between $Q_{p,k}$ and $\text{int}[Q_{p,k}]$, namely, $\beta = Q_{p,k} - \text{int}[Q_{p,k}]$ is a measure of the distance of this interpolated point from q_B towards the point at q_A. The value of β always satisfies $0 < \beta < 1$.

14C.4.1.4 The components of the stress or strain tensor of the interpolated point can be determined from the value of β by linearly interpolating between the stress or strain components at q_B and q_A. For instance, the value of any stress component σ_{ij} at any interpolated point is determined from $\sigma_{ij} = {}^{q_B}\sigma_{ij} + \beta \cdot \left({}^{q_A}\sigma_{ij} - {}^{q_B}\sigma_{ij}\right)$.

14C.4.1.5 A step-by-step procedure for performing Wang-Brown cycle counting, which results in a list of ordered indices $Q_{p,k}$ for each path p is presented below, and a basic flowchart for this algorithm is provided in Figure 14C.9. The steps presented below use indicial notation and are written to facilitate implementation in a computer programming language due to the obvious complexity. This approach handles many special cases and includes many details that have been left out of other, less precise descriptions of this algorithm. An example that demonstrates the use of this algorithm is included in WRC Bulletin 550 [1].

a) STEP 1 – Obtain a loading history of N_{LH} sequential values of the stress or strain tensor at some location at the corresponding times ${}^{q}t$, where $q = 1, \ldots, N_{LH}$. For a stress-based approach, the corresponding stress components are denoted by ${}^{q}\sigma_{ij}$. For a strain-based approach, the corresponding strain components are denoted by ${}^{q}\varepsilon_{ij}$.

b) STEP 2 – Define a generic loading variable ${}^{q}L_{ij}$ to contain either the stress or strain values, depending on whether a stress or strain based approach is being performed. If a stress-based approach is desired, then use Equation (14C.64) to set the values of the generic loading values. If a strain-based approach is desired, then use Equation (14C.65).

$$ {}^{q}L_{ij} = {}^{q}\sigma_{ij} \qquad \left(stress\text{-}based\ approach\right) \tag{14C.64} $$

$$ {}^{q}L_{ij} = {}^{q}\varepsilon_{ij} \qquad \left(strain\text{-}based\ approach\right) \tag{14C.65} $$

c) STEP 3 – Calculate the Mises stress or Mises strain from the generic loading values ${}^{q}L_{ij}$ for each time index $q = 1, \ldots, N_{LH}$ in the original loading history by using Equation (14C.66) for a stress-based approach or Equation (14C.67) for a strain-based approach. The effective Poisson's constant accounting for partial plasticity is assumed to have the value $v_{eff} = 0.4$, which is typical, see reference [18].

$$ {}^{q}L_{eq} = \left[\frac{\left({}^{q}L_{11} - {}^{q}L_{22}\right)^2 + \left({}^{q}L_{22} - {}^{q}L_{33}\right)^2 + \left({}^{q}L_{11} - {}^{q}L_{33}\right)^2 + 6\left({}^{q}L_{12}^2 + {}^{q}L_{13}^2 + {}^{q}L_{23}^2\right)}{2} \right]^{0.5} \qquad \left(stress\text{-}based\ approach\right) \tag{14C.66} $$

$$ {}^{q}L_{eq} = \left[\frac{\left({}^{q}L_{11} - {}^{q}L_{22}\right)^2 + \left({}^{q}L_{22} - {}^{q}L_{33}{}^{2}\right) + \left({}^{q}L_{11} - {}^{q}L_{33}\right)^2 + C_{\gamma} \cdot \left({}^{q}L_{12}^2 + {}^{q}L_{13}^2 + {}^{q}L_{23}^2\right)}{2\left(1 + v_{eff}\right)^2} \right]^{0.5} \qquad \left(strain\text{-}based\ approach\right) \tag{14C.67} $$

d) STEP 4 – Find the particular value of $q = q_{\max}$ that corresponds to the maximum value of ${}^{q}L_{eq}$ over all possible values of q. Reorder the original loading history points so that the point with index $q_{\max}$ occurs first by defining a new reordering index $q' = 1, \ldots, N_{LH} + 1$ that is related to the original index q as follows (in

addition to reordering, this scheme also replicates the first point at the end of the loading history to enforce periodicity):

$$q = q' + q_{\max} - 1 \qquad \text{if } 1 \le q' \le N_{LH} - q_{\max} + 1 \tag{14C.68}$$

$$q = q' - N_{LH} + q_{\max} - 1 \qquad \text{if } N_{LH} - q_{\max} + 1 \le q' \le N_{LH} + 1 \tag{14C.69}$$

e) STEP 5 – Set the first and last indices for the initial path search to the following values, which encompasses the entire range of history points to start out with (the range is restricted for subsequent iterations).

$$q'_F = 1 \tag{14C.70}$$

$$q'_L = N_{LH} + 1 \tag{14C.71}$$

f) STEP 6 – Initialize the trailing interpolation factor β_T to one.

$$\beta^T = 1 \tag{14C.72}$$

g) STEP 7 – Set the total number of paths to zero, $N_{TP} = 0$.

h) STEP 8 – Increment the total number of paths, $N_{TP} = N_{TP} + 1$ and set $p = N_{TP}$. Set the number of interior blocks of points that are skipped over but need to be counted afterwards to zero, $N_{IB,p} = 0$.

i) STEP 9 – Calculate the Relative Mises values for all q' between q'_F and q'_L with respect to the first point at q'_F. That is, for each point $q' = q'_F, \ldots, q'_L$, find the corresponding value of q and the value of q_F corresponding to q'_F by using Equation (14C.68) or (14C.69), as appropriate, and then calculate the *relative* Mises stress or strain with respect to the first point q_F using either Equation (14C.73) for a stress-based approach or Equation (14C.74) for a strain-based approach using the generic loading differences defined by Equation (14C.75). In the following equations, the value $\beta = 1$ should be used for each value of q' except when $q' = q'_L$, in which case it should be set equal to the terminal value $\beta = \beta^T$.

$${}^{q'}L^R_{eq} = \left[\frac{\begin{array}{c}\left(\Delta L_{11} - \Delta L_{22}\right)^2 + \left(\Delta L_{22} - \Delta L_{33}\right)^2 + \\ \left(\Delta L_{11} - \Delta L_{33}\right)^2 + 6\left(\Delta L_{12}^2 + \Delta L_{13}^2 + \Delta L_{23}^2\right)\end{array}}{2} \right]^{0.5} \qquad \left(stress\text{-}based\ approach\right) \tag{14C.73}$$

$${}^{q'}L^R_{eq} = \left[\frac{\begin{array}{c}\left(\Delta L_{11} - \Delta L_{22}\right)^2 + \left(\Delta L_{22} - \Delta L_{33}\right)^2 + \\ \left(\Delta L_{11} - \Delta L_{33}\right)^2 + C_\gamma \cdot \left(\Delta L_{12}^2 + \Delta L_{13}^2 + \Delta L_{23}^2\right)\end{array}}{2\left(1 + \nu_{eff}\right)^2} \right]^{0.5} \qquad \left(strain\text{-}based\ approach\right) \tag{14C.74}$$

$$\Delta L_{ij} = {}^{q-1}L_{ij} + \beta \cdot \left({}^{q}L_{ij} - {}^{q-1}L_{ij}\right) - {}^{q_F}L_{ij} \qquad \text{for } i, j = 1, 2, 3 \tag{14C.75}$$

j) STEP 10 – Always add the first point q'_F to the current path by setting the number of points in the current path to one, $N_p = 1$, and then setting $Q_{p,N_p} = q_F$, where q_F is determined from q'_F by using either Equation (14C.68) or (14C.69), as appropriate.

k) STEP 11 – Find the next peak in the Relative Mises values ${}^{q'}L^R_{eq}$ computed in STEP 9 that occurs after q'_F but before q'_L. If there is such a peak, set the index q'_P to the index of the first peak in ${}^{q'}L^R_{eq}$ where

$q'_F < q'_P < q'_L$ (does not include end points). If there is no peak that satisfies this condition, then just set $q'_P = -1$. Keep track of this Last Peak (LP) index for later use by setting $q'_{LP,p} = q'_P$.

l) STEP 12 – If there are no more peaks ($q'_P = -1$), then go to STEP 13. Otherwise, go to STEP 16.

m) STEP 13 – If $\beta^T = 1$ (the list of points considered for the current path search does not end in an interpolated point), then go to STEP 14. Otherwise, go to STEP 15.

n) STEP 14 – Add the last point q'_L to the current path by incrementing the number of points in the current path, $N_p = N_p + 1$, and then setting $Q_{p,N_p} = q_L$, where q_L is determined from q'_L by using either Equation (14C.68) or (14C.69), as appropriate. Then, go to STEP 24.

o) STEP 15 – Add the interpolated point from a previous path that terminates the present set of points being searched through by incrementing the number of points in this path, $N_p = N_p + 1$, and then setting $Q_{p,N_p} = q_L - 1 + \beta^T$, where q_L is determined from q'_L by using either Equation (14C.68) or (14C.69), as appropriate. Then, go to STEP 24.

p) STEP 16 – If there is another peak ($q'_P > 0$), then go to STEP 17. Otherwise, go to STEP 24.

q) STEP 17 – Add the peak point q'_P to the current path by incrementing the number of points in the current path, $N_p = N_p + 1$, and then setting $Q_{p,N_p} = q_P$, where q_P is determined from q'_P by using either Equation (14C.68) or (14C.69), as appropriate. Keep track of this Last Peak (LP) index for later use by setting $q'_{LP,p} = q'_P$.

r) STEP 18 – Find the first index $q'_{\geq P}$ greater than q'_P such that the Relative Mises value ${}^{q'_{\geq P}}L^R_{eq}$ at this point is equal to or exceeds the value at the last peak, i.e., ${}^{q'_{\geq P}}L^R_{eq} \geq {}^{q'_P}L^R_{eq}$. If there is such a point, continue on with STEP 19. Otherwise, if no such point exists, then go to STEP 24.

s) STEP 19 – If point $q'_{\geq P}$ corresponds to an existing point from the original loading history, which would be the case if ${}^{q'_{\geq P}}L^R_{eq} = {}^{q'_P}L^R_{eq}$, then continue on with STEP 20. Otherwise, go to STEP 21.

t) STEP 20 – Add the existing point $q'_{\geq P}$ to the current path by incrementing the number of points in the current path, $N_p = N_p + 1$, and then setting $Q_{p,N_p} = q_{\geq P}$, where $q_{\geq P}$ is determined from $q'_{\geq P}$ by using either Equation (14C.68) or (14C.69), as appropriate. Set $\beta^T = 1$ since this is not an interpolated point. Go to STEP 22.

u) STEP 21 – Create a new, interpolated point and add it to the current path. This new point is interpolated between the two points corresponding to the indices $q'_{\geq P} - 1$ and $q'_{\geq P}$ such that it's Relative Mises value is the same as that at the last peak corresponding to q'_P. To do this, first determine the interpolating factor β^T such that the value of the Relative Mises computed at this point is equal to the value ${}^{q'_P}L^R_{eq}$. This is done by using a non-linear root finder method (such as the method of bisection) to find the particular value of β^T that satisfies either Equation (14.76) for a stress-based approach or Equation (14C.77) for a strain-based approach with the loading differences defined by Equation (14C.78).

$$ {}^{q'_P}L^R_{eq} = \left[\frac{\left(\Delta L_{11} - \Delta L_{22}\right)^2 + \left(\Delta L_{22} - \Delta L_{33}\right)^2 + \left(\Delta L_{11} - \Delta L_{33}\right)^2 + 6\left(\Delta L_{12}^2 + \Delta L_{13}^2 + \Delta L_{23}^2\right)}{2} \right]^{0.5} \quad \left(stress\text{-}based\ approach\right) \qquad (14C.76) $$

$$ {}^{q'_P}L^R_{eq} = \left[\frac{\left(\Delta L_{11} - \Delta L_{22}\right)^2 + \left(\Delta L_{22} - \Delta L_{33}\right)^2 + \left(\Delta L_{11} - \Delta L_{33}\right)^2 + C_\gamma \cdot \left(\Delta L_{12}^2 + \Delta L_{13}^2 + \Delta L_{23}^2\right)}{2\left(1+\nu_{eff}\right)^2} \right]^{0.5} \quad \left(strain\text{-}based\ approach\right) \qquad \text{(14C.77)} $$

$$ \Delta L_{ij} = {}^{q'_{\geq P}-1}L_{ij} + \beta^T \cdot \left({}^{q'_{\geq P}}L_{ij} - {}^{q'_{\geq P}-1}L_{ij} \right) - {}^{q_F}L_{ij} \qquad \text{for } i, j = 1, 2, 3 \qquad \text{(14C.78)} $$

Once β^T is determined, this new, interpolated point is added to the current path by incrementing the number of points in the current path, $N_p = N_p + 1$, and then setting $Q_{p,N_p} = q_{\geq P} - 1 + \beta^T$, where $q_{\geq P}$ is determined from $q'_{\geq P}$ by using either Equation (14C.68) or (14C.69), as appropriate.

v) STEP 22 – Increment the number of interior blocks of points that need to be counted recursively later, $N_{IB,p} = N_{IB,p} + 1$, and then set the starting and ending indices for this block to $q'_{F,p,N_{IB}} = q'_P$, $q'_{L,p,N_{IB}} = q'_{\geq P}$ and $\beta^T_{p,N_{IB}} = \beta^T$. This block of points lies between the last peak and this newly interpolated point and will be counted later.

w) STEP 23 – If $q'_{\geq P}$ is a peak, then set the next peak index to this value, $q'_P = q'_{\geq P}$. Otherwise, find the next peak between $q'_{\geq P}$ and q'_L and set q'_P to this value. If there are no more peaks, set $q'_P = -1$. Then, go back to STEP 16.

x) STEP 24 – All blocks of interior points that were previously skipped over now need to be counted if $N_{IB,p} > 0$ by iterating through each index $r_p = 1, \ldots, N_{IB,p}$, setting $q'_F = q'_{F,p,r_p}$, $q'_L = q'_{L,p,r_p}$, and $\beta^T = \beta^T_{p,r_p}$ and go back to STEP 8. If $N_{IB,p} = 0$, go to STEP 25.

y) STEP 25 – If there was at least one peak ($q'_{LP,p} > 0$), then set $q'_F = q'_{LP,p}$ and go back to STEP 8 in order to count all points that come after the last peak. Otherwise, continue with STEP 26.

z) STEP 26 – The total list of N_{TP} paths have been obtained.

1) For each path $p = 1, \ldots, N_{TP}$, the number of points per path is denoted by N_p. The ordered indices for each point in the path $k = 1, \ldots, N_p$ are denoted by $Q_{p,k}$. If $Q_{p,k}$ is an integer, then this point comes from the original history list. Otherwise, the point was interpolated between two existing points from the original history list.

2) Obtain the loading (stress or strain) ranges for each path by looping through all the points contained within each path and finding the minimum and maximum value of each stress or strain component and then taking the difference between these values. This is done for each path p by determining all values of the index q that lie within the designated path. This corresponds to all the values of q that satisfy $Q_{p,1} \leq q \leq Q_{p,N_p}$. The loading ranges are then determined from the following equations:

$$ \Delta L_{ij,p} = \max_{q \text{ in path p}} \left[{}^{q}L_{ij} \right] - \min_{q \text{ in path p}} \left[{}^{q}L_{ij} \right] \qquad \text{(14C.79)} $$

14C.4.1.6 Using the recorded cycle count data (loading ranges) obtained by using the WBCC method outlined above, the fatigue damage is calculated in accordance with a Level 2 Method A (stress-based) in Part 14, Paragraph 14.4.3.2.2 or Level 2 Method B (strain-based) in Part 14, Paragraph 14.4.3.3.2 Assessment. Additional details for implementation of the appropriate multiaxial damage model are included in WRC Bulletin 550 [1].

14C.4.1.7 The loading range for each path represents a half cycle as the loading and unloading sequences are counted separately, unlike uniaxial Rainflow, see Paragraph 14C.3, which counts full cycles directly. As a result, the damage for each path must be divided by a factor of 2. This factor of 2 should be incorporated into the

denominator of Equation (14.20) in Part 14, Paragraph 14.4.3.2.2 for a Level 2 Method A (stress-based) or Equation (14.32) in Part 14, Paragraph 14.4.3.3.2 for a Level 2 Method B (strain-based) Assessment.

14C.4.2 Critical Plane Cycle Counting

14C.4.2.1 The Critical Plane Cycle Counting (CPCC) method considers multiple candidate planes and defines the plane that experiences the maximum damage as the critical plane. CPCC is recommended to determine the time points representing individual half cycles for situations where the variation in time of loading, stress, or strain cannot be represented by a single parameter, see references [8], [19], [20], and [21]. This cycle counting method is applicable for non-proportional loading, where the plane of maximum loading is unknown (both tensile and shear failure modes are considered), and is recommended for a Level 3 Assessment, as described in Part 14, Paragraph 14.4.4. A detailed step-by-step procedure for the CPCC algorithm is given below. A flowchart for this procedure is provided in Figure 14C.10.

14C.4.2.2 CPCC involves sequentially choosing a number of candidate planes by rotating the original (unprimed) coordinate system to a new orientation (using primed coordinates) as shown in Figure 14C.11. The normal and shear stresses and strains are computed with respect to this rotated coordinate system, and then a multichannel Rainflow method is used to calculate damage on each plane in terms of these planar values. The maximum damage plane is considered to be the critical plane and limits the fatigue life.

14C.4.2.3 A step-by-step procedure for CPCC is shown below. An example that demonstrates the use of this algorithm is included in WRC Bulletin 550 [1].

a) STEP 1 – Obtain a loading history of N_{LH} values of stress or strain at the corresponding times ${}^{q}t$, where $q = 1, \ldots, N_{LH}$. For a stress-based approach, the necessary stress components are denoted by ${}^{q}\sigma_{ij}$. For a strain-based approach, the necessary strain components are denoted by ${}^{q}\varepsilon_{ij}$.

b) STEP 2 – Decide on an appropriate discretization of the angles θ and ϕ by choosing sufficiently small increments of these angles, $\Delta\theta$ and $\Delta\phi$. Recommended values are $\Delta\theta = 5°$ and $\Delta\phi = 5°$ but any other, sufficiently small values can be used instead. The smaller the increments, the more accurate the determination of the fatigue life will be.

c) STEP 3 – Initialize θ and ϕ to be zero.

$$\theta = 0^{\circ} \tag{14C.80}$$

$$\phi = 0^{\circ} \tag{14C.81}$$

d) STEP 4 – If $\theta \leq 180°$, continue on with STEP 5. Otherwise go to STEP 21.

e) STEP 5 – If $\phi \leq 180°$, continue on with STEP 6. Otherwise go to STEP 20.

f) STEP 6 – Calculate the direction cosines between the original and primed coordinate axes in terms of the angles θ and ϕ as follows (the first subscript, which can be either 1, 2, and 3, refers to the rotated coordinate axes x', y', and z', while the second subscript refers to the original axes x, y, and z).

$$d_{11} = \cos\theta \cdot \sin\phi \tag{14C.82}$$

$$d_{12} = \sin\theta \cdot \sin\phi \tag{14C.83}$$

$$d_{13} = \cos\phi \tag{14C.84}$$

$$d_{21} = -\sin\theta \tag{14C.85}$$

$$d_{22} = \cos\theta \tag{14C.86}$$

$$d_{23} = 0 \tag{14C.87}$$

$$d_{31} = -\cos\theta \cdot \cos\phi \tag{14C.88}$$

$$d_{32} = -\sin\theta \cdot \cos\phi \tag{14C.89}$$

$$d_{33} = \sin\phi \tag{14C.90}$$

g) STEP 7 – For each time point q, calculate the stress normal to the rotated plane, ${}^{q}\sigma_N$, and the shear stress components within the rotated plane, in-plane shear stress ${}^{q}\tau'_{12}$ and out-of-plane shear stress ${}^{q}\tau'_{13}$, using the direction cosines from STEP 6.

$${}^{q}\sigma_N = {}^{q}\sigma'_{11} = {}^{q}\sigma_{11}d_{11}^2 + {}^{q}\sigma_{33}d_{13}^2 + {}^{q}\sigma_{22}d_{12}^2 + 2\left({}^{q}\sigma_{12}d_{11}d_{12} + {}^{q}\sigma_{13}d_{11}d_{13} + {}^{q}\sigma_{23}d_{13}d_{12}\right) \tag{14C.91}$$

$${}^{q}\tau'_{12} = \left[\begin{array}{r} {}^{q}\sigma_{11}d_{11}d_{21} + {}^{q}\sigma_{22}d_{12}d_{22} + {}^{q}\sigma_{33}d_{13}d_{23} + {}^{q}\sigma_{12}\cdot\left(d_{11}d_{22} + d_{12}d_{21}\right) \\ + {}^{q}\sigma_{13}\cdot\left(d_{13}d_{21} + d_{11}d_{23}\right) + {}^{q}\sigma_{23}\cdot\left(d_{12}d_{23} + d_{13}d_{22}\right) \end{array}\right] \tag{14C.92}$$

$${}^{q}\tau'_{13} = \left[\begin{array}{r} {}^{q}\sigma_{11}d_{11}d_{31} + {}^{q}\sigma_{22}d_{12}d_{32} + {}^{q}\sigma_{33}d_{13}d_{33} + {}^{q}\sigma_{12}\cdot\left(d_{11}d_{32} + d_{12}d_{31}\right) \\ + {}^{q}\sigma_{13}\cdot\left(d_{13}d_{31} + d_{11}d_{33}\right) + {}^{q}\sigma_{23}\cdot\left(d_{12}d_{33} + d_{13}d_{32}\right) \end{array}\right] \tag{14C.93}$$

h) STEP 8 – For each time point q, calculate the strain normal to the rotated plane, ${}^{q}\varepsilon_N$, and the shear strain components within the rotated plane, in-plane shear strain ${}^{q}\gamma'_{12}$ and out-of-plane shear strain ${}^{q}\gamma'_{13}$, using the direction cosines from STEP 6. Equations (14C.94) through (14C.96) assume that ${}^{q}\varepsilon_{ij}$ is the true strain tensor. If instead the engineering strain tensor is used, then make the following substitution in Equations (14C.94) through (14C.96), i.e., ${}^{q}\varepsilon_{ij} = 0.5 \cdot {}^{q}\gamma'_{ij}$ for $i \neq j$. The derivation of the true and engineering strain transformations is included in Annex B of WRC 550 [1].

$${}^{q}\varepsilon_N = {}^{q}\varepsilon'_{11} = {}^{q}\varepsilon_{11}d_{11}^2 + {}^{q}\varepsilon_{33}d_{13}^2 + {}^{q}\varepsilon_{22}d_{12}^2 + 2\left({}^{q}\varepsilon_{12}d_{11}d_{12} + {}^{q}\varepsilon_{13}d_{11}d_{13} + {}^{q}\varepsilon_{23}d_{13}d_{12}\right) \tag{14C.94}$$

$$\frac{{}^{q}\gamma'_{12}}{2} = \left[\begin{array}{r} {}^{q}\varepsilon_{11}d_{11}d_{21} + {}^{q}\varepsilon_{22}d_{12}d_{22} + {}^{q}\varepsilon_{33}d_{13}d_{23} + {}^{q}\varepsilon_{12}\cdot\left(d_{11}d_{22} + d_{12}d_{21}\right) \\ + {}^{q}\varepsilon_{13}\cdot\left(d_{13}d_{21} + d_{11}d_{23}\right) + {}^{q}\varepsilon_{23}\cdot\left(d_{12}d_{23} + d_{13}d_{22}\right) \end{array}\right] \tag{14C.95}$$

$$\frac{{}^{q}\gamma'_{13}}{2} = \left[\begin{array}{r} {}^{q}\varepsilon_{11}d_{11}d_{31} + {}^{q}\varepsilon_{22}d_{12}d_{32} + {}^{q}\varepsilon_{33}d_{13}d_{33} + {}^{q}\varepsilon_{12}\cdot\left(d_{11}d_{32} + d_{12}d_{31}\right) \\ + {}^{q}\varepsilon_{13}\cdot\left(d_{13}d_{31} + d_{11}d_{33}\right) + {}^{q}\varepsilon_{23}\cdot\left(d_{12}d_{33} + d_{13}d_{32}\right) \end{array}\right] \tag{14C.96}$$

STEP 9 – Decide the appropriate main and auxiliary channel components for the fatigue damage model that is selected. For the purpose of illustration, assume here that the Brown-Miller strain-based fatigue damage model is used. To determine the cumulative fatigue damage for the current candidate plane, two cycle counts shall be performed, where each shear strain component within the rotated plane (i.e., ${}^{q}\gamma'_{12}$ and ${}^{q}\gamma'_{13}$) is individually considered as the main channel component while all other stress/strain components within the rotated plane are considered as auxiliary channel components. Initialize the cycle count identifier, i.e., let $CC = 0$, and proceed to STEP 10.

i) STEP 10 – If $CC = 0$, let ${}^{q}\gamma_{CC}^{main} = {}^{q}\gamma'_{12}$ and ${}^{q}\gamma_{CC}^{aux} = {}^{q}\gamma'_{13}$. If $CC = 1$, let ${}^{q}\gamma_{CC}^{main} = {}^{q}\gamma'_{13}$ and ${}^{q}\gamma_{CC}^{aux} = {}^{q}\gamma'_{12}$.

j) STEP 11 – Count the main channel component values ${}^{q}\gamma_{CC}^{main}$ using the uniaxial RCC algorithm from Paragraph 14C.3.1. This results in a list of M_{CC} counted cycles for the candidate plane of interest.

k) STEP 12 – For each cycle $k_{CC} = 1, \ldots, M_{CC}$, determine the minimum and maximum of the main channel component values over that cycle, denoted by $\gamma_{\min,k_{CC}}^{main}$ and $\gamma_{\max,k_{CC}}^{main}$, the minimum and maximum of the auxiliary component values over that cycle, denoted by $\gamma_{\min,k_{CC}}^{aux}$ and $\gamma_{\max,k_{CC}}^{aux}$, and the minimum and maximum of the strain normal to the rotated plane over that cycle, denoted by $\varepsilon_{N,\min,k_{CC}}$ and $\varepsilon_{N,\max,k_{CC}}$.

l) STEP 13 – For each cycle $k_{CC} = 1, \ldots, M_{CC}$, compute the shear strain range using Equation (14C.97) through (14C.99) and the normal strain range using Equation (14C.100).

$$\Delta\gamma_{k_{CC}}^{main} = \left|\gamma_{\max,k_{CC}}^{main} - \gamma_{\min,k_{CC}}^{main}\right| \tag{14C.97}$$

$$\Delta\gamma_{k_{CC}}^{aux} = \left|\gamma_{\max,k_{CC}}^{aux} - \gamma_{\min,k_{CC}}^{aux}\right| \tag{14C.98}$$

$$\Delta\gamma_{k_{CC}} = \sqrt{(\Delta\gamma_{k_{CC}}^{main})^2 + (\Delta\gamma_{k_{CC}}^{aux})^2} \tag{14C.99}$$

$$\Delta\varepsilon_{N,k_{CC}} = \left|\varepsilon_{N,\max,k_{CC}} - \varepsilon_{N,\min,k_{CC}}\right| \tag{14C.100}$$

m) STEP 14 – If mean stress effects have not been accounted for, compute the maximum, minimum, and mean stress over all points q contained within each cycle $k_{CC} = 1, \ldots, M_{CC}$, using Equations (14C.101) through (14C.103).

$$\sigma_{N,\max,k_{CC}} = \max_{q \text{ in cycle } k_{CC}} \left[{}^{q}\sigma_{N} \right] \tag{14C.101}$$

$$\sigma_{N,\min,k_{CC}} = \min_{q \text{ in cycle } k_{CC}} \left[{}^{q}\sigma_{N} \right] \tag{14C.102}$$

$$\sigma_{N,\text{mean},k_{CC}} = 0.5 \cdot \left[\sigma_{N,\max,k_{CC}} + \sigma_{N,\min,k_{CC}} \right] \tag{14C.103}$$

n) STEP 15 – For each cycle $k_{CC} = 1, \ldots, M_{CC}$, use an appropriate fatigue damage model to obtain the permissible number of reversals (half-cycles) for cycle k_{CC}, $N_{f,k_{CC}}$ in terms of the values of $\Delta\gamma_{k_{CC}}$ and $\Delta\varepsilon_{N,k_{CC}}$ determined previously in STEP 13 and the Morrow mean stress correction using the mean stress $\sigma_{N,\text{mean},k_{CC}}$ computed in STEP 14. Assuming the Brown-Miller fatigue life model, this is done by iteratively solving Equation (14C.104) for $N_{f,k_{CC}}$ by using a non-linear, numerical root finding procedure, assuming the left hand side and the material specific fatigue parameters $\sigma'_{f,k_{CC}}$, $\varepsilon'_{f,k_{CC}}$, $E_{k_{CC}}$, $b_{k_{CC}}$, and $c_{k_{CC}}$ are known. Note that if the material specific fatigue parameters have been determined from fatigue data that already includes the effect of mean stress, let $\sigma_{N,\text{mean},k_{CC}} = 0.0$.

$$\frac{\Delta\gamma_{k_{CC}}}{2} + \frac{\Delta\varepsilon_{N,k_{CC}}}{2} = 1.65 \cdot \left(\frac{\sigma'_{f,k_{CC}} - \sigma_{N,\text{mean},k_{CC}}}{E_{k_{CC}}} \right) \left(2N_{f,k_{CC}}\right)^{b_{k_{CC}}} + 1.75 \cdot \varepsilon'_{f,k_{CC}} \left(2N_{f,k_{CC}}\right)^{c_{k_{CC}}} \tag{14C.104}$$

o) STEP 16 – Determine the net fatigue damage parameter $D_{f,\theta,\phi}^{CC}$ for the current candidate plane by summing over the inverse of all the permissible number of cycles. The number of repetitions of the k_{CC}^{th} cycle is $n_{k_{CC}}$ and the fatigue knockdown factor is f_{ND}.

$$D_{f,\theta,\phi}^{CC} = \sum_{k_{CC}=1}^{M_{CC}} \frac{n_{k_{CC}}}{\left(\frac{N_{f,k_{CC}}}{f_{ND}}\right)} \leq 1.0 \qquad \left(f_{ND} \geq 1.0\right) \tag{14C.105}$$

p) STEP 17 – If $CC = 0$, increment the cycle count identifier by one, i.e., let $CC = 1$, and go back to STEP 10. Otherwise proceed to STEP 18.

q) STEP 18 – Determine the maximum of the net fatigue damage parameters $D_{f,\theta,\phi}^{CC}$ using Equation (14C.106).

$$D_{f,\theta,\phi} = \max\left(D_{f,\theta,\phi}^{0}, D_{f,\theta,\phi}^{1}\right) \tag{14C.106}$$

r) STEP 19 – Increment the angle ϕ and go back to STEP 5.

$$\phi = \phi + \Delta\phi \tag{14C.107}$$

s) STEP 20 – Increment the angle θ, set $\phi = 0°$, and go back to STEP 4.

$$\theta = \theta + \Delta\theta \tag{14C.108}$$

t) STEP 21 – The critical plane is defined as the plane with the maximum damage factor, $\underset{\theta,\phi}{max}\left[D_{f,\theta,\phi}\right]$, where the maximum is taken over all the values of θ and ϕ that were considered. The total number of cycles to failure for this critical plane, N_f, is given by Equation (14C.109).

$$N_f = \frac{1}{\max\limits_{\theta,\phi}\left[D_{f,\theta,\phi}\right]} \tag{14C.109}$$

14C.5 Nomenclature

a_{ij}	deviatoric back stress components, $i,j = 1,2,3$.
a_{ij}^{k}	decomposed deviatoric back stress components, $k = 1,2,3,4$ and $i,j = 1,2,3$.
α_{ij}	back stress components, $i,j = 1,2,3$.
α_{ij}^{k}	decomposed back stress components, $k = 1,2,3,4$ and $i,j = 1,2,3$.
b	material specific isotropic hardening parameter.
b_k	average fatigue strength exponent for the k^{th} cycle.
c	fatigue ductility exponent.
c_k	average fatigue ductility exponent for the k^{th} cycle.
CC	cycle count identifier used in critical plane cycle counting to keep track of the two cycle counts that are performed on each candidate plane.
C_γ	coefficient in elastic and plastic effective strain equations. $C = 1.5$ if shear strains are engineering strain values and $C = 6.0$ if the shear strains are tensor values.

d_{ij} direction cosines between the rotated coordinate axes, $i = 1,2,3$ and the original axes $j = 1,2,3$.

D_f cumulative fatigue damage factor that must be less than or equal to 1.

$D_{f,P}$ cumulative fatigue damage factor that must be less than or equal to 1 for candidate plane P.

$D_{f,P}^{CC}$ cumulative fatigue damage factor for cycle count CC on candidate plane P.

δ_{ij} Kronecker delta function, $\delta_{ij} = 1$ when $i = j$, otherwise, $\delta_{ij} = 0$ when $i \neq j$.

$\Delta\varepsilon_{eq}$ actual equivalent strain increment (Von Mises).

$\Delta\varepsilon_{ij}$ actual components of the strain tensor increment, where the diagonal components of the strain tensor are normal strain increment and the symmetric upper and lower components are shear strain increments, $i, j = 1,2,3$.

$\Delta\varepsilon_{ij}^{e}$ elastic components of the strain tensor increment, where the diagonal components of the strain tensor are normal strain increment and the symmetric upper and lower components are shear strain increments, $i, j = 1,2,3$.

$\Delta\varepsilon_N$ normal strain range on the plane of $\Delta\gamma_{\max}$.

$\Delta\varepsilon_{N,k}$ normal strain range on the plane of $\Delta\gamma_{\max,k}$ for the k^{th} cycle.

$\Delta\varepsilon_k$ normal strain range of the k^{th} cycle.

$\Delta\gamma_{\max}$ maximum shear strain range.

$\Delta\gamma_k$ shear strain range for the k^{th} cycle.

$\Delta\gamma_k^{aux}$ auxiliary channel shear strain range for the k^{th} cycle.

$\Delta\gamma_k^{main}$ main channel shear strain range for the k^{th} cycle.

ΔL_i relative i^{th} directional component of the normal loading with respect to q'_{PV}.

ΔL_{ij} relative i^{th} directional component of the shear loading with respect to q'_{PV}, $i, j = 1,2,3$.

$\Delta\sigma_{eq}$ actual equivalent stress increment (Von Mises).

$\Delta\sigma_{ij}$ actual components of the stress tensor increment, where the diagonal components of the stress tensor are normal stress increment and the symmetric upper and lower components are shear stress increments, $i, j = 1,2,3$.

$\Delta\sigma_{ij}^{e}$ elastic components of the stress tensor increment, where the diagonal components of the stress tensor are normal stress increment and the symmetric upper and lower components are shear stress increments, $i, j = 1,2,3$.

$\Delta\sigma_N$ normal stress range on the plane of $\Delta\tau_{\max}$.

$\Delta\sigma_k$ normal stress range of the k^{th} cycle.

ΔS increments of actual of the deviatoric stress tensor.

$\Delta\tau_{\max}$ maximum shear stress range.

$d\lambda$ plastic multiplier.

dp effective plastic strain rate.

ε actual uniaxial strain component.

${}^{q}\varepsilon$ single parameter value of strain at time index q.

${}^{m}\varepsilon_{k}$ strain at start of k^{th} cycle.

${}^{n}\varepsilon_{k}$ strain at end of k^{th} cycle.

ε_{ij} actual components of the strain tensor, where the diagonal components of the strain tensor are normal strain and the symmetric upper and lower components are shear strain, $i, j = 1,2,3$.

${}^{q}\varepsilon_{ij}$ actual components of the strain tensor, ε_{ij}, at time index $q, i, j = 1,2,3$.

ε_{ij}^{e} elastic components of the strain tensor, where the diagonal components of the strain tensor are normal strain and the symmetric upper and lower components are shear strain, $i, j = 1,2,3$.

${}^{qe}\varepsilon_{ij}^{e}$ elastic components of the strain tensor, ε_{ij}^{e}, at time index qe, $i, j = 1,2,3$.

${}^{qi}\tilde{\varepsilon}_{ij}^{e}$ components of the elastic strain tensor, $\tilde{\varepsilon}_{ij}$, at interpolated time index qi, $i, j = 1,2,3$.

ε_{i} normal strain components of the strain tensor, $i = 1,2,3$.

${}^{q}\varepsilon_{i}$ normal strain components of the strain tensor at time index q, $i = 1,2,3$.

ε_{eq} actual equivalent strain (Von Mises).

ε_{eq}^{e} elastic equivalent strain (Von Mises).

${}^{q}\varepsilon_{eq}$ equivalent strain (Von Mises) for time index q.

ε_{N} normal strain on the plane of $\gamma_{\max}$.

$\varepsilon_{N,\max}$ maximum normal strain on the plane of $\gamma_{\max}$.

$\varepsilon_{N,\max,k}$ maximum normal strain on the plane of $\gamma_{\max}$ for the k^{th} cycle.

$\varepsilon_{N,\min}$ minimum normal strain on the plane of $\gamma_{\max}$.

$\varepsilon_{N,\min,k}$ minimum normal strain on the plane of $\gamma_{\max}$ for the k^{th} cycle.

ε' local strain on the candidate plane of interest.

$\varepsilon_{ij}{}'$ actual components of the strain tensor, where the diagonal components of the strain tensor are normal strain and the symmetric upper and lower components are shear strain on the current transformed candidate plane, $i, j = 1,2,3$.

$\varepsilon_{i}{}'$ normal strain components of the strain tensor on the current transformed candidate plane.

ε_{f}' fatigue ductility coefficient.

$\varepsilon_{f,k}'$ average fatigue ductility coefficient for the k^{th} cycle.

E modulus of elasticity of the material under consideration.

E_{k} average modulus of elasticity of the material under consideration for the k^{th} cycle.

f yield function.

f_{ND} fatigue knockdown factor.

γ_{ij} shear strain components of the strain tensor, $i, j = 1,2,3$.

γ_{ij}' shear strain components of the strain tensor on the current transformed candidate plane, $i, j = 1,2,3$.

${}^{q}\gamma_{ij}$ shear strain components of the strain tensor at time index q, $i, j = 1,2,3$.

$\gamma_{\max}$ maximum shear strain.

$\gamma_{\max,k}$ maximum shear strain for the k^{th} cycle.

$\gamma_{\max,k}^{aux}$ auxiliary channel maximum shear strain for the k^{th} cycle.

$\gamma_{\max,k}^{main}$ main channel maximum shear strain for the k^{th} cycle.

$\gamma_{\min,k}$ minimum shear strain for the k^{th} cycle.

$\gamma_{\min,k}^{aux}$ auxiliary channel minimum shear strain for the k^{th} cycle.

$\gamma_{\min,k}^{main}$ main channel minimum shear strain for the k^{th} cycle.

H plastic modulus.

$\mathrm{int}[\cdot]$ function that returns the truncated integer portion of a floating point number.

k cycle index.

k_{CC} cycle index for cycle count CC.

K material specific constant describing the hardening behavior.

${}^{q}L_{i}$ normal loading components of the stress/strain loading tensor at time index q.

${}^{q}L_{ij}$ shear loading components of the stress/strain loading tensor at time index q, $i, j = 1,2,3$.

${}^{q}L_{eq}$ Von Mises from the generic loading values at time index q.

${}^{q'}L_{eq}^{R}$ *relative* Von Mises with respect to the reference peak or valley index q'_{PV}.

$\max[\cdot,\cdot]$ function that returns the maximum value of its two arguments.

M total number of counted cycles.

M_{CC} total number of counted cycles for cycle count CC.

$M_{\theta,\phi}$ total number of counted cycles on the θ, ϕ candidate plane of interest.

n material specific constant describing the hardening behavior (exponential).

n_k number of repetitions of the k^{th} cycle.

$\hat{n}$ normal vector of the critical plane.

N_f number of cycles to failure.

$N_{f,k}$ number of cycles to failure for the k^{th} cycle.

N_k number of points in the cycle.

N_E total number of points in the elastic loading history.

N_{EP} total number of elastic-plastic points in the output of the plasticity correction algorithm.

N_{EI} number of elastic stress sub-increments in the plasticity correction algorithm.

N_{LH} total number of points in the loading history.

ν Poisson's ratio.

ν_{eff} effective Poisson's coefficient.

p path number.

P candidate plane index.

q time index.

qe time index of the elastic loading history.

qi sub-increment counter index.

$q_{\max}$ values of q that lead to a maximum value of ${}^{q}L_{eq}$.

q' reordered time index with the point $q_{\max}$ occurring first.

q'_{PV} time index of the next peak or valley.

ϕ rotation angle about the x axis.

Q material specific isotropic hardening parameter.

$Q_{p,k}$ list of ordered indices for the $k = 1, \ldots, N_p$ points belonging to the path p.

r isotropic hardening function.

S_{ij} actual components of the deviatoric stress tensor.

S_{ij}^{T} components of the trial deviatoric stress tensor.

σ actual uniaxial stress component.

σ_{ij} actual components of the stress tensor, where the diagonal components of the stress tensor are normal stress and the symmetric upper and lower components are shear stress.

σ_{ij}^{e} components of the elastic stress tensor, where the diagonal components of the stress tensor are normal stress and the symmetric upper and lower components are shear stress, $i, j = 1,2,3$.

${}^{qe}\sigma_{ij}^{e}$ components of the elastic stress tensor, σ_{ij}^{e}, at time index qe, $i, j = 1,2,3$.

${}^{q}\sigma_{ij}$ actual components of the elastic-plastic stress tensor, σ_{ij}, at time index q, $i, j = 1,2,3$.

${}^{qi}\tilde{\sigma}_{ij}$ components of the elastic stress tensor, $\tilde{\sigma}_{ij}$, at interpolated time index qi, $i, j = 1,2,3$.

σ_{i} normal stress components of the stress tensor.

${}^{q}\sigma_{i}$ normal stress components of the stress tensor at time index q.

${}^{q}\sigma_{\mathbf{n}}$ stress normal to a plane with normal vector n at time index q.

σ_{eq} actual equivalent stress (Von Mises).

σ_{eq}^{e} elastic equivalent stress (Von Mises).

${}^{q}\sigma_{eq}$ equivalent stress (Von Mises) for time index q.

$\sigma_{N,mean,k}$ Morrow mean stress correction term.

σ' local stress on the candidate plane of interest.

σ_{ij}' actual components of the stress tensor, where the diagonal components of the stress tensor are normal stress and the symmetric upper and lower components are shear stress on the current transformed candidate plane, $i, j = 1,2,3$.

σ_i' normal stress components of the stress tensor on the current transformed candidate plane.

σ_f' fatigue strength coefficient.

$\sigma_{f,k}'$ average fatigue strength coefficient for the k^{th} cycle.

${}^q\sigma$ single parameter value of stress at time index q.

${}^m\sigma_k$ stress at start of k^{th} cycle.

${}^m\sigma_{ij,k}$ single component of the stress tensor at start of k^{th} cycle, $i, j = 1,2,3$.

${}^n\sigma_k$ stress at end of k^{th} cycle.

${}^n\sigma_{ij,k}$ single component of the stress tensor at end of k^{th} cycle, $i, j = 1,2,3$.

σ_0 yield stress.

τ_{ij} shear stress components of the stress tensor.

τ_{ij}' shear stress components of the stress tensor on the current transformed candidate plane.

${}^q\tau_{ij}$ shear stress components of the stress tensor at time index q.

$\tau_{\max}$ maximum shear stress.

${}^qt$ time point in the loading history corresponding to time index q.

${}^mt_k$ starting time for the k^{th} cycle.

${}^nt_k$ ending time for the k^{th} cycle.

θ rotation angle about the y axis.

x, y, z global Cartesian coordinate system.

x', y', z' transformed coordinate system.

X absolute value of the loading range in consideration using the Rainflow Cycle Counting method.

Y absolute value of the previous loading range adjacent to X using the Rainflow Cycle Counting method.

Y_e yield stress from combined hardening.

Y_0 yield stress.

Y_1 increased yield stress from isotropic hardening.

14C.6 References

1. Stenta, A., Gassama, E., Panzarella, C., Cochran, J. and Osage, D.A., *Standardization of Fatigue Methods for Use in API 579-1/ASME FFS-1*, WRC Bulletin 550, Revision 1, Welding Research Council, Inc., New York, NY, 2018.
2. J.A. Bannantine, J.J. Corner, and J.L. Handrock, *Fundamentals of metal fatigue analysis*. 1990.
3. A. Ince, G. Glinka, and A. Buczynski, "Computational modeling of multiaxial elasto-plastic stress-strain response for notched components under non-proportional loading," *Int. J. Fatigue*, vol. 62, pp. 42–52, 2014.
4. F. Dunne and N. Petrinic, *Introduction to computational plasticity,* Oxford University Press, 2005.
5. J.L. Chaboche, "Constitutive equations for cyclic plasticity and cyclic viscoplasticity," *Int. J. Plast.*, vol. 5, no. 3, pp. 247–302, 1989.
6. J.L. Chaboche, "On some modifications of kinematic hardening to improve the description of ratchetting effects," *International Journal of Plasticity*, vol. 7, no. 7. pp. 661–678, 1991.
7. J. Chaboche, "A review of some plasticity and viscoplasticity.pdf," *Intern. J. Plast.*, vol. 24, pp. 1642–1693, 2008.
8. J. A. Bannantine, "A variable amplitude multiaxial fatigue life prediction method," The University of Illinois at Urbana-Champaign, 1989.
9. S. Bari, "Constitutive modeling for cyclic plasticity and ratcheting," 2001.
10. S. Krishna, "Unified constitutive modeling for proportional and nonproportional cyclic plasticity responses," 2009.
11. A. Ince, "Development of computational multiaxial fatigue modelling for notched components," 2012.
12. S. Downing and D. Socie, "Simple rainflow counting algorithms," *Int. J. Fatigue*, vol. 4, no. 1, pp. 31–40, 1982.
13. "Standard practices for cycle counting in fatigue analysis," *ASTM Standard E 1049-85*. Philadelphia: ASTM, 2005.
14. Y.-L. Lee, M.E. Barkey, and H.-T. Kang, *Rainflow cycle counting techniques*. 2012.
15. C.H. Wang and M.W. Brown, "Multiaxial random load fatigue: life prediction techniques and experiments," *Multiaxial Fatigue Des.*, vol. 21, pp. 513–527, 1996.
16. Y. Lee, T. Tjhung, and A. Jordan, "A life prediction model for welded joints under multiaxial variable amplitude loading histories," *Int. J. Fatigue*, vol. 29, no. 6, pp. 1162–1173, 2007.
17. P. Dong, Z. Wei, and J.K. Hong, "A path-dependent cycle counting method for variable-amplitude multi-axial loading," *Int. J. Fatigue*, vol. 32, no. 4, pp. 720–734, 2010.
18. M.A. Meggiolaro and J.T.P. De Castro, "An improved multiaxial rainflow algorithm for non-proportional stress or strain histories - Part II: The Modified Wang-Brown method," *Int. J. Fatigue*, vol. 42, pp. 217–226, 2012.
19. D.F. Socie and G.B. Marquis, *Multiaxial Fatigue*. Warrendale, PA: Society of Automotive Engineers, 2000.
20. T. Langlais, "Computational methods for multiaxial fatigue analysis," PhD Thesis, University of Minnesota, 1999.
21. J. Draper, *Modern Metal Fatigue Analysis*, Published by EMAS Publications (2008).

14C.7 Figures

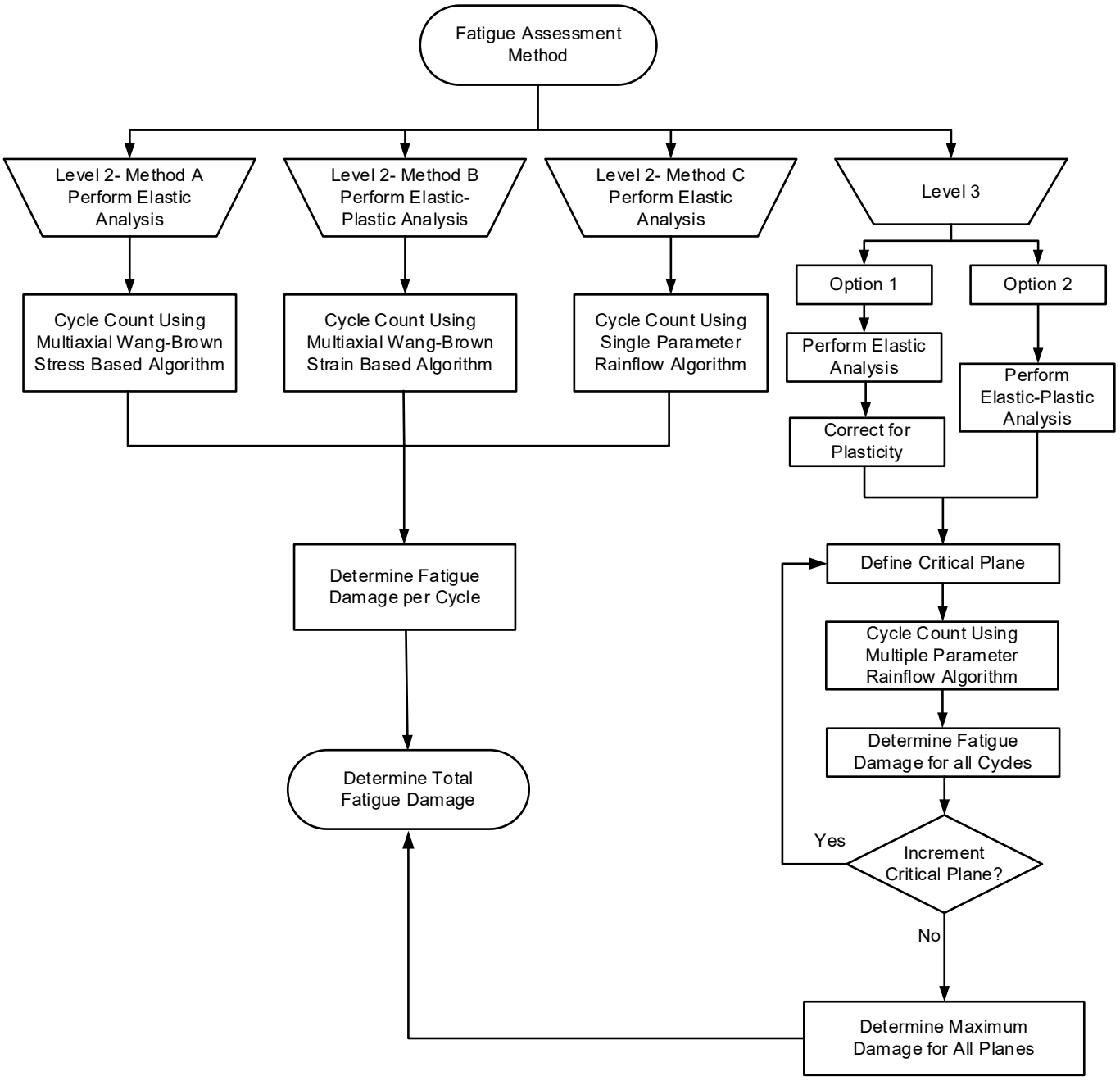

Figure 14C.1 – General Procedure for the Fatigue Assessment Method that Incorporates the Cycle Counting Algorithms Described in this Annex

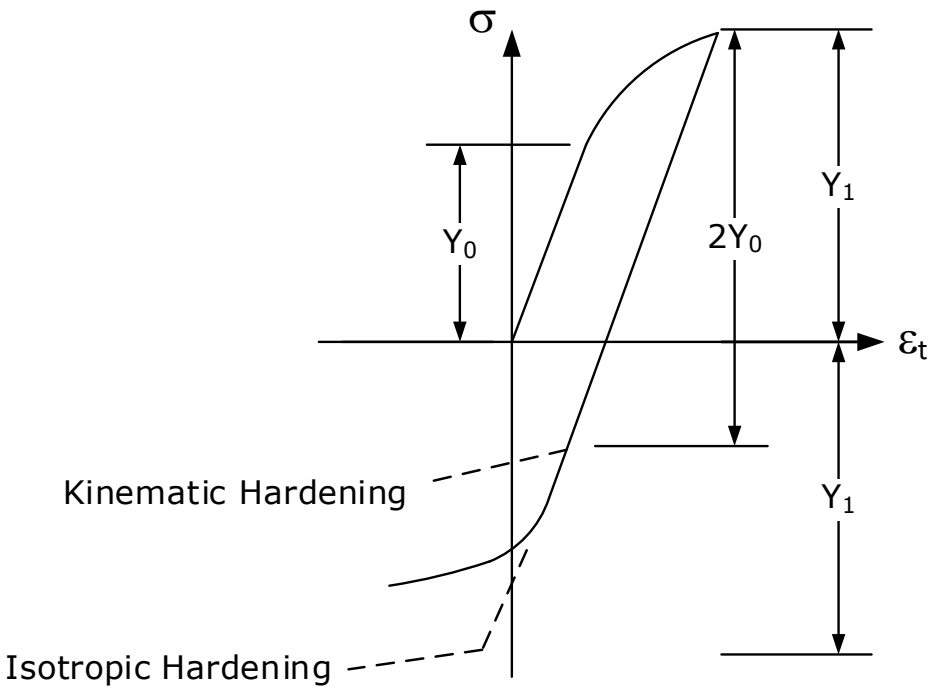

Figure 14C.2 – The Bauschinger Effect in Materials

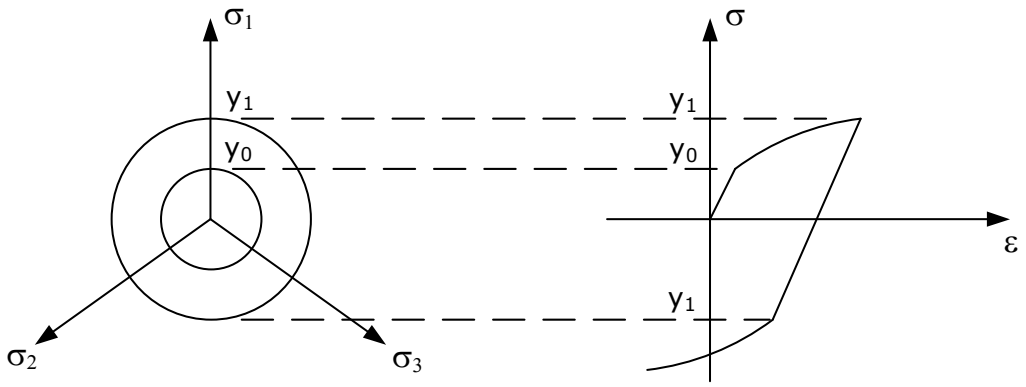

(a) Isotropic Strain Hardening Model

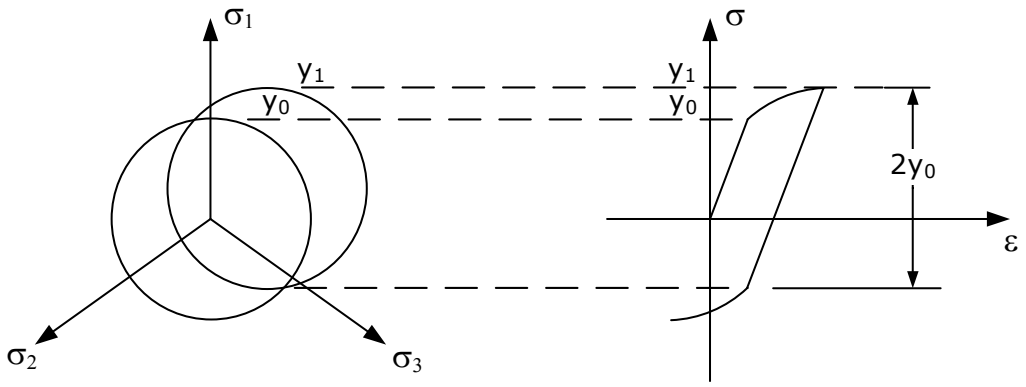

(b) Kinematic Strain Hardening Model

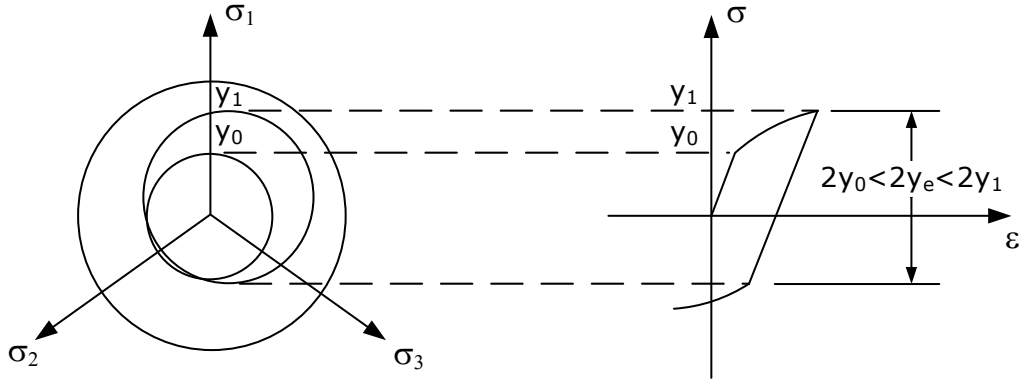

(c) Combined Strain Hardening Model

Figure 14C.3 – Plasticity Models

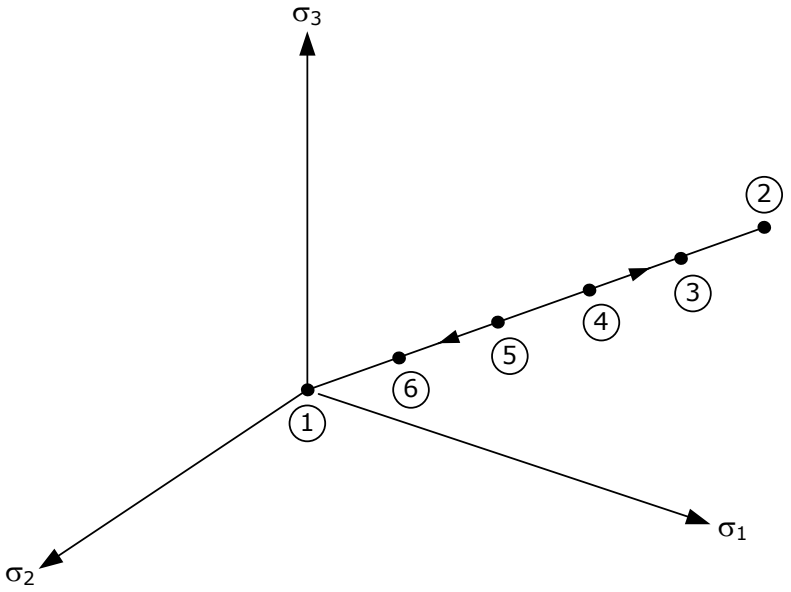

(a) Proportional Loading

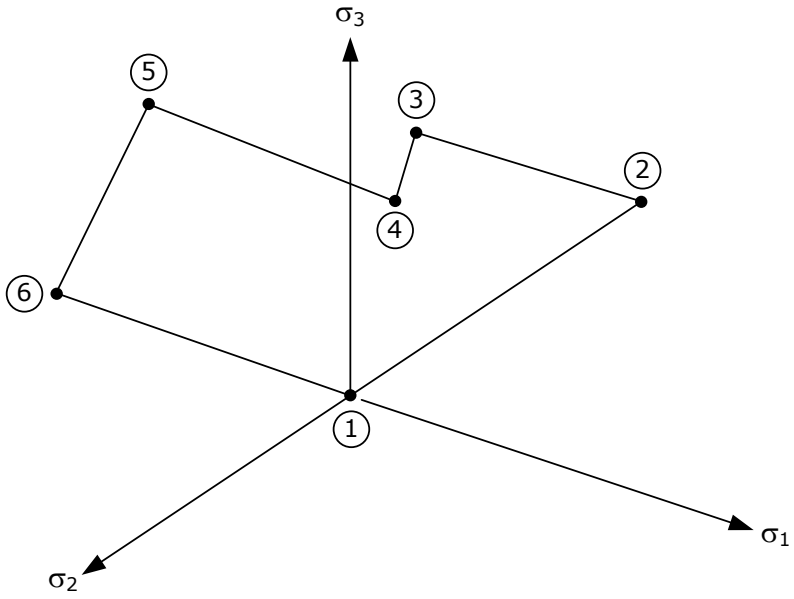

(b) Non-Proportional Loading

Figure 14C.4 – Visual Interpretation of Proportional vs. Non-proportional Loading History

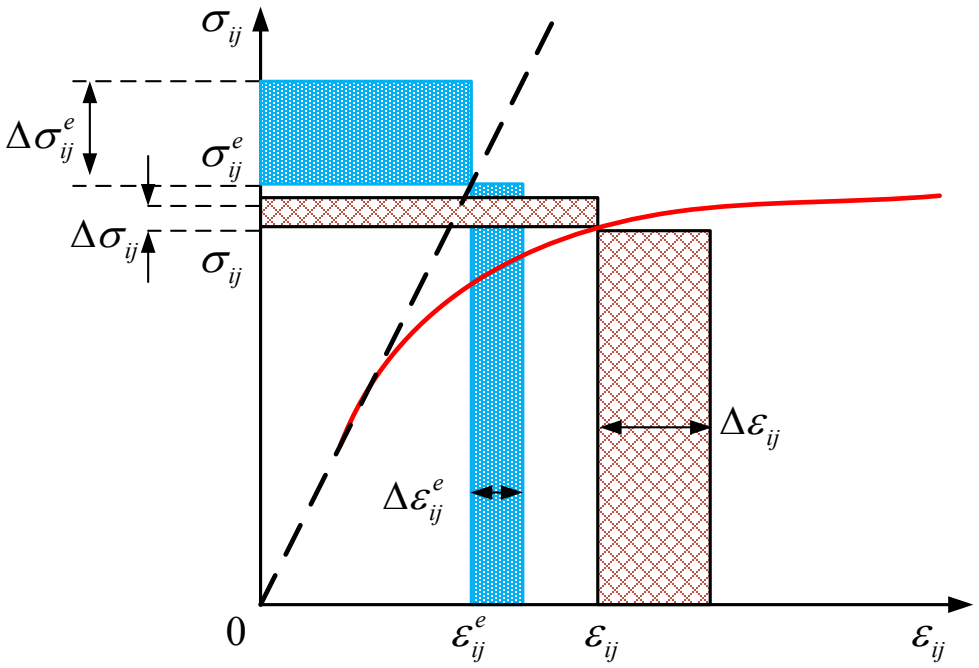

Figure 14C.5 – Visual Representation of the Incremental Neuber's Rule

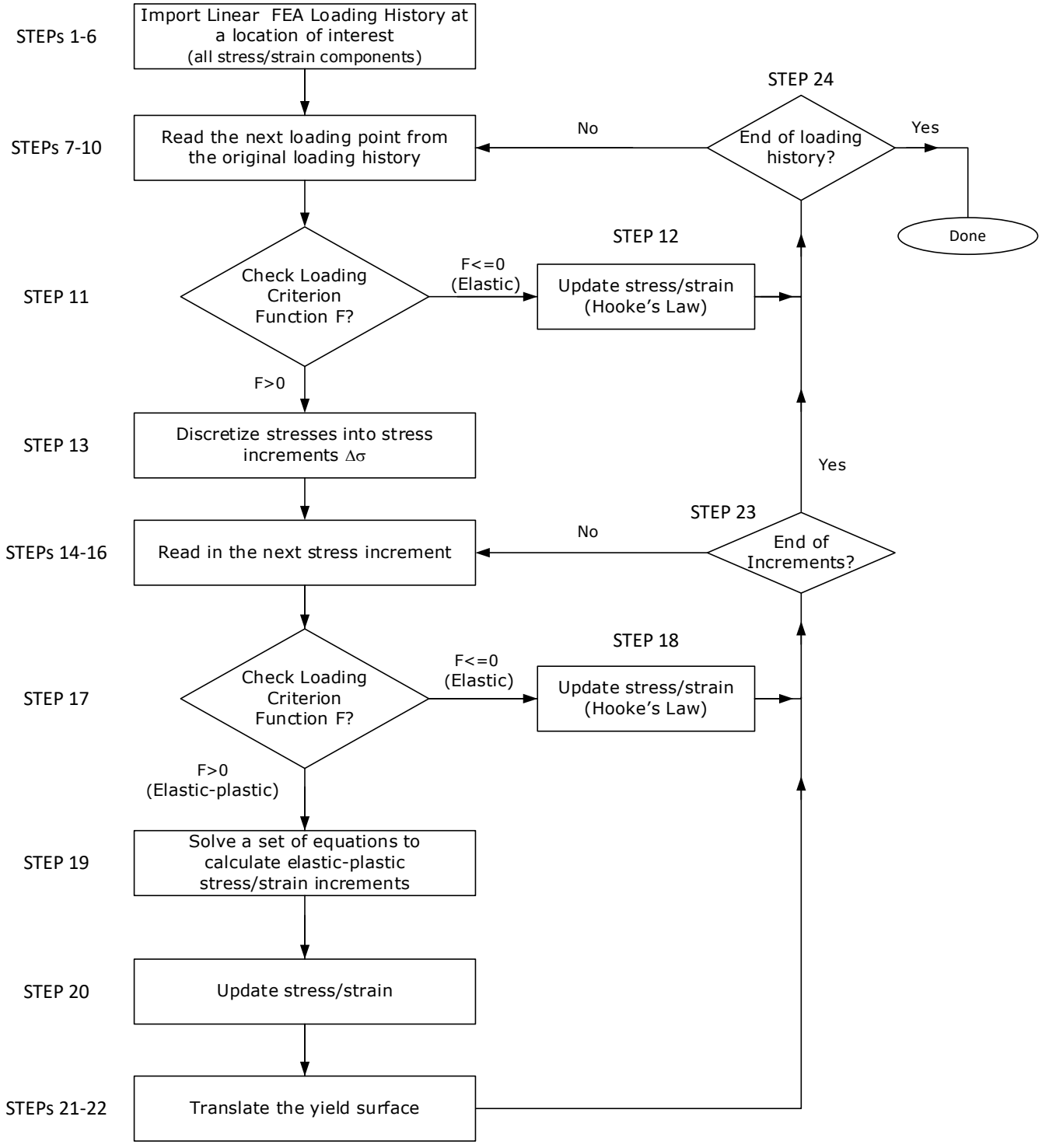

Figure 14C.6 – Multiaxial, Non-proportional, Incremental Neuber's Rule for Plasticity Correction

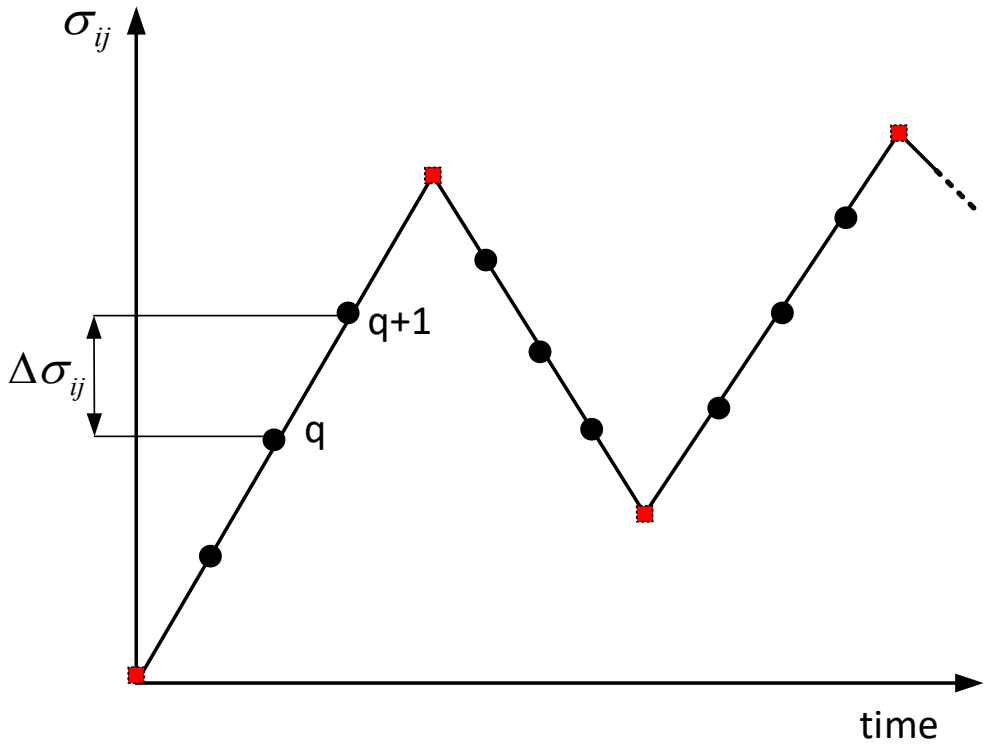

Figure 14C.7 – Example of an elastic loading history obtained by running a linear elastic FEA analysis and used as input to the Neuber plasticity correction algorithm. The red squares are the original FEA results while the black circles are the interpolated values used in the plasticity correction algorithm.

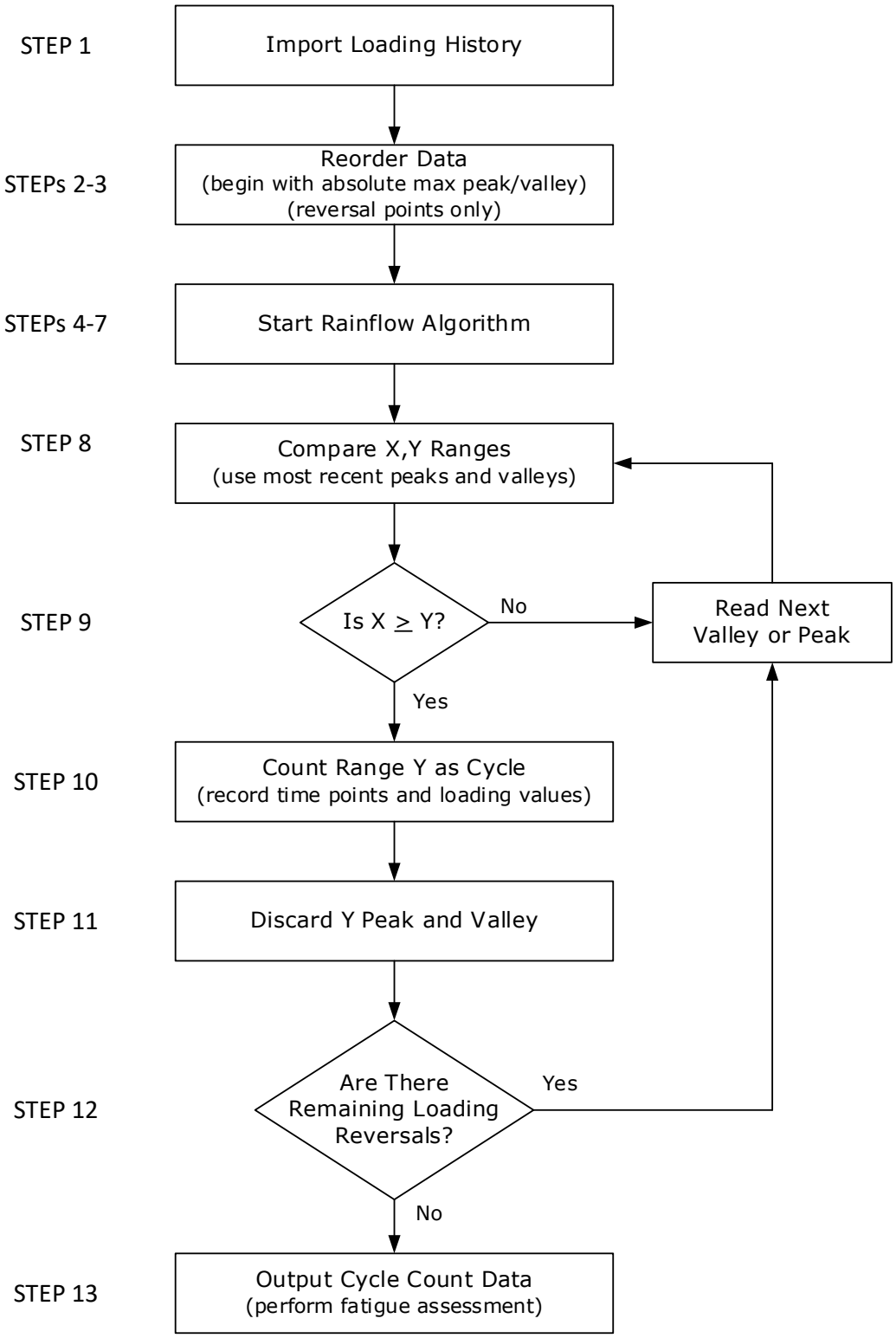

Figure 14C.8 – Procedure for the Uniaxial Rainflow Cycle Counting Algorithm

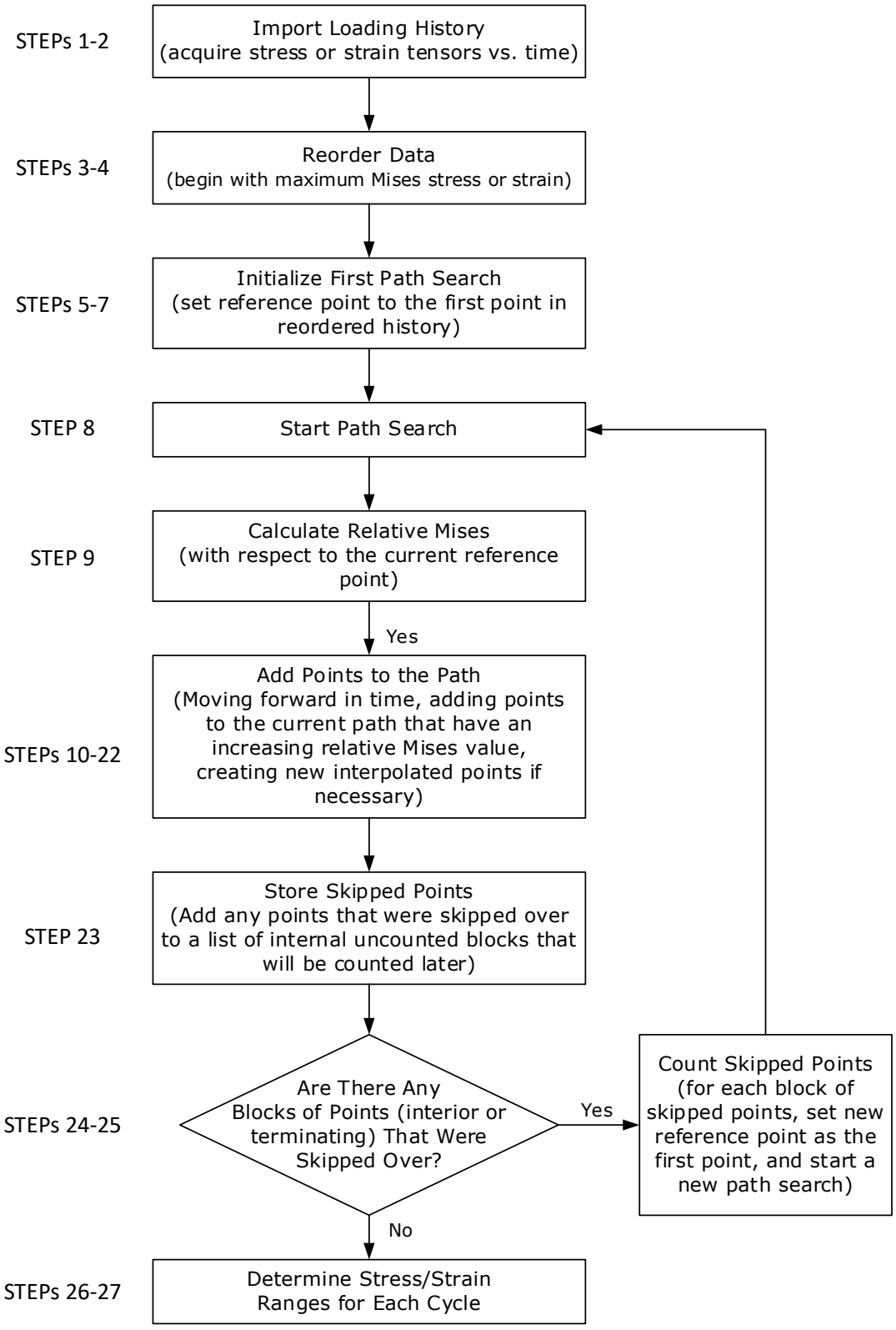

Figure 14C.9 – Procedure for the Multiaxial Wang Brown Cycle Counting Algorithm

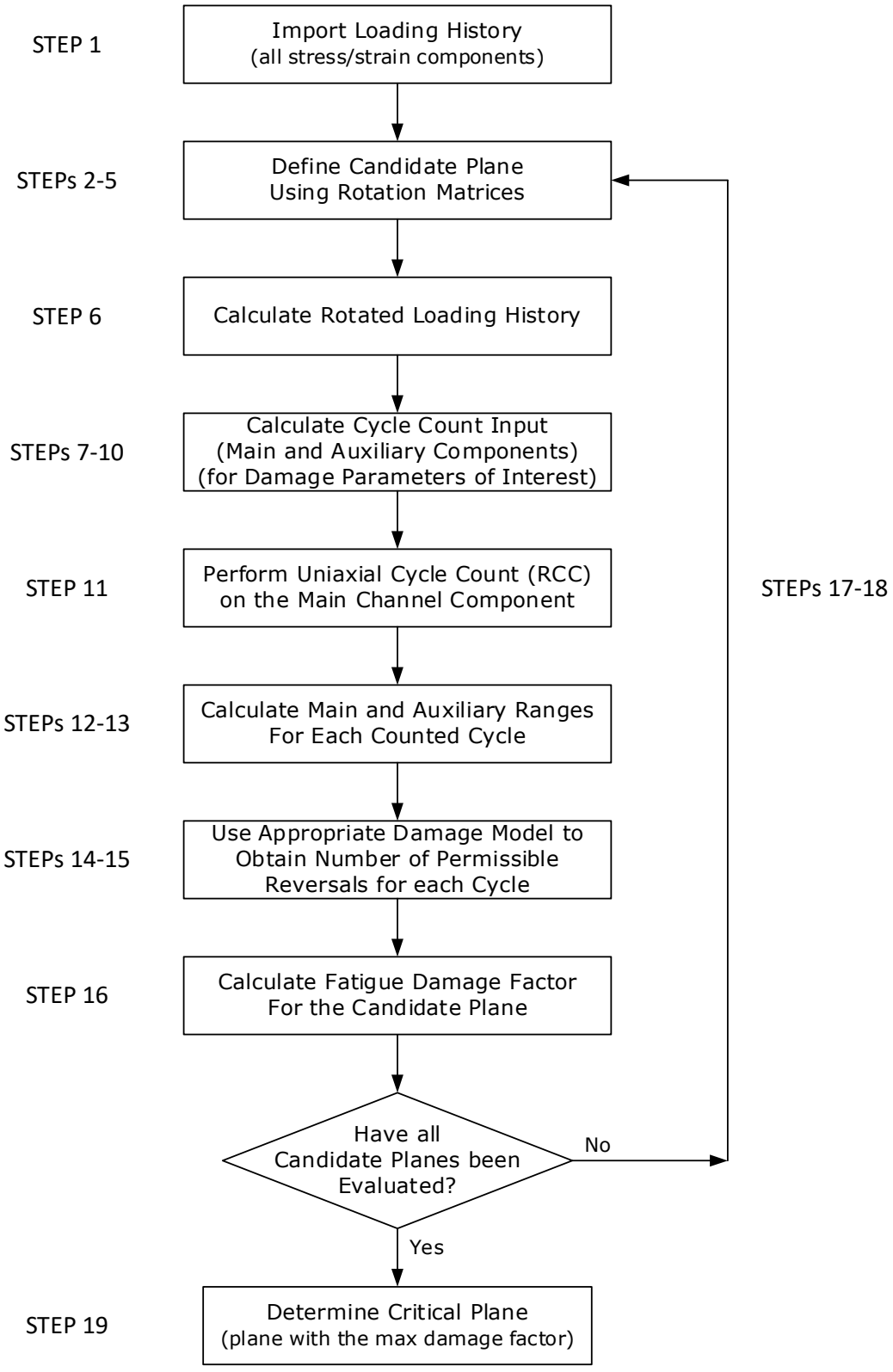

Figure 14C.10 – Procedure for the Multiaxial Critical Plane Cycle Counting Algorithm

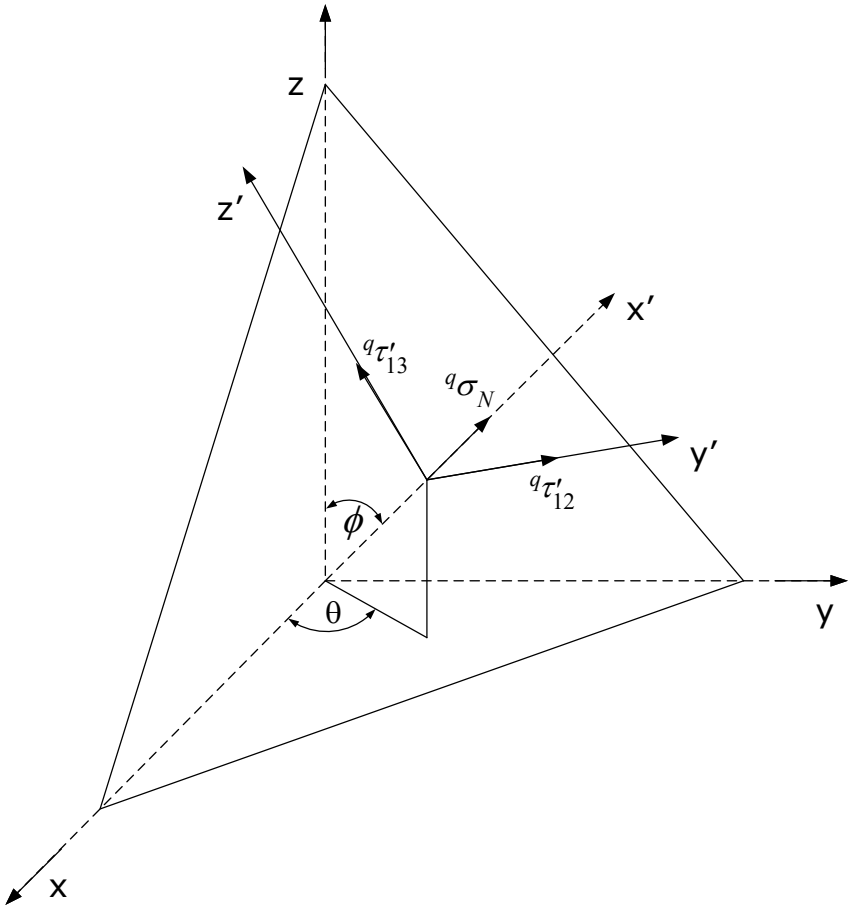

Figure 14C.11 – Transformation of the Cartesian coordinate system to the primed coordinate system for use in the Critical Plane Cycle Counting algorithm. The coordinate axis x' is normal to the candidate plane in consideration.

[Inentionally Left Blank]

[Intentionally Left Blank]

200 Massachusetts Avenue, NW
Suite 1100
Washington, DC 20001-5571
USA

202-682-8000

For additional information and to order:
Phone: 1.800.THE.ASME
(1.800.843.2763)
Email: customercare@asme.org
Website: asme.org

Additional copies are available online at www.api.org/pubs

Phone Orders: 1-800-854-7179 (Toll-free in the U.S. and Canada)
303-397-7956 (Local and International)
Fax Orders: 303-397-2740

Information about API publications, programs and services is available on the web at www.api.org.

Product No. C57904

ISBN 978-0-7918-7449-3